

Peter Laznicka

Giant Metallic Deposits

Future Sources of Industrial Metals

Peter Laznicka

Giant Metallic Deposits

Future Sources
of Industrial Metals

With 458 Figures and a CD-ROM

Peter Laznicka
64 Lochside Drive
5021 West Lakes
Australia

www.Totalmetallogeny.com

Library of Congress Control Number: 2006922186

ISBN-10 3-540-33091-7 Springer Berlin Heidelberg New York
ISBN-13 978-3-540-33091-2 Springer Berlin Heidelberg New York

This work is subject to copyright. All rights are reserved, whether the whole or part of the material is concerned, specifically the rights of translation, reprinting, reuse of illustrations, recitation, broadcasting, reproduction on microfilm or in any other way, and storage in data banks. Duplication of this publication or parts thereof is permitted only under the provisions of the German Copyright Law of September 9, 1965, in its current version, and permission for use must always be obtained from Springer-Verlag. Violations are liable to prosecution under the German Copyright Law.

Springer is a part of Springer Science+Business Media
Springeronline.com
© Springer-Verlag Berlin Heidelberg 2006
Printed in Germany

The use of general descriptive names, registered names, trademarks, etc. in this publication does not imply, even in the absence of a specific statement, that such names are exempt from the relevant protective laws and regulations and therefore free for general use.

Cover design: E. Kirchner, Heidelberg
Layout: Camera-ready by author
Production: Almas Schimmel
Printing: Krips bv, Meppel
Binding: Stürtz AG, Würzburg

Printed on acid-free paper 30/3141/as 5 4 3 2 1 0

Preface

This book has been written for those interested in, and concerned about, the future sources of metals for the industry, and through it for the rapidly growing population of the world. The poverty eradication, possible by 2025 according to Jeffrey Sachs, and the increase of living standards, will require a lot of new metals. At present over 95% of the industrial metals come from mines situated on land and the exceptionally large (giant or world-class) deposits contribute the bulk, regardless of where they are located: one of the most practically relevant lessons of globalization. This role of the oversize deposits is projected to persist until at least the end of this century, but finding them is going to be increasingly more costly and will require all the sophistication and effort the exploration community could muster. This requires a solid broad knowledge as the chance of finding an orebody by accidentally stumbling upon it, or by unsophisticated prospecting, has by now been severely reduced. As mineral exploration is, and will continue to be, mainly precedent-oriented activity, there has been a need for a comprehensive text to provide essential facts about the global distribution of metals now and in the future, above the textbook level.

This book consists of three parts (and a CD-ROM), although the parts are not explicitly marked as such. Part I (Chapters 1-3) starts with a short review of the changing sources and utilization of industrial metals, and it explains the various approaches to magnitude classification of ore deposits as related to geochemical backgrounds. Part II (the main body of the book; Chapters 4-14) is a factual review of the "giant" deposits in a rather loose empirical framework of depositional environments and rock associations. The spectrum of the geological settings follows the plate tectonic arrangement, but the plate tectonic concepts, as related to the actual ore formation, are used sparingly because many are still in the hypothetical domain, they change rapidly, and there is the ubiquitous multiplicity of interpretations. The emphasis here is on the demonstrable, lasting "facts" one can actually see in the field. The closing Part III (Chapters 15-17) deals with the common geological attributes of the "giants" and how they relate to the industrial needs. It ends up with some revelations as to how and where the future "giants" might be found.

In writing this book I have made a good use of the over 40 years long experience in the ore deposits field, and personal familiarity with at least 4,000 ore sites in some 140 countries and large territories, along with a multilingual reading capability. I have compressed many "facts" into a series of "inventory diagrams" of rocks and ore occurrences in close to 80 lithotectonic settings, interspersed throughout this book. The diagrams came from my electronic book "Total Metallogeny" and they also show the place of the ore types considered of limited significance, together with the "giants". This alleviates somewhat my feeling of guilt of catering to the "big and rich" only. The small deposits are, moreover, often indicators of the larger ore presence and have to be recognized and interpreted as such. Unfortunately the printing costs make it impractical to have the graphics printed in full color in the book, but this has been solved by repeating these graphs, in color, in the companion CD-ROM. Also on the CD-ROM is a fairly complete (more than 1000 entries) database of the "giant" and "world class" metal deposits of the world. I believe this book and database cover at least 90% of the eligible deposits and regions, including many of the metal sources of the future.

Although this book ends at page 732, the search for relevant ore information may have just started for some of the readers, willing to move farther on. The bulk of the 300 plus figures (mostly simplified cross-sections of ore deposits) have all

been uniformly drafted and modified after the original materials, referenced to the respective authors. They are all represented in the physical collection of geological materials called Data Metallogenica (more than 70,000 individual samples from almost 4,000 ore deposits of the world), presently installed in Adelaide, South Australia, and usually open for a free on-site inspection. There, the reader can actually see the "real thing" (samples are the "second best" source of knowledge after an actual mine visit) about which he/she reads, and even perform non-destructive tests and access the dedicated information folders.

Even before the journey down-under one can obtain an extensive supplementary visual experience by visiting www.Datametallogenica.com, an internet-based counterpart of the above collection, now operated by Amira International out of Melbourne. The website shows representative miniaturized rock/ore sample sets called LITHOTHEQUE, arranged in a unique way and stored library-style, as well as detailed images of thousands of samples photographed at an extremely high resolution. Each figure in the present book based on LITHOTHEQUE includes its corresponding number in Data Metallogenica, so finding it is a matter of minutes. Also available on the website are field photos and graphics from my sampling expeditions, and those supplied by the industry, governments and academia. Data Metallogenica is a non-profit undertaking, but it has to pay for itself so there is a subscription fee. Even without subscription, anyone can access the extensive free information preview in the Datametallogenica.com website.

Acknowledgments: The more than 1,500 references in this book make it clear that this is a collective undertaking, an extract of knowledge generated by hundreds of thousands of colleagues in the industry, governments and academia. The shared purpose and enthusiasm of my international peers supported a wonderful, politically neutral fellowship, very helpful in alleviating the antagonism that divides this world along political, religious, racial, wealth and other lines. My thanks thus go to the thousands of persons and organizations who provided direct or indirect help to keep my project moving, and all I can do is to print a short list of names, the tip of an iceberg. The main supporters were: Amira International, Christian Amstutz, Anglo-American Corporation, Australian Mineral Foundation, Australian Selection Ltd., Chris Bates, Rob Bills, BP Minerals, Alfred Bogaers, Bill Brisbin, Chen Guoda, Roy Corrans; CVRD Ltd., Directorate of Mineral Resources Jeddah, Peter Freeman, Geoscience Australia, Magnus Garson, Alan Goode, David Groves, G. von Gruenewaldt, Greg Hall, Paul Heithersay and PIRSA Adelaide, INCO Ltd., Mel Kneeshaw, Jan Kutina, Jim Lalor, Don Mustard, Národní Museum Praha, Normandy Ltd., Kerry O'Sullivan, Zdeněk's Pertold and Poubá, Rio Tinto Ltd., Dimitri Rundkvist, Phil Seccombe, Nikos Skarpelis, Art Soregaroli, Teck Ltd., Jim Teller, Universities of Manitoba, Charles (Prague), Heidelberg, Moscow State, New England, Oriente, Western Australia and Zimbabwe; Richard Viljoen, Western Mining Ltd, HDB Wilson, Karl Wolf, Roy Woodall, Zhai Yusheng.

The actual book writing has been a lonely affair, as one of the organizations that brought me to Australia (AMF) went out of business, so I have had to do without technical assistance from anywhere: a source of immense frustration in struggling with the computer while physically manufacturing the ready to print document. I am grateful to Springer-Verlag in Heidelberg for agreeing to publish my book, and thank Ms. Almas Schimmel for bringing it into production. Karl Wolf, as many times before, contributed his meticulous editing skills. My geological wife Šárka, a most reliable co-worker, deserves the greatest thanks.

Peter Laznicka, Adelaide, January 2006

Contents

Explanations, Abbreviations, Units.....	1
Context	1
Explanations, abbreviations.....	4
1 Civilization based on metals	7
1.1 Past and present sources of industrial metals.....	7
1.1.1 Introduction	7
1.1.2 History of metal supplies	7
1.1.3 Present metal supplies.....	11
1.2 Metal prices	12
1.3 Future metal supplies.....	15
1.3.1 How much metals will be needed?	15
1.3.2 Reducing demand for "new" metals	19
1.4 Conclusion: future supplies of metals and giant deposits	29
2 Data on metallic deposits and magnitude categories: the giant and world class deposits	35
2.1 Data sources and databases.....	35
2.2 Giant and world class ore deposits: definition and characteristics	38
2.3 Dimension, complexity and hierarchy of metallic deposits	44
2.4 The share of "giant" metal accumulations in global metal supplies	47
3 From trace metals to giant deposits	55
3.1 Introduction	55
3.2 Extraterrestrial metals and ore formation resulting from meteorite impact.....	56
3.3 Lithospheric evolution and geochemical backgrounds to metals concentration and accumulation	59
Introduction to Chapters 4 to 14	65
4 Mantle to oceans	71
4.1 The mantle	71
4.1.1 Mantle metallogeny	72
4.2 Oceanic crust, ocean floor	73

4.2.1	Oceanic spreading ridges	73
4.3	Intraplate volcanic islands, seamounts and plateaux on oceanic crust	77
4.4	Sea water as source of metals	77
4.5	Ocean floor sediments.....	78
5	Young island arcs.....	81
5.1	Island arc metallogeny and giant deposits	82
5.2	Island arc-trench components and ore-forming processes	83
5.3	Porphyry Cu-Au-(Mo) deposits in young island arcs	90
5.4	Epithermal Au-(Ag) deposits.....	94
5.5	Young subaqueous-hydrothermal (Fe)-Zn-Pb-Cu (and Ag,Au-Sb,As) deposits (VMS, kuroko-type).....	97
5.6	Magnetite beach sands	100
6	Andean-type margins	101
6.1	Introduction.....	101
6.2	Metals fluxing and metallogenesis.....	104
6.2.1	Ores in predominantly continental sediments	107
6.2.2	Ores in contemporaneous and "young" subaerial volcanics	109
6.2.3	Ores in ancient continental margin volcanics, predominantly andesite	115
6.2.4	"Red beds" in andean margins	118
6.2.5	Ores in andean margin rhyolites	118
6.3	Epithermal deposits and hot springs	120
6.3.1	Hot spring deposits	121
6.4	High-sulfidation epithermal ores	122
6.4.1	Low-grade ("bulk"), low-sulfide Au-Ag deposits	123
6.4.2	Transition to sulfides-rich high-sulfidation Au-Ag systems.....	125
6.4.3	Diatreme-dome complexes with enargite-gold centers surrounded by pyrite, Zn-Pb-Ag carbonate replacements	126
6.4.4	Combined high sulfidation/porphyry Cu-Au-Ag systems.....	129
6.5	Low sulfidation (LS) deposits.....	131
6.5.1	Au-dominated low-sulfidation ores	132
6.5.2	Au-(Te)>Ag alkaline association	135
6.5.3	Bonanza Ag >> Au	136
6.5.4	Epithermal to mesothermal Pb, Zn (Cu), Au, Ag deposits	139
6.5.5	Other epithermal deposits: Mo, W, Bi, U, As, Sb, Te.....	140
6.5.6	LS deposits as part of a system: other related mineralization?	142
6.5.7	"Bolivian-type" porphyry Sn-bonanza Ag composite association.....	143
6.6	Carlin-type micron-size Au (As, Hg, Sb) deposits.....	147
6.6.1	"Invisible gold" in the Great Basin	149
6.6.2	"Carlin-type" gold outside the U.S.A.....	152

7 Cordilleran granitoids.....	153
7.1 Introduction	153
7.2 Metallogeny	154
7.3 Porphyry deposits	157
7.3.1 General and calc-alkaline	157
7.3.2 Breccias in porphyry systems	159
7.3.3 Evolution of mineralized calc-alkaline "porphyry" systems, alterations, ores	164
7.3.4 Alkaline (diorite-model) porphyry Cu	165
7.3.5 Combined porphyry Cu (Mo, Au)-skarn deposits	168
7.3.6 Precambrian porphyry-style Cu, Mo, Au deposits.....	171
7.3.7 Supergene modification of porphyry deposits	171
7.3.8 Porphyry Cu: global distribution and deposit descriptions.....	180
7.4 Stockwork molybdenum deposits	199
7.4.1 Differentiated monzogranite Mo suite	200
7.4.2 High-silica rhyolite suite (Climax-type).....	201
7.4.3 Stockwork Mo in the alkaline "rift" association	204
7.4.4 Precambrian stockwork Mo "giants"	204
7.4.5 Mo-dominated skarn deposits.....	205
7.5 Stockwork, vein and skarn Mo-W-Bi	207
7.6 Scheelite skarn deposits.....	209
7.7 Cordilleran Pb-Zn-Ag (Sb) deposits.....	212
7.7.1 High-temperature Zn, Pb, Ag replacements in carbonates	212
7.7.2 Mesothermal Pb-Zn-Ag (Sb) veins.....	218
7.8 Hydrothermal Fe, Mn, Sb, Sn, B, U, Th deposits in, and associated with, Cordilleran granitoids	220
 8 Volcano-sedimentary orogens.....	 225
8.1 Introduction	225
8.1.1 Growth and evolution of composite eugeoclinal orogens as exemplified by the Canadian Cordillera	227
8.2 Ophiolite allochthons, melanges and alpine serpentinites	229
8.3 Oceanic successions	233
8.4 Mafic and bimodal marine volcanic-sedimentary successions	235
8.4.1 VMS deposits	235
8.4.2 Sedimentary rocks-hosted Fe, Cu, Zn, Pb ores	242
8.4.3 Au-Ag deposits	243
8.5 Differentiated mafic-ultramafic intrusions (Alaska- Urals type)	243
8.6 Calc-alkaline and shoshonitic volcanic-sedimentary successions	245
8.7 Sundry metallic ores	249
 9 Precambrian greenstone-granite terrains	 252
9.1 Introduction	252

9.1.1	Abitibi Subprovince (greenstone belt), Canadian Shield	253
9.2	Komatiite association and Ni ores	256
9.3	Early Proterozoic paleo-ophiolites	260
9.4	Mafic and bimodal greenstone sequences: Fe-ores and Cu-Zn VMS deposits	
9.4.1	Mafic (meta-basalt) sequences and banded iron formations	262
9.4.2	VMS deposits in bimodal and sequentially differentiated volcanic-sedimentary sequences.....	264
9.5	Granitoid plutons and older Precambrian "porphyry" deposits	272
9.6	(Syn)orogenic hydrothermal Au-(As, Sb, Cu) in greenstone terrains	273
9.7	Synorogenic Cu (U, Ni, Au, Ag) deposits overprinting greenstone belts	290
9.8	Ores in late orogenic sedimentary rocks in greenstone belts.....	292

10 Intracratonic orogens, granites, hydrothermal deposits 295

10.1	Introduction.....	295
10.1.1.	Granitoids in orogenic setting.....	296
10.2	Massif anorthosite association: Fe-Ti-V and Ni-Cu deposits	303
10.3	Ores closely associated with granites.....	305
10.3.1	Rare metals pegmatites	305
10.3.2	Zr, Nb, Ta, Y, REE, Th, Be association in peralkaline granites.....	310
10.3.3.	Uraniferous leucogranites, aplites, pegmatites.....	312
10.3.4	Granite-related wolframite deposits (Jiangxi-type).....	313
10.3.5	Granite-related tin deposits	315
10.3.6	Cassiterite regoliths and placers.....	321
10.3.7	Multi-metal zoned Sn, Mo, W, Bi, Be, Pb, Zn skarn-greisen-vein systems	323
10.3.8	Hydrothermal U deposits	327
10.4	Mesothermal gold	331
10.4.1	Intrusion ("granite")-related Au veins, stockworks, disseminations	
10.4.2	Gold skarns	333
10.4.3	Transition of granite-related to (syn)orogenic Au deposits	335
10.5	Dominantly orogenic Au deposits.....	339
10.5.1	(Syn)orogenic gold veins and stockworks	339
10.6	Gold placers	346
10.7	(Syn)orogenic Sb and Hg deposits.....	349
10.7.1	Antimony deposits	349
10.7.2	Mercury deposits.....	355
10.8	Pb, Zn, Ag veins and replacements	358

11. Proterozoic Intracratonic Orogens and Basins:	
Extension, Sedimentation, Magmatism	367
11.1	Introduction367
11.2	Metallogeny and giant deposits369
11.3	Proterozoic Pb-Zn-Ag "sedex" deposits374
11.4	Strata controlled Proterozoic copper deposits in (meta)sedimentary rocks.....377
11.5	Au and U in quartz-rich conglomerate (Witwatersrand- type).....385
11.6	Fe in Superior-type banded iron formations (BIF)394
11.7	Fe (BIF) and Mn in diamictites.....403
11.8	Bedded and residual Mn deposits406
11.9	Miscellaneous, complex Zn, Pb, Cu, Co, V, Ag, Ge Ga, (U) sulfide deposits409
11.10	Oxidic (nonsulfide) Zn and Pb deposits.....411
11.11	Unconformity uranium deposits412
11.12	Hydrothermal Fe-oxide deposits with Cu, or U, or Au, or REE (Olympic Dam-type).....415
12 Rifts, paleo-rifts, rifted margins, mantle plumes, anorogenic and alkaline magmatism.....	425
12.1	Introduction425
12.2	Young rifts, hydrothermal activity.....428
12.3	Mantle plumes, continental breakup, rifted continental margins430
12.3.1	Hot spots and mantle plumes430
12.3.2	Rifted (Atlantic-type) continental margins430
12.3.3	Intraplate and rift margin mafic to bimodal magmatism.....432
12.4	Plateau (flood) basalts.....434
12.4.1	Ni-Cu sulfide deposits in intrusions associated with plateau basalt provinces434
12.4.2	Lateritic bauxite on basalt.....439
12.5	Diabase, gabbro, rare peridotite dikes and sills440
12.6	Bushveld-style layered intrusions443
12.7	Sudbury complex Ni, Cu, Co, PGE, Ontario: an enigma.455
12.8	Alkaline magmatic association459
12.8.1	Introduction459
12.8.2	Alkaline metallogeny and giant deposits461
12.8.3	Alkaline volcanic and subvolcanic centers462
12.8.4	Nepheline syenite-dominated intrusions.....463
12.8.5	Alkaline pyroxene-nepheline series and alkaline ultramafics467
12.9	Carbonatites470
13 Sedimentary associations and regolith	
13.1	Introduction480
13.2	Marine clastics481
13.2.1	Ore formation482

13.2.2	Detrital (clastic) ores: coastal and shelf heavy mineral sands and paleoplacers of Fe, Ti, Zr, REE, Th	484
13.3	Combined clastic and chemical bedded sedimentary deposits	487
13.3.1	Particulate (oolitic) ironstones	487
13.3.2	Bedded Mn deposits (Phanerozoic)	490
13.3.3	Mineralized carbonaceous pelites ("black shales")	492
13.3.4	Phosphorite-black shale association.....	497
13.3.5	Cu, Ag (Pb, Zn, Au, PGE) associated with reduced marine units above "redbeds" (Kupferschiefer or copper shale-type).....	500
13.3.6	Sedex Pb-Zn-Ag deposits in basinal shale near carbonate platform	503
13.4	Marine carbonates and evaporites	509
13.4.1	Introduction.....	509
13.4.2	Warm current (Florida-type) phosphorites and their uranium enrichment	512
13.4.3	Bedded Mn deposits in "basinal" (reduced) carbonates	513
13.4.4.	Low-temperature Zn-Pb deposits in carbonates	513
13.4.5	Discordant (vein) Zn-Pb orebodies of "MVT affiliation"	522
13.4.6	Stratabound cinnabar deposits in carbonates	522
13.4.7	Metallic ores in karst on carbonates.....	523
13.5	Marine evaporites and metallic ores	525
13.6	Hydrocarbons as a source of metals.....	526
13.7	Regolith and continental sediments	528
13.7.1	Introduction.....	528
13.7.2	Glaciation and ores in glaciogenic (cryogenic) materials and structures, related talus and glacio-fluvial deposits	529
13.7.3	Humid tropical regoliths	529
13.7.4	Supergene Cu ores and leaching/precipitation profiles	538
13.7.5	Paleo-regoliths, paleosols and basal sequences at unconformities	541
13.7.6	Humid alluvial environments: placer deposits	542
13.7.7	Lakes and lacustrine sequences.....	544
13.7.8	Arid regoliths and sediments.....	545
13.7.9	Sandstone-dominated continental sequences: "gray" and "red"	548
13.7.10	Metals recoverable from coal.....	549
13.7.11	Infiltrations from meteoric waters: "sandstone U (V)" deposits	550
13.7.12	Cu-sandstone deposits in red and gray (varicolored) beds	555
13.7.13	Sandstone Pb-(Zn) deposits	556
13.8	Anthropogenic metal sources.....	559
14	Higher-grade metamorphic associations	561
14.1	Introduction	
14.2	Metallogeny	563
14.3	High-grade associations and ores.....	565

14.4	High-grade metamorphosed banded iron formations (BIF)	567
14.5	Pb-Zn-Ag sulfide orebodies in gneiss >> marble, Ca-Mg-Mn silicates: Broken Hill-type	568
14.6	Zn, Pb sulfide orebodies in marble and Ca-Mg silicates, and Zn-Mn oxide orebodies in marble	571
14.7	Zn, Cu, Pb sulfide deposits in gneiss, schist, marble (meta-VMS?)	574
14.8	Disseminated Cu sulfide deposits in gneiss, schist and marble	576
14.9	Scheelite, uraniferous phosphates, magnesite, borates in marble and Ca-Mg silicate gneiss	577
14.10	High-grade metamorphic mafic-(ultramafic) associations	579
14.11	Structures subjected to retrograde metamorphism and metasomatism	584
15 Giant deposits in geological context		589
15.1	Origin of the giant deposits	589
15.1.1.	Genetic coding and ore varieties	590
15.1.2	Giant deposits and their genetic and host rock associations	598
15.2	Giant metallic deposits: geotectonic setting	605
15.3	Giant metal accumulations in geological time	606
15.4	Why "giants" are so big and are where they are?	610
16 Giant deposits: industry, economics, politics		613
16.1	Historical background	613
16.2	Giant deposits and corporations	616
16.3	Giants' economics	620
17 Finding or acquiring giant deposits		628
17.1	Introduction	628
17.2	History of discovery of giant ore deposits/districts	631
17.3	Acquiring giant deposits for tomorrow	640
17.3.1	Acquisition of an existing deposit	641
17.3.2.	International risk assessment	642
17.3.3	Acquiring "giants": geology perspective	646
References		649
Locality index		707
Subject index		719

CD-ROM (attached):**Supplementary materials to accompany the book Giant Metallic Deposits and Future Sources of Industrial Metals**

Peter Laznicka (2006)

README

This CD-ROM contains materials that supplement the text, presented in my book "Giant Metallic Deposits", that would be impractical or too costly to have in the book itself. There are two parts: 1) a database, and 2) selection of 79 rock/ore inventory diagrams, interspersed as black-and-white figures throughout the book, here repeated in color.

CONTENTS

Note: the CD-ROM has an independent page numbering

Part 1, Database GiantdepShort

Introduction	2
Explanations	2
Table 1, organized by book page numbers	4
Table 2, organized by metals and localities	25
Table 3, organized by localities (deposits, areas)	46

Part 2, Total Metallogeny Geosites (book figures in color)

Introduction	67
Directory of Geosites organized by book Chapter and Figure numbers	67
Directory of Geosites organized by the "G" numbers (as in Total Metallogeny)	69
Geosites (Figures) pages: total 79.....	71

Explanations, Abbreviations, Units

Context

As explained in Preface, this book is a self-contained member of a broader knowledge system on the world's mineral deposits and their settings I have been developing and experimenting with for more than 40 years. It is a product of global first-hand information gathering in the field and "data mining" from the literature, followed by sorting and organization into interrelated sets searchable and accessible by the rapidly evolving techniques of modern information technology. From day one geological tangibles, rocks and ores, have been an important (in fact, fundamental) component of the knowledge system, because of their ability to preserve the "objective and permanent truth" that does not change with continuously mutating concepts. Miniaturization, unique organization and progress in electronic image transfer have made it possible for a reader to instantly move from reading printed information in a traditional book into high-resolution displays of images of representative rock/ore sets and site photographs and graphics, all in bright color and continuously updated. If convinced, he or she can even visit and peruse the original material and perform non-destructive tests!

This book, in particular, is closely related to three members of the "ore knowledge family" with which it shares the presentation philosophy and some materials such as figures. They are briefly reviewed below:

1. A set of Empirical Metallogeny books (Laznicka, 1985, 1993) where mineral deposits of the world are organized by formational environments and lithologic associations in which they occur. The emphasis is on factual information that form the background of search for analogues in the field. Although the 1985 book especially is now rather dated, both books contain data on a myriad of lesser size deposits not included in the present volume.

2. Total Metallogeny-Geosites (Laznicka, 2004), a graphic knowledge base that provides basic geological and metallogenic information on 240 depositional environments and rock associations, and shows the usual sites of ore deposits (Fig. A.1). In addition to brief, database-style description, the work (a hardcopy book and a 3x1 m poster, both in

color and also available on DVD-ROM) comprise 240 color graphs (graphics). The graphs are stylized cross-sections reminiscent of ore deposit models widely available from the literature, but their main role is to provide inventory of the rocks and ores to be encountered in a given setting. For that reason I refer to them as "inventory diagrams". They are most helpful for browsing and ideas gathering by explorationists and for people engaged in evaluation of territories for mineral prospectivity. The diagrams include all metallic deposits (not only the "giants" treated here) which is essential in order to gain a balanced picture about ore distribution, as many lesser ore occurrences have an indicative value in search for the "elephants". 70 of these Total Metallogeny diagrams have been reprinted here, in black and white, and they appear in color in the attached CD-ROM. Complete information is available from the original reference (Laznicka, 2004). For more information, please visit www.Totalmetallogeny.com.

3. LITHOTHEQUE, a "rock library", is a collection of some 3,400 page-size aluminum plates, each of which contains up to 20 permanently attached miniature rock and ore samples. Most plates provide a tangible record (documentation) of mostly visually recognizable materials present in an ore deposit (or a lithologic association, environment), arranged in a uniform way, thus ideal for comparisons (Fig. A.2). I have collected 95% of the material that comes from almost 4,000 deposits and occurrences in 144 countries and large territories of the world, and assembled all of them in the period of 35 years (between 1970 and 2005). Many of the deposits represented have been mined out and reclaimed so they are no longer accessible.

Every LITHOTHEQUE plate is equipped with an explanation sheet that comprises a graph (usually a cross-section of a deposit), legend describing the numbered units and ore types shown in the graph, and identifying the individual samples actually present on the plate (Fig. A.3). The graphs are based on published literature, some unpublished material (mostly mine handouts) and several original field sketches. All have been prepared in a uniform way to facilitate comparison.

ARCS 3 (continental)

← GEOSET
GEOSITE

31. ANDESITE-DACITE-RHYOLITE & PLUTONICS 32. RHYODACITE-RHYOLITE GRANODIORITE-GRANITE 33. LATITE-TRACHYTE MONZONITE-SYENITE

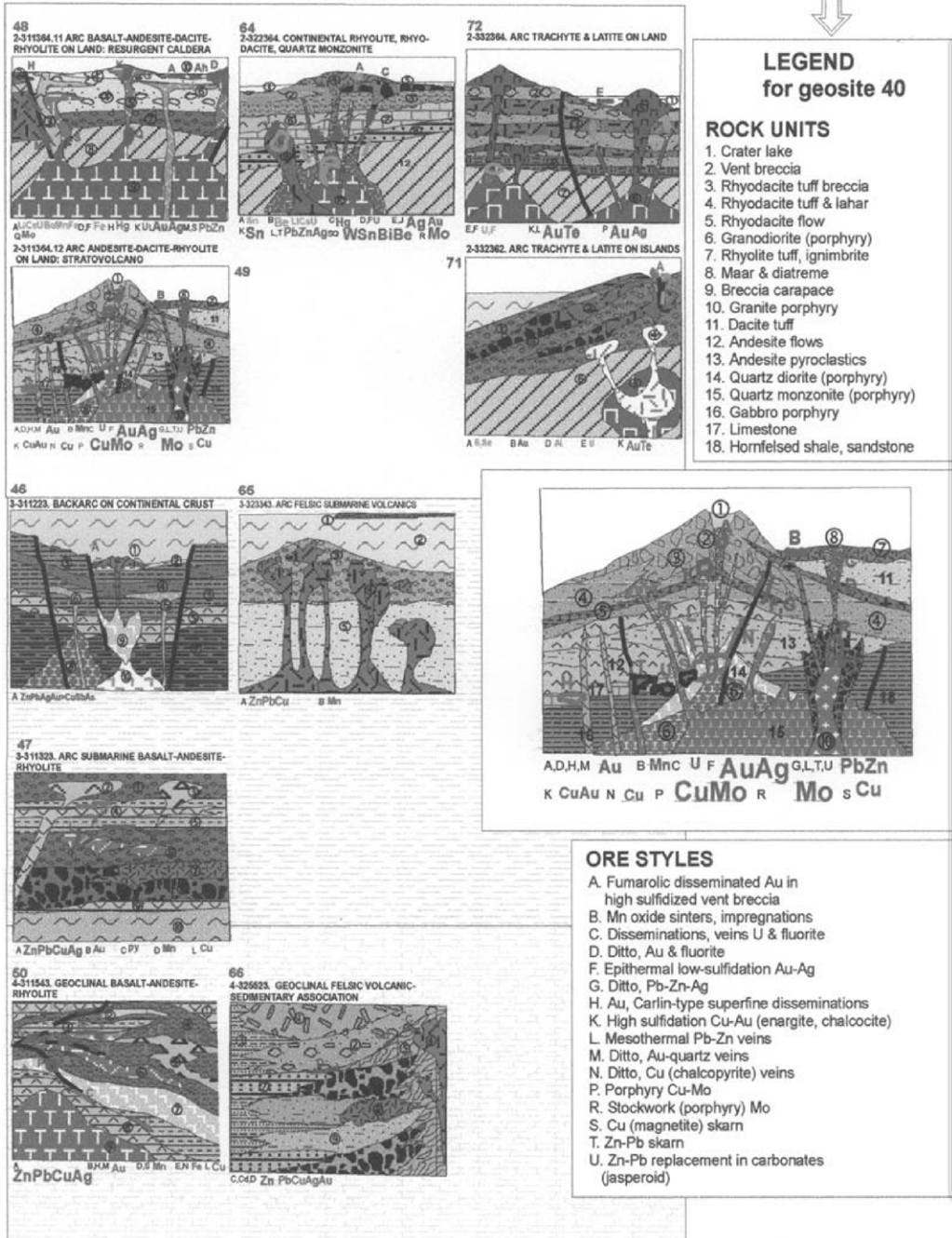


Figure A.1. Selection of rock and ore inventory diagrams in the division of magmatic arcs established on continental crust, some of which have been reprinted in this book. From Laznicka (2004), Total Metallogeny

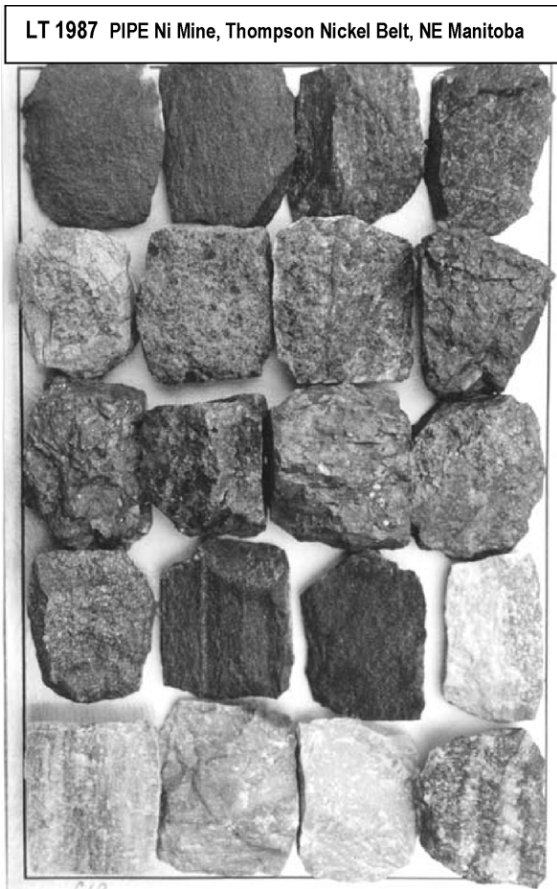


Figure A.2. Photograph of an average LITHOTHEQUE set (about 18 x 28 cm size) with twenty miniature rock and ore samples permanently attached to an aluminum plate and arranged in a standard order (oxidized ores - primary ores - alterations - host rocks) to facilitate comparison. This plate is of the Pipe Mine in the Thompson Nickel Belt, Manitoba and is a part of the Data Metallogenica knowledge base.

Although most of the graphs are based on, and referenced to, the original authors, the figures have been modified, often to a substantial degree, to maintain uniformity and be up to date. I accept responsibility for the inevitable errors that could be present: do not blame the original authors!

Most of the cross-sections of ore deposits that appear in this book have been reprinted from the Lithotheque explanatory sheets, together with shortened and edited legends, and referenced as "from LITHOTHEQUE No. 2563" followed by references to the original source(s). The copyright of the original explanatory sheets of which the graph is a part is thus vested with the Lithotheque collection and its owner, that can change with time.

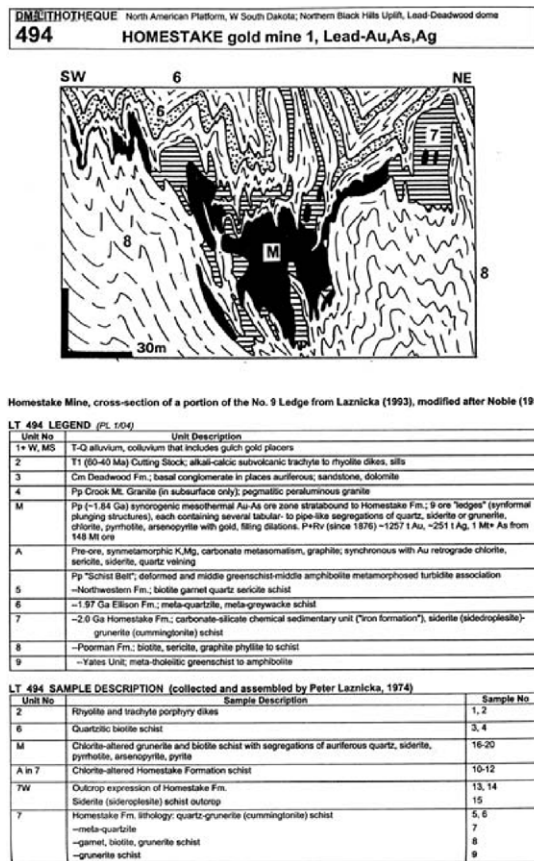


Figure A.3. Example of an explanation sheet of a Lithotheque sample plate (this one applies to the Homestake Au mine, South Dakota). Under the title with a plate number is a simplified cross-section of the orebody. The top text paragraph under the graph is a legend to the numbered and lettered units shown in the graph, whereas the bottom paragraph identifies and briefly describes the samples attached to this Lithotheque plate. Figures reprinted in this book correspond to the graph with edited legend only, whereas the entire explanation sheet can be downloaded and printed, by subscribers, from www.Datametallogenica.com.

At present (2005) Lithotheque is the "flagship" of Data Metallogenica, a broader knowledge system presently owned by Amira International of Melbourne (www.amira.com.au). The physical collection, that also includes an extensive suite of conventional size samples (Macrotheque) and archive of dedicated reprints, notes and photos, is in Adelaide, South Australia, and can be visited free of charge (Fig. A.4). The images of entire Lithotheque plates as well as a number of individual samples, photographed at a very high resolution, are available from the Data Metallogenica website (www.Datametallogenica.com) accessible by

subscription (but with an extensive free preview and list of included deposits). This site also offers printable explanation sheets for all Lithotheque plates.



Figure A.4. Data Metallogenica collection installed in Adelaide, South Australia. More than 3,400 Lithotheque plates are stored, library-style, in slotted cabinets and have an instant accessibility.

Explanations of uniform styles, numbering and lettering used in figures marked "from LITHOTHEQUE"

Numbers	Rock units, arranged from the youngest to the oldest
M	Mineralization; sites of metal accumulation, in most cases economic orebodies. Massive to densely distributed ores are shown in solid black; disseminated, stringer, etc. ores are shown by outline
M1, M2...	Various styles of mineralization
MW	Weathering-modified "primary" orebodies, e.g. gossans, oxidation zones
A	Hydrothermally altered rocks
A1, A2....	Various types of alteration
MA	Mineralization and alteration considered jointly
F	Fault filling rocks (e.g. gouge, breccia, mylonite, phyllonite, etc.); fault traces are shown as wavy lines, usually not labeled
FA	Hydrothermally altered fault rocks
Bx	Breccias
W	Weathered rocks (and ores)
W3, 5W....	Weathered numbered rock units

Geological ages

They are widely abbreviated in figures, tables and lists as letter codes, or they have the form of Ma (millions of years ago) or Ga (billions of years ago). In explanations to the "from LITHOTHEQUE" graphs letter abbreviations (e.g. Pe=Permian; Cm=Cambrian) or Ma/Ga values appear at the start of the explanatory sentence, e.g. Cm3 Bonnetterre Formation limestone. 1, 2, 3 stand for Lower, Middle and Upper, e.g. Cm3=Upper Cambrian. For list of abbreviations please see Table A.1.

Table A.1. Abbreviations of geological ages used in figures, tables and lists. Most abbreviations correspond to Series but if this is not available (or the age spans several Series) a System, Erathem or Eonothem are used. The geochronology is after the International Union of Geological Sciences 1989 Global Stratigraphic Chart.

Stratigraphic division	Age Ma	Abbreviation
Phanerozoic		PhZ
Cainozoic		CZ
Quaternary	1.6	Q
Tertiary		T
Pliocene	5.3 (4.8)	Pl
Miocene	23 (23.7)	Mi
Oligocene	36.5	Ol
Eocene	53 (57.8)	Eo
Paleocene	65 (64.4)	Pc
Mesozoic		MZ
Cretaceous	135 (140)	Cr
Jurassic	205	J
Triassic	250	Tr
Paleozoic		PZ
Permian	290	Pe
Carboniferous	355	Cb
Devonian	410	D
Silurian	438	S
Ordovician	510	Or
Cambrian	570 (540)	Cm
Precambrian		PCm
Proterozoic		Pt
Neoproterozoic	1000	Np
Mesoproterozoic	1600	Mp
Paleoproterozoic	2500	Pp
Archean	~4200	Ar

Ma figures are the lower age boundaries of each division

Miscellaneous abbreviations

BIF	Banded iron formation
MORB	Mid-ocean ridge basalt
MVT	Mississippi Valley Type
VMS	Volcanic-associated massive sulfides (also spelled VHMS)
sedex	Sedimentary-exhalational

Quoting tonnages of ore, contained metal(s), and grades

Standard tonnage data entries for ore deposits (in text and tables) have one of the following forms:

- tonnage of ore followed by ore grade(s) and metal(s) content(s) in a deposit, e.g.
-52 mt @ 1.5% Cu, 2 g/t Au for 780 kt Cu, 104 t Au
-52 mt/1.5% Cu, 2 g/t Au for 780 kt Cu, 104 t Au
- tonnes of metal(s) stored in a deposit followed by grade(s), e.g.
-2.5 mt Cu @ 0.75%; 96 t Au @ 3.5%
-2.5 mt Cu/0.75%; 96 t Au/3.5%

NOTE: The tonnages of ore and contained metal(s) need not add as the metals may have been derived from different ore types, captured from different information sources, based on incomplete data, etc. Ideally, the tonnage figures should be close to geological reserves (or the U.S. reserve base), that is the tonnages on metal(s) present in the deposit before the mining has started (pre-mining reserves). The data quality, however, depends of the published (and some oral, archival) sources that deteriorate rapidly away from Australia, Canada, U.S.A. and South Africa (read Chapter 2). Obviously unreliable tonnages have been edited.

Status of tonnages (indicated occasionally):

P, Pt	production, total production
Rv	reserves
Rc	resources

Tonnage units and abbreviations

All tonnages have been recalculated to metric tons (tonnes), abbreviated "t". 120 t = 120 tons; 120 kt = 120 thousand tons; 120 mt = 120 million tons; 1.2 bt = 1.2 billion tons. The grades are either in percent (1.2% Cu; 6.8% Pb) or in grams per ton (the same as ppm; e.g. 12 g/t Au). Conversion factors used to calculate tonnages quoted in various traditional non-metric units:

1 short ton	0.9072 t
1 long ton	1.016 t
1 pound (lb)	0.4536 kg
1 Troy ounce (oz)	31.10 grams
1 Flask (Hg)	34.47 kg

Pure metals converted from various compounds

Al metal grades and tonnages in this book (with few exceptions) are expressed as pure elements (Au, Cu, Fe, Al) rather than compounds (Al₂O₃; WO₃; Li₂O) or, even worse, archaic units incomprehensible to the public ("short ton units of WO₃"). The conversion constants (gravimetric factors) are below:

Al ₂ O ₃	x	0.52923	=	Al
As ₂ O ₃	x	0.75736	=	As
BeO	x	0.36	=	Be
Bi ₂ S ₃	x	0.813	=	Bi
Ce ₂ O ₃	x	0.85377	=	Ce
CdS	x	0.778	=	Cd
Cr ₂ O ₃	x	0.684	=	Cr
Cs ₂ O	x	0.94323	=	Cs
Fe ₂ O ₃	x	0.69944	=	Fe
HfO ₂	x	0.94797	=	Hf
HgS	x	0.862	=	Hg
Li ₂ O	x	0.4645	=	Li
MnO ₂	x	0.632	=	Mn
MoS ₂	x	0.599	=	Mo
Nb ₂ O ₅	x	0.699	=	Nb
NiO	x	0.7858	=	Ni
PbS	x	0.866	=	Pb
Rb ₂ O	x	0.91441	=	Rb
RE ₂ O ₃ *	x	0.538	=	REE
SnO ₂	x	0.788	=	Sn
Ta ₂ O ₅	x	0.819	=	Ta
ThO ₂	x	0.879	=	Th
TiO ₂	x	0.5995	=	Ti
U ₃ O ₈	x	0.848	=	U
V ₂ O ₅	x	0.56	=	V
WO ₃	x	0.793	=	W
Y ₂ O ₃	x	0.78744	=	Y
ZnS	x	0.671	=	Zn
ZrO ₂	x	0.7403	=	Zr

* Group REE factor taken as of Ce

Some special terms and usages

"Giant(s)", "giant deposit", "large deposit", "near-giant", "Au-giant" etc., spelled in quotation marks, correspond to magnitude categories as defined in Table 2.3.

"Geochemical giant" is sometimes used to characterize ore deposit that is "giant" in terms of geochemical accumulation, but of much lesser economic significance (it applies mostly to Sb, Hg and As deposits).

Locality names printed in **bold** introduce descriptions of "giant" (and some "world class") deposits, e.g. **Olympic Dam**

Metallogene refers to a distinct geological setting, environment, condition, control, etc. selectively influencing local metal(s) accumulation (ore formation); very close to the terms metallogenic province and metallotect.

1 Civilization Based on Metals

1.1. Past and present sources of industrial metals

1.1.1. Introduction

Metals are one category of a trio of geological materials on which is based our present industrial civilization. The other two categories are mineral fuels like coal, petroleum and natural gas, and nonmetallics (industrial minerals) like stone, sand and gravel, salt or clays. Fuels and nonmetallics (with some exceptions where metallic ore is also a nuclear fuel such as uranium, and where metallic ore has alternative applications as an industrial mineral from which the metal component is not extracted) are not treated in this book as there is voluminous literature that provides this information.

Since the Bronze Age, our evolving civilization has depended on metals and this will continue in the future, despite the increasing competition metals are now receiving from organic and organometallic synthetics (e.g. plastics, silicone, graphite) and composite materials. The first metals in human possession came from geological materials: initially from few native metals found in an almost "ready to use" state, then from easy to process ores, followed by complex ores that required advanced technology, and finally from various materials increasingly different from the classical metallic-looking ores ("unconventional ores"). Shortly after the "geological" metals had been produced and utilized, recycling of the no longer needed objects took place and since then, recycled metals joined the "new" (mine) metals as an important component of global metals supply. The alternative metals supplies are briefly reviewed below, but the main body of this book deals with the "new" metals supplies obtained from geological materials, especially from mineral deposits of exceptional, "giant" magnitude that supply the greatest share of industrial metals now, and probably in the near future.

In 2002 mines of the world produced ores containing 495 million tons of "new" iron ("new" metals are produced from ores for the first time and are not recycled); 35.25 million tons of "new" aluminum contained in bauxite; 9.217 million tons of "new" copper; 7.170 million tons of "new" zinc; 7.6 million tons of "new" manganese (a metal invisible to the consumer as its main role is an

essential steel ingredient). Also produced were 42,219 t of uranium (1990 figure); 2,170 tons of gold; 171 tons of platinum; 23.1 tons of rhenium. No recent figures are available on the rarest and costliest naturally occurring metal, radium. In 1937, 40 grams of radium had been produced globally, at \$ 30,000 per gram! That was after a price drop from \$ 70,000/g in the previous year (Dahlkamp, 1993). Radium was then used for radiotherapy of the rich, an application taken over, after 1945, by synthetic radioisotopes. Overall, less than 1 kg of Ra has been globally produced by now, most of it as an unrecovered trace component of uranium.

The above figures and also Table 1.1., Fig. 1.1. clearly indicate the highly variable rates of utilization of metals by society. Industrial metals are now subdivided into the following categories:

Ferrous metals	Fe, Mn, (Cr)
Light metals	Al, Mg, (Ti)
Base metals	Cu, Zn, Pb, (Ni, Co, Sb)
Rare metals	Sn, W, Mo, V, Nb, REE
Very rare metals	Ta, Be, Ga, Ge, In
Radioactive metals	U, Th, actinides and transuranides
Precious metals	Au, Ag, Pt group (PGE)
Metalloids	As, Sb, Se, Te
Alkaline & alkaline earths metals	Li, Rb, Cs (the rest is not treated)

As this is a rather inexact, utilitarian organization, place of the remaining metals is subjective and at times controversial. Craig et al. (1988) used, in their popular textbook, two alternative classes of abundant and geochemically scarce metals, the latter further subdivided into ferroalloy, base, precious and specialty metals, respectively. Uranium and thorium are treated as nuclear energy resources.

1.1.2. History of metal supplies

There are six metals known and utilized since antiquity: gold, copper, silver, iron, lead and tin (also possibly antimony and arsenic). Of these gold, copper and meteoric iron-nickel alloy occur in native state in nature and were likely known to the hunter-gatherer societies.

Table 1.1. History, importance and value of industrial metals (in millions US\$)

Metal	Year of discovery, discoverer	Beginning of industrial use	Main uses today	Value 1996/7 product	Ct
Iron (ore)	Since antiquity	Since iron ages	General industry, construction, transport	17,900	1
Aluminum, metal	1809 Davy	1880s	Transport, construction, packaging	34,900	1
Copper	Since prehistory	Since prehistory	Electricals, construction, transport	28,900	1
Gold	Since prehistory	Since prehistory	Jewelery, investments, electronics, dentistry	24,600	1
Zinc	500 BC brass artifacts	Brass, 1 AD	Galvanizing, alloys, die-casting	9,800	1
Nickel	1751 Cronstedt	1880s	Steel, alloys, electroplating	7,140	2
Lead	Since antiquity	Since 5000 BC	Batteries, solders, pigments	3,860	2
Platinum group	1800s Wollaston	300 AD	Catalysts, jewelery, electronics	2,700	2
Silver	Since antiquity	Since antiquity	Photography, silverware, electronics	2,330	2
Manganese	1774 Scheele	1839	Steel, alloys, pigments	1,770	2
Cobalt	1780 Bergman	1907 metal	Superalloys, steel, magnets; earlier pigments	1,550	2
Magnesium metal.	1808 Davy	1850s	Alloys, transport, Fe smelting	1,520	2
Tin	Bronze since antiquity	Since antiquity	Tinplate, solders, alloys	1,310	2
Uranium	1789 Klaproth	1890s	Energy, weapons, earlier pigments	1,250	2
Molybdenum	1778 Scheele	1894	Steel, alloys, tools	1,220	2
Titanium metal	1790 Gregor	1890s	Alloys, steel	960	3
Chromium	1797 Vaquelin	1850s	Steel, alloys, electroplating, earlier pigments	830	3
Vanadium	1830 Sefstrom	1905	Steel, alloys, tools	737	3
Tungsten	1780s	1850s	Steel, alloys, tools, ceramic carbide	455	3
Boron compounds	1808 Gay-Lussac	1200s	Glass, detergents, chemicals; compounds	432	3
Zirconium compounds	1824	1914	Ceramics, refractory foundry sand (compounds)	385	3
Lithium	1817 Arfvedson	1890s	Ceramics, light alloys, batteries, chemicals	359	3
Strontium compounds	1790 Crawford	1790s	Ceramics, glass chemicals (compounds)	300	3
Beryllium	1797 Vaquelin	1920s	Electronics, light alloys, defence	265	3
Rare Earths	1794 Gadolin, others	1880s	Catalysts, phosphors, alloys, electronics	264	3
Antimony	Since antiquity	4000 BC	Flame retardant, batteries, alloys, pigments	170	3
Niobium	1801 Hatchett	1930s	Steel, alloys	134	3
Indium	1863 Reich & Richter	1920s	Electronics, electroplating, solders	54	4
Germanium	1886 Winkler	1930s	Fibre optics, electronics	49	4
Tantalum	1802 Ekeberg	1900s	Capacitors, electronics, alloys, bulbs	40	4
Arsenic oxide	Since antiquity	1800s	Wood preserver, chemicals, toxins	39	4
Bismuth	Since Middle Ages	1833	Chemicals, pharmaceuticals, alloys	27	4
Rhenium	1925 Noddack et al.	1930s	Petrochemical catalyst, alloys	23	4
Cadmium	1817 Strohmeyer	1870s	Batteries, pigments, electroplating, alloys	22	4
Gallium	1875 de Boisbaudran	1940s	Electronics, photocells	19	4
Mercury	Since antiquity	1500s	Electrolysis, electronics, batteries, amalgams	13	4
Selenium	1817 Berzelius	1940s	Photocells, electronics, glass, chemicals	13	4
Tellurium	1872 Mueller v.R.	1930s	Alloys, metallurgy, catalyst	12	4
Rubidium	1861 Kirchhoff	1920s	Photoelectrics, glass, chemicals	n.a.	5
Cesium	1860 Bunsen	1960s	Ditto	n.a.	5

Table 1.1. (continued)

Metal	Year of discovery discoverer	Beginning of industrial use	Main uses today	Value of 1996/7 product	Ct
Thorium	1828 Berzelius	1885	Incandescent lamps; possible nuclear fuel	n.a.	5
Thallium	1861 Crookes	1896	Chemicals, toxins	n.a.	5
Scandium	1879	1950s	Metal halide lighting	n.a.	5
Yttrium	1794 Gadolin, others	1940s	TV phosphors, laser crystals	n.a.	5
Hafnium	1922 de Hevesy	1953	Nuclear reactor control rods	n.a.	5

NOTES: Column Ct, "Importance category" of metals is based on the recent value of global production (not tonnage!) as follows: 1, fundamental metals, \$ 10 billion plus; 2, very important metals, \$ 1 billion plus; 3, important metals, \$ 100 million plus; 4, minor (specialty) metals, \$ 10 million plus; 5, very minor specialty metals, less than \$ 10 million.

The latter occupied territories where these metals occurred (e.g. Asia Minor for copper, Eastern Desert of Egypt and Sudan for gold). Tin, silver and lead required primitive smelting to separate from ores, a process almost certainly discovered by accident. Silver does occur as a native metal in nature but at outcrop it is tarnished black and unappealing. Accidental joint smelting of tin and copper ores resulted in bronze, an alloy with physical properties much superior to those of pure copper, that gave rise to the Bronze Age.

Although the bulk of early native metals (especially gold) came from scattered finds of megascopic particles (nuggets, grains) resting at the surface, early mining soon developed by following the ore outcrops to depth. Before 3000 B.C. there were probably no more than ten "mines" at bona fide ore deposits in the Old World (outside of China), with an intermittent production of several tons of copper and several kilograms of gold. The number of mines increased exponentially in the age of Sumerian, Phoenician, Greek, Etruscan, Roman, Celtic, Chinese, Middle Eastern, Central and South American and other states and empires when metallic deposits had been discovered not only at the home turf, but in territories invaded by conquering armies as well. Probably the earliest recorded metal mining and recovery from what are present-day metallic deposits is attributed to the Sumerians, mining and processing copper in south-central Iran around 3,500-3,000 B.C. (Kuřvart, 1990). This included oxidation zone of the "giant" porphyry copper Sar Chesmeh (Chapter 7), subsequently forgotten then rediscovered in the 1900's. In the Pharaonic times the Egyptians, or their vassals, mined copper in Sinai and possibly Hijaz, gold in the Eastern Desert and Nubia. The Phoenicians, around 1,100-800 B.C., mined or traded silver at several locations around the Mediterranean basin as in the Spanish Meseta,

Cartagena, and Lavrion in Attica, as well as copper in Asia Minor and Cyprus. Lavrion (Chapter 10) then became a "world class" silver and partly lead source to the Athenian state, especially under Pericles around 480 B.C., and a source of much of its wealth.

Additional metals: antimony, arsenic and mercury, had already been utilized before the onset of Middle Ages (that is, around the end of the 5th Century A.D.), more in the form of compounds (pigments such as vermilion and antimony sulfides, poisons like arsenic trioxide) than native metals. In the Middle Ages these metals were joined by bismuth, found in native form in some silver mines; cobalt compounds used in glass and ceramic pigments; and zinc to alloy with copper to form brass, but probably not pure zinc. Several ferroalloy metals such as manganese, chromium and nickel participated in medieval iron weapons and utensils smelted at several locations known for superior quality of their wares. The iron ores came from several deposits enriched in the alloy metals (e.g. lateritic Fe ores formed on ultramafics and enriched in Cr and Ni; gossanous limonite over siderite veins enriched in Mn), although the presence of such metals was not recognized and analytically proven then.

It was not until the 1750s and the onset of the Industrial Revolution with modern chemistry emerging, when the process of discovery and isolation of new metals (and other chemical elements) started and rapidly gained in strength so that between 1751 and the end of the 19th century 49 new metals were added to the Periodic Table itself compiled, between 1890 and 1895, by Mendeleyev. There have been few naturally occurring elements left to be added in the 20th century: Hafnium in 1922 and rhenium in 1925.

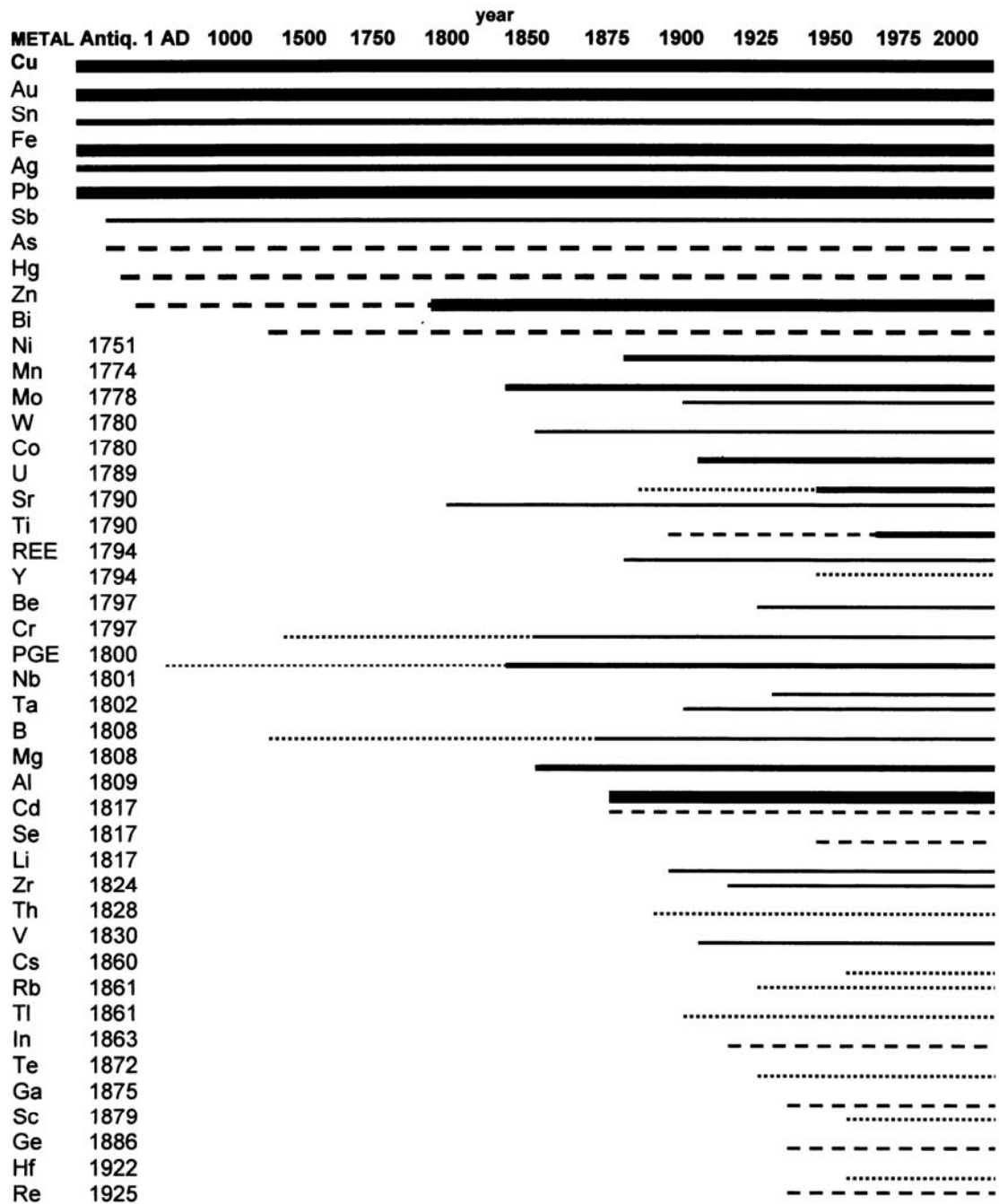


Figure 1.1. History and importance of industrial metals (based on data in Table 1.1). NOTES: Year in the 2nd column is the year of metal discovery. Bars show the period of industrial metals utilization and metal importance, based on the 1996-1997 US\$ value of the world production as follows: \$ 10 billion + (thickest solid line); \$ 1 billion + (medium solid line); \$100 million + (thin solid line); \$ 10 million + (dashed line); under \$ 10 million (dotted line). Antiq = metal known since antiquity

All new elements discovered afterwards have been the impermanent transuranic products of radioactive decay series, both those occurring in the nature and those confined to the laboratory.

Many new element discoverers did not simultaneously isolate the element in its pure form and this resulted in some controversy as to the authorship and the exact year of discovery of several metals. This subject is sufficiently covered in literature on the history of chemistry and in reference works and will not be discussed here. In the period of rapidly accelerating science and industrial technology driven by the Industrial Revolution, major wars and most recently breakthroughs in nuclear physics, electronics and biotechnology, industrial (practical) application of the newly recognized metals followed discoveries. The lead time between the discovery and application of metals kept, in most cases, shrinking. Aluminum was discovered in 1808 but it was not until the 1880s when the mass production of this metal has started, continuously increasing to make Al the #2 industrial metal, after iron. It has taken even longer for molybdenum to become an indispensable component of specialty steels: 138 years since its discovery in 1778, through the period of small-scale utilization in the 1890s, to the rapidly growing demand of Mo as an ingredient of a steel used as armor plate in World War I. With the war over, the demand for molybdenum suddenly dropped dramatically, to return at the onset of another great war and then to stay.

With the full and final complement of metals now in place, industrial applications of and demand for individual metals remain almost steady, grow or shrink. The mineral industry responds and the result is the never ending fluctuation of metal prices, production figures and exploration rushes. Table 1.1. and its graphic representation in Figure 1.1. show the present-day relative importance of industrial metals based on the 1996/7 values of global production. Iron, aluminum, copper and gold are the heavyweights, worth more than \$ 10 billion per year. They are followed by zinc, nickel, lead, platinum elements, silver, manganese, cobalt, metallic magnesium, tin, uranium and molybdenum, each worth \$ 1 billion plus. Seven metals at the end of the spectrum (this does not include individual metals in the rare elements and platinoid groups) are probably worth several million dollars or less per year, but precise production and value figures are lacking.

1.1.3. Present metals supplies

Present supplies of industrial metals can be primary, secondary or both. This distinction is important as it influences production statistics and determines demand for new metals supplied by the mining industry each year.

Primary or “new” metals are recovered from newly mined, or stockpiled, ores, then added to the existing inventory of industrial metals for the first time. Most primary metals have been extracted at or near sites of source ore deposits and are credited, in statistics, to a certain country or territory (e.g. copper production of Chile; gold production of Nevada). Such production figures are geologically meaningful as they indicate local mineral endowment and/or “specialization” on a certain metal. In a minority of cases metals are produced from imported ores and the metal production is credited to the country where the smelter is located. The best examples are Canada and Norway, both important producers of aluminum, 100% locally smelted from bauxite ore imported from overseas. Neither country has domestic bauxite deposits and there is virtually no likelihood that any would be found in the future, but both countries have cheap and abundant electric power that constitutes about 60% of the cost of “new” aluminum. It is thus economic to import bauxite from Guinea or Jamaica using cheap sea transport, add local energy, then export the surplus aluminum not required by domestic industry. Should it become economic to recover aluminum from hard silicate rocks such as anorthosite or nepheline syenite in the future, Canada and Norway would become self-sufficient in the required raw materials. Many if not most rare and specialty metals such as the rare earth elements, indium, scandium, thallium, tellurium and other metals are by-products smelted and refined from ores imported from many sources for the recovery of the more abundant metals (e.g. copper, lead, zinc, titanium, zirconium) in specialized smelters and refineries in Europe (e.g. Hoboken in Belgium), Peru (Oroya), Australia (Port Pirie), United States, Japan and China.

Secondary (recycled) metals once entered human civilization as primary metals where they assumed residence lasting from several days (as with “new”, pre-consumer scrap) to several millenia (metallic objects from the distant prehistory now in museums). Metals that are a part of the cumulative “civilization inventory” are in plain view all around us (vehicles, rails, utensils, coins) or they are concealed (construction steel in buildings, electric wiring, gold reserves in central banks) and they

have a variable “service life” during which most suffer partial dispersion (such as weight reduction of coins and rails due to wear). At the end of their lifetime metals are either wasted, recycled or reallocated. Wasted metals are lost from inventory whereas recycled and reallocated metals join and enlarge the supply of primary metals in any given year.

Recently, the Minerals Yearbook, now published by the U.S. Geological Survey (previously by the now defunct U.S. Bureau of Mines) started to compile and publish statistics on the “release to environment” (read waste) and “transfers”(recycling and reallocation) of industrial metals. The data, yet incomplete, are instructive but, unfortunately, applicable to the United States only. An example: of the total 1995 U.S. supply of (entirely imported) chromium of 1,790,000 tons, 10,500 tons was released into the environment (i.e. lost), 8,460 tons was impounded to land (i.e. it ended up in garbage dumps and landfill). 69,300 t of the Cr was transferred, the bulk (56,700 t) through recycling. Most of the transferred chromium reappeared as a component of the next years metal supply, reducing the demand for primary chromium by less than 4%. This is very minor compared with lead 66.8% of which was recycled, in the United States, in 1996 (read below). Metals transfer statistics for the rest of the world are very sketchy.

Reallocated metals include two main categories: 1) metals (and other commodities) released from United States’ (and some other governments) strategic stockpiles, and sold on the open market; 2) periodic sales of precious metals such as gold, platinum and silver held by central banks or hoarded by investors (or royal houses).

1.2. Metal prices

Industrial metals are mineral commodities, that is articles of trade or commerce. Metal prices are widely used in statistics and quantitative studies, including this book, but one must know what the numbers mean and as to whether they are appropriate for the given purpose. Also, a great accuracy should not be expected despite the quantitative figures, and conclusions reached should be considered approximate only.

Commodity prices in general are established at stock exchanges, based on supply and demand in a particular time. In the minerals trade most processed pure metals are a commodity, but various alloys (e.g. ferroalloys like ferronickel), compounds

(like alumina), raw metals (like blister copper or titanium sponge), mineral concentrates, ores (like bauxite, chromite or iron ore) are listed and marketed commodities as well. Most global metal prices are determined at the London Metals Exchange (LME) and widely published in specialized bulletins, trade journals and, in case of the common metals, in many daily newspapers. The prices change on daily basis and the recent price movements, as well as historical data, are extensively covered in the literature (for example in the U.S. Geological Survey Mineral Yearbooks; in Mining Annual Reviews; in Crowson’s “Minerals Handbooks”, e.g. Crowson, 1998), together with graphs. Reference literature usually provides an average price of a metal (commodity) in a given year and, sometimes, a period average (several years, decade). Averaged period prices of the common industrial metals, corrected for inflation (e.g. quoted in constant 1990 dollars) change relatively little, but specialty metals often undergo wild swings as their stocks fluctuate and their momentary applications come and go. The peak price of \$ 30/lb Mo in 1979 went down to \$ 3/lb the following year, causing mines closures and preventing development of the “giant” Quartz Hill Mo deposit in Alaska (Ashleman et al., 1997). Substitutes are inevitably found for metals the price of which went out of hand, causing drastic drop in demand and price collapse (example: substitution of silicon for Ge in electronics in the 1960s-1970s).

Metal prices clearly influence profitability so they are a paramount variable in feasibility studies and all sorts of forward planning and speculation. High metal prices make it possible to mine low-grade ores, hence the cut-off grade could be placed quite low. Low metal prices cause deferment of mine projects and start-ups and cause operating mines caught in sharply declining price spiral to resort to “high-grading” or at least momentary mining of the higher-grade blocks, leaving the low-grade material for better times. Some of the heavily regulated metals of strategic importance, like uranium, have had their resources quoted in terms of several fixed cost categories; these were, in the 1960s-1970s, as follows: 1. <\$ 80/kg U; 2. \$ 80-130/kg U; \$ 130-260/kg U (Dahlkamp, 1993).

Tin is the only metal subjected to several attempts by the producing countries, successful over a period of time, to stabilize, control and increase the world price of this commodity. The beginnings of the tin cartel go back seventy years when the International Tin Committee applied a set of supply controls to reduce wild price fluctuation during the Great Depression. Its post-war successor, the

International Tin Council, was established in 1956 and it included both major tin producing and consuming countries. A series of agreements for five year periods established floor, ceiling, and average price for tin applied to transactions among the members. Price equilibrium was maintained by means of export controls based on production quotas assigned to each member country and by buffer stocks. The buffer stock, into which the member countries contributed, had to purchase tin on the global market when the world price of tin approached, or fell below, the floor of the agreement price. If the world price exceeded the agreement ceiling, the stock had to sell tin.

The tin agreements worked quite well for over 25 years, bridging several price declines of other metals such as copper, zinc and lead. The tin price ceiling, at US\$ 1.10/lb in 1956, reached the unrealistic US\$ 7.25/lb in late 1981 (the 1997 tin price was about US\$ 2.50/lb), yet the Agreement price was never reduced. The 1981-1982 recession sharply depressed tin consumption and the artificially high price prevented recovery. The consumers reduced tin use or resorted to substitutes, non-members of Tin Council increased supplies, and there were illegal tin exports. The buffer stock had to pay high price to buy abundant tin offerings, borrowing money in the process and finally running out of cash. The end came in 1985 when the International Tin Agreement collapsed. The tin price plunged, the accumulated tin in buffer stock was insufficient to pay back the loan, creditors lost money, mine closures followed, and tin exploration died out.

Table 1.2. and Fig. 1.2 show mineral commodity prices, that include metals, based on late 1980s-early 1990s averages as recorded in the U.S. Bureau of Mines Mineral Yearbooks. An enormous range of industrial metals prices is instantly apparent, spread over nine orders of magnitude (or 15 orders if ultra-rare metals like radium are included). There is a general correlation between metal price and metal scarcity as it follows from geochemical abundances (discussed in Chapter 3) where, as expected, the rare metals like gold are more expensive than the common metals like aluminum and iron. There are, however, numerous exceptions where some abundant metals appear overpriced (e.g. titanium) and some scarce metals underpriced (like antimony or mercury). In case of titanium this is clearly the consequence of a very high cost of production of a geochemically abundant metallic titanium (Ti compounds such as titania, TiO₂, are much cheaper). The low price of antimony and mercury is the consequence of market forces (both

metals are on the losing side of industrial applications hence the demand is decreasing), and also the fact that both metals form high-grade deposits that are cheap to mine and process. There might be some geochemical factors involved as well. One of them is the possibly inaccurate Sb and Hg clarkes (too low? read Chapter 3), the other an exceptional metallogenetic productivity, in other words natural tendency to form highly concentrated local metal accumulations (orebodies) from geochemically widely dispersed substances.

Metal prices, as reviewed above, are widely used to put value on orebodies in ground (e.g. a deposit with 1 million tons of copper could be said to be worth \$ 2 billion using the approximate average price of 1t Cu=\$ 2,000; it could be worth even more if there are by-product Mo, Ag and Au), value of unmined resources in a territory, value of ore metal(s) per square kilometer or per unit of population, and similar. The results look accurate and convincing to some and are sometimes used in planning and prediction of industrial potential but they are not “real world” indicators of economic viability and profitability because it costs a lot to find a viable orebody, then to mine the ore and extract the metals. The profit equals the sale price of metal (commodity) minus the costs and the profit margins tend to be slim for most metals and occasionally negative. The next paragraph shows how the hypothetical costs of successive products in a typical “hot” copper extraction process rapidly increase when value is added, to eventually reach the LME price for electrolytic copper. Some semi-products could be marketable commodities in their own way, for example Cu ore sold to a nearby mill owned by another company; concentrate shipped overseas; smelter copper.

1. Bulk (low-grade, e.g. 0.5%) copper ore, \$ 15.00/t
2. Medium grade ore, e.g. 3% Cu, \$ 50.00/t
3. Handpicked, almost pure chalcopyrite lump concentrate; 20% Cu, \$ 200.00/t
4. Chalcopyrite mill concentrate; 30% Cu, \$ 600.00/t
5. Blister copper, \$ 1000.00/t
6. Copper scrap (urban, inhomogeneous) \$ 1100.00/t
7. Copper scrap, industrial, homogeneous \$ 1900.00/t
8. Electrolytic copper, cathodes \$ 2000.00/t
9. Electrolytic copper, casted bars or rolled wire \$ 2100.00+/t

It is also obvious that profitability of a deposit could increase enormously when a cheaper extraction technology (or an economy of scale) is applied, and some of the production steps listed above are eliminated. In case of copper this has been achieved by the technology of direct orebody, or heap, acid leaching followed by copper electrowinning from solution. There, three stages in the traditional hot (i.e. involving smelting) technology have been eliminated. The real value of the copper contained in one ton of Cu ore, in terms of return on investment, is thus substantially lower than the LME price of an equal amount of refined metal. Historical statistics of actual commodity sales, especially if converted into constant dollars, are thus more accurate indicators of value and profitability.

Table 1.2. Typical mineral commodity prices as they had been in the 1980s and 1990s. Compiled from data listed in the U.S. Geological Survey reports. The prices are in U.S. dollars.

Commodity	Price \$/t
Sand and Gravel	\$5.00
Stone, crushed	\$5.00
Helium*	\$11.00
Gypsum	\$12.00
Sand, chemical	\$18.00
Iron ore	\$27.00
Dolomite	\$35.00
Bentonite	\$40.00
Nepheline & phonolite	\$43.00
Chromite	\$50.00
Limestone	\$50.00
Iron	\$55.00
Cement	\$56.00
Feldspar	\$60.00
Potash	\$60.00
Slate (roofing)	\$60.00
Ilmenite concentrate	\$62.00
Clays	\$70.00
Phosphates	\$70.00
Pyrophyllite	\$70.00
Mica	\$80.00
Sodium carbonate	\$83.00
Barite	\$90.00
Perlite	\$90.00
Sodium sulfate	\$95.00
Magnesite	\$120.00
Ocher	\$130.00
Nitrates	\$140.00
Zircon concentrate	\$148.00
Fluorite	\$150.00
Salt (halite)	\$150.00
Sulfur	\$150.00

Andalusite	\$160.00
Bauxite	\$160.00
Halloysite	\$180.00
Pumice	\$190.00
Kaolin	\$200.00
Kyanite	\$240.00
Nitrate (Chilean)	\$240.00
Sillimanite	\$240.00
Talc	\$260.00
Vermiculite	\$260.00
Wollastonite	\$300.00
Diatomite	\$330.00
Garnet	\$340.00
Corundum & emery	\$400.00
Spodumene	\$400.00
Rubidium	\$450.00
Asbestos	\$500.00
Graphite	\$500.00
Rutile concentrate	\$550.00
Monazite	\$600.00
Alumina	\$700.00
Pyrite	\$700.00
Borax	\$800.00
Lead	\$800.00
Strontium	\$800.00
Zinc	\$880.00
Manganese	\$900.00
Mn oxide	\$900.00
Quartz crystal	\$1,200.00
Aluminum	\$1,505.00
Cesium	\$2,300.00
Copper	\$2,400.00
Cadmium	\$2,800.00
Titania	\$2,800.00
Boron	\$3,200.00
Antimony	\$3,240.00
Li carbonate	\$3,300.00
Magnesium	\$4,300.00
Arsenic	\$4,500.00
Rare Earths	\$4,500.00
Tin	\$6,400.00
Selenium	\$7,530.00
Bromine	\$7,700.00
Bismuth	\$7,800.00
Nickel	\$7,800.00
Lithium	\$8,000.00
Mercury	\$9,320.00
Molybdenum	\$10,000.00
Tellurium	\$10,000.00
Chromium	\$11,400.00
Titanium	\$13,000.00
Tungsten	\$14,000.00
Vanadium	\$14,000.00
Iodine	\$15,000.00
Neodymium	\$19,700.00
Lanthanum	\$23,000.00

Cerium	\$28,500.00
Uranium	\$33,000.00
Praseodymium	\$38,850.00
Tantalum	\$60,000.00
Cobalt	\$61,000.00
Thorium	\$70,000.00
Scandium	\$90,000.00
Thallium	\$90,000.00
Yttrium	\$90,000.00
Indium	\$112,000.00
Dysprosium	\$132,000.00
Gadolinium	\$136,500.00
Silver	\$170,000.00
Samarium	\$175,000.00
Erbium	\$190,000.00
Ytterbium	\$230,000.00
Hafnium	\$308,000.00
Beryllium	\$340,000.00
Palladium	\$410,000.00
Holmium	\$510,000.00
Gallium	\$520,000.00
Rhenium	\$800,000.00
Terbium	\$880,000.00
Germanium	\$900,000.00
Ruthenium	\$1,200,000.00
Europium	\$1,650,000.00
Thulium	\$3,600,000.00
Lutetium	\$7,000,000.00
Rhodium	\$9,000,000.00
Gold	\$12,000,000.00
Osmium	\$12,600,000.00
Platinum	\$12,800,000.00
Iridium	\$15,000,000.00
Diamond	\$225,000,000.00

1.3. Future metal supplies

1.3.1. How much metals will be needed?

Government planners, corporations, investors, speculators, futurists would all like to know what the future societal needs of commodities, in our case metals, will be and, once this is known, where the required supplies will come from. In this paragraph we will focus on the first half of the question, making use of the time-tested approach of projecting the past. We are particularly interested in the future supplies of "new" (mine/smelter) metals and this requires consideration to be given to supplies of the "secondary" metals, as well as to the means of reducing the anticipated demand. This is treated in some detail below.

U.S. Geological Survey (previously U.S. Bureau of Mines) Mineral Yearbooks, Mineral Facts and

Problems and most recently Mineral Commodity Summaries available on internet (<http://minerals.usgs.gov/minerals/pubs/mcs/2003>) have been providing, for several decades, the best available United States' and global statistics on provenance of industrial metals. The same publications, and several other sources (mostly mining journals and related annual reviews; global to national yearbooks and statistical compilations) also keep providing information and opinions about short term metals demand, price and supply forecasts. The accuracy and reliability of information varies and the conclusions reached apply at best to some two or three immediately following years. To make a case for the future of minerals industry that includes the risky business of exploration, long term forecasts are needed.

Published forecasts rely mostly on projections of historical trends supported by assumptions popular in the period. Most projections made in the past, as in the 1970s (e.g. Mineral Resources Perspectives 1975; U.S. Geological Survey Professional Paper 940) turned out to be grossly inaccurate to outright wrong, which compares favorably with political predictions made in about the same time: none of them (except for few dissidents) predicted dissolution of the Soviet Union and disintegration of the world's communist block! Having no better means at hand, this book has to follow the same forecasting pattern, although we will consider a greater range of alternative scenarios.

Figure 1.3. graphs the rates of world's yearly productions (not a cumulative production!) of seven selected metals, from antiquity to the year 2003. The reliability of data decreases with age and the very old figures are just guesstimates supported by a small number of historical information. Sustained, locally almost exponential growth of yearly productions is apparent since the start of the Industrial Revolution to approximately the 1950s. This applies equally to the "metals of antiquity" (Au, Cu, Fe, Sn, Pb) as well as the newcomers like aluminum and nickel. After 1950 the production growth curve for tin has reached a plateau and lead seems to have peaked in the mid-1970s, with mine production decreasing since. The total yearly lead supply, however, still increases slightly but this is due to contributions from recycled lead. Is the plateauing, or reversal of the rate of metal production, a preview of the eventual trend for most metals, especially those hurt by cheaper and often more effective substitutes?

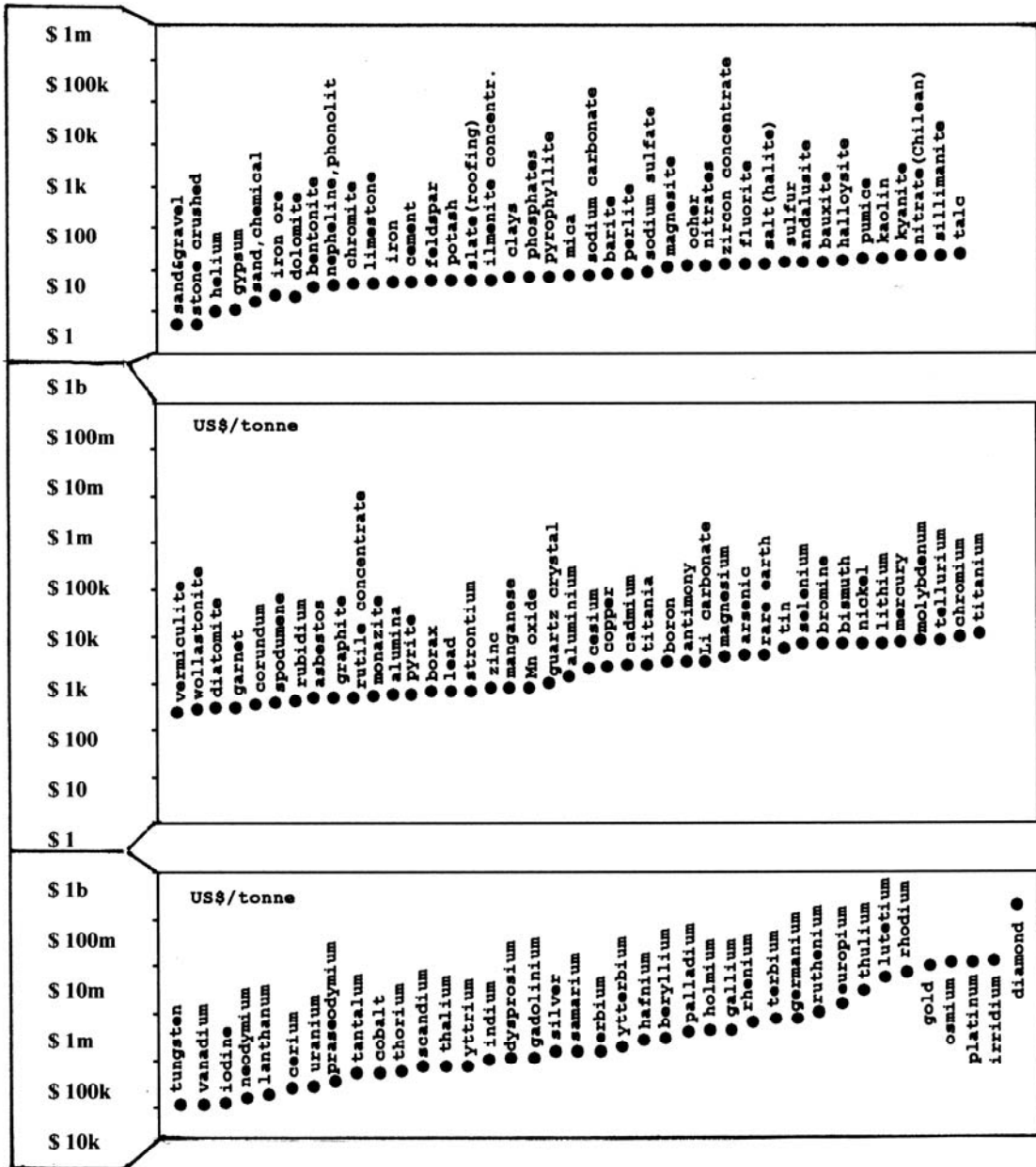


Figure 1.2. Graphical representation of the typical metal prices of all mineral commodities in the 1980s-1990s, as listed in Table 1.2. The prices are in US\$ per one ton, except for gases (e.g. helium) that are per cubic meter

To make a case for the continuing existence of mining and smelting industry (Barton, 1980), a popular villain in the age in which environmentalism has become important political issue and media topic (Beck, 1991), future material needs of the rapidly growing global population are routinely invoked (compare the introductory chapters of recent textbooks on mineral resources

like Craig et al.1988; Kesler, 1994, Holland and Petersen, 1995 and several recent papers; even the enlightened environmentalists like Jared Diamond of the "Collapse" fame [Penguin Books, 2005] recognize the essential role of mining when practiced sensibly). Numerous population growth projections now circulate in the public domain.

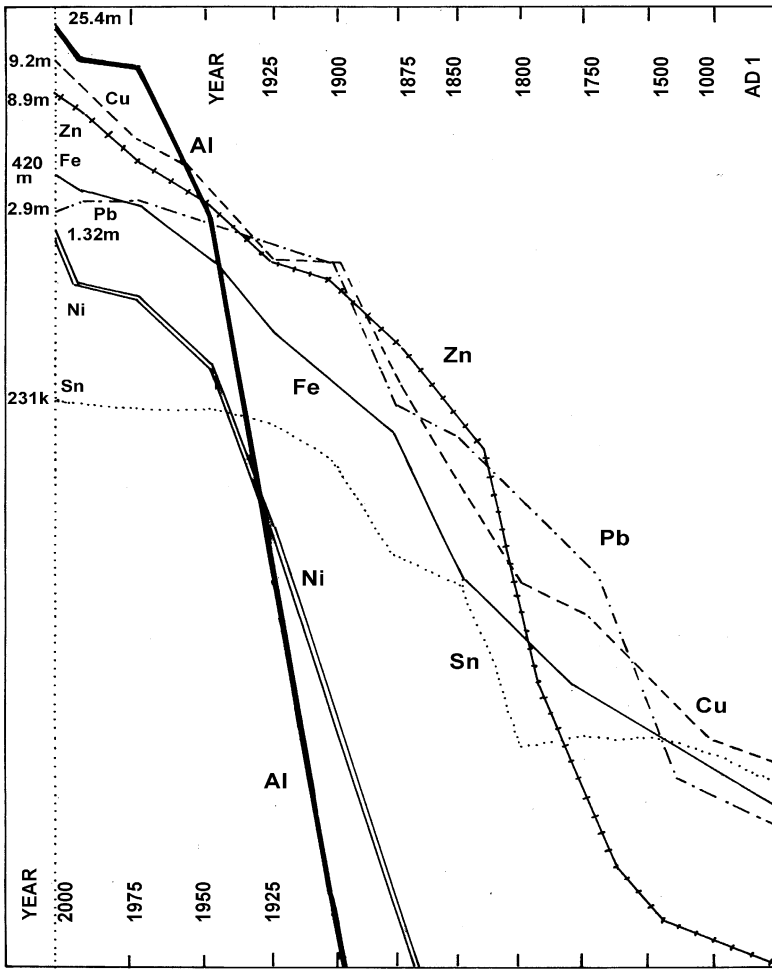


Figure 1.3. Trends of generally rapidly increasing annual production (not cumulative production) of seven selected metals, from antiquity to about the year 2000

Although their figures differ, they all conclude that the present exponential population growth will continue for at least several more generations to finally stabilize towards the end of the 21st century. By that time the Earth would have to support some 12 billion people or more, that is at least twice the present population count of 6.5 billion. Unless this teeming mass of humanity partially self-destruct (Diamond, 2005), it will require at least the present amounts of per-capita mineral supplies. If there is a two or three-fold population increase between now and 2050, the commodity demand in 2050 will be approximately equal to the present demand times two or three; in concrete terms for copper some 16 or 24 million tons Cu.

Consumption per capita: In developed countries consumption of commodities per capita has increased rapidly in the post-World War 2 period,

sometimes dramatically, resulting in overconsumption and increasing production of waste. The consumption increased substantially in the underdeveloped countries as well, but the gain has been wiped out by the exponential population growth. The reality is that even if the world's population stabilizes in the future (it has stabilized in some "mature" countries like Italy, Germany, France, Russia or Hungary where, however, it is being reversed by immigration from the rapidly growing populations), the consumption is predicted to continue to grow together with increasing affluence. Under the predominantly market philosophy that guides the present world "growth is good", hence consumption is good, the demand for mineral resources is bound to increase.

The consumption of mineral commodities, however, does not increase regularly and uniformly but in the form of localized bursts driven by rapid

industrialization, growth of national prosperity measured by per-capita share of the gross national product, and export-oriented manufacturing. Presently, China followed by India provide the fastest growing commodity market. Since 1990 copper consumption in China has grown at a rate of 12% per year and aluminum at 14% per year, making the country the world's second largest Cu and Al consumer (Humphreys, 2002). India, despite its image of a poor overpopulated country, is the world's largest consumer of gold. Previous consumption related to rapid industrialization bursts took place in Japan (1960s-1970s) and in South Korea, Taiwan and Singapore (1970s-1980s).

There is, however, a great inequality around the world in consumption of goods that include minerals, as "one quarter of the world's population that inhabits industrialized countries absorbs more than three-fourths of the world's nonfuel minerals production" (Barney et al., 1980, The Global 2000 Report to the President), leaving the rest of humanity undersupplied. Baring drastic changes to lifestyle in the "post-industrial" society into a paradise-like high-tech playground as imagined by some futurists (e.g. O'Neill, 1981), or more likely a fragmented world periodically lashed by calamities like wars, pandemics or famine (Ophuls, 1977). It could be realistically assumed that consumption of metals will increase at least twice or three times by the year 2050.

At least 50% of supply will have to be "new" metals. If so, the mineral industry will have to deliver, between now (2005) and 2050, some 22,275 mt of iron, 1,451 mt of aluminum, 418 mt of copper, 323 mt of zinc, 113,850.t of gold. Figure 1.4. shows the historically accumulated inventory, known reserves and estimated resources of gold in a variety of source materials, and gold demand based on zero % and 4.1%/y, growth. A massive change of public attitude such as "one cannot eat gold", and fashion, could cause a sharp drop in gold demand, leaving the yellow metal with some 20% of the projected demand only that has practical industrial application, and crippling markets for such non-productive gold applications like treasury hoards and, partly, jewelry.

Adequacy of future metal supplies: To address future supplies of metals, most classical texts plunge, without preliminaries, into the topic of geological aspects that control ore formation and occurrence. This indeed is the principal mission of this book but we will address it later, once the numerous other factors bearing on adequacy of

future metal supplies outside geology, geochemistry and metallogeny fields have been examined.

Metals' and minerals' production is driven by industry and consumers' demand ("the markets") and the demand has been increasing steadily for most commodities, but not in a very predictable way for some of them. Antimony, lead and mercury, strategic metals in times of World War 2, have lost much of their industrial applications, in case of Pb and Hg mainly on the basis of their toxicity to humans and the environment. Asbestos, a nonmetallic commodity, suffered similar fate. This drop in demand, resulting in reduced production hence in extension of the static life of resources known then, had not been correctly predicted (forecasted) mainly because environmental awareness counted for little in the 1940s and 1950s.

Consumption of other metals, on the other hand, advanced rapidly and demand matched by production grew steadily and almost exponentially (aluminum). Others, mainly some minor and specialty metals, have experienced short bursts of phenomenal demand and price increase, followed by sudden drop in demand, price collapse and in many cases return to the pre-peak insignificance. This happened, in the period between 1950 and 2005, to germanium, beryllium, tantalum, gallium, and to a lesser degree uranium, platinum metals, tungsten. Radium, the pre-World War II expensive miracle metal, has suffered total wipeout. Some metals still wait for a meaningful industrial application (thorium), others are underutilized with huge known resources but relatively low demand (niobium, most rare earth elements).

Commodity demand and price forecasting is thus a risky and uncertain business and the assessment of resources adequacy double so. At the present level of industrial efficiency and affluence achieved by developed countries it appears that any industrial metal required could be supplied by the globalized industry to anyone who can pay, from existing or newly discovered deposits, so far always found in time to meet the demand. No long-term shortages of industrial metals are anticipated in the near future, based on the contemporary philosophy. This is very different from the supply situation in the not too distant past, especially in times of war, where the need for strategic minerals (and even more so energy resources) often determined the military campaigns. As late as in the 1970s, numerous government and private studies predicted severe supply shortages of various commodities due to exhaustion of available deposits, on the global or national (especially United States') basis.

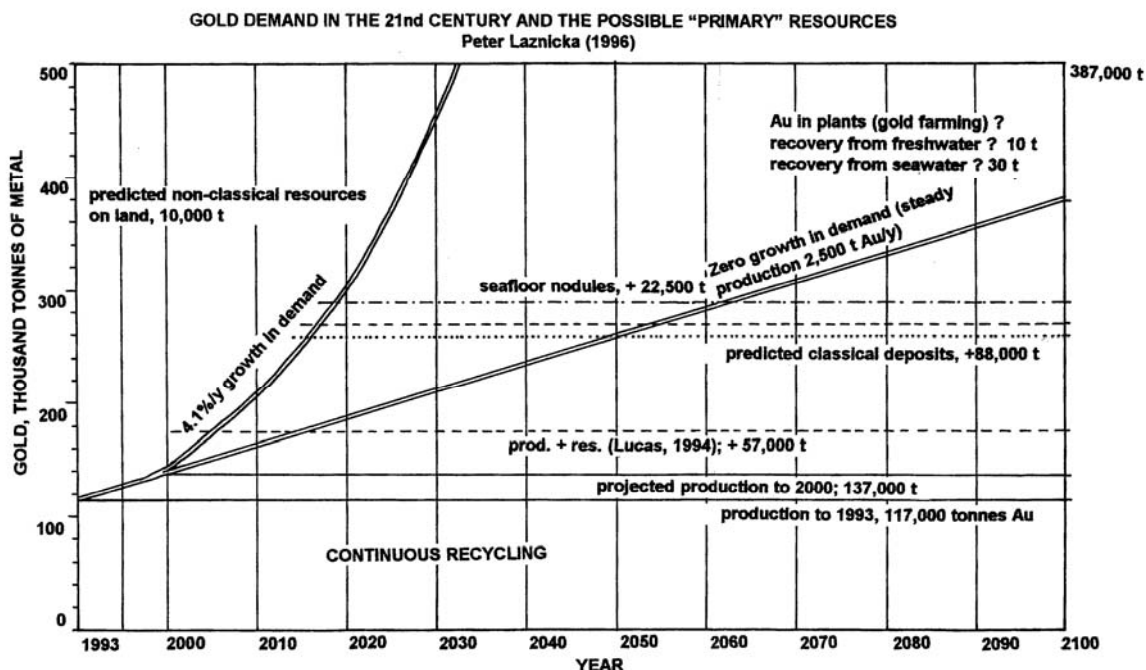


Figure 1.4. Various speculative scenarios about the future demand and supply of gold based on projection of the present trends. From Laznicka (1996)

So, according to the Club of Rome, 1972, in *Limits of Growth*; Brobst and Pratt, eds. (1973); Morgan, (1976) and others, by 1990 the world should have ran out of antimony, tungsten, silver, and some other metals. These assumptions have generally been proven wrong in the following decades (Bender, 1977, 1982) and the opposite happened. There has been an oversupply of mineral commodities for the past 20 years and a steady decrease of the real price of most metals. Kesler (1994) provided a very readable explanation for this situation in the introductory chapter of his textbook and warned that this state of affairs was temporary. So did Holland and Petersen (1995).

1.3.2. Reducing demand for "new" metals

Although this book makes a point that future demand for industrial metals is going to continue, the question of importance for the primary metal producers (and ore finders) is how much metals will probably be needed and what proportion of the supply will have come from the traditional mine/smelter providers of "new" metals. To make an acceptable educated guess, we have to briefly review some of the conditions that reduce the

demand for "new" metals now and possibly in the future, as well as alternative sources of other than "new" metals likely to contribute to future supply. Recycling is already the most obvious and relevant contributor to metal supply and it is growing because of environmental concerns and improving organization of scrap collecting. It is also possible that with the growing inventory of metals in active use, cumulatively contributed by mining industry over the years, a point might be reached when the world's metals inventory develops into an almost closed system constantly renewing and recycling itself, with only a small quantity of "new" metals needed to replenish losses caused by wear and tear and to supply new growth. This scenario needs to be seriously considered by planners should the "no growth" state of human population and economy, advocated by some futurists (e.g. Ophuls, 1977), ever come. The following is a selection of mechanisms capable of reducing the "new" metals supplies, now and in the future.

Recycling

Recycling is the single largest source of secondary metals added to annual metals supply (Henstock, 1996). Because of the recent publicity given to

recycling, considered mainly from the premise of environmental conservation rather than extending metals supply, there is a widespread public perception that recycling is a modern phenomenon. This is false. In the past, when most metals constituted a scarce and costly commodity produced in small quantities and when labor was cheap, virtually no metals were wasted and metallic objects at the end of their productive life were mostly reconstituted (reshaped) by local tradesmen, outside the realm of national statistics. This practice still persists in developing countries but in the rich industrialized societies this is limited, if at all, to precious metals (e.g. refabrication of jewelry). The more recent state-organized recycling, that had the purpose to extend the supply of strategic metals under conditions of restricted supply, took place in times of emergency such as wars. Germany and Great Britain during World War II achieved the greatest efficiency.

Mass industrial production in the post-World War II years, rapid increase of wealth in western industrialized countries, introduction of disposable consumer packaging (food and beverage cans) and mass ownership of automobile has resulted in a rapidly increasing volume of waste that included metals. A peak was reached in the 1960s-1970s, symbolized by the (mostly American) car cemeteries. This trend has started to reverse following the "environmental decade" of the 1970s; the car cemeteries are gone, transferred to wrecker and recycler yards, but as recently as in 1986 the municipal waste in the United States has still contained 8.8% of metals representing 864 kg/year per capita. Comparative figures have been 8% of metals in waste in Great Britain; 7% in Australia; 3.2% in Germany; 1.3% in Japan (World Resources 1992-93). The situation now (in 2004) is about 40% improved.

Although not yet perfect, mass recycling in industrialized countries is now better organized and universal, and it contributes increasingly more significant quantities of secondary metals to national and global metal supplies via scrap processing (Rao et al, eds, 1995). Minerals Yearbook discriminated between "new" (pre-consumer) and "old" (post-consumer) scrap. The former is generated in smelters, refineries and fabrication plants, is invisible to the public, and much of it is recycled in the same enterprise (the rest is sold). The latter consist of domestically recycled metals of which 78 million tons worth \$ 18 billion have been generated, in 1996, in the United States alone. The 1996 U.S. metal supply contained the following percentages of recycled metals: lead,

66.8%; metallic titanium, 48%; aluminum, 39%; iron, 39%; copper, 35.1%; metallic magnesium, 35%; nickel, 32.4%; tin, 29%; zinc, 26.1%; selenium, 29%; chromium, 20.5%; tantalum, 20% (Minerals Yearbook, 1996). This is an improvement on the situation in 1983, shown on Table 1.3. Metals with few applications that absorb most of the yearly metal supply such as lead (for storage batteries) achieve the best recycling rates, especially when the metal component is sealed, protected from dispersal, and collected by a single industry (automotive servicing). Recycling data for the rest of the world are incomplete and with few exceptions (Germany, Japan, Switzerland, Scandinavia) lower to much lower than the U.S. results. As an example, the 1996 world supply contained 16% of recycled copper; 17% of aluminum; about 35% of (mostly reallocated) gold. The percentage of recycled metals in yearly global commodity supplies keeps increasing, although not uniformly: many metals, especially minor components of alloys, are dispersed or recycled without a record. It is not clear when a recycling peak is going to be reached and what would its magnitude be. What is clear is that secondary metals are a significant component of the present supply of industrial metals, that their importance is increasing, and that the geological/exploration community should pay attention that has been hitherto minimal.

Table 1.3. Proportion of "old scrap" (recycled, used and discarded metals) in the total yearly supply of industrial metals, as in 1983. Calculated from data in the U.S. Bureau of Mines "Mineral Facts and Problems", 1985 edition.

Metal	% of old scrap, USA	% of old scrap, world
Steel (Fe)	46%	
Lead	45%	38%
Antimony	43%	54.5%
Tungsten	31.9%	20.6%
Mercury	27.6%	14.8%
Nickel	25%	25%
Copper	22%	22.6%
Silver	21.5%	44.2%
Aluminum	15.13%	8.8%
Platinum metals	14.8%	15.2%
Magnesium	13%	
Zinc	7.24%	5.57%
Gold	5-10%	
Tin	3.16%	2.17%
Cobalt	2.9%	

Product downsizing

Consumer products that underwent significant downsizing in the affluent societies in the past thirty years, hence material saving, include automobiles and electronic products such as radios and computers. Products that underwent increase in size or volume include houses and daily food consumption. This is reflected in the per capita increased demand for construction materials (most of which are nonmetallics) and decreased per capita demand for metals in the 1990s.

Elimination of products and constituent materials

It is hard to imagine that as late as during the World War 2 commodities such as sheet mica and antimony were on the strategic minerals list, i.e. critically important and in short supply. Muscovite had been used as an insulator, especially as a non-conductive base for copper conductors in many electrical applications. Sb+Pb alloy was the mainstay of typography. Most insulators are now synthetic while computerized phototypesetting, xerography and other printing techniques eliminated the need for antimony. These metals have now been marginalized and their production depressed or eliminated altogether.

In the mid-1980s a technological change in manufacturing of the ubiquitous 450g or similar steel "soup can", used for food packaging, took place. The old can model with soldered seam, each consuming several grams of tin, has been substituted by a one-piece pressed model. This eliminated some 50% of world's tin demand and, combined with collapse of the International Tin Agreement (read above), devastated the world's tin industry.

Substitution

Markets can suddenly develop or collapse with material substitution, an event that has far-reaching consequences for the commodity supplier (Jewett, 1986). This has several causes: a) the newly applied material is superior to the older; b) the price of the original ingredient increased so the manufacturers have turned to a substitute, even if inferior; c) deposits of the original raw material became exhausted; d) supply was interrupted or greatly reduced; e) government legislation interfered with markets, for example by putting toxic or otherwise harmful commodities outside the law.

a) is exemplified by rapid change of the principal materials used in aircraft manufacturing in the past twenty years. Airbus Industries alone used 76% aluminum, 8% steel, 8% titanium, 5% other materials, and 3% composites in 1980s whereas the consumption projection for the year 2000 has been 46% composites, 34% aluminum, 9% titanium, 6% steel, and 4% other materials.

b) In the mid-1970s the price of copper suddenly increased so manufacturers of the standard house electrical wire started to market the cheaper aluminum wire. This caused some troubles resulting in several fires (by short circuits), widely publicized by the media. The house insurance increased for Al-wired residences and demand for aluminum wire dropped. Soon the copper price returned to normal and with it the time-tested copper wire.

c) It is little known that the most successful technology of aluminum recovery, hot electrolysis, uses molten Al fluoride bath and that the original natural ingredient, the mineral cryolite (Na_3AlF_6), came from a single known mineral deposit in the world, Ivigtut in Greenland, now exhausted. The aluminum industry, started on cryolite, had to develop an early substitute, a synthetic Al fluoride, from the available more abundant raw materials: bauxite (calcined and refined to alumina) and fluorite.

d) Supply reduction or interruption of raw materials flow is most intense and pressing in the time of major conflicts, so it is not a surprise that many new, now universal technologies of commodity manufacturing, have been developed in times of war initially as a measure to alleviate shortages caused by interrupted supply. About the greatest technological achievement of World War 1, from which the mankind benefits, has been the process of manufacturing synthetic nitrates from atmospheric nitrogen, developed in Germany. The direct impetus for this was the interruption of supply of natural Chilean nitrates that were essential for the war effort (nitrates were the main ingredient of classical explosives and gunpowder). World War 2 contributed much more. In addition to the utilization of nuclear power, first for destructive purposes and later for power generation which inaugurated uranium as a commodity in instant demand, it contributed a viable process of gasoline manufacturing from coal developed in Germany (then temporarily abandoned over most of the world except South Africa in the post-war period), and the process of extraction of metallic magnesium from sea water developed in Great Britain. It is interesting to trace the changing uses of uranium

throughout the ages, and the demand it created (Dahlkamp, 1993):

- 1500s: Pitchblende, the heavy but then useless companion of silver in some Erzgebirge deposits (Jáchymov, Johanngeorgenstadt), was dumped
- 1789: Klaproth discovered U as a new element
- 1825-1900: U used as glass and porcelain color pigment (fluorescent yellow, orange, green) and about 750 t U were produced from mines in the Erzgebirge, Cornwall, western United States
- 1898: P. and M. Curie discovered radium in pitchblende from Jáchymov and shortly afterward radium was used for radiation therapy of the very rich. The 1906 price for 1 gram Ra of \$ 10 million came down to \$ 120k in 1913 and \$ 70k in 1926. Known and newly discovered uranium mines of the ~1906-1938 period produced Ra (about 547 grams were produced worldwide in this period), with little use for the uranium co-product
- 1939-1960: Discovery of nuclear fission and a promise of powerful weaponry led to accelerated exploration, exploitation and extraction of U²³⁵ and synthesis of plutonium through chain reaction, with world's production reaching 10⁵ tons U/year;
- 1951-present: First nuclear power plants have been born and, gradually, demand for uranium as nuclear fuel has taken over U supplies for military uses. Even the depleted U (mostly U²³⁸) found a use as armor-piercing shells.

e) Government regulations. Some governments regulated, to some extent, mining and processing of strongly toxic substances such as arsenic and mercury already in the distant past, but the mass preoccupation with the real as well as imaginary health hazards related to minerals is largely a legacy of the 1970s, the Environmental Decade. The content of Hg and As in consumer products like thermometers or rat poison has been reduced to a minimum or outlawed entirely. Restriction on the use of the less toxic metals such as lead, cadmium, thallium (including the toxic as well as radioactive uranium) resulted in elimination of such formerly common consumer products like lead ingredient in gasoline, cadmium-based paints, and thallium-containing rodent killers. Lead has been virtually eliminated in the paint pigment market with exception of pigments used in industrial primers, as in ship hull preparation. The universal substitute in the important category of white household pigment has become titania and this created tremendous demand for TiO₂, the bulk of which comes from beach sand deposits. The future of the lead shot used by Canadian sports hunters is also bleak as more ducks are said to die from lead poisoning by ingesting spent ammunition than by being hit by it. The solution? Probably silver-coated lead pellets!

1.3.3. Où sont les métaux por avenir? Future ore deposits, conventional and non-conventional

The French quotation above (“where are the metals for the future”) is borrowed from the title of Pierre Routhier’s book (Routhier, 1980). There, Professor Routhier tied the future metals supply directly to geological sources in discrete ore deposits formulated in terms of the then relatively new plate tectonic model, heralded as the principal intellectual tool of future metals discoveries. The reality of future ore finding is more complex and in addition to the classical ore deposits numerous non-traditional geological metal sources will likely contribute a share of metals (Figure 1.5). The main body of this book is dominated by giant conventional deposits although unconventional resources are also discussed in the context of depositional environments and lithologic associations. They are briefly summarized below.

Unconventional mineral commodity sources

What are unconventional metal sources? They could be geological materials (i.e. rocks and aggregates) that contain metals in (much) lower concentrations than the conventional ores; they could be geological materials utilized for other purpose than metal extraction (e.g. as energy sources, such as coal or petroleum), the trace metal content of which could be recovered during processing; it could be seawater, atmospheric air, plants (Table 1.4). Some unconventional sources have been around for a long time, others are new, and a next generation of such sources could be developed in the future (Shanks, ed., 1983).

Mineral commodities from seawater and other liquids: Surely the oldest non-conventional mineral commodity source still in use is sea water (or lake water) from which salt (halite) is produced in salinas. The seawater can be “ordinary” (i.e. with the average NaCl content of about 3.4%), or enriched as in some restricted marine basins in the arid belt (e.g. Gulf of Persia) or in saline lakes. Climate is the principal condition that controls location of salinas whose bulk is along flat arid coasts, but even fairly wet or seasonally dry coasts as north of Bangkok, Thailand, can successfully operate when there is a local market. This salt resource is inexhaustible. Not considering the occasional utilization of bitterns, the KCl and MgCl₂ enriched brines that remain after halite

harvesting, metallic magnesium has been the second and bromine the third commodity industrially recovered from seawater up to the present.

Normal seawater contains 0.13% of dissolved Mg as chloride, and industrial recovery by electrolysis started in the early 1940s in response to the immediate wartime need. It stayed and at present between 30% and 60% of metallic magnesium is produced from seawater whereas magnesite, the earlier Mg ore, is now mostly processed into Mg compounds such as refractories (Kramer, 1985).

What are the principal requirements for selecting the site of a plant for Mg recovery from sea water? Not considering the economic and political factors (such as cost of electricity, environmental acceptance of the industry), the main requirement is an efficient natural removal of the processed (Mg-depleted) seawater and continuing supply of the undepleted water. This works best in straits with continuous, monodirectional (i.e. not tidal) and strong sea currents as, for example, along the English Channel (La Manche). In contrast with the classical ores, there is no emphasis on a "high-grade" seawater, although waters that are highly diluted by fresh water brought in by streams (such as in the Baltic or Caspian Seas) are not suitable.

The magnitude of metal concentration in seawater, however, could be important in the future should recovery of other metals, such as Au and U, becomes reality (Mero, 1965). Sites in the world ocean where the water is enriched in certain trace metal will be sought as it is known that trace element concentrations in sea water sometimes vary with location (e.g. Fe, Mn, Cu and Zn are enriched near sites of discharge of hydrothermal brines as at spreading ridges). There is, however, no overall survey yet. So far, trace metals recovery from seawater has been achieved in the laboratory and future economic projections have been made, but the low metal prices through the 1980s and 1990s have brought further experimentation to a standstill. Although the resource of dissolved uranium in the world ocean is estimated at about 5 billion tons of U and 6 million tons of Au (Llewelyn, 1976), no profitable recovery process has so far been found, although it was tried (e.g. by the Metal Mining Agency in Japan; International Mining, August 1986). Economic viability of seawater thus remains uncertain. Metal recovery circuits attached to desalination plants of which there are some 7000 today around the world, appear to be the economically most viable solution for seawater utilization as a metal source. If so, metals from seawater would provide one of several competing metal sources and with the exception of magnesium it does not appear that any of the metals recovered from seawater would ever dominate the market.

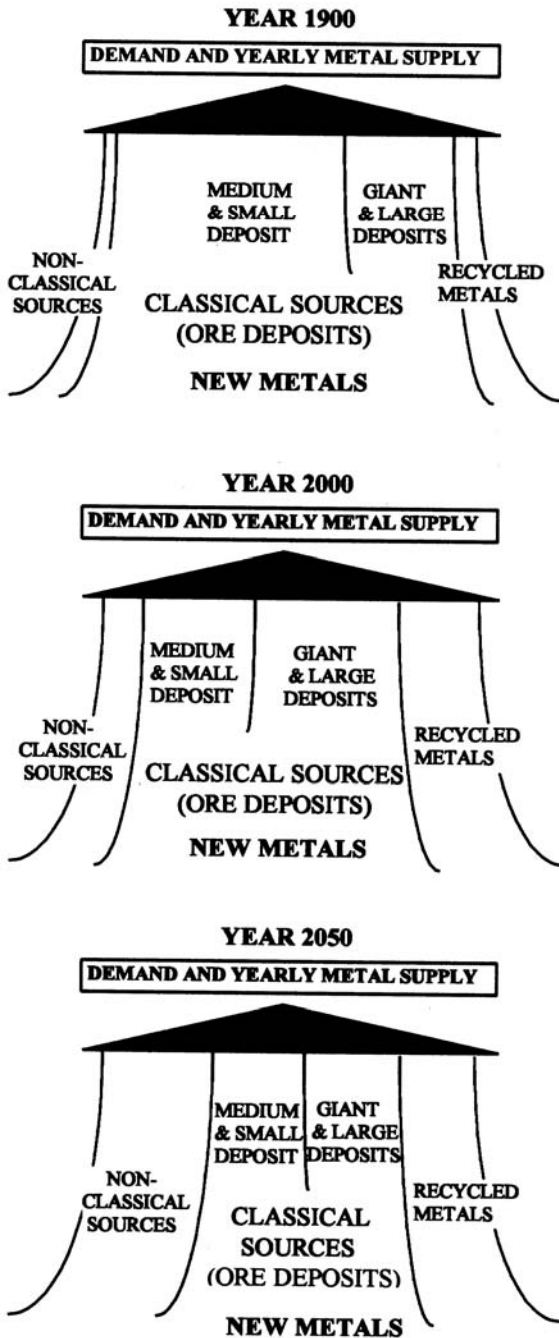


Figure 1.5. Presumed future metal sources. Modified from Laznicka (1996), computer graphics by Prof. C. Schejbal

Table 1.4. Selected unconventional sources of industrial metals

Metal source	Area, locality	Resources, geology, references	Grade	Reserve resource
Mg recovered from seawater	World ocean	Mg in MgCl ₂ dissolved in sea water; Kramer (1985)	0.13% Mg	n x 10 ¹³ t
Metals dissolved in hydrothermal fluid	Salton Sea, California	Active deep hydrothermal system in rift; White (1981)	540 ppm Zn 102 ppm Pb 1.4 ppm Ag	5 mt Zn, 900 kt Pb, 120 kt As, 10 kt Ag
B dissolved in hydrothermal fluid, in steam	Larderello geothermal center, Tuscany, Italy	Fluid reservoir in 160-700 m depth above granitic intrusions; Pichler (1970)		P _{to 1936} 7-8 mt H ₃ BO ₃
Li recovered from playa brine	Salar de Atacama, Chile	Li dissolved in brine interstitial to salt; Ferrell (1985)	0.14% Li	1.35mt Li
	Clayton Valley, Nevada	As above, Li also in hectorite, salts	0.023% Li	4 mt Li
	Salar de Hombre Muerto, Argentina	Li dissolved in brine; Minerals Yearbook, 1996		1.5 mt Li ₂ CO ₃
Li, Cs, U, Hg dispersed in lake beds, tuff	McDermitt Caldera, Nevada and Oregon	High trace metals content in fill of peralkaline rhyolite caldera; Rytuba and Glanzman (1985)	236 ppm Li 27 ppm U 0.29 ppm Hg	
W, As recoverable from playa brine	Searles Lake, California, U.S.A.	W dissolved in brine interstitial to salt (with As); Smith (1979)	32 ppm W; 100 ppm As	68 kt W 210 kt As
Mg from evaporites and brine	Makola & Youbi areas, SW Congo	Carnallite-rich evaporite deposit, solution mining; Mining Annual Review 1999		800 bt of Mg salts
	Brazzaville			
V recovered from petroleum	Venezuela and other countries	V resides in hydrocarbons, concentrates in ashes; Kuck (1985)	100-464 ppm V	9 kt V
Hg recovered from natural gas	Groningen gas field, Netherlands; former E. Germany	Hg vapors in gas from reservoirs in Zechstein; Ozerova (1981)	2 mg Hg/m ³	3 kt Hg
V recovered from tar sands	Athabasca Oil Sands area, Alberta	Dispersed V>Ni in bitumen matrix to Cretaceous sand, in clay fraction; Scott et al. (1954)	240 ppm V	3.0 mt V 750 mt Ti 8 bt Al
Al by-product of oil shale processing	Piceance Basin, Colorado	Al in authigenic dawsonite and nordstrandite in shale; Smith and Milton (1966)	2.15% Al	3.1 bt Al
Ge recovered from residua after coal burning	British Carboniferous coals and elsewhere	Trace Ge partitions into ash and flue dust up to a maximum of 2% Ge (Paone, 1970)	7 ppm Ge mean	200 kt Ge
Ditto	Novikovskoye, Sakhalin; Shkotovskoye, Primorye, Russia	Ge recovered from residua in power plants; Kats et al. (1998)	296 & 610 ppm Ge in raw coal	
U as by-product of phosphorite processing	Florida Land Pebble Phosphate Province	Trace U in fluorapatite of the pebble concentrate; Fountain & Hayes (1979)	85 ppm U mean	1.5 mt U
	Ditto	U in supergene Al phosphates	150 ppm U	400 kt U
Ga recovered from bauxite residua	Jamaica bauxite province; elsewhere	Ga accumulates in red mud processing residue; Petkof (1985)	50 Ga, 153 Sc, 100 Th, 1900 REE; all ppm	10 kt Ga, 30 kt Sc, 20 kt Th, 200 kt RE
Ti, Zr in low-grade dune sands	North Stradbroke Island dunes, Queensland	Ilmenite > rutile, zircon in heavy mineral fraction; 1.5-2% heavies, cutoff 0.75%; Wallis and Oakes (1990)	0.5% Ti 0.18% Zr	4.8 mt Ti 460 kt Zr
B from tourmalinite	Sullivan Pb,Zn,Ag mine, British Columbia, Canada	Tourmalinite is an alteration product in footwall of sedex orebody; Hamilton (1982)	4% B ₂ O ₃	200 mt B ₂ O ₃

Table 1.4. (continued)

Metal source	Area, locality	Resources, geology, references	Grade	Reserve, resource
Mn in nodules from Cretaceous shale	Chamberlain, South Dakota; area 240 km x 180 m	Diagenetic nodules with 15.5% Mn make up 5.5% of 13 m shale interval; Pesonen et al. (1949)	0.85% Mn	11 mt Mn

More unconventional deposits in the oceanic domain are described in Chapter 4

Waters (brines) of saline lakes such as Dead Sea, pore waters in the subsurface of saline lakes or dry playas (as under Searles Lake, California; Salar de Atacama, Chile), various formational brines associated with deep intracrustal reservoirs of petroleum as well as with independent brine pools, and geothermal hot springs (as in Larderello, Italy) have supplied a variety of mineral commodities for over a century. These sources are transitional into classical ores when solid salts form by evaporation of brines, or mineral sinters develop by precipitation from hot springs. Salts precipitated from brines are either permanent (they form bedded, buried deposits), or ephemeral (salt crusts in playa lakes cover the lake floor in the dry season, saline brine fill the basin in the wet period). Of the numerous products extracted from saline brines one can mention Na carbonates (trona, nahcolite), Na and Mg sulfates (mirabilite and epsomite), Na chloride (halite), Na and Ca borates (borax, colemanite, ulexite), Br, J, Li compounds (Salar de Atacama, Dead Sea), even tungsten (Searles Lake, California; Smith, 1979).

Mineral commodities extracted from air and earth gases: Gas mixtures present in the ordinary air, in hydrocarbon gases, in volcanic emissions, have long been utilized for selective recovery of pure elemental gases (i.e. O₂, N₂, He, Ne, Ar, Kr, F, Cl), gaseous compounds (CO₂, CH₄) and for recovery of various solid commodities that are present in gases as either aerosols or as gaseous compounds (e.g. SO₂, H₂S, H₃BO₃). Since the mid-1910s air has been the source of nitrogen for production of synthetic nitrates. Sulfur recovered from sour natural gas by scrubbing, which is a purification process applied at source to remove sulfur pollutants from the gas before it is piped to consumers, has elevated Canada into third place among the world's sulfur producers. This created market surplus that has made pyrite mining for sulfuric acid production in North America uneconomic and similar developments elsewhere

have greatly restricted pyrite mining in the rest of the world. Pyrite concentrate, at several mines where it has to be recovered from complex massive sulfide ores in order to liberate Cu, Zn and Pb sulfides, has become a liability as, in the absence of a market, it has to be disposed off and maintained to prevent oxidation and escape of acid compounds into the environment.

Several metals have been industrially recovered from various gases, or there is a potential to do so in the future and, as with sulfur, environmental protection is the principal incentive. Ozerova (1981) reported the presence of 2 mg Hg/m³ in the Groningen gas field in the Netherlands and in several fields in the former East Germany, derived from reservoirs in the metalliferous Upper Permian (Zechstein) strata. She estimated a mercury resource there of about 3,000 t Hg. A small portion of Hg may have already been recovered.

Metals from living organisms ("metal harvesting", "phytomining"): Trace element (metal) contents in various living organisms and their body parts (e.g. flesh, blood, bones, shells, tissue, wood, resins, etc.) have been reported for over a century and a sizeable database can be assembled from the literature (e.g. up to 560 ppm V in ash of Tunicates; up to 1% Zn and 0.1% Pb in fish bones; up to 0.5% I in ash of Laminaria seaweed; Mero, 1965). Although some trace metal contents in selected organisms approach the metal contents in industrial classical ores, an oyster or even an oyster colony will not yet make an orebody. Some communities of living organisms, however, have yielded small quantities of economic minerals after harvesting and processing (Leblanc et al, 1999); consequently, there is a possibility that some mineral compounds could be harvested in the future. The pre-industrial potash (K₂O) supply, for example, was produced by precipitation from solutes derived by leaching wood ash of some trees ("pot-of-ash"). Later on, a small quantity of copper was recovered from ash of peat in a small bog accumulated in the valley under the Coed-y-Brenin

porphyry copper deposit in Wales (Turf Mine); more Cu-impregnated peat deposits have been reported (e.g. the Tantramar Swamp, New Brunswick; Fraser, 1961), and uranium has also been recovered/reported from peat (Masugnsbyn, Sweden; California). Finally, iodine was produced in the last century from ash of sea weeds harvested off Great Britain (Mero, 1965; Lefond, ed., 1975).

Are we going to industrially harvest some metals soon? So far, there have been few encouraging signs, as the research in biotechnology is pointing in another direction: towards organisms-assisted containment of pollutants (phytoremediation), that is in-situ use of plants to extract heavy metals from contaminated sites using hyperaccumulator plants. Anderson et al. (1999) reported that a small shrub *Alyssum bertolonii* can remove over 100 kg Ni per year per hectare from substrate enriched in Ni above the mean crust content (they experimented with residual soil over ultramafics with 0.42% Ni). The plant-extracted metals are then recovered from ashes after incineration. A trial nickel phytomining in California achieved mean nickel concentration of 0.53% Ni in the plant *Streptanthus polygaloides* and a potential return of \$ 513/ha to the grower was calculated as achievable under optimum conditions.

Biomining (Barrett et al., 1993; Rawlings, ed., 1997) is a bacterial metal recovery from solution or sludge. It is a rapidly growing processing technology (usually a component of hydrometallurgy as it follows leaching) rather than a means of "making ore".

Trace metals in and recovered from fossil fuels-coal: In several cases, coals are so enriched in some trace metals such as uranium that the U-grade approaches the grade of other types of U ores, hence such a coal becomes a uranium ore in its own right. In most cases, however, plans have been drawn to utilize the metalliferous coal as a source of energy first (by burning it), then extract (leach) uranium from the residue (ash, slag, cinders). The better known deposits of uraniferous coals are in the U.S. Midwest (South Dakota, North Dakota, Montana; Denson and Gill, 1965), in northern Czech Republic (Radvaňovice), and elsewhere (Laznicka, 1985d). At several places in China (e.g. Wujiao in Hunan) sapropelic "stone coals", locally burned for energy, are highly anomalous in V, Cu, Ni, Ag, Mo and other recoverable trace metals and grade into metalliferous black shales (Chapter 13).

In addition to the rare coals strongly enriched in some trace metals (metal concentration factors are greater than about 50), there is a much greater abundance of slightly metal enriched coals

(concentration factors between about 5 and 50; Bouška, 1981). Although these coals could not be economically mined as metal ores, the non-volatile metals (i.e. most trace metals except Hg, As, Tl, partly Pb) remain in the residue after coal burning, from which they can be recovered mainly by leaching. This has several advantages: a) the residue had already been mined and delivered to the industrial complex at no extra cost; b) it has to be eventually disposed off; c) the trace metal concentrations have increased, after burning, several times relative to the coal; d) many trace metals can be easily and cheaply leached. Materials like this are sometimes called technological ores. The "germanium rush" of the 1950s (Paone, 1970) provides the best case history. Unfortunately, only small quantities of metals have been recovered from coal residua so far and the main reason seems to be that the power generating companies just do not want to bother.

Trace metals recovered from hydrocarbons: Like coals, hydrocarbons are often enriched in some trace metals (predominantly vanadium), which concentrate in ashes (Valkovic, 1978). It is, however, virtually impossible to collect the ash remaining after hydrocarbon combustion so the extraction of trace metals sometimes takes place in refineries that are equipped for this task (Kuck, 1985). It seems more feasible to recover trace metals from solid hydrocarbons like the Athabasca tar sands of Alberta, Canada (Scott et al., 1954) or from oil shales in the Piceance Basin, Colorado. The Alberta tar sands contain on the average 240 ppm V and 80 ppm Ni in bitumen that binds together quartz sands in a Cretaceous sand. Because of the enormous tar resource there is about 3 million tons of contained vanadium but only a fraction is recovered at present. The Piceance Basin oil shale (Chapter 13) contains, in some units, authigenic dawsonite and nordstrandite ($\text{NaAl}(\text{CO}_3)(\text{OH})_2$) and although the average recoverable aluminum content in such units is only 2.15% Al (i.e. less than one third of the Al clarke value) aluminum recovery might be feasible if it becomes a part of the overall industrial process of oil recovery. If so, there is a resource of some 3.1 billion tons of Al (Smith and Milton, 1966).

Metals on the deep sea floor: Ferromanganese nodules were first reported in 1891 by Murray, the geologist/oceanographer of the British Challenger expedition. Massive research into nodule distribution, origin, exploitation and processing took place during the Decade of Oceanography in

the 1960s and 1970s (Mero, 1965) but has petered down since. Even so a massive database of several thousand reports and journal articles exists (Haynes et al., 1986; McKelvey, 1986; Chapter 4). The nodules are, with variable density, scattered on top of abyssal oceanic clay and rapidly decrease in concentration with depth. They thus form a sea floor blanket that can be harvested by remote suction machinery (giant vacuum cleaners), washed, and shipped for metallurgical processing onshore. The Pacific nodules contain on the average 18% Mn and 17% Fe but the profit makers of nodule mining would be the trace elements, especially Co, Ni and Cu (followed by marginally enriched REE, Mo, V, Pb). The "good grade" concentrations are about 1.2% Co, 1.5% Ni and 1.2% Cu but the trace metals are unevenly distributed. Two best studied and economically most feasible nodule fields are in the equatorial and southern Pacific; the former is south of Hawaii between the Clarion and Clipperton fracture zones, and it is estimated to hold between 5 and 10.4 billion tons of nodules over an area of 6 million square kilometers, containing between 42 and 90 mt Ni and 35-76 mt Cu (Thiry et al., 1977). No actual production has, so far, taken place (except for experimental recovery of several thousand tons of nodules by the large resource corporations) and exploitation in the near future does not appear likely because of the political problems (ownership and sovereignty) and the generally unfavorable economics of metals supply.

Ferromanganese crusts that are valuable for their generally high trace cobalt contents are another variety of hydrogenous metal resources at the deep ocean floor (Toth, 1980; Hein et al., 1985; Chapter 4). They coat rock outcrops at seamounts, walls of submarine canyons and island pedestals and their mining would be many times more expensive than nodule mining as it would require selective scraping of hard rock surfaces. The positive side of Mn-Co crusts mining, however, would be the location as some are in the United States' (e.g. Johnson Island) or Micronesian Federation territorial waters; this would remove one of the political constraints on mining. Metalliferous muds produced at oceanic spreading ridges and subsequently carried away during ocean spreading have a bulk enrichment of Mn (around 0.6% Mn) and some trace metals and could also become a low-grade metal source in distant future (Field et al., 1983).

Accumulations of hydrothermal base, precious and rare metals sulfides together with Fe and Mn oxides are now known from more than hundred localities oceanwide, mostly from oceanic spreading ridges (Chapter 4) and less frequently

from back-arc basins, island arcs and seamounts (Rona, 1988; Fouquet et al., 1993; Chapter 5). The first deposit of hydrothermal metalliferous muds, that also appears economically viable, has been discovered in the 1960s in the Atlantis II Deep, in the axial graben of the Red Sea (resource of some 1.7 million tons of zinc, 400 thousand tons copper, and other metals in a 4-8 m thick mud layer distributed over 4.5 km² of seafloor; Degens and Ross, eds., 1969; Chapter 12). The oceanic spreading-ridge massive sulfides have mostly been added in the 1970s and 1980s, whereas the 1990s are marked by accelerated research in the island arc and backarc systems (e.g. the Lau Basin; Herzig and Hannington, 1995). So far, with the exception of Atlantis II Deep where experimental exploitation and feasibility have been performed, little economic resource evaluation and testing have been attempted.

The perspective of future hydrothermal sea floor sulfide and gold mining appears uncertain. The sulfide fields exposed on the bare sea floor are mostly small whereas the larger accumulations of gold (hundreds of tons of gold in material with a grade of 18 g/t Au is estimated to be present on a seamount 10 km south of the Lihir Island off New Ireland, in a depth of 1100 m; Peter Herzig, lecture, 1998) and of sulfides in sediments (as on the Escanaba and Juan de Fuca Ridges in eastern Pacific and in the Gulf of California; Koski et al., 1984; Goodfellow and Zierenberg, 1997) are partly buried. They would require deep underwater underground mining in unconsolidated and seismically active grounds. The outlook is thus less promising relative to nodule mining, although some of the reported deposits are in territorial waters of Papua New Guinea, Canada, the United States, and Mexico which is an important political advantage.

Metals recovered from very low grade orebodies and metalliferous units on land: The average and minimum (cut-off) grades of all metals have decreased with time, some drastically so (the average grade of the world's copper ores around 1900 was about 2% Cu and the lowest mined Cu ore had about 1 % Cu; in the 1990s the average Cu grade is about 0.8% Cu and the lowest grade of a predominantly Cu deposit, although with Au co-product, is 0.17% Cu and 0.79 g/t Au at Cadia Hill, New South Wales; Newcrest Mining Staff, 1998; Chapter 8). As a consequence the protore and some of the metal-rich "rocks" of yesterday are industrial ores of today. This trend will continue influenced, naturally, by demand and price. Most metals and nonmetallic commodities, in addition to the

inventory of the presently economic deposits and past producers repeatedly treated in databases, also include several known occurrences of presently uneconomic low-grade materials. Most of these occurrences have not been thoroughly explored hence they are not delineated and lack published ore reserves (although resource estimates are often quoted). They, however, represent the next logical step for the resource industry to turn to and mine, utilizing to a considerable degree the existing infrastructure

The numerous examples from the history of mining, when the industry has turned to materials with substantially lower grade than what was there mined before and succeeded, include: porphyry coppers whose exploitation in the western United States around the turn of the 20th century has initiated the concept of large tonnage "bulk mining" and processing of base metals; the "raw" or "lean" banded iron formations with some 20-30% Fe that are upgraded into 65% Fe pellets; the very low-grade "bulk" gold ores processed by heap leaching; and others.

The "low grade ores of the future" to watch include:

- Metalliferous "shales" (this includes slates, schists, even gneisses), examples: The 1600 km long metalliferous shale belt in south-eastern China (e.g. in the Hunan and Guizhou Provinces) where some shale occurrences contain up to 5% Mo, 7% Ni, 2% Zn, 1 ppm PGE, 0.55 Au (Coveney et al, 1992; Fan Delian et al., 1992); the Permian Phosphoria Formation in Idaho and Montana mined for phosphates, is also a large repository of V, Mo, Zn, Ag and other elements, not yet tapped, Chapter 13; the Alum Shale of southern Sweden with a large resource of U, V and Mo (Andersson et al., 1983). The bituminous, phosphatic Chattanooga Shale of Tennessee has elevated trace uranium but not enough to support economic recovery. If, however, all the shale constituents were separated, recovered and marketed, the operation would likely be profitable and a case for total resource utilization and no-waste mining could be established. Under the present legislation, however, the project would not be approved on environmental grounds.
- Sub-grade (that is, under 0.2% Cu and no Au) disseminated Cu, Mo and Au "porphyry" deposits;
- Low-grade (0.5-1% Zn+Pb) Zn- and Pb-mineralized altered carbonates as in the

Triassic "Ore Dolomite", Silesia-Kraków region of Poland;

- Disseminated rare metal minerals in alkaline complexes and carbonatites;
- Super-low grade heavy minerals sands as in the dune deposits at Stradbroke Island, Queensland (around 0.7% of heavy minerals);
- others.

Metals recovered from "rocks": Concentration histograms of any metal clearly indicate that the greatest proportion of metals resident in the crust is stored in rocks with the mean crust content concentration. It is, however, unlikely that rocks containing the Clarke values of 25 ppm Cu, 130 ppm Cr or 55 ppm Ni will ever be mined and processed for the recovery of Cu, Cr and Ni as there are certain "ordinary rocks" whose trace metal content is several orders of magnitude greater than the average trace contents. This is most strikingly illustrated by the group of elements enriched in ultramafics: Cr (average content 0.2% Cr, i.e. 15.4 times the Cr mean crust content of 130 ppm); Ni 0.2%; Co 50-100 ppm. The average Ni content in ultramafics like serpentinite is only four times lesser than the present average grade of Ni in the world's ores (about 0.8% Ni) and 5.5 times lesser than the average Ni grade in the presently mined laterite/saprolite deposits (about 1.1% Ni). It is thus likely that the "ordinary" ultramafics are going to become viable sources of Ni and also Cr, Mg and Co by-products by, say, 2050. The need to dispose of environmental liabilities such as large waste dumps could enhance the potential of "common rocks" as metal sources; for example, the large dumps of crushed or milled ultramafics accumulated after a century of asbestos mining in the Eastern Townships of Québec (e.g. Thetford Mines-Black River; Asbestos) recently started to be processed for the recovery of magnesium; Ni and Cr could follow.

Ultrabasics are geochemically unique and most of the remaining ore metals do not reside in "high grade ordinary rocks" although some come close: Zr, REE, Nb, Ta and others metals anomalously concentrate in alkaline rocks and carbonatites (Chapter 12); high Zn is in some shales and pelitic carbonates (Chapter 13); U in high-K, silicic granites (Chapter 19), black shales, phosphorites; Li in lithionite granites; and others. By far the most widespread category of metal-enriched rocks are various shales and their metamorphic equivalents, especially those high in carbon ("black shales") that can accumulate Ag, As, Au, Be, Bi, Cd, Co, Cu, Ga, Ge, Hg, Li, Mn, Ni, Pb, PGE, Rb, REE, Sb, Se, Sn,

Tl, Th, U, V, W, Y and Zn, although shales "specialize" and different elements are enriched at different sites. There is a gradual and continuous sequence of increasing metal concentrations from "trace metal-rich rocks" (this category) through "metalliferous rocks" (e.g. shales) to "ores"; the "typical" concentration limits for uranium in such a sequence would be about 10-20 ppm, 60-150 ppm, and 300 ppm plus, respectively. For copper it would be about 200-300 ppm, 0.1-0.2%, and 0.4% plus, respectively.

1.4. Conclusion: future supplies of metals and giant deposits

Review of the non-conventional ores above makes it clear that the future commodity supplies are going to come from a mixed bag, more mixed than anything we have experienced so far (Figs. 1.6, 1.7). It seems that the heterogeneity of supplies will at least be preserved at the present level, and more likely increased but we do not believe a supply monopoly would develop in which all (or most) metals would come from a single source such as seawater. Even individual commodities are most likely to come from more than a single source as is, presently, the case with metallic magnesium (about 60% comes from seawater, 20% from magnesite, 25% from dolomite, 4% from brucite, 1% from ultramafic waste). There is certainly going to be a competition in future commodity supplies, and local comparative advantage in geology, combined with environmental and political considerations, will allow profitable existence of local raw material producers that might appear marginal and be overlooked in grand global forecasts; however, the share of small to medium deposits in global supply of the common industrial metals will likely come down to less than 10%, fairly soon. The present share of giant deposits in the world's metals supply will likely increase to peak some 30 to 50 years from now, once the existing "giants" are gradually exhausted and the new generation of "giants" will almost entirely consist of the shallowly, then deeply-buried orebodies.

Apart from the greatly increased exploration costs to find such deposits, their abundance and variety will likely decrease with the increasing depth. First to disappear are likely to be the supergene enriched and unconsolidated clastic ores, the present mainstay of the Al, Fe, Mn, Ti, Zr, partly Au, Sn, Cu, U, supplies. Only their paleo-equivalents at buried unconformities, paleoplacers (Witwatersrand) will be left once the solid bedrock

is reached, under the unconsolidated or friable cover and regolith.

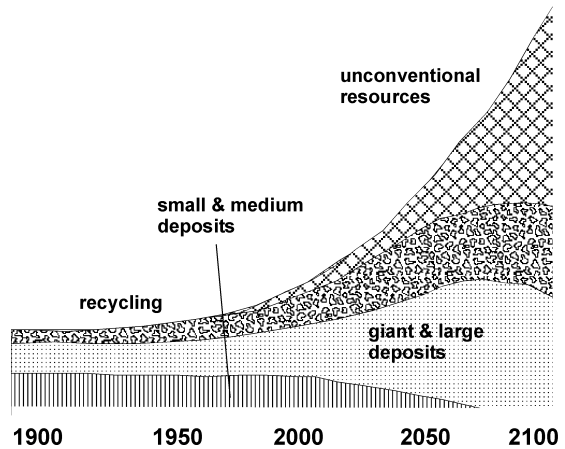


Figure 1.6. Projected anticipated main source categories of industrial metals

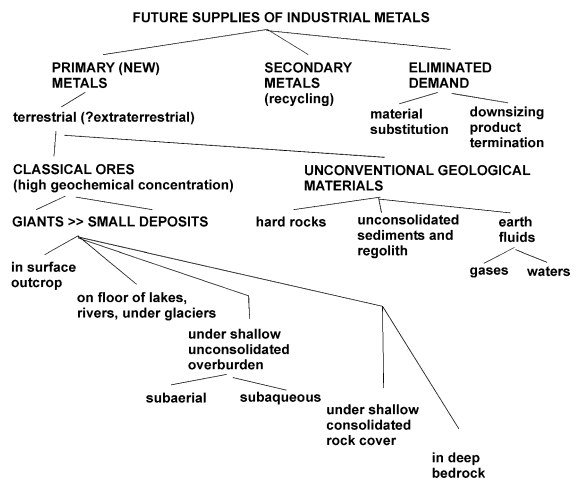


Figure 1.7. Categories of the future metal supplies expected to grow at the expense of the classical (highly geochemically concentrated and in surface outcrop) deposits

In the same time, epithermal deposits will disappear. It can be argued that deposits that originated in greater depth like the mesothermal deposits (e.g. the orogenic "shear-Au"), Bushveld-type Cr, Ni, Fe, Ti, PGE or Broken Hill-type Pb-Zn-Ag might be discovered under the present metallogenes dominated by the high level deposits, but apart from the exploration costs mining in depths exceeding some 2000 m would be so costly to eliminate profit margins. The present deep Witwatersrand mining, at the average depth exceeding 2000m and reaching down to almost 4000m, is rapidly becoming unprofitable despite the

fact that the "reefs" in the established fields require relatively little of deep exploration and have to be merely followed.

Sober analysis indicates that the present exponential growth of almost everything: population, consumption, resources exhaustion, pollution, environmental degradation, is unsustainable. Drastic measures and new, revolutionary approach will be required to establish sustainable levels, if at all possible. The first test is going to come within the next 30 to 50 years when the forthcoming depletion of hydrocarbons will have forced drastic rethink of the automobile culture and transportation in general. If the car production is greatly reduced, it will lower the demand for metals; this will extend the lifetime of existing ore deposits (the argument that metals might be substituted by plastics and composites is only a half-truth; plastics are produced from hydrocarbons and coal, commodities that undergo depletion as well). So as the future energy costs are going to increase, so will metal prices. This will encourage recycling to reach its maximum practical limits (still some 20 to 40% to go) and it will make economic metal recovery from the "nonconventional resources" like sea water and "ordinary rocks" increasingly attractive.

The "new approach" to mineral resources will induce a variety of cost- and environment-saving arrangements and symbiotic establishments recovering metals and nonmetallics from sea water in units attached to desalination plants, 100% (no waste) utilization of geological materials, mining as a by-product of earth works and habitat creation (e.g. excavation for underground factories, transportation and storage facilities with utilization of the excavated rock as construction material or an ore). There is already a mine of the future in operation. It is the Felbertal tungsten mine in the Austrian Alps (Chapter 14), the largest ("giant") European W deposit, quietly operating deep under an alpine valley unnoticed by tourists. This mine still depends on the classical geochemically enriched ore, though.

We believe the future mineral commodity supplier, be it a "vertically integrated" corporation or a one-person business, will be required to handle, simultaneously, three types of tasks (not considering product marketing): 1) "inventing" the type of raw material suitable for an industrial application presently in demand; alternatively, developing an application (a product) to be manufactured from an existing raw material already in the company's portfolio, in a "no objections" setting; 2) finding the required raw material by

exploration or otherwise; 3) processing the material in an economic and innovative way so that profit is made.

Large integrated corporations maintain special divisions developing and marketing new applications for their products; for example Molycorp, Inc., the owner and operator of the giant Mountain Pass rare earths deposit in California (Chapter 12), has developed many new industrial applications for their products and created market and demand where there was none before. So did INCO, Ltd. for nickel; AMAX, Inc. for molybdenum; Brush Wellman, Inc. for beryllium. The new application developers have to work closely with exploration departments (or with exploration consultants) at all stages of the project to be kept aware as to what kind of raw materials would be possibly available and which would be more economic to procure and exploit if there is a choice. Exploration geologists, in turn, have to be continuously on the lookout not only for orebodies required to replace deposits of existing materials that are being depleted, but also for alternative materials that might possibly substitute for them as well. Many small, locally based junior mining companies, whose main business is mineral exploration, do very well when they are flexible and knowledgeable about new products and applications, new markets, new technologies and continuously vary their ore finding programs and property portfolios to take advantage of changing markets, demands and prices. This, in turn, might encourage better technical education and knowledge preservation, a sorely needed task.

Global resources of metals at the start of the 21st century: the U.S. Geological Survey data

These are compiled, with minor modifications, in Table 1.5.

No-waste resource exploitation: hypothetical utilization of the Chattanooga Shale, Tennessee

Waste dumps, tailings ponds, dissolved solids in waste waters, aerosols that result from mining, are pollutants and eyesores. They are also a liability that have to be handled during reclamation, and they cause material loss. Utilisation of everything that has to be extracted during mining, when practicable, can add value and reduce or eliminate the environmental impact. The idea is not entirely new as the "clean" waste rock from hardrock mines has been used as crushed stone for road and other construction for some time. Clean quartz tailings after gold-quartz vein processing can substitute for glass sand.

Table 1.5. Official but recalculated and edited 2002 U.S. Geological Survey data on global metals production, price, endowment and reserve life

Metal	World production	Approximate metal price	World reserve	World re-serve base	World resource	Static re-serve life
Al ^a	32.25 mt	\$ 1,500/t	5.5 bt	8.25 bt	16.25 bt	156y
Ag	18.8 kt	\$ 145/kg	270 kt	520 kt		14.36y
Au	2,530 t	\$ 9,912/kg	42.5 kt	89 kt	100 kt	16.8y
As	26.5 kt	\$ 600/t	530 kt	795 kt		20.78y
Be	160 t	\$ 360/kg	30 kt?		80 kt	187.5y
Bi	3,900 t	\$ 8030/t ^b	330 kt	680 kt		84.6y
Cd	18,7 kt	\$ 660/t	600 kt	1.8 mt		32.1
Co	36.9 kt	\$ 14,300/t	6.7 mt	13 mt	15 mt	181.6y
Cr ^c	3.913 mt	\$ 249/t	482 mt	2.137 bt	3.612 bt	12.3
Cs	~100 t?	\$ 13,700/kg	1.4 mt	2.2 mt		372.3y
Cu	9.217 mt ^d	\$ 1,540/t	480 mt	950 mt	1,600 mt	52.1
Fe ^e	495 mt	\$ 50/t	67 bt	148 bt	360 bt	135.4
Ga ^b	55 t	\$ 425/kg	30 kt?		1 mt?	545y
Ge	68 t	\$ 1,700 ^f	100 kt?			1,471y
Hf	90 t ^g	\$ 130/kg	517 kt	933 kt	1 mt	574y
Hg	1,400 t	\$ 4,200/t	120 kt	240 kt	600 kt	86y
In ^b	200 t	\$ 210/kg	690 t			3.45y
Li	15.1 kt	\$ 16/kg ^h	4.1 mt	11 mt	13 mt	272y
Mg ^j	422 kt	\$ 1,875/t				unlimited
Mn	7.6 mt	\$ 250/t ^b	300 mt	5,000 mt		39.5
Mo	128 kt	\$ 8,300/t	8.6 mt	19 mt		67.2
Nb	25.7 kt	\$ 6,776/t	4.4 mt	5.2 mt		171y
Ni	1.32 mt	\$ 6,776/t	61 mt	140 mt		46.2y
Pb	2.9 mt	\$ 970/t	68 mt	140 mt	1,500 mt	23.4y
PGE ^k	400 t	\$ 15,000/kg	71 kt	80 kt	100 kt	177y
Pd	193 t	\$ 10,610/kg				
Pt	171 t	\$ 18,000/kg				
Ir		\$ 5,065/kg ^m				
Os		\$ 12800/kg ^m				
Rh		\$ 24150/kg				
Ru		\$ 1,930/kg				
Ra	40 g ⁿ	\$ 30,000 n				
Rb	300 t?	\$ 9,980/kg	150 kt?			500y?
Re	23.1 t	\$ 1,069/kg	2,400 t	10,000 t		104y
REE ^o	68 kt	\$ 230/t	70 mt	120 mt		1029y
Ce	34 kt	\$ 23.75/kg				
Dy	204 t	\$ 81.35/kg				
Er	340 t	\$ 187.50/kg				
Eu	102 t	\$ 875/kg				
Gd	238 t	\$ 143/kg				
Ho	68 t	\$ 606/kg				
La	24 kt	\$ 28.75/kg				
Lu	6.8 t	\$ 5,625/kg				
Nd	9.52 kt	\$ 27.50/kg				
Pr	3,128 t	\$ 40/kg				
Sm	544 t	\$ 93.75/kg				
Tb	68 t	\$ 856/kg				
Tu	136 t	\$ 4,500/kg				
Yb	6.8 t	\$ 287.50/kg				
Sb	141 kt	\$ 1,474/t	1.8 mt	3.9 mt		12.7y
Sc ^b	1,800 t	\$ 198/kg	300 kt?			167y?
Se	1,460 t	\$ 8,540/t	84 kt	180 kt		57.5y

Table 1.5. (continued)

Metal	World production	Approximate metal price	World reserve	World reserve base	World resource	Static reserve life
Sn	231 kt	\$ 4,000/t	6.1 mt	11 mt		26.4 y
Sr ^p	158 kt	\$ 62/t	3.0 mt	52.8 mt	440 mt	19y
Ta	1,530 t	\$ 165/kg	39 Kt	110 kt		25.5y
Te	130 t	\$ 37.4/kg	21 Kt	47 kt		161y
Th	300 t?	\$ 93/kg	1.2 Mt	1.4 mt	2.5 mt	883y
Ti ^q	2.94 mt	\$ 7,770/t	282 Mt	492 mt	738 mt	96y
Tl	15 t	\$ 1,250/kg	380 t	650 t	17,000 t	25y
U ^r	42,219 t	\$ 26/kg ^s	2 Mt ^t	2.87 mt	4.63 mt	47y
V	67 kt	\$ 5,500/t	13 Mt	38 mt	63 mt	279y
W	46.6 kt	\$ 9,730/t ^b	2.9 Mt	6.2 mt		62y
Y	2,400 t	\$ 105/kg	540 Kt	610 kt		225y
Zn	7.17 mt	\$ 880/t	200 Mt	450 mt	1,900 mt	28y
Zr ^u	910 kt	\$ 25/kg	27.4 Mt	53.3 mt	44 mt	30y

NOTES: Data in this table are from U.S. Geological Survey Commodity Summaries 2003, and except for figures marked with question mark that are my estimates, they are true quotes recalculated to uniform metric units of pure metals. The original data were, as is the American tradition, in a chaotic mix of units that included metric tons, short tons, kilograms, pounds, Troy ounces, flasks of mercury, units of WO₃. Most of the commodities were shown as pure metals, but also as compounds (mostly oxides) or shipping products such as Ti sponge, bauxite, Fe ore and Mn ore. The reliability of data at source varies as the U.S. Government often withheld proprietary data when there was a single U.S. producer only (as with beryllium), then filled the gaps by estimate (or not at all). The Summaries also applied estimates to generate production figures for countries that did not publish their data (e.g. the former USSR, China).

To fill the metal prices column posed a special challenge not only because of the variety of units, but also because there is a wide range of prices depending on the form, purity and degree of processing of metals; it was occasionally unclear what the quoted prices actually represent. When a range of prices was given, I entered the lowest price. Some information gaps have been filled by price quotes for other years and this is clearly marked in the table. The table is hardly accurate, especially for the fringe metals, but in the absence of better data the figures here provide a rough approximation which is better than nothing. The reader will note that there is a variable degree of discrepancy between the U.S. Geological Survey figures and figures applied in the metallogeny-related chapters in this book that I have generated from data available for individual metallic deposits.

Indexed notes: **a:** Al content in bauxite taken as 25% Al; **b:** 1996 data; **c:** Cr content in chromite ore; **d:** smelter (primary) copper; **e:** Fe content in ore @ 45% Fe; **f:** 1997 data; **g:** 1983 production; **h:** Li content in lithium carbonate; **j:** magnesium metal only produced from different materials including sea water; virtually unlimited resource of materials suitable for Mg recovery; **k:** group figure for platinum group metals; **m:** 1992 price; **n:** 1937 price; **o:** "mischmetal", a mixture of rare earth elements dominated by Ce and La and marketed mainly as oxides. The prices of RE metals were calculated from the 1996 prices of RE oxides with 80% of metal and the production tonnages calc-estimated using ratios for bastnaesite concentrate; **p:** Sr content in celestite; **q:** Ti in titanium sponge; **r:** 1990 U production; **s:** 1997 U price; **t:** 1989 figures from Crowson (1992); **u:** Zr content in compounds, price for Zr sponge

Magnesium and possibly chromite and trace nickel extraction from dumps and tailings after asbestos mining has recently started.

The following account deals with a hypothetical example of a no-waste open pit mining and processing of the, on the average 5 m thick, Gassaway black shale member of the late Devonian Chattanooga Shale along the Eastern Highland Rim in Tennessee (near Nashville). This unit (Conant and Swanson, 1961; Fig. 1.8) is distributed over a large area and it is in a shallow subsurface of less than 66 m under the surface over an area of some 1295 square kilometers. This "orebody" was drilled and investigated in the 1950s and 1960s mostly as a possible source of low-grade uranium. If it is ever mined (this is unlikely in the near future because of the severe environmental constraints), it will be likely processed for multiple commodities: petroleum (this is a

low-yield "oil shale"), sulfur in pyrite, trace U, Mo, V and perhaps Ni, Se substantially enriched in the shale. Phosphates could be produced from phosphoric horizons immediately above and below the black shale. The commodities listed above represent less than 10% of volume of the "ore" (shale), the remainder of which (pulp) is very suitable for production of expanded shale for lightweight aggregates. As thermal expansion of the shale pulp result in increased volume and reduced specific gravity, the product volume would be about twice the volume of the shale mined.

Table 1.6. gives the calculated "in ground" values of marketable commodities, but the processing costs would be high. The shale is self-energizing as it burns, leaving behind more than 95% of residue. If the bitumen contained in the shale is used up as fuel, there would be little hydrocarbons left to extract as "oil".

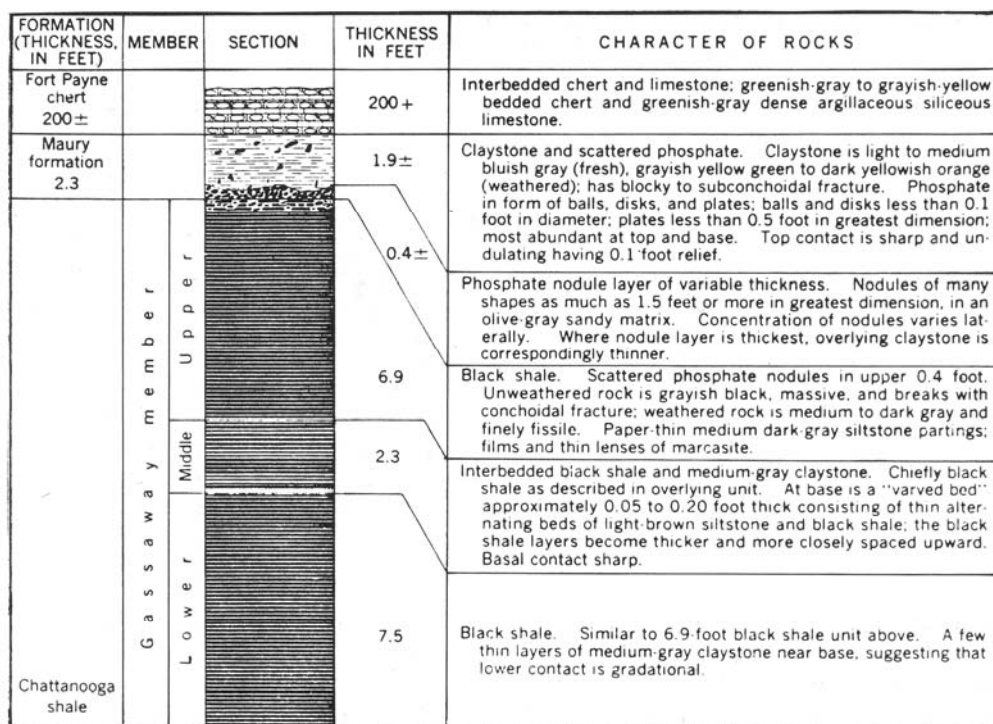


Figure 1.8. Detailed section of the uraniferous Gassaway Member in Tennessee, from Conant and Swanson (1961), U.S. Geological Survey

Table 1.6. Inventory of commodities in the Gassaway black shale unit in Tennessee. Area 1295 km², average thickness 5 m, specific gravity 2.3. Estimated values are in U.S. dollars, 1990s prices

Commodity	grade	units	price per unit	quantity	value (USD)
Expanded shale	90% +	m3	\$50	6.5 billion	\$ 325 billion
Sulfur (from pyrite)	5.5%	tons	\$90	825 million	\$ 74 billion
Oil (liquid hydrocarbons)	7.6 l/t	barrels	\$30	714 million	\$ 21 billion
Uranium (trace metal)	60 ppm	tons	\$20,000	900,000	\$ 18 billion
Molybdenum (trace metal)	160 ppm	tons	\$9,000	2,4 million	\$ 21 billion
Vanadium (trace metal)	160 ppm	tons	\$20,000	2.4 million	\$ 48 billion
TOTAL					\$ 507 billion

In the energy-hungry, environmentally indifferent 1950s and 1960s a megaproject like this would have received serious consideration and literature of the period would consider this as a future of resource exploitation. The "green wave" of the 1970s and beyond has extinguished similar hopes.

2 Data on Metallic Deposits and Magnitude Categories: the Giant and World Class Deposits

2.1. Data sources and databases

This book strives to be quantitative. It is based on data from mineral deposits, gathered over a period of 40 years and assembled in an unpublished database called GIANTDEP, in my books (Laznicka, 1985, 1993, 2004) and in Data Metallogenica (read above). The data have limitations, they change (improve) with time, and are only as good as their original sources. Readers familiar with a large volume of literature that quotes numerical data from mineral deposits are aware about the constant change and discrepancies. Data used in this book have been reconciled and edited in a uniform way so that discrepancies have been “smoothed”, but not eliminated.

Numerical data

Not considering geographic coordinates, distances and dimensions (length, width, depth, thickness) of orebodies, the principal numerical units that characterize ore deposits are ore tonnage and average metal(s) grade. From this can be calculated the economic content of metals in a deposit. The ideal figures would correspond to proven quantities of metals present in a delineated ore deposit before mining started (i.e. pre-mining reserves) and not subsequently modified afterwards. Orebodies with gradational (assay) boundaries against the host rocks also require information about the cut-off grade, as various cut-offs determine the tonnage of material classified as ore. Although ideal tonnage/grade figures, capable to withstand scrutiny, do exist, the majority of data scattered in the literature, including this book, assume to be close to the ideal figures, but offer no background check. Such data are sometimes known as metal(s) endowment and they could be the quantities of ore or metals actually produced during the lifetime of a presently exhausted mine, past production and remaining reserves, calculated quantities of metals never recovered, and similar. In this book, I have endeavored to build the economic metal(s) tonnage figures in a deposit to the highest, realistic levels often from fragments of data, with minor gaps filled by estimates. In some cases when making numerical

comparisons the minimum assured metal quantities, and the maximum extrapolated or estimated quantities, were used side-by-side as alternatives.

Apart from data variation and uncertainty caused by the dimensional category and complexity of a metal accumulation (read below), the data vary by representing either production (cumulative to date or for a period of time only), reserves or resources. The resource figures are always greater (and less certain) than reserve figures. There are several categories of reserves and resources in international use of which two: the “western” ones (defined by the U.S. Geological Survey and used, with modification, by the “western” mining industry) and the “eastern” ones (developed in the former Soviet Union and used in the socialist and some third world countries), have been most widely used.

Cumulative metal tonnage/grade figures recorded during the lifetime of a past producer and from unmined orebodies for which reserve figures have been calculated, are generally final and do not change with time. Figures from operating mines and from prospects undergoing active exploration do change: they mostly grow. Sometimes the growth is phenomenal and figures quoted in the review and reference literature lag behind. The Mount Leyshon low-grade gold stockwork in Queensland went into production in 1986, with published reserves of 23.1 t Au, to deliver more than 3 million ounces (93.3 t) Au by the time of mine closure and rehabilitation in 2002. (Teale and Lynch, 2004).

The copper endowment of the huge El Teniente copper deposit in central Chile has gone from 3 mt Cu quoted in the pre-1940 literature through 6 mt Cu in 1960, 9.6 mt Cu in 1975 (Camus, 1975) to 50 mt in 1980, 55 mt in 1996, to the latest figure of 94.4 mt Cu quoted by Cooke et al. (2004). There are two reasons for it: 1) continuous production and exploration that result in a steady increase of metal produced and proven; 2) the nature of quoted figures. Whereas the pre-1980 figures represented production to date, the more recent figures incorporate past production and resources that include a much lower grade material than what was the case in the past (average grade of 0.63% Cu for the 2004 figure versus about 2% Cu for the “classical” ore). Unfortunately, the nature of the tonnage/grade data available for the bulk of the

world deposits is not always available so what we have are generic figures of variable accuracy. Continuous refinement of mineral databases is thus essential, but in the meantime we have to use data far from perfect to reach quantitative conclusions, as in this book. The novice reader, in particular, has to realize that numbers, as in the tonnage/grade figures, only appear accurate but in many cases they are not.

Data sources

With very few exceptions the ore/metals tonnage and grade figures represent delineated metal accumulations of actual or potentially economic interest. Delineation (that is, exact establishment of limits of an orebody) is essential, as it marks the boundary between the "ore" and the "normal rock". There is no controversy when there is a sharp drop in metal concentration between the ore and the "rock", but orebodies with gradational boundaries often change shape and dimension as the cut-off grade (the minimum grade mined) changes with economic conditions. Some obvious and well-known metal accumulations are not presently delineated, hence they are usually not included in mineral deposit databases and compared with the "classical" deposits: they are open-ended. Perhaps the best known example of non-delineated orebodies are the seafloor fields of Fe-Mn nodules. Others are massifs, zones or continuous units of rocks from which metals could be extracted (e.g. serpentinite as a source of Mg, Cr and Ni; anorthosite or nepheline syenite as a source of Al; beach or dune sands for heavy minerals), of which only portions have been delineated as economic orebodies, mostly on politico-technologic or environmental grounds.

Tonnage/grade data for delineated classical deposits come from published literature like international research journals (*Economic Geology*, *Mineralium Deposita*, *Ore Geology Reviews*); trade journals (*Mining Journal*; *Engineering and Mining Journal*; *CIM Bulletin*); government publications (U.S. Geological Survey Professional Papers, *Bulletins and Mineral Yearbooks*; *COMRATE*, 1975, report); compilations of ore deposit models (Cox and Singer, eds, 1986; du Bray, ed, 1995; Kuznetsov, ed, 1983; Roberts and Sheahan, eds, 1988; Kirkham et al, eds, 1993); conference and symposia volumes; annual reports of publicly listed corporations; and others. Data in text- and reference books retain validity for the traditional deposits, but become rapidly outdated where they deal with recent discoveries and actively explored properties.

Increasingly, last minute tonnage/grade data are posted at company web pages. Regurgitated data can be found in numerous databases, manual and electronic (e.g. CRIB/MRDS of the U.S. Geological Survey; LODE database of large European deposits; GEODE), but not many are publicly available, at least not for an affordable cost.

The "mainstream data" published in and by organizations domiciled in the developed English-speaking countries (the United States, Canada, Australia, South Africa) are most abundant, accessible and consistent. They have a hundred year long tradition. Information from countries that publish in major European languages is less consistent, scattered and often hard to reach outside the countries of origin, but it does exist and circulate at least in compilations. Data in the literature printed in cyrillic (former USSR, Bulgaria, Serbia, Mongolia) and especially in Asian and Arabic scripts, can be read by few, so only English translations or review articles circulate widely and enter the Western awareness. The traditional Anglophone disinterest about the literature outside the mainstream has been further compounded by foreign governments' secretiveness and censorship, prevalent especially in the literature from communist and socialist countries between about 1940 and 1990 (compare Laznicka, 1985b). In the past ten years or so, with globalization and international investments booming, a wealth of tonnage/grade data has been seeping out of the former Soviet Union, China, Eastern Europe, Mongolia and Vietnam, leaving North Korea as the last remaining no-data recluse. Capture and utilization of such data, however, still remains incomplete.

GIANTDEP database: This database supports the numerical conclusions reached in this book. The database is continuously evolving, hence the conclusions change slightly with time. This book presents conclusions based on the 1997-1998 state of GIANTDEP and published in Laznicka (1999), as well as conclusions based on the most recent, 2003-2005 version. In this database each entry represents an exceptional accumulation of one ore metal only in an orebody, ore deposit, ore field, district or basin, identified as a locality (the internal complexity and dimensions of the various types of "localities" are reviewed below). In most cases there is one database entry per locality (for example, the giant Kirkland Lake gold ore zone in Ontario is a single entry locality, as only gold is accumulated above the giant deposit threshold). When one locality stores exceptional tonnages of more than one metal, it is entered two or more times (Table 2.1).

Table 2.1. Deposits and districts with exceptional accumulations of two or more metals; updated from Laznicka (1999)

Metals	Number of localities	Example locality	Metals	Number of localities	Example locality
2 metals			3 metals		
Au, Ag	1	Pachuca, Mexico	Ag, Pb, Zn	6	Sullivan, Canada
Ag, Cu	2	Lubin (Kupferschiefer), Poland	Ag, Pb, Au	1	Beregovo, Ukraine
Ag, Pb	6	Santa Eulalia, Mexico	Ag, Cu, Mo	1	Butte, Montana, U.S.A.
Ag, Sn	3	Potosi, Bolivia	Ag, Cu, Zn	1	Kidd Creek, Canada
Ag, Zn	1	Rajpura-Dariba, India	Au, Cu, Mo	2	Petaquilla, Panama
As, V	1	Kerch Fe Basin, Ukraine	Bi, Sn, W	1	Shizhouyuan, China
Au, As	2	Vasil'kovskoye, Kazakhstan	Cu, As, Se	1	Rio Tinto ore field, Spain
Au, Cu	13	Grasberg, Indonesia	Cu, Ni, PGE	2	Sudbury Complex, Ontario ¹⁾
Au, Te	2	Cripple Creek, Colorado, U.S.A.	Au, U	1	Witwatersrand, S. Africa ¹⁾
Pb, Cd, As	1	Tsumeb, Namibia			
Bi, Sn	1	Gejiu, China	PGE, Ni, Au	2	Merensky Reef, South Africa
Cr, PGE	2	Great Dyke, Zimbabwe ¹⁾	Ti, Fe, V	1	Bushveld Magnetite, S. Africa
Cu, Mo	10	Chuquicamata, Chile	W, Bi, Te	1	Verkhnye Qairakty, Kaz.
Cu, Co	1	Katanga (Shaba) Copperbelt	Zr, Nb, REE	1	Ilímaussaq, Greenland ¹⁾
Cu, Ni	2	Jinchuan, China			
Fe, Mn	1	Urucúm (Corumbá), Brazil	4 metals		
Fe, V	1	Bakchar ore field, Russia	Cu,U,Au,Ag	1	Olympic Dam, South Australia
Mo, U	1	Billingen (Alum Shale), Sweden	Ag, Mo, Cu, Au	1	Bingham porphyry, U.S.A.
Nb, REE	1	Bayan Obo, China	Pb, Zn, Ag, Cu	1	Mount Isa, Australia
Nb, Th	1	Araxá, Brazil	Zn, Pb, Ag, Bi	1	Brunswick # 6, 12; Canada
Nb, Zr	1	Lovozero Complex, Russia ¹⁾	REE, Y, Nb, Sc	1	Tomtor, Anabar Massif, Russia
Ni, Co	1	New Caledonia laterites			
Pb, Sb	1	Bawdwin, Myanmar (Burma)	5 metals		
Pb, Zn	8	Century, Australia	Zn, Pb, Ag, As, Sb	1	Cerro de Pasco, Peru

¹⁾ Cumulative tonnage of several deposits in a mineralized complex

The number of entries in GIANTDEP is thus larger than the number of localities. The huge Olympic Dam deposit in South Australia is an example of a four-metals "supergiant" reported to contain, in the 2004 global resource of 2.6 billion tons, 33.8 mt Cu @ 1.3%, 1300 t Au @ 0.5 g/t, 832kt U @ 0.032% and 7540 t Ag @ 2.9 g/t (Skirrow et al., 2002). Two additional metals: Fe (676 mt @ 26%) and Ce-La rare earths (13 mt @ 0.5%) are below the giant threshold (they are "large" metal accumulations). The total calculated value of the contained metals, at average prices, is of the order of US\$ 160 billion, although not all the metals are recoverable. Olympic Dam is the single largest U deposit in the world; the largest U and Cu resource in Australia; 2nd largest Australian gold; and the world's 6th largest Cu deposit.

Most localities in the GIANTDEP file are single deposits or sometimes composite entities (ore fields, districts, ore zones, belts and systems), the metal content of which is a sum of metals in several orebodies or deposits that, individually, are not of the "giant" magnitude. A minority of localities are members of hierarchically arranged sets in which

the lower rank metal accumulations (orebodies, ore deposits) are included in higher rank groupings like ore fields, districts or basins. Witwatersrand is a typical example: it is a "basin" (e.i. the first-order division) subdivided into several goldfields (second-order division, e.g. West Wits), some of which contain still lesser, third-order divisions such as individual "reefs" (=orebodies like Vaal Reef). The locality rank is clearly listed in GIANTDEP and further discussed below.

Visualization of ore deposits and their host associations-Data Metallogena: In terms of realism (essential for the growth of a practicing, field-oriented geologist) the sources of geological knowledge rank as follows (from the most realistic down): 1. Field visit or study (with literature background); 2) Comprehensive sets of geological samples (including drill core) with photos, notes, some analytical data, literature; 3) Literature study only; 4) Databases compiled from literature.

Field visits are costly and time consuming and few geologists are lucky enough to visit a sufficient number and variety of deposits in their lifetime to

reach the geo-nirvana: that is, a balanced understanding (or at least a "feeling", hunch) of where ores tend to be and where to look for the new ones. Serendipity, often mentioned as a factor in ore discovery (e.g. Woodall, 1983, 1984, 1994), works best with experienced geologists. This leaves the second best option, the locally assembled real rocks, as the more accessible realistic learning alternative. Central, state museums are rarely on the itinerary of knowledge-seeking practical geologists because of the belief that they only concentrate on curiosity objects. This belief is wrong (compare Laznicka, 1985b) but the truth remains that to capture the gems of practical knowledge stored in museums one has to penetrate the officialdom to reach collections behind the public galleries. Small company or mine museums are more user friendly and sometimes excellent (many used to exist in the former U.S.S.R.), but they keep disappearing rapidly.

Since about 1970 several enlightened governments invested into drill core libraries and these have proven their worth by now; some are excellent and they provide a first-rate service, usually at no cost (examples: South Australian core library in Adelaide; Western sedimentary basins library in Calgary, Alberta). The problem with museums and core libraries is that there is too much material of variable relevance, and a lack of portability. There was a need for a more compact alternative to provide an introductory (first-stage, equivalent to a publication abstract) yet comprehensive visual information on the actual rock and ore materials from which the many types of mineral deposits, and their host associations, are assembled. Such alternative is now available in the form of Data Metallogena (DM), briefly introduced above. Images of geological materials with explanatory sheets and complementary information can now be accessed by internet worldwide (www.Datametallogena.com), and the actual samples are open for inspection and nondestructive testing in DM's home in Adelaide. Book readers can thus gain an immediate on-line access to DM to have the written world extended by images of the real geological materials, field photos and graphs. In a rapidly growing number of cases a DM online visit comes close to a virtual field visit.

2.2. Giant and world class ore deposits: definition and characteristics

Concept history

Metallic ore deposits and districts have been known and exploited since antiquity and their number steadily grew. As, before the Industrial Revolution, only ten metals had been known and utilized (gold, copper, tin, iron, lead, silver, mercury, antimony, arsenic, bismuth, partly zinc for alloys) the number of mines and their geological variety had been small. Some ancient deposits or mines were famous because of the contribution they made to the wealth and power of the local state, territory or royalty, and/or because of their importance for the economy and trade of the medieval and earlier world. Selection of the famous mines of antiquity and of medieval times include Sar Chesmeh, Iran; Queen Sheba gold mine in Yemen; the King Solomon copper mines near Timna, Israel; the Laurium (Lavriion) silver mines in Greece, the principal wealth source of the Athens state; the Kolkhida gold area in the Caucasus; the Transylvania gold region (Roşia Montană, Brad) in Romania; the Cornish tinfield in Great Britain; the Erzgebirge tin and silver region (Freiberg, Schneeberg, Jáchymov, Cínovec); the Kutná Hora silver mines in Bohemia; the silver mines of the Spanish Meseta and Almadén mercury deposit; and many others.

In the old days mineral deposits were neither systematically explored and their reserves calculated and published, nor were there systematic and reliable records of cumulative metal production, hence quantification was impossible. In retrospect we now know that the Queen Sheba and King Solomon mines were small deposits; Lavriion, Kutná Hora, Jáchymov, Freiberg were medium to large deposits; and only Roşia Montană, Almadén, Cornwall and Iberian Meseta as a whole, were giant or world-class deposits as defined below. A large influx of giant deposits followed the conquest of the Americas (e.g. Potosí and Cerro de Pasco in Bolivia and Peru; Guanajuato, Zacatecas and Pachuca in Mexico; Morro Velho in Brazil) and, of course, the Industrial Revolution when the number of industrial metals discovered and later utilized kept rapidly growing. Quantitative data on mineral deposits (grade and tonnage) were, however, entering the literature very slowly and most were incomplete figures for short periods of production. De Launay (1913) and the earlier issues of *Economic Geology* (from 1907 through 1940) quoted quantitative data

very sparingly. Ore reserve figures became available relatively late, in the 1930s, pioneered by the data generated in the large, bulk mined porphyry copper deposits of the American West (e.g. Bingham, Morenci) and published mostly in the U.S. Geological Survey Professional Papers and Bulletins. For a brief period of time before World War 2 government agencies in the former USSR (e.g. Ural'skaya Planovaya Komissia, 1934), also published ore reserve figures. The latter publications, in Russian, are virtually unknown and unread in the West, and they were soon terminated and replaced by secrecy in their home country.

It was not until the early 1960s and the onset of computerization when data became sufficiently abundant to construct global databases and perform numerical analyses. Metallogeny, based on geotectonic models of the day (geosynclines & orogenic belts until 1968, plate tectonics afterwards), became popular and its most colorful expression was the early generation of metallogenic maps published between 1955 and 1985 (e.g. Shatalov et al., 1966; Laffitte et al., 1970; Grushevoi et al., 1971; Guild et al., 1981; read Foose and Bryant, 1993, for bibliography). Probably the earliest quantitative map of the world's mineral deposits was published by Laffitte and Rouveyrol (1964, 1965). The magnitude of ore deposits (districts), taken as the percentage of global endowment of each commodity, was shown by the size of the symbol; for example, of the 280 million tons of cumulative world copper production and reserves in 116 deposits, 5 deposits contained 38% of the total copper and were shown by large symbols. Most of the largest symbols in Laffitte and Rouveyrol (1964) map corresponded to giant deposits defined below, as known in the 1960s, although some "deposits" were, in fact, large mineralized provinces (e.g. the African Copperbelt, Arizona-New Mexico Cu province). Since the 1960s the number of ore "giants" has almost doubled.

Several quantitative databases of the world's ore deposits (e.g. MANIFILE, Laznicka, 1973; CRIB, later renamed MRDS, database of the U.S. Geological Survey, Calkins et al., 1973; U.S. Geological Survey, 1988) and national/regional ore deposits (e.g. CANMINDEX of Canada, Picklyk et al., 1978; Mindep of British Columbia and Yukon) were initiated in the late 1960s-1970s and some have been later used with geographic information systems (GIS; e.g. Sinclair et al., 1999). The magnitude of ore deposits followed from figures and, more strikingly, from graphic plots. It was thus possible to separate the "exceptional" deposits from

the "normal" ones but there was no special terminology for the exceptional deposits and/or a magnitude classification.

Magnitude terminology for deposits of geological resources has been first developed by the petroleum industry (e.g. Klemme et al., 1970) and the United States' literature uses the following terms applied to quantities of recoverable petroleum in ground (Hobson and Tiratsoo, 1981):

- Significant oilfield 1 million barrels plus
- Major oilfield 25 million barrels plus
- Giant oilfield 100 million barrels plus
- Supergiant oilfield 10 billion barrels plus

A barrel contains 42 U.S. gallons or 159 litres of fluid. The international magnitude limit of giant oilfields is larger than the U.S. counterpart (500 million barrels plus) and there were 187 giant and 17 supergiant oilfields in the world, in the 1970s (Hobson and Tiratsoo, 1981). The above count included 33 giant and supergiant fields and these, although they represented mere 0.1% of the significant and larger petroleum accumulations, held more than a quarter of the estimated ultimately recoverable oil resources of the world.

The Russian book edited by Favorskaya and Tomson (1974) used the designation "krupnye mestorozhdeniya" (=large ore deposits) in its title and is generally considered to be the initiator of selective treatment of only the exceptional ore deposits. True to the secrecy that applied to grade/tonnage information in the former Soviet Union, the book is non-quantitative. In about the 1980s, the geological and mineral industry jargon has been enriched by inclusion of the highly subjective term "world class deposits" that rapidly infected even the serious and precise research literature and conference proceedings of the 1990s and beyond (e.g. Cox and Singer, 1986; Whiting et al., 1993; Clark, 1995; Keith and Swan, 1996; Naldrett, 1999). The term seems to be mainly an attention catching and marketing tool and is so relative that it conveys no real information about the magnitude of the deposit and cannot be used for comparison purposes (the "worldclassiness" is in the eyes of the beholder). Alternative non-quantified magnitude terms used in the Chinese literature are "large", "superlarge" as well as "giant" and "supergiant" deposits (e.g. Pei Rongfu, editor, 1997). Russian literature has used, interchangeably, terms like "unique", "large", "exceptional" and "giant" (e.g. Litvinenko et al., 1996; Epstein et al., 1994). Because of state

ensorship and unavailability of production/reserve figures in communist countries until recently, the use of non-quantified magnitude figures had some justification.

Mining operations are characterized and ranked on the basis of ore tonnage and/or production per day, month, year. This is widely used in planning and engineering management but is not of much use in economic geology as a small, high-grade deposit could contain more metal than a large, low-grade deposit. Greatness of a metal accumulation can be further expressed by a magnitude rank based on the tonnage of ore in reserve or, better, by tonnage + grade at a certain cut-off grade. This gives best results when applied to populations of mutually comparable deposits (same metals, same type) like porphyry coppers. Such an information is best displayed in grade/tonnage graphs (e.g. Cox and Singer, eds., 1986).

The remaining quantitative indicator of an orebody greatness is its monetary (usually U.S. dollar) value, applied to the "value" of metal(s) in the economic ore derived by multiplying the tonnage of the contained metal(s) by the present LME price (for example, the Olympic Dam deposit had a value of about \$ 162 billion in the late 1990s). As with the ore tonnages above, dollar values are most helpful when used for comparison of contemporary deposits of the same metals and similar styles.

Several attempts to classify magnitude categories of ore deposits and introduce precise terminology have been made, since the 1980s, on the basis of 1) share of the known global endowment of a commodity (e.g. copper) held by a deposit (e.g. Singer, 1995), an economic geologic premise; 2) magnitude of ore metal accumulation in relation to the mean crustal content of elements (e.g. Laznicka, 1983), a geochemical premise; 3) dollar values, an economic premise.

Economic geologic premise: the world class deposits (WCD)

Singer (1995) pointed out that the recently popular term "world class deposit" had been overused and had no frame of reference whatsoever. Using data assembled in the U.S. Geological Survey databases (already applied in preparation of the mineral deposit models and grade/tonnage graphs; Cox and Singer, eds, 1986; du Bray, ed, 1995), he proposed a quantitative definition where WCD's are those in the "upper 10 percent of deposits in terms of contained metal", a magnitude comparable with his alternative term "giant". A "super-giant" would

apply to the upper 1% of deposits. Singer (1995) placed the lower limits of WCD's of the five metals he processed at 100 t Au, 2,400 t Ag, 2 mt Cu, 1.7 mt Zn, 1.0 mt Pb, hence there is some discrepancy in respect to the "giant" and "super-giant" thresholds proposed by Laznicka (1999) and followed in this book (these are: 250 t Au, 7,000 t Ag, 2.5 mt Cu, 6.7 mt Zn, 1.5 mt Pb).

Singer's approach requires accurate and finite numbers of deposits together with their grades and tonnages, but there is likely a discrepancy between the numbers of deposits in the USGS databases and the objective reality. The U.S. Geological Survey database used by Singer, for example, included 1,325 Cu deposits whereas in my personal database there are more than 2,000 Cu entries and I am still aware that this number is incomplete. I suspect that the USGS databases become progressively undernourished in ore deposit entries as one moves away from the United States and from countries where the USGS personnel worked as advisers (e.g. the Arabian Peninsula), and that this undernourishment becomes significant in the C.I.S. countries and China. Moreover, Singer (1995) did not carry on his exercise beyond the five metals and as the source database is not available, it is not possible to extend the WCD magnitude terminology to deposits of other metals.

WCD's are clearly economic geologic, rather than metallogenic, entities so they are influenced by price, demand, markets that do not directly correlate with the geochemical magnitudes of metal concentration and accumulation on which is based the "giant" deposit terminology pursued here (it is explained below). Singer's (1995) WCD's of the "unwanted" (like Th, As) and limited demand (Nb, REE) metals that have few database entries would be hardly comparable with deposits of the eagerly sought metals like Au, Cu, Zn endowed with thousands of deposits each. Given the lack of perfect databases, I suggest to utilize the term "world class" in the subjective, informal and approximate way as is the case with many comparable terms in geosciences and mining. Alternatively, top ten deposits (rather than top 10% of deposits) of each metal could be declared as of "world class", and the magnitude of the tenth entry selected as the WCD threshold until a new major discovery is made that would move the threshold one notch up. Example: ten largest Cu deposits & ore fields ranked by metal endowment:

1. El Teniente, 94.5 mt
2. Chuquicamata, 87 mt
3. Kolwezi, 67 mt
4. Rio Blanco-Los Bronces, 59 mt

5. Olympic Dam, 46 mt
6. Tenke-Fungurume, 45.6 mt
7. Ertsberg-Grasberg, 44 mt
8. Collahuasi, 29.5 mt
9. Escondida, 26 mt
10. Udokan, 24 mt

The "world class" threshold thus would be 24 million tons of copper.

An alternative to the "world class" characterization of an ore deposit could be the share (percentage) of the world's endowment of the same metal, a deposit stores. So the Kalahari Mn Basin stores some 48% of the world's on-land Mn, Olympic Dam is credited with 37% of the world's U, Almadén has some 29% of the world's Hg. Surely these figures would vary with various authorities and change with time, but so do all quantities based on mining data. Laffitte and Rouveyrol (1964) used this approach successfully in constructing what was one of the first quantitative maps of the world's ore deposits (metallic and nonmetallic).

The geochemical premise: giant and super-giant deposits

Shortly after first estimates of elements abundances in the crust had been published (Clarke, 1924), it became obvious that metal concentrations in ore deposits are closely related to them. Fersman (1933) coined the term "clarke" as a unit of the mean crust content (for example, clarke of copper was then 30 ppm Cu), as well as the term "clarke of concentration" (CC) alias concentration factor, which is an ore grade divided by clarke. So CC of a 1.0% Cu ore is $10,000 \text{ ppm} / 30 = 333$.

McKelvey (1960) devised a relationship between crustal abundances and potential United States' ore reserves, expressed as $R=A \times 10^{9-10}$, where R=reserve in short tons; A=clarke in percent. In case of lead, using the Pb clarke of 0.0013%, the U.S. lead resources fell into the range of 1.3 to 13 million tons (or 1.6 to 16 million tons if the more commonly quoted Pb clarke of 16 ppm were used). As this was lower than the 1960 reality of 31.8 million tons of lead in the U.S. reserves, Erickson (1973) introduced the factor of 2.54 to modify the McKelvey's formula as $2.54A \times 10^{9-10}$. This was based on the 31.8 mt of Pb resource divided by McKelvey's 13 mt Pb. Erickson (1973) claimed that this formula represented "the potential recoverable resource for most elements".

Increasing globalization of mineral deposit data, and the realization that metallogeny is really a

geochemistry of exceptional metal accumulations, required a common denominator that would make it possible to compare and rank deposits of the various metals according to the effectiveness of ore forming processes, as well as favorability of settings in which these processes took place plus their preservation history. In simple words, there was a need to compare deposits of metals with highly variable clarke values such as iron, copper, tin, uranium and gold by magnitude of their geochemical accumulation process to assign the top contender the rank of a "geochemical giant".

Magnitude of metals' accumulation: This task clearly could not have been accomplished by comparing straight economic tonnages of metals in orebodies, as a 1000 ton gold orebody is clearly more exceptional and it took more effort to form than a 1000 ton deposit of tin, copper or iron. The only means to measure and compare the geochemical effectiveness would be with the help of derived, artificial units, such as tonnages of a hypothetical rock that would accommodate those thousand ton contents of various metals in clarke concentrations. Such a unit is called tonnage accumulation index (tai; Laznicka, 1983, 1999) and is derived by dividing the economic metal content in a deposit by metal clarke.

After calculating tonnage accumulation indexes for thousands of metallic deposits in a database, several classes of magnitude in terms of metal accumulation effectiveness became apparent. The top ones, with tai's of the order of $n \times 10^{11}$ and $n \times 10^{12}$, have been named giant and supergiant (Laznicka, 1983, 1999). Magnitude thresholds are different for every metal because every metal has a different clarke, so a giant iron deposit starts at 4.3 billion tons of Fe, a copper giant starts at 2.5 million tons of Cu, a gold giant requires at least 250 t Au. The problem of the enormous range of tonnage magnitudes within one division of a log scale (e.g. between 2.5 and 25 million tons of copper) has been rectified by subdividing each log interval into three equal portions that are referred to as "low", "mid" and "high". So a 5 mt Cu deposit would be a "low giant"; a 12 mt Cu deposit would be a "mid giant"; a 20 mt Cu deposit would be a "high giant". The same applies to subdivisions in the "large" and "supergiant" divisions. Names of the accumulation magnitude divisions follow from Table 2.2; Table 2.3. lists thresholds of magnitude divisions for each metal.

Table 2.2. Terminology of metal accumulations (deposits, districts) based on tonnage accumulation index (tai), exemplified by Cu (Cu clarke=25 ppm)

magnitude term	tai: lower threshold	corresponding Cu tonnage
Supergiant (deposit)		
high supergiant	6.6×10^{12}	165 mt (unknown)
mid supergiant	3.3×10^{12}	82.5 mt
low supergiant	1×10^{12}	25 mt
Giant (deposit)		
high giant	6.6×10^{11}	16.5 mt
mid giant	3.3×10^{11}	8.25 mt
low giant	1×10^{11}	2.5 mt
Large (deposit)	1×10^{10}	250 kt
Medium (deposit)	1×10^9	25 kt
Small (deposit)	1×10^8	2,500 t
Very small (deposit)	1×10^7	250 t

Concentration factor (clarke of concentration):

Tonnage accumulation values say nothing about metal concentration although it is assumed that the delineated deposits listed in the literature have sufficient grades to be of economic interest. As classical ore deposits are also exceptional concentrations of metals expressed in reports as ore grade (in percent, ppm, ounces per ton), a unit of clarke-related concentration is needed to work together with tai. This unit is the already mentioned clarke of concentration, CC (Fersman, 1933) and the proposed terminology of the metal concentration magnitudes follows from Table 2.4.

Clarke-normalized quantitative data from metal deposits have the advantage of being completely devoid of the politico-economic and technological influences, hence any metal accumulation can be accommodated and compared. This makes it possible to maintain continuity in the treatment of both "ores" and "rocks".

Most giant and supergiant deposits defined by relation to metal clarkes are also the world class deposits of Singer (1995), but there are exceptions. The geochemically most abundant metals Fe, Al and Mg form ore deposits with very low clarkes of concentration (between 3 and 10; in case of Mg recovered from sea water CC is negative, i.e. Mg concentration in seawater is less than Mg clarke), hence an iron deposit needs a resource of at least 4.3 billion tons of Fe to become a "geochemical giant". Corresponding tonnages for Al are 8 billion tons and for Mg 3.2 billion tons. There are few iron accumulations that qualify (e.g. the Snake River Fe deposit, Yukon, 11.62 bt of Fe), but none of aluminum recovered from bauxite. The largest

listed bauxite district, Boké-Gaoual in Guinea, has Al content of 3.88 billion tons, hence it is a "mid-large" accumulation. If, in the future, anorthosite should become an industrial Al ore, many anorthosite massifs will become giant deposits. Deposits of several metals with limited demand like thorium also lack giant deposits because none have been delineated. The remaining metals without "giants": Be, Ga, Ge, In, Sc, Ta and Tl have limited industrial demand and also have poor geochemical ability to locally accumulate. Their largest deposits, however of small to medium-size only, would attain the "world class" rank of Singer (1995) because of the way his definition is worded (10% of largest deposits, regardless of size). Although this book applies uniformly the geochemical accumulation magnitude divisions to maintain consistency, it is not fundamentalist and the largest deposits of giants-lacking metals are treated as well.

Clarke values used to determine magnitudes of metal concentration and accumulation: Although free of economic and technologic bias, tai and CC figures are influenced by clarke values. These, unfortunately, are not uniform and they change with the progress of science in time and, for the worse, with individual roughly contemporary authorities (please see the table of metal abundances and further discussion in Chapter 3). Clarke values for continental crust calculated by Wedepohl (1995), illustrated here by several trace metals, are 56 ppm Ni, 25 ppm Cu, 14.8 ppm Pb, 1.7 ppm U, and 2.5 ppb Au. Corresponding clarke values from Rudnick and Fountain (1995) are 51 ppm Ni, 24 ppm Cu, 12.6 ppm Pb, and 1.42 ppm U. In contrast, Taylor and McLennan (1995) credit their "bulk continental crust" with 105 ppm Ni, 75 ppm Cu, 8 ppm Pb, 0.91 ppm U, and 3.0 ppb Au. The discrepancy in the crucial elements like Ni is about 200 percent, Cu 300 percent, Pb and U under 200 percent. The main reason for this discrepancy are the various proportions of the lower and upper continental crusts selected by the authors, and a controversy about the composition of the lower continental crust (is it mostly "basaltic"?). Taylor and McLennan (1995) gave more weight to the mafic component in the lower crust, hence their high clarke values for the siderophile and chalcophile metals like Ni and Cu.

In this study are used the clarke values of Wedepohl (1995); Fig. 2.1. It is obvious that if clarke estimated by different authorities are used to calculate tai's and CC's, the definition and number of "geochemical giants" will change.

Figure 2.3. Crustal abundances (clarkes), thresholds and range of the "large", "giant" and "super-giant" accumulations of metals. Modified from Laznicka (1999)

metal	clarke ppm	Large deposits			Giant deposits			Supergiant deposits		
		low	mid	high	low	mid	high	low	mid	high
Al	8.0×10^4	8.0×10^8	3.2×10^9	5.6×10^9	8.0×10^9	3.2×10^{10}	5.6×10^{10}	8.0×10^{10}	3.2×10^{11}	5.6×10^{11}
Fe	4.3×10^4	4.3×10^8	1.7×10^9	3.0×10^9	4.3×10^9	1.7×10^{10}	3.0×10^{10}	4.3×10^{10}	1.7×10^{11}	3.0×10^{11}
Ti	4.0×10^3	4.0×10^7	1.6×10^8	2.8×10^8	4.0×10^8	1.6×10^9	2.8×10^9	4.0×10^9	1.6×10^{10}	2.8×10^{10}
Mn	7.2×10^2	7.2×10^6	2.9×10^7	5.0×10^7	7.2×10^7	2.9×10^8	5.0×10^8	7.2×10^8	2.9×10^9	5.0×10^9
Zr	2.0×10^2	2.0×10^6	8.0×10^6	1.4×10^7	2.0×10^7	8.0×10^7	1.4×10^8	2.0×10^8	8.0×10^8	1.4×10^9
REE	1.5×10^2	1.5×10^6	6.0×10^6	1.1×10^7	1.5×10^7	6.0×10^7	1.1×10^8	1.5×10^8	6.0×10^8	1.1×10^9
Cr	1.3×10^2	1.3×10^6	5.2×10^6	9.1×10^6	1.3×10^7	5.2×10^7	9.1×10^7	1.3×10^8	5.2×10^8	9.1×10^8
V	1.0×10^2	1.0×10^6	4.0×10^6	7.0×10^6	1.0×10^7	4.0×10^7	7.0×10^7	1.0×10^8	4.0×10^8	7.0×10^8
Zn	6.5×10^1	6.5×10^5	2.6×10^6	4.6×10^6	6.5×10^6	2.6×10^7	4.6×10^7	6.5×10^7	2.6×10^8	4.6×10^8
Ni	5.5×10^1	5.5×10^5	2.2×10^6	3.9×10^6	5.5×10^6	2.2×10^7	3.9×10^7	5.5×10^7	2.2×10^8	3.9×10^8
Cu	2.5×10^1	2.5×10^5	1.0×10^6	1.8×10^6	2.5×10^6	1.0×10^7	1.8×10^7	2.5×10^7	1.0×10^8	1.8×10^8
Co	2.4×10^1	2.4×10^5	9.6×10^5	1.7×10^6	2.4×10^6	9.6×10^6	1.7×10^7	2.4×10^7	9.6×10^7	1.7×10^8
Y	2.4×10^1	2.4×10^5	9.6×10^5	1.7×10^6	2.4×10^6	9.6×10^6	1.7×10^7	2.4×10^7	9.6×10^7	1.7×10^8
Nb	1.9×10^1	1.9×10^5	7.6×10^5	1.3×10^6	1.9×10^6	7.6×10^6	1.3×10^7	1.9×10^7	7.6×10^7	1.3×10^8
Li	1.8×10^1	1.8×10^5	7.2×10^5	1.3×10^6	1.8×10^6	7.2×10^6	1.3×10^7	1.8×10^7	7.2×10^7	1.3×10^8
Sc	1.6×10^1	1.6×10^5	6.4×10^5	1.1×10^6	1.6×10^6	6.4×10^6	1.1×10^7	1.6×10^7	6.4×10^7	1.1×10^8
Ga	1.5×10^1	1.5×10^5	6.0×10^5	1.1×10^6	1.5×10^6	6.0×10^6	1.1×10^7	1.5×10^7	6.0×10^7	1.1×10^8
Pb	1.5×10^1	1.5×10^5	6.0×10^5	1.1×10^6	1.5×10^6	6.0×10^6	1.1×10^7	1.5×10^7	6.0×10^7	1.1×10^8
Th	8.5×10	8.5×10^4	3.4×10^5	6.0×10^5	8.5×10^5	3.4×10^6	6.0×10^6	8.5×10^6	3.4×10^7	6.0×10^7
Cs	3.4×10	3.4×10^4	1.4×10^5	2.4×10^5	3.4×10^5	1.4×10^6	2.4×10^6	3.4×10^6	1.4×10^7	2.4×10^7
Be	2.4×10	2.4×10^4	9.6×10^4	1.7×10^5	2.4×10^5	9.6×10^5	1.7×10^6	2.4×10^6	9.6×10^6	1.7×10^7
Sn	2.3×10	2.3×10^4	9.2×10^4	1.6×10^5	2.3×10^5	9.2×10^5	1.6×10^6	2.3×10^6	9.2×10^6	1.6×10^7
As	1.7×10	1.7×10^4	6.8×10^4	1.2×10^5	1.7×10^5	6.8×10^5	1.2×10^6	1.7×10^6	6.8×10^6	1.2×10^7
U	1.7×10	1.7×10^4	6.8×10^4	1.2×10^5	1.7×10^5	6.8×10^5	1.2×10^6	1.7×10^6	6.8×10^6	1.2×10^7
Ge	1.4×10	1.4×10^4	5.6×10^4	9.8×10^4	1.4×10^5	5.6×10^5	9.8×10^5	1.4×10^6	5.6×10^6	9.8×10^6
Ta	1.1×10	1.1×10^4	4.4×10^4	7.7×10^4	1.1×10^5	4.4×10^5	7.7×10^5	1.1×10^6	4.4×10^6	7.7×10^6
Mo	1.1×10	1.1×10^4	4.4×10^4	7.7×10^4	1.1×10^5	4.4×10^5	7.7×10^5	1.1×10^6	4.4×10^6	7.7×10^6
W	1.0×10	1.0×10^4	4.0×10^4	7.0×10^4	1.0×10^5	4.0×10^5	7.0×10^5	1.0×10^6	4.0×10^6	7.0×10^6
Tl	5.0×10^{-1}	5.0×10^3	2.0×10^4	3.5×10^4	5.0×10^4	2.0×10^5	3.5×10^5	5.0×10^5	2.0×10^6	3.5×10^6
Sb	3.0×10^{-1}	3.0×10^3	1.2×10^4	2.1×10^4	3.0×10^4	1.2×10^5	2.1×10^5	3.0×10^5	1.2×10^6	2.1×10^6
Se	1.2×10^{-1}	1.2×10^3	4.8×10^3	8.4×10^3	1.2×10^4	4.8×10^4	8.4×10^4	1.2×10^5	4.8×10^5	8.4×10^5
Cd	1.0×10^{-1}	1.0×10^3	4.0×10^3	7.0×10^3	1.0×10^4	4.0×10^4	7.0×10^4	1.0×10^5	4.0×10^5	7.0×10^5
Bi	8.5×10^{-2}	8.5×10^2	3.4×10^3	6.0×10^3	8.5×10^3	3.4×10^4	6.0×10^4	8.5×10^4	3.4×10^5	6.0×10^5
Ag	7.0×10^{-2}	7.0×10^2	2.8×10^3	4.9×10^3	7.0×10^3	2.8×10^4	4.9×10^4	7.0×10^4	2.8×10^5	4.9×10^5
In	5.0×10^{-2}	5.0×10^2	2.0×10^3	3.5×10^3	5.0×10^3	2.0×10^4	3.5×10^4	5.0×10^4	2.0×10^5	3.5×10^5
Hg	4.0×10^{-2}	4.0×10^2	1.6×10^3	2.8×10^3	4.0×10^3	1.6×10^4	2.8×10^4	4.0×10^4	1.6×10^5	2.8×10^5
PGE	1.3×10^{-3}	1.3×10^1	5.2×10^1	9.1×10^1	1.3×10^2	5.2×10^2	9.1×10^2	1.3×10^3	5.2×10^3	9.1×10^3
Te	5.0×10^{-3}	5.0×10^1	2.0×10^2	3.5×10^2	5.0×10^2	2.0×10^3	3.5×10^3	5.0×10^3	2.0×10^4	3.5×10^4
Au	2.5×10^{-3}	2.5×10^1	1.0×10^2	1.8×10^2	2.5×10^2	1.0×10^3	1.8×10^3	2.5×10^3	1.0×10^4	1.8×10^4
Re	4.0×10^{-4}	4.0×10^0	1.6×10^1	2.8×10^1	4.0×10^1	1.6×10^2	2.8×10^2	4.0×10^2	1.6×10^3	2.8×10^3

Clarke values are after Wedepohl (1995), metals arranged by decreasing clarkes

With Taylor and McLennan (1995) clarkes the number of nickel, copper and gold giants would decrease, the number of lead and uranium giants would increase.

Table 2.4. Proposed terminology of metal concentration in ore deposits based on clarkes of concentration (CC) (concentration factor)

CC lower threshold	Term	Examples of Cu deposits
1×10^5	extremely high	25%
1×10^4	very high	2.5%
1×10^3	high	0.25%
1×10^2	moderate	250 ppm
1×10^1	low	25 ppm
1×10^{-1}	sub-clarkes	2.5 ppm

NOTE: this is a terminology applicable uniformly to all metals, but uneven ability of metals to concentrate and resource economics result in different terms applied to specific metals in economic ores. The lowest cut-off grade of the "bulk mineable" Cu ores (e.g. porphyry coppers) is about 0.2% Cu now, so ores with average grade of 0.3-0.5% would be called low-grade, 2-5% Cu high grade, 10% plus extremely high grade.

2.3. Dimension, complexity and hierarchy of metallic "deposits"

Metallic "deposits" (a generic term), the names of which are recorded in databases and named in the literature, are highly nonuniform in terms of dimension and internal complexity. Seven examples of actual deposits below illustrate this point (Figs. 2.2 a-d):

1. The giant Mountain Pass rare earth deposit in California (Section 12.9) is an ideal "simple giant": it is a single, internally homogeneous lonely orebody that measures about 760x70 m and has a sharp boundary against its wallrocks.
2. Kidd Creek, the massive sulfide Zn, Cu, Ag giant in Ontario (Chapter 9), is also easy to deal with but the deposit is internally complex (it consists of a massive sulfide lens floored by stringer stockwork) and the continuity is interrupted by deformation.
3. Broken Hill supergiant Pb, Zn, Ag zone in Australia (Chapter 14) is a 7 km long virtually continuous mass of eight coalescing separate high-grade lodes of comparable character, but with varying metal ratios ("Lead" and "Zinc" lodes plus several lower-grade bodies). The uniformity is further complicated by the

presence of oxidation zone (gossan), and sulfides remobilized along shears.

4. Collahuasi, in the Chilean Andes (Chapter 7) is a composite ore field (called district in Masterman et al., 2004) that measures about 15 x 10 km across and consists of several deposits of different types: disseminated porphyry Cu with hypogene, secondary sulfide, and oxide copper intervals; Cu, Au, Ag veins; and exotic infiltration Cu deposits in gravels.
5. Faro-Anvil Pb, Zn, Ag district in Yukon (Chapter 13) is an elongated NW-SE trending zone about 50 x 10 km across that contains seven delineated massive sulfide orebodies and scattered ore occurrences.
6. Witwatersrand (Chapter 11) is a remnant of a late Archean predominantly sedimentary basin measuring about 500 x 300 km that contains nine areas of concentrated mineralization ("goldfields") and several scattered lonely ore occurrences. Most of the surficial outcrop in the Witwatersrand is, however, occupied by younger geological units largely devoid of mineralization, and the gold is virtually confined to the Central Rand Group that has the best continuity in the (often deep) subsurface. Each named Goldfield measures between 20 and 100 km along its longer axis (so it corresponds to a "district") and it consists of several extensive sheet-like orebodies of auriferous conglomerates, there called "reefs".
7. The central Andean copper and gold belt (Chapters 6, 7) is a 2500 km long, 500 km wide linear north-south zone of densely scattered predominantly Meso-Cenozoic Cu, Mo, Au, Ag deposits of several types (but predominantly porphyry Cu-Mo) formed within a long lasting consuming continental margin. It is bordered by gaps in, or absence of, strong mineralization.

The above examples demonstrate the considerable range of dimensions (only the length and width dimensions are considered above, to which should be added the depth dimension), complexity and hierarchy of sites of metal accumulation, yet all the above categories tend to be jointly manipulated in order to reach various metallogenic conclusions. Accepting at par and comparing the Mountain Pass-like single orebodies with Witwatersrand-type basins exceeds the proverbial comparison of apples and oranges: it is more like comparing a single wheel with a locomotive. In this book and the GIANTDEP database the rank of entries (localities, "deposits") is always indicated.

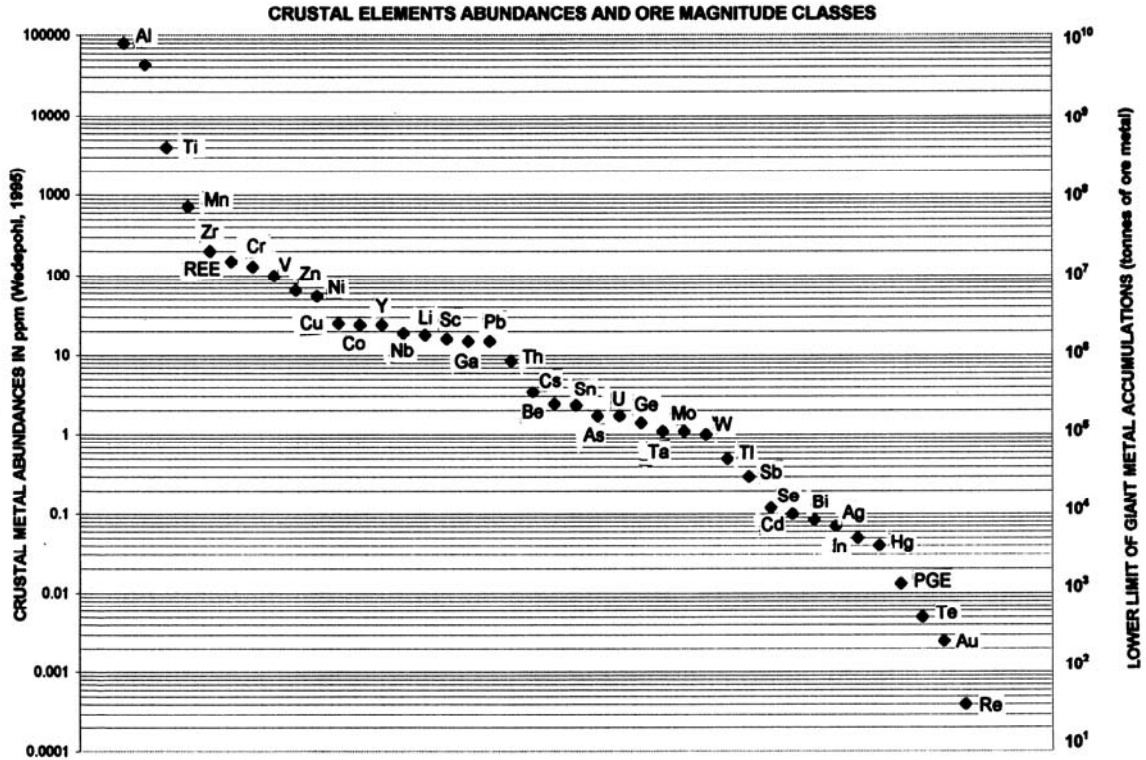


Figure 2.1. Graph showing lower limits (thresholds) of giant deposits (right scale) as related to crustal abundances (clarkes) of metals

Hierarchical listing is frequently used (in GIANTDEP, the Witwatersrand entries occupy three ranks: Witwatersrand basin-> Klerksdorp Goldfield -> Vaal Reef).

There is more discrepancies in many reviews of metallic deposits and in databases sourced from the heterogeneous, especially international, literature. The wide reach of the term "ore deposit" has been mentioned above and the same applies to "district". The term "district" is, moreover, used as i) a purely political administrative unit (e.g. Keonjhar district, India); ii) as a territory administered by a mine registrar (e.g. Robinson district in Nevada that includes the Ely ore field); iii) as a territory of densely distributed and/or mutually related ore occurrences (e.g. the Faro-Anvil district, the preferred usage here). There are more terms in the literature that require scrutiny. Mine is a producing facility and/or a property and it may i) coincide with a single orebody or an ore deposit; ii) include several ore deposits (e.g. the Kosaka or Hanaoka mines in the Hokuroku district of Honshu) or iii) include a portion of a continuous ore deposit within a mine lease (e.g. the Hemlo gold ore deposit is

subdivided into three properties, the Broken Hill NSW lode had up to seven major properties in various times). The Russian term "ore knot" (rudnyi uzel) corresponds to ore field or ore district and the same applies to the western term "goldfield". Zone (ore zone), trend (e.g. Carlin Trend), belt (e.g. Whitehorse copper belt) are usually used for elongate (linear) ore-bearing territories in the ore field, district, regional (e.g. the African Copperbelt) to continental (e.g. the Andean Copper Belt) ranks.

There are more ore site terms that have a genetic connotation, or are used in the context of a specific theory, branch of science or a model. The term "province" (e.g. metallogenic province in general like Abitibi in Canada; Bolivian tin province) refers to a region with a distinct mineralization, especially one dominated by a single metal. Metallotect, popular in the European literature of the 1970s-1980s, has a distinct tectonic connotation that implies prominent fault control. This does not work well with deposits formed in sedimentary basins or at the paleosurface where other controls are predominant.

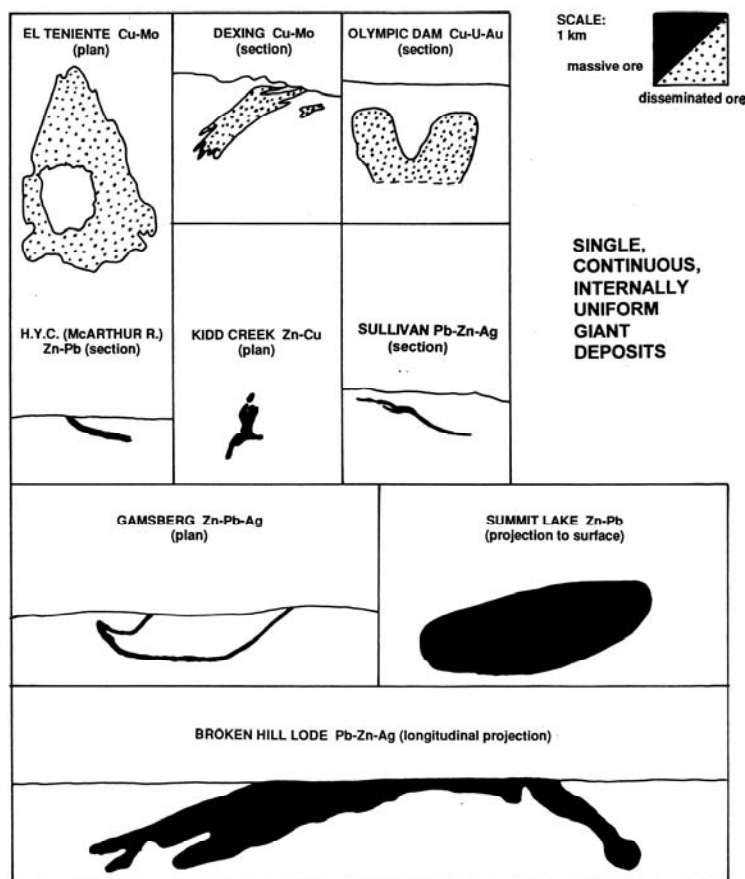


Figure 2.2a. Configuration, complexity and "footprint" of selected examples of "giant" deposits: single, continuous, internally uniform orebodies

In this book the term metallogene is used for a set of processes, conditions and environments working together to produce a distinct metallogenic pattern, and the affected territory itself (e.g. the Bushveld metallogene incorporates the processes of derivation, differentiation, fractionation, emplacement and cooling of mafic-ultramafic magmas responsible for the distinct Cr, Fe, Ni, Ti, V, and PGE metallogeny).

Traditional names of localities common in the literature like Victoria Goldfields, Carlin Trend, African Copperbelt, and others are retained in this work but they are provided with a rank qualifier in the GIANTDEP database and in tables and diagrams. Only localities of corresponding rank are mutually contrasted, compared and employed to reach quantitative conclusions. Ranks of sites of industrial metal(s) accumulations ("localities", "deposits") used in this book, from small and simple to large and complex, are summarized in Table 2.5 and Fig. 2.3.

Configuration of giant localities in database entries: Simple internally homogeneous deposits like Mountain Pass enter database as they are, their magnitude expressed by ore tonnage, grade, and/or metal content. Composite deposits like porphyry coppers with reserves residing in both hypogene and secondary-enriched or oxidized portions, are entered as a whole or as two, or three, separate entries. This is most useful when all components are of giant magnitude. Giant size localities (ore field, district, belt, etc.) that are composites of two or more orebodies/ore deposits, allow a variety of possible configurations. Some contain one or more giant members of lower rank (deposits or orebodies), plus deposits of lesser than giant size. Others contain only deposits of sub-giant size that reach the required "giant" threshold only after addition.

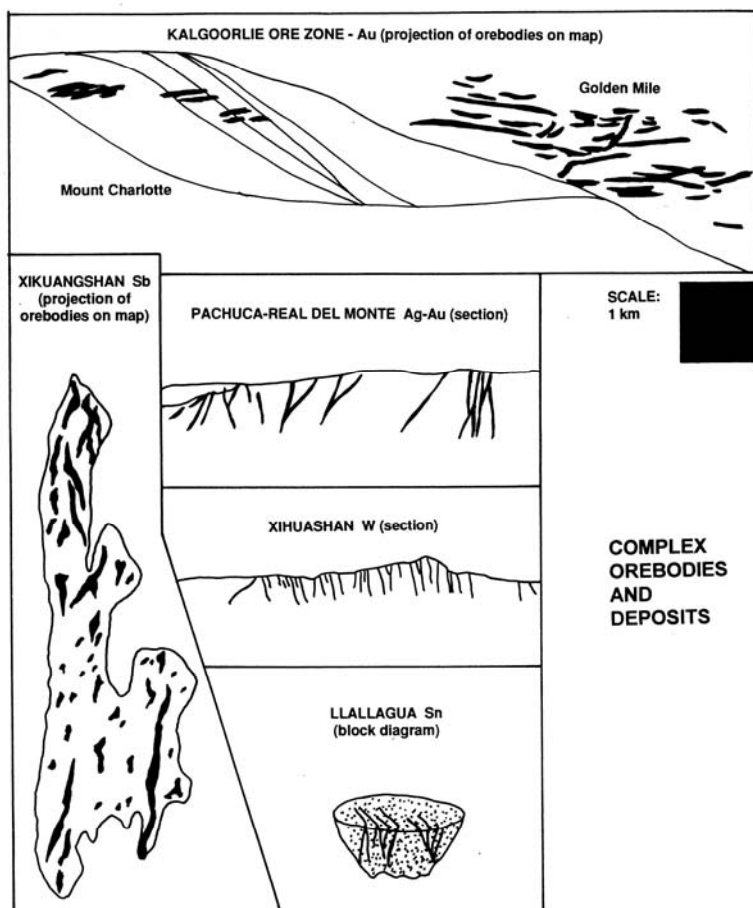


Figure 2.2b. Configuration, "footprint" and internal complexity of "giants": complex orebodies and deposits

In the absence of clear and natural delimiters such as prominent gaps in ore density, geological change or different age/style of deposits, "giant manufacturing" is a highly subjective process, and it accounts for the many discrepancies in published statistics related to ore deposits of exceptional size.

Expressions used in text and tables: The ore magnitude terms based on Clarke values are used consistently in this book and the magnitude terms are shown in quotation marks ("giant", "giant deposit", "large orebody", "super-giant district"). The term "near-giant" is used for deposits not yet of the giant rank, but close to it and likely to become a "giant" in the near future while the exploration continues. In few instances the term "geochemical giant" is used for metal accumulations of the geochemically "giant" magnitude, but with lesser to none industrial (economic) importance under the present conditions.

2.4. The share of "giant" metal accumulations in global metal supplies

Based on the quantitative criteria outlined above, there were 486 entries (records) that qualify as "giant", and 61 entries that qualify as "supergiant", in the 1999 version of the GIANTDEP database, on which were based the conclusion in Laznicka (1999). New additions (up to mid-2005) are included in the attached CD-ROM file version, but have not been used for new calculations. The database entries (one entry per metal/locality, hence when one locality contains giant accumulations of three metals, it is listed three times) translate into 446 "localities". The localities that range in dimension and complexity from simple, single ore deposits to large composite metalliferous "basins" are sometimes arranged hierarchically.



Figure 2.2c. Configuration, "footprint" and internal complexity of "giants": ore fields, districts, horizons, shears

That is, the greater, first or second order divisions include smaller, third order units that correspond to the bulk of independent (non-hierarchical) primary entries in the database). There were 547 primary entries, 51 second order divisions and one first order division (the Witwatersrand "Basin"). Although the bulk of entries are the "classical" (highly geochemically enriched) deposits or districts, there are 57 entries that are low-grade or otherwise unsuitable for immediate production, but they represent a significant local accumulation of metals to be perhaps exploited in the future. This does not include the metalliferous materials on ocean floor or sea water (Chapter 4).

Table 2.6. shows the global endowment (that is cumulative past production and remaining or new reserves and resources) of all industrial metals. The endowment used here corresponds to the "maximum endowment" shown in column 4, Table 4 in Laznicka (1999), as the available data are still

insufficient to produce an absolutely accurate figures (compare the values assembled by the U.S. Geological Survey shown here in Table 1.5). Fig. 2.6. indicates the very uneven numbers of giant deposits of the various metals, and the impressive share of the giant and super-giant deposits in storing the world's resources of industrial metals (the figures include both the past production and the metals that remain, hence they are not indicative of what is still left in ground). The dominant role of the "giants" as the warehouse of metals in present time follows quite convincingly from the numbers, despite the limited accuracy.

As expected, the absolute magnitude of metal accumulations generally increases with the increasing geochemical abundance of elements (the McKelvey's Law, McKelvey, 1960; Erickson, 1973), but the increase is not systematic.

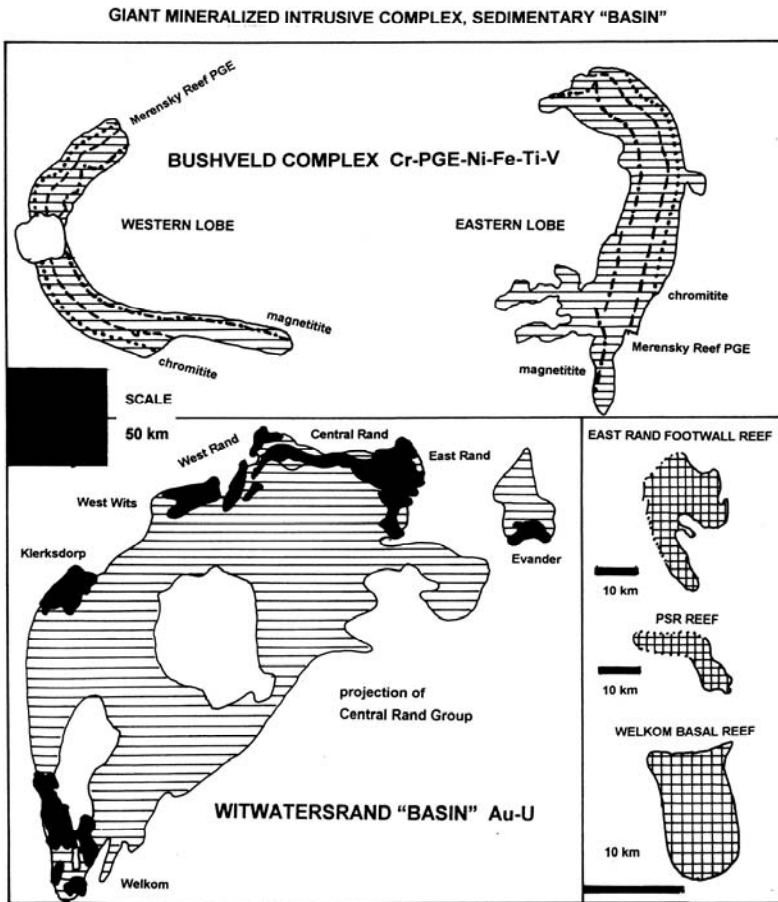


Figure 2.2d. Configuration, internal complexity of "giants": large magmatic complexes and sedimentary basins

This is due to several causes some of which are entirely extraneous to geology, while the others are probably the consequence of the geochemical behaviour of elements in the various rock- and ore-forming systems.

One obviously extraneous factor influencing the frequency of "giants" of several metals is the differences in price and market demand, which do not closely correlate with crustal abundances of elements. The high-demand metals like Fe, Cu, Zn, Au have been eagerly sought and exploited for centuries, hence every newly found deposit usually goes into production within few years and the inventory of localities grows. The limited-demand metals such as Zr, Nb, REE are mined and supplied by several specialty producers serving captive markets. The already known but substantially unexploited resources of the latter metals are sufficient for several hundred years at the present rate of consumption, so there is little incentive for vigorous exploration, hence the inventory of known

deposits increases slowly if at all. The inventory of deposits of the almost nil-demand metals like thorium is stagnant and fragmentary. The largest recorded Th resources are in complex deposits where other metal is the principal economic commodity and the Th quantities, that are not being recovered at present, have been calculated from published analyses. Examples include the U-conglomerates at Elliot Lake, Ontario; the Nb-carbonatite at Araxá; and others.

Certain "cheap" metals are grossly undervalued in relation to their geochemical scarcity. The most striking example is antimony: Sb that has clark of only 0.3 ppm sells for about USD 4.0/kilo in contrast with the more abundant Ni, with clark of 55 ppm, that normally sells for about USD 7/kilo. The main reason for the poor performance of antimony is the loss of its principal past use in typography, hence a collapse of demand. Another reason for the antimony bargain price is that it forms highly concentrated deposits that are cheap

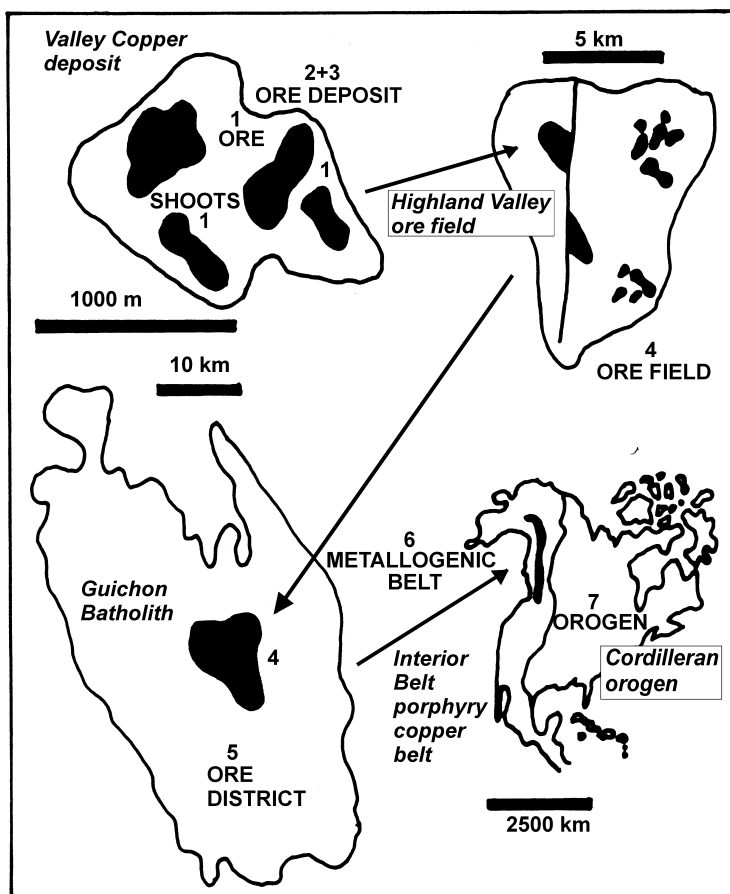


Figure 2.3. Ranks and hierarchy of mineralized objects exemplified by the Highland Valley porphyry Cu ore field, British Columbia, Canada (read Chapter 7 for description)

Table 2.5. Ranks and hierarchy of metals accumulations

Rank	Common names	Dimensions	Characteristics
1	Ore shoot, component of composite orebody	X-X00 m	Entity within or immediately adjacent to an orebody (rank 2) with some special characteristics (e.g. high grade, different metals) or a different style in composite orebodies (e.g. footwall stockwork in VMS, oxidation zone, band of sheared ore)
2	Orebody, ore bed, ore layer	X0-X000 m	Single body of ore material like massive sulfide lens, ore vein, sedimentary ore bed, mass of altered rock with disseminated sulfides, residual ore blanket
3	Ore deposit (deposit, e.g. Cu deposit). Also used as general term in lists of various ranks	X00-X000 m	Equivalent to orebody in single body ore deposits or a set of close orebodies of the same (e.g. vein swarm) or different (e.g. veins, replacements, breccia bodies, enrichment blankets) styles and ore metals
4	Ore field; ore center; ore knot; ore complex	~5 to ~20 km	Group of two or more orebodies/ore deposits of the same or different types, but usually genetically related
5	Ore district (district); large ore complex, trend, zone	~10 to 100 km	Territory containing one or more repetitive and usually genetically related styles of orebodies; strong administrative influence

Table 2.5. (continued)

Rank	Common names	Dimensions	Characteristics
6	Mineralized region, belt, basin, geological division, province	~50 to 500 km	Territory or geological division, structure with numerous deposits of one or few metals of repetitive style. Witwatersrand "basin", Victorian Goldfields province, Iberian Pyrite Belt, African Copperbelt
7	Continental scale ore belts, provinces, basins	~300 to 5000 km	Distinctly and/or densely mineralised continuous territories that can be shown on page-size world maps. Andean Cu-Au belt and its segments (e.g. Central Chile Cu-Au Belt); SE Asian Tin Belt; Basin-and-Range ore province (in USA and Mexico)

NOTES: 1 = smallest rank. X stands for several, e.g. X km = several kilometers. Extensive, formerly continuous ore horizons, beds, layers and units such as the chromitite bands, Merensky Reef and Magnetite layers of the Bushveld complex combine characteristics of an orebody (Rank 2) with dimensions of a mineralized region (Rank 6). The same applies to the Cretaceous West Siberian ironstone horizon, Eastern Australian (Pacific) heavy minerals sands province, Guinea bauxite province, Pacific floor Fe-Mn nodules province

to mine and process; the largest deposits are in countries with low cost labor and logistics (China, South Africa, Bolivia). Antimony and mercury deposits in fact, especially the three super-giants Almadén-Hg, Spain; Idrija-Hg, Slovenia; Xikuangshan-Sb, Hunan, China, have achieved the greatest magnitudes of the relative metal concentration and accumulation ever recorded! (compare the plot of Almadén [Hg] and Xikuangshan [Sb] on Fig. 2.5, high in the 10^4 and 10^5 range of concentration factors and in the 10^{12} area of accumulation magnitudes).

Column four in Table 2.6 gives the number of giant and super-giant deposits of each metal included in the GIANTDEP database. Copper is the undisputed winner followed by gold. The number-of-giants sequence, arranged by decreasing number of entries, is as follows (numbers of entries, out of 523, from Table 2.6 are in brackets): Cu (103); Au (99); Pb (55); Ag (43); Mo (41); Sb (24); Sn (22); Zn (21); Hg (19); W (12); Fe (11); As (9); U (9); Mn (9); Ni (8); PGE (7); Nb (6); REE (5); Bi (5); Co (3); Cr (3); Zr (3); V (2); Cd (1); Th (1); Ti (1); Y (1). The following metals have not reached the "giant" threshold: Al, Be, Ga, Ge, In, Sc, Se, Ta, Te, and Tl, for a variety of reasons. Aluminum is too geochemically abundant (it is the most abundant metal in the crust with Clarke of 8%, not counting Si), hence the threshold for the giant magnitude of Al deposits is 8 billion tons of contained Al. No deposit or even an extensive area of bauxite, presently the only viable Al ore, approaches such an endowment. Once anorthosite becomes an industrial aluminum ore, many anorthosite massifs of today will achieve the "giant" status. Ta, as geochemically abundant as Mo (1.1 ppm); and Ga and Sc, as geochemically abundant as Pb (15 ppm), tend to

remain dispersed and substitute for other elements in minerals' lattices. Ta forms low concentrated accumulations in the highest fractionated granitic and alkaline systems, but Ge and Sc rarely form minerals of their own. Gallite is a mineralogical rarity known from two localities only and so is thortveitite; besides, market for Ga and Sc is extremely limited. Se, Tl, Te and In are rare to moderately rare metals that accumulate in sulfide deposits and are recovered from electrolytic residue, to supply the very small market (Staff, U.S. Bureau of Mines, 1985).

The largest accumulations of each metal

Table 2.7. lists and Fig. 2.4. show graphically the single largest deposits or districts for each industrial metal. When more than one locality example for a single metal are listed, usually the first entry has the highest magnitude of metal accumulation but a very low-grade which renders it currently uneconomic (e.g. the Chattanooga Shale, Tennessee-U; Chapters 1 and 13). The second entry (and the rest of single entries) is (are) the presently economically viable "classical" metal deposits (e.g. Olympic Dam, South Australia-U). Fig. 2.5. is a plot of these deposits on a graph that contrasts metal concentrations (as Clarke of concentration; vertical axis) and metal accumulations (as tonnage accumulation index; horizontal axis). As already mentioned, two Hg and Sb deposits stand out from the rest in terms of the magnitude of metal accumulation, at substantial metal grades. The rest of metal entries plots as what looks like a random cluster with some general trends faintly suggested.

Table 2.6. Global endowment of ore metals and share of the giant and supergiant deposits modified from Laznicka (1999), reprinted from *Economic Geology* v.94, Table 4, p. 460

Metal	Total world production, t	Global endowment maximum, t	Number of giants	Metal content in all giants
Al	505 mt	1.2 bt	0	0
Fe	34 bt	3,000 bt	11	2,510 bt
Ti	153 mt	12 bt	1	9.50 bt
Mn	835 mt	7.7 bt	9	7.44 bt
Zr	18.6 mt	470 mt	3	435 mt
REE	1.04 mt	280 mt	5	98 mt
Cr	430 mt	9.2 bt	3	4.18 bt
V	861 kt	2.10 mt	2	2.06 bt
Zn	225 mt	620 mt	21	315 mt
Ni	28.3 mt	145 mt	8	121 mt
Cu	354 mt	1.35 bt	103	1.23 bt
Co	1.15 mt	15 mt	3	12 mt
Y	14 kt	5 mt	1	3.0 mt
Nb	272 kt	110 mt	6	104 mt
Ga	1,103 t	110 kt	0	0
Pb	170 mt	338 mt	55	302 mt
Th	13 kt	1.62 mt	1	1.16 mt
Hf	X00 t	X0 kt	0	0
Be	12.8 kt	81.6 kt	0	0
Sn	12.5 mt	26 mt	22	23.8 mt
As	3.32 mt	21 mt	9	8.65 mt
U	1.86 mt	32 mt	9	3.45 mt
Ge	1,100 t	110 kt	0	0
Ta	4,700 t	400 kt	0	0
Mo	2.43 mt	28.4 mt	41	27.4 mt
W	500 kt	4.7 mt	12	3.63 mt
Tl	310 t	17 kt	0	0
Sb	2.49 mt	7.5 mt	24	6.97 mt
Se	56.6 kt	750 kt	1	225 kt
Cd	744 kt	2.2 mt	1	1.08 mt
Bi	167 kt	600 kt	5	520 kt
Ag	947 kt	1.37 mt	43	859 kt
In	2,800 t	12 kt	0	0
Hg	413 kt	980 kt	19	950 kt
PGE	7,160 t	103 kt	7	90.8 kt
Te	4,900 t	42 kt	1	1,000 t
Au	99.5 kt	177 kt	99	97.2 kt
Re	X00 t	X0,000 t	0	X,000 t

NOTES: Metals are arranged by decreasing clarke values. Total recorded global production to 1992, compiled by S.M. Laznicka from *Minerals Yearbook*. Gaps filled by extrapolation

Maximum global endowment = compiled sums of global past production of ore metals plus remaining or new reserves and some resources of delineated deposits, with several calculated metal contents of geological bodies like the Bushveld metalliferous layers, and calculated contents of some unrecovered trace and associated metals in ores mined for other elements. Because of incompleteness of the global endowment data the values shown are considered as maxima. To reduce confusion, metal tonnages are shown in tons (t), thousand tons (kt), million tons (mt) and billion tons (bt)

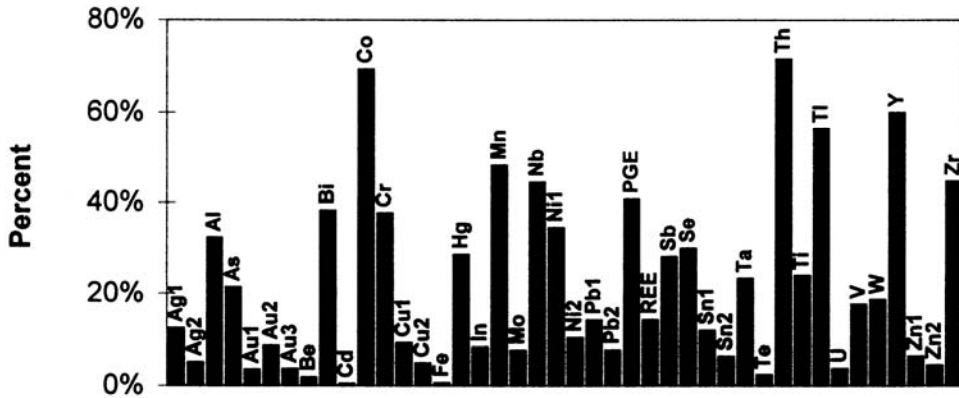


Figure 2.4. Share of giant deposits of the global ore metals endowment (compare Table 2.6). From Laznicka (1999), reprinted from Economic Geology, v.94, Fig. 1, p.462

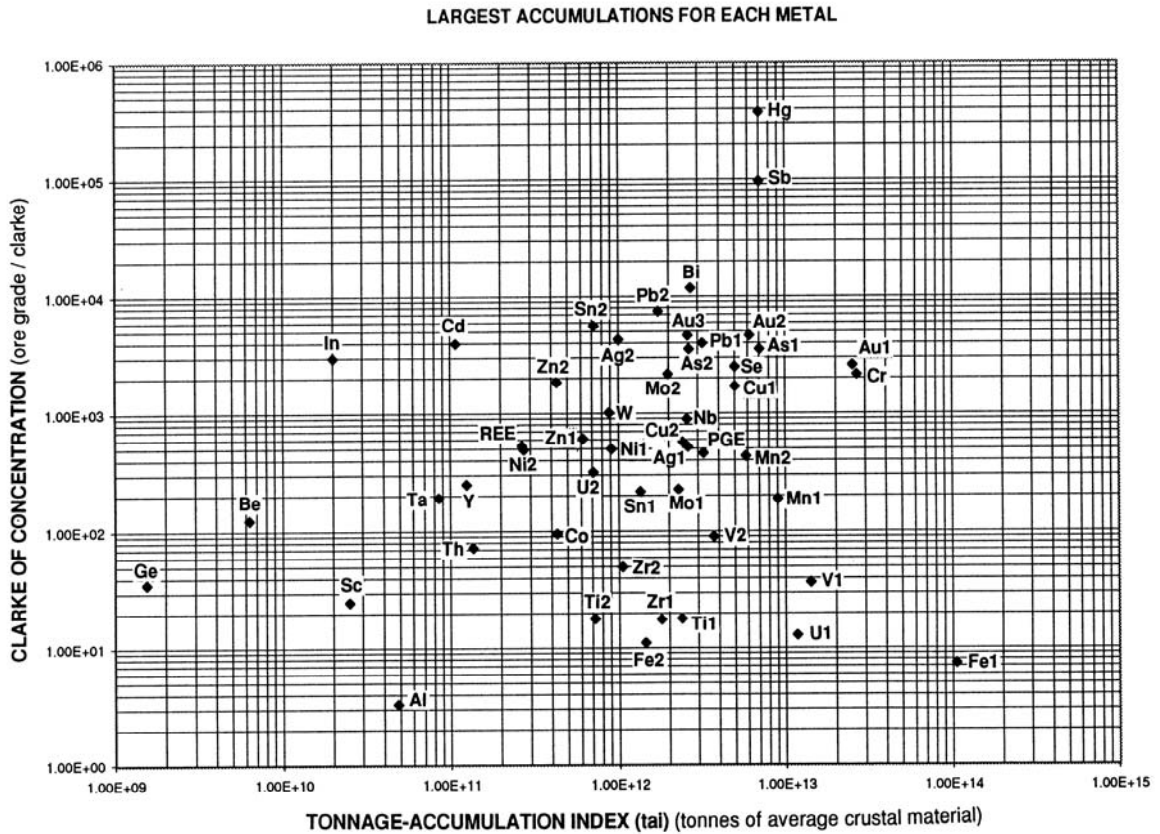


Figure 2.5. Plot of the largest deposits/districts of industrial metals into a clarke of concentration versus tonnage accumulation index graph

Table 2.7. Single largest deposits/districts of the industrial metals and their share of global endowment

Metal	Largest deposit/district	Object	Metal content, t	Grade	% of max. endowment
Al	Boké-Gaoual, Guinea	area	3.88 bt	26.5 %	32.33
Fe	Alegria, Brazil*	deposit	62 bt	48.0 %	0.62
Ti	Bushveld Main Magnetite Seam, South Africa	unit	2.88 bt	7.2 %	24.00
Mn	Kalahari-Mamatwan, South Africa	deposit	4.19 bt	31.3 %	48.16
Zr	Lovozero eudialyte lujavrite unit, Russia	unit	210 mt	1.0 %	44.68
REE	Tomtor, Anabar Shield, Russia	deposit	40 mt	8.0 %	14.29
Cr	Bushveld chromitite seams, South Africa	unit	3.47 bt	28.0 %	37.72
V	Bushveld Main Magnetite Seam, South Africa	unit	371 mt	0.9 %	17.67
Zn-1	Kraków-Silesia Muschelkalk Basin, Poland	basin	40 mt	4.0 %	6.45
Zn-2	Broken Hill, N.S.W., Australia	ore zone	28 mt	12.0 %	4.52
Ni-1	New Caledonia laterite-saprolite blanket	area	50 mt	2.75 %	34.48
Ni-2	Talnakh-Oktyabrskoye, Russia	ore field	15 mt	2.7 %	10.34
Cu-1	Copperbelt, Katanga portion, DRC Congo	ore belt	125 mt	4.25 %	9.26
Cu-2	El Teniente, Chile	deposit	66 mt	1.31 %	4.89
Co	Copperbelt, Katanga portion, DRC Congo	belt	10.4 mt	0.23 %	69.33
Y	Tomtor, Anabar Shield, Russia	deposit	3 mt	0.6 %	60.00
Nb	Seis Lagos, Brazil	deposit	48.9 mt	1.7 %	44.45
Ga	Brockman, Western Australia, Australia	deposit	640 t	150 ppm	0.6
Pb-1	Viburnum Trend, S.E. Missouri, U.S.A.	ore zone	48 mt	4.0 %	14.20
Pb-2	Broken Hill, N.S.W., Australia	ore zone	26 mt	11.3 %	7.69
Th	Araxá, Brazil	deposit	1.16 mt	0.62 %	71.60
Be	Strange Lake, Labrador, Canada	deposit	15.1 kt	300 ppm	1.85
Sn-1	Kinta Valley placers, Ipoh, Malaysia	area	3.10 mt	0.05 %	11.92
Sn-2	Dachang, Jiangxi, China	ore field	1.65 mt	1.3 %	6.35
As	Río Tinto, Spain	ore field	4.50 mt	0.6 %	21.43
U	Olympic Dam, South Australia	deposit	1.20 mt	540 ppm	37.5
Ge	Tsumeb, Namibia	deposit	2,160 t	5 ppm	2.0
Ta	Ghurayyah, Saudi Arabia	deposit	93.3 kt	212 ppm	23.33
Mo	Climax, Colorado, U.S.A.	deposit	2.18 mt	0.24 %	7.68
W	Verkhnye Qairakty, Kazakhstan	deposit	880 kt	0.102 %	18.72
Tl	Meggen, Germany	deposit	960 t	24 ppm	56.47
Sb	Xikuangshan, Hunan, China	ore field	2.11 mt	2.9 %	28.13
Se	Río Tinto, Spain	ore field	225 kt	30 ppm	30.00
Cd	Tsumeb, Namibia	deposit	10.8 kt	40 ppm	0.49
Bi	Shizhouyuan, Hunan, China	deposit	230 kt	100 ppm	38.33
Ag-1	Lubin Kupferschiefer district, Poland	district	170 kt	4 ppm	12.44
Ag-2	Potosí (Cerro Rico), Bolivia	deposit	70 kt	30 ppm	5.12
In	Mount Pleasant, New Brunswick, Canada	ore field	100 t	15 ppm	8.33
Hg	Almadén, Spain	deposit	280 kt	0.15 %	28.57
PGE	Merensky Reef, Bushveld, South Africa	unit	42 kt	6.0 ppm	40.78
Te	Cripple Creek, Colorado, U.S.A.	ore field	1000 t	8.5 ppm	2.38
Au-1	Central Rand Group, Witwatersrand, S. Africa	basin	63 kt	6.5 ppm	35.60
Au-2	Welkom Goldfield, Witwatersrand, South Africa	ore field	15.3 kt	11.6 ppm	8.64

* There is probably an order of magnitude error in the original source; the Fe content is more likely 6.2 bt

The metals that prefer dispersal to local concentration are on the left, the high-clarke metals (Al, Fe) near the bottom, the high-grade ore forming metals (most of which are hydrothermal) in the upper half. It should be realized that the plot represents single most exceptional localities out of exceptional populations, hence most of these deposits are in some way unique and not necessarily representative of the remaining "giants" and lesser

size deposits of corresponding metals. The geological reasons for metals superaccumulation, as much as they can be determined or at least guessed, are discussed in Chapter 15.

3 From trace metals to giant deposits

3.1. Introduction

Classical ore deposits are exceptional local accumulations of highly concentrated metals of actual or potential industrial interest. This concept of exceptionality is relative to the geochemical background of ore-hosting environments. In the presumably iron-nickel Earth's core, Fe+Ni are predominant hence their accumulation is "normal". Local accumulations of oxygen, nitrogen and hydrogen would be exceptional. In biosphere where we live, the situation is reversed. Two end-member mechanisms are capable of causing exceptional local accumulations of metals within the present human habitat and its present technical reach (the anthroposphere):

1. An instant import of already concentrated metals from outside the biosphere and lithosphere. Metals could arrive from the outer space, derived from asteroids or space debris, in the form of meteorites or cosmic dust. Such mechanism exists, has been repeatedly observed, but has not yet produced a confirmed economic deposit (read below). Another alternative is an import of a preconcentrated metal(s) from the earth's core (hardly viable) or from the deep mantle. There is a convincing evidence that diamonds originate below the graphite/diamond stability boundary at depths greater than 150 km and are brought to the upper crust, as xenocrysts, by kimberlitic and lamproitic magmas that also originate in similar depth (Mitchell, 1986). Except for several metals that are geochemically enriched in such magmas like titanium and chromium, there is no indication that metallic deposits in the crust have formed by a similar process.

2. Local metal concentration and accumulation from dispersed metals within the lithosphere, or at interfaces between mantle, hydrosphere, biosphere and atmosphere with continental crust. Myriad of such processes have been directly observed in action (such as accumulation of heavy minerals along shorelines; precipitation of metallic minerals from hot springs), others have been credibly duplicated by experiment, and the rest is still controversial in the realm of a hypothesis or at best theory. R.D. Stanton has made an important statement that "ores are but rare rocks", in the time

when petrology and metallogeny had been pursued as two different independent schools of learning. This follows convincingly from histograms of metals inventory in the crust where the bulk of every metal is stored in rocks at mean crust content concentrations (clarkes). The highly concentrated metals in ores are at the end of the spectrum and the "rock"/"ore" boundary is flexible as it moves with demand and progress in extraction technology (Fig. 3.1). Geochemistry, petrology and metallogenesis try to determine how metals concentration and accumulation happened. Structural and regional geology, and metallogeny, study where and when that happened and where we can find the products, including giant deposits. This is the principal subject matter treated in the main body of this book (Part II), but before we get to it, two additional introductory topics have to be dealt with:

- 1) Establishment of geochemical background abundances, especially of trace (and some major) metals, in geological domains within which, out of which, or through which the ore forming metal fluxes operated;

- 2) Recognition that few ore deposits are the product of an instant, and/or a single stage process and that most orebodies have had a protracted and complex history of gradual metal accumulation, modification and post-formational ore preservation. This is essential to consider yet it does not clearly follow from traditional textbook ore classifications. An improvement could be achieved by adopting and using a simplified, abbreviated "ore history recording" explained in Chapter 15.

It has already been mentioned that most, if not all, ore giants are the top members in a sequence of comparable ore type members, statistically dominated by lesser magnitude deposits. If so, the origin of the ore giants has not been substantially different from the origin of the "normal" deposits, hence "giants" owe their existence to quantitative, rather than qualitative, factors: stronger (i.e. higher energy) processes, richer metal sources, longer process duration, multiple ore stages, most favorable setting and timing, most efficient ore preservation. These factors are summarized in Chapter 15.

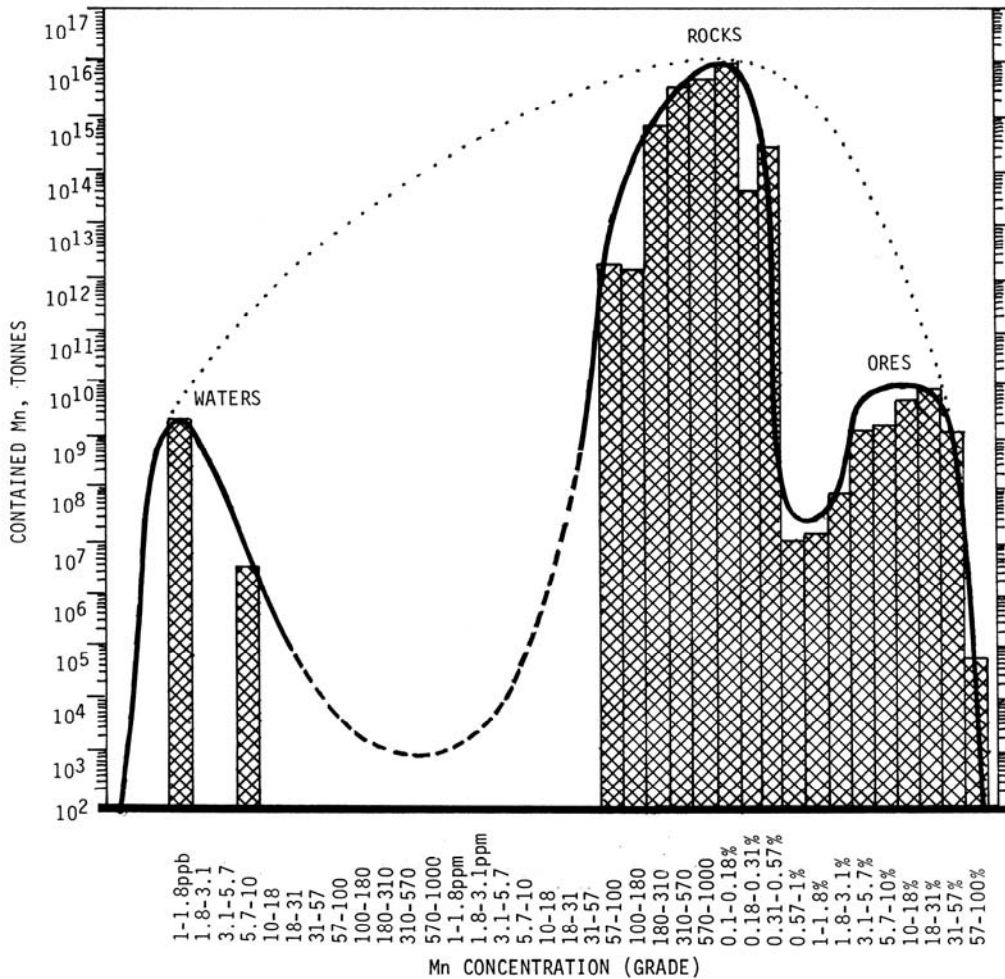


Figure 3.1. Graph contrasting concentration (grade) and tonnage of stored manganese in the Earth's geological materials (including sea water) that is probably applicable to other trace metals as well. From Laznicka (1992), reprinted courtesy of Elsevier B.V., Amsterdam. The graph shows clearly the three modes of Mn concentration: the sub-clarke dissolved Mn in sea water, the Mn in rocks, the concentrated Mn in ores. The lack of grade continuity between the rocks and waters is due either to the lack of published data, or is real, or both. The thin dotted curve would apply to a near-lognormal Mn distribution, applicable if the waters/rock gap did not exist

In contrast to the voluminous literature, especially the text/reference books that deal with ore genesis, the approach here is selective: the processes and settings that favor or potentially favor formation and occurrence of "giants" are emphasized, the rest subdued or ignored altogether.

3.2. Extraterrestrial metals and ore formation resulting from meteorite impact

We are not going to deal here with possible metal accumulations on the Moon, on planets or in asteroids but only with the extraterrestrial materials that have actually landed at the earth surface (or the sea floor) and with the metallogenic interaction of an impact with local terrestrial (or marine) rocks.

Meteorites

Iron meteorites would be an excellent source of iron, nickel and platinumoids as they contain, on average, about 90% Fe, 7-20% Ni, 0.5-1% Co and several ppm of platinum metals (Mason, 1979). Unfortunately, the world's total recorded tonnage of recovered iron meteorites is 460 tons only and the largest meteorite found so far, the Hoba, weighs 60 tons and it contains 16.4% Ni. The actually observed 1947 multiple fall of meteoritic irons in Sikhote Alin in the Russian Primor'e region yielded over 400 pieces with the total weight of 23 tons. The dispersed iron debris resulting from the Arizona Crater (Canyon Diablo) impact some 50,000 years ago amounts to 11.5 tons recovered so far, and there is still some 8,000 to 12,000 tons of dispersed fine Fe-Ni alloy particles left in ground (Shoemaker, 1963; Buchwald, 1975); Fig. 3.2.

Chondrites, silicate rocks of ultramafic composition, are rich in nickel (1.03% Ni) and are greatly enriched in platinum metals (Pt 1.01 ppm; Ir 0.51 ppm; Os 0.48 ppm; Pd 0.49 ppm; Rh 0.25 ppm; Ru 0.69 ppm, for a total platinum group elements' content of 3.43 ppm (the data are for the C1 carbonaceous chondrite from Mason, 1979). They would thus be an excellent PGE and Ni ore if they were present in substantial quantity, which they are not. Cosmic dust with similar trace metals and of which substantial amounts land continuously at the earth surface, remains in dispersed form. The iridium enrichment at paleosurfaces believed contemporaneous with past meteoritic impacts and widely quoted in the "extinctionist" literature (e.g. Alvarez et al., 1980) have concentrations of at most 10 times the Ir clarkite of 0.54 ppb; Ir would be difficult to economically recover from the several cm thick clayous horizons. Because of the high energy impacts of the celestial bodies much of their mass vaporizes and is returned to the outer space. What remains on Earth is dispersed and it is difficult to imagine the existence of a significant, geologically young local accumulation of meteoritic material on earth to develop into a metallic deposit, especially a giant one.

Impact sites and paleo-astroblemes

It is easy to agree that meteorite impacts that create astroblemes can also modify, mainly structurally, existing ore deposits if any were present in the target area (examples considered in the literature include the Pervomaiskoye Fe deposit in the Krivoi Rog district, Ukraine; Nikol'skiy et al., 1983; uranium deposits in the Carswell Structure,

Saskatchewan; Baudemont and Fedorowich, 1996). Impacts can also create basins that fill by fallback and post-impact deposits (as in the Ries Crater, Bavaria; Fig. 3.3), some of which have accumulated industrial minerals (e.g. Grieve and Masaitis, 1994). The 100 km diameter Eocene Popigay astrobleme in Siberia is filled by fallback breccia that contains between 0.5 and 5 carats (0.2 and 1 grams per ton) of industrial (not gem quality) impact diamonds of potentially economic interest. Impacts also contribute to structural burial of earlier ore deposits as in the "Au super-giant" Witwatersrand "basin", thus assisting in ore preservation (McCarthy et al., 1990). The 2.0 Ga Vredefort impact event in South Africa is credited with possibly driving fluids that caused partial gold remobilization within the original Witwatersrand paleoplacer. In several cases, meteorite impacts have been considered responsible for triggering ascent of mafic or alkaline magmas from depth or with producing neomagmas from crustal rocks in the target area (Lightfoot et al., 1997). Contemporaneous or subsequent evolution of such magmas could have produced Fe-Ni-Cu sulfide ores, as in Sudbury (Chapter 12).

Only in the case of Sudbury, Ontario, 1.85 billion years old presumably impact structure, suggestions have been made that the Ni, Cu and platinumoids-bearing sulfide ore itself is of extraterrestrial origin (Dietz, 1972; Morrison, 1984; Stöffler et al., 1994). This idea is not universally accepted although the role of an ancient impact in producing the elliptical Sudbury structure, a variety of breccias, shatter cones and unusual rocks, has been debated for more than 30 years with no end in sight (read a more detailed description of the Sudbury mineralized complex in Chapter 12). In his recent models, Naldrett (1989a, 1999a,b) assumed a Paleoproterozoic impact that excavated deep crater, shattered and pulverized local rocks (Archean granite-gneiss and Proterozoic greenstones and metasediments), and triggered ascent of mafic magma from a reservoir under the present Sudbury Basin. The magma so created assimilated crustal debris, mixed with the impact melt, and exsolved Fe, Ni and Cu sulfide melt that simultaneously, in several centers, filtered down by gravity through the shattered rocks and breccias. As the melt descended it fractionated, depositing the Ni- and Cu-rich sulfide fraction in the Sublayer with the more mobile liquid penetrating deep into the basement to form essentially copper-bearing footwall orebodies. The Sublayer, a possible impact crater liner, is now an inhomogeneous hybrid breccia compositionally approaching quartz diorite to granodiorite.

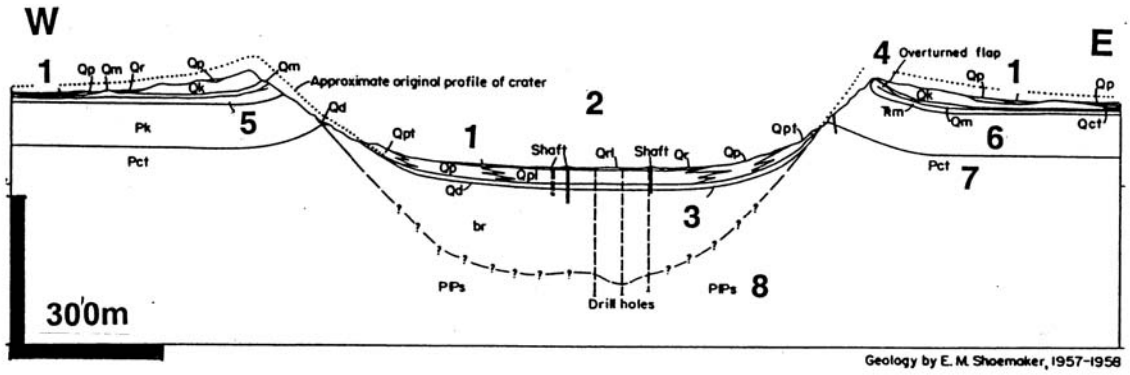


Figure 3.2. Cross-section of the Arizona Meteor Crater (Canyon Diablo), from Shoemaker (1987; U.S. Geological Survey; also from LITHOTHEQUE No. 1662). This is the only locality with more than 10 kt of metal (iron) of demonstrably extraterrestrial origin, dispersed in impactites and surficial sediments. Not a "giant", the contained iron amounts to less than one day's production of a large open pit iron mine

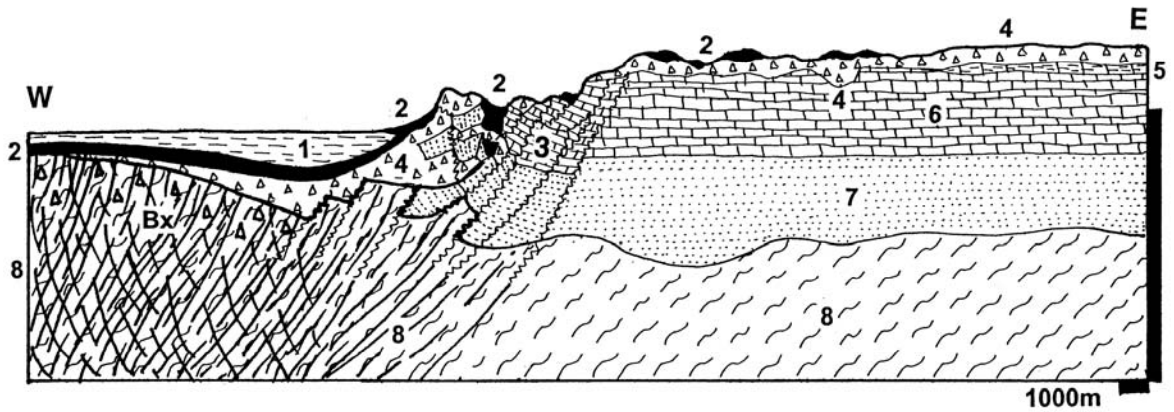


Figure 3.3. Cross-section of the eastern rim and part of the crater of the Miocene Ries impact structure near Nördlingen, Bavaria. From LITHOTHEQUE No. 1773, modified after Pohl et al. (1977). The section shows the characteristic distribution of impactites, breccias and target rocks in an only slightly eroded structure. Except for some construction materials, there are no mineral deposits and only local trace metal enrichment of the extraterrestrial Ni and Ir. Explanations: 1. Mi3-Q post-impact fluviatile and limnic sediments. Products of the 14.8 Ma impact: 2. Suevite breccia, heterolithologic layer of shock metamorphosed and vesiculated fragments with some impact melt, coesite and stishovite; 3. Megabreccia of impact-jumbled and displaced target rocks; 4. Bunte Breccia: as above, but smaller, heterolithologic fragments; Bx. Partly impact melted crater floor gradational to shock metamorphosed subfloor breccia; 5. OI-Mi pre-impact molasse clastics; 6. J platformic sandstone, shale, limestone, marl; 7. Tr sandstone, shale, limestone; 8. Pre-Pe Variscan crystalline basement

It hosts the bulk of massive, breccia and matrix Fe, Ni, Cu sulfide ores. If this scenario is correct, the Sudbury ores would be synchronous with the impact, although not directly brought in from the outer space (Grieve and Therriault, 2000).

Impact sites as a lead to giant deposits?

It is unlikely that economically interesting relics of an extraterrestrial metalliferous material will ever be found, although there remains a remote

possibility that deep water impact targets could have somehow cushioned the kinetic and thermal energy of the impact and facilitated preservation of a fraction of the cosmic metals. Nothing has, however, been reported from the few recent and presumed ancient underwater impact sites, so far. The origin of the Sudbury ores remains controversial and regardless of conditions created by the postulated Proterozoic impact the Fe, Ni, Cu sulfide ore demonstrably appears to be the product of separation from fractionating contaminated mafic

magma, the ore style and setting of which does not substantially differ from similar systems that lack the impact diversion, like Noril'sk in Siberia (Lightfoot et al., 1997). The empirical characteristics at Noril'sk are thus relevant in the search for Sudbury Ni-Cu analogs but it would not work the other way, starting with and insisting on the presence of impact indicators. The idea that powerful impacts may have triggered mantle plumes and hot spots and possibly related ores may have some merit, but it is easier, as above, to concentrate directly on the search of rocks associated with plume activity than approaching the problem indirectly via impact sites.

3.3. Lithospheric evolution and geochemical backgrounds to metals concentration and accumulation

The "geological" stage of the solid Earth is presently believed to have started some 4.6 billion years ago (Nisbet, 1987). The oldest dated terrestrial minerals, zircons, crystallized around 4.2 Ga (Myers, 1988). The oldest dated rocks are close to 3,930 Ma; Black et al. (1986). The oldest dated ore deposits are the 3.8 Ga old chromites in South Greenland ultramafics (Chadwick and Crewe, 1986). The oldest ore "giant" is probably the Antimony Line in the Murchison Greenstone belt, South Africa, dated at 3.02 Ga (Saager and Köppel, 1976). Compare also the "calendar" of Precambrian lithogenetic and ore forming events in Laznicka, (1993, p. 63). The bulk of preserved ore deposits of any age formed by local accumulation of metals within the lithosphere, although few had probably formed within the mantle (this includes both the lithospheric mantle and the asthenosphere) and were later incorporated into the lithosphere as fragments and melts. Lithosphere and its divisions (domains, envelopes), and partly the mantle, have been the metal sources and also the sites of ore formation and deposition. They had been there before the ores and they influenced greatly the selection of ore metals to accumulate and styles of ore deposits. A brief story tracing the evolution of terrestrial domains, as it is interpreted today, is thus relevant, as the ore formation is ultimately related to the development of the major lithospheric domains although it was a very minor and local diversion.

Earth evolution and geochemistry

Interpretations of the bulk geochemistry and evolution of the early Earth (Carlson, ed., 2004)

usually start with solar element abundances, determined spectroscopically. The pre-geological Earth is now believed to have been a body that grew by successive impacts and accretion of microplanets, planetesimals and cosmic dust (Allégre et al., 1995; Palme and O'Neill, 2004). Two types of microplanets are considered. The first type was differentiated into Fe and Ni-rich metallic core and silicate (chondrite) outer layer. Iron meteorites and chondrites, respectively, recently recovered at the Earth's surface, are considered to be fragments of disrupted planetesimals that arrived too late to be accreted into the developing Earth. The second type of microplanets likely consisted of chondrite only. The source of the rare palasite meteorites (olivine in Fe-Ni metallic matrix) is uncertain. Most of the reported "meteorites" of unusual composition like copper or Cu-Ni sulfides have been proven as "meteo-wrongs" so there is no clear evidence that materials such as equivalents of the Sudbury Fe-Ni-Cu sulfide ores exist in space.

The accreted Earth underwent melting and metallic core separation shortly after accretion (Wänke et al., 1984; Newsom, 1990). The refractory siderophile metals (Fe, Ni, Cr; platinumoids) and some moderately siderophile elements (Mo, W, Sc) preferentially partitioned into the core, depleting the "solar mix" (Anders and Grevesse, 1989). A thick envelope of undepleted mantle surrounded the core. The mantle is considered to have been compositionally close to carbonaceous chondrites (C1; Table 3.1), although Shen-su Sun (1982) estimated abundances of refractory lithophile elements (Al, Ca, Ti, Zr, Y, Sc, REE) in the primitive mantle to have been about two times of ordinary chondrites. Opinions differ as to whether, at the early stage, there had already been a thin veneer of a material enriched in incompatible and moderately volatile elements, enveloping the early mantle, to evolve into the continental crust, or whether the crust formed gradually by repeated partial melting of mantle followed by ascent of the more mobile components by a mechanism of hot-spot melting or subduction (Palme and O'Neill, 2004; Morris and Ryan, 2004). The idea of a continental crust formed before 4 Ga and remaining constant in mass since (Bowring and Housh, 1995) is particularly attractive to a globally versed field geologist (compare Laznicka, 1993), although the truth is probably somewhere between the two competing schools of thought. The early continental mass suffered repeated fragmentation followed by amalgamation.

Table 3.1. Major and trace metal abundances in chondrite, primitive mantle, oceanic basalt and average continental crust

METAL	C1 chondrite P&O 2004	Earth's Primitive Mantle; P&O 2004	MORB (oceanic basalt); A.H. 1988	Continental Crust P&O 2004
Li (ppm)	1.49	1.60	*3.30	1.30
Be (ppm)	0.025	0.07		1.50
B (ppm)	0.69	0.26		1.50
Mg (%)	9.61	22.17	4.57	3.20
Al (%)	8.50	2.38	8.08	8.41
Sc (ppm)	5.90	16.50	41.37	
Ti (ppm)	458.00	1280.00	*7600.00	5440.00
V (ppm)	54.30	86.00		230.00
Cr (ppm)	2646.00	2520.00		185.00
Mn (ppm)	1933.00	1050.00		1400.00
Fe (%)	18.43	6.30	9.36	7.07
Co (ppm)	506.00	102.00	47.07	29.00
Ni (ppm)	10770.00	1860.00	149.50	105.00
Cu (ppm)	131.00	20.00	74.4	75.00
Zn (ppm)	323.00	53.50		80.00
Ga (ppm)	9.71	4.40		
Ge (ppm)	32.60	1.20		
As (ppm)	1.81	0.066		1.00
Se (ppm)	21.40	0.08		
Rb (ppm)	2.32	0.605	1.26	260.00
Sr (ppm)	7.26	20.3	113.20	260.00
Y (ppm)	1.56	4.37	35.82	
Zr (ppm)	3.86	10.81	104.24	100.00
Nb (ppm)	0.247	0.588	3.51	11.00
Mo (ppm)	0.928	0.039	*0.31	1.00
Ru (ppb)	683	4.55		
Rh (ppb)	140	0.93		
Pd (ppb)	556	3.27		
Ag (ppb)	197	4		80
Cd (ppb)	680	64		
In (ppb)	78	13		
Sn (ppm)	1.68	0.138	1.38	2.50
Sb (ppb)	133	12	*10	200
Te (ppb)	2270	8		
Cs (ppb)	188	18	14	1000
REE (ppb)	2599	7286	43491	
-La (ppb)	245	686	3895	16000
-Ce (ppb)	638	1786	*7500	
-Nd (ppb)	474	1327	2074	
Hf (ppb)	107	300	2974	
Ta (ppb)	14	40	*132	1000
W (ppb)	90	16	*10	1000
Re (ppb)	39	0.3		
PGE (ppb)	3347	22		
Os (ppb)	506	3.4		
Ir (ppb)	480	3.2		
Pt (ppb)	982	6.6		
Au (ppb)	148	0.88		3
Hg (ppb)	310	6		
Tl (ppb)	143	3	*1.4	360
Pb (ppm)	2.53	0.185	0.49	8.00
Bi (ppb)	111	5		
Th (ppb)	30	83	120	3500
U (ppb)	7.8	21.8	71	910

Data sources: P&O = Palme and O'Neill (2004); A.H. = Hofmann (1988), * = Sun and McDonough (1989)

Table 3.2. Major and trace metal abundances in the continental crust

METAL	Lower Continental Crust (W 1995)	Lower Continental Crust (T&M 1995)	Upper Continental Crust (W 1995)	Upper Continental Crust (T&M 1995)	Bulk Continental Crust (R&G 2004)
Li (ppm)	13.0	11.0	22.0	20.0	21.0
Be (ppm)	1.7	1.0	3.1	3.0	2.1
B (ppm)	5.0	8.3	17	15.0	17.0
Mg (%)	3.15	3.8	1.35	1.33	
Al (%)	8.21	8.52	7.74	8.04	
Sc (ppm)	25.0	36.0	7.0	11.0	14.0
Ti (ppm)	5010.0	6000.0	3117.0	3000.0	
V (ppm)	149.0	285.0	53.0	60.0	97.0
Cr (ppm)	228.0	235.0	35.0	35.0	92.0
Mn (ppm)	929.0	1700.0	527.0	600.0	
Fe (%)	5.71	8.24	3.09	3.50	
Co (ppm)	38.0	35.0	11.6	10.0	17.3
Ni (ppm)	99.0	135.0	18.6	20.0	47.0
Cu (ppm)	37.4	90.0	14.3	25.0	28.0
Zn (ppm)	79.0	83.0	52.0	71.0	67.0
Ga (ppm)	17.0	18.0	14.0	17.0	17.5
Ge (ppm)	1.4	1.6	1.4	1.6	1.4
As (ppm)	1.3	0.8	2.0	1.5	4.8
Se (ppm)	0.17	50.0	0.083	50.0	0.09
Rb (ppm)	41.0	5.3	110.0	112.0	84.0
Sr (ppm)	352.0	230.0	316.0	350.0	320.0
Y (ppm)	27.2	19.0	20.7	22.0	21.0
Zr (ppm)	165.0	70	237.0	190.0	193.0
Nb (ppm)	11.3	6.0	26.0	25.0	12.0
Mo (ppm)	0.6	0.8	1.4	1.5	1.1
Ru (ppb)					0.34
Rh (ppb)					?0.4
Pd (ppb)		1		0.5	0.52
Ag (ppb)	80	90	55	50	53
Cd (ppm)	0.1	0.1	0.1	0.1	0.09
In (ppb)	52	50	61	50	56
Sn (ppm)	2.1	1.5	2.5	5.5	2.1
Sb (ppm)	0.3	0.2	0.31	0.2	0.4
Te (ppb)					?12
Cs (ppm)	0.8	0.1	5.8	3.7	4.9
REE (ppm)	138.0	56.0	147.0	116.0	148.0
-La (ppm)	26.8	11	32.3	30.0	31.0
-Ce (ppm)	53.1	23	65.7	64.0	63.0
-Nd (ppm)	28.1	12.7	25.9	26.0	27.0
Hf (ppm)	4.0	2.1	5.8	5.8	5.3
Ta (ppm)	0.84	0.6	1.5	2.2	0.9
W (ppm)	0.6	0.7	1.4	2.0	1.9
Re (ppb)		0.4		0.4	0.2
PGE (ppb)					1.41
Os (ppb)		0.05		0.05	0.031
Ir (ppb)		0.13		0.02	0.022
Pt (ppb)					0.5
Au (ppb)		3.4		1.8	1.5
Hg (ppb)	21		56		0.05
Tl (ppm)	0.26	0.23	0.75	0.75	0.9
Pb (ppm)	12.5	4.0	17.0	20.0	17.00
Bi (ppb)	37	38	123	127	160
Th (ppm)	6.6	1.06	10.3	10.7	10.5
U (ppm)	0.93	0.28	2.5	2.8	2.7

Data sources: W 1995 = Wedepohl (1995); T&M 1995 = Taylor and McLennan (1995); R&G = Rudnick and Gao (2004)

Mantle-derived juvenile crust has been continuously added at plate margins throughout the ages and the process is active and well documented today.

Mid-ocean ridge basalt (MORB tholeiite; Table 3.1), the principal constituent of the modern oceanic crust, is interpreted as partial melt derived from heterogeneous mantle depleted in the incompatible metals during repeated subduction and cycling (Bennett, 2004). The displaced metals have been added to the continental crust (Hofmann, 2004). The intraplate basalts found at oceanic islands like Hawaii, in plateaux, seamounts as well as in continental flood and rift basalts, are compositionally different from MORB. They have higher complement of incompatible elements and most are alkali basalts with local development of intermediate and acid volcanic members. This is attributed to the activity of magma plumes established deep in the undepleted mantle from which they scavenged the incompatible elements (Hofmann, 2004), although inheritance of continental crust components is also likely for complexes that originated in intracontinental rifts.

Although it is not known how far back in history can subduction be traced, it is a powerful mechanism to which is attributed extraction of the predominantly incompatible elements from the mantle and their transfer into the continental crust (Bennett, 2004). Subduction is also considered responsible for contamination of the mantle by crustal elements that include organic carbon, and by introduction of water into great depths, perhaps even into the subcrustal levels. The subducting plates undergo elements distillation as pressure and temperature increase during plate descent and some elements start to return back to the oceans and continental crust. Morris and Ryan (2004) have established a relative order of efficiency of element extraction from the subducting slab, with nearly 100% of boron extracted and returned to the lithosphere early, followed by Cs, As, Sb, Pb (50-75% extraction rate) and Rb, Ba, Sr, Be (20-30% extraction rate). The extracted metals are believed mostly released within the island arc window as magma component. Some can build up in the upper mantle wedge at base of the continental crust, while the surviving elements are released to the upper mantle at a depth of about 225 km. Dehydration and decarbonation during subduction, with transfer of incompatible elements into the overlying mantle wedge, cause mantle metasomatism (Hofmann, 2004). Partial melting of the metasomatized intervals or flushing of selected elements by ascending fluids is believed responsible for

generation of alkaline magmas and volatile streaming.

Continental crust

Continental crust (Wedepohl, 1991, 1995) is a component of lithosphere between 0 and as much as 70 km thick. Traditionally, it has been subdivided into the upper and lower continental crusts. The Upper Crust (Table Table 3.2) is dominated by unmetamorphosed through amphibolite grade metamorphosed sedimentary and volcanic rocks intruded by high and intermediate level granitoids and gabbroids. The predominant lithologies originated by deposition on stabilized cratons (platformic sequences) and their downwarped flanks ("miogeoclines"), as well as along consuming plate margins and rifts. The Lower Crust (Taylor and McLennan, 1985, 1995; Table 3.2) is dominated by granulite-facies metamorphics with some migmatites that range from felsic (e.g. garnet-feldspar granulite, minor meta-quartzite) to mafic (garnet amphibolite to eclogite) and there are bodies of anorthosite, meta-gabbroids, ultramafics as well as metasedimentary marble. The 1970s models considered the Lower Crust as mainly high-grade metamorphosed oceanic crust (the "basaltic layer" of Russian authors), rather orderly disposed, with increasing metamorphic grade down to the MOHO boundary against the mantle. Modern research over Precambrian cratons (Rudnick and Fountain, 1995), aided by deep seismic profiling, indicates extensive subhorizontal contraction tectonics with numerous interleaved thrust sheets and slices of merging meta-supracrustals and magmatites, interspersed with mylonitic intervals.

Geochemical background to the presence of ore deposits

The origin of lithosphere and mantle as briefly reviewed above, and the ore deposition there, have resulted from complex processes not yet well understood. The material base of Earth's evolution is thus fundamental and tables of element abundances for average crust, for the various lithospheric divisions, for the mantle, hydrosphere and biosphere have been published at frequent intervals by various authorities since the pioneering work of Clarke (1924). As research techniques improve and accumulated data grow almost exponentially the classical elements abundance estimates of the 1960s have been refined, but this has not removed discrepancies among data tables produced by the various authors and research

schools. There is not a "correct" choice so one has to select a table most in agreement with one's past experience. Continental crust abundances by Wedepohl (1995) have been selected as a basis for calculating tonnage accumulation indexes in Laznicka (1999) and throughout this book (see Table 2.3. in Chapter 2), together with the alternative figures of Rudnick and Gao (2004) for comparison. Data on chondrite, mantle, and crust abundances from Palme and O'Neill (2004), mid-ocean ridge basalts by Hofmann (1988); Sun & McDonough (1989), and on lower/upper continental crust by both Wedepohl (1995) and Taylor & McLennan (1995), appear in the same table. Although the geochemical data are not ideal (Rollinson, 1993, used 352 pages to tell us what is wrong with them), they are the only ones we have so they have to be used. The quantitative conclusions in the field of metallogeny are thus based on conclusions reached by geochemists and petrologists and when these data change the ore-related data have to change too. Despite

discrepancies in values, it is apparent that each lithospheric and crustal domain has one or more distinct groups of elements (metals) that are moderately to strongly enriched in respect to the other domains, as follows:

- Mantle: Mg, Cr, Ni, Co, PGE
- Oceanic crust: Fe, Cu, Mn, Zn
- Lower Continental crust: Al, Zr, REE, Th
- Upper Continental Crust: Sn, W, Mo, Li, Rb, Be, Bi, Ta, Nb, Pb, U

It can be statistically demonstrated that ore deposits of the same metals prefer the geochemically enriched domains either directly (they are hosted by them) or indirectly (metals derived from Domain A now hosted by Domain B). Although trace metal enrichment of the environment is not the only component of successful ore prediction, it is where the interpretative process should start.

Introduction to Chapters 4 to 14

Ever since De Launay's monumental *Traité de Métallogénie* published in 1913, writers of text- and reference books in economic geology (Lindgren, 1933; Schneiderhöhn, 1941; Bateman, 1950; Smirnov, 1976; Guilbert and Park, 1985) experimented with organization of book contents which, in turn, reflected classifications of mineral deposits popular in their times. The books organization has gradually shifted from purely genetic one (orthomagmatic, mesothermal, sedimentary, etc. deposits) to those that emphasize host rock associations (Stanton, 1972; Laznicka, 1985, 1993) or geotectonic setting: first based on the geosynclinal model (Bilibin, 1955), later on plate tectonics (Routhier, 1980; Mitchell and Garson, 1981; Sawkins, 1990). Thanks to the extreme nonuniformity of metallic deposits, no single subject organization has been capable of providing a "democratic" framework in which all types of ores would receive equal attention and provide the student with an unbiased outlook required to go out and search for ores. Every organizational framework favors the deposits that "fit" into a popular pigeonhole (or correspond to a popular model) and it tends to marginalize or completely ignore deposits that do not fit or, even worse, forces the latter into classes for which they are ill suited (is it not like governments, religions and political doctrines operate?).

Stanton (1972) pioneered the organization of ores based on host rock associations, but hydrothermal veins that are not controlled by uniform host rocks refused to cooperate so Dick put them into a "vein association". How do you go around looking for areally extensive "vein rocks"? In the plate tectonic models young (active) oceanic spreading ridges and back-arcs have provided the most convincing settings for some types of ores, some of which have been directly observed in the process of formation: an ultimate proof in geology!. This clarity and reliability of genetic interpretation, however, grows gradually weaker as one moves into the geologically older and deeper-seated rock associations, and away from the plate margins. There, hypothesizing so dear to the geologists (note the ubiquitous paragraphs reviewing the often conflicting interpretations based on the same sets of data that nowadays adorn almost every research paper or reference book) overshadows the facts. Popular models are put to action whether they help

or not. How important are the plate tectonic settings for the formation of ore laterites or placers? Not much.

For the purpose of general teaching and academic research "streamlined" ore classifications and organizations are fine, in fact essential for presentation to the 3rd or 4th year geology students and still preserving their sanity. They serve also well to academic researchers who enjoy the luxury to concentrate on a selected topic or a method and to keep them "refining" it under the security of tenure and a research grant. The practicing geologist faced with the task of placing into suitable pigeonholes all mineralizations that occur in his/her territory, or an explorationist expected to find new orebodies rather than to research those found by others, need a different assistance. Exploration is still precedent (analogue) driven, even given that many of the future orebodies are to be found under a deep cover by drilling geophysical anomalies. One still needs the ability to "read the rocks" and interpret the "facts" revealed in the drill core to position the next hole creatively to find a mine for a minimum expenditure.

In mineral exploration "everything goes" as long as it leads to a new orebody and no single framework, model or idea is a panacea equally suitable for all types of deposits (Hodgson, 1993; Woodall, 1984, 1994). This "geo-multiculturalism" should be reflected in a text primarily written for the practitioners, so what is the most suitable framework of organization applied to all metallic deposits, anywhere, and preferably of a large magnitude?

I believe it is the combination of plate tectonics (to start with, and for the geologically young orebodies in the "key" settings; Table II.1), depositional environments (e.g. meandering rivers, anywhere), lithologic associations (e.g. alkaline rocks; redbeds; Table II.2), geological age groups (e.g. Archean "greenstone" association), intensity/style of deformation and metamorphism (e.g. shear zones, breccias), supergene modification (e.g. Au-gossans), genetic groupings of deposits (e.g. deposits attributed to "basinal brines" flowing through aquifers), and ore types (e.g. Broken Hill-type Pb-Zn).

Table II.1. Young (active, recent) plate tectonic environments and book chapters; only those that contain ore "giants" are reviewed

Chapter No., environment	Example	Processes	Rock formation	Ore formation
4. Ocean spreading ridges	Mid-Atlantic Ridge Iceland	Spreading of central rift, outpouring of mantle generated lavas	MORB basalt lavas, breccias, ~sediments; diabase in depth	Massive Fe,Zn,Cu>Ag,Au sulfide mounds; metalliferous Fe,Mn enriched sediment
4. Abyssal ocean floor	Central Pacific Ocean	Pelagic sedimentation on oceanic crust foundation; some hemipelagic	Red abyssal clay, calcareous or siliceous ooze	Mn-Fe oxide nodules and crusts ~ with elevated Cu,Co,Ni
4. Mid-plate oceanic islands and seamounts	Hawaii Nauru	Central and chain eruptions of lavas to form shield volcanoes, seamounts; coral islands, atolls	Tholeiitic basalt > alkaline basalts > andesites, trachyte Coral and platform limestone	Mn,Co crusts > rare massive sulfides at some seamounts; phosphate (trace U) in coral islands; Fe,Al laterite
N.A. Trenches and accretionary wedges	Aleutian, Peru-Chile trenches; Barbados	Oceanic & terrigenous sediments fill trench, accrete against trench wall, oceanic crust subducts	Mixture of pelagic, hemipelagic, terrigenous, volcanics sed; slices of oceanic basalt, serpentinite	Reworked discontinuous oceanic ores: Mn-rich seds, chromite in serpentinite, Cyprus-type VMS
5. Ensismatic (Mariana-type) island arcs	Mariana Islands	Oceanic crust carrying seamounts, debris subducts under oceanic plate	Arc basalt volcanism, accretion of basalt & peridotite seamounts	Traces of oceanic ores as above in accreted blocks & debris
5. Island arcs with continental basement (Japan-type)	Japanese islands	Subaerial and submarine volcanism above subduction zone; accretion, sediment aprons	Arc basalt < andesite > dacite, rhyolite in stratovolcanoes, calderas; volcanic sediments	Au enriched in some hot springs, also Fe,Mn; massive pyrite, sulfur; magnetite beach sands
5. Back arcs, interarc rifts	Japan Sea, Lau Basin, Okinawa Basin	Volcanic, terrigenous, biogenic sedimentation, minor volcanism, submarine hydrotherms	Marine sediment, mostly mud, marl; basalt > andesite > rhyolite; hydrothermal sediments	Rare submarine massive Fe > Cu,Zn,Pb sulfides, ~Ag,Au
6. Andean-type (continental) magmatic arcs	High Andes from Colombia to Peru	Calc-alkaline magmas melted above subduction zone ascend to form stratovolcanoes, calderas	Arc andesite > basalt, dacite, rhyolite lavas & pyroclastics; volcanic lake sediments	Sulfur lavas; Au-Ag and Hg in some hpt spring systems; alteration alunite; borates, Li, Mn in lake sediments
13. Mid-plate stable shelf, epicontinental marine basins	Baltic Sea; Sahul Shelf	Detrital and/or carbonate sedimentation	Mud, sand > gravel; biogenic carbonate muds, coral; evaporites	Bedded Fe>Mn oxides, phosphatic sediments; halite
13. Mid-plate stable continental environments, humid & arid	Greenland; Lake Superior; Sahara	Erosion of mountains, river & lake & rift basin filling, regolith and soil formation	Glacial sediment (till, outwash); gravel, sand, mud; soil & laterite; aeolian sand, loess	Au,Sn,Cu,W, etc. ore blocks in drift; alluvial placers Au,Sn; lake Fe,Mn ores; Fe,Al,Ni,Mn,Co laterites
10. Collisions, Himalayan type	Himalayas, Tibet Plateau, Ganges Foreland Basin	Rapid land rise, deformation, erosion; melting in depth produces granite, rare volcanism	At surface rock debris; sand, mud, peat in foreland basins; lake sediments, evaporites	Li, borates in playas in Tibet
12. Early stage of intra-continental rifts	East African Rift system	Faults-bounded extension, flanks bounded uplift; volcanism, basin filling	Flood basalt and bimodal, later alkaline volcanism > carbonatite; lake sediments, playas	Soda lakes (Natron, Magadi); diatomite; fluorite

Table II.1. (continued)

Chapter No., environment	Example	Processes	Rock formation	Ore formation
12. Advanced rift-drift stage (oceanic crust appears)	Red Sea	Crustal extension changing to ocean opening and drift; seafloor hot springs	Early evaporites, carbonates; later mud; MORB basalt at sea floor in axial zone, sialic flanks	Metalliferous muds and hot springs brines enriched in Zn,Cu,Ag,Mn,Fe
N.A. Transcurrent fault plate margins	San Andreas Fault system	Strike-slip movement of two lithospheric plates; earthquakes	Fault rocks (gouge, breccia), debris in depressions	Traces of Au in hot springs (Alpine Fault, New Zealand)

Table II.2. Examples of interpreted ancient plate tectonic environments and selected "giant" deposits they contain

Chapter No., plate environment	Commodity & type	Examples of ore deposits (described "giants" and some "large" deposits are shown in bold)
8, 9 (14). Oceanic lithosphere, ophiolites (many ophiolites are suprasubduction, formed in back arcs floored by oceanic lithosphere)	Cr, podiform chromite Cu (Zn), Cyprus-type mass. sulfides Cu (Zn), Besshi-type mass. sulfides Fe,Mn metalliferous sediments #Hg, cinnabar from springs #Chrysotile asbestos in serpentinite #Au,Ag,Co arsenides in listvenite #Fe,Ni,Co,Cr laterite and saprolite #Mg, nodular and lake magnesite	Turkey (e.g. Guleman); Kempirsai , Kazakhstan Cyprus (e.g. Mavrovouni); Semail, Oman Besshi, Sazare, Japan; Windy Craggy , Canada Cyprus, Troodos Complex ochers and umbers New Almadén, Mayacmas , California Thetford Mines, Black Lake, Asbestos, Québec Bou Azzer-Graara belt, Morocco New Caledonia peridotite allochthons Kununurra , Queensland
8, 9 (7, 13, 14). Oceanic, pelagic, hemipelagic sedimentary rocks	Mn, nodular and bedded #Au, micron-size disseminated	Austrian Alps, Timor, Olympic Peninsula, WA Gold Quarry , Carlin Trend, Nevada
8, 9, 10. Accretionary wedges	#Au, orogenic hydrothermal lodes	Juneau Au belt , Alaska; Mother Lode , California
8, 9. Subduction melange & blueschist	same as in ophiolite	New Almadén-Hg , California
8, 9. Ensismatic island arc	Cu,Au porphyry deposits Cu,Au high sulfidation (enargite) Au,Ag low sulfidation epithermal Cu veins Pb-Zn-Ag epithermal veins Au, epithermal low sulfidation	Santo Tomas , Dizon, Philippines Lepanto (Mankayan) , Philippines Baguio Au district (Antamok) , Philippines Osarizawa, Japan Toyoha, Hosokura: Japan Chitose, Sado: Japan
8, 9. Back arc and interarc rifts	Zn,Pb,Cu,Ag kuroko massive sulfide pyrite >Cu,Zn,Pb mass.sulf. in seds Cu,Au stockworks in porphyry	Hokuroku district, Japan; Buchans, Canada Iberian pyrite belt (Rio Tinto, Corvo-Neves) Rio Tinto, Cerro Colorado orebody , Spain El Teniente, Rio Blanco , Chile
6, 7. Andean magmatic arc, axial zone	Cu,Mo porphyry and breccias Cu,As enargite high sulfidation	El Indio-Tambo , Chile
7, 10. Cordilleran arc (inner side of principal magmatic arcs)	Cu,Mo porphyry and skarn Pb,Zn skarn, carbonate replacement Pb,Zn mesothermal veins W, scheelite skarn Mo, stockwork in quartz monzonite Au, micron-size disseminated Au, mesothermal veins Au, epithermal veins, stockworks Ag (Au) bonanza epithermal veins Sb (Au) stibnite veins Fe, magnetite-actinolite lavas, sheets	Bingham , Utah; Cananea , Mexico Leadville , Colorado; Santa Eulalia , Mexico Parral, Concepción del Oro: Mexico Cantung, Mactung , NWT, Canada Endako , Boss Mountain: B.C., Canada Carlin and Getchell Trends , Nevada Central City, Colorado; Boulder Batholith, MT Round Mountain , NV; Cripple Creek , CO Guanajuato, Pachuca, Zacatecas : Mexico Hillgrove , N.S.W., Australia El Lago, Pedernales: Chile; Durango, Mexico

Table II.2. (continued)

Chapter No., plate environment	Commodity & type	Examples of ore deposits (described "giants" and some "large" deposits are shown in bold)
7, 10. Arcs on thick sialic crust predating rifting	Sn, cassiterite veins Sn "porphyry", disseminated Ag,Sn epithermal vein arrays Mo (W) Climax-type stockworks	Llallagua , Bolivia; Kavalerovo district, Russia Cerro Rico and Oruro , deeper levels: Bolivia Cerro Rico , Summit: Bolivia Climax, Henderson, Mt. Emmons , Colorado Jos & Bauchi Plateaus, Nigeria; Pitinga , Brazil Nairn anorthosites, Canada; Åna Sira massiv, (Tellnes), Norway Voisey's Bay , Labrador, Canada Olympic Dam , South Australia
10, 11, 12. Intraplate "hot spots" and sialic doming predating rifting (anorogenic magmatism)	Sn, veins, greisens in granite Fe,Ti oxides: massive, disseminated in anorthosite Cu,Ni in troctolite near anorthosite Cu,Au,U in hematite-matrix breccia	Bushveld, magnetitite seams; South Africa Bushveld, Merensky and UG2 Reefs ; S. Africa Bushveld , South Africa; Great Dyke , Zimbabwe Stillwater , Montana; Muskox, northern Canada Noril'sk and Talnakh , Siberia, Russia Michigan Cu district , U.S.A. Kupferschiefer of Poland, Mansfeld-Sangerhausen , Germany Zhezkazgan , Kazakhstan
7, 11, 12. Intracontinental rifts & "hot spots"	Fe,Ti,V in layered mf-umf intrusions PGE dissem. in magm. layer, ditto Cr, chromitite magmatic layers, ditto Ni,Cu sulfides at base of intrusions Cu,Ni,PGE in & close to gabbro sills #Cu, native Cu in meta-basalt #Cu sulfides in black shale on redbeds #Cu sulfides in gray sandstone in redbeds Zr,REE,Nb in layered apgaitic syenite Ta,REE,Y,Th,U in peralkaline granites Ta,Be,U,Th in alkali pegmatites, veins REE,Nb,Cu disseminated in carbonatite	Ilímaussaq , Greenland; Lovozero , Russia Ghurayyah , Jebel Sayid: Saudi Arabia Ilímaussaq , Greenland; Lovozero , Russia Mountain Pass , California; Araxá , Brazil
11, 12, 13. Passive continental margins and intracratonic basins	Fe, bedded particulate ironstone Mn, bedded oxides or carbonates P(U), bedded or nodular phosphorite #U, unconformity U in basement, cover #U(V), sandstone infiltrations #U, infiltrations in lignite and coal #Zn,Pb, Mississippi Valley-type Zn,Pb,Ag sediments hosted (sedex)	Birmingham , Alabama; Minette Basin, France Nikopol' , Takmak : Ukraine; Kalahari , S. Africa Morocco ; Phosphoria Fm. , Montana; Florida Athabasca Basin , Canada; Alligator Rivers Australia Colorado Plateau, San Juan Basin : U.S.A. Cave Hills, South Dakota; Montana, N. Dakota S.E.Missouri, Tri-State, E. & C. Tennessee, Red Dog , Alaska; Mount Isa & Century , Australia; Sullivan , B.C., Canada
11, 12, 13. Rifting & extension in passive margins		
10, 14. Collisional systems	Sn,W hydrothermal in/near granites #Sn, regoliths & placers U, pegmatitic & hydrothermal veins	Cornwall , U.K.; Erzgebirge , Germany & Czech Republic Burma, Thailand, Malaya, Billiton belt, S. Asia Rössing , Namibia; Příbram, Jáchymov: Czech R.
6. Transform faults 12. Meteorite impacts related metallogenesis	Au,Sb,Hg hot springs precipitates Cu,Ni,PGE sulfides in hybrid gabbroids	McLaughlin, Sulfur Bank , California Sudbury , Ontario (alternative genetic explanation)

NOTE: # indicates ore origin by a superimposed process (postdating the indicated plate tectonic environment)

In a flexible framework of organization either of the eight or so aspects (premises) of organization takes precedence whenever it is the single most important controlling factor for a certain type of ores. The emphasis here is on the empirical, factual characteristics and indicators that one can actually

see in the field and map, although concepts are essential to "think ahead", predict and tie together the various "facts" that initially do not seem to have much in common (a sort of a forensic work).

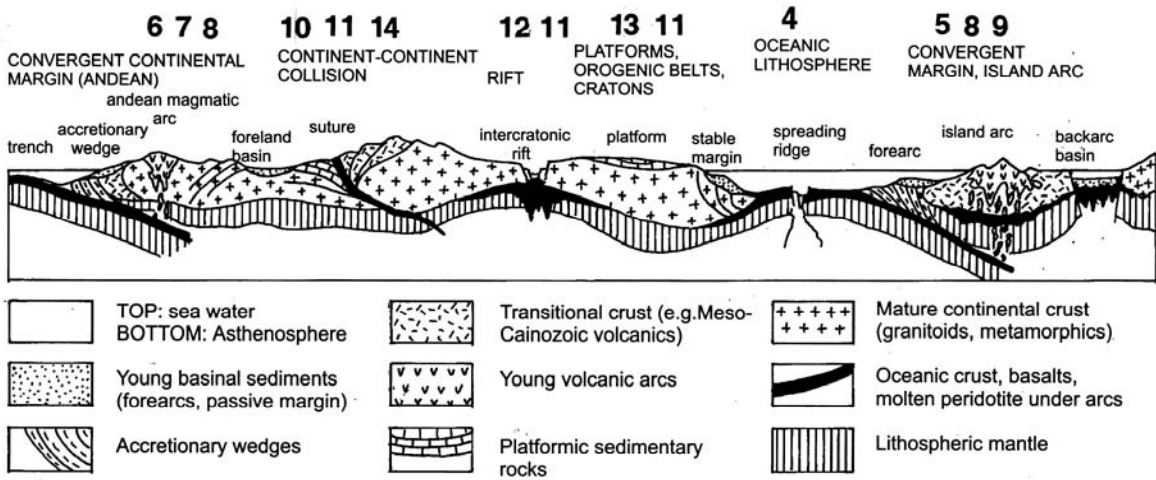


Figure II.1. Very much simplified diagrammatic cross-section showing the approximate place of Chapters 4 to 14 in global geotectonic subdivisions

After a lifetime of experimentation with ore organization on a global basis I have created a realistic system of 241 empirical pigeonholes ("geosites"), based on the various local combinations of depositional environments, rock associations and genetic factors, ready to accommodate all sorts of ores discovered so far and possibly predict the place of some future ones. It is called Total Metallogeny-Geosites (TM; Laznicka, 2001, 2004) and it is hardly a neat and rational classification as it is full of overlaps and transitions. It comes, however, close to what ore geology really is. TM is an inventory of precedents of ore setting and host rock assembly and can be used as a catalogue for browsing and generation of exploration ideas. I have tried to construct this book on similar principles, although the selection of settings is reduced as only those suitable for the "giant" deposits are considered.

Chapters in Part II thus loosely follow the progression of plate tectonic regimes and settings from oceans through the consuming margins to continental interiors and rifts (Fig. II.1), but a distinction is made between the "young" environments (still active or recently active, visually recognizable) and their presumed counterparts now preserved in orogens and cratons. The chapters and their names are not sacrosanct and should not be confused with classifications. Their main purpose has been to break down the large amount of information into manageable units. Certainly there is an overlap and imperfections in my efforts to impose some order on the gifts of Mother Nature and I can only hope that my successors will do better. In the meantime cross-references are widely used to put the reader back on track, in case he/she gets lost.

4 Mantle to oceans

4.1 The mantle

Earth's mantle is the intermediate region between the metallic core and lithosphere. It is the thickest (about 2,850 km) and most voluminous (82% of Earth's volume, 68% of mass) Earth division composed of ferromagnesian ultramafic silicate rocks. The traditional mantle boundaries (Ringwood, 1975) have been placed on distinct seismic discontinuities. The bottom discontinuity, at about 2900 km depth, separates the Lower Mantle from the Core. Between the 400 km and 900 km depth is the Transitional Zone, above which is the Upper Mantle that is in contact with the continental crust in depths ranging from about 30 to 70 km, and with the oceanic crust in depths between 12 and 16 km. Mantle petrology and processes, mainly from the theoretical point of view, are well reviewed in petrology texts (e.g. Maaløe, 1985; Hess, 1989).

The mantle is subdivided into the solid, rigid, lithospheric mantle, and plastic ("molten") asthenosphere that undergoes convective flowage. The lithosphere/asthenosphere boundary is uneven and further complicated by the presence of mantle plumes that are rising, subvertical columns or cones of buoyant magma the internal temperature of which is some 200-250° C greater than that of the surrounding asthenosphere. A "typical" plume originates near the thermal boundary layer at the core interface (Davies, 1998b) and this has been confirmed by high resolution tomography of the plume beneath Iceland, but other plumes have much shallower roots and are rather narrow (Nataf, 2000). The surface projections of plumes are called "hot spots" and they are believed responsible for continental breakup, development of rifts, and partial melting of mantle materials to form basaltic and alkaline magmas emplaced into continental and oceanic crusts. Plateau basalt is the best known product (White and Mackenzie, 1995).

The classical view of a mantle stratified by rock composition and packing density of minerals is no longer popular, although some stratification could have been in place before the onset of subduction in the Archean and perhaps earliest Proterozoic, when the mantle was some 200-300°C hotter. The modern mantle has been contaminated by convection-driven subduction and plume activity (Campbell, 1998) so much of the upper mantle, at least, is now a "well-

stirred" heterogeneous mixture and even the more homogeneous lower mantle presumably contains patches of reconstituted oceanic crust detached from subducted slabs (O'Neill and Palme, 1998). The depth reached by the subducted material, before it dissipates, is not known. The older estimate of some 250 km under surface has now been extended beyond the 660 km depth seismic discontinuity and many believe that some slabs make it to the mantle/core boundary (Davies, 1998).

The principal constituents of the subducting slab are hydrated Mid Ocean Ridge basalt (MORB) with its partially altered diabase, gabbro and mafic-ultramafic cumulate infrastructure, plus the harzburgitic mantle residue under MOHO. The latter changes with increasing depth into a "normal" mantle lherzolite. There is also a component of ocean floor sediments derived from the altered MORB, themselves carried down the subduction zone, but significantly modified by prolonged contact with ordinary or hydrothermally-conditioned seawater (Hékinian, 1982). A variable proportion of subductible continental crustal materials such as windblown quartz sand and silt (a very high proportion is on the Atlantic floor; Emery and Uchupi, 1984) and biogenic carbonate, silicite and phosphate, are also present in oceanic sediments. The result is a significant but heterogeneous contamination of the pristine mantle by many of the incompatible and other elements previously removed from the mantle to form the continental crust early in geological history. Many of these elements are returned to the crust under consuming plate margins during dehydration and partial melting of the subducting slab, but some remain and are added to the mantle.

The cardinal question of mantle geochemistry and petrogenesis which, in turn, influences the nature of mantle-initiated magmatism (and metallogeny) within the crust, is the place and behaviour of incompatible elements in the mantle (Faure, 2001). The 1960s-1970s vintage mantle models, proposed before the universal acceptance of plate tectonics and subduction, assumed the existence of depleted (of incompatible elements) mantle at shallower levels, and undepleted mantle of or close to chondritic composition, still holding its incompatible complement, at greater depth, especially in the lower mantle. According to this

model the basaltic parent magmas emplaced into the crust at mid-ocean ridges or in rifts were derived by decompression melting in the depleted lithospheric mantle (Wilkinson, 1982), whereas the alkaline magmas originated in the undepleted mantle in greater depths or, alternatively, resulted from crustal contamination.

The classical concept has undergone change in the past 30 years (Hofmann, 1997; Faure, 2001 for review). Although the existence of depleted and undepleted mantle still holds, it is now accepted that much of the mantle has been contaminated by many cycles of subduction and convective overturn and possibly some assimilation of continental crust near its base. This resulted in mantle heterogeneity so that incompatible elements-enriched regions could be found at many different places; these regions are called "fertile mantle" by some authors. The most popular interpretations of the source regions of alkaline magmas, based to some extent on empirical observation derived from mantle xenoliths in deeply sourced basalts, kimberlites and lamprophyres, assume the role of mantle metasomatism (Roden and Murthy, 1985). Mantle metasomatism, as summarized in the ever popular Geological Society of America Special Paper 215 (Morris and Pasteris, 1987), is produced by recharging of the mantle, previously depleted in the LIL (=large ion lithophile) elements, by asthenospheric injections of melts of uncertain origin (possibly derived from hydrated and carbonated peridotite), or from residual melts and fluids derived from trapped alkaline basalt at the MOHO discontinuity (Roden and Murthy, 1985). Metasomatic effects in mantle xenoliths and in few ultramafic blocks tectonically emplaced into the oceanic crust as at St. Paul Rocks in the equatorial Atlantic, range from visually obvious to cryptic. The obvious metasomatic effects range from veins and altered patches of hydrous and alkaline minerals such as phlogopite, alkali amphiboles and feldspars, to xenoliths of rocks dominated by these minerals such as glimmerite, carbonatite or potassic minette. The cryptic effects are only analytically detectable.

Magmas generated by partial melting of metasomatized mantle are greatly enriched in LIL elements, Fe, Al, alkalis, H₂O, CO₂, F and other elements and compounds and when emplaced into the crust they produce, after fractionation, alkaline provinces with a variety of rare rocks and distinct metallic deposits (Chapter 12). Intracrustal alkaline provinces can either be contemporaneous with mantle metasomatism in depth, or they may postdate metasomatism of the magma source region

by billions of years. Typical alkaline provinces seem to coincide with the existence of mantle "hot spots" in their time of origin.

4.1.1 Mantle metallogeny

The mantle is geochemically enriched in Mg, Fe and siderophile trace metals such as Cr, Ni, Co plus platinum group elements (see Table 3.1, column 3) but little is known about the existence of local super-accumulations of these elements to call orebodies. The only metallic "ore" samples delivered from inside the mantle come from rare chromite-enriched dunite xenoliths in kimberlites (diamond xenocrysts in kimberlite and lamproite are not considered in this book). Even if peridotite is, in the future, used as a source of industrial magnesium, and even if significant accumulations of chromite, Fe-Ni-Co sulfides and perhaps platinoids do exist in the mantle, their existence is academic as mantle is outside the reach of the present exploration and mining technology. The tonnage of mantle xenoliths available near the present land surface is insignificant. The mantle is, however, the ultimate source of almost all metals that form ore deposits within the crust, some of which are of giant magnitude.

The relation of rock associations (and their ores) in the crust to the mantle ranges from immediate and intimate, to distant and largely irrelevant. With perhaps few rare exceptions, all the ultramafic "mantle" rocks exposed in the crust are not samples derived from the unmodified mantle itself, but residua after fused mantle peridotite from which the basaltic melt had been extracted (the harzburgitic component of oceanic lithosphere and ophiolites), plus cumulates produced by differentiation of mantle-derived basaltic magma, present in the same setting. The initially geochemically preselected metals in the mantle had been further interactively developed after incorporation into the crust, to produce a distinct suite of ore deposits some of which are of the "giant" magnitude (e.g. Ni laterite/saprolite as in New Caledonia). The dismembered ultramafic "dike" that hosts the giant Jinchuan Ni,Co,PGE deposit in China (Chapter 12), considered by some as a mineralized mantle slice, is now considered a root zone of a Great Dyke-style intrusion related to magnesian basalt magma (Naldrett, 1999). The rift and crustal extension-controlled association of plateau basalt and related Bushveld style intrusions and the alkaline silicates-carbonatite association (Chapter 12) are even richer in exceptional metal accumulations than the MORB

systems. The basalts are usually attributed to magmas produced by melting of the depleted mantle, the alkaline melts came from the undepleted and/or metasomatized mantle intervals.

4.2. Oceanic crust, ocean floor

Present knowledge about the oceanic crust and its ancient, modified equivalents, evolved independently from two sources of experience: oceanic and continental. The oceanic experience goes back to Charles Darwin's Beagle expedition in 1831, then to the 1872-1876 Challenger voyages recorded in the writings of Murray and Renard. The continental line of research may have originated with Brongniart's naming of ophiolite in 1813, followed by recognition of the distinct radiolarite, pillow basalt, serpentinite association by Steinmann in 1927 ("Steinmann Trinity"). It was only shortly before the 1968 formulation of plate tectonics when the fundamental genetic correspondence of the present oceanic crust and ophiolites had been recognized by Brunn (1959), Gass (1968), Coleman (1977) and others.

Modern understanding of oceans, ocean floor, oceanic lithosphere, and ophiolites is supported by extensive and rapidly growing literature to which the reader is referred (e.g. Basaltic Volcanism Study Project, 1981; Hékinian, 1982; Emery and Uchupi, 1984; Keating et al., eds., 1987; Dilek et al., eds., 2000; Floyd, ed., 1991). This book thus moves directly to the brief review of ore metals fluxes and local mineral accumulations, and briefly reviews the most promising ore-hosting sub-environments. This chapter deals with the presently active, and recently active ("young") systems and settings where several ore metals can be directly observed in the process of accumulation, although "giant" deposits of the classic type are virtually nonexistent. The ancient oceanic rocks associations preserved on land, ophiolites, are of more interest as a site of ore "giants" and they are treated in Chapter 8.

4.2.1. Oceanic spreading ridges

The principal source material from which is generated the bulk of the oceanic crust is the upper mantle. Mantle convection causes the ascent of asthenosphere, through thinned mantle lithosphere, into shallow depth under oceanic spreading ridges. There, partial melting of the mantle lherzolite (olivine and ortho-, clinopyroxene peridotite) takes place in depth. The product is refractory ultramafic

residue of harzburgitic (olivine + orthopyroxene) and dunitic (olivine only) composition, and basaltic melt. The refractory peridotite constitutes a unit between the predominantly basaltic oceanic layer on the top, and lherzolitic sub-oceanic mantle below, to form the relatively rigid lithosphere (BVSP 1981; read also Chapters 6 to 8 in Hess, 1989 and most modern texts on petrology).

The bulk of the new oceanic lithosphere forms along oceanic spreading ridges all of which, with the exception of the Neovolcanic Zone of Iceland, are deep submarine. Lesser quantity of oceanic rocks accumulate in extensional systems above subduction zones, in back-arcs ("suprasubduction" oceanic association and ophiolites). The upper parts of spreading systems are sites of vigorous interaction of magma with seawater during which basalts are altered, partially hydrated and metasomatized. Sea floor sediments form by direct precipitation from hydrotherms ("exhalites"), by biogenic processes, and by reworking of the volcanic products. There is a range of spreading ridge configurations ranging from the purely volcanic to those filled by a thin layer of sediment. The back-arcs (Chapter 5) are floored by the continental crust outside the spreading axis and are all sediment-rich.

The shallow subsurface under active spreading ridges contains short-lived magma chambers and systems of magma conduits where limited differentiation and fractionation is taking place to produce a range of ultramafic to mafic cumulates. Some of these are preserved on land as usually dismembered, impersistent layered intrusions, sills or dikes. Sheeted diabase dike arrays, former feeders of the submarine basalt flows, are preserved in most ophiolite complexes. Post-cumulus gabbros, and minor plagiogranites that grade to albitites and Na-Mg metasomatites (Coleman and Peterman, 1975), are also present.

After its rapid and dynamic formation the oceanic crust is passively carried away from spreading ridges towards lithospheric plate margins where it is subducted. Relatively minor quantities of oceanic materials are scraped or sliced away at plate margins and added to the continental crust. During its passive residence under the floor of oceans, the spreading ridge volcanics and synvolcanic sediments are gradually buried under the cover of seafloor sediments of pelagic (from oceans, e.g. biogenic), hemipelagic, and some volcanic and terrigenous (land-derived) provenance. The ocean floor sequence is also pierced by magmas related to

the intraplate magma plumes under "hot spots" that produce oceanic islands, seamounts and plateaux.

Ore metals fluxing and accumulation

The process of bulk conversion of mantle peridotite into oceanic (MORB) basalt plus ultramafic residue is a major geochemical event. Compared with the "primitive mantle" (see Table 3.1.) the basaltic (MORB) magma is enriched in Al (~3.5x), Ti (7x), Sc (3x), Cu (3.5x), Y (9x), Zr (10x), Nb (6x), Mo (9x), Sn (10x), REE group (7x), Ta (3x), Pb (2x) and U (3.5x). It is impoverished in Mg (-5x), Cr (-5-7x), Ni (-12x) and Co (-2x). MORB basalts are thus compositionally about intermediate between the "primitive mantle" and continental crust. Hofmann (1988) recognized a "simple, two stage model of extracting first continental and then oceanic crust from the initially primitive mantle", in which the latter has achieved only moderate (up to a factor of 10) concentrations of mainly moderately incompatible elements, compared with the 50 to 100 times maximum concentrations of the highly incompatible elements such as Cs, Rb in the continental crust (the alternative explanation is that the "continental" elements have been progressively and cumulatively extracted from the oceanic crust). MORB formation alone thus does not result in extreme partition of some major and trace metals to produce first stage ores or significant metals preconcentrations. The basalts became the source of ore metals only when subjected to interaction with hydrothermal systems, seawater leaching, or weathering.

The residual refractory peridotite is a stronger repository of pre-enriched metals like Cu, Ni and Co. Although disseminated to rarely massive chromite has been recovered from several dredge hauls at oceanic ridges, it is unlikely that an economic deposits might be discovered. It, however, confirms the oceanic origin of ophiolite-hosted chromitites (Chapter 8). In addition to chromite, synmagmatic accumulations of Fe, Ni, Co sulfides with or without platinoids and titanomagnetite or ilmenite, also known from ophiolites, have also been detected in mid-ocean ridge cumulates but the presence of economic ores is highly unlikely.

Hydrothermal systems at and under sea floor

The extra-magmatic phase of metals fluxing at spreading ridges, still broadly synvolcanic, is the result of a very dynamic interaction of heated seawater convecting through basalts and/or sediments in the sub-sea floor region. These hydrotherms selectively leach major and trace metals from rocks en-route, then deposit them at the sea floor as true hydrothermal sediments (exhalites) or as replacements of the pre-existing sediments or volcanics. Alternatively, metals precipitate in the shallow subsurface as dilation fillings and replacements of highly altered rocks. The ideal deposits correspond to the VMS (or VHMS) model, that is volcanic or volcanic-hosted massive sulfide deposits, proposed by Schneiderhöhn, Oftung, Stanton in the 1940s-1950s and subsequently repeatedly updated as a result of discovery of the active seafloor systems (e.g. Ishihara, ed., 1974; Sangster and Scott, 1976; Franklin, 1993). An ideal VMS set consists of 1) stratiform layer, lens or mound of massive sulfides deposited at the sea floor; 2) mineralized sub-seafloor feeder system that could be a stockwork of veins, veinlets or stringers, or mineralized breccia, in strongly altered rocks. There are many variations of the basic VMS model in terms of syn-depositional architecture, setting and mineral composition. The architectural variations include the presence of broad ("distal") haloes of ore metals in "metalliferous sediments" (see below); sea floor "gossans"; clastic orebodies (typically conglomeratic) of VMS reworked down the paleoslope; transitional orebodies formed in water-filled dilations, as in rubble under the sea floor, or by early diagenetic replacement of unconsolidated, water-saturated sediments. The geotectonic setting of VMS deposits ranges from those formed in basalt-dominated systems at spreading ridges and in some back-arc basins, plus their counterparts in ophiolites ("Cyprus-type" when in volcanics, "Besshi-type" when in sediments), to VMS systems where acid volcanics are prominent (kuroko, Noranda and Rio Tinto ore types). The latter formed in island arc/back-arc settings and in some rift systems. The mineralogical composition of sulfides usually correlates with the geotectonic setting where the Cyprus-type deposits are predominantly pyritic or pyrrhotitic with or without chalcopyrite and rare sphalerite, whereas the kuroko and similar deposits are dominated by sphalerite, galena and lesser chalcopyrite. Surprisingly, the recently formed VMS's on the

ocean floor (read below) are much richer in Zn, Pb, Ag and Au than their ancient counterparts.

Although close to 50 sulfide occurrences have been recorded at the present sea floor above oceanic crust by now (Rona, 1988; Herzig and Hannington, 1995), very few (such as the Middle Valley, Davis et al., 1992 and TAG hydrothermal mound, Petersen et al., 2000) have been drilled and ore tonnages estimated. Only the **Middle Valley VMS field** in the Eastern Pacific is demonstrably of the "large" magnitude in terms of Zn, Cu and Au, and could be a silver "giant" holding between 7,100 and 14,200 t Ag (Herzig and Hannington, 1995). Additional future discoveries are likely, the sediment-filled ridges being more promising although ores would be more difficult to find under sedimentary cover. VMS occurrences in the back-arc setting and the Red Sea "metalliferous muds", the latter approaching the "giant" magnitude, are described in Chapters 5 and 12, respectively

The ancient oceanic VMS deposits (Cyprus and Besshi types) in ophiolites on land (Chapter 8) are quite numerous but small and only aggregate tonnages of districts or regions like the Troodos Complex of Cyprus or Semail Ophiolite in Oman could bring them into the "large" category.

Sulfide deposits at oceanic ridges

Figure 4.1. shows idealized inventory cartoons of sediment-free and sediment-filled oceanic spreading ridges, with sites of metal accumulation. The oceanic ridge morphology is influenced by the spreading rate and evolutionary phase as most ridge complexes are cyclic. In a typical cycle (Gente et al., 1986) a slow- to medium-spreading ridge evolves from an initial set of fissures and collapsing slabs through graben formation to graben filling by basaltic lava into, ultimately, a dome or ridge formation. Some grabens fill by sediment. In modern, active or recently active spreading systems, the processes taking place at the top of the system such as tectonism, volcanism, heat flow, sedimentation and ore formation, and their products, have been observed, sampled and drilled from submersibles and are extensively described in the literature. Information about what happens in the subsurface is mostly interpretational and based on analogy with ophiolites, except for the limited observation of features on graben walls and in fault scarps, in dredge hauls, and limited drill core (e.g. in the TAG field; Petersen et al., 2000).

Spreading ridges are an important metallogene dominated by Fe, Mn, Cu, Zn, Ag, Au

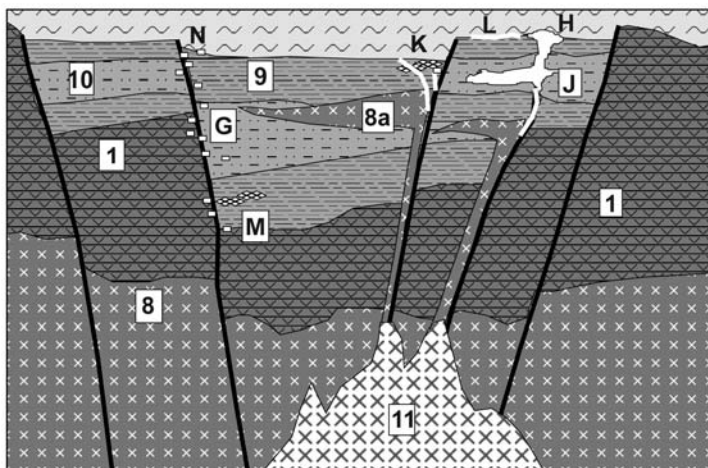
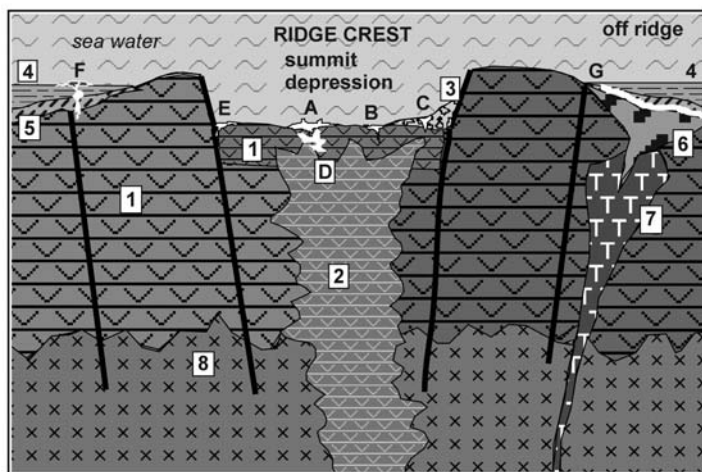
accumulations resulting from heated seawater/basalt interaction and having the form of VMS-style sulfides and metalliferous sediments. The first actively forming sulfide occurrences, indicated by the presence of "black smokers", ore chimneys, and worms, were reported by Francheteau et al. (1979) from the East Pacific Rise. More ore discoveries followed shortly, located in sediment-free ("bare") ridges as on the Mid-Atlantic Ridge (TAG and Snake Pit sulfide fields; German et al., 1993; Fouquet et al., 1993), Galapagos Rift (Haymon, 1989); Explorer Ridge off British Columbia (Hannington et al., 1991), Juan de Fuca and Gorda Ridges off Oregon and California (Koski et al., 1984) and elsewhere. Mineralized sediment-filled spreading systems are represented by the northern Juan de Fuca Ridge (Kappel and Franklin, 1989), Escanaba Trough off California (Zierenberg et al., 1993) and the Guaymas Basin in Mexico (Koski et al., 1985). Further descriptions appear in the review papers of Rona (1984), Rona and Scott, eds. (1993), Herzig and Hannington (1995).

The sulfide ores precipitate from 260° to 360° C hot brines of heated seawater, in water depths between 3700 and 1500 m. The water column provides hydrostatic pressure needed to prevent boiling. At the "bare" ridges, sulfides precipitate continuously almost anywhere within the graben, ridge crest and flanks, subsidiary structures, concurrent seamounts. They form chimneys, fields of broken chimneys, mounds, saucer or bowl shaped masses, ore rubble on the sea floor or breccia fill in the porous basaltic rubble in the shallow subsurface. In the TAG field (Petersen et al., 2000) the orebody is a 50m high massive and breccia pyrite-rich circular mound with a diameter of 200m, estimated to contain some 3.9 mt of material with 2.1% Cu and 0.6% Zn. The mound is mineralogically zoned around the anhydrite-rich core impoverished in base metals due to continued zone refining. It is floored by quartz, anhydrite and pyrite breccias in silicified and chlorite and paragonite altered basalt. Elsewhere, the principal hypogene ore minerals are pyrite, marcasite, pyrrhotite, sphalerite or wurtzite, chalcopyrite, cubanite, rare galena and occasional exotic minerals like Pb, Sb, Ag sulfosalts. Quartz, opal, anhydrite, barite and smectites are the principal gangues. The near-ore quartz, chlorite, smectite wallrock alteration gives way to intensely chlorite, epidote, albite altered basalt in depth that corresponds to the greenschist facies (Mottl, 1983). Metal ratios in sulfide deposits as well as the content of precious metals vary from field to field as well as within a

field. Fouquet and Herzig (1991) gave the average composition of 33 base metals-rich sulfide samples as ~26% Fe, 7.83% Cu, 8.17% Zn, 0.05% Pb, 960 ppm Co, 233 ppm Cd, 154 ppm As, 163 ppm Se, 50 ppm Mo, 49 ppm Ag, 0.26 ppm Au.

In the sediment-filled spreading systems, hemipelagic, turbiditic, lesser pelagic and

hydrothermal sediment prisms are invaded by basalt dikes and sills. Sulfides, dominated by pyrite and pyrrhotite, range from dispersed component of mud to clastic grains and fragments, replacement lenses



1. MORB basalt
2. Hydrothermally altered basalt
3. Submarine talus
4. Pelagic sediments (clay, oozes)
5. Metalliferous hydrothermal sediment
6. Albitized dacite (ketarophyre)
7. Trondhjemite (plagiogranite)
8. Sheeted diabase dikes
- 8a. Diabase & gabbro dikes, sills, stocks
9. Pelagic or hemipelagic mud, clay
10. Lithic & volcanic turbiditic sand
11. Active basalt magma chamber
- A. Ridge crest submarine hydrothermal field: mounds, chimneys, VMS
- B. Fe, Mn, Cu, Zn in hot brine pools
- C. Sulfides in veins, stockworks in talus
- D. Sulfide stockworks, veins, breccias in altered basalt
- E. Low-temperature venting of water; worm colonies, some Fe-Mn crusts
- F. Off-ridge medium temperature spring vents, mounds with Fe-Mn oxides
- G. Mixed hydrothermal and hydrogenous clay, Mn-Fe oxide crusts
- H. Sulfide mounds above fluid vents
- J. Alteration and minor sulfides in wet unconsolidated sediments
- K. Diffuse outflow of moderately hot fluids, alteration, barite, silica
- L. Metalliferous sediment
- M. Diffuse disseminations of pyrrhotite, rare Zn, Cu sulfides near faults
- N. Fe hydroxides, rare Cu, Zn sulfides in talus
- P. Fe > Zn, Cu sulfides in altered basalt near faults

Figure 4.1. Diagrammatic inventory of lithologies and ore types in bare (top) and sedimented (bottom) oceanic ridges. From Laznicka (2004), Total Metallogeny sites G4 and G5

and sheets in the subsurface, to sulfide mounds and "smokers" projecting on the sea floor. At the best studied and economically most promising **Bent Hill field in the Middle Valley** near the northern termination of the Juan de Fuca Ridge off Vancouver Island (Goodfellow and Franklin, 1993), mounds of sediment rich in sulfide fragments are altered, replaced and permeated by sfalerite, Fe oxides, silica, clays and barite. Scattered, mostly anhydrite chimneys, vent 184° to 274°C hot fluids. The fluids, evolved and metallized in the basaltic subsurface, have been modified by reaction with the water-saturated sediments. Herzig and Hannington (1995) estimated the up to 96m thick sulfidic resource in the Middle Valley to be of the order of 50 to 100 mt of material with an average grade of 4.7% Zn, 1.3% Cu, 142 g/t Ag and 0.8 g/t Au.

Sea floor sulfide accumulations left in contact with water are gradually modified by supergene processes. Crusts and precipitates of Fe hydroxides, jarosite, opal, atacamite may form, up to the point of gradual destruction of the sulfide body (Halbach et al., 1998). The subaqueous gossan over the TAG field (Hannington et al., 1991) is enriched in residual gold, up to a grade of 23 g/t Au.

Most seafloor sulfide ore fields have Fe and Mn enriched haloes produced by gradual settling of particles emitted in the "black smoke" and hydrothermally precipitated to form a thin, irregular layer of oceanic "metalliferous sediment" at the basalt/oceanic sediments contact or within the spreading ridge fill. Off the Galapagos Ridge (Honnorez and Von Herzen et al., 1981) low-temperature brines in sediment mounds precipitate todorokite crusts and fragments interspersed with Fe hydroxides and grading into nontronitic and celadonic clays.

4.3. Intraplate volcanic islands, seamounts and plateaux on oceanic crust

Intraplate volcanic islands built on oceanic lithosphere are attributed to mantle "hot spots": buoyant plumes of hot asthenospheric melts of substantially smaller dimension and potency than those at spreading ridges. Stationary plumes over which the lithosphere drifts are marked by chains of islands or seamounts, a case exemplified by the

Hawaiian archipelago (Macdonald, 1968). The cumulative surface area of oceanic islands is very small and environmentally sensitive.

The islands lack completely economic minerals except for small ferruginous laterite deposits on the Kauai Island (Hawaii) and have almost zero ore discovery potential. The predominant rocks on the islands are tholeiitic and alkali basalts enriched in incompatible elements, and several islands have rare intermediate to acid differentiates like hawaiite, trachyte and rhyolite. The latter are best developed in the central volcanoes of Iceland where the "hot spot" volcanism overlaps with MORB effusions (Gudmundsson, 2000). A rare carbonatite occurrence is known in the Cape Verde Islands.

Seamounts, the submerged equivalents of islands, are more numerous and they are economically interesting as sites of preferential precipitation of hydrogenous ferromanganese crusts (read below). The crusts are greatly enriched in cobalt and cumulatively represent a substantial Co and Mn resource, although a viable extraction technology is not yet in place. The mineral potential of oceanic plateaux, some with a very large area (e.g. the Ontong Java Plateau in western Pacific) is unknown. Most plateaux are submarine sheet flows of tholeiitic basalt similar to MORB but slightly enriched in incompatible metals (Floyd, 1989) that include copper. As they are almost unaltered, the plateau basalts retain most of their trace Cu and this might enhance copper fluxing when subjected to melting in subduction zone. Alternatively, oceanic islands and plateaux, upon reaching the consuming plate margin, are accreted rather than subducted, contributing to the basalts variety there. Those enriched in K approach the "shoshonitic suite" considered a favourable host to magmatic-hydrothermal Cu-Au and Au deposits (Chapter 5).

4.4. Sea water as source of metals

Average sea water contains 3.5% of dissolved solids and, since antiquity, it has been a source of salt (halite) obtained by evaporation. Nowadays, seawater is the source of 90% of bromine and a significant proportion of metallic magnesium. In the 1980s the United States produced 120,000 t Mg/year from sea water in six plants. During the period of high metals demand in the 1970s sea water was declared as a metals resource of the future, the large quantities of dissolved metals

calculated and publicized (e.g. an estimated resource of 4 billion tons of U in the world ocean, at a concentration of 3.3 ppb U; Bloch, 1980), and supply projections were made. The interest waned during the period of decreasing commodity prices and demand for metals afterwards. The half-hearted experiments brought disappointing results and the publicity stopped. It is likely that one of the future industrial cycles endowed with a new technology (e.g. of concurrent water desalination and selected metals extraction), combined with enlightened politics, will usher in a renewed interest in oceanic resources. In addition to U and Au popular in the 1970s (Koide et al, 1988), the following metals that are both in demand and are relatively enriched in seawater, will likely be recovered (average contents in seawater, in ppb, are in brackets; data are from Garrels et al., 1975): B (4450); Li (170); Rb (120); Mo (10); Ni (6.6); U (3.3); Cu, Zn (2); V (1.9). Contrary to the popular belief about geochemical uniformity of seawater the trace metal contents vary with depth, temperature and location and future research will most likely outline "high-grade" water intervals where the "seawater mining" would start. Gold, with the average sea water content of 0.011 ppb Au, ranges from 0.001 to 44 ppb Au (Lucas, 1985) so if gold extraction from seawater starts at all the "high grade" water areas will have to be identified and "mined" first. The viability of metals extraction from seawater could be further enhanced by new technologies of biogenic and bacteriogenic recovery ("metal farming"); iodine and copper were recovered from ashes of marine plants in the past.

4.5. Ocean floor sediments

More than three quarters of the World Ocean has a basement of MORB basalt covered by unconsolidated to moderately consolidated (in depth) sediments, the age of which ranges from Jurassic to contemporaneous. Oceanic sediments start to accumulate at spreading ridges and the earliest generation that rests directly on basalt has the closest "oceanic" affiliation. As the oceanic plate moves away from the spreading ridge the sedimentary cover thickness increases and the oceanic signature is diluted. Turbidites, biogenic sediments, hemipelagic sediments become dominant and are governed more by climate, bathymetry and sediment sources than by the presence of oceanic basement.

There is an extensive literature devoted to oceanic sediments (e.g. Lisitsyn, 1971; Emery & Uchupi, 1984; Heezen and Hollister, 1971; Einsele, 1992) and their mineral resources (Mero, 1965; Cronan, 1980; Meylan et al., 1981;

McKelvey, 1986). As a gross oversimplification, the abyssal (depths greater than 5000 m) equatorial oceanic sedimentary stratigraphy starts with the basal hydrothermal and mixed sediments originating at spreading ridges and resting on basalt, topped by pelagic "red clay". Above it are siliceous oozes (radiolarian and diatomaceous) locally cemented to chert topped, above the calcite compensation depth, by calcareous oozes. Carbonates are missing in the high latitudes. Ancient sediments, still under the ocean floor, also record several past anoxic periods (most significant in Cretaceous) when highly carbonaceous, reduced sediments formed.

Oceanic biogenic carbonates and most of the silicites are depleted in trace metals, but the ancient "black" sediments are phosphatic and enriched in V, Mo and U. The extremely slowly depositing abyssal red clays of combined volcanic (from decomposed basalts) and terrigenous (from blown dust) provenance are greatly enriched in trace Mn (0.43%), Cu (230 ppm), Ni (210 ppm), Co (110 ppm), Zn (170 ppm) and some other elements (data from Bischoff and Piper, eds., 1979), compared with crustal clarkes. Contents of 0.2% Cu or Ni have been locally reported. The trace metals association, plus iron, appears even more enriched in the three oceanic metallogenesis briefly reviewed below, in which the metal concentrations reach or exceed grades of ores mined on land, and the stored quantity greatly surpass the inventories of metals in terrestrial deposits. The metals are clearly transition metals released by hydrothermal percolation of basalts on spreading ridges, and by underwater weathering (halmyrolysis) of MORB and oceanic island basalts and their glasses.

The mode of metals' precipitation, however, varies. At or near spreading ridges the metals are hydrothermal ("exhalative"), precipitated during hot brine cooling and reaction with seawater. Away from the ridge, metals settled from suspension of particulate matter, for example of constituents of the "black smoke", to enrich the pelagic clays up to 600 km from the spreading ridge (Leinen, 1992). At the abyssal floor and on seamounts and their flanks the metals slowly precipitated from sea water either directly (hydrogenous sediments; Piper and Heath, 1989) or by redistribution during early diagenesis in the uppermost layer of the water-saturated sediment. At and under the ocean floor are the true, almost inexhaustible Mn, Ni, Cu, Co resources of the

future, but they are difficult to delineate and even more to mine (Cronan, ed, 2000). In terms of increasing grade they are 1) metalliferous sediments; 2) ferromanganese nodules; 3) ferromanganese crusts.

1. Metalliferous sediments (clays): These, together with the Fe-Mn nodules, were first recovered and described by the Challenger Expedition (1872-1876), then re-discovered in the late 1960s and later at several locations in the Pacific Ocean notably at the Nazca Plate west of South America (Dymond et al., 1973). The reddish-brown oxidized, carbonate-free clays are composed mostly of terrigenous illite or volcanogenic smectite with zeolites (phillipsite) and amorphous Fe-Mn hydroxides. Fe and Mn hydro-oxides and the trace metals are dispersed throughout or reside in micronodules that could be mechanically separated. The average metal content of an East Pacific metalliferous sediment given by Field et al., (1983) is 15% Fe, 5% Mn, 0.11% Cu, 0.10% Ni, 0.04% Zn, 0.02% Co, 0.015% Mo, valued at \$ 67.50/ton at 1980 prices (over \$ 100 now). The Bauer Deep alone stores, over an area of about 0.5 million km², "millions to billion tons of most transition metals" (Field et al., 1983). The sediment recovery from 5 km depths and processing of the super-fine mixture of 7 to 10 recoverable metals would be extremely costly and not expected to take place in the foreseeable future. More recently the abyssal red clay became of interest as a repository of radioactive waste (McKelvey, 1986).

2. Ferromanganese nodules: These are the single best known and most publicized oceanic resource (Mero, 1965; Bischoff et al., 1979; Glasby and Read, 1976; Baturin, 1988). The nodules are potato-shaped, structureless or internally-zoned segregations of finely-crystalline Mn oxy-hydroxides (or manganates) such as vernadite, todorokite, buserite, birnessite and Fe hydroxides, ranging from millimeters to more than 10 cm in diameter. They rest on the seafloor where their density and size could be photographed, and rapidly diminish in size and concentration within few centimetres into the host sediment. Fe-Mn oxide nodules occur in the entire World Ocean, including shelves and epicontinental seas, but economically interesting concentrations are known only from the abyssal floor of the Pacific and

Indian (less Atlantic) oceans where the prevalent sediment is pelagic red clay and partly siliceous ooze. It is believed that the nodules are product of an extremely slow hydrogenous precipitation from "normal" seawater, perhaps with microbial assistance, where the initially precipitated Mn and Fe hydro-oxides absorb and locally accumulate a long list of trace metals. Ni, Cu and Co reach the highest concentrations of 0.89%/0.1-2.0%; 0.66%/0.01-2.0%; 0.44%/0.05-2.50%, respectively (mean contents in Pacific nodules/range, Haynes et al., 1986). Trace metals concentration together with nodule density determine the economic potential of a nodule field (the mean Mn content of 21.6% is of lesser importance). Other significantly concentrated trace metals in nodules are Zn (0.11%), Pb (0.072%), Mo (0.041%), Te (216 ppm), Tl (169 ppm), As, REE, PGE.

In the 1960-1980s exploitation of oceanic nodules was a hot topic: the distribution of nodules and their Ni, Co, Cu contents had been mapped (compare Figure 1 in Piper and Heath, 1989 showing the nodule distribution in NE and E Pacific), extraction and processing technology developed and tested. No actual mining has yet taken place. The main reasons are insufficient profitability at the low end-of-the-century commodity prices and, even more so, politics. The Law of the Sea passed by the United Nations and opposition of the major Mn and Co producers are here to make any attempt on mining a long and costly hassle (McKelvey, 1986). The metalliferous nodules, however, remain a distinct and extremely significant resource for the future. What quantities of metals are stored there?

Mero (1965) estimated, perhaps too generously, the nodule resource in the Pacific Ocean only, at 1.66×10^{12} t that store 400 bt Mn, 16.4 bt Ni, 8.8 bt Cu, 5.8 bt Co. The Soviet calculation (Bezrukov et al., 1970) based on 36.13 million km² of the most prospective Pacific floor, came with an overall resource of 3.4×10^{11} tons of nodules containing 71 bt Mn, 2.3 bt Ni, 1.0 bt Co and 1.9 bt Cu. They outlined seven higher-grade "ore zones" with the average content of 9.4 kg/m² of nodules. The most prospective nodule area is in the NW equatorial Pacific in the vicinity of Clarion and Clipperton transform faults, SE of Hawaii (about 8°30' to 10° N, 131° 30' to 150° W). The frequently quoted nodule resources there depend on the area selected to delineate this "orebody". Dean (1983) estimated that 2.5 km² of

the Pacific floor there contains over 20 bt of nodules @ 28.8% Mn, 1.2% Ni, 0.99% Cu, 0.23% Co, 0.13% Zn and 0.048% Mo that translates into a resource of 5.76 bt Mn, 240 mt Ni, 198 mt Cu, 46 mt Co, 26 mt Zn and 9.6 mt Mo. The nodules occur in an approximately 10 cm thick Quaternary surface layer of radiolarian ooze or pelagic red clay resting on mottled clay, in water depths between 5000 and 6000 meters. Several production estimates prepared in the 1970s assumed an optimal production of some 3 mt dry weight of nodules per year which, at 50% recovery, would yield a yearly output of 20.3 kt Ni, 20.3 kt Cu, 2.7 kt Co and 405 kt Mn (Hubred, 1975).

3. Ferromanganese crusts: Described by Halbach et al. (1982), Dean (1983), Piper and Heath (1989), Hein et al (2000) and others, these are one millimeter to at most 25 cm thick black, hard encrustations of Mn and Fe oxy-hydroxides (todorokite, birnessite, goethite) that coat exposed submarine hard rock surfaces and talus on tops or flanks of oceanic islands, ridges, seamounts and guyots. In this they are complementary to the ferromanganese nodules that rest on the surface of soft sediments. Some crusts are hydrothermal precipitates formed in areas of active volcanism at spreading ridges, but the bulk is halmyrolic or hydrogenous (precipitated from seawater). The

hydrothermal crusts are high in iron and low in trace metals, the hydrogenous crusts have Mn > Fe and are highly enriched in Co (0.2 to 2.0% Co) with a possible by-product Ni (around 0.4%), Ti (around 1.2%) and, locally, Pt (around 0.5-1 ppm). Copper is low.

The economically interesting crusts formed in water depths that are much shallower compared with the abyssal nodules (about 3500-1000 m) and the Co grade is highest in shallow water depths. This, as well as the fact that substantial metalliferous crusts deposits exist within the U.S. Exclusive Economic Zone (EEZ) in extension of the Hawaiian Archipelago, Johnston Island, Midway as well as in EEZ's of other Pacific island nations (Micronesia, Kiribati, Tuvalu), simplifies access and the permitting politics. In contrast to scooping or vacuuming the loose seafloor nodules, however, the metalliferous crusts would require underwater hard-rock mining, a technology not yet available. The most favorable Hawaii-Johnston-Palmyra Islands zone of Mn-Co crusts is estimated to contain a resource of some 190 mt Mn and 1-2 mt Co. Ritchey (1987) provided estimated tonnage data for two Central Pacific submarine ore deposits (or ore fields). The Horizon Guyot has a resource of about 75.5 mt of crusts containing 18 mt Mn, 581 kt Co, 340 kt Ni and 46 t Pt. The S.P. Lee Guyots are credited with 24 mt of crusts with 6.9 mt Mn, 286 kt Co, 130 kt Ni and 15.5 t Pt.

5 Young Island Arcs

Island arc systems are one form of subduction-influenced convergent continental margins as they appear at the surface, on the ocean floor and in shallow subsurface. The other form, entirely on land, is called here for brevity "andean-type margins" or "andean margins" and is included in Chapters 6 & 7. Accretionary complexes are common to both systems and here they are lumped together with the island arc systems. Although both island arc and andean systems are shaped by processes taking place above subduction zones, in the former case this happens predominantly in and close to marine environment and there is a high proportion of juvenile crust formed, for the first time, by conversion from the mantle. In the andean margins most of the visible action like volcanism, that accompany active subduction, is subaerial and there is a much greater proportion of mature continental crust underneath. Many landforms (such as stratovolcanoes, subaerial calderas) are common to both the island and andean domains and the differences are quantitative rather than qualitative; the former are generally less "mature" (slightly behind along the path of the prolonged mantle-to-crust conversion) and this is reflected in the petrology and metallogeny. The "giant" ore deposits in island arcs are dominated by the basaltophile (or siderophile & chalcophile) metals like Fe, Cu, Au, Zn, related to magmas with a high mantle contribution (e.g. porphyry Cu-Au; Cyprus, Besshi and kuroko VMS; Figure 5.1.), whereas the andean terrains have a much higher proportion of the more lithophile metals like W, Mo, Sn, Li and Be. The overlap between both types of convergent margins is minimized by descriptions of common features in one chapter only, followed by cross-referencing.

Geological age, post-depositional modification and depth of erosion: Geological age correlates, in general, with the depth of erosion and this, in turn, exposes progressively deeper levels of rock formation and modification, and changes the frequency and type of metallic ores. Most textbooks and reference works apply the genetic premise and treat deposits, presumably related to subduction (and other mechanisms as well), as an age/depth continuum regardless of changes resulting from the post-subduction evolution.

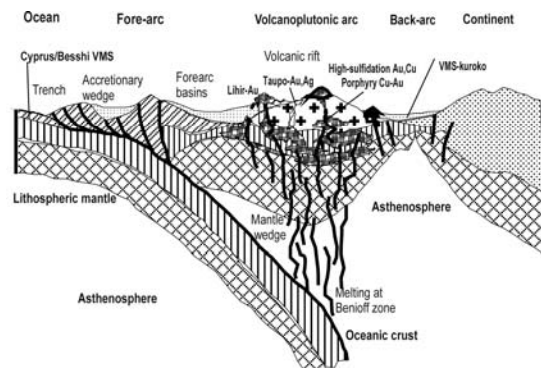


Fig. 5.1 Generalized model of an island-arc system, showing setting of the "giant" and "large" metallic deposits

For practical purpose it is more useful to distinguish between the 1) "young" systems, some of which are still active or if not, the syn-depositional stage can still be credibly interpreted (this chapter), and 2) the "old" systems where the early materials have been overprinted, modified, dismembered and repositioned so that there is little resemblance to what they once were. The "young" versus "old" boundary is subjective but most "young", "pristine" systems (that is ones that are unmetamorphosed, little deformed and still at the site of origin) are late Cenozoic. The "old" counterparts of island arc and andean margin assemblages in Phanerozoic to middle Precambrian orogenic belts, appear in Chapter 8. Early Precambrian greenstone-granite terrains have a chapter of their own (9) and so have the high-grade metamorphosed terrains regardless of age (Chapter 13). Island arc systems have an extensive literature (Mitchell and Bell, 1973; Dewey, 1980; Gill, 1981; Carlile and Mitchell, 1994; Hamilton, 1995; Corbett and Leach, 1998). Warmly recommended, for field practitioners, is reading that emphasizes facts and field observation in the classical island arc terrains such as Indonesia, Japan and the western Pacific margin (e.g. Van Bemmelen, 1949; Hamilton, 1979).

5.1 Island arc metallogeny and giant deposits

At convergent continental margins new continental crust is generated by chemical conversion of oceanic crust and portions of mantle by subduction-related processes, and by physical accretion of lithospheric fragments piggybacked in on top of the descending plate. The crust generation is not direct and uniform and a myriad of lesser order processes and variations intervene to make convergent plate margins and their eventual successors, the "eugeoclinal" orogenic belts, the most complex and still imperfectly understood lithospheric domains.

Although lithospheric convergence and subduction are the dominant first order rock forming regimes, second and lesser order crustal extension (rifting), collision and transcurrent faulting operate simultaneously or follow shortly. Considered in isolation and at local scale, the latter have more in common with other lithospheric domains than with subductive margins. One example: back-arc basins, extensional structures that produce in their most advanced segments MORB-like assemblages and ophiolites, hence they are really oceanic spreading ridges in miniature.

Island arc systems as a group are mostly composed of transitional crust, that is a crust that is in the process of a long-term conversion of oceanic crust (itself derived from the mantle) into the sialic mature continental crust. Much of the transitional crust is juvenile, that is added to the continents for the first time although recycled, second generation materials occur in many settings (it has also to be realized that the mantle itself is not "pristine", but contaminated by the many cycles of subduction of oceanic and some crustal materials such as terrestrial seaborne dust accumulated in oceanic sediments). Most of the arc magmatism is andesitic (Gill, 1981). The magmas are believed generated by melting at and above the Benioff zone, in depths greater than 100 km. Hess (1989) summarized the evolution of arc magmatic suites that can change with time and increasing depth to the Benioff zone, from the low-K tholeiite through the increasingly more potassic calc-alkaline series to local shoshonites. There is a number of research publications where essentially the same geochemical data provide basis for conflicting interpretations (e.g. Kay, 1980; Perfit et al, 1980; Coulon and Thorpe, 1981). Hamilton (1995) relied on empirical field observations combined with geophysical data to dispel the myth that "subducting oceanic plates slide down fixed slots" as shown in textbooks, and pointed out that basaltic melts

formed in depth are the starting material for the entire subsequent lithogenesis (and metallogenesis as well). Such basalts melts initially pond at the base of the arc from where "all more evolved rock types are generated in the crust by fractionation, secondary melting and contamination". The basalts that have not made it higher up remain, in equilibrium with the prevalent pressure-temperature conditions, at the base of the continental crust and as a part of the ancient lower crust.

Although magmatism is at the center of island arc metallogenesis, orthomagmatic deposits are rare here and the ones recorded formed in depth, so they only appear after a substantial deformation, uplift and erosion. Such deposits are thus part of the ancient "eugeoclinal" orogens (Chapter 8) rarely apparent in the "live" arcs. Magmatic-hydrothermal deposits like porphyry Cu-(Au,Mo) are moderately common in volcano-plutonic centers of the "young" arcs but require rapid exposure to appear in their "pristine" form, unmodified by orogenic modifications that places them into older orogens (Chapter 8). Young porphyry deposits like Panguna (Bougainville) are included in this chapter, but to avoid repetition other examples are treated jointly with the more numerous "porphyries" in the andean-type margins (Chapters 6 & 7).

About the most productive metal accumulating mechanism in island arcs is magma (or hot rock) interaction with an external fluid. Convecting sea water, heated by magmatic (volcanic) heat, leaches the weakly-bound trace metals mostly from hydrated volcanics, then precipitates them at- or under the sea floor as massive to disseminated sulfides (VMS) and Fe, Mn oxidic "exhalites". Additional forms of ore accumulation include replacements of unconsolidated sediments; veins, breccias, as well as replacements of consolidated rocks under sea floor. The trace elements involved are of the "basaltophile" group (Fe,Mn,Cu,Zn,Pb,Ag,Au) with the lithophile elements practically missing. VMS occurrences, actively forming in "young" (pristine) island arc systems, are being discovered at the seafloor with increasing frequency (Fouquet et al., 1993; Rona and Scott, eds., 1993; Binns and Scott, 1993; Herzig and Hannington, 1995) but none has, so far, approached the "giant" magnitude. The ancient VMS counterparts, however, now in Phanerozoic orogens or in Precambrian greenstone belts, are significant and they are treated in Chapters 8 and 9. Unexpectedly, active to recently active submarine epithermal systems (e.g. the Conical Seamount close to Lihir Island with its "giant" on-land gold deposit; Herzig et al., 1990; read below), both of

the low-sulfidation and high-sulfidation types and greatly enriched in Au and Ag, are the most likely candidates to reach the "giant" rank once there is enough data to delineate the deposits and estimate the resources.

Sedimentogenic deposits in island arcs, like magnetite beach sands, are at best of the "large" magnitude.

5.2. Island arc-trench components and ore forming processes

Present convergent margins vary from the relatively simple and regular ("smooth") predominantly non-accretionary margins with a distinct on-land magmatic arc marked by a string of almost regularly spaced stratovolcanoes (the Andean margin in northern Chile), to increasingly complex and confused island arc margins marked by frequent flips of subduction dip and migrating subduction zones as in the Indonesia-Philippine region and western Pacific (Hamilton, 1979; Hutchison, 1989; Carlile and Mitchell, 1994). This results in several generations of remnant magmatic arcs under- and above water, rift systems and sedimentary basins. Most margins have a protracted history, further complicated by accretion of successive terranes generated outside their present location and genetically unrelated, in their pre-accretionary history, to their neighbours (Coney, 1989). Accretionary margins as along the Pacific margin of North America could be hundreds- to a thousand km wide and most consist of earlier generations of rocks formed dominantly in island arc systems now situated more inland than similar later generations. The brief review below is a summary of basic characteristics of the sub-environments in trench-arc-backarc systems (as shown in Fig. 5.1.) with emphasis on the ore forming processes that may result in giant accumulations of metals.

Trenches, subduction complexes, high pressure metamorphic belts

The oceanic domain reviewed in Chapter 4 terminates at the outer edge of an ocean trench, which is the entry point of the mafic oceanic crustal slab, with portion of its sediment cover, into the subduction zone (Leggett, ed, 1982). Active and recently active trenches range from the sediment-starved, non-accretionary, intraoceanic ones (Marianas type; Fryer and Hussong, 1981; Fryer, 1996) to sedimented trenches at accretionary margins (e.g. Japan and Nankai Trenches facing the

Japanese accretionary prisms; Java Trench; Middle America Trench; Einsele, 1992; Watkins, 1989). The trench sediments are a mixture of oceanic pelagic and hemipelagic clays and terrigenous and volcanic turbidites. There is no viable process of ore formation at work, although both trench varieties receive some mineralized material generated elsewhere (at spreading ridges, in seamounts) and carried on the oceanic plate (e.g. chromite, VMS detritus, metalliferous sediment, Fe-Mn nodules).

The material that enters the subduction zone (hydrated oceanic crust with portions of mantle topped by hydrothermal, pelagic and hemipelagic sediments) suffer dismemberment and deformation to produce subduction melange and megabreccia (Raymond, ed, 1984). Progressive dehydration and high-pressure metamorphism take place with increasing depth (Peacock, 1990). The most common variety of subduction melange consists of a scaly slate matrix with scattered blocks of graywacke and/or ophiolite lithologies and there is a gradation into a melange with silvery serpentinite matrix. Large blocks of MORB basalt ("knockers") are often present, as in the Franciscan complex of California.

At a depth greater than about 30 km the high-pressure metamorphic assemblage starts to form. This includes blueschist and, in much greater depth, eclogite after metabasites, and aragonite-lawsonite, jadeite rocks after sediments, especially graywacke. Several subduction complexes have been locally uplifted and exhumed to reach the surface and blueschist belts as old as 800 Ma are known, associated with ophiolites (Goodwin, 1991). The high-pressure metamorphism has no ore-forming role, except for the metamorphic conversion of Ti minerals (mainly titanite) into rutile that frequently accumulates in eclogites (Blake and Morgan, 1976). Subducted synvolcanic deposits like the Cyprus and Besshi-types are sometimes preserved in blueschist-metamorphosed hosts (e.g. the small Island Mountain Cu, Zn mine in California; Arna Unit-Cu, Zn, Pb in the Peloponnesos, Greece; Skarpelis and Mantzos, 1990), or in melange (Ergani Maden-Cu, Co; Turkey).

Forearcs (arc-trench gaps)

Like trenches, forearcs range from non-accretionary to accretionary varieties complicated by a frequently thick imbricate wedges of sediments scraped from the descending plate. Both forearc varieties often contain depositional basins (Vessell and Davies, 1981) filled by little disturbed clastics, usually of sandy turbidites up to 3 km thick. Some

basins and their flanks are the sites of low volume submarine to subaerial volcanism of contrasting composition that preceded, paralleled or postdated magmatism in the main island arc. Boninite, first described from the Izu-Mariana Arc, is the most often quoted volcanic type (Crawford, ed., 1989). This is a high-Mg basalt to andesite suite produced by small degree melting of depleted spinel harzburgite. No mineralisation is known from its young occurrences although boninite has been described as associated with some ancient VMS deposits as in the Troodos Complex of Cyprus or in the Urals (Buribay-Baymak).

The Miocene to Quaternary New Ireland Basin off the northern Papua New Guinea is filled by up to 7 km thick sediment prism, pierced by several seamounts and islands in the Tabar-Feni group, composed of alkaline volcano-plutonic association (Exon et al., 1986). Several subaerial and one submarine hydrothermal gold occurrences are known, of which the Ladolam ore field on Lihir Island is of giant magnitude (read below).

Fryer et al. (2000) described submarine mud volcanoes from the Mariana forearc venting and depositing serpentine mud with serpentinite, blueschist, chert and metabasite debris, probably derived from the top of a descending subducted oceanic slab and adjacent mantle. The debris was propelled by a 250-150°C hot fluid. Future analytical data might provide information on fluxing of some metals such as mercury and antimony from active subduction zones, known to be associated with "detrital serpentinite" (e.g. at Abbott Springs, California; Moiseyev, 1968).

Accretionary wedges

Ocean floor materials that are not subducted (pelagic and hemi-pelagic sediments, minor basalt, volcanic and terrigenous turbidites) are gradually scraped off against the inner wall of the trench, or underplate forearc basins to form a growing, imbricate sedimentary wedge often of large areal extent (the Makran subduction-accretion complex in Baludzhistan is 900 km wide; Şengör, 1987). A portion of the wedge material is supplied by tectonic erosion of continental crust of the upper plate (von Huene and Scholl, 1991). The deformed sediments are interlaced with tectonic slices of oceanic metabasalt and ophiolite (Isozaki et al., 1990). There is no clear case of actively forming major mineralization in young accretionary wedges except for rare rhodochrosite veinlets in the Barbados wedge, although small relic "oceanic" ores occur peripherally (for example, bedded Mn

ores in the Eocene Crescent Formation, Olympic Peninsula, Washington State; Tabor and Cady, 1978). The well documented mass expulsions of fluids (formational waters, methane) from accretionary wedges are of interest and it is likely that small amounts of diagenetic pyrite form during dewatering to possibly participate later, during orogeny, in formation of the (syn)orogenic gold deposits common in the ancient, lithified accretionary wedge associations. Extensive barren synorogenic veining and crack-sealing by quartz, locally with albite, chlorite, zeolites and carbonates, is common in cleaved low-grade metasediments, worldwide. The occurrences in the Cretaceous Kodiak accretionary wedge in Alaska (Fisher, 1996) are attributed to precipitation from expelled seawater and CO₂-rich, dehydration-released fluids at depths of 8-12 km under surface where no gold is present. For gold to form, a deeper level of gold release and transport by fluids, produced during metamorphic devolatilization of hydrous minerals, is required. This takes place mainly near the amphibolite to greenschist facies transition in still greater depth, in the presence of arc or collisional granitoids, as in the Juneau gold belt, Alaska (~310 t Au; Goldfarb et al., 1997; Chapter 8).

Accreted and "suspect" terranes

Accreted terranes are common to both island arc (e.g. the Shimanto Belt in Shikoku; Taira et al., 1988) and andean systems (Chapter 6); this paragraph applies to both. In the late 1970s the concept of "suspect terrane" accretion was proposed and tested along the western continental margin of North America (Saleeby, 1983). An extensive collage of displaced terranes, brought in from the offshore together with the pre-accretion ore deposits they carried, has been recognized and named in the broad swath of Cordilleran-Pacific territory between the Bering Strait and Baja California. The small terranes accreted to the North American plate quietly whereas the composite superterranes collided along sutures, causing major orogenies. Synorogenic and later granitoids stitched the terranes together. Collision-related strike-slip movements produced a series of narrow fault basins filled by thick piles of monotonous turbidites. One of those, the Cretaceous Kuskokwim Basin in SW Alaska, hosts the large epithermal, fault-controlled vein and stockwork Donlin Creek gold deposit, related to high-level felsic dikes (790 t Au; Goldfarb et al., 2004; Chapter 6).

The majority of western Cordilleran terranes are of oceanic or island arc derivation. Some are related

to rifting, and the Yakutat Block in SE Alaska is an actively accreting microcontinent impinging on the North American continent. The andesitic Wrangell volcanic field was produced above the subducting Pacific plate transporting, piggyback-style, the microcontinent (Kienle and Nye, 1990).

The pre-accretion metallogeny of each terrane has to be considered separately as there are substantial differences. This is exemplified by two adjacent terranes in southern Alaska (Goldfarb and Miller, eds, 1997). Both terranes are the product of Triassic rifting episodes in the offshore of which the earlier episode produced the Alexander Terrane, host of the giant **Windy Craggy Fe,Cu,Co deposit** in British Columbia (190 Mt @ 1.6% Cu, 0.09% Co, 0.2 g/t Au). This is a stratabound massive sulfide body developed along the contact of basalt and marine clastics and is usually interpreted as of Besshi-type. The **Greens Creek massive sulfide deposit** on Admiralty Island south of Juneau, Alaska (12.5 Mt @ 12.8% Zn, 4.0% Pb, 0.4% Cu, 456 g/t Ag and 4.1 g/t Au; Goldfarb and Miller, eds, 1997) is a "silver near-giant" (5700 t Ag) and the second largest United States' silver producer of the past decade. It has very similar setting to Windy Craggy but is entirely enveloped by black meta-argillite that, in turn, rests on meta-basalt. The younger Triassic rift-related subaerial meta-basalt flows in the adjacent Wrangellia Terrane contributed their high trace Cu content (160 ppm Cu) to form the high-grade hydrothermal chalcocite replacements in Triassic carbonates at **Kennecott, Alaska** (544 kt Cu and 280 t Ag produced between 1913 and 1938; Bateman and McLaughlin, 1920), during the Cretaceous accretion, by proximal hydrothermal transfer by a convecting fluid heated by nearby granitoids. A portion of the ore came from detritus embedded in a glacier.

The Sierra Nevada Foothills of California (Duffield and Sharp, 1975; Chapter 7), home of the famous **Mother Lode gold system**, is an example of a composite multiphase Paleozoic and Mesozoic terrane that accreted to the North American Plate over a period of 300 million years, terminating in the Jurassic (Landefeld, 1988). The Triassic-Jurassic immature arc and basin metamorphics host several small massive Cu, Zn sulfide deposits and are penetratively deformed and intersected by numerous shears and melange zones. The Melones Fault Zone is interpreted as a tectonic melange established during accretion, along which portion of the arc basement tectonically intruded the arc and basin assemblages. At present, the Sierra Nevada Foothills are a remnant of metamorphosed supracrustals intruded by the multiphase, Jurassic-

Cretaceous Sierra Nevada granitic batholith, of which some 7-10 km thickness has been lost to erosion since the Cretaceous.

Predominantly sedimentary basins in convergent margins

In active island arc-dominated convergent margins and in offshore of the andean-type belts (Chapter 6), high percentage of the total area consists of marine basins where active sedimentation takes place. This is not apparent from the literature dealing with metallic deposits as the sediments have a low prospectivity, although the petroleum-focused literature fills this gap. Major works on regional geology, such as the compilations of the Indonesian region (van Bemmelen, 1949; Hamilton, 1979), provide a balanced picture.

The recent sediments and their basins range from those that are specific to convergent margins (such as inter-arc basins filled by sediment with a high proportion of pyroclastic detritus), to those that are non-specific and common to several geotectonic domains (e.g. terrigenous shelf and slope sediments; carbonate reef environments). Most basins and sediments are in-between. The majority of convergence-specific basins have a magmatic component, other than detritus. This ranges from isolated, mostly basaltic sills or flows emplaced into wet sediments, felsic sills or small domes, pyroclastic flows, to isolated subaqueous volcanic centres and, finally, subaqueous to partly subaerial volcanic arcs. The literature favours back-arcs in which the greatest variety of materials of contrasting derivation (continental, pelagic, MORB, arc) interact and in which several interesting metallic deposits actively form at present. Although non-spectacular as ore hosts, the recent sediments have an important role as analogues for interpretation of the ancient "eugeoclinal" rocks, many of which contain giant orebodies. Brief selection of the young basin varieties follows:

- Continental shelves and slopes adjacent to convergent margins as off California. They consist of monotonous hemipelagic to pelagic mud locally interrupted by turbiditic tongues and/or slumps and debris flows (counterparts of olistostromes). In the tropical belt patchy carbonate buildups could be present with related forereef breccias. Hydrogenous phosphorite nodules (with trace U) in the California offshore are a potentially significant resource with some 1 billion tons of phosphorite in place (Emery, 1960).

- Turbiditic fans of terrigenous derivation consist of alternating sand and mud sets. The Bengal Fan (Einsele, 1992) extends for a distance of several thousand km from its source in the Bay of Bengal into the forearc of the Sunda Arc (off Sumatra). Smaller turbiditic fans dominated by pyroclastic and epiclastic detritus form a part of volcanoclastic aprons adjacent to explosive island volcanoes and arcs. No ore occurrences are known.
- Fringing and barrier reefs surround volcanic islands, and carbonate sediments accumulate in small lagoons, in tropical environments. A young emergent reef on Efate, Vanuatu, participated in the entrapment of Mn oxides, displaced from local mafic volcanics, to form the small Forari Mn deposit (Warden, 1970). On Vaghena and Rennell Islands in the Solomons Archipelago airborne volcanic ash trapped in lagoons has diagenetically converted to an unusual form of clayous bauxite (Taylor and Hughes, 1975). These are small deposits. There is, however, a link to the "world class" deposits of young, unconsolidated (earthy) gibbsitic bauxite in Jamaica (~1.5 bt of ~50% Al₂O₃; Comer, 1974). This bauxite forms blankets in numerous karst sinks dissolved in Eocene limestone resting on paleo-arc volcanics and is interpreted, as in the Solomons, as an allitized volcanic ash blown in from the Lesser Antillean volcanoes. Reef and other shallow marine carbonates facilitate formation of metalliferous skarns at contact with intrusions.

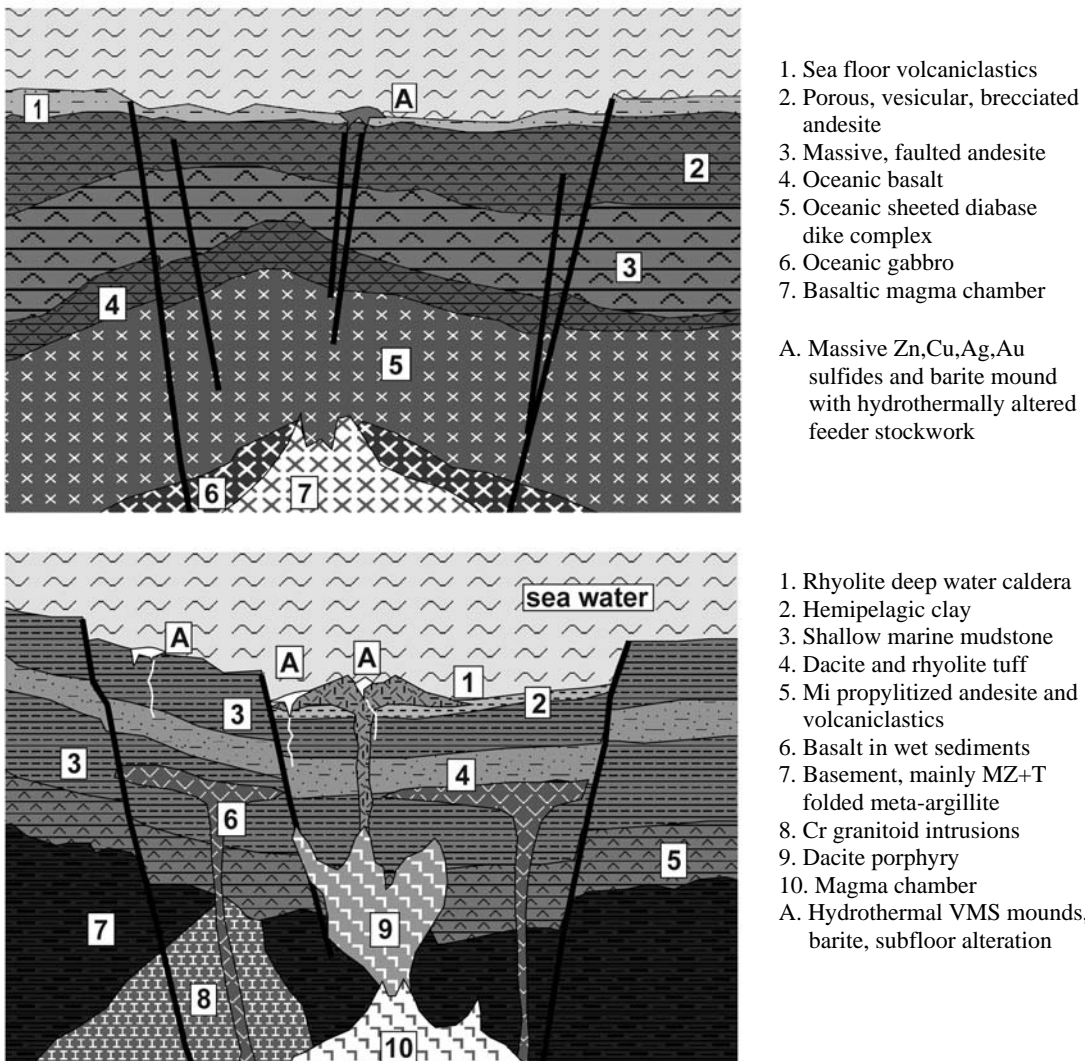
Back-arc, inter-arc, and other extensional basins

Back-arc basins formed by lithospheric extension of the upper plate above subduction zone (Karig, 1974; Saunders and Tarney, 1991; Marsaglia, 1995). Most, like Mariana Trough or Lau Basin (Fig. 5.2) are intraoceanic, flooded by tholeiitic basalt similar to MORB and covered by a variable but mostly small thickness of sediment (von Stackelberg et al., 1990; Fouquet et al., 1993). Ensialic back-arc basins (Fig. 5.3) as in the Sea of Japan, Okinawa Trough (Halbach et al., 1993) and Manus back-arc (Binns and Scott, 1993) have been established on attenuated and rifted continental crust. Off Japan this took place between the parent continent (eastern Asia) and mature island arc (the Japan archipelago), where the arc volcanism

overprints an older (as old as 1.6 Ga in Japan) basement. Alternatively, rifting and extension affected an earlier arc that split into an inactive remnant arc and a new magmatic arc (Smith and Landis, 1995). The Sea of Japan is also a marginal sea (or basin), but some back-arc systems continue on land to form, for example, the Taupo Neovolcanic zone of New Zealand (read below). Pull-apart transform basins (Gulf of California) and trapped basins (Aleutian Basin) complete the lot (Saunders and Tarney, 1991).

Spreading above a mantle diapir terminates with production of suprasubduction ophiolite described in Section 8.2, a near-equivalent of the Mid-Ocean Ridge association, but not all backarc basins have reached this stage and not all ophiolites are complete. The Cretaceous Rocas Verdes assemblage in southern Chile, interpreted as a back-arc ophiolite (Saunders et al., 1979), formed in a basin on extended continental crust, has gabbro, sheeted dikes, plagiogranite, abundant basalt, but lacks peridotite. The basalts are overlain by and are intercalated with thin shale that contains some chert and jasper, and this changes facies into a thick pile of volcanoclastics. Many "eugeoclinal" associations (Chapter 8) are like this and the Triassic Alexander Terrane in SE Alaska, mentioned above as the host of the giant Windy Craggy and Greens Creek massive sulfides, comes to mind. There are more sediment varieties, especially in the narrow basins bordered, or still flooded (Okinawa Basin), by continental crust. They include: debris flows and lahars; turbidite fans; hemipelagic and pelagic clays; pelagic siliceous and carbonate sediments; tuff. The sediments are often intruded by basalt dikes and sills and magma emplaced into wet sediments produced peperite.

The sediment variety in back-arcs is sometimes matched by the presence of more evolved volcanics such as andesite, dacite, rhyodacite and rhyolite in the form of domes, sills, short viscous flows and debris flows and these, in turn, are associated with massive sulfides (Rona and Scott, eds, 1993; Herzig and Hannington, 1995). Seafloor massive sulfide occurrences comparable in architecture (chimneys, mounds, talus) with those at mid-ocean ridges (Section 4.3.1), but different in composition and gold-rich, have been described from the Lau Basin SE of Fiji (Fouquet et al., 1993; Herzig et al., 1993), Manus Basin in northern Papua New Guinea (Scott



Figures 5.2 Models of recent back-arc lithologies and mineralisations; top: constructed on oceanic crust (Lau Basin-type); bottom: constructed on attenuated continental crust (Okinawa Basin-type). From Laznicka (2004), Total Metallogeny plates G37 and G46

and Binns, 1992) and from the Central Okinawa Trough off SW Japan (JADE deposit; Halbach et al., 1993). The JADE deposit in the depth of 1,340 to 1,450 m, in argillized rhyolite hosts, has an inner massive sulfide core fringed by barite and native sulfur. The seafloor sulfide occurrences are attractive for their high precious metals content but their magnitude has not yet been established. They are scientifically important as an analogue of the kuroko-type and similar VMS deposits in the "eugeoclinal" associations (Chapter 8).

Magmatic (volcano-plutonic) arcs

Magmatic arcs are the resting places of volcanic and plutonic rocks crystallized from magmas believed generated at the top and above the descending lithospheric slab (at and above the Benioff-Wadati seismic interval), and transported into the upper lithosphere. There is a voluminous literature on petrogenesis (reviewed in Hess, 1989), geochemistry and metallogenesis (reviewed in Sawkins, 1990; Stanton, 1994) of magmatic arcs. Sillitoe (1972) has been the first to propose that porphyry Cu-Mo deposits formed from melts generated during subduction, presumably from

melting and recycling of the trace metal content of metalliferous oceanic muds. The melting, driven by dehydration, friction and increasing geothermal gradient starts at depths of about 100 km under the present magmatic arc and the initially basaltic batches of melt (BVTP, 1981) gradually rise towards the surface triggering zone melting of mantle and crustal rocks, and magma mixing and differentiation along the way (Kay, 1980; Maaløe and Petersen, 1981; Wilson and Davidson, 1984).

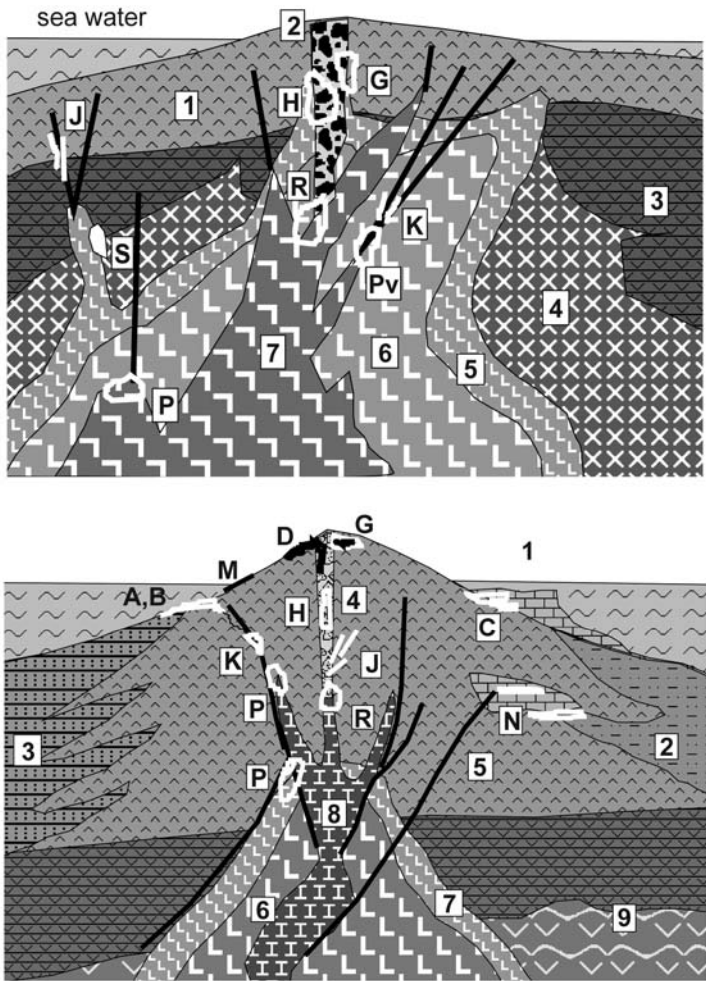
Although there is a controversy as to exactly which materials undergo subduction-related melting and how the melts make it through the at least 100 km thick overburden to the near-surface, there is an abundant accumulated empirical knowledge about the type of magmas that have reached the upper 5 km of the crust where hydrothermal fluids start to separate, the rock varieties the melts produced, and the ores that are sometimes associated. There is a distinct trend of "maturation" of the magmas (that is, advancement from the least evolved mafic, silica and alkalis-poor magmas compositionally close to the mantle and oceanic basalt, to the silica and potassium-rich magmas close to the "granitic" continental crust) in relative time and space (Gill, 1981). As a rule, the most "immature" basalt-dominated tholeiitic magmas are dominant in the ensimatic and intraoceanic magmatic, mostly island, arcs such as the Marianas. Bimodal association is usually associated with intra-arc rifting. More evolved arcs have an andesite-dominated calc-alkaline suite. Magmas emplaced into regions with mature continental crust in microcontinents or in Japan-style island arc interiors have widespread rhyolite. There is a good correlation of arc magmas with the nature and thickness of the lithosphere through which the melts (or just heat fronts) passed and with which they interacted. This, together with isotopic and petrogenetic trace metal evidence, supports magma derivation from sources that are much closer to the final resting places of the upper crustal magmatic rocks than the magic 100 km deep Benioff interface.

Island arc maturity: Arc maturity (degree of advancement of crustal evolution) correlates with the most recent igneous series which, in turn, partly determines the metallogeny.

The most immature arcs form when two oceanic plates converge along a steep Benioff zone (e.g. the Marianas, Tonga arcs). Most of the action here is under the sea and islands, if at all present, are small and low. Some islands and submarine ridges are remnant arcs from the earlier stages of evolution. The volcanics are members of the low-K island arc

tholeiite and boninite series and predominant submarine (pillowed or massive) lavas, hyaloclastites and breccias often incorporate MORB and serpentinized mantle peridotite blocks, rafts and debris together with ocean floor sediments (BVSP, 1981; Fryer et al., 2000). The volcanics are hydrated and affected by syn- to early-postvolcanic Na, Ca, Mg metasomatism like spilitization. Bimodal associations result when rare felsic volcanics are present as in the NE Caribbean (Donnelly and Rodgers, 1980) and if so, Na-metasomatism of dacite or rhyolite produces "keratophyre" and albitophyre. Plutonic equivalents are rarely exposed in young arcs and when they are they are mostly gabbros and diabase dikes, sometimes diorite or quartz diorite, trondhjemite ("plagiogranite"). Some basaltic stratovolcanoes are underlain in depth of some 3 km by cumulate gabbro, dunite and harzburgite. These correspond to the Alaska-Urals complexes in eugeoclinal terrains. No economic ores are known from the "young" arcs, and in the eugeoclinal equivalents (Chapter 8) they are mainly the Cyprus- and Besshi-type VMS. The basalts, high in trace Cu, could have contributed metals to the more evolved plutonic systems related to the "Philippine-type" of porphyry Cu-Au deposits (read below).

Semi-mature arcs form on top of older oceanic arcs or back-arcs, or on transitional crust. Commonly they form major islands (as in the Philippine and Indonesian archipelagos; Carlile and Mitchell, 1994) and they also build narrow isthmuses that connect continents (e.g. Panama). The volcanics belong to the calc-alkaline series dominated by andesite although basalt, dacite and rhyolite are also widespread. Inherited oceanic and MORB remnants crop-out in erosion-dissected composite terrains. This is the most visible magmatic series in the Pacific region exposed in stratovolcanoes and occasional calderas. Pyroclastics are more voluminous than lavas and much of the tephra as well as eroded debris from older volcanics have been multiply reworked and resedimented into thick submarine turbiditic aprons around islands. Subvolcanic and plutonic members of semi-mature arcs belong to the I-type (magnetite) diorite, quartz diorite and granodiorite. These host porphyry Cu-(Au,Mo) deposits (e.g. Waisoi, Fiji), sometimes with high-sulfidation enargite-gold deposits (e.g. Mankayan district in Luzon, Tapanakan; read below). Low-sulfidation epithermal gold veins and disseminations are also common in Kyushu (Hishikari), northern Luzon (Baguio district) and elsewhere.



- 1. Andesite lavas & pyroclastics
 - 2. Vent & diatreme breccia
 - 3. Tholeiitic basalt flows
 - 4. Gabbro; 5. Microdiorite; 6. Diorite
 - 7. Tonalite and tonalite porphyry
 - 8. Black bars: porphyry dikes
 - G. Alunite replacements, disseminations
 - H. Epithermal Au in diatreme, breccias
 - J. Epithermal Au-(Ag) veins
 - K. High sulfidation epithermal Cu-Au
 - P. "Diorite model" porphyry Cu-Au
 - Py. Ditto, exocontact ore in volcanics
 - R. Porphyry-Au
 - S. Magnetite-apatite replacements
-
- 1. Reef, carbonate sediments
 - 2. Volcaniclastics in lagoon
 - 3. Volcanic sandy turbidite
 - 4. Vent facies, andesite-dacite
 - 5. Andesite lavas, pyroclastics
 - 6. Synvolcanic diorite (early phase)
 - 7. Microdiorite, marginal facies
 - 8. Late synvolcanic tonalite, granodiorite
 - 9. Basalt to amphibolite, early arc stage
 - A. Fe-(Mn) submarine hot spring precip.
 - B. Ditto, Fe sulfides (some with Au)
 - C. Mn oxide impregnations in tuff
 - D. Hot spring Au in vent breccia
 - G. Alunite, sulfur impregnations
 - H. Epithermal Au in diatreme, breccia
 - J. Epithermal Au-(Ag) veins
 - K. High sulfidation Cu-Au
 - M. Magnetite beach sands
 - N. Mn oxides in tuff, limestone
 - P. Porphyry Cu-Au in/near diorite
 - R. Ditto, porphyry Au

Figure 5.3. Metallic mineralization in island arc volcanic centers cored by comagmatic high-level intrusions. Top: Philippine-style diorite/tonalite intrusions emplaced to basalt/andesite; ore types H,J,K,P,Py include "giants". Bottom: more evolved variant with latest granodiorite; ore types H,J,K,P,R include "giants". From Laznicka (2004), Total Metallogeny sites G40 and G39

High-K shoshonitic series occasionally appears in the form of central volcanoes as in Tambora, Indonesia (van Bemmelen, 1949) and in the New Guinea Highlands, or in caldera complexes. The shoshonitic Tavua caldera in Fiji hosts the "giant" Au-Te Emperor Mine in Vatukoula, formed along the faulted caldera margin (read below). Shoshonitic to alkaline suite of trachyandesite, trachyte, monzonite and syenite in the Tabar-Feni islands chain off New Ireland (PNG) grades to undersaturated basanite, tephrite, nephelinite and phonolite. The K/Na ratio is between 0.5 and 1 (McInnes and Cameron, 1994). The dissected Luise caldera on Lihir island hosts the "giant" Ladolam porphyry/epithermal gold deposit (read below).

Alkaline basalt seamounts and islands are in the Tyrrhenian Sea (e.g. Ustica Island, Pichler 1981) and peralkaline rhyolites are known from Pantelleria in the Mediterranean and D'Entrecasteaux Islands, PNG.

The mature (Honshu- or Japan-type) arcs have a thick, old continental crustal basement or form over a microcontinent (e.g. the Taupo "rift" and the Hauraki Goldfield, North Island, New Zealand; Cas and Wright, 1987). The mature basement consists of blocks detached from contiguous continents by extension and rifting which, in Japan, faces its source area across the Sea of Japan, a marginal sea (back-arc). The basement often comprises an older generation of subduction or collision generated

granitoids and volcanics with relict metallic deposits formed while in the former continental location. The youngest island arc-stage volcanism that overprints older arcs usually belong to the calc-alkalic series. The least evolved basaltic andesite formed from magmas melted in the deeper reaches of Benioff zone with minimal contribution from the continental crust, but increasingly potassic and siliceous members appear as the mature basement itself contributed melts. Dacite, rhyodacite, rhyolite pierced by comagmatic granodiorite and quartz monzonite and rarely monzogranite are quite common and they are indistinguishable from comparable magmatic rocks in the andean margins (Chapter 6). Several prominent calderas are known (e.g. the Lake Toba, Sumatra). VMS deposits as in the "Green Tuff" region in Japan (kuroko-type Zn, Pb, Cu, Ag deposits; read below) are associated with submarine volcanic centers, whereas epithermal Pb, Zn, Ag; Cu; Au-Ag; Mn; vein, replacement and disseminated deposits are in mostly subaerial volcanic piles pierced by high-level intrusions. Japan hosts several deposits of metals that are uncommon in island arcs such as Sn (Ikuno, Akenobe), W, Mo and U. Most of such deposits formed in continental setting and have been partly modified, following incorporation into the island arc environment.

Highly potassic (in places ultrapotassic) lavas and pyroclastics, dominated by rhyolite and trachyte, are prominently developed in the Aeolian and Aegean arcs (off Greece and southern Italy), especially in the Roman igneous province and Tuscany (Percerillo, 1985). They are greatly enriched in fluorine, boron and in places uranium; these metals form subeconomic accumulations in volcanoclastics (especially lacustrine sediments). Larderello is a famous geothermal area and a "world class" producer of boric acid from hot brines heated by a young granite apex in depth.

5.3 Porphyry Cu-Au-(Mo) deposits in young island arcs

Porphyry deposits in young island arcs represent probably no more than 15-20% of comparable deposits recorded from the andean margins (Chapter 6), yet they are economically important, especially because of the high gold content. In times of high Au prices, the value of gold in some deposits exceed the value of copper. Eight "giants" occur in the Indonesia-Pacific region and if Panama is considered equivalent to island arc, there are two

additional "giants". In addition to the high Au:Cu and very high Au:Mo ratios the island arc "porphyries" differ from the "andean" porphyries by associating with diorite or quartz diorite stocks emplaced into comagmatic or slightly older andesite (the "diorite model" of Hollister, 1978). The diorite/andesite contacts are often diffuse and much of the ore tends to reside in the volcanics (hence many deposits are also classified as "volcanic" porphyry Cu). The parent stocks are columnar, tabular or irregular and the alteration zoning is less regular than in the "andean" porphyries, is overlapping and often indistinct. Joint porphyry Cu-Au/high sulfidation Cu-Au occurrences are very common and these two types either occur side-by-side (e.g. Lepanto-Far South East) or the high sulfidation overprints earlier porphyry (e.g. Tampakan). Economically significant oxidation and secondary sulfides zones are rare and small which is a function of the physiographic development and climatic history, as all these deposits are located in areas of rapid uplift in high-rainfall setting.

Philippine porphyry Cu-Au province

Philippine archipelago contains 5 porphyry "giants" and at least 13 "large" deposits that store close to 40 Mt Cu (Divis, 1983). Sillitoe and Gappe (1984) summarized characteristics of 48 deposits and compiled a "Philippine porphyry model", further modified by Corbett and Leach (1994). The modern Philippines are an active island arc complex influenced by two major and several minor subduction zones; the former comprise the west-dipping zone initiated in the Philippine Trench, and the east-dipping zone extending from the Manila Trench. There is an almost continued andesitic central magmatic arc in the vicinity of the Philippine Fault. There is a number of active volcanoes and geothermal areas where fluid movements cause alteration and embryonal Cu-Au mineralization comparable with the earlier systems associated with economic ores (Corbett and Leach, 1994).

Continuous island arc evolution in the Philippines started in the Cretaceous, on predominantly amphibolitic basement locally exposed in the western part of the archipelago. The earliest Philippine porphyry Cu-Mo is the Middle Cretaceous (95-100 Ma) **Toledo (Atlas)** group on Cebu (Divis, 1983; 1.38 bt @ 0.45% Cu, 0.24 g/t Au for 6.215 mt Cu, 331 t Au, 100 kt Mo, 2,624 t Ag), comprised of three deposits of multistage stockworks and disseminations of Cu sulfides with minor molybdenite in K-feldspar, biotite,

magnetite-altered Lower Cretaceous andesite, basalt and clastics intruded by quartz diorite. There is a strong gypsum-anhydrite overprint negatively influencing the stability of open pits.

Except for the 30 Ma old deposit **Sipalay** on Negros Occidental, the rest of the Philippine porphyries are Miocene to Pliocene with the youngest economic deposit (Santo Tomas) less than 1.4 Ma old. The remaining largest deposits occur in five clusters (from north to south): Mankayan (Far South-East) and Baguio (Santo Tomas) districts of northern Luzon; Pinatubo massif of NW Luzon (Dizon); Batangas-Marinduque area (Taysan, Marinduque); and SE Mindanao (Tampakan). The orebodies are associated with diorite, diorite porphyry, quartz diorite, dacite porphyry, rarely granodiorite stocks, plugs and dikes emplaced into andesite. Breccias and intramineral intrusions are common.

Corbett and Leach (1994) described in detail the often overlapping sequence of alteration-mineralization phases in the youngest Philippine porphyries. 1) Prograde alteration due to magmatic fluid produced minor K-silicate (biotite >> K-feldspar) alteration grading to actinolite, then epidote, chlorite, albite, pyrite fringe. Fracture stockworks and breccia-cementing quartz with some K-feldspar, biotite, magnetite and specularite formed. Some deposits suffered intense silicification, attributed to vapor-dominated phase and this may progress into argillic alteration of sericite, andalusite, tourmaline, pyrophyllite, diaspore with alunite and kaolinite. Cu introduction followed quartz veining, and chalcopryite with bornite filled cracks. 2) Retrograde alteration was due to 400-300°C meteoric waters. Sericite, quartz > chlorite, carbonates and anhydrite overprint the earlier phase and may be accompanied by a second generation of pyrite, chalcopryite and hematite in thin veinlets or disseminations in altered wallrocks. 3) Argillic overprint due to low-temperature sulfate, bicarbonate or neutral groundwaters during uplift and unroofing produced clay minerals: kaolinite, dickite, pyrophyllite, chlorite, smectite and illite. 4) High sulfidation overprint due to magmatic fluids issued from subvolcanic intrusions caused extensive silicification and alunite, pyrophyllite, dickite, illite alteration. Bornite, covellite, enargite, luzonite, tennantite sometimes formed. This overprint usually relates to a separate pulse of fluids. Low sulfidation gold-quartz veins and stockworks of variable magnitude, spatially associated with the porphyry deposits in most districts, are always younger. Those in the Baguio district (Antamok and Acupan) are of the (near) "giant" magnitude.

Santo Tomas II (Philex) (UND Programme, 1987; 511 mt ore @ 0.32% Cu, 0.7 g/t Au, 0.2 g/t PGE for 340 t Au, 1.6 Mt Cu, calculated 102 t PGE) is the largest porphyry deposit in the Baguio district, NW Luzon and a typical "uncomplicated" Philippine porphyry (Fig. 5.4). It is a Late Pliocene to Quaternary, subvertical, 700 m deep Cu-Au system with platinoid values associated with the Santo Tomas calc-alkaline quartz diorite porphyry stock emplaced into Oligo-Miocene tectonized, hornfelsed and biotite, chlorite, actinolite altered andesite. The central mineralized fracture stockwork consists of veinlets of bornite, chalcopryite and magnetite superimposed on biotite-altered, quartz veined and locally silicified diorite porphyry and andesite. This changes into pyrite, chalcopryite and hematite in biotite, sericite, actinolite assemblage along margins. Late stage fractures are filled, and the whole complex permeated, by anhydrite that hydrates into gypsum. There is a clay, silica, goethite and jarosite -bearing leached capping over the ore outcrop with some residual gold, but almost no supergene oxide or secondary sulfide mineralization. Other Philippine "giants":

- **Marinduque Island (Marcopper)-Cu,Au**, Philippines * 3.241 mt Cu and 82 t Au in two orebodies: San Antonio (Rc 611 mt @ 0.38% Cu, 0.1 g/t Au, 0.003% Mo), Tapian (P+Rv 177 mt @ 0.52% Cu, 0.12 g/t Au, 0.004% Mo) * 15-20 Ma flat N-S elongated quartz, chalcopryite stockwork and > disseminations in K-silicate and sericite; oxidation zone * ore in Mi quartz diorite porphyry emplaced to Eo-Mi clastics & andesite * Loudon (1976).
- **Sipalay-Cu,Au**, Negros Occidental, Philippines * Rc 884 mt @ 0.5% Cu, 0.34 g/t Au containing 4.42 mt Cu, 300 t Au * 30 Ma steep-dipping tabular zone of quartz, pyrite, chalcopryite > bornite veinlets; minor chalcocite blanket * ore is in biotite & sericite altered Eo-Ol quartz diorite emplaced to metalvolcanics * Wolff (1978).
- **Hinoban-Cu,Au**, Negros Occidental, Philippines * Rc 650 mt @ 0.5% Cu, 0.24 g/t Au containing 3.25 mt Cu, 156 t Au * Ol? subhorizontal body of quartz, chalcopryite, pyrite veinlets, disseminations * ore is in silicified, sericitized quartz diorite emplaced to "keratophyre" * Asian Journal of Mining, May 1997.

Porphyry/high sulfidation overlap in the Philippines: Mankayan ore field in northern Luzon is the site of the **Lepanto** high-sulfidation Cu-Au deposit, mined since the 16th century until late 1990s (Hedenquist et al., 1998; Pt 36.3 mt ore @ 2.9% Cu, 3.4 g/t Au for ~740 kt Cu and 115 t Au). Lepanto is a fault-controlled, 3 km long gently dipping brecciated zone of early stage pyrite, enargite and luzonite

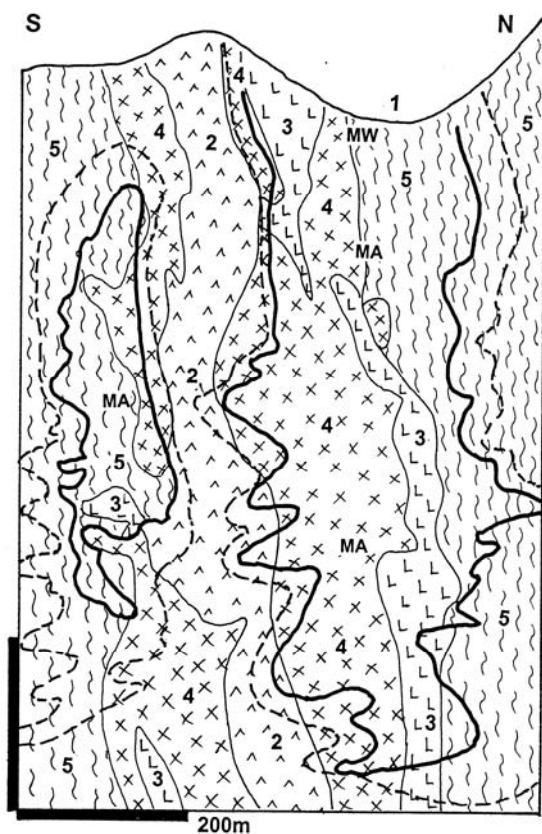


Figure 5.4. Santo Tomas II (Philex) porphyry Cu-Au, Baguio district, Luzon: a cross-section. 1. Q cover & regolith; 2. Intrusion and intrusive breccia; 3. 2.1 Ma andesite porphyry; 4. Biotite, chlorite, actinolite-altered porphyry; 5. Ol-Mi hornfelsed and tectonized andesite. MW, leached zone; MA, Pl_3 -Q fracture veinlet to disseminated Cu sulfides in K-altered hosts (solid black line outlines the orebody). From LITHOTHEQUE 2125, modified after Philex Mine Staff (1994)

followed by later pyrite with tennantite, chalcopyrite, Pb-Zn sulfides, Au-Ag tellurides, Bi, Sn and Se minerals, and electrum in anhydrite, barite, vuggy quartz and alunite gangue. The host late Pliocene dacite and andesite tuff, diatreme breccia and dacite porphyry dikes as well as the Cretaceous-Eocene metavolcanics under unconformity are altered by ore-proximal alunite changing away into kaolinite, nacrite and dickite, then into chlorite and smectite. In 1980, the existence of a buried porphyry Cu-Au deposit, the **Far South-East**, was recognized. This is hosted by altered basement metavolcanics, diatreme breccia and Plio-Pleistocene quartz diorite porphyry dikes, 650 m under the surface. The bell-shaped disseminated and stockwork orebody (Hedenquist et

al., 1998; 650 Mt @ 0.65% Cu and 1.33 g/t Au for 4.225 Mt Cu and 864 t Au) is in pervasively biotite, magnetite, minor K-feldspar alteration assemblage overprinting the earlier chlorite-sericite alteration veined by vitreous quartz. Chalcopyrite and bornite are in later-stage veinlets and disseminations with anhydrite, pyrite, white mica and hematite associated with euhedral quartz (Fig. 5.5).

More orebodies have been found in the Mankayan ore field subsequently, including another buried porphyry Cu-Au (Guinaoang; 500 mt @ 0.4% Cu, 0.4 g/t Au) and the Victoria low-sulfidation vein gold deposit (65 t Au; Claveria et al., 1999) so this ore field has entered the new millennium with a pre-mining resource of some 7 mt Cu and 1,240 t Au or more (if the recently quoted resource of 1,423 mt @ 0.4% Cu and 0.6 g/t Au for the Far South-East is included). Hedenquist et al. (1998) have concluded that the Lepanto-Far South-East pair of orebodies is contemporaneous, formed between about 1.42 and 1.30 Ma, under alunite-altered paleosurface, in depths ranging from about 700m to 2000m measured to the tops of orebodies. The porphyry deposits formed from hot, high salinity magmatic hydrothermal fluids, subsequently cooled and diluted by meteoric water into a lower salinity acidic fluid moving laterally via permeability zones to form the Lepanto orebody.

Tampakan Cu-Au deposit is in southern Mindanao north of General Santos City (Middleton et al., 2004; Rc 1,104 mt ore @ 0.65% Cu and 0.26 g/t Au for 4.98 mt Cu and 286 t Au). It was found by WMC Resources in 1992, during a systematic exploration program. The deposit is located at the northern end of an active magmatic arc (an active volcano is 12 km away), superimposed on thrust-faulted and folded Miocene andesitic basement. The ore zone is controlled by a splay from a major WNW-trending fault zone, a product of Miocene-Pliocene collision. The host association is a deeply dissected Pliocene stratovolcano complex composed predominantly of pyroxene andesite flows. These are intruded by hornblende diorite porphyry stocks and dikes with diatreme and hydrothermal breccias. Post-mineralization andesitic and dacitic plugs and flow domes intrude and overlie the entire sequence.

At surface the deposit is indicated by silica and argillic lithocap. The most widespread zone of advanced argillic alteration underlies illite-smectite-chlorite altered andesites and it hosts most of the copper and gold. The zone is up to 400 m thick, it has the form of an almost flat-lying tabular body

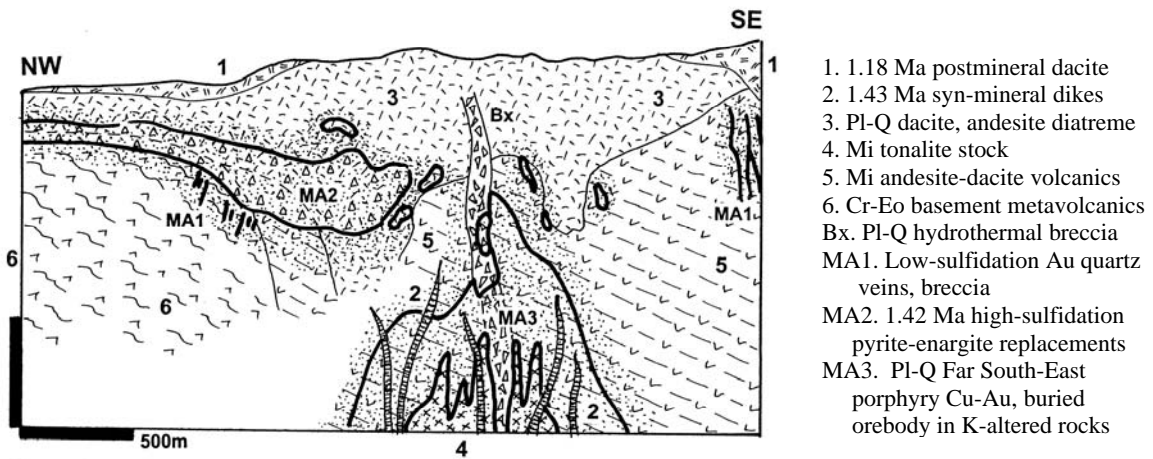


Figure 5.5. Lepanto and Far South-East deposits, Mankayan ore field, diagrammatic cross-section modified after Concepción and Cinco (1989), Garcia (1991), Hedenquist et al. (1998). From LITHOTHEQUE No. 3265

controlled by fault intersections and intravolcanic unconformity and it consists, from top to bottom, of silica, silica-clay and clay-silica subtypes. The "clays" are predominantly kaolinite, dickite, rutile and alunite with local pyrophyllite and diasporite, in company of vuggy silica. There are ghosts of an earlier stage quartz stockwork that increase with depth, eventually turning into a porphyry-style mineralization of fracture quartz veinlets with disseminated pyrite, chalcocopyrite and minor bornite overprinted by anhydrite-gypsum.

The main ore zone is 200 to 400 m thick, subhorizontal, composed of advanced argillic assemblage mineralized by several generations of sulfides filling vugs in silica, disseminated in the "clay" and changing, with depth, into subvertical feeder breccias. The sulfides comprise early pyrite, enargite and later digenite and bornite. Luzonite, chalcocopyrite, molybdenite are less common. Supergene sooty chalcocite is minor, and oxidic Cu minerals (chrysocolla, rare malachite and azurite) occur in mineralogical quantities because of the steep terrain and rapid erosion.

Other Indonesia-West Pacific porphyry Cu-Au

Three porphyry Cu-Au "giants" found in the Indonesia-Pacific region: Batu Hijau, Indonesia (read below); Panguna, Bougainville, and Waisoi (Namosi), Fiji, are all very similar in style and setting to the Philippine porphyries, being related to diorite/quartz diorite emplaced into island arc andesite (Corbett and Leach, 1998). At Panguna the intrusions differentiated as far as granodiorite.

Batu Hijau Cu-Au deposit is near the SW coast of Sumbawa Island in the Sunda archipelago of

Indonesia (Clode et al., 1999; 1.494 bt @ 0.52% Cu, 0.4 g/t Au for 7.77 mt Cu and 598 t Au). Sumbawa Island is best known for Tambora Volcano, a site of the 1815 catastrophic eruption, about the largest in recent history. This volcano is shoshonitic and located on the northern coast of the island. The Batu Hijau deposit (Fig. 5.6) was discovered by stream geochemistry and bulk leach for gold, and only after a target had been outlined spectacular green staining was discovered in a gully. The area is underlain by a succession of middle Miocene arc andesite volcanics and volcanoclastics with a prominent limestone unit, an is intruded by several generations of low-K quartz diorite (tonalite) porphyries with some intrusion breccias. There are three phases of Late Miocene-Pliocene tonalitic stocks associated with quartz-sulfide veining and porphyry Cu mineralization. Contrary to the usual situation where the youngest phases are mineralized, here the Old Tonalite has the greatest quartz-magnetite vein abundance and the Intermediate Tonalite stores most of the ore. The youngest phase carries only feeble mineralization.

The orebody has a subvertical columnar shape in cross section and the ore, centered on the young tonalite stocks, surrounds a barren core. The multistage mineralization started with the emplacement of quartz, biotite, magnetite veinlets in pervasively biotitized host rocks, with some disseminated chalcocite, digenite, bornite and chalcocopyrite. Andalusite and anthophyllite occur at the fringe. Late feldspar-destructive alteration produced sericite with albite, chlorite and calcite on fringe. This grades into and is followed by the advanced argillic association and late stage

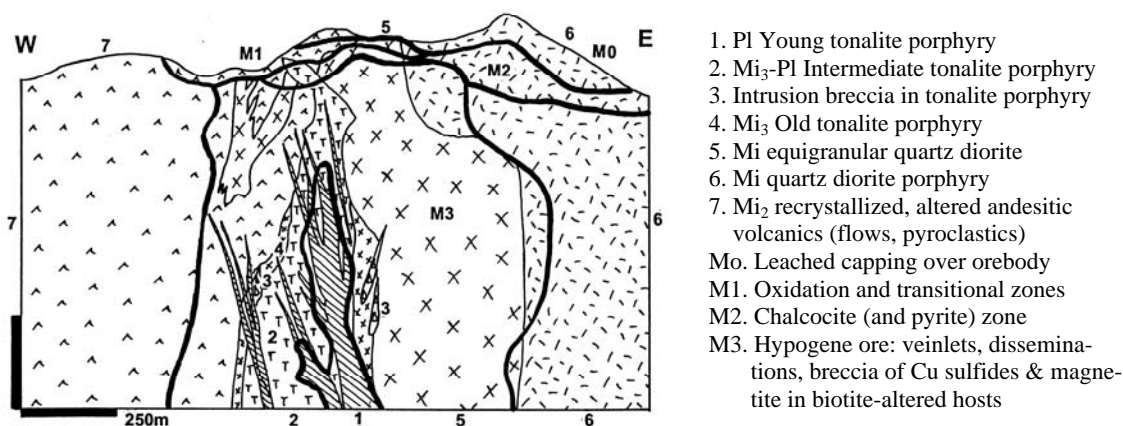


Figure 5.6. Batu Hijau porphyry Cu-Au deposit, Sumbawa, Indonesia. Diagrammatic cross-section modified after Clode et al. (1999) and Newmont Nusa Tenggara Ltd. (2002), from LITHOTHEQUE No. 2465

smectite, sericite and chlorite with minor veinlets of Pb, Zn, Cu sulfides and tennantite. The secondary enrichment zone is thin and discontinuous and mostly consists of supergene chalcocite, covellite and native copper topped by brochantite, chrysocolla, pseudomalachite and other oxidized minerals. More western Pacific "giants":

- **Panguna Cu-Au deposit**, Kieta, Bougainville Island, PNG * 1.4 bt @ 0.53% Cu, 0.63 g/t Au contains 5.84 mt Cu and 632 t Au * Pl porphyry Cu-Au, hypogene ore * pyrite, chalcopyrite, magnetite, quartz in biotite alteration envelope * Pl granodiorite & quartz diorite stocks in Mi quartz diorite pluton and OI hornfelsed andesite * Clark (1990).
- **Waisoi Cu-Au deposit**, Namosi district, Viti Levu, Fiji * Rc 1.1 bt @ 0.45% Cu, 0.13 g/t Au, 0.005% Mo containing 4.95 Mt Cu, 143 t Au * 6 Ma "diorite model" porphyry Cu-Au * in Pl stocks of tonalite porphyry emplaced to andesite volcanic center * Colley and Flint (1995).

5.4. Epithermal Au-(Ag) deposits

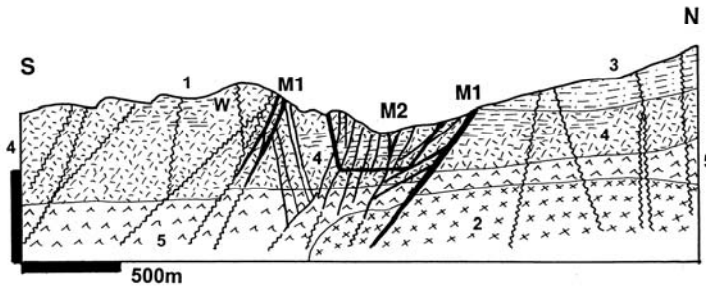
Epithermal Au-Ag deposits are widespread in the "young" island arcs and the "common variety" of low-sulfidation gold-quartz fissure veins, stockworks or mineralized faults does not substantially differ from comparable deposits in the andean margin setting (Chapter 6), where they are described in greater detail. The veins form during extensional episodes in island arcs and often occur together with porphyry Cu-Au deposits (as in the Baguio district, Luzon), but when they do they are substantially younger (Mitchell and Leach, 1991). Gold-only deposits with variable silver content such as Paracale, Acupan, Gosowong and others grade into deposits with moderate (although rarely recovered) Pb-Zn (Waihi) or Cu sulfides

(Antamok), and eventually into Pb-Zn-Ag veins (Toyoha, Hosokura, Cikotok) or Cu veins (Osarizawa). The "giant" magnitude was achieved by few deposits only, like Antamok, Philippines (304 t Au; read below) and Hishikari, Kyushu, Japan (326 t Au). Acupan in the Baguio district, Luzon, is a "near-giant" (200 t Au). Some epithermal gold deposits are very young (Hishikari: 1 Ma; Acupan: 0.65 Ma) and others are probably still actively forming in depth, under hot spring systems as in the Taupo Zone in New Zealand.

There is a special category of gold deposits associated with potassic (shoshonitic) plutonic rocks (Muller and Groves, 1997). Of the frequently quoted examples two "giants" qualify for membership in the "young" island arcs setting. They are the Emperor Mine in the Tavua caldera in Fiji (read below), and the Ladolam deposit on the Lihir Island, PNG (read below). The latter is, moreover, an example of telescoped porphyry- and epithermal-style ores. Porgera in the PNG Highlands is in a setting closer to collided andean margins and appears in Chapter 6.

High-sulfidation Au and Cu-Au deposits are fairly common in island arcs (Corbett and Leach, 1994), but most are either small or associated with porphyry coppers (Mankayan, Tampakan; read above). The "large" high sulfidation Chinkuashih (Jinguashi) Cu-Au ore field in northern Taiwan still lacks associated porphyry Cu-Au.

Antamok mine (Damasco and Balboa, 1992; 304 t Au @ 3.5 g/t, 335 t Ag) is in the Baguio district of northern Luzon in a company of, but younger than, several porphyry Cu-Au. It is a 3.5 to 1.1 Ma sericite-adularia (low sulfidation) epithermal system of three major NW-trending fault controlled veins, up to 2 km long and 20 m wide, filled by white and



1. ~2.1 Ma andesite and dacite plugs
2. ~8 Ma hybrid diorite stock
- 3+4. $Mi_3?$ volcaniclastics, andesite
5. Mi_{1-2} andesite, dacite, pyroclastics
6. Eo basalt to andesite flows
7. Cr-T₁ schistose meta-volcanics
- M1. Three major quartz, Cu sulfides, anhydrite, electrum veins
- M2. Bulk mineable low-grade ore

Figure 5.7. Antamok gold mine, Baguio district, Luzon: diagrammatic cross-section modified after Damasco & Balboa (1992), and Benguet Corporation (1994); from LITHOTHEQUE No. 2123

gray quartz, rhodonite, bornite, chalcopyrite, anhydrite and electrum in sericite-illite altered Miocene andesite, dacite, pyroclastics and diorite (Fig. 5.7). These higher-grade veins were mined from underground workings and exhausted in the past. More recently blocks of short, thin tensional quartz-pyrite veins and veinlets in argillized rocks between the main ore veins have been bulk-mined from an open pit. The average grade was 2.5 g/t Au.

- **Hishikari-Au** (326 t Au @ 60 g/t; Izawa et al., 1990) is the largest and richest deposit of the Plio-Pleistocene hot spring and epithermal deposits in the Kyushu volcanic province, Japan. The 1.0 Ma old deposit comprises three zones of massive, banded and vuggy quartz-adularia fault and fissure veins with pyrite and native gold in smectite-altered Quaternary dacite and andesite, resting on sedimentary rocks of the Shimanto accretionary complex.
- **Waihi (Martha mine)**, North Island, New Zealand (Brathwaite et al., 1989; P+Rv ~15 Mt @ 3.2 g/t Au, 33 g/t Ag containing 232 t Au, 9,147 t Ag) is the largest deposit and the only "giant" in the Hauraki Goldfield. Multiple Miocene steeply dipping quartz, chalcedony > adularia veins with pyrite, sphalerite, galena, acanthite and electrum follow normal faults in near-vein adularia-sericite, and regionally propylitically altered Miocene andesite and dacite.
- **Morobe Goldfield** (Wau, Eddie Creek), P+Rc 264 t Au (Sillitoe et al., 1984) is a predominantly placer field in NE Papua New Guinea. Several Plio-Pleistocene zones of quartz, chalcedony, adularia, pyrite, electrum veins, stockworks and silicified breccias are related to dacite plugs and diatremes emplaced to Miocene granodiorite and Mesozoic metamorphics.

Tavua Caldera and Emperor (Vatukoula) Au-Ag mine, Fiji (Colley and Flint, 1995; Eaton and Setterfield, 1993; P+Rc 338 t Au @ 10 g/t Au). Tavua Caldera in northern Viti Levu Island, is erosional remnant of a caldera underlain by Miocene-Pliocene shoshonitic volcanics. The pre-caldera shield volcano stage consists of early

subaqueous, later subaerial absarokite (=shoshonitic augite-olivine basalt) lavas with minor tuff and interflow sediments, resting on earlier volcanic arc basement. This is overlain by caldera-stage shoshonite (=K-rich andesite) and banakite (=biotite trachyandesite) flows, tuff, volcanic and caldera collapse breccias. These are intruded by several monzonite plugs and a trachyandesitic "fused agglomerate". A small Pliocene monzonite stock approximately in the centre of the caldera hosts subeconomic porphyry-style disseminated chalcopyrite mineralization (Nasivi Prospect) in albitized core overprinted by silica-alunite and anhydrite cap.

The **Emperor Mine** is a low-sulfidation mineralized system along the western margin of the caldera (Fig. 5.8). The lode structures are both steep and gentle ("flatmakes") narrow faults and fractures filled by dilational veins, and fault intersections surrounded by bulk-mineable "shatter zones". The quartz > carbonates, albite, pyrite, minor galena, sphalerite, Au-tellurides, gold veins and veinlets are enveloped by quartz, adularia, sericite, illite and roscoelite alteration assemblage that grades into a district-wide propylitization.

Lihir Island and Ladolam Au deposit, Papua New Guinea. Lihir (alias Niolam) is an island in the Tabar-Feni group of small shoshonitic to alkaline (predominantly trachybasaltic) volcanic islands formed along local extensional structures in the New Ireland Basin north of, and parallel with, the New Ireland Island (Kennedy et al., 1990). The setting is a forearc in the Manus arc-trench system and it contains several Pliocene to Quaternary volcanoes, some of which project as islands (e.g. Lihir), while others remain submerged as seamounts (Fig 5.10).

Lihir Island measures 20x13 km across and is a composite of three young volcanoes constructed on remnants of a late Miocene submarine stratovolcano

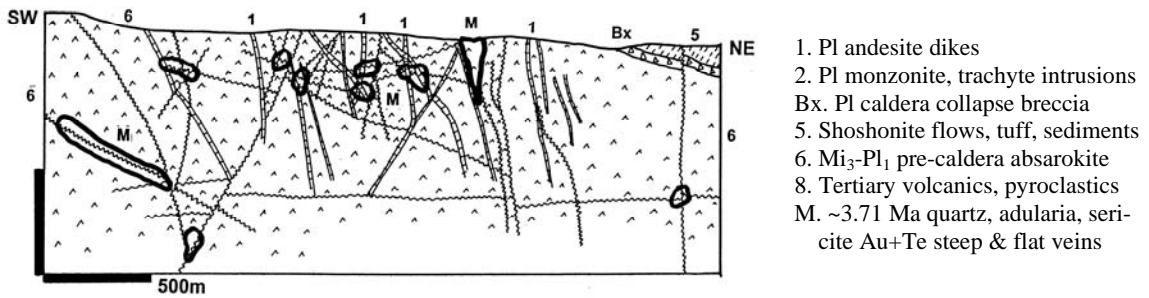


Figure 5.8. Emperor gold mine, Vatukoula, Viti Levu, Fiji, diagrammatic cross-section. From LITHOTHEQUE No. 2862, modified after Eaton and Setterfield (1993), Emperor Gold Mines Ltd. information, 2002

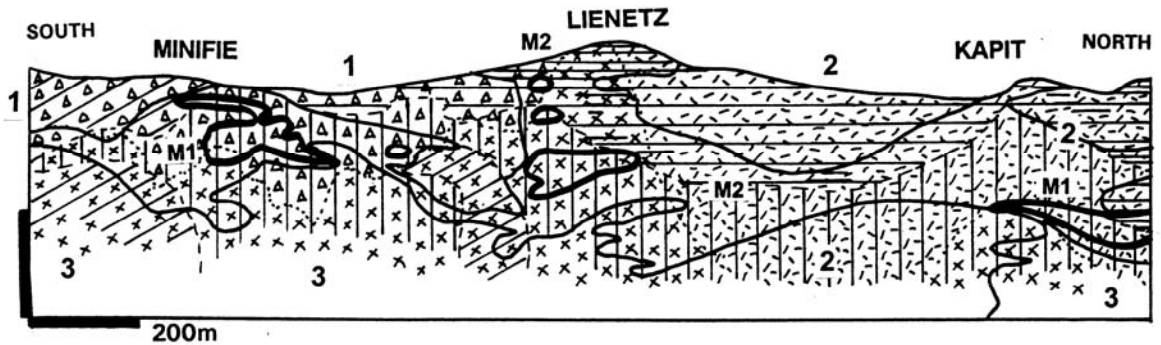


Figure 5.9. Ladolam gold deposit, Lihir Island, Papua New Guinea. Diagrammatic cross-section from LITHOTHEQUE No. 2242, modified after Moyle et al. (1990), Lihir Ltd. on-site information, 1994. 1. P1-Q predominantly pyroclastic and hydrothermal breccia; 2. Predominantly volcanic flows: trachybasalt, trachyte, andesite, latite; 3. Predominantly intrusive rocks: diorite > monzonite, syenite. M1: disseminated higher-grade Au ore (5 g/t Au plus), bold outline; M2: low-grade (1-5 g/t Au) disseminated ore, thin outline. Line patterns show superimposed hydrothermal alteration. Horizontal: argillic > advanced argillic; oblique: propylitic; vertical: potassic (K-feldspar and biotite, sericite)

(Moyle et al., 1990). The Pleistocene Luise Volcano, composed of flows, tuff breccia and tuff of alkali basalt and trachybasalt composition, is marked by an elliptical, steep-walled crater ("caldera") attributed to sector collapse and decapitation of stratovolcano top at around 0.35 Ma, followed by phreatic and phreatomagmatic eruptions. The collapse is believed to have removed up to 1 km thickness of the former volcanic cone, exposing the pre-collapse monzodiorite core and its porphyry-style mineralization, and juxtaposed it against the shallower crustal levels producing and hosting epithermal-style ores (Sillitoe 1994). The Luise "caldera" is partly breached and opened towards the sea, facing a 10 km long submarine avalanche fan. A series of northward-dipping arcuate structures resulting from collapse provided conduit for ascent and mixing of hydrothermal fluids, and in combination with permeable units host the gold mineralization.

Ladolam gold deposit (Moyle et al., 1990; Kidd and Robinson, 2004; Rc₂₀₀₄ 442 Mt of ore @ 3.14 g/t Au for 1,389 t Au, plus past production) was discovered in 1982 by a combination of regional geochemical sampling and detailed examination of a coastal outcrop of silicified pyritic breccia (Fig. 5.9). This resulted in progressive discovery of five economic orebodies with diffuse outlines, delineated on basis of the cut-off grade (currently 1.7 g/t Au). The original lithologies in the deposit evolve from trachybasaltic, latitic, andesitic and trachytic lava flows and interlayered fragmentals in the basement, to a breccia complex in the center of the "caldera". The basement is intruded by equigranular biotite monzonite with minor leucogabbro, pyroxene diorite and biotite syenite. All rocks are pervasively altered, often beyond recognition. The early potassic alteration (biotite, K-feldspar, anhydrite), laterally grading to propylitization, is associated with intrusions and occurs as relics. This is overprinted by epithermal-

style adularia, illite-kaolinite clays, anhydrite, pyrite, marcasite and other minerals. Active geothermal activity (hot springs) at and near the surface are still active, and up to 300°C ground temperatures have been reached during exploration drilling and mining. This requires blowout prevention and a system of steam discharge relief wells.

The diffuse and overlapping orebodies are largely subhorizontal to gently dipping, hosted by permeable units adjacent to feeder faults, and confined by impermeable basement volcanics and clay horizons. Kidd and Robinson (2004) recognized two principal varieties of ore: 1) refractory K-feldspar, sulfide mineralization; here, submicron gold is held in very fine-grained sulfides of dark-gray sooty appearance that uniformly permeate the altered rocks and constitute up to 6% of the ore. Pyrite and marcasite are predominant, followed by arsenian pyrite and arsenopyrite. Secondary porosity due to alkaline leaching produced cavities of up to 10 m across in some orebodies; 2) low-sulfidation quartz, chlorite, bladed anhydrite with free gold in fracture veins and veinlets, developed through all deposit levels and attributed to mixing of magmatic and meteoric fluids. The near-surface ore is oxidized and residual gold is dispersed in "limonite" and clays.

Au,Ag,Pb,Zn,Cu,Sb,As,Hg-mineralized seamounts near Lihir Island: In 1994, a research party aboard the ship Sonne discovered widespread signs of submarine hydrothermal activity on southern flanks of Lihir Island, in depths ranging from 1000 to 1500 m (Petersen et al., 2002). The predominantly mafic, potassic to Na-alkalic submarine volcanics consist of alkali-olivine, clinopyroxene, and porphyritic phlogopite basalt, and one ejecta blanket with mantle-derived mafic to ultramafic xenoliths. The vent field near Edison Seamount contains several clam beds and dark sulfidic sediment together with methane anomalies.

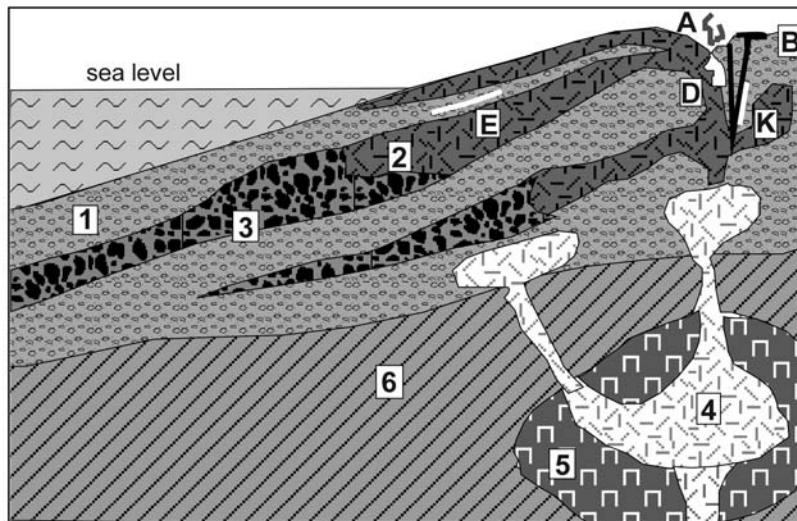
The largest and best studied **Conical Seamount**, 10 km south of Lihir, stands more than 600 m above its sea floor base, with top in a depth of 1050 m (Herzig et al., 1999). The small summit platform hosts a recent zoned alteration-mineralization system that combines features of subaerial low-sulfidation epithermal complexes and submarine "exhalative" systems. It also has the highest concentrations of gold and silver ever reported from the modern sea floor (average 26 ppm, maximum 230 ppm Au; average 216 ppm, maximum 1200 ppm Ag). The principal mineralization styles include a central clay, silica, and pyrite stockwork

with fine-grained Zn, Pb, Cu sulfides, gold and electrum, and late-stage fracture veins of amorphous silica (opal) with stibnite, realgar, orpiment, and Fe, Pb, As, Sb, Hg sulfides. The host volcanics are strongly argillized (illite, smectite, chlorite, sericite) with minor adularia, carbonates and silica.

5.5. Young subaqueous-hydrothermal (Fe)-Zn-Pb-Cu (and Ag,Au,~Sb,As) deposits (VMS, kuroko-type)

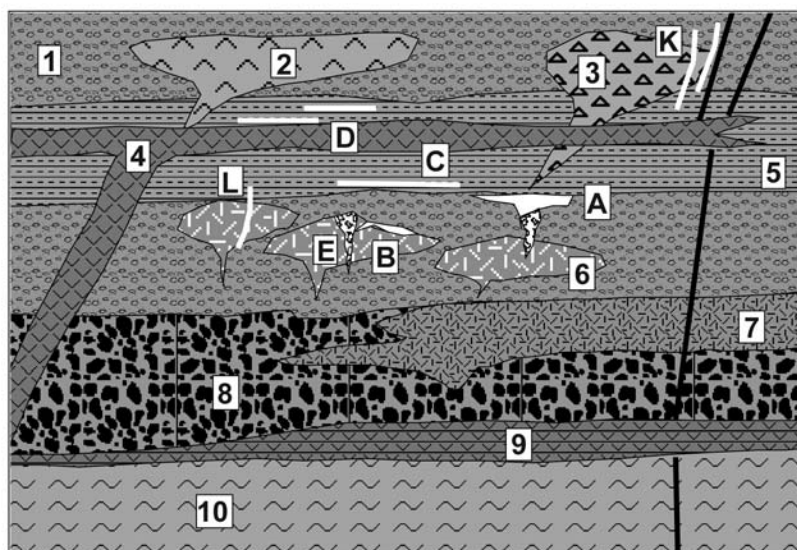
Volcanics-(associated) massive (Fe), Cu, Zn, Pb deposits (VMS or VHMS) in orogenic belts puzzled the 1900-1960 vintage geologists, who usually placed them into the granite-related replacement category. Alternative origins, such as the Schneiderhöhn's "submarine exhalative", remained a fringe opinion until the mid-1960s when the geologic community firmly embraced the synvolcanic-hydrothermal origin of such deposits at, or under, the sea floor. A special role in this change of ideas played the young (Miocene) Japanese kuroko-type deposits set in a relatively pristine and still active island arc complex, that are free from major post-depositional deformation and metamorphism that obscures the formational characteristics of most VMS in orogenic belts. Here are reviewed the "young" VMS deposits now accessible on land, whereas their older deformed counterparts appear in Chapter 8.

The synvolcanic-hydrothermal origin of VMS and kuroko deposits has been confirmed beyond doubt in the 1970s and subsequent years when similar type of ores has been found on the seafloor, some still actively forming. The first such ores were discovered in young intercontinental rifts (Red Sea; Chapter 12), followed by finds at oceanic spreading ridges (Chapter 4) and, finally, in island arc systems (especially back-arcs). Selected examples of the "still under water", active or recently active VMS-forming systems, are of paramount scientific interest but no sufficient quantitative data are available so far to identify a "giant" accumulation. So, regretfully, the reader is referred to the abundant, and rapidly growing literature (Herzig et al., 1990, 1993; Scott and Binns, 1992; Fouquet et al., 1993; Rona and Scott, eds., 1993; Halbach et al., 1993; Herzig and Hannington, 1995). "Shallow" (that includes depths between 0 and 2000m) submarine hot springs and hydrothermal deposits on the sea floor are tabulated, and partly described in Hannington et al. (1999).



1. Bedded trachyandesite, latite, shoshonite tuff
2. Ditto, lavas, domes, vent breccias
3. Hyaloclastite, debris flow
4. Active magma chambers
5. Earlier syenite, monzonite
6. Basement
- A. Fumaroles, sublimates of S, Se, traces Cu, Co, Pb, Zn, Au
- B. Hot spring systems: Hg, Au, Ag, As, Sb
- D. Pervasively altered volcanics, disseminated Au, Ag
- E. U impregnations in altered tuff
- K. Epithermal Au-Ag, Te

Figure 5.10. Young alkaline island arc centre (modelled after the Tabar-Feni group, Papua New Guinea), rocks and ores inventory cross-section from Laznicka (2004), Total Metallogeny Site G71



1. Felsic subaqueous tuff
2. Andesite
3. Dacite lava dome
4. Basalt/diabase dike, sill
5. Mudstone, shale
6. Rhyolite lava domes
7. Submarine rhyolite flow
8. Felsic subaqueous tuff breccia
9. Basalt flow
10. Basement: folded & intrusive rocks
- A. Kuroko-type VMS, massive lens and footwall stockwork
- B. Au-rich, pyritic VMS
- C. Bedded pyrite
- D. Bedded Mn (Fe)
- E. Stockwork Cu, Au
- K. Epithermal Au-Ag, Pb-Zn
- L. Epithermal Cu (Au) veins, stockworks, breccias replacements

Figure 5.11. Inventory diagram of a young basalt-andesite-dacite-rhyolite submarine volcanic-sedimentary association (comparable with the Green Tuff of Japan), intruded by felsic domes and mineralized by kuroko-type VMS. From Laznicka (2004), Total Metallogeny Site G 47

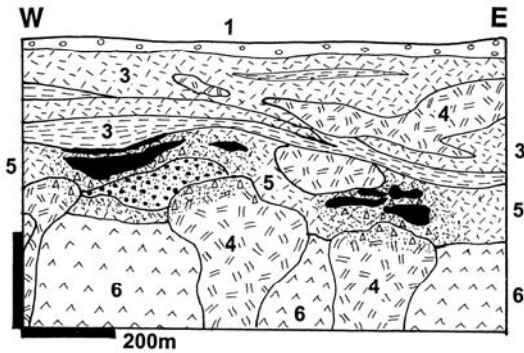


Figure 5.12. Simplified cross-section of the Matsumine and Shakanai kuroko deposits (Hokuroku district, Honshu). After Dowa and Nippon Ltd. materials; from LITHOTHEQUE No. 3306. 1. Pl-Q pumice, tuff, cover sediments; 2. Mi₂₋₃ post-ore diabase sill; 3. Mi₃ mudstone; 4. Mi_{2,3} subvolcanic "White Rhyolite" domes; 5. Ditto, caldera-stage submarine felsic volcanics and breccias; 6. Mi_{1,2} basalt domes & flows. Black: ~13 Ma VMS lenses, some with footwall stockworks, in alteration envelopes

Hokuroku (kuroko) Zn, Pb, Cu, Ag, Au district of Japan is an about 60 km long belt centered on the town of Ohdate in NW Honshu, in the Green Tuff region. This is the principal, and type, area of the Miocene "kuroko-type" massive sulfide deposits (Ishihara, ed., 1974; Ohmoto and Skinner, eds., 1983; Fig. 5.11., 5.12). Less important kuroko deposits also occur in Hokkaido and central Honshu. Up to one hundred of mostly small orebodies, with aggregate tonnage of about 140 mt at an average grade of 3% Zn, 1.5% Cu and 1% Pb, stored some 5.1 Mt Zn, 2.04 Mt Cu, 1.53 Mt Pb, 9,700 t Ag and 152 t Au, so Hokuroku qualifies as a Pb+Ag "giant district". The largest Hanaoka ore field stored 1.8 mt Zn @ 3.7%, 1.13 mt Cu @ 2.2% and 420 kt Pb.

The ores are hosted by an up to 5 km thick Miocene Green Tuff sequence of island arc volcanics, sediments and minor plutonic rocks. The initial, Lower Miocene magmatic arc formed on folded Permian carbonaceous phyllite and chert basement and it is dominated by subaerial andesite. By Middle Miocene the Hokuroku belt became a deep marine graben subparallel with the present Honshu coast, marked by eruption of subaqueous dacite flows, volcanic breccias and volcanoclastics (mainly mudstone) as well as subvolcanic "White Rhyolite" domes. The altered (albitized, silicified) domes and related breccias are intimately associated with the VMS deposits, some of which are rooted in them by their footwall stockworks, or occur on flanks and above. The felsic volcanism was

followed by tholeiitic basalt flows and more mudstone. The volcanics of norther Honshu suffered subgreenschist to lower-greenschist alteration (mostly zeolites, clay minerals, celadonite) responsible for the greyish-green coloration (hence "Green Tuff"). Much of the alteration is diagenetic (breakdown of volcanic glass and unstable silicates) and partly due to pervasive hydrothermal flushing by convecting sea water driven by the heat of buried intrusions, but is not directly related to mineralization.

The model Middle Miocene (~14-13 Ma) "kuroko-type" VMS have a sharp hangingwall contact against unaltered sediments or post-ore volcanics, marked by a siliceous unit that varies from quartz-hematite (jasper) to quartz-pyrite. Underneath is a massive sulfide body that ranges from broadly stratabound sheets to thick lenses and irregular, potato-shaped bodies. In most mining areas such bodies come in clusters, ranging from mere ore boulders to large masses (e.g. the Motoyama orebody in the Kosaka ore field stored 360 kt Zn, 176 kt Cu, 64 kt Pb). The upper portion of the massive sulfide body is dominated by dark sphalerite (marmatite) and galena in barite or silica gangue (black ore=kuroko in Japanese), whereas the lower part is mostly pyrite and chalcopyrite. The mineral transition is gradational and never complete. Most massive ore lenses have funnel-shaped stockworks and disseminations of pyrite and chalcopyrite in strongly silicified footwall in sericite, chlorite and clay envelopes. Masses of gypsum and anhydrite with erratic sulfides are sometimes positioned between the sulfide mass and footwall stockwork, but rarely contribute economic ore. Pyrite-only masses, some high in gold, occur rarely in comparable setting but all are small.

Popular interpretations place the sites of kuroko formation into underwater calderas, although explosive volcanism is unlikely in water depths exceeding 2-3 km, theoretically required for the ore formation. The ~300-90°C ore fluid was a convecting sea water leaching trace metals from the volcanic pile en-route and possibly also from the carbonaceous rocks in the basement. It was heated by small quartz diorite to granodiorite intrusions anticipated in depth. Copper (Osarizawa) and lead-zinc (Toyoha, Hosokura) vein ore fields formed on fringe of VMS-mineralized ore fields

5.6. Magnetite beach sands

Detrital Ti-magnetite is ubiquitous in beach sands along high-energy coasts of island arcs and andean margins with active, explosive andesitic volcanism as in Indonesia, the Philippines, Japan, Kuriles and Aleutians, New Guinea, Melanesia, New Zealand and others. There, magnetite is reworked from recently deposited ash (pyroxene, amphibole and sanidine crystals are still fresh). This is augmented and/or substituted by epiclastic magnetite released from eroded, weathering decomposed and softened tuffs and lavas although much of the "old" rock-

forming magnetite oxidizes to hematite and is dispersed. The proportion of magnetite in sand varies from several percent to 60% and although very low-grade sands were exploited in Japan during World War 2, there has been little sustained mining elsewhere except in New Zealand, where such sands represent the principal national iron source. The "black sand" beaches in the Taranaki and Auckland Provinces, North Island, store some 570 mt Fe @ 12-20% Fe and 54 mt Ti @ 2-5% Ti, hence a "large" metal accumulation (Williams, 1965).

6 Andean-type Margins

6.1 Introduction

Andean-type continental margins and their metallogeny are magnificently displayed in the cordilleras of South and North America, especially in the portion of the Andes between Ecuador and Santiago. The latter is thus a model of a long-lasting, persistent (for 570 million years; Petersen, 1999) convergent continental plate margin that is easy to delineate. This is not the case of the numerous older disrupted margins that have been repositioned and re-integrated since their origin; the Kazakhstan or Iran-Afghanistan Blocks (microcontinents?) come to mind. As this is a "convenience" chapter, the emphasis is on the rock- and ore-forming environments and processes that are characteristic of the model Andean arcs, that are: broad magmatic arcs developed over cratonward thickening continental crust; subaerial volcanism; terrestrial sedimentation in mountainous setting. Included here are components that normally belong to other chapters in this book when they are (almost) identical, such as the continental crust-influenced magmatism in mature (Japan-style) island arcs. In the ancient terrains influenced by dispersion and accretion in particular, it is virtually impossible to distinguish between magmatic arcs formerly attached to a continent and those in the island arc setting. Virtually all marine rock- and ore-forming environments (as in the marine forearc), even if attached to andean margins, are described in Chapter 5.

Limits of andean margin-based products against the intracrustal, collision and extension-driven magmatic systems are even more difficult to establish; they seem to be clear only in book titles (e.g. Seltmann et al., eds., 1994) but once inside the reader is faced with an overlap and interplay of all three major mechanisms associated with generation of mostly granitoid magmas (subduction, collision, extension-rifting) and non-uniform interpretations highly influenced by tradition and schools of thought. All three mechanisms tend to be represented in an average "continental margin" or orogenic belt ("orogen") as both terms are used interchangeably in the literature, depending on premise. Collision and rifting operated in subductive margins as well at a variety of scales and in several phases (e.g. during formation of the

basement over which an andean margin is superimposed), but as the emphasis in this chapter is on subduction-driven magmatism, the bulk of collision and rifting-assisted magmatic rocks are treated in Chapters 10 and 12, respectively. There is, however, a generous overlap.

The present chapter provides introduction to the overall andean metallogenesis, then it treats the predominantly supracrustal depositional environments and resulting rock associations. The intracrustal associations and ores (mostly granitoids) have been placed into Chapter 7 in order to subdivide the large body of "andean" information into more manageable parts (the andean margins have produced and host the largest number of ore "giants").

Origin of andean margins: An andean-type margins is a crustal domain believed produced from magmas melted above a subduction zone dipping under a continent, then emplaced into heterogeneous continental basement rock associations formed, over variable lengths of time, in a variety of environments. The subduction, and magma-generating principles are identical with the other form of subductive convergent margins, island arcs, treated in Chapter 5. There is an extensive literature about andean margins reviewed in general texts on geotectonics (Condie, 1982), petrology (Maaløe, 1985; Hess, 1989) and metallogeny (Sawkins, 1990), as well as in regional descriptions particularly of the two principal type areas: the Andes (Ericksen et al., eds., 1989; Corvalán, 1989; Mpodozis and Ramos, 1989, 1990; Lamb et al., 1997) and the North American Cordillera (McMillan, 1991; Gabrielse and Yorath, eds, 1992; Dawson et al., 1992; Burchfiel et al., 1992; Barton, 1996).

The single most important ingredient of andean metallogeny is magmatism (Harmon and Rapela, eds., 1991) which, in turn, drove hydrothermal systems. The magmatic melts generated closest to a moderately to steeply-dipping subduction zone in subcrustal depths are believed initially derived from the mantle (especially the asthenospheric mantle wedge), variously hydrated mafic oceanic crust, and oceanic sediments. They resulted in little evolved magmas with mantle signatures comparable with those at intra-oceanic island arcs (Chapter 5), like

low-K island arc tholeiite. These rocks are quite rare in andean arcs where they are most often found in accreted terranes originally formed in the island arc setting, and in intra-andean rifts. The dominant andean volcanic rock, progressively more potassic calc-alkaline andesite (Gill, 1991), is variably attributed to fractionation and crustal contamination of the initial mafic melt and/or melting within the continental crust. Since the melting at Wadati-Benioff zones starts at depths exceeding 100 km, the magma generation is spread over a thick column of materials that include between 20 and 70 km of continental crust. The mantle parentage of melts is thus strongest where the continental crust is thinnest. As, in a typical Andean margin, the magmatic arc is situated far inland where the continental crust is already quite thick, various theories have been advanced for bringing the mantle closer to the surface or increasing its contribution, so that the partially mantle-sourced melts could reach the top 2-5 km under the surface where the bulk of hydrothermal ores is produced. There, the mantle-derived trace metals can separate from the metaluminous magma and form ore deposits such as porphyry coppers. Recently, the slab window and other configurations, resulting from subduction of aseismic oceanic ridges or seamounts, have been most popular (Greene and Wong, 1989; Skewes and Stern, 1995). Other frequently debated topic bearing on magma generation in subductive margins is the "flat" (versus steep) subduction. The "flat" subduction of a low-dip downgoing plate, that reaches far into the continental interior (as far as the cordilleran foreland; Burchfiel et al., 1992), is of particular interest in metallogeny as it is believed associated with crustally melted acidic magmas and related Au, Mo, W, Sn, Li and other deposits.

Tensional episodes ("rifting") that overlap with, or postdate subduction in composite andean margins, are believed accompanied by basalt produced by partial melting of the mantle. Such magmas underplate and heat the continental crust where they trigger intracrustal melting and production of felsic magmas (Lipman, 1992b). Alternatively, the basaltic magma reaches the near-surface region where the continental crust is thin (attenuated) or absent, or where major tensional systems provide conduits. Coexisting basaltic melts and crustal acidic magmas produce bimodal

magmatic associations.

In the moderately to deeply-eroded andean margins the most striking feature is the widespread presence of granitoids, ranging from small stocks to regional batholiths (Pitcher, 1978). As the average 40 km thick continental crust has about the quartz diorite or granodiorite composition, these two plutonic rocks are also most common there. The metaluminous (I-type) granitoids are generally considered melted from mafic to intermediate intracrustal materials (earlier igneous rocks and metamorphics), the peraluminous (S-type) granites melted from former sediments. The crustally melted magmas are further influenced by the nature of the source region (mafic versus felsic), the degree of contamination, differentiation and fractionation, and the emplacement level.

Subenvironments in the andean margins

A typical Andean margin starts with a trench where the oceanic plate is subducted (Fig. 6.1). From there on, two end-members of margins can be distinguished: 1) "smooth" margins where, after a narrow submarine interval, the fore-arc is mostly subaerial, represented by mature rock associations of the older uplifted basement (in relation to the young, active volcanic arc) interspersed with young sedimentary basins. The type area is the Andean margin off northern Chile, although the narrow belt of Jurassic to Cretaceous marine sediments and largely mantle-derived volcanics (basalt, andesite) in the Coast Ranges, attributed to an intracrustal rift, provides conditions for magma and ore generation comparable with the following category; 2) composite margins where one or more generations of successively accreted terranes broaden the width of what some call transitional crust, before the edge of the contiguous continent is reached. The broad fore-arc often consists of islands separated by marine waterways before the contiguous land is reached, and the magmatic arc usually overprints an accreted terrane or forms along boundaries of several terranes. This is well developed along the Cordilleran margin off British Columbia. Both end-member patterns are complicated by transcurrent faulting that produce margins entirely of their own as in southern California, and multiphase crustal extension capable

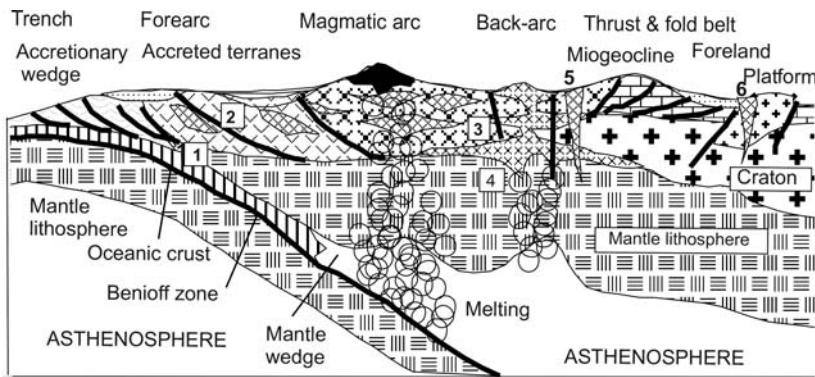


Figure 6.1. Diagrammatic cross-section of an andean-type convergent continental margin showing the usual sub-environments. Numbers indicate magmatic families: 1. Oceanic (MORB basalts, diabase, gabbro, differentiated mafic-ultramafic intrusions, Na-series basaltoids (spilite) and dacite (keratophyre); 2. Island arc suites: rare boninite, arc tholeiite & bimodal sets, low-K calc-alkaline; 3. Andean arc suite: average-K calc-alkaline granitoids (quartz diorite, granodiorite, monzogranite), I- and S-type; 4. Rift-related tholeiitic basalt, diabase, gabbro; granite and rhyolite, syenite and trachyte, foidites; 5+6. Anorogenic small intrusions: K-granite & rhyolite, peralkaline granite & syenite, foidites, kimberlite and lamproite

of doubling the width of the andean margin (or orogenic system). Western United States between Denver and San Francisco is an outstanding, well described example (Burchfiel et al., 1992).

An active magmatic arc has, ideally, the form of a row of regularly spaced active stratovolcanoes (as in the High Andes and the High Cascades), separated by non-volcanic sectors attributed to non-subduction. Most volcanic arcs have migrated over the time and narrow, focussed arcs grade into a diffuse pattern of scattered volcano-plutonic centers distributed over large areas. The extensive Laramide (Cr₃-Pc) magmatic province in the western United States measures 1000 km across the E-W axis and it controls a number of "giant" porphyry Cu-Mo deposits (Miller et al., 1992; Keith and Swan, 1996). In the Andes, there have been two subparallel magmatic arcs marked by active volcanoes throughout much of the Phanerozoic history (Petersen, 1999): the Main Andean and East Andean arcs. The 200 km space between both arcs suffered crustal extension with ascent of basaltic magmas. This and similar terrains are sometimes called (continental) back-arcs, or interarcs. There are superficially similar, although mostly submarine, extensional grabens in the forearc setting as in the Jurassic-Cretaceous Cañete Basin of western Peru and comparable basins in Chile. Along the North American Pacific margin these are substituted by predominantly oceanic, ophiolitic, island arc and backarc lithologies in a number of accreted terranes (Saleeby, 1983; Gabrielse and Yorath, eds., 1992).

Magmatic arcs are emplaced into a variety of

basements ranging from uplifted fragments of Precambrian granitoids and metamorphics (Laramide intrusions in SW Arizona-N Sonora) through Phanerozoic eugeoclinal volcanic-sedimentary suites of accreted terranes to miogeoclinal sediments, to comagmatic volcanics (Boulder Batholith, Montana). The Sierra Nevada batholith of California is interpreted as a deep (depth of emplacement ~25 km under the J-Cr paleosurface) root of a magmatic arc, intruded mostly into a collisional suture (Cowan and Bruhn, 1992). The area continentward from the magmatic arc and its foundation of uplifted folded continental basement progresses into a thrust and fold belt dominated by miogeoclinal carbonates and clastics, bordered by foreland depressions (basins) against the craton. Some forelands (the Tertiary Wyoming, Montana, to South Dakota province; Christiansen, Yeats et al., 1992; Sierras Pampeanas in Argentina; Jordan and Allmendinger, 1986) comprise alternating basement uplifts and fault-bounded (mostly continental) sedimentary basins.

This ideal picture is complicated by the presence of earlier generations of now inactive magmatic arcs, metamorphism, major transcurrent and/or extensional faults, terrane displacements, uneven erosion and prolonged history. In the western United States Tertiary extension superimposed on a long-lasting andean margin has produced a variety of contrasting styles such as metamorphic core complexes (Crittenden et al, 1980), detachments, uplifted plateaux (Colorado Plateau), basin-and-range extensions (Great Basin mostly in Utah, Nevada and Arizona; Eaton, 1982; Lister and Davis,

1989; Gans et al., 1989), predominantly flood basalt-filled plateaux and grabens (e.g. Snake River), bimodal volcanic systems (Yellowknife) and rift grabens. All are blessed with a rich and varied metallogeny that includes many "giants" (Table 6.1).

The resulting continental margin (without accreted terranes) is thus a mixture of basement outcrop, magmatic arc rocks of several generations exposed at various emplacement levels from volcanic to plutonic, generally narrow zones of littoral, shelf to slope sedimentary basins, and a variety of usually small continental sedimentary basins. The width of the magmatic arc is influenced by the dip of the Benioff zone. Steep dips result in narrow, focused arcs; flat to subhorizontal dips make up broad, diffuse areas of migrating volcanic and/or plutonic belts as in the "Laramide" west-central United States. The subduction-related magmatism terminates when subduction stops or reaches a great depth, and after a transitional period it is sometimes substituted by magmatism related to extension (rifting) or collision.

A young andean-type margin has a distinct magmatic polarity, although where accreted terranes are present this can be locally disturbed by the presence of "misfit" crustal types such as sialic microcontinents among the predominantly oceanic and island-arc basaltic and andesitic lithologies. The basement (pre-subduction) lithologies usually progress, away from the ocean towards the craton, from ophiolite, oceanic tholeiite, tectonized rocks in the accretionary wedge, arc andesite, volcanic turbidite and other "eugeoclinal" supracrustals, with or without comagmatic plutonic rocks, into stable margin (miogeoclinal) shales, sandstones and carbonates. These are intruded by collisional granites and floored by medium to high-grade metamorphics. In the American Cordillera, at the latitude of British Columbia, the intermediate volcanics-dominated Pacific-side "eugeocline", assembled from accreted terranes, strikingly contrasts with the Rocky Mountains "miogeocline" (stable western continental margin of North America), but similar contrast is not apparent in the central Andes. The British Columbia "eugeocline", moreover, contains abundant ophiolite and alpine serpentinite occurrences, especially along the collisional sutures that separate the accreted terranes; these are virtually missing in the central Andes. The two contrasting (eu- and miogeoclinal) assemblages do not correspond to the pair of two major types of adjacent geosynclinal basins as modelled by Marshall Kay, Jean Auboin and others, as they are not contemporaneous. The usual

progression of lithofacies across convergent margins, however, still corresponds to the pattern recognized by Hans Stille in the 1940s and then developed by Bilibin (1951) as a framework for organization of the major metallic deposits. Although the geosynclinal model is now recognized as flawed, the empirical recognition of lithofacies-controlled metallogeny had enhanced mine finding in the 1950s and beyond, especially in the former U.S.S.R.

To summarize, the usual compositional polarity (ocean to craton) of the andean basements has a parallel in the polarity of subduction-related magmatic rocks formed during the convergent margin evolution. The pre-accretion magmas and rocks emplaced into the accreted oceanic/immature arc suites as in the Coast Batholith of British Columbia and in the Klamath Mountains of Oregon and northern California, are Na and Ca-rich tonalites-trondhjemites with some gabbros. The large, deeply eroded batholiths that mark the position of persistent magmatic arcs like Sierra Nevada are predominantly of metaluminous granodiorite with some quartz diorite and granite; the comagmatic volcanics, where preserved, are mainly andesite with some dacite and minor rhyolite. Smaller and usually younger differentiated plutons are mostly metaluminous and increasingly potassic granodiorite-quartz monzonite whereas rhyolitic and rhyodacitic caldera-related and ignimbritic volcanism predominate, together with subcrustally derived basalts, in the "back-arc" setting over extended thick continental crust progressing into the foreland. Peraluminous adamellite and granite are in or close to migmatitic and gneissic projections of thickened continental crust as in the metamorphic core complexes, and their volcanic equivalents (rhyolites) are relatively rare. Alkaline rocks are most common in small volcano-plutonic centres scattered on the fringe of magmatic arcs especially in the foreland, or they are members of the extensional (rifting) regimes superimposed on the andean margins after subduction termination.

6.2. Metals fluxing and metallogenesis

Andean-type margins, that can be credibly delineated, contain the greatest proportion of the world's copper and molybdenum resources, the bulk of which resides in giant and supergiant deposits (Laznicka, 1999). The North American Cordillera alone stores some 230 Mt Cu and 12 Mt Mo in 3 Mo "supergiants", 25 Mo "giants" and 23 Cu "giants". Gold, silver, zinc and lead follow.

Table 6.1. Examples of Meso-Cenozoic (late Triassic to Quaternary) "giant" deposits in the andean-type continental margin of the North American Cordillera, arranged by sub-environments

Sub-environment	Ore type	Deposit/district	Age	Metals content
Island/isthmus magmatic arc ¹	calc-alk porphyry Cu	Petaquilla, PN Cerro Colorado, PN	O11 Mi3	Cu 14.4m; Mo 437k; Au 305t Cu 13.3m; Mo 199k; Au 155k
Forearc				
intrusion into turbidites	calc-alk porphyry Cu	Pebble, AK	~38	Cu 3.06m; Au 404t
hydrothermal over ophiolite and turbidites	silica-carbonate Hg	New Almaden, CA	Pl	Hg 19k
	ditto	New Idria, CA	Pl	Hg 19k
	ditto	Mayacmas, CA	Pl	Hg 13k
volcanic-sedimentary basin	Besshi-type VMS?	Windy Craggy, BC	Tr3	Cu 4.16m; Co 88k
	ditto	Greens Creek, AK	Tr3	Ag 16k (Zn 3.36m, Pb 1.23m)
accretionary complex	meso-epithermal vein	Donlin Creek, AK	70	Au 777t
Accreted terranes ²				
pre-andean island magmatic arc	diorite/syenite porphyry Cu-Au	Galore Creek, BC	J1	Cu 2.81m; Au 169t
	calc-alk porphyry Cu	Schaft Creek, BC	J1	Cu 2.73t; Mo 227k; Au 182t
	ditto	Gibralter, BC	J1	Cu 2.88m
	ditto	Highland Valley BC	J1	Cu 9.0m
Magmatic arcs				
in comagmatic volcanics	calc-alk porphyry Cu porphyry, epith. vein	Safford, AZ Butte, MT	Cr3-T 78-73	Cu 7.4m Cu 10.4m; Ag 21.8k; Mo 201k; As 143k; Bi 1.8k
in Precambrian basement	porph/vein/placer Au	Fairbanks distr., AK	Cr,T	Au 433t
	calc-alk porphyry Cu	Ray, AZ	Pc	Cu 8.5m
	ditto	Bagdad, AZ	Cr3	Cu 6.4m; Mo 192k
	ditto	Cananea, MX	Cr3	Cu 17.1m; Mo 320k
	mesothermal vein	Coeur d'Alene, ID	Cr3-T	Ag 34k; Pb 8.035m
in volc-sedim-granite mix	calc-alk porphyry Cu	Ajo, AZ	Cr3-T	Cu 4.06m
	ditto & skarn	Pima (Tucson) AZ	Pc	Cu 16.9m
	ditto	Yerington, AZ	J	Cu 6.0m
	ditto	Bisbee, AZ	130	Cu 4.4m
	calc-alk porphyry Cu	San Manuel-AZ	70	Cu 8.2m
	ditto	Globe-Miami, AZ	Pc	Cu 8.1m
	porphyry Cu-Mo	Taurus, AK	Cr3-T	Mo 315k; Cu 2.25m
	ditto	Casino, YT	71	Mo 162k; Au 324t; Cu 1.7m
	stockwork W-Mo	Logtung, BC	Cr1	W 191k; Mo 69k
	stockwork Mo	Buckingham, ID	86	Mo 752k
	ditto	Thompson Cr., ID	88	Mo 324k
	ditto	Endako, BC	138	Mo 292k
	ditto	Hudson Bay Mt. BC	63	Mo 164k
	ditto	Quartz Hill, AK	30-27	Mo 1.204m
	ditto	Alice Arm, BC	55-49	Mo 138k
	ditto	Adanac, BC	75-71	Mo 121k
	ditto	Cumo, ID	52-45	Mo 742k
	ditto	Mt. Tolman, WA	60-50	Mo 396k
	ditto	Red Mountain, YT	87	Mo 187m
	Climax-type Mo	Mount Hope, NV	38	Mo 510k
	shear Sb-scheelite-Au	Yellow Pine, ID	T	Sb 85l; Au 250t
	Carlin-type Au	Getchell, NV	39	Au 435t
	ditto	Twin Creeks, NV	42	Au 340t
	epith. bonanza Au Ag	Guanajuato, MX	O1	Ag 38,850t; Au 175t
	ditto	Zacatecas, MX	O1	Ag 26k
	ditto	Pachuca, MX	20.3	Ag 46.5k; Au 215k
	ditto	Tayoltita, MX	43-40	Ag 15k; Au 304t
	ditto	Comstock, NV	13	Ag 7260t; Au 312t

Table 6.1. Continued

Sub-environment	Ore type	Deposit/district	Age	Metals content
in miogeocline (sediments)	epi-meso stockw. Au	Round Mt, NV	O1	Au 441t
	porphyry-skarn Cu	Bingham, UT	38	Cu 27.4m; Mo 820k; Au 1570t; Ag 9500t
	ditto	Ely, AZ	111	Cu 4.88m; Au 200t
	ditto	Santa Rita, NM	Cr3-T	Cu 6.5m
	ditto	Morenci, AZ	67	Cu 17.7m
	mesoth. veins/replac.	Bingham, UT	38	Pb 2.41m (Zn 1.65m)
	ditto	Park City, UT	36-33	Ag 7868t; Pb 1.215m
	ditto	Leadville, CO	O1	Ag 7961t; Pb 1.3m
	ditto	Tintic, UT	31	Ag 8100t; (Pb 913k)
	ditto	Santa Eulalia, MX	O1	Pb 3.11m; Ag 13.6k
	ditto	Fresnillo, MX	O1-Mi	Ag 13093t
	skarn, mesoth. vein	San Martin, MX	O1	Ag 12k; (Zn 5.0m; Cu 1.0m)
	meso-epithermal vein	S. Francisco, MX	Eo-O1	Ag 13k; (Zn 2.5m)
	scheelite skarn	Cantung, NWT	91	W 116k
	ditto	Mactung, NWT	97	W 235k
	Carlin-type Au	Carlin Trend, NV	~39	Au 3328t
	ditto	Cortez-Pipeline NV	Eo-O1	Au 289t
	ditto	Jerritt Canyon, NV	Eo-O1	Au 470t
	replacement stibnite	Wadley, MX	O1?	Sb 90k
	bertrandite tuff	Spor Mountain, UT	6	Be 24k
Shears, sutures, fault zones	(syn)orogenic Au	Juneau, AK	57-54	Au 369t
	ditto	Grass Valley, CA	J-Cr	Au 330t
	ditto	Mother Lode, CA	J-Cr	Au 803t
	ditto, placers	Sra Nevada Fh., CA	T-Q	Au 1770t
	ditto	Klondike, YT	T-Q	Au 380t
fault disseminated Hg	Pinchi Lake, BC	Eo-O1	Hg 9.5k	
Foreland intrusion in basement uplift	Climax-type Mo	Climax, CO	30	Mo 2.7m; W 281k
	ditto	Henderson, CO	28	Mo 1.243m
	ditto	Mt. Emmons, CO	18	Mo 372k
	ditto	Rico, CO	4	Mo 124k
	ditto	Questa, NM	25-24	Mo 400k
	epithermal Au-Te	Cripple Creek, CO	O1	Au 817t
	dissem. rare metals	Round Top, TX	36	Zr 1.76m; Li 784k; Th 320k
	sedimentary basins	Grants, NM	Cr	U 390k V 160k
	ditto	Wyoming Foreland	O1-Q	U 212k
	ditto	Piceance Bs., CO	Eo	Al 3.18b (low-grade)
Rifts, volcanism, hydrotherm	metalliferous fluid	Salton Sea, CA	Q	Ag 10.9k; Zn 6.0m
	mantos in tuff	Santa Rosalia, MX	Mi-Pl	Cu 3.92m; Co 287k
Basin-and-Range extension	disseminated Hg	McDermitt, NV	18-15	Hg 17,250t (U,Li,Cs)
	bedded lacustr. borate	Kramer, CA	Mi2	B ₂ O ₃ 50m
	playa brines	Silver Peak, NV	T-Q	Li ~1.0m

1. Refers to Panama Isthmus; 2. Ores in accreted terranes formed during island arc residence, during docking, and during subduction after accretion. Tonnages: t=tons, k=kilotons, m=million tons, b=billion tons

Minor metals that are significantly to exclusively related to the Andean margins include bismuth, tellurium, beryllium, lithium, boron and others. Tungsten and tin dominate metallogeny of the collisional/extensional systems (Chapter 10), but

three of the world's ten largest tin deposits (Llallagua, Potosí, San Rafael) sit in the middle of the East Andean magmatic arc. Most of the Andean margin ore metals are moderately to strongly incompatible (with the rock-forming silicates) and

characteristic of the intermediate, metaluminous calc-alkaline magma series with local sprinkling of peraluminous and alkalic systems.

The bulk of the andean margin ore deposits are members of a metal fluxing system (metallogene) that spans several crustal levels, from the deepest levels where magmas are generated and charged with trace metals to the supergene products at the surface. It is important, especially for research purposes and for greenfields ore search, to consider such systems as a whole and this philosophy is followed here in terms of magmatic families and metal associations. Many one-of-a-kind ore deposits, however, are not members of conventional lithogenetic systems or their membership has not yet been recognized. A brief review of the various environments and rock associations common in subaerial andean arcs follows.

6.2.1. Ores in predominantly continental sediments

Most sedimentary basins in the Andean margins are fault controlled and a high proportion is influenced by contemporaneous explosive volcanism that supplies detritus, and drives hot springs sometimes discharging into lakes. There is a great variety of basins controlled by climate (hot versus cold; humid versus arid) and environment (talus, alluvial fans, glacial, fluvial, lacustrine; marine environments are considered in Chapter 5). Metal accumulations that include several "giants" are the result of 1) "normal" sedimentation of ore substance in, usually, lake basins; 2) physical wasting and gravity transfer of detritus, including an ore component, from adjacent, exposed "primary" deposits; 3) chemical transfer of metals in solution, leached from nearby primary deposits; 4) diagenetic precipitation of metals released from volcanic glass during devitrification, and unstable minerals (e.g. olivine, augite, sanidine) during hydration; 5) introduction of dissolved metals in hot spring brines discharging into a basin; 6) combination of several processes.

1) "Normal" sediments of depositional basins: Several major nonmetallic deposits in the andean margins formed by chemical precipitation from lake or ground waters. They include the extensive deposits of young natural nitrates in the Chilean Atacama "salars" (Ericksen, 1993; Ericksen and Salas, 1989; over 10 bt of NaNO₃ produced, 2.5 bt of "caliche" with 7% NaNO₃ remains), large deposits of soda (trona and nahcolite) in the Eocene lacustrine Green River Formation in Wyoming (Bradley and Eugster, 1969; some 100 bt plus of

Na-carbonates), and large reserves of oil shale in the same formation in several basins in Colorado. The **Piceance Basin near Rifle, Colorado**, contains a 170 m thick oil shale section, distributed over some 640 km², with accessory dawsonite. This is an authigenic Na-Al carbonate that contains 18.7% of acid-extractable aluminum, possibly recoverable as a by-product of oil shale processing. If so, the Al resource in the Piceance Basin is about 3.18 bt Al (Smith and Milton, 1966).

2) Ores in materials derived by physical wasting from primary deposit: glacials and placers:

Continental glaciation is thought of as an ore-destructive process eroding, denuding and dispersing ore substance from earlier deposits although, occasionally, glacial materials "gently" buried bedrock deposits and enhanced their preservation (e.g. some gold placers in the "black slate" association in the Lena-Bodaibo region, and elsewhere in Siberia; Bilibin, 1955). Glacial drift is sometimes enriched in metalliferous component to such an extent that it constitutes an economic ore. The ore metals are present as separate mineral grains or mineralized boulders and several glaciogenic deposits are known worldwide (not all are in the andean margins). Examples: uraninite in drift over the Key Lake U deposit, Saskatchewan; scheelite-bearing talus on flanks of the Felbertal deposit, Austria; high-grade Cu ore embedded in "live" glacier and in talus under Kennecott, Alaska; cassiterite-bearing moraine at **Rodeo, Bolivia**; and others (read review in Laznicka, 1985a, p. 740). Many of these deposits have been mined in the past and the yield recorded jointly with their bedrock parents as, considered separately, they were of the small to medium-size except for Rodeo that may hold as much as 300kt of low-grade Sn (Putzer, 1976). The "giant" **La Quinoa-Au** orebody has gold dispersed in 50-100 m thick glacial moraine gravels discovered, in 1997, in the "supergiant" Yanacocha ore field in Peru (420 t Au, 2,923 t Ag @ 0.8-1.6 g/t Au; Bartra, 1999). The gold resides in Fe-hydroxides, relics of pyrite and Cu sulfides, and in quartz veinlet clasts derived from oxidized high-sulfidation ore upslope. Only the material that can be traced to its source in the Cerro Yanacocha area is of ore grade (the cut-off grade is 0.35 g/t Au), the rest of the moraine is barren.

The "**pallacas**" at foot of **Cerro Rico** in Potosí, Bolivia, are aprons of debris flow and talus derived from the richly Ag-Sn mineralized summit and flanks of the mountain. They store 9,520 t Ag in a resource of 80 mt @ 119 g/t Ag, plus tin values (Bartos, 2000). This is in addition to the unknown

quantities of silver produced in the past. Elsewhere, especially in Canada, Scandinavia and Russia, the metalliferous glacials are thought of more as indicators of possible orebody presence up-drift (Outokumpu-Cu and several other deposits have been discovered by glacial boulder tracing), than as sites of an economic orebody. But one never knows.

Fluvial and partly glaciofluvial processes of pickup, transport, enrichment and redeposition of ore particles from weathering-disaggregated, oxidized and softened primary orebodies to form placer deposits, is a more efficient process credited with generation of several giant accumulations of resistate minerals such as gold or cassiterite. Not all Au/Sn placers are, however, in the andean margins. In the arid regions the first site where ore particles come to rest are alluvial fans and piedmont gravels, but only small deposits have been recorded (e.g. Jicarilla, New Mexico). Gulch placers that fill valleys of small creeks in terrains with a well developed humid regolith grade into more extensive but lower-grade auriferous terrace gravels; these are scattered throughout the North American Cordillera (Boyle, 1979). In parts of Alaska and Yukon placers are restricted to the lands that escaped Quaternary glaciation so that the earlier regolith had been protected from glacial erosion. The aggregate tonnage of several placer goldfields in the northern Cordillera has reached the giant magnitude in the Fairbanks Goldfield, Alaska (275 t Au) and Klondike (Dawson City) Goldfields in the Yukon (390 t Au). Farther south, giant alluvial placer goldfields are in the Sierra Nevada Foothills of California (1,770 t Au), Colombia (1,500 t Au; especially the Chocó area), San Antonio de Poto, Peru (501 t Au). Elsewhere, gold placers at least partly sourced in the andean-type margins, include the Central Kolyma district 400 km north of Magadan, Russia (2,600 t Au). The bulk of the placer gold came from the syn-orogenic (mesothermal) lode systems like the Mother Lode in California (Chapter 10), so collision and transcurrent faulting, widespread throughout the world, controlled the ore formation and the deposits are not unique to the andean margins. Gold placers derived from primary deposits related to the andean-type magmatism are mostly small.

3) *Metals leached from primary deposits and precipitated from meteoric waters:* Primary ore deposits subjected to oxidation and erosion in humid environments soon lose most of their more soluble and mobile metals, leaving behind residuum that is sometimes metalliferous (Chapter 13). In arid regions where evaporation greatly exceeds

precipitation most of the metalliferous leachate moves downslope and through permeable rocks as groundwater. Metals like copper may precipitate to form "exotic" deposits. Many porphyry coppers in Chile have one or more such deposits in alluvial fans and piedmont gravels downslope from the metal source, sometimes covered by ignimbrite. Several exotic deposits are "large", and Mina Sur (formerly Exotica), downslope from the "super-giant" porphyry Cu-Mo Chuquicamata, is itself a "giant" (310 mt @ 1.17% Cu for 3.63 mt Cu content). Some exotic deposits like the chrysocolla deposit Sagasca in Chile (Rc 400 mt @ 0.5-2% Cu) and partly Tesoro (175 mt @ 0.72% Cu) do not have a known major primary source. The Chilean exotic deposits have been recently reviewed by Münchmeyer (1996) and those attached to giant porphyry coppers are briefly described below.

4) *Diagenetic precipitates of metals released from volcanic glass and ash during devitrification:* Many subaerial volcanics, especially the rapidly quenched rhyolites and their pyroclastics or flood basalts, retain their "frozen" trace metal content that failed to partition into the magmatic-hydrothermal fluid phase. The "left behind" trace metals could later be released, transported and reconcentrated by both hypogene and supergene processes. Here we consider the case where metals released during diagenetic devitrification of volcanic glass and/or groundwater leaching from decomposing volcanics precipitate in porous tuffs, argillized/zeolitized volcanoclastic "lake beds", in adjacent/subjacent alluvial fan or "wash", or in any other porous or receptive material nearby. The metals usually did not migrate far from source. The potential for formation of a significant deposit correlates with the syn-magmatic trace metal enrichment in the source rock, many of which formed in the rift stage postdating subduction. Mafic to intermediate source rocks (basalt, andesite) contribute Mn to form small Mn oxide deposits (e.g. Three Kids near Las Vegas, Nevada); highly fractionated rhyolites may contribute U, Li, Be, Rb, Cs. The actually mined infiltrational deposits of this type include the small Anderson U mine in Arizona hosted by Miocene carbonaceous volcanic mudstone and, especially, some of the "sandstone uranium" deposits around the world. In the South Texas Coastal Plain district the U infiltration was sourced in Upper Eocene through Lower Miocene vitric volcanoclastics; the uraniumiferous lignites of South Dakota and adjacent Montana were mineralized by U leached from Miocene air-fall tuff. The large U deposits in the San Juan Basin of New Mexico (Laguna and

Ambrosia Lake) comprise dispersed U oxides and silicates precipitated on humate reductants (review in Dahlkamp, 1993; Chapter 13). Elsewhere, the diagenetically released then fixed trace metals provide metalliferous rock intervals but not yet economic orebodies like the Li, Cs and U enriched volcanoclastics that fill the McDermitt Caldera in Nevada/Oregon, described below. This category overlaps with the following mineralization and distinction cannot often be made.

5) Mineralized "lake beds" and "salars": This is a counterpart of the submarine-exhalational deposits (VMS) in the marine domain. Here, the ore minerals precipitated in shallow continental lacustrine setting or in wet tuff-filled depressions. The metals-carrying spring (brine) temperatures here were much lower, the hydrostatic pressures close to zero. The selection of metals and nonmetallic precipitate is also very different from the deep marine systems. As in the previous category, most of the ore metals accumulated in the "lake beds" were derived by leaching extremely fractionated volcanics like topaz rhyolite by both descending waters subsequently heated in depth, or by ascending meteoric waters. In contrast with category 4 the metal source rocks are often buried, hence not apparent at the surface. Hot springs that are part of epithermal systems are reviewed later (Section 6.3.1).

Recent (active) playa lakes and "salars" that have accumulated ore metals or nonmetallic minerals believed introduced into the system by hot brines include the lithium "giants" in Chile, Argentina, Bolivia (Erickson and Salas, 1989) and Nevada. The soda, potash and boron deposit **Searles Lake in California** (50 mt B_2O_3 ; Smith, 1979) also contains 150 ppm Li_2O , ~100 ppm As and 32 ppm W dissolved in brine and stored in the salts. The calculated tungsten content there is about 68 kt (a "large" accumulation), probably leached from the basement known for scheelite skarns in the area. The United States' playa deposits coincide with the Basin-and-Range extension postdating the Cordilleran subduction.

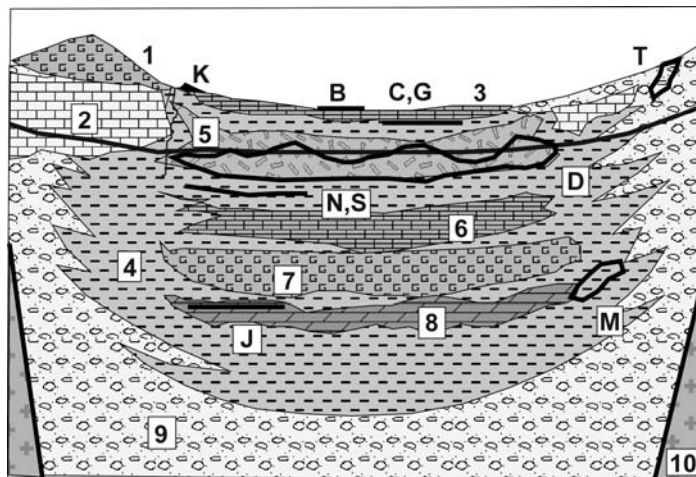
Salar de Atacama is a large playa lake between the Andean Main Range and Cordillera Domeyko, in northern Chile. It is a basin filled by Cenozoic lacustrine volcanoclastics interbedded with evaporites (halite, gypsum, thenardite), that has an over 250 m thick nucleus of almost pure halite (Ide and Kunasz, 1990). The top of the halite mass is

porous, karsted by repeated dissolution and reprecipitation by infrequent rain. The playa that is mostly dry at the surface is a reservoir of saline brine anomalous in lithium (0.15% Li) and potassium (1.8% K). This brine body alone is credited with a resource of 4.6 mt Li. Twice this amount of Li may reside in dilute brines in the rest of the salar. The source of Li is clearly in the anomalously Li-enriched Late Miocene to Holocene acidic tuffs and derived sediments in the area (29-89 ppm Li, maximum 493 ppm Li) that release Li into groundwater. The water is transported by short ephemeral mostly underground streams into the basin where it undergoes rapid evaporation; more Li-enriched brine is added from scattered hot springs. The El Tatio Geysir north of the basin contains up to 47 ppm Li. The **Clayton Valley Li** brine deposit in Nevada, the largest source of Li in the United States, has a comparable origin. Fresh rhyolite flows and tuffs there contain up to 228 ppm Li and this has been reduced to about half in the altered and weathered rocks, indicating transfer of Li into the undrained basin. The resource there is of the order of 2 mt Li.

The "giant" Miocene **Boron-Kramer borate deposit** is a fossil lacustrine evaporite in the Mojave Desert of California. It is a roughly lenticular, 100-150 thick mass of crystalline borates, interbedded with volcanic mudstone and resting on a vesicular basalt flow. The core of the orebody is composed of sodium borates borax and kernite (P+R ~200 mt @ 25% B_2O_3) enveloped by a Ca-borate fringe of colemanite and ulexite (Barnard and Kistler, 1956). J.F. Siefke (oral communication, 1982) interpreted the borate deposit as an evaporite precipitated in a shallow permanent (not playa) lake saturated by Na and B; these elements were supplied by nearby volcanic-heated thermal springs. There are no metallic occurrences except for occasional realgar on mudstone fractures and minor stibnite in the hangingwall. The folded and deformed probable equivalent of Kramer, the borate deposit Tincalayu in NW Argentina, has an estimated resource of about 5 mt of borax (Erickson, 1993).

6.2.2. Ores in contemporaneous and "young" subaerial volcanics

Active volcanoes are highly visible and dynamic systems that we might rightly associate with ore formation, but much of the action takes place at the



1. Gypsum sand dune; 2. Pedogenic calcrete; 3. Salts crusts on playa surface; 4. Playa mud; 5. Brine-saturated mud, displacive crystals and nodules of evaporite minerals; 6. Massive salts body; 7. Nodular to massive gypsum; 8. Lacustrine dolomite; 9. Conglomerate, alluvial sand, talus; 10. Bedrock.
B. Authigenic alunite; C. Li in hectorite, bentonitic clay; D. Li, B, As, W anomalously enriched in subsurface brine; G. Pyritic or S-rich euxinic horizon enriched in Li, As; J. Bedded magnesite; K. Mn, W in spring aprons; M. Bedded borates in clay; N. F, (U) in reworked felsic ash; S. Mn oxide infiltrations; T. Oxidic U infiltrations in surficial playa sediments.

Figure 6.2. Diagrammatic inventory of sediments and economic minerals in young arid playas in subaerial volcanic areas. Some sediments under the surface may have precipitated in perennial salt lakes. Ore types D (Li) and M (B) have known "giant" counterparts. From Laznicka (2004), Total Metallogeny site G204

subvolcanic and plutonic levels where some epithermal and magmatic-hydrothermal ores form; these are described below. The direct ore forming potential of young surficial volcanism is small to negligible, although the magnitude of metal fluxes is sometimes remarkable (read below). Hedenquist (1995) believes this is due to the lack of efficient trapping mechanism. The volcanic landforms, as seen at the surface, may influence or control ore deposition in depth so their understanding is important. Sillitoe (1977) and Sillitoe and Bonham (1984) reviewed the metallic mineralization affiliated with subaerial volcanism with emphasis on controls of the epithermal and porphyry deposits in neo-volcanic terrains. In the Andes and to a lesser degree in the Cordillera, young (Neogene and Quaternary) volcanics cover a large area of a densely mineralized "basement" (over 300,000 km² in the Andean hinterland; Ericksen et al., 1987) and being largely post-mineralization they are considered a hindrance to exploration. Ericksen et al. (1987) think otherwise and they suggest a "deeper" look at the young eruptive centers that may conceal buried orebodies, using geochemistry, geophysics and geological investigations.

Stratovolcanoes

These are distinct, often imposing symmetrical conical edifices produced by repeated eruptions from a central vent (Cas and Wright, 1987). They comprise steeply dipping pyroclastics interstratified with lava flows. The most common rocks are andesite, basaltic andesite, dacite. Some stratovolcanoes have small summit calderas,

parasitic craters and diatremes. Dikes, breccia columns, pipes and small intrusive domes and stocks appear at the subvolcanic level, the top of which is sometimes exposed in glacier-dissected volcanoes as on the Puna plateau in Bolivia and Argentina (Sillitoe, 1975). The volcano interiors also come close to the surface in explosively decapitated volcanoes as determined in the Lihir Island, Papua-New Guinea (Chapter 5). In some volcanoes large masses of rocks, especially in the vent area, are acid sulfate altered and permeated by sublimed or melted sulfur. Such sulfur is locally mined (e.g. from the Ollagüe volcano in Bolivia; ~50 mt of sulfur ore), but there are not yet economic deposits of metals formed in active volcanoes.

In the humid climatic belt as in Indonesia, Japan or Colombia many craters support small acidic lakes associated with active gold precipitation. In the recently active Osorezan Volcano at the northernmost tip of Honshu, a lake filled by metalliferous sediment developed in a shrinking crater from hot springs that accompany hydrothermal eruptions. The ore minerals in the lake sediments are vertically zoned from the earliest and deepest Pb-Zn sulfides through Au, Hg, Te, Pb, Sb, As sulfides to As-S; Hg-S; and S (Izawa and Aoki, 1992). The highest metal values there are 0.65% Au, 0.55% Hg, 1.05% Te, 0.37% As. The ore minerals have precipitated from heated waters with neutral pH and variable salinity, so they are the top of a low-sulfidation epithermal system. The Galeras Volcano in Colombia, in contrast, emits up to 360° hot fumaroles near margin of the active central vent. The fluids are acid waters rich in CO₂,

SO₂, H₂S and HF mixed with up to 80% of magmatic water vapor (Goff et al., 1994). These fumaroles intensely alter the andesite, itself anomalous in trace gold, to the acid sulfate assemblage, and deposit Au, Cu, As, Ag and Se-rich sublimates. The magmatic fluid itself contains about 0.07 g/t Au and it releases some 0.5 kg of gold per day to the environment (also 1.89 t As!). It is believed that the fumarolic activity indicates a gold-pyrite-enargite deposit actively forming (or in the process of degradation) in the subsurface. Acid hot springs simultaneously active at flanks of the volcano also carry and precipitate gold, but the concentrations are an order of magnitude lesser.

It is believed that active formation of epithermal (especially high sulfidation), porphyry and skarn

deposits is also taking place under the vent area of the Lascar stratovolcano in northern Chile (Matthews et al., 1996), in depths between 300-500 m (Sillitoe, 1973, 1976). Notwithstanding ores, some active volcanoes dissipate significant quantities of metals into the atmosphere or hydrosphere. The White Island, New Zealand, releases 110 t Cu and 36 kg Au/year; Mount Etna in Sicily annually wastes 580 t Cu, 4700 t Zn and 84 kg Au (Hedenquist, 1995).

Table 6.2. contains a selection of "giant" ore deposits interpreted as having formed in stratovolcanoes. Island arc examples (Chapter 5) are also included. Fig. 6.3. provides inventory of the various ore types in and around stratovolcanoes.

Table 6.2. Selected "giant" deposits interpreted as having formed in stratovolcanoes.

Age, Ma	ore deposit	ore type	size	references
Mi	Cerro Casale, Chile	diorite porphyry Au-Cu	3.1 mt Cu, 837 t Au	Vila & Sillitoe, 1991
Eo	Recsk, Hungary	porphyry/high sulfid. Cu	5.3 mt Cu	Baksa et al., 1980
Mi3	Brad (Barza), Romania	low sulfid. Au, porph. Cu	?1000 t Au	Ianovici & Borcoş 82
Mi3	Roşia Montană, Rom.	ditto	501 t Au	O'Connor et al., 2001
Mi	Roşia Poieni, Romania	porphyry Cu	4.0 mt Cu	Ianovici & Borcos 82
0.9-0.35	Ladlam, Lihir, PNG	porphyry & epithermal Au	1389 t Au	Kidd, Robinson 2004
4.25	Tampakan, Philippines	porph. & high-sulf. Cu, Au	7.18 mt Cu, 287t Au	Middleton et al. 2004

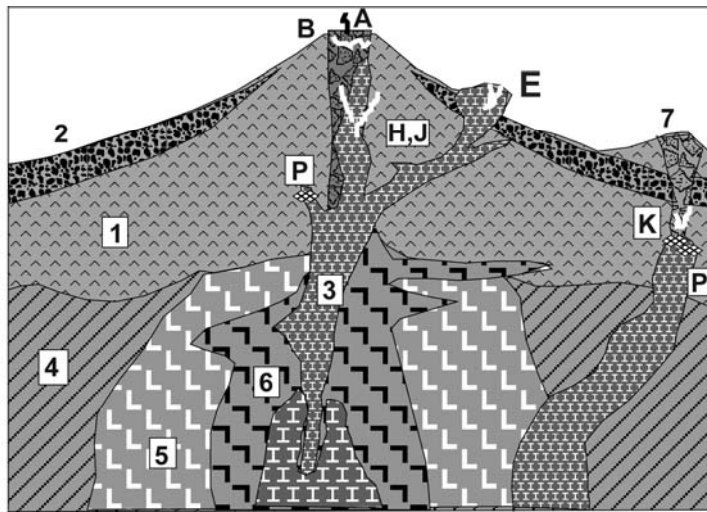
Table 6.3. Selected "giant" deposits interpreted as having formed in calderas

age, Ma	caldera/volcanic field	deposit	ore type	size	reference
26-18	Latir, New Mexico	Questa	porphyry Mo	400 kt Mo	Lipman 1992a
73-69	Silver Bell, Arizona	Silver Bell	porphyry Cu	800 kt Cu	Lipman 1992a
73-69	Sierrita, Arizona	Pima group	porphyry Cu	16.9 mt Cu	Lipman 1992a
26-25	Mt. Jefferson-Toquima, Nevada	Round Mountain	epithermal Au	441 t Au	Rytuba 1994
16-15	McDermitt, Nevada & Oregon	McDermitt & others	epithermal Hg infiltr. Li, U	17,250 t Hg	Rytuba & Glanzman 1979
Mi	Banska Štiavnica, Slovakia	Banska Štiavnica Hodruša	epithermal Au, Ag, Pb, Zn	?333 t Au 6000 t Ag	Lexa et al. 1999
8	San Cristobal, Bolivia	San Cristobal	epithermal Ag	14,900 t Ag	Kamenov et al., 2002
3.7	Tavua Caldera	Emperor	epitherm. Au, Te	338 t Au	Colley, Flint 95
J3	Tulukuyev Caldera, Transbaikal, Russia	Streltsovka-U	vein, stockw. U	280 kt U	Chabiron et al. 2003

Calderas

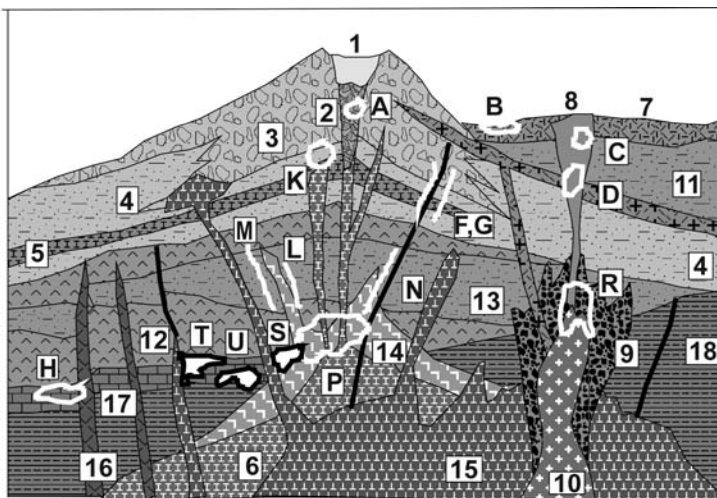
Calderas are composite circular or elliptical structures formed by collapse of volcanic edifices into voids created by magma evacuation from shallow magma chambers (Fig. 6.4). The widely quoted model of ash-flow calderas of Lipman

(1984, 1992a) has three stages. Stage 1 is marked by precollapse volcanism where clustered andesitic-dacitic stratovolcanoes grow over small high-level intrusive stocks. In Stage 2 vertically zoned magma chamber (felsic magma on top) rose and produced ash-flow eruptions that spread laterally and fill the depression resulting from caldera collapse. The



1. Andesite lava, pyroclastics
 2. Lahars
 3. Granodiorite, quartz latite porphyry
 4. Continental crust basement
 5. Diorite, diorite porphyry
 6. Quartz diorite, quartz diorite porphyry
 7. Diatreme and vent breccia
- A. Metalliferous fumarolic precipitates
 B. Native sulfur, Se, sublimates, lavas
 E. Mn oxide hot spring veins, crusts
 H. Epithermal Au-Ag veins, breccias
 J. Ditto, Pb-Zn-Ag
 K. High sulfidation Cu-As-Au masses, veins in advanced argillic alteration
 P. Porphyry Cu (Au,Mo)

Figure 6.3. Predominantly andesitic/dioritic stratovolcano showing mineralization types. H, K and P ore types may include "giant" equivalents. From Laznicka (2004) Total Metallogeny site G38

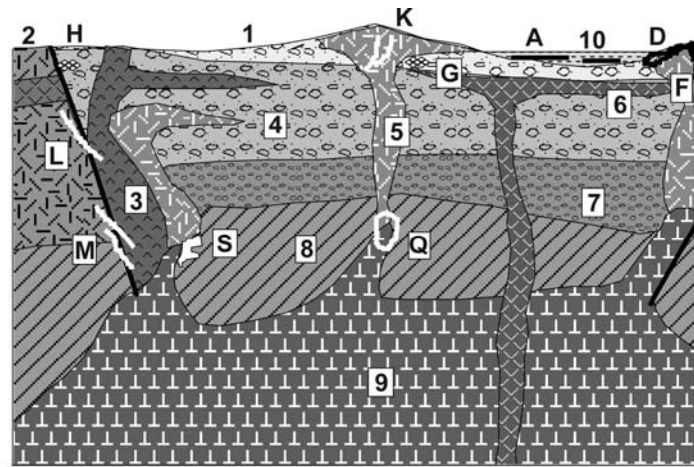


1. Crater lake; 2. Vent breccia;
3. Rhyodacite tuff breccia; 4. Ditto, tuff & lahar; 5. Rhyodacite flow;
6. Granodiorite porphyry; 7. Rhyolite tuff, ignimbrite; 8. Maar and diatreme;
9. Carapace breccia; 10. Granite porphyry; 11. Dacite tuff; 12. Andesite flows; 13. Andesite pyroclastics;
14. Quartz diorite porphyry; 15. Quartz monzonite porphyry; 16. Gabbro;
17. Limestone; 18. Hornfelsed shale, sandstone; A. Fumarolic Au in sulfidized vent breccia; B. Mn oxides;
- C. Fluorite, U veins, disseminations; D. Ditto, Au and fluorite; F. Low sulfidation Au-Ag; G. Ditto, Pb-Zn-Ag; H. Micron-size Au disseminations; K. High sulfidation Cu, Au; L. Mesothermal Pb-Zn; M. Ditto, Au-quartz veins;
- N. Ditto, Cu sulfide veins; P. Porphyry Cu-Mo; R. Stock-work Mo; S. Cu skarn; T. Zn-Pb skarn; U. Zn-Pb carbonate replacement (with jasperoid).

Figure 6.4. Complex, highly evolved stratovolcano built on mature continental crust. Ore types F, G, H, K, L, M, P, R, S, T, U may include "giant" equivalents. From Laznicka (2004) Total Metallogeny site G49

earlier volcanoes cave into the depression and caldera walls collapse to produce breccias that interfinger with the acid tuff fill. Stage 3 is marked by uplift and resurgence above rising magma chamber and magma intrudes the cogenetic volcanic pile in its roof. Small felsic volcanic domes also form. The central intra-caldera uplift is surrounded by a ring of caldera-fill sediments (moat). Hydrothermal activity and mineralization are widespread late in this cycle and are controlled

by ring fractures, radial faults and extensional grabens, as well as by high porosity units such as pumice or breccias. Epithermal deposits of Au, Ag, Pb, Zn, Cu and other metals form over intermediate calc-alkaline intrusions. Sn, Be, U are related to silicic, potassic, peraluminous and peralkaline magmas. Massive, breccia-forming to stockwork magnetite with actinolite, diopside and apatite, mined from the still recognizable caldera at El Laco in northern Chile (Frutos and Oyarzún, 1975) and



1. Felsic tuff (non-welded) and moat fill; 2. Ignimbrite; 3. Andesite porphyry; 4. Andesite tuff; 5. Resurgent domes of rhyodacite, rhyolite, quartz latite; 6. Basalt flow and dike; 7. Felsic tuff; 8. Basement rocks; 9. Quartz monzonite or granodiorite stock; 10. Volcanic lake beds. A. Impregnations, sinters of Mn, Li, Cs, U, Be in lake beds; Ah=hematite. D. Magnetite lavas; F. Subvolcanic magnetite vents, breccias; G. Alunite; H. Cinnabar disseminations, opalite; K. Epithermal U veins; L. Epithermal Au-Ag veins, breccias; M. Ditto Pb,Zn,Ag,Au and replacements in basement; Q. Stockwork Mo; S. Pb-Zn replacements in basement carbonates.

Figure 6.5. Model of a resurgent caldera on mature continental crust, showing mineralization types. Types H, K, L, M, Q, S have known "giant" equivalents. From Laznicka (2004) Total Metallogeny site G48

Table 6.4. Selected examples of "giant" deposits associated with domes and dome complexes.

Age	deposit	ore type	tonnage	references
Mi	Oruro, Bolivia	epithermal Sn-Ag veins, replac.	8.5 kt Ag; Sn	Sillitoe & Bonham, 1984
Mi	Apuseni Mts. Romania	epithermal Au	?2000 t Au	Ianovici et al., 1976
20 Ma	Llallagua, Bolivia	vein/porphyry Sn	2 mt Sn	Grant et al., 1980
13 Ma	Cerro Rico, Bolivia	porphyry Sn/epithermal Ag veins	84 kt Ag 1 mt Sn	Bartos, 2000
12 Ma	Yanacocha, Peru	high-sulfidation disseminated Au	1804 t Au	Turner, 1999
19	Monywa, Myanmar	porphyry & high-sulfidation Cu-Au	4.1 mt Cu	Win & Kirwin, 1998

Table 6.5. Selected examples of "giant" deposits associated with diatremes

Ore deposit & type	age & tonnage	diatreme details	references
Cresson (Cripple Creek, Colorado) low sulfidation Au	32-28 Ma 817 t Au	heterolithic vent breccia topped by maar filled by lacustrine sediments	Kelley et al., 1998
Colquijirca, Peru; high-sulfidation Cu-Au & Pb-Zn-Ag mantos	Mi; 8.2 mt Zn, 2.26 mt Pb	dacitic diatreme-dome complex intruded carbonates and clastics; high-sulfidation bedded replacements of sediments	Bendezú et al. 2003
Cerro de Pasco, Peru; pyritic Pb-Zn-Ag replacement, Cu-Ag veins	Mi; 8.6 mt Zn, 20.2 kt Ag	dacitic diatreme-dome complex intruded limestone, black phyllite, clastics; high-sulfidation endocontact, exocont. replac.	Einaudi, 1977
El Teniente, Chile; porphyry Cu-Mo breccias, stockwork	4.6 Ma; 94 mt Cu, 2.5 mt Mo	post-ore diatreme funnel filled by matrix-supported breccia is enveloped by mineralized brecciated andesite	Skewes & Stern, 1996
Rio Blanco-Los Bronces, Chile; porphyry Cu-Mo in breccias	6-4.6 Ma; 59 mt Cu	series of diatreme and hydrothermal breccia bodies in roof of buried stock	Skewes & Stern, 1996
Roşia Montană, Romania; low-sulfidation Au veins, disseminations	Mi-Pl; 501 t Au	diatreme-dome complex within a stratovolcano; disseminated Au in heterolithic breccia, fracture veins	O'Connor et al. (2001)
Acupan Au mine, Philippines; low-sulfidation Au veins	1 Ma; 200 t Au	Balatoc altered diatreme above dacite plug, intersected by gold-quartz veins	Cooke et al. 1996
Trepča Pb-Zn-Ag mine, Kosovo	T; 3.45 mt Pb, 5100 t Ag	Pb-Zn-Ag-Bi carbonate replacements at contact of heterolithic breccia pipe	Janković, 1980

from the moderately eroded Oligocene Chupaderos caldera near Durango, Mexico (Lyons, 1988) are interpreted as ore lavas or injected melts. Alternative interpretations prefer metasomatic replacement

Economic metal accumulations are practically absent from recent calderas and in older, eroded calderas and cauldrons most hydrothermal ores greatly postdate caldera collapse and relate to intrusions that are not genetically connected with the caldera cycle (Rytuba, 1994). Table 6.3. has a selection of caldera-associated "giant" deposits.

Ignimbrite fields (sheets)

Densely welded subaerial ash-flow sheets issued from calderas or fissure eruptions blanket large areas in young volcanic fields at andean-type margins and remain, uneroded, in terrains as old as Mesoproterozoic (e.g. the Gawler Range Volcanics, South Australia; these, however, are in intracratonic extensional setting). The volcanics vary in composition from alkalic rhyolite to andesite, but calc-alkaline rhyolite to rhyodacite are most common in the andean setting. The rapid emplacement and cooling from viscous magmas denied magmatic fluids the opportunity to condense and separate, hence the trace metals content once present in magmas remains virtually undepleted. Some ignimbrites derived from highly fractionated magmatic systems, and even more small associated subvolcanic domes, stocks and laccoliths, contain large low-grade resources of lithophile metals, perhaps of future economic interest (e.g. Zr, Rb, Li, Th, Y, Cs, Be in the Round Top Laccolith, Texas; Price et al., 1990; read below). In addition to their role as future resource, metalliferous ignimbrites may have served as a source rock releasing trace metals to superimposed metallogenesis. They also provided cover to various mineralizations that formed at paleosurface such as oxidized and enriched porphyry coppers; this prevented removal of the bedrock deposits by erosion.

Lava and subvolcanic domes and dome complexes

Viscous (rhyolitic and dacitic, some andesitic) lavas extruded at the surface form lava domes and stubby flows; Showa Shinzan on Hokkaido (in an island arc setting; Chapter 5) is one of the best contemporary examples whose birth has been observed and recorded in detail. There, synvolcanic metalliferous fumaroles deposited mineralogical quantities of Cu, Fe, Zn, Pb, Ag, Au in sublimates.

Many if not most Cenozoic domes are, however, volcanic crater plugs, stubs of solidified lava or plugs of non-vented magma, exhumed by erosion from their soft and easily erodable surroundings (Cas and Wright, 1987). The main metallogenetic role of domes is in providing brittle dilations to be subsequently filled by hydrothermal ores. Such dilations are abundant in expanded and brecciated dome carapaces and in systems of brittle fractures. Selected "giant" deposits associated with domes or dome complexes are in Table 6.4.

Maars, tuff rings, tuff cones, diatremes

Maars are volcanic structures resulting from phreatomagmatic explosive eruptions. They are most common in the intracontinental extensional (rift-related) settings (Chapter 12). Ore-related maars as a 2nd or 3rd order structures associated with stratovolcanoes and composite volcanic fields have also been interpreted, mostly from island arcs (e.g. Eddie Creek-Au, Papua New Guinea; Sillitoe and Bonham, 1984). At the Kawah Ijen Volcano in easternmost Java (Delmelle and Bernard, 1994), the extremely acidic and minerals-rich crater lake (pH 0.4) triggers occasional phreatic eruptions. The lake is rich in native sulfur spherules that enclose sulfides (enargite), suggesting active ore deposition in depth. In the American Cordillera, maars are associated with the post-subduction Basin-and-Range extension and intracratonic rifting. Mineralization, when present, formed at the subvolcanic level in diatreme breccias the exposure of which required deeper levels of erosion. It is difficult to distinguish true phreatomagmatic diatremes from explosive breccia columns excavated and infilled, under vents, by magmatic gases or expanding hydrotherms. Selection of "giant" deposits associated with diatremes and breccia columns is in Table 6.5.

General subaerial volcanics as hosts to ores

The majority of hydrothermal deposits in the andean-type margins relies on local structural and sometimes lithological controls that are unrelated to physiography in place during the active stage of volcanism. The ores, usually younger to much younger than the active volcanism, are about equally common in the andean volcanics as in the pre-volcanic basement: the high-level ores (hot spring and epithermal) are more frequent in the volcanics, the intermediate level ores like mesothermal veins and replacements prefer the basement. The porphyry deposits are in between. In

many mineralized areas the youngest volcanics are post-ore and although they conceal ore occurrences they also protect the earlier-formed deposits from being eroded away.

In a typical, long-lasting andean-type paleovolcanic terrain as in the Mexican Sierra Madre Occidental (Clark et al., 1979), several thick stacked volcanic series comprise predominantly high-K calc-alkaline andesitic ash-flow tuffs intercalated with andesite and dacite flows and domes, with local rhyolitic flow domes and ignimbrite sheets. Basalts are rare, although flood basalts are dominant in the bimodal rift association that often postdates the subduction-related volcanism as in the western North American Basin and Range Province. The andean volcanics are intruded by comagmatic dikes and small stocks of quartz diorite (dacite), granodiorite and quartz-monzonite porphyry and by granitoid plutons. The youngest generations of volcanics are unaltered and unmetamorphosed but the older successions at the bottom of the volcanic pile tend to be overprinted by the sub-greenschist to greenschist mineral assemblages (zeolites, albite, chlorite, conspicuous epidote, carbonates). This "propylitization" is attributed to load metamorphism or metasomatism in the roof of granitoids that can have a regional extent. Zones of silicification and argillization along faults are also common and in the humid tropics the former are often selectively exhumed. In the Sierra Madre and elsewhere the predominant ore type are Au-Ag or Pb-Zn-Ag fissure veins.

6.2.3. Ores in ancient continental margin volcanics, predominantly andesite

In a convergent margin with more than 500 million years permanence like the Andes the distinction between "young" and "old" rocks is difficult to make. The deformed, Mesozoic and older rock associations should be more properly treated as part of the "eugeoclinal orogenic belts" (Chapter 8). As this would lead to much repetition, many of the older "andinotype" volcano-plutonic features, that include granitoids and related ores, are uniformly reviewed here regardless of age.

Cu-dominated "mantos" in/near andesite

Although the Andes and especially Chile are famous for the huge porphyry coppers, the region is also a type area for various Cu, Fe, Mn and Au mineralizations in (meta)andesites that are neither "model" epithermal or mesothermal deposits precipitated from channelled, external fluids

(described below), nor the VMS's treated in Chapters 4, 6 and 8. All these deposits are genetically enigmatic and their unifying empirical features are predominantly andesite-dominated host lithology, disseminated "manto"-like orebodies, and a belief that the andesite was an essential component of the mineralization system (most likely as a metal source, as unaltered equivalents of the host volcanics have above-clarke trace Cu contents), rather than an accidental host (Vidal et al., 1990). Most of the deposits are small to medium-size but there are at least three Cu and Au "giants" and some future discovery potential remains. In the review literature examples of the andesitic deposits are scattered under numerous headings.

The "manto-style" (=stratabound blanket or sheet) bodies of disseminated Cu sulfides are hosted by massive (meta)andesite lavas (Lo Aguirre, Chile; ~200 kt Cu); occur along basaltic andesite lava flowtops (Buena Esperanza, Chile; ~300 kt Cu plus); are disseminated in laharc breccias and conglomerates (Sustut, British Columbia; 352 kt Cu; Wilton and Sinclair, 1988) or are in detrital sedimentary rocks interbedded with andesites (Cerro Negro-Diablo field, Chile; ~250 kt Cu; Camus, 1985). The host volcanics are low-grade metamorphosed with abundant epidote, albite, chlorite, sometimes prehnite and zeolites and there is an abundant evidence of synmetamorphic copper outmigration during burial or thermal (in granitoid roof) metamorphism. There is some similarity with the Keweenawan-style native Cu deposits described under the "rifts" heading (Chapter 12).

Boleo Cu>Co, Zn, Mn "manto" deposit near Santa Rosalía, BS, Mexico, is a lonely giant in this category (Wilson, 1955; McInnes, 1995). The old Boleo concession produced 760 kt Cu and 20 kt Co from 19 mt of high-grade ore (4.8% Cu). Recent work has established a large low-grade resource of 167 mt @ 1.25% Cu, 0.075% Co (or 445 mt grading 0.71% Cu, 0.06% Co and 0.69% Zn) for a total endowment of 3.92 mt Cu and 287 kt Co, with a by-product Zn, Mn and Ag. This enigmatic deposit consists of five stratabound, persistent ore horizons within a 11 x 3 km large, NW-SE elongated area subparallel with the Gulf of California (Fig. 6.6). The host unit, Mi₃ to Pl₁ Boleo Formation is 140 m thick on the average and consists of several cycles of interbedded shallow marine andesitic ash-fall tuff and tuffaceous conglomerate, floored by a deltaic? polymictic basal conglomerate, litharenite and gypsum. This unit

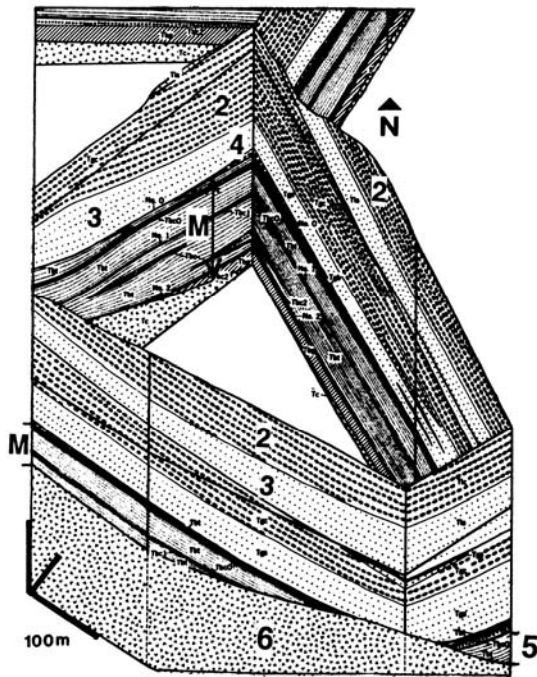


Figure 6.6. Boleo Cu > Co, Zn deposit, Baja California Sur, Mexico; cross-section detail from Wilson (1955); also LITHOTHEQUE No. 947. M: ore horizons of Cu sulfides dispersed in montmorillonitic tuff; 2, 3. Pl sandstone, conglomerate; 4. Pl Upper Boleo Fm., limestone and gypsum with sandstone lenses; 5. Lower Boleo Fm., latite to andesite tuff over nonmarine basal conglomerate; 6. Mi subaerial andesite & basalt flows, tuff, minor volcanoclastics

rests unconformably on subaerial tholeiite flows of the Miocene Comondú Volcanics. A full cycle starts with the conglomerate or with manganeseiferous basal limestone and changes upward into bentonitic tuff or tuffaceous sandstone. The copper-bearing horizons are located at base of the tuff units at contact with the conglomerate. The very finely disseminated ore minerals: chalcocite with minor chalcopyrite, bornite, covellite, native copper, pyrite, sphalerite and galena, interspersed with Mn-oxides (cryptomelane), are virtually invisible in the dark-coloured, unoxidized host rock despite the high grade. The low-grade material is even more elusive. Chrysocolla and malachite, replacing the sulfide grains and coating fractures and bedding planes, makes the oxidized ore easier to recognize. The Boleo origin is puzzling and attributed to late Tertiary intracratonic rifting responsible for opening of the Gulf of California.

The following category of Cu deposits is (meta)andesite-hosted, at least partly of the "manto" style, but the ore emplacement has been recently

attributed to magmatic-hydrothermal or convecting fluids emanating from, or driven by, intrusions that need not be comagmatic with the host andesite. The "giant" **El Soldado-Cu** "manto" deposit in Chile (P+Rv 200 mt @ 1.4% Cu for 2.8 mt Cu; Boric et al., 2002) has recently been interpreted as a stratabound mesothermal replacement of a Lower Cretaceous calc-alkaline basalt-rhyodacite unit interbedded with black shale and volcanic arenite. The vein-like discordant and zoned pyrite, chalcopyrite, bornite, chalcocite and hematite bodies with calcite, albite, K-feldspar and chlorite gangue follow faults in a brittle shear system, where they intersect the favorable strata.

In the "large" **Punta del Cobre** ore field south of Copiapó, Chile (~1.8 mt Cu @ 1.5% Cu; Leveille and Marschik, 1999) Cu-sulfide mantos in albitized flows of Neocomian andesite, and fracture veins/breccias in dacite domes, are considered epigenetic. The volcanics are members of the highly productive, andesite-dominated transitional marine-continental Jurassic-Cretaceous facies of Central Chile attributed, like the Casma-Huarmey belt in Peru, to andean margin extension (aborted marginal basin on thinned continental crust; Mpodozis and Allmendinger, 1993). This facies belt can be traced along the Andean coast from central Chile to the Ecuador border. The central Peru segment of this belt (Cañete Basin) contains several groups of Cu sulfide "manto" deposits in thermally metamorphosed volcanics and sediments (e.g. Cerro Lindo-Cu; Raúl and Condestable-Cu in the Mala group, SE of Lima; ~600 kt Cu). These deposits are intermediate between the Chilean "mantos in andesite" and skarn, and distinct for the presence of alteration amphibole ("amphibolitic Cu-Fe skarns" of Vidal et al., 1990). The large Marcona magnetite deposit in southern Peru is credited with 1.5 Mt Cu resource, much of which is unrecoverable.

There are a number of hydrothermal copper sulfide deposits predominantly associated with andesites, but also with more acid volcanics and small plutons, that are transitional between the mineralized mantos, "volcanic" porphyry coppers, skarn and VMS. They range from stratabound disseminations in altered volcanics to bedding-discordant stockworks and zones of disseminated sulfides. Lahanos and Murgul in Turkey (~600 kt Cu) and Sam Goosly (Equity) in British Columbia (~500 kt Cu, 1980 t Ag) are examples of the "large" deposits. Candelaria and Mantos Blancos in Chile are the "giants".

(La) **Candelaria-Cu, Au**, a recently discovered "giant" deposit also near Copiapó, Chile (Ryan et al., 1995; Rv 366 mt of ore @ 1.29% Cu, 0.26 g/t

Au, 4.5 g/t Ag for 4.72 mt Cu content) is a transition between an "andesitic manto" and skarn, with some porphyry-Cu features (Fig. 6.7).

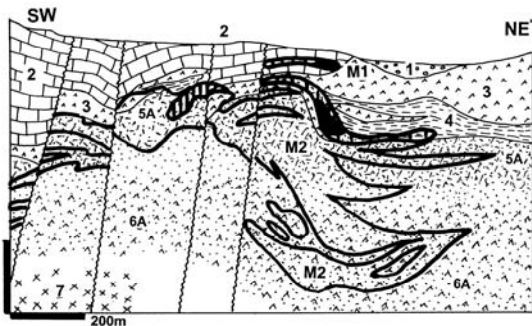


Figure 6.7. Candelaria Cu-Au deposit, Tierra Amarilla, Chile; cross section from LITHOTHEQUE No. 2427, modified after Ryan et al. (1995). 1. Q fluvial gravel; 2. Cr hornfelsed and skarned limestone, volcanoclastics; 3. J3-Cr1 basaltic andesite; 4. Ditto, andesite tuff and volcanoclastic member; 5. Ditto, altered massive dacite; 6. Ditto, altered lower andesite member; 7. Cr buried batholith (hypothetical); M1. Marginal Cu ore replacing metasediments, solid black is massive pyrrhotite; M2. Main orebodies: chalcopyrite with magnetite "mantos" in early K-silicate (mainly biotite) altered andesite, overprinted by Ca-Na alteration synchronous with Cu

It has been popularized in the recent literature as member of the loosely defined IOGC (=iron oxide-copper-gold) "family" (Sillitoe, 2003). Since its discovery in 1985 by Phelps Dodge it has become an exploration model and its equivalents eagerly sought in the Andes and beyond. Candelaria is hosted by Lower Cretaceous andesite and tuff topped by limestone and fine-grained volcanoclastics. All these rocks are thermally metamorphosed (hornfelsed and skarned) in the roof and 1 km from contact with the Copiapó Batholith. The top of the mineralization system consists of magnetite-amphibole skarn in calcareous meta-tuff with pyrrhotite, pyrite and chalcopyrite. The garnet skarn occurrences grading to marble are virtually free of ore. The main ore reserves, at greater depth and stratigraphically lower, are in biotite, K-feldspar and amphibole-altered andesite and tuff and have the form of stacked subhorizontal bodies of chalcopyrite disseminated in and veining magnetite-replaced breccias. The 119-116 Ma mesothermal deposit is broadly contemporaneous with granodiorite of the Copiapó Batholith but it is not clear whether the batholith was the source of the

ore components or merely a heat source driving convecting hydrotherms with copper sourced from the andesitic volcanic pile.

Mantos Blancos Cu-Ag deposit 45 km NE of Antofagasta (Rc 405 mt of ore @ 1.5% Cu and 17 g/t Ag containing 4.6 mt Cu and 7,650 t Ag; Rodriguez, 1996) is a hydrothermal replacement and disseminated semi-stratabound Cu sulfide deposit in pervasively albite, quartz-altered Triassic acidic meta-volcanics intruded by Jurassic andesite, dacite and microgranite. The Triassic host rocks are members of a thick, rift-controlled continental volcanic redbeds sequence (Flint et al., 1993) and they crop out in the Miocene-Holocene Salar basin (Atacama evaporitic playas); this may explain the thick, Cl-rich oxidation zone dominated by atacamite and chrysocolla.

Fe oxides-Cu-(Au) deposits in andean setting

Metals other than copper associated with andesites and forming manto-type orebodies include manganese and iron. Small Mn deposits of this style are moderately common around the world (e.g. in the northern flanks of Sierra Madre, Eastern Cuba; ~3 Mt Mn; in the Coquimbo Province Mn belt, Chile; ~7.5 Mt Mn) but they are all minor. The iron deposits ("neither a skarn, nor a vein") in the Coast Ranges of central Chile (e.g. El Romeral, El Tofo, Algarrobo) are also small, but have recently received attention as one of the possible links in explaining the origin of the "IOGC" ore deposit "family" (Hitzman et al., 1992). They are predominantly replacement masses of magnetite in mylonitic andesite and diorite in and close to the dip-slip and strike-slip Atacama fault system (Brown et al., 1993). The Early Cretaceous Fe ores formed in depths close to the brittle-ductile transition, in a deformational regime contemporaneous with development of the magmatic arc.

The "giant" copper deposit **Manto Verde (Mantoverde)** and satellites (Vila et al., 1996; Rc 230 mt of oxide ore @ 0.55% Cu and 0.11 g/t Au, plus >400 mt of sulfide ore @ 0.52% Cu for a total of 3.345 mt Cu) has a similar setting (Fig. 6.8). It is a 123-117 Ma old disseminated hematite, magnetite, pyrite and chalcopyrite replacement and dilations-filling "manto" in K-feldspar, sericite and chlorite-altered fault rocks developed over andesite lavas and volcanoclastics in the Atacama deformation zone.

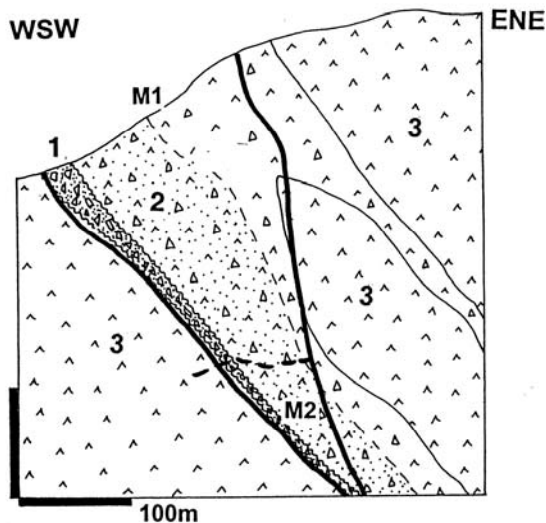


Figure 6.8. Mantoverde Cu deposit, Chile; cross-section from LITHOTHEQUE No. 2424, modified after Vila et al. (1996). 1. Mantoverde chaotic fault breccia, locally friction milled down to sandstone grain size; 2. Dis-aggregated Manto Atacama Breccia in fault hangingwall, over chloritized and K-altered andesite; 3. Cr₁ altered andesite intruded by diorite. M1. Oxidation zone, infiltrated chrysocolla; M2. Hypogene ore, scattered and dilations-filling chalcocite > bornite with specularite or magnetite in breccia

6.2.4. "Red beds" in andean margins

Red (or varicolored) beds are an oxidized, hematite-pigmented predominantly detrital continental sedimentary association of mostly alluvial conglomerate, litharenite or arkose, mudstone (Turner, 1980). They may grade into, or contain interbeds of, evaporites (mostly gypsum or anhydrite) and/or lacustrine carbonates, and change facies into more humid (coal-bearing) successions. The "typical" red beds are preserved in intracratonic extensional grabens (rifts; Chapter 12) but they also occur in second- or third-order grabens in the andean-type margins as in the Palocene-Eocene sequence on the Puna-Altiplano plateau. There, the epiclastic detritals derived from crystalline basement or unroofed granitoids mix with tuffaceous volcanoclastics and/or they are interstratified or intruded by members of the bimodal rift association: basalt and rhyolite. The rocks are also synchronous with the andesitic volcanism in the magmatic arc, and emplacement of the earlier generation of the Andean porphyry coppers. In the Cuzco area in southern Peru (Soncco

Formation; Perelló et al., 2003) the basal tuffaceous sandstone includes several meters thick horizon with hypogene chalcocite and bornite. The economic potential is unknown. Farther south, in Bolivia, a younger, Oligocene-Miocene succession of volcanic red beds hosts the "large" Corocoro ore field (774 kt Cu @ 1.3-5% Cu; Ljunggren and Meyer, 1964); this consists of several chalcocite and native copper-bearing horizons ("mantos") in reduced, grey litharenite and reworked tuff, intersected by a fault. The Andean redbeds present a challenge to the explorationist on basis of some similarity with the giant Dzhezkazgan (Zhezqazgan) ore field in Kazakhstan (35 Mt Cu; Chapter 12) which, although in an intracontinental basin, is synchronous with the Carboniferous porphyry coppers in the Balkhash province nearby.

6.2.5. Ores in andean margin rhyolites

Ancient continental rhyolites form several extensive ignimbritic outcrop areas around the world, complete with flow domes and subvolcanic intrusions. Most are in the bimodal, rift-related intracratonic setting. In addition to the Cordilleran and Andean belts in the Americas, continental margin paleo-rhyolites are known, among others, from the Permocarbiniferous of eastern Kazakhstan and NE Queensland. Most of the associated Sn, W, Mo, Au and Cu ore deposits, however, are hydrothermal and genetically related to hypabyssal plutons. These are described in Chapter 7. Here, the emphasis is on occurrences where the felsic volcanics host ores, or are directly genetically associated with mineralisations so that rhyolite presence is an essential empirical indicator in exploration.

Peraluminous rhyolite in andean margin settings

Peraluminous magmas have more Al than what can be accommodated in feldspars and are the product of remelting of crustal materials, mainly fine clastics. Most peraluminous magmas never vent and instead solidified in depth to form intracrustal batholiths. A small number of young peraluminous silicic volcanic centers are known in the andean margins, where they are associated with distinct Sn, Li, and Be enrichment or mineralization (e.g. in the Macusani and Morococala volcanic fields in Peru and Bolivia, respectively, or in Sierra Blanca, West Texas). Peraluminous rhyolite is considered by some to be the extrusive equivalent of rare metals pegmatites. The Eocene **Round Top laccolith** in Sierra Blanca, Texas, 140 km SE of El Paso (Price,

2004), with its rhyolitic carapace, intrudes Cretaceous limestone and shale. The extrusive and especially the shallow intrusive rhyolite are greatly enriched in lithophile trace metals, most of which form their own sparsely disseminated Li, Sn, Be, Nb, Th, Y, REE and Zr minerals like cassiterite, changbaiite, cryolite, thorite, yttrocerite, together with several unusual fluorine-rich phases. Price et al. (1990) have estimated a resource of some 1.6 bt of material in the laccolith alone, grading 490 ppm Li, 1900 ppm Rb, 210 ppm Y, 200 ppm Th, 58 ppm Be, 62 ppm Cs, 39 ppm Th and 47 ppm U, perhaps suitable for future bulk mining and complex extraction of the rare metals. The recent exploration, however, targeted small Be-rich skarn and fluorite replacement bodies in the limestone exocontact, where most Be resides in the rare mineral behoite (Be hydroxide). The 36 Ma rhyolite is attributed to crustal melting above flat slab, far inland from the edge of the American Plate.

Topaz rhyolite and F, Be, U mineralizations

Topaz rhyolite is popular with American geologists (Christensen et al., 1986) and although similar to the Sierra Blanca rhyolite in its enrichment of lithophile trace metals and with high F, it is considered metaluminous, mostly post-subduction (related to crustal extension), and petrochemically closer to the Climax-type Mo-forming magmas than to tin granites. Topaz rhyolite is silicic, extremely fractionated fluorine-enriched rock found as small endogenous lava domes and flows throughout the U.S. Cordillera. Of the anomalous trace elements Be, U, Sn and fluorite locally entered a variety of genetically related ore deposit types, although only beryllium produced a "world class" deposit, Spor Mountain in Utah.

Rhyolite in the Toano Range in NE Nevada (Price, 2004) has 87 ppm of trace U and 46 ppm Th that qualifies it as a "future resource", although under the present environmental mentality it is more of a nuisance because of the high alpha-particles emittance. Uranium released during devitrification and hydration in the supergene zone sometimes re-precipitated at redox interfaces in nearby aquifers and channels as in the small Yellow Chief deposit in the Thomas Range, Utah; more substantial but still small U deposits in Chihuahua, Mexico (Sierra Peña Blanca) owe their origin to postmagmatic reconcentration of the U extracted from rhyolite by hydrothermal or supergene processes. Equally miniature in size are the occurrences of topaz with cassiterite, beryl, hematite and other minerals precipitated from vapor-phase and fumaroles in

miarolitic cavities (e.g. Thomas Range, Utah). Fumarolic cassiterite and a later-stage, low-temperature cassiterite that includes the metacolloform "wood tin", accumulated in fissure veins (e.g. Taylor Creek Rhyolite in SW New Mexico; Durango tin deposits, Mexico).

Spor Mountain Be ore field north of Delta, Utah (P+Rv at least ~8.5 mt ore @ 0.3% Be containing ~24 kt Be; Lindsey 1977, Christiansen et al., 1986, Davis, 1991) is the world's largest beryllium accumulation that also contains a substantial resource of U (at 0.012 % U), fluorine, lithium (in smectite=hectorite), zinc and other metals. The ore, mined from at least eight pits, is hosted by three subparallel horizons of coarse felsic lithic tuff now interpreted as lahar or talus, that contain abundant fragments of dolomite derived from the Ordovician and Silurian miogeoclinal basement (Fig. 6.9). The ore horizons, in turn, are enclosed in Miocene (21 Ma) "beryllium tuff" of the Spor Mountain Formation that rests on Eocene rhyodacite and Oligocene rhyolitic ash-flow tuff although, over basement ridges, the "beryllium tuff" rests directly on the basement carbonates. The ore sequence interfingers with, or is covered by, porphyritic rhyolite member. The Be ore is represented by very fine-grained, invisible and inconspicuous bertrandite $\{Be_4Si_2O_7(OH)_2\}$ dispersed throughout the argillized and adularia-altered coarse tuff and replacing, with fluorite and opal, the dolomite fragments. The bulk of bertrandite is believed younger than 6 Ma, epithermal (250°C fluids) and genetically related to emplacement of the nearby 7-6 Ma Topaz Mountain rhyolite flows and plugs. The other mined Be deposit in the Western Utah Beryllium Province is Gold Hill (1,750 t Be @ 0.175%), a discordant set of epithermal quartz, adularia, calcite, bertrandite veins and disseminations in silicified and argillized quartz monzonite.

Peralkaline rhyolite-related Hg, Li, Cs, U mineralization: McDermitt Caldera, NV & OR

The 45 km diameter McDermitt caldera complex straddles the Nevada-Oregon state line in the Basin and Range Province (Rytuba and Glanzman, 1985; Noble et al., 1988). It is a complex of overlapping and nested calderas and rhyolitic ring domes erupted between 17.9 and 15.8 Ma, and a member of the bimodal post-subduction volcanic suite controlled by crustal extension. The many generations of rhyolite ash-flow tuff and extrusive/subvolcanic rhyolite have an excess of alkalis over aluminium, hence are members of the

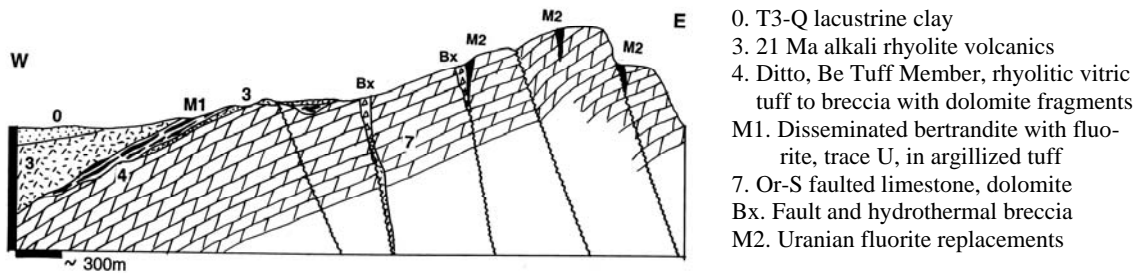


Figure 6.9. Spor Mountain area, Utah, diagrammatic representation of the Be metallogene. From LITHOTHEQUE No. 674.1, based on Lindsey (1977), Brush Wellman Inc.

peralkaline suite (comendite). The Caldera coincides with the Opalite alias McDermitt mercury ore field, mined since 1924 and hosting, until recently, the last remaining operating Hg mine in North America. Mercury (P+R ~17,250 t) came from five mines (McDermitt Mine is the largest and a "geochemical giant" with 10,300 t Hg), three of which, including the McDermitt Mine, are situated in tuffaceous lake beds filling the caldera moat whereas two deposits are in volcanics near the ring fracture. The orebodies are disseminations and impregnations of cinnabar and, locally, corderoite ($\text{Hg}_3\text{S}_2\text{Cl}_2$) in opalized and adularia, zeolites, smectite and cristobalite-altered host rocks along fractures. The ores are interpreted as typical hot spring deposits. Hg could have been extracted from local tuff and volcanoclastics where it is anomalously enriched (0.29 ppm and 0.26 ppm, respectively; Rytuba and Glanzman, 1985).

The Hg enrichment is unusual, compared with the enrichment in lithophile elements Li (236 & 300 ppm), Cs, and U (20-22 ppm) that are expected in peralkaline magmas. Uranium is concentrated at several places within the caldera and forms two small deposits (Aurora and Moonlight); the latter is related to the brecciated contact of intrusive rhyolite and caldera wall. Li is concentrated in hectorite (Li-smectite), up to a grade of 0.68% Li, in the zeolitized resedimented tuff in the caldera moat. The orebody has a substantial thickness and is a significant future resource.

The late Jurassic Tulukuyev Caldera in the Russian Transbaikalia (Chabiron et al., 2003) is in many respects similar to the McDermitt Caldera, but is deeply eroded so that the much older granitic basement is mineralized together with the overlying, F and U enriched highly fractionated rhyolite. The largest, and last producing Russian U ore field **Streltsovka** (Streltsovskoye, ~280 kt U; Section 10.11) formed by transfer of the trace U in rhyolite into brittle structures in both volcanics and basement granites.

6.3. Epithermal deposits and hot springs

Epithermal (Lindgren, 1933) and hot spring deposits represent the least temperate (<300°C) and shallow (formation depths from 0 to 1,500 m under the surface) hydrothermal deposits. They are transitional, as a class, into the deeper-seated and higher temperature mesothermal deposits via the transitional "porphyry" group, and sometimes into the volcanics-hosted or associated (VMS) sulfide deposits. Because epithermal deposits form at high crustal levels and in settings undergoing uplift, they erode fast hence the majority of them exposed at the present surface formed during Cenozoic. The "prime time" of formation, that is the age of deposits to be most commonly found in the present outcrop, is Quaternary to Miocene for the hot spring ores and Miocene to Eocene for the "typical" epithermals. Some striking exceptions do occur, though. The mineralized auriferous sinter deposits in the Drummond Basin of Queensland (e.g. Wirralie, Glen Eva; reviewed in Solomon and Groves, 1994), credibly interpreted as of hot spring origin, are Devonian. The convincingly epithermal Mahd-adh-Dhahab Au-Ag deposit in the Arabian Shield is Neoproterozoic. The genetically enigmatic As-Au-Cu deposit Boliden in Sweden (Weiheid et al., 1996) is Paleoproterozoic. Penczak and Mason (1999) recently interpreted the Campbell Red Lake Au deposit in Archean greenstones in Ontario as a metamorphosed epithermal system, a concept not readily accepted by many geologists; but if so this would be about the oldest epithermal deposit known.

The conventional first-order division of epithermal deposits into two subclasses is based on alteration and ore mineralogy, which also imply the fluid nature and derivation (Heald et al., 1987):

- 1) High sulfidation (HS) alias acid sulphate alias alunite-kaolinite; and

2) Low sulfidation (LS), alias adularia-sericite.

High sulfidation deposits are the product of interaction of acid, oxidized, sulfur-rich fluids typically produced by condensation of wet, SO₂-rich magmatic volatiles like those vented by active volcanoes, with surrounding rocks. Low sulfidation deposits formed mostly from variously mineralized heated meteoric waters. Transitions, overlaps and joint occurrences of both epithermal varieties abound, and Sillitoe (1993) listed many actual examples. The two subdivisions of epithermal deposits provide explorationists with several empirical facts:

1) The high-sulfidation deposits are practically confined to areas of volcanism broadly contemporaneous with mineralization; the fluids were influenced by the volcanic style and magma composition (this determined the selection of ore metals). The HS deposits are in the upper part of a vertically zoned hydrothermal systems and often situated above porphyry-type deposits, hence they have a predictive value in ore search. The nature of rocks into which were the HS deposits emplaced is of lesser importance, although the selection of hosts is limited (most are coeval volcanics).

2) The low-sulfidation deposits require a geothermal system (heat) to drive the fluid convection and this could be volcanism (usually the waning stages of) or, most often, hot intrusions or magma chambers in depth. Less frequently the heat is generated by radioactive decay (in "hot" granites), geothermal gradient or, exceptionally, meteorite impact. As a consequence LS deposits found in volcanic areas tend to be younger to much younger than the main stage of volcanism (and the HS deposits) and often there is no genetic relation to volcanism at all. The LS deposits are also materially influenced by the rocks through which the fluids circulated that were the source of ore metals, and rocks into which they were emplaced. Although some LS deposits (e.g. Cu, Au, Ag, Pb-Zn veins and replacements) are associated in space with some magmatic-hydrothermal systems such as porphyry coppers against which they are zonally arranged, they are of little predictive value because most LS deposits occur independently.

6.3.1. Hot spring deposits

Active hot springs, or what is left from inactive but geologically young hot spring systems after erosion, are the (near) surface expression of an epithermal

system in depth. Their study, particularly where drilled to explore for geothermal energy as in the Taupo Zone of New Zealand, in the Philippines, and elsewhere, has provided a wealth of direct information on the nature of convective hydrothermal systems down to some 750 m depths (Hedenquist and Henley, 1985; Simmons and Browne, 2000 and references therein). Although the bulk of the convecting fluid is meteoric water, small percentages of juvenile magmatic water could be present in some locations and it is possible that a portion of sulfur, CO₂, and some volatiles (Hg, Se) in the system could be of magmatic origin. Most of the spring fluids are neutral to slightly alkaline CO₂-rich chloride waters corresponding to the low-sulfidation epithermal systems in depth, but acid sulfate springs also form by atmospheric oxidation of H₂S in condensed vapor, released in depth by boiling. The latter is responsible for weak advanced argillic alteration. The fluid, some 300°C hot in depths greater than 1000 m, rises to the surface and boiling occurs along the way. This results in phase separation, mineral precipitation and alteration. The precipitation is most intense at the onset of boiling in the "epithermal depths" of around 750-500 m under the surface, but continues, with diminishing efficiency, up to the surface. Precious metals, with As, Sb and Hg sulfides have accumulated in silica sinters precipitated from hot water pools and in "muds" at several locations, but despite some locally impressive grades (80 g/t Au and 175 g/t Ag in a sinter at Waiotapu, New Zealand, precipitating in a hot pool above a hydrothermal eruption breccia; Weissberg, 1969; Hedenquist and Henley, 1985) a sufficient tonnage is lacking. Epithermal accumulations of Ag-Au (at the higher levels) and Pb-Zn-Ag (at the deeper levels), however, could be discovered in depth by drilling into the recent and young hot spring systems. Krupp and Seward (1987) studied the Rotokawa hot springs in the Taupo zone, a site of a small-scale mining of sulfur in lacustrine muds, which also contain a small resource of about 250 kg Au at 1 g/t Au concentration in the bright colored, As and Sb-rich muds. They have calculated that up to 370 t Au could have been cumulatively transported into the region beneath the hydrothermal eruption crater by a fluid saturated with 7.2 mg/kg Au, over the past 6,060 years, to possibly form a giant accumulation at a depth of several hundred meters.

It is thus unlikely that a major Ag-Au deposit, precipitated from fluids depleted by boiling in depth, would be found at or near the present surface (but read the exception below), but this restriction does not apply to mercury (and sulfur) transported

as a volatile gas. This ore forming mechanism is responsible for the Quaternary **Sulfur Bank S-Hg** deposit in the Geysers-Clear Lake geothermal area in California (Fig. 6.10), a "geochemical giant" (7,000 t Hg; White and Roberson, 1962). There, cinnabar with sulfur, pyrite, marcasite, zeolites and smectite impregnate silicified and argillized Quaternary andesite flow, landslide rubble and talus, resting unconformably on Mesozoic sedimentary rocks and Franciscan ophiolite. The ore zone is peneconcordant with the present surface, the mineralization persists to a depth of 75 m, and the ore deposition has continued, periodically, since 44,000 years ago.

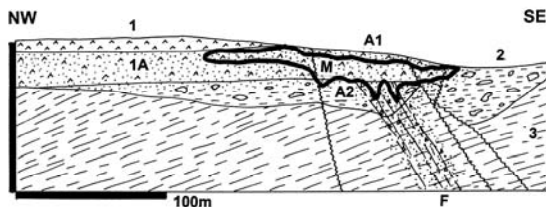


Figure 6.10. Sulfur Bank S-Hg deposit, Clear Lake, California, produced by recently active hot springs. From LITHOTHEQUE No 1156, modified after White and Roberson (1962). 1. 44,500 y old augite andesite flows; 1A, A1. Ditto, leached by hot springs to opaline silica residue; M. Recent sulfur replacements and dilation fill, cinnabar impregnations; A2. Deeper spring alteration, partially to totally argillized andesite; F. Fault gouge and breccia; 2. Q lacustrine and landslide sediments; 3. J₃-Cr₃ Franciscan and Great Valley litharenite.

A similar geothermal system, 2.5 million years ago, produced the "large" **McLaughlin Au-Sb-Hg** deposit (93 t Au @ 5.21 g/t Au plus Sb, Hg; Lehrman, 1987). This is a fossil, disrupted hot spring system controlled by a major fault in the Mesozoic Franciscan assemblage. Cinnabar, in sinter, occurs at the highest level, followed to depth by gold-stibnite ore in sinter and a variety of breccias, interpreted to formed above the depth of 200 m under the paleosurface, from heated connate brines derived from Franciscan sediments. The ancient gold deposits elsewhere, interpreted as of hot spring origin, are mostly small to medium size, with the possible exception of Round Mountain, Nevada (P+Rc 441 t Au @ 1.15 g/t Au; Henry et al., 1997) where, however, the hot spring characteristics are difficult to visualize.

High-temperature, rift-related geothermal system, Salton Sea

Salton Sea depression in SW California has formed

within the Cordilleran continental margin, in the on-land continuation of the rift system in the Gulf of California. Drilling for geothermal resources in the 1960s encountered a large, hot (maximum temperature 365°C), high-salinity liquid-dominated geothermal system that contains a large quantity of dissolved metals and actively alters the reservoir rocks (McKibben et al, 1988). High-grade sulfides of Cu with Ag, Au values actively precipitate as scales in geothermal wells. The brine pool is estimated to contain 6 Mt Zn, 10,885 t Ag, and other metals; a "giant" metal accumulation indeed.

6.4. High-sulfidation epithermal ores

One giant (Butte, Montana), three "large" (Goldfield, Nevada; Lepanto, Luzon; and Chinkuashih, Taiwan) and one small (Lahocsa, Hungary) enargite-rich Cu-Au-As deposits were mined in the past and described in the classical literature as a variety of epi- or mesothermal vein or massive sulfide deposits. More "giant" deposits (Monywa, Pueblo Viejo) are considered high-sulfidation but are not enargite rich. Still others (Cerro de Pasco, Colquijirca) do have small enargite orebodies but the principal ore is in Pb-Zn-Ag replacements. In the Butte ore field (described below) enargite is a component of the high level "horse tail" fissure vein swarm on top of a large porphyry copper deposit (Berkeley Pit). In Lepanto (island arc setting; total production 36.3 Mt ore @ 2.9% Cu, 3.4 g/t Au, 10 g/t Ag; Chapter 5) enargite with luzonite, tennantite, Au-Ag tellurides and other minerals in chalcedonic quartz gangue form a 2 km long pencil-shaped replacement zone adjacent to a diatreme. Several blind porphyry Cu-Au deposits in the Mankayan ore field (the Far South-East, Guinaoang and Victoria), totalling more than 1.5 Bt of ore, have been discovered in depth, in the past 20 years (Hedenquist et al., 1998). The Lahocsa deposit, in the Hungarian Mátra Mountains, also led to discovery of the large buried Récsk porphyry copper. Only Goldfield, Nevada (118 t Au; Ashley and Keith, 1976) and Chinkuashih, Taiwan, are so far without known porphyry copper counterparts. Goldfield consists of numerous gently dipping "ledges" (narrow fracture zones mineralized by chalcedonic quartz with scattered famatinite, enargite, bismuthinite, gold and other minerals) in silicified and alunite, pyrite, clay-altered Miocene dacite and andesite, and some of the ledges reach into the underlying Cambrian carbonaceous slate. These classical enargite deposits have been found by unsophisticated visual prospecting.

The high-sulfidation subclass of epithermal deposits introduced in the 1980s (Heald et al., 1987) gave new identity to the enargite deposits mentioned above, and went farther to explain and characterize deposits of comparable origin, that lack the conspicuous sulfides, on the basis of fundamental, ore-proximal alteration assemblages. This has been of particular importance for understanding the new generation of (very) low-grade, "bulk-tonnage" Au-Ag deposits like Yanacocha, Pierina, La Coipa, Pueblo Viejo and others where the ore can rarely be visually recognized, where the orebodies have assay boundaries, and where ore finding relies on geochemistry applied in the context of a conceptual model. Recently, a mineral spectra analysis (PIMA) that can rapidly and non-destructively identify the invariably fine-grained and white alteration minerals, has entered the field.

In neovolcanic areas with an abundance of barren ridges and summits as in the High Andes of Peru and Chile, or in tropical areas rich in landslide scars as north of Baguio, Luzon, extensive hydrothermal alteration has the form of prominent chalky-white or yellow patches with occasional ledges of resistant silica (chalcedonic quartz). Most of the alteration is due to clays (kaolinite or smectite) that could be the result of supergene alteration and that are common in the low-sulfidation environments as well. The type acid-sulfate alteration minerals are finely crystalline, white or pinkish alunite (fine powdery and chalky alunite is a product of acid leaching or supergene processes unrelated to ore; Sillitoe, 1993), talc-like pyrophyllite, silica, sometimes native sulfur, gypsum and barite. Alunite and pyrophyllite alone do not guarantee gold presence as both form major deposits devoid of metals (Zaglik in the Caucasus and Foxtrap in Newfoundland, respectively), but when gold is present it is fine-grained (invisible), in pyrite (that itself can be so fine-grained as to resemble a black mud) or in/with enargite, luzonite, Ag-sulfosalts and other sulfides when these are present. Gold may also reside in the distinctive "vuggy silica", without sulfides. As most of the recently bulk-mined gold ore, processed by heap leaching, comes from the oxidation zone (e.g. 80% of the Pierina ore), no sulfides are in sight and gold has been transferred into Fe-hydroxides that coat fractures or impregnate the material, or it remains locked in silica.

High-sulfidation orebodies are controlled by structure (vents, breccia zones that conducted acid fluids from the volcanic source) and, sometimes, lithology (porous aquifers for open space ore deposition, replaceable rocks such as interbedded

carbonates at Colquijirca). Orebodies range from quartz-dominated "bonanza" Au-Ag veins through enargite-rich massive sulfide veins (El Indio) to funnel-shaped mineralized breccias (Pueblo Viejo), irregular subhorizontal impregnations (Pierina, most of Yanacocha orebodies), subvertical diatremes. The subhorizontal gold orebodies are sometimes confused by the presence of opaline, chalcedonic or quartz-containing zones of silicification related to water table positions in the past, and acid-leached intervals produced by steam-heated groundwater marked by the advanced argillic assemblage grading to an almost pure residual SiO₂ (as cristobalite, tridymite or opal) and porous leached zones. They are rarely economically mineralized except for minor occurrences of cinnabar and realgar-orpiment, but could be locally gold-bearing where they accommodate gold displaced from the principal ore zone (e.g. at Pierina). Sillitoe (1993), Corbett and Leach (1994), Carlile and Mitchell (1994) and others provide more detail.

6.4.1. Low-grade ("bulk"), low-sulfide Au-Ag deposits

Yanacocha Au,Ag, ore field, northern Peru, is the world's largest high sulfidation Au resource and it has recently been the largest South American gold producer. Located ~20 km north of Cajamarca, the first orebody was discovered in 1985 by drilling a geochemical anomaly. Several tens of individual, low-grade, open-pit and heap-leachable deposits have been discovered since, over an area of ~120 km² (Turner, 1999; Harvey et al., 1999; Bartra, 1999). The ore tonnage figures increase on the monthly basis and 1,804 t Au @ ~1.0 g/t, with several times as much Ag, is probably close to the recent geological resource. The Rc₁₉₉₉ in oxide ore only was 840 t Au. Most of silver is probably lost, as the doré contains about 70% Au, 25% Ag and 5% Zn+Cu (Harvey et al., 1999).

The Yanacocha goldfield measures 17x6 km along the ENE axis and is divided into two portions by the Quinua basin, filled by Quaternary glacial drift. The folded basement of Cretaceous limestone is unconformably topped by Eocene and younger? rhyolitic pyroclastics and, around Yanacocha, further topped by predominantly intermediate volcanic and subvolcanic rocks of the Miocene (12.5-11.8 Ma) Yanacocha Volcanic Complex (YVC; Turner, 1999). This strongly hydrothermally altered assemblage hosts all Au deposits in the goldfield, and is a part of a NE structural corridor in northern Peru, almost perpendicular to the Andean structural grain. The YVC is an erosional

remnant of an extensive volcanic field, the preserved thickness of which reaches about 1,400 m. The basal section is dominated by feldsparphyric andesite to dacite lava flows and domes. Above is a predominantly fragmental sequence of generally unwelded subhorizontal layers of crystalline tuff to tuff breccia, interbedded with phreatomagmatic deposits. The latter are commonly silicified. Several crosscutting, subvertical but comagmatic bodies of matrix-supported, heterolithic breccia are interpreted as diatremes. They contain high proportion of hydrothermally altered fragments in matrix of finely porphyritic andesite or rock flour, and overlap with mineralization. YVC evolution terminated with emplacement of small subvertical andesitic to dacitic feldspar porphyry bodies and eventually unaltered rhyodacite domes.

Hydrothermal alteration dated between 11.5 and 10.9 Ma (Turner, 1999) defines the Yanacocha goldfield and it envelopes all orebodies (Fig. 6.11). Although classified as acid-sulfate it is dominated by silica that forms large masses exposed as cerros (buttes), e.g. the Cerro Yanacocha. The silica (quartz, locally relic chalcedony) has several forms, and their interpretation aids exploration. Granular silica, with alunite and native sulfur, forms often extensive subhorizontal tabular bodies produced by leaching of volcanics above hydrothermal cells. It often tops vuggy silica of cavernous fine quartz, believed produced by condensation of magmatic vapors at contact with meteoric water-saturated rocks. It forms irregular, thick subhorizontal bodies. Massive silica fills and replace wallrocks in up to 450 m thick subhorizontal masses. Silica-Fe oxide breccia (hematite, goethite) grades into quartz-pyrite breccia in depth, and it forms dike-like subvertical to flat-lying bodies at intermediate levels (beneath granular silica). The soft members of the advanced argillic alteration suite are situated outward and downward from the silicified centers and are dominated by a great variety of alunite (most proximal), pyrophyllite and kaolinite mixtures, with variable proportion of quartz. Montmorillonitic (clay, argillic) and propylitic (silica, chlorite, montmorillonite, illite) alteration zones are along the fringe of the mineralized area (Fig. 6.11).

Gold (and a fraction of silver) is presently recovered from the oxidized ore only, which is locally developed to some 300 m depth under the present erosional surface. The oxidation is pre-Quaternary and the regolith thickness has been reduced by alpine glaciation. The oxidized ore is inconspicuous and the invisible finely dispersed

gold is in residual "limonite", or as free gold in granular or vuggy silica. With increasing depth jarosite appears with relics of the primary sulfides, mostly disseminated and fracture-coating pyrite with some enargite and bornite; the primary ores average 0.1% Cu. Most of the oxidized gold appears residual with neither enrichment nor impoverishment throughout the regolith (Ag, however, is depleted in the oxidized ore). The very low-grade ore (typical grade range is 0.8-1.6 g/t Au, usual cutoff is 0.35 g/t Au) occurs in eight emission centers in the district, **Cerro Yanacocha** being the largest (Harvey et al., 1999; P+Rv 429 t Au, 9,734 t Ag). The tabular semi-stratabound ore zones are flat-lying to gently dipping, up to 2,000 m long and 400 m wide, and in most cases confined to zones of silicification. Only small gold amounts come from the alunite-rich material, although alunite-silica altered volcanics envelop the orebodies. Of the silica varieties the granular silica hosts most of the gold, followed by vuggy silica and the silica-iron breccias. There is only a limited correlation between the pre-alteration lithology and ores, although the porous and permeable rocks had a better chance. The magmatic-hydrothermal mineralization was a long-lasting process that progressed in several pulses. The gold transported by fumaroles precipitated under fluctuating water tables, in acid-leached and silicified volcanics.

Alpine-type, Quaternary glaciation has physically removed portion of exposed ore from the Cerro Yanacocha center and redeposited it downslope to form the "giant" La Quinoa deposit (50-100 m thick, Rc 420 t Au, 2923 t Ag)

Pierina-Au,Ag, NE Peru (Volkert et al., 1999; P+Rc 110 mt ore @ 2.8 g/t Au, 22 g/t Ag for 308 t Au, 2420 t Ag). Pierina is a single, relatively compact deposit (~900 x 300m) perched on a ridge high above the Rio Santa graben and 18 km NW of Huaraz, in the Cordillera Negra (Fig. 6.12). It is a mostly oxidized low-grade disseminated multistage high-sulfidation Au-Ag deposit underlain in depth by higher-grade hypogene veins and stockworks. The hosts are late Eocene to Miocene andesite flows, overlain by Miocene rhyodacite pumice tuff deposited in a restricted graben. Above are remnants of lithic tuff. The structurally controlled mineralization is believed located on flanks of a vent or dome, predominantly in zonally altered pumice tuff. Most gold is residual, disseminated in a thick subhorizontal vuggy silica blanket believed to commence above the feeder vent. Some gold continues into the adjacent alunite zone with minor

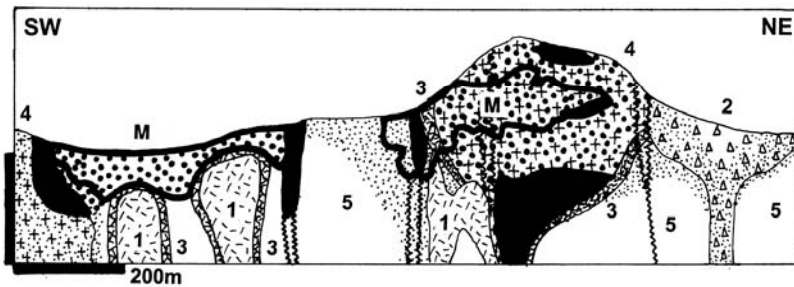


Figure 6.11. Yanacocha ore field, Peru, Carachugo Sur (left) and Este (right) deposits. From LITHOTHEQUE No. 2481, modified after Minera Yanacocha and Harvey et al. (1999)

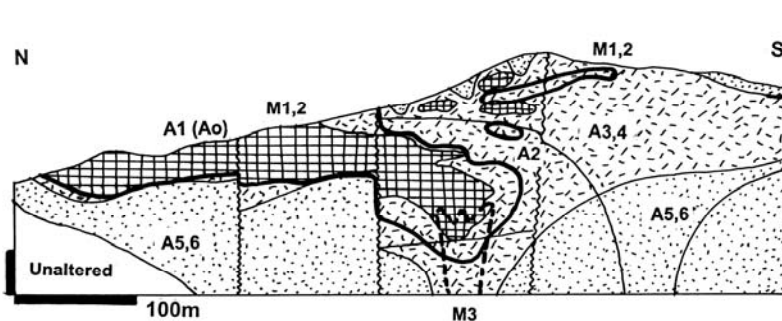


Figure 6.12. Pierina Au deposit, Huaraz, Peru. Disseminated gold in oxidized acid sulfate altered felsic pyroclastics. From LITHOTHEQUE No. 2494, modified after Volkert et al. (1999) and Barrick Pierina Staff (2000)

pyrophyllite and dickite, but disappears completely when the kaolinitic and illitic clay alteration zone is reached. The recently mined heap leach ore has been coming from the oxidation zone, where micrometer-size gold is dispersed in Fe hydroxides and remains in quartz. Kernels of partly oxidized pyrite, enargite, covellite and/or sulfur, locally encountered in the oxidized ore, are considered hypogene remnants of the early mineralization stage. The hypogene alunite has been dated at 14.5 Ma.

6.4.2. Transition to sulfides-rich high-sulfidation Au-Ag systems

Yanacocha and Pierina appear low in sulfides but this is mainly the consequence of supergene oxidation of much of the ore, and very low Au-grades. Elsewhere, the sulfides : (Au+Ag) ratio in ore increases sharply and some orebodies become pyritic massive sulfides with enargite, a case of El Indio described below. Similar enargite-rich sulfide bodies occur in other associations as with Zn-Pb (Cerro de Pasco, Colquijirca; read below) or porphyry-Cu (Agua Rica in the andean setting; Mankayan, Tampakan, and others in island arcs).

1. Mi₃ late dacite, andesite plugs; 2. Diatreme, heterolithic breccia with porphyry fragments; 3. Carapace, rim & hydrothermal breccia; 4. Dacite domes; 5. Felsic pyroclastics. BLACK: massive silica; DOTS: vuggy & granular silica; STIPPLES: alunite & clay alteration; M: disseminated Au-Ag ores

M1,2. Mi-Pi dispersed gold in residual Fe hydroxide and relicts of M3. M3. Pyrite, enargite, gold in silicified tuff. Dominant alteration: A1. Vuggy silica & Au (Ao=steam alteration); A2. Quartz-alunite; A3. Dickite; A4. Pyrophyllite; A5. Kaolinite, smectite, sericite; A6. propylite. Unaltered Mi felsic pyroclastics

El Indio-Pascua Au-Ag-Cu belt, Chile and Argentina (Bissig et al., 2002; belt total P+Rc ~1,358 t Au; 28,746 t Ag; min. 2 mt Cu) started with El Indio, the first "giant" gold discovery in Chile, only developed in the 1980s. More discoveries followed in the about 60 km long north-south trending El Indio-Pascua belt, now the second Au+Ag zone of importance in Latin America (after Yanacocha). This belt follows the Chile-Argentina border (also the Pacific-Atlantic divide) in the High Andes. It is in a structural block with late Paleozoic volcano-plutonic basement, intruded by Eocene diorite. The area became site of late Oligocene to late Miocene (27-6.2 Ma) predominantly andesitic to dacitic explosive volcanism with coeval subvolcanic activity. The closing pulse of this stage, between 9.4 and 6.2 Ma, was associated with widespread hydrothermal activity driven by small dacitic domes and plugs. Effects of the resulting hydrothermal alteration are strikingly visible from the air, exposed on the barren arid outcrop surface. Two phases of younger volcanics in the area are free of mineralization. Bissig et al. (2002) made a case for the important role of pediplains (planar erosional surfaces) as one of the controls of shallow hydrothermal mineralization in northern Chile, and

concluded that all important Ag-Au depositing hydrothermal activity in the belt took place immediately below the Los Rios pediplain (the youngest of a set of three).

El Indio-Tambo Au-Ag-Cu ore field (P+Rc 295 t Au, 2,000 t Ag, 1.8 mt Cu; Siddeley and Araneda, 1986; Jannas et al., 1999) is about 180 km east of La Serena. The mineralization, in the form of numerous fault and fracture veins and hydrothermal breccias, is both north of (El Indio) and south of (Tambo) Cerro Canto, a thick pile of dacitic tuffs considered a vent area. The Miocene volcanics comprise two generations of andesite (older and younger) and dacitic to rhyolitic pyroclastics. The latter are strongly hydrothermally argillized and in places silicified, and they host most of the orebodies. Hypogene and supergene alunite and jarosite, with or without native sulfur and gypsum, are more localized and controlled by fault zones and breccias. The earlier and deeper-seated reduced ore stage, prevalent at El Indio, produced systems of straight or anastomosing massive pyrite-enargite fault and fissure veins, gradational to stockworks. Luzonite, chalcopyrite, tennantite and tetrahedrite are minor. There are almost no gangue minerals, and some wallrock breccia fragments. Typical grades of the El Viento vein system range from 6-12% Cu, 4-10 g/t Au and 60-120 g/t Ag (Siddeley and Araneda, 1986). Some veins border pervasively silicified wallrocks, but much of the volcanics and fault fragmentites are argillized, with variable content of alunite.

The younger generation of El Indio-Tambo veins formed under oxidizing conditions at higher crustal levels. The "medium-sulfidation" quartz veins with some alunite and pyrophyllite carry free gold (especially in the "bonanza" shoots, as in the Indio Sur vein that yielded 120 kt of ore @ 250 g/t Au; Siddeley and Araneda, 1986). Minor amounts of pyrite, enargite and tennantite are accompanied by a list of rarer sulfides, arsenides and tellurides. Ore grades vary rapidly within the range of ~4-12 g/t Au, 66-130 g/t Ag, 7-10% Cu and 0.5-2.0% As. A 20 kt ore package from the high-grade Indio Sur vein also contained 0.13% Sb, 0.12% Pb, 100 ppm Te and 30 ppm Hg plus Bi, Se.

At **Tambo** breccia and short vein orebodies have barite, alunite, gold association with the rare telluride rodalquilarite, enveloped by silicified breccia. When not pervasively silicified, the wallrocks are altered into the sericite, kaolinite, pyrophyllite, illite assemblage.

The contiguous Pascua-Lama and Veladero ore fields are at the northern end of the El Indio belt, on both sides of the Chile-Argentina border (Bissig et

al., 2002). **Pascua (Chile)-Lama (Argentina)-Au,Ag** ore field (Rc 578.5 t Au; 19,593 t Ag) is in uplifted basement complex west of the Miocene volcanic pile. The host rocks are late Paleozoic granitoids and minor rhyolite tuff. The "giant" quantities of precious metals reside in clusters of hydrothermal breccia pipes, adjacent quartz stockworks, and tabular zones of silicification enveloped by quartz-alunite alteration. The **Veladero Au-Ag field** in Argentina (485 t Au; 7,153 t Ag), ~4 km SE of Pascua, is in Miocene volcanics.

La Coipa Ag-Au, the "near-giant" high-sulfidation deposit close to the northern end of the Maricunga ore belt farther north in the Chilean Andes (Oviedo et al., 1991; P+Rv 4,710 t Ag, 84 t Au), is dominated by silver. The bulk of silver is in enargite, disseminated with gold in silicified and advanced argillic-altered Miocene dacitic pyroclastics and subvolcanics and Triassic black argillite. Ag is enriched in the oxidation zone, in cerargyrite and Ag-iodates.

6.4.3. Diatreme-dome complexes with enargite-gold centers surrounded by pyrite, Zn-Pb-Ag carbonate replacements

Another famous Miocene mineralized belt in the long-known and highly productive Cerro de Pasco-Colquijirca region on the central Peruvian pampa, recently underwent a drastic genetic re-interpretation partly as a result of discovery of the concealed San Gregorio Pb-Zn orebody (Fontboté and Bendejú, 1999).

Colquijirca ore field (Yaringaño et al., 1999; Bendejú et al., 2003; P+Rv 8.2 mt Zn, 2.26 mt Pb, 1 mt Cu, 4,294 t Ag, ~20 t Au) is centered 12 km south of Cerro de Pasco in a thrust and normally faulted succession of Devonian to Eocene miogeoclinal rocks. South of Colquijirca the bedded rocks are pierced by a Miocene (12.7 to 12.4 Ma), predominantly dacitic diatreme dome complex, exposed in Cerro Marcapunta. A portion of the sedimentary stratigraphy, that included the Mitu redbeds, collapsed into the cavity. The diatreme is filled by pyroclastics, followed by brecciated lava flows that spread laterally, and crackle-brecciated lava domes.

The diatreme volcanics are hydrothermally altered and host a small disseminated stockwork Au-Ag orebody in depth of 60 m under the Marcapunta summit. The "giant" Zn+Pb and "large" Cu+Ag contents in the ore field, however, come

from stratabound replacement bodies in carbonates north (Smelter, Colquijirca; dated at 10.8-10.6 Ma), and south (San Gregorio; dated 11.6-11.3 Ma) of the diatreme (Bendezú et al., 2003). The northern orebodies are hosted by Eocene limestone and marl with conglomerate at base that rest, disconformably, on Permian redbed sandstone. Outward from the diatreme the orebodies are zoned in terms of ore metals (Cu, Au - Zn, Pb, Ag), ore mineralogy (pyrite, enargite, quartz in the Smelter deposit; pyrite, sphalerite, galena, minor chalcopyrite, siderite in Colquijirca), and alteration assemblages (proximal quartz-alunite, distal dickite, kaolinite); Fig. 6.13.

Smelter (or Marcapunta) Cu-Au deposit (~50 mt @ 1.0% Cu, 0.33 g/t Au; Bendezú et al., 2003) is a tabular body of massive to vuggy and brecciated pyrite and enargite with variable quartz and alunite. The (old) **Colquijirca Zn-Pb-Ag deposit** (Yaringaño et al., 1999; ~30 mt @ ~7.9% Zn, 1.5% Pb, 48 g/t Ag) is a set of stacked massive to densely disseminated sphalerite, lesser galena, pyrite mantos with barite, dolomite, calcite gangue, interspersed with alteration clay and passing upward into a thick oxidation zone. Narrow, subvertical veins of pyrite, enargite, quartz, alunite, pyrophyllite, in depth under the manto orebodies, are considered by Bendezú et al. (2003) as feeders, rooted in the diatreme complex.

South of Cerro Marcapunta, under Quaternary alluvium of the Pampa de Junín, the old San Gregorio mine produced several tons of bismuth from blocks of residual Bi-carbonates enclosed in clay. The "giant" concealed **San Gregorio replacement Zn-Pb orebody** has been found in the 1990s (Bendezú et al., 2003; 86 mt containing 5.82 mt Zn, 1.82 mt Pb, 2854 t Ag. Of this, 11 mt is a low-Zn, Pb but high Ag and Bi oxidized material). In contrast to the northern orebodies, San Gregorio is in the Lower Jurassic Pucará limestone, its mantos are thicker and less regular, and the host dolomitized limestone is decarbonated and converted into a mixture of quartz, alunite and clay interspersed with sulfides: extremely fine-grained sphalerite and lesser galena with minor pyrite and marcasite. Massive zincian rhodochrosite occurs along the ore-relict dolomite contacts.

The Colquijirca Zn-Pb-Ag orebodies, at times considered stratiform or remobilized from Devonian carbonaceous phyllite, are now rather convincingly interpreted as a hitherto uncommon variant of low-temperature (~300°C to 150°; hence epithermal) carbonate replacements related to high-sulfidation systems (Fontboté and Bendezú, 1999). As major

Zn-Pb accumulations are unusual in high-sulfidation systems, Colquijirca remains an intriguing anomaly.

Cerro de Pasco Zn-Pb-Ag-Cu mineralized center, Peru (Einaudi, 1977; Rivera, 1997; 8.59 mt Zn; 2.97 mt Pb; 20,240 t Ag; 1.1 mt Cu). Cerro de Pasco is 172 km NE of Lima in central Peru, at an elevation of ~4,300m. It is a famous deposit originally mined for silver by the natives, then by the colonists. Modern mining started in 1906 first for copper and silver, then (and presently) for Pb-Zn-Ag. This is a polygenetic mineralization in which several highly productive ore types overlap in an area little larger than 3x2 km. Not all the ores are high-sulfidation and there does not seem to have been a single central fluid-emitting center as envisaged for Colquirica, despite many similarities (Cheney, 1991; Rivera, 1997); Fig. 6.14.

The lithologic succession from Colquijirca continues northward towards Cerro de Pasco, although the Eocene sediments are almost missing except for small remnants along the Cerro de Pasco "vent". The principal sedimentary lithologies at Cerro are Devonian carbonaceous phyllite (Excelsior) with some quartzite interbeds, overthrust from the east by the massive Pucará Limestone. The strata, exposed in northerly striking folds, are intruded by Miocene diatreme-dome complex (the "Vent"), comparable with Marcapunta at Colquijirca, but with a strong development of quartz monzonite stocks and dikes. Except for massive, quartz-sericite-pyrite altered dacitic volcanics, the diatreme is filled by crudely bedded upward-fining fragmentites composed of the local rocks: black phyllite, dark "chert", Pucará Limestone, rare altered granitoids and massive pyrite, in sandy matrix. An alternative explanation of the fragmentite origin is that this might be the downdropped Eocene Shuco Member, an alluvial fan deposit.

Cerro de Pasco used to have a thick blanket and irregular patches enriched in Ag and Cu, with a variety of rare minerals, developed collectively over a variety of ore types by epithermal leaching followed by supergene processes. It is now mined out. There are three principal hypogene ore types, with additional subtypes at Cerro (Einaudi, 1977), but opinions differ as to their timing and origin. Cheney (1991) and Rivera (1997) distinguished at least two major stages of mineralization, the earlier one having taken place before the diatreme emplacement and thrusting, the later being

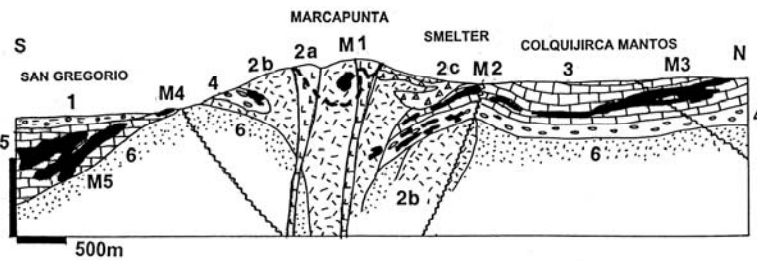


Figure 6.13. Colquijirca ore field, Peru; from LITHOTHEQUE No. 913, modified after Minera Brocal (2000), Fontboté and Bendejú (1999). LITHOLOGY: 1. Q alluvial cover sediments; 2a. Mi acid volcanic-subvolcanic complex, domes; 2a. Ditto, quartz latite and dacite flows; 2c. Ditto, diatreme breccia and pyroclastics; 3. Eo limestone; 4. Eo conglomerate; 5. Tr₃-J₁ limestone and dolomite; 6. Pe-Tr redbed sandstone

- M1. Concealed HS Au-Ag orebody;
- M2. Massive to disseminated pyrite, enargite;
- M3. Replacement pyrite, galena, sphalerite "mantos";
- M4. Bi-enriched gossan;
- M5. HS Pb-Zn-Ag limestone replacement.

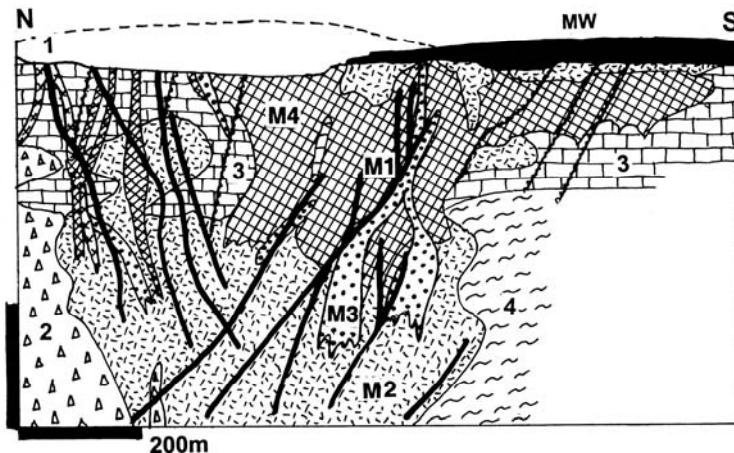


Figure 6.14. Cerro de Pasco deposit, Peru. Cross-section from LITHOTHEQUE No. 914, modified after Cerro de Pasco Corporation (later Centromin), 1965

- MW. Gossan & oxidation zone
- M1. Pyrite-enargite veins
- M2. Massive pyrite
- M3. Massive pyrrhotite pipes
- M4. Massive Zn,Pb replacement
- 1. 15-14 Ma quartz monzonite dikes
- 2. Mi "Vent", upward fining heterolithologic breccia
- 3. Tr-J Pucará Limestone, chert
- 4. D Excelsior Fm. biotite phyllite, metaquartzite

genetically related to (magmatic)-hydrothermal processes coeval with the diatreme.

- 1) Massive silica-pyrite body, 1800 m long and ~300 m thick, dips ~70% west along the eastern margin of the diatreme and continues for ~820 m downdip. Anhedral pyrite forms a steely mass or a vuggy aggregate, and encloses fragments (remnants?) of dark "chert". The closest resemblance of this orebody is to jasperoid-associated hydrothermal carbonate replacements. The pyritite itself has been of little value other than source of sulfur, although it stores a large quantity of subgrade metals (calculated contents: ~130 kt As, ~80 kt Sb, ~15 kt Bi, ~2.5 kt Te, ~15 t Au). The pyrite mass is cut by pyrrhotite pipes and veined by pyrite-enargite and other minerals.
- 2) Massive fine-grained gray sphalerite, pyrite, galena, calcite bodies are adjacent to, and overlap with, the silica-pyrite bodies in the east. They replace tectonized Pucará Limestone. They store the bulk of Cerro de

Pasco's ore metals (P+Rv ~80 mt @ 9.2% Zn, 3.5% Pb and 101 g/t Ag; Cheney, 1991) and appear to be the oldest mineralization that predates the fault and diatreme. Interpretations range from diagenetic replacement ("Irish-type") to mesothermal replacement in the roof of an earlier (pre-diatreme) granitoid intrusion. Rivera (1997) argued that the pyrite body is younger than the Zn-Pb ores, which it partly degrades.

- 3) Pyrite-enargite and luzonite (quartz) veins and local pipes follow mainly east-west fractures formed after the diatreme emplacement. They intersect all local lithologies that include the pyritite and Zn-Pb orebodies. These genuinely high-sulfidation veins account for the bulk of Cerro's Cu and a share of Ag (P+Rv ~35 mt @ 2.47% Cu, 124 g/t Ag). Apparently there were several generations of veins, some associated with advanced argillic alteration (alunite, dickite, quartz) and sericitization when in silicate hosts. The veins age is bracketed by the

14.2 Ma albitized quartz monzonite dikes that intersect some veins.

6.4.4. Combined high sulfidation / porphyry Cu-Au-Ag systems

High-sulfidation epithermal deposits coexist with porphyry copper's in several ore fields around the world. The closeness of the respective ore types varies: some overlap in space to form continuous composite ore zones (Agua Rica, Butte), elsewhere both ore types form separate deposits, with porphyry Cu in greater depth (Mankayan, Récsk). In most cases HS deposits are the smaller (sub-giant) ones, although in Agua Rica the younger high-sulfidation assemblage that contains the bulk of economic ore overprints, and almost completely destroys, the earlier porphyry Cu-Au-Mo. The timing of formation of the coexisting ore types also varies; in Butte, Agua Rica and Tampakan the high-sulfidation orebodies are younger than the porphyry Cu, in the remaining "giants" the ore porphyries are younger. It does not appear that most HS deposits are simple high-level equivalents of contemporaneous porphyry deposits in depth and both may have been members of two different systems that accidentally joined at the present location. Most smaller HS deposits as listed by Arribas (1995) lack porphyry Cu neighbours and this also applies to the majority of porphyry coppers. Despite the lack of guarantee that a HS deposit will have a "porphyry" brother below or somewhere in the area, this possible association is an important exploration lead worth testing. Reading about the important known deposits is the first step.

Butte, Montana, Cu-Ag-Mo ore field ("the richest hill on Earth"; Marcus, 2000. The same epithet is also claimed by Cerro Rico Ag-Sn in Bolivia and Broken Hill Pb-Zn-Ag in Australia). This is certainly the world's largest enargite-dominated high-grade vein system credited with total production of 296 mt ore @ 2.5% Cu and 68 g/t Ag. This represents some 7.4 mt of contained Cu; 20,128 t Ag; as well as 143 kt As (not recovered), 1,833 t Bi; 89 t Au; 144 t Se; and 108 t Te (Tooker, 1990). The total geological resource (most of it unrecoverable) of the central Butte ore field, quoted by Marcus (2000), is 5.05 bt of material with 0.44% Cu, 0.03% Mo and 3.6 g/t Ag which, if the past production is added, comes to the total endowment of some 6 bt of material with 31.254 mt Cu; 1.7 mt Mo; and 40 kt Ag; with As a quadruple "giant" indeed.

Butte is a metal-zoned ore field entirely hosted by the late Cretaceous, epizonal quartz monzonite intruded into its own rhyolite ejecta (by now erosion removed; Hamilton and Myers, 1967). The parent Boulder Batholith is controlled by major lineaments within the Precambrian basement of the Wyoming Shield and its platformic cover. A major hydrothermal system at Butte was active between 64 and 57 Ma, probably sourced and/or driven by a buried intrusion in depth. It produced two overlapping vein/stockwork complexes (Fig. 6.15). The earlier complex called, in the literature, "Pre-main stage" (PMS) produced a huge, although relatively low-grade (0.24% Cu in the Continental Pit reserve) dome-shaped porphyry Cu-Mo bodies in K-feldspar and biotite-altered quartz monzonite. This ore has been mined in the Berkeley and Continental open pits, partly from the chalcocite-dominated blanket of secondary sulfides. This was followed, after some 5 m.y. break, by ores of the "Main Stage" (elsewhere, this would be called "Late Stage") that consist of two sets of NE and NW veins and vein zones that fill fissures and faults in quartz monzonite and reach into the upper portion of the porphyry Cu-Mo system. These 6 to 30 m wide veins in the district centre have a quartz-pyrite gangue associated with an almost massive hypogene chalcocite and enargite, lesser bornite, covellite, digenite, djurleite and other minerals. These veins averaged 4.5% Cu and over 130 g/t Au but the grade decreased with depth. Towards south-east the veins split and change into a system of closely spaced veinlets of the same minerals to form the well-known Butte "horse tail" pattern. The wallrocks have zoned alteration envelopes where sericite zone immediately adjacent to the vein, sometimes with dickite, pyrophyllite and topaz, grades outward into kaolinite-, then montmorillonite-altered monzonite. At the ore field scale, veins with pyrite, chalcopyrite and sphalerite, and with rhodochrosite, galena, sphalerite, define distinct metal zones that surround the porphyry center. Brimhall (1979) concluded that the Main Stage veins formed by progressive hypogene leaching of, and selective metals redistribution from, the earlier porphyry Cu-Mo, under epithermal conditions.

Récsk-Lahocsa HS epithermal and porphyry/skarn Cu-Au deposits. This ore pair is located in the Mátra Mountains in north-central Hungary, where the Triassic miogeoclinal limestone, dolomite, shale and quartzite basement is overlain by Upper Eocene marine andesite, volcanoclastics, limestone and marl. The andesite had been intruded by

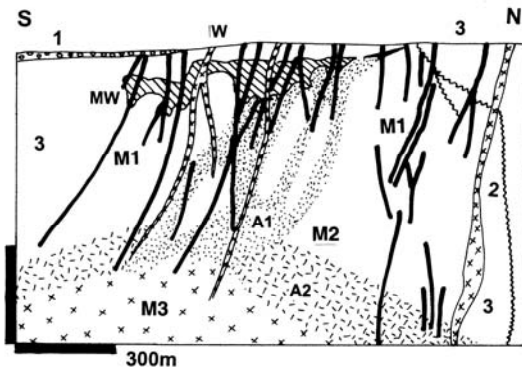


Figure 6.15. Butte ore field, Montana, cross-section through the central part (Berkeley Pit). From LITHOTHEQUE No. 860, modified after Anaconda Ltd., Brimhall (1979), Tooker (1990). 1. Q gravel; 2. T₁ quartz porphyry dikes; 3. Cr₃ Boulder Batholith quartz monzonite, variously altered. W. Leached capping and oxidation zone; MW. Secondary sulfides zone (chalcocite and covellite); M1. Main Stage, enargite-pyrite veins in sericite altered hosts (A1); M2. Hypogene zone, porphyry Cu-Mo stockwork, disseminations; A2. Pervasive biotite alteration; M3. Quartz-molybdenite rich core of the zoned Pre-Main Stage porphyry mineralization

comagmatic diorite to andesite porphyry followed by widespread magmatic-hydrothermal and epithermal mineralization around 35 Ma. The Lahocza Hill high-sulfidation deposit was discovered in the mid-1800s and intermittently mined; the total production and reserves have been some 50 kt Cu and 14 t Au only (Gatter et al., 1999), although the Engineering and Mining Journal (February 1996) quoted a resource of 99 t Au @ 2.1 g/t in "enargite ore". The Lahocza orebody is a silicified zone with advanced argillic lithocap that contains several small stocks and breccia bodies mineralized by pyrite, enargite, luzonite, tennantite and other rarer minerals. The deep-seated Récsk ore group was discovered in the 1960s during oil exploration (Baksa et al., 1980; Rv 800 mt @ 0.66% Cu, 0.006% Mo for 5.3 mt Cu and 49 kt Mo). It consists of several irregular bodies of stockwork and disseminated pyrite, chalcopyrite, minor sphalerite, and molybdenite in sericite and "propylite" (calcic-sodic) altered diorite, wrapped around the silicified core. The hydrous alteration assemblages overprint earlier potassic alteration and had probably been influenced by carbonate contacts and relict connate fluids in the marine sediments and volcanics. About 30% of the ore resources is in pyrrhotite, pyrite, chalcopyrite, bornite, magnetite and sphalerite masses in exoskarn and partly endoskarn immediately at the intrusion contact, whereas Zn-Pb rich skarn and marble replacement bodies are farther from the contact.

Agua Rica Cu, Mo, Au deposit near Andalgalá, NW Argentina (Rc 1,714 mt @ 0.43% Cu, 0.17 g/t Au, 0.032% Mo for 7.37 mt Cu at 0.2% Cu cutoff, 291 t Au and 548 kt Mo; Landtwing et al., 2002) is a multistage Miocene subvolcanic center in Sierras Pampeanas. A series of hornblende, biotite and feldspar porphyries and a variety of breccias intrude the Neoproterozoic or lower Paleozoic basement metasediments. The magmatic activity was paralleled by protracted mineralogenesis and alteration which, between 8.56 Ma and 3.5 Ma, changed from magmatic-hydrothermal into the high-sulfidation and supergene enrichment stages, as the site was undergoing uplift, erosion and explosive unroofing.

The earliest porphyry Cu, Mo and Au mineralization in potassic-altered host, associated with feldspar porphyry, is present as relicts. The bulk of the hypogene ore is in veins and matrix of hydrothermal breccia dominated by covellite, some enargite, minor sphalerite, galena and molybdenite, overprinting the earlier "porphyry" ore. The associated advanced argillic alteration is marked by silicification, vuggy silica, alunite and pyrophyllite. Supergene chalcocite and covellite have spotty distribution as remnants of an erosion-dissected enrichment blanket.

Additional examples of the "giant" and some "large" high sulfidation/porphyry sets include Tampakan and Mankayan in the Philippines described in Chapter 5. Monywa in Myanmar, Nena-Frieda River in PNG and Bor in Serbia are briefly characterized below.

- **Monywa Cu ore field, Myanmar** * Rc 1 bt @ 0.41% Cu for 4.1 mt Cu * 19 Ma high-sulfidation disseminated and fracture chalcocite with pyrite in sericite, alunite, diasporite, pyrophyllite altered breccias related to dacite porphyry * in Ol andesite of the Burma Volcanic Arc * Win and Kirwin (1998).
- **Bor Cu-Au ore field, Serbia** * P+Rc ~990 mt @ 0.6-1% Cu for ~5.6 mt Cu, ~190t Au * 1. Cr₃ massive to stockwork pyritic high-sulfidation body with lesser covellite, chalcocite, bornite, enargite in silica, sericite & advanced argillized andesite. 2. Cr₃ porphyry Cu-Mo in K-silicite & sericite-altered andesite in depth, above diorite * Cr₃ Timok andesite-diorite complex * Janković et al. (1980).
- **Chelopech Au-Cu-As deposit, Panagurishte district, Bulgaria** * Rv 32 mt @ 5.3 g/t Au, 1.38% Cu, 0.15% As; +P for total ~225 t Au (or 360 t), 600 kt Cu, 50 kt As * Cr, 20 steeply dipping massive to disseminated pyrite > enargite, tennantite, bornite, chalcopyrite lenses in breccia pipes in silicified and advanced argillic altered andesite * Cr calc-alkaline andesite, dacite, diorite complex * Bogdanov (1983),

Popov et al. (1983); Bonev et al (2002).

- **Frieda River-Nena Cu-Au ore field, PNG** * Rc (Frieda) 1.0 bt @ 0.47% Cu, 0.28 g/t Au; Nena Rc 60 mt @ 2% Cu, 0.6 g/t Au * Mi; Frieda: 5 porphyry Cu-Au orebodies, pyrite, chalcocopyrite, magnetite > bornite fracture stockwork in biotite altered diorite; Nena: high-sulfidation pyrite, enargite, luzonite etc. in residual silica altered core in silicified and advanced argillized breccias * Mi andesite-diorite arc complex, remnant of Mi2 stratovolcano * Morrison et al. (1999).

6.5. Low sulfidation (LS) deposits

Low-sulfidation epithermal deposits contain more "giants" than the high-sulfidation category. They include the world's largest silver deposit (Cerro Rico-Potosí, 86,000 t Ag) and 4 out of 10 world's largest silver accumulations. They also store a major proportion of world's gold resources (Cooke and Simmons, 2000), significant share of lead and zinc, and some Hg, Sb, Sn. Sillitoe (1993) tabulated characteristics of alkalic, sub-alkalic rhyolite, and sub-alkalic andesite-rhyodacite LS sub-categories by rock association. Of these, the deposits associated with alkaline igneous complexes have some unique features although of the four "giants" recorded two (Cripple Creek and Emperor) are in a potassic (shoshonitic) suite whereas the other two (Porgera and Ladolam) are in a sodic suite. The alkaline-related LS deposits have been reviewed by Richards (1995) and, together with other types of deposits, by Mutschler and Mooney (1993). The two calc-alkaline sub-associations of Sillitoe (1993) are considered jointly, as their characteristics overlap and are rarely fully developed to define a group; besides, as LS deposits depend on convection of heated meteoric water, the source of heat is often "anonymous": not in sight and not necessarily related to the volcanic suite which may host the orebodies. To those above should be added the rarely occurring peraluminous felsic volcanic suite dominated by rhyolite and lithophile metals, where related "classical" epithermal deposits are small and scattered. The subvolcanic and plutonic levels of peraluminous suites have, however, produced important deposits in the Bolivian Tin Belt. Descriptive treatment of the LS deposits followed in this book is best based on the ore metals: Au-Ag rich, Pb-Zn-Ag rich, and the rest.

The young, "typical" LS deposits hosted by andesite or dacite come as fissure or fault-controlled crustiform, massive or breccia veins of quartz (chalcedonic, white crystalline, sometimes amethyst), with or without adularia, Mn-carbonate

(rhodochrosite) and rhodonite, calcite, barite and fluorite gangue interspersed with bands or scattered grains of ore minerals. Discrete veins often split into zones of subparallel or anastomosing second-order veins, stockworks or breccias. Long, persistent fault structures like the Veta Madre in Guanajuato (25 km long) or the Comstock Fault (7 km long) contain a variety of discontinuous orebodies separated by barren, or pyritized, gouge. In many instances the selvage of altered rock bordering a discrete high-grade quartz vein has low-grade gold values (mostly in pyrite) and in deposits that consist of numerous subparallel quartz veins formerly mined individually from underground (e.g. Antamok, Waihi), the modern open-pit operations bulk-mine everything including the old stopes and pillars.

In addition to veins disseminated, usually low-grade pyritic Au-Ag orebodies in altered porous rocks (tuff, coarse fragmentals, fault or diatreme breccias), make up several "giants". The generally low-grade ore zones could be blanket-like, "stratabound", such as the unwelded mineralized felsic tuff at Round Mountain enclosed in densely welded altered ignimbrite, or replacements of terrigenous sandstone horizons in vein extensions in the Balei goldfield, Siberia (Lozovskii et al., 1960). Subvertical mineralized breccia structures are represented by the Cresson diatreme in the Cripple Creek goldfield and by the Dealul Cetate diatreme at Roşia Montană.

LS veins often reach into the basement under volcanics, or crop out entirely within the basement rocks when the volcanics have been removed by erosion. The pre-volcanic rocks can have a substantial influence on the form of orebodies: veins or fluid conduits that intersect carbonate horizons may change into replacements (mantos), impervious horizons such as shale or clay-sealed unconformities may force ascending fluids to pond and produce orebodies laterally extending from a fissure. Epithermal pyritic or galena-sphalerite carbonate replacements with silica (jasperoid) gangue are difficult to distinguish from mesothermal replacements. Epithermal deposits intersecting or interacting with pyritic carbonaceous rocks (black slates, phyllites) as in Guanajuato, or earlier massive sulfide orebodies, are a special case periodically causing a debate as to whether these rocks supplied the ore metals, or sulfur, now found in the epithermal veins.

The ore mineralogy of LS deposits ranges from finely dispersed ("invisible") gold or electrum in white quartz without sulfides (Mt. Skukum, Yukon; not a "giant!") through low-sulfide gold-quartz

veins with gold in quartz or with pyrite (arsenopyrite is rare in epithermal deposits), to gold-dominated "bonanza" veins (Hishikari), or "silver bonanzas" with argentite/acanthite, Ag-sulfosalts and electrum (Mexican-type deposits like Guanajuato). Most LS Pb, Zn, Cu sulfides-rich veins yield by-product Au and Ag (Creede-type). Often, as in the Veta Madre in Guanajuato or in Zacatecas, the bonanza ore shoots are superimposed on the dominant and persistent quartz lodes with sparse Pb, Zn, Cu sulfides. Au-Ag tellurides occur locally and are most widespread in the alkaline LS sub-type (Cripple Creek, Porgera). Selenides (naumannite) are rarely present (e.g. in Kochbulak), whereas molybdenite, stibnite, cassiterite, stannite occur as accessories or form orebodies of their own. In oxidized outcrop the low-sulfide gold-quartz veins are leached, sulfides removed and converted into Fe hydroxide coatings where the residual gold is retained but rarely enriched. Outcrops of bonanza Ag-veins and veins rich in argentiferous galena often contained masses of almost pure Ag-halides (chlorargyrite, bromargyrite) or their mixtures with Mn oxides (residual after the rhodochrosite gangue). The high-sulfide Pb, Zn, Cu veins formed standard Fe- and Mn-hydroxides rich gossans grading downward to oxidation and (Ag-rich) secondary sulfide zones on top of the hypogene orebody.

Young, pristine epithermal deposits in volcanics may be capped by remnants of laminated silica sinter changing laterally to acid leached zones and downward into soft argillized intervals that suffer rapid erosion. Various exhumed zones of subsurface silicification may also be present in outcrop (Sillitoe, 1993).

LS veins in depth, unmodified by supergene processes, will have the immediate wallrock adjacent to a vein silicified or altered to adularia, sericite or illite, smectite and/or chlorite, sometimes anhydrite. The outer alteration envelope, often of regional extent, will be "propylitized", i.e. altered to chlorite, albite, pyrite, calcite, epidote and/or clinozoisite. Minerals characteristic for the HS association like alunite, pyrophyllite and diasporite often intervene as well (e.g. in the Comstock Lode). Alkaline systems like Cripple Creek (Thompson et al., 1985) and Porgera have adularia, dolomite, roscoelite (greenish vanadate mica) and pyrite in the inner alteration zone; sericite, smectite, magnetite, minor adularia and pyrite in the outer zone. Veins in rhyolite lack the "propylitic" envelope and chlorite/epidote only occur in place of biotite. At Round Mountain (Sander and Einaudi, 1987) the alteration of felsic tuff passed through

several stages and is now dominated by selective replacement of sanidine phenocrysts by adularia and the plagioclase groundmass by albite. Elsewhere, silicification is most common and kaolinite substitutes for smectite.

6.5.1. Au-dominated low-sulfidation ores

These have been reviewed in detail by Cooke and Simmons (2000). There is an almost uninterrupted sequence of LS deposits between the gold-only (e.g. Round Mountain) and silver-only (e.g. Batopilas) end-members, with most deposits in-between. The exact genetic cause is unknown, but usually attributed to lithologic variations in the subsurface where the convecting fluids extracted their metals (example: ophiolitic basements as under the Apuseni Mountains gold province in Romania tend to support high Au:Ag ratio ores; "black shale" basements as under the Mexican Ag "bonanzas" breed high Ag:Au ratio ores). Because of the lower silver dollar values relative to gold, many "gold" deposits in the public mind, like the Comstock Lode, are in fact Ag>>Au deposits.

Round Mountain-Au, Nevada (Sander and Einaudi, 1990; Henry et al., 1997; P+Rc 453 t Au @ 1.15 g/t, ~150 t Ag). This is a "giant" low-grade gold deposit discovered in 1906, but large-scale mining (open pit and heap leach) started only in 1977 when profitable technology became available. In the literature Round Mountain tends to be listed under "hot springs", "stockwork" or "disseminated" gold, none a satisfactory designation.

Situated in the Basin-and-Range Province, this deposit is hosted by variably welded Oligocene rhyolitic ash-flow tuff issued from a caldera and probably overlying caldera ring fracture. Lower poorly welded tuff is capped by densely welded ignimbrite, in turn topped by erosional remnants of another non-welded unit. The "bulk" mineralization, oxidized to a depth of 400 m, resides in the lower and middle tuff units. In the welded ignimbrite gold is controlled by zones of short, parallel (sheeted) brittle fractures in unaltered or slightly previously silicified and/or K-altered tuff. The fracture density is of the order of 3 to 5 per 1m. Most fractures are "clean", with or without thin sericite rims, but some are filled by clay gouge, coated by Fe-hydroxides (after pyrite), or covered by flat adularia crystals. Gold comes as scattered crystals plus "moss gold". Coarse gold nuggets are common in the clay gouge and require gravity separation.

The lower, non-welded tuff contains the main Au resource in predominantly unoxidized refractory ore

that form stratabound blanket-like orebody. Electrum, free or in pyrite, is associated with pyrite cubes sparsely scattered (1-3% by volume) in sericite and adularia-altered tuff matrix and in some lithic fragments. Scattered higher-grade (to bonanza-grade) fissure veins were selectively mined in the area before the bulk mining, but the production was very minor. Gold precipitated during a brief hydrothermal event around 26.0 Ma, shortly after cooling of the pyroclastics, from low-salinity fluids at and below 275°C (Henry et al., 1997). The "bulk" Au mineralization is inconspicuous as there are no associated intrusive dikes or stocks in the area (no caldera resurgence). The mineralization predates the basin-and-range extension in Nevada which, however, contributed to the deposit preservation on a pediment surface. Minor fan conglomerate and alluvial gold placers formed most recently.

Metaliferi (South Apuseni) Mountains Au-Ag province, western Romania

This is the most productive gold province of Europe, exploited at least since the times of the Roman occupation (A.D. 100; Ianovici et al., 1976; Ianovici and Borcoş, 1982; Alderton and Fallick, 2000; P+Rc ~1,800 t Au plus Ag, Te). Like the Erzgebirge, this is also an area of classic 18th to 19th centuries studies (von Cotta, Pošepný) that provided factual foundation on which has been built the science of Economic Geology. Unfortunately the lack of English literature in the past seventy years, due to political changes more than to the decline of mining, condemned this province to obscurity from which it is only now emerging.

The richly mineralized area measures about 600 km² and it is an about 60 km long, NE-extending wedge north of Deva; the main mining centers are Brad and Roşia Montană. This is a part of the historic Transylvania and many of its localities are known in the literature under the former Hungarian names; this applies to some mineral names e.g. nagyagite, named after Nagyag, now Săcăramb). Apuseni Mountains are one of the blocks that rises above the flats of the Cenozoic Transylvanian and Pannonian Basins, on the inner side of the Carpathian Foldbelt arc (a component of the Alpine orogen; Heinrich and Neubauer, 2002). There is a Carboniferous and older (Variscan) metamorphic basement covered by NW-verging nappes of Jurassic, predominantly basaltic ophiolites, and Cretaceous flysch (turbidite). They are attributed to the closure of Tethyan Basin and incorporation of scattered blocks and basins into the European plate,

during a series of diachronous collisions (Alpine orogeny; Mitchell, 1996).

Two economically important magmatic episodes, attributed to subduction, took place and their products are widely scattered in this part of Europe. The late Cretaceous to Eocene "banatite" episode produced porphyry Cu-Mo deposits in Banat and East Serbia; the Miocene-Pliocene episode produced calc-alkaline subaerial volcanics associated with epithermal Au-Ag and Pb-Zn, some with porphyry-Cu in depth. Configuration of the Miocene continental (micro)plates is uncertain.

The Metaliferi Mts. contain five Au-Ag ore fields (or districts), each of which except one also have porphyry Cu-(Au) prospects in depth. All are genetically associated with late Miocene-early Pliocene andesites and their subvolcanic equivalents. One porphyry prospect (Roşia Poieni, ~4 Mt Cu) is of the "giant" magnitude, but only two porphyry Cu were actually mined: Deva, in the Mureş Valley south of the gold province. The abundant porphyry-Cu occurrences seem to confirm the conclusion based on O and H isotopes (Alderton and Fallick, 2000) that the mineralizing fluids to the epithermal veins were largely of magmatic derivation, with barely any meteoric water to prove. The total prehistoric and historic gold production of the entire province is estimated at some 1,260 t Au (Muzeul Aurului, Brad, oral information, 1994) but the record is fragmentary and cannot be subdivided to credit individual deposits of which there is close to 40. The Brad (Barza) and Roşia Montană goldfields are the largest and demonstrably stored "giant" quantities of gold.

Brad goldfield (?1000 t Au; Ianovici and Borcoş, 1982) has several groups of dominantly NNW and NE-trending fissure veins in an E-W zone about 10 km long, centered on the Barza paleo-volcano. The host rocks form a chain of middle-late Miocene plugs and vents of hornblende andesite, and coalescing andesite flows with rare pyroclastics and volcanoclastics, usually at base. The vents intruded Jurassic ophiolitic (mostly basaltic) basement and some veins persist there. In the Musariu Nou mine the auriferous veins in the ophiolite are high in base metal sulfides and there is a porphyry Cu-(Au) orebody in andesite porphyries near contact with ophiolites. The steeply-dipping fissure veins comprise massive, drusy, locally banded white or amethystine quartz grading to breccias. Carbonates (calcite, dolomite, rhodochrosite), adularia, and barite are common gangue minerals and most veins have a moderate content of Pb, Zn and Cu sulfides. Gold comes partly as electrum, partly as Au-Ag tellurides most

of which have been first described from here (krennerite, hessite, petzite, sylvanite, nagyagite). In **the Săcăramb Au-Ag-Te deposit** (Alderton and Fallick, 2000) tellurides are the main ore carrier. There, a 14 Ma andesite stock, andesite flows, and rarely Miocene sandstone above Carboniferous schist basement, are intersected by 13 major NNW and NNE vein groups. The thin (average 0.3 m) and steep fissure veins are 500-600 m long and reach into a depth of 600 m. They are vuggy, grade to breccia, and composed of quartz with Ca-Mg carbonates, barite, pyrite, Pb, Zn, Cu sulfides, As-Sb sulfosalts, and tellurides. The veins have thin (~1-1.5 m) quartz, sericite, adularia, clay alteration envelopes, in regionally propylitized andesite.

Roșia Montană-Au,Ag ore field (Ianovici et al., 1976; O'Connor et al., 2001; P+Rc ~450 mt of ore containing ~501 t Au, 2400 t Ag) has been active at least since A.D. 100. The old miners selectively mined the high-grade vein and breccia intervals, leaving behind over 140 km of underground drives, stopes and glory holes, many hand- and fire-excavated. O'Connor et al. (2001) estimated the total amount of gold produced from Roșia at mere 28 t Au, a way too little! The gold endowment has greatly increased with delineation of the low-grade resource of 344 Mt @ 1.3 g/t Au and 6 g/t Ag, to be mined from six areas (O'Connor et al., 2001).

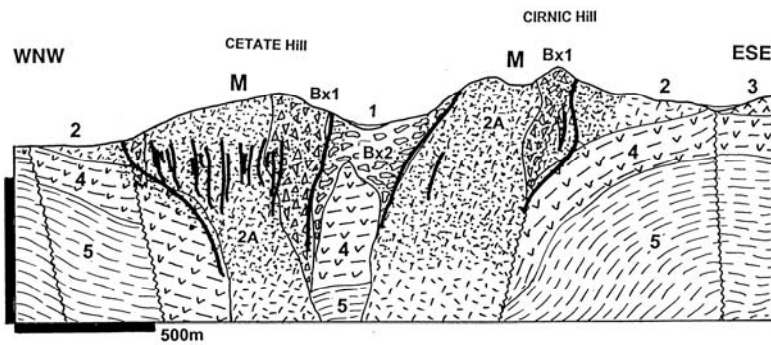
Roșia Montană orebodies are a part of a Miocene rhyodacitic (dacitic) volcanic center (a diatreme-dome complex interpreted as a core of stratovolcano), emplaced through late Cretaceous carbonaceous shale. The latter is a member of turbiditic suite and it contains lenses of grey pelitic limestone. The shale is covered by acid to intermediate volcanoclastics of the first Miocene eruptive phase (Badenian). Two prominent hills with mine workings above Roșia Montană, Dealul Cetate and Dealul Cîrnic, are cored by thoroughly altered rhyodacite with corroded bipyramidal quartz phenocrysts in quartz-sericite-matrix, emplaced into heterolithic "vent breccia". More breccia varieties are present. "Black breccia" forms an unmineralized pipe between both hills, and there are thin phreatomagmatic? subvertical breccia columns in rhyodacite, mostly composed of rhyodacite fragments in adularia, quartz, illite, and pyrite altered matrix (Fig. 6.16).

The old-time miners worked high-grade but thin fissure veins, stockworks and silicified breccias filled with quartz (often amethystine), rhodochrosite, pyrite, tetrahedrite, alabandite, Pb-Zn-Cu sulfides, Ag-sulfosalts and electrum. The low-grade "bulk" ore comprise fine-grained electrum disseminated with pyrite in altered

rhyodacite and breccias. The mineralization is interpreted as a "porphyry-Au" precipitated from boiling magmatic-hydrothermal fluid, although still at the epithermal range of temperatures (~266-230°C).

Additional Au-dominated LS "giants": These are briefly tabulated below; some are recent discoveries for which information is lacking.

- **Donlin Creek** ore field, SW Alaska * Rc 777.5 t Au * 70 Ma, 12 vein & stockwork orebodies of quartz, carbonate, arsenopyrite, pyrite, stibnite, gold in sericite, pyrite, carbonates altered faults; transition to orogenic Au * Cr turbidites of accretionary complex cut by rhyodacite dikes * Goldfarb et al. (2004).
- **McDonald Au deposit** 65 km NW of Helena, Montana * Rc 375 mt @ 0.67 g/t Au for 251 t Au * T, stockwork of quartz-adularia veinlets and replacements of permeable tuff layers, stratabound silica sinter on top; a hot-spring deposit?
- **Alto Chicama**, N-C Peru * Rc 295 t Au, 1.54 g/t * epithermal, "in quartzite" * SEG Newsletter No. 58, 2004.
- **Kochbulak-Kairagach** (Angren) Au-Ag-Te ore field, Kurama Range, Uzbekistan * ?290 t Au + Ag, Te * Cb-Pe, several zones of steeply dipping gold-quartz veins and silicified diatremes with complex As,Bi,W,Cu,Pb,Zn,Sb association, tellurides and gold; quartz, sericite, propylite alteration * In Cb₂ andesite, tuff, dacite cut by stocks of syenodiorite * Borodaevskaya & Rozhkov (1974).
- **Balei ore field (Taseevka deposit)**, Eastern Transbaikalia, Russia * P+Rv 80 mt @ 3.3-16 g/t Au for 458 t Au * Cr, quartz, chalcedony, adularia, carbonates, pyrite, chalcopyrite, pyrrargyrite, electrum veins to stockworks; quartz, sericite alteration * in Pt to PZ basement gneiss & granitoids, Tr-Cr continental sediments, J granodiorite * Lozovskii et al. (1960).
- **Hishikari Au deposit**, Kyushu, Japan * 326 t Au @ 60 g/t * 1 Ma, bladed quartz, adularia, pyrite, gold; several fissure & fault, vein groups in silicified & smectite-altered volcanics * Q andesite, dacite near unconformity over Shimanto accretionary prism sediments, above molten magma chamber * Izawa et al. (1992).
- **Morobe Goldfield** (Wau, Bulolo, Eddie Creek), PNG * 264 t Au, much from placers * Pl-Q, several groups of quartz, adularia, pyrite gold veins, stockworks, disseminations in silicified & sericite-altered diatreme and faults; alluvial placers * in Pl-Q dacite plugs & domes, Mi granodiorite, MZ metamorphics * Sillitoe et al. (1984).



1. Q alluvium & colluvium, include Au placers; 2. Mi₂₋₃ rhyodacite porphyry stocks; 3. Mi quartz andesite; 4. Felsic volcaniclastics; 5. Cr₃ black shale, minor limestone. Bx1. Altered phreatomagmatic? breccia; Bx2. "Vent" ("Black") breccia: maar lake deposit? A. Hydrothermal alteration: silica, adularia, illite, pyrite, clay

Figure 6.16. Roșia Montană Au ore field, Apuseni Mts., Romania. Cross-section from LITHOTHEQUE No. 2080, modified after Borcoș in Ianovici et al. (1976), O'Connor et al. (2001). ORES: M. Thin low-sulfidation higher-grade fissure veins and mineralized breccias (black lines) enveloped by blocks of disseminated low-grade gold in altered rhyodacite and breccias (outlined)

6.5.2. Au-(Te)>Ag alkaline association

These deposits, now mostly interpreted as low-sulfidation magmatic-epithermal, have been reviewed by Müller and Groves (1997). Cripple Creek and partly Porgera are the best known "giants" in the cordilleran and collisional settings, briefly reviewed here. Their counterparts in the young island arcs, Emperor and Ladolam (Lihir), are in Chapter 5.

Cripple Creek Au-Te goldfield, central Colorado (Lindgren and Ransome, 1906; Thompson et al., 1985; Kelley et al., 1998; P+Rc 817 t Au plus Te) is in the southern Rocky Mountains, east of the Rio Grande Rift. The regional rocks are Proterozoic schists and gneisses intruded by several generations of granitoids. The goldfield coincides with an elliptical NW-elongated basin with an area of 18 km², considered as an early diatreme. It has a very heterogeneous fill known under the group name of Cripple Creek Breccia (CCB; Thompson et al., 1985). The most magma-proximal members are coarse, fragment-supported heterolithologic vent? breccias of mixed basement, Tertiary volcanic, and sedimentary fragments. These breccias grade to matrix-dominated bedded fragmentites interstratified with lacustrine and fluvial clastics. Water-lain sediments have been found down to a depth of 1000 m under the surface. The present explanation is that the CCB started as an early diatreme (maar?) followed by subsidence and fluvial and lacustrine sedimentation, interrupted by renewed explosive eruptions. The CCB is intruded by a suite of Oligocene (32.5-28.7 Ma) intrusions dominated by phonolite, with lesser trachyandesite and rare mafic to ultramafic members. Some

intrusions have remnants of subaerial flows, but most are dikes poorly exposed at the surface. The rocks are attributed to fractionation of alkali basalt magma contaminated by lower crustal materials (Kelley et al., 1998). Also present are small, subvertical breccia pipes interpreted as phreatomagmatic eruptions. The Cresson Blowout is the best known and well mineralized example. It is a breccia pipe filled by fragments of basement and alkaline rocks in lamprophyre and rock flour matrix.

Cripple Creek is a famous goldfield discovered in 1891 and largely deserted by the 1960s. The cumulative past production of 653t Au has been derived from thin fault and fracture lodes, and from vug-filling ores in the Cresson breccia. In both types of orebodies gold resided almost exclusively in tellurides, free gold being rare and mostly "secondary". The lodes are composite structures 0.5 to 3 m thick, assembled from a number of narrow subparallel vuggy veinlets typically adjacent to phonolite dikes. The fill is multistage, but the dominant early assemblage has quartz, biotite, K-feldspar, fluorite, dolomite and pyrite gangue. The Cresson vugs were often lined by ore minerals only, with not much gangue. One "mega-vug" there yielded nearly 2 t Au. The ore minerals are pyrite, lesser galena and sphalerite, and a variety of rarer Cu, As, Sb, Hg sulfides that are locally present. The tellurides are dominated by calaverite (AuTe₂) with lesser krennerite, sylvanite and petzite. The alteration is erratic with K-feldspar and pyrite dominant. Narrow alteration envelopes around the veins with tellurides have sericite, pyrite, roscoelite, adularia, magnetite and fluorite.

In the 1980s have been discovered near-surface zones of finely disseminated gold at fault

intersections or along major NW shears. These added further 164 t Au to the goldfield total, although grades are within the 1.0-3.0 g/t Au range. Microcrystalline gold is free or enclosed in pyrite, in fluorite, quartz, barite gangue. Permeable zones are enclosed in adularia, pyrite and sericite altered wallrock. The largest Cresson deposit is in vicinity of the famous Blowout orebody, but unrelated to it.

The Cripple Creek Au mineralization is multistage, believed formed from early magmatic-hydrothermal fluids within the temperature range of 250°-105°C, between 31.3 and 28.2 Ma (Kelley et al., 1998).

Porgera Au-Ag-(Zn,Pb) ore field, Papua New Guinea (Handley and Henry, 1990; Richards and Kerrich, 1993; Ronacher et al., 1999; 613 t Au, ~1,800 t Ag). Porgera has been discovered in 1938 in the PNG Highlands, 130 km WNW of Mt. Hagen, to join much later the league of the New Guinean Au and Cu "giants". Although popularly recognized as a rather unique "porphyry-Au" or "epithermal bonanza" associated with alkaline mafic magmatism, it departs from the above images. First, the alkaline complex is sodic (that is, of splilitic affinity) rather than potassic as in shoshonites, and at least a portion of the sodic character is due to alteration (especially of the peperites, produced by mingling of high-level magmas with wet marine sediments). Second, the "porphyry-Au" is really a disseminated Au-pyrite mostly in calcareous black mudstone above porphyry intrusions, grading to Fe-Zn-Pb veining; a rather common mesothermal ore variety. This leaves us with the truly epithermal fault veins that contain Au-bonanza ore shoots (Fig. 6.17).

Porgera is in Cretaceous carbonaceous and calcareous mudstone, a shelf association deposited on the passive margin of the Australian Plate. Presently this is a late Miocene, early Pliocene fold and thrust belt resulting from collision. The sediments are intruded, along NW and NE fault intersections, by about 6 Ma high-level porphyritic hornblende and augite diorite (gabbro), later andesite (alkali basalt), and latest-stage feldspar porphyry dikes. The magmatic rocks are epidote, chlorite and carbonate-altered and they produce slight induration in their roof rocks. The latter are strongly folded and faulted with gradations to tectonic melange.

Hydrothermal ore deposits are associated with the porphyry phases and are structurally controlled. The early-stage, low-grade bulk-mined orebodies (104 mt @ 3.6 g/t Au) consist of disseminated auriferous pyrite gradational to pyrite, sphalerite,

galena veinlets or veins in sericite-carbonate altered sediments and partly porphyry. In depth, these are joined by masses of magnetite, chalcopyrite and pyrrhotite in biotite, actinolite, anhydrite-altered hosts (Ronacher et al., 1999). The late-stage epithermal (250-145°C) mineralized breccias and veins are mostly confined to the Roamane Fault. They comprise quartz, pyrite, minor tetrahedrite, adularia, roscoelite, native gold and Au-Ag tellurides. Bonanza shoots may exceed grades of 1% Au over short intervals and they contain spectacular coarse specimen gold. The ore formation took place at ~5.7 Ma (Richards and Kerrich, 1993).

6.5.3. Bonanza Ag >> Au

Low-sulfidation epithermal deposits of precious metals, including "giants", can be assembled into a continuous sequence between the Au and Ag end-members (this is most convincing when based on the tonnage-accumulation index ratios; also on the monetary values of each metal). The results are sometimes influenced by oxidation, where the mined oxidized ore depleted in silver (e.g. in Yanacocha) has Au > Ag, whereas the hypogene ore has a reverse ratio. Many heap leach operations do not recover silver, hence Ag does not appear in statistics. It is not known what causes the Au : Ag variations but there is a distinct Au or Ag provincialism and the Mexican Silver Province, in particular, is world famous. This section focuses on deposits where silver is dominant.

Comstock Lode (Virginia City goldfield) Ag-Au, Nevada (Vikre, 1989; Hudson, 2003; Berger et al., 2003; Pt ~19 mt of ore containing 312 t Au @ ~14 g/t; 7,260 t Ag @ ~340 g/t). Discovered in 1859 and located 24 km SE of Reno, this is one of the icons of the American West, still worth visiting to savor the spirit. The area is near the western limit of the Great Basin, where Mesozoic basement is overlain by lavas and pyroclastics resulting from several pulses of a Miocene stratovolcano. The basal andesites (18-15 Ma) are intruded by 15.2 Ma diorite and overlain by 14.7-12 dacite to rhyodacite (Kate Peak Formation), coeval with the epithermal mineralization. The widespread alteration and mineralization is structurally controlled and two (or three) prominent normal fault zones: the Comstock Fault and the Silver City Fault, controlled most of the metals produced. Comstock Fault (also called Lode) is a 15 km long N15°E striking, 30-50° east dipping repeatedly reactivated brittle fault zone up to 100 m wide. It is filled by silicified fault breccia and gouge and/or

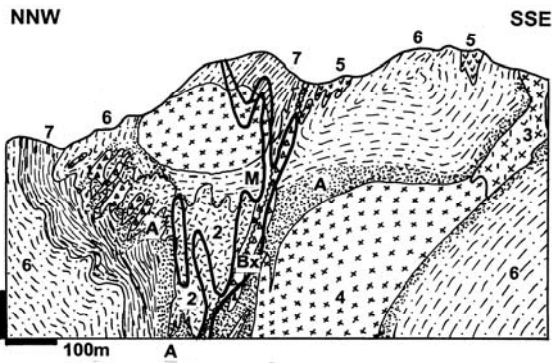


Figure 6.17. Porgera Au ore field, New Guinea Highlands. Cross-section from LITHOTHEQUE No. 2245, modified after Porgera Joint Venture (Placer Pacific, Ltd.), 1997. 2. ~6 Ma feldspar porphyry dikes; 3. "Augite diorite" (melanogabbro); 4. "Hornblende diorite" (gabbro); 5. Alkali basalt to trachyandesite; 6. Cr₃ Fine clastics, carbonaceous mudstone; 7. Ditto, calcareous to dolomitic siltstone & sandstone; 8. Ditto, sericite-dolomite altered. M. 6.0-5.7 Ma multistage Au mineralization (description in text); Bx. Fault, hydrothermal and diatreme? breccias

hydrothermal stockwork of predominantly quartz with some adularia, with an upward increasing carbonate content. Near Virginia City the Kate Peak andesite is in the hangingwall, Davidson Granodiorite in footwall. Much of the fault zone fill is barren or at most slightly pyritic. The ore-bearing sections, when developed, are only about 2-5 m wide. In them, individual "bonanza" veins are from 2 mm to 3 cm wide and they consist of several generations of pyrite, argentite, electrum, galena, sphalerite, and chalcopyrite. The mineralization occurs in compartments or in ore shoots branching from the Lode. Big Bonanza, an ore shoot that was 300 m wide, 217 m tall and 66 m wide (stope width) produced 1.4 mt of ore that yielded 75 t Au and 1,400 t Ag, between 1873 and 1882. The main mineralization stage has been dated at 13 Ma, the low-salinity fluids varied between 300°C and 235°C..

The Comstock goldfield is extensively hydrothermally altered and alunite-rich ledges, sometimes with pyrophyllite, are widespread, although without mineralization. Of the 12 alteration assemblages recognized (Hudson, 2003) silicification, adularia and sericite-illite are immediately adjacent to the lodes, whereas propylitization (this is its type area) is areally distributed.

Mexican silver province (belt)

A broad, 2000 km long mineralized belt extends from Rio Grande in the north to Mexico City in the south. It contains eight "giant" silver ore fields, and more deposits of the "large" magnitude. All are related to Tertiary calc-alkaline magmatism. Three deposits (Santa Eulalia, San Francisco del Oro, partly Fresnillo) are of the high-temperature Zn-Pb sulfide replacement type with Ag by-product. Six deposits (Tayoltita, Pachuca, Zacatecas, Guanajuato, Batopilas, partly Fresnillo) are of the low-sulfidation vein and stockwork type with a minor proportion of base metal sulfides (Zn, Pb and Cu are not normally recovered). Of the latter, Batopilas is silver-only, whereas Tayoltita also produces significant gold.

Pachuca-Real del Monte Ag-Au ore field (Fries, 1991; P+Rv 42,452 t Ag, 215 t Au). This is the world's second largest epithermal silver accumulation after Potosí, discovered in 1522, 100 km NNE of Mexico City. Located at margin of the Mexican Neovolcanic province, the geology comprises subhorizontal units of early Oligocene and late Pliocene subaerial andesites, resting on Mesozoic miogeoclinal carbonates in greater than 700m depth (outside the limit of mining). The volcanics are block-faulted and intruded by Pliocene rhyolite and dacite dikes, probably coeval with mineralization. The relatively compact ore field (~10 x 8 km) contains numerous sets of NW and NNE-trending, steeply-dipping extensional veins, controlled by faults. The veins consist of vuggy quartz with adularia, calcite, low proportion of Pb, Zn, Cu sulfides, acanthite, argentite and Ag-Sb-As sulfosalts. The present grades are of the order of 180 g/t Ag and 1.2 g/t Au, but they were much higher in the past coming from bonanza ore shoots and Ag halides in the oxidation zone. The veins have albite, sericite, and carbonates alteration envelopes, in regionally propylitized volcanics.

Guanajuato Ag-Au district, central Mexico (Gross, 1975; Querol et al., 1991; P_{to} 1984 31,700 t Ag, 135 t Au). Although only the second-largest, this is the most historical and cultural of the Mexican silver cities (and districts); Fig. 6.18. Discovered in 1548, the district occupies an area of about 20x16 km in the Mesa Central metallogenic region. The folded, greenschist metamorphosed basement is represented by Triassic to Cretaceous Esperanza Formation of gray to carbonaceous phyllite with interbedded marble and greenstone, and diorite intrusions. It crops out, in places, in the Veta Madre footwall. Gross (1975) reported anomalous trace values of Ag (8.3 ppm Ag) and Au

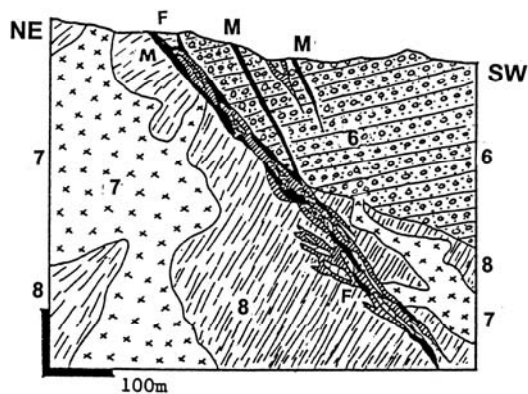


Figure 6.8. Guanajuato, Mexico, cross-section of the Veta Madre near the Las Torres Mine. From LITHOTHEQUE No. 1089, modified after Guiza (1956). M. 29-27 Ma low-sulfidation "Ag-bonanza" veins. F. Fault zone; 6. Eo-Ol red conglomerate; 7. Cr₃-T1 granite to diorite, local gabbro; 8. J-Cr black phyllite, minor marble and greenstone

(0.15 ppm Au) in the black phyllite, the ratios of which closely approximate metal ratios in the lodes, hence these rocks could have acted as source beds during mineralization. This basement is intruded by the probably "Laramide" granitoids of the La Luz Complex in the NW and unconformably overlain by Eocene red bed conglomerate and sandstone which, in turn, are capped by Oligocene mainly rhyolitic and dacitic pyroclastics, lavas, domes and "lake beds". These units are intruded by andesite and rhyolite dikes considered feeders to the Oligocene volcanics and probably coeval with the 30.7-27.4 Ma epithermal veins in the area.

The ore field is situated on the NE flank of a NW-trending regional syncline and although the Eocene and younger units are flat-lying to gently dipping, they are intensely faulted and these faults control the metallic deposits. Three NW-trending mineralized fault systems are most prominent in the district, each of which also constitutes a mineralized subdivision: La Luz in the NW, Veta Madre in the center, La Sierra (Peregrina) in the NE (Querol et al., 1991). The 25 km long Veta Madre fault zone (system) dips 35° to 55° SW, is most persistent, and it accounts for at least ¾ of the precious metals produced from the field.

Veta Madre Ag-Au zone (Gross, 1975) is a brittle deformation zone (normal fault) up to 100 m wide filled by blocks (slivers) of wallrocks interspersed with tectonic breccia and gouge. The rocks are variously silicified, chloritized and quartz-calcite veined, then re-brecciated. The Veta Madre Ag-Au deposit is a zone of discontinuous

(compartmentalized) mineralized segments and "bonanza" shoots within the fault, that varies in thickness from few cm to 30 m. The narrow orebodies have the form of sharply outlined tabular veins, the thick orebodies are internally stockworks of anastomosing veins. The veins consist of quartz (commonly chalcedonic or amethystine), calcite and adularia with scattered pyrite and Zn, Pb, Cu sulfides. Silver accumulates in dark gray bands or diffuse patches of fine-grained silver minerals, with a high proportion of selenides. The main Ag minerals are acanthite and aguilarite, followed by Ag-As-Sb sulfosalts. Wallrocks and breccia fragments in veins are argillized and sericite-adularia altered, in addition to the pervasive silicification. Outside the veins the rocks are propylitized, the redbed conglomerates are bleached and reduced. The homogenization temperatures range from 385° to 160° C, with an average of 230°C (Querol et al., 1991).

Additional Ag >> Au "giants":

- **Batopilas-Ag**, Chihuahua, NW Mexico * Pt 9,360 t Ag * Ol?, groups of thin, short fissure and fault veins of calcite with irregular pods of native silver; slight silica, chlorite, actinolite wallrock alteration, proximity to porphyry-Cu prospect * in Ol andesite, dacite, granodiorite * Wilkerson et al. (1988).
- **Tayoltita-Ag, Au** (San Dimas), Sinaloa, NW Mexico * Pt ~14,337 t Ag, 304 t Au * 43-40 Ma, groups of quartz, adularia, rhodochrosite, calcite with scattered Cu, Zn, Pb sulfides, Ag-sulfosalts, electrum in sericite altered hosts * in Cr-Mi rhyolite, andesite, granodiorite * Clarke & Tittley (1988).
- **Metates-Ag, Au**, Durango, N. Mexico * Rc 434 Mt @ 18.6 g/t Ag, 0.75 g/t Au for 8072 t Ag, 325 t Au * presumably stockwork/disseminations in altered volcanics * Mining Annual Review, 1999.
- **Zacatecas-Ag**, N-C Mexico * Pt 23,236 t Ag @ ~10 g/t + Zn, Pb, Cu, Au * Ol, three groups of quartz, calcite, pyrite, Zn, Pb, Cu sulfides, freibergite, acanthite & Ag-sulfosalts fissure & fault veins; quartz, sericite, clay alteration * in Eo-Ol latite, rhyolite in deeply eroded caldera on Cr microdiorite, Pe-Tr supracrustals * Ponce & Clark (1988).
- **Waihi-Ag, Au ore field**, Hauraki Goldfield, New Zealand * P+Rv ~9,500 t Ag, 252 t Au; most in Martha mine * Mi, conjugate system of quartz, adularia, calcite, rhodochrosite, pyrite, Pb, Zn, Cu sulfides, pyrrargyrite, acanthite, electrum veins in sericite, clay altered hosts * Mi andesite topped by post-ore rhyolite * Williams (1965).
- **Dukat-Ag, Au**, Omsukchan district, Magadan Oblast, E. Russia * Rv 30 mt @ 360 g/t Ag, 1 g/t Au for 10,800 t Ag, 30 t Au + Pb, Zn * 87-78 Ma, thirty quartz, chlorite, adularia, rhodochrosite, rhodonite, galena, sfalerite, acanthite, Ag sulfosalts shoots in fault veins; quartz, sericite, chlorite alteration * in Cr

rhyolite, volcanic dome flooded by leucogranite * Konstantinov (1993).

- **Prognoz-Ag,Pb,Zn**, Yana Basin, NE Siberia, Russia * ~10,000 t Ag * Cr, 12 zones of quartz, siderite, tetrahedrite, pyrrargyrite fracture veins * Elevatorski (1996).

6.5.4. Epithermal to mesothermal Pb, Zn, (Cu), Au, Ag deposits

LS epithermal vein deposits dominated by Pb, Zn, Ag with some Cu and by-product Au are known in the United States as "Creede-type" (Cox and Singer, eds., 1986). **Creede** is a Miocene (25.1 Ma) 8 km long adularia-sericite type vein ore field in the San Juan Mountains of Colorado, controlled by a structural graben external to caldera. Although Creede is only a "large" deposit (Pt 4.88 mt of ore containing 2,643 t Ag, 141 kt Pb, 45 kt Zn, 2.7 kt Cu and 4.82 t Au), it has been repeatedly studied and modeled in a minute detail (Barton et al, 1977). A porphyry Mo deposit, under a barren gap, had been predicted from past research results and actually intersected in a drillhole, although its economic worth is unknown.

There are over a thousand vein deposits of this type around the world, but most are of small to medium size. Only few are "large" (Toyoha and Hosokura in Japan, Pulacayo in Bolivia, Casapalca in Peru, Parral district in Mexico) although the aggregate production of the Romanian **Baia Mare district** (6 mt Pb+Zn; Grancea et al, 2002) that comprises Baia Mare, Baia Sprie, Cavnica, and lesser deposits, would exceed the "giants" threshold. The **Huarón Mine in central Peru** (Thouvenin, 1984; P+Rv ~28 mt ore containing 10,000 t Ag, 1.25 mt Zn, 736 kt Pb, 185 kt Cu), in operation since 1912, is a confirmed vein "giant". It is a zone of more than 70 fissure veins with minor replacement intervals where the veins intersect limestone, and it postdates Miocene monzonite dikes. The other vein "giant", **Beregovo** in the Ukrainian Transcarpathia, is credited with a reserve of 300 mt @ 1.5 g/t Au, 15 g/t Ag, 1.5% Pb and 2.1% Zn, published in *Economic Geology* (Vityk et al., 1994); if true, this would represent 450 t Au, 4.5 mt Pb and 6.3 mt Zn; a figure hard to believe for a vein deposit. This could be an error in decimals but if not, the essential information is below.

The large **Trepča-Pb, Zn deposit** near Kosovska Mitrovica, Kosovo (Schumacher, 1954; P+Rv ~50 mt @ 6.9% Pb, 4.2% Zn, 102 g/t Ag and 0.76% As) has a calculated content of 3.45 mt Pb, 2.1 mt Zn, 5100 t Ag, 380 kt As and 5350 t Bi. This is a galena, sphalerite, tetrahedrite, Ag-sulfosalts

replacement of marble at contact with an explosive breccia pipe related to Tertiary "trachyte".

The important **La Unión Pb-Zn-Ag ore field** in the Cartagena district, SW Spain, has been mined since the Roman or even Phoenician times (modern P+Rv were ~240 mt @ 3.8% Zn and 3.2% Pb for 9.12 mt Zn and 7.68 mt Pb; Oen et al., 1975) but there is no reliable record about the tonnage of silver taken from the oxidation zone. The ore field is in the Betic Cordillera, where the Variscan metamorphic basement is covered by a complex of stacked nappes produced by the Alpine orogeny, and capped by Miocene-Pliocene shallow marine sediments. In the basement Paleozoic micaschists alternate with marble, metaquartzite and amphibolite. The allochthon is dominated by Permo-Triassic phyllite, meta-quartzite, calcitic and dolomitic marble, evaporites and minor meta-dolerite. On top are remnants of Miocene-Pliocene subaerial volcanics (andesite, trachyandesite, latite) and hypabyssal stocks (Fig. 6.19).

In antiquity, high-grade silver-rich and easy to sort Miocene (~10.4 Ma) low-sulfidation epithermal fissure and fault veins, and residual oxidic Pb-Ag ores, were the principal object of mining. The veins formed mostly NW-trending swarms, zonally arranged in respect to volcanic centers. Ag-rich galena, sphalerite, pyrite, chalcopyrite, tetrahedrite, minor cassiterite, Ag-sulfosalts in silicified, argillized and propylitized volcanics graded to replacements when intersecting carbonate hosts. Modern mining in the 1960s to 1980s has been dominated by complex stratabound mantos in carbonate rocks adjacent to faults and phyllitic screen units, mined from a NE-SW line of open pits in the allochthon. The mantos, composed of scattered to locally massive galena and sphalerite ores with pyrite, magnetite, siderite and greenalite, were interpreted as either late Tertiary low-temperature hydrothermal replacements (Oen et al., 1975) or as syn-depositional (exhalative?) precipitates, later remobilized (Pavillon, 1969).

San Cristóbal Ag-Pb-Zn ore field, Bolivia (Kamenov et al., 2002; Rc 240 mt @ 62 g/t Ag, 1.67% Zn, 0.58% Pb for 14,880 t Ag, 4.01 mt Zn, 139 kt Pb). San Cristóbal is a newly developed "bulk-mineable" ore field in the Bolivian Altiplano south of the Salar de Uyuni. It is related to a Miocene subvolcanic center of andesite and dacite porphyry emplaced into mid-Tertiary continental red beds and volcanoclastics. This is a low-grade silver deposit sometimes referred to as "porphyry-Ag". First discovered in the 1630s, San Cristóbal is a mixture of small, higher grade veins of quartz, barite, siderite, hematite, tetrahedrite, stromeyerite

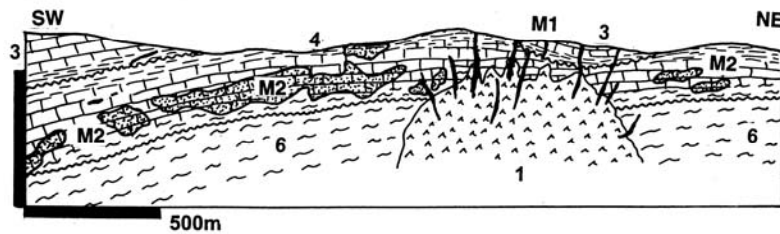


Figure 6.19. La Unión Pb-Zn-Ag ore field, Cartagena district, SE Spain. Diagrammatic cross-section from LITHOTHEQUE No. 1745, modified after Oen et al. (1975), Arribas Jr. & Tosdal (1994)

M1. 10.4 Ma low-sulfidation Pb-Zn-Ag fault and fissure veins; M2. Mantos of Pb,Zn sulfides, magnetite, greenalite in limestone; 1. Mi-Pl subvolcanic stock; 3. Allochthon: Tr carbonates over phyllite; 4. Pe-Tr bimodal meta-volcanics over schist; 6. Autochthon, Pt+PZ metamorphics

and native silver interspersed with stockworks of Ag-bearing pyrite veinlets (Toldos deposit), and vein, stockwork and disseminated Ag-galena, sphalerite, pyrite and chalcopyrite in silicified and adularia, sericite, clay altered intrusive and partly sedimentary hosts.

Additional Pb,Zn,Ag "giants":

- **Banska Štiavnica-Hodruša** Au,Ag,Pb,Zn,Cu ore field, Slovakia * 333? t Au, 6 kt Ag, 1.6 mt Zn, 1.12 mt Pb +Cu * Mi, ~120 fault and fissure veins of quartz, carbonate, Pb,Zn,Cu sulfides, electrum in quartz, sericite altered hosts; small porphyry-Cu, Fe skarn in depth * Mi eroded caldera andesite, rhyolite, granodiorite on MZ carbonate basement * Lexa et al. (1999).
- **Baia Mare Pb,Zn,Ag,Au district**, NW Romania * 3.5 mt Pb?, 2.5 mt Zn?, 9 kt Ag? * Mi-Pl, series of ore fields along 60 km long E-W belt (Baia Mare, Baia Sprie, Cavnic); X00 fault and fissure veins of quartz, carbonates, adularia, Pb,Zn,Cu sulfides, tetrahedrite, Ag-sulfosalts in quartz, sericite altered hosts * in Mi-Pl andesite, dacite, rhyolite; Eo-Mi sediments * Lang (1979); Grancea et al (2002).

6.5.5. Other epithermal deposits: Mo, W, Bi, U, As, Sb, Te, Hg; Mn

The above metals do form epithermal deposits some of which are "geochemical giants", but the metals either command a limited demand (Bi, As, Sb, Te, Hg), are overshadowed by other than epithermal deposits (Mo, W, U), or both, so the epithermal examples remain largely obscure. Bi, As, Te and partly Sb are also components of several giant deposits mined chiefly for other commodities. For example, the giant Cerro de Pasco, mined for Zn, Pb, Ag and Cu, also has a calculated content of ~130 kt As, 80 kt Sb, 15 kt Bi and 2.5 kt Te, all of which rank as a "giant" accumulation, but only a fraction is actually recovered in the Oroya smelter. The Cripple Creek Au "giant" is also a Te "giant", but virtually no Te production is recorded. The industrial demand for the listed metals can,

however, change rapidly and in the ensuing exploration the epithermals would be one of the ore types of interest, hence this brief section should be considered as an index of possibilities.

Molybdenum is rarely accumulated in the epithermal environment but Petrachenko (1995) reports widespread occurrence of low-temperature (150-100°C) molybdenite on Paramushir and Iturup Islands in the Kuriles island arc. Rather than being of economic interest themselves, these occurrences may indicate presence of a more important Mo accumulation at the plutonic level. Similar occurrences of metacolloform MoS₂ and jordisite in propylitized Devonian volcanics at the Shaitan-Simess locality in Kazakhstan (Shcherba et al., 1972) change with depth into a stockwork of molybdenite veinlets in quartz-sericite altered intrusion.

Tungsten. High-level W vein deposits carry either ferberite or hübnerite, or scheelite, in a gangue of chalcedonic quartz, barite and fluorite. The most frequently quoted locality is the Nederland deposit in the Boulder County near Denver, Colorado. W also participates in several complex As, Sb, Hg deposits precipitated from hot springs, recently or in the past (e.g. Niğde, Turkey). In Golconda, Nevada, W co-precipitated with Mn hydro-oxides from a recent spring and some 48 kt of tungsten is dissolved in the Searles Lake brine, a playa lake in the Mojave Desert of California. All these deposits are small.

Bismuth, other than as a component of complex deposits, forms rare high-level deposits where Bi is the major accumulated metal. (**Cerro Tasna** in the Bolivian Tin Belt is the best known example (Ahlfeld and Schneider-Scherbina, 1964). The small San Gregorio deposit of Bi oxides near Colquijirca, Peru, mined in the 1930s, has turned out to be part of the oxidation zone of the "giant" San Gregorio Pb-Zn-Ag deposit, discovered subsequently.

Uranium. Miocene chaledonic quartz, fluorite and pyrite veins to stockworks with pitchblende, coffinite and locally jordanite and molybdenite were mined, on a small scale, from alkali rhyolite domes at Marysvale, Utah (Cunningham et al., 1982). This, and the vein or disseminated U-(Mo) deposits in felsic volcanics (Ben Lomond and Maureen in Queensland; Sierra Peña Blanca in Chihuahua, Mexico) are all small, but a giant U accumulation exists in the Strel'tsovsk (Strel'tsovskoye) ore field in the late Jurassic Tulukuyev Caldera, in the Russian Transbaikalia. (Andreeva and Golovin, 1999; ~280 kt U). This is the largest and presently the only producing Russian U resource. The orebodies are mostly fracture-controlled albitites with disseminated pitchblende and brannerite in quartz, carbonates, sericite and clay-altered zones hosted by a F-rich, peralkaline rhyolite, dacite and granosyenite porphyry suite.

Antimony. Significant Sb mineralization, with the "geochemical giant" status, is present in several deposits in the convergent plate margins. In the Pliocene to early Pleistocene **McLaughlin-Au, Sb, Hg hot spring deposit** in California (Lehrman, 1987) stibnite occurs with gold in multiply disrupted chaledonic silica veins and disseminations in a diatreme breccia, superimposed on a tectonic melange that brings together the Franciscan ophiolite in the footwall and sediments of the Great Valley sequence in the hangingwall. Also present are disrupted and altered 2.2 Ma plugs of olivine-pyroxene basalt. The gold endowment of 107 t makes this a "large" Au deposit, but the 22 mt ore reserve contains at least 2% Sb that is not included in the published reserves and is not recovered. If so, this would represent some 40 kt Sb. Also recovered in the past, when the upper levels of this deposit were mined by the small Manhattan Mine, was 589 t of mercury.

Sierra de Catorce Sb district, central Mexico, contains the interesting San José Mine near the Wadley railway station (White and Gonzáles, 1946; Zarate-Del Valle, 1996; ~90 kt Sb). This is a set of eight almost perfectly stratabound mantos replacing beds of Jurassic limestone, cut by a fault with discordant ore veins. Evaporitic anhydrite and gypsum beds abound in the basal portion which, in turn, rests of Triassic-Jurassic red beds enriched in Sb. Eocene-Oligocene (35 Ma) quartz diorite dikes occur in the area. The Sb-mantos consist of crystalline stibnite with minor pyrite, marcasite and cinnabar in chaledonic silica and calcite gangue, under carbonaceous argillite screens, in solution-thinned and cavernous limestone. The mantos grade

laterally into jasperoid with scattered stibnite. Much of the near-surface ore is oxidized into stibiconite, cervantite and valentinite.

Bolivian Sb belt (Pt ~300 kt Sb) is located between Potosí, Tupiza and the Argentinian border in southern Bolivia and has been for many years important producer of antimony coming from tens of mostly small simple stibnite vein deposits controlled by faults in Paleozoic slate (Ahlfeld and Schneider-Scherbina, 1964). The Chilcobija Mine (Pt ~70 kt Sb) has been the largest producer.

In the **Bau district in Sarawak**, NW Borneo (Mustard, 1997; Pt 91 kt Sb, 1110 t Hg, 93 t Au) stibnite, sarabauite, kermesite and other minerals occur in Miocene fault-controlled quartz, calcite, pyrite, native arsenic, realgar and orpiment veins and limestone replacements that also contain submicroscopic gold. Much of the metals came from the oxidation zone, especially from residual clay filling karst.

Arsenic. Arsenic is presently an undesirable component of many epithermal gold-silver and copper deposits and although it is rarely recovered and marketed, it imparts a "geochemical giant" status on many deposits because of its low clark value. In the young epithermals, most As is stored in enargite, arsenian pyrite and/or realgar and orpiment; the complex deposits Trepča, Cerro de Pasco, and Pueblo Viejo store some 380 kt, 130 kt, and 150 kt As, respectively. The Paleoproterozoic Boliden deposit in Sweden (Chapter 9), with its endowment of 600 kt As a portion of which was actually recovered and sold in the past, is one of the three arsenic "supergiants" known. In this metamorphosed deposit As is in arsenopyrite.

Mercury. In addition to the three hot-spring related Hg deposits mentioned above (Sulfur Bank) and in Chapter 8 (New Almaden, New Idria), at least three other Hg "giants" are in the convergent margin setting. Monte Amiata, Italy; Huancavelica, Peru; and Terlingua, Texas.

Monte Amiata Hg-Sb district, Italy (~80 kt Hg @ 0.8% Hg) is a part of the Tuscan calc-alkaline to K-alkaline late Miocene to Pleistocene magmatic province (Pichler, 1970); there, several geothermal areas are still active today (e.g. the Larderello wells that produce boric acid in addition to geothermal energy). Flows and domes of rhyolite, quartz latite and trachyte, related to the 0.43 Ma Mount Amiata volcanic centre, are emplaced into and rest unconformably on deformed Cretaceous to Eocene varicoloured shale and limestone and, partly, on Cretaceous turbidites and slate-dominated melange

of the Ligurian Nappe. The principal Hg deposit **Abbadia San Salvatore** is an elongated zone of lens-like orebodies of disseminated, fracture filling and replacement cinnabar with some pyrite, marcasite, native mercury, realgar and orpiment, in karsted limestone breccia and residual clay within the thrust. It is covered by Quaternary ignimbrite and interpreted as a late Pliocene-Pleistocene hot spring deposit.

Huancavelica-Hg ore field, Peru (Noble and Vidal, 1990; Pt 51 kt Hg) contains a number of small mines (the largest: Santa Barbara) of disseminated cinnabar with variable quantities of pyrite, locally realgar, orpiment, arsenopyrite and stibnite and with frequent traces of hydrocarbons. The low-temperature late Miocene minerals impregnate Cretaceous quartz sandstone, replace Jurassic limestone, and fill fractures in Miocene dacite. Clay minerals, calcite and quartz are the most common gangues. The mineralization is very irregular, not amenable to bulk mining although a resource remains.

Terlingua-Hg ore field, Texas (Yates and Thompson, 1959; Pt 5,100 t Hg) is located in the Big Bend of Rio Grande. It comprises 20 small, now abandoned mines. Cinnabar with calcite, clays, hydrocarbon traces and pyrite impregnate Cretaceous limestone and Tertiary clastics along brittle faults, near Tertiary soda-alkaline laccolith, dikes and breccia pipes.

Tellurium is an occasional by-product of processing of the Cerro de Pasco complex ores (2,500 t Te calculated content) and it is also concentrated in the alkaline epithermal gold deposits, although rarely recovered. There, Te resides in the Au-Ag tellurides like krennerite, hessite, sylvanite and others, and as rare native Te. Official reserve figures for Te are not available but the calculated amounts of Te in the Cripple Creek ores exceed 1000 t. In the Săcărâmb deposit in Romania there is probably more than 500 t Te, and about the same amount is in the Emperor Mine, Fiji and Kochbulak in Uzbekistan.

6.5.6. LS deposits as part of a system: other related mineralization?

In several hydrothermal deposits epithermal orebodies overlap with ores formed in greater depth such as skarn, porphyry copper, replacements, and this can be explained as a multistage mineralization in which the crustal levels, where the ore deposition was taking place, rose or subsided. This can be exemplified by the recently developed "large" Au-

Cu deposit **El Valle-Boinás**, in the Rio Narcea district in western Asturias, NW Spain (Rc 14.2 t ore @ 4.3 g/t Au, 0.41% Cu, 12.27 g/t Ag in both oxidized and sulfide ore); Fig. 6.20. There, the mineralization formed in two major hydrothermal stages: 1) the older stage, at 285 Ma (Permian), produced calcic and magnesian exoskarn with magnetite, pyrrhotite, chalcopyrite, bornite, arsenopyrite, Bi-sulfides and electrum. The ore is in Cambrian limestone at rhyodacite porphyry dike contacts, in roof of a Permo-Carboniferous granodiorite, and at the supra-plutonic level. 2) The younger stage, at 255 Ma, produced low sulfidation epithermal, low sulfide Au-Ag quartz, carbonate, adularia veins, breccias and replacements superimposed on the earlier rocks that include skarn. More cases of ore telescoping and overlap are described below.

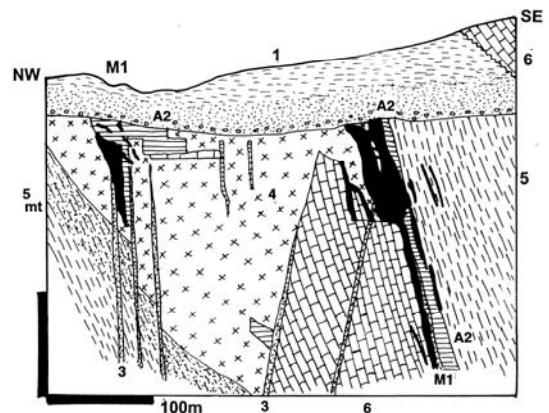


Figure 6.20. El Valle-Boinás Au, Cu deposit, Asturias, northern Spain, showing overprinting of older Cu-Au skarn by LS epithermal Au ore. Cross-section from LITHOTHEQUE No. 3017 modified after Rio Narcea Gold Mines, Ltd., on-site information, 2000. 1. T cover sediments & regolith; A2. ~255 Ma carbonatized & serpentinized diabase dike; 3. ~285 Ma altered rhyodacite porphyry dikes; 4. ~303 Ma quartz monzonite, granodiorite; 5(mt). Cm₃ slate, litharenite, trachybasalt, thermally metamorphosed; 6 (mt). Cm₁₋₂ limestone, dolomite to marble. M1. ~255 Ma low-sulfides epithermal Au veins, breccia, replacement superimposed on ~286 Ma Cu-Au exoskarn.

Many LS deposits were discovered in the past by visual prospecting. Once found, they became the starting point of search for undiscovered deposits. The most obvious ones are orebodies of the same type farther afield and under cover, as many LS veins come in groups. Structures (faults, fracture sets) are the main control here. The shape and nature of orebodies could change with variation in

structure style and host lithology: for example, a fissure vein in brittle silicate rocks could change into replacement in carbonate or disseminated orebody in porous or densely fractured rocks. Young LS deposits like hot springs could have produced derivative deposits such as stratabound ores in adjacent lake sediments, rarely in stream sediments. Older deposits exposed at surface may have contributed metals or mineralized fragments to regolith or secondary deposits such as glacial drift, talus or alluvial fans.

As LS fluids derive their metal load from wallrocks in shallow depth, such rocks (or members of their association) may crop out at the present surface, be intersected by drilling in the subsurface, or may be predicted on the basis of local stratigraphy and magmatism. Of special interest are the carbonaceous rocks (black slate, phyllite, schist) as they are often metalliferous to the point that they themselves might become an orebody. Older massive sulfide occurrences can also be found.

It is potentially possible to predict, then find, blind orebodies of other types such as the porphyry deposits that may have been a part of the same hydrothermal system responsible for the known LS ores. The epithermal/porphyry association is not as close here as among the HS deposits, but it sometimes exists. Porphyry or skarn Cu-Mo and Cu-Au deposits, although not always economic, have been discovered by accident in mining works like crosscuts, or by drilling for LS ores, in the Apuseni Mountains of Romania (e.g. the Musaria Nou porphyry Cu near Brad, Roşia Poieni porphyry Cu near the Roşia Montană LS ore field; Berbelec and David, 1982), in the Banská Štiavnica district in Slovakia (Hodruša, Vyhne) and elsewhere. The intense research applied to the Creede epithermal system in Colorado contributed early results applicable to practical predictive metallogeny. Barton et al. (1977) determined that fluids in a freely convecting hydrothermal system as in Creede precipitated minerals with normal solubilities (that is, those more soluble in hot solutions) near the top of the convecting cell as a consequence of boiling, loss of acid components and fluid mixing. These are capped by sericite-altered wallrocks. Minerals with retrograde solubility like anhydrite and molybdenite had been experimentally determined to have concentrated in the hottest parts of the system in greater depths; a porphyry Mo was predicted to be possibly present under Creede, but separated by a barren interval between the shallow and deep mineralizations. Subsequent test drilling has demonstrated existence of a Mo mineralization there, as predicted.

6.5.7. "Bolivian-type" porphyry Sn-bonanza Ag composite association

Bolivia has been long famous for the unique association and overlap of disseminated cassiterite in altered rhyodacite domes and bonanza silver veins. This overlap is manifested not only on the ore province, district and deposit scales, but even on the ore mineral scale where rare Sn, Pb and Ag sulfosalts formed. The Bolivian Tin Belt (BTB; Turneure, 1971), that also includes portions in southern Peru and NW Argentina, is an 800 km long arcuate mineralized belt in the Eastern Cordillera (Cordillera Oriental) of the Andes, established over the early Paleozoic "miogeocline" that rests on Precambrian metamorphic basement. This belt has been a significant producer of silver and tin from numerous deposits, some of which had been found and worked by the local Aymará before the arrival of Europeans (total endowment is of the order of 5 mt Sn and 100 kt Ag). The province comprises 4 "Sn-giants", one "Ag-giant" and one "Ag-supergiant" and it has an extensive classical to modern literature (Turneure 1960, 1971; Ahlfeld and Schneider-Scherbina, 1964; Sillitoe et al., 1975; Grant et al., 1980; and others).

The magmatism and associated mineralization culminated in two phases. In the older phase, Triassic to Jurassic batholiths and related Sn, W and Pb-Zn-Ag deposits, formed on a continental basement undergoing extension at the onset, or before, the Andean subduction cycle. They have been since eroded to the upper- to middle- plutonic levels. The plutons are thus comparable with the intracontinental granites treated in Chapter 10. The second, younger magmatic and metallogenetic period commenced in late Oligocene and continued until present (Avila-Salinas, 1991). Throughout this period the BTB has been an integral part of the Andean convergent margin, associated with the Eastern magmatic arc separated from the Main (Western) arc by the Puna/Altiplano extensional terrain. Although the magma generation in the Eastern arc is usually attributed to crustal melting above a flat subduction zone, both magmatic cycles (Mesozoic and late Cenozoic) may have shared the same melt source regions. The fundamental difference between the Tr-J and OI-Q magmatic/metallogenetic cycles is thus the depth level of evolution and emplacement of magmas and related ores which, in the younger phase, range from epizonal plutonic (as in the deeper-eroded Cordillera Quimsa Cruz that has small Sn-W deposits similar in style with the older phase) through epizonal plutonic ("porphyry") to subaerial

volcanic. The bulk of the highest level magmatites and ores are concentrated south of Oruro (the Southern Tin Belt of Grant et al., 1980), but there are exceptions, one of which is the "giant" San Rafael Sn-Cu deposit NW of Lake Titicaca.

The Southern Tin Belt is a broad series of crustal blocks dotted by small granitoid plutons and stocks, partially eroded volcano-plutonic centers, rare active volcanoes, and extensive tuff and ignimbrite blankets interspersed with outcrops of the Ordovician and Silurian (meta)sedimentary basement. The magma series is variously interpreted as metaluminous to weakly peraluminous, with strong local peraluminous suites as in the Macusani Volcanics in Peru (Pichavant et al., 1988) and in the Morococala volcanic field in southern Bolivia (Morgan et al., 1998). Ore deposits in the Eastern arc range from 1) classical "Cornwall-style" (but without Cu except for San Rafael) quartz-cassiterite veins in epizonal plutons, related dikes, or basement (San Rafael, Colquirí, Huanuni); 2) higher-grade Sn veins and vein swarms in isolated porphyry stocks and breccia columns where the altered breccia also contains disseminated low-grade cassiterite (Lallagua); and 3) volcanic-subvolcanic complexes (probably original stratovolcanoes) with erosion exhumed hydro-thermally altered rhyodacitic domes (stocks) and probable vent breccias. Porphyry-style cassiterite with pyrite is disseminated or forms fracture stockworks in the intrusion or in breccias, in the roof of which formed hydrothermal fracture veins mineralized by cassiterite, Sn-Pb-Ag sulfosalts, and "bonanza" Ag (the latter still upgraded in the supergene zone). The Chorolque deposit is a tin-only deposit, the "giants" Cerro Rico and Oruro are tin-silver. The remaining category 4), as distinguished by Grant et al. (1980), comprises little eroded volcanic complexes lacking intrusive rocks other than porphyry dikes. The Sn-Ag deposits are of small to medium size although the recently developed, low-grade Ag-Pb-Zn "giant" San Cristobal, described above, may be a member of this category (Fig. 6.21).

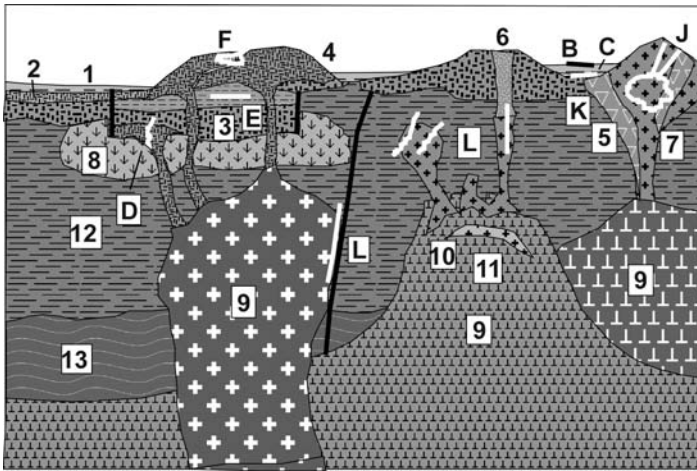
The early tin introduction is believed to have been magmatic-hydrothermal, subsequently partly redistributed by convecting meteoric waters as the system evolved. The bonanza Ag veins have traditionally been interpreted as precipitates from heated meteoric waters, although Sillitoe et al. (1998) considered the Ag-mineralized vuggy silica lithocap at the Cerro Rico summit as of high-sulfidation origin. Never mind the controversy, a

brief description of the "giants" follows.

Cerro Rico, Potosí Ag-Sn-(W,Bi,Pb-Zn) centre, Bolivia (Ahlfeld and Schneider-Scherbina, 1964; Grant et al., 1980; Sillitoe et al., 1998; Bartos, 2000; global endowment ~84,000 k Ag, ~1 Mt Sn). Cerro Rico is the world's largest "Ag-supergiant", a prominent landmark just south of the high city of Potosí, and the only "giant" the image of which participates in a state seal (of Bolivia) and appear on the national currency. Officially discovered in 1545 (unofficially long before that) it yielded phenomenally silver-rich ores from the near-surface workings that later moved underground, and since the late 1800s also tin. Exact production/reserve data are not available; the remaining resource of 143 mt of open-pit material grading 174 g/t Ag and 0.1-0.25% Sn (Bartos, 2000) is not representative of the rich ores mined earlier, and is blocked on socio-political grounds.

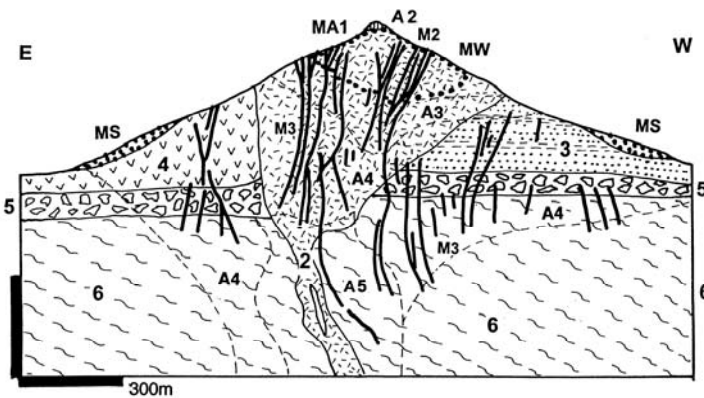
The prominent conical landmark Cerro Rico is erosional remnant of an elliptical (~800 m diameter) 13.8 Ma (Miocene) dacitic or rhyodacitic dome, believed emplaced into crater wall of a stratovolcano (Grant et al., 1980; Bartos, 2000). The subhorizontal wallrocks, preserved at high levels, are Miocene subaerial felsic tuffs, lacustrine sandstone to mudstone and a phreatomagmatic explosion breccia. They rest unconformably on folded, slightly pyritic Ordovician black slate with minor litharenite. The stock is surrounded by Quaternary landslide debris, talus and debris flow conglomerate that grade to alluvium, and these materials contain recoverable Ag and Sn in clasts, mined from "pallacas" (Bartos, 2000); themselves a "giant" deposit (Section 6.2.1.); Fig. 6.22.

The mushroom-shaped Cerro Rico stock (dome) is pervasively altered and mineralized, and mineralogically and geochemically zoned within depth interval of 1,150 m beneath the summit, reached by mine openings. Cunningham et al. (1996) argued that the bulk of the ore metals had been introduced within 300,000 years after dome emplacement, the mineralization episode was short-lived (13.76-12.5 Ma) and largely driven by magmatic fluids. Subsequent hydrothermal episodes were minor. The main hydrothermal phase pervasively altered the porphyry into a mixture of sericite, kaolinite, chlorite, quartz, and in deeper parts tourmaline, with relics of magmatic quartz phenocrysts. It also produced, on top, a 400 m thick zone of subhorizontal silicification floored by argillic alteration (lithocap; Sillitoe et al., 1998) and



1. Volcanic lake beds; 2. Ash-flows; 3. Felsic tuff; 4. Rhyolite domes; 5. Intrusion and hydrothermal breccia; 6. Diatreme; 7. Felsic porphyries; 8. Caldera-related pluton; 9. Peraluminous granite plutons; 10. Pegmatite, leucogranite; 11. Albitized apogranite; 12. (Meta)sediments & volcanics; 13. Crystalline basement. B. Borates at playa surface; C. Li in brine, lacustrine sediments; U. infiltrations; bedded borates; D. Epithermal U veins; E. Be, Li, Rb, Cs, fluorite disseminations in tuff, subvolcanics; F. Fumarolic cassiterite; J. Epithermal Sn-Ag veins; K. Porphyry Sn; L. Cassiterite (~Cu) veins.

Figure 6.21. Inventory model of ores in dominantly peraluminous volcanic-subvolcanic systems. From Laznicka (2004) Total Metallogeny site G74. Ore types C, E, J, K, L include "giant" deposits



MS & 1. "Pallacas", detrital cassiterite; MA1. Lithocap of vuggy residual silica; MW. High-Ag grade oxidation zone; M2. Swarm of Ag & Sn veinlets in altered porphyry; M3. Sets of high-grade fissure Ag, Sn, Pb, Sb, As veins, sheeted at upper levels; surrounded by veinlet & disseminated ("porphyry") cassiterite. A: Dominant alteration minerals: A1 silica; A2 jasperoid; A3 advanced argillic; A4 sericite-pyrite; A5 quartz-tourmaline. 2. 13.8 Ma altered dacite porphyry dome, to breccia; 3, 4. Mi tuff, volcanoclastics; 5. Explosion breccia; 6. Or phyllite > litharenite

Figure 6.22. Cerro Rico Ag-Sn ore complex, Potosí, Bolivia. Cross-section from LITHOTHEQUE No. 900, modified after Comibol Staff (1977), Sillitoe et al. (1998) and Bartos (2000)

equated with products of high-sulfidation regimes. Cunningham et al. (1996) considered this cap a supergene acid-leached member of the overall quartz-sericite-pyrite complex.

The very top of Cerro Rico is protected by remnant of a massive chalcedonic jasperoid. Below is a 250 m thick porous zone of vuggy silica with locally apparent relic quartz phenocrysts and empty or residue-filled vugs after feldspars. This silica contains between 200 and 350 g/t Ag and ~0.1% Sn in disseminated argentite and acanthite with barite, and fragments of this material are the major components of "pallacas" (Bartos, 2000). Beneath the silica is a 150 m thick zone of quartz, dickite, illite, kaolinite, some pyrophyllite and svanbergite alteration. The lithocap is cut by a 170 m wide zone of sheeted veins with "bonanza" silver contents in

argentite, pyrargyrite, native silver and supergene chlorargyrite.

Overall, there are 35 main steeply dipping veins and vein sets in the upper part of Cerro Rico that range from 10 to 60 cm in width, and they merge into five principal vein systems in depth (Bartos, 2000). The hosts include the altered porphyry as well as cover fragmentites (breccias) and basement dark phyllites. The veins in the core are rich in Sn, As, Bi and W, are of higher temperature (~330-240°C), and comprise quartz, pyrite, cassiterite, arsenopyrite, wolframite and bismuthinite. The lower-temperature peripheral veins are high in base metals and comprise quartz, pyrite, stannite, sphalerite (marmatite), chalcopyrite, tetrahedrite, galena and Ag-Sb-As and Pb-Sb sulfosalts. Massive alunite veins that crosscut the sulfide veins near the

lithocap base are attributed to magmatic steam, although supergene alunite veinlets also occur in the oxidation zone (Cunningham et al., 1996).

Oruro Sn-Ag ore field, Altiplano, Bolivia (Chace, 1948; Sillitoe et al., 1975; P+Rv 12,000 t Ag, 120 kt Sn, 80 kt Pb in veins, Rc 400? kt Sn @ 0.3% in porphyry). Oruro is closest to Potosí in style and is famous for the presence of rare Sn-sulfosalts (franckeite, teallite). Two vein groups (Itos and San José) are associated with 16 Ma rhyodacite to quartz monzonite porphyry stocks and hydrothermal intrusive breccia (or diatreme?) emplaced into S-D₁ black slate and minor litharenite. Steeply dipping "bonanza" fissure and replacement veins in porphyry, breccia and slate contain pyrite, cassiterite, arsenopyrite, galena, sphalerite, stannite, chalcocopyrite, tetrahedrite, franckeite and teallite in quartz gangue. The wallrocks are quartz, sericite and pyrite altered. A porphyry-style low-grade body of disseminated cassiterite is in sericite (quartz, tourmaline) altered porphyry.

Llallagua (Catavi) Sn ore field, Bolivia (Turneaure, 1935; Vargas, 1970; Sillitoe et al., 1975; Grant et al., 1980; global P+Rc ~2 mt Sn). This is the largest tin deposit of Bolivia and probably of the world, although accurate statistics are missing. It is located in the same Southern Bolivian Tin Belt as Potosí, but it belongs to the deeper-eroded variety (class "C" of Grant et al., 1980) that lacks associated extrusives. It is also a "straight-Sn" deposit ("porphyry-Sn" of Sillitoe et al., 1975), without silver (Fig. 6.23). The ores are associated with, and largely hosted by, the small (1,730 to 1,050m at the surface), downward-tapering, elliptical Salvadora stock, emplaced into middle Silurian to early Devonian turbiditic litharenite and shale. The Lower Miocene (20 Ma) stock is interpreted as a subvolcanic fill of a vent of originally quartz-latite porphyry composition, but it is now pervasively altered. The alteration is predominantly of the quartz-sericite type changing to tourmaline with depth, and into (supergene?) illite and kaolinite near the surface. The stock is also intensely crackle- to mosaic-brecciated throughout and this is overprinted by more "open" irregular masses, pipes and dikes of breccia. The breccias range from fault, diatreme or intrusive (with wallrock fragments), through hydraulic to hydrothermal and are rich in quartz and tourmaline cements.

The whole altered stock contains "porphyry-style" disseminations and fracture veinlets of cassiterite, with or without pyrite and quartz. The

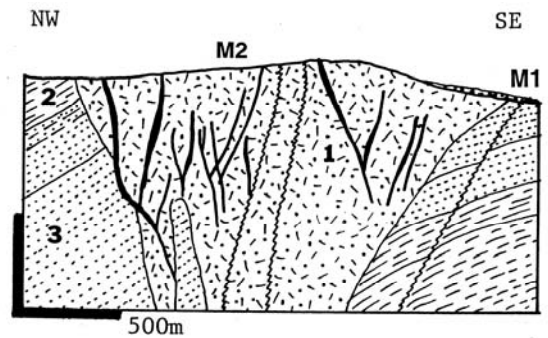


Figure 6.23. Llallagua (Catavi) tinfield in Salvadora Stock. Cross-section from LITHOTHEQUE No. 898 modified after Turneaure (1935), Comibol Catavi Staff (1977). M1. Cassiterite placers; 1. Mi-Pl pervasively sericitized quartz latite porphyry stock, grading to intrusion breccia. M2. Disseminated porphyry-style cassiterite in Salvadora stock, intersected by quartz, cassiterite veins; 2. D₁ shale; 3. S₂₋₃ litharenite.

average grade is 0.3% Sn that slightly increases (to ~0.5% Sn) in the limonite-stained supergene zone near the surface, and decreases with depth as tourmaline becomes dominant. The proven reserve was about 100 mt @ 0.3% Sn but the actual resource is greater. Superimposed on the above are sets of steeply-dipping fissure or fault veins. Most trend NE and some continue beyond the porphyry limits. The veins supplied most of the historically produced tin, are 30-80 cm wide, composed of quartz with cassiterite and variable amounts of bismuthinite, franckeite, chalcocopyrite, arsenopyrite, stannite and other minerals (Turneaure, 1935). The mineralization is attributed to magmatic fluids with a temperature range of ~400-260°C (Grants et al., 1980). A significant quantity of tin has been won from small scale workings in talus, colluvium and alluvial placers.

San Rafael-Sn, Cu, SE Peru (Mlynarczyk et al., 2003; P+Rv ~ 1 mt Sn content @ 4.7%, ~280 kt Cu @ 0.16%). San Rafael is a highly productive, high-grade ore field at the northern extremity of the Bolivian Tin Belt, in the Puno department of Peru. It is a 3.5 km long, 1,200 m deep a NE-dipping quartz lode with subparallel veins, genetically related to a late Oligocene (25 Ma) granite stock emplaced into Lower Paleozoic, partly hornfelsed slate. The stock is of peraluminous biotite- and cordierite-bearing potassic monzogranite and leucogranite. Tin is produced from densely scattered, sometimes banded or massive brown cassiterite with chlorite in lode quartz. The wallrock granite displays chloritic alteration that overprints

earlier sericitization and quartz-tourmaline veining. Cu in chalcopyrite is zonally enriched above cassiterite, and in veins that cut through slate. The mineralization is attributed to mixing of magmatic and meteoric fluids.

(Cerro) Tasna-Bi in Bolivia is known as the world's largest deposit mined primarily for bismuth (Sillitoe et al., 1998; P+Rc ~12,000 t Bi?; RV₁₉₉₈ 500 kt @ 1.47% Bi, 1.28% Cu), although several complex deposit in China (Shizhouyuan) and elsewhere greatly exceed this Bi tonnage. It is an eroded Miocene dome complex where dacitic stocks and dikes cut Lower Paleozoic slate. A series of quartz, tourmaline, bismuthinite, chalcopyrite, arsenopyrite, wolframite veins in silicified and tourmalinized selvages has advanced argillic lithocap.

Ancient (deformed, some metamorphosed) epithermal deposits

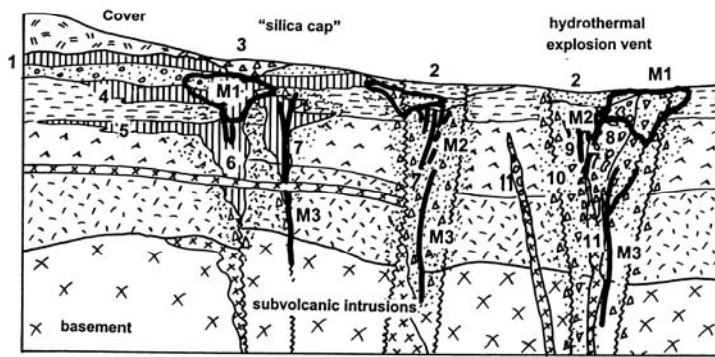
Most epithermal deposits formed within a narrow depth interval under the paleosurface (between about 200 and 1,500 m) and are soon removed by erosion so pre-Mesozoic deposits are rare. Old, unmetamorphosed epithermal deposits retain their original mineralogy, i.e. the chalcedonic quartz, adularia, alunite, pyrophyllite, and the general orebody shape. Erosion-resistant components such as siliceous sinters or silicified fault or porous aquifer zones also remain. Metamorphosed HS epithermals are usually associated with a suite of high-alumina silicates (andalusite; also kyanite and sillimanite) and oxides (diaspore and corundum), some of which have formed nonmetallic deposits of their own like the (now exhausted) Semiz-Bugu diaspore/corundum deposit in Kazakhstan. These minerals are widespread in association with centers of silicification ("secondary quartzites") interpreted as remains of former advanced argillic lithocaps (Sillitoe, 1995). Some "secondary quartzites" indicate the presence of Carboniferous porphyry Cu-Mo in the Kazakhstan Block (north of Lake Balkhash; Nakovnik, 1968) and are probably the product of acid leaching adjacent to porphyry systems. The same or similar mineral assemblages could have formed by many other mechanisms such as thermal metamorphism of aluminous sediments, metamorphism of regoliths, or metamorphism of alteration envelopes around subaqueous VMS systems. The paleo-epithermal occurrences are thus always controversial and their interpretation changes. The following "large" and "giant" deposits/districts have been interpreted as

preserved, variously modified ancient epithermal systems by some authors:

- Jurassic-Cretaceous: Sam Goosly (Equity) Cu, Ag, Au, British Columbia
- Devonian: Drummond Basin-Au (e.g. Wirralie, Glen Eva, Pajingo; Fig. 6.24)
- Devonian: Lake Cowal-Au, New South Wales
- Neoproterozoic: Mahd adh Dhahab-Au, Ag, Saudi Arabia
- Neoproterozoic: Imiter-Ag, Morocco
- Paleoproterozoic: Boliden-As, Au, Cu, Sweden
- Archean: Bousquet-Au, Quebec
- Archean: Campbell-Dickinson mines, Red Lake district, Ontario

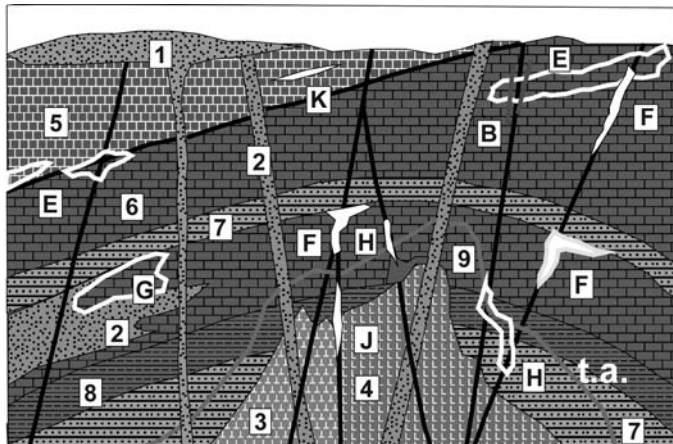
6.6. Carlin-type micron-size Au (As, Hg, Sb) deposits

This is a very heterogeneous group of gold deposits that defies accurate definition (Hofstra and Cline, 2000). Their principal characteristic is the presence of disseminated submicroscopic gold (invisible megascopically and under the microscope) held in arsenian pyrite, that replaces a variety of rocks. There is no direct, obvious and conspicuous association with igneous systems (Cline, 2004). In the early stages of recognition (1960s-1970s) these deposits were characterized as stratabound replacements in carbonates under a thrust plate screen ("sediment-hosted gold"). This was adequate for the first and model deposit found, the (Old) Carlin. Following the wave of new discoveries and re-interpretation of several previously known deposits as of "Carlin-type" in the 1970s and 1980s, it has been found that much of the disseminated gold is fault-controlled and discordant to bedding, that it also resides in non-carbonate rocks like siliceous slate, meta-basalt, older diorite and felsic volcanics. The genetic interpretation also drifted from deep-seated (3 km plus; middle plutonic level) to shallow (hot spring to upper epithermal level); from magmatic-hydrothermal possibly related to porphyry copper systems to epithermal; from magmatic-hydrothermal through metamorphic-hydrothermal to basinal fluids product, from Devonian to late Tertiary; from subduction-related to collision or extension-controlled. Probably no other ore type has recently generated so much genetic controversy so the term "Carlin-type" is convenient, as it has the capacity to accommodate many very dissimilar deposits of finely dispersed gold that do not fit into any of the more distinct ore categories (Fig. 6.25).



1. Silica sinter deposited on surface;
2. Silicified & argillized mud, fallback from hydrothermal eruptions;
3. Sinter related breccias;
4. Silica sinter deposited in subsurface;
5. Bedded jasperoid;
6. Silica in the hot spring roots;
7. Hydrothermal veining, stockworks, breccia;
8. Hydrothermal explosion breccia;
9. Matrix-supported lithic breccia;
10. Reworked, altered wall-rock fault breccia;
11. Subvolcanic porphyry dikes, plugs.

Figure 6.24. Diagrammatic cross-section (not to scale) showing the preserved features and products of fossil hot spring systems, including mineralization. From LITHOTHEQUE No. 2945, based on D₂-Cb Drummond Basin in Queensland (Pajingo, Wirralie, Glen Eva and other deposits). Although cumulatively this is only a "large" Au province, there is some potential of discovery of "giant" equivalents. M1. Disseminated, "invisible" gold, almost no sulfides; M2. Upper epithermal chalcidonic Au-(Ag) veins & mineralized breccias; M3. Lower low-sulfidation Au-(Ag) epithermal veins, the proportion of sulfides increases



1. Rhyodacite;
 2. Subvolcanic & epizonal porphyries;
 3. Granodiorite, quartz monzonite;
 4. Diorite to granodiorite;
 5. "Basinal" siliceous slate, chert (allochthon);
 6. Miogeoclinal carbonates, shale, minor sandstone;
 7. Sandstone (quartzite);
 8. Shale, siltstone;
 9. Skarn and contact hornfels; t.a. thermal aureole.
- B. Barite veins, replacements; E. Carlin-type micron-size Au orebodies in inconspicuously altered hosts (mostly carbonates), various configurations; F. Au disseminated in jasperoid; G. Au replacements near intrusions; H. Carlin-type disseminations, stockworks in older intrusions; J. Au in silicified fault breccia; K. Bedded barite; V in "black slate"

Figure 6.25. Inventory model of ore types expected in settings comparable with the Nevada Carlin-type Au province. From Laznicka (2004), Total Metallogeny site G167. Ore types E, F, G, H, J alone or in combination, have produced "giant" deposits

Recently, a new ore type has been announced: "distal disseminated deposits" (Hofstra and Cline, 2000; Cline, 2004). These are supposed to be demonstrably magmatic-hydrothermal ores in sedimentary hosts, distal to porphyry-Cu or skarn systems. The McCoy (skarn) and Cove (distal) pair in the Battle Mountain district in Nevada is quoted as an example. At Getchell, gold was introduced at least four times: first into the skarned exocontact of a Cretaceous granodiorite, then into fault structures in response to successive hydrothermal events, the latest dated at ~42 Ma (Groff et al., 1997).

The Carlin-type origin has been reviewed many times (Seedorf, 1991; Kuehn and Rose, 1995; Arehart, 1996; Simon et al., 1999; Hofstra and Cline, 2000) and the many fine genetic points will

not be discussed further as they provide little to assist discovery. The "mainstream" 1990s-2000s vintage opinion applicable to the type area in north-central and north-eastern Nevada, is as follows:

- 1) Most Au deposits formed between 42 and 30 Ma (Eocene-Lower Oligocene), in about the time of formation of the "supergiant" Bingham porphyry/skarn Cu-Mo-Au deposit in Utah (where there are two small "Carlin-type" deposits in the district, Barney's Canyon and Melco; Presnell and Parry, 1996, however, argued that they were Jurassic, predating Bingham). Flat subduction that produced many scattered volcano-plutonic centers in Nevada

and Utah was possibly instrumental. The Au orebodies predate the Basin-and-Range extension;

- 2) The prevalent fluid temperatures were in the epithermal range (~250-120°C) and mesothermal temperatures were reached in scattered skarn and mesothermal vein deposits related to Jurassic plutons, genetically unrelated to Carlin;
- 3) The ore fluids were indistinct, of uncertain provenance, probably a mixture of meteoric, metamorphic and magmatic waters;
- 4) The submicroscopic gold is both free, residing in a variety of ore or non-ore minerals, as well as bound in the lattice of pyrite or arsenian pyrite. Arsenopyrite is rare in the type area and realgar-orpiment with stibnite, although widespread, postdate the main gold phase; the ores are low in silver;
- 5) There is a combined structural and lithologic control. The fluids were channeled by dilatant fracture systems and gold orebodies developed in the steep, cross-cutting faults themselves, or they spread laterally replacing favourable horizons to form manto-style orebodies (argillaceous and carbonaceous limestone in Old Carlin);
- 6) The most widespread alteration in carbonate hosts caused solution removal of calcite (decalcification), slight argillization and slight silicification grading to replacement jasperoid;
- 7) The characteristic geochemical signature of the Carlin-type includes As, Sb, Hg, Tl, Cu, Zn-Pb-Ag are enriched locally (most polymetallic ore occurrences in the area predate the Carlin-type);
- 8) Most Carlin-type orebodies have diffuse assay boundaries (unless bounded by faults) and a range of grades from 0.5 g/t Au (the lowest cut-off grade) to 34 g/t Au orebody average (at Deep Star, P+Rv 50 t Au) with local "bonanza" intervals. The single largest Betze orebody (900 t Au) grades 7.5 g/t Au;
- 9) All known Carlin-type deposits are shallow (maximum 500 m under the present surface), bulk mined by open pits with the only exception of the high-grade underground Meikle mine;
- 10) Some orebodies (Old Carlin) have a high proportion of oxidized ore with gold dispersed in saprock or in limonite-coated fractures; the deeper orebodies are unoxidized and refractory.

6.6.1. "Invisible gold" in the Great Basin

"Invisible gold" deposits have been known and mined in the Great Basin, in western United States, since 1891 when the first successful cyanide leaching plant in the United States commenced operation in Mercur, Utah (Kornze, 1987). **Mercur-Au, Ag, Hg ore field**, 24 km south of the Bingham porphyry Cu-Mo "supergiant", is a "large" deposit (P+Rc ~147 t Au @ 4 g/t Au) whose high-grade but small secondary Ag deposit was discovered in 1870, and exhausted within two years. Subsequently, a small quantity of cinnabar was produced. Gold was identified by assay and then mined from several stratabound replacement bodies in decalcified and silicified Lower Carboniferous limestone. The Cortez gold cluster in central Nevada had a similar history: secondary silver was found at outcrop in 1862 and briefly mined, followed by discovery of disseminated gold in silicified sedimentary rocks in Gold Acres (Radtke et al., 1987). The third historic deposit in the region is **Getchell**, discovered in 1934 on flanks of the Osgood Mountains (known for numerous small deposits of scheelite skarn related to Cretaceous granodiorite; Nanna et al., 1987). The gold ore initially mined in Getchell was a mixture of Fe and As oxides that changed with depth into a complex assemblage of As, Sb, Cu, Pb, Hg, Bi, Tl, Ag, Hg sulfides and sulfosalts in veins and in mineralized fault rocks, controlled by a 3 km long NNW deformation zone. Getchell used to be a rewarding mineralogical locality famous for the striking, large masses of realgar and orpiment. There, the early stage ultrafine disseminated gold was partly remobilized to a 10 micron and larger size, providing a limited response to prospectors equipped with panning dish. Before the (Old) Carlin discovery the three mined deposits of the Carlin type have produced, or stored in reserves, about 90 t Au: a tip of an iceberg given the present endowment of the Carlin-type gold in Nevada and Utah of some 5,200 t Au.

The (Old) Carlin deposit 50 km west of Elko, Nevada, was discovered by Newmont Inc. in 1961, using geochemical reconnaissance, with a remarkable foresight given the period when the price of gold was US\$ 33/Troy oz and the surviving U.S. gold mines devastated by the wartime ban of gold mining (Teal and Jackson, 1997). Newmont was influenced by findings of Ralph Roberts of the U.S. Geological Survey who noted that many small ore fields in NW Nevada were hosted by carbonate rocks of the Cordilleran miogeoclinal autochthon, in erosional windows under the Roberts Mountains

thrust plate of eugeoclinal siliceous slate. Carlin, with an initial reserve of 100 t Au, has been found in the Lynn Window. In the same year, Newmont acquired the old Maggie Creek Cu, Pb, barite and turquoise diggings south-east from the (Old) Carlin that has eventually developed into the "giant" Gold Quarry mine. This deposit is partly in the Upper Plate meta-sediments. Gold exploration in Nevada accelerated after 1980 when gold price peaked at more than US\$ 800/oz and, gradually, two subparallel NNW alignments of Carlin-type deposits emerged in Nevada: the western Getchell Trend and the eastern Carlin Trend. Some latest discoveries are located outside these trends. The greatest scoop in the Nevada gold history, against which even the find of the Comstock Lode pales into insignificance, has been the 1987 acquisition of the small Goldstrike property NNW of the Old Carlin by a small company Barrick Resources (Bettles, 2002). In 1987 Goldstrike had a reserve of 31 t Au. Nine years and hundreds of km of drill holes later, the Goldstrike property stores 1,617 t Au (52 Moz), rivalling the richest mines on the Witwatersrand but mined for a fraction of costs, and Barrick Inc. is now the world's #3 gold miner.

Nevada Carlin-type gold province

Considered jointly, this is the world's 2nd largest gold repository after Witwatersrand (Thompson et al., 2002; ~6,000 t Au). Carlin-type gold accumulations are notoriously difficult to delineate and break down into discrete "deposits", as they form interconnected trends interrupted by gaps; in this respect they resemble the MVT deposits as in the Tri-State district. Separation by properties goes against the geological logic, but this is what tonnage figures are based on. The literature is inconsistent, for example the "Carlin Trend" is 40 miles long to some, 160 miles long to others and definitions are not always provided. The famous Goldstrike (property) is either in Central, or Northern Carlin trend or, alternatively, in the Bluestar Subdistrict. For consistency the geographically defined groupings are considered here and only the "giants" are included.

All the Carlin-type deposits in Nevada (there are few outside the state) are situated in the Great Basin (or Basin-and-Range province) marked by the famous late Cenozoic extensional tectonics. The disseminated gold deposits, however, are older (42-36 Ma, Eocene) and the bulk is hosted by supracrustal rocks that are members of two domains: 1. Autochthon ("lower plate") that comprises Silurian and Devonian miogeoclinal

carbonates and fine clastics (that include carbonaceous argillites) of the stable continental margin flooded by Precambrian craton; 2. Allochthon comprised of Ordovician to Devonian "basinal" (or continental slope, oceanic, eugeoclinal) fine siliceous clastics with chert, some impure carbonates and local greenstone metabasalts. These rocks occur in several thrust sheets, members of the Roberts Mountains thrust system (Burchfiel et al., 1992), transported from the west over the autochthon. The low-angle Roberts Mountain Thrust brought rocks from as much as 200 km away into the area where they constitute the "upper plate". Erosional windows in the upper plate expose the autochthon at several places, especially around Carlin. Scattered Meso-Cenozoic intrusions were emplaced into both supracrustal domains and locally (e.g. in the Goldstrike deposit) passively host a portion of the gold ore.

On the grand scale the gold deposits are controlled by deep-seated structures that project to the present surface as trends of gold occurrences of various degrees of continuity. The NNW-oriented Carlin trend is most consistent; other trends include Getchell and Battle Mountain-Eureka trends, as well as less extensive districts not called "trend" (Jerritt Canyon, Alligator Ridge).

NW Carlin trend ("Old" Carlin-Goldstrike-Dee deposits): Carlin Trend is about 60 km long and stores some 3,328 t Au, of which some 2,177 t Au is in the 30 km long north-western section NNW of the town of Carlin (Christensen, 1993; Teal and Jackson, 1997). This 30 km long NNW-trending segment comprises an almost uninterrupted string of overlapping gold deposits, in various host rocks and at several stratigraphic levels. The original 1961 Newmont Ltd. discovery, "Old Carlin", is near the SE end, the largest property, Goldstrike, is slightly north of centre. The geology here is dominated by Cambrian to Devonian shelf carbonates of the autochthon (lower plate) and Ordovician "eugeoclinal" siliceous clastics and chert of the allochthon (upper plate). Lower Carboniferous synorogenic sedimentary rocks of the overlap assemblage are less important. These units are locally intruded by Jurassic, Cretaceous to Eocene granitoids and all rocks can be gold-mineralized.

The "Old" Carlin Au deposit (Radtke, 1985; Pt ~120 t Au @ 6.0 g/t; Fig.6.26) is in the lower plate, exposed in an erosional window through the upper plate and about 70-80 m under the thrust sole. The now exhausted orebodies are stratabound blankets with diffuse boundaries in dark-gray Devonian thin

bedded laminated silty dolomitic micritic limestone with bioclastic interbeds. The sedimentary rocks are

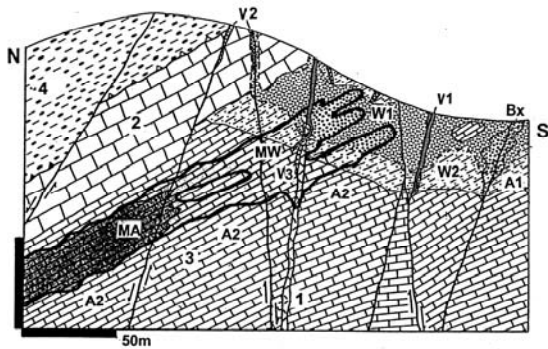


Figure 6.26. "Old" Carlin deposit adopted from Radtke et al. (1980) and Rye (1985) of the U.S. Geological Survey (also LITHOTHEQUE No. 693) and re-keyed. W. Supergene alteration: with leaching (W1), without or with limited leaching (W2); V. Post-gold fracture & fault veins: V1 barite, V2 quartz, V3 sparry calcite; Bx, Fault breccia; A. Hydrothermal alteration: A1 silicification (jasperoid), A3 decalcification and illite; 1. Eo₃-Ol felsic dikes; 2. Lower Plate, D grey thick-bedded limestone; S₃-D₁ dark thin-bedded limestone; 4. Upper Plate, Or allochthon; siliceous slate, chert

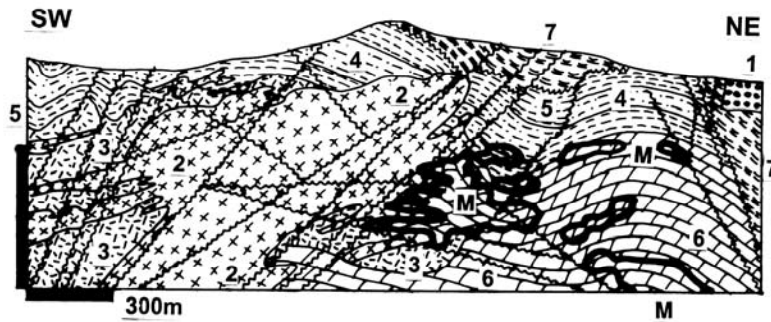
block faulted and some faults have silicification (jasperoid) rims, or control barite or sparry calcite veins. The disseminated gold orebody is 2,100 m long and 20-50 m thick. Au resides in arsenian pyrite that is sparsely disseminated in decalcified, slightly silicified impure carbonate. The ore and alteration are visually unrecognizable and the only occasionally visible mineral is orange realgar filling fractures in limestone. The upper 50 m of exposed rocks in the Carlin pit are oxidized and leached into a beige, brown or red-pigmented inconspicuous material. Pyrite is decomposed and the dispersed gold resided mostly in Fe hydroxides.

Goldstrike (Post-Betze) Au deposit (Leonardson and Rahn, 1996; Bettles, 2000; P+Rc 1,617t Au plus). Situated 8 km NW of the "Old" Carlin, Goldstrike is the largest U.S. gold deposit, on par with the largest Witwatersrand gold mines. It consists of several overlapping and adjacent, shallow and deep stacked orebodies (Post, Betze, Screamer, Rodeo, Meikle), progressively discovered and developed since 1962 (Fig. 6.27). Between 1974 and 1995 the ore was derived from no less than 25 individual pits (Leonardson and Rahn, 1996); mining has been since consolidated to several mega-pits and, at Meikle, an underground mine. The bulk of mineralization is in the lower plate, especially in footwall of a set of high-angle, NNW-striking faults. The host rocks are Devonian

calcareous black shales and brecciated limestones, but also Jurassic diorite intrusions and Ca-silicate exocontact hornfels. The granitoids are passive hosts to the gold introduced much later (around 36 Ma). The ore mineralogy is everywhere the same, a micron-size gold carried by arsenian pyrite, in decarbonated and slightly silicified or argillized limestone or silicified, argillized shale or diorite. The near-surface orebodies are oxidized. Compared with the "Old" Carlin, the orebodies occur at several depth levels, are less regular, and although predominantly stratabound and gently dipping they cross lithologic boundaries. Higher local Au grades are in steeper strongly fractured, brecciated, hydrothermally veined structures with quartz, calcite, kaolinite or illite, pyrite, barite, realgar, orpiment and stibnite. The average grade of the Post oxide orebody was 1.74 g/t Au and 0.56 g/t Ag. The largest continuous Lower Post-Betze refractory orebody stored 16 million ounces (498 t Au) of gold in the 1995 ore reserves of 64 mt and it graded 7.77 g/t Au, 1.24 g/t Ag, 0.17% As, 20 ppm Hg, 19 ppm Tl, 442 ppm Zn, 22 ppm Se and 4 ppm Te (Volk et al., 1996). Contents of the unrecovered trace metals, in this partial reserve only, correspond to "large" accumulations of As (109 kt); Hg (1,282 t); Se (1,410); Te (256 t) and a "medium" accumulation of Tl (1,218 t). These amounts would more than triple if the entire Goldstrike endowment of non-oxidized ore were considered.

Meikle Au orebody (Emsbo et al., 2003; 8 mt @ 24.5 g/t Au for 224 t Au) was drill intersected in depth of 398 m and it is a higher-grade mineralization mined from underground. It is hosted by silicified limestone collapse breccia in Devonian Popovich and Roberts Mountain carbonates near high-angle faults; Eocene-Oligocene biotite feldspar porphyry and rhyolite dikes are present. The collapse is attributed to syn-mineralization thinning of strata due to decarbonatization, or it could have been partly earlier.

Gold Quarry-Maggie Creek Au ore field (Rota, 1996; 760 t Au @ 1.25 g/t). Gold Quarry is the second largest "giant" after Goldstrike, located 16 km NW of Carlin (town). Maggie Creek had been a site of small-scale Cu, Pb, Ag, Au mining since 1870 but, following modern exploration after 1960, the concealed Main Gold Quarry orebody has been found only in 1979 and open pit mining started in 1980. Gold Quarry is located at the southern edge of the Carlin Window and earlier descriptions considered the mineralization to had been in siliceous rocks of the upper plate (Ordovician Vinini Formation). Although this is still partly true,



1. Mi friable silt, tuff, gravel; 2. J diorite; 3. Hornfelsed & skarned S+D sediments in exocontact; 4. D Rodeo Creek Unit, siltstone, sandstone; 5. Ditto, argillite; 6. D Popovich massive limestone, some mudstone; 7. Upper Plate, Or Vinini Fm. mudstone, siltstone, chert. M. Carlin-type micron-size disseminated gold

Figure 6.27. Goldstrike (Betze-Post) deposit, Carlin Trend, Nevada. Cross-section from LITHOTHEQUE No. 2315, modified after Leonardson and Rahn (1996) and Barrick Goldstrike Staff, 1999 tour

the bulk of gold is now believed to be in Devonian silicified carbonates and slates of the autochthon, and probably also in the early Carboniferous? rocks of the overlap assemblage (Rodeo Formation?; Rota, 1996). The rocks are strongly deformed and the stratigraphy is probably thinned due to volume loss during hydrothermal decarbonatization.

90% of the ore is in hangingwall of the SE-dipping Chukar Gulch Fault, in a wedge-shaped fault block that preserves 400 m thick section of mineralized strata. Rota (1996) distinguished three ore styles: 1) fracture and quartz veinlet stockworks in silicified sediments (Main orebody); 2) disseminated gold in stratabound silicified and argillized strata; 3) Deep Feeder-steep subvertical structure with a higher-grade (~3.5 g/t) ore. As elsewhere, micron-size gold is mostly held in arsenian pyrite overgrowths of sparsely scattered pyrite grains, and is slightly enriched in the carbonaceous intervals. Alteration (quartz, illite, sericite, kaolinite, calcite leaching) are stronger than in the "Old" Carlin. The main stage mineralization is attributed to 210-150°C hot reduced fluids active around 35 Ma, and it may have been followed by a late-stage hydrothermal leaching and oxidation that deposited hematite in the subsurface, before the supergene oxidation. This is a very low-grade deposit where the cut-off grade of the heap-leach oxide ore was mere 0.2 g/t Au.

The remaining four Carlin-type "giants" are briefly summarized below:

- **Getchell & Turquoise Ridge**, NW Nevada * Rc 436 t Au * 95-39 Ma multistage skarn, pyrite, stibnite, realgar, orpiment, gold in tabular orebodies along 5 km long fault zone; micron-size Au in decalcified & silicified carbonates * Cm limestone and shale, intruded by Cr granodiorite * Groff et al. (1997).
- **Twin Creeks**, Getchell Trend, NW Nevada * 340 t Au * 42 Ma, several subhorizontal bodies of micron-size Au in disseminated arsenian pyrite > stibnite, orpiment in various decalcified, silicified, sericitized

hosts near thrusts * Or greenstone & phyllite, D-Pe carbonates * Stenger et al. (1998).

- **Jerritt Canyon field**, NE Nevada * 470 t Au * 42-30 Ma, 11 tabular orebodies of micron-size Au in pyrite, near faults, in decalcified carbonaceous limestone & siltstone, partly jasperoid * PZ laminated siltstone, carbonates in the lower plate * Hofstra et al. (1999).
- **Cortez cluster (incl. Pipeline & Gold Acres)**, central Nevada * 350 t Au * T₂, three groups of low-angle tabular zones adjacent to fault, of submicron disseminated gold with pyrite in decalcified, silicified hosts * S carbonates and siltstone/shale in the lower plate * Foo et al. (1996).

6.6.2. "Carlin-type" gold outside the U.S.A.

Curiously, after more than 30 years of intense worldwide search, there is not yet a confirmed "Carlin-type" giant, anywhere in the world, so there must be something special under northern Nevada that is not duplicated elsewhere. Medium- to "large" Carlin-like discoveries have been reported from Guangdong and Guizhou in China; from the North Takab geothermal area, Iran (Zarshuran deposit, 100 t Au @ 3-4 g/t Au; Daliran et al., 1999); from the Potrerillos ore field in Chile (Jeronimo), close to the porphyry Cu-Mo; from Mesel, northern Sulawesi, Indonesia; from Alšar, Yugoslav Macedonia (Alšar has the world's highest concentration of thallium; Percival et al., 1994). World's deposits that share some characteristics with the "classical Carlin", like stratabound ore horizons in pelitic carbonates that lack direct intrusion contacts (but not the submicroscopic gold) include the Pilgrim's Rest district in South Africa and the "giant" Telfer in NW Australia (Chapter 11).

7 Cordilleran Granitoids

7.1. Introduction

Cordilleran granitoids are best developed, you guess it! in the North American Cordillera, especially in the Canadian and NW USA portion where the mountain system is not much affected by the post-orogenic extension. The term "Cordilleran" is used in the literature rather informally for the North American orogenic system and comparable terrains elsewhere, especially for those with dominantly subduction-related granitoids emplaced into continental crustal basement (Pitcher, 1982, coined the term "andinotype" for this granitoid variety). Here the term serves mainly as a brief chapter heading for the deeper-seated form of magmatism in andean-type margins.

We are fortunate that this segment has an excellent, recent, comprehensive descriptive literature under three single covers, in the following volumes of the Decade of North American Geology series: Plafker & Berg, eds (1994) for Alaska; Gabrielse and Yorath, eds. (1992) for the Canadian Cordillera; Burchfiel et al., eds. (1992) for the United States' Cordillera. The size of these volumes is proportional to the geologic and metallogenic complexity to be expected in this setting, a fact not apparent from the "telegraphic" selection of topics provided in this chapter. Cordilleran granitoids and the almost exclusively hydrothermal deposits in this setting have the largest complement of "giants" of all divisions treated in this book.

As with other chapters, this is not a sharply delineated entity. The difference between the contents in this and Chapters 5, 6, 8 10 and 12, especially, is more quantitative than qualitative and it is a matter of emphasis. In respect to Chapter 6, this chapter focuses on what is below the predominantly young, near-surface and undisturbed andean volcanics. In relation to Chapter 10, the typical granitoids and their ores, treated here, are related to subduction under convergent continental margins. The typical ore metal here is Cu. In Chapter 10 the typical granitoids are related to orogeny and the typical metals are Sn and U. Mo, W, Zn, Pb, Au and Ag are common in both settings. In practice, however, the andean-type continental margins incorporate all genetic varieties of granitoids that overlap and mingle in a collage of rock groupings collected over the span of 500 m.y.

or more. Despite the frequent departures from the "model" and existence of local irregularities, there is a repetitive overall trend across the Cordilleran-type systems where the granitoids and associated ores become more mature, fractionated, and potassic away from the ocean and towards the continental interior.

There is another point that requires clarification: the meaning and role of orogeny and orogen. Orogeny is a timed upheaval that deforms, repositions and metamorphoses rocks and that produces structural complexes called orogens; the American Cordillera is one such orogen. At the introductory level as in textbooks and university courses, as well as in specialist studies focused on processes acting in a restricted time interval, it is quite possible to treat separately the rocks and ores related to ocean spreading, subduction, collision and extension. The island arc (Chapter 5) and andean-type margins (Chapter 6) focus on rocks/ores created during the existence and as a part of the respective regime. An orogeny later created a new geological entity (orogen) that incorporates components formed earlier in one of the above mentioned settings. Orogeny modified (deformed, metamorphosed) the earlier rocks and also created brand new "orogenic" rocks and ores that had not been there before. So andean margins can be the same thing as cordilleran orogens, depending on premise.

In the study of granitoids and associated ores it is customary to distinguish pre-orogenic, syn-orogenic (orogenic), post-orogenic and anorogenic granitoids, all of which can be found in the same orogen (e.g. the Cordilleran orogen), sometimes even within a single composite batholith (e.g. Sierra Nevada). Most pre-orogenic granitoids are also synvolcanic, formed both in island arcs and andean-type margins. In this chapter the emphasis is on the latter. In the "real world", however, there is no sharp boundary between the subduction-influenced (mostly syn-volcanic, but many magmas did not reach the surface) and orogenic granitoids. This genetic overlap is well illustrated by the great Sierra Nevada Batholith in California (Bateman et al, 1963). The bulk of this Jurassic-Cretaceous composite intrusion is composed of metaluminous phases (granodiorite is dominant) presently attributed to subduction-related melting. There, as well as farther east of the main magmatic arc in

Arizona, also occur peraluminous granites formed by intracrustal melting as a consequence of crustal compression and thickening under a thermal blanket of overthrust sheets (Miller et al., 1992). The crustal silicic melts rose and intruded the metamorphics in the batholith roof. The melting, although attributed to the thermal energy from mantle, was contemporaneous with or shortly postdated the peak of orogeny. This process is thus identical with formation of anatectic granites in the purely collisional orogens (Chapter 10).

Sometimes, in orogens with multiple accretionary terranes as in British Columbia (Dawson et al., 1992) granitoids and ores are classified in respect to the time of amalgamation (docking) to an ancestral craton or an earlier superterrane, as pre-, syn- and post-accretionary.

Cordilleran granitoid varieties and settings

The granitoid varieties in orogens based on presumed magma sources (I, S, S-I, M, A) are briefly reviewed in Section 10.1. Figure 7.1. shows diagrammatically the usual setting of granitoids in the various facies and structural divisions of a typical Cordilleran orogen. The visually recognizable (mappable) setting has a considerable influence on petrology, expected magma family, style and metallogeny of most granitoids, although some granitoids seem to be almost oblivious to the nature of the immediate wallrocks (e.g. the porphyry Cu-Mo related granitoids). There can be a considerable local heterogeneity in granitoid type, and related mineralization. Keith et al. (1991) noted that, in Nevada alone, "within any given mountain range as many as ten distinct mineral systems may be present in a limited geographic area". In each setting, further variation is due to the relative timing (pre-, syn-, post-orogenic and anorogenic) and the level of granitoid emplacement (and exposure at the present erosional surface). The latter range from the highest level subvolcanic intrusions (~0.3-1.5 km under the paleosurface) through the "porphyry" and epizonal granite levels (~1-5 km depths) to mesozonal (~5-15) and katazonal (15 km plus) granitoids (Buddington, 1959).

7.2. Metallogeny

Ore deposits related to granitoid plutonism form by far the greatest proportion of the giant metal accumulations (Laznicka, 1999). Of these, the porphyry Cu-Mo and the zonally arranged Pb-Zn veins and replacements demonstrably formed within

the Andean-type margins are the strongest group but there is a controversy as to the setting of many of the hydrothermal Mo, Zn-Pb-Ag, Au, W and Sn giants affiliated to granitoids. Some are subduction-related, others formed during collision or extension but as Cobbing (1990) and others have correctly stated, the granitoid-related metallogeny is influenced mainly by the magma variety and the melt sources that could be identical in both subductive, collisional and extensional settings.

There is little doubt that the ultimate provenance of metals in ores changes from the predominant mantle/oceanic sources to the continental sources as the continental crust thickens in the cratonward direction and this results in a distinct zonality of preferentially accumulated metals across the continental margin and orogen, typically (from the ocean to the craton centre): Fe (Cr, Ni, Hg, Sb, Au) - Cu, Au (Zn, Ag, Au) - Cu, Mo (Zn, Pb, Ag, Au) - Mo, W - Sn, U (W, Mo, Bi, Be, Li). This zonality is best developed across the North American Cordillera and across the northern Chile-Bolivia transect in the Andes, but numerous local exceptions and reversals occur as a consequence of accretion of pre-subduction mineralized terranes, different timing, local environments, depths of emplacement, and other factors.

Magmatic deposits

Orthomagmatic ores, directly separated from magmas in the course of magmatic crystallization and fractionation, are uncommon, small and sometimes controversial in convergent margins. The only metallogene with some magmatic ore potential are the scattered occurrences of mafic and rarely ultramafic rocks, outside the ophiolite association. They are both pre-orogenic and syn-orogenic. The former are exemplified by small synvolcanic Alaska-Ural complexes that formed at base of island arc volcanic sequences. The fully differentiated complexes are zoned from dunite core to pyroxenite, gabbro and diorite, but they grade into a single rock (mostly gabbro) occurrences and/or into the alkaline-ultramafic association (e.g. Inagly in Siberia). They are frequently mineralized and the most common ore is Ti-magnetite, usually associated with pyroxenite. The **Kemuk Mountain** blind iron deposit in Alaska has a large, but sub-economic resource of 2.2 Bt @ 16% Fe and 2.5% TiO₂ (Foley et al., 1997). Other accumulated metals include Cu (e.g. Volkovskoye in the Urals), chromite, Ni sulfides and platinoids. The PGE occurrences in the Urals, especially around Nizhny

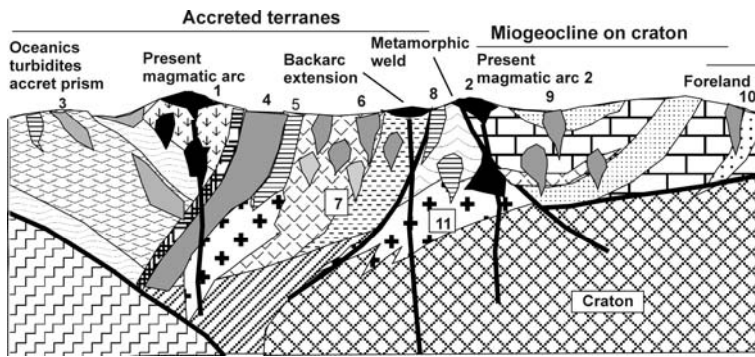


Figure 7.1. Generalized cross-section across a Cordilleran orogen showing granitoid varieties and their setting

Usual granitoid varieties

1. Calc-alkaline andesite, diorite, quartz diorite, granodiorite; 2. Rhyo-dacite, granodiorite, quartz monzonite; 3. Gabbro, tonalite, trondhjemite in oceanic association; 4. Calc-alkaline, metaluminous suite of large batholiths (Sierra Nevada); 5. Peraluminous (two-mica) granite; 6. Post-accretion granodiorite; 7. Pre-accretion quartz diorite, granodiorite; 8. Peraluminous granite, pegmatite; 9. Quartz monzonite; 10. Granite, syenite, quartz monzonite

Tagil where Pt recovery from placers started in the 19th century, are associated with chromite-bearing dunite and remain an enigma. The PGE potential of Alaska-Ural complexes is unknown and is probably in the "large" category.

Synorogenic gabbroids most often occur in the vicinity of major faults, or are the early members of composite plutons. The small Brady Glacier layered gabbro-peridotite pluton in SE Alaska has a resource of 91 Mt @ 0.5% Ni and 0.3% Cu (Foley et al. 1997).

Magmatic-hydrothermal deposits

Magma acquire their trace metal complement from a variety of subcrustal and crustal materials. Hydrated, oxidized, S and Cl-enriched oceanic crust together with the metasomatized and "normal" mantle provide the initial partial melts enriched in the siderophile and chalcophile metals (Fe, Ni, Cu, Co, Zn, Pb, Mo) and volatiles. As the melting along the Benioff zone propagates into the lower and eventually middle crust the magmas acquire the lithophile metals (Sn, U, Ta, Be, Li, Rb, Cs). The deep seated intrusions retain their trace metals in average concentrations bound in minerals with which the elements are compatible; most are silicates like olivine, pyroxenes, amphiboles, feldspars, but also magnetite, sulfides (mainly pyrrhotite), ilmenite, monazite.

Partitioning of trace metals into melt requires fractionation followed by rapid ascent of the water-saturated magma into shallow crustal levels (<6 km under the surface) where the confining pressure is reduced. There, aqueous fluid separates, transfers to the upper reaches of the magma chamber and, eventually, into dilations or replaceable rocks in the granite apex or roof where the ore minerals can precipitate (Candela, 1989, 1991). There are numerous factors that can enhance, or suppress, the

ore-forming potential of a magmatic system. For example, porphyry Cu-Mo formation requires hydrous oxidized magma with a high Cl/H₂O ratio that facilitates early water saturation and partition of a large proportion of Cu (and Mo) into this fluid. In less oxidized and reduced magmas Cu and Mo are partitioned into accessory sulfides, Ti minerals, and magnetite that prevent metals' entry into the residual fluid. The intake of W and Sn by fluids in reduced magmas and eventual mineralization are, on the other hand, enhanced.

Barton et al. (1991) argued that the ability of a magmatic system to produce orebodies depends primarily on the availability of water; "dry" intrusions cannot transfer and locally accumulate metals even when they are geochemically enriched in some. Anomalously trace metal enriched "wet" intrusions, however, have an increased ore forming potential. The system "wetness" can be judged by the type and intensity of alteration aureoles around and above intrusions and by rock textures, and it is important to be able to tell the purely thermal aureoles (e.g. hornfelsed shales; likely to be barren, although their brittleness facilitates fracturing that may provide sites of ore deposition) from hydrothermal alteration aureoles marked by K- and Na-feldspars, quartz, biotite, sericite, chlorite and other minerals. Students of porphyry Cu deposits in particular are well versed in the importance of alteration recognition in exploration.

Anomalous enrichment of some magmatic systems in ore metals, well above the average for the given rock type, is also intensely researched in order to explain and predict the ore formation, particularly of the giant deposits. A metal enrichment can be established already within the mantle source (e.g. in metasomatized mantle). Many investigators consider mantle wedge within the upper plate, under the crust, the principal source of the "fertile" magmas responsible for porphyry

copper belts. Several interactive mechanisms have been proposed to explain the enhanced local metallogenic productivity, for example opening of a "slab window" above a subducting but still diverging plate; this happens when an active spreading centre is subducted. Slab window facilitates upward flow of hot asthenosphere unrestricted by a thick lithospheric lid (Sisson et al., 2003). Alternatively, anomalous metal levels in magmas can build up gradually during differentiation and fractionation, often influenced by wallrock contamination and absorbed intracrustal fluids. Contamination renders some metals like copper incompatible to remain in the lattice of silicates (e.g. pyroxenes, amphiboles) or oxides (magnetite) forcing them to accumulate in the residual melt and finally magmatic water. This is followed by precipitation as a consequence of pressure/temperature drop, boiling or fluids mixing. In some cases metals enter evolving magma along its ascent, or result from remobilization of earlier ores. Alternatively, ore metals are displaced and transferred from a metal-enriched but inactive intrusive body, by hydrothermal convection driven by the heat from another intrusion in depth, often a younger phase of the same system. In the latter case the presumed deep-seated intrusion is not always proven because of the reluctance of mining companies to drill to test theories, although in several cases such drilling resulted in important discoveries of buried deposits (e.g. the "giant" Henderson-Mo deposit in Colorado discovered by drilling under the small surficial Urad-Mo deposit).

Certain metals or metals groups are systematically affiliated to distinct magmatic families. This had been repeatedly confirmed since the times of Lindgren, Emmons, Fersman, Schneiderhöhn, Shand and Peacock in the 1930s-1940s, refined by Abdullayev and others in the 1960s ("petrometallogenic series") and further perfected in the past 20 years. Keith et al. (1991) demonstrated the remarkably consistent correlation between magma chemistry in the Cordilleran region of the western United States and elsewhere (Table 7.1.) and identified 24 distinct magma series specialized in various metals, in north-central Nevada only. For example, oxidized metaluminous calc-alkaline diorite-granodiorite magma series specialize in copper (Yerington and other porphyry Cu deposits), or in gold when reduced (Getchell, Gold Acres and Goldstrike; the latter interpretation is controversial).

Hydrothermal-convective systems and deposits

Ore bodies form by precipitation of metals from fluids derived from heated seawater (VMS deposits), meteoric water (epithermal deposits), formational (connate) water or brine, water released by metamorphic dehydration, and others. The chemistry (especially salinity) of convecting fluids vary, from the high salinity fluids characteristic for base metal deposits to the low-salinity but CO₂-rich fluids responsible for gold precipitation. The temperature also varies from mesothermal (~400-300°C) through epithermal and deep sea floor brines (~300-100°C) to hot springs (<100°C). The fluid circulation is driven by magmatic heat emanating from intrusions or magma chambers below, by geothermal heat, by heat from radioactive decay (e.g. "hot granites") or by combination of all. Ore metals are scavenged from rocks along the fluid path and precipitated by boiling, fluid mixing or cooling. In some ore-forming systems as in porphyry Cu-Mo emplaced into a thick continental crust, the magmatic-hydrothermal ores in, or immediately adjacent to the parent intrusion, are surrounded by convectively precipitated pyritic Cu ore in hydrolytically (sericite) altered wallrocks or in skarn & carbonate replacements. There are often zonally arranged vein, replacement or disseminated Zn, Pb, Ag and sometimes Au deposits.

Many convectively precipitated ore bodies, however, lack identifiable heat source. The practice prevalent in the 1950s to automatically assign ore formation to the nearest granite does not hold, especially in case of the mesothermal gold veins as in the Victoria Goldfields province of Australia or Sierra Nevada Foothills where most of the veins are older than the local granites (Chapter 10). Metal sources to convecting hydrotherms are usually also indistinct, although influenced by the geotectonic setting and sometimes by the "metal provincialism". The former case applies to the seafloor-generated VMS deposits (especially their ancient equivalents; Chapters 8, 9), the ore metals of which were scavenged from the "volcanic pile". Those formed at spreading ridges or in intraoceanic arcs are dominated by copper ("Cyprus-type"), those formed in settings with continental crust as in the mature island arcs and backarcs are Zn, Pb, Cu, Ag-rich ("kuroko", Rio Tinto and Noranda-types). The case of "metal provinces", in which some metals such as W, Sb, U, Cu, Zn, Pb, Ag and others entered a variety of ore types formed over a long time period, is attributed to metal scavenging from shallow crustal sources (typically "black schists") enriched in certain metals at an early stage, and such source

Table 7.1. Granitoid magma series and associated "giant" deposits (selection)

Magma series	Ore type	Example deposits
Peraluminous calcic ("S" type)	scheelite (pyrrhotite) exoskarn; quartz monzonite	Mactung, Cantung
Peraluminous calc-alkalic	gold-quartz stockwork in indurated clastics	Muruntau (Uzbekistan)
Metaluminous calc-alkalic ("I" type); oxidized	meso-epithermal Ag veins to stockworks porphyry Cu-Mo & skarns in granodiorite/quartz monzonite	Rochester (Nevada) Bingham, Butte, Chuquibambilla, Escondida, Pima-Mission
Ditto, reduced	high-sulfidation (enargite) Cu-Au veins, replacements	El Indio
Metaluminous, alkalic-calcic	Carlin-type micron-size disseminated gold Climax-type molybdenite stockworks in porphyry	Carlin Trend, Jerritt Canyon Climax, Henderson, Urad
Ditto, quartz-alkalic	"porphyry-Sn" to quartz-cassiterite veins; epith. Ag replacement Zn-Pb-Ag in carbonates	Potosí, Llallagua Cerro de Pasco, Tintic
Peralkaline	porphyry Cu-Mo, skarn, jasperoid Cu,Au,Pb-Zn disseminated bertrandite in tuff	Ely (Robinson) Spor Mountain, UT
Alkalic	infiltrations & dispersed Li,U,Cs; fracture Hg stockwork molybdenite in porphyry	McDermitt Caldera Malmbjerg, Rico
	porphyry and low-sulfidation Au vein, disseminations	Lihir, Emperor (Fiji)

Applies to all magmas-related deposits (Chapters 5, 6, 10). Based on Keith et al. (1991), more examples added

rocks can sometimes be analytically confirmed. More often, however, the contrasting metal sources are hypothetical and attributed to the "deep crust" or mantle inhomogeneities, communicating with the near-surface via the deep fault systems. Most concrete cases apply to the syn-orogenic deposits reviewed in Chapter 10.

7.3. Porphyry deposits

7.3.1. General and calc-alkaline

This is a famous class of metallic deposits that contains most "giants" (101) and "supergiants" (8) and is easily the most researched and publicized class of metal accumulations. There is an extensive review literature (Titley and Beane, 1981; Titley, ed. 1982) as well as literature on the classical mineralized regions ("The Great Laramide Porphyry Cu Cluster"; Keith and Swan, 1996; Schroeter, ed., 1995) and individual deposits. Porphyry coppers are internationally distributed and store some 1.2 billion tons of Cu, about 70% of the world's total and in contrast to the alternative Cu ores (e.g. strata-related) they have had a much faster rate of discovery in the past fifty years. Porphyry deposits have been classified from many premises, the one based on the recoverable metals being the most unequivocal one. The other premises include geotectonic setting, magma chemistry, district-scale ore metal zoning, architecture of parent intrusions and related orebodies, evolutionary history of

mineralized systems with alteration varieties, and supergene enrichment or impoverishment of orebodies. These characteristics combine and overlap to make up the individual deposits, accounting for the great local variety in what otherwise would be a well defined "family" of ores.

Geotectonic setting and magma series

Porphyry coppers are confined to convergent continental margins, both island arc (Chapter 5) and Andean-type (Chapter 6; general aspects of all porphyry coppers are treated jointly here), where they are synchronized with periods of subduction (Richards, 2003). They are absent in the intracrustal collisional and extensional systems except for few small porphyry-like examples (e.g. Tribag, Ontario; Chapter 12). The parent intrusions follow the "maturation trend" of magmas emplaced into the thickening wedge of the continental crust (Fig. 1). Stockworks resembling embryonal porphyry Cu started to form in the immature island arcs, often in association with the VMS deposits, and some may be comparable with the footwall stockworks under VMS (e.g. the Cerro Colorado at Rio Tinto, Blyava in southern Urals; Chapter 8). They are associated with sodic (plagiogranite, albitophyre) magmas some of which at least are the product of seawater metasomatism overprinting tholeiitic magmatic rocks. There are several deposits transitional between pyritic massive sulfides, stockworks and porphyry deposits such as Mount Morgan, Queensland (Chapter 8). The "diorite model"

(Hollister, 1978) alias "alkaline suite" (Barr et al., 1976), quartz-deficient porphyry Cu- and Cu-Au deposits (e.g. Galore Creek, British Columbia) formed in immature island arcs from arc tholeiitic to calc-alkaline magmas (Lang et al., 1995), rarely in subaqueous setting. Close counterparts of island arc-emplaced porphyry Cu-Au have been discovered even in mature Andean-type margins with a thick continental crust, as in the Maricunga belt in Chile (Vila and Sillitoe, 1991). At the other end of the igneous spectrum, alkaline magmas are characteristic for rifts (Chapter 12) and although the associated metals there are substantially different from the "Andean suite", especially deficient in Cu and Au, there are (as always!) exceptions that invalidate this statement. The giant Palabora Cu stockwork in carbonatite, in terms of mining and processing technology, is a "bulk" mineable orebody little different from porphyry coppers. Viable Cu, and especially Au, accumulations in alkaline intrusions near the subduction-related andean-type margin limit thus cannot be excluded. Some are already there, for example in the Cordilleran Foreland east of the Rocky Mountains.

The bulk of porphyry Cu (Mo, Au) deposits is related to calc-alkaline, metaluminous magmas predominantly of granodiorite-quartz monzonite composition (Table 7.1). They started to form in semi-mature to mature island arcs and culminated in the andean-type margins. In continental margins rich in accreted terranes as in British Columbia, porphyry Cu-Mo formed before, during and after accretion (Dawson et al., 1992). The proportion of Mo in porphyry deposits generally increases with the magma "maturation", and local sediments-dominated settings. The transitional Mo=Cu and Mo>Cu category of porphyry deposits is mostly in quartz monzonite porphyry hosts. The most evolved alkali-calcic siliceous metaluminous magmas, transitional between the subduction and rifting regimes, produced the "Climax-type" Mo deposits that are poor in Cu and Au but enriched in W and Sn. Logtung, British Columbia, is an uncommon type of Mo-W stockwork deposits with affinities to the Central Asian deposits (Chapter 10).

District-scale metal zoning

Most porphyry Cu deposits occur alone or in clusters and they lack major coeval deposits of other metals and other but supergene ore types (e.g. El Teniente, Chuquicamata, Highland Valley districts). Some plutonic "porphyries" are associated with mesothermal gold in veins and replacements (e.g. in Andacollo, Chile, Au-bearing

"mantos" are adjacent to a porphyry Cu; Reyes, 1991). Au-Cu association, along with As and Ag, is particularly striking in the few cases where the near-surface high-sulfidation enargite-rich Au-Cu deposits (e.g. the Mankayan and Récsk ore fields) have deeper-seated porphyry Cu-Au equivalents. Some porphyry Cu have low-sulfidation epithermal Au deposits in their roof (e.g. Brad, Romania). The most complex coeval district zoning patterns, however, have formed around the centrally located porphyry Cu (Mo, Au) deposits in mature continental settings over old (Precambrian in Cananea, Butte) basement or over miogeoclinal assemblages (Bingham, Fig. 7.3, 7.4; Santa Rita, Morococha, Fig. 7.5). In Bingham the large porphyry Cu (Mo, Au) orebody, with a Mo-rich silicic core, is fringed by Cu-skarn, Zn-Pb-Ag replacements and "Carlin-type" Au deposits within a radius of some 10 km from the Bingham pit (Cunningham et al., 2004; read below). In the Almalyk (Olmalyk) ore field in Uzbekistan, small mesothermal Au vein deposits are adjacent immediately to the porphyry Cu (Mo, Au), followed by Zn-Pb replacements (Kurgashinkan). In Kazakhstan, the Kounrad (Qonyrat) porphyry Cu-Mo is adjacent to the East Kounrad stockwork Mo.

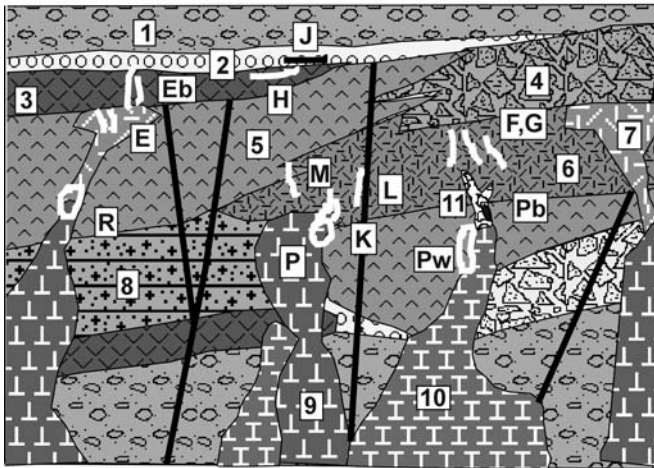
Architecture of parent intrusions and related orebodies

In a widely quoted paper, Sutherland-Brown (1976) has described the ideal changes in architecture of the parent intrusions and related porphyry Cu (Mo, Au) deposits with increasing depth of emplacement. At the highest levels formed the "volcanic" deposits where the orebodies reside in altered volcanic rocks (andesite, basaltic andesite, dacite, sometimes rhyolite) interspersed with dikes of coeval andesite or dacite porphyry, microdiorite, monzonite, syenite and other porphyries (examples: Copper Mountain-Ingerbelle, British Columbia; Lang et al., 1995; Safford, Arizona; Robinson and Cook, 1966; Refugio, Chile; Vila and Sillitoe, 1991). Ores (partly) hosted in non-coeval (older) volcanics and any other rocks unrelated to the ore-bearing system (including granitoids as in San Manuel-Kalamazoo) are, by contrast, sometimes called "wallrock porphyries".

At the intermediate emplacement level formed hypabyssal (stock or "phallic") porphyry Cu (Mo, Au); Nielsen (1976), Sutherland Brown (1976), Hollister (1978). There, the orebodies are associated with epizonal composite porphyritic granitoid intrusions emplaced into coeval volcanic pile in a subaerial structure, typically a stratovolcano. In

many cases the volcanics have been eroded away and the stocks are surrounded by, and may interact with, genetically unrelated rocks in the basement. The intrusions are a variety of small plugs, dikes, magmatic and hydrothermal breccias. They have a

substantial vertical extent but a small footprint (projection at surface). The porphyry Cu (Mo, Au) deposits concentrate in the apical region of the youngest, most evolved intrusion phases and occur within or immediately adjacent to or above the



1. Intermediate to felsic tuff; 2. Gravels;
 3. Flood basalt; 4. Volcanic fanglomerate;
 5. Andesite flow, tuff; 6. Rhyolite-rhyodacite ignimbrite; 7. Rhyolite domes; 8. Volcanic redbeds; 9. Quartz monzonite porphyry; 10. Granodiorite porphyry; 11. Diatreme breccia.
- E. Epithermal Ag veins; Eb. Disseminated Ag in breccia; F. Low sulfidation epithermal Au-Ag; G. Ditto, Pb-Zn-Ag; H. Cu in subgreen-schist amygdaloidal basalt; J. Cu infiltrated in redbeds; K. High sulfidation (pyrite-enargite) Cu,Au; L. Mesothermal Zn-Pb veins & replacements; P. Porphyry Cu-Mo; Pb. Porphyry Cu in breccia; Pw. "Wallrock" porphyry Cu; R. Stockwork Mo > Cu in quartz monzonite.

Figure 7.2. Porphyry Cu-Mo dominated mineralization in moderately eroded andesite-rich volcano-plutonic belts in andean-type convergent margins. Inventory diagram from Laznicka (2004), Total Metallogeny site G51

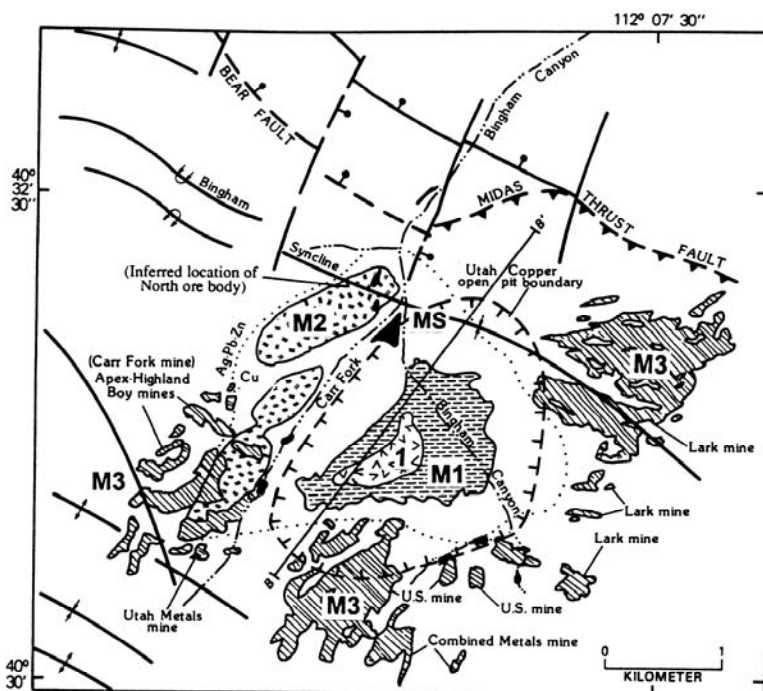
parent intrusion. The alteration-mineralization patterns are broadly concentric and centered on the intrusion.

At the lowest erosional level of unroofed major batholiths the "plutonic" or "batholithic" porphyry Cu (Mo, Au) occur, but there are few major deposits that have actually formed at the mesozonal level; the batholiths mostly acted as wallrocks to a younger magmatic system after having risen into the epizonal niveau. There, the mesozonal granite is the dominant unit and its former roof rocks occur mainly as erosional relics, as rafts and xenoliths, or as hybrid and restite-enriched intervals typically at or near contacts. The orebodies, when present, are associated with deformation and fracture zones and with the youngest, highest level, most differentiated and usually most felsic (often aplitic) phases emplaced into the more mafic (tonalitic or granodioritic) mass of the batholith. The porphyry Cu (Mo, Au) orebodies have often tabular outlines ("linear" porphyries), controlled by intensity of fracturing. Broad areas of the batholith are often weakly hydrothermally altered and contain patches of subeconomic mineralization, overprinted by the higher-grade orebodies. The disseminated ore minerals are sometimes intersected by quartz-veined sheeted zones and solitary quartz veins, with

or without metallic mineralization. The opinion differs as to how far the porphyry Cu (Mo, Au) model can be stretched and whether or not the quartz-Cu sulfide veins could still be classified as porphyry deposits. The giant Precambrian Malanjkhanda Cu deposit in India has recently been the subject of such controversy (Sarkar et al., 1996; Panigrahi and Mookherjee, 1997).

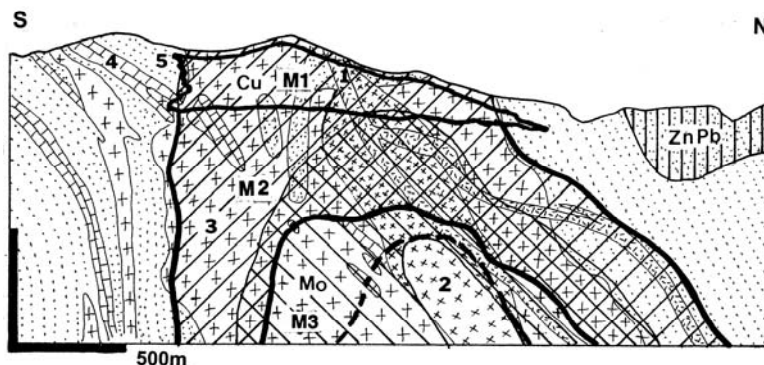
7.3.2. Breccias in porphyry systems

Breccias are ubiquitous in and around "porphyry" systems. Some giant and many more lesser size Cu-(Mo, Au) deposits are predominantly hosted by breccias (e.g. Los Bronces and Sur Sur deposits in the Rio Blanco ore field, Chile; Skewes and Stern, 1995; Bisbee, Arizona; Bryant, 1968; Toquepala, Peru; Zweng and Clark, 1995) so they sometimes appear, in the literature, under a "breccia" heading instead of porphyry-Cu. This is misleading because there are no orebodies confined exclusively to breccias as this is a matter of percentages: orebodies may range from 90%+ to 0% in terms of breccia hosting. Breccias are an extremely important component for genetic interpretation, and one of the most economical visual leads to ore provided they



- 1. Centrally located Oligocene quartz monzonite porphyry stock, a core of an alteration, metal, and ore-style zoned hydrothermal ore field
- MS. Gold placers
- M1. Disseminated Cu sulfide mineralization in K-silicate altered porphyry; Mo increases with depth and degree of silicification
- M2. Projection of Cu exoskarns
- M3. Projection of vein and replacement Pb-Zn-Ag deposits in mainly Upper Carboniferous carbonates and clastics
- BLANK: thermally metamorphosed folded Paleozoic sedimentary rocks (limestone, shale, quartzite)

Figure 7.3. Map showing metals and ore-type zonation in the Bingham porphyry-centered ore field, Utah. From Tooker (1990), U.S. Geological Survey Bulletin 1857-E



1. Eo rhyolite, latite dikes, plugs
 2. 39 Ma Bingham Stock, multi-phase quartz monzonite porphyry
 3. Ditto, biotite (augite) monzonite
 4. Cb₃ limestone, calcar. pelites
 5. Ditto, quartzite
- M1. Thick chalcocite blanket
 M2. Main Cu>Mo hypogene sulfide ore in K-silicate alteration
 M3. Mo>Cu sulfides in K-silicate & silicified porphyry around barren core rich in magnetite

Figure 7.4. Bingham Canyon zoned porphyry Cu-Mo-Au deposit, Utah; cross-section from LITHOTHEQUE No. 682 modified after John (1978)

are satisfactorily interpreted and sensibly named in reports.

Breccias have a voluminous, but fragmented literature. Laznicka (1988) provided a summary of all breccias so a breccia student has more than 1000 examples to choose from and match. Sillitoe (1985) and Baker et al. (1986) have published widely used breccia classifications applicable to volcano-plutonic complexes that include porphyry coppers. Most breccia interpretations and names are based on

a combination of genesis (e.g. tectonic/fault, magmatic, hydrothermal, phreatomagmatic, hydraulic, etc.); presumed site of formation or deposition (vent, diatreme, maar), form (breccia pipe, dyke), texture (fragments or matrix supported), and composition (relative: mono- versus hetero-lithologic; petrographic: rhyolite breccia). Virtually all breccias in porphyry systems (except the accidentally present host rocks that comprise conglomerates, talus, laharc and other volcanic

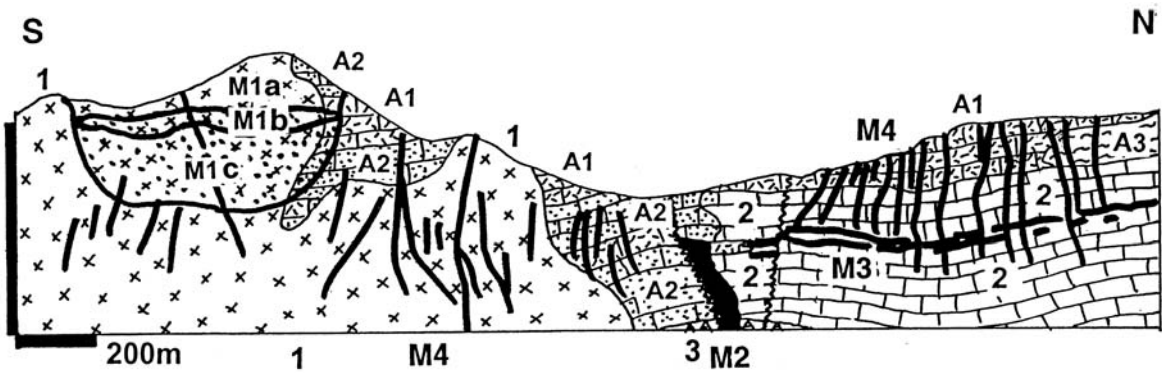


Figure 7.5. Morococha ore field, central Peru. A zoned polymetallic system centered on Miocene intrusions emplaced to thick carbonate, metapelite and redbed sequence. From LITHOTHEQUE No. 2483, modified after Centromin (1977). M1. Porphyry-style ores in endocontact: M1a=leached capping; M1b=chalcocite blanket; M1c=hypogene Cu>Mo sulfides, stockwork & disseminations in K-silicate and sericite-altered intrusion. M2. High-sulfidation, proximal pyrite, enargite, tennantite, etc. veins, breccias, replacements; M3. Pb-Zn stratabound replacement mantos, chimneys. M4. Metal zoned fissure veins: Fe-Cu > Pb,Zn,Ag > Ag,Sb. 1. 8 Ma diorite, granodiorite, quartz monzonite; 2. Tr-J limestone & dolomite; 3. Ditto, basal anhydrite member; 4. Ditto, basalt flows; Pe subaerial andesite, dacite; 6. Dark phyllite to slate

breccias) are members of the disaggregated fragmentite sequence (Laznicka, 1989) formed by fracturing of the source rock followed by fragment loosening, separation, mixing and outward transport; they are not clastic breccias formed by local accumulation of fragments brought in from outside. The textural terms applicable to members of an evolving disaggregated sequence: crackle - mosaic - rubble - melange breccia are also commonly used.

Most breccias are multistage and have a history. To start, a three-dimensional fracture network has to form in a solid rock. In most cases this is tectonic, and fracture networks form along brittle faults. Hydraulic fracturing (by "lifting" or "pushing" unsupported rock slabs in a pressurized hydrothermal system) is also common. Both systems of fractures could continue evolving or, alternatively, another mechanism may take over to expand, rotate, mix and transport the fragments. In magmatic or intrusion breccias the fragments are carried by the still molten and moving magma as xenoliths and remain, after cooling, embedded in magmatic matrix. In intrusive or fluidized breccias (Bryant, 1968) a slurry of fragments is transported by pressurized fluid and rammed into dilations. The result is a mixture of macrofragments in a rock-flour matrix. In hydrothermal breccias overheated pressurized fluid not only causes eruptions and particle transport, but also simultaneous (or subsequent) fragment alteration, cement generation and ore minerals precipitation. Skewes and Stern (1996) argued that hydrothermal breccias prominent in some porphyry systems formed by expanding

high temperature gases exsolved from magmas, and as they slightly postdate the adjacent plutons they have to be related to younger intrusions in depth, not yet unroofed. "Chemical breccias" (Sawkins, 1990) may have formed by hydrothermal corrosion and in-situ (without transport) void infilling. Collapse breccias derived their fragments from above, usually by foundering of an unsupported roof into a void.

In relation to ore formation, breccias are pre-, syn- and post-ore. The pre- and syn-ore breccias are beneficial as they provide permeability pathways for fluids to move, and dilations for ores to precipitate. Typical mineralized breccias consist of completely, or around the rim only, altered rock fragments in hydrothermal quartz cement, with scattered ore minerals. Multistage breccias may consist of ore grade blocks in a younger generation hydrothermal cement. The post-ore breccias may play a negative role as they indicate removal and dispersion of existing orebodies. The best documented case comes from El Teniente (Camus, 1975), where the circular phreatomagmatic breccia pipe (Braden Pipe) shot through the earlier orebody and took a portion of it away, but still left enough in place to make El Teniente the world's largest Cu "supergiant". A similar event took place in the La Copa diatreme, Rio Blanco field (Warnaars et al., 1985).

There may be a positive side of the post-ore breccias, though. Copper sulfides disseminated in the "intrusive breccia" at Bisbee, Arizona, formed elsewhere and were transported to the present location as a slurry (Bryant, 1968). A diatreme may

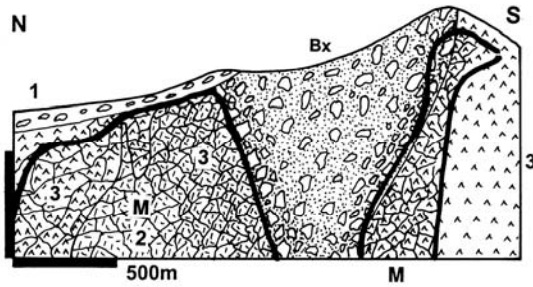


Figure 7.6. El Teniente Cu-Mo deposit, Chile. Cross-section through the Braden Breccia, a late-stage vent filled by matrix-supported, heterolithic concrete-looking breccia (Bx). It is bordered by progressively tighter disaggregated breccia, grading to hydraulic/hydrothermal breccia in biotitized andesite hosting the bulk of the ore stockwork. 1. Q cover sediments; 2. Pl dacite porphyry; 3. Mi andesite, quartz diorite. From LITHOTHEQUE No. 2287, modified after Camus (1975), Codelco Ltd. (1977)

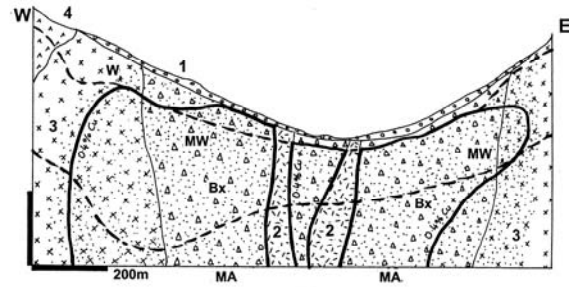


Figure 7.8. Los Pelambres porphyry Cu-Mo, Chile. From LITHOTHEQUE No. 2420 modified after Atkinson et al. (1996). 1. Q talus & gravels; 2. Mi intramineral quartz monzonite porphyry dikes; 3. Quartz diorite; 4. Cr1 hornfelsed andesite; W. Leached capping and remnants of oxidation zone; MW. Secondary sulfide zone, chalcocite > covellite; MA. Disseminated Cu, Fe, Mo sulfides in K-silicates and anhydrite-altered breccia

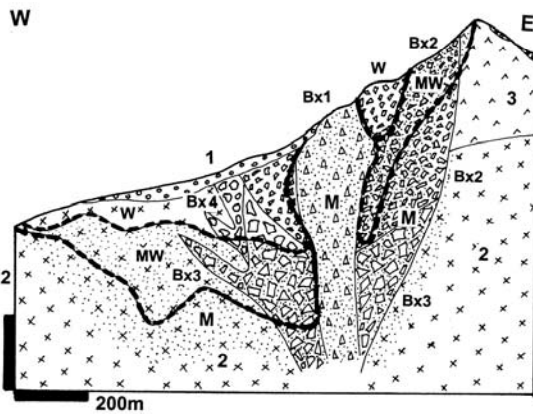


Figure 7.7. Los Bronces (western) sector of the Rio Blanco-Disputada Cu-Mo ore field where several mineralized breccia bodies alone host "giant" metal accumulations. 1. Q glaciofluvial sediments; 2. Mi quartz monzonite; W. Leached capping; MW. Secondary chalcocite zone; M. 5.4-5.2 Ma disseminated Cu,Fe,Mo sulfides in K-silicate altered matrix of breccias, grading to low-grade haloes in granitoids. Breccias from youngest to oldest: Bx1, Anhydrite Breccia; Bx2, Infiernillo Breccia; Bx3, Western Breccia; Bx 4, Central Breccia. All are heterolithic, matrix-infilled breccias with angular to subrounded fragments (read description in Warnaars et al., 1985). From LITHOTHEQUE No. 2404, modified after Warnaars et al. (1985) and Codelco, Ltd. (2000)

contain mineralized fragments brought in from the unexplored depth and trigger exploration drilling or even mining. Even more complex history is

recorded by Sillitoe (1995) from the Maykayan field, Luzon (Chapter 5): there, a porphyry Cu-Au ore fragments were discovered by a consultant in pyroclastic breccia in the Lepanto high-sulfidation mine. The low-angle cross-bedded breccia was interpreted as a base surge deposit of a maar-diatreme complex. Subsequent drilling (based on additional pieces of evidence) found the blind, giant Far Southeast porphyry Cu-Au deposit. A selection of "giant" porphyry Cu (Mo, Au)-related breccias follows:

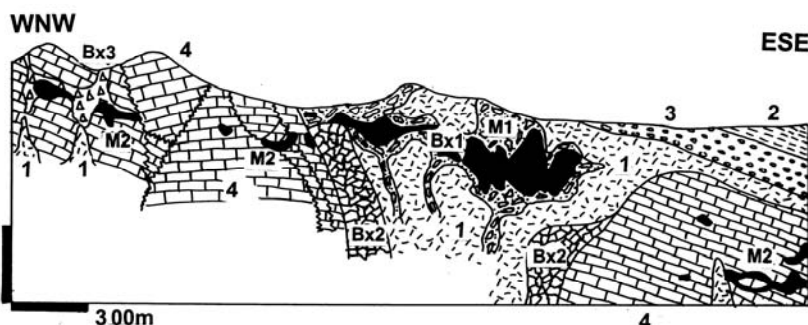
- **El Teniente, Chile, Braden Breccia.** 4.6 Ma tourmaline-rich heterolithic breccia fills inverted cone with an almost circular diameter of 1,200 m and 1,800 m vertical extent. Resembling concrete, the centre consists of a mix of abraded rock fragments (some mineralized) in sericite-altered rock flour matrix. Near margin is a 50-60m wide zone of Cu-enriched breccia of less mixed andesitic wallrock fragments with tourmaline, anhydrite, quartz, chalcocopyrite cement. Interpreted as vent or diatreme, largely post-mineralization (intersects and removes a portion of earlier Cu-Mo orebody). Camus (1975), Skewes and Stern (1996).
- **El Teniente, Chile, Ore Breccia.** Hydraulic & hydrothermal disaggregated breccia (crackle, mosaic, rubble) in biotite-altered andesite with chalcocopyrite > bornite fracture stockwork. Irregular body, principal host to ore. Camus (1975).
- **Rio Blanco-Los Bronces, Chile.** 7.3-4.9 Ma breccias emplaced in 20-8 Ma andesite and quartz monzonite. 5 x 1 km semi-continuous zone of ten main columnar, conical to irregular, mostly subvertical, mostly monolithic breccia bodies composed of disaggregated to transported K-feldspar and biotite altered fragments in the same minerals plus tourmaline-altered rock flour matrix or (also anhydrite) void infill. Disseminated chalcocopyrite,

molybdenite. Interpreted as magmatic-hydrothermal, grading to diatreme. Skewes & Stern (1996).

- **Los Pelambres-El Pachón**, Chile & Argentina. 10.0-8.9 Ma irregular body of K-feldspar & biotite altered angular volcanic and plutonic rock fragments emplaced into a quartz diorite porphyry stock. Disseminated Cu-Mo sulfides. Interpreted as produced by exsolved magmatic fluids (=magmatic-hydrothermal, intrusive breccia); Atkinson et al. (1996).
- **Toquepala**, SW Peru. 58 Ma chimney 700 m in diameter and traceable to 1000 m depth, filled by disaggregated to transported breccia of K-feldspar, biotite, tourmaline, anhydrite altered fragments and infill, related to dacite porphyry. Uniformly disseminated and veinlet chalcopyrite in breccia, 1.1 km diameter halo of low-grade Cu in sericite-altered rocks. Zweng & Clark (1995), Mattos & Valle (1999).
- **Toromocho** porphyry Cu, Morococha, Peru. Mi hydrothermal breccia of predominantly K-silicates and sericite altered granitoid fragments infilled by scattered chalcopyrite, pyrite, tennantite, sphalerite, Bi-minerals; Alvarez (1999).
- **Agua Rica**, Argentina. 6.3-4.9 Ma hydrothermal breccia grade downward into intrusion breccia and porphyry. Overprints and disrupts earlier porphyry-style mineralization and hosts the bulk of high-sulfidation disseminated Cu-Au ore. Advanced argillic alteration. Landtwing (2000).
- **Agua Rica**, late stage diatreme. Unmineralized post-ore phreatomagmatic breccia destroyed portion of the earlier orebody and infilled crater. Landtwing et al (2000).
- **Cananea** Cu, Mo, Zn, Pb ore field, Mexico. A number of subvertical, mostly subrounded to elliptical breccia pipes in a NW trending zone, intersecting Precambrian basement granite, Paleozoic sedimentary rocks and early Tertiary quartz porphyry stocks. La Colorada Pipe was near

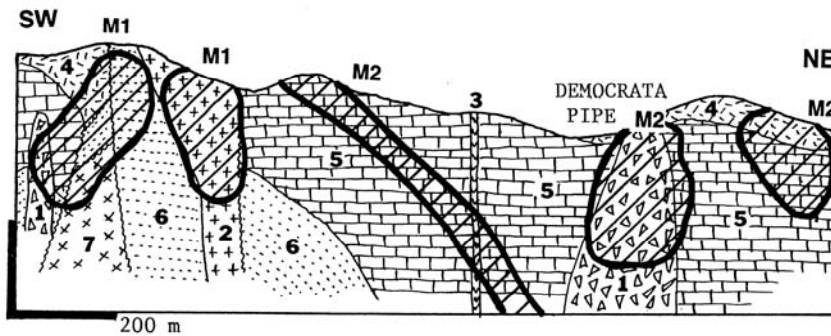
the apex of a porphyry plug emplaced to volcanics, composed of porphyry fragments altered and successively infilled by massive Cu sulfides and molybdenite, then late pyrite-alunite with high-sulfidation minerals (luzonite, tennantite, covellite, etc.). The pipe is enclosed in quartz-phlogopite sheath and has a quartz, sericite, alunite halo. Capote Pipe is a subvertical breccia body passing through granite, quartzite into limestone near the top. It is filled by angular fragments of altered porphyry with porphyry-style Cu-Mo mineralization that grades into massive Fe, Cu, Zn, Pb replacement bodies in carbonates. Most Cananea breccias hosted a very high grade, locally massive sulfide mineralization. Velasco (1966), Bushnell (1988).

- **Bisbee**, Arizona. 178-163 Ma heterolithic, matrix-rich intrusive breccia was forcefully injected into dilations and low-pressure areas in quartz porphyry, in turn emplaced into Paleozoic limestone and dolomite (Fig. 7.9). The breccia a porphyry are pervasively quartz, pyrophyllite, sericite-altered and massive pyrite-bornite ore forms irregular pods in breccia. Pyrite-chalcopyrite veinlets are in sericitized adjacent porphyry. More Fe-Cu sulfides replace silicified or recrystallized carbonates. Bryant (1968).
- **Kounrad** (Qonyrat), central Kazakhstan. Cb2 heterolithic breccia of slightly attrition-rounded fragments in quartz-sericite altered matrix cuts earlier advanced argillic altered wallrocks. Interpreted as hydrothermal vent with disseminated pyrite, chalcopyrite, bornite. Kudryavtsev (1966).



1. 130 Ma altered quartz-feldspar porphyry; 2. Cr2 red shale & sandstone; 3. Cr1 red conglomerate; Cm-Cb1 mio-geoclinal carbonates; 5. Mp schist; Bx1. Intrusion (fluidized) heterolithic breccia; Bx2. intrusion contact breccia; Bx3. Breccia in silicified exocontact carbonates

Figure 7.9. Bisbee, Arizona. M1: Scattered pods of pyrite, bornite, disseminated Cu sulfides and oxides, believed at least partly clastic and transported in a slurry, in quartz-sericite altered intrusive (fluidized) breccia. M2 are massive quartz (jasperoid) and Fe, Cu, Zn, Pb sulfide replacements in exocontact carbonates. From LITHOTHEQUE No. 1647, based on Bryant and Metz (1966)



1. Mineralized and barren breccia pipes related to porphyry stocks; 2. T1 granodiorite, quartz monzonite porphyry; 3. T1 diabase; 4. Cr3-Eo andesite, dacite, rhyolite; Cm-Cb3 mioecoclinal carbonates; 6. Cm quartzite; 7. 1.44 Ga quartz monzonite

Figure 7.10. Cananea ore field, Sonora, N Mexico. Cross-section from LITHOTHEQUE No. 956.1, modified after Velasco (1966). A complex ~53 Ma porphyry-style Cu-Mo sulfide fracture stockworks and disseminations in K-silicate altered silicate rocks (M1), and Cu, Zn, Pb sulfide replacements in carbonates. Sulfides in breccias replace matrix and some hosted high-grade, almost massive ore (La Colorada Pipe)

7.3.3. Evolution of mineralized calc-alkaline "porphyry" systems, alterations, ores

As late as 1946, the hydrothermal origin of the alteration K-feldspar and biotite in porphyry Cu deposits had not been recognized, so some writers interpreted porphyry copper's as magmatic segregation deposits in syenite. Lowell and Guilbert (1970) introduced their alteration zoning model of porphyry coppers, based on observation in the San Manuel-Kalamazoo deposit in Arizona. This neatly integrated hitherto scattered pieces of alteration information, but also fostered an unrealistic expectation about the simplicity and regularity of alterations. The meticulous paper by Gustafson and Hunt (1975) on the El Salvador deposit in Chile fostered awareness about multistage, prograde and retrograde processes. In the mid-1970s, John Proffett found that the Jurassic Yerington composite pluton in Arizona, that hosts several porphyry Cu and skarn deposits, had been tilted about 90° during the Tertiary basin-and-range extension so the present erosional surface exposes some 8 km deep vertical profile through a pluton/alteration/ore system. This has made it possible to combine laboratory determinations with direct empirical observations and mapping in the field (an approach hitherto common in the study of the Precambrian VMS deposits in greenstone belts, many of which are also exposed at an angle of 90° in respect to their depositional setting) and numerous studies have resulted (Dilles, 1987). The modern research on porphyry deposits as members of magmatic-hydrothermal systems is gaining

momentum and several such systems as at Bingham, Utah (Einaudi, 1992; Cunningham et al., 2004; Redmont et al., 2004); Butte, Montana (Brimhall, 1979); El Salvador (Gustafson and Hunt, 1975); Alumbraera, Argentina (Proffett, 2003), and others have by now been extensively studied. This has advanced our understanding but also demonstrated the difficulty of preparing credible simplified summaries.

In a typical "porphyry" system hydrous fluid-rich intrusive bodies, usually small porphyritic stocks or swarms of non-venting dikes, are emplaced in shallow depth (2-3 km), above a larger pluton (magma chamber) in a depth of 5-6 km. Some 1.4 to 2 km under the surface as at Bingham, the magmas exsolved vapor and 700-560° hot boiling hypersaline brine (38-50% NaCl equivalent) with extremely high contents of dissolved ore metals (1,000 ppm Cu plus); Inan and Einaudi (2002). The fluids penetrated densely fractured roof rocks and precipitated vitreous or granular quartz veinlets with minor K-feldspar and biotite, and scattered chalcopyrite, bornite and digenite. In silicate rocks potassic alteration produced halos of hydrothermal K-feldspar, biotite (phlogopite), sometimes magnetite, muscovitic phengite, anhydrite, andalusite, tourmaline. The alteration propagated through networks of macrofractures and microfractures resulting in large blocks of pervasively altered rocks. In carbonate wallrocks the same fluids produced exoskarn, zoned from proximal andradite with salite (diopsidic clinopyroxene) through a wollastonite front into recrystallized marble. Chalcopyrite, pyrite and

magnetite masses replaced marble relics in skarn and partly the silicates, and filled brittle fracture in the skarn. Outward from the potassic zone the same magmatic fluid, cooled to near its lower limit of 350°C, produced sodic-calcic alteration assemblage of quartz veinlets with actinolite, albite, epidote, titanite (Dilles et al., 1995) and/or sodic-potassic assemblage. The sphalerite-galena replacement bodies in carbonates and veins in clastic sedimentary rocks in the Bingham district and elsewhere probably also formed from similar fluids (Inan and Einaudi, 2002; Cunningham et al., 2004).

The shallow intrusions heated the roof rocks, at Bingham within a radius of some 10 km from the centre, causing convection of fluids stored in and acquired by the predominantly sedimentary rocks, but mostly meteoric water. These 350-250°C hot, low-salinity fluids reacted with the earlier altered, as well as unaltered rocks, causing feldspar-destructive hydrolytic sericite, quartz, pyrite (phyllitic) alteration in granitoids, and retrograde chlorite, talc, tremolite, pyrite and smectite association in skarn, as well as local remobilization of sulfides. Localized advanced and intermediate argillic alteration produced pyrophyllite, illite, smectite. Small, low-temperature "Carlin-like" deposits formed 6-8 km from the Bingham system center (Cunningham et al., 2004); alternatively, they formed earlier. The evolution, alteration assemblages and mineralization are somewhat different in the alkaline porphyry systems, reviewed below.

High-level porphyry copper systems that developed under cover of coeval volcanics in stratovolcanoes or flow domes grade upward into, or are capped by, the high-sulfidation products described in Chapter 6. Enargite-dominated Cu-As-Au orebodies formed at several locations preserved from erosion (described below), but elsewhere only erosional relics, or deeper parts of this assemblage remain, which Sillitoe (1995) called lithocaps. Lithocaps are not confined to porphyry coppers as probably the most visually striking example sits on top of the Sn-Ag system at Cerro Rico above Potosí, Bolivia (Chapter 6).

In the featureless Kazakh Steppe north of Lake Balkhash, lithocaps marked by exhumed silicification ledges ("secondary quartzites") at the surface and andalusite, diasporite, pyrophyllite, sericite and rare zunyite and dumortierite in the subsurface, dot the terrain and they provided an early lead in the search for ores in the 1930s. Of the 500 major occurrences of "secondary quartzites" in the North Balkhash region, 60 are associated with porphyry Cu occurrences (Yesenov, ed., 1972) that

include the "giant" Kounrad (Qonyrat) and several "large" deposits. This area is further described below. Sillitoe (1995) briefly reviewed characteristics of the Kazakh relict lithocaps, their supergene modification and importance in exploration, as the classical literature is mostly in Russian and hard to get (e.g. Nakovnik, 1941).

7.3.4. Alkaline (diorite model) porphyry Cu

This is a heterogeneous group of deposits gradational into, or overlapping into some "porphyry Cu-Au" and "porphyry Au", as well as some of the "volcanic porphyry-Cu". It has also links to the magnetite-rich feldspathites with Cu and Au that constitute the presently popular "iron oxide gold copper family" (Hitzman et al., 1992) and the Candelaria Cu-Au deposit in Chile (Chapter 6). The terms "alkaline" and "diorite" porphyry-Cu was born, and circulate widely, in British Columbia (B.C.) where some ten "medium" to "large", and one "giant" (Galore Creek) Cu-Au deposits of this type occur in the Stikinia and Quesnellia accreted terranes (Barr et al., 1976; Lang et al., 1995). They store some 6 Mt Cu and 530 t Au. All these deposits are of Upper Triassic-Lower Jurassic age and are hosted by late Triassic marine to continental (meta)andesite and shoshonitic suite of intraoceanic island arc, and broadly coeval but more evolved (fractionated) dioritic to syenitic intrusions. The ore deposits and their setting are mostly unweathered thanks to their exposure in a formerly glaciated terrain. They are indeed substantially different from the contemporaneous "classical" porphyry copper's like Highland Valley, that are predominant in the province.

The largest of the British Columbia's alkaline Cu-Au deposits is **Galore Creek** in the Stikine River basin, NW B.C. (Logan & Koyanagi, 1994; Rc 385 mt @ 0.73% Cu, 5.7 g/t Ag, 0.44 g/t Au for 2.81 mt Cu, 2,194 t Ag, 169 t Au). It is hosted by late Triassic potassic (shoshonitic) basaltic andesite breccias, flows and pyroclastics with pseudoleucite trachyte (or phonolite) units. These are intruded and partly replaced by several generations of hybrid K-feldspar syenite, syenite porphyry, and predominantly syenitic to lamprophyric dikes contaminated by epidote, diopside, amphibole, biotite and other minerals. The intrusions grade into magnetite-veined breccias and garnet, diopside, hornblende, biotite, anhydrite endoskarn and metasomatized volcanic fragmentites. Cu-Au mineralization is scattered throughout the complex and the largest Central Zone is a structurally controlled zone of disseminated and veinlet

chalcopyrite with minor bornite in a variety of lithologies. The richest ores are in overlapping syenite, K and Ca metasomatites, and disseminated Cu and Fe sulfides in K-feldspathized rocks.

In the early mined and best accessible **Copper Mountain-Ingerbelle** group of orebodies near Princeton (1.06 mt Cu, 37.6 t Au; Fig. 7.11), and in the Iron Mask pluton near Kamloops that contains at least nine small deposits (532 kt Cu, 31.2 t Au), late Triassic arc andesites with abundant breccias are intruded and metasomatized by Lower Jurassic diorite-syenite suite and affected by alternating Na-Ca (albite, chlorite, epidote, diopside with embryonal garnet skarn development) and K (K-feldspar, biotite) metasomatism. Copper in chalcopyrite and bornite with variable gold content is disseminated in fracture-controlled zones and, at Copper Mountain, in short "pegmatoidal" K-feldspar, biotite fracture veins (Lang et al., 1995). **Mount Milligan** is the largest "alkalic/diorite" Au-Cu deposit in British Columbia (417 mt @ 0.221 Cu, 0.49 g/t Au for 922 kt Cu and 204 t Au) although the grade is hardly impressive. The richest ore concentrations are located in biotite and chlorite-overprinted garnet skarn. The rest of Mount Milligan orebodies are in a 1.9 km long zone of sparsely disseminated chalcopyrite, bornite and magnetite in K-feldspar and biotite-altered monzonite, feldspar porphyry and breccias, enveloped by propylitization.

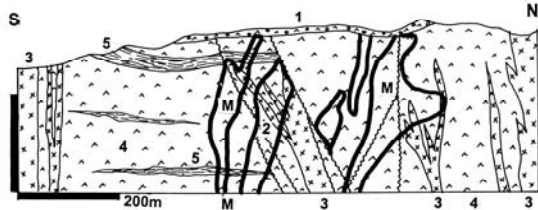


Figure 7.11. Ingerbelle Mine near Princeton, British Columbia, a "large" diorite model Cu, Au, Ag deposit (M) grading to skarn. From LITHOTHEQUE No. 182, modified after Macauley (1973). 1. Eo subaerial volcanic cover; 2. Cr3-T1 porphyry dikes; J1 diorite, monzonite, syenite; 4. Tr3 augite andesite volcanics; 5. Tr3 argillite, volcanarenite

The next significant concentration of the "diorite model" Cu-Au deposits is in the **Maricunga Au-Cu ore belt of east-central Chile** (Vila and Sillitoe, 1991). The igneous hosts are calc-alkaline and the ores have plenty of quartz; the extremely high Au:Cu ratios, however, result in true gold porphyries. This significant mineral belt, discovered in the 1980s, stores some 1,300 t Au and 3.85 mt Cu in very low grade, bulk-mineable "porphyry"

deposits only; more gold and especially silver are in the epithermal La Coipa (Chapter 6). Maricunga area is the axial zone of the Main Andean volcanic belt as it was in Miocene, before it shifted its location farther east. The belt is marked by remnants of dissected andesitic stratovolcanoes intruded by small diorite and locally quartz diorite stocks. Several very high level porphyry Au-Cu deposits and prospects, in 14 zones, preserve remnants of advanced argillic lithocaps that are well apparent from the air in the barren, formerly partly glaciated terrain. The largest "giant" **Cerro Casale-Au,Cu** (Aldebaran; Vila and Sillitoe, 1991; Rv 952 mt @ 0.71 g/t Au, 0.26 % Cu storing a resource of 837 t Au and 3.1 mt Cu) is a stockwork of quartz, magnetite, hematite, pyrite, minor chalcopyrite veinlets and veins in K-silicates altered andesite above diorite porphyry stock. The deposit is partly leached (~6% of the ore is oxidic) and capped by remnants of an advanced argillic lithocap. The smaller but still "giant" **Refugio-Au, Cu** (Vila and Sillitoe, 1991; Rv 297 mt @ 0.86 g/t Au with 259 t Au and 750? kt Cu) has three zones of quartz-sulfide veinlets in a chlorite-altered andesite above early Miocene quartz diorite porphyry stock. The chlorite is believed to overprint the earlier alteration biotite. Finally, the adjacent **Marte and Lobo** deposits hold jointly 194 t Au in 126 mt ore @ 1.43-1.6 g/t (Vila and Sillitoe, 1991) and they are almost pure Au end-members of the porphyry Au-Cu series. There, stockwork of quartz-pyrite veinlets with lesser magnetite and hematite is in argillic-altered diorite emplaced into andesite. The argillization overprints earlier K-silicates. Vila and Sillitoe (1991) considered the Maricunga Au-rich porphyries comparable with similar deposits in the Philippines, although there is much greater variability and age range (Miocene to Cretaceous).

The last examples of "diorite model" deposits come from the Upper Ordovician-Lower Silurian shoshonitic magmatic centers in the Molong oceanic volcanic arc, Lachlan Foldbelt, New South Wales (Scheibner and Basden, 1998). The smaller **Goonumbla (Northparkes)** center (Heithersay and Walshe, 1995; 132 mt @ 1.1 % Cu, 0.5 g/t Au for 1.45 mt Cu and 66 t Au) is a narrow, subvertical cluster of orebodies explored to depth of 1400 m. The ore is a network of quartz, K-feldspar, chalcopyrite, bornite and gold orebodies in biotite, K-feldspar, magnetite, and hematite-altered monzodiorite sheets emplaced into monzonite and quartz monzonite bodies that intruded basaltic andesite to trachyandesite lavas, sills and peperite.

Cadia Au, Cu ore field near Orange is a cluster of five stockwork, vein and disseminated Au-Cu deposits and two Fe, Au, Cu skarns (Holliday et al., 2002; Forster et al., 2004; total P+Rc 574 t Au, 4.4 mt Cu; Fig. 7.12) that together achieve the "giant" magnitude. Individually, the deposits range in size from 8 mt to 352 mt of ore and they are low- to extremely low grade, lacking significant supergene enrichment (the largest Cadia Hill deposit has P+Rv 352 mt @ 0.16% Cu and 0.63 g/t; the "best" orebody, Ridgeway, has Rc 54 mt @ 0.77% Cu, 2.5 g/t Au). Of Ordovician age (438 Ma) this is about the oldest "giant" Cu-Au porphyry-skarn system, not counting Haib and Malanjhand (Chapter 9; the latter is more a vein-type). Development of Cadia into a profitable operation provided encouragement for the search of comparable mineralized systems in Paleozoic orogens elsewhere, the potential of which is rarely acknowledged in the traditional porphyry-Cu literature.

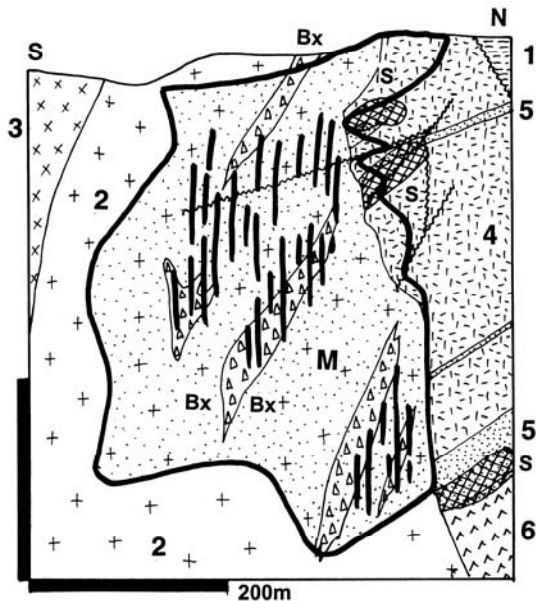


Figure 7.12. Cadia Quarry Cu-Au low-grade vein and fracture stockwork orebody in Or3 quartz monzonite and minor skarn (M; 0.2% Cu, 0.2 g/t Au outline). From LITHOTHEQUE No. 2377 modified after Forster et al. (2004), Newcrest Mining Staff (1998). 1. S sandstone & shale; 2. Or3 quartz monzonite; 3. Or diorite, monzodiorite; 4. Or coarse andesitic volcanoclastics; 5. Ditto, sandstone & limestone interbeds; 6. Or augite andesite; Bx syn-plutonic biotite-altered magmatic-hydrothermal breccia of pegmatoidal appearance; S. Garnet endoskarn

The mineralization is genetically related to the late Ordovician shoshonitic Cadia Intrusive Complex,

emplaced into near-comagmatic pyroxene basaltic andesite to latite. The predominantly marine, sub-greenschist metamorphosed volcanics contain volcanoclastic and limestone units. The intrusive rocks range from diorite to aplite or even pegmatite (or metasomatic pegmatoid?), although quartz monzonite porphyry is the main phase and ore associate. Although several small deposits (mainly Fe, Cu, Au skarns) had been found and mined in the area since 1851, the "large" Cadia Hill deposit has been discovered only in 1991, and developed shortly afterwards. Cadia Hill and the adjacent Cadia Quarry deposits mined jointly from an open pit, are a system of sheeted quartz veins and stockworks predominantly hosted by a pinkish, leucocratic quartz monzonite grading to quartz syenite. Pyrite, chalcopyrite, bornite are sparsely scattered in quartz and on Na-Ca silicates altered fractures. The highest density of the ore minerals is in steep breccia bodies of pegmatitic appearance, composed of porphyry fragments infilled by coarse biotite, K-feldspar, quartz, and plagioclase. The richest orebody, Ridgeway, is a quartz stockwork in K-feldspar, biotite, epidote, chlorite altered monzonite and hornfelsed volcanics, whereas the two Fe, Cu, Au skarns are small orebodies.

This brief review indicates the high degree of complexity within this group of "alkaline" Cu-Au deposits. In terms of geotectonics they come from a wide range of settings: intraoceanic arc interacting with highly evolved potassic magmatic hydrothermal system; principal andesitic magmatic arc on mature continental crust, yet with dioritic stocks that are more at home in immature island arcs. Missing from the list are alkaline syenitic complexes formed within a thick continental crust near termination of a flat subducting slab, of the Cripple Creek variety (Chapter 6). Cripple Creek is a "giant" epithermal gold accumulation but a porphyry-style Au-Cu equivalent is not yet known. The Allard Stock porphyry Cu, Au, Ag prospect in the La Plata Mountains, Colorado (Werle et al., 1984) comes close.

This review also confirms the lack of sericitization superimposed on the magmatic hydrothermal potassic alteration, that changes laterally into Na-Ca "propylitization" and embryonal garnet-pyroxene skarnization. The rapid alternation between sodic (albite) and potassic (K-feldspar, biotite) hydrothermal alteration fluxes in some deposits support the idea that fluids causing albitization may have exchanged Na for K to cause K-feldspathization farther down, and vice versa.

7.3.5. Combined porphyry Cu (Mo, Au) - skarn deposits

High level, predominantly "dry" plutons intruded into sedimentary sequences cause thermal (contact) metamorphism: shale converts into biotite-plagioclase hornfels, pure limestone or dolomite recrystallizes to marble, impure carbonate usually changes to finely crystalline plagioclase-diopside (garnet, wollastonite, biotite) hornfels (sometimes described as skarnoid), andesite into hornblende-plagioclase hornfels (Barton et al., 1991). In volatile-rich ("wet") intrusion systems like those that result in porphyry copper deposits, the early thermal metamorphism is followed by multistage hydrothermal metasomatism that can be correlated with events and alterations in the pluton (Einaudi, 1982; Einaudi et al., 1981). The early potassic alteration in porphyry correlates with the early oxidized prograde calcic exoskarn zoned, away from the contact, from andradite with salitic diopside to wollastonite to marble. Magnesian exoskarn after dolomite has prograde forsterite (Mg-olivine) and diopside, retrograde tremolite, actinolite, talc, serpentinite, phlogopite, chlorite and anhydrite. Magnetite may be present. Chalcopyrite and bornite replace marble relics in skarn, skarn itself, or fill fractures in skarn and adjacent hornfels. When mineralized porphyry directly borders exoskarn the Cu (Mo, Au) mineralization continues without interruption and large combined porphyry/skarn orebodies result. Endocontacts on the intrusion side usually carry the standard "porphyry" alteration assemblages (that is, K-silicate adjacent to prograde exoskarns and phyllic or propylitic near retrograded skarns), although some contacts are gradational and minerals of the skarn association (Ca-Fe garnets, pyroxenes) also occur in the hybrid "porphyry" varieties to form endoskarn. Endoskarns are commonly Cu-mineralized but large discrete orebodies are uncommon.

Convecting fluids causing sericitization in porphyry are responsible for skarn retrogradation, silicification, pyritization and argillization. Small amounts of sphalerite and galena may precipitate in the skarn at porphyry contact, but larger Zn-Pb deposits form in separate bodies outside the contact, still in skarn or in marble with or without jasperoid. In the Central mining district, New Mexico, the "giant", enriched Santa Rita (Chino) porphyry copper deposit borders on a "porphyry-Cu related skarn" with characteristic andradite-diopside association (Einaudi, 1982). This skarn is Cu-dominant and mined together with the porphyry

ores; sphalerite is minor, at marble contact. Zn-dominant skarns in the Central district (Oswaldo, Empire, Pewabic mines; Jones et al., 1967), all small deposits, have the Mn-hedenbergite, bustamite, rhodonite association and are situated at the andradite-marble contact (Einaudi, 1982). The huge Antamina Cu-Zn deposit in Peru may be an exception but there, porphyry-hosted Cu sulfide bodies are very subordinate (Fig. 7.13).

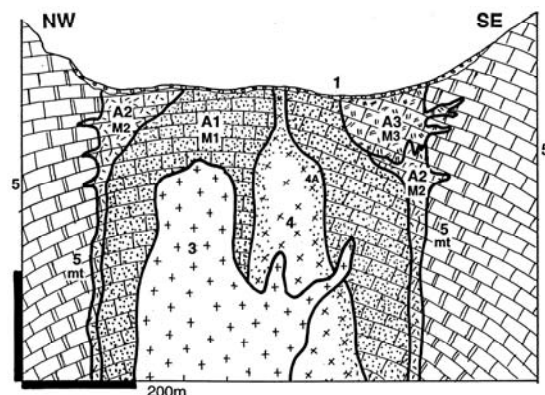


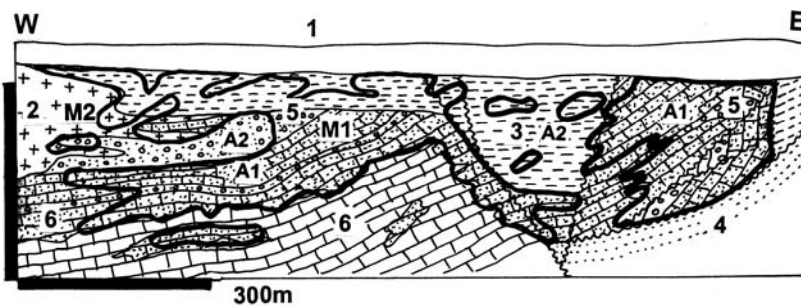
Figure 7.13. Antamina Cu-Zn deposit, Peru. This is a "giant" Cu-Zn skarn in the exocontact of a quartz monzonite stock that hosts only a minor porphyry-style Cu mineralization. From LITHOTHEQUE No. 3201, modified after O'Connor (2000). 1. Q overburden; 2. Mi-P1 andesite dikes; 3. Mi3 intermineral & postmineral granodiorite; 4. Mi2 quartz monzonite porphyry; 4A. Endoskarn in porphyry; 5. Cr3 limestone, 5mt is marble near contact. A1, brown grossularite skarn, hosts chalcopyrite-dominated replacements; A2, green garnet skarn, hosts M2, mostly sphalerite. A3, wollastonite skarn, hosts bornite-rich ores

In addition to single continuous Cu skarn-porphyry deposits like Mission (Fig. 7.14) or Twin Buttes in Arizona, porphyry and skarn often form separate orebodies yet this rarely follows from simple database entries and production statistics. Regardless, when carbonate wallrocks are present, mineralized Cu-porphyry is an excellent indicator of possible skarn presence, and vice-versa. Table 7.2 is a list of joint "giant" porphyry and skarn deposits or ore fields, arranged by decreasing skarn percentages.

There are hundreds of Cu-skarns without Cu-porphyries, but most are small although there are perhaps 30 "large" ones (>250 kt Cu). Those associated with phaneritic plutons are probably eroded to the "mesozonal" granite depths where porphyry copper deposits rarely form and, instead,

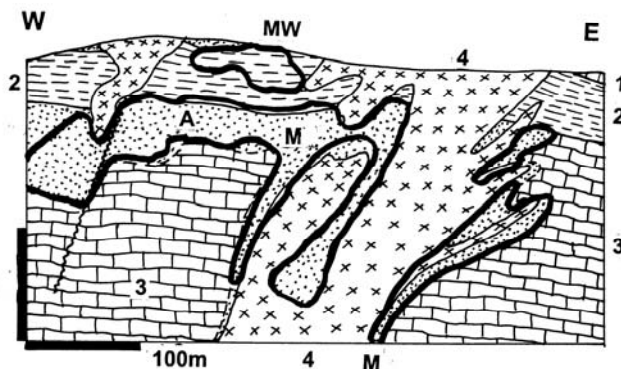
Table 7.2. List of joint "giant" porphyry and skarn copper deposits, arranged by decreasing skarn proportion

Deposit/ore field	Intrusion & ore age, Ma	Skarn host age	Cu, million tons	Other metals, tons	% Cu in skarn
Tintaya, Peru	Ol	Tr, J	1.932		100%
Antamina, Peru	9.8	Cr ₃	9.9	Zn 7.6mt; Ag 10.6 kt	95%
Pima-Mission, Arizona	60	PZ-MZ	7.87	Ag 3840 t	80%
Twin Buttes, Arizona	Eo	Pe	5.7	Mo 128 kt	80%
Bisbee, Arizona	130	Cm-Pe	4.4		65%
Gaspé, Quebec	D ₃ -Cb ₁	D ₁	3.31		50%?
Ertsberg-Grasberg, Indon.	4-2.5	Cr-Mi	43.7	Ag 14.8 kt; Au 4063 t	35%?
Ok Tedi, PNG	4-1.2	Ol-Mi	4.68	Au 138 t	30%
Cananea, Mexico	T ₁	Cm-Cb	17.1	Zn 400 kt; Mo 300 kt	25%
Ely (Robinson), Arizona	110	D-Pe	4.88	Au 200 t	20%
Santa Rita, New Mexico	56	Cb ₂	6.5	Au 120 t	20%
Veliki Krivelj, Serbia	Cr ₃	Cr	3.3	Mo 112 kt	20%?
Sungun, Iran	Mi	Cr	5.16	Mo 129 kt	20%?
Bingham ore field, Utah	39-37	Cb ₂	22.6	Ag 8829 t; Au 1014 t	16%
Lakeshore, Arizona	64	Cr ₃	3.53		12%
Yerington district, Arizona	J	Tr	6.0		10%
Cadia, NSW, Australia	Or ₃	Or	4.4		10%
Récsk, Hungary	Eo ₃	Tr	10.185		10%?
Morococha, Peru	7.2-8.2	J	5.75	Zn 150 kt; Ag 9631 t	5%?



1. T3-Q fanglomerate; 2. T1 quartz monzonite porphyry; 3. Cr arkose, shale; 4. Tr-Cr red beds; 5. PZ (Pe) quartzite, shale; 6. PZ miogeoclinal carbonates; A1. Exoskarn and silicate marble; A2. K-silicates and sericite altered hornfels & intrusion

Figure 7.14. Mission deposit, Pima (Tucson-south) district, where most Cu concentrate comes from exoskarn. From LITHOTHEQUE No. 534, modified after Kinnison (1966). M1 is pyrite, chalcopyrite > bornite ore in skarn, M2 is a fracture stockwork in porphyry and biotite hornfels



- MW. Au in residual Fe hydroxides; heap leach ore
- M. Au in disseminated replacive pyrite > chalcopyrite, Fe, Zn, Pb sulfides in exoskarn
- A. Prograde & retrograde exoskarn;
1. Tr limestone;
2. Tr hornfelsed clastics;
3. Ditto, carbonate member thermally recrystallized to marble;
4. T1 hornblende-biotite granodiorite & porphyry

Figure 7.15. McCoy-Cove Au skarn deposit, Battle Mountain district, Nevada. From LITHOTHEQUE No. 2313, modified after Kuyper (1988)

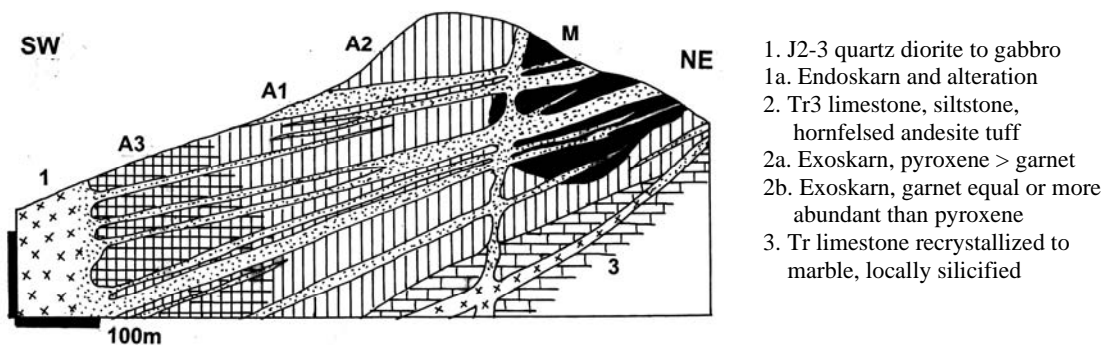


Figure 7.16. Hedley, British Columbia, As-Au skarn (an "As-giant"). M: Sheet-like, overlapping en-echelon bodies of exoskarn with massive to scattered arsenopyrite that encloses refractory gold. From LITHOTHEQUE No. 181, modified after Ettlinger et al. (1992)

mesothermal Cu (and Pb-Zn-Ag and Au) veins coexist. Alternatively, porphyry Cu deposits may still be discovered and there are several encouraging case histories where Cu skarns were long known and mined before porphyry coppers have been discovered (e.g. Grasberg Cu-Au porphyry in the Ertsberg Fe-Cu skarn group, Papua (Irian Jaya); Antapacay porphyry in the Tintaya Cu skarn district, Peru; Cadia Hill Au-Cu porphyry in the Old Cadia Fe-Cu skarn field, New South Wales).

After 1980, exploration accelerated for gold skarns (as well as mesothermal Au vein) deposits in porphyry Cu districts. No major gold skarn has been recorded in continuity with porphyry coppers but several "large" gold skarns have been found near (e.g. Fortitude Au skarn, 75 t Au & 286 t Ag; McCoy-Cove, 58 t Au, 2,581 t Ag; both in the Battle Mountain district in Nevada; Theodore et al., 1990; Fig. 7.15). The "giant" **Wabu Ridge** gold skarn, 35 km north of Grasberg, Irian Jaya, (310 t Au; O'Connor et al., 1999), in Jurassic-Cretaceous limestone exocontact, is proximal to a Miocene-Pliocene porphyry intrusion but the intrusion is not mineralized. Gold occurs with arsenopyrite, pyrrhotite and Bi minerals in biotite, K-feldspar, tourmaline, axinite and datolite-altered retrograde skarn. Several "large" Au-skarns worldwide lack associated porphyry deposits (e.g. Hedley, British Columbia, P+Rv ~61.3 t Au @ 7.3 g/t and at least 200 kt As in arsenopyrite; Fig. 7.16). Theodore et al. (1991) recorded 90 gold skarn deposits worldwide having median tonnage and grade of 279 kt ore @ 5.7 g/t Au.

Deformed and metamorphosed porphyry deposits (Phanerozoic)

In contrast to many types of metallic deposits such as massive sulfides, most porphyry copper deposits remain "pristine" and in the original growth position. Faulting often offset porphyry orebodies (as in the San Manuel-Kalamazoo set, Arizona) and sometimes remove parts of them that are now being searched for (e.g. the lost western portion of the Chuquicamata orebody, Chile, displaced by the Falla Oeste fault). In the Basin-and-Range province of the western United States the extensional faulting caused tilting of porphyry Cu-mineralized blocks, from slight (e.g. 30° at Bingham) to severe (~90° in Yerington). The orebodies, however, remain unmetamorphosed and free of penetrative deformation. There are few Phanerozoic "giant" and "large" deposits where this does not apply.

Gibraltar (or Gibraltar; Drummond et al, 1976; P+Rc 934 Mt @ 0.29% Cu, 0.007% Mo for 2.881 Mt Cu) is in the Intermontane Belt of British Columbia. It is a north-west elongated zone of several orebodies in a composite, locally sheared Jurassic-Cretaceous predominantly dioritic to tonalitic pluton with local aplite and quartz-feldspar porphyry. The pluton has a strong regional cataclastic foliation in a shear zone and is retrograded into a greenschist assemblage of sericite, chlorite and epidote. This metamorphic assemblage merges with the hydrothermal alteration minerals (sericite, chlorite, quartz, albite, pyrite) in the Gibraltar ore zone, resulting in elongated orebodies composed of sets of unidirectional quartz, pyrite, chalcopyrite and molybdenite veinlets and

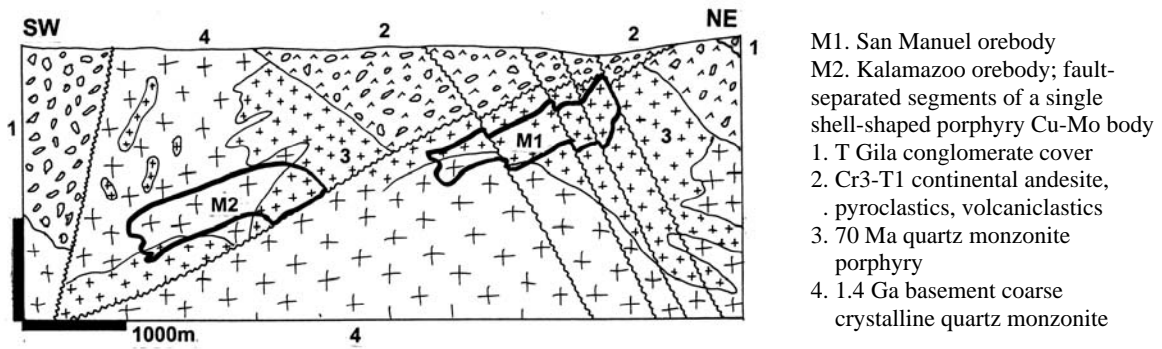


Figure 7.17. San Manuel-Kalamazoo deposit, Arizona, cross-section from LITHOTHEQUE No. 525, modified after Lowell (1968) and Chaffee (1982)

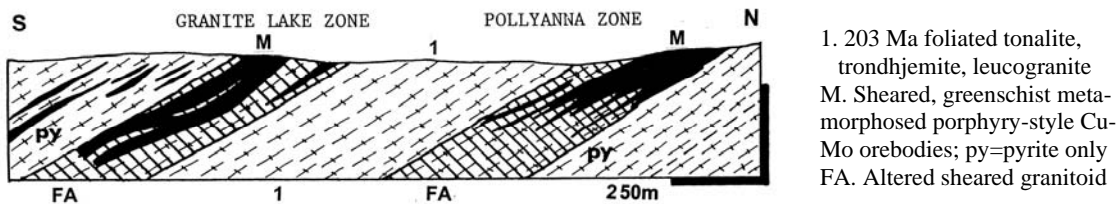


Figure 7.18. Gibraltar deformed and retrograded porphyry Cu-Mo, British Columbia; cross-section of two ore zones from LITHOTHEQUE No. 201, modified after Drummond et al. (1976)

stringers ("parallel stockwork"). There is a controversy as to whether this is a remobilized, metamorphosed pre-tectonic, or syntectonic, mineralization.

7.3.6. Precambrian porphyry-style Cu, Mo, Au deposits

As expected, deformed and metamorphosed deposits are dominant among the few surviving Precambrian porphyry-style deposits and some appear in Chapter 9. As the "porphyry deposits" are high-level metal accumulations emplaced into rising (in contrast to subsiding) settings, they are rapidly eroded away. The "prime-time" of epithermal deposits is Miocene, of porphyry Cu-Mo deposits it is late Cretaceous-Oligocene. Everything older becomes increasingly rare and this applies to the "giant" deposits in particular: the "gerontocratic tail" of porphyry deposits are mostly small marginal occurrences, although there are few exceptions.

Another problem is of classification and naming. The geological age, that broadly correlates with increasing deformation, metamorphism, dislocation of formerly continuous systems and evolutionary changes as one moves back in time, makes many genetic interpretations of orebodies uncertain and subjective. The first question is: how far back can

one trace the subductive continental margins? The second thing is: how can one tell apart sheared and metamorphosed porphyry Cu from equally modified sub-VMS stockworks or even sheared "copper sandstone"? The literature is inconsistent and often misleading. To compensate, the controversial deposits in "greenstone belts" are treated under a genetically neutral heading in Chapter 9. The deeply eroded Precambrian granitoids are almost devoid of genetically related ores so there is not much to cover. Both settings, however, contain rare disseminated or stockwork deposits usually designated as "porphyry-style", some of which could be of economic importance hence worth searching for. These are treated in Chapter 9 and they even include two "giants" and several "large" deposits.

7.3.7. Supergene modification of porphyry deposits

Porphyry copper deposits exhumed by erosion and exposed at surface rapidly undergo supergene modification. Physical weathering as in glaciated, mountainous or desert settings is not known to have produced an economic deposit; dispersion of the ore material into the regolith, however, is an important aid to exploration.

Chemical weathering in the presence of meteoric water, especially when such water has been acidified as a result of oxidation of sulfides, especially pyrite, is an extremely important agent. It is a factor that has to be considered in exploration for porphyry deposits, because most of them are concealed under leached cappings. Even more importantly, it is a factor that may influence the economic viability and profitability of a deposit, and determine the ore processing method. Considerations reviewed here apply to all porphyry deposits, regardless of size, but the selection of examples is restricted to the “giant” and several “large” deposits.

Porphyry copper outcrops and leached cappings

In recently deglaciated areas as in Alaska, much of Canada, Scandinavia and Siberia, the rocks (when they are not covered by glacial drift) are fresh and free of deep oxidation. Thin, surficial stains of the green Cu oxidic minerals (chrysocolla, malachite, azurite), however, form within few hundred years after exposure (or under porous gravels) and they alert the prospector. Most Canadian outcropping porphyries have been found in this manner. Exceptions to this rule, of deposits with thick mature leached cappings and supergene zones like Casino in the Yukon (Bower et al., 1995), are usually explained as pre-glaciation alterations preserved in non-glaciated areas or as uneroded relics. Panteleyev (1981), however, believed that the 38m thick leached capping over the chalcocite-enriched zone, that closely parallels the post-glacial physiography at the Berg porphyry-Cu in British Columbia, is post-glacial. If so, it has been produced within the past 10,000 years and is still forming.

On the opposite side of the spectrum are “porphyry” outcrops in the tropics that are masked by laterite and deep regolith from which copper is almost entirely leached out so there may be no geochemical response. In mountainous humid tropics, however, rapid erosion and landslides often temporarily expose limonitic gossans and occasional green oxidic patches; “giants” Ok Tedi (PNG) and Batu Hijau (Sumbawa Island, Indonesia) crop out in this fashion. Batu Hijau means “green rock”.

The “standard” porphyry Cu outcrops and regoliths, however, as considered in the literature and based mostly on experience from the western United States (Locke, 1926; Blanchard, 1968), start with a fossil (non-recent) leached cap of variable thickness. The cap developed cumulatively in the

past over a porphyry Cu deposit, and has been preserved until now because of its increased resistance to erosion. Many porphyry coppers are also concealed, in addition to the leached cap, under alluvial fans or young volcanics. The latter provide increased protection from erosion; Livingston et al. (1968) determined that 15 largest western U.S. porphyry Cu deposits are located within 10 km of the erosional edge of potential young cover volcanics, from which they have been only recently exhumed. Most of the newly discovered deposits such as Escondida have had the cover still in place when found.

Supergene modification of porphyry (and other) ores exposed at the (paleo)surface requires meteoric water to leach, transfer and re-precipitate metals, but once have the secondary deposits formed the water flow has to be reduced to prevent removal and dissipation of the enriched ores. This requires a fortuitous interplay of local presence of large hypogene Cu orebodies, uplift, rates of erosion sufficient to dissect pediplains and unroof the tops of porphyry deposits, precipitation, permeability, and movement of water table to optimize the ore formation and preservation conditions. In northern Chile such interplay was most favourable in the period between about 18 and 14 Ma (Lower to Middle Miocene) under sufficiently humid conditions when supergene enriched ores formed at La Escondida and elsewhere, and have been preserved thanks to sudden dessication after 14 Ma that initiated the present arid condition in the Atacama desert (Alpers and Brimhall, 1988). Comparable conditions that left behind supergene enriched porphyry coppers probably prevailed at other times elsewhere. Examples include the late Cambrian enrichment at Bozchakol, Kazakhstan (Kudryavtsev, 1996); Jurassic enrichment in Bisbee, Arizona; Eocene-Oligocene enrichment of many porphyry Cu deposits in the American West (Titley, 1993a).

A textbook supergene profile over a pyrite-rich Arizona porphyry Cu deposit would look as follows (from top to bottom): 1) genetically unrelated surface cover (transported soil, alluvium, young volcanics); 2) siliceous, variably “limonite” (=mixture of goethite, hematite and jarosite) stained and impregnated leached capping, devoid of copper. With increasing depth may appear fracture coatings of clay (kaolinite), Cu-oxides stained clay, rare turquoise, supergene alunite and jarosite; 3) upper oxidation zone of chrysocolla, with atacamite and/or brochantite, antlerite in arid setting marked by saline playas as in northern Chile. Malachite and azurite mostly occur when skarn or carbonate

wallrocks are present. Yellow Mo “ochers” (ferrimolybdate) indicate Mo-rich orebodies; 4) Lower oxidation zone of cuprite, native copper; 5) secondary sulfide zone of “chalcocite” (that could be a mixture of several mineral varieties like djurleite, digenite), sometimes covellite, completely replacing the hypogene minerals; 6) supergene/hypogene transition with chalcocite-coated pyrite, chalcopyrite; and 7) hypogene zone of chalcopyrite, bornite, pyrite.

Anderson (1982) reviewed the western American leached cappings in greater detail and made practical suggestions of using empirical characteristics to estimate the approximate sulfide mineralogy and total sulfide content in the hypogene deposit, the remnants of which could still be in depth.

Oxidation zone and oxidic Cu orebodies

Locally rich and easy to smelt near-surface occurrences of oxidized Cu minerals (malachite, azurite, native copper, cuprite) over porphyry copper deposits had been discovered and mined early (some already in antiquity, e.g. Sar Cheshmeh in Persia). They were also mined during the early stages of exploitation of deposits located in the arid or semi-arid settings as in the western United States and northern Chile, in the late 1800s and early 1900s. The oxidic ore mining practically terminated by the 1960s because of exhaustion, with few exceptions (Inspiration Mine in Arizona, Fig. 7.19, practiced and perfected heap and in-situ leaching of the low-grade oxidic ores). The mass production of concentrate from porphyry coppers in the 1960s through 1980s relied mostly on sulfide ores, treated by flotation.

Interest in oxidic orebodies has returned in the 1990s, because of 1) new discoveries of “giant” and “large”, mostly concealed oxidic orebodies (e.g. El Abra, Radomiro Tomic at Chuquicamata); 2) perfection of solvent extraction of copper followed by electrowinning as a low-cost technology; 3) environmental friendliness, as electrowinning eliminates hot smelting, hence the release of SO₂ into the atmosphere which has been the most polluting by-product of copper industries, responsible for a rash of smelter closures in the 1980s and 1990s. The many industrial forms of acid and bacterial leaching (leaching of dumps of mined, crushed and stacked ore; waste dump leaching; in-situ leaching after induced fragmentation; in-situ leaching of naturally permeable material) have profoundly reduced the cost of copper (and partly

gold) recovery and drastically lowered the cut-off grade of ores, hence increased reserves. At Toquepala, Peru (Mattos and Valle, 1999) the cut-off grade of the in-situ leach ore is now 0.1% Cu and this has added 700 mt of 0.2% Cu material to the existing reserve of 300 mt @ 0.83% Cu and 0.07% Mo (the total P+Rv at Toquepala are 9.637 mt Cu and ~686 kt Mo). Although oxidic-Cu leaching is more economical, faster, and has a higher recovery rate, much of the Toquepala leach ore is sulfidic.

The dimension of porphyry-Cu related oxidic orebodies ranges from several hundred tons to “giant” accumulations (Table 7.3). Except for the (old) Chuquicamata oxidic “giant” (18.57 mt Cu), the other “giants” are all recent discoveries, or newly delineated substantial orebodies previously indicated by small outcrops or mined using primitive technology. The “giant” orebodies include Radomiro Tomić, a concealed deposit north of Chuquicamata (5.6 t Cu) and El Abra (4.22 mt Cu; Fig. 7.20), both in northern Chile. The “large” oxidic orebodies are in Zaldivar (1.132 t Cu); Escondida (2.22 mt or 780 kt Cu) and Escondida Norte (~980 kt Cu), all in the La Escondida cluster in northern Chile. This, taken together, total between 2.9 mt and 4.3 mt oxidic Cu. Oxidic Cu ores are generally depleted in Au and Mo relative to the hypogene ores.

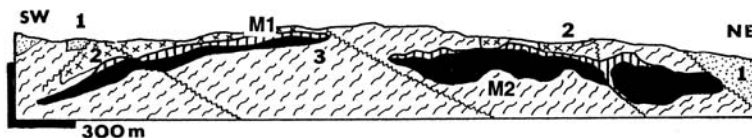
Transported Cu oxidic ores: exotic deposits

Exotic deposits have already been briefly mentioned above as an example of ore infiltrations in subaerial sediments. There, the emphasis was on the “stand alone” deposits like Sagasca and El Tesoro (Fig. 7.21) that lack associated major porphyry Cu deposits. There are more exotic deposits in the Cordillera Domeyko porphyry copper belt in northern Chile that include Chuquicamata; in fact, most “giant” deposits there seem to have exotic Cu cohorts (Münchmeyer, 1996; Table 7.4). In northern Chile only, the “exotics” store some 8 mt of copper. The largest deposit and the only one of the “giant” magnitude (3.5 t Cu), the appropriately named Exotica (now Mina Sur), starts right at the edge of the in-situ oxide blanket of the Chuquicamata porphyry Cu-Mo “supergiant”.

Exotica (Chuquicamata-Mina Sur) (Mortimer et al., 1977; Münchmeyer, 1996; 310 mt @ 1.17% Cu for 3.63 mt Cu; Fig. 7.22) is a paleochannel-type infiltrational Cu (and Mn) oxidic orebody traceable,

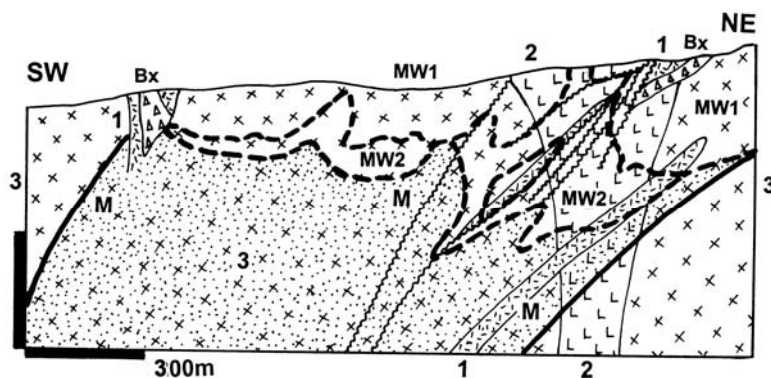
Table 7.3. Oxidic ore component in published total resources of porphyry copper deposits

No.	Deposit/ore field	Total Cu in ores, tons	Cu in oxidic ore, tons	Oxidic Cu grade, %	% of oxidic Cu
4	Casino, Yukon	1.55 mt	30 kt		2.0
18	Inspiration (Globe-Miami), Arizona	3.95 mt	985 kt	0.43	25
22	Lakeshore, Arizona	3.19 mt	3.19 mt	1.0	100
24	San Manuel-Kalamazoo, Arizona	8.576 mt	2.03 mt	0.58	24
29	Morenci-Metcalf, Arizona	18.2 mt	3.663	0.88	20
32	Cananea, Sonora, Mexico	17.0 mt	3.1 mt	0.26	18
51	Cerro Colorado, Chile	4.05 mt	4.05 mt	0.9	100
52	El Abra, Chile	4.7 mt	4.22 mt	0.55	90
53	Chuquicamata (deposit), Chile	67 mt	18.57 mt	0.91	27.7
53	Radomiro Tomić, Chuquicamata, Chile	13.75 mt	5.5 mt	0.56	40
54	La Escondida, Chile	26.013 mt	2.22 mt	0.68	8.5
54	La Escondida Norte, Chile	12.95 mt	980 kt	0.7	7.5
54	Zaldivar (Escondida cluster), Chile	3.813 mt	1.132 mt	0.57	30
56	Mantos Blancos (not porphyry), Chile	4.6 mt	2.694 mt	1.58	58.5
57	Mantoverde (not porphyry), Chile	3.345 mt	1.265 mt	0.55	38
62	Fortuna de Cobre, Chile	4.0 mt	2.53 mt	0.23	63
62	Regalito, Chile	4.122 mt	550 kt	0.2	13
85	Batu Hijau, Sumbawa, Indonesia	7.77 mt	211 kt	0.37	2.7
108	Bozchakol, Kazakhstan	1.27 mt	36 kt	1.13	2.8



1. T Gila Conglomerate
2. 61.2 Ma Schulze Granodiorite
3. Pt Pinal Schist, schist to gneiss

Figure 7.19. Miami-Inspiration deposit, Arizona, successfully practiced early copper leaching and recovery since the 1930s. Cross-section from LITHOTHEQUE No. 532, modified after Peterson (1962). M1. Chrysocolla > azurite acid leach ore; M2. Sooty chalcocite supergene sulfide blanket over low-grade veinlet and disseminated hypogene ore



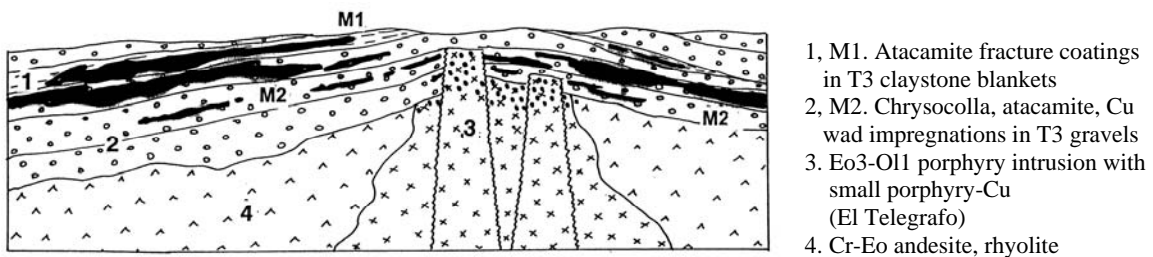
- Bx. Biotite-altered intrusion breccia
- MW1. Chrysocolla > brochantite leach ore, principal Cu source
- MW2. Relics of chalcocite blanket
- M. Hypogene fracture and breccia bornite, chalcopyrite ore
1. 34 Ma quartz monzonite porphyry
2. Eo "Dark diorite"
3. Eo quartz diorite

Figure 7.20. El Abra, Chile, "giant" porphyry copper where the metal is recovered (in 2000) mainly by leaching oxidic ore. From LITHOTHEQUE No. 2458, modified after El Abra Staff (2000)

Table 7.4. Exotic copper deposits derived from "giant" porphyry-Cu systems (all are in northern Chile)

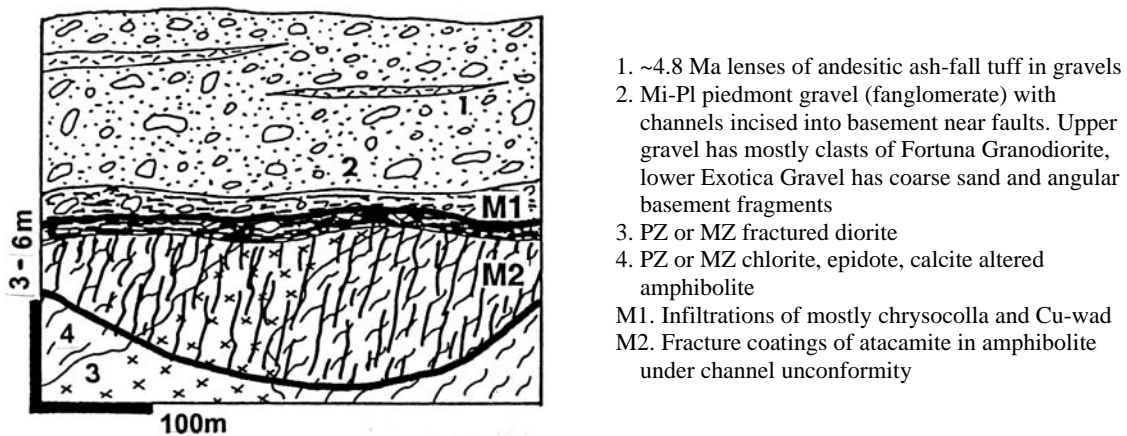
Parent deposit	Age of ore	Cu resource	Exotic deposit	Age of ore	Type	Cu resource
Chuquicamata deposit	31 Ma	67 mt	Mina Sur (Exótica)	T	channel	3.63 mt
Radomiro Tomić, Chile	31 Ma	13.7 mt	Radomiro Tomić	T	horiz. blanket	5.57 mt
Unknown			Sagasca Madre	T	blanket	?3.0 mt
El Telégrafo prospect	Eo-Ol	?X0 kt	El Tesoro	T	alluvial fan	1.26 mt
Collahuasi-Rosario	34 Ma	19.6 mt	Huinquintipa	T2-3	channel	X00 kt
Collahuasi-Ujina	35 Ma	5.9 mt	Ujina	T2-3	channel	X0 kt
El Abra	Ol	4.7 mt	Ichuno	T	channel, fault z.	X00 kt
			Lagarto	T	channel	X0 kt
El Salvador	42 Ma	10.8 mt	Damiana	T	blanket, channel	X00 kt

X in the last column stands for "several" (X00 kt = several thousand tons)



- 1, M1. Atacamite fracture coatings in T3 claystone blankets
- 2, M2. Chrysocolla, atacamite, Cu wad impregnations in T3 gravels
3. Eo3-Ol1 porphyry intrusion with small porphyry-Cu (El Telegrafo)
4. Cr-Eo andesite, rhyolite

Figure 7.21. El Tesoro exotic (infiltrational) Cu deposit, Chile; diagrammatic cross-section from LITHOTHEQUE No. 2450, modified after Münchmeyer (1996)



1. ~4.8 Ma lenses of andesitic ash-fall tuff in gravels
 2. Mi-Pl piedmont gravel (fanglomerate) with channels incised into basement near faults. Upper gravel has mostly clasts of Fortuna Granodiorite, lower Exotica Gravel has coarse sand and angular basement fragments
 3. PZ or MZ fractured diorite
 4. PZ or MZ chlorite, epidote, calcite altered amphibolite
- M1. Infiltrations of mostly chrysocolla and Cu-wad
M2. Fracture coatings of atacamite in amphibolite under channel unconformity

Figure 7.22. Mina Sur (Exótica) diagrammatic cross-section from LITHOTHEQUE No. 893

from its origin at the edge of the Chuquicamata deposit, for 6.6 km downslope in the SE direction, to fade away under 200 m thick cover of barren Miocene arid talus and mudflows. The channel is eroded into Paleozoic basement metamorphics, initially along the Falla Occidental fault zone, and filled by alluvial gravel. The 1,200 m long and up to 110 m thick mineable portion of the deposit is a

stratabound impregnation of chrysocolla, cupriferous wad, atacamite and gypsum in kaolinized and smectite-altered epiclastic gravel with minor volcanic ash fall. At the basement unconformity atacamite forms fracture infiltrations reaching, along fractures and small faults, into the bedrock. As the bedrock amphibolite and diorite are chloritized and locally albitized and epidotized, it

would be natural to interpret this situation, as seen in a drill core, as an oxidized top of a porphyry copper orebody. It is generally accepted that the dominant chrysocolla has formed by reaction of copper sulfate-rich waters with amorphous silica released from volcanic ash undergoing diagenetic devitrification. Wet chrysocolla paste continues to precipitate on walls of the Mina Sur pit, forming spectacular blue cascades.

In addition to mineralized channels which are the most common form, oxidic Cu and Mn minerals also precipitate in thin but laterally extensive alluvial fans (Damiana Cu deposit south-west from the El Salvador porphyry copper), or along basement faults (El Abra, Fig. 7.23). Münchmeyer (1996) described the mineral zoning sometimes developed. In the near-source (proximal) region, some exotic deposits include supergene chalcocite impregnations in reduced pyritic gravel.

Exotic deposits are virtually unknown outside of northern Chile, which is puzzling. The Great Basin in the western United States and Mexico, with its many porphyry Cu deposits endowed by well-developed supergene zones, thick piles of fault-bounded porous continental sediments and volcanics, and a history of changing climatic and hydrologic regimes, would seem to be the prime candidate. **Casa Grande deposit** in Arizona (Titley, 1993; 319 mt @ 1% Cu) of "Cu oxides in valley fill and enriched over deeply buried pluton" is probably at least partly exotic. The rest are just small occurrences.

Auriferous gossans

A special form of residual deposits over porphyry/skarn Cu-Au systems are goethite-rich gossans mineralized by dispersed residual gold. In contrast to the supergene chalcocite blankets (read below) that form over pyritic sericite-altered orebodies, auriferous gossans and goethite-rich leached cappings prefer low-pyrite potassic-altered substrate as in the "alkalic porphyry Cu-Au" (or diorite model deposits; read above), or Fe-Cu-Au skarns. Associated carbonates neutralize the acidic fluids. The largest residual gold deposit recorded is the "capping ore" at Ok Tedi, Papua New Guinea (Bamford, 1972; 114.3 mt ore @ 1.2 g/t Au for 138 t Au; Fig. 7.24).

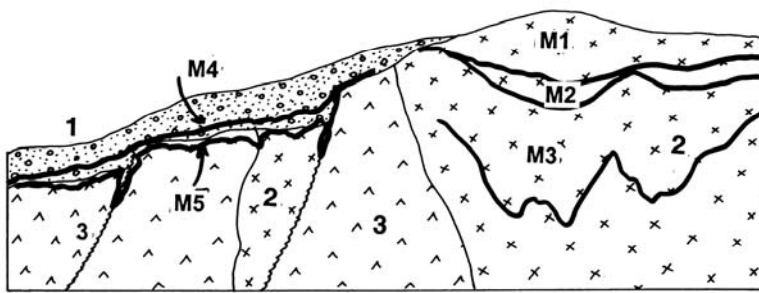
The famous "Au gossans" at Cerro Colorado in the Rio Tinto ore field in Spain (Chapter 8), sometimes treated under the heading "porphyry Cu-Au" in the literature, formed over Fe-Cu sulfides in breccias and stringer stockworks in footwall of VMS deposits.

Supergene sulfide blankets

"Bulk" mining of copper ores from open pits started in the United States around the turn of the 20th century (in 1906 at Bingham), based on what were then "low-grade" ores (around 2% Cu). The ore was distributed in subhorizontal blankets in shallow subsurface and this made open pitting possible. All the early 1900s American open pits started in the chalcocite-dominated enriched zones over porphyry coppers, with some oxidic ore, whereas the hypogene (primary) porphyry Cu-Mo material was of no use, in many cases not even recognized. This was as well, given the contrast in grade values between the enriched Cu orebodies and the non-enriched protore as tabulated by Titley (1993; Table 7.5). These grades correspond to ores mined in the 1960s to 1980s when 0.8% Cu was considered a good grade. In those years the 2% Cu plus grades of selectively mined, locally almost massive chalcocite, were long gone. It comes as a surprise to realize that the second largest American "porphyry", Morenci-Metcalf in Arizona (P+Rc 17.693 t Cu) formed over a 0.1-0.15% Cu protore.

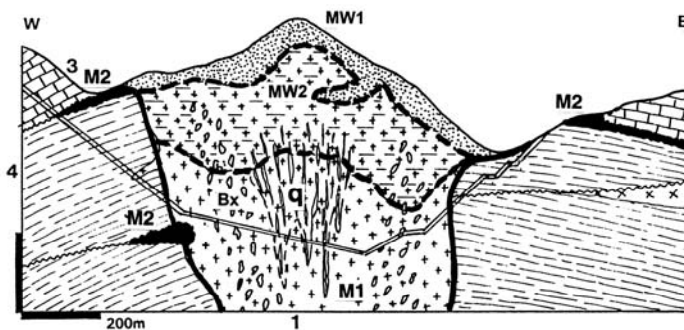
Supergene sulfides formed, in the geological past, under water tables, beneath oxidation zones and/or leached cappings, by precipitation from descending, acidic meteoric waters in reducing environment. The acidity was produced by oxidation of pyrite and the copper was acquired from the primary sulfides decomposed in the oxidation zone. Destruction of chalcopyrite or bornite partitioned copper into solution leaving much of the iron behind, in the leached capping or gossan, hence the "secondary sulfides" are predominantly members of the chalcocite group (Cu₂S), sometimes with covellite; they make up a superior copper concentrate (up to 78% Cu versus the ~30% Cu for chalcopyrite concentrate).

"Secondary sulfide" or "enriched" orebodies form subhorizontal blankets (unless tilted by a post-depositional tectonism like the extensional faulting in the Great Basin) of disseminated, fracture coating or almost massive "sooty" chalcocite. The host rocks are weathering argillized (kaolinized), previously sericitized, rocks of any composition ranging from a "porphyry" through volcanics to older silicate rocks of the basement. This sooty chalcocite ore is visually unimpressive and, unless in the early stages of oxidation that produces the greenish Cu oxidic minerals, it is virtually unrecognizable from argillized material stained by Mn oxides. Much of the chalcocite is an in-situ replacement of the original chalcopyrite or pyrite, and most chalcocite



M1. Present oxidation zone; M2, M3. Chalcocite blanket and hypogene sulfides zone; M4. Exotic Cu infiltrations in coluvial and fanglomerate gravel: chrysocolla, Cu-wad; M5. Exotic Cu minerals infiltrated along faults & fractures; 1. Poorly sorted gravel; 2. Eo-Ol granitoids; 3. Cr & T1 andesite & volcanics

Figure 7.23. El Abra porphyry Cu deposit, Chile. Diagrammatic cross-section showing the place of exotic Cu deposits as related to their metal source in oxidized porphyry-Cu upslope. From LITHOTHEQUE No. 2461, field sketch



MW1. Au-bearing gossan over skarn and leached capping on porphyry; MW2. Oxidized (malachite) chalcocite blanket; M1. Hypogene quartz-chalcopyrite stockwork in biotite altered porphyry. q=sheeted quartz veins; M2. Cu-mineralized exoskarn; Bx. Intrusion breccia; 1. 2.6 Ma monzonite porphyry; 2. 2.6 Ma monzodiorite; 3. Cr limestone and marble; 4. Ditto, siltstone

Figure 7.24. Ok Tedi Cu-Mo-Au deposit, SW Papua New Guinea, showing the important auriferous gossan (MW1). From LITHOTHEQUE No. 2247, modified after Section 424200 N (Courtesy of Ok Tedi Mining Ltd., 1997)

blankets grade downwards into hypogene ores through a mixed zone of relic pyrite and chalcopyrite grains coated by chalcocite. The upper boundary of the "secondary sulfides" against the oxides was relatively sharp in the time of origin, but has become more gradational due to the fluctuating water table and post-depositional encroachment of the oxidation front. Many oxidic orebodies are predominantly pseudomorphic replacements of the former secondary sulfide ores.

Because of the required fluid acidity, enriched zones form preferentially over pyrite-rich protore, typically those in the sericite (phyllitic) alteration zones that tend to have lower Cu grades; this explains the feeble protore grades recorded by Titley (1993). The chalcopyrite/bornite dominated, low-pyrite K-feldspar/biotite altered zones in porphyry deposits do not respond so well to secondary enrichment, unless they are configured to be in a way of the acid waters flow. Exhaustion of the initial enriched ores in some deposits caused the production to turn into the primary ores in the potassic altered zones (typical grades between 0.35

and 0.6% Cu), bypassing the 0.1-0.2% Cu pyritic protore. The latest trend, made possible by perfection of the in-situ leaching technology, has resulted in lowering the cut-off grade of ores down to 0.1% Cu. This has made many protore economic (as mentioned for Toquepala, above). The "alkalic" Cu-Au "porphyries" that lack the sericite zones and are low in pyrite, and skarns, also do not respond well to the formation of chalcocite blankets and instead support, under favourable conditions, formation of gold-rich goethitic gossans (Sillitoe, 1993).

"Chalcocite blankets", considered alone, include at least 20 deposits of the "giant" magnitude (Table 7.5). The supergene orebodies in the Chuquicamata and Escondida deposits held 33 mt and 18.73 mt of copper, respectively. The deposits range from the "classical" orebodies where bulk mining of the enriched ores started in the first half of the 20th century (e.g. Bingham, Morenci; Fig. 7.25, Chuquicamata), to the new generation discoveries of mostly concealed orebodies found and developed in the past thirty years (El Salvador, Fig. 7.26; La

Table 7.5. Secondary sulfide ore component of "giant" porphyry-Cu deposits; selected examples

No	Deposit/ore field	Ore age	Total Cu tons	Grade % Cu*	Cu in superg. sulf.	Grade % Cu	% superg. Cu
4	Casino, Yukon	Cr ₂	1.69 mt	0.23	512 kt	0.43	32
14	Bingham Canyon deposit, Utah	39-37 Ma	17.42 mt	0.67	7.2 mt	1.75	41
15	Ely (Robinson), Nevada	111 Ma	4.88 mt		2.55 mt	1.0	52
17	Bagdad, Arizona	76-72 Ma	6.4 mt		587 kt	0.64	9.1
18	Miami-Inspiration, Arizona	59 Ma	6.68 mt	0.57	3.95 mt	1.3	59
19	Ray, Arizona	Pc	13.5 mt	0.15	2,536 mt	0.85	19
25	Esperanza (Pima distr.), Arizona	Pc	2.8 mt	0.3	298 kt	0.62	10.6
29	Morenci-Metcalf, Arizona	67 Ma	18.2 mt	0.1	14.53 mt	0.8	80
30	Tyrone, New Mexico	56 Ma	2.8 mt		2.8 mt	0.8	100
31	Santa Rita (Chino), New Mexico	Pc	6.5 mt	0.2	2.53 mt	0.85	39
32	Cananea, Sonora, Mexico	T ₁	17.1 mt		3.8 mt	1.0	22
33	Caridad, Sonora, Mexico	Eo ₁	7.8 mt	0.2	4.8 mt	0.64	61.5
46	Cerro Verde, southern Peru	59-56 Ma	6.0 mt		1.72 mt	0.52	29
47	Cuajone, Peru	51 Ma	13.08 mt		2,061 mt	0.97	16
48	Quellaveco, Peru	54 Ma	6.33 mt		3.34 mt	0.65	53
50	Collahuasi ore field, Chile	34 Ma	29.5 mt	0.81	26.23 mt	1.66	80-90
51	Cerro Colorado, Chile	Eo-Ol	4.05 mt		4.06 mt		100
52	Spence, Chile	Eo-Ol	4.0 mt		4.0 mt	1.0	100
53	Chuquicamata deposit, Chile	31.1 Ma	67 mt	0.51	33 mt	1.37	49
53	Radomiro Tomić, Chile	31 Ma	13.75 mt		2.87 mt	0.83	21
54	Escondida deposit, Chile	Eo-Ol	26.0 mt		23.78 mt	1.31	91.5
54	Zaldivar, Chile	Eo-Ol	5.7 mt		2,681 mt	0.57	47
67	Los Pelambres, Chile	9.9 Ma	20.8 mt		5.21 mt	0.93	25
80	Sar Cheshmeh, Iran	20-19 Ma	12.5 mt	0.9	5,625 mt	2.0	75

*Very low protore grades for Ray, Esperanza, Morenci, Chino and Caridad are from Titley (1993), quoted to demonstrate the extremes of supergene enrichment; there is no guarantee that the entire supergene Cu resources or these and other deposits formed uniformly from such protores. At the majority of deposits grades of the hypogene precursors to chalcocite blankets have not been determined.

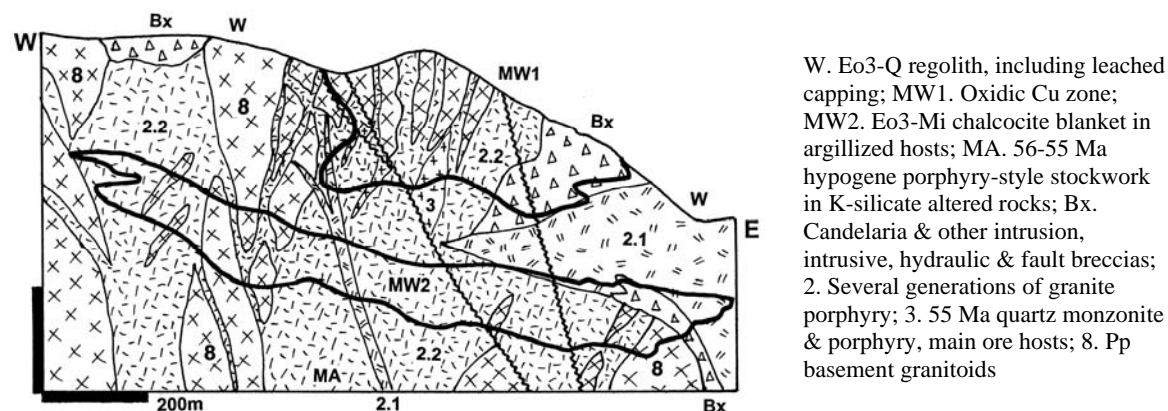
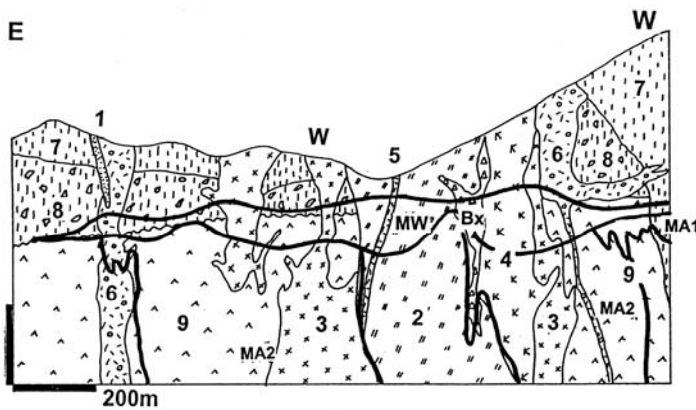
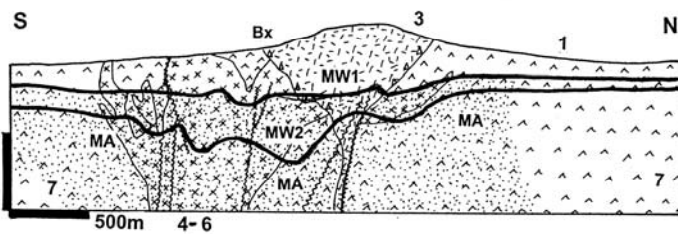


Figure 7.25. Morenci-Metcalf complex, cross-section of the NW Extension deposit from LITHOTHEQUE No. 522 modified after Preece (1989), Melchiorre & Enders (2003), Phelps Dodge Morenci. This is one of the three largest U.S. porphyry coppers with a total P+Rc of ~6.7 bt @ 0.42% Cu for 28 mt Cu, most of which resides in several chalcocite blankets distributed over an area of ~25 km².



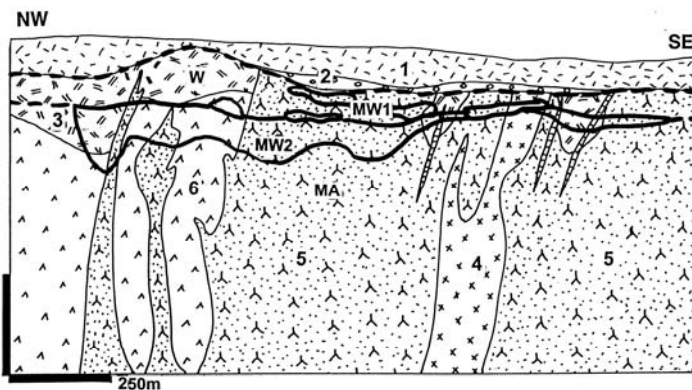
W. Leached capping and relics of oxidation zone; MW. Sooty chalcocite blanket; MA1. Minor enargite-pyrite HS ore in advanced argillic altered hosts; MA2. 42-41 Ma hypogene quartz, Cu-Mo sulfides stockwork; 1. Postmineral dacite & pebble dikes; 2. 41.2 Ma "L" granodiorite porphyry; 3. 41.6 Ma "X" granodiorite porphyry coeval with ores; 4. 41.9 Ma "K" granodiorite porphyry; 5. "A" biotite dacite porphyry; 6. Quartz plagioclase, quartz eye rhyolite porphyry; 7. 58 Ma rhyolite domes; 8. 63-30 rhyolite ignimbrite; 9. PZ-MZ basement, Cr3 andesitic volcanics

Figure 7.26. El Salvador porphyry Cu-Mo, Chile, an "intermediate generation" chalcocite blanket deposit. Cross-section from LITHOTHEQUE No. 2439, modified after Codelco El Salvador Staff (1998)



1. T3-Q fanglomerate, ash; MW1. T2-Q leached capping with oxidic Cu near base and along faults; MW2. 18-14.7 Ma chalcocite blanket; MA. Eo3-O11 multi-stage porphyry-style stockwork in K-silicate & sericite altered hosts with terminal acid sulfate stage; 2. Post-ore quartz monzonite (continued below)

Figure 7.27. La Escondida, Chile, a "late generation" chalcocite blanket deposit discovered under cover in the Falla Domeyko trend between El Salvador and Chuquicamata. Cross-section from LITHOTHEQUE No. 2455 modified after Padilla et al. (2001). Legend continued: 3. 35-32 Ma subvolcanic rhyolite stock and extrusive dome fringed by breccia; 4-6 Eo3-O11 multiphase quartz monzonite & granodiorite stock; Bx. At least four types of volcanic, igneous, hydrothermal, fault breccias; 7. Pc propylitized andesite



1. 0.75 Ma ignimbrite; 2. T3-Q fanglomerate; W. Buried leached capping; MW1. T2-3 oxidation and mixed zone; MW2. Chalcocite blanket, principal ore; MA. ~33 Ma substantially eroded disseminated and stockwork porphyry Cu; 3. 9.4 Ma ignimbrite; 4. 33 Ma granodiorite porphyry; 5. 35 Ma feldsparphyric granodiorite porphyry stock; 6. Pe-Tr andesite flows with minor sedimentary interbeds

Figure 7.28. Ujina deposit in the Collahuasi cluster, Chile; another late generation chalcocite blanket discovered under ignimbrite cover. Cross-section from LITHOTHEQUE No. 2463, modified after Bisso et al. (1998)

Escondida, Fig. 7.27; Collahuasi, Fig. 7.28). The statistics also indicate a big increase in the lower grade Cu-ore resources in the many "classical" deposits as the original chalcocite orebodies are

nearing exhaustion, or are already exhausted, so the mining operation moves into the lower-grade hypogene ores not even noted 100 years ago. This causes, occasionally, oversupply of the by-product

molybdenum, more abundant in the potassically-altered primary ores than in chalcocite blankets.

7.3.8 Porphyry Cu: global distribution and deposit descriptions

Porphyry coppers are the single ore type with the greatest number of 101 "giant" and 8 "super-giant" members (25 Mt Cu plus; Butte, Bingham, Collahuasi, La Escondida, Chuquicamata, Rio Blanco, El Teniente, Ertsberg-Grasberg). The conservative, minimum cumulative Cu content was 445 Mt Cu (Laznicka, 1999), whereas the more speculative figure based on geological resources (this book) exceeds 1 billion tons Cu. The porphyry-Cu are also the most consistent indicator of presence of past subductive plate margins, as well as a measure of the approximate depth of erosion since the time of ore formation (the presently outcropping orebodies required removal of about 2 to 3 km of the former rock cover, less for some 10 porphyry Cu "giants" that remained concealed in the time of discovery). Ages of exposed porphyry coppers are thus good indicators of the local cumulative rate of erosion (Table 7.6. and Figure 7.29).

Table 7.6. Formation of porphyry Cu (Mo, Au) "giants" and "supergiants" in time

Time	Cu, mt	Mo, mt	Au, t
Mi-Q	415.90	7.796	12,026
Eo ₃ -Ol	285.11	5.013	2,100
Cr ₃ -T1	231.65	4.023	2,825
J-Cr	43.00	0.435	616
Tr-J ₁	18.38	0.387	--
Cb-Pe	45.00	0.229	2,041
Cm-D	25.97	0.225	917
Pp	9.71	--	--
TOTAL	1,074.72	14.178	20,525

Cu tonnages in 108 deposits are most complete; Mo and Au include only "giant" and few "large" accumulations (110+ kt Mo, 250+ t Au) in porphyry-Cu "giants". Stockwork Mo deposits and gold in deposits of other types are not included.

The youngest porphyries (Ok Tedi, 1.2 Ma; Grasberg, 3.2-2.5 Ma; Panguna, 3.4 Ma; Baguio district, 2-1.5 Ma) are in active or recently collided subductive margins that undergo rapid uplift and erosion in heavy rainfall tropical regions of Papua New Guinea, Melanesia and the Philippines. They are followed by porphyries in rapidly rising plate edges above "bulges" on the subducting plate,

thickened by incorporation of a spreading ridge or an oceanic platform (Chilean Andes at Santiago latitude: El Teniente, Rio Blanco; 6-4.5 Ma).

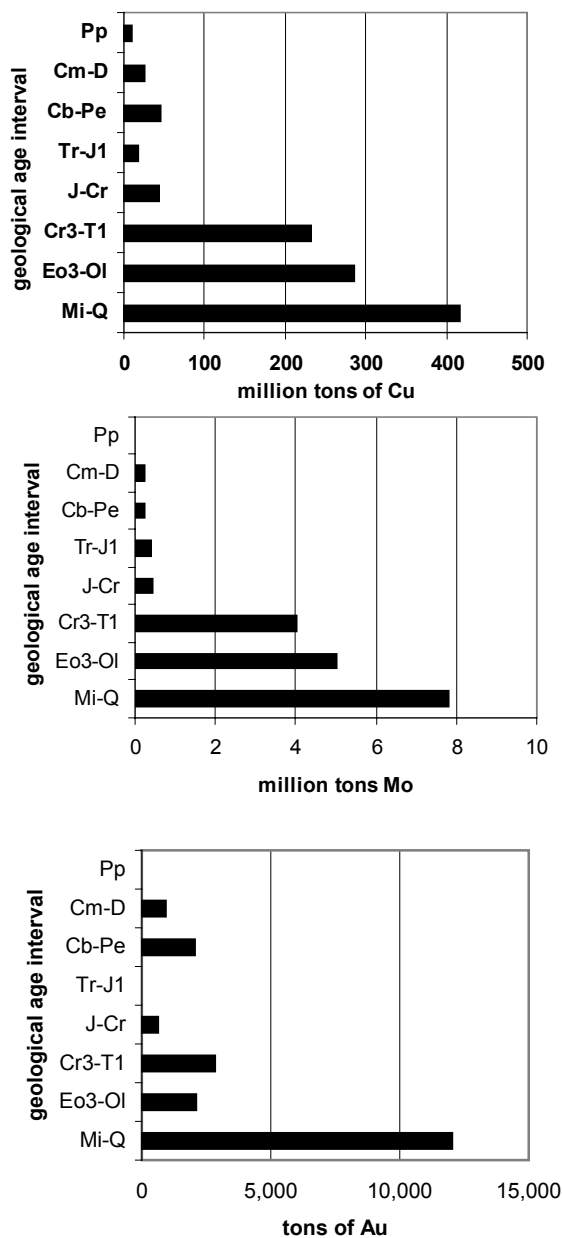


Figure 7.29. Distribution of ages of formation of "giant" and "super-giant" porphyry Cu (Mo, Au) deposits; n=109. Top: "Giant" magnitude based on Cu content in a deposit or ore field. Middle: "Giant" Mo accumulations in porphyry Cu-Mo. Bottom: "Giant" Au accumulations in porphyry Cu-Au

The "prime times" (ore formation ages that have the maximum exposure in the present outcrop) of porphyry coppers are between late Cretaceous and Miocene (~70-10 Ma) and outcrop belts of such deposits have the best continuity. With increasing formational ages the porphyry-Cu belts become fragmentary and eventually degenerate into isolated single relic occurrences. The oldest bona fide "giant" porphyry-Cu is Haib, Namibia (about 1.81 Ga; Minnitt, 1986) and even smaller "typical" porphyry coppers disappear in the early Paleoproterozoic, sometimes to be substituted by a variety of "impersonator deposits".

The most prolific "giant" porphyry-Cu belts and terrains, with their metal endowment, are listed in Table 7.7. and plotted in Fig. 7.30. There, both the "andean" and "island arc" settings are treated jointly. All entries are porphyry coppers with minor exceptions of "giant" deposits of other types ("mantos" in metavolcanics; mineralized deformation zones) that occur in porphyry-Cu provinces (northern Chile) and their supergene zones are unrecognizable from the true "porphyries". An "entry" in Table 7.7. can be a single deposit, or a cluster of nearby and closely related deposits (i.e. an ore field).

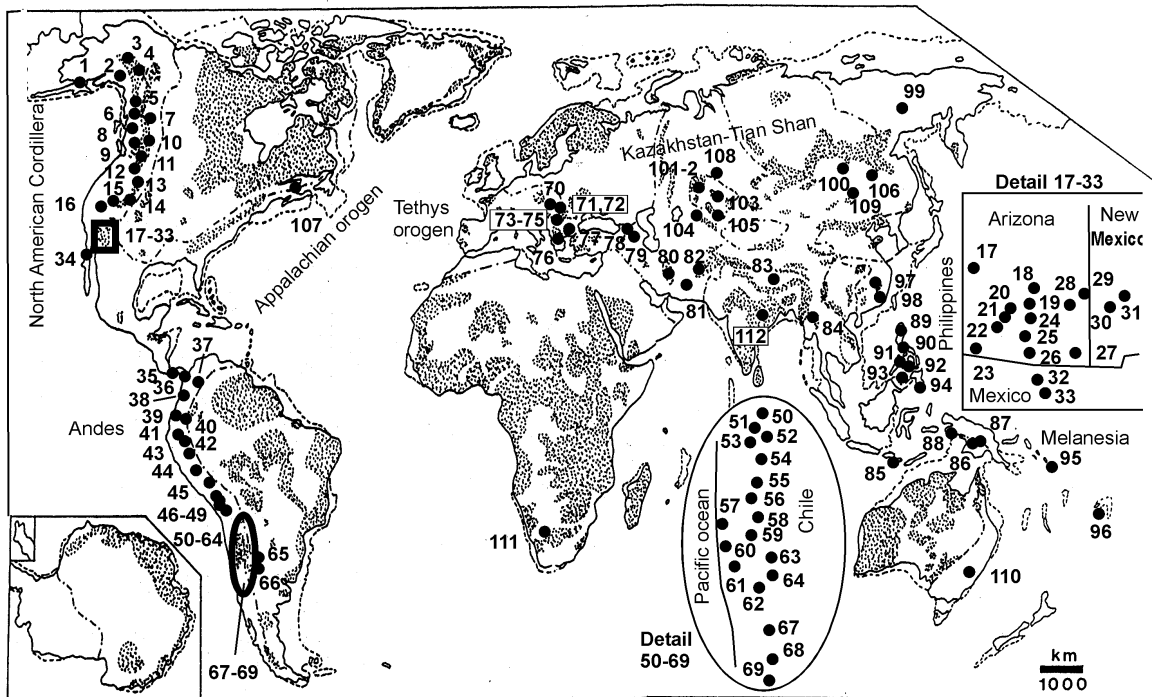


Figure 7.30. Global distribution of "giant" and "super-giant" porphyry Cu (Mo, Au) deposits and ore fields. The numbered deposits are named and briefly described at the end of this section and in Table 7.7.

Given the huge number of porphyry-Cu "giants", it is impossible to describe in reasonable detail most of them: not even the supergiants. The reader is thus referred to the brief information paragraphs at the end of this section. Examples described below in greater detail include El Teniente, the largest porphyry-Cu where the bulk of ores is hypogene; Chuquicamata, almost as large, a cluster of orebodies formed simultaneously with movement along a major dextral fault and significantly supergene enriched and modified; Rio Blanco-Los Bronces, dominated by magmatic-hydrothermal

breccias; Bingham, an example of metal zoned (Cu,Mo,Ag,Au,Pb,Zn) ore field; Ertsberg-Grasberg, a symbiosis of porphyry and skarn ores. Also described, elsewhere in this book, is Butte as an example of a high-sulfidation phase superimposed on earlier porphyry-Cu in an andean margin setting (Chapter 6), and another joint porphyry-high sulfidation set in the island arc setting (Mankayan; Chapter 5).

Table 7.7. Distribution of "giant" porphyry Cu (Mo, Au) deposits in the most productive ore belts and regions of the world (see also world map plot in Fig. 7.30).

Belt/terrain	ore age	deposit/ore field	Cu, mt	Mo, kt	Au, t	
Cordilleran orogen						
• Alaska-Yukon	Cr3-T1	Pebble, AK	8.47	454	968	
		Orange Hill-Bond Cr., AK	2.62	164		
		Casino, YT	1.55	134	174	
		Taurus, AK	2.25	315	172	
		total	9.89	1,067	1,314	
	• British Columbia-northern Washington	Tr3-J1	Schaft Creek, BC	2.913	160	136
			Galore Creek, BC	2.73	227	182
			Kemess, BC	0.86		220
			Gibraltar, BC	2.88	65	
		Highland Valley, BC	9.00			
	Cr3-Eo	Berg, BC	1.6	200		
		Mi	Glacier Peak, WA	6.68	153	
	total	26.66	805	538		
	• Western United States Northern Mexico	Ol	Bingham, UT	21.27	1,560	958
		Cr3-T1	Butte, MT	17.70	201	200
Ely, NV			4.88			
Bagdad, AZ			6.40	191		
Globe-Miami, AZ			8.10			
Ray, AZ			13.50			
Poston Butte, AZ			2.90			
Casa Grande, AZ			3.50			
Lakeshore, AZ			3.50			
Ajo, AZ			4.06			
San Manuel-Kalamazoo, AZ			5.58			
Pima (Tucson-South), AZ			16.90	343		
Helvetia, AZ			2.58			
Safford, AZ			7.38			
Morenci-Metcalf, AZ		18.20	256			
Tyrone, NM		2.80				
Santa Rita (Chino), NM		6.60				
Cananea, MEX		17.10	300			
La Caridad, MEX		7.80	666			
El Arco, MEX	3.60					
J	Yerington, NV	6.00				
	Bisbee (Warren), AZ	4.40				
total	187.36	3517	1,278			
Central America, Panama	Ol-Mi	Cerro Colorado, PAN	13.26	199		
		Cerro Petaquilla, PAN	14.40	437	305	
		total	27.66	636	305	

Table 7.7. (continued)

Belt/terrain	Ore age	deposit/ore field	Cu, mt	Mo, kt	Au, t
The Andes, • Colombia to southern Peru	Mi-Pl J	Pantanos-Pedagorcito, CO	9.70		
		Chaucha, EC	1.70		
		La Granja, PE	13.57	345	
		Michiquillay, PE	4.55	210	
		Perol (Minas Conga), PE	1.05		280
		Galena, PE	2.92		73
		Antamina, PE	18.00	450	
		Toromocho, PE	5.75	181	
		Mocoa, CO	2.60		
		Corriente, EC	4.86		
	Cr ₃ -Eo	Antapaccay, PE	3.41		63
		Cerro Verde-Santa Rosa, PE	6.00		
		Cuajone, PE	13.08	365	
		Quellaveco, PE	6.33	205	
		Toquepala, PE	10.40	117	
		total	103.82	1,873	280
• Chile, Argentina	Eo ₃ -Ol ₁	Collahuasi, CH	29.50	1,400	
		Quebrada Blanca, CH	7.94		
		Cerro Colorado, CH	4.05		
		El Abra, CH	4.70		
		Chuquicamata, CH	87.00	997	
		La Escondida, CH	70.00	500	
		Spence, CH	4.00		
		El Salvador, CH	10.80	119	
		Potrerrillos, CH	4.18		
		Andacollo, CH	2.45		305
	Mi-Pl	La Fortuna, CH	2.85		
		Regalito, CH	4.12		
		Refugio, CH	0.75		259
		Cerro Casale, CH	3.10		837
		Bajo de la Alumbreira, AR	4.06		523
		Agua Rica, AR	4.65	277	180
		Los Pelambres, CH	20.79	528	
		El Pachón, AR	5.49	126	
		Rio Blanco-Los Bronces, CH	59.30	1,380	
		El Teniente, CH	94.40	2,480	434
	total	424.14	7,807	2,770	
Tethys orogenic system	Mi-Q	Roşia Poieni, RO	4.00		
		Buçium Tarniţa, RO	3.30		
		Skouries, GR	2.67		477
		Kadzharan, ARM	77.20	7500	
		Sungun, IRAN	5.16	129	
		Sar Chesmeh, IRAN	12.50	600	450
		Reko Diq, PK	5.38		328
		Barit, PK	3.60		
		Yulong, CHINA	8.50	238	297
		Récsk, HU	10.18		
	Cr ₃ -Ol	Majdanpek, SRB	6.00		300
		Velikij Krivelj, SRB	3.30	112	
		Bor, SRB	5.60		240
		Panagurishte district, BG	4.14		320
		total	71.35	1,579	2,412

Table 7.7. (continued)

Belt/terrain	Ore age	Deposit/ore field	Cu, mt	Mo, kt	Au, t
Myanmar-Indonesia-PNG-Melanesia	Mi-Pl	Monywa, MY	4.50		
		Batu Hijau, INDO	7.77		598
		Grasberg-Ertsberg, INDO	43.70		4,063
		Ok Tedi, PNG	4.68		522
		Frieda River, PNG	4.70		280
		Panguna, PNG	5.84		632
		Waisoi, FIJI	4.95		143
		total	76.14		6,095
Philippines	Mi-Pl	Mankayan, PH	8.00		1,240
		Santo Tomas II, PH	1.60		340
		Marinduque, PH	3.24		82
		Tampakan, PH	4.98		286
	Cr ₃ -Ol	Toledo, PH	6.21		331
		Sipalay, PH	4.42	100	300
		Hinoban, PH	3.25		156
		total	25.49		2,166
Miscellaneous Asia	J-Cr	Dexing, CHINA	8.60	150	240
		Zijinshan, CHINA	3.18		149
		Peschanka, RU	3.76		376
		Erdenet, MONG	9.61	285	
	Cb-Pe	Kounrad (Qonyrat), KAZ	3.75		
		Samarka, KAZ	3.00		100
		Aktogai-Aiderly, KAZ	12.50		
		Almalyk (Olmalyk), UZB	18.70	229	2,049
		Yuwa-Yandong, CHINA	4.70		
	Cm-D	Duobaoshan, CHINA	2.35		
		Bozchakol, KAZ	3.20		
		Oyu Tolgoi, MONG	15.06		343
		total	88.40	664	3,000
Australia, Canada, Namibia, India	D	Cadia, NSW, AUS	4.40		574
		Gaspé (Murdochville), CAN	3.31	225	
	Pp	Haib River, Namibia	3.10		
		Malanjkhand, India	6.61		
		total	17.42	225	574
GRAND TOTAL		108 entries	1,074.72	14,178	20525

Au and Mo tonnages lesser than the "giant" threshold (250t and 110kt, respectively) are not included in totals

El Teniente-Cu,Mo, central Chile (Howell and Molloy, 1960; Camus, 1975; Cuadra, 1986; global P+Rc 12.4 bt of ore @ 0.63% Cu, 0.02% Mo, 0.035 g/t Au containing 94.4 mt Cu, 2.48 mt Mo, 434 t Au; Cooke et al., 2004; Fig. 7.6). El Teniente (formerly Braden) deposit is the southernmost major Chilean porphyry-Cu, located 37 km E of Rancagua and ~90 km south of Santiago, in rugged setting of the High Andes. The largest porphyry-Cu "super-giant", it is also the single world's largest copper deposit and one where the near-equivalent tonnage of copper in the Zambian Copperbelt is cramped into a north-pointing triangular area that measures 3x2 km and has a proven depth of mineralization of 1,600m. The deposit had been discovered and mined on a small scale in the 1500s, then rediscovered by a lieutenant (el teniente) in

1706. Large-scale mining by block caving started in 1909, marked by a huge glory hole today.

The mineralization is hosted by a largely subaerial, calc-alkaline andesitic Farellones Formation (Miocene; ~14 Ma), the lower member of which is a set of massive feldspar-phyric pyroxene-hornblende andesite flows, now thermally metamorphosed and hydrothermally altered to biotite (albite, anhydrite) hornfels. The middle and upper Farellones Members are epidotized andesites with lacustrine intercalations, and basalt/andesite flows with pyroclastic units, respectively. The volcanics are intruded by the 9-6 Ma Sewell Diorite that has its own phase of potassic alteration dated between 7.5 and 7 Ma. This was followed in short succession, between about 4.7 and 4.5 Ma, by a series of subvolcanic dacite porphyry intrusions, a

variety of breccias, alteration and mineralization. The Braden Breccia and the post-mineral latite, andesite and lamprophyre dikes are dated around 3.8 Ma (Cuadra, 1986).

The El Teniente orebody is a part of one of the regional volcanic centers, aligned along the north-south axis. Its triangular outline has a barren core, represented by an almost perfectly circular, late- to post-ore Braden Pipe, an explosive diatreme. The Pipe has shape of an inverted cone with surface diameter of 1,200 m and 1,800 m depth extent. It is filled by a gray, friable, concrete-looking heterolithologic breccia of attrition-subrounded poorly sorted fragments of the majority of local rocks, supported by sericite-altered rock-flour matrix. There are occasional empty cavities in the breccia, some lined with large crystals of the late-stage minerals. The Pipe pierced and destroyed the earlier orebody and it contains a proportion of mineralized fragments, of no economic value. Fragments of breccia from the Braden Pipe are, in turn, still contained in the latest-stage, slightly mineralized tourmaline breccia. The orebody had clearly been a site of prolonged, repeated brecciation and volatiles streaming responsible for a succession of probable initial tectonic breccias (at fault intersections) followed by magmatic, hydraulic, hydrothermal, phreatomagmatic (diatreme, vent) and possibly collapse breccias.

Copper mineralization has the form of subparallel (less anastomosing) chalcopyrite, pyrite, bornite, tennantite-tetrahedrite and molybdenite fracture veins and veinlets, with or without quartz, sericite, tourmaline, K-feldspar, biotite, anhydrite, chlorite gangue. This grades into diffuse disseminations of the same minerals in K-silicates altered wallrocks. Alternatively, the hydrothermal minerals fill breccia voids and spread into the fragments. The typical ore grades varied in the past between 1.5 and 2.0% Cu, when 9.6 mt of copper was produced from 490 mt of ore to the end of 1974 (Camus, 1975). They are lower now but the resources have greatly increased with lowering of the cut-off grade (presently around 0.4% Cu).

The ore minerals are zoned horizontally, away from the center of the orebody, from bornite-chalcopyrite through dominant chalcopyrite to dominant pyrite. Zoning in time (oldest to youngest) is similar. Camus (1975) distinguished four mineralization stages with the bulk of Cu and Mo emplaced during the Main hydrothermal phase around 4.7-4.5 Ma when quartz, sericite, anhydrite and chlorite assemblage partly overprinted the earlier biotite, K-feldspar alteration. The dominant wallrock is the fractured and brecciated biotite-

altered Farellones andesite converted into the Marginal Breccia in a narrow rim around the Braden Pipe, with Sewell Diorite in the east and south-east, and Teniente dacite porphyry in the north.

Supergene stage, preserved in a 2.4 km long central depression over the orebody, is up to 600 m thick and comprises leached capping, zone of sporadic oxidized Cu minerals, and discontinuous chalcocite blanket in argillized wallrocks collapsed (or expanded) as a consequence of anhydrite hydration to gypsum and/or gypsum leaching. Given the huge tonnage of the hypogene ore the supergene mineralization has been of little significance.

Chuquicamata Cu-Mo ore field, northern Chile

(Lopez, 1939; Jarrell, 1944; Lindsay et al., 1995; global P+Rc, whole field 11.4 bt @ 0.76% Cu for 86.64 mt Cu, Ossandón et al., 2001). Chuquicamata ore field, 240 km NE of Antofagasta in the Atacama Desert, is a 30 km long narrow north-south string of orebodies along the West Fault structure; from north to south: Radomiro Tomić, Chuquí Norte, Chuquicamata Mine, Mina Sur-Exotica, Mansa Mina-MM, the approximate center of which is the first discovered (by the indigenous miners before European settlement), and largest, Chuquicamata (Chuquí) Mine. The other orebodies have been progressively discovered later. The ore field is at par with El Teniente as one of the two world's largest copper repositories, whereas the Chuquicamata Mine (orebody) is the #2 after El Teniente (with 8.5 bt @ 0.79% Cu for 67.03 mt Cu, 997+ kt Mo, ~45 kt Ag, ~333 t Re; the minor metals are not all recovered).

Chuquicamata is the flagship of the late Eocene-early Oligocene grouping of porphyry-Cu deposits in the Precordillera of northern Chile, controlled by the N-S trending West Fault structure (Falla Occidental in the Cordillera Domeyko) that also control La Escondida and El Salvador. In Chuquicamata, this long-lasting, ductile to brittle transcurrent and reverse fault separates the virtually barren rocks in the west (Jurassic-Cretaceous complex Fortuna Intrusion of coarse granodiorite to adamellite), from mineralized rocks in the east. The latter have a pre-Oligocene basement of Paleozoic metamorphics (retrograded granite gneiss, amphibolite, diorites), overlain by Mesozoic volcanics and sediments. This is intruded by several generations of subvolcanic porphyries of the Eocene-Oligocene Chuquí Porphyry Complex. The latter comprise four named "porphyries" of probably dacitic derivation, dated between 38 and

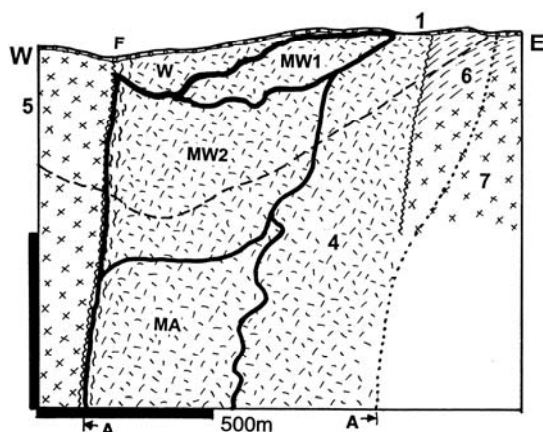


Figure 7.31. Chuquicamata Cu-Mo deposit, Chile, a cross-section showing the deep-reaching supergene zones. From LITHOTHEQUE No. 892, generalized and modified after Ossandón (2001) and Codelco Ltd. information. 1. T3-Q cover; F. West Fault (Falla Occidental); W. Mi leached capping; MW1. Mi oxidized Cu zone (brochantite, atacamite, chrysocolla, etc.); MW2. Secondary sulfides zone: chalcocite, covellite increases with depth; MA. 34-31 Ma hypogene pyrite, chalcopyrite, bornite fracture stockwork in phyllic alteration overprinting K-silicates and terminated by a HS epithermal pulse. "A" shows the extent of hydrothermal alteration. 4. 34.8 monzogranite porphyry (main ore host); 5. ~35 Ma Fortuna Granodiorite, barren; 6. Tr3-J clastics over andesite & dacite; 7. Tr2 granodiorite

33 Ma, but they are all strongly deformed by early ductile, then cataclastic and finally repeated brittle syntectonic deformation and concurrent alteration, that their boundaries are difficult to determine.

Hypogene alteration and mineralization in Chuquicamata is subdivided into two major stages. The Early Stage is marked by K-feldspar and albite alteration of the magmatic feldspar and biotitization of amphibole. Propylitization (chlorite) is superimposed. The alteration affects all porphyries and it is associated with weak chalcopyrite and bornite mineralization. The Main Stage (31.1 Ma) was controlled by repeatedly reactivated and remobilized structures subparallel with the West Fault. Veins, veinlets, breccia fill are dominated by quartz, pyrite, chalcopyrite and bornite in sericite-altered wallrocks and there are widespread quartz-molybdenite veins. Many are sheared. The Main Stage terminated with local enargite, digenite, covellite, pyrite veins in sericitized wallrocks, and local alunite veins.

Supergene effects have been well preserved in the dry Atacama desert climate, and they can be traced to depths of 800m along permeable faults.

Under relics of a leached capping, oxidation zone with a great variety of secondary minerals (atacamite, antlerite, chrysocolla, brochantite) replace the secondary sulfides. Massive to sooty chalcocite formed a subhorizontal blanket with keels of high-grade to massive chalcocite reaching deep along faults and linear tectonic breccias.

Radomiro Tomiá (Pampa Norte) Cu deposit is 5 km north of Chuquicamata Mine, concealed under 30 to 150 m of unconsolidated gravel (Cuadra and Rojas, 2001; Rc 1 bt @ 0.55 Cu in oxidation zone, 350 mt @ 0.93% Cu in secondary sulfides, 1.3 bt @ 0.53% in hypogene sulfides). The acid-soluble oxide orebody is a structure-controlled blanket 150-200 m thick that starts immediately under the bottom of the gravel and rests on a 20-150 m thick chalcocite and covellite blanket. The oxides comprise mostly atacamite with subordinate Cu-clays, chrysocolla, Cu-wad, kaolinite and montmorillonite. The hypogene bornite, chalcopyrite, pyrite mineralization is entirely in quartz, K-feldspar veinlets in potassically altered Chuquí Porphyry east of the West Fault. It is not economic at present.

The large infiltration Cu deposit **Mina Sur (Exotica)**, downslope from Chuquicamata, has been described earlier. The crucial problem of Chuquicamata exploration is where, if anywhere, is the hypothetical western portion of the ore zone, displaced by the West fault, the cumulative sinistral displacement of which is about 35 km (Ossandón et al., 2001).

Rio Blanco-Los Bronces Cu-Mo ore field, central Chile (Warnaars et al., 1985; Serrano et al., 1996; P+Rc 6.9 bt @ 0.86% Cu, 0.02% Mo, 0.035 g/t Au for ~59.3 mt Cu). This ore field, 70 km east of Santiago in the rugged High Andes, is shared by two corporations with properties on opposite sides of a mountain ridge (Fig. 7.7). The area is underlain by a deeply eroded Miocene quartz monzonite batholith with thermally metamorphosed remnants of Cretaceous and Miocene andesitic volcanics and volcanoclastics in its roof. A series of small late Miocene-Pliocene high-level porphyry stocks and breccias have been emplaced along a 6 km long NNW zone of weakness, and they are associated with Cu-Mo mineralization that is about equally hosted by potassically-altered porphyries and wallrock granitoids, and breccia bodies.

Skewes et al. (2003) counted at least 15 mineralized breccias in the ore field, some of which are composite, and they distinguished four major breccia generations and styles. The earliest (~14.2 Ma) monolithologic breccias were emplaced at a

depth greater than 3,000 m into the batholith. They are dominated by Fe-Mg silicates (amphibole, pyroxene, biotite) and magnetite in the matrix, and they are poor in sulfides. The higher level, mineralized breccias formed around 5.2 and 4.9 Ma, simultaneously with and shortly after the stockwork and Cu mineralization. They form subvertical bodies with outcrop areas of up to 2 x 0.7 km (most have diameters of several hundred meters) and they reach into considerable depths. The breccias are predominantly monolithologic, assembled from angular wallrock fragments in 5-25% of rock flour matrix. The matrix is hydrothermally altered and permeated by quartz, biotite and/or tourmaline, chlorite, magnetite, chalcopyrite, bornite, molybdenite and pyrite. The wallrocks contain identical alteration silicates and the breccia fragments are often sericitized. The Cu sulfides often dominate the matrix, grading 10% Cu or more. The two largest breccia bodies: Sur-Sur and Donoso each store 10 mt Cu plus. Two sub-categories of breccias are sometimes distinguished: the earlier one dominated by biotite, the later with tourmaline. Fluid temperatures of between 690-400°C support the magmatic-hydrothermal origin from expanding, upward-streaming fluids exsolved from a cooling intrusion in depth (Warnaars et al., 1985; Skewes et al., 2003). Post-emplacment fragment settling and compaction in some breccias simulate a collapse origin.

Intrusions of small silicic porphyries shortly followed the biotite and tourmaline breccias and they are believed associated with the later-stage sericitization and silicification, and partial redistribution of the earlier Fe, Cu and Mo sulfides. They may have been coeval with the next generation of matrix-rich, heterolithologic (vent) breccias with attrition (sub)rounded fragments, such as the La Coipa vent. These breccias correspond to the Braden Breccia in El Teniente and are largely post-mineral, dated at 4.9 and 3.9 Ma. Supergene alteration and chalcocite are minor in this still glaciated, deeply dissected terrain, although sometimes preserved down to about 200 m along permeable faults and breccias.

Bingham Cu,Mo,Au,Ag,Pb,Zn ore field, Utah (Economic Geology special issue, 1978; James, 1978; John, 1978; P+Rv_{whole field} 21.27 mt Cu, 1.56 mt Mo, 958 t Au, 47,082 t Ag, Babcock et al., 1995; read Table 7.6. for alternative tonnages). Bingham is in the Oquirrh Mountains, about 32 km SW of Sault Lake City. Discovered in 1863 it was the first deposit where open pit, bulk-mining of a "low-grade" (then <2% Cu) ore commenced in 1906. By

1996 the porphyry-Cu deposit alone produced 14 Mt Cu and this resulted in one of the largest, deepest and most picturesque open pits in the world. The ore field is quite compact (6 x 4 km) and within this area it contains four or five varieties of ores and groupings of deposits, zonally arranged around the central monzonite stock (Figs. 7.3, 7.4).

Bingham is situated near the eastern margin of the Great Basin, in folded and thrust-faulted late Carboniferous succession of alternating quartzite and limestone, intruded by a series of late Eocene (49-38.8) granitoid stocks. The centrally-located, approximately triangular multiphase Bingham Stock has an earlier equigranular monzonite intruded by quartz monzonite porphyry and late-stage latite porphyry dikes. The sedimentary rocks in the roof are thermally metamorphosed and the carbonates locally converted to skarn. The polymetallic mineralization is related to, and zonally arranged around, the Bingham Stock with the general metal maxima Mo - Cu, Au, Ag - Pb, Zn, Ag - Au. The ore emplacement coincided with hydrothermal alteration that had two principal phases. The earlier magmatic-hydrothermal phase (<600°C) produced potassic alteration within and immediately adjacent to the stock (K-feldspar & biotite in silicate rocks, prograde skarn in carbonates), and the bulk of the porphyry- and skarn-style Cu, Mo, Au ores. The potassic zone is bordered by the propylitic assemblage (actinolite, epidote, chlorite). The later phase, attributed to convecting meteoric waters coeval with latite dikes, overprinted the former to produce sericite, pyrite, quartz envelopes and selvages to quartz, pyrite, galena, sphalerite, Pb-sulfosalts veins and limestone replacements in the outer (exocontact) zone.

Bingham Canyon porphyry Cu-Mo deposit is the single largest metal repository in the ore field (2.6 bt ore @ 0.67% Cu, 0.06% Mo, 0.31 g/t Au and 15.g/t Ag for 17.42 mt Cu, 1.56 mt Mo, 806 t Au, 39,000 t Ag content; Babcock et al., 1995; Inan and Einaudi, 2002, quote 27.5 mt Cu, 1.3 mt Mo and 1,610 t Au for the same). Fracture veinlet to disseminated chalcopyrite, bornite, pyrite come with alteration biotite, K-feldspar and quartz dominantly hosted by the granitoids. Mo increases with depth and the frequency of quartz veining. A small proportion of this continuous orebody is in exocontact carbonates (as skarn) and metaquartzite. At the NE margin of the Bingham Stock, a zone with a resource of 90 mt @ 0.8% Cu is in metaquartzite and is rich in nukundamite. This is a Cu-Fe sulfide close to, and visually unrecognizable from, bornite (Inan and Einaudi, 2002). The Bingham orebody, at the start of operations, had a

discontinuous oxidation zone and an enriched chalcocite blanket.

Skarn Cu-Au-Ag orebodies in the Bingham ore field (Atkinson and Einaudi, 1978) are in the immediate exocontact of granitoid stocks and the two principal deposits: North Ore Shoot and Carr Fork, respectively, contributed jointly 124 mt of ore and 3.124 t of Cu to the ore field total (Babcock et al., 1995). The vein and replacement mesothermal Pb-Zn-Ag deposits, in the outer exocontact (e.g. Lark and U.S. Mine), contributed 2.167 mt Pb, a "giant" resource in its own way. The small Barneys Canyon and Melco Carlin-type deposits in the sedimentary rocks outside of the central mineralized area are sometimes listed as the most "distal" products of the Bingham magmatic-hydrothermal centre (Babcock et al., 1995).

Ertsberg (Gunung Bijih)-Grasberg Fe, Cu, Au, Ag ore field, eastern Indonesia (MacDonald and Arnold, 1994; Rubin and Kyle, 1997; Meinert et al., 1997; Widodo et al., 1999; global P+Rc₂₀₀₂ 2.6 bt @ 1.13% Cu, 1.05 g/t Au, 3.72 g/t Ag for 23.8 mt Cu, 2,006 t Au, 14,715 t Ag). The ore field is located in the Central Range of New Guinea, in Papua (Irian Jaya) and about 5 km WNW of Puncak Jaya (4883 m), the highest peak in this part of Australasia. It measures about 10 x 5 km along the WNW axis. The setting is a recently collided northern stable continental margin of the Australian Plate, composed of a series of 50-70° north-dipping thrust sheets of Jurassic-Cretaceous clastics and Paleocene to Oligocene platform carbonates. This was intruded by several high-level Pliocene stocks, the largest being the 4.4-2.6 Ma equigranular Ertsberg pluton composed mostly of dioritic rocks, and the multistage 3.23-2.83 Ma Grasberg complex that also includes its presumed volcanic equivalents. Ertsberg pluton and its satellites are unmineralized, but contain five Fe-Cu-Au-Ag exoskarn deposits in its roof and wallrocks. The Grasberg complex, in turn, hosts a "near-supergiant" porphyry-style Cu-Au-Ag deposit.

Fe-Cu-Ag-Au skarns. The "large" (P_t 750 t Cu) **Ertsberg** magnetite-copper orebody was discovered in 1936, by accident, and went into production only in 1972, under difficult conditions (Mealey, 1996, recorded the technical history in a very readable book). Four more skarn orebodies have been found between 1976 and 1996 and the biggest price, the Grasberg porphyry deposit, arrived in 1988. The skarn orebodies all contain Cu, Ag and Au in chalcopyrite and bornite. Kucing Liar is the largest, a "giant" of 320 mt of ore storing 4.48 mt Cu (Widodo et al., 1999). The skarns are in a

diorite-proximal exocontact in garnet, clinopyroxene, monticellite, magnetite prograde skarn in Tertiary carbonates. At the Big Gossan deposit, galena and sphalerite replace marble along fringe of the Fe-Cu-Au skarn (Meinert et al., 1997).

Grasberg disseminated Cu-Ag-Au (MacDonald and Arnold, 1994; Rubin and Kyle, 1997; Rv₁₉₉₉ 1.9 bt @ 1.04% Cu, 3.05 g/t Ag, 1.0 g/t Au for 19.76 mt Cu, 1,900 t Au, 5,795 t Ag); Fig. 7.32. Grasberg Complex is a sub-circular concentric intrusion with a composite, multiphase Pliocene quartz monzodiorite core emplaced into Dalam Diatreme. The latter is an upward-flaring matrix-supported andesitic or trachyandesitic breccia interpreted as a vent or maar infrastructure. With increasing depth the breccias become tighter, the fragments more angular, and they grade into a diorite dike swarm. At the upper levels the Diatreme is pervasively sericite and anhydrite altered, it contains around 5% pyrite, and erratically disseminated chalcopyrite. The alteration changes into argillic and propylitic away from the centre. In a depth below 800 m formed a cupola intersected by a stockwork of Cu-Au mineralized quartz veins in K-silicates envelope (MacDonald and Arnold, 1994). Emplacement of the Main Grasberg phase hornblende-biotite monzodiorite porphyries was shortly followed by magmatic-hydrothermal (600°C plus) K-silicate alteration and formation of sheeted quartz-magnetite fracture veins to stockworks in porphyry and adjacent Dalam rocks. These veins also carry chalcopyrite, bornite and pyrite or, alternatively, later independent thin fracture veinlets of Cu sulfides with biotite and K-feldspar intersect the earlier veins and the host rocks. The latest quartz, pyrite, sericite, chalcopyrite, bornite, digenite and covellite veins overlap with the youngest generation of porphyry dikes. Minor supergene chalcocite coats grains of hypogene sulfides and is, with native copper, preserved along permeability structures to a depth of about 30m. The Grasberg orebody has the form of a subvertical column extending from the surface (elevation of 4,200 m) to a depth of at least 1,500 m. It comprises two nested coaxial porphyry orebodies: the deep, earlier Dalam Stage stockwork in predominantly fragmental rocks and the upper, Main Grasberg stage fracture stockwork predominantly in porphyries (MacDonald and Arnold, 1994). At Grasberg, ore reserves have been separately calculated for the open pit and underground units.

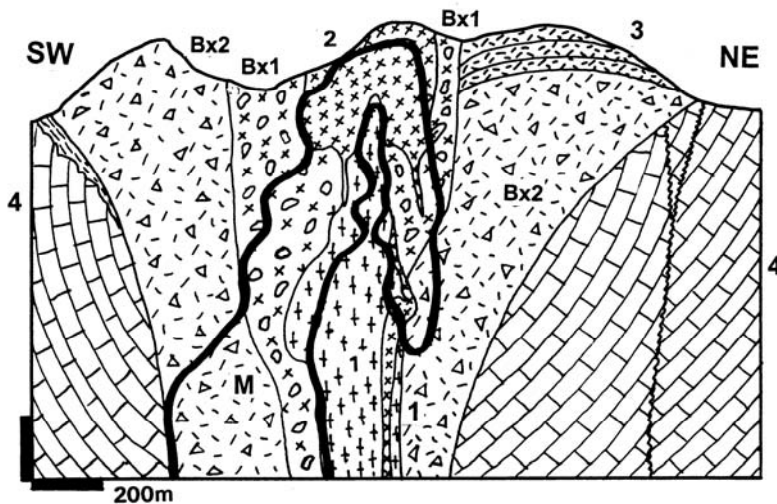


Figure 7.32. Grasberg Cu-Au-Mo stockwork, Papua (Irian Jaya), eastern Indonesia. Cross-section from LITHOTHEQUE No. 2239 based on 1997 materials courtesy of PT Freeport Indonesia.

- M. Fracture chalcopyrite > bornite stockwork with K-silicates over quartz, K-feldspar, magnetite stockwork
 Bx1. Dalam Diatreme, quartz monzodiorite intrusion breccia
 Bx2. Trachyandesite tuff & breccia in vent?
 1. Pl feldspar-crowded quartz monzonite dikes
 2. Quartz monzodiorite porphyry dikes
 3. Argillized volcanics
 4. T limestone recrystallized at contact

Remaining porphyry-Cu (Mo, Au) "giants"

It is impossible to provide standard length descriptions for the 101 porphyry Cu "giants" and 8 "super-giants" of the world (Table 7.6. and Fig. 7.3) so they are listed in an abbreviated form below. There, the information is arranged in the following order, separated by asterisks:

- Number on Fig. 7.3, name, status, country
 - Ore deposit: subtype, C-A=calc alkaline, ALK=alkaline (diorite model), N-A=Na alkaline (albite); ore distribution, style
 - Ore mineralogy: H hypogene, S supergene, O oxides and leached capping. Numbers indicate importance of each: 0=zero; 1=slight; 3=moderate; 5=complete. Abbreviations: ST=standard mineralogy, pyrite & chalcopyrite; STQ=ditto, plus quartz veining
 - Alterations; ST=standard zoned alteration K-silicate, sericite, propylitic
 - Parent intrusion: age, lithology; actual ore hosts underlined
 - Other wallrocks: age, lithology, hosts underlined
 - Ore tonnage & grades; contained metals. The figures need not add (different data sources, timing)
 - Selected references.
1. **Pebble** deposit, SW Alaska * C-A, dissem. & stockw. * H5, STQ + moly * ST alteration * 97-90 Ma granodiorite porphyry * J3-Cr3 turbidites * Rv 460 mt @ 0.35% Cu, 0.015% Mo, 0.37 g/t Au for 3.06 mt Cu, 404 t Au; Rc 3.026 bt for 8.47 mt Cu, 454 kt Mo, 968 t Au * Nokleberg et al. (1995), Young et al. (1997), Ashleman et al. (1997).
 2. **Orange Hill & Bond Creek**, Nabesna, E-C Alaska * C-A, veins, dissem. in porph. & skarn * H5, STQ + bornite, magnetite * ST + exoskarn * 113 Ma qz.

diorite, granod. porph. * Cb2-Tr & J3-Cr1 mafics, limest., turbidites * O.H.: 320 mt @ 0.35% Cu, 0.02% Mo; B.C.: 500 mt @ 0.3% Cu, 0.02% Mo. Total: 2.62 mt Cu, 164 kt Mo * Nokleberg et al. (1995).

3. **Taurus** deposit, Tanana Valley, E-C Alaska * C-A, dissem. & stockw. * H5, STQ + moly * ST alteration * T1 granod. porphyry, rhyol. porph. stock * PCm schist, gneiss * 450 mt @ 0.35% Cu, 0.02% Mo, 0.41 g/t Au for 2.25 mt Cu, 315 kt Mo, 172 t Au * Young et al. (1997), Ashleman et al. (1997).
4. **Casino** deposit, Dawson Range, W-C Yukon * C-A, stockw. & dissem., steep ovoid brecc. pipe * H3, S1, O1; STQ * ST, supergene leaching * 74-72 Ma in Cr2 breccia, granodior. * PCm mafic gneiss * 558 mt, hypogene 445 mt @ 0.23% Cu, 0.024% Mo, 0.27 g/t Au. Total 1.55 mt Cu, 134 kt Mo, 174 t Au * Bower et al. (1995).
5. **Schaft Creek** ore field, NW British Columbia * C-A, 3 zones, dissem. stockw. & breccia * H5, STQ * ST alteration * 220 Ma feldsp. porph. dikes * Tr3 hornfelsed andes., pyrocl., intruded by Tr3-J2 pluton * 971 mt @ 0.3% Cu, 0.0165% Mo, 14 g/t Au, 1.2 g/t Ag for 2.913 mt Cu, 160 kt Mo, 136 t Au * Spilsbury (1995).
6. **Galore Creek** ore field, NW British Columbia * ALK, stockw., dissem. > skarn * H5, ST * K-silic, propyl, minor skarn * J1, 220 Ma syenite * Tr3 andesite, siltstone * 910 mt @ 0.3% Cu, 0.025% Mo, 0.2 g/t Au, 1.5 g/t Ag for 2.73 mt Cu, 227 kt Mo, 182 t Au * Dawson et al. (1992).
7. **Kemess North & South** ore field, N-C British Columbia * C-A, two zones, stockw. & dissem. * H4, O1, STQ, Au left in leached zone * K-silicates overprint phyllic * J1 qtz. monzon., feldsp. porph. * Tr3-J1 hornfelsed mafic flows, pyrocl. * 425 mt @

- 0.2% Cu, 0.37-0.62 g/t Au for 220 t Au, 865 kt Cu * Rebagliati et al. (1995).
8. **Berg** deposit, Tahtsa Range, W-C British Columbia * C-A, two zones, veins, stockw. > dissemin. * H4, S+O 1; STQ * ST alteration, leached cap * 50 Ma qz. monzonite porph. * J2 hornfelsed andesite, pyroclastics, clastics * 400 mt @ 0.4% Cu, 0.05% Mo for 1.6 mt Cu, 200 k Mo * Heberlein (1995).
 9. **Fish Lake** deposit, W-C British Columbia * C-A, oval deep column; stockwork > dissemin. * H5, minor bornite * ST alteration * Cr3 qz diorite stock, swarm of qz porph dikes * Cr1 hornfelsed andesite, volcanoclast. * 1,148 mt @ 0.22% Cu, 0.41 g/t Au for 2.53 mt Cu, 471 t Au * Caira et al. (1995).
 10. **Gibraltar** ore field, central British Columbia (Fig. 7.18) * C-A to N-A, deformed & retrograded, 6 linear zones; stringers stockwork, dissemin. * H5, ST + moly * qz, seric, chlorite, epidote, carbonate * synorogenic, peralumin. Na-alkaline (trondhjemitic), propyl. assoc. & sericite * Tr3 synorog. tonalite, trondhjemitic; sheared, greensch. metam * Pe oceanic & melange assoc. * 934 mt @ ~0.3% Cu, 0.008% Mo for 2.88 mt Cu, 65 kt Mo * Drummond et al. (1976)
 11. **Highland Valley** ore field, S-C British Columbia (Fig. 7.33) * C-A, cluster of plutonic oreb., some breccias; stockw > dissemin, veins * H, STQ + bornite * ST alteration, silicif., but most ore in phyllic * 202-192 Ma ores in ~210 Ma composite batholith; granodior > breccias * Tr3 andesite, volcanoclast. * ~2 bt @ 0.45% Cu, 0.007 Mo for ~9 mt Cu * Casselman et al. (1995).
 12. **Glacier Peak** ore field, N-C Washington * C-A, cluster of irreg. & tabular oreb. * H4 S1, chalcop, moly, scheelite * quartz, K-feldspar alteration * 21 Ma ore in dacite porph. breccia, qz diorite plug in Mi qz monzonite pluton * schist, gneiss * 1.7 bt @ 0.334% Cu, 0.009% Mo for 5.678 mt Cu, 153 kt Mo, ~1 kt W * Lasmanis (1995).
 13. **Butte composite zoned ore field**, W-C Montana * C-A, multistage. Central zone swarm of Cu-As-Ag HS veins intersect stockw-dissemin porph Cu-Mo. On fringe Zn-Pb-Ag veins * H3, S+O2; veins pyrite, enargite, chalcocite; porphyry ST; superg. chalcocite * ST in porphyry, seric near veins * 58-57 veins in 78-73 Ma qz monzonite pluton * Total P+Rc ~2,083 mt @ 0.85% Cu for 17.7 mt Cu, but Pt+Rv ~10.4 mt Cu, 201 kt Mo, 21,850 t Ag, 143 kt As, 1819 t Bi. Of this HS veins Pt 296 mt @ 2.5% Cu, 68 g/t Ag for 7.4 mt Cu; Pb-Zn not included here * read text, Chapter 6.
 14. **Bingham composite zoned ore field**, Utah (Fig. 7.3, 7.4) * C-A, multistage. Central deep cylindrical porphyry Cu-Mo stockw > dissemin, veins with M-rich core bordered by 2 major proximal Cu skarns, fringed by Zn-Pb-Ag veins, replacements * H2, S2, O1; porph STQ + moly, bornite, garnet-px exoskarn * ST alter. in porphyry, high-silica core envel. by K-silicate, superimp phyllic; skarn * 38-37 qz monzon porph stock * Cb2 hornfelsed, skarned, marbled limest. sandst. shale * District total 21.27 (or 27?) mt Cu, 958 t Au; porphyry: 2.7 bt @ 0.7% Cu, 0.04% Mo, 2.64 g/t Ag, 0.31 g/t Au for 18.9 mt Cu, 1.56 mt Mo, 7137 t Ag, 837 t Au; skarns 130 mt containing 3.6 mt Cu * read text, this Chapter.
 15. **Ely** (Robinson) ore field, Nevada * C-A dissemin. in porph, veinlets in retrograde skarn, jasperoid replac. in marble * H3, S2; STQ in porph., qz, pyrite, chalcocopyrite, magnetite veinlets in skarn; py, chalcop. replac. in silicif. marble; periph. pyritic Au * K-silic alter. in porph., later phyllic; retrograde (actinolite, saponite, clays) in skarn; jasperoid in marble * 111 Ma porphyry plugs * D-Pe hornfelsed shale, limest. sandst. * 600 mt @ 0.55-1.0% Cu for 4.88 mt Cu, 200 t Au, 600 t Ag * James (1976); Einaudi (1982).
 16. **Yerington** ore field, SW Nevada * C-A cluster of ~5 porphyry, 2 Cu-skarn deposits; stockw., replac. * H4, S1; STQ, magnetite, bornite * ST alter. in porph., exoskarn in limest. * J qz monzodiorite, granodior, latite stocks * Tr3 andes. volcanoclast, limest. * 1.162 bt @ 0.4% Cu, total ~6.0 mt Cu * Dilles, 1987; Einaudi, 1982.
 17. **Bagdad** deposit, Arizona * C-A stockw, veins * H4 S1; STQ + moly > tetrahedrite * 76-72 Ma ore in Cr3 granod & qz monzon. stocks * ST alteration * 1.6 bt @ 0.53-0.37% Cu, 0.012% Mo for 6.4 mt Cu, 191 kt Mo * Anderson et al. (1955); Barra et al. (2003).
 18. **Globe-Miami ore field**, S-C Arizona (includes Miami-Inspiration, Fig. 7.19; Copper Cities, Castle Dome, Pinto Valley deposits) * C-A, 8 deposits, stockw, dissemin, vein, infiltr * H2, S+O3 * ST alteration * 61 Ma granod & qz monzon porph * 1.06 Ga diabase, 1.6-1.4 granite * Total ~8.1 mt Cu * Peterson (1962); Creasey (1980).
 19. **Ray** ore field, S-C Arizona, Fig. 7.34; * C-A, stockw, dissemin ores at fault intersection * H3, S+O2 ST + moly * ST alter, biotite over diabase * 65 Ma ore in 70-60 Ma multiphase qz dior. granodior porph pluton * Pp-Mp schist, qz monzonite, quartzite, diabase * P+Rc ~1.7 bt @ 0.6-0.8% Cu for 13.5 mt Cu * Phillips et al. (1974); Long (1995).
 20. **Poston Butte** deposit, S-C Arizona * C-A stockw, dissemin * H,S,O; ST mineralogy * ST alteration * 64 Ma ore in Cr3 granod. pluton-dike complex * Pt schist, granite * Rc 725 mt @ 0.4% Cu for 2.9 mt Cu * Nason et al. (1982).
 21. **Casa Grande** deposit, S-C Arizona * C-A, stockw. & dissemin * T alteration * Cr3 granod, qz monzon * Rc 350 mt @ 1.0 Cu for 3.5 mt Cu * Min. Eng., June 1979.
 22. **Lakeshore** deposit, S-C Arizona * C-A, blind orebody, stockwork & dissemin.; 5% skarn * H5, ST ; * ST alteration * 64.1 Ma ore in Cr3 granodior. stock * Cr3 andesitic volcanoclastics * 500 mt @ 0.7% Cu for 3.5 mt Cu * Huyck (1990), Cook (1988).
 23. **Ajo** (New Cornelia), SW Arizona * C-A, stockw & dissemin * H4, S+O1; STQ * ST alteration * 65-55 qz monzon. porph stock, dikes * Pp qz monzonite * 580 mt @ 0.7% Cu, 0.001% Mo, 1.57 g/t Ag, 0.125 g/t

- Au for 4.06 mt Cu * Gilluly (1946); Wadsworth (1968).
24. **San Manuel-Kalamazoo** deposit, S-C Arizona; Fig. 7.17. * C-A, two parts of a cylindrical oreb. separate by fault; stockw, vein, dissem. * H3, S+O2; STQ + moly * ST concentric alter., quartz core * Cr3 qz monzonite porph * Mp porph. monzogranite * 1.303 bt @ 0.63% Cu for 6.576 mt Cu * Lowell (1968).
 25. **Pima (Tucson-South)** ore field, S-C Arizona (incorporates major deposits Pima-Mission, 7.87 mt Cu, Fig. 7.14; Twin Buttes, 6.694 mt Cu; Sierrita-Esperanza, 2.8 mt Cu) * C-A, stockwork & dissem. (porphyry), major exoskarn * H4, S1; STQ + moly, bornite * ST alter in porph, retrogr. skarn alter. * Pc qz monzon, granodior, rhyodac porph * Tr-Eo andes, rhyol; Pe limest * total 3.065 bt @ 0.54% Cu for 16.9 mt Cu, 343 kt Mo, ~6000 t Ag * Jansen (1982); West & Aiken (1982); Einaudi (1982).
 26. **Helvetia (Rosemont)**, S-C Arizona * C-A, H4, O1 in skarn * magnetite, chalcopyrite, pyrite, moly * exoskarn * Cr3-T1 granodior., qz monzon. porph. * PZ limestone, marble, skarn * 325 mt @ 0.54% Cu, 2.58 mt Cu * Creasey & Quick (1955).
 27. **Bisbee (Warren)** ore field, S-C Arizona; Fig. 7.9. * C-A dissem. in porph, intrus. breccia, replac. in skarn, jasperoid * H2, S+O3; STQ in porph., pyrite, chalcop, bornite, magnetite in carbonates * seric, pyrite in porph., jasperoid, some skarn * 130 Ma ore, breccias & porphyry * Pp schist, PZ therm. metam. limest., hornfels * 330 mt @ 0.4-2.3% Cu for 4.4 mt Cu and Ag, Au * Bryant & Metz (1966); Bryant (1968).
 28. **Safford (Lone Star)** ore deposit, Arizona * C-A, "volcanic, wallrock" porph. deposit; veinlets, dissem., brecc * H5; STQ + bornite * silicif., K-silic, seric, propyl (epidote) * 67-52 Ma small granod, qz monz. plags, stocks * Cr3 comagma. andes, dacite flows, pyrocl * 1.8 bt @ 0.41% Cu for 7.38 mt Cu * Robinson & Cook (1966).
Dos Pobres deposit, Safford distr., SE Arizona * C-A, as in Safford * 363 mt @ 0.72% Cu, 0.01% Mo for 2.614 mt Cu * Langton & Williams (1982).
 29. **Morenci-Metcalf** ore field, SE Arizona; Fig. 7.25. * C-A, dissem. + stockw. chalcoc. blanket, oxid. leach ore, new hypog. resource; some skarn * H0-3, S+O5-2; STQ * seric, pyrite over K-silicate * 67 Ma hypog. ore in breccia, qz monz. porphyry * PCm schist, PZ hornfelsed sedim. * 2.932 bt @ 0.62% Cu, 0.086 Mo, 1.2 g/t Ag for 18.2 mt Cu, ~256 kt Mo * Moolick & Durek (1966).
 30. **Tyrone** deposit, SW New Mexico * C-A, stockw. & dissem. all in chalcocite blanket * S>O5; chalcosite, pyrite, chrysocolla * sericite, pyrit over K-silicate * 56 Ma qz monzonite porph stock * PCm basement complex * 400 mt @ 0.7% Cu for 2.8 mt Cu * Titley (1993).
 31. **Santa Rita (Chino)** deposit, Central district, SW New Mexico * C-A, chalcoc. blanket over stockw, dissem empl. to fault zone; some skarn * H1, S+O4; STQ + moly, bornite * St alter., silicif, skarn * 70-56 Ma ore, granod qz monz. porph * PZ, MZ thermally metam limest, clastics * 859 m t @ 0.75% Cu for 6.6 mt Cu * Reynolds & Beane (1985).
 32. **Cananea** ore field, Sonora, NW Mexico; Fig. 7.10. * C-A; many orebodies along 14 km zone; dissem., stockw., veins in porph; high-grade replac in breccia pipes; skarn; chalcoc. blankets * H3, S+O2; STQ in porph + bornite, moly; +sphalerite, galena in replacements * ST in porph., skarn, jasperoid in carbonates * 69-64 Ma qz monzon, breccia * Mp qz monzonite; Cm-Cb2 limest, dolom, shale, quartzite; MZ contin. volc. * total 3.35 bt @ ~0.7 Cu for 17.1 mt Cu, 300 kt Mo * Bushnell (1988).
 33. **La Caridad** deposit, Sonora, NW Mexico * C-A, stockw., dissem., breccia; chalcoc. blanket * H2, S3; STQ + moly * ST alteration * Eo1 qz monzon porph stocks * Cr-T1 diorite, granodior * 1.754 bt @ 0.44% Cu, 0.038 Mo for 7.8 mt Cu, 666 kt Mo * Saegart et al. (1974).
 34. **El Arco** deposit, Baja California, NW Mexico * C-A, stockw., dissem * H4, S1 STQ * ST alteration * Cr granod, qz monzon porph * Cr1 greenschist-metam hornfelsed andesite, diorite * 600 mt @ 0.6% Cu, 0.2 g/t Au for 3.6 mt Cu, 120 t Au * Coolbaugh et al. (1995)
 35. **Cerro Colorado** deposit, Panama * C-A; dissem, stockw., irreg. orebody * H4, S1; pyrite, chalcop., bornite, moly * phyllic alter. * Mi3-Pl qz latite, rhyol, rhyodac, qz-feldsp porph * Ol subaer. andesite flows * 2.21 mt @ 0.6% Cu, 0.009% Mo, 4.7 g/t Ag, 0.07 g/tr Au for 13.26 mt Cu, 199 kt Mo, 10,387 t Ag * Kesler et al. (1977).
 36. **(Cerro) Petaquilla** deposit, Panama * C-A, stockw. & dissem. * H5; chalcopyrite > magnetite, pyrite, bornite * ST alteration * O11 granodior. * Ol andesitic volcanics * 3.7 bt @ 0.5% Cu, 0.016% Mo, 0.09 g/t Au for 14.4 mt Cu, 437 kt Mo, 305 t Au * Mining Ann. Rev. 1999
 37. **Pantanos-Pegadorcito** ore field, NW Colombia * C-A, stockw & dissem * H4; STQ, moly * ST alteration * Ol-Mi dacite porph, breccia, diori & qz monzon. porph * Ol tonalite, T andesite, dacite * 9.7 mt Cu @ 0.5% * Sillitoe et al. (1982).
 38. **Mocoa**, SW Colombia * C-A stockw, breccia, dissem; thick leach cap, no enrichm. * H5; ST + moly, bornite * K-silicate & propyl overprinted by sericite * J1-2 biotite dacite porph stock * J1-2 comagmatic dacite, andesite * 260 mt @ 1.0% Cu for 2.6 mt Cu; Mo * Sillitoe et al. (1984).
 39. **Chaucha**, Ecuador * C-A; stockw, dissem, breccias * H4, S+O1; STQ + moly * phyllic alter. * 12-9 Ma ore, qz monzon. & granodior porph * T andesite, granodior * 1.6 mt Cu @ 0.7% * Goosens & Hollister (1973)
 40. **Corriente**, Eastern Cordillera, Ecuador * C-A * J granitoids * 600 mt @ 0.8% Cu for 4.86 mt Cu * Soc. Econ. Geol. News 58 (2004).
 41. **La Granja**, N Peru * C-A stockw, dissem, brecc > skarn * H3, S+O2; pyrite, chalcop > enargite, sphaler, moly * sericite, adv. argillic * Mi2-3 qz-feldsp porph. stock * 2.3 bt @ 0.59% Cu, 0.015%

- Mo, 5 g/t Ag for 13.57 mt Cu, 345 kt Mo, 11,500 t Ag * Schwartz (1982).
42. **Cajamarca porphyry province**, N Peru:
Michiquillay deposit * C-A stockw, veins, dissem * H4, S1; ST + moly * phyllic, argillic alter. * 20.6 Ma ore & qz monzon porph stock in shear zone * Cr quartzite, limestone * 700 mt @ 0.65% Cu, 0.03% Mo, 0.1-0.5 g/t Au for 4.55 mt Cu, 210 k Mo * Hollister & Sirvas (1974).
Perol deposit (Minas Conga) * C-A, stockw, dissem, skarn * H5, STQ; Zn-Pb sulfides in skarn * K-silic & propyl overpr. by sericite * Mi1 qz diorite, porphyry stocks * Cr3 carbonates * 350 mt @ 0.3% Cu, 0.8 g/t Au for 1.05 mt Cu, 280 t Au * Llosa et al. (1999).
Galeno deposit * similar to above * 486 mt @ 0.6% Cu, 0.15 g/t Au for 2.92 mt Cu, 73 t Au.
43. **Antamina** deposit, N-C Peru; Fig. 7.13. * C-A, Cu-Zn skarn replac >> porph. Cu * H5; skarn: chalcop, sphaler, pyr, pyrrh > galena, moly; porph: ST + moly * exoskarn; K-silic * 10 Ma monzogranite porph stock * Cr skarned, marbled limest * 1.5 bt @ 1.2% Cu, 1.0% Zn, 0.03% Mo, 70 ppm Bi, 13 g/t Ag for 18 mt Cu, 15 mt Zn, 450 kt Mo, 103 kt Bi, 19,500 t Ag * O'Connor (1999).
44. **Toromocho** porphyry Cu, Morococha ore field, Peru; Fig. 7.5. * C-A porph. stockw, dissem grading to exoskarn, envel. by Zn-Pb-Ag vein, replac * H5; pyrite, chalcop, tennantite, moly in porph * ST alteration > skarn > adv. argillic * 8.2-7.1 Ma dior, granod, qz monzon porph * J marbled limest, hornfels, skarn * 1.259 bt @ 0.4% Cu, 0.013% Mo, 47 g/t Bi, 8.45 g/t Ag for 5.75 mt Cu, 181 kt Mo, 9,631 t Ag * Alvarez (1999)
45. **Tintaya-skarn & Agacapay porphyry** Cu, Peru
Tintaya deposit * exoskarn, 139 mt @ 1.39% Cu, 0.23 g/t Au for 1.93 mt Cu.
Antapaccay deposit * C-A porph stockw, veins > skarn * H5; STQ * K-silic, sericite > skarn * Eo-Ol qz diorite, granod porph * Cr limest, hornfels * 420 mt @ 0.82% Cu, 0.15 g/t Au for 3.41 mt Cu, 63 t Au * Perelló et al. (2003).
46. **Cerro Verde-Santa Rosa**, SW Peru * C-A, stockw, superg blanket * H3, S+O2; AST hypogene + moly, bornite; brochantite, chrysocolla over chalcocite * ST alteration * 59-56 dacite porph stock * granite gneiss * 1 bt @ 0.6% Cu for 6 mt Cu * Chan et al. (2003).
47. **Cuajone** deposit, SW Peru * C-A stockw > oxide blanket * H5 (minor Ox), STQ * K-silic. alteration * 51 Ma qz latite porph stock * Eo andesite * 1.825 bt @ 0.64% Cu, 0.02% Mo for 13.08 mt Cu, 365 kt Mo * Concha & Valle (1999).
48. **Quellaveco** deposit, SW Peru * C-A stockw, breccia, chalcoc & oxidic blanket * H3, S+O2; STQ + moly; chrysocolla, brochantite over chalcocite * ST alteration * 54 Ma qz monzon porph, breccia * Cr andesite * 974 mt @ 0.65% Cu, 0.021% Mo for 6.33 mt Cu, 205 kt Mo * Estrada (1975).
49. **Toquepala** deposit, SW Peru * C-A stockw, breccias, dissem; low-grade oxidic leach ore * H4, S+O1; STQ + moly, tourmaline in breccia * K-feldspar, biotite, anhydrite, tourmaline * 58 Ma dacite porph, breccia * Cr andesite * 900 mt @ 1.0% Cu, 0.013% Mo for 9.0 mt Cu, 117 kt Mo + 1.4 mt Cu @ 0.2% * Clark (1990), Zweng & Clark (1995).
50. **Collahuasi** ore cluster, N Chile; **Rosario, Ujina**; Fig. 7.28, **Quebrada Blanca** giant deposits * C-A, rich chalcocite blankets over stockw & dissem in porphyry; superimp. Butte-style HS Cu-As-Ag veins; partly under ignimbrite cover * H2, S3; ST + bornite, moly; enargite in veins * ST alteration locally adv. argillic * 34.6-33 Ma miner. & granod porph * Pe-J andes, rhyol, clastics * total ~4.7 bt @ 0.82% Cu, ~0.003% Mo, ~6 g/t Ag for 29.5 mt Cu, ?1.4 mt Mo, ?28 kt Ag; Rosario ~26.2 mt Cu, Ujina 5.85 mt, + Mo, Ag; Quebrada Blanca additional 836 mt @ 0.95% Cu for 7.94 mt Cu * Clark et al. (1998).
51. **Cerro Colorado** deposit, N Chile * C-A, mostly chalcoc blanket + oxides over stockw * S4, O1; chalcocite, pyrite, chrysocolla, atacamite * sericite, clays * Eo-Ol dacite porph stock * 450 mt @ 0.9% Cu for 4.05 mt Cu *
52. **El Abra** deposit; N Chile; Fig. 7.20, 7.23. * C-A breccia, stockw, oxid. > chalcoc blanket * H1, S1, O3; hypog. chalcop > bornite, moly; chalcocite; chrysocolla, brochantite * K-silicate * 34 Ma intrus breccia, qz monzon porph * Eo diorite, qz diorite * 800 mt @ 0.55% Cu (oxides) for 4.7 mt Cu * Ambrus (1977).
53. **Chuquicamata** ore cluster, N Chile, includes **Chuquicamata**; Fig. 7.31, **Radomiro Tomic, Mansa Mina, Mina Sur**; Fig. 7.22, giant deposits * C-A, 30 km N-S mineraliz. zone along major fault; dissem, stockw, chalcoc blankets, oxides blankets; exotic deposit * H2, S2, O1; hypog. STQ + moly, bornite > tennantite-tetrahedrite; chalcocite, covellite, chrysocolla, atacamite, brochantite * STQ hypogene, seric-pyr, grades to local adv. argillic * 35-31 Ma two stage ore, O11 granod to dacite porph * Tr-J hornf. shale, siltst, litharen, andesite, dacite, granodior * total ~11.4 bt @ 0.76% Cu, ~0.014% Mo, 4 g/t Ag for 87 mt Cu, ~997 kt Mo, 45 kt Ag, 333 t Re * Ossandón et al. (2001).
54. **La Escondida** ore cluster, N Chile; Fig. 7.27. * include giant deposits **La Escondida, Escondida Norte, Zaldivar** & "large" **Chimborazo** * C-A, several chalcocite > oxidic blankets over stockwork, dissem. > breccia * H2, S2, O1; ST + moly, born in primary ore; chalcoc., covellite, atacamite, brochantite * ST hypog. alter., sericite with chalcoc., argillic with oxides * 34-31 Ma qz diorite porph, rhyolite porph, breccias * Cr-Pc andesite, PZ-MZ basement sedi, & volc. rocks * total ~5 bt @ 0.5-2.2% Cu, 0.01% Mo, 4 g/t Ag for 70 mt Cu, 2500 kt Mo, 22 kt Ag * Alpers & Brimhall (1988), Padilla et al. (2001).
55. **Sierra Gorda and Spence** deposits, N Chile * C-A, dissem in breccia, stockw * H5, Spence S+O5 STQ * STQ alteration * Eo-Ol breccias, porphyries * Spence 400 mt @ 1.0% Cu for 4 mt Cu.

56. **Mantos Blancos** deposit, N Chile * not a porphyry Cu, oxidized replacement mantos in Tr acidic volcanics (Chapter 6); 405 mt @ 1.5% Cu, 17 g/t Ag for 4.6 mt Cu, 7,650 t Ag; Rodrigues (1996).
57. **Mantoverde** deposit, N Chile * not a porphyry Cu, oxidized disseminated Fe oxides-Cu sulfides in brittle shear. ~630 mt @ 0.53% Cu, 0.11 g/t Au for 3.345 mt Cu. Chapter 6. Vila et al. (1996).
58. **El Salvador** ore field, N Chile; Fig. 7.26. * C-A, stockw. & dissem, breccias, chalcoc blanket * H2, S3, STQ hypog. + moly, bornite; minor ox., exotic * STQ hypog. alter. * 42-41 ore & several granod & dacite porph. rhyolite * Cr3-Pc rhyolite domes, ignimbr; Cr3 andesite, volcanoclastics; PZ-MZ basement * ~700 mt @ 0.9-2.4% Cu, 0.017% Mo for 10.8 Mt Cu, 119 kt Mo * Gustafson & Hunt (1975).
59. **Potrerrillos** deposit, N Chile * C-A, stockw and dissem, minor skarn, chalcocite blanket * H2, S3; STQ + moly, bornite * ST alteration * 34 Ma qz diorite, granod porph stock * J hornfelses siltst, sandst, limest * 390 mt @ 1.1% Cu for 4.18 mt Cu, 95 t Au * Marsh et al. (1997).
60. **Candelaria** deposit, N Chile * not a porphyry Cu; "mantos" of magnetite, chalcopyrite, bornite in biotite-altered andesites in intrusion roof (Chapter 6). 366 mt @ 1.29% Cu, 0.26 g/t Au, 4.5 g/t Ag for 4.72 mt Cu. Ryan et al. (1995).
61. **Andacollo** ore field, N Chile * C-A to diorite model; dissem, stockw; chalcocite blanket; peripheral replac. Au mantos * H2, S3; STQ + moly * ST alteration * Cr3 dior. qz dior porphyry * Cr andesite, dacite, pyroclastics * 300 mt @ 0.7% Cu, 0.153 g/t Au for 2.45 mt Cu, 305 t Au * Reyes (1991).
62. **La Fortuna; Regalito** deposits, N Chile * C-A, dissem, stockw; chalcocite and oxidic blankets * H2, S+O3 (Regalito entirely oxidized) * ST alteration * T porphyries * La Fortuna 465 mt @ 0.61% Cu, 0.5 g/t Au for 2.84 mt Cu, 232 t Au; Regalito 628 mt @ 0.43% Cu for 4.122 mt Cu * SEG Newsletter 61 (2005).
63. **Refugio** deposit, Maricunga belt, NE Chile * ALK (diorite model) to C-A, 3 stockw zones above diorite stock * H5; pyrite, magnetite, chalcop, bornite., moly * chlorite overpr. biotite * Mi1 qz diorite stock * Mi andesite * 297 mt @ 0.86 g/t Au for 259 t Au, 7750 kt Cu * Vila & Sillitoe (1991).
64. **Cerro Casale** (Aldebaran) deposit, Maricunga belt, NE Chile * ALK (diorite model) to C-A; stockw, veins in eroded stratovolcano * H5; quartz, magnet, hemat > chalcop * K-silic altered diorite capped by adv. argillic vein envelopes in breccia * Mi diorite porph stock * Mi andesite, breccia * 952 mt @ 0.26% Cu, 0.71 g/t Au for 3.1 mt Cu, 837 t Au * Vila & Sillitoe (1991).
65. **Bajo de la Alumbreira** deposit, NW Argentina; Fig. 7.35. * C-A, conc. zoned stockw, dissem * H5; ST + moly, bornite, magnetite * K-feldspar, biotite, magnetite to propylitic, concentr. zoned * 7 Ma ore in Mi3 cluster of small dacite porph emplaced to andesite * Mi andesite * 780 mt @ 0.52% Cu, 0.67 g/t Au for 4.056 mt Cu, 523 t Au * Proffett (2003).
66. **Agua Rica** (Mi Vida) deposit, Andalgalá, NW Argentina; Fig. 7.36. * C-A to ALK, multiphase porph. overprinted by HS epith.; breccias, veins, stockw, dissem. + chalcoc. blanket * H2, S3; pyrite > enargite, covellite, bornite over earlier STQ porphyry + moly * adv. argillic overprints earlier sericite & K-silic. alteration * 6.3-4.9 Ma ore & hydroth breccias, dacite to monzonite porph. * 8.56 Ma syenodior., Np-PZ phyllite, quartzite, schist, gneiss * 750 mt @ 0.62% Cu, 0.037% Mo, 0.24 g/t Au for 4.65 mt Cu, 277 kt Mo, 180 t Au * Rojas et al. (1998).
67. **Los Pelambres-El Pachón** ore field, Chile-Argentina; Fig. 7.8. * C-A, dissem & veinlets in breccia, porphyry; minor skarn; thick chalcocite blanket * H1, S4; + bornite, moly * ST alteration, chalcoc blanket sericite + pyrite * 9.9 Ma ore, small qz diorite, qz monzon stock * Cr andesites * Los Pelambres sector 3.3 bt @ 0.63% Cu, 0.016% Mo for 20.79 mt Cu, 528 kt Mo. Pachón sector (Argentina) 900 mt @ 0.61% Cu, 0.014% Mo for 5.49 mt Cu, 126 kt Mo * Atkinson et al. (1996).
68. **Rio Blanco-Los Bronces** cluster, E-C Chile; Fig. 7.7. * C-A, series of huge breccia pipes, stockw & dissem, minor chalcocite * H5; STQ + tourmaline, moly, bornite * ST alter., dominant K-silicates, sericite * 6-4.5 Ma ore, breccias, qz monzon, dacite porph * Mi hornfelses andesite * 6.9 mt @ 0.86% Cu, 0.02% Mo, 0.035 g/t Au for 59.3 mt Cu, 1.38 mt Mo * Warnars et al. (1985).
69. **El Teniente** deposit, E-C Chile; Fig. 7.6. * C-A, stockw & dissem in hydraulic breccia pierced by post-ore diatreme * H4, S+O1; chalcop, bornite, moly * K-silic, mostly biotite, some silicif, tourmaline * Mi3-Pl breccia, qz diorite, dacite porph * Mi hornfelses & biotitized andesite * 12.4 bt @ 0.63% Cu, 0.02% Mo, 0.035 g/t Au for 94.4 mt Cu, 2.48 mt Mo, 434 t Au * Camus (1975), Cuadra (1986).
70. **Récsk-Lahocza** ore field, Matra Mts., Hungary * "Diorite model" porphyry-Cu stockw. in depth, some skarn, HS epitherm. Cu-Au veins, replac near surface * H5; chalcop, pyrite, bornite, moly in porph., pyrite, enargite, luzonite in HD * K-silic (biotite) in porph, sericite, adv argillic in HS * Eo3 diorite, subvolc andesite * Tr limestone, shale * 700 mt @ 0.66% Cu for 10.185 mt Cu * Morvai (1982).
71. **Roşia Poieni** deposit, Apuseni Mts, Romania * Diorite model, columnar stockwork, transition to HS epitherm * H4, S+O1; pyrite, magnetite, chalcop, bornite, moly in porph; pyrite, enargite, galena, sphalerite in HS * ST in porph., sericite-adv argillic alunite, anhydrite * Mi microdiorite, andesite porph * Mi andesite paleovolcano, Cr turbidites * 1.0 bt @ 0.4% Cu for 4 mt Cu * Heinrich & Neubauer (2002).
72. **Buçium Tarniţa** deposit, Apuseni Mts, Romania * adjacent to Rosia Poieni, comparable geology * 1.0 bt @ 0.32% Cu for 3.3 mt Cu * Mining Journal, May 1999.
73. **Majdanpek** deposit, E Serbia * Diorite model to C-A; "volcanic porph-Cu", linear stockw & veins along

- fault zone; massive pyrite, magnetite replac in andesite * H5; ST in porph + magnetite, moly, galena, sphalerite * K-silic, sericite, silicification, propyl * Cr3 post-ore diorite, andesite porph * J limest, Pt schist, marble * 1 bt @ 0.6% Cu, 0.3 g/t Au for 6 mt Cu, 300 t Au, ~3,600 t Ag * Janković (1982), Herrington et al. (1998).
74. **Veliki Krivelj** deposit, E Serbia * Diorite model, "volcanic porph", dissem & stockw; minor skarn * H4, S+O1; chalcop, pyrite, chalcocite * biotite > sericite, silicif, anhydrite * Cr3 qz diorite porph, andesite porph * Cr andesite * 750 mt @ 0.44% Cu, 0.015% Mo, 0.08 g/t Au for 3.3 mt Cu, 112 kt Mo * Janković (1982), Herrington et al. (1998).
75. **Bor** ore field, E Serbia * Cluster of orebodies, diorite model, "volcanic porph", HS epithermal veins/replac * H5; pyrite, magnetite, chalcop in porph, massive pyrite, chalcop, enargite replac * biotite to seric, adv. argillic, silicif * Cr3 diorite & andesite porph * Cr andesite, pyroclastics * 540 mt @ 0.67% Cu, 0.2 g/t Au for ~5.6 mt Cu, ?240 t Au * Janković et al. (1980), Janković (1982), Herrington et al. (1998).
76. **Skouries** deposit, Chalkidiki, N Greece * ALK (shoshonitic) stockw in syen. plugs empl. to gneiss dome * H5; ST miner. + bornite, Au * biotite alter. * 18 Ma ore, Mi syenite plugs, dikes * gneiss dome * 568 mt @ 0.47% Cu, 0.8 g/t Au for 2.67 mt Cu, 477 t Au * Tobey et al. (1998).
77. **Panagurishte** district, W-C Bulgaria (includes "large" Cu-Au porphyry & HS deposits **Elatsite**, **Assarel**, **Medet**, **Chelopech**) * Diorite model porph stockw, dissem & HS veins, replac. * H4, S1; ST minerals in porph; pyrite, enargite in HS * biotite to sericite, propylite; adv. argillic * Cr3 diorite, granod > qz monzon. porph * Cr3 andesite & volcanoclast., Ct gneiss, PZ granitoids * total 4.14 mt Cu, 320 t Au; Chelopech only, HS veins + replac.: ~220 t Au, 600 kt Cu, ~60 kt As * Bogdanov (1983), Popov et al. (1983).
78. **Kadzharan** deposit, Armenia * C-E, stockw. and dissem * H5; STQ + moly * ST alteration, silicification * Ol or Mi qz-feldspar porph. * Eo hornfelsed andesite, dacite, rhyolite & volcanoclastics * Rc 1.8 bt for 7.2 mt Cu, ?500 kt Mo * Pidzhyan (1975), Mining Ann. Rev. (1999)
79. **Sungun** deposit, Iranian Azerbaidzhan * C-A, stockw in porph & skarn * H5?; STQ + moly * ST alter., exoskarn * Mi diorite to qz monzonite stock * Cr limest, Eo volcanoclastics * Rc 860 mt @ 0.6% Cu, 0.015% Mo for 5.16 mt Cu, 129 kt Mo * Hezarkhani & Williams-Jones (1998).
80. **Sar Cheshmeh** deposit, S-C Iran * C-A, stockw, dissem, veins * H2, S3?; STQ + moly * ST alteration * 12.5 Ma hornbl & qz-feldspar porph, granodior * Eo andesite, pyroclastics * total 12.5 mt Cu, ?600 kt Mo, ?450 t Au, 5 kt Ag; Rc₁₉₉₉ 1.25 bt @ 0.6% Cu, 0.03% Mo, 0.27 g/t Au, 3.9 g/t Ag * Waterman & Hamilton (1975).
81. **Reko Diq** ore field, Chagai Hills, Balujistan, NW Pakistan * C-A, 19 deposits in 15 km struct zone; enrich. blanket under leached cam * S5; STQ mineralogy * K-silic in protote, sericite in chalcocite zone * 10-22 Ma qz diorite, granod porph * T1 volcanics, sediments * Rc 840 mt @ 0.64% Cu, 0.39 g/t Au for 5.376 mt Cu, 328 t Au * Tethyan Copper Ltd. website (2005).
82. **Barit (Gilgit)** ore field, NW Pakistan * porphyry Cu-Au * Rc 360 mt @ 0.7-1.2% Cu for 3.6 mt Cu * Mining Ann. Rev. (1999).
83. **Yulong (Qulong)**, Xizang (Tibet), W China * C-A, stockw in porph + skarn, 5 orebodies in tect zone * Rc 850 mt @ 0.99% Cu, 0.028% Mo, 0.35 g/t Au for 8.5 mt Cu, 238 kt Mo, 297 t Au * Hou et al (2003).
84. **Monywa** ore field, central Myanmar (Burma) * Diorite model to C-A, HS veins, replac, dissem, stockw superimp on porph Cu-Au; **Letpadaung** "giant" deposit * H1, S4?; superg. & hypog. chalcoc, digenite, covellite; in porph. Cu-Mo ST & moly * adv. argillic, + sericite overprint K-silicate * 19 Ma andesite porph, breccias * Mi andesite, pyroclastics * Rc (Letpadaung) 1.069 bt @ 0.4% Cu for 4.5 mt Cu * Win & Kirwin (1998).
85. **Batu Hijau** deposit, Sumbawa, Indonesia * Diorite model to C-A, stockw, dissem * H5, minor S+O; STQ miner + magnetite * ST alter * Mi3-Pl multiphase tonalite porph * Mi2 island arc andesite * 1.494 mt @ 0.52% Cu, 0.4 g/t Au for 7.77 mt Cu, 598 t Au * Clode et al. (1999); read Chapter 5.
86. **Ok Tedi (Mt. Fubilan)** deposit, Tabubil, SW PNG; Fig. 7.24. * Diorite model to C-A, stockw > skarn, Au gossan * H5; STQ + moly, bornite, magnetite * ST alter + exoskarn * 1.2-4.0 Ma ore + monzonite, qz monzon stock, diorite pluton * Ol-Mi limestone, MZ-T fine clastics * 777 mtore (543 mt porph. @ 0.6% Cu, 0.5% Au) for total 4.68 mt Cu, 552 t Au * Bamford (1972).
87. **Frieda River-Nena** ore field, W-C PNG * Diorite model to C-A Frieda porph. stockw, Nena HS veins, replac * H5; STQ minerals + bornite, moly > enargite * K-silicate in porph, seric & adv. argillic in Nena * Mi2 porph. microdiorite, diorite * Cr-Eo shale, phyllite, ophiolite ultramaf, basalt * Rc (Frieda) 1.0 bt @ 0.47% Cu, 0.28 g/t Au for 4.7 mt Cu, 280 t Au; Nena is small * Morrison et al. (1999).
88. **Ertsberg-Grasberg** ore field, Tembagapura, Papua, Indonesia (includes **Grasberg** porph. Cu-Au; Fig. 7.32, **Ertsberg** group skarns, **Kucing Liar** skarn "giants") * C-A, central Grasberg stockw, vein, dissem porph-Cu surrounded by 5 major exoskarn Fe,Cu,Au deposits * H5; STQ + moly, bornite, magnetite; ST skarn * ST alter in porph, exoskarn * 2.5 Ma ore, Pl granod porph, diatreme breccia * MZ-CZ marbled limest, skarn, hornfels * Grasberg 3.87 bt @ 1.13% Cu, 1.05 g/t Au, 3.83 g/t Ag for 43.73 mt Cu, 4,063 t Au, 14,822 t Ag * Rubin & Kyle (1997).
89. **Mankayan** ore field, N Luzon, Philippines (includes historical HS **Lepanto-Cu,Au**, 2 buried porph. Cu-Au **Far South-East** & **Guinaoang**, minor Au veins * Diorite model to C-A, porph. stockw, breccia, dissem; HS replac, veins * STQ + magnetite,

- bornite, moly in porph.; pyrite, enargite, luzonite in HS * K-silicate, seric-chlorite in porph; adv. argillic + sericite in HS * 1.42-1.3 Ma ores, porph. in Mi3 qz diorite, diatreme breccias * Mi2 island arc andesite, volcanoclastics * total field ~8 mt Cu, 1,240 t Au; Far South-East Rc 1.423 bt @ 0.4% Cu, 0.6 g/t Au for 5.69 mt Cu, 854 t Au * Hedenquist et al. (1998).
90. **Baguio** district porphyries, Luzon, Philippines (district includes 6 "large" porph Cu-Au, 1 "giant-Au" **Santo Tomas**; major LS vein Au) * Santo Tomas: Diorite model to C-A subvertical stockw, dissem * H5; bornite, chalcop, magnetite, pyrite, chalcop, hematite * K-silic, chlorite, seric-actinolite, anhydrite * Pl3-Q qz diorite porph stock * Ol-Mi hornfelsed, altered andesite * 511 mt @ 0.32% Cu, 0.7 g/t Au, 0.2 g/t PGE for 1.6 mt Cu, 340 t Au, 102 t PGE * UND Programme (1987).
91. **Marinduque** Island ore field, Philippines * Diorite model to C-A, to large stockw-dissem deposits * H5; STQ minerals * ST alter * 15-20 Ma qz diorite porph * Eo-Mi clastics, andesite * 3.241 mt Cu @ 0.38-0.52% Cu, 82t Au * Loudon (1976).
92. **Toledo (Atlas)** ore field, Cebu, C Philippines; Fig. 7.37. * Diorite model to C-A, 3 major deposits, stockw, dissem * H5; ST minerals * ST alter. * Cr (59.7 Ma?) diorite porph * Cr metabasalt * 1.38 mt @ 0.45% Cu, 0.24 g/t Au for 6.215 mt Cu, 331 t Au * Bryner (1969).
93. **Sipalay** ore field, Negros Occidental, Philippines * Diorite model to C-A, steeply dipping tabular stockwork > dissem * H5; STQ + bornite * biotite, sericite, propylitic * 30 Ma qz diorite porph * Cr-T1 mafic volcanics * 884 mt @ 0.5% Cu, 0.34 g/t Au, 0.015% Mo for 4.42 mt Cu, 100 kt Mo, 300 t Au * Bryner (1969), Wolff (1978).
- Hinoban deposit**, Negros Occidental, Philippines (see Chapter 5); 650 mt @ 0.5% Cu, 0.24 g/t Au for 3.25 mt Cu, 156 t Au.
94. **Tampakan** deposit, S Mindanao, Philippines * Diorite model, "volcanic"porph Cu-Au in eroded stratovolcano; flat-lying zone at fault intersct., porph Cu-Au in depth overprinted by HS veins, replac * H5; pyrite, chalcop, moly in porphyry; pyrite, enargite, bornite, digenite in HS * silica lithocap, ad, argillic, remn of K-silic in depth * Pl hornbl. diorite stocks * Mi andesite flows * 1.104 bt @ 0.65% Cu, 0.26 g/t Au for 4.98 mt Cu, 286 t Au * Middleton et al. (2004).
95. **Panguna deposit**, Bougainville, PNG * C-A stockw, breccia, dissem * H5, minor S+O; STQ miner + magnetite, moly, bornite * 3.4 Ma ore in granod + qz diorite porph, breccia * Ol hornfelsed andesite * 1.397 bt @ 0.53% Cu, 0.63 g/t Au for 5.84 mt Cu, 632 t Au * Clark (1990).
96. **Waisoi** deposit, Namosi, Viti Levu, Fiji * Diorite model to C-A, stockw zone in dissected volc centre * H5; ST mineral * ST alteration * Pl qz diorite * Mi-Pl andesite, pyroclastics * 1.1 bt @ 0.45% Cu, 0.13 g/t Au for 4.95 mt Cu, 143 t Au * Colley & Flint (1995).
97. **Dexing** ore field, Jiangxi, E-C China * C-A stockw, dissem * H5; STQ + moly, bornite * ST alter * 170-148 Ma granod porph stock * 1.4 Ga phyllite, volc-sedim assoc * 1.6 bt @ 0.47% Cu, 0.01% Mo, 0.2 g/t Au for 8.6 mt Cu, 150 kt Mo, 240 t Au * Yan & Hu (1980).
98. **Zijinshan** ore field, E-C China * porphyry Cu-Au, second. enrichment * Rc 650 mt @ 0.49% Cu for 3.185 mt Cu, 149 t Au * Asian J. of Mining, July-August 1997.
99. **Peschanka** deposit, NE Kolyma, E Siberia, Russia * ALK, stockwork * H5?; chalcop, bornite, pyrite, magnetite * K-silicate, propyl * J3-Cr1 qz monzonite porph * J3 gabbro, monzonite, syenite pluton * Rc 940 mt @ 0.51% Cu, 0.4 g/t Au for 3.76 mt Cu, 376 t Au * Abzalov (1999).
100. **Erdenet** deposit, N-C Mongolia * C-A stockw, dissem, chalcoc. blanket over hypog. ore * H2?, S3?; STQ + moly * seric overprints K-silic * 207 Ma granod, granosyen porph * Pe basalt, andesite, rhyolite; Cm metavolcanics * total ~14 mt Cu, Rc 1.78 bt @ 0.54% Cu, 0.016% Mo, 0.01 g/t Au for 9.612 mt Cu, 285 kt Mo * Lamb & Cox (1998).
101. **Kounrad (Qonyrat)** deposit, C Kazakhstan * C-A, stockw, dissem, breccia; chalcoc. blanket * H2, S3?; ST porph. miner. + moly overprinted by HS enargite, tetrahedrite, chalcocite * silicif, sericite, adv. argillic overprint K-silic * Cb2 granod porph * Cb2 rhyolite, tuff * P+Rv 3,748 mt Cu (recent grades 0.34% Cu, 0.005% Mo, 0.017 g/t Au) * Sotnikov et al. (1977), Abdulin et al. (1978), Kudryavtsev (1996).
102. **Samarka** deposit, C Kazakhstan * C-A stockw, breccia, dissem * ST miner. * ST alter. + silica capping * D1 granod porph * S3-D1 qz diorite batholith * 3 mt Cu @ 1.5% Cu, ~100 t Au * Sokolov (1998).
103. **Aktogai-Aiderly** ore field, E-C Kazakhstan * C-A, breccia, stockw, dissem STQ minerals + moly * ST alter, silicif. * Cb3 breccia, granod porph * Cb gabbro, diorite, granod pluton emplac. to volcanics * Rc 1.5 bt @ 0.39% Cu for 12.5 mt Cu * Sotnikov et al. (1977), Abdulin et al., (1978), Zvezdov et al. (1993).
104. **Almalyk (Olmal'yk)**, Kurama Range, Uzbekistan; comprise **Kal'makyr** and (buried) **Dalnee** deposits; Fig. 7.38. * ALK to C-A, stockw around barren porph; zoned at fringe Au veins, Zn-Pb replac * H3?, S+O2?; STQ + moly, bornite * ST alter * Cb3 porph syenodiorite, granod porph * D3 limestone, D1 meta-rhyolite * total 18.7 mt Cu (+ calculated 229 kt Mo, 2041 t Au, 12,522 t Ag, 13,230 t Se, 1,098 t Te, 566 t Re); Kal'makyr recent grades 0.54% Cu, 0.051% Mo, 0.5 g/t Au; Dalnee Rc 2.5 bt @ 0.38% Cu, 0.4 g/t Au * Sotnikov et al. (1977), Samonov & Pozharisky (1974).
105. **Tuwu-Yandong** ore zone, Xinjiang, NW China * ALK to C-A, stockw + dissem in elongated structure * H5?; ST + moly, bornite, covellite * K-silic, silicif, sericite * 323 Ma ore, 333 Ma monzonite porph,

- diorite porph * Cb island arc andesite, tuff, sedim. * Rc 4.7 mt Cu @ 0.67% * Mao et al. (2004).
- 106. Duobaoshan**, Heilongjiang, NE China * Diorite model to C-A? stockw * H5?, ST miner. * K-silic, silicif, propylite * 292-178 (mostly Pe) miner. in granod. porph. in gabbro, tonalite, trondhj. pluton * Or2 metavolcanics * P+Rc 500 mt @ 0.47% Cu, 0.14 g/t Au for 2.35 mt Cu, 70t Au * Mu & Lin, lecture (1996).
- 107. Gaspé** (Murdochville) ore field, SE Quebec; 2 adjacent deposits; Fig. 7.39. * C-A dissem, stockw in porph & skarn * H5, minor S+O; ST minerals + moly, bornite * ST in porph, skarn, anhydrite * D3-Cb1 rhyodac porph plug, dikes * D1 calcar limestone to siltst, Ca-silicate hornf, skarn * 344 mt @ 0.8% Cu, 0.08% Mo for 3.308 mt Cu, 225 kt Mo * Meinert et al. (2003).
- 108. Bozshakol** deposit, N Kazakhstan * Diorite model to C-A, stockw + dissem * H5?, S+O minor; ST + magnetite, moly > sphalerite * Earlu K-silic, magnetite, hematite, later ST * Cm2 tonalite porph * Cm1-2 meta-basalt, andesite, tuff * Rv₁₉₈₄ 179 mt @ 0.72% Cu, 0.014% Mo, 0.28 g/t Au, Rc ?3.2 mt Cu * Abdulin et al. (1978), Kudryavtsev (1996).
- 109. Oyu Tolgoi** ore field, S-C Mongolia; Fig. 7.40. * Diorite model to C-A, 3 mineraliz zones, multiphase stockw + breccia porph-Cu overprinted by HS; chalcoc. blanket * H2, S3?; STQ in porph, hypog. chalcocite, covellite, tennantite in HS * STQ in porph, sericite + adv. argillic in HS * Cr enrich. blanket on 411 Ma multiphase hornbl-feldsp porph * S-D arc andesite, basalt, sedim * Rc2003 2.45 bt @ 0.61% Cu, 0.14 g./t Au for 15.06 mt Cu, 343 t Au * Perelló et al. (2001), Kirwin et al. (2003).
- 110. Cadia** ore field, NSW, E-C Australia; Fig. 7.12. * ALK, 5 porphyry & 2 skarn deposits; sheeted veins, fract stockw, dissem, skarn * H5; qz, chalcop, bornite, magnetite * K-feldsp, biot, actinol, epidote in porph; skarn * 438 Ma monzonite to monzodior, qz monzon porph stocks * Or andesite, volcaniclastics * total 4.4 mt Cu, 574 t Au; Cadia Hill deposit Rc 350 mt @ 0.16% Cu, 0.68 g/t Au * Forster et al. (2004).
- 111. Haib River** ore field, S Namibia * C-A, linear zone of dissem & stockw miner * STQ minerals + moly * ST alteration * Pp qz feldsp porph stock * Pp granite, meta-andesite, rhyolite * 1.28 bt @ 0.41-0.19% Cu for 3.1 mt Cu * Minnitt (1986).
- 112. Malanjkhand** deposit, Madhya Pradesh, C India * Steeply dipping, arcuate shear zone, silicified and veined by qtz, chalcopyrite, pyrite veins grading to stockwork, in 1.82 to 1.68 Ga biotite granite. 120 m thicj supergene zone (oxidic Cu and chalcocite). Interpreted by some as porphyry-Cu. 6.61 mt Cu @ 0.83%, 4,734 t Ag @ 6 g/t, 158 t Au @ 0.2 g/t. Sikka et al. (1991).

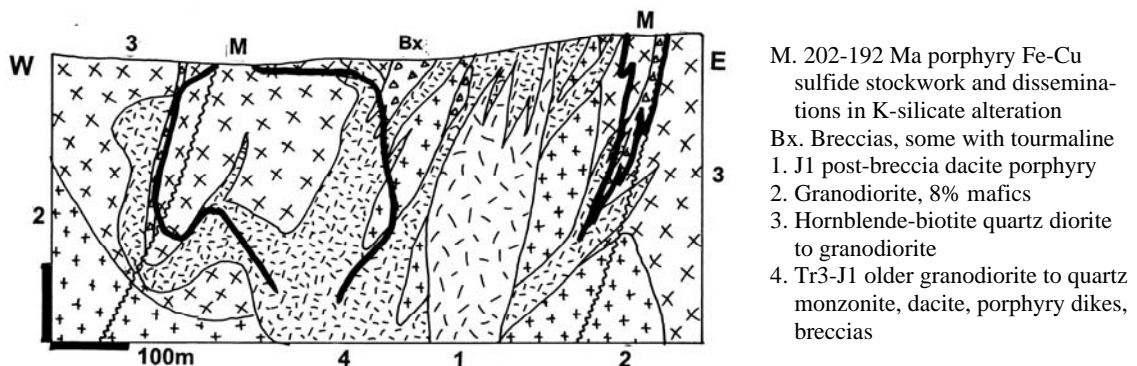
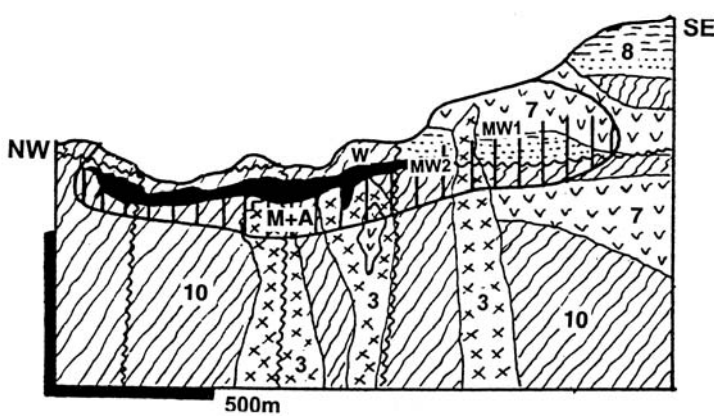
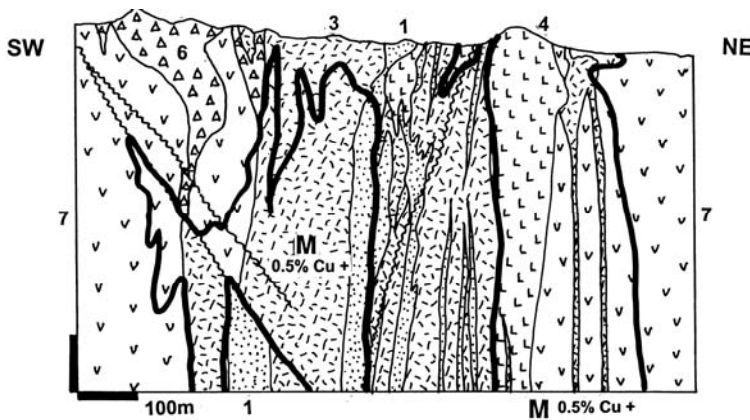


Figure 7.33. Highland Valley porphyry Cu cluster, British Columbia: an example of western Canadian Cu porphyry lacking supergene modifications (removed by glacial erosion). Jersey pits cross-section from LITHOTHEQUE No. 2067, modified after Carr (1966)



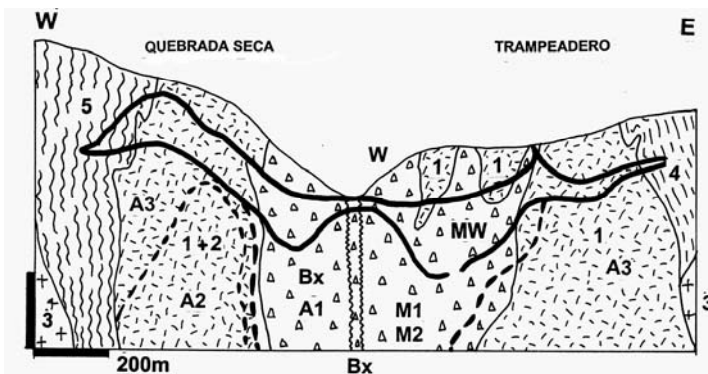
- W. Regolith & leached capping
- MW1. Oxidation zone, blankets of chrysocolla, malachite, azurite
- MW2. Sooty chalcocite blankets
- M. ~60 Ma cluster of chalcopyrite, bornite > molybdenite fracture stockwork bodies in various K-silicate altered hosts
- 3. 60.8 Ma quartz monzonite porphyry, ore-related
- 7. 1.14 Ga diabase
- 8. Mp quartzitic clastics
- 10. 1.7 Ga metasedimentary and metarhyolite schist

Figure 7.34. Ray porphyry Cu-Mo cluster, Arizona: example of an almost indiscriminate porphyry-style mineralization in a variety of K-silicate altered Proterozoic rocks, related to the voluminously minor Laramide parent intrusions. Cross-section of the old pit from LITHOTHEQUE No. 528, modified after Metz and Rose (1966)



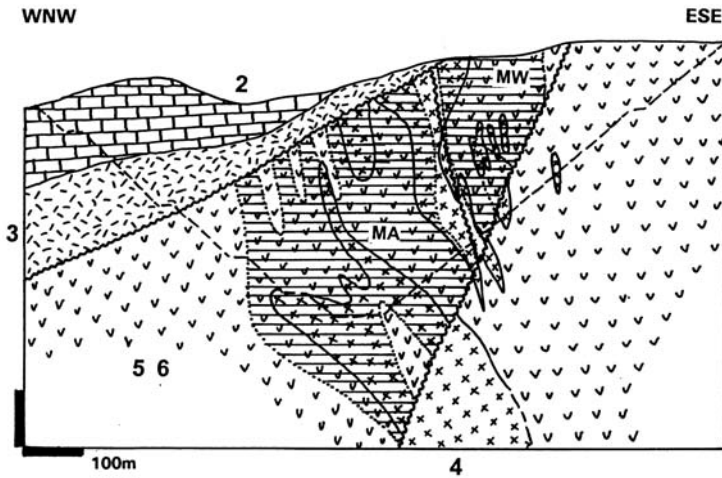
- M. 7.1 Ma veinlet & disseminated Cu-Mo sulfides in K-silicate alteration over quartz-magnetite veining
- 1. Late dacite, rhyodacite porphyries
- 3. 7.1-6.8 Ma main syn-ore dacite porphyry
- 4. 7.1 Ma dacite porphyry stock synchronous with the early ore stage
- 6. Igneous breccia in andesite
- 7. Mi andesite flows, tuff, breccia

Figure 7.35. Bajo de la Alumbrera porphyry Cu-Au-Mo deposit in Sierras Pampeñas, Argentina, has the shape of an annulus around a low-grade core. Cross-section from LITHOTHEQUE No. 2509, modified after Proffett (2000) and materials provided courtesy of Minera Alumbrera, 2000



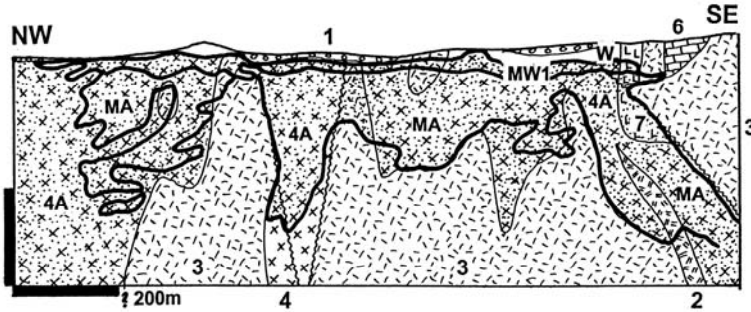
- W. Leached capping; MW. 3.9 Ma supergene sulfides: chalcocite at top, covellite at bottom; M1. 6.29-4.88 Ma Main Stage, HS disseminations, veinlets, breccia bodies of pyrite >> enargite, covellite, bornite in advanced argillic envelope overprinting the earlier porphyry-style (M2). Alterations: A1, advanced argillic; A2, K-silicates; A3, phyllic. 1. Mi3-P11 porphyry complex; 2. 8.56 Ma syeno-granodiorite; 3. Or-S coarse monzogranite; 4. Np-PZ1 phyllite; 5. Np-PZ schist, gneiss, migmatite

Figure 7.36. Agua Rica Cu-Au-Mo, Andalgalá, Argentina: a multistage deposit where the high-sulfidation Main Stage overprints relics of the earlier porphyry-style Cu-Mo. From LITHOTHEQUE No. 2517, modified after Rojas et al. (1998)



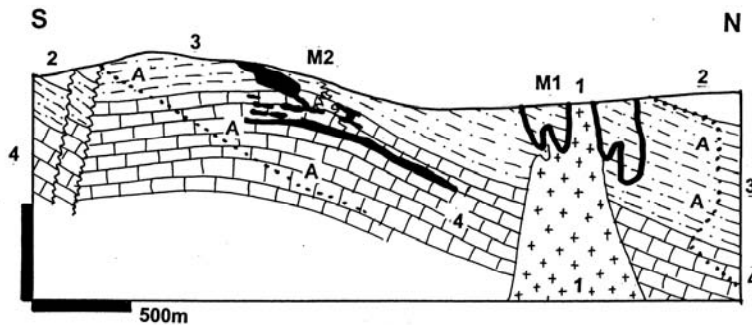
MW. Erratic patches of secondary sulfides under leached capping with minor oxidic Cu minerals
 MA. Multistage stockwork and disseminations of Fe-Cu > Mo sulfides in K-silicate envelope overprinted by silicification, sericite and anhydrite-gypsum
 1. Regolith and cover sediments
 2. Mi1 limestone and clastics
 3. Cr1 andesitic pyroclastics and dikes
 4. 108 Ma quartz diorite
 5. Cr1 hornfelsed andesite to basalt
 6. Cr1 conglomerate, volcanite, slate interbeds in basalt

Figure 7.37. Toledo (Atlas) ore field, Cebu, Philippines: example of the largest early generation Philippine porphyry Cu. Carmen orebody from LITHOTHEQUE No. 2131, modified after Reyes et al. (1981) and Atlas Corporation materials



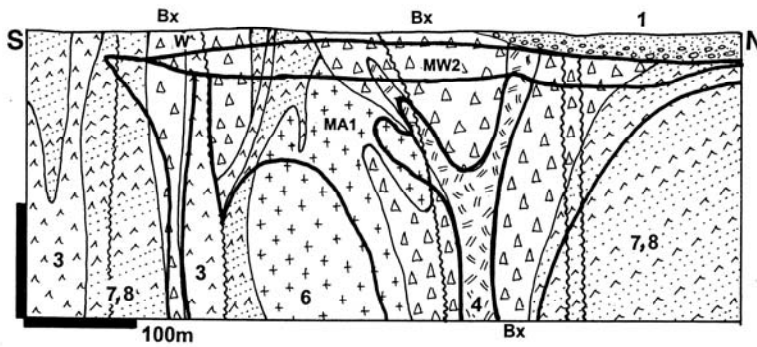
1. Colluvium & regolith
 W. Leached capping; MW1. Oxidation zone; MW2. Poorly developed chalcocite zone; MA. Concentrically zoned conical Cu-Mo-Au stockwork in syenodiorite (4) around almost barren porphyry (3). 2. Cb3 dacite porphyry dikes; 3. Cb3 granodiorite porphyry; 4. Cb3 syenodiorite; 6. D3 marble

Figure 7.38. Almalyk (Olmalyk) ore field, Kurama Range, Uzbekistan, the largest Cu-Au-Mo "giant" of the former U.S.S.R. marked by a silicified outcrop ("secondary quartzite"). Kal'makyr deposit, cross-section from LITHOTHEQUE No. 3263 modified after But'yeva et al. in Samonov and Pozharisky (1974) and materials courtesy of the Almalykskaya Ekspeditsiya, 1994



M1. "Wallrock porphyry": brittle fracture Fe-Cu>Mo sulfides stockwork in altered silicate rocks
 M2. Replacement pyrite, chalcopyrite disseminated in retrograde skarn and "porcellanite"
 1. D3-Cb1 rhyodacite porphyry
 2. D1 feldspathic sandstone, shale
 3+4. D1 hornfelsed calcareous siltstone and skarned impure limestone ore hosts

Figure 7.39. Gaspé ore field, Murdochville, SE Québec, example of a low-grade disseminated Fe-Cu>Mo sulfides predominantly in calcareous sedimentary rocks close to a mineralizing porphyry stock. Cross-section from LITHOTHEQUE No. 119, modified after Allcock (1982)



W. Regolith and leached capping; MW1. Oxidation zone (poorly developed); MW2. Cr1-2 chalcocite blanket; MA1. Late stage HS sulfides in advanced argillic assemblage overprint earlier phyllic and K-silicate porphyry-style Cu-Au stockwork; 1. Cr3-T1 sedimentary cover; 3. S-D postmineral dikes; 6. S-D main feldspar porphyry; 7,8. S-D island arc basalt, andesite, volcaniclastics

Figure 7.40. Devonian Oyu Tolgoi 15 million tons Cu plus porphyry Cu-Au field, Gobi, southern Mongolia, proven in the early 2000's. Cross-section of the Central Oyu deposit from LITHOTHEQUE No. 3235 modified after Perelló et al. (2001) and materials provided courtesy of Ivanhoe Mines Ltd., 2003

7.4. Stockwork molybdenum deposits

Molybdenum is a relatively rare trace metal (Clarke 1.1 ppm), so every deposit with more than 110,000 Mo is a "giant". Mo has also a tendency to superaccumulate locally and the result is a list of 33 Mo "giants" and 4 Mo "super-giants" (Climax, 2.18 Mt Mo; Henderson-Urad, 1.243 Mt Mo, both in Colorado; Quartz Creek, Alaska, 1.207 Mt Mo; Mount Tolman, Washington, 1.175 Mt Mo). The true magnitude of the Chinese deposits is uncertain although Luanchuan in Henan has been credited with 2.06 Mt Mo (Mining Annual Review, 1999) and Nannihu-Sandaozhuang and Jinduicheng contain the greatest share of the "many million tons of Mo" in the East Qinling Mo Belt. All 35 "giants" listed here are of the "stockwork-Mo" type, with minor associated skarn. This makes porphyry molybdenum the second largest congregation of "giant" deposits after porphyry coppers. In addition to this Mo is also recovered from the porphyry Cu-Mo deposits (Table 7.7) where copper is the principal commodity, and in terms of Mo content 38 deposits fall into the "Mo giant", and 4 deposits or ore fields (Bingham, Collahuasi, Rio Blanco, El Teniente) into the "Mo supergiant" categories. Virtually the entire enormous localized Mo resources are situated within the andean-type margins where their origin is coeval with subduction; the Climax-type deposits are in the outer (pericratonic) fringe of andean margins, close to the presumed terminus of a flatly subducting slab where the overall compressional regime changes into extension (rifting); Fig. 7.42. Two Mo "giants" are in entirely intracontinental rifts (Chapter 12) and

two are in Precambrian terrains with uncertain affiliation (Chapter 9).

All porphyry Mo are high-temperature magmatic-hydrothermal deposits associated with differentiated metaluminous granitic magmas. There is some uncertainty about the mantle component of such magmas, but the prevalent opinion is that these magmas originated within a thick Precambrian lithosphere, most likely in the lower continental crust. Carten et al. (1993) reviewed this problem in some detail.

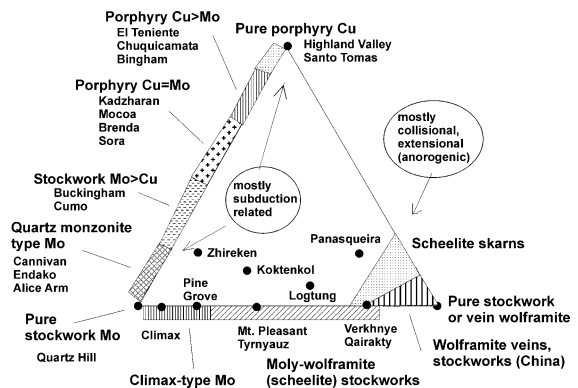


Figure 7.41. Variety of stockwork and disseminated ore types in the system Cu-Mo-W

As with the other magmatic-hydrothermal systems, there is a good correlation between the selection of the preferentially accumulated metals and magma suites, and a distinct trend is apparent. Porphyry Mo have an intermediate position between porphyry Cu-Mo and high-level granite-related

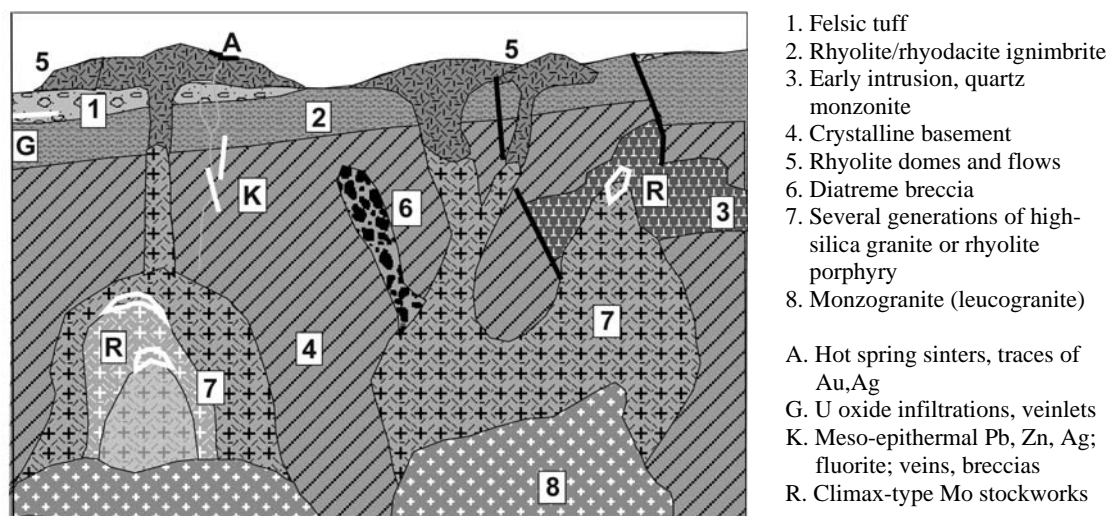


Figure 7.42. Inventory cross-section of high-silica metaluminous granite & rhyolite. Ore type R yields "giant" deposits. From Laznicka (2004), Total Metallogeny set G59

wolframite/scheelite stockworks (Fig. 7.41). Mo in the metaluminous magma series can accumulate alone, to form purely Mo deposits (e.g. Quartz Creek); combine with copper to form a transitional sequence between the Cu-only porphyry (e.g. Highland Valley), porphyry Cu>Mo (e.g. Bingham), porphyry Mo>Cu (e.g. Mount Tolman), and porphyry Mo; or combine with tungsten to form a series of Mo>W (e.g. Nannihu-Sandaozhuang) to W>Mo (Logtung) "giants" that include skarns. Mo and W jointly accumulated in ore fields can either form mixed orebodies (e.g. Logtung), or be separated: Mo preferring stockworks in porphyry or biotite-altered clastics, W forming scheelite skarn in carbonates (e.g. Tyrnyauz). The geotectonic setting of many W deposits, particularly the most productive ones as in China, is controversial and attributed mostly to the collision-generated magmas treated, in this book, in Chapter 10.

Porphyry-Mo deposits have been for a long time a purely American phenomenon as the United States is the home of 16 "Mo giants" and "Mo supergiants", leads in the tonnage of Mo resources and production, and contains the type area of the "Climax-type" in the Colorado Rocky Mountains. The economic porphyry-Mo monopoly has been recently weakened following the discovery and development of the "super-large" Mo deposits in Shaanxi and Henan, China, but the intellectual monopoly remains as there has been very little written about the Chinese deposits outside of China. Apart from the literature on individual deposits, several recent reviews of porphyry-Mo are

available. Reviews by Westra and Keith (1981) and Carten et al. (1993) are widely used and they contain lists of deposits and extensive references.

There are several competing classifications of the porphyry-Mo deposits but three subgroups have been recognized, under different names, by most investigators and their "giants" are briefly reviewed below.

7.4.1. Differentiated monzogranite Mo suite

These are systems that are a part of the calc-alkaline quartz diorite, granodiorite, quartz monzonite, granite magmatic assemblages. There, the "granodiorite molybdenite systems" (Mutschler et al., 1981), "calc-alkaline Mo", quartz-monzonite Mo" and "differentiated monzogranite Mo" (Carten et al., 1993) are close cousins of porphyry coppers. In the "Morenci Assemblage" of Keith and Swan (1996), the most Cu-Mo productive Laramide (late Cretaceous to Paleocene) magmatic suite of the American Cordillera, porphyry Cu-Mo deposits correlate with the hydrous, iron-poor, oxidized, late stage high-level biotite granodiorite intrusions that postdate biotite-hornblende granodiorite precursors in subduction-related metaluminous suites. There, molybdenite either occurs as a minority component of the ordinary disseminated or stockwork copper ore (typical Mo contents in a 0.8% Cu ore are of the order of 0.02-0.04% Mo), or as a major component in a high Mo:Cu ratio ore from a usually later-stage and/or deeper and/or centrally located high-silica intrusive phase ("felsic porphyry", "aplite") as in

Bingham, Utah (this is outside the Laramide suite proper). The very high Mo:Cu ratio porphyry deposits just seem to have a greater proportion of such "Mo-aplites" although the site of the Mo component rarely follows from tonnage figures. Also, they show preference for hornfelsed clastics as wallrocks to intrusions whereas the Cu-rich porphyries favor andesitic volcanics, when present.

There is some terminological confusion. The "quartz monzonite-Mo" of Westra and Keith (1981) comprise the same deposits as the "differentiated monzogranite" of Carten et al. (1993). This is mostly a matter of context. The quartz monzonite (or granodiorite) applies to the broader rock association, although the actual Mo host rock may be a minor monzogranite or even high-silica rhyolite intrusion (this is well illustrated in the Hudson Bay Mountain deposit shown below; Fig. 7.43). The "monzogranite-Mo" addresses the minority host rock directly.

Endako Mo deposit, central British Columbia (Bysouth and Wong, 1995; Kimura et al, 1976; P+Rc 336 Mt @ 0.087 Mo for 292,320 t Mo; Fig. 7.44). This largest Canadian Mo producer is located 160 km west of Prince George, in the Stikinia Triassic island arc terrane near its boundary with the "oceanic" Cache Creek terrane. The deposit is enclosed entirely in a coarse quartz monzonite, a middle phase of a composite late Jurassic-early Cretaceous (166-137) pluton. The NW-trending, 3.4 km long ore zone is up to 370 m wide and it is mined from several open pits. There are two generations of ore. The earlier and minor, higher-temperature (~440°C) magmatic-hydrothermal stockwork of quartz, molybdenite, pyrite veins has K-feldspar alteration selvages. The mineralization ages (~154-145 Ma) overlap with ages of host rocks, indicating close relationship. The later, dominant mineralization is a system of sheeted, ribbon-textured steeply SW-dipping veins ranging in thickness from several cm to about 1m. Within each vein of strained to brecciated quartz are numerous thin parallel laminae of molybdenite with accessory magnetite and pyrite. The sericite-altered selvages pass into slabs of unaltered, or slightly argillized quartz monzonite. There are several generations of post-mineral dikes and the ore zone is faulted. The Mo laminae sometimes acted as slip surfaces and are smeared, and there has also been some movement along the vein/wallrock contacts, filled by gouge and overprinted by kaolinization of the cataclastic monzonite.

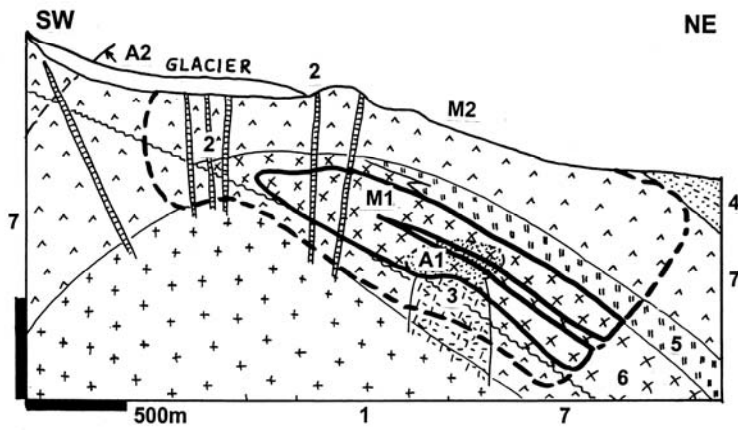
Quartz Hill Mo deposit, SE Alaska (Ashleman et al., 1997; Rc 1.584 Bt @ 0.076% Mo for 1.204 Mt Mo). Quartz Hill is an unmined Mo "super-giant" located 70 km east of Ketchikan. It is associated with a small (3x5 km) composite peraluminous leucogranite and rhyolite stock, a lonely Oligocene (30 Ma) post-orogenic intrusion emplaced, along faults intersections, into gneiss and migmatite of the Coast Batholith. This late Jurassic to Eocene batholith welds together two accreted Cordilleran superterranes. The early porphyritic biotite granite grades to leucogranite, in turn intersected by quartz-feldspar porphyry and rhyolite plugs and dikes, complete with a variety of breccias (intrusion, diatreme, hydrothermal breccias).

The Mo orebody is a 2,800 m long, 1,500 m wide and up to 500 m deep tabular zone with assay boundaries (cut-off grade is 0.05% Mo) in apical part of the Quartz Hill complex. Dated at 27 Ma, this is a multistage fracture stockwork of quartz, fine molybdenite (or molybdenite-only), pyrite, frequent magnetite, and local Pb,Zn,Cu sulfides in the porphyries. As the hosts are themselves silicic and potassic the ore-stage quartz and K-feldspar alteration is quite indistinct and merge with the partially autometasomatized hosts.

Ashleman et al. (1997) pointed out that Quartz Hill share characteristics of both the monzogranite suite, and the high-F, high-silica rhyolite-alkalic suite (Climax-type) of stockwork Mo deposits, without clearly fitting into either category. The origin is attributed to rifting-generated magma emplaced into thickened continental margin, in a period of change from subduction to oblique subduction and strike-slip motion.

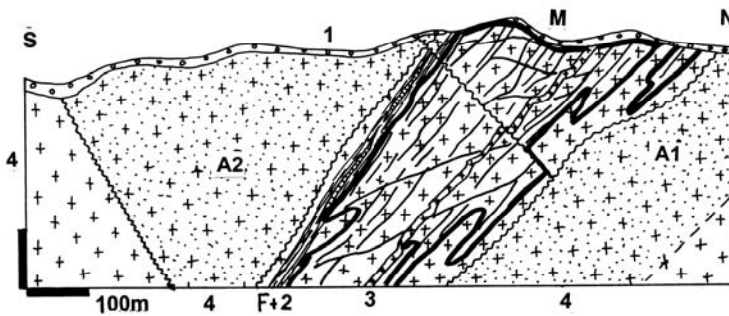
7.4.2. High-silica rhyolite suite (Climax type)

Systems related to highly evolved and fractionated high silica rhyolite are instantly recognizable by absence of the calc-alkaline suite of intermediate to felsic granitoids; the rhyolite-felsic porphyry-granite members occur alone. The "high-silica rhyolite-alkalic suite" has been further subdivided by Carten et al. (1993) into Climax (Fig. 7.45), transitional, and alkalic subtypes. This is a specialist's classification that turns a bit confusing and controversial if applied in the field, especially to geologically old occurrences. For practical purposes it is easier to retain the popular "Climax-type" term for the Mo deposits deficient in copper and related to granite-derived high-silica porphyry or "aplite", of calc-alkalic or alkali-calcic derivation, and treat separately only the porphyry Mo's in the truly



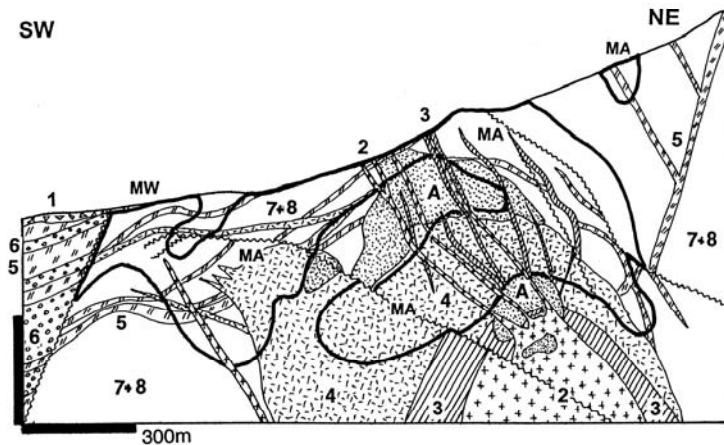
- M1 (high-grade core), M2 (low-grade fringe) ~60 Ma multiphase quartz-molybdenite stockwork and veins in roof above plug
- A1. Strong silicification
- A2. Multiphase overlapping K-, Na-silicate, sericite, quartz alteration
- 1. Cr3 quartz monzonite
- 2. Quartz-feldspar porphyry
- 3. Rhyolite porphyry plug
- 4. Cr1 clastics, minor coal
- 5. J2-3 leucogranodiorite sill
- 6. Ditto, porphyritic granodiorite
- 7. J1-2 andesitic volcanics

Figure 7.43. Glacier Gulch Mo deposit, Hudson Bay Mountain near Smithers, British Columbia. Example of a multiphase Mo stockwork mainly in older granitoids, in roof of an inconspicuous rhyolite porphyry plug. Much of the deposit is under a small alpine glacier. From LITHOTHEQUE No. 1129, modified after Atkinson (1995)



- M. Cr1 zone of quartz-molybdenite sheeted veins and stockwork
- F+2. Brittle fault partly intruded by Eo-Mi post-ore basalt dike
- 1. Q glacial sediments cover
- A1. K-feldspar veinlet alteration
- A2. Sericitic vein selvages
- 3. Cr porphyry dikes
- 4. J3-Cr1 biotite granodiorite & monzogranite

Figure 7.44. Endako, British Columbia, example of a fault-controlled zone of sheeted quartz-molybdenite veins grading to "linear stockwork". From LITHOTHEQUE No. 803, modified after Kimura et al. (1976)



- MW. Oxidation zone and leached capping with ferrimolybdenite
- 2. OI3 post-ore granite, rhyolite
- MA. 33-24 Ma, three overlapping shells of Mo stockwork around successive porphyry intrusions
- A. High silica zone and quartz-topaz alteration changes to sericitization
- 3. Aplitic porphyry, intramineral dikes
- 4. High Si rhyolite & biotite porphyry
- 5. Eo quartz monzonite porphyry sills
- 6. Cb2 arkosic sandstone, conglomerate
- 7+8. Pp biotite schist, gneiss

Figure 7.45. Climax Mo deposit, Fremont Pass, Colorado, a multiphase stockwork-Mo "super-giant". Cross-section from LITHOTHEQUE No. 651, modified after Wallace et al (1968), White et al. (1981) and AMAX Inc. on-site information, 1976

alkaline association of trachyte, syenite, and sometimes feldspathoidal rocks in fully evolved rift systems (next paragraph and Chapter 12).

The Climax-type parent intrusions form small stocks or cupolas believed to be the most fractionated, volatiles-enriched protuberances "on the back" of larger, deeper plutons, and they often come as sets of multiple intrusions. Intrusion and hydrothermal breccias are common. Other complexes are fault-controlled and have an elongated, sheet-like form, or are a swarm of parallel or anastomosing dikes. Some intrusions still preserve remnants of comagmatic volcanics as in Questa, New Mexico, believed controlled by a caldera margin fault. The stock apexes tend to be silicified and enriched in fluorite and topaz (greisen alteration) and this persists into the roof rocks, changing into K-feldspar, biotite and sericite-pyrite alteration. Stockworks of quartz, molybdenite, pyrite veinlets or hairthin sulfide veinlets without quartz are superimposed. Leached cappings over porphyry Mo, when developed, resemble those over porphyry-Cu but tend to be less ferruginous. Oxidation zones are indistinct, marked by yellow ferrimolybdate coatings, but none form economic orebodies in their own right. Secondary sulfides do not exist.

The Climax-type systems, although attributed to the "rift environment" by Carten et al. (1993), have still more affinities to the andean-type margins than to the East Africa-type rifts; perhaps the term "proto-rift" would be more appropriate to transitional situations that fill the void between subduction termination and the onset of extension, as on the still thick Precambrian continental crust (50 km crustal thickness in the Climax-Henderson area). Bookstrom (1981) attributed this transition to the subduction rollback or slab foundering, accompanied by melt generation in the lower crust.

Climax Mo deposit in Colorado (Wallace, 1995; P+Rc 1,125 Mt @ 0.24% Mo, 0.025% W for 2.7 Mt Mo, 281 kt W [calculated]) is the first porphyry Mo deposit discovered, developed and studied; the largest Mo "super-giant"; and type locality (Fig. 7.45). Located at the altitude of more than 3,000 m in the Colorado Rocky Mountains north of Leadville, it had been first staked in 1879 as a graphite prospect. Production started in 1918 as a delayed response to the sudden World War 1 demand for molybdenum needed for armour steel, but the demand soon subsided. It was not until the World War 2 years when the mine assumed full-scale production. Although not yet exhausted,

Climax has gone through several stop and go cycles recently, caused by fluctuating demand and environmental problems.

The Climax deposit is a complex of three coaxial Oligocene (33-24 Ma) intrusions of granite and rhyolite porphyry, emplaced into Paleoproterozoic biotite gneiss and Mesoproterozoic quartz monzonite basement. The intrusions are arranged in such a way that each progressively younger phase was emplaced at a lower level into the roof of an older intrusion. Porphyry dikes corresponding to each phase as well as the mineralization and alteration are in the roof area above each intrusive phase. There are two separate, arcuate, annular ore shells over the apex of the two lower (younger) intrusive stocks, and an erosional remnant of a third (upper) shell. Taken together, these orebodies form an inverted hollow cone with upper and lower diameters of 1,400 and 750 m, respectively, and a height of about 450 m.

An orebody is composed of a stockwork of crisscrossing quartz, molybdenite and pyrite veinlets less than 3 mm thick changing to hairthin fractures filled by molybdenite-only, in silicified and K-feldspar altered porphyry. Quartz, sericite and pyrite alteration marks the outer fringe and there is a thoroughly silicified ("metasomatic quartzite") core in each stock, grading to quartz-topaz greisen. Each Mo orebody is accompanied by a tungsten zone located above, from which the by-product hübnerite and minor cassiterite are recovered. In the pre-Quaternary oxidation zone ferrimolybdate, Mo-"limonite" and Mo-jarosite substitute for molybdenite, without a marked enrichment or impoverishment in Mo.

Henderson-Urad twin deposit, Colorado (White et al., 1981; Wallace, 1995; Rc 727 Mt @ 0.171% Mo for 1.243 Mt Mo) is the second largest Climax-type Mo system preserved on flanks (the small, outcropping Urad deposit) and inside (Henderson) Red Mountain, near Berthoud Pass on fringe of the Colorado Mineral Belt. Twelve non-venting stocks of Oligocene high silica and fluorine rhyolite intrude older porphyry phases which, in turn, are emplaced into the Mesoproterozoic (1.4 Ga) anorogenic granite. The molybdenite orebody is a composite of three overlapping ore shells related to the productive porphyry stocks. Molybdenite, in a stockwork of high-temperature hydrothermal veinlets is the only major ore mineral.

Alteration and metal zoning in the Climax-type deposits is not so well developed and predictable as in porphyry coppers. In the Henderson system (Seedorf and Einaudi, 2004), which is entirely

concealed so it had evolved as an almost closed magmatic-hydrothermal system, the high-temperature mineralization-alteration assemblages (quartz-fluorite and quartz, K-feldspar, molybdenite, some magnetite) formed in multiple cycles near the apex of several Oligocene rhyolite stocks. The same fluids continued upward to produce sericitic assemblage with pyrite, local topaz, magnetite and elevated tungsten values with rare wolframite. This zone grades, in turn, into an intermediate argillic assemblage (pyrite, clay, spessartite garnet, rhodochrosite) with minor sphalerite and galena occurrences. The lower-temperature alteration envelope had formed during a single cycle and Seedorff and Einaudi (2004a, b) found no evidence for convective circulation of fluid, nor redeposition, of the earlier ores.

The third largest porphyry-Mo mineralized system in the Colorado Rocky Mountains, concealed inside **Mount Emmons** near the Crested Butte ski resort, has been discovered after 1970 in the course of mining and exploration for small Pb-Zn sulfide veins (Thomas and Galey, 1982; Rv 141 Mt @ 0.264 Mo, for 372 kt Mo in the Mt. Emmons deposit only). The three Climax-type stockwork Mo orebodies are controlled by cupolas of Miocene (18 Ma) rhyolite porphyry and hornfelsed roof rocks. Only in the middle of the drill-proving campaign it was found that the blind orebodies were indicated by ore fragments found in an outcropping breccia pipe above the Redwell porphyry stock, and by high-grade Mo material present on the dump of a small Keystone Pb-Zn mine (Rostad, 1991). The ore discovery has been followed by a period of Mo oversupply and low prices and, most recently, by environmental objections so the deposit has not been developed.

7.4.3. Stockwork Mo in the alkaline "rift" association

This small population of deposits includes two "giants": Malmbjerg in Greenland and Nørkli in the Oslo Rift, Norway. Except for their broad geotectonic setting, these deposits correspond closely to the "Climax-type". The 25.7 Ma Malmbjerg deposit in east-central coastal Greenland has been recently dated by Brooks et al., 2004 (181 Mt @ 0.15% Mo for 271,500 t Mo). This is the largest of three Mo deposits near the Paleogene multistage Werner Bjerger alkaline complex composed of alkali gabbros, syenites, granite and remnants of feldspar porphyry roof. The small 25.8 Ma granite, aplite and feldspar porphyry stock is, however, not directly related. Molybdenite occurs

in a fracture stockwork that envelopes the intrusion apex, and disseminated in flat-lying greisen veins.

7.4.4. Precambrian stockwork Mo "giants"

There are three significant variously deformed and metamorphosed stockwork molybdenite deposits in Precambrian greenstone belts comparable, in many respects, with the young porphyry molybdenum systems. Lobash is in Mesoproterozoic potassic granite emplaced into Archean greenstone, hence there is no genetic association with the greenstones. The deposit has some resemblance to the Climax-type, or even more to the young fractionated granitic intrusions emplaced into older basements, like Quartz Lake-Mo, Alaska. Archean Coppin Gap and Setting Net Lake are close to the Phanerozoic granodiorite-quartz porphyry-Mo subclass.

The "giant" Mo stockwork **Lobash** in Russian Karelia (130 kt Mo content @ 0.06-0.09 % Mo; Pokalov and Semenova, 1993) is predominantly hosted in Archean greenstone meta-volcanics, but is genetically related to the apex of a Mesoproterozoic post-orogenic K-alkaline biotite granite. The interstratified amphibolite facies metamorphosed andesite, dacite and basalt are intruded by dikes of rhyolite porphyry. The granite cupola has muscovite-altered (greisenized) endocontact and biotite-altered, previously thermally metamorphosed exocontact. The orebody is an elongated stockwork of quartz, molybdenite, pyrite, pyrrhotite, magnetite and minor chalcopyrite, 90% of which is in the metavolcanics. The best mineralization is 100 m above the granite contact. The orebody has an assay boundary and broad Mo halo exists outside the cutoff grade of 0.03% Mo. The 1.7-1.5 granite and Mo age are attributed to the Karelian tectonomagmatic activation.

The "near giant" **Coppin Gap** deposit in the Pilbara Province of NW Australia comes close (Barley, 1982; Jones, 1990; 107 kt Mo @ 0.105%, 155 kt Cu @ 0.152%). It is a blind orebody composed of several generations of gray quartz with molybdenite selvages, and pyrite, chalcopyrite disseminations along fractures in strongly silicified and sericitized Archean meta-basalt, intrusive dacite porphyry and granodiorite. This 2.98 Ga mineralization is believed associated with injections of late-orogenic calc-alkaline magmas into deformed and thermally indurated meta-volcanics above a high-level apophysis of a buried granite batholith.

The last "large" deposit in this category is **Setting Net Lake** in NW Ontario (Ayres et al., 1982; 48,980 t Mo @ 0.054% Mo). This is a 2,500

m long zone of closely spaced quartz-molybdenite veinlets in weakly sericitized Archean (2.643 Ma) porphyritic granodiorite stock intruded into greenstone metabasalt and metasediments.

7.4.5. Mo-dominated skarn deposits

As with the porphyry-Cu systems, mineralized exoskarns form when carbonate and some non-carbonate replaceable wallrocks are present; this applies to the porphyry-Mo as well. Even so, deposits that include Mo skarns are quite rare (Einaudi et al., 1981, tabulated 11 localities), but three "Mo giants" with at least a portion of Mo in skarn, can be identified: they are Rossland-Red Mountain, British Columbia (Dawson et al., 1991; Rc 187 Mt @ 0.1% Mo), Cannivan Gulch, or Mountain, Idaho (Einaudi et al., 1981; 185 Mt @ 0.096% Mo); Pine Nut, Nevada (Einaudi et al., 1981; 181 Mt @ 0.06% Mo). Exoskarns associated with Mo accumulations do not appreciably differ from other skarns, and could be both calcic and magnesian, oxidized or reduced. At Cannivan (Einaudi, 1981) the magnesian skarn formed in dolomite and it has prograde forsterite (Mg-olivine) and tremolite, retrograde serpentinite. Molybdenite veinlets occur both in the late Cretaceous granite endocontact, as well as in the skarn, with magnetite, pyrite and minor chalcopyrite. At the Red Mountain deposit near Rossland the skarn and adjacent contact hornfels formed after pelites provided brittly fractured wallrocks, healed by quartz, molybdenite, pyrite, minor chalcopyrite fracture stockwork.

Brief descriptions of Mo-stockwork and skarn "giants" in Cordilleran setting

These descriptions follows format established earlier for porphyry coppers (p. 37) and the numbered localities are plotted in Fig. 7.45. Mo accumulations in porphyry Cu-Mo deposits, even when Mo is the "giant" accumulation, are assembled in Table 7.7 and Fig. 7.30. All localities have the rank of a "deposit" unless indicated otherwise. CL=Climax-type; MZ=monzogranite type; ALK=alkalic. All ores are hypogene, ST mineralogy is quartz, molybdenite, pyrite.

1. **Quartz Hill**, Alaska * MZ to CL fracture stockw in porphyry apex * ST miner + magnetite * K-silicates, silicif. * 30 Ma peraluminous leucogranite & rhyolite porph stock * PZ-MZ metamorphics * Rc 1.584 bt @ 0.0762% Mo for 1.207 mt Mo * Nokleberg et al. (1995), Ashleman et al. (1997).
2. **Alice Arm** ore field, B.C. (includes Kitsault, Ajax and Roundy Creek deposits) * MZ, ring-shaped stockw around porph stock * ST miner, fringe Pb-Zn

- veins * K-silic envel by sericite * 55-49 Ma diorite to qz monzonite stock * J hornfelsed graywacke, shale * 125 MT @ 0.115% Mo for 144 kt Mo in Kitsault, 201 mt @ 0.006% Mo in Ajax for 120 kt Mo * Hodgson (1995).
3. **Red Mountain, Big Salmon Range**, S-C Yukon * MZ, multistage vein, stockw, breccias * ST miner * zoned K-feldspar, sericite, propyl alter * Cr qz monzon porph, breccias * PZ-MZ cataclastic rocks * 187 mt @ 0.1% Mo for 187 kt Mo * Brown & Kahlert (1995).
4. **Adanac (Ruby Creek)**, Atlin, B.C. * MZ, stockw in ring peripheral to cupola * ST multiphase miner * K-silic, sericite, silicif * 72-70 Ma qz monzonite * Cr3 older qz monzonite phases * 152 Mt @ 0.063% Mo for 96 kt Mo * Pinsent & Christopher (1995).
5. **Logtung**, north-central B.C. * MZ multistage fracture stockwork and veins * quartz, molybdoscheelite, moly, scheelite, arsenop, fluorite * K-silicate, skarn * 118 Ma monzodiorite stock * PZ-MZ meta-clastics, reaction skarn * 230 mt @ 0.03% Mo, 0.083% W for 191 kt W, 69 kt Mo * Noble et al. (1995).
6. **Hudson Bay Mt (Glacier Gulch)**, Smithers, B.C. * MZ to CL fract stockw in roof of rhyolite plug & breccia * ST, minor scheelite * silicif overprint K-silicates * 63 Ma qz porphyry plug emplaced to early granod sheet * J hornfelsed andesite, Cr clastics * 92 mt @ 0.178% Mo, 0.05% W for 164 kt Mo * Atkinson (1995).
7. **Endako ore field**, B.C. * MZ, zone of sheeted quartz veins with moly on selvages * ST miner * quartz-sericite overprint early K-silic * 138 Ma qz monzonite, qz-feldsp porph dikes * earlier granodiorite * 308 mt @ 0.084% Mo for 292 kt Mo * Bysouth & Wong (1995).
8. **Rossland (Red Mountain)**, south-central B.C. * MZ fract stockw * ST miner * silicif, retrogr skarn * J1 granodior * Tr-J hornfelsed andesite, clastics * 187 mt @ 0.1% Mo for 187 kt Mo * Dawson et al. (1992).
9. **Mount Tolman** (Keller), N-C Washington * MZ zoned multiphase fract stockw & veins * ST, late stage Cu, Pb, Zn sulfide veins * K-silic to propyl, overprinted by sericite * 52-57 Ma miner in 61-55 Ma biot granite to granodior * Or-Cb hornfelsed clastics * 2.18 bt @ 0.056% Mo for 1.216 mt Mo * Lasmanis (1995),
10. **Big Ben**, Little Belt Mts., Montana * CL, stockw * ST miner * K-silic, silicif * 51-50 Ma synvolc. high-Si rhyolite porph * Eo acid volc * 376 mt @ 0.1% Mo for 376 kt Mo * Carten et al. (1993)
11. **Cannivan**, W Montana * MZ, stockw & exoskarn * ST miner + chalcopyrite * K-silic, silicif, retroskarn * 64-61 Ma biot qz monzonite * Cm dolom, Mg-skarn * 185 mt @ 0.096% Mo for 178 kt Mo * Carten et al. (1993), Einaudi et al. (1981).

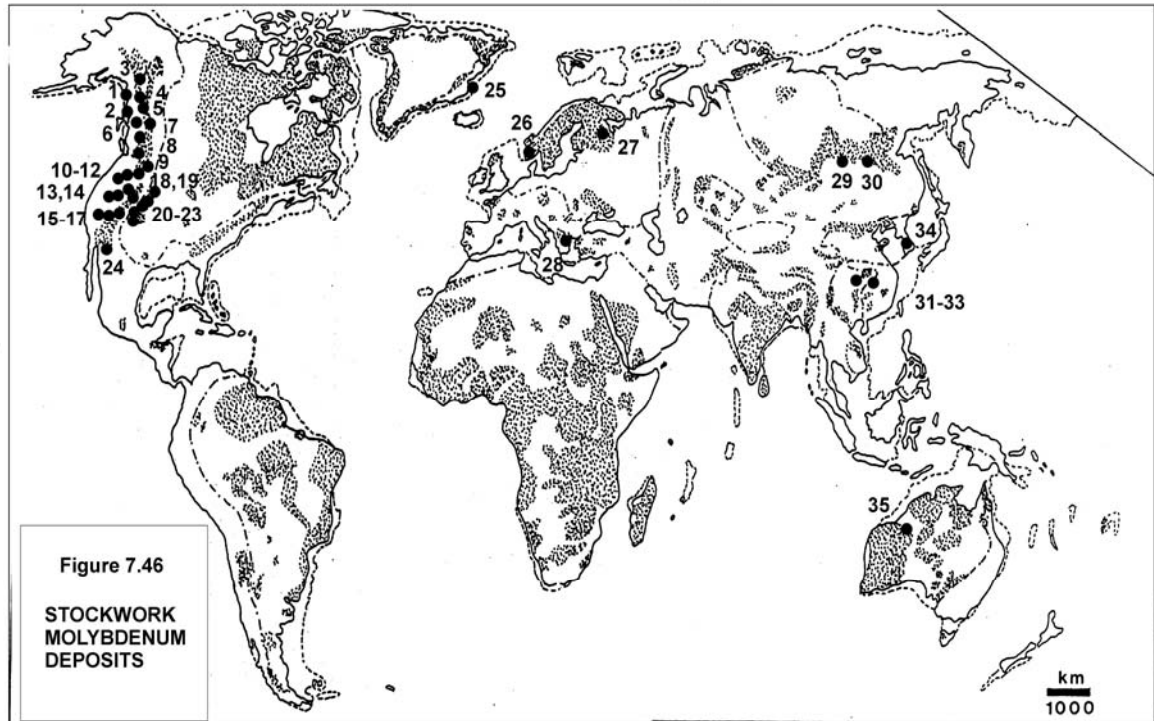


Figure 7.46. Worldwide distribution of the "giant" and "super-giant" stockwork Mo deposits

12. **Thompson Creek**, Idaho * MZ tabular to hood-like stockw * ST miner * K-silic, silicif * 88 Ma biot granite to qz monzon * Cb1 hornfelsed black argillite * 300 mt @ 0.108% Mo for 324 kt Mo * Schmidt et al. (1991).
13. **Cumo**, Idaho * MZ, stockw in granite * ST mine * K-silic, silicif * 52-45 Ma monzogranite porph * older granitoids * 1.258 bt @ 0.059% Mo, 0.074% Cu for 742 kt Mo * Carten et al. (1993).
14. **Pine Nut**, Nevada * MZ, Mo stockwork * ST miner * K-silic, silicif * T1? qz monzonite porph * 181 mt @ 0.06% Mo for 109 kt Mo; Carten et al. (1993).
15. **Buckingham**, Battle Mt. district, Nevada * MZ, stockwork * ST miner, fringe Pb-Zn-Ag veins * K-silicate, sericite, silicif * 86 Ma monzogranite porph * Cm3 hornfelsed sediments * 1.3 bt * 0.06% Mo for 742 kt Mo * Theodore et al. (1992).
16. **Mount Hope**, Nevada * CL, stockw in two stacked shells * ST miner * K-silicate, silicif * 38 Ma high-Si rhyol. aplite, granite porph * Or hornfelsed clastics, carbonates * 451 mt @ 0.09% Mo for 510 kt Mo * Westra & Riedell (1996).
17. **Hall** (Nevada Moly), Nevada * MZ, stockw. in cylinder around porph stock * ST miner, Pb-Ag veins on fringe * zoned K-silic, seric, silicif, topaz * 23 Ma rhyol porph plug * Cm hornfelsed clastics, marble * 200 mt @ 0.091% Mo for 180 kt Mo * Shaver (1986).
18. **Pine Grove**, Wah Wah Mts, SW Utah * CL, dissem to stockw Mo emplaced to vent * qtz, moly, topaz, fluorite > hübnerite * silicif, K-silic, argilliz * 23-22 Ma qz porphyry * Ol-Mi ash-flow tuff, trachyandes flows, PCm & Cm quartzite, shale * 125 mt @ 0.17% Mo for 212 kt Mo * Keith et al. (1986).
19. **Rico (Silver Creek)** Colorado * CL, stockw in apex of porphyry stock >> skarn * ST + Pb-Zn replac on fringe * K-silic, silicif * 3.9-3.4 Ma alaskite porph stock * D-Cb1 limest, Pt granitoids, greenst * 40 mt @ 0.31% Mo for 124 kt Mo (Rc 682 kt Mo) * Naeser et al. (1980).
20. **Henderson-Urad (Red Mountain)** ore field, Colorado * CL; Henderson is buried set of 3 overlapping stockw zones above multiple non-venting stocks * ST miner, Pb-Zn-Ag veins on fringe * K-silic, silicif * 28 Ma high-Si rhyol porph * 727 mt @ 0.171% Mo for 1.243 mt Mo * Seedorf & Einaudi (2004).
21. **Climax**, Tenmile Range, Colorado * CL, 3 coalescing shells of stockw above cupolas * ST miner + wolfr. * silicif, K-silic, sericite * 30 Ma ore, 33-24 Ma high-Si rhyol porph * 907 mt @ 0.24% Mo for 2.7 mt Mo * Wallace (1995).
22. **Mt. Emmons-Redwell Basin** ore field, Colorado * CL, 3 buried orebodies, stock in cupola roof, breccia pipes * ST + hübnerite, fluorite, Pb-Zn veins on fringe * K-feldsp, silicif, seric * 18 Ma high-Si rhyol

- porph * hornfels * 141 mt @ 0.264% Mo for 372 kt Mo * Thomas & Galey (1982).
23. **Questa**, New Mexico * CL, stockw at linear to arcuate contact * ST miner * K-silic, silicif, seric * 25-24 Ma biot leucogranite, aplite, rhyol porph * T2 volcanics, Pt gneiss, pegmat * 277 mt @ 0.144% Mo for 400 kt Mo * Johnson et al. (1990).
 24. **El Creston (Opodepe)**, Sonora, N Mexico * MZ, Mo stockw * ST miner * silicif, K-silic * 181 mt @ 0.06% Mo for 109 kt Mo * Carten et al. (1993).
 25. **Malmbjerg**, Werner Bjerge, E Greenland * ALK, stockw above porph stock * ST, Pb-Zn veins on fringe * silicif, K-silic * 26 Ma high-Si rhyol, trachyte, feldsp & syenite porph * Cb hornfelsed sedim * 181 mt @ 0.15% Mo for 271 kt Mo * Gleadow & Brooks (1979); Brooks et al. (2004)
 26. **Nordli**, Hurdal, Oslo Rift, Norway * ALK, stockw & breccia in cupola * ST miner * K-silic, silicif * 280-247 Ma high-Si rhyolite * 181 mt @ 0.084% Mo for 152 kt Mo * Pedersen (1986).
 27. **Lobash**, Karelia, NW Russia * MZ, linear Mo stockw in hornfelsed greenst above granite stock * ST miner + >magnetite, scheelite * silicif, K-silic, seric * Pp rhyol porph on top of granite * Ar greenstones * Rc 230 kt Mo @ 0.063% + 0.01-1.4% W, 1-10 g/t Au * Pokalov & Semenova (1993).
 28. **Mačkatica-Surdulica** ore field, Serbia * MZ, pipe-like stockw * ST miner * silicif, seric * 40-36 Ma dacite porph * Eo granodior, PZ gneiss, schist * 181 mt @ 0.078% Mo for 141 kt Mo * Janković (1982).
 29. **Sora (Sorskoye)**, Kuznetsk Alatau, Russia * MZ, stockw and dissem in breccia, veins * quartz, moly, chalcop, fluorite * K-feldspar, albite * 335-318 Ma qz feldsp porph, breccias, granosyenite * D diorite, Mp, Cm mafic metavolc, metasedim * ?120 kt Mo * Sotnikov & Berzina (1968).
 30. **Zhireken**, E. Transbaikalia, Russia * MZ stockw to qz veins in stock exocont * ST miner, minor chalcopyrite, wolfr * K-silic, silicif * J3 granite porph * J2 granodior, PZ granite bathol * ?150 kt Mo * Pokalov (1974); Sotnikov et al. (1977).
 31. **Jinduicheng**, E. Qinling belt, China * MZ to CL stockw in roof of porph stock * ST miner + fluorite silicif, K-silic * 124 Ma monzogranite porph * Pt biot. hornfels after spilite * 907 mt @ 0.1% Mo for 907 kt Mo * Nie (1994).
 32. **Nannihu-Sandaozhuang ore field**, E. Qinling belt, China * MZ, stockw Mo in hornfels, W-Mo skarn * multistage, ST + hubnerite, scheelite * K-silic, retrogr. skarn, silicif * J-Cr monzogranite, leucogranite * Np marble, skarn, biot hornfels * ?1 mt Mo+ * Ren et al. (1995).
 33. **Luanchuan County Mo district**, E. Qinling belt: other deposits, Henan, China * MZ, stockw in hornfels + skarn * ST + hubnerite, scheelite * K-silic, retrogr. skarn, silicif * J-Cr monzogran, granite porph * Np mafic metavolc, metaseds, hornfelsed * X00 kt Mo * Nie (1994), Ren et al. (1995).
 34. **Yongwol**, South Korea * MZ, Mo stockwork * ST miner * silicif, K-silic * T monzogran porph * 192 kt Mo @ 0.24% Mo.

35. **Coppin's Gap**, Pilbara, Western Australia * MZ stockwork to veins, metamorphosed * quartz, moly, pyrite, chalcop * silicif, sericite * 2.98 Ga ore, 3.06 Ga plagiocl porph., granodior * Ar greenstone metavolc * 145 mt @ 0.15% Cu, 0.09% Mo for 130 kt Mo * Barley (1982).

7.5. Stockwork, vein and skarn Mo-W-Bi

This is a small group of little known deposits which, however, includes at least five "giant" and several "large" deposits of Mo, and/or W, and/or Bi. All these deposits produce or contain molybdenum, but only in Koktenkol' (430 kt Mo) and probably Nannihu-Sandaozhuang, is molybdenum the principal metal recovered; elsewhere Mo is a by-product of tungsten mining, although it's content could still be of the "giant" magnitude.

These deposits are transitional in all respects. In terms of geotectonics, some clearly correlate with active subduction in an andean-type margin (Logtung in British Columbia). This is less clear in Central Kazakhstan, which is the type area of the magmatic-hydrothermal Mo-W deposits that store at least 1,250 kt W, 650 kt Mo, 250 kt Bi and 20 kt Be in at least seven "giant" and "large" deposits (not necessarily economically mineable in the 2000s). These deposits, of late Carboniferous to lower Permian age, are associated with leucogranites which Heinhorst et al. (1996) attributed to crustal melting resulting from "internal collision", followed by extension. Serykh (1996), in the same volume but writing on behalf of the indigenous Russian school, distinguishes between the 1) "synorogenic" (corresponding to syn-subduction) calc-alkaline magmatic series of lower-middle Carboniferous quartz diorite, granodiorite and quartz monzonite associated with the numerous porphyry Cu-Mo deposits like Kounrad/Qonyrat, and 2) its late, metaluminous (magnetitic) leucogranitic differentiates followed by a separate postorogenic series of "alaskite" (=high-silica alkali rhyolite) of mainly lower Permian age. According to Serykh (1996) the W-Mo deposits are associated with the older suite of calc-alkaline leucogranites, whereas the later alaskites remain virtually barren.

There is almost no tin associated with the leucogranite-related Central Kazakh deposits which Serykh (1996) attributed, as would Keith and Swan (1996), to the reducing nature of the Sn-bearing systems. In Kazakhstan, granite-related "large" Sn deposits appear on the fringe, near Kokchetav (Kokshetau) and in the Kalba Mountains. Sn and W, however, accumulate jointly in the predominantly peraluminous systems attributed to

intracontinental collisions as in Cornwall, the Erzgebirge, SE Asian tin belt and the Lachlan Foldbelt (Chapter 10).

The Mo-W deposits are also transitional in style: they range from swarms of subparallel (sheeted) veins controlled by fault zones (Boguty) to greisen-rimmed vein swarms in, above and around small leucogranite cupolas (Verknee Kairakty/Qairaqty) to thin fracture networks or disseminations in greisenized or silicified hosts. The alteration ranges from potassic (K-feldspar > biotite), muscovite ("mica-greisen"), quartz-topaz greisen, to prevalent silicification and skarn alteration in carbonates. The ore minerals are predominantly wolframite and/or scheelite with molybdenite and the orebodies tend to have high Bi content, sometimes also Be, Cu, Ag. When carbonates are present in the exocontact, mineralized skarns form readily. If so, W and Mo tend to develop contrasting orebodies in the same deposit or ore field, although transitions are common. W in scheelite most often precipitates in the garnet-clinopyroxene exoskarn, whereas molybdenite prefers filling, with quartz, brittle fracture stockworks in granitoids, hornfelsed roof meta-pelites or brittly fractured exoskarns. The mineralized skarns are of the high-level (epizonal), oxidized variety; similar skarns in the "super-giant" Shizhuyuan W, Bi, Mo, Be deposit in Hunan are in the centre of a metal-zoned polymetallic ore field (Chapter 10).

Verknee Kairakty/Qairaqty is the largest W-Mo-Bi deposit in Central Kazakhstan (Russsikh and Shatov, 1996; ~900 mt ore @ 0.102% W, 0.024 % Bi, 0.004% Mo for 880 kt W, 216 kt Bi, 36 kt Mo, 880 t Te). It is located in greenschist-metamorphosed Siluro-Devonian terrigenous turbidites, intruded by buried late Carboniferous biotite granite pluton in depth. There are several leucogranite cupolas under and near the ore field, but at least 500 m under the present erosional level. The roof above cupolas is thermally metamorphosed (cordierite hornfels in depth grading to biotite-plagioclase hornfels higher up) and hydrothermally altered by biotite, quartz, fluorite. This is overprinted by fault-controlled quartz, muscovite > fluorite, topaz, green biotite, pyrite greisen in the ore zone. The ore deposit has a 2.3 x 1.7 km large elliptical outline with a narrower, tabular orebody tapering with depth. This contains stockwork of fracture veinlets grading to veins and composed of quartz, K-feldspar, muscovite, scheelite, pyrite and lesser wolframite, fluorite, chalcopyrite, Bi sulfides and tellurides. The formation temperatures ranged from 415° to 180° C. There is a 5-40 m thick clay-sericite leached

capping grading to oxidation zone with tungstite, ferrimolybdenite and other minerals. Despite the presence of several rare minerals (e.g. creedite), the oxidation zone is uneconomic.

The nearby **Koktenkol'** deposit contains more Mo than W and a significant portion of the resource is in residual clay in the oxidation zone (Mazurov, 1996; 605 mt @ 0.071% Mo, 0.025% W for 430 kt Mo, 151 kt W, 253 kt Cu, Bi). The deposit is yet to be developed. The host rocks are Upper Devonian andesitic to rhyolitic volcanics, pyroclastics and volcanoclastics with limestone on top. These are intruded by three leucogranite cupolas rooted in an Upper Carboniferous biotite granite pluton. The roof rocks are thermally and hydrothermally metamorphosed. Alteration biotite and K-feldspar veinlets are in the silicate rocks, the carbonate is recrystallized to marble and converted to garnet, vesuvianite, bustamite and wollastonite exoskarn. The bulk of Mo is in a multistage fracture stockwork of quartz, K-feldspar, muscovite, molybdenite, pyrite, wolframite, Bi-sulfides veinlets; scheelite replaces and fills fractures in the skarn. The post-Triassic humid regolith contains substantial tungsten resource in an up to 220 m thick clay zone, thickest where it tops the karsted carbonate and skarn. W is bound in clays, in dispersed tungstite, and residual scheelite.

Akchatau/Aqshatau, the first major tungsten deposit discovered in Central Kazakhstan, also contains a recent reserve of 16 kt Be in addition to 52.4 kt W and 17.5 kt Mo, in a system of more than 300 greisen veins (Beskin et al., 1996). It is probably a "W-giant" as it has been in production since the late 1940s, but the past production figure is not available.

Leaving Kazakhstan for China, the "super-large" **Nannihu-Sandaozhuang** ore field is in the Eastern Qinling porphyry Mo province in Shaanxi, north-central China (Ren et al., 1995). This province supplies the bulk of Chinese Mo and it is said that in terms of resources it rivals the Colorado Rockies metallogene. The ore field consists of stocks of Jurassic-Cretaceous granite porphyry emplaced into Neoproterozoic meta-sedimentary rocks. The Nannihu orebody is a 2,400 m long, 144 m thick tabular stockwork of quartz, feldspar, muscovite, molybdenite, magnetite and fluorite in porphyry apex, in hornfelsed clastics, and in Ca-Mg silicate hornfels. The Sandaozhuang orebody is an early andradite, diopside, wollastonite exoskarn, retrograded to amphibole, epidote, chlorite hydrous skarn, and subsequently veined and replaced by

pyrite, pyrrhotite, magnetite, fluorite, scheelite and molybdenite.

Tyrnyauz-W, Mo ore field used to be the largest Soviet tungsten producer, discovered in 1934 and in operation since 1940 (Kurdyukov, 1980; ?300 kt W, ?80 kt Mo, ?5 kt Bi). It is located in the Caucasus Front Range, Russia, and belongs to the complex association of scheelite skarn with Mo values (~77%), and stockwork/disseminated molybdenite in biotite hornfels and granitoids. The folded and thrust-faulted Middle Paleozoic and Lower Jurassic hornfelsed litharenite, black slate and marble are intruded by Jurassic or older leucogranite, and they form a roof pendant above late Tertiary biotite granite. Most of the tabular and lenticular scheelite skarn orebodies occur along the marble/hornfels contact. Apparently, several mineralization ages are represented, ranging from Devonian through Jurassic to Tertiary.

Mount Pleasant ore field in southern New Brunswick, Atlantic Canada, is in the Appalachian orogen (Sinclair, 1994; Dagger, 1972; Fig. 7.47). It has several ore zones of contrasting style and composition storing about 60 kt W @ 0.2% W, 30 kt Mo @ 0.1%, 30 kt Bi @ 0.1%, plus 50 kt Sn in one zone making it a "Bi-giant". There is also a resource of ~90 t of indium and a by-product Zn, Pb and Cu. The ores are genetically associated with two high-level plugs of Lower Carboniferous quartz porphyry emplaced into comagmatic rhyodacite, latite and feldspar porphyry flows rich in basement rafts and xenoliths, attributed to a late Devonian caldera. The intrusions postdate a post-orogenic porphyritic granite pluton, in turn intruded into folded hornfelsed Ordovician to Silurian graywacke and slate. The early stage wolframite, molybdenite, bismuth, bismuthinite and other minerals form stockworks and disseminations in greisenized porphyry. They are followed by sulfides-rich (sphalerite, galena, chalcopyrite, arsenopyrite, tennantite, stannite) fracture veins, replacements and mineralized breccias with cassiterite, with abundant fluorite. The bulk of cassiterite is late, disseminated in endogreisen in porphyry and in veins in the exocontact.

Remaining Mo-W stockwork "giants": There are not many left, except possibly in China from where reliable information is hard to get. The **Riviera** prospect in Western Cape, South Africa is a "near-giant" with 46 mt @ 0.216% W, 0.02% Mo for 99.36 kt Q and 9.2 kt Mo (Rozendaal et al., 1994). It is a concealed greisen with pyrrhotite-rich endoskarn pods and veins with scheelite, molybdenite and pyrite. **Yangchuling** disseminated, veinlet and breccia W-Mo deposit in China (Yan et al., 1980) is probably of a "giant" magnitude. The ore is in

hornfelsed shale and sandstone in roof of a granodiorite porphyry stock. The **Xinglokang** "porphyry W-Mo" credited with 140 kt W @ 0.15%, is probably similar. The Diaodaban-Gulangxia district in the North Qilian metallogenic zone in Gansu has four "W-Pb-Zn deposits" supposedly storing 316 kt W (China Geological Survey brochure, 2004). The East Kounrad Mo>W deposit in Kazakhstan, adjacent to the Kounrad (Qonyrat) porphyry Cu, is probably a "Mo-giant" often mentioned in the Soviet literature from the 1970s (e.g. Pokalov, 1974). It is a system of quartz, molybdenite > wolframite veins grading to stockworks in ~302 Ma leucogranite sheets.

7.6. Scheelite skarn deposits

Before World War 2 the few scheelite skarns known were considered a curiosity, as tungsten demand was easily met from wolframite vein deposits in China, or largely by-product tungsten from tin-mining regions. The wartime strategic considerations, mostly in the United States but in the Soviet Union and the British Empire as well, contributed to accelerated exploration during which hundreds of small to medium size scheelite deposits found in the United States and elsewhere assured a temporary self-sufficiency in this metal. Throughout the 1960s and 1970s, with erratic tungsten supplies from China, the price of tungsten was good and more deposits had been found, worldwide. The present tungsten price and demand are low, hence there is little exploration. Although more than 1000 scheelite skarn occurrences are now known worldwide and they have a cumulative endowment of some 1 mt W, there are just four "scheelite-giants" (Mactung and Cantung, Canada; Sangdong, South Korea; King Island, Tasmania), unless Shizhuyuan and Tyrnyauz are counted (the latter is described in Section 7.5., the latter in Chapter 10). Of the four "giants" the Canadian deposits, located in the miogeoclinal domain of the north-eastern Cordillera, are in a convergent margin setting as are the numerous, but smaller, deposits in the United States' Cordillera.

Scheelite skarns (Einaudi et al., 1981; Newberry and Swanson, 1986; Ray and Webster, 1991; Meinert, 1993) are almost monometallic deposits, as except for small quantities of Mo (in powellite or molybdo-scheelite) and Cu (in chalcopyrite) no other by-product metals are recovered. They also stand isolated, lacking systematically associated deposits of other types and metals although many W-skarns occur in broadly defined gold provinces as in west-central Nevada (Osgood Mountains, close to the Getchell Carlin-type deposit), eastern Uzbekistan to Kyrgyzstan, and elsewhere. The "simple" scheelite skarns are relatively deep-seated, absent from the

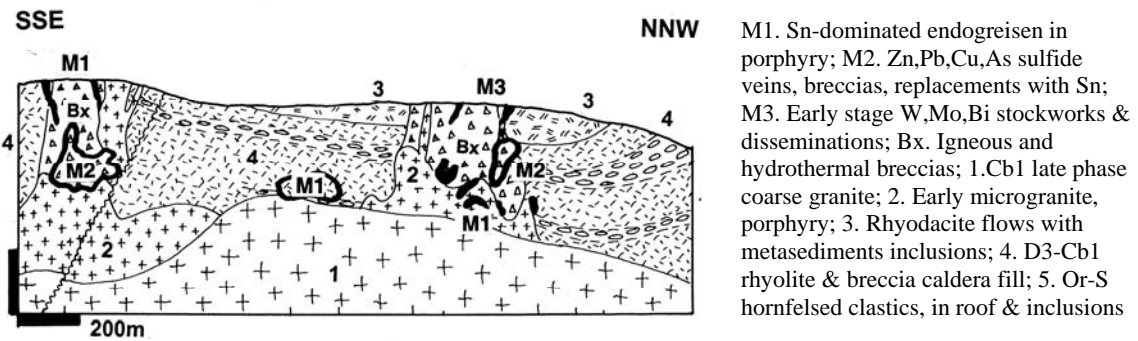


Figure 7.47. Mount Pleasant complex ore field, New Brunswick, Canada. From LITHOTHEQUE No. 126, modified after Dagger (1972), Koilman et al. (1986) and Sinclair (1994). Orebodies (from SSE to NNW): Fire Tower, Saddle, North Zone, projected on the line of section

"porphyry" group and instead associated with equigranular, mesozonal granitoids in the endocontact. The complex skarns, related to high-level granites in Sn-Pb-Zn ore fields as in Dongpo (Shizhouyuan deposit) and partly Dachang, are described in Chapter 10. The "simple" skarns are considered predominantly magmatic-hydrothermal, mesothermal, related to metaluminous to weakly peraluminous calc-alkaline granodiorite to biotite monzogranite, sometimes with an aplitic to pegmatitic fringe near the contact. They are intermediate between the systems with a greater mantle/oceanic component that produced Fe, Au, Cu and Zn skarns, and magmas generated within a thick, mature crust associated with Sn, Be and partly Mo skarns (Meinert, 1995). The magmatic-hydrothermal systems are more often reduced than oxidized.

The skarns are situated close to parent granitoids, either in the immediate exocontact directly adjacent to an intrusive pluton, stock or a dike, or some distance away ("distal skarn"). The latter have a dual control: a fault as a conduit of the ore-forming fluids, and a "favourable" host rock, most often a carbonate. Some skarn carbonate replacements are highly selective and pseudomorphically replace a single carbonate bed, resembling stratiform deposits. The "giant" Sangdong deposit in Korea was long considered "stratiform" as there was no parent intrusion in sight, until found in some depth under the orebody recently (Fletcher, 1984).

Scheelite skarns are located in thermally metamorphosed roof rocks above or laterally to intrusions and most replace calcic marbles and Ca-Mg silicate rocks, although some are in entirely silicate rocks. Carbonaceous rocks ("black" slate) are particularly favourable hosts to reduced skarns (Einaudi et al., 1981). Some exocontact rock mixtures such as ferruginous marls produce rocks

composed of the skarn minerals (that is, Ca-garnet and clinopyroxene) by isochemical thermal metamorphism alone (reaction skarn or skarnoid) but typical mineralized skarns are hydrothermal metasomatites. A standard profile of a contact skarn starts with endoskarn within the intrusion, that is equivalent to calcic alteration: K-feldspar is replaced by plagioclase, biotite by diopside and titanite (sphene), and there could be also present garnet, amphibole, quartz, chlorite, epidote, calcite and often some chalcopryrite. Prograde, higher temperature exoskarn (~500-400°C) has the standard garnet (almandine-rich in reduced skarns, andraditic in oxidized skarns) and clinopyroxene (diopside to hedenbergite) composition with or without vesuvianite, magnetite and pyrrhotite, and usually some amphibole or biotite ("hydrous skarn" of Bowman et al., 1985). This is bordered by recrystallized marble. The younger, superimposed and fracture-controlled retrograde skarn (retroskarn), when developed, consists of amphibole, epidote, albite, chlorite, calcite and other minerals.

In the tungsten ore, inconspicuous whitish scheelite occurs scattered in all skarn varieties, difficult to tell from feldspar, quartz or calcite without ultraviolet light (this is a standard ore evaluation technique underground but a bit awkward at surface, although night traverses have been performed). In reduced skarns scheelite is usually associated with pyrrhotite masses, stringers and disseminations. Invisible powellite (CaMoO_4), and frequently present chalcopryrite, also occur.

Cantung (Canada Tungsten; Bowman et al., 1985; Dawson et al., 1992; P+Rc 116 kt W @ ~1.2 % W; Fig. 7.48) is the only past producer in the 300 km long, NNW-trending arcuate belt of seven scheelite

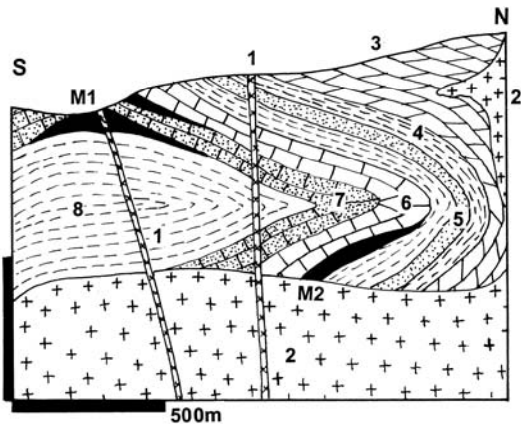


Figure 7.48. Cantung deposit, NWT, Canada. Cross-section from LITHOTHEQUE No.707, modified after Bowman et al. (1985) and Canada Tungsten Ltd. M. Disseminated scheelite in pyrrhotite-rich exoskarn, Pit Orebody (top left) and E-Zone (bottom); 1. Porphyry dikes; 2. 92-90 Ma biotite quartz monzonite; 3. Cm-D2 basal sequence: dolomite; 4. hornfelsed argillite; 5. metaquartzite; 6. marble; 7. Ca-Mg silicate hornfels; 8. Np phyllite & contact hornfels

skarn deposits in SE Yukon and adjacent Northwest Territories, in the Canadian Cordillera; the total resources of this belt are of the order of 400 to 600 kt W. Most of the exoskarns are located in Lower Cambrian limestones interbedded with argillite, carbonaceous argillite and quartzite, situated close to the shelf- to basin- transition in the Paleozoic Cordilleran miogeocline. This sedimentary sequence, that rests on thick Precambrian basement, is intruded by a string of small Middle to Late Cretaceous quartz monzonite plutons enveloped by a wide thermal aureole of hornfels, marble and locally skarn.

Cantung contains two outcropping and one buried scheelite skarn orebodies immediately adjacent to the 91.6 Ma old quartz monzonite contact with limestone and then following the limestone horizon above and below a screen of hornfelsed meta-argillite (Fig. 7.48), in a recumbent anticline. Scheelite is disseminated in pyrrhotite-rich portions of prograde proximal garnet-pyroxene and more distal amphibole, biotite skarn. The quartz monzonite stock has an extensive marginal facies of aplite and this rock also forms abundant dikes that intersect the orebodies and the thermally metamorphosed sedimentary rocks.

Mactung (Macmillan Pass Tungsten; Dick and Hodgson, 1982; Atkinson and Baker, 1986; Rv 32 Mt @ 0.736% W for 235 kt [or ?479 kt] of contained W) is the largest scheelite skarn in the Cordilleran belt, situated in an alpine tundra about 175 km NW of Cantung. The host rocks are

limestone beds in the Lower Cambrian sequence of alternating hornfelsed micaceous phyllite, slate and impure limestone. The 97.5 Ma old scheelite orebodies have a form of persistent, stratabound bands of exoskarn, replacing two limestone horizons some distance from the nearest granite. The main body of the Mactung biotite quartz monzonite stock (92.1 Ma), one apophysis of which intersects the ore zone, is not considered to be the source of the ore fluid; probably an earlier phase was. In the orebodies scheelite with abundant pyrrhotite and minor chalcopyrite with molybdenite are disseminated in almandine-rich garnet and pyroxene prograde skarn with a variable content of quartz and biotite. Quartz veins parallel to bedding or cleavage in hornfelsed meta-pelites have narrow quartz, muscovite and tourmaline envelopes and some scattered scheelite and molybdenite. Their contribution to the overall W resource is minimal.

Sangdong scheelite deposit in South Korea (Fletcher, 1984; Kwak, 1987; 120 kt W @ 0.56%, 10 kt Bi, 7 kt Mo) is an internationally known Korean deposit characterized, in the classical literature, as an epigenetic "distal skarn", or a "stratiform" (presumably exhalitic) tungsten mineralization. The principal ore zone is a narrow, 3.5-5 m thick and 1.5 km long horizon in a Lower Cambrian carbonate unit interbedded with hornfelsed shale and sandstone. The central unit in this horizon has a quartz, biotite, muscovite assemblage grading outward to hornblende-quartz, minor biotite, and ultimately to garnet-diopside skarn. The ore consists of closely spaced quartz-scheelite and quartz, scheelite, Bi, Mo, Cu sulfide veinlets in quartz-mica core, that grades 1.2-2.0 % W. This drops to 0.24-1.2 W in the hornblende-quartz zone, and to sub-economic values in the skarn. Deep drilling in the 1980s intersected an Upper Cretaceous (85-83 Ma) peraluminous granite stock enriched in W, Mo and Bi, 500 m under the ore horizon (Moon, 1989) and also a quartz-molybdenite stockwork (16 Mt @ 0.24% Mo for 38.4 kt Mo) 300 m below the scheelite orebody. This makes Sangdong comparable with the group of W-Mo ore systems described above.

Additional "giant" scheelite skarns: Other than Tyrnyauz described above and Shizhuyuan included in Chapter 10, the **Grassy (King Island, Dolphin)** ore field off NW Tasmania is the only example (Kwak and Tan, 1981; review in Solomon and Groves, 1994; ~14 mt @ 0.64% W for 105 kt W, 4.2 kt Mo; Fig. 7.49). There, Mo-rich scheelite is disseminated in several lenses of andradite-clinopyroxene and grossularite-calcite skarn controlled by two horizons of Cambrian limestone enclosed in

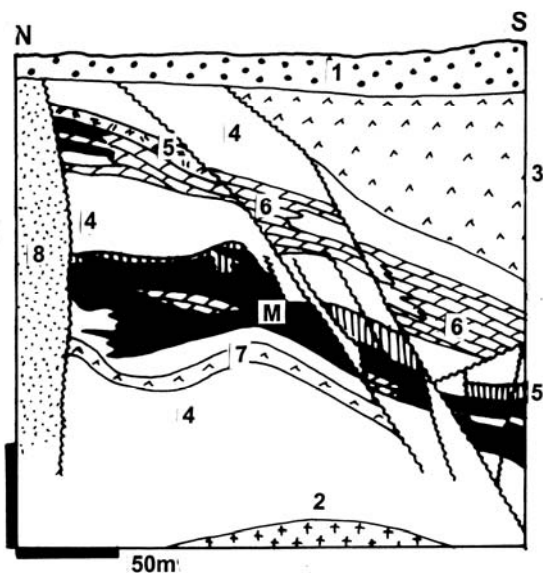


Figure 7.49. Dolphin (Grassy, King Island) scheelite deposit, Tasmania. Cross-section from LITHOTHEQUE No. 1321, modified after Geopeko Ltd. (1981). M. Cb1 disseminated scheelite with pyrrhotite in exoskarn; 1. Q cover sediments; 2. Cb1 granodiorite, adamellite; 3. Cm2 meta-komatiitic peridotite, basalt, diabase; 4. Hornfelsed metapelite; 5. Pyroxene-garnet hornfels; 6. Marble to silicate marble; 7. Cm Lower Volcanics meta-komatiite, basalt; 8. Np quartzite

hornfelsed shale and meta-spilite. Lower Carboniferous quartz monzonite stock is the source intrusion. The almost total pseudomorphic replacement of the limestone band by skarn was the reason for frequent placement of this deposit into the stratiform family, in the 1970s.

The largest United States' scheelite skarn field near **Pine Creek** in the Sierra Nevada contained about 16 mt @ 0.48% W and 0.15% Mo for ~80 kt W. It was in rafts of marble embedded in 90 Ma granites of the Sierra Nevada Batholith (Newbery and Swanson, 1986).

7.7. Cordilleran Pb-Zn-Ag (Sb) deposits

7.7.1. High-temperature Zn, Pb, Ag replacements in carbonates

North American “manto” and/or “chimney”-style replacement Pb, Zn, Ag deposits in carbonates, like Leadville and Santa Eulalia, have been one of the pillars of classical economic geology (Lindgren, 1933). They provided opportunity for an endless genetic debate and a variety of classifications from many premises which, unfortunately, is not yet over although the prevalent opinion now follows the ideas and terminology introduced by Megaw et al. (1988), Tittley (1993b) and others. As usually, the

group characteristics are based on “typical” example deposits but there are always transitions and exceptions, and there are many deposits that just do not fit. In this book some of the “Pb-Zn-Ag giants” not included here may be found in Chapters 6 and 10.

The deposit examples treated here are bona fide “Cordilleran”, as they are coeval with active subduction-related granitoid magmatism; this can be empirically demonstrated by the zonal arrangement of Pb-Zn-Ag orebodies around porphyry coppers (as in Butte, Bingham, Tintic, Morococha, Cassandra and Kurama Mts. ore fields or districts). Although moderate-size Pb-Zn-Ag occurrences occur where the coeval granitoid intrusions were emplaced into the “eugeoclinal” (volcanic-sedimentary) basements (Fig. 7.50), the bulk of the Pb-Zn-Ag “giants” associate with intrusions into sedimentary rocks of the miogeocline (Fig. 7.51), resting on a (usually Precambrian) crystalline basement.

Some Zn-Pb-Ag deposits in exoskarns or marbled carbonates occur at the immediate intrusion contact, whereas others are situated at some distance away from the contact (“distal” orebodies), but still within a broader thermal and hydrothermal aureole. In the 1930s and well into the early 1960s, when the idealized Emmons’ metal zoning model around granite intrusion was considered universally valid, any nearby granite used to be automatically considered as the supplier of ore metals. In the 1970s-1980s the role of intrusions close to the Cordilleran Pb-Zn-Ag deposits was reduced to a heat source only. Heated convecting fluids presumably extracted the metals from crustal rocks (an equivalent of processes better documented in the VMS and epithermal models). Most recently the Cordilleran Pb, Zn, Ag replacements and vein deposits, especially those around porphyry copper-bearing stocks, are credited to magmas that contribute a significant proportion of magmatic waters to the ore-forming fluid (e.g. Inan and Einaudi, 2002, but read the discussion in Tittley, 1993b, p.607). The nearest granite need not have been, and usually was not, the fluid source (D.M. Smith, 1996). The ore-coeval granite is more often hidden in depth.

In some of the Pb-Zn-Ag deposits coeval with porphyry coppers (e.g. Tintic, Utah) the porphyry-Cu is rather feeble. Elsewhere, none is in sight. Leadville in Colorado is adjacent to the Colorado porphyry Mo belt so Mo “specialized” intrusions may substitute. In plutonic tin provinces, reviewed in the collision and extension shaped orogens

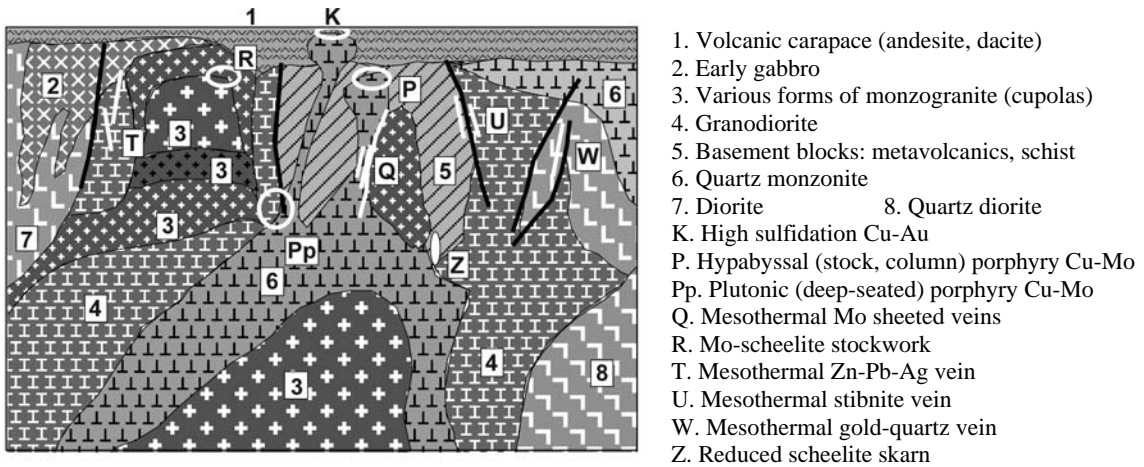


Figure 7.50. Inventory of ores associated with calc-alkaline granitoids emplaced into old volcanic-sedimentary basement. From Laznicka (2004) Total Metallogeny site G52. All ore types shown can reach the "giant" magnitude

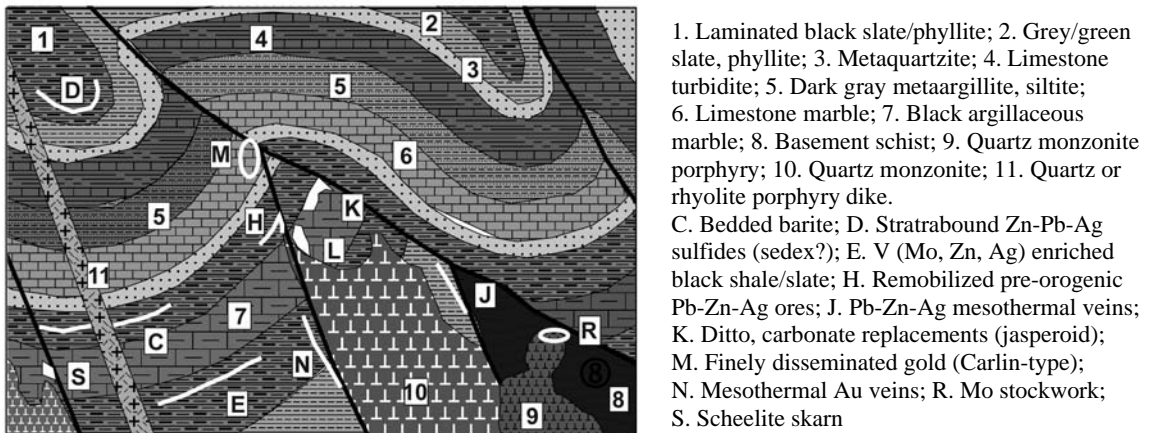


Figure 7.51. Inventory of rocks and ores close to the shelf/carbonate platform and "basinal" facies transition (margin of miogeoclinal domain) in orogens intruded by granitoids. From Laznicka (2004), Total Metallogeny site G160. Ore types C, D, J, K, M, N, R and S can reach the "giant" magnitude

(Chapter 10), Pb-Zn-Ag skarns and replacements are present as well. It appears that a thick, mature basement of Precambrian metamorphics was essential, as major Pb-Zn-Ag deposits are lacking where the basement is comprised of accreted, mainly immature oceanic or island arc lithologies. In the traditional literature this group of deposits is treated in terms of Pb-Zn-Ag skarns, high- and medium-temperature carbonate replacements and veins, but in many ore districts there is a continuum and overlap of orebody forms. This is further complicated by the fact that some VMS (Chapter 8), "sedex", and Mississippi Valley-type Zn-Pb

deposits, especially when deformed and metamorphosed, mimic the Cordilleran orebodies.

The truly "high-temperature" Pb-Zn-Ag carbonate replacements (Megaw et al., 1988; Titley, 1993b) are contemporaneous with formation of the early prograde exoskarn assemblage (these ores are different from those superimposed on the skarn later). They form at temperatures between about 680° C and some 400°C, followed by cooler (mesothermal to epithermal) mineral phases. Einaudi et al. (1981) compiled a sequence of skarns arranged by increasing distance and intimacy from the "causative" intrusion as follows (from proximal to distal): skarns at contacts of batholiths; granitoid

stocks; porphyry dikes; outside of direct granite contact; carbonate veins with the "skarn" minerals. Meinert (1987) studied the Pb-Zn-Ag skarn/replacements zonality at the Groundhog deposit in the Central (Santa Rita) district of New Mexico and distinguished: 1) proximal skarns with garnet-pyroxene ratio of about 1:1; 2) intermediate (central) skarn with the same ratio of 1:20; and distal skarn-free replacement Zn-Pb mantos in marble or silicified marble. Replacement systems that lack skarn are hosted by silicified carbonates (jasperoid) only, or by recrystallized carbonates (marble) enriched in Fe and Mn e.g. in manganosiderite. The latter alteration can best be visually appreciated in oxidized or completely leached gossanous outcrops pigmented brown or black by Fe and Mn hydro-oxides, as in Leadville.

The prograde Zn-Pb mineralized skarns contain hedenbergite to johannsenite (Mn) pyroxenes, abundant pyrrhotite, marmatitic (Fe-rich, dark) sphalerite and minor galena (e.g. at Kamioka, Dal'negorsk, in the high-pyroxene type) and andradite to slightly spessartitic (Mn) garnet, diopside, pyrite, pyrrhotite, sphalerite and galena (Meinert, 1993). The sulfides are younger than the skarn silicates to which they are interstitial, and often replace marble relics. The same minerals occur in retrograded (hydrated) amphibole, epidote, actinolite skarn. There, the orebodies are irregular and most commonly follow contacts of skarn and marble. The marble or jasperoid replacement bodies tend to be mineralogically simple (mostly sphalerite, galena, pyrite) and are structurally and/or lithologically controlled. The "mantos" (blankets) are peneconcordant with bedded carbonates and in extreme cases completely replace thin carbonate belts so they appear "stratiform". The "chimneys" are subvertical replacements or dilation filling bodies usually controlled by fault intersections, often hosted by breccias. Additional orebody varieties are found in "hydrothermal karst"; in such a setting the "high temperature" replacements emulate the Mississippi Valley-type (MVT) deposits. De Voto (1983) considered the paleokarst-controlled deposits in Colorado (Leadville, Gillman, Aspen) as earlier, low-temperature deposits overprinted in the magmatic-hydrothermal environment. MVT deposits, however, are very low in silver, whereas Leadville is an "Ag-giant" (7,961 t Ag).

Hydrothermal replacements are an economically important source of Pb, Zn and Ag, although in the past decades they have been overshadowed by the large "sedex" deposits and the Mississippi Valley-type (Chapter 13). There are about 20 "giants" in

this genetic group, but as their setting may be different they appear, in this book, under different headings. So those in the andean systems (e.g. Cerro de Pasco) are in Chapter 6, those in the intraplate orogens in Chapter 10.

Most "giants" owe their magnitude rank to the content of silver (7,000 t Ag+; 10 deposits) followed by lead (1.5 Mt Pb+; 6 deposits), but except for Cerro de Pasco and Antamina (7 mt and 15 mt Zn, respectively) no other deposit qualifies as a "Zn-giant"; that is, it does not exceed the required 6.5 Mt Zn endowment. To compensate, several deposits from the "Zn-large" category are considered and listed below. The Kassandra ore field in Greece, with ores containing some 120 to 250 kt of arsenic that is not recovered and rarely listed, has the dubious honor of being an "As-geochemical giant".

Many skarn and replacement Zn-Pb-Ag deposits overlap with fault or fissure veins and the veins tend to be especially high in silver ("bonanza-Ag"), as in the Park City and Lavrion (Laurium) ore fields. The N70°E/65°N trending Mayflower vein in the Park City field consists of quartz, lesser calcite, rhodochrosite, rhodonite, pyrite, sphalerite, galena and small bonanza shoots of enargite, tetrahedrite, Ag-sulphosalts and chalcopyrite. The carbonate wallrocks are silicified, the quartz diorite quartz-sericite-pyrite altered.

Most of the Pb-Zn-Ag deposits, especially those in the semi-arid western United States and northern Mexico, had distinct goethite and black Mn-oxides rich gossans, enriched in "invisible" silver (Blanchard, 1968). Extremely rich masses of Ag haloids, mostly chlorargyrite, had been mined from oxidation zones in the early stages of exploitation; with depth they often graded into patchy blankets enriched in supergene Ag sulfides (argentite, acanthite) and native silver (Emmons, 1913). Lead was represented by cerussite, anglesite and residual galena. Zn accumulated in smithsonite or hemimorphite at the deeper regolith levels, sometimes transported into karsted carbonates nearby to form small exotic deposits.

Predominantly skarn deposits

Antamina Cu-Zn-Ag-Mo deposit, San Marcos, Peru (O'Connor, 1999; Rc 760 mt @ 1.3% Cu, 1.0 % Zn, 14 g/t Ag, 0.03% Mo, 70 ppm Bi for 9.88 mt Cu, 7.6 mt Zn, 10,640 t Ag, 228 kt Mo, 53 kt Bi; see Fig. 7.13). Antamina is located in the northern part of the Central Peru mineral belt, in a recently deglaciated valley in the late Eocene east-verging Marañon Fold and Thrust Belt. It is the world's

largest continuous Cu-Zn skarn (2.5 x 1 km, ~1 km deep). Discovered by the Incas, it went into a large scale production in 2001.

The host rocks are folded and thrust late Cretaceous (~88-84 Ma) marine shale, marl and limestone in core of a NW-trending regional synclinorium. This is intruded by multiphase stocks of Miocene (~9.8 Ma) granodiorite porphyry exposed in their apical areas. The dominant variety is the earliest "crowded plagioclase porphyry", the later phases have more K-feldspar phenocrysts. The porphyries contain relics of K-silicate alteration (mainly biotitization), silicification, and quartz veining with patches of molybdenite and/or chalcopyrite, much of which were obliterated by the superimposed Ca-metasomatism (skarnization).

Extensive rock metasomatism has affected both the porphyry endocontact (endoskarn) and exocontact (exoskarn after carbonates, biotite hornfels after shale). A typical zoning pattern from the porphyry into limestone is: coarse garnet-plagioclase endoskarn, fine-grained pink garnet endoskarn, transitional skarn, brown garnet exoskarn, green garnet exoskarn, wollastonite skarn, marble, limestone. Both brown and green garnets are grossularite. There are widespread hydrothermal breccias in all lithologies.

The ore metals are quite evenly distributed throughout the entire altered porphyry and skarn body, rather than to form high-grade masses. Copper as chalcopyrite and bornite, with associated minor Bi sulfides and sulfosalts, form patches and veins with epidote, chlorite, magnetite and pyrite in the retrograded endoskarn, and then continue through the exoskarn to the marble contact. Disseminated chalcopyrite and bornite are common in the wollastonite skarn. Zn in sphalerite is dominant in the green garnet skarn. There are neither secondary sulfides, nor gossans as the oxidation zone has been removed by glaciers and partly incorporated into moraine.

Naica in Chihuahua, northern Mexico, is a "large", frequently quoted Zn, Pb, Cu, Ag skarn deposit where "mantos" and "chimneys" are well developed (Stone, 1959; Megaw et al., 1988; ~20 mt of ore @ 4.2% Pb, 3.5% Zn, 0.39% Cu, 148 g/t Ag, 0.19 g/t Au for 840 kt Pb, 700 kt Zn and 2,960 t Ag; Fig. 7.52). It is also one of the "hottest" Zn-Pb skarns with up to 680° homogenization temperatures of fluid inclusions, which is surprising as the only igneous component exposed at the mine level are thin, albitized rhyolite porphyry dikes. Presumably, a buried intrusive stock is in the

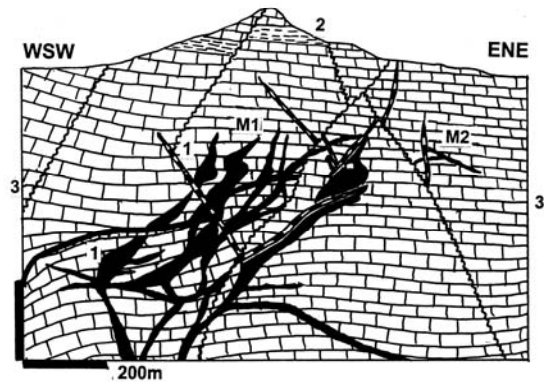


Figure 7.52. Naica skarn deposit, Mexico, cross-section from LITHOTHEQUE No. 1107.2 modified after Bravo in De Hoyos (1988). M1. 26 Ma Zn-Pb-Cu skarn orebodies grading to limestone replacements; M2. Fracture filling Fe-Zn-Pb sulfide veins; 1. ~26 Ma albitized rhyolite or rhyodacite dikes; 2. Cr1 calcareous pyritic shale; Cr1 limestone recrystallized to marble

subsurface. The host rocks are generally gray Cretaceous limestones of several formations, interbedded with minor clastics. In the vicinity of mineralized structures they are bleached and recrystallized into a white marble. The thin (~4 m thick) mantos are gently dipping, persistent sheets of zoned exoskarn, laced with sulfides: pyrite, sphalerite, galena, fluorite, local chalcopyrite, arsenopyrite and other minerals. The central zone of wollastonite, grossularite and vesuvianite grades laterally to Mn-hedenbergite, quartz and calcite. The chimney orebodies are steeper fault and fracture replacements that cut the mantos, when in contact. Some are filled by exoskarn with sulfides as in the mantos, others are filled by pyrrhotite-dominated massive sulfide ore. There was an up to 120 m thick gossan at the start of mining and oxidation zone had formed over the orebody that consisted of goethite, Mn-oxides, cerussite, anglesite and Ag-halides but was almost completely devoid of zinc. Stone (1959) calculated that at least 50,000 t of Zn has been leached out.

Kamioka, the largest zinc ore field in Japan (Nishiwaki et al., 1970; 90 mt @ 5% Zn, 0.7% Pb, 30 g/t Ag containing 4.5 Mt Zn, 630 kt Pb, 2,700 t Ag, 6,300 t Bi, 338 t Te), is located in the Mesoproterozoic Hida metamorphic terrain of north-central Honshu. There are close to 60 irregular orebodies in three deposits. They formed by replacement of marble and Ca-Mg silicate units interbedded with biotite-sillimanite gneiss and migmatite of the Hida complex, intruded by pegmatite, gabbro, diorite, monzonite and syenite

before separation from the Asian continent. The hydrothermal mineralization is late Cretaceous, associated with quartz-feldspar porphyry dikes and small stocks, some of which are locally K-feldspar, sericite and quartz altered and contain disseminated molybdenite. Most of the ore minerals: marmatitic sphalerite, galena, lesser pyrite, chalcocopyrite, arsenopyrite, Ag-sulfosalts replace hedenbergite, garnet, epidote skarn. Less important are sulfide replacements of silicified marble and late stage calcite fracture veins.

Bingham (described earlier), Tintic, and Morococha are examples of ore fields where Cu, Zn-Pb skarns and replacements are zonally arranged around high-level intrusions, mineralized by porphyry copper.

Predominantly no-skarn Pb-Zn-Ag replacements

Tintic ore field around Eureka, Utah (Lindgren and Loughlin, 1919; Morris, 1987; Pt 17.5 mt of ore containing 8,500 t Ag, 1.05 mt Pb, 205 kt Zn, 116 kt Cu and 86.5 t Au with additional metal resources in depth); Fig. 7.53, is a classical representative of a multistage magmatic-hydrothermal centre. It brings together several ore associations and styles. The centre is located in a fault block near the eastern margin of the Great Basin in central Utah. The rocks there are Neoproterozoic quartzite and slate covered by a 3.3 km thick section of Cambrian to Permian miogeoclinal sedimentary rocks dominated by limestone and dolomite, with a less widespread quartzite and sandstone near base. In late Cretaceous these rocks had been thrust and carried eastward for as much as 160 km, then block-faulted. In Oligocene a composite volcano that included a caldera stage buried the sedimentary pile under a thick cover of latite and quartz latite ash-flow tuff, flows and agglomerate. Several small quartz monzonite stocks, plugs and dikes intruded. Widespread hydrothermal activity followed emplacement of the Silver City quartz monzonite. The earliest hydrothermal phase converted many faulted carbonate bodies into hydrothermal dolomite and this created extensive solution porosity ("hydrothermal karst"). Callahan (1977), however, considered a possible presence of an earlier paleokarst, complete with the Mississippi Valley-type Zn-Pb orebodies. The volcanics were partly propylitized (chlorite, albite, calcite, epidote).

The early postmagmatic solutions produced a recently discovered porphyry Cu-Mo in depth, in the contact area of a quartz monzonite stock. The fluids rose into the sedimentary roof along a system of NNE-trending fissures marked by monzonite and

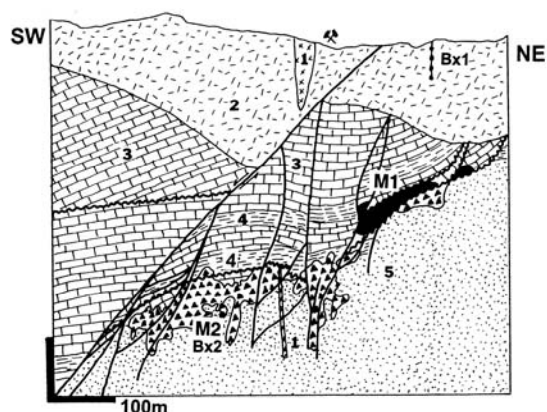


Figure 7.53. Tintic ore field, Utah, North Lily Mine cross-section from LITHOTHEQUE No. 678, modified after Morris and Lovering (1979). M1. ~31 Ma Pb-Zn-Ag sulfide replacements in jasperoid and recrystallized limestone; M2. Ag-Au-Cu high-sulfidation (enargite) breccia bodies. Bx1. Pebble dikes; Bx2. Hydrothermal and solution collapse breccia. 1. Oligocene quartz monzonite porphyry; 2. Oligocene subaerial volcanics; 3. Cambrian-Permian dolomite and limestone; 4. Cambrian shale; 5. Cambrian quartzite

"pebble" dikes (i.e. intrusive breccias) to produce five major ore zones ("runs"). The earlier fluids of the acid sulphate type caused widespread silicification and advanced argillic alteration of the silicate and partly carbonate rocks (zunnite, pyrophyllite, alunite, and especially a large body of halloysite clay mined in the 1970s-1980s). The fluids also precipitated a suite of high-sulfidation Cu, As, Bi, Ag, Au minerals (enargite, famatinite, luzonite, tennantite, tetrahedrite, Ag sulphosalts, Au-Ag tellurides and electrum in quartz, chalcedony, barite, rhodochrosite gangue) in fracture and breccia-controlled open-spaces in silicate rocks, overlapping with galena and sphalerite replacements in the partially silicified dolomitized limestone. The high sulfidation ores came from four major mines (e.g. Mammoth, Trixie) and they account for the Cu, Au and portion of Ag produced from the Tintic field.

The predominant Tintic orebodies, however, are Pb, Zn, Fe sulfide replacements in carbonates. The large, fault and fracture-controlled steep columnar ore masses ("chimneys") are located along avenues of fluid ascent where the principal minerals galena, sphalerite and pyrite in cherty jasperoid, barite and rhodochrosite gangue accommodate a minority of the high sulfidation ores. The partly stratabound "mantos", runs and pods of extremely variable size in carbonates, produced by fluids advancing away from faults, are mineralogically more simple. The

oxidation zone in Tintic is very deep and the early production had been derived from a great variety of secondary minerals of Pb, Zn, Cu, As, Sb, and Bi, greatly enriched in silver.

Leadville Ag, Pb, Zn, Au, Cu ore field, Colorado (Emmons et al., 1927; Thompson, 1990; P+Rv 24.6 mt ore containing 7,961 t Ag, 1.3 mt Pb, 780 kt Zn, 89 t Au; Fig. 7.54). Leadville is a classic locality meticulously described in the early memoirs of the U.S. Geological Survey (S.F. Emmons and others), from where it entered the textbook literature. It is also type locality of the "intrusion-related, carbonate-hosted" Pb-Zn deposits (Titley, 1993b), especially those formed in or near block-fault depositional basins in the western United States' late Paleozoic carbonate platform (D.M. Smith, 1996).

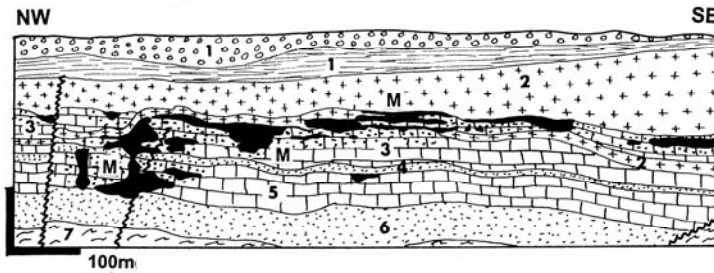
Leadville is near the center of the NE-trending Colorado Mineral Belt that crosses the NNW grain of the Rocky Mountains ranges. The thin section of Ordovician to Lower Carboniferous, predominantly carbonate rocks on eastern flanks of the Sawatch Proterozoic basement uplift, is intruded by a series of hypabyssal porphyry intrusions ranging in age from late Cretaceous to Oligocene. Most intrusions predate mineralization. Pb-Zn replacement orebodies in the Leadville (town) ore field are west of the Brece Hill porphyry stock and the porphyry intrusions have mostly the form of thick sills.

Thompson (1990) distinguished seven ore types in the Leadville district, of which the "Leadville-type" Pb-Zn-Ag dolomite-hosted replacement bodies have been of greatest importance and interest. These are individual or stacked massive pyrite or pyrrhotite replacements with variable proportion of Fe-sphalerite (marmatite), galena, minor chalcopyrite and tetrahedrite in Mn-enriched (rhodochrosite or manganosiderite) gangue and/or alteration envelope. Semi-stratabound mantos project into zones up to 1,200 m long and 200 m wide, that range in thickness from a few meters to 60m. Late Cretaceous to Eocene White Porphyry sills parallel, envelop or terminate the ore mantos and/or the host carbonates, but they are pre-ore, intersected by frequent fault and fissure veins considered fluid conduits. The most common ore host is the Lower Carboniferous Leadville Limestone. Thompson (1990) determined the filling temperatures of the Pb-Zn-Ag mantos as between 328 and 270°C, and the age of mineralization as 33.8 Ma. Silver-rich supergene orebodies of cerussite, smithsonite and Mn-oxides formed near surface and contributed to the high silver yields in the early mines.

Lavrion (Laurium) Ag-Pb-Zn ore field, Greece (Marinou and Petrascheck, 1956; N. Skarpelis, tour & oral communication, 1995; P+Rc ~3 mt Pb, ~3 mt Zn, ~6,000 t Ag). Lavrion is one of the few "giants" discovered and mined in the very distant past (since about 1,000 B.C., then by the Athenian State under Pericles, 500-400 B.C.; Konofagou, 1980). This is also the best preserved mining and metallurgical archeological site about 50 km SE of Athens, in Attika. The ancients mined a rich and mineralogically interesting oxidation zone (hemimorphite, smithsonite, cerussite, adamite, Ag-halides, native silver) in gossanous paleokarst, partly pseudomorphically replacing Pb, Zn, Ag sulfides and partly redeposited in fractures and cavities in the footwall as "exotic" accumulations. The ancient miners also exploited the rich portions of the hypogene silver-rich sulfide ore. The ancient grades reported by Konofagou (1980) were 20% Pb and 400 g/t Ag and the miners left behind large dumps of the lower-grade material and metalliferous slag, largely reprocessed after 1875.

The Triassic-Jurassic host metamorphics (several horizons of marble intercalated with micaschist and amphibolite) are topped by relics of high-pressure metamorphosed allochthon. The metamorphics were intruded by Miocene (~9 Ma) hornblende-biotite granodiorite stock and dacite dikes and sills. In the immediate intrusion exocontact formed the Plaka skarn deposit (magnetite, pyrrhotite, scheelite, Pb, Zn, Cu sulfides) of minor economic importance. Most of the Lavrion wealth came from the Kamareza deposit that includes several subhorizontal mantos of massive to disseminated sulfides in marble or marble breccia under schist screen. The marble is recrystallized, ankeritized and pyritic. The dominant ore minerals are sphalerite, galena, pyrite, arsenopyrite, tetrahedrite, Pb-Sb sulfosalts and Ag-sulfosalts in gangue of barite, ankerite, calcite and quartz.

There are many variations among the remaining Pb-Zn-Ag replacement "giants", ranging from the "full-spectrum" ore fields (central porphyry stock with porphyry-style Cu-Mo, endo/exoskarn with Cu, Zn-(Pb), Zn-Pb mantos or chimneys in marble or silicified carbonate [jasperoid], Zn-Pb veins) to "simple" Pb-Zn replacements in carbonates only. The former are exemplified by Morococha, Dal'negorsk (Tetyukhe), the latter by Santa Eulalia-West field.



1. Q gravels and lacustrine silt;
- M. ~34 Ma Pb-Zn-Ag replacement mantos and chimneys in carbonates;
2. T1 porphyry sills; 3. Cb1 limestone, D3 dolomite; 4. D3 Parting Quartzite
5. Or1 dolomite; 6. Cm3 quartzite;
7. Mp schist, gneiss, granitoids

Figure 7.54. Leadville, Colorado, California Gulch Pb-Zn-Ag mantos; cross-section from LITHOTHEQUE No. 653, modified after Emmons et al. (1927)

7.7.2. Mesothermal Pb-Zn-Ag (Sb) veins

"Mesothermal" fracture or fault-filling Pb-Zn-Ag veins are universally present in most geotectonic settings that have a thick continental crust basement, brittle fractures or faults, and a history of hydrothermal fluid convection. In the andean (cordilleran-)type margins intruded by magmas related to subduction, postmagmatic polymetallic veins are associated with epizonal granitoids in space and time. The veins occur in the outer metal zones surrounding porphyry coppers (as in Butte), or in roof rocks above small granitoid intrusions (San Francisco del Oro-Santa Barbara). Opinions differ as to the proportion of magmatic component in the fluid if any, considered predominantly as derived from meteoric waters or "basinal fluids". Most dilation-filling veins are in silicate rocks (but these can be replaced as well) and some are in carbonates. In ore fields where silicate and carbonate host rocks alternate the former are preferentially veined, the latter replaced, by contemporaneous fluids (as in Tintic); alternatively, several generations and styles of Pb-Zn-Ag ores may be present (as in Fresnillo).

Single, strong, thick and persistent veins do occur, but most ore fields consist of vein arrays and groups, usually trending in one or more preferential directions. The vein textures range from massive ore to banded (crustiform) veins of alternating ore and gangue bands, to breccia veins, and veins composed of gangue with scattered sulfides. Most common gangues are crystalline quartz, carbonates (siderite, ankerite, dolomite, calcite or Mn-carbonates), frequently barite, sometimes fluorite. The sulfides are sphalerite, galena, pyrite with usually subordinate chalcopyrite, tetrahedrite, Ag-sulfosalts. Quartz-sericite alteration, silicification and carbonatization are most common alterations. Sometimes there is a gradation into sulfides-rich gold-quartz veins. Thousands of mostly small to

medium magnitude veins have been mined through the history mainly for silver and lead (zinc was of less value, especially in the remote locations) but there are few "giants"; even so, most production/reserve figures are aggregate tonnages derived from many individual veins in an ore field or a district. Comparable veins in the collisional orogens are described in Chapter 10.

By far the largest Cordilleran Pb-Zn-Ag vein district, Coeur d'Alene in northern Idaho, is controversial. The most recent interpretations (Leach et al., 1998) indicate that the two principal groupings of orebodies there: 1) the older, deformed and metamorphosed predominantly Zn-Pb orebodies like Bunker Hill, are Neoproterozoic (around 1.0 Ga); 2) the younger, high Ag-Cu-Sb (tetrahedrite) lodes are "Laramide", that is late Cretaceous-early Tertiary. Both, moreover, are (syn)orogenic, and unrelated to the older granodiorite-quartz monzonite stocks in the area. Coeur d'Alene veins are thus the genetic analogue of the (syn)orogenic gold deposits that also crop out in the andean-type margins (read below), but have no connection with the subduction-driven magmatism. The ore forming fluids had most likely been released during metamorphic dehydration in depth.

Coeur d'Alene district (Fryklund, 1964; Gott and Cathrall, 1980; $P_{1884-2004}$ 34,000 t Ag; 8.035 mt Pb; 3.05 mt Zn; 170 kt Cu; ~70 kt Sb; 16 t Au) is located well east of the Coeur d'Alene city, Idaho, in the country around Kellogg, Burke and Mullan. The district measures 40x20 km. It is on both sides of the WNW-trending Osburn strike-slip fault with up to 26 km lateral displacement and 5,000 m of vertical offset. There are 12 broadly subparallel "mineral belts" (WNW trending zones of densely distributed separate orebodies), most of which belong to the Pb-Zn group. The 12 km long Silver Belt west of Wallace contains the richest vein deposit in the District, the Sunshine Mine. With the

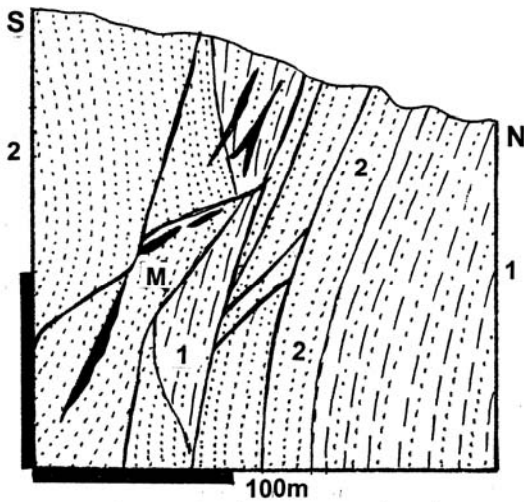


Figure 7.55. Bunker Hill Pb-Zn-Ag deposit, Kellogg, Coeur d'Alene district, Idaho. Cross-section from LITHOTHEQUE modified after Fryklund (1964). M. Steep tabular bodies of massive to disseminated sulfides in sericite-siderite altered quartzite along faults; 1. Mp St. Regis Fm. varicolored clastics; 2. Mp Revett Fm. thick-bedded quartzite

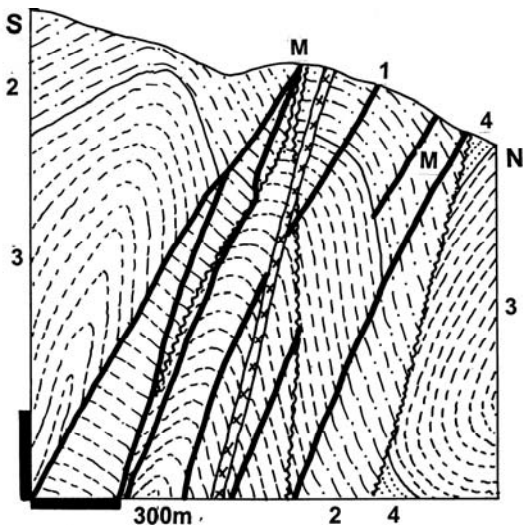


Figure 7.56. Polaris Mine, Coeur d'Alene district, Idaho, an example of a "Silver Belt" deposit. Cross-section from LITHOTHEQUE No. 1640, modified after Mitcham (1952). M. Ag-rich siderite, Ag-tetrahedrite fault-controlled replacement veins; 1. Diabase dikes; 2. Mp Wallace Fm. argillite to siltite, minor dolomite & limestone; 3. Mp St. Regis Fm. varicolored clastics; 4. Mp Revett Fm. thick bedded quartzite

exception of several scattered early Cretaceous granodiorite-quartz monzonite stocks, the area is

underlain by up to 20,000 m thick pile of strongly deformed, greenschist-metamorphosed, largely non-volcanic clastics of the Mesoproterozoic (1.5-1.25 Ga) Belt Supergroup. The rather monotonous meta-sediments are dominated by gray or maroon siliceous slate, sericite phyllite, sericite quartzite, locally with impure meta-carbonate interbeds.

The low-silver Zn-Pb belts have steeply dipping mineralogically simple quartz, sericite, siderite, ankerite, galena, sphalerite, specular hematite, magnetite, pyrrhotite replacement veins, most of which occur in faults (shears) and fractures along axial planes of major folds. Biotite, garnet and grünerite are locally present. Most of the ores, as in the largest mine in the Pb-Zn group, **Bunker Hill** (P+Rv 39 Mt ore; Fig. 7.55), are fine-grained, metamorphosed and plastically deformed. The prevalent wallrock alteration is "bleaching", i.e. low-temperature discoloration of rocks containing metamorphic sericite, with additional hydrothermal sericite. Decalcification, hydration of hematite pigment, and siderite-ankerite carbonatization are associated.

The high-silver lodes in the "Silver Belt" (Fig. 7.56) are richest in the "giant" **Sunshine Mine** near Wallace (Harris et al., 1981; Wavra et al., 1994; P₁₀ 1994 10,574 t Ag; 45 kt Cu; 63 kt Pb; 29 kt Sb). The mineralized zone is 3.2 km long, 2.3 km deep and 800 m wide. It consists of some 30 replacive, structurally controlled veins in bleached meta-argillite, siltite, quartzite and minor carbonates. The veins are composed of crystalline siderite with variable proportion of quartz and ankerite, and scattered or veinlet Ag-rich tetrahedrite, arsenopyrite, pyrite, chalcopyrite and galena. Rich ore shoots in meta-quartzite are filled by massive Ag-tetrahedrite with minor Fe, Cu, Pb sulfides.

Additional Pb-Zn-Ag "giants" associated with Cordilleran granitoid: Not counting vein and replacement deposits reviewed in Chapter 6 and Chapter 10, ten Pb-Zn-Ag deposits and districts qualify as "giants" in the Cordilleran setting. San Martin, Karamazar West, Cove, and Kassandra have dominant skarns; Santa Eulalia West and Bingham are carbonate replacements; Park City and Fresno have both replacements and veins; Butte and Keno Hill have veins; Bawdwin is controversial (read also the summary table of hydrothermal Pb-Zn-Ag deposits in Chapter 10). Of the ten localities listed, Karamazar, Kassandra, Bingham and Butte are in districts with one or more coeval porphyry coppers.

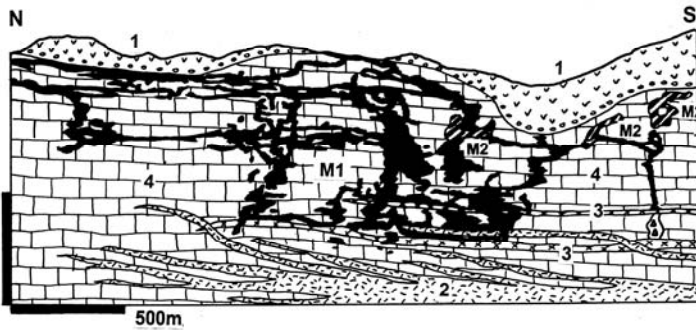
- **San Martin-Sabinas**, Zacatecas, N Mexico (Megaw et al., 1998; P+Rv ~100 mt @ 5% Zn, 1% Cu, 0.4% Pb, 120 g/t Ag for 5 mt Zn, 12,000 t Ag). Predominantly massive to disseminated pyrrhotite,

- sphalerite, pyrite > chalcopyrite > galena in garnet-pyroxene endo- and exoskarn in MZ limestone at contact with composite Ol-Mi diorite to granite stock. Mantos, chimneys > veins, fault control.
- **Karamazar Range West** (deposits Kansai, Altyn Topkan, Kurusai etc.), NW Tadjikistan (Smirnov & Gorzhevsky, 1974; estim. 3 mt Zn, 1.5 mt Pb, 10 kt Ag). This is an area of numerous structurally controlled exoskarns lining immediately adjacent Cb3-Pe dikes of granodiorite porphyries in roof of the Kurama Batholith. The hosts are D-Cb1 carbonates and hornfelsed clastics, the orebodies are dominated by sphalerite & galena and grade to jasperoid replacements and veins.
 - **Cove, Battle Mountain district**, Nevada (Brooks et al., 1991; Rv 60 mt @ 120 g/t Ag, 2.2 g/t Au for 7,200 t Ag, 146 t Au). Oxidized, pyritic distal disseminated replacements of Pb,Zn,Cu,Sb,Ag sulfides in Tr limestone, jasperoid and clastics near Eo? granodiorite & quartz monzonite sills & dikes; Au-skarn at nearby McCoy deposit.
 - **Kassandra ore field**, Chalkidiki, N Greece (Gilg & Frei, 1994; largest deposit Olympias, Rv 16 mt @ 5% Zn, 3.3% Pb, ~0.3-2% As, 120 g/t Ag, 5.5 g/t Au, and Madem Lakos: 4.7 mt at similar grades). Total about 1 mt Pb, 1.2 mt Zn, 2,800 t Ag, min. 120 kt As ("As-giant"). 25-24 Ma Ca and Mg exoskarn mantos in basement marble, related to granodiorite porphyry, in roof of Ol-Mi pluton. Multistage Zn-Cu-Pb-Ag-Au mineralization is rich in sphalerite and arsenopyrite and is near sericite-altered porphyry Cu-style showing.
 - **Santa Eulalia**, Chihuahua, northern Mexico: S.E. West (major) is a carbonate replacement, S.E. East is a skarn (Megaw et al. 1988; P_{to 1980s} 37 mt @ 8% Pb, 7.1% Zn, 320 g Ag; total 3.2 mt Pb, 3.52 mt Zn, 13,580 t Ag; Fig. 7.57). Stacked Pb, Zn sulfide replacement mantos up to 4 km long and chimney in Cr limestone, without or with jasperoid. Cut by rhyolite porphyry dikes, above Ol-Mi pluton.
 - **Bingham Pb-Zn deposits**, Utah (Rubright & Hart, 1968; Pt 25.2 mt @ 8.6% Pb, 6.6% Zn, 155 g/t Ag, 1.21 g/t Au for 2.17 mt Pb, 1.66 mt Zn, 3,906 t Ag, 80 t Au; Fig. 7.58). Ring of Pb-Zn sulfide replacements in Cb3 carbonate bands confined by clastics, in the outer (distal) zone of hydrothermal mineralization around the porphyry Cu-Mo mineralized 38.5 Ma quartz monzonite stock. Manto, chimney, some veins in silicified or recrystallized marble hosts, skarn rare.
 - **Park City ore field**, Utah (Bromfield, 1989; Pt ~15 mt ore with 1.216 mt Pb, 675 kt Zn, 9,575 t Ag). 36-33 Ma thin Pb-Zn sulfide mantos in Cb3-Pe carbonates; high-Ag "bonanza" fissure and fault veins in hornfelsed shale, clastics near Ol diorite porphyry dikes and stocks.
 - **Fresnillo ore field**, Zacatecas, Mexico (Ruvalcaba-Ruiz & Thompson, 1988; P+Rv 13,093 t Ag; Pt ~1.2 mt Pb, 1.7 mt Zn; Fig. 7.59). Over 150 fissure high-Ag Pb-Zn sulfide veins, several manto and chimney Pb-Zn sulfide replacements, in Cr limestone, shale and volcanics zoned around small 32-28 Ma quartz monzonite stock. Multistage, "bonanza" Ag intervals. High-Ag oxidation zone mined in the past.
 - **Butte Zn-Pb-Mn veins**, Montana (Meyer et al., 1968; 2.2 mt Zn). 58-57 Ma rhodochrosite-sphalerite fissure veins in quartz monzonite, in the outer (distal) metal zone around porphyry-Cu and high-sulfidation vein swarm (Chapter 6).
 - **Karamazar Range East, Kanimansoor** Ag deposit, N Tadjikistan (Lukin et al., 1968; Elevatorski, 1996; old Ag production, new resource quoted as 39 mt @ 108 g/t Ag, 0.25 g/t Au; low-grade disseminated resource ?990 mt @ 51.7 g/t Ag, 0.4% Zn, 0.44% Pb). Cb3-Pe veins & steep narrow replacement zones along quartz porphyry dikes in Cb3 continental volcanics. High-Ag "bonanza" shoots.
 - **Keno Hill-Elsa** ore field, Yukon (Boyle, 1965; Pt ~4.7 mt ore @ 1,412 g/t Ag, 6.84% Pb, 4.6% Zn for 6,769 t Ag). 28 mainly NE narrow gouge-filled fault and fissure vein zones in schist, phyllite, quartzite, diabase sills around Cr3 quartz monzonite stock. High-Ag "bonanza" veins, up to 200 m deep relic oxidation zone.
 - **Bawdwin**, North Shan State, Myanmar (Hutchison, 1996; calculated totals 4.1 mt Pb, 3.6 mt Zn, 218 kt Sb, 218 kt Cu, 130 kt As, 10.4 kt Bi, 8 kt Ag + Co, Ni; grades vary). An enigmatic deposit dominated by 4 km long NW-SE Pb-Zn sulfide zone with Cu-Pb-Ag-As lodes, barite. Prominent oxidation zone. Main host is Or sericitized and silicified rhyolite intruded by 211 Ma quartz-feldspar porphyry. Believed Tr hydrothermal, perhaps partly remobilized older ores.

7.8. Hydrothermal Fe, Mn, Sb, Sn, B, U, Th deposits in, and associated with, Cordilleran granitoids

The above metals form "giant" concentrations in other than andean-margin settings and these are described in other sections. Isolated deposits, however, do occur here but are, at most, of the "medium" to "large" magnitude.

Iron, in magnetite skarns and "Chile-type" hydrothermal deposits, has provided the resource base of important national steel industries (as in Magnitogorsk, the Urals) and an exportable commodity when near the coast (e.g. Marcona, Peru; Tasu Sound, British Columbia). In terms of geochemical Fe accumulation the close to thousand recorded Fe skarns are small to medium-size deposits with few "large" ones (430 mt Fe plus) and no "giants". The largest skarn and replacement examples are Marcona, Peru; the Turgai district, Kazakhstan ; Magnitogorsk, Russia.



M1. ~47-26 Ma Pb-Zn-Ag replacement bodies in recrystallized but little altered limestone; M2. Minor bodies of exoskarn with Fe-Zn-Pb sulfides near porphyry dikes; 1. Eo-Ol conglomerate topped by continental volcanics; 2. Ol rhyolite dikes and sills; 3. ~37 Ma diabase and diorite dikes; 4. Cr1 microcrystalline platform limestone

Figure 7.57. Santa Eulalia West, Chihuahua, Mexico, cross-section from LITHOTHEQUE No. 1108, modified after Megaw et al. (1988)

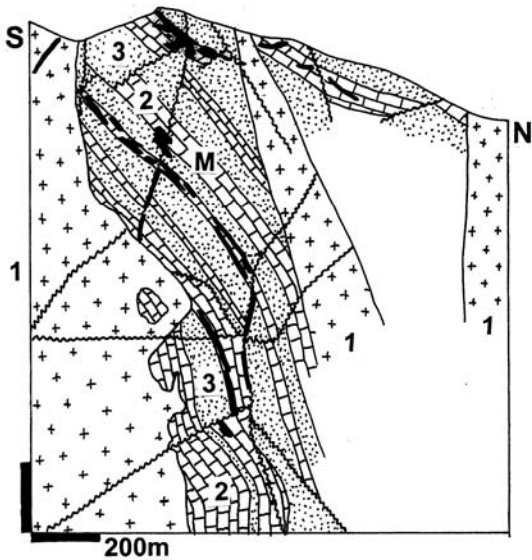


Figure 7.58. Bingham ore field, Utah, U.S.S.M. Pb-Zn-Ag mine; cross-section from LITHOTHEQUE No. 684 modified after Rubright and Hart (1968). M. Pb-Zn-Ag sulfides selectively replace limestone; 1. ~39 Ma quartz monzonite porphyry; 2. Cb3 limestone and hornfelsed calcareous shale grade to Ca-silicate hornfels and skarn; 3. Cb3 quartzite

Manganese accumulations in andean margins are small and insignificant and have the form of veins (Butte) or replacements (Philipsburg, Montana).

Antimony, because of its low clarke (0.3 ppm), forms numerous "geochemical giants" once a deposit exceeds 30 kt Sb. The following examples are in andean margins where the role of granitoids in their genesis is uncertain; some are probably (syn)orogenic deposits precipitated from metamorphic fluids. Southern Bolivia (between Tupiza and Potosi), mostly simple stibnite veins; Sierra de Catorce, Mexico, stibnite replacive mantos in limestone; Yellow Pine, Idaho: mineralized altered fault zone in silicate rocks.

Tin in the large Tertiary Bolivian "porphyry-Sn" deposits is clearly a part of the andean margin metallogene in the eastern magmatic belt. This is not the case of the Triassic Sn deposits in the central portion of the Bolivian Tin Belt (around La Paz), comparable with the collision-related tin provinces (e.g. Malaya). Other Sn provinces are in the same, transitional setting and are jointly treated in Chapter 10.

Boron in silicate minerals and complex oxides (e.g. datolite, szajbelyite, ludwigite, axinite, tourmaline, etc.) provides a low-grade, high-recovery-cost alternative to the evaporitic and hot-spring type B deposits as in the Mojave Desert of California. For the sake of self-sufficiency and strategic necessity deposits of this type have been developed in Korea, Liaoning Province of eastern China, and Sikhote Alin in the Russian Pacific area. There, the Dal'negorsk borate skarn deposit, cogenetic with the Pb-Zn-Ag skarns and replacements in the same ore field, is of interest (read Chapter 10).

Uranium forms, sporadically, small vein and disseminated deposits associated with highly fractionated leucogranites and syenites and small secondary deposits derived from them; the small Bokan Mountain deposit in SE Alaska is frequently mentioned. The more significant hydrothermal U deposits are reviewed in Chapter 10.

Thorium, recorded from andean margins, forms small insignificant vein deposits in the western U.S. Cordillera (e.g. Lemhi Pass), probably related to alkaline complexes.

Deposits in andean-margins related to tectonism and metamorphism (metamorphic-hydrothermal deposits)

Several important (syn)orogenic goldfields (e.g. Juneau, Alaska) and mineralized zones (e.g. the Mother Lode belt, California) also occur in the andean margins. There they are synchronous with collisions that accompanied "docking" of the "suspect terranes" in times of accretionary margin

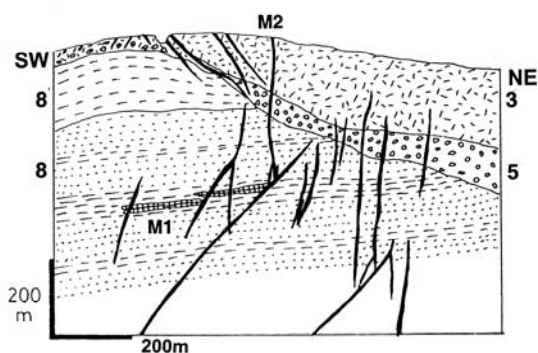


Figure 7.59. Fresnillo ore field, Mexico, cross-section of the Fortuna, Proaño and Populo ore zones from LITHOTHEQUE No. 1096.1, modified after Compañía Fresnillo S.A., 1985. M1. ~31-29 Ma Pb-Zn-Ag replacement mantos in marble and jasperoid; M2. Pb-Zn-Ag fault and fissure veins; 3. Ol quartz monzonite; 5. Ol2 continental conglomerate, paleotalus, tuff; 8. Cr1 graywacke, siltstone, shale > limestone

assembly. Collisions, combined with terrane convergence and subduction, produced geothermal regimes that facilitated magma generation, metamorphism and hydrothermal fluid movement (Goldfarb et al., 1993). Although the formation of large batholiths (e.g. the Coast Batholith of British Columbia; parts of the Sierra Nevada Batholith of California) and the ore fluids movement were broadly synchronous, the (syn)orogenic gold deposits like Alaska Juneau are now considered as metamorphic-hydrothermal, although "intrinsic" magmatic-hydrothermal deposits related to plutons, also occur (Newberry et al., 1995). Collision-related mesothermal gold deposits are reviewed, as a group, in Chapter 10.

Deposits of other metals, of (syn)orogenic origin, include the Coeur d'Alene Pb-Zn-Ag-Sb veins described above and comparable deposits elsewhere; disseminated sulfide deposits in shears mined mostly for silver (Candelaria in Nevada); small Ni sulfide deposits in sutures and shears with, or intersecting, ultramafics; Au, Sb and W deposits in shear zones; disseminated cinnabar deposit. All such deposits are of lesser magnitude, although Yellow Pine is a "large" gold deposit and a "Sb-giant". The Pinchi Lake cinnabar deposit in British Columbia (6,000 t Hg) is a "geochemical giant".

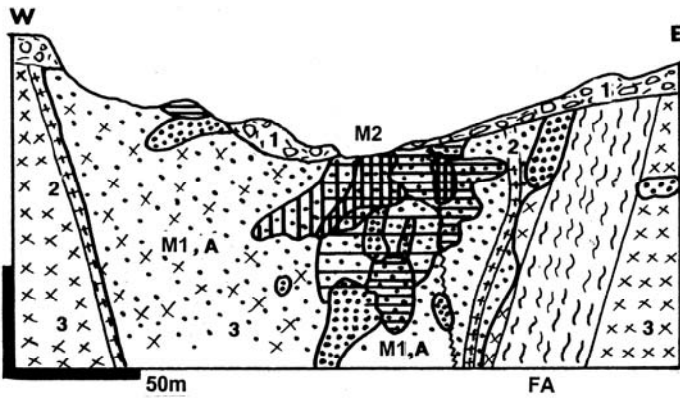
Yellow Pine, or Stibnite, ore field in central Idaho (Cooper, 1951; 79 kt Sb, 206 t Au, 6,365 t W, 170 t Ag; Fig.7.60) is controlled by the NE-trending

Meadow Creek Fault. The host rocks belong to a Jurassic to Cretaceous mesozonal pluton of slightly foliated biotite quartz monzonite, emplaced into lower Paleozoic carbonates and clastic meta-sediments, and intersected by numerous aplite dikes. About 50 m wide center of the fault is filled by gouge and breccia, and fracturing and shearing continues into the hangingwall quartz monzonite. The multistage mineralization broadly coincide with emplacement of Tertiary quartz latite, diorite and gabbro dikes. The earliest hydrothermal phase produced a broad zone of sparsely disseminated pyrite and arsenopyrite with gold values ranging from 1.4 g/t to 6.53 g/t, in sericitized, silicified and carbonate-altered fractured quartz monzonite. This was recently mined as a low-grade "bulk" orebody containing invisible gold, reminiscent of the Carlin-type. A small, high-grade (1.7% W) fine-grained scheelite orebody formed in the second stage. This is enveloped and overlapped by disseminations, thin veinlets, stockworks, lenses and small veins of stibnite ore selectively mined during World War 2 when the average grade was 4% Sb. Large amount of material with 0.81% Sb remains in ground.

Pinchi Lake deposit (Paterson, 1977; ~6,000 t Hg @ 0.75% Hg) is located in central British Columbia, in and along the margin of an important terrane boundary, the Pinchi Fault. Cinnabar with minor pyrite forms fracture coatings and veinlets in silicate fault rocks, and disseminated replacements when the host is marble. The wall rocks are a melange of late Carboniferous chert, marble, ophiolitic meta-basalt and serpentinite, plus Triassic-Jurassic graywacke, siltstone and limestone. Blueschist has a spotty distribution.

Common types of "inherited" deposits commonly present in andean-margins, but genetically unrelated to andean subduction and magmatism

Andean margins have been assembled from, and constructed on, a variety of rocks generated in the very distant past, in many environments. These basement rocks carry with them surviving pre-andean mineralizations, unmodified or modified (for example, remobilized) by subsequent lithogenesis and ore formation. These deposits are treated jointly with comparable deposits elsewhere in the framework of environments and rock associations in which they formed, rather than



- M1, A. Low-grade, disseminated "invisible" gold in quartz, sericite, clay altered cataclastic granitoids;
 M2. Higher-grade stibnite (horizontal ruling) and scheelite (vertical ruling) orebodies with diffuse boundaries in cataclastic granitoids and fault rocks (breccia and gouge). Au: dot pattern.
 FA. Brittle to ductile shear zone, variably silicified and sericite, clay altered.
1. Q landslides, glacial drift, alluvium;
 2. Eo latite, rhyolite dikes;
 3. Cr granodiorite, leucogranite,

Figure 7.60. Yellow Pine ore field, Idaho, Meadow Creek Sb-W-Au Mine. Cross-section from LITHOTHEQUE No. 1531, modified after Cooper (1951)

where they are now. The most common examples include the (marine) volcanics-associated massive Fe, Cu, Zn, Pb sulfides; banded iron formations; "sedex" Zn-Pb deposits; metalliferous phosphorites; Mississippi Valley-type Zn-Pb deposits; "sandstone uranium"; and others. Many are "giant" deposits.

8 Volcano-Sedimentary Orogens

Brief orientation: This chapter concentrates on deformed volcanic-sedimentary rock and ore associations that constitute the "eugeoclinal" domain (megafacies) of orogens. Their recent and "young" counterparts are in Chapters 4, 5 and 6, the old (Precambrian) equivalents in Chapter 9. Subduction-related granitoids that intrude these orogens and their mostly hydrothermal ores are in Chapter 7, high-grade metamorphics of all sorts in Chapter 14. There could be components of rift associations (Chapter 12) and intracratonic orogens (Chapters 10, 11). The eugeoclinal domain borders on the sediments-dominated miogeocline and platform (Chapter 13). The lithologic variety in this setting is immense and can be best visualized if one imagines the present Indonesian Domain (Hamilton, 1979) squeezed, after collision, between the SE Asian and Australian rigid cratonic complexes. To avoid repetition, the dominant "giants"-forming ore types pursued here are the Phanerozoic VMS; the (syn)orogenic Au, also abundant in this setting, are summarized in Chapters 9 and 10.

8.1. Introduction

Components of the "young" (Chapters 5, 6) convergent continental margins of accretionary, island-arc or andean-types earlier or later collide with, and accrete to, a continent or another arc, and undergo shortening and deformation as a result of such a collision. These island arc-dominated components are joined by slices of the oceanic crust and mantle that escaped subduction and all amalgamate, together with the predominantly continental basement, into an orogenic belt (orogen). Orogens are regional to continental, linear systems (collages) of deformed (folded, faulted) and variously metamorphosed rocks of many provenances. They also incorporate pre-, syn- and post-collision granitoid and other plutons. Orogenies, the collision events, have been traditionally named and dated and orogens named after the "strongest" orogeny (e.g. Variscan, Caledonian, Appalachian Orogen alias Variscides, Caledonides). Composite terrains resulting from several orogenies form orogenic complexes (e.g. Lachlan orogenic belt, Altaides) but, for the sake of brevity, the term "orogen" is used here for a variety of deformed belts in general.

There is a great selection of orogen settings, ranging from ensimatic (established on or incorporating oceanic crust) through transitional

(over predominantly island arc collages) to ensialic (intracontinental, intracrustal). There is even more orogenic styles based on what collided with what and how, recently classified and described by Şengör (1987), Şengör and Natal'in (1996). It is, however, not the purpose of this book to plunge into geotectonic polemics as our organization is based primarily on contrasting rock associations.

A classical, long-lasting continental margin orogenic system of constant polarity (growth and evolutionary trends have repeatedly progressed from the ocean in the west to the craton in the east) is exemplified by the American Cordillera or the Andes. One stage of development of these orogens, that of subduction-related volcanism (Chapter 6) and plutonism (Chapter 7) largely taking place while the orogen is welded to a craton, has already been reviewed. The present chapter deals mostly with rocks and ores that formed before, when the constantly growing orogen provided a docking edge for accretion of terranes being brought in, piggyback-style, from the oceanic domain by the subducting plate. Accretion commenced, in the Cordillera, as early as in Ordovician, first volcanic island arcs arrived in Middle Triassic. Together, the terranes added some 600 km wide swath of land to the Ancestral North America. As, statistically, the accreted terranes are mostly of oceanic, accretionary wedge, turbidite and island arc derivation with some mantle slices in collisional sutures, the mostly juvenile (that is, generated for the first time rather than recycled) volcanic-sedimentary rock association is of intermediate bulk composition (approaching quartz diorite). In the 1950s vintage geotectonics (Kay, 1951; Auboin, 1965) this was referred to as eugeosynclinal (later shortened to eugeoclinal) megafacies, in contrast to the miogeoclinal megafacies that is non-volcanic and deposited in sedimentary basins established on stable continental crust (Fig. 8.1). A miogeoclinal assemblage (Chapter 13) comprises the eastern portion of the Cordillera (e.g. the Rocky Mountains), established on Precambrian basement of the Canadian Shield. It is important to realise that the Cordilleran eu- and mio- domains are not contemporaneous, hence they formed under different conditions far apart.

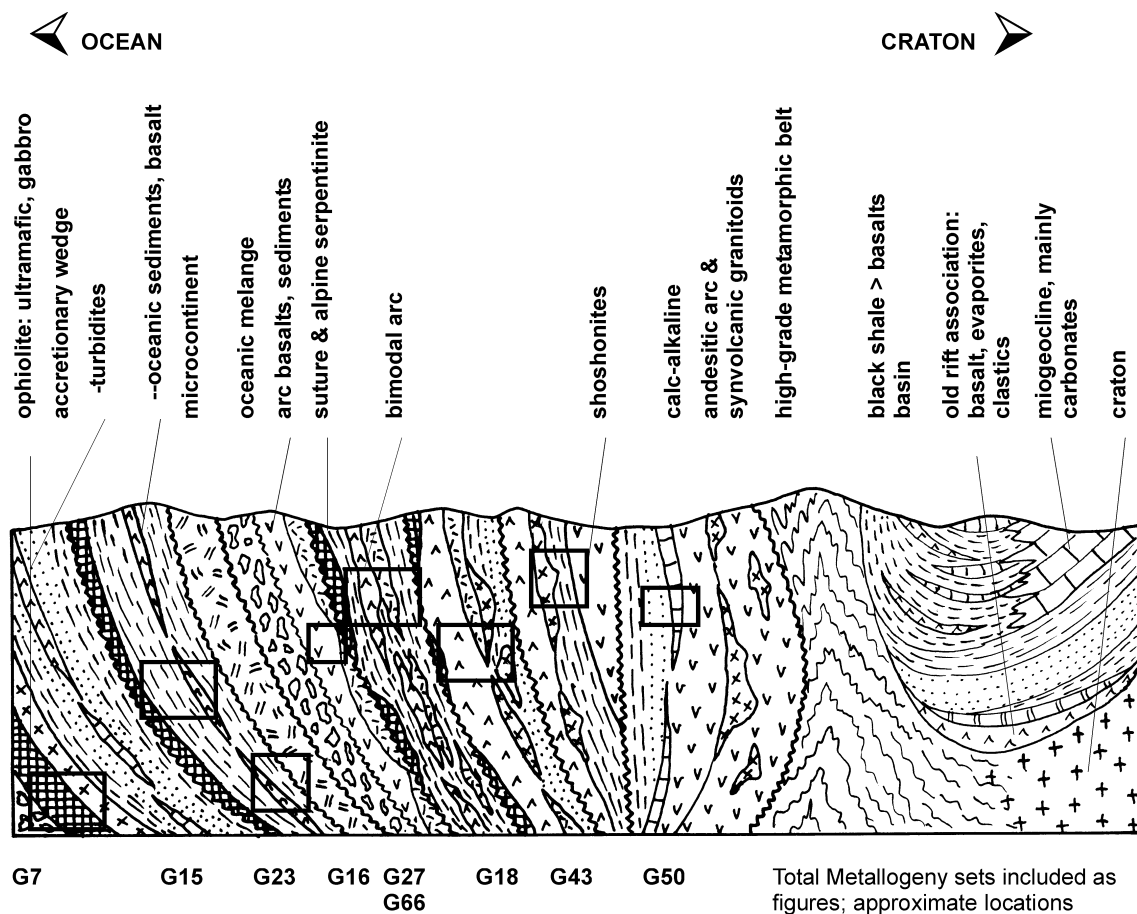


Figure 8.1. Inventory diagram (cross-section) showing rock associations expected in a late Precambrian to Phanerozoic volcanic-sedimentary orogenic belt (orogen) with single polarity (one progression of lithofacies from ocean on the left, to craton on the right). The actual place of the associations may vary, especially in composite orogens largely assembled by accretion and displaced by thrusting and strike-slip faulting. Not to scale. The more detailed "inventory diagrams" of rocks/ores appear as figures below, as follows: G7=Fig. 8.3; G15=Fig. 8.6; G23=Fig. 8.7; G16=Fig. 8.20; G27=Fig. 8.8; G43=Fig. 8.22; G50=Fig. 8.21.

Although the geosynclinal model and corresponding geotectonic cycle are now outdated and, since 1968, replaced by plate tectonics, the "eu" and "mio" terms continue to be officially used as a shortcut for the two contrasting lithologic mega-associations. They have been extensively applied in the *Geology of North America* volumes (Palmer and Wheeler, eds., 1980s-1990s). This chapter deals predominantly with the volcanic-sedimentary supracrustal component of orogenic belts and partly with the synvolcanic (pre-orogenic) plutonic rocks that are intimately associated. Ores genetically related to orogenic and post-orogenic granitoids and hydrothermal systems are in Chapters 6 and 7, although there is an overlap and often some interaction between the "basement" and the invading younger magmas. The early Precambrian

"greenstone belt" counterparts of eugeoclinal assemblages are not fundamentally different from the Phanerozoic except that they are more deeply eroded and there are some relatively minor differences caused by secular change. They have been placed into a separate Chapter 9 mostly to preserve a convention. High-grade metamorphics, anywhere, are in Chapter 14 as their original setting and genesis are often uncertain. The "young", and not significantly disturbed older rock associations related to rifts, with a high degree of individuality, are in Chapter 12, but extension-controlled lithologies subsequently incorporated into orogens, with which they shared the later part of history, appear in this chapter. Rifting and subduction-related rocks in orogens are notoriously difficult to

distinguish, especially when rifting is a second-order tectonic regime in subductive terrains.

8.1.1. Growth and evolution of composite eugeoclinal orogens as exemplified by the Canadian Cordillera

Although the central theme of this chapter are the volcanic-sedimentary (eugeoclinal) rock assemblages, a long-lasting orogen is a collage of lithologic associations that formed in many different environments that are, in this book, treated in several chapters. Although, for the purpose of classification and description, this helps to break a complex orogen into better manageable lesser components that are then treated separately, it obscures interactions between the many contrasting units. Such interaction is essential for formation of many types of ores.

In a nutshell one can distinguish, within a composite orogen, ores formed with their parent rock units before incorporation into the orogen (e.g. synvolcanic "Cyprus-type" VMS formed at oceanic spreading ridges), and ores hosted by a pre-collision unit, but formed during or after incorporation into the orogen (e.g. orogenic gold deposits, Ni-laterites). Still more orebodies are related to intrusions emplaced into orogens during and after the peak of deformation that are little influenced by the nature of the older basement (Fig. 8.2).

The Canadian Cordillera, evolution and ores:

Compositional heterogeneity of long-lasting orogens and its bearing on the variety of ore deposits is illustrated by geological history of the British Columbia and Yukon portion of the North American Cordillera in Canada, and adjacent Alaska. This review is based on Gabrielse and Yorath, eds. (1992) and Dawson et al. (1992), but only the "giant" and several "large" deposits are included as examples.

- pre-1.7 Ga. Formation of Canadian Shield, the continental basement; the Cordilleran Orogen evolved on its western margin.
- 1.7-0.78 Ga. Deposition of predominantly intracratonic and craton-margin detrital and lesser carbonate sedimentary basins on the Shield basement, with limited granitic plutonism. The "giant", presumably sedimentary-exhalational Sullivan Pb-Zn-Ag deposit (Chapter 11), and the synorogenic portion of Pb-Zn-Ag veins in the Coeur d'Alene district farther south in Idaho (Chapter 7), formed.
- 0.78-0.57 Ga. Formation of a rifted continental margin accompanied by minor mafic flows and dikes, carbonates, rare evaporites, red beds and glaciogenic diamictites, with more widespread monotonous "gray" detrital sequences. The "large"

Crest Fe deposit in diamictites and Coates Lake stratabound Cu in pelitic dolomite formed.

- Cambrian to Middle Devonian. Cordilleran miogeocline was established at the passive continental margin. Thick sequence of predominantly carbonates with lesser shale and sandstone gradually change facies from near-shore (carbonate platform to shelf) to off-shore (deeper basin), from east to west. Subordinate mafic submarine volcanics in the basinal facies are controlled by extension. Two "giant" Zn,Pb,Ag "sedex" deposits/ore zones (Howard's Pass, Faro-Anvil) formed in carbonaceous shales of the basinal facies (Chapter 13).
- Upper Devonian to Middle Triassic. Accretion in the west (at Pacific edge) initiated growth of the Cordilleran eugeoclinal megafacies, while the miogeoclinal megafacies continued its separate development in the east (in the Ancestral North American terrane). The carbonaceous shale basinal facies hosts two Zn-Pb-Ag sedex "giants" (Macmillan Pass in Canada, Red Dog in Alaska), and two "large" deposits of the same type (Gataga, B.C.; Lik-Sue, Alaska). The accreted terranes comprise predominantly oceanic lithologies (mafic meta-volcanics, siliceous slate, chert, reef limestone, ophiolitic melanges) with gabbro and diorite intrusions, and immature island arc successions with local shallow water sedimentary rocks. No "giant" deposits are known but Myra Falls is a "large" VMS field of Zn, Pb, Cu, Ag, Au in Devonian island arc volcanics.
- Middle Triassic to Oligocene. Predominantly andesitic island arc terranes started to accrete in the west (Nicola, Takla and Nikolai Groups), and coeval to slightly younger diorite to granodiorite and quartz monzonite intrusions produced series of porphyry Cu-Mo and Cu-Au deposits that include five "giants" (Highland Valley, Shaft Creek, Gibraltar, Kemess, Fish Lake; Chapter 7). In the "oceanic" Alexander Terrane formed the "Besshi-type" "giant" Windy Craggy and the nearby "Ag-giant" Greens Creek VMS. Terrane amalgamation and subduction continued, converting the rest of the Cordillera into an andean-type margin with andesitic, dacitic and rhyolitic volcanism on land. Sedimentary "successor basins" formed in fault depressions. Dextral transcurrent faults along terrane boundaries contain slivers of alpine-type serpentinite associated with the Hg "geochemical giant", Pinchi Lake. Stockwork-Mo "giants" (Endako, Alice Arm, Adanac, Rosslund, Smithers in B.C., Quartz Hill in Alaska) and three scheelite "giants" (Logtung, Cantung, Mactung) are related to granitic intrusions (Chapter 7). Two regional tectonic welts produced by compressional thickening of crustal rocks during or after collision of two superterranes in Jurassic and Cretaceous comprise high-grade metamorphic belts intruded and migmatitized by granitoids (Chapter 14). Only few "medium" to "large" Broken Hill-type Zn-Pb deposits are known. The "giant" orogenic Juneau

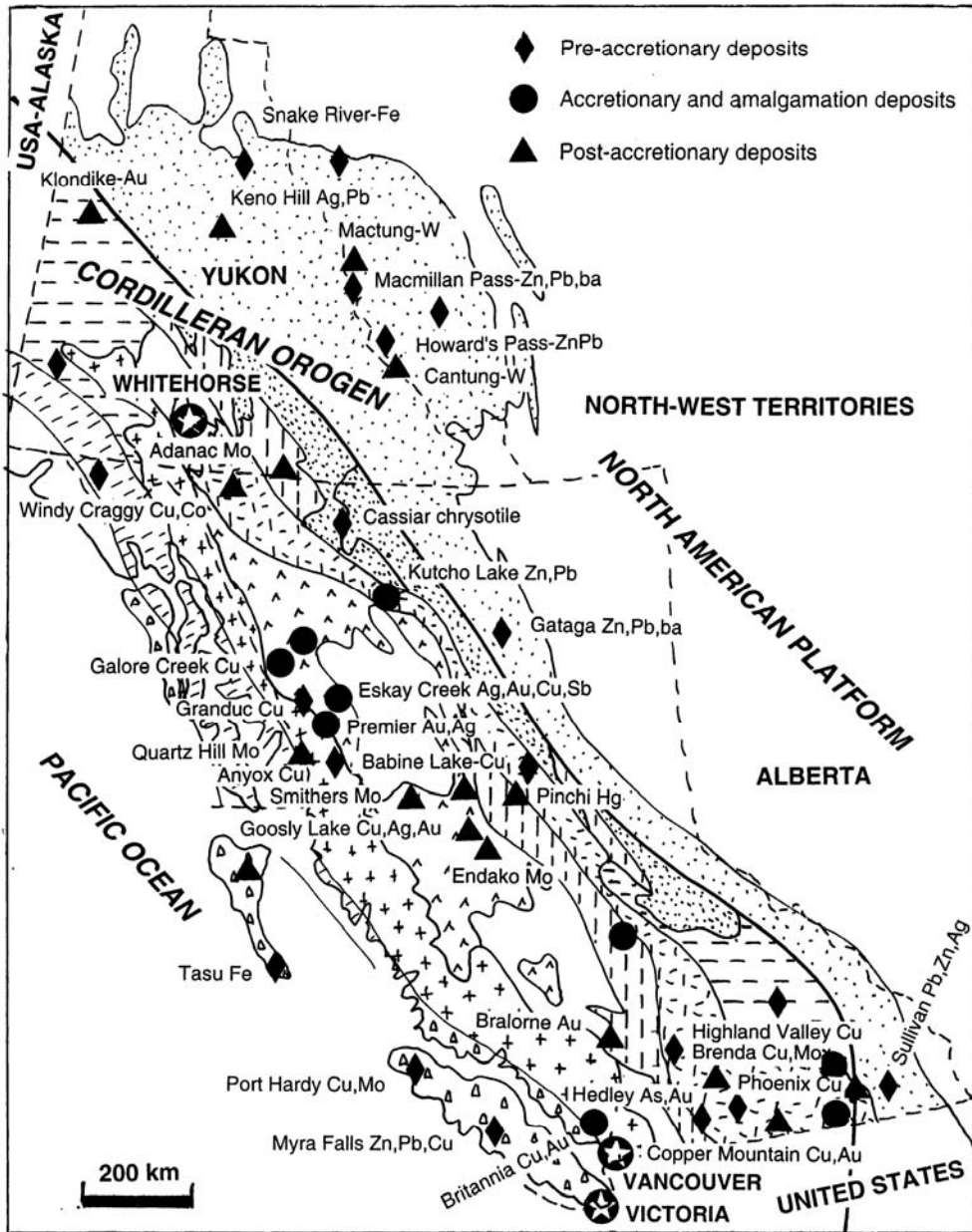


Figure 8.2. Map of the Canadian Cordillera showing the megafacies belts (domains) and prominent metallic deposits classified by timing of emplacement (pre-, syn- and post-accretion). Most of the deposits are granite-related and described in Chapter 7. Based on data in Geology of Canada no. 4 (Gabrielse and Yorath, eds., 1992), especially in Dawson et al. (1992)

gold belt is adjacent to the Coastal Batholith in Alaska (Chapter 10).

- Oligocene to Present. Subduction continued along several sectors of the Pacific coast, driving andean-type volcanoes in the Cascade Range. Extension in the Cordilleran interior belt facilitated extrusion of flood basalts. Stream erosion of the regolith over

vein gold occurrences produced placer gold, but "giant" goldfields (Klondike, Fairbanks) survived only in the non-glaciated regions of the Cordillera. Quaternary glaciation formed alpine valleys, thick drift fill and lakes but no metal concentrations.

Unfortunately, the Cordillera is not very rich in the VMS and Besshi-type deposits, a "flagship" of this chapter.

These seem most abundant in bimodal volcanic-sedimentary settings, usually interpreted as related to crustal extension in back-arcs or intra-margin rifts. The Cambrian volcanic-sedimentary sequences in Tasmania, Devonian in the Rudnyi Altai, and Lower Carboniferous in the Iberian Pyrite Belt are better endowed in VMS deposits and are described below.

Volcanic-sedimentary ("eugeoclinal") sub-associations: The brief review of Cordilleran evolution above mentioned most of the rock associations to be expected in eugeoclinal orogenms. This rest of this chapter provides more detail about the volcanic-sedimentary and pre-accretion plutonic sub-associations, minus those already reviewed in Chapters 6 and 7. The most important ore type here: VMS/Besshi is only briefly mentioned in the host lithology context here, but is treated in a greater detail in a special paragraph below. The principal lithologic associations are:

- ophiolite allochthons, melanges and alpine serpentinite
- oceanic successions
- mafic and bimodal predominantly marine volcanic-sedimentary sequences
- mafic-ultramafic intrusions
- calc-alkaline volcanic-sedimentary successions
- felsic volcanic-sedimentary successions
- turbidites
- slate/schist, carbonates, chemical sediments

7.2. Ophiolite allochthons, melanges and alpine serpentinite

Since the 1970s it has been firmly established that the ophiolite association (serpentinized peridotite, gabbro, diabase, tholeiitic basalt, chert/jasper) are samples of ancient oceanic crust with corresponding stratigraphy (Chapter 4), saved from disappearance down subduction zone by tectonic emplacement onto the continental crust (Dewey and Bird, 1971). The majority, if not all, examples of the ophiolite association are thus allochthonous, variably tectonized and dismembered. Tectonic slivers of serpentinite alone, sometimes grading into melange, are known as "alpine serpentinite" in the literature. The strong deformation, metamorphism and alteration affected ophiolites first in the time of formation at and under spreading ridges, then again during the emplacement onto the continental margin by tectonic underplating, incorporation into a subduction complex followed by exhumation, accretion of MORB and seamounts, overthrusting and obduction, extrusion into collisional sutures.

Many ophiolites have further been variably modified during residence within the continental crust. Bona fide ophiolites range in age from Tertiary to Neoproterozoic; Meso- and Paleoproterozoic ophiolites are rare, controversial, incomplete and usually strongly metamorphosed. Archean ophiolites are unknown and ultramafic occurrences there are members of the komatiite association or intrusions into the crust (read below).

Although the early interpretations automatically assumed that ophiolites were accreted remnants of former mid-ocean ridges, more recent research favors formation of many (if not most) ophiolite complexes in extensional structures above subduction zones, as in back-arc and some fore-arc basins ("suprasubduction ophiolites"). The "mid-ocean" ophiolites often contain a lherzolite component (a former mantle) as in the Jurassic western ophiolite belt in Albania (Beccaluva, ed., 1994). The suprasubduction ophiolites like the Josephine Complex in Oregon (Harper, 1984; Alexander and Harper, 1992), California Coast Range (Coleman, 2000), Zambales Range in Luzon (Hawkins and Evans, 1983), Mayarí-Baracoa area of eastern Cuba (Proenza et al., 1999) and many others, are dominated by the residual harzburgitic tectonite. Although the fully developed ophiolites in the suprasubduction setting have the right "oceanic" lithology, the broadly associated rocks are increasingly "continental" or "nondescript" and reviewed below.

Like the modern oceanic association, ophiolites are geochemically enriched in Mg, Fe, Cr, Mn, Ni, Co, Cu and PGE, sometimes to such an extent that some "rocks" themselves become potential ores of the future (e.g. the Coto, Luzon, harzburgite has up to 0.315% Ni and 0.61% Cr; Hawkins and Evans, 1983). These elements accumulate in numerous occurrences most of which are of small size. The common ore types originally established at spreading centers then preserved in ophiolite allochthons, usually in a highly tectonized form, include podiform chromites; "Cyprus" and "Besshi"-type Fe, Cu, (Zn, Co) massive and stockwork sulfides; Mn oxides and silicates associated with chert and jasper. Ores that resulted from interaction of tectonism (e.g. shearing) and hydrothermal activity with members of the ophiolite association include gold (also Co, Ag) "listvenite", chrysotile asbestos fracture stockworks in serpentinite, and "California-type" cinnabar deposits. Ores that resulted from weathering-upgraded geochemically enriched metals in rocks, especially in the ultramafics, include Fe, Ni, Mn, Co, Cr and possibly PGE. The following ore types have

reached the "giant" magnitude in ophiolites or there is a possibility that they might so (Fig. 8.3):

- Podiform chromite
- California-type (silica-carbonate) Hg deposits
- Ni (Co) laterite/saprolite

Metals from raw ultramafics

Refractory peridotite is a strong repository of geochemically pre-enriched metals such as Cr, Ni and Co. Its on-land equivalents in ophiolite and alpine serpentinite associations came close to become one of the industrial sources of magnesium, so far realized only when the "environmental money" subsidize the cost of Mg extraction from silicates as in processing the serpentinite waste dumps left after chrysotile asbestos mining (e.g. in the Black Lake-Thetford Mines field, Quebec). Although serpentinite contains between 37 and 52% MgO, the Mg silicate bond requires more energy to break than what is needed for Mg recovery from carbonate or chloride. With the average 0.2% of trace Ni and 0.2-0.5% of trace Cr ophiolitic/alpine peridotite is only a small step away from becoming industrial source of these metals in the near future. When this happens politico-economic factors will determine the location of deposits. At present, only 4 to 6 times enrichment of peridotite trace metals content is needed to produce economic Ni, Co, Cr and Fe orebodies, some of which are of "giant" magnitude, from ophiolitic ultramafics in the lateritic weathering environment (read below).

Podiform chromite

Cr enrichment of mantle peridotites in general and the refractory peridotite in particular is visually demonstrated by the presence of ubiquitous scattered chromite grains; they locally aggregate to form podiform chromite deposits. Of several thousand recorded deposits of this type the majority is small and only aggregate ore tonnages of districts or whole regions (such as "Turkey", "Albania") ever achieve the "large" magnitude. The largest **Kempirsai Cr district** in Kazakhstan has a resource of 300 mt of chromite (Melcher et al., 1999). In the Main Ore Field near Khromtau Alpoor magnesiochromite forms up to 2 km long and 230 m thick lenses, sheets and pods in a 25 km long belt. The host rock is mostly serpentinitized harzburgite. The 420-400 Ma old, metamorphosed Kempirsai ophiolite massif is located in the southern extension of the Urals Mountains and is

interpreted as exhumed from a site more than 50 km deep in a subduction zone.

Opinions differ as to the origin of ophiolitic chromites, although they are clearly syngmatic. The traditional genetic models assumed chromite segregation in the mantle, followed by plastic deformation, then dismemberment in a MORB conduit still within the mantle, or during obduction. More recent models (e.g. Edwards et al., 2000) favor separation of chromite from basaltic melts passing through the upper mantle below a spreading ridge as a result of magma mixing, contamination or hydration. The well layered varieties of chromite in ophiolitic cumulates probably formed as chromite-olivine cumulus in basaltic magma chambers, synchronous with MORB extrusions. Apparently the largest podiform chromite deposits as in the Zambales Range in Luzon and in the Kempirsai district (Melcher et al., 1999) formed in the suprasubduction setting. In addition to chromite, syngmatic accumulations of Fe, Ni, Co sulfides with or without platinoids, as well as titanomagnetite or ilmenite, are also known from presumed MORB cumulates. Although they closely resemble the Bushveld-type ores (Chapter 12) all are small deposits. Although discovery of larger deposits is possible, the very dynamic nature of the MORB systems and small volume of their land-based equivalents makes discovery of giant Cr deposits highly unlikely.

Cyprus and Besshi-type VMS

Although these Fe > Cu, Zn sulfide types are very popular in the literature (type areas are the Troodos Complex in Cyprus, Semail Ophiolite in Oman, and the Sambagawa terrane in Shikoku, Japan; Slack, 1993), most deposits are small to medium-size and very few reach the "large" magnitude; if so, published figures are mostly aggregate tonnages of many smaller deposits distributed over a large area (e.g. the Troodos Complex in Cyprus stored about 900 kt Cu in more than 20 deposits). Ducktown, Tennessee (1.63 mt Cu); Besshi, Japan (700 kt Cu); Ergani Maden, Turkey (680 kt Cu, 25 Kt Co). Other Cu, Co, Zn massive sulfides associated with submarine meta-basalts and/or sediments, listed as of Cyprus or Besshi types, reside in overall "eugeoclinal" associations short of the exact ophiolite model. In their review of ophiolite-hosted volcanogenic massive sulfides, Galley and Koski (1999) listed some 70 localities assembled from some 200 ophiolite occurrences around the (Western) world but all are small to "medium" size. Løkken is the only "large" deposit.

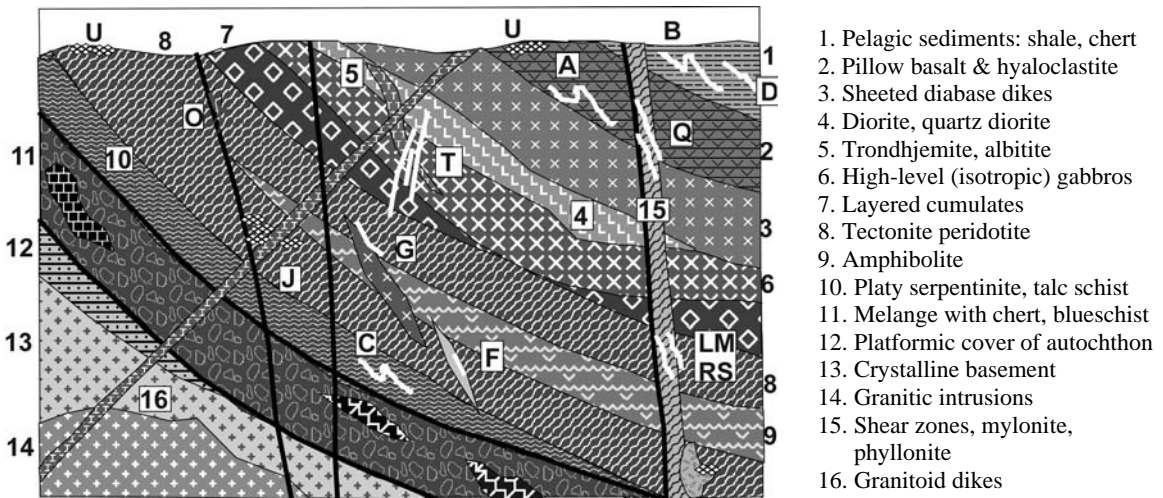


Figure 8.3. Ophiolite allochthon, rocks & ores inventory diagram from Laznicka (2004), Total Metallogeny site G7. ORE TYPES: A. Metamorphosed Cyprus-type VMS; B. Metamorphosed Besshi-type Cu, Zn; C. Sheared chromitite; D. Tectonized sedimentary Mn; F. Emerald, chrysoberyl at pegmatite/ultramafic contacts; G. Ni, Cu, PGE sulfides at gabbro contacts; J. Chrysotile asbestos fracture stockworks; L. "Listvenite" (silica-carbonate) Au; M. Co, As, Ag in altered sheared serpentinite; N. Mesothermal Pb-Zn-Ag replacing carbonatized ultramafics; O. California-type cinnabar; Q. Chalcopyrite stringers in sheared basalt; S. Ni (Co, Cu) sulfide mobilizates in shears; U. Metalliferous laterite & saprolite (mostly Fe, Ni, Co, Cr, Al, Au); W. Resedimented regoliths. Ore types B, O, U include "giant" equivalents

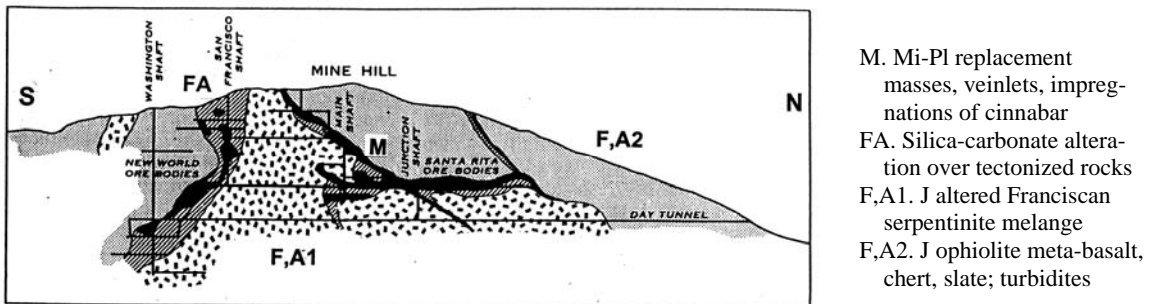


Figure 8.4. New Almaden Hg ore field, metropolitan San José, California.. Historic cross-section of the Day Tunnel Mine after Schuette, reprinted from Bailey and Everhart (1964), U.S. Geological Survey

- M. Mi-Pl replacement masses, veinlets, impregnations of cinnabar
- FA. Silica-carbonate alteration over tectonized rocks
- F,A1. J altered Franciscan serpentinite melange
- F,A2. J ophiolite meta-basalt, chert, slate; turbidites

There seems to be some potential for additional greenfield discoveries of major stratabound Fe, Cu (Co, Zn) deposits associated with ophiolites and the type to watch for are presumably synsedimentary (alternatively synorogenic?) nickel deposits spatially associated with ophiolitic serpentinite of which, so far, only several small representatives are known (e.g. Rolette, Québec; Jabal Mardah, Saudi Arabia; Carten and Tayeb, 1990). The latter is a 10 km long ore zone within the Neoproterozoic Darb Zubaydah ophiolite that contains several massive, disseminated and stockwork bodies of pyrite, millerite, polydymite and/or vaesite in greenschist-metamorphosed basaltic turbidites. The largest

orebody contains 1.5 mt ore @ 0.8% Ni and is interpreted as having formed in a submarine canyon or in an inter-fan setting in a spreading centre.

Silica-carbonate (or California-type) cinnabar deposits

Although demand and price of mercury are at a historically low at present, many economically little significant Hg deposits qualify as "geochemical giants" because of the extremely high Hg tonnage accumulation index. A substantial proportion of cinnabar deposits are spatially associated with serpentinite (Fig. 8.4), although they are younger,

low-temperature hydrothermal ("hot spring"), and controlled by major fault or melange zones (Henderson, 1969). The type example is the **New Almaden Hg ore field** in suburban San José, California (38,090 t Hg @ 2.21% Hg; Bailey and Everhart, 1964). There, fine-grained to microcrystalline cinnabar replaces or fills fractures in silica-carbonate altered Franciscan serpentinite and associated rocks. The ore is the product of a Pliocene hot spring system controlled by fracture and interfragmental permeability in a melange body, confined by impervious screen of clay fault gouge. **New Idria** (19 kt Hg) and **Mayacmas** (13 kt Hg) are similar deposits in California, although the host rocks are mainly turbidites. Although mercury itself is of little interest now, cinnabar and trace Hg are one of the favorable indicators of the "hot spring" Au (Ag, Sb) deposits. The "large" McLaughlin deposit in Napa Valley, California (91 t Au @ 5.4 g/t, estimated ~34 kt Sb; Lehrman, 1987) has been discovered under the small Manhattan cinnabar mine.

Fe, Ni, Mn, Co, Cr in laterite and saprolite

Humid tropical weathering of any (not only ophiolitic) ultramafic rock causes removal of silica and magnesia, leaving residue further enriched in Fe, Ni, Co and Cr over the already high preconcentration of these elements in the parent rock. Under favorable physiographic conditions and with a suitable protection from erosion (for example, under ferricrete capping/cuirasse), large residual Ni deposits can form and survive. Nickel laterite/saprolite deposits are now the second largest source of nickel after Ni sulfide deposits (e.g. Sudbury, Noril'sk), and they contain larger Ni resource. Several "Ni laterites" are true giants.

New Caledonia lateritic Ni province, western Pacific.

The island of New Caledonia is the largest and richest Ni laterite/saprolite province in the world and also one where industrial extraction of Ni from hydrosilicates has been going on since 1908. The island (Paris, 1981) measures about 400 x 50 km and is composed of Permian to Lower Tertiary continental margin sediments, volcanics and metamorphics. These are locally topped by Eocene tholeiitic basalt on which rest numerous allochthonous massifs (klippen) of peridotite emplaced in late Eocene. The ultramafics cover nearly 30% (6,000 km²) of the island. The peridotite massifs are mostly harzburgite with some dunite

and lherzolite and are associated with minor slices of serpentinite and ultramafic/mafic cumulates.

The fossil (Oligocene and younger) humid weathering profile (regolith) is developed over most peridotite massifs and is protected by an up to 30m thick ferruginous duricrust (cuirasse) topping plateaux. This is in itself a major metal accumulation that stores some 15 bt of 30-65% Fe, so far non-utilized. The lateritic carapace under the duricrust consists of soft pink zone of Fe-oxide microconcretions in clay matrix that change with depth into mottled zone and yellow to green smectitic saprolite resting on leached and locally silicified (saprock) and eventually fresh peridotite. Nickel concentration increases steadily downward from the carapace and is highest in the greenish-brown saprolite. There it is represented by dispersed to fracture-filling Ni-hydrosilicates ("garnierite", pimelite) with grades between 2-3% Ni and 0.05-0.08% Co. Spectacular green Ni-hydrosilicate fracture infiltration veins grade up to 10% Ni and reach deep into the saprock. The overlying "yellow laterite" is of substantially lower grade (~1.3-1.6% Ni) but it is rich in Mn oxides and patches of asbolite (Co-enriched Mn oxides). Hitherto rarely exploited, the yellow laterite is the principal ore in the "world class" **Goro** deposit, presently under development.

The New Caledonian Ni ores are exposed high on flanks of eroded plateaux ("mines hautes") close to remnants of the protective cuirasse, but have been removed by erosion farther downslope. The total New Caledonia metals resource is of a "super-giant" magnitude and it has been variously estimated as between 50 and 80 mt Ni and ~2.5 mt Co (Paris, 1981). More ore remains under the plateau interior. Data for individual workings are hard to get; for example, the recently developed Goro concession is credited with reserves of 165 mt @ 1.6% Ni and 0.16% Co for 2.64 mt Ni..

In the rest of the world, based on imperfect data, there are two "Ni-giants" (Moa, Cuba; 9.8 mt Ni; Palawan, Philippines, 6.3 mt Ni) and at least ten "large" deposits/districts of Ni-laterite/saprolite with 2 mt Ni plus (Soroako, Indonesia, 4.4 mt Ni; Biankouma-Touba, Ivory Coast, 4.3 mt Ni; Davao, Philippines, 4 mt Ni; Gag Island, Indonesia, 3.93 mt Ni; Ramu River, PNG, 3.5 mt Ni; Murrin Murrin, Australia, 2.9 mt Ni; Marlborough, Australia, 2.142 mt Ni; Nicaro, Cuba, 2.1 mt Ni; San Felipe, Cuba, 2 mt Ni; Pinares de Mayarí, Cuba, 2 mt Ni; Falcondo, Dominican Republic, 2 mt Ni). The Western Australian deposits (Murrin Murrin near Laverton, Cawse and Bulong near Kalgoorlie) formed on Archean komatiitic ultramafics.

Resedimented Mg, Fe, Ni, Co regoliths on ultramafics

Residual metalliferous weathering crusts undergo erosion and mass wasting, which sometimes produce resedimented deposits. In New Caledonia these include Ni (Co) mineralised talus and coluvium, alluvium, hematite beach sands, and nickeliferous lagoonar clays (compare Laznicka, 1985) but because of the abundance and richness of the in-situ regolith these occurrences are not of economic interest now. Elsewhere, as in the Greek Larymna and Evia districts, in the Urals, Kosovo and Macedonia, Ni-hydrosilicates have been redeposited and are now karst and/or Ni-Co rich goethitic iron ores. Both types of deposits are, however, of the "medium" magnitude at best.

Microcrystalline ("amorphous") magnesite

Microcrystalline magnesite is one of the common residual minerals to form in lateritic regoliths on ultramafics, but the numerous occurrences are small and erratic. In **Kunwarara, Queensland** (Milburn and Wilcock, 1998; Rc ~1.2 bt magnesite concentrate at 20% MgCO₃ cutoff, for 345 mt Mg; Figure 8.5) such magnesite has been reworked and reprecipitated in nodular form to form a shallow, easy to mine stratiform flat lying "world class" orebody.

8.3. Oceanic successions

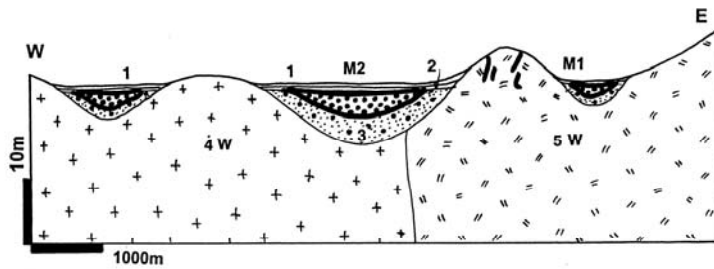
This term enjoys a liberal use in the literature but well preserved, little disturbed equivalents of the ocean floor stratigraphy have rarely been preserved in orogenic belts. Most "oceanic terrains" are allochthonous, in disrupted and heavily tectonized accreted terranes or in thrust sheets and nappes transported onto the continental margin or earlier allochthons. Some "oceanic" successions are complementary to ophiolites, to which they are the stratigraphically higher members. They include mid-ocean ridge basalts, pelagic and hemipelagic silicites (cherts), red claystones, pelagic limestones. Some meta-basalts and frequent units of shallow water limestones are interpreted as accreted seamounts or Hawaii-type oceanic islands with limestone reef caps.

In the Canadian Cordillera the Devonian to Triassic Slide Mountain Terrane (Monger et al., 1991) is the first accreted allochthon thrust over the western margin of the Cordilleran miogeocline. This, and the similar Cache Creek Terrane, have

masses of shallow-water fusulinid limestone enveloped by radiolarian chert, silvery argillite, siliceous slate, turbiditic wacke with discontinuous units and blocks of tholeiitic basalt, gabbro and alpine serpentinite. There is also a complement of rare granitic rocks and mature sediments. Stacked and imbricated thrust sheets grade into melange. The "incompatible" lithologies resulted from basement incorporation during tectonic transport, or came from flanks of intracontinental backarc basins. The Cretaceous Rocas Verdes assemblage in Patagonia interpreted by Saunders et al. (1979) as a succession formed in a basin on extended continental crust, is a transition between ophiolite (lacking the ultramafic members) and the Cordilleran oceanic suites mentioned above.

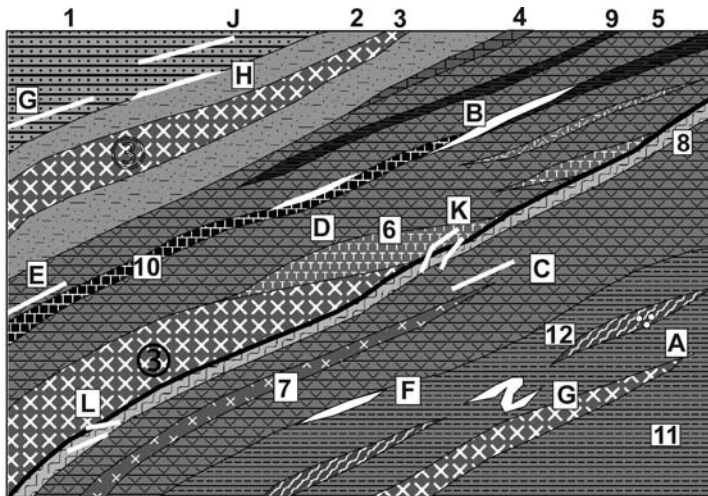
The "oceanic" metallogeny merges with one related to immature island arc and back-arc assemblages and it is impossible to separate them (Figures 8.6. & 8.7). The ore content consists of scattered small deposits of sedimentary Mn oxides, carbonates and silicates; podiform chromite in serpentinite; "Cyprus-type" Cu-rich VMS in and along meta-basalt contacts.

Subaerial to shallow marine basalt, cover carbonates, and the Kennecott-type Cu-Ag deposits: The subaerial to shallow submarine Triassic Nikolai Greenstone in SE Alaska, the similar Karmutsen Group basalts on Vancouver Island, and the comparable, although younger, Comodú Volcanics in Baja California, are an anomaly among the predominantly deep-water oceanic and island arc accreted terranes. The Nikolai Greenstone (MacKevett et al., 1997) is an up to 1.8 km thick sequence of mostly subaerial, green to purple (oxidized) basalt flows of uncertain origin (an accreted oceanic plateau like Ontong Java? accreted pre-MORB Iceland style volcanics?). The Nikolai basalts are high in trace Cu (at 155 ppm six times the Clarke), that still resides in the rocks in contrast to the copper in Na-altered submarine basalts that lost much of it to the environment. At **Kennecott Mines near McCarthy**, Alaska (MacKevett et al., 1997; P_{to 1938} 4.017 mt ore @ 13% Cu for 536 kt Cu, ~100 t Ag) the basalt is overlain by intertidal to shelf-type late Triassic limestone that, in turn, hosts replacement Cu sulfide deposits. The orebodies fill and replace steeply dipping fissures and adjacent breccia, enlarged near base. Massive chalcocite and djurleite are dominant and there are minor relics of earlier pyrite, chalcopyrite and bornite. 95% of the ore precipitated from 90°C hot fluids at sites of mixing of oxidized Cu-rich brines rising from the Nikolai



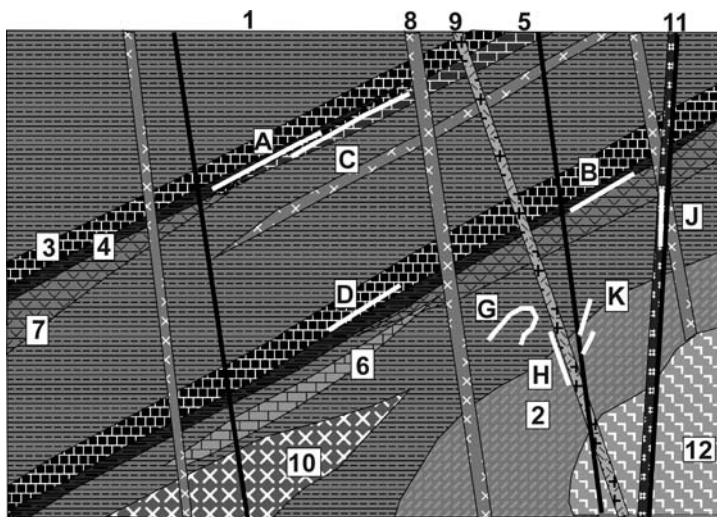
- 1. Q2 black clayous soil
- 2. Mi-Q1 channel mudstone on regolith
- 3. Ditto, sandy clay
- M2 in 3. Microcrystalline magnesite, locally dolomite nodules in sediment
- M1 in 5W. "Amorphous" magnesite veins in ultramafic regolith
- 4W. Weathered Pe3-Tr1 plutonics
- 5W. Weathered ~562 Ma ophiolites

Figure 8.5. Kunwarara magnesite in regolith over the Marlborough ophiolite complex, Queensland. Diagrammatic cross-section from LITHOTHEQUE No 2959 based on data in Milburn and Wilcock (1998) and field visit



- 1. Turbidites (sandstone & shale); 2. Subaqueous basalt tuff; 3. Gabbro; 4. Limestone; 5. Submarine basalt flows & hyaloclastites; 6. Trondhjemite, keratophyre; 7. Diabase dikes & sills; 8. Chloritic schist in shear zone; 9. Black slate, phyllite; 10. (Meta)chert; 11. Footwall schist, phyllite; 12. Serpentinite slivers.
- A. Podiform chromite; B. Bedded Fe sulfides in volcanics; C. VMS Cyprus type in volcanics; D. Bedded Fe in volcanics; E. Ditto, cherty Mn; F. Besshi-type VMS; G. Bedded Fe in sediments; H. Bedded pyrite/pyrrhotite in sediments; J. Bedded Mn in sediments; K. Mesothermal Au veins; L. Ditto, Cu sulfides, veins

Figure 8.6. Basalt-dominated marine "geoclinal" assemblage (mixed oceanic, back-arc, immature arc components) and the recorded ores (C, F and K types have "giant" equivalents). From Laznicka (2004) Total Metallogeny site G15



- 1. Slate to phyllite, litharenite
- 2. Thermally hornfelsed slate
- 3. Black (carbonaceous) chert
- 4. Black slate
- 5. Bedded Mn carbonates
- 6. Pelitic limestone
- 7. Spilite (albitized basalt)
- 8. Diabase dikes, sills
- 9. Quartz diorite porphyry
- 10. Synvolcanic gabbro
- 11. Late orogenic lamprophyre
- 12. Synorogenic quartz diorite
- A. Stratiform pyrite/pyrrhotite
- B. Bedded siliceous Mn in chert
- C. Bedded pyritic Mn carbonate
- D. Metalliferous black slate or chert
- G. Synorogenic Au (Cu, Sb, As) lodes
- H. Au (Sb) mesothermal veins
- J & K. Pb-Zn-Ag & U veins

Figure 8.7. "Eueoclinal" slate-dominated association from Laznicka (2004), Total Metallogeny site G23. Ore types C, G and H have known "giant" equivalents

basalt, and evaporitic S-rich fluids from the limestone and dolomite, during the Cretaceous.

8.4. Mafic and bimodal marine volcanic-sedimentary successions

Marine sequences dominated by tholeiitic basalt units, monotonous meta-pelite, immature wacke, ribbon chert, occasional deep-water or shallow water limestone, are usually interpreted as of immature island arc origin, although the bimodality is suggestive of rifting; perhaps in back-arc basin or intra-arc rift and there could be some "oceanic" components (Figs. 8.6., 8.7). Gabbro or diorite stocks are common and felsic rocks (dacite, rhyolite, plagiogranite) form flows, flow breccia, peperite, pyroclastic and volcanoclastic units, small intrusions and plutons. The magmatic rocks are predominantly sodic (spilite=Na metabasalt; keratophyre=Na dacite; trondhjemite=Na granodiorite) and this used to be attributed to a distinct magmatic series, although metasomatism through magma-sea water interaction is now the mainstream interpretation (Fig. 8.8). Both bedded and transgressive albitites occur.

8.4.1. VMS deposits

VMS is the most common and economically important ore type in this setting. The terms VMS (volcanic or volcanogenic massive sulfides), alternatively VHMS (volcanics-hosted massive sulfides) are frequently used incorrectly, as many of the prominent examples like Brunswick No. 12 and many deposits in the Iberian Pyrite Belt are actually in sedimentary rocks (hence corresponding to the Besshi-type). Some deposits like Greens Creek (Taylor et al., 1999) are considered a VMS-sedex hybrid. VMS have a rich literature (Large, 1992; Barrie and Hannington, 1999) so no extensive introduction is needed here. The popular models and their type deposits are briefly described in Chapters 4 (recent sulfides at oceanic ridges), 5 (deposits formed in back-arc including kuroko), this Chapter 8 (Cyprus, Besshi, Rio Tinto), Chapter 9 (VMS in greenstone belts, e.g. Noranda). VMS are greatly modified by deformation and metamorphism, the intensity of which is statistically proportional to age. The "young" (pre-orogenic deposits like those in Chapter 5) are "pristine": undeformed and still in a setting and position in which they formed, whereas in the strongly deformed and metamorphosed deposits the syndepositional features have been weakened or obliterated altogether and overprinted by deformational textures and structures and metamorphic minerals. The "secondary" characteristics often mimic the "primary" ones (e.g. VMS and sedex banding is frequently

metamorphic, not sedimentary; compare McClay, 1983; original breccias are obscured by fragment stretching and flattening) that makes many early interpretations unreliable.

Of the VMS host rock associations distinguished by Barrie and Hannington (1999) the bimodal-mafic, partly bimodal-felsic, bimodal-siliclastic and partly mafic-siliclastic associate with the majority of deposits that include "giants". The felsic members seem to be essential for ore genesis and Hart et al. (2004) tried to determine, using trace element geochemistry and petrogenesis, which felsic varieties are favorable to associate with ores, and which are likely to remain barren. They found tholeiitic rhyolite depleted (in the ore metals); high-silica rhyolite favourable; alkali dacite-rhyodacite barren; and most calc-alkaline felsics in-between.

In the Caledonian orogen in Norway and Sweden (Grenne et al., 1999) the Ordovician and Silurian Gula, Støren, and Stekenjokk-Fundsjø sequences of the above type host abundant Cu-Zn VMS and Besshi-type deposits most of which are small to medium, although Stekenjokk (663 kt Zn, 372 kt Cu, 1300 t Ag) and Løkken (690 kt Cu; 540 kt Zn; 1500 t Se) are of the "large" magnitude. Ordovician to Lower Carboniferous massive sulfides in meta-volcanics are also widespread in the Urals (Prokin et al., 1998), in what is probably the world's longest (2,000 km) VMS belt in Russia and Kazakhstan. The Uralian VMS can be subdivided into those associated with bimodal and calc-alkaline suites, respectively. The former is dominant and include the largest deposits. **Deptyarka** (Magak'yan, 1968; 120 mt ore plus), 40 km SW of Yekaterinburg, is a flat, 4800 m long tabular body of fine-grained pyrite with subordinate chalcopyrite, sphalerite and rare bornite, tetrahedrite, galena and arsenopyrite in late Silurian-early Devonian keratophyre and quartz-sericite schist. A significant proportion of copper (estimated at about 1.5 mt Cu) came from the zone of secondary sulfides rich in chalcocite. Other significant VMS ore fields in the Urals include **Uchaly** (Rc 113 mt @ 1.08% Cu, 3.73% Zn, 18 g/t Ag and 1.26 g/t Au for 4.215 mt Zn, 1.22 mt Cu, 2,034 t Ag and 142 t Au), **Gai, Buribay, Sibay and Blyava**. Reliable tonnage figures are hard to get; at least Uchaly, Buribay and Sibay are likely of the "giant" magnitude. Other predominantly meta-volcanics-hosted Phanerozoic VMS in bimodal suites include those in the Cambrian Tulgheş Series in the Romanian Carpathians (e.g. Baia Borşa, ~100 Mt ore plus), Fundul Moldovei,

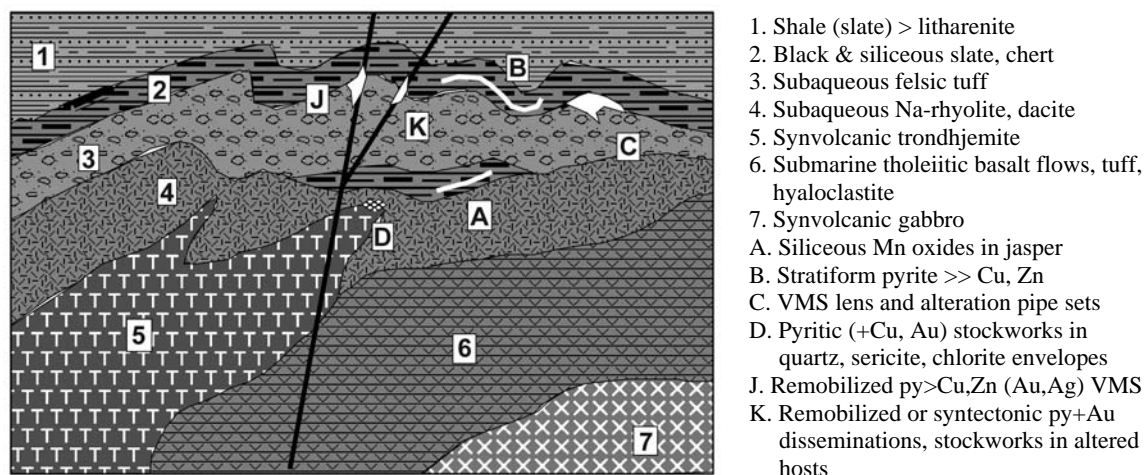


Figure 8.8. "Geoclinal", submarine bimodal volcano-plutonic and sedimentary association. Rocks and ores inventory from Laznicka (2004), Total Metallogeny set G27. Ore types C, D may have "giant" equivalents

Leşul Urşului; the selenium-rich pyritic VMS Yanahara in Honshu (32 mt @ 1.2% Cu and 0.01% Se for 3,200 t Se content); the newly discovered **San Nicolas** in Zacatecas, Mexico (100 mt of ore containing 1.6 mt Zn, 1.36 mt Cu, 150 kt Pb, 2400 t Ag and 41 t Au). The important, "giants" containing VMS belts and districts of South Iberia, western Tasmania, New Brunswick and Rudnyi Altai are briefly described below.

Iberian Pyrite Belt

This is by far the world's biggest and most consistent VMS-mineralized terrain in SW Spain (north of Huelva) and SE Portugal (Sáez et al., 1996; Barriga and Carvalho, eds., 1997; Leistel et al., 1998). It is an about 250 km long, up to 70 km wide east-west trending, folded and faulted Upper Devonian to Middle Carboniferous volcano-sedimentary belt in the Variscan Orogen that contains 80 plus VMS deposits (Fig. 8.9., Table 8.1). The pyrite-dominated orebodies range in size from several thousand tons to more than 100 mt. There are eight Cu, Zn or Pb "giants" (not counting the pyrite resources and the negatively valued arsenic) and the total known metal endowment of the belt is estimated to be of the order of 1.7 bt with an average grade of 2.3% Zn, 0.92% Cu, 0.77% Pb, 0.4% As, 29 g/t Ag and 0.58 g/t Au. This corresponds to some 35 mt Zn, 14.6 mt Cu, 13 mt Pb, 6.8 mt As, 46,100 t Ag and 920 t Au. The base metals are not uniformly distributed in all deposits and have not been always recovered. Sb, Bi, Co, Se and Te are also anomalously enriched.

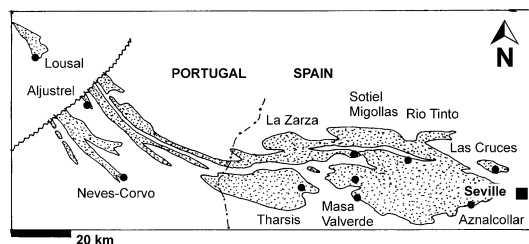


Figure 8.9. South Iberian Pyrite Belt, a map showing location of the "giant" and several "large" VMS, stockwork and Au-gossan deposits listed in Table 8.1.

The Belt has an extensive literature (e.g. Soriano and Martí, 1999, and references therein). It has a late Devonian phyllite and quartzite basement overlain by the ore-hosting Upper Devonian to Lower Carboniferous (Famennian to Viséan; ~360 to 342 Ma) volcano-sedimentary (VS) complex. This, in turn, is overlain by turbidites of the post-volcanic, post-mineralization Middle Carboniferous Culm Group. The VS complex is strictly bimodal, composed of marine siliclastics and volcanoclastics (predominantly slate and litharenite) intercalated with submarine sodic silicic and mafic ("spilite" and "keratophyre") lavas, sills emplaced into wet unconsolidated sediments, non-explosive breccias, and peperites. The rocks are subgreenschist to lower greenschist metamorphosed, complexly deformed (folds, thrusts), but there are no exposed granitic intrusions within the belt and they only appear north and east of it (Fig. 8.10).

Table 8.1. "Giant" and selected "large" deposits in the Iberian Pyrite Belt

Deposit/cluster	N.D	"Giant" of	style/host	Tonnage/grade; metals content
Lousal, PT	16	--	MS, black slate under spilite	Pt ~100 kt Cu, 140 kt Zn, 80 kt Pb
Aljustrel, PT (Fig. 8.11, 8.12)	5	Zn, Pb, Ag	MS	Rv 250 mt @ 3.0% Zn, 1.0% Pb, 0.8% Cu, 38 g/t Ag, 0.84 g/t Au for 7.5 mt Zn, 2.5 mt Pb, 2 mt Cu, 9,500 t Ag, 200 t Au
Neves-Corvo, PT (Fig. 8.13)	5	Cu,Zn, Pb,Sn,Ag	MS; black slate above felsics	Rv 220 mt @ 4.11% Zn, 3.12% Cu, 0.74% Pb, 0.22% Sn, 37 g/t Ag for 6.86 mt Cu, 9.042 mt Zn, 1.63 mt Pb, 484 kt Sn, 8,140 t Ag
--ditto, low-grade ore				Rc 138 mt @ 0.51% Cu, 0.23% Zn for 704 kt Cu
São Domingos, PT	1	--	MS; gossan; black slate	Pt 25 mt @ 2.5% Zn, 1.25% Cu for 625 kt Zn, 312 kt Cu
Tharsis (Norte), SP (Fig. 8.14)	5	Au, As	MS; gossan; black slate, tuff	Rc 110 mt @ 2.7% Zn, 0.7% Cu, 0.8% Pb, 0.33% As, 23 g/t Ag, 2.6 g/t Au for 2.97 mt Zn, 660 kt Pb, 550 kt Cu, 363 kt As, 5,490 t Ag, 284 t Au
La Zarza, SP	1	Pb, Ag, Au	MS; black slate on felsics	P+Rc 164 mt @ 2.49% Zn, 1.24% Cu, 1.09% Pb, 47 g/t Ag, 1.7 g/t Au for 4.08 mt Zn, 2.034 mt Cu, 1.79 mt Pb, 7,708 t Ag, 294 t Au
Sotiel Migollas, SP	2	Pb	MS; black slate	Rc 133 mt @ 2.76% Zn, 1.24% Pb, 0.7% Cu for 3.67 mt Zn, 1.65 mt Pb, 931 kt Cu
Masa Valverde, SP	1	Pb, Zn	MS; black slate	Rc 120 mt @ 5.2% Zn, 1.9% Pb, 0.6% Cu for 6.24 mt Zn, 2.28 mt Pb, 720 kt Cu
Rio Tinto ore field --massive sulfides (Fig. 8.15)	6+	Cu,Zn,Pb, Ag,Au	MS; black slate on felsics	P+Rv ~500 mt @ 2.1% Zn, 0.9% Cu, 0.8% Pb, 26 g/t Ag, 0.5 g/t Au for 10.54 mt Zn, 4 mt Pb, 4.5 mt Cu, 13 kt Ag, 250 t Au
--Cerro Colorado (Fig. 8.16)	1	--	Stockwork; rhyolite, spilite	Rv ~200 mt @ 0.6% Cu for 1.2 mt Cu; protore ~2 bt @ 0.15% Cu, 0.15% Zn, 0.06% Pb, 7 g/t Ag, 0.07 g/t Au
----ditto, gossan	1	Au, Ag	Gossan	Rc 100 mt @ 57 g/t Ag, 2.05 g/t Au for 5,700 t Ag, 205 t Au
Aznalcóllar, SP	2	Pb, Ag	MS; black slate, felsics	166 mt @ 2.7% Zn, 1.43% Pb, 0.44% Cu for 4.35 mt Zn, 2.3 mt Pb, 730 kt Cu
Las Cruces, SP (Fig. 8.17)	1	--	MS, second. sulfides., oxides	41.3 mt @ 6.18-0.6% Cu, 5.86-0.77% Pb, 4.3% Zn, 140-27 g/t Ag, 6.7-0.4 g/t Au for 1.077 mt Cu, 1.075 mt Zn, 553 kt Pb, 598 t Ag, 19 t Au
Iberian Pyrite Belt total, PT & SP	>80	py,Cu,Zn, Pb,Au,Ag	MS>stockworks gossans	P+Rv ~1.7 bt @ average 0.92% Cu, 2.3% Zn, 0.77% Pb, 0.4% As, 29 g/t Ag, 0.58 g/t Au for ~35 mt Zn, 14.6 mt Cu, 13 mt Pb, 46 kt Ag, 920 t Au

Data from Strauss et al. (1977); deCarvalho (1991); Barriga & deCarvalho, eds. (1997); Silva et al. (1997); Leistel et al. (1998); Sáez et al. (1999); Tornos, written communication (2002); GEODE website (2003). Abbreviations: in second column, N.D. means number of deposits (orebodies) in a cluster; MS=massive sulfide lenses

Orebodies, both in outcrop and concealed, are scattered throughout the belt and the most significant ones come in clusters. The most productive orebodies are stratiform lenses to sheets of pyritic massive ore typically located at felsic volcanic/slate contacts, or entirely within carbonaceous slate (Sotiel, Tharsis). The former are usually associated with ore fluid conduits in the footwall (alteration pipes, stockworks) and are referred to as "proximal" or "autochthonous". The latter lack the feeders and are designated "distal" or "allochthonous" (corresponding to the Besshi-type).

Many sulfide lenses are pyrite-only, with the base metals present in concentrations around and under 0.1% or only locally accumulated, so they have low economic value. Other deposits contain mixed pyrite, sphalerite, galena and chalcocopyrite ore throughout, or as banded ore in the lower parts of pyritic orebodies (Sotiel, Aznalcóllar). The Corvo orebody is unusual as it contains a significant proportion of cassiterite in the pyritic ore.

The Iberian deposits have an almost standard VMS stratigraphy, with siliceous slates grading to jasper at the top, followed by massive pyrite with

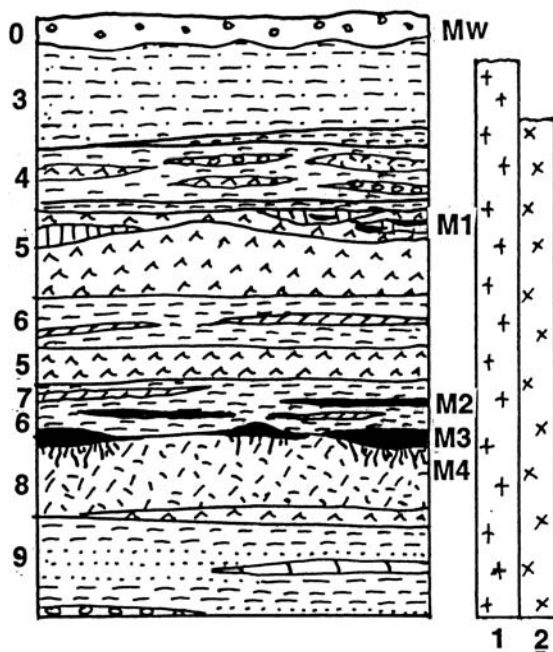
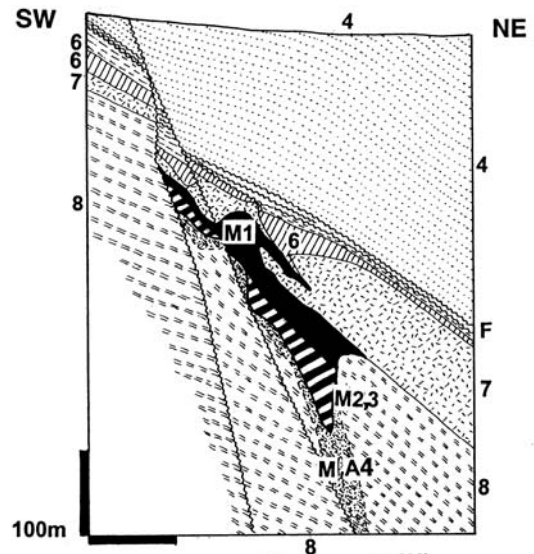
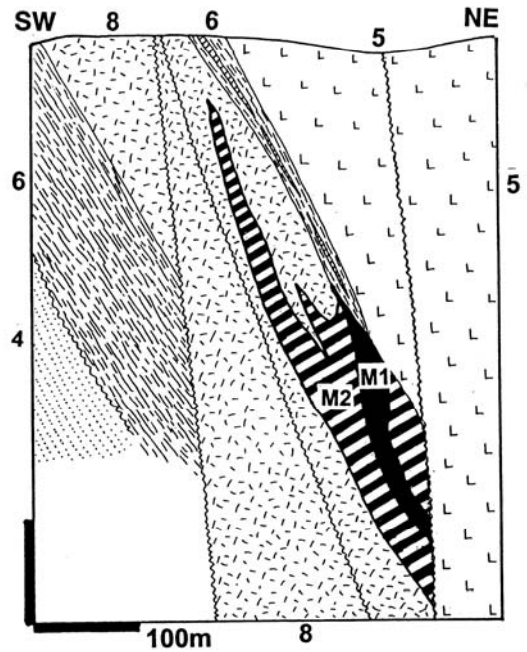
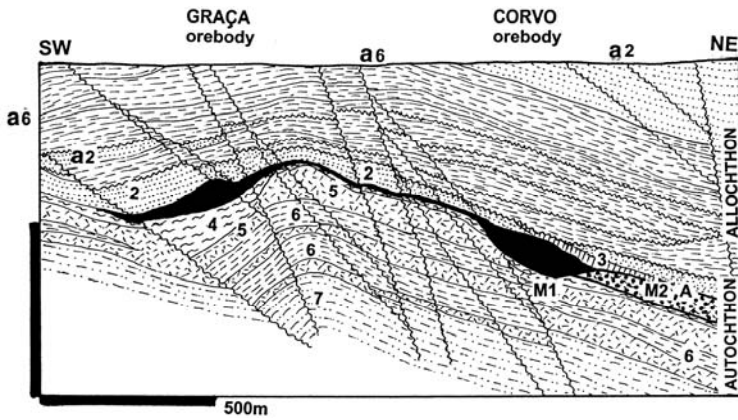


Figure 8.10. Iberian Pyrite Belt, simplified lithostratigraphic column showing the stratigraphically controlled ore-bearing horizons. From LITHOTHEQUE No. 3055, based on data in Strauss & Gray (1986), Leistel et al. (1998), and Sáez et al. (1999). 0. Mi-Q cover sediments and anthropogenic deposits; 1. Cb granitoids; 2. D3-Cb gabbro; 3. Cb1-2 Culm Group turbidites; 4-9: D3-Cb1 Volcanic-Sedimentary (or Siliceous) Complex. 4. Mixed epiclastics, some volcanics; 5. Mafic units, spilitic tholeiitic basalt flows, dikes; M1 in 6. Synvolcanic siliceous Fe & Mn oxides; 6. Varicolored slate, siliceous slate, jasper; M2 in 7. Bedded pyritic deposits with Zn,Cu,Pb in slate, close to the Besshi model 7. Black carbonaceous slate; 8. Na-altered (keratophyre) rhyolite to dacite flows, sills, pyroclastics, strongly altered; M3 in 8. Classical "Rio Tinto-type" VMS, lenticular pyritic masses in or over felsic units, some with footwall stockworks (M4). 9. D3 Phyllite-Quartzite Formation

the base metals enriched intervals (when present) below. Tens of small Mn-oxide deposits had been mined in the past from oxidation zones over rhodochrosite or rhodonite lenses in jasper. The base of many massive sulfide lenses is copper-rich and transitional into the footwall stockwork. It is also enriched in Bi and Co (Marcoux et al., 1996) and sometimes gold. The footwall stockworks have the form of anastomosing quartz veinlets with scattered Fe and Cu sulfides, breccia, or thin chalcopryrite stringers and/or porphyroblastic pyrite in heavily chloritized and often sheared, or silicified wallrock. The Cu-rich stockworks are either mined together with the massive sulfide ore, or they form separate

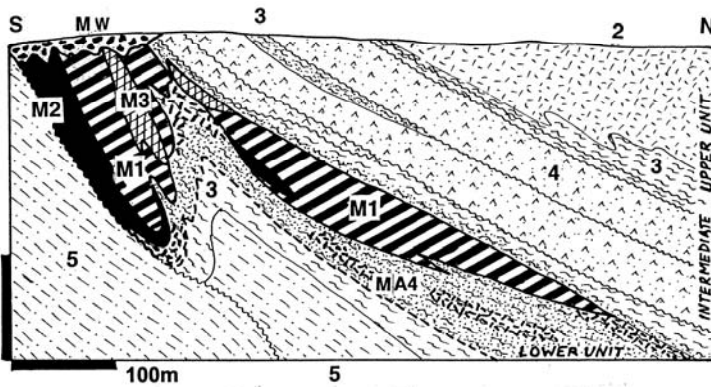


Figures 8.11, 8.12. Moinho (top) and Feitais (bottom) deposits, Aljustrel cluster, Portugal. Example of a metal-zoned VMS lenses in acid submarine volcanics close to a subvolcanic rhyolite porphyry intrusion. From LITHOTHEQUE No. 3029 & 3031, modified after EuroZinc in Dawson et al. (2003). M1: Sphalerite-rich zone; M2: massive or banded pyrite, low in Zn, Cu; M3: chalcopryrite-rich massive pyrite; M+A4 chalcopryrite-rich stringer stockwork in chlorite-altered, sheared footwall rhyolite (Feitais) 4. Cb2 Culm Group turbidites; 5. Cb1 quartz-feldspar phyric subvolcanic rhyolite; 6. Cb1 chert, jasper, varicolored slate; 7. Cb1 Hangingwall rhyolite and tuff; 8. Cb1 massive rhyolite flows with hyaloclastite, peperite, minor shale



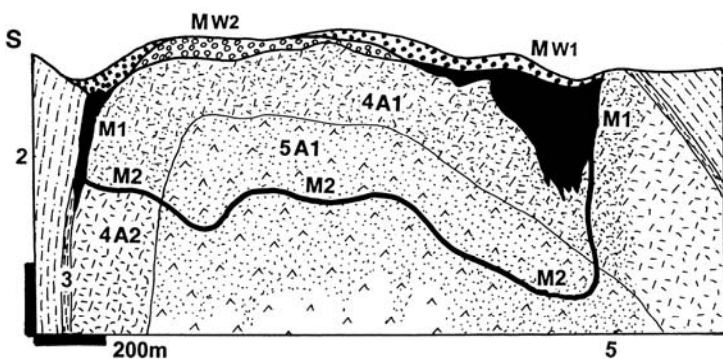
- 1. MZ? diabase dikes (not shown);
- 2. Cb2 turbidites
- 3. D3 Volcanic-Siliceous Complex, jasper and carbonate: 4, black slate; 5, felsic flows and domes; 6, Lower Slate with carbonates;
- a6. D3-Cb1 allochthon: black, siliceous, purple slate, minor felsic volcanics;
- 7. D3 Phyllite-Quartzite Group.
- M1. 360-342 Ma stratabound VMS lenses high in cassiterite;
- M2+A. Thin intervals of pyrite, chalcopyrite in altered footwall to VMS bodies

Figure 8.13. Corvo-Neves VMS cluster, cross-section of two orebodies from LITHOTHEQUE No. 3034, modified after deCarvalho (1991) and SOMINCOR Ltd.



- 2. MZ? diabase sill
- D3 Volcanic-Siliceous Complex:
- 3. Rhyodacite sill; 4. Black slate and tuff; 5. Carbonatized metabasalt (spilite); 6. D3 Phyllite-Quartzite Gr.
- MW. Goethitic gossan with Au values
- M1. Massive low-Cu pyrite
- M2. Complex ore, pyrite, sphalerite, galena, siderite in slate;
- M3. Breccia of fine pyrite & siderite, 1.5-2.0 g/t Au
- MA4. Altered footwall with Fe,Cu > Co,Bi sulfides in veins & stockworks

Figure 8.14. Tharsis VMS cluster, Filon Norte and Guillermo orebodies. From LITHOTHEQUE No. 3039, modified after Strauss and Beck (1990) and Tornos (2003). Example of orebodies predominantly in carbonaceous slate



- MW1. Residual Au gossan over VMS; MW2. Ditto, over stockworks.
- M1. Pyritic VMS lenses; M2. Stockworks, altered breccia in M1 footwall; pyrite, chalcopyrite;
- 2. Cb1 Culm Group turbidites; D3-Cb1 Volcanic-Sedimentary Complex:
- 3. Transitional mixed felsic tuff, volcanoclastics, jasper, slate; 4. Acid volcanics; 5. Spilitic basalt; 6. D3 Phyllite-Quartzite Group.
- Alterations: A1 mainly chlorite; A2 mainly sericite.

Figure 8.15. Rio Tinto ore field, Cerro Colorado stockwork and auriferous gossan. Cross-section from LITHOTHEQUE No. 3048, modified after Rambaud (1969), Sobol et al. (1977) and Garcia Palomero (1992)

bodies as at Cerro Colorado in the Rio Tinto field. The outcropping orebodies have well developed

goethitic gossans, some of which have been partially reworked into young (Cainozoic) colluvial

and alluvial gravels. Gossans near Tharsis and especially over the Cerro Colorado stockwork are enriched in gold and silver and have been intermittently mined since the Roman times.

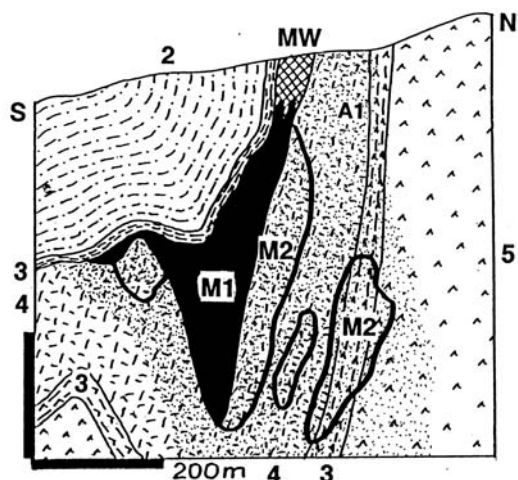


Figure 8.16. Rio Tinto ore field, San Dionisio and Filon Norte VMS deposit from LITHOTHEQUE No. 3051, modified after IGME Dirección de Recursos Naturales, García Palomero (1979), Sáez et al. (1999). MW. Auriferous gossan; M1. VMS, pyrite-dominated stratabound lenticular masses in or draped over felsic units; M2. Footwall stockwork and breccia with pyrite, chalcopyrite in chlorite, sericite, quartz altered rocks; 2. Cb1 Culm Group turbidites; D3-Cb1 Volcanic-Sedimentary Complex: 3. acid tuff, volcaniclastics, jasper, purple slate; 4. Acid flows, hyaloclastite, peperite, sills emplaced to wet sediments; 5. Spilitic mafic volcanics; A1. Chloritic alteration

Cerro Colorado gossan had a 1984 resource of ~100 mt ore @ 1.8-2.5 g/t Au containing some 101 t Au and 5700 t Ag (Fig.8.15). Much unrecorded gold was, moreover, won in the past centuries. Viable secondary sulfide zones are rare in the Belt, with the exception of the recently discovered concealed **Las Cruces** deposit near Seville (Fig. 8.17). This one has a blanket of predominantly sooty chalcocite (15 mt of 6.18% Cu and 27.4 g/t Ag) sandwiched between an Au, Ag and Pb-rich gossan above, and a pyritic Zn, Pb, Cu mass below. The Iberian "giant" deposits are summarized in Table 8.1. and the largest ones: Rio Tinto and Neves-Corvo, briefly described below.

Rio Tinto ore field, Huelva Province, SW Spain, has the largest metals accumulation in the Iberian Pyrite Belt, over an area of about 8 km² (Sáez et al., 1999; P+Rv are quoted as either 234 mt or 334 mt

of ore @ 2.5% Zn, 1.0% Cu, 1.0% Pb, 0.3% As, 30 g/t Ag, 0.3 g/t Au for some 5 mt Zn, 2.5 mt Cu, 2.5 mt Pb, 1 mt As, 7500 t Ag and 100 t Au). There, the VS complex is partly concealed under erosional remnants of the Culm turbiditic slate and litharenite, separated by the Transitional Series of mixed acid tuff and volcanic/epiclastic conglomerate, arenite, purple slate and chert. The largest San Dionisio VMS orebody (Fig. 8.16), mined in the now exhausted Atalaya Pit, is a folded pyritite mass with minor chalcopyrite, sphalerite and galena in, or draped over, silicified and chlorite-altered felsic volcanics. These, in turn, rest on spilitic metabasalt. The footwall stockwork has the form of breccia in quartz, sericite, chlorite altered "keratophyre" with stringers and disseminations of pyrite and chalcopyrite. There is a small, porous goethitic gossan at the ore outcrop. The smaller San Antonio VMS orebody is a thin, long pyritite sheet downslope from the Planes Pipe: a semi-massive pyrite, chalcopyrite-replaced footwall breccia pipe.

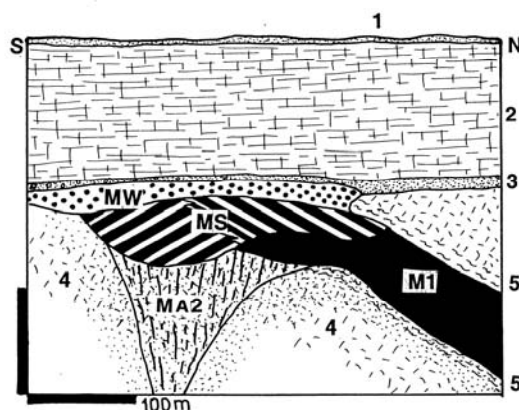


Figure 8.17. Las Cruces deposit, Gerena, cross-section from LITHOTHEQUE No. 3053 modified after Knight et al. (1999), Doyle (2003), Cobre Las Cruces Ltd. website, 2003. 1. Mi3-Q sedimentary cover, upper sand; 2. Ditto, marl; 3. Ditto, friable basal glauconitic sandstone; MW. Au-Ag rich gossan and oxidation zone; MS. Secondary Cu sulfides blanket; M1. Rio Tinto-type VMS pyritic lens; MA2. Footwall stockwork of pyrite, chalcopyrite in chloritized black slate and volcanics; 4. D3-Cb1 Volcanic-Sedimentary Complex, felsic volcaniclastics; 5. Ditto, black slate

Cerro Colorado is a dome with a meta-basalt (spilite) core enveloped by a thick felsic volcanic-sedimentary unit with the thin Transitional Series on top (Fig. 8.15). The center of the dome is eroded so that the mineralized felsic unit is exposed and covered by a thick gossan, whereas remnants of

massive pyritite are preserved along the flanks. The core of the dome is intensely chlorite and sericite-quartz-pyrite altered, and crisscrossed by a network of quartz and/or pyrite, chalcopyrite veinlets and disseminations. In the older literature, Cerro Colorado was often listed as an example of "porphyry copper". The stockwork resource has recently been quoted as 200 mt of material with 0.6% Cu (for 1.2 mt Cu), with some 100 t Au and 5700 t Ag in the gossan.

Neves Corvo ore field is in the southern Portugal portion of the Belt, near Castro Verde (de Carvalho, 1991; deCarvalho et al., 1999; P+Rc ~270 mt of ore, variable grades, containing ~4.3 mt Cu, 171 kt Sn, 3.8 mt Zn, 400 kt Pb, 2,664 t Ag; Fig. 8.13). With the first discovery made in 1977 by drilling a Bouguer anomaly under some 300 m of cover, it is one of the latest finds in the Iberian Pyrite Belt and one with the highest Cu grades (42 mt @ 7.6% Cu). It is also the only VMS known that contains cassiterite in large quantities and high concentrations (4.3 mt @ 2.5% Sn of tin ore, plus Sn in Cu ores).

The ore field is a cluster of five lenticular stratabound massive sulfide orebodies floored by footwall stockworks, entirely enveloped by sedimentary rocks (mostly black phyllite; e.g. Corvo orebody), or in sediments on top of acid volcanics (quenched rhyolite grading to hyaloclastite and peperite). These rocks are members of the Volcanic-Sedimentary (VS) succession and are here dated as uppermost Devonian. VS (and some orebodies) are covered by the Lower Carboniferous Culm turbidites. The orebodies have the usual VMS stratigraphy. The very top is a thin jasper and/or carbonate band, followed by barren pyrite underneath. A portion of the pyritite still contains a large resource of 0.5% Cu ore. The lower portion of the massive sulfide bodies is Zn > Pb rich (in sphalerite, galena), whereas the basal portion is Cu-rich throughout (Cu is in chalcopyrite, minor tetrahedrite/tennantite and bornite), and intermittently Sn-rich (as visible or invisible brown cassiterite, minor stannite). The gangue is quartz with variable proportion of chlorite, sericite, dolomite, siderite and barite. The footwall stockwork and breccia in slate and/or rhyolite has veinlets and disseminations of chalcopyrite with local cassiterite and sphalerite, in pyritic quartz, chlorite or sericite-altered rocks. Banded ("rubané") ore of pyrite, chalcopyrite, sphalerite, locally cassiterite bands alternating with carbonaceous slate occurs in the hangingwall region of some orebodies (especially Corvo) and is interpreted as tectonically emplaced.

Bathurst-Newcastle district, New Brunswick

This is a portion of the Appalachian Orogen in eastern Canada that contains, within a sub-circular area with a diameter of 50 km, over 100 Zn, Pb, Cu, and Ag occurrences (McCutcheon, 1992; Goodfellow et al., eds., 2003). Of these, 37 orebodies have a published ore tonnage and 11 are, or were, producers. All these deposits are of the VMS, VMS-related stockwork, or Besshi types, and almost all are syn-depositional and hosted by a narrow stratigraphic interval (about 468-464 Ma) in the Middle Ordovician bimodal Tetagouche Group. There is one Zn, Pb, Ag "giant" (Brunswick No. 12; Fig. 8.18) that contains more metals than the rest of the deposits combined, and several "large" deposits. The three largest deposits Brunswick No. 12 and No. 6, Heath Steele) are in felsic volcanic meta-sediments (now schists), hence they are of the Besshi-type. Their metal ratios are close to the Hokuroku orebodies (Chapter 5). The host configuration (discontinuous lenticular bodies of massive meta-rhyolite and quartz-feldspar augen schist {=metacrystic rhyolite} in the regionally distributed felsic meta-hyaloclastite, tuffite, wacke and meta-pelite) is reminiscent of the VS succession in the Iberian Pyrite Belt. The underlying quartzite-slate and the upper metabasalt-slate successions strengthen the similarity, but except for the higher metamorphic grade (upper greenschist) and penetrative deformation, the New Brunswick orebodies have much lower pyrite:base metal ratios, hence much greater per-ton ore value.

The "giant" **Brunswick No. 12** orebody (Fig. 8.18) was discovered in 1953, one year after the Brunswick No. 6 discovery which, in turn, had been found by testing a previously known "exhalative" iron deposit (Lentz, 1999; P+Rv 148 mt @ 8.82% Zn, 3.51% Pb, 0.33% Cu, 99 g/t Ag for 13.054 mt Zn, 5.195 mt Pb, 49 kt Cu and 14,652 t Ag). This is a single, multiply folded and metamorphosed stratabound lens of massive pyrite, sphalerite, galena, pyrrhotite, chalcopyrite in sericite-chlorite altered "greenish-gray meta-siltstone", now biotite and sericite schist, situated on top of a submarine "felsic volcanic pile". The sulfides are imperfectly mineralogically zoned from massive pyrite through banded Zn, Pb, Cu sulfide to massive pyrite, pyrrhotite and basal Cu-rich zone in chlorite, stilpnomelane altered schist believed to be the footwall stockwork. In the stratigraphic hangingwall, there is a discrete body of "exhalitic" iron formation of meta-chert and jasper, magnetite, hematite, pyrite and siderite. The host unit is interfolded with massive meta-rhyolite and felsic

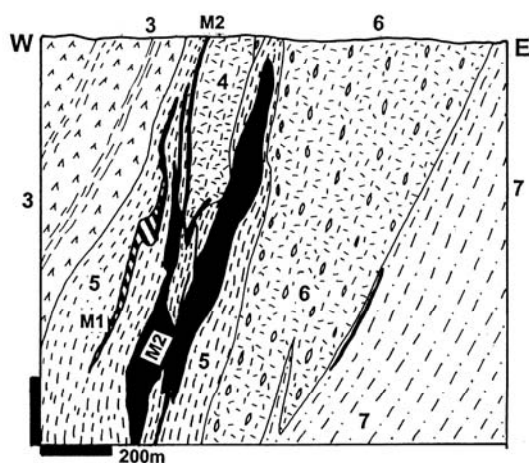


Figure 8.18. Bathurst-Newcastle district, New Brunswick, Canada. Brunswick No. 12 deposit from LITHOTHEQUE No. 3268, modified after Luff (1977), Van Staal and Williams (1984). 3. Or1-2 graywacke-slate interbedded with basalt; 4. Or Tetagouche Group, massive rhyolite, felsic hyaloclastite; 5. Ditto, meta-volcanic clastics; 6. Lower felsic volcanic fragmentals, quartz-feldspar porphyry (now "augen schist"); M1. Iron Formation in VMS hangingwall; M2. Stratabound lenses to deformed sheets of massive Fe, Zn, Pb, Cu sulfides in altered volcanic clastics; 7. Or1 quartzite-phyllite unit

hyaloclastite, and underlined by more schists interpreted as volcanic wacke, with a prominent unit of quartz-feldspar augen schist (porphyry), probably a rhyolite flow or sill. Back-arc floored by continental crust, or rifted mature island arc, are the presently popular environmental interpretations.

8.4.2. Sedimentary rocks-hosted Fe, Cu, Zn, Pb ores

The VMS deposits hosted predominantly by (meta)sedimentary rocks in submarine volcanic association (this is what distinguishes them from the "sedex" deposits, Chapter 13, although there are some transitions) are popularly known as Besshi-type (Slack, 1993). There seems to be more sediment-hosted VMS deposits not listed as "Besshi-type" in the literature, including "giant" deposits like Tharsis and Sotiel, Spain and Brunswick No.12 in Canada. The type locality **Besshi** (Banno et al, 1970; 30 mt @ 1.2% Cu, 0.3% Zn, 6.6 g/t Ag, 0.2 g/t Au for 360 kt Cu) is a "large" deposit in the Jurassic Sambagawa terrane in Shikoku. The thin, tabular, stratabound body of massive to interbanded pyrite, chalcopyrite, minor sphalerite, bornite, magnetite and hematite, with or

without quartz gangue, persists to a depth of 3.5 km down plunge. Pyrrhotite increases with depth. The immediate host is carbonaceous schist sandwiched between chlorite-amphibolite schist, originally basalt.

Windy Craggy Cu-Co-Au deposit, in the Tatshenshini valley in the remote NW corner of British Columbia, is better known in the exploration circles for the permitting fiasco than for its geology. This is said to be the largest "Besshi-type" deposit and one of its few "giants" (Peter and Scott, 1999; Rc 297 mt @ 1.38% Cu, 0.08% Co, ~2 g/t Au for 4.1 mt Cu, 240 kt Co, ~600 t Au). First the fiasco (McDougall, 1991). Windy Craggy was discovered in 1958 by tracing moraine float but not much happened until 1988, so the politically favourable period for mine permitting in this part of Canada was missed. The 1988-1991 exploration campaign completed 65 km of drill holes and over 4 km of underground development at considerable cost due to difficult access, just to be denied mining permit by the British Columbia Government at the end. UNESCO then rushed in to declare this rarely visited corner a World Heritage Area, an honour no other unmined orebody has received so far!

Two ore zones are in Triassic bimodal volcanic-sedimentary suite that unconformably overlies Neoproterozoic to Permian succession of the largely "oceanic" Alexander accreted terrane. The host association consists of several cyclic basalt flow and sill-dominated units alternating with tuffaceous, calcareous and/or carbonaceous argillite. Two main zones of folded, steeply-dipping stratabound massive sulfide bodies have meta-basalt in the stratigraphic footwall and calcareous siltstone to argillite with interbedded tuff in the hangingwall. There is a well developed stockwork/stringer zone in the footwall composed of quartz, carbonate, pyrrhotite, minor chalcopyrite veins and veinlets in chloritized and locally silicified meta-basalt. The massive sulfide lenses consist of pyrite-rich core enveloped by pyrrhotite-dominated mass with lesser chalcopyrite, magnetite and local sphalerite. The sulfides are capped by siliceous and calcareous, locally laminated "exhalite" with framboidal pyrite, gradational to sulfidic argillite. A portion of the "exhalite" is enriched in gold (up to 14.7 g/t over 29.7 m interval). There is no supergene alteration left and gossan development started only several hundred years ago, following deglaciation.

Greens Creek deposit, SE Alaska (Taylor et al., 1999; Rv 24.2 mt @ 13.9% Zn, 5.1% Pb, 665 g/t Ag and 5.3 g/t Au for 3.36 mt Zn, 1.235 mt Pb, 16.1 kt Ag and 128 t Au) has recently been the largest U.S. silver producer. It is located in the same

Alexander accreted terrane as Windy Craggy, on Admiralty Island 29 km south of Juneau. The immediate host rock is a thinly laminated carbonaceous phyllite at or near contact with metabasalt flow and tuff. These rocks are members of the Triassic (~211 Ma) bimodal island arc suite. The overturned quartz, pyrite and sericite altered rocks contain lenticular masses of pyrite, sphalerite and galena in silica-carbonate and barite groundmass, and grade to disseminated ore rich in Cu, Sb, As, Ag sulfosalts (chalcopyrite, freibergite, pyrargyrite). The latter are responsible for the "bonanza" magnitude silver grades.

8.4.3. Au-Ag deposits

Virtually all VMS and Besshi-type deposits contain some silver and gold, recoverable in most cases. The grades vary between about 5 and 100 g/t Ag and 0.05-6 g/t Au; Franklin (1993) calculated the mean values of Canadian VMS's (much of which are Precambrian) as 0.8 and 2.0 g/t Au, and 19.0 and 79.0 g/t Ag. The precious metals values are higher in the Zn-Pb-Cu group of Franklin (1993), where the Ag grade correlates with Pb (presence of galena). Gold rarely shows a clear correlation. With a virtual disappearance of demand for pyrite as a raw material, several "pyrite-only" deposits with 1 g/t or more gold could be re-labelled as gold deposits. In contrast with disseminated gold deposits with less than 5% pyrite amenable to heap leaching, however, processing of the massive pyrite ores for gold only would greatly increase costs and cause serious environmental problems, although higher Au grades and a semi-massive style of ore can make the "pyrite-only" VMS profitable (e.g. in the Precambrian Bousquet ore field; Chapter 9). Gold and silver also accumulate in goethitic gossans over pyritic deposits, where the problem of excessive ore acidity does not exist. Several "large" Au-rich gossans over VMS exist (e.g. Rio Tinto, Tharsis).

In addition to Bousquet, several major Au (Ag) deposits exist in the same "eugeoclinal" setting as VMS and this includes the "As-giant" Boliden (Chapter 9) and "Au-Ag giant" Pueblo Viejo. Pueblo Viejo, in particular, is interesting as a case of gradual revelation of the "geological truth" as mining has progressed from the deep regolith with oxidic Ag-Au ores into the primary zone. The results seem to indicate the existence of an Au (Ag)-rich transitional ore type between VMS and epithermal (high sulfidation) models, or even a "pure" submarine high-sulfidation variety (Kesler et al., 2005).

Pueblo Viejo Ag-Au-Zn ore field, Dominican Republic (Nelson, 2000; Kesler et al., 2003; Pt oxide ore 759 t Ag, 166 t Au; Rc sulfide ore at 1 g/t Au cutoff: 544 mt @ 1.98 g/t Au, 11.76 g/t Ag for 1,078 t Au, 6397 t Ag. Total: 7,156 t Ag, 1,244 t Au. Also present but not recovered are ~1.9-3 mt Zn @ ~0.35-0.5%, over 200 kt As, 16 kt Hg and 11

kt Te). Mining in Pueblo Viejo started in 1975 in a featureless blanket of bulk mineable disseminated Au and Ag in regolith (gossan) rich in residual silica fragments. The host sequence are bimodal submarine volcanics (Na-metasomatized basaltic andesite and dacite), pyroclastics and volcanoclastics of the Lower Cretaceous Los Ranchos Formation. This is interpreted as an immature island arc sequence that form basement to much of the Greater Antilles Arc. In the Pueblo Viejo ore field that consists of at least eight separate deposits so far (there is some style resemblance to the wholly subaerial Yanacocha; Chapter 6), the highly pyritic and carbonaceous bedded rocks are interrupted by various discordant structures interpreted as diatremes and/or domes. Nelson (2000) recognized a series of volcanic centers/domes of andesitic to dacitic composition with fragmental quartz porphyry units, mantled by breccia and surrounded by resedimented clastics (Fig. 8.19). These centers are strongly silicified and overprinted by advanced argillic (pyrophyllite > alunite, diaspore) and argillic (kaolinite) alteration. Au and Ag reside in quartz >> pyrite, sphalerite, galena, enargite veins and stockworks controlled by steep syndepositional faults. The orebodies dated at around 115 Ma are considered coeval with deposition of the upper Los Ranchos Formation, but are overprinted by several later thermal events (~77-35 Ma; Kesler et al., 2005).

8.5. Differentiated mafic-ultramafic intrusions (Alaska-Urals type)

Gabbros and diabase dikes/sills, other than components of ophiolite, are common in eugeoclinal orogens either as synvolcanic equivalents of mafic volcanics or as minor components of synorogenic granitoid plutons. Independent intrusions also occur, especially in or near collisional sutures. No major metallic deposits are known. Small differentiated mafic-ultramafic intrusions, on the other hand, had been more successful in metal accumulation and although a "giant" is yet to be discovered, several "large" deposits of Fe (Ti), Cu and PGE, and one "near-large" Ni, are known. The iron in most intrusions resides in Ti-magnetite and although the material is of very low-grade (16% Fe plus in Klukwan and Kachkanar) it is a "soluble iron" present in large, consistent masses of rock (pyroxenite) in which it is disseminated.

Urals-Alaska type complexes (Foley et al., 1997; Fig. 8.20) are small, usually subcircular intrusions,

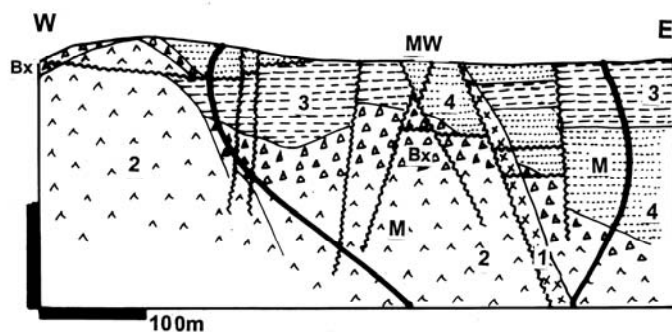


Figure 8.19. Pueblo Viejo Ag-Au ore field, Dominican Republic. Cross-section of Monte Negro South from LITHOTHEQUE No. 1193, modified after Nelson (2000)

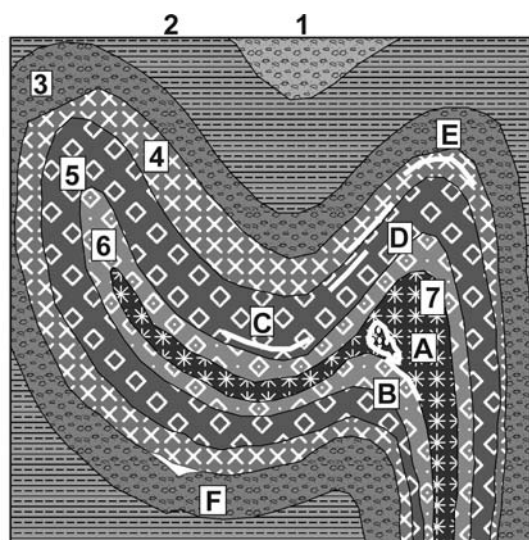


Figure 8.20. Alaska-Urals ultramafic-mafic complex, inventory diagram (cross-section) from Laznicka (2004), Total Metallogeny site G16. 1. Mafic tuff; 2. Argillite, shale, slate; 3. Contact hornfels; 4. Hornblende gabbro; 5. Clinopyroxenite; 6. Wehrlite; 7. Dunite. A. Ni-Cu-PGE, chromite disseminations, pipes in peridotite; B. Ditto, in troctolite and along contacts; C. Cu-Pd>Pt disseminations, veinlets in pyroxenite; D. Fe-Ti layered disseminations in pyroxenite; E. Cu, Pd, bornite layered disseminations in pyroxene gabbro; F. Ni-Cu sulfides in norite; M. PGE placers

some of which are compositionally zoned. A typical zoned intrusion has dunite or peridotite core changing outward into pyroxenite, olivine gabbro, gabbro and sometimes diorite. The intrusions are interpreted to have formed at base of island arcs by mantle and oceanic crust melting at subduction zones. Those in SE Alaska are Jurassic to Oligocene, those in the Urals are Silurian-

MW. Oxidized ore; spongy gold in quartz, Ag-halides enriched near base; M. Fracture & fault quartz vein sets flare to disseminated Au with Zn, Pb, Cu sulfides, enargite in advanced argillic alteration; CrI Los Ranchos Fm.: 1. Andesite dike; 2. Spilitized andesite domes; Bx. Matrix supported heterolithic breccia; 3. Carbonaceous siltstone; 4. Carbonaceous litharenite

Devonian. The Cretaceous **Klukwan Complex** north of Haines, SE Alaska, has a 5x2 km outcrop area and it comprises clinopyroxenite surrounded by epidotized hornblende diorite. There is a resource of some 3.15 bt of pyroxenite with disseminated Ti-magnetite (16.8% of soluble iron), and further 900 mt @ 10.8% Fe is in alluvium and colluvium for a total of 626 mt Fe content (Foley et al., 1997). There are sections locally enriched in platinum metals. The best mineralized Lower Silurian **Kachkanar Complex** in central Urals (Reshit'ko, 1967) is a group of three lenticular massifs emplaced to amphibolite and chlorite schist in a shear zone. The cores are occupied by dunite that grades outward into peridotite, olivine pyroxenite, clinopyroxenite, olivine gabbro, gabbro-norite, diorite and syenite. Platinum alloys form small scattered disseminated grains in olivine pyroxenite and wehrlite, whereas Pt-Pd sulfides prefer diallagite and magnetite-rich pyroxenite. The former minerals are enriched in alluvial placers, the latter can be recovered by magnetic separation. Kachkanar holds the greatest share of the Uralian PGE resources (some 700 t PGE plus). Vanadiferous Ti-magnetite with subordinate ilmenite form extensive uniform disseminations in pyroxenite layers (20-30% magnetite) that translates into an average grade of 16.64% of soluble iron. There is a resource of 12.2 bt of material containing 2.03 bt Fe (Rundkvist, ed., 1978). The Ti content is a mere 1-2%.

Nizhnyi Tagil, in the same belt as Kachkanar, is the most famous platinum deposit in the Urals that supplied metal for the world's first and only Russian platinum coinage in the 1800s; a minimum of some 300 t Pt has been produced (Rundkvist, ed., 1978). Platinum metals are bound in Pt-Fe and Os-Ir alloys that form minute, irregular disseminations in dunite. These are most common in chromite-rich schlieren

and in steeply dipping pipes with diffuse outlines that postdate crystallization of the host dunite, probably emplaced in the manner of the Bushveld PGE pipes (e.g. Driekop). The chromite zones are most common in faulted sections and are sometimes associated with dunitic pegmatites. Most of the past PGE production came from regolith and alluvial placers.

Volkovskoe (Volkovo) massif lies between Tagil and Kachkanar (Samonov and Pozharisky, 1974; about 600 kt Cu @ 0.85% Cu, ~300 t Pd). This is a Late Silurian NNW-elongated zoned olivine gabbro, gabbro, gabbrodiorite, diorite and quartz diorite intrusion emplaced into mafic meta-volcanics. The copper is in disseminated chalcopyrite and bornite, in lenses that overlap with disseminated Ti-magnetite and apatite zones. About 200 individual ore lenses have been recorded in pyroxene gabbros over a strike length of 3 km. Pd and Au are recovered as a by-product.

8.6. Calc-alkaline and shoshonitic volcanic-sedimentary successions

Calc-alkaline magmatism in island arc systems is associated with semi-mature arcs, constructed on the earlier-formed immature arc (and partly oceanic) basement (“transitional crust”), and/or on fragments of continental crust previously detached from a continent, as in Japan (Chapter 5). The magmatism over the transitional crust is mostly andesitic/dioritic, with magmatic differentiation adding some dacite, quartz diorite and granodiorite. Continental crust basement supports the entire magmatic range from diorite to monzogranite. The “eugeoclinal” portion of orogens as in the northern Cordillera, assembled from a mosaic of accreted terranes, has largely a bulk transitional crustal basement supporting mostly andesitic volcanism, in both the pre-collisional island arc setting and the post-collisional andean margin setting (Fig. 8.21). Here and there, however, more felsic and/or shoshonitic magmas intervene (Fig. 8.22). The fully evolved calc-alkaline suites consist of the entire differentiated sequence basalt-andesite-dacite-rhyolite, but mafic-only, bimodal, and felsic-only associations form simultaneously in extensional structures (back-arcs, interarc rifts). Often, evolution from tholeiitic and/or bimodal to calc-alkaline successions is realized within a single structure and if mineralization (usually VMS) is present, it may be difficult to assign it to a single magmatic family. Most VMS deposits here are

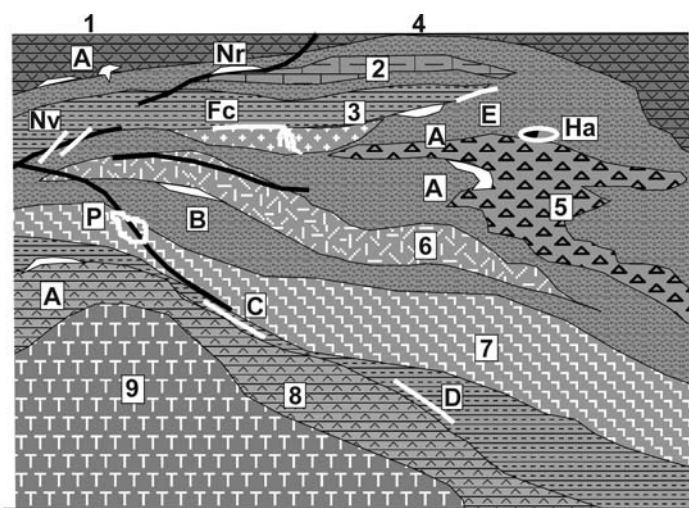
members of the bimodal-felsic association of Barrie and Hannington (1999) that includes >50% felsic volcanics and <15% volcanoclastics. Few VMS's are associated mainly with andesite (e.g. Tambo Grande), but andesite-dominated terrains support most porphyry Cu-(Mo,Au) deposits related to calc-alkaline intrusions (Chapter 7).

Quesnellia terrane, Canadian Cordillera

This is a member of the Intermontane Superterrane that accreted to the North American Plate in late Jurassic (Souther, 1992). It has a late Paleozoic basement interpreted as remnant of an immature volcanic arc, unconformably overlain by the Upper Triassic, partly emergent, predominantly andesitic island arc sequence (Nicola and Takla Groups). The western facies of mainly calc-alkalic andesite flows and local ignimbrite, interpreted as magmatic arc (Souther, 1992), changes in the easterly direction into feldspar- and augite-feldspar volcanoclastics and a thick pile of subalkaline (shoshonitic) augite andesite pillow lavas and volcanoclastics with impure limestone units. This is interpreted as a back-arc basin sequence above easterly subducting oceanic plate. Similar subalkaline andesites erupted later (in Lower Jurassic) farther east to form the Rossland Group where ankaramitic members associate with andesite. The accretion of Quesnellia was completed by mid-Cretaceous (Souther, 1992) and was followed by transcurrent faulting.

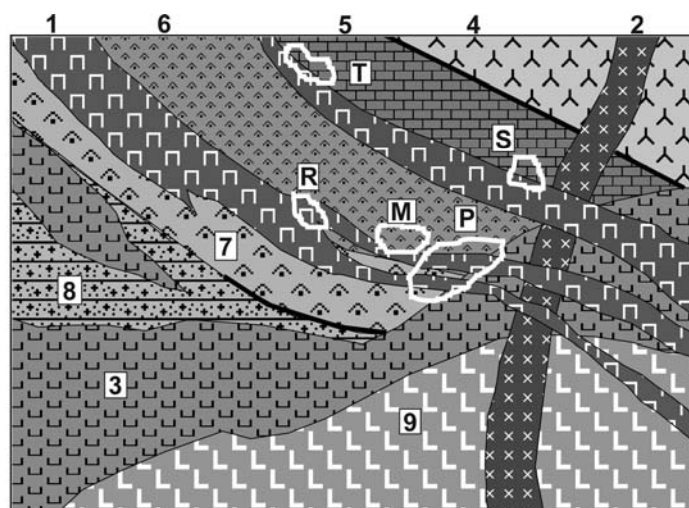
Quesnellia is the most consistently mineralized and productive accreted terrane in British Columbia (Dawson et al., 1992). The pre-accretion metallogenesis, while in an island arc setting, produced both “alkaline” and calc-alkaline porphyry Cu-(Au, Mo) deposits that include the “giant” Highland Valley ore field, one “giant” stockwork-Mo (Rossland-Red Mountain), several “large” Cu-Fe and As-Au skarns (Phoenix, Hedley) (Chapter 7). The post-accretion mineralizations include one “large” mesothermal Cu, Au, Ag field (Rossland) and an Ag, Pb, Zn vein district (Slocan). Stikinia, another accreted terrane separated from Quesnellia by the Cache Creek “oceanic” assemblage (read above) is very close to Quesnellia. It hosts one “giant” porphyry Cu-Mo (Schaft Creek), one “giant” (Endako) and several “large” stockwork-Mo's, as well as Sustut that is a stratabound deposit of Cu sulfides disseminated in subgreenschist-metamorphosed andesitic volcanoclastics.

There are barely any synvolcanic metal accumulations in this setting except for the enigmatic Ag-Au “bonanza” at Eskay Creek,



1. (Meta)basalt; 2. Limestone; 3. Shale, slate; 4. Felsic submarine tuff; 5. Dacite porphyry; 6. Rhyolite and quartz porphyry; 7. Tonalite; 8. Massive andesite submarine flows; 9. Trondhjemite, synvolcanic intrusions.
- A. VMS kuroko-style, and resedimented downslope; B. Au-rich pyritic VMS; C. Bedded pyrite; D. Bedded sedimentary Mn; E. Fe exhalite, oxide; Fc. Bonanza Ag>Au, Zn, Pb bedded sulfides; H. Synvolcanic stockwork pyrite, Au; L. Syntectonic quartz-pyrite-chalcopyrite stockwork in volcanics; M. Ditto, quartz, pyrite, Au; Nr. Syntectonic siderite replacements; Nv. Ditto, veins plus Cu, Ag, Sb, Hg; P. Porphyry-style Cu

Figure 8.21. Calc-alkaline, sequentially differentiated island arc basalt-andesite-rhyolite suite and coeval plutons; inventory diagram (cross-section) from Laznicka (2004), Total Metallogeny Site 50. Ore types A, B, H, Ha, Nv, P have known "giant"equivalents



1. Syenite porphyry or trachyte dikes; 2. Diabase dike; 3. Monzonite porphyry; 4. Latite lavas; 5. Limestone; 6. Alkaline andesite, shoshonitic pyroclastics; 7. Andesite/shoshonite flows; 8. Volcaniclastics; 9. Diorite to monzonite.
- M. Cu-Au magnetite, pyrite, calcite veins in volcanics near dikes; P. Cu-Au porphyry in K-silicate altered andesite, monzonite, syenite; R. Au>Cu stockworks in syenite, monzonite, shoshonitic volcanics; S. Cu-Au skarn grading to P; T. Au-As exoskarn at diorite contacts

Figure 8.22. Island arc type, quartz deficient (shoshonitic) intermediate volcano-plutonic and sedimentary complexes. Rocks & ores inventory from Laznicka (2004), Total Metallogeny Site G43. Ore types P, R and S have known "giant"equivalents.

probably because of the shallow water depths. This, however, is compensated by the wealth of ores related to the metaaluminous and/or shoshonitic epizonal to mesozonal intrusions that intrude the comagmatic andesites. This contrasts with the Miocene andesitic Green Tuff association of Honshu (Chapter 5) that hosts the important and widespread "kuroko-type" VMS. Apparently, these formed in a deep-water sub-environment rifted off the main arc. There are, on the other hand, neither

porphyry-Cu nor porphyry-Mo of significance in the Japanese archipelago.

Eskay Creek is an enigmatic, complex "large" deposit in the Iskut River area in NW British Columbia, famous for its "bonanza" Ag-Au ore and unconventional mineralogy (Roth et al., 1999; P+Rv 3,662 t Ag, 86 t Au in four orebodies). It is hosted by, and genetically associated with, a Middle Jurassic bimodal volcanic-sedimentary unit interpreted as having formed in an intra-arc

extensional graben within the predominantly andesitic, calc-alkaline Hazelton Goup. In the ore field there are at least eight orebodies, both stratabound lenses in sedimentary rocks and stockworks in altered footwall rhyolite. The ore hosting shale is a member of a pillow basalt and volcanic breccia-shale hangingwall assemblage. Of the several orebodies the bulk of metals came from the 21B Zone, a 900 m long, 60 to 200 m wide and up to 20m thick tabular body grading up to 2% Ag and 200 g/t Au (the average grade of the 21B Zone was 2930 g/t Ag, 65.5 g/t Au, 5.6% Zn, 2.89% Pb, 0.77% Cu plus Sb, As, Hg). There, resedimented ore is in a paleochannel filled by cobble- to pebble-sized clasts of sphalerite, tetrahedrite, freibergite, galena, Pb-sulfosalts and rare electrum with amalgam in barite and silica gangue. Also present among clasts is pervasively sericite-chlorite altered and locally stockwork-mineralized footwall rhyolite, barite and calcite. Stibnite veining and partial clast replacements occur near the centre of the orebody.

The even more mineralogically enigmatic but lower grade 21A Zone is a small stratabound lens at the rhyolite-shale contact with a reserve of 1.06 mt @ 8.9 g/t Au and 96 g/t Ag (Roth et al., 1999). The ore is, however, dominated by Sb, As > Hg not included in the published reserve. It consists of semi-massive stibnite, realgar, lesser cinnabar and arsenopyrite in shale, above disseminated stibnite, arsenopyrite, and tetrahedrite in sericitized footwall rhyolite. The Eskay Creek ores precipitated from sea water-dominated, low-temperature (210-120°C) fluids in an actively faulting basin intruded by rhyolite domes, in depths as shallow as 160 m. It is thus an example of shallow water VMS deposits where boiling was not suppressed by hydrostatic pressure of a 2 km plus thick water column. The clastic ore is clearly of local derivation, although its exact source has not been determined.

The Andes

Elsewhere, VMS deposits in calc-alkaline terrains prefer intervals where the predominant andesitic flows and pyroclastics give way to marine volcanoclastics with chemical sedimentary component (silica, pyrite, carbon) intercalated with andesite or dacite flows, felsic domes and quenched acid brecciated lavas with debris flows that are intruded by dikes and sills. Tambo Grande in NW Peru and Cerro Lindo in west-central Peru are two "large" ore fields that exemplify submarine metallogenesis in predominantly subaerial, andean-type volcano-plutonic arcs. Both deposits are in Cretaceous volcanoclastics, deposited in a series of

Jurassic to Cretaceous marine basins (e.g. Cañete Basin) in extensional grabens, produced by rifting in the Andean fore-arc (read also Chapter 6). **Tambo Grande** (Tegart et al., 2000; 182 mt of ore containing 1.86 mt Cu, 2.0 mt Zn, 4468t Ag and 165 t Au) has footwall of andesitic flows and pyroclastics with local pyrite and chalcopyrite stockworks in silicified, chloritized and sericitized andesite, topped by several sulfides-dominated, barite-capped mounds. Each thick, flat-lying mound has pyrite core with a number of peripheral or internal zones of chalcopyrite, sphalerite, minor tennantite. On the top is a hematitic gossan, covered by Miocene to Quaternary sediments. **Cerro Lindo** (Zevallos, 1999; 75 mt of ore with 2.13 mt Zn, 705 kt Cu, 270 kt Pb, 3300 t Ag) is a NE-trending, 8 km long zone of dismembered orebodies very similar to Tambo in thermally metamorphosed bedded Cretaceous volcanoclastics in roof of the Coastal Batholith. This setting proximal to younger granites influenced the past interpretation of similar deposits as plutons-related replacements.

Buchans, Newfoundland

Buchans in Newfoundland (Swanson et al., eds., 1981; 15.81 mt of ore containing 2.31 mt Zn, 1.202 mt Pb, 206 kt Cu, 2,055 t Ag and 23.7 t Au) is a "large" ore field very similar to the Japanese kuroko in setting, style and metal ratios. The host is a cyclic, calc-alkaline mature island arc association of basalt in the footwall, andesite in the hangingwall, with three cycles of submarine dacite fragmentals and volcanic siltstone sandwiched in-between. Number of stratabound lenses of massive, breccia and streaky-textured pyrite, sphalerite, chalcopyrite, galena and barite are present, some with footwall stockworks of disseminated and stringer pyrite with lesser sphalerite and chalcopyrite in strongly silicified and chloritized hosts. Buchans is famous for the almost model presence of resedimented ores in paleochannels formed on the submarine paleosurface, downslope from and shortly after formation of the earlier, "rooted" orebodies. The clastic ore is an unsorted conglomerate to breccia composed of a mixture of sulfide fragments, barite, silicified and unaltered wallrocks. All Buchans orebodies are disrupted and tectonized in a complex thrust system, then intruded by swarms of post-orogenic diabase dikes.

Rudnyi Altai VMS region

Rudnyi Altai is a part of the Late Paleozoic (Hercynian) Zaisan orogen in NE Kazakhstan and

southern Siberia. It used to be the principal lead, zinc and silver producer of the former U.S.S.R. of which, after partition, some 80% of capacity is now in Kazakhstan, 20% in Russia. The ore region, east of Oskemen (formerly Ust'-Kamenogorsk) contains some 40 major Devonian polymetallic massive sulfide deposits that include at least two "giants" (Leninogor and Zyr'yanovsk).

Leninogor (Leninogorsk) ore field has several deposits dominated by the "giant" Ridder-Sokol'noye multistage Pb, Zn, Ag, Cu, Au complex (Bublichenko et al., 1972; Pokrovskaya and Kovrigo, 1983; P+Rv 150 mt ore plus, of which 112 mt remains in reprocessable tailings with 5.3 g/t Ag and 0.62 g/t Au; Elevatorski, 1996; estimated P+R ~7.5 mt Zn, 5.5 mt Pb, 750kt Cu, 7000 t Ag, 200 t Au). The Middle Devonian (Eifelian) volcanic-sedimentary assemblage rests unconformably on Ordovician basement and represents a tectonic block ("graben-syncline"). Although placed into the bimodal suite, mafics are rare in the ore-bearing association and they are andesitic. Cu- and polymetallic mineralization occurs at several horizons. The most productive uppermost horizon is dominated by submarine flows and domes of sodic rhyolite ("keratophyre") alternating with and emplaced into siltstone and shale with tuff interbeds. There is a significant hydrothermal-sedimentary component (silica, calcite, barite) that grade into entirely chemical sedimentary and replacement bodies ("exhalites"). The latter have the form of mounds or stratabound sheets that rest on marker horizons of dolomite, chlorite and sericite tuff or tuffite, and have their feeder roots in thoroughly silicified ("secondary quartzite") rhyolite. Lenticular massive pyrite, sphalerite, galena, tetrahedrite, minor chalcopyrite bodies occur in the basal portion of silica-barite mounds, and grade into disseminated ores. The ores and host rocks are almost unmetamorphosed and not penetratively deformed. There is one stratiform orebody of resedimented clastic sulfides, and a system of subvertical sphalerite-chalcopyrite and auriferous quartz-sulfide veins under the main mound in central part of the orebody.

Zyr'yanovsk ore field (Bublichenko et al., 1972; at least 150 mt ore, grades and setting similar to Leninogor) is second in importance in Rudnyi Altai. It has a series of subparallel massive sphalerite, pyrite, galena, minor chalcopyrite lenses controlled by cleavage in silicified and sericitized Devonian rhyolite, dacite and siltstone, above albitized rhyodacite dome.

In the Irtysh deformation zone in the same region, the VMS deposits (e.g. Berezovsk-

Byelousovka) are metamorphosed and penetratively deformed.

Mount Read Volcanics VMS belt

This is an arcuate, 200 x 20 km N-S belt of Middle Cambrian volcanic, sedimentary and minor intrusive rocks in western Tasmania (Corbett and Solomon, 1989; Corbett, 1992; Solomon and Groves, 1994). The central portion of which is densely mineralized and it stores some 7.2 mt Zn, 2.9 mt Pb, 1.7 mt Cu, 9 kt Ag and 200 t Au. Most of these metals are in two "near-giant" massive sulfide deposits Rosebery and Que River-Hellyer, and in the "large" Cu ore field Mount Lyell. This relatively compact area, in temperate rainforest, is well accessible and it has been extensively studied from a variety of premises.

The volcanic belt borders on the Proterozoic Tyennan massif in the east and interfingers with the flyschoid sediments of Dundas Trough in the west. Several small synvolcanic granitoid massifs intruded along the eastern margin of volcanics. The Cambrian volcanics suffered local early post-volcanic hydrothermal alteration and had been strongly cleaved and lower greenschist metamorphosed during the Devonian orogeny. Corbett (1992) distinguished seven lithologic associations among the volcanics, ranging from high-K alkaline andesite, dacite and rhyolite to rifting-related andesite-basalt and rare shoshonites. The Central Volcanic Complex hosts all the important ore deposits. In it, the early rhyolitic-dacitic volcanism was followed by andesite and basalt. McPhie and Allen (1992) demonstrated the local association of massive sulfides with pumiceous submarine mass flow volcanoclastics.

Rosebery (Green et al., 1981; P+Rc 28.3 mt @ 14.3% Zn, 4.5% Pb, 0.6% Cu, 145 g/t Ag, 2.4 g/t Au for 4.405 mt Zn, 1.27 mt Pb, 4,103 t Ag and 68 t Au) is the largest and earliest found VMS deposit (Fig. 8.23). It is a sheeted stratabound zone of at least 16 ore lenses and pods. Massive to banded pyrite, sphalerite, galena, pyrrhotite, arsenopyrite, chalcopyrite and tetrahedrite are in gangue of barite, quartz, carbonates, chlorite and sericite. The footwall is a thick, massive, feldspar-bearing pumice breccia and the orebody rests on its graded, fine-grained top. The hangingwall is a black pyritic mudstone above which are feldspar and minor quartz-bearing pumiceous pyroclastics.

The more recently discovered **Hellyer** VMS deposit and the smaller **Que River** orebody nearby (McArthur and Dronseika, 1990; 20 mt ore containing 2.75 mt Zn, 1.447 mt Pb, 3,442 t Ag, 87

kt Cu and 53 t Au) are in mixed, coarse fragmental sequence with dacite and black shale sandwiched between lower andesites and basalts in the footwall, and comparable sequence dominated by pillow lavas in the hangingwall. The massive Fe, Zn, Pb, Cu sulfides body grades upward into massive barite, and has a sericite-chlorite altered footwall stockwork zone.

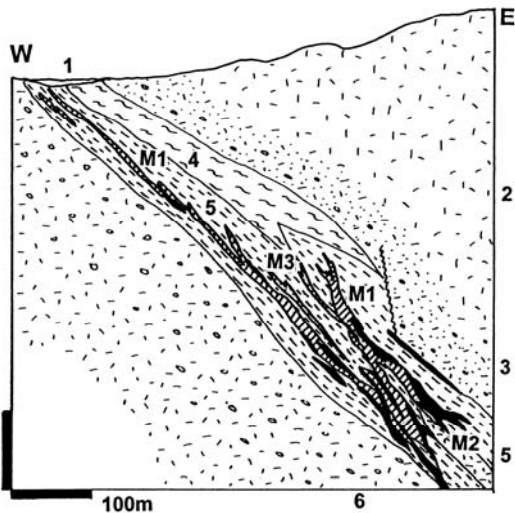


Figure 8.23. Rosebery VMS deposit, western Tasmania; cross-section from LITHOTHEQUE No. 3303 modified after Green et al. (1981), Rosebery Mine Staff. 1. Q unconsolidated sediments; Cm2-3 Mt. Read Volcanics: 2. Rhyolite, dacite flows, pumice breccia; 3. Hangingwall, rhyolitic pumiceous mass-flow deposits; 4. Black slate; 5. Ore host: stratified felsic volcanoclastic sandstone, altered; M. Partly remobilized, deformed kuroko-style Zn,Pb,Cu VMS zone; M1, predominantly Zn,Pb sulfides; M2, predominantly pyrite-chalcocopyrite; M3, predominantly barite (sphalerite, galena); 6. Footwall rhyolite and dacite pumice breccia, subvolcanic sill

Mount Lyell Cu ore field near Queenstown (Hills, 1990; Pt ~108 mt of ore for 1.404 mt Cu, 1,050 t Ag and 45 t Au) contains a variety of orebodies enclosed in sericite, chlorite and quartz-altered, strongly cleaved mainly felsic tuffs, lavas and breccias. Most and the largest orebodies (Prince Lyell) are of disseminated pyrite with lesser chalcocopyrite in chloritized rhyolite. There is one small massive pyrite-chalcocopyrite orebody (The Blow) and a body of bornite-rich siliceous ore believed resulting from Devonian synorogenic remobilization (North Lyell).

Mount Morgan Cu-Au, Queensland

Mount Morgan ore field in central Queensland (Messenger et al., 1998; ~50 mt @ 0.7% Cu, 5 g/t Au for 280 t Au and 370 kt Cu) had been the largest former gold producer in Queensland for many years (Fig 8.24). It is also a genetically enigmatic deposit interpreted as either of synvolcanic exhalative origin (Messenger et al., 1998 and earlier authors) or tonalite-related hydrothermal replacement (Arnold and Sillitoe, 1989). The "boot-shaped" orebody in the subvertical Main Pipe and perpendicularly disposed subhorizontal Sugarloaf zone is in a fault-bounded roof pendant of Middle Devonian rhyolitic to dacitic volcanic-sedimentary sequence, much similar to the VS succession at Rio Tinto. The pendant is surrounded, and thermally metamorphosed, by Upper Devonian trondhjemite to tonalite. The Main Pipe has massive pyrite with lesser chalcocopyrite and minor sphalerite cut by anastomosing quartz veins and high-grade gold-tellurides shoots. The Sugarloaf orebody has disseminated and veinlet pyrite, pyrrhotite and chalcocopyrite in quartz, sericite, chlorite-altered volcanics. There was a goethitic gossan with high residual gold values (Pt ~2.4 mt ore with 72 t Au).

8.7. Sundry metallic ores

Synvolcanic "exhalative" deposits of other metals than Fe, Cu, Zn, Pb, Ag and Au do occur, but many are controversial or of small to medium size. The "giant" Sn accumulation in the Neves Corvo VMS ore field is a lonely exception. Synvolcanic, submarine-hydrothermal origin is often applied to the scheelite deposits in Felbertal, Austria, but from the empirical premise of host lithology they are more at home among high-grade metamorphics (Chapter 14). So are the "Broken Hill-type" Pb-Zn deposits, whatever they had been before the metamorphism, and the small Co deposits north of Salmon, Idaho. Exhalitic Fe and Mn ore deposits are widespread and, in fact, the German Devonian Lahn-Dill type Fe deposits had been the first ore type interpreted by Schneiderhöhn, back in the 1940s, as submarine-exhalative. They are all small, however, although some of their Archean counterparts (Chapter 9) reach the "large" magnitude. The same applies to some siderite deposits in combined "eugeoclinal" volcanic-sedimentary and carbonate setting like the Styrian **Erzberg** in Austria. Although important in the context of European siderurgy, it is a mere "medium" size deposit of 214 mt Fe @ 39% Fe.

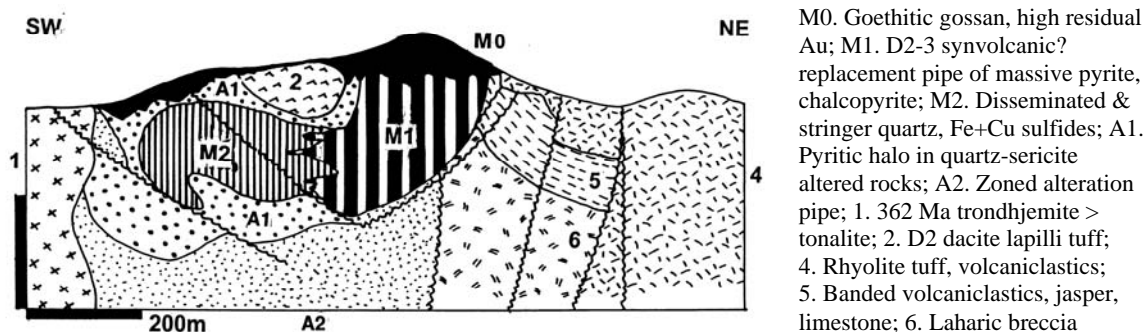


Figure 8.24. Mount Morgan massive and disseminated pyrite, Au, Cu deposit, Queensland. Cross-section from LITHOTHEQUE No. 308, modified after Messenger et al. (1998)

Some Fe (Magnitogorsk, Turgai) and Cu (Tur'ya) skarn deposits are alternatively interpreted as synvolcanic, metamorphosed and remobilized near granite contacts but, likewise, they are "undersize". The Turgai Fe province in NW Kazakhstan, considered collectively, is a "large district" with 3.0 bt Fe (Baklayev, 1973). The widespread "exhalative" Mn deposits are all small.

Syngenetic-diagenetic and sedimentary-exhalative deposits in carbonaceous pelites and carbonates, as well as the various "metalliferous shales", are treated in Chapter 13 although some of the host units border on, or are even a part of, the

"eugeoclinal" orogens. The many sedimentary lithofacies of the latter such as turbidites, (meta)pelites and carbonates do not contain major metal accumulations.

Syn- and post-orogenic hydrothermal vein, replacement and disseminated deposits of Au-Ag, Cu, Pb-Zn-Ag, Sb, W, Mo, Sn and other metals, partly superimposed on and hosted by (meta)volcanic and sedimentary associations, appear in Chapters 6, 7 and 10. Synvolcanic and early postvolcanic veins and replacements do occur, but none alone reach the "giant" magnitude.

9 Precambrian Greenstone-Granite Terrains

9.1. Introduction

"Greenstone belt" (Condie, 1981) is the popular, although quite inaccurate term for relatively low-grade metamorphosed volcanic-sedimentary successions of mostly Early Precambrian age, exposed in the old cratons, shields and blocks. "Schist belt" is used as a synonym, or a name for predominantly meta-sediments dominated equivalents of the "greenstone belts". De Wit and Ashwal (1995, 1997) identified at least 260 Archean belts worldwide, Murchison (Western Australia; 120,000 km²) and Abitibi (Canadian Shield; 115,000 km²) being the largest ones.

Long-lasting erosion and denudation, combined with uplift, removed upper levels of orogens composed of supracrustal successions and epizonal intrusions, and exposed the deep basement of katazonal granites, migmatites and gneisses. The depth of erosion is roughly proportional to geological age so Paleoproterozoic and Archean terrains are eroded to a much greater depth than Phanerozoic ones. The erosion and denudation follow, intermittently, tectonic consolidation and stabilization ("cratonization"), which incorporated remnants of formerly independent volcanic-sedimentary orogens and their basements into blocks (cratons) that continued as rigid units throughout the rest of geological history. In the pre-1968 models cratons and orogenic belts outside them were treated as qualitatively different entities. They still are, in structural sense, but in terms of lithologic associations and much of metallogeny Archean greenstone belts are the equivalent of Phanerozoic "eugeoclines" with some variations due to evolution (Condie, 1981; Goodwin, 1991).

The bulk of Early Precambrian shields consists of "granite-greenstone terrains" where the greatly predominant "granite" (~70-80% by area in Archean shields, usually shown in pink on geological maps) is a mix of mainly tonalitic, less metasedimentary gneiss grading to migmatite and granite gneiss, intruded by mostly katazonal granitic plutons and batholiths of several generations. Metavolcanic ("greenstone"), metasedimentary ("schist") and mixed lithologies form numerous shallow (some 6 km maximum thickness) erosional remnants on the "granite" basement, and have the

form of short, irregular, winding or anastomosing belts to small patches. Formerly considered keel-like in cross-section, it now appears that perhaps the majority of greenstone belts are thin sheets, with a high degree of structural repetition of their stratigraphy (de Wit and Ashwal, 1995). The metamorphic grade is typically greenschist to lower amphibolite, increasing to middle-upper amphibolite around syn- to post-orogenic intrusions. Subgreenschist grade is rare among Archean greenstones but it does occur (e.g. in the Noranda area, Québec). Higher-grade greenstone equivalents, amphibolites and mafic granulites, are treated in Chapter 14.

The geotectonic setting of the (especially Archean) greenstone belts and related magmatic rocks has been continuously debated (e.g. Ayres, ed., 1985; Goodwin, 1991). Shortly after introduction of plate tectonics in the 1970s the majority opinion favoured oceanic or island arc origin of the "greenstones", and the greatly predominant bimodal sequences that contain komatiites were compared with immature, intraoceanic island arcs. The alternative opinion favoured "rifts", both initially intracontinental (Atlantic margin-type) and intra-oceanic, or intra-arc type. It is not certain as to whether subduction operated in the Archean, and/or when it started. As in the young island arc systems (Chapter 5) subduction and rifting go hand-in-hand, so the distinction is academic yet used in the empirical grouping of geological regions and their metallogenies. The Proterozoic Mount Isa Inlier in Queensland, an area with several prominent ore "giants", is an orogenic system in which the "rift" characteristics are stronger than the typical features attributed to subduction-related island arcs, so there is a preference in the literature to treat such complexes under the heading of "paleorifts" or similar. Internally, greenstone supracrustals are intruded by both synvolcanic and syn- to post-orogenic plutons (Ayres and Černý, 1982; Fig. 9.1). As in the eugeoclinal belts the relative timing of "greenstone" metallogenesis can be 1) pre-greenstone, 2) contemporaneous with greenstone deposition (syn-depositional, syn-volcanic or syn-sedimentary), and

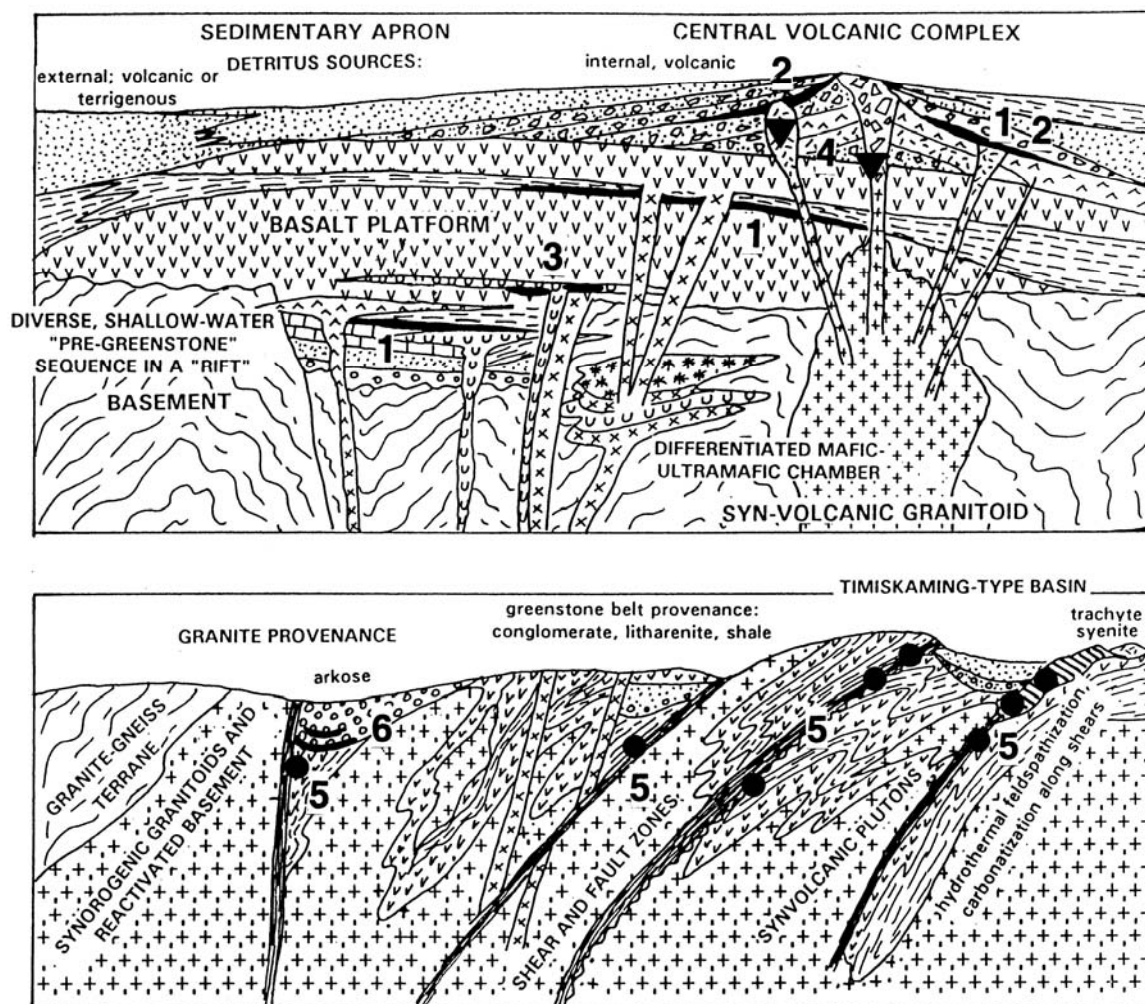


Figure 9.1. Usual lithologic association included in early Precambrian greenstone terrains, showing the place of "giant" metallic deposits. TOP: Units assembly as it was before major orogeny and now no-longer preserved; the major synvolcanic "giants" are shown: 1. Algoma-type BIF; 2. VMS deposits ("Noranda-type"); 3. Ni sulfides associated with komatiites. BOTTOM: Post-orogenic assembly complete with many shear zones. The synorogenic "giants" include 5. Shear-related (syn)orogenic Au >As, Sb, Cu deposits; 5. Auriferous conglomerates in syn- to early post-orogenic basins on greenstone belts (Tarkwa). Modified from Laznicka (1991, 1993)

3) post-greenstone (syn-orogenic to post-orogenic, related to structures and intrusions). Pre-orogenic metallogensis was active in time of formation of the "greenstone" basement, but as the basement is often uncertain, invisible or very deeply eroded, few ore occurrences have been recorded there and almost all are insignificant. There is, however, some discovery potential, for example of the Witwatersrand- and Elliot Lake-type basal auriferous or uraniferous conglomerates resting on mature basement. This ore type could be expected in the platformal/rift sequences locally present at base of some greenstone successions (Thurston and

Chivers, 1990). The syn-greenstone metallogensis is emphasized in this chapter. Although the syn- and post-orogenic ore formation in Phanerozoic and Late Proterozoic settings is treated separately in Chapter 10, the Early Precambrian counterparts have been included in this chapter for the sake of continuity and to accommodate the many links (and uncertainties) that exist among the pre-, syn-, and post-orogenic mineralizations.

Compared with the metallogeny of the Phanerozoic "eugeoclinal" orogens, "greenstone" metallogeny appears more simple because much of the high-level mineralizations have been removed

by erosion, and probably also because some of the more evolved ore styles did not form that early in the earth's history. The three dominant syn-depositional ore types that contribute "giants" in greenstone belts are banded iron formations, massive Fe, Cu, Zn, Pb sulfides, and "komatiitic" Ni sulfides. Syn- and post-orogenic ores are dominated by the orogenic Au association. Other ore types are one-of-a-kind or rare.

There is an abundant literature about the greenstone belts in general (e.g. Windley, ed., 1976; Nisbet, 1987; Condie, 1981; Goodwin, 1991, De Wit and Ashwal, eds., 1997) and on regions where they are prominently developed (Thurston et al., eds., 1992; Tankard et al., 1982; De Ronde and De Wit, 1994; Geological Survey of West Australia, 1990). "Greenstone" metallogeny is covered in several global reviews (e.g. Hutchinson, 1981, 1984; Sokolov, 1984; Naqvi, ed., 1990; Laznicka, 1993, p. 105-632), regional reviews (e.g. Anhaeusser and Viljoen, 1986; Groves and Batt, 1984) and commodity/ore type reviews (e.g. Hutchinson et al., eds., 1982; Barrie and Hannington, eds, 1999, of VMS; Foster, ed, 1991, of gold). Our story starts with brief description of the Abitibi Subprovince of the Canadian Shield. This is followed by review of the rock associations hosting "giants" (Fig. 9.1), and/or ore types that are not controlled by the host lithology.

9.1.1. Abitibi Subprovince (greenstone belt), Canadian Shield

Abitibi is the largest and most "typical" Archean greenstone belt in the Canadian Shield, and probably in the world (Ludden et al., 1986; Jensen, 1985; Thurston et al., eds., 1992; geological map MERQ-OGS, 1984; Figures 9.2, 9.3). The subprovince measures about 750x250 km along its median line, it crosses the Ontario-Québec provincial boundary, and it is defined by numerous mining towns the largest being Timmins, Noranda, Val d'Or and Chibougamau. The internally complex belt includes some 80% of features recognized globally in Archean greenstone belts, except for deep regolith stripped away during four successive Quaternary glaciations. This eliminates from consideration, with few exceptions, the economic ore types prevalent in greenstones exposed in the tropics such as enriched iron formations, gold placers and residual Mn oxides. Although the Abitibi rocks are virtually free of weathering, the exposure is limited due to extensive drift cover.

The Subprovince is bordered by two major collisional structures and it terminates in the north

and south at the appearance of granite-gneiss terrains. The supracrustals have an east-west structural grain and an "anastomosing motif that coincides with lozenge-shaped blocks, each enclosing one or several volcanic complexes or gneissic-granitic terranes" (Hubert and Marquis, 1989). Two principal (Northern and Southern) Volcanic Zones are subdivided by Central Granite-Gneiss Zone that preserves relics of a thin blanket of monotonous tholeiitic "plateau-like" metabasalt. The Abitibi volcanic zones are a collage of coalescing multistage semi-mature volcanic > sedimentary piles dated around 2.72-2.69 Ga, pierced by comagmatic intrusions and resting on "subaqueous lava plains" of tholeiitic meta-basalt (Thurston and Chivers, 1990). The volcanic piles evolved during four cycles; a complete cycle has up to four magmatic associations, from base to the top (Goodwin, 1982; MERQ-OGS, 1983): a) komatiitic units (peridotitic to basaltic komatiite with feeder dikes, sills, minor intrusions); b) tholeiitic basalt and rare andesite units of the monotonous "basalt plains", with rare tholeiitic rhyolite; c) calc-alkaline units that are either bimodal (basalt-dacite/rhyolite) or sequentially differentiated (basalt, andesite, dacite, rhyolite). The volume of pyroclastics and volcanics greatly exceeds the volume of lavas. Many central volcanic complexes are cored by large synvolcanic tonalite and trondhjemite plutons. Thermal aureoles around plutons are indistinct, but the stocks and their environs are fractured and hydrothermally altered; d) alkaline units of shoshonitic trachyte, trachyandesite, syenite, with rare pseudoleucite trachyte. The latter are spatially associated with remnants of conglomerate and litharenite-slate turbidite suite (Temiskaming Assemblage), particularly common near regional shear zones.

The Archean volcanic pile rests on an earlier high-grade metamorphic basement. Two early anorthosite-dominated layered intrusions (Lac Doré Complex) are reminiscent of the cratonic Bushveld Complex. The greenstone volcanic pile had been first deformed and metamorphosed to the dominant greenschist rank during the 2.65 Ga Kenoran Orogeny, when prominent east-west trending steep regional shear zones ("breaks") formed. The shearing was followed by emplacement of syn- to post-orogenic plutons and batholiths. In the southwest, the Archean rocks are unconformably overlain by the predominantly sedimentary Paleoproterozoic Huronian Supergroup intruded, in the Cobalt-Haileybury area, by thick diabase and gabbro sheets (Nipissing diabase).

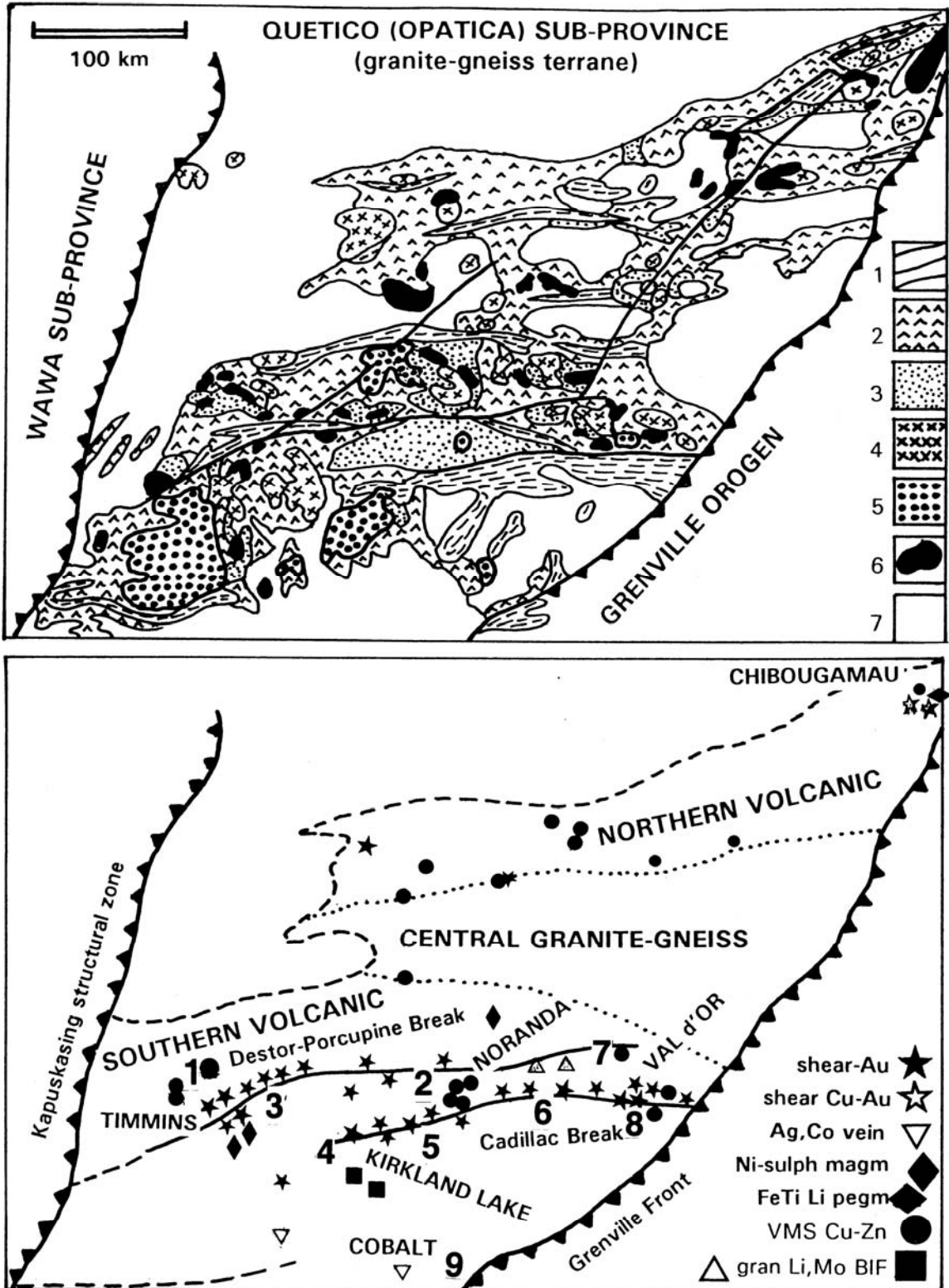


Figure 9.2. Abitibi Subprovince, Canadian Shield, geology and ores (Laznicka, 1991; explanations are on facing page)

Figure 9.2. (continued). TOP, map legend: 1. High-grade metasediments, contemporaneous with metavolcanics (schist to gneiss); 2. Mafic to (rare) intermediate volcanics; 3. Felsic metavolcanics and subvolcanics; 4. Synvolcanic granitoids; 6. Gabbro and ultramafic intrusions; 7. Basement (Archean granite gneiss, migmatite, granitoids) and post-Abitibi (Pp Huronian Supergroup) rock units. BOTTOM: Plot of principal Abitibi ore deposits; the "giant" deposits are numbered: 1. Kidd Creek-VMS; 2. Noranda VMS cluster that includes the Horne "Au-giant"; 3. Timmins-Porcupine-Au; 4. Kirkland Lake-Au; 5. Kerr Addison-Au; 6. Bousquet-Cadillac, Au; 7. Malartic-Au; 8. Val d'Or-Au; 9. Cobalt-Ag, As, Co, Ni, Bi

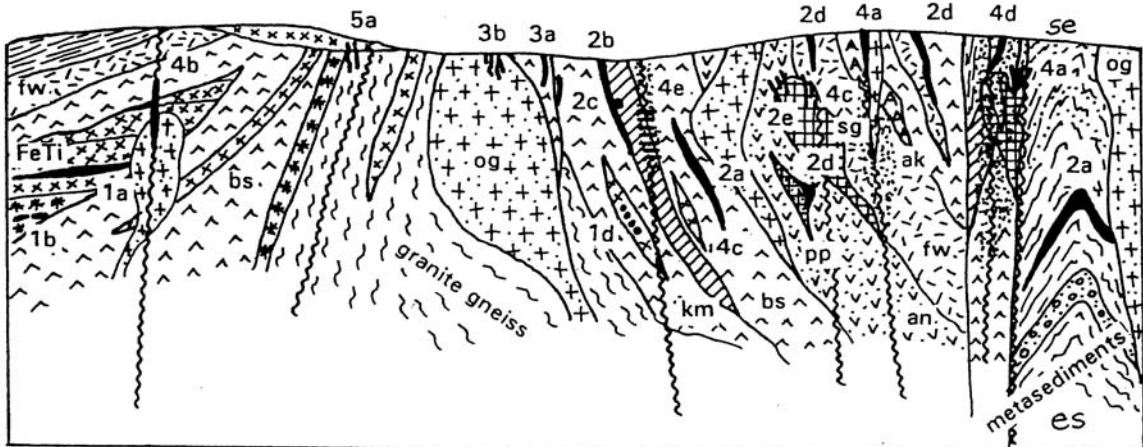


Figure 9.3. Inventory diagram (cross-section) showing the place of metallic deposit types (numbered) and main rock associations (letter codes) in the Abitibi Subprovince in Ontario and Québec, from Laznicka (1991, 1993). Not to scale. The following ore types contain "giant" members: 2d, 4a and 5a. Explanations of rock codes: an=andesite; ak=albitic porphyries; bs=metabasalt; es=epiclastic metasediments; fw=felsic metavolcanics; og=orogenic granitoids; sg=synvolcanic granitoids. Ore types. 1: Ultramafic & mafic intrusion hosts, 1a=Ti-magnetite, ilmenite; 1b=Cr & PGE; 1c=disseminated chromite; 1d=disseminated komatiitic Ni. 2: Synvolcanic and synsedimentary ores, 2a=Algoma-type BIF; 2b=stratiform Fe sulfides; 2c=komatiitic Ni contact deposits; 2d=Fe,Zn,Cu VMS; 2e=subvolcanic Zn, Cu, Au. 3: Ores related to orogenic granitoids, 1a=rare metals pegmatites; 2b=Mo veins, stockworks. 4: Orogenic hydrothermal deposits, 4a=Au only lodes; 4b=Cu, Au shear lodes; 4c=Cu (Au,Mo) veins, stockworks in granitoids; 4d=Au (Cu) in feldspathized fault rocks; 4e=magnesite replacements. 5: Post-orogenic deposits, 5a=Cobalt type Ag,As,Co,Ni veins; 5b=relics of mineralized regoliths.

Abitibi metallogeny: The Abitibi Subprovince contains about 3,000 recorded ore occurrences and 265 present and past mines, in Ontario and Quebec (Thurston et al., 1992). It has the world's second largest gold endowment after Witwatersrand (5,091 t Au), of which some 1,850 t Au alone came from the Timmins-Porcupine goldfield. Production and reserves of other metals total 180 mt Fe, 7.02 mt Ti, 196 kt V, 15,571 mt Zn, 8.7 mt Cu, 297 kt Pb, 1,808 mt Ni, 16,422 t Ag (compare Laznicka, 1993, p.140). There are 12 "giant" deposits and zones ("camps"): eight "Au-giants" (Hollinger-Coniaurum in Timmins, 995 t Au; Kirkland Lake, 786 t Au; Val d'Or, 388 t Au; Dome-Preston in the Porcupine field, 386 t Au; Bousquet, 336 t Au; Kerr Addison, 331 t Au; Horne in Noranda, 330 t Au; Malartic, 323 t Au); two "Ag-giants" (Kidd Creek, 14,640 t Ag; Cobalt camp, 15,500 t Ag); one "Cu giant" (Kidd Creek, 3.5 Mt Cu) and one "Zn-giant" (Kidd Creek, 11.7 Mt Zn). There are 6 "large" Au deposits

(100 t Au plus), 2 "large Ag", 1 "large Ni", 6 "large Cu", 3 "large Zn" and one "large Sn" (Kidd Creek, 142 kt of contained Sn). In terms of ore styles, there are 6/5 (i.e. "giant"/"large") synorogenic Au, 1/1 post-orogenic Ag,As,Co,Ni; 2/1 VMS-Au, 1/5 VMS-Cu, 0/1 synorogenic Cu, 1/3 VMS-Zn, 1/1 VMS-Ag; 0/1 komatiitic Ni.

The numerous, although individually mostly small Zn-Cu dominated VMS deposits ("Noranda-type") are associated with bimodal central volcanic-sedimentary complexes, especially with their felsic members. The deposits form clusters, often controlled by marker horizons of "exhalite". Volcanic stratigraphy, facies and geochemistry are the best tools of predictive metallogeny.

The (syn)orogenic gold deposits are even more widespread than the VMS and all the "giants" are located near, although not necessarily within, prominent shear zones ("breaks") like the Destor-Porcupine Break, Kirkland-Larder Lake Break, and

Cadillac Break. The host rock lithology appears to have had a limited control on gold deposition, although some lithologies are more favourable to host Au deposits (e.g. komatiite), others are less favourable (e.g. the homogeneous synorogenic plutons and batholiths). In the Bousquet zone in Québec gold accumulated in both synvolcanic (pyritic VMS) and superimposed synorogenic (vein, stockwork) structures, but the concept of "exhalitic" gold, strong in the 1970s, is much weaker now.

There are virtually no economic ores in the granite-gneiss basement. The Proterozoic basinal clastics contain the important Elliot Lake district of basal uraniferous conglomerates situated outside the Abitibi Sub-province, and the idiosyncratic Cobalt camp has hundreds of individually small post-orogenic "bonanza" Ag, As, Co, Ni, Bi fissure veins in, and in the contact aureole of, the Nipissing mafic sill. These veins are always close to, or sometimes within, the Abitibi Archean basement that contains earlier syndepositional mineralization. The most prominent Abitibi deposits or "camps" are described in some detail below.

9.2. Komatiite association and Ni ores

In 1969, the Viljoen brothers discovered and interpreted submarine ultramafic lavas in the Komati River region (Barberton Mountain Land, South Africa) that they named komatiite. Since that time, komatiites have been found in all major Archean and some Proterozoic greenstone belts (Fig. 9.4). Arndt and Nisbet, eds. (1982) defined komatiite as an ultramafic volcanic rock that contains between 18 and 32% of MgO. Komatiitic peridotite may grade into, or be associated, with komatiitic basalt, and olivine-rich cumulates that form hypabyssal layered intrusions. There are also komatiite dikes and sills, hard to tell from the massive flows. The lavas are all submarine, sometimes interbedded with sediments. They may grade into flow breccias, but tuffs are rare. A typical flow unit of komatiite has massive to knobby peridotite at base, followed by spinifex-textured serpentinized olivine (a conspicuous skeletal quench texture), and topped by chilled and fractured flowtop. Komatiitic basalts are visually unrecognizable from tholeiitic basalts and they come as massive to pillowed flows, breccias, hyaloclastites. Barrie et al. (1999) interpreted komatiites as products of partial melting of primitive (Al-undepleted) mantle, or of partial melting of refractory harzburgite that underwent previous basalt extraction.

Komatiitic ultramafics, like other ultramafics, have systematically high average trace contents of several metals: Cr (0.12-0.25%), Ni (0.1-0.25%), Co (60-180 ppm). Locally, the trace contents increase up to about 0.35% Ni, but as long as this is a silicate Ni (bound in olivine lattice) it is not economically recoverable. 0.34% Ni stored in sulfides (disseminated pentlandite with pyrrhotite), however, may qualify as an orebody, although still uneconomic at present (e.g. the Dumont Sill with a resource of 1.635 mt Ni). A factor of concentration of mere 3, and sulfidation of the silicate Ni, are required to convert a "rock" komatiite into an economic ore presently mined at Mount Keith in Western Australia (0.6% Ni). As komatiitic magmas are low in S, sulfur derived from adjacent rocks can be assimilated by magma and this seems to be indicated by the frequent presence of pyritic carbonaceous phyllite (slate) in the footwall of many Ni sulfidic orebodies. An alternative mechanism of enrichment of the trace Ni in komatiite is the supergene process. Ni laterite and saprolite grading 1.0% plus Ni constitutes a viable ore, equivalent to Ni laterites formed over ophiolites (Chapter 8). Because Ni grade is rather high (55 ppm), a "Ni-giant" needs to contain 5.5Mt Ni plus and this has not been achieved by any deposit in the present category. As komatiitic Ni (and related laterites) are still economically important and some are of the "world class", selected "large" Ni deposits (550 kt Ni+) are briefly described below.

Komatiitic Ni sulfide deposits

Barnes and Brand (1999) distinguished the following field categories of komatiitic occurrences: 1) Thin differentiated spinifex-textured flows (e.g. Munro Township, Ontario); 2) channelized sheet flows with thick olivine-rich cumulate base, flanked by thin differentiated units (e.g. Kambalda); 3) dunitic channelized sheet flows with central lenses of olivine adcumulate (e.g. Mount Keith); 4) thick dunitic sheet flows and layered lava lobes and/or sills. The stratigraphically higher zones include pyroxenite and gabbro (e.g. the Wiluna ultramafic complex, Forresteria). The above scheme overlaps with classification of komatiitic Ni-sulfide deposits by host rock and ore style of Lesher (1989), who distinguished komatiitic peridotite-hosted, and komatiitic dunite-hosted deposits. The Ni ore in each class are further subdivided into two styles: 1) "stratiform" (high-grade massive, breccia to network sulfide deposits at the base of flows) and "stratabound" (disseminated to blebby sulfides

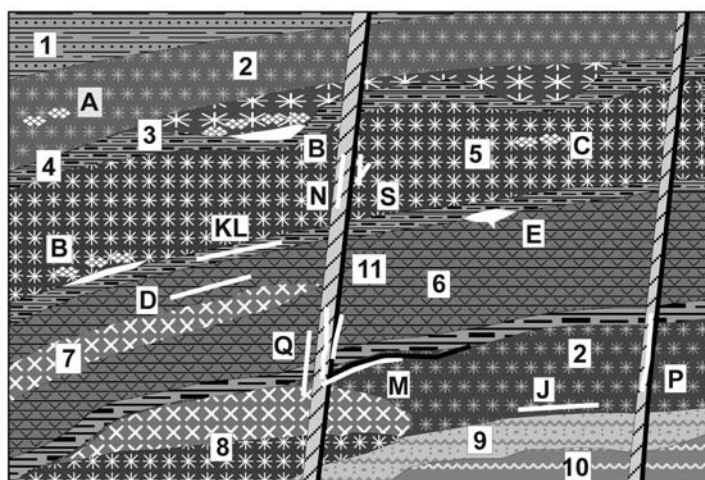


Figure 9.4. Inventory diagram of ore deposits that may be present in the early Precambrian komatiite association. From Laznicka (2004) Total Metallogeny site G21. Ore types E, M, Q, R have "giant" equivalents

1. Metasediments; 2. Peridotite flow; 3. Dunite cumulate at base of flow; 4. Interflow sediments; 5. Peridotitic sill; 6. Tholeiitic basalt; 7. Gabbro sill; 8. Layered intrusion: top gabbro, bottom peridotite; 9. Archean basal platformic sediments; 10. Archean crystalline basement. A. Ni sulfides disseminated in umafic interior; B. Ditto & massive sulfides at contacts; C. PNG & Ni disseminated in ultramafic sill; E. Fe,Cu VMS; J. BIF; K. Increased Cu,Co,As,-Ni,Zn in metalliferous schist; L. Fe-Ni sulfides in black schist; M. Au superimposed on "exhalite"; N. Remobilized Ni arsenides; P. Ditto in sheared komatiite; Q. Au in silica-carbonate-fuchsite metasomatite; R. Sb in altered shears; S. Chrysotile; X. Ni laterite; Y. Residual chromite

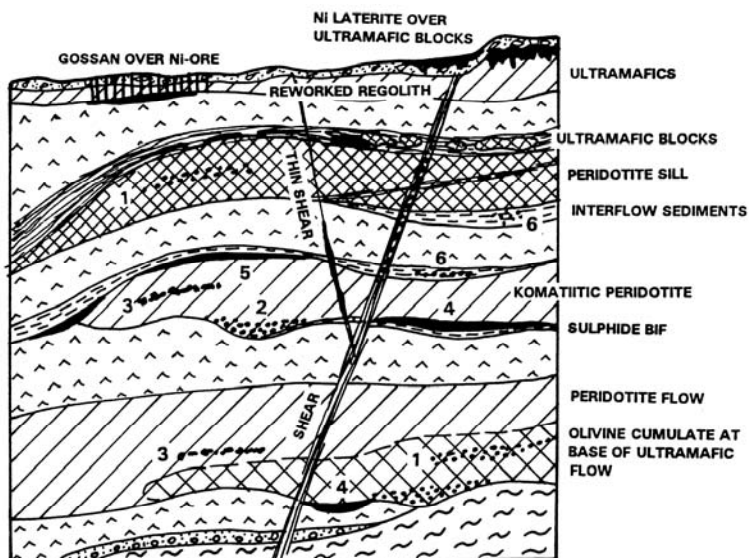
within a peridotite body). I find this stratiform/stratabound difference rather confusing as the terms "basal", "footwall" or "contact" (in rare cases hangingwall) high-grade Ni ore, versus disseminated intra-komatiite ore, would provide a clearer image (Fig. 9.5). The ore mineralogy of massive, breccia, network and disseminated sulfides is simple and repetitive, dominated by pyrrhotite with lesser pentlandite and chalcopyrite. Pyrite, cubanite and magnetite may be present in small amounts and violarite dominates the supergene sulfide zones. Gossans (oxidation zones) over sulfide orebodies are depleted in Ni and the apple green minerals (gaspéite, garnierite) are present in mineralogical quantities only.

Kambalda Dome deposits (Gresham and Loftus-Hills, 1981; Stone and Masterman, 1998; P+Rc 67 Mt @ 2.9% Ni, 0.25% Cu for 1.943 Mt Ni, ~90 kt Cu, ~29 kt Co; this includes some outlying deposits). Kambalda is 60 km south of Kalgoorlie, Western Australia, in the Archean Yilgarn Craton. The first orebody there (Lunnon) was drill-intersected in 1966 and this started the Australian nickel industry, presently the fifth in the world. Kambalda Dome refers to a discontinuous outcrops of two members of ~2.88 Ga komatiitic ultramafics, sandwiched between meta-basalt units, in a structural dome cored by granitoid intrusions. The supracrustals are metamorphosed between the upper greenschist and lower amphibolite grades. 24 ore "shoots" (a local term for an orebody or a group of orebodies), ranging in size from several thousand tons to 1 mt plus of ore, are scattered over an area

of 400 km². The orebodies are of the channelized flow type, in the Lower Ultramafic Member. 80% of the high-grade massive, breccia and minor matrix sulfides fill elongated troughs (embayments) in footwall basalt, under sheet flows of the peridotitic Upper Member. The remaining orebodies are near the hanging-wall contact (e.g. Jan shoot; Fig. 9.6), at base of the second or third ultramafic flow, higher up in the sequence. The original stratiform, contact ore sheets are disrupted into multiple ore surfaces in most deposits. Interflow albitic metasediments of cherty appearance contain pyrite and pyrrhotite, and are slightly nickeliferous when adjacent to the contact orebodies. The usual sulfides (pyrrhotite, pentlandite, pyrite, minor chalcopyrite) are strongly deformed, recrystallized and locally remobilized. The host ultramafics are in places carbonated and/or converted into talc-tremolite schist. Millerite is present locally.

Perseverance alias Agnew-Ni ore field near Leinster, Western Australia, is the largest komatiitic "contact" Fe>Ni>Cu deposit (Billington, 1984; 2.62 mt Ni @ 0.7-2.5% Ni; Fig. 9.7). The massive to breccia lenticular to sheet-like bodies of pyrrhotite, pentlandite, minor chalcopyrite follow sheared basal ultramafic contact against metasedimentary schist. The ore has Durchbewegung fabrics and is believed to be syntectonically remobilized. Disseminated to net-textured sulfides are in the peridotitic accumulate in the hangingwall.

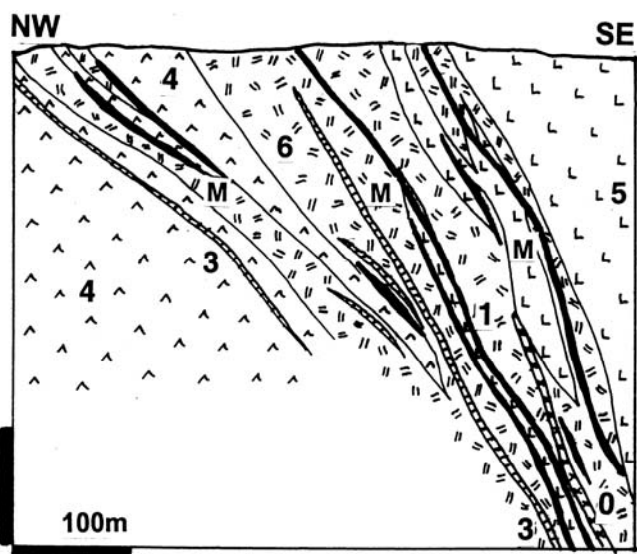
Mount Keith, 1100 km NE of Perth in Western Australia (Donaldson et al., 1986; 478 mt @ 0.5-0.6% Ni for 2.75 mt Ni; Fig. 9.8) is an example of



Ni ore types (all are pyrrhotite > pentlandite > chalcopyrite)

1. Disseminated sulfides inside ultramafic flow or sill
2. Disseminated sulfides along basal contact of ultramafics
3. Intra-flow massive to breccia ore
4. Massive breccia to matrix ore along basal ultramafic contacts
5. Ditto, along the hangingwall contact
6. Disseminated, stringer, breccia to massive ore in interflow, basal or hangingwall metasediments

Figure 9.5. Variety of Fe-Ni-(Cu) sulfide deposits in the early Precambrian komatiitic association. Laznicka (1991, 1993)

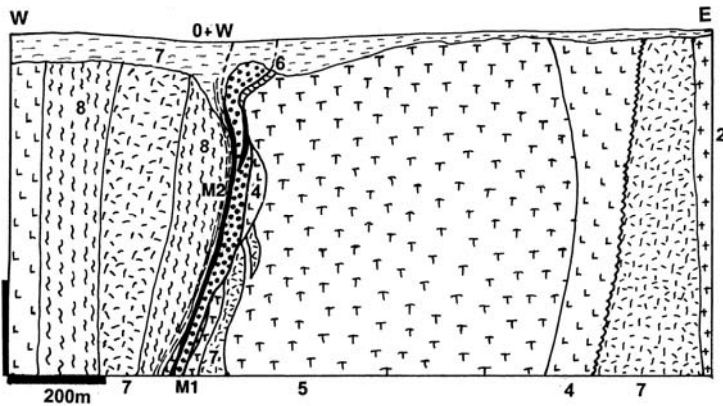


0. Post-ore diabase dike
1. Porphyry intrusions and dikes
3. Interflow metasediments;
4. Tholeiitic pillowed and massive metabasalt
5. Ultramafic komatiite with spinifex, less thick cumulate flows
6. Ditto, thick cumulate lava channels with ore, thinner barren flows flanking footwall interflow sediment
- M. Massive, breccia, matrix, stringer disseminated Fe, Ni > Cu sulfides; both basal and hangingwall orebodies
7. Lunnon Basalt, tholeiitic flows and hyaloclastites

Figure 9.6. Kambalda Ni cluster, cross-section of the Jan Shoot, one of the 24 individual deposits around the Kambalda Dome. Example of a deposit with orebodies in the komatiite hangingwall. From LITHOTHEQUE No. 1372, modified after Marston (1984) and WMC Corporation handout

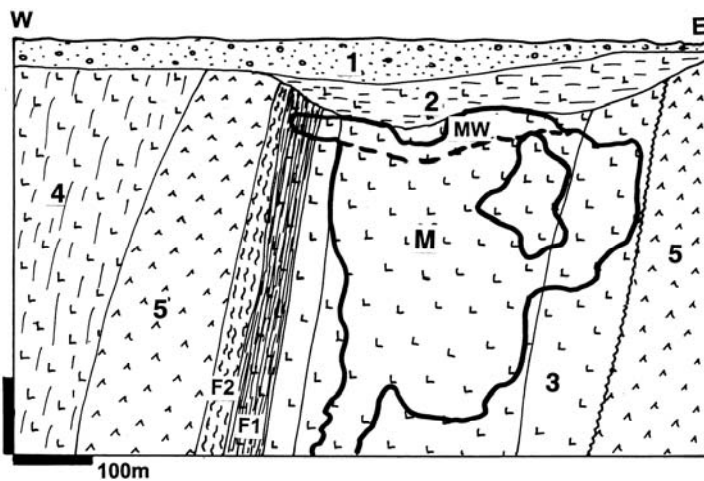
the disseminated, dunite-hosted ore type. It is a lenticular body of serpentinized, upper greenschist-metamorphosed and strongly deformed (sheared) adcumulate to mesocumulate Archean dunite. The ore minerals (predominantly pentlandite) are evenly and sparsely disseminated throughout. The pyrrhotite-rich ore near the stratigraphic top grades into pyrrhotite-free ore beneath. Millerite with

pentlandite dominate the intensely sheared and talc-magnesite altered ultrabasics. Near surface, the Fe-Ni sulfides are leached out but conspicuous purple stichtite replaces accessory chromite grains. In the 60 to 90 m depth, in the zone of secondary sulfides, violarite with minor pyrite substitute for pentlandite. The **Yakabindie** deposit, 20 km south of Mount Keith in the same komatiitic belt, stores



- 0+W. Regolith and T-Q sediments;
 2. Basement granite gneiss; 4. Ar metakomatiite, now mostly silicate schist locally retrograded to serpentinite; 5. Serpentinized peridotite cumulate; 6. Actinolite marker; 7. Meta-dacite, rhyolite and felsic pyroclastics; 8. Metasedimentary schist; M1. Disseminated to net-textured Fe, Ni sulfides in adcumulate; M2. Massive to breccia Fe, Ni > Cu sulfides along sheared contacts

Figure 9.7. Perseverance (Agnew) Ni deposit near Leinster, Western Australia: the single largest "contact" deposit. From LITHOTHEQUE No. 2662, modified after Billington (1984)



1. T-Q transported overburden
 2. T saprolite on dunite
 MW. T, supergene sulfides violarite, marcasite and millerite replace pentlandite; stichtite after chromite
 M. Large tonnage of evenly and sparsely disseminated pyrrhotite, pentlandite in dunite adcumulate
 3. Ar dunitic ad- and meso-cumulate in the center enveloped by orthocumulate
 4. Ar komatiitic ultramafics, undivided; F1, F2. Altered mylonite and phyllonite in shear;
 5. Ar mafic and bimodal greenstone

Figure 9.8. Mount Keith disseminated Ni deposit, Western Australia from LITHOTHEQUE No. 1380, modified after WMC Corporation handout, 1981, and Burt & Sheppy (1975)

1.54 mt Ni in a 0.5% Ni ore. **Dumont Sill** in the Abitibi Subprovince is the largest, but low-grade (1.635 mt Ni @ 0.34%) example of the Mount Keith-type of disseminated Fe-Ni-Cu sulfides in komatiitic peridotite, in Canada. All the remaining komatiitic Ni occurrences in the rest of the world store less than 1 mt Ni.

Silicate and oxide Ni in laterite/saprolite over komatiite

Ni-enriched humid tropical weathering profiles ("Ni-laterite") form on any ultramafic rock with a high silicate trace Ni content (0.2-0.3% Ni), and have already been described in Chapter 8 where the parent rocks were members of the Phanerozoic

ophiolite association. In the early Precambrian greenstone belts the main ultrabasic parent rocks are komatiitic peridotites, especially the olivine-rich cumulates. Some of these, in addition to Ni in olivine lattice, contain some Ni in disseminated sulfide phase (pentlandite), but in low concentrations that are not sufficient to produce deposits of the Mount Keith-type. The sulfide component contributes to the Ni content of the residual ore to produce what is a mixture of laterite and gossan.

"Ni-laterites" on komatiite have been discovered much later than the classical deposits on ophiolites and alpine serpentinites (in the 1970s) and, so far, brought into production only in Western Australia where there are presently three integrated mining

and processing complexes (Murrin Murrin, Bulong and Cawse), with few more under construction. The Ni extraction technology used is acid pressure leach and the product is metallic Ni and Co in pellets. The Western Australian metalliferous regolith formed between late Cretaceous and Miocene under humid climatic conditions. It is preserved as discontinuous relics under Quaternary alluvium and colluvium, locally overprinted by silcrete and calcrete. There are no natural outcrops in the generally flat terrain and the "Ni-laterites" have been first encountered in excavations for vein gold (e.g. Ora Banda), later by exploration drilling. The parent ultramafics are members of the Archean komatiitic suite extensively developed in the Norseman-Wiluna belt, especially near Kalgoorlie and Leonora.

Murrin Murrin ore field 60 km east of Leonora (Fazakerley and Monti, 1998; Rc 215 mt @ 1.02% Ni, 0.065% Co for 2.193 mt Ni, 140 kt Co; Fig. 9.9) is presently the largest "Ni-laterite" field and complex in Australia. The ores are in a flat featureless plain dissected by shallow valleys of seasonal streams that separate several ridges with relic laterite profile over ultramafics. There are some 14 separate orebodies within an area of about 20x6 km, in two groups. The relic Cainozoic regolith starts under thin veneer of coluvium and local calcrete and has the following zones (from surface down): 1) remnants of ferruginous duricrust; 2) ferruginous laterite zone of powdery and concretionary goethite with minor clay; 3) smectite zone dominated by apple green, brown, black mixture of nontronite with lesser montmorillonite, saponite, chlorite and serpentinite. The black pigmentation is due to Mn oxides and to a lesser degree to residual magnetite; 4) saprolite zone of argillized (smectite), chloritized, and locally silicified serpentinitized peridotite with preserved primary textures of the parent peridotite beneath. Infiltration veinlets and patches of chalcedonic silica, magnesite, palygorskite and other minerals are common.

Nickel does not form detectable minerals of its own and resides in the lattice of hydrosilicates (mostly nontronite; up to 4% Ni, less in montmorillonite and chlorite) and Fe/Mn oxides. Intervals high in black sooty wad are enriched in Co ("asbolite") and Ni as well. The orebodies have assay boundaries (the initial cutoff grade was 0.8% Ni) and they include the bottom of the ferruginous zone, the smectite zone and the top of saprolite.

Additional "large" (1 million tons of Ni content plus) Ni laterite/saprolite deposits on komatiitic peridotite, all in Western Australia, are:

- Bulong, 1.4 mt Ni

- Cawse, 1.37 mt Ni
- Mount Margaret, 1.14 mt Ni
- Ravensthorpe, 1.1 mt Ni
- Wiluna, 834 kt Ni.

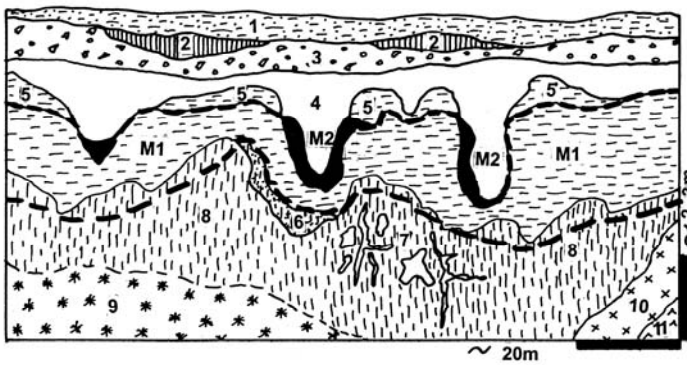
More deposits are being discovered and proven and this includes two megaprojects the capital costs of which exceed \$ 1 billion (Kalgoorlie area and Ravensthorpe). Ni laterite/saprolite deposits are also summarized in Chapter 12.

Miscellaneous mineralizations associated with or superimposed on komatiites:

There is a number of small to medium deposits and ore occurrences, some "with potential", spatially associated with komatiites (reviewed in Laznicka, 1993, p.274-292). They include many forms of remobilized Ni ores; banded iron formations (e.g. Koolyanobbing, Western Australia); sulfidic schists; residual magnesite and Fe, Cr, Mn, Co accumulations. The only "giants" are among the (syn)orogenic "shear-Au" and comparable Sb, As deposits superimposed on members of the komatiite association along tectonic structures. Despite their relative rarity (komatiites constitute between 1 and 5% of Archean greenstone belts), komatiites and associated iron formations host up to 20% of synorogenic gold in some regions; about 17% of the Zimbabwe gold came from ultramafics. Sheared and hydrothermally altered komatiite converts to talc-tremolite schist, silica-carbonate or quartz only rock with visually striking green fuchsite, or pure dolomitic, ankeritic and magnesitic carbonate. The latter had often been interpreted as metasediments ("exhalites"). The following synorogenic "Au-giants" are fully or partly hosted by komatiites: Kolar, India (800 t Au); Porcupine (Timmins) sub-goldfield (559 t Au), Balmertown (550+ t Au), Kerr-Addison (331 t Au; Fig. 9.10), Malartic (310 t Au), all in Canada; Morro Velho, Brazil (408 t Au); Murchison Range, South Africa (600 kt Sb, 12 t Au); Kilo-Moto, Congo (270 t Au) and others.

9.3. Early Proterozoic pale-ophiolites

Recently, several Paleoproterozoic rock associations that include lithologies reminiscent of the younger ophiolites (especially serpentinitized peridotite and graphitic schist) have been interpreted as ophiolite in the literature (Fig. 9.11). None correspond to the complete ophiolite model and the multiphase deformation, metamorphism and metasomatism allow for a multiplicity of genetic interpretations. The Purtuniqu Ophiolite in the Cape Smith belt of northern Labrador (Scott et al., 1989)



1. T-Q unconsolidated cover;
- T regolith (laterite/saprolite):
2. remnants of ferricrete; 3. red laterite; 4. Brown montmorillonitic laterite to saprolite; 5. Ditto, yellow saprolite; M2. Asbolite-rich saprolite; M1. Nontronite and Ni-hydroxylsilicates rich green saprolite; 6. Ferruginous saprolite; 7. Silica & magnesite secretions and veins; 8. Sapolite (general); 9. Ar serpentinized dunite, harzburgite, pyroxenite; 10. Gabbro; 11. Greenstone basalt

Figure 9.9. Murrin Murrin Ni-Co laterite/saprolite, Western Australia. Diagrammatic cross-section from LITHOTHEQUE No. 2637, based on 2001 tour with Mark Gifford, Anaconda Ltd.

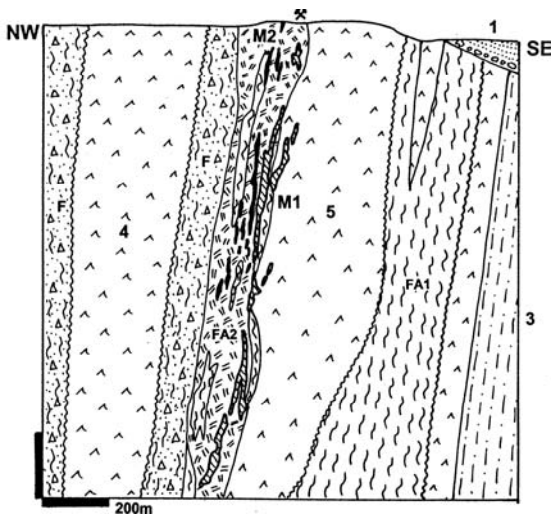


Figure 9.10. Kerr Addison Au mine, Virginiatown, Ontario, cross-section from LITHOTHEQUE No. 449, modified after Kerr Addison Staff (1967). One ore zone (M1) is in spectacular green fuchsitic metasomatite. 1. Pp Cobalt Group clastics; M1. "Carbonate ore", free gold in quartz-carbonate stockwork over fuchsite-carbonate altered sheared peridotite; M2. "Flow Ore", pyritic, in altered tholeiitic metabasalt & conglomerate; Alteration: FA1, chlorite-talc phyllonite; FA2, pervasive carbonatization; 2. Ar Timiskaming syenite, lamprophyre (shoshonitic) plugs; 3. Ditto, graywacke; 4. Ar Boston Assemblage tholeiitic metabasalt; 5. Ar Larder Lake komatiitic basalt & peridotite

is a member of a much broader package of ultramafic and mafic rocks that also include komatiites and continental rift-type tholeiites. The Ni-Cu sulfide mineralization there (e.g. Katiniq) is related to komatiite.

The Kalevian (2.1-1.9 Ga) assemblage in the Kainuu Schist Belt in Karelia of E-C Finland is

another candidate (Loukola-Ruskeeniemi et al., 1991). There, the Jormua Complex (Kontinen, 1987) consists of several fault-bounded remnants of serpentinite and talc-tremolite-carbonate schist intruded by cumulate gabbros and associated with a mafic dike complex and pillowed meta-basalt. This is in tectonic contact with Archean? granite gneiss basement and with Kalevian metasedimentary schist sequence. The ordinary micaschist contains intervals of pyritic and pyrrhotitic black schist which, in turn, encloses bands enriched in base and rare metals. At **Talvivaara**, a resource of 300 mt of subeconomic ore @ 0.26% Ni, 0.53% Zn, 0.14% Cu, 0.02% Co, 630 ppm V, 103 ppm Mo and 2.6 ppm Ag has been outlined (Loukola-Ruskeeniemi et al., 1991); this represents 780 kt of sulfidic nickel plus a variety of by-product metals. This suggests the possible existence of a "stratabound-Ni" ore style, more productive examples of which might be discovered in the future.

Outokumpu lithologic assemblage located in the same belt (Koistinen, 1981) is complicated by a complex alpinotype tectonics that brought together a large body of serpentinite, graphitic schist, metabasite, metaquartzite and Ca-Mg-Cr silicate rock usually designated as "skarn" (Fig. 9.11). The origin of these rocks is suspect and although some could be metamorphosed original lithologies (quartzite, former metachert?), the "skarn" looks much like carbonatized ultramafic, subsequently metamorphosed. This is an interesting rock, full of chromian varieties of the common silicates (e.g. chromdiopside, uvarovite, Cr-amphiboles). The now exhausted original Outokumpu massive pyrite, pyrrhotite, chalcopyrite and sfalerite lens in the Keretti mine has produced 1.06 mt Cu, 280 kt Zn and 22.4 t Au. There is a fringe of disseminated pyrrhotite and pentlandite in the quartzite and

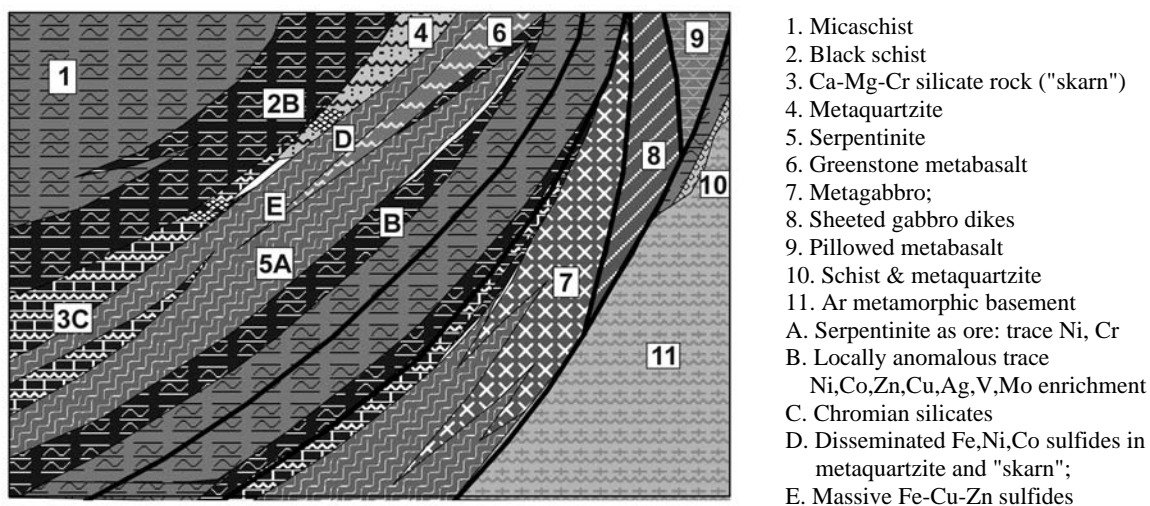


Figure 9.11. Inventory diagram of rocks and ores in Paleoproterozoic serpentinite-black schist association (based on the Outokumpu Assemblage). From Laznicka (2004), Total Metallogeny site G9

"skarn" with a resource of 64 kt Ni and 79 kt Co. The latter was mined in the Vuonos open pit.

9.4. Mafic and bimodal greenstone sequences: Fe-ores and Cu-Zn VMS deposits

Original stratigraphy of greenstone belts is difficult to determine due to the extensive tectonic stacking and duplication of units (de Wit and Ashwal, 1995), although precision zircon ages help considerably (Ludden et al., 1986). Lithostratigraphic associations thus assume the main role for organization and prediction of metallic deposits (Fig. 9.12). Of the four associations distinguished by Thurston and Chivers (1990), their categories "mafic-ultramafic volcanic sequences" (with komatiites, partly reviewed above), and "mafic to felsic volcanic cycles", are treated here. The latter hosts the majority of pre-orogenic ore deposits in greenstones.

9.4.1. Mafic (meta-basalt) sequences and banded iron formations

The Superior Province in Canada (Thurston and Chivers, 1990) and similar terrains elsewhere contain relatively monotonous, laterally extensive, originally gently dipping tholeiitic and komatiitic flows. Many have a gabbroic central facies, some hyaloclastites and non-explosive fragmental units with rare interflow chert, jasper, banded iron formation and/or argillite. Substantial metallic

deposits are uncommon in the predominantly tholeiitic successions (komatiites are reviewed above) and world class deposits include only the "Algoma-type" (exhalative) banded iron formation. VMS deposits of the Cyprus-type are virtually unknown (there is a tiny representative in the Potter Mine, Munro Township, NE Ontario) but some gabbro-anorthosite intrusions, probably magma chambers to basalts, have a Bushveld-style layered Ti-magnetite enrichment (Lac Doré, Chibougamau, Québec). There are hundreds of small vein to disseminated occurrences of pyrite, pyrrhotite, chalcopyrite, gold, and Ni-sulfides but nothing major.

Algoma-type iron formations (Gross, 1980) occur in several Archean and Paleoproterozoic lithologic associations (bimodal, turbiditic) and their high-grade metamorphic equivalents (Chapter 14). Hundreds of occurrences are known and several small non-enriched deposits (e.g. Adams Mine near Kirkland Lake, Sherman Mine near Timagami, Griffith Mine south of Red Lake, all in Ontario) had been mined and beneficiated in the 1960s-1970s. The mines lost to the competition of supergene enriched ore imported mainly from Brazil, presently the world's largest exporter of this kind of ore.

Serra dos Carajás in Pará, NE Brazil, was the site of "greenfields" discovery of the first iron deposit, on a plateau with stunted vegetation in 1967, to become about the most significant metallogenic province in Brazil since (Beisiegel, 1982; Fig. 9.13). The deposits, estimated to contain

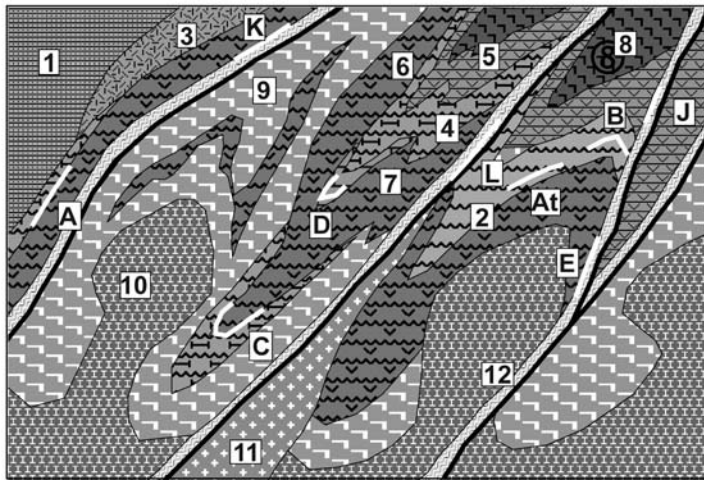


Figure 9.12. Greenstone bimodal metavolcanics intruded by synorogenic granitoids; rocks and ores inventory diagram from Laznicka (2004), Total Metallogeny site G30. Ore types C,D,J,K,L have known "giant" counterparts

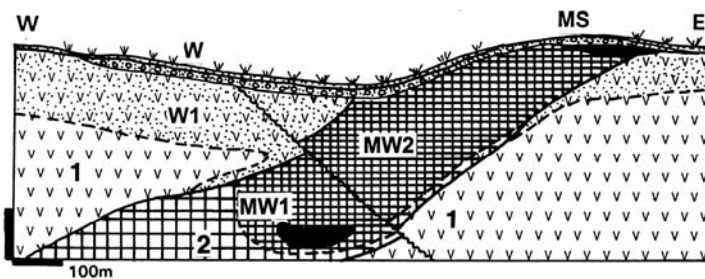


Figure 9.13. Serra dos Carajás, Pará, Brazil, cross-section of the Plató N4E iron deposit. From LITHOTHEQUE No 1967, modified after Beisiegel (1982) and DOCEGEO company literature and on-site information, 1990

a minimum of 11.82 bt of iron in a 66.1% Fe direct shipping ore (a "giant province"), crop out in three ranges within the Serra dos Carajás (Serra Norte, Serra Sul, Serra Leste) and in the adjacent Serra São Félix. The largest single deposits are the Plató S11 in the Serra Sul (6.82 bt Fe @ 66%, a "giant"), the Plató N4E (2.086 bt Fe @ 61.1-66.6) and the Plató N5 (1.045 bt Fe @ 60.1-67.1% Fe) in the Serra Norte. Plató N4E has, so far, been the only producing deposit the ore from which is railed to the port of São Luis for export.

Plató N4E deposit near the new Carajás township (Beisiegel, 1982; Fig. 9.13) is a supergene modified top of a N-S trending, multiphase deformed siliceous BIF horizon, sandwiched between units of a generally massive, locally chloritized Archean meta-basalt of the Amazonas Craton. The enriched orebody, over 200 m thick, substitute some 400-500 m thick primary BIF that

originally contained between 35 and 45% Fe. The anomalous BIF thickness is probably due to structural multiplication. The supergene profile starts, at the top, with a thin blanket of infertile soil with blocks of Fe and bauxitic laterite, exposed in a natural clearing (clareira) in the Amazon rainforest. Below is a discontinuous blanket of in-situ massive or pisolitic ferruginous duricrust with scattered hematite fragments. This grades into colluvial breccia of angular massive hematite fragments, subrounded blocks of redeposited laterite, and transported soil concretions in matrix of brown ocher. These materials are usually collectively described as canga and are part of the tropical weathering profile. The Fe content is about 45-55% Fe and these materials are not presently mined.

The bulk of the enriched orebody underneath is a gray friable hematite that forms a thick, unsupported mass. This is interpreted as an in-situ

uncemented residue of the original specularite and martitized hematite crystals, remaining after pre-Cenozoic removal of silica from the metamorphosed BIF ("itabirite"). The friable hematite encloses blocks of cohesive, massive hematite, and relics of partially leached original BIF. The ore variety called platy hematite (plaquette) is composed of a dense aggregate of cryptocrystalline or recrystallized hematite mosaic, sometimes cementing residual Fe-oxide grains.

All remaining Algoma-type iron ore deposits in the rest of the world, supergene enriched and "raw", are much smaller than Carajás and not even of the "large" magnitude. They are overshadowed by the sediments-hosted BIF (Superior-type), although some volcanics-associated BIF are extensive but uneconomic to mine at present (low grade in the region of 15-20% Fe, insufficiently supergene enriched, thin and distributed over large areas, and lacking magnetite). The high-grade metamorphosed equivalents appear in Chapter 14.

Siderite/pyrite Fe ore: Although the model Algoma-type BIF is composed of Fe oxides in matrix of or interbanded with quartz, there are few deposits where the primary iron is in carbonates (siderite, ankerite) and/or pyrite, pyrrhotite. The **Wawa iron field** in Ontario is an example, barely on the threshold of the "large" magnitude category (Goodwin et al., 1976; 420 mt Fe @ ~33%; Fig. 9.14). It is briefly described here as it is probably the largest non-sedimentary siderite deposit in the world.

The deposit is a part of the NE-trending, 2.75 to 2.7 Ga Michipicoten Iron Range near the shore of Lake Superior. The iron carrier is the intravolcanic Helen Iron Formation (HIF), recently interpreted as a massive exhalative siderite-pyrite unit resting on top of intensely hydrothermally altered rhyolite-dacite pyroclastics that enclose an otterite (Mn-chloritoid) alteration pipe (Morton and Nebel, 1984). The orebody is now interpreted as a product of exhalative venting in freshly accumulated felsic pyroclastics on the seafloor (Goodwin et al., 1985) and a close equivalent to some Fe-Zn-Cu VMS deposits.

The HIF is member of a cyclic bimodal submarine volcanic sequence where it tops the lowest mafic-felsic cycle. It rests on a pile of rhyolite-dacite massive or bedded pyroclastic flows, block and ash flows, lava flows and domes. The sequence is overturned and greenschist metamorphosed. The siderite-pyrite interval crops out in a discontinuous 25 km long belt segmented

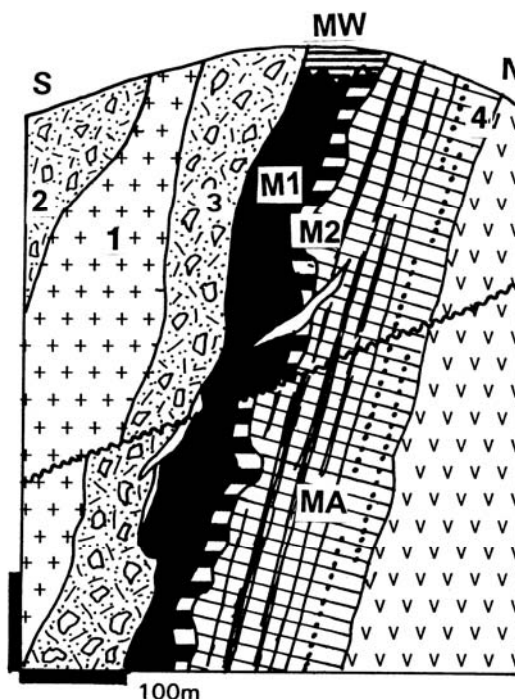


Figure 9.14. Helen Fe Mine, Wawa, Ontario, cross-section from LITHOTHEQUE No 1007, based on data in Goodwin et al. (1976). MW. Goethite in oxidation zone; M1. Ar, massive siderite; M2. Pyrite >> siderite; MA. Massive, banded or brecciated chert > siderite, black phyllite; 1. Ar metadiorite; 2. Sericite altered felsic metavolcanics; 3. Ditto, felsic pyroclastics; 4. Chert with locally disseminated magnetite (siliceous BIF)

by faults. In the main Helen Range near Wawa it is about 60 m thick. The lower 35-40 m is a buff, fine-grained massive siderite with chert bands. This changes into a 22 m thick massive pyrite or locally pyrrhotite body with some siderite and granular chert. On top is a 350 m thick, chert-dominated heterogeneous unit interlayered with black phyllite, siderite bands and disseminated magnetite. Iron mining near Wawa started in the oxidation zone, with goethitic ore derived from supergene alteration of both siderite and pyrite. Subsequently, the massive siderite became the selectively mined shipping ore.

9.4.2. VMS deposits in bimodal and sequentially differentiated volcanic-sedimentary sequences

The areally extensive "mafic plain" volcanics give locally way to lithologically more diverse, central and usually cyclic mafic-felsic volcanic complexes.

Bimodal (compositionally contrasting; Thurston et al., 1985; Ayres and Thurston, 1985) volcanic sets consist of a mafic member (basalt to basaltic andesite, up to about 60% SiO₂) and a felsic member (dacite, rhyodacite, rhyolite with >70% SiO₂), separated by a compositional gap. The volcanic members can form simultaneously, or sequentially where felsics are the younger component. Although fractionation of the mantle-derived basaltic magmas probably took a part, the acid magmas are believed derived primarily by melting of transitional (tonalitic?) or continental crust, then stored temporarily in compositionally zoned magma chambers. Sequentially differentiated basalt-andesite-dacite-rhyolite sets, present in a limited number of Archean terrains, are probably a product of mixing and fractionation of basaltic parent magmas and rhyolitic derivatives.

The central, cyclic complexes are dominated by andesitic to dacitic ash-flow volcanics (tuffs) with intercalated mass-flow deposits, and shallowing-upward facies terminating with subaerially deposited material (Ayres and Thurston, 1985). Lava flows (except basalts at the beginning of each cycle) are less common. The subaerial acid explosive volcanism is mostly reflected in the abundant volcanoclastic sediments (mostly quartz-rich litharenite=graywacke) that form thick turbiditic aprons around, and over eroded volcanoes. Erosion has removed most of the subaerial volcanic tops so few are left in the greenstone belts today. Synvolcanic plutonic rocks come as layered intrusions (gabbro, anorthosite, diorite) and diorite, tonalite, trondhjemite, granodiorite plutons (Fig. 9.15; 9.16).

As in the Phanerozoic eugeoclinal terrains (Chapter 8), submarine bimodal volcanics and associated sedimentary rocks hold bulk of the predominantly (Fe)-Zn-Cu early Precambrian massive sulfide deposits. The 1980s models favoured underwater calderas as the preferential sites of VMS deposition (e.g. Gibson and Watkinson, 1989), but the required shallow water setting of submarine explosive volcanism (>500 m water depth) contrasts with the 2000 m plus depth in which VMS are supposed to form.

Volcanics-hosted massive Fe, Cu, Zn sulfide deposits (VMS)

Archean VMS deposits have abundant and popular literature (e.g. Sangster and Scott, 1976; Franklin et al., 1981; Franklin, 1993) influenced by examples from the Canadian Shield (especially the Abitibi Subprovince) where this type is widespread and

well developed. Outside Canada and Scandinavia, however, Early Precambrian VMS deposits are rare to non-existent. Of the several hundred recorded deposits (compare Franklin et al., 1981) most are individually small to medium in size, but usually come in clusters. Based on the accumulation index alone, there are only six "giant" metal accumulations of which three are in the single Kidd Creek deposit (10,468 mt Zn, 3.58 mt Cu, 12,371 t Ag). The remaining "giants" are the Bousquet goldfield (278 t Au in VMS only) and the Horne Mine (319 t Au). Cumulative metal tonnages in ore districts would add Noranda (2.54 mt Cu), Flin Flon-Snow Lake (2.5 mt Cu) and Skellefte (7,567 t Ag, 1.288 mt As) to the list of "giant districts", where ore from many lesser deposits is processed in one central smelter. The purely geochemical magnitudes of metal accumulation, however, do not give sufficient credit to the economic value of VMS ore, which is very high. Being complex deposits, VMS typically yield four or more metals from one ton of ore (Kidd Creek yields Zn, Cu, Pb, Sn, Ag, Au, Cd, Bi, Se, Te, In, Ga), so they have a high unit value. Curiously, the elements most concentrated in VMS, iron and sulfur in pyrite and pyrrhotite, are rarely mentioned and they are de-emphasized in statistics. An ore with 1.5% Cu and 3% Zn may appear "lean", but in most cases the remainder is pyrite or pyrrhotite so the material is a true, heavy, metallic-looking massive sulfide. As the market for Fe sulfides is very limited now, they are often a liability that requires costly disposal to satisfy environmental regulations.

Setting and emplacement models: The bulk of the early Precambrian VMS are in bimodal suites of tholeiitic basalt and rhyolite that may exhibit pseudo calc-alkaline trends as a consequence of hydrothermal alteration (MacGeehan, 1978). VMS in andesite-dominated suites (e.g. in the Lac Dufault field) are rare. Most massive orebodies of the Cu-Zn Noranda Type (Franklin, 1993) are in, or on top of, rhyolite breccia and are floored by feeder stockwork in altered footwall rocks. Unless dismembered and severely deformed they have the typical VMS internal zoning: siliceous and/or ferruginous, often laminated, "exhalite" on top, changing to pyrite or pyrite-sphalerite rich mass with pyrrhotite-chalcopyrite base, above chloritic alteration pipe with chalcopyrite stringers. In the same sub-district (Knuckey et al., 1982) the "mushroom" configured orebody sets come in groups controlled by one or more marker horizons of "tuffaceous exhalite". In the "Mattabi-type" VMS (Morton and Franklin, 1987), in contrast, the

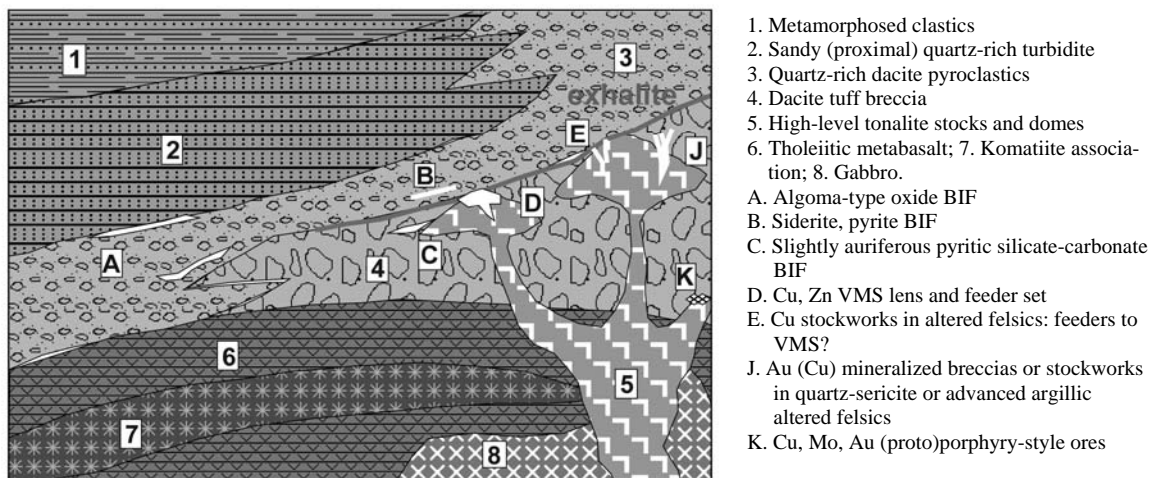


Figure 9.15. Bimodal volcano-plutonic submarine center, probable depositional configuration (before deformation). Rocks and ores inventory diagram from Laznicka (2004), Total Metallogeny site G29. Ore types A, D, J may contain "giant" members

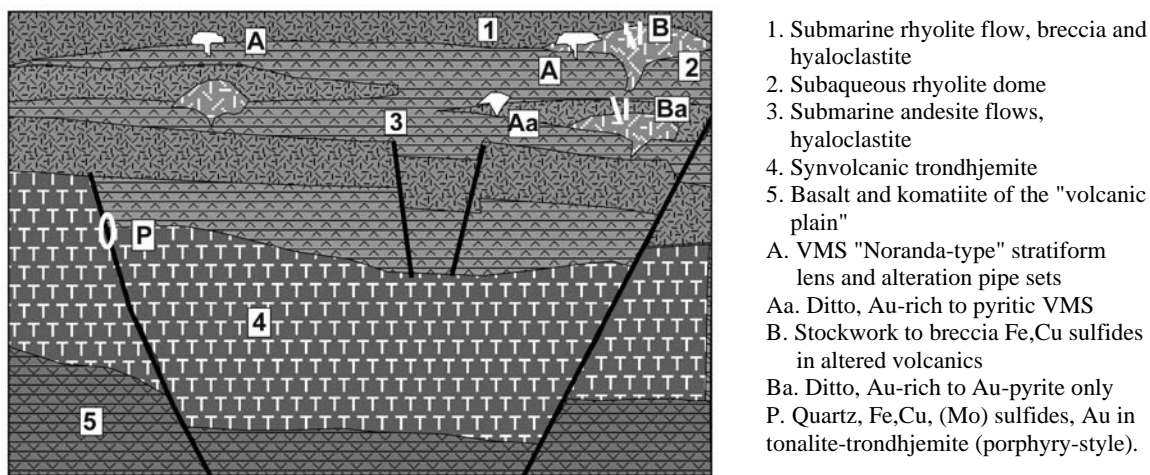


Figure 9.16. Early Precambrian rocks and ores in a calc-alkaline, andesite-dominated submarine paleocaldera (e.g. Noranda). A model before deformation. From Laznicka (2004), Total Metallogeny site G56. Ore types A and Aa may have "giant" members

stratabound massive sulfide lens is flooded by a broad, semiconformable and diffuse area of zoned footwall alteration (chlorite and sericite).

Subvolcanic bodies of tonalite or trondhjemite, considered a heat source driving convecting hydrotherms under the sea floor, are expected to occur in depth under the stratigraphic VMS footwall, but are not always in sight. The idealized model of the Archean VMS by Sangster (1972) that resembles the kuroko model (Chapter 5) and its many subsequent renditions, are based on the Lac Dufault (Waite-Amulet) subdistrict north of

Noranda, where at least 17 medium-size orebodies are preserved in growth position in sub-greenschist metamorphosed, non-penetratively deformed, and only 30° tilted host andesite-rhyolite sequence (Fig. 9.17). This is a rarity as most of the world's VMS's are sheared and metamorphosed so that the ideal model has to be painstakingly put together, sometimes with a great deal of fantasy. In the Sangster model the VMS massive lens, resting on or enveloped by "exhalite", is shown as covered by post-ore volcanics, typically andesite. In many VMS, especially the Paleoproterozoic ones as in the

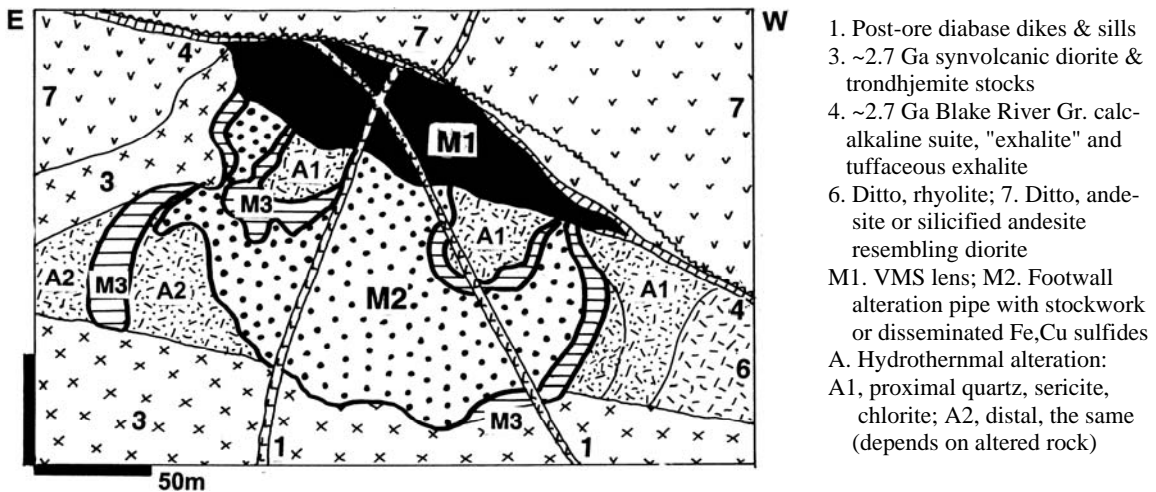


Figure 9.17. Norbec deposit in the Lac Dufault VMS cluster near Noranda, Québec: example of a subgreenschist-metamorphosed, non-penetratively deformed and only slightly tilted "Noranda-type" Cu, Zn VMS. From LITHOTHEQUE No. 1883, modified after Purdie (1967)

Skellefte and Flin-Flon districts, the orebodies are in, or covered by, volcanic sediments (now typically carbonaceous slate or phyllite).

Noranda Volcanic Complex ("Caldera"), Abitibi Sub-province, Québec (Kerr and Gibson, 1993). This is the youngest and best preserved, central volcanic complex in the Archean Blake River Group. The complex is 7-9 km thick, has a diameter of about 35 km, and it had once been probably a large shield volcano. There are five packages of conformable volcanics (basalt < andesite < rhyolite flows, minor pyroclastics) of which the ~2.698 Ga "Mine Sequence" is believed erupted in time of cauldron subsidence. The former magma chamber is now represented by the Flavrian Pluton that has a high-level sill-like intrusion in its core. The adjacent Dufault synvolcanic pluton (2.69 Ga) is of calc-alkaline biotite granodiorite, with a thermal aureole in the roof volcanics. The subsidence resulted in formation of a 15-20 km large area north of Noranda, filled by eight cycles of fissure-fed andesite-basalt and rhyolite flows and pyroclastics. These host 17 almost pristine "lens and stem"-type VMS deposits in the Lac Dufault sub-district (less than 5 Mt of ore each), and the 13.8 mt Quemont deposit on the outskirts of Noranda.

The Horne block is a tectonic wedge of subvertically tilted units of a north-facing rhyolite, cut by quartz-feldspar porphyry dikes. There are some volcanoclastics and Kerr and Gibson (1993) assumed shallow water depths (500 to 100 m) during formation of the Horne deposit, an "Au-

giant". The **Horne Cu-Au-(Zn)** mine (Maclean and Hoy, 1991; Pt 60.26 mt @ 2.2% Cu, 5.29 g/t Au, 13 g/t Ag for 1.325 mt Cu and 319 t Au plus Rc 24 t @ 1.2% Zn, 0.15% Cu, 1.5 g/t Au in the subeconomic #5 Zone) is at site of the present Noranda smelter complex. Horne deposit is a scattering of some 30 individual cylindrical to podiform and tabular bodies of massive and some stringer chalcopyrite, pyrrhotite, pyrite and quartz in a subvertical structure that consists of at least three stratigraphic intervals. The massive tholeiitic rhyolite, breccias and tuff are pervasively quartz, quartz-sericite and sericite-chlorite altered. The deep #5 Zone contains large, but low-grade massive pyrite bodies in breccia interpreted as a syndepositional slump. The pyrite contains low Zn and Au values.

Post-depositional modifications of VMS: Many if not most early Proterozoic VMS deposits depart from the ideal model to the point of becoming "nondescript". Most of the massive orebodies are deformed, significantly more than the regionally present rocks, as the highly ductile sulfides "invite" often multiphase deformation followed by recrystallization in shears. Many massive and banded pyrrhotite, sphalerite and galena bodies are in fact "ore mylonites" that grade into semi-ductile breccias; there the more brittle materials (wallrocks, pyrite and magnetite porphyroblasts) are embedded in a paste of the ductile sulfides with *Durchbewegung* fabrics. The deformed VMS orebodies often occur in subvertical position in highly strained (schisted) metavolcanics, mainly

chlorite- and sericite schists. Kidd Creek is an example of a moderately strained (extended) orebody that has the form of a schistosity-conformable lens and its length to thickness ratio is about 8 to 10. The Golden Manitou orebody has corresponding ratio of about 40, and the Normétal orebody (ratio 100 to 200) is a thin sulfide sheet in strained wallrocks. There is a potential to confuse the thin, foliation-parallel sulfide sheets with laterally extensive sea floor "exhalites". Many VMS are metamorphosed (Chapter 14), but there is very little mineralogical change as the Fe, Zn, Cu, Pb sulfides remain the same. The altered wallrocks, however, change to biotite, muscovite, garnet, anthophyllite, cordierite and other schists.

Kidd Creek deposit (Barrie et al., 1999; Hannington and Barrie, eds, 1999; P+Rc 156 mt @ 6.5% Zn, 2.35% Cu, 0.23% Pb, 89 g/t Ag, 0.1% Sn for 10.468 mt Zn, 3.581 mt Cu, 12,371 t Ag, 320 kt Pb, 142 kt Sn) is the largest Precambrian VMS, located 25 km north of Timmins, Ontario (Fig. 9.18). The deposit, the top of which is under mere 6 m cover of glacial drift, was discovered in 1963 by drilling an airborne electromagnetic anomaly. It is a single, although segmented, orebody about 700 m long and up to 150 m wide. It persists to a depth of 3,000 meters. The orebody is interpreted as deposited in a structural graben within the 2.72-2.71 Ga old Kidd-Munro Assemblage, one that comprise a wide range of volcanics and subvolcanic sills ranging from serpentinite through picrite, tholeiitic basalt, dacite, high-Si rhyolite and minor argillite. The rocks are greenschist metamorphosed and steeply dipping, facing west.

The footwall rocks in Kidd Creek are serpentinized peridotitic flows or sills intercalated with, and topped by, rhyolite. Argillite (a real meta-pelite or phyllonite?) occurs locally. The Mine Rhyolite is the immediate footwall to the orebody and it grades from massive, flow-banded rhyolite to fragmental rocks (breccias; Sangster's "millrock") and presumably epiclastic polymictic source-proximal conglomerate with rhyolite, basalt and sulfide fragments. The rhyolite is strongly silicified, sericite, chlorite and carbonate altered, and it hosts chalcopyrite-rich stringer stockwork. Above the felsic footwall lie three massive sulfide segments with a Cu-rich lower portion and Zn-rich (sphalerite) upper portion that ranges from an almost pure pyrite to almost massive brown sphalerite. The central and south orebodies also have replacement bodies of volcanic and massive to

semi-massive fragments replaced by pyrite, pyrrhotite and chalcopyrite. The hanging wall succession consists of fragmental quartz porphyries, basalt, and gabbro dikes and sills. Because of the glacial erosion and drift cover, there is neither oxidation zone (other than the shallow surficial "rusting") nor secondary sulfide zone.

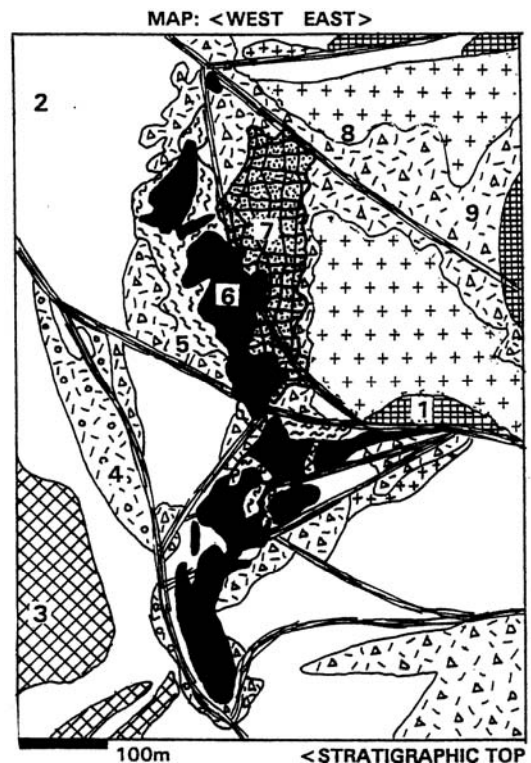


Figure 9.18. Kidd Creek VMS deposit near Timmins, Ontario. Map from LITHOTHEQUE No. 454, modified after Falconbridge Kidd Creek Mine materials and on-site visit, 1985. All rocks are members of the 2715-2716 Kidd-Munro Assemblage. 1. Komatiitic ultramafics; 2. High-Fe gabbro sill; 3. "Dacite"; 4. Quartz-eye porphyry (sericite schist); 5. "Graphitic schist" (phyllonite?), grade to tectonic breccia; 6=M1. Several lenses of deformed and metamorphosed VMS; 7=M2. Footwall stringer stockwork (pyrrhotite-chalcopyrite) in altered felsic metavolcanics; 8. Massive metarhyolite; 9. Coarse rhyolite volcaniclastics

This is hardly a model VMS; Kidd Creek had a protracted and dynamic emplacement history (2.7-2.8 million years long) with overlapping "syngenetic" (seafloor deposition?) and hydrothermal metasomatic events. It is difficult to distinguish true metasedimentary rocks and ores (epiclastic fragmentals, argillites) from visually equivalent tectonites like fault breccia, mylonite and

phyllosite. The alteration overprint makes this task even more difficult.

Additional major VMS deposits: Despite the popularity of the VMS model, it is surprising there are no more "giants" in the early Precambrian greenstone belts in addition to those described above. **Flin Flon Zn-Cu-Ag-Au ore field** in Manitoba comes closest to becoming one, as active exploration continues and new orebodies are being found directly under the town (Galley et al., 1990; ore field total 3.912 mt Zn, 2.012 mt Cu, 3247 t Ag, 196 t Au; Fig. 9.19). Flin Flon is the site of a smelter provided by feed from some 35 intermittently producing VMS deposits in the Flin Flon-Snow Lake district, of which three are within the town area. The largest **Flin Flon deposit** (Koo and Mossman, 1975; Pt 64 mt @ 4.4% Zn, 2.2% Cu, 41.5 g/t Ag, 2.6 g/t Au for 2.82 mt Zn, 1.41 mt Cu, 2,614 t Ag and 164 t Au) is in a greenschist-metamorphosed Paleoproterozoic island arc-type bimodal succession. In the deposit there are six steeply dipping orebodies that are, on the average, 21 m thick and 270 m long. Massive chalcopyrite is dominant near the base, sphalerite and pyrite prevail near the top. The massive ore is underlain by disseminated chalcopyrite and pyrite in the footwall, in chloritized massive to brecciated meta-rhyolite and pillowed greenstone basalt (Galley et al., 1990).

The remaining "large" greenstone belt VMS with 1 mt Zn or Cu plus and/or more than 100 t Au, include:

- Mattagami, Québec; Archean, 3.6 mt Zn, 312 kt Cu;
- Crandon, Wisconsin; Paleoproterozoic, 3.92 mt Zn, 770 kt Cu, 2590 t Ag, 70 t Au;
- Jerome, Arizona; Paleoproterozoic, 1.63 mt Cu, 1.1 mt Zn; 1500 t Ag; 61 t Au;
- Kristineberg, Sweden; Proterozoic, 1.04 mt Zn, 240 kt Cu (the entire Skellefte greenstone belt stores 4.83 mt Zn, 240 kt Cu, 644 kt Pb and 7567 t Ag; the Rakkejaure VMS deposit is exceptionally rich in arsenopyrite with the As content of 1.3%, and although it is the largest VMS in the region its 142 kt of contained As makes it unattractive to mine, for environmental reasons; Fig. 9.20);
- Golden Grove, Western Australia; Archean, 1.23 mt Zn, 105 kt Cu.

The "large" high-grade metamorphosed 1 million ton plus deposits (Manitouwadge, Izok Lake, Vihanti, Prieska, Falun and Ämmeberg) appear in Chapter 14. More detail about the lesser VMS deposits is in Laznicka (1993), and in the reviews quoted above.

Gold-rich VMS: Most polymetallic VMS deposits contain between 0.1 and 1.0 g/t Au, recovered as a by-product. Small number of VMS deposits contain more gold (e.g. Quemont, 5.4 g/t Au; Horne, 6.1 g/t

Au) so gold becomes the principal money earner in periods of high gold prices. At the end of the spectrum, there are essentially pyrite-only auriferous VMS mined for gold alone. The Bousquet (Cadillac) zone is the only "giant" of this type recorded, although this is not a "purebred" VMS but a polygenetic system of probably synvolcanic massive pyrite, advanced argillic altered felsics, and syn-orogenic hydrothermally altered shear zone. The equally enigmatic Boliden deposit in Sweden was a "large" gold producer, and an "As-giant". Both are briefly described below.

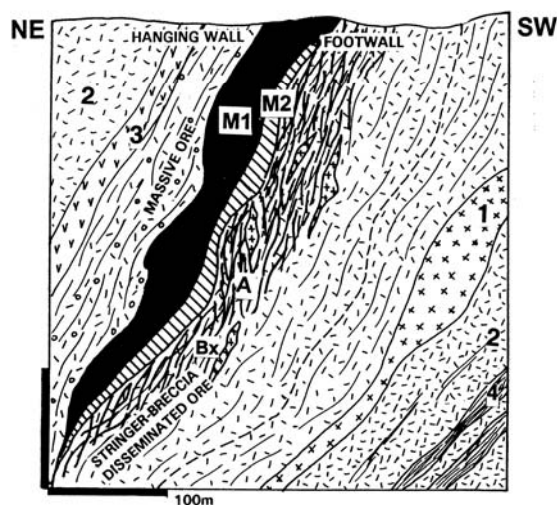


Figure 9.19. Flin Flon VMS ore field, Manitoba, Trout Lake deposit; cross-section from LITHOTHEQUE No. 1735 based on information from C.B. Koo, 1989. An example of a deformed (Durchbewegung) massive Zn-Cu sulfide lens (M1) floored by sheared & chloritized footwall with Fe-Cu sulfide stringers (M2). A. Chlorite >> sericite alteration; Bx. Fault breccia; 1. Pp diorite & gabbro dikes; 2. Pp bimodal tholeiitic felsic volcanics converted to quartz-sericite schist; 3. ~1.886 Ga greenstone basalt to andesite pillowed flows, hyaloclastite; 4. Graphitic schist (phyllosite?)

Bousquet and five other major Au deposits are controlled by the almost east-west trending Dumagami Structural Zone (DSZ), parallel with the Cadillac Break 20 km ENE of Noranda (Tourigny et al., 1989; 336 t Au whole zone, 278 t Au pre-D₂ deformation deposits; Fig. 9.21). The zone is about 12 km long and 500 m wide steeply south-dipping high-strain (shear) zone superimposed on fine-grained felsic pyroclastics, felsic flows and subvolcanic porphyries of the about 2.7 Ga Blake River Group (that also hosts the Noranda VMS).

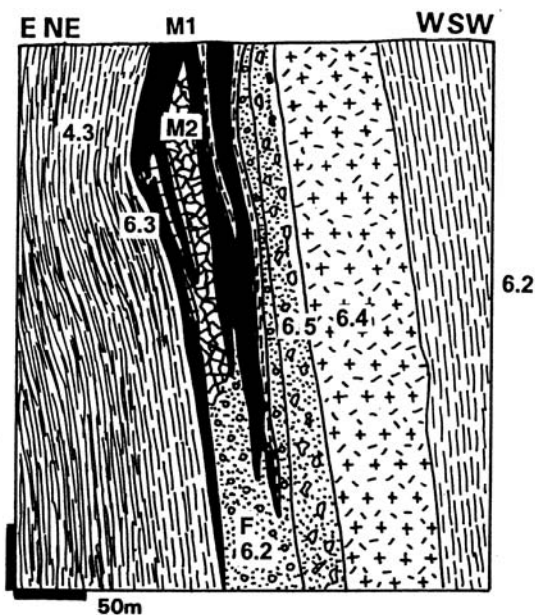


Figure 9.20. Rakkejaure As-rich Zn, Cu, Pb, Ag VMS deposit, Skellefte district, Sweden. Cross-section from LITHOTHEQUE No. 604, modified after Svansson in Boliden AB materials, 1986. 1. Q glacial sediments; 4.3. ~1.875 Ga gray to graphitic metapelite; 6: 1.9-1.88 Ga rhyolite > dacite, andesite, basalt submarine metavolcanics; 6.2. sheared felsic volcanics; 6.3. marble lenses; 6.3 massive quartz-eye porphyry; 6.5. volcanic breccia to conglomerate. M1. Steeply dipping massive Fe,As,Zn,Pb sulfides with Durchbewegung along contact of sheared, altered volcanics and schist; M2. Fe, Cu sulfide veins & stringers in sericite, chlorite altered rocks

The DSZ is transected by straight or anastomosing zones of shears and fractures filled by phyllonite (sericite schist), mylonite and syntectonic hydrothermal minerals. The faults are peneconcordant with and younger than the D_2 regional foliation. Gold is concentrated discontinuously throughout the DSZ at irregular intervals. Orebodies in the eastern part (Dumagami, Bousquet 2) have more synvolcanic characteristics, those in the centre (Bousquet 1) are transitional, whereas the Doyon deposit in the west produces from veins oblique to foliation. The final stage of gold fixing at its present sites was clearly (syn)orogenic, but it is believed that at least a portion of the gold is syn-volcanic, co-precipitated with pyrite, Cu, and local Zn, Pb in a VMS system. In the Dumagami deposit (Marquis et al., 1990) massive pyrite bodies have a ruler-like form and are composed of fine to medium-crystalline, recrystallized and foliated pyrite that encloses

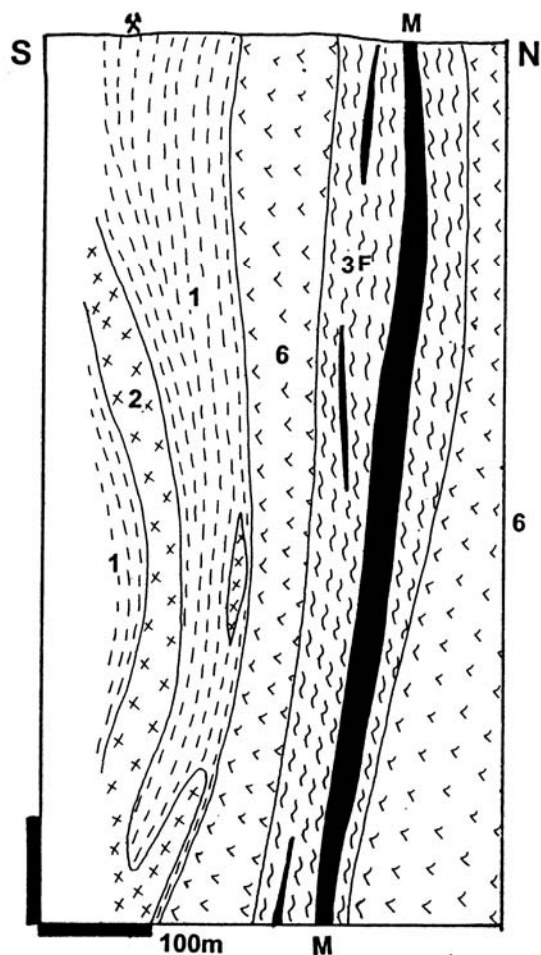


Figure 9.21. Bousquet Au ore zone, Dumagami Mine; cross-section from LITHOTHEQUE No. 2275 modified after Marquis et al. (1990). M. Ar deformed & metamorphosed auriferous pyrite-dominated VMS in shear phyllonite gradational to synorogenic quartz stringers & disseminations. 1. Ar amphibolite facies volcanoclastics; 2. Metagabbro; 3-5 ~2.7 Ga Blake River Group, bimodal metavolcanics; 3, massive porphyries, biotite schist; 4, quartz-muscovite schist; 5, andalusite-quartz rock; 6, metabasalt

silicified wallrock fragments. Some bodies have Durchbewegung fabrics and grade into pyrite veinlets and disseminations. Sphalerite and galena are enriched in the outer zone. The pyritic lenses are enveloped by an up to 30 m thick zone of massive and schistose andalusite-quartz rock that is, in turn, enveloped by sericite (muscovite) schist. The host rock is massive to schistose "quartz-eye porphyry". The gold is associated with retrograde (synorogenic) pyrophyllite, diaspore, kaolinite and quartz assemblage and is accompanied by chalcopyrite, bornite, galena and Cu-Ag sulfosalts.

Farther west, laminated veins or zones of disseminated pyrite parallel with foliation change into schistose wallrock inclusions. The veins are commonly boudinaged, pinching and swelling. They contain disseminated subhedral to euhedral pyrite usually accompanied by chalcopyrite and by minor amounts of quartz, muscovite, kyanite, chloritoid and chlorite. With decrease in the sulfide content the veins change into linear, diffuse zones containing up to 10% of disseminated pyrite, some of which is gold-bearing.

Boliden, one of the first metallic deposits discovered in the Skellefte VMS zone in northern Sweden, has an interesting combination of features and a controversial origin (Weiherd et al., 1996; Pt 8.34 mt @ 6.9% As, 1.41% Cu and 15.2 g/t Au for calculated content of 575 kt As, 117 kt Cu, 127 t Au, 75 kt Zn, 25 kt Pb, 401 t Ag, 3,300 t Se plus Co, Bi, Te; Fig. 9.22). The Paleoproterozoic (~1.8 Ga) host sequence comprises predominantly felsic, sodic submarine metavolcanics that are tightly isoclinally folded and sheared. Three major deformation phases are recognizable, and the regional greenschist metamorphism is overprinted by thermal metamorphism attributed to the late orogenic, 1.75 Ga Revsund Granite.

The east-west trending, vertical deposit is a lens of massive, locally banded fine-grained pyrite 600 m long, 40 m wide, and it bottoms in the depth of about 250 m. Its contacts against the quartz-sericite schist wallrock are sharp and generally peneconcordant with foliation. In places, the ore has a form of breccia, enclosing and partly replacing fragments of wallrocks. The massive pyrite that locally grades into pyrrhotite encloses a number of arsenopyrite masses irregularly distributed in the central part of the ore zone. More arsenopyrite is found outside the pyrite mass, in sericite schists. The fine-grained compact arsenopyrite grades into breccia, or into a cavernous ore attributed to late-stage hydrothermal leaching. The interfragmental voids in breccia and the cavities are filled by minerals of the younger generation that include Fe and Zn, Pb, Cu sulfides, Cu, Pb, Ni, Co arsenides and antimonides, Bi-tellurides and native gold. Quartz, calcite, rutile, apatite, andalusite and sericite are the most common gangue minerals. Some gangue minerals form anomalous local concentrations like the "rutile rock" that also contains high concentrations of Bi, Te, Sn, Au and Se. Outside the massive sulfide body gold occurs with some of the sulfosalts and tellurides in quartz-

tourmaline veins in chloritized and feldspathized mafic intrusive dikes.

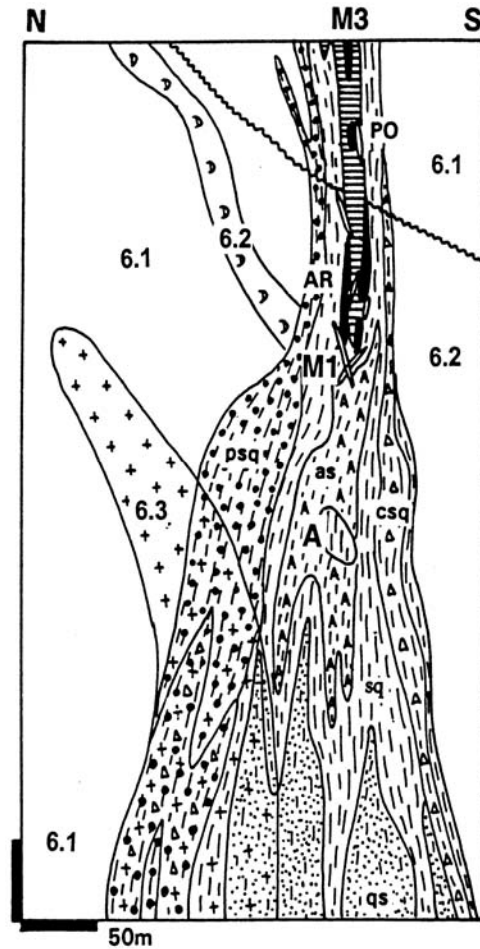


Figure 9.22. Boliden Au,As,Cu deposit, Skellefte district, Sweden. Cross-section from LITHOTHEQUE No. 601, modified after Nilsson (1986), Weiherd et al. (1996) and Boliden AB handout. 6: 1.9-1.85 Ga Skellefte Group, amphibolite-grade rhyolite > dacite, andesite, basalt submarine volcanics: 6.1, subvolcanic dacite; 6.2, basalt & andesite sills; 6.3, quartz porphyry stock. M1. 1.85-1.822 synorogenic quartz-Au-tourmaline veins; M2. Quartz, chalcopyrite, etc. veins in brecciated arsenopyrite; M3. 1.852 Ga subvertical zone of partly remobilized massive pyrite; local massive arsenopyrite (AR) and pyrrhotite (PO) pods. A. Pipe-like zoned aluminous alteration envelope

The ore zone is surrounded by a broad alteration envelope superimposed on the strained felsics and interpreted as an alteration pipe. In the deep core of the pipe the wallrocks are almost completely silicified and converted into "secondary quartzite".

This changes upward into a massive or schistose "andalusite rock" that forms irregular lenses enveloped by sericite schist. The "andalusite rock" has abundant scattered rutile and local patches of diasporite, corundum and clay minerals. As expected the genetic interpretation keeps changing. Weihed et al. (1996) proposed a high sulfidation epithermal or shallow-water VMS-related stockwork origin, associated with high level intrusions of dacite and andesite, subsequently deformed and metamorphosed to lower amphibolite grade.

9.5. Granitoid plutons and older Precambrian "porphyry" deposits

A typical porphyry-Cu or stockwork-Mo deposit is geologically young (most formed between Cretaceous and Miocene) and they are described in some detail in Chapter 7. This chapter deals mainly with the leftovers that include early Precambrian disseminated and stockwork Cu, Mo, Au deposits in and close to granitoids (Ayres and Černý, 1982). They resemble the true Phanerozoic porphyry deposits and some have probably formed in a similar way. Others mimic the porphyry deposits in their external appearance, but formed by different mechanisms elsewhere. Some could be of economic importance hence worth searching for. They even include two "giants" and a small number of "large" deposits. Several varieties of the "porphyry-style" deposits and their host associations can be distinguished: 1) Deposits related to the early "porphyries" associated with synvolcanic intrusions emplaced into coeval volcanics in a mostly subaqueous island arcs? 2) Deposits related to synorogenic and post-orogenic intrusions; 3) Deposits associated with calc-alkaline subaerial volcano-plutonic complexes comparable with those in the andean margins (Chapter 6).

Porphyry Cu, Mo and Au occurrences in Precambrian greenstone belts are reviewed in Laznicka (1993, p. 480 and references therein). Although there are some 50 frequently mentioned occurrences worldwide, many are controversial and only resemble the Phanerozoic "porphyries" in some way.

1. Synvolcanic disseminated & stockwork Cu-Au deposits and synorogenic deposits that resemble them

Demonstrably synvolcanic, Precambrian porphyry-style Cu (Au, Mo) deposits are uncommon and most of those so interpreted

examples are now considered late post-volcanic to synorogenic. The primary (bedrock) zone of the "giant" **Boddington Au>Cu>Mo** deposit 100 km SE of Perth, Western Australia (Allibone et al., 1998) used to be placed here, until more recent research has demonstrated the late-orogenic formation of the bedrock mineralization. This deposit, discovered in 1980 by testing a gold geochemical anomaly in bauxite, is described below.

Somewhat similar to Boddington are probably the "medium" to "large" disseminated or stockwork Cu, Mo and Au deposits in the laterite-covered silicified and "propylitized" diorite porphyry in Goren and Gaoua in Burkina Faso (Zeegers et al., 1981). Also associated with a 1.88 Ga old diorite porphyry is the medium-size Tallberg porphyry Cu-Mo located north of the Skellefte massive sulfide belt in northern Sweden (Weihed et al., 1992; 118 kt Cu @ 0.27% Cu, 4,380 t Mo).

A transitional category of intrusions in Precambrian greenstone belts is usually designated in the literature as "late postvolcanic". These intrusions are neither coeval with the main body of the mainly submarine bimodal or, less frequently, basalt-andesite-rhyolite volcanics, nor are they members of the typical batholith-forming synorogenic granites. In Archean greenstone belts small porphyry intrusions, usually heavily albitized, sericitized or carbonate-altered, are often associated with (syn)orogenic gold deposits, creating controversy as to whether they are genetically related to the gold, or just passively hydrothermally altered together with other wallrocks (Burrows and Spooner, 1986). In the former **McIntyre gold mine** near Timmins, Ontario, the often quoted Pearl Lake Porphyry (Davies and Luhta, 1982; 92 kt Cu @ 0.64%; 7,000 t Mo @ 0.05%; 14 t Au @ 1.0 g/t) contained a small zone of disseminated chalcopyrite, bornite and tetrahedrite in albite, quartz, anhydrite, hematite-altered shear zone, within the "giant" Hollinger-Coniaurum (syn)orogenic gold zone that stored almost 1,000 t Au.

The Archean **Chibougamau Cu-Au** district in the eastern Abitibi greenstone province in Québec is well known for the presence of shear and fracture controlled pyrrhotite-chalcopyrite veins (48 mt of ore @ 1.83% Cu and 2 g/t Au produced from 16 mines) and several small porphyry-style occurrences. The veins had been traditionally considered synorogenic but recently Pilote et al. (1998) used precision dating to demonstrate that the orebodies were coeval with synvolcanic tonalitic dykes dated between 2.716 and 2.714 Ga. The

newly proven Lac Clark-type quartz, pyrite, chalcopyrite, molybdenite stockwork and breccia occurrences are a part of the same system. The **Lac Troilus Au deposit**, recently discovered 120 km north of Chibougamau (Fraser, 1993; 60 mt ore containing 60 kt Cu, 93 t Ag and 78 t Au), is of the "large" magnitude and considered a member of an Archean "porphyry" system. There, chalcopyrite, pyrite and pyrrhotite are disseminated in biotite-altered intermediate greenstone metavolcanics, in hanging-wall of a large felsic dike. Further into the hanging-wall the alteration becomes more sodic and the Au:Cu ratio increases.

2. Disseminated Mo, Cu, Au deposits in synorogenic to postorogenic intrusions in greenstone belts

This group is represented by the "giant" Mo stockwork Lobash in Russian Karelia (130 kt Mo content @ 0.06-0.09 % Mo; Pokalov and Semenova, 1993) in a 1.7-1.5 granite, and the "near giant" Coppin Gap deposit in the Pilbara Province of NW Australia (Jones, 1990; 107 kt Mo @ 0.105%, 155 kt Cu @ 0.152%). Both are briefly described in Chapter 7, as is the "large" Setting Net Lake deposit in NW Ontario (Ayres et al., 1982; 48,980 t Mo @ 0.054% Mo).

3. Disseminated Cu, Au, Mo deposits in presumed andean-type setting

About the only "giant" Precambrian porphyry deposit, known from the andean-style setting, is **Haib** in southern Namibia (Minnitt, 1986; 303 mt @ 0.41% Cu plus 978 mt @ 0.19 for a low-grade total of 3.1 mt Cu). Haib is located in the Paleoproterozoic Richtersveld Province, composed of up to 8 km thick, 2.0 Ga old andesite-dominated calc-alkaline volcanics of the Oranje River Group, intruded by the comagmatic Vioolsdrif Plutonic Suite (VPS; Reid, 1979; Reid et al, 1987). The VPS consists of four composite batholiths emplaced into their volcanic roof between 1.96 and 1.81 Ga. The older plutonic phase consists of granodiorite, tonalite and diorite, the younger phase comprises quartz monzonite and leucogranite. The plutons are intruded in places by swarms of quartz-feldspar porphyry dikes and stocks and the Haib deposit is associated with one such intrusion emplaced into granite and meta-volcanics. The orebody is a linear zone where disseminated and veinlet pyrite, chalcopyrite and minor molybdenite occur in K-feldspar and biotite-altered zone enveloped by sericite, pyrite, quartz which, in turn, is surrounded

by an extensive chlorite, epidote and carbonate alteration. There is a 40 m thick supergene enriched zone.

9.6. (Syn)orogenic hydrothermal Au-(As, Sb, Cu) in greenstone terrains

9.6.1. Introduction to orogenic deposits

This section about (syn)orogenic deposits differs from the rest of the greenstone-belt deposits in that host lithology is no longer the leading premise for classification, naming and ore search. With the exception of the Witwatersrand-type Au in conglomerates (Chapter 11) that is not considered here, all remaining early Precambrian gold deposits of some importance are confined to greenstone belts, but once there they can be hosted by any rock type. These deposits, dominated by gold and designated as mesothermal (some, previously, kata- or hypothermal), shear-type Au (Hodgson, 1989, 1993), syn-orogenic or orogenic (Groves et al., 1989, 1991; Goldfarb et al., 2001) represent at least 10,000 database entries globally and they share the following characteristics: 1) hydrothermal origin of the majority of "straight gold" deposits from CO₂-rich, low salinity fluids, in the 400-250° temperature range (hence "mesothermal-Au"); 2) strong structural control, especially by major shear zones in the proximity (hence "shear-Au") and local linear structures filled by quartz or sulfide veins, stockworks and disseminations ("lode-Au"); 3) timing of formation that broadly correlates with an orogeny (hence "orogenic" or "syn-orogenic" Au). All type designations mentioned above are used, interchangeably, in the literature. Of course there are some deposits that do not share all the majority characteristics and they are considered separately below (Groves et al., 2003). First, however, some magnitude statistics:

There are 26 "giant" deposits and "camps" (goldfields) in the early Precambrian greenstone terrains (Fig. 9.23, Table 9.1), of which Kalgoorlie approaches the super-giant magnitude (P+Rc 2,380 or 2,458 t Au, depending on data source). Even so, these deposits are inferior in magnitude to the Witwatersrand goldfields, and to the single Phanerozoic deposit Muruntau of a comparable type (4,000 t Au plus; Chapter 10). Of the total, 22 "giants" are Archean and 4 Paleoproterozoic. Of the 22 Archean deposits or goldfields one is predominantly in turbiditic meta-sediments (Sheba-Fairview), one overprints granitoids, dikes and sills

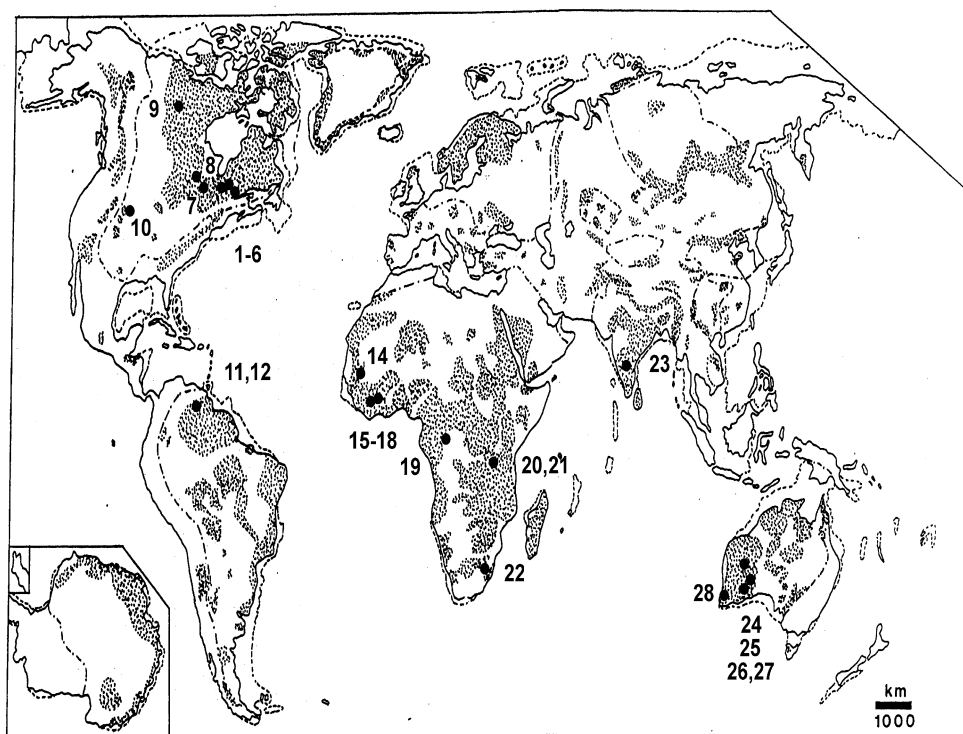


Figure 9.23. "Giant" orogenic deposits and goldfields, global distribution. Numbered localities are explained in Table 9.1.

(Val d'Or), two are superimposed on subvolcanic porphyries (Hollinger and Dome), one is hosted by differentiated mafic sill (Golden Mile). The remaining 18 Archean deposits are mainly in meta-basalts and associated rocks. All four Paleoproterozoic "giants" are hosted predominantly by meta-sedimentary rocks. Many of the "Au-giants" are also "As-giants" (starting at 170 kt As), although arsenic tonnages in gold deposits are never listed, and grades are quoted sparingly. Calculations based on data fragments reveal the following "As-giants": Obuasi, ~1.2 mt As; Homestake, 1 mt As plus; Yellowknife, Balmertown-Red Lake, Prestea, Golden Mile, Morro Velho: 200 kt As plus each. Antimony is the only associate of gold in "shear-Au" type deposits that has achieved a "giant" status, or even more: the Murchison Range "Antimony Line" is a "Sb-supergiant", where the 630 kt Sb resource greatly exceeds the 40 t Au. The "giant" Olimpiada deposit in Siberia is also a "Sb-Au giant" although the exact Sb tonnage there is not known. Copper, although associated with gold in several deposits, has not achieved the "giant" magnitude of accumulation. The "large" "shear Cu-Au" Chibougamau "camp" in Québec total 1.125 mt Cu

in 17 orebodies, of which 496 kt Cu and 14 t Au is in the largest Campbell Chibougamau deposit.

Some of the greenstones-hosted orogenic "Au-giants" are briefly described below and the rest follows in abbreviated form. Ranked by magnitude, they are (the figures refer to tons of gold; ON=Ontario, WA=Western Australia): Kalgoorlie "camp", WA, 2,380 or 2,458 t; Homestake, USA, 1,319 t; Obuasi, Ghana, 1,275 t; Hollinger-McIntyre (Timmins), ON, 995 t; Kolar, India, 825 t; Kirkland Lake, ON, 786 t; Hemlo, ON, 632 t; Boddington, WA, 589 t; NE Porcupine (including Dome), ON, 559 t; Balmertown (Red Lake), ON, 554 t; Yellowknife, NWT Canada, 499 t; Morro Velho, Brazil, 470 t; Moto, Congo, 463 t; Geita, Tanzania, 455 t; Prestea, Ghana, 412 t; Val d'Or, Québec, 388 t; Las Christinas, Venezuela, 373 t; Kerr Addison, ON, 340 t; Kambalda-St. Ives, WA, 336 t; Malartic, Québec, 323 t; Bulyanhulu, Tanzania, 274 t; Plutonic, WA, 265 t; Sheba-Fairview, South Africa, 262 t; Sadiola, Mali, 403 t; Sunrise Dam, WA, 250+ t. The total tonnage of gold stored in the greenstone belts-hosted "Au-giants" is about 16,000 t Au.

Table 9.1. Early Precambrian (syn)orogenic deposits/goldfields of the world

No	Geological division	Deposit, goldfield	Age	Geology	Tonnage	References
1.1	Canadian Shield --Superior Prov. --Ontario	Timmins --Hollinger- McIntyre	Ar	Au in pyrite adjacent to quartz veined, sheared & altered porphyry and greenstone metabasalt along shear	995 t Au 9.8 g	Wood et al. (1986)
1.2		Timmins --Dome, Preston	Ar	Au in low-sulfide quartz, numerous orebodies in greenstone basalt, meta-sediments around porphyry intrusion	393 t Au	Rogers (1982)
2		Kirkland Lake	Ar	~6 km long zone of low sulfide Au-quartz vein arrays in brittle syenite, trachyte & porphyry along shear	786 t Au	Kerrich & Watson (1984)
3		Kerr Addison	Ar	Au in pyrite, arsenop in qz veins to stockw and dissem, in silica-carbonate altered komatiite, metasedim. in shear	340 t Au	Kerr Addison Staff (1967)
4	----Québec	Bousquet	Ar	Au in massive pyritite (VMS) overprinted by Au-qz veins, stockworks in deform. zone over porphyry, greenst	336 t Au	Tourigny et al. (1993)
5		Malartic	Ar	Many vein, stockw, dissem Au-quartz & pyrite, arsenop bodies in/near syenite stocks, greenst along major shear zone	323 t Au	Sansfaçon (1986)
6		Val d'Or: Sigma-Lamaque	Ar	Low-sulfide Au quartz, tourmaline brittle veins & stockworks in diorite & porph dikes, greenstone basalt	291 t Au ~5.5 g	Roberts & Brown (1986)
7	----Ontario	Hemlo	Ar	Au in dissem pyrite with molybdenite, barite band in foliation // zone of muscovite, quartz, K-feldsp schist	632 t Au 8.2 g	Muir et al. (1995)
8		Balmertown, Red Lake dist.	Ar	qz-arsenop-Au veins in greenst basalt, dissem qz-sulfides replacements in carbonated komatiite	554 t Au 10-18 g Au; As	Penczak & Mason (1999)
9	--Slave Prov. --NWT	Yellowknife	Ar	qz-arsenopyrite-Au veins to stockw in altered sheared greenstone basalt	499 t Au ~10 g Au	Henderson (1970)
10	--Wyoming Pr. --S. Dakota	Homestake	Pp	Au in qz-arsenop "ledges" superimp. on Ca-Fe-Mg carbonate & cummingtonite "BIF" unit in mostly metasedim setting	1319 t Au	Noble (1950)
11	Guyana Shield --Venezuela	El Callao	Pp	Scattered Au-qz veins > dissem, shears in greenst basalt, gabbro, schist	350 t Au	Channer et al. (2005)
12.1		Km 88: Las Cristinas	Pp	Au+pyrite disseminated in 2 km long broad shear zone in greenstone basalt	400 t Au 1.2 g Au 0.13% Cu	ditto
12.2		Km 88: Brisas	Pp	Au+pyrite > chalcopyrite dissem & veinlets in epidote-carbonate altered shear zone in greenstone mafic tuff	286 t Au 0.69 g Au 0.13% Cu	ditto
13	Brazilian Shield --Minas Geraes	Morro Velho	Ar	Au dissem with pyrite, arsenop in silica-carbonate zone ("BIF") along altered shear in greenstone basalt	470 t Au	Vieira, de Oliveira (1988)
14	West African Craton; Mali	Sadiola Hill	Pp	Au dissem in pyrite, arsenop, etc. in skarn & biotite altered greywacke in ductile-brittle shear zone	403 t Au 2.86 g	Milési et al. (1992)
15	--Ghana	Obuasi (Ashanti)	Pp	8 km long shear zone in turbiditic metasediments, Au in qz lodes enveloped by dissem arsenopyrite	1648 t Au ~8 g Au ~2.7% As	Oberthür et al. (1996)
16		Prestea	Pp	Au in arsenop dissem & in qz lodes in 10 km zone of sheared, silicif m-sedim > m-basalt schists	412 t Au 10.3 g + As	Leube et al. (1990)
17		Bogosu	Pp	As above, high proportion of oxidized ore	331 t Au	ditto

Table 9.1. (continued)

No	Geological division	Deposit goldfield	Age	Geology	Tonnage	References
18		Tarkwa	Pp	Several stratiform "reefs" of dissem. Au, pyrite in synorogenic quartz-rich conglomerate resting on greenstones	670 t 1.3-6 g	Sestini (1973)
19	Central African (Congo) Craton --Congo	Moto	Ar	Mineralized shear zone in greenstone, past production ~50% from placers and regolith	463 t Au 3.1 g Au	Lavreau (1984)
20	Tanzanian Craton, Tanzania	Geita, Lake Victoria	Ar	Au-quartz lodes in shears in greenstone metabasalt; dissem Au with pyrite, pyrrhotite, arsenop in sheared BIF	455 t Au 4.1 g	Kuehn et al. (1990)
21		Bulyanhulu, Lake Victoria	Ar	Several subparallel Au-quartz and dissem. Au-pyrite zones in felsic & mafic greenstone. "exhalite"	274 t Au 13 g	Kenyon (1998)
22	Kaapvaal Craton; S. Africa	Barberton:Sheba-Fairview	Ar	Sheba: 25 tabular fracture zones of Au in pyrite, arsenop replacem. in silicif, carbonated komatiite + graywacke	262 t Au	Wagner & Wiegand (1986)
23	Dharwar Craton --India	Kolar	Ar	Persistent low-sulfide Au-quartz lodes along shears in amphib facies metam basalt	825 t Au 16.5 g	Hamilton & Hodgson (1986)
24	Yilgarn Craton --Western Australia	Plutonic	Ar	Subparallel zones of qz veining & dissem Au in arsenopyrite, pyrite in altered shears in greenst basalt > sedim	265 t Au 3.6 g Au	Vickery et al. (1998)
25		Granny Smith Sunrise	Ar	A number of Au-quartz, pyrite, arsenop. lodes and replacem in high-strain zone in altered metavolc and plutonic dikes	270+ t Au	Acacia Resources (2000)
26		Kalgoorlie	Ar	Golden Mile: ~2 km wide zone of brittle dilatational qz>pyrite, Au, telluride veins, veinlets in deformed mafic sill	2230 t Au	Clout et al. (1990)
27		Kambalda-St.Ives zone	Ar	30 km long zone of Au-quartz lodes to stockw in sheared greenst basalt, komatiite, porphyry	368 t Au 3.47 g	Watchorn (1998)
28	Western Gneiss	Boddington	Ar	Late orogenic (undefomed) qz, actinol, biot, pyrite, arsenop stockw in shear over m-andesite; Au laterite capping	589 t Au 0.8-1.8 g	Allibone et al. (1998)

Additional "near-giants" that are being actively mined and explored so they are likely to reach the "giant" magnitude sometimes soon, include the following ore fields and centers (camps): Akim and Yamfo, Ghana; Mt. Magnet, Leonora, Yandal-Nimary, Norseman in Western Australia. Some entries in this table corresponds to one or few zones within a larger goldfield (e.g. Sigma-Lamaque in the Val d'Or camp; Balmertown in the Red Lake camp; Golden Mile in the Kalgoorlie camp), so the Au endowments are lesser than of the entire goldfields

Setting of deposits: The early Precambrian lode gold deposits are not fundamentally different from those in the younger orogenic belts (Chapter 10), and are treated separately mainly because of the established convention. This class of deposits has a comprehensive, global review in Laznicka (1993, p. 152-169, 385-449 and references therein) so only a short introduction and update are needed before the brief description of selected "giant" example deposits. Because all greenstone belt lithologies can host gold deposits in the presence of favourable structures, Au deposits are much more widespread and more regularly distributed than the lithologically highly selective VMS (read above). They thus occur

widely in the "basalt plain" and turbidite settings devoid of other deposits, as well as in bimodal successions where they coexist with VMS although the latter are older and genetically unrelated. In the Bousquet goldfield (read above) the orogenic gold overprints the presumably synvolcanic mineralization. Although Au lodes are common in komatiites where they may mingle with Ni sulfide deposits (e.g. in the Kambalda-St. Ives zone), there is likewise no genetic connection. Gold lodes, however, have a special affinity for the "Algoma-type" oxide iron formations, as gold co-precipitates with pyrrhotite, pyrite or arsenopyrite formed by sulfidation of the iron oxides (Kerswill, 1996).

There are numerous "medium" and "large" deposits of this type (e.g. Raposos, Cuiabá and São Bento in Brazil; Ladeira, 1988; Mount Magnet, Western Australia; Geraldton, Pickle Crow in Ontario) but no "giants" except for the Geita goldfield in Tanzania. Homestake, Morro Velho and partly Balmertown are in what used to be interpreted as "sulfide iron formation" and "exhalite" in the 1970s, but has since been reinterpreted at many localities as zones of metasomatic silicification and carbonatization, usually with Fe sulfides. Granitoids, more the synvolcanic than the synorogenic variety, do host lode gold but most deposits are small and they greatly postdate granite emplacement. Some earlier "shear-Au" lodes in supracrustals, on the other hand, are intersected by later granitoids. Alkali rocks such as syenite and trachyte, some of which are truly magmatic while others are Na- (albitite) and K-feldspar metasomatites, also host more gold deposits than what is their outcrop share and this includes the "giant" Kirkland Lake, Ontario.

Orebody styles: Shear zones are the principal district-scale controlling features of lode gold deposits (Hodgson, 1989; Colvine et al., 1988). When they themselves host gold the mineralization is usually multistage. Bonnemaïson (1986) recognized three commonly represented stages. In Stage 1 formed the mylonitic fill. Simultaneous hydration, carbonatization or silicification converted the ultramafic and mafic mylonite (phylionite) into serpentinite, talc, or chlorite, silica, carbonate assemblages. Felsic hosts underwent similar alteration except for lacking serpentinite and talc. Gold pre-concentrated in pyrrhotite. In Stage 2 the shear zone had been invaded by diorite to leucogranite dikes and by veins of milky quartz, produced by lateral secretion of silica. The sugary ("bucky") quartz partly replaced carbonatized wallrocks. In Stage 3 formed quartz lodes and stockworks mineralized by main stage gold, pyrite, arsenopyrite and base metals sulfides.

There is a bewildering variety of possible lode varieties (Fig. 9.24), often within a single deposit or even a single lode, so a meaningful "pigeonholing" of the gold deposits is practically impossible. About the most sensitive way is to tabulate the many discrete orebody characteristics, then use them for comparison of the various deposits. Several end-member progressions of the many ore attributes can be recognized, as follows:

- STRUCTURES: compressional (e.g. shears) to tensional (dilations);

- ORE EMPLACEMENT: open space filling to replacement;
- GANGUE: abundant quartz to no quartz
- SULFIDES: no sulfides in vein (quartz only)-low, moderate, only sulfides
- THE PLACE OF GOLD: in vein, in selvages, in both
- THE STATE OF GOLD: free milling to refractory (in sulfides)
- GOLD PURITY: high purity (up to ~980 per mil) to low purity (electrum)
- VEIN TYPE: discrete veins, parallel vein sets, stockworks, disseminations
- CONFORMITY WITH STRUCTURES: bedding/foliation parallel, crosscutting
- WALLROCKS: unstrained to mylonite, phyllonite, breccia
- ALTERATION INTENSITY: fresh to pervasively altered wallrocks
- VEIN ATTITUDE: vertical to "flat" (low angle), rarely horizontal
- OXIDATION: ferruginous regolith with relic gold versus fresh outcrop
- TIMING: pre-, syn- to post-orogenic
- METAMORPHISM: unmetamorphosed to metamorphosed.

Vein types and their geometries have been classified and described by Hodgson (1989) and are summarized in Figure 9.24. In major deposits several styles coexist. A classical visual structural analysis is applied to discover and trace the traditional quartz veins but most of those in outcrop have already been found by traditional prospectors. The modern ore types that have revitalized the gold industry in Canada, Australia, Brazil and elsewhere are dominated by low-grade deposits with refractory gold in disseminated sulfides, and free but dispersed gold in deep oxidation zones amenable to heap leaching (especially in Australia), "sulfidic schists" (e.g. Hemlo), Au-mineralized banded iron formations and "exhalites", plus the classical veins discovered under cover and the known ones followed to a great depth.

Ore genesis: Genetic interpretation of the "shear-Au" deposits keeps changing with times (Boyle, 1979), from the classical pre-1950 granite-postmagmatic model, through the emphasis on synvolcanic/synsedimentary processes (stratiform deposits) in the 1970s, metamorphic dehydration in depth of the 1990s, to the present genetic postmodernism (that is, admission that all the above mechanisms could have been end-members in a










	1 QUARTZ GANGUE	2 QUARTZ + INTERVENING ROCK	3 FAULT- AND WALL ROCK ONLY
A FOLD CONTROL	saddle, leg, neck reefs and spurs	ditto, sets of parallel veinlets to stockworks	mineralized alterites to metasomatites, massive sulphide bodies
B BRITTLE EXTENSIONAL FISSURES AND VEINS, within and outside shears	fracture/fissure veins, sheets, bulges and vein arrays; quartz breccia bodies	sets of extensional quartz veinlets; breccias of wallrock fragments cemented by quartz; stockworks of quartz veinlets	
C DUCTILE SHEARS; OREBODIES WITHIN AND CONFORMABLE WITH SHEARS	laminated, dilation filling or replacement veins: pre-, syn- and post-metamorphic; straight (planar), folded, sheared	banded quartz-wallrock sets; thin quartz lenses to stringers in wallrocks (schists); straight, planar sheets; folded zones	Au exhalites, pseudoexhalites, sulphide-silicate facies BIF; Au superimposed on oxide BIF; Au "sulphide schist" orebodies
D COMBINATION AND OTHER CONTROLS	irregular quartz masses in shears and at various contacts	irregular quartz-wallrock masses in shears and at contacts	as above, irregular masses
			
			
			

Figure 9.24. (Syn)orogenic Au deposits in greenstone belts organized by mineralogy and structure. From Laznicka (1991).

complex gold-depositing system). The bulk of the "typical" (syn)orogenic deposits are still attributed to low-salinity mesothermal fluids released by metamorphic dehydration in depth during or following shortly collisional events, and contemporaneously with metamorphism of the local rocks (prograde or retrograde); Groves et al. (1988, 1993; Kerrich & Cassidy, 1994). The fluids circulation may have been assisted by heat from granitoids. The fluids were rising into higher crustal levels and precipitated gold on cooling, pressure drop, and reaction with wallrocks (particularly those with "extreme" compositions like BIF, pyritic schists, carbon-rich rocks). The gold deposition was predominantly a deep-seated process (~10 km depths or more) although Groves (1993) demonstrated a continuum of gold precipitation in the Yilgarn Craton spanning some 15 km or more of crustal thickness. The greenschist metamorphic zone, however, contains statistically most gold deposits and although they occur throughout the whole range of metamorphic intensities from granulite to sub-greenschist, the frequency of occurrence and size diminish at both (too shallow, too deep) ends. The range of fluid temperatures above and below the mesothermal necessitated introduction of another term, hypozonal, to accommodate this variation (Groves et al., 1989). In empirical classifications it is useful to consider two end members of lode gold deposits, in any setting: 1) those predating the main stage of orogeny, hence deformed, metamorphosed and variously reconstituted (e.g. Balmertown, Golden Mile, Hemlo); 2) the late-stage, post-orogenic ones, almost free of post-ore modifications (e.g. Boddington, Sigma-Lamaque).

The less "typical" Au deposits require some departure from the prevalent model. The "activation"-type deposits as in the important Shandong goldfields of eastern China are Mesozoic, but superimposed on Archean greenstones and metamorphics. There is thus no relationship between ore formation and host metamorphism (read Chapter 10). The depth level of ore formation is another point of contention, especially for metamorphosed gold systems. Penczak and Mason (1999) argued for an epithermal origin of the "giant" Balmertown ore zone in the Red Lake district, Ontario, but their model is not widely accepted. The magmatic-hydrothermal gold derivation, especially the various "porphyry gold" models (both pre-orogenic and late metamorphosed, and syn-, post-orogenic) are still around although they continuously mutate (Spooner, 1993). One problem here is the confusion between true

magmatic intrusions and Na- and K-metasomatites that may mimic them (pseudointrusions). Groves et al. (2003) considered several such examples that include several "giants", namely Boddington in Western Australia, Hollinger-McIntyre and Dome deposits near Timmins, Ontario and the Hemlo "sulfidic schist", also in Ontario. These deposits are briefly described below. Finally, the problem of "stratiform" (synvolcanic, synsedimentary) gold, popular in the 1970s, remains and is best illustrated by the Bousquet goldfield, reviewed above.

Gold in meta-volcanics and mafic sills, early stage (deformed, metamorphosed orebodies)

Balmertown ore zone (Campbell & former Dickenson mines), Red Lake district, NW Ontario (Corfu and Andrews, 1987; Penczak and Mason, 1999; ~554 t Au @ ~14 g/t Au, min. 250 kt As). This is a set of two deep underground mining properties exploiting numerous Au orebodies in a NW-trending continuous deformation zone. The Red Lake greenstone belt here is represented mainly by 3.0 to 2.87 Ga tholeiitic meta-basalt with minor felsic meta-volcanics, komatiitic ultramafics, meta-sediments and diorite deformed, metamorphosed and probably intruded in depth by granitoids between about 2.73 and 2.70 Ga. The supracrustals are thermally metamorphosed and modified by a multistage alteration that includes pervasive biotitization, silicification and aluminous alteration (local andalusite, garnet, cordierite, chloritoid) of meta-basalt, and talc-carbonate alteration and silicification of the ultramafics.

The principal ore style of the multiple orebodies are dilation-filling zones consisting of early-stage dolomite-ankerite veins subparallel with foliation. These had been folded, sheared, fractured and brecciated and finally invaded by late quartz, sulfides (arsenopyrite, pyrite, pyrrhotite) and native gold with alteration chlorite. The F and A Zones are 0.3 to 2 m thick. The foliation-oblique veins grade into quartz, arsenopyrite, stibnite replacement bodies up to 20 m wide, situated along the contact of, or within, ultramafics. The banded metacolloform, crustification and cockade structures of vein and alteration carbonates, accompanied by a "cherty" quartz, were interpreted as "exhalites" in the 1980s. More recently, Penczak and Mason (1999) favored pre-metamorphic alteration and mineralization and they suggested that this was a deformed and metamorphosed low-sulfidation epithermal deposit. There is little support for this idea among the Shield geologists.

Kalgoorlie Goldfield, Western Australia (Phillips, 1986; Clout et al., 1990; P+Rv Golden Mile only: 2,230 t Au; Mount Charlotte: 150 t Au for a total of 2,380 t Au, or 2,458 t Au, ?1,000+ t Te). This is the largest Au vein system in Archean greenstones, predominantly hosted by a differentiated dolerite (diabase, microgabbro) sill emplaced into ~2.69 Ga meta-basalts (Fig. 9.25). The goldfield measures about 10x2 km of which the Golden Mile orebody, the "richest mile on earth", is about 1x3 km. Since the discovery by Pat Hannan's party in 1893 the deposit was selectively mined from numerous underground workings under different ownership, and in the past decades from a consolidated Superpit, the largest open pit operation in Australia.

The Golden Mile Dolerite (GMD) is a persistent, more than 20 km long and 400-800 m thick differentiated intrusion. Travis et al. (1971) distinguished ten magmatic layers predominantly composed of diabase, with 60 m of quartz-rich granophyre unit. The GMD had been regionally metamorphosed into the actinolite-albite assemblage and later pervasively hydrothermally altered. The multiphase orebodies are structurally controlled. The Golden Mile ore zone is a shear system with numerous NNW-striking and SW dipping "lodes". A "lode" is defined by Clout et al. (1990) as "an area of auriferous and pyritic hydrothermal alteration developed within and flanking selective parts of more extensive shear zones". The lodes vary from 30 to 1,800 m in length, are 1-10 cm wide, have 30-1,160 m vertical extent, and comprise between 20 and 50% of the ore zone. Previously selectively mined with grades of 10 g/t Au plus, the bulk mined remnants in the Superpit run 2.5 g/t Au after dilution.

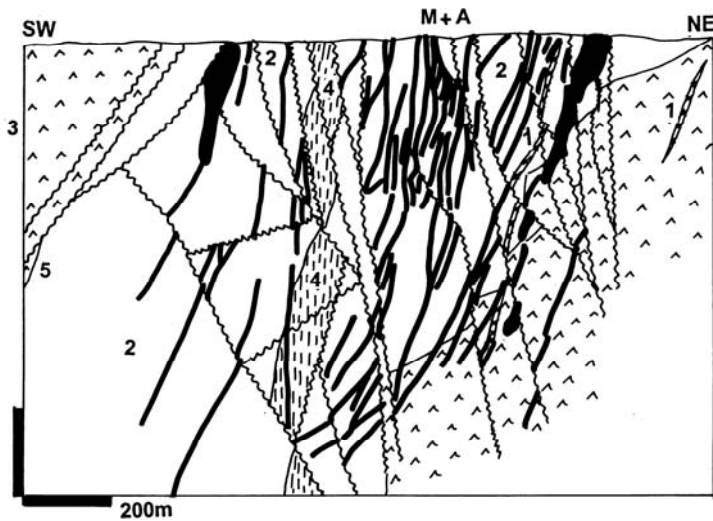
The lode fill varies from site to site and it includes altered mylonite, phyllonite, ductile and dilational (disaggregated) multiphase breccia. Hydrothermal alteration is usually symmetrically distributed around a lode, ranging from a narrow, 1.5 cm thick core of intense pyritization, sericitization and carbonatization that grades into ankerite and siderite zone, then into an envelope of regional pervasive chloritization and mild carbonatization. Vanadian silicates and oxides (mainly V-muscovite), with extremely high gold grades, form shoots in the inner zone. Gold resides mostly in pyrite that has the form of disseminations, scattered euhedral crystals and veinlets that grade into almost solid sulfide lenses in some lodes. There are no discrete gold-quartz veins. Au and Ag tellurides store about 15-20% of the gold. The richest telluride shoots run up to 0.15% Au in the

former Oroya Mine, hosted by carbon-rich interflow meta-sediments in the Paringa Basalt.

At the Mount Charlotte Mine north of the Golden Mile Superpit (Clout et al., 1990), a low-grade auriferous stockwork formed in the brittle granophyre unit of the GMD and in albite porphyry dikes. The stockwork consists of 2 to 50 cm thick coarse crystalline quartz veins enveloped by ankerite, sericite and pyrite alteration haloes. The bulk of gold is in pyrite, disseminated in altered wallrocks.

Timmins-Porcupine gold district, Ontario (Ferguson, 1968; Pyke, 1982; P_{to 2001} 1,928 t Au, P+Rc ~2100 t Au). This is the second richest "greenstone" gold district and the largest Canadian producer. Located in the western Abitibi Subprovince, the district contains numerous scattered Au deposits in a broad NE-trending zone that measures about 20x12 km. Two closely related groups of mines: the NE-trending 5 km long Hollinger-Coniaurum zone NE of Timmins (Fig. 9.26), and the Porcupine cluster (Dome-Preston), have each a "giant" ore field status. This district is an example of multistage gold mineralization and of close association of gold with "porphyries", although the metallogenetic role of the latter is controversial (Spooner, 1993). Equivalent situation, however, is common in many world's gold regions.

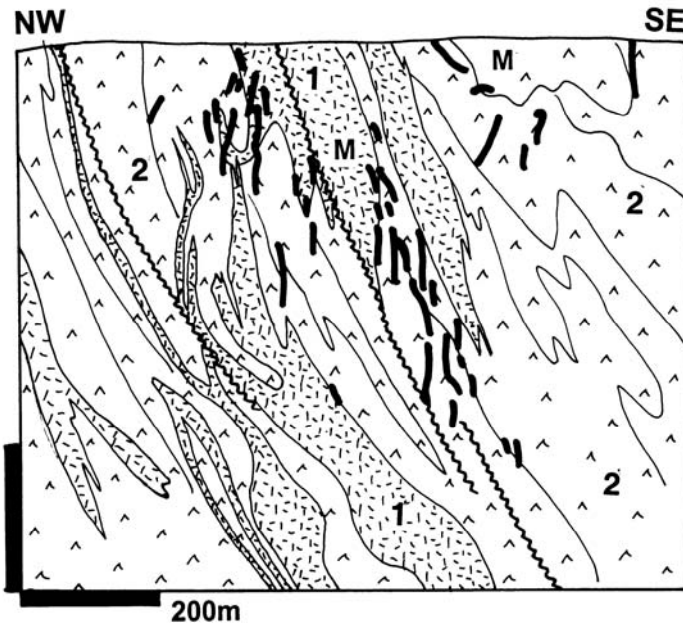
The oldest rocks in the district are in a thick, ~2.7 Ga komatiitic and tholeiitic succession of greenstone-metamorphosed basalt and minor peridotite (Tisdale Group) that produced several small "komatiite-Ni" type deposits and that hosts the majority of younger Au veins. This is overlain by felsic volcanoclastics, especially in the SE portion of the district, that contain minor iron formation but are devoid of gold ores. These "basement" rocks were folded and thrust. The most important ore-controlling structure is the NE-trending Porcupine-Destor Fault, one of the major Abitibi "Breaks". Synorogenic turbiditic sediments of the Timiskaming Group settled in fault basins and are now preserved in a long, narrow erosional remnant adjacent to the Porcupine-Destor Fault. Several subvolcanic stocks of trondhjemite porphyries and later albite dikes, believed genetically related to gold, had been emplaced around ~2.69 Ga into the folded basement and their maximum occurrence coincides with the two most productive Au-mineralized centers. The subsequent main phase of the Kenoran orogeny produced penetrative deformation, strong foliation, greenschist metamorphism, zones of sericitization



M+A. More than 400 discrete and coalescing sericite & carbonate altered, pyrite, Au, tellurides mineralized shears, most in mafic intrusion, along 2 km NW zone

1. Albite porphyry dikes
2. ~2.7 Ga Golden Mile Dolerite, differentiated tholeiitic diabase sill, granophyre margins
3. Ar Devon Consols komatiitic pillowed metabasalt
4. Tuff, volcanoclastics
5. Ar Paringa tholeiitic to komatiitic metabasalt

Figure 9.25. Golden Mile ore zone, Kalgoorlie, Western Australia; cross-section from LITHOTHEQUE No. 1294, modified after Clout et al. (1990)



M. Structurally controlled orogenic (or porphyry-related, modified) folded ribbon to massive quartz veins enveloped by auriferous pyrite in sericitized wallrocks

1. Ar Pearl Lake and other quartz-feldspar porphyry bodies, variously albitized and sheared to quartz-sericite schist
2. Ar, several map units of greenstone metabasalt with thin interbeds of volcanoclastics

Figure 9.26. Generalized cross-section of the former Hollinger Mine, Timmins, Ontario from LITHOTHEQUE No. 1851, modified after Ferguson (1968)

and emplacement of syn- to post-orogenic plutons in the broader area.

The Timmins genetic controversy is mainly a matter of semantics: the main ore-forming phase is pre-orogenic in respect to the Kenoran orogeny, but syn- to early post-orogenic in respect to deformation that produced the Timiskaming unconformity. Shearing overprinted older generation of gold deposits, whatever their origin (some were porphyry-related?), and produced a younger, syn-orogenic Au generation. The multiple

ore origins then overlap and merge, resulting in a sweeping generalization of the Timmins district as a "shear-Au" or "orogenic-Au" example. Groves et al. (2003) placed the Hollinger-McIntyre deposit, together with Boddington and Hemlo, into the category of "probably modified porphyry-epithermal systems".

Gray and Hutchinson (2001) found auriferous pyritic clasts in Timiskaming conglomerates that indicate presence of possibly synvolcanic gold accumulations in the area, nowhere known from a

mine or outcrop. The largest gold deposits: Hollinger-McIntyre and Dome are spatially associated with albitized and locally sericitized porphyries and breccias, and the porphyries are anomalously enriched in Cu, Au and Mo; a small Cu-Au orebody in albite, sericite, quartz and anhydrite-altered porphyry was mined in the former McIntyre mine and it has received widespread publicity as an Archean "porphyry-Cu". The gold veins, as in the largest Hollinger Mine on the outskirts of Timmins, are younger than the porphyries which they overprint in the form of S-shaped quartz and/or pyritic stringers in schisted basement greenstones and porphyry alike. There, en-echelon, centipede and gash-vein arrays, showing all stages of syntectonic crack-seal quartz emplacement, are in evidence. The quartz contains irregularly scattered grains and bunches of beige scheelite but is almost free of gold. 95% of the gold produced came from pyrite adjacent to quartz, disseminated in the sericite, albite and ankerite-altered wallrocks. In the adjacent McIntyre Mine (Wood et al., 1986) sheared sericitized "pyritic dacite" contains 5-15% of auriferous pyrite in the form of evenly disseminated cubes.

In the southern, Porcupine mine cluster, an intense metasomatic carbonatization is in evidence, where the host rocks are komatiite and greenstone basalt. Zones of total dolomite-ankerite replacement are peneconcordant with selected flows so they appear as stratigraphic units, interpreted as "exhalite" in the past. At former Delnite, Aunor and Buffalo Ankerite mines the carbonate horizons grade into gold-bearing quartz, tourmaline, ankerite, pyrite orebodies. In the "giant" Dome Mine (Rogers, 1982; Pt 393 t Au) the ore zones are stockworks of quartz, carbonate, tourmaline veins sometimes with fuchsite, parallel or oblique to foliation, in a wide range of rocks that also include felsic pyroclastics and flows. Most orebodies are in schisted rocks, with the exception of the "dacite-type ore". The latter is en-echelon array of lenticular quartz veins with disseminated auriferous pyrite and pyrrhotite. Moderately carbonatized and bleached dacite is also locally gold-bearing.

The problem of overlap of magmatism (especially of porphyry and lamprophyre dikes) and orogenesis (ductile to brittle deformation) and their influence on mesothermal gold deposition exists at many other deposits. At the "near-giant" **Sunrise-Cleo** deposit in the rapidly developing Granny Smith cluster in the Northeastern Goldfields, Western Australia (Acacia Resources, 2000; Fig. 9.27) several styles of gold orebodies appear at least partly coeval with syn-mineralization porphyry

dikes, but also replace and infill ductile to brittle shears in older greenstone and replace iron formation bands.

The historic **Morro Velho Mine** in Nova Lima, Brazil (Vieira and de Oliveira, 1988; Pt 470 t Au; Fig. 9.28) is another example deposit where carbonatized horizon ("Lapa Sêca") in Archean mafic/ultramafic meta-volcanics controls gold orebodies. Lapa Sêca is a 3 to 100 m thick and up to 14 km long, banded to massive ferrous dolomite, ankerite, microcrystalline quartz unit that has a variable proportion of sericite, fuchsite, Cr-chlorite, albite, epidote and stilpnomelane. It replaces and is interlayered with sheared greenstone and graphitic phyllite. Gold with a high content of silver is in banded disseminations and masses of pyrrhotite, pyrite, arsenopyrite and minor Cu, Zn, Pb, Sb sulfides. The entire band is not continuously mineralized; sulfidic orebodies are concentrated in a series of overlapping folded lenses and ESE-dipping sheets, traceable down plunge for almost 4,800 m.

Kolar Goldfield in Karnataka, India (Hamilton and Hodgson, 1986; 825 t Au @ 16.5 g/t) is an example of a low-sulfide gold-quartz lode system metamorphosed to middle or upper amphibolite grade. It is confined to a small greenstone relic enveloped by a "sea" of tonalitic granite gneiss. The north-south trending ore zone is 10 km long, 2 km wide and has been followed into a 3,000 m depth. It is hosted by Archean tholeiitic and komatiitic amphibolite with interbeds of banded iron formation, pyrite/pyrrhotite and graphite-rich schist (phylionite?), and meta-pyroxenite. 97% of gold came from the Champion Reef system of low-sulfide quartz veins and lodes filled with subparallel quartz veinlets alternating with schisted host rocks. Wallrocks adjacent to veins display a zonally arranged metamorphosed alteration zones, from the lode outward: diopside, hornblende, biotite. The productive orebodies are localized by intersections of N-S and NNW reverse shears. The lode quartz is predominantly of the laminated (ribbon) variety, in which bands of translucent quartz with free-milling gold are interleaved with ribbons of schist. Central parts of wider lodes contain massive ("bucky"), coarse crystalline, white to dark gray strained quartz. Only about 3% of the production has come from zones of disseminated auriferous sulfides.

Gold in meta-volcanics, late stage veins

Boddington, Western Australia (Symons et al., 1990; Allibone et al., 1998; P₁₀ 2002 140 t Au from

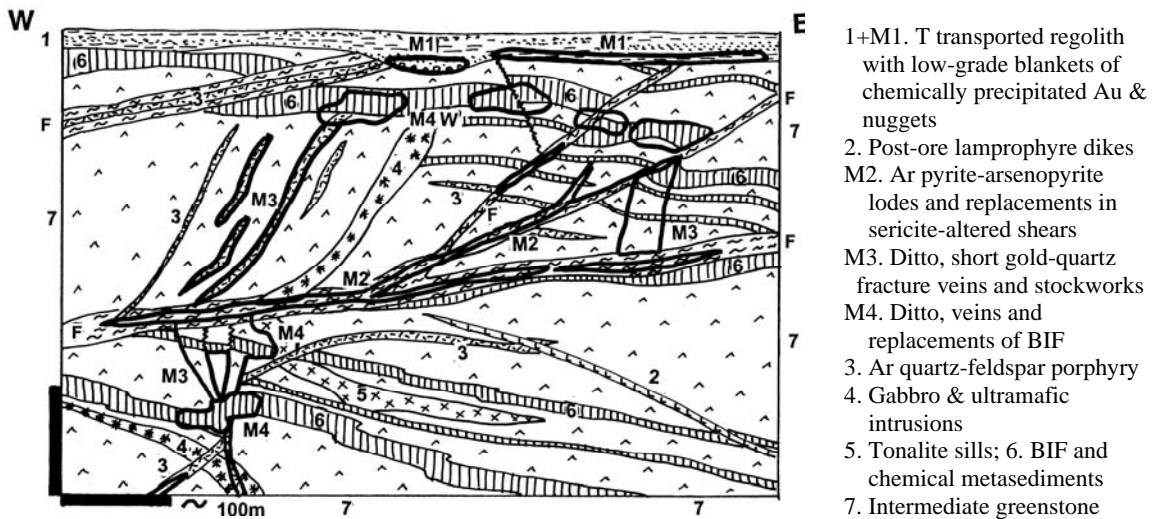


Figure 9.27. Sunrise Dam Au deposit, Granny Smith cluster, Western Australia; cross-section from LITHOTHEQUE No. 2629, modified after Acacia Resources (2000)

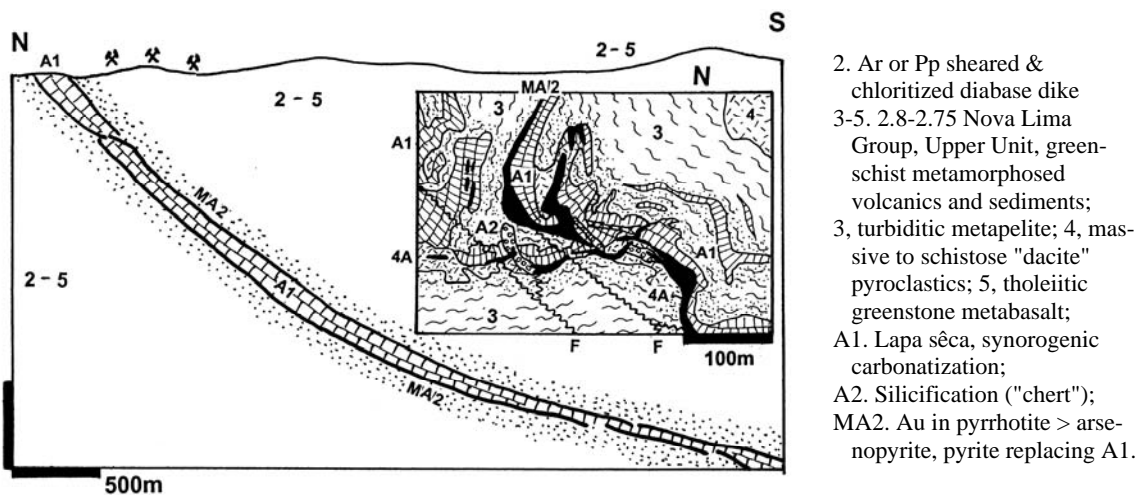


Figure 9.28. Morro Velho Mine, Nova Lima, MG Brazil. Cross-sectional projection of the ore zone (after Vieira & de Oliveira, 1988) with inset showing detail from the geological map of the 10th mine level. From LITHOTHEQUE No. 1199

laterite, Rv 271 t primary gold for 411, or 589 t Au plus Cu; Fig. 9.29). Boddington is 120 km SE of Perth, in the Darling Ranges lateritic bauxite province. It was an accidental discovery: an aluminum smelter's concern about traces of heavy metals in the Boddington bauxite in the early 1980s led to analytical work, during which high gold contents were found. Mining this auriferous bauxite, together with a portion of regolith beneath started in 1987, based on an initial reserve of 45 t @

1.8 g/t Au with 0.5 g/t cutoff grade, and terminated in 2001 when the supergene materials have been exhausted after producing 140 t Au. Large resource of hypogene Au and Cu ore remains in depth. Before Boddington, another important discovery had been made: that of the small, fault-bounded Archean Saddleback greenstone belt surrounded by high-grade metamorphics of the Western Gneiss Terrain, entirely concealed by a thick lateritic cover. This belt is the Boddington's host.

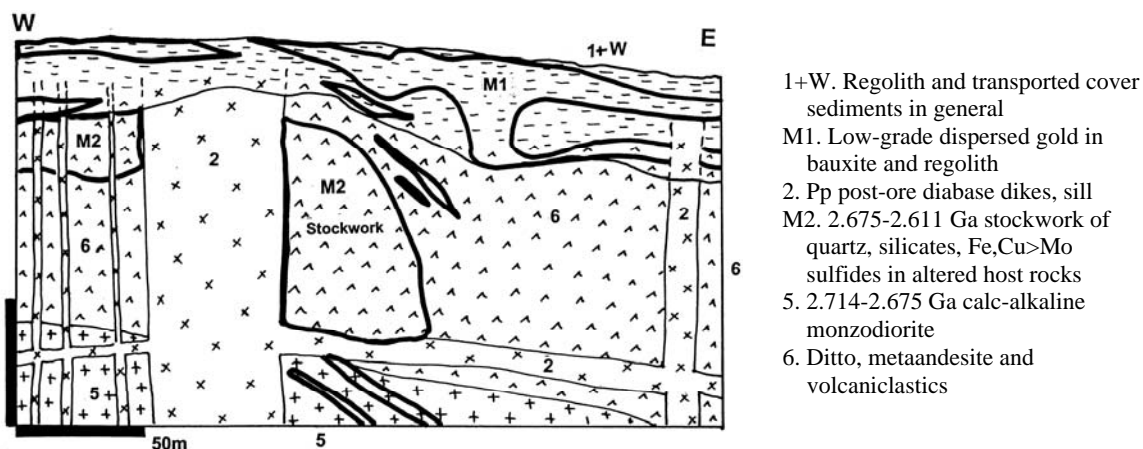


Figure 9.29. Boddington Au laterite (bauxite) and bedrock deposit, Western Australia; cross-section of the Pit A. From LITHOTHEQUE No. 2693, modified after Worsley Alumina materials and site visits in 1994, 2001

First, the supergene ore. The mature, Cenozoic lateritic weathering profile at Boddington developed partly on a slope, so the weathering zones are inclined. From top to bottom, the profile consists of 1) unconsolidated gravel of Fe-rich gibbsite pisoliths; 2) indurated ferruginous and bauxitic hardcap composed of gibbsite, hematite and goethite pisoliths and regolith fragments; 3) friable, unconsolidated bauxitic laterite gravel; 4) variously ferruginized predominantly kaolinitic clayous saprolite; 5) green clayous lower saprolite with bedrock relics (Symons et al., 1990). Dispersed, invisible but free gold of high fineness (990+) is in the three top zones of the profile where it forms a semicontinuous blanket 3 to 12 m thick. This stores some 30% of supergene gold. The gold mostly precipitated at a redox front near the Cenozoic water table. 70% of the gold reserve was in the lower clay and saprolite where the Au content was highly variable. Auriferous clay mixed with mineralized relics of the primary veins and goethitic gossanous material.

In the early stages of mining, the hypogene materials recovered from drill core suggested porphyry-style mineralization related to early synvolcanic intrusions, particularly of the diorite Cu-Au model (Symons et al., 1990). As the pit progressed and the unweathered materials became available, that model has been substituted by the late stage "orogenic-Au" model in which mesothermal fluids, channeled by the D4 faults, may have been coeval with the emplacement of synorogenic granitoids at 2,611 Ma in the area, without being genetically related to them (Allibone et al., 1998). Boddington orebodies are multistage, hosted by a variety of rocks formed during five

phases of igneous activity between about 2.714 and 2.611 Ga. The host rocks include greenstone basalt, andesite, minor felsic volcanics, two suites of ultramafic dikes (komatiitic pyroxenite), synvolcanic high-level monzodiorite, and a great variety of fault rocks ranging from mylonite, phyllonite to brittle breccias and complicated by hydrothermal alteration. These have all been cut by the late orogenic plutons, and again by Paleoproterozoic post-ore diabase dikes and sills. Several generations of hydrothermal alteration and veining have been recorded, of which only the latest veins and stockworks, related to evolution of the D4 faults between 2,675 Ma and 2,611 Ma, represent economic ore (Allibone et al., 1998). The veins are non-foliated and crosscut three generations of ductile shears, some previously mineralized. The veins are dominated by quartz with variable contents of pyrite, molybdenite, chalcopyrite, pyrrhotite, gold, and silicates clinozoisite, biotite and actinolite. The same silicates provide alteration haloes.

Sigma-Lamaque mines, Val d'Or goldfield, Quebec (Robert and Brown, 1986; 291 t Au). These two adjacent mines have been the largest gold producers in the Val d'Or "camp" in the Québec portion of the Abitibi Subprovince. They are also about the youngest among the Abitibi "shear-Au" deposits, dated between 2.592 and 2.579 Ma (Fyon et al., 1992) that is some 90 m.y. later than emplacement of the major synorogenic plutons in the area. At Sigma, gold is in a vein network in Archean (2,705 Ma) meta-andesite intruded by comagmatic porphyritic diorite and slightly younger swarm of feldspar porphyry dikes, then by

synorogenic quartz diorite. Lamaque is famous for its "ladder veins" in a diorite dike. The orebodies range from laminated low-sulfide gold-quartz veins in shears to quartz-tourmaline extensional veins, breccias and stockworks extending from shears into brittle rocks. The narrow alteration envelopes around veins have inner pyrite-sericite, sometimes with ore-grade gold concentrations, and outer carbonate (ankerite) zones. Albite is locally present. The close association of diorite plugs and dikes with some orebodies resulted in several interpretations of magmatic-hydrothermal or two-stage origin of the veins, but Robert and Brown (1986) demonstrated, by cross-cutting relationships and replacement of metamorphic minerals by the mesothermal alteration assemblage, the post-metamorphic peak emplacement of these veins.

Gold veins in syenite and trachyte

In the Abitibi Subprovince, potassic (shoshonitic) volcanics occur at the top of some pre-orogenic volcanic cycles. The most widespread K-alkaline rocks in Abitibi are, however, closely associated with the "breaks" (prominent deformation zones), especially the Larder Lake-Cadillac "Break". There the trachyte and syenite are in, and interact with, Timiskaming synorogenic sediments (Cooke and Moorhouse, 1969). In addition to true volcanic and plutonic rocks, however, there is a wide range of potassic (K-feldspar) and sodic (albite) metasomatites, usually pigmented by hematite (hence orange, brick red or maroon in color) that have the form of diffuse fronts gradually altering and replacing adjacent rocks, especially Timiskaming graywacke. Some metasomatites mimic the magmatic rocks (pseudotrachyte, pseudosyenite) from which they are virtually unrecognizable (Fig. 9.30).

Kirkland Lake, Ontario (Ward et al., 1948; Kerrich and Watson, 1984; 786 t Au; Fig. 9.31) is the largest goldfield in the Abitibi in this association. The north-east striking mineralized zone is controlled by a steeply south dipping thrust fault, 2 km north of and subparallel with the regional Larder Lake-Cadillac Break. The host rocks are syenite, augite syenite and syenite porphyry intruding and locally replacing conglomerate and graywacke of the ~2.68 Ga Timiskaming Group. At least a portion of the "trachyte tuff" is probably a (partial) K-metasomatite. The Main ore zone is, for much of its 5 km long course and explored depth to almost 3,000 m, a clean-cut fault represented by a single fault plane, locally changing into a set of two or

three planes or into a bow-like arrangement of parallel and crossover faults up to 600 m wide. Because of the brittle host rocks the amount of mylonite fill and wallrock "schisting" is minimal, which accounts for the "clean" nature of the low sulfide gold-quartz veins. The veins of white quartz with some carbonate have narrow sericitic and silicification envelopes, and broader carbonatization zones. They range from single dilational veins through composite veins to mineralized brittle fault breccias and stockworks. The largest, continuous stopping length of ore measured 2,150 m. Gold was present as scattered coarse native gold and in tellurides, in the company of pyrite with minor galena, sphalerite, chalcopyrite and arsenopyrite. The sulfide content has never exceeded 2% of the vein filling. During the period of vigorous mining in the first half of the 20th century, there were seven operating properties of which the Lake Shore Mine alone was a "giant", having produced 265 t Au. By now the Kirkland Main ore zone is almost exhausted.

Metasediments-hosted gold lodes

Homestake Mine, Lead, South Dakota (Noble, 1950; P+Rv ~160 mt ore containing 1,319 t Au, ~420 t Ag, at least 1 mt As; Fig. 9.32). This was the largest gold producer in the United States, until the development of the Carlin Trend in the 1980s. It is a widely quoted example of a gold system controlled by combined stratigraphy/lithology and structure, in a Paleoproterozoic "schist" (that is, metasediments-dominated) belt. The northern Black Hills is a part of a basement uplift near the centre of the North American Platform, reactivated in the early Tertiary. In the NW Black Hills, near Lead and Deadwood, up to 3.5 km thick Paleoproterozoic succession of monotonous phyllite, quartzite and local graphitic schist rest on Archean basement and a thin rift association. This is topped by a 60 to 100 m thick chemical metasedimentary unit (silicate-carbonate "banded iron formation"), the Homestake Formation, that hosts the Au ore zone. Above is a 1.97 Ga interbedded quartzite and phyllite with minor meta-chert, BIF and meta-basalt terminated by a gray sericitic phyllite. The succession is polyphase deformed and metamorphosed to biotite or staurolite grades. The Precambrian rocks are deeply eroded and unconformably capped by Late Cambrian basal limestone and dolomite conglomerate, siltstone and shale that change upward into a succession of platformic sediments. These represent, with several hiatus, all systems between Ordovician and Jurassic.

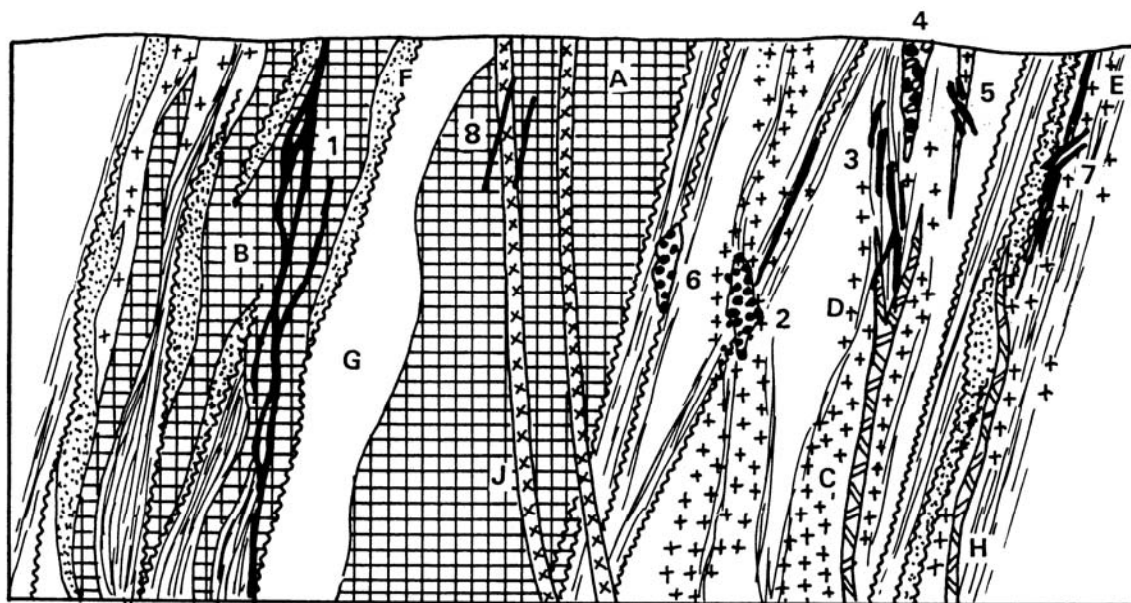


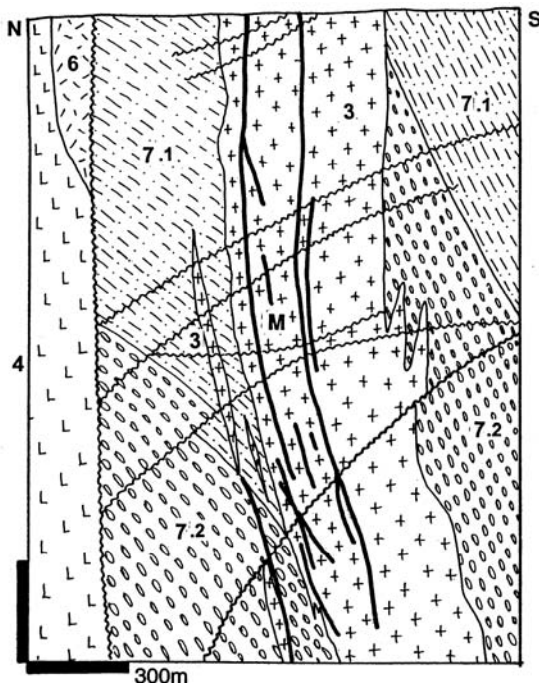
Figure 9.30. Lithology and ore styles in the Archean trachyte-syenite (alkaline, shoshonitic) association as in the western Abitibi Subprovince, NE Ontario. Diagrammatic and not to scale, from Laznicka (1991); also Laznicka (1993, p.442).

- A. Massive, internally homogeneous brittle syenite or monzonite plutons and stocks, sharp contacts
- B. Composite anastomosing sheets of feldspar syenite, augite & contaminated syenite, porphyry; sharp to diffuse contacts
- C. Minor stocks, dikes of syenite or syenite porphyry, sharp to diffuse contacts
- D. Zones of diffuse feldspathization along discrete syenite intrusions
- E. Ditto, along fault zones and shears
- F. Trachyte; can be partly or completely feldspathized supracrustals or fault rocks
- G. Archean mafic metavolcanics, mostly greenstone basalt, komatiite
- H. Lamprophyre dikes; most are intensely altered (K- and Na-feldspathized)
- J. Post-tectonic diabase dikes
- 1. Extensive fissure vein systems in brittle syenite and alteration-indurated wallrocks (Kirkland Lake)
- 2. Disseminated Au-pyrite in syenite porphyry and metasomatic feldspathites
- 3. Shear and fracture veins and vein systems in altered supracrustals intruded by K- and Na- feldspar porphyries
- 4. Breccia pipes with scattered auriferous pyrite in groundmass
- 5. Stockworks and disseminations of pyrite, chalcopyrite, molybdenite in and near syenite stocks
- 6. Disseminated to massive pyrite > chalcopyrite, Au in silicified supracrustals near syenite
- 7. Extensive linear fault-controlled zones of strong alteration and metasomatism along structural breaks. Au is in metasomatized ductile-brittle shears or in fractures (Kerr Addison)
- 8. Small fracture veins of Au with quartz, barite, carbonates, minor Cu, Zn, Pb sulfides

Both the basement and cover have been intruded by Lower Tertiary stocks, laccoliths, sills, and dikes of high-level anorogenic monzonite, rhyolite, phonolite and aegirine rhyolite.

The Deadwood-Lead district started as a gulch placer goldfield. Of the bedrock gold 94% was stored in the Homestake Mine and the rest came from numerous, though small, replacement and vein deposits related to Tertiary magmatism. The district is an outstanding example of "inheritance metallogeny" as it is believed that gold in the Phanerozoic deposits was recycled from the Homestake system (Norton, 1989).

The Homestake As-Au ore zone is controlled by an about 12 km long fold structure in the Homestake Formation composed of graphitic ankerite ("sideroplesite") schist, an "exhalite" that changes with increasing metamorphic grade into cummingtonite-quartz schist. Redden and French (1989) considered the 1.97 Ga Homestake Formation as the original source of gold, later deformed and metamorphosed at around 1.6 Ga. Metamorphic remobilization produced the actual orebodies that are elongate, very irregular pods of ore that form "ledges" in the tectonically thickened Homestake Formation along SE-plunging crossfolds. The latter, in turn, modify earlier NNW-

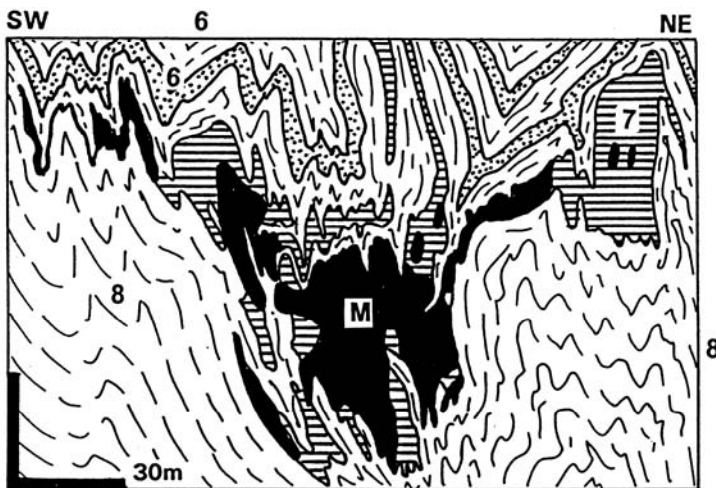


M. Ar arrays of steep, subparallel synorogenic multistage gold-quartz veins along faults and brittle fractures in syenitic rocks

Ar3 (2686-2677 Ma) Timiskaming Assemblage:

- 3. Syenite, syenite (feldspar) porphyry
- 4. Augite syenite to syenogabbro
- 6. Trachyte to trachybasalt flows, tuff, agglomerate; some "trachytes" are feldspathized clastics
- 7.1. Turbiditic litharenite
- 7.2. Polymictic conglomerate

Figure 9.31. Kirkland Lake goldfield, Ontario, cross-section through the former Wright-Hargreaves Mine. From LITHOTHEQUE No. 451, modified after Ward et al. (1948) and Hopkins (1949)



M. ~1.84 Ga synorogenic mesothermal quartz, siderite, grunerite, arsenopyrite, gold "ledges" stratabound to Unit 7

- 6-8 Pp Homestake Schist Belt, metaturbidites with chemical sedimentary units:
- 6, metaquartzite, schist
- 7, 2.0 Ga Homestake Fm., siderite-grunerite (cumingtonite) iron formation
- 8. Poorman Fm., phyllite to schist

Figure 9.32. Homestake Mine, Lead, South Dakota; cross-section of a portion of the No. 9 Ledge from LITHOTHEQUE No. 494, modified after Noble (1950)

striking folds. The ore consists of disseminations, scattered grains, blebs, veinlets and small masses of pyrrhotite, pyrite and arsenopyrite in matrix of recrystallized "chert", ankerite schist or cumingtonite-garnet-biotite schist. Visible gold is rare in the richest intervals only. There was an oxidation zone with low-grade residual gold in

"limonite" mined from an open pit at the end of the mine lifetime.

The largest of the Lower Tertiary satellite hydrothermal deposits adjacent to Homestake is Bald Mountain, 4 km W of Lead (Norton, 1989; P+R 215 t Au). The Carlin-type ore there is in subhorizontal ore shoots in Cambro-Ordovician

dolomitized limestone above, or immediately at, the sub-Cambrian unconformity. The ore zone is confined by impervious shale. The ore replacements (mantos) are up to 1.5 km long, 100 m wide and 6 m thick and are adjacent to subvertical brittle deformed columns interpreted as feeders of hydrothermal fluids. The submicroscopic gold resides in fine-grained disseminated pyrite replacements in partly silicified dolomite (jasperoid). Much of the ore has been oxidized into hematite- or goethite-rich material with low-grade refractory gold, amenable to heap leaching.

Obuasi (Ashanti) goldfield, Ghana (Oberthür et al., 1996; P+Rc 1,275 t Au @ 22.5 g/t Au, min. 1.2 mt As @ 1.4-4.1% As; Fig. 9.33). This is the richest goldfield in Ghana, and the largest (syn)orogenic-Au in Africa. Located about 80 km south of Kumasi the goldfield is in low-grade metamorphosed, folded and cleaved turbidites of the 2.2-2.1 Ga Birrimian Supergroup (Leube et al., 1990). The almost continuous orebodies are controlled by a 8 km long NNE-trending shear zone in litharenite and graphitic phyllite, sporadically intruded by diabase and gabbro dikes that resemble, after shearing and alteration, mafic meta-volcanics. Up to 50 m wide orebodies consist of low-sulfide quartz lodes with scattered free-milling gold. The sulfides are arsenopyrite, minor pyrite, sphalerite, galena, tetrahedrite, chalcopyrite and rare tellurides. The quartz veins are enveloped by quartz, sericite, chlorite, carbonate-altered mylonitic and phyllonitic wallrocks (especially black graphitic phyllonite and gouge), impregnated by disseminated arsenopyrite that stores "invisible" gold. There is a thin oxidation zone with residual gold.

"Sulfidic schist" orebodies

Mineralized "K-feldspar schist" at the "large" Big Bell deposit in Western Australia (Handley and Cary, 1990; 103 t Au @ 3.4-7.8 g/t Au, 34 g/t Ag) puzzled geologists for some time, but it was not until the Hemlo discovery that "sulfidic schist Au-deposits" have become a popular exploration target. Card et al. (1989) defined this type as one "characterized by a dominance of sulfide mineralization over quartz veins and by a paraconcordant position within their host volcanic-sedimentary sequence", with "ores (that) typically comprise disseminated and vein pyrite in sericite schists, which are the result of potassium metasomatism".

Hemlo gold deposit (Hugon, 1986; Kuhns et al., 1986; Muir et al., 1995; 632 t Au @ 8.2 g/t, 70 kt Mo @ 0.16% Mo, 3.8 mt BaSO₄) has been proven

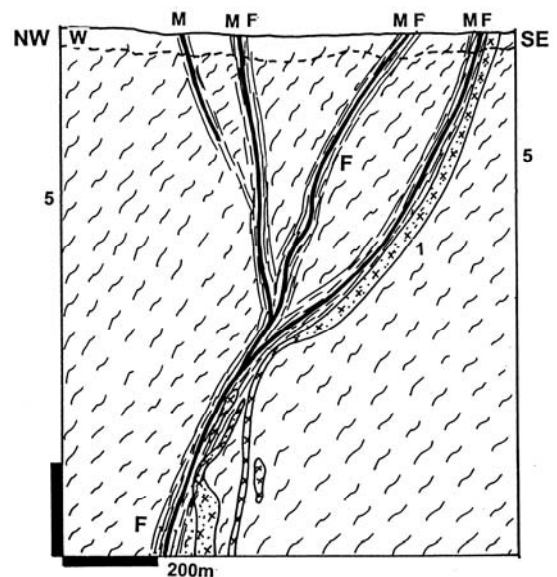


Figure 9.33. Obuasi (Ashanti) ore field, Ghana, cross-section from LITHOTHEQUE No. 2779, modified after Gyapong and Amanor (2000). W. Tropical humid regolith; M. Gold-quartz lodes with free-milling gold and minor Fe,Pb,Zn,Cu sulfides enveloped by sheared wallrocks with disseminated auriferous arsenopyrite. F. Fault rocks (mylonite, phyllonite); 1. Massive to sheared diabase; 5. Pp Lower Birrimian turbiditic volcanoclastics

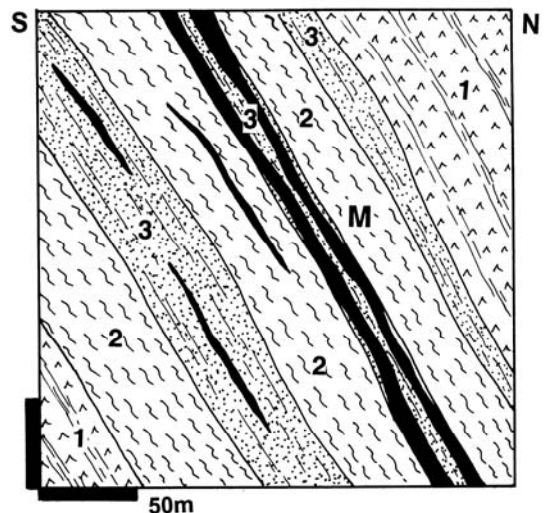


Figure 9.34. Hemlo ore zone, Ontario, cross-section of the Page-Williams Mine; from LITHOTHEQUE No. 2285. Modified after Burk et al. (1986) and Kuhns et al. (1994). 2.772-2.695 Ga units of the Cedar Lake Formation. 1. Hornblende-biotite schist to amphibolite; 2. Biotite schist to granofels with local Ca-Mg silicates; 3. Muscovite-microcline schist to granofels, locally with kyanite, sillimanite, V-Ti muscovite. M. Quartz, pyrite, gold disseminated foliation parallel orebodies locally with molybdenite and barite band

in the early 1980s on site of a perennial prospect partly transected by the Trans-Canada Highway, and it became the largest gold deposit developed in Canada in fifty years (Fig. 9.34). Hemlo is 35 km east of Marathon, central Ontario, in a local Archean (~2.77 Ga) greenstone belt that is a part of the Wawa Subprovince, Canadian Shield. The WNW-ESE trending, 3 km long and about 500 m wide, steeply north dipping Hemlo ore zone supports three underground properties. The ore zone, close to and parallel with the Hemlo Shear Zone, is in tightly folded volcanoclastics with a "porphyry" unit, but because the rocks had been multiphase deformed and metamorphosed (prograde amphibolite grade, locally retrograde greenschist overprint), then feldspathized, there is a great deal of lithologic mimicry and uncertain rock identifications. Post-ore feldspar porphyry and diorite dikes, however, intersect the ore zone and the 2.69 Ga synorogenic Cedar Lake pluton is less than 1 km north of the ore zone.

The Main ore zone is a persistent tabular body traceable through all three properties. On the Golden Giant property (Kuhns et al., 1986) the zone is 24 m wide on the average and it has been explored for 1,500 m downdip. It has the following composition (from hangingwall to the footwall):

1. Banded quartz- or feldspar-rich biotite schist to granofels with hornblende-rich to amphibolite bands. Garnet and lesser staurolite porphyroblasts are common and there are abundant chloritized and bleached retrograde bands.
2. Bands of a whitish quartz-muscovite & feldspathic schist ("rhyolite") appear. The Barich microcline forms porphyroblasts, veinlets and indurated rock layers that have the appearance of porphyry.
3. The schist becomes thinly foliated (phyllonitic) and finely dispersed bluish molybdenite appears. Molybdenite smeared on numerous slip surfaces, sometimes with spots of orange realgar, gives the rock an appearance of a graphite schist. Gold values start to appear. Massive Ba-microcline, quartz, muscovite, green roscoelite (V-muscovite) and rutile granofels are often brittly fragmented and the fragments cemented by barite, pyrite, quartz or sulfides. Quartz pods may carry stibnite or cinnabar.
4. Fine quartz ("chert") impregnated by molybdenite with pyrite and white crystalline bands and swelling lenses of barite appear. A green vanadian muscovite forms thin seams in muscovite schist. Disseminated pyrite carries

gold and rare scattered grains of native gold and aurostibnite are also present.

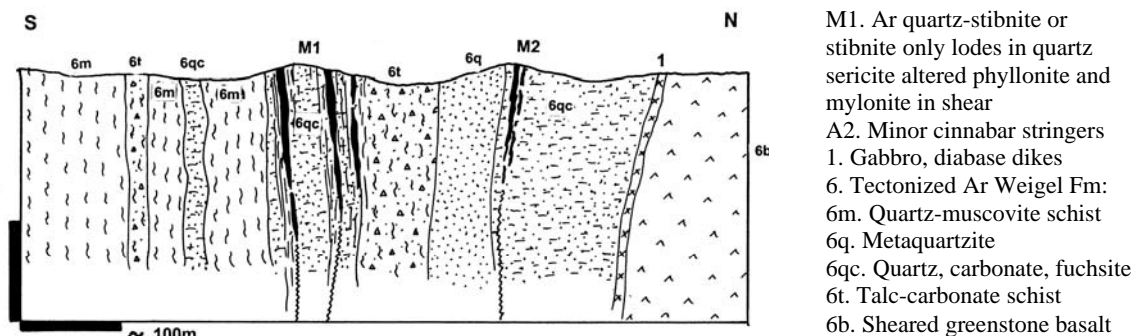
5. Feldspar porphyroblasts in schists increase in abundance to form a pseudo-porphyry, subdivided by quartz-muscovite schist seams and some tourmaline. Genuine strained porphyry sills may also be present.

Local ore varieties at Hemlo include fracture stockworks of auriferous pyrite with molybdenite in low-strain areas, and an up to 30 cm thick zone of massive pyrite, lesser pyrrhotite and arsenopyrite at the Page-Williams property. The shorter ore zones parallel with the Main zone are comparable, but less complete. Hemlo mineralogy and geochemistry are certainly unconventional and hard to explain, especially for the presence of minerals characteristic for the low-temperature, low-pressure associations like realgar and cinnabar. The average composition of Hemlo gold grains is 86.2% Au, 6.5% Hg and 5.9% Ag (Harris, 1986). Hemlo has been blessed with a rich collection of genetic interpretations in the literature. It is most likely a pre-metamorphic mineralization, extensively remobilized.

Synorogenic Sb-Au deposits in Archean greenstone belts

Other than arsenic that forms several unreported "geochemical giants" among the "shear-Au" deposits, antimony is a metal frequently present in minor amounts (e.g. in the Balmertown ore zone, Ontario; in the "large" Wiluna goldfield, Western Australia; in the Kadoma and Kwekwe goldfields, Zimbabwe), but rarely recovered. The Murchison greenstone belt in former Transvaal, NE South Africa, is an exception as it hosts a "Sb-supergiant" that is a variant of the Archean "shear-Au" style anomalously enriched in Sb and also Hg, with only minor gold.

Antimony Line, Murchison Goldfield near Gravelotte (Pearson and Viljoen, 1986; 640 kt Sb, 44 t Au; Fig. 9.35) has been a significant antimony producer, second largest after Xikuangshan in China. The Line coincides with a high-strain zone with prominent ENE-trending schistosity, fold axes and cleavage. All Sb (Au, Hg) orebodies are in the Weigel Formation composed of multiphase deformed, metamorphosed and hydrothermally altered members of an about 3.0 Ga komatiitic and tholeiitic association. The host rocks, as they are now, are chloritic schist, meta-quartzite, muscovite schist, talc-chlorite schist, carbonatized komatiite, banded iron formation and strained greenstone. The Antimony Line ore zone is in locally pyritic,



M1. Ar quartz-stibnite or stibnite only lodes in quartz sericite altered phyllonite and mylonite in shear
 A2. Minor cinnabar stringers
 1. Gabbro, diabase dikes
 6. Tectonized Ar Weigel Fm:
 6m. Quartz-muscovite schist
 6q. Metaquartzite
 6qc. Quartz, carbonate, fuchsite
 6t. Talc-carbonate schist
 6b. Sheared greenstone basalt

Figure 9.35. Antimony Line, South Africa, cross-section through Weigel and Monarch-Hg mines. From LITHOTHEQUE No. 260, based on Pearton (1986), Pearton and Viljoen (1986), site visits

talc-carbonate and silica-carbonate metasomatized ultramafics enclosed in quartz-chlorite and quartz-muscovite schist (phyllonite). Fuchsite is widespread. Although high trace Sb contents occur throughout the entire zone, the mineable orebodies are in several discontinuous carbonate-rich nodes. There, the orebodies are zones of quartz veining with stibnite disseminations, stringers and discrete quartz, carbonate, stibnite lenses.

The largest single Sb-Au deposit is the Alpha-Gravelotte complex (Abbott et al., 1986; $P_{to 1948}$ 446 kt Sb @ 5%, 10 t Au). There, stibnite with lesser berthierite, pyrite and minor amounts of Fe, Ni, Co arsenides, scheelite and gold, occur in zones of irregular quartz veining and breccia cementation in a "cherty", green to gray magnesian and fuchsitic quartz-carbonate and talc-carbonate metasomatized komatiite. All orebodies are in a steeply north dipping, up to 200 m wide zone. The largest Gravelotte Main Reef is several meters thick tabular body, 650 m long. The small Monarch cinnabar mine (240 t Hg @ 0.16% Hg; Pearton, 1986) is a metallogenic curiosity as it is the world's oldest Hg deposit. It is a short schistosity-parallel zone of disseminated and stringer cinnabar with some Sb and Cu sulfides in a structure adjacent to and parallel with the Antimony Line. The host rocks are quartz, ankerite and fuchsite altered, quartz veined, schisted komatiitic meta-basalts.

9.7. Synorogenic Cu (U, Ni, Au, Ag) deposits overprinting greenstone belts

Small chalcopyrite deposits and occurrences, usually with pyrrhotite or pyrite, are ubiquitous where hydrothermally altered shears intersect metabasalt greenstones (Ni in pentlandite is additional where the hosts are peridotitic komatiite

or ultramafic intrusions). An examples of a "large" deposit is the Thierry Mine near Pickle Lake, Ontario (216 kt Cu, 13.7 kt Ni, 72 t Pd). Similar ore style is also common in the "paleorift" setting, reviewed in Chapter 12. "Giant" Cu accumulations are uncommon, although the Singhbhum Cu belt and the Salobo deposit can be placed into this category. The former, however, although often referred to as a "world class deposit", is a 200 km long mineralized structure, hence a "giant Cu belt".

Singhbhum Copper Belt, Bihar, India (Sarkar, 1982; 3.5 mt Cu @ 0.74-2.5% Cu, 54 kt U, 40.35 kt Ni in 14 larger deposits) used to be the main source of Indian copper before Malanjkhand discovery. It is a multiphase, 30° to 50° north-dipping ductile overthrust system ranging from several hundred meters to 15 km in width, along which a Paleoproterozoic (2.4 to 2.3 Ga) greenstone belt-style volcanic-sedimentary sequence had been thrust over the Archean Singhbhum Craton. Copper and the less important uranium mineralization occur discontinuously along almost the entire length of the structure in 500m to 9,000 m long intervals.

All Cu orebodies are hosted by ductile, altered tectonites formed in place of 2.3 Ga metabasalts (Dhanjori Volcanics) and, to a lesser degree, metapelitic schist. The ore shears are filled by biotite-chlorite-quartz and locally muscovite phyllonite grading to "epidiorite" (tectonized metabasalt with albite porphyroblasts), and into partially to fully albitized equivalents ("soda granite" of the earlier authors). The "copper lodes" are several centimeters to meters thick, up to several kilometers long sheets or lenses of ore-grade tectonites. Between Badia and Surda the continuously mineralized interval is 8 km long. Two parallel Cu lodes are mined in the Mosaboni

Mine, four at Pathagora, and up to nine in Rakha. The principal mineral is chalcopyrite with variable amounts of pyrite and pyrrhotite, with locally present magnetite, ilmenite, pentlandite, uraninite, molybdenite and other minerals. The minerals occur as disseminations, scattered pyrite porphyroblasts, stringers and braided veinlets subparallel with foliation and strain-slip cleavage planes of the host tectonite. Sulfide nests, small masses and late stage fracture veins occur locally.

Mosaboni, 45 km SE of Jamshedpur (Sarkar, 1982; 740 kt Cu @ 1.7% Cu; Fig. 9.37) is the oldest continuously operating mine in the belt. It has two lode zones 20-50 m apart, dipping 25-30° NE, peneconcordant with foliation and up to 11 m thick. The continuous orebody is about 7 km long and 2 km wide. In the footwall is the moderately deformed to epidioritic Dhanjori metabasalt, whereas the hangingwall has gneissic albitite overlain by metasedimentary schist with metaquartzite interbeds. The ore shear is between 500 and 1000 m wide and filled by biotite-chlorite phyllonite gradational into sheared albitite with lozenge-shaped massive albitite resister blocks. Chalcopyrite, pyrite and pyrrhotite form stringers in chlorite schist, and veinlets, blebs and bunches along margins of quartz and albitite lenses. The nearby **Rakha Mine** (1.5 Mt Cu @ 1.02% Cu) has the largest Cu reserve in the Singhbhum Copper belt and up to nine orebodies 1-9 m thick and up to 2 km long.

The Singhbhum shear zone also contains the bulk of Indian uranium resources, although of low grade. Uraninite with minor magnetite, allanite, xenotime, millerite and other minerals are disseminated in phyllonite and merge with the copper lodes (some 11,500 t U has accumulated in the Mosaboni mill tailings). The most important predominantly U deposits (Jaduguda, Jublatola) are stratigraphically higher than copper, in tectonized metasediments. Ni sulfides are present in sectors where the shear overprints komatiites and there are scattered occurrences of magnetite with apatite and xenotime.

(Igarapé Salobo deposit (Vieira et al., 1988; Villas and Santos, 2001; Rc at 0.4% Cu cutoff: 1.3 bt @ 0.74% Cu, 0.43 g/t Au for 9.62 mt Cu, 559 t Au, ~156 t Ag, ~70 kt Mo, min. 300 mt Fe) is the largest copper and gold deposit in Brazil (Fig. 9.36). It is located in the Serra dos Carajás mineral province of SE Pará, in Amazon jungle 60 km WSW of the Carajás townsite. The host sequence is a NW trending multistage ductile to brittle deformation zone superimposed on Archean greenstone-style assemblage of amphibolite

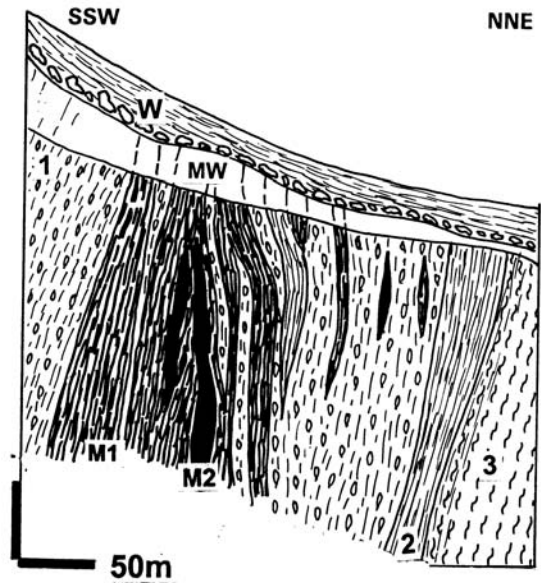
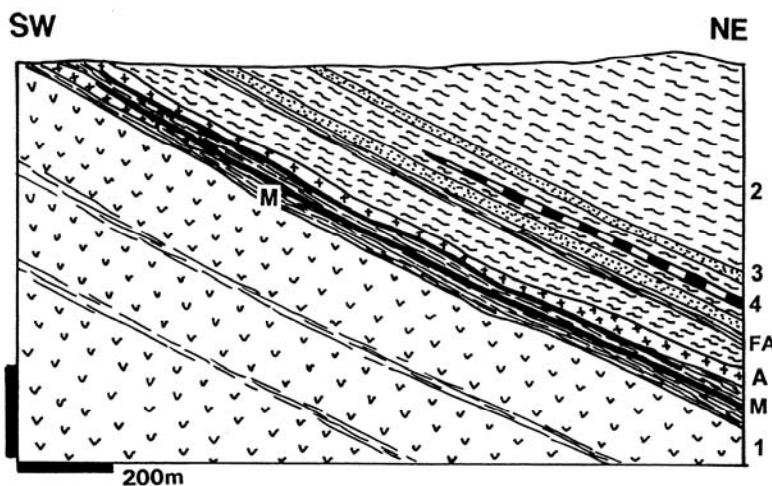


Figure 9.36. Igarapé Salobo Fe-Cu-Au deposit, Pará, Brazil; cross-section from LITHOTHEQUE No. 1969, modified after Farias and Saueressig (1982) and Vieira et al. (1988). W. T-Q regolith, colluvium; MW. Oxidation and secondary sulfides zone; M. Lenticular and sheet-like bodies of magnetite with disseminated chalcocite, bornite > chalcopyrite and sulfide stringers in schist. Mineralized retrograded and altered (feldspathization, biotite, grünerite, biotite) shear. M1, ~10-50% magnetite; M2, massive magnetite. Ar Igarapé Salobo Group, phyllonitic schists: 1. Porphyroblastic biotite, garnet, amphibole, quartz schist; 2. Fine-grained, lepidoblastic plagioclase-biotite-amphibole schist; 3. Chloritized biotite (sillimanite) gneiss

(metabasalt), metagraywacke schist and metaquartzite intruded by 2.57 Ga granitoids. This assemblage forms a relic surrounded by the Xingú basement complex. The Salobo deposit is a 4000 m long NW-SE trending zone of subvertical lenticular replacement bodies of massive to disseminated magnetite in mylonite overprinted by coarse ("pegmatoidal") alteration assemblage of K-feldspar, biotite, oligoclase, grünerite-cummingtonite and garnet, followed by retrograde chloritization. The ore minerals: chalcocite, bornite, chalcopyrite with minor molybdenite postdate magnetite in which they are enclosed, or they are disseminated and as stringers in the silicates. There is a 60 m thick regolith with relics of martitized magnetite in an earthy saprolite with largely "invisible" copper values (Rv 107 mt @ 0.75% Cu). There, copper resides in interspersed hydrous ferric oxide and partly in hydrated biotite (Veiga et al., 1991). The latest genetic interpretation favors granitoids-related synorogenic ore emplacement



1. ~2.3 Ga Dhanjori metaarenite, amphibolite; 2. ~2.3 Ga Chaibasa biotite schist; 3. Ditto, metaquartzite; 4. Ditto, magnetite and magnetite-apatite band and lenses;

M. ~1.68-1.63 Ma schistosity-conformable tabular zones of disseminated to stringer Cu,Fe>Ni,Mo sulfides in quartz, chlorite, biotite-altered phyllonitic schist in ductile shear;

A. ~2.2 Ga massive albitized "Soda Granite";
FA=altered fault rocks

Figure 9.37. Mosaboni Mine, Singhbhum Copper Belt, Bihar, India. Cross-section from LITHOTHEQUE No. 1814, modified after Sarkar (1982), Hindustan Copper Ltd. materials and on-site visit, 1987

corresponding to the Fe oxide-Cu-Au "family". The more recently discovered "giants": Alemão deposit in the Igarapé Bahia ore field (170 mt @ 1.5% Cu, 0.8 g/t Au for 2.55 mt Cu and 136 t Au) and Cristalino (Rv 200 mt @ 1.6% Cu and 0.25 g/t Au for 3.2 mt Cu and 500 t Au), both briefly described by Villas and Santos (2001) are also in greenstone setting in the Carajás province and presumably of similar origin.

9.8. Ores in late orogenic sedimentary rocks in greenstone belts

Alluvial to shallow marine mature sedimentary rocks, comparable with the alpine molasse, postdate most orogenies and settle in intermontane and/or foreland basins of greenstone-dominated foldbelts as one of the latest lithofacies. Although the frequency of occurrence and outcrop area of the Precambrian "molasse" increases with decreasing age, the earliest lithofacies with "molasse" characteristics is the 3.2-3.3 Ga Moodies Group in the Barberton Mountain Land, Kaapvaal Craton (Tankard et al., 1982). This is a shallow water succession of immature to submature quartz-rich litharenite and feldspatic quartzite with local intervals of supermature quartz arenite. It rests unconformably on (or has fault contacts with) greenstones of the Onverwacht Group and/or turbidites of the Fig Tree Group, and there are rare intervals of jaspillite, banded iron formation and volcanics. The Group is a passive host to mostly small orogenic Au-vein deposits. The only

stratigraphy/lithology controlled ore type to be expected in this setting is a Witwatersrand-style gold paleoplacer (read Chapter 11). A dozen of occurrences and small deposits of this type have been recorded, but the only "giant" recognized so far is the Tarkwa Goldfield in Ghana.

Tarkwa Goldfield (Sestini, 1973; Milési et al., 1992; $P_{to 2000}$ 250 t Au @ 6 g/t, Rc 420 t Au @ 1.3 g/t) is the second largest goldfield in Ghana, and the only gold conglomerate "giant" outside of the Witwatersrand (Fig. 9.38). The mature, shallow water clastics are members of the 2.1 Ga Tarkwaian System, a 250 km long SW-NE synclinal "basin" that rests unconformably on the Birrimian greenstone-schist belt. The latter is richly mineralized by lode gold deposits throughout. The molassic sediments have been deposited in a collision-generated basin and deformed by transcurrent faulting shortly afterwards.

In Tarkwa and in the adjacent Teberebie, Iduapriem and Abooso sectors the Tarkwaian is up to 2,400 m thick succession of litharenite, metaquartzite, phyllite and minor conglomerate. The gold mineralization is confined to the 120-600 m thick Banket Member situated in about mid-section. It consists of fine to medium-grained mature sericitic quartzite with a number of conglomeratic lenses and horizons ("reefs"). In Tarkwa there are three persistent subparallel "reefs" with the bulk of gold in the Basal Reef. In Teberebie there are up to five reefs, two of which are marginally economic. Metamorphic grade ranges from greenschist to lower amphibolite and

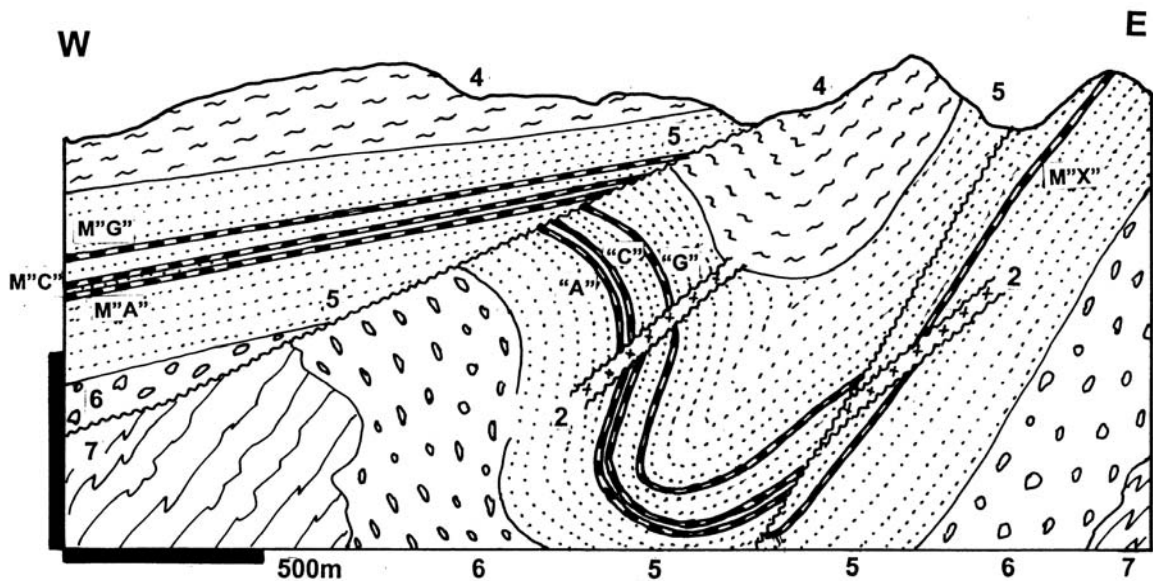


Figure 9.38. Tarkwa Au deposit, Tarkwa Syncline western limb; cross-section from LITHOTHEQUE No. 2799, modified after Gold Fields Ghana Ltd., 2001. 2. Pp diabase sill and dike (post-ore); Pp Tarkwaian Group; 3. Huni fine feldspathic quartzite to phyllite; 4. Tarkwa phyllite; 5. Banket Series, quartzite with units of quartz-pebble conglomerate that includes M: sparsely disseminated gold in matrix of quartz conglomerate in four "reefs"; A=Main Reef; B=B Zone Reef; C=West Reef; G=Breccia Reef; X=Composite Reef. Pp Kawere Group, metagraywacke, phyllite, polymictic conglomerate; 7. 2.2-2.1 Ga Birrimian Supergroup basement, a greenstone-schist belt

there are numerous diabase and gabbro bodies emplaced into the ore interval.

The Basal Reef contains two to ten 1 to 10 m thick discontinuous lenses of mature conglomerate, composed of 90% rounded quartz pebbles in quartz, hematite, sericite, magnetite matrix. The hematite content ranges from 2 to 60% and is interpreted as a product of oxidation of original clastic magnetite, later recrystallized to euhedral grains and porphyroblasts (Milési et al., 1989). The conglomerate lenses pass laterally into crossbedded pebbly meta-arenite. The Middle Reef has higher content of angular schist fragments and hematite or martitized magnetite seams with small scale crossbedding. The uppermost Breccia Reef has abundant angular fragments of locally recycled schist and phyllite.

Gold in Tarkwa forms small (10-15 microns) equidimensional grains. It is most common in the matrix of conglomerate that contains more than 20% of hematite. The gold grade varies and the traditional underground ore with about 6 g/t Au came from several cm to 2 m thick shoots near the floor of the Basal Reef. The modern open pits mine and process the reefs in bulk, achieving grades between 1 and 2 g/t Au. As in the Witwatersrand, over 80% of the gold particles are neoformed,

synmetamorphic and contemporaneous with the S2 schistosity (Milési et al., 1989), so the paleoplacer origin is occasionally questioned.

The Damang Au deposit, situated on the eastern limb of Tarkwa Syncline and recently mined from an open pit, has an interesting style. The host is the Banket conglomerate, enclosed in fine-grained feldspathic quartzite to phyllite grading to pebbly wacke. These metasediments are interbedded with phyllite to chloritoid schist, and intruded by a set of gabbro (diabase) sills. The conglomerate contains erratic gold disseminated in the matrix, that is economically recoverable only from oxidized material with >1 g/t Au. The main gold production is derived from altered wallrocks adjacent to late (D3) subhorizontal dilational sheeted quartz veins controlled by easterly-dipping thrusts. The veins are barren whereas gold resides in pyrite > pyrrhotite disseminated in quartz, sericite, chlorite, biotite and carbonate-altered wallrocks. The average grade is 2.09 g/t Au and the sulfides are believed to be the result of hydrothermal sulfidation of clastic magnetite and/or hematite.

10 Intracratonic Orogens, Granites, Hydrothermal Deposits

10.1. Introduction

This chapter emphasizes predominantly hydrothermal metallic deposits in orogenic belts presumably related, directly or indirectly, to granitoids emplaced into a thick, mature continental crust as a consequence of collision and crustal extension. The emphasis is on the rock-ore association rather than process, hence (syn)orogenic deposits in- or related to granitoids appear here, whereas comparable deposits in, for example, Precambrian greenstone belts appear in Chapter 9. The boundary of the present category against largely subduction-related Cordilleran granitoids (Chapter 7) is vague as there are transitional types that would fit equally well into either category. Anorogenic granitoids are included here, but strongly alkaline rocks with feldspathoids are considered in Chapter 12. The supracrustal rock associations that form basement or cover to the syn- and postorogenic granitoids and to hydrothermal deposits are reviewed in separate Chapters 8 and 13 for the volcanic-sedimentary ("eugeoclinal") and nonvolcanic ("miogeoclinal") mega-facies, respectively.

Orogenic belts and systems (orogens) are linear belts of deformed, variously metamorphosed and commonly granitoid-intruded rocks, of usually continental or multi-continental magnitude. They are one of the pillars of regional geology and global geotectonics and although their descriptions have changed little in the past hundred years, their interpretation continued changing, most profoundly after 1968 when plate tectonics replaced the geosynclines-based geotectonic cycle. Orogenies have been timed and named and there are tens of them in a major orogen: most are local, but there are several periods of almost synchronous global upheaval.

In the present context orogenies are explained as products of collision. Small collisions, such as arc/arc or arc/continent, produce a minor orogeny, but usually extinguish the existing subduction zone and reposition it at the edge of the outermost arc. This results in a situation that subduction-related magmas form above the new subduction zone whereas collision-related magmas form simultaneously close to the collisional suture, often

only several hundred kilometers apart. Both types of magmas and associated ores need not be much different. In the andean-type margin of the Canadian Cordillera (Samson and Patchett, 1991) comparable porphyry Cu-Mo deposits formed by pre-, syn-, and post-collision events (Dawson et al., 1992) and these collisions, within an overall regime of subduction, have not influenced much the metallogenesis of the overall mega-orogen (in the above case the Cordilleran, Andean, or Circumpacific convergent continental margins).

Major collisions, such as continent/continent, cause much greater upheavals and trigger magma generation and/or hydrothermal ore formation (Coward and Ries, eds., 1986). Şengör (1990, 1992) distinguished three major styles of such collisions and resulting orogens. In Himalayan-type orogens neither of the two colliding continents override the other at shallow levels, although the suture fill can be extruded to form a nappe. The collision sutures are often steep, straight and gently curved and incorporate products of long-lived and well-developed magmatic arcs, as well as ophiolites. Alpine-type orogens involve extensive override of one continent by another at shallow structural levels (<15 km). There are low-angle dipping, often sinuous sutures and remnants of pre-collisional magmatic arcs are poorly represented. Turkic-type orogens (Şengör and Natalín, 1996), characteristic for the Tethys orogen, result from subduction of extensive oceanic areas covered by a thick sedimentary pile. Large accretionary prisms are converted into metasedimentary basement complexes that contain infaulted shreds and rarely nappes of ophiolites.

Classical collisional orogens or orogenic systems are sandwiched between Precambrian cratons, themselves collages of pre-consolidation orogens. The Mesozoic-Cainozoic Alpine/Tethys orogen of Europe and Asia is slightly to moderately eroded collage of shifted terranes squeezed between the cratonic blocks of Laurasia (in the north) and Gondwana (in the south). It displays a divergent progression of lithofacies away from the central axis (Auboin, 1965). The Paleozoic Caledonian/Variscan (Hercynian) orogen in Europe and its eastern continuation in Asia, the Altaides (Şengör et al., 1993; alias Central Asian Orogenic

Belt of Jahn et al., 2000) is a collage of moderately eroded terranes between the East European and Siberian Cratons in the north, and Tarim and North China Cratons in the south. Such collages contain "everything", from relic Precambrian blocks (microcontinents) to oceanic, rift, island arc, andean-type margin, miogeocline and platform assemblages of various ages, in various stages of deformation and metamorphism, eroded to non-uniform depths. Metallogenic analysis is difficult here.

If the entire orogen is considered as a "collisional metallogene", as is sometimes the case in short presentations, the ore formation and distribution become blurred and the only credible feature that would differentiate a deposit A from deposit B would be the accumulated metals and their ratios. The alternative is to break the orogenic collage into constituent parts to pick up the identifiable components (e.g. porphyry coppers and the distinct rock assemblages that accompany them) and treat each separately (the Map of Magmatic Associations of the former U.S.S.R.: Kharkevich, ed., 1968, is an excellent tool to accomplish this). Such selection and sorting has been attempted in this book, but although this "works" for the distinct ore types/rock associations (like ophiolitic ultramafics), there always remains a large residue of ore deposits and/or lithofacies difficult to place into the correct pigeonhole, unless one forces it (or has an up-to-date, reliable literature about the many distant lands).

Some of the pre-orogenic deposits that include "giants", and settings described in the earlier Chapters, had a complex history and they are included in this Chapter when the orogenic effects (that is deformation, metamorphism, magmatism, remobilization) created a virtually new "personality" of a deposit, leaving the original (pre-orogenic) form open to interpretation. A typical example are the Pb-Zn-Ag deposits of the Broken Hill-type, now residing in high-grade metamorphics (Chapter 14). There are about ten or more conflicting interpretations as to what they were and where they had formed originally. In Chapter 14 as well as here such deposits are treated as synorogenic deposits in metamorphics, an empirical reality required by the explorationist to search for analogues elsewhere. It is up to the academic researchers to determine and argue the origin. To lump Broken Hill together with the "exhalites" presently forming on the sea floor, one of the published interpretations, may entertain students for a while, but it may be a disservice to future

exploration geologists as various classroom dogmas are difficult to forget.

In addition to the pre-orogenic deposits incorporated into orogens with or without modification, there are the syn-orogenic and post-orogenic ores that formed for the first time as a consequence of orogeny. There are two broad groups: 1) The ores are, directly or indirectly, associated with distinct rocks, in the present case mostly collision-related or anorogenic granitoids. The search for ore analogues to known models in the field thus starts with recognition and mapping of such associated rocks, after which it moves into recognition of additional ore controls like structure or host rock lithology. 2) The ores are associated with structures (e.g. faults) and processes (hydrothermal activity) that are universal (potentially present in any setting and rock association), but they are best developed and repeatedly present in certain rock associations. The (syn)orogenic (mesothermal) gold deposits are related to orogeny and their first order control is structure, lithology coming second. The Phanerozoic and late Precambrian deposits are summarized here, whereas those in Precambrian greenstone belts are in Chapter 9. In equivocal cases, in respect to ore deposit placement (and there are many), reference to important deposits is made in two or more chapters.

10.1.1. Granitoids in orogenic setting

Granitoids suffer from classifications based on a multitude of premises. The classification based on the presumed magma source: I (igneous) alias magnetite series, versus S (sedimentary), alias ilmenite series, have already been discussed in Chapter 7. The A (anorogenic) granites could be of any derivation (most are I), emplaced without orogenic assistance. The magma series have been assigned to geotectonic mega-environments: initially, the subductive margins were credited with the I-type, the collisional systems with the S-type, rifts and crustal extensions with the A-type. This assignment applies to prevalent situations only, as exceptions have been found on both sides. As several I or S assignments did not exactly fit, a new variety "S-like" (Suarez et al., 1990) or "S-I" have been introduced. Geochemical characteristics of granitoids have also been applied (Harris et al., 1986).

In the Chinese literature on regional metallogeny magmatic series: i) of crustal derivation; ii) of mixed derivation; and of iii) mantle derivation have been recognized, based on geochemical

parameters. These have been quite successful in separating, for example, granitoids associated with the magmatic-hydrothermal deposits of Sn and W, on one hand, and Cu-Mo deposits, on the other. Although not perfect, the three granitoid categories are quite useful tools in the initial stage of predictive metallogeny, but detailed analysis should follow.

The organization of granite types by geotectonic setting developed by Pitcher (1978, 1983) is widely used in regional and field geology (e.g. Scheibner and Basden, 1998). Of the four "orogenic granite-types" of Pitcher (1983), the Pacific-type and the Andinotype granites are related to subduction and applicable to Chapters 5 to 9. The Hercynotype and Caledonian-type granites apply here, plus the anorogenic granites. Some European authors (e. g. Seltmann and Faragher, 1994) here also include "Alpinotype" granites, emplaced to "pericontinental trenches of eugeoclinal basins". Scheibner and Basden (1998) added the Lachlan-type alias extensional back arc granitoid class, somewhat transitional between the Andinotype and Caledonian types. What are the characteristics of these "granites"?

Hercynotype granites

Also designated as syn-collisional or syn-orogenic, these granitoids form in thickened segments of metasediments-dominated upper continental crust (attributed, by some authors, to the "A-subduction", that is underthrusting of continental slabs), under low-pressure, high-temperature metamorphic conditions that produce the series biotite (sillimanite) gneiss - migmatite - anatectic granite. The resulting S-type granites have broad, diffuse contacts with migmatites at the "katozonal" (generative) level but change into diapiric batholiths and plutons as they rise (Barton et al., 1991). There are abundant "common" (non-fractionated) pegmatites and aplites, inclusions or rafts of refractory rocks such as gabbro, amphibolite, sometimes marble or Ca-Mg silicate gneiss. Pitcher (1979) gave the ratio of gabbro : diorite/tonalite : granodiorite/granite in Hercynotype complexes as about 2 : 18 : 80, but typical batholiths are monotonous and predominantly of equigranular to porphyritic adamellite (quartz monzonite) to biotite granite. Most plutons froze at depth before reaching the surface and silicic lavas are extremely rare. Metallic ores are rarely associated.

Caledonian-type granites

They postdate the peak of orogeny (hence are early- to late-orogenic or post-orogenic), controlled by "post-closure uplift", alias relaxation during the gradual uplift and erosion of an orogenic belt. Uplift led to rapid unroofing of plutons and metamorphics formed in depth, brittle faulting and fracturing, and formation of intra-orogenic (intermontane) and orogen-margin basins. They filled with mostly continental detritus (molasse). The granitic magmas are interpreted as melted by adiabatic decompression and by heat transfer from basaltic magmas that rose to underplate the continental crust, locally infilling the distended areas, and partly mixing with the anatectic melts; afterwards they differentiated. The melt sources are deeper than in the Hercynotype association, mostly in the tonalitic lower crust, with a variable mantle contribution.

The plutons are discordant, have contrasting, narrow thermal aureoles, and although the S-type is predominant, I-type granitoids are common. The rocks are more basic than in the previous group (granodiorite to biotite adamellite), but differentiation and fractionation of the parent magmas has produced a wide range of rocks ranging from gabbro to alaskite. Plutons and batholiths tend to be multiphase, with the youngest phases most evolved. The evolved, volatile-rich melts selectively rise and often form cupolas "on the back" of regional batholiths that rose high into the crust. Highly fractionated pegmatites occur, and magmatic-hydrothermal ores (Sn, W, Mo, Bi, Be, Li, Rb, Cs), grading to the Pb-Zn-Ag association, are characteristic. Intrusion-related Au, Sb, As, U deposits also occur, but hydrothermal Cu is generally rare although there are important exceptions (e.g. in Cornwall, England). There is an overlap with, and gradation into, the magma-ore associations formed near transition of the "flat slab subduction" into extension (rifting). This took place in the most external (that is, closest to continental craton) portion of the Cordilleran (e.g. Colorado Rockies and Trans-Pecos Texas) and Andean (Cordillera Occidental in Bolivia, Peru and Argentina) convergent margins (Chapters 6, 7). This is one of the reasons for uncertainty in interpreting the former setting of continental fragments incorporated into orogenic collages.

Anorogenic granites

These are emplaced during periods of "tectonic calm" into any brittle crust, at sites of local extension (dilation). This chapter deals with

anorogenic magmatism within cratons that are still flooded by continental crust, although the crust could be thinned (extended, attenuated), and with silica-oversaturated to about saturated magmas. Full-fledged rift association and undersaturated magmatic rocks are treated in Chapter 12. Anorogenic granitoids form small plutons, central complexes, resurgent cauldrons, stocks, ring complexes, dikes, commonly associated with intrusion, phreatomagmatic or hydrothermal breccias. They are usually explained as a product of decompression melting, or melting by heat from underplating basaltic magma or mantle plume, having the material source in the granulitic lower crust with variable mantle contribution. Some writers seek the source of A-granites in the asthenosphere. The rocks range from calc-alkaline, alkali-calcic to alkaline biotite granite, alkali granite, syenite.

Venting intrusions have comagmatic acid volcanic cover of rhyolitic, rhyodacitic, or trachytic flows and ignimbrites. Surprisingly, the anorogenic volcanics are commonly preserved in sequences as old as Mesoproterozoic and older (e.g. the Gawler Range Volcanics of South Australia; St. Francois Mountains in Missouri), whereas comparable volcanics in the andean-type belts are long gone, removed by erosion. The majority of A-granites have characteristics of I-type granites. Although their magmas are said to have been "dry" (some intrusions carry presumably asthenospheric fluids involved, after fractionation, in formation of magmatic-hydrothermal deposits of rare metals), extensive breccia and hydrothermal alteration-mineralization systems locally developed near the paleosurface. Those in the Gawler Craton of South Australia (e.g. Olympic Dam) survived under younger platformic cover.

Metallogeny of the acid anorogenic complexes is intermediate between the evolved (fractionated) Caledonian-type postorogenic intrusions (Fig. 10.1), and rift-related systems. Sn with Li, Rb, Cs, Be, sometimes W and Mo, Ta-Nb, U, sometimes Zr, REE, Y, Th are associated with A-granites. The high Fe, Olympic Dam-style complexes with Cu, Au and U seem to require bimodal systems where granite or syenite are associated with gabbro.

Research literature and conference presentations put too much emphasis on determining the geotectonic setting of ancient granitoid suites with often inconclusive or controversial results. To put this problem into a more realistic context, let me quote the "Conclusion" in Cobbing (1990):

"Although distinct tectonic settings such as subduction-related volcanic arc, rift associated, and

continental collision/collage are commonly recognized and may be characterized by a distinctive granite plutonism, such plutonism in any one setting may overlap compositionally with that from others, depending on the kind and proportion of crustal material involved in magma genesis. Similar compositional overlap may also be achieved within a single subduction-related setting by a proportional crustal increment with increased arc maturity. The result is that similar kinds of granites may be produced by tectonic settings that are different in kind but convergent in effect, depending on the kind of crustal material mobilized".

Metallogeny of collisional orogens

Compared with subduction-influenced convergent margins (Chapters 5-7), intracontinental orogens are poorer in ores with Cu, Mo and Ag; about equal in Au, Pb, Zn, Li, Sn (when the Bolivian Sn giants are included in Chapter 7); slightly richer in W; and much richer in U, Sn (if the Bolivian Sn giants are included here). If, however, the presumably subduction mantle-derived metals in magmatic-hydrothermal deposits (MT) are contrasted with the crust-sourced metals (CR), the contrast will be much stronger in the key metals: Cu (for MT) >> Sn, Pb, Li, U (for CR). This contrast follows very strikingly from map plots of metallic deposits distributed along the length of the single polarity orogens (those evolved during a long-lasting accretion and evolution from ocean on one side to continent on the other as the American Cordilleran and Andean orogens). There, especially along the length of the Canadian Cordillera, an imaginary copper-lead line (Laznicka and Wilson, 1972) separates the "copper domain" at the Pacific (western) side where Pb deposits are rare to non-existent, from the "lead domain" at the Rocky Mountains (eastern) side where there are virtually no hydrothermal Cu deposits. The same "line" roughly coincides with the "diorite line" (diorite domain in the west, granodiorite in the east) and both lines mark approximately the limit of the Ancestral North America in the east against the accreted terranes in the west (Dawson et al., 1992). Similar metal polarity is not well developed in the bipolar orogens (orogens between two cratonic blocks) such as the European Hercynides.

As in the andean-type margins (Chapters 6, 7), mafic-ultramafic intrusions coeval with collisions are very minor, unless inherited from the pre-collision stages of development (oceanic and rift associations) and granitoids dominate the metallogenesis. Mafic-ultramafic intrusions and plateau basalts related to rifting, however, often intrude or cover the collisional orogens; they appear

in Chapter 12). The lack of mafic/ultramafic lithologies also means the virtual absence of orthomagmatic deposits of Cr, Ni, Co, Cu and PGE.

Although, in the case of the granodiorite-quartz monzonite association that dominates the Andinotype-granites of Pitcher (1979), it was correct to state that granitic intrusions lack magmatic (orthomagmatic) deposits, this does not fully apply to the acid and alkali-rich magmas and products of their fractionation in collisional setting. Rare metal pegmatites are the prime example, although some writers question as to whether these products of residual melts, charged with volatiles and then (hydrothermally?) metasomatized, are true intrusions. If so, pegmatites are an example of late magmatic ore deposits as they accumulate economically interesting quantities of Li, Rb, Cs, Sn, Ta-Nb and Be that include several "giants". Although typical pegmatites are confined to the mesozonal and katazonal granite levels, the less typical ones, like the "Stockscheider" rims of leucogranite cupolas, reach into the granite epizone. Even more, the rare fluorine- and alkalis-rich albite, lithionite (zinnwaldite), topaz granites (ongonites in the Russian literature) are so enriched in some trace elements as to constitute "ores of the future". The Cínovec (Zinnwald) granite has 1-1.5% F, 1,000-2,000 ppm Rb, 800-1500 ppm Li, 100-150 ppm Cs and 30-50 ppm Sn (Breiter, 1994). These metals are mostly bound in mica (zinnwaldite or lithionite, rarely lepidolite), in an inconspicuous equigranular granitic rock. Magmatogene cassiterite, disseminated in some late-stage leucogranites in Cornwall (Stone and Exley, 1985, p.584), is at the beginning of a series of tin ore accumulations. This series continues as magmatic-hydrothermal (in greisens and high-temperature exoskarns) through convecting meteoric waters-deposited mesothermal (Cornwall cassiterite-Cu sulfides veins) to, exceptionally, epithermal (e.g. "wood tin") Sn deposits (Lehmann, 1990). One should mention that most of the historical production of granite-related tin came from regolith ("eluvial placers") and alluvial placers, a very last stage product in the tin accumulation process.

The bulk of economic metals in the "bedrock" division of collisional orogens (the sedimentary cover sequences are reviewed in Chapter 13), except for the relic deposits formed in various other environments before, reside in hydrothermal deposits. These form a genetic series between two end-members: 1) granite-related, and 2) independent of granite. Such a series can best be

demonstrated on an local examples for which the Erzgebirge/Krušné Hory metallogene has been selected. Much of the information here comes from the volume edited by Seltmann et al. (1994).

Erzgebirge (German name) or **Krušné Hory** (Czech name) is a highland fault block around 10,000 km² in area located across the German-Czech boundary south of Chemnitz and Dresden, north of Karlovy Vary and Teplice (Fig. 10.2.). It is a part of the late Paleozoic Hercynian (Variscan) orogen at the NW margin of the Czech (Bohemian) Massif: a Proterozoic rigid block within a collage of predominantly E-W trending fold belts. This is a "sacred territory" to a historian of world currencies, chemistry, mining and mining education, geological concepts, mineralogy, and economic geology, because:

--the term *dollar* came from here, based on *tollar* (Thaller), a 16th century silver currency mined and minted in Jáchymov (Joachimsthal); Fig. 10.3.

--the first textbook on mining, ore beneficiation and exploration technology, by Georgius Agricola (1556), is based on observation from the same place; Agricola (alias Georg Bauer) was a medical doctor in Jáchymov and a keen observer of activities in the local extractive industries;

--the first mining academy was established in Freiberg in 1756;

--this school made a contribution to general geology (Werner: neptunist concepts), and became a cradle and centre of Economic Geology teaching and research, until this discipline relocated to North America at the turn of the 20th century;

--Jáchymov (Joachimsthal) was the first, and for a long time only, known deposit of uranium. U was found by Klapproth in ore from Johanngeorgenstadt, whereas radium and polonium were discovered by Pierre & Marie Curie in the Jáchymov pitchblende. Radioactivity, discovered by Becquerel, was first observed in the same material. The first batch of uranium minerals identified and described came from here too, although none is named after this place.

Although mined for over a millenium, the last metal mines in the Erzgebirge stopped production in the early 1990s (some have been converted to tourist mines), although brown coal mining still continues on its flanks. Over the ages this has been an "ancient world class" source of silver and tin, then Cold War uranium. Most of the 1,000 plus ore

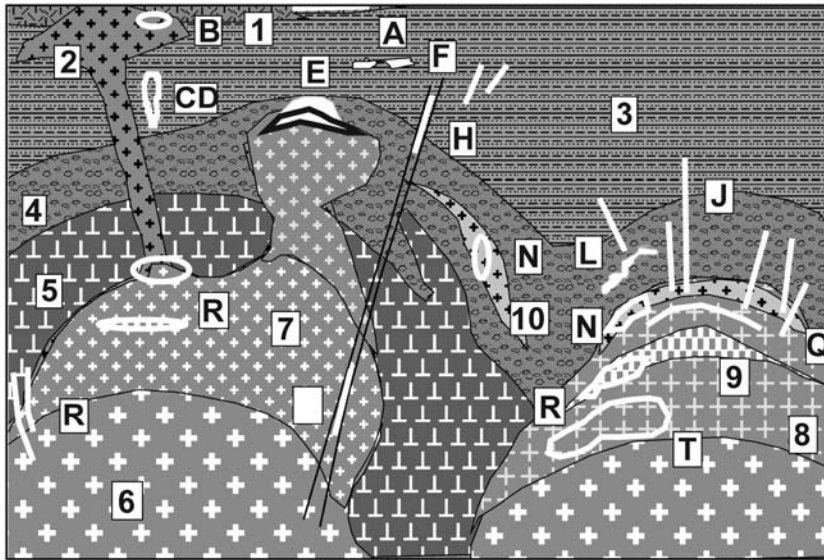


Figure 10.1. Late- to post-orogenic suite of evolved (potassic and silicic) predominantly peraluminous granites approximately corresponding to Pitcher's "Caledonian-type"; these are common in Cornwall and the Erzgebirge where they carry important Sn, W, Bi, etc. mineralization (read below). From Laznicka (2004), Total Metallogeny site G75. Explanations (continued): F. Mesothermal Pb-Zn-Ag veins, replacements; G. U in episyenite along faults; J. Sn, W, Mo, Bi veins and stockworks; L. Sn carbonate replacements; M. Sn, W, etc. oxidized exoskarn; N. Sn, W, Bi scattered in pegmatite; Q. Sn, W, etc. disseminated in greisen; R. W, Mo, Bi porphyry- and stockwork-type deposits; T. Bulk low-grade Li, Rb, Cs in lithionite or zinnwaldite granite. Ore types C, F, J, L, M, Q, R have "giant" members

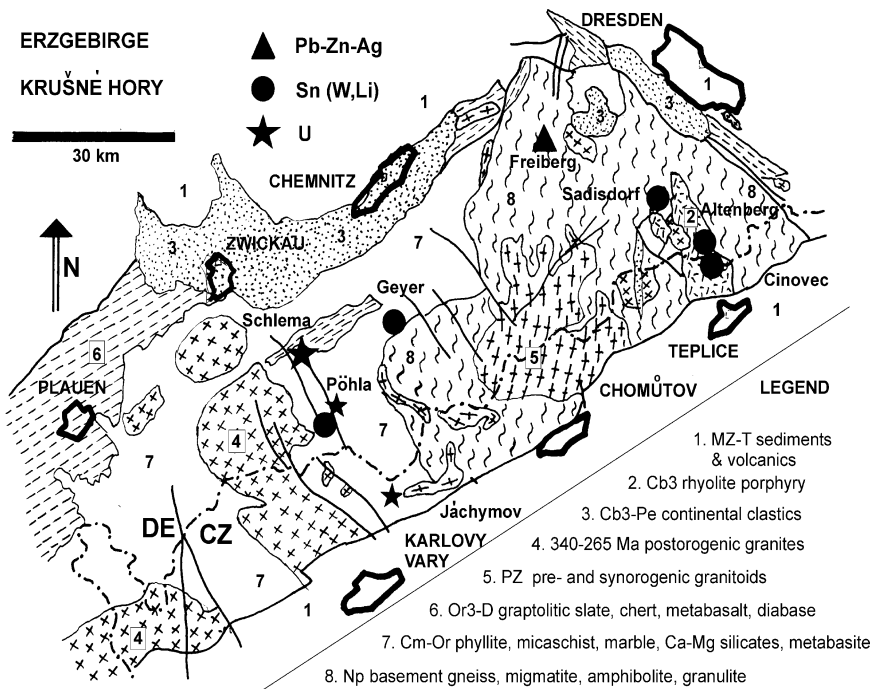


Figure 10.2. Simplified map of the Erzgebirge/Krušné Hory region showing location of the "giant" and some "large" metallic deposits mentioned in text. DE=Germany; CZ=Czech Republic



Figure 10.3. Jáchymov (Joachimsthal) coat of arms and scenery as seen by the artist. Courtesy of the Jáchymov Town Council

deposits and occurrences were small to medium size, including Jáchymov itself (~1,500 t Ag, 12,000 t U). There are just four "giants" (Freiberg, 7,000 t Ag, 1.7 Mt Pb; Altenberg, 290 kt Sn; Pöhla, ~300 kt Sn; Cínovec, 210 kt Sn) and five "large" Sn, Li, two "large" U, one "large" Ag deposit.

The Erzgebirge has a Proterozoic, high-grade metamorphic basement, topped by "eugeoclinal" metapelite-dominated schists related to Cambro-Ordovician extension. Despite this, it is an ensialic orogen with "acidic crust" and a prominent regional gravity low (Bankwitz and Bankwitz, 1994). Subduction during Silurian and Devonian was followed by a Lower Carboniferous orogeny (collision) accompanied by regional metamorphism and, after some 40-50 million years and partial uplift, by emplacement of several phases of late-orogenic granites (Seltmann and Faragher, 1994). These granites are believed to form a composite batholith under the entire Erzgebirge, exposed at the surface in several epizonal massifs. Coeval volcanics and subvolcanics are rare, preserved only in erosional remnants of the Permian Altenberg

Caldera. Earlier synorogenic granites, that initiated the melting in the lower to middle crust, are suspected in depth but are not exposed in this region.

The post-orogenic granites form two complexes (Tischendorf, 1989; Tischendorf and Förster, 1990). The predominant, earlier complex is a biotite S-type granite with local muscovite-biotite phases. It lacks widespread associated mineralization except for several small wolframite deposits in greisen and quartz veins, in the western part of the district. The younger, highly evolved fluorine-rich I- or A-type granite forms small massifs and cupolas, further modified by late-stage alkali metasomatism (albitization and K-feldspathization; apogranite). It is a topaz, albite, Li-mica (lithionite or zinnwaldite) leucogranite enriched in Li, Rb, Cs, Sn, Nb, Ta, Y and HREE. The granites are interpreted as products of several intracrustal melting episodes, complete with remelting of the earlier phases, followed by fractionation (Seltmann and Faragher, 1994). Throughout this process, the alternating partitioning of trace metals into the various mineral phases, such as mica and feldspar, followed by their destruction, influenced the timing and style of the Sn and rare metals economic mineralization. Apparently the metals' partitioned into the fluid phase produced the early generation of pegmatitic (in Stockscheider rims) and disseminated/stockwork cassiterite and associated minerals in endocontact greisens (quartz-mica, sometimes topaz, metasomatites). A special form of orebodies in Cínovec/Zinnwald (read below) are flat lodes of quartz with scattered cassiterite and wolframite, rimmed by coarse zinnwaldite, then by fine-grained greisen, parallel with the granite cupola outline.

In the later mineral stages, especially in fissure veins emplaced into the roof rocks (exocontact), the ratio of cassiterite to sulfides decreased and eventually sulfides became dominant. This is particularly well developed in Cornwall where, based on isotopic analysis, magmatic waters were only isotopically detected in pegmatites and calc-silicate hornfels veins, whereas the Main Stage veins precipitated from convecting meteoric waters (Sheppard, 1994), often after a large time lag in respect to the host or adjacent granite emplacement (Stone and Exley, 1985). The heat required to drive the convecting cells is believed generated by radioactive decay of accessory minerals in the high heat-producing granites, like uraninite, monazite, zircon, radioactive potassium in feldspars, and others. Tin was scavenged from the granite, especially where it had been stored in micas, so the lack of early Sn partition into the residual melt to

form early magmatic hydrothermal ores was here offset by the availability of postmagmatically extractable trace tin. Metal scavenging by late fluids can operate in other rocks than granites as well, such as greenstone, diabase and gabbro, and these sources of extractable trace Cu could explain the large amounts of copper that accompanies tin, and in places dominates veins, in the Cornish tin field.

In the Erzgebirge late postmagmatic Sn veins are not as common as in Cornwall, but they are substituted by the mesothermal carbonate-pitchblende veins. These veins and vein systems are controlled by deep lineaments and zones of brittle fracturing and occur near the tin granites, although not directly related to them (Štemprok and Seltmann, 1994). The more complex veins have an early quartz, pyrite, pyrrhotite stage, followed by the main stage that has several generations of dolomite and calcite, pitchblende, pyrite, and locally Cu-selenides. If granite is the host (rarely), it is sericitized and argillized; wallrock schists are silicified, sericitized, chloritized, carbonate veined, and there is the distinct "reddening": hematite pigmentation. A huge uranium vein system in Schlema-Alberoda near Aue (Pt 80 kt U; read below) had been the largest U vein deposit supplying the Soviet industrial-military complex in times of the Cold War. Although the high heat producing granites may have been the source of heat to drive the late-stage meteoric water convection and perhaps to supply some U, most of the U had likely come from the carbonaceous meta-sediments abundant in the area; the "black" lithologies also acted as a reductant, and a source of sulfur. In Ronneburg, at the NW fringe of the Erzgebirge near Gera, a large synsedimentary accumulation of trace U in Silurian graptolitic shale required only a minor remobilization of U into fractures to become by far the largest U deposit of the former Communist block (read below); there are no granites around.

In France, where most hydrothermal U deposits are in granite, the gap between the trace U-enriched granite emplacement and formation of economic pitchblende veins has been precision dated. In the St. Sylvestre complex near Limoges (Cuney and Raimbault, 1991) leucogranites had been emplaced at 325 Ma; the first barren hydrothermal stage to form episyenites (porous feldspathic rocks after hydrothermally desilicified granites), quartz veins and silicified ("chert") breccias took place at 301 Ma; the quartz, carbonate, pitchblende veins (Fanay and Margnac deposits) formed around 280 Ma.

The Erzgebirge uranium lodes, especially those near Jáchymov, Johanngeorgenstadt and

Schneeberg, are overprinted by shoots of the "five elements" (Ag, As, Co, Ni, Bi) mineral association. Here, native silver, argentite/acanthite, Ag-sulfosalts come with native arsenic, löllingite, Ni- and Co-arsenides and Bi minerals in quartz-carbonate gangue. The metal tonnages were minimal measured by present standards, yet significant enough to ensure Medieval prosperity to several of the "silver cities", as well as a steady supply of cobalt for blue pigments in the local porcelain industry (e.g. Meissen and Karlovy Vary). These are low temperature, meteoric waters-based veins, the metal sources of which are puzzling; perhaps skarns or "black schists"?

Mesothermal Pb-Zn-Ag veins are scattered throughout the Erzgebirge, but are of major significance only in the Freiberg-Brand ore field SW of Dresden (Pt ~7,000 t Ag, 1.7 Mt Pb from close to 1,000 veins; read below). The vein filling is of several generations marked by decreasing temperature of precipitation, formed over a protracted period of time (over 100 million years). The last variety of low-temperature hydrothermal deposits are fluorite and/or barite veins with quartz or calcite gangue, filling faults. The youngest fluorite impregnations of late Cretaceous sandstone at Sněžník are Tertiary, and barite/fluorite still actively precipitate from the mineral hot springs in the Teplice spa.

As it follows from the Erzgebirge example, intrusions (granites) have a diminishing role in ore formation over the time. They could be the source of a) heat, fluids, and metals (Sn and rare metals pegmatites; Sn, W, Li, Be disseminations and stockworks in high-temperature endocontacts in granite cupolas and some veins; b) source of heat (residual magmatic heat or radioactive decay) and extractable metals; the fluids are external (Cornwall-type Sn-Cu lodes; partly mesothermal U; partly Fe oxides Cu, U, Au; c) sources of heat only, the fluids and metal sources being external; partly China-type W veins, mesothermal U, mesothermal Pb-Zn-Ag; partly mesothermal Au. As, Sb; d) source of extractable metals, the heat and fluid being external; partly Fe oxides-Cu, U, Au; partly unconformity U; and e) of no genetic consequence (partly mesothermal Au, As, Sb; Ag, As, Ni, Co, Bi veins. As one moves away from granites into the more distal and lower temperature ore systems, the structural control and rock alteration (e.g. albitization, carbonatization, chloritization) increase in importance and become the principal tools of prediction and search for ores.

10.2. Massif anorthosite association: Fe-Ti-V and Ni-Cu deposits

Anorthosite is a rare rock composed of 90% plus calcic plagioclase (Hess, 1989). Anorthosite association includes anorthosite itself plus other rocks, some of which are very minor and inconspicuous but can be important ore hosts. Of several anorthosite associations and styles, two are most important for ore search: 1) anorthosites of layered (Bushveld-style) complexes; and 2) massif anorthosites. Both are parents to important Fe, Ti, V oxide deposits but have a different setting. The former anorthosites appear in Chapter 12, the latter are described here (Fig. 10.4).

Anorogenic and unmetamorphosed massif anorthosites range from monomineralic masses through compositionally zoned to layered bodies that form small to large circular intrusions emplaced into low-grade metamorphic terrains undergoing extension (e.g. in northern Labrador), to foliated, gneissic sheets and massifs in granulite facies metamorphic belts. The latter range from pre-metamorphic to syn-metamorphic deep-seated intrusions melted within, and emplaced into, the lower continental crust. The youngest, Jurassic, "pristine" anorthosite is a rare component of small anorogenic granite intrusions in Nigeria. The "prime time" of massif anorthosite emplacement, however, had been between about 1.7 and 0.9 Ga when the two best studied and mineralized provinces in eastern Canada and SW Norway formed.

There are three petrologic varieties of anorthosite: labradorite, andesine and "alkalic" (containing antiperthite and 3-4% K₂O). The first two are associated with pyroxene-bearing rocks ranging from norite (a gabbro) through jotunite (monzodiorite), mangerite (monzonite) to orthopyroxene granite (charnockite). Troctolite (olivine-plagioclase) also occurs. The "alkalic" anorthosite comes with gabbros and also "nelsonite" dikes (=ilmenite-apatite with variable amounts of rutile).

The origin of massif anorthosite is not yet fully understood and ideas of deep intracrustal metasomatism contrast with magmatic differentiation of parent magmas producing cumulate rock bodies of different composition. Duchesne (1999) developed a model based on the Fe-Ti rich Rogaland anorthosite province of southern Norway, but applicable outside it as well. There, anorthosite massifs are the product of emplacement of large diapirs of plagioclase-rich mush that crystallized during ascent and

simultaneously suffered brittle deformation. This explains the well-known "shattered image" texture of many anorthosites. The pyroxene (and rarely olivine)-rich cumulates separated during the ascent within and along margins of the diapir, or crystallized from melts expelled into the roof and wallrocks as dikes or small massifs with chilled margins.

Fe-Ti oxides (Ti-magnetite, ilmenite, ulvöspinel, hematite-ilmenite intergrowths) with P (in apatite) and elevated V and/or Cr had been a part of the differentiation and cumulus separation process, in association with ferromagmas (these crystallized as ferrodiorite, ferromonzonite, ferrosyenite). The metallic melts either solidified in situ to form disseminations, or separated as a residual liquid injected into low-pressure areas and dilations within and outside the intrusion. These formed high-grade, partly massive orebodies. Fe-Ti oxide disseminations in rocks, like ferrodiorite, are universally present (the typical contents are around 3% TiO₂ and 15% FeO), but additional enrichment was required to produce ore grades and sufficient tonnage. In the homogeneous ilmenite norite (or jotunite) dike that hosts the "large" Tellnes orebody (read below), the ore cumulate was enriched by crystal sorting in a noritic melt (Duchesne, 1999). The coarse "shattered anorthosite" facies, in contrast, remains unmineralized except when injected by the ore melt.

The rare olivine-bearing differentiates (troctolite, rare peridotite) are not always present in and near anorthosite complexes and if so they are small, inconspicuous, and often overburden-covered. They are geochemically enriched in Cr, Ni, Co, Cu, PGE but before the 1994 discovery of the Voisey's Bay Ni-Cu deposit in Labrador the olivine-rich differentiates were rarely targeted by explorationists; now they are! The disseminated to massive Fe, Ni, Cu sulfides formed by liquid separation from mafic melt, presumably assisted by contamination of magma reacting with the wallrocks, in a process comparable with formation of Noril'sk, Sudbury, and other magmatic Ni-Cu deposits. Fe, Ti and V are geochemically abundant metals, so huge local metal accumulations are required to produce a "giant" deposit (4.3 bt Fe, 400 mt Ti, 10 mt V, respectively). This has rarely been achieved; hence there are no "giant" deposits here so only five "large" Fe-Ti-(V) localities and one "large" Ni-Cu deposit are briefly described here (they are still, however, of the "world class"). In the economic sense, however, massive anorthosite association is a globally significant source of Ti.

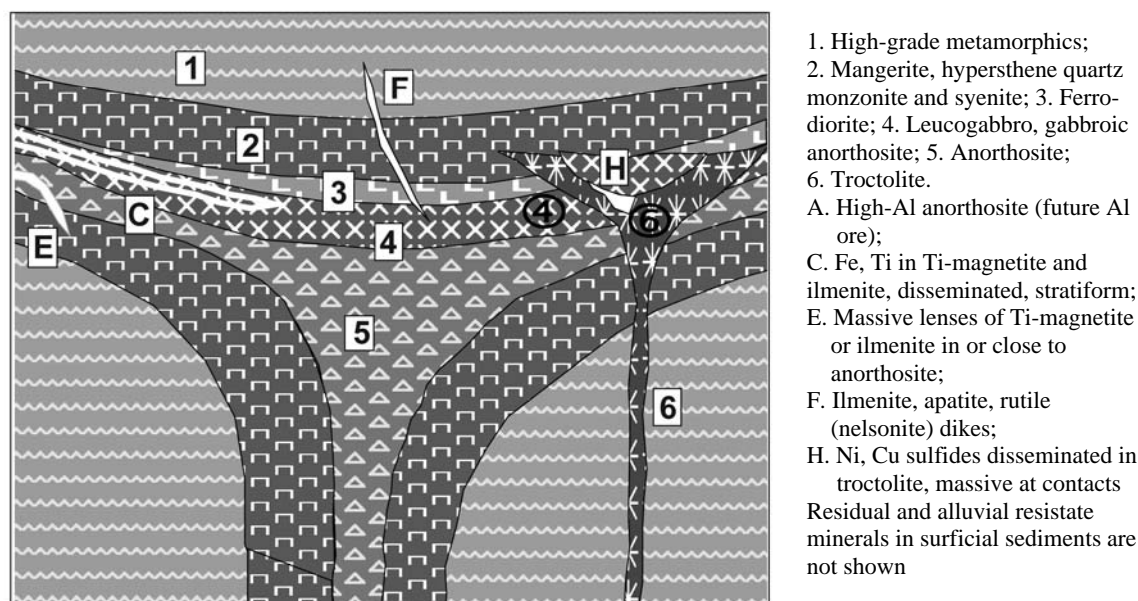


Figure 10.4. Anorogenic massif anorthosite, gabbro and troctolite association, before deformation; rocks/ores inventory diagram from Laznicka (2004), Total Metallogeny Site G98. Until the Voisey's Bay Ni-Cu discovery the small separate ultramafic intrusions often associated with anorthosites were rarely considered as of economic interest

SE Canadian Shield massif anorthosite region.

The Grenville and Nain Proterozoic and Archean structural provinces in Labrador, NE Québec, E Ontario and NE New York probably contain over 75% of the world's anorthosites, distributed in about 15 larger and many smaller plutons. The bulk of these plutons had been emplaced between 1.46 and 1.27 Ga, so they predate the ~1.1 Ga Grenville collisional orogeny in the Grenville province, and postdate the ~1.8 Ga Torngat collision in Nain (Ryan et al., 1995). Anorthosites in the 1.35-1.29 Ga Nain Plutonic Suite are believed emplaced above a mantle "hot spot" and they remain undeformed and unmetamorphosed. Anorthosites in the Grenville province had been exposed to metamorphic conditions as high as granulite facies, yet they largely retain their massive appearance despite widespread recrystallization, granulation and localized shearing. The intrusions have irregular distribution as single independent bodies, or clusters in a broad WSW-ESE belt. Near the eastern terminus the anorthosite belt turns north as it enters the Nain province. There is little ore in the Nain, but the Grenville anorthosites store some 765 mt Fe and 185 mt Ti in past production and reserves, and some 1.5 bt Fe and 350 mt Ti in resources mined from five major areas.

Magpie Mountain Fe, Ti, V deposit is the largest one (Valée and Raby, 1971; P+R ~1 bt of ore with 42.0% Fe, 6.3% Ti, 0.1% V for 475 mt Fe, 70 mt Ti, 952 kt V; Rc 1,075 mt Fe, 150 mt Ti, 2.5 mt V). It is located 200 km NE of the port of Sept Iles, in terrain underlain by migmatitic gneiss and granite. The N-S trending, 6 km long and up to 500 m thick ore zone is a wedge-like, steeply dipping body of massive ore injected into granite gneiss and gabbro-anorthosite, and in places intersected by post-ore granite. The main ore mineral is fine-grained (0.2-0.4 mm) Ti-magnetite (75%) intergrown with 5-10% of ilmenite lamellae and 10% of ulvöspinel. The remainder is silicate gangue. The second largest **Lac Allard-Lac Tio** ore field lies about 45 km NNE of Havre St. Pierre, eastern Québec (Bergeron, 1972; 133 mt Fe @ 38%, 73.5 mt Ti @ 21%, 608 kt V @ 0.174%). There, the anorthosite host is medium-grained, ilmenite-rich. The ore is composed of coarse crystalline massive ilmenite with exsolved hematite. The orebodies are a series of narrow tabular zones and irregular lenses, believed injected into an already solid anorthosite as a residual magmatic liquid. The 1.2 x 1.0 km large orebody is intersected by flat-lying or gently-dipping bands of anorthosite with densely disseminated ilmenite.

Rogaland anorthosite province, southern Norway. Three major massifs of anorthosite and associated norite, jotunite (monzonorite) and mangerite crop out along the coast of southern Norway (Korneliussen et al., 1985; Duchesne, 1999). These rocks, exposed over an area of 1,200 km², had probably been emplaced in the same time as the Nain/Grenville anorthosite in Canada, and the published ages of 1,050 and 960 Ma probably reflect the age of metamorphism (most anorthosites and the Fe-Ti oxide deposits they host have been deformed and metamorphosed), although the Tellnes deposit and its host dike are post-orogenic (930-920 Ma). Of fifty small Fe-Ti deposits intermittently exploited in the past, only the largest deposit, Tellnes, in the Åna-Sira massif, is still in production.

Tellnes (Krause et al., 1985; Duchesne, 1999; ~400 mt ore @ 31% Fe, 10.2% Ti for 93 mt Fe, 43.2 mt Ti; Fig. 10.5) is 10 km east of Sokndal and it is a 2,700 m long, up to 400 m wide SW-plunging arcuate mass of fine-grained ilmenite norite. At both ends, this mass extends into a dike of jotunite to quartz mangerite, 14 km long. The orebody has a sharp contact with the older medium- to coarse-grained massif anorthosite. The ilmenite is finely disseminated in a rock with the average composition of 53.2% An₄₄ plagioclase, 28.6% ilmenite, and 10.2% orthopyroxene. The ilmenite contains 10-15% of exsolved hematite and some Zn-rich spinel. Accessory minerals include pyrrhotite, pentlandite, chalcopyrite and baddeleyite.

Two remaining anorthosite complexes of the world, with a "large" Fe or Ti endowment, are:

- **Liganga**, 180 km SE of Mbeya in Tanzania (Harris, 1961; 615 mt Fe @ 50%, 96 mt Ti @ 7.8% and 4.614 mt V @ 0.375%); a Neoproterozoic anorthosite intrusion into Archean basement.
- **Dzhugdzhur Range**, eastern Siberia, Russia (Rundkvist, ed., 1978; 425 mt Fe @ 17%, 100 mt @ 4%); disseminated apatite, ilmenite and Ti-magnetite in a 1.7 Ga gabbro, pyroxenite and anorthosite complex emplaced to high-grade Archean metamorphics.

Small ultramafic intrusions in massif anorthosite provinces: **Voisey's Bay Ni-Cu-Co** deposit, Labrador (Ryan et al., 1995; Naldrett et al., 1996; Rc 150 mt @ 1.9% Ni, 1.1% Cu, 0.08% Co for 2.85 mt Ni, 1.65 mt Cu, 120 kt Co). Voisey's Bay is 35 km SW of the coastal town of Nain, in the Newfoundland sector of Labrador. The area is dominated by the 1.35-1.29 Ga old post-orogenic Nain Plutonic Suite of anorthosite, granite, diorite,

with several troctolite intrusions (Kiglapait layered intrusion is the largest) and dikes. This suite straddles the 1.86 Ga collisional boundary between the Archean Nain province in the east, and Paleoproterozoic Churchill province in the west. The area was mapped and investigated by the government in the 1980s but considered unfavorable to host major ore accumulations.

In 1993 geologists Al Chislett and Chris Verbiski landed on a gossanous outcrop, noted some chalcopyrite relics and took geochemical samples. Four holes drilled the following year delivered excellent results, including 103.4 m intersection in massive Fe, Ni, Cu sulfides. An unprecedented staking rush followed what is described as the richest mineral discovery in Canada in 40 years. Properties changed hands, and politics got into a way of speedy development.

The deposit is at, and below the entry of, a troctolite feeder sheet (dike) into base of layered, 12 km long Reid Brook troctolite intrusion. This east-west trending troctolitic complex is emplaced into Archean sulfidic gneiss, but straddles and extends beyond the collisional suture into the Churchill province. The intrusion is dissected by a fault and consists of an older, layered section and a younger, massive portion. The latter troctolite has modal composition of 75% plagioclase, 20% olivine and 5% orthopyroxene, so it is a relatively light-colored xenolithic rock, reminiscent of Merensky and J-M reefs. It grades into olivine gabbro. Sulfides (~75% pyrrhotite, 12% pentlandite, 8% chalcopyrite & cubanite, 5% magnetite) occur at three sites near base of the 30-100 m thick troctolite sequence, in and above footwall breccia. The single richest orebody is the Ovoid Zone, a body of massive to breccia sulfides that measures 520x300x100 m. Its reserve is 31.7 mt @ 2.83% Ni, 1.68% Cu, 0.12% Co and there is a halo of disseminated sulfides present. The mineralisation is interpreted as sulfide melt separated from a batch of metals-enriched magma, contaminated by sulfur from the gneiss it traversed, accumulated at the base of magma chamber, then sunk back into the feeder dike (Naldrett et al., 1996).

10.3. Ores closely associated with granites

10.3.1. Rare metals pegmatites

As there is little difference between Precambrian and Phanerozoic pegmatites, all pegmatites are included in this Chapter (Fig. 10.6). Granitic

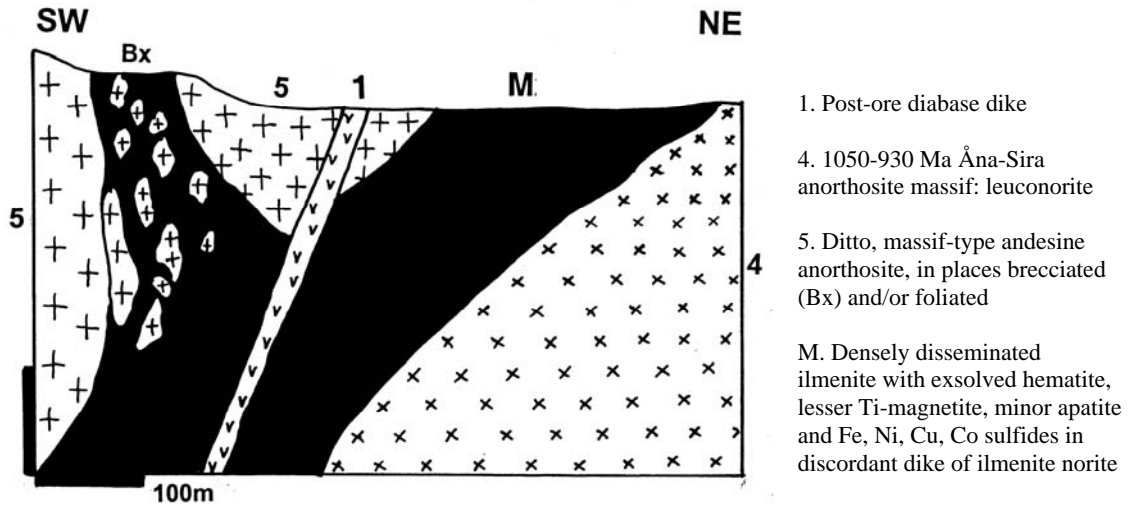


Figure 10.5. Tellnes Fe-Ti deposit, southern Norway. Cross-section from LITHOTHEQE No. 1689.2, modified after Krause et al. (1985)

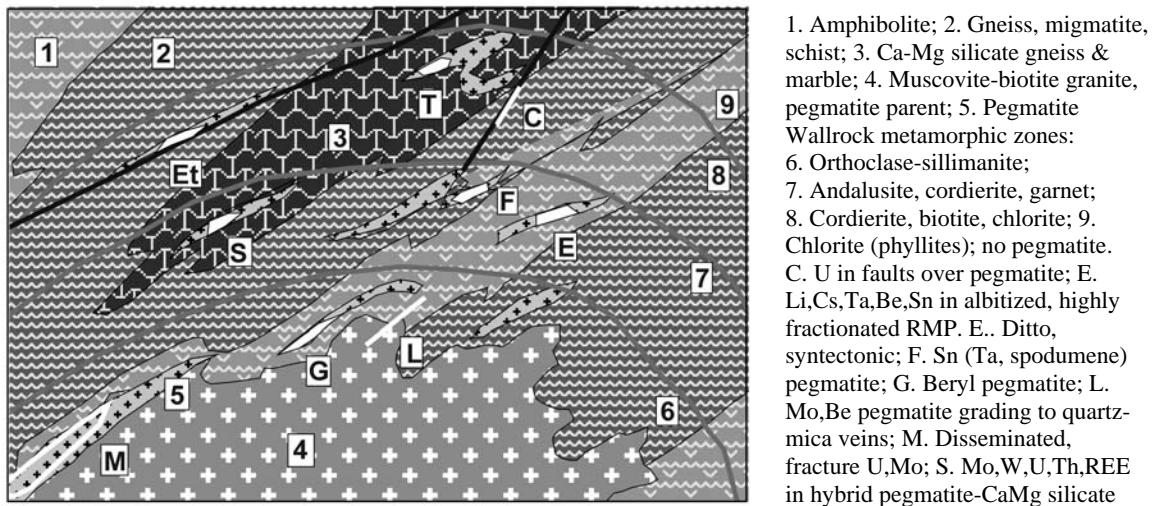


Figure 10.6. The place of rare metals pegmatites in relation to the (presumed) parent intrusion. From Laznicka (2004), Total Metallogeny site G79. Explanations (continued): T. Corundum in desilicified pegmatite and its wallrocks; X. Sn, Ta, spodumene resistates in pegmatite regolith (not shown); Y. Sn, Ta in alluvial placers (not shown)

pegmatite is a coarsely to very coarsely crystalline quartzo-feldspathic rock predominantly related to anatexitic granite. The most widespread are in-situ pegmatites, formed by local separation of partial melt in zones of granitization. Melts derived from Archean tonalitic or granodioritic gneiss had I-type signatures and formed numerous lenses, patches, short dikes and stockworks at or near the melt sites, ranging from pink or white aplite to coarse pegmatite. There are no major associated metallic

deposits. Pegmatites formed by partial melting of metasedimentary sequences (peraluminous or S-type) start as diffuse patches of quartzo-feldspathic mobilizate in migmatite, then collect in low-pressure areas as simple quartz, feldspar (predominantly microcline), mica (predominantly biotite) small pegmatite bodies, sometimes with accessory aluminous minerals like garnet, cordierite, sillimanite, and andalusite. These pegmatites are non-fractionated but possess a

limited mobility to mingle with various metallic ores undergoing dynamic metamorphism when present, typically in shears. Broken Hill Pb-Zn, Thompson Ni-Cu, Franklin Mn-Zn and other deposits have their share of "ore pegmatites" (Chapter 14).

Transported pegmatites form by collection and movement of the partial melt (mobilizate) away from the source, followed by deposition in dilations: semi-brittle to brittle fractures, shear zones, cores of anticlines, lithologic contrasts. These are "common pegmatites" and although some large bodies develop zoning based on grain size of the constituents (finer-grained marginal facies to coarse crystalline, even "blocky" center), there are no rare minerals. Thousands of such pegmatites, however, have been quarried for feldspar and some also for quartz and mica. Some are high in tourmaline, a potential future source of boron.

Rare metals pegmatites, RMP (a term that originated in the Russian literature, e.g. Vlasov, ed., 1968; Gordiyenko, 1970; Kuz'menko, ed., 1976, and later adopted in the West, e.g. Černý, ed., 1982) are highly fractionated pegmatites that can contain economic accumulations of one, or more, "rare metals" like Sn, Ta-Nb, Be, Li, Rb, Cs, REE, Th, U, Sc, and others. They represent less than 0.1% of pegmatite occurrences, of which the bulk resides in the "intermediate depth" zone marked by the cordierite-amphibole or andalusite-sillimanite

metamorphic assemblages. These pegmatites are considered differentiates of highly fractionated granitic magma, enhanced by late metasomatic processes, and occur in the roof or vicinity of a "fertile" parent granite intrusion. A more detailed review for a non-specialist is in Laznicka (1993, p.1080-1119), that also contains abundant references.

As an economic commodity, granitic pegmatites are the principal source of nonmetallics like K-feldspar, sheet mica, spodumene, petalite and beryl. Until the late 1950s pegmatites, and their weathering products in regolith, had also been the only source of Li, Rb, Cs, Be, Ta, Nb, Sc, REE and Y. This has changed recently with the arrival of the various low-grade "bulk" ore resources like disseminated ores in apogranites (Ta, Y), carbonatites (Nb, REE), diagenetic and epithermal ores related to acid volcanics (Li, Cs, Rb, Be), lacustrine brines (Li), and by-products (e.g Ta as a by-product of tin smelting). Despite this change, however, pegmatites still remain important as an alternative resource, as a base for specialty products, and as a mineral repository capable to rapidly respond to short-term surges in materials' demand (e.g. the "coltan", i.e. columbium-tantalum concentrate rush of the late 1990s, triggered by the sudden demand for Ta for use in capacitors in mobile telephones).

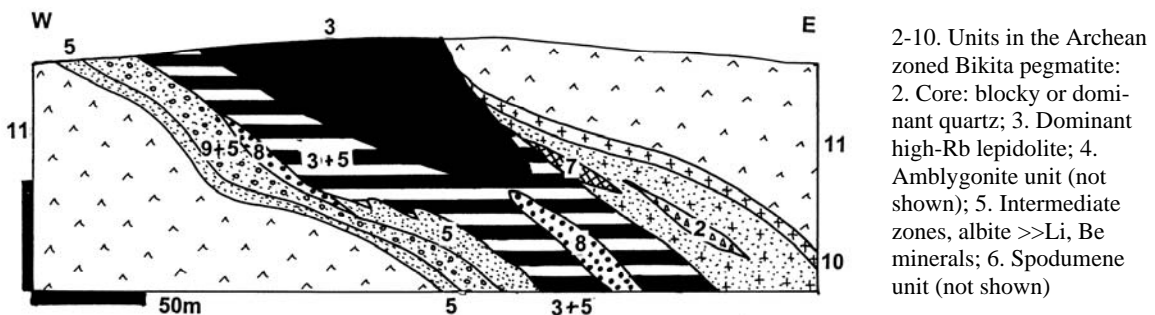


Figure 10.7. Bikita pegmatite, Zimbabwe, cross-section of the Main (Lepidolite) Quarry as an example of mineralogically (commodity) zoned rare metals pegmatite. From LITHOTHEQUE No. 2709, modified after Cooper (1961) and Martin (1964). Explanations (continued): 7. Pollucite unit; 8. Petalite, eucryptite unit; 9. Beryl unit; 10. Simple wall zone pegmatite; 11. Ar amphibolite (metabasalt)

Many of the "rare metals", however, are not particularly rare in terms of their crustal clarkes: e.g. Rb, 60 ppm; Li, 18 ppm; Ta, 1.1 ppm, which is about as much as Zn, Pb and Mo, respectively, but they do not form local accumulations so readily. Because of this, the "world class" pegmatite

deposits, such as Bernic Lake (Tanco), Bikita (Fig. 10.7), Greenbushes (Fig. 10.8), and Wodgina, are only "medium" to "large" in terms of the magnitude of geochemical accumulation, adopted here. There is only one "giant": Manono in Congo, with a resource of 292 kt of tin. Despite this, the largest

metalliferous pegmatite deposits are briefly described below.

Setting: About 80% of pegmatites, including the RMP, and all the important ones, are in Precambrian terrains. This is mostly a function of deeper cumulative erosion that has exposed the deep (mesozonal to katazonal) levels where these pegmatites originated. The majority of pegmatites are in orogenic belts with continental crustal basement, although the older Precambrian belts are now constituents of cratons. Most of the largest rare metal pegmatites are of intracrustal peraluminous derivation (some are related to the A-type intrusions), and many are emplaced into greenstone belts, which is another consequence of the depth of erosion: the mesozonal level has simply been eroded away from the vast tracts of Precambrian granite-gneiss terrains.

The RMP's in greenstone sequences have sharp, contrasting contacts against the metabasites, sometimes with holmquistite (Li-amphibole) in the exocontact. The pegmatite bodies range from schistosity-peneconcordant lenses and sheets to cross-cutting tabular bodies, "blows", pipes, and irregular bodies. They are affiliated to late-orogenic to post-orogenic highly fractionated peraluminous (leuco)granites, frequently emplaced during or after a retrograde event that took place at higher crustal levels and was accompanied by development of ductile to ductile-brittle shear zones. Such pegmatites are massive, undeformed and unmetamorphosed, often marked by the presence of giant crystals (e.g. huge spodumene crystals in the Keystone quarries, South Dakota).

Economically important syntectonic, foliated RMP's are less common, but they do occur. Two outstanding examples are the "large" **Greenbushes Li, Sn, Ta, Nb deposit** in Western Australia (Hatcher and Clynick, 1990; 110 kt Li, 40 kt Sn, 8,522 t Ta; Fig. 10.8) and the **Uis Tinfield** in Namibia (Richards, 1986; 106 kt Sn; Fig. 10.9). Groves et al. (1986) pointed out that the Greenbushes pegmatite is not only deformed, lacking a specialized granite parent, and containing disseminated ore minerals in the sodic (albitic) zone with no well-defined metasomatic units, but that it occurs in a polymetamorphic high-grade Barrovian-type belt, controlled by a major shear zone.

RMP's are very selective in respect to the metamorphic isograds of the host rock metamorphics into which they were emplaced. This is most obvious in pegmatite fields in which the various pegmatite bodies are concentrically zoned around the parent intrusion, as in the southern Black

Hills, South Dakota (Redden et al., 1982). There, the 1.72 Ga or 1.697 Ga Harney Peak Granite is emplaced into a Paleoproterozoic schist terrain that forms a structural dome.

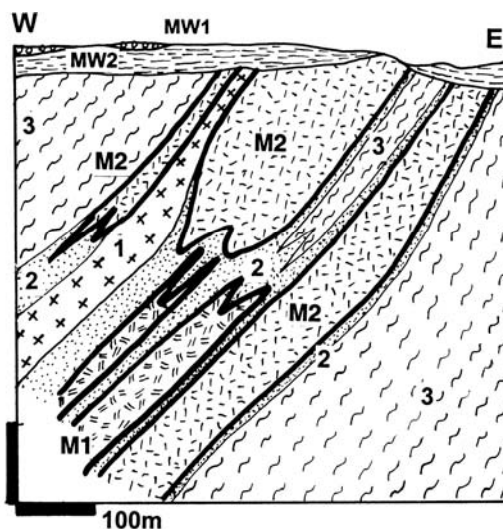


Figure 10.8. Greenbushes synorogenic spodumene, Sn, Ta pegmatite, Western Australia. Cross-section from LITHOTHEQUE No. 2140, modified after Hatcher and Clynick (1990). MW1. T3, discontinuous patches of gibbsite-goethite laterite; MW2. Argillized pegmatite saprolite with resistate cassiterite, Ta minerals. 1. Mafic sill; 2. ~2.65 Ga pegmatite, undifferentated foliated microcline, albite, muscovite quartz; M1. Albite pegmatite with tourmaline, muscovite, scattered Sn, Ta minerals and beryl; M2. Spodumene pegmatite; 3. Argabbroamphibolite and hornblende-biotite schist with holmquistite at spodumene contact

The composite inhomogeneous peraluminous leucogranite and pegmatitic granite are enveloped by a concentric sillimanite zone, changing outward into staurolite and subsequently garnet zones. Of the 20,000 recorded pegmatite bodies in the Black Hills (Norton, 1975; the cumulative production of Li, Sn, Be, and Ta-Nb has been less than "medium"), the bulk of occurrences are unzoned "common" pegmatites found in the "high-sillimanite" zone immediately adjacent to the granite. About 200 zoned pegmatites were mined. Of these, mica and/or beryl pegmatites prevail in the "low sillimanite" zone, whereas the RMP's (most with spodumene) are found along the outer fringe of the pegmatite field, in the staurolite zone. No pegmatites occur in the garnet zone.

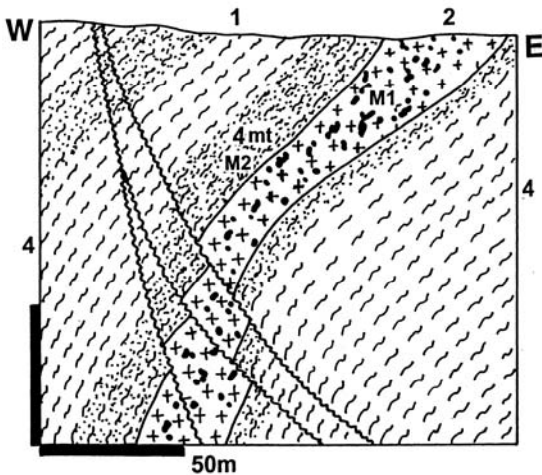


Figure 10.9. Uis tinfield, SW Namibia, typical Sn-pegmatite cross-section. From LITHOTHEQUE No. 292, modified after Richards (1986). 1. Regolith that includes cassiterite placers; 2. 550-460 Ma pegmatite swarm; M1. One of ~100 bodies of late syntectonic unzoned albitized pegmatite with scattered cassiterite; M2. Cassiterite-tourmaline schist at exocontact. 4. Np metaturbiditic schist; 4mt. Knotted Schist, diablastic and porphyroblastic

Internal zoning: Most RMP's are internally zoned. The zoning is textural, mineralogical or combined. Cameron et al. (1949) distinguished four repetitively present zones in the intermediate depth pegmatites that have a character of "successive shells concentric about an innermost zone or core". This he attributed to in-situ differentiation of pegmatitic magma in a closed system. From the outer contact of the pegmatite body inward, the zones are: 1) border zone; 2) wall zone; 3) intermediate zone; and 4) core. The zones are marked by increasing crystal size toward the centre accompanied by the appearance of albite, beryl, spodumene, and rare metals minerals, when present. Nikitin (1968), in contrast, stressed the role of postmagmatic, mainly sodic hydrothermal fluids interacting with the earlier, predominantly K-feldspar pegmatite to create albite-dominated metasomatic zones in an open system. The metasomatites are irregular, overprint the various earlier zones, but surprisingly do not extend beyond the pegmatite. Most of the Li, Rb, Cs, Be, Sn, Ta, and Nb minerals are in the albitic metasomatites, although scattered beryl and spodumene can also be found in the K-feldspar-dominated early phases.

Supergene modification of ore pegmatites

Non-outcropping pegmatites buried in bedrock (e.g. Bernic Lake) or pegmatites exposed in the glacially scoured terrain as in Canada, Scandinavia or Siberia are completely fresh (unweathered). The rest is modified in the zone of weathering, to a variable degree. Most pegmatite minerals decompose to form clay and such clay is mostly eroded away, together with the originally present metals, representing a net material loss. A portion of saprolite, gradational to spodumene pegmatite, contains recoverable Li utilized in Greenbushes and in Manono. Resistate minerals, like cassiterite and columbite-tantalite, wadginite, and others remain, little modified by weathering, in residual clay or saprolite to form "eluvial placers", or are reworked into alluvial gravel and sand. These form valuable, cheap-to-mine orebodies, exploited in the early phase of mining in Greenbushes and still successfully mined in Uis, Manono, and many other lesser localities. Sn placers can produce economic concentrations from scattered small occurrences of metalliferous pegmatites that would be uneconomic to mine on their own. Pegmatite sources account for a small proportion of the regolithic tin in SE Asia (Thailand, Malaysia, Indonesia), being most important in the Western Belt in Thailand (e.g. Phuket). Pegmatitic source of placers is usually indicated by high tantalite : cassiterite ratios. There are no zones of "secondary enrichment" in the ore pegmatites outside the hydrated/oxidized zone.

Bernic Lake (Tanco) pegmatite near Lac du Bonnet in south-eastern Manitoba (Trueman and Turnock, 1982; 116 kt Li @ 1.28%, 76,657 t Cs, 7,065 t Rb, 3,668 t Ta @ 0.1278%) is a completely blind, subhorizontal lenticular body discovered, under a lake, by exploratory drilling in the 1930s. It intrudes Archaean meta-gabbro and it terminates in a series of parallel dikes. The pegmatite has been traditionally subdivided into nine mineral assemblage zones (Crouse et al., 1979), interpreted as a concentric set resulting from primary crystallization (microcline, perthite, quartz, petalite, amblygonite, spodumene, pollucite). This was overprinted by metasomatic assemblage of albite > muscovite, lepidolite, beryl and complex Ta-oxides. The present production of spodumene, tantalite, wadginite, Rb-lepidolite, pollucite, amblygonite, and potentially beryl concentrates comes from six zones. The almost monomineralic pollucite body has a reserve of 350 kt of material grading 21.97% Cs₂O, and it is the world's largest, high-grade cesium resource. The delicately rhythmically

banded saccharoidal metasomatic albite, on the eastern flank of the deposit, contains disseminated complex Ta-oxides and scattered lepidolite along the margin. This is a pegmatite specialist's mine as the many minerals, except for lepidolite and the Ta-oxides are white, yet recognizable by a trained eye. The large petalite deposit discovered recently at Separation Rapids in NW Ontario is in the same pegmatite belt. The **Bikita pegmatite field** in Zimbabwe (Martin, 1964) is the closest match to Bernic Lake in terms of mineralogy, but it has more cassiterite and a regolith that includes tin placers.

Greenbushes Sn, Ta, Li deposit (Hatcher and Clynick, 1990; 110 kt Li @ 1.86%, 39,828 t Sn, 8,522 t Ta) is in a high-grade metamorphic belt in the south-western corner of the Archean Yilgarn block, Western Australia. The pegmatite outcrop is weathered to a depth of 50 m where the pegmatite has been converted to a mixture of kaolinite after feldspar and halloysite after spodumene. Residual grains of cassiterite and tantalite are enclosed. A portion of the regolith has been reworked into alluvium that contains cassiterite placers. The 2.5 Ga Greenbushes pegmatite consists of a N-S striking, 40-50° west dipping main body that is 3.3 km long and controlled by a major shear zone. The wallrock gneiss, meta-quartzite and amphibolite have sharp, often boudinaged or mylonitic contacts against the pegmatite, with biotite-holmquistite reaction rims at amphibolite exocontact. The gneissic, deformed and recrystallized pegmatite is interpreted as a syntectonic intrusion (Groves et al., 1986). Although a sort of mineralogical zoning is apparent, the zones are discontinuous, asymmetric and gradational, interrupted by wallrock rafts and a mafic sill. The blocky microcline perthite zone lacks rare metals. The albite > quartz, tourmaline, muscovite zone is fine grained, and it contains scattered spodumene and beryl; it hosts the disseminated cassiterite and tantalite orebody. Several subzones up to 80m thick contain between 30% and 50% spodumene, intergrown with quartz. The pegmatite lacks a distinct core, Li-mica, pollucite and other minerals, and there is no obvious parent granite.

Manono-Kitotolo deposit in Katanga, DRC-Congo (Bassot and Morio, 1989; 837 kt Li @ 2.8%, 292 kt Sn and at least 14 kt Ta) is in an up to 14 km long, 140 m thick, subhorizontal pegmatite "laccolith" emplaced into Kibaran (Mesoproterozoic) micaschist, meta-quartzite and meta-diabase. The wallrocks had been syntectonically granitized at 1.3 Ga and intruded by post-orogenic muscovite leucogranite dated between 947 and 906 Ma. The granite is considered

parental to the 910 to 880 Ma pegmatite, interpreted as situated in or near the roof of a granite cupola. The pegmatite is internally homogeneous, the exocontact is tourmalinized (in schist) or biotitized (in meta-diabase). In places is developed quartz, Li-muscovite, topaz greisen with disseminated cassiterite. The greisen often grades to saccharoidal albite with lepidolite and cassiterite disseminations. The main pegmatite body is composed of a mixture of quartz, microcline, albite, spodumene and mica in various proportions. Along the hanging wall contact, spodumene crystals up to several meters long are oriented perpendicularly to the pegmatite surface. Locally present are 505 Ma old quartz, feldspar, thoreaulite, tantalite and wolframite veins. The "hard", unweathered pegmatite grades between 186 and 1,400 ppm Sn and the highest grades are along the contact. Most of the past production came from pegmatite saprolite, yielding kaolin as a by-product, and from placers. Huge Li, Sn and Ta resource in fresh pegmatite remains.

Other significant rare metal pegmatites include São João del Rei, MG, Brazil (311 kt Li, ~8 kt Ta in regolith); Borborema district in NE Brazil (~113 kt Li); Yellowknife field, NW Canada (75 kt Li); Wodgina in the Pilbara, NW Australia (Rv 508 t Ta, much larger Rc); Koktogai in northern Xinjiang, China; and others.

10.3.2. Zr, Nb, Ta, Y, REE, Th, Be association in peralkaline granites

Apogranite, a term common in the Russian literature (Beus, 1968) and sometimes used in English as well, is a highly fractionated hypersolvus (i.e. free of magmatic plagioclase) partly or fully albitized granite or syenite. Apogranites related to tin leucogranites carry Sn, Ta, Li, Rb (e.g. Pitinga, Cínovec; read above). Peralkaline granites (those with molecular excess of alkalis over alumina) are low in tin (although they often occur in predominantly tin provinces like the Jos-Bauchi in Nigeria, and there are some exceptions) and instead accumulate Zr and one or more of the rare metals listed in the heading. The predominantly feldspathic (albite, K-feldspar) rocks may contain quartz, scattered Na-pyroxenes and amphiboles (aegirine, arfvedsonite, riebeckite) and sometimes fayalite (=Fe olivine). High-silica peralkaline granites are enriched in Be (6-56 ppm), Ga (28-45 ppm), Nb (69-670 ppm), La (95-580 ppm), Y (73-490 ppm), Th (17-23 ppm); Bowden et al (1987). The trace metal contents are still higher in lattices of selected silicates (e.g. aegirine, amphibole) or they form accessory minerals of their own (e.g. zircon, pyrochlore, monazite, xenotime, euxenite,

columbite). Such minerals are considered late magmatic to early postmagmatic (deuteric, autometasomatic) and tend to be evenly distributed. They range from fine-grained "invisible" disseminations to coarse megascopic minerals scattered in the pegmatite facies. As the capacity of these metals to accumulate is rather low, few deposits qualify as "giants" (only one, Abu Dhabbab is a "Ta-giant"). The remaining significant deposits are briefly characterized at the end of this section.

Most peralkaline apogranites are anorogenic to postorogenic, forming small cupolas, stocks, ring complexes, dikes and sills. The majority is undeformed and unmetamorphosed. Few localities have deformed apogranite grading to alkalic migmatite. The favorite setting of these rocks are extensional structures in Precambrian cratons and shoulders of intracratonic rift systems. The type area is on both sides of the Red Sea and in Nigeria.

Zr, Nb, REE, Y, Ta, Th, U peralkaline granites of the Arabian Shield. This large territory in Saudi Arabia only contains about 70 massifs dominated by peralkaline granite, ranging in age from 686 to 517 Ma. The granites postdate continental accretion and are emplaced into foldbelts of island arc derivation. Five of the best mineralized Saudi granites, explored before 1984, contain a cumulative resource of about 4.66 mt Zr, 1.09 mt

Nb, 738 kt Y, 206 kt Th, 98 kt Ta and 54 kt U. The orebodies have the form of low-grade disseminations of ore minerals in "deutericly altered granite" (Ghurayyah), in apical sheets of aplite or pegmatite (Jabal Sa'yid), in pegmatite, quartz pods, veins and apophyses in the roof exocontact (Jabal Hamra), and in the matrix of intrusion breccia (Zubaydah).

The largest **Ghurayyah** deposit near the Red Sea coast in NW Saudi Arabia contains over 80% of the rare metals resource of the entire province (Drysdall et al., 1984; 440 mt of ore containing 3.784 mt Zr, 993 kt Nb, 583 kt Y, 176 kt Th, 93 kt Ta and 51 kt U; Fig. 10.10). Bringing this deposit into operation as a supplier of the more desirable metals (Ta, U) would flood the very limited market with some co-product metals like Y, and a way would have to be devised of how to stockpile the presently unwanted metals like Th. The Ghurayyah stock has a diameter of 900 m with steep contacts and is emplaced into Proterozoic metamorphics. It is composed of peralkaline porphyritic leucogranite cut by a breccia pipe. The granite contains veins and pods of pegmatite, metasomatic quartz, veinlets of fluorite, and up to 5% of disseminated minerals that include zircon, columbite-tantalite, pyrochlore, samarskite, aeschnyrite, xenotime, monazite, thorite and uraninite. Hydrothermal alteration is inconspicuous, represented by albitization, local silicification and chloritization.

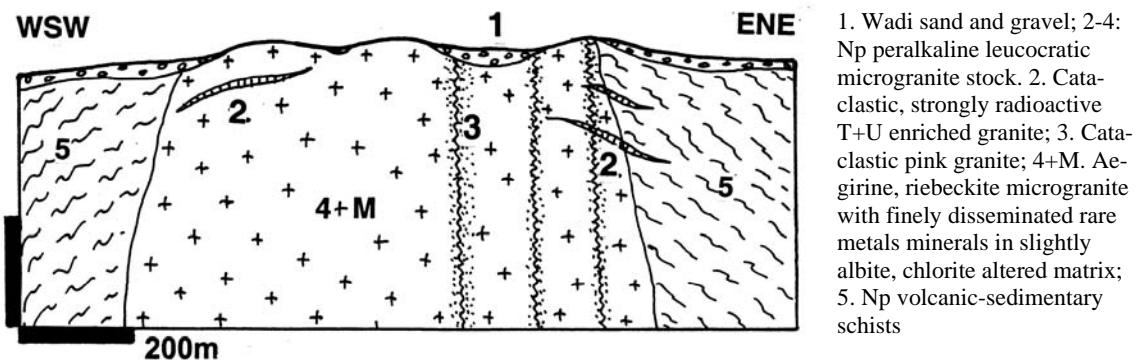


Figure 10.10. Ghurayyah peralkaline intrusion with disseminated minerals of rare metals, NW Saudi Arabia. Cross-section from LITHOTHEQUE No. 2171, based on data in Collenette and Grainger, eds. (1994), Drysdall et al. (1984)

Blachford Lake Complex, NW Canada: Zr, REE, Nb, Ta, Be. This is a 2.6 to 2.3 Ga intrusion emplaced into an Archean greenstone belt about 100 km SE of Yellowknife (Davidson, 1982). The complex is subcircular and concentric, with a diameter of about 25 km. It is composed of several

successively intruded plutonic phases. The earliest phase includes gabbro that grades into anorthosite and ferrodiorite. This is intruded by xenolithic syenite to granite. The latest core of the complex consists mostly of riebeckite granite with internal

core of peralkaline syenite (Thor Lake syenite) and breccia.

This syenite hosts the **Thor Lake ore field** (Trueman, 1983; Rv ~70 mt @ 3.5% Zr, 0.4% Nb, 1.7% REE+Y, 0.03% Ta for 2.45 mt Zr, 280 kt Nb, 1.19 mt REE+Y, 21 kt Ta). The estimated resource is more than 2.4 bt of ore and there is also 1.6 mt @ 0.76% BeO for 14,100 t Be. This ore field comprises at least five separate mineralized zones along the granite-syenite contact, and a 1.5 km long, N-S trending "T-zone", which is saucer-shaped in cross-section. This zone is surrounded by granite and it branches from the pegmatitic syenite. The entire ore field is enriched in rare metals, but they tend to selectively accumulate in separate zones and structures. The largest "bulk" orebody is in the central breccia where columbite-tantalite, zircon and bastnäsite are scattered in magnetite and fluorite matrix. The "T-zone" contains at least five subzones of anomalously concentrated phenacite in the magnetite-albite-riebeckite association, replacing pegmatite. Y and Th are accumulated in quartz-fluorite metasomatite with scattered xenotime and thorite crystals. Large accumulations of Li-mica with up to 7% Li and 0.5% Rb are in a subhorizontally banded body under the central quartz mass. The brecciated quartz contains bastnäsite and parisite in matrix.

Motzfeldt Center ore field in the Igaliko intrusive complex, Gardar province in SW Greenland. There, Nb-Ta mineralized peralkaline granite is a member of the 1.31 Ga alkaline suite (Tukiainen, 1988; ~50 mt @ 0.28-0.7% Nb, 250-820 ppm Ta for about 250 kt Nb and 25 kt Ta; the "conservative estimate" of 410 kt Ta @ 0.41% [Mining Magazine, April 1986] is probably an error in decimal point). This is a ring complex that comprises three steep-sided intrusions of peralkaline and nepheline syenite, emplaced into Mesoproterozoic continental quartz arenite containing mafic to intermediate volcanic interbeds. The outer ring zone has a quartz-normative character, a consequence of magma contaminated by assimilation of the roof arenite. Semi-assimilated blocks of quartzite are common and magma fractionation produced peralkaline residue emplaced as late stage sheets of microsyenite and pegmatite. The latter rocks are reddish-brown, miarolitic, hydrothermally hematitized and albitized. The altered microsyenite contains arfvedsonite, abundant fluorite, disseminated zircon, thorite and patches enriched in pyrochlore. The pyrochlore is enriched in Ta at the deeper levels and in Nb at the upper levels.

Other significant deposits of this type include **Abu Dhabbab** in Egypt (131 kt Ta @ 0.274%, 55 kt Nb @ 0.114%; **Nuweibi** in Egypt (746 kt Nb @ 0.91%, 4,920 t Ta @ 164 ppm); **Strange Lake** in Labrador (52 mt @ 2.17% Zr, 0.24% Y, 0.27% Nb, 0.45% REE, 290 ppm Be for 125 kt Y and 15 kt Be). The Jurassic **Jos-Bukuru Complex** in Nigeria, a major Sn province where cassiterite is won from regolith over tin granites, has also produced ~2 kt Ta. 235 kt Nb @ 0.21% is in the riebeckite granite of a ring complex emplaced into Precambrian metamorphics.

10.3.3. Uraniferous leucogranites, aplites, pegmatites

Highly fractionated granites, especially peraluminous "tin granites", can produce local trace U (and Th) concentrations of the order of 30-50 ppm U or more by purely intramagmatic processes. Such U-anomalous granites are not yet industrial U ores, but they can supply heat to hydrothermal convection and become repositories of uranium liberated and further concentrated/accumulated by a variety of postmagmatic geological processes. These include hydrothermal circulation to form vein deposits, leaching by groundwater for subsequent precipitation at redox interfaces to form "sandstone uranium", transfer to arid duricrusts.

The U concentration has sometimes been enhanced, still within the evolutionary cycle of the parent magmatic system (rather than by a superimposed process), to achieve values approaching economic ores, as in Namaqualand, South Africa; Namibia (Jacob et al., 1986); and elsewhere. The result are uraniferous leucogranites, aplites, pegmatites and alaskites of which the so far only delineated and producing deposit is the "large" (but economically "world class") **Rössing** in Namibia (Berning et al., 1976; 138 kt U @ 280-360 ppm U). This deposit, north-east of Swakopmund, is in high-grade metamorphosed and migmatitic supracrustals of the Neoproterozoic Damara Sequence. The host rocks include biotite-cordierite gneiss, hornblende-biotite gneiss, pyroxene-hornblende gneiss, marble and minor skarn. Partial melting in the upper continental crust produced a large quantity of quartz-feldspathic mobilizate that underwent further fractionation and possibly initial separation of the hydrous phase to produce a U-mineralized "alaskite". The Rössing alaskite is a deep-level intrusion that would be described elsewhere as pegmatite, but it differs from a typical rare metal pegmatite by its disorganized nature, lack of zoning and gradational contacts.

This high-silica light-colour material varies in size from fine crystalline aplite to coarse pegmatite

and it forms injections, replacements, infills of low pressure shadows and dilations, large irregular masses and dikes in two ore zones, each some 500-600 m in length and open at depth. Berning (1986) considered the "alaskite" to have been a syntectite derived by partial melting in depth and epigenetically introduced into its present site at around 468 Ma, separately from the older in-situ synorogenic neosome. The alaskite, nevertheless, replaces and encloses semi-assimilated biotite gneiss inclusions, although the contacts against marble and Ca-Mg silicates are sharp. Uraninite is the main U mineral and it forms micron-size to 0.3 mm large grains enclosed in the rock-forming minerals as well as interstitially. Monazite, zircon and betafite are the associated minerals. Secondary U minerals, mainly beta-uranophane, form pseudomorphic replacements of uraninite grains in the oxidation zone and coat fractures. They accounted for 40% of recovered uranium in the upper mine levels.

Only a fraction of the "alaskites" in the mine area and their biotite-rich inclusions are significantly uranium mineralized so that careful grade control and selective mining are necessary. Economic ore cannot be reliably visually identified, although the uraniferous rocks tend to be darker, usually reddish on the weathered surface, the quartz is often of the "smoky" variety, and there are brightly yellow coatings of secondary minerals. The open pit mine at Rössing has operated successfully since 1978, despite having the absolutely lowest U grade of all deposits mined. Several secondary carnotite deposits in west-central Namibia (the largest is Langer Heinrich) precipitated in calcrete and gypsum-cemented gravels in ephemeral streams, from U leached from uraniferous alaskites.

The peralkaline granite at Ghurayyah, Saudi Arabia (read above) stores some 51.5 kt of disseminated U, partially recoverable should this multiple rare metals complex ever enter production.

10.3.4. Granite-related wolframite deposits (Jiangxi-type)

South-eastern China (Jiangxi, formerly Kiangsi, and adjacent Hunan, Fujian, Guangxi and Guangdong Provinces) store more than 50% of the world's tungsten (some 5.5 mt W plus) in several hundred granite-related, predominantly wolframite, and mostly vein deposits (Kazanskii, 1972; Hepworth and Zhang, eds, 1982; Elliott, 1992). This tungsten (and also Sn, Be, Sb) province, also known as Nanling Metallogenic Subprovince (Kang et al., 1992), contains the greatest share of the 1,500

known tungsten deposits in China, including 25 that are "large and supergiant" (in Chinese magnitude classification). These are distributed in numerous clusters that comprise deposits of variable size, a small percentage of which is of the exceptional magnitude. In the Dayu and Panguan areas, each of which contains "giants", 185 W deposits are in an area of 7,800 km² and 111 deposits are in 11,000 km², respectively (Kang et al., 1992). Unfortunately, up-to date quantitative information is still hard to get from China.

Basement of the **Nanling tungsten province** is the Caledonian orogenic belt, rifted from Gondwana (or ancestral Australian Plate) and accreted to the Yangtze (Cathaysian) platform in the north, in late Ordovician-Silurian time (Hutchison, 1996). The oldest supracrustal rocks are Neoproterozoic (Sinian) and Cambrian low-grade turbiditic meta-sediments with minor meta-carbonate interbeds, intruded by late Silurian granites. These are locally unconformably overlain by Devonian to Carboniferous conglomerate, sandstone and shale, deformed during Permo-Triassic by the Indosinian Orogeny (collision). Widespread Yanshanian (Jurassic-Cretaceous) plutonism in Jiangxi and adjacent provinces had been in response to Mesozoic collisions or, alternatively, to subduction from the south-east that produced the extensive, mostly Cretaceous andesitic magmatic belt traceable from southern China through Sikhote Alin to Alaska.

The Yanshanian granites range from I-type (associated with porphyry W-Mo deposits like Yangchuling; Yan et al., 1980) to the predominant S-type (called in the Chinese literature "transformation granite"). The classical Jiangxi wolframite deposits are associated with the latter granites, and there is a widespread belief among the Chinese geologists that a strong ancient syn-sedimentary or syn-volcanic trace tungsten pre-enrichment in supracrustals had been incorporated into the Yanshanian granite melts and super-concentrated in the course of magma fractionation. Certainly, the trace W contents in the meta-sediments there are anomalous (in the region of 6 to 17 ppm W, hence 6 to 17 times the W clark of 1.0 ppm), and are highest in sediments of the Jurassic fault-bounded basins, broadly contemporaneous with the granitic magmatism (Li Yidou, 1993).

It is believed that much of the eastern Chinese W (and Sn, Be) province is floored, in depth, by large buried mesozonal granitic batholiths (as in the Erzgebirge) and that high-level cupolas of fractionated leucogranites were the "emanative centers" responsible for mineralization. Although

there are local variations, Hu Shouxi et al. (1984) have presented an alteration-mineralization model of an ideal leucogranitic cupola, as follows: 1) the "normal" biotite monzogranite in depth gradually changed to muscovite-biotite granite, then muscovite leucogranite in the core of cupola; 2) the cupola was terminated by a K-feldspar > albite, quartz, mica pegmatoid (=Stockscheider), "armed" with a quartz crust against the hornfelsed meta-sediments; the quartz contains patches of muscovite, fluorite, triplite, wolframite, and base metal sulfides; 3) the early post-magmatic alteration-mineralization started in depth, producing a potassic zone (K-feldspar > quartz, biotite) superimposed on leucogranite; 4) this was overprinted by a K-Na assemblage of K-feldspar, albite, with some quartz and muscovite; 5) Na-metasomatism followed, dominated by albite ("apogranite") with some quartz, Li-muscovite, topaz, lepidolite; 6) greisenization (alkali removal) came next and quartz, muscovite, topaz, fluorite assemblage formed in the uppermost endocontact, and disseminated or stockwork mineralization with wolframite and cassiterite formed at some deposits; 7) predominantly quartz veins filled tensional fractures in both granite and hornfelsed roof rocks.

Different deposits in Jiangxi have different preferences and either granite is the principal host (e.g. Dahutang), or the meta-sediments are (e.g. Xihuashan). The endocontact mineralization is commonly disseminated or stockwork, and magmatic-hydrothermal. The vein filling, at least in the later stages, is the product of convecting meteoric fluids. Hu Shouxi et al. (1984) pointed out that strong greisenization was a prerequisite of a strong W mineralization to form. Simple veins at small deposits are quartz-wolframite only, whereas at large deposits like Xihuashan (read below) the veins are multiphase and vertically zoned. The minority assemblages of composite veins at tungsten deposits, such as Ta-Nb-(Sn), Be, Li, Mo, Bi, Pb-Zn-Ag, appear to be sub-economic, but they form their own accumulations elsewhere as in the "supergiant" Shizhuyuan deposit in Hunan, or in the zoned cassiterite-sulfide centers like Dachang and Gejiu (read below).

Xihuashan (formerly Sihuashan) deposit in the Dayu (Tayu) ore field, Jiangxi (McKee et al., 1987; Giuliani, 1985; Kang et al., 1992; 891 kt W @ 0.88% W) is the largest tungsten "giant" and type locality of vertically zoned exocontact veins. It is genetically related to late Jurassic (151-147 Ma) composite biotite S-granite pluton cut by aplite and pegmatite dikes and emplaced into thermally metamorphosed Neoproterozoic to Cambrian

clastics. Together the five granite phases of the pluton outline an imperfect cupola, but the youngest and most fractionated and altered G-5 granite cuts across the older granites as an irregular, subvertical dike/stock. The earliest equigranular leucocratic (1-5% biotite) granite has the highest Sr, Ba and Ce and lowest Rb, Y and Nb trace contents, plus ore metals. Y, REE, Rb and W, Sn, Be increase into the younger granite phases, but there is a slight depletion as the youngest G-5 phase is reached. This is explained (McKee et al., 1987) as a consequence of partition of these elements into the vapor phase, removal from the residual melt, and transfer into the subsequently formed ore greisens and veins. The G-5 granite is a fine-grained porphyritic leucogranite overprinted by "episyenite" (albitite and microcline alteration patches) with variable amounts of accessory garnet, ilmenite, fluorite, tourmaline, topaz and W, Sn, REE minerals. It is locally capped by a "Stockscheider" pegmatite, and shortly followed by greisenization.

A set of 615 productive, thin (0.4-2 m thick) subparallel fracture veins in a 2.5 km long zone, mostly in the roof of intrusion, is rooted in the G-5 granite and greisen. The veins are vertically zoned, but the zoning is reversed from what one would expect (the most temperate, magmatic-hydrothermal phases are at the upper levels, the low-temperature base metals with fluorite and calcite are at the lowest levels). This is attributed to progressive vein filling under conditions of decreasing fluid temperature, from the initial 420° C to the final 150° C (Giuliani et al., 1988) and increasing involvement of meteoric water. The upper parts of veins carry mainly cassiterite, topaz, beryl and helvite. The middle, most productive parts, have wolframite with minor molybdenite and bismuthinite in quartz, K-feldspar gangue. The lower part of veins is dominated by carbonate and fluorite gangue with arsenopyrite, pyrite, pyrrhotite and Pb, Zn, Cu sulfides. Some veins have narrow greisen envelopes, others a narrow muscovite liner against the wallrock.

Dajishan (formerly Tachishan; Shi and Hu, 1988; Kang et al., 1992; veins Pt 52 kt W @ ~2% W, overall Pt about 102 kt W) has been in operation since 1918, with production coming from several sets of WNW-trending, steeply north dipping fracture veins in Cambrian meta-arenite in granite roof, hence a configuration comparable with Xihuashan. In the 1970s a blind body of mineralized granite has been discovered at depth. The granite has the form of a convex cap, detached from the main body of a pluton about 300 vertical meters below. The composite intrusion ranges from

a 167 Ma biotite granite through biotite-muscovite granite to a 159 Ma muscovite granite, which hosts a complex disseminated and stockwork W, Be, Nb, Ta mineralization formed shortly after emplacement of the host granite. The vein system, in contrast, is younger, dated around 142 Ma. Whereas the rare metals are uniformly disseminated throughout the feldspathized granite (apogranite), late wolframite forms scattered superimposed nests and patches contemporaneous with the exocontact veins.

Additional tungsten "giants" in the Nanling Subprovince, and mostly in Jiangxi, include the **Piaotang** deposit (also in the Dayu district) said to have a large reserve; **Pangushan** (112 kt W @ 1.2% W; subvertical fissure veins in Devonian clastics); **Yachishan** (118 kt W in exocontact veins); and **Gueimeishan** (107 kt W; sheeted quartz-wolframite veins). The tonnages are from the old paper by Ke-Chin Hsu (1943) (alias Xu Keqin), and are rather obsolete now. The more recent literature provides some geological descriptions, but no tonnage (Kang et al., 1992). They, however, rank Jubankeng in Guangdong as the "largest quartz-W vein"; Xingluokeng in Fujian as the "largest veinlet-disseminated W in granite"; and Damingshan in Guangxi as the largest "stratoid" tungsten deposit. Presumably the deposits (an others) are of our "giant" magnitude.

There is an emerging tungsten province in the **North Qilian Orogen** in Gansu, north-central China (Kang et al., 1992; Mao Jingwen et al., 1998), in which two "giant" deposits (Xiaoliugou and Ta'ergou) are credited with the endowment of 200,000 t W each. They are supposedly related to Ordovician (442 Ma) I-type granodiorite to biotite granite emplaced into Paleoproterozoic marble, schist, amphibolite and gneiss; Meso- to Neoproterozoic ophiolite, phyllite and meta-carbonates; and Ordovician mafic metavolcanics. **Xiaoliugou** is a quartz-wolframite, muscovite, fluorite, beryl, arsenopyrite vein and greisen deposit (~180 veins grading between 0.3% and 5.1% W, 0.03-0.54% BeO); **Ta'ergou** is an exoskarn with endogreisen with quartz, fluorite, scheelite, wolframite, cassiterite, beryl, grading 0.144% to 0.48% W and 0.003-0.3% BeO.

The **East Qinling Metallogenic Subbelt** in east-central China (Kang et al., 1992; west of Zhengzhou) is another emerging tungsten province mostly mineralized by Mo-W (scheelite) stockworks and skarns (compare Section 7.5 above). The **Sandaozhuan W-Mo** deposit is ranked as a "W-supergiant" in the Chinese literature, one of the four largest tungsten repositories in the country.

The most recent major tungsten discoveries in China, according to the China Geological Survey 2004 brochure, are in the Qinghai Province, in the West Kunlun orogen. The **Baigan Lake** area supposedly contains 24 orebodies in two 15 km long, 2-4 km wide Sn-W belts credited with 500 kt W @ 0.3% and 200 kt Sn @ 0.23%.

There do not seem to be any wolframite vein/stockwork "giants" outside China. The nearest candidate, **Panasqueira in Portugal** (Kelly and Rye, 1979; Fig. 10.11), has an endowment of 75 kt W; Hemerdon wolframite stockwork in Cornwall, England, stores 60.5 kt W in 42 mt of ore grading 0.144% W. The largest European tungsten deposit, Felbertal in Austria, is an enigmatic stratabound scheelite dissemination in metamorphics (Chapter 14). Genetic affiliation to a granite cannot be excluded, although credible evidence is missing.

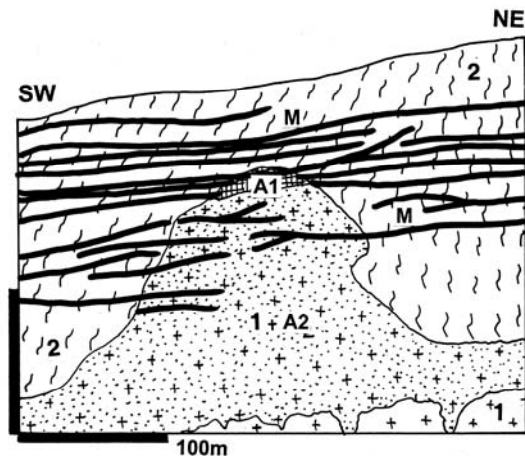


Figure 10.11. Panasqueira wolframite deposit, Beira Baixa, W-C Portugal. Cross-section from LITHOTHEQUE No. 101, modified after Kelly and Rye (1979). M. Post-290 Ma swarm of subhorizontal multiphase quartz, muscovite, ferberite, arsenopyrite, chalcopyrite, etc. dilational veins in hornfelsed roof above granite cupola; 1. ~290 Ma peraluminous muscovite leucogranite; A1. Silicified quartz cap in cupola apex; A2. Greisen-altered cupola; 2. Cm metapelitic schist, hornfels near granite contact

10.3.5. Granite-related tin deposits

If subvolcanic "porphyry-Sn" and vein deposits (Llallagua, Potosi, Oruro, San Rafael. Morococala; Chapter 6) are excluded the rest of the world's tin endowment is related, directly or indirectly, to granites. When the "porphyry-Sn" are included (as they are ultimately related to granitic systems in depth as well), the world's total ore tin tonnage is of

the order of 30 mt Sn. Deposits that store this tin are dominated by "giants" and can be subdivided into the following sub-categories (see also Fig. 10.1):

- subvolcanic "porphyry-Sn" and related veins; about 5 mt Sn (read Chapter 6)
- rare metals (Li, Rb, Cs, Ta, Nb, Sn, Be) pegmatites; about 800 kt Sn (read above)
- "Cornwall-type" Sn (~W, Cu, Mo, Bi, Be) vein, stockwork and disseminated deposits in granites and silicate wallrocks; about 4.7 mt Sn
- "Pitinga-type" or "Jos-Bauchi (Nigeria)-type" complex Sn, Ta, Nb disseminated deposits in albitized cupolas; about 1.5 mt Sn
- Skarn and replacement Sn deposits; about 2.5 mt Sn
- Cassiterite (and minor tantalite-columbite) regoliths and placers; about 15 mt Sn

The above groups are not sharply delineated and there are transitions; for example, the skarn/replacement orebodies are members of a system that includes granite as well (obvious or concealed), often simultaneously mineralized. The tonnage figures for tin placers apply to often large mineralized areas and they may include tin derived from small bedrock deposits as well.

Cornwall-type granite-related Sn (W, Cu, Mo, Bi, Be) veins and stockworks in silicate rocks: Genetic background to these deposits has already been provided in the introduction to the collisional granite metallogeny above, on the example of the Erzgebirge/Krušné Hory metallogene. This subgroup includes about six "giant" deposits or ore fields (Redruth-Camborne, 310 kt Sn; Altenberg, 210 kt Sn; Cínovec, 260 kt Sn; Krásno, 290 kt Sn; Komsomolsk na Amure, 300 kt Sn; Khapcheranga, 240 kt Sn). Of these the magnitude of Khapcheranga is uncertain, perhaps exaggerated. Deposits/ore fields Deputat and Kavalerovo in eastern Russia may be of the "giant" magnitude, but no reliable figures are available. There are about 7 or 8 "large" deposits, some approaching "giants". Cumulative tin endowments for districts and regions, such as Cornwall (2.5 mt Sn), include placers as well as bedrock deposits and they are summarized under Sn placers. All these deposits are related to peraluminous (S-type) leucogranites, fractionated from biotite granites and the orebodies are 1) in cogenetic granites, which they shortly postdate; 2) in roof rocks above the source granites; 3) in both; and 4) in older host rocks (including granites), with no potential source granite in sight.

Cínovec (in Czech Republic) and **Zinnwald** (across the border in Saxony), in eastern Erzgebirge

(Štemprok and Šulcek, 1969; Štemprok et al., 1995; P+Rv ~150 kt Sn, 30 kt W plus low-grade Rc ~55 mt ore @ 0.2% Sn, 0.045% W for total of 260 kt Sn, 54 kt W. Potential resource in zinnwaldite granite: 550 mt @ 0.25% Li, 0.18% Rb, 0.01% Cs, 67 ppm Th and 32 ppm U for 1.43 mt Li, 990 kt Rb, 55 kt Cs and 36,850 t Th). This is in an almost ideal late Carboniferous to Permian broad leucogranite cupola related to medium-grained porphyritic granite to microgranite emplaced into comagmatic rhyolite and ignimbrite issued from the nearby Altenberg Caldera (Seltmann, 1994). The elliptical cupola dips gently (30°) in the north and south, steeply (80°) in the west. Late magmatic to postmagmatic autometasomatic alteration starts imperceptibly in a depth of about 730 m under the cupola roof with the appearance of initially intercrystalline, later K-feldspar destructive albite, and with the formation of protolithionite. The intensity of metasomatism increases upward and the albitization is locally total, producing albitite lenses and pipes associated with zinnwaldite. The most common rock variety is albitized and partly sericitized, kaolinized lithian granite composed of quartz, K-feldspar and zinnwaldite with accessory fluorite, topaz and low-grade disseminated cassiterite, zircon, columbite and other minerals. In about the middle of the albitized granite appear irregular bodies of K-feldspathite (metasomatic syenite) and the roof contact of the cupola is represented by K-feldspar pegmatite liner (Stockscheider). The Na-, then K-alteration and low-grade Sn, Li mineralization are early postmagmatic-hydrothermal. There is no obvious structural control.

Shortly after cupola emplacement several flat ore lodes filled planes of contraction parallel with the cupola roof, enveloped or connected by quartz, zinnwaldite, lesser topaz and fluorite greisen. The lodes are up to 1 m thick, often symmetrical, with core of quartz with scattered large crystals of cassiterite, wolframite and occasional rarer minerals like scheelite, stolzite, arsenopyrite, galena, sphalerite and others. A regular, coarse ("pegmatitic") zinnwaldite selvages line the lode quartz against the greisen envelope. The greisen interval in Cínovec is 200-300 m thick and contains a large resource of low-grade Sn, Li, Rb and Cs material.

Altenberg in Saxony, about 5 km north of Cínovec (Fig. 10.12), has been the largest Erzgebirge tin producer (Chrt and Bolduan, 1966; Rösler et al., 1968; P+Rv ~50 mt @ 0.3% Sn, 0.18% Li, 0.244% Rb, 117 ppm Bi for 150 kt Sn, plus remaining low-grade Rc of ~60 kt Sn for 210 kt Sn total) and about the most spectacular one.

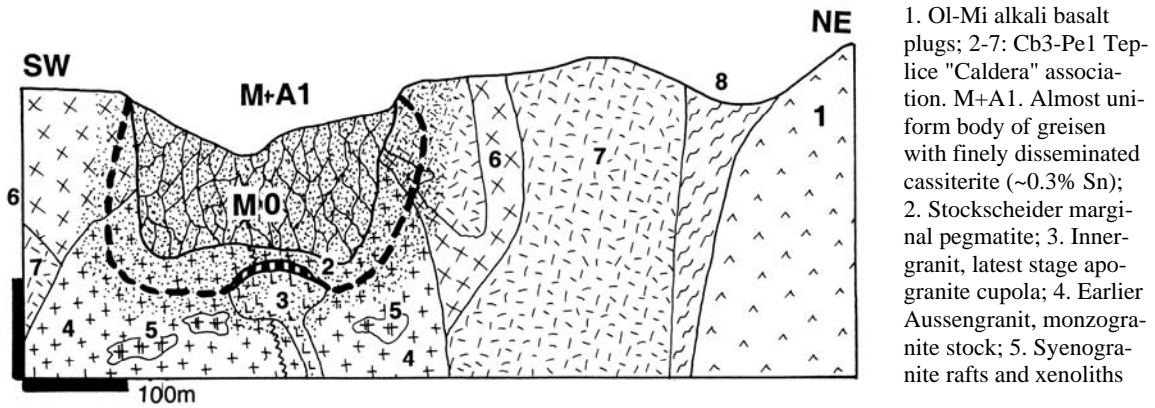


Figure 10.12. Altenberg tin granite cupola and greisen Sn orebody. Cross-section from LITHOTHEQUE No. 3101, modified after Seltmann and Schilka (1995), Ossenkopf & Helbig (1965). Explanations (continued): 6. Older porphyritic granite; 7. Cb3 Teplice Quartz Porphyry, rhyolite flow and subvolcanics; 8. Np gneiss to migmatite

Seltmann (1994) interpreted Altenberg setting as a late Carboniferous caldera, formed by collapse into the magmatic chamber of the older (barren) "Gebirge" biotite granite. This triggered extrusion of rhyolitic ignimbrite, emplacement of granite porphyry dikes, and resurgent granite cupolas. The earlier cupola was thoroughly greisenized shortly after emplacement, and again following intrusion of a ridge-shaped stock of highly fractionated albitized leucogranite ("Inner Granite") with its own greisen envelope. The latter is capped by a thin pegmatitic Stockscheider almost entirely autometasomatically converted into pure, columnar topaz ("pyknite"). The earlier greisen is a dark gray topaz, quartz, Li-biotite rock (locally called "Zwitter"), the younger greisen is a light, bleached, hematite-pigmented rock. Cassiterite with lesser wolframite, molybdenite, bismuthinite, bismuth, arsenopyrite and rarer minerals come as filling of hairthin (0.06-0.1 mm) fractures in the greisen, giving the whole mass an average grade of 0.3% Sn. Altenberg has been the site of medieval mining that persisted, with some breaks, until 1992. Initially, the richer portions of Zwitter had been selectively mined and gravity separated. A catastrophic roof caving into the underground workings created a steep-walled, rubble-filled depression called Pinge, a tourist attraction until recently (the Pinge has now been fenced), and the post-collapse mining was essentially an ore withdrawal from this unplanned block caving.

Krásno (formerly Schönfeld) and **Čistá** (Litrbachy) deposits in the Horní Slavkov-Krásno ore field (Chrt and Bolduan, 1969; Jarchovský, 1994; P + low-grade resources ~290 kt Sn) are in an

about 10 km long NE-SW line of albitized (apogranite) and locally greisenized Permian-Carboniferous leucogranite cupolas emplaced into migmatitized Proterozoic paragneiss in NW Czech Republic. This block is separated from the Erzgebirge, in the north, by the Tertiary Ohře River graben, but is an extension of the Erzgebirge metallogene. Two adjacent mineralized stocks near Krásno, emplaced into hydraulically brecciated gneiss roof, produced from massive and up to 200m thick quartz, topaz, zinnwaldite greisen bodies laced by a thin fracture stockwork and disseminations of cassiterite, wolframite, arsenopyrite, molybdenite and chalcopyrite; the Hüberstock alone is estimated to have originally contained about 150 kt Sn and 70 kt W. With increasing depth the greisen passes, through a transitional zone, into albitized granite, leucogranite and eventually unaltered K-feldspar monzogranite. The transitional zone contains intervals of hypogene argillization (kaolinite). Several mineralogically complex Sn, W, Cu, Pb, Zn veins and carbonate-pitchblende veins occur in the stock aureole. The Čistá deposit, discovered in the 1960s, is a low-grade (between 0.2-0.3% Sn), concealed deposit of disseminated cassiterite with a relatively high Ta content, in elongated bodies of greisen superimposed on a laccolithic Li-mica granite (3-6% protolithionite to zinnwaldite) with accessory topaz (Jarchovský, 1994).

Cornwall (and part of Devonshire), in SW England (Dines, ed, 1956; Dunham et al., 1978; Halliday, 1980; Halls, 1994; 2.5 mt Sn, 2 mt Cu), has about the same area as the Erzgebirge, but much greater cumulative tin and copper production making it a

Sn "giant district". This district has been mined, with interruptions, since the Celtic prehistory, then by the Romans, and eventually by the modern industry. The last operating mine, South Crofty in Camborne, survived until the late 1990s. Much of the early tin came from alluvials and there are no sufficient records to assign the total Sn and Cu production to the individual ore fields, with exception of the Camborne-Redruth Sn+Cu field, the only undisputable "giant".

The peninsula is underlain by a folded, thrust, faulted and locally thermally metamorphosed sequence of monotonous Devonian to Lower Carboniferous shale, siltstone and sandstone with local meta-basalt (spilite) units and rare carbonates. These were intruded by five large diachronous Permian (293-274 Ma) biotite S-granite cupolas carried "on the back" of a more extensive batholith in depth. Each cupola is believed to have evolved independently, with its own associated early mineralization, followed by more regional, late stage ores. Halliday (1980) demonstrated the at least 75 million years long history of metallic ore formation, postdating granite emplacement and not directly related to it (the supposed direct genetic association of granite and hydrothermal ores, as in Cornwall, was the basis of the metal zoning model around granitic intrusions, popular in the 1930s to 1950s). Using "typical" ages, some of the 293 Ma plutons evolved, around 285-280 Ma, rare endocontact greisens with sheeted quartz, cassiterite and/or wolframite stockworks (e.g. Hemerdon); around 280-275 Ma, after fracturing, were emplaced granite porphyry dikes ("elvans"), followed shortly by the Main Stage of Sn, W and Cu lode mineralization. This stage is responsible for the bulk of the Cornish tin and copper; at around 270 Ma formed minor Pb, Zn, Sb, Ag, Cu veins; between 230 and 220 Ma originated the remaining low-temperature polymetallic, uranium, fluorite and barite veins. Minor remobilization events persisted through the Tertiary, alongside regolith development and placers formation. Except for the earliest and highest temperature magmatic-hydrothermal ores, the vein deposits are meso- to epithermal, precipitated from heated basinal fluids and meteoric waters preferentially channelled by the "crosscourses" (NW-trending faults; Halls, 1994). There is a general consensus that Sn was derived from the granites, particularly the highly fractionated leucogranites, during alteration, whereas copper came from the "greenstones" that are rich in trace Cu (43-115 ppm Cu).

The "giant" **Redruth-Camborne** ore field (P+Rv ~310 kt Sn, 850 kt Cu; Soft Crofty Mine

alone had P+R 115.5 kt Sn @ 1.5% Sn, 34 kt Cu; Fig. 10.13) is immediately north of the Carnmenellis granite pluton (and cupola), considered one of the "emanative centers" (Dines, 1956) of ore fluids. It has a thick swarm of subparallel, ENE-trending fault, fissure and breccia lodes partly hosted by the granite, porphyry dikes, but mainly by Devonian turbidites and metabasites. The earlier greisen-bordered fractures at granite edge are filled with quartz, K-feldspar, muscovite, cassiterite, wolframite, arsenopyrite, löllingite. The later, complex, Main Stage lodes have cassiterite, chalcopyrite, chalcocite, arsenopyrite, sphalerite, hematite and other minerals in gangue of tourmaline, quartz, chlorite and fluorite. The veins are tabular, several centimeters to 12 m wide, traceable along strike for 500-1,000 m and exceptionally up to 6 km. Some have been mined down to depths of 750 m. The Sn:Cu ratio varied. The Dolcoath Vein has produced 355 kt Cu and 93.5 kt Sn, whereas other veins carried exclusively chalcopyrite and chalcocite (e.g. Devon Great Consols, 776 kt Cu).

The Dolcoath Main Lode near Camborne, the most productive vein in Cornwall, is a 50-90° SW dipping structure that continues for 1.5 km. The thickness varies between 0.3 and 12 m and the lode is filled by brecciated quartz, tourmaline and cassiterite in depth where granite is the host rock, and by comb quartz, pyrite and chalcopyrite near the surface, in slate and greenstone wallrocks. The wallrock alteration includes silicification and tourmalinization in granite, sericitization and chloritization in the sedimentary rocks.

Additional deposits or tinfields of the Cornish-type already mentioned, as well as those in eastern Australia, appear in Table 10.1.

Pitanga-type disseminated Sn, Li, Be, Ta, Nb deposits in albitized cupolas: This is a subtype of the leucogranite-related deposits that is not entirely unique as it merges with the "tin granite" category reviewed above; separate treatment is just a matter of preference and emphasis. In terms of composition, complexes of this type are close equivalents of the "rare metals" pegmatites (read above) at epizonal to, locally, subvolcanic crustal levels. Although Pitanga in Brazil is the "giant" representative, it is not well exposed because of the intensive tropical weathering and clastic reworking. The best studied locality of this type is **Echassières** in the French Massif Central (Fig. 10.14) which, unfortunately, is far from being a giant.

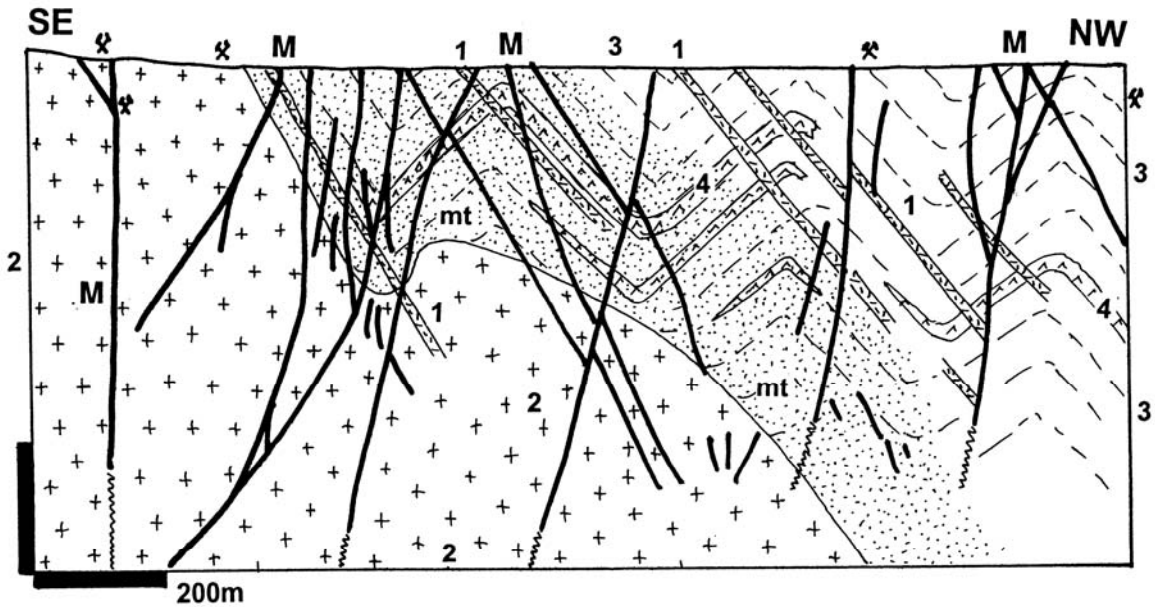
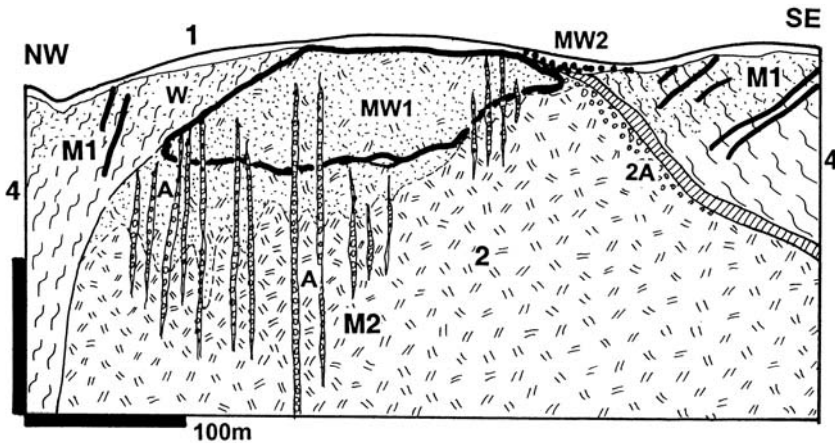


Figure 10.13. Camborne-Redruth Sn-Cu ore field, Cornwall, SW England. Cross-section from LITHOTHEQUE No. 2108 between the old Dolcoath and Roskear mines, modified after Dines (1956). Greenstone bodies and "killas" positions are diagrammatic. 1. ~270 Ma "elvans", granite porphyry dikes; 2. ~285 Ma Carn Brea peraluminous porphyritic muscovite-biotite monzogranite; M. ~286-280 Ma array of subparallel NE-trending Sn-Cu mineralized fault & fissure veins and lodes crossed by a NW-trending set. Dotted: hydrothermal alteration, mt=thermal metamorphism (hornfelsing). 3. D "killas", slate to phyllite; 4. D metabasalt and metadiabase sills



1. T-Q unconsolidated sediment with MW2=Sn placers; W. Regolith, especially MW1=kaolinitic clay; M1. Cb quartz-wolframite fissure veins; 2, M2. ~305 Ma cupola of epizonal albite, topaz, lepidolite apogranite with scattered cassiterite and Li, Be, Ta minerals; 2A. Marginal pegmatite; A. Li-muscovite greisen-altered fractures; 4. Np biotite-staurolite schist

Figure 10.14. Beauvoir apogranite cupola near Echassières, Massif Central, France. Cross-section from LITHOTHEQUE No. 1770, modified after Burnol et al. (1980)

The Beauvoir granite intrusion at this locality includes ~21 mt of material with 0.13% Sn, 0.8% Li₂O, 500 ppm BeO, 300 ppm Nb+Ta and 117 ppm W (Burnol et al., 1980; Cuney et al., 1992). This is a Permian peraluminous biotite granite cupola intruded by several highly fractionated younger intrusive phases that include the Beauvoir albite-

lithionite granite. Lithionite makes up to 20% of the granite and there are disseminated cassiterite, herderite, montebrasite, microlite and topaz. This granite is deeply weathered and residual kaolin is the main product of present mining.

Pitinga, located in the Amazon forest 250 km north of Manaus, Brazil, is a rich alluvial and

residual cassiterite and tantalite deposit (El Koury and Junior, 1988; Rv 269 kt Sn, 1.7 mt Zr, 210 kt Nb, 24.6 kt Ta; Rc is 575 kt Sn in placers containing, on the average, 2.1 kg/m³ Sn). The present production of tin and tantalum comes exclusively from the deep tropical regolith and there is a large future resource in the fresh granite underneath. Disseminated cassiterite and the Zr, Nb, Ta, Be minerals are in greisen and adjacent albitic stock within a Mesoproterozoic (1.69 Ga) cupola of rapakivi-like biotite granite.

Yanbei in southern Jiangxi, China, the "largest porphyry tin in China" (Liu et al., 1999; 300 mt ? @ 0.5-1.5% Sn, 0.13-0.37% Cu, 78 ppm Nb, 10.25 ppm Ta), is a deposit of disseminated cassiterite, chalcopyrite, columbite and other minerals in peraluminous topaz granite pluton emplaced into rhyolite in a fault zone. The high Cu content is unusual in this ore type.

Replacement Sn deposits in carbonates: Even this sub-category is not completely unique, as all Sn replacements in carbonates are related to granite as the most likely source of tin and hydrothermal heat, if not always of the mineralizing fluid as well. Most such granites, when recognized, also host some mineralization themselves. As before, it is a matter of proportions as many of the Sn systems in silicate rocks reviewed above also include some carbonate Sn replacements, even if economically insignificant.

Sn-skarns

Einaudi et al. (1981) have reviewed the sub-group of "tin-tungsten skarns" and concluded that they are very rare, ranging from 0.1 to 3 mt in size. They are associated with extensive greisen in the endocontact, with prominent idocrase and Mn-rich garnet in the prograde skarn assemblage, and with Sn-titanite malayite in addition to cassiterite. Simple tin skarns are indeed small and rare (perhaps with the exception of Pöhla-Hämmerlein), but the literature headings usually apply to complex polymetallic systems that also include skarn (often not even tin-bearing) among the many varieties of other orebodies. The zoned Sn-polymetallic ore fields of Gejiu and Dachang in China, and especially the "super-giant" Shizhuyuan in Hunan, are among the world's largest tin repositories of this sort.

In the true skarn silicate association tin can be bound 1) in the lattice of silicates (up to 4.75% Sn in Ca-garnets, up to 2.4% Sn in some amphiboles) or in malayite CaSnSiO₅, most widespread in wollastonite skarns; this mineral may be more

common but it is difficult to recognize as it resembles titanite or grossularite; 2) as fine, "invisible" cassiterite dispersed in a carrier ore mineral like pyrrhotite or magnetite; 3) as megascopic cassiterite on fractures and in veinlets of skarn minerals. Laznicka (1985, p. 1186-1190) reviewed several small Sn-skarn deposits, to which should be added the only recognized "giant" **Pöhla-Hämmerlein** on the German side of the Erzgebirge. This deposit (Velichkin and Malyshev, 1993; Rv 58 kt Sn @ 0.42% in the Hämmerlein section only, Rc of ~300 kt Sn and 48 kt W in the low-grade material; R. Seltmann, oral communication, 1995; Fig. 10.15) was discovered during the secretive vein uranium mining and exploration in the 1970s-1980s. This probably kept it too long away from development, until it was too late (Pöhla is now a "Gastbergwerk"). The Sn orebody is pyroxene-garnet and pyroxene-epidote skarn with disseminated replacive and fracture-filling pyrrhotite, sphalerite and cassiterite in carbonate-containing Cambro-Ordovician schist and marble sequence, in roof of a Permian tin granite cupola. There is a minor development of quartz-cassiterite veins and veinlets in granite, some with greisen rims. Uranium veins that made Pöhla the second largest U deposit in the Erzgebirge, are dated at 270 Ma and they carry pitchblende with minor sphalerite, galena and local Ni-Co arsenides with Ag sulfosalts in gangue of quartz, calcite and fluorite. They are controlled by major faults.

Cassiterite replacements in marble, no skarn

This type, also called "distal skarn" (this is not a good term as "skarn" refers to a Ca-Mg silicate assemblage) is best developed in the Western Tasmanian tin province, Australia, where it is related to Devonian post-orogenic peraluminous granites emplaced into a Cambro-Ordovician orogenic belt. Where exposed (e.g. at Heemskirk) these granites carry small cassiterite vein- and greisen deposits. Where granite cupolas or porphyry dikes are emplaced into a roof that consists of alternating clastics and carbonate beds, sulfide-rich cassiterite replacements formed in thermally metamorphosed marble and associated feeder fractures. The first deposit of this type, **Mount Bischoff** near Waratah (Groves, 1972; P+Rv 10.3 mt @ 1.13% Sn for 116 kt Sn) started as a very high-grade operation in a sandy cassiterite-quartz regolith, remaining on top of the replacement ore.

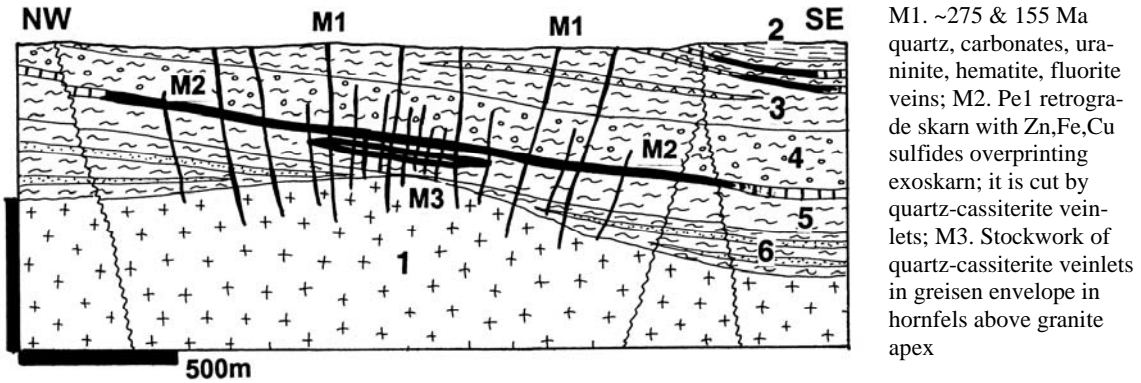


Figure 10.15. Hämmerlein Sn, U, Zn deposit, Erzgebirge in Saxony; cross-section from LITHOTHEQUE No. 2201, modified after Velichkin and Malyshev (1993). Explanations (continued): 1. Cb3 adamellite overprinted by leucogranite; 2. Cm3 metaturbiditic phyllite with quartzite interbeds; 3. Cm2 quartz, biotite, muscovite schist with marble and amphibolite lenses; 4. Ditto, quartz, garnet, muscovite schist; 5. Cm1-2 schist with marble and skarn lenses; 6. Cm1 micaschist with quartzite horizons

The largest deposit in the belt and the only "giant" is Renison Bell, discovered in 1890 and still active (with interruptions).

Renison Bell (Patterson et al., 1981; P+Rv 287 kt Sn @ 1.4% Sn, possibly up to 400 kt of contained tin) is located on eastern flank of a NW-SE trending anticline, intersected by a subparallel, longitudinal fault. A small granite outcrop is about 3 km SE of the orebodies, which, however, are believed to lie above a granite ledge in depth. The roof rocks are thermally metamorphosed Lower Cambrian fine clastics (sandstone, siltstone, shale) interbedded with massive to laminated dolomite. The principal orebodies are bedded replacements of three dolomite horizons; the replacement ranges from complete to partial and the metasomatic fronts advance from the Federal-Bassett Fault. The ore is composed of massive pyrrhotite with dispersed, mostly "invisible" cassiterite, and variable but small amounts of chalcopyrite, pyrite, arsenopyrite, stannite and other minerals. The alteration minerals and gangue are the same (tourmaline, quartz, tremolite, talc, siderite and fluorite), with the metasomatic front rimmed by talc. The steeply dipping fault zone is veined by quartz with coarser-grained cassiterite and sulfides. The fluid temperatures ranged from 390° to 130° and most are in the mesothermal category.

10.3.6. Cassiterite regoliths and placers

Cassiterite is a chemically and mechanically resistant mineral so it survives both tropical chemical weathering that produces soft, easily

erodable regolith, and stream transport that forms alluvial placers. Marine beach cassiterite placers also occur, but most of the offshore cassiterite resources are in buried alluvial channels under the near-shore marine sediments. This combined weathering-ressedimentation mechanism has produced areally extensive tin deposits that are easy and cheap to mine using primitive technology, over and around cassiterite-mineralized granite systems. Some such systems contained sufficiently rich and locally accumulated primary Sn (plus other metals) orebodies to be mined on their own, simultaneously with the regolith mining or after exhaustion of the secondary resources. There are numerous examples, including the "giants" (Cornwall, Erzgebirge, Gejiu; also the "porphyry-Sn" deposits of Bolivia). Other granite-related Sn ore systems consisted of scattered small deposits of various types, but mostly of small quartz-cassiterite veins, disseminated cassiterite in greisen, and disseminated cassiterite in albitized "apogranites". The latter would be uneconomic to mine on their own, in the hard-rock primary zone. It is possible that undiscovered major bedrock tin deposits still remain, masked by the thick tropical regolith in the SE Asian Tin Belt, Rondônia, and elsewhere.

The secondary cassiterite occurrences are of many types, divisible into the following first order categories: 1) in-situ cassiterite-bearing regoliths ("eluvial placers"); 2) alluvial (stream) placers; 3) lacustrine and marine placers; and 4) glacial and fluvio-glacial unsorted detrital deposits changing to placers. The many varieties of the secondary Sn deposits in the humid tropical coastal setting, as in

Thailand, Malaysia and Indonesia are described and classified by Hosking (1969, 1979). Significant cassiterite resources, however, also occur in the less known places as in Siberia, along the Arctic Ocean coasts (Patyk-Kara, 1999); there, they are the relics of regoliths formed under warmer climates before the Quaternary glaciation and preserved either in the non-glaciated tracts of land, or under the protective cover of a "gentle" glacial drift or nearshore sediments.

Placer deposit of any type are usually difficult to delineate as hundreds of small placers and regoliths coalesce to form large regional systems that follow the drainage patterns, sometimes subdivided on the basis of political boundaries that do not correlate with geology. It is also difficult to differentiate between the primary and secondary tin, as many production and reserve statistics do not provide a breakdown. Table 10.1 thus may not be accurate and exhaustive and formulation of "giant" metal accumulations is sometimes quite subjective, depending on where one draws the boundary.

In the 2,800 km long, 400 km wide Sundaland or Southeast Asian Tin Belt (Myanmar, Malaya, Indonesia; Batchelor, 1979; Schwartz et al., 1995; ~9.6 mt Sn) several generations of cassiterite deposits in regolith and resedimented clastics have been forming since Miocene. Despite centuries of intensive mining substantial tin resources are believed to still remain in the subsurface and in offshore. Over 55% of the total tin production came from the Main Belt in Malaya and southern Thailand. The earliest, pre-Miocene regolith over the Triassic and Cretaceous tin-mineralized complex first shed colluvial placers. These formed under savanna conditions of alternating wet- and dry- seasons and some remain preserved as a cover over paleo-stream divides, a few hundred meters downslope from their bedrock source. These were succeeded by Pliocene piedmont fan placers and "debris flows of sodden stanniferous regolith including core boulders and talus" (Batchelor, 1979). They form discontinuous massive wedges along valley sides and are particularly well developed in the Kinta Valley (read below). Cassiterite in both types of slope placers is angular, sometimes intergrown with quartz. Further sorting and rounding of the clastic material in streams produced alluvial placers, both buried and exposed.

Kinta Valley near Ipoh, Perak, Malaya (Rajah, 1979; Schwartz et al., 1995; P₁₈₇₆₋₁₉₇₆ 1.98 mt Sn; Fig. 10.16) is the most famous and one of the most productive tinfields in the Sundalands, where 130 years of continuous mining has resulted in a large

amount of unconsolidated cover removed which has exposed scattered mineralized bedrock exposures.

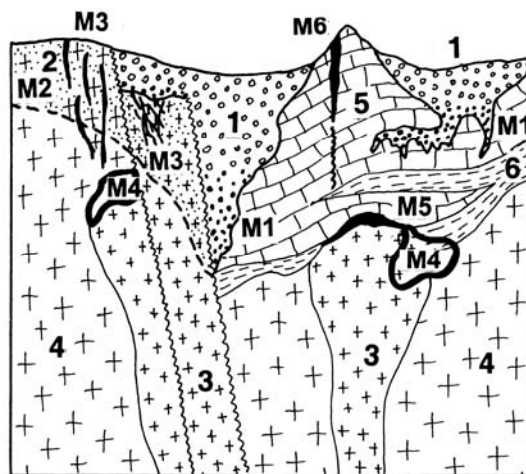


Figure 10.16. Kinta Valley near Ipoh, Perak, Malaysia; diagrammatic cross-section of the Tekka Mine in Lahat from LITHOTHEQUE No. 2291 (P. Laznicka, visit, 1998). 1+M1. T3-Q alluvium and colluvium partly filling fault and karst depressions, with cassiterite placer; 2+M2. T3-Q humid tropical regolith, disseminated residual cassiterite in argillized greisenized granite and M3-M5 regolith; M3. Tr cassiterite in veins, stockworks, pegmatite; M4. Tr disseminated cassiterite in greisen; M5. Disseminated cassiterite with Fe, Cu sulfides and magnetite in skarn and marble; M6. Tr hydrothermal massive hematite veins. 3. Tr peraluminous tin granite, younger phase; 4. Ditto, older phase biotite granite to adamellite; 5. Pe distal turbidite, hornfelsed; 6. Pe limestone recrystallized to marble in granite roof

There, a system of Triassic peraluminous granite cupolas consists of regionally distributed older megacrystic biotite granite to adamellite phase, locally intruded by a younger, highly fractionated muscovite and/or tourmaline leucogranite stocks and dikes. Thermally metamorphosed Devonian to Permian supracrustals, now hornfelsed turbidite and limestone marble, form rafts in granite and remnants of the roof. Scattered small cassiterite occurrences form small lodes, disseminations in endo-, less often exo-greisen and quartz, tourmaline, muscovite, K-feldspar, cassiterite veins in hornfelsed meta-sediments. Small Sn-Cu exoskarn and sulfide replacements are in marble near granite. Low-temperature, late-stage massive hematite veins replace marble and breccias along faults. The marble is karsted and sinkholes, caves and collapse breccia have provided excellent traps to preserve cassiterite-bearing gravels.

Placers that contain "Sn-giants", or reach the "giant" magnitude, appear in Table 10.1. and Fig. 10.17.

10.3.7. Multi-metal zoned Sn, Mo, W, Bi, Be, Pb, Zn skarn-greisen-vein systems

The principal "giant" representative of this subgroup is the **Shizhuyuan** (also spelled Xi-zhoyouang) deposit in the Dongpo ore field near Chenzhou, southern Hunan (in the Nanling Range; Kwak, 1987; Lu, 2003; Fig. 10.18). The "main orebody" reserve is quoted as 170 mt of ore that contains 600 kt W, 490 kt Sn, 300 kt Bi, 200 kt Be, 130 kt Mo, 76 mt CaF₂ plus Ta (~1,000 t) and Nb (~3,000 t) in wolframite, Re (~174 t) in molybdenite and there are additional resources in other orebodies like Pb, Zn, Ag, Sb in distal veins and replacements. It is thus a "Bi super-giant", W, Sn, Mo "giant" and a "large" Be deposit (but the world's largest beryllium accumulation reported).

The ores are genetically related to a composite Jurassic (162-150 Ma) intrusion of epizonal to subvolcanic peraluminous biotite to muscovite-biotite granite and quartz-porphry dikes, emplaced into Upper Devonian thin-bedded argillaceous micritic limestone and dolomite thermally metamorphosed to marble in the granite roof. The roof rocks are thrust and faulted against Devonian sandstone and Neoproterozoic (Sinian) meta-sediments. The granite and porphyry intruded in three phases, accompanied by hydrothermal mineralization.

Although there are scattered occurrences of pegmatitic phase, aplite and albite-lithionite leucogranite, Shizhoyuan is not a typical granite cupola. Quartz, topaz, muscovite, beryl endogreisen in a granite porphyry dike with disseminated and vein scheelite, wolframite, molybdenite and bismuthinite is one form of mineralization, but not the most important one.

The principal ore zone has the form of a thick, multistage mineralized subhorizontal exoskarn blanket resting on granite and intruded by porphyry dikes. The dimensions are 1,000 m in length, up to 800 m in width, and up to 500 m in thickness although the average thickness is of the order of 200-300m. The banded argillaceous limestone is converted to grossularite, vesuvianite, wollastonite exoskarn that changes, at the distal end, into a banded garnet/calclitic marble mixtite. Dolomitized limestone is converted into diopside-garnet skarn. Grossularite > vesuvianite is the main host to disseminated replacive scheelite, and superimposed wolframite, bismuthinite, molybdenite associated

with amphibole, oligoclase, sericite retrograde skarn, and intense fluorite alteration. There are at least seven recognizable mineralization stages. The lower part of the skarn orebody was subsequently brittly fractured, and infilled by a network of 10-40 cm thick exogreisen veins. The greisen composition is quartz, topaz, muscovite with disseminated cassiterite, arsenopyrite, beryl, wolframite, scheelite and molybdenite. Fractures-controlled sulfides-rich stockwork in marble at the skarn fringe contains quartz, tourmaline, fluorite, cassiterite, stannite, chalcopyrite and arsenopyrite. Pyrite, sphalerite, galena replacements in jasperoid are mined from the distal zone and some stibnite-rich veins occur at fringe of the ore field.

Multi-metal zoned Sn, Cu, Pb, Zn, Ag granite-skarn-replacement-vein-placer systems

Here belong two "giant" metals supermarkets in China, Gejiu and Dachang. They are both multiphase, complexly zoned and overlapping hydrothermal ore systems centered on a high-level peraluminous ("tin granite") stocks or cupolas, emplaced into carbonate-rich roof associations. There is some analogy in style, although not in the selection of metals, with the porphyry Cu-Mo centered systems such as Bingham (Chapter 7), where Cu is in place of Sn here. The metaluminous granitoid-related system in Bingham is, moreover, rich in gold, which is virtually nonexistent around the S-granites. Pb, Zn, Ag, however, accumulated on the mesothermal flanks, in both systems. Also different is the widespread presence of residual tin ores (placers and oxidized/leached ores) based on relic cassiterite.

Gejiu (formerly spelled Kochiu) 300 km south of Kunming, Yunnan (Meng et al., 1937; Li Xiji et al, 1992; 1.0 or 1.6 mt Sn content in the early orebodies grading 3.65% Sn, plus W, Cu, Be, Pb, Zn) is a small district with five major but internally complex constituent metal-zoned ore fields. Laochang is the most important one. The rich supergene accumulations of cassiterite in clay filling karst sinks, residual after Sn-replaced carbonates, have been mined for over 400 years. Modern mining of the complex primary ores started only after 1950. The geology consists of over 3,000 m thick sequence of folded and faulted, locally evaporitic Middle Triassic miogeoclinal carbonates, resting on older clastics and ultimately on Precambrian gneiss.

Table 10.1. Tin-mineralized regions of the world that include "giant" deposits

No/ Sect	Deposit, district	Age	Type, geology	Tonnage kt Sn
Brazilian Shield				
1/10.3	Pitinga, Amazonas, Brazil	1.69 Ga	Placer, regolith over disseminated cassiterite, zircon, Ta-Nb in peralkaline apogranite	575 (+25 kt Ta)
2/10.3	Rondônia State placers, BR	Np	Placers, regolith over tin granite cupolas	1,850
3/10.3	Cordillera Real Tr ores, Bolivia	Tr	Sn (W) veins to stockworks related to monzogranite plutons; some placers	~400
Andean margin & orogen				
4/6.5	San Rafael, Peru	Mi	High-grade Sn-Cu veins in andean volcanic association related to epizonal granite	1,000
5/6.5	Oruro, Bolivia	Mi	Disseminated low-grade Sn in subvolcanic porphyry, epithermal Sn,Ag,Pb,Sb veins	~520
6/6.5	Llallagua, Bolivia	Mi	Sn in vein swarm and disseminated in subvolcanic porphyry; minor placers	~2,000
7/6.5	Potosí-Cerro Rico, Bolivia	Mi	Sn-Ag epithermal veins to stockwork, cassiterite disseminated in altered subvolcanic porphyry stock; Sn colluvium	~1,000
Variscan orogen, Euroasia				
8/10.3	Cornwall-Devon, Great Britain; total	Cb3-Pe	Many granite cupolas with exocontact Sn-(Cu) veins, endocontact stockworks, placers	2,500
	--Camborne-Redruth field	Ditto	System of deep quartz, chlorite, cassiterite, Cu sulfide veins in supracrustals in roof of granite cupolas; porphyry dikes	310
9/10.3	Spain & Portugal granites	Cb3-Pe	Widely scattered granite plutons and cupolas; endo- & exocontact veins, stockworks, placers	~200
10/8.4	Neves Corvo, Portugal; Sn in VMS	D3-Cb1	Cassiterite disseminated in pyritic, high-Cu VMS in acid submarine volcanics	484
11/10.3	Erzgebirge, GE&CZ, total	Cb3-Pe	Sn in veins, greisens in exo- and endocontact of tin granite cupolas; minor placers	~1,100
	--Cínovec/Zinnwald, CZ+GE	Cb3-Pe	Contact-parallel flat Sn (Li, W, Mo, Bi) greisen-rimmed quartz lodes in apogranite cupola; low-grade disseminated zinnwaldite	260 + ~1.43 mt Li
	--Altenberg, Germany	Ditto	Stockwork/disseminated cassiterite in several generations of endogranitic greisen	210+
	--Krásno, Czech Republic	Ditto	Sn disseminated in greisenized granite cupola, in endocontact Sn,W,Mo,Cu,U veins	290
	--Pöhla-Hämmerlein, GE	Ditto	Sn in fracture stockwork over Zn-rich exoskarn	~300
12/10.3	Kokchetau Block, Kazakhstan	Ditto	Syrymbet, Donetskoe deposits; quartz-cassiterite exocontact veins, endogreisen	?250
Africa, miscellaneous				
13/10.3	Jos Plateau, Nigeria	J	Extensive alluvial placers over anorogenic tin granite cupolas with dissem. & stockwork Sn	~810
14/10.3	Kivu-Maniema-Katanga placers, Congo (Kinshasa)	Np	Alluvial and regolith cassiterite & Ta, Li in rare metals pegmatite over wide areas	~650
	--Manono-Kitotolo zone	Np	Sn disseminated in rare metal (spodumene) pegmatite and its argillized regolith	297; 828 kt Li 14 kt Ta
15/10.3	Uis, Namibia	Cm-Or	Syntectonic Sn pegmatite veins, veinlets	106
NE Asia-Mesozoic belts				
16/10.3	East Arctic Shelf placers, Russia	J-Cr	Sn in buried alluvial channels under beaches & offshore, beach Sn placers	~250
17/10.3	Yakutia, (Sacha Republic), Kolyma; Russia	J-Cr	Scattered centers of granite-related vein, stockwork Sn (Deputat, Ege-Khaya) over large area; alluvial placers	?300
18/10.3	Chukotka-Seward Peninsula: Russia & W Alaska	Cr-T1	As above, includes buried alluvial channel placers in offshore, beach placers; Pevek, Valkumei, Lost River	?300

Table 10.1. (continued)

No/Sect	Deposit, district	Age	Geology	Tonnage
19/10.3	East Transbaikalia, Russia	J-Cr	Scattered Sn vein/stockwork groups, placers	?400
	--Khapcheranga	Ditto	20 exocontact fault veins in granite roof	240+
20/10.3	Komsomolsk na Amure ore field, eastern Russia	Cr3	Tourmaline-cassiterite exocontact veins, endocontact stockworks	?300
21/10.3	Sikhote Alin-Kavalerovo ore field, Primor'ye, Russia	Eo	Sn in fault & fracture veins in biotitized roof above granite stocks	?250
22/10.3.	Qinghai Province, W China		Baigan Lake, E. Kunlun belt; W>Sn veins	200
23/10.3.	Nanling Range, SE China	J-Cr	Exocontact W>Sn veins, skarn, replacements; endocontact veins, stockworks; placers	?2,200
	--Shizhouyuan ore field, Hunan	J	Complex W,Sn,Mo,Bi,Be,Pb-Zn skarn, greisen, exocontact veins above granite cupolas	490
	--Furong ore field, Hunan	J	Similar to above	820
	--Bailashui ore field, Hunan	J	Sn skarn, replacements, veins	510
	--Yanbei, Jiangxi	J-Cr	"Porphyry-Sn"and endogranite stockwork in topaz granite, some greisen	?250
24/10.3.	Yunnan, China			
	--Gejiu ore field	Cr3	Sn skarn, marble replacement, stockwork over skarn; zoned Sn,Cu,Pb,Zn,Ag around granite	1,000 (or 1,600)
	--Changpo deposit	Cr3	Ditto	750
	--Dulong	Cr	Similar to Gejiu	?500
	SE Asia Tin Belt	Tr-T1	System of 3 or 4 subparallel Sn N-S, NW-SE Sn belts; most Sn from placers, regolith	~9,600
25/10.3	Main Range (Malaya-Thailand)	Tr2-J1	Widespread alluvial & regolith placers over granite & mineralized roof, also offshore	5,280
	--Kinta Valley, Ipoh	Ditto	Ditto, largest single tinfield	2,000
26/10.3.	Western Granite Province Myanmar-W. Thailand	J3-O1	As above, minor regolithic rare metals pegmatite (Phuket), wolframite veins	1,340
27/10.3.	Indonesian Tin Islands	Tr2-J1	Extensive alluvial, also offshore placers, over mineralized granite + roof regolith	2,690
	--Bangka, Indonesia	217 Ma	Ditto	1,500
	--Belitung, Indonesia	Tr2-J1	Ditto	650+
	Tasman Orogen, Australia			
28/10.3	NE Queensland	Pe3	Sn in veins, greisen stockworks, placers	~250
29/10.3	New England, Qld+NSW, Australia	Pe3	Extensive exogranite veins, endogranite stockworks & greisens, placers related to tin granite and leucogranite	210
30/10.3	Western Tasmania	D	2 major Sn-pyrrhotite replacement deposits in carbonates above tin granite stocks, some with endogranitic greisen, vein Sn; placers	~520
	--Renison Bell	347 Ma	Ditto, several pyrrhotite-cassiterite mantos in dolomite, replacements in feeder fault	287

Areas without individual "giant" Sn deposits, or where the tinfield total is less than 230 kt Sn, are not included yet this table is believed to represent >90% of the world's tin endowment; Sn in "Geology" also stands for cassiterite, the only major Sn mineral. "No/Sect" in the heading indicate number on the map of world Sn deposits (Fig. 10.17) and Section in this book where the deposit is described. "Age" indicates approximate age of the primary Sn mineralization

Meta-diorite sills intrude the carbonates locally and they probably contributed copper to the system. Much of the district is in the thermal aureole of a Cretaceous peraluminous biotite granite pluton that sends several cupolas and stocks of fractionated two-mica and tourmaline granite towards the surface. As in Cornwall, orebodies are distributed zonally around granite stocks and 90% of resources are in the exocontact thermally recrystallized

limestone and dolomite, controlled by NNE-trending anticlinoria and fault systems. Deposits in granite appear of limited importance and they are endogreisens with disseminated cassiterite and stockworks of quartz, tourmaline, cassiterite veinlets. Sn-Cu skarn with vesuvianite and wollastonite occurs at the immediate granite exocontact in depth.

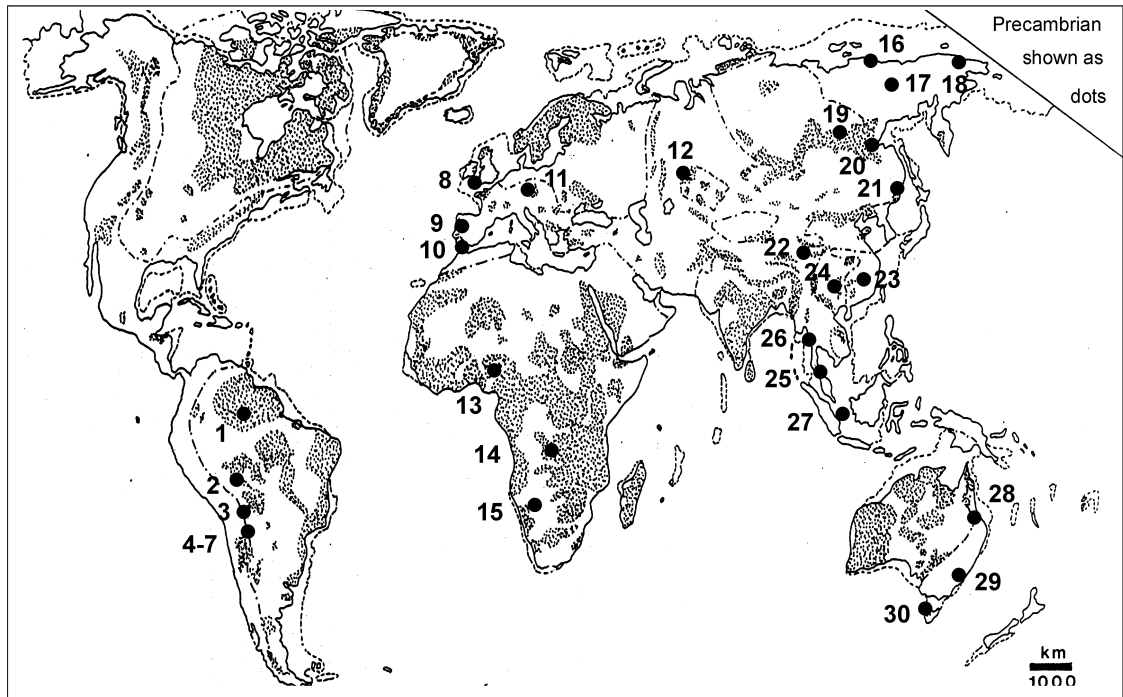


Figure 10.17. Distribution of the "Sn-giants" around the world (read Table 10.1 for locality names and data)

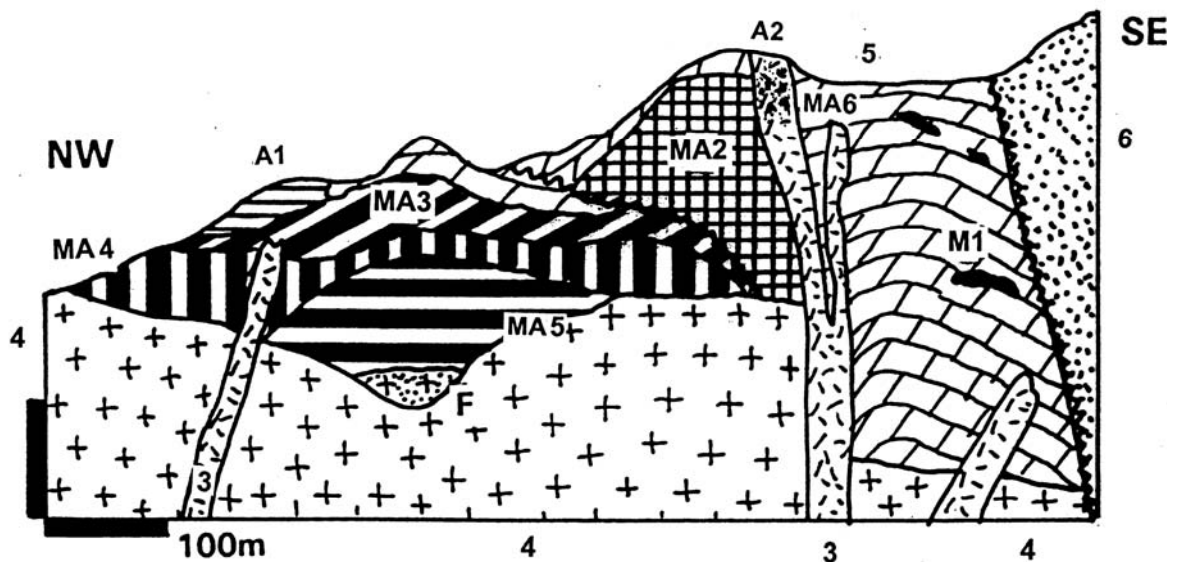


Figure 10.18. Shizhouyuan in the Dongpo multi-metals ore field, Hunan, China; cross-section from LITHOTHEQUE No. 1812, modified after, Lu (2003), Wang Changlie mine staff tour, 1993. M1. 146-144 Ma galena, sphalerite, pyrite marble replacements and quartz-pyrite veins; Main mineralization and alteration period at 187-157 Ma related to epizonal granitic magmatism. MA2. Quartz, tourmaline, fluorite, cassiterite, etc. stockwork in marble; MA3. Bi in oxidized and partly retrograded exoskarn; MA4. W, Bi, Mo in exoskarn; MA5. Disseminated wolframite, scheelite, cassiterite, Mo & Bi sulfides, topaz, beryl in grossularite exoskarn (main ore type); MA6. W, Sn, Mo, Bi, Be in endogreisen; A1. Oxidized skarn; A2. Greisens; 2. J post-ore diabase dikes; 3. J monzogranite & quartz porphyry dikes; 4. 172-139 Ma peraluminous leucogranite; 5. D3 argillaceous limestone recrystallized to marble; 6. D sandstone

Economically most important are the stratabound replacement mantos in carbonates and their mineralized feeder faults and fractures in granite roof. They are rich in sulfides with hematite, cassiterite, arsenopyrite, pyrite, sphalerite, galena and they grade into low-grade disseminated replacements of cassiterite in carbonate (~0.4% Sn). Fault and fracture Cornwall-type quartz, tourmaline, cassiterite, chalcopyrite veins is another major ore type. Small scheelite skarns, Li, Be, Ta-Nb deposits associated with albitized leucogranite and rare nepheline syenite, also occur.

Dachang ore field, in Guangxi WNW of Guangdong, is very similar in style to Gejiu and it is credited with ~100 mt of ore @ 1% Sn (Tanelli and Lattanzi, 1985; Fu et al., 1991). In addition, there is a significant by-production of Zn > Pb > Sb > Cu plus numerous rare metals. Much of the Pb+Sb comes from boulangerite and jamesonite-rich orebodies, sulfosalts that rarely occur in greater than mineralogical quantities elsewhere. The core of the system in the ore field is a Cretaceous (91 Ma and older) intrusion of peraluminous biotite granite, much of which is concealed, and also diorite and granite porphyry. The intrusives are exposed at surface as narrow linear bodies rather than as a central stock. The roof rocks are Devonian to Triassic miogeoclinal limestones interstratified with marl, shale, sandstone and quartzite. A considerable proportion of the sedimentary rocks are carbonaceous ("black"), variously graphitized in the thermal aureole. The ore field contains six large composite orebodies and more small ones; Changpo-Tongkeng is the largest and best known. As in Gejiu, the orebodies are zonally arranged in respect to granite and granite porphyry, although there does not seem to be an important mineralization in the granite itself. Zn-Cu exoskarns (Lamo and other deposits) have chalcopyrite and sphalerite with pyrite, pyrrhotite in diopside, andradite, epidote and wollastonite association. The principal ore type in Dachang are cassiterite-sulfide ores, mined from the largest deposits. The ores come as fracture stockworks, veins and irregular masses in sedimentary rocks and some grade, with increasing depth, into stratabound replacement mantos. They are composed of pyrite, pyrrhotite, arsenopyrite, sphalerite, cassiterite, jamesonite, franckeite, stannite, boulangerite and other minerals, in gangue of quartz, calcite and sometimes fluorite. A possibility of remobilized and Sn, Sb, As enhanced stratiform (sedex? or "Irish-type"?) orebodies has been suggested. The remaining ore types are fault or fracture quartz, fluorite, calcite, stibnite, wolframite, scheelite

veins, and residual cassiterite in pockets of clay in regolith, as in Gejiu.

Several complex ore fields with huge (exaggerated?) Sn endowments discovered more recently and mentioned in a Geological Survey of China 2004 brochure, lack accessible literature. They (e.g. Furong and Bailashui in the Nanling Range and Dulong in Yunnan) are probably of the Gejiu/Dachang style and are included in Table 10.1.

10.3.8. Hydrothermal U deposits

Deposits genetically related to intrusions

A small number of U deposits, other than the U-leucogranites reviewed above, appear to be closely related to the immediate postmagmatic hydrothermal activity of an intrusion (or a volcano-plutonic complex). They are thus an end-member of a spectrum of granite-ore relationships at the other end of which are U deposits emplaced long after the cooling of intrusion.

Streltsovka (settlement) or **Streltsovskoye** (deposit) is a U-Mo mineralized volcano-plutonic complex (dissected caldera) in the Pri-Argun ore district in SE Russia, near the Chinese and Mongolian borders. The administrative/processing center is Krasnokamensk (Chabiron et al., 2003; ~280,000 t U @ 0.2% U+). The roughly circular, block-faulted remnant of a caldera has a diameter of about 20 km and is filled by about 1 km thick Late Jurassic continental volcanic and sedimentary rocks, unconformably resting on Late Carboniferous granite. The volcanics consist of an older basalt, andesite and trachyandesite, whereas the youngest mildly peralkaline, highly fractionated rhyolite occurs near the centre. Fresh rhyolite is enriched in fluorine (1.4-2.7% F) and uranium (15-23 ppm) and is strongly altered. Chabiron et al. (2003) considered rhyolite the principal source of U in orebodies, together with a subsidiary U source in the basement granites.

The Streltsovka ore field contains twenty productive deposits. The largest Streltsovskoye underground mine (60 kt U) is producing from veins in both the basement and volcanics, crossing the unconformity. The next largest Tulukuevskoe deposit (30 kt U) is a stockwork in volcanics, mined from an open pit. The mesothermal (390-290°C) multistage mineralization is Lower Cretaceous (139-130 Ma) and ranges from structurally-controlled disseminations through stockworks to fault and fracture veins in hydromica (illite, phengite) altered wallrocks. Early barren quartz, carbonate, pyrite, hydromica veins are followed by

the main quartz, molybdenite, pitchblende stage. This is a postmagmatic mineralization probably related to a leucogranite intrusion, indicated by albitization in depth. The "large" deposits Dornot in Mongolia (33 kt U @ 0.28% U) and Xiangshan in Jiangxi, China (26 kt U @ 0.1-0.3% U) are said to be comparable with Strel'tsovka in setting and style of mineralization (Chabiron et al., 2003).

Skarn and replacement uranium deposits are uncommon and small, although the best known examples: **Mary Kathleen** in Queensland (Battey et al., 1987; ~10 kt U @ 0.1%, 200 kt REE @ 2.1%) and **Mina Fé** in Spain (Both et al., 1994; 16 kt U) were important in local economies. Mary Kathleen, a predominantly rare earths deposit, had uraninite superimposed on Mesoproterozoic allanite and stillwellite skarn. In **Mina Fé** near Ciudad Rodrigo, low-temperature pitchblende and other minerals fill dilations in fractured carbonaceous unit in turbidites and although occasionally listed as "replacement", even "skarn", this deposit is close to the much larger "black shale" Ronneburg ore field described above. The "large" U deposit **Pöhla** in the German Erzgebirge (~40 kt U; Fig. 10.15 above) is associated in space with a major Sn-Zn-W skarn (read above), but it is a younger, mesothermal vein system (read below).

Deposits related to structures

Much of what had been known about uranium deposits by the end of the 1980s has been compiled in the excellent book of Dahlkamp (1993). Little new information has been added in the West in the past 20 year period when uranium has been in disfavor, but new formerly secret quantitative information is now entering from the former U.S.S.R. and its satellites, following disintegration of the empire after 1990.

Uranium, a typical product of repeated magmatic and sedimentogenic differentiation and fractionation with highest trace contents in the super-mature continental crust, concentrates and accumulates in many ways that are dissimilar from other metals. This is, most of all, influenced by the very different behaviour of tetravalent and hexavalent U where changes in the redox state influence uranium mobility. Uranium is one of the most restless elements that moves readily across geological systems and environments and its deposits, once formed, frequently reform, enlarge or reduce, or dissipate altogether. A typical uranium deposit thus records ages of more than one event in its genetic history.

Hydrothermal U deposits formed from fluids within the 440°C to ~120°C range (mesothermal to epithermal, although the term epithermal is rarely used outside of volcanic settings; "low temperature fluid" is preferred), of meteoric, basinal and metamorphic derivation. U-carrying fluids were both ascending (e.g. granite-heated meteoric waters) and moving laterally/descending (heated "basinal fluids"). Trace U was leached from potassic granites and granite-gneisses (e.g. Limousin district, Alligator Rivers province); from rhyolites (Strel'tsovskoye); from quartz-rich sandstones (Athabasca U province), from "black shales" (Ciudad Rodrigo); from combined sources; or from "unknown" (Olympic Dam). U precipitated in carbon-rich structures (Příbram, Athabasca U Province), in Mg-carbonate rich settings (Rabbit Lake, Ranger), in Fe-oxides (Olympic Dam) and elsewhere as a consequence of reduction, two fluids mixing, loss of solubility, reaction with wallrocks.

Basement/cover unconformities provided important control in the time of ore formation, not only to the "unconformity-U" deposits but also to a variety of vein, breccia and shear U-deposits. Whether uranium orebodies formed above or under unconformity is not in doubt when the above-unconformity rocks are still preserved, but is not obvious for U veins in the basement from which the cover rocks have been removed by erosion. This causes some classification ambiguities.

The classification of uranium deposits by Dahlkamp (1993) is still the most logical and widely used one, although some deposits are ambiguous and can be placed equally well into two or more groups (for example, "metasomatite" and "breccia complex" types can also be "unconformity" or "volcanic", depending on their geological setting). In this chapter the Dahlkamp's "Vein-type U" (Type 3) is retained and reserved for deposits presumably formed from the slightly higher temperature (~370-250°C) ascending hydrotherms in intracontinental orogens. Comparable deposits in prominent volcanic setting (e.g. in dissected calderas as Strel'tsovskoye) are reviewed above and in Chapter 6. The "Unconformity" and "Subunconformity" deposits (Types 1, 2 of Dahlkamp) formed from lower-temperature (~240-120°C) "basinal fluids" and as the prominent examples are all Proterozoic, they appear in Chapter 11. The same applies to the "Breccia complex" (Type 8) deposits exemplified by Olympic Dam, reviewed under the heading "Fe-oxide plus Cu, Au, U, REE hydrothermal deposits" in Chapter 11. The "Metasomatite deposits" (Type 12), in high-grade metamorphic setting, are

included in Chapter 14. Hydrothermal U deposits of all categories contain just six “geochemical giants”, whereas many economically important deposits are only of the “large” magnitude, yet selectively and briefly described below.

Hydrothermal uranium veins, disseminations and replacements: Dahlkamp (1993) distinguished granite-related and granite-unrelated deposits, but it now appears that in this group granites were 1) mainly the source of heat to drive convecting meteoric fluids; such U deposits are early post-magmatic, slightly younger than the granite (e.g. Strel'tsovskoye); and 2) mostly the source of trace U, anomalously enriched during an often protracted history of fractionation to leucogranites, pegmatites and early alteration; the U veins formed long after cooling of such granites, by leaching of their trace U content by genetically unrelated fluids (e.g. in the Limousin district the host granite is 325 Ma, the U veins 275-270 Ma).

Limousin (La Crouzille) district, about 20 km north of Limoges, France, is the most studied “large” granite-associated vein uranium system (Leroy, 1978; ~38 kt U @ 0.1-0.6% U). Most orebodies are in Carboniferous S-type biotite granite emplaced into Neoproterozoic metamorphics, usually in the vicinity of lamprophyre dikes that postdate the granite. Pitchblende with pyrite, coffinite, fluorite are in fracture and breccia veins in granite along faults, or disseminated in “episyenite” (porous orthoclase-muscovite residual and alteration material remaining after dissolution of quartz and plagioclase in granite). The early hydrous potassic alteration in a narrow rim of granite adjacent to a vein caused muscovitization of feldspars, chloritization of the mafic minerals, pyritization of lamprophyre. The second stage alteration produced hematite pigment (“reddening”), montmorillonite, minor adularia and microcrystalline silica in wallrocks adjacent to fissures and resembling veins. Secondary U minerals, mostly autunite and torbernite, formed in the oxidation zone.

Příbram in the Czech Republic, 60 km southwest of Prague, is a historical Pb, Zn, Ag ore field, where uranium mining started in 1948 (Kolektiv, 1984; Kříbek et al., 1999; Pt 41,742 t U; Fig. 10.19). This is a 24 x 2 km SW-NE trending fault system along the NW margin of the Carboniferous Central Bohemian pluton that contains several hundred mostly transversal (NW-SE) fracture veins

in granite roof composed of hornfelsed Neoproterozoic slate and graywacke. As in France, the vein emplacement (278-275 Ma) greatly postdated the granite (345-335 Ma). The veins grade to stockworks and consist of quartz with several generations of white and pink carbonates (calcite, dolomite), shoots and veinlets of uraninite (pitchblende) and pyrite. Pb, Zn, Cu sulfides and Ni, Co arsenides, locally with native silver, occur intermittently. The wallrocks are chloritized and hematite-pigmented. The Příbram U veins are interesting for they have very high bitumen content, and some 15% of U production came from bitumen-uraninite ores (Kříbek et al., 1999). Although the carbon was mobilized from the carbonaceous members of the roof rocks, the bitumens in veins are younger than the main portion of the U ores and are attributed to polymerization of gaseous and liquid pyrolysates, infiltrated into the mineralized fractures.

(Nieder)schlema-Alberoda ore zone near Aue, Erzgebirge, Germany, is the largest European vein uranium deposit with 80 kt U produced (Vlasov et al., 1993; Fig. 10.20). It is a uranium-rich portion of an 8 km long NE-trending zone of brittle deformation and veining between the historic silver-mining center of Schneeberg and Schlema. The zone is a complex of subparallel individual veins to veinlet stockworks in faults filled by altered and partly gangue-cemented breccia, ductile tectonite slivers and rock flour, and laced by brittle tensional fractures. The host rocks are Ordovician to Devonian metamorphosed supracrustals that include micaschist to phyllite, graphitic schist, some meta-quartzite, minor dolomite grading to skarn, “mafic schists” (metabasites), albite-chlorite rocks and meta-diorite, all sheared in the deformation zone. These are intruded by Carboniferous porphyritic monzogranite, aplite and lamprophyre. The multiphase vein mineralization consists of the earliest Sn-W veins and greisens, followed by Pb, Zn, Cu sulfide veins. The latest phase has Ni-Co arsenides, Ag sulfosalts and Bi sulfides superimposed on the earlier phases. The non-uranium ores, important around Schneeberg in the past, have not been systematically followed after the World War 2, in what has been a reckless mining campaign in a densely populated urban environment with the sole purpose of providing uranium for export to the U.S.S.R. The former mines, that include enormous dumps, are now largely rehabilitated.

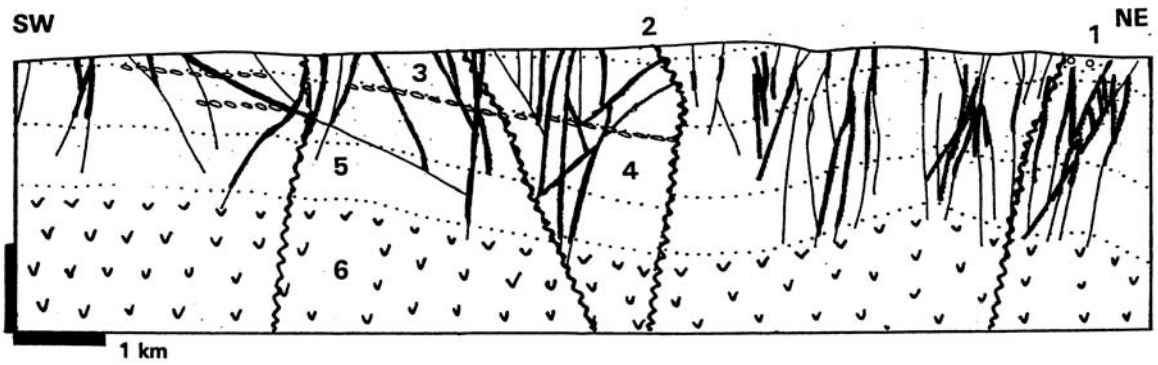


Figure 10.19. Příbram U zone, Czech Republic; cross-section from LITHOTHEQUE No. 2117 modified after Kolektiv (1984). BLACK: ~270 Ma carbonate-pitchblende veins; 1. Cm conglomerate and lithic sandstone; 2. Np argillite-siltstone unit; 3. Ditto, siltstone-litharenite unit; 4. Ditto, litharenite-conglomerate unit; 5. Ditto, basal siltstone-argillite unit; 6. Ditto, greenstone metabasalt, slate

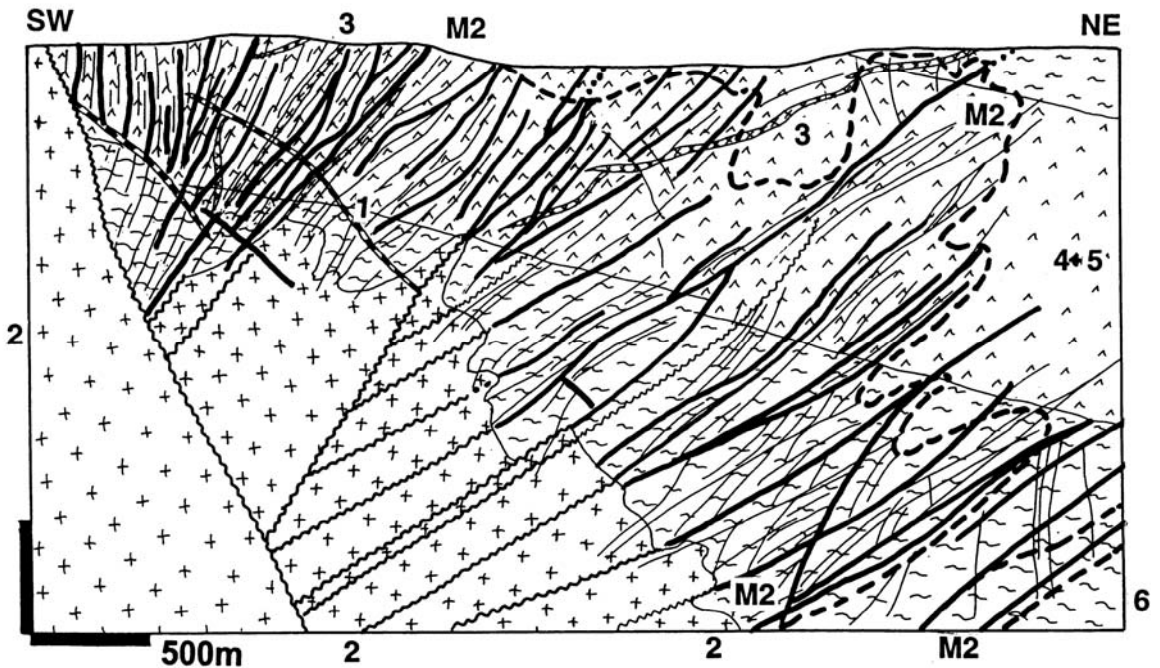


Figure 10.20. Niederschlema-Alberoda U zone near Aue, Erzgebirge, Saxony; cross-section from LITHOTHEQUE No. 3107 modified after Vlasov et al. (1993). M1. MZ-T late stage carbonate, Ni, Co, Bi, Ag, As veins (of limited economic importance but they supported medieval mining in Schneeberg); M2. ~275-270 Ma system of ~200+ quartz, carbonates, pitchblende, pyrite > coffinite, etc. fault veins grading to stockworks. M3. Cb early stage Sn-W and Cu, Pb, Zn veins and greisen (not economic); 1. Cb thick barren quartz veins in faults; 2. ~340-320 Ma porphyritic monzogranite; 3. ~346-320 Ma tectonized kersantite dikes; 4. D mafic schists, greenstone, metadiabase; 5. Or3-S carbonaceous phyllite, minor carbonate lenses, skarn; Or. Micaschist to phyllite

The Phase 2 of the Schlema mineralization (275-270 Ma) produced more than 200 composite south-west dipping veins of quartz, several generations of carbonates, pitchblende, pyrite, minor coffinite and

other minerals in quartz, sericite, graphite, chlorite, hematite, and carbonate-altered supracrustals. The veins quickly faded away, changing into barren or quartz-filled and/or altered faults, upon reaching

granite in depths ranging from about 1,000 to 1,800 m. The granite apex contained showings of Sn-W in greisen and fracture veins of no economic importance.

10.4. Mesothermal gold

Hydrothermal, predominantly mesothermal gold deposits in Phanerozoic and late Proterozoic setting (those in early Precambrian greenstone belts are included in Chapter 9) make up a huge database of deposits. They are extremely difficult to compartmentalize, as there is a choice of premises many of which are overlapping. For example, the "orogenic" (or synorogenic) class introduced by Groves et al. (1997), serves its purpose in separating the synvolcanic deposits (like VMS), formed broadly contemporaneously with volcanic or sedimentary rocks, from the orogenic deposits formed in the same setting later, during or after deformation and orogenic magmatism. In this sense, most Au deposits in the latter group are (syn)orogenic or post-orogenic so we can now move to the second order of division.

Some orogenic deposits appear genetically related to intrusions, others are not. There is no clear-cut division and, worst of all, genetic relationships are difficult to prove beyond doubt, as even fluid inclusions and stable isotopes are not absolutely conclusive. Magmatic-hydrothermal deposits, where the metals, fluids and heat were all supplied by an intrusion, are an ideal end-member in a sequence of diminishing genetic association between intrusions and hydrothermal ores. As is the case of porphyry Cu-Mo (Chapter 7) and the high-temperature Sn-W deposits (read above), it is practically useful to identify such "productive" intrusions as an exploration aid. The genetic connection between hydrothermal gold and a pluton (stock, dike) is best demonstrated by the "porphyry-Au" hosted by synvolcanic intrusions in subductive magmatic arcs (Chapters 5-7), but this is more controversial in collisional orogens. The possible variations follow from Fig. 10.21.

There, varieties No. 1&2 would, in the past, be automatically considered as precipitated from hydrothermal fluids exsolved by the host intrusion itself, or by a slightly younger phase of the same complex presumably hidden in some depth. This could be the case and "porphyry", "stockwork", or "intrusion-related" Au deposits result. The "granite" parentage, however, has to be proven as in probably more cases the intrusion hosting gold veins may have been cool and dead at the time of ore emplacement and had nothing to do with the vein

origin, except providing dilutions (No. 5 in Figure 10.21). Such "granite" is thus of limited exploration importance as equivalent veins can occur in any kind of brittle rock. Nos. 3&4 in Fig. 10.21. are transitional situations where the gold veins are structurally controlled by a fault or shear, but the presence of granitoid porphyry dikes, thermal metamorphism, and other tell-tale signs suggest that another "granite" in depth may have provided at least the heat if not the fluid and metals, to drive hydrothermal convection that formed the vein. A "dead" granitoid may have even contributed some trace metals to the scavenging fluids.

The progression of ore styles in Fig. 10.21 may ideally indicate an initially magmatic-hydrothermal fluid gradually mixing and eventually changing into convecting heated meteoric and formational waters and, eventually, to fluids released at depth by metamorphic dehydration. The heat contribution from plutons, however, may still be a component of the deep dehydration process; the "giant" Juneau goldfield in SE Alaska, considered as an example of the orogenic metamorphic-hydrothermal mineralization, is merely 10 km from the nearest outcrop of the large Coast Batholith, broadly contemporaneous with the vein formation (Goldfarb et al., 1997). The Mother Lode structure in California may be in comparable situation in respect to the Sierra Nevada batholith (Landefeld and Silberman, 1987).

10.4.1. Intrusion ("granite")-related Au veins, stockworks, disseminations

These are neither "porphyry-gold", nor "(syn)orogenic" or "Carlin-type" deposits. In the late 1990s (e.g. McCoy et al., 1997; Thompson et al., 1999) a transitional group has been created that bring together presumably magmatic-hydrothermal, mesothermal gold deposits hosted by, ore close to, high-level granitoid intrusions to which they may be source-related. Most members of this group are in collisional orogenic belts, although some are at home in the Cordilleran setting as well (Chapter 7). Newberry et al. (1995) named such deposits, in Alaska, as "intrinsic", to differentiate them from the mainly metamorphic-hydrothermal deposits which, even where there is a "granite" in sight, lack a demonstrated metal source relationship. This seems to be a recurrent problem worldwide, reaching back to gold deposits in the Archean greenstone belts (Chapter 9).

Thompson et al. (1999) had specifically in mind deposits associated with tin and/or tungsten provinces that also include Bi, As, Mo, Te and Sb

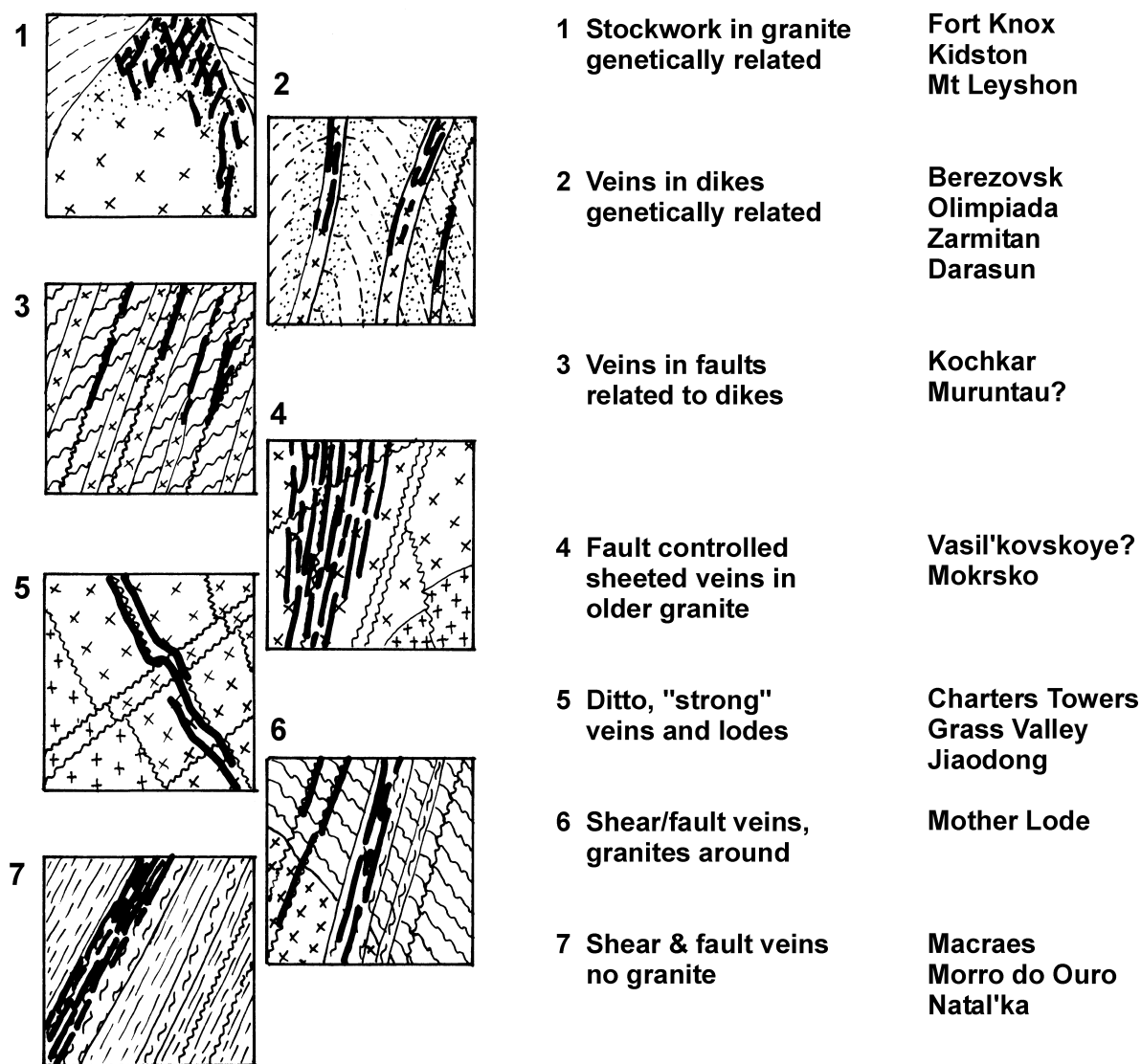


Figure 10.21. Varieties of styles of Phanerozoic and late Precambrian hydrothermal gold deposits

deposits, some of which are reviewed above and in Chapter 7. The parent granitoids crystallized from crustal melts (I or S) emplaced into cratonic margins in either the landward regions of andean-type systems, or in collisional settings. Of the list of deposits they quoted three "large" deposits qualify for membership in the andean-type margins: Fort Knox near Fairbanks, Alaska (~210 t Au); Dublin Gulch near Dawson, Yukon (46.5 t Au); and Kori Kollo in the La Jolla ore field, Bolivia (151 t Au). To this could probably be added Pogo, Alaska (170 t Au); Nezhdaninskoye in NE Siberia (~500 t Au); and others. A major problem is where to draw a

boundary between these presumably genetically "granite-related" structurally-controlled gold deposits and gold veins/stockworks which formed later, from metamorphic-hydrothermal fluids, for which the granitoids are but passive hosts (No. 4 in Fig. 10.21). The following examples of selected "giant" and "large" Au vein/stockwork deposits are presently considered synchronous with and genetically related to intrusions:

Fort Knox near Fairbanks, Alaska (Bakke, 1995; 158 mt @ 0.83 g/t Au for 131 t Au; with nearby placers it is the main contributor to some 250 t Au plus credited to the Fairbanks goldfield;

also some Bi, W, Te). Fort Knox is associated with Cretaceous (95-86 Ma) granodiorite to granite plutons, intruded into metapelitic schist and gneiss of the Yukon-Tanana Terrane. The plutons are moderately peraluminous and suggestive of a mesozonal pluton rather than a high-level intrusion. The "pegmatite" bodies described in the literature are more likely fracture-controlled zones of microcline alteration. Native gold is scattered in quartz, in a series of sub-parallel sheeted quartz veins that are 2-15 cm thick, 10 to 50 cm apart, with narrow alteration envelopes of K-feldspar, biotite, albite, muscovite and local dumortierite, grading to sericite. The veins have less than 0.5% of sulfides: pyrite, pyrrhotite, arsenopyrite, bismuthinite and molybdenite, as well as scheelite and wolframite, and fall into the mesothermal range (330-270° C).

Vasil'kovskoye deposit, an Au-As-Bi "giant", is located 17 km NW of the regional centre Kokshetau (Kokchetav) in northern Kazakhstan, a city of 150,000 (Abishev et al., 1972; Abdulin et al., 1980; 138 mt @ 2.8 g/t Au, 1.28-8.5% As, 50-125 ppm Bi plus Te, W for 386 t Au, 1.5 mt As plus, ~12,420 t Bi; Fig. 10.21). The deposit is hosted by early Ordovician hornblende gabbrodiorite to diorite, overprinted across a tectonic contact by a 468-456 Ma hornblende-biotite granodiorite. The latter is crowded by pink microcline porphyroblasts resulting from an early K-metasomatism. The intrusions are emplaced into metamorphics along the northern margin of the Kokchetav Block. The granitoid mass is faulted, brittle fractured and cut by several north-east trending sets of subparallel sheeted veins. The veins are filled by quartz-arsenopyrite or arsenopyrite only, with minor amounts of pyrite, bismuthinite, chalcocopyrite, sphalerite and other minerals, in quartz-sericite alteration envelopes. Gold is both free but fine-grained, and refractory. The fine-grained arsenopyrite contains up to 110 g/t Au, whereas the coarse arsenopyrite averages a mere 2.2 g/t (Abishev et al., 1972). The sericite has been dated at 443 Ma (late Ordovician to Silurian). The ore fluids were in the mesothermal range (370-270°C). Atmospheric weathering leached the uppermost 5 to 10 m, removing arsenopyrite but leaving quartz and gold behind.

Lesser gold deposits listed by Thompson et al. (1999) that may be genetically related to granitoids include Mount Leyshon near Charters Towers (Pt 111 t Au; Fig. 10.22) and Kidston (155 t Au), both in Queensland; Mokrsko-Čelina in the Czech Republic (100 t Au); Kori Kollo in Bolivia (133 t Au), but the list hardly ends here and there are more potential candidates (Table 10.21).

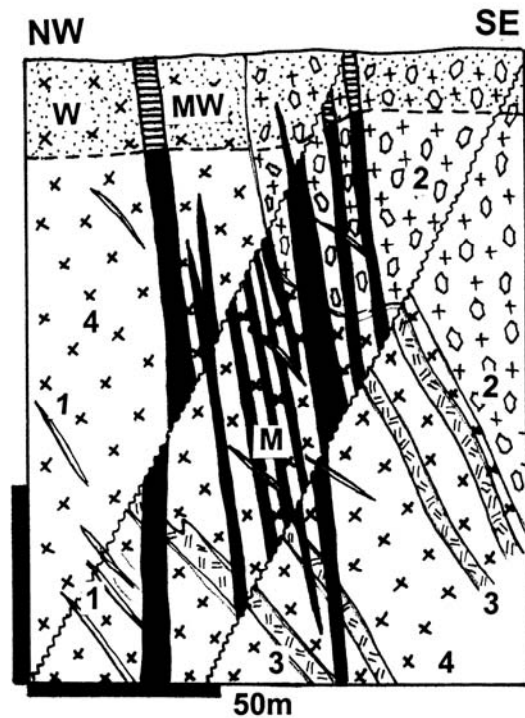


Figure 10.22. Vasil'kovskoye As-Au deposit near Kokshetau, NW Kazakhstan; cross-section from LITHOTHEQUE, modified after Abdulin et al. (1980). W. Leached granite in regolith; MW. Oxidized ore, Au in limonite, skorodite at transition to hypogene ore; M. Sets of subparallel sheeted fracture (joint) veins of Au in arsenopyrite (quartz); 1. Post ore porphyry dikes; 2. D granodiorite with microcline porphyroblasts; 3. Or-S leucogabbro and diorite dikes; 4. Or-S. Hybrid mixture of gabbro, quartz diorite, microdiorite

10.4.2. Gold skarns

Gold skarns are included in reviews of metalliferous skarns (Einaudi et al., 1981; Meinert, 1993) and those in the porphyry-Cu provinces have been briefly mentioned in Section 7.3.5. There are few "gold only" skarns and the examples listed in literature are small, medium to, at best, "large". Most are in the Cordilleran orogens (Chapter 7).

Except for the Wabu Ridge deposit in Papua (Irian Jaya) where gold is the main commodity, several "giant" Au accumulations reside in copper-dominated skarns related to porphyry Cu-(Au, Mo) systems. In the Ertsberg-Grasberg cluster in Irian Jaya (Chapter 7) the recently discovered Kucing Liar orebody stores 448 t Au and 1,696 t Ag in a reserve of 320 mt @ 1.4 g/t Au, 5.3 g/t Ag, 1.4% Cu (Widodo et al., 1999).

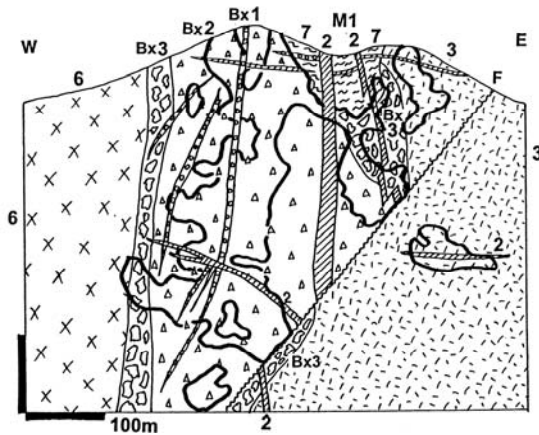


Figure 10.23. Mount Leyshon Au deposit, NE Queensland, cross-section from LITHOTHEQUE No. 2926, modified after Orr (1995). Ore outline is based on 0.8 g/t Au cut-off. M1. ~280 Ma porphyry-level disseminated, breccia filling and replacement fine free gold with pyrite in sericite-altered porphyries and breccias. Breccias: Bx1. Heterolithologic intrusive breccia (attrition-rounded fragments); Bx2. Fragment-supported heterolithologic breccia, principal host; Bx3. 1.6 km diameter breccia pipe with basement fragments in 30-100% of rock flour matrix. 1. Cover sediments; 2. Pe1 late porphyry and trachyandesite dikes; 3. Cb3-Pe1 quartz-feldspar phyr pyrophy, aphanitic matrix; 6. Or-S granite and porphyry; 7. Cm-Or1 metasilstone and litharenite

Some porphyry Cu-(Au, Mo) deposits contain separate gold skarn orebodies the value of which greatly exceeds the copper value. In the Battle Mountain district, Nevada, the Copper Canyon ore field contains one very small, although past producing, porphyry Cu-(Au, Mo) deposit and two recently discovered and mined gold skarns: Fortitude (14.5 mt @ 5.14 g/t Au and 29.8 g/t Ag) and the smaller Tomboy-Minnie, for a total endowment of 103 t Au. The McCoy-Cove deposit, 50 km SW of Battle Mountain, contains another 120 t Au and 3,550 t Ag, but not all in a "true" skarn. Elsewhere, Cu is subordinate to Au in skarn as in Kuru-Tegerek in Kyrgyzstan (97 t Au @ 0.56 g/t Au), El Valle-Boinás and Carlés in the Rio Narcea belt, NW Spain (61 t Au and 16 t Au, respectively), Bermejil, Guerrero, Mexico (47 t Au), probably Olkhovskoye, Russia. In the Natal'ka "Au-giant" in the Magadan area, Russia, skarn is a minor component in a predominantly shear-controlled gold-quartz vein system.

Skarn dominated by arsenopyrite with gold is a distinct variety of which several examples are known. Two, Hedley in British Columbia and Złoty

Stok in Poland, are only "large" and "medium" gold accumulations, but "geochemical As-giants". Hedley (Barr, 1980; 8.4 mt @ 7.3 g/t Au and 3-5% As for 61.3 t Au and a ?minimum of 200 kt As; see also Fig. 7.16 above) is in folded and thermally metamorphosed Upper Triassic arc association of andesite tuff, breccia and volcanoclastics with argillite and impure limestone interbeds. There are also probably comagmatic augite diorite and quartz gabbro, although these rocks could be hybrids. The supracrustals are intruded by Jurassic and Cretaceous quartz diorite and granodiorite stocks and dikes. The limestone was converted to garnet, hedenbergite, axinite and epidote skarn. In the original Nickel Plate zone, the orebodies are tabular, overlapping en-echelon masses of exoskarn situated about 80 m from the marble front, mineralized by disseminations, scattered grains and masses of arsenopyrite with minor pyrite and sphalerite. Gold is enclosed in arsenopyrite.

Złoty Stok in Silesia, Poland (formerly Reichenstein; Schneiderhöhn, 1941; Mikulski et al., 1999; P+Rc 97 t Au, 900 kt As) is a historical small mining town with an enigmatic gold-bearing Fe-As sulfides-dominated magnesian "distal skarn" (replacement of silicate marble). The orebodies are in diopside, tremolite, chondrodite, forsterite dolomitic marble, retrogressively hydrated and largely converted to para-serpentinite. Masses of high-temperature (530-400°C) löllingite, arsenopyrite, pyrrhotite, magnetite and chalcopyrite are in a compact 40x35 m ore lens grading between 5 and 35 g/t Au and 35-40% As, and in more recently discovered orebodies with a much lower grade. The gold is in arsenopyrite and in the skarn silicates. The host association comprises Neoproterozoic to lower Paleozoic schist, amphibolite and marble, intruded by Late Carboniferous syenite and diorite.

The giant **Wabu Ridge** gold skarn in Papua (Irian Jaya; O'Connor et al., 1999; 310 t Au) is only 35 km north of the Grasberg porphyry/skarn Cu-Au complex, but the high-boron As, Bi, Au association is more compatible with the collisional setting as it is located in the Central thrust belt. The K-feldspar, biotite, apatite, tourmaline, axinite, datolite, pyrrhotite, arsenopyrite, Bi sulfides and sphalerite ore zones are superimposed on retrograde skarn along contact of a Mi-Pl volcano-plutonic complex and J-Cr carbonates.

10.4.3. Transition of granite-related to (syn)orogenic Au deposits

Gold in reactivated cratons and orogens: The concept of tectono-magmatic reactivation of old, previously consolidated (cratonized) blocks of continental crust is an important component of the classical Soviet and Chinese metallogenic systematics (e.g. Shcheglov, 1967). The Russian Transbaikalia and the East China Craton are, indeed, type areas of this concept. Several important goldfields in eastern China that includes the largest Chinese gold-only province, the Shandong Peninsula, are in Mesozoic (Yenshanian orogeny) structures, coeval with or shortly postdating emplacement of Jurassic to Cretaceous granitoids, and superimposed on Archean or Paleoproterozoic granite-greenstone terrains. There is a strong belief that the gold is remobilized from the Precambrian rocks and, in some cases, from Precambrian mesothermal deposits in reactivated old shears. In the Niuxinshan deposit in the Eastern Hebei goldfield (Trumbull et al., 1992) the fault-controlled gold-quartz veining is associated with greisenized margins of Jurassic granodiorite and diorite porphyry dikes, where it predates the younger generation of trachyte and lamprophyre dikes. This brackets the gold emplacement and suggests, together with the isotopic evidence, that at least a portion of this ore is magmatic-hydrothermal. In the "large" Niuxinshan deposit (~53 t Au; Yao et al., 1999), the 190-175 Ma gold-quartz veins in greisenized and sericitized granodiorite contain pyrite, but are low in other sulfides. Veins in Archean amphibolite have a substantial content of pyrite, chalcopyrite, galena, sphalerite, Bi minerals and scheelite.

In the **Jiaodong** (East Jiao Peninsula) gold district in the Shandong Province, eastern China (Zhai Yusheng et al., 1997; P+Rc 1,030 t Au plus) several north-east trending gold-mineralized deformation zones are in Archean and Paleoproterozoic granite-greenstone basement, granitized and intruded by Lower Cretaceous granodiorite, adamellite and abundant diorite to granite porphyry and lamprophyre dikes. The basement gneiss, amphibolite and schist, as well as the Mesozoic granitoids, are intersected by fault zones some of which are earlier ductile shears reactivated under brittle conditions at higher crustal levels. They are filled by tectonic breccia and rock flour cemented by quartz and hydrothermal alteration minerals: sericite, pyrite, less common K-feldspar, biotite, local fuchsite. Chinese geologists

recognize two principal styles of mineralization, Linglong and Jiaojia.

Linglong (Rv 127 t Au @ ~9.7 g/t Au) is the single largest orebody in the province, and a representative of the relatively simple, low-sulfides gold-quartz fault lodes. The lode is up to 3 km long, persistent, up to 6 m wide and traced to a depth of 600 m. For most of its course it is in the Cretaceous granite, at or near contact with Archean amphibolite.

Jiaojia deposit is in the intermediate deformation zone (some 20 km W of Linglong), and the gold is disseminated and in quartz-gold veinlets in silicified and sericitized fault rocks. The Cangshang and Sanshandao ore zone at the western Jiaodong fringe, adjacent to the Bohai Sea, is of the veinlet-disseminated type, along a sheared contact of Archean (2.53 Ga) amphibolite and Jurassic granodiorite in the footwall. The mesothermal ore is of Jurassic age (154 Ma). **Cangshang** (53 t Au @ 4.81 g/t) is mined by an open pit, presumably the largest gold-producing pit in China (Zhang et al., 2003).

Wulashan (also known as Hadamengou) deposit 25 km WNW of the steel centre Baotou in Inner Mongolia (Nie and Bjørlykke, 1994) is only of the "large" magnitude so far (25 t Au plus @ 5.19 t g/t Au), but is interesting for its conspicuous orange K-feldspar-quartz lodes and zones of feldspathization resembling pegmatite. These veins, on hillslopes above a major highway, were in plain sight for quite long but they have been identified as part of a gold system only in the mid-1980s. The host-rocks are high-grade Archean metamorphics (amphibolite, migmatite, gneiss, marble) intruded by late Paleozoic granitic plutons. The low-sulfides K-feldspar, quartz, pyrite, arsenopyrite, galena, gold veins fill faults and fractures.

Gold deposits related to, or associated with, granitoid dikes

Intrusive dikes related to mostly mesothermal granitoid plutons (diorite to granodiorite porphyry, diabase, granite porphyry, aplite, lamprophyres like minette and kersantite) are extremely common in many goldfields (Abdullaev, 1957) and they are often closely related to fault and fissure gold-quartz veins. Some dikes are heavily feldspathized (albitized, microclinized) and gradational into hydrothermally feldspathized fault rocks or fissure margins that are sometimes confused with true dikes. The dike/vein relationship ranges from intimate and genetic (when the dike itself encloses a presumably magmatic-hydrothermal early

postmagmatic gold stockworks, disseminations or veins usually in K-feldspar and biotite alteration envelope), to fortuitous (when both dikes and veins share the same faults or fractures, or where the dike provided a brittleness contrast in heterogeneous settings). Dikes combined with thermal induration of supracrustals (read below) are suggestive of a granitoid body below, a setting repeated at many giant goldfields.

The two historical "giant" goldfields in the Urals, Russia: Berezovsk and Kochkar, are textbook examples of the dike/vein association. The **Berezovsk** goldfield (Baksheev et al., 1999; P+Rv ~700 t Au @ 2.5-18 g/t Au) is 12 km north-east of Yekaterinburg (Sverdlovsk), in central Urals. The surrounding rocks are Siluro-Devonian phyllites and greenstones intruded by gabbro and serpentinite, in a main collisional suture. These rocks were intruded by a 320-310 Ma diorite to granodiorite pluton and a swarm of granodiorite and monzonite porphyry and lamprophyre dikes. Some dikes are albitized and this predates the ore stage. The predominantly N-S striking dikes are densely fractured and about 40% of them are quartz, biotite, sericite, pyrite altered and mineralized. The principal orebodies have the form of dense stockworks of thin quartz, sulfides, gold veinlets confined to dikes, with few through-going veins. The minority of short quartz veins reach into the gabbro and serpentinite where they are enveloped by "listvenite" (this is its type locality), that is talc, quartz, carbonate, fuchsite alteration. There are two multistage vein associations. The more important one has quartz, pyrite, galena, chalcocopyrite, tetrahedrite, and gold. The second association is dominated by quartz and tourmaline with abundant scheelite, pyrite, and the same sulfides as above. Most gold in veins is native, very irregularly distributed. The predominantly sericitic alteration envelopes contain about 2 g/t of disseminated gold.

Kochkar goldfield (Kisters et al., 2000; Pt >300 t Au, Rc ~400 t Au) is in the town of Plast 80 km SW of Chelyabinsk in southern Urals. The host rocks are members of a deeply eroded tonalitic and trondhjemitic gneiss dome permeated by lower Carboniferous porphyritic granodiorite, and intersected by several generations of dikes of variable composition. The ore is in a dense ENE-trending swarm of more than 2000 repeatedly altered, deformed and metamorphosed, schistose mafic dikes composed of biotite, hornblende, plagioclase, K-feldspar, quartz and other minerals. Over 1200 steep, tabular quartz-sulfide lodes (only about 200 are productive) are adjacent to, or parallel with, the dikes, in a 15 km long and 5 km

wide north-south zone. The veins are 0.4 to 2 m wide and tens to hundreds of meters long. The filling is of quartz with lesser tourmaline, ankerite, calcite, pyrite, arsenopyrite, galena, chalcocopyrite and tellurides. Gold is both free milling and refractory, the latter is in pyrite and arsenopyrite, and the gold bullion contains up to 10% of platinum metals. Contrary to the usual situation where late-stage dikes provided the brittle medium for fracture development and vein formation, in Kochkar the dikes had been the softer and less competent component reactivated into a set of conjugate shear zones bordered by brittly fractured, permeable granitoids (Kisters et al., 2000). The granitoids are thus mineralized whereas the dikes are barren. The Permian mesothermal gold-quartz lodes, formed close to the peak of upper greenschist-lower amphibolite metamorphism, were subsequently retrograde metamorphosed and overprinted by a younger generation of brittle faults and post-ore alteration.

Gold veins and stockworks in sheared, thermally indurated supracrustals above intrusion

The main example deposit (or ore field) here is Muruntau in Uzbekistan, the largest hydrothermal gold deposit known and one comparable in magnitude with the largest Witwatersrand conglomerate orebodies. **Muruntau** (Aleshin and Uspenskii, 1991; Marakushev and Khokhlov, 1992; Drew and Berger, 1996; P+Rc ~4,300 or 5,100 t Au @ 2.5-3 g/t Au; Fig. 10.24) was discovered in 1957 as a by-product of uranium search in the Kyzyl-Kum desert of western Uzbekistan. Kyzyl-Kum is at the western outcrop extremity of the North Tian Shan orogen that continues, in the subsurface, north-west to eventually merge with the Uralides. The bedrock outcrop in the low desert hills is limited (some 20-25%) and the rest of the area is covered by Cretaceous and Tertiary, mostly continental sandstone-shale sequence, that contains the important Navoi-Uchkuduk "sandstone-uranium" province.

The oldest bedrock unit is the Neoproterozoic Tazkazgan Suite of medium-grade metamorphosed siliceous, locally carbonaceous schist, mafic metavolcanics and dolomite with local U-V ore occurrences. The overlying Cambro-Ordovician Besopan Suite is a greenschist-metamorphosed unit dominated by quartz-rich marine lithic arenite, siltstone and shale. It hosts the Muruntau orebody that crops out close to the erosional edge of Silurian-Devonian limestone and ophiolite allochthon. The meta-sediments passed through at

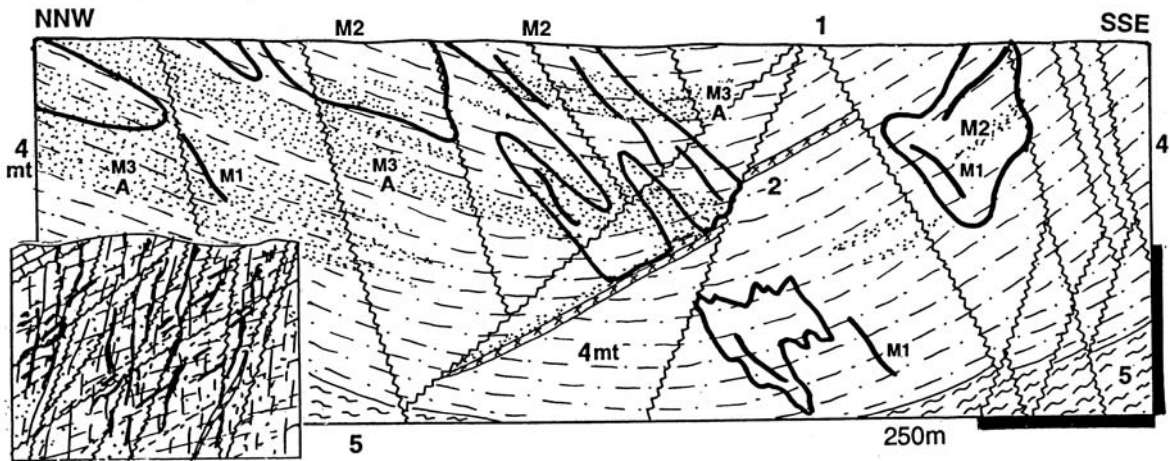


Figure 10.24. Muruntau Au deposit, Kyzyl Kums, Uzbekistan; cross-section from LITHOTHEQUE No. 2069, based on data in Aleshin and Uspenskii (1991), Marakushev and Khokhlov (1992), on-site visit, 1993. M. ~245-220 Ma low-sulfide mesothermal mineralization. M1, discrete short and lenticular Au-quartz pyrite, arsenopyrite veins; M2, stockworks of thin short mostly steep gold-quartz veinlets with thin sericite or chlorite selvages superimposed on flat Au-enriched zones; M3, quartz-scheelite veinlets in feldspar, biotite, quartz altered hosts. A. District-wide biotite alteration, localized quartz, chlorite, feldspar > Mg tourmaline. 1. Q cover sediment and regolith; 2. Pe buried leucogranite; 3. D1-Cb1 limestone, dolomite; 4. Or-S Besapan Suite "distal turbidite", mainly monotonous siltstone; 5. Lower Besapan, chlorite-sericite slate to phyllite

least four deformation stages, probably starting in Ordovician and terminating by the late Carboniferous-early Permian (Hercynian) collision and accretion that provided the future Muruntau site with enhanced permeability at the intersection of NW and NE-trending regional shear zones. Several small Permian post-orogenic S-type granite plutons have been mapped in the area, the nearest outcrop being about 12 km south-east of Muruntau. A 4 km deep drill hole near the present mine pit encountered deformed leucogranite dikes near the bottom, probably indicating a large parent intrusion beneath responsible for thermal metamorphism in the mine area. The metamorphism is slight near the surface (general induration of the meta-sediments grading to spotted schist with biotite and chlorite spots), but it intensifies with depth with the appearance of cordierite and sillimanite. There are several dikes of albitized granite porphyry in the pit.

The early alteration by 400-350°C fluids produced a lenticular linear zone of a fine-grained quartz, albite, phlogopite, chlorite, oligoclase assemblage adjacent to a shear, with minor pyrite, quartz veining and subeconomic gold (0.1-2 g/t Au). The Main ore stage, of several substages, produced the Muruntau orebody that has an assay boundary and projects at the surface as an approximately 3.5 x 2.5 km ellipse with an east-west axis. The associate alteration has K- and Na

feldspars, biotite, quartz and local Mg-tourmaline (dravite). The smaller Myutenbai orebody (Rc 325 mt @ 1.9 g/t Au for 620 t Au) is in a prong in the south-eastern continuation of the main ore zone.

The low-grade Muruntau orebody is selectively bulk-mined from an enormous open pit presently about 400 m deep, crushed in the pit, and railed to a state-of-the art mill and processing plant about 6 km away. The plant produces around 60 t of gold per year and the cumulative production since 1962 is now of the order of 1,500 t Au. Material with >1.5 g/t Au, down to the flexible cut-off grade now around 0.5 g/t, is stockpiled and heap-leached by Newmont, Inc, using proprietary technology.

The predominant mineralization style is an extensive yet non-uniform fracture network of thin, short, mostly steeply-dipping low sulfide gold-quartz veinlets with thin sericite or chlorite selvages superimposed on "flat" biotite (phlogopite) altered zones enriched in gold during the earlier alteration-mineralization stage. The sparse sulfides are pyrite and arsenopyrite. The quartz stockwork is in turn intersected by a small number of through-going, but usually short, lenticular quartz, pyrite, arsenopyrite, gold veins in faults and fractures. Scheelite occurs locally in shoots within both steep and flat quartz veins, associated with strong K-silicate alteration. There is a relatively thin zone of supergene leaching near the surface, with residual gold in limonite.

There is nothing strikingly unusual to explain such an enormous local accumulation of gold, that would be different from thousands of less fortunate deposits around the world, in similar setting. Drew and Berger (1996) put the excellent permeability of the host rocks, in making for a long period of time, as the number one factor. If Muruntau were discovered 100 years ago, it would have been a site of some 4 or 5 underground mines selectively extracting the higher-grade through-going veins, cumulatively producing some 100-200 t Au over a period of fifty years. A million of years ago, the deposit would have been buried under the Devonian limestone thrust sheet.

Kyzyl-Kum gold province contains more significant gold deposits, but reliable descriptions are scarce and tonnage figures vastly inaccurate, apparently inflated to attract investors. Daugyztau (?135 mt @ 4 g/t Au) and close-by Amantaitau (?60 mt @ 3 g/t Au) are on the extension of the Muruntau fault zone 50 km SW of Muruntau. **Kokpataz** (?175 mt @ 3.5 g/t Au) is a system of low-sulfide gold-quartz veins associated with diorite porphyry and lamprophyre dikes, and of bulk-mineable gold in disseminated pyrite, arsenopyrite in quartz-sericite altered shear. The host rocks are tectonized Neoproterozoic mafic to intermediate meta-volcanics interbedded with dolomitized limestone and carbonaceous schist. **Zarmitan** (or Charmitan; Rc ?80 mt @ 3 g/t Au for 240 t Au) is in the Nuratau Range, NE of Samarkand.

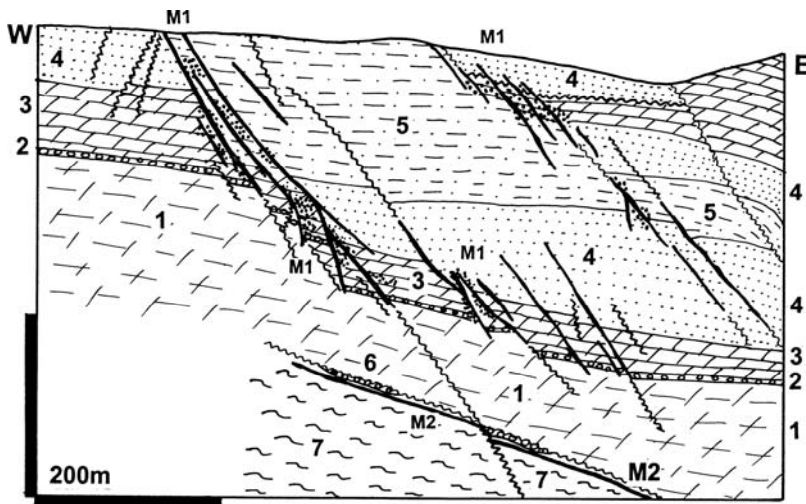
Natal'ka (Natal'inskoe) deposit in the Omchak ore field (Eremin et al., 1994; P+Rv ~130 mt @ 4 g/t Au, ?0.4% As for 525 t Au, ~520 kt As) share with Muruntau a setting in thermally metamorphosed clastics, above intrusions, with a strong fault control. This is the largest primary gold deposit in the infamous (Gulag Archipelago!) Yana-Kolyma ore belt in north-eastern Russia. The host rocks are Permian quartz-rich meta-graywacke, siltstone and argillite with a unit of diamictite (pebbly mudstone). Cretaceous S-granite plutons are present in the area but are not directly in the ore zone, which, however, contains pre-ore mafic, intermediate and felsic dikes. Mineralization is controlled by a strong NNE-trending fault system. 99 individual ore zones, of this 8 major, have been recognized; the main zone can be traced for up to 5 km and is up to 600 m wide. It consists of quartz veins and stringers with, on the average, 2% of pyrite and arsenopyrite plus subordinate Pb, Zn, Cu, Sb, As sulfides and sulfosalts. Wallrock alteration is variable and silicification, carbonatization with

pyrite and arsenopyrite enriched selvages are predominant in sediments, whereas porphyry dikes are albitized or K-feldspar altered in the proximal zone.

Salsigne in the Montagne Noire, the largest French Au deposit and for a time the world's largest arsenic producer (Reynolds, 1965; Bonnemaïson et al., 1986; P+Rc 270 t Au, 603 kt As, 5157 t Bi; Fig. 10.25), has had a long history of mining. The classical orebodies are steeply dipping sets of fracture and fault quartz, arsenopyrite, pyrite, minor Bi-minerals veins and discontinuous stratabound replacements in K-silicate altered Carboniferous to Devonian clastics with interbeds of massive dolomitic limestone. These rocks are members of two nappes, thrust over the Cambro-Ordovician schist basement. More recently discovered has been the Lower Deposit: a gently west dipping 2-3 m thick bedding-parallel replacement along thrust. Mostly refractory gold is in arsenopyrite and associated Fe, Cu, Zn, Bi sulfides, in silicified fault rocks, interpreted as "exhalite" in the 1980s. The ~300 Ma ores are synorogenic, possibly related to a concealed intrusion.

Olimpiad (Olimpiadinskoye) Au-As-Sb deposit (Genkin et al., 1994; 750 t Au @ 2.5-8 g/t Au + X00 kt As) was a 1950s antimony discovery; the presence of gold has been recognized in the 1970s. It is the largest deposit in the Neoproterozoic schist belt of the Yenisei Range in western Siberia. Fine-grained refractory gold is mostly in massive to disseminated arsenopyrite and pyrrhotite that replace quartz, sericite and carbonate-altered carbonaceous schist, marble and exoskarn in a fault zone. The 856 to 792 Ma mineralization has fluid inclusion temperatures between 490 and 240°C and is believed genetically related to a concealed intrusion in depth of about 1000 m under the orebody.

The **Nezhdaninskoye Au-Ag-As deposit** in the Allakh Yun Basin, Verkhoyansk-Kolyma orogen in eastern Siberia, is somewhat similar (Bortnikov et al., 1998; 336 or 480 t Au @ 3.0 g/t, 2,000 t Ag). Fine refractory gold is in pyrite and arsenopyrite, in turn disseminated and in veinlets in a 10 km long, steeply dipping fault zone. The host Permian turbidites are quartz, sericite, carbonate altered and intruded by Mesozoic granodiorite, quartz diorite and lamprophyre dikes.



M1. ~300 Ma mesothermal fault-fracture high-sulfide (arsenopyrite, pyrite, etc.) quartz veins and replacements; M2. Stratabound quartz, arsenopyrite, etc. replacement zone along thrust. Salsigne-Fournes Nappe: 1. D1 calcareous clastics; 2. D1 basal sandstone over dolomitic shale; 3. Cm massive dolomitic limestone; 4. Cm interbedded siltstone, limestone, diabase dikes; 5. Cm1 siltstone, sandstone. Autochthon: 6. Or3-D1 clastics; 7. Metaturbiditic schists

Figure 10.25. Salsigne Au-As deposit, Aude, southern France; cross-section from LITHOTHEQUE No. 1741, modified after Crouzet et al. (1979), Bonnemaïson et al. (1986)

10.5. Dominantly orogenic Au deposits

10.5.1. (Syn)orogenic gold veins and stockworks

Gold veins predominantly in older plutons:

Mesothermal gold-quartz veins that fill faults and brittle fractures in granitoid masses are relatively uncommon compared with gold in sheared supracrustals, and there are few "giants". One of them is the **Grass Valley-Nevada City** goldfield (Johnston, 1940; Pt 330 t Au @ 7-14 g/t, 90 t Ag) in northern segment of the Sierra Nevada Foothills gold belt near Sacramento, California. The host is a Jurassic mesozonal granodiorite pluton emplaced into polyphase deformed late Paleozoic and Mesozoic slate, litharenite, greenstone metavolcanics and serpentinite in a collisional suture belt. Numerous low sulfide gold, ankerite, calcite, pyrite, arsenopyrite veins with minor galena, chalcocopyrite, sphalerite and gold form a north and north-west striking conjugate system. Veins in granodiorite have gentle dips (average 35°), those in supracrustals are steep. The veins fill normal and reverse faults, crush zones and fissures in strongly sericitic, quartz, pyrite altered and carbonatized wallrocks. Some veins are remarkably persistent and traceable over a vertical interval of more than 1,300 m without change in mineralogy. This deposit contributed a fair share of detrital gold to the extensive placers in the Sierra Nevada Foothills.

The "almost giant" **Charters Towers** goldfield 120 km SW of Townsville in northern Queensland

(Levingston, 1972; 224 t Au @ 34 g/t Au in historical lodes) has several groups of narrow high-grade quartz veins with low to moderate sulfide content (pyrite, galena, sphalerite, arsenopyrite, chalcocopyrite) filling "clean" brittle fissures (there is just one small orebody in a shear zone). Gold is free and in places very visible. The veins are Devonian, hosted predominantly by late Ordovician to Silurian (470-426 Ma) equigranular mesozonal hornblende-biotite tonalite and granodiorite and they have narrow greenish sericite and pink smectite alteration rims. Lower Carboniferous (335 Ma) hornblende porphyry dikes are post-ore. The plutons intruded Neoproterozoic to Cambrian meta-sedimentary gneiss to migmatite.

Gold associated with carbonaceous meta-sediments ("black slate"): Carbonaceous ("black", graphitic) rocks are widespread in many mesothermal goldfields and in some they are the dominant feature believed of prime importance in ore genesis. Many carbonaceous rocks are controversial and their origin, as well as the possible role of carbon in ore genesis, vary. The following varieties of gold/carbon associations can be distinguished:

1) Carbonaceous sedimentary rocks (argillite, slate, phyllite, schist), usually pyritic, with a synsedimentary or diagenetic (also "exhalative") low-grade gold content in sulfides (pyrite, arsenopyrite) or dispersed, possibly held in the C-rich substance. There is no major gold deposit known where an unmodified (that is not

penetratively deformed and/or hydrothermally veined) "black slate" would constitute an ore, although minor presence of such a rock in several goldfields has been frequently recorded. In others (Sukhoi Log) it is considered a protore to the superimposed mineralization (Bur'yak, 1975).

2) Penetratively deformed and/or sheared low-grade carbonaceous (graphitic) metamorphics (phyllite, biotite schist) mineralized by "invisible" dispersed gold, or gold bound in pyrite or arsenopyrite porphyroblasts or patches, or gold in thin quartz and quartz-sulfide stringers. There could be some silicification but otherwise obvious hydrothermal alteration rims are rare. The orebodies are long, linear zones of shearing. The gold origin is uncertain: remobilized original (syngenetic) gold? synorogenic hydrothermal gold introduced into a shear and precipitated in reducing and sulfur-rich environment? Morro do Ouro, Brazil, is the best "giant" example briefly described below.

3) Carbonaceous (meta)sediments-rich rock association, usually sheared and/or faulted, with dilational gold-quartz (pyrite, arsenopyrite) veins, stockworks, lenses, saddle reefs. Granitoid plutons may be present in the area, but there is no apparent genetic association. The gold is most often attributed to precipitation from metamorphic-hydrothermal fluids, in local reducing and sulfur-rich (in pyrite, arsenopyrite) environment. The orebodies range from persistent tabular quartz veins to vein arrays and stockworks in linear deformation zones and shears, to predominantly dilation-controlled orebodies in tight folds.

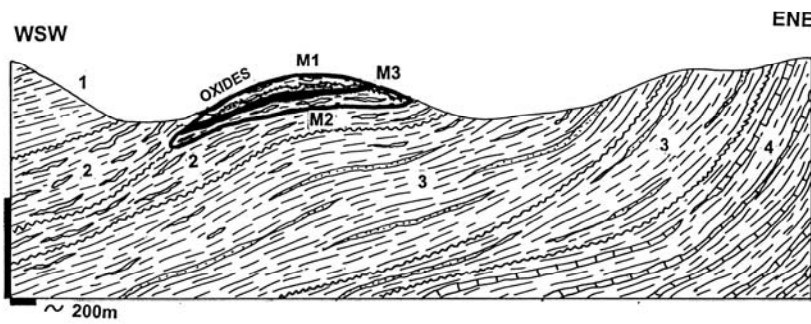
4) Hydrothermally altered faults and shear zones where carbon (graphite) is considered an alteration substance, introduced by fluids from outside (Daugyzttau and Amantaitau, Uzbekistan).

Morro do Ouro deposit near Paracatú, Minas Gerais, Brazil (Zini et al., 1988; Freitas-Silva et al. (1991; P+Rc 654 mt @ 0.444 g/t Au, 0.17% As for 290 t Au, 1.112 mt As; the cut-off grade in 2001 was 0.3 g/t Au; Fig. 10.26). This is about the world's lowest grade hard rock gold deposit ever mined. Gold placers and subsequently gold in the oxidation zone were intermittently mined on a small scale by the locals since 1734. Large-scale open pit mining has started in the 1980s. The about 6 km long ore zone is hosted by metamorphosed clastics of the Meso-Neoproterozoic Paracatú Formation, a miogeoclinal sequence that is in tectonic contact with a probably contemporaneous meta-carbonate unit. The clastics consist of gray phyllite with thin meta-quartzite horizons and lenses, and a prominent band of carbonaceous phyllite or phyllonite that

contains the ore. This structure is probably a trace of a low-angle to almost flat, ENE-directed thrust (Freitas-Silva et al., 1991). The sequence, especially the carbon-rich band, is penetratively deformed, has a strong mylonitic foliation, and contains boudins of competent materials like quartzite and vein quartz.

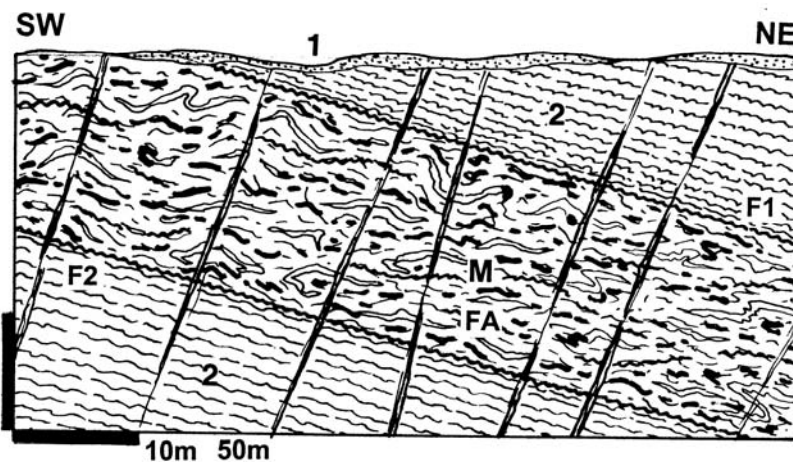
The "high-grade" zone (0.6 g/t Au and 0.25% As plus) coincides with the interval richest in carbon and consists of 1) microfractures filled by arsenopyrite, pyrite and pyrrhotite that contain ultra-fine refractory gold; 2) of small masses of arsenopyrite with minor galena, sphalerite and pyrite grading to scattered metacrysts of arsenopyrite in foliation planes and to thin sulphide laminae; and 3) of gold encapsulated by quartz in quartz boudins and occasional short through-going veins. This interval is enveloped by a low-grade zone in gray sericitic to slightly graphitic phyllite with intricately folded, foliation-parallel discontinuous veinlets and laminae of quartz and/or pyrite with arsenopyrite. Most of the early production came from the oxidation zone where gold was dispersed in powdery and fracture-encrusting limonite. The present style of the primary orebody is interpreted as a syn-orogenic dispersion of ultra-fine gold in an about 680-650 Ma graphitic fault structure that also contains dismembered earlier quartz veins. Most of the veins contain only sub-grade gold values. If this is a pre-orogenic orebody ("Carlin-type"?) the original appearance, alteration and regional setting have been obliterated by the superimposed tectonism.

Macraes ore field in Otago, New Zealand (Craw et al., 1999; P+Rc ~125 mt @ 1.44 g/t Au for ~186 t Au; Fig.10.27) is a gold-mineralized portion of an overthrust structure. It is filled by carbonaceous gold ore without quartz and there are some similarities to Morro do Ouro. The ore zone is in upper greenschist metamorphosed meta-turbidites of the Mesozoic Torlesse accreted terrane, in the Otago Schist Belt. About 10 orebodies are distributed in a 10 km long interval of a NW-trending, 30 km long Hyde-Macraes shear zone. In the main open pit this zone is a 10 to 120 m thick duplex with well-developed hangingwall and footwall bounding shears. In between is the Intrashear Schist, a shale-resembling graphitic fault rock that is either free of silicate impurities, or it contains minor quartz slivers and boudins. The schist carries ultrafine dispersed gold with an average grade of 1.5 g/t, and is mined in bulk. Quartz stockworks and quartz lodes concordant with the shear formed in brittle structures during uplift and exhumation.



M1. Residual gold dispersed in regolith; M2. Lowest-grade, low-sulfides Au dispersed in schist (phyllonite); M3. Higher-grade refractory Au in sulfides, most in quartz boudins; 1. Pt2-3 phyllite intercalated with black phyllite, quartzite; 2. Quartz boudins-rich horizon in black phyllonite; 3. Phyllite; 4. Calcareous phyllite, schist

Figure 10.26. Morro do Ouro Au deposit, Paracatú, MG, Brazil; cross-section from LITHOTHEQUE No. 2500, modified after Freitas-Silva et al. (1991) and Rio Tinto Paracatú Staff, site visit 2000



1. Q unconsolidated sediments; 2. Cb-J Haast Schist, greenschist-metamorphosed turbiditic schist, phyllonitic near the shear, with greenstone lenses and interbeds; M, FA. Thick, low-angle overthrust duplex filled by phyllonite and semi-ductile fault breccia crowded with discontinuous, low-sulfide quartz lenses and boudins grading to ribboned phyllonite replacements; some scheelite

Figure 10.27. Macraes Au mine, Orago, New Zealand; diagrammatic cross-section from LITHOTHEQUE No. 2228. P.Laznicka, 1998 visit assisted by Ross Mining Macraes Staff

Sukhoi Log deposit, ~15 km NW of Kropotkin, central Siberia (Bur'yak, 1987; Rundkvist et al., 1992; Rv 365 mt @ 2.6 g/t Au, 205 mt @ 0.8 g/t Au for 1,113 t Au). This is as yet undeveloped, largest gold deposit in Russia, located in the Baikal-Patom Foldbelt about 120 km NNE of Bodaibo. Bodaibo has been a center of placer mining since 1840 ("Lena Goldfield"), but several bedrock gold deposits, especially in the Kropotkin sub-district farther north, have been discovered only in the 1960s-1970s. Sukhoi Log is a polygenetic, low-grade mineralization believed gradually evolved over a period of some 700 million years. The earliest recorded event had been late Mesoproterozoic or early Neoproterozoic rifting marked by bimodal volcanism and sedimentation; the "giant" Kholodnina Pb-Zn deposit, reminiscent of the Broken Hill-type, formed in this period. The Neoproterozoic downwarp that succeeded the rift (a

sag stage) filled with a thick succession of carbonaceous shale, quartz-rich litharenite and interbedded limestone. It is believed that the initial gold enrichment in "black shale" also took place. The late Neoproterozoic-Lower Cambrian orogeny (~570-520 Ma) deformed and metamorphosed this sedimentary pile under biotite to garnet/staurolite isograd conditions into phyllite, schist and marble. The biotite-grade phyllite became the preferential host to Au-sulfide ores, whereas the garnet/staurolite schist hosts the gold-quartz veins. The present form of the Sukhoi Log orebodies has been established in the Carboniferous (350-312 Ma; equivalent of the Hercynian orogeny in Europe), during a "tectono-magmatic activation" event when small stocks of adamellite and lamprophyre dikes intruded as close as 6 km from the ore zone.

The Sukhoi Log orebody is a 2.5 km long, 200-300 m thick, gentle NE dipping interval of sheared

and fractured alternating carbonaceous schist and marble that enclose fracture stockwork of thin low-grade quartz-pyrite veinlets. These grade into disseminations and replacement patches rich in sulfides: pyrite, arsenopyrite, pyrrothite, chalcopyrite, sphalerite, galena. Most of the gold is in pyrite (2 to 50 ppm Au). Platinum is enriched in the hanging wall region of the gold orebody and continues beyond the economic Au limit (Laverov et al., 1998). Cross-cutting quartz-carbonate veins with sulfides and gold formed last. The central part of the ore zone has magnesite, siderite, ankerite, chlorite, pyrite alteration, then fades away into magnesite-siderite metacrysts scattered throughout the schist, and pyrite (Bur'yak, 1987).

Between Jurassic and Miocene the Sukhoi Log goldfield has undergone uplift, peneplanation, formation of regolith, and partial reworking of the oxidation zone into karst and alluvial placers. There are three additional bedrock gold ore fields in the district.

Mesothermal Au lodes in turbidites and slate-litharenite sequences: Gold-only, syntectonic deposits in turbidites are widespread in the Lachlan Foldbelt in eastern Australia (Solomon et al., 1994), especially in the famous Victoria Goldfields. Surprisingly, there is just one "giant" hypogene ore field, Bendigo (Pt 540 t lode Au, Rc 34 mt @ 12 g/t Au; Johansen, 1998; for a total of 948 t Au. Further 157 t Au came from placers in the area). The second most famous Victorian ore field, Ballarat, stored just 117 t lode gold in lodes, plus 343 t Au in placers, for a total of 430 t Au.

Bendigo goldfield (Sharpe and MacGeehan, 1990; Schaubs and Wilson, 2002 and references therein; Figs. 10.28, 29) is in central Victoria, Australia, hosted by Lower Ordovician quartz-rich turbiditic litharenite, siltstone and slate. The rocks are sub-greenschist metamorphosed and folded into narrow, tight upright anticlinal zones that correspond to some 70% shortening. There are small Devonian granite massifs in the area, but they are unrelated to the anticlines; one intrusion intersect the gold lodes. The Au mineralization is in 15 parallel north-south trending lines of lodes in and close to anticlinal axes, separated by 100-400 m wide barren intervals. The lodes have a simple composition: the dominant form comprise laminated or "bucky" (massive, coarse-grained) quartz with some ankerite, 0.5-2.5% pyrite, arsenopyrite, local galena, sphalerite and abundant coarse visible gold. The veins are enveloped by a distinct and broad sericite (muscovite), ankerite,

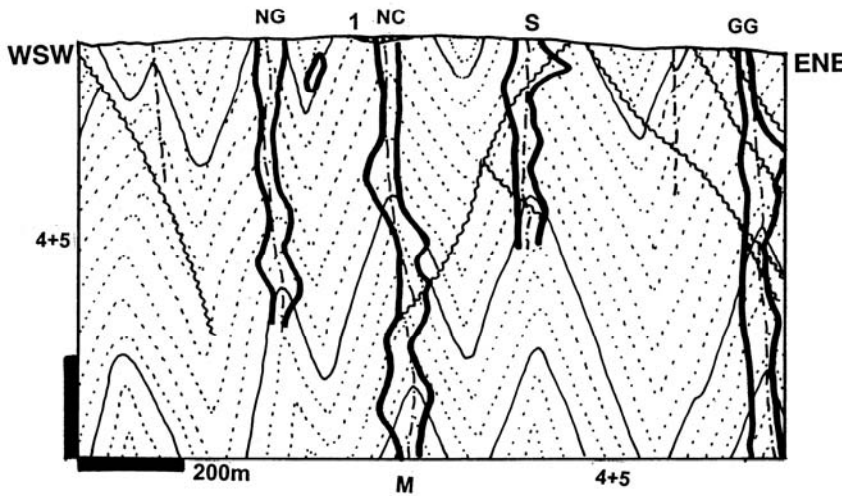
chlorite and albite alteration halo when in litharenite, but there is almost no visible alteration when the veins are bordered by a strained, sometimes tectonically polished black argillite. Pyrite and arsenopyrite metacrysts are scattered near the vein.

Although Bendigo has been made popular by textbook images of saddle reefs and associated bedding-parallel lodes in anticlines, not all orebodies are like that. Johansen (2001) described what happened: "As the folds (parallel anticlines) tightened they "locked-up" and continued compression resulted in reverse faulting and thrust faulting. The faulting occurred at regular intervals at depth down the anticlines creating horizontal zones of structural complexity called "ribbons". The position of the ribbons is controlled by the location of bedding-parallel laminated veins, which created foci for later faulting. The ribbons were the loci for quartz reef formation and were mined on average to 500 metres, and in parts of the field to 1,400 metres, beneath the surface. There was no evidence of a drop off in gold grade with depth, and the tenor of mineralization and the size of reefs stay relatively constant with depth".

The Bendigo lodes are believed emplaced in at least two periods, the older (450-420 Ma) coeval with regional metamorphism and thrusting, the younger (410-370 Ma) following relaxation and granite emplacement in the broader area. The veins are mesothermal, precipitated from ~350°C fluids released by metamorphic dehydration in depth and reacting with the wallrocks, especially with their accessory pyrite.

Stratabound Au-(Cu,Ag) replacements in faulted miogeoclinal sequences: Telfer ore field at the edge of the Great Sandy Desert in Western Australia is an enigmatic deposit (Rowins et al., 1997; P+R in 1996 about 250 mt @ 1.4 g/t Au for 363 t Au; 2003 Rv+Rc in deep orebodies added 360 mt @ 1.5 g/t Au and 0.19% Cu for 1,381 t Au content). It is hosted by the Neoproterozoic Yeneena Supergroup, a succession of generally gently folded (but faulted and thrust) alternating miogeoclinal siltstone, quartz-rich sandstone, pelitic limestone and dolomite resting on Paleoproterozoic metamorphic complex. It has been deformed and greenschist- to sub-greenschist metamorphosed during the 700-600 Ma orogeny, accompanied by emplacement of small granite plutons. No pluton, however, has been so far discovered within or under the ore field.

The Au orebodies are in a set of two en-echelon, double plunging asymmetric anticlines (domes) and



M. D-Cb1 dilatant to replacement low-sulfides gold-quartz bodies controlled by several parallel N-S anticlinal axial zones; 1. T-Q alluvial gravels with placer gold; 4. J thin lamprophyre dikes; 5. Or1 turbiditic litharenite alternating with siltstone, slate; strong cleavage. ANTICLINES: NG. Nell Gwynne NC. New Chum S. Sheepshear GG. Garden Gully

Figure 10.28. Bendigo, Victoria Goldfields, Victoria Hill cross-section from LITHOTHEQUE No. 2829, modified after Willman and Wilkinson (1992)

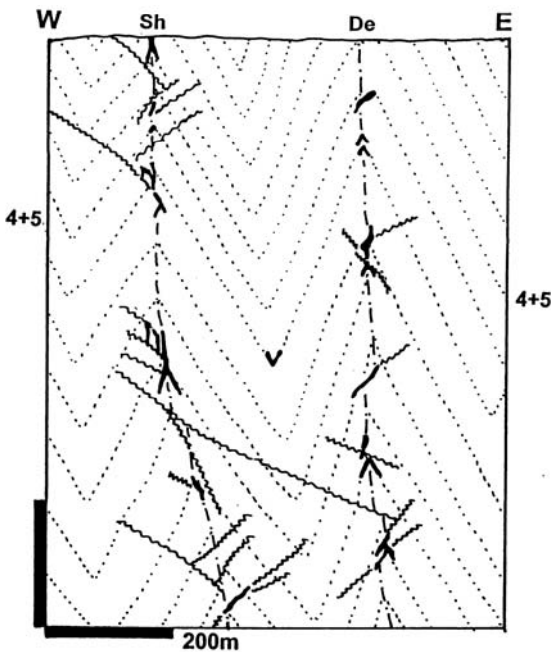


Figure 10.29. Bendigo Goldfield, Sheepshead and Deborah Anticlines. Cross-section from LITHOTHEQUE No. 2831 showing the true size and discontinuous nature of the orebodies (in black). Based on information from Bendigo Mines NL, 2000, derived from their new decline. 4+5. Or1 turbidites, alternating litharenite and slate. Sh=Sheepshead, De=Deborah Anticlines

(pyrite with minor chalcocopyrite, pyrrhotite, galena, sphalerite, free gold) with interstitial quartz, or separate bedding-parallel quartz veins with scattered sulfides. Some “reefs” are very extensive: the Middle Valley Reef, 0.5 m wide, extends over 10 km². Fracture stockworks of comparable composition are in both the hangingwall and footwall of a “reef”, and sometimes link reefs situated at different stratigraphic levels. Vearncombe and Hill (1993) argued for the ubiquity of strata-parallel shear zones that resulted in shortening, that control synorogenic structure-controlled epigenetic mineralization and mimic syn-sedimentary stratiform ore beds. Rowins et al. (1997) considered the ore fluid to have been of marine evaporitic origin derived, with the ore metals, from the sedimentary pile and possibly heated by synorogenic to postorogenic granites. Telfer has a thick oxidation and leached zone and the first phase of mining was based on heap leaching of gold dispersed in residual limonite and locked in quartz. Locally, the oxidation zone was enriched in chrysocolla, malachite, cuprite and native copper.

Gold belts in accretionary terranes, sutures, along terrane boundaries: Accretionary terranes outboard of magmatic arcs in combined subduction/collision settings bring together a variety of lithologies of mostly mantle (e.g. serpentinite), oceanic, island arc and turbidite derivation interspersed with sutures, fault systems, and a variety of plutons. Superimposed over such composite assemblages that are, typically, greenschist metamorphosed, are

in thin high-grade stratabound units at depth. Most are persistent, bedding-conformable sheets (“reefs”) of crudely banded massive to disseminated sulfides

very long (100 km plus), narrow belts of structurally controlled, discontinuous mesothermal gold deposits. The deposits range from dilational gold-quartz veins and stockworks to shear-replacing quartz lodes and sometimes disseminated auriferous pyrite bodies in altered (mostly albitized) wallrocks. The ores are nonselective in terms of their host rocks: every rock can form a wallrock and the host rock frequency is usually close to the proportion of rock types in the area. As meta-turbidites (graywacke, slate) are most widespread they are also the most common ore hosts, followed by greenstone meta-basalt, diorite to granodiorite, gabbro and serpentinite. Carbonate hosts are rare.

Rather than being confined to a single major fault the orebodies follow a trend of subparallel, mutually linked or independent fault arrays. Individual orebodies are usually small to medium, irregularly spaced, with distribution maxima followed by "gaps". The aggregate tonnage of contained gold in an entire belt, as listed in the literature, could be significant (e.g. Mother Lode, 803 t Au), but it should be realized that this represents a length of 196 km and that there is not a single "giant" deposit or ore field along this length. In the Juneau gold belt in Alaska there is one "A-giant". Even though productive orebodies in "gold belts" are discontinuous, there is a better continuity of hydrothermally altered rocks and sericitized, silicified, chloritized and carbonatized rocks that often bridge short barren gaps. Most prominent gold belts shed a quantity of detrital gold into the environment to form mostly alluvial placers, sometimes exceeding the quantity of gold won from lodes. Placers widen the mineralized area and conceal some non-mineralized gaps.

The gold deposition required a number of preparatory steps, but then occurred suddenly, usually during a period of relaxation and extension that postdated the peak of compressional orogeny, or during change from a compression to transpression and strike-slip faulting. The genetic interpretations about the sources of gold and fluids keeps changing from granite-related magmatic of the 1950s to metamorphic dehydration theories of the 1990s. The more recent interpretations increasingly favor a collective effort during "thermal events": for example, release of a gold-bearing metamorphic pore fluid at the greenschist-amphibolite facies' transition, which is then driven into relaxing thrust faults by heat from the nearby batholith (Goldfarb et al., 1997, for the Juneau Gold Belt).

Mother Lode Au belt in California is a 196 km long narrow (1-1.5 km wide when not twinned) NNW-trending deformation (fault) zone west of, and parallel with, the Sierra Nevada range and Jurassic-Cretaceous magmatic arc (Knopf, 1929; Landefeld and Silberman, 1987; Pt 803 t Au, 150 t Ag between Georgetown and Mariposa, or 415 t Au between Cosumnes River and Mariposa). The most productive ore field was a 16 km long segment between Jackson and Plymouth that yielded ~200 t Au. Mother Lode occupies the central and southern portion of the much longer Sierra Nevada Foothills Foldbelt the northern part of which contains the important Alleghany and Grass Valley-Nevada City districts (read above). The Foothills Foldbelt comprises Paleozoic and Mesozoic rocks accreted to the Cordilleran margin and penetratively deformed by the late Jurassic orogeny: a major collisional event. The predominant lithologies in the belt are members of Triassic to Jurassic dismembered ophiolite with alpine serpentinite slivers; greenstone metabasalt to basaltic andesite with related volcanoclastics; volcanic and epiclastic litharenite, siltstone to slate; hemipelagic to pelagic carbon-rich slate. The metamorphic grade varies from prehnite-pumpellyite to amphibolite. Jurassic-Cretaceous granodiorite plutons related to the Sierra Nevada magmatic arc intrude the belt near its southern end.

The central feature of the Mother Lode gold belt is the late Jurassic Melones Fault Zone (MFZ) and adjacent melange belt (Duffield and Sharp, 1975). Interpretations of MFZ vary. Landefeld and Silberman (1987) interpreted MFZ as a zone of failure formed during accretion, that juxtaposes Jurassic-Triassic volcanic arc and basin elements and incorporates tectonically intruded fragments of the sub-arc basement. In the southern part of the belt MFZ is a 3.5 km wide tectonic melange with serpentinite matrix that changes, farther north, into a broad shear zone and eventually about 1 km wide mylonite-phyllonite zone. The Jurassic accretion was accompanied by predominantly ductile deformation that changed into semi-brittle shearing and brittle faulting, following uplift. MFZ is the continuous first-order structure that controls the orebodies, comparable with the "breaks" (e.g. Cadillac Break) in many Archean gold belts (Chapter 9). The gold orebodies are in brittle structures superimposed on MFZ, or in adjacent rocks. Knopf (1929) described the principal Mother Lode mineralization styles and example deposits and his descriptions are still valid.

1) Veins. Quartz veins are usually of the shear lode variety, subparallel with the local structural

grain. The dip of most veins is less steep than is the cleavage, with dips ranging between 50-70°. The vein filling is a coarse milky-white quartz that forms lenticular masses as much as 17 m thick and 2.2 km long. The solid quartz orebodies sometimes change into a large number of thin subparallel quartz stringers in slate (schist). Quartz veins hosted by slate or phyllite are usually ribboned, with widespread screens of slate in quartz. Greenstone host rocks, in turn, host clean and homogeneous quartz masses. Ribboning, abundance of crack-seal structures, grayish tint and the presence of sulfides distinguish lode quartz from the locally abundant metamorphic milky quartz. Most gold-quartz lodes have also ankerite, sericite and albite and occasionally green fuchsite (locally called mariposite), sometimes scheelite. Pyrite is the most common sulfide followed by arsenopyrite and rare chalcopyrite, galena, sphalerite. Gold is mostly free, often coarse and nuggety. Au-Ag tellurides occur locally. The average grade of veins was about 9 g/t Au, of 839-899 fineness. Pervasive wallrock alteration (sericite, pyrite, ankerite) is strong in graywacke and greenstone. In slate it is substituted by quartz, ankerite, chlorite stringers and veining. When serpentinite is the host rock the veins widen, split and become diffuse or merge with the talc, chlorite, magnesite, quartz, carbonate alteration assemblage ("listvenite").

2) Disseminations, veinlets. The greenstone-hosted "gray ore" (e.g. Fremont, Keystone, Bunker Hill mines) consists of pervasively quartz, sericite, albite and ankerite altered meta-basalt that contains 3-4% of scattered auriferous pyrite or arsenopyrite. The grade averaged 7 g/t Au and most orebodies were adjacent to strong quartz vein systems. The "mineralized schist" ore type (e.g. Melones, Carson Hill mines) are sheared metavolcanics, now amphibolite or chlorite schist. They may carry about 3 g/t Au in a sericite-pyrite altered rock, enveloped by quartz and ankerite veinlets. The refractory gold is mostly in pyrite veinlets, stringers and scattered cube metacrysts. Albitized massive rocks (typically diorite or gabbro) are locally slightly auriferous, but have been, so far, of little economic importance.

Landefeld and Silberman (1987) attributed the Mother Lode gold mineralization to fluids released by metamorphic dehydration in depth at the onset of the thermal event that subsequently caused partial melting in the crust and ascent of granitic magmas. The ores postdate the metamorphic and orogenic peak, but some are affected by post-ore brittle faulting.

Juneau gold belt in south-eastern Alaska (P+Rc 423 t Au plus placer gold) has much in common with the Mother Lode belt. The belt is 160 km long, NNW-trending, in an accretionary terrane complex assembled from greenschist-metamorphosed Permian to Cretaceous sedimentary and volcanic rocks (phyllite, graphitic phyllite, greenstone metabasalt and meta-andesite, minor marble and quartzite). These are intruded by several generations of gabbro to granodiorite plutons (Berg and Cobb, 1967; Goldfarb et al., 1997). The belt has a dense agglomeration of narrow terranes bounded by ductile to brittle sutures, thrusts, shears, strike-slip and normal faults resulting from repeated collision events. 70 Ma (Upper Cretaceous) and younger strain relaxation facilitated intrusion of small granodioritic plutons in the gold belt, and of the huge Coast Batholith 10 km away. Barrovian (low pressure, high temperature) metamorphism overprinted the previously regionally metamorphosed supracrustals, and gold lodes filled brittle dilational faults and fissures. Several gold-quartz vein deposits of Mother Lode-style are scattered throughout the belt of which the Juneau goldfield stores the bulk of gold (369 t Au). This gold came from two adjacent mines: the "giant" Alaska Juneau (P+Rc ~209 mt ore @ 1.62 g/t Au for 279 t Au) and Treadwell (25 mt ore containing 90 t Au).

Alaska Juneau mine (Spencer, 1906), in operation during the early 1900s, was then the world's lowest grade underground hardrock gold mine (the overall grade was 1.23 g/t Au). The mine is in interfaulted Triassic graphitic phyllite and greenstone, intruded by several Cretaceous diorite stocks. The rocks are biotite, albite and ankerite altered. The steeply dipping ore zone is 530 m long and 250 m wide and it consists of a large number of thin quartz veinlets and veins parallel with cleavage that strikes about N70°W, but the veins cross the cleavage dip. The ore consists of quartz, minor ankerite with calcite, sericite, pyrrhotite, pyrite, sphalerite, galena, chalcopyrite and although selected samples of sulfides-rich material ran as high as 14 to 35 g/t Au the bulk ore, after dilution, graded between 1.2 and 1.5 g/t Au. In the Treadwell mine on Douglas Island, close to Alaska Juneau, but in a different terrane (Gravina belt), gold is associated with pyrite disseminated in chlorite-sericite and ankerite-altered greenstone. There are 2-4% of sulfides and the ore grade was about 3 g/t Au.

10.6. Gold placers

Gold placers have contributed significant proportion of gold produced by now and there are some 2-3,000 t Au still left in remaining resources. Placers are typical secondary (resedimented) deposits and they could only form where primary gold, released at source and transported, was available. Gold has specific gravity around 19 (depending on purity) and to be recoverable by traditional gravity techniques, it has to be coarse enough. Unfortunately, coarse gold does not travel far from source because of its softness (some 15 km at most by gravity or water transport; Boyle, 1979), although glacial, debris flow or pyroclastic transport can extend this limit. The bulk of detrital gold deposits, however, are alluvial so the maximum distance from source generally applies.

Placer proximity to bedrock gold sources assures that detrital gold does not move far beyond the limit of hardrock gold provinces, but it spreads laterally and downstream to form placer fields and placer-filled channels. These are difficult to delineate, name and quantify and except for small placer goldfields bordered by barren gaps (e.g. Klondike/Dawson City, Yukon) placer fields coalesce to form huge gold provinces (regions) that include both gold placers and bedrock deposits (e.g. the Victoria Goldfields Province, Australia). Krivtsov and Migachev (1998) distinguished 23 such provinces in the Russian Federation, most of them in a broad belt bordering the Siberian Platform in the south and terminated by political boundaries (against Kazakhstan, Mongolia and China) and Pacific Ocean. Political boundaries are frequently used to delineate placer fields which is unfortunate as this has little regard for geology.

Placer gold is often said to be a yesterday's resource as most historical placers are exhausted or considerably depleted by now, but an amount equivalent to several "giant" deposits is still known to be left in ground and additional speculative resources likely remain in buried channels in the offshore, and under Quaternary glacial sediments and young lava fields. Approximate recalculation of the percentage data in Krivtsov and Migachev (1998) indicates that of the approximately 10,000 t of gold historically produced in Russia (within the present boundaries), some 80% came from Siberian and Far East placers, the rest from hardrock deposits. In terms of reserves and resources (these are estimated to be of the order of 4,000 t Au) the hardrock gold reserves/resources in Russia are 2.9 times greater than in placers. Except for Russia, placer deposits are still extensively exploited in

Brazil (the Amazon Basin) and isolated placers or small workings are still producing in Alaska (Valdez Creek), Canada (Klondike), Brazil, the Guyanas, Venezuela, Colombia, Bolivia, Ghana, Tanzania, China, Australia, New Zealand and elsewhere.

Styles and settings of gold placers: Review literature on gold placers is a disappointment as most writers would rather elaborate on the mysteries of the Witwatersrand than provide practical information on the young placers required by exploration geologist. Boyle (1979) book provides the best start, despite the lack of graphics. Bilbin (1955) and Bykhovskii et al. (1981) prepared about the most useful texts, unfortunately in Russian. This section deals with the neo-placers only, formed between about Eocene and Quaternary and still insufficiently consolidated. Paleoplacers are treated in Chapters 11 and 13.

Before placers can form, gold has to be released from its hardrock host which, in most cases, are quartz veins. With the exception of glaciers grinding fresh bedrock and transferring gold particles into the drift, this requires deep humid weathering and mature physiography. Gold particles so released are transferred into colluvium or alluvial fans, directly eroded by gulch creeks from the decomposed bedrock and concentrated at the channel bottom, or reworked by streams from unsorted sediment, such as colluvium and glacial drift. Gold in placers can be free, or enclosed in quartz. The latter is virtually nowhere recovered. There are very few hardrock gold sources to placers other than lodes, as replacement deposits of ultrafine gold (like the Carlin-type) do not yield particles large enough to be mechanically recovered. Because of this, Carlin was missed by the oldtimer prospectors.

The first-order placer classifications differentiate between alluvial and beach placers. Although minor Au beach gravel deposits are known (Nome in western Alaska being most popular; Nelson and Hopkins, 1972), not a single "giant" has been found in this setting so far. The stream and delta placers are subdivided by Boyle (1979) into the present-day (actively forming) placers, and fossil elevated and depressed equivalents. Elevated placers are all Quaternary, mostly Holocene, and present in or at the bottom of surficial gravel piles. They are vulnerable to erosion. Depressed placers are deeply buried under a pile of younger deposits, volcanic flows or pyroclastics, or glacial sediments that protected them from erosion. Many are of Tertiary

age, have no surficial expression and reflect ancient drainage that may have changed by now.

The least mature and source proximal placers are gulch and creek channel gravels. Many soon develop into sediments of meandering streams. There, channel lag deposits consist of gravels that lagged behind while the finer and/or lighter fraction (sand) moved farther downstream as a bed load. These are enriched in gold and form discontinuous lenticular patches in deeper parts of the channel, commonly resting on the bedrock. Channel lags are the most productive repository of gold and other heavy minerals. The richest paystreaks lie directly at the bedrock bottom where gold is often trapped in cracks and other irregularities. The paystreaks may persist for several meters upward, the gold flakes being in the gravel matrix. "False bottom" paystreaks (intraformational gravels usually resting on clay bottom) are less frequent and difficult to predict. In deposits of inactive streams the lag gravels are covered by the finer sand of point bars and eventually buried under the alluvial plain.

Point bar deposits form at convex sides of meanders. They may contain gold when it is locally abundant, but the gold tends to be fine and insufficiently localized so the single-stage paystreaks are low-grade, although relatively extensive. Repeated reworking of the point bar placers during the successive stages of stream downcutting can considerably upgrade the paystreaks by winnowing out much of the light detrital constituents. Many bench and terrace gravels that fringe river valleys are modified former point bar deposits. Flood plains and flood basin deposits are mostly of fine silt and clay rich in organic matter, and interrupted by sand intercalations. These do not contain detrital placer gold that can be physically recovered, but there is a possibility that fine to very fine ("colloidal") gold can form very low-grade but relatively extensive accumulations in floodplains and possibly represent a future resource recoverable by solvent leaching. Minard (1971) reported up to 1.2 ppm gold in floodplain sediments near Jefferson, South Carolina, in an area with known gold mineralization in a bedrock regolith.

Super-fine gold results from mechanical attrition of coarser gold particles, but also from the liberated gold previously held in sulfides, or finely dispersed as in Carlin. Such gold, transported mainly in suspension with density currents saturated in mud ("flotational gold") can migrate into porous gravels below. Super-fine gold may also provide gold to accrete into nuggets in soil profiles.

Buried alluvial placers: deep leads: Although almost every young placer is buried to some extent and excavation is needed to reach the near-bottom paystreak, buried placers as treated in the literature require at least several tens of meters of overburden (unless partially exhumed) and be geologically older than the modern deposits, to qualify. Especially challenging are placers unrelated to the present drainage, the majority of which are Tertiary. Buried placers may be either unconsolidated to partly cemented, and with increasing age and cementation they change into paleo-placers (Chapters 11, 13). Most buried placers are former lag deposits in paleochannels and, in contrast with most modern placers, they are diagenetically altered. The most common alteration product is clay resulting from argillization of unstable silicate clasts and matrix, hence the buried old placers are often clay choked and this complicates processing. The clay used to be removed by a variety of means such as hydraulic mining and "puddling" in the past, causing a substantial environmental damage by choking streams which, in turn, became prone to flooding. This triggered early government intervention as in the ancestral Yuba River placers near Sacramento, California. There, a 1884 court injunction banned the placer mining (Yeend, 1974). In about the same time in Bendigo, a similar problem required diversion of the clay sludge into the Bendigo Creek floodplain where the old preserved sludge now contains up to 4 g/m³ of fine gold. Deep leads also tend to be "limonite" rich, the iron having been derived from the soil profile by leaching mafic silicates and oxides. Under strong reducing conditions as under swamps and bogs authigenic siderite and pyrite may have formed.

Sierra Nevada Foothills deep lead gold placers, California (Yeend, 1974; 1,562 t Au). Placers are responsible for about 40% of California's gold production and this production came from both Tertiary fluvial gravels in buried channels, as well as from Quaternary gulch and river placers. Both placer groups derived their gold from abundant mesothermal vein deposits (like the Mother Lode vein system; read above) subjected to humid weathering, uplift and erosion. Tertiary deep leads formed in valleys of rivers that flowed southwestward. Lindgren (1911) pointed out the close correlation of the economic gold placers with the metasedimentary, metavolcanic and ultramafic rocks in the basement. In contrast, gravels over granitoid plutons were barren.

In the **ancestral Yuba River gravels** (Yeend, 1974), 153 tons of gold is believed still in place, saved from mining by the 1884 injunction. There,

the Eocene gravel rests on Paleozoic phyllite containing minor fault-bounded slivers of serpentinite, intruded by granodiorite. In the North Columbia diggings the auriferous gravel thickness ranged from 100 to 150 m, and the bottom 24-30 m of slate-dominated boulder and cobble gravel contained most of the gold. The overall grade was less than 1 g/t Au per cubic yard, and the richest 60 cm thick paystreak contained about 6 g/t Au. The gravel was largely situated under the water table, was reduced ("blue"), with locally common authigenic pyrite. The "upper gravel" contained abundant silt and clay units, dominant milky quartz and quartzite clasts, and low gold content. The gravels were buried under Tertiary andesite tuff, volcanic mudflows, and locally under a biotite-rich rhyolite tuff.

Klondike placers, Dawson City, Yukon, Canada. Klondike River is a tributary of the Yukon River near Dawson City, and extensive placers distributed over about 2,500 km² have yielded some 373 t of gold so far (Boyle, 1979). The goldfield is in a thoroughly dissected upland marked by rounded hills and numerous stream tributaries (gulches) to the main watercourse. The area was not recently glaciated, but is in the present permafrost zone frozen down to 70 m depth. This somewhat facilitated, shortly after the goldfield discovery in 1896, the early underground mining from shallow shafts as it increased stability, but then the material had to be defrosted. Following property consolidations in the 1930s, dredging became the principal mining technique and the ground had to be thawed before dredging could start, by injecting steam into holes drilled on a grid.

The Klondike bedrock is composed of metamorphics of the Yukon-Tanana terrane and it comprises predominantly muscovite schist with graphitic schist, greenstone and serpentinite slivers, locally tectonized and altered. The gold is believed to have come from numerous small quartz veins and stringers in faults. The alluvial gravels are at several levels. The high elevation, Tertiary White Channel gravels are areally extensive and contain widespread but low-grade detrital gold. Much of this gold has been reworked into low-level gravels at bottom of the present creeks and gulches. The valley gravels are 1.2-3.3 m thick, rest on the bedrock schist, and had high gold grades throughout. The gravel is topped by 0.5-10 m thick blanket of black frozen organic-rich muck.

Victoria Goldfields placers. Central and eastern Victoria, Australia, is composed of several subparallel, north-south trending structural belts that are all members of the Paleozoic Lachlan

orogenic belt. Most of these belts contain scattered small deposits of gold, but the bulk (~75%) of the past Victorian gold production of over 2,500 t Au came from the Bendigo-Ballarat belt (or gold Subprovince; Phillips and Hughes, 1996). The Devonian lode deposits there have produced over 1,000 t Au and are dominated by a single "giant" (Bendigo goldfield, reviewed above). Detrital gold deposits account for some 1,470 t Au and most of this gold was produced between the time of discovery in 1851 and 1910. After a virtual gap in activity between 1915 and early 1980s exploration resumed and in 2002 there were at least five intermittent small placer operations.

Of the 1,470 t of placer gold perhaps 200 t came from buried "deep leads", the rest from shallow "diggings" and dredged areas (Canavan, 1988). The Bendigo-Ballarat gold sub-province contains thirteen combined placer/lode goldfields, of which one placer goldfield (Ballarat, 343 t placer Au) is a "giant" and three are "large" (Bendigo, 157 t Au; Fig. 10.30; Castlemaine, 146 t Au; Creswick, 81 t Au; all alluvial gold only). Gold was discovered at or close to the surface near stream headwaters and followed into progressively greater depths. The Recent (Quaternary) placers have been found in gullies and valleys where they rested on deeply weathered bedrock. They supplied the bulk of the gold recovered. The placers often merged with gossans and regoliths of the lode deposits. A small gold production came from probably Pliocene high-level terrace deposits found above the present streams. The rest of gold has been derived from the "deep leads" some of which are as old as Eocene. About the most interesting are "deep leads" capped by basalt flows, as in Ballarat.

Ballarat Goldfield, 120 km NW of Melbourne, is about 14 km long (N-S) and 5 km wide (Baragwanath, 1923; P+R 438 t Au of which 343 t is from total placer, 70 t from deep leads). It consists of three strike-parallel zones of quartz "reefs" in Ordovician turbidites, concealed under thick overburden of Cainozoic gravel and sand subdivided by flows of Pliocene-Pleistocene basalt. Mining started in shallow alluvial gravels rich in nuggets and gradually moved into "deep leads". Some deep leads were mined from underground workings reaching the depth of 150 m and accessed through four basalt flows. Payable placers were located directly on the basement floor, were between 1 and 12 m thick, and consisted of a quartz-rich gravelly "wash" with coarse gold, covered by barren gravel and sand, or by basalt. Gravels sandwiched between basalt flows were in

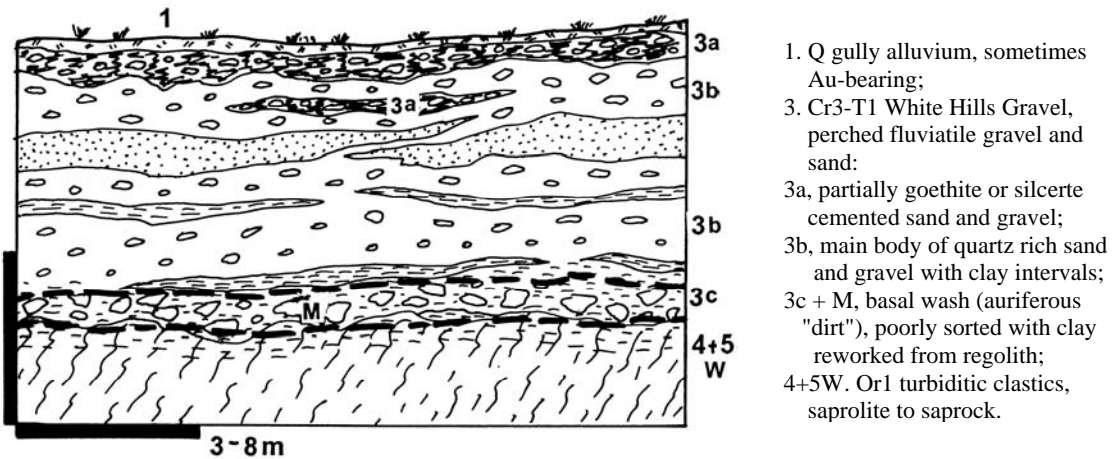


Figure 10.30. Bendigo, Victoria Goldfields, White Hills gravels and paleoplacer. Diagrammatic section from LITHOTHEQUE No. 2833; P. Laznicka, field sketch 2000

most cases barren. The gold placer-filled channels follow sinuous courses branching into tributaries, and tracing them beneath basalt was extremely costly and uncertain. Hundreds of holes drilled at random around Ballarat found nothing.

Victorian Goldfield yielded a large number of nuggets, including the largest ever recorded Welcome Stranger (71.07 kg Au) found near Moliagul. The second largest nugget (68.27 kg), came from Ballarat.

Conclusion on mesothermal gold and placers: Figures 10. 31, 32 and Tables 10.2 and 3 show and list the worldwide distribution of Phanerozoic and late Precambrian Au lode "giants" and placers, respectively. Their early Precambrian counterparts are in Chapter 9.

10.7. (Syn)orogenic Sb & Hg deposits

10.7.1. Antimony deposits

Antimony is worth about \$4-6/kg and it is a low-demand metal today. But it is geochemically rare, with a clarke of 0.3 ppm and because of it every deposit with 30,000 Sb plus is a "geochemical giant". There are at least 21 of them, plus 3 "super-giants" with 300 kt Sb plus and this does not include deposits in Precambrian greenstone belts (Chapter 9), and additional complex deposits where Sb is a by-product (like the Coeur d'Alene district with ~70 kt Sb, mostly in tetrahedrite; Chapter 7). This contrasts, for example, with nickel worth between \$7 and \$10/kg; yet Ni with the clarke of 55 ppm is 183 times more abundant than antimony.

Hence a Ni "giant" starts at 5.5 Mt Ni, which in financial terms is 3,033 times more than the 30 kt "Sb-giant". This is about the most striking case of discrepancy between the geochemical and economic premises of rating magnitudes of metal accumulation, and the way out is to reduce the coverage given to the Sb "giants" and extend the Ni coverage to include the "large" deposits. This is exactly what I have done, hence the identifiable "Sb-giants" are all listed in Table 10.4, but the more detailed description is kept short.

All economic Sb deposits are hydrothermal, ranging from epithermal to mesothermal with the latter predominant. Except for the tetrahedrite and Cu, Pb, Ag sulfosalts-rich deposits described above, the bulk of antimony is stored in what the U.S. Geological Survey (Cox and Singer, eds., 1986) term "Simple Sb deposits". The simplicity lies in the fact that most such deposits are just stibnite without or with few other metals and minerals like pyrite and arsenopyrite. The "simple-Sb's" grade into Sb-Au, Sb-As and Sb-W deposits and their combinations, again not counting the ores with Sb-sulfosalts. In the Au-Sb deposits (gold being the main cash earner), stibnite substitutes for the usual arsenopyrite as the major sulfide (as in Hillgrove, La Lucette, Yellow Pine). The Siberian "giant" gold deposit Olimpiada holds 40% of Russian Sb reserves. Most Sb deposits are (syn)orogenic, not directly related to granitoids (yet often sharing structures with granitoid porphyries and lamprophyres), and with a special affinity for major fault zones filled by high-level fault rocks (that is, fault breccia, gouge, "fault slate" rather than mylonite), especially ones rich in carbon. Sb deposits form separate groupings (belts) or they

Table 10.2. Summary of Phanerozoic and late Proterozoic "giant" hydrothermal gold deposits (includes several "As-giants" marked *)

No. on map	Deposit, district	Age	Type, geology	Tons Au
1	Fort Knox, Fairbanks, Alaska	Cr	Intrusion-related; low-grade sheeted veins, stockwork to disseminated Au with sulfides in granitoid stock	200
2	Juneau goldfield, SE Alaska (Alaska Juneau & Treadwell mines)	Eo1	Orogenic; low-grade Au-quartz veining to disseminations in altered shears	369
3	*Headley As-Au, British Columbia	J1-2	Au-As arsenopyrite-rich exoskarn	61 200 kt As
4	Lincoln, Montana; McDonald-Au	Cr3-T	Intrusion-related or orogenic, veins & stockworks in granitoids	255
5	Grass Valley-Nevada City, CA	J-Cr	Orogenic; Au-quartz veining in fractured granitoid massif	330
	Allegheny goldfield, California	J-Cr	Orogenic; Au-quartz veins in fault zone in metamorphics, disseminated Au in albitized wallrock granitoids	280
6	Mother Lode belt, California	J-Cr	Orogenic; long fault zone with discontinuous intervals of Au-quartz veining	803
7	*Morro do Ouro, Paracatu, Brazil	Np	Orogenic; very low grade disseminated Au with As, Fe sulfides in graphitic phyllonite along low-angle thrust	290 1.112 mt As
8	*Salsigne ore field, France	Cb3	Orogenic; system of Au-quartz fissure and fault veins; Au in stratabound Fe,As,Bi sulfides replacement	270 603 kt As
9	*Zloty Stock, Lower Silesia, Poland	Cb3	Au-As loellingite and arsenopyrite-rich exoskarn near granodiorite contact	97 900 kt As
10	Berezovsk, Urals, Russia	Cb1- Tr2	350 steep fault & fracture Au-quartz, sulfide veinlet stockworks near porphyry dikes in sericitized eugeoclinal wallrocks	700
11	Kochkar ore field, Plast, Urals, Russia	Cb	Orogenic; system of steep Au-quartz, sulfide lodes along mafic dikes in a shear zone in granite gneiss	400
12	*Vasil'kovskoye deposit, Kokschetau Block, NW Kazakhstan	Or3 or D	Intrusion-related; set of sheeted Au-quartz-arsenopyrite veins to stockworks in K-feldspar & sericite altered multiphase intrusion	420 1.5 mt As
13	Muruntau, Kyzyl-Kum, Uzbekistan	Pe	Orogenic; Au-quartz stockwork in indurated & altered clastics above intrusion	4,300
	Myutenbai, Kyzyl Kum, Uzbekistan	Pe	Ditto	620
	Kokpataz, Kyzyl Kum, Uzbekistan	Pe	Orogenic; Au-quartz and arsenopyrite veins, replacements in hornfelsed clastics	612
	Zarmitan, Uzbekistan	Pe	Intrusion related over orogenic? Au-quartz, K-feldspar & As,Fe,Bi sulfides + scheelite stockworks & veins in clastics near granosyenite	240
14	Bakyrchik, Kalba, Kazakhstan	D-Cb	Orogenic; Au-quartz stockwork & disseminated As, Fe sulfides in steep shear zone in carbonaceous metasediments	260
15	Kumtor deposit, Tian Shan, Kyrgyzstan	Np	Orogenic; multiphase Au-quartz veins and breccia in hangingwall of brittle-ductile fault	517
16	*Olimpiada, Yenisei Range, Russia	Np	Intrusion related over orogenic; fine disseminated Au in Fe,Sb,As sulfides in altered, sheared black schist, marble and skarn above concealed intrusions	550 ?70 kt Sb
17	Sukhoi Log, Kropotkin, Lena Goldfield, Russia	Np	Orogenic; stratabound zone of Au-quartz & sulfide veinlets to disseminations in sheared black slate	1,113

Figure 10. 2. (continued)

No. on map	Deposit/district	Age	Type, geology	Tons Au
18	Balei (Taseevka deposit) East Transbaikal, Russia	Cr	Intrusion-related; meso-to epithermal sheeted Au-quartz veins to stockworks along faults in PZ basement granitoids disseminated strata-bound Au replace Cr conglomerate in graben	458
19	Nezhdaninskoye, Alakh Yun, Sakha (Yakutia), Russia	J-Cr	Intrusion-related over orogenic? Fine disseminated Au in Fe,As sulfides in steep persistent altered fault zone in clastics intruded by granitoid stocks & lamprophyre	336
20	*Natal'ka, Omchak goldfield, Magadan region, E. Russia	Cr	Orogenic; persistent Au-quartz veining and disseminated Fe, As sulfides in shear	525 520 kt As
21	Maiskoye, central Chukotka, Russia	Cr	Disseminated micron-size Au with Fe, As sulfides in sheared silicified (black) shale	374
22	Niuxinshan, E. Hebei, China	J3-Cr1	Intrusion-related; Au-quartz & Fe,As,Cu,Zn,Pb sulfide veins in shear in metamorphics near greisenized granite	?300
	Xiaoqinling district, Shaanxi, China	J-Cr	Intrusion related? Series of Au-quartz veins in Precambrian metamorphics in faults near Mesozoic granitoid stocks	380
23	Jiaodong Au province, Shandong, China (Linglong, Jiaojia, Cangshang deposits)	Cr1	Intrusion-related over orogenic; series of Au-quartz vein deposits in shear zones in Precambrian granites and metamorphics, near Mesozoic granitoid stocks & dikes; also disseminated Au in altered fault fill	1,030
24	Wabu Ridge, Papua, Indonesia	Mi-Pl	Intrusion-related retrograde skarn in porphyry exocontact, disseminated, fracture, replacement Au with Fe, As, Bi sulfides	310
25	Kucing Liar skarn, Ertsberg, Papua, Indonesia	Mi-Pl	Au-Cu skarn adjacent to major (Grasberg) porphyry Cu-Au-Mo	448
26	Telfer, Western Australia	Np	Orogenic; stratabound horizons of quartz veining and disseminated Fe,Cu,As sulfides along bedding shears in fine clastics and carbonates	1,381
27	Charters Towers, Queensland, Australia	Cb1	Orogenic; several sets of fault and fracture Au-quartz veins in granitoids	224
28	Bendigo, Victoria, Australia	D	Orogenic; several zones of Au-quartz lodes in anticlines in turbidites	948
29	Macraes, Otago, New Zealand		Orogenic; disseminated Au in breccia, gouge, phyllonite in a shear duplex	186

occur at the fringe of tungsten provinces (as in China); alternatively they are part of Pb-Zn-Ag or Au provinces. The lithology of wallrocks determines whether the Sb orebodies are either veins (in silicate rocks) or replacements ("mantos") in carbonates; in many ore fields veins/replacements are interchangeable. The silicate rocks-hosted Sb deposits form a progression from stibnite stringers and impregnations of fault gouge and breccia with virtually no gangue, through stockworks of quartz-stibnite stringers in fault rocks, to predominantly quartz veins enclosing massive stibnite.

Xikuangshan (also spelled Hsi-K'uang-Shan or Si-Kon-Shan) is a "super-giant" ore field in Hunan, China, which alone holds some 30% of the world's Sb endowment; this makes China the principal producer and storage house of antimony. It is also a candidate for deposit with the world's largest tonnage accumulation index, of all metals. Xikuangshan (Tegengren, 1921; Wu Jiada et al., 1990; Yi Jianbin and Shan Yehua, 1995; over 2 mt Sb content with grade of about 3% Sb) is the example of a predominantly carbonate replacement ("manto") complex. The deposit is about 200 km WSW of Changsha, in the Paleozoic platformic cover over the Yangtze Platform.



Figure 10.31. The worldwide distribution of Phanerozoic-late Proterozoic Au "giants" (see table 10.2. for deposit names and characteristics)

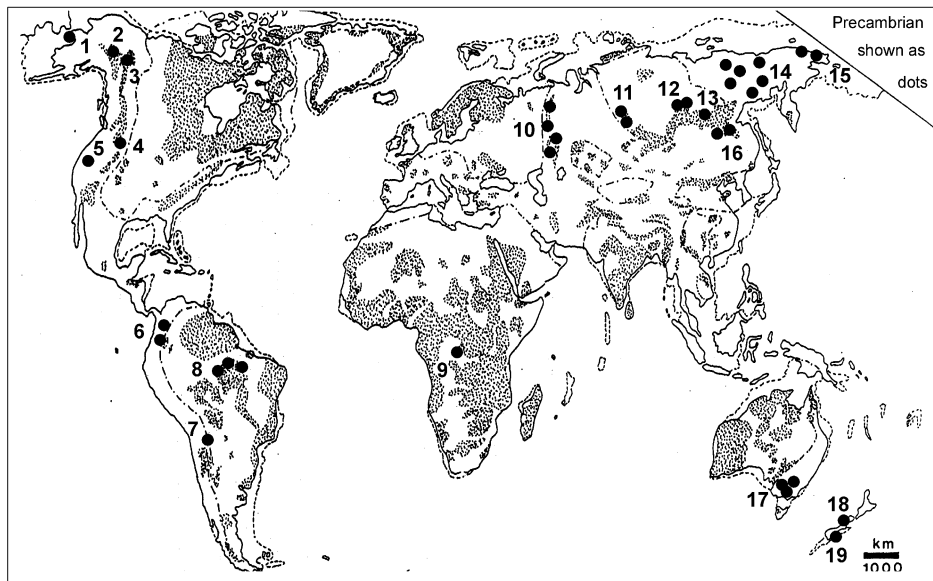


Figure 10.32. Global distribution of "giant" gold placers (see Table 10.3. for names and characteristics of numbered localities)

The open-folded, but thrust and faulted, host sequence consists of bedded, shallow-water limestone with some dolomite, alternating with shale and quartz-rich sandstone. Except for few lonely kersantite dikes, there are no signs of major intrusive activity. The NNE-trending ore zone,

about 8 km long, intersect a NE-plunging anticline in Upper Devonian limestone with interbedded shale that terminates with sandstone-rich units at the top and bottom. The mineralization has the form of multiple stratabound "mantos" in several limestone beds screened by shale.

Table 10.3. "Giant" (total production/reserves 250 t Au plus) gold placers and placers regions of the world

No	Placer/region	Type	Gold, tons
1	Nome, Seward Peninsula, W Alaska	alluvial, glaciofluvial, beach, offshore	194
2	Fairbanks placers, Alaska	alluvial, glaciofluvial	233
3	Klondike (Dawson City), Yukon	alluvial, gulch and high terrace; in permafrost	373
4	Western Montana, USA	alluvial, mostly gulch	270
5	Sierra Nevada Foothills, California	alluvial, gulch	1,717
6	Colombia placers (total)	alluvial	1,500
	--Chocó region	alluvial	1,072
7	Tipuani placers, Bolivia	alluvial	300
8	Rio Tapajóz Basin, Amazon Basin, Brazil	alluvial	5,632
9	Kilo-Moto placers, N-C DRC Congo	alluvial	250
10	Urals placers, Russia	alluvial	500
11	Yenisei Range, Russia	alluvial	460
12-16	Eastern Siberian placers, Russia		Pt 5,500
12	Bodaibo (Vitim R. Basin, Lena Goldfields)	alluvial, deep leads under glacials	1,000
13	Central Aldan goldfield, Russia	alluvial	300
14	Upper Kolyma Basin, Russia	alluvial and glaciofluvial, some deep leads	2,643
	--Susuman placers	ditto	1,057
	--Yagadnoye placers	ditto	809
15	Chukotka Peninsula placers	alluvial, buried channel, beach	
	--Chaun Bay	ditto	715
16	Amur (Heilongjiang) Basin placers, RU+CH	alluvial	2,500
17	Victoria Goldfields, placers, Australia	alluvial, channel, terrace, deep leads	1,500
	--Ballarat placers	ditto, deep leads under basalt flows	343
18	Westland and Nelson placers, New Zealand	glaciofluvial, alluvial, minor beach	910
19	Otago placers, New Zealand	glaciofluvial, alluvial	568

It extends from the footwall of a major NNE-striking, NW-dipping normal fault. The ore is multistage with the early stage of extensive silicification (jasperoid) accompanied by fine-grained stibnite replacements, followed by the second stage of coarsely crystalline, dilations (fractures and vugs)-filling stibnite. Impressive mineralogical specimens of stibnite adorn many world's museums. The epigenetic mineralization is Jurassic or later, contemporaneous with crustal extension and fault basin formation (activation or "diwa" regime), with fluid temperatures dropping from the initial 300°C plus to around 100°C. Chinese geologists think strongly about the proximal (local) sources of antimony, extracted from the trace Sb-enriched rocks traversed by convecting fluids. Much of the ore in the uppermost manto is oxidized to a mixture of cervantite, stibiconite, valentinite and kermesite stored in karsted limestone regolith. Xikuangshan is merely the largest ore zone in a larger area with numerous other Sb deposits (compare locality map in Wu Jiada et al., 1990).

The **Wadley** replacement deposit (Sierra de Catorce, Mexico), described in Chapter 6 in the andean-margin context, is very similar in form.

Also similar is the "giant" Kadamzhai deposit in Kyrgyzstan, in the former Soviet Central Asia, that had been for many years the principal source of Soviet antimony. **Kadamzhai** (Nikiforov et al., 1962; ~300 kt Sb; Fig. 10.33) is in the South Ferghana fold- and Hg-Sb belt, a Paleozoic accretionary complex dotted by hundreds of Sb and Hg deposits and occurrences; the belt is described below, under mercury. The deposit consists of an up to 5 km long stratabound ore zone in brecciated and silicified Lower Carboniferous limestone, confined under a screen of Lower Devonian shale and argillite. This is intersected by a series of faults, considered feeders of the ore fluid. Stibnite is the principal mineral with rare pyrite, marcasite, realgar and orpiment directly scattered in jasperoid, or associated with later stage breccia zones and fracture veins. The latter have quartz, calcite, barite and fluorite gangue.

Turhal ore field in north-central Turkey (Gokçe and Spiro, 1991; minimum 100 kt Sb) is an example of a composite Sb-ore field in which a variety of ore styles are represented. The field is predominantly located in Permian to Jurassic eugeoclinal succession in the Pontic (northern Turkic) foldbelt, composed of phyllite (locally carbonaceous) with

greenstone meta-basalt intercalations, topped by Mesozoic limestone. The earliest of some 37 different orebodies are stratabound stibnite and pyrite lenses in carbonaceous phyllite and subeconomic stibnite disseminations in calcareous quartzite. Most of the remaining orebodies are cross-cutting fault and fracture veins in phyllite and greenstone with stibnite in quartz and carbonate gangue.

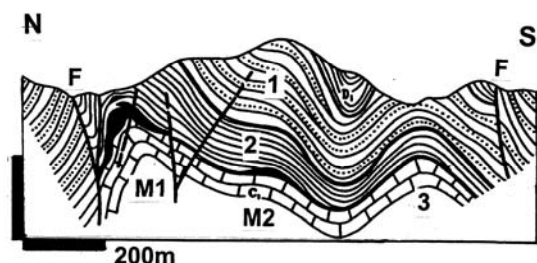


Figure 10.33. Kadamzhai Sb deposit, Kyrgyzstan, cross-section from LITHOTHEQUE No. 2206 modified from Nikiforov et al. (1962). M1. Oxidized (valentinite, senarmontite) and primary stibnite in jasperoid and breccia; M2. Stibnite and calcite replace limestone. 1. Allochthon: S shale to litharenite; 2. D1 argillite; 3. Cb1 massive limestone; F. Faults

Hillgrove Sb, Au, W ore field in New South Wales is an example of stibnite-dominated veins with significant gold- and some scheelite- byproduct (Ashley and Craw, 2004; P+Rc ~80 kt Sb, 33 t Au, 2,100 t W). There are about 204 individual veins, mineralized fault breccias and stockworks in a field that measures 8 x 5 km, explored over a vertical span of 1000 m. The orebodies are hosted by Carboniferous turbidites, thermally metamorphosed to biotite hornfels, and by Permocarboferous diorite, granodiorite and S-type monzogranite. Steeply north-east dipping multistage veins fill brittle faults and fractures and sometimes branch into adjacent stockworks up to 20 m wide. The early stages have quartz, scheelite, arsenopyrite, pyrite with gold and minor Pb, Zn sulfides. This is overprinted by quartz, stibnite with gold, arsenopyrite and rare aurostibnite. Gold is both free and refractory in arsenopyrite, concentrated in haloes adjacent to some veins. The alteration is sericite, ankerite, quartz; the 250° to 100°C fluids deposited the ores between 255 and 247 Ma, contemporaneously with infrequent lamprophyre dikes.

As "Sb-giants" need only 30 kt Sb to qualify, there are at least 40 deposits of this magnitude around the world and probably more in China, for which tonnage data are

not available. Also not readily available are data on Sb content in complex Pb, Zn, Ag, Cu, Au and other deposits. Table 10.4. below is thus not complete (also missing is the Archean Murchison Range-Sb in South Africa).

Table 10.4. "Giant" Phanerozoic and late Precambrian hydrothermal antimony deposits of the world

Deposit/district	Type	kt Sb
North American Cordillera		
Coeur d'Alene, Idaho	complex veins	70
Yellow Pine, Idaho	complex Sb-Au-W in shear zone	79
McLaughlin, California	hot spring Sb-Au	*40
Sierra de Catorce, Mexico	simple Sb bedded carbonate replacement	90
The Andes		
Bolivian Sb belt --Potosi area	simple stibnite fault veins	*300
(Chilcobija mine)		70
--Tupiza area		230
Variscan orogen, Europe		
La Lucette, France	quartz Sb-Au veins	42
Brioude-Massiac, FR	simple Sb fault veins	40
Krásná Hora-Milešov, Czech Republic	quartz Sb-Au veins	50
Appalachian orogen, Canada		
Lake George, NB	simple Sb veins	55
Beaver Brook, NFDI	simple Sb veins	42
Tethyan (Alps-Himalayas) orogen		
Stadt Schläining, Aust	simple Sb veins	*100
Krupanj-Zajača, Serbia	Sb karsted carbonate replacements, veins	70
Turhal, Turkey		+100
Central Asia (Altai, Tian Shan, Tadjikistan)		
Kadamzhai, Kyrgyzstan	Sb carbonate reemplacements	300
Nichkesu, Kyrgyzstan	complex Sb-Au-Pb-Cu veins	*100
Savoyardy, Kyrgyzstan & Xinjiang	Ditto, Sb-Au veins	*70
Chatkal Range, Kazakh stan & Uzbekistan	Ditto	*100
Jijikrut, Tadjikistan	Ditto + simple Sb	183
Chulboi, Tadjikistan	Ditto	463
Yenisei Ridge		
Olimpiada, Russia	simple quartz-Sb vein marginal to Au-Sb-As shear zone	*300
Verkhoyansk-Chukotka orogens in Russia		
Sentachau, Sacha	simple Sb veins	70
Qinling orogen, N-C China		
Yawan, Gansu	simple Sb veins	*50

Table 10.4 (continued)

SE China (Hunan, Guizhou, Guangxi)		
Xikuangshan, Hunan	replacement mantos in carbonates > veins	2000
Gaoguashan, Hunan	complex Sb-W veins	*70
	complex Sb-Au-W bedded replac, veins	*100
Qinglong, SW Guizhou	simple Sb bedded & steep veins	0
Banpo, Guizhou	simple Sb bedded & steep veins	*70
Dachang, Guangxi	complex zoned Sn,Pb, Zn,Sb ore field	*150
Burma, Malaya, Borneo		
Bawdwin, Shan State	complex Pb,Zn,Sb, Cu,Co,Ni replacem.	218
Bau, Sarawak	complex Au-Sb veins	91
Tasman orogen, E Australia		
Hillgrove, NSW	complex Sb > Au,W quartz veins	80
Costerfield, Victoria	simple Sb (Au) veins	40

* asterisk indicates tonnage estimate

10.7.2. Mercury deposits

Mercury is a member of the quintet of metal villains: As, Hg, Cd, Pb and U (and the newcomers Be and Tl) ostracized by the risk averse society for their toxicity. While lead and uranium quietly thrive, demand for arsenic and mercury took a strong dive in decades past. It is unfortunate as mercury is so special, the only metal liquid at room temperature. Even more than antimony, Hg is geochemically rare (clarke of 40 ppb), hence 4,000 t Hg accumulation is a "geochemical giant". There are seven "Hg-giants" and three "Hg super-giants" (Almadén, 276 kt Hg; Idrija, 170 kt Hg; Huancavelica, 51 kt Hg). Four additional "giants" (New Almaden, New Idria, Sulfur Bank, Monte Amiata) are described with hot spring deposits (Chapter 6) and ophiolites (Chapter 8). This demonstrates the unparalleled ability of mercury to locally super-accumulate to reach a record tonnage accumulation index.

The bulk of mercury deposits precipitated from low-temperature hydrothermal fluids and this process is still much in evidence; cinnabar actively precipitates in Coso Hot Springs, California, and Steamboat Springs, Nevada, and has barely stopped precipitating at the Puhupuhi (New Zealand), Sulfur Bank (California), and few other Quaternary hot spring deposits. New Almaden and New Idria are only slightly older. The rest of Hg deposits are "fossil", shown by the fluid inclusion research as precipitated mostly at temperatures between 150°

and 50° C. The principal Hg ore mineral is cinnabar, and native mercury, metacinnabar, corderoite and livingstonite are local rarities adding no more than 2% to the global Hg endowment. The only alternative Hg-carrier responsible for one or two "Hg-giants" is Hg-tetrahedrite (schwarzite) that won the "giant" title to the medium-size vein siderite-barite deposit Rudňany in Slovakia (Pt 4,217 t Hg plus @ 0.025% Hg).

Most cinnabar deposits occur in or near brittle faults the high levels of which have been preserved from erosion. Like antimony, cinnabar in silicate fault rocks occurs as gouge impregnations and stringers without gangue minerals, with dickite or kaolinite, or in veins, stockworks and breccias cemented by quartz (chalcedony), carbonates, zeolites, celadonite, and others. Porous rocks adjacent to faults like sandstone or conglomerate are impregnated by cinnabar. In sheared and talc, carbonate, silica altered alpine serpentinite ("listvenite") cinnabar replaces alteration carbonates and forms stringers in the remaining materials. Cinnabar hosted by carbonates, adjacent to feeder faults, form replacements or open-space disseminations in clay-filled or empty dissolution (karst) voids. The orebodies range from irregular and discordant tabular bodies along faults and fractures, to stratabound replacements ("mantos"). At the Wanshan deposit, Guizhou, China, up to seven carbonate horizons are mineralized. Residual cinnabar occurs in clay fill of karst sinks and collapse breccias and is even occasionally reworked into placers because of its chemical stability (but poor resistance to abrasion).

The two "Hg super-giants" Almadén (and three lesser deposits in the Almadenejos field) and partly Idrija, are different as they have (some) orebodies with a high degree of stratigraphic control so their genetic interpretation has kept changing, like politics, from synsedimentary-diagenetic (or "exhalative") to synorogenic-epigenetic. This is discussed in greater detail below. Most mercury deposits are isolated or form clusters and there are few "Hg-belts". Two most prominent belts are the discontinuous Hg belt in coastal California associated with the Franciscan Assemblage (ophiolite, ultramafics, melanges, hot springs) and the South Ferghana Hg-Sb belt in Kyrgyzstan and Tajikistan.

South Ferghana Hg-Sb belt is a 500 km long east-west zone in the Tian Shan orogen (a member of the Altaiides), located along the southern margin of Ferghana Intermontane Basin filled by "molasse". This was the principal source of Hg and Sb in the former U.S.S.R (Fig. 10.34).

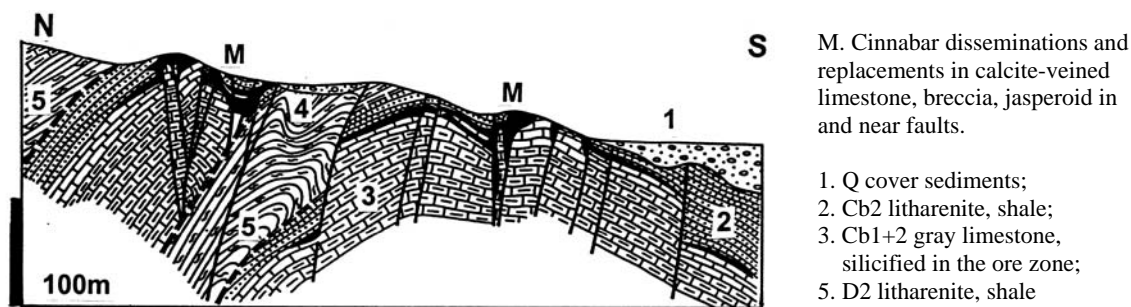


Figure 10.34. Khaidarkan Hg deposit, Kyrgyzstan, cross-section from LITHOTHEQUE No. 2207 modified from Nikiforov et al. (1962)

It contains several hundred deposits and occurrences of these metals that probably total more than 150 kt Hg and 500 kt Sb (Nikiforov et al., 1962; Nikiforov 1970). The belt, a late Paleozoic accretionary complex, comprises Silurian to Middle Carboniferous supracrustals. The northernmost facies zone has a thick sequence of Devonian oceanic meta-basalts. South of it, Devonian to Middle Carboniferous dolomite and limestone rest conformably on Silurian terrigenous clastics of a stable continental margin. Middle Carboniferous clastics in successor basins top both earlier lithofacies.

The foldbelt is subdivided into a series of narrow east-west slices by numerous parallel faults that resulted from three phases of tectogenesis: 1) Devonian normal extensional faulting (rifting) that established the depositional trough; 2) Lower Carboniferous collision that resulted in a series of overthrusts and tectonic emplacement of serpentinite slices; and 3) late Carboniferous and Permian block faulting accompanied by calc-alkaline plutonism in the southern zone, and minor alkaline intrusions (syenodiorite, monzonite) in the north.

The Hg and Sb deposits are probably Mesozoic, postdating late Paleozoic block faulting, but predating Alpine deformation. The ore belts have the form of "coulisses": long and narrow east-west screens of concentrated mineralization on both sides of faults. Nikiforov (1970) distinguished three parallel mineralization zones. The northernmost zone (Chonkoi, Sarytash deposits) contains Hg orebodies in mafic volcanics, ultramafics and interbedded sedimentary rocks. Economically most important is the central zone. There, most of the orebodies are confined to hydrothermally silicified fractured carbonates directly under the impervious Carboniferous shales, in cores of thrust-modified anticlines (e.g. Khaidarkan, Kadamzhai). The

stratabound ore zones have impregnations, stockworks and patches of calcite, dolomite, with stibnite and cinnabar. Less productive discordant ore zones along faults have simple calcite-cinnabar replacements, stockworks and veins (Symap). The southern zone carries complex Sb, Hg and W, As, Pb, Zn, Ag, Au and Cu ores (mostly veins) in thermal aureole of plutons. This is an emerging mineral province that contains major resources of antimony with gold, silver and base metals mostly in Tadjikistan.

The largest Hg ore field in the central zone is **Khaidarkan** (Nikiforov et al., 1962; Pt 29,820 t Hg + Sb, fluorite). This is a stratabound zone hosted by silicified limestone breccia in footwall of the north-dipping Ishmetau Thrust. The east-west zone is about 15 km long and about 1 km wide. Orebodies are controlled by third-order anticlines and occur along faults in the Lower Carboniferous limestone, just under the Middle Carboniferous shale. About 80% of the rich orebodies (2-5% Hg, some Sb) are located within 30-40 m under the contact. The ore is composed of nests and patches of cinnabar and stibnite in quartz, fluorite and calcite gangue. Realgar and orpiment are common and dominate the small orebodies scattered throughout the hangingwall shale. The rich ores are usually floored by low-grade disseminated and veinlet cinnabar and stibnite in silicified and argillized host rocks.

Almadén deposit in central Spain, 120 km north of Cordoba (Fig. 10.35), is a most enigmatic mineral system at par with the Witwatersrand (Saupé, 1990; Hernández et al., 1999; 276 kt Hg @ 8-1% Hg). NOTE: the Almadén Hg endowment quote keeps changing, downward from figures as high as 650 kt presented in the 1960s-1970s literature. It was 487 kt in Laznicka, (1985). It is the largest Hg "super-giant" that stores close to 30-40% of mercury of the world's endowment.

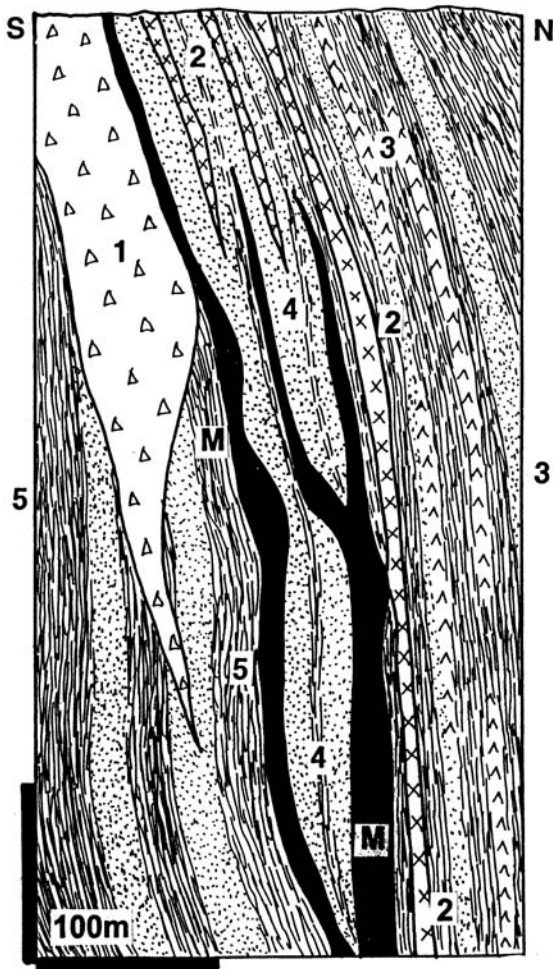


Figure 10.35. Almadén Hg deposit, Spain, diagrammatic cross-section from LITHOTHEQUE No. 104, based on Schuette's 1931 rendering, Saupé (1990), Hernandez et al. (1999). M1. S? stratabound cinnabar, minor pyrite impregnations and replacements in the Criadero Quartzite, near Frailesca. Three flat subvertical orebodies. 1 (Bx). Or-D Frailesca, fragmentite of altered olivine basalt and sediment fragments in matrix; interpreted as alkali diatreme emplaced to wet sediments; 2. Or-D diabase; 3. S-D alternating quartzite, shale, metabasalt; 4. S Criadero Quartzite, white and black members separated by shale; 5. Or Footwall Shale

It is also the number 1 deposit in terms of geochemical magnitude of accumulation, of all metals. Despite this, there is no satisfactory explanation where this mercury had come from, and why it had accumulated in this geologically almost "normal" setting.

Almadén is the principal and largest deposit in a more extensive Hg ore district that contains three smaller deposits near Almadenejos south-east of

Almadén, and one small La Cueva deposit north-east of town Jébrak & Hernandez, 1995). Two of the former deposits are of the stratabound variety like Almadén, the latter one is a discordant stockwork in volcanics. Almadén has more than 2,000 years long mining history initially as a producer of pigments, later of metallic mercury used in Au and Ag recovery from ores by amalgamation. Most recently mercury has been a major technology metal. The mercury price and demand, and corresponding rate of production, have fluctuated widely. These days, near the bottom of mercury demand, the Almadén mines are barely alive and considered practically exhausted, although they could probably still respond to a sudden surge in demand. The economic problems are exacerbated by environmental considerations as Almadén is clearly the most mercury polluted town in the world, although it does not really show in this bustling country town.

This is a part of the Iberian Massif, a Hercynian (late Paleozoic) orogenic system floored by a rigid Proterozoic continental block. The ore hosts are members of Ordovician to Devonian predominantly sedimentary sequence of sub-greenschist metamorphosed, folded and faulted quartz-rich litharenite, siltstone and shale with several bands of orthoquartzite, deposited in an intracratonic marine basin. The sedimentation was accompanied by an almost continuous, although small volume, submarine and sub-sea floor magmatism attributed to alkaline (basanite/nephelinite to trachybasalt, trachyte, rhyolite) and tholeiitic (diabase) series. The most voluminous non-clastic rocks are altered heterolithologic breccias that contain basalt and shale/sandstone fragments in altered matrix ("frailesca") interpreted as diatremes, but resembling teschenitic peperites and granulates with analcite. Hernández et al. (1999) noted that the "frailesca" bodies have rather nebulous outlines, suggestive of emplacement into wet, not entirely consolidated sub-seafloor sediments. The rest of the magmatic rocks are true dikes and sills. The Almadén Hg orebodies, although rarely hosted by "frailesca", occur in vicinity and seem to be genetically related.

The principal Hg orebodies are in the Silurian Criadero Quartzite, a unit composed of two horizons of quartzite: the upper black (carbonaceous), the lower white (quartz-only). The quartzites are folded to a vertical position and disrupted into three flat bodies adjacent to the "frailesca" lens (Saupé, 1990). The ore consists of cinnabar-impregnated and replaced quartzite grading to reticulate (network of healed diffusely

mineralized fractures) to almost massive cinnabar. Pyrite is the only minor metallic mineral of importance. The sedimentary hosts are virtually unaltered, whereas in the mafic volcanics the early spilitization (Na-metasomatism) is overprinted by Fe-Mg carbonatization and slight sericitization. The cinnabar emplacement appears to have been early, predating full lithification of the host quartzite (some cinnabar is enclosed in presumably diagenetic quartz cement), but the homogenization temperatures between 375° and 150°C (Hernández et al., 1999) preclude ordinary diagenesis. The most suitable explanation is a syndiagenetic introduction of Hg by an externally derived fluid. The Hg source is not known; Saupé (1990) suggested mobilization of mercury from the "black shales" present in the sequence. Hernández et al. (1999) preferred an indirect mantle source, via the "frailesca" intrusive activity.

Idrija ore field is in Slovenia, 50 km west of Ljubljana, and it is the second largest "Hg-supergiant" (Bercé, 1958; Lavrić and Spengenberg, 2003; P+Rc 170 kt Hg; Fig. 10.36). The field is in a complex tectonic structure that involves Carboniferous to late Triassic allochthon of carbonaceous shale and limestone, a variety of light limestones and dolomites, shale and sandstone, thrust over Jurassic-Cretaceous limestone and Eocene turbidites. The most critical is the Middle Triassic association of "oceanic" mafic volcanoclastics with radiolarian chert resting on basal sandstone and conglomerate, that also includes carbonaceous Skonca Shale. This shale hosts uniform cinnabar impregnations conformable with shale laminations, considered synsedimentary by most authors and usually attributed to the contemporary submarine volcanism. Outside this shale a variety of rocks are impregnated, veined or replaced by cinnabar with or without pyrite, dolomite, calcite, quartz or chalcedony gangue, controlled by faults and structural dilations. This multistage mineralization is most abundant at the footwall side of thrusts.

An important Hg province is in **Guizhou, SE China** (He Lixian and Zeng Ruolan, 1992), although the tonnage data are hard to get. The most often mentioned classical deposit Wanshan was credited with 10 kt Hg in the pre-World War II literature and more deposits have been found and/or explored after establishment of the People's Republic. Presumably the "gigantic" deposits of the Chinese would clear our "Hg-giant" threshold. All except two are in Guizhou and they are Muiyouchang, Wanshan, Dadongla, Shuiyinchang.

Gongguan and Yangshikeng are in Shaanxi and Sichuan, respectively. All the Chinese "Hg-giants" are cinnabar replacements in carbonate rocks.

The possibly largest Hg ore field in Guizhou is **Muiyouchang** in the Wuchuan County (He Lixian and Zeng Ruolan, 1992; ?50 kt Hg plus). There, fine-grained cinnabar with minor stibnite, sphalerite, realgar are uniformly disseminated in Lower Cambrian gypsiferous dolomite with anhydrite beds. The ore forms stratabound mantos along the anticlinal axis in a zone 4 km long and up to 150 thick, under an argillaceous dolomite screen. Calcite, quartz, barite and sparry dolomite are the gangue minerals, gradational to the locally silicified (jasperoid) and calcitized wallrock dolomite. The low-temperature mineralization is attributed to basinal fluids, reduced by methane.

Table 10.5. is a brief survey of the world's Hg "giants", some of which have already been described in Chapters 6, 7 and 8.

10.8. Pb, Zn, Ag veins and replacements

Polymetallic deposits have about the most widespread and "typical" hydrothermal ores in the intracratonic orogens. Exact, even approximate number of them is impossible to give as the prevalent type of orebodies are veins most of which are, individually, small. Groups of veins are mined together and congregate to form ore deposits, fields and districts. Various configurations, many subjective, are possible to create a "locality" that enters a database. In the Freiberg ore field, for example, there are 1,100 individual veins. Another problem is to delineate the present Pb, Zn, Ag category. The classics had it easy: Lindgren (1933) would place these deposits into his "mesothermal Pb-Zn" with the assumption that the ores were genetically related to granites. Some probably still are, but granite is now considered mostly a heat source to drive convecting fluids rather than the source of metals. Below is a sequence of types of polymetallic deposits arranged by diminishing influence of granites on their formation, from high to nil:

- 1) Pb-Zn veins and/or replacements, zoned around intrusions that produced magmatic-hydrothermal deposits of Cu-(Mo) (porphyry coppers) or Sn-(Li, W, Be);
- 2) mesothermal Pb-Zn veins in the roof or aureole of intrusions lacking magmatic-hydrothermal deposits;

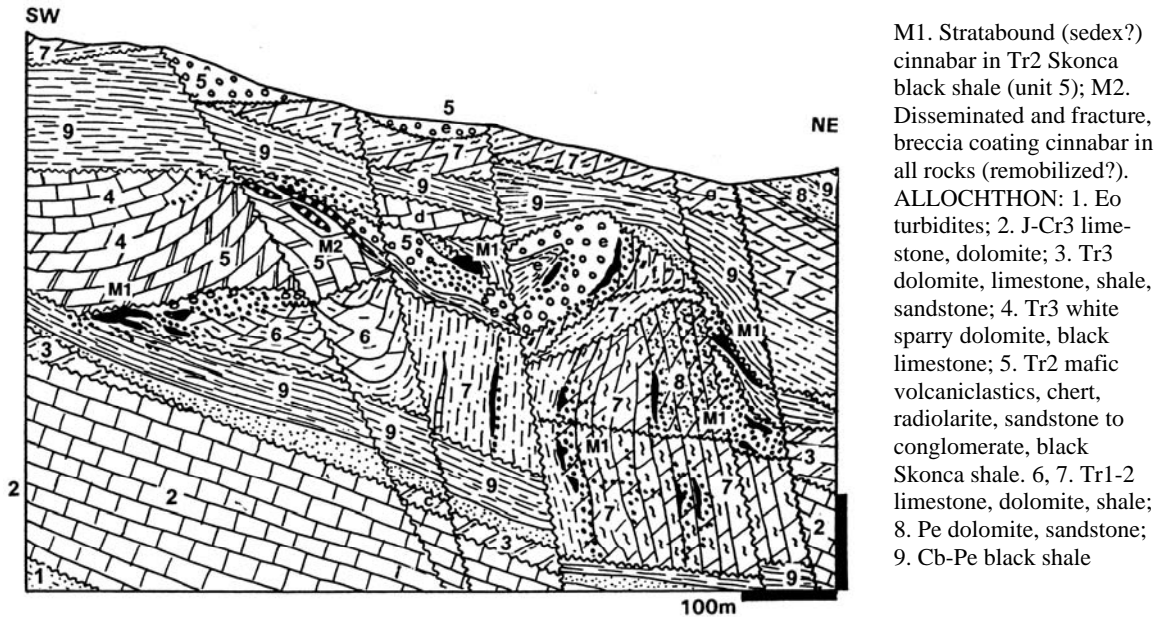


Figure 10.36. Idrija Hg ore field, Slovenia, cross-section modified after Bercé (1958), Mlakar and Drovenik (1972)

Table 10.5. Survey of the world's "giant" Hg deposits

Deposit/district	Type	kt Hg
North American Cordillera & the Andes		
Pinchi Lake, B.C.	impregnations, stringers in fault zone	9.5
McDermitt & Cordero, Nevada	impregnations in tuff & volcanoclastics	14
New Almaden, California	impregnations in altered serpentinite	38.1
New Idria, California	ditto, in turbidites near fault	19
Mayacmas, California	impregnations in serpentinite melange	13
Sulfur Bank, California	impregnations in hot spring sinter, andesite	7
Huancavelica, Peru	limestone replacem., sandstone impregn.	51
Variscan orogen, Europe		
Almadén, Spain	impregnations of quartzite near diatreme?	276
Almadenejos, Spain	ditto	16.5
Las Cuevas, Spain	impregnations in volcanic breccia	5.2
Nikitovka, Ukraine	impregnations in sandstone	33.7
Tethyan (Alps-Himalayas) orogen		
Monte Amiata, Italy	replacements in limestone, impregn.	80
Idrija, Slovenia	stratiform + fault impregnations	170

Draževici, Bosnia	impregnations in carbonates	4.2
Rudňany, Slovakia	Hg in schwazite in siderite veins	4.2
Karareis & Kalecik, Turkey	impregnations in fault and ophiolite melange	*12
Altaiides of Asia (Tan Shan, etc.)		
South Ferghana Sb-Hg belt, Kyrgyzstan	impregnations in fault zones	*150
--Khaidarkan deposit	ditto	30
China		
Wanshan, Guizhou	replacements in carbonates, karst	+10
Muyouchang, Guizhou	replacem. in dolomite under shale screen	*+50
Dadongla, Guizhou	replacements in carbonates	*20
Shuiyinchang, Guizhou	ditto	*20
Gongguan, Shaanxi	ditto, with Sb	*20
Yangshikeng, Sichuan	replacements in carbonates	*20

Cinnabar is the principal Hg mineral, unless noted otherwise; *asterisk indicates estimate

3) These probably precipitated from convecting meteoric waters in the postmagmatic period (driven by heat of cooling intrusions) or afterwards (driven by heat produced by radiogenic decay in the high heat granites, or by other form of geothermal heat);

- 4) structurally controlled (syn)orogenic Pb-Zn deposits probably precipitated from metamorphic-hydrothermal fluids; and
- 5) structurally controlled Pb-Zn veins in the "basement", mesothermal to low-temperature, broadly coeval with "sedex", "Irish", or "Mississippi Valley" types formed in the sedimentary cover above and probably deposited from "basinal fluids" reaching under unconformity. Granites are absent or only accidentally present.

Pb-Zn deposits that are an important part of metallogeny of the Cordilleran belts (mostly Type 1, partly Type 3 like Coeur d'Alene) are reviewed in Chapter 7, although there is an overlap. Type 4-related deposits in sedimentary cover sequences appear in Chapter 13. Pb-Zn deposits in the high-grade metamorphics ("Broken Hill-type") are treated in Chapter 14. Type 2 is prevalent in the present context. Both fault and fissure veins and carbonate replacements occur, although high-temperature ores in exoskarn are less common here than in the Cordilleran setting. There are about 16 Pb-Zn-Ag "giants" and most are ore fields or districts; there are few individual orebodies or compact deposits to reach the "giant" magnitude. In addition to above, the Olympias deposit in Greece is an "As-giant". Bawdwin in Myanmar (Burma), of controversial origin, is a Pb, Ag, As and Bi "giant". There is not a single "Zn-giant" (6.5 Mt Zn plus) and zinc deposits are of substantially less importance and value in this setting than elsewhere. This is partly due to the fact that most of these deposits have long histories of mining and until about the mid-1800s zinc was of limited industrial importance and not recovered.

Pb-Zn-Ag veins

Fissure and less frequently fault and shear veins formed in brittle, predominantly silicate rocks and they are the most distinct type of polymetallic deposits. Tensional (dilatant) veins that fill smooth, straight fissure in homogeneous brittle rocks, such as older granite massifs or hornfelsed supracrustals in granite roof, are the textbook example. Sometimes fissures are filled by granitoid porphyry, lamprophyre or diabase dikes and the dikes, their contacts, or fissures in continuation of dikes are filled by veins. The veins range from simple, single-stage (e.g. quartz vein with scattered crystals of galena) to composite, multi-stage and zoned veins. In the 1960s there was a debate as to whether the zoned veins formed from a progressively cooling

single fluid, or from a series of fluid pulses, each (as a rule) cooler than the previous one, depositing different assemblages. The classical veins are symmetrically or asymmetrically banded with a distinct mineral paragenesis (sequence of mineral deposition). Paragenetic studies originated in Freiberg (read below) and became the preoccupation of the pre-1970 literature. The majority of fissure veins are steeply dipping but flat veins also occur.

Fissures (no movement of adjacent blocks) grade to faults and many veins fill faults or subsidiary tensional fractures to form kilometers long vein systems; those in Grund (Harz, Germany) are up to 20 km long and 100 m wide, intermittently mineralized. The early stages of fault veins had usually been deformed by continuous fault movements, the late stages remain undeformed. Shears, thrusts and other compressional structures carry asymmetrical veins, arrays of stringers, dynamometamorphosed ore shoots.

Most mesothermal veins are dominated by gangue minerals (quartz, carbonates: siderite, dolomite, calcite, rare rhodochrosite; barite, fluorite). The ore minerals are galena, sphalerite, pyrite, pyrrhotite, chalcopyrite, tetrahedrite and Pb, Cu, Ag sulfosalts like boulangerite, jamesonite, pyrargyrite; stibnite. Metal zoned veins tend to be Pb, Ag-rich at the upper levels and increase in Zn, then Cu, Au with depth. Abundant gangue carbonates at upper levels change with depth into eventually barren quartz, and also the proportion of Fe-sulfides increases. Wallrock alteration is predominantly quartz and sericite, also chlorite, and there are common Fe, Mn carbonatization haloes.

Replacements

Characteristics applicable to deposits in the Cordilleran belts (Chapter 7) apply here too, except that the proportion of high-temperature exoskarns is much lower and most replacement orebodies occur in silicified (jasperoid) or only recrystallized and/or slightly Fe/Mn carbonate-altered limestone or dolomite units adjacent to faults. In some instances silicate rocks are also replaced, often by a two-stage process; for example, ultramafic rock or basalt or diabase are first carbonatized, then the carbonate is replaced by sulfides. A special case of silicate host replacement is exemplified by the Cobar-type Zn, Pb, Ag, (Cu) deposits (read below) in which sulfide masses are controlled by cleavage, axial planes of tight folds, and anticlines in turbiditic sedimentary rocks.

Selected example deposits (Pb-Zn-Ag veins & carbonate replacements)

Linares-La Carolina district, Sierra Morena, Spain: long, persistent Pb-Zn-Ag fault veins.

This district (Vázquez Guzmán, 1989; ~3.0 mt Pb @ 4-15%; ~1.0 mt Zn; 7,500 t Ag) is in the Iberian Massif, a part of the Hercynian orogen. The area consists of folded Ordovician to Lower Carboniferous monotonous clastics resting on Proterozoic metamorphics, all intruded by Permo-Carboniferous plutons. The district contains several clusters of subvertical veins; those in the Linares field in the south trend mainly NNE, those near La Carolina about 45 km north strike E-W. Around the turn of the 20th century this was the principal European lead supplier with production coming from some 1300 mines.

The veins cut both granite and the clastics (slate & quartz-rich graywacke) hornfelsed in the granite roof. The Guindo vein has been traced for 10 km, the richest Arrayanes Vein for 12 km. The latter vein alone is credited with about 1 mt Pb. It is 1 to 5 m thick and has a multiphase, repeatedly brecciated quartz, ankerite, calcite, galena, sphalerite, boulangerite fill in quartz, sericite, clay altered hosts. The veins postdate the emplacement of the batholith, hence are late Permian or Mesozoic.

Freiberg, Germany: multiple Pb, Ag-rich veins in a metamorphic dome above buried pluton. The Freiberg ore field is in Saxony, in the north-eastern flank of the Erzgebirge. This is a historic, long-lasting mining area and a cradle of Economic Geology taught, first in the world, in the Bergakademie (Mining Academy). The school is still there, only it is now a Technical University (TU Bergakademie Freiberg). The ore field (Baumann, 1976; 1.7 mt Pb, 7,000 t Ag plus Cu, Zn, Sb, Bi) and its vein system intersect a dome composed of monotonous Proterozoic biotite gneiss believed to be underlain in depth by a Permo-Carboniferous granite pluton. The ore field contains about 1,100 discrete fissure veins, of which about 100 were productive and mined from several dozens shafts. The bulk of the veins occur within a 5x12 km long NNE-trending belt situated approximately in the center of the dome. The remaining veins are in a less distinct east-west system along the dome fringe.

Baumann (1976) distinguished two types of fissures, which he interpreted as shear joints and feather joints. The former have a great strike length (up to 20 km) and dip vertically. The vein widths are up to 6 m and the fissures are filled by fault breccia, rock flour and gouge often impregnated by

ore minerals. The feather joints trend NW-SE, dip 30-70° to SW, are shorter (average 2 km) and filled by massive to banded veins. The vein filling in Freiberg formed during two major cycles: 1) Permo-Carboniferous postmagmatic cycle driven by heat from cooling intrusion; 2) Triassic to Tertiary cycle related to high-level, low temperature fluids in the period of tectonic "activation" of the Bohemian Massif. Two major vein associations formed in the first cycle: a) quartz, arsenopyrite, pyrite, sphalerite, galena, and b) siderite, pyrite, galena, freibergite, jamesonite, Ag-sulfosalts, native silver. The wallrocks displays a slight sericite, quartz and carbonate alteration. The second cycle resulted in the following associations: c) fluorite-barite, hematite, lesser galena, sphalerite and marcasite; d) cherty or chalcedonic quartz, carbonates, skutterudite, niccolite, proustite, argyrodite, and e) quartz, hematite, Mn-oxides. The wallrocks were slightly bleached, argillized and silicified. The overall zoning pattern is indistinct, approximately from the centre outward: Zn, Pb-Ag, Ag-Pb, Sb.

Oberharz, Germany: a system of persistent, subparallel, ore-veined strike slip faults.

Oberharz alias Clausthal-Zellerfeld district is a Pb, Zn, Ag mineralized area about 22x25 km in size, in the north-western extremity of the Harz Mountains (Buschendorf et al., 1971; Pt, without Rammelsberg, ~1.8 mt Pb, 700 kt Zn, 4,700 t Ag). This is a part of the late Paleozoic Variscan collisional orogen composed of a thick sequence of Devonian marine sandstone, slate and limestone with bimodal sodic volcanics and subvolcanic intrusions (spilite-keratophyre suite), unconformably topped by Lower Carboniferous (Kulm) synorogenic turbiditic siliceous slate and quartz-rich litharenite. The Middle Devonian carbonaceous slate hosts the important "sedex" deposit Rammelsberg (Chapter 13). The late Devonian to Carboniferous orogeny was followed by intrusion of post-orogenic granite stocks and it was disrupted by a system of subparallel WNW-trending strike-slip faults. The fault-controlled ores formed during four or more phases of vein filling and intra-vein metasomatism. The vein structures are up to 20 km long and up to 50 m wide, filled by tectonic breccia and gouge, but the vein mineralization is not continuous and is restricted to sectors up to 6 km long.

(Bad) Grund, the most recently active vein sector, has alone produced 950 kt Pb, 400 kt Zn and 2,000 t Ag (Sperling, 1973; Fig. 10.37). There, the ore shoots consist of mineralized fault breccia, banded veins, and linear stockworks in faults.

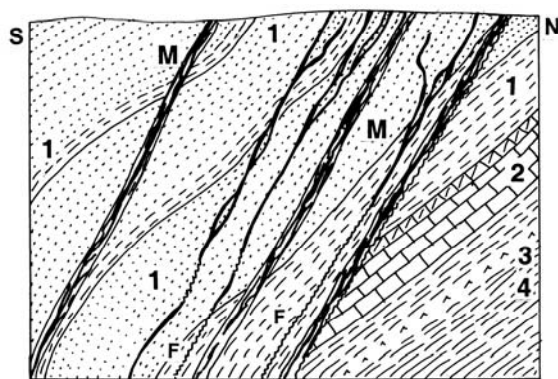


Figure 10.37. Bad Grund Pb-Zn-Ag deposit, Harz Mts., Germany: diagrammatic cross-section of a portion of the vein system from LITHOTHEQUE No. 579, based on data in Sperling (1973) and Preussag AG. Not to scale. M. Cb-Pe (minor J-Cr) quartz, carbonates, Pb, Zn sulfides, minor Ag-sulfosalts fault and fissure veins. F=faults. 1. ~Cb1 Kulm facies turbiditic clastics; 2. D3 limestone, calcareous shale; 3. D shale, argillite, minor chert; 4. D bimodal but mainly mafic submarine volcanic and sedimentary rocks (spilite-keratophyre association)

The veins consist of several generations of sphalerite and galena, lesser bournonite, boulangierite, tetrahedrite and Ag-sulfosalts, in predominantly quartz gangue with a lesser proportion of siderite, calcite and barite. The wallrocks are slightly sericitized, silicified and carbonatized, or laced by ankerite, siderite stringers in bleached wallrocks.

Dal'negorsk (formerly Tetyukhe) (Ratkin, 1995; min. 1.6 mt Pb, 70 mt @ 7-10% B₂O₃). This has been the most important Pb, Zn, Ag producer in the Russian Far East (in Sikhote Alin, NE of Vladivostok), based mostly on massive Pb-Zn sulfide replacements and skarns in olistolithic Triassic marble enveloped by Cretaceous clastics and cut by ~70 Ma post-accretionary granitoids. Recently an interesting borate deposit has been discovered in skarn. There, fine-grained datolite and danburite form retrograde replacements of the earlier exoskarn around faults, gradational into veins in marble.

Kamioka (Fig. 10.38), the largest Zn deposit in Japan, originated in a setting similar to Dal'negorsk although at present it is a part of the Japan island arc. It is briefly characterized in Chapter 7.

Pb-Zn-Ag "giants" summary. Table 10.6. and Fig. 10.40. list the world's "giant" mesothermal Pb-Zn-Ag deposits, including those briefly described in Chapter 7.

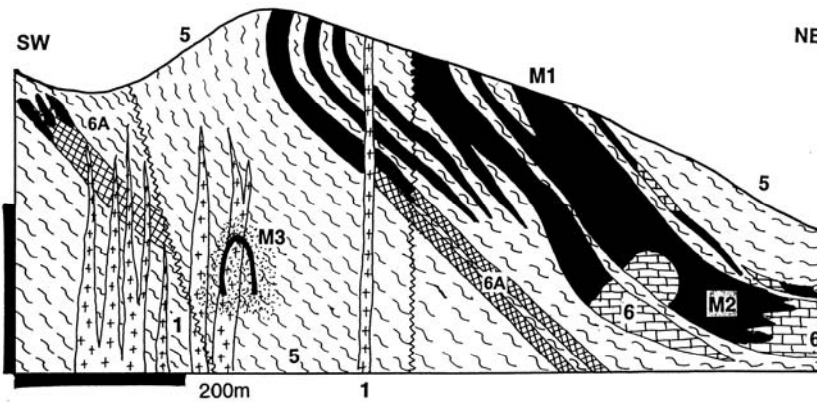
Cobar-type synorogenic Zn-Pb replacements in deformed turbidites

Cobar-Elura Zn, Pb, Ag and Au district (a comprehensive review is in Solomon and Groves, 1994, p. 703-713, and references therein) is in Lower Devonian quartz-rich turbidites formed in a transtensional marine basin, and polyphase deformed shortly afterwards. Overlapping Cu-Au and Pb-Zn orebodies formed along the eastern, isoclinally folded and strongly cleaved margin of the Cobar Basin to form an almost continuous string of narrow lenticular auriferous quartz-sulfide orebodies south-east of Cobar, and the isolated "near-giant" **C.S.A. Pb, Zn, Ag deposit** 12 km NNW of Cobar (Scott and Phillips, 1990). C.S.A. orebodies are situated in a high-strain zone in a lower greenschist-metamorphosed siltstone that is strongly cleaved, quartz veined and intersected by steep, chlorite-filled shears. The ores form several sets of coalescing lenses of massive sulfides enveloped by chlorite, quartz and pyrrhotite, plus several quartz-sulfide veins. Pb-Zn-(Cu) lenses are more common than Cu-Zn lenses. The main ore minerals are pyrite, pyrrhotite, sphalerite, galena in the former, pyrrhotite, chalcocopyrite, magnetite, quartz, chlorite in the latter assemblage. The ores are much deformed with *Durchbewegung* fabrics. The fluid temperatures were in the range of 350-245°C and the laboratory evidence indicates that the orebodies are syn-deformational replacements of silicate wallrocks rather than reconstituted VMS.

Elura deposit is 40 km NW of Cobar (de Roo, 1989; 29 or 50 mt ore @ 5.3% Pb, 8.5% Zn for 3.825 mt Zn, 2.385 mt Pb, 3105 t Ag; Fig. 10.39). It is in the same belt and the same host rocks as C.S.A. The deposit consists of two subvertical, ellipsoidal bodies of massive pyrite, sphalerite, galena, and siderite with minor Cu sulfides, chlorite, barite and Ba-silicates above a zone of quartz-rich siliceous ore with the same minerals. In the ore endocontact are preserved unreplaced wallrock inclusions, but continuity of bedding across these inclusions indicates that the orebody is a metasomatized hinge of an axially cleaved anticline. Dynamometamorphic fabrics, semi-brittle breccias, and crack-seal veins and veinlets support the syn-deformational replacement origin of Elura.

High-grade silver deposits

All mesothermal Pb-Zn veins and replacements produce silver as a by-product. Silver is mostly stored in galena and is recovered from PbS concentrates, during lead smelting.



M. Close to fifty 64-63 Ma skarn and mesothermal replacement Zn>Pb orebodies in the Hida metamorphic basement complex. M1. Zn, Fe sulfides superimposed on exoskarn; M2. Sulfides replace silicified marble; M3. Minor porphyry-style molybdenite in porphyry.

Figure 10.38. Kamioka Zn ore field, Honshu, Japan, cross-section from LITHOTHEQUE No. 158 modified after Nishiwaki et al. (1970). Explanations (continued): 1. ~65 Ma quartz-feldspar porphyry; 5. 1.8-1.5 Ga Hida Gneiss Complex gneiss, migmatite; 6. Ditto, marble and Ca-Mg silicate converted to exoskarn (6A)

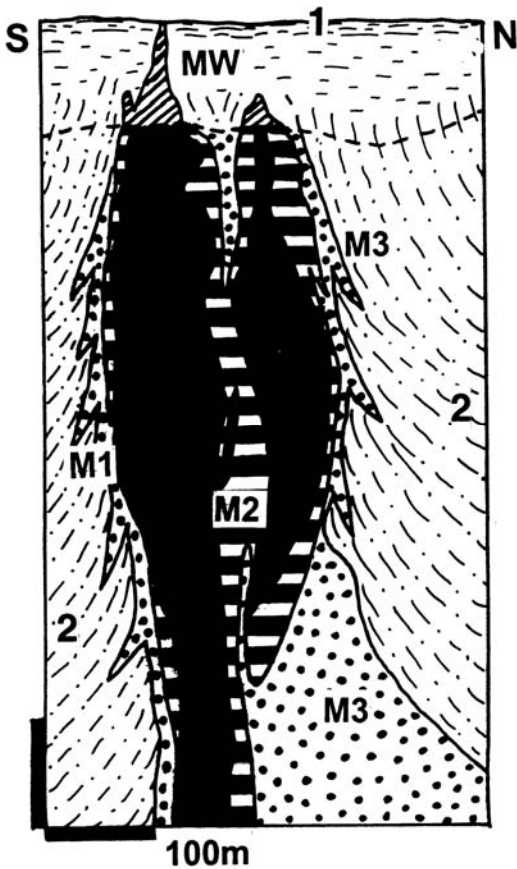


Figure 10.39. Elura Pb-Zn-Ag deposit, NSW, Australia, cross-section from LITHOTHEQUE No. 1261 modified after De Roo (1989). MW. Gossan and oxidized ore; M1. D syntectonic concentrically zoned vertical pipes of massive Fe, Zn, Pb > Cu sulfides; M2. Siliceous rims of M1 with disseminated sulfides; 2. D1 dark siltstone to shale, fine sandstone bands

Ag is less common in tetrahedrite, and least common in Ag-sulfosalts or in argentite/acanthite present as rare minerals in standard polymetallic deposits. When Ag grades in a Pb-Zn ore (not galena concentrate) reach about 280 g/t, the deposit is usually listed as Ag-Pb in databases. Alternatively, separate veins or ore shoots that are low in base metal sulfides, but (relatively) high in the Ag-minerals, are a component of some polymetallic ore systems as in Freiberg (read above); Kutná Hora, Czech Republic (13th-17th century production of ~2,500 t Ag from ~10 mt ore with 400-500 g/t Ag); or the "near-giant" Ag-Pb-Zn Keno Hill district, Yukon (6,563 t Ag @ 1,412 g/t Ag). Alternatively, stand-alone Ag vein systems are known, although most are at best "large" (e.g. Hiendelaencina, Spain, ~3,500 t Ag; Chañarcillo, Chile; 2,300 t Ag), regardless of their historical importance and fame (e.g. Kongsberg, Norway; 1,400 t Ag). Ag-tetrahedrite (Sunshine Mine, Idaho) and epithermal "bonanza" Ag-(Au) deposits (e.g. Guanajuato) are described in Chapters 7 and 6, respectively. Silver deposits of the "five elements" association (Ag, As, Co, Ni, Bi), some with uranium, are also of the "large" magnitude at best (Jachymov, about 1,500 t Ag), never mind their medieval importance and lasting fascination of mineralogists. The only "Ag-giant" in this group is Cobalt, Ontario, reviewed in Chapter 12. Deposits in the Bou Azzer belt in Morocco produced silver and gold as a by-product of cobalt mining and although the cobalt endowment is at best of the "medium" magnitude, this is an "As-giant" and a very distinct mineralized collisional system.

Table 10.5. Summary of hydrothermal Pb-Zn-Ag "giants"

No/ Sect	Deposit, district, area	Age	Type	Tonnage
1/7.7	Elsa-Keno Hill, Yukon	Cr3	Mesothermal fault/fissure veins in silicate rocks	6769 t Ag, 380 kt Pb
2/7.7	Coeur d'Alene, Idaho	Cr3	Ditto	8,035 mt Pb, 4.05 mt Zn, 34 kt Ag
3/7.7	Bingham Pb-Zn, Utah	OI	Mesothermal Pb-Zn replacements zoned around porphyry Cu-Mo	2.41 mt Pb, 1.7 mt Zn, 3906 t Ag
4/7.7	Tintic, Utah	OI	Ditto	1.05 mt Pb, 2.05 mt Zn, 8500 t Ag
5/7.7	Park City, Utah	OI	Mesothermal veins in sediments, replacements in carbonates	1.216 mt Pb, 675 kt Zn, 9575 t Ag
6/7.7	Leadville, Colorado	OI	Mesothermal replacements, some veins	1.3 mt Pb, 780 kt Zn, 7961 t Ag
7/7.7	Santa Eulalia, Chihuahua, Mexico	OI	Carbonate replacements (West), skarn (East)	3.2 mt Pb, 3.52 mt Zn, 13,579 t Ag
8/7.7	San Martín, Chihuahua, Mexico	OI	Skarn > carbonate replacements > veins	5 mt Zn, 400 kt Pb, 12 kt Ag
9/7.7	Fresnillo, Zacatecas, Mexico	OI-Mi	Carbonate replacements, meso-epithermal veins	1.3 mt Pb, 1.7 mt Zn, 13,093 t Ag
10/6.4	Cerro de Pasco, Peru	Mi	Carbonate replacement adjacent to intrusion; high-sulfid. veins	8.59 mt Zn, 2.97 mt Pb, 20,240 t Ag
11/6.4	Colquijirca, Peru	Mi	High-sulfidation replacement mantos	8.2 mt Zn, 2.26 mt Pb, 4294 t Ag
12/6.5	Huarón, Peru	Mi	Meso-epithermal fault & fissure veins > replacements	1.25 mt Zn, 736 kt Pb, 10 kt Ag
13/7.7	Antamina, Peru	Mi	Exoskarn Zn-Cu around porphyry Cu-Mo stock	7.6 mt Zn, 10,640 t Ag + Cu, Mo, Bi
14/7.7	Aguilar, Argentina	Or?,T	Deformed & remobilized sedex?	1.39 mt Pb, 1.8 mt Zn, 7,000 t Ag
15/6.5	San Cristóbal, Bolivia	Mi	Epithermal stockwork & low grade disseminations in volcanics	4.01 mt Zn, 139 kt Pb, 14,880 t Ag
16/10.8	NE Wales district, Great Britain	Cb-Pe	Mesothermal fault & fracture veins in clastics	1.62 mt Pb
17/10.8	Oberharz district, Germany	Cb-Pe	Ditto	1.82 mt Pb, 1.22 mt Zn, 5,000 t Ag
18/10.8	Freiberg, Germany	Pe-MZ	1100 fault & fissure veins in gneiss & schist	1.7 mt Pb, 7,000 t Ag
19/6.5	La Unión (Cartagena), Spain	Mi	Carbonate replacements > skarn > epithermal veins	9.12 mt Zn, 7.68 mt Pb
20/10.8	Linares-La Carolina, Spain	Pe-MZ	Fault & fracture veins in granite and clastics	~3 mt Pb, ~1 mt Zn, ~7500 t Ag
21/6.5	Banska Štiavnica-Hodruša, Slovakia	Mi	Epithermal veins > replacements in caldera around porphyry stock	1.12 mt Pb, 1.6 mt Zn, ~6 kt Ag
22/6.5	Baia Mare district, Romania	Mi-Pl	Series of fault and fracture veins	?3.5 mt Pb, ?2.5 mt Zn, ?9 kt Ag
23/6.5	Trepča, Kosovo	Mi	Carbonate replacements adjacent to diatreme/volcanic center	3.45 mt Pb, 2.1 mt Zn, 5,100 t Ag
24/10.8	Southern Rhodopen, Bulgaria	Mi	44 groups of fault-fissure veins	2.77 mt Pb, 2.18 mt Zn, 4,000 t Ag
25/7.7	Kassandra ore field, Greece	Mi	Skarn, carbonate replacements, veins near porphyry Cu stocks	1.0 mt Pb, 1.2 mt Zn, 2.8 kt Ag, 120 kt As
26/7.7	Lavrion, Attika, Greece	Mi	Carbonate replacements > skarn, oxidation zone around intrusion	?3 mt Pb, ?3 mt Zn, 5200 t Ag
27/10.8	Angouran, Iran	OI-Mi	Oxidation zone, mixed ore, sulfide replacements	5.7 mt Zn, 811 kt Pb

Table 10.5 (continued)

No/Sect	Deposit, district, area	Age	Type	Tonnage
28/10.8	Mehdiabad, Iran	Ol-Mi	Ditto	4.29 mt Zn, 1.105 mt Pb, 3,102 t Ag
29/7.7	Karamazar West, Tajikistan	Pe	Skarn, carbonate replacements around porphyry Cu intrusions	?3 mt Zn, ?1.5 mt Pb, ?10 kt Ag
30/7.7	Karamazar East, Tajikistan	Pe	Meso-epithermal veins & disseminations in volcanics	?38000 t Ag (in Kanimansur)
31/10.8	Nerchinsk (Argun River), Russia	J2-3	500 orebodies in district, carbonate replacements > veins	2.3 mt Pb, 1.5 mt Zn, 800 t Ag
32/7.7	Bawdwin, Shan State, Myanmar	Tr	Replacements & veins in silicified older rhyolite	4.1 mt Pb, 3.6 mt Zn, 8 kt Ag, 218 kt Sb
33/7.7	Dal'negorsk (Tetyukhe), Russia	Cr	Skarn > carbonate replacements > veins	min. 1.6 mt Pb, 1.8 mt Zn
34/7.7	Kamioka, Honshu, Japan	Cr3	Skarn in marble near intrusion	4.5 mt Zn, 2,700 t Ag
35/10.8	Shuikoushan, Hunan, China	Cr1	Carbonate replacements, minor skarn around intrusion	2 mt Pb
36/10.8	Elura, NSW, Australia	D	Replacement of clastics // cleavage, adjacent to fault	2.385 mt Pb, 3.825 mt Zn, 3,105 t Ag

No/Sect=number on map (Fig. 10.40) and number of the Section in this book where the deposit is described; Age=age of ore deposition. Tonnages are of contained metals

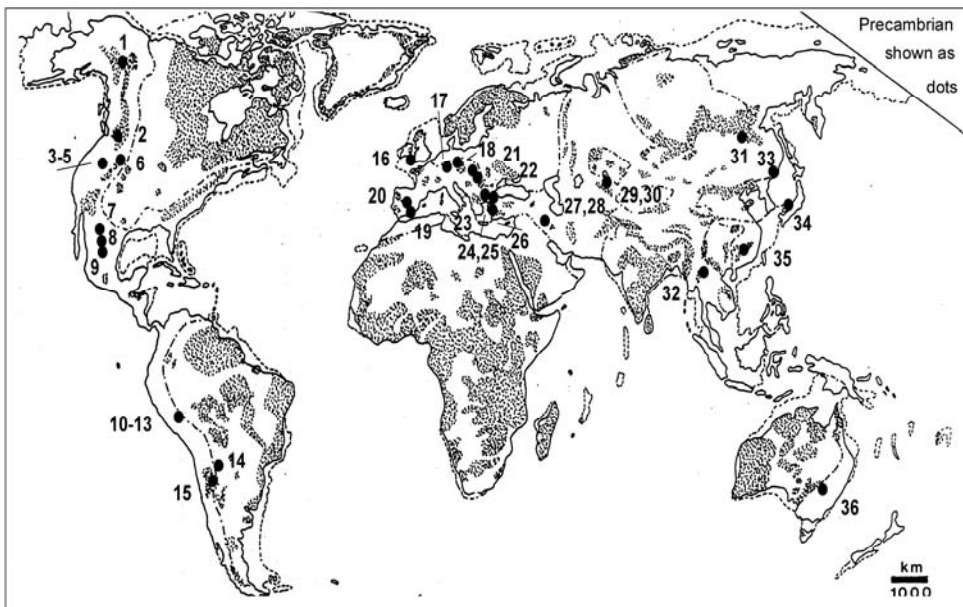


Figure 10.40. "Giant" mesothermal Pb-Zn-Ag deposits of the world (see Table 10.5. for locality names and brief characteristics)

11 Proterozoic Intracratonic Orogens and Basins: Extension, Sedimentation, Magmatism

11.1. Introduction

Early Precambrian greenstone belts (Chapter 9) are relatively uniform and "simple". This is the consequence of less diversified early crustal evolution, as well as deep erosion that has progressively removed the more varied upper levels. Although the model, greenschist-metamorphosed greenstone belts rest on or border older, high-grade metamorphosed "basement complexes" (Chapter 14) and must have been initiated by rifting, the distinct stages of rifted margin development (Chapter 12), and metallogenesis resulting from interaction of the early stages of "greenstone" evolution with the old basement, are not emphasized in the literature. They, however, exist, although as an exception in the form of the mature "pre-greenstone" association of quartz arenites or conglomerates, carbonates, possible evaporites, terrigenous detrital sediments, interspersed with at least partly subaerial basalt flows and sometimes rhyolitic ignimbrites (e.g. Thurston and Chivers, 1990). By the Proterozoic (or even earlier as in the Kaapvaal Craton; Tankard et al., 1982) the frequency and, especially, preservation of the intracratonic rock- and ore-forming environments, sustained by repeated extension of the continental crust combined with periodic influx of mantle-generated magmas from depth, have increased considerably. Some authors (e.g. Hutchinson, 1981) thus formulated the Proterozoic style of metallogeny as a distinct and different one in respect to the Archean "greenstone" metallogeny. This, however, is only partly true as "greenstones" continued their separate existence along continental margins through the Proterozoic, to merge with the Phanerozoic "eugeoclinal" belts (Chapter 8) and volcanic arcs (Chapters 5, 6).

This chapter brings together several apparently disparate metallogenesis that share the following common characteristics: 1) mature Precambrian continental crustal basement that underwent extension simultaneously with new rocks formation; 2) components of the "rift cycle"; 3) anorogenic volcanism; 4) abundant subaerial or shallow water lithogenesis; 5) subsequent orogenic deformation, metamorphism and granitoid plutonism; 6) none or low- to medium-grade metamorphism; and 7)

predominantly Proterozoic age. The emphasis is on interaction. Some distinct settings and ore types reviewed here, and summarized in the global context in Laznicka (1993, Chapter 3, p.633-672), include metallogenesis resulting from orogenic interaction with "rift" volcanics (e.g. Mount Isa-Cu), intracratonic breccia metasomatites and related Fe oxides-rich Cu, Au, U systems (Olympic Dam); unconformity-U deposits; Kiruna-type Fe; Witwatersrand-style Au and U conglomerates; Proterozoic "sedex" basins (Mount Isa, McArthur River); and the African Copperbelt-style Cu systems. Separately treated are the "rift" basalts & Bushveld-style intrusions (Chapter 12); alkaline magmatism (Chapter 12); high grade metamorphosed equivalents (Chapter 14); younger rifts and rift margins (Chapter 12) and Phanerozoic platformic/miogeoclinal sequences (Chapter 13). Metallogeny associated with collisional to anorogenic granitoids in intracontinental orogens is included in Chapter 10.

Example areas where most of the features of the present group can be found include the Mount Isa Inlier in northern Queensland (Blake, 1987; Blake et al., 1990); the "Witwatersrand Triad" in southern Africa (Tankard et al., 1982); the Huronian Supergroup of Ontario (Bennett et al., 1991; Fyon et al., 1992), the Windermere Assemblage in the Canadian Cordillera (Gabrielse and Campbell, 1992; Souther, 1992); portions of the Pine Creek "Geosyncline", northern Australia (Ferguson and Goleby, eds., 1980); Gawler Craton of South Australia (Drexel et al., eds., 1993); the Lufilian Arc of central Africa (Unrug, 1988).

Composition and assembly: Paleoproterozoic and especially Meso- and Neoproterozoic terrains with a relatively thick continental crust support successions deposited in extensional intracratonic basins. They were reviewed and their metallogeny briefly characterized in Laznicka (1993) under the heading "Diverse (land-to-shelf) metasedimentary association" (Fig. 11.1). These rock groupings are in many respects comparable with those deposited in younger rift-initiated basins except that during and after completion of the supracrustal deposition the basal sequences were substantially deformed, intruded by plutons, and metamorphosed.

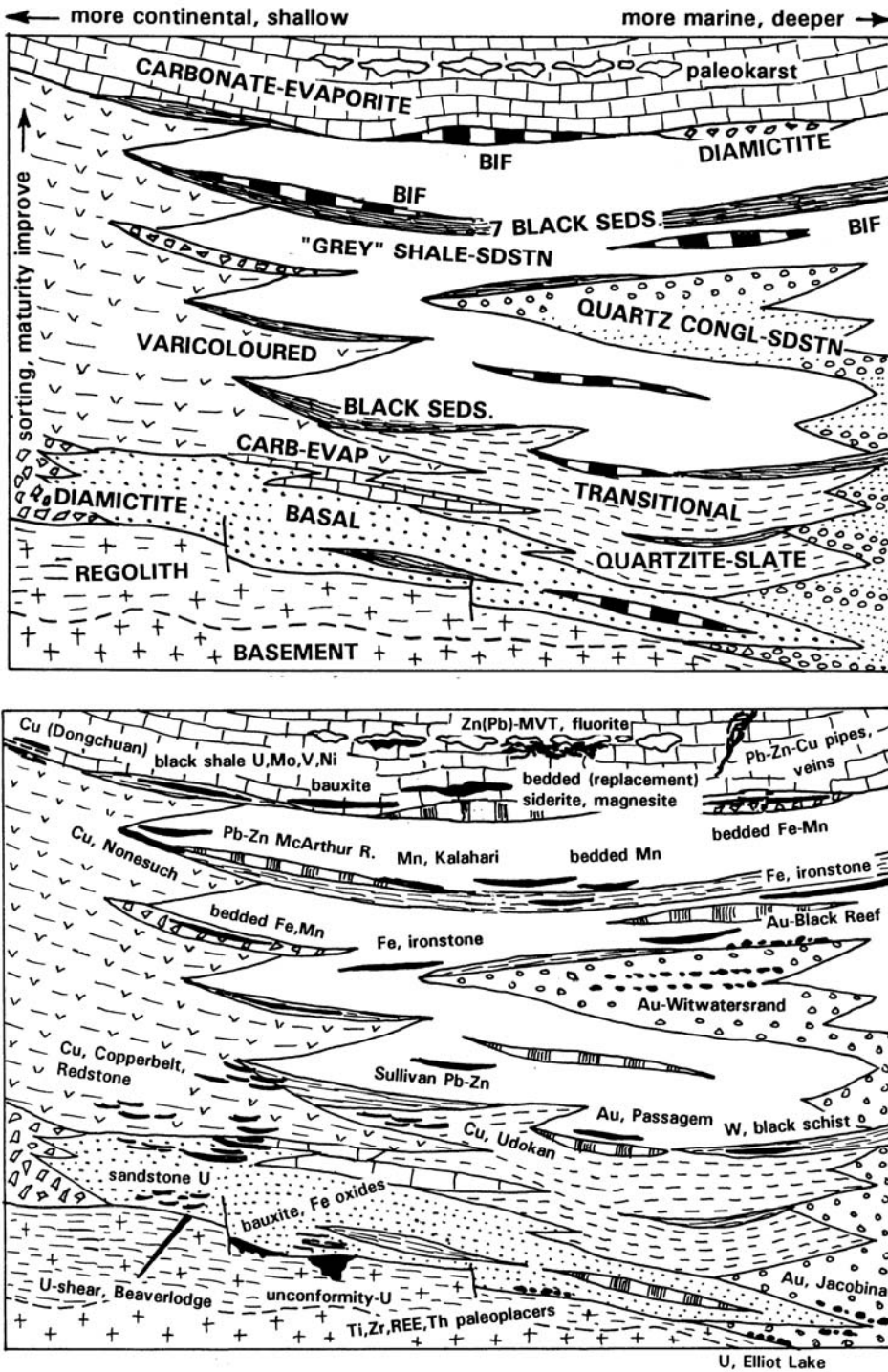


Figure 11.1. Diverse supracrustal rock associations characteristically developed in the mid- to late-Proterozoic intracratonic setting (TOP) and a selection of representative ore types (below). Diagrammatic, not to scale, effects of orogenic deformation, metamorphism and plutonism removed. From Laznicka (1991, 1993)

There is a broad spectrum of styles of the basal sequences ranging from the gently folded, faulted,

subgreenschist ones (as in the Mesoproterozoic MacArthur Basin in Australia) through greenschist-

metamorphosed and pluton-intruded ones (Mesoproterozoic Mount Isa Group) to the amphibolite-facies, heavily plutonized equivalents (Chapter 14). The extensional intracratonic basins as in the Mount Isa Inlier contain up to three cycles of "cover sequences" (e.g. supracrustals) resting on a stabilized, eroded orogen (Blake, 1987). Each cycle starts with a rift facies, then changes into a sag/thermal subsidence facies with laterally more extensive finer and more mature clastics containing carbonates and indicators of hypersaline conditions, and terminates with a turbidite/basin collapse facies of quartz-rich terrigenous to volcanoclastic flysch. Each cycle is followed by orogeny and a peak in granite emplacement (Fig. 11.2).

The rift phase (treated in more detail in Chapter 12) commences with felsic to bimodal, usually subaerial, volcanics that interfinger with coarse, immature clastics (fanglomerate) rapidly changing into arkose and quartz-rich blanket sandstone. Substantial proportion of sedimentary rocks are of subaerial origin, deposited under arid conditions hence they are oxidized (varicolored or red-beds association). Carbonate buildups (e.g. stromatolite "reefs") and iron rich sediments could be present, but are not typical. Proterozoic evaporites deposited in restricted marine basins, or in rift lakes, are much rarer than their Phanerozoic counterparts, and are degraded by repeated periods of dissolution. Because of this Proterozoic halite is almost non-existent and except for anhydrite (sometimes hydrated to gypsum) the old evaporites are often substituted by the less soluble minerals (silica, barite) that replaced them diagenetically. Alternatively, the sites of vanished evaporites ("the evaporite that was" of Warren, 1999) are now filled by a variety of collapsed or subsided materials (mainly breccias), some of them mineralized. Unconformities on commonly regolithic older basement are important surfaces of movement and interaction of fluids, and the basal sedimentary units comprise the greatest variety of lithologies influenced by detritus sources in the basement.

The sag phase consists of alternating relatively mature clastics (quartz arenite-quartzite, siltstone to shale/slate, sometimes carbon-rich argillite) and carbonates (dolomite >> limestone). There is a high proportion of mixed lithologies such as marls, dolomitic marls, carbonate-permeated siltstone and sandstone, with gradual transitions. Hypersaline indicators are common (gypsum, anhydrite, halite

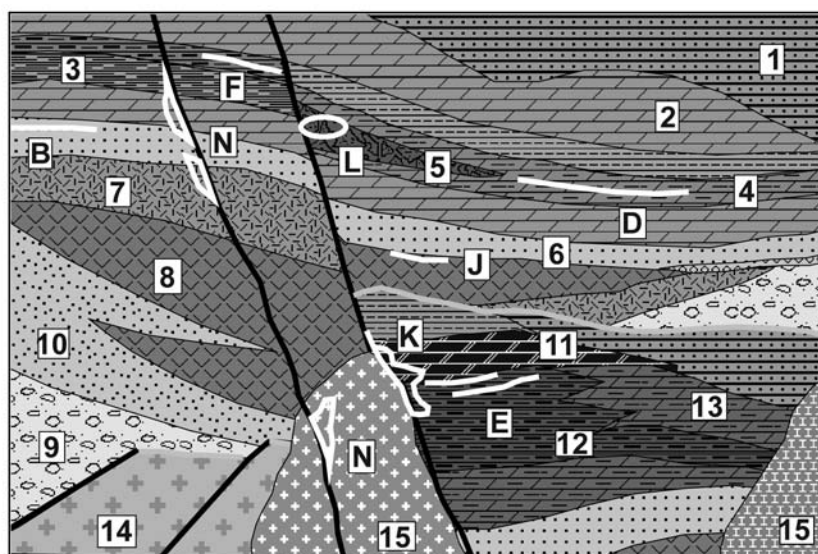
casts) although evaporites are rare. One of the least metamorphosed examples quoted in the literature, the HYC Pb-Zn mineralized marl in the McArthur Basin of Australia, is bituminous and yields the oldest extractable hydrocarbons (1.69 Ga). In the greenschist-metamorphosed units as in the Urquhart Shale at Mount Isa, the carbon comes as a finely dispersed graphite. Layers of airborne tuff are common and they mix with sediments in all proportions. The sediment thickness and early diagenesis may have been greatly influenced by the activity of growth faults. Synsedimentary faulting was responsible for coexisting areas of thin, flat sedimentary covers ("platforms", as the Lawn Hill Platform) and up to 10 km thick adjacent "trough" sequences (e.g. the Batten Trough in the McArthur Basin).

The turbidite phase consists of quartz-rich, "distal" turbidites with some volcanoclastics. The predominantly sedimentary post-rift sequences correspond to the Phanerozoic platform and miogeoclinal successions treated in Chapter 13.

11.2. Metallogeny and giant deposits

Proterozoic intracratonic ores included in this chapter store a significant proportion of the world's supply of U, Cu, Pb, Zn, Au, Ag and Co in "giant" deposits. The deposits display strong provincialism, that is they frequent relatively small local geological or structural terrains in which deposits of a certain metal and certain type are abundant and large, but comparable deposits are almost completely missing outside such terrains. The well known examples include the Witwatersrand Basin (over of world's gold) with 7 "supergiant" and 3 "giant" goldfields, and no other "giant" of comparable type outside, except for Tarkwa in Ghana (Chapter 9). Uranium resides in three Proterozoic provinces that store more than 95% of the given type, with nothing major outside them. The same applies to deposits of Cu, Zn, Pb, Ag and Co.

With possible exception of the Kiruna-type Fe ores, all the metal accumulations are recycled from mostly upper crustal source rocks and from mantle-derived mafics. Magmatic and magmatic-hydrothermal ores are practically missing as those related to granites, mafic intrusions and alkaline intrusions are considered in different Chapters (10 and 12, respectively).



1. (Meta)turbidite; 2. (meta)-dolomite; 3. Black pelite; 4. Slate, phyllite; 5. Black dolomitic marl with growth fault talus breccia; 6. Quartzite; 7. Felsic (meta)volcanics; 8. Mafic (meta)volcanics; 10. Funglomerate, talus; 10. Blanket sandstone (quartzite); 11. Siliceous (meta)dolomite; 12. Black slate, phyllite; 13. Dolomitic slate, phyllite; 14. Crystalline basement; 15. Syn- to postorogenic granites.
- B. Oolitic ironstone; D. Pb, Zn, Ag sedex deposits, subgreenschist; E. Ditto, in black pyritic slate; F. Ditto, in high-grade metamorphics;

Figure 11-2. Mixed Proterozoic rift-sag-turbidite association intruded by syn- to postorogenic granites. Effects of orogenic deformation removed. Rocks/ores inventory cross-section from Laznicka (2004) Total Metallogeny site G226. Explanations (continued): J. Cu in metabasalt flowtops; K. Cu sulfides replacing silica-carbonate near fault contact with greenstones (Mount Isa); L. Zn-Pb in carbonate breccia near fault. Ore types D, E, F include "giant" equivalents

The enigmatic hydrothermal epigenetic Fe-oxide breccia and vein deposits with variably co-precipitated Cu, or U, or Au-Ag (Olympic Dam-type) are associated with high-level anorogenic volcano-plutonic centers, but the volcanics may be eroded and the magmatic association not clearly displayed. This group of deposits is treated separately at the end of this chapter. Supergene physical recycling probably produced Au and U deposits of the Witwatersrand and Elliot Lake types, although the source rocks of primary metals have not yet been convincingly identified. Chemical recycling of metals leached from source rocks, then precipitated in suitable traps, has been repeatedly suggested in the literature.

The fluids involved in generation of the various sedimentary-hosted, chemically precipitated metallic deposits have been interpreted as heated meteoric waters, heated marine brines, heated saline basinal brines, hydrothermal metamorphic fluids (Mount Isa, Cu; Perkins, 1984; Hannan et al., 1993), and other. Ore genesis, as it applies to the Australian terrains, is extensively discussed in Solomon et al. (1996). Evaporites in sedimentary successions may have contributed to saline brine formation so their presence is considered favorable in ore search (Warren, 1999). The heat required to drive brine circulation is considered to have been due to the ordinary geothermal gradient, enhanced

gradient available above high heat producing granites (Solomon and Heinrich, 1992), volcanic heat, heat from shallow mafic (gabbro, diabase) sills, granite or alkaline intrusions.

The Proterozoic metallic deposits discussed here range from presumed syngenetic clastic (Au, U paleoplacers) through sedimentary-diagenetic, sedimentary-exhalative to syn- or post-orogenic dilation fillings and replacements. There are many genetically controversial orebodies like the Witwatersrand, although the "modified placer" origin seems to best account for the observed features, provides an effective exploration tool, and has most adherents. Elsewhere, as in Mount Isa, genetic controversy persists between the advocates of syngenetic-diagenetic and synorogenic hydrothermal formation of the Cu and Pb-Zn-Ag orebodies (e.g. Painter et al., 1999).

Copper "giants": the (meta)basalt connection: Tholeiitic basalt and its plutonic equivalents (diabase, gabbro), abundantly emplaced during the "rift stage", are powerful metallogenes. The magmatic and magmatic-hydrothermal deposits of Ni, Cu, PGE (Noril'sk, Sudbury, Bushveld), associated with intrusions and resulting from active fractionation in the time of magma emplacement, are treated in Chapter 12. Here the focus is on the subaerial or shallow subaqueous basalts that

generated no ready-made ores in the time of emplacement, but that introduced into the system, and retained, high trace Cu contents (of the order of 100-150 ppm Cu) to be redistributed and sometimes locally accumulated by superimposed processes. These include: 1. Supergene Cu leaching followed by precipitation of the metal from channeled leachate in a redox environment; 2. synorogenic Cu displacement from parent rocks followed by reprecipitation from metamorphic hydrotherms; and 3. other processes. Subaerially extruded basalts are better capable than their marine counterparts to retain trace Cu, which is normally depleted in seawater-altered (spilitized, i.e. Na- and Mg-metasomatized and hydrated) submarine basalts. Subaerial basalt flows are, moreover, associated with continental sediments such as conglomerates and first-cycle arenites that may later provide permeable and porous sites for ore precipitation, or act as an intermediate stage in inheriting portion of the basaltic Cu in detritus, or Cu held in the interstitial Fe oxides or clays. For this reason the sediments associated with basalt need to be of the arid variety (red or varicoloured beds), as Cu is leached out during humid sedimentogenesis. This leads to the "volcanic redbeds" class of Cu deposits of Kirkham (1996b) and other authors.

The copper/basalt field association is an excellent empirical exploration indicator that has contributed to ore discoveries (e.g. of Olympic Dam) and it has often been suggested in the literature. The basalt (gabbro) Cu source rocks need not be exposed at the surface, but could be in depth, possibly indicated by coincident magnetic and gravity anomalies. In terms of intimacy, the basalt/Cu association form an end-member sequence starting with Cu accumulated in the basalt itself (not necessarily, however, at the depth level from which the copper has been displaced as in the Keweenaw Cu province; Chapter 12) and terminating with Cu in sediments only. At the latter end, the basalt input is difficult to demonstrate and may have been absent (read below).

Mount Isa Inlier, Queensland: juxtaposed Cu and sedex Pb-Zn-Ag

Mount Isa Inlier is a Proterozoic intracratonic orogenic belt (Blake, 1987; Fig.11.3) exposed in an erosional window surrounded by Neoproterozoic and Phanerozoic platformic sediments. The Inlier has been subdivided into four blocks separated by N-S trending faults. The westernmost Lawn Hill Platform hosts the "giant" Century Zn-Pb deposit (read below), the Western Fold Belt contains the

string of three Zn-Pb-Ag "giants" and one "Cu-giant" of the Mount Isa ore field. The Central Belt comprises high-grade metamorphosed felsics intruded by plutons and lacking major ore deposits, whereas the Eastern Belt near Cloncurry hosts the Pb-Zn-Ag "giant" Cannington (in high-grade metamorphics, included in Chapter 14) and the "large" deposits Ernest Henry (Cu-Au), and Dugald River (Zn>Pb). The description immediately below concerns the Western Belt and its Mount Isa ore field. The "Basement" of the Inlier consists of high-grade metamorphics produced by the 1.89-1.87 Barramundi Orogeny. It is topped by three "cover sequences" that contain components of the rift-sag cycle. In the Western Belt the Cover Sequence 2 (sequence #1 is not developed there) starts with basal conglomerate, arkose, minor basalt and mature quartz arenite topped by at least 7.5 km thick Eastern Creek Volcanics. These are trace Cu-rich, greenschist-metamorphosed locally amygdaloidal tholeiitic meta-basalts with flow-top breccias, fluvial sandstone or conglomerate interbeds and with indicators of former evaporite presence. The mafics are also interspersed with bands of epidosite and chlorite schist interpreted as products of synmetamorphic hydration (Hannan et al., 1993). The metavolcanics are overlain by arenites and grade upward into shallow marine, locally dolomitic terrigenous sediments, intruded by 1.75-1.67 Ga granite plutons. The Cover Sequence 3 includes the about 1.67 Ga Mount Isa Group (Blake, 1987), a sedimentary sequence with mature quartz arenite in the basal portion, fining-upward into dolomitic siltstone with local tuffaceous and "chert" interbeds. This includes the Urquhart Shale, host to the Mount Isa orebodies. These sedimentary rocks were, shortly afterwards, deformed and greenschist metamorphosed during the Isan Orogeny.

Mount Isa Pb-Zn-Ag deposit in NW Queensland (Mathias and Clark, 1975; P+Rc 7.363 mt Pb, 6.82 mt Zn, 17,890 t Ag) was discovered in 1923, and this was followed by discovery of the **Mount Isa Cu** orebodies underground (Perkins, 1990; P+Rv 255 mt @ 3.3% Cu for 10.026 mt Cu, 120 kt+ Co; Fig. 11.4). **Hilton Mine**, 20 km north of Mount Isa, was found in 1947 (Forrestal, 1990; P+Rv 49 mt @ 9.3% Zn, 6.5% Pb, 151 g/t Ag for 4.557 mt Zn, 3.185 mt Pb and 7,399 t Ag; Fig. 11.5). **George Fisher Mine**, 2 km north of Hilton, has been delineated in 1992 (Chapman, 2004; Rc 108 mt @ 11.0% Zn, 5.4% Pb, 93 g/t Ag for 10.787 mt Zn, 5.05 mt Pb, 8,659 t Ag). The 25 km long Mount Isa ore zone thus stored 23.7 mt Zn, 15.6 mt Pb and 34 kt Ag.

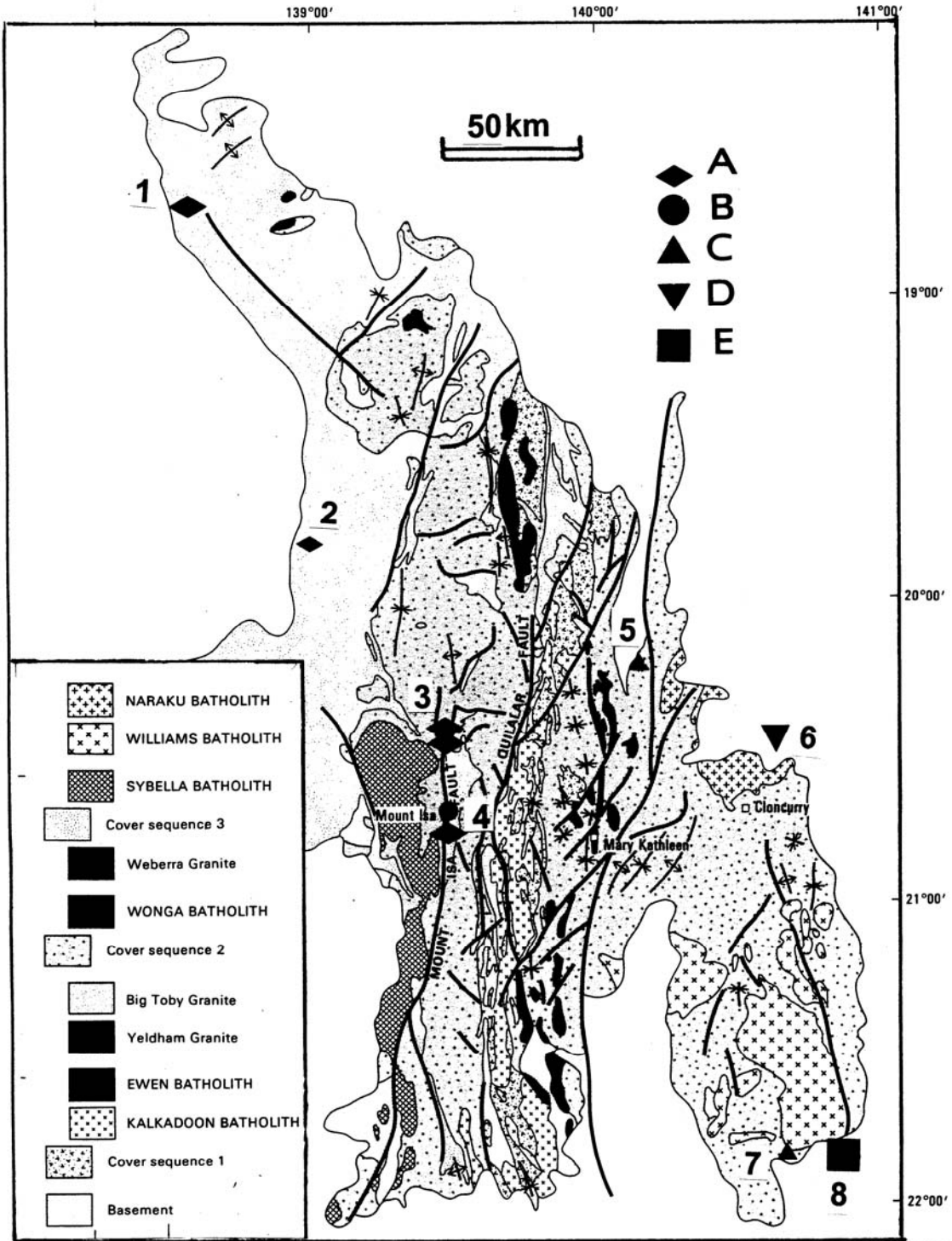


Figure 11.3. Mount Isa Inlier, Queensland, geological map from Blake et al. (1990) reprinted courtesy of The Australasian Institute of Mining and Metallurgy. "Giant" and several "large" deposits added: 1. Century, Zn-Pb-Ag; 2. Mount Loretta-Zn; 3. Hilton and George Fisher Pb-Zn-Ag; 4. Mount Isa Pb-Zn-Ag and Cu; 5. Dugald River-Zn; 6. Ernest Henry-Cu, Au; 7. Pegmont, Zn-Pb; 8. Cannington Pb-Zn-Ag. Symbols: A. Sedex Pb-Zn-Ag; B. Synorogenic Cu replacements; C. Shear-hosted Zn-Pb; D. Shear-hosted magnetite-Cu-Au; E. Broken Hill-type Pb-Zn-Ag in high-grade metamorphics

Mount Isa is unique by the presence of separate, although interdigitated, Zn-Pb-Ag and Cu orebodies hosted by the same sequence but controversial in origin. The ore host is the about 1,000 m thick Urquhart Shale. It is composed of a delicately laminated greenschist-metamorphosed dolomitic, pyritic siltstone ranging in color from light-gray (the dolomite-rich bands) to black (carbonaceous "shale" = phyllite). The sedimentary package crops out in a narrow, fault-bounded north-south trending, 65° west dipping band subjected to three deformational events. At Mount Isa this band is modified by the north-plunging asymmetric Mount Isa Fold, the western limb of which contains most of the orebodies. In the east, the orebodies are terminated by two major NNW-trending shear zones.

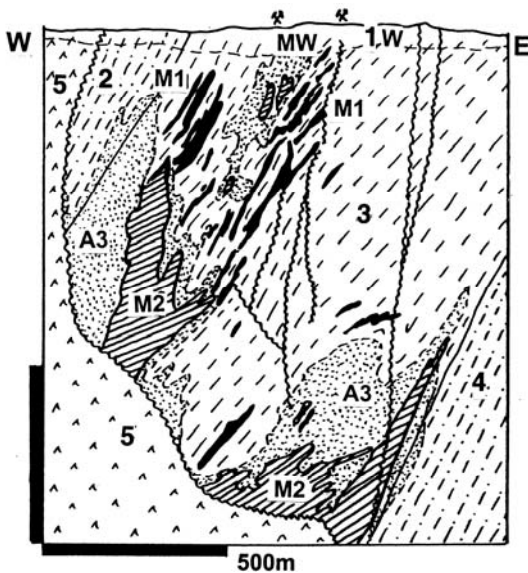


Figure 11.4. Mount Isa Mine cross-section showing both the Pb-Zn-Ag and Cu orebodies. From LITHOTHEQUE No. 1462, modified after Burns (1993), Perkins (1997) and Mount Isa Mines Staff, 1981 visit. MW. Oxidation zone that includes gossan; M1. Stratabound Pb-Zn-Ag orebodies in Urquhart Shale, interpreted as sedex; M2. Replacement, cross-cutting Cu orebodies in silica-dolomite alteration (A3). 1. W. T-Q cover sediments and regolith; 2. 1.67 Ga Mount Isa Group (Cover Sequence 3), Spear Siltstone; 3. Ditto, Urquhart Shale; 4. Ditto, Native Bee Siltstone; 5. ~1.7 Ga Eastern Creek Volcanics, meta-basalt altered along the Paroo Fault

Pb-Zn-Ag orebodies. On the map, the "lead orebodies" (Forrestal, 1990) appear as multiple thin, parallel, bedding-conformable folded bands or lenses in the Urquhart Shale. The richly mineralized

ore interval measures 1,600x650 m at surface and 1,200 m down dip. The individual sulfide bands are between 1mm and 1m thick and mineable orebodies (about 30 numbered orebodies in the Mount Isa Mine) include the thicker ore bands, or groups of bands. The ore is composed of fine-grained, densely disseminated galena, sphalerite, pyrite and pyrrhotite in the "shale" matrix, grading to massive sulfides. The bands are almost perfectly conformable with bedding except for the disharmonically folded intervals where galena is enriched in fold hinges, flowage structures and injections into pressure shadows.

At **Hilton** (Fig. 11.5), the orebodies are in the same stratigraphic position as at Mount Isa, after 20 km long barren interval. They are confined to a narrower zone (110 to 250 m thick), are more deformed, and richer in chalcopyrite although the Cu grades are only of the order of 0.5%. The **George Fisher** orebodies (Chapman, 2004), 400 m below surface, are in a N18°W trending, 50-80° west dipping, 450 m thick mineralized sequence, traceable for 1,200 m along strike. 10 separate orebodies of pyrite, sphalerite, galena, pyrrhotite are in calcite, Fe-dolomite, sericite, feldspar, quartz matrix in the "shale". Although the Mount Isa Pb-Zn-Ag orebodies are one of the founding members of the sedex family (Goodfellow et al., 1993), that is synsedimentary-hydrothermal type of deposits, alternative genetic interpretations do exist. About the most convincing alternative is post-depositional replacement of diagenetic Fe sulfides in shale by the epigenetic Zn, Pb sulfides (compare Solomon et al., 1994, for discussion).

Mount Isa Cu orebodies. The Mount Isa Cu orebodies (Perkins, 1990; Fig. 11.4.) are confined to "silica-dolomite", which is a lighter-colored, inhomogeneous (brecciated, pseudobrecciated) metasomatite composed of sparry dolomite replacing the Urquhart Shale. The dolomite is, in turn, partially replaced by microcrystalline quartz ("chert"), whereas chlorite, biotite and stilpnomelane replace the pelitic component. Chalcopyrite, pyrrhotite, pyrite, minor cobaltite come as fine to coarse grains, blebs, streaks, veinlets and stringers mainly replacing the dolomite. The silica-dolomite is clearly a syntectonic metasomatite and it envelopes the Pb-Zn zone mainly in the south, and in its footwall region. Its border against the Urquhart Shale and the Pb zone is gradational, but in depth it is cut by a shear zone that has juxtaposed the Urquhart Shale against the stratigraphically much deeper Eastern Creek Volcanics. The meta-volcanics adjacent to the shear zone are converted to chlorite schist and

depleted in much of the trace copper. They are considered the probable source of the ore copper, carried into the orebodies by a hybrid metamorphic fluid (Hannan et al., 1993).

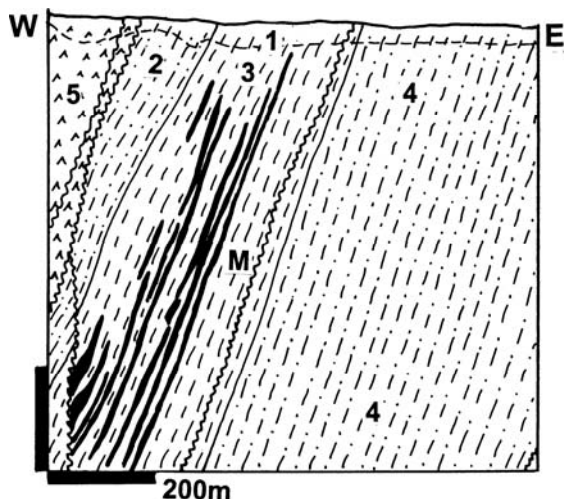


Figure 11.5. Hilton deposit, Mount Isa ore zone, composed of virtually only Pb-Zn-Ag orebodies. From LITHOTHEQUE No. 1464, modified after Forrestal (1990) and Mount Isa Mines Staff, 1981 visit. 1. T-Q cover sediments and regolith; M. Pb-Zn-Ag stratabound orebodies in Urquhart Shale interpreted as sedex. 2. ~1.67 Ga Mount Isa Group, Spear Siltstone; 3. Ditto, Urquhart Shale; 4. Ditto, Native Bee Siltstone; 5. ~1.7 Ga Eastern Creek Volcanics, meta-basalt

Mount Isa Inlier is a distinct Cu (as well as Zn-Pb-Ag) province with some 800 copper occurrences recorded in both the Western and Eastern Belts. Those in the Western Belt (such as the Gunpowder group), traceable for more than 200 km north of Mount Isa, are replacements, veins and disseminations in metasediments and the source relationship to Eastern Creek Volcanics seems to hold.

11.3. Proterozoic Pb-Zn-Ag "sedex" deposits

Hydrothermal-sedimentary or **SED**imentary-**EX**halational model assumes precipitation of sulfides (and also barite) from medium-temperature basinal brines, on the seafloor, in the time of sedimentation or early diagenesis (Goodfellow et al., 1993, and references therein). As usually, concepts keep changing. In terms of host lithologic association there is a choice of placement of these

deposits. Those in Phanerozoic terrains preferentially occur in detrital "basinal" sequences oceanward from carbonate platforms (e.g. the Selwyn Basin) so they are reviewed in the context of the miogeoclinal megafacies (Chapter 13). The Proterozoic sedex deposits are not much different, but as the continental facies progression is interrupted by deformation and longer lasting erosion, demonstration of intracratonic extension to create depositional basins increases in importance and influences formulation of exploration models. Selected sedex (or sedex-like) "giants" are thus reviewed here and one (Mount Isa) has already been described above. Deposits of the Broken Hill Pb-Zn type in high-grade metamorphics, considered by some authors as meta-sedex, are treated in Chapter 14. About nine Proterozoic "giants" with sedex characteristics store some 72 Mt Zn, 44 Mt Pb and 63 kt Ag. Of these, seven are in Australia; three in the Mount Isa ore field alone.

McArthur River (H.Y.C.) Zn-Pb-Ag deposit, northern Australia. This "giant" deposit (Logan et al., 1990; Rv 237 mt @ 9.2% Zn, 4.1% Pb, 41 g/t Ag for 22.5 mt Zn, 9.5 mt Pb, 9,551 t Ag) is broadly contemporaneous with Mount Isa. It is in sub-greenschist metamorphosed and very little deformed sedimentary rocks, so that it provides a popular genetic model. The deposit was discovered in 1955, based on the "concept of association of mineralisation with specific sediments" (Logan et al., 1990). Because of the extremely fine grained nature of the ore minerals, hence high recovery costs, exploitation was delayed until the 1990s.

The H.Y.C. (Here's Your Chance) deposit is 592 km NW of Mount Isa, under 20m of unconsolidated alluvial cover. The orebodies are in a thickened interval of dolomite to shale, siltstone and minor evaporite succession in the 1.69 to 1.65 Ga McArthur Group, in the north-trending Batten Trough (a paleorift). The stratiform orebody is hosted by a 55 m thick unit of thinly interbedded, K₂O-rich carbonaceous and pyritic dolomitic siltstone, subaqueous slump to debris flow breccia (dolomite fragments embedded in black shale matrix), and recrystallized feldspar-rich tuff. The rocks are interpreted as lacustrine or sabkha deposits. 1.5 km east of the orebody, separated by a dolomitic (talus?) breccia, is the NNW-trending Emu Fault, interpreted as a growth fault. The small Ridge Pb-Zn deposit is situated on top of the breccia.

The McArthur ore zone comprises seven subparallel ore horizons separated by barren breccia and siltstone. The sulfides (sphalerite > galena >

pyrite >> chalcopyrite) are extremely fine-grained and have the form of laminae, disseminations, scattered crystals and massive lenses. The ore minerals are so inconspicuous as to be visually almost unrecognizable so the best indication of ore grade is the presence of coarse, remobilized sulfide veinlets and scattered grains on joints and in fractures. Equally inconspicuous was the oxidized outcrop of the deposit, of limonite-stained, cream colored hemimorphite.

Century Zn-Pb-Ag deposit, Lawn Hill district, NW Queensland (Broadbent and Waltho, 1998; Rc 167.5 mt @ 8.24% Zn, 1.23% Pb, 33 g/t Ag for 13.8 mt Zn, 2.06 mt Pb, 5,527 t Ag; Fig. 11.6). This is the most recently proven "giant" in the westernmost belt of the Mount Isa Inlier: the Lawn Hill Platform. Century is the first stratabound Zn-Pb deposit found in a district with tens of small Pb-Zn vein deposits known for over 100 years. The orebody outcrop itself was successively included in nine exploration tenements to be recognized only after reverse circulation drilling of geochemical targets by CRA Ltd. in 1990. The host rock is the 1,595 Ma Lawn Hill Formation, the youngest unit of the same sequence that hosts Mount Isa. It is a 850 m thick sequence of subgreenschist-metamorphosed, gently folded but intensely block-faulted terrigenous siltstone and sandstone rich in carbonaceous shale units. In contrast with the dolomitic units that host Mount Isa and McArthur River deposits, the sediments here are purely siliclastic except for discordant carbonate breccias along fractures. The subhorizontal to gently dipping ore zone consists of two sets of delicately laminated bands of fine grained sphalerite and lesser galena with pyrobitumen and siderite gangue in black shale bands, separated by barren stylolitic siltstone interval. There is a pyrite halo. Although stratabound, in detail the mineralization transgresses bedding. Broadbent and Waltho (1998) proposed a syn-diagenetic replacive, rather than sedex, model of origin of the ore.

The **Dugald River** "near Zn-giant" deposit is near Cloncurry, in the eastern portion of the Mount Isa Inlier (Xu, 1996; Rc 60 mt @ 10% Zn, 1% Pb, 30 g/t Ag for 6.05 mt Zn, 950 kt Pb, 2050 t Ag). It is in a shear zone that intersects the Mesoproterozoic Corella Formation, synchronous with the D4 deformation phase, hence the ore emplacement was (syn)orogenic (Xu, 1996).

Sullivan Pb-Zn-Ag deposit, Kimberley, SE British Columbia (Hamilton et al., 1982; Lydon et al., eds., 2000; P+Rv 162 mt @ 6.5% Pb, 5.6% Zn, 67 g/t Ag

for 10.53 mt Pb, 9.56 mt Zn, 10,854 t Ag, 50 kt Sn, 134 kt As; Fig. 11.7). Sullivan, which is a single complex deposit, is one of the "founding fathers" of the sedex model. Located, at the continental scale, in the present Cordilleran orogen in a "distal turbidite" association, it does not seem to have much in common with rifting. Recently, however, it has been demonstrated that Sullivan and the host Aldridge Formation were deposited in a Mesoproterozoic (~1.45 Ga) lacustrine or marine intracratonic rift basin near margin of the North American craton, complete with a thick set of gabbro dikes and sills intruded into wet, unconsolidated sediments (Høy, 1993).

The Belt-Purcell Basin and Supergroup in SW Canada and NW United States (Aitken and McMechan, 1991) comprise an up to 20 km thick sequence of clastics with rare carbonates at the margin and minor interbedded metabasalts (but with abundant gabbro-diorite sills), generally interpreted as a pull-apart basin. Although much of the Supergroup is devoid of ore occurrences, the middle mature sequence contains several "large" stratabound Cu deposits in quartzite (Spar Lake, Rock Creek in Montana), whereas the lower, slate-litharenite division, hosts much of the Coeur d'Alene Ag-Pb-Zn vein district in Idaho (Chapter 7) and the stratabound Sullivan orebody in Canada.

Sullivan was discovered in 1892 and finally exhausted in 1991. It has had an exciting industrial history in parallel with the continuously changing genetic concepts (Lydon et al., eds., 2000). The host Aldridge Formation is a gray, monotonous, rusty weathering flyschoid sequence of rhythmically banded quartz-rich wacke interbedded with slate and topped by a sheet of polymictic intraformational conglomerate. The conglomerate lens is in the immediate footwall of the Sullivan stratabound orebody and is, in turn, overlain by graywacke, pyrrhotite-laminated slate and several sets of slate bands alternating with wacke. A thick gabbro sill is about 500 m beneath the orebody.

The Sullivan orebody is a saucer-shaped composite lens of partly separate, partly coalescing sulfide lenses with a maximum thickness of 100 m, and is approximately circular in plan with a diameter between 1.6 and 2.0 km. In the west the orebody is thickest, and is massive to poorly layered with minor interbeds of clastics. Towards the east the clastic component increases and delicately laminated sulfide bands alternate with sulfide-poor graywacke and slate. The ore zone and its environs contain evidence of several phases of overlapping brittle fragmentation (brecciation), hydrothermal alteration and mineralization.

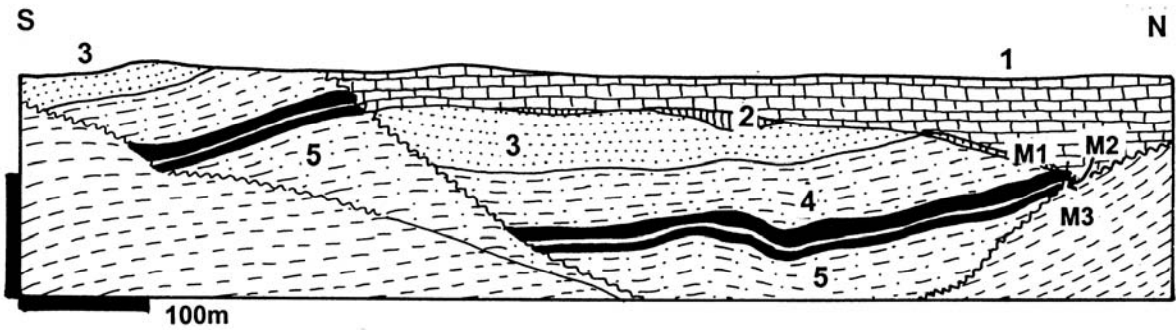
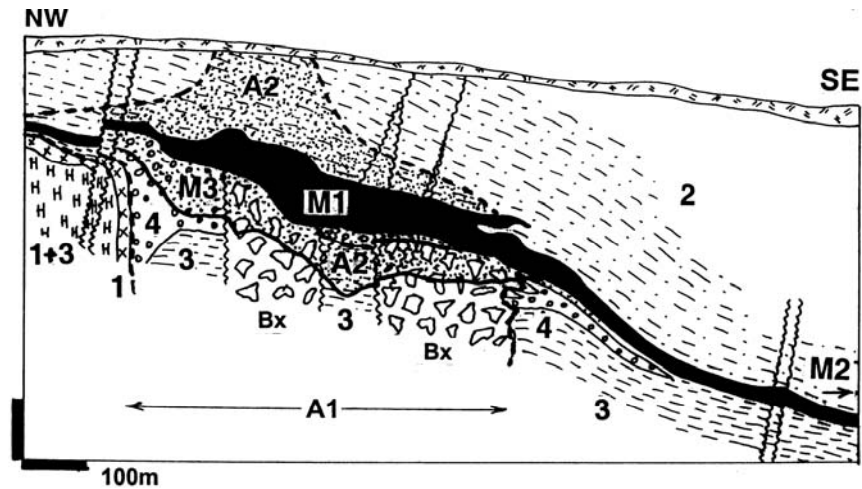


Figure 11.6. Century Pb-Zn-Ag deposit, Lawn Hill ore field, NW Queensland. Cross-section from LITHOTHEQUE No. 2996, modified after Broadbent and Waltho (1998). 1. Cm Georgina Basin limestone (cover); 2. Sub-Cambrian unconformity and paleogolith with residual deposits, karsting, phosphates; 3. ~1,595 Lawn Hill Fm. Unit Pmh5: siltstone, shale, sandstone; 4. Ditto, Unit Pmh4, ore-bearing; M. Two major sets of delicately laminated stratiform bands of fine Pb-Zn-Fe sulfides with siderite gangue in carbonaceous shale: M1, Upper Ore Zone; M2, barren shale and siltstone; M3, Lower Ore Zone. 5. Footwall units, alternating shale and siltstone with subeconomic sphalerite or barren floored by carbonaceous shale



M1. Main massive Fe-Pb-Zn sulfide mass, sheared then recovered; M2. Eastern Zone, five conformable Fe-Pb-Zn sulfide bands interbedded with sediments; M3. Footwall complex, a vent? zone veined and replaced by pyrrhotite, Zn, Pb sulfides, cassiterite; A1. Tourmaline alteration; A2. albite, chlorite alteration; 1. Mp gabbro dikes;

Figure 11.7. Sullivan Pb-Zn-Ag Mine, Kimberley, British Columbia; cross-section from LITHOTHEQUE No. 1468, modified after Hamilton et al. (1982). Explanations (continued): 2. ~1.45 Ga Middle Aldridge Fm., quartz-rich wacke; 3. Ditto, meta-argillite, minor wacke; 4. Ditto, intraformational conglomerate

In contrast with the classical sedex model the fragmentation and alteration, although most intense in the footwall, persist through the orebody into the hangingwall but some wallrocks remain virtually unaltered. In the west the footwall sequence is intersected by masses of breccia and it was collectively altered into as much as 40 m thick zone of fine, cherty-looking tourmalinite enveloped by chloritized and sericitized wallrocks and overlain by pyrrhotite >> sphalerite and galena laminated chloritic metasediments. Discordant quartz, calcite, and predominantly Fe, Zn, Pb sulfide veins also contain chalcopyrite, arsenopyrite and cassiterite. Given the large Sullivan tonnage, the average 310

ppm Sn in the ore represents some 50 kt of stored tin, although only a fraction of it has been recovered. This makes Sullivan the second largest tin deposit in Canada. The Main orebody in the western sector is a more than 50m thick abruptly thinning sulfide mass, dominated by pyrrhotite. The brecciated hangingwall is pervasively albite, chlorite, pyrite and carbonate altered.

In the east, the orebody is at most 36 m thick and it consists of four sulfide bands. The lowest Main ore band overlies the "Footwall Shale" (a phyllonite) with a sharp, unconformable contact. It consists of dense, fine-grained massive sulfide bands in which either pyrrhotite, sphalerite or

galena is the dominant sulfide. Sulfides compose up to 75% of the ore, the rest being quartz, some 15% calcite, minor chlorite, muscovite, local garnet and scapolite. Wallrock inclusions, attrition-rounded pyrite porphyroblasts and *Durchbewegung* fabrics are common and they grade into brittle breccia. The stratigraphically higher bands are more regular, fine grained, delicately laminated.

The deposit, with an approximate average time of emplacement quoted as 1.47 Ga, was multiply deformed between Mesoproterozoic and Eocene. The sulfides have been inhomogeneously retextured under predominantly ductile conditions to form spectacular folds known from museum specimens and textbook photos. The hangingwall sequence was transported to the NNE relative to the footwall along a low-angle overthrust and the ductile orebody acted as a *décollement* horizon. It has acquired inhomogeneously distributed tectonite fabric, deformational banding and fragmental character that includes the "ball ore" (McClay, 1983). The sedex genetic model is still considered valid (Lydon et al., eds., 2000) but the ore deposition was not simple and instant. The superimposed deformation and retexturing has produced post-depositional structures and textures that often visually mimic the syn-depositional ones, and disrupt the early deposit architecture.

Sedex-type Pb-Zn-Ag deposits, regardless of age, are summarized in Table 13.5, Fig. 13.23, Chapter 13.

11.4. Strata controlled Proterozoic copper deposits in (meta)sedimentary rocks

Copper in sedimentary rocks is a famous category of deposits, the second most important source of copper after the porphyry deposits (23.4% of the world's Cu, according to Singer, 1995). They are typified by the European Kupferschiefer (or Cu-shale) type; Cu-sandstone exemplified by the giant Dzhezkazgan, Kazakhstan (these two localities are Phanerozoic ore complexes described in Chapter 13); and the African Copperbelt (read below); Bartholomé, ed (174); Boyle et al, eds (1989). Some high-grade metamorphic Cu deposits, the origin of which is controversial (e.g. Aitik), appear in Chapter 14. In addition to sandstone, shale and their metamorphic equivalents, dolomite and mixed dolomite/clastics host many of the deposits included with the above types (Fig. 11.8).

The first order controls of the sediment-hosted Cu are the host lithology and stratigraphy, the second order is structure, the third order is the

presence of Cu source rocks along the direction of movement of the ore forming fluids. As discussed above, the latter are in many cases mafics undepleted in trace Cu, although the source relationship need not have been direct (e.g. basalt -> Cu deposit) but could have had an intermediary (e.g. basalt -> redbed sandstone -> Cu deposit). Although the classical models for the Cu-shale deposits assumed "syngensis" (that is introduction of copper with the host sediment during deposition followed by diagenetic fixing), and post-lithification Cu infiltration into porous sediments, new research leans more towards the post-sedimentation, epigenetic models. If so, publication titles that include the term "stratiform" (e.g. Boyle et al, eds, 1989) are basically incorrect, although this point usually disappears once the reader gets down to the actual detail in research papers. In Laznicka (1993, p.813-842) these deposits are included in a section entitled "Varicolored sedimentary association" to emphasize lithologic control and linkage to deposits of other metals like U, Pb, Zn, Ag. The African Copperbelt is described in some detail here as the outstanding type region.

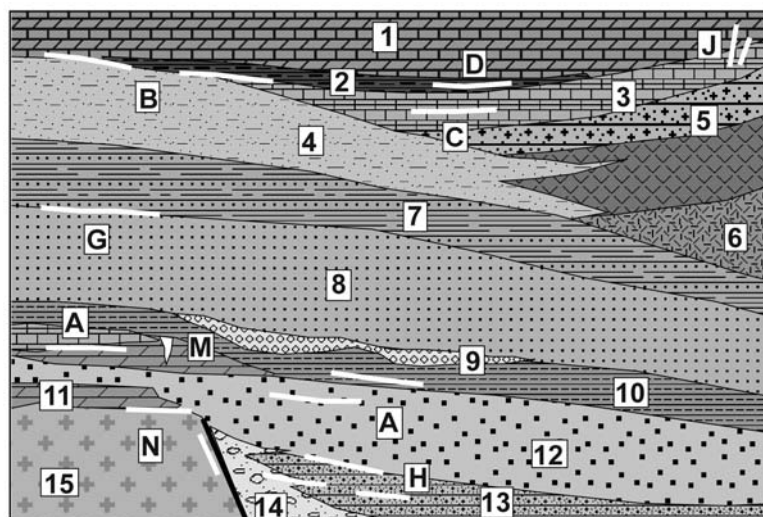
Deposits that qualify for membership in this category are quite common, but most are small. There are just two "supergiant Cu provinces" (African Copperbelt, ~219 mt Cu and 11 mt Co; Chara-Udokan, some 27 mt Cu), plus three "supergiant" and fourteen "giant" deposits and ore fields, twelve of which are included in the African Copperbelt. This indicates the scarcity and extreme irregularity of large metal accumulations of this ore type.

Lufilian Arc and the African Copperbelt

Lufilian Arc (Unrug, 1988; Fig. 11.9) is a Neoproterozoic, predominantly sedimentary intracratonic orogenic belt exposed in eastern Angola, in Shaba (alias the Katanga province of SE Congo-D.R.C.), and northern Zambia. The arcuate structure is up to 800 km long. It consists of the 1,100 to 600 Ma Katangan Supergroup with several basement inliers, and it hosts the African Copperbelt ores. The Copperbelt is a 520 km long, NW-trending metallogenic belt subdivided by political boundary into the Congo and Zambia portions. This is also a language boundary that affects the geological literature (French for Congo, English for Zambia) and, surprisingly, also an ore style boundary as the Congolese deposits (except for Musoshi) are in dolomitic hosts and have high cobalt contents, whereas the Zambian deposits are in low-carbonate "shale", "sandstone" and

"graywacke". I have put these lithologies into quotation marks as these rocks are, on the Zambian side, substantially metamorphosed so that a visitor to Mufulira, expecting to see a graywacke, is faced

with an amphibolite grade schist. But terminology based on the original lithology persists by tradition.



1. Limestone, dolomite, anhydrite; 2. Black metapelite; 3. Paleosabkha: mudstone, dolomite, evaporite clasts; 4. Arkose; 5. Basalt and volcaniclastics; 6. Rhyolite; 7. Interbedded sandstone, shale; 8. Red sandstone, subarkose; 9. Quartz-pebble conglomerate; 10. Siltstone, shale; 11. Dolomite; 12. Coarse arkose; 13. "Wash" to better-sorted sandstone; 14. Talus, fanglomerate; 15. Crystalline basement.

A. Cu, Co stratabound sulfide orebodies; B. Cu in dolomite at redox interface; C. Pb, Zn stratabound ores in laminated dolomite.

Figure 11.8. Proterozoic redbed and associated lithologies, diagrammatic cross sectional rocks and ores inventory from Laznicka (2004), Total Metallogeny Site G201. The rocks are mostly metamorphosed and deformed (the prefix meta- is omitted), but shown in their pre-deformational state. Explanations (continued): D. Metalliferous black pelites; G. Cu sandstone; H. U, Cu infiltrations in clastics; J. Cu replacements and veins in carbonates; M. Zn, Pb, Cu, etc. in breccia in carbonates ("Kipushi-type"). N. Cu fault and fissure veins, replacements

The up to 10 km thick Katangan Supergroup is subdivided into three Groups: the basal Roan, the middle Lower Kundelungu, and the upper Upper Kundelungu (François, 1974; Unrug, 1988). The Roan Group, up to 1,500 m thick and about 1,100-900 Ma old, is a lithologically very diverse "rift sequence" of thin basal continental clastics, followed by shallow marine terrigenous clastics and topped by chemical and biochemical sediments of carbonate platform and hypersaline lagoon. This is the principal host to the Copperbelt ores. The ~890 Ma, 3 km thick Lower Kundelungu is a glaciomarine succession grading to a monotonous shale and quartzite with local carbonate units. The ~700-600 Ma Upper Kundelungu is an about 3 km thick sequence of shallow-water sandstone, shale and minor carbonates. Deformed and altered mafic intrusions occur in the two lower groups.

The African Copperbelt is a major source of global copper (about 25%) and provides up to 80% of cobalt supply (Table 11.1). There are also two "large" Zn-Pb deposits (Kipushi and Kabwe) and a "large" and historically important uranium deposit

Shinkolobwe. The precious metals contents in the Copperbelt Cu-Co ores are very low. Most of the Shaba deposits had spectacular malachite stained outcrops and were known to the local population, although large scale mining started only around the year 1910. In Zambia, the orebodies in siliclastics are deeply leached and covered by a thick regolith so only two small deposits were known to the locals, the rest has been discovered by exploration later. The presence of "copper clearings" and Cu indicator plants helped.

Zambian Copperbelt

The SE-trending, south-eastern portion of the Copperbelt in Zambia is about 160 km long and 50 km wide (Mendelsohn, ed., 1961; Fleischer et al., 1976; Annels, 1984; ~88 mt Cu, 1.0 mt Co). Clusters of Cu-Co deposits occur on both limbs of the NW-trending Kafue Anticline, in two or three subparallel zones. A short zone of "Footwall arenite orebodies" (in meta-quartzite) is on the outer SW-margin of the Kafue Anticline (Chingola, Chibuluma, Kalulushi).

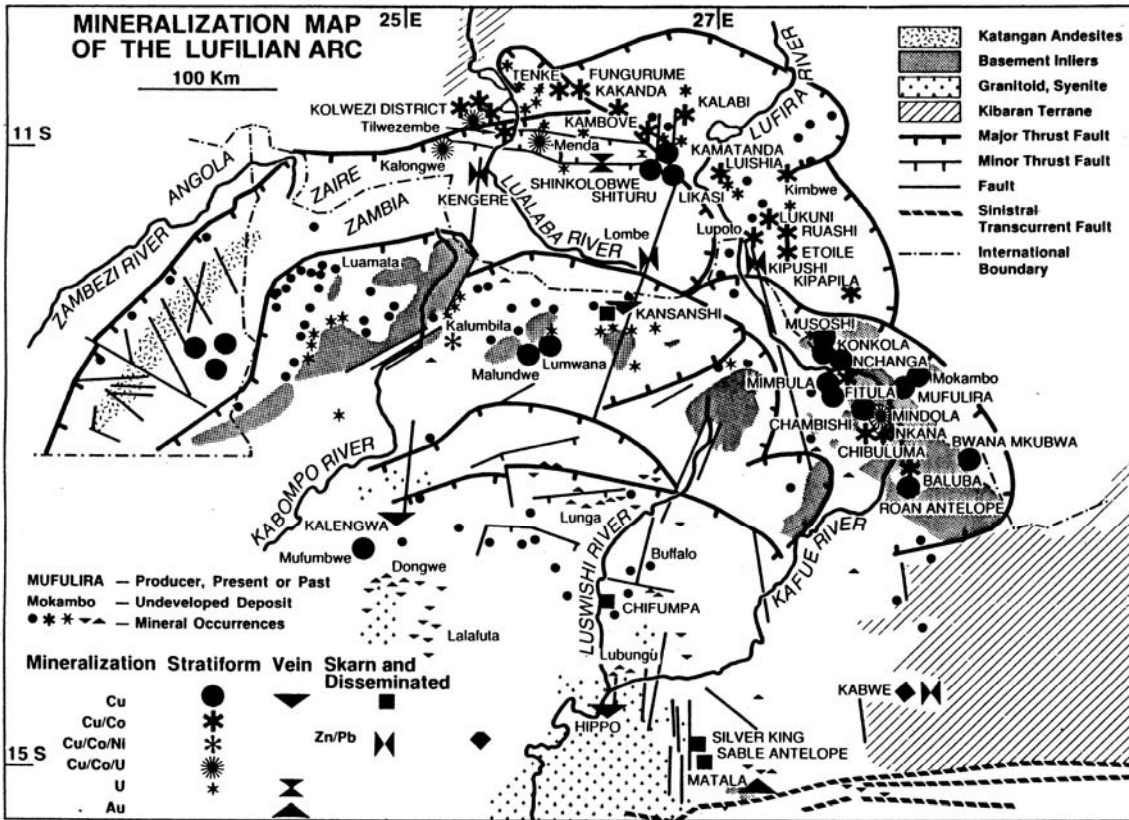


Figure 11.9. Map of the Lufilian Arc in Angola, D.R.C. Congo and Zambia, showing distribution of the Katanga Supergroup and its metallic deposits. From Unrug (1988), courtesy Economic Geology v.83:6, Fig. 3, p. 1250

It flanks the major "Ore Shale belt" on the inner side (Konkola, Chililabombwe, Nchanga, Chambishi, Nkana, Luanshya; Figs. 11.10, 11.11). The NE flank of the Kafue Anticline (Mufulira) contains "Sandstone orebodies" (in metagraywacke schist). The orebodies in many deposits are vertically stacked at several stratigraphic horizons and this contributes to a high degree of lithologic variability.

The pre-1.36 Ga basement is exposed in several structural domes. It consists of frequently sheared Lufubu biotite and hornblende gneiss, a variety of granites and gabbros, and remnants of the Muva metaquartzite and schist on top. There is a widespread although scattered and, so far, uneconomic copper mineralization in the basement that has the form of veins and stockworks in metamorphics, and stockworks and disseminations in granitoids. The Nchanga "red" granite directly under the productive portion of the Copperbelt has erratically distributed, but extensive, Cu sulfides and oxides in fractures above a shear (Garlick,

1973). The Samba "porphyry-Cu" (Rc 189 kt Cu @ 1.1%; Wakefield, 1978) comprises pyrite, chalcopyrite and bornite disseminations and veinlets in schist and biotite-muscovite metaquartzite. It is interpreted as metamorphosed quartz monzonite to granodiorite porphyry.

The ore-bearing Roan Group has been subdivided into the about 1,000 m thick Lower Roan, and 500-800 m thick Upper Roan (Mendelsohn, ed., 1961). Lower Roan is a continental to marine clastic sequence. It is close to the "rift stage" sequence (lacking, however, volcanics) deposited on a rugged, block faulted basement in a system of deep troughs interrupted by hills. As a consequence it rapidly changes facies over small areas and its lithology is influenced by local provenance of detritus (Gartlick, 1967). It hosts all the major copper orebodies described below. Upper Roan, on the other hand, is a dolomitic sequence interpreted as deposited on carbonate platform and as it lacks ores it is not further considered here.

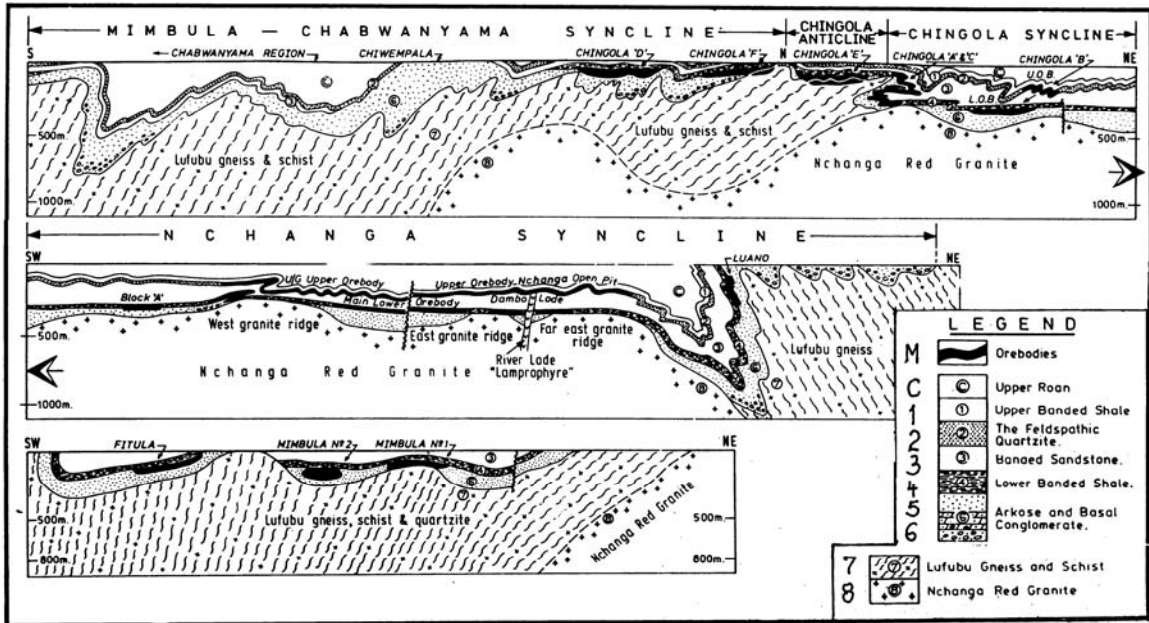


Figure 11.10. Cu orebodies in the Ore Shale Belt on the inner side of the Kafue Anticline, in the Nchanga ore field. Cross-sections from Diederix (1977), courtesy of the N.C.C.M. Corporation, Zambia

Footwall Arenite Orebodies. The **Chingola "F"** orebody (133 kt Cu @ 3.9%; Diederix, 1977) straddles the Katangan-Lufubu Gneiss nonconformity and is the most basal Cu orebody in the Copperbelt. Chalcopyrite and bornite precipitated in basal conglomerate and partly in the overlying arkose, as well as in the regolithic gneiss and schist under unconformity. The sulfides in gneiss form schistosity-parallel stringers and disseminations in the poorly sorted Lower Roan clastics. The orebody is 550 m long and has a high proportion of oxide ore, as well as refractory Cu held in hydrated mica. The somewhat similar **Mimbula II** orebody is a series of stacked ore lenses in a steep NW trending syncline of Lower Roan feldspathic metaquartzite with schist interbeds. The orebodies are rod-like shoots parallel to plunge and the set is 900 m long and about 150 m thick. An orebody has a core of disseminated bornite, chalcopyrite and chalcocite enveloped by malachite-chrysocolla oxide ore and by "invisible" refractory ore with Cu residing in vermiculite. The latter material is difficult and costly to process.

Ore Shale Belt: At the SW side of the Kafue Anticline the sedimentary succession generally starts with the Basal or Boulder Conglomerate that grades (on granite basement) into an "arkose", or

(over gneiss or schist) into micaceous phyllarenite. These are very immature, first cycle sediments, often gradational into their regolithic basement source rocks. Higher up, alluvial conglomerate and quartzite are better sorted and aeolian quartz arenite is locally present. "Transitional beds", believed of lagunar origin, comprise clastics with abundant anhydrite cement. On top of the transitional beds rests the "Ore Shale", an important marker and an ore host traceable for over 125 km. Orebodies are often designated as "footwall" or "hangingwall" in respect to the Ore Shale. The Shale is a 5 to 50 m thick grayish-green meta-argillite, laterally changing into carbonaceous meta-argillite. Anhydrite concretions are sometimes present.

Nchanga-Chingola ore field or Syncline (Fleischer et al., 1976; Diederix, 1977; 22.5 mt Cu @ 1.2-5.03%, 177 kt Co @ 0.3-0.49%) has orebodies in five stratigraphic intervals over a vertical range of 200 to 300 m. Of this, 32% of reserves are in the Footwall, 23% are in the Ore Shale, 31% are in the Hangingwall. 14% of Cu in the low-grade refractory material is in the capping. The **Nchanga Main Lower orebody** is one of the largest single orebodies in the Copperbelt, in which 55% of ore is in the Ore Shale proper, the rest is in the footwall arkose. Ore Shale here is a fine-grained, black micaceous siltstone to shale

mineralized by finely disseminated chalcocite laterally changing into chalcopyrite and ultimately into pyrite on the fringe. The Shale is up to 30 m thick and locally high in cobalt (up to 1% Co) in carrolite. The "arkose" hosted ore has disseminated chalcopyrite, cupriferous pyrite, minor bornite and chalcocite in a well sorted feldspathic metaquartzite. The **Nchanga Upper orebody** (Diederix, 1977) is on the southern limb of the Nchanga Syncline, has a total strike length of over 7 km, is about 30m thick and has been followed to a depth of 450 m. Crenulated Feldspathic Quartzite and basal portion of the Upper Banded Shale are tightly folded and locally overturned. The primary ore has disseminated bornite that changes with increasing depth into chalcopyrite with some carrolite. Secondary chalcocite gives way to cuprite, malachite and chrysocolla near surface.

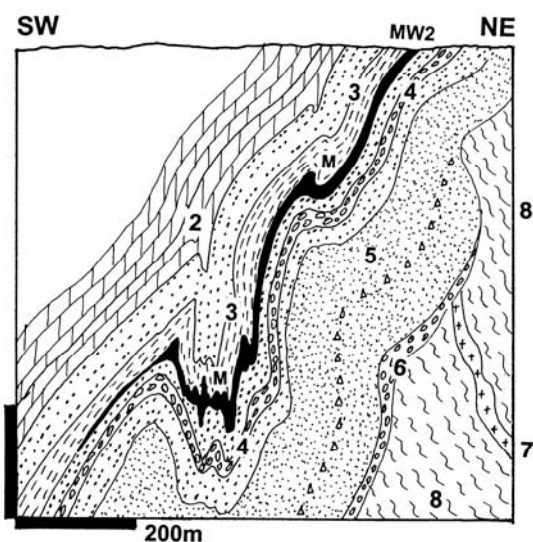


Figure 11.11. Zambian Copperbelt, Cu orebodies in the Nkana Syncline (Kitwe ore field). Cross-section from LITHOTHEQUE No. 1518, modified after Garlick (1976). M. Five major folded stratabound orebodies in two horizons, in the Ore Shale. MW. Oxidized ore; 2. Upper Roan, green pyritic meta-argillite, arenite, dolomite; 3. Lower Roan, hangingwall, similar rocks; 4=M, Ore Formation; mineralized meta-argillite with anhydritic mica arenite, arkose; 5. Footwall sequence, meta-arenite, aeolian quartzite; 6. Ditto, basal conglomerate; 7. Basement, Pp granodiorite, diorite; 8. Pp (~2.0 Ga) Lufubu schists

Sandstone Orebodies: **Mufulira** (Mendelsohn, ed., 1961; Fleisher et al., 1976; 11.07 mt Cu @ 1.18-7.28%) is the principal example in this group, located on the eastern side of the Kafue Anticline. The host rocks are relatively coarse fragmental

meta-arenites, underlain by a discontinuous unit of gypsum and anhydrite-bearing crossbedded aeolian quartzite that fills depressions in the Lufubu Schist. There are three stacked ore zones and numerous interhorizons (21 in total) with an aggregate thickness of 50-60m. The typical host is a "carbonaceous wacke", a greenschist-metamorphosed feldspathic and lithic phyllarenite. Pyrite, chalcopyrite, bornite and chalcocite change from fine disseminations into coarse blebs and small replacement masses, in hosts ranging from meta-argillite to conglomerate.

Shaba (Katanga) Copperbelt

This north-western portion of the African Copperbelt in SE Congo (D.R.C.) (Lombard and Nicolini, eds., 1962; François, 1974; 125 mt Cu, 10.30 mt Co) is about 250 km long and 70 km wide belt approximately between Kolwezi and Lubumbashi (formerly Elizabethville). About 236 Cu-Co occurrences there include 72 economic deposits and four large mining centers. The structural style there is different from the one in Zambia and it is a thin-skin tectonics (Unrug, 1988) combined with "extrusions" (diapirs) of the lower Roan rocks through the Kundelungu cover. These structures have the form of tight upward or northward-verging antiforms, some of which are thrust (e.g. the "Avancée de Kambowe"). All rocks are brecciated at a variety of scales.

In Shaba Copperbelt the contact of the lowermost Katangan with the crystalline basement is not exposed. The Roan Group is 1.3 to 1.8 km thick and subdivided into three formations. The basal R1 (or R.A.T. for roches argilo-talqueuses) is a hematitic dolomite shale to siltstone with sandstone and dolomite interbeds. The middle R2 (or Mines Formation) is a rhythmically banded detrital-carbonate succession and it hosts most of the Cu-Co orebodies. The upper R3 (Dipeta) Formation is a thick sequence of interbedded pelitic arenite and dolomite. The ore-bearing R2 has a Lower Ore Zone that consists of chloritic dolomite, locally with conglomerate lenses, resting on erosional disconformity, and of magnesite-rich and cherty dolomite. The Upper Ore Zone has dolomitic sandstone and dolomite interbedded with black pyritic slate. Both mineralized zones are separated by a usually barren R.S.C. interval (roche siliceuse cellulaire), which is a massive to bedded, often stromatolitic, porous siliceous dolomite. R1 is usually correlated with the mineralized Lower Roan in Zambia (François, 1974), and the Upper Ore Zone is "indistinguishable from the Ore Shale of

Zambia (Mendelsohn, 1989). Lefebvre (1989), on the other hand, considered the ore hosts in Shaba to be younger than those in Zambia. The style of Shaba mineralization follows from description of two contrasting examples below.

Kolwezi "lambeau": mineralized thin-skinned thrust sheets. **Kolwezi ore district** near the NW limit of Shaba Copperbelt (Bartholomé et al., 1973; François, 1962; 67 mt Cu @ 4-4.5%, 6.24 mt Co @ 0.4% Co) stores over 50% of copper and cobalt in the Shaba Copperbelt. This is an erosional remnant of a composite deformed thrust sheet of Lower Roan rocks, resting on the Kundelungu autochthon. The structure measures 25 x 12 km along the ENE axis and is believed tectonically transported to north-west for more than 60 km (François, 1962). The sole of the allochthon has an up to 100 m thick gouge to thrust sole breccia. Above is a "megabreccia", a collection of slices and blocks of the R2 dolomite-shale sets embedded in the R1 red hematitic and chloritic sandstone, topped by a thin conglomerate. A portion of the R1 is an internal breccia. The constituent ore fields: Musonoi, Kamoto, Kolwezi, Ruwe, Dikuluwe-Mashamba correspond to individual slices of the allochthon or to groups of slices, most of which have low dips.

The orebodies are stratabound sheets of chalcocite, digenite, bornite, chalcopyrite, pyrite and carrolite capped with a thick, spectacularly green oxidation zone. They occur at one or two stratigraphic horizons. The Lower Orebodies are in a massive chloritized and silicified dolomite just above the R1 red sandstone, along a redox interface comparable with one in the European Zechstein (Chapter 13). The Upper Orebodies, not always economic, are at the base of the S.D. Dolomitic Shale, a 35-90m thick unit of alternating laminated black dolomitic shale and siltstone (Bartholomé et al., 1973).

Avancée de Kambowe: ore-bearing brecciated and thrust-faulted cores of antiforms. **Kambowe ore field** (François, 1962; 8 mt Cu, 250 kt Co) is 20 km NW of Likasi (formerly Jadotville) in central part of the Shaba Copperbelt. This is a WNW-trending, 5.5 km long and 1 to 2 km wide anticlinal culmination, overturned and thrust over the monotonous Upper Kundelungu detritals. Internally this is a megabreccia assembled from numerous jumbled blocks and slices of the more competent R2 Formation, infilled and enveloped by meso- to microbreccia of the R1 to R3 and partly Kundelungu units. The numerous orebodies are disseminations and replacements of chalcopyrite, bornite, chalcocite, digenite and carrolite at three dolomite horizons of the R2 (cumulative thickness

70 m), separated by a 30-40m thick interval of barren shale to dolomite. The sulfides are extensively oxidized into malachite and chrysocolla at and near surface. Each megabreccia block or slice may contain folded or brecciated sheet-like orebodies bound to a favorable stratigraphic horizon, although not all blocks are mineralized. Table 11.1. is a summary of the Copperbelt deposits.

Kodar-Udokan Cu province, E-C Siberia.

This remote area is located about 320 km SE of Bodaibo (Lena Goldfield), in a short NW-trending Udokan Range SE of the Chara River, and the Kodar Range NW of the river. Most of the relevant literature is in Russian (Fedorovskii, 1972; Bogdanov et al., 1973), but there are some English translations, mostly specialist reports (Bogdanov and Golubchina, 1971; Samonov and Pozharisky, 1974). The up to 11 km thick intracratonic Proterozoic Udokan Series, similar in lithology to the Belt-Purcell Supergroup in North America, rests on Archean metamorphic basement. Of the three constituent sub-series most mineralized is the uppermost Kemen Group. In the western Udokan Range its 1 km thick lower division is a quartz-rich meta-arenite with abundant heavy mineral laminae and "black beds", interpreted as a subaqueous delta deposit. The central Upper Sakukan Formation is a 650m thick cyclic sequence of crossbedded feldspathic quartz arenite with calcitic cement and it hosts the Udokan Cu orebody. The overlying Namingu Formation is a gray to green metasiltstone with units of fine sandstone. Several "Cu-shale" interbeds are also known. The rocks are open-folded and greenschist metamorphosed, except near granitic intrusions where the amphibolite facies prevail.

Udokan Cu deposit, Namingu district (Krendelev et al., 1983; 1.2 bt ore @ 2% Cu for 24 mt Cu content) is a continuous WNW-trending mineralized horizon exposed in a structure about 10 km long, 3-4 km wide and 140 to 330 m thick. It is exposed in a symmetrical brachysyncline the northern limb of which dips 10-30° SW, whereas the southern limb is steep and locally overturned. The footwall and hangingwall sequences are both composed of crossbedded arkosic meta-arenite with several interbeds of slightly pyritic meta-siltstone. Detrital magnetite is abundant and several beds contain up to 20% of it. The copper orebodies have diffuse outlines.

Table 11.1. African Copperbelt, brief data on the principal Cu (Co) ore fields and deposits

Deposit/ore field	Geology, ores, references	Tons Cu /grade Tons Co/grade
NW portion of the Copperbelt (all in Shaba/Katanga, D.R.C. Congo)		
Kolwezi Thrust Plate (ore fields: Musonoi, Kamoto, Kolwezi, Ruwe); 270 km NW of Lubumbashi	Sub-greenschist; Lower Roan, complex allochthon thrust NW over Kundelungu. Megabreccia, slices of ore dolomite, 2 stratabound ore horizons; Ore Shale and Footwall orebodies equivalents; rich oxidation zone. Bartholomé et al. (1973); François (1974)	67 mt Cu/4.-4.5% 6.24 mt Co/0.4% Kamoto, 11.25 mt Cu Dikulwe, 10.8 mt Cu
Tenke-Fungurume ore field, 190 km NW of Lubumbashi	Sub-greenschist; Lower Roan, E-W synclinal thrust slice resting on Kundelungu. Two stratabound Cu-Co horizons on base of R2. Substantial oxidation zone (100 mt oxides). Demesmaeker (1962)	45.6 mt Cu/2.5-4.5% 3.27 mt Co/0.2%
Kambove and other fields, Likasi area, 145 km NW of Lubumbashi	Sub-greenschist; Lower Roan anticline composed of megabreccia thrust to NW over Kundelungu. Two stratabound Cu-Co horizons at base of R2. Substantial oxidation. Demesmaeker (1962).	~8.0 mt Cu ~250 kt Co
Lubumbashi district (Étoile and other ore fields)	Sub-greenschist to greenschist; Lower Roan in anticline thrust over Kundelungu. Two horizons of stratabound Cu on base of R2. Substantial oxidation zone	~6.0 mt Cu ~150 kt Co
SE portion of the Copperbelt in Zambia (Musoshi and Kinsenda are in Shaba/Katanga)		
Kinsenda, Congo; 70 km NNW of Kitwe	Lower Roan; four superimposed lenses in conglomerate under schist near basement granite. Lefebvre (1989)	1.36 mt Cu/4.5%
Mufulira, 30 km N of Kitwe	Lower Roan; 3 major ore zones, minor mineralization in 21 lithologic horizons; hosts: coarse "greywacke" (meta-phyllarenite) > schist, dolomite, quartzite; high proportion of anhydrite. Mendelsohn, ed. (1961); Fleischer et al. (1976)	11.07 mt Cu/1.18-7.28% Cu
Bwana Mkubwa (Ndola), 56 km ESE of Kitwe	Lower Roan; ore is in W-plunging tightly folded feldspathic and argillaceous metaquartzite above the Muva Quartzite basement. Mendelsohn, ed. (1961)	256 kt Cu/3.62%
Musoshi (Congo), 85 km NW of Kitwe	Lower Roan; footwall mineralization in "arkose" on NE flank of the Konkola Dome, E-W syncline. Cailteaux (1974)	4.62 mt Cu/2.1%
Konkola (Bancroft), Zambia and Chililabombwe, 75 km NW of Kitwe --Konkola Deep --Konkola North	Greenschist; Lower Roan; mineralized Ore Shale (siliceous schist) to dolomitic argillite on the E side of the Konkola Dome. Mendelsohn (1961), Cailteaux (1974)	17.03 mt Cu/3.06-4.06% Cu 12.92 mt Cu/3.8% 3.16 mt Cu/2.15%
Nchanga-Chingola, 50 km NW of Kitwe	Greenschist to kyanite, cordierite; Lower Roan, 2 synclines trending E-W north of Nchanga Granite dome; 32% Cu is in Footwall Orebodies, 23% in Ore Shale, 31% in Hanging-wall; large resource of refractory Cu in dolomitic mica-schist above Nchanga Orebody. Diederix (1977)	19.02 mt Cu/2.22%-5.03%. 177 kt Co 3.48 mt Cu/1.2% in refractory ore
Mimbula, 45 km WNW of Kitwe	Greenschist; Lower Roan; overfolded asymmetric complex, fold plunging NW; Footwall Orebodies at several horizons, 6 superimposed ore lenses over NW basement ridge. Diederix (1977)	243 kt Cu/2.7%

Table 11.1. (continued)

Deposit/ore field	Geology, ores, references	Tons Cu/grade Tons Co/grade
Fitula, 40 km WNW of Kitwe	Greenschist; Lower Roan; NW-SE asymmetric basin, Footwall orebodies in arkose on Lufubu Schist. Diederix (1977)	239 kt Cu/5.28%
Nkana (Rhokana), 5 km S of Kitwe	Greenschist; Lower Roan; NW-plunging syncline, 13 m thick ore formation rests on basal conglomerate+sandstone in Ore Shale; folded, W dipping. Fleischer et al. (1976)	14.69 mt Cu/2.22-3.37% 417 kt Co/0.15%
Chibuluma South Chibuluma (Kalulushi), 15 km W of Kitwe	Greenschist; Lower Roan, Footwall orebodies in a WNW syncline; in sericite-rich quartzite with basal conglomerate, main mineral is chalcopyrite. Arcuate orebodies on S flank of the Basin. Fleischer et al. (1976)	2.51 mt Cu/1.36-4.74%
Chambishi, 25 km NW of Kitwe	Greenschist; Lower Roan; major orebody is in the Ore Shale, in a WNW syncline; 2 minor orebodies are in Footwall and Hangingwall. Fleischer et al. (1976)	3.88 mt Cu/2.31-2.88%
Baluba, 33 km SSE of Kitwe	Lower amphibolite facies, scapolitized rocks; Lower Roan; 2 orebodies in Ore Shale, at perimeter of a WNW Basin, hosted by scapolitic micaschist, dolomite, tremolite schist. Fleischer et al. (1976)	2.27 mt Cu/2.35-2.56% 112 kt Co/0.16%
Luanshya (Roan Antelope), 40 km SSE of Kitwe	Lower amphibolite facies; Lower Roan; tight NW syncline, mineralized Ore Shale horizon on both limbs. Brummer (1955), Fleischer et al. (1976)	7.75 mt Cu/2.41-2.91%

All deposits contain chalcopyrite, bornite and chalcocite; those with Co also carrollite

They are discontinuous tongues, lenses and anastomosing sheets of mineralized rock within the ore horizon. The multistage mineralization has up to seven generations of sulfides (predominantly chalcopyrite and pyrite, some bornite) and associated minerals (Krendeliev et al., 1983). The early generation of disseminated sulfides is interpreted as diagenetic, ranging from authigenic to late diagenetic replacing early cements, pyrite and clastic magnetite. Subsequent generations of Cu minerals come in short fracture veinlets and are attributed to fluids active during "katagenesis" (post-lithification diagenesis) and thermal metamorphism due to granite and diabase intrusions in the area. Postmagmatic hydrothermal activity produced some fracture-controlled K-feldspathization and quartz-K feldspar veining, followed by retrograde sericitization and chloritization. Quartz, chlorite, calcite, magnetite, chalcopyrite, bornite and chalcocite veinlets formed as well. The oxidation zone is thin and spotty, deeply eroded and mostly removed by Quaternary glaciation.

The second largest Cu deposit in the area, **Krasnoye** (Narkelyun et al., 1977) is about 60 km

ENE of Udokan and some 4,000 m stratigraphically below. The ore-bearing succession here is 750-1,000 m thick and it hosts seventeen 1.6 to 23 m thick mineralized lenses in a NE-trending syncline. Chalcopyrite and pyrrhotite are the main minerals, bornite and pyrite are less frequent.

Additional "Cu-giants": There are not many Proterozoic deposits that would qualify left. **White Pine Mine** in Michigan (10.3 mt Cu @ 1.2%) has two stratabound horizons of shale and sandstone with chalcocite and native copper, respectively, in Neoproterozoic lacustrine sediments. They are members of the Keweenaw Rift succession described in Chapter 12. The undeveloped **Kona Dolomite Cu** horizon, also in Michigan (Kirkham, 1989), has Rc of 1 bt of material @ 0.3% Cu disseminated in Paleoproterozoic arenite unit on top of dolomite and metapelite that, in turn, rest on granitic basement. Spar Lake and Rock Creek in Montana; Nifty in the Patterson Ranges of Western Australia; and Redstone in the Canadian Cordillera are "large" deposits. The **Dongchuan belt** in Yunnan is probably a "giant" (? 6 mt Cu), with Cu sulfides replacing reduced carbonate resting on redbed clastics.

11.5. Au and U in quartz-rich conglomerates (Witwatersrand-type)

Mature quartz-rich, well-sorted, probably fluvial conglomerates, comparable with the Witwatersrand Au+U "reefs", are known from at least 30 regions of the world and they have been repeatedly investigated for Au and U. Almost all are Proterozoic or "Proterozoic-like", as the type area in South Africa is now known to be Late Archean. So far, however, only one "Au-giant" (Tarkwa; Chapter 9), one "large" gold deposit (Jacobina), and one "giant" uranium district (Elliot Lake) of comparable type have been discovered outside the Rand. Steady new discoveries and extensions of existing orebodies, however, have continued in the Witwatersrand confirming the effectiveness of the "brownfield" exploration.

These conglomerates consist of well-rounded clasts of white, gray and occasionally black quartz of vein and pegmatite derivation, sometimes "chert". Unstable lithic clasts and angular quartz clasts are minor, but indicative of multiple provenance. The matrix is a mixture of quartz grains and muscovite, sericite or chlorite. Mature, clast-supported conglomerates grade into matrix-supported rocks where the matrix is believed to be epimatrix, that is product of late diagenetic to metamorphic disaggregation and conversion of the original unstable (lithic) clasts. There is a variable proportion of heavy minerals like ilmenite, zircon, monazite, rutile, chromite, sometimes magnetite, and pyrite that come in many forms (clasts, nodules, replacements, veinlets, etc.). High carbon substance and fuchsite are common.

The bulk of conglomerates are basal members of the upward-fining sequences, resting on mature (cratonic, high-grade metamorphic) basement unconformity either directly, or as lithosomes in a sedimentary suite that also includes sandstone, shale, carbonates and lava flows (Fig. 11.12). Many conglomerates are members of the rift association, or they occur in fault-bounded grabens. Mineralized "paleoplacers" of this type include Elliot Lake (U), Jacobina (Au, U), Dominion Reef (Au, U) and Pongola (Au). The minority of conglomerates are intraformational, but as they include all the "reefs" in the Central Rand Group they store the bulk of gold and about one half of uranium. These conglomerates occur at low-angle (up to 4°) disconformities within a cyclic sequence of quartz-rich sandstone, "poudingue" (scattered quartz pebbles in sandstone), some shale and occasional basalt flows.

Witwatersrand Basin Au-U province

Witwatersrand "Basin" is an elliptical area measuring about 350 km along the NE axis, 200 km along the NW axis, occupied by the Late Archean Witwatersrand Supergroup (Fig. 11.13). The present "Basin" bears little resemblance to the original depositional basin and, most recently, it has been interpreted as an erosional remnant of a Paleoproterozoic uplift triggered by the Vredefort meteorite impact event. Much of the Supergroup is in deep subcrop, with outcrop and shallow subcrop present only in a discontinuous arc along its northern (Johannesburg, Klerksdorp) and southwestern (Welkom) margins, and around the Vredefort Dome in the centre. The area of the Witwatersrand Supergroup outcrop/shallow subcrop is estimated at about 13,000 km² and it contains seven major areas of concentrated Au-U mineralization (called goldfields) plus a dozen of scattered minor deposits and occurrences (Table 11.2). Until 2004, the Rand has produced about 52,000 t gold out of the estimated 130,000 cumulative world gold production, and it is credited with the past production plus resources of 109,000 t Au (JCL Ltd. Annual Report, August 1997); I have managed to account for some 76,390 t Au by adding the reasonably reliable production and resource figures from the individual goldfields. Whatever the true figure, there is no doubt that the Rand is an exceptional metallogene without parallel, yet an extremely enigmatic one. Continuing research and flood of publications keeps refining our knowledge about sedimentogenesis of the Rand conglomerates and about the mechanism and timing of gold emplacement, but what remains as elusive as ever is the "Factor X": what was the source of gold, and what caused such a phenomenal local supply of gold within a relatively brief period of earth history.

The Witwatersrand literature is overwhelming and it falls between two end-members of essentially descriptive "facts", and specialist interpretations. Blocks of "facts" are gathered in Haughton, ed. (1964) and Anhaeusser and Maske, eds. (1986). Facts have not changed much with time. Tankard et al. (1982) treated the Witwatersrand Triad in the context of evolution of southern Africa. Pretorius (1991), Robb et al. (1997) and Robb & Robb (1998) have written good summary papers that include the interpretations to start with. The brief but comprehensive review in Laznicka (1993, p.776) provides list of selected references until 1990 classified by subject.

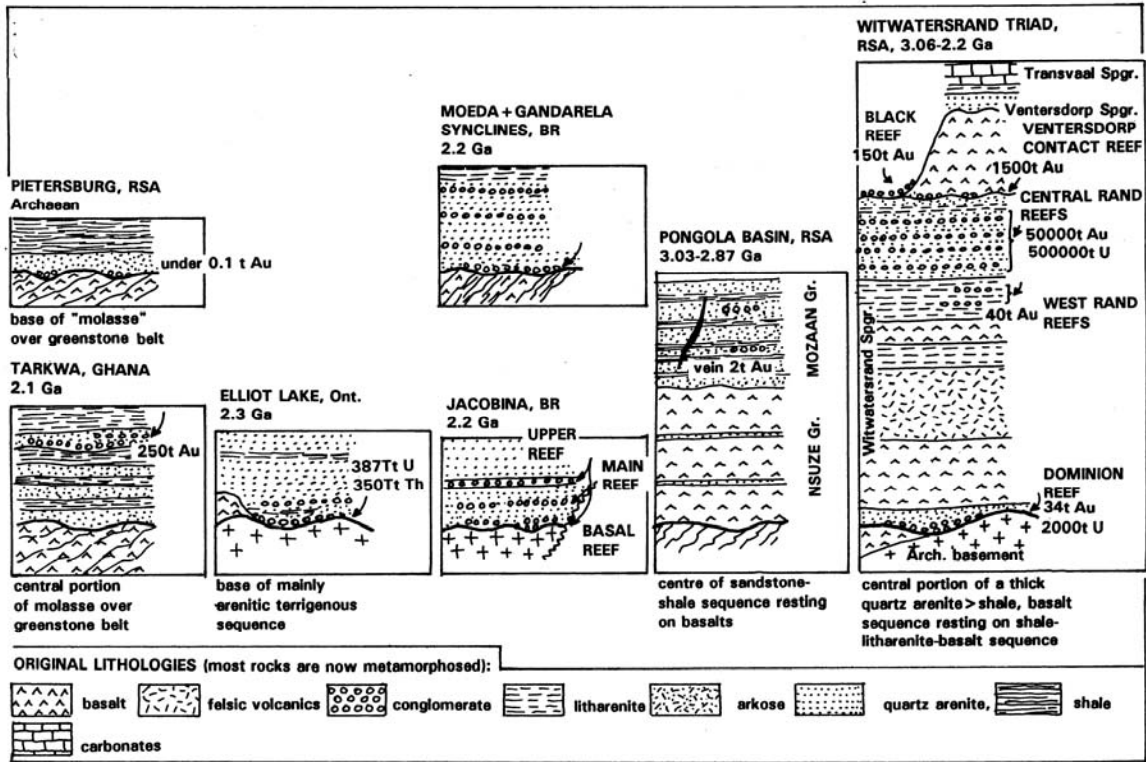


Figure 11.12. Diagrammatic representation of setting of the Witwatersrand-like Au, U and PGE-bearing mature quartz conglomerates. From Laznicka (1991, 1993)

Setting, stratigraphy, lithology: The Late Archean (2,914 to 2,780 Ma) Witwatersrand Supergroup is the middle member of the Witwatersrand Triad (Tankard et al., 1982), an up to 18 km thick mature, intracratonic-style sedimentary and volcanic sequence deposited in a system of progressively widening basins on the previously consolidated Kaapvaal Craton. The basement is a typical Archean granite-gneiss terrain with small greenstone belt relics, intruded by synorogenic to postorogenic granites as young as 2.68 Ga but none that intrudes the Triad succession.

The earliest **Dominion Group** (3.06 Ga; Minter et al., 1988) is up to 2,710 m thick and it is a distinct "rift sequence". The 60 m thick clastic unit includes two conglomerate beds interpreted as channel bars, with small paleoplacer deposits. The up to 3 m thick basal placer contains erratically distributed gold and uraninite but the total production recorded from the Klerksdorp goldfield was only 25.75 t Au and 1,931 t U. The terrigenous basal unit is overlain by 1,100 m of continental amygdaloidal basalt flows with minor tuff,

separated by paleosol and quartzite horizons, on top of which is a 1,550 m thick pile of rhyolite and dacite flows, breccias, tuff and paleosol.

The **Witwatersrand Supergroup** consists of the lower, predominantly tidal to shallow marine, West Rand Group and upper, predominantly fluvial-deltaic, Central Rand Group. The **West Rand Group** underlies the entire Basin. It varies from 830m to 7,500m in thickness and it consists of marine shale and semi-mature arenite with several thin deltaic to fluvial conglomerate interbeds. Three conglomeratic units ("reefs") are slightly auriferous, with some 40 t Au recovered so far. There is also a 250m thick unit of amygdaloidal basalt flows with flow breccia on top. In the lower part of the Group is the "contorted iron formation", a thin laminated magnetite-rich siliceous argillite contorted along a décollement plane of a small thrust. Although the Fe content is only 35%, this is an important marker horizon that crops out in the metropolitan Johannesburg (near the Witwatersrand University), and a unit with distinct magnetic signature that can be traced in the subsurface.

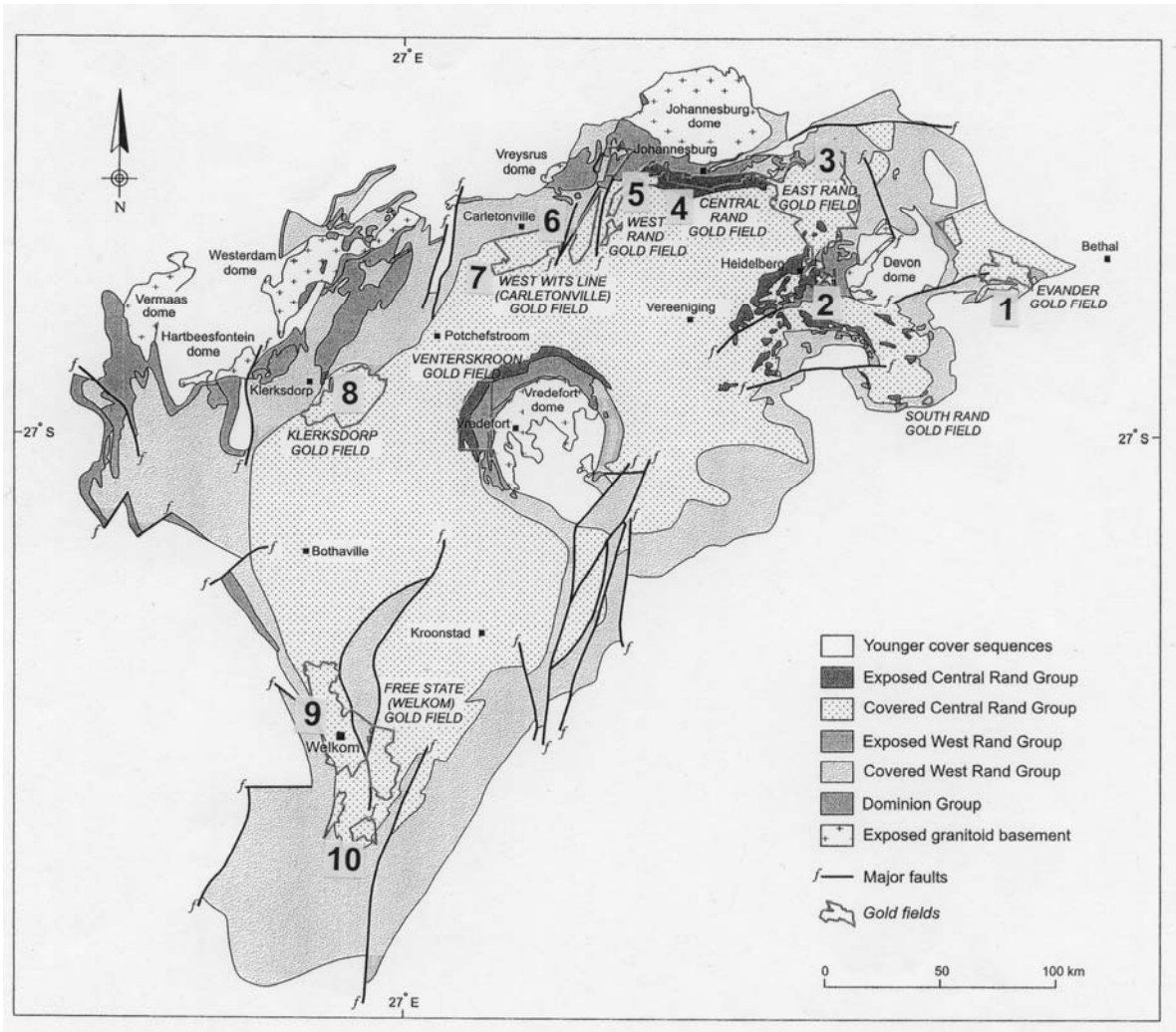


Figure 11.13. Map of the present outcrop and subcrop of the Witwatersrand Supergroup in the Kaapvaal Craton, South Africa. Reprinted from Robb and Robb (1998), courtesy of the South African Council for Geology, Pretoria. Numbers of the significant goldfields and deposits have been added and they correspond to the entries in Table 11.2

Central Rand Group is the principal host to the Witwatersrand Au-U conglomerate horizons ("reefs"). The Group has a discontinuous distribution, believed deposited, under compressional conditions, in many small sub-basins located on subsiding fault-bounded blocks. About 18 such blocks have been recognized so far (Meyer et al., 1990) and recognition of the fragmentary nature of basins is important in search of additional possibly mineralised "forgotten outliers". The small basins accumulated up to 2,880 m of strata dominated by quartz sandstone with minor conglomeratic units, two or more thin amygdaloidal basalt flows, and infrequent slate. The gold everywhere resides in conglomerate sheets and

there are several tens of such sheets in three major groups within the Central Rand Group, and one (the Ventersdorp Contact Reef, VCR) on top of it. The intraformational "reefs" are aggradational sediment packages resting on low-angle (<4°) erosional disconformities, believed deposited in alluvial fan or braidplain, although some authors consider lacustrine or marine delta or even shallow offshore. The VCR is a degradational feature, a gravel mantle on incised piedmont, captured while "on the move" and preserved under contemporaneous lava flows (Reimold and Viljoen, eds., 1994).

Table 11.2. Brief summary of the Witwatersrand goldfields (P+Rc >250 t Au)

No	Goldfield	Location	Discovered (mined since)	P+Rc, tons Au
1	Evander (Kinross)	120 km ESE of Johannesburg	1951 (1958)	2,772
2	Nigel Reef	40 km SE of Johannesburg		642 t
3	East Rand	25-60 km ESE of Johannesburg	1890s	9,511
4	Central Rand	Johannesburg metropolitan area	1886 (1888)	9,072
5	West Rand	25-40 km W of Johannesburg	1890s	9,710
6	West Wits (Carletonville)	35 km W of Johannesburg	1934	19,936
7	Far West Rand (Eilandsrand, Deelkraal Mines)	50 km WSW of Johannesburg	1990s	2,019
8	Klerksdorp	160 km SW of Johannesburg	1886	7,174
9	Free State (Welkom)	270 km SW of Johannesburg	1934 (1946)	16,196
10	South Free State (Joel & Beatrix Mines)	20 km SW of Virginia	1970s-1980s	1,331
	Witwatersrand total		1886	65,500

All gold production and resources in the goldfields with more than 250 t Au came from reefs in the Central Rand Group and from the Ventersdorp Contact Reef

The Central Rand sedimentary rocks range from supermature, well-sorted and locally crossbedded quartz arenite through matrix-rich quartz wacke to lithic arenite. Although the bulk of sediments is terrigenous, some of the massive greenish-brown weathering mudstones and diamictites could be argillized mafic flows. The shale horizons, many of which are eroded disconformity surfaces topped by new upward-fining cycles, are often highly aluminous and regolithic attaining up to 35.8% Al₂O₃ and 30.3% TiO₂ in places.

Ventersdorp Supergroup is the areally extensive (~200,000 km²) and up to 7,860m thick cover sequence of the productive strata, barren of metals. It is composed predominantly of 2.74 Ga continental basalt flows with interbedded clastics, emplaced under conditions of crustal extension.

Au and U mineralization, the Witwatersrand conglomerate "reefs": Surprisingly, there is no other style of mineralization than the "reefs", not counting the potential resource of a very low-grade gold (~1 g/t Au and less) in some quartzites and shales adjacent to the payable "reefs" (Phillips, 1987), and perhaps also in the West Rand Group. Although 1 g/t Au is now a viable ore in many parts of the world, the great depth and difficult geotechnical conditions render this resource in the Witwatersrand uneconomic for a long time to come. Moreover, 98% of Au and U is in, and on top of, the Central Rand Subgroup with very small quantities in the Dominion Group, West Rand Subgroup, and Black Reef Group.

The first viable ore discovery was made by George Harrison in 1886, in an oxidized conglomerate outcrop on the farm Langlaagte near present day Johannesburg in the Central Rand; the site has been preserved. Mining started the next year and similar outcrop discoveries followed near Klerksdorp and in East and West Rand. After a period of following the outcropping and adjacent reefs into great depth, a period of "greenfield" discoveries of concealed reefs started in the 1930s with discovery of the West Wits and later Welkom (Free State) goldfields. In this, the early application of magnetometry helped to trace the Magnetic Shale marker in depth west from its shallow subcrop area in West Rand, then drill for the Central Rand strata stratigraphically above it. The deep search continues with gold resources at the Western Ultra Deep Levels proven to 5,000 m depths.

The Witwatersrand production and resources of 76,390 t Au are shared by seven (or eight) major goldfields in the Gauteng, Mpumalanga and Free State Provinces (formerly Transvaal and Orange Free State). West Wits (Carletonville) Goldfield has the greatest share (19,936 t Au) followed by Welkom with its extension near Virginia (16,196 t Au), and Central, East and West Rand (each 9,000 t Au plus). The gold grade varied from about 5 to 21 g/t Au, the average being 7.5 g/t in the 1990s (Robb and Robb, 1998). About 120 mines have operated in the Rand throughout the history. Every goldfield, except Evander, has produced from more than one reef so it is difficult to collect data for individual reefs that constitute true continuous orebodies. The Basal Reef (Welkom Goldfield; 4,500 t Au) is

probably the world's richest single continuous orebody, followed by the Carbon Leader (West Wits Goldfield, 3,164 t Au). The Main Reef conglomerate group, 6-45 m thick, continues for about 160 km and has produced 22,107 t Au. It is followed by the Bird Reef group (11,392 t Au). About 120 kt of uranium has been produced until the late 1990s (Pretorius, 1998) and there is a theoretical resource of some 473 kt U left although it is doubtful that much more would be actually recovered as U has always been a by-product of Au mining. The U grade varies from about 80 to 500 ppm; it has been 183 ppm in the Klerksdorp Goldfield (46 kt U produced), 358 g/t in West Rand.

Reefs and reef packages within the Central Rand Subgroup: Most of the Witwatersrand gold is in 1-2 m thick "reef packages" distributed along the northern and (Welkom) south-western extremity of the Central Rand outcrop and subcrop area, near basement granite domes and close to the points of entry of sedimentary detritus into the basin. About 30 reef packages (reefs, placers) are known. Some are very extensive: the Basal and Steyn Placers in the Welkom Goldfield cover 400 km². The Vaal Reef in the Klerksdorp Goldfield covers 256 km², is up to 1.6 m thick, and has an average content of 500 ppm U and 15 g/t Au (Antrobus et al., 1986).

A typical reef package (Minter et al., 1988; Fig. 11. 14) consists of a footwall of shale or quartzite topped by a low-angle unconformity (erosion surface). The sub-unconformity surface is often scoured and leached (paleoregolith) and often coated by carbon. The carbon is interpreted as an algal? residue or infiltrated pyrobitumen that postdated the reef formation. Almost pure carbon forms black seams and lenses with columnar partition and it grades into conglomerate or arenite with carbon matrix. The carbon tends to be enriched in Au, U and other metals with locally extreme values. The conglomerate rests above the carbon seam or directly on the unconformity. This is a 5 to 30 cm thick blanket composed of white, gray to black well-rounded vein quartz clasts with a variable proportion of lithic clasts. The matrix is a mixture of quartz grains with silicates (metamorphic sericite, chlorite, chloritoid), some heavy minerals, pyrite and gold. Gold is predominantly free-milling, in particles scattered throughout the matrix and in/on pyrite. The shape of gold ranges from demonstrably clastic, rounded or toroid-shaped particles (Minter, 1999) through pseudoclastic grains where gold replaces fully or partially detrital grains like quartz or magnetite, to chemically precipitated microfracture fillings, pyrite

coatings, filaments. Colloidal gold resides in carbon. U resides in uraninite and minor brannerite.

Several reef packages combine with products of intense erosional channeling which either predated the reef deposition, or postdate and erode the reef. In the East Rand Goldfield (Antrobus and Whiteside, 1964) channels formed in Jeppetown Shale under the Main Reef Leader contained up to 100m thick and 1,660 m long fill of usually pyritic quartzite with scattered pebbles and conglomeratic lenses. Although erratically distributed, 24.4 t Au was recovered from channels at the Brakpan property.

Ventersdorp Contact Reef (VCR). VCR (Reimold and Viljoen, eds., 1994; 3,062 t Au produced mainly from the West Wits and Klerksdorp Goldfields; Fig. 11.15) is the stratigraphically highest reef formed along the low-angle unconformity between the Witwatersrand Supergroup below and the Ventersdorp Supergroup above, especially under its lower Klipriviersberg basalt pile. The Reef varies in thickness from zero to about 5 m (anomalous thicknesses are reached over synsedimentary faults) and it is gold-bearing only when it truncates the auriferous portion of the Central Rand Subgroup. VCR is thus a "secondary" placer produced by cannibalization of earlier placers, and the only reef the gold source of which is known. In contrast to the Central Rand reefs VCR is interpreted as a gravel arrested in transit by contemporaneous Westonia komatiitic lava flows, without which it would have self-destructed. The placer consists of locally derived gravels present in a fluvial channel and terrace system cut into pediment. There is a locally intense hydrothermal alteration dominated by chlorite with some albite, sericite and carbonates with minor pyrrhotite, chalcopyrite, sphalerite and galena. This is attributed to high permeability that provided conduit for later stage hydrothermal fluids.

Witwatersrand origin and history: Like most enigmatic ore deposits, published genetic interpretations have kept changing with times, popular models of the day, and bias of the investigators. As usually, selected evidence has often been used to make a case even if the rest of the evidence suggested otherwise. The history of genetic concepts until the late 1980s has been critically reviewed by Pretorius (1991). Although the clastic nature of the reef conglomerates was recognized early and has rarely been in doubt, opinions have differed on the source, mechanism and timing of gold and uranium introduction.

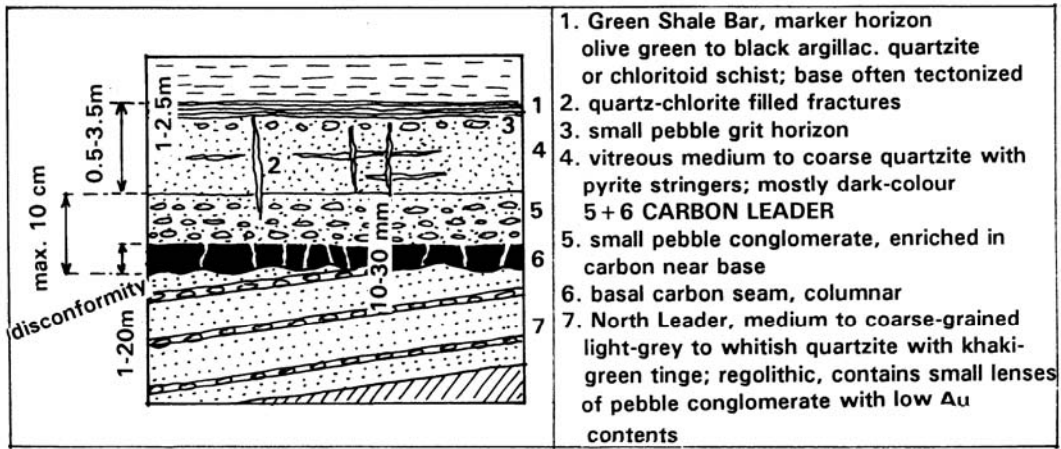


Figure 11.14. A typical "reef package" representative of the Carbon Leader, West Wits Goldfield. From Laznicka (1991, 1993), based on data in Engelbrecht et al. (1986)

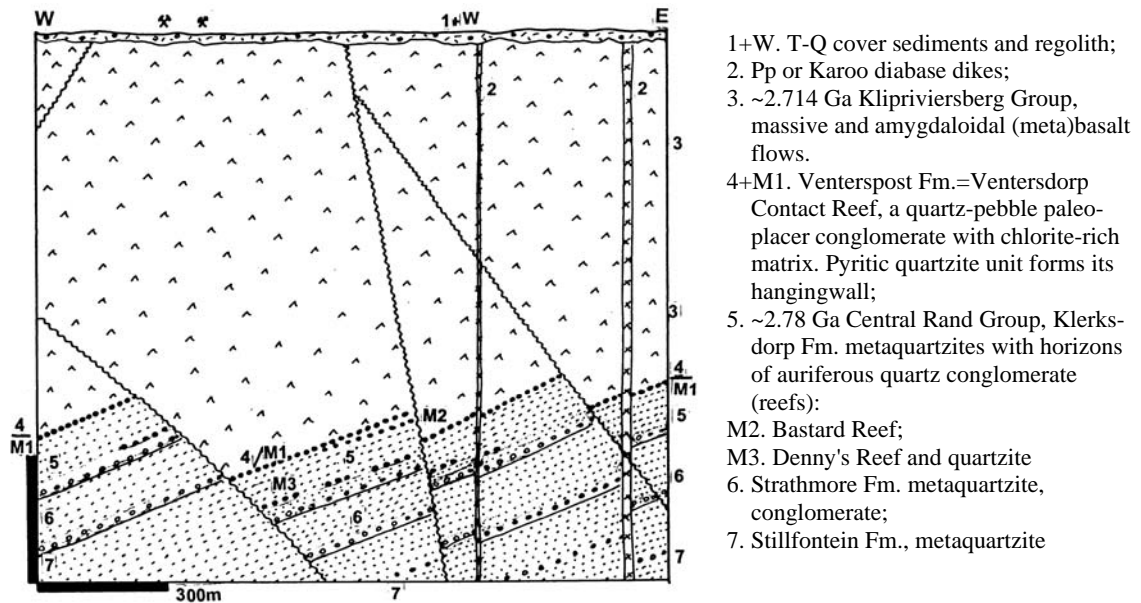


Figure 11.15. Klerksdorp Goldfield, Tau Lekoa (Vaal Reefs #10) mine, showing the Ventersdorp Contact Reef (VCR) segmented by faults. Cross-section from LITHOTHEQUE No. 2758, based on de Vries (2001), Gartz and Frimmel (1999) and 2001 visit

Except for a brief attempt to apply submarine exhalations to the Rand origin, the contest has been between the proponents of clastic gold and uraninite (e.g. Minter, 1999: "irrefutable detrital origin") and hydrothermal emplacement (e.g. Phillips and Myers (1989). In the past decades a compromise "modified detrital" model has developed that takes into account the multistage and polygenetic nature of the orebodies and record/interpret the changes that took place during the long "active" history of the reefs.

Robb et al. (1997) recognized the following stages of reef evolution:

- 1) Clastic sedimentation between 2,894 and 2,714 Ma. Introduction of epiclastic gold, uraninite, pyrite and a variety of detrital minerals into a largely subaerial alluvial system to produce several giant paleoplacers. This was shortly followed by early diagenetic growth of authigenic minerals (e.g. pyrite) and modification of some ore clasts, including gold,

by dissolution/precipitation. The Cenozoic "deep leads" in the Victorian goldfields (Chapter 10), many preserved under basaltic flows, demonstrate the viability of this concept as they contain both clastic gold, (semi)authigenic nuggets, as well as pyrite formed in reducing microenvironments. The stability of uraninite under subaerial conditions, however, required reducing atmosphere: a subject of many papers published in the 1970s. The incredibly productive Au and U source rocks, however, have not been identified and remain hypothetical.

- 2) Early intrabasinal authigenesis around 2,550 Ma, perhaps assisted by the heat from granites in the area. More pyrite formed.
- 3) Intrabasinal maturation of syndepositional (e.g. algal) and migratory hydrocarbons around 2,350 Ma. Redistribution of some local metals into bituminous nodules; hydrocarbon attack and encapsulation of some uraninite clasts.
- 4) Peak metamorphism (to greenschist facies) of the Witwatersrand Supergroup around 2,050 Ma (about contemporaneously with emplacement of the Bushveld complex) and 2,025 (Vredefort impact event). Late sulfides formed (pyrite, pyrrotite, chalcopyrite, galena, sphalerite, gersdorffite) and metamorphic fluid circulation produced locally intense alteration (such as chlorite, albite, sericite, carbonates) in the Ventersdorp Contact Reef and widespread reprecipitation of gold. This stage accounts for most of the metamorphic, hydrothermal and epigenetic features observed in the ores.
- 5) Since about 2.0 Ga the system was in mothballs, until the Cenozoic exposure of a small portion of the ores at the surface, oxidation and leaching. Due to the generally flat nature of the Witwatersrand, no major recent placers formed.

Example Witwatersrand goldfields

Central Rand. This discovery goldfield (P+Rc 9,072 t Au @ 8.33 g/t) is a 50 km long east-west strip centered on Johannesburg (Fig. 11.16). Here, the Witwatersrand Triad rests on Archean basement of the Johannesburg Dome and dips 60° to the south. The central Rand Subgroup is 2,860 m thick and it hosts six reef groups. The principal Main Reef, 1.5 m thick on the average, is overlain by the Main Reef Leader. The Reef is continuously mineralized over a strike length of 36 km. Several mines between Roodepoort and Boksburg produced gold from banded pyritic quartzite interpreted as

channel fill deposits. Central Rand was a region of early mining responsible for tailing dumps that are part of the scenery at the southern fringe of Johannesburg. It included the most productive property of the Rand's mid-life period, the Crown Mines (Pt 1,412 t Au).

West Wits Line (Carletonville Goldfield; Engelbrecht et al., 1986; P+Rc 19,936 t Au). This entirely concealed goldfield merges with the West Rand Goldfield and it contains the Rand's largest and deepest mines: Driefontein Consolidated and Western Deep Levels. Following the drill discovery in the 1930s exploitation was long delayed while awaiting the arrival of technology capable of penetrating and sealing the aquifer in the Transvaal dolomite that blanket most of the area. The goldfield is subdivided into three major fault blocks that coincide with depositional sub-basins, each of which contains different selection of productive reefs. Most of the historical gold came from the Carbon Leader (~3,164 t Au @ 20.9 g/t; Fig. 11.17). This is a high-grade graphite and quartz-pyrite conglomerate seam that is rarely thicker than 10 cm, situated near base of the Randfontein Formation. Second in importance is the Ventersdorp Contact Reef (older production ~1,331 t Au @ 15 g/t). It is up to 2.5 m thick and highly variable in thickness, pebble size, and gold distribution. It is also intermingled with the Westonia mafic flows, and in places intensely hydrothermally altered (chlorite is predominant).

Welkom (Free State) Goldfield (Minter et al., 1986; P+Rc 16,196 t Au @ ~11.6 g/t; Fig. 11.18). This is the latest goldfield discovered, situated 270 km SW of Johannesburg. It is completely concealed under thick Karoo and partly Ventersdorp cover. The goldfield coincides with a north-south trending syncline that is broken into blocks and segments by numerous normal and some reverse faults. The production comes from a large number of reefs at five stratigraphic levels, the most important being the Basal Reef. This Reef is a pebbly siliceous, slightly pyritic quartzite horizon that contains intervals of polymictic (Steyn Placer) and quartz (Basal Placer) conglomerates. About 11% of Au+U came from quartzite. In the southerly direction, around Virginia, the Central Rand Subgroup rapidly thins, changes facies and suffers substantial basin-edge overfolding. Profitable mines (Beisa, Beatrix), however, have been developed there in the past few decades.

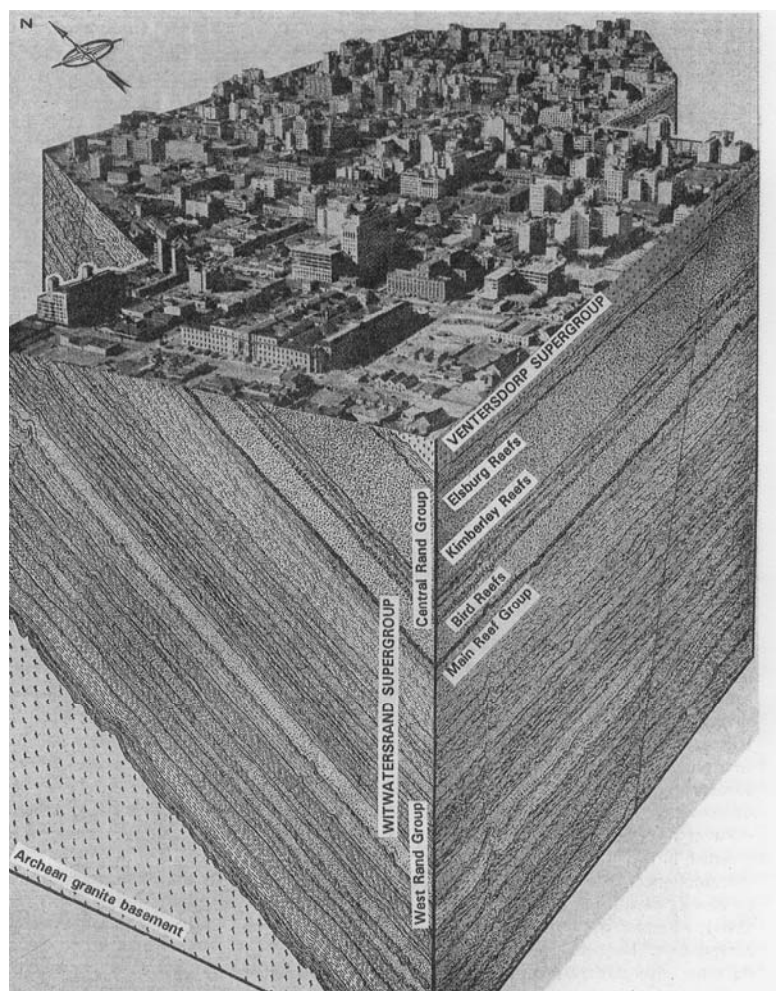


Figure 11.16. Central Rand Goldfield under the city of Johannesburg (as it was in the late 1940s). Four Reef groups are shown, all in the Central Rand Group mature clastics that rest on the predominantly marine West Rand Group (meta)sediments. Reprinted from *The Mining Survey*, v.3, No.4, September 1951, a Transvaal Chamber of Mines publication

Elliot Lake (Blind River) U-(Th, REE, Y) paleoplacers, Ontario

This district, about 130 km west of Sudbury in Central Ontario, was the principal uranium producer in Canada before discovery of the rich Athabasca Plateau deposits (Robertson, 1981; Roscoe, 1996; $P_{1957-1992}$ 140.5 kt U @ 0.09%, pre-mining Rc ~432 kt U, 350 kt Th, ~180 kt REE+Y). The ore host, 2.45 Ga Matinenda Formation, is a unit in the Paleoproterozoic Huronian Supergroup that unconformably overlies Archean greenstones of the Superior Province, Canadian Shield. The Matinenda is up to 210 m thick and consists of sericitic meta-arkose, locally floored by metabasalt flows, that rest on Archean paleoregolith complete with sericite-

rich metamorphosed paleosol. The meta-arkose encloses lenticular quartz-pebble conglomerate sheets at several stratigraphic levels, interpreted as continental valley fill to braid fan. The succession was open folded, block faulted and greenschist metamorphosed during the 1.9 Ga orogeny. U mineralization occurs in two WNW-trending zones (Quirke Lake and Nordic) at margins of the Quirke Syncline, and in the small Pronto outlier in the south. The northern Quirke Lake Zone measures 10x3.5 km and has been followed 1,200 m downdip (Fig. 11.19). The southern Nordic Zone measures 6x2 km and has three productive conglomerate units ("reefs") in a 30 m thick package.

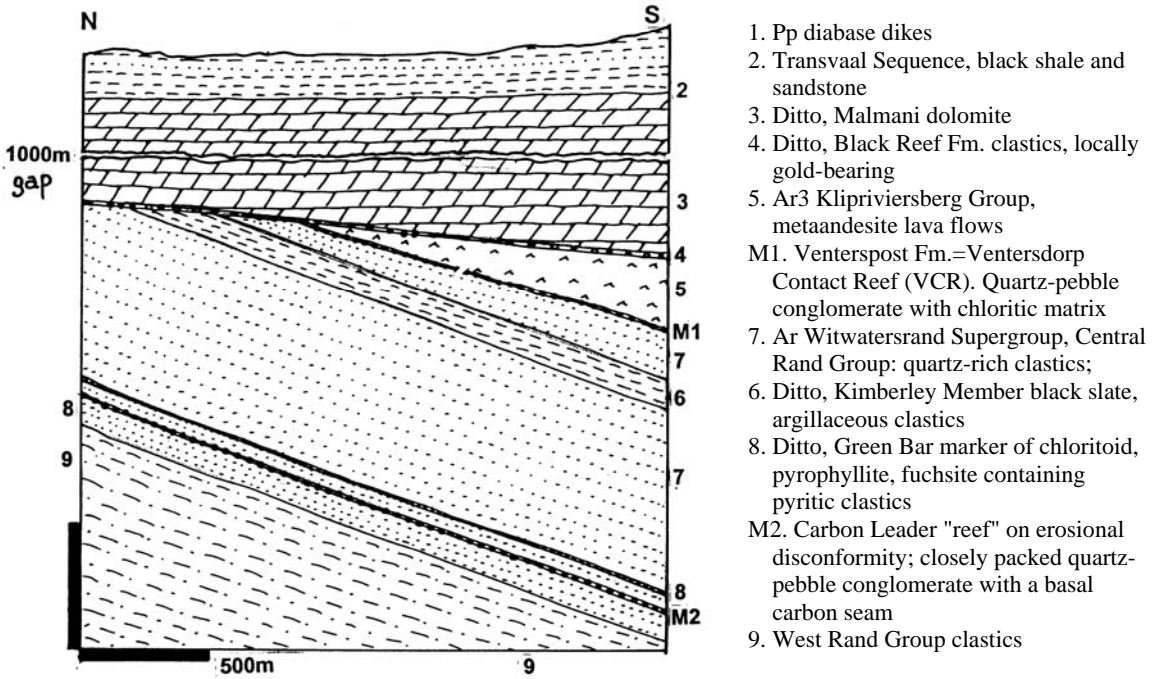


Figure 11.17. West Wits Goldfield, Western Deep Levels Mine cross-section from LITHOTHEQUE No. 2754, compiled from literature data. The world's deepest mine produces from two principal reefs, more than 1000 m apart

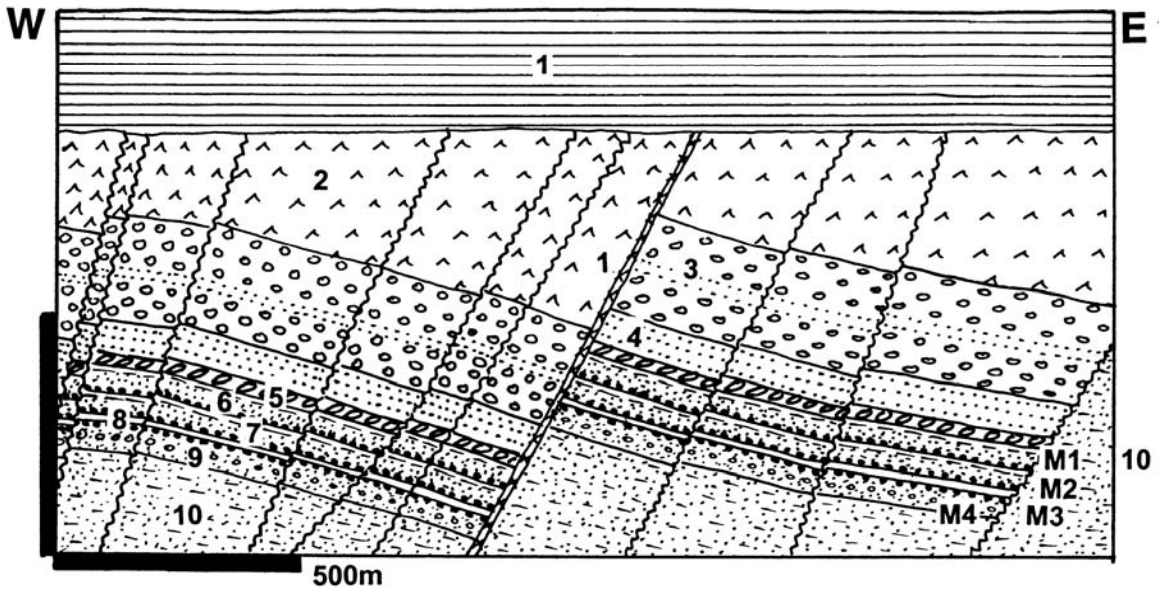


Figure 11.18. Welkom (Free State) Goldfield, a typical cross-section through the northern (classical) portion. From LITHOTHEQUE No. 279, modified after McKinney et al. (1964). 1. MZ Karoo diabase dikes; 2. Ar3 Klipriviersberg Group, metaandesite lavas; 3. Ar3 Witwatersrand Supergroup, Central Rand Group: eight fluvial fan formations. Eldorado Fm. upper quartz-rich polymictic conglomerate; 4. Ditto, lower quartzite; 5. Ditto, Aandenk diamictite conglomerate, black slate; 6. Polymictic conglomerate, quartzite, argillite in B Reef hangingwall. M. Five producing reefs. M1=B Reef; M2=Leader Reef; M3=Saaiplaas Placer; M4=Basal and Steyn Reefs. 7. Dagbreek Fm. sandstone and shale; 8. Harmony Fm. diamictite and green shale; 9. Welkom Fm. quartzite, conglomerate fan; 10. West Rand Group, argillaceous quartzite

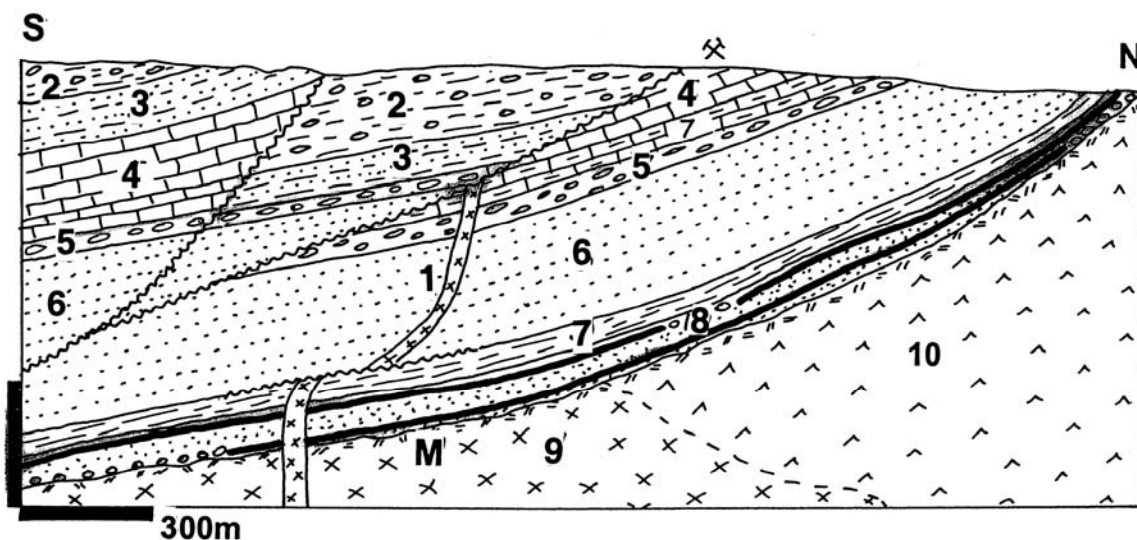


Figure 11.19. Elliot Lake uranium district, Ontario, Quirke Syncline. Cross-section through the Quirke 2 Mine from LITHOTHEQUE No. 1584, based on mine documentation. 1. Pp diabase dikes; 2. Pp Huronian Supergroup, Gowganda Fm., diamictite, purple clastics; 3. Serpent Fm. arkose and subgraywacke; 4. Espanola Fm. limestone, dolomite, siltstone; 5. Bruce Fm., conglomerate, graywacke, limestone; 6. Mississagi Fm., coarse subarkose; 7. Pecors and Ramsay Lake Fms., argillite to conglomerate; 8. Matinenda Fm., subarkose with conglomeratic horizons and basal paleosol; M. Two horizons of quartz-rich pyritic U, Th, REE, Y-bearing basal conglomerate; 9. Ar basement tonalite, regolithic under unconformity; 10. Ditto, greenstone

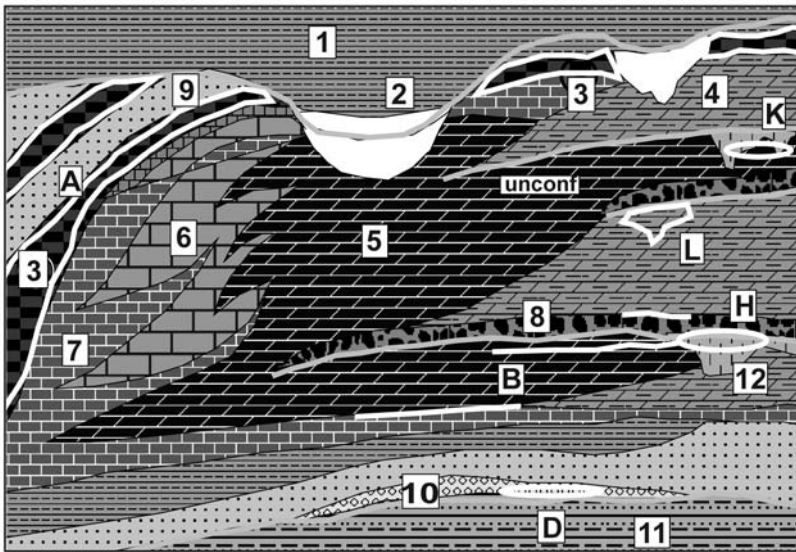
The mineralized reefs have a variable persistency and intricate lensing is common. The most persistent Rio Algom-Denison Reef comprises two conglomerate zones each 1.8 to 3.6 m thick, separated by a 0.6 to 2.4 m thick barren meta-arkose. The conglomerate has well-rounded vein quartz clasts in sericite matrix with pyrite that constitutes 3-15% and locally up to 30% of the rock. The principal ore minerals are uraninite, brannerite and monazite, and the uraninite : monazite ratio decreases down paleoslope. The ore minerals are fine-grained, invisible, and partly permeated by carbon. Under the microscope abraded uraninite crystals and monazite suggest detrital origin and there are locally developed carbon nodules enriched in base metals, filling fissures.

11.6. Fe in Superior-type banded iron formations (BIF)

James (1954) defined BIF as "a chemical sediment, typically thin-bedded or laminated, containing 15% or more iron of sedimentary origin, commonly but not necessarily layers of chert". This identifies BIF as a "rock", a mapable lithologic unit. The primary (diagenetic) BIF come in oxide (quartz: chert or

hematite-pigmented jaspillite, hematite or magnetite), carbonate (siderite or ankerite), silicate (chamosite, greenalite) and sulfide (pyrite, pyrrhotite) facies. Quartz, magnetite, hematite, Fe sulfides recrystallize under conditions of increasing metamorphism but retain their mineralogical composition, whereas Fe ore and gangue silicates change to minnesotaite, grünerite, cummingtonite and orthopyroxene. Although at textbook level the BIF facies are often taken as indicative of basal depths and distance from shore (oxides nearshore, sulfides "basal"), the rapid changes in mineralogy within a single BIF unit more likely reflect microenvironmental variations in fluid chemistry, reaction with host rocks, diagenetic changes and metasomatism. Most BIF are members of clastic basal sequences that rest on eroded and sometimes partly regolithic greenstone belt basement. Some are close to the clastic-carbonate transition (Fig. 11.20).

Every BIF, however, does not constitute an ore in economic sense as much more is needed to assure profitability and with it a status of a delineated ore deposit that could be quantified, compared and ranked. Apart from the politico-economic conditions, the profitability of a Fe orebody is governed by several geological factors.



1. Shale of the upper sequence;
 2. Resedimented ironstone;
 3. Ironstone slump breccia;
 4. Cherty algal dolomite;
 5. Subtidal stromatolitic dolomite;
 6. Platform edge limestone;
 7. Basinal limestone;
 8. Residual chert breccia;
 9. Sandstone;
 10. Conglomerate;
 11. Clastics of the lower sequence;
 12. Karst under unconformity.
- A. Sediment-hosted BIF; B. Mn-enriched dolomite; D. Basal Au paleoplacer; G. Enriched Fe ore in slumps; H. Residual Mn oxides in karst over Mn dolomite; K. Fluorite (Pb, Zn) replacements in dolomite; L. Zn, Pb MVT ores in paleo-karst under unconformity;

Figure 11.20. Usual lithofacies present in a Proterozoic intracratonic basin (as in the Transvaal Sequence of South Africa; Tankard et al., 1982; Beukes, 1986) and the common metallic deposits dominated by Fe (in BIF) and Mn. Inventory cross-section from Laznicka (2004), Total Metallogeny Site G168. Explanations (continued): S. Resedimented ironstone at base of a top sequence above unconformity; T. Ditto, Mn oxidic ores resedimented above unconformity

They are sufficient size and grade; near-surface orebodies amenable to open pit mining; low-cost of iron recovery; absence of harmful impurities. These factors combine and although an ideal Fe deposit would be large, thick, high-grade, cropping out as an ore hill or a range, this is not always the case and special local conditions intervene to economically utilize orebodies inferior in various ways. The frequently substantial contrasts in the style of Fe orebodies, especially those that are supergene enriched and those that are not, do not follow from simple tonnage statistics and this influences the determination of "giants" (Fig. 11.21). An example:

Mesabi iron range in Minnesota (Marsden, 1968; described below) has been then principal ore supplier to the United States' steel industry since 1890. The mining started in supergene enriched ore containing, on average, 54% Fe. By the 1970s this ore was exhausted, after some 3 bt of ore had been produced. As this was a major ore supplier with established markets, the producers started, after a profound change in technology, to mine and process the primary BIF locally called taconite. The average grade of taconite is a mere 27% Fe (even a 22% Fe material is mined) and its resource is of the order of 60 bt. To compete, however, with the imported direct shipping ore from Brazil that contains 65% Fe, the Mesabi Range industries have had to absorb the extra cost of ore beneficiation (milling, magnetic

separation, agglomeration) to supply Fe oxide pellets with approximately the same ~65% Fe grade. This could only have been achieved by economy of scale (milling up to 500,000 t ore/day) and by utilizing only magnetite BIF that can be magnetically separated. Hematite and Fe-Mg silicate BIF do not qualify as ore at present. This leaves us with the following set of tonnage figures for the Mesabi Range (Marsden, 1968):

- 1) Total past production of enriched ore: 3 bt @ 54% for 1.62 bt Fe
- 2) Production and resources of magnetite taconite: 45 bt @ 25% for 11.25 bt Fe
- 3) Resources of Fe in "common" (non-magnetic) taconite: 15 bt @ 25% for 3.75 bt Fe
- 4) Total enriched and non-enriched Fe ore - 17.82 bt of Fe content.

Mesabi Range is thus a "large" ore region in terms of enriched ore and "giant" region in total Fe. This applies to other deposits listed in Table 11.3. where similar distinction is used, when the available data allow it. Otherwise the general ore tonnages quoted in literature usually correspond to the mineable, enriched ore.

Varieties of BIF and origin of Fe ores: Banded iron formations (BIF) have an extensive literature summarized and classified in Laznicka (1993, p. 956-986 and references therein).

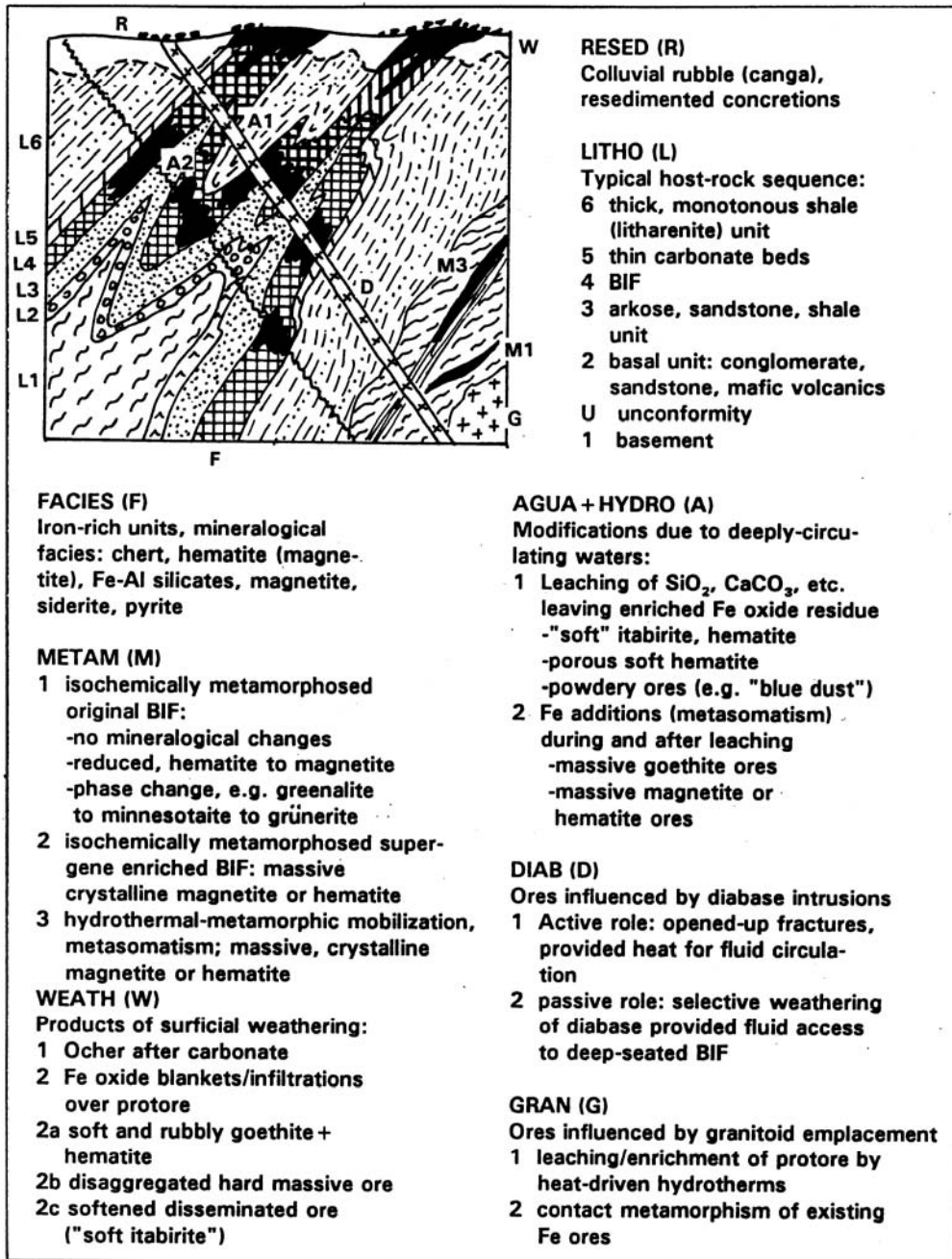


Figure 11.21. Varieties of industrial Fe ores derived from the initial Superior-type BIF, produced by post-depositional agents like deformation, metamorphism, igneous intrusion and supergenesis. From Laznicka (1991 and 1993). Abbreviations of the metallogenes (ore-forming or modifying factors) are self-explaining and correspond to the scheme described in Laznicka (1993. FACIES=refers to lithofacies established before lithification; METAM=metamorphic effects; WEATH=surficial supergenesis due to weathering; RESED=clastic resedimentation; LITHO=refers to the BIF host lithologies; AQUA+HYDRO=heated basinal and/or hydrothermal fluids operating underground; DIAB=influence of the post-BIF diabase and gabbro dikes; GRAN=thermal effects due to igneous intrusions: mostly granitoids but also gabbroids (e.g. Duluth Complex)

A typical BIF is a chemical sediment (or partly hydrothermal, volcanic sediment-"exhalite") gradational into, and often indistinguishable from, a soft sediment or volcanoclastic replacement. It forms stratiform horizons and units compositionally banded at a variety of scales (micro-, meso-, macro), often delicately folded and microfaulted. In the popular BIF classification based on host lithology Algoma-type stands for BIF associated with mafic, less felsic (meta)volcanics, (Lake) Superior-type is in (meta)sediments. Gross (1996) has added the Rapitan-type for BIF associated with presumably glaciogenic diamictites and then there are BIF's hosted by turbidites that are considered either a Superior sub-type or an independent type.

At best, these BIF types are end-members as there is a transition between the volcanic and non-volcanic categories. At worst, the stratiformity of the precursors to the near-surface, oxidized, Fe enriched ores (although not of the regionally associated "rock" BIF) is being increasingly questioned at a number of important deposits. There, as the mining and exploration reach into the deeper levels under the supergene enriched hematite blankets, the "primary" ore is often revealed as a stratabound or entirely discordant hydrothermal hematite or magnetite replacement in or above carbonates (usually dolomite), sometimes with talc, tremolite and/or other silicates. The replacements are associated with altered sediments or volcanics, as well as with diabase dikes and sills. Dalstra and Guedes (2004) specified several deposits in the Hamersley (Tom Price; Fig. 11.22) and Carajás Provinces where the discordant ores are intermediate in grade (45-55% Fe) between the raw BIF (30-35% Fe) and the high-grade enriched ore (65-69% Fe). Other districts listed by Dalstra and Guedes include the Cuadrilátero Ferrífero, Krivoi Rog, Thabazimbi and Bailadila. The deep magnetite or hematite-carbonate ores under the enriched Iron Duke deposit, and especially several prospects in the emerging Mount Woods Fe ore province in South Australia (e.g. Prominent Hill; read above) suggest link with the Olympic Dam-style Fe oxide, Cu, Au, U type (read above). At Bayan Obo in China (Chapter 12) the Fe oxide replacements in dolomite are, moreover, greatly enriched in bastnäsite, monazite, pyrochlore and other minerals to constitute a significant Nb resource and the world's largest rare earths repository.

Although simple, usually ocherous goethite or porous hematite-rich iron deposits can form by a single stage Meso-Cenozoic enrichment of a BIF outcrop modified by lateritic weathering, many of the large, deep and rich Fe deposits have had a long

and complex history of modifications that started shortly after deposition in the Precambrian. Many Fe ore districts, moreover, contain second-stage deposits produced by physical and chemical reworking and redeposition of the early in-situ ores. This is best demonstrated by the selected regional examples below.

Hamersley Iron Province, Western Australia

This is a WNW-elongated, 570 by 170 km large iron ore province situated south of the shipping ports of Karratha/Dampier and Port Hedland in NW Western Australia, along the southern margin of the Pilbara Archean Block (Shield) (Trendall, 1983; Harmsworth et al., 1990). The 2,500 m thick 2.6 to 2.45 Ga Hamersley Group rests on mafic meta-volcanics and immature clastics of the Fortescue Group. Hamersley Group is dominated by BIF (~40%) and although this BIF appears entirely "sedimentary", deposited on a "submarine platform", the top of the Group has a thick section of bimodal volcanics and there are abundant diabase feeder dikes indicating near-contemporaneity of the Fe-rich chemical sedimentation and distal? volcanism around 2.47 Ga (Taylor et al., 2001).

There are six lithostratigraphic units that contain iron formations, of which two are presently of main economic interest: the basal, about 230 m thick Marra Mamba IF and the 142 m thick Dales Gorge Member of the Brockman IF, situated about 250 m higher in the stratigraphic column. There are numerous units and bands of tuffaceous shale, and the Wittenoom Dolomite Formation. The Hamersley Iron Province is folded and lower greenschist to sub-greenschist metamorphosed.

There is a tremendous amount of iron in the Hamersley Province accumulated as the raw BIF (of the order of 10,000 bt Fe @ 22.5-30% Fe) but the presently economic ores (cut-off grade ~55% Fe) store only a fraction of this tonnage, estimated at between 15.0 and 19.5 bt Fe. There are many varieties of ores described by Harmsworth et al. (1990) ranging from simple ones produced by Meso-Cenozoic supergene processes that are shallow, blanket-like, non-metamorphosed goethite-rich and still related to the present land surface, to genetically complex, thick and deep high-grade hematite bodies enriched during the Proterozoic. Both types rest on or within the solution thinned original BIF's.

Marra Mamba IF orebodies (Rc ~8.8 bt ore @ ~60% Fe; Harmsworth et al., 1990) belong to the shallow supergene ores developed on the oldest (basal) 2.6 Ga BIF within the Hamersley Group.

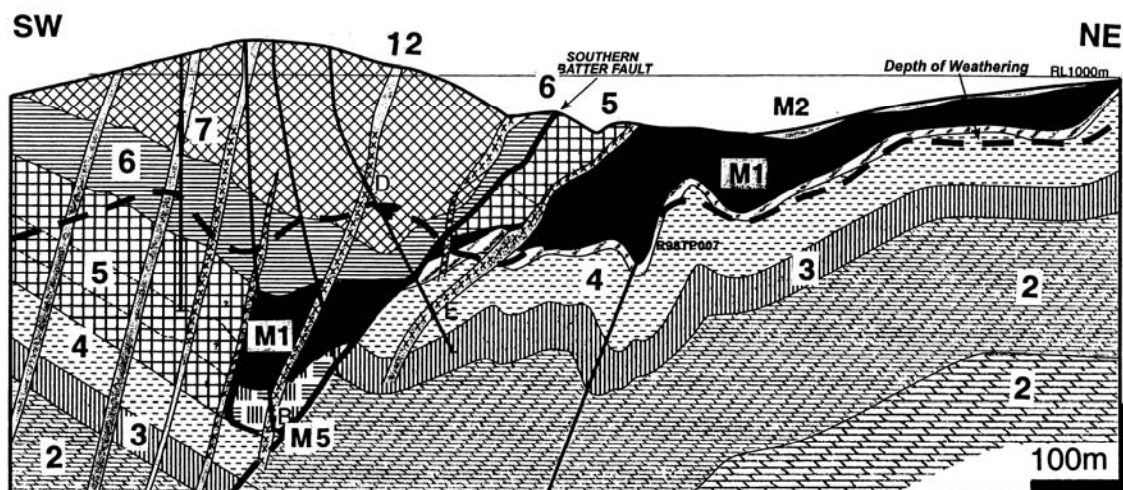


Figure 11.22. Mount Tom Price iron deposit, Hamersley Range, Western Australia, reprinted from Taylor et al. (2001), *Economic Geology* v. 96:4, Fig. 5, p. 845. Example of a multistage enriched initially Superior-style BIF. Original legend slightly modified to suit LITHOTHEQUE No. 2563. M1. High-grade microplaty hematite (martite), ~65% Fe; M2. Hydrated supergene hematite with a variable proportion of goethite; M5. Primary magnetite and siderite-magnetite BIF relics. 2. ~2.6 Ga Hamersley Group, Wittenoom Fm. dolomite, argillite; 3. Mt. Sylvia Fm. BIF separated by chert and shale; 4. Mount McRae Shale, pyritic black slate with chert; 5. Brockman IF, Dales Gorge Member, BIF; 6. Whaleback Shale Member shale, chert, local BIF; 7. Joffre Member BIF; 12. Pp diabase and gabbro dikes

At the presently mined Marandoo deposit near the Mount Bruce landmark the soft and friable martite-ocherous goethite gradational to a more indurated martite-goethite ores form a 20-30m thick, almost flat blanket on the Mount Newman BIF Member, when the latter is exposed at the surface or in shallow subsurface. Portion of the orebody is concealed under Tertiary alluvium filling a paleovalley.

Brockman IF orebodies (19 bt+ of ore at 55% Fe plus; Harmsworth et al., 1990) also include young supergene martite-goethite ores (e.g. in the Rhodes Ridge ore field; Rc 1.0 bt @ 61.6% Fe), but the two richest deposits: Mount Whaleback near Newman (1.7 bt @ 64% Fe for 1.09 bt Fe) and Mount Tom Price (900 mt @ 64% Fe for 576 mt Fe) are of the complex hematite variety. The widely quoted CSIRO-AMIRA polygenetic model (Morris, 1987) traced the history of post-depositional BIF enrichment back to about 2.0 Ga. There, the diagenetic magnetite in BIF first converted into hematite (martite) or into kenomagnetite (=a metastable phase between magnetite and maghemite) by near-surface as well as deep supergene processes related to meteoric (or "basinal"?) waters. The chert was partly or completely leached. The in-depth oxidation required efficient circulation of groundwater in a presumed artesian system controlled by structure.

The silica leaching alternated with void filling and/or quartz replacement by secondary Fe oxides in a cyclic reduction-oxidation system at the end of which formed bodies composed chiefly of goethite. The goethite, in turn, was metamorphosed into microplaty hematite around 1.85 Ga, which was then partly exhumed and eroded around 1.7 Ga to contribute hematite detritus to the Mount McGrath conglomerate. The final episode of unroofing of the partially enriched Hamersley Group iron formations in Mesozoic and Cenozoic subjected these materials to the third cycle of weathering under humid tropical conditions. Unmetamorphosed martite-powdery goethite ores have formed from the unmodified BIF's, especially those rich in Fe-carbonates. The powdery "blue dust" martite-hematite ores resulted from supergene leaching of silica and goethite from formerly compact ores. The subrecently formed ores coexist with unmodified relics of the Proterozoic ores like the 2.0 Ga metasomatic goethite and the slightly younger high-grade microplate hematite.

The alternative genetic interpretation of the rich Hamersley ores, especially the microplaty hematite at Tom Price, assumes structurally controlled hydrothermal metasomatism and upgrading of BIF in depth prior to unroofing, during which magnetite, hematite, carbonate, apatite precursors had formed. Subsequent removal of carbonate and apatite by

leaching, oxidation of magnetite, and compaction produced the high-grade hematite (Taylor et al., 2001; Dalstra and Guedes, 2004).

Tertiary Fe channel gravels. The Meso-Cenozoic humid weathering produced a thick lateritic capping over the Hamersley outcrop complete with rubble (canga) deposits on flanks, but laterites have been largely eroded away by now, following uplift. A substantial proportion of the pedogenic hematite-goethite microconcretions ("pisoliths") have been reworked and deposited in channels of several stream systems that drained the northern flanks of the Hamersley Range. The Miocene Robe Formation, now exposed in the Robe River (Fig. 11.23) and Marillana (Yandicoogina) channel systems, has a resource of some 4.7 bt of 58% Fe ore (i.e. 2.73 bt Fe; Hall and Kneeshaw, 1990). The bedded, semi-consolidated, granular ore is exposed in a series of low mesas and is between 25 and 45 m thick, very economic to mine.

Lake Superior (Animikie) iron province, United States (partly Canada)

This is a classical area of iron metallogeny (Van Hise and Leith, 1911) where concepts and terminology have been generated and industrial application of BIF ores initiated and perfected. The extensive (~220,000 km²) area is situated west and east of the Lake Superior over which the ore from Minnesota, Wisconsin and Michigan is shipped to the blast furnaces in Ohio and Pennsylvania. BIF and related Fe orebodies are in the lower portions of Paleoproterozoic (2.2-1.85 Ga) Animikie and Marquette Range Supergroups deposited over the Archean basement of the southern Canadian Shield. There, they are separated by rocks and structures of the younger Proterozoic Midcontinent Rift into three separate areas each of which contains one or more BIF units and iron mining districts locally called "Ranges". The following Iron Ranges have been economically most important (the iron tonnages indicate the approximate Fe content in mineable enriched or magnetite taconite ores, but not in the raw BIF): Mesabi Range (12.87 bt Fe) and Cuyuna Range (82 mt Fe), both in Minnesota; Gogebic Range (170 mt Fe), Wisconsin; Marquette Range (1.175 bt Fe) and Menominee Range (148 mt Fe), both in Michigan.

The Animikie/Marquette sedimentary succession that hosts the BIF comprises, in the north-west (e.g. in Mesabi), shallow water (shelf) sedimentary rocks transgressively deposited over Archaean metamorphic basement along a stable continental

margin. The sedimentary rocks are thin (0-1,500 m), almost flat-lying, subgreenschist-metamorphosed. The thicker (1,500 to 6,000 m) sediments in Michigan were deposited in a synorogenic foredeep and they partly overstep the Archean basement in the NW. They are deformed, generally steeply-dipping and greenschist-metamorphosed. All BIF's were supergene enriched in several stages (between Proterozoic and Cretaceous) but, compared with their counterparts in Australia and Brazil, the regolith thickness has been substantially reduced by Quaternary glaciations and the softest near-surface ores removed. Both relatively thin, near-surface enrichment ore blankets, and structurally controlled deep-seated enriched ores produced by groundwater circulation, are represented.

Mesabi Range, NE Minnesota (Marsden, 1968; 17.28 bt total Fe) is a 192 km long, 0.5 to 5 km wide ENE-trending outcrop belt with Hibbing and Virginia City as the main mining centers. The Biwabik IF ranges from 30 to 225 m in thickness and it rests on a thin veneer of quartzite or argillite transgressive over the Archean basement. The cyclic BIF is subdivided into two "cherty" and two "slaty" units. The "cherty" (jaspillitic) units consist of bands of chert, jasper or recrystallized quartzite that alternate with bands of magnetite, hematite, siderite, ankerite, greenalite, minnesotaite and stilpnomelane in various proportions. The Fe-Al silicates occur as granules or in matrix, whereas the Fe oxides and carbonates are mostly in the matrix or as siderite spherulites. The "slaty" bands are dark, laminated, non-granular aggregates of fine (pelitic) chert, magnetite, Fe silicates and siderite, alternating with chert microbands. As there is no pelitic component the name shale is a misnomer.

The Mesabi Range has produced, since 1890, about 3 bt of direct shipping ore with an average grade of 54%, exhausted by the 1970s. The enriched ore came as relics of soft, friable and rubbly hematite and goethite blankets, trough filling and fissure infiltrations within the BIF. A small portion of the regolith was reworked into the basal conglomerate beds of the Cretaceous cover. The present large tonnage bulk mining depends on the raw, low-grade BIF ("taconite") that contains magnetite, as magnetite can be economically magnetically separated and processed into pellets. Only the "cherty" units qualify as ore; there, magnetite forms diffuse bands, mottles and schlieren in the matrix of recrystallized (quartzitic) BIF. The best beds of magnetite taconite are in the middle portion of the Lower Cherty Member and they range in thickness from 0.6 to 83 m.

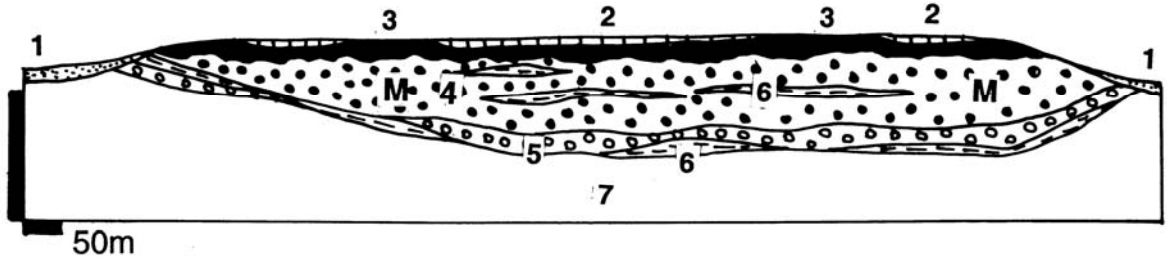


Figure 11.23. Robe River Fe ore field, Western Australia, Mesa J cross-section. From LITHOTHEQUE No. 2578. Based on data from Robe Ltd. Staff, Pannavonica (2000 visit). 1. Q alluvium, colluvium; 2. T2-Q weathered pisolite and laterite relics; 3. T2-3 hardcap rich in vitreous goethite, some silica infiltration. Locally selectively mined as ore. 4=M. T2 ore pisolite, relatively homogeneous, usually friable hematite and goethite particles in limonite and clay matrix; 5. Low-grade basal pisolite; 6. Intraformational or basal clay-rich unit; 7. Ar & Pp regolithic basement, bedrock to the Fe ore channels

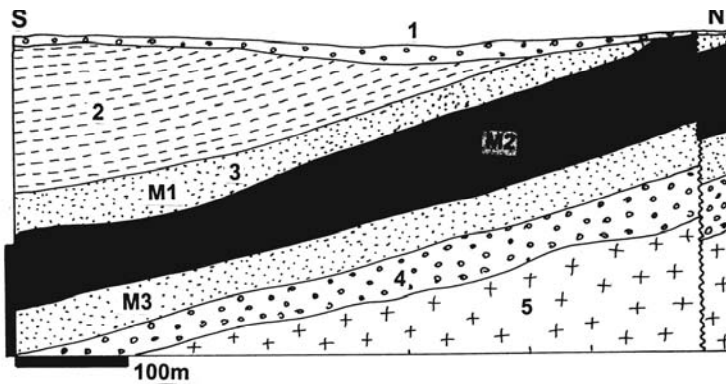
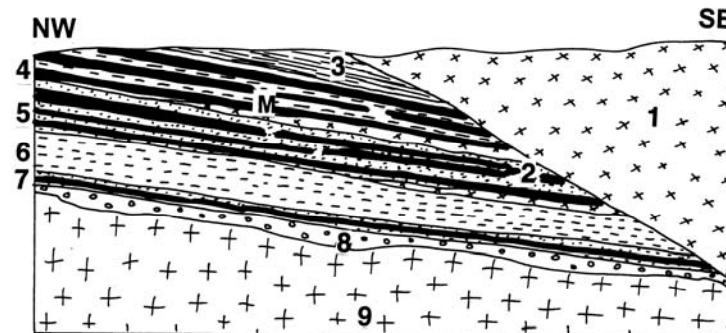


Figure 11.24. Mahoning Mine, Hibbing, cross-section from LITHOTHEQUE No. 1991, based on data from Hibbing Taconite Company Inc. This is the largest Fe ore operation in the Mesabi Range, Minnesota, producing pellets shipped to the steel mills of Pennsylvania and Ohio. 1. Q glacial sediments; 2. Pp Biwabik Iron Formation, Lower Slaty Member; 3+M. Ditto, Lower Cherty Member. M1=low-grade taconite; M2=mottled, magnetite-rich taconite (principal ore); C=lean taconite; 4. Pp Pokegama Quartzite and basal conglomerate; 8. Archean basement



1. ~1.1 Ga Duluth Complex, gabbro; 2. Mp diabase dikes & sills; 3. Pp Virginia Fm. slate, hornfelsed near gabbro contact; 4. Pp Biwabik Iron Formation, Upper Slaty Member; 5+M. Ditto, Upper Cherty Member, thermally metamorphosed to magnetite quartzite; 6. Ditto, Lower Slaty Member; 7+M. Ditto, Lower Cherty Member with magnetite quartzite; 8. Pp Pokegama quartzite, conglomerate; 9. Ar basement.

Figure 11.25. Cross-section of the Aurora Mine, Mesabi Range, producing from thermally upgraded magnetite BIF near gabbro contact. From LITHOTHEQUE No. 1992, based on information from Aurora Mine Staff

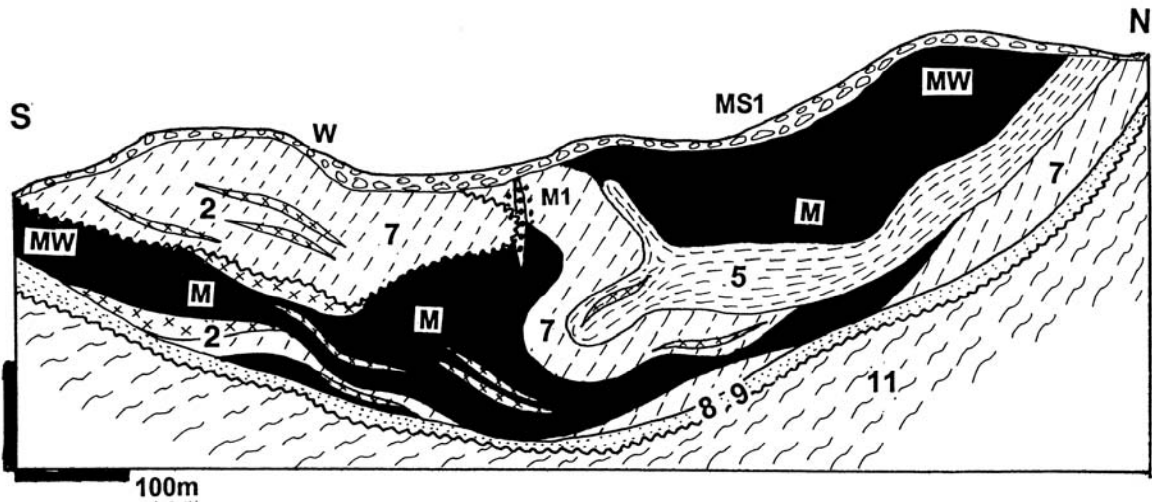


Figure 11.26. Caê Mine cross-section, Itabira, MG, Brazil. From LITHOTHEQUE No. 1975, modified after Santana and Polonia (1982). QW. T-Q laterite and saprolite; MS1. Canga, unconsolidated scree or goethite-cemented blanket of hematite blocks; 2. Pp dikes and sills of metadiabase; M1. Small Au-quartz veins and stringers in shears; 5. Pp Piracicaba Group schist, phyllite, quartzite; 7. Pp Itabira Group, Caê Itabirite; greenschist-metamorphosed quartz-hematite BIF; MW. Soft hematite, powdery mass of loose specularite flakes; M. Hard hematite, massive, 67% Fe; 8+9. Pp Batatal Fm., sericitic phyllite and Moeda metaquartzite; 11. Ar Rio das Velhas chlorite schist

The ore in the largest mine in Hibbing contains between 20 and 45% of magnetite (14-32% Fe; Fig. 11.24).

Near the NE extremity of Mesabi Range near Babbitt (Bonnichsen, 1975) the Biwabik IF was intruded by a tongue of the 1.1 Ga Duluth mafic intrusion and thermally metamorphosed to pyroxene hornfels facies. The metamorphic assemblage includes ortho- and clinopyroxene, fayalite, cummingtonite, hornblende, quartz and magnetite and, with 25-30% of magnetic iron, it qualifies as an economic Fe ore. East of Aurora the BIF underwent thermal recrystallization that enlarged the magnetite grain size (Fig. 11.25). This improved the processing characteristics so the BIF units that are presently uneconomic in the Mesabi Range became "ore" here.

Quadrilátero Ferrífero, Minas Gerais, Brazil (Dorr, 1969; Klein and Ladeira, 2000; minimum 150 bt Fe @ 40% or 16 bt Fe @ 55+ %) was the principal and oldest Fe-mining district of Brazil; now it competes with the more recently discovered Carajás Fe province in Pará. The Quadrilátero has a relatively compact area of just 7,000 km², SE of Belo Horizonte and the principal BIF unit, Caê Itabirite, is a member of the pre-2.0 Ga Minas Supergroup. The shallow marine terrigenous, chemical and carbonate succession rests on Archean greenstones (Nova Lima group, host of the Morro

Velho "Au-giant"; Chapter 9) and granite-gneiss terrain. Caê Itabirite ranges in thickness between 30 and 2,000 m (average 350 m). It is floored by Batatal Formation phyllite, and topped by Gandarela dolomite, dolomitic iron formation and phyllite. The "itabirite" is a greenschist to lower amphibolite metamorphosed BIF exposed in several narrow synclinal belts interrupted by basement uplifts, and composed of alternating white quartzite (meta-chert) and quartz-specularite granofels bands. The itabirite has an unusually high average content of 37% Fe that represents a huge future resource, but as the Fe carrier is largely hematite the recovery would be too costly hence all the mining to-date has been from the enriched orebodies.

As elsewhere in humid tropics, supergene Fe enrichment in the Cretaceous and younger regolith is most widespread and it has resulted in a variety of near-surface, friable, unmetamorphosed ores. The topmost material is "canga", a rubbly or concretionary goethite-hematite ferricrete found in-situ or transported downslope. It grades between 45 and 65% Fe. The most voluminous enriched ore is the "soft hematite" gradational into a powdery or flaky "blue dust" hematite. This gray, directly mineable (without blasting) material with 60 to 67% Fe is believed produced by supergene leaching of silica from the ordinary, or previously enriched, itabirite (Fig. 11.26).

The pre- to synorogenic "hard hematite" (up to 67% Fe) is the most valuable local ore composed of 98-99% pure, fine to coarse steely hematite. Tabular or lenticular orebodies are controlled by zones of tight folding, axial planes, cleavage and ductile shears and they commonly transgress the original bedding. Dorr and Barbosa (1963) interpreted the "hard hematite" as a synmetamorphic replacement from up to 332°C hot hydrothermal fluids, driven by the heat of synorogenic granites.

Russian Platform: the Krivoi Rog (Ukraine) and Kursk (Russia) BIF regions

The Paleoproterozoic succession that crops out in the Ukrainian Shield, and is present in a shallow subcrop under Phanerozoic platformic cover in the Kursk-Voronezh Massif, contains by far the largest portion of the world's iron (estimated at more than 40 trillion of raw BIF and some 19 bt Fe in 55% plus Fe ores). The Western awareness about this resource is limited as the most comprehensive descriptive literature is in Russian only (e.g. Polishchuk et al., 1970; Belevtsev, ed., 1962) and is hard to get here. There is a brief review in Laznicka (1993, p. 980-994) with literature selection.

Krivoi Rog (Kriviy Rih) "Basin", Ukraine. Krivoi Rog (Sokolov and Grigor'ev, 1974; Belevtsev et al., 1983) is a famous European iron ore district variously credited with some 2.8 bt of Fe in rich ores (57.6% Fe), further 6.5 bt Fe in ~36% Fe ores marginally economic in times when Ukraine was a part of the USSR, and some 100 bt Fe in a 25-30% Fe raw BIF. It is in the central part of the Archean-Paleoproterozoic Ukrainian Shield, in a N-S trending Krivoi Rog-Kremenchuk fault-bounded metallogenic belt. The belt contains several narrow, discontinuous "basins" of Paleoproterozoic supracrustals, exposing a 3.5 to 6.5 km thick stratigraphic column.

The Paleoproterozoic supracrustals in the Krivoi Rog "Basin" rest unconformably on Archean metamorphic basement. The 100 to 200 m thick basal unit is a distinct "rift association" of widespread mafic metavolcanics (now amphibolite) with minor metaquartzite and conglomerate. This is unconformably overlain by meta-arkose, gray and black phyllite, and carbonate-chlorite-talc schist. The middle Saksagan Suite is an up to 1,400 m thick succession of mainly chemical sediments that contain up to 7 macrobands of predominantly oxide BIF, interbanded with quartz-sericite, amphibole, chlorite, carbonate and graphite schist of combined volcanic and terrigenous provenance. The upper sequence starts with basal conglomerate and

continues into metaquartzite, schists and lesser dolomite. All three divisions are intruded by diabase dikes and granitoids. The Krivoi Rog BIF comprises alternating mesobands of "chert" (now metaquartzite) and bands with variable content of magnetite, hematite, siderite, pyrite, Fe chlorites, cummingtonite, sericite, chlorite and local riebeckite and aegirine. The "regular" BIF contains the bulk of iron in low-grade material (around 30% Fe), a small portion of which is supergene enriched near the surface.

As in the iron districts reviewed above, the best Krivoi Rog ore mined to-date is the "Saksagan-type" massive gray magnetite, martite, hematite and sometimes amphibole ore that averages 57.5% Fe and has been mined 1,500 m downdip from an array of underground mines. Interpreted as synorogenic, hydrothermal-metasomatic, this ore is superimposed on the BIF along ductile shears, tight anticlines, crossfolds, cleavage and faults. The orebodies have the form of steeply-dipping lenses persistent for hundreds of meters along strike and more than 2,000 m downdip, and of irregular shoots, pipes and stockworks. The Saksagan-type ores probably formed during the mid-Proterozoic orogeny, by redeposition of the local iron by convecting fluids driven by heat from granite intrusions. Some orebodies have been modified by Meso-Cenozoic supergene processes. From the surface down, the supergene zones are as follows: 1) surficial, resedimented concretionary and infiltrational goethite; 2) residual hydrohematite-goethite rubble and soft, porous ore saprolite; 3) earthy and friable hematite-martite ores in place of the "hard" ore.

About 4% of the rich ores in the main Krivoi Rog (Saksagan) Basin, and most ores in the small Zheltye Vody Basin to the north, are associated with sodic metasomatites that overprint BIF along high-strain structures (Belevtsev, ed., 1974). These ores occur in depths exceeding 1,500 m and grade into the "Saksagan-type" higher up. The principal mineral is massive magnetite intergrown with aegirine, enveloped by zones of albitization and carbonatization. U, Zr, REE, Sc, and V mineralization (Tarkhanov et al., 1991), associated with the sodic metasomatites, has made Zheltye Vody the largest Ukrainian uranium deposit, and a significant source of scandium.

Kursk Magnetic Anomaly (KMA) Fe region, SW Russia (Sokolov and Grigor'ev, 1974; Chaykin, 1985; about 15 bt Fe in ~55% Fe ore plus ~4.6 bt Fe in 32% Fe pelletable magnetite BIF). KMA measures about 450 km along the NW axis and is 150 km wide. This has been a prominent magnetic anomaly detected by travellers as early as

in the 1600s. The magnetism is due to extensive Paleoproterozoic BIF, buried under 37 to 550m of Phanerozoic sedimentary cover of the Russian Platform. There are two almost continuous belts of BIF: the longer Belgorod belt in the south-west, and the shorter Oskol belt in the north-east, with the city of Kursk approximately in-between.

The largely terrigenous 1.9 Ga Kursk Series rests unconformably on the 3.0-2.7 Ga Archean greenstone and granite gneiss basement of the Voronezh Massif. The synclinal or trough-like zones of the Paleoproterozoic metasediments are sometimes interfolded with the Archean greenstones, which creates an illusion of widespread Proterozoic volcanism. The tightly folded and greenschist metamorphosed Kursk Series has a lower division of arkosic meta-arenite and phyllite; middle division dominated by BIF; and upper phyllite division. Because of the young cover, the pre-Devonian regolith has been protected from recent erosion and it includes a thick blanket of supergene enriched Fe ores preserved on both sides of the unconformity. The primary ore is imperfectly known and considered comparable with Krivoi Rog, except for the greater representation of magnetite in the BIF. Several mined orebodies in KMA are of enormous size. The "giant" **Yakovlevo** deposit in the Belgorod district (Sokolov and Grigor'yev, 1974; 6 bt Fe @ 60.5% Fe) is 200 to 400 m wide in plan and it has been traced for 50 km along strike, without thinning out. The **Mikhailovka** deposit 100 km NW of Kursk (Chaykin, 1985; 3,614 mt Fe @ 38.8% Fe) is in a steeply east-plunging syncline several hundred meters stratigraphically above Archean greenstones and, in places, in a shear contact with them. The sheared talc, serpentinite and tremolite phyllonite after Archean komatiites contains up to 0.6% Ni, recoverable as a by-product of iron mining (Rundkvist, ed., 1978).

BIF global distribution. Significant Superior-type BIF iron ore regions of the world are summarized in Table 11.3 and located in Fig. 11.27. The "Algoma-type" BIF are not included (read Chapter 9).

11.7. Fe (BIF) and Mn in diamictites

Diamictite is "any nonsorted or poorly sorted terrigenous sediment that consists of sand and/or larger particles in a muddy matrix" (Flint et al., 1960; read also Laznicka, 1985, p.837-842 and Laznicka, 1993, p.898-915 for comprehensive metallogeny review). Paraconglomerate and conglomeratic mudstone are substitute terms.

Although most young unconsolidated diamictites are glaciogenic (e.g. subglacial till and partly glacier fringe drift, glaciomarine silt with dropstones), interpretations become less certain in ancient, consolidated and dismembered diamictite successions not all of which are necessarily glaciogenic tillites. Interpretations are made more uncertain by a high degree of geological mimicry when, for example, tectonic melanges and fault rocks as well as volcanic mudflows (lahars), that resemble tillites, are uncritically interpreted as such.

Quaternary glacial diamictite (till) is one of the most metallogenically sterile materials the role of which is dispersal and wasting of former locally accumulated metals in the bedrock, but portion of the ore minerals from the bedrock deposits may be still left in the drift in sufficient quantities to allow economic recovery. This includes two "giants": the Quinua detrital gold deposit in drift below Yanacocha, Peru, and the Ag-Sn "pallacas" on flanks of the Cerro Rico, Potosí, Bolivia (Chapter 6). Large volumes of glacial drift, moreover, can store cumulatively large quantities of detrital gold in subeconomic concentrations (e.g. west of the Alpine Fault, New Zealand; Nome area, Alaska; NE Siberia) available for local enrichment in fluvial channels or in beach sediments. There are no significant ancient equivalents of detrital ores in diamictites known, although glaciogeny is one of the metallogenic agents worthy of consideration in explaining the Witwatersrand origin.

Several Proterozoic successions have a distinct diamictite component and some are, directly or indirectly, associated with chemical sedimentary ore accumulations like bedded Fe and Mn, and less importantly phosphorite, pyrite, Cu, Mo, V, U and Au. The cumulative ore metal content in the Proterozoic diamictite association is about 43 bt Fe and 226 mt Mn (Laznicka, 1993), whereas there is virtually nothing in the Phanerozoic equivalents. The most interesting is the enigmatic diamictite-carbonate association in which the presumably glacial deposits are preceded, immediately followed or interbedded with carbonates interpreted as deposits of tropical carbonate platforms. Also of interest are diamictites associated with synchronous volcanism (Fig. 11.28). BIF and partly Mn in diamictite association account for the Neoproterozoic peak in a histogram that shows distribution of Fe deposits in geological time. The main peak, of course, is between 2.2 and 1.8 Ga when the bulk of the Superior-type BIF formed, which is explained by gradual change of the reducing atmosphere and hydrosphere into an oxidizing one.

Table 11.3. Summary of the "large" (430+ mt Fe) and "giant" (4.3+ bt Fe) Superior-type iron formations (locations are plotted on Fig. 11.27).

No	District, deposit	Raw BIF, tons Fe/grade	Upgradeable BIF, tons Fe/grade	Enriched BIF, tons Fe/grade
1-5	Lake Superior Fe province, USA	70 bt/26%	24 bt/28%	3.6 bt/50%
1	--Mesabi Range, Minnesota	15 bt/25%	11.25 bt/25%	3.0 bt/54%
2	--Cuyuna Range, Minnesota	1.41 bt/32%		82 mt/55.5%
3	--Gogebic Range, Wisconsin	2.48 bt/32%		170 mt/55%
4	--Marquette Range, Michigan	4.55 mt/26%	1.0 bt/26%	173 mt/51%
5	--Menominee Range, Michigan	1.38 bt/32%		148 mt/51%
6	Labrador Fe province, Canada	trillion tons/20-30%		
7	--Wabush Range, Quebec*		1.15 bt/38%	
8-9	Kursk Magnetic Anomaly, Russia	10 trillion/25-30%	4.6 bt/32%	16 bt/55%
8	--Belgorod deposit			5.93 bt/60.5%
9	--Mikhailovka deposit		3.614 bt/39%	partly included
10	Krivoi Rog, Ukraine	100 bt+/25-30%	6.543 bt/35.7%	2.784 bt/57.6%
11	East Hebei Fe province, China		1.2 bt/35%	
12	Bailadila Fe district, India			998 mt/66.5%
13-14	Quadrilátero Ferrífero, Brazil	150 bt/40%		16 bt/55%
13	--Itabira ore field		1.363/47%	1.15 bt/67%
14	--Alegria ore field		8.5 bt/50%	150 mt/64%
15	Serra do Urucum, Brazil***	15 bt		560 mt/63% canga
16	Tiris, Mauritania		562 mt/38%	
17	Tasiat, Mauritania		2.1 bt/35%	
18	Sishen, North Cape, South Africa			1.3 bt/65%
19-27	Hamersley province, Australia	5.2 trillion t/22.5%		19.25 bt/55%
19	--Mount Whaleback, Newman			1.09/64%
20	--Tom Price			576 mt/64%
21	--Ophtalmia Range			472 mt/63%
22	--Rhodes Ridge			616 mt/61.6%
23	--Marra Mamba (several deposits)			4.84 bt/55%
24	--Mining Area C		2.4 bt	542 mt/61.6%
25	--Robe River Tertiary clastics**			1.45 bt/58%
26	--Marillana Channels (Yandi)**			873 mt/58.2%

All figures are tonnages of contained Fe in ore (not of ore) and all entries are of the (Lake) Superior-type (except #15) and Paleoproterozoic (~2.2-1.8 Ga). Upgradeable ores are presently economic to mine for pre-smelter upgrading (mainly pelletization) and most contain magnetite. Enriched ores are both supergene and probably hypogene, mostly of hematite or goethite. *—high metamorphic grade; **—alluvial ferruginous gravel deposits ("pisolith"), reworked from lateritic profiles over BIF. ***—Fe in diamicite association. Based on Table 4-13 in Laznicka (1993) with updates. Not included here are the "Algoma-type" deposits (Chapter 9), high-grade metamorphosed deposits (Chapter 14), deposits in diamicites (read text) and Phanerozoic ironstones (Chapter 13)

Presumably, global glaciation with anoxic basins capped by ice sheets and accumulating Fe (and Mn) in solution, to be later precipitated en-masse during interglacials or postglacials, had a similar effect (Klein and Beukes, 1993). BIF iron deposits associated with diamicites are known from Neoproterozoic successions in the Flinders Ranges of South Australia; in the Corumbá-Mutún Fe-Mn district in Brazil and Bolivia (10-20 bt Fe @ 45-58% Fe and a "Mn-giant" with 171 mt Mn @ 45%; Haralyi and Walde, 1986); in the Rio Peixe Bravo in Minas Gerais, Brazil (1.225 bt Fe @ 35%); in the Kaokoveld of Namibia; in the Dzhetym and Naryn Ranges of SE Kyrgyzstan. The Mackenzie

Mountains "redbed mixtites" in NW Canada host the "Fe giant" Crest deposit.

Crest (Snake River) Fe deposit (Yeo, 1981; 11.62 bt Fe @ 46%; Fig. 11.29) is in the outer fold and thrust belt of the NE Canadian Cordillera. The basal Meso- to Neoproterozoic "rift association" and platform carbonates are unconformably overlain by the 790-770 Ma Rapitan Group. This is a 300 to 1,000 m thick varicoloured detrital sequence with diamicites, traceable for over 650 km along strike. The Rapitan is gently open folded, faulted and subgreenschist metamorphosed. It consists of a cyclic alternation of maroon or light green diamicite with gray to varicolored mudstone,

siltstone, sandstone and orthoconglomerate. The diamictites consist of angular to subangular pebbles of local siltstone with minor clasts from the underlying rocks, but there are no abundant exotic

clasts. The diamictites range from fragmentites with around 60% of megaclasts to siltstones with some 5-10% of dropstones.

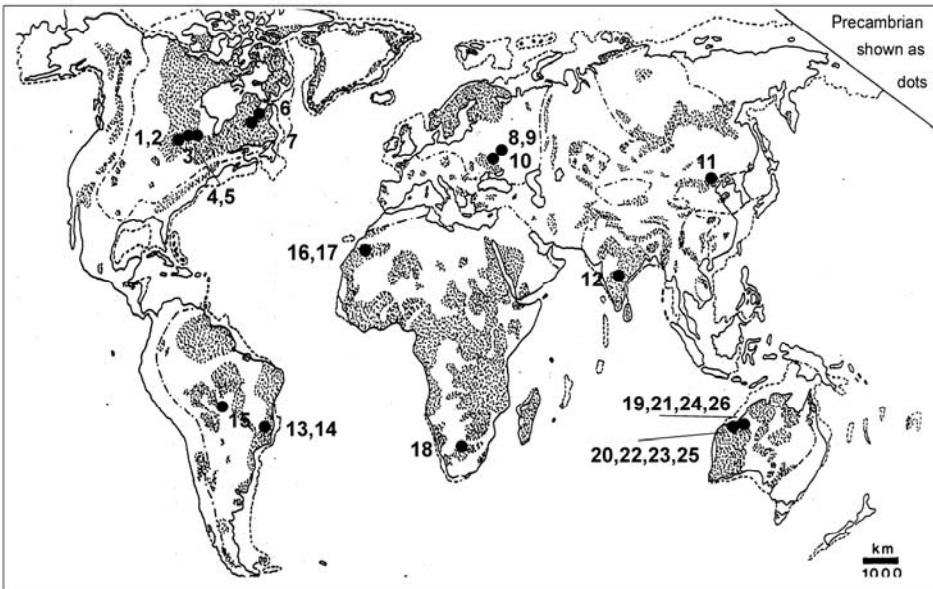
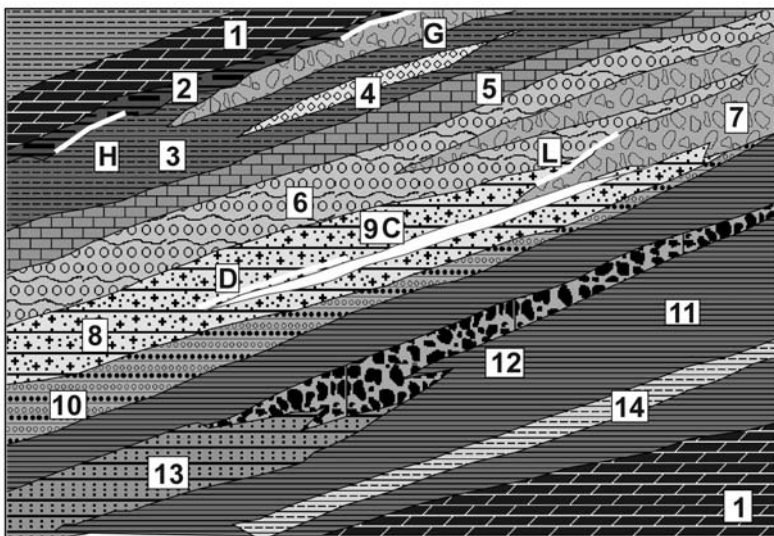


Figure 11.27. Significant Superior-type Fe deposits and districts of the world. Numbers refer to localities listed and characterized in Table 11.3



- 1. Gray dolomite; 2. Black shale/slate; 3. Gray marine shale; 4. Channel conglomerate; 5. Thinly-bedded limestone; 6. Stratified diamictite; 7. Massive diamictite; 8. Wacke, matrix-rich arkose; 9. Chemical sedimentary unit; 10. Laminated siltstone with dropstones; 11. Laminated siltstone; 12. Debris flow; 13. Turbidites; 14. Varicolored shale, siltstone.
- C. Rapitan-type cherty BIF; D. Stratiform siliceous Mn formation; G. Metalliferous phosphorite, carbonaceous schist; H. Bedded Mn, pyrite; L. Heavy mineral paleoplacers; V. Supergene enriched BIF

Figure 11.28. Ancient diamictite association, cross-sectional inventory of lithologies and ores from Laznicka (2004), Total Metallogeny Site G184

The iron enrichment that has regionally the form of hematite pigment and bands of hematite shale changes into ore-grade BIF at several stratigraphic levels. At the Crest property, the Sayunei Iron

Formation is up to 165 m thick and 51 km long. More than ten, up to 24 m thick, Fe-rich subzones have been recognized and the calculated Fe resources are in up to three thickest beds of the 40-

50% Fe laminated hematite-jasper ore. In the local variety of "nodular iron formation", sharply outlined jasper nodules are scattered in the banded ore, whereas the "mixtite iron formation" (Yeo, 1981) is a diamictite with hematite mudstone matrix. Ore genesis and iron source at Crest are enigmatic, although the preferred 1980s interpretation invoked an "exhalitic" contribution. There is no supergene modification whatsoever in an area deglaciated only several thousand years ago. Crest, discovered in the 1960s, remains undeveloped because of isolation (hence transportation problem) combined with environmental considerations, yet it is probably the last undeveloped major Fe resource remaining along the Pacific Rim.

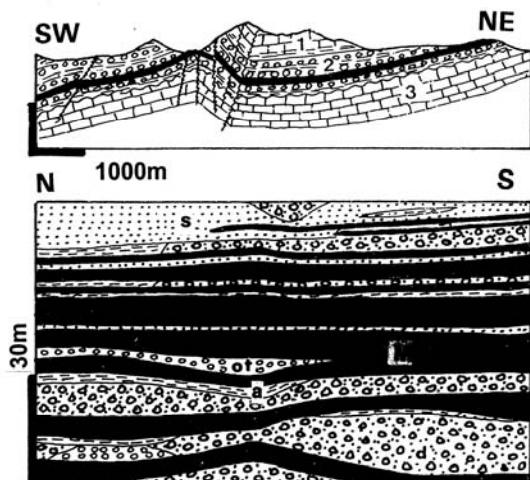


Figure 11.29. Snake River (Crest) siliceous BIF in Rapitan diamictite association. Regional and detailed cross-sections from LITHOTHEQUE No. 754, based on materials compiled by the Crest Exploration Ltd. in 1964. 1. Np Twitya Fm. limestone, dolomite, argillite; 2. ~755-730 Ma Rapitan group diamictite association: a=argillite; s=lithic sandstone; ot=quartzite; d=diamictite. M (black), red jasper interbedded with steely hematite; 3. Np Little Dal dolomite

11.8. Bedded and residual Mn deposits

The bulk of the world's manganese supply comes from, and all giant deposits are, bedded (stratiform) or weathering-enriched bedded deposits. Of this, more than 75% of the contained Mn are in Proterozoic deposits, the rest being in Phanerozoic deposits. No major Archean Mn deposits are known.

There is a transition between BIF with high-Mn content (~10% Mn plus, usually in separate orebodies from the iron ones) through low-Mn BIF

where the Mn is a component of the iron ore, to almost Fe-free bedded Mn orebodies. BIF or at least jaspillite, however, are usually there as well: stratigraphically below the Mn (as in the Kuruman province) or in the presumed source area to detritus and leachate from a Mn-rich bedrock undergoing humid tropical weathering (e.g. Paleoproterozoic BIF as a source to the Oligocene Nikopol' Mn province; Chapter 13). BIF are thus important in the predictive metallogeny of Mn, and so are (meta)basalts or mafic volcanics that are high in trace Mn (around 0.1% Mn), that is readily leached out during both hydrothermal and supergene hydration and alteration (e.g. Ongeluk basalt in the Kuruman area). This is similar to the behaviour of copper, although "giants" Mn-Cu deposits are not known; the bedded Cu, Co, Zn, Mn deposit Boléo in Baja California (Chapter 6) comes closest. Carbonaceous lithologies (black shale, black limestone) are also important repositories of Mn, reaching "giant" magnitude in Moanda (Gabon) and Molango (Mexico; Chapter 13).

The sedimentary Mn metallogenesis resembles one of iron, except that Mn is more mobile hence it "goes faster and farther", forming accumulations more "distal" than Fe. As expected, there has been a debate as to whether bedded Mn deposits are hydrothermal-sedimentary ("exhalitic", e.g. R.W. Hutchinson's line), syngenetic-diagenetic (e.g. Force and Cannon, 1988), or in-between. The latter authors argue for syngenetic precipitation of Mn in shallow marine sediments along the redox interface between the oxidized sediments on land (e.g. red beds) and in the nearshore, and reduced "black shale basins". No model, however, provides plausible explanation for the exceptional local Mn accumulations as in the Kuruman Basin in South Africa that alone stores more than 50% of the world's on-land Mn resources. Brief factual description is the best way out.

Transvaal Supergroup and Kalahari Mn field, South Africa

Transvaal Supergroup (or Sequence) is an up to 15 km thick, 2.65-2.05 supracrustal succession (80-90% of sedimentary rocks, 10-20% of volcanics) deposited in a "vast epeiric basin covering at least 500,000 km² of the Archean Kaapvaal Craton" (Tankard et al., 1982). It is the world's oldest, most extensive, fully developed "miogeoclinal" and platform association enlivened by several volcanic units related to crustal extension. The latter have a major influence on metallogeny. This account is restricted to features present in the south-western

Transvaal sub-basin (Griqualand West), in the North Cape Province.

The Griqualand West sequence (Beukes, 1983) starts with a thick basal platformic carbonate (mostly dolomite) with minor shale, overlain by a cyclic sequence of three banded and clastic-textured iron formations with a 50-150 m thick Magkayene Formation (presumably glaciomarine diamictite). Above is a 500 to 1,000 m thick pile of, on top, subaqueous basaltic andesite flows (Ongeluk Formation) with pillows, hyaloclastites and rare chert interbeds. This, in turn, is conformably overlain by the predominantly chemical sedimentary, 2.3-2.2 Ga Hotazel Formation that comprises four units of siliceous (jaspilitic) banded iron formation interlayered with three low-iron Mn ore layers. The base of Hotazel is between 2,700 to 4,200 m above the Archean basement unconformity, so it is entirely intraformational and it grades upward into ferruginous limestone, minor dolomite and chert.

Kalahari Mn field (Nel et al., 1986; Tsikos and Moore, 1997; Tsikos et al., 2003; 4,194 mt Mn @ 31% Mn) is located about 60 km NW of Kuruman and is served from the Hotazel company town (Figs. 11.30, 31). Kalahari should not be confused with the much smaller, and older, Postmasburg Mn field farther south. The discovery outcrop, the Black Rock kopje, was first noted in 1941 and subsequently the entire ore field that measures 34 km along the NW axis, concealed under thin cover of the Tertiary Kalahari Formation, has been outlined by drilling and excavations. In analogy with many iron deposits that consist of an earlier, stratiform, lower grade banded iron formation followed by superimposed, structurally controlled high-grade "deep" Fe orebodies (read above), similar situation exist in the Kalahari Mn field. There, the bedded Mamatwan-type ore (after the largest Mamatwan open pit mine; Nel et al., 1986) is a microcrystalline, bedded, banded, stratiform braunite, kutnahorite, minor hausmannite ore with hematite and calcite gangue that grades in the 30% Mn range. It constitutes the bulk of the Kalahari Mn resources. The higher-grade Wessels-type ore (Gutzmer and Beukes, 1995) is restricted to the NW part of the field. It consists of coarse, massive to vuggy hausmannite, braunite, bixbyite in chlorite, andradite, calcite etc. matrix superimposed on the stratiform ore along faults. This ~50% Mn ore is mined from underground and it was remobilized by 200-400° C hot fluids. Supergene alteration has affected near-surface portions of both ore types.

Rocks of the earliest Hotazel chemical sedimentary cycle rest on bleached, silicified,

hematitized and/or epidotized Ongeluk meta-basalt and hyaloclastite and they have the form of a jasper to banded chert-hematite BIF. This changes upward into a 6 m thick, low-grade (~30% Mn) jacobsonite-rich basal Mn-Fe layer that is not being mined. The almost flat lying middle Mn unit (bed) is 19.7 m thick in the Mamatwan pit and it has an average grade of 38% Mn. The ore is an inconspicuous dark brownish-gray, fine-grained, nonmetallic looking massive or banded Mn "mudstone", the manganiferous nature of which is "revealed" only in the oxidation zone where it is coated, or replaced, by black cryptomelane or pyrolusite. Fragments of oxidized Mn ore are abundant near base of the Kalahari gravels and calcrete and there are also pockets of pedogenic, concretionary Mn oxides. The upper Mn ore layer is 19 m thick and as it is low-grade (20-30% Mn) it is stockpiled or not mined. In the small Hotazel deposit situated in a fault-bounded outlier of the main Kalahari field, three mainly braunite Mn ore layers with a cryptomelane-enriched top are intruded by a small bostonite laccolith, brecciated and slumped.

The Kalahari Mn genesis is an enigma. Although the sedimentary-diagenetic origin of the bedded Mn ores and the associated BIF appears convincingly demonstrated (Tsikos et al., 2003), the Mn source is unclear and it would be tempting to consider the spilitized, locally silicified and hematitized Ongeluk Basalt, with 0.1% Mn when unaltered, as the Mn source. Although "exhalite feeders", "footwall stockworks" and MORB paraphernalia have been from time to time invoked, Tsikos et al. (2003) argued that these are syn-orogenic features superimposed on the Hotazel rocks and ores during the Meso- to Neoproterozoic time.

Moanda Mn district, Gabon (Weber, 1969, 1973; 275 mt Mn @ 35% Mn in enriched lateritic ore; Rc ~6.5 bt Mn @ 13.5% Mn in protore). This "Mn supergiant" matches the Kalahari Basin in total Mn content, but the bulk is in low-grade rhodochrosite protore not economic now. Moanda is located 40 km WNW of Franceville in eastern Gabon and it exploits unconsolidated lateritic blanket with supergene enriched Mn oxides on top of tropical plateaux (Okouma, Bangombe). The Mn blanket is developed on erosional relics of an almost flat lying Paleoproterozoic sedimentary Mn unit preserved in several downfaulted blocks. The supergene blanket is 8 to 17 m thick. The leached thin soil horizon on top is underlain by a 5-6 m thick allitic layer with microconcretions of gibbsite, goethite and lithiophorite in clay, gibbsite and goethite matrix.

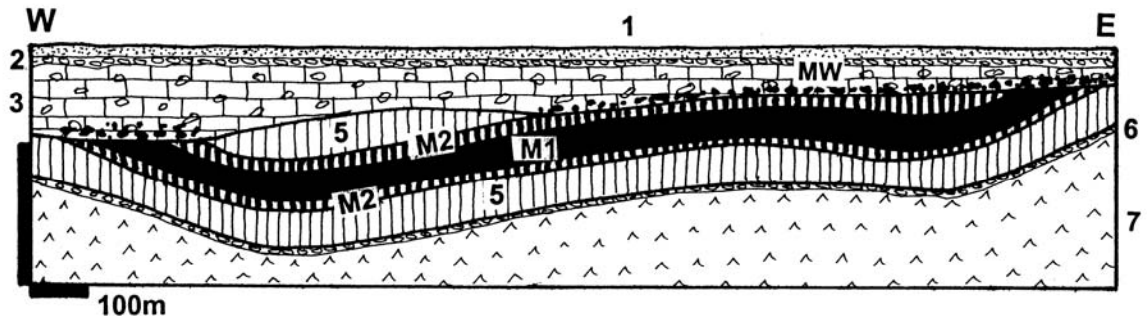
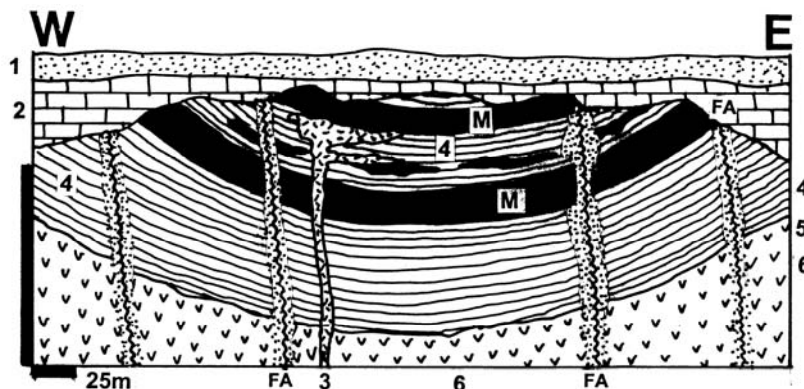


Figure 11.30. Kalahari Mn Basin, Mamatwan Mine, North Cape, South Africa. Cross-section from LITHOTHEQUE No. 1962, modified after Nel et al. (1986). 1. Q aeolian sand; 2. T3-Q loose gravel; 3. Mi-Q massive calcrete limestone and calcrete-cemented debris; MV. Supergene Mn oxides in and under calcrete; 4. Trachyte and microsyenite dikes; 5. Pp (~2.22 Ga) Hotazel Fm., rhythmically banded jaspillite enclosing up to three layers (lenses) of Mn ore; M. Stratiform horizons of Mn ore. M1. Pelitic braunite > hausmannite, kutnahorite, the main mined bed; M2. Pelitic hematite and jacobsonite, marginal. 6. Pp Ongeluk Fm. basaltic andesite flows and hyaloclastite, hyaloclastite bed on top; 7. Ditto, mafic flows



1. T-Q aeolian sand, loose gravel; 2. Mi-Q massive calcrete limestone to breccia; MW. Supergene cryptomelane > manganite at base of calcrete; 3. Trachyte, microsyenite dikes; 4. ~2.22 Ga Hotazel Fm. rhythmically banded jaspillite with three Mn horizons; M. Layers of massive or banded braunite > hausmannite, Mn-carbonate; FA. Bleached and oxidized jaspillite along faults;

Figure 11.31. Hotazel Mn mine, North Cape, South Africa. Cross-section from LITHOTHEQUE No. 1963, based on SAMANCOR Ltd. materials, 1990. Explanations (continued): 5. Pp Ongeluk Fm., ferruginous hyaloclastite; 6. Ditto, subaqueous flows of pillowed tholeiitic basaltic andesite

This layer contains ~15% Mn and is not recovered. The productive horizon below is a 3-9m thick saprolite composed of tablets ("plaquettes") of manganite, pyrolusite, nsutite and cryptomelane in matrix of Fe and Al hydroxides. Lenses of massive ore of the same composition and Mn-impregnated relics of sandstone and shale occur throughout. A compact pyrolusite layer marks the base of the enriched zone.

The primary protore below is an almost unmetamorphosed ~2.1 Ga member of the Francevillian Supergroup that rest unconformably on Archean crystalline basement (Bonhomme et al., 1982). The basal Francevillian consists of varicoloured continental strata that host several medium-size "sandstone-U" deposits (Mounana, Oklo). Above is a marine pelitic unit with sandstone channels, dolomite, occasional mafic volcanics,

chert and carbonate, silicate and sulfide iron formation (siderite, greenalite, stilpnomelane, pyrite) that becomes increasingly carbonaceous upward, locally reaching up to 20% of organic carbon. The preserved uppermost 70m of this unit are manganiferous and constitute the Mn protore. Mn resides in rhodochrosite that evolves from/replaces dolomite, cements sandstone and is interlaminated with black pyritic illite-chlorite shale. Locally, there are lenses containing up to 90% of "black rhodochrosite". The Moanda Mn association is interpreted as early diagenetic, deposited in an anoxic basin greatly enriched in Mn dissolved in seawater. The anomalous local supply of Mn remains unexplained, although Weber (1973) assumed some sort of Mn source connection with the contemporaneous spilitic submarine volcanism in the Okondja Basin, 70 km to the NE.

In the **Corumbá-Mutún** Fe and Mn province in the border area of Brazil and Bolivia (171 mt Mn @ 45%; Haralyi and Walde, 1986) "giant" Fe and Mn deposits are in the 990-950 Ma Jacadigo Group. This is a diamictite-rich association where Fe is accumulated in several horizons of siliceous BIF. Mutún produces only Fe ore (mostly from enriched colluvial gravel), whereas at Corumbá 2-5 m thick beds of siliceous Mn oxides (cryptomelane) occur in arkose and diamictite just below the BIF.

11.9. Miscellaneous, complex Zn, Pb, Cu, Co, V, Ag, Ge, Ga, (U) sulfide deposits

An assortment of hard to classify and interpret, Pb-Zn and/or Cu-dominated sulfide deposits rich in various rare metals, occurs in some carbonate-containing Proterozoic sequences. The deposits combine characteristics of the Mississippi Valley (the largest Proterozoic MVT deposits are Gayna River with 2.4 mt Zn and 200 kt Pb, and Goz Creek with 827 kt Zn, both in the NW Canadian Cordillera; Pering in South Africa with 648 kt Zn), sedex, "black shale", replacement and vein types and are jointly controlled by structure (faults, unconformities) and lithology. The genesis varies, although the majority of deposits would be nowadays attributed to the low-temperature hydrothermal "basinal fluids". Seven Pb or Zn "giants" have been recognized.

Tsumeb in northern Namibia (Lombaard et al., 1986; Frimmel et al., 1996; Kamona et al., 1999; Fig. 11.32) is a famous, recently closed mine and mineralogical locality and also the source of 23 (or 27) mt ore grading 10% Pb, 4.3% Cu, 3.5% Zn, 1.0% As and 95 g/t Ag containing 2.7 mt Pb, 1.16 mt Cu, 945 kt Zn, 230 kt As and 2,565 t Ag. Also present in the orebody and sometimes recovered has been 13.5 kt Mo (0.05%), 10.8 kt Cd (0.04%), 2,700 t Hg (0.01%), 2,160 t Ge, 1,350 t Se, and 540 t Te.

Tsumeb is located in the northern foreland fold and thrust belt of the Damara orogen, in the Neoproterozoic Otavi Group dolomite interpreted as deposited in an intracontinental rift graben. The 3,000 m thick predominantly dolomite succession with minor limestone, anhydrite and gypsum changes facies to shale, and rest on the Chuos diamictite. The carbonates are unconformably overlain by terrigenous clastics of the Mulden Group. The strata are open along E-W axes, lower greenschist metamorphosed and moderately faulted.

Local brittle faults and breccia zones, however, control the mineralized structures but are often obscured by solution and alteration.

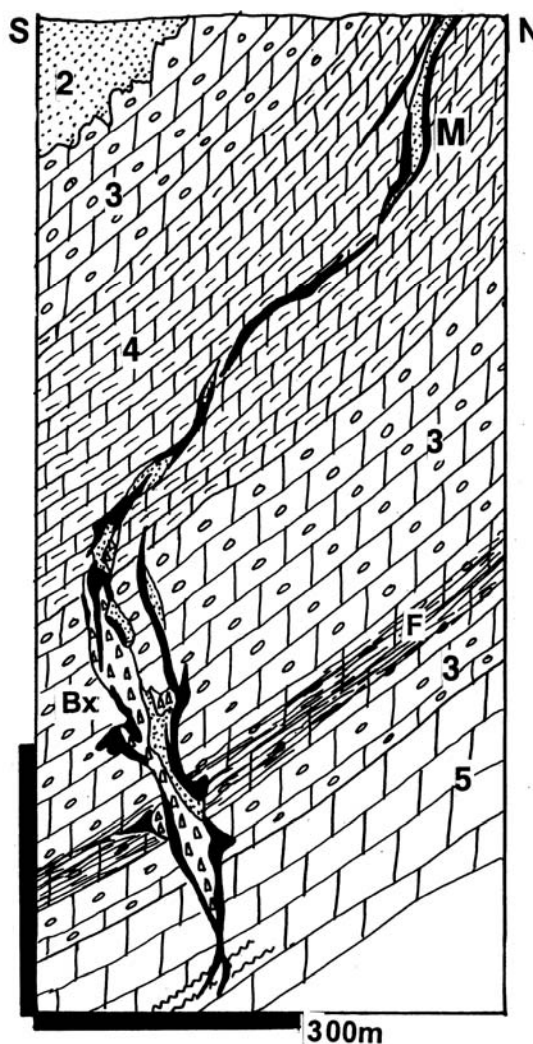


Figure 11.32. Tsumeb Mine, Otavi, NW Namibia, cross-section from LITHOTHEQUE No. 1940, modified after Lombaard et al. (1986), Tsumeb Mines materials. M. ~580-550 Ma synorogenic mineralized steeply dipping structure filled by breccia (Bx) and influvium of Unit 2. Replacements and disseminations of Zn,Pb,Cu,As, etc. sulfides overprinted by deep oxidation; 1. Np-Cm1 Mulden Group slate to phyllite (not shown); 2. Ditto, feldspathic sandstone; 3. ~600-545 Ma light gray dolomite with chert; 4. Ditto, dark gray bedded dolomite; 5. Massive light-gray dolomite

The Tsumeb ores are confined to a steep pipe-like structure formed under the Mulden unconformity. The pipe is elliptical to tabular in cross-section,

measuring 200x100 m at the surface but diminishing with depth until its termination 1,716 m under the surface. The pipe is filled by several varieties of breccia that range from in-situ disaggregated breccia in the wallrocks to collapse or intrusive breccias filling the central void. Externally derived breccia components are rare and much of them are a quartz-feldspar influvium ("pseudoaplite") derived from basal clastics of the Mulden Group. The complex orebody consists of massive Pb, Cu, Zn sulfide replacements in pipe walls that extend as mantos (bedding subparallel masses) into the adjacent dolomite. The remainder are disseminations and stringers in breccias and calcitized, in depth silicified, wallrocks. The main ore sulfides are galena, tennantite, sphalerite, chalcocite group, bornite and enargite and there are numerous Ge, Ga, V, Sn and W minerals for many of which Tsumeb is the type, or only, locality. A body of almost massive germanite encountered on the 6th level totalled 28 tons. There was a prominent supergene zone reaching, with diminishing intensity, into the depth of more than 1,600 m under the surface: a world record! Cerussite, malachite, cuprite, mimetite, wulfenite, smithsonite and willemite provided the bulk of ore mined from the oxidation zone, whereas chalcocite, djurleite, digenite and covellite formed in the secondary sulfide zone. The oxidation zone contributed many rare minerals of the list of 213 species described from here. Frimmel et al. (1996) considered the Tsumeb sulfides as relatively high-temperature (450°C), precipitates from (syn)orogenic basinal fluids injected into the foreland around 570-560 Ma.

Kipushi-Zn,Cu,Pb,Ag (formerly Prince Leopold Mine) is a mined-out deposit 30 km WSW of Lubumbashi, in the Shaba/Katanga (DRC Congo) Copperbelt (De Magnée and François, 1988; Kamona et al., 1999; P+Rv 55 mt ore with 7.59 mt Zn @ 13.8%, 1.155 mt Cu @ 2.1%). The deposit is younger than the copper orebodies in the Roan Group (read above) and not directly related to them. The ore zone is a steeply NW-dipping deformation structure that has the Lower Kundelungu Kakontwe Dolomite in the footwall, and a tectonic slice of silty dolomitic shale in the hangingwall. The structure is located along the eastern contact of a diapiric megabreccia composed of the Roan Group rocks, extruded from depth. There are also bodies of altered meta-gabbro.

Massive to disseminated sulfides fill and replace breccias and wallrock carbonates in the deformation zone under impermeable screen of the hangingwall

shale, and they extend into breccias in the footwall dolomite. The multiphase mineralization started with formation of pyrite, arsenopyrite and sphalerite orebodies, followed by at least four phases of precipitation of cobaltian chalcopyrite, molybdenite, chalcocite, tennantite, Ag-rich bornite, and other minerals. There is an about 100 m deep oxidation and secondary sulfides zone with turquoise impregnations in the hangingwall shale, and pseudomorphic replacements as well as infiltrations of many supergene minerals in the paleokarsted footwall dolomite. Kipushi is, like Tsumeb, a famous mineralogical locality noted for many rare Pb, Mo, W, V, Ge, Ga and In minerals.

Zawar, India: Zn, Pb mineralized deformed, metamorphosed, mineralized carbonate horizon.

The Zawar ore field in Rajasthan is a segment in the 30 km long Zn-Pb ore belt south of Udaipur (Basu, 1982; Hindustan Zinc, Ltd., tour 1988; 3.172 mt Zn, 1.744 mt Pb in four major ore deposits). The area consists of greenschist-metamorphosed clastics and carbonates of the pre-2.0 Ga Aravalli Supergroup. All ore deposits are confined to a dolomite unit bordered by a gray to black phyllite (partly phyllonite) and meta-graywacke. Diabase dikes are locally abundant. The meta-sediments have been deformed in at least four phases. The earliest deformation around 2.0 Ga produced a north-plunging anticlinorium that defines the Zawar belt. The subsequent 1.7-1.5 Ga deformation was responsible for the east-west trending and west-plunging overturned anticline. Of the four major deposits, Mochia and Balaria are on the northern limb of the east-west fold, Zawarmala and Baroi are on both limbs of the north-south structure.

Within the sheared, penetratively deformed and repeatedly recrystallized dolomite unit the orebodies are structurally controlled. The ores range from replacement disseminations and stringers of sphalerite, pyrite, galena and lesser Fe, Cu, As, Sb sulfides to massive bodies of the same composition. The massive sulfides range from crystalline masses with a simple annealed mosaic texture to protoclastites or ductile breccias with well developed *Durchbewegung* fabrics. The orebodies have a form of stringers, ductile veins, boudins, lenses, flattened pipes, schlieren, and irregular blocks of disseminated minerals. Ore filling brittle fractures and dilations are minor. The orebodies are controlled by axial cleavage, anticlinal noses, shears and lithology. The Balaria orebody has the shape of a "branching tree" related to shear and slip surface intersections, and to the screen effect of phyllonite seams.

Brown's Pb, Cu, Co, Ni deposit near Batchelor, in the former Rum Jungle uranium ore field south of Darwin, Australia, is a "Pb-giant" with an unusual combination of ore metals in Paleoproterozoic metasediments (McCready et al., 2004; Rc 82 mt ore @ 2.2% Pb, 0.77% Cu, 0.12% Co, 0.11% Ni containing 1.804 mt Pb, 634 kt Cu, 98 kt Co, 90 kt Ni). The extremely fine-grained galena, sphalerite, chalcopyrite, pyrite and siegenite form dense disseminations in an almost unaltered graphitic phyllite, flooded by magnesian dolomite and intruded by a diabase sill. The supracrustals mantle a set of two Archean basement domes. The Brown's deposit is interpreted as a bedding-parallel synsedimentary-diagenetic mineralization, substantially remobilized during the 1.8 Ga orogeny into crosscutting stringers, veinlets and patches of the same but coarser-grained minerals. Several discontinuous, steeply SSE-dipping lenticular orebodies occurs in the NE-trending Embayment Zone, intersected by a series of faults. Post-orogenic uranium mineralization sourced in the Archean basement, mined from the field in the 1960s-1970s, locally overprints the base metal ores. There is a 20+ meters thick oxidation and secondary sulfides zone on top of the Brown's orebody. The "large" (8 mt of ore containing 968 kt Zn, 440 kt Pb, 880 t Ag) Woodcutters deposit 10 km east from Brown's is a synorogenic vein hosted by the same rock association.

Abra Pb, Ba, Ag deposit is located 170 km SW of Newman in Western Australia, in the Mesoproterozoic Bangemall Basin (Boddington, 1990; Rc 200 mt of ore with 1.8% Pb, 0.18% Cu, 6% Ba, 6 g/t Ag for 3.6 mt Pb, 360 kt Cu, 1,200 t Ag plus barite). The open folded but faulted, almost unmetamorphosed succession of submature sandstone, shale and carbonates is intruded by diabase sills and it overlies the 2.0 to 1.7 Ga Capricorn orogen and ultimately the buried suture zone between the Pilbara and Yilgarn Archean cratons. The Abra deposit is situated in a sub-basin interpreted as a graben established during the rift phase, in laminated dolomitic siltstone, sandstone and stromatolitic dolomite with chert and jasper interbeds. The top of the complex ore zone is a stratabound 23m thick unit of metacolloform hematite, barite, quartz and dolomite. Some bands also contain scattered galena, pyrite and chalcopyrite and the same minerals occur as veins and cross-cutting breccias. This changes with depth into red jasperoid-dominated material with some magnetite and hematite and eventually into an up to 350 m thick footwall zone of chloritized and locally

silicified, dolomitized and barite-replaced rocks. The latter is extensively veined by galena-barite and chalcopyrite-magnetite. Scheelite and gold are locally enriched and constitute a separate, low-grade ore zone (~150 mt @ 0.13 g/t Au). As expected genetic interpretation of this buried deposit changes with seasons and the majority of investigators assume introduction of low-temperature mineralizing fluids into a sedimentary pile undergoing diagenesis under the seafloor (a variety of the sedex model).

11.10. Oxidic (nonsulfide) Zn and Pb deposits

Most sphalerite and galena deposits exposed in areas free of Quaternary glaciation have in-situ or transported (exotic) oxidation zones with oxidic Zn and/or Pb minerals (smithsonite, hemimorphite, hydrozincite, cerussite, anglesite, pyromorphite, plumbojarosite). Cumulative tonnages of the oxidic Zn or Pb ores vary, but most are (were) in the small to medium range. At the recently discovered **Scorpion Zn** deposit in southern Namibia (Borg et al., 2003; 6.81 mt Zn @ 7-10.6% Zn), however, smithsonite and hemimorphite hold a greater share of the complex oxide-sulfide orebody. Several entirely or almost entirely nonsulfide Zn deposits, interpreted as hypogene (Hitzman et al., 2003), are known from Proterozoic sequences. Beltana and Aroona in South Australia are of small to medium size, Vazante in Brazil is a "near-giant". The high-grade metamorphosed "large" to "giant" equivalents, Franklin and Sterling in New Jersey, appear in Chapter 14.

Vazante Zn ore field is about 350 km SE of Brasília, in Neoproterozoic platformic carbonate cover of the São Francisco Craton, deformed during the Brasiliano Orogeny (Monteiro et al., 2000; P+Rv 19.2 mt ore @ 21% Zn for 4.56 mt Zn; Fig. 11.33). This is the largest Zn deposit of Brazil and the largest unmetamorphosed oxidic Zn deposit of the world. The more than 10 km long NE-trending thrust intersects subgreenschist-metamorphosed massive dolomite with minor interbeds of sericitic and pyritic carbonaceous slate to phyllite. The 50-75° NW dipping fault zone consists of sheared and recrystallized, locally chloritic dolomite grading into up to 100 m thick heterogenous fault breccia zone in the hangingwall. There is a diffuse Fe-dolomite alteration envelope. The Zn ore forms a system of discontinuous lenticular veins in the fault and subparallel with it. They range from few cm to 5 m in thickness and the largest vein continues for

some 5 km along strike. Masses of cream-colored willemite or red willemite-hematite mixture contain patches of greenish-brown sphalerite with galena. Quartz, Fe-dolomite and siderite are the gangue minerals. The blind willemite orebody is capped by a solution collapse breccia with residual chert rubble and boxwork of residual and infiltrated hemimorphite, smithsonite and hydrozincite. The deep willemite bodies are considered synorogenic, low-temperature (80-200° C) hypogene carbonate replacements, produced by mixing of basinal fluids (Hitzman et al., 2003).

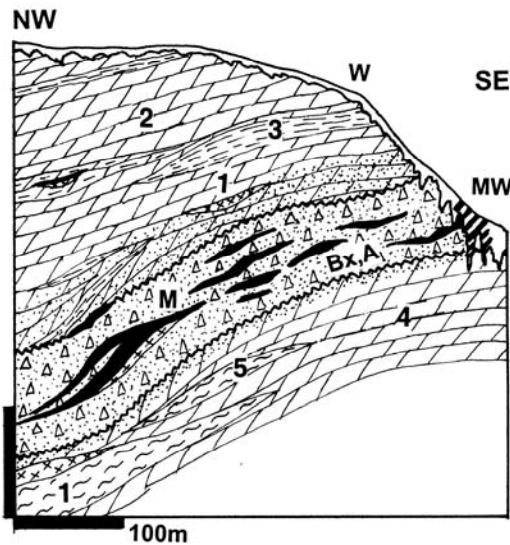


Figure 11.33. Vazante oxidized Zn deposit, MG, Brazil, cross-section from LITHOTHEQUE No. 2503 modified after Monteiro et al. (2000), Companhia Mineira de Metais (T.F. DeOliveira) site visit, 2000. W. Regolith, karst over carbonates; MW. In-situ and infiltrated hemimorphite, hydrozincite in karst breccias; M. Np pure and hematitic willemite with quartz, dolomite, siderite, lenticular bodies in altered breccia (Bx,A) in shear; 1. Np Vazante Fm., metasbasite lenses; 2. Pamplona Member dolomite > phyllite; 3. Ditto, quartz-sericite phyllite > dolomite; 4. Morro do Pinheiro Member, dark argillaceous metadolomite; 5. Ditto, carbonaceous phyllite to phyllonite

Stand-alone oxidic Pb deposits of substantial size have not been recognized until the discovery of the "giant" **Magellan-Pb** deposit in Western Australia, in 1991 (Pirajno and Preston, 1998; Rc 210 mt of ore @ 1.8% Pb containing 3.78 mt Pb). This deposit is in sedimentary rocks of the Paleoproterozoic Napperu Basin that straddles the northern outcrop of the Archean Yilgarn Block in Western Australia. The Pb minerals (cerussite > anglesite, plattnerite,

pyromorphite) mixed with clay residue form matrix of a quartz boxwork in stromatolitic dolomite, situated above metals-enriched carbonaceous metapelite. The 1.65 Ga deposit is interpreted as a mineralized solution collapse breccia.

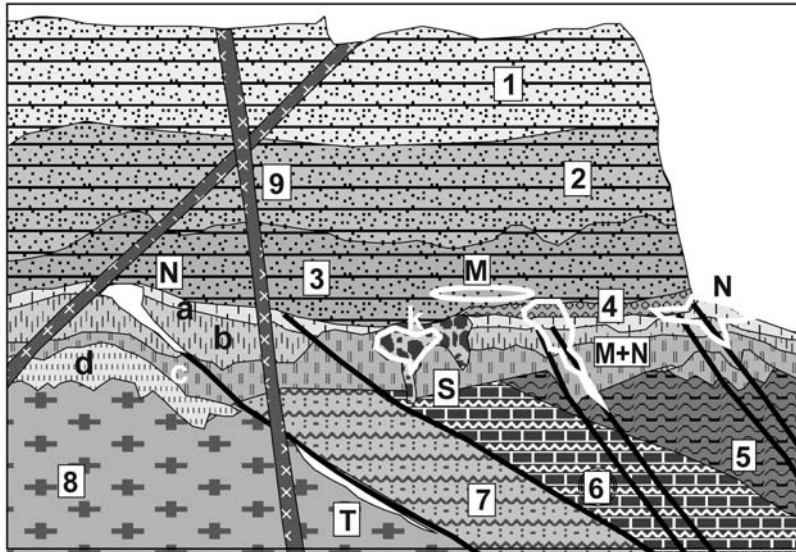
11.11. Unconformity uranium deposits

Rabbit Lake U deposit in Saskatchewan was discovered in 1968 and not knowing much about origin of what was then a new ore type, Duncan Derry coined the nongenetic term "unconformity uranium" (UU), based on the actually observable setting in the field (Fig. 11.34). At present UU's are the highest-grade U deposits recognized (12.7% U in the McArthur River deposit and 7.9% in the Cigar Lake deposit) that have the form of irregular uraninite-rich pods, lenses, sheets and wedges rather than classical ore veins, and are of limited vertical extent, hence mineable from open pits when in outcrop. The wisdom that UU deposits are restricted to immediate proximity of platform edge, or occur under platform, has proven valid and guided exploration for the next third of a century. The UU genesis is still not clear, except for a consensus that UU comprise hydrothermal ores precipitated from fluids with temperatures between 300° to 95°. Most orebodies are multistage, with a series of ages determined for the various events. The two principal UU provinces: The Athabasca Basin and fringe in Saskatchewan (Cameron, ed., 1983; Fogwill, 1985; cumulative endowment ~610 kt U) and the Alligator Rivers region in Northern Territory, Australia (Battey et al., 1987; Ferguson and Goleby, eds., 1980; ~370 kt U) are both "giant provinces". The former province contains one "giant" (McArthur River; 189 kt U), one "near-giant" (Cigar Lake, 155 kt U) and three "large" U ore zones (Rabbit Lake-Collins Bay; 104 kt U), Key Lake (76 kt U); and Midwest Lake (41.65 kt U). The rest are "medium" size deposits. The Alligator Rivers province has one "giant" (Jabiluka, 176 kt U), one "near-giant" (Ranger, 160 kt U), and three "medium" deposits. There are virtually no UU deposits outside those two provinces listed above; Kintyre (Western Australia; 30.6 kt U) is one of the exceptions.

Dahlkamp (1993) subdivided the UU deposits into his "contact type" (Type 1) that includes most of the Athabasca Basin deposits, and "sub-unconformity-epimetamorphic type" (Type 2) reserved for the Alligator Rivers deposits. The Type 1 has discordant, fault and fracture-controlled orebodies associated with graphitic tectonites and Ca-Mg silicates in the basement; or pod, lense or

blanket-like bodies resting directly at unconformity, in a clay envelope under the sedimentary sandstone cover. Tails of the latter deposits can extend high into the cover sandstone to form infiltrations

comparable with the "sandstone-U" type (Chapter 13). Some small orebodies in the area are sandstone infiltrations alone.



1. Platformic quartz arenite, white; 2. Ditto, sandy color; 3. Ditto, mottled, hematitic or limonitic; 4. Basal conglomerate; 5. Graphitic paragneiss or schist; 6. Dolomitic marble to Ca-Mg silicate gneiss; 7. Feldspathic gneiss (meta-arkose?); 8. Basement complex gneiss, granite; 9. Diabase dikes; Alterations: a=white bleaching; b=hematite pigmentation; c=Mg chlorite to hematite-chlorite; d=discoloration; k=karsting, solution and tectonic brecciation. M. U oxides, infiltrations in sandstone above unconformity; N. U (Ni,Co,As, Au) ores under unconformity in tectonized basement;

Figure 11.34. Inventory diagram (cross-section) of unconformity U ores modelled on the eastern margin of the Athabasca Plateau, Saskatchewan, Canada. From Laznicka (2004), Total Metallogeny Site G205. Explanations (continued): S. U in collophanite (apatite) in paleokarsted marbles (Itataia); T. U oxides disseminated in albitized rocks near faults

Both types of UU deposits are either monometallic (uraninite with some coffinite, pyrite, marcasite, secondary minerals in the oxidation zone) or polymetallic: U-minerals as above plus pods of Fe, Ni, Co arsenides (löllingite, smaltite, gersdorffite, rammelsbergite, niccolite). As usually, a healthy choice of genetic interpretations is offered in the literature, that include convection of syn-diagenetic heated basinal fluids, hypogene hydrotherms, diagenesis-overprinted paleosurface regolith. Dahlkamp's verdict: polyphase evolution, fluid temperatures between 230-127°C. The Type 2 of the UU's is controlled by fault structures and is strata-bound to a suite of Paleoproterozoic retrograded muscovite-chlorite and graphitic schists (or phyllonites) close to Archean granite-gneiss domes with high trace U. Mesoproterozoic cover sandstones with rhyolitic ignimbrite are present, but the cover/basement interaction is less straightforward in Australia than in Canada. Solomon and Groves (1994, pages 287-343) provided a comprehensive review of the Alligator Rivers province, focused on ore genesis.

Athabasca Basin U province, northern Saskatchewan, Canada. Six groups of U deposits are associated with unconformity under the mainly flat-lying quartz-rich continental to shallow-marine sedimentary rocks of the Mesoproterozoic (1.7-1.5 Ga) Athabasca Basin. The basin rests on several Canadian and Proterozoic divisions of the western Canadian Shield of which the most important is the Paleoproterozoic Wollaston Domain (Sibbald, 1987). This is a polyphase deformed, amphibolite grade-metamorphosed complex of mature quartzite, conglomerate and arkose with local graphitic metapelite, metabasite, Ca-Mg silicates and marble. The complex is retrograded along fault zones with albite, chlorite, graphite altered intervals. The Athabasca Basin sediments rest unconformably on an up to 50 m thick regolith, interpreted as mainly the saprolite portion of a fossil laterite profile (Macdonald, 1985). The predominant quartz arenite with minor conglomerate, siltstone and shale intervals is intersected by 1.4 and 1.1 Ga gabbro and diabase dikes.

Rabbit Lake-Collins Bay zone (Ward, 1989; P+Rv ~104 kt U). Rabbit Lake orebody, the first

greenfield discovery, was found by boulder tracing in shallow subcrop in the regolithic basement less than 1 km from the Athabasca sandstone erosional edge, near the western shore of Wollaston Lake. Subsequently, a dozen more deposits have been found in a 20 km long NE-trending zone along the Collins Bay Fault. The Rabbit Lake orebodies are in a wedge-like block outlined by two NE and NNE-trending, SE-dipping graphite-rich faults. The ore is entirely in metamorphics, overprinted by sodic metasomatism in the pre-ore stage. The host rocks are meta-quartzite, "plagioclase" (a metasomatite), diopside-plagioclase rocks, marble and graphitic schist. On top is biotite-sillimanite paragneiss with amphibolite layers. The rocks are tectonized, repeatedly brecciated and retrograded. The sequence of progressively younger alteration minerals includes chlorite, tourmaline, Na-feldspar, quartz, dolomite, hematite, clays. Supergene argillization is still progressing. The hematite is partly hydrothermal, partly the product of regolith development. The orebody has the shape of a flattened pipe plunging 20° to 40° NE, and it has several high-grade pods surrounded by a lower-grade ore. The ore minerals are pitchblende and coffinite in the form of blebs, veinlets and disseminations in the altered rocks. The main stage of ore emplacement has been dated at 1,281 Ma. Eagle Point is the largest group of two orebodies in this zone (59 kt U). This is a blind deposit covered by a thin veneer of glacial drift and partly by waters of Wollaston Lake. The Paleoproterozoic host schists with meta-quartzite bands rest on Archean granitic basement. They are intersected by a 300 m wide system of subparallel, 40° SE dipping faults. Lenticular orebodies of disseminated sooty pitchblende with coffinite follow faults and have been traced to a depth of 450 m under the surface.

Cigar Lake deposit, a "near-giant" (Bruneton, 1987; 154,600 t U @ 7.9% U) is a blind deposit, found in 1981 under 410 m of Athabasca sandstone and thin veneer of glacial sediments by drilling an electromagnetic conductor. It is about 60 km SW of Rabbit Lake and an example of a deposit at, and above, unconformity. The Paleoproterozoic basement under the orebody consists of meta-pelitic biotite to cordierite and sillimanite gneiss with common pegmatite and quartz-feldspathic mobilizate and Ca-Mg silicate gneiss layers. The rocks are tectonized and retrograded (chloritic), and in place mylonitized, graphitic and pyritic, especially the "augen gneiss" directly under the ore pod. A paleo-regolith predates hydrothermal alteration and uranium deposition and it grades into conglomeratic quartz arenite of the Athabasca

Group. The laterally extensive, 2,150 m long and up to 20 m thick orebody is in strongly clay-altered sandstone, immediately above an east-west basement ridge that appears to be a projection of a fault zone. The highest-grade East Zone contains 110 kt U in a 12.3% U ore that also contains 1.16% Pb, 0.96% Ni, 1.67% As, 0.7% Cu, 0.15% Co and 0.14% Mo. This is surrounded by a low-grade ore envelope. The multiphase mineralization consists of locally almost solid mixture of uraninite, Ni-Co arsenides and minor Cu, Pb, Zn sulfides in Fe and Mg chlorite, kaolinite and illite matrix. The orebody is capped by massive hematitic illite clay with siderite and traces of hydrocarbons. Hydrothermal alteration continues both under and above the orebody and several U-ore patches extend upward, along steep faults, into the Athabasca sandstone (Bruneton, 1987).

The even larger and richer **McArthur River** deposit 70 km NE of Key Lake (McCready et al, 1999; Rc 189 kt U @ 12.7% U) has been discovered in 1988, in depth of 500-700 m under the surface. The 1,521 Ma old ore consists of massive pods of uraninite with some pyrite, galena and sphalerite, controlled by a fault zone in Athabasca sandstone, above unconformity.

Alligator Rivers uranium province, Northern Territory, Australia

Uranium was first discovered, in the Paleoproterozoic Pine Creek orogen, near Rum Jungle in 1953. This has been followed by the Alligator Rivers discoveries in 1970 and afterwards (Needham et al., 1980). The U province is about 220 km east of Darwin, around the residential and administrative center Jabiru. 72 uranium deposits and occurrences have been recorded in an area of 3,000 km² and of the approximately 370 kt of U content some 47% is in the only "giant" Jabiluka.

The low-lying area of poor outcrop is dominated by the 2.5 Ga to 1.8 Ga Nanambu Complex. This is interpreted as a dome of Archean granitic gneiss mantled by up to 5,600 m thick Paleoproterozoic continental to shallow marine meta-sediments, deformed and metamorphosed during the 1.8 Ga orogeny. The dome is flanked by a wide belt of repeatedly deformed rocks of the Cahill Formation dominated by micaschist and meta-quartzite with amphibolite, Ca-Mg silicate rocks, and dolomitic marble. Pyritic, graphitic and chloritic schists abound and at least some are retrograded and tectonized lithologies. Cahill hosts about 50% of the U occurrences and over 90% of contained uranium (Needham, 1985). Prominent escarpment marking

the erosional edge of the Mesoproterozoic cover units, especially the Kombolgie quartz-rich sandstone, is everywhere in sight and although the four largest U deposits are situated within 5 km from the escarpment, several U showings lie more than 30 km away. The sub-Kombolgie paleoregolith is less distinct than in Saskatchewan because it is overprinted by and merges with the thick Cenozoic tropical regolith. The bulk of economic mineralization in the area is in the basement under unconformity, but this may be the consequence of politics as the Arnhem Land plateau is an Aboriginal land and environmentally protected territory where exploration has been banned or discouraged.

The Alligator Rivers U deposits are remarkably similar in shape, style, setting and composition to those around the Athabasca Basin. Most ores are in tectonic breccias, some modified by solution and collapse, in and along faults. The breccias are altered, predominantly by chlorite accompanied by hematite and also sericite, illite, silica, graphite and carbonate. The intense Mg metasomatism is attributed to the presence of evaporites in the cover units. The main ore minerals are sooty to colloform or massive uraninite, minor brannerite, pyrite, but Ni-Co arsenides are uncommon. Most deposits contain traces of gold, but only in Jabiluka this constitutes a mineable resource. The oxidation zone is from 10-60 m thick and secondary U minerals provided important mill feed in the early stages of mining at Ranger. The ores are multistage and timing of the initial, and main, U introduction ranges from 1,750 Ma to 1,600 Ma (Maas, 1989). Of this, Ranger orebodies formed earlier, prior to deposition of the cover sequence. Jabiluka, Nabarlek and other deposits postdate the Kombolgie deposition and formed from 300°-200°C hot fluids in depth of about 2 km under the paleosurface (Wilde et al., 1998). The uranium source is not known with certainty but was most likely in the basement rocks, especially in the U-enriched Nanambu Complex, and in the cover sequence, especially in its rhyolite component.

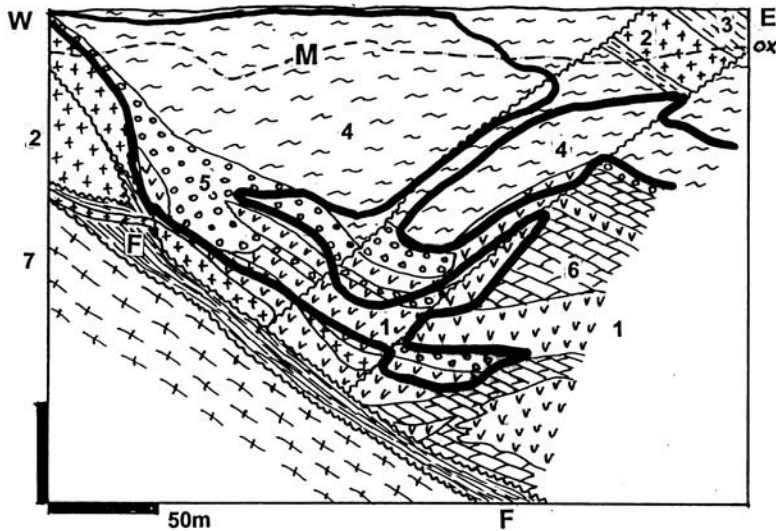
Ranger ore field near Jabiru (Kendall, 1990; P+Rv ~160 kt U @ 0.24-0.37% U; Fig. 11.35) is, at present, the only operating complex that consists of a cluster of orebodies. Ranger I is in tectonized and heavily altered quartz-mica schist of the Cahill Formation, underlain by chlorite-altered dolomite, tectonized pegmatite and metasomatic chloritite. All these rocks are in the hangingwall of a 30° east-dipping bedding-parallel shear that separates them from schists and gneisses of the Nanambu Complex

in the footwall. A pre-ore diabase sill is also present. The 60m thick oxidation zone has mostly saleeite and sklodowskite infiltrations, fracture coatings and pseudomorphic replacements of uraninite. The hypogene ore is disseminated and fracture-filling uraninite with some apatite, less than 0.5% of pyrite and base metals sulfides, and graphite. The higher-grade intervals are in strongly brecciated zones and in quartz-chlorite veins. The Ranger I orebody is an extremely irregular, assay-bounded basin-like structure, and although predominantly in schist it continues into dolomite and in places diabase. The orebody irregularity is attributed to solution collapse into the space previously occupied by dolomite.

Jabiluka, 25 km north of Jabiru, is the only "U-giant" in the region (Hancock et al., 1990; 176 kt U @ 0.33% U, 11.77 t Au) and it also contains a small gold orebody and traces of platinoids. Two separate orebodies: the small, near-surface Jabiluka I and the large, concealed Jabiluka II, are situated along a WNW-trending brecciated, retrograde metamorphosed and hydrothermally altered deformation zone. The Cahill Formation hosts comprise alternating quartz, muscovite, biotite, chlorite and graphite-retrograded biotite-sillimanite gneiss with a magnesite and dolomite interval. Jabiluka II is over 1,000 m long, 400 m wide and up to 135 m thick. It consists of veins and fracture veinlets, disseminations and replacements of uraninite with pyrite and minor coffinite, brannerite, chalcopyrite and galena, at four horizons. The gold orebody is a separate, 2 to 12 m thick breccia-hosted body. The ore zone persists from the sub-Kombolgie unconformity to a depth of at least 600m. The primary U mineralization has been dated at 1,614 Ma (Maas, 1989), shortly postdating deposition of the 1,650 Ma old sandstone and rhyolite cover.

11.12. Hydrothermal Fe oxide deposits with Cu, or U, or Au, or REE (Olympic Dam-type)

If, as it is often stated, Witwatersrand was the discovery of the 19th Century, Olympic Dam finding in 1975, under 300 m of solid rocks cover, has certainly been a discovery of the 20th century: at least its second half (Fig. 11.36). Not only has it introduced a new, highly productive ore type eagerly sought since, but it contributed a case history illustrative of the modern technology of exploration for deeply buried orebodies.



1. ~1.37 Ga diabase dikes and sills; 2. Mp pegmatite; M, ox: outline of the oxidation zone, saleeite, gummite, etc. M. ~1.737 Ga disseminated sooty uraninite, pyrite, etc. in Mg-chlorite, quartz, sericite altered sheared marble and schists. Irregular orebodies above footwall shear; 3. Pre-1.87 Ga Cahill Fm., hangingwall muscovite-chlorite schist (phyllo-nite); 4. Upper Mine Sequence quartz, chlorite, muscovite schist; 5. Lower Mine Sequence "chert" (silicified carbonate), schist; 6. Ditto, marble; F. Footwall shear phyllonite, breccia; 7. Ar Nanambu Complex

Figure 11.35. Ranger 1 deposit, Jabiru, NT, Australia. Cross-section from LITHOTHEQUE No. 1210, modified after Eupene et al. (1975), Needham (1985), Savory (1994) and Ranger Mine Staff, 1981 visit

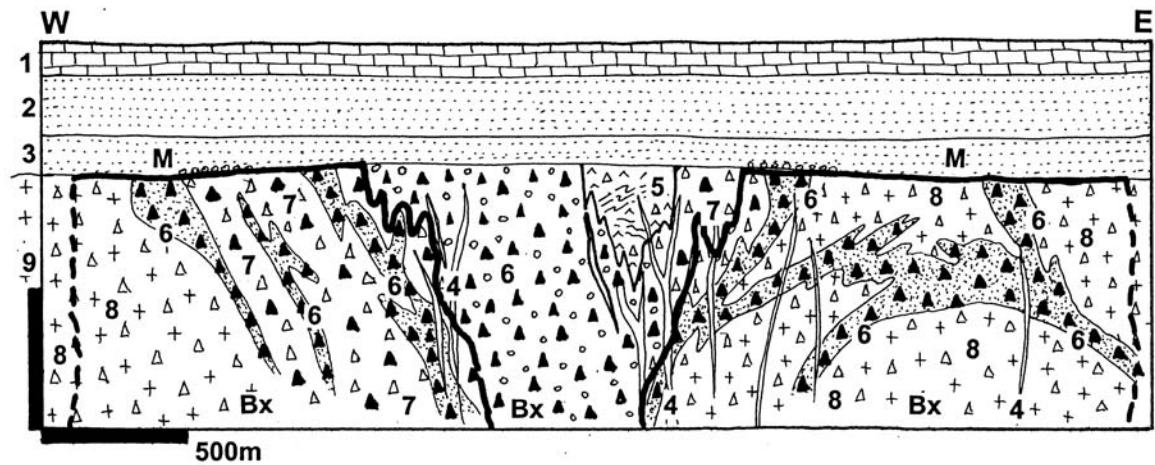


Figure 11.36. Olympic Dam deposit, South Australia, diagrammatic cross-section from LITHOTHEQUE No. 1785, modified from Reeve et al. (1990), Haynes et al. (1995), WMC Olympic Dam Staff, visit 1988. 1. Platform cover: Cm1 limestone; 2. Np quartzite; 3. Np sandstone with conglomerate lenses at unconformity. M. ~1.59 Ga Olympic Dam Breccia Complex overprinted by disseminated Cu sulfides, U oxides and finely dispersed gold in hematite-saturated, chlorite, sericite, quartz altered breccias. All sub-units below are altered and mineralized: 4. Mafic, ultramafic?, felsic dikes; 5. Mixed volcanoclastics?, laminated quartz-hematite sediment in diatreme?; 6. Barren hematite-quartz breccia; 7. Hematite-rich multistage breccias with Cu minerals; 8. Hematite breccia with abundant granite fragments (proximal to wallrock source); 9. Low- or no-hematite "granite breccia" disaggregated series ranging from crackle to melange, sericite, chlorite, carbonate altered; 9. ~1.59 Ga Roxby Downs coarse pink granite, member of the Hiltaba Suite

The success has been earned thanks to the teamwork of many talented specialists and enlightened management (and also good luck!); read Section 17.2. Olympic Dam is a breccia complex permeated and replaced by hematite, with Cu sulfides and "invisible" gold, uranium, silver

and rare earth minerals disseminated throughout. The metal combination is rather weird and the happy coexistence of sulfides with their highly oxidized environment requires reconsideration of some genetic rules. It seems as if the Creator borrowed parts from some ten previously known

ore types, then scrambled them together in one place, in a rather chaotic way. Before Olympic Dam (OD) discovery, several small known deposits consisted of material with close resemblance to OD to such an extent that samples removed from them, then tossed around OD, would not be recognized as coming from the outside. The deposits are Mount Painter-U in South Australia, Bear (Pagisteel)-Fe in Yukon, and Pea Ridge-Fe in Missouri. These are thus bona fide "Olympic Dam-type" deposits. Subsequently discovered "large" deposits Ernest Henry in Queensland and Prominent Hill in South Australia (read below), and perhaps the "giant" Alemão in the Carajás region of Brazil, have also more than 75% points of similarity with OD to qualify for membership in this ore type. Hundreds of other deposits are similar to OD in some respects but dissimilar in others (Haynes, 2000). Many such deposits have been incorporated into the "iron oxide (Cu-U-Au-REE) "family" by Hitzman et al. (1992), which mutated into the IOCG (=iron oxide, copper, gold) grouping presently popular in Australia (Porter, ed., 2000, 2002).

Although comparison of the various ore types on the basis of certain common features is an inspirational exercise, it could also be misleading if carried too far. So this section starts with description of Olympic Dam as the prototype, followed by several closer analogues, then several "large" and "giant" deposits with some important points of OD similarity. Iron-only deposits, whether hydrothermal or magmatic, are reviewed as the Kiruna-type. Deposits in carbonatite or related to alkalic systems like Palabora and Bayan Obo are treated in Chapter 12. Fe-Cu skarns and Cu sulfides with magnetite in biotite-altered andesites of the andean margins (Candelaria, Chile) are in Chapter 6. Deposits in prominent shear zones overprinting greenstone belts like the Singhbhum Cu-U belt in India and Salobo, Alemão and others in the Carajás province of Brazil, are in Chapter 9.

Olympic Dam and the Gawler Craton Fe-oxides Cu,Au,U province

Gawler Craton is an Archean to Mesoproterozoic block that occupies much of central and western South Australia (Drexel et al. 1993), west of the Adelaide "Geosyncline". Around the turn of the 20th Century the Moonta-Wallaroo ore field (Fig. 11.37), near the SE margin of the Craton, was a significant copper producer (Pt 367 kt Cu, 4 t Au) but production terminated in 1923. In the early 1970s Western Mining Corporation initiated a search for stratabound copper deposits in Stuart Shelf, the

eastern margin of the Craton covered by platformic sedimentary rocks. They followed a model developed by D.W. Haynes that postulated accumulation of Cu, released from oxidized and altered basalts, in reducing sedimentary environment. In an area of thick cover, such basalts would be indicated by coincident gravity and magnetic anomalies. Two such anomalies, along a tectonic lineament considered favorable, were drilled in 1975. The first hole passed through 38 m of 1.0% Cu with virtually invisible chalcocite disseminated in a breccia and the 9th hole, completed in 1976, intersected 170 m @ 2.1% Cu and 0.5% U. Production at OD started in 1988.

Olympic Dam (Fig. 11.36) is the most prominent deposit in a 500 km long, arcuate belt of scattered Fe, Cu, Au, U deposits and prospects recognized along the eastern margin of the Gawler Craton, that encompasses two geological "domains": Mount Woods Domain in the north-west (100 km SE of Coober Pedy), and Olympic Domain in the east (Ferris et al., 2002). In both domains basement outcrops are poor to non-existent (concealed by a thick sedimentary cover) and most information comes from drilling. The Mount Woods Domain consists of pre-1.75 Ga granulite to amphibolite facies metamorphosed metapelites, Ca-Mg silicate gneiss with dolomite marble, and is intruded by several generations of granitoids. The youngest granite generation, Balta Granite (1584 Ma), is considered to be a member of the anorogenic Hiltaba suite. There is one "large" Fe, Cu, Au, U deposit Prominent Hill (read below) delineated so far, and several prospects. The Domain holds large iron resources in banded iron formation.

The Olympic Domain consists of pre-1.86 Ga metamorphosed clastics with Ca-Mg silicate members, overlain by deformed felsic meta-volcanics and a younger generation of finely laminated meta-siltstone, meta-arkose, Ca-Mg silicate and amphibolite. These are, in turn, topped by almost flat-lying, little deformed and unmetamorphosed Gawler Range Volcanics dated at 1592-1591 Ga. The latter are mostly felsic lavas with basalt near base, and precursor of the 1595-1575 Hiltaba Magmatic Event (Ferris et al., 2002) and related Hiltaba Granite Suite (HGS). HGS is widely distributed throughout the Gawler Craton and it is a post-orogenic to anorogenic suite of highly fractionated Rb, Y, Zr, Th, U enriched granites that include several masses of "hot" granites investigated as a "dry heat" energy resource. The typical HGS lithology is a coarse, pink, K-feldspar rich epizonal monzogranite, locally grading to quartz monzonite and quartz syenite.

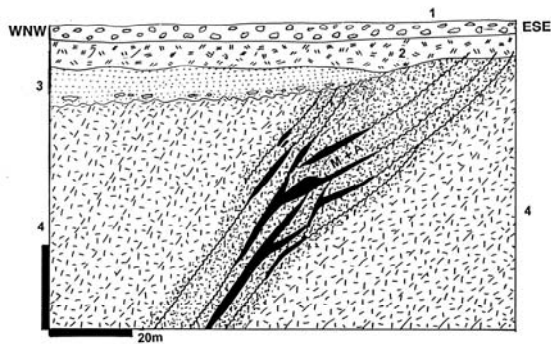


Figure 11.37. Moonta, Wheal Hughes Mine, cross-section from LITHOTHEQUE No. 2535, modified after Hafer (1991), site visit 2001. This formerly enigmatic deposit, the largest Australian Cu producer of the 1900s, has recently been interpreted as a member of the Fe-oxides & Cu "family" with an affinity to Olympic Dam. 1. T-Q unconsolidated and calcrete-cemented cover; 2. Mixed calcrete and residual clay; 3. Cm1 platformic sandstone with conglomerate near base; M+A. Structurally controlled dilation filling and replacements of Cu sulfides with magnetite & hematite in brittle shears intersecting K-silicates, tourmaline and chlorite-altered "porphyry". 4. ~1740-1737 Ma Moonta Porphyry, felsic to intermediate volcanics and subvolcanics that grade to breccia, K-silicate altered; portions could be feldspathic metasomatite

There is a possibility that HGS is the felsic component of a bimodal suite with gabbros not yet intersected.

The Fe, Cu, Au, U province is rich in breccia occurrences most of which are, or started as, high level fault breccias, followed by extensive hydrothermal alteration probably coeval with the HGS emplacement. Skirrow et al. (2002) distinguished three, progressively younger and locally overprinting alteration associations (from early to late): 1) skarn-K feldspar or albite ~ magnetite, locally Cu sulfides; 2) magnetite-biotite, local Cu sulfides; and 3) hematite, sericite, chlorite, carbonates, locally Cu sulfides and U, REE minerals. Associations 1 and 2 are most common in the Mount Woods Inlier, 3 is predominant at Olympic Dam. The HSC granites are believed to be genetically associated with the Fe, Cu, Au, U occurrences, but although the granites are widespread throughout Gawler Craton, only those in the eastern mineral belt accompany such ores. This is attributed to the possible presence of deep crustal fractures in this belt, that contributed mantle-derived fluids (Ferris et al., 2002).

Olympic Dam (OD) ore deposit, underground mine and integrated processing complex, are located

north-east of the mining community Roxby Downs, in central South Australia about 560 km NW of Adelaide (Reynolds, 2000). The OD deposit consists of a single, continuous, irregular orebody that extends in the subsurface for about 3 km along the NW-SE axis and has, so far, been proven to a depth of more than 500 m under its subcrop. The top of the orebody is 300m or more under Neoproterozoic and younger sedimentary rocks (Fig. 11.36). The October 2004 reserves have been quoted as 2.95 bt of ore with 1.2% Cu, 0.34% U, 0.5 g/t Au and 2.6 g/t Ag, but the recently announced "29% increase in resources" (Shierlaw in The Advertiser, 18. 12. 2004), together with the production since 1988, would result in a total endowment of about 46 mt Cu, 1.4 mt U, 1900 t Au, 9,900 t Ag with ~750 mt Fe (30% Fe is in the mined ore, unrecovered) and ~10 mt REE (0.27% Ce and 0.17% La in the ore). OD is thus a Cu "super-giant"; U, Au, Ag "giant"; and REE "large" deposit. It has the world's largest U resource (estimated at over 30%) and is the largest Cu, REE and second largest Au accumulation in Australia. OD has a growing literature (Reeve et al., 1990; Oreskes and Einaudi, 1990; Haynes et al., 1995; Skirrow et al., 2002; and references therein).

The OD orebody of disseminated to dispersed Cu, U, Au, REE minerals is hosted entirely by the Olympic Dam Breccia Complex (ODBC) which, in turn, is fully enclosed in and coeval with the Mesoproterozoic Roxby Downs Granite, a member of the Hiltaba Suite. The breccia starts as a crackle breccia in fractured granite and then the granite fragments gradually loosen, rotate, and mix in a fashion common with the disaggregated breccia series (Laznicka, 1988, 1989). The breccia also progressively changes from a monolithologic to a heterolithologic fragmentite. The fragmentation process, probably initiated by tectonic brecciation along a regional WNW fault, was accelerated and eventually entirely driven by high-pressure gas and fluid streaming, attributed to phreatomagmatic eruptions (and/or initial non-venting fluid exsolution from magma, and vaporization). This resulted in hydrothermal alteration concurrent with brecciation (mostly sericite and silica) and introduction of Fe oxide and ore components. The disaggregated and variously altered breccias were repeatedly re-brecciated and re-altered and locally rammed into temporary dilations, in the manner reminiscent of the intrusive breccias described by Bryant (1968). These form sedimentary-looking sets of laminated hematitic microfragmental siltstone grading to breccia. An orthosedimentary origin for these rocks has also been proposed. The

exotic components of the ODBC, mentioned in the literature as felsic, mafic to ultramafic volcanics and dikes, are controversial because, in such a thoroughly intermixed and repeatedly altered system, lithologic mimicry is strong. Any chloritized material could pose as meta-basalt. The existence of a maar topping the OD system, hence the possibility of incorporation of material from the crater facies, has been sometimes invoked.

The dominant hydrothermal alteration at OD corresponds to the type 2) mentioned above (Skirrow et al., 2002), with type 1) increasing with depth and type 3) prominent towards the top and centre, where it contributes to the central quartz-hematite altered barren zone. The principal ore minerals, other than the omnipresent hematite, are Cu sulfides. Blebs and visible grains of bornite and lesser chalcopyrite are scattered throughout the breccia, whereas the fine-grained chalcocite is virtually invisible. Uraninite with minor coffinite and brannerite, likewise dispersed and invisible, are the main U carriers. Bastnäsite and monazite contribute most of the rare earths (Oreskes and Hitzman, 1993). Microscopic gold is free, enclosed in sulfides or dispersed in the matrix. The gangue minerals include quartz, sericite, chlorite, carbonates, fluorite and barite overwhelmed by black and red hematite.

The granite emplacement, brecciation and mineralization all overlap within the age range of 1590 and 1588 Ma so there is little doubt that OD is genetically related to magmatic evolution of the Hiltaba granite suite. Although the granite is also credited as the source of the ore metals, it is unlikely that this is a magmatic-hydrothermal alteration and mineralization, especially if this is indeed a diatreme-maar system and the breccias are phreatomagmatic. Alteration K-feldspar and biotite are missing. Haynes et al. (1995) attributed the ore emplacement to mixing of two 250° to 150° hot fluids, hence sub-mesothermal conditions. There is no clear evidence of regolith under the Mesoproterozoic paleosurface, and remnants of the higher-level rocks possibly in place in the time of mineralization (a possible source of some of the metals?). Several OD-like prospects have been drilled in the area but none appears economic so far. The best known one, Acropolis, is dominated by magnetite.

Prominent Hill Fe, Cu, Au, U deposit, Mount Woods Inlier (Belperio and Freeman, 2004; Rc 107 mt @ 1.94% Cu, 0.65 g/t Au, ~100 ppm U for 2.076 mt Cu, 70 t Au, 9,700 t U). This deposit, concealed under about 100 m of cover sediments about 150

km NW of Olympic Dam, is the second viable deposit of the Olympic Dam-type, discovered in South Australia. It has been found in 2001 by drilling a linear gravity anomaly. Like Olympic Dam, this is a breccia complex with disseminated Cu sulfides and gold in hematite matrix, grading to densely hematitized fragmentites. The Au:Cu ratio is much higher, the U:Cu ratio much lower, than at OD. The greatest difference is in lithology. This east-west tabular zone, framed by two steeply north-dipping faults, is in the high-grade Paleoproterozoic basement metamorphics topped by a low-grade metamorphosed Mesoproterozoic volcanic and sedimentary rocks correlated with the Gawler Range Volcanics. The supracrustals rest in what Belperio and Freeman (2004) believe was a structural graben. A significant proportion of the supracrustals is dolomitic and intrusions are represented by apophyses of altered quartz diorite rather than granite, and a variety of dikes. The deposit is still open in the east and below 500 m so there is a chance of reaching the "giant" magnitude once the mining starts (it is planned for 2008).

Ernest Henry, about 35 km NE of Cloncurry, is the largest deposit of the Fe-oxide-Cu-Au "family" in the Eastern Fold Belt of the Mount Isa Inlier, NW Queensland (Ryan, 1998; Rv 167 mt @ 1.1% Cu, 0.05% Co, 0.54 g/t Au for 1.84 mt Cu, ~60 kt Co, 90 t Au; the ore zone is still open at depth). It has been discovered in 1991 by drilling an electromagnetic anomaly under thin sedimentary cover. The host rocks are Paleoproterozoic intermediate to felsic brecciated meta-volcanics, overprinted by areal Na-Ca metasomatism (mainly albite). Small slivers of carbonaceous "siltstone", adjacent to the shear and composed of foliated biotite and chlorite, are probably a phyllonite. The supracrustals are intruded by diorite. The pipelike orebody is associated with a 350 m wide, SSE-dipping breccia zone bordered on both sides by mylonitic shears. As in Olympic Dam there is a gradation, from the ore zone margin, of crackle-brecciated meta-volcanics through rubble and melange breccias into the central part. There, the fragmental nature of the ore hosts gives way to a "massive matrix", formed by mechanical attrition in an active fault combined with concurrent alteration and mineralization. The breccia has two compositional end-members. The less common "marble matrix breccia", near the footwall, consists of Na- and K-silicate altered wallrock fragments rimmed by biotite, magnetite and chlorite, in calcite-rich matrix. The predominant "orebody breccia" has a magnetite, biotite, chlorite

assemblage. In the hypogene zone, chalcopyrite and minor pyrite are disseminated in magnetite-carbonate gangue. The thick supergene zone under unconformity has a clay to chlorite-rich leached capping impregnated by Fe-hydroxides and a blanket of secondary sulfides near base that account for 12% of the reserve. The predominant minerals are the chalcocite group, bornite, chalcopyrite, native copper, plus rarer minerals. The mineralization is variably timed between 1.51 Ga and 1.48 Ga and explained by mixing of fluids one of which may have had a magmatic component (Mark et al., 2000). The hydrothermal systems in the Cloncurry area are believed to have been driven by ~1.5 Ga post-orogenic to anorogenic potassic intrusions, like the Naraku Batholith.

Great Bear Lake region, NW Canada: Sue-Dianne and NICO prospects. The Paleoproterozoic Bear structural province of Canadian Shield is famous for the Port Radium vein Ag-U deposit, an important radium producer in the 1930s. It also hosts the Sue-Dianne prospect, the only convincing Canadian Olympic Dam-type Fe-Cu breccia, and its "giant" As, Bi, Co, Au consort NICO (Goad et al., 2000). Both deposits are in the Mazenod Lake area, some 160 km NW of Yellowknife. The Great Bear magmatic zone consists of a series of Paleoproterozoic (~1.9-1.85 Ga) calc-alkaline granitoid plutons ranging from synorogenic to postorogenic, emplaced into shelf-to slope clastic metasediments and locally capped by comagmatic subaerial volcanics with subvolcanic dikes. The volcanics range from andesite through dacite to rhyolite and rest unconformably on folded meta-sediments. The youngest rapakivi-type granites intrude across the unconformity.

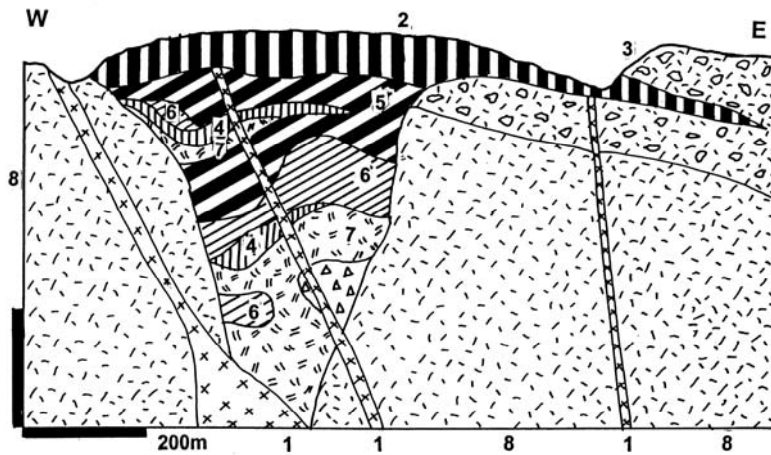
The southern part of the Great Bear magmatic zone is an As, U, Cu, Co, Bi, Au, Ag metallic province, with numerous showings of these metals, and with a past U producer (Rayrock; compare Fig. 2 in Goad et al., 2000). The **Sue-Dianne** prospect is a hydrothermal diatreme breccia complex marked by intense K-feldspathization and hematite, magnetite introduction into stockwork fractures. Cu, as disseminated chalcopyrite and lesser bornite, is in intensely K- and Na, Ca, Mg silicates and hematite altered breccias in the core of the system. Unfortunately, this is a "medium" size deposit only (28 mt @ 0.7-0.96% Cu for 225 kt Cu).

The **NICO** deposit in the same zone is an As and Bi "giant", although in terms of economics cobalt and gold are the main payable ingredients (Goad et al., 2000; 106 mt in four zones with ~0.75% As,

0.12% Bi, 0.1% Co for 795 kt As, 127 kt Bi, 106 kt Co, ~90 t Au). This is a most unusual metals association with some features reminiscent of skarn. The ores are in four zones, traceable for 7 km along strike. They are controlled by an unconformity that separates the hornfelsed meta-graywacke and siltstone basement cut by porphyry dikes, and rhyolite cover. In the largest Bowl zone the orebodies are in stacked stratabound north-dipping sulfide-bearing lenses of metasomatic "ironstone" (amphibole, magnetite, biotite) capped by K-feldspar altered rhyolite. Disseminated and fracture-filling magnetite, hematite, Co-arsenopyrite, bismuth, bismuthinite, Bi-tellurides and gold are in gangue of prograde and retrograde silicates. The prograde assemblage has ferro-hornblende, biotite, magnetite, K-feldspar, minor diopside-hedenbergite. The retrograde minerals are ferro-actinolite, biotite 2, chlorite, hematite, local tourmaline.

Bushveld complex roof, South Africa: Vergenoeg fluorite & Fe deposit. Vergenoeg (or Kromdraai) mine and mineralized breccia pipe system is near Rust de Winter, 65 km NNE of Pretoria, in the Paleoproterozoic felsic assemblage in roof of the Bushveld Complex (Crocker, 1985; Fourie, 2000; Rc 174 mt @ 28.1% CaF₂ for 48.9 mt CaF₂, or 23.72 mt F; 195 mt @ 42% Fe; + Y, REE, Th, U; Fig. 11.38). This is one of the world's largest fluorine accumulations, although still only a "large" deposit in terms of geochemical accumulation (a "F-giant" would need 62.5 Mt F), but there is no bigger fluorine deposit reported. This is an incredibly well preserved, almost undeformed and unmetamorphosed hydrothermal mineralized breccia complex, hosted by subaerial rhyolite flows, pyroclastics and volcanoclastics. The many near-surface features still in place suggest the suprastructure that could have been present above the Olympic Dam structure, before burial.

The breccia pipe complex called Vergenoeg Suite (VS; Crocker, 1985), dated at 1.95 Ga, intrudes and partly overlies flow-banded rhyolite of the Rooiberg Group and overlaps with diabase/dolerite dikes some of which are younger, some older. VS is exposed along the erosional edge of the Waterberg Group, from which it has been recently exhumed. The centre of the system is a downward tapering, discordant, subvertical volcanic pipe that has a diameter of about 900 m at the surface. The pipe is filled with felsic pyroclastics.



1. Mp diabase dikes; 2-7+M: Units (including ore types) that are members of the ~1.95 Ga Vergenoeg Suite, a subvertical funnel-shaped volcanic breccia pipe with relics of stratified ejecta at paleosurface. 2. Principal fluorite and Fe ore in gossan, F-hematite cap, massive specularite sheets; 3. Stratified felsic pyroclastics and basal ignimbrite; 4. Fluorite-filled crackle breccia, siderite or pyrite-rich bodies; 5. Magnetite-fluorite body to magnetite plug;

Figure 11.38. Vergenoeg fluorite and Fe deposit, Bushveld Complex roof, South Africa. Cross-section of the Vergenoeg pipe from LITHOTHEQUE No. 2733, modified after Crocker et al. (1988), Fourie (2000), 2001 site visit. Explanations (continued): 6. Magnetite-fayalite body; 7. Almost monomineralic fayalite (ferrodunite); 8. ~2,066 Ma Rooiberg Group, massive rhyolite

It is also permeated and replaced by a vertical funnel-shaped massive and breccia-cementing, multistage hydrothermal assemblage (Borrok et al., 1998). The early, high-temperature (~500°C) magmatic-hydrothermal fayalite (=Fe olivine), fluorite, ilmenite assemblage was soon retrograded by 500-150°C fluids interpreted as a magmatic/meteoric waters mix. This resulted in an earlier ferroactinolite, grünerite, Ti-magnetite, and later siderite, hematite, magnetite and other minerals. Groups of hypogene minerals form overlapping fayalite (a hydrothermal Fe-dunite), magnetite-fayalite, magnetite-fluorite, siderite, and hematite-fluorite bodies within the pipe that are separately mined, or rejected as waste. Masses of pyrite and pyrrhotite (or local fluorite-pyrite composite ores) are widely distributed throughout the pipe. There are also minor Zn, Pb, Cu sulfides, and dispersed accessory minerals of REE, Y, Nb, Th and U. Near the surface the breccia pipe flares upward and changes into units of stratified mineralized ejecta and bedded volcanic-sediments, now preserved as relics. Some constitute ore, like the Plattekop massive hematite body with scattered fluorite metacrysts, and the Naauwpoort fluorite-mineralised outwash fan placer (Crocker, 1985). The top of the Vergenoeg ore system is oxidized, leached and converted to gossan of goethite, secondary hematite and fluorite, with relic sulfides in the deeper part. The gossan is enriched in resistate accessory minerals of rare metals. There is a consensus that the structure and the initially high-temperature ores are related to the Bobbejaankop

highly fractionated anorogenic potassic granite, a parent to several Bushveld tin deposits.

Kiruna-type iron deposits

Kiruna-Gällivare iron province in northern Sweden has been the principal supplier of quality iron ore to European industry for over a century. The massive magnetite deposits especially, such as the “flagship” orebody Kiirunavaara, have puzzled geologists for about as long, and the end is still not in sight. Ore descriptions stand, but genetic interpretations keep changing. Not counting the temporarily popular models like submarine exhalations, there has been a long lasting controversy as to whether the Kiruna ores are magmatic melts, or hydrothermal replacements. The second crucial problem related to the previous one is of metasomatism versus primary magmatism (volcanism). Kiruna is well endowed in albitic rocks that look like Na-trachyte, Na-porphyr, Na-syenite so orthomagmatic terms are being used for these rocks and they are reported as alkalic. Is the albite magmatic or metasomatic?

Discovery of the young (2.1 Ma) magnetite deposits in andean volcanics at El Laco, northern Chile (Frutos and Oyarzún, 1975), initially interpreted as ore lavas by Park, has provided material for genetic comparisons with Kiruna. Unfortunately, the magmatic versus hydrothermal controversy persists at El Laco as well. So, Kiruna-type deposits could be best defined as follows:

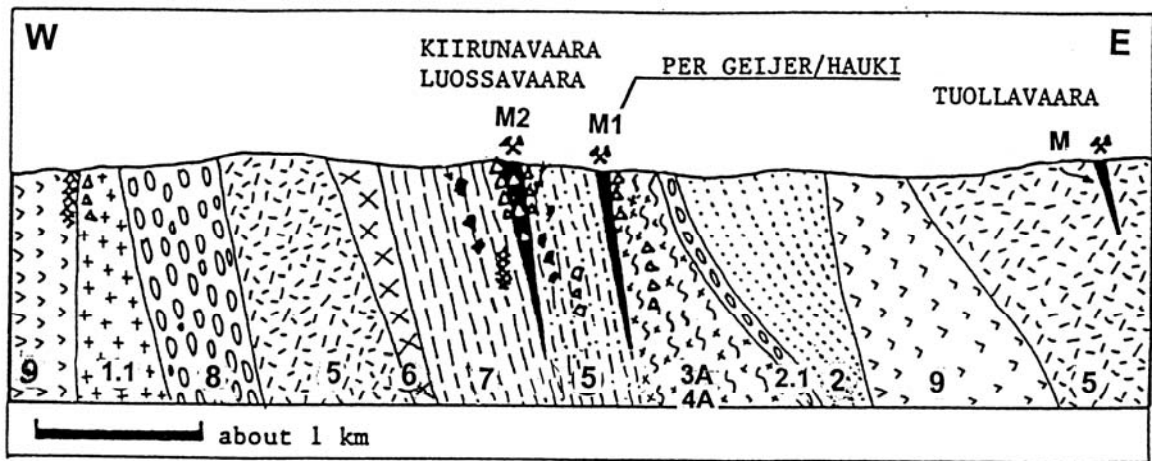


Figure 11.39. Kiruna iron ore field, Norrbotten, Sweden, generalised cross-section from LITHOTHEQUE No. 606, modified after Forsell and Godin (1980), Parák (site visits, 1986), and LKAB Ltd. materials updated after Cliff et al. (1990). 1.1. ~1,792 post-orogenic granite and syenite; 2-8: ~1.9-1.88 Ga Kiruna Porphyry Group (complex): 2. Hauki Quartzite, grading to disaggregated breccia (2.1); 3. Lower Hauki silicified felsic tuff? with hematite-rich intervals and local metabasalt; M1. "Per Geijer Ores", apatite-rich hematite-dominated tabular bodies along faults grading to metasomatites and breccia; 4. Rektorn Porphyry, partly or entirely albitic metasomatite; 5. "Quartz Keratophyre", albitized rhyodacite to dacite pyroclastics; M2. Kiirunavaara and Luossavaara massive magnetite-apatite orebodies; 6. Syenite sill (or metasomatic feldspathite ?); 7. Syenite porphyry, trachybasalt to trachyandesite (or feldspathized volcanics?), local magnetite-rich "porphyry". 8. Kurravaara Conglomerate, polymictic conglomerate or heterolithologic breccia. A (as in 3A, 4A) is for alteration (widespread albitic, also silica, K-feldspar, actinolite) superimposed on all rocks; it mimics igneous appearance. 9. ~2.1-1.93 Kiiruna Greenstone Group metabasalt

Accumulations of Fe-oxides (magnetite and hematite) in volcanics or intrusions, or in deformation zones, that are neither sedimentary nor seafloor-exhalative. Their empirical characteristics follow from description of the type locality below, and from notes on several important deposits elsewhere. Because of the high Fe clark, not a single deposit, even a district, has the rank of a "geochemical giant". Even Kiirunavaara, the largest one, is only "large", but economically of the "world class".

Kiruna-Gällivare (Norrbotten) Fe province is in northern Sweden (Cliff et al., 1990; ~3.5 bt Fe in eight major deposits and groups). The orebodies are members of a Paleoproterozoic volcano-plutonic and minor sedimentary association developed along the rifted margin of an Archean block, exposed north of Kiruna (Fig. 11.39). The earliest Greenstone Group (2.5-2.1 Ga) consists of tholeiitic meta-basalt and minor metasediments that contain several small "exhalative" Fe deposits and the "medium" Viscaria Cu deposit in albitites. The Middle Sedimentary Group of quartzite, conglomerate and micaschist on top is, in turn, overlain by the Porphyry Group (1.9-1.86 Ma). In

the Kiruna area the Porphyry Group consists of Na-alkalic (or metasomatized?) rhyolite, trachyte, trachybasalt, syenite (or albite pseudosyenite), and leucogabbro. The youngest unit is the 1.75 Ga Upper Sedimentary Group of quartzite and feldspathic quartzite.

In the Kiruna city area there are two groups of Fe orebodies: the more important Kiirunavaara-Luossavaara couple of massive magnetite (Fig. 11.40), and the "Per Geijer" orebodies of predominantly hematite, higher up in the stratigraphy (Fig. 11.41). The latter are of limited economic importance (~55 mt Fe @ 33-50%), are high in phosphorus, and have many characteristics of metasomatic replacement of breccia near faults, in an area of strong albitization (compare Laznicka, 1988, p. 705-710).

Kiirunavaara (Forsell and Godin, 1980) is the main and most important orebody (2.6 bt Fe @ 60%+) on Kiruna outskirts (Fig. 11.40). This is a 4 km long, 90 m wide, 60° east-dipping tabular to lenticular body explored to a depth of 2,000m, now mined entirely from underground in what is said to be the world's largest underground metal mine. The ore consists of solid magnetite with minor apatite

(~1% P) and variable amounts of actinolite. The orebody is conformable with lithological contacts.

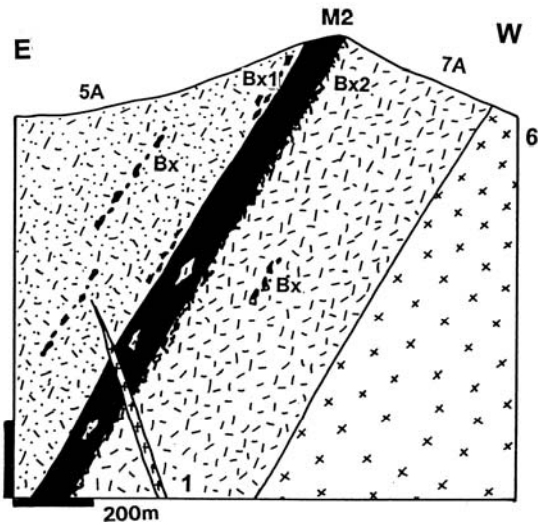


Figure 11.40. Kiirunavaara magnetite-apatite orebody, Kiruna, Sweden, diagrammatic cross-section from LITHOTHEQUE No. 607, modified after LKAB Ltd. materials & site visit 1986, updated after Cliff et al. (1990). 1. ~1.88 or 1.79 Ga microgranite and granophyre dikes; M2. ~1.9-1.88 massive magnetite-apatite orebody; Bx. Disaggregated breccias in Units 5 & 7, many veined by magnetite; Bx1: breccia in orebody hangingwall; Bx2: ditto, in footwall; 5. "Quartz keratophyre" in the hangingwall, probably albitized rhyodacite to dacite pyroclastics; 6. Syenite sill (may be partly or entirely albite metasomatite); 7. Footwall "Syenite Porphyry", probably feldspathized volcanics, locally magnetite-rich. "A" stands for alteration, mostly feldspathization

In the hangingwall is porphyritic Na-rhyolite ("keratophyre"), in the footwall is a "syenite porphyry", also described as albitic trachyandesite (Na-metasomatites?). The footwall contact is a magnetite-veined breccia. The orebody dated at 1.89-1.88 Ga (Cliff et al., 1990) is intersected by syenite or granophyre dikes dated at 1,792 Ma. The ~600°C temperature of ore formation is attributed to a "high-temperature fluid process as well as conventional magmatic crystallization" (Cliff et al., 1990). There is a widespread Na-Ca alteration (albite, scapolite, actinolite) affecting rocks in the region, and opinions differ as to its timing; the alternatives are early postmagmatic? around 1.5 Ga? "Caledonian" (=mid-Paleozoic)?.

Scattered Fe deposits of the "Kiruna-type" are widely distributed in northern Sweden. The Svappavaara group 35 km SE of Kiruna has about

400 mt of 55-60% Fe ore in three major deposits. The second largest group of some 18 orebodies is around Malmberget (Gällivare district), about 100 km SSE of Kiruna (930 mt @ 55% Fe). There, the orebodies and host rocks are gneissic, highly deformed and metamorphosed.

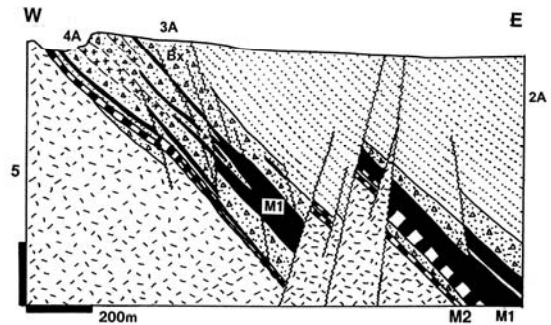


Figure 11.41. Cross-section of the "Per Geijer-type" (hematitic) Fe orebodies, Kiruna, Sweden. From LITHOTHEQUE No. 1713, modified after Parák (1975) and site visit, 1986. All units are members of the ~1.9-1.88 Ga Kiruna Porphyry Group. 2A. Hauki Quartzite, variously altered; 3A. Lower Hauki, silicified, hematite-replaced and feldspathized brecciated felsic tuff?; M1. Apatite-rich, siliceous hematite orebodies grading to metasomatites and breccias; 4A. Rektorn Porphyry, partly or entirely albitic metasomatite?; 5. "Quartz Keratophyre", albitized rhyodacite to dacite pyroclastics

Kiruna-type elsewhere. Fe deposits in some respects comparable with Kiruna are scattered around the world, but most are small to "medium", even in terms of cumulative district Fe tonnages. There are three "large" deposits of interest (430 mt Fe plus): Marcona, Peru (2.65 bt Fe @ 60% Fe, largest of the "Chile-type"), El Laco, Chile (~500 mt Fe). Both these deposits are members of the andean-margin metallogene (Chapter 6). Other important Fe districts/deposits include: Bafq-Saghand district in central Iran (~1.5 bt Fe) with the Chador Malu deposit (568 mt @ 58% Fe); Grängesberg in the Bergslagen province, central Sweden (220 mt Fe); the Ozarks (SE Missouri) Fe province (~190 mt Fe), Cerro Mercado, Durango, Mexico; and few others.

12 Rifts, Paleo-rifts, Rifted Margins, Mantle Plumes, Anorogenic and Alkaline Magmatism

12.1. Introduction

The term "rift" was introduced, in 1896, by Gregory for a structural graben in Africa (now the Gregory Rift), then for the entire continental system of grabens of which this was a part (the East African Rift system). Since then, until the onset of plate tectonics in 1968, "riftology" became an established branch of geotectonics and a fairly mature one in terms of global inventarization and description of the visually discernible (i.e. mostly geologically young) physiographic rifts. Since 1968 "riftology" has continued its evolution as an integral part of the New Global Tectonics.

Rifts are products of lithospheric extension active, at various stages of evolution, in all terrestrial geotectonic divisions of all geological ages: in oceans, within magmatic arc systems, in orogens, within cratons and platforms. Because of this, it can be argued that some three quarters of ore deposits are in some way related to rifting, hence "rift-related metallogeny" is a frequent component of regional and global ore classifications and descriptions, especially in textbooks and review papers. The problem is to establish a limit beyond which the association of ores with rifting is minor, secondary or irrelevant and stop there. This, of course, is highly subjective.

Rifting is a geodynamic mechanism that generates extensional structures (basins) that fill with rocks that are often lithologically selective and arranged in a distinct order ("rift association"; compare Chapters 10, 11). It also triggers magma formation and evolution in depth (especially in the mantle) and facilitates ascent of distinct magmas to the near-surface levels. Metals accumulation is a part of the lithogenetic process so it is more logical to threat ore deposits in the context of rock associations with which they formed and where they remain, even when all traces of the rift physiography are gone. The characteristic rift (or extension)-related rock associations are alkaline magmatic, continental flood basalts, diabase and bimodal suites, Bushveld-style differentiated complexes, supracrustal "rift associations" and their many varieties (e.g. red beds, evaporites; Chapter 13). Most of these rock associations also form outside of rifts (e.g. in relation to "hot spots" alias

mantle plumes) and in other lithotectonic settings covered in virtually all chapters of this book.

This chapter makes a brief introduction to show how the various rock groupings are related to rifting and mantle plume activity, and provides description of the traditional "rift-related lithofacies" and their "giant" deposits. It starts with the "young", preferentially still active systems endowed with substantial metal accumulations that are intimately associated with active intracontinental rifting (Salton Sea), and the early stages of oceanic extension (Red Sea). There, the rifting is a directly observable and measurable process together with the resulting structures, rocks, and the few recorded ore occurrences. Also apparent and analytically demonstrable is the supporting role of the adjacent continental rocks on the rift lithogenesis and metallogenesis (as in the Red Sea "Deeps"). In the latter case rifting is the primary attribute in respect to ore formation, the host lithology secondary. With increasing geological age and related tectonic disruption, overprinting, metamorphism, weathering and other agents the rift/ore association becomes increasingly more tenuous to become, eventually, a matter of faith. As one moves into the ancient, it is more productive to select the lithology as the primary attribute in the search of ores, never mind the rifting. In the present chapter the intra- and inter-continental rifting only is considered, although there is a transition into the intraoceanic extensional systems (oceanic spreading ridges). The latter are discussed in Chapter 4.

Varieties of rift systems: Some authors differentiate between passive and active rifting (Morgan and Baker, eds., 1983). Passive rifting is the consequence of tensional stretching of the crust, graben formation and thinning of the continental lithosphere that brings the mantle closer to the surface. Active rifting is initiated in the asthenosphere where the rising mantle plume melts its way up closer to the surface, creating "hot spots". Hot spots may be associated with stretching and graben formation (as in the Afar Triangle and the Ethiopian basalt field; Burke, 1996), or not (as in the Cameroon Line).

A practically important aspect is the place of the (mainly passive, extensional) rifting in the

continent-ocean evolutionary sequence. 1) The least evolved rifts are just fault-bounded grabens entirely within the continental crust, lacking directly associated magmatic activity. They are filled by sedimentary prisms that are thicker than the strata on flanks, but the lithology is indistinct. Some such structures provide reservoirs to hydrocarbons. Segments of the Rhine Graben in Germany come close (e.g. the post-Eocene graben fill near Karlsruhe; Einsele, 1992). 2) The semi-evolved rifts are still entirely within the continental crust (they bottom in it), but there is abundant coeval magmatism based on both mantle-derived and crustally melted magmas (Figs. 12.1, 12.2). The East African Rift system is the type area of slightly extended systems (~10-20%), the Great Basin in Nevada is a strongly extended, broad, multiple stretch system (50% and more). The Great Basin crustal extension, however, involved detachment and significant horizontal movement of plates where the lower plate was pulled out from beneath the upper plate without a visible discontinuity in the upper plate (Wernicke, 1992). 3) Fully evolved rifts have split the continental crust into two blocks facing each other across an axial zone floored by oceanic crust and mantle. Separation achieved, further spreading results in continental drift and formation of a progressively wider ocean. Red Sea and the Gulf of Suez (Landon et al., 1994) record several stages of this process.

Stages of riftogenesis, resulting rocks and ores:

The literature sometimes uses terms pre-, syn- and post-rift stages but in a non-uniform way, and in either the regional context or in respect to the actual rift fill. The pre-rift stage, especially in cratonic plates stationary for a long time as in the post-30 Ma Africa (Burke, 1996) results in a system of swells and shallow sags filled by sediments of epicratonic basins. Sedimentary ores may also settle in such basins (e.g. bedded Fe ores). Stream systems sometimes produce alluvial placers, and often long-distance flow of basinal fluids in aquifers may form the Mississippi Valley-type Zn-Pb ores in the subsurface (Chapter 13). Occasional anorogenic granite/syenite complexes and hot-spot or fissure-related mafic or alkaline magmas may intrude the swells. Although the above pattern need not be followed by rifting, Burke (1996) pointed out that the majority of Jurassic and younger African rifts originated over traces of the reactivated Pan-African intracrustal orogen, exposed in swells. This also explains the frequently observed coincidence in space (but not in time) of older deposits of lithophile metals (e.g. Sn, Mo, Be, Nb, Ta) related

to late-orogenic and anorogenic granites, in and near much younger rifts.

In the Colorado and New Mexico Rocky Mountains the pre-rift stage of the Rio Grande Rift is marked by a string of Oligocene "Mo-giants" of the Climax-type (Henderson, Climax, Mount Emmons, Questa; Chapter 6). Although placed into the "rift environment" by Carten et al. (1993), the deposits rest within a thick continental crust and are alternatively attributed to the waning stages of the "flat" Cordilleran plate subduction (Bookstrom, 1981). Cripple Creek-Au in Colorado, another Oligocene "giant", is also close to the Rio Grande Rift and affiliated with a small high-level alkaline intrusive complex (Chapter 6).

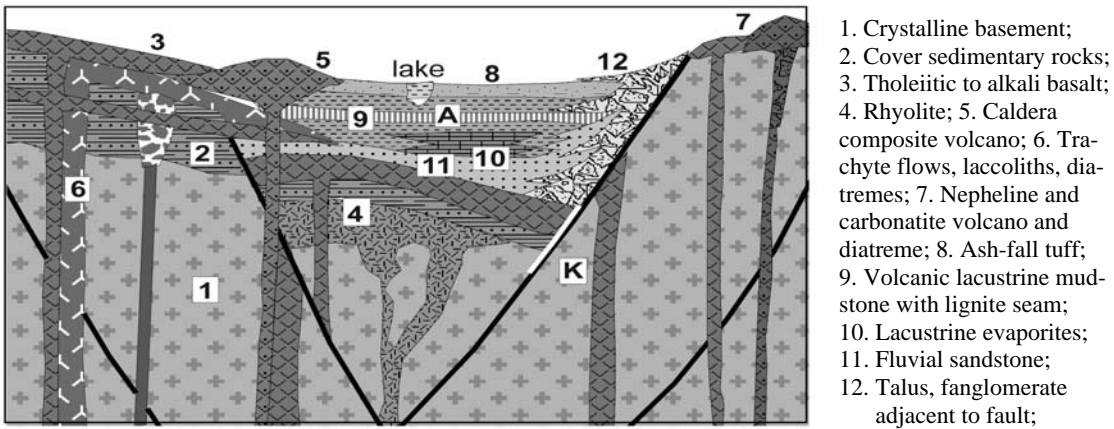
In the late pre-rift stage initial tensional fissuring provided conduits and sites of emplacement for magmas from depth, especially basaltic magma to form flood basalts preserved on flanks of many rifts, and/or swarms of diabase dikes and sills. Felsic and alkaline magmas are also present, and this volcanism continued throughout the rift stage (e.g. Pallister, 1987).

The rift stage coincides with the formation and evolution of structural grabens and basins (Einsele, 1992, p.429). The "rift lithofacies" usually starts with terrestrial rocks, changing upward into marine ones. A complete rift lithologic association is expected to include:

- 1) a basement regolith under unconformity;
- 2) coarse immature proximal terrestrial clastics such as talus breccia, fanglomerate and "wash" derived from the steep valley walls and floor;
- 3) terrestrial, less often subaqueous, lava flows with minor pyroclastics of: a) mantle-derived tholeiitic to high-alumina basalt; a) calc-alkaline to peralkaline rhyolite, trachyte, c) alkaline suite (basanite, phonolite, nephelinite, rare carbonatite);
- 4) fluvial or lacustrine sediments;
- 5) hypersaline tidal or lagoonal evaporites, sabkha-type gypsum-dolomite-mudstone sets;
- 6) marine halite, anhydrite, gypsum with reef carbonates.

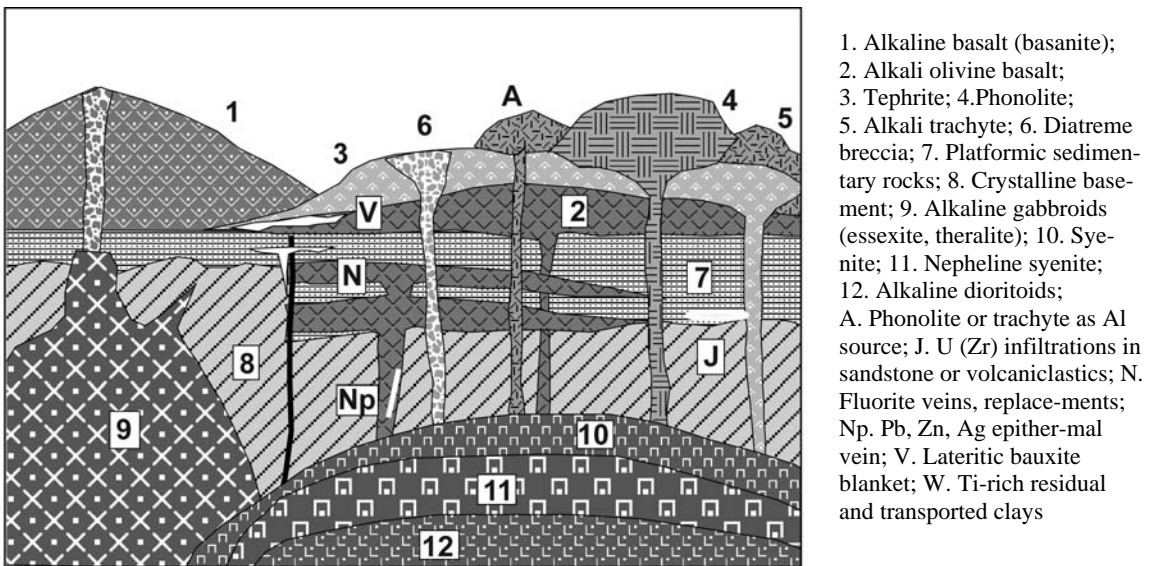
The East African Rift system is the type area (McConnell, 1972; Kampunzu and Lubala, eds., 1991), unfortunately no giant metallic deposits are known from there.

Post-rift evolution varies with the type of structures left behind at the end of the rift stage. Most published models invoke post-rift thermal subsidence (sag or downwarping stage) that creates broad, smooth basins.



1. Crystalline basement;
2. Cover sedimentary rocks;
3. Tholeiitic to alkali basalt;
4. Rhyolite; 5. Caldera composite volcano; 6. Trachyte flows, laccoliths, diatremes; 7. Nepheline and carbonatite volcano and diatreme; 8. Ash-fall tuff; 9. Volcanic lacustrine mudstone with lignite seam; 10. Lacustrine evaporites; 11. Fluvial sandstone; 12. Talus, fanglomerate adjacent to fault;

Figure 12.1. Slightly extended young (recent) intracontinental rift (e.g. East African Rift) with subaerial mafic, bimodal and alkaline volcanism and lacustrine sedimentation. From Laznicka (2004) Total Metallogeny Site G222. Explanations (continued): A. Zn, Mn, Pb, Hg, As, enrichment in hydrothermal brines discharging on lake floor; K. Fluorite veins, replacements



1. Alkaline basalt (basanite); 2. Alkali olivine basalt; 3. Tephrite; 4. Phonolite; 5. Alkali trachyte; 6. Diatreme breccia; 7. Platformic sedimentary rocks; 8. Crystalline basement; 9. Alkaline gabbroids (essexite, theralite); 10. Syenite; 11. Nepheline syenite; 12. Alkaline dioritoids; A. Phonolite or trachyte as Al source; J. U (Zr) infiltrations in sandstone or volcanoclastics; N. Fluorite veins, replacements; Np. Pb, Zn, Ag epithermal vein; V. Lateritic bauxite blanket; W. Ti-rich residual and transported clays

Figure 12.2. Young (e.g. Miocene) but inactive, slightly extended intracontinental volcanic rift (graben) like Auvergne, České Středohoří, Hopi Buttes. Erosion removed volcano tops and most of loose tephra and the hills are mostly exhumed high-level domes, dikes and diatremes originally emplaced into soft sediments or pyroclastics. From Laznicka (2004), Total Metallogeny Site 101. No conventional metallic "giants" are expected, except for large tracts of phonolite or clays mined in bulk for Al, Ti recovery

These are filled by a variety of sediments that are finer-grained, more mature and also more monotonous than those from the rift stage. "Distal turbidites" are common. Shale, sublitharenite, carbonates, some evaporites are dominant and volcanic component, if any, is more often airborne ash coming from distant eruptions rather than local

volcanic centers. The post-rift successions merge with the "normal" sediments of platforms and miogeoclines (Chapter 13) and the distinction is subjective. Regional geologic interpretations in terms of rift stages are locally popular (for example in the Mount Isa Inlier in northern Australia; Blake, 1987; read Chapter 11) and if so, the post-rift stages

are associated with formation of giant sedex deposits there (McArthur River-Zn, Pb; Mount Isa-Hilton; Century), and bedded Fe deposits elsewhere. Completed rift successions either remain virtually unmodified (except for erosion) within continental platforms, or are incorporated into collisional orogens or subductive convergent margins.

12.2. Young rifts, hydrothermal activity

This subject has been recently reviewed by McKibben and Hardie (1997). Hot springs and deep-seated hydrothermal systems are widespread in many types of dilational structures permeated by heated water of which rifts are just one variety. Of the thousands recorded hot spring occurrences, some of which are enriched in or deposit small quantities of base and precious metals, the Salton Sea geothermal system stands out as its cumulative content of Zn, Pb, As dissolved in brine is of the "large" to "giant" rank.

Salton Sea Geothermal System (SSGS)

SSGS is in Imperial Valley in the south-eastern corner of California and it crosses the border into Mexico (McKibben and Elders, 1985; McKibben et al., 1988a, b). Salton Sea is a recent shallow valley lake filled by freshwater from the Colorado River, in a depression separated from the actively extending Gulf of California by prograding delta. The depression and the underlying sedimentary prism occupy a pull-apart structure opened up by a right-lateral movement along two faults, in the SE extremity of the San Andreas fault system. This takes place within the overall regime of rifting and crustal thinning in the landward extension of the East Pacific Rise oceanic spreading system. The thick Pliocene to Quaternary sedimentary pile in the subsurface includes fluvial-deltaic and lacustrine semi-consolidated mudstone, siltstone and sandstone with bedded non-marine anhydrite, intruded by contemporaneous rhyolite domes. These subvolcanic rocks are believed related to a composite intrusion in depth and they are jointly responsible for a substantial thermal and hydrothermal metamorphism of sediments.

The magmatic heat drives a hydrothermal system of circulating Na-Ca-K-Cl brine that contains 20-26% of total dissolved solids and this also supports the largest developed hot-water dominated geothermal field in North America. The solids have been derived by dissolution of sedimentary evaporites and wallrock leaching. The brine that is

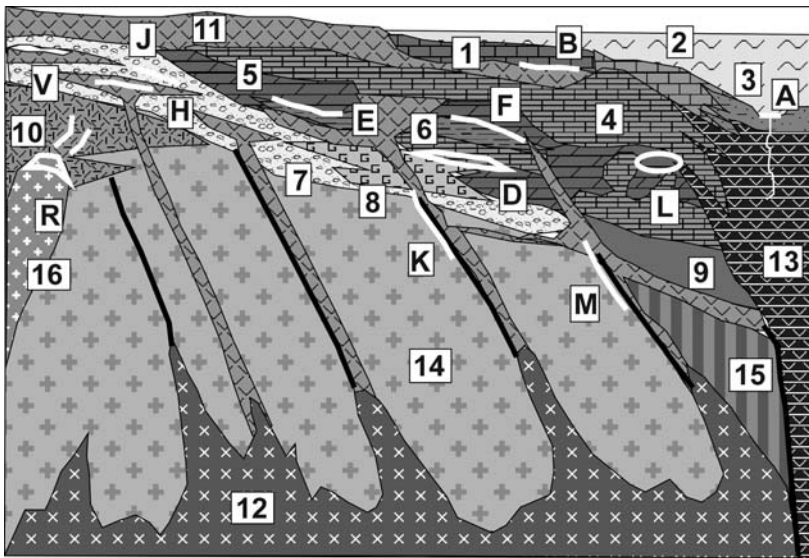
365°C hot in depth of 2,200 m is overlain by a cooler, low-salinity brine. The high-temperature brine contains, in solution, 0.17% Fe, 0.15% Mn, ~510 ppm Zn, ~100 ppm Pb, X00 ppm As, 1 ppm Ag, but only ~6 ppm Cu, which translates into a "large" and "giant" contents of 6 mt Zn, 1.2 mt Pb and 10,885 t Ag. The alteration assemblages in the reservoir rocks are zoned from the highest level epidote, albite, chlorite, calcite, quartz zone through a biotite zone, clinopyroxene zone, to the deepest and highest temperature garnet (skarn) zone. Except for the recently precipitated high-grade ore scales described from wells and pipes, solid metallic minerals have been rarely detected in drill holes. They are Fe, Zn, Pb, As and Cu sulfides in quartz, calcite, epidote, chlorite and hematite veins and veinlets that fill minor fractures.

Young rift-drift transition: the Red Sea

The present Red Sea area (Pallister, 1987; Coleman, 1993) has been an extensional rift system and depositional basin for the past 25 million years. During the last 4 m.y. sea floor spreading has been initiated at several sites in the axial trough, the deepest part of the system. The present arid African and Arabian coasts are fringed by mud and salt flats (sabkhas), raised coral, infrequent beaches: all interrupted by widespread flood basalt tongues. The arid tropical carbonate shelf lithofacies with patchy fringing reef has a significant pelagic component and it grades into pelagic ooze in the main deep water marine trough. In the shallow subsurface, resting on attenuated continental crust, is a progression of Miocene to Pliocene sediments that changes from red continental clastics into algal and reefal carbonates and marls. There is also a thick unit of salt (Fig. 12.3).

The magmatic activity and influence are pervasive and significant. In the long pre-rift stage that postdated the Pan-African orogeny, intracrustal melting had produced highly fractionated A-granite and comagmatic rhyolite. This was followed and accompanied by outpourings of basalts. Swarms of diabase dikes, fed by expanding and advancing magma chambers, filled fractures in the continental rocks and fed extensive lava fields (harrats) on top of the Arabian Platform and throughout the Red Sea graben. Central volcanoes are uncommon. The lavas are mainly alkali olivine basalt, changing into tholeiite with depth and towards the main trough.

The oceanic crust exposed in the Red Sea axial valley is, in contrast, compositionally close to MORB.



1. Carbonate shelf sediments; 2. Carbonate reef; 3. Deep water pelagic ooze; 4. Salt, minor anhydrite; 5. Algal and reefal limestone, dolomite; 6. Carbonaceous mudstone; 7. Terrigenous clastics; 8. Gypsiferous mud (sabkha); 9. Pelagic limestone; 10. Rhyolite and related A-granite; 11. Basalt flows, dikes; 12. Tholeiitic and alkali basalt front to diabase dikes; 13. MORB-like spreading ridge basalt; 14. Rifted continental crust; 15. Transitional crust; 16. Alkaline and peralkaline intrusions; A. Fe, Mn, Zn, Cu, Ag metalliferous brines, pools and muds; B. Fe, Mn, Ba submarine hydrothermal crusts on top of basalt;

Figure 12.3. Red Sea-style rift-drift transition with young oceanic crust in the axial zone. Ore type A has one "near-giant" equivalent (Atlantis II Deep). From Laznicka (2004), Total Metallogeny Site 231. Explanations (continued): D. Early diagenetic Mn, Cu, Zn, Pb in sabkha sediments; E. Oolitic ironstone; F. U in marine phosphorites; H. Cu in altered basalt flowtops; J. Cu oxide and sulfide infiltrations in reduced portions of redbeds; K. Pb, Zn, Cu, Mn, F, Ba hydrothermal fault veins; L. Ditto, void filling or carbonate replacing sulfides (MVT-type); R. REE, Y, Zr, U, Nb, Ta, Sn in alkaline and peralkaline intrusions

There, the magmatic heat drives hydrothermal circulation and saline brines accumulate in several deep pools on the seafloor where they locally precipitate hydrothermal and mixed metalliferous sediments. About twenty such "deeps" are known by now (Guennoc et al., 1988), ranging in depth from 1,200 to 2,850 m. About one half of the "deeps" have an active discharge of slightly metalliferous thermal brines on the seafloor, which results in enrichment of trace Mn, Zn, Cu, Pb, Co and Ag in muds. So far, only one "large" metalliferous deposit of industrial interest, Atlantis II Deep, has been discovered and tested.

Atlantis II Deep is in the axial zone of the Red Sea, midway between Saudi Arabia and Soudan (Degens and Ross, eds., 1969; Blissenbach and Nawab, 1982; 693 mt of bulk sediment containing 91.7 mt of dry salt-free material @ 2.06% Zn, 0.46% Cu, 41 g/t Ag, 0.512 g/t Au for 1.89 mt Zn, 425 kt Cu, 3,755 t Ag, 47 t Au; Guney et al., 1988). Temperature and salinity anomalies in the Red Sea axial zone were first noted in the 1950s, and occurrences of hot sea floor brine pools and metalliferous sediments in several sub-basins ("Deeps") were discovered by oceanographic cruises in the 1960s and 1970s. Atlantis II was the first "deep" where the metalliferous sediments have

been found, in 1965, by the vessel R/V Atlantis II. The early, yet in many respects definitive, reports are published in the volume edited by Degens and Ross, eds. (1969). The discovery has had an enormous impact on understanding of ore forming processes and came in the right time when the concept of "stratiformity" of ores was the king. The Atlantis II slow-spreading geothermal system has been active for the past 25,000 years and the ore metals so far accumulated in the bottom muds have sufficient grade and tonnage of Zn, Cu, Pb, Ag and Au to qualify as a "large" ore field in the magnitude classification adopted here.

The Atlantis II "ore field" is defined by the hot brine pool that occupies a portion of the "deep" (a sub-basin in the Red Sea median valley floored by MORB-like basalt in ~2,000 m depth) that measures 14 km along the NNW axis and is 5 km wide. The brine pool is about 200 m thick and is density stratified. The Lower Brine has an average present temperature of around 62°C and 25.7% salinity, but the temperature fluctuated over the time; it is highest near the seafloor entry points of the incoming hydrothermal fluid, up to 270°C hot. The hydrotherms bring dissolved metals, leached mostly from the young oceanic basalt, to the pool. The metals precipitate, upon cooling and mixing

with the sulfate-rich pool brine, as a metalliferous sediment (“mud”). The “mud” thickness ranges from several meters to the maximum of 25 m (average 8.5 to 11 m; Guney et al., 1988) and it is estimated that there is some 696 mt of “bulk” sediment containing 227 mt of wet “metalliferous mud” irregularly distributed in eight sub-basins.

The metalliferous sediment is unconsolidated, brightly colored, very fine-grained, laminated, compositionally zoned mixture of bioclastic carbonate, Ca-sulfates and hydrosilicate nonmetallic “gangue” minerals, Fe and Mn gangue minerals, and base/precious metals. The gangue minerals include montmorillonite, siderite, rhodochrosite, anhydrite, Mn oxides, Fe hydroxides, magnetite, hematite and pyrite. The base and precious metals component is dominated by a very finely dispersed sphalerite and chalcopyrite accumulated in two black sulfide layers (there are local spots grading up to 25% Zn) separated by ocherous oxidic layers and terminated on the top by a layer of amorphous silicates. Hydrothermal vents and cross-cutting veins are locally present, some associated with high-temperature (250-400°C) metamorphic assemblages in the host sediments (ilvaite, mushketovite). Laterally, the ore layers change facies into Fe-hydroxides and manganite-rich sediments.

12.3. Mantle plumes, continental breakup, rifted continental margins

12.3.1. Hot spots and mantle plumes

Hot spots are the surficial expression of asthenospheric mantle plumes that rise and impact the base of the crust (both oceanic and continental). There the plumes heat the lithosphere contributing to isostatic uplift. Some plumes penetrate the crust bringing along the subcrustally generated magmas, causing intracrustal melting and further ascent of magmas so generated, or both. The mantle plumes are usually considered to be long-lasting and stationary so when a lithospheric plate moves over (above) them, they leave a track (“hotline”) in the form of a discontinuous chain of volcanic islands (Hawaii) or on-land volcanoes (Cameroon Line, Snake River-Yellowstone). Under stationary plates (as in the post-30 m.y. Africa; Burke, 1996) the plumes feed multiphase volcanic centers.

The idea of mantle plumes was proposed in the 1960s by Tuzo Wilson, further documented by Morgan in the 1970s, and widely applied since. Every recent textbook on petrology provides introduction and references (try Faure, 2001, p.56)

Mantle plumes vary in size and they are irregularly spaced. They are separate from and independent of rifts but may cause rifting (extension; read above), they may overlap with rift or MORB magmatism (as in Iceland), or congregate in the vicinity of major rift systems. Hot spots/mantle plumes do not produce ores as such, but drive magmatic systems (e.g. alkaline complexes, carbonatites, kimberlites) with associated mineralisation (Pirajno, 2001). As there is an overlap between rift and hot spot magmatism, magmas generated by either system are usually treated jointly in the literature, including this book.

12.3.2. Rifted (Atlantic-type) continental margins

When continents separate and drift apart, they face each other over oceanic crust-floored seas that could be narrow (e.g. the Red Sea) or wide (e.g. the Atlantic Ocean between North America and Africa). Rotation, further fragmentation, strike-slip offsets, collisions rapidly destroy continental outlines so the former connections are hard to make and increasingly become hypothetical (Fig. 12.4).

The rifted margins become passive (Atlantic-type) continental margins where the continental crust gradually thins to zero and the oceanic crust takes over. Ideally, a continental margin profile should correspond to a cross-section from the continental edge near the rift axis to the continental interior, as at the time of separation. This is often the case, but more frequently erosion removes the upper crustal levels and post-rift, especially marine, sedimentation buries the margin under a succession of young strata. On the other hand, cumulative erosion exposes deeper levels of the former rifted margins and exposes feeder systems to volcanoes such as diabase dikes and sills, and plutonic cores of central volcanic complexes. A variety of aborted extensional grabens (unsuccessful attempts at separation that include aulacogenes) is more abundant than remnants of former successful rifts.

From the ore exploration premise, there are several end-member characteristics of rifted margins that have some bearing on ore prediction: 1) exposed versus buried (under post-rift sediments and/or sea water) margins; and 2) volcanic versus non-volcanic margins. Needless to say, well-exposed rifting-stage lithologies as along the coasts of Greenland are directly accessible to visual exploration. The deeply concealed rift assemblages, in addition to possibly preserving ores formed during the rift stage, provide a potent mix of contrasting lithologies.

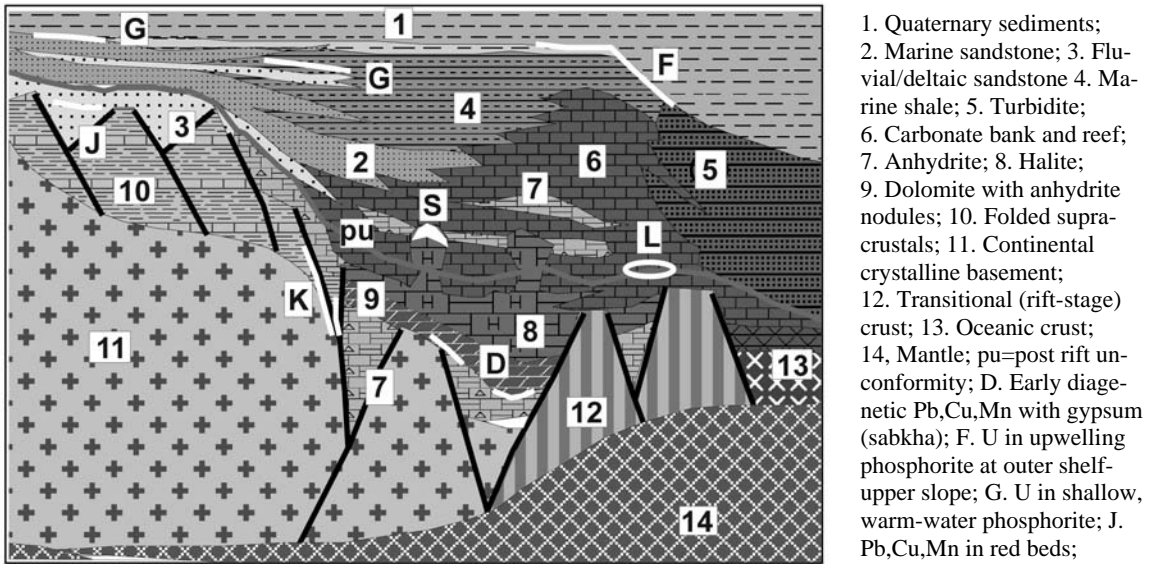


Figure 12.4. Rifted continental margins, as under the Atlantic coast of North America. F, G and L ore types have known "giant" equivalents. From Laznicka (2004), Total Metallogeny site 232. Explanations (continued): K. Hydrothermal Pb,Zn,Cu,Mn,Ba,F veins; L. Ditto, void fillings or carbonate replacements (MVT-type); S. Sr,U,Pb,Zn, sulfur in caprock of salt domes

These are rich in trace metals (Cu in basalts) or in complexing components of fluids (NaCl in evaporites) available for post-rift metallogenesis. These could have provided a favorable setting for processes that acted in depth (magmatism, metamorphism) or near-surface (circulation of basinal fluids) and resulted in capture, transfer and reconcentration of some trace metals to produce a new generation of ores at higher crustal levels. Awareness about the existence and condition of former rift lithologies in depth is thus an essential component of regional metallogenic analysis.

The non-volcanic to moderately-volcanic, mostly buried rifted margin successions are exemplified by the Triassic rift association in subsurface of the Atlantic continental margin of North America (Chapter 13). The young, well-exposed, volcano-plutonic rift assemblage is preserved in the North Atlantic borderland, especially along the coast of Greenland. Its Proterozoic counterparts are best developed in the Gardar Zone of Greenland and in the Mid-Century Rift in the north-central United States, briefly reviewed with the Michigan copper province (read below).

North American Atlantic-type rift-initiated continental margins: Atlantic continental margin along the coast of eastern United States includes the type area of passive continental margins initiated by

rifting (Dewey and Bird, 1970; Klitgord et al., 1988). The margins history goes back to Upper Triassic when the Pangea breakup started on site of the earlier Appalachian accretionary orogen. The Atlantic margin deposits are over 90% sedimentary and they have accumulated in a string of marginal basins, platforms and embayments subparallel with the coast, on increasingly thinned and attenuated continental, transitional and partly oceanic crust in the offshore. The physiography of the present Atlantic margin comprises coastal plain, continental shelf with offshore platforms (e.g. the Blake Plateau), continental slope, and continental rise. The basement to the margin sediments is a 30-40 km thick continental crust that has the form of a pre-rift sedimentary platform cover resting on crystalline basement, or in places the bare basement itself. This crust offshore from the hinge thins to 20-10 km and changes into stretched and faulted rifted continental crust (still recognisable as such), then into a transitional rift-stage crust, strongly modified by mantle influence (remobilized and infilled by mafic dikes). The oceanic domain starts with the marginal oceanic crust, the first new oceanic lithosphere formed in the time of drift initiation in lower Jurassic, and eventually the ordinary oceanic crust represented by layers 2 (basalts) and 3 (gabbroids); Klitgord et al. (1988).

The sedimentary record preserved in the North American Atlantic margin can be subdivided into the pre-rift, syn-rift and post-rift stages. The pre-rift rocks are not emphasized here. The syn-rift deposits (sediments >> volcanics) accumulated under conditions of active crustal extension, graben formation and minor igneous intrusion. Rocks formed in two sets of basins: 1) landward, initially onshore basins filled by immature alluvial sediments grading to lacustrine muds with tholeiitic basalt flows and diabase/gabbro hypabyssal intrusions; 2) seaward basins in which the basal land sediments are overlain by coastal and shallow water carbonates, sabkha sequences and thick evaporites (halite, anhydrite): a close counterpart of the pre-drift portion of the present Red Sea. The syn-rift deposits are terminated by the post-rift unconformity (pu in Figure 12.4) that marks initiation of spreading (drift).

The much thicker (up to 20-25 km) deposits of the post-rift (drift) stage were laid down on an alternatively prograding and retreating shelf, slope, and rise. The inner and middle shelf sediments are mixed terrigenous-carbonate sandstones, siltstones and shales interrupted by several continental sandstone tongues. The Jurassic-Cretaceous shelf break is marked by a massive carbonate pile accumulated in reefs and carbonate banks. It contains anhydrite-rich units and is in places intruded by diapirs of the syn-rift salt deposits.

The present Atlantic continental slope is dissected by submarine canyons and interrupted by slumps, slide scars and debris flows of carbonate and generally fine terrigenous detritus. The continental rise is predominantly a depositional environment dominated by fine grained contourites. Although the lithology of the pre-Quaternary Atlantic sediments is influenced by climate and bathymetry (the carbonate: terrigenous clastics ratio increases southward), the greatest contrast is among the Quaternary sediments. The northern shelf (off eastern Canada) is covered by an up to 200 m thick layer of glaciomarine deposits, whereas the southern extremity (Bahamas) is a highly productive tropical carbonate platform.

12.3.3. Intraplate and rift margin mafic to bimodal magmatism

This section provides a brief introduction to the characteristic magmatic families that accompany rifting, and related significant metallic deposits. Although basalts dominate the rift settings, also present are the less common felsic rocks in bimodal suites and differentiated mafic-ultramafic

complexes (Bushveld-type) considered to be the magma chambers of basalts. The frequency of plutonic rocks in outcrop increases with geological age as erosion exposes the deep-seated roots of magmatic systems that are out of sight in the young rifts. The predominantly tholeiitic, olivine and alkali basalts overlap, in many provinces, with alkaline magmatic rocks treated in Section 12.8.

In this chapter, "age is not a barrier" and Quaternary basalts are treated jointly with their Precambrian counterparts. Mafics in the oceanic domain, in subduction-related plate margins and in "greenstone belts" have their place in Chapters 4, 5 and 8, respectively. Several examples of rift-related igneous rocks can also be found in Chapter 11 (Proterozoic intracratonic orogens) where the mafics often played the role of passive contributors of trace metals (especially Cu) now accumulated in synorogenic orebodies. High-grade metamorphosed equivalents of the magmatic rift association appear in Chapter 14.

North Atlantic Borderland: Lower Tertiary rifting-related magmatic province: This Province consists of scattered outcrop areas of ~65-50 Ma magmatic rocks related to continental breakup and formation of rifted continental margin on both sides of the Atlantic Ocean and Labrador Sea. Excellent coastal outcrops exist along the western and eastern coasts of Greenland, on Baffin Island, in the Faeroes, NW Britain and northern Ireland. Subaerial volcanics often change into submarine ones, interbedded with marine sediments and deposited in several basins now preserved in the Atlantic and the Labrador Sea (Fig. 12.5). There is an extensive literature on this Province (Morton and Parson, eds., 1988; Upton, 1988 and references therein; read also extensive reviews in petrology textbooks like Faure, 2001, p. 196-212). Although there are no known giant metallic deposits (except Malmbjerg-Mo, related to younger anorogenic granite; Chapter 10) and only few minor and one potentially interesting "large" ore occurrence (Skaergaard-Au, PGE), this Province provides a very complete inventory of the various lithologies, styles and settings repeatedly encountered in many comparable provinces elsewhere.

Northern Laurasia had been under tensional regime since at least the Triassic (e.g. Newark Trough) and there were several episodes of extension afterwards that culminated with continental breakup. The extension and lithosphere thinning created numerous sediment-filled grabens in the hinterland and on the Atlantic floor.

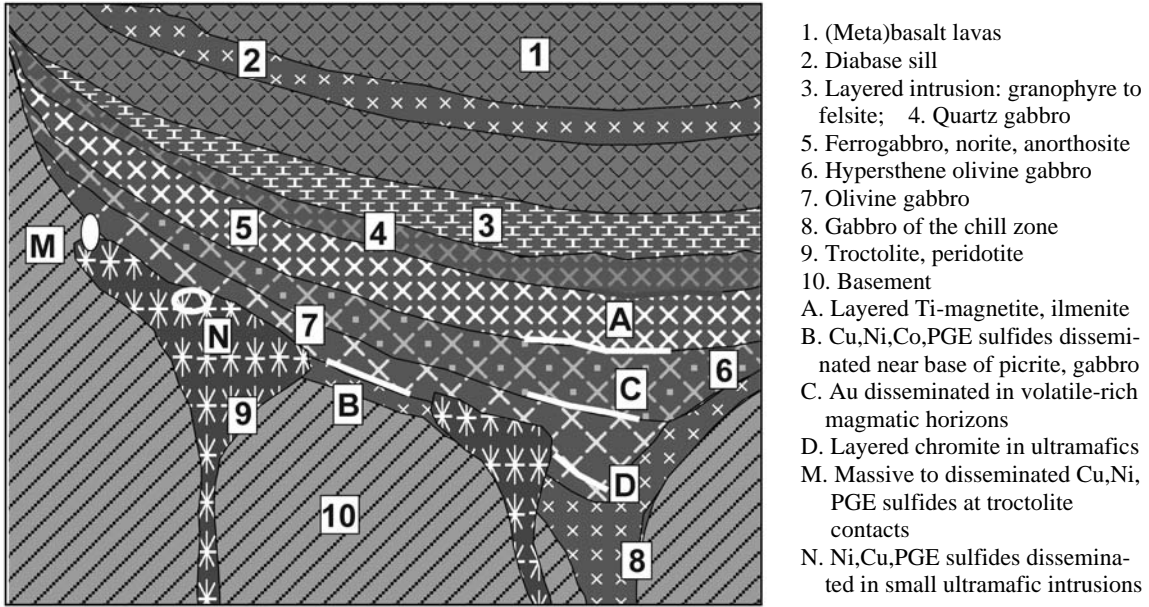


Figure 12.5. Layered differentiated intrusion under comagmatic basalts, modelled on the example of Skaergaard (and partly Duluth). Inventory diagram of rocks and ores from Laznicka (2004) Total Metallogeny Site G89

This facilitated emplacement of widespread diabase dike or sill swarms. The breakup was diachronous and it took place between about 65 and 50 Ma. The plateau basalt-dominated volcanic phase started with fissure eruptions of high-Mg, olivine-rich rocks (picrite, olivine-rich tholeiite) that soon changed into the dominant tholeiitic and/or quartz tholeiitic basalt. The latter produced thick plateaux composed of numerous subaerial lava flows gradational into pillowed flows, peperites and hyaloclastites when emplaced into or under water. Mildly to strongly alkaline basalts mark the transition into the predominantly alkaline provinces. Felsic volcanics (rhyolite, trachyte) and rare andesite participate in locally present bimodal associations.

The fissure eruptions were followed by formation of central volcano-plutonic complexes most of which are cored by simple tholeiitic gabbro, but some are multiphase layered intrusions with several varieties of olivine, ortho- and clinopyroxene and plagioclase cumulates in the layered units. Granophyre is common in intrusion roofs and border zones. The 54.6 Ma **Skaergaard Intrusion** in the Kangerdlugssuaq basalt region, East Greenland, is a classical locality first described in the 1939 memoir of Wager and Brown, and studied repeatedly afterwards (e.g. McBirney, 1996). The funnel-shaped intrusion drove a large

hydrothermal system convecting within the intrusion and in its roof, causing metasomatism. The intrusion contains at least ten stratabound zones ("reefs") enriched in precious metals, of which one (Platinova Reef; Andersen et al., 1998; Brooks et al., 1999; 91 mt @ 1.83 g/t Au, 1.8 g/t Pd for 166 t Au, 160 t Pd) or two are presently of economic interest. These "reefs" are in banded mesogabbro, at top of the Middle Zone, in the Layered Series. There, small scattered interstitial grains of pyrrhotite, chalcopyrite, bornite, digenite and chalcopyrite enclose gold and PGE minerals. Genetic interpretations of this ore range from immiscible sulfide melt settled into cumulates, to early postmagmatic hydrothermal replacement of favorable horizons.

Some erosion-dissected central complexes contain wide range of lithologies. The 50 Ma Kangerdlugssuaq complex in the same area as Skaergaard has early gabbro followed by quartz syenite, syenite and nepheline syenite. The nearby Gardiner ring complex is exposed in an eroded nephelinitic volcano and consist of ultramafic cumulates, agpaite syenites and carbonatite. Well-studied central complexes are particularly common in the Inner Hebrides of NW Scotland. The Skye Island (reviewed in Faure, 2001, p. 197) has Precambrian basement with Cambrian limestone and Mesozoic sandstone on top, overlain by up to

2,300 m of Paleocene-Eocene alkali olivine basalt, hawaiite, mugearite and trachyte. There is a layered mafic-ultramafic intrusion (Cuillin Hills) and several granite and granophyre ring dikes, cone sheets and stocks interpreted as products of melting of the Archean basement. Basement contamination of the mantle-derived melts at Skye (and elsewhere) is widespread, and so is hydrothermal alteration (Thompson, 1982). Surprisingly, no significant mineralization resulted.

12.4. Plateau (flood) basalts

Flood basalt occurrences range from single short basalt flows in valleys and isolated cinder cones, to extensive plateau basalt ("trap") provinces. Basalts in the largest Triassic Tunguzka Basin in north-central Siberia cover about 1.5 million km², the smaller 149-119 Ma Paraná Basin in Brazil has about 1.2 million km²; the 70-63 Ma Deccan Plateau in India measures 518 thousand km². The geologically young, subaerial basalts are gray, extremely monotonous, and completely devoid of metallic mineralization (except when tropically weathered into lateritic bauxite). They are a hindrance to visual exploration as they cover large tracts of a frequently well mineralized basement (e.g. in Tasmania, Victoria goldfields of Australia). On the positive side, basalt flows have protected alluvial gold placers from erosion and some of the preserved "deep leads" (e.g. in Ballarat; Chapter 9) are of the "giant" magnitude. Also "giant" are some Early Precambrian paleoplacers such as the Ventersdorp Contact Reef in the Witwatersrand, preserved under the Klipriviersberg basaltic pile (Chapter 11).

The latter, however, are "green" basalts that are geologically older, and have suffered diagenetic, burial, hydrothermal or metamorphic hydration of olivine and pyroxenes to actinolite and/or chlorite, and albitization of plagioclase. "Green" basalts also cover large tracts of potentially mineralized basement, hence they play the same role as the gray basalts, but their main role in ore formation was as a source of trace Cu and partly Ag released, transported and locally accumulated by a variety of post-volcanic mechanisms. Of the flood basalt varieties, tholeiitic basalts have the highest trace Cu contents (70 to 250 ppm, i.e. 3 to 10 times clarke), whereas alkali basalts are low in Cu. Copper in hydrothermal fluids migrates readily out of hydrated basalts and small scattered occurrences of Cu sulfides, native copper, malachite, azurite and chrysocolla are ubiquitous in and near such basalts. Several "Cu-giants" sourced from the "green"

plateau (meta)basalts are known, and described in Chapter 11. In the Michigan native copper province (total ~ 6 mt Cu in ores) stratabound, low-temperature hydrothermal deposits of native copper in prehnite, quartz, calcite, pumpellyite, zeolite, etc. gangue fill porous, scoriaceous basalt flowtops, or porous interflow conglomerate horizons. The copper accumulated in the upper levels of the ~5 km thick pile of tholeiitic lava flows, that also supplied the trace Cu, by precipitation along the hydrated prehnite-pumpellyite interface, from fluids released by dehydration in the epidote zone underneath (Jolly, 1974). In the "giant" Mount Isa Cu orebodies in Queensland (Chapter 11), copper from the deformed Eastern Creek Volcanics (continental tholeiitic metabasalt) was transferred by syn-orogenic hydrothermal fluids into the dolomitic, carbonaceous Urquhart Shale in fault contact with the volcanics.

12.4.1. Ni-Cu sulfide deposits in intrusions associated with plateau basalt provinces

Intracratonic mafic-(ultramafic) systems contain the bulk of the world's economic platinum metals, a significant share of nickel, and important copper, but all known deposits are in the intrusive phases (Naldrett, 1989). In contrast with the Ni-sulfides hosted by komatiites (Chapter 9) no Ni-mineralized volcanics, and no true ultramafic lavas, have been recognized in the flood basalt setting. The most primitive parent magmas to several mineralized intrusions produced olivine-rich picrites and picritic basalts; those in the Tertiary Baffin Island (Canada) and Swartenhuk (W. Greenland) basalt fields contain 0.18-0.22% Cr₂O₃ and 0.1-0.12% NiO (Clarke, 1977), which is substantially less than the common 0.2% Ni in ultramafic komatiite flows. The Ni-bearing intrusions range from those that are closely associated with comagmatic basalts (hence the basalts provide important exploration indicators, e.g. in the Noril'sk-Talnakh district), and those where no basalts are present (e.g. Bushveld, Great Dyke). The first group is reviewed here, the second one in Section 12.6.

Siberian Platform plateau basalt province and the Noril'sk-Talnakh Ni, Cu, PGE district, Russia

The Siberian Platform contains the world's most extensive continuous plateau basalt cover, estimated to exceed 1.5 million km² (Bilibina et al., 1976). The Platform has Precambrian cratonic basement exposed along its fringe and in the centre (Anabar

Shield), covered by Ordovician to Permian platformic sedimentary succession. The basaltic ("trap") magmatism lasted from late Permian (~250 Ma) to late Triassic (~205 Ma). Several small alkaline basalt and alkaline-ultramafic complexes formed afterwards. The latter (Maymecha Suite) contains kimberlites that produce most Russian diamonds.

The centre of the plateau basalt province is the Tunguzka Basin, a broad depression filled by fissures-fed subaerial basaltic lavas with locally high proportion of tuff issued from central volcanoes and diatremes. Tholeiitic basalt is dominant, alkali olivine basalt less common. Diabase dike swarms are widespread along the fringe of the Plateau. The early stage intrusive equivalents mostly comprise undifferentiated diabase. This forms sills or basin-like concordant intrusions controlled by bedding or formational boundaries of the enclosing Paleozoic sedimentary rocks (Zolotukhin, 1964). In the middle and late stages of the magmatism in Triassic, cross-cutting, more steeply inclined plutons became common. The dominant gabbro-d diabase grades into picrite, troctolite, local teschenite and analcite dolerite. The Siberian basalt province has the most complete selection of Cu, Ni, PGE, Fe, Pb-Zn ore varieties to be expected in this setting, of which Noril'sk and Talnakh are "giant" Ni, Cu, PGE ore fields. The diatremes-related Angara-Ilim Fe province is of the "large" magnitude. The remainder are mostly small ore occurrences. Mineralized regolith is completely missing.

Noril'sk-Talnakh ore district. This is the principal Russian producer of Ni, Cu and platinum metals and second largest PGE (after Bushveld) and sulfide Ni (after Sudbury) repository of the world. Naldrett (1999), however, put the Noril'sk Ni endowment ahead of Sudbury, although the average grade of 2.7% Ni for the whole district is probably too high. The first orebody was discovered near Noril'sk in 1920. The present city of Noril'sk is built on permafrost about 100 km east from the shipping port of Dudinka on the lower Yenisei River, in north-central Siberia. The past and present production comes from the Noril'sk ore field in the south, and from the Talnakh ore field 30 km NNE of Noril'sk, discovered in 1962. There is a voluminous literature, mostly in Russian; the recent English literature is dominated by Naldrett (1998, 1999a), Naldrett et al (1996) and the volume edited by Lightfoot and Naldrett (1990, 1994). This literature is preoccupied with laboratory data and genetic models, with few decent orebody descriptions (Russian texts from the Soviet era

deliver more detail, e.g. Sobolev et al, 1978, but they lack scales, locations and grade/tonnage data). Naldrett (1999a) credited the district with P+Rv of 900 mt @ 2.7 % Ni for 24.3 mt Ni content, with perhaps 30 mt Cu, 240 kt Co, 1,980 t Pd @ 2.2 g/t and 855 t Pt @ 0.95 g/t. The grades in the Talnakh (Oktyabr'skoe deposit) 100% massive sulfide ore are 10.9 % Cu, 7.6% Ni and 0.15% Co, whereas the Medvezhaya Rechka open pit mined, in 1997, material with 0.28% Cu, 0.23% Ni and 4.5 g/t PGE (Goldie in Naldrett, 1998). There is thus a huge difference between the rich massive and lean disseminated ores. The rich orebodies in the district appear to be approaching exhaustion and new discoveries are being made in some 200 km long NNE belt along the Kharayelakh Fault.

Noril'sk-Talnakh district is located near the NW margin of the Siberian Platform, in an area intersected by several Neoproterozoic rift grabens in the subsurface, covered by Ordovician to Permian platformic supracrustals that include Devonian carbonates and evaporites (anhydrite, gypsum, halite) and Permo-Carboniferous coal association. The plateau basalt volcanism is represented by the second, Triassic volcanic phase the products of which fill a series of elliptical basins subdivided by basement "highs". There are several hundred sites of former paleovolcanoes and their subvolcanic-plutonic equivalents. The majority of intrusions are simple gabbrodiabase sills and about 1% of them are differentiated within the gabbrodiorite-troctolite range. Felsic differentiates are rare and separate ultramafic bodies are not known. The ore-bearing intrusions are subhorizontal 100-300 m thick lenses and sheets, peneconcordant with the sedimentary or mafic lava wallrocks (Fig. 12.6). They are members of the high-Mg olivine suite and have a high trace Ni content (0.11-0.2% Ni).

The ore minerals are hosted by both the intrusions and by the thermally and hydrothermally altered supracrustals. Pyrrhotite, pentlandite, chalcopyrite, bornite, cubanite and a number of rare Ni, Cu, Pt-Pd, Bi, Sb, Te minerals occur as: 1) low-grade (<0.8 % Ni) disseminations in troctolite, gabbro-d diabase or "taxite" (noritoid, or crustally-contaminated, inclusions crowded gabbrodiabase) intrusions; 2) massive and breccia ore above the basal endocontact; and 3) veinlet, stringer and disseminated ore in altered sedimentary rocks below or above the intrusions. These have high Cu:Ni ratios or lack Ni altogether. The dominant and most widespread alteration in the wallrock sandstone and gabbros is albitization, skarnization in carbonates, thermal hornfelsing in shales.

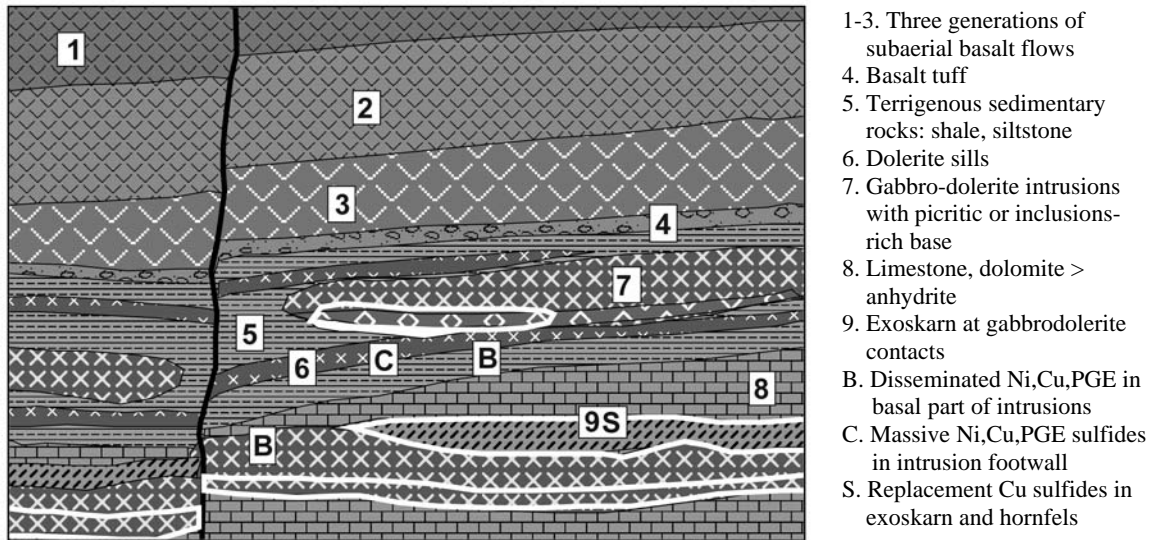


Figure 12.6. Mineralized subvolcanic gabbro-diorite sills emplaced into platformic sedimentary rocks that include carbonates and anhydrite as in the Noril'sk-Talnakh district, Russia. From Laznicka (2004) Total Metallogeny Site G88

Gabbros are locally biotitized, scapolite occurs locally, chlorite is abundant in faults.

The basalt and tuff fill of the Noril'sk and Kharayelakh Basins is over 3,000 m thick. The lowermost and earliest 500 m of the sequence is depleted in Cu, Ni and PGE which Naldrett (1999a) attributed to the loss of these metals as the basaltic magma exited the magma chamber and reacted with the evaporitic, sulfur-rich wallrocks. The lost metals became locally concentrated to eventually achieve ore grades. The progressively younger magma pulses that produced the stratigraphically higher basalt units in the basin lost a lesser percentage of the trace metals. The Noril'sk ores are generally interpreted as products of repeated separation and local accumulation of immiscible Fe, Ni, Cu sulfide melt followed by a hydrothermal stage. Most of the ore sulfur is interpreted as derived from the wallrock anhydrite or coal.

Pechenga (Petsamo) Ni, Cu, Co, PGE zone, Nikel', NW Russia (Haapala, 1968; Gorbunov et al., 1985; Rv₁₉₈₉ 150 mt ore containing 915 kt Ni, Abzalov and Both, 1997; estimated P+Rc ~2.2 mt Ni, 1.00 mt Cu, 100 kt Co, 120 t PGE). This strategically important "world class" Ni ore zone was discovered in 1921 when this was a part of Finland (Petsamo), then incorporated into the U.S.S.R. and developed. It is located in the NW corner of the Kola Peninsula, in what is interpreted as a Paleoproterozoic (1.98 Ga) "rift sequence"

developed on extended high-grade metamorphic Archean basement. The host Pechenga Series is a 10 km thick fan-shaped unit of basal conglomerate topped by four cycles of ferropicrite (olivine-rich metabasalt) interlayered with, and underlaid by, phyllite and metagraywacke. Ni-Cu sulfide mineralization is confined to an arcuate, 70 km long belt of tectonized carbonaceous phyllite (partly phyllonite), crowded with some 220 lenticular gabbro or zoned wehrlite, pyroxenite, gabbro intrusions in the form of 2-700 m thick and 200 to 7,000 m long sheets, slices, lenses and boudins (tectonically dismembered sills?). The intrusions are tectonized, serpentinitized and talc, carbonate, chlorite altered. At least 22 Ni-Cu sulfide orebodies (pyrrhotite, pentlandite, chalcopyrite, cubanite) occur along both sides of the carbonaceous and pyritic phyllite contact with serpentinite. The orebodies change upwards from 0.1 to 10 m thick massive and breccia sulfide ore at base into low-grade sulfide disseminations in serpentinite; the latter is the dominant style of mineralization. The footwall phyllite is laced with chalcopyrite-rich stringers in a zone 0.3 to 2 m thick. Late-stage quartz-calcite veins with pyrite and chalcopyrite fill dilations. The most persistent orebodies (e.g. the Kaula deposit) are developed along the sole of overthrusts, along tectonic contacts between the footwall phyllite and hangingwall serpentinitized intrusion.

Pechenga is difficult to classify; it combines characteristics of Noril'sk, the Outokumpu assemblage, komatiitic suite, and Thompson stripped of its high-grade metamorphic overprint. It is a synorogenic mineralization with Ni-Cu source in the mafic/ultramafic intrusions but it is unclear as to whether the sulfides are synmagmatic, later deformed and remobilized, or syntectonic, produced by sulfidation of trace Ni by sulfur from pyritic metapelites.

Keweenaw (1.1 Ga) flood basalt province, Lake Superior Basin

This is an extensive region well exposed along the southern and western (in Michigan), and northern (in Ontario) shores of Lake Superior, where the basalt/copper connection is demonstrated by hundreds of Cu occurrences at both ends of the basalt/sediment spectrum. This includes one "giant Cu province" (Michigan-Cu) with two resident "giants" (Calumet-Hecla, 2.7 mt Cu; White Pine, ~10.5 mt Cu) and five "large" Cu deposits; plus one "large", though uneconomic, Cu ore field in Ontario (Batchawana). Not included here is the Cu-Ni "giant" associated with the intrusive Duluth Complex (read Section 12.6). This Province is a member of the Mesoproterozoic Midcontinent Rift, traceable for about 3,000 km across North America (Nicholson et al, 1992; Fig. 12.7). It is a system of linked half-grabens on the Paleoproterozoic and Archean orogenic basement, filled by up to 20 km of continental basalt flows followed by sediments (Hoffman, 1989; Wallace, 1981). The pre-rift continental to shallow marine sediments were followed by massive outpouring of Keweenaw lavas that lasted about 20 m.y. (from about 1.14 to 1.12 Ga; Green, 1982) and emplacement of intrusive equivalents in depth. The volcanics are predominantly olivine and quartz tholeiite with locally abundant rhyolite (5-25% of the volcanics), and they form a series of seven partly overlapping lava plateaux between 0.12 and 12 km thick. The greatest thickness was reached in the Keweenaw Peninsula in Michigan, which coincides with the Michigan native copper district.

The mafic flows are entirely subaerial, on the average 7 to 12 m thick and zoned from a massive central layer through an amygdaloidal upper third into a scoriaceous or brecciated flowtop. Some flows are topped by lenses or thin layers of interflow sediments like polymictic conglomerate rich in rhyolite clasts, brown sandstone or shale. The gently dipping individual basalt flows are remarkably persistent, almost undeformed except

for block faults, and affected by load metamorphism ranging from zeolite to upper greenschist (Jolly, 1974). In Michigan, the volcanic activity was followed by sedimentation and up to 10 km thick succession of fluvial, lacustrine and shallow marine sediments accumulated in the basin. The oldest unit, Copper Harbour Conglomerate, is more than 2,000 thick redbed polymictic conglomerate that is conformably overlain by the Nonesuch Formation. The latter is an about 2000 m thick, locally exposed lens of carbonaceous (even bituminous in places) interbedded litharenite, mudstone and dolomitic laminite. It is topped by a thick, monotonous Freda Sandstone.

Keweenaw Peninsula native copper district, Michigan (Butler and Burbank, 1929; White, 1968; P+Rv ~6.33 mt Cu). This is the world's largest, and the only significant, Cu accumulation represented, with one exception, by native copper. The "zeolite copper deposits" of Emmons were actively mined around the turn of the 20th century but there is not much activity now. The orebodies are stratabound tabular bodies controlled by the extensively prehnite, pumpellyite, chlorite, epidote, K-feldspar, quartz, calcite and zeolites-altered and infilled basalt flowtops, or by interflow sediments modified by the same alteration assemblage (Fig. 12.8). There are six major stacked "amygdaloidal" ore horizons and four "conglomerate" ore horizons in the district, in a 45 km long segment of the NE-trending ore belt. One or more horizons were mined from a single property. The "amygdaloids" supported most workings and contributed about 65% of the Cu production, but the Calumet-Hecla conglomerate deposit was the largest and only continuous "giant" orebody in the district (P+R 114 mt @ 2.4 % Cu, for 2.736 mt Cu content; Kirkham, 1996b). The Cu ore there consisted of scattered grains, wires, blebs and plates of native copper enclosed in altered amygdaloidal basalt, in masses of alteration or gangue minerals dominated by white or pale green prehnite interstitial to the flowtop breccia, or in groundmass of conglomerate or sandstone. The orebodies were several centimeters to 5 m thick blankets ("mantos"). Fissure veins with the same mineral association or with chalcocite (Mount Bohemia) are exceptional and insignificant. The currently held genetic model (Jolly, 1974) assumed extraction of the trace Cu from basalts in depth during metamorphic dehydration, followed by fluid ascent along faults and precipitation at the prehnite, pumpellyite, laumontite and chlorite interface higher up, along the interflow permeability surfaces. The mineralization postdated the basalt emplacement by some 60-70 m.y.

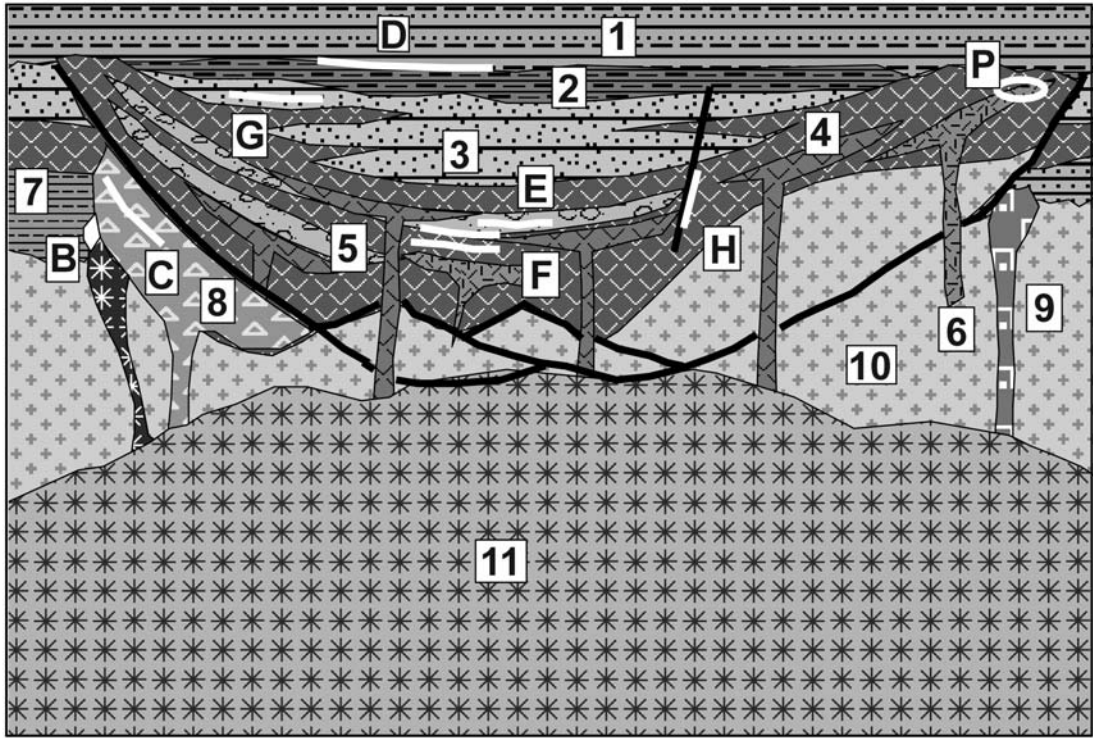


Figure 12.7. Diagrammatic representation of the North American Mid-Century Rift and its Keweenaw volcanic succession showing the rocks and ores inventory. From Laznicka (2004) Total Metallogeny Site 220. 1. Cyclic platformic sandstone, shale; 2. Black bituminous lacustrine shale; 3. Alluvial redbed sandstone, conglomerate; 4. Continental flood basalts with feeder dikes; 5. Red interflow conglomerate; 6. Rhyolite and porphyry; 7. Pre-rift sedimentary rocks; 8. Gabbro-anorthosite layered intrusion (on right) with associated troctolite stock (on left); 9. Alkaline intrusion; 10. Siliceous crystalline basement; 11. Mantle and underplating basalt; B. Cu-Ni sulfides at gabbro, troctolite and sulfidic sediment contacts; C. Disseminated and layered Fe,Ti,V oxides in gabbro, anorthosite; D. Stratabound Cu,Ag sulfides in lacustrine sediments; E. Disseminated Cu in interflow conglomerate; F. Native Cu in basalt flowtops; G. Cu sandstone in reduced redbeds; H. Cu in fracture and fault veins; P. Disseminated Cu (Mo,Au) in breccia and A-granite, porphyry, rhyolite. Ore types B, D, E and F have known "giant" members

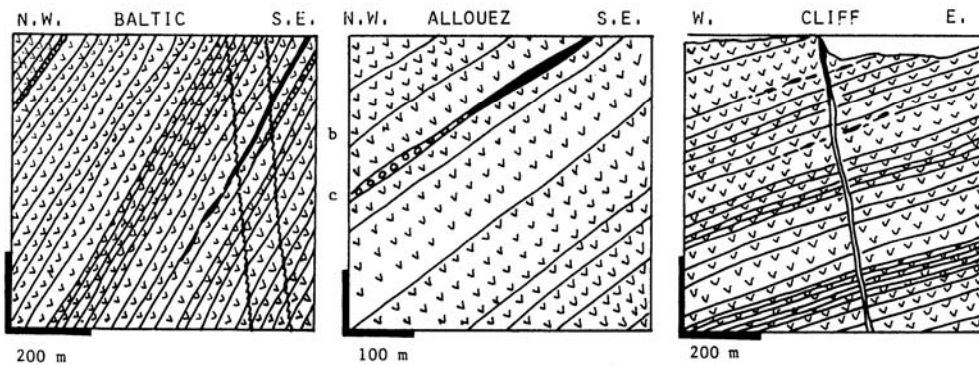
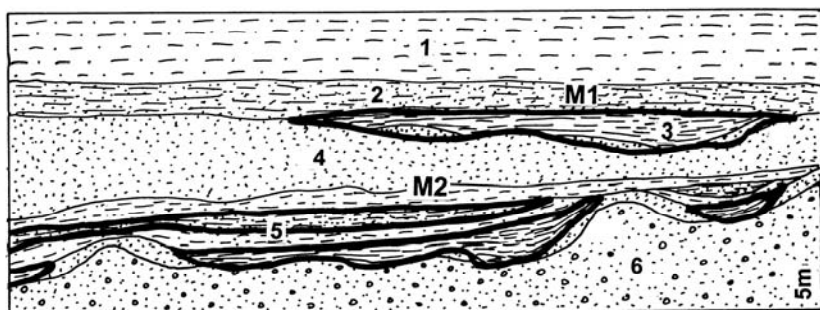


Figure 12.8. Examples of the three principal styles of the Michigan-type native Cu deposits related to subaerial metabasalt flows, Keweenaw Peninsula, Michigan. From LITHOTHEQUE (also Laznicka, 1985) based on data in Butler and Burbank (1929). Baltic Mine (left) has Cu-mineralized prehnite-pumpellyite altered basalt flowtops; Allouez Mine (centre) has native Cu scattered in red interflow conglomerate; Cliff Mine (right), a small deposit, is a crosscutting Cu vein. Explanations: b=metabasalt; c=conglomerate; black=orebodies



1. Np white quartz sandstone; 2. Np lacustrine Nonesuch Shale, upper siltstone; 3. Ditto, bituminous shale; 4. Ditto, light lithic sandstone with red shale partings; 5. Ditto, Parting Shale, dark shale to siltstone intercalated with reddish siltstone; 6. Copper Harbor redbeds

Figure 12.9. White Pine Mine, Michigan, diagrammatic cross section from LITHOTHEQUE No. 815 modified after Ensign and Patrick (1968), White Pine geology staff handouts, 1971. Explanations (continued): M1. Upper Orebodies, chalcocite disseminated in siltstone; M2. Lower Orebodies, disseminated chalcocite and native copper in chloritic sandstone and shale

White Pine mine, Ontonagan County, Michigan (Brown, 1971; P+Rv 322 mt @ 1.1 % Cu, 7.5 g/t Ag for 3.59 mt Cu, 2,415 t Ag; Rc 6.72 mt Cu; Fig. 12.9). The redbed-type Copper Harbor Conglomerate in Michigan hosts only small Cu occurrences, although globally this would be a common setting for the "sandstone-Cu" type. The base of the overlying Nonesuch Shale, however, has a reduced, lacustrine carbonaceous shale/litharenite unit that host the important subhorizontal stratabound White Pine deposit. At base of the unit is chloritic sandstone to shale, mineralized by disseminated chalcocite with interstitial native copper in sandstone matrix. As in the similar Kupferschiefer (Chapter 13), a small quantity of Cu sulfides and oxides infiltrated the top of the partly reduced redbeds beneath. In the upward direction native copper disappears and chalcocite becomes the only ore mineral, until it abruptly terminates. Above, the only sulfide present is pyrite, although Zn and Pb are strongly enriched. Genetic interpretations range from single stage syngensis/diagenesis through epigenetic replacement of syngenetic pyrite by fluids carrying copper, to a single stage epigenesis. There is no visible direct connection with basalts in depth.

Cu breccias and porphyry Cu-Mo showings, Batchawana area, Ontario. Batchawana area in central Ontario, at the east shore of Lake Superior, was the site of three past mines producing from small Cu deposits in sediments, metabasalts, and breccia pipes. The breccia pipes and associated uneconomic very low-grade Cu-(Mo) porphyry deposits in the **Tribag group** (Norman and Sawkins, 1985; ~280 mt of material with 0.13-2.75% Cu) are located along the margin of Keweenawan basalts over the Archean greenstone belt-type basement, intruded by a small anorogenic

granite stock and several heterolithologic breccia pipes. At least three subvertical breccia bodies consist of a jumble of basalt and diabase fragments supported by rock flour matrix and cemented by chlorite, quartz and carbonates, with scattered grains of pyrite, chalcopyrite and magnetite. There is virtually no wallrock alteration in the near-surface area, but propylitization and sericitization increase with depth. Norman and Sawkins (1985) interpreted the pipes as a result of roof collapse into open space, created by magmatic-hydrothermal fluids in depth. The small 1.055 Ga granite stock contains an embryonal, sub-grade porphyry style disseminated Cu-Mo mineralization, one of the few occurrences of this type in the world associated with rifting.

12.4.2. Lateritic bauxite on basalt

Lateritic bauxite (Bárdossy and Aleva, 1990) mined for the production of alumina which, in turn, is smelted to obtain aluminium, favours basalts of any geological age and any setting as parent rock. Of the global bauxite resource of 54 bt (about 12.64 bt Al content) in the 1980s quoted by Bárdossy and Aleva (1990) (the figure has not changed much since), 19% of tonnage (that is 10.26 bt of bauxite with ~2.4 bt Al) formed on basalts. The majority of parent basalts are subhorizontal plateau basalt flow units, peneconcordant with planation surfaces, topped by bauxitic (gibbsitic) duricrusts that continue for many kilometers. Lateritic bauxites on basalts are always ferruginous (red), of lower grade and purity than the "karst bauxites" or laterites formed on low-Fe parents like nepheline syenite, shale or arkose, and they may grade into ferricrete duricrusts (cuirasses; Chapter 13). Of the 22 bauxite districts or regions entirely or completely on basalts

reviewed by Bárdossy and Aleva (1990), the following are of "world class" (400 mt Al plus):

- **Central Highlands of South Vietnam**; recent gibbsitic bauxite developed on Late Pliocene to Pleistocene flood basalt (Rc ~3.2 bt @ 21.2% Al for 678 mt Al).
- **Adamaoua (Ngaoundere) plateau** in NE Cameroun, Cenozoic bauxite on Upper Cretaceous and Lower Tertiary basalt flows (Rc 1,825 mt @ 23.4% Al for 427 mt Al).

12.5. Diabase, gabbro, rare peridotite dikes and sills

The common diabase (often called dolerite) is a hypabyssal equivalent of tholeiitic or quartz tholeiitic basalt that form dikes and sills of variable thickness. It is a greenish, massive, uniform rock of simple composition (Ca plagioclase, clinopyroxene, accessory magnetite). The pyroxene is frequently converted to actinolite or chlorite, the plagioclase is partly or entirely albitized. The Ca released during this conversion accumulated in calcite fracture veins, ubiquitous in most diabase bodies. Diabase is gradational to gabbro and/or diorite dikes and sills. Most diabase bodies are uniform throughout (some have finer-grained chilled contacts) but few are internally differentiated. Differentiation is most common in very thick gabbro sills such as the Golden Mile Dolerite in Kalgoorlie (Chapter 9) or the Nipissing Sill in Ontario (Lightfoot and Naldrett, 1996); if so, marginal granophyre is the most common differentiate. There is a transition between gabbro sills/dikes and Bushveld-style layered intrusions; the Great Dyke of Zimbabwe is, in fact, a layered intrusion and the true feeder dike (or dikes) are expected underneath. Peridotite dikes or sills are rare.

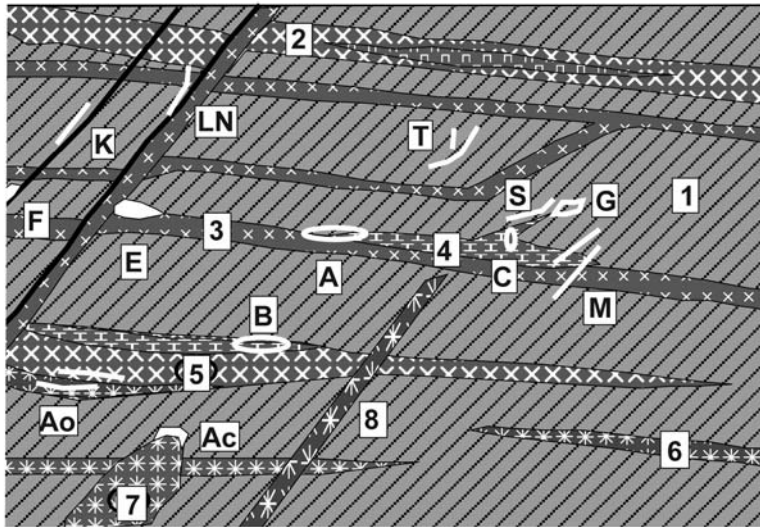
From the premise of field geology and exploration it is convenient to differentiate between diabase/gabbro dikes/sills that are visible members of a broader lithologic association (e.g. sheeted diabase dikes in the ophiolite association; feeder dikes in flood or "geoclinal" basalt sequences) and independent dikes/sills. Only the latter are considered in this section. Of the independent dikes/sills a greater portion was never associated with coeval volcanics at the surface and the magma infilled tensional dilations entirely in the subsurface. A minority was a part of the feeder system to extrusive basalts, but erosion has removed the surface equivalents. In deeply eroded terrains these two varieties cannot be distinguished.

Diabase/gabbro dikes and sills (further referred to as "mafic dikes") have usually narrow rims of thermally metamorphosed rocks in the exocontact, and occur as single bodies or as members of dike swarms (Halls and Fahrig, eds., 1987). Dike swarms are most common in the hinterland of rifts and paleorifts and in the vicinity of triple junctions and aulacogenes, but an almost regular network of dikes of several generations criss-cross large cratons and shields, like the Canadian Shield. Some individual mafic dikes there are remarkably persistent; the 1.14 Ga Great Abitibi Dike in Ontario and Québec is subvertical, up to 600 km long and up to 250 m wide. Its composition ranges from olivine gabbro to monzodiorite, emplaced in two pulses (Goodwin, 1991)

Metallogeny: (Compare the comprehensive reviews in Laznicka, 1985 and 1993, p. 1123-1138). The bulk of mafic dikes encountered in the field (they tend to have good outcrops and are a favourable material for crushed stone, hence exposed in many quarries) are completely devoid of ore indications. Directly associated ore occurrences formed as a by-product of magmatic evolution of the mafic body, mostly by separation of immiscible ore liquid to form local Fe, Ti, V oxide and/or Fe, Cu, Ni sulfide accumulations in a manner comparable with the Bushveld-type intrusions (read below). Such occurrences are infrequent, small, and confined to the thickest, best differentiated sills transitional to layered complexes. The highly productive differentiated sills in the infrastructure of some plateau basalt fields as in Noril'sk are exceptional and described above. No "giant" magmatogene deposits are associated with the "ordinary" mafic dikes/sills.

Ore occurrences indirectly related to mafic dikes/sills formed:

- 1) When the intrusion provided selectively more favorable structural conditions (e.g. brittle fractures) for ore deposition from genetically unrelated later, epigenetic fluids. The Golden Mile-Mount Charlotte "Au-giant" near Kalgoorlie (Chapter 9), and many other "large" vein Au deposits, have mafic dike hosts;
- 2) When a mafic intrusion, typically crystallized from anhydrous, sulfur-poor melt, supplied heat that energized external fluids in the roof rocks and sustained convection. The ore metals were scavenged by the fluids from wallrocks and/or partly or in full from the cooling mafic body itself. The Cobalt, Ontario Ag, As, Co, Ni vein district is a "giant" example.



1. Wallrocks; 2. "Giant gabbro sill"; 3. Tholeiitic diabase, gabbro sills; 4. Granophyre; 5. Gabbro sill changing to layered intrusion (ultramafic bottom, granophyre top); 6. Peridotite sill; 7. Picritic gabbro plug and sill; 8. Troctolite dike; A. Cu-Ni sulfides in gabbro or granophyre; Ao. Ditto, in olivine-rich members; Ac. Ditto, at diabase contacts; B. Au, erratically disseminated in granophyre, gabbro; C. Cu,Co sulfides in granophyre rims; E. Magnetite-pyrite exoskarn; F. Magnetite, actinolite, apatite veins, pods; G. Massive magnetite or hematite, disseminated Cu,Au,U in altered breccia;

Figure 12.10. Inventory diagram of metallic ores associated with diabase, gabbro and related dikes in extensional (rift) settings. From Laznicka (2004) Total Metallogeny Site 83. Explanations (continued): K. Quartz, carbonate, chalcopryrite veins; L. Pb,Zn,Ag veins; M. As,Ag,Co,Ni,Bi (U) fault and fissure veins, quartz-carbonate gangue (Cobalt-type); N. Ditto, native Ag only, carbonate gangue; S. Pitchblende veins, breccias; T. Th-REE veins and metasomatites. Ore types G and M have known "giant" members

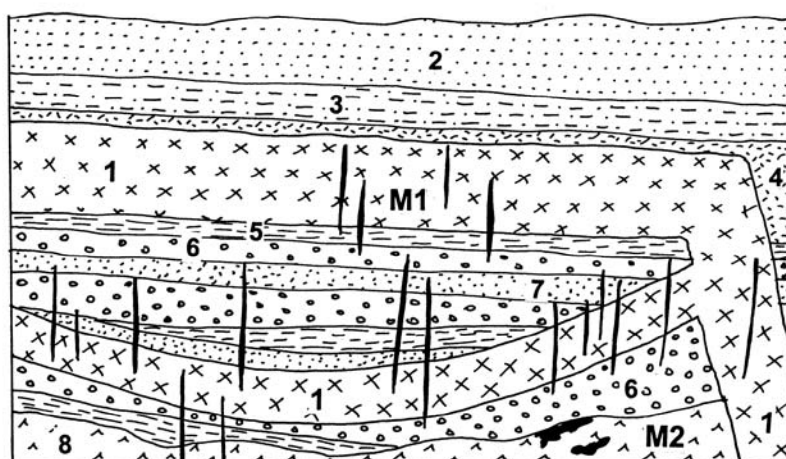
- 3) When the mafic intrusion served as a passive metal source (e.g. of Cu, Ni, Co) selectively extracted, removed, then reprecipitated by genetically unrelated hydrotherms; and
- 4) When supergene leaching and pedogenesis transferred a mafic intrusion into lateritic bauxite or residual ironstone. Several "world class" bauxite ore fields formed over diabase dikes/sills. Selected examples of significant mineralizations related to mafic dikes follow.

Nipissing gabbro Sill and Cobalt-Gowganda Ag, As, Co, Ni, Bi district, Ontario

The "giant" Cobalt ore field (and three smaller fields nearby) in NE Ontario are located in the Cobalt Embayment, the northernmost, little deformed and almost unmetamorphosed portion of the 2.48-2.22 Ga Huronian Supergroup prism and foldbelt (Bennett et al., 1991). There, the clastics of the uppermost Huronian sedimentary cycle (Cobalt Group) are basal diamictites and siltstones with rafted pebbles grading into "red" wacke, siltstone and shale. The sedimentary rocks rest unconformably on folded greenstones of the Archean Abitibi Subprovince, and both successions are cut by the 2.22-2.19 Ga Nipissing Sill. The Sill is actually a set of several hundred meters thick intrusive sheets and dike swarms mainly composed of ortho- and

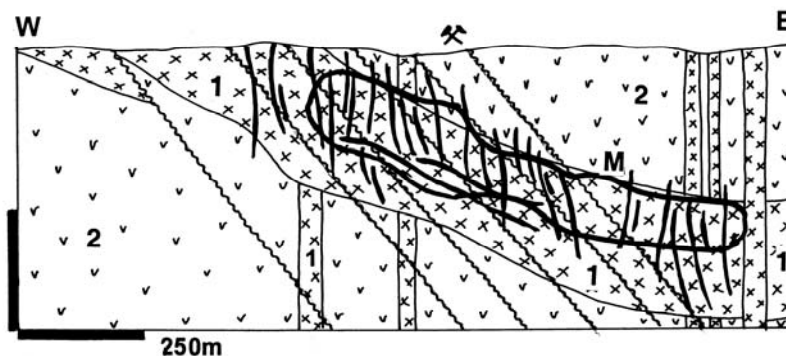
clinopyroxene gabbro with minor feldspathic pyroxenite, gabbro-anorthosite, and leucocratic ("pink") granophyre phase near the top. Several hundred mostly short steeply-dipping low-temperature hydrothermal veins fill faults and fractures in a broad area, divided into four ore fields. The Cobalt ore field has been the most productive, followed by the Gowganda field (Pt ~1,700 t Ag).

Cobalt ore field (or camp) (Berry, ed, 1971; Petruk et al., 1972; Boyle, 1976; Andrews et al., 1986; Pt ~16,000 t Ag, 11,250 t Co, 675 t Cu, plus calculated content of ~60 kt As, 6.5 kt Ni, some Bi) was discovered in 1903 and produced from more than 60 small mines up to now (Figs. 12. 11 & 12.12). The Archean basement is an isoclinally folded greenschist-metamorphosed succession of metabasalt, volcanoclastics and interflow sediments. The latter include stratabound black sulfidic interflow meta-argillite enriched in pyrite, chalcopryrite, sphalerite and galena and there are some shears mineralized by the same metals. Huronian clastics rest unconformably on the Archean and the Nipissing Sill is emplaced along, or close to the unconformity. All ore veins are near the unconformity and within 200 m of the dike contact. Most are hosted by the clastics and gabbro, although some continue into the basement.



M1. Carbonate, quartz, silver, Ni-Co arsenides, etc. fault and fissure veins; M2. Massive and disseminated Fe,Cu,Zn,Pb sulfides in Archean greenstones and schists; 1. ~2.2 Ga Nipissing Sill gabbros; 2. Pp Huronian Supergroup, Lorrain quartzite; 3. Ditto sandstone; 4. Gowganda Fm. graywacke; 5. Ditto, shale; 6. Ditto, conglomerate; 7. Ditto, sandstone; 8. Ar greenstone metabasalt, phyllite

Figure 12.11. Cobalt-Gowganda silver district, Ontario, diagrammatic lithology and ore vein sites. From LITHOTHEQUE No. 1894, based on literature data and site visits



M. Narrow calcite, silver, Fe, Co, Ni arsenides, tetrahedrite, etc. fault and fissure veins with sharp slickensided contacts; 1. ~2.2 Ga Nipissing gabbro sheets and dikes; 2. Ar Abitibi greenstone belt metabasalts and metapelites enriched in Fe, Cu, Zn, Pb sulfides

Figure 12.12. Gowganda-Miller Lake ore field, Ontario, cross-section through Siscoe Shaft # 6. From LITHOTHEQUE No. 988, modified after Hester (1988). The vein position is diagrammatic

A single controlling structure can contain several types of ore veins: fissure (dilatant) veins free of deformation; shear veins with a strong penetrative fabric parallel with the vein walls; and replacement veins in carbonatized comminuted wallrocks with disseminated sulfides. The veins vary in thickness from 1 cm to over 30 m and they have thin selvages of quartz, chlorite, actinolite, microcline, albite and epidote adjacent to a 2-5 cm wide chlorite-calcite alteration halo in the wallrock. Some veins are associated with patches of pink Na- or K-feldspathization ("red rock", "pseudosyenite"). The vein centers are filled by calcite with or without pink dolomite.

Many veins are barren but when ore shoots are present they form bands, small masses and disseminations on the inner side of the silicate selvage, or small masses, clusters to disseminations anywhere in the vein. The "silver shoots" grade around 750 g/t Ag and their terminations are

enriched in arsenopyrite, chalcopyrite and tetrahedrite. The complex assemblages of metallic gray Fe, Co and Ni arsenides are indicated in outcrop and in exposed workings by rapidly forming powdery coatings of pink erythrite, apple green annabergite and "khaki" scorodite. The most common ore minerals in veins are löllingite, safflorite, skutterudite, cobaltite, niccolite, arsenopyrite, rammelsbergite, gersdorffite and bismuth. Native silver forms rosettes, wires, and plates in fractures. Base metals sulfides occur as scattered grains in calcite veinlets that are most common along vein contacts.

The Cobalt veins are reminiscent of the European "five-elements association" that is common in the German and Czech Erzgebirge (Chapter 10), but they lack uranium. U, on the other hand, forms "giant" concentrations in conglomerates in the Blind River-Elliott Lake district SW of Cobalt, at the base of Huronian

above the same unconformity (Chapter 11). Cobalt veins have been traditionally interpreted as a product of scavenging of trace metals from local lithologies by meteoric or formational fluids heated by the Nipissing intrusion (Boyle, 1976). Andrews et al. (1986) emphasized structural control and mineralization that postdated the gabbro, with ore metals derived mostly from the Archean basement although Co and Ni came more likely from the gabbro.

The "Ag-giant" Imiter (Chapter 8) in the Moroccan Anti-Atlas, has some mineralogical and structural similarities with Cobalt but is not closely associated with diabase or gabbro. **Imiter** is in the Saghro Massif (Cheilletz et al., 2002; Rc ~8,000 t Ag), controlled by a 7 km long fault zone in Neoproterozoic black phyllite and andesite intruded by a 572 Ma granodiorite and remnants of 550 Ma rhyolitic volcanics. Supergene enriched bonanza veining that comprise native silver, amalgam, Ag-Hg sulfosalts in dolomite gangue is superimposed over earlier Pb, Zn, Cu, Co, Ni, As mineralization in quartz-sericite altered wallrocks. Cheilletz et al. (2002) considered this an epithermal mineralization, genetically associated with the 550 Ma rhyolites.

Lateritic bauxite over diabase (dolerite) sills and dikes

After basalt (read above), diabase is the second most important parent to residual bauxite deposits, with 17.1% of global tonnage in 16 districts/areas (Bárdossy and Aleva, 1990). This corresponds to some 9.234 bt of bauxite and ~2.16 bt Al. There are six "world class" districts (400 mt Al plus) where the lateritic bauxite formed entirely or partially on diabase, five of which are in Guinea and one in the Darling Ranges of Western Australia (Table 12.1).

Guinea bauxite subprovince (Bárdossy and Aleva, 1990) contains the world's largest proven reserves of bauxite (9.1 bt) that cap lateritic plateaux belonging to the "African" (Late Cretaceous-Early Tertiary) planation surface. The bauxite continued to form from Cretaceous to the present. The source rocks are Mesozoic diabase sills and dikes emplaced during the continental breakup and drift of South America away from Africa, as well as the adjacent Devonian and Silurian shale and siltstone. These stable margin sedimentary rocks rest on and surround the Guinean and Leo arches of the Precambrian basement. Gibbsite bauxite forms almost continuous blanket on top of the erosion-dissected plateaux. Boké-Goual is the largest bauxite region in NW Guinea that covers an

area of 150x70 km. The bauxite resource is quoted as 2.65 bt, containing some 662 mt Al.

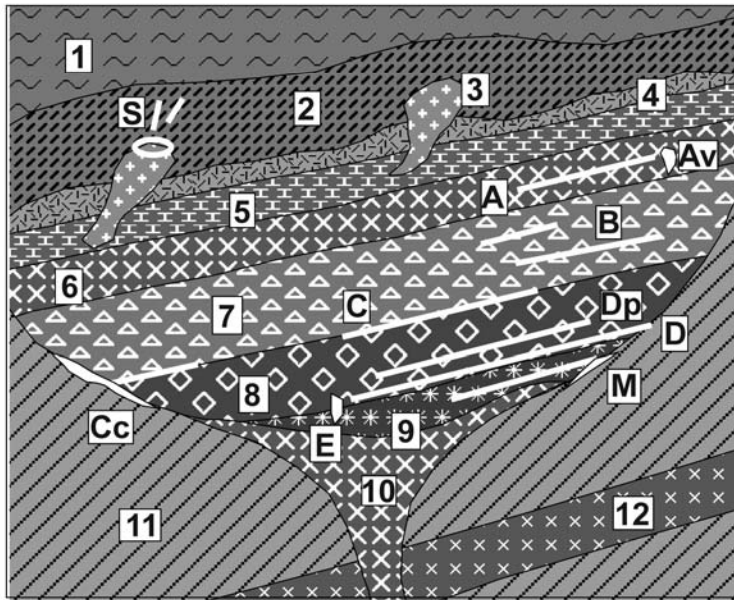
12.6. Bushveld-style layered intrusions

Bushveld-type intrusions store the greatest proportion of the world's inventory of platinum metals and chromite, plus significant proportion of the world's nickel and vanadium. The bulk of these resources is in just three complexes: Bushveld (a multiple metals supergiant), Great Dyke, and Sudbury. Two other significant members of the Ni-PGE club, the Phanerozoic Noril'sk and ultramafic Jinchuan, are described above and below, respectively.

Layered mafic-ultramafic intrusions are generally thought of as former magma chambers to mafic and possibly some ultramafic (komatiitic) extrusive rocks, although such association is not apparent in the three major complexes listed above: either the volcanic levels have been completely eroded, or they had never formed. The magmatic complexes have been classified from a variety of premises (compare Naldrett, 1989b, 1993) of which the one based on lithotectonic setting is most useful for exploration. Based on this premise, the following Precambrian categories of intrusions are briefly reviewed in Laznicka (1993; pages 540-553 and 1138-1202): 1) dominantly Archean complexes that appear in or near greenstone terrains (e.g. Lac Doré, Fox River Sill, Mashava, and others). None of them contains giant orebodies; and 2) dominantly Proterozoic, anorogenic layered intracratonic complexes (Bushveld-type; Fig. 12.13), plus Sudbury that departs from the Bushveld model and has been recently treated under the heading "Astrobleme-associated Ni-Cu" (Eckstrand, 1996). Only category 2) is considered in this section, which also includes metamorphosed, but non-penetratively deformed examples like Stillwater. The very high-grade metamorphosed equivalents that merge with the surrounding supracrustal metamorphics (e.g. Fiskenaeset-Cr, partly Selebi-Phikwe and Thompson Ni, Cu) belong to Chapter 14.

Bushveld igneous complex, South Africa, and its Cr, Ni, Cu, PGE, V "giants"

The 2.06 Ga Bushveld complex is a global geological anomaly: an outstanding petrologic model and the world's largest known (and most valuable) source of at least six industrial metals.



1. Slate, phyllite; 2. Thermally hornfelsed sediments; 3. Anorogenic granite; 4. Felsite, rhyolite; 5. Granophyre; 6. Gabbro, quartz gabbro, diorite; 7. Anorthosite, ferrogabbro, norite; 8. Layered series: bronzitite, anorthosite, norite; 9. Ultramafics (mostly harzburgite); 10. Chilled contaminated intrusive endocontacts; 11. Basement rocks; 12. Gabbro dike. A. Layered magnetite or ilmenite in gabbro; Av. Discordant Fe-Ti-V pipes; B. PGE in olivine-rich pegmatoid layers in anorthosite; C. PGE, Ni, Cu in bronzitite in cyclic units; Cc. Ditto, hybrid contacts with PGE, Ni, Cu; D. Chromite layers in ultramafic cyclic units; Dp. Ditto, high PGE in chromitite; E. PGE in dunitic pipes; M. Ni, Cu sulfides at basal contacts; S. Hydrothermal Sn veins, disseminations, replacements

Figure 12.13. Diagrammatic representation of rocks and ores in Bushveld-type mafic-ultramafic complexes. From Laznicka (2004), Total Metallogeny Site 90

If all six platinum metals were considered separately, this number would increase to eleven. Because of this, all the remaining complexes/deposits are usually described and interpreted with reference to Bushveld, a practice followed here as well. This causes some problems. Because Bushveld is so big and regular it is, for example, difficult to delineate, quantify and compare its mineral deposits. The literature struggles with this as witnessed by the enormous range of published Bushveld metal tonnages, none of which is final (e.g. to 100m, 300m, 1200m depths). This is influenced by economics of the day (e.g. minimum thickness of a mineable chromitite seam) and degree of exploration. The problem is illustrated by the painstaking process of estimation of chromite resources, undertaken by Vermaak (1986). This author calculated that all mineable chromitite seams in the Bushveld complex thicker than 20 cm, with the average grade of 44.19% Cr₂O₃, contain 708 mt of ore to the depth of 30 m (=reserves); 1,714 mt ore to the depth of 100 m (=indicated reserves); 9.05 bt of ore to the depth of 500 m (=inferred reserves) and 11.475 bt of ore as total reserve; this translates into some 3.468 bt of Cr content. If the latter figure is extrapolated to include the ore possibly present to the depth of 1,500 m, the figure will triple to 10.4 bt Cr. Although the deep-seated chromite is presently uneconomic to exploit

for Cr only, the platinumiferous UG2 Reef is now being extracted from depths greater than 1,500 m and at the Northam Mine its reserves have been calculated to a depth of 2,700 m. In terms of speculative geological resources, the entire Bushveld contains at least 20 bt Cr.

Table 6-1 in Laznicka (1993) provides several alternative tonnages of the Bushveld metals endowment, of which only two are listed here, as follows:

- 1) Whole Bushveld, past production and all categories of presently industrial reserves and resources in "economic" depths (metal content/average grade): Cr: 2.7 bt/28%; Fe, 3.0 bt/50%; Ti, 400 mt/7.2%; V, 50 mt/0.8%; Ni, 12 mt/0.3%; Cu, 6 mt/0.2%; PGE, 50,000 t/2 ppm (in it: 24 kt Pt, 16 kt Pd, 5.2 kt Ru, 3.2 kt Rh, 2.8 kt Ir, 600 t Os); 850 t Au.
- 2) Whole Bushveld, projected geological resources to 3,000 m depth: Cr, 20.8 bt; Fe, 132 bt; Ti, 19.01 bt; V, 1.77 bt; Ni, 23 mt; Cu, 13 mt; PGE, 121 kt (in it: 60 kt Pt; 40 kt Pd; 11 kt Ru; 7 kt Rh; 4800 t Ir; 1200 t Os); 1800 t Au.

Because of the enormity of the Bushveld mineralized layers, the conventional ore terminology and hierarchy do not work well here. For example, the Merensky "Reef" in the Western Lobe is a magmatic layer several cm to 2 m thick,

yet traceable for some 240 km along strike (not counting the interruption by the younger Pilansberg intrusion). Is this an orebody, a district, a belt? A delineation of ore deposits, based on present mine properties (e.g. Atok, Northam), is against the geological logic (the mines exploit ownership-defined intervals of continuous ore horizons), it is here generally avoided and the entire ore horizons are treated as single deposits.

Bushveld complex has an elliptical outcrop measuring about 460x330 km with an area of 67,340 km², just north of Pretoria in former Transvaal, NE South Africa (Willemse, 1964; Tankard et al., 1982; Von Gruenewaldt, 1977; Vermaak, 1986; Anhaeusser and Maske, eds., 1986; Economic Geology Special Issues No. 1, v.71, 1976 & No. 4, v.80, 1985; Eales and Cawthorn, 1996; Cawthorn and Walraven, 1998). It is an agglomeration of medium- to high-level ultramafic-mafic magmatic bodies of the Rustenburg Layered Suite (RLS; Von Gruenewaldt et al., 1986; Vermaak and Von Gruenewaldt, 1986) intruded into Paleoproterozoic supracrustals of the Transvaal Group and partly (in the Potgietersrus area) into the Archean basement. The suite is "pristine", preserved close to its original position in the time of emplacement, and is virtually unmetamorphosed. The magma emplacement was controlled by intersections of NNE and E-W lineaments and the magma supply is attributed to a mantle plume under the Kaapvaal Craton. Magmas migrated towards the surface along two concentric, ellipsoidal, inverted conical fractures and along seven feeders. Cawthorn and Walraven (1998) favored RLS formation by crystallization of successive injections of magma, closely spaced in time so that each earlier magma batch had not entirely cooled and differentiated before the addition of the next batch. The entire RLS was emplaced in some 75,000 years.

Rustenburg Layered Suite (RLS) is about 8 km thick and discontinuously exposed in five outcrop areas ("compartments") separated by remnants of the roof meta-sediments, felsic meta-volcanics, granophyre units and the 2.0 to 1.65 Ga anorogenic Lebowa Granite Suite. The latter contains several "medium" to "large" Sn and fluorite deposits, is not genetically related to RLS, and is not considered here. The RLS compartments have an almost identical stratigraphy suggesting original continuity, but not all magmatic layers are present everywhere. The compartments include:

- 1) The Far Western Limb north of Zeerust;
- 2) The Western Limb (Lobe), a semi-circular outcrop with a 60 km radius and 10-15° dips

to east between Pretoria, Rustenburg and Thabazimbi;

- 3) The Potgietersrus Limb (Prong) in the north;
- 4) The Eastern Limb (Lobe) along the Drakenberg Escarpment north and south of Steelpoort, dipping to west; and
- 5) The Southeastern (or Bethal) Lobe present in subcrop.

Rustenburg Layered Suite stratigraphy and related ores (from base to the top):

The widely used classical zonal stratigraphy of Willemse (1969) based, in turn, on earlier writing, has more recently been extended by addition of new lithostratigraphic subunits (Kent, ed., 1980). The traditionally named zones, however, have been preserved and continue to be used in the general literature, particularly the one "for export". The principal RLS zones, and the giant metals accumulations they host (in brackets) are, from base and margin to the top, as follows:

1. Marginal Zone (Platreef-PGE, Ni, Cu)
2. Lower Zone
3. Critical Zone (Lower and Upper chromitites; UG2-Cr, PGE; Merensky Reef-PGE, Ni, Cu)
4. Main Zone
5. Upper Zone (magnetite seams-Fe, Ti, V).

(1) The chill and marginal zones at base of RLS.

The transgressive contact of the RLS against rocks of the Pretoria Subgroup has an interface of marginal rocks of variable thickness. The basal and lower Critical Zone is generally bordered by pyroxenites. The upper Critical and Main Zones are bordered by gabbroids, especially norites (Sharpe, 1982). These rocks are compositionally close to the mafic dikes complex that is under, and marginal to, RLS. There are some hybrid, inclusions-crowded rocks. Although the marginal rocks are enriched in noble metals and mineralogical quantities of Fe, Cu, Ni sulfides, no significant basal massive or disseminated sulfide orebodies, common in many layered complexes around the world, have been found so far. This is attributed to the sulfur-poor magmas and a lack of pyritic wallrocks. The only significant "giant" along the Bushveld contact (but corresponding to the Critical Zone) is Platreef in the Potgietersrus Limb.

Platreef PGE, Ni, Cu deposit (zone) (White, 1994; resources in a 54 km long interval quoted by Cabri and Naldrett: 2.2 bt ore @ 6.3 g/t PGE+Au, 0.36% Ni, 0.18% Cu for 5,296 t Pt, 5,792 t Pd, 496 t Rh, 372 t Ru, 99 t Ir, 62 t Os, 430 t Au, 7.5 mt Ni, 3.75 mt Cu. Reserves/resources in the operating Angloplat Mine between Sandsloot and Overysel

are quoted as 28.8 mt @ 5.73 g/t PGE+Au and 151 mt @ 4.98 g/t PGE+Au).

This is an about 60 km long, NNW trending west-dipping interval along the basal contact of the Potgietersrus Limb, best exposed about 30 km NNW of Potgietersrus (Fig. 12.17). There, 713 kg of PGE-Au bullion was produced from diggings at the Tweefontein farm, from an up to 100 m thick "pyroxenite package" called Platreef, before World War 2. After many unsuccessful later attempts, large scale modern mining has started in the 1990s in the Sandsloot open pit. Platreef is the stratigraphic equivalent of the upper Critical Zone (that in other limbs hosts the Merensky Reef), here directly transgressing over the Transvaal (meta)sediments in the south and Archean basement in the north. The RLS Lower Zone and parts of the Critical Zone are absent. At Tweefontein the Bushveld footwall is represented by the Penge banded iron formation, at Sandsloot it is the Malmani Dolomite, at Overysel it is Archean granite and gneiss.

Reaction of the basic magma with basement rocks resulted in an interval of contaminated pyroxenites, hybrid rocks and metasomatites that varies in thickness from several meters to 100 m (this against the most reactive carbonate wallrocks). The pyroxenitic interval is overlain by gabbro-norite and anorthositic norite of the Main Zone. At Sandsloot, the Platreef is interrupted by a truncated diapir of Malmani Dolomite injected into the magma chamber (White, 1994). There, the west-dipping footwall dolomite is recrystallized into marble that changes upward into a hybrid exocontact sequence (exoskarn) of mainly dolomite with variable monticellite, wollastonite and serpentinite haloes. This interval contains erratically disseminated replacement Fe, Ni and Cu sulfides with PGE values. This material is presently stockpiled. The first endocontact interval above is the "A Reef", a remnant of basal (marginal) contaminated pyroxenite with dolomite rafts and inclusions. This is succeeded upward by the "B Reef", an orthopyroxenite with or without feldspar and, finally, "C Reef" of enstatitic and bronzitic pyroxenite. The three "Reefs" constitute the entire mineralized interval (Platreef) that is 60-100 m thick. The best and most consistent mineralization is in the "B Reef". The ore minerals comprise scattered visible grains (blebs) of pyrrhotite, lesser pentlandite and chalcopyrite. The sulfides enclose microscopic Pt and Pd minerals (ferroplatinum and PGE tellurides, sulfides, arsenides and Pd alloys) and minor gold. The supergene sulfide zone contains violarite, millerite and godlevskite. The

oxidation zone is indistinct, diluted by karsting and carbonate infiltrations, and is not processed. At Tweefontein, the iron formation exocontact was converted into Fe-rich pyroxenite. There, sperrylite has been reported to occur in shears and in sheared pegmatite injections.

2. Lower (Basal) Zone. This zone is dominated by bronzitite with harzburgite units and rare, thin intervals of norite. Wallrock xenoliths and endocontact contamination are common and the ultramafics are often serpentinized. Economic chromite and PGE-Ni mineralization is known only from the 1,600 m thick Lower Zone in the Potgietersrus Limb. There, two sets of high-grade chromitite layers at Grasvally (Fig. 12.15) and Zoetveld are in olivine-chromite cumulate (dunite) and partly olivine pyroxenite (Hulbert and Von Gruenewaldt, 1986). The metallurgical-grade chromite is similar to chromite from the Great Dyke, is of high quality, but the seams are strongly deformed and impersistent. Two platiniferous sulfide horizons have been drilled in the same area and they are the stratigraphically lowermost PGE occurrences in the RLS.

3. Critical Zone. This is the economically most important zone in the RLS. It is over 1,500 m thick in the Eastern Limb and slightly thinner in the west. The lower part is dominated by pyroxenite, especially a medium-crystalline, brown bronzitite that grades into feldspathic bronzitite. There are several harzburgite and dunite layers. The 800 m thick upper part commences with the appearance of cumulus plagioclase and consists of about eight spectacularly layered cyclic units ranging from chromitite, through orthopyroxenite to norite and anorthosite (Cawthorn and Walraven, 1998).

Chromitite layers. Bushveld complex has the world's greatest resource of chromite, estimated at about 3.6 bt of contained Cr to a depth of 500 m (Vermaak, 1986), and at least 20 bt Cr, presently uneconomic, in the entire Complex. With exception of the small stratigraphically lower Grasvally deposit (read above) the chromite is entirely in the Critical Zone and exploited from tens of mines in both the Western and Eastern Limbs (Fig. 12.15). The main center of mining is around Steelpoort in the Eastern Limb where up to 29 discrete chromitite layers have been recorded.

The chromitite layers (Cousins, 1964; Cousins and Feringa, 1964) start with the Lower layers (LG) in orthopyroxenite hosts.

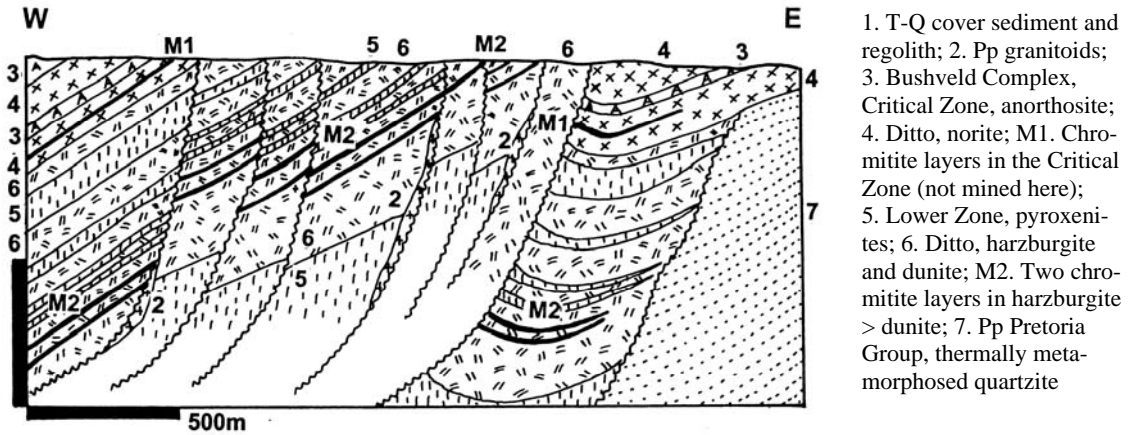


Figure 12.14. Grasvally chromite mine, Potgietersrus Prong, South Africa, cross-section from LITHOTHEQUE No. 2726 modified after Hulbert and von Gruenewaldt (1986). Example of metallurgical-grade chromite in the Lower Zone

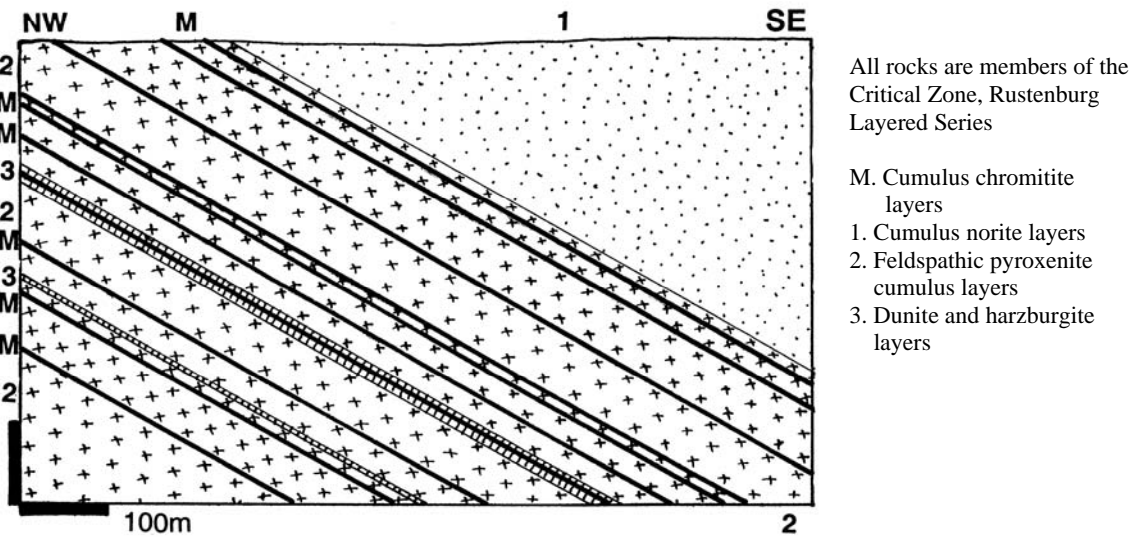
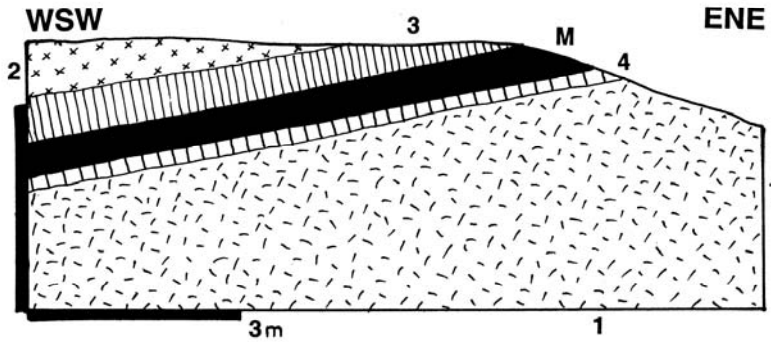


Figure 12.15. Zwartkop chromite mine, West Lobe, diagrammatic cross-section from LITHOTHEQUE No. 1952, based on data in von Gruenewaldt and Worst (1986). Example of chromitite layers in the Critical Zone

Middle layers (MG) are in the pyroxenite/anorthosite transition, and Upper layers (UG) in the anorthosite to norite cycles. The layers are numbered consecutively from the stratigraphic bottom to the top (e.g. UG1 is the lowermost chromitite layer in the Upper division). A typical chromitite is a sharply outlined magmatic stratiform band composed of densely disseminated (~60 to 80%) dark brown to black subhedral to euhedral crystals of Cr-spinel (chromite) cumulus suspended in olivine, bronzite and plagioclase matrix.

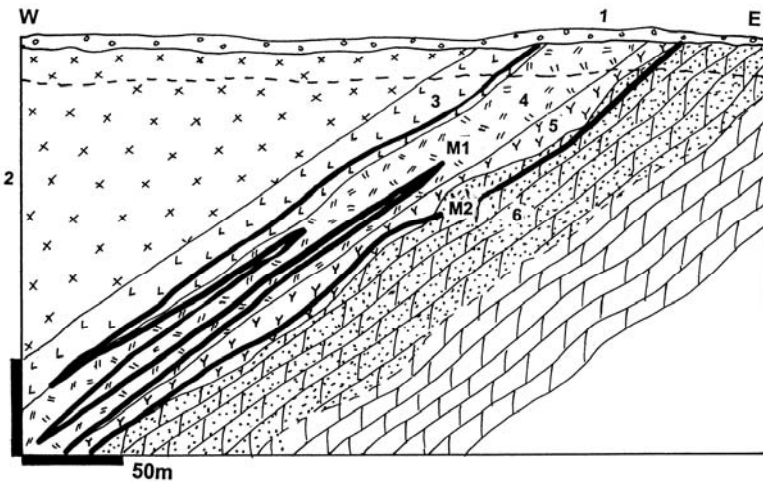
Many chromitite layers are composite; they split, anastomose, show plastic deformation or contain xenoliths. The grade ranges from about 38% to 51% Cr₂O₃ and the chromite is of chemical grade (FeO

between 21% and 30.4%), that is a material inferior in quality to the metallurgical grade. The ore layers range from several cm to 6.55 m in thickness, although the average thickness is between 0.5 and 1 m. Abundant magmatic layers with weakly disseminated chromite are not economic at present. Some layers have a great stratigraphic persistency and the 1.05 m thick LG6 (Steelpoort Layer) has been traced for 85 km along strike. All chromitites are enriched in platinum metals but only few selected layers have PGE grades high enough to pay for recovery. The UG2 layer ("reef") has the highest PGE content, the value of which greatly exceeds the value of chromite (that becomes a mere "gangue").



- 1. ~2060 Ma Rustenburg Layered Suite, Critical Zone anorthositic
- 2. Ditto, norite
- 3. Ditto, bronzitite
- 4. Ditto, bronzitite pegmatoid
- M. UG2 Reef, platiniferous chromitite seam in layered pyroxenite

Figure 12.16. UG2 platiniferous reef, outcrop near Hackney; cross-section from LITHOTHEQUE No. 1950, based on literature data and outcrop visit with G. von Gruenewaldt, 1990



- 1. T+Q unconsolidated sediments and regolith; 2. Rustenburg Layered Series in the Potgietersrus Prong, Main Zone gabbro, norite; 3. Ditto, Platreef interval, stratigraphic equivalent of Critical Zone; C Reef; 4. Ditto, B Reef; orthopyroxenite, main PGE host; 5. Ditto, A Reef, remnants of contaminated basal pyroxenite, dolomite inclusions; M1. Syn-to late-magmatic scattered Fe, Ni, Cu sulfides with PGE in a 60-100 m thick interval; 6. Hybrid basal Ca-Mg silicate (skarn) exocontact in Malmani Dolomite;

Figure 12.17. Platreef PGE zone in the Sandsloot (Amplats) deposit north of Potgietersrus. Cross-section from LITHOTHEQUE No. 2722, based on Amplats Ltd. materials, 2001. Explanations (continued): M2. Fe, Ni, Cu sulfides with inclusions of PGE minerals, erratic disseminations in Unit 6. 7. Pp Malmani Dolomite, thermally recrystallized marble

It rivals the Merensky Reef as a major Bushveld platinoids carrier.

UG2 Reef platiniferous chromitite. The UG2 layer averages 1.22m in thickness, has an average Cr₂O₃ content of 43.67%, and Cr/Fe ratio of 1.35 (Vermaak, 1986); Fig. 12.16. The precious metals content ranges from about 6 to 7 g/t and this includes between 0.2 and 1.4 g/t Au (Hiemstra, 1985). The layer is very persistent and present in most Bushveld compartments. In the Amandelbult and adjacent Northam mines in the Western Limb the 1.0 to 1.2 m thick UG2 layer is split into a 60-80 cm thick main band and two or three 11 cm thick "leaders" above, separated by poikilitic pyroxenite with accessory chromite. The immediate footwall and hangingwall of the UG2 is an up to 70 cm thick

pegmatoidal feldspathic bronzitite. The bulk of the precious metals in the chromitite layer is associated with fine-grained, inconspicuous interstitial pentlandite, pyrrhotite, chalcopyrite and pyrite. 5-20% is in silicates and 0-10% in chromite. Over 30 PGE minerals have been identified by microprobe; the most common minerals being laurite (RuS₂), cooperite (PtS), braggite ([Pt,Pd,Ni]S), vysotskite (PdS) and others. Their selection and abundance vary from place to place. The UG2 reserve figures for the properties where this "reef" is mined have rarely been published. The Northam Mine is an exception and it contains 319 mt of ore @ 6.6 g/t PGE+Au (2,105 t PGE+Au content) to a depth of 2,700 m (International Mining, September 1986). The whole Bushveld is credited with 3.726 bt of ore in UG 2 @ 3.65 g/t Pt and 3.05 g/t Pd for 13,600 t

Pt and 11,300 Pd content (Stribrny et al., 2000), but many alternative estimates are also available.

Merensky platinumiferous Reef (Wagner, 1929; Vermaak, 1976; Kruger and Marsh, 1982); P+Rc to 2,400 m depth, calculated tonnages from Laznicka, 1993, p.1148; metal content/usual grade: 16.16 mt Ni/0.24%; 9.2 mt Cu/0.1%; 22,044 t Pt/3.5 ppm; 8,742 Pd/2 ppm; 2,978 t Ru/0.6 ppm; 1,126 t Rh/0.4 ppm; 398 t Ir/0.15 ppm; 330 t Os/0.1 ppm; 1192 t Au/0.14 ppm. The South African Department of Mines quoted the 1998 reserve base as 37,200 t PGE and inferred resource as 28,600 t PGE..

Merensky Reef (MR) was discovered in 1925. It is a 5 cm to 1.5 m thick magmatic band of feldspathic bronzite traceable for 130 km along strike in the Western Limb, and 120 km in the Eastern Limb (Figs. 12.18, 12.19). MR granularity, internal stratigraphy and mineralogy vary slightly, and Viljoen (1994) distinguished two principal facies in the Western Lobe: the pegmatoidal Rustenburg Facies and the equigranular Swartklip Facies. The Reef is situated at base of the 9 to 10 m thick Merensky cyclic unit, which is a second layered unit under the base of the Main Zone (that is, it is near the top of the Critical Zone). In the Rustenburg area this unit rests on the "Boulder Bed", which is a horizon comprised of ellipsoidal masses of pyroxenite resting on anorthosite. Merensky Reef above starts with a thin chromitite band, immediately overlain by the pegmatoidal layer. The latter consists of subhedral to euhedral bronzite crystals with interstitial plagioclase and scattered sulfides that grade upward into a fine-grained rock of the same composition, terminating with another thin chromitite band. This, in turn, is overlaid by medium-grained poikilitic pyroxenite with feldspathic pyroxenite at the top. Above is a thin norite, followed by mottled anorthosite.

Near Rustenburg and elsewhere, MR is marked by major "pothole structures" (Viljoen and Hieber, 1986). These are circular areas that vary in size from a few meters to about 400-500 meters, in which MR is depressed into the footwall units up to 100 m below its normal stratigraphic position. Some potholes are associated with elevated "reef" sections, slumped intervals and downslope transported breccias. The potholes are usually attributed to the action of late-stage volatiles.

The PGE values are associated with scattered single grains, blebs and rarely small masses of pyrrhotite > pentlandite, chalcopyrite and pyrite, interstitial to silicates or enclosing subrounded feldspar and bronzite inclusions. The sulfides are

usually coarse enough to be megascopically recognizable and they are important visual indicators of the presence of precious metals. The PGE minerals are mostly microscopic and masked by the common sulfides, although specimen samples (e.g. of sperrylite) are occasionally found. In the Rustenburg area the mineralogy is dominated by braggite and cooperite (81%), sperrylite (6%), laurite (5.2%), electrum (3.3%), Pt-Pd tellurides (2.6%) and Pt-Fe alloys (1.7%; Viljoen and Hieber, 1986). At Amandelbult, in contrast, 31.3% of PGE are in Pt-Fe alloys, 19.6% in tellurides, 19% in Pt-Pd sulfides and 17.5% in laurite. The bullion comprises 54.43% Pt, 30.05% Pd, 6.69% Ru, 3.97% Rh, 2.6% Au, 1.24% Ir, and 1.02% Os.

4. Main Zone. Main zone starts at the top of the last cyclic unit and in the lower 2,000 m it is composed of feldspathic rocks (mostly norite and gabbro) with few anorthosite and feldspathic pyroxenite bands and a 1,600 m thick mass of monotonous, homogeneous massive gabbro-norite in the centre. There is a pyroxenite marker in the upper part that indicates addition of a new magma batch (Cawthorn and Walraven, 1998). There is no significant metallic mineralization.

5. Upper Zone. This zone starts with fine-grained norite at base and several meters above the Lower Magnetite Layer 1, the first of up to 30 magmatic magnetite layers in this zone. The differentiated sequence is dominated by gabbro, olivine diorite, minor anorthosite and troctolite. Cawthorn and Walraven (1998) calculated that a 1,500 m thick volume of residual magma was lost from the chamber which explains the complete absence of quartz and K-feldspar near the stratigraphic top of the Bushveld RLS (these minerals, however, occur in the roof granophyres). The cumulus magnetite in this zone occurs either as a dispersed, rock-forming component of gabbroids, or it is concentrated into stratiform layers of massive magnetite the cumulative thickness of which exceeds 20 m (Cawthorn and Molyneux, 1986).

Vanadiferous titanomagnetite layers (Willemse, 1969; Molyneux, 1970; Reynolds, 1986; calculated metal contents from Laznicka, 1993, p.1149, all magnetite layers to 300 m depth [reserve]: 13.2 bt Fe/50%, 1,901 bt Ti/7.2%, 177 mt V/0.8%. All magnetite layers to 1,500 m depth: 66 bt Fe; 9,505 bt Ti; 885 mt V).

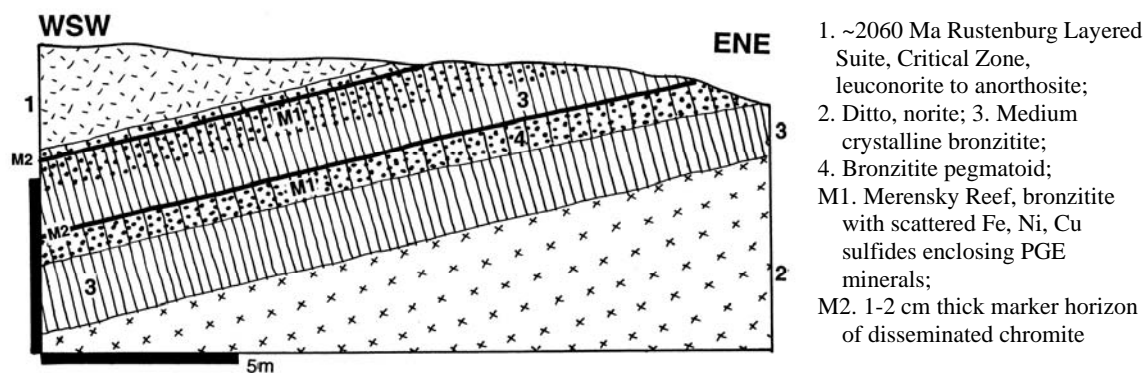


Figure 12.18. Merensky Reef, diagrammatic cross-section of an outcrop near Winnarshoek, Eastern Lobe. From LITHOTHEQUE No. 1951, based on site visit with G. von Gruenewaldt, 1990

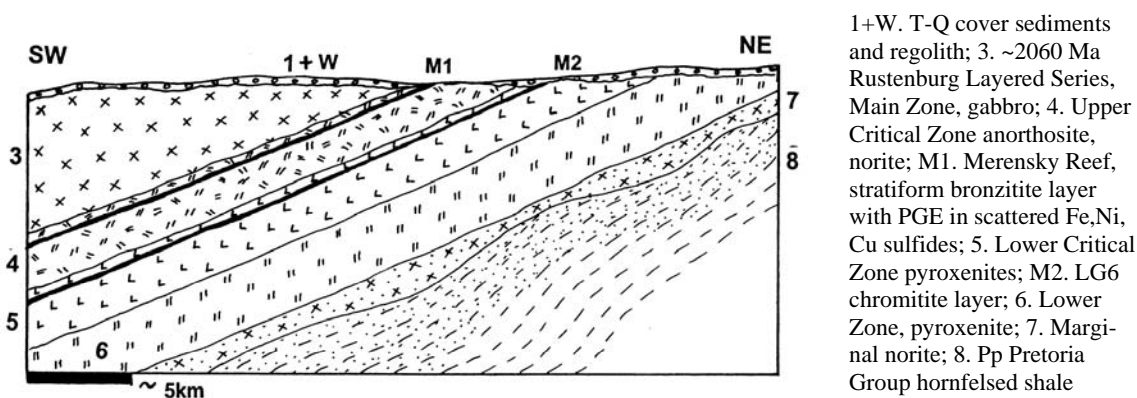


Figure 12.19. Lebowa (Atok) PGE Mine, Olifants River, Eastern Lobe, cross-section from LITHOTHEQUE No. 2724 based on data in Mossom (1986)

Three sets of centimetres to 10 m thick, remarkably persistent magnetite layers are developed in the ferrogabbro members of the Upper Zone. They have been traced for 175 km along strike in the Western Limb, and for 160 km in the Eastern Limb where up to 30 layers have been counted. The fresh magnetite is a massive black rock with a metallic luster, composed of fine to coarse, closely packed polygonal magnetite crystals with well developed tripple junctions. The magnetite is intergrown with ilmenite, ulvöspinel, and there is a variable proportion of matrix silicates. At outcrop, the magnetite is martitized. These layers constitute an enormous resource of a complex Fe-Ti-V ore, but so far there have been only two open pit mines exploiting the oxidized Main Magnetite Seam (MMS).

The gently dipping MMS is best developed in the Eastern Limb where it ranges in thickness from 1.2 to 2.7 m. In the area of best exposure near Magnet Heights the 1.5 m thick seam dips 20° west and is

traceable for nearly 60 km along strike. It has a sharp lower contact against gabbro and a more diffuse upper contact, gradational through feldspathic magnetite to gabbro with disseminated magnetite. There is an about 5 cm thick troctolite layer below the magnetite. The ore grade of the MMS is between 55.8 and 57.5% Fe, 12.1-13.9% TiO₂ and 1.6% V₂O₅. The tonnage available to the depth of 30 m only in the former eastern Transvaal has been conservatively estimated at 149 mt of ore (Cawthorn and Molyneux, 1986). Von Gruenewaldt (1977) estimated 1 bt of ore to be in the same unit. Intervals with sparsely disseminated Fe, Cu and Ni sulfides occur in the Upper Zone, but no economic orebody has been outlined, so far.

The remaining ore deposits and occurrences in the Bushveld complex: There is a number of magmatic, hydrothermal and residual deposits and occurrences of Ni, Cu, V, PGE and magnesite in the Complex but all are small to medium size. The Bushveld exocontact is, however, an important source of andalusite mined

from thermally metamorphosed shales of the Pretoria Subgroup, and of extensive replacement and vein deposits of fluorite hosted by Malmani Dolomite in the Zeerust area.

Great Dyke of Zimbabwe Cr, PGE

Great Dyke (Worst, 1960; Wilson, 1982; Prendergast, 1987; Rv+Rc 899 mt Cr @ 36.42%; Vermaak, 1986; Rc 4,130 t Pt, 2,936 t Pd, 367 t Rh, 367 t Ru, 46 t Ir, 46 t Os; Naldrett et al., 1987; plus ~6.5 mt Ni @ 0.24%, ~3.8 mt Cu @ 0.14%). This is a prominent NNE trending ~550 km long and 3-11 km wide structure. It is a layered mafic-ultramafic intrusion emplaced into Archean metamorphics and granitoids of the Zimbabwe craton. Its age is quoted within the range of 2.58 and 2.46 Ga. The Dyke is close to a lopolith with a basinal structure in cross-section, in which the magmatic layers dip towards the centre at angles of around 30°. The maximum stratigraphic thickness of the layered rocks is about 3,300 m and it is believed that a feeder dike is underneath. The Dyke is very little deformed, subgreenschist metamorphosed, and close to its original position in the time of emplacement. Along the long axis, the Dyke is subdivided into four narrow Y-shaped ultramafic-mafic complexes (magma chambers or sub-chambers) of which the Hartley (Chegutu) complex (Darwendale Subchamber) is the longest (312 km), most complete, best studied and most mineralized one.

Each complex consists of lower ultramafic and upper mafic sequences. The ultramafic sequence is preserved throughout the entire Dyke length, whereas the mafic sequence is a series of discontinuous erosional remnants. The ultramafic sequence starts with norite at base. This is overlaid by 14 cycles of dunite - harzburgite - bronzitite. The topmost bronzitite passes upward into websterite of the mafic sequence (Wilson, 1982). The mafic sequence is up to 1,000 m thick in the Hartley complex but much thinner elsewhere, and it is dominated by norite followed by gabbro and anorthositic gabbro. Quartz gabbro is most common in the southernmost Wedza complex. Rafts and xenoliths of roof rocks are widespread.

Chromite. Great Dyke as a whole is a "supergiant" repository of Cr and platinum metals, accumulated in large elongated magma chambers repeatedly replenished by injections of primitive magma (Prendergast and Jones, eds, 1989). Cr is accumulated in the ultramafic sequence that contains up to 0.77% of trace Cr, and is mined from up to 12 magmatic layers of chromitite. The layers are substantially thinner than those in the Bushveld

but of higher grade (up to 54% Cr₂O₃) and with a higher Cr/Fe ratio (up to 3.9), hence of the metallurgical type. The ultramafic sequence contains 4 chromitite units in the upper (bronzitite) succession that contain 36-49% Cr₂O₃. Each unit comes as a single layer or a set of several layers of densely disseminated chromite in serpentinized harzburgite, 5 to 100 cm thick. The lower (dunite) succession contains 7 layers at base of each cycle. The layers are thin (10-15 cm on the average), almost massive and sharply outlined, with 43-54% Cr₂O₃, in serpentinized dunite. Although the quantity of contained Cr in the entire Great Dyke is enormous (Prendergast, 1987 estimates 10 billion tons of chromite, that is some 2.6 bt Cr) the mining economics is precarious and, so far, the ore came from dozens of small (near) surface diggings and shallow underground mines that relied on very low labour costs.

Platinoids and Fe-Ni-Cu sulfide "reefs". The presence of platinum metals near the top of the ultramafic sequence was known for a long time (Wagner, 1929; Worst, 1960) but accelerated exploration has taken place only in the 1980s and modern mining has started in the 1990s. The principal PGE accumulation is in the Pyroxenite #1 Layer on top of the Cyclic Unit 1, just below the base of gabbros. The layer consists of a mottled diallag (augite) norite or feldspathic bronzitite that resembles the Merensky Reef as developed in the Bushveld Eastern Limb. One or two PGE-bearing horizons are present in this setting, in all four Great Dyke complexes. In the more important Main Sulfide Zone (MSZ; Prendergast and Jones, eds, 1989) the host bronzite is "deuterically" altered (i.e. suffered a late magmatic-hydrothermal overprint) and it contains augite, plagioclase, biotite, potash feldspar and quartz. Visible scattered blebs and finely disseminated pyrrhotite > pentlandite, chalcopyrite enclose or accompany sperrylite, moncheite, merenskyite, hollingworthite and gold. The MSZ thickness is usually between 1 and 3 m (maximum 12 m); Prendergast and Jones, eds (1989) estimated a speculative resource of 4.4 bt @ 3.5 g/t Pt, 1 g/t Pd, 1 g/t Au and 0.35% Ni to be available in the entire complex. Stribny et al. (2000) quoted 1.128 bt of ore with 2,592 t Pt/2.3 ppm and 1,728 t Pd/1.53 ppm. The largest and longest operating Hartley Platinum mine near Selous, 70 km SW of Harare, has a published resource of 168 mt of ore @ 2.376 g/t Pt, 1.867 g/t Pd, 0.422 g/t Au, 0.18 g/t Rh, 0.21% Ni and 0.14% Cu in a 18° dipping, 1.3 m thick "reef" (Fig. 12.20).

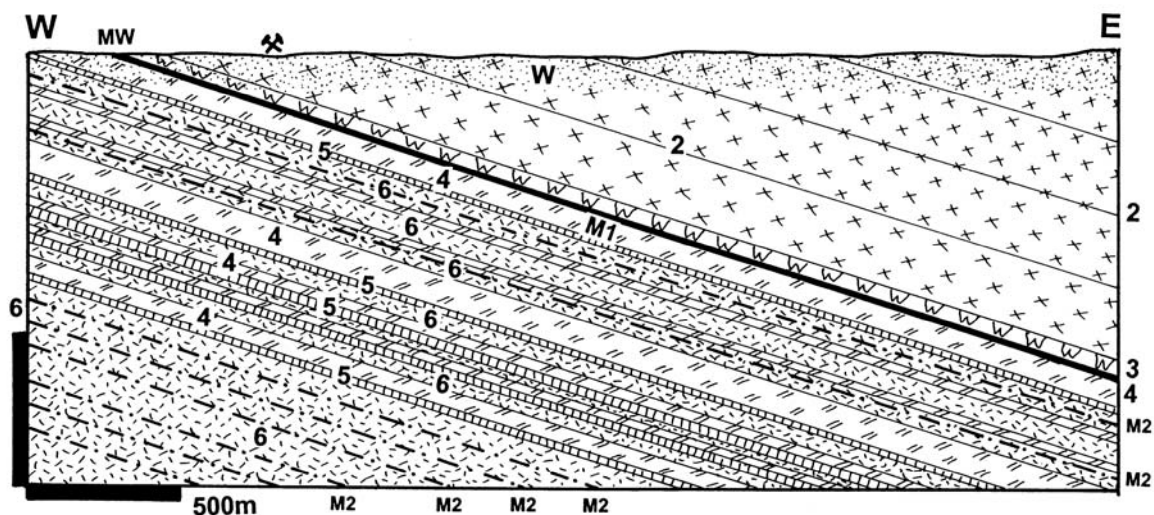


Figure 12.20. Great Dyke, Hartley PGE Mine, Selous, Zimbabwe. Cross-section from LITHOTHEQUE No. 2360, based on data in Prendergast (1987) and materials from Delta Ltd., Hartley Mine Staff. 1+W. T-Q sediment cover and regolith; MW. Oxidized ore, residual PGE and Au disseminated in saprock; 2. ~2.461 Ga Great Dyke layered intrusion, Upper Mafic Sequence gabbro-norite, gabbro; 3. Lower Ultramafic Sequence, websterite; M1 at Units 3/4 contact, 3 zones of PGE enrichment. The 2-5 m thick Main Sulfide zone is economic and has PGE minerals in Fe,Ni,Cu sulfide blebs scattered in deuterically altered bronzitite; 4. Bronzitite; 5. Sheared and serpentinized thin olivine bronzitite layers; 6. Granular and poikilitic harzburgite, dunite; M2. Chromitite seams

The Lower Sulfide Zone, sporadically developed, could be as much as 35-80 m thick but the mineralization is erratic and low-grade.

Duluth Complex Cu-Ni mineralization

The ~1.2 Ga Duluth differentiated intrusion in northern Minnesota is a component of the Mesoproterozoic North American Mid-Continent Rift, and one of the chambers that supplied magma to form the thick and extensive Keweenaw flood basalt province. The Keweenaw basalts and minor felsic volcanics crop out, discontinuously, around the present Lake Superior and they host the "giant" Michigan native copper district (read above). The Duluth Complex has an area of 4,715 km² and it is a composite pluton that comprises a dominant, continuous gabbro-anorthosite body accompanied by a group of small troctolite-norite massifs distributed along the NW margin of the main intrusion (Bonnichsen, 1972).

The troctolite association is more petrologically variable than the gabbro-anorthosite and it hosts Cu-Ni sulfide orebodies. The dominant troctolite and augite troctolite also include local bodies of gabbro, ferrogabbro, norite, picrite, dunite, peridotite, and some intermediate to felsic rocks. Hornfelsed inclusions of wallrock metasediments

are abundant along the contact, and the magmatic rocks are contaminated by silica, alumina and alkalis from digested wallrocks. Graphite is abundant where the Virginia "black slate" is in contact.

Duluth Complex was emplaced into an area of thinned Archean continental crust of the Canadian Shield. The Archean rocks, locally in contact, are granitoids and greenstone belt lithologies. The latter are unconformably and transgressively overlaid by sedimentary rocks deposited in the Animikie Basin (a Paleoproterozoic stable margin succession) that include the Biwabik Iron Formation (this hosts the Mesabi Range BIF; Chapter 11). This, in turn, is overlaid by the Virginia Formation graphitic slate. Both have local contacts with the Duluth intrusion.

Duluth NW Margin Cu-Ni sulfide zone. Drilling and some underground mining exploration has outlined a large Cu and Ni resource in a series of discontinuous ore deposits distributed in a 55 km long and 3.2 km wide belt between Hoyt Lakes and the area east of Ely (Bonnichsen, 1972). The published resource estimates vary widely, mostly as a consequence of different cut-off grades applied. Listerud and Meineke (1977) calculated that 3.96 bt of ore was available in units more than 17 m thick, with a cutoff grade of 0.5% Cu+Ni, and an average grade of 0.66% Cu and 0.2% Ni. This represents

26.13 mt Cu, 7.92 mt Ni, plus approximate quantities of by-product metals: 554 kt Co @ 0.014%, 360 t Pd @ 0.09 g/t, 176 t Pt @ 0.032 g/t and 92 t Au @ 0.014 g/t. The largest single deposit, Minnamax east of Babbitt, is alone a "giant" credited with 2.671 mt Cu @ 0.8-3% and 661 kt Ni @ 0.2-0.6%.

The Cu-Ni mineralized zone follows the north-western contact of Duluth and dips about 25° SE under the edge of the intrusion. The intrusive ore hosts are members of the 100-150 m thick Basal Zone and consist of inclusion-rich dunite, augite troctolite, olivine gabbro and gabbro-norite (Mainwaring and Naldrett, 1977; Tyson and Chang, 1984). The ore intrusions are emplaced into either of the three Precambrian associations listed above that are thermally metamorphosed in the exocontact, whereas the intrusive endocontact is contaminated. The originally pyritic shale of the Virginia Formation was of greatest importance as a source of sulfur, and graphite contaminant in the Cu-Ni sulfides (Ripley, 1981) and all explored orebodies are close to the Virginia shale contact. The Virginia shale in the exocontact is now a cordierite-biotite hornfels that grades into an inhomogeneous brecciated interphase along the intrusion/sediment contact. This interphase is composed of olivine, ortho- and clinopyroxene, graphite, cordierite, Al-spinel, biotite, plagioclase and K-feldspar with disseminations, veinlets, blebs, ore-cemented wallrock breccia and small masses of pyrrhotite, chalcopyrite and pentlandite. The interphase is alternatively interpreted as a contaminated and inclusions-choked Duluth endocontact (Mainwaring and Naldrett, 1977) similar to the Norl'sk taxitic gabbrodiabase; as a possibly separate small intrusion comparable with the Sudbury Sublayer (read below); or as an in-situ metasomatized Virginia meta-sediment (M. Foose, oral communication).

Although the Duluth ore discoveries go back into the 1960s and 1970s, they are in an environmentally sensitive area of lakes and forests, and politics rather than the geological or technical factors, have so far prevented the mine development.

Stillwater complex PGE, Cr, Ni, Cu, Montana

It seems incomprehensible that Stillwater, with its modest endowment of 2.14 mt Cr @ 27.2% (Howland et al., 1949), has the largest chromite resource in the Americas. Chromite mining there started late during World War 2 for the sake of self sufficiency, but terminated shortly after the war when the much cheaper chromite imports became

available again. The concentrate produced and the ore in place are still there, a part of the U.S. Government strategic reserve. The platinoid story is different. Until the 1970s Sudbury, with its modest endowment of some 300 t PGE, was the largest platinoid resource in North and South America. Then the J-M Reef has been discovered and drilled to become, with its 1,651 t PGE reserve and possible 6,000 t PGE resource, the only American "PGE giant".

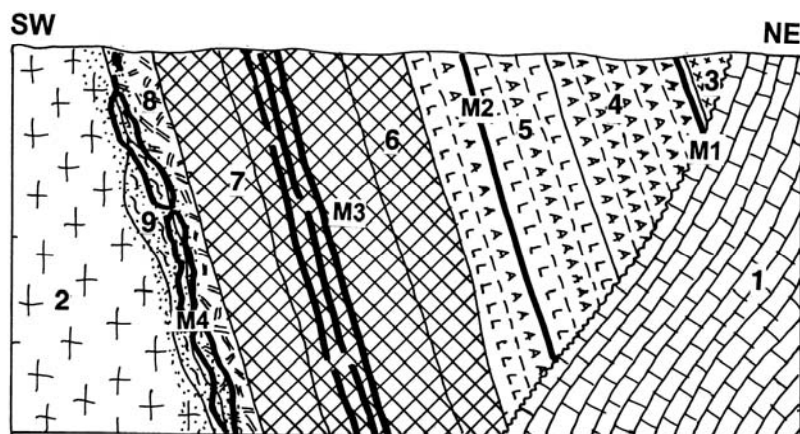
Stillwater complex in the Beartooth Mountains, 80 km SW of Billings, south-central Montana, is an erosional relic of a 2.7 Ga sill-like layered intrusion emplaced into the 3.3 Ga granite and high-grade metasedimentary terrain of the Archean Wyoming Province (Jackson, 1961; Page, 1977; Zientek et al., 1985; Czamanske and Zientek, eds., 1985). It is a 45 km long and up to 7.4 km wide, WNW-striking and generally steeply dipping rigid tabular magmatic mass. The Complex is substantially thrust- and block faulted and locally sheared, but it is free of penetrative deformation and wholesale metamorphic recrystallization despite having survived an orogeny that metamorphosed the enclosing supracrustals into granulite grade. At the hand sample and outcrop scales Stillwater materials are thus frequently indistinguishable from those from Bushveld (Fig. 12.21).

The maximum stratigraphic thickness of the Stillwater is about 6,000 m and its subdivisions, from the base up, are as follows (Zientek et al., 1985):

- 1) The Basal Series, about 50 m thick, composed of norite and bronzitite. There are abundant semi-assimilated wallrock inclusions and the magmatic rocks are contaminated. There is a broad thermal metamorphic aureole in the exocontact with cordierite and hypersthene hornfels. The entire basal contact is enriched in pyrrhotite >> pentlandite, chalcopyrite in small masses, stringers and disseminations credited with a resource of some 375 kt Ni @ 0.25% and 375 kt Cu @ 0.25% (Ross and Travis, 1981).
- 2) The Ultramafic Series above has a lower, 670 m thick cyclic Peridotite Zone (dunite, harzburgite, bronzitite) and an upper, 400 m thick Bronzitite Zone. It contains up to 13 tabular layers of olivine cumulate enriched in chromite, the proportion of which ranges from about 10% (sparse disseminations) to 80% (almost massive chromitite). Despite tectonic segmentation the individual chromitite seams have a great continuity. The "G chromitite" has been traced, with interruptions, for some 40

km. In the wartime Mouad Mine the "G chromitite" ranged from 1 to 4 m in thickness and the grade was a mere 12 to 15% Cr. All Stillwater chromitites have an increased content of precious metals, but only the "A chromitite" has some economic potential; it grades 3.5 ppm PGE (0.99 ppm Pt, 2.29 ppm Pd, 0.25 ppm Rh; Page, 1977). The platinumoids are in sperrylite and in Fe-Pt alloy inclusions in chromite.

3) The Banded Series is 4,500 m thick and its basal contact is marked by the first appearance of cumulus plagioclase overlaid by banded norite, two-pyroxene gabbro, and anorthosite. Cumulus olivine reappears in five thin intervals of troctolite to olivine anorthosite and two such intervals contain Bushveld-style scattered Fe, Ni, Cu sulfides and associated platinumoids.



1. PZ sedimentary rocks of the Cordilleran miogeocline; 2. Ar granitoids (post-Stillwater); 3. 2.7 Ga Stillwater Complex, Upper Zone, gabbro, pigeonite gabbro; 4. Ditto, anorthosite, troctolite, olivine gabbro; 5. Norite, anorthosite, gabbro; M1. Picket Pin PGE Reef, marginal; M2. J-M PGE Reef, olivine-bronzite-plagioclase pegmatoid, PGE in blebs of Fe,Ni, Cu sulfides

Figure 12.21. Diagrammatic cross-section of the Stillwater Complex near Nye, Montana, from LITHOTHEQUE No. 491 compiled from literature. Explanations (continued): 6. Ultramafic Zone, bronzitite; 7. Ditto, harzburgite; M3. Chromitite seams; 8. Basal Zone and endocontact, inhomogeneous norite, gabbro, bronzitite; M4. Massive, stringer and disseminated pyrrhotite > pentlandite, chalcopyrite in hybrid rocks along basal contact; 9. Relics of pyroxene hornfels metamorphosed Archean rocks

J-M Reef and "reef package". Named after Johns-Manville, the asbestos mining company that made the discovery (Todd et al., 1982) the J-M Reef contains the entire precious metals resource currently quoted from Stillwater (some 421 mt @ 14.83 g/t Pd, 4.24 g/t Pt with by-product Au and Ni). J-M Reef and its extension, Howland Reef, are 350 to 400 m above the Banded Series contact, in the stratigraphically lowest olivine-bearing layer. The "reef package" is about 60 m thick, composed of olivine anorthosite to troctolite, and is traceable throughout most of the Stillwater outcrop although the actual mineable "reef" is preserved only in two 6.75 km and 5.5 km long segments. The spotted light-gray and dark green rock, in places pegmatitic, contains between 0.5 and 2% of scattered visible grains and blebs of pyrrhotite > pentlandite and chalcopyrite, and microscopic braggite, vysotskite and other PGE minerals, plus gold. The orebodies are magmatic stratiform sheets within the entire "reef package", and Raedeke and Vian (1986) have

recognized six such horizons in the Minneapolis Adit area, dipping 70° NE. Most of the high-grade ore is in the Main Zone of orebodies spaced at intervals of 60 to 90 m and having a lateral dimension of 3 to 80 m. The more recently discovered Picket Pin PGE horizon (Boudreau and McCallum, 1986) is in anorthosite about 3,000 m stratigraphically above the J-M Reef. It is extensive and thick, but discontinuous with erratic PGE values.

Jinchuan, Gansu, China: Ni, Cu, PGE

Jinchuan (Chai and Naldrett, 1992; 510 mt @ 1.07% Ni, 0.67% Cu, 1 g/t PGE+Au for 5.5 mt Ni, 3.42 mt Cu, 115 kt Co, 280 t PGE+Au) is a remnant of an intrusion that has some similarity with the Great Dyke in being dominated by peridotite, but it hosts Ni-Cu sulfide orebodies rather than Cr and platinumoids. The NW trending, 6.5 km long ore zone is interpreted as a deeply eroded 1.501 Ga layered

intrusion emplaced into Paleoproterozoic migmatite, marble and gneiss along the southern margin of the Sino-Korean craton. The zone consists of three subchambers, each of which exposes a zoned ultramafic body of serpentized dunite enveloped by lherzolite and websterite. The dunite is mineralized throughout by low-grade disseminated blebs of pyrrhotite, pentlandite and chalcopyrite and there is a number of lenticular bodies of net-textured sulfides, crosscutting vein-like sulfide masses up to 20 m thick, and some replacement bodies in the wallrocks. These resemble skarn at marble contacts. Chai and Naldrett (1992) interpreted Jinchuan as a root zone of a mafic-ultramafic intrusion related to magma with the initial composition of magnesian basalt, the gabbroic top of which has been eroded away.

Additional significant Cr, Ni, PGE deposits: There are no "giants" left in addition to the deposits described above and few "large" deposits (Naldrett, 2004). The string of Paleoproterozoic layered intrusions in northern Finland (Kemi, Penikat, Koillismaa, Suhanko and others; Papunen and Vormaa, 1985) is an emerging metals province, with the operating Kemi chromite mine (36 mt Cr) and several PGE prospects (Suhanko, Rc 448 t PGE). Aganozero in the Russian portion of Karelia has a reserve of 15.73 mt Cr. Lac des Iles deposit in NW Ontario has a resource of 159 mt @ 1.55 g/t Pd, 0.17 g/t Pt and 0.12 g/t Au for 274 t PGE total (247 t Pd, 27 t Pt). The precious metals are, with Fe, Ni and Cu sulfides, erratically disseminated in hybrid synorogenic gabbroids, in an Archean greenstone belt that also contains several peridotite bodies. Hattori and Cameron (2004) interpreted this ore as of "supersolidus mixing type".

12.7. Sudbury complex Ni, Cu, Co, PGE, Ontario: an enigma

Sudbury complex has been the principal supplier of the world's nickel for almost a century and until recently it was the number one Ni-sulfide "giant district". (Pye et al., ed., 1984; Lightfoot and Naldrett, eds., 1994; Lightfoot et al., 1997a, b; Naldrett, 1989a, 1999b; P+Rv 1,648 mt @ 1.2% Ni, 1.03 % Cu, 0.04 % Co, ~4 g/t Ag, 0.14 g/t Au, 0.4 g/t Pt, 0.4 g/t Pd for 19.78 mt Ni, 17 mt Cu, 659 kt Co, 5,792 t Ag, 579 t Pt, 579 t Pd, 231 t Au; Naldrett, 2004). The recently released data, however, indicate that Sudbury is actually number two, ranking closely behind Noril'sk-Talnakh in Siberia (read above).

Located in north-central Ontario at the juncture of Superior, Southern and Grenville Provinces of

the Canadian Shield, Sudbury is many things in one (Figs.12.22, 12.23).

1. An ore district: It is an oval ring measuring about 65x25 km (along an ENE axis) with several tens of Fe-Ni-Cu sulfide orebodies, of comparable mineralogical composition and close in style and setting, scattered along its perimeter. The greatest accumulation (clustering) of orebodies is along the northern (North Range) and southern (South Range) margins, although the eastern and western extremities of the ring also contain scattered deposits. Cumulatively, Sudbury is a Ni and Cu "giant district", but not a single deposit reaches the required giant magnitude for Ni (5.5 mt Ni), although the two largest deposits (Creighton and Frood-Stobie) qualify as "Cu-giants". It is, however, difficult to impossible to obtain tonnage data for the individual deposits as all are shared by two corporations (INCO and Falconbridge) who prefer to lump such data together in reports, even including properties outside Sudbury. The "district endowment" (read above) thus makes it impossible to compare ore accumulations of the same rank (i.e. deposit to deposit), yet this is exactly what the literature does (e.g. Mount Keith, a single deposit versus Sudbury, a region of some 1,200 km²).

2) A structure (basin) and stratigraphic succession: At the 1960 through 1980s state of knowledge Sudbury was presented as a basin (brachysyncline) filled by supracrustals of the 1.85 Ga and younger Whitewater Group, resting on conformable and symmetrically disposed magmatic layers of the Sudbury Igneous Complex (SIC). This, in turn, unconformably overlies older Paleoproterozoic (2.2 Ga plus) folded (meta)sediments and (meta)volcanics of the Huronian Supergroup in the south, and Archean basement metamorphics in the north. More recent cross-sections based on deep seismic data (e.g. Cowan et al., 1999; Boerner and Milkereit, 1999) still show symmetrical disposition of the two uppermost units of the basin fill (the Chelmsford sandstone and Onwatin phyllite, both carbon-rich), whereas the underlying Onaping Formation, interpreted as an impact-related fallback breccia to dust, and the underlying SIC magmatic sheets, preserve their basal symmetry in the north but appear overturned in the south. The entire Sudbury complex, traceable geophysically to a depth of 11 km, is asymmetrical and plunges to the south. This is mostly explained by the post-emplacement, northward thrusting of the South Range lithologies along the South Range Shear Zone.

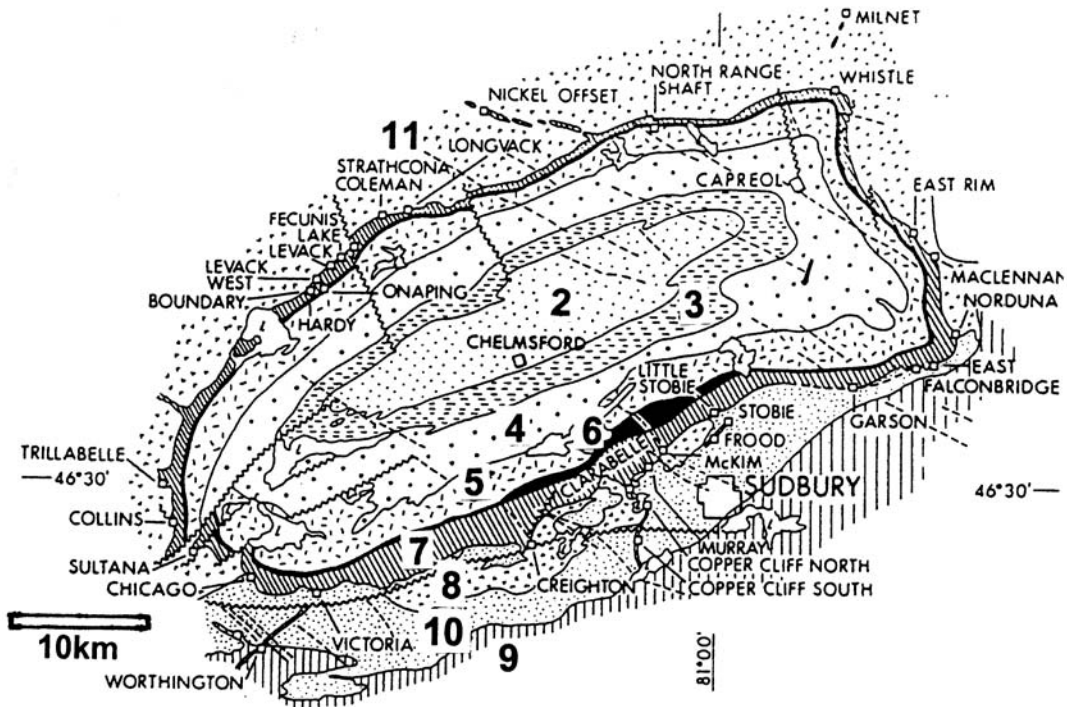


Figure 12.22. Sudbury Basin and Igneous Complex, map from Naldrett et al. (1985) reprinted courtesy of the Ontario Geological Survey. 1. Diabase dikes (not shown); 2. Pp Chelmsford sandstone; 3. Onwatin Fm., phyllite; 4. Onaping Fm. fallback braccia. Sudbury Igneous Complex: 5. Granophyre; 6. Quartz-rich gabbro; 7. Norite and Sublayer; Pp granite and gneiss; 9. Pp quartzite; 10. Pp graywacke; 11. Ar gneiss, migmatite

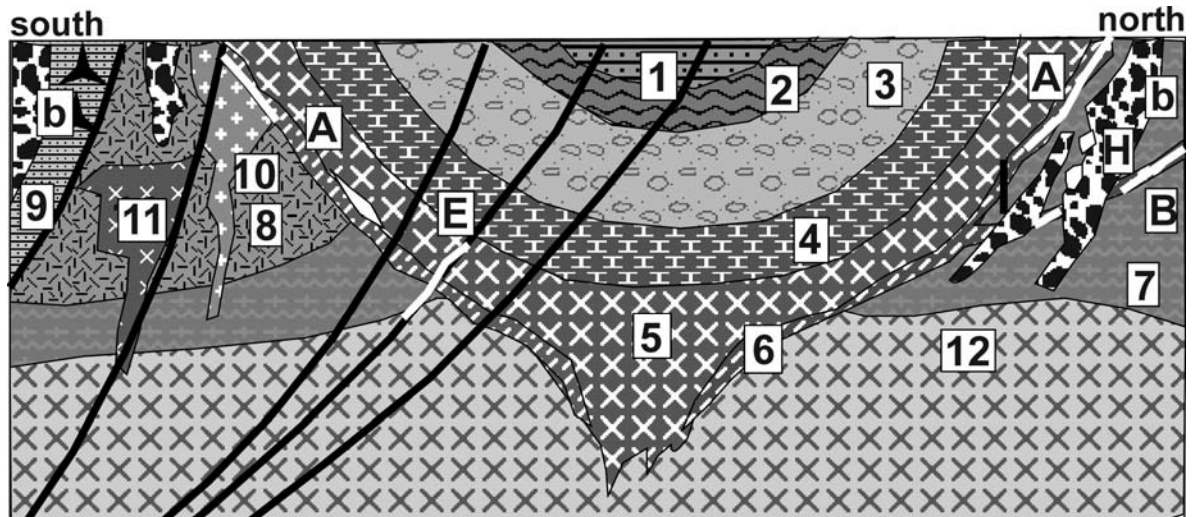


Figure 12.23. "Sudbury Astrobleme", rocks and ores inventory diagrammatic cross-section from Laznicka (2004), Total Metallogeny Site G236. 1. Chelmsford high-C sandstone; 2. Onwatin phyllite; 3. Onaping fallback breccia; 4. Granophyre; 5. Norite, quartz gabbro; 6. Sudbury Sublayer, inhomogeneous quartz diorite to gabbro; 7. Ar granite gneiss; 8. Pp felsic metavolcanics; 9. Pp quartzite; 10. Pp granite; 11. Pp gabbro, diabase; 12. Geophysically indicated mafic-ultramafic intrusion; b. Sudbury Breccia. Ores: pyrrhotite > pentlandite, chalcopyrite massive, breccia, matrix, disseminated orebodies: A. In Sublayer and in basal norite; B. In offset dikes; E. Ductile ore breccia along shears that intersect ore horizons; F. Mineralized faults (here also millerite, gersdorffite). H. Cu, massive to breccia chalcopyrite in deep footwall

3) As a magmatic association (complex): Sudbury is clearly a differentiated magmatic body, although not cyclic and delicately banded like Bushveld and Stillwater. The Main Mass is a 2.5 km thick layered mafic to felsic slab and it is underlain by thin, discontinuous and rather inhomogeneous Sublayer of approximately noritic composition with slightly more felsic (quartz dioritic) Offset Dikes radiating from it. The Main Mass starts at the top, just under the inclusions-crowded igneous-textured "melt rock" (base of the Onaping Formation; read below) and it comprises a) granophyre grading to plagioclase granophyre; b) quartz gabbro; c) South Range norite and felsic norite; d) marginal quartz-rich norite of the South Range and mafic norite of the North Range; and e) Sublayer (Naldrett, 1997).

All Fe-Ni-Cu sulfide deposits occur in the Sublayer, in the related Offset Dikes, and to a lesser degree along both Sublayer contacts so they are close to the "basal contact orebodies" recorded from many, if not most, differentiated intrusions (e.g. Stillwater). The Main Mass is devoid of ores. The laboratory research has provided increasing evidence for crustal derivation of much or all of the SIC melts (Lightfoot et al., 1997a, b) and it is presently popular to interpret the Main Mass as an impact melt sheet differentiated in-situ into its norite, gabbro and granophyre members. The remaining problem is finding the presumed source rocks of suitable composition (preferably mafic and Ni, Cu enriched) in the impact target area. There, Paleoproterozoic gabbroids (e.g. the 2.2 Ga Nipissing gabbro) or Archean mafic intrusions are frequently invoked. Derivation of the Sublayer is more problematic as it contains occasional ultramafic xenoliths; extreme interpretations invoke extraterrestrial origin of the whole or parts of the Sublayer, and/or its sulfide ores.

4) As a site of a 1.85 Ga asteroid impact (paleo-astrobleme): Dietz (1964), in his search for ancient equivalents of young meteor impact sites like the Cañon Diablo in Arizona, visited Sudbury and registered several pieces of evidence suggestive of impact origin of the structure and possibly its rocks and ores. The idea has germinated, gaining increasing acceptance, to reach a point of no return in the 1990s and figuring (perhaps prematurely) in headings like "Astrobleme-associated Ni-Cu" (Canadian Ore Type 27.1a; Eckstrand, 1996).

Naldrett (1997) summarized the local geological aspects suggestive of "an explosion of unusually large intensity", of which he believed that "meteorite impact is the more likely origin". The aspects are: a) basal shape of the structure; b)

shock metamorphic features around the structure, especially shatter cones; c) Sudbury Breccia composed of unsorted country rock fragments showing signs of incipient melting (pseudotachylite), and present in the basement around the SIC perimeter; d) Footwall Breccia in basement rocks beneath the SIC, Sublayer and orebodies. It reaches its greatest thickness (and partly hosts the Ni-Cu ores) in the North Range; e) evidence of shock metamorphism in country rock inclusions in the Onaping Formation that include rare occurrences of microdiamonds; and f) the 1,800 m thick Onaping Formation. This is a heterolithic fragmentite composed of country rock fragments in a matrix of plastically deformed glassy shards. The "Green Onaping" at the top grades into "Black Onaping" (carbon-rich) below and eventually into an igneous-textured "melt rock" in the basal section. Onaping is usually interpreted as a meteorite fall-back breccia.

The sulfide ores are "genetically neutral" and their interpretations range from being a direct component of the impacting body plastered over the crater walls, especially in "embayments" (trough-like depressions in footwall rocks) (Dietz, 1964; Morrison, 1984), to immiscible melts separated from the differentiating magma (of whatever origin). As an exploration analogue, Sudbury orebodies are in the "right" setting typical for the bona fide magmatogenic Ni-Cu-PGE deposits such as Duluth or Noril'sk-Talnakh (read above), namely at a contact between mafic magmatic body above and brecciated and thermally metamorphosed basement below, and hosted by contaminated and xenolithic gabbroid with signs of ultramafic involvement.

Sudbury ores: The Fe-Ni-Cu sulfide ores in Sudbury deposits are dominated by pyrrhotine with about equal proportion of lesser pentlandite and chalcopyrite (1-5%) and variable amounts of pyrite, magnetite, cubanite, sphalerite and galena. Remobilized ores along shears, as in the Falconbridge mine, also contain millerite, niccolite, gersdorffite and cobaltite. The principal Pt carrier is sperrylite, whereas Pd is mainly in michenerite. Textures range from massive sulfide ore to brittle ore breccias in which the sulfides provide matrix to generally angular wallrock fragments. With decreasing ore:rock ratio this grades into "matrix" and "ragged disseminated" ores and, eventually, into low-grade, fine-grained sulfide disseminations in Sublayer and other hosts. Mineralized breccias and short, discontinuous veins also occur in the

"deep footwall" orebodies that are dominated by copper.

Orebody caught in shears (Falconbridge, Garson) have the distinct "ball" ores of the attrition rounded more brittle rock fragments like norite, with porphyroblasts of pyrite or magnetite, suspended in the "paste" of pyrrhotite and Ni-Cu sulfides that show *Durchbewegung* fabrics. This ore grades into stringers. Partial remobilization resulted in chalcopyrite moving into pressure shadows, and the appearance of Ni sulfides and arsenides. Schisted wallrocks (phylionites) are altered to actinolite, biotite, chlorite.

There is virtually no oxidation zone left behind, following several cycles of Quaternary glaciation and outcrop scouring (some orebodies have been covered by a thin till veneer). The rusty postglacial goethitic gossan preserved until the 1970s at the discovery site near the Murray Mine had a virtually fresh ore under 10 to 30 cm of goethitic and jarositic material.

Literature descriptions of the Sudbury ore deposits usually differentiate between those situated in the longer known South Range, and the more recently discovered North Range (Pye et al., 1984; Dressler et al., 1991).

South Range deposits. Sudbury ores had been discovered twice: first by a surveyor in 1856 (followed by inaction), then by a railway construction crew in 1883. Mining started in 1886, first for copper only, later for nickel as well. **Murray Mine** 8 km west of Sudbury, near the discovery site, is a 45° north-dipping tabular zone of predominantly low-grade disseminated Fe-Ni-Cu sulfides in inclusions-crowded quartz diorite (or quartz norite) of the Sublayer. The inclusions comprise unmineralized peridotite, pyroxenite and gabbro of uncertain provenance, as well as material derived from the immediate Paleoproterozoic greenstone, granite and gabbro footwall rocks. The "inclusion massive sulfide ore" has subrounded, unmineralized wallrock fragments in *Durchbewegte* sulfide matrix. Sparsely disseminated sulfides persist for several meters into the hangingwall Main Mass norite.

Creighton Mine 12 km WSW of Sudbury (Souch et al., 1969; Fig. 12.24) is one of the two largest Sudbury Ni-Cu deposits and a typical "embayment orebody" emplaced in a trough-like depression in Paleoproterozoic granite and gabbro footwall, along the NW-dipping Sublayer/basement contact. Mineralization has been proven to a depth of 2,400 m. Souch et al. (1969) characterized the ore types as follows: the "ragged disseminated" ore,

typical for ore in the Sublayer hangingwall, has sulfide blebs and discontinuous interstitial fillings in a breccia composed of closely packed rock inclusions in a quartz-rich norite matrix.

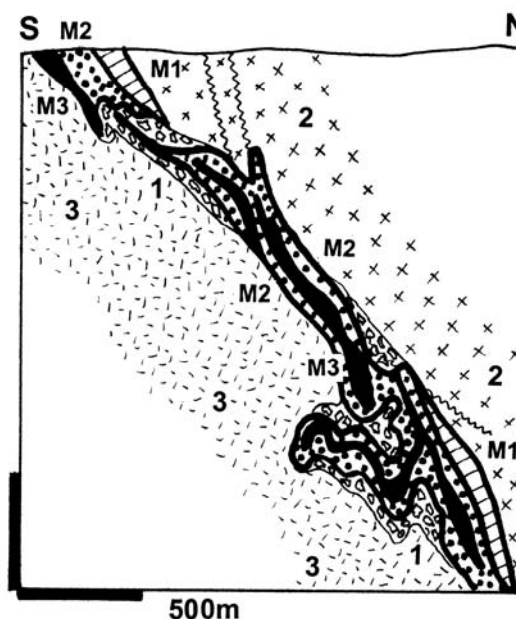


Figure 12.24. Creighton Mine, Sudbury, cross-section from LITHOTHEQUE No. 2252, modified after Souch et al. (1969). Example of a Sublayer deposit partly modified by shearing. 1. Sublayer, inhomogeneous inclusions-rich diorite to norite, grading to breccia; 2. Norite; 3. Pp Creighton Granite and Huronian meta-sediments. Ni-Cu sulfide ores: M1, disseminated in Sublayer and Footwall Breccia; M2, massive and sheared, mylonitic ore; M3, sulfides disseminated in norite

The ore grades downward into a "gabbro-peridotite inclusion sulfide", which is a breccia of magmatic fragments, often exceeding 1 m in size. Irregular masses of norite with minor microcline (presumably fragments, with quartz, derived from footwall granite) contain "interstitial sulfides" that fill spaces between euhedral plagioclase and pyroxene. The "inclusion massive sulfide" ore forms irregular, discontinuous bodies along the footwall contact. It contains angular fragments of footwall rocks in a relatively unstrained massive sulfide matrix. The basal Sublayer contact is gradational and the ore continues into the footwall as stringers and pods. A portion of the Creighton ore zone is sheared and filled by "contorted schist inclusion sulfide", where twisted phylionite fragments and subrounded quartz grains rest in "sulfide paste".

North Range deposits (Levack, Onaping, Strathcona, and other mines). This is a 10 km long NE-trending belt of closely spaced deposits about

25 km NW of Sudbury (Naldrett and Kullerud, 1967; Cowan, 1968; Coats and Snajdr, 1984). The basement here consists of Archean high-grade metamorphics and granitized rocks converted into pyroxene, hornblende and albite-epidote hornfels in a broad alteration zone adjacent to the SIC contact. Much of the Fe-Ni-Cu sulfides form disseminations, veinlets, stringers and small masses in the light-colored Footwall Breccia that dips 40° SE. The Sublayer here is a fine- to medium-crystalline heterogeneous norite, crowded by compositionally very variable inclusions (felsic to ultramafic). The sixteen orebodies here are mostly associated with "embayments". There is a substantial Cu-only ore within the footwall rocks (Archean basement) that has the form of massive bodies, veins and networks. Chalcopyrite is the principal mineral and there is some bornite.

Fault-related deposits: Falconbridge Mine (Pt 36 mt @ 1.72% Ni, 0.89% Cu for 619 kt Ni, 320 kt Cu, 79 kt Co, 19 t PGE and 2 t Au). This deposit, 10 km ENE of Sudbury, had originally been covered by glacial overburden and it was detected geophysically by T.A. Edison in 1899 (Owen and Coats, 1984). The ores are in a set of two east-striking, subvertical mineralized shears along or close to the contact of the South Range Norite and Paleoproterozoic greenstone. The "Southwall Zone" was entirely in greenstone and it contained local accumulations of early gersdorffite. The Main Zone orebody was in a shear complicated by later faults, that has been followed down to 1,800 m. This contained recrystallized tectonized mixture of pyrrhotite, pentlandite and chalcopyrite that enclosed subangular to rounded wallrock inclusions.

Offset dike orebodies: the Frood-Stobie ore zone. There are five major quartz diorite offset dikes that branch perpendicularly or obliquely from the Sublayer (Foy Dike, 28 km long; Copper Cliff dike, 19 km long) and five short, subparallel dikes (Frood-Stobie, Vermilion) (Grant and Bite, 1984). The Frood-Stobie ore zone, 3 km long, is the largest offset deposit and one of the two largest deposits in the Sudbury district (Souch et al., 1969; P_{to 1947} 54 mt ore @ 2.39% Ni, 3.62 % Cu, 2.2 g/t PGE plus Rc 91 mt of low-grade ore; Fig. 12.25). The NE-trending ore zone is hosted by a 70° NW dipping mass of chaotic breccia to megabreccia composed of attrition-subrounded fragments and megablocks of the Huronian basement supracrustals, infilled by either recrystallized rock flour, or by quartz diorite. In the footwall, the structure is bordered by a

ductile shear filled by "contorted schist inclusion sulfide" similar to the one at Creighton. The largest resource, however, comprises disseminated sulfide blebs in quartz diorite and massive replacements in breccia matrix. The Frood section alone is 1,430 m long, 1,700 m deep and 300 m wide at the surface.

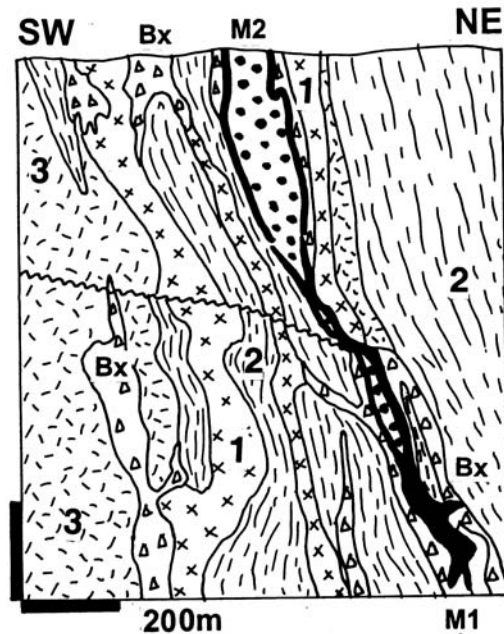


Figure 12.25. Frood Mine, Sudbury, cross-section from LITHOTHEQUE No. 1592, modified after Souch et al. (1969). 1. Pp Offset Dike, an inhomogeneous inclusions-rich quartz diorite gradational to altered breccia (Bx), amphibolite and gabbroids; 2. Pp Huronian Supergroup, Stobie Fm. metabasalt. schist; 3. Pp Copper Cliff Rhyolite; M1. Massive and breccia-cementing Fe,Ni,Cu sulfides; M2. Ditto, stringers and disseminations

12.8. Alkaline magmatic association

12.8.1. Introduction

Alkaline (or alkalic) rocks have many definitions and the one by Currie (1974) is most relevant for the practical mission of this book. It reads: "alkaline igneous rocks are characterized by the presence of feldspathoids and/or alkali pyroxenes and amphiboles, either in the rock itself or in the chemical analysis recalculated into the C.I.P.W. norm". Certain rare rocks like carbonatites, kimberlites and sometimes associated dunites are traditionally included with the alkaline family although, in their pure form, they do not contain alkalies at all. They are, however, transitional into

alkaline rocks (e.g. through alkaline carbonatite, phlogopitic kimberlite, alkaline pyroxenite) so they can be considered end-members of the alkaline series. Most importantly, they are usually associated with alkaline rocks in the field, they favor alkaline igneous provinces, and they share the geotectonic setting and petrogenesis with the alkalis. Carbonatites prefer association with the sodic alkaline series (nepheline-dominated associations), kimberlites with the potassic series (leucite-rich rocks). Some rocks, like kimberlites, however, do come as small solitary, monolithologic occurrences but, as this book does not deal with diamonds, the only mineral commodity associated with kimberlites and of which many are "world class" deposits, kimberlites are not even considered here.

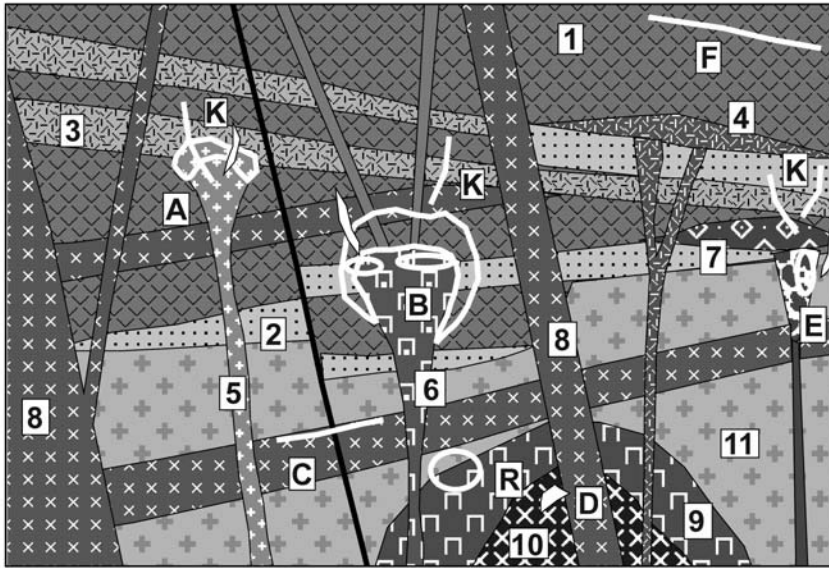
Alkaline rocks are rare (less than 1% of magmatic rocks by volume and area of occurrence) and the majority of them concentrate in regions of stable continental crust undergoing thinning and extension, especially graben/horst formation and rifting. For that reason the alkalines occur in association with other rocks that favor similar setting such as plateau basalts and their plutonic counterparts (Sections 12.4, 12.6). As most are intracratonic (intraplate), Chapters 10 and 11 are also relevant to alkaline rocks occurrence. Alkaline rocks in the oceanic setting (in Hawaiian-type islands) are mentioned in Chapter 4, but none are associated with giant deposits there. Some rocks in convergent continental margins, "eugeoclinal" orogens and greenstone belts have "alkaline tendencies" (e. g. the shoshonitic association; Chapters 5-9), but feldspathoidal rocks there are exceptional unless they are genetically unrelated, much younger occurrences. Finally some lamprophyres like minette and kersantite are placed by some authors into the alkaline family; there, most come as late stage dikes in syn- and post-orogenic granitoid terrains (Chapters 7, 10). The very rare high-grade metamorphosed alkaline rocks are included in Chapter 14.

The frequency of alkaline rocks decreases with increasing age, hence Archean alkalines are exceptional and the few recorded occurrences are mostly (high-grade) metamorphosed. This is partly due to secular evolution (alkaline rocks tend to form in the latest stages of magmatic evolution in stable cratons), partly to preservation. Alkaline volcanics, the bulk of which is Cenozoic, are rapidly eroded away and become increasingly rare in geologically older settings. Because many characteristic

magmatic rock-forming and accessory minerals in alkaline rocks (like K- and Na-feldspars, Na-amphiboles and pyroxenes, some feldspathoids, phlogopite, magnetite) can also form by hydrothermal metasomatism or metamorphism, many so formed rocks mimic the truly magmatic alkaline rocks. Some metasomatic fenites adjacent to carbonatites are indistinguishable from orthomagmatic nepheline syenites, and many metasedimentary marbles metasomatically enriched in Nb, rare earths, and the "right" Sr isotopes are unrecognizable from magmatic carbonatites (and vice versa). Understanding alkaline metasomatism and its products is important in mineral exploration as many major metallic deposits are part of the process, yet many petrology texts stick to the magmatic orthodoxy and do not consider the important role of postmagmatic metasomatism.

Alkaline associations and provinces: Sørensen (1974) recognized the following alkaline associations:

- 1) Alkaline-ultrabasic association. This association comprises dunite, pyroxenite, pyroxene-nepheline series (ijolite, urtite, melteigite), grading to nepheline syenite. Carbonatite may be present. The rocks form small, concentrically zoned intrusions cored by dunite and enveloped by alkalic pyroxenites, gabbroids and syenites (e.g. Inagly massif, Siberia; Kovdor, Kola Peninsula). Differentiated intrusions dominated by the nepheline-rich members (e.g. Khibiny) and rare layered differentiated intrusions of predominantly syenitic composition (Lovozero) may be associated in space. The Cambrian to Devonian magmatic province in the Kola Peninsula, Russia, is considered as the type area although the Russian literature (e.g. Rundkvist, ed., 1978) prefers the Permian Meimecha-Kotui province of the Siberian Shield, or the Cambro-Ordovician (older) suite in the Kola Peninsula (Kovdor, Afrikanda).
- 2) Gabbro-syenite alkaline association. This association overlaps with plateau basalt provinces and comprises "normal" and alkaline gabbros and syenites, nepheline syenite and peralkaline granite. It is typified by the Mesoproterozoic Gardar Province in southern Greenland (Fig. 12.26), famous for the spectacularly layered syenitic intrusions like Ilímaussaq.



1. Plateau basalt flows; 2. Quartz arenite; 3. Trachyte tuff; 4. Trachyte laccolith, stocks; 5. Quartz syenite and granite; 6. Foyaitic nepheline syenite; 7. Alkaline ultramafics, carbonatite, flooded by diatreme; 8. Giant gabbro dikes; 9. Syenite; 10. Gabbro; 11. Pre-rift sialic basement. A. Ta,Nb,Be,U,Th disseminated in peralkaline stock, in pegmatite, metasomatites; B. Zr,REE,Y,Nb,Th,Be,Ta as above, in fractionated nepheline syenites; C. Ti-magnetite or ilmenite in gabbroids; D. Fe,Ni,Cu sulfides in gabbro

Figure 12.26. Rocks/ores cross-sectional inventory based on the Mesoproterozoic "Gardar Rift" in southern Greenland. From Laznicka (2004) Total Metallogeny Site G225. Explanations (continued): E. Nb,REE,Ti,Th,U,Sc disseminated in carbonatite and alkaline metasomatites; K. Cu in subgreenschist basalt; K. Be,REE,Th,U in alkaline hydrothermal veins; R. Mo stockwork in quartz syenite, granite. Ore types A, B, E, R have known "giant" equivalents

- 3) These intrusions are also greatly enriched in rare metals like Zr, REE, Ta, Be, Th and U.
- 4) Granitoid association. This association has a scarcity of basic rocks and is typified by peralkaline granite gradational to calc-alkaline granite (especially the potassic "tin-granite") with minor nepheline syenite, fayalite granite, anorthosite and other rocks. The Permian to Tertiary "Younger Granite Province" in West Africa, especially the Jos-Bukuru complex in Nigeria (MacLeod et al., 1971), is considered the type area. It is enriched in Sn, Ta and Nb. Peralkaline granites, that include several "giants", are reviewed in Chapter 10.

Other authors formulate alkaline associations in many different ways (compare petrology textbooks, e.g. Carmichael et al., 1974; Hess, 1989; Faure, 2001) and also discuss at length igneous petrogenesis. There is, furthermore, a specialized literature on ultrapotassic rocks (Gupta and Yagi, 1980), kimberlites, lamproites and diamonds (Mitchell, 1986); lamprophyres (Rock et al., 1991) and carbonatites (read below). The Russian authors, Currie (1974) and others distinguish, among the silica-undersaturated rocks, the miaskitic ($\text{Na}+\text{K}:\text{Al}$ less than 1) and agpaitic ($\text{Na}+\text{K}:\text{Al}$ greater than 1) petrochemical classes. From the

exploration point of view it is more practical to focus on the level of exposure and differentiate among the predominantly volcanic provinces (e.g. the East African Rift; the Cenozoic central and western European Province, e.g. the České Středohoří), and the predominantly plutonic provinces (compare Laznicka, 1985, p. 1473).

12.8.2. Alkaline metallogeny and giant deposits

Alkaline magmas are greatly enriched in many predominantly incompatible, lithophile elements and rare metals like Nb, Ta, Zr, REE+Y, Th, U, Be, Hf. Sources and geochemical histories of some of these metals, that are of value in interpreting igneous petrogenesis, are extensively discussed in the petrologic literature (compare Faure, 2001 for review and references). Opinion on the source of these metals is split between those favoring origin in the metasomatized or undepleted mantle (the existence of which is mostly supported by phlogopite and other minerals contained in mantle xenoliths), and those who prefer the continental crust as the metal source, perhaps by releasing its trace metals into passing mantle-derived melts. The melts' origin is usually attributed to mantle plumes (hot spots) originating in the asthenosphere

(Chapter 4). The mantle-sourced melts, upon reaching the crust, are then modified by differentiation and fractionation when the trace metals (and also some major metals like Al and Ti) preferentially partition into some of the members in the usual (ultra)mafic to felsic differentiated series. Diamond (and its indicator minerals, not treated in this book) is anomalous as it is brought as ready-made xenocrysts, from its original source in greater than 150 km depth.

Some rare "rocks" (as opposed to classical "ores") are so enriched in rare metals that they would constitute a "bulk mineable" deposit (at par with porphyry coppers or some disseminated gold deposits) if prices of these metals were better and if there were sufficient markets. This applies to the enormous accumulations of zirconium in some magmatic units in the Ilímaussaq, Lovozero and other complexes, in concentrations around 1.0 % Zr (that is, with a concentration factor of 50 in respect to Zr clarkite); and to highly Nb, REE and other metals enriched carbonatites. The grade-tonnage relationships follow from the example in Laznicka (1985, p.1520) based on Zr in the Lovozero (Russia) and Ilímaussaq (Greenland) complexes. The whole Lovozero is estimated to store 360 mt Zr at 0.355% Zr average concentration; 210 mt Zr in eudialyte lujavrite at 1.0% Zr; 30 mt Zr in the eudialyte layers @ 5.7% Zr; and 25 mt Zr in the 10.16% Zr eudialyte concentrate (eudialyte formula is $[\text{Na,Ca,Fe}]_6\text{Zr}[\text{OH,Cl}][\text{SiO}_3]_6$).

The Ilímaussaq example is even more striking (read below). If the Lovozero or Ilímaussaq were bulk-mined for the recovery of all the anomalously enriched trace metals they carry (Zr, REE, Y, Th, U, Be, Ta), they would provide a long-lasting, "(super)-giant" resource. This would, however, lead to overproduction, hence price lowering for metals with limited demand (REE, Y, Th) alongside the "in demand" metals (Ta, U, Be), not considering the environmental, technological and political constraints. It is, however, likely that these presently "unconventional resources" are the ores of the future. The felsic alkaline lithologies like phonolite and nepheline syenite have also high aluminum content (of the order of 20% Al_2O_3) with some varieties reaching 23.09% Al_2O_3 (Laacher See, Germany; Wimmenauer, 1974) which comes close to 50% of the grade of some presently mined bauxites. This makes these silicate rocks another potential ore of the future, of Al. Nepheline concentrate obtained as a by-product of apatite recovery from the Khibiny complex in NW Russia already is (or was?) smelted for aluminium under the Soviet economic conditions.

Given the high "regular" enrichment in trace metals of some alkaline rocks, a relatively weak geological "next step", capable of local upgrading of the trace or major (Al, Ti) metals, can result in an economic deposit. Supergene enrichment is the least controversial "small step" and this has already produced economic deposits of bauxite in Arkansas and Poços de Caldas, Brazil (on "regular" nepheline syenite). "Giant" deposits of Nb, REE and Th, and "large" deposits of the same metals plus Ta, Ti, U, Y and Sc, formed on previously "slightly" enriched alkaline rocks and, especially, carbonatites (e.g. Nb, REE, Th over the Seis Lagos, Araxá, Tomtor and Mount Weld carbonatites). The non-supergene "slight" metal upgrading includes extreme magmatic differentiation and fractionation in silicate rocks (e.g. Zr in eudialyte as in Ilímaussaq and Lovozero; REE, Y, Nb in apatite as in Khibiny, loparite and steenstrupine as in Lovozero, Ti in perowskite as in Tapira and Catalão), and in carbonatites (Araxá). REE, Nb metasomatism (replacement) as in Bayan Obo and Cu replacement in Palabora has a similar effect. The "extreme" metal enrichment is exemplified by the highly variable collection of small to medium-size late stage pegmatites, metasomatites and hydrothermal veins present in virtually all alkaline complexes. More detail on the alkaline and carbonatite metallogeny and lists of ore deposits, most of which are lesser magnitude metallic occurrences, are in Semenov (1974), Deans (1966), Richardson and Birkett (1996a,b) and have been summarized in Laznicka (1985, p. 1473-1582) and Laznicka (1993, pages 1222-1245).

Alkaline rocks and especially carbonatites contain one "super-giant" deposit (of Nb; Seis Lagos), 15 "giant" entries (that is, accumulations of a single metal) that correspond to 9 deposits (some contain multiple "giant" metal accumulations, e.g. Araxá Nb, REE, Th; Lovozero Nb, REE, Zr; Tomtor Nb, REE); and 27 "large" entries corresponding to 13 "large" deposits, some of multiple metals. Given their rarity (silicate alkaline rocks crop out at less than 1% of earth's surface; carbonatites have been recorded from less than 400 occurrences, worldwide), these rocks host by far the highest number of metal "giants" per rock occurrence (Laznicka, 1999).

12.8.3. Alkaline volcanic and subvolcanic centers

It is interesting to note that the most extensive and famous alkaline volcanic provinces around the East African Rift, West- and Central-Europe, and

American Mid-West, contain virtually no metallic occurrences. As mentioned above some phonolites (especially the areally extensive "plateau phonolite" of eastern Africa) might become potential Al ores of the future, possibly of giant magnitude. The alumina content in phonolite is upgraded in tropical regoliths to form lateritic bauxite, but even an incomplete supergenesis that produces hydrosilicate clays rather than Al hydroxides may result in alumina enrichment and alternative Al source of the future. Clays and claystones, already excavated as a by-product of coal mining, are particularly attractive future metal sources as processing them reduces the amount of waste. Some footwall clays under the Miocene brown coal in the Chomútov coal basin, NW Czech Republic, contain up to 30-40% Al₂O₃, 4-15% TiO₂ and 0.2-0.4% V (Sattran et al., 1966). They formed as saprolite over phonolite (Braňany), or by reworking and argillization of phonolite regolith and ash-fall beds.

Uranium is commonly enriched in alkaline volcanic terrains, mostly as stratabound or discordant infiltrations of U oxides, released by breakdown of volcanic glass and unstable carrier minerals during diagenesis or low-temperature hydrothermal activity (e.g. Poços de Caldas district, Brazil). "Sandstone-U" deposits (Chapter 13) are the most common example of traps of migrating uranium, but their majority have mixed U sources that also include granitic and metamorphic basement in addition to the alkaline volcanics. "Large" uranium fields with the metal sourced largely from alkaline volcanics include Hamr-Mimoň in the Czech Republic, U-lignites in South Dakota and Montana, deposits in the Wyoming U-province. Grants (Ambrosia Lake) region, San Juan Basin, New Mexico, is a "giant U district".

Inconspicuous, yet substantial rare metals accumulations (Zr, Nb, REE, Y, Ta) are increasingly found in unusual alkaline settings and associations. One example is the **Toongi deposit** near Dubbo, New South Wales (Rc 83 mt @ 1.406% Zr, 0.315% Nb, 0.11% Y, 0.025% Ta, 0.61% REE and 0.034% Hf to a depth of 100m; Alkane NL website, 2002). This is a 600x400 m large elliptical stock of inconspicuously altered, fine grained Jurassic alkali trachyte emplaced into the Lachlan Foldbelt orogenic basement, covered by erosional remains of Jurassic platformic sediments and trachyte, olivine basalt lavas. The micron-size (invisible) evenly disseminated Zr-silicates eudialyte, natroniobite and bastnäsite would make this a bulk-mineable orebody of "large" magnitude if the resources were extended to 200 or 300m depth. The same company has explored the

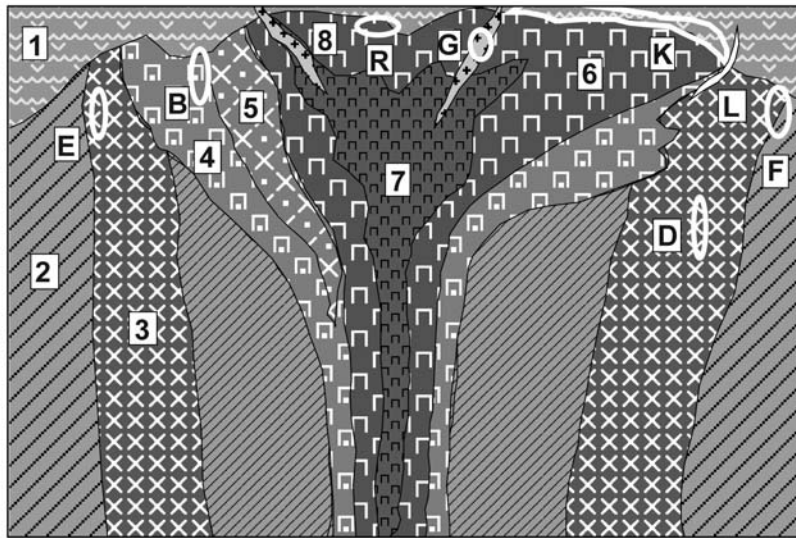
enigmatic **Brockman deposit near Halls Creek**, NE Western Australia (Chalmers, 1990; Rv 4.29 mt of ore @ 0.77% Zr, 0.31% Nb, 0.098% REE, 0.03% Hf, 0.022% Ta and 0.011% Ga). The inferred and indicated resources there are quoted as additional 45 mt of ore which is still not enough to clear the "large" deposit threshold, yet the entire package of rare metals makes Brockman an attractive potential source of Ta, Hf and Ga (Rc ~9,400 t Ta, 12,870 t Hf, 4,720 t Ga). The deposit is located in the Paleoproterozoic Hall's Creek greenstone belt that hosts several small shear zone-style orogenic gold deposits, and it consists of extremely fine grained disseminated zircon, columbite, Y-niobates, minor bertrandite, bastnäsite and parisite in an altered "trachytic ash-flow tuff". This is a NE-trending, steeply dipping to vertical 5-35m thick unit traceable for 3.5 km along strike, within a mafic to bimodal meta-volcanic and meta-sedimentary "greenstone" association. Chalmers (1990) interpreted this mineralization as "syngenetic but modified by F-rich solutions soon after deposition", although synorogenic alkaline metasomatism appears equally attractive.

The "giant" Cripple Creek epithermal goldfield in the Colorado Rockies in alkaline rocks, as well as gold deposits in the shoshonitic association, appear in Chapters 6 and 7.

12.8.4. Nepheline syenite-dominated intrusions

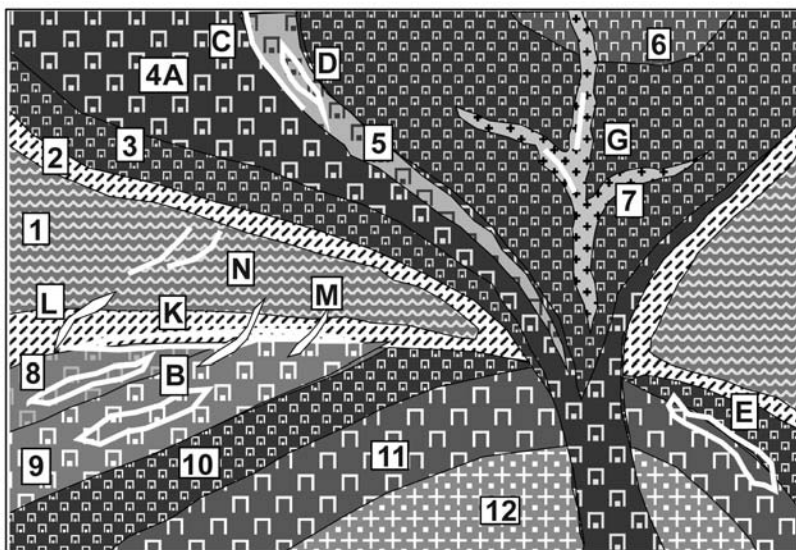
Nepheline syenite intrusions can be subdivided into the less alkaline miaskitic (Na₂O+K₂O/Al₂O₃<1), Fig.12.27; and more alkaline agpaitic (Na₂O+K₂O/Al₂O₃ <1); Fig.12.28; families. Although this seems rather academic, there is a significant difference between both categories in appearance, lithologic association, mineralogy, and the type of commonly associated ores. Agpaitic nepheline syenites are low in Ca, Mg, CO₂; high in Fe, and exceptionally high in trace metals Nb, Be, Li, REE, Y, Th, U, Ta, as well as Cl and F. Common accessory minerals are eudialyte and F-arfvedsonite. Agpaitic members associate with, or evolve from, miaskitic complexes with which they share the circular, zoned, multiply overlapping centers (ring complexes, cauldrons), or they often form the outer zones of ijolite - pyroxenite - carbonatite complexes; some of the nepheline rocks there are metasomatic fenites.

Agpaitic syenites are best known from the few well studied and publicized multiphase partly layered intrusions like Ilímaussaq and Lovozero.



1. Thermally metamorphosed roof rocks;
 2. Crystalline wall-rocks;
 3. Gabbro, outer ring;
 4. Miaskitic nepheline syenite ring;
 5. Alkaline gabbro;
 6. Amphibole-augite syenite;
 7. Quartz-amphibole syenite;
 8. Syenite pegmatite;
- B. Nb,Ta,Zr,REE,Y,Th in pyrochlore disseminated in foyaite; D. Cu,Ni,PGE sulfides disseminated in pegmatitic gabbro; E. Ditto, postmagmatic stringers, breccia; F. Ditto, stringers and disseminations in contact hybrids; G. REE,Nb,Y Zr disseminated in syenite pegmatite; K. Ditto, in alkaline metasomatites;

Figure 12.27. Inventory cross-section of rocks and ores in a composite miaskitic ring complex; from Laznicka (2004) Total Metallogeny Site G103. Explanations (continued): L. REE,Th,F in britholite, disseminated in vein alkaline metasomatites; R. Mo stockwork in quartz syenite



1. Gneiss;
 2. Fenite envelope;
 3. Foyaite;
 4. Coarse agpaite nepheline syenite;
 5. Ijolite-urtite;
 6. Pulaskite;
 7. Ultra-alkaline pegmatite and metasomatites;
 8. Naujaite (extremely fractionated nepheline syenite);
 9. Lujavrite;
 10. Miaskitic nepheline syenite;
 11. Quartz syenite, nordmarkite;
 12. Peralkaline granite.
- A. Nepheline syenite as Al ore; B. Zr>Ta,Nb,REE,Be disseminated in highly fractionated nepheline syenite; C. Apatite > REE, Zr in urtite; D. REE>Nb>Ta,Th in loparite, pyrochlore disseminated in urtite, juvite; E. Ta,Nb>Th,REE in contaminated microsyenite; G. Be,REE,Nb,Th,U,Ta in agpaite pegmatite;

Figure 11.28. Rocks and ores inventory cross-section in a moderately eroded agpaite alkaline central complex. From Laznicka (2004) Total Metallogeny Site G106. Explanations (continued): K. Zr,Th,U,Cs,Rb,Li,V disseminated in fenite exocontacts; L. Be,REE,Ta,Nb,Th in alkaline metasomatite veins; M. Be,REE,Th,U late stage veins related to lujavrite; N. U,Th,Ti,REE exocontact hydrothermal veins. Ore types B, D, E have known "giant" equivalents

There, extremely fractionated syenitoids crystallized as chamber floor cumulates (kakortokites at Ilímaussaq), cumulates under the intrusion roof (naujaite), late residual melts (lujavrite), pegmatites, metasomatites and veins. Mappable magmatic units within a composite

intrusion differ not only by composition, but also by grain size and crystallinity. Medium- to coarse-crystalline syenites with megascopically recognizable alkali feldspars, nepheline, alkali pyroxene (aegirine), Na-amphibole, sometimes sodalite, arfvedsonite or eudialyte grade into fine

crystalline foyaite, where tablets of alkali feldspar rest in matrix of nepheline and mafic minerals.

Ilímaussaq intrusion, Greenland (Ferguson, 1964; Bailey et al., 1981; Larsen and Sørensen, 1987; 38 mt Zr, 43 kt U, 86 kt Th). This is a portion (~150 km²) of a Mesoproterozoic (1,168 or 1,020 Ma) intrusion exposed along the rocky shores of southern Greenland. It is a member of the Gardar igneous province dominated by tholeiitic basalt and gabbro magmatism controlled by intracratonic extension and rifting, with enhanced alkalinity during the late stages. The igneous petrology is related to volatiles-rich (F, Cl, CO₂) benmoreitic residual magmas (Upton and Emeléus, 1987). The basaltic magma preferentially produced swarms of giant dikes, whereas the alkaline and peralkaline melts accumulated in ten or more steep-sided central plutonic complexes. There, salic intrusions comprise 87% of the total outcrop, gabbroids 13%. Ilímaussaq and Motzfeldt are two salic complexes with significant accumulations of rare metals.

The high-level Ilímaussaq intrusion measures about 17 x 8 km and cuts both the basement granite as well as the unconformable remnants of Mesoproterozoic sandstone and basaltic roof. Larsen and Sørensen (1987) argued that agpaite magma filled a narrow, perhaps 1,500 m thick zone on top of a large stratified basalt-syenite chamber at depth. It differentiated and fractionated as an essentially closed system, cooling from the top so the rocks crystallized successively downward from the roof (hence the lowermost agpaite unit crystallized last). The chamber floor rocks are rhythmically layered cumulate kakortokites and lujavrites greatly enriched in Zr, the roof cumulates are represented by foyaite (=intergranular-textured nepheline syenite) and naujaite (=poikilitic sodalite-nepheline syenite). The lujavrite (=trachtyoid nepheline syenite) horizon in-between pierced and brecciated the already solidified roof cumulates, causing widespread metasomatism, diking, hydrothermal alteration and veining.

The ~230 to 400 m thick basal kakortokite unit (Nielsen, 1973) consists of several rhythms of alternating colourful bands of different mineralogical composition. In ascending order, the black bands are arfvedsonite-rich, the red bands eudialyte-rich, the white bands alkali feldspar and nepheline-rich. The black bands grade 1.14% ZrO₂, the red eudialyte bands 7.07% ZrO₂, the white bands 1.02% ZrO₂. The corresponding Nb₂O₅ contents are 0.05%, 0.56%, and 0.1%, respectively. The average content of the entire kakortokite unit is ~1.3% ZrO₂ and about 0.13% Nb₂O₅, which

translates into the 38 mt of Zr content listed above. Sphalerite is a widely distributed accessory mineral here, with 0.1% Zn present over large areas. Kakortokites are bordered by a pegmatite against the marginal augite syenite (Bohse et al., 1971). The pegmatite is about 50m thick, of the same composition as kakortokite but more heterogeneous. The mean ZrO₂ content is 2.0%.

A variety of unusual mineralized metasomatites has been described from the Ilímaussaq roof (Engell et al., 1971). "Lujavritized syenite" is composed of albite and arfvedsonite, replacing nepheline syenite. Aegirine-replaced naujaite has metasomatic aegirine, partially or completely replacing a sodalite-rich nepheline syenite. A portion carries scattered crystals of chkalovite (Na₂(BeSi₂O₆)). Analcite-replaced naujaite is a porous light-colored rock with chkalovite, epistolite and Li-mica in crystal-lined miaroles. Albitized arfvedsonite nepheline syenite dike in the Taseq area contains large number of Be minerals of several generations. The metasomatites grade into shear and fissure-filling mineral veins.

Be-rich hydrothermal veins in the Kvanefjeld area (Engell et al., 1971) consist of albite and natrolite gangue that contains scattered Be minerals chkalovite, tugtupite, beryllite and bertrandite, with several Nb, REE, Th and U minerals. In veins extending into the mafic lava, anorthosite and augite syenite roof, analcrite is the principal gangue and the veins grade 0.6% Nb₂O₅ and 0.008% Ta₂O₅. Nb and Ta reside in pyrochlore, epistolite and murmanite. The largest, potentially economic Be accumulation in Ilímaussaq is in the Taseq slope area (Engell et al., 1971; 180 kt ore @ 0.1% BeO). There, a zone of hydrothermal veins and veinlets is superimposed on arfvedsonite nepheline syenite dikes containing steenstrupine. The main Be mineral is chkalovite in albite-fluorite gangue. Be with U and Th are also enriched in many thin but persistent hydrothermal veins in the fenitized exocontact along the NE side of the Ilímaussaq intrusion (Hansen, 1968).

The Kvanefjeld area near the NW contact of Ilímaussaq contains a late lujavrite dike that intrudes earlier brecciated lithologies and then extends into the exocontact (Nielsen, 1973). The dike is enriched in steenstrupine and lesser amounts of monazite, thorite and uraninite. The whole rock contains 100-800 ppm U, 200-2,000 ppm Th, 1.2% REE. The reserves are currently estimated to be at least 18 mt of ore, containing 43 kt U and 86 kt Th.

Motzfeldt Centre Ta, Nb, Zr, Th, U, REE, Greenland (Tukiainen, 1985; Rc ~50 mt @ 0.28-

0.7% Nb and 250-820 ppm Ta for about 250 kt Nb @ 0.5% and 25 kt Ta @ 500 ppm. Alternative, probably erroneous estimates go as high as 410 kt Ta @ 0.41% Ta). Motzfeldt is one of several composite salic intrusive centers within the Igaliko complex, itself one of the intrusions within the Gardar Igneous Province of SSW Greenland (Upton and Emeleus, 1987). Motzfeldt has been dated at 1.31 Ga and it is a ring complex of three steep-sided, outward-dipping intrusions of peralkaline, nepheline and arfvedsonite syenite, emplaced into Mesoproterozoic continental quartz arenite roof with basalt interbeds. The outer ring zone has a quartz-normative character, a consequence of magma contamination by the assimilated quartzite from the roof. Semi-assimilated quartzite blocks are common and magma fractionation produced peralkaline residue emplaced as late stage sheets of microsyenite and pegmatite. The latter rocks are reddish-brown, miarolitic, hydrothermally albitized and hematitized.

The altered microsyenite contains arfvedsonite, abundant fluorite, disseminated zircon, thorite, and patches enriched in pyrochlore. The euhedral pyrochlore grains are enriched in Ta at the deeper levels and represent a considerable Ta and Nb resource.

Lovozero alkaline massif, Russia (Vlasov et al., 1959; Gerasimovsky et al., 1974; Kogarko, 1987; possible Rc ~20 mt Zr, 7 mt Nb, 5.5 mt REE, 80 kt Ta, 30 kt Th., etc.). This is a composite, 650 km² agpaitic intrusion in the Kola alkaline province of NW Russia dated at 370 Ma (Upper Devonian), emplaced into the Byelomoride Archean granite-gneiss basement. The intrusion has a subcircular outline, sharp contacts, a stock-like shape in depth topped by a laccolith-like differentiated sequence. The concentrically zoned intrusion resulted from four successive magmatic phases. Metamorphosed and metasomatized nepheline syenites of Phase 1 are preserved mostly as rafts and xenoliths. Phase 2 produced a cyclic, rhythmically layered sequence of (from bottom to top of each cycle) urtite, foyaite, lujavrite. Phase 3 comprises coarsely crystalline layered lujavrite with a prominent zone of eudialyte lujavrite in the central part of the massif. Phase 4 emplaced alkaline dikes (monchiquite, camptonite, tinguaitite).

The Lovozero rocks are extremely agpaitic (the Na₂O+K₂O/Al₂O₃ ratio is 1.44), dominantly sodic, and anomalously enriched in Zr (0.48% ZrO₂ is the whole complex average) and other rare elements. The prime candidate for bulk-mineable sources of industrial metals are syenites with a high content of

eudialyte (for Zr, Nb, Ta, REE), loparite-rich urtite horizons, and steenstrupine and lovozerite-bearing lujavrites (for Ta, Nb).

Layered eudialytic lujavrite (mesocratic nepheline syenite) constitutes 18% of the intrusion and forms a rhythmic sequence 150 to 500 m thick, with an average content of 1.36% ZrO₂. Each rhythm consists of successive bands of leucocratic, mesocratic and melanocratic varieties, with gradual transition from one to the other. Dark red bands, highly enriched in eudialyte, contain up to 75% of eudialyte crystals in nepheline matrix, and they form lenticular intercalations 0 to 40 cm thick. In the Chivruai valley 13 eudialytite bands form about 40% of a 3 m thick section of lujavrite. Eudialytites contain 6.76 to 8.68% ZrO₂, 0.39-0.93% (Ta,Nb)₂O₅ and 1.01-1.56% REE₂O₃. This represents a resource of 10 to 100 kt Ta, 1 mt Nb, 100 kt to 1 mt REE and some 4 to 40 mt Zr (Rundkvist, ed., 1978).

Loparite (REE,Na,Ca)₂(Ti,Nb)₂O₆ is another important carrier of rare metals. It forms scattered black xenomorphic grains in urtite and juvite, and its concentrate contains 8-10% Nb₂O₅, 0.65-0.75% Ta₂O₅, 0.62-0.76% ThO₂ and 16-17% REE₂O₃. When loparite content approaches about 10%, the intrusive layer can be selectively mined as a complex ore. According to Rundkvist et al. (1978) such layers may potentially contain as much as 25% of the world's resources of Ta (between 5 and 60 kt Ta) and 12% of Nb resources (some 5-8 mt Nb), as well as between 1 and 10 mt of REE and perhaps 500 to 800 kt Th. Although the global percentages seem a bit too ambitious, there is no doubt that the Lovozero loparite accumulations represent a "giant" resource of Ta, Nb and Th. Additional resources of the same metals are in steenstrupine and lovozerite-bearing lujavrites. Steenstrupine (REE,Th,Ca,Na)₂(Mn,Fe)(SiO₃)₄.5H₂O contains 14% REE₂O₃, 10.23% ThO₂, 4.37% Nb₂O₅ and 1.28% Ta₂O₅. Lovozerite (Na,Ca)₂(Zr,Ti)Si₆O₃(OH)₆. 3H₂O contains 16.54% ZrO₂ and 0.56% REE₂O₃ (Vlasov et al., 1959). Other than as rare minerals in pegmatites, these hydrosilicates are enriched in several lujavrite layers where a rock with 1 to 2% steenstrupine could become an industrial ore with 0.015 to 0.025% Ta, 0.2-0.3% Nb, 0.5% REE and 0.X% Th (Rundkvist, ed., 1978).

Pegmatites are widespread in nepheline syenite complexes and they contain many rare minerals, often of specimen quality. In Lovozero, Vlasov et al. (1959) distinguished patchy and layered pegmatites. Some of the layered pegmatites, most of which occur at boundaries of magmatic units, are of economic interest. The pegmatitic horizon beneath

the ijolitic urtite unit consists of up to six subparallel pegmatitic layers as much as 2.5 m thick, traceable for several kilometers. The pegmatites are usually mineralogically zoned, with typomorphic minerals to identify each zone and its suitability as an ore. Murmanite ($\text{Na}_2[\text{Ta,Ti,Nb}]_2\text{Si}_2\text{O}_9$), one of the Lovozero Ta carriers, may constitute up to 10% in the intermediate pegmatite zone.

12.8.5. Alkaline pyroxene-nepheline series and alkaline ultramafics

Khibiny massif and apatite, Ti, REE, Zr deposits. Urtite (82-86% nepheline, 12-16% aegirine), ijolite (~50% each nepheline and pyroxene) and melteigite (70-90% pyroxene, rest nepheline) are members of the magmatic series intermediate between nepheline syenite and pyroxenite. The Khibiny intrusion in the Kola Peninsula, NW Russia, is the type locality and it is also the world's largest composite alkaline intrusive complex (1,327 km²) that contains the largest magmatogene apatite deposit (Vlasov et al., 1959; Ivanova, 1963; Kogarko, 1987; 2.7 bt @ 18% P_2O_5 containing 44 mt REE, Al in nepheline concentrate, Zr, Ti; Fig. 12.29). This Devonian (367-365 Ma) complex is exposed as an almost perfect hollow ring in the tundra, its center concealed under Quaternary glacial sediments. In the depth this concentrically zoned intrusion is a lopolith filled by some 20 km thick layered series, emplaced into fenitized Archean metamorphic basement. The magmatic layers dip some 20° towards the center and become steeper near the eastern margin. Kramm and Kogarko (1994), using Sr isotope analysis, demonstrated the existence of two separate intrusions, believed produced by fractional crystallization of two magma batches almost free of crustal contamination. The principal Group I complex has a core of foyaite enveloped by cone sheets of ijolite, urtite, malignite, rischorrite (K-feldspar, nepheline, aegirine, arfvedsonite, biotite), khibinite (K-feldspar, nepheline, aegirine, arfvedsonite) and nepheline syenite. The Group II has a large core of carbonatite concealed under drift and karsted, surrounded by tinguaita, pyroxenite and ijolite.

The apatite deposits are controlled by a zone of brecciated ijolite and urtite peneconcordant with the gently east dipping igneous layering, cemented by light-green crystalline apatite. The best ore is in a zone about 2.4 km long and 160 m thick that contains up to 65% of apatite with lesser quantities of Ti-magnetite, brown titanite (sphene) and

eudialyte. The latter three minerals are recovered as by-products (Ivanova, 1963), together with nepheline concentrate used as a nonconventional Al ore. The titanite-rich orebodies in hangingwall of the apatite orebody contain 8-11% TiO_2 over a thickness of 5 to 30m, whereas the titanite concentrate grades 26% TiO_2 . The apatite concentrate is high in rare earths (up to 5% of REE_2O_3), recovered during chemical processing of apatite. Based on the published apatite reserves, this represents some 44 mt REE. Rare earths are also significantly concentrated in pegmatite veins and those at the Yukspor locality near Kirovsk had been mined for their REE content. The principal REE mineral was a dark yellow to brown lovorrite ($\text{Na}_2\text{Ca}_4[\text{Ce,Lu}][\text{Ti,Nb}][\text{Si}_2\text{O}_7]_2[\text{F,OH}]_4$).

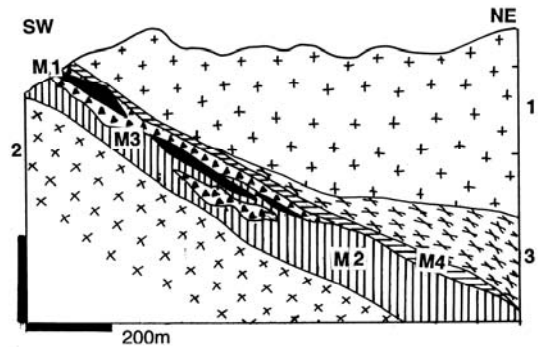


Figure 12.29. Khibiny apatite deposit, Kola, NW Russia, cross-section from LITHOTHEQUE No. 869 modified after Dudkin (1993). 1. ~373 Ma Khibiny Complex, poikilitic nepheline syenite; 2. Massive urtite, ijolite, melteigite; 3. Gneissic ijolite-urtite; M1. Massive apatite-nepheline ore; M2. Banded and lenticular apatite-nepheline; M3. Breccia of apatite > nepheline cemented by aegirine, nepheline, apatite, eudialyte; M4. Titanite, nepheline, apatite, aegirine ore

Alkaline ultramafic association: This association is dominated by pyroxenites, the bulk of which is diopside, augite and/or aegirine alkaline clinopyroxenite. These are variously associated with olivine pyroxenite, peridotite and dunite at the more mafic end (there the alkalinity is often manifested by the presence of phlogopite). The pyroxene-nepheline series (ijolite, urtite, melteigite) and nepheline syenite prevail at the salic end of the spectrum. Carbonatites are frequently present (read below) and virtually all major pyroxenite complexes have at least one carbonatite occurrence. Every member of the association can occur alone (e.g. small dunite or clinopyroxenite stocks or dikes), most often in a defined alkaline-ultramafic

province, but complex, multiphase intrusions with the (almost) full spectrum of ultrabasic to salic members "under one roof" are most popular with the petrologists and are best mineralized. The lithologic variability is reflected in the selection of ore metals and types.

Ultramafics are enriched in trace Cr and Ni as their counterparts in the non-alkaline setting and small ore occurrences of these metals plus platinoids have been recorded. No "giants" are known and probably the only "large" Ni accumulation is the 100 mt @ 1.5% Ni resource quoted for a group of small laterite/saprolite deposits developed over the Cretaceous Iporá Group dunites along the Paraná Basin fringe in Goiás, Brazil (Danni, 1976).

Pyroxenites retain their tendency to accumulate Fe (in magnetite) and Ti (in titanomagnetite); perovskite (CaTiO_3) becomes another important Ti-carrier. Apatite is also commonly concentrated, especially in foskorite (an olivine, magnetite, apatite rock). Copper sulfides are common in small showings but only some Palabora pyroxenites and foskorites contain disseminated bornite, adjacent to the latest stage "giant" Cu accumulation in transgressive carbonatite. Alkaline pyroxenites, however, often "borrow" metals and minerals normally associated with the salic (nephelinitic) alkaline lithologies, like Zr (in baddeleyite, common in Palabora and Kovdor), REE, Ta, Nb, Th (Kovdor). This is usually due to overprint of younger, more salic or carbonatitic magmatic phases and/or to metasomatism. Some alkaline pyroxenites are metasomatic fenites.

Many economic mineralizations in alkaline-ultramafic complexes are products of supergene processes, interacting with the "primary" protores. The effects are both physical (loosening of resistate minerals from the hard rock, mechanical enrichment) and chemical (e.g. conversion of phlogopite to vermiculite; breakdown of perovskite into TiO_2 [anatase]).

Palabora (Phalaborwa) Fe, P, Cu, REE, Zr, South Africa. Palabora, in the former eastern Transvaal, is the largest open pit metal mine in South Africa, a "world class" magmatic phosphate producer, and a "Cu giant" (Hanekom et al., 1965; Fourie and De Jager, 1986; Eriksson, 1989; Wilson, 1998; P+Rc 2.25 bt @ 0.52% Cu, 18% Fe for 11.7 mt Cu, 405 mt Fe in carbonatite; estimated 5 bt of apatite-Fe ore to 1,700 m depth with calculated ~5 mt REE; by-product Zr, U, Th). Although Palabora is usually listed with carbonatites that carry the bulk of Cu, it is an alkaline ultramafic complex

dominated by clinopyroxenite with a late-stage carbonatite stock of a limited extent.

The 2.03 Ga alkaline complex with an area of 16 km² consists of three concentrically zoned, subcircular, coalescing intrusions extending for a distance of over 6.6 km along a N-S axis. The intrusions plunge 76-80° east into the Archean metamorphic basement of the Kaapvaal Craton. Each multistage intrusion has a diameter of about 2 km. The northern and southern intrusions are composed entirely of pyroxenite. They range from a fine-grained, homogeneous diopside pyroxenite through a pegmatoidal variety into phlogopite, apatite, feldspar pyroxenite, phlogopitic glimmerite, and serpentinized forsterite-phlogopite pegmatoid. Only the central intrusion, Loolekop, has carbonatite core with Cu mineralization.

Phosphate and vermiculite deposits. In Palabora, phosphate comes from two major sources: 1) apatite-rich phlogopite pyroxenite, and 2) foskorite; Fourie and De Jager (1986). 1) Phlogopite pyroxenite, present in the northern intrusion, has an average content of 9% P_2O_5 . Apatite is interstitial to diopside and it contains 0.64% REE (the ore has ~0.12% REE). 2) Foskorite in the Loolekop intrusion is a rock composed of variable proportions of forsterite, magnetite and apatite, with minor calcite, baddeleyite and locally disseminated bornite or chalcocite replacing calcite. It forms pipe-like bodies between the central carbonatite and the outer pyroxenite. Foskorite averages 10.5% P_2O_5 and about 25-28% Fe, with 0.5-0.6 REE. Vermiculite, in one of the world's largest deposits, is in the upper levels of pegmatoidal pyroxenite where it formed by hydration of metasomatic phlogopite that replaced the earliest brecciated dunite plug.

Loolekop disseminated Cu deposit (Eriksson, 1989). The Loolekop intrusive pipe contains a carbonatite core, the youngest intrusive phase immediately adjacent to, and partly transitional into, foskorite. The outer zone consists of vertically concentrically zoned medium to coarse crystalline Mg-calcitic and partly dolomitic carbonatite with some scattered forsterite, magnetite, phlogopite, monazite and clinohumite. Bornite forms disseminated grains, inclusions in olivine and magnetite, massive patches and lenses. It is interpreted as orthomagmatic segregation from sulfide-rich magma. The banded (older) carbonatite is intersected by dike, vein and stockwork-like transgressive, massive, magnetite-rich carbonatite controlled by NW and NE-striking fracture sets, forming a W-E elongated curvilinear zone. The younger carbonatite is mineralized by the main,

postmagmatic hydrothermal phase of chalcopyrite in the form of disseminated grains and small masses along NW and NE fractures. The average grade here is around 1% Cu but abundant thin fracture coatings of valeriite in the pit area reduce concentrate recovery. The ore is diluted by thick post-ore diabase dikes.

Palabora is the only copper deposit in carbonatite ever mined and its giant size and ore distribution is comparable with major porphyry coppers. In contrast to most carbonatites, the Loolekop orebody has Sr and Nd isotopes indicative of crustal input (Eriksson, 1989); this suggests the possibility of Cu derivation from crustal rocks (e.g. greenstones, gabbroids, amphibolites) intersected in depth during the upward passage of the volatiles-rich alkaline and carbonatitic magma.

Kovdor Massif Fe, P, Zr, Russia (Borovikov and L'vova, 1962; Ilyin, 1989; 708 mt @ 35% Fe, 6.6% P₂O₅, 0.3% Zr, Ta, Nb). This is a composite alkaline-ultramafic intrusion with carbonatite in the Kola alkaline province of NW Russia, a member of the older (than Khibiny and Lovozero) group which also includes the Afrikanda massif with Ti ores. The broadly elliptical multiphase massif measures 40.5 km² and is emplaced into the Archean Byelomoride gneiss, with up to 1,500 m wide fenitized envelope in the exocontact. The core is composed of the earliest dunite, discontinuously enveloped by jacupirangite, ijolite and melilitic rocks (turyaites). As in Palabora, the early dunite had been brecciated and converted into a variety of metasomatites that merge and overlap with the orthomagmatic, mostly nepheline-bearing phases. Phlogopitic glimmerite is widespread, and it is converted into vermiculite in the locally thick supergene zone. Aegirine, diopside, monticellite, garnet, amphibole, K-feldspar, phlogopite in variable proportions constitute the rest of metasomatites. Ijolite-melteigite form the peripheral ring and merge with fenites (or is a fenite). Two generations of aegirine, diopside and phlogopite-bearing calcitic carbonatite form several steep, late-stage linear bodies with diffuse outlines and gradations into metasomatites.

The principal metal resource mined since 1962 from the SW periphery of the intrusion is a low-Ti magnetite; the ore is close to the Palabora foskorite and comprise ~45% magnetite, 25% forsterite, 15-20% apatite, 5-10% calcite, some phlogopite and accessory baddeleyite. Additional low-grade magnetite resources are along the fringe of the dunite core where one 1.5 km long, 250 m wide zone grades ~16% Fe and 0.15 to 0.25% Ni. The phlogopite glimmerite, when mined and

beneficated, yield 20-25% of Ti-magnetite with 0.17-0.21% V.

Kovdor is an example of a mineralized complex with a great variety of low-grade mineralizations suitable for bulk mining and multi-commodity beneficiation. The principal product is a calcic magnetite ore suitable for blending with siliceous magnetite derived from BIF's in the area. In addition to Zr in baddeleyite there seems to be a substantial resource of a very low-grade Nb and Ta (Rundkvist, ed., 1978), further enriched in the late stage dikes and structurally controlled replacements.

Residual Ti oxide deposits in regolith

Tapira (Fig. 12.30) and Catalão in Brazil are two examples out of several Cretaceous rifting-related alkaline-ultramafic complexes, intruded into the São Francisco Craton of SE Brazil, at fringe of the Paraná Basin. Both contain pyroxenite with a high content of perowskite and apatite, as well as independent intrusions of carbonatite with disseminated pyrochlore. There is a late Tertiary humid tropical regolith as thick as 100 m that blankets both complexes and its metalliferous intrusions. In the regolith supergene decalcification of perowskite took place that left behind free TiO₂ in the form of disseminated and "hard" (crystalline) anatase, with relic apatite, in saprolite and pyroxenite saprock. Saprolite over carbonatite at both localities consists, as in Araxá, of clayous limonitic residue with scattered relics of pyrochlore and products of its decomposition. **Tapira** (Herz, 1976) is credited with a reserve of 200 mt @ 13.2% Ti, 750 mt @ 8.5% P₂O₅ and 113 mt @ 0.6% Nb. **Catalão** (Putzer, 1976) is credited with 170 mt of anatase containing 102 mt Ti, ~1.4 mt REE ore @ 1.7%, and 45 mt of carbonatite with 0.4-1.3% Nb₂O₅.

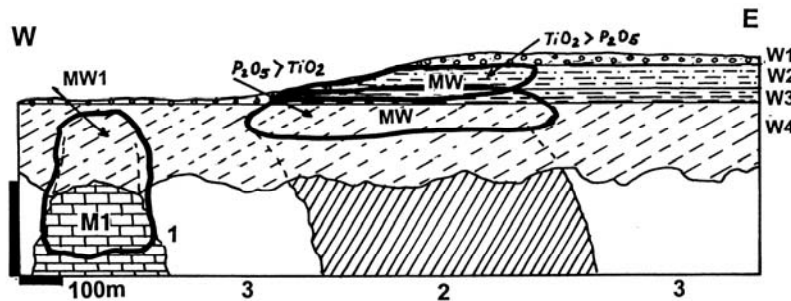
Additional significant metallic deposits in the alkaline association: There are no known "giants" other than those described above, and only a few "large" deposits. The **Powderhorn Complex** in SW Colorado is a small Cambrian pyroxenite, nepheline syenite and carbonatite intrusion emplaced into Precambrian granitoids in the Cordilleran basement (Temple and Grogan, 1965). The biotite pyroxenite contains a large Ti resource in perowskite (1.642 mt of ore @ ~7% Ti for ~138 mt Ti) and also ~2.5 mt REE, 290 kt Nb and 26 kt Th in carbonatite. The perowskite ore has some similarity with the primary ore in Tapira (read above), but there is no regolith with easy to mine and process residual material at Powderhorn. The environmental sensitivity there interferes with development. This does not seem to

be much of a problem at **Afrikanda** (~49 mt Ti) in NW Russia, a small pipe-like dunite and pyroxenite alkaline ultramafic intrusion, with Ti in disseminated perowskite and Ti-magnetite (Sokolov and Grigor'yev, 1974).

The 1.19 Ga **Strange Lake** intrusion in central Labrador, NE Canada (Miller, 1988) has a reserve of 52 mt @ 2.17% Zr, 0.24% Y, 0.27% Nb, 0.45% REE and 0.029% Be; this corresponds to globally significant 125 kt Y and 15 kt Be contents but in terms of geochemical accumulation this is merely a "medium size" deposit. The rare minerals (elpidite, gittinsite, pyrochlore, etc.) are disseminated in a stock of aegirine and riebeckite-bearing

peralkaline granite (read also Chapter 10). The Mushugai deposit in southern Mongolia is sometimes reported as an "REE giant", with some similarity to Bayan Obo (carbonatized alkaline intrusion or carbonatite?).

Dunite members of the alkaline-ultramafic suite are, like other ultramafics, high in trace Cr and Ni. The small Cretaceous intrusions on fringe of the Paraná Basin in Goiás, Brazil (Iporá area; Danni, 1976) collectively store some 100 mt of lateritic ore @ 1.5% Ni.



~70 Ma Tapira alkaline ultramafic complex: regolith. W1. Ferricrete cap; W2. Brown mottled saprolite; W3. Green to brown saprolite, silica blocks; W4. Green saprock on pyroxenite; MW. Densely disseminated authigenic anatase; 1. Carbonatite intrusion; M1+MW1. Disseminated pyrochlore; 2+M2. Perowskite in pyroxenite; 3. Dunite, syenite; 4A. Fenite (schist)

Figure 12.30. Tapira Ti & Nb deposit, MG, Brazil, diagrammatic cross-section from LITHOTHEQUE No. 1196, based on information from P. de Tarso, 1980, and site visit

12.9. Carbonatites

Hogböm, in his 1884 study of the Alnö alkaline complex in Sweden, wondered about the possible magmatic origin of the "marble" there, and Brøgger in his 1921 work on the Fen complex in Norway introduced the terms carbonatite and fenite. It was not until the 1950s, however, that the case for magmatic carbonate rocks has been confirmed beyond reasonable doubt, universally accepted, and summaries with definitions published (Heinrich, 1966; Tuttle and Gittins, eds., 1966). Unfortunately, this also resulted in an uncritical interpretation of every marble with some geochemical correspondence to carbonatite (Sr isotopes, high Nb or REE) as magmatic and mantle-related, although there is a growing body of evidence that many carbonatites formed from volatiles-charged rest magmas grading to magmatic-hydrothermal systems (much like some rare metals granitic pegmatites) that veined, replaced and altered the wallrocks. The boundary between orthomagmatic and metasomatic rocks is often difficult to determine and the reader is left confused when identical rocks are listed and interpreted under different names, depending on the author's genetic preference. As a general rule, the Western literature

of the 1960s-1990s period preferred the orthomagmatic bias, whereas the Soviet literature was strong on metasomatism. As concepts influence search for new orebodies, exploration geologists should be aware about this controversy. Several "carbonatite" occurrences appear to be meta-sedimentary marbles, metasomatically "carbonatitized" (that is, enriched in carbonatite trace metals and some of the petrogenetic isotopes). The Bayan Obo iron ore deposit and a "giant" REE accumulation is a prime example (read below). Hydrothermal systems triggered by evolution of alkaline magmas, with or without carbonatites, mutate and mix as they move away from source and assume many forms where their initial alkaline affiliation is no longer obvious. This may apply to some orebodies associated with albitites (e.g. of U, Th), Olympic Dam-style ferruginous breccias, fluorite and soda deposits, and others.

Setting, origin and varieties: All "true" carbonatites are associated with predominantly intracontinental alkaline magmatic complexes, even if such connection is not easily apparent as in tectonically dismembered and/or metamorphosed terrains (for high-grade metamorphosed carbonatites read Chapter 14). Intraoceanic

carbonatites are rare, but they do occur in the Hawaiian-type island setting (e.g. Cape Verde). The bulk of intracratonic carbonatites are controlled by extensional structures like grabens and rifts, as are the alkaline rocks (read above), and they appear to be differentiates of melts produced above mantle plumes (Bell, ed., 1989; Woolley, 1989).

The bulk of "registered" carbonatites (there are some 400, possibly 500 worldwide) are "plutonic" and geologically old; erosion has exposed the subsurface levels in which carbonatites formed, ranging from perhaps 500m to some 12 km depths. These are the "typical" carbonatites treated in the literature, including this book. The bulk of carbonatites is composed of an interlocking mosaic of carbonate crystals of fine to coarse grain size. The most common are calcitic carbonatites (sövite), followed by calcite-dolomite to dolomite carbonatites ("rauhaugite", "beforsite") and iron-rich carbonatites (ankerite, siderite, sometimes oxidized to hematite). Sr (strontianite) carbonatites are exceptional (Kangankunde, Malawi). There is a transition from pure carbonatites through silicate carbonatites (with phlogopite, forsterite, diopside, Na-amphibole, monticellite, etc.) into silicate plutonic rocks with carbonate matrix or accessory carbonate (read above). Many carbonatites or their contacts are breccias or replacements of brecciated rocks.

The most common and "typical" form of high-level plutonic carbonatites are cylindrical or conical pipes of massive, breccia or vein/stockwork carbonatite that are the latest members of concentrically zoned alkaline-ultramafic complexes. Those centrally located are believed to represent the central plug of former nephelinite volcanoes. In the "normally" zoned alkaline complex (Smirnov, 1968) the youngest carbonatite core is enveloped by ijolite-urtite, alkali pyroxenite, and fenitized wallrocks (Fig. 12.31). The latter range from orthoclase feldspathite (usually a breccia) through metasomatic albitite, nepheline syenite, into Na-amphibole (e.g. richterite, crossite, riebeckite) and pyroxene (aegirine) rocks. In other complexes, however, carbonatite plugs have an off-centre location and/or occur independently of immediately associated alkalic rocks as plugs, dikes, stockworks and replacements.

Alkali and volcanic carbonatites: Oldoinyo Lengai volcano, Tanzania (Dawson, 1966; Dawson et al., 1987). Oldoinyo Lengai is the first active volcano observed to issue carbonatitic lavas. It is a steep cone with a diameter of 8 km, towering 2,100 m above the surrounding plain in the Gregory

Rift of northern Tanzania. The cone is composed of ijolitic pyroclastics and ash reinforced by thin screens of phonolite and nephelinite lavas, dissected by erosional gullies and stained by white powdery calcite. The summit crater emits natrocarbonatite lavas accompanied by ash eruptions at almost regular intervals (every 7 years or so). The unusually low-temperature "foamy" lavas (around 500°C) do not glow, are initially black, but turn rapidly gray and eventually decompose into whitish calcitic residuum as the soluble Na carbonate component is dissolved and leached out by runoff. The principal minerals in the fresh lava are Na-Ca carbonates nyerereite and gregoryite. The Na₂CO₃-rich runoff reaches the nearby Lake Natron, a playa lake, where it accumulates in brine and encrusts the dry lake floor. In the nearby Lake Magadi farther north in Kenya, trona is mined and processed. The Oldoinyo Lengai natrocarbonatite is anomalously enriched in Sr (1.12%), REE (0.15%), Li (189 ppm), U (46 ppm) and depleted in Ti and Nb, compared with the "typical" carbonatite.

The CaCO₃ residue remaining after the removal of Na-carbonates is compositionally close to the "normal" calcitic carbonatite. In the nearby but slightly older, inactive Kerimasi Volcano the natrocarbonatite tephra has been converted into supergene Ca-carbonatite that mingles with calcrete. Under endogenic conditions in depth, it is possible that the natrocarbonatite melts dissociate to cause fenitization (alkali metasomatism) in wallrocks; it has been suggested that natrocarbonatitic magmas are the cause of strong fenitized aureoles (Dawson et al., 1987). It is not yet clear how this influences carbonatite metallogenesis.

Geochemistry and metallogeny: Carbonatites are greatly enriched in trace Nb (~1,951 ppm, 1000x clarke), REE (~2,000 ppm, 13x clarke), Zr (1,120 ppm, ~6x clarke), Mo (42 ppm, 38x clarke), Y, Th and U, and impoverished in Ni, Cu, Cr, Au and other elements. This correlates quite well with the empirical knowledge of carbonatite-associated metallic deposits that are also dominated by Nb and REE. The trace Zr and Mo enrichment, on the other hand, does not have counterparts in major orebodies (the Zr production coming from Palabora is a by-product of Cu and phosphate mining and would not be economic in itself). Copper, on the other hand, forms the only carbonatite hosted "giant" (Palabora), despite its trace content in carbonatites being ten times lower than clarke.

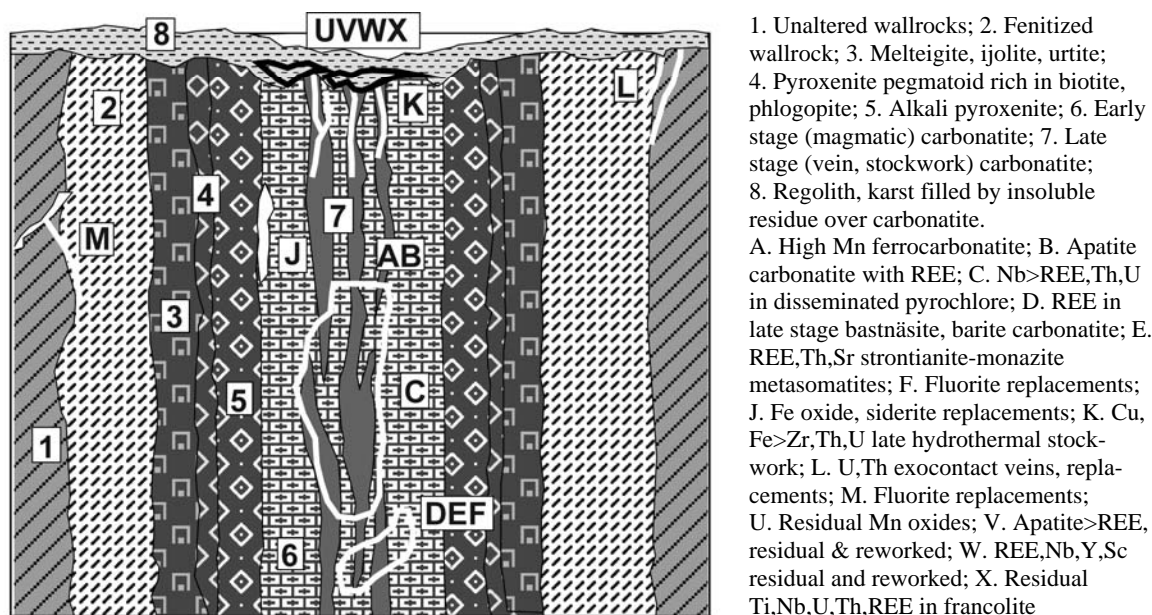


Figure 12.31. Rock/ore cross-sectional inventory in eroded meso-epizonal composite alkaline-carbonatite ring complex, from Laznicka (2004) Total Metallogeny Site G114

Of the nine carbonatite “giant” and one “supergiant” entries, four are of Nb, five of REE, one of Cu. Of the eleven “large” entries, Nb accounts for 4 deposits, REE for 3 deposits, U for two deposits, Y and Ta for one deposit each. Based on data in the GIANTDEP database (now updated), of a total of 350 recorded carbonatite occurrences in the world, five host “giant” or “supergiant” deposits, and additional five carbonatites host “large” deposits (Laznicka, 1999). This corresponds to 2.86% of the global inventory of carbonatites. Because some of these deposits are multiple “giants” (they contain more than one metal as a “giant” accumulation), the “giant” and “large” accumulations of metals in carbonatites total 21 database entries. No other rock type or association comes close.

Most of the trace metal enrichment in carbonatites is considered to be orthomagmatic, established in the mantle. In pure carbonatites the principal trace metals (Nb, REE) partitioned into finely dispersed minerals like pyrochlore, monazite, bastnäsite and others, interstitial to the rock-forming carbonates. In silicate- and apatite-rich carbonatites a portion of the trace metals resides in the non-carbonate minerals, especially in apatite that is usually enriched in REE and U. The content, variety and grain size of the rare minerals tend to increase in the late-stage magmatic phases, in ferrous carbonatites, in metasomatites. Carbonatite-related dikes and veins tend to be particularly rich in a

variety of rare minerals, but their size and persistency are low, so they have limited economic importance. Very late stage hydrothermal processes are important ore forming agents responsible for Cu sulfide mineralisation at Palabora, and Fe, REE, Nb replacements in Bayan Obo.

Supergene process of carbonate dissolution that leaves behind insoluble residue enriched in most rare metals is, after the magmatogene enrichment, the second most important carbonatite metallogene. Of the 21 GIANTDEP entries of “giant” and “large” metal accumulations in carbonatites, 14 are influenced by supergene enriched orebodies. Although, as expected, the majority of residual REE, Nb, Y, Th, U, Sc and other minerals are in weathering and leaching profiles in humid tropics (e.g. in the Amazon rainforest as Seis Lagos), some are relic profiles preserved in the present boreal environments of Siberia, Scandinavia and Canada; there, the mineralized paleokarst has been preserved in depressions under glacial drift. The multiple “giant” Tomtor in Siberia contains extremely rich layers of resistate rare metals minerals reworked from the supergene residue and resedimented by stream and wave action. Quaternary lacustrine beach deposits of apatite sand in the Cargill complex in Ontario formed by post-glacial reworking of pre-glacial paleokarst on carbonatite.

Hypogene-only carbonatite ores

Mountain Pass REE, barite; California (Olson et al., 1954; Rowan et al., 1986; P+Rc ~130 mt ore @ 4.25-6.5% REE for 6.23 mt REE). Mountain Pass is 100 km SW of Las Vegas, at the NW margin of Mojave desert where a wedge-like fault block of Proterozoic basement is exposed within the Cordilleran orogen. The older sillimanite, garnet, biotite paragneiss and granite gneiss are intruded by a Mesoproterozoic (~1.52-1.375 Ga) potassic suite that includes a variety of augite, biotite, microcline syenites (shonkinite), leucosyenite and granite. These intrusions form small discordant plutons and dikes in a 10 x 3 km long NW-trending belt. Also present are swarms of numerous short, lenticular calcite > dolomite, ankerite, siderite veins and pods, some of which carry inconspicuous rare earth minerals. Several claims were staked here in the 1940s, 1950s and earlier, based on minor scattered occurrences of galena and sphalerite, but neither the presence of carbonatite nor its rare earths mineralization were then recognized until after completion of the U.S. Geological Survey project (Olson et al., 1954). The old Sulfide Queen prospect was then rediscovered as the then world's richest known rare earths deposit and open pit mining started afterwards. In the 1980s Mountain Pass had been the leading source of rare earths supply, a position subsequently shared with the Bayan Obo deposit in China (read below).

Sulfide Queen carbonatite is an over 70 m thick, 760 m long N-S striking, 40° west dipping tabular body that thins towards the north (Fig. 12.32). It is structurally controlled and it cuts foliation of the enclosing granitic augen gneiss, but its contact is irregular and the carbonatite grades into fenite. The pinkish carbonatite is foliated and it contains numerous partly assimilated wallrock rafts and patches of shonkinite, suggesting emplacement into a fault zone by magma injection and wallrock replacement. The fenitized inclusions and wallrocks have a striking appearance because of the fracture-controlled lavender blue riebeckite on the pink background of feldspathite and carbonatite. The ore-grade carbonatite is a medium- to coarse-crystalline pink rock composed of about 40% calcite, 25% barite, 10% strontianite, 12% bastnäsite, 8% quartz and a small amount of accessory minerals like celestite, florencite, monazite, allanite, galena and others. Bastnäsite (REE[CO₃]F), the main REE carrier, has a nonmetallic appearance and its densely scattered crystalline grains range in color from light tan to honey yellow to reddish-brown. Bastnäsite has a

resinous luster, but is difficult to tell from the surrounding minerals, especially barite. The bastnäsite concentrate (Molycorp Inc. oral information, 1982) contains between 60-70% rare earths oxides, of which 99.49% comprise the light REE (La, Ce, Pr, Nd, Sm, Eu) and mere 0.318% is shared among the heavy REE (Gd, Tb, Dy, Ho, Er, Tm, Yb, Lu) and Y. The following are the percentages of REE oxides recalculated to 100% of REE oxides content in the Molycorp bastnäsite concentrate: La, 33.2%; Ce, 49.1%; Pr, 4.3%; Nd, 12.0%; Sm, 0.78%; Eu, 0.11%; Gd, 0.17%; Tb, 0.016%; Dy, 0.031%; Ho, 0.005%; Er, 0.0035%; Tm, 0.0008%; Yb, 0.0013%; Lu, 0.0001%; Y, 0.09%.

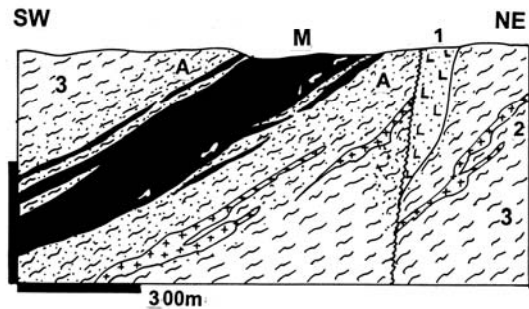


Figure 12.32. Mountain Pass, California, cross-section of the Sulfide Queen rare elements carbonatite from LITHOTHEQUE No 1433, based on data from Molycorp Inc, 1976. 1. Mp inhomogeneous K-feldspar syenite; 2. Pegmatite; 3. Migmatite; A. Fenite

Bayan Obo, China, Fe, REE, Nb replacement or meta-carbonatite (Chao et al., 1989, 1997 and references therein; 1.5 bt Fe [or 35% Fe ore?], 30 or 85 mt REE content, 1 or 3 mt Nb content). Bayan Obo (old spelling: Pai-yun-o-po) is in the Yinshan Range, in Inner Mongolia, N-C China (Fig. 12.33). This is the world's largest REE resource discovered so far. Two ore fields occur in a zone of deep faults between the northern margin of the Sino-Korean Shield and southern margin of a late Paleozoic foldbelt crossing the border from Mongolia. The orebodies are in the Mesoproterozoic (~1.65 to 1.35 Ga) Bayan Obo Group, a thick clastic-carbonate sequence unconformably resting on the late Archean gneiss basement. The immediate ore hosting unit is the H8 dolomitic marble and partly the overlying H9 feldspathized graphitic schist in the hangingwall. The H6 clastics in the stratigraphic footwall are also feldspathized and veined by alteration minerals. The host units are exposed in an 18 km long, 2 km wide E-W to NNE-trending syncline with steep limbs, deformed and low-grade metamorphosed during its protracted post-depositional history. The metasediments, including

the Archean basement outside the immediate mineralized area, are intersected by numerous short and narrow, predominantly calcitic carbonatite dikes of Mesoproterozoic and/or Lower Paleozoic age. Some dikes have spectacular dark aegirine, Na-amphibole, albite and/or K-feldspar fenitic rims. Some references mention the presence of probably Early Paleozoic gabbroids in the area, and there are Permian syn- and post-orogenic granite plutons.

Magnetite and hematite had been discovered in the area in 1927 and the first REE minerals identified in 1935, although the local fairy has it that the rare earths were discovered only after the Fe ores, smelted in the Baotou steel works in the 1960s or 1970s, resulted in a "funny steel" and this inspired mineralogists to investigate. Iron, rare earths, and niobium ore are now selectively mined from large open pits in the Main and East Orebodies. Nb is confined to the western portion of the ore zone and it resides in disseminated Nb-rutile and columbite in marble, associated with Fe ores. Chao et al. (1997) distinguished two principal bulk-mined mixed Fe-REE ore types, plus late-stage superimposed veins and metasomatites with often spectacular specimen minerals (170 mineral species have been identified, of this 18 new minerals described from here) but of limited economic importance. Supergene alteration is minor.

The principal ore type (1) is the banded ore, mined from both pits, that consists of stratabound lenses of very fine-grained and micro- to meso-scale laminated and banded magnetite and/or hematite near the top of the H8 dolomite, enveloped by (2) disseminated and stockwork ore. The orebodies are up to 1,200 m long, up to 400 m thick, and have been followed to a depth of 900 m and more. The ore grades and minerals are irregularly distributed and this requires selective mining. The banded REE-free units of magnetite-hematite iron ore, railed 100 km to Baotou blast furnaces, run 20 to 55% Fe (average 35%). They grade to Fe oxides mixed with disseminated monazite and bastnäsite, and to iron-free monazite and bastnäsite ore with or without fluorite gangue. The REE minerals in the bulk ore are mostly very fine-grained, "invisible". Bastnäsite and monazite in a coarser form occur in the late-stage breccias, stockworks or veins accompanied by aeschynite, huangheite (=Ba-REE-fluorocarbonate), aegirine, and the rarer minerals plus minor Fe, Zn, Pb sulfides. There is a generous selection of alteration assemblages. The hangingwall metapelites (partly shear phyllonites?) suffered multistage feldspathization: an earlier albite superseded by Ba-feldspars and microcline, together with biotite. The

footwall is intensely albitized and riebeckite, aegirine-altered.

The Bayan Obo host rocks and ore genesis remain controversial, to which the recent explosion of "isotopist" literature contributes a lion's share (read references in Chao et al., 1997). The first controversy is the origin of the host marble; the spectrum of opinions ranges from orthosedimentary ("platform carbonate"), through volcanic-sedimentary ("carbonatitic tuffite"), to carbonatized lithologies, to magmatic (meta)carbonatite. Chao et al. (1997) favored sedimentary marble overprinted by hydrothermal alteration/mineralization. The second controversy is as to whether the ores are synchronous with the host dolomite, or synchronous & remobilized, or entirely epigenetic (introduced). The mineralization is clearly multistage and polygenetic and there is a range of radiometric ages between 1.42 Ga and 220 Ma the meaning of which is fiercely debated by the isotopes/fluid inclusions specialists. Chao et al. (1997) suggested 430-420 Ma as the most likely time of the main mineralization stage. There is an overwhelming evidence for the "alkaline influence" throughout, but (not yet) a clear, visible, unequivocal genetic association with a major alkaline magmatic body. There is some similarity with Mountain Pass (read above) and with the small "Bastnäsite-type" Fe-REE orebodies in the Swedish Bergslagen (reviewed in Laznicka, 1993), but hardly with the "Fe oxide-Cu-Au-U" (Olympic Dam-type), the latest fad, as Cu, Au and U are virtually nonexistent here. Bayan Obo has clearly a unique combination of features. Careful recording of visual and microscopic facts would be the best contribution to its understanding.

Weathering-enriched carbonatite ores

Araxá Nb, REE, Th, U + barite, phosphates. Araxá in Minas Gerais, Brazil (Fig. 12.34), used to be the world's largest Nb deposit; now it ranks second (after Seis Lagos), yet it is still the world's #1 Nb producer (Grossi Sad and Torres, 1978; Wooley, 1987; P+Rv, residual ore, 462 mt @ 2.1% Nb, ~2.8% REE; Rc primary ore 936 mt @ 1.1% Nb; total contents about 19.9 mt Nb, 17.5 mt REE, 1.67 mt Th, 135 kt U). The Barreiro alkaline-ultramafic complex near Araxá is a Late Cretaceous (91 Ma) circular, 16 km², zoned intrusion emplaced into metaquartzite and biotite schist of the Paleoproterozoic (~1.8 Ga) Araxá Group. The early ultramafics had been brecciated, converted to phlogopite glimmerite with relics of olivine and diopside, and invaded/replaced by ferruginous dolomitic carbonatite veined by calcitic carbonatite.

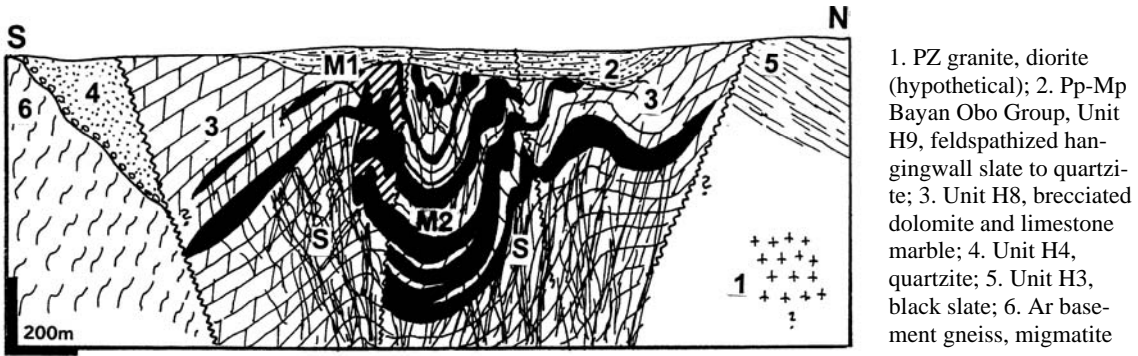


Figure 12.33. Bayan Obo Fe, REE, Nb ore field, Nei Mongol, China. Diagrammatic cross-section from LITHOTHEQUE No. 2118, modified after Chen Guoda (1982), Tu Guangzhi (1984), Chao et al. (1989) and Drew et al. (1989). Explanations (continued): M1. High-grade REE orebodies of disseminated replacive monazite, bastnäsite in fluorite and hematite gangue; M2. Massive to densely disseminated replacive hematite and magnetite in H8 dolomite; S. Carbonate veining, stockworks, breccia cement mostly in the footwall

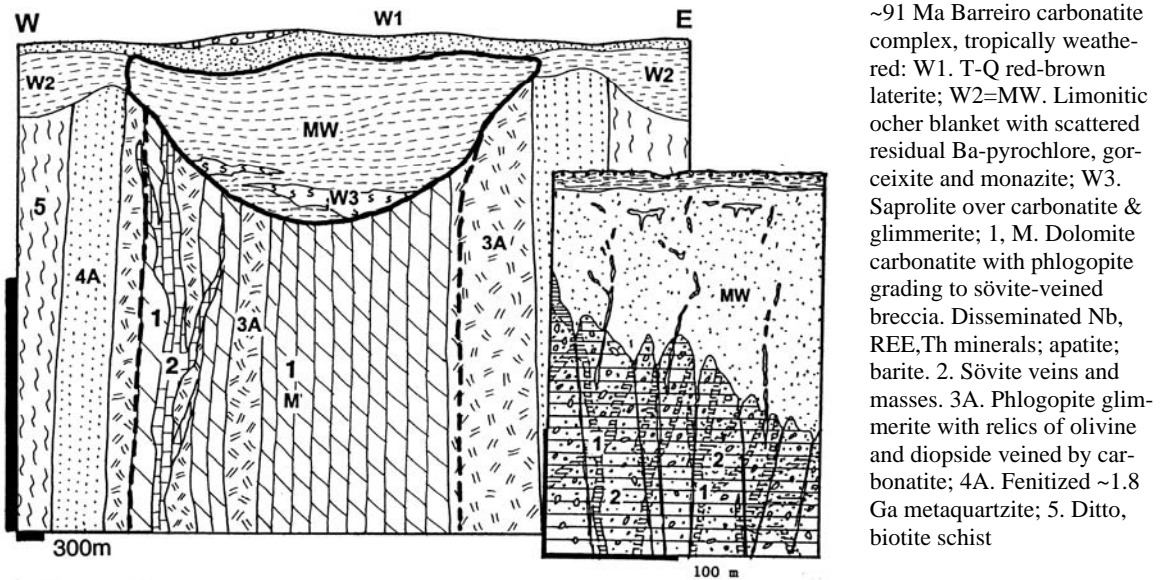


Figure 12.34. Araxá Nb, REE, Th deposit in regolith over carbonatite; cross-section from LITHOTHEQUE No. 1194, based on data in Barcellos (1986); Betz, oral communication during site visit in 1980.

The intrusion is bordered by a narrow ring of incipient fenite, fracture veined by arfvedsonite, aegirine, calcite, microcline, apatite and quartz. The complex is deeply weathered, and a portion of the fresh carbonatite reached by drilling is a breccia of partly digested glimmerite permeated and cemented by carbonatite. This contains disseminated magnetite, bariopyrochlore, monazite and other Nb, Ti, REE, Th, U minerals together with apatite. This constitutes a substantial ore resource, so far untouched by mining.

The carbonatite and glimmerite are capped by a 150-230 m thick humid tropical regolith that rests on karsted carbonatite in depth. At the surface is a thin layer of red-brown lateritic soil with local relics of transported ferricrete and silcrete. This is removed as overburden during open pit mining. Beneath, in a depth of several meters, is the relatively uniform thick blanket of light-brown limonitic ocher, the in-situ ferruginous residue (saprolite) remaining after complete dissolution and removal of the Ca and Mg carbonate component. This contains scattered relic blocks of barite

grading, with increasing depth, into barite fracture veins. The typical composition of the ocher is 35% goethite, 20% barite, 16% magnetite, the rest being fine-grained ("invisible") partly oxidized bariopyrochlore, monazite, gorceixite, relic apatite with crandallite and other minerals. This is the principal ore mined in the open pit, and site of the 462 mt reserve of Nb ore. The average, cheap to mine (no blasting!) ore grades between 2.5 and 3% Nb₂O₅, 4.0% REE₂O₃, 30-40% Fe, 10-20% barite, with high Th and moderate U values. (W. Betz, oral communication, 1980). A resource of 375 mt @ 14.5% P₂O₅, formed over apatite-magnetite rocks similar to foskorite, is saprolitic clay with a high content of secondary carbonate apatite, mined in the NW and SE parts of the complex. A small body of exceptionally REE-rich residue (800 kt @ 13% REE₂O₃) is in the NE sector of the complex and it contains finely dispersed monazite and goyazite.

(Morro dos) Seis Lagos-Nb,REE; Amazonas, Brazil (Issler, 1978; de Souza, 1996; Rc 2.9 bt @ 2.0% Nb, 1.5% REE for 57 mt Nb and 43.5 mt REE). This is the world's largest Nb accumulation, and a "super-giant", located in the Amazon forest 850 km NW of Manaus. The mineralization is partly exposed in three low hills that rise from the Rio Negro plain and was discovered by airborne radiometry with ground follow-up. The hills correspond to three circular alkaline-carbonatite intrusions of Mesozoic age, emplaced into Mesoproterozoic hornblende and biotite gneiss basement. The carbonatite includes calcitic and sideritic varieties with disseminated pyrochlore and monazite, whereas pyroxenite contributes ilmenite, zircon, titanite and rutile. There is an up to 230 m thick, Late Tertiary to recent lateritic weathering profile, of which the 110 to 155 m thick limonitic saprolite constitutes the ore. The ore is dominated by Fe and minor Mn hydroxides and oxides with disseminated fine grained Nb-rutile, Nb-brookite, cerianite, and relics of monazite and pyrochlore that increase with depth.

Tomtor complex, Siberia-Nb, REE, Y, Sc, V, U (Epstein et al., 1994; Kravchenko and Pokrovsky, 1995; Kravchenko et al., 1996). Tomtor alkaline-ultramafic massif is a 350 km² composite intrusion emplaced into Meso- to Neoproterozoic sedimentary cover of the Siberian Platform, east of the Archean Anabar Shield. The location is extremely inaccessible and much of the intrusion is covered by Permian coal association, Jurassic marine clastics, and Cenozoic alluvium that complicate field study. The first striking feature is

the protracted history of magmatic emplacement. Entin et al. quoted in Kravchenko and Pokrovsky (1995) distinguished 13 magmatic pulses that span the period of 560 million years, from ~800 Ma to 240 Ma. The 2-6 km thick outer ring is composed predominantly of nepheline syenite varieties, separated by a 1-3 km wide jacupirangite-ijolite ring from the central 12 km² carbonatite core, dated between 660-510 Ma. The carbonatite is overlain by downfaulted blocks of intensely altered nepheline, Na-pyroxene, olivine, apatite, magnetite, K-feldspar rocks that Kravchenko and Pokrovsky (1995) tentatively interpret as paleovolcanics, but that can equally well be alkaline metasomatites in fenitized roof exocontact. The complex, and especially the carbonatite core, are intruded by a great variety of overlapping plugs and dikes of picrite, alnöite, nepheline syenite, melilite rocks, phoscorite, and apatite, magnetite and monticellite rocks. These grade into a variety of metasomatites, especially carbonatized rocks and metasomatic carbonatites. The carbonatite core itself comprises an unmineralized calcite-dolomite perimeter with a youngest core of Nb, REE, Zr and U bearing calcite, dolomite and ankerite carbonatites and metasomatites.

Kravchenko, in his many papers and notes, suggests that this might be the world's largest and richest Nb,Y and Sc deposit that contains "several hundred million tons of ore", but more specific tonnage figures are not supplied although some published ore grades are now available. The ores are buried under Meso-Cenozoic sedimentary rocks of the Siberian Platform that unconformably blankets erosional remnants of the Permian coal-bearing succession. There are three successively deeper mineralized zones that change from the uppermost resedimented horizon through the intermediate in-situ mineralized regolith to hypogene ores in magmatic-hydrothermal metasomatites, and ultimately into disseminated magmatic minerals in carbonatites and pyroxenites. The grade decreases with depth.

The Upper Ore Horizon, 3 to 25 m thick, contains locally extremely rich ores. It is immediately below the Middle Permian sandstone and conglomerate; the conglomerate contains accessory pyrochlore clasts. The subhorizontal orebodies, although faulted, are tabular, bedded or have the form of blankets in siltstone-fine sandstone association interpreted as lacustrine or paludal. The thinly banded ore consists of alternating "light" and "dark" mineral bands or laminae. The light bands consist of fine-grained monazite, rhabdophane and scattered pyrochlore grains in matrix of florencite.

The dark layers have pyrite, anatase, rutile, ilmenorutile. The bedded ore, interpreted as lacustrine paleoplacer, change facies into conglomerate and talus breccia deposits formed on paleoslope. These fragmentals are mineralized by alumophosphates (florencite, minor gorceixite or goyazite) with pyrochlore bands. The Upper Horizon ores range from porous to compacted and have been affected by several phases of hydrothermal and groundwater (diagenetic) alteration. The mean grade of the rich ores, quoted by Kravchenko, is 13.8% REE, 5.4% Nb, 0.8% Y, 0.04% Sc plus 0.61-0.68% V and up to 0.61% U.

The Lower Ore Horizon is composite, up to 50 m thick (as much as 300 m in sinkholes) and most likely a paleoregolith that incorporates the lowermost saprock of previously metasomatized alkaline rocks, in-situ sapolite, and local proximally reworked weathered material on top. It is complicated by post-depositional faulting, syn-depositional collapse and slumping into paleokarst, and several stages of hydrothermal and diagenetic metasomatism. The main minerals there are authigenic francolite and siderite that infill and partly replace metasomatized saprock remnants, that carry their own complement of relic ore minerals. Of the long list of ore minerals, pyrochlore and columbite are of the greatest economic interest. Average contents of the potentially economic metals in this horizon, listed in Kravchenko and Pokrovsky (1995), are about 1.2% REE, 0.44% Nb, 248 ppm Th and 89 ppm Sc. These are overall metal contents rather than ore grades, as economic orebodies have not yet been defined and there the grades would be much higher.

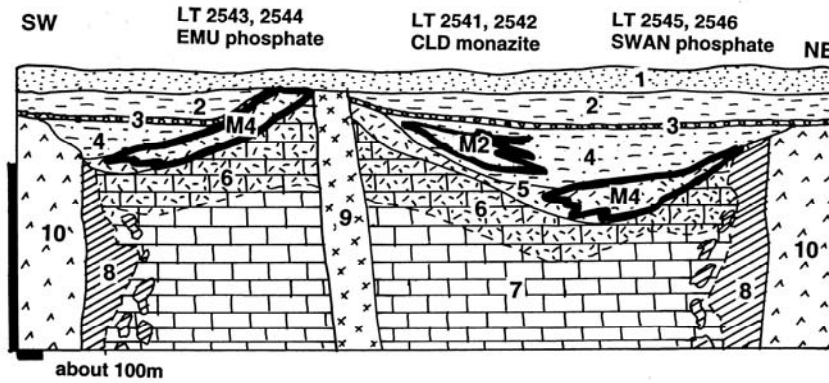
The "primary" mineralization in Tomtor consists of a number of minerals disseminated in carbonatite, in the various metasomatites, and in later stage dikes. It is poorly known and probably

marginal as an ore resource, although it contains all the metals enriched in the two "secondary" horizons above but in much lower concentrations. The orebodies comprise the "standard" disseminated pyrochlore, especially in the central ankerite carbonatite, accompanied by apatite, magnetite and richterite. Apatite-rich intervals (e.g. phoscorite), phlogopitic glimmerite, and other types of potentially economic materials have not yet been outlined.

Additional carbonatite-related significant deposits:

There is a number of important accumulations of REE, Nb and Ti in carbonatites, but none is a "geochemical giant". The 2.064 (or 2.021?) Ga **Mount Weld** near Laverton in Western Australia (Duncan and Willett, 1990; Fig.12.35) has a deep regolith with the usual mixture of residual clays enriched in apatite, REE (1.47 mt), Nb, Y, Ta (40,426 t), unusual for carbonatite, is the most valuable component (Rc 145 mt @ 0.034% Ta₂O₅). The poorly known **Phong Tho** ore field in Vietnam has three deposits of bastnäsite, credited with 7.97 mt of contained REE (Minerals Yearbook, 1996). The first mined Nb carbonatite in Oka near Montreal probably stored some 735 kt Nb before mining, whereas the reserve at Mabounie, Gabon, is conservatively estimated at some 378 kt Nb.

There are more titania deposits in residual clays over both carbonatite and pyroxenite (Tapira-style), produced by decomposition of perowskite. The Salitre and Serra Negra deposits near Patrocinio, Minas Gerais, Brazil (Richardson and Birkett, 1996) are jointly credited with a resource of 88.3 Mt Ti (grades around 16% Ti). The Serra de Maicuru deposit in Pará, Brazil, has 450 mt of ore @ 11.4% Ti for 51.3 mt Ti content, in anatase after perowskite.



1. OI-Q alluvium; 2. Cr3-Eo lacustrine clay; 3. Post-Pe relics of ferruginous laterite; 4: Regolith over carbonatite, subzones, 4a. Crandallite-goyazite; 4b+M1. Limonite, local pyrochlore (Nb); 4c+M2. Crandallite & monazite (REE, Y); 4d+M3. Crandallite, local Nb,Ta,Y,U, REE. 5+M4. Karst with apatite ore;

Figure 12.35. Mount Weld phosphate, REE, Nb, Ta, Y, Th, U deposit in regolith on carbonatite, Western Australia. Cross-section from LITHOTHEQUE No. 2541, modified after Jockel (2002), site visit. Explanations (continued): 7+M5. ~2,021 Ma subvertical cylindrical body of carbonatite and breccia with irregularly distributed apatite, pyrochlore and other rare metals minerals; 8. Fenite (mainly phlogopite); 9. Pp diabase dike; 10. Ar greenstones, mostly metabasalt.

13 Sedimentary Associations and Regolith

13.1. Introduction

Sediments and sedimentary rocks as hosts to giant metallic deposits have already been invoked in several earlier chapters like oceanic sediments (Chapter 4); sediments in island arcs and andean margins (Chapters 5 and 6, respectively), sedimentary rocks in the eugeoclinal orogens (Chapter 8) and in early Precambrian greenstone belts (Chapter 9), in Proterozoic intracratonic orogens (Chapter 11) and in rift settings (Chapter 12). In all these chapters the sediments or sedimentary rocks, and processes that formed them, have been treated as second-order divisions, subordinated to the first-order categories based on geotectonic and lithotectonic premises.

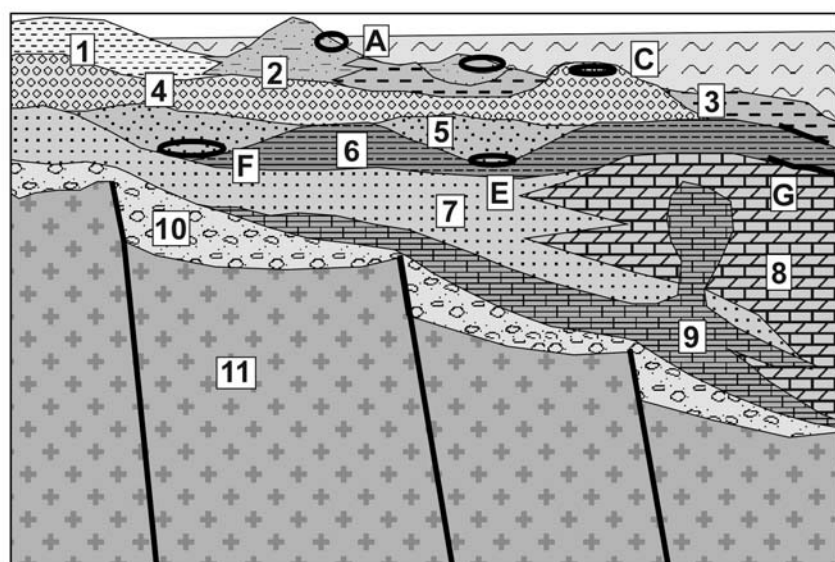
In this Chapter only sediments (with few exceptions where a volcanic component is present), sedimentary rocks, products of weathering, and their depositional environments are treated. The bulk has formed along stable (Atlantic-type) continental margins, in epeiric seas, in intracontinental basins or as regoliths. The predominantly Phanerozoic and some late Precambrian sedimentary rocks are now members of the platformic sequences and miogeoclinal orogens. Figures 13.1-13.3. give a preview of the characteristic sites of metallic deposits in the "stable" depositional settings of the young Atlantic-type continental margins (Fig. 13.1), in the "deep basin" division of miogeoclinal orogens near the transition to "eugeoclines" (Fig. 13.2), and in complex platformal sequences (Fig. 13.3).

Most of the metallic ores these environments generate or host are products of "intrabasinal" processes that contrast with the predominantly hydrothermal epigenetic deposits which, even if hosted by sedimentary rocks, resulted from metal supplies and/or process driving energies that came from outside the "basin", mostly from igneous intrusions or deep seated (metamorphogenic) geothermal heat and were controlled by structures. The latter deposits are considered in the earlier chapters. This does not imply that all metal accumulations in sediments are necessarily synsedimentary or diagenetic. Epigenetic, post-lithification deposits occur in abundance here, but they are attributed to "basinal fluids" or meteoric, ground waters closely related to the basin evolution.

Of course there are transitions to the extrabasinally sourced ores, and in some cases we simply do not know.

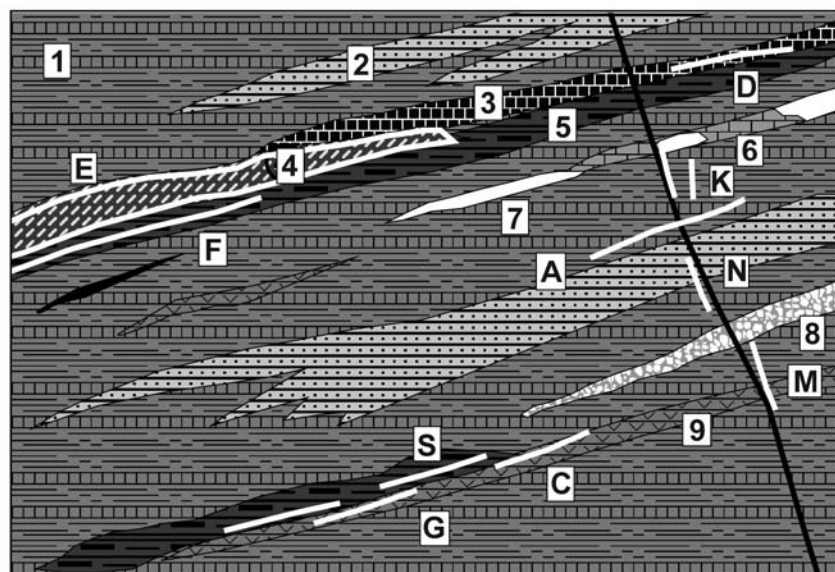
At least 80% of sedimentogenic and stratigraphic information in the literature (e.g. Einsele, 1992; Reading, ed, 1986) apply to the ore-hosting environments and rock associations considered below. Specialized sedimentologic literature, and its applied version, basin analysis, dominated by the needs of petroleum geology, concentrate on the most common and "typical" processes, environments and the "normal" sedimentary rocks. 99% of such rocks, however, are devoid of metallic ores. The remaining 1% is treated in sedimentology texts as a "special facies" (e.g. sedimentary ironstones), (late) diagenetic effects (e.g. the MVT deposits), or is not considered at all. Situations in which, for example, some epigenetic deposits (included in the preceding chapters), superimposed on sedimentary rocks, are also partly controlled by the sedimentary lithology (e.g. replacement Zn-Pb sulfide "mantos" that require carbonate hosts) are rarely noted. Although sedimentologic literature provides basis for an explorationist searching for ores in sediments, much of the specialist detail there is not essential (or has a local application only) or is too ambiguous as a tool of ore finding, so it is not considered here. The sections below are selective, biased towards settings and processes that contain or generated giant "ores in sediments" (e.g. Amstutz and Bernard, eds., 1973) or strata-related ores (e.g. Wolf, ed., 1976-1985). More detail about the lesser deposits is scattered in the literature and in textbooks on both sedimentology and economic geology (compare Laznicka, 1985, 1993).

The organization of sections in this Chapter is based on combined lithology and depositional environment as the first order of division (Marine Clastics, Marine Carbonates and Evaporites; Regoliths and Paleoregoliths, Continental Sediments). The second order of division is based on the selection of accumulated ore metals and/or ore deposit types. Most ores and their settings, however, can be organized from a variety of premises so similar ore deposits can appear under different headings scattered in several chapters in this book. The only way of how to prevent the reader from becoming lost is through cross-referencing in the text and intelligent indexing.



1. Coastal, partly subaerial sediments of marsh, tidal flat, lagoon; 2. Quartz sand of barrier islands, bottom sands; 3. Sea floor mud; 4. Relic sand, gravel, till; 5. Relic buried alluvial channels; 6. Marine shale on shelf; 7. Marine deltaic to shelf sandstone; 8. Shelf carbonates; 9. Evaporites; 10. Coarse continental sediments of the rift stage; 11. Continental crust basement; A. Fe, Ti, Zr, REE in heavy minerals sand; C. Au winnowed from relic till or outwash on shelf; F. Ditto, cassiterite; G. U in sea floor phosphorite

Figure 13.1. Usual association of sediments and sedimentary rocks along the non-volcanic Atlantic-type continental margins and sites of the common metallic deposits. Ore types A and F have known "giant" members. From Laznicka (2004), Total Metallogeny Site G148

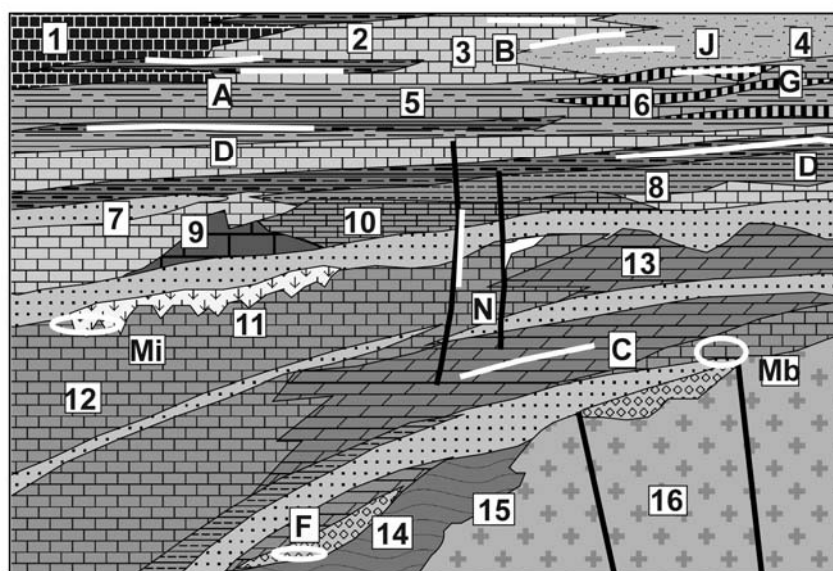


1. Thick argillite and chert sequence; 2. Quartzite; 3. Ribbon chert; 4. Phosphorite; 5. Black shale; 6. Basinal limestone; 7. Bedded barite; 8. Debris flow; 9. Pillow basalt (spilite), hyaloclastite, diabase sill; A. Bedded siderite, ankerite; B. Bedded Mn carbonate, silicates; C. Besshi- or Cyprus-type VMS; D. Bedded barite; E. "Basinal" phosphorite & U, V, Mo etc.; F. Metalliferous black shale; G. Zn, Pb, Ag sedex; K. Siderite veins, replacements & Cu, Hg, Sb; L. Crystalline magnesite;

Figure 13.2. "Basinal" sequences of the miogeoclinal domain in orogenic belts, inventory of the usual rocks and ore deposits. From Laznicka (2004), Total Metallogeny Site 139. Ore types D, E, G, K, N have known "giant" members. Explanations (continued): M. Chalcopyrite in siderite, quartz veins and replacements; N. Stibnite veins; S. W (Sb), scheelite or ferberite, stibnite veins and replacements

Rock associations treated here range from "recent" (Holocene to late Tertiary, i.e. late Cenozoic) to approximately Neoproterozoic; older equivalents appear in Chapters 9 and 11. The rocks also range

from unconsolidated (e.g. clay, mud) through consolidated (mudstone, shale) to slightly or moderately metamorphosed (slate, phyllite, some schists).



1. Chert; 2. Black shale & phosphorite; 3. Carbonates; 4. Redbeds; 5. Marine/palaeozoic cyclothem; 6. Coal seams; 7. Marine sandstone; 8. Marine shale; 9. Carbonate reef, bioherm; 10. Evaporites; 11. Karst under unconformity; 12. Limestone; 13. Dolomite; 14. Basal conglomerate; 15. Basement schist; 16. Basement granitoids; A. "Upwelling" phosphorite with V,U,etc.; B. Warm water phosphorite with U; C. Bedded & nodular barite; D. U,V,Mo,Zn dispersed in black shale; F. Au paleoplacers in basal sequences;

Figure 13.3. Inventory of rocks and ores present in complex sequences of stable platforms (e.g. North American interior); cross-section from Laznicka (2004), Total Metallogeny Site G149. Explanations (continued): G. Coal enriched in Ga,Ge,U,Sc, etc.; J. Cu shale or sandstone in redbeds or at redox interfaces; Mi. Intraformational MVT (Mississippi Valley-type) Zn,Pb; Mb. Ditto, near basement unconformity; N. Fluorite, barite (Pb,Zn) breccia and fracture veins; Not shown: V. U in residual and resedimented phosphorite; W. Residual barite; X. Fluorite residual over N

High-grade metamorphosed equivalents are in Chapter 14. The rock associations here are predominantly nonvolcanic, although 10-20% of volcanics or syndepositional intrusions (e.g. basalt sills emplaced into wet sediments) could be present in some transitional associations. Postdepositional intrusions as well as faults and hydrothermal systems are treated as extraneous interactors: briefly mentioned here, then referred for more detail into one of the earlier chapters.

13.2. Marine clastics

Marine clastics have been deposited in a variety of environments within the slope-shelf-coast continental margin, and epicontinental sea basin-shelf-coast, progressions of environments and facies (Reineck and Singh, 1980; Scholle et al, eds., 1982; Galloway and Hobday, 1983; Reading, ed., 1986; Einsele, 1992). The sediments then passed gradually through several stages of diagenesis to become lithified sedimentary rocks. This took place under the floor of marine basins or, alternatively, in a subaerially exposed sediment pile. Afterwards, the completed sedimentary rocks remained buried under an increasing load of new sediment being continuously added at the top to eventually undergo

static load metamorphism. Sedimentary sequences of this type are preserved in platforms and in some intracratonic basins, but few are thick enough to change into substantially metamorphosed equivalents in depth. Platformic sequences cover large areas in stable cratonic interiors, are almost flat-lying or gently inclined, and virtually undeformed. Their stratigraphy is quite predictable except for hiati and, above the basal interval typically resting on crystalline basement, they comprise several upward fining sequences of mature clastics alternating with carbonates. This is the playground of the sequence stratigrapher. Syn-sedimentary volcanics are exceptional in the "normal" platformic sequences, although they increase with the proximity to the regions of extension (rifting; Chapter 12). Almost all extensive platform sequences are pierced by scattered anorogenic volcano-plutonic complexes or intrusions alone, diked by diabase, and locally covered by flood basalts. In addition to the usual alternating sag basins and swells, fault-bounded extensional grabens are present on platforms, evolving with increasing intensity into failed rifts (aulacogenes) and active rifts that eventually result in continental breakup and ocean spreading (Chapter 12).

Most of the relatively monotonous and predictable shelf-slope sediments at stable (Atlantic-type) continental margins (Heezen, 1974; Fig. 13.1) rest on and bury earlier rift sequences, and partly prograde over the oceanic crust. The rift sequences (Chapter 12), volcanic or nonvolcanic, are very variable and rapidly change facies. Once buried, they need not influence much the continuing sedimentation at sea floor, but they influence the post-depositional processes within the sedimentary pile both structurally and materially. Deep formational fluids of high salinity originate in the rift-stage evaporites, and fluids interacting with mafic volcanics can leach out and transport trace elements like copper. Thick syn-rift evaporites, especially halite-rich sequences, furthermore, produce salt diapirs that pierce and dam shelf sediments and actively influence sedimentation. They are particularly common along the Atlantic margins of North America and Africa (Emery and Uchupi, 1984; Schlee, 1980).

A variety of environments in rapidly subsiding systems and basins as along and over the buried rifted continental margins, in forelands to orogenic fronts, in the shelf-slope progressions of all sorts, accumulate thick prisms of sediments most of which are eventually deformed and incorporated into orogenic belts (Mitchell and Reading, 1986). There, they constitute the non-volcanic miogeoclinal domain (or mega-facies).

13.2.1. Ore formation

The bulk of passive margin clastics have terrigenous (land-derived), epiclastic provenance and they are brought into the basin by streams, wave erosion, wind or ice transport (Reading, ed., 1986; Walker, ed., 1984; Allen and Allen, 1980). Most of the source rocks from which the clasts are derived are on land and are chemically weathered in the regolith, so only the resistate minerals and rocks (mainly quartz, micas, chert and hydrated clay minerals as mud) enter the sedimentary basin to provide clasts and matrix. Lesser proportion of clasts comes from essentially unweathered mechanically abraded source rocks as in glacial sediments (till), some desert sediments, and as clasts derived by submarine erosion. Resedimented clastics like turbidites are another category. Volcanic clasts are rare and mostly derived from airborne ash or from floating pumice that can travel thousands of kilometers from source, or occasionally from the rift-stage volcanics. Most volcanic fragments in platformic and miogeoclinal sediments are epiclastic, removed by erosion from

older volcanics exposed on land. Finally, there are intrabasally generated carbonate or silica bioclasts and dispersed cosmic dust and micrometeorites.

Depending on sediment maturity and distance from source, the coarsest and most heterogeneous, immature clastic assemblages are in the basal units of sedimentary sequences above basement unconformities (nonconformities), particularly in fault-bounded basins with steep gradients. Much of these sediments are non-marine and, in most cases, members of the rift sequences. Farther from source the clast size decreases (except for a variety of intrabasinal and gravity-driven materials like olistostromes, "wildflysch" blocks, and rafted pebbles), and the clast composition becomes more uniform. Most pelites have an undecipherable particles provenance, further obscured by authigenesis. Resedimented materials like coarse turbidites go half way. Diagenesis (Larsen and Chillingar, 1979; McDonald and Surdam, eds., 1984; Mumpton, ed., 1986), with its many stages, starts immediately after clast deposition. A portion of matrix forms (e.g. by breakdown of unstable silicates and silicate rocks) and the gradual process of cementation starts. Chemical sediments like evaporites are "just cement".

In a model sedimentogenesis, sea water provides the medium of detritus transport, and as entrapped formational (connate) fluid it becomes the principal agent of diagenesis, long after burial. This fluid evolves by reaction with sediments, especially with its soluble components (e.g. halite) and it circulates, even in lithified sequences, utilizing porous and permeable units and structures. Much of our understanding of deep fluid movements is a by-product of petroleum studies. In shallow aquifers connate fluids mix with or are substituted by meteoric waters.

In special situations, extraneous heated fluids (brines) become a part of sedimentogenesis and this can happen during all stages: during clastic sedimentation, early diagenesis when the sediments are still wet and unconsolidated, or after lithification. The fluids have a range of temperatures (zero to about 300°C; temperatures between about 100-140° are most common with the MVT deposits-forming systems), derivations and controls. Most are connate fluids heated by geothermal heat, others are sea, connate or meteoric waters heated by intrusions (e.g. basalt sills emplaced into wet sediments), some of which may have a small magmatic (juvenile) component. The fluids move along porosity and permeability channels and are most prominent along fault zones. Mineral and metal fluxes, some of which result in

ore formation that includes several "giants", take place in a variety of settings and during all stages of sedimentogenesis (Maynard, 1983; Gregor et al., 1988).

Clastic ores: Genetically least controversial are physical accumulations of resistate heavy minerals derived from the basement, or reworked and usually enriched from an earlier generation of mineralized sediments (e.g. conglomerates); Miall (1978). The "heavy heavy" minerals (gold, platinoids, cassiterite) concentrate predominantly in alluvial placers. They are preserved in the marine realm either in their original setting of stream channels found buried under younger marine sediments in the offshore, or the minerals are brought by streams onto the beach environment and enriched there by wave action. Buried stream channels with economic cassiterite deposits are well developed in the offshore of NE Siberia (Patyk-Kara, 1999), Malaya, and Bangka Island that include several "giants" (e.g. Kuala Langat, 300 kt Sn; Batchelor, 1979). Gold placers, both in buried alluvial channels, in beach gravels and also as lag deposits on the shelf are quite rare and small; only in the Nome goldfield in western Alaska the marine placers, mostly in raised beaches, account for greater share of the 170 t Au produced (Nelson and Hopkins, 1972). The "heavy heavies" do not travel far from source and in Alaska, northern Siberia, Westland Province of New Zealand and elsewhere the gold in beach placers has been partly reworked from glacial till that swept large areas mineralized by bedrock gold (Boyle, 1979; Craw et al., 1999). Because of the hydraulic factor, "heavy heavies" occur in gravels (or conglomerates) rather than sands.

The "light heavies" (ilmenite, rutile, zircon, monazite) are widespread in beach placers (heavy minerals sands) but rather rare in alluvial systems. Derived primarily from tropically weathered metamorphic, plutonic and volcanic rocks they form extensive tracts along active as well as fossil (raised) beaches and adjacent coastal dunes, often traceable for hundreds of kilometers. Because Fe, Ti, Zr and REE are geochemically abundant metals, there are few truly "giant" accumulations (read below).

Some other ore minerals form clastic accumulations. The magnetite beach sands from Taranaki and Auckland Provinces, New Zealand, are mentioned in Chapter 5. A small beach deposit composed of well sorted hematite granules winnowed from lateritic profile near Monéo, New Caledonia, is briefly described in Laznicka (1985, p.100-103). Although economically insignificant, it

provides a very convincing model of possible formation of some Phanerozoic "oolitic" ironstones (read below).

Extrabasinal, transported metalliferous mud or colloids: Mud- or clay-size particles of Fe and Mn oxides and hydroxides derived by erosion and denudation of lateritic ferricrete or earlier enriched iron ores (e.g. BIF; Chapter 11) are carried in suspension to eventually settle on the sea floor. There, they are diagenetically modified and cemented by the intrabasinally formed authigenic minerals into bedded deposits (Maynard, 1983).

Extrabasinally derived trace metals brought in solution, precipitated in reducing or sulfidizing syndiagenetic microenvironments: Metals like Mn, Cu, Zn, Pb, Sb, Mo, Ni, V, U, As, Hg, Ag and Au are released by weathering on land and brought into the marine environment in solution. From there they gradually and selectively accumulate in carbonaceous, pyritic or phosphoritic sediments, especially in the anaerobic, euxinic environment. Some "black shales", extremely enriched in selected trace metals, came close to becoming ores in their own way (e.g. the Swedish "Alum Shale", a "giant" U deposit; read below); others (e.g. the Chattanooga Shale) are potential "ores of the future". Still other enriched carbonaceous rocks provide fertile ground for generation of the next generation of deposits by metals remobilization. In an opposite way, Mn dissolved in seawater accumulated in oxidizing environments around euxinic basins (Force and Cannon, 1988) to produce "giant" deposits as in the Ukraine (read below). In a variation on this theme, that probably formed the Kupferschiefer Cu "super-giant" (read below), oxidizing groundwaters with Cu in solution ascended from a "red bed" aquifer and precipitated the metal as they encountered the redox interface of a pyritic carbonaceous shale.

Authigenic (syndiagenetic) granules, oolites, intraclasts, crusts: Oceanic Fe-Mn nodules are the best understood granule to pebble-size particles that form by hydrogenous precipitation of metallic minerals on the sea floor, or in the upper layers of wet sediment (Chapter 4). Subaqueous phosphorite (Baturin, 1982) and barite nodules, crusts and pavements and oceanic Mn-Co metalliferous crusts are other examples of authigenic materials precipitated in-situ. Such particles or crusts either remain in place or they are reworked to form granular deposits. About the best known ore type composed of ore particles presumably constituted within the basin (but read above), then redeposited

into a bedded microconglomerate, are the so called oolitic (better term is "particulate") ironstones (read below) and also some bedded Mn deposits. The origin of hematite, chamosite, goethite or siderite "ooliths" is controversial because of the lack of a clear recent examples (but compare Kimberley, 1979); however, the frequent nuclei of fossil fragments in "ooliths", enveloped by precipitated ore minerals, suggest intrabasinal formation (Maynard, 1983).

"Exhalitic" syndimentary ore precipitates: Heated metalliferous "basinal fluids" entering sedimentary basin from below, along growth faults or breccia zones (or flowing downslope from the site of discharge), precipitated bedded "ore sediment" (of barite, pyrite, Zn-Pb sulfides, rarely Cu, Ni) either directly, or by replacing/mixing with existing sediment (read about "sedex" deposits, with numerous "giants", below).

Post-lithification (epigenetic) hydrothermal replacements and porosity, dilation fillings: This is a variation on the "sedex" theme, sometimes indistinguishable from it. The sedimentary pile may have provided a "favourable" bed/unit (e.g. carbonate, anhydrite or gypsum) selectively replaced or impregnated by ore precipitated from extraneous hydrothermal fluids. Important deposits are described in preceding chapters.

Post-lithification impregnation, fracture filling and cement replacement by descending meteoric fluids: Porous sandstones host impregnation deposits of U(V), Cu, Pb-Zn and some other metals, of which the "sandstone-U" deposits have been extensively studied (Galloway and Hobday, 1983; read below). The "story" assumes hexavalent U in meteoric water solution, derived by leaching of felsic volcanic glass or leucogranites, to migrate down until it encounters a reductant to precipitate as U_3O_8 (pitchblende) or coffinite. Cu in "Cu sandstones" probably behaves in a similar manner, whereas Pb(Zn) in "Pb sandstone" precipitate more likely from low-temperature basinal fluids, the same that precipitate the MVT deposits in carbonates (Maynard, 1983; read below). Several U, Cu and Pb "giants" fit into this category.

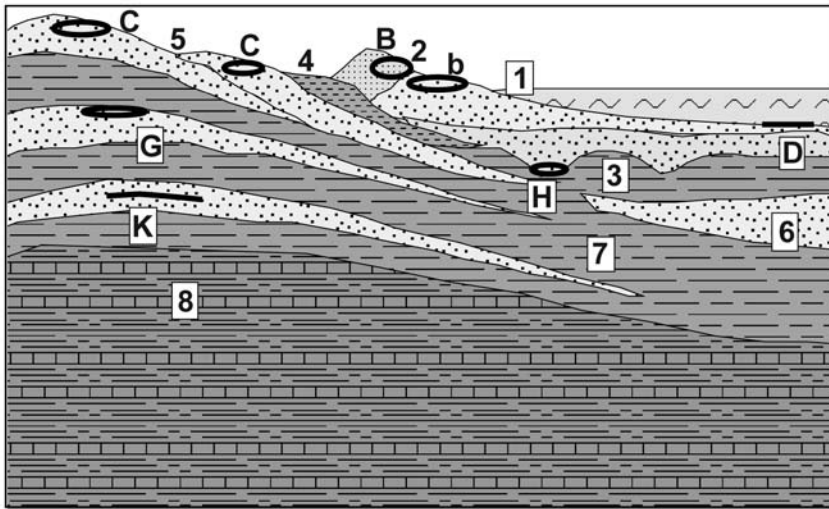
Supergene processes: Supergene processes, both under humid and arid conditions, generated significant residual deposits of some metals and also released ore mineral clasts and metals in solution to enter sedimentary basins and accumulate to form ore deposits. Supergene superimposed on

already existing sedimentary deposits can produce numerous changes, ranging from enrichment to impoverishment of the metal content. Lateritic bauxites formed on kaolinitic clays, shales or limestones are the best example not only of a total Al enrichment, but also of mineralogical conversion of a costly to smelt alumosilicates to Al hydroxides.

13.2.2. Detrital (clastic) ores: coastal and shelf heavy mineral sands and paleoplacers of Fe, Ti, Zr, REE, Th

Placer accumulations of the "heavy heavy" minerals like gold and cassiterite have been described together with their bedrock sources in Chapters 7-10 and will not be repeated here. The present emphasis is on the "light heavy" minerals like ilmenite and leucoxene (partly magnetite), rutile, zircon and monazite and associated industrial minerals like garnet and staurolite. These are derived from deeply weathered common rocks within a broad source area (rather than from primary orebodies, hence they are not linked to a specific ore source), have specific gravity around or under 5, and accumulate in mature sands rather than in gravels. The source rocks could be either "primary" (first generation; i.e. metamorphics, granitoids, volcanics) or "secondary" (earlier sands or sandstones containing the heavy minerals in lower concentrations). Although alluvial deposits of the same minerals are known, they are smaller and not considered in this book.

The heavy minerals are all unaltered resistates (except for ilmenite that is often converted to leucoxene), released by deep chemical weathering from parent rocks in the hinterland, then carried by streams and runoff to the coast where they are sorted by waves. The minerals are all very fine grained and collectively (due to dominant ilmenite) "black". Black streaks of heavy minerals can be seen on many beaches composed of mature quartz sand, but not all beaches contain sufficient quantities of heavies to qualify as mineral deposits, not considering the non-geological constraints (read below). The "classical" heavy mineral deposits formed (and still form) during transgressions, on moderate-high energy wave-dominated coasts, on active beaches adjacent to land or forming barriers to coastal lagoons. The favorable sites of accumulation are berm crests and the back beach, with portions of adjacent coastal dunes (Fig. 13.4). Roy (1999) went into a greater detail and distinguished three types of heavy mineral placers along the Pacific coast of Australia.



1. Modern beach quartz sand, b=backshore; 2. Modern sand dune, fine quartz sand; 3. Buried beach with alluvial channels; 4. Lagoon filled by organics-rich mud, silt; 5. Raised quartz sand beaches; 6. Sand bodies, shelf facies; 7. Shelf mud, mudstone, clay; 8. Undifferentiated shelf sediments. Heavy Fe,Ti, Zr,REE mineral sands setting: A. Recent beach; B. Dune sand; C. Raised fossil beach tracts (paleostrands); D. Ditto, in submerged relic beach sand;

Figure 13.4. High- to moderate energy (beach-dune dominated) young coastal environments and rock associations, rock/ore inventory diagram from Laznicka (2004), Total Metallogeny Site G173. Explanations (continued): G. Heavy minerals in buried beach sands; H. Ditto, in buried alluvial channels; K. Ditto, heavy minerals are now in a lithified sandstone. Each setting can accumulate "world class" equivalents and usually more than one setting contributes to an aggregate ore tonnage figure. Detrital Au, Sn, diamonds may also be present

It was (and locally still is) easy to mine heavy minerals from active beaches by primitive techniques, especially the very rich ones (up to 70% heavies) that tend to replenish after storm (this suggest additional heavy mineral resource in the offshore). Such mining took place near Jacksonville in Florida, along the coast of Kerala (SW India), near Pulmoddai in NE Sri Lanka. Exhaustion of active beaches, and even more environmental objections, led the miners to concentrate on alternative sources of heavy mineral sands: 1) fossil strand lines inland and associated parallel dune tracts that are mined by techniques common with alluvial mining (McDonald, 1985; Fig. 13.5); and 2) offshore resources. Although the rich (visibly "black") heavy mineral sands are highly valued, the ore grade alone is no longer the most important consideration as modern technology can cheaply recover the heavy minerals concentrate from "ore" that does not require crushing, by gravity (often accomplished on floating dredge-factories). This is followed by magnetic or electrostatic minerals separation. What is more important is the location of mining sites out of public view, in underutilized areas, with low thickness of overburden and easy restorability. The profitably mined high-dune sand near Amity Point, Stradbroke Island offshore from Brisbane, grades between 0.7% and 1% of

"heavies" hence, recalculated to the contained titanium, it is less than the Ti clarkie of 0.4%!

If the 1970s and 1980s marked the rush of explorers away from beaches to the fossil (but still mostly Pleistocene, marking the high sea water stands) raised strands several km inland from the present beach, the 1990s and 2000s have seen a rush to discover largely buried and levelled sand horizons in Tertiary basins like the Murray Basin in Victoria and South Australia (Roy et al., 2000; Fig. 13.6), and most recently the Eucla Basin that crosses the South- and Western Australian borders. The **WIM 150** deposit near Horsham in western Victoria has a resource of 4.9 bt of sand with 2.8% of extremely fine-grained heavies in a 22 m thick Pliocene sand unit (Roy et al., 2000). The Soviets, however, were first to mine heavy minerals from Meso-Cenozoic sands on the Russian Platform (Rundkvist et al., 1978). Ultimately, due to the growing demand for titania (for household paint!) some of the long-known but unmined "hardrock" paleoplacers are now considered for production. This includes the Late Permian (Karoo) Fe, Ti, REE paleoplacer near Bothaville, Free State, South Africa (Behr, 1965; Rc ~185 mt of ore; Mining Journal, November 1997; Fig. 13.7).

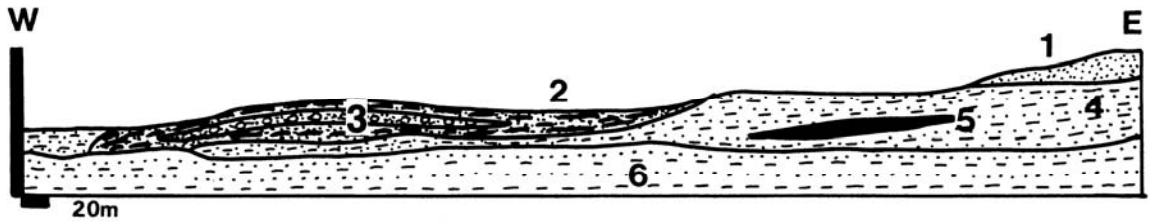


Figure 13.5. Capel heavy mineral sands deposit south of Perth, Western Australia, of the raised beach and dune variety. From LITHOTHEQUE No. 2232 modified after Welch et al. (1975). 1. Q yellow dune sand, 5-15% of heavy minerals; 2. Q raised beach, foreshore and dune sands, 10-30% heavies; 3. Q indurated sand with ferruginous cement ("coffee rock"); Q. Clay sand; 5. Q high-grade foreshore sand with >30% of ilmenite > rutile, zircon > monazite. 6. MZ clay sand

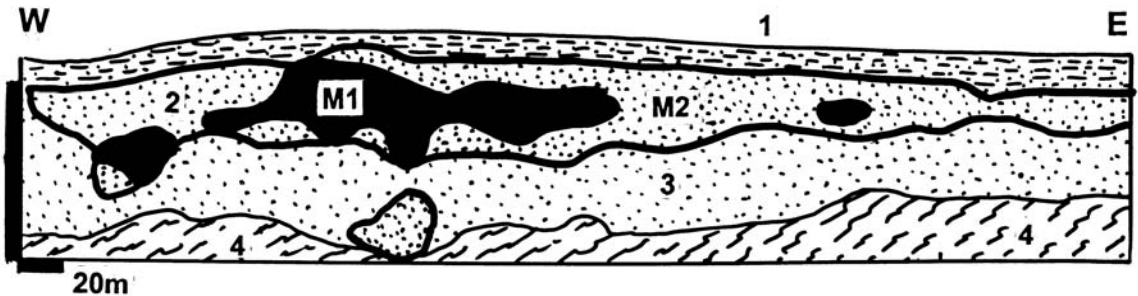
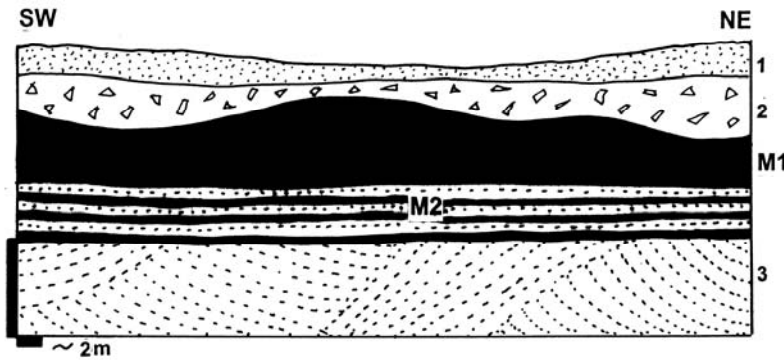


Figure 13.6. Bondi paleostrand in the Balmoral-Douglas heavy minerals deposit in the Murray Basin, W-C Victoria: example of a fossil beach-type deposit very distant from the present coast. From LITHOTHEQUE No. 2817, based on documents provided by Basin Minerals Ltd. in 2001. 1. Pl-Q overburden topsoil and sandy clay; 2+M. Pl Loxton-Parilla Sand, beach to lagoonal sand with 4.6% of heavy minerals (ilmenite >> leucoxene, zircon, rutile). M1=ore with >20% of heavies; M2=3-20% heavies. 3. Pl yellow quartz-rich sand; 4. Cm-Or basement of folded clastics



1. T-Q sand, relics of laterite; 2. Ditto, sandstone rubble with some heavy minerals; 3. Pe Karoo fluvial-deltaic and littoral mature quartz sandstone with several paleo-strand lines rich in heavies; M1, High-grade heavy minerals sandstone (ilmenite & leucoxene > hematite > rutile > zircon > monazite); M2. Low-grade heavy minerals laminated sandstone

Figure 13.7. Great Fortune orebody, Bothaville heavy minerals district in Karoo sandstone, central South Africa. Diagrammatic cross-section sketch from LITHOTHEQUE No. 2739 based on data in Behr (1965) and site visit, 2001

Heavy mineral sands mined in Australia and Florida are commonly economic with 1.2-1.5% of heavies, depending on the mineralogical composition (rutile is more valuable than ilmenite). Higher grades are, of course, welcome. Because of the industry capability to overcome the standard grade constraints on defining an orebody, and also for the

lack of reliable data, it is extremely difficult to delineate, quantify and rank heavy mineral deposits. Because of this and also because of the high geochemical abundances of the recoverable Fe, Ti, Zr and REE, there are no known "geochemical giants" and it is even difficult to agree on which are the "world class" deposits.

Table 13.1. Selected examples of major onshore heavy mineral sand deposits and regions

Locality	Tonnage of sand or concentrate	HM grade	Ilmenite & leucoxene	Rutile	Zircon	Monazite
Trail Ridge, Florida	200 mt	4%	38 mt		12 mt	
Sherbo, Sierra Leone				30 mt		
Nile Delta, Egypt			540 mt		16.2 mt	5.4 mt
Sokoke, Kenya	1,200 mt	3%	10 mt	1.54 mt	1.2 mt	
Micaune, Mozambique			22mt	0.6 mt	2.4 mt	0.3 mt
Port Dauphin, Madag.			2.0 mt		0.1 mt	0.1 mt
Richards Bay, S. Africa	1,000 mt	6%	60 mt	3 mt	5 mt	
Quilon, Kerala, India			17.5 mt	1.3 mt	10 mt	2.9 mt
Pulmoddai, Sri Lanka			2.5 mt	0.6 mt		0.02 mt
Cooljarloo N of Perth	620 mt	3.2%	11,2 mt	0.732 mt	2.01 mt	0.183 mt
Eneabba N of Perth			18.5 mt	3.9 mt	7 mt	0.18 mt
Capel etc. S of Perth			25 mt		2.2 mt	0.16 mt
Eucla Basin, S. Austr.	108 mt	6%	1.4 mt	0.455 mt	3,3 mt	
Centr. Murray Bs., Vic.	140 mt	1.9-5%	2 mt	0.85 mt	0.5 mt	
WIM 150, Victoria	4,900 mt	2.8%	43.3 mt	12 mt	18.2 mt	1.92 mt
Eastern Australia			13.4 mt	6.3 mt	6.2 mt	
N. Stradbroke, Qld			6 mt	3.07 mt	2.53 mt	0.003 mt

Note: Compiled from fragmentary data in the literature. The localities range from ~5 square km properties to 500 km long coastal tracts and are not mutually comparable

Table 13.1. lists selected localities most of which are rather extensive regions. It is difficult to decide which one is the "largest" and "best".

Richards Bay Fe-Ti-Zr, KwaZulu-Natal, South Africa (Bartlett, 1987; P+Rv ~ 1 bt @ 5-6% ilmenite, 0.3% rutile, 0.4-0.65% zircon). Richards Bay is the largest of a string of heavy mineral deposits along the Indian Ocean coast between East London and Mozambique border. Located about 200 km NE of Durban it is an inland Pleistocene fossil dune system, parallel with the present coast, 17 km long and 2 km wide. Up to 180 m high dunes rest on a raised beach and the economic sand orebodies are 30 m thick on the average. At base there is an about 5 m thick interval of a well layered beach sand, covered by a finer, massive dune sand. The sands have been mined since 1977, initially for rutile and zircon only, but after 1978 ilmenite has been locally processed into titania slag (85% TiO₂). The ore sand is continuously dredged using integrated floating excavation and concentration plant that extracts the heavy mineral fraction and returns the light fraction for instant reclamation. The concentrate is magnetically and electrostatically separated and rutile, zircon and monazite concentrates exported, whereas ilmenite is smelted locally in electric furnace to produce titania slag and pig iron.

13.3. Combined clastic and chemical bedded sedimentary deposits

13.3.1. Particulate (oolitic) ironstones

"Oolitic" ironstones, together with coal, started the industrial revolution in Western Europe, England and eastern United States but have recently been eclipsed and virtually displaced by the present mainstay of iron ores, the naturally enriched or beneficiated Precambrian banded iron formations. Although relatively low-grade (30-40% Fe), mostly non-magnetic, and rarely supergene enriched to the present industrial specifications, there are still substantial ironstone resources left in sparsely populated areas where mining and beneficiation would raise minimal objections (e.g. in western Siberia, northern Alberta, Libyan desert). In the densely populated developed countries, former mine sites are now more valuable as housing estates, parks or at best "Gastbergwerks", than sources of raw material. In addition to the remaining industrial potential, ironstones are a classical ore type the origin of which has not yet been unequivocally explained so research continues (Maynard, 1983; Young and Taylor, eds., 1989).

As with banded iron formations (Chapters 9, 11), ironstone deposits are difficult to delineate, hence to determine their magnitude. Like the BIF's they

consist of a single sedimentary bed or a set of beds that may continue for a long distance (the West Siberian Basin has an area of 66,000 km²) but that are not economic to mine throughout. Ore deposits or districts are sections where the ore beds are anomalously thick or where more than one bed congregate. Because of the high geochemical abundance of iron (Fe clarkite is 4.4%) a “Fe giant” has the lower limit of 4.4 bt Fe, attained by only one “ore field” (Bakchar in the West Siberian Fe Basin, itself a “Fe super-giant” basin). The Fe deposits/basins summarized in Table 13.2. are all “large”, i.e. with 440 Mt Fe plus. There are few (potential) by-product metals in ironstones forming significant accumulations. They include increased Mn, V and As, the latter being rather undesirable, in some ores but they are rarely systematically recovered. The Kerch iron field in the Ukraine is credited with a calculated resource of 600 mt Fe @ 35%, 57 mt Mn @ 3%, 11.4 mt V @ 0.67% and 2.2 mt As @ 0.13% (Sokolov and Grigor'yev, 1974) so this field would qualify as an As and V “giant”, but the unusually high V content is probably not present throughout. On the other hand, the Soviets used to recover Ge and Sc from certain Fe ores.

Mineralogy and geology: A typical “oolitic ironstone” is composed of ferruginous particles (goethite, hematite, chamosite, thuringite, siderite, rarely magnetite, pyrite) resting in a non-ore (clay minerals, clastic quartz, carbonate cements), or ore (“muddy” hematite or goethite, siderite, ankerite) groundmass. Ideally, the usually rounded, uniform size (~1-3 mm diameter) particles are internally concentrically laminated and have sometimes a core of a “marine substance”, usually fossil fragments. These are interpreted as true ooids (ooliths), intrabasinal allochemical components, produced either by direct iron precipitation or by diagenetic replacement of carbonate ooids by iron. Formation of the heavy ferruginous ooids is difficult to explain by an analogy to the “repeated suspension in carbonate cloud” that applies to aragonite ooids. Repeated movement and frequent particle repositioning on the sea floor are more likely (Maynard, 1983). Many if not most ferruginous particles are, however, internally structureless, of irregular shape, and of a relatively large size. These were likely derived by winnowing and sorting of particles brought in from land, most likely from lateritic weathering profiles (read above). In the Birmingham, Alabama ores, hematite encloses or partly replaces fossils and a portion of the ore has a high calcite content so it is self-fluxing. Some particulate ironstones grade into hematitic shale or

sandstone; the latter is a quartz-rich sandstone with clasts coated, or cemented, by a Fe mineral (usually hematite).

Ironstone formational environments are interpreted as islands-dotted or coast-proximal shallow tropical inland seas (Kimberley, 1978), coastal marsh, lagoon, barrier bar environments (Maynard, 1983), delta fronts, shelves or even lakes (compare Einsele, 1992, for review). Many iron sequences are cyclic with a common (but not the only one!) upward progression from basinal shale through prodelta siltstone and quartz-rich litharenite to shallow subtidal siltstone and sandstone, ironstone bed, carbonaceous shale (often pyritic) (Young and Taylor, eds., 1989). The latter is sometimes substituted by bioclastic limestone. The geologically young ironstones (Jurassic to Eocene; e.g. the “Minette” of Lorraine and Luxembourg; Fig. 13.8) have usually goethite, sometimes chamosite and/or siderite ooids. The older (typically Ordovician to Devonian) ironstones are mostly “red” (hematitic), although chamosite is often present or it forms small monomineralic deposits. The above ironstone varieties are exclusively sedimentary-diagenetic, confined to stable shelves or epicontinental seas, and are treated as such in the sedimentologic literature.

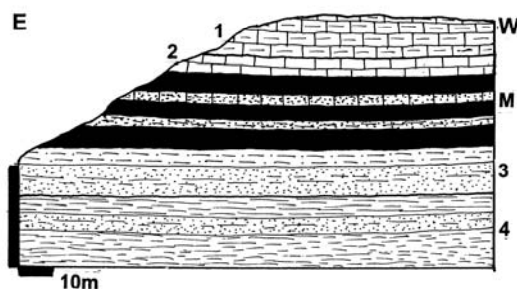


Figure 13.8. Dudelange-Tétange “minette” Fe ore deposit, Luxembourg, cross-section sketch from LITHOTHEQUE No. 1017, based on field visit in 1978. 1. J2 marl; 2. Ditto, red bioclastic calcirudite to calcarenite; M. J2-3 “Minette” ironstone, several productive beds of goethite, leptochlorite, hematite particles in calcitic sandstone; average grade 27% Fe; 3. J1 greenish-gray mica sandstone and siltstone; 4. J1 mudstone, siltstone

Some Fe deposits (e.g. in the German and Moravian Devonian, Ordovician in the Czech Barrandian), however, are closely associated with intracratonic submarine basaltic or bimodal (“spilite-keratophyre association”) volcanism.

Table 13.2. Selected "large" (430 mt Fe plus) to "giant" bedded ironstone districts (stratigraphic units)

District/unit	Age	Grade Fe	Contained Fe	Other metals
Clear Hills, Swift Creek; NW Alberta, CA	Cr3	33%	520 mt	V 3 mt @ 0.2%
Birmingham, Alabama	S2	30%	1,200 mt	
Wabana (Bell Island), Newfoundland	Or1	51.3%	1,300 mt	
Northampton Sand Ironstone, U.K.	J1	31%	470 mt	
Lorraine (France)-Luxembourg "Minette"	J1	29%	3,700 mt	
South German ironstone region	J2	18-30%	1,000 mt	
Gifhorn Basin, NW Germany	J2	32%	500 mt	
Salzgitter, northern Germany	Cr1	31.5%	500 mt	
Kerch Peninsula, Ukraine	J	35%	600 mt	57 mt Mn @ 3% 11.4 mt V @ 0.67% 2.21 mt As @ 0.13%
Ayat (Turgai) district, NW Kazakhstan	Cr3	37.1%	2,500 mt	
West Siberian Basin, Russia	Cr3	30%	300,000 mt	
---Bakchar ore field	Cr3	37.4%	10,500 mt	V 3.64 mt V @ 0.13%
Ningshiang Fe-ore type, central China	D2-3	50%	900 mt	
Gara Djebilet, SW Algeria	D1	45%	1,300 mt	
Wadi Shati, southern Libya	Cb1	40%	1,520 mt	
Pretoria Ironstone, South Africa	2.2 Ga	46%	X,000 mt	

There is a facies progression from the clearly "exhalative" hematite bodies associated with red or green "jasper" (the Lahn-Dill Typus of Schneiderhöhn, 1941) through massive hematite lenses in shales at or near the volcanic top, to red hematitic particulate ironstones entirely in sediments, stratigraphically above the volcanics. Alternatively, the ironstone could be dominated by siderite, thuringite, sometimes magnetite and grade into the entirely sideritic ores like the Romanian Teliuc-Ghelar Type of Krautner (1977).

West Siberian Fe ore Basin and the Bakchar Fe,V deposit (Tomsкая Kompleksnaya Ekspeditsiya, 1964; Rc whole basin ~900 bt @ 30% Fe for ~300 bt Fe content; Rc Bakchar only 10.5 bt Fe content @ 37.4%, 3.64 mt V content @ 0.13%). This Basin is centered on Tomsk in western Siberia and it has an Upper Cretaceous iron-bearing suite 80-500 m thick, that includes (from bottom to top) the following units: 1) Basal Unit, 20-50 m thick, mostly composed of sandy to shaly continental and marine sedimentary rocks. There are several thin lenses of nearshore marine Fe ores. 2) Middle Unit, 10-400 m thick, of cyclically alternating tongues of sandy to shaly, continental to marine sediments. There are five important horizons of Fe ore in the marine tongues. 3) Upper Unit of greenish-gray, marine, thin-bedded mudstone with sporadic siderite lenses.

Each iron-ore horizon 2-35 m thick has a distinct facies and grade distribution pattern. The nearshore sandstone contains less than 15% Fe in cement, to

culminate with a 30% Fe particulate ironstone of predominantly Fe-chloritic and sideritic composition. The ironstones formed during regression, have an easterly detritus provenance and originated in a wide tract of shallow water. The largest **Bakchar deposit** 180 km NW of Tomsk has three exceptionally favorably developed ore horizons that coalesce and produce ore zone with an aggregate thickness of between 60 and 120 m. The flat-lying host sequence is of Santonian to Maastrichtian age and rests on Turonian sandstones and lignite succession with a slight disconformity. Each ore-bearing cycle has a distinct fining-upward progression of sediments, from basal terrigenous granule conglomerate to sandy or particulate ironstone, to shale or claystone on top. The most common medium-grained ore variety has a dark-brown or greenish-black colour and is composed of goethite, chamosite-strigovite, and glauconite ooids, granules and clastic fragments (about 70% by volume), cemented by leptochlorites. Additional ore varieties include reworked, sandy to conglomeratic ore at base of the overlying Paleogene sediments; sideritic ore, and siderite or goethite-cemented sandstone. There are local sedimentary lenses enriched in glauconite, hisingerite, vivianite, and phosphorite.

Birmingham Fe district, Alabama (Simpson and Gray, 1968; Rc ~4.05 bt ore @ ~30% Fe for ~1.2 bt Fe). This is an example of the older, "red" (hematite) ironstones and the largest ore field in the

Appalachian "Clinton-type" ore association. The entire sequence is spectacularly displayed for posterity (when the mining has ceased) in cuts of the Red Mountain Expressway in metro Birmingham. The ore field is located in the gently folded and thrust-faulted Valley and Ridge Province, in the Appalachian orogen. The 100 to 170 m thick Silurian ore sequence rests on Ordovician limestone and consists of units of alternating crossbedded lenticular quartz-rich sublitharenite (quartzite) and greenish-gray shale. The ironstone forms several parallel lenticular seams. In the former Vulcan Mine the basal Irondale Seam included about 1.7 m of ferruginous sandstone. This was overlaid by 1.3 m of flat pebble feruginous or calcareous sandstone, in turn topped by the Big Seam ore layer, 6 m thick. The stratigraphically highest Ida Seam rests on about 10 m thick barren sandstone.

The recently mined Big Seam is composed of numerous lenses of interstratified hematite, sandstone, shale and limestone and this accounts for the low (32% Fe) overall grade. Red, pelitic hematite is the dominant mineral and it forms flat particles with rounded edges and usually a concentric microstructure. Hematite also forms the matrix and replaces calcitic bioclasts and fossils. There are four ore varieties: 1) fine-grained conglomerate or sandstone with hematite-coated quartz clasts and with hematite-calcite cement; 2) hematitized fossil fragments and hematite ooids cemented by hematite (the highest-grade type); 3) hematite ooids in calcite matrix or cement; and 4) flattened concretions and pebbles of red hematite. In the weathering zone the ore is friable because of the loss of cementing and skeletal calcite.

13.3.2. Bedded Mn deposits (Phanerozoic)

After the oceanic Mn-Fe nodules (nowhere mined yet; Chapter 4) and the super-giant Proterozoic Kalahari and Moanda bedded Mn's reviewed in Chapter 11, bedded Phanerozoic Mn deposits are next in importance. Historically, they are the most significant ones and they have extensive literature dominated by Russian works (Strakhov, 1962; Strakhov et al., 1968; Varentsov and Rakhmanov, 1974; Maynard, 1983). Table 13.3. lists two "super-giant" Mn districts (Nikopol-Tokmak and Molango; the latter is in carbonates hence described in Section 13.4) and four "giants" (two additional "giants" are included in the Nikopol-Tokmak district).

Bedded Mn deposits are somewhat similar to particulate ironstones (read above), but their Mn-oxide particles, when present, are larger than ooids

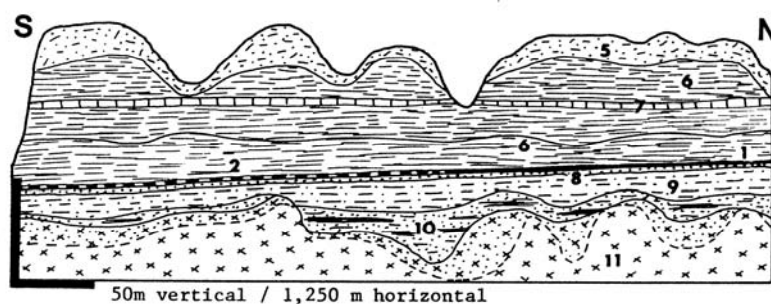
(microconcretions or pisoliths). There is an inconclusive debate as to whether they are "primary" and marine (formed on the sea floor by syndiagenetic accretion like the oceanic nodules) or "secondary", formed in weathering profiles on land. The latter can still be subdivided into pisoliths formed in lateritic profiles on land then physically reworked into a marine basin, or originally marine Mn-carbonate deposits oxidized in-situ after subaerial exposure. The very near-shore Mn oxide (cryptomelane, pyrolusite) deposits grade into offshore ("basinal") bedded Mn carbonate deposits composed of pelitic rhodochrosite, kutnahorite, or Mn-calcite. The latter are massive, sometimes laminated ores, hosted by reduced, often carbonaceous ("black") pelites or carbonates and fading away at pinchouts into strings of concretions. The bedded Mn carbonate ores are fine-grained and gray (the characteristic pink rhodochrosite appears only in younger remobilized fracture veinlets when present) and easily overlooked in non-oxidized rocks as in drill core. In outcrop the ore is marked by secondary Mn oxides that also formed many small enriched high-grade Mn deposits, mined in the past.

In the presently popular model, Force and Cannon (1986) interpreted syngenetic Mn deposits as having formed by chemical precipitation of Mn dissolved in anoxic basins (e.g. of the present Black Sea type), by oxidation and water mixing in shallow near shore settings along the deep basin fringe. To form a Mn deposit, iron co-precipitation and detrital influx had to be prevented or reduced and the best conditions for this existed during highstands of a transgressive-regressive wedge, where Mn accumulated at black shale pinchouts. This model seems best applicable to the marine Mn carbonate deposits that could be termed distal, as there is not much consideration given to the proximity to primary Mn sources. Many bedded Mn deposits, including the largest ones in the South Ukrainian Basin and in the Northern Urals-Novaya Zemlya Mn Province, are in basal sequences transgressive over (meta)basalts, siliceous ("exhalative") Mn protores and/or Mn-rich Precambrian banded iron formations, that show numerous signs of trace Mn withdrawal in the time of bedded Mn deposition. These rocks had been the likely Mn source and Mn deposits did not form elsewhere in the same type of basins, without the Mn-providing bedrocks.

Nikopol-Bol'shoy Tokmak district, South Ukrainian Mn Basin; Strakhov et al. (1968), Varentsov and Rakhmanov (1974); P+Rv~1.65 bt Mn @ 24-30% Mn.

Table 13.3. "Giant" (72 mt Mn plus) Phanerozoic bedded sedimentary Mn ore districts

District	Age	Brief geology	Mn content/grade	Reference
South Ukrainian Basin	O1	Upper nodular Mn oxide over pelitic Mn carbonate	P+Rv ~1.65 bt/24-30%	Varentsov & Rakhmanov (1974)
---Nikopol	O1	Ditto	940 mt/24-30%	Ditto
---Bol'shoi Tokmak	O1	Massive bedded pelitic Mn carbonate, minor oxides, in subsurface	Rc 490 mt/24.5%	Ditto
Sulmenev, N. Novaya Zemlya, Russia	T1	Bedded Mn carbonate	121 mt/13-14%	Ivanova and Ushakov (1998)
Rogachev-Tainin, S. Novaya Zemlya, Russia	T1	Ditto	243 mt/13-14%	Ditto
North Urals Basin	Pc	Pelitic & concretionary Mn carbonates over Cr sediments and PZ volcanics	75 mt/21%	Varentsov and Rakhmanov (1974)
Chiatura, Georgia	O1	Several Mn oxide > carbonate beds over karsted limestone	600 mt/20%	Ditto
Molango, Mexico	J3	Beds of finely crystalline rhodochrosite in carbonate association	1.6 bt/10%	Okita (1992)
Groote Eylandt, NT, Australia	Cr2	Blanket of friable concretionary Mn oxides on basement regolith	220 mt/46%	Frakes and Bolton (1992)



ORE: 1. Oxidic and mixed ore; 2. Mn carbonate ore.
 5. Q sedimentary cover; 6. Mi-Pl mudstone, marl; 7. Limestone bed; 8. O1 quartz-glaucou-nite sandstone; 9. Ditto, siltstone; 10. Ditto, basal claystone, siltstone, lignite; 11. Regolith Precambrian basement

Figure 13.9. Nikopol ore field, South Ukrainian Mn ore basin, cross-section of the Grushevsko-Vasan area modified after Strakhov et al. (1968)

This is a segment of the belt of Oligocene nearshore sediments preserved along the perimeter of the present Black Sea in Bulgaria, Romania and southern Ukraine and situated south and east of the "giant" Proterozoic Krivoi Rog iron ore "basin". There, the Proterozoic greenstone and granite-gneiss basement with a thick post-Carboniferous regolith is unconformably overlain by a transgressive sequence of poorly sorted sandy to clayous "wash" (reworked regolith), changing upwards into marine siltstone to claystone. The latter contain discontinuous units of friable glauconitic quartz-rich litharenite with shell banks topped by the Mn horizon which, in turn, is overlain by fine-grained, greenish-gray smectitic claystone and, eventually, marly claystone.

The "Mn-basin" is a group of three discontinuous outcrop (around Nikopol, in the west) and subcrop

(around Bol'shoi Tokmak, in the east) occurrences of a single Mn ore horizon, in an arcuate belt about 250 km long. The **Nikopol ore field** (Fig. 13.9) has an area around 230 km² and the subhorizontal, slightly synclinal ore bed is between 0.75 and 3 m thick (average 2.18m). It accounts for the bulk of past production and remaining reserves of the "rich" ore (about 30-40% Mn). The ore horizon is subdivided into three facies: oxide, mixed (or "concretionary") and carbonate. The oxide facies comprises friable, earthy mixture of cryptomelane, wad and minor pyrolusite and is interpreted as "secondary" (oxidation zone or enriched residue). The mixed zone consists of Mn oxide (mainly manganite and/or pyrolusite) nodules that range in size from 0.1 to 1 cm, in a matrix of pelitic carbonate or mudstone. The nodules are partly corroded by the carbonate that indicates their earlier

deposition on the sea floor, which Byelous and Selin (1975) compared with the syn-diagenetic origin of the recent nodules in Loch Fyne off Scotland (the sea should have been warmer to precipitate the associated glauconite).

The carbonate ore facies is nodular to lumpy and the nodules are composed of a very fine-grained, pelitic gray rhodochrosite or oligonite gradational to Mn-calcite in mudstone matrix with glauconite and abundant pelagic (micro)fossils. The carbonate facies is of much lower grade than the oxides and it is minor in Nikopol where it occupies the deeper buried portions of the orebody. It is, however, the only facies in the most extensive, entirely buried **Bol'shoi Tokmak** ore zone, where the resource probably exceeds 1 billion tons of ore. The associated siltstones in the entire zone are enriched in Mn (0.23-1.7%) and contain the Myezhdurechye deposit that stores some 180 mt Mn @ 20% Mn concentration.

The "giant" **Chiatura** deposit in Georgia and the "near-giant" Mn zone in the **Mangyshlak Peninsula** now in Kazakhstan (Table 13.3) are members of the same facies belt, discontinuously distributed along the present Caspian Basin.

Groote Eylandt, NT, Australia (Ostwald, 1981; Frakes and Bolton, 1992; ~450 mt ore @ 46% Mn for ~220 mt Mn; Fig. 13.10) is the only Australian "Mn giant". It is located on an island in the Gulf of Carpentaria, close to the mainland, and hosted by relics of a thin Mid-Cretaceous marine sedimentary sequence that rests unconformably on Proterozoic metaquartzite. The high-grade subhorizontal Mn ore blanket is up to 9 m thick, composed of loose to poorly cemented pyrolusite and cryptomelane pisoliths (microconcretions) topped by a hardcap. The layer rests directly on the basement or on a thin interface of sand and glauconitic clay. The elaborate facies models popular in the literature would be much simplified if it were accepted (Dammer et al., 1996) that the rich pisolitic orebodies are likely the product of an almost total supergene reworking of a low-grade Cretaceous primary mineralization in marine sediments, during several stages. The original pyritic, glauconitic clay with Mn carbonate occurs as relics in the southern sub-basin, presently considered uneconomic to mine.

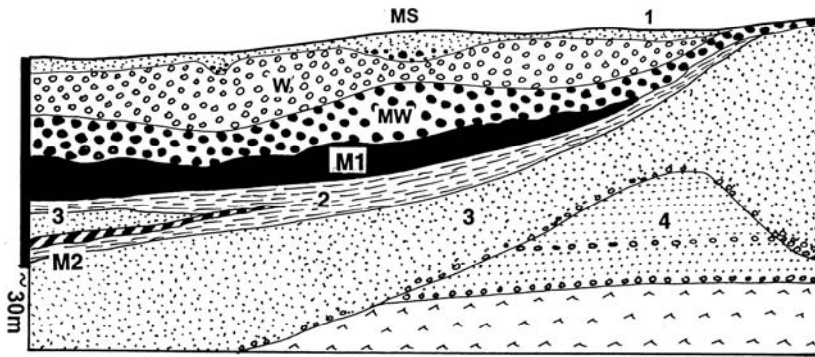
13.3.3. Mineralized carbonaceous pelites ("black shales")

"Black shale" is a popular term for dark organic carbon-rich pelites. The Huyck's definition (quoted

by Schultz, 1991) reads "a dark-colored, laminated, fine-grained, clastic sediment that contains 50% or more particles sized less than 0,062 mm equivalent spherical diameter (i.e., silt or clay) and greater than 0.5% organic carbon shale". A "metalliferous black shale" is a shale 2x enriched, with some exceptions, in trace metals relative to the USGS Standard SDO-1 Ohio Devonian Shale. The above definitions are suitable for the "typical" rocks, but too restrictive for the rest that appears in the literature under the "black shale" heading that also includes massive mudstone, pelitic carbonate, silicite (chert), carbonaceous sandstone, slate, schists, young bituminous rocks that are not black at all, and the recent progenitors, the euxinic black muds. This section considers "black shales" in the broader sense and the equivalents in carbonate rocks are in Section 13.4. below (there are many transitions). There are also transitions into phosphorites, also reviewed below (Fig. 13.11).

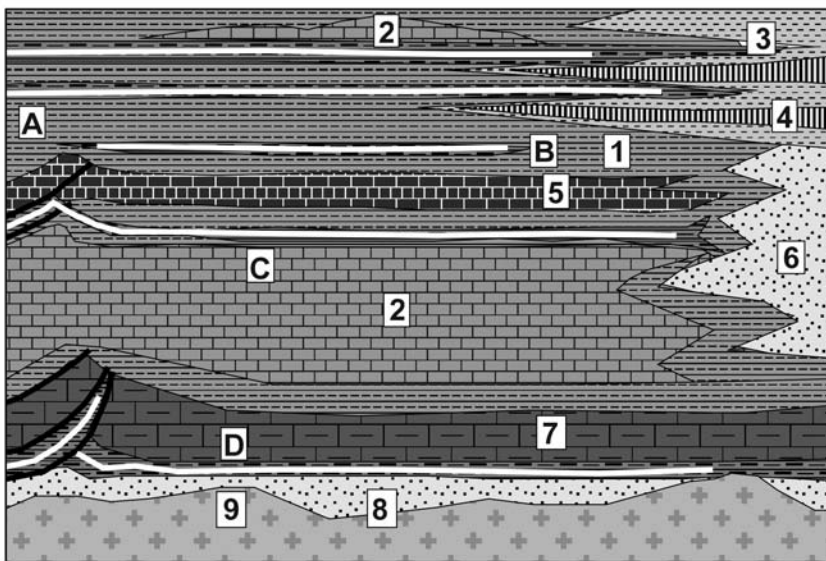
A "typical" black shale consists of a fine-grained partly clastic (e.g. quartz, clay minerals, magnetite, rare heavy minerals), partly authigenic (silica, clay minerals, feldspars, chlorite, carbonates, pyrite) "body", with organic carbon that is a residue after decomposed organic tissues. The organic bodies were micro- and less commonly macro-organisms (plankton, benthos, algae, etc.) in the marine domain, or plant or pollen material in terrestrial coaly sediments (Section 13.7). The existence of the plant-based carbon residue goes back to Devonian, whereas the aqueous microorganic carbon can be traced to at least the Late Archean (e.g. to the Witwatersrand; Chapter 11). The organic carbon species of marine or lacustrine provenance range from sapropel in unconsolidated sediments through benzen-soluble hydrocarbons to kerogen and finally graphite. The proportion of organic carbon in shales varies widely from the definition minimum of 0.5% C to well over 50% C. Some of the carbon-dominated marine rocks are combustible and range from the little metamorphosed "stone coal" (widespread in China) to the higher metamorphosed shungite (native to the Baltic Shield) and highest metamorphosed graphite.

Preservation of organic carbon in sediments requires anoxic conditions (waters and interstitial fluids depleted in oxygen) and this is best realized in euxinic basins (Einsele, 1992).



1+MS. Cr3-Q reworked sediments with some Mn oxide grains; W. T ferruginous laterite; MW. Mn oxides from M1 modified by pedogenesis; M1. Cr1-2 shallow marine sheet of friable particulate Mn oxides in sand and clay matrix; M2. Relics of Mn carbonates in marl; 2. Cr1-2 marine claystone to siltstone; 3. Ditto, quartz-rich sand; 4. Pp sandstone over basalt and diorite

Figure 13.10. Groote Eylandt Mn complex, NT, northern Australia, diagrammatic cross-section from LITHOTHEQUE No. 3198 based on data in Pracejus et al. (1988), Pracejus and Bolton (1992)



1. Marine shale; 2. Marine limestone; 3. Brackish-freshwater mudstone; 4. Paralic coal; 5. Siliceous, cherty limestone; 6. Coastal sandstone; 7. Glauconitic limestone; 8. Basal sandstone; 9. Pp crystalline basement.
METALLIFEROUS BLACK SHALES: A. In coal cyclothem (Indiana); B. Monotonous epeiric shale (Pierre Shale); C. Shale as facies of delta redbeds (Chattanooga); D. Shale near base of sequence (Kolm Shale)

Figure 13.11. Inventory cross-section of metalliferous carbonaceous pelites in Phanerozoic platformic sequences. From Laznicka (2004), Total Metallogeny Site G154

Such basins require a stratified water body that can only develop under the wave base, generally in water columns deeper than 50m. The type area of a present euxinic basin and sediments is the Black Sea and its deep Mud Layer C (Degens and Ross, eds., 1974) that has 3.5% of organic carbon. Carbon can also be protected from oxidation by rapid burial (Leventhal, 1998) and although this can still provide source rocks for hydrocarbons, the high sedimentation rates dilute the organic content and retard the trace elements absorption from seawater during early diagenesis. Black sediments, and especially the metalliferous black shales, thus require slow to almost nil sedimentation ("starved basins") and H₂S-poisoned environment that restricts macro-organic activity; microorganisms like sulfate-reducing bacteria, however, still thrive. Sediments formed in euxinic environments are thus identified, in addition to the organic carbon content and structures, by the lack of macrofossils and trace fossils (e.g. burrows).

Although the Black Sea and the deepest portion of the Caspian Sea are generally considered as inland or intracratonic seas, they have developed on sites of earlier back-arc basins and have oceanic crust under the sedimentary cover.

Table 13.4. Selection of trace metals-rich carbonaceous shales and phosphorites

District/unit	Age	Type	Ore tonnage	Grades	Metal content
Rapid Creek, NWT, Canada	Cr	Pyrite, phosphate, ironstone beds grading to black shale	27 bt	21.5% Fe 14% Px	5.805 bt Fe 3.8 bt Px
Western Phosphate Field, USA (Phosphoria Formation)	Pe	Deeper marine bedded phosphorite		18% Px+ 90 ppm U 300 ppm V 1000 ppm Y	15-20 bt Px 3-10 mt U 10-30 mt V
---Soda Springs (Conda)	Pe	Ditto	22 bt	27.7% Px 90 ppm U	6.1 bt Px 2 mt U
North Carolina shelf offshore	Mi	Warm water phosphorite	4.53 bt	~30% Px ~60 ppm U	1.36 mt Px 272 kt U
Aurora District (on land), NC	Mi	Ditto	1 bt	30% Px 60 ppm U	300 mt Px 60 kt U
Florida & Georgia phosphates	Mi-Pl	Ditto, residual phosphorite (land-pebble)		60-110 ppm U	7.16 mt U
Blake Plateau, Atlantic Ocean	T-Q	Seafloor phosphatic pavements, pebbles	2 bt	22% Px 60 ppm U	440 mt Px 120 kt U
Morocco phosphate province	Cr	Bedded warm water phosphorite	60 bt	35% Px 80 ppm U	21 bt Px 2.4 mt U
NW Karatau, Kazakhstan	Cm1	Deeper marine bedded phosphorite, black shale	200 mt	28% Px 0.23% V	56 mt Px 460 kt V
Georgina Basin, Queensland	Cm2	Deeper water bedded phosphorite	3.8 bt	16% Px 78 ppm U	608 mt Px 296 kt U
Julia Creek, Queensland	Cr1	Oxidized and unoxidized oil shale	1.8 bt	0.21% V	3.78 mt V
Chatham Rise, South Pacific	Q	Phosphatic nodules on sea floor	100 mt	24% Px 230 ppm U	24 mt Px 23 kt U

Abbreviations: Px=P₂O₅

This is not typical for the majority of black shale occurrences, such as those in the epicontinental basins of the North American Platform. Euxinic sub-environments of the present and black shale producing sites of the past existed in a great variety of geotectonic settings and depositional environments; there, most were confined to restricted basins or fault-bounded troughs. They are common in the oceanic, convergent and rift continental margins, with or without associated volcanics; in the slope-to-shore progression at stable continental margins where they have been recorded from all divisions. Most lack contemporaneous volcanism. Black shales are widespread in the intracratonic basins (the type environment) and some rifts (Chapter 12) as well as in lakes. In playa lakes, reduced sulfurous black muds exist in the depth of several cm, without the commonly quoted requirement of at least 50 m of water column. Environmental interpretation of black shale occurrences is thus highly controversial.

Trace metals, metalliferous black shales and related metallic deposits: Ordinary shales are

enriched in many trace metals in relation to Clarke values. Metalliferous black shales are enriched even more in one or more trace metals (Leventhal, 1998). Such “normal” (that is, syngenetic-diagenetic) metal enrichment may sometimes reach or exceed the economic threshold so that a “shale” becomes a mineable “ore” in its own way. Up to now, there have been few cases when this has happened, most notable being the Scandinavian Alum Shale that had actually experienced a brief period of exploitation as the principal Swedish energy resource (the shale has 300 ppm U, as much as the successfully mined pegmatitic U deposit Rössing in Namibia; Chapter 10). The mining was stopped on environmental grounds. Unmodified black shales highly enriched in Mo, V, Ni, Cu, Ag, Mn and other metals are intermittently mined, on a small scale, at several locations in China (Fig. 13.12).

As the cut-off grade of many metallic ores is being continuously lowered, a number of known black shale occurrences will achieve the economic ore status sometimes in the future. Foremost among them will be the “totally consumable” shales able to provide several economic commodities with no

waste left behind. Although low-grade, the cumulative value of several products will add on, to result in a significant per-ton value of the ore. The often quoted example is the Devonian-Lower Carboniferous Chattanooga Shale of Tennessee and adjacent states. The shale averages 60 ppm U, it contains P_2O_5 , extractable hydrocarbons, and the pulp can be utilized as expanded construction material. Over its area of distribution in east-central Tennessee (~12,000 km²) the shale is estimated to contain about 6 Mt of uranium. It is not yet close to being an economic resource, although in the 1960s-1970s, when the uranium prices and demand were at an all-time high, it was widely quoted as being close to become one. Once the Chattanooga Shale will have achieved the economic status, environmental protection will become the paramount obstacle to mine permitting.

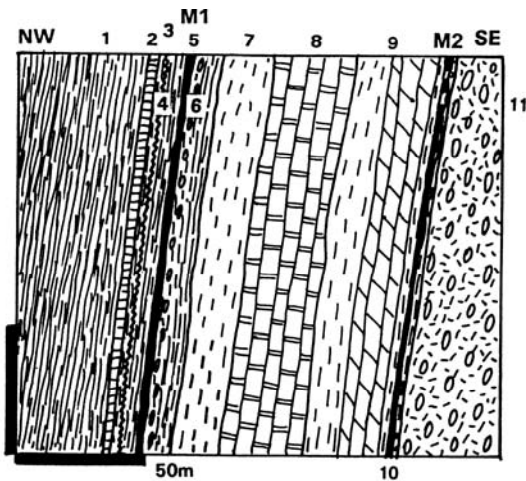


Figure 13.12. Metalliferous (V, Mo, Cu, Ni) black shale exposed in a quarry near Wujiaao reservoir, Hunan, China. From LITHOTHEQUE No. 1811, sketch based on field visit and data in Fan Delian (1988). 1. Cm1 Niutitang Fm. black shale with chert; 2. "stone coal"; 3. Gossanous metalliferous shale from shear; 4. Gray sericite shale; 5+M1. Phosphatic metalliferous slightly pyritic shale; 5. Black shale with phosphorite concretions; 7. Np Liuchapo Fm., sericitic slate; 8. Black chert; 9. Np Doushantuo Fm., sericitic slate and calcareous dolomite; 10+M2. Massive to banded pyrite in black slate; 11. Np (~750 Ma) Nantuo Fm. diamictite and siltstone with rafted pebbles

There are more shales like this, the best known being those in the Phosphoria Formation, here treated in the phosphorite section (read below). The Late Jurassic-Early Cretaceous **Bazhenov Formation in the West Siberian Basin** (Gavshin and Zakharov, 1996) is an enormous repository of

organic carbon and potential by-product metals; unfortunately it is in a depth of 2 to 3 km. This is a siliceous black argillite with 8% $orgC$, comparable with the Black Sea floor sapropel. It stores up to 18 trillion tons of organic matter and contains up to 104 ppm U over 15 m, 285 ppm Mo over 6m, 1015 ppm V over 6m and 1188 ppm Zn over 21m. The U resource in the entire formation is of the order of 6 billion tons (more than U dissolved in the world ocean). If mined and complexly processed, the shale would provide the present supply of U and V for many centuries and would seriously compete with the hydrothermal Mo producers.

The selection of metals enriched in black shales varies considerably (Table 13.4) and is virtually impossible to explain and attribute to a source; as a general rule, the non-calcic shales have a preference for U, Mo and V, the calcic shales for Zn, Pb, Ag, Cu but there are exceptions. In some cases geochemically contrasting rocks in the vicinity could be considered the likely metal source (e.g. Ni and Cr near ultramafics) but this logic is lacking in most other cases. The trace metals in black shales reside in minerals of the "pulp" (rarely), absorbed (dispersed) in carbon, incorporated into pyrite, or forming micro- or macroscopic minerals of their own in the rock (e.g. as microconcretions, metacrysts, cements, microfracture veinlets). These are sometimes unexpected and inconspicuous, like the authigenic gray monazite in the Belgian Stavelot Massif (Burnotte et al., 1989). The metals may have entered the system during sedimentation, during the early diagenesis when still on the sea floor or in wet sediment, during late diagenesis, during or after lithification. There may have been a metal contribution from external sources, by means of metal-bearing hydrothermal fluids. The sedimentary-exhalational deposits, formed in this way, are treated in a separate section below and they are likely transitional into the shales metallized from the sedimentogenic sources only.

Economic grade orebodies within, at contact, or genetically influenced by black shales: Black shales, even when not themselves mineralized to reach an economic grade, are often associated with metallic orebodies that are of much higher grade, but also of a much smaller size. Here belong the often quoted high-grade Mo-Ni ore beds in Lower Cambrian of southern China (near Zunyi in Guizhou: average 2.5% Ni, 5.8% Mo, 1.59% As, 0.27% Se, 141 ppm U, 0.2 ppm Pt, 0.29 ppm Au; near Dayong in Hunan: average 2.63% Ni, 2.77% Mo, 1.02% As, 0.27 ppm Pd; Coveney et al., 1994), and in the Devonian Ni ore band in the Selwyn

Basin, Canada (Nick prospect: 5.3% Ni, 0.73% Zn, up to 61 ppm Re, 0.77 ppm PGE+Au; Hulbert et al., 1992). Unfortunately, the thickness of such high-grade ore beds is only several cm (5-15 cm thick sulfide bands in a 2 m thick black shale horizon near Zunyi, 3 cm thick band at Nick) and the continuity is limited, hence these are "small" to "medium" magnitude orebodies. The origin of such metalliferous beds is attributed to "internal distillation" (gangue volume shrinkage) during diagenesis, or to hydrothermal supply in the vicinity of faults (hence a form of sedex deposits).

Black shales are periodically invoked as the source rocks of base, rare and precious metals in hydrothermal veins and replacements (e.g. some Chinese Sb and W deposits; gold deposits as in the Lena Goldfield in Siberia; Bur'yak, 1983, or Bakyrchik, Kazakhstan; pitchblende veins in the Příbram district, Czech Republic; Křibek, 1989; Ronneburg in Germany, Mina Fe in Spain), or as a reducing or sulfurizing microenvironment that facilitated precipitation of metals from passing fluids (e.g. the pyritic Kupferschiefer, read below; several Carlin-type deposits in Nevada, Chapter 7). Many metal "giants" of highly variable origin are spatially associated with black shales, so the shales are a valuable metallogene to be noted and interpreted during exploration. The "giants" examples below include a "pure" syn-diagenetic metalliferous shale (Alum Shale) and an internally remobilization-enriched black shale (Ronneburg). More black shale-associated ores appear in section on mineralized redox interfaces (Kupferschiefer), phosphorites and sedex deposits below.

Alum (Kolm) Shale-U, V, Mo, Sweden (Andersson et al., 1985). The Proterozoic Sveconorwegian metamorphic basement in southern Sweden is covered by scattered erosional remnants of Cambrian and Ordovician platformic sediments, sometimes capped by (and preserved under) Permo-Carboniferous diabase sills. The largest Billingen-Falbygden remnant has a gently westerly dipping Lower-Middle Cambrian basal sandstone overlaid by a thin interval of Middle-Upper Cambrian Alum Shale on top of which is, in turn, a thick unit of Lower Ordovician limestone with a shale horizon. The 22-23 m thick Alum Shale is enriched in U (70 ppm), Mo and V and the 2.5 to 4 m thick Peltura scarabeoides zone within, at Mount Billingen, is a bituminous black shale with 15.5% of organic carbon (partly recoverable as hydrocarbons) and 13% pyrite. It also contains ~300 ppm U, 750 ppm V and 350 ppm Mo. About 90% of the uranium is "invisible", evenly disseminated in the seam and the

rest is in "kolm", a nodular, carbon-rich substance similar to anthracite that averages 0.45% U. Also present, in footwall of the highest-grade unit, is the Great Stinkstone Band of lenses and megaconcretions of coarse crystalline diagenetic bituminous limestone.

The partially mined Ranstad deposit (area about 500 km²; Fig. 13.13) has a reserve of ~300 kt U and the high-grade unit distributed over the entire Billingen remnant has a resource of 3.4 bt of a 292 ppm U shale, for 993 kt of contained U. The entire Alum Shale in Sweden stores 8.2 bt of material with 213 ppm U, 680 ppm V, 270 ppm Mo and 1.4 ppm Ag for ~1.7 mt U, 5.576 mt V, 2.214 mt Mo and 11,480 t Ag: a quadruple "giant". The Närke Alum Shale area west and south of Örebro stores further 180 kt U in shale that contains between 145 and 2445 ppm U (Andersson et al., 1985).

Ronneburg-Kauern uranium ore field, Thuringia, Germany (Vinokurov and Rybalov, 1992; Dahlkamp, 1993; 160 kt U @ 0.07-0.14% U; Fig. 13.14). This used to be the largest uranium resource in the Soviet Block outside the USSR, yet fairly obscure (the above Russian reference does not even name it), despite the large conical dumps visible from the Autobahn 20 km SE of Gera, Thuringia, in the former East Germany (DDR). Mining ceased in the 1990s and the site is presently under reclamation. The deposit is in the Variscan (late Paleozoic) Saxothuringian intracratonic folded belt, north of the Erzgebirge. The host to ores is a 350 to 500 m thick folded and faulted Upper Ordovician to Devonian succession of black slates interstratified with grayish-green clay slate, black siliceous slate, quartz-rich litharenite and dolomitized limestone. These are intruded by Devonian diabase and amygdaloidal basalt sills. The carbonaceous sediments, that contain an average of 7% _{org}C, are enriched in trace U, Mo, V, Ni, Cu and Pb and the greatest enrichment (50 to 130 ppm U) is within a 70-100 m thick stratiform horizon of Lower Devonian-Silurian siliceous black slate and carbonate. The ore field has an area of 164 km² and is in a zone of repeatedly reactivated N-S faulting. The earlier faults are synsedimentary. Vinokurov & Rybalov (1992) assumed structurally controlled hydrothermal supply of metals into the basin, above the "normal" supply from seawater by diagenetic absorption. This metal enrichment was repeatedly remobilized (and possibly still increased) during several deformation phases, mostly in Permian (late stages of the Variscan orogeny) and Mesozoic.

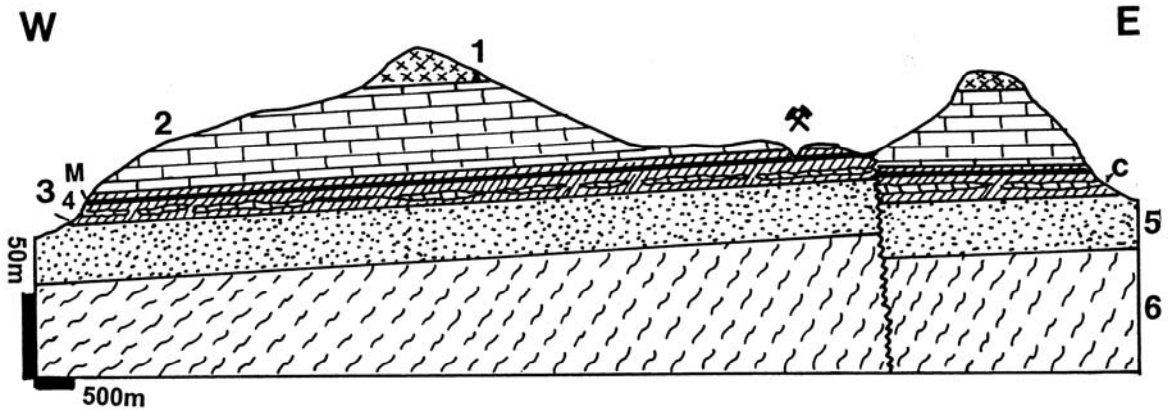


Figure 13.13. Ranstad U deposit, Häggum, Billingen Hills, S. Sweden, cross-section from LITHOTHEQUE No. 1726 modified after Andersson et al. (1985) and site visit. 1. Cb-Pe diabase sill, erosional remnant; 2. Or1 limestone and gray to reddish shale horizon; 3. Cm2-3 Alum Shale Fm., carbonaceous shale; M in 3. 4-5 m thick pyritic black shale horizon with ~300 ppm U; 4. Great Stinkstone band, bituminous limestone megaconcretions and lenses; 5. Cm1-2 basal sandstone; 6. Pt Sveconorwegian gneiss basement

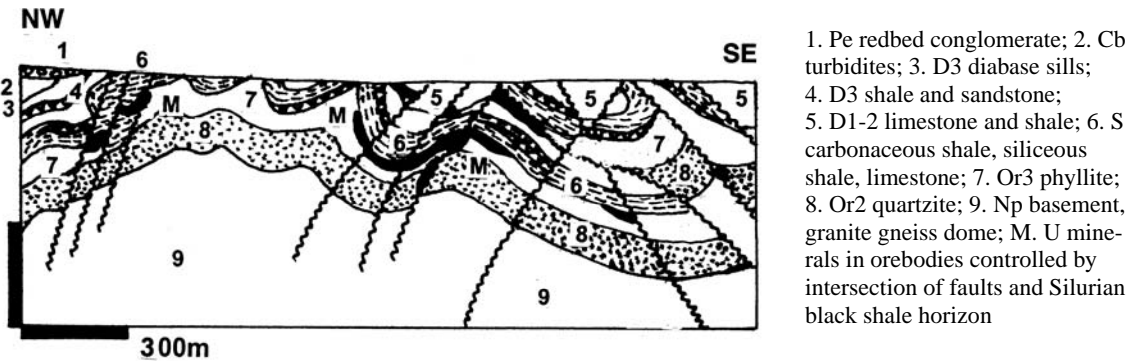


Figure 13.14. Ronneburg-Kauern U ore field near Gera, Thuringia, Germany, cross-section from LITHOTHEQUE No. 3109 modified after Vinokurov and Rybalov (1992), information from Wismut GmbH and site visit

The orebodies are broadly stratabound, with most of the ore accumulated in an about 100 m thick interval. Several elongated, assay-determined ore zones hundreds of meters long contain irregular bodies composed of dense stockworks of microfractures filled by pitchblende, overprinted by a younger generation of carbonate veinlets with scattered or sooty pitchblende, pyrite and rare Cu, As, Ni, Co minerals. There is a slight pervasive silicification, chloritization and bleaching within the ore blocks and narrow carbonatization and hematization aureoles along the stronger veins. The style is quite reminiscent of the Mina Fé near Ciudad Rodrigo in Spain. This is an almost entirely blind mineralization, without a well developed oxidation zone.

13.3.4. Phosphorite-black shale association

Many, if not most, black shale sequences are also high in P_2O_5 and they grade into successions where the phosphatic rock is the subject of mining and the interstratified or adjacent sedimentary rocks that include black shale, chert, and siliceous limestone, are the "waste". Both the phosphorite and, even more, the associated black slate, may be metalliferous and vanadium is the most often enriched metal. Phosphorites are themselves transitional between the presumably deeper-water, black shale and chert-rich end-member typified by the Phosphoria Formation (read below), and the warm, shallow-water phosphorites predominantly in carbonates, as in Florida (Section 13.4). In the early version of the U.S. Geological Survey ore deposit types (Cox and Singer, eds., 1986) the former phosphorites went under the heading "Upwelling-

type phosphates", the latter under "Warm water phosphates" (or Florida-type).

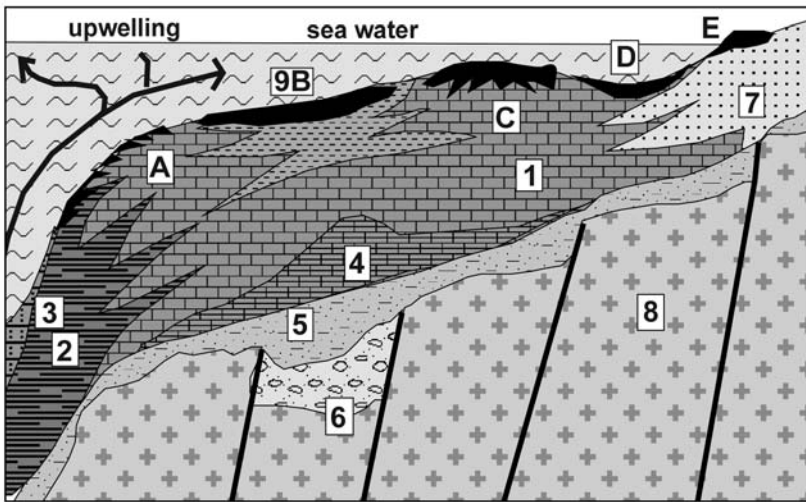
Wind- and currents-driven upwelling of cool, nutrients-rich ocean waters is presently (and since at least the Cretaceous) widespread along west-facing continental margins as off northern Africa, Namibia, Peru. Its role in phosphogenesis has been first proposed by Kazakov in 1937, and repeatedly refined since (compare Einsele, 1992, p. 198; Chandler and Christie, 1996; Fig. 13.15). The waters are slightly enriched in dissolved P_2O_5 but more importantly nourish abundant plankton (and related food chain). The skeletons, organic remains, coprolites that are further enriched in phosphorus in relation to sea water, settle at submarine plateaux, along the upper slope and outer shelf edges and on the shelf, at sites of low clastic deposition, to eventually produce condensed phosphatic sequences. During early diagenesis phosphorus is released from the organics and reprecipitated as francolite (carbonate fluorapatite) pellets, nodules, crusts or carbonate replacements. These are frequently physically reworked and/or enriched by clay winnowing, and often cemented to form sea floor pavements. In areas of strong upwelling as off Peru, phosphorite accumulates in the transitional zone between laminated organic-rich black muds with diagenetic chert nodules or beds, and the more oxygenated sediments seaward or landward (Einsele, 1992). This strongly approximates facies progression in the Phosphoria Formation (Fig. 13.16). Alternative mechanisms of marine phosphogenesis do exist (Bentor, ed., 1980).

Marine phosphorites, both the young ones still on the sea floor (e.g. off California, Chatham Rise) and in ancient sequences, are high in fluorine and in several trace metals. Of these, uranium is most consistently enriched in concentrations of between 50 and 150 ppm U. Although this is hardly an economic concentration, U is a potentially important by-product of phosphorite beneficiation. So far, very little uranium has actually been recovered in this way outside of Florida and possibly Kazakhstan, despite the large volume of phosphates processed annually in countries like Morocco. This may soon change. With the increasingly stringent regulations on content of toxic trace metals in fertilizers the producers will have to remove much of the trace U and other elements, and this may saturate the market in the same fashion elemental sulfur, produced by scrubbing sour natural gas at source, did decades ago especially in Canada. Countries with enormous phosphorite resources will thus join the ranks of U producers.

There are more trace metals present in/potentially recoverable from phosphorites, but their concentrations are highly unpredictable. The spot maxima like 210 ppm Ag, 1,700 ppm REE+Y, 7,260 ppm V, 110 ppm Sc, and others listed by Altschuler (1980) for the Georgina Basin phosphorites in Queensland look interesting, but average contents of trace elements present in the same setting, with greater than 2x clark values, are more practically important. They are: 1.5 ppm Ag, 15 ppm As, 6 ppm Mo, 10 ppm Sc, 3.7 ppm Se, 105 ppm U, 18 ppm Cd, 70 ppm V, 190 ppm Zn and 450 ppm REE. Many "phosphorite" trace metal values listed in the literature actually correspond to the associated black shales (especially of V). If tonnages of only few of these trace metals in phosphorites were accurately quantified and considered as "unconventional mineral resources", many phosphorite basins would attain the rank of a "giant", even "super-giant" accumulation. These and additional examples are in Table 13.5.

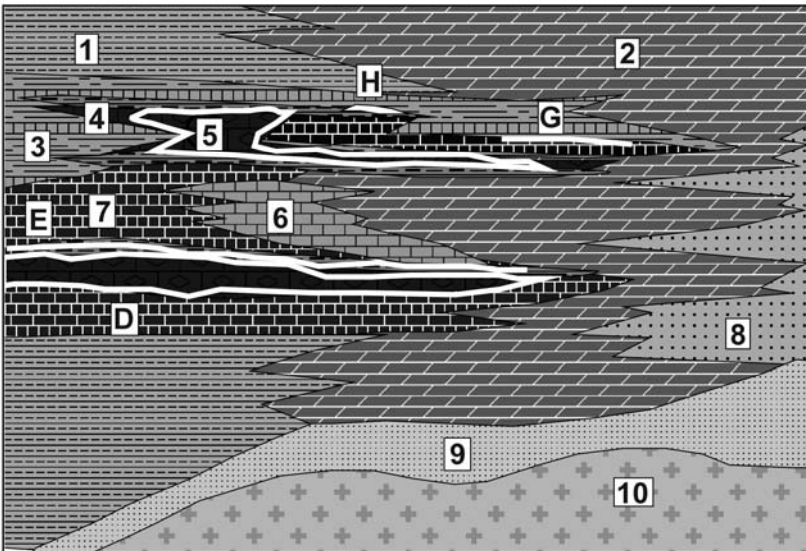
Phosphoria Formation in the Western Phosphate Field, U.S.A. (McKelvey et al., 1959, 1986; Cressman & Swanson, 1964; Swanson, 1973; 15-20 bt P_2O_5). The Western Phosphate Field is an area of some 346,000 km² in W. Montana, SE Idaho, NE Utah and SE Wyoming where the host Phosphoria Formation occurs in outcrop or subcrop. The Middle to Late Permian Phosphoria formed in the Cordilleran miogeocline, along facies transition from the deeper "basinal" facies dominated by shale, chert and phosphorite in the west, and a broad carbonate shelf in the east rapidly changing into "red beds" farther on. It is a strongly folded and thrust-faulted, almost unmetamorphosed thin unit rich in chemical sediments, with rapidly changing alternating lithologies dominated by chert, siliceous and carbonaceous (black) shale to argillite, siltstone, quartz-rich litharenite and minor dolomite and limestone. P_2O_5 is greatly enriched in two members: the stratigraphically lower Meade Peak Member, and the higher Retort Member. Four open pit and underground mines currently produce phosphorite from both Members and the field is second in importance, after Florida, as United States' phosphate supplier.

In the **Meade Peak Member** dark carbonaceous shale and phosphorite are the end-members of a succession that also includes fine pelletal phosphatic shale, structureless (pelitic) phosphorite, bioclastic phosphorite that includes fish scales, and pelletal phosphatic dolomite or limestone.



1. Shelf carbonates; 2. Basinal shale-chert; 3. Slope turbidites; 4. Evaporites; 5. Rift-stage arkose, litharenite; 6. Rift-stage basal conglomerate; 7. Beach, barrier, delta sands; 8. Crystalline basement; 9. Phosphorite. PHOSPHORITE SITES: A. Upper slope pavements, carbonate replacements; B. Offshore shelf, pellets and cements with glauconite; C. Replacements of carbonate mounds; D. Pellets and beds in warm shallow basin; E. Shallow coastal hardgrounds, reworked phosphorite

Figure 13.15. Cartoon showing the various phosphorite facies along upwelling-influenced continental margin. From Laznicka (2004) Total Metallogeny Site G142



1. Shale and mudstone
2. Dolomite
3. Siliceous, phosphatic shale
4. Black metalliferous shale
5. Pelletal, oolitic, pelitic phosphorite
6. Gray to black limestone
7. Chert, black or phosphatic
8. Lagoonar-deltaic redbeds sandstone, mudstone, anhydrite, gypsum, dolomite
9. Alluvial and beach sandstone
10. Basement
D. Pelletal to oolitic phosphorite with F, U
E. V,Mo,Ag,Se etc. rich metalliferous shale
G. Bedded barite

Figure 13.16. Place of the "upwelling" (basinal) phosphorite in the continent to basin transition as developed in the Western Phosphate Basin, U.S.A. From Laznicka (2004) Total Metallogeny Site G143

The thickness ranges from zero to about 15m and the Member is mined in bulk in open cuts when the grade exceeds the usual cutoff of 18% P₂O₅, or selectively from underground. Conda in SE Idaho is the largest and best known mine (Gulbrandsen and Krier, 1980). Vanadium is only moderately enriched in phosphorite (except for a 2.3 m thick phosphatic bed near the Meade Peak footwall at

Conda that grades 0.28% V₂O₅), but makes for an important resource in a black shale unit near the top of the Member (McKelvey et al., 1986). The Vanadiferous Zone is distributed over an area of about 11,500 km² in the border region of Wyoming, Idaho and Utah and it is an about 3.3 m thick package of a lower black shale, middle phosphorite and upper siltstone that averages 0.5% V.

Subeconomic resources quoted in McKelvey et al. (1986) for a portion of this zones are 37 mt @ 0.5% V for mere 185 kt V (a "medium" size deposit) but the geological resources are much greater.

The **Retort Member** crops out mostly in Montana and is similar to the Meade Peak, although the rocks are more thinly bedded with a tendency to form rhythmically alternating sandstone, chert and carbonate sets. The pelite contains up to 25% of organic carbon and a portion of the Member is an oil shale. Near Melrose, Montana, the member is 9 m thick and rich in uranium (average 0.015% U).

Phosphoria Formation is a giant, complex repository of fluorine (1.5-2 bt F) that is being partially extracted from phosphorite with accessory fluorite during processing, and many highly enriched, probably eventually recoverable metals for which information is patchy (U.S. Department of Interior Release, 1981). Foremost are uranium (estimated total content of 3 to 10 mt U in phosphorite and associated black shale) followed by vanadium, with the following highest average values recorded for selected units: 0.5% V, 150 ppm U, 0.5% Zn, 900 ppm Ni, 820 ppm Mo, 110 ppm Se.

The **Cambrian phosphate province of the former Soviet Central Asia** in southern Kazakhstan and adjacent Kyrgyzstan (Garkovets et al., 1979; Eganov et al., 1986) is comparable in lithology and facies relationship with the Phosphoria Formation, but is much more extensive (a 2,000 km long discontinuous NNW-SSE belt with 100 km long most productive segment in the Malyi Karatau Range in Kazakhstan). There, the phosphorite unit is about 70 m thick and contains some 0.21% V. The highest V values (up to 0.63% V) are reported from a horizon of black chert immediately underlying the phosphatic unit, interbedded with dolomite. Vanadium is absorbed in anthraxolite, V-sericite and roscoelite. The same horizon is enriched in Ba, Cr, Mo, Se, Re, Cu and U. Tonnages of the enriched trace metals are not available but probably amount to several million tons of V, and hundreds of thousand tons of Mo and U. Additional trace metals-rich phosphate localities are in Table 13.4. above.

13.3.5. Cu, Ag (Pb, Zn, Au, PGE) associated with reduced marine units above "redbeds" (Kupferschiefer or copper shale-type)

The German Kupferschiefer (KS), mined since the Medieval times, is one of the famous mineral deposit types and the largest repository of copper in Europe (if the most inflated resource estimate of

350 mt of contained Cu were true, KS would store about one quarter of the world's copper!). KF has also provided an outstanding case of a tight lithostratigraphic control to ore, originally considered stratiform (synsedimentary), now demoted to stratabound (postdepositional, epigenetic). Its setting is also an excellent empirical model for metals accumulated in the first reduced marine or lacustrine unit above oxidized clastics repeated, with some variations, around the world. Maynard (1983, 1991a) placed KF among the "products of diagenesis in rifted basins". Characteristics of this ore style follow best from description of the type area in central Europe.

The Kupferschiefer is a thin (zero to about 2 m thick) lithostratigraphic unit and a marker horizon on base of the Upper Permian Zechstein (or Marl Slate in Britain) carbonate-evaporite sequence that, over much of its subcrop and rare outcrop area, rests disconformably on Lower Permian continental arenites of the Rotliegendes (and locally Weissliegendes) succession. The latter contains intermittently bimodal volcanic "rift" association mostly of subaerial basalt ("melaphyre") and rhyolite, rhyodacite flows, hence KS is also a member of the rift association (Chapter 12). KS has been traced in subcrop from SE England through the Netherlands, central Germany to Poland along a 1,500 km long profile and over an area of 600,000 km² (Wedepohl, 1971). Wedepohl also estimated that more than 6,000 km² of KS carries 0.3% Cu plus, mined over a productive area of 1,200 km², plus 30,000 km² that grades 0.3+% Zn. Pb is also widespread and precious metals have recently been discovered in deep mines in Poland. Copper (and associated metals) has been mined from four major areas (the Hessen Depression, especially Richelsdorfer Gebirge, SE of Kassel; the Mansfeld-Sangerhausen district in the Harz Foreland, NW of Halle; the North Sudetic Syncline in SW Poland; the Fore Sudetic Monocline with its Lubin-Sieroszowice district west of Wroclaw). The first three areas crop out, the last one is entirely concealed in the subsurface in a flat country. The second area is a "Cu-giant", the first and third are "large" Cu accumulations, and the last area is a "Cu super-giant" (Table 13.7).

Mansfeld-Sangerhausen Cu district (Jung and Knitzschke, 1976; ~2.5 mt Cu @ 1.6-2.9%, ~12,800 t Ag @ 191 g/t) is developed in one of the post-orogenic ("molasse") basins in foreland of one branch (Harz) of the Variscan orogen. The extensional ("rift") basin is filled by the Lower Permian Rotliegendes continental "redbed"

succession of fluvial red sandstone with minor conglomerate and bimodal volcanics, transitional into a less colorful Weissliegendes near the top, interpreted as dune sand. Kupferschiefer (KS) is the first, Upper Permian (Zechstein) marine euxinic sediment rapidly deposited on top of the continental sandstone, on floor of a restricted evaporitic basin. It is a 30-40 cm thick unit that underlies some 200 km² in the ore district. It thins or is entirely missing above several sandstone highs (sand dunes or sandbars). From base to the top KS changes from a band of sandy, highly bituminous black shale into strongly, then slightly bituminous dolomitic marl. This changes upward into a 3-6 m thick dolomite and limestone with anhydritic nodules (Zechsteinkalk). Above is the Werra Anhydrite with 45-65 m of mostly anhydrite, locally hydrated to gypsum, and evaporitic dolomite (Fig. 13.17). Elsewhere in the North German Zechstein Basin, the corresponding unit contains a thick sequence of halite and K-Mg salts mined near Stassfurt.

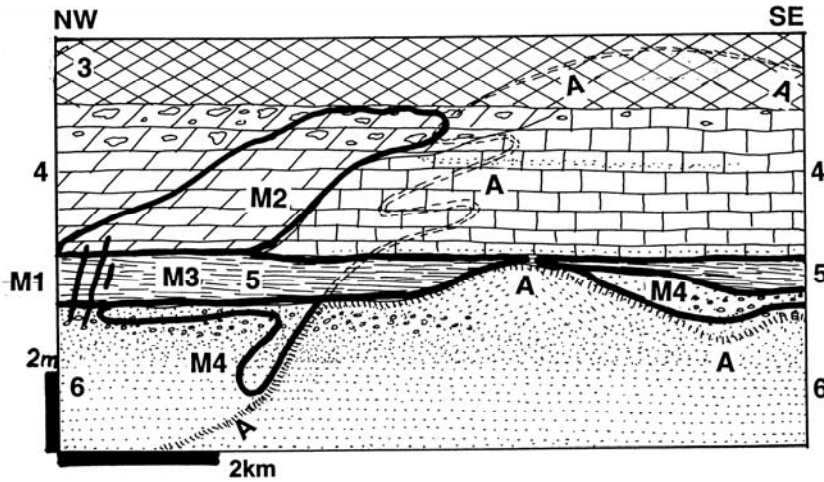
KS and its immediate footwall and hangingwall are persistently mineralized by Cu, Fe, Pb and Zn sulfides that form very fine-grained, largely "invisible" disseminations in the KS grading into discontinuous laminae and small sulfide patches, nodules and lenses. Green coatings of secondary Cu minerals that form shortly after exposure are the best visual indicators of ore presence. Minerals of the chalcocite group and bornite are dominant, chalcopyrite is less common. Galena and sphalerite increase with stratigraphy and their strongest development is in the Zechsteinkalk, but they have rarely been recovered. "Sanderz" (sandy ore) has a discontinuous distribution in the Weissliegende sandstone in the immediate KS footwall and it comprises bornite and chalcocite that replace calcitic matrix, and sometimes clasts, in sandstone or conglomerate. Most of the Sanderz is oxidized into pseudomorphic or infiltrated malachite, azurite, tenorite or chrysocolla. "Rücken" are late-stage crosscutting fracture veinlets and veins of barite, carbonates or quartz with Ni, Cu, Co arsenides and native silver.

The Cu-Ag mineralization is epigenetic, probably Triassic, and only developed immediately above "Rote Fäule" that is a slightly altered, diffuse, hematite pigmented rock. The alteration crosscuts, usually at a low angle, bedding and sedimentary laminations. Rote Fäule is barren and, although most characteristic in the footwall sandstone, it persists through the KS and Zechsteinkalk into the anhydrite unit.

The early mining started around Mansfeld in the NE portion of the district where the orebody had been exposed at the surface, and then it changed into underground operations in the south-westerly direction towards Sangerhausen. The mining near Mansfeld terminated in the 1970s, leaving behind sizable waste dumps now rapidly disappearing, and terminated near Sangerhausen in the 1990s.

Lubin district, SW Poland (Kucha, 1982; Jovett, 1986; Oszczepalski, 1999; P+Rv ~2.6 bt @ 2.0% Cu, 40 g/t Ag, 0.2% Pb, 0.1% Zn, for ~68 mt Cu, 170 kt Ag, 5.2 mt Pb, 5.0 mt Zn). Centered about 75 km NW of Wroclav, this is an about 50 km long, narrow NW-trending zone of predominantly Cu mineralization at base of Zechstein, at the NW-dipping limb of the Fore-Sudetic Monocline (Fig. 13.18). The presently mined continuous deposit (operating mines, from SW to NE: Lubin, Połkowice, Rudna, Sieroszowice) has an area of about 600 km², thickness between 0.4 and 26 m (average about 4 m), and is open in depth (Kucha and Przybyłowicz, 1999). The basic stratigraphy is comparable with the one at Mansfeld (read above) with some exceptions, and the ore is predominantly in the Kupferschiefer (KS) and partly in the immediately adjacent Zechsteinkalk above, and Weissliegendes below, in reduced pyritic and carbonaceous sedimentary rocks above the hematitic Rote Fäule alteration envelope. The white Weissliegendes sandstone here is immediately overlain by a 0.3-0.5 m thick liner of basal limestone or dolomite, on top of which is the KS, a black fissile carbonaceous shale. KS changes upwards and is sometimes substituted by a dark gray dolomitic shale followed by dark gray dolomite, dolomitic limestone and anhydrite. The Rote Fäule alteration overprint modifies rocks appearance; for example, the oxidized KS becomes a red to reddish-gray shale strongly depleted in organic carbon with abundant hematite, rare relics of sulfides, and enrichment in noble metals (Oszczepalski, 1999).

The main Cu-Ag mineralization is zoned and strongest at the reduced side of the redox boundary and mostly in the KS, where the chalcocite series are the dominant minerals. Away from contact the proportion of bornite and chalcopyrite increases and so does galena, sphalerite, pyrite and marcasite. The remainder of the 70 plus minerals identified in the district is of less importance. Pb and Zn become locally abundant to form separate orebodies in the hangingwall carbonates, most of which are in the Rudna Mine sector.



M1. Fracture veins of barite, Ni,Co,Cu arsenides; 3. Pe3 Zechstein, Werra Anhydrite with dolomite; 4. Zechstein Limestone & dolomite, anhydritic; M2. Disseminated and replacive Zn-Pb sulfides; 5. Kupferschiefer, 30-40 cm thick carbonaceous laminated dolomitic marl. M3. Disseminations & laminae of Cu sulfides in Unit 5; A. Rote Fäule red hematitic alteration;

Figure 13.17. Cross-sectional model of the Kupferschiefer in the Mansfeld-Sangerhausen district, Germany, from LITHOTHEQUE No. 3110 modified after Rentzsch (1974). Explanations (continued): M4. Sanderz, Cu sulfides replace calcite matrix in footwall sandstone or conglomerate; 6. Pe1 Upper Rotliegendes, top of red beds composed of bleached white, grey and red conglomerate and sandstone

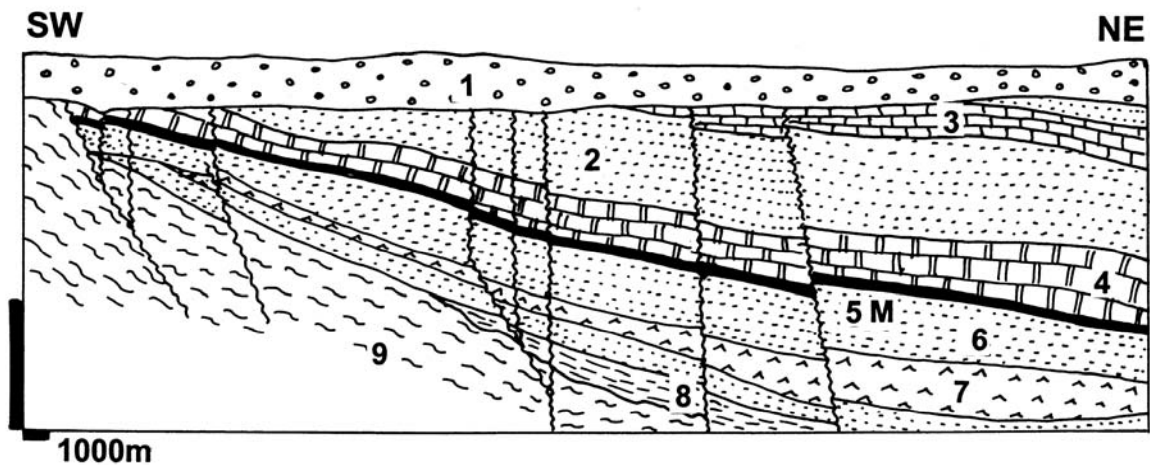


Figure 13.18. Cross-section of the Fore-Sudetic Monocline in the Lubin Cu district, Silesia, SW Poland. From LITHOTHEQUE No. 2021, modified after Wodzicki and Piestrzynski (1994). 1. Q-T cover sediment; 2. Tr sandstone; 3. Tr Limestone; Pe3 Zechstein evaporites, basal dolomite under anhydrite and halite; 5+M. Kupferschiefer black dolomitic marl, disseminated Cu sulfides; 6. Pe1 Rotliegendes red sandstone > conglomerate; 7. Pe1 bimodal continental volcanics; 8. Cb3 coal measures; 2. Pt to Cb1 folded and metamorphic basement

Lubin district produces some 0.6 t Au and 0.15 t Pd+Pt per year, recovered during copper refining. This comes from the contact zone where the precious metals are dispersed at both sides of the redox boundary. Two preferred sites of precious metals enrichment (sometimes called orebodies) have been identified, both of which are at the base of KS. The earlier reported site is in the **Lubin West Mine** (Kucha, 1982), where the "Noble Metals-bearing Shale" is an up to 10 cm thick band between the "pitchy shale" and the basal dolomite,

above the Weissliegende sandstone. There the gold content reaches up to 3,000 ppm in places and there is also up to 700 ppm Pt, 400 ppm Pd, 0.1% Se plus variable quantities of Hg, Bi and U. The noble metals reside in mooihoeite and haycockite, in turn confined to red lenses rich in Fe-Ca phosphates in the black shale, or are dispersed in the organic shale component. The subsequently discovered precious metals site in the **Polkowice West Mine** (Piestrzynski and Wodzicki, 2000; Rc ~150 t Au @ 1.5 g/t, 17 t Pt @ 0.2 g/t, 7 t Pd @ 0.1 g/t) is a 0.2-

0.8 m thick tabular body situated below the main Cu-Ag ore zone and extending over an area of 60 km². The zone lies within the redox transition, predominantly in the Weissliegendes hematite-stained sandstone, but it locally transgresses into the KS and Werra Dolomite above. Finely disseminated gold and electrum are associated with sparsely scattered Cu and Fe sulfides, Ni arsenides, and selenides (clausthalite).

As all orebodies in the district are concealed, there are no oxidation or secondary sulfide zones. As in Mansfeld, the mineralization is considered epigenetic, probably coeval with Triassic rifting in the area, produced by substitution of diagenetic pyrite in shale by Cu and other metals carried by oxidized basinal fluids. The fluids originated in the permeable red sandstone below, and were confined by the shale and evaporitic aquaclude above along which they spread.

13.3.6. Sedex Pb-Zn-Ag deposits in basinal shale near carbonate platform

Sedex (sedimentary-exhalational) deposits (Goodfellow et al., 1993; Lydon, 1996) are the dominant source of zinc and lead. The "exhalational" origin was first suggested by Schneiderhöhn, using the "classics" Rammelsberg (Fig. 13.19) and Meggen (Fig. 13.20) in Germany as a model, and the concept has reached the peak of popularity in the past thirty years. There are two frequency peaks of occurrence of the Zn-Pb "sedex" (and their presumed high-grade metamorphic equivalents like Broken Hill; Chapter 14): Mesoproterozoic (the great Australian deposits, Sullivan) and Middle-Upper Paleozoic (northern Cordillera and Germany). The former are treated in Chapter 11, the latter here.

All the Paleozoic "sedex" are in black shale (slate)-dominated condensed sequences usually interpreted as having formed in starved, (semi)-euxinic submarine rift basins along or within stable (miogeoclinal) continental margins. There are usually minor submarine volcanics (e.g. Na, Ca-metasomatized basalts=spilites and Na-dacite or rhyolite=keratophyre); Fig. 13.21. Some successions have continental clastics underneath. Also present in the vicinity of the black shale basins are "clean" platform carbonates, which causes rapid facies change. Carbonates in the black shale successions have the form of interbeds of dark-gray "basinal" limestone, carbonate component in shale, and resedimented (allodapic) limestone turbidites, slumps or debris-flow breccias. Carbonate platform to black shale basin transition is spectacularly

developed in the Northern Cordillera, in the Selwyn and Kechika basins in Canada (MacIntyre, 1991; Gordey et al., 1992) and in the Brooks Ranges of NW Alaska (Schmidt, 1997a,b). It is also well developed in the Devonian "Schwelle und Trog" facies in the German Rheinische Schiefergebirge and in Harz (Large and Walcher, 1999).

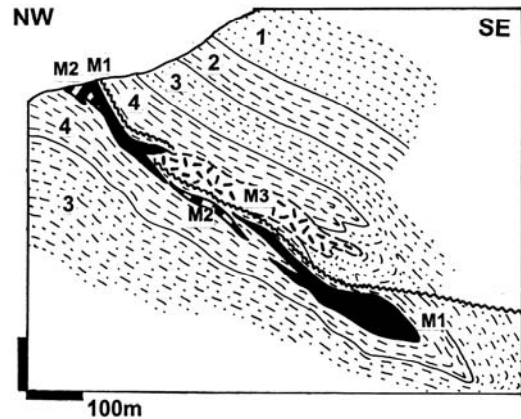
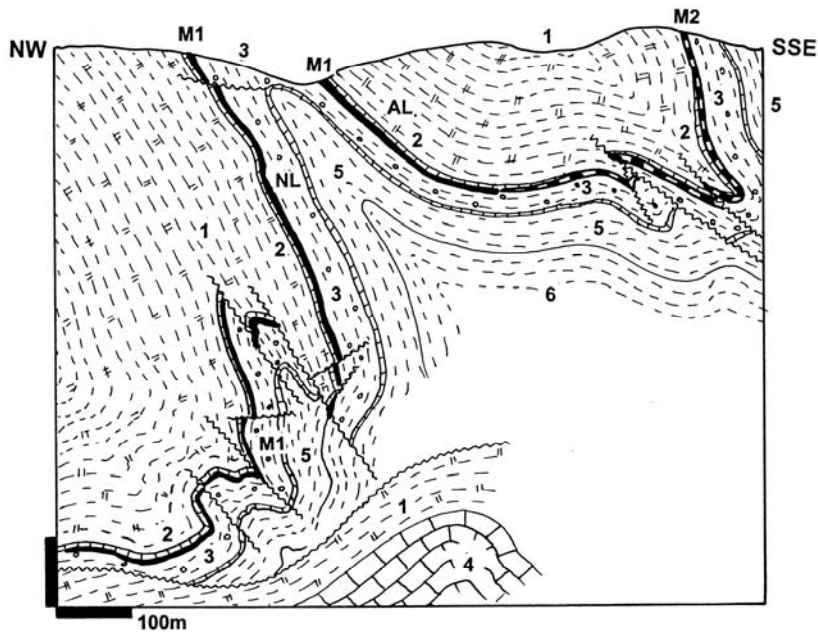


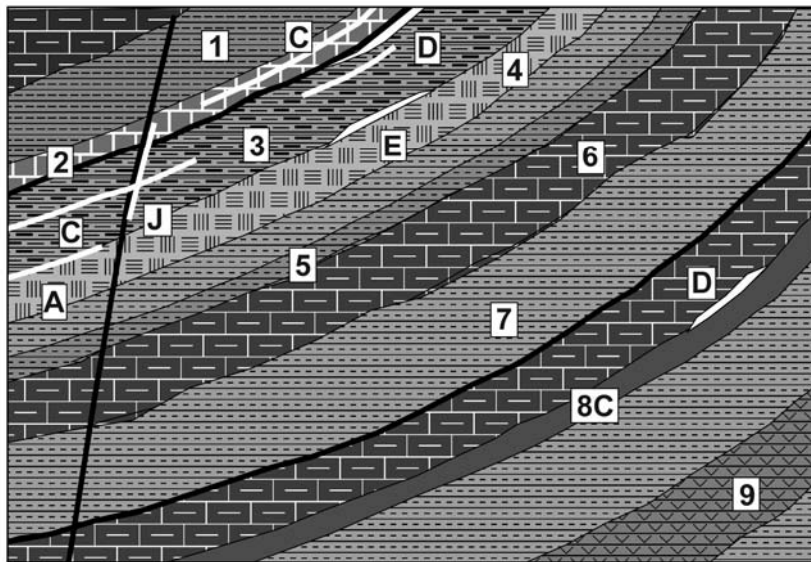
Figure 13.19. Rammelsberg Pb, Zn, Ag and barite deposit near Goslar, Harz Mts., Germany, an early prototype of the submarine-exhalational origin. Cross-section from LITHOTHEQUE No. 581, modified after Kraume (1955), Sperling and Walcher (1990). 1. D1 litharenite; 2. D1-2 Calceola Slate metapelite to arenite; 3. D2 lower Wissenbacher Schiefer, slate with sandy interbeds; 4. D2 upper Wissenbacher Schiefer, carbonaceous argillite to slate; M1-3 D2 synsedimentary hydrothermal mineralization: M1 stratiform massive Zn-Pb sulfide lens; M2. Massive barite lens; M3. Kniest, Cu-sulfides rich stockwork and disseminations in altered slate in stratigraphic footwall of the massive ore

Most of the Zn-Pb "sedex" deposits are associated with bedded barite which, in the Anarraaq deposit in Alaska, represent a gigantic accumulation of perhaps 2 billion tons BaSO₄. In contrast with the Mississippi Valley-type deposits in platform carbonates (that are usually not very far; compare Schmidt, 1997a,b), the "sedex" deposits are quite high in silver. The "Irish-type" Zn-Pb deposits (Hitzman and Beaty, 1996) are in many respects transitional between sedex and MVT, but occur in dominantly carbonate sequences (Section 13.4). The last controversial subject of "sedex" is distinction between the proximal (that include crosscutting footwall fluid feeders under stratiform bodies, as with the VMS) and distal (no feeders) orebodies. The Rammelsberg deposit (read below) is the "proximal" variety as the bedded barite on top gives way to stratabound Zn-Pb beneath and there is discordant Cu in the footwall.



- 1. D3 greenish shale with calcareous bands;
- 2. D2-3 thin pelagic limestone marker in the immediate ore hangingwall;
- M1. D2-3 "Kieslager" stratiform massive pyrite > sphalerite > galena;
- AL=Alters Lager, NL=Neues Lager orebodies;
- M2. Massive gray to black barite layer;
- 3. D2 basal dark shale with sandstone interbeds, reef detritus and limestone marker at base;
- 4. D2 Meggen Reef facies, biogenic limestone;
- 5. D2 Tentaculite shale;
- 6. D2 Wissenbacher Schiefer, gray to black shale

Figure 13.20. Meggen barite and pyritic Zn > Pb deposit, Lennestadt, Sauerland, Germany. Cross-section from LITHOTHEQUE No. 551 modified after Ehrenberg et al. (1954), Weisser (1972), Krebs (1972)



- 1. Siltstone
- 2. Chert, siliceous slate
- 3. Carbonaceous shale
- 4. Na-dacite (keratophyre)
- 5. Felsic tuffaceous shale
- 6. Dark basal argillaceous limestone
- 7. Shale
- 8. Bedded barite
- 9. Submarine basalt (spilite) flows, diabase sills
- A. Ironstone and siliceous iron formation (Lahn-Dill)
- C. Bedded barite
- D. Stratiform massive Zn,Pb sulfides (sedex) in shale
- E. Ditto, in felsic volcanics or at contacts
- J. Barite, Pb-Zn remobilized veins and replacements

Figure 13.21. "Basinal" black shale, chert, dark limestone > spilite, keratophyre association in orogenic belts (as in the Rheinische Schiefergebirge, Germany); rocks and ores inventory cross-section from Laznicka (2004), Total Metallogeny Site G144

The discordant Cu-rich "Kniest" stockwork in the footwall. Red Dog is more likely the "distal" variety and the quartz-sulfide veins in the ore field are considered synorogenic.

The basic premise of "sedex" origin has not changed since the Schneiderhöhn's days (in the 1940s): it is still a product of a low-temperature (less than 300°C, usually ~150-250° C)

hydrothermal fluid discharged and precipitated on the sea floor, or injected into the still unconsolidated sediments. Opinions vary about the sources of heat (magmatic, from deep granites, or "rift" magmatism; non-magmatic geothermal), fluid origin (sea water; formational fluids; metamorphic fluids), fluid channels (growth faults) and timing of ore formation. The comprehensive "story" recently worked out in the Red Dog district in Alaska (Kelley and Jennings, 2004) assumes underwater expulsion of Ba-rich pore fluids along seeps in the basin paleoslope and vents at the seafloor, followed by overlapping methane plus H₂S discharges, and high-salinity metalliferous fluids that precipitate metals by replacement of barite, carbonates, or the carbonaceous, siliclastic sediment. Copper is generally rare in the "sedex" ores, although chalcopyrite or tetrahedrite veins, stockworks or replacements are sometimes spatially associated (e.g. Matahambre, Cuba).

Rammelsberg Zn, Pb, Ag, Cu & barite deposit, Goslar, Germany (Kraume, 1955; Sperling and Walcher, 1990; Large and Walcher, 1999; P₁₀ 1989 ~28mt @ 14% Zn, 6% Pb, 2% Cu, 140 g/t Ag, 1 g/t Au, 20% BaSO₄, 800 ppm Sb, 500 ppm As, 70 ppm Bi for 5.1 mt Zn, 2.1 mt Pb, 560 kt Cu, 3,920 t Ag, 22.4 kt Sb, 14 kt As, 1,960 t Bi). Rammelsberg is a hill on the outskirts of Goslar, located at the foot of the Harz Mountains in north-central Germany. The mining there continued since at least AD 968 until the mine closure in 1989. The deposit is a part of the uplifted Harz Massif, in the Rhenohercynikum, a terrane within the late Paleozoic Variscan Orogen. It is situated close to the hinge between the Devonian Goslar Trough and Rammelsberg Rise (the Trog und Schwelle arrangement). The continuous "miogeoclinal" succession starts with Middle Devonian interbedded shale, sandstone and quartzite changing into calcareous shale, then Middle Devonian Wissenbacher Schiefer, a monotonous shale succession and the ore-hosting unit. Above are Upper Devonian shales and limestones topped by Lower Carboniferous (Kulm) turbidites with basal siliceous shale and chert. There are rare horizons of acidic ("keratophyre") tuffite, and perhaps synsedimentary diabase sills in the Upper Devonian strata. The succession is sub-greenschist metamorphosed, isoclinally folded with a strong axial cleavage, and intersected by a series of subvertical faults some of which control mostly Mesozoic Pb-Zn-Ag fissure veins in the Oberharz district (e.g. Grund, Clausthal-Zellerfeld).

The Rammelsberg ore zone, interpreted as "proximal sedex", is in the Wissenbacher Schiefer

unit of dark gray (slightly carbonaceous) shale to argillite with minor interbeds of litharenite and carbonates, interpreted as "distal turbidite". The lateral stratigraphic equivalent to ore is the Erzbandschiefer, a pin-stripe ankerite-laminated pyritic shale, geochemically enriched in Pb, Zn for many kilometers along strike. The 50-60° SE dipping ore package comprises four major and several minor stratiform and stratabound orebodies, plus minor crosscutting late stage veins. The original discovery, the Old (Altes Lager) orebody, is a 600 m long and 12 m thick strongly internally deformed and partly remobilized lens of massive sulfides, mined to a depth of 300 m. It comprises mostly fine grained pyrite, sphalerite, galena, minor chalcopyrite in barite, ankerite, pelite gangue.

The New (Neues Lager) Orebody was found in 1859 in depth; it is 8 to 40 m thick, comparable in composition with the Altes Lager. The grade is between 21-24% Zn+Pb+Cu. In footwall of a portion of the above orebodies is the Kniest, a stratabound zone of veinlets, lenses, disseminations of low-grade Zn, Pb, Cu sulfides (but relatively enriched in chalcopyrite) with quartz, ankerite, calcite and chlorite gangue, in silicified shale. On top of the ore package is a gray barite-rich zone with scattered low-grade Zn-Pb sulfides. Little is known about the gossan and presumably silver-rich enriched zone, mined-out long time ago in the "pre-literature" ages.

Rammelsberg appears close to the Goodfellow et al. (1993) model of "vent" (or proximal) sedex, with Kniest being the vent and the massive sulfide bodies the laterally spreading hydrothermal-sedimentary facies. The other German "sedex", the "large" **Meggen Zn-Pb-barite** deposit in the Rheinische Schiefergebirge, has a similar setting but it is a 6 km long, fairly uniform sheet of pyritic sphalerite, minor galena, topped by a large barite layer (Krebs, 1972; Fig. 12.20).

Red Dog Zn, Pb, Ag ore field, Alaska (Moore et al., 1986; Schmidt, 1997a; Kelley and Jennings, 2004 & references therein; 148 mt ore @ 16.6% Zn, 4.6% Pb, 83 g/t Ag for 24.6 mt Zn, 6.81 mt Pb, 12,284 t Ag). Red Dog is located in the western Brooks Range of NW Arctic Alaska, in tundra 135 km north of Kotzebue. Rusty stains were first noted in 1955, examined in 1968, and explored during the 1980s (Fig. 13.22). Mining of the Main orebody started in 1989 and subsequently three additional, stacked orebodies have been discovered within the Red Dog thrust plate (Aqqaluk, Paalaaq and Qanaiaq).

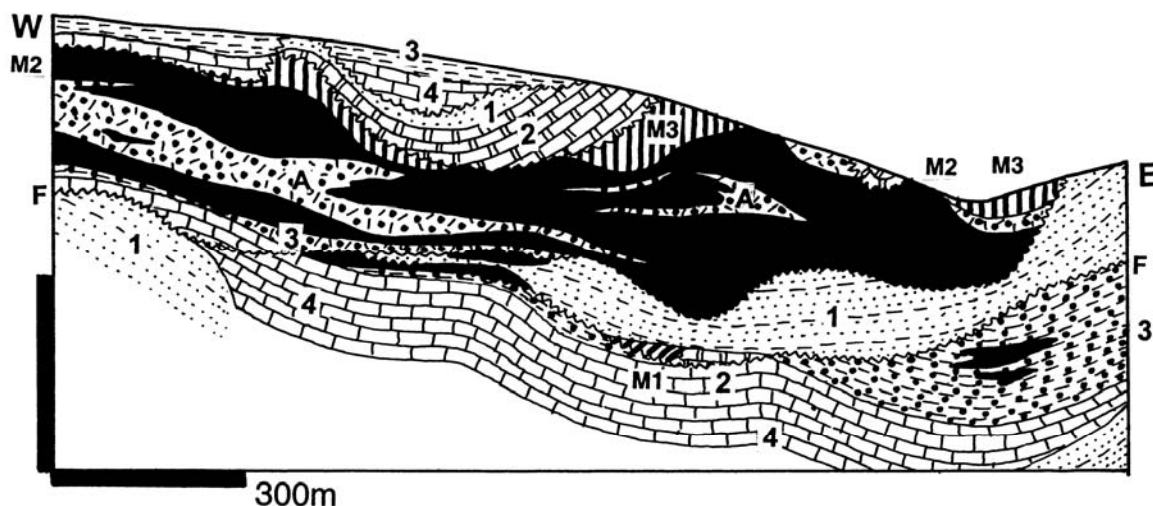


Figure 13.22. Red Dog Main deposit, Brooks Range, NW Alaska; cross-section from LITHOTHEQUE No. 3250, modified after Moore et al. (1986). 1. Cr1 Okpikruak Fm. sandstone, shale; Brooks Range Allochthon, three stacked thrust slices: 2. Cb3-Tr1 Siksikuk Fm., light-green shale, chert, host to M1. M1. Up to 30 m thick stratabound barite horizon in chert; 3. Cb1-Cb3 Ikalukrok Unit, laminated siliceous black argillite with bedded chert; host to M2. M2. Stack of almost flat lying elongated lenses of massive to semi-massive sphalerite > galena > Fe, Cu sulfides in quartz and barite gangue. Chaotic to breccia structures, tectonized during thrusting. Black dots in A: sub-grade disseminated sulfides in silicified rocks; 4. Cb1-Cb3 Kivalina Unit rhythmic gray shale and calcarenite; F=faults and thrusts

Two additional major deposits (Sue-Lik and Anarraaq) are within a 15 km radius to constitute the Red Dog ore field.

The orebodies are all hosted by the Lower Carboniferous (Mississippian) Kuna Formation, which is a 120 m thick sequence of thinly interbedded calcareous shale with minor bioclastic limestone, overlaid by 30-240 m thick unit of siliceous shale, black phosphatic shale, radiolarite and calcareous turbidite. Kuna Formation formed in a restricted, sediment-starved anoxic basin rimmed by a carbonate platform and floored by Late Devonian-Early Carboniferous Endicott Group of shallow marine siliclastics, that also include fluvial redbeds. There are minor syndimentary mafic volcanics. The sedimentary succession formed at a passive continental margin but was deformed during the 170-100 Ma Brooks Orogeny, and afterwards. The orebodies are now in three subhorizontally stacked, imbricated and internally deformed allochthon sheets and are practically unmetamorphosed despite the burial depth of 9 km or more before unroofing.

The Red Dog ore zone comprises four stacked and complexly deformed orebodies in a shallow dipping duplex structure. The orebodies range from stratabound, 90-175 m thick lenses of banded sulfides (several generations of sphalerite, galena, lesser pyrite or marcasite in quartz or barite gangue) grading to sphalerite and quartz-cemented breccia.

The ore grain changes from fine to coarse. The Main orebody is zoned, from top to bottom: 1) barite; 2) barite with sulfides; 3) silicified barite; 4) massive Zn-Pb sulfide; and 5) quartz-sulfide veins mainly in the Endicott Group beneath the orebody. The ore zone is enveloped by silica-rich rocks interpreted as either biogenic sediments (radiolarites, spiculites), or products of hydrothermal alteration. The silicites are also greatly enriched in thallium (up to 1.22% in some samples). The main stage of mineralization has been timed at around 338 Ma, and it was preceded by, and overlaps with, extensive barite precipitation in the region. The ores range from syndeositional to diagenetic and are attributed to low-temperature (~250-100°C) high-salinity, methane and Ba-rich basinal fluids expelled from the sedimentary pile undergoing compaction, and probably injected into still unconsolidated wet sediments in shallow depth under the sea floor. The quartz-sulfide veins in the area, of little economic importance, are mostly syngenetic.

Anarraaq deposit, 10 km NW of Red Dog (Kelley and Jennings, 2004; 1 or 2 bt barite, 18 mt ore @ 18% Zn, 5.4% Pb, 85 g/t Ag), has the world's largest barite resource and is also a "near-giant" Zn-Pb orebody. Discovered in 1999, it is a 6 km long zone in Lower Carboniferous carbonaceous and siliceous shale with interbeds of basinal carbonate and carbonate turbidite. The host is the Kuna

Formation as in Red Dog, but Anarraaq is lower in the stratigraphy.

Selwyn Basin Zn, Pb, NW Canada. Selwyn Basin is a NNW-elongated composite sequence of Cambrian to Lower Carboniferous sedimentary rocks deposited near the western margin of the Cordilleran miogeocline along the boundary of southern Yukon and Northwest Territories. The Basin narrows and continues south into British Columbia as Kechika Trough (Fritz et al., 1991). The sedimentary rocks now crop out in a series of imbricate thrust sheets east of the Tintina Trench, a prominent strike-slip fault. Throughout its Paleozoic history the miogeocline consisted of an easterly tapering prism of "clean" carbonate platform and shallow shelf limestone, dolomite with minor mature sandstone and shale, deposited on stable North American Platform floored by the Canadian Shield. These rocks now constitute the Cordilleran Foreland belt (Mackenzie and Rocky Mountains). The platform succession changes facies, often quite abruptly, into an assemblage of carbonaceous shale, siliceous shale, chert, thinly bedded dark "basinal" limestone and calcareous siltstone with locally developed submarine (meta)basalt flows and tuff. These rocks are interpreted to have formed in a series of deeper marine basins and troughs in the outer shelf and slope. Tectonic instability between Upper Devonian and Lower Carboniferous, marked by local emplacement of granitoids into the orogen, resulted in a turbiditic clastic wedge of chert sandstone and conglomerate, interbedded with black shale (Gordey, 1991). The platform edge then moved farther east.

Selwyn Basin contains three prominent "giant" Pb, Zn, Ag "camps" (groups of deposits larger than ore field) and a large resource of bedded barite, both interpreted as the syosedimentary "sedex" type formed by ore precipitation on the sea floor, or in unconsolidated wet sediments, from basinal brines channeled by growth faults (Godfellow et al., 1993). The oldest, Upper Cambrian **Faro-Anvil** "camp" (Jennings and Jilson, 1986) has 120 mt of ore @ 5.6% Zn, 3.7% Pb, 45-50 g/t Ag for 6.72 mt Zn, 4.44 mt Pb, 5,640 t Ag in seven deposits, in a 45 km long NW-trending zone. A series of thick massive Fe, Zn, Pb lenticular bodies are in graphitic and quartz-rich phyllite of the Rabbitkettle Assemblage, that also contains submarine greenstone basalt flows and tuff at stratigraphically higher levels.

Howard Pass (also known as Summit Lake) is a 28 km long, 20-50 m thick NE-SW trending narrow

ore zone that comprises three orebodies. This is the largest Canadian Zn-Pb deposit, not yet mined (Lydon, 1995; Rv+Rc 478 mt @ 5%Zn, 2% Pb for 23.9 mt Zn, 9.56 mt Pb). This Lower Silurian mineralization (Fritz et al., 1991) could be the closest example of the "distal sedex" type. It is interpreted as precipitated from a 220°C hot chloride-bicarbonate brine discharged on the sea floor. The mineralization comprises laminae of extremely fine-grained mixture of sphalerite and galena with minor pyrite, alternating with laminae of gray siliceous and calcareous shale to locally chert, in a rather indistinct, monotonous regional succession of gray to black shale to slate. The host succession is unusual in having only a minor pyrite content. Better apparent Zn-Pb sulfides occur in thin and short remobilized veinlets controlled by cleavage. Even an ore with 20% of sulfides is virtually unrecognizable in outcrop and local tales mention unsuspecting geological parties who walked over the orebody without noticing anything unusual. The visual obscurity of the ore, exposed on the frost-heaved barren alpine tundra surface, is made still more difficult by the presence of chalky white coatings of hydrozincite, indistinguishable from the similarly looking calcitic encrustations. The 1972 discovery was a follow-up on a Zn-anomalous lithochemical sample randomly collected in 1968. Despite the prospecting rush this triggered, nothing comparable has been found yet.

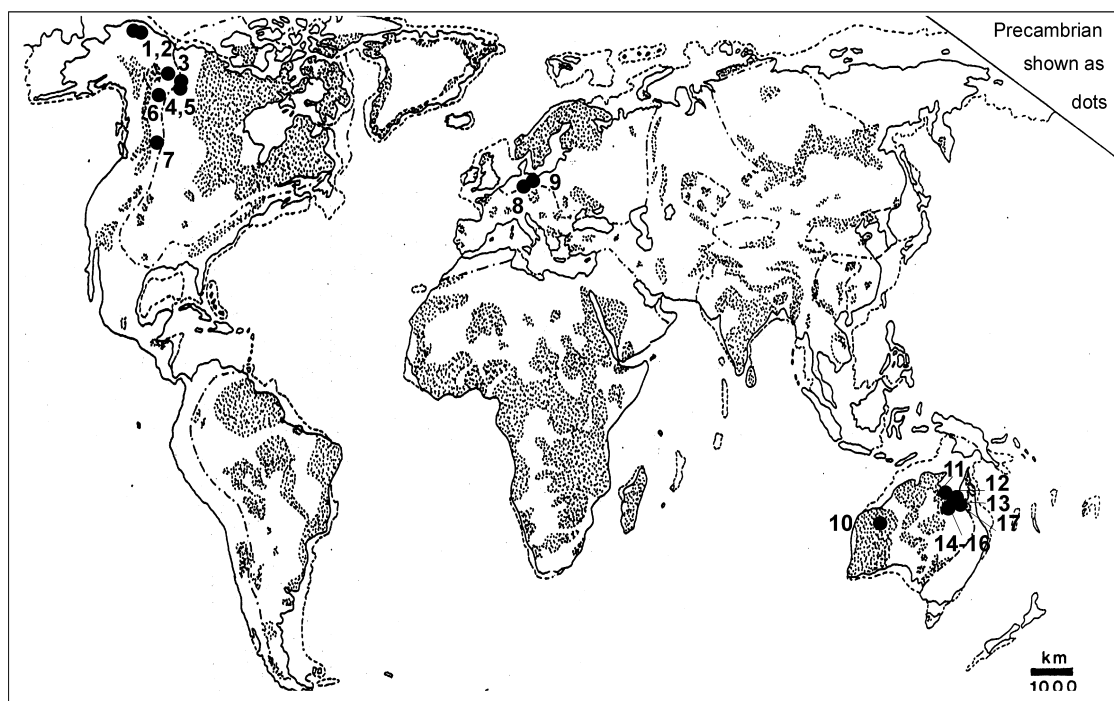
The youngest "sedex" deposits in the Canadian Cordillera are hosted by the Upper Devonian clastic wedge (Earn Group) in the **Macmillan Pass** area (Gordey, 1991), along the strategic World War 2 Canol Road. The structurally separated twin deposits **Tom and Jason** (McClay and Bidwell, 1986; Bailes et al., 1986) together store 30 mt of ore with 6.57-7.0% Zn, 4.6 to 7.09% Pb and 49-80 g/t Ag, for 2.025 mt Zn, 1.722 mt Pb and 1,897 t Ag. Both deposits are hosted by carbonaceous shale and shale with sandstone bands ("distal turbidite") and partly by polymictic and chert conglomerate (debris flows), close to a growth fault. The source proximal stratabound orebodies are thick lenses of massive pyrrhotite, galena, sphalerite, pyrite, minor chalcopyrite. These change into more laterally extensive, stratiform banded ore of the same minerals but dominated by pyrite and barite. Bedded barite deposits changing into trains of barite concretions and lenses in black slate are widespread in the Macmillan Pass area.

Table 13.5. and Fig. 13.23 list the world's major sedex deposits of all ages.

Table 13.5. Summary of the major Pb-Zn-Ag deposits in fine clastics interpreted as sedex

No	Deposit/ore field	Age	Pb, mt	Zn, mt	Ag, t	BaSO ₄ .mt
1	Red Dog (ore field), Alaska	Cb1	6.81	24.6	12,284	
2	Anarraaq (deposit), Alaska	Cb1	0.972	3.24	1,530	~1,500
3	Faro-Anvil (ore field), Yukon	Cm3	4.44	6.72	5,640	
4	Howard's Pass, Yukon & NWT	S1	9.56	23.9		
5	Macmillan Pass (Tom & Jason), Yukon	D3	1.72	2.025	1,897	
6	Gataga (ore field), British Columbia	D2-3	1.1	3.5	1,536	23.0
7	Sullivan, Kimberley, British Columbia	1.45 Ga	10.53	9.56	10,854	
8	Meggen deposit, Germany	D2-3	3.4	10.7		10.0
9	Rammelsberg deposit, Germany	D2	2.1	5.1	3,920	5.6
10	Abra deposit, Western Australia	Mp	3.6		1,200	12.0
11	McArthur River (HYC deposit), NT, Australia	1.65 Ga	9.5	22.5	9,551	
12	Century deposit, Queensland	1.595 Ga	2.06	13.8	5,527	
13	Lady Loretta deposit, Queensland	Mp	0.74	1.6	1,053	
14	George Fisher dep, Mt Isa distr, Queensland	1.67 Ga	5.05	10.787	8,659	
15	Hilton dep, Mt Isa distr, Queensland	1.67 Ga	3.185	4.557	7,399	
16	Mount Isa deposit, Queensland	1.67 Ga	7.363	6.82	17,890	
17	Dugald River deposit, Queensland	Mp	0.95	6.05	2,050	

Proterozoic deposits are described in Section 11.3

**Figure 13.23.** Map of the major Pb-Zn-Ag deposits interpreted as sedex

13.4. Marine carbonates and evaporites

13.4.1. Introduction

Carbonates and evaporites are fascinating rocks provided with an extensive and rapidly growing literature that appears overwhelming to an explorer searching for metallic deposits. Fortunately, much of the sedimentogenic detail (e.g. the paleontological nature of buildups or bioclasts) is of little relevance for ore presence (it is of more importance in petroleum geology) and can be greatly reduced for the purpose of predictive metallogeny. Various marginal and "special" factors such as unusual depositional environments, atypical settings, hydro(geo)logy, extraneous influences such as magmatism or heated brines, coincidences and contrasting contacts (e.g. oxidizing against reducing), and others become of paramount importance. These aspects are rarely treated in the literature based on the sedimentogenic premise, hence the "carbonate-evaporite" literature should provide a base on which to assemble multicomponental models but is not the end in itself. The book of John Warren (1999) "Evaporites" is an excellent example of a treatise that starts from the sedimentologist's premise, then explores many of the "exceptional circumstances" where evaporites influenced, directly or indirectly, the accumulation of ore metals. Consequently, the (former) evaporite presence ("an evaporite that was") should be sought and treated in the predictive metallogeny context, even when the evaporites themselves do not host the metals. The drawback of this kind of literature and follow-up analysis is that it tends to go too far (perhaps 50% of known ores can be shown to be somehow influenced by evaporites), so conceptualization has to stop at some point.

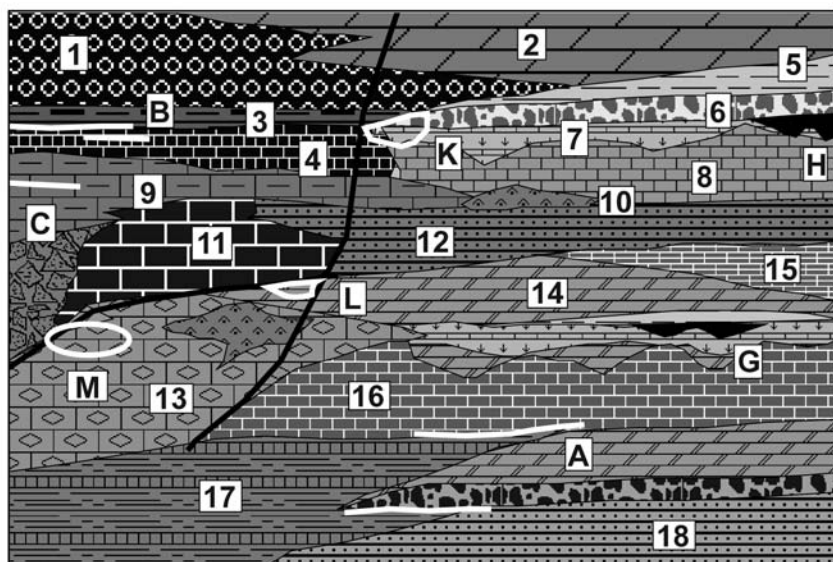
Ores in or related to carbonates briefly figure in Chapters 6, 7 and 10 where carbonates provided replaceable hosts to extraneous hydrothermal fluids (e.g. skarn, jasperoid, Carlin-type deposits) and Chapter 11 that specialize in Proterozoic (meta)carbonates. Ocean floor carbonates are briefly mentioned in Chapter 4. Continental evaporites and pedogenic carbonates (calcrete) follow. High-grade metamorphic equivalents of carbonates and rare evaporites are in Chapter 14.

Marine carbonates and evaporites setting, environments, evolution, metallogenesis: Global and regional descriptions and models of carbonate and evaporite environments, petrology and post-depositional evolution (diagenesis) are available from the literature and will not be repeated here (e.g. Bathurst, 1975; Wilson, 1975; Scholle, 1978;

Scholle et al., 1983; Moore, 1989; Einsele, 1992; Warren, 1999). The appearance of both lithologic groups goes back to the Proterozoic, although there is some evidence of early Archean evaporites (now preserved as barite, e.g. at North Pole, Western Australia) and carbonates in some Archean "rift sequences" and, of course, as hydrothermal sediments or carbonatized volcanics in Archean greenstone belts (Chapter 9). In this chapter only the Neoproterozoic to recent associations are considered.

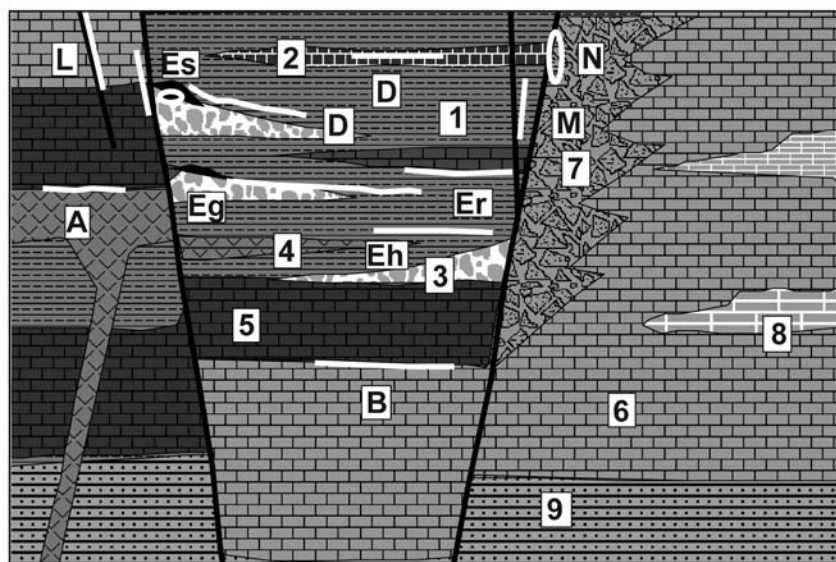
Present carbonate-depositing environments are dominated by carbonate buildups and reef-lagoon complexes that, together with other shallow marine forms like carbonate sand beaches and dunes, and calcareous shelf sediments, produced the "carbonate platform" assemblages of the past (Fig. 13.24). The latter are usually contrasted with the "basinal facies" of evenly thin-bedded dark (carbonaceous) limestone interbedded with, or changing facies into, shales. Einsele (1992) has summarized the concept of carbonate ramp in which the facies progression from shallow to deep water takes place on a gently sloping sea floor without a distinct shelf edge, although barrier reef bordered edges also exist. There, the reef sheds debris into the fore-slope and the open marine basinal pelagic sediments, both carbonate and siliclastic. The carbonate platform-basin interface is an important metallogene with Zn-Pb sulfide deposits, preferentially accumulated on both sides of it. In the literature on ore deposits the bathymetric contrasts that produced two different adjacent sedimentary lithofacies are usually attributed to faulting (rifting) along the margin and within a carbonate platform (Fig. 13.25). Evaporites form in a similar settings (Fig. 13.26) where they overlap with carbonates, although the origin of the "salt giants" and deep-water evaporites remains controversial (compare Einsele, 1992, p.242).

In terms of geochemistry pure carbonates and evaporites are among the most "refined" rocks that, together with the supermature quartz arenites, have the lowest contents of trace metals; the high-purity limestones average 0.35% Fe, 0.22% Al, 0.14% Mn, 0.1 ppm Co, 20 ppm Ni, 4 ppm Cu, 0.44 ppm Mo, 1 ppm Sn, 11 ppm Cr (Rösler and Lange, 1972). They are thus unproductive as metals source rocks (with some exceptions like manganoan carbonates and impure carbonates that leave aluminous residue), but provide excellent reservoirs to entrap metals migrating from outside. In terms of major metals, however, carbonates (magnesite and dolomite) and carnallitic evaporites, are sources of extractable Mg. The Makola and Youbi areas near Pointe Noire, Congo Brazzaville, store a large quantity of Mg in the 800 bt of carnallite (Mining Annual Review, 1999).



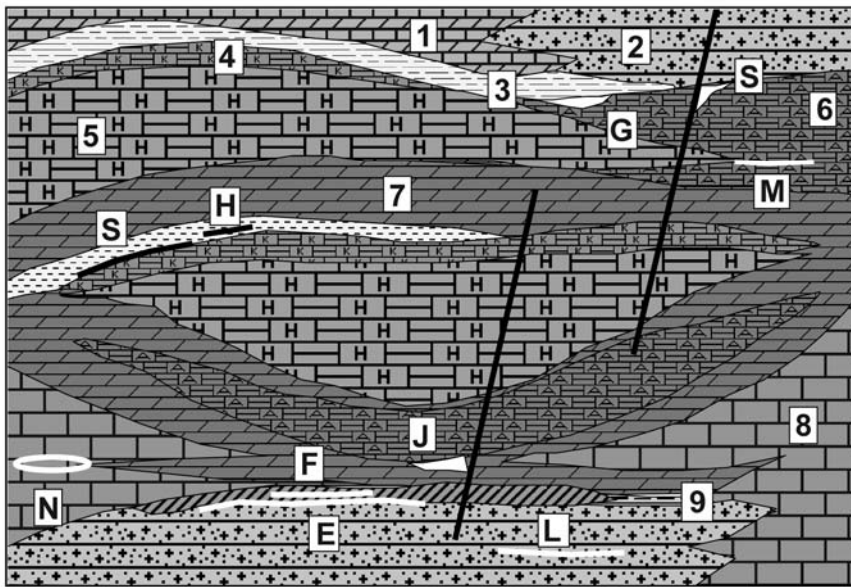
1. Gray nodular limestone;
 2. Dolomite; 3. Black shale;
 4. Siliceous limestone;
 5. Varicolored clay; 6. Residual breccia at unconformity;
 7. Karst, solution breccia; 8. Gray limestone;
 9. Dark marl to mudstone;
 10. Mafic flows, sills;
 11. Reef limestone; 12. Laminated calcarenite;
 13. Nodular marly limestone;
 14. Laminated dolomite;
 15. Evaporites; 16. Massive limestone;
 17. Calcareous shale; 18. Sandstone;
- A. Bedded hematite, siderite; B. Barite nodules, lenses; C. Bedded Mn carbonate or oxides;

Figure 13.24. Rocks and ores of a carbonate platform (on right) changing to a "basinal sequence" (left); inventory diagram from Laznicka (2004), Total Metallogeny Site G166. Explanations (continued): G. Mediterranean type bauxite at unconformity; H. Fe (Ni,Co) in transported laterite filling karst; K. Mississippi Valley (MVT) Zn-Pb type; L. Fluorite, barite replacements; M. Fe (Mn) siderite replacements of carbonates. Deposit types C and Fe have known "giant" members



1. Gray to black pyritic argillite;
 2. Gray ribbon chert;
 3. Debris flows, breccia, diamictite;
 4. Submarine basalt flows, diabase sill;
 5. Dark siliceous basinal limestone;
 6. Light platform limestone and dolomite;
 7. Carbonate breccia;
 8. Evaporite;
 9. Sandstone;
- A. Exhalative Lahn-Dill type iron formation; B. Bedded Mn in carbonates; D. Bedded barite; E. Sedex Zn,Pb,Ag; Eg. Ditto, associated with growth fault breccias; Eh. Ditto, monotonous fine-grained sulfide horizon in shale; Er. Ditto, at contact of shale and limestone near reef; Es. Ditto, Pb-Zn lens floored by Cu sulfides;

Figure 13.25. Basinal clastic > carbonate facies in a fault trough (graben) within a shallow marine carbonate platform, rocks and ores inventory from Laznicka (2004), Total Metallogeny Site G159. Explanations (continued): L. Siderite, hematite veins; M. Pb,Zn,Ag quartz-siderite veins; N. Ditto, disseminated replacements in carbonate breccia. Ore types B and E (all varieties) have known "giant" members



1. Platform carbonate; 2. Redbeds; 3. Red or green claystone; 4. K-Mg marine evaporites; 5. Halite; 6. Anhydrite; 7. Evaporitic and diagenetic dolomite; 8. Reef limestone; 9. Euxinic marl, black shale; E. Stratabound Cu (Ag) at redox interfaces (Kupferschiefer); F. Stratabound Pb-Zn replacements in dolomite; G. Native sulfur in gypsum, marl; H. Pb, Zn in gypsum & marl; J. Baryte, Mn, Pb, Zn, Ag replacements; L. Sandstone Cu; M. Mn marl interbeds in anhydrite; N. Zn-Pb of MVT type; S. Cu, Sb, Ag sulfide replacements

Figure 13.26. Thick carbonate-evaporite sequence, rocks and ores inventory from Laznicka (2004), Total Metallogeny Site G161. Ore types E, F, N have known "giant" members

The few syngenetic and diagenetic metallic deposits to form in carbonate depositing environments like U in phosphorites, bedded Mn carbonates, and replacement Zn-Pb sulfides ("Irish-type"; read below), also owe their origin to external metal fluxes that include heated basinal brines. The same applies to evaporites.

Early and late carbonate diagenesis is marked by extensive movement of basinal fluids that include hydrocarbons. Dolomitization and also silicification are common diagenetic products associated with many epigenetic ore deposits in carbonates, especially the Mississippi Valley-type Zn-Pb. The relationship of metasomatic dolomite and Zn-Pb sulfides remains controversial. Petroleum and gas maturation and migration is related to ore genesis directly (hydrocarbons as a source of recoverable trace metals like V and U; this is of a minor importance) or, more frequently, indirectly as a process parallel with migration of metalliferous brines, and as a reductant (e.g. to fix uranium moving in oxidizing solutions). When evaporites, especially halite, are present, the formation of salt domes creates dilations utilized by migrating fluids for ore deposition (e.g. Nikitovka-Hg), or it supports formation of native sulfur deposits by bacterial activity. Although "world class" sulfur deposits formed in this way (e.g. in the Gulf Province, especially in Louisiana), no major metal accumulations are associated.

Late diagenesis (supergeneration, hypergenesis) under subaerial and near-surface conditions, like carbonate dissolution by meteoric waters to form karst, is an important metallogene. The less important effect is residual enrichment of earlier formed metal accumulations in carbonates (e.g. Mn oxides, Zn-Pb sulfates, carbonates and silicates), the more important effect is creation of open spaces to be filled by ore material brought in from outside such as bauxite, Fe-Ni transported laterites, and others. In halite-rich evaporite successions salt dissolution was more rapid and more thorough than carbonate dissolution and it left behind large voids filled by collapse and contraction. A variety of breccias had resulted (compare Laznicka, 1988), some of which were later (rarely simultaneously with the dissolution) overprinted by products of hydrothermal alteration and mineralization. Warren (1999) devoted a chapter, and extensive discussion, to such "evaporites that were" and their ores.

Post-diagenetic epigenesis produced a variety of deposits of Au (Carlin and Kuranakh-types); Hg, As, Sb, Fe, Zn-Pb, Cu, Sb, W, Sn (skarn and hydrothermal replacements) related to external hydrothermal systems, where the carbonates provided a passive replaceable medium, or voids to be filled.

Carbonate-hosted "giants" specialise in a small selection of ore metals. The Zn-Pb giants are dominant.

13.4.2. Warm-current (Florida-type) phosphorites and their uranium enrichment

“Warm current phosphorites”, as they are headlined in Cox and Singer, eds. (1986), are at one end of the marine phosphorite facies series, the other being the “upwelling-type” phosphates (read above). In practice this is a transitional series the middle members of which share the characteristics of both end members (e.g. the NW African phosphates). Warm water phosphorites are enriched in several trace metals like their “basinal” counterparts, although the selection of metals varies. Those in the Central Florida district average 111 ppm Sb, 42 ppm As, 29 ppm W, 19 ppm V, 16 ppm Mo, 11 ppb Re and 60-110 ppm U (Riggs et al, 1985). Of these, Sb, Re and U have the greatest concentration clarkes, but uranium is the only metal recovered. In the 1980s, the district had an annual production capacity of around 1,150 t U.

Florida Phosphate province (Cathcart, 1963; Riggs et al, 1985). Phosphate mining started in the “Land-Pebble phosphate district” (Fig. 13.27) of central and southern Florida, east of Tampa, in the 1880s and since then Florida has been the principal phosphate producer of the United States, and second in the world (after Morocco; Fig. 13.27). The “Land Pebble district” is just a fraction of the extensive Atlantic Coastal Plain and adjacent shelf phosphate complex that extends from southern Florida to North Carolina (south of Washington, D.C.) and as far into the Atlantic offshore as the Blake Plateau. The phosphate tonnage estimates vary widely between 4 and 9 bt of identified resource, and 4.1 to 10.7 bt of resource potential of phosphate concentrate (around 31% P_2O_5) for Florida only, and more than 47 bt of concentrate for the whole region. The concentrate alone does not provide measure of P_2O_5 content in the actual “ore”, that could run from about 5% to 30% of P_2O_5 . The region stores up to 7.16 mt of by-product U, in concentrations between 60 and 110 ppm U in the phosphorite concentrate and about 185 to 350 ppm in P_2O_5 (Riggs, 1991). The actually recoverable U tonnage would be a fraction of this.

The bulk of this resource is in Miocene sediments and sedimentary rocks that formed in a wide range of environments ranging from upwelling-influenced continental slope to shelf to nearshore lagoons. The most productive phosphatic environment have been shallow-water platforms that project onto the continental shelf. The original chemically precipitated phosphorite (Ca fluorapatite) has the form of sand- to pebble-sized

pellets (intraclasts) and these are repeatedly reworked into a variety of host sediments (both carbonate and siliclastic), or they remain on the sea floor as scattered grains or pavements cemented by authigenic phosphorite. The principal phosphorite carriers in Florida are the Miocene Hawthorn and Pungo River assemblages composed of both terrigenous shelf and platform carbonate facies. In Florida they are overlaid by the Pliocene Bone Valley Formation, which is a fluvial facies on land that grades downslope into estuarine to shallow marine sediments.

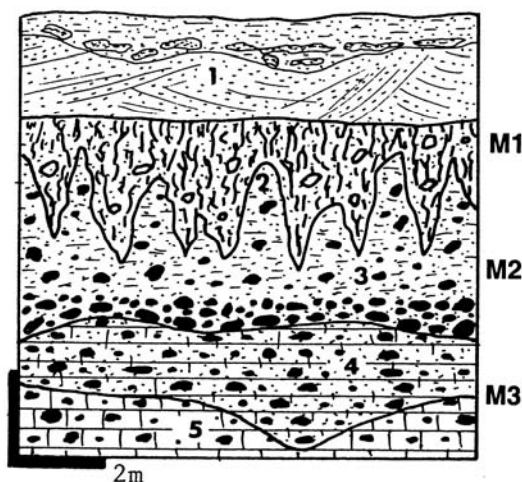


Figure 13. 27. Diagrammatic cross-section of a Land Pebble phosphate deposit, Fort Meade area, Florida. From LITHOTHEQUE No. 328, based on 1974 field visit. 1. Q dune sand, hardpan; M1. Zone of infiltrated and grain-cementing Al phosphates in recent regolith; 2. Pl Bone Valley Fm., unconsolidated clay, sand, gravel with phosphate nodules; 3+M2. Main zone of residual fluorapatite nodules reworked from M3. 4. Regolith over Unit 5, calcareous sandy clay saprolite; 5+M3. Mi Hawthorn Fm. biomicrite with scattered fluorapatite nodules

The present phosphate mining takes place on land, in four Florida to southern Georgia districts, and one (Aurora) North Carolina district. In Florida the Central and South Florida districts (the original Land Pebble region) measure some 7,000 km² and are located south and SE of the Ocala Upland, a subaerially exposed area of non-deposition in Miocene. The Hawthorn succession there is represented by a 4 to 40 m thick white biosparite limestone that changes into a hard dolomite towards the north. There is a thin non-calcareous sandstone and claystone unit on top. The low P content (2-5% P_2O_5) in the original carbonate has the form of dispersed “mud” apatite as well as apatite pellets (Riggs, 1985). The grains and pellets range in size

from 1 to 30 mm, are structureless, yellowish-brown, with a smooth, shiny surface. This has not been an economic ore so far and all the production came from the supergene enriched material on top. In the small North Florida district the subaerial enrichment produced the "hard rock phosphate", a secondary apatite that replaced the host carbonate and precipitated in karst cavities. In the rest of Florida the principal ores are apatite nodules ("pebbles") reworked into the Bone Valley clastics.

The Bone Valley Formation ranges from 0 to 17 m in thickness. The basal 2-4 m, the main ore horizon, comprise unconsolidated sand, clay and gravel with a high content of phosphatic nodules. The nodules average 20-30% P_2O_5 and between 110 and 160 ppm U. Tropical weathering and leaching superimposed on the Bone Valley sediments produced a blanket of infiltrated and grain-cementing Al and minor Fe phosphates crandallite, millsite and wavellite. The Al-phosphates may constitute up to 30% of the ore horizon. They are impoverished in P_2O_5 , but enriched in U to 90-300 ppm.

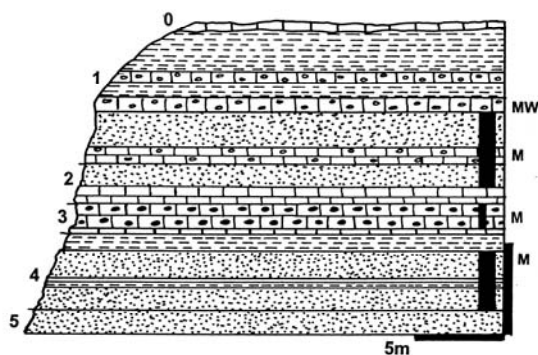


Figure 13.28. Oued Zem phosphate deposit, Morocco, cross section from LITHOTHEQUE No. 1750, modified after Aramboug et al. (1952). 0. T platformic limestone cover; MW. "Silix phosphate", phosphatic chert; M. Cr3-Eo three horizons of diagenetic and partly supergene phosphatic sediments that include sandstone with fluorapatite grains with francolite, staffelite, clay matrix that grade to phosphatic limestone; 1. Eo limestone with chert and marl; 2. Pc3 sandy phosphorite, phosphatic limestone; 3. Pc2 phosphatic limestone; 4. Cr3 sandy phosphorite interbedded with limestone; 5. Cr3 sandstone.

Other phosphorite deposits of the world contain trace uranium (the average U content in phosphorites is usually quoted as between 50 and 100 ppm), even when the exact values are rarely available from the literature and the U is not recovered. If the phosphorite resource of Morocco (Fig. 13.28), estimated at some 60 bt with around

60% of concentrate (that is, some 36 bt of concentrate; calculated from data in the Engineering and Mining Journal, September 1986) contained 80 ppm U in concentrate, the total U content would be 2.9 mt U.

13.4.3. Bedded Mn deposits in "basinal" (reduced) carbonates

Molango, Mexico (Okita, 1992; Force and Maynard, 1991; Rv ~203 mt Mn @ 27%, Rc 1.5 bt Mn @ 10%). This is the largest Mn accumulation in the Americas, located in the Cordilleran miogeocline of central Mexico. Okita (1992) suggested a similarity of Molango with the early diagenetic Mn carbonates presently forming in the mildly anoxic bottom muds in the Baltic Sea. The Baltic, however, is a shallow siliclastic inland sea whereas the Upper Jurassic sedimentary rocks that host Molango have been assigned to the continental slope depositional environment by Force and Maynard (1991).

Molango Mn district, in the Sierra Madre Oriental, occupies an area of about 50 x 25 km. There a ~9 m thick Mn ore bed, and its 50 m thick Mn-enriched "package", intermittently crop out at surface. The ore is composed of finely laminated dark gray carbonaceous rhodochrosite, virtually indistinguishable from the overlying limestone. The rhodochrosite ore ranges from pelitic to clotted to pelletal or intraclastic. Pyrite is conspicuously rare in and near the Mn bed. The Mn orebody has been mined from four deposits, of which only the Nonoalco Mine in the south also produces battery-grade oxide ore from the regolith, mostly composed of pyrolusite and ramsdellite. "Basinal" limestone occurs both in the hangingwall and footwall with calcareous shale, siltstone, conglomerate, red bed sandstone and rare basalt (rift association) below.

Okita (1992) interpreted the Mn ore as early diagenetic, where Mn present in pore waters, assisted by organic matter and pyrite, replaced the original limestone. Force and Maynard (1991) proposed diagenetic reduction of the original Mn oxides: an idea supported by the presence of magnetite and some fauna in the ore. Molango is similar to the Proterozoic "Mn giant" Moanda described in Chapter 11. There, however, the oxidized ore is most prominent.

13.4.4. Low-temperature Zn-Pb deposits in carbonates

Shallow water carbonates (of platforms and miogeoclines) are an important repository of zinc

and lead sulfide deposits that store a high proportion of the world's Zn, less Pb but, characteristically, very little Ag. Table 13.6 lists one Pb "super-giant" (the S.E. Missouri district or the Viburnum Subdistrict), 10 "Pb giants", 6 "Zn giants", 9 "large" Pb entries, 12 "large" Zn entries and 2 "large" Ag entries. Over the years an elaborate "type" terminology has developed, but the type definitions are unable to keep with the rapid progress of new interpretations and re-interpretations and are even less able to agree on the type definition and limits. A single Zn-Pb deposit like Bleiberg in Austria (Fig. 13.29) can, and has been placed, into the Alpine, Appalachian, Irish and Mississippi Valley types, by various authors and in various times. This is compounded by the fact that several "ore types" can coexist within a single deposit or ore field/district. Perhaps the Mississippi Valley, MVT (itself lacking a distinct single type locality) should be used as a shortcut for low-temperature, mostly stratabound sphalerite and galena deposits in carbonates that are not genetically associated with epi-, meso- and hypothermal hydrothermal systems, the latter affiliated, at least indirectly, with magmatism (Chapters 6, 7, 10). What are the key characteristics of the named MVT varieties?

1. The original MVT-type (Brown, ed., 1967) evolved as an alternative of Lindgren's and others' classes of "telemagmatic" and "cryptomagmatic" deposits in times when most base metals ores were considered hydrothermal and granite-related (compare Wolf, 1981). The original MVT-type locality was the Upper Mississippi Valley Zn-Pb province (at 7,800 km² much larger than a district) dotted by some 400 individual deposits that range in size from several tons of ore to about 3 mt, and cumulatively store some 1.6 mt Zn and 750 kt Pb (Heyl et al., 1959). These deposits range from bedding parallel blankets to discordant veins and their common characteristics include limestone hosts (usually dolomitized), strong stratigraphic control, simple mineralogy (low-Fe sphalerite [brown to yellow], galena, pyrite or marcasite), low silver content, low temperature high salinity fluids (~60-140°C), and lack of genetically associated magmatic rocks. In the more modern usage (e.g. Leach and Sangster, 1993 and references therein) a "typical" MVT is, furthermore, located in platforms, is epigenetic and mostly open-space filling. The ore minerals crystallized, after host rocks lithification, from basinal brines (often petroleum-related; Sverjensky, 1984) or from groundwater brines that

migrated, like birds, across continents (e.g. Bethke and Marshak, 1990; Garven et al., 1998; Appold and Garven, 1999), or formed regional paleoaquifers (Kesler, 1996).

2. The Appalachian (in America; e.g. East Tennessee-Zn; Hoagland, 1976) **and Alpine** (in Europe; e.g. Bleiberg, Mežica; Maynard, 1983) **Zn-Pb types** were varieties of MVT located in miogeoclines, in deformed and sometimes slightly metamorphosed successions. They were interpreted as pre-, syn- and post-orogenic. Recent literature added syntectonic expulsion of basinal fluids during deformation and/or syndepositional hydrothermal fluids (sedex in carbonates) as additional ore-forming components (e.g. Velasco et al., 1994; Kesler, 1996).

3. The Irish type (e.g. Hitzman and Beaty, 1996) emphasized the bedded and apparently syn-depositional or diagenetic replacement nature of the Zn-Pb deposits, produced early by sea water, "basinal" or extraneous hydrothermal fluids channelled along growth faults. In Navan (Anderson et al., 1998) the strongest evidence for the early (syn-diagenetic) mineralization has been furnished by the presence of ore clasts in the Boulder Conglomerate, unconformably resting on the ore-bearing Pale Beds (read below). Pearce and Wallace (2000), however, demonstrated that, in Navan, all mineralization postdated the erosion surface and was younger, post-lithification. Additional characteristic of the Irish type was the presence of oxidized clastics (red beds) under the carbonates, with which they communicated via faults (Fig. 13.30). The latter feature brought the Irish type close to the Kupferschiefer (read above) that also has Pb-Zn sulfides in marine carbonates above redbeds, the only difference being the presence of a reduced basal marine unit enriched in copper.

4. The Illinois-Kentucky (or vein-MVT; Hall and Friedman, 1963) **type** is exemplified by the predominantly fluorite-barite and minor Zn-Pb crosscutting veins in the above-mentioned district (also in the English Pennines and elsewhere), that have all the fluid and temperature characteristics of the MVT, but lack the stratiformity. The veins cut all types of wallrocks, clastics as well as carbonates, although they often spread laterally to form stratabound "mantos" when passing through a carbonate unit.

Table 13.6. Selection of major ("giant" and several "large") low-temperature Zn, Pb deposits in carbonates: Mississippi Valley, Irish, Appalachian, Alpine and similar types.

Deposit/district	Geology	Metal tonnages	References
Polaris, Little Cornwallis Island, northern Canada Pine Point, NWT, Canada	Gently dipping irregular body of sfalerite, galena filling voids and fractures in karsted D3 limestone; underlain by veins and breccia; in permafrost 65 km long E-W belt of 87 deposits of void and fracture filling sphalerite & galena in coarse D2 metasomatic dolomite	22 mt @ 14% Zn, 4% Pb for 3.08 mt Zn and 880 k Pb 95 mt @ 6.2% Zn, 2.5% Pb for 5.8 mt Zn, 2.4 mt Pb	Symons and Sangster (1992) Kyle (1981)
East Tennessee (Mascot-Jefferson City) district, U.S.A. Central Tennessee (Elmwood), United States South-Eastern Missouri district, U.S.A.: Old Lead Belt Ditto, Viburnum Trend	Broadly stratabound zones of yellow sphalerite in solution collapse breccias and under unconformity, in Or2 dolomitized limestone Reddish sphalerite scattered in peneconcordant solution collapse breccia under Or2 unconformity, in Or1 coarse dolomitized limestone 19 km long NW-SE area of scattered and nest-like galena in subhorizontal assay-bounded bodies in Cb reef-influenced limestone, dolomite with shale 64 km N-S zone of near continuous partly zoned galena >> sphalerite > Cu sulfide along a reef-influenced tract of Cm carbonates	P+Rc 250 mt @ 3.0% Zn for 7.5 mt Zn, 10.5 kt Cd 75 mt @ 4.3% for 3.2 mt Zn 369 mt @ 3.0% Pb for 10.2 mt Pb 454 mt @ 5+% Pb, 0.8% Zn, for 32 mt Pb	Briskey et al. (1986) Callahan (1977) Misra et al. (1996) Hagni (1989) Hagni (1989)
Ditto, Mine La Motte, Fredericktown	Narrow linear bodies of scattered galena > pyrite > siegenite in ferruginous Cm dolomite and top of carbonates-cemented sandstone	P+Rc 2 mt Pb, 55 kt Ni, 10 kt Co	Snyder and Gerdemann (1968)
Tri State district, central United States	Extensive area of low-grade scattered sphalerite > galena, Fe bisulfides in stratabound brecciated and partly silicified, dolomitized Cb1 limestone. Picher field alone: 7.3 mt Zn, 1.8 mt Pb	~500 mt @ 2.3% Zn, 0.6% Pb for 11.5 mt Zn, 3.0 mt Pb	McKnight and Fischer (1970)
Navan ore field, Irish Midlands	Series of stratabound replacement > open space filling sfalerite, galena, pyrite lenses in shallow Cb1 limestone under deeper water limestone, near faults	70 mt @ 10.9% Zn, 2.6% Pb for 7.63 mt Zn, 1.84 mt Pb	Hitzman and Beaty (1996)
Reocin, Torrelavega, Santander Province northern Spain	Stratabound lenticular and tabular bodies of scattered > replacive galena, sphalerite, Fe sulfides in brecciated Cr1 dolomitized limestone; oxides	~80 mt @ 10% Zn, 1% Pb for 8.55 mt Zn, 0.8 mt Pb	Grandia et al. (1999)
Iglesiente district, SW Sardinia, Italy	Stratabound void-filling and replacive sphalerite, galena, Fe sulfides in Cm1 paleokarsted carbonates under Tr unconformity; fracture veins, breccias	~4.8 mt Pb, ?3 mt Zn + barite	Boni (1985) Boni et al (1996)
Bleiberg-Kreuth ore field, Carinthia, Austria	Stratabound bodies of scattered sphalerite, galena, Fe-sulfides in rhythmic dolomitized limestone interbedded with shale; breccias, faults	P+Rv 4.2 mt Zn, 800 kt Pb, 16 kt Cd, 1600 t Ge	Holzer and Stumpfl (1980)
Silesia-Kraków ore region (Bytom, Olkusz, Chrzanów), Poland	Large area of Tr2 limestone and several generations of dolomite with clusters of stratabound tabular & breccia sphalerite > galena bodies; hydrothermal karst, faults, oxidation zones	P+Rv ~500 mt @ 3.8% Zn, 1.6% Pb for 28 mt Zn, 8 mt Pb	Sass-Gustkiewicz et al. (1982); Leach et al. (1996)
Touissit-Bou Bekker, NE Morocco	Stratabound tabular bodies of paleokarst breccia filling > replacing sphalerite, galena, Fe sulfides in J dolomitized limestone under clastic screen	Pt 67 mt @ 7% Pb, 3% Zn for 4.7 mt Pb, 2 mt Zn	Bouabdellah et al. (1996)
Fankou, northern Guangdong, SE China	Replacement > void filling bodies (mantos) of low-temperature galena, sphalerite, pyrite with minor As,Cu,Hg,Sb sulfides in D dolomite & limestone	3.36 mt Zn, 1.65 mt Pb, 3,180 t Ag	Song Shuhe, ed. (1990)
Admiral Bay, Canning Basin, NNW Australia	Several deeply buried zones of ribbon-like stratabound massive to disseminated replacive galena, sphalerite in Or2 dolomitized limestone	140 mt ore with 7.76% Zn, 6.14% Pb, 4,980 t Ag	Williams in Ferguson (1999)

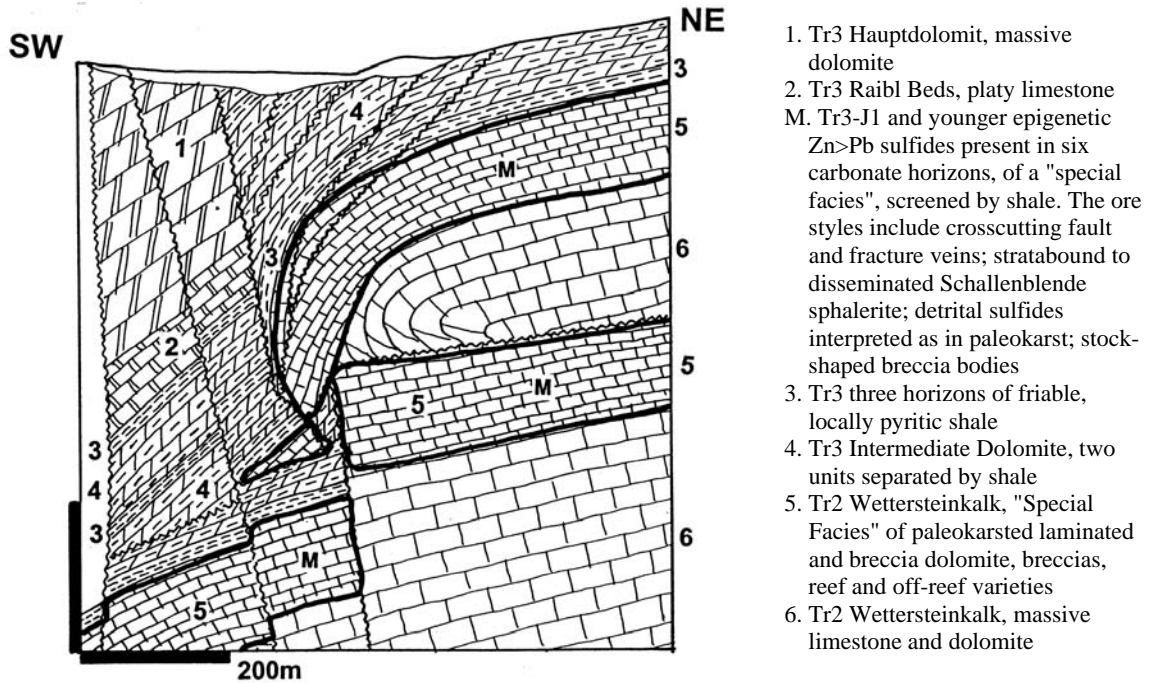


Figure 13.29. Bleiberg-Kreuth ore field, Drauzug, Carinthia, Austria, representative of stratigraphically-controlled, but epigenetic mostly void-filling MVT deposits. Cross-section from LITHOTHEQUE No. 3295, modified after Höller (1953) and Schulz (1966)

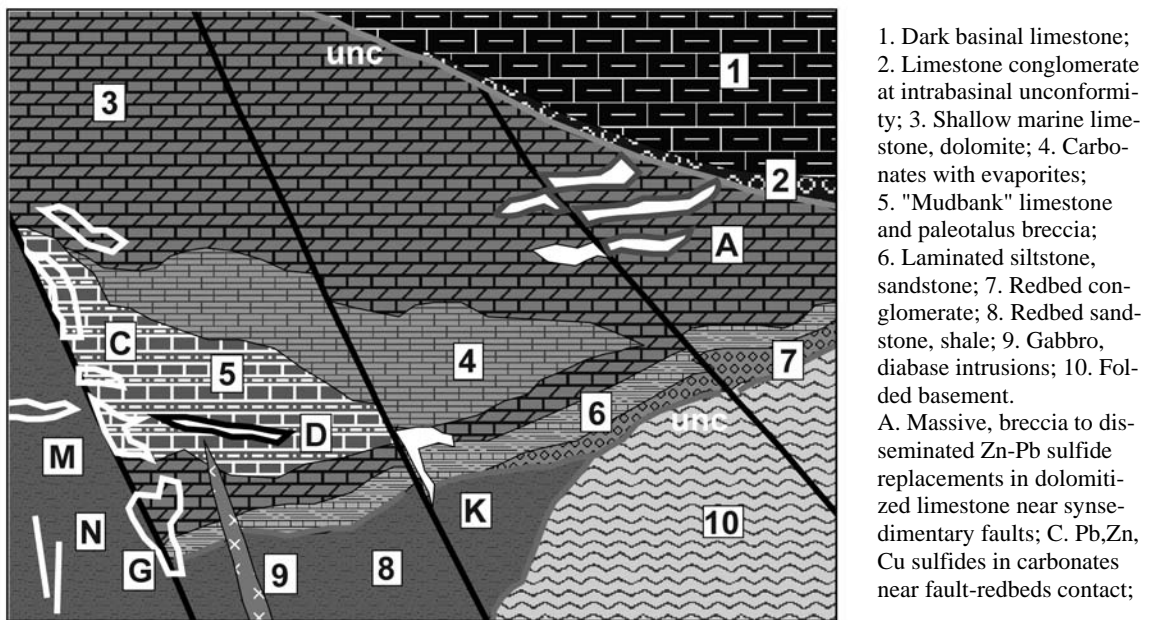


Figure 13.30. Inventory cross-section of rocks and ores in Pb-Zn mineralized carbonates resting on continental redbeds and influenced by syndepositional (growth) faulting, as in the Irish Midlands. From Laznicka (2004), Total Metallogeny Site G162. Explanations (continued): D. Cherty siliceous hematite replacement; G. Bornite, tennantite disseminated in brecciated carbonate near fault contact with redbeds; K. Replacive barite with some Pb,Zn,Ag sulfides in Mn-siderite altered carbonates near fault; M. Cu-sandstone in reduced redbeds; N. Quartz-chalcopyrite fracture veins; U. Oxidic Pb-Zn under paleosurface. Ore types A and C have known "giant" members

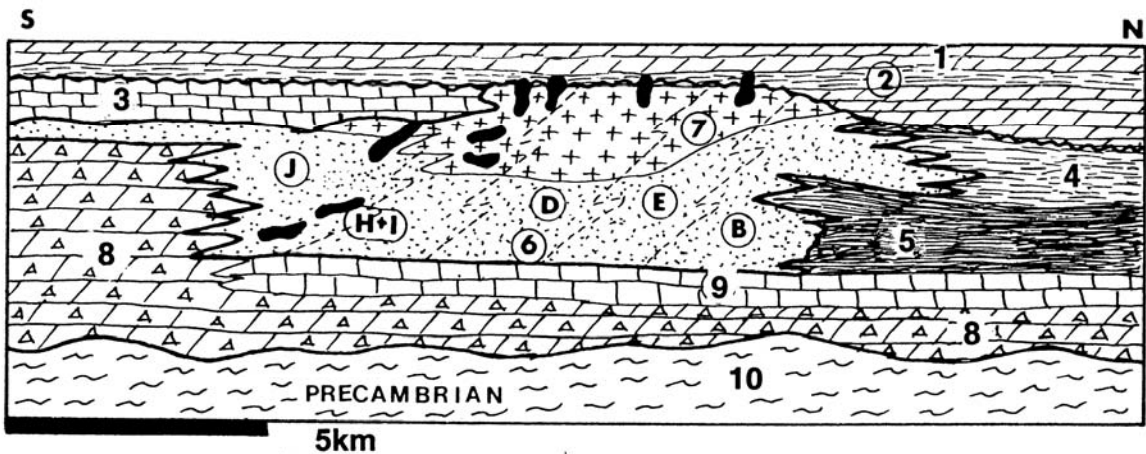


Figure 13.31. Pine Point Zn-Pb district, NWT, Canada, diagrammatic cross-section showing depositional and alteration facies and setting of the orebodies. From LITHOTHEQUE No. 537, based on data in Irvine (1972), Kyle (1981), Cominco Ltd. Staff, 1975 tour. M (shown solid black): scattered to semi-massive (in breccia) sphalerite, galena and Fe sulfides form lower-grade bedding-peneconcordant tabular bodies in dolomite and higher-grade discordant breccias. 1. D2 limestone; 2. D2 shale marker horizon; 3. D2 limestone; 4. D2 basinal shale; 5. D2 dark basinal calcareous shale to argillaceous limestone; 6. D2 fine to medium-grained dolomitized limestone. Paleoenvironmental interpretation by Kyle: B=basin; D=barrier reef; E=foreereef; H+I backreef to lagoon; J=southern reef flank. 7. Coarse crystalline, porous metasomatic dolomite mass ("Presquille Facies"); 8. D2 evaporitic dolomite, gypsum, anhydrite; 9. D2 fine dolomite; 10. Precambrian crystalline basement of the Canadian Shield

Although individual MVT deposits show preferences for one of the above "types", most actual examples are mixtures of several styles: high-grade stratabound ore layers, scattered sphalerite or galena crystals in (usually) dolomitized and sometimes silicified porous limestones or breccias (e.g. Pine Point, Fig. 13.31), "hydrothermal karst" with large cavities and solution-collapse breccias lined by metacolloform "Schallenblende"-type sphalerite, and mineralized fracture veins. This is further complicated by the post-depositional reworking such as gravity collapse into voids and/or oxidation that created "calamine" (hemimorphite), hydrozincite, smithsonite and cerussite ores. Better than to engage in descriptions of the various transitional "types" with the associated controversy, several distinct "giant" deposits and areas are characterized below, with emphasis on the empirical facts.

South-Eastern (SE) Missouri Pb province (Snyder and Gerdemann, 1968; Hagni, 1995; Ohle, 1996; ~970 mt of ore containing ~46 mt Pb + calculated 7.2 mt Zn, 1.26 mt Cu, 6,750 t Ag). This Province, located south-east of St. Louis, stores the world's largest accumulation of lead in ores and is exceptional among the MVT deposits, most of

which are dominated by zinc. The mineralization is discontinuously distributed over an area of 15,000 km², in three "(super)-giant" districts and three lesser ore fields. This area is a part of the North American Platform and the mineralization, hosted by Cambrian sedimentary rocks, surrounds the Ozark Uplift (dome). The latter has a core of Mesoproterozoic anorogenic granite and rhyolite, mineralized by several small to medium-size Fe oxide vein and breccia deposits.

The Cambrian strata start with the basal Lamotte Sandstone, a quartz arenite to arkose with scattered boulders near base where it pinches out against basement granite knobs. It is up to 120 m thick and overlaid by the 50 to 140 m thick Bonneterre limestone, dolomitized above and near the basement highs. The Bonneterre has a high degree of facies variability, with algal reefs, oolitic grainstones, calcarenite bars with shaly partitions. These facies, especially their porosity and permeability, influenced ore emplacement so they are important for ore prediction. The bulk of ores is hosted by the dolomitized Bonneterre, and partly the Lamotte Sandstone below. The Davis Formation overlies the Bonneterre and it consists of alternating dolomite and shale beds. It is unmineralized and may have provided an impermeable screen to the ore fluids.

Fredericktown ore field (Snyder and Gerdemann, 1968; ~2 mt Pb, 55 kt Ni, 10 kt Co), the first Pb deposit discovered in 1720, is in the extreme SE of the province and it is unusual for its content of Ni and Co (a possibly significant Co resource remains). There, galena with minor pyrite, chalcopyrite and siegenite form small masses and dense disseminations grading to single scattered crystals in linear orebodies (sand ridges). The hosts are the ferruginous dolomite in the lowermost 17 m of the Bonneterre, and the uppermost, dolomite-cemented Lamotte. The grade varies between 1 and 10% Pb and the minor siegenite contributes about 0.5% Ni and 0.15% Co to the ore. The most intensely mineralized intervals lie immediately above or near the Lamotte pinchout and the orebodies have a narrow, linear and arcuate form, encircling a knob of Proterozoic granite.

Old Lead Belt Pb district (Snyder and Gerdemann, 1968; Pt 369 mt @ ~3% Pb for ~10.2 mt Pb) was in production between 1864 and the 1970s when the production ceased. This is a system of largely interconnected, subhorizontal low-grade orebodies distributed over an area that measures 19 km in the NW-SE direction, NE of the Ozark Dome. There is a great variety of orebody forms (mineralized pinchouts encircling basement knobs; mineralized ridges and bars in coarse calcarenite and algal reef confined by lagoonal black shale; bar-reef structures; disconformities; mineralized slides and slump breccias). The ground has several generations of block faults. The primary ore is dominated by galena in bedded orebodies, both of open space and replacement origin, rapidly changing into crystalline aggregates and disseminated crystals. Pyrite and marcasite are finely disseminated in gray shaly carbonate beds, and associated with galena as small masses, scattered grains, fracture veinlets. Sphalerite, chalcopyrite, siegenite and bravoite occur locally but have not been recovered. Although almost all the ore is in dolomite, dolomitization is considered as diagenetic, earlier than the introduction of metals. Little is known about the oxidation zone, formed over the outcropping orebodies (near Bonne Terre) and presumably dominated by cerussite. It was mined out during the earliest phase of mining

Viburnum Trend (Economic Geology Special Issue v.3/72, 1977; Sverjensky, 1981; Hagni, 1995; 454 mt of ore with 5% plus Pb, ~0.8% Zn, 0.14% Cu, 7.5 g/t Ag for ~32 mt Pb); Fig. 13.32. This is a narrow N-S trending, 64 km long near-continuous ore zone located west of and above the buried flanks of the Ozark Dome. Discovered in 1955, this has been the principal U.S. lead producer for 45

years. The blanket-like orebodies, on average 6-7 m thick, are in the upper part of the Bonneterre, immediately under or close to a 60 cm to 3.5 m thick Sullivan siltstone marker that provided an impervious screen to the mineralizing brines. The partly dolomitized limestone has a high degree of facies variability marked by barrier reefs (controlled by basement faults) and interreef lagoonal lithologies. Porous oolitic grainstone and clastic carbonate units are the preferred ore hosts.

Although lead is still the dominant metal, the contents of Zn, Cu and Ni-Co are higher than in the Old Lead Belt. The ore minerals are multistage; Fe sulfides are early, followed by the main stage of Pb, Zn, Cu sulfides, and terminated by late siegenite (Ni-Co). The mineralogically zoned orebodies have chalcopyrite and bornite at bottom, galena and sphalerite in the middle, Fe sulfides on top. The epigenetic mineralization is now interpreted as Permian, precipitated from basinal fluids sourced in foreland basins adjacent to the Ouachita orogenic front in the south. The deep basinal brines migrated during compression and uplift and deposited their load within the permeability horizons around the Ozark Dome (Garven et al., 1999).

Kraków-Silesia (or Upper Silesia) Zn-Pb region (Sass-Gustkiewicz et al., 1982; Leach et al., 1996; P+R >500 mt of ore averaging ~3.8% Zn, 1.6% Pb for ~28 mt Zn, 8 mt Pb). This is the second MVT region of global importance but, in contrast with SE Missouri, Zn is the dominant metal here. As in Missouri, the mineralization is irregularly distributed and there are three major clusters (districts) of orebodies mined for a long time (Bytom, Chrzanów and Olkusz; Fig. 13.33) and one more recently discovered cluster near Zawiercze. Most of the ores are in an about 200 m thick succession of Middle Triassic carbonates (Muschelkalk), a platformic cover that partly overlaps the coal-bearing Carboniferous "molasse" in the Variscan Foredeep, and protruding relics of Devonian carbonates. The latter are locally ore-bearing as well.

The dominant ore style has the form of tabular replacement bodies of sphalerite, galena and Fe sulfides in hydrothermally dolomitized limestone ("Ore Dolomite") that postdates the earlier diagenetic dolomite. The tabular bodies are overprinted by and grade into spectacular mineralized solution collapse breccias (hydrothermal karst of Sass-Gustkiewicz et al., 1982) lined by metacolloform sphalerite (Schallenblende).

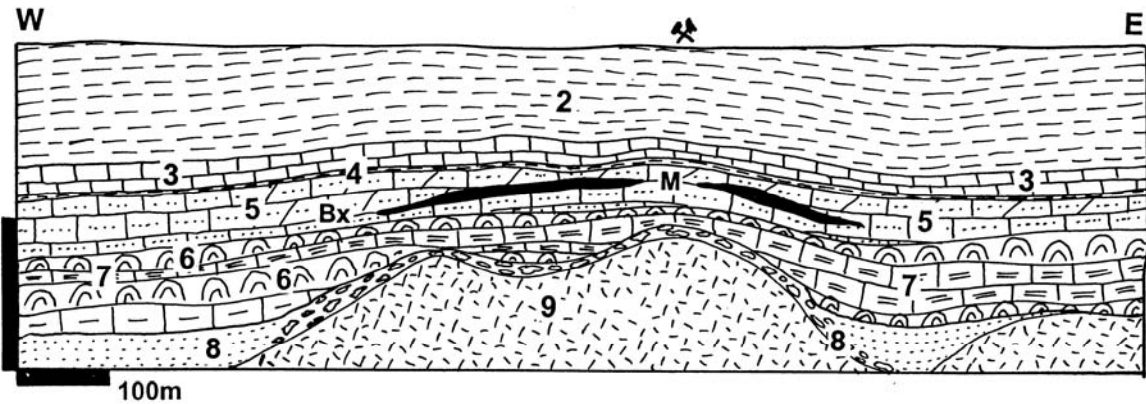


Figure 13.32. Viburnum Trend, S.E. Missouri, cross-section of the Fletcher Mine. From LITHOTHEQUE No. 3253, modified after Paarlberg and Evans (1977). 2. Cm3 Davis Fm. interbedded shale, impure limestone and dolomite; 3-7: Cm3 Bonneterre Fm., reef-influenced carbonate platform. 3. Thin-bedded limestone grainstone, mudstone; 4. Thinly laminated quartz siltstone marker; 5. Calcarenite (ORE HOST); M. Replacive and pore filling galena > Fe sulfides > sfalerite, chalcopyrite and bornite in a blanket in dolomitized calcarenite under siltstone screen; 6. Reef facies; 7. Backreef facies, algal boundstone and burrowed lime mudstone; 8. Cm1 Lamotte Sandstone, quartz arenite and basal conglomerate; 9. Mp basement, anorogenic felsic volcano-plutonic complex

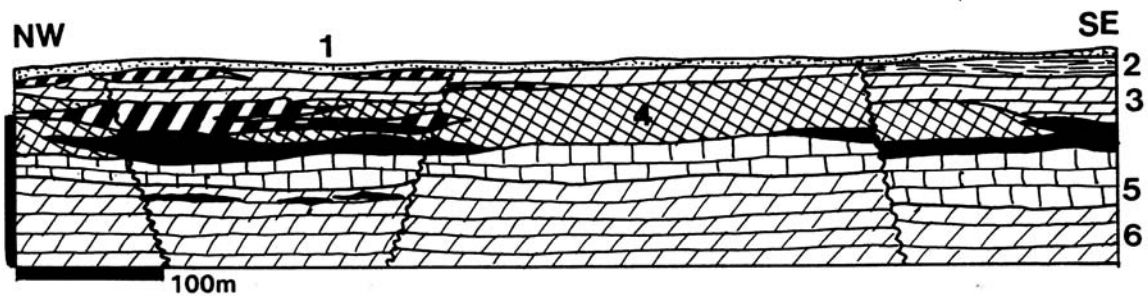


Figure 13.33. Silesia-Kraków Zn-Pb region, Olkusz ore field; cross-section from LITHOTHEQUE No. 2025, modified after Radwanek-Bak (1985) and 1992 site visit. 1. Q sediment cover; M (solid black). Sphalerite (Schallenblende), Fe sulfides > galena in peneconcordant metasomatic dolomite breccia; MW (striped). Oxidation zone, hemimorphite, smithsonite, cerussite; 2. Tr3 Keuper mudstone, siltstone, basal karst breccia; 3. Tr2 Diplopora Dolomite; 4. Tr2 metasomatic Ore Dolomite with high trace Zn content; 5. Tr2 Gogolin Limestone; 6. Tr1 Rhaetian dolomite

The high-salinity fluids have homogenization temperatures between 40° and 156° C and as expected, there is a continuous genetic controversy as to the ore timing and derivation. One group favors an early (late Triassic-early Jurassic) ascent of fluids from the basement along an important NW-SE deformation zone and Caledonian terrane boundary; late Paleozoic porphyry-type Mo, W, Cu and Cu-skarn bodies have recently been discovered under the Zawiercze MVT ores. The other school of thought (Leach et al., 1996; Heijlen et al, 2003) prefers ore precipitation from Late Alpine (that is, Cretaceous to Tertiary) hot Zn-Pb bearing basinal brines expelled from Carpathian foreland basins, by mixing with fluids from local aquifers.

Tri-State Zn-Pb region (district) is a discontinuously mineralized territory of about 5,000 km² in the Kansas, Missouri and Oklahoma borderland (Hagni, 1976; Ragan et al., 1996; Pt 11 mt Zn, 2.65 mt Pb). The bulk of production came from 25 km² of ground in the **Picher ore field** in NE Oklahoma (McKnight and Fischer, 1970; 7.3 mt Zn, 1.8 mt Pb; Fig. 13.34) that had the distinction of being the lowest-grade major Zn-Pb deposit ever mined (1.99% Zn+Pb in the early 1940s). The ore is in Lower Carboniferous (Mississippian) limestone situated several hundred meters above the Precambrian crystalline basement of the North American Platform, and topped by erosional remnants of Late Carboniferous (Pennsylvanian) paralic coal-bearing cyclothem. The latter contains

Pb and Zn-enriched black mudstone. The Mississippian host carbonates are rather monotonous, slightly argillaceous biomicrites rich in chert nodules or interbedded with lenticular chert bodies. There are minor oolitic limestone and greenish to black shale interbeds. In the Picher field, 15 carbonate beds are preferentially mineralized.

The principal ore mineral is sphalerite that forms small replacement masses and grains, and loose crystals scattered in and coating the surface of numerous vugs and voids in breccia ("snow-on-roof" texture). The sphalerite crystals are ruby red in the center, with an almost black outer zone. Galena is less common, and chalcopyrite, enargite and luzonite are exceptional. Pyrite, marcasite, coarse sparry calcite and crystalline dolomite are the major gangue minerals and the host rocks are dolomitized and substantially silicified (chert). The most common orebodies ("runs") are confined to several numbered stratigraphic intervals and have a curvilinear trend controlled by joint systems. Superjacent runs may locally coalesce and adjacent runs may unite to form irregular blanket deposits ("sheet grounds"). The former grade into "circle grounds", that are roughly circular brecciated, silicified and dolomitized solution collapse structures. They are most common under the Pennsylvanian unconformity and are compositionally zoned. The center is composed of crystalline dolomite replacing limestone. This is surrounded by silicified rim bordered by zone of limestone dissolution, filled by residual chert rubble ("boulder ground"). Sphalerite is most common along the dolomite contact. The 60°-135° hot basinal fluids caused substantial silicification, uncommon in most MVT districts. The possible reason is reprecipitation of the abundant early diagenetic silica in chert nodules.

Irish Midlands and Limerick Zn-Pb province (Hitzman and Beaty, 1996) stored some 15 mt Zn and 4.7 mt Pb in one Pb-Zn "giant" (Navan), four "large" Pb-Zn deposits, and more than 15 small deposits and prospects (Fig. 13.35). Silvermines was the only historical deposit, the rest has been discovered between the 1960s and 1990 when Lisheen, the last significant deposit, has been found.

The central Irish Plain is a generally flat area with poor outcrop (with exception of the Silvermines Mountain), underlain by flat-lying to gently dipping (but substantially faulted) Lower Carboniferous carbonates. The carbonates rest unconformably on Devonian red beds (Old Red Sandstone) which in turn blanket folded rocks of

the Caledonian orogenic basement. The Carboniferous carbonates comprise several sequences of rather monotonous shallow to deep water micritic and bioclastic limestones, calcareous shales and diagenetic dolomites, of which two divisions host most of the ores. The lower one, the Courceyan Pale Beds, comprise a shallow water limestone that hosts the bulk of Navan ores. The upper sequence is the deep-water Waulsortian carbonate mudbank facies that hosts the rest of the "large" deposits. Typical Irish Zn-Pb deposits are stratabound, replacive to void-filling sheets and lenses of sphalerite, galena, pyrite and marcasite, with dolomite, calcite and locally barite gangue. A separate thick barite body was mined in Silvermines. All orebodies show close relationship with faults and in Tynagh Carboniferous carbonates are in fault contact with the red beds (this increases the mineralogical variability with the appearance of Cu, Ag and Hg in the ore). The 1970s vintage genetic interpretations favoured the exhalitic model, with hydrothermal ore fluids delivered via growth faults to precipitate in the depositional basin. The occasional presence of jasper or banded ironstone as in Tynagh and filamentous pyritic mounds at Silvermines supplied the best evidence, but more recently Cruise (1996) demonstrated that the ironstones were post-lithification replacements. The subsequent models favoured syndiagenetic introduction of metals in low-temperature basinal brines; recently, there has been a move towards post-lithification replacement (e.g. Pearce and Wallace, 2000).

Navan (Tara) Zn-Pb deposit (Anderson et al., 1998; ~70 mt of ore @ 10.9% Zn, 2.6% Pb for 7.63 mt Zn, 1.84 mt Pb). Navan, 50 km NW of Dublin, is a concealed ore complex discovered in 1970, and one of the three largest Zn resources in Europe (the others are Reocin and Upper Silesia). The Lower Carboniferous (Courceyan) succession of predominantly shallow marine carbonates rests on thin laminated Carboniferous siliclastics, Devonian redbeds and Ordovician-Silurian basement. 97% of the Zn-Pb mineralization discovered so far is in the middle of the sequence, in the Pale Beds of the Navan Group. Except for minor Tertiary dolerite dikes, there are no magmatic rocks in the ore field. The Pale Beds comprise a sequence of limestones (micrite, wackestone, grainstone, packstone) deposited in progressively deepening water, interstratified with beds of diagenetic dolomite and several marker horizons. They are also frequently channelled, which accounts for the common lateral textural variation and formation of limestone conglomerate, a favorite host of ore.

dominated by a brown and yellow sphalerite, subordinate galena and minor pyrite, marcasite with calcite, dolomite and locally barite gangue. The ore minerals are both of replacement and open space-filling types and they range from an almost massive to disseminated ore. Large cavities, collapse breccias, scattered crystals of ore minerals characteristic for many MVT deposits are missing. The Boulder Conglomerate contains abundant early (syndimentary to diagenetic) framboidal pyrite. The Zn-Pb sulfide ore in the Conglomerate has a higher proportion of Fe sulfides than ore in the Pale beds, and gangue of saddle dolomite. There is a controversy as to the origin and timing of this ore, considered as reworked earlier ore from the Pale Beds (Anderson et al., 1998), or a replacement contemporaneous with the main orebodies (Pearce and Wallace, 2000). All investigators, however, agree that the mineralization is epigenetic, probably multistage, introduced by a hydrothermal fluid high in seawater sulfate relatively early in the post-compactional history of the carbonate pile, in proximity to faults, around 345 Ma, 343 Ma, or slightly later.

13.4.5. Discordant (vein) Zn-Pb orebodies of "MVT affiliation"

Discordant, steep to vertical structures filled by low-temperature hydrothermal minerals with MVT-comparable "signatures" are present in almost every major MVT deposit or complex. They are usually attributed to remobilization (when they postdate the stratabound Zn-Pb orebodies) or are alternatively interpreted as feeders and ore fluid conduits. In the **Illinois-Kentucky mining district** (Grogan and Bradbury, 1968; 9.5 mt CaF_2 , 122 kt Zn, 54 kt Pb) subvertical fault or fracture veins are dominant whereas stratabound replacement bodies, comparable with the MVT type, are rare (e.g. Cave in Rock). This district has been a significant fluorite producer, but a feeble source of metals. In the **Upper Mississippi Valley Zn-Pb district** (or mineralized area; Heyl et al., 1959; 1.6 mt Zn, 750 kt Pb) stratabound Zn-Pb bodies prevail but discordant structures are significant. Hundreds of relatively small subvertical Pb-Zn veins, mineralized fractures, replacements along small reverse faults, occur at several stratigraphic levels in Paleozoic platformic carbonates. Arnold et al. (1996) attributed the Permian (270 Ma) mineralization to a gravity-driven discharge of heated groundwater fluids (75-220°C) within a regional paleo-hydrogeological system.

North Pennines (Ineson, 1976; 20 mt CaF_2 , 4 mt Pb) and **South Pennines** (Ford, 1976) ore regions in central United Kingdom had a significant past production of lead. Zinc was of little interest in the distant past and often not recovered. The more productive North Penine region has an area of about 1,600 km^2 , where numerous steeply dipping epigenetic veins filled by carbonates, fluorite, barite, galena and sphalerite are hosted by a Carboniferous sedimentary sequence composed of dominant marine limestone with minor shale, sandstone and paralic coal association. There are abundant diabase sills and dikes that occupy the same structures as ore veins. Peneconcordant replacement orebodies in ankeritized limestone adjacent to feeder veins or fissures have the form of "flats", "wings" or "mantos". They are best developed where limestones are confined under an impermeable shale screen.

Pillara (Blendevalle) Zn-Pb mine in the Lennard Shelf (Canning Basin) MVT province of northern Australia (Murphy, 1990; P+Rv 20 mt @ 8% Zn, 2.4% Pb; Fig. 13.36) is about the largest single deposit where a "typical" MVT-style ore fills steeply dipping faults. There, epigenetic sphalerite, galena, pyrite and marcasite with calcite and locally barite gangue replace fragments and matrix in 2-30 m wide sheets of solution-modified fault breccia, and encrust open voids in the breccia. The host rocks are members of the late Devonian algal and stromatoporoidal reef facies series, resting on Paleoproterozoic basement.

13.4.6. Stratabound cinnabar deposits in carbonates

Several carbonates-hosted disseminated and replacement cinnabar deposits in areas with young volcanism (Terlingua, Texas; Monte Amiata, Italy) are attributed to magmatic heat-driven hot springs activity (Chapter 6). In the Guizhou mercury province in south-central China that represents perhaps 100,000 t of Hg in ores (reliable tonnage figures are not yet available), however, numerous stratabound cinnabar disseminations in Cambrian platformic carbonates are attributed to low-temperature high-salinity oil brines that supplied both the mercury (original source unknown) plus H_2S and methane reductant. The orebodies formed in porous, often evaporitic dolomites under impermeable black shale or argillaceous dolomite screen (He Lixian and Zeng Ruolan, 1992).

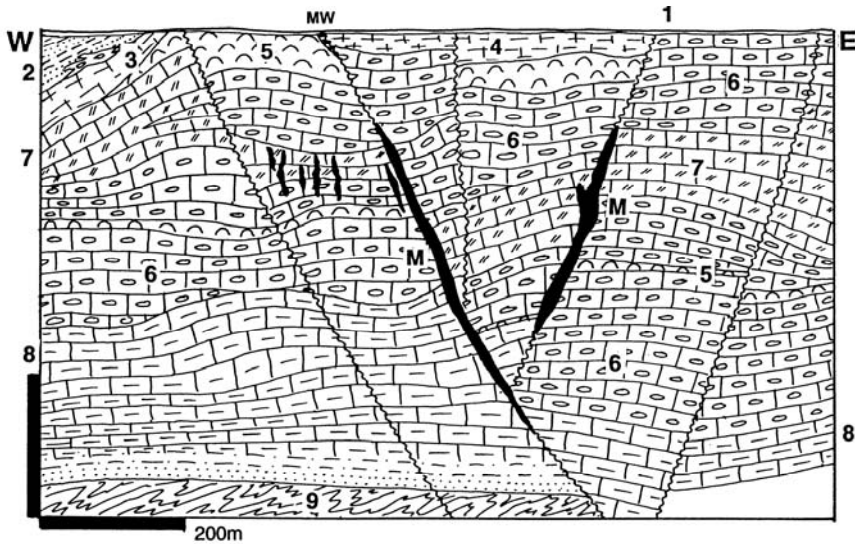


Figure 13.36. Pillara (Blendevalle) Zn-Pb Mine, Canning Basin, NE Western Australia. Cross-section from LITHOTHEQUE No. 3149, modified after Western Metals Ltd., 2003 visit. Explanations (continued): 6. Coarse stromatoporoidal bioclastic limestone; 7. Fenestral *Amphipora* algal limestone; 8. Flaggy calcareous shale, argillaceous limestone, basal siltstone and arkose; 9. Pp crystalline basement

Fenghuang-Xinhuang Anticline Hg zone, Guizhou, S-C China (Dadongla, Wanshan, Jiudiantang Hg ore fields) (He Lixian and Zeng Ruolan, 1992; estimated 50,000 t Hg plus). This is some 50 km long NNE-trending anticline in folded and faulted Cambrian strata on the Yangtze Paraplatform. The main anticline is overfolded by several WNW-trending second order anticlines that contain several ore fields, generally parallel with the anticlinal axes. The best known “classical” ore field **Wanshan** (10,000 t Hg @ 0.3%, old data) contain several manto-style impregnation and replacement cinnabar bodies in almost flat-lying Lower-Middle Cambrian dolomitized limestone. The mineralogy is simple, dominated by cinnabar with some pyrite, stibnite, As-sulfides and traces of hydrocarbons. The host rocks are silicified and calcitized by 62-162° hot brines. The early Hg production came from the residual material in karst.

Muyouchang Hg ore field, Wuchuan County, Guizhou (He Lixian and Zeng Ruolan, 1992; estimated 20-30 kt Hg) is a “gigantic deposit”, perhaps the largest in China, that extends for 4,000 m along a NE-trending anticline. The ore interval in Lower-Middle Cambrian anhydritic and gypsiferous cavernous dolomite contains several stratabound orebodies, usually screened by a dense argillaceous dolomite. Some orebodies of disseminated and fracture filling cinnabar are hosted by anhydrite beds. Cinnabar is the dominant mineral accompanied by minor stibnite, sphalerite and

realgar, in calcite, quartz, barite and dolomite gangue. The host rocks are slightly silicified and calcitized. The ore precipitation is attributed to methane reduction of Hg dissolved in oil field brine.

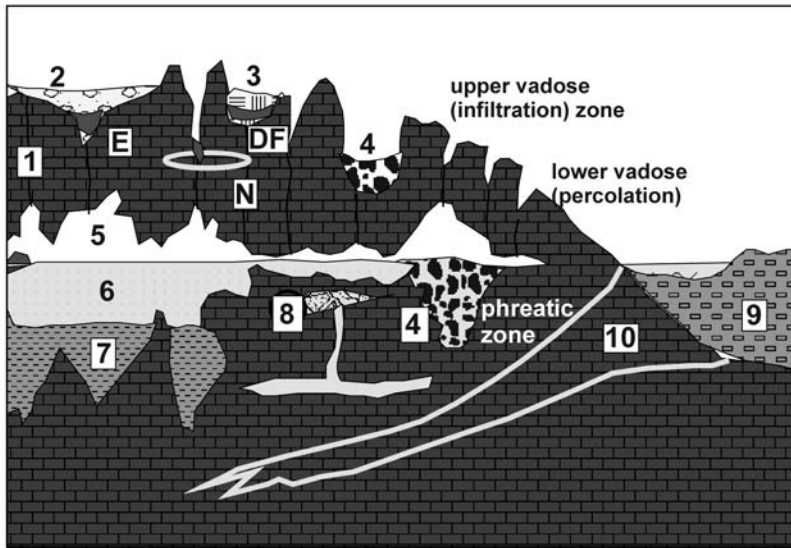
13.4.7. Metallic ores in karst on carbonates

Karst and paleokarst are forms of a regolith dominated by carbonate dissolution and reprecipitation by action of descending meteoric waters (Fig. 13.37). Karsting alone does not generate orebodies, yet karst is an important metallogene in two principal ways: 1) as a supergene modifier of the primary carbonates-hosted ores; and 2) as an agent of generation of voids (e.g. caves, cavities, solution collapse breccias) and basins (depressions, sinks) that fill by ore material that need not be genetically related to the carbonate progenitors.

1) Residual karst-type ores

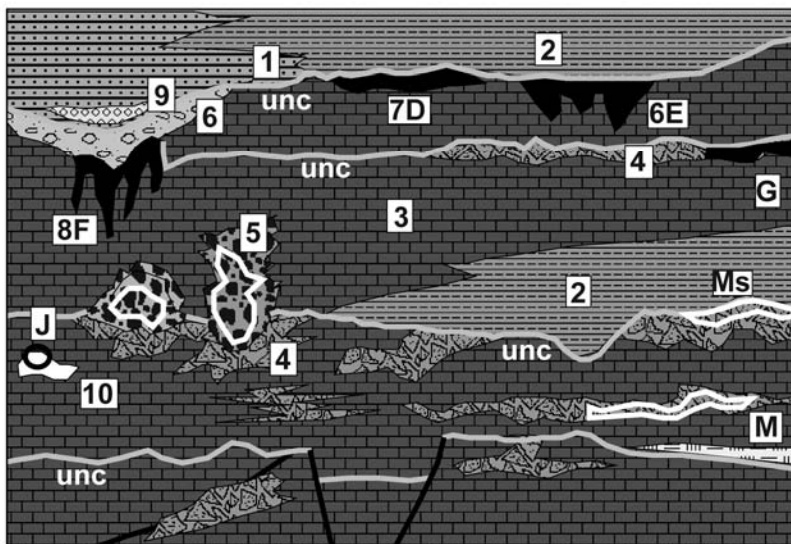
These require primary orebodies on which to form. Because karsting also creates spaces for ore deposition much better protected from erosion than regoliths on silicate rocks, the generally soft residual ores are preserved near the present surface, or on paleosurface now represented by unconformity (Fig. 13.38).

1. Residual red & brown soil, karst; MW. Partly oxidized Zn-Pb ore; M. Post-D3 sphalerite, galena, Fe sulfides with calcite and local barite gangue fill and replace solution-modified fault breccia; 2. D3 mudstone, sandstone turbidite; 3. D3 thin bedded calcareous siltstone; 4. marginal slope facies, calcareous siltstone to sedimentary breccia; 5-8 D2-3 Pillara Fm., platform limestone: 5. Massive stromatoporoidal limestone;



1. Ancient (rock) carbonate;
2. Residual rubble in sink;
3. Residual soil; 4. Collapse rubble; 5. Air-filled cave system; 6. Water filled caves;
7. Cave floor sediment;
8. Solution breccias and porosity; 9. Exposure surface on young carbonate sediments;
10. Brackish (mixed) water zone; A. Trace U in recent guano on cave floor (phosphate); D. Sinkhole fill by gibbsitic bauxite; E. Residue of primary barite, Fe,Mn,Pb,Zn,Sn,Sb,Hg replacement ores; F. Fe,Ni,Co transported laterite in sinks; N. Redeposited residual Pb,Zn, Sn,Sb etc. ores from karst

Figure 13.37. Inventory of features and ores in recent (active) karst system from Laznicka (2004), Total Metallogeny Site G170



1. Sandstone; 2. Shale; 3. Carbonates; 4. Paleokarst breccia, solution features, cements;
5. Solution collapse breccia; 6. Coarse lag residue under unconformity; 7. Paleosol (e.g. bauxite); 8. Infiltrations under unconformity; 9. Residual karst debris reworked into basal sediments; 10. Unfilled cavern; unc=unconformity.
- D. Karst-type bauxite; E. Residual barite, phosphorite; F. Fe oxides in karst under unconformity; G. Mn oxides infiltrations; J. U,V, barite, etc. cave incrustations; K. Descloizite (V) in solution collapse breccia; M. MVT-type Zn,Pb; Mb in breccia, Ms under shale

Figure 13.38. Inventory of rocks, features and ores associated with unconformities (paleosurfaces) in carbonate-dominated, mainly platformic sequences. From Laznicka (2004), Total Metallogeny Site G171

Most “giant” deposits in karst formed on carbonatites (e.g. Nb, REE, etc. deposits Araxa, Seis Lagos, Tomtor; Chapter 12) and the ore minerals come as resistates (e.g. pyrochlore, monazite, baddeleyite) or “converted resistates” (e.g. anatase after perowskite). Many outcropping MVT deposits have karsted tops, filled by hemimorphite (“calamine”), hydrozincite, smithsonite, cerussite, anglesite and pyromorphite.

Not a single karst orebody considered alone, however, has achieved the “giant” magnitude.

2) Ore-filled karst structures

Karst (Mediterranean) bauxite (Bárdossy, 1982). The first aluminum produced from bauxite came from Les Baux in the Haute Var bauxite district in southern France: a karst bauxite. Because of the

high geochemical abundance of Al, the “giant” threshold of 8 bt Al has nowhere been achieved, but lesser bauxite accumulations are still of the “world class”. Of the latter group the largest deposits are bauxitic laterites on silicate rocks (Section 13.7 and partly Chapter 12), whereas karst bauxites, even as cumulative regional tonnages, are much smaller. They, however, supported national aluminum industries of France, Italy, Russia, Hungary, Serbia-Montenegro and Greece for some time, although most deposits are now substantially depleted. The largest karst bauxites in Jamaica still continue as a major exporter.

Karst bauxites fill depressions in carbonates (mostly limestones). The geologically young depressions with bauxite (as sinkholes in the tropical karst in Jamaica; Fig. 13.39) are exposed, never buried, hence the bauxite is an unconsolidated variety of red soil. The geologically older bauxites (the oldest known bauxite is Neoproterozoic) are preserved at unconformities and they either remain concealed in depth, or are exposed at the present surface after erosional unroofing. The karst bauxite origin varies from place to place and remains controversial in some cases (Bárdossy, 1982). The old models interpreted bauxite as the accumulated insoluble aluminous residue, originally present in the parent limestone as a silicate impurity. It was, however, difficult to account for the large bauxite resources resting on high purity limestones, as in Jamaica. Comer (1974) argued that the source of the Jamaica bauxite was Miocene airborne ash issued from volcanoes in the Lesser Antilles arc that blanketed the limestone surface, from where it has been gradually washed into the karst depressions. The Al source was thus allogenic, although the pedogenic allitization (removal of silica, formation of gibbsite and Fe oxides/hydroxides) took place in situ, in the late Cenozoic. This model is probably applicable to many of the geologically older bauxites, although the volcanic ash may have been substituted by a residue or detritus of aluminosilicate rocks upslope from the bauxite resting place, the same source that gave rise to lateritic bauxites.

Of the global bauxite resource of 45 bt calculated by Bárdossy (1982), only 5.5 bt is shared by karst bauxites of which almost one half are the “red soil”-type gibbsitic bauxites that form blankets in depressions in the tropical karst of central **Jamaica**. There, they rest on Middle Eocene to Lower Miocene limestone (Comer, 1974; ~ 2 bt of 50% Al_2O_3). All the remaining deposits listed by Bárdossy (1982) are of small to medium magnitude,

the largest being the late Cretaceous bauxite field of Kiona, Parnassos, in Greece (250 mt of bauxite).

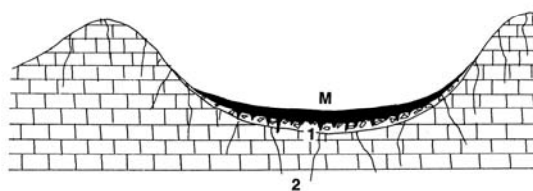


Figure 13.39. Tobolski bauxite mine, Jamaica, cross-section from LITHOTHEQUE No. 824; field sketch, 1976. M. Mi-Q earthy to friable pisolitic gibbsitic bauxite, residual fill of sinkhole; 1. Limestone residue and rubble changing to fractured karsted limestone; 2. Eo2-Mi1 pure carbonate platform limestone

Karst structures on Phanerozoic carbonates also accommodate deposits of Fe, Mn, Ni-Co, U, Pb-Zn and Au all of which are small, or at best of medium size. Some of the largest ones are on Precambrian meta-carbonates (Chapters 11, 14).

13.5. Marine evaporites and metallic ores

Evaporites include 1) those readily soluble under atmospheric conditions like halite and K/Mg chlorides, hence absent from outcrop (except for the rare Iranian “salt glaciers”), and 2) those less soluble ones like anhydrite or gypsum. Very few minor ore occurrences are hosted by evaporites (e.g. the Huitzucó, Mexico Hg-Sb livingstonite deposit in anhydrite; Ulutelyak-Mn, Russia; magnetite related to basalt diatremes in the Angara-Ilim district, Siberia) and such association is a local coincidence, of little use in general exploration. The only “geochemical giants” in evaporitic successions are some of the cinnabar deposits in Guizhou, China, like Muyouchang (read above).

More metallic deposits, including “giants”, are believed to have formed in settings that included evaporites, where the evaporites provided some partial or indirect assistance to the ore forming process. Warren (1999, his Chapter 8) reviewed this topic in some detail and his examples of evaporites facilitating ore genesis include the “giant” Cu mineralizations Boléo, Dzhzhkazgan, Dongchuan, and Kupferschiefer in Germany and Poland, and the “large” Pb-Zn deposits San Vicente, L’Argentière and Bou Grine. The principal genetic role of evaporites was to enhance brine salinity, and/or brine sulfatization, sulfurization and reduction capabilities.

Salt domes, diapirs and cappings

The metallogenic role of evaporites is enhanced around salt domes and diapirs (Braunstein and O'Brien, eds., 1968), which also provide structural control, trap hydrocarbons, and biogenically transform anhydrite into limestone plus sulfur (Fig. 13.40). "World class" sulfur deposits form in this way (not treated here), whereas the limestone provides a replaceable medium and abundant porosity (in breccias) for fluid mixing and chemical precipitation. Some oil field brines that are anomalously rich in Zn and Pb precipitate sulfides in caprocks, producing mineralizations with MVT affinity (Kyle and Saunders, 1996). The Hockley Dome in Texas contains 12 mt of ore @ 4.2% Pb+Zn: a medium magnitude orebody.

(Jebel) Bou Grine-Zn, Pb, Tunisia (Orgeval et al., 1989; ~10 mt of ore @ 7.3% Zn, 2.4% Pb) is a "large" east-dipping ore structure at periphery of the Jebel Lorbeus diapir. It is located in the Domes belt of the Tunisian Atlas, where over a dozen of small to medium-size Pb-Zn, barite-fluorite and replacement iron deposits are associated with Triassic saline diapirs forcibly intruded into Cretaceous limestones and marls. The Jebel Lorbeus diapir comprises core of Triassic gypsum to gypsiferous mudstone with some halite, flanked by a transition zone interpreted as a caprock. This consists of a lower unit of pyritic shale; zebra-banded calcite; calcite, dolomite and shale breccia with gypsum and celestite. This zone contains small lenticular bodies of Fe sulfides, sphalerite, calcite and minor galena. The main stratabound orebodies are higher-up, in Upper Cretaceous carbonaceous foraminiferal limestone, laminated limestone and calcareous shale. A very fine-grained Fe, Zn, Cu sulfide laminites in the black limestone grades to semi-massive sphalerite and galena in brecciated limestone. The mineralization is attributed to hot saline basinal brines that rose along faults to produce syngenetic ores near the sediment-seawater interface, followed by late diagenetic replacements in breccia. Shallow old workings exploited hemimorphite-dominated fracture veins near surface.

Solution fronts of bedded evaporites

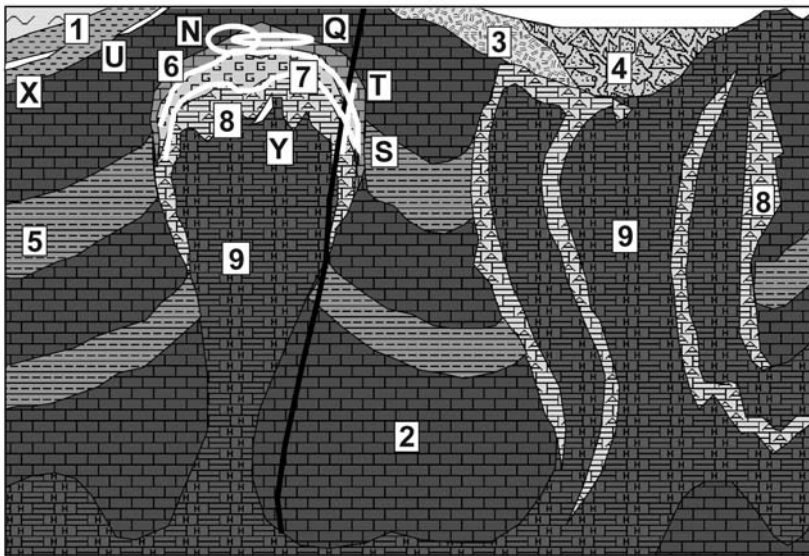
Halite and K, Mg chlorides-rich bedded evaporites exposed at surface or in shallow permeable subsurface undergo dissolution that triggers collapse of the overlying rocks. In the Western Canadian Sedimentary Basin in SW Manitoba, SE Saskatchewan and NE Alberta the extensive, broad

solution fronts above the Devonian Prairie Evaporite are marked by a widespread occurrence of cool saline springs. Slight enrichment in trace metals was found associated with some springs. Feng and Abercrombie (1994) recognized the presence of micron-size disseminated gold, accompanied by a variety of base and precious metals sulfides, near Fort McKay in Alberta. This they registered as a new "Prairie-type" gold mineralization. Subsequently, similar occurrences have been found in SW Manitoba, in solution chimneys in Devonian platformic limestone partly filled by Quaternary glacial sediments (Fedikow et al., 1996). The metals are associated with siliceous sinters and rinds and the site is near the projection of the Precambrian Churchill-Superior Provinces structural boundary in the basement. Although no economic deposit has been found so far, this is an interesting case of post-glacial Quaternary metallogenesis based on saline brines less than 100°C hot.

13.6. Hydrocarbons as a source of metals

Hydrocarbons (natural gas, petroleum, solid bitumens) and some associated substances (e.g. oilfield waters; H₂S, CH₄, CO₂-rich gases) contain a variety of minor (sulfur) and trace (metals) elements. There is no known case where a minor/trace element concentration and accumulation would be of such a magnitude as to convert an hydrocarbon reservoir into an ore deposit (that is, one exploited primarily for its metal or sulfur content), especially of "giant" magnitude. But once a hydrocarbon deposit is actively exploited and the raw material processed, usually for its energy content, it is possible to simultaneously retrieve the minor/trace elements, even when their concentrations are far lower ("technological ores") than the minimum grades of "classical" metal ores. Sometimes, such recovery is even required by law as in the case of polluting elements (S) or toxic metals (Hg, As, Cd, Pb). Elements so recovered then contribute to the overall mineral supply and compete with corresponding elements produced from classical ores.

Sulfur is the only element the environmentally mandated recovery from sour natural gas at source has influenced global supply, and put many former dedicated S resources (especially pyrite deposits) out of business. Mercury recovered from natural gas (e.g. in the Groningen field, the Netherlands; in former East Germany; Ozerova, 1981) is another example.



1. Sedimentary fill of rim syncline; 2. Carbonates; 3. Residual carapace of gypsum, black shale, dolomite; 4. Solution collapse breccia; 5. Shale; 6. Fine limestone in caprock; 7. Transitional caprock zone: gypsum, calcite, sulfur; 8. Anhydrite; 9. Salt stocks (diapirs) with inclusions of anhydrite, dolomite.
- N. MVT-type Zn-Pb sulfides in breccia or caprock fractures; Q. U infiltrations in asphaltite; S. Sulfur impregnations and masses; T. Cinnabar, sulfur, fluorite, bitumen veins; U. Fe siderite in rim syncline near mud volcanoes;

Figure 13.40. Salt structures: domes, diapirs, extrusions: inventory of rock and ore types from Laznicka (2004), Total Metallogeny Site G169. Explanations (continued): X. Cu sulfide impregnations in peridiapiric breccia; Y. Mg borates replacement masses

Although liquid petroleum has often interesting trace metal contents that vary regionally (e.g. high V in Venezuela, high Hg and Ni in California), their industrial recovery has so far been at a small scale and intermittent. These metals by-product might slightly influence the global metal supply, but the contained quantity of trace metals is insufficient to declare an oil field a "giant" metal repository.

Deposits of solid hydrocarbons (Parnell, 1988) have a better chance to contribute to global supply of V, Ti and Zr through by-product recovery, although only the **Athabasca Tar Sands deposit in Canada** clears the "giant resource" threshold. This deposit (Johnson and McMillan, 1993) is the largest of a group of Lower Cretaceous oil sand accumulations in east-central Alberta. The industrial center there is Fort McMurray and the bitumen resource is estimated at $268 \times 10^9 \text{ m}^3$ which, with a density ranging from 965 to 1010 kg/m^3 , is close to the same amount in tons. The deposit is a continuous surface blanket of nonmarine quartz sand, up to 35 m thick, impregnated by semi-solid black bitumen. It rests unconformably on Devonian limestone that also contains hydrocarbons. Bitumen content in the mineable deposit ranges from 10 to 18% by weight. The bitumen has an average trace content of 240 ppm V and 100 ppm Ni (Scott et al., 1954). This translates into 64.3 mt of contained vanadium but only a fraction is likely to be recovered. The V resides mostly in fly ash and

residual coke remaining after refining, in distant refineries that receive the "synthetic crude", the end-product at Fort McMurray. The second recoverable metallic resource in the tar sands are heavy minerals ilmenite, leucosene, rutile and zircon that remain in the detrital fraction of the sand in centrifuge tailings, once the bitumen has been removed. The heavy minerals grade varies between 2 and 3.5% and although the Canadian Mining Journal (June, 1997) claims 5% of the world's supply of Ti and Zr "is locked in Athabasca tailings", accurate figures are not available; perhaps 1 bt Ti and 20 mt Zr. 15 bt Al_2O_3 could be recovered from the clay fraction

Oilfield brines: Saline formational waters that underlie liquid hydrocarbons in oil pools have frequently elevated trace metal contents and are often invoked as the metalliferous brines that produced MVT deposits in the past. Some are in a process of forming modern MVT equivalents at present (e.g. Kyle and Saunders, 1996). The metalliferous nature of some hot oilfield brines is indicated by scales and incrustations of ore minerals in pipes and wells. At the classical locality of Cheleken Peninsula in the Caspian Sea (Lebedev, 1973) the annual discharge of heavy metals from brine seepages amounts to 300-360 t Pb, ~50 t Zn, 24-35 t Cu, 18-24 t Cd and 6-8 t As. The metal concentrations in brines vary and even the highly

metalliferous fluids (e.g. in the Raleigh oilfield, Mississippi: 222 mg/l Zn, 53 mg/l Pb; Saunders and Rowan, 1990) cannot be assigned to a deposit magnitude class as the volume of the brine is not available.

13.7. Regolith and continental sediments

13.7.1. Introduction

Recent (that is, presently forming and near past) weathering crusts and mostly unconsolidated sediments are the least controversial of the many lithologic associations (Ollier and Pain, 1996). Depositional environments of the geological materials need not be painstakingly interpreted with all the uncertainty this entails and with the multitude of competing models, because they are seen in action and can be just described. The degree of interpretational uncertainty, however, increases rapidly with depth and time so the paleoenvironments of the ancient regolith rock associations have to be interpreted in the same painstaking way as of any other assemblage of rocks the formation of which is impossible to directly observe today.

Recent (Quaternary and the latest Tertiary) environments and materials associations do form, and store, metal accumulations some of which have achieved the "giant" status, but the majority of such ores are "secondary", that is derived by reconstitution of an earlier "primary" deposit. A portion of the "secondary" deposits is directly and clearly related to discrete, identifiable "primary" sources, for example Ni laterites to ultramafics, "eluvial" cassiterite placers to tin granites, proximal gold placers to gold-quartz veins in the bedrock. In some cases the metal source/regolith deposit relationship is obscure or unknown.

Although most "secondary" deposits are enriched in respect to their source rock or ore, the Clarke concentration (enrichment factor) is low, usually less than 10 (it is, for example, 2 to 3 for lateritic bauxites on phonolite, 4 to 7 for Ni laterites on peridotite). This style of deposits can be approached (organized, described, searched) from two equally important premises: from that of the primary rock source, and from the environment or process producing the "secondary" ore. In this book the "secondary" deposits as above are treated as a variant of the "primary" ores, so the principal descriptions are scattered through many chapters. In this chapter the "secondary" deposits are briefly

tabulated and cross-referenced, following a short description of their environments, settings and styles.

For a large group of primary deposits, supergene modification (weathering, erosion, denudation) is a case of "negative metallogenesis" that gradually destroys and removes an earlier orebody, but pockets of economically viable material may temporarily remain along the "path of destruction", to produce ore deposits of their own. The most common example are ores in talus, landslides, slumps, alluvial fans or source-proximal moraine downslope from "giant" deposits; at least two such "pockets" are of the "giant" magnitude themselves (the Quinua Au deposit in moraine under Yanacocha, Peru; the Ag-Sn bearing "pallacas" under Cerro Rico, Bolivia; Chapter 6). Metalliferous alluvial placers are an extension of this type of ore concentrations. Although gold, cassiterite and platinoids do not travel far from their primary source, the exact parent deposit may be difficult to pinpoint. Dispersed products of supergene wasting of primary ores, uneconomic on their own, are nevertheless of fundamental importance in physical (ore boulders tracing, panning concentrate analysis) and geochemical search for the "primary" deposits.

The remaining category of supergene ore accumulations lacks identifiable primary metal sources, although the overall "bedrock" or "basin" nature still influences at least the metal selection preferences. Orebodies form as local concentrations of previously dispersed metals in many continental sedimentary environments, as a variant of common sediments (e.g. heavy mineral alluvial sands), or as a substance brought in solution from outside and precipitated in the sediment before or after lithification (e.g. the "surficial U deposits" in unconsolidated sediments and their counterparts, "sandstone-U" in solid rocks). The near-surface precipitation of metals from descending meteoric waters (or ascending groundwaters in arid pedogenic systems) are still an extension of the supergene metallogenesis, but with greater depth the formational waters and hydrothermal fluids take over and continental sedimentary rocks become hosts to genetically unrelated epigenetic deposits (e.g. veins, impregnations, replacements) like any other rock. Continental supergene environments are not directly controlled by plate tectonics, or only a very little (the parent "bedrocks", however, usually are) and instead are influenced by the standard physico-geographic (geomorphologic) factors such as physiography and climate (temperature and humidity).

13.7.2. Glaciation and ores in glaciogenic (cryogenic) materials and structures, related talus and glaciofluvial deposits

Glaciogenesis is a supergene system dominated by physical erosion, transportation and deposition with negligible chemical component (Eyles and Miall, 1984; Goldthwait and Matsch, 1989). The initial glacial sediment, till, is the worst sorted sediment known but it undergoes a degree of sorting and winnowing of the fine detrital fraction by running water: within and under a glacier (to form eskers), in front of glacier tongues (outwash), or by subsequent reworking by streams or coastal waves. There, several varieties of glaciofluvial and glaciomarine sediments form. Glaciers moving over substantial bedrock ore deposits erode, incorporate and carry and eventually disperse the primary ore substance. As mentioned above, a portion of such material is sometimes salvaged to form economic orebodies of their own, downslope from the primary deposits. The **Quinua Au deposit** under the epithermal "giant" Yanacocha in the Peruvian Andes (Turner, 1999; Harvey et al., 1999; 420 t Au, 2923 t Ag; Chapter 6) is one of the three recorded "giant" deposits related to glaciation. The deposit is in a depression between two primary gold mineralized ridges and it is a 50-100 m thick mixture of glacial, alluvial, landslide and debris flow materials with assay boundaries. The precious metals are in fragments of the oxidized high-sulfidation ore, as well as dispersed in matrix. The metals recovery is by heap leaching.

The other potential "giant" is the **El Rodeo Sn-mineralized moraine near Viloco** in the Cordillera Quimsa Cruz in Bolivia (Ahlfeld and Schneider-Scherbina, 1964). This is a virtually flat body of unsorted till, composed of a chaotic mixture of locally derived granite, metamorphics, vein quartz, cassiterite, magnetite and minor gold. It is interpreted as a Quaternary ground moraine, subsequently uplifted and dissected by the Rio Yaco. The contained cassiterite resides in fragments of the original gangue (from which it has to be recovered by milling and gravity concentration) as well as separate sand-size grains. The latter is recoverable by primitive artisanal mining techniques, despite the low average grade of some 200 g/t Sn. The mined portion of El Rodeo stores some 48 kt Sn. The overall tin resource in El Rodeo is estimated by Putzer (1976) to be some 500 mt of material grading 0.02-0.1% Sn, containing perhaps 300 kt Sn. The third glaciation-related "giant" are the "pallacas" at foot of the **Cerro Rico in Potosí, Bolivia** (Murillo et al., 1968; Bartos, 2000; Rc

~100 mt of material @ 119 g/t Ag for 11.9 kt Ag and ~10 kt Sn) mentioned in Chapter 6. This is a glaciation-assisted mixture of talus and landslide rubble with Sn and Ag values contained mostly in silicified ore fragments, derived from the extensive epithermal mineralization at the Cerro summit and on slopes. Bartos (2000) outlined six individual deposits, mined by the locals using primitive techniques.

Glacier-redeposited ores have many more forms; for example at the "large" Kennecott ore field in Alaska (Bateman and McLaughlin, 1920), blocks of rich chalcocite ore were embedded in ice of a small alpine glacier, as well as in talus, under slope outcrops of the primary ore.

Small first generation glaciers that recede and eventually melt are most favorable to produce "secondary" deposits as described above. Drift produced by continental glaciers of several generations has a low potential. The gold-rich Abitibi mineral province in the Canadian Shield, most likely covered by a proximal auriferous regolith before the Quaternary glaciation, is now partially covered by drift resulting from the fourth, Wisconsinian glaciation that stripped bare the bedrock already swept three times before. It is possible that some of this gold still exists in sediments formed during the first glacial advance, somewhere. Alluvial (e.g. in the Sacha/Yakutia Republic in Siberia; New Zealand) and beach (e.g. Nome in Alaska) gold placers reworked from drift are locally important and may approach the "giant" magnitude (compare Laznicka, 1985, p. 737-750; Boyle, 1979, 1987; Bilibin, 1955).

Paleo-glaciogenic associations are treated in the context of diamictites (that could be also of other that glacial origin) in Chapter 11, as those that host important orebodies (of Fe and Mn, as Snake River-Yukon and Corumbá-Brazil) are Proterozoic. Also Proterozoic is the "large" Cu ore field Mount Gunson, South Australia (Williams and Tonkin, 1985; Drexel et al., 1993). This has predominantly chalcocite infiltrations in breccias and fractured ground interpreted as of periglacial origin, along a Neo- to Meso-Proterozoic unconformity.

13.7.3. Humid tropical regoliths

As with other varieties of "secondary" mineralizations, weathering does not create new ore deposits "out of nothing" but it requires earlier orebodies, or "rocks", geochemically enriched in some major or trace metal, to operate. Search for "metalliferous laterites", for example, is thus a binary effort that has to start from two ends:

1) identification of metal(s) enriched bedrock geology; and 2) identification of suitable climatic and physiographic environment, present or past. This philosophy also applies in this book where the "secondary" deposits are described jointly with their "primary" sources. This reduces this chapter to a brief directory.

Secondary deposits range from those still in the process of active formation (this may take place in some depth under rainforest floor so that it may not be directly apparent), through young deposits barely exposed by erosion, to variously degraded ore relics. The oldest weathering-formed deposits are found at unconformities, preserved under the protective cover of younger rocks.

Many "secondary" deposits discovered first often resulted in later finding, or developing, the "primary" deposits underneath or nearby. Often the "primary" deposits have been developed after exhaustion of the "secondaries" (e.g. the "taconite" iron ores of the Mesabi Range, Minnesota; Chapter 11). Reverse situations are also common, especially when arrival of new technology has made profitable mining of very low-grade materials, such as ~1 g/t Au ores or 0.2% Cu ores: both processable by heap- or in situ leaching.

Chemical weathering in the wet tropics goes hand in hand with physical erosion and denudation, hence more existing primary deposits exposed at surface are destroyed than new "secondary" deposits are created. Even when economic "secondary" deposits form, they are always only the transitional stages in the process of overall mass wasting where, usually, more of the metal(s) stored in the "primary" source is lost than temporarily preserved. The classical secondary deposits like the "ore laterites", however, have a higher grade than their primary sources (e.g. 50 to 65% Fe in the enriched Fe ores versus ~25-35% Fe in banded iron formations), and are cheaper/easier to mine and process. The concentration factors achieved, however, are very small: usually less than 10. Typical secondary deposits are residual, that is they formed in-situ by removal of the unwanted substance (typically SiO₂, CaCO₃, MgO, alkalis) which increases the relative concentration of the valuable substance left behind (typically Fe, Al, Ni, Mn, Sn, etc.). Often there is some limited migration of substances within the weathering profile itself (e.g. Ni leached from ultramafics descending to the saprolite or leached rocks levels to form infiltrations), or physical reworking and transport that produces "tertiary" (redeposited) deposits, usually in alluvial systems (e.g. the "pisolite" Fe

gravels in the Hamersleys, Chapter 11; cassiterite placers; read below).

Many weathering-generated or modified metallic deposits are "giants", or "world class" (all major bauxite and many enriched Fe districts are "world class" as they are economically important but have not reached threshold of the "geochemical giants" of 8 bt Al and 4.3 bt Fe). The deposits listed in Table 13.7. are either entirely "secondary" (all bauxite deposits, Ni laterites), or they are the "secondary" component of binary (that is primary and secondary) deposits (most of the rest). The significant deposits have already been described in other chapters so only a reference is made here.

Weathering and related metallogenesis (Fig. 13.41) have an extensive literature both general and related to specific metals or types of ores (Emmons 1917, McFarlane, 1976; Lelong et al., 1976; Mabbut, 1980; Butt, 1989) and there is a brief review in Laznicka (1985, p.677-727).

Fe ores

The dominant iron ore of the 2000s, exported from Brazil and Western Australia, comes from enriched banded iron formations. The direct shipping (non-pelletized) ores run about 65% Fe mainly as hematite, and they are the product of secondary supergene enrichment of the original "lean" banded iron formations (~20-45% Fe). These BIF's come from both the (meta)volcanic association (Algoma type-e.g. Serra dos Carajás, Chapter 9) and (meta)sedimentary association (Superior type, e.g. Mesabi Range; Chapter 11). Many iron formations share characteristics of both associations. The simplest enriched BIF formed by supergene leaching of silica in humid tropics, usually with conversion of the original magnetite to hematite and goethite (e.g. the Marra Mamba ores of the Hamersley Range). Orebodies rich in massive high-grade "hard hematite" or specularitic "blue hematite", like many of the Hamersley orebodies (Mt. Tom Price; Mt. Whaleback; Chapter 11) have a more complex, multistage origin that may have involved hydrothermal transfer and metamorphic conditioning. The "giants" listed in Table 11.3 are all Fe districts or provinces. The primary BIF resources of some run into trillions of tons of iron (especially the Kursk Magnetic Anomaly of Russia and the Australian Hamersley Range).

Aggregate resources of ferricrete caps (cuirasse) of some lateritic terrains formed on ultramafics or basalts (as in New Caledonia) also qualify as "giants".

Table 13.7. Brief summary of "giant" and "near-giant" metallic deposits in regolith (selection); most are described in text in several chapters

Metal	Deposit/district	Type of ore in regolith	Metal content/grade
Fe	New Caledonia cuirasse	Fe oxides (30-65% Fe) hardcap on top of laterite on peridotite klippen; several areas	15 bt Fe/30-65%
	Kursk Magnetic Anomaly, Russia	Several enriched Fe deposits in pre-Carboniferous regolith over raw Pp mainly oxide BIF	27 bt Fe/50-60%
	---Yakovlevo ore field only	Ditto	16 bt Fe/60%
	Hamersley Range, Australia	Tertiary and Proterozoic high-grade supergene hematite, combined with possibly "basinal fluid" ore over Pp mostly oxide BIF	19.25 bt Fe/60-65%
	---Marra Mamba type ore	Mostly goethitic and hematitic supergene ore	8.8 bt Fe/50-62%
	Quadrilátero Ferrífero, Minas Gerais, Brazil	Several varieties of colluvial & lateritic (canga), supergene and "basinal fluid" enriched hematitic ores over Pp metamorphosed siliceous BIF	32 bt Fe/60-65%
	Serra dos Carajás, Pará, Brazil	Two lines of discontinuous "plateaux" of supergene hematite and canga on Ar Algoma-type BIF	11.82 bt Fe/60-66%
Mn	Mesabi Range, Minnesota	Relics of supergene enriched hematite and goethite over Pp siliceous BIF ("taconite")	3 bt Fe/50-60%
	Corumba-Mutún, W Brazil and SE Bolivia	Residual and transported (plaquette, canga) hematite over Np BIF (jaspillite) in diamictite association	10-20 bt Fe/50-60%
	Moanda, Gabon	Residual Mn oxides in lateritic capping of several dissected plateaux, developed over Pp Mn carbonate	275 mt Mn/35%
	Nikopol, Ukraine	Concretionary Mn oxides gradational to Oligocene bedded Mn carbonates; partly or entirely supergene	940 mt Mn
Al	Groote Eylandt, Australia	Blanket of concretionary Mn oxides in thin Cr sediments over basement regolith; partly or fully supergene?	222 mt Mn
	Weipa, Australia	Young lateritic concretionary gibbsitic bauxite, over kaolinized sedimentary basement cover	875 mt Al/29.15
	Central Highlands, Vietnam	Ferruginous lateritic bauxite blanket over flood basalt	678 mt Al/21.2
	Boké-Goual, Guinea	Ferruginous laterite blanket on several dissected plateaux formed on Cr dolerite, shale	622 mt Al/25%
	Touque, Guinea	Ditto	533 mt Al/23.16%
	Adamaoua, Cameroon	Ditto, bauxite on basalt and granitic gneiss	427 mt Al/23.4%
	Darling Ranges, Western Australia (S of Perth)	Gibbsitic laterite blanket over greenstones of the Ar Saddleback belt	480 mt Al/~16%
Ti	Pakaraima Mts., Guyana	Lateritic bauxite blankets on sandstone, schist	?1,119 mt Al/15.9%
	Los Pijiguaos, Venezuela	Ditto, bauxite on granite and schist	?1,160 mt Al/20%
	Tapira, MG, Brazil	Regolithic anatase formed in lateritic blanket over perovskite-rich pyroxenite	26.4 mt Ti/13.2%
Cr	Catalão, MG, Brazil	Ditto	102 mt Ti
	Surigao Norte, Mindanao, Philippines	Residual chromite in laterite and saprolite over ophiolitic serpentinite	12.3 mt Cr/2.85%
Mg	Kunwarara, Queensland	Nodular "amorphous" magnesite partly reworked from serpentinite regolith, partly authigenic in T lacustrine basin fed by runoff	1.2 bt MgCO ₃ /20% ++ or 345 mt Mg
Ni,Co	New Caledonia	Limonitic Ni laterite (with asbolite) and Ni hydrosilicates-rich saprolite over Eo peridotite klippen in 3 major dissected plateaux	50-80 mt Ni 2.5 mt Co
	---Goro deposit only	Ditto, predominantly limonitic laterite to mine	2.64 mt Ni/1.6% + Co
	Moa, Holguín Prov., Cuba	Limonitic laterite and Ni hydrosilicates saprolite over Cr ophiolitic serpentinite	9.8 mt Ni/1.4%
	Niquelândia Complex, Brazil	Limonitic laterite and Ni hydrosilicates saprolite over peridotites of Pp differentiated layered intrusion	6.5 mt Ni/1.3% (Rc) 650 kt Co/0.13%
	Palawan Island, Philippines	Ni laterite and saprolite over ophiolitic serpentinite	6.3 mt Ni/1.8%
Surigao Norte, Mindanao	Ni laterite and saprolite on Eo ophiolitic serpentinite	5 mt Ni/1.22%	
Soroako, Sulawesi	Ni laterite and saprolite on on ophiolitic serpentinite	4.4 mt Ni/1.67%	

Table 13.7 (continued)

Metal	Deposit/district	Type of ore in regolith	Metal content/grade
Ni,Co	Biankouma-Touba, Côte d'Ivoire	Laterite and saprolite over ophiolite and alpine-type serpentinite in 10 deposits	4.3 mt Ni/1.5% 300 kt Co/0.11%
	Pujada, Davao, S Mindanao	Ni laterite and saprolite on ophiolitic serpentinite	4 mt Ni
	Gag Island, Papua, Indonesia	Ni laterite and saprolite on ophiolitic serpentinite and melange	3.93 mt Ni/1.51%
	Ramu River, PNG	Ditto	3.5 mt Ni/1.4%
	Weda Bay, Halmahera, Indonesia	Ni hydrosilicates in saprolite over ophiolitic serpentinite	2.96 mt Ni/1.37% 259 kt Co/0.12%
	Murrin Murrin, Western Australia	Ni hydrosilicates in saprolite over Ar komatiitic peridotite in ~22 separate orebodies	2.9 mt Ni/1.04% 223 kt Co/0.08%
	Marlborough, Queensland	Ni hydrosilicates in saprolite over ophiolitic serpentinite	2.142 mt Ni/1.02%
	Nicaró, Holquín Pr., Cuba	Ni laterite and Ni-hydrosilicates in saprolite over Cr ophiolitic serpentinite	2.1 mt Ni/1.4%
	San Felipe, Camagüey Cuba	Ditto	2.0 mt Ni/1% 200 kt Co/0.1%
	Pinares de Mayari, Cuba	Ditto	2.0 mt Ni/1.3% 200 kt Co/0.1%
	Falcondo, Dominican Rep.	Ditto	2.0 mt Ni
	Wingellina, W. Australia	Relics of Ni saprolite on ultramafics of metamorphosed Mp mafic-ultramafic layered intrusion	2.0 mt Ni
	Cu		Chalcocite blankets over porphyry Cu: see Table 7.5 Oxidic Cu in exotic deposits over porphyry Cu: see Table 7.4 Oxidic Cu over porphyry Cu, see Table 7.3
Katanga (Shaba) Copperbelt		Oxidic ore over near-surface orebodies in Np dolomitic hosts	at least 30% of 127 mt Cu
Zambia Copperbelt		Ditto, oxidic ore over silicate rock hosts	at least 15% of 88 Mt Cu
---		Nchanga-Chingola, Cu in refractory ore in residual hydrosilicates	3.48 mt Cu/~1.0-1.5%
Zn,Pb	Skorpion, S. Namibia	Sauconite, tarbuttite, hydrozincite, smithsonite on partly karsted sulfide-mineralized marble units	2.61 mt Zn/10.6%
	Mehdiabad, Iran	Smithsonite, hemimorphite in oxidation zone and mixed with primary sulfide replacements	portion of total 15.7 mt Zn, 5.014 mt Pb, 11,118 t Ag
	Silesia-Krakow, Poland	Smithsonite, hemimorphite (calamine) ores in karsted oxidation zone over MVT sulfide deposits in Tr dolomitized limestone; 3 major ore fields	3.941 mt Zn
	Magellan deposit near Wiluna, W. Australia	Supergene cerussite orebody in residual breccias in Pp dolomite, wacke, black schist	3.78 mt Pb/7.1%
Sn	Broken Hill, NSW, Australia	Gossan and oxidation zone over Pp massive Pb-Zn sulfide orebody in high-grade metamorphics	at least 2 mt Pb, 5,000 t Ag from regolith
	Peninsular Malaya, Malaysia	Alluvial placers grading to in-situ regoliths ("eluvial placers") of resistate cassiterite over granites; 3 belts	3.6 mt Sn
	---Kinta Valley, Ipoh, Perak, Malaysia	Alluvial placers grading to in-situ regolith with scattered residual cassiterite over granite-related primary sources; much ore in karst sinks	1.411 mt Sn
	Ranong-Phuket belt, Thailand	As in Malaya; all Sn deposits are in Western and Central tin belts	1.57 mt Sn
	Bangka Island, Indonesia	Ditto, also offshore placers	1.5+ mt Sn
	Belitung Isl., Indonesia	Ditto	650+ kt Sn
	Rondônia State, NW Brazil	Alluvial and residual cassiterite in placers and regolith over Mp tin granites	1.85 mt Sn
	Pitinga, Amazonas, Brazil	Alluvial and residual cassiterite over apogranite and greisen primary mineralization	575 kt Sn
Maniema Province, Congo	As above, over rare metals pegmatites	265 kt Sn	

Table 13.7. (continued)

Metal	Deposit/district	Type of ore in regolith	Metal content/grade
Nb,Ta REE	Araxá, MG, Brazil	Relic and converted relic Nb (REE,Th,U) minerals dispersed in limonitic ocher residual after silicate carbonatite	9.7 mt Nb + U, Th, REE
	Seis Lagos, Amazonas, Brazil	Residual Nb (REE,Ta,Th,U) minerals in regolith over carbonatite; minor placers	Most of 57 mt Nb 43.5 mt REE
	Tomtor, Siberia, Russia	Multistage complex of lacustrine placer, regolith, primary carbonatite with scattered minerals of Nb, REE, Y, Sc, Th, U, Ta in carbonatite	?10.8 mt Nb ?27 mt REE ?45 kt Sc
U Au, Ag	Itataia, Ceará, NE Brazil	U in colophonite infiltrations in Pt marble	121 kt U
	Pueblo Viejo, Dominican Republic	Residual oxidized blanket with relic gold and Ag halides over high-sulfidation primary deposit	455 t Au
	Telfer, Western Australia	Residual Au in oxide zone over low-grade, primary veins, stockwork, replacements in Pt rocks	363 t Au
	Boddington, W. Australia	Residual Au in lateritic bauxite and underlying silicate regolith over Au-(Cu) vein, stockwork, disseminated bedrock orebody in Ar greenstones	140 t Au
	Carlin Trend, Nevada	Au in limonitic fracture coatings residual after "Carlin-type" disseminated replacement ores	at least 20% of 3,328 t Au
	Rio Tinto, Cerro Colorado gossan Ok Tedi, PNG	Residual Au in limonitic gossan after Fe+Cu sulfide stockwork in Cb felsic volcanics Residual Au dispersed in limonitic gossan relic after Fe-Cu-Au skarn and Cu-Au porphyry Cu	101++ t Au 138 t Au

NOTE: Tonnage figures represent metals stored in the "secondary", supergene, residual, etc. components in mixed orebodies only

The low- to medium-grade (~30-40% Fe) particulate (oolitic) ironstones started the industrial revolution but are nowadays mined for local consumption only. Although many are locally supergene enriched the enrichment is inconsistent and ineffective because of the high proportion of siliclastic fraction that remains in the residue. Carbonate-cemented ironstone (as partly in Birmingham, Alabama) produced the best residual ores by removing the carbonate component (which, on the other hand, made the Alabama ores self-fluxing) but the size of orebodies was at best of the "medium" magnitude.

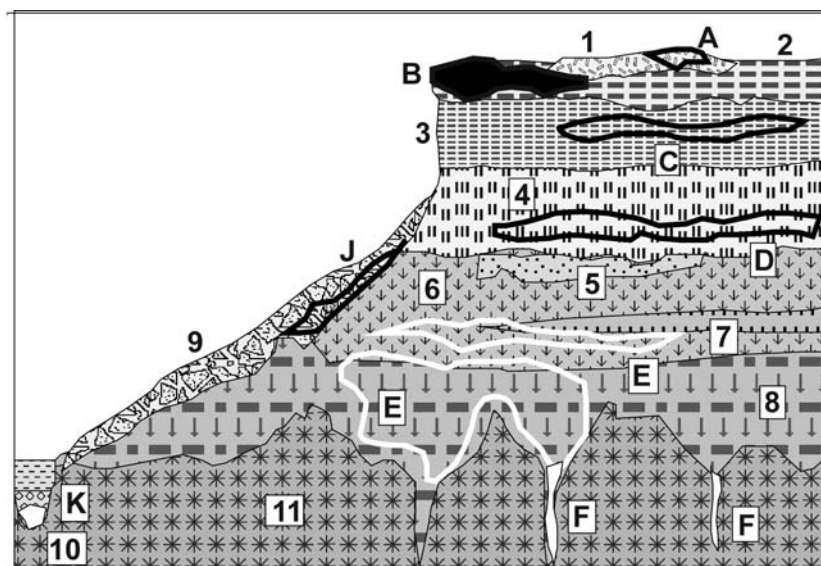
Mn ores

Undiluted supergene Mn oxides (pyrolusite, cryptomelane) produce "battery-grade" shipping materials (65% Mn plus), most of which are the product of selective and labor intensive mining and beneficiation (often hand sorting). Deposits of this type formed on the bedded Mn deposits in the combined clastic and chemical sedimentary successions often associated with BIF (Chapters 9, 11), on volcanic-sedimentary "exhalites" (Chapter

8) and on carbonates. Most deposits were of the small to medium-size. The supergene "Mn giants" Moanda and Groote Eylandt formed on low-grade rhodochrosite-rich protorees. The Mn oxide ores at Nikopol (Section 13.4) are partly supergene, partly primary diagenetic. In contrast with iron, more economic Mn resides in, and is mined from, non-enriched bedded Mn in both siliclastics (Kalahari) and carbonates (Molango).

Al ores: bauxite

Bauxite still holds a 98% monopoly as the preferred aluminum ore. Of the 54 bt of global bauxite resources in the 1980s quoted by Bárdossy and Aleva (1990) (the resources may have increased to about 60 bt in 2004), the bulk are young, in-situ lateritic bauxites some of which (in western Africa) are still forming. Transported bauxites (the majority of the karst bauxites; Bárdossy, 1988) hold a much lesser share of resources. The largest "world class" residual gibbsitic blankets preserved on dissected plateaux in Guinea (Boké-Goual, Fria, Touque; Chapter 12) as well as bauxites in Cameroon and Vietnam, formed on diabase, basalt and shale.



1. Reworked laterite, soil, rubble; A. Fe, Al, P, Mn residual rubble; 2. Lateritic duricrust capping; B. Fe, Al, P, Mn, Ti, Au solid metalliferous crusts to breccia (e.g. bauxite, Fe oxides); 3. Carapace, hematite concretions in pink clay; C. Metals as in B, concretionary ore particles in oxidized clay; 4. Mottled zone; D. Mn, Ni, Co, Au-rich soil (laterite); 5. Patchy silicification, opal, chalcedony; 6. Lithomarge, fine clayous saprolite; E. Ni, Co hydrosilicate infiltrations in reduced saprolite; 7. Greenish nontronitic clay; 8. Coarse saprolite; 9. Colluvium and rubble;

Figure 13.41. Humid tropical (laterite, saprolite) regolith on silicate rocks (especially mafics, ultramafics), inventory diagram from Laznicka (2004), Total Metallogeny Site G181. Explanations (continued): F. Magnesite, Ni hydrosilicates par descensum veins, fracture fillings; J. Fe, Al, Mn, P transported in talus (e.g. canga); 10. Stream channel, sorted resistate gravel and sand; K. Fe, Al, Mn, P stream reworked resistate gravel; 11. Bleached (saprock), then fresh, silicate bedrock. Ore types B, D, E have known "giant" equivalents

The extensive "peneplain" (or platform) bauxite sheets as in NE Australia (Weipa-Aurukun, Gove; Fig. 13.42), Brazil (Trombetas, Paragominas) and the Guyanas (Fig. 13.43), formed by allitization of young claystone, mudstone or arkosic sandstone.

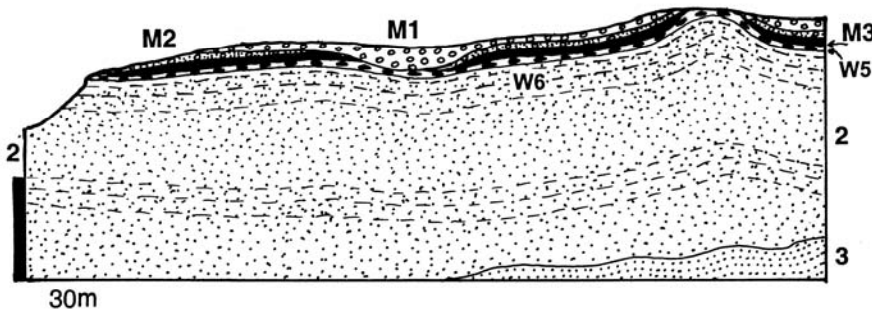
Weipa (Evans, 1975; Schaap, 1990; ~3 bt of bauxite @ 29.15% Al, for 875 mt Al content) is located along the western coast of the remote Cape York Peninsula in northern Queensland. The "red cliffs" had been sighted by Captain Matthew Flinders in 1802, but it was not until the 1960s when this was recognized as an extensive blanket of bauxite. The blanket is between 1.5 and 10 m thick, composed of gibbsite and boehmite pisoliths with about 12% of Fe oxides and traces of kaolinite. The blanket has a thin, patchy cover of soil with scattered loose pisoliths, and it rests on kaolinitic clay that is also a marketable commodity. This is further underlaid by friable arkosic sandstone and more claystone and mudstone interpreted as of Jurassic-Cretaceous age, resting on Mesoproterozoic metamorphic basement. The flat-lying shallow marine sediments are believed bauxitized between late Cretaceous and Oligocene, so the regolith is fossil and partially eroded. Additional large bauxite resource exists south of Weipa near the Aurukun community.

Supergene TiO_2

Titania is enriched in most residual bauxites formed on gabbro, diabase and basalt where the average TiO_2 content is around 4-5% (Bárdossy and Aleva, 1990), but it is almost never recovered. The only humid tropical regoliths mined for titanium are the anatase-rich residua on alkaline pyroxenite in Tapira and Catalão in Brazil, both of which are "large" accumulations (Chapter 12). Anatase (TiO_2) formed by the breakdown of perowskite (CaTiO_3), enriched in pyroxenite.

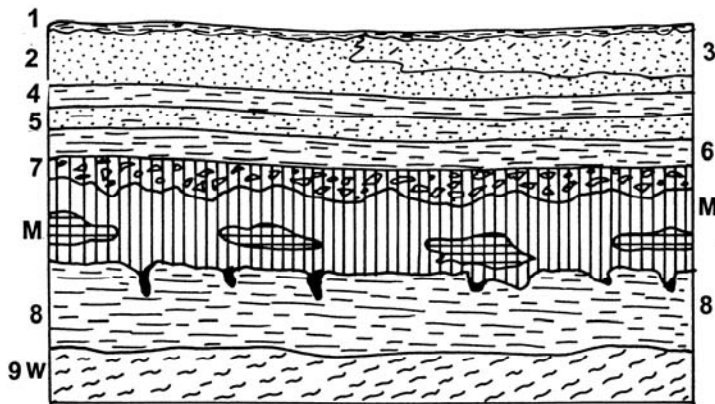
Mg in "secondary" magnesite

White, microcrystalline ("amorphous") magnesite forms by carbonatization of olivine (forsterite) and the serpentine minerals in ultramafic regoliths, most commonly in the ophiolite association. The chalky white magnesite, often strengthened by dispersed opal or chalcedony, forms nodules, fracture veins, infiltrations and "magcrete" (equivalent to calcrete) in ultramafic saprolite and saprock (=leached rock). Thousands of small magnesite occurrences occur around the world, but few "world class" deposits of "amorphous" magnesite have formed.



T1 in-situ and transported bauxite regolith: M1. Loose pisolithic bauxite; M2. Cemented pisolith; M3. Tubular bauxite, anastomosing vesicular cavities filled by cement; M4. Loosely cemented nodular bauxite; W5. Nodular ironstone;

Figure 13.42. Gove (Nhulunbuy) bauxite plateau, NE Arnhem land, northern Australia; cross-section from LITHOTHEQUE No. 3199, based on Somm (1975). Explanations (continued): W6. Mottled kaolinitic zone and kaolinitic saprolite; 2. Cr1 kaolinized fluvial arkosic and quartz sandstone, minor lignite; 3. Pp gneiss, migmatite, granite



1. Q topsoil; 2. Q white quartz sand; 3. Yellow quartz sand; 4. T3-Q gray clay; 5. Ditto, sand or sandy clay with reworked bauxite concretions; 6. T3 gray lignitic clay with pyrite concretions; 7 (M) Top of bauxite horizon, 1-4 m thick zone of partial re-silicification; nodular gibbsite in kaolinitic clay; M. Main bauxite horizon, low- to intermediate Fe earthy, structureless to concrectionary gibbsitic bauxite; 8. T white kaolinitic clay; 9W. Pcm saprolitic basement gneiss, granodiorite

Figure 13.43. Linden bauxite ore field, Guyana, cross-section from LITHOTHEQUE No. 1064; 1981 field visit sketch

The largest accumulations resulted when the nodules and magnesite dust, augmented by authigenic magnesite, have been reworked and deposited as bedded fluvial or lacustrine deposits.

Kunwarara magnesite deposit (Milburn and Wilcock, 1998; 1.2 bt of material with 35% of magnesite) is 60 km NW of Rockhampton in central Queensland (see Fig. 8.5). The semi-consolidated late Tertiary to Quaternary fluvial to lacustrine sediments lap on regolithic serpentinite of the mid-Paleozoic Marlborough ultramafic ophiolite complex. The serpentinite itself contains abundant "amorphous" magnesite occurrences. The up to 40 m thick sediments fine upward from basal gravel through sandstone to siltstone, and are overlaid by 1 to 6 m of recent black clay. The magnesite ore lens, about 12 m thick, consists of an upper zone of very large white porcellanous magnesite nodules, with minor dolomite, in clay and friable authigenic magnesite matrix. This fades downward into medium to small nodules scattered in fine grained

sand. The magnesite nodules are partly of clastic, partly of authigenic origin showing evidence of displacive growth in the present medium. The orebody is locally channelled and partially silicified near the top. Presently used in the refractories industry, the Kunwarara magnesite is expected to provide feed to the planned Queensland magnesium smelter.

Ni (and Co, Cr) laterite and saprolite

Oxide and silicate-based nickel is an alternative to sulfidic Ni ores. As Ni recovery from "laterite" costs more than recovery from sulfides, these materials require a higher grade (1% Ni plus) and greater tonnage to form economic deposits. In New Caledonia, rich lateritic Ni ores have been successfully smelted since 1908.

Humid tropical weathering profiles on ultrabasics (both ophiolitic; Chapter 8 and komatiitic; Chapter 9, peridotites) are distinctly vertically zoned. Under a thin surficial cover is an

erosion-resistant sheet of hematitic duricrust (ferricrete or cuirasse), often found capping dissected plateaux. Beneath it is a soft reddish or pinkish zone of hematite microconcretions (pisoliths, buckshot) in powdery Fe oxide and clay matrix that changes downward into a yellow or brown spotted (mottled) clay zone rich in Fe hydroxides. These zones are interpreted as laterite, a tropical soil, in which the parent rock texture has been completely destroyed. The lower laterite zone is enriched in Mn, Ni and Co concentrated in Fe and Mn oxides and hydroxides. Ni-grades (typically around 1% Ni) are lower than in the underlying saprolite and lateritic ores used to be avoided during selective mining in the past. Some new mining developments that include the "large" **Goro deposit in New Caledonia** (Rv 165 mt of ore @ 1.6% Ni, 0.16% Co for 2.64 mt Ni and 264 kt Co), are predominantly in the "yellow laterite".

The saprolite (lithomarge) below laterite consists of a greenish residual montmorillonitic (nontronitic) clay with preserved parent rock texture that grades into the underlying, leached ultrabasic rock. There are common fracture infiltrations of silica (opal to chalcedony, often green chrysoprase) and magnesite. Ni resides in silicates substituting for Mg and Fe (Ni-montmorillonite, Ni-chlorite) and is either dispersed, "invisible", or accumulated in light-green infiltration veinlets of "garnierite" (a nickeliferous smectite, saponite, chalcedony, etc. mixture). This is the most desirable kind of Ni ore grading more than 1% Ni (the New Caledonia saprolites averaged 3% Ni; Chapter 8). In partially eroded regoliths this is the only nickeliferous zone left and it could be strongly degraded by silicification.

Table 13.7. lists over twenty "large" continuous or closely grouped deposits that store between 1.0 mt and 5.5 mt Ni (5.5 mt Ni being the lower "giant" limit). Two of them (Moa Bay, Cuba: 9.8 mt Ni; Rio Tuba, Palawan, Philippines: 6.3 mt Ni) qualify as "giants". The often quoted Ni mega-tonnage of New Caledonia (~32 mt Ni) comes from numerous deposits formed over a series of discontinuous peridotite massifs is a 400 km long island (Paris, 1981). The massifs are remnants of an Eocene allochthon.

Cobalt accompanies nickel in residual ores on ultramafics (the usual Ni:Co ratio is about 10:1), but is not always recovered. The cumulative content of cobalt in the New Caledonia "laterites" is usually quoted as 2 mt Co; the Goro deposit contains 264 kt Co @ 0.16%. Co is mostly enriched in the limonitic laterite where it is absorbed on Mn hydro-oxides to form "asbolite". Residual chromite and magnetite

occur disseminated through lateritic profiles, but are rarely recovered during Ni mining. Accumulations of residual chromite, usually over the "podiform chromite" or layered chromite deposits, rarely reach the "medium" magnitude.

Residual Sn deposits

Cassiterite, the dominant Sn carrier, is a chemically and physically resistant mineral that remains disseminated in weathering-softened and thinned intervals of "tin granites" that would be too low grade to mine as a hardrock. Cassiterite is also selectively liberated from complex veins and replacements. Deposits of in-situ residual cassiterite are usually designated "eluvial placers" and they are mined, in SE Asia, jointly with the cassiterite placer deposits produced by regolith reworking. As the usual mining method is high pressure water monitoring, the Sn tonnages in the eluvial and alluvial placers are usually quoted jointly. They include the SE Asian "giant" tinfields like Kinta Valley, Bangka and Belitung, as well as the deposits in Rondônia and Amazonas (Pitinga) in Brazil.

Residual Nb and REE (Th,U) deposits

The three largest ("giant" and "super-giant") Nb deposits (Seis Lagos, Tomtor and Araxá) are in residual clay and powdery limonite formed by weathering of carbonatite (Chapter 12). Because of the total dissolution and removal of the carbonate component the enrichment factor of the residual fraction, that includes the ore minerals, is very high. Fine grains of pyrochlore, columbite, monazite and products of their partial or total decomposition are evenly dispersed in the brown clay residue. Also residually enriched are barite (when present in the primary carbonatite) and apatite (or its varieties francolite or collophanite). The "large" U deposit Itataia in Brazil (Angeiras, 1988; Chapter 14) contains uranian collophanite in marble, a portion of which could be residual.

Residual Au (Ag) deposits

Gold, because of its low solubility, resists leaching from weathering profiles and can remain, in the pre-weathering concentration or enriched, in its original place of occurrence from which other metals (except Fe) have been removed and sulfides decomposed. Weathering breaks down sulfides (mainly pyrite and arsenopyrite) that previously held gold in refractory ores and the gold is

liberated, usually dispersed in Fe "limonite" or present as independent grains or as fracture coatings. Such material is amenable to heap or in-situ leaching and hundreds of mostly small leaching operations have appeared in the past twenty years, many to cease working once the oxidized material has been exhausted. When large resources of the primary (sulfidic and usually refractory) ore remained, a complete change of the mining and processing technology has been needed, requiring a substantial investment. Telfer, Pueblo Viejo, Boddington, several Carlin Trend mines, are examples of "giants" that have had to pass through this costly change. In the literature, the "secondary" gold deposits are usually classified as either "Au gossans" (or oxidation zones), or "Au laterites", although there is a transition.

"*Au gossans*" are exemplified by the **Cerro Colorado gossans** in the Rio Tinto ore field (Chapter 8) formed on top of a pyrite-chalcopyrite stockwork. Gossans are a form of oxidation zone comprised of a dense accumulation of residual goethite, formed over Fe sulfides-rich ores. It rests directly on the hypogene ore (like the immature gossans formed over glacier-swept orebodies in the Canadian Shield), or it caps and protects from erosion the softer oxidation or secondary sulfides zones underneath, in the same way ferricrete protects the soft laterite. Most gossans are in-situ replacements of the original orebody and when auriferous the gold is residual, possibly enriched in relation to the gangue or soluble minerals leached out. Most sulfidic Au deposits outside the boreal zone had gossans or oxidation zones with recoverable gold, but this rarely follows from statistics. Table 13.7. lists examples of "giant" (Telfer, Pueblo Viejo) and "large" (Ok Tedi, Cerro Colorado at Rio Tinto) deposits where the Au gossans/oxidized orebodies had enough individuality to be treated separately.

"*Au laterites*" have gained popularity with the unexpected discovery of gold values in lateritic bauxite at **Boddington**, Western Australia (Allibone et al., 1998; Chapter 9). Boddington has produced 140 t Au from the supergene material grading about 1.8 g/t Au, with a 0.5 g/t Au cutoff; 271 t Au remain in the hypogene zone, to be developed. "Large" gold deposits, where Au-laterite contributes significantly to the overall Au resource, include Igarapé Bahia in Brazil and Omai in Guyana. A typical deep regolith that overprints Archean, greenstone-hosted, shear-controlled gold deposits in Western Australia, the type area, has

two end-members (Butt, 1989; Mann and Webster, 1990; read also the review in Solomon et al., 1994, p. 779 and in Laznicka, 1993, p.565): a) the lateritic variety developed under conditions of humid tropical weathering and preserved, or renewed, in the high rainfall savanna climatic zone near the coast (e.g. in the bauxite province of Darling Ranges south of Perth); and b) relic lateritic profiles modified by declining water tables in the arid region (e.g. the Eastern Goldfields) where calcrete presently forms.

In a humid tropical weathering profile over auriferous substratum the following zones can be distinguished (from top to bottom): 1) Thin residual or transported soil, loam, windblown sand, volcanic ash, colluvium and similar; 2) Ferruginous zone high in Fe oxides and hydroxides, but usually lacking the hard, plateaux-capping ferricrete. In most cases this is a mixture of loose goethite, hematite or maghemite microconcretions ("buckshot") and locally gibbsite. In the arid belt the ferruginous material is enveloped or entirely displaced by calcrete or silcrete. 3) Mottled zone that comprise kaolinitic or smectitic clay to claystone with ferric microconcretions near the top. 4) Saprolite is the in-situ argillized and hydrated bedrock composed of kaolinite over quartzofeldspathic rocks, smectite and chlorite over metabasite and ultramafics. In subsequently arid climates the earlier saprolite underwent leaching and/or precipitation of silica (silcrete and "cherty" cements), groundwater calcrete, and sometimes gypsum and halite. 5) The bottom zone is composed of partly weathered (bleached) rock fringe and, ultimately, the fresh bedrock. Along faults and fracture zones and along the more rapidly decomposing rocks like diabase dikes, the saprolitization reaches depths of 100 m and more.

Dispersion of gold into the regolith and formation of Au-laterite depends on the nature of the orebody. Low-sulfide solid quartz veins rich in coarse free milling gold rarely produce gold-enriched supergene haloes. This, however, is common around vein orebodies with granulated and leached quartz in outcrop, in low- or no-quartz ores where the gold is in hydrothermally altered selvages, in silicate or carbonate veins, replacements and disseminations.

Butt (1989) demonstrated that the low-grade secondary gold accumulations in regoliths have two concentration maxima, separated by a depleted interval ("barren gap"). The secondary gold accumulations higher in the profile (the Au-laterite) are usually subhorizontal zones just under the surface, in the ferruginous horizon. Gold may also

accumulate in calcrete when it is present, although this rarely results in a mineable orebody but it aids geochemical exploration. Gold laterite contains finely dispersed, invisible gold; there are rarely any visual indicators to tell a gold-bearing laterite from a barren one. Small amount of gold could be present as megascopic particles like small nuggets sometimes enclosed in pisoliths, scattered tiny octahedral gold crystals (visually reminiscent of pyrite), gold smears or "paint gold" on fractures or slip surfaces. The size and shape of the Au-laterite orebodies is proportional to the size of the primary gold deposit. Mineralized shear zones produce linear ore zones ("troughs") 5 to 30 m deep. Authigenic gold particles like nuggets can be found near the surface.

The second gold enrichment interval deep in the regolith (the "Au-saprolite") is more closely related to the primary gold source and is narrower around steep structures, although it often evolves into subhorizontal zones higher in the profile (Butt, 1989). The gold tends to be coarser, with a greater proportion of visible crystals, wires and plates. The Au-laterite and Au-saprolite over sulfides-rich orebodies change into Au-gossans with increasing depth.

13.7.4. Supergene Cu ores and leaching/reprecipitation profiles

Copper is highly mobile in aqueous systems. As most primary Cu deposits have sulfide mineralogy, weathering-assisted decomposition of sulfides produces H_2SO_4 that lowers the pH of descending meteoric waters, which increases their reactivity and leaching capability. Copper is leached at higher levels in a supergene profile and removed in solution, impoverishing and wasting the original orebody. This process is particularly strong in rapidly eroding mountainous humid tropics like New Guinea, Indonesia and the Philippines. In (formerly) semi-arid to arid settings where runoff is reduced, much of the rainwater in permeable (porous or densely fractured) rocks percolates to the underground where groundwater table and a hydrologic system are established. This results in a zoned supergene leaching, alteration and reprecipitation system that is best developed over porphyry Cu deposits, where it is superimposed on the hypogene Cu mineralization and associated hypogene alteration zones. Because the uppermost, near-surface zone, the leached capping, is depleted in Cu, empirical techniques have been developed to predict the nature of economic Cu mineralization in depth based on interpretation of the residual mineral

assemblages (mainly Fe hydro-oxides and jarosite) left behind in the leached capping (Locke, 1926; Blanchard, 1968; Anderson, 1982). These and other studies advanced our understanding of the secondary (supergene) Cu accumulations formed above hypogene orebodies, some of which (e.g. Morenci, 0.1-0.15% Cu) have such low grades as to be uneconomic to mine now, and in the near future.

Supergene Cu deposits are of two types: oxidic and of (secondary) sulfides and their magnitude, in relation to hypogene orebodies, varies. Some ("giant") porphyry deposits, like Highland Valley in British Columbia, have only hypogene ores; the supergene zones have been removed by glaciers. Others have strong oxidation zones that could be of lower grade, but they respond well to the modern heap or in-situ leaching and electrowinning technology (e.g. El Abra, Chile). There are at least eight porphyry Cu systems where the oxidic Cu orebodies alone have reached the "giant" magnitude (Table 7.3). More "Cu oxidic giants" are members of other ore systems, like the Copperbelt-style stratabound ores in (meta)sediments; there, the Katanga/Shaba orebodies have a particularly strong and spectacular oxidic development. The secondary sulfide orebodies (blankets), dominated by minerals of the chalcocite group, are often spectacularly rich and they had been the mainstay of the bulk open pit mining in the western United States, in the early 1900s (at Bingham, Morenci, Santa Rita). There are at least 18 porphyry Cu's worldwide where the supergene sulfide orebodies alone qualify as "giants" (Table 7.5) and most of them are in the western United States, Chile and Peru.

Supergene Cu oxidic orebodies

Oxidic Cu minerals (malachite, azurite, chrysocolla) are ubiquitous in outcrop and near surface of most Cu sulfide deposits, except for the highly pyritic ones. To form a "giant" supergene Cu oxidic accumulation, however, a "giant" sulfide-Cu precursor, favorable setting, and the "right" conditions are needed. Supergene over porphyry copper systems is influenced by climate and topography. Humid climates produce high water tables that prevent deep oxidation and the usually high rate of erosion rapidly removes the supergene zones already formed. "Giant" porphyries in humid tropics like Ok Tedi, Batu Hijau and Grasberg thus have feeble to non-existent supergene orebodies (Ok Tedi, however, has a "large" "Au-gossan"). Semi-arid climates are about the most suitable as the periodically recharging low water tables facilitate leaching, deep oxidation and enrichment

(Anderson, 1982). The extremely arid zones as in the Atacama desert slow down or entirely inhibit supergenesis, but preserve the existing secondary orebodies while deep oxidation is still taking place.

Supergene leaching and oxidation are cyclic, controlled by fluctuation of the groundwater table. The Cu enrichment blankets (both oxidic and sulfide) are multistage and migrate downward with continuing erosion. Anderson (1982) recognized six mineralogical types of supergene cappings. His primary malachite (azurite), goethite capping forms in the presence of carbonates that neutralize the acid solutions, and is common in porphyry Cu systems transitional into skarns or in skarns only (e.g. Mission, partly Bingham). The resulting orebodies are minor in the porphyry Cu systems, but major and spectacularly developed over the Katanga stratabound orebodies hosted by dolomite or dolomitic "shale" (Chapter 11). Over porphyry Cu, most oxidic minerals belong to the antlerite-brochantite (also chrysocolla, malachite) association of Anderson (1982), considered secondary and formed by oxidation of an earlier chalcocite blanket following lowering of the water table. A spectacular oxidation zone with many rare mineral species developed over the Chuquicamata chalcocite blanket; unfortunately, it was mined away long time ago (Zentilli et al., 1996). The exotic (transported) deposit Mina Sur, downslope from Chuquicamata, has been sourced in this zone (Chapter 7). A "giant" subhorizontal Cu oxidic blanket, 4.3 km long and 180-200 m thick, is presently mined from the **Radomiro Tomic orebody** north of the "classical" Chuquicamata pit (Cuadra and Camus, 1998; 363 mt @ 0.7% Cu, for 2.54 mt Cu content, in the oxide zone only). This orebody is dominated by chrysocolla near the top that grades to atacamite at the bottom where it changes into a mixed oxidic-chalcocite ore. The in-situ oxides continue laterally into an exotic (transported) deposit in alluvial gravels.

El Abra Cu deposit NE of Chuquicamata (Ambrus, 1977, Chapter 7; Rv 767 mt @ 0.55% Cu for 4.7 mt Cu content) presently produces electrowon copper from an entirely oxidic ore. The oxidation zone there comprises fracture infiltrations and pseudomorphic replacements of earlier chalcocite (and partly hypogene chalcopyrite) by chrysocolla, lesser brochantite and minor cuprite. There are remnants of a secondary sulfide blanket with chalcocite in sericite and clay altered hosts, formed over a fracture and breccia-controlled hypogene chalcopyrite, bornite, molybdenite mineralization in biotite and K-feldspar altered late Eocene quartz monzonite porphyry. The Ichuno

exotic deposit downslope from El Abra has impregnations of chrysocolla and Cu-wad in colluvial and conglomerate gravels, grading into fracture infiltrations in basement volcanics and granitoids.

Cu oxidic orebodies, in style and genetic history comparable with those in the porphyry copper systems, are also a part of other "giant" Cu sulfide accumulations like stockworks in albitized breccias over felsic volcanics (Mantos Blancos; 2.694 mt Cu in atacamite, chrysocolla blanket; Chapter 6) and hydrothermally altered brittle deformation zones (Manto Verde; 1.265 mt Cu in oxidic ores. A relatively little known form of oxidic Cu mineralization is in refractory ores, where Cu is absorbed in phyllosilicates (vermiculite, biotite, phlogopite) or in argillized feldspar and the bond is so strong that the conventional acid leaching beneficiation technology does not work here. There is a "giant" resource of the refractory Cu ore (3.48 mt Cu content @ 1.2%; Diederix, 1977) in dolomitic micaschist above the Nchanga orebody in the Zambian Copperbelt.

Supergene (secondary) Cu sulfide orebodies

"Giant" orebodies of secondary sulfides (predominantly of the chalcocite group) are virtually confined to porphyry Cu systems, although the recently discovered Las Cruces VMS deposit near Seville (915 kt Cu @ 6.18% Cu; Chapter 8) comes close. In altered pyrite-chalcopyrite porphyry Cu systems rich in K-silicates, the initial chalcocite blanket forms during the 1st cycle of oxidation and leaching (Anderson, 1982). After this, most of the very rich ore blankets (including the "giants") grew by repeated Cu additions as the blanket gradually descended into the lower levels, following the dropping water table. The chalcocite blankets left above the water table have been oxidized to produce some of the oxidic orebodies described above, or have been degraded, leaving behind the diagnostic hematite capping in the leached zone (this is visually very apparent in some open pit mines like Chino-Santa Rita, Morenci, Toquepala and others; compare photos in Anderson, 1982). The high-pyrite phyllic (sericite-pyrite) altered hypogene zones are the preferential loci of chalcocite precipitation.

In the **Morenci-Metcalf Cu field** in Arizona (P+Rc 17.7 mt Cu @ ~0.8%) virtually the entire 16 to 330 m thick orebody is a chalcocite blanket over the subeconomic protore, but the sooty black chalcocite, alone or replacing fracture veinlets of pyrite and chalcopyrite, is evenly dispersed rather

than massive. The situation is similar at **La Escondida, Chile** (Padilla et al., 2001; 26.0 mt total Cu, 23.78 Mt supergene Cu; Chapter 7) where 91.5% of Cu ore reserve is in the chalcocite blanket. Lenses of almost massive chalcocite grading between 25% and 40% Cu provided a "bonanza" during the early stages of open pit mining in Bingham, Santa Rita, and other deposits in the American South-West.

Supergene Zn and Pb oxidic ores

Like copper, the bulk of primary Zn and Pb ores comes as sulfides (sphalerite and galena) while presumably hypogene oxidic ores are exceptional (e.g. Vazante, Brazil; Chapter 11) and reviewed in Hitzman et al. (2003). Most outcropping Zn and Pb deposits outside the area of Quaternary glaciation (and some even there!) had at least some secondary Zn and Pb minerals in the oxidation zone, mined in the earliest period mainly for lead and residual silver. Before 1900, smithsonite and partly hemimorphite (calamine) were the principal sources of metallic zinc, itself used mostly for brass manufacturing but with the arrival of flotation in the 1920s sphalerite concentrates became the dominant Zn source (Large, 2001). Only a very limited production of oxidic Zn-Pb ores continued afterward, although there were some exceptions.

Hitzman et al. (2003) subdivided supergene zinc (and also lead) deposits into direct replacement, wall-rock replacement, and residual plus karst fill varieties, although they are transitional and larger deposits may comprise more than one variety. Direct replacements are pseudomorphic substitutions of sphalerite and galena by smithsonite, hemimorphite and cerussite or anglesite. Such ores form mostly after the MVT deposits, they tend to be pigmented by Fe and Mn hydro-oxides, and enclose relics of galena and frequently chert or jasperoid. They include the Iranian "giant" Mehdiabad and "near giant" Angouran deposits, oxidation zone of the Jinding "sandstone-Pb" deposit in Yunnan, China (read below) and the cerussite-anglesite deposit Magellan in Western Australia (Chapter 11).

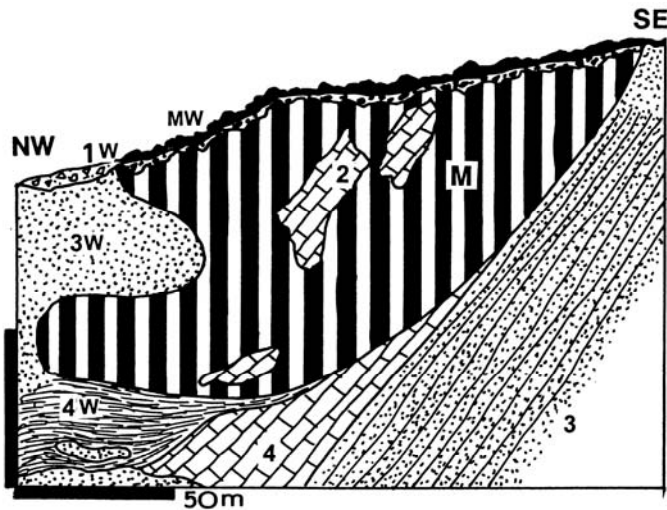
The wall-rock replacement type is the equivalent of "exotic deposits", where a hypogene orebody, presumably of sphalerite, was dissolved by acidic waters produced by oxidation of Fe-sulfides, and the Zn-rich leachate travelled downward to replace limestone or dolomite wallrocks along the way. The ore minerals are the same as above but the orebodies are more homogeneous and relatively "clean". The largest example of this type, Skorpion

in Namibia, has still some connection with its sulfidic precursor, believed to have been a VMS-type mineralization comparable with the nearby Rosh Pinah (Borg et al., 2003). Many other oxidic Zn bodies, all small to medium, have lost such a connection.

The karst/residual type is a chaotic mixture of Zn or Pb oxidic minerals with residual ferruginous clays, Fe-Mn hydro-oxides, relic galena, and silicites in karst depressions (sinkholes) and solution-collapse breccias. The best known **Padaeng deposit**, the principal source of ore for the Tak zinc smelter in west-central Thailand, is of the "near-large" magnitude (5.1 mt ore @ 12% Zn; Reynolds et al., 2003; Fig. 13.44).

Mehdiabad Zn,Pb,Ag deposit, Iran (Union Capital Ltd., 2001, in Hitzman et al., 2003; 218 mt ore @ 7.2% Zn, 2.3% Pb, 51 g/t Ag for 15.7 mt Zn, 5.014 mt Pb, 11,118 t Ag in mixed sulfide-oxide ore) is the largest supergene "Zn giant". Like the smaller Angouran deposit, it is located in the Zagros collisional belt of west-central Iran, hosted by early Paleozoic carbonates. Although tentatively interpreted as of the MVT type, the high silver content makes this unlikely and hydrothermal replacement seems more probable. The young smithsonite and hemimorphite capping replaces much of the primary sphalerite and galena.

Skorpion Zn deposit, SW Namibia (Borg et al., 2003; Rc 24.6 mt @ 10.6 Zn for 2.6076 mt Zn in oxidic ore, 6.91 mt Zn total resource) is located in the Gariiep Foldbelt, NW of the Rosh Pinah mine. The hosts are Neoproterozoic moderately metamorphosed felsic volcanics and volcanoclastics with a thick marble unit. They are folded and thrust and host up to 25 m thick presumably stratabound zones of disseminated to massive pyrite, pyrrhotite and sphalerite in silicified metavolcanics (VMS-type?). The oxidic-Zn orebody, presently mined, occurs partly above the sulfides and partly above locally karsted marble, itself unmineralized. The host rock is identified as a "meta-arkose" which, in the unmineralized extension, has abundant calcitic cement. The lenticular orebodies are dominated by inconspicuous fine-grained sauconite (Zn-smectite) and hemimorphite that fill voids after feldspar and replace biotite. Hemimorphite, smithsonite, tarbuttite (Zn-phosphate) and stolzite are megascopically more conspicuous where they fill voids in breccia or fractures. The Zn oxide ore is post-deformational, hence clearly younger and superimposed on the pre-metamorphic sulfides.



- 1W. Alluvium, transported laterite
- MW. Smithsonite cap and hemimorphite-rich duricrust;
- M. Mi2-P1 stratabound body of crystalline hemimorphite, lesser smithsonite, goethite floored by smithsonite-rich karstic ore with clay residue in Unit 4.
- 2. J2 bioclastic limestone and dolomite relics
- 3. J2 calcareous dolomitic sandstone;
- 4. J2 hydrothermally dolomitized sandy dolomite
- 4W. Residual clay after karsted Unit 4.
- 5. J2 black argillaceous limestone

Figure 13.44. Padaeng oxidic zinc deposit, Mae Tao, W-C Thailand, cross-section from LITHOTHEQUE No. 1783 based on Padaeng Industry Ltd. reports and site visit in 1988, modified after Reynolds et al. (2003)

This is attributed to groundwater sulfide oxidation and replacement. Its age is pre-Miocene.

13.7.5. Paleo-regoliths, paleosols and basal sequences at unconformities

Paleosols (Retallack, 1986; Reinhardt and Sigleo, eds., 1988; Wright, ed., 1986), paleokarst (James and Choquette, eds., 1987), "evaporites that were" (now mostly breccias; Warren, 1999) and paleoclimates (Holland, 1984; Frakes et al., 1992) have an extensive literature that sometimes touches on mineral deposits. The products and consequences that include metallic deposits are preserved along unconformities, either still buried in depth or exhumed. Unconformities and their varieties play an important role in metallogeny (Laznicka, 1985c): 1) They preserve rocks and modifications (alterations, textural changes) formed under the paleosurface (regoliths) and above (basal sequences), before their deep burial. Today's unconformities were yesterday's erosional subaerial land surfaces, subjected to interaction with atmosphere and hydrosphere of the period. Subaqueous unconformities interacted with the ancient sea- or lake water; 2) Unconformities are important discontinuities more permeable than the adjacent rocks, and often provide lithologically contrasting boundaries that channel fluids, provide screens and geochemical (e.g. redox) barriers. The related ores formed in depth, after unconformity burial. Unconformities are thus preferentially associated with a variety of metal accumulations

that include several "giant" deposits. Because most unconformity-related "giant" deposits have already been described in other chapters, here is only a brief summary.

Paleo-regoliths under unconformity and basal clastics, pre-burial mineralization

"Karst" (or Mediterranean-type) bauxites (Bárdossy, 1982; read above.) are a textbook example of unconformity-related deposits, but they are all small (compare Laznicka, 1985a). Pre-Cenozoic enriched Fe deposits formed on banded iron formations (Chapter 11) are all unconformity related, although there is a controversy as to whether the enrichment was related to paleoclimates before burial, or hydrothermal activity after burial. "World-class" enriched Fe deposits include orebodies in the Hamersley Range, Yakovlevo in the Kursk Magnetic Anomaly under Carboniferous cover, and others. The "large" Sishen-Fe deposit in the North Cape, South Africa, is one of the many Fe and Mn mineralizations that resulted from Proterozoic weathering along the sub-Pretoria/Postmasburg unconformity (Beukes, 1983).

The "basal" variety of the Witwatersrand-style Au-U conglomerates includes mostly deposits of lesser magnitude (e.g. Dominion Reef, Jacobina). The Elliot Lake-U district (Chapter 11) is a lonely "giant". At most basal conglomerate deposits the sericite-pyrite (sometimes fuchsite) altered sub-unconformity regolith (that includes a paleosol; Button and Tyler, 1981) provided matrix

incorporated into the first basal detrital unit of conglomerate. The reduced nature of this regolith, at Paleoproterozoic and Archean unconformities, is one of the pillars for the theory of early Precambrian reducing atmosphere. The highly Au+U productive Central Rand conglomerates rest on low-angle unconformities but the stratigraphically highest Ventersdorp Contact Reef is a true clastic unit at base of a volcanic rift sequence, with its own (chlorite-rich) regolith and angular unconformity against the Central Rand basement, the source of gold.

An interesting, up to 5 m thick sericite-pyrite altered regolith (paleosol) on the Hekpoort Basalt, a member of the Pretoria Group, extends over more than 100,000 km² of the former Transvaal (South Africa) and stores some 10¹¹ to 10¹² t of material with 30% Al₂O₃ (16% Al) (Button 1979). This represents some 500 bt of contained aluminum, a "super-giant" low-grade Al accumulation should it be ever exploited. More recently, Martini (1986) recorded erratic gold occurrences in the same unit. More unconformity-related mineralizations in southern Africa are reviewed in Button and Tyler (1981).

Numerous metallic deposits, including "giants", are buried under unconformably overlying units, typically platformic sequences, that act as mere passive covers that have protected mineralizations at and under paleosurfaces from erosion, without modifying in any way the ores already there (for example, no reworked and upgraded ore material from the basement incorporated into basal units of the cover). The Cu, Au, U "super-giant" Olympic Dam (Chapter 11), under 300 m of platformic cover, is an outstanding example. Exploration for buried deposits under such "uninvolved" thick covers is costly and unpredictable, dependent on drilling deep geophysical targets.

Paleo-regoliths under unconformity and basal units, post-burial mineralizations

The "unconformity-U" deposits (Chapter 11) are the most obvious example as the term unconformity appears in the title. There, the basement/sandstone cover unconformity with well-developed regolith (paleosols) provided a hydrologic surface and a geochemical (redox) barrier to circulating U-loaded fluids. Orebodies (including the "giants" Cigar Lake, McArthur River-U, Ranger and Jabiluka) formed at, below and above unconformity. Along the sub-Roan unconformity in the African Copperbelt (Chapter 11), the copper likely derived from the basement predominantly accumulated in

the cover sedimentary sequence (Katanga Supergroup) with only minor, largely uneconomic mineralization in the basement (Button and Tyler, 1981). The Kupferschiefer (read above) is somewhat similar, with the bulk of Cu (and Ag, Pb, Zn) accumulated in the first reducing unit of the cover sequence above unconformity. Unconformities provided an outstanding control to the MVT deposits in carbonates (read above) precipitated in solution collapse breccias under unconformity (e.g. the East Tennessee Zn district) and in reef sequences above unconformity (e.g. SE Missouri-Pb).

13.7.6. Humid alluvial environments: placer deposits

Alluvium is a "general term for clay, silt, sand, gravel or similar unconsolidated detrital material deposited by a stream or other body of running water as a sorted or unsorted sediment in the bed of the stream or on its flood plain or delta, or as a cone or fan at the base of a mountain slope" (A.G.I. Glossary of Geology). There is an extensive sedimentologic literature (Miall, 1978; Einsele, 1992), as usually too rich in detail for an exploration geologist as there is only a relatively small number of situations where ores form and reside. Several sub-environments can be recognized, based on temperature and physiography, each with its own facies series of sediments. In addition to the uneven effectiveness of the various sedimentary sub-environments to trap and accumulate metals, the composition and preparation of the detritus source area is of paramount importance. First, it has to be anomalously enriched in the ore metal(s). Second, the metals have to be liberated and sometimes pre-conditioned.

In settings dominated by physical weathering, mechanical grinding (as along the sole of a glacier) is non-selective and the resulting detritus is compositionally a replica of the source area's lithology. The ore minerals, originally residing in the parent rock, will remain dispersed in the detritus: 1) as either liberated mineral grains in the sand fraction, or 2) as ore or mineralized rock fragments in the coarse fraction. There will be a high proportion of fines with unrecoverable ore component

In deeply chemically weathered source terrains the thick regolith is enriched in residue remaining after decomposition (hydration and oxidation) of the unstable minerals, and partial removal of the product in solution or fine suspension. Chemically

stable minerals are liberated and pre-enriched in the regolith, sometimes to such a degree that the regolith becomes an "eluvial (in-situ) placer". In most cases, however, the regolith is further reworked in an alluvial system.

Humid alluvial metallogenesis "specializes" in physical sorting of clastic mineral grains by specific gravity, the main product of which are heavy mineral placer deposits (Fig. 13.45). Although the "light heavies" (e.g. ilmenite, rutile, zircon, monazite) do accumulate in alluvial systems, especially in the floodplain sub-environment (e.g. the fluvial monazite placers in the Inner Piedmont of the SE United States; Overstreet et al., 1968), the deposits are small and subordinate in importance to the beach and dune placers (read above). The "heavy heavies" (gold, platinoids, cassiterite), on the other hand, are predominant in alluvials and the deposits are very close to the bedrock source (within about 15 km for the bulk of coarse gold deposits). For that reason it is logical to treat the Au, Sn and PGE placers as derivatives of the bedrock deposits and treat them jointly in Chapters 7 and 10).

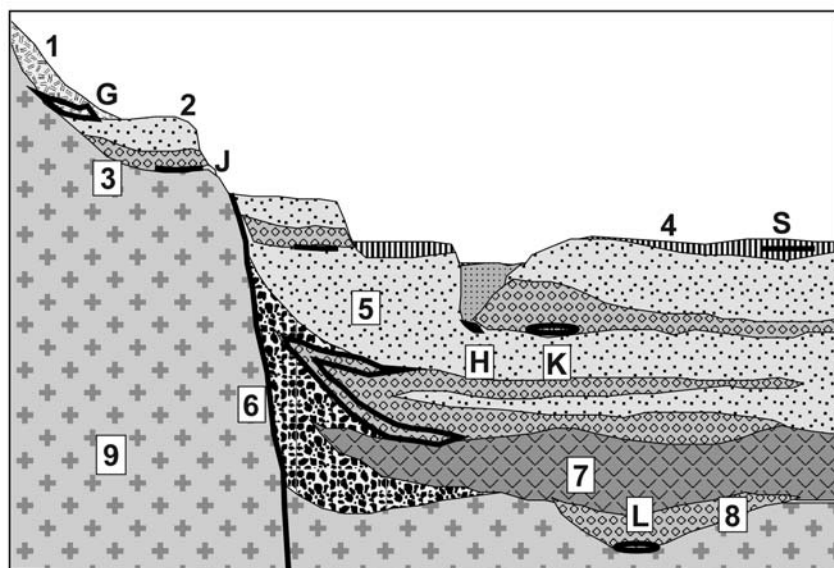
Heavy mineral placers have areal distribution and are extremely difficult to delineate and quantify. The metal or ore mineral particles typically accumulate in channels (river bed sediment), so a channel is the "ore deposit", but the economic sites ("paystreaks") are discontinuous. In addition to channels, the ores also accumulate in terrace gravels. The channels themselves branch, form extensive drainage networks, and change upstream into gulches: valleys filled by poorly sorted colluvium alternating with creek alluvium. In rich bedrock gold or tin provinces everything is, discontinuously, Au- or Sn-bearing. A single bedrock giant goldfield like the Homestake in South Dakota shed detritus to form paleo-placers in Cambrian basal conglomerate, then again in Cenozoic gravels. The young placers, although initially rich (as near Deadwood) have been almost insignificant in relation to the huge Homestake ore zone (1,319 t Au versus 5.5 t Au). Elsewhere, as in the **Klondike (Dawson City) goldfield** in the Yukon (Boyle, 1979, 1987; Mortensen, 1990; >398 t Au), virtually no bedrock gold deposit has been discovered so far and the gold is believed to have been collectively sourced from a large number of small fracture veins and veinlets in the area, or from a higher level Au mineralization now removed by erosion.

The situation in Siberia and the Russian Far East (Krivtsov and Migachev, 1998) is intermediate between the two extremes above. The "goldfields"

there cover huge territories (something like a quarter of Europe) that results in substantial cumulative production figures (e.g. Amur Goldfield-5,445 t Au; Upper Kolyma Basin-2,643 t Au; Lena Goldfield-1,000+ t Au). Although these figures are incomplete and inaccurate, and they should be subdivided into lesser territorial divisions, the fact remains that due to the areal distribution and interconnectedness of placers geologically justifiable limits of goldfields are difficult to establish. The Siberian gold placers started to produce several centuries back but discoveries and exploitation of the primary deposits came much later. The ratio of placer gold to bedrock gold thus decreased with time. In the Rio Tapajós Basin, Brazil (~5,632 t Au) the ratio is close to 100:0, as in Klondike. In the Lena Goldfield, the discovery of Sukhoi Log (~1,113 t Au) changed the placers : lodes ratio from about 100:1 to about 50:50. In the Victoria goldfields of Australia (P+Rv of ~2,600 t Au, with about ~1,500 t Au from placers) the ratio of about 60:40, as it was before the comeback of Victorian mining in the 1980s, is now changing in favor of the lode gold.

Although still alive, placer gold mining in the world rapidly declines as the resources are finite, and the "last frontier", offshore mining, is not as promising as previously thought. This situation is a little different with tin mining in the humid tropical belt of south-eastern Asia (except for China), where the hard rock cassiterite mining, never very important, has come to a virtual stop. Following exhaustion of the extensive mixed eluvial and alluvial placers onshore, new resources are being discovered offshore mostly as alluvial channels (valley placers) buried under shelf sediments (e.g. off Banka Island, NW Indonesia and western Malaya; Batchelor, 1979). Similar buried placers that include "giants" occur under the Arctic shelf of northern Siberia and the Far East, Russia (Patyk-Kara, 1999). Platinoid placers are all small and localized, lacking "giants".

Geology of the Au, Sn and PGE placers has been reviewed by Bilibin (1955), Hails (1976), Batchelor (1987), Boyle (1979 and 1987), Bykhovskii et al. (1981), MacDonald (1983), Laznicka (1985, p.751-780), Youngson and Craw (1999) and others. Examples of placer "Au giants" are briefly summarized in Chapter 10 and Table 10.3, the detrital "Sn giants" are included in Section 10.3. and Table 10.1.



1. Unsorted colluvium;
 2. Cross-bedded sand in terraces and point bars;
 3. Ditto, lag gravel;
 4. Mud, peat, organics of floodplains;
 5. Fine to coarse sand and gravel deposited by braided streams;
 6. Talus and alluvial fan adjacent to fault scarp;
 7. Valley flood basalt;
 8. Buried gravel, sand channel;
 9. Bedrock.
- Placers of coarse heavy minerals (Au, Sn, PGE) based on metal availability in the bedrock: A. Deluvial and proluvial; H. Channel gravel; J. Lag gravel in terraces; K. Point bar gravel;

Figure 13.45. Gravel and sand-dominated humid alluvium and colluvium, rocks and ores inventory from Laznicka (2004) Total Metallogeny Site G189. Explanations (continued): L. Buried channel gravels; M. Alluvial fan, sheet flow, near growth fault; S. Superfine Au dispersed in fine sand, mud. "Giant" heavy mineral deposits usually consist of more than one type of placer

13.7.7. Lakes and lacustrine sequences

In terms of clastic sedimentation, large lakes are not much different from seas and their sediments are hard to tell from marine deposits in the geological record. In terms of chemical sedimentation, salt lakes with water composition approaching that of seawater are qualitatively indistinguishable from marine sediments, but have a greater proportion of shallow water and restricted basin successions. Freshwater lakes contribute little to chemical sedimentation whereas saline lakes (other than $\text{NaCl} \gg \text{KCl}$, MgCl_2 ; Warren, 1999) deposit unusual evaporites (e.g. Na and Mg sulfates, Na or Mg carbonates, boron minerals) and some authigenic mineral suites. They are strongly influenced by composition and nature of their watersheds that may include synchronous explosive volcanism. This directly delivers pyroclastic detritus into the lake, undepleted in elements normally leached during the epiclastic lithogenesis (e.g. U, Li, B). Some dissolved elements are brought by groundwater springs and hydrothermal discharges. Through dessication, permanent lakes eventually convert into playas or salars (read below).

In economic terms, lakes of all kinds "specialize" in nonmetallics and account for several "world class" sources of these commodities. Examples: The Dead Sea contains a dissolved resource of 2 bt KCl,

1 bt MgBr_2 and 20 bt MgCl_2 (Bentor and Mart, 1984); the recent semi-dry Lake Magadi in Kenya stores 30 bt of trona; the Eocene Green River Formation contains the huge Na-carbonate deposits in Wyoming (75 bt of trona, 30 bt of nahcolite; Bradley and Eugster, 1969), and oil shale in Colorado. Lake Kuchuk near Novosibirsk in Siberia contains 600 mt of Na_2SO_4 in brines and underlying strata (Warren, 1999). Several metals are now, or are potentially recoverable, from lake brines or ancient lacustrine sediments. They include co-products (Mg from the Dead Sea), potential by-products (Al from dawsonite in oil shale; U) or Li, Rb, Cs, etc. as possible economic products from some Tibetan saline lakes the resource magnitude of which is unknown (Zheng Mianping et al., 1981; compare Chapter 6 describing Li & B in synvolcanic brines and sediments in the andean setting). The metal accumulations mentioned above may be available in huge quantities, but they are of super-low grades (often lesser than corresponding clark values) and would fit into the category of "technological ores" or "ores of the future". Selected examples follow.

Dead Sea, Palestine and Israel-Mg (Bentor and Mart, 1984; Einsele, 1992 ~12 bt Mg dissolved). Dead Sea is a saline lake (salinity is 31.5%), 400 m deep, with an area of 143 km², in the north-south rift graben. It is fed by the Jordan river and by

springs that leach salts from thick Pleistocene salt deposits in the subsurface. Mg chloride and bromide compose about 50% of the dissolved salts.

Piceance basin, Colorado, Al in oil shale (Smith and Milton, 1966; ~3.18 bt Al content; Fig. 13.46). Piceance Basin is one of the four "basins" on the Colorado Plateau, filled by Eocene lacustrine sequence of the Green River Formation (Bradley and Eugster, 1969; the same unit that contains the Na-carbonate evaporites in Wyoming). The Formation has three Members, of which the lower and upper members are monotonous mudstone, tuffaceous near the top. The middle Wilkins Peak Member is a more interesting cyclic unit of seven alternating lithofacies, interpreted by some as a playa lake complex (Eugster and Hardie, 1975). They are (from bottom to top): 1) Flat pebble conglomerate of dolomitic mudstone composition; 2) calcarenite and mud-cracked dolomitic mudstone; 3) laminated and thin-bedded dolomitic mudstone; 4) "oil shale" (kerogen-containing dolomitic marl laminite); 5) salt facies of halite, trona, nahcolite, shortite, northupite; 6) well-sorted channel sandstone; and 7) felsic tuff.

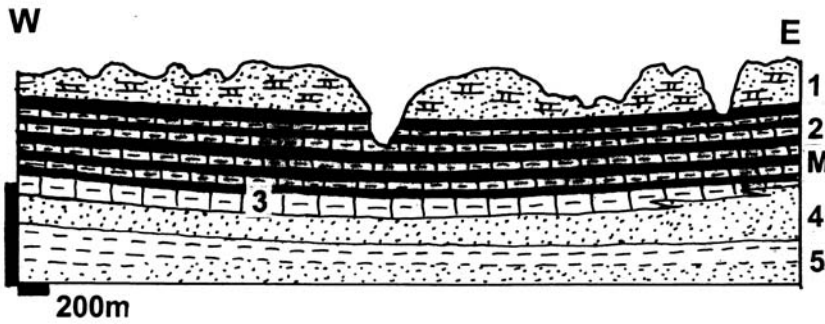
Other than evaporitic salts, the Wilkins Peak Member contains a huge resource of oil shale (Eugster, 1985). The shale is most favorably disposed in the Piceance Basin in Colorado (near the town of Rifle), where its development has been a series of stop-and-go efforts that correlate with the fluctuating oil prices. In addition to petroleum, the same shale that would have to be quarried, transported and thermally processed to extract the hydrocarbons, contains the inconspicuous and largely microscopic mineral dawsonite ($\text{NaAl}[\text{OH}]_2\text{CO}_3$). Dawsonite contains 35.4% Al_2O_3 or 18.7% Al (Smith and Milton, 1966) and is distributed, in a 230 m thick section, over an area of about 640 km^2 . 10 to 15.5 volume percent of dawsonite (minimum dawsonite content in rocks is 8%) forms an admixture in the dolomitic marl and there is a slightly more massive 15 m thick and 2.4 km long unit that contains 50% or more of dawsonite. Based on the minimum dawsonite content, there is some 3.18 bt Al in dawsonite in Piceance Basin, potentially recoverable as a by-product during oil shale processing. Dawsonite is interpreted as product of diagenetic reconstitution of analcite, that had in turn formed by devitrification of the tuffaceous component (Sullivan, 1985). Uranium is slightly enriched (average 50 ppm U, maximum 0.15% U; Mott and Drever, 1983) in radioactive phosphatic zones closely associated with the trona horizons. 25 zones

ranging in thickness from 7 cm to 2 m have been recognized.

Modern lake and bog sediments contain accumulations of Fe or Mn hydro-oxides as lake floor nodules or "bog ores"; U or Cu infiltrations; and others. Ancient lacustrine sequences host uranium (Lodève, France); copper (Klein Aub, Namibia; Nonesuch Shale, Michigan); pisolithic Fe ores (Tula and Lipetsk on the Russian Platform, Lisakovsk in the Turgay Basin, Kazakhstan); nodular magnesite; some redeposited bauxite deposits (Sangaredi, Guinea). Most are small, few are "large". The Mesoproterozoic White Pine Cu deposit (Chapter 11) is of "giant" magnitude.

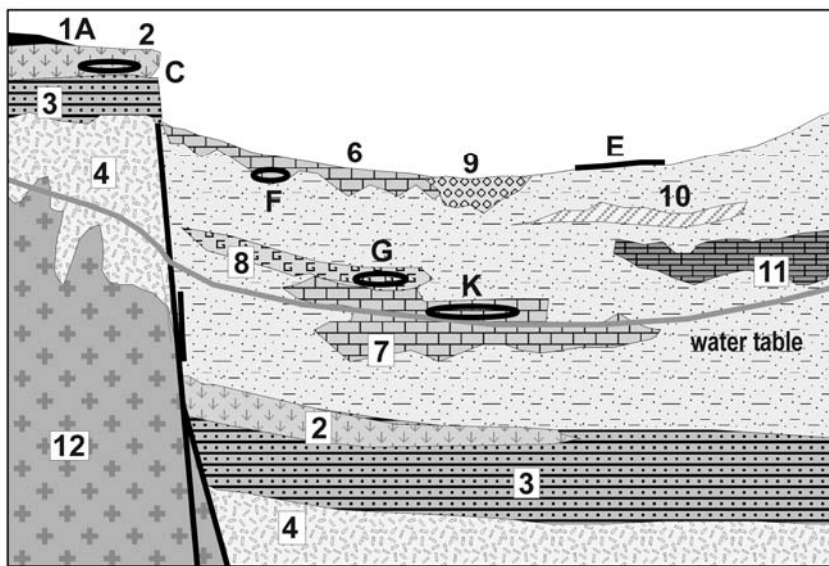
13.7.8. Arid regoliths and sediments

Arid depositional environments are, in the literature, usually treated under the heading "Deserts" (e.g. Collinson, 1978) but many of the sub-environments and processes important for metal accumulation do not require a true desert to operate. The fundamental characteristic of arid lands is that evaporation greatly exceeds precipitation; this makes surficial water scarce and groundwater to move up, by capillarity. Physical weathering is dominant, but some chemical weathering takes place too so the desert sediments are not as pristine as the freshly manufactured glacial till. Although initial leaching of desert outcrops and clastic grains cause surficial decomposition of the unstable silicates and partial leaching (this is indicated by grain surfaces coated by Fe hydroxides and oxides), most mineral and rock fragments retain their complement of trace metals much of which, in humid environments, are leached out. Such metals, and those absorbed on the grain coating Fe oxides, become available for release and redeposition during diagenesis in depth (Fig. 13.47). Arid clastics are derived from the bedrock (first cycle sediments) from volcanic ash or from repeatedly reworked earlier clastics, mostly mature sandstones. They are transported and deposited by wind (to form dune sand to silt), gravity (talus) and water during infrequent storms and flash floods. The sediments settle in shallow, gently sagging cratonic basins, or in fault-bounded rapidly subsiding basins as in the Basin and Range Province of western North America. Active faults create gradients, and bring fresh undepleted basement rocks to the surface together with their ore deposits, if there are any (there may be plenty; every bedrock range in Nevada, Arizona, northern Mexico, Atacama Desert in Chile and elsewhere has a number of mostly abandoned mines).



Eocene Green River Fm.
 1. Sandstone, marl, siltstone; 2=M Parachute Creek Member oil shale in marl, with dawsonite content; 3. Marl, paper shale, limestone, sandstone; 4. Massive sandstone, shale, marl; 5. Eo Wasatch Fm. redbeds

Figure 13.46. Portion of the Piceance Basin at Parachute Creek, Colorado, with oil shale containing dawsonite as a potential Al resource of the future. Cross-section from LITHOTHEQUE No. 1450, modified after Donnell (1961)



1. Ferricrete relics; 2. Silcrete; 3. Kaolinized sandstone; 4. Granite regolith; 5. Undivided alluvium, dune sand, fanglomerate
 6. Pedogenic calcrete
 7. Groundwater calcrete
 8. Gypsicrete; 9. Wadi channel gravel; 10. Pedogenic nitrates; 11. Pedogenic halite; 12. Basement.
 A. Fe in ferricrete relics; C. Ti enrichment in silcrete; E. U in phoscrete crusts and nodules; F. U infiltrations in pedogenic calcrete; G. U infiltrations in gypsicrete; K. U in groundwater calcrete; L. Exotic Cu,U,Mn,Co oxidic infiltrations

Figure 13.47. Arid regolith and duricrusts, inventory of materials and ores from Laznicka (2004), Total Metallogeny Site G197

At the foot of the bedrock range short ephemeral streams deposit alluvial fans that prograde, across the pediment and basement block faults, into the alluvium-filled basin. Mud pans and playas form in the lowest parts of undrained basins, some of which are underlain by thick prisms of salts. The ideal arid physiography is substantially complicated by the presence of contemporary volcanics (read Chapter 6).

Because of the lack of running water, detrital orebodies like placers are rare and insignificant (e.g. Jicarilla Au placer, New Mexico, in fanglomerate; 7.2 t Au). Gold particles may have been once common at deflated surfaces of serirs in the vicinity of vein outcrops in Egypt, Sudan and Saudi Arabia, but have been depleted in the earliest stage of

exploitation. All significant metallic deposits in young arid terrains, that include several "giants" and "large" accumulations, are chemical precipitates and all depend on a special supply of the ore metal not available under conditions of model sedimentogenesis.

Arid duricrusts: calcrete

Calcrete is the principal arid duricrust known to host one (Yeelirrie) or two (Langer Heinrich, Namibia) "large" uranium deposits, although more than 100 small occurrences of this type have been recorded worldwide. Silcrete, gypcrete and phoscrete are also locally uraniumiferous but the known tonnages of ore material are very small. The more

common pedogenic calcrete formed near surface in a soil profile and has the form of friable nodules, dusting, gravel and rubble cement. It may be uraniferous in areas of anomalous U supply, for example from a component of felsic volcanic ash undergoing devitrification (e.g. the shroekingierite deposit in Lost Creek, Wyoming; Sheridan et al., 1961). The groundwater valley and playa calcretes are less apparent but locally accumulated more uranium in two principal provinces: central Western Australia (Butt, 1988) and Namibia (Hambleton-Jones, 1982).

Yeelirrie Homestead-U,V is SW of Wiluna, Western Australia (Mann and Horwitz, 1979; Cameron, 1990; 44,625 t U @ 0.13% U; Fig. 13.48). It is a 6 km long segment of a deep, Miocene to Quaternary groundwater channel that periodically drains the partly silcreted old planation surface composed of Archean granitic bedrock, and discharges into a playa. The deeply weathered granite is slightly enriched in U. The NW-trending Yeelirrie channel is filled by 20 to 85 m of alluvial clay with some quartz, feldspar and windblown sand. Groundwater calcrete forms discontinuous lenses of dense calcitic to dolomitic duricrust, 8 m thick, near Yeelirrie. There, under several centimeters of a red, silty loam, isolated nodules of pedogenic calcrete start to appear, and they grade downward through laminated calcrete crusts and foamy, earthy or fragmental calcrete into a hard, white, porcellaneous groundwater calcrete that is locally dolomitized. With increasing depth this calcrete becomes conglomeratic or brecciated and ultimately changes into a basal, brown, silty carbonate transitional into a breccia of red siltstone fragments enclosed in a light-brown calcrete matrix. Underneath is an unconsolidated, non-calcareous reddish-brown alluvial sandy clay to silt. Bright yellow to greenish-yellow carnotite forms coatings and impregnations in most varieties of the groundwater calcrete. The orebody is 3-7 m thick, up to 750 m wide and 6 km long.

Exotic Cu deposits

These deposits are close equivalents of orebodies precipitated in groundwater drainage channels in arid regions and influenced by anomalous local supply of metals, in the present case copper. In contrast to the uraniferous calcretes where U is sourced from dispersed trace metal, exotic deposits are a form of transported oxidation zone derived from major primary sulfidic deposits, especially porphyry coppers, and precipitated from

groundwater leachate downslope from the source. Several tens of small exotic Cu occurrences are known around the world, but only in the Atacama Desert of northern Chile they reach prominence as they store some 8 mt of Cu. The largest deposit **Mina Sur (Exotica)** downslope from the "super-giant" Chuquicamata porphyry Cu-Mo is itself a "giant" (Münchmeyer, 1996; 310 mt ore @ 1.17% Cu for 3.63 mt Cu); El Tesoro and Sagasca are "near-giants". Most of the Chilean exotic deposits are directly associated with major porphyry coppers, but the Cu source to Sagasca and partly El Tesoro remains unknown. Exotic Cu deposits are described in the porphyry Cu context (Chapter 7, Table 7.4).

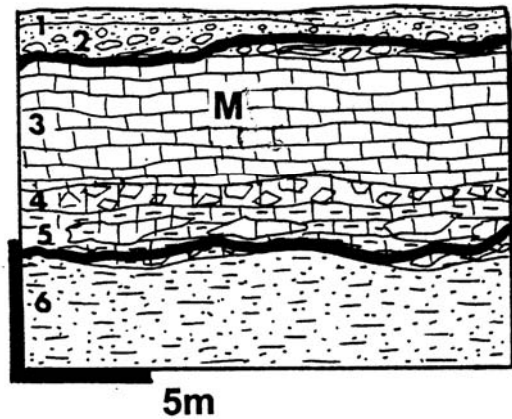


Figure 13.47. Yeelirrie carnotite deposit in groundwater calcrete near Wiluna, Western Australia; cross-section from LITHOTHEQUE No. 1219, 1981 field sketch. M. Bright yellow carnotite infiltrations and fracture coatings in slightly karsted groundwater calcrete; 1. T3-Q red silty loam; 2. Nodular, earthy pedogenic calcrete; 3. White, porous groundwater calcrete and dolomite; 4. Recemented conglomeratic calcrete; 5. Brown silty calcrete grading to breccia of siltstone fragments in calcrete matrix; 6. Brown alluvial sandy silt to clay

Playas and salars

Playas are depressions in arid regions filled by fine detritus brought in by ephemeral streams (sometimes also by argillized volcanic ash) and salts. During wet season (or in wet years) they fill by saline water but this soon evaporates leaving behind salt crusts covering the playa floor. Salar resemble (and are transitional into) playas, but they are more a form of duricrusts formed from evaporating groundwater in underground channels and deltas that are never (or rarely) covered by lake water; alternatively, they are considered floors of

dessicated lakes. In central Andes the term is often used interchangeably for playas. The most famous mineral deposit type associated with salars is the Chilean nitrate mined in the Atacama Desert.

In addition to the occasional rainwater fill and surficial salt incrustations, most playas have underground brine pools, some are fed by groundwater springs that could be thermal (grading to hydrothermal fluids), and many are underlaid by layers to thick masses of accumulated salts. Playas are an important source of nonmetallic commodities like halite, gypsum, trona and mirabilite. The Searles Lake, California, brine contains 32 ppm W (Carpenter and Garrett, 1959) that translates into a "resource" of 68,000 t W, a "large" accumulation. This is an isolated case due to anomalous tungsten enrichment in the catchment area (the Cordilleran scheelite belt). Some playas are, however, important repositories of boron and lithium, both of which have ultimately volcanic sources. These metals are recovered from brines, from salts on playa floors (e.g. ulexite), or from montmorillonitic clays (Li in hectorite). All the important Li and B deposits that include several "giants" are in the andean-type continental margins (Nevada, California, Chile, Argentina, Bolivia) or in Turkic-style orogens (Turkey) and described in Chapters 6 and 10, respectively. Searles Lake is described below as a complex producer of many commodities.

Searles Lake, eastern California (Smith, 1979) is a playa located in a fault-bounded graben in the Mohave Desert, a part of the Basin and Range province of Cainozoic crustal extension. The salts-encrusted or muddy playa floor is underlaid by a prism of Quaternary sediments several thousand meters thick, of which the uppermost 270 metres of interbedded salt and mudstone have been drilled and studied in detail. The salts are composed of Na-Ca carbonates and sulfates, halite and borax. Interstitial brine occurs in two evaporite horizons in the subsurface; it is pumped out, and treated in two large chemical plants. The cumulative value of mineral production was \$ 1 billion in 1979, and is about tripple that amount now (no heavy metals have been recovered so far). In 1979, there was a significant salt and brine resource left that contained some 50 mt B₂O₃ and 150 ppm Li₂O, as well as 98-102 ppm As. The salts are both the product of rain and runoff water evaporation and subsurface (hot) springs discharge.

13.7.9. Sandstone-dominated continental sequences: "gray" and "red"

Introduction

Pre-Quaternary and usually consolidated sandstone-dominated sequences formed in a variety of depositional environments, some of which have already been reviewed above (the Proterozoic equivalents are reviewed in Chapter 11). They include alluvial (mostly fluvial), deltaic, eolian and lacustrine successions that partly overlap with the coastal and nearshore marine deposits. There is an extensive literature from the dual premise of sedimentology (Miall, 1985; Einsele, 1992) and "ores in sediments" (Wolf, ed., 1981-1986; Maynard, 1983; Galloway and Hobday, 1983; Force et al., 1991) that provides extensive background. As already mentioned, our understanding of continental metallogenesis is about the most complete, as the system of metals accumulation can be directly observed, at least in respect to the syndepositional clastic ores (e.g. placers). The system components and their role are supported by observation and interpretations change little in time, except for minor refinements. The recent clastic ores also demonstrate most convincingly the basic tenet of metallogenesis: that ore formation is an add-on to the common rock lithogenesis and although the latter provides an essential framework, the "extreme" (or special) conditions have to be met in order to get the orebody. Example: fluvial gravels are everywhere, but only those in close proximity to primary gold orebodies (or older placers) can accumulate placer gold.

This section puts emphasis on medium- to coarse-grained clastics (sandstone to conglomerate) although fine clastics (mudstone, shale) and (bio)chemical sedimentary rocks (carbonates, evaporites) are additional members of the package and have an important role to play. Also important are volcanic additions, in most cases of airborne ash transported for large distances. The literature usually treats continental clastics in terms of humid and arid end members, to which should be added glacial sediments. The aridity, combined with physiography, influences petrology of the initial sediment and usually also the quality of sorting. Unstable clasts (Fe-Mg silicates, feldspars, carbonates) are depleted in humid sediments whereas arid sediments retain much of them (some, however, are diagenetically regenerated like many Na- and K-feldspars). Arid sediments exposed on surface for some time develop Fe-hydroxide patina ("desert varnish") and this is behind the traditional

belief that the hematite-pigmented "red beds" are all desert sediments. In reality the hues of clastics, particularly sandstones, are mostly a diagenetic effect due to groundwater. This is spectacularly demonstrated in some "sandstone-U" mines where the oxidized "pink" sandstone changes into the reduced (and uraniferous) greenish-gray sandstone, within few meters. On the Colorado Plateau the "red" sandstones are never far away from the "gray" coal-bearing association. "Red" (better "varicolored"; Fig. 13.49) suites are, however, important for certain varieties of diagenetic ores, like the "Cu-sandstone".

Metallogenesis in continental clastics

Formation of continental sedimentary rocks progresses in the same fashion and produces equivalent lithofacies and rocks regardless of the plate tectonic domain. The latter, however, influences the selection of bedrocks to supply detritus and solutes to fill the continental basin and the selection of metals to possibly accumulate there. Some of the preferred tectonic settings include rifts and extensional grabens (Cu, Pb-Zn, U), foreland basins (sandstone U), intracratonic uplifts, some with anorogenic granitoids or alkaline rocks, zones of tectono-magmatic activation, and combinations of the above

Syn-sedimentary clastic ores are dominated by paleo-placers of resistate heavy minerals, and by reworked, transported metalliferous weathering crusts. Gold paleo-placers, older than the Cenozoic unconsolidated "deep leads" (Chapter 10) and Precambrian Witwatersrand-type Au and U deposits (Chapter 11) are uncommon and small (e.g. the Deadwood, South Dakota, paleoplacer in Cambrian basal conglomerate located at the erosional unconformity over the Homestake gold deposit). The regional gold enrichment in late Cretaceous-Paleogene conglomerates in the NW Wyoming foreland (47-222 ppb Au; Antweiler and Love, 1967) could become a "resource of the future" that theoretically stores some 100,000 t Au. Platinoid paleo-placers (e.g. Adamsfield, Tasmania) are exceptional and tiny. Most of the "light heavy minerals" paleoplacers are marine beach and nearshore deposits, although alluvial placers also occur in proximity of basement uplifts as around the Korosten anorthositic massif in Ukraine.

Redeposited "soft" residual Fe ores are locally of the "world class" importance. Those derived from the Precambrian Hamersley Range in Western Australia fill Tertiary stream paleochannels with hematitic and goethitic microconcretions

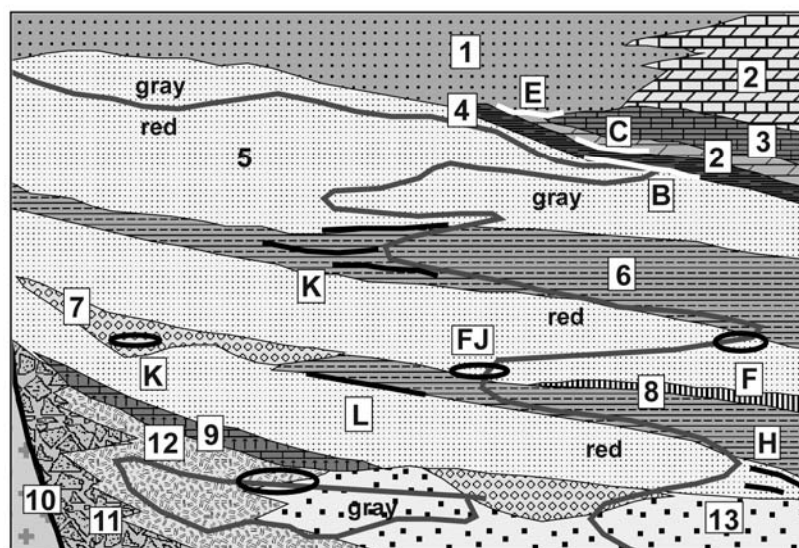
("pisoliths") of uniform size and represent a resource of 4.7 bt of a 58% Fe material (Hall and Kneeshaw, 1990). The Robe River and Yandicoogina channels are "large" Fe deposits that jointly store 2.76 bt Fe. Similar Fe "gravelites" in Oligocene channels in the Lisakovsk deposit (Turgai Downwarp, NW Kazakhstan; Sokolov and Grigor'yev, 1974) store some 700 mt Fe. Redeposited bauxite locally preserved in alluvial to lacustrine (but not marine!) suites is of limited economic importance, except in China where mostly Carboniferous allochthonous diasporic bauxite is sometimes associated with coal deposits (Xiuwen subtype, e.g. Xiaoshanba deposit in Guizhou; Liao Shifan et al., 1990).

13.7.10. Metals recoverable from coal

The bulk of coals are organic carbonaceous rocks derived from terrestrial plant remains, subjected to a variable degree of diagenetic coalification (Galloway and Hobday, 1983). Marine coals ("stony coal") of algal and other derivation are mentioned in Section 13.3. Coal geochemistry and metallogenesis are reviewed in Bouška (1981) and Laznicka (1985a,d). From the production point of view industrial metals obtainable from coal can be subdivided into 1) those in materials physically separable during mining; 2) those chemically recoverable from coal or residues after burning.

Category 1) is represented by pyrite (marcasite) and siderite. The early diagenetic siderite has the form of "blackband" (microcrystalline pelitic siderite pigmented by or interdigitated with coal seams) and pelosiderite in concretions and lenticular beds. Both used to be recovered and utilized in the times of industrial revolution mainly in Great Britain and Germany, despite their low-grade (<30% Fe). Cumulative tonnages of such siderite would place some coalfields into the "large" Fe ore magnitude class (e.g. the South Wales Coalfield stored 5 bt of Fe ore; Wright et al., 1968). Their present economic importance is virtually nil.

Category 2) includes a variety of dispersed (invisible) trace elements some of which are concentrated to such a degree that their value (usually in the high-demand periods only) exceed the value of coal, hence the coal is mined as a metallic ore. This happened briefly in the 1960s and 1970s, under conditions of command economy, when some Soviet, Czech (Radvaňovice), East German and Hungarian (Mécsek) coals were mined for their uranium content.



1. White marine quartz arenite;
 2. Marine limestone (top), dolomite (bottom);
 3. Marine evaporites;
 4. Marine black marl, slate;
 5. Fine alluvial quartz arenite, gray or red;
 6. Alluvial mudstone;
 7. Fluvial channel conglomerate;
 8. Coal (lignite);
 9. Pedogenic calcrete;
 10. Crystalline basement;
 11. Talus;
 12. Fanglomerate, "wash";
 13. Coarse cross-bedded arkose;
- B. Stratabound Cu (Ag) at redox interface;
 C. Stratabound Pb,Zn in marine pelitic or laminated carbonate;
 E. Mn oxide impregnations;
 F. Sandstone Pb-Zn;
 J. Cu-sandstone;
 K. Ditto, in reduced redbeds; sandstone

Figure 13.49. Rocks and ores inventory in predominantly continental varicolored sedimentary sequences (redbeds); from Laznicka (2004) Total Metallogeny Site G200. Explanations (continued): L. Cu sandstone, disseminations in white and gray sandstone intervals with organic reductant; H. Sandstone U-V. Ore types B, F, H, K have known "giant" members

Normally, however, the trace metals are recovered (or potentially recoverable) from the slag, ashes and flue dust remaining after coal burning, to constitute a "technological ore". The trace metals "recovery rushes" in the post-1945 period coincided with temporary peak demands (most notably for U, Ge and Ga) that usually subsided as fast as they arose and a sustained, long-term production has rarely been achieved except, perhaps, in the centrally planned economies as in the former U.S.S.R. and China. Large state enterprises that burned coal from several mines in central power plants were best positioned to gather the residua and recover the trace metals.

The sudden Ge demand for the semiconductor industry in the 1950s identified the highest Ge-enriched residue: the flue dust with up to 2% Ge (in contrast to the average trace Ge content in coals of 7 ppm) (Aubrey, 1955) and it was estimated that in the United Kingdom alone up to 2,000 t Ge could be recovered annually from wastes remaining after burning ordinary coal (Paone, 1970). The Ge resource in British coals was estimated at 200 kt Ge in materials with >0.1% Ge and at least 1 mt in ashes with >0.01% Ge: a "giant resource" equivalent. In 2005 there is very little domestic coal industry left in Great Britain, hence the remaining Ge resource is almost inaccessible. Other countries that continue (and accelerate) coal burning for energy purposes such as China are now in a position

to utilize this resource in times of need. Other trace metals enriched in coal ashes (in ppm) are: Ag 1-10; As 100-900; Be 1-30; Ga 25-180; Mo 10-200; Ni 50-800; Pb 5-600; V 100-1000; Zn 300-5000. Volatile toxic metals like As, Hg, Pb, Tl, Cd will likely need to be removed from the marketed coal at source in the near future for environmental reasons. These metals will augment the existing global supply.

Trace metals in coals are absorbed, or form organometallic compounds, in the organic fraction; constitute own accessory minerals (e.g. sphalerite, galena); or accumulate in the inorganic ash. The metals entered the system at various times starting with the plant metabolism in a swamp, during early diagenesis, by infiltration from above or from below. Strongly metalliferous coals often coincide with earlier orebodies enriched in corresponding metals (compare Laznicka, 1985d).

13.7.11. Infiltrations from meteoric waters: "sandstone-U (V)" deposits

Early mineralogical occurrences of uranium and vanadium minerals like carnotite had been known from the Colorado Plateau in the western United States, and sporadically mined for vanadium, and later for radium, in the first three decades of the 20th century (Rautman, 1983). The principal early U-V district was Uravan in south-western Colorado

where carnotite and other minerals impregnated fluvial sandstone and this provided the convenient name "sandstone-U-V" (also "Western States U"; Rackley, 1976) for this ore type. There was little use for uranium up to about 1941 and much of it ended up in tailings, after vanadium recovery. This changed with the rapidly advancing utilization of nuclear energy, first for military and later for peaceful purposes. A series of exploration rushes resulted in discovery of numerous U-producing deposits and districts along the entire Cordilleran foreland. This ore type has become the principal U source in the United States (P+Rv ~850 kt U @ 0.085% U plus) and its deposits have established a model publicized in extensive literature (Finch, 1967; Galloway et al., 1979; Dahlkamp, 1993 and references therein). Except for the "giant" Niger U province (~350 kt U) and the emerging province of the Tian Shan foreland in Kazakhstan and Uzbekistan (?600 kt U plus), the remaining "sandstone U-V" regions of the world store only "medium" to "large" quantities of U; Table 13.8.

Within a sandstone-U district or province, the individual orebodies are quite small (X00-X000 t of U content) and ore from several mines is usually processed in a central plant. The mineral economy depends on the U price of the day which, in the 1960s, was quite high (~\$ 80/kg U), and reserve tonnages in that period were quoted based on this price (or even on \$130/kg U). In the 1980s-1990s, however, the spot market prices hovered around \$10-20/kg U, although the U price is now increasing. The wide range of U price fluctuations is responsible for the uncertainty built into the published tonnage figures of uranium deposits.

Origin: Sandstone-U (V) deposits precipitate in permeable rocks from mostly descending or laterally circulating meteoric waters less than 100°C hot that carry dissolved U in greater than average concentrations. To enrich such water elevated concentrations of leachable U have to be present in the recharge area. The most common U sources are "hot" potassic leucogranites, U-veins or black shales, acid volcanics. Particularly U-productive are felsic ash-fall tuffs or tuffaceous sediments derived from volcanic eruptions hundreds of km downwind, common in the Cordilleran foreland. U is released from the ash by diagenetic devitrification and leaching, and carried in solution downward.

U is removed from the generally oxidized circulating groundwater in the subsurface and precipitated upon encountering a reductant, or reacting with Ti-Fe oxides (e.g. Ti-magnetite, ilmenite, leucoxene), some clays, carbonates, pyritic

rocks. The literature usually distinguish between the intrinsic (internal) reductants that had been in place before the U precipitation (e.g. plant debris, coalified wood trash, logs) and extrinsic (external) reductants introduced from outside like hydrocarbons (petroleum or methane), CO, ascending reducing fluids. Some reductants, like the humates that impregnate sandstone in the Grants district of New Mexico (Fig. 13.50) and correlate with economic U orebodies, are about intermediate between both categories mentioned above.

U in sandstones precipitated as hexavalent U in urano-vanadates carnotite or tyuyamunite (the same minerals are common in calcrete; read above) or as tetravalent silicate coffinite, uraninite or U-organometallic compounds. Many carnotite occurrences are products of secondary oxidation and reprecipitation of the earlier uraninite or coffinite after uplift and erosion. The ore minerals coat quartz grains, infiltrate or replace sandstone matrix or cement, or organic materials. Coalified wood logs in otherwise unmineralized sandstone often contain high-grade U. The U⁺⁴ oxidic minerals are generally invisible and finely dispersed, visually indicated only after oxidation when colorful greenish or yellowish secondary U minerals start to form shortly after exposure. Alteration zones tend to be, however, visible and sometimes strikingly so (read below).

Typical hosts to sandstone-U are alluvial quartz-rich sandstones, particularly in sequences interbedded with shale or in channels incised into and covered by mudstone. Marine sandstone (Texas U province), alluvial conglomerate, limestone or dolomite sometimes host U ores as well. The U orebodies come as tabular lenses, sometimes stacked and/or coalescing, often arranged into persistent trends. Although most are intraformational some are close to, or rest directly, on regolithic basement above unconformity (e.g. Stráž Block, Czech republic; Fig. 13.51). The roll, or roll-front orebodies are popular in the literature, although they are widespread only in the Wyoming basins, especially Shirley (Harshman, 1972) and Powder River Basins (e.g. Highland; Fig. 13.52). The rolls are ideally C-shaped redox edges of oxidized sandstone tongues, developed discordantly within a single sandstone bed and usually confined by a relatively impermeable mudstone or shale. The oxidized sandstone is greenish-yellow or beige, pink (in the Highland open pit), with abundant limonite staining. It is depleted in pyrite, calcite and uranium.

Table 13.8. Selection of "giant" to "large" (world class) "sandstone-U" districts and provinces

District/province	Hosts age	Geology	Tons U/grade
Colorado Plateau Province; Utah, Arizona, Colorado	Tr3	Tabular and channel infiltrations of U-V oxides in gray Chinle Fm. sandstone and conglomerate; mostly intrinsic (coalified wood trash) reductants	45.2 kt U
San Juan Basin, New Mexico	J3	Stacked peneconcordant tabular bodies of infiltrated U oxides in clastics of the Morrison Fm., confined by mudstone; humate reductants	~450 kt U
---Grants District	J3	Ditto, pod-like and tabular orebodies	390 kt U/0.1% 160 kt V
Wyoming Foreland U Province	T1	Several scattered fields of infiltrated U oxides in T1 continental clastic basins; roll-fronts widespread	212 kt U
Texas Coastal Plain	Eo-Mi	Peneconcordant blankets, channels, roll-fronts of U oxides in fluvial-marine hosts with bentonitic layers; mostly extrinsic (methane, hydrocarbons) reductants	65 kt U/0.1-0.2
Agadés Basin (Air Massif Foreland), Niger	Cb-Cr1	Peneconcordant blankets, rolls with infiltrated U oxides in sandstone, U derived from anorogenic granites and volcanics of Air Massif	210 kt U
Stráž Block, Czech Republic	Cr2	Tabular infiltrational bodies of U oxides with Zr in reduced continental sandstone & channels	Rc ~80 kt U
Balkhash Basin, Kazakhstan	J	U oxide infiltrations in sandstone, in coal (Nizhne Iliiskoe deposit)	?30 kt U/>0.05% ?20 kt Mo/0.03%
Chu-Sarysu Basin, Kazakhstan	T1(Eo)	Tabular bodies of infiltrated U oxides in sandstone screened by mudstone (largest: Kanzhugan-Torktuduk deposit)	?350-500 kt U
Central Kyzylkum Basin, Uzbekistan	Cr3-T1	Tabular U oxide infiltrations in clastic basin between a mosaic of basement blocks (Wyoming Foreland-style); high Se in ores. Uchkuduk, Surgaly, Navoi fields	55 kt U
Amalat Plateau (N of Chita), Transbaikalia, Russia	Mi	Clastic channels in paleovalleys in block faulted granitic basement; U infiltrations in sandstone and lignite, some covered by Q flood basalt	100 kt U/0.05%

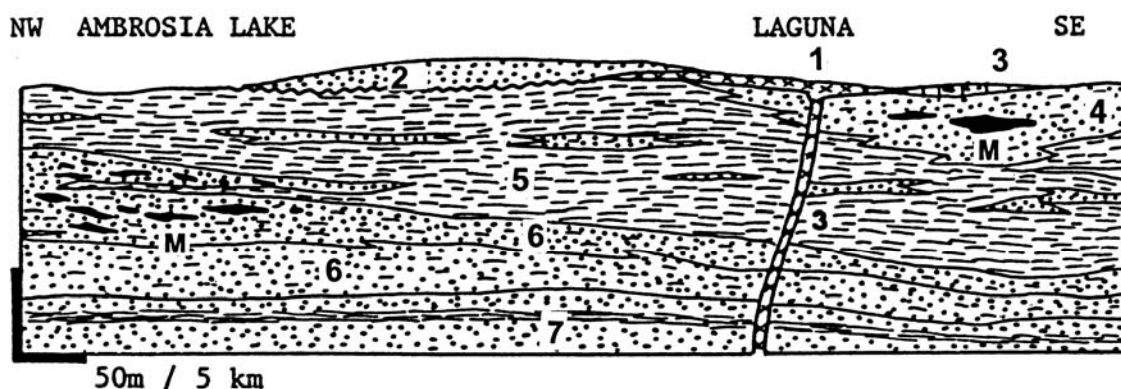
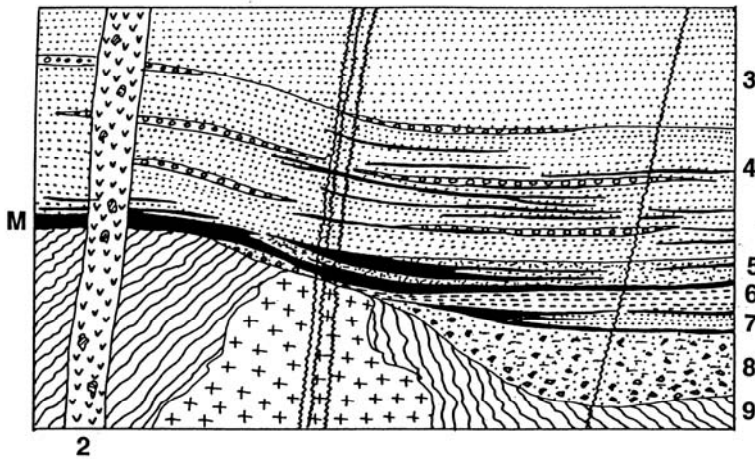
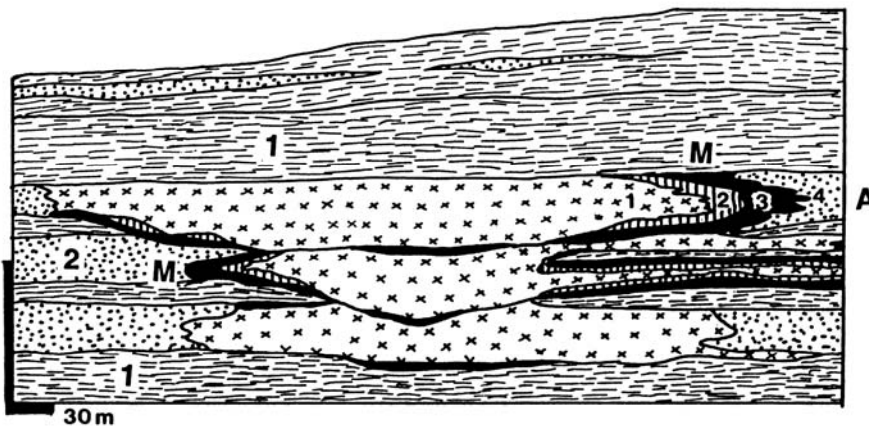


Figure 13.50. Grant U district, New Mexico, simplified cross-section of the Ambrosia Lake and Laguna ore fields. From LITHOTHEQUE No. 533, modified after Hilpert (1969). 1. T basalt dike; 2. Cr quartz sandstone; M. J-T1 trend (tabular)-type peneconcordant infiltrational U orebodies in reduced host sandstone; 3. J Todilto Limestone; 4. J3 Morrison Fm., Jackpile Sandstone 5. Ditto, Brushy Basin Member lacustrine tuffaceous mudstone with sandstone lenses; 6. Ditto, Westwater Canyon member, feldspathic and montmorillonitic sandstone, siltstone; 7. J Recapture Sandstone



M. Tabular to lenticular subhorizontal bodies of uraninite > hydrozircon impregnations; 2. Pc-Pl alkaline mafic dikes; 3. Cr3 Turonian blocky quartz sandstone > siltstone, marl; 4. Cr3 marine Cenomanian, quartz sandstone; 5. Ditto, channel sandstone, reworked Unit 6 sandstone at base of Unit 5, main U host; 6. Cr3 continental Cenomanian, organics-rich freshwater siltstone, mudstone; 7. Ditto, fluvial quartz sandstone; 8. Ditto, basal wash; 9. Pre-Cr basement, regolith on top

Figure 13.51. Diagrammatic cross-section of the Stráž pod Ralskem-Hamr uranium infiltration orebodies, Czech Republic. From LITHOTHEQUE No. 3104, modified after Sýka et al. (1978); Pavel Veselý, DIAMO, 2003 visit



1. Eo Wasatch Fm. fluvial-paludal mudstone; 2. Ditto, sandstone; M. Uraninite and coffinite finely dispersed at redox roll fronts in arkose tongues confined by mudstone. Alteration (small numbers): 1. Pink oxidized sandstone; 2, 3. Redox roll; 4. Unaltered sandstone

Figure 13.52. Highland uranium deposit, Powder River Basin, Wyoming, an example of visually striking roll-style of the "sandstone-U" deposits. Diagrammatic section of the pit wall from LITHOTHEQUE No. 1174, based on Dahl and Hagmaier (1974), Langen and Kidwell (1974), 1980 mine tour

The mineralized roll, several meters thick, is dark gray, greenish gray to black and it contains dispersed pitchblende and coffinite mixed with pyrite and often high trace Mo and Se. Calcite cements and concretions are common, especially along the contact with unaltered gray sandstone. Sets of stacked rolls or coalescing rolls from two or more adjacent sandstone beds are common.

Colorado Plateau uranium province, western United States

Colorado Plateau is an elliptical area of little deformed almost flat-lying monoclines of Permian to Jurassic continental clastics resting on

Paleoproterozoic basement, enveloped by folded units of the Cordilleran orogen (Cowan and Bruhn, 1992). The clastics interfinger with miogeoclinal limestone in the west. The very scenic redbeds (e.g. in Monument Valley, Arizona) comprise fluvial, deltaic, lacustrine and shallow tidal flat sandstone with red tuffaceous siltstone and mudstone. They change upward into more "gray" sedimentary rocks of the foreland basin.

Finch (1967) counted some 4,000 individual U and/or V orebodies in Colorado Plateau, concentrated in several mining districts and belts at two main stratigraphic levels (Granger and Finch, 1988). The lower level in the Upper Triassic Chinle Formation is mineralized mainly in SE Utah and

northernmost Arizona (Lisbon Valley, White Canyon, Monument Valley) and it accounts for some 42.5 kt U produced (Dahlkamp, 1993). Tabular orebodies peneconcordant with bedding are in channel sandstones rich in coalified plant trash. The upper mineralized level is in the late Jurassic Morrison Formation, the earliest foreland basin succession formed east of a broad orogenic highland in the west (Cowan and Bruhn, 1992). Uravan and Grants mineral belts store the bulk of the Colorado Plateau U and V endowment.

Uravan U-V belt (Motica, 1968; Dahlkamp, 1993; Pt 36 kt U @ ~0.17%, 180 kt V @ ~0.8%) is an arcuate N-S zone of numerous U-V orebodies in westernmost Colorado. It is the oldest U mining area in the United States, hosted by the Salt Wash sandstone member of the Jurassic Morrison Formation. The semiarid fluvial sandstone in channels incised into a broad alluvial plain is locally crowded with coalified plant remains and is overlain by oxidized (red) tuffaceous mudstone. The tabular and local roll-front orebodies in reduced sandstone were, when discovered, completely oxidized near the surface into a bright colored mixture of yellow carnotite and tyuyamunite with brown to red vanadates. The unoxidized zone in coaly sandstone in depth contained sooty pitchblende, coffinite, montroseite, rauvite, and vanadian chlorites and hydromicas (e.g. roscelite). The highest grade ore along the redox boundary is bordered by a thin bleached zone against oxidized hematitic sandstone, and is rich in Se.

Grants uranium region, New Mexico (~390 kt U @ 0.085+%U, ~160 kt V; Moench and Schlee, 1967; Dahlkamp, 1993). This is the most productive U.S. uranium region and a model of U oxide infiltrations in black carbonaceous humate, itself introduced into the sandstone shortly before or during the primary U mineralization. The region measures about 150 km along the NW axis and is ~30 km wide. It is in Upper Jurassic strata (Morrison Formation) of the San Juan Basin, west of Albuquerque and it is subdivided into seven ore fields of which the Ambrosia Lake ore field accounts for the bulk of production. The numerous tabular and pod-like U orebodies are stacked at several levels in sandstones that belong to two members. The lower Westwater Canyon Member is a medium- to coarse-grained feldspathic arenite interpreted as a braided stream deposit. The overlying Brushy Basin Member is predominantly tuffaceous shale believed deposited in a mudflat and playa lake, with sandstone tongues (Jackpile and Poison Canyon Sandstones). Maynard (1991b) argued that the best orebodies in the Westwater

sandstone formed where the overlying Brushy Basin sediments are diagenetically altered to smectite, whereas the zeolite-altered ash beds, that retain their trace U, rest on barren sandstone.

The bulk of orebodies is unoxidized and the principal U mineral is coffinite with some sooty pitchblende and amorphous uraniferous humate, dispersed and co-extensive with the black sooty organic matter that fills pores in sandstone. A portion of the primary U was redistributed near steeply dipping faults to form small stack and roll-front orebodies. The U source is believed to have been in the felsic tuff component in the Westwater sandstone itself, the humates and fluids were likely expelled from the Brushy Basin mudflat succession during compaction. The earliest primary mineralization accompanied and shortly postdated the host diagenesis (~130-100 Ma) but portions of the orebodies have been repeatedly remobilized.

Wyoming Foreland U province (Harshman, 1972; Dahlkamp, 1993; P+Rc ~212 kt U @ 0.04-0.22% U). This is the second most productive U.S. uranium province, which is very low in associated vanadium. Discovered later than the Colorado Plateau ores, it covers much of central Wyoming, SW and NE of Casper. The Basins are a part of the Cordilleran Foreland, a mosaic of thrust-faulted uplifts of basement-cored mountain ranges interspersed with basins filled by synorogenic sediments (Miller et al., 1992). The basement belongs to the Archean Wyoming Province and comprises greenstone belts, granite-gneiss and syn- to post-orogenic granite. The intermontane basins shortly postdate crustal shortening produced by the Laramide orogeny that terminated around 55 Ma, and they are filled by Paleocene and Eocene alluvial fan, fluvial and lacustrine "gray" sediments that include coal (lignite) measures. There are scattered Eocene to Oligocene alkaline and felsic magmatic centers that contributed ash fall component to the basinal sediments. Tuffs of the Oligocene White River Formation were the major contributor of the trace uranium now in ores.

Hundreds of individual small roll-front U orebodies constitute ten defined ore fields, scattered in the following Basins: Wind River (Gas Hills); Powder River (Highland-Box Creek); Shirley Basin; Great Divide Basin. **Gas Hills** (~60 kt U), **Shirley Basin** (~120 kt U) and **Highland** (~20 kt U; Fig. 13.51) ore fields stored the bulk of the U reserves (Harshman, 1972). Almost all orebodies are in the redox fronts of intraformational tongues of groundwater-altered sandstone, separated by mudstone interbeds and enriched in coal-related

carbonaceous substance. The principal ore minerals that coat sand grains in the altered redox fronts are coffinite and sooty pitchblende and there is a locally substantial content of Mo and Se. The U has been derived from Tertiary tuffaceous component as well as from Archean potassic granite regolith, either directly or after reworking to form the host arkosic sandstone. Uranium precipitated in response to both intrinsic (carbonaceous substance in sandstone) and extrinsic (hydrocarbons and H₂S-rich gas seeps) reductants. The first discovered orebodies were oxidized with limonite and carnotite (e.g. Pumpkin Buttes) but the bulk of U came from the "primary", although repeatedly redistributed orebodies, dated between Oligocene and recent.

The remaining "giant" and "large" sandstone-U regions are briefly characterized in Table 13.7.

13.7.12. Cu-sandstone deposits in red and gray (varicolored) beds

Oxidized continental predominantly clastic successions (red beds; Turner, 1980) are almost synonymous with occurrences of the "Cu-sandstone" (redbed-Cu; Kirkham, 1996a) ore type. These deposits are quite comparable in style with the "sandstone-U" (in Lisbon Valley, Utah, both types overlap), from which they differ mainly in terms of trace metal availability. Copper is almost always derived from intermediate to mafic magmatic sources, common in paleorift systems or along andean-type margins. The purely sedimentary setting is transitional into the "volcanic redbeds" (Kirkham, 1996b) that include mineralized volcanics themselves, most prominently in the Proterozoic Keweenaw native Cu province in Michigan (Chapter 11). The "giant" stratabound Cu deposit Boléo in Mexico is related to andesitic volcanism in an andean-type continental margin (Chapter 6).

Although widespread and very predictable (coatings of malachite or chrysocolla are almost a standard feature whenever there is a reduced [light green or gray] interval or patch in a redbed succession), Cu-sandstone occurrences are mostly of small to medium size. Kirkham (1989) assembled 290 occurrences in his database that included also the Kupferschiefer-type Cu ores. There is just one "giant" ore field (Dzhezkazgan) and 6 or 7 "large" Phanerozoic deposits or ore fields. Several persistent stratigraphic units are known to contain tens to hundreds of Cu-sandstone (and "Cu-shale") occurrences over thousands of square kilometers that store "large" to "giant" total Cu contents, but precise figures are rarely available.

Examples include the Lena (Angara) Basin in central Siberia; the Permian Cu province in western Cis-Uralia, Russia; the South Tadjik Depression. Various metamorphosed Proterozoic counterparts of the Cu-sandstone and Cu-shale types (e.g. the African Copperbelt) appear in Chapter 11.

As with the "sandstone-U", the sedimentary Cu-hosting successions range from reworked arid basement regolith ("wash") through poorly sorted fanglomerate of alluvial fans to stream (wadi) sandstone to lacustrine or marine deltas. Interbedded are often tuffaceous mudstones and sediments of (playa) lakes with evaporites and lacustrine dolomite. There are transitions to shallow marine sediments. Within a thick redbed sequence there are reduced intervals some of which are syndepositional (e.g. carbonaceous lacustrine mudstone), but most are post-lithification, related to past aquifers or to circulating "basinal fluids".

The "redbed" copper deposits are epigenetic, low-temperature (<100°C), precipitated from aqueous solutions. Although some metal-transporting fluids could have been meteoric waters mowing downslope (comparable with fluids that formed the "exotic deposits" downslope from porphyry coppers; Chapter 7), there is a consensus that the majority of ore fluids were saline brines circulating horizontally or upslope (Kirkham, 1996a). The salinity was mainly the result of dissolution of rock evaporites by meteoric waters. The Cu in solute was largely derived by diagenetic release of trace Cu from unstable clasts undergoing decomposition and oxidation (mainly pyroxene and magnetite), in turn derived from mafic volcanics. Alternatively, copper was released by in-situ leaching of volcanics (e.g. amygdaloidal basalt flows) and in some cases of Cu sulfides present in earlier hydrothermal deposits. Precipitation of Cu from chloride complexes in oxidized fluid required reductants. Coalified plant trash (ubiquitous in Nacimiento, New Mexico), carbonaceous substance or diagenetic pyrite provided intrinsic reductants; coalbed or petroleum methane, H₂S, CO and hydrocarbons diffusively streaming from below acted as extrinsic reductants (envisioned by Gablina, 1981, for the Dzhezkazgan origin). Alternatively, Cu precipitated as a result of mixing of fluids of various provenances.

A typical Cu-sandstone deposit consists of disseminated chalcocite, bornite, chalcopyrite and/or malachite, azurite, chrysocolla or atacamite in pores of reduced sandstone. The minerals either fill intergranular voids, or they replace earlier, e.g. calcitic, cements. The oxidic minerals are either the primary precipitates (typical for near-surface

descending fluids as in exotic deposits) or late products of retrograde sulfide oxidation. Pb and Zn have sometimes accumulated in adjacent zones. The same ore minerals may occur in greenish, gray or black mudstones where they form fine dispersions (e.g. in Creta, Oklahoma) or small nodules, veinlets. Reduced Cu-mineralized pelites within redbed sequences overlap with the Cu sandstone and are usually treated jointly in the literature. Reduced pelites ("black shale") at boundaries of continental redbeds in the footwall and marine successions in the hangingwall are of the Kupferschiefer-type, reviewed above. Occasionally, Cu resides in, or along contact with, dolomitic members of the redbed sequence (e.g. in Dongchuan, Yunnan). In Timna in the Dead Sea Rift (Segev and Sass, 1989; 530 kt Cu) chrysocolla and other oxidic Cu minerals reside in a siliclastic sandstone produced by karstification and carbonate removal from a Cu-enriched Cambrian dolomite, during rifting.

Dzhezkazgan (Zhezkazgan) Cu (+Pb, Zn) ore field, Kazakhstan (Bogdanov et al., 1973; Samonov and Pozharisky, 1974; Gablina, 1981; 730 mt Cu) used to be the main source of Soviet copper, before the U.S.S.R. demise. The spectacularly green oxidation zone was worked by the ancients, rediscovered by the Cossacks in the mid-1880s, then intermittently mined under financing by the Russian and British capital until developed into a major industrial complex in the pre-World War II years. The ores are located in a graben near the southern closure of the Dzhezkazgan Permo-Carboniferous basin, at the northern edge of the first-order Chu-Sarysu Basin of central Kazakhstan. The Ulutau Precambrian basement uplift is west of the Dzhezkazgan Basin and the ore-bearing strata are situated above a basement high. The Basin contains several stratabound Cu and also Pb-Zn and U zones (Cu is present throughout a 70 km long belt with an area of 600 km²) of which the Dzhezkazgan ore field is the largest one.

The ore-bearing Middle-Upper Carboniferous Dzhezkazgan Suite comprises rhythmically alternating gray and red lithic sandstone units that change facies into siltstone. Minor evaporites and dolomite are present. Druzhinin (1973) interpreted the paleo-environment as a regressive cyclic sequence of alluvial coastal plain (the red beds) grading to paralic deltas with lagoons and shallow marine sediments (the gray beds). The more recent interpretation (Gablina, 1981) is of a closed intermontane basin with alluvial, deltaic-lagoonal and saline lake facies. The red-gray rhythms (there

are at least 51 rhythms in the mineralized interval, each 2-42 m thick) are alternatively attributed to post-lithification reduction in aquifers possibly by circulating oilfield waters, and/or hydrocarbon and H₂S seepage from the underlying, Lower Carboniferous marine carbonates. The source of Cu is unclear, usually attributed to the regionally distributed Devonian-Lower Carboniferous andesitic volcanics of the Central Kazakhstan andean-type margin (the Balkhash porphyry-Cu province, broadly contemporaneous with the Cu sandstones, is several hundred km farther east). The sedimentary rocks are gently open-folded and block faulted.

There are 26 stratabound ore horizons in the gray units, with up to 2 km long and 18 m thick lenticular orebodies. The ore consists of densely disseminated chalcopyrite, bornite and chalcocite in sandstone and partly shale, and there are separate galena and light sphalerite mineralized orebodies stratigraphically above the copper. The Cu sulfides have a high rhenium content.

13.7.13. Sandstone-Pb (Zn) deposits

This is a rare (less than 20 deposits worldwide) yet locally highly productive ore type (Laisvall-largest Pb deposit in Scandinavia; Mechernich-largest Pb resource in Germany; Jinding-largest Pb deposit in China) that includes five "giants". Bjørlykke and Sangster (1981) and Sangster (1996) provided a comprehensive review. A typical sandstone-Pb deposit consists of dominant disseminated galena, interstitial to quartz clasts in sandstone and replacing cement (typically calcitic) and matrix. "Knotten", poikilitic galena spots and schlieren, are most characteristic. Sphalerite is subordinate and usually zonally arranged in respect to galena (in the hangingwall area in Laisvall). The stratabound blanket-like (manto) or tabular orebodies are relatively low-grade (1-5% Pb) but the "giants" are extensive and of a large tonnage.

Although superficially similar to the "Cu-sandstones" (read above), some of which have Pb-Zn rich fringe (e.g. Dzhezkazgan), "sandstone Pb" have closer genetic affiliation with the MVT deposits (read above) such as high-salinity "basinal" brines, fluid temperatures between 100° and 160°C, lead sources in granitic basement or Pb-mineralized sedimentary sequences. Some orebodies in the basal Lamotte Sandstone in the SE Missouri MVT region are comparable with "sandstone-Pb". In l'Argentière (Samama, 1968; 303 kt Pb @ 3.7%) galena disseminated in Triassic feldspathic sandstone of "redbed" affiliation changes upward

into replacements in lagoonar dolomite. Most sandstone-Pb deposits are in non-volcanic transgressive basal sequences that include both continental redbeds (Salmon River, l'Argentière) or lacustrine sequences (Jinding), and nearshore-marine (deltaic, lagoonar, beach; Laisvall) rocks. The mainstream genetic model (Bjørlykke and Sangster, 1981) assumes lead, extracted from the basement and transported in saline brine through porous sandstone aquifer, precipitated by H₂S at sites enriched in organic matter (coalified wood trash in continental sediments) and/or pyrite. Mechernich, Laisvall and Jinding, briefly described below, exemplify disseminated Pb (Zn) deposits in continental redbeds, marine mature sandstone, and complex settings, respectively.

Mechernich & Maubach (Eifel district) Pb-Zn, Germany (Walther, 1984; Schneider et al., 1999; P+Rc ~4.124 mt Pb, ~3.2 mt Zn, ~920 t Ag, including unrecovered, mostly Zn, content; Fig. 13.53). In the 1800s and earlier, when massive galena deposits of 10+% Pb were the norm, the mined disseminated deposits at Mechernich (~2% Pb) had been a global anomaly. They, however, produced between 1.5 and 2 mt Pb until 1977, although with large losses and virtually no zinc recovered. The Eifel district is SW of Köln (Cologne), in the Rhenohercynian fold- and thrust belt of the late Paleozoic Variscan orogen. The Devonian "basement" siliclastics and carbonates are overprinted by a N-S lineament crossed by a series of NW faults, that border a small triangular relic (basin) of the Triassic "molasse" facies. The Middle Bundsandstein redbed sandstone and conglomerate unconformably overlie Devonian rocks, and grade upwards into Middle and Upper Triassic carbonates and marls. Several low-temperature (~140°C) fault-controlled vein galena deposits (Bleialf and Rescheid; ~400 kt Pb) intersect the basement, and isotopically corresponding high-salinity fluids also precipitated the much more extensive disseminated Pb & Zn sulfides in the Mechernich and Maubach ore fields (Schneider et al., 1999). The most likely ore forming event is dated around 170 Ma (Jurassic).

Mechernich Pb-Zn ore field, the larger one (Schröder, 1954; ~250 mt ore @ 0.57-2.5% Pb for ~3.8 mt Pb, 3.1 mt Zn, 820 t Ag content) is a 10 km long, 1 km wide NE trending zone along the SE margin of the Triassic outcrop. There, the weathered Devonian basement graywacke is unconformably overlaid by basal friable sandy "wash", topped by a set of four beds of white quartz sandstone each topped by a conglomerate. Above is

a white and red sandstone interbedded with red mudstone, grading to shale, carbonates and evaporites of the Upper Bundsandstein. The lenticular and blanket-like assay-defined Pb-Zn orebodies are in the lower white sandstone beds. There, galena with minor yellow sphalerite forms "knotten" that replace carbonate cement in slightly silicified sandstone. Disseminated yellow sphalerite and minor pyrite, bravoite and chalcopyrite predated galena emplacement. The oxidation zone was dominated by cerussite. In the much smaller **Maubach Pb-Zn deposit** (von Behrend, 1950; ~12 mt @ 2.7% Pb, 0.9% Zn for 324 kt Pb, 108 kt Zn plus ~24 kt Co in bravoite) the Triassic host unit is coarse, conglomeratic and the dominant galena forms crystals that line cement-solution voids after cement dissolution, fracture fill, or scattered spots.

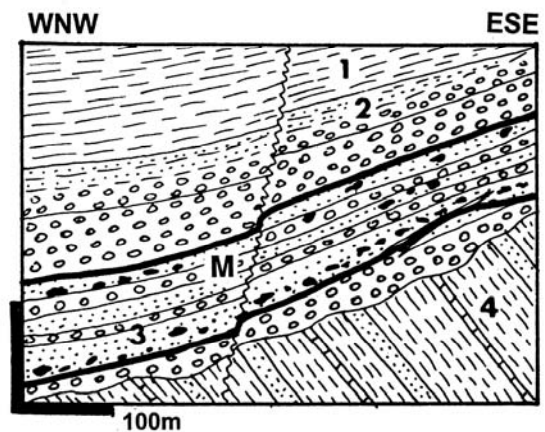


Figure 13.53. Mechernich disseminated Pb deposit, Eifel, Germany, diagrammatic cross-section from LITHOTHEQUE No. 549 based on data in von Behrend (1950), Schröder (1954). M. Disseminated and nodular galena >> sphalerite in reduced red sandstone; 1. Tr1-2 marl, dolomite, siltstone; 2. Tr1 Middle Bundsandstein redbed sandstone and conglomerate with whitish reduced mineralized interval; 4. D1 folded basement slate, litharenite, minor impure limestone

Laisvall Pb>Zn deposit, NW Sweden (Rickard et al., 1979; Bjørlykke and Sangster, 1981; P+Rv 108 mt @ 3.9% Pb, 0.5% Zn, 8 g/t Ag for 5.4 mt Pb; Fig. 13.54). Laisvall is the largest of a group of sandstone-Pb deposits in the Lower Cambrian platformic sedimentary rocks resting on the Baltic Shield basement, along the eastern front of the Caledonian orogen. Laisvall and Vassbo are in the autochthon, Dorotea is in the lowermost Caledonian nappe. The basement in Laisvall is a Neoproterozoic granite topped by thin Vendian

(~640 Ma) diamictite, feldspathic sandstone and siltstone with rafted pebbles.

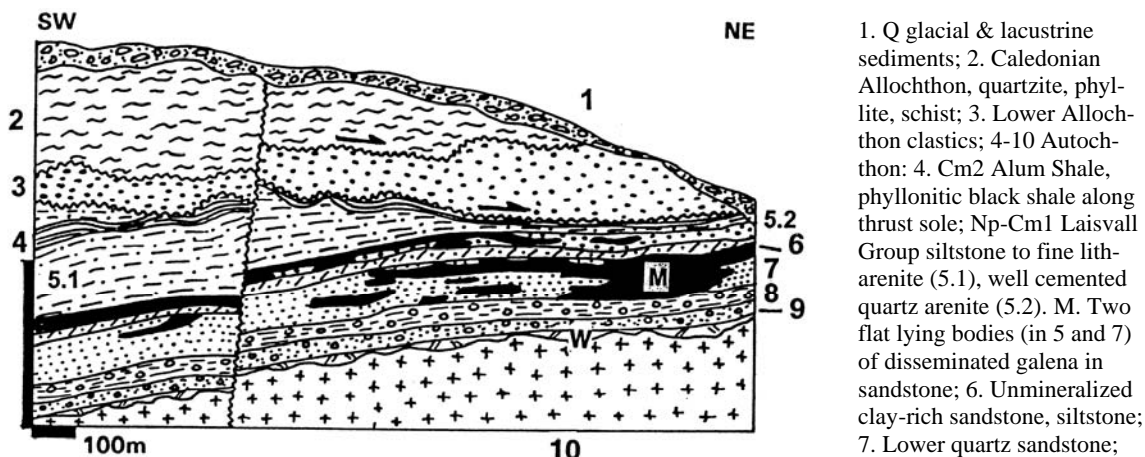


Figure 13.54. Laisvall lead sandstone deposit, Norrbotten, NW Sweden; longitudinal section from LITHOTHEQUE No. 612.2 modified after Lilljequist (1973), Rickard (1983). Explanations (continued): 8. Np-Cm1 "Pebbly Shale" diamictite grading to arkose; 9. Ditto, basal conglomerate to arkose; W. Paleoregolith under unconformity; 10. Pp Sorsele Granite basement

Above is 40-45 m of transgressive nearshore marine Lower Cambrian (~560 Ma) succession. This consists of locally conglomeratic quartz arenite, the ore host, intercalated with light green shale and overlain by more siltstone topped by Middle Cambrian black (Alum) Shale; the latter is interrupted by the Caledonian lower nappe. Stratabound tabular to lenticular Pb orebodies, traceable for 6.5 km along strike, occur at two horizons in sandstone (quartzite) and they are dominated by disseminated galena accompanied by slight silicification. Disseminated yellow sphalerite with pyrite increase into the hangingwall and some fractures are filled by remobilized galena or sphalerite veinlets.

Jinding (Lanping) Zn-Pb-(Sr) deposit, SW Yunnan, China (Li and Kyle, 1997; Rv 140 mt ore with 11.02 mt Zn, 1.94 mt Pb, 176 kt Cd, 1,276 t Ag, 610 kt SrSO₄). This "triple giant" (Zn, Pb, Cd) is the largest Zn-Pb deposit in China, discovered in the 1960s in the Nujiang Prefecture. It is also the most complex "sandstone-Pb" with dual lithologic and structural controls (growth fault). The orebodies are hosted by Paleocene-Eocene continental succession interpreted as a siliclastic fan-delta and debris flow facies rich in calcitic cement and Triassic limestone blocks in breccias. This rests on top of a Triassic-Jurassic volcanic-sedimentary redbed rift sequence which, in turn, is floored by Ordovician to Permian supracrustals. The Tertiary ore hosts are overthrust by Jurassic redbeds and Triassic limestone. The geotectonic interpretation is

of a sutures-bounded microplate along the collision zone between the Indian Plate and Yangtze Platform.

The north-dipping ore zone is 1,450 m long along strike, over 1,000 m downdip, and up to 54 m thick. It is in the immediate footwall of the Pijiang growth fault. The upper orebody consists of fine disseminated sphalerite and galena that replace calcitic cement in a well-sorted, fine-grained lithic arenite (phyllarenite composed of quartz and metamorphic rock fragments). The lower, parallel orebody comprise massive pyrite, celestite, fine-grained galena and sphalerite, veining and replacing carbonate blocks in breccia and in sandstone. There is a substantial oxidation zone of hemimorphite, smithsonite and cerussite (50 mt @ 8% Zn, 1% Pb). The Tertiary low-temperature (90-160°C) mineralization is attributed to high-salinity brines ascending along growth faults and mixing with descending meteoric waters.

Additional "sandstone Pb-Zn "giants":

Dorotea (Bjørlykke and Sangster, 1981; Rc 3.1 mt Pb) is in the Lower Cambrian allochthon along the Caledonian front, hundreds of km SSW of Laisvall. Galena is disseminated in coarse quartzite resting on granitic basement, under siltstone cap.

Salmon River (Yava, Silvermines, Talisman) is in the Cape Breton Island, Nova Scotia, Canada (Sangster and Vaillancourt, 1990; Sangster, 1996; Rc 71.2 mt @ 2.09% Pb for 1.48 mt Pb). Galena with minor pyrite and sphalerite are disseminated, in pores, and as replacement of coalified plant trash in late Carboniferous sandstone. There are three stratabound zones in channels separated by fault-bounded basement ridges.

13.8. Anthropogenic metal sources

Anthropogenic (human-made) metal resources are marginal to the mission of this book that deals with the geological (nature-made) materials. If considered in the extreme, the entire metals inventory this society possess, in active use or in largely dead storage (e.g. gold in banks and national treasuries vaults; strategic stockpiles of governments), would qualify as a resource, as one day a portion of it might become a component of industrial metals supply. The gold sales by government treasuries in the 1990s and 2000s represented a significant proportion of the world's gold supplies that helped to reduce demand for the "new" (newly mined) gold and depress prices over several years. Similar effect have had the occasional sales of metals from the U.S. government strategic stockpile. These matters will not be pursued further.

Waste from mineral (ore) processing, however, is a different story as it accumulates in what are "secondary" (or tertiary?) deposits of metals that could be mined and reprocessed. The origin of such deposits approximates natural rocks formation: waste dumps and tailings are detrital sediments, where the ore metals reside in (or are) the clasts, and there is often a proportion of chemically precipitated metals. Metalliferous slags are akin to volcanic lavas.

Waste dumps and tailings on mine sites represent production losses and they have nothing to do with the geological magnitude of an ore deposit from which they came. Where the tonnage and grade of mine waste had been known, it was added to the total production figure of a mine in order to establish the pre-mining metal reserve: the principal variable employed throughout this book (in many cases the pre-mining reserves have already been published, not including the losses). In terms of mineral economics, however, metalliferous dumps, tailings and slags are repositories of metals akin to natural metallic deposits and they are subject to the same procedures of acquisition, reserve estimation, development, mining and processing as are the geological deposits.

Some deposits of waste materials are no longer at the mine sites, but at sites of processing facilities located elsewhere. Typically, large central processing plants used to treat ore or concentrate from several deposits so the tailings or slag there had a group input and their metal content can no longer be added to increase the pre-mining reserve of the original ore deposits.

Magnitude of metal resources in waste deposits

Every metallic deposit suffers from ore and metal losses during mining (e.g. by leaving pillars and unmined ore remnants in ground; by dumping a proportion of ore together with waste; by loss into dust, mud, effluents), transportation, milling, concentration, smelting and refining. The losses vary greatly between about 5 to 75%, and there are losses of up to 100% of metals not utilized in the times of mining such as zinc in the Ag-Pb-Zn ore in Lavrion mined under Pericles, and uranium in pitchblende dumped during the medieval silver mining in the Erzgebirge.

The ancient practice of not recovering all metals present in complex ore deposits has sometimes been recently reversed; for example, the reckless uranium mining for shipment to the U.S.S.R., from the Erzgebirge mines in the 1950s to 1980s, did not recover silver and proustite-rich material ended up in the Jáchmov's waste dumps. The non-recovery of some ore metals from mined ores continues, the most striking example being As (in gold ores, e.g. in Morro do Ouro, Red Lake, Muruntau) for which there is no market at present. Should a market develop centuries from now, the As in waste will likely be extracted, provided that the waste repositories remain and can be identified. In contrast to the yesterday's mining that left behind waste dumps and tailings, the contemporary waste is often removed, especially when it contains a toxic substance like arsenic. The percentage of metal losses from the mined ore depends on the type of ore, mining technique and processing technology. Obviously, the greater the past losses the more likely it is to find an economic anthropogenic deposit at or near the former mine site.

It is estimated that before the widespread application of flotation for disseminated or intergrown (as in the VMS) base metal sulfide ores, the losses were a minimum of 15-20%, so that a fully mined out "giant" Cu deposit of, say, 3 mt Cu left behind between 450 and 600 kt Cu in waste (a "large" accumulation). The gold (and silver) recovery from good grade ores, before the application of hot pressure leaching in autoclaves, was also no better than 80% so some 20% of gold remained in tailings. To accumulate an anthropogenic metal resource of a "giant" magnitude thus required at least 5 to 10 times the metal tonnage in the primary deposit, or in a group of primary deposits the ore from which was processed in a central plant. There are few identified "waste giants"; the largest ones, of gold (and uranium), were the waste and slime dumps that

were, until the 1970s-1980s, a part of scenery of every goldfield on the Witwatersrand veld. The dumps have been gradually reprocessed and in the 1990s they provided 45% of the South African gold output of 470 t Au (that is, 211.5 t Au). The average grade in tailings was 3 g/t Au and the cost per ton milled \$ 22, versus the \$ 70 milling cost of the about twice as rich primary ore from the underground (Dixon, 1998). Having produced about 48,000 t Au by the year 2000, at 20% processing losses (my estimate), there must have been some 12,000 t of the lost gold around the Witwatersrand: a "super-giant" indeed!

No other goldfield could match the Witwatersrand "waste ore" magnitude and a "giant" (250 t plus) Au resource in waste can only be credited to Muruntau (the <1 g/t Au material heap-leached by Newmont probably contains a 250+ t Au resource, but the material comes from a low-grade stockpile rather than waste dump), and possibly Kalgoorlie. Tailings from the Leninogor (Kazakhstan) base metals smelter in the Rudnyi Altai Pb, Zn, Ag district, accumulated over a period of 200 years or more, store a "large" or possibly "giant" resource of silver and gold. This was conservatively estimated at ~851 t Ag @ 4.34 g/t and 84 t Au @ 0.56 g/t (Canadian Minerals Yearbook, 1993) It is unlikely there is a "giant" anthropogenic deposit of ferrous, base or rare metals left anywhere in the world, although several "large" and "world class" accumulations have been identified and some of them already mined. A brief review of the identified anthropogenic metal "deposits":

Waste dumps: At most large historical mines, dumps have been reprocessed many times, especially if acid-soluble Cu or cyanide-soluble Au were present. The Erdenet, Mongolia, porphyry Cu-Mo dumps remaining in 1996 have contained 688 kt Cu recoverable by solvent extraction and electrowinning.

Tailings: The Kambove-Kakanda tailings (Katanga Copperbelt) contained 61.17 mt of dolomitic silt and sludge grading 0.98% Cu and 0.19% Co (containing 600 kt Cu and 116 kt Co; Panorama Ltd., 1996 Annual Report). The Kachkanar iron works in the Urals have accumulated 800 mt of tailings after wet magnetic separation of magnetite, with recoverable trace scandium. Estimated grade of 10 to 20 ppm Sc would represent between 8 and 16 kt of contained Sc. At Fort McMurray, Alberta (Athabasca Tar Sands) the froth treatment tailings contain about 6.7% Ti and ~1.8% Zr in ilmenite,

rutile and zircon (Owen and Tipman, 1999). At the rate of ~100 kt Ti/year and ~30 kt Zr/year this would represent a co-product to hydrocarbons of ~5 mt Ti and 1.5 mt Zr in fifty years, by a single company. The Elliot Lake district, Ontario (Robertson, 1981) produced some 100 mt of tailings during its lifetime, grading 0.09% Th and 0.04% REE, for 90 kt Th and 40 kt REE content. These metals are mainly in monazite and partly in brannerite and uraninite.

The red residual muds remaining after bauxite treatment by the Bayer process store a large number of trace metals and have recently been an important industrial source of gallium. The Jonquière smelter in Québec has produced some 15-20 t Ga/year since 1989, from imported ore (Canadian Mining Journal, March 1989). In Jamaica, around 13.25 mt of red mud is produced each year and it contains 31.5% Fe, 5.1% Ti, 0.31% V₂O₅, 0.19% REE, 0.14% Zr and 92 ppm Ga₂O₃ (Wagh and Pinnock, 1987). 300 mt of such mud, accumulated in some 25 years, thus contains ~2,760 t Ga₂O₃.

The Noril'sk central concentrator in Siberia has accumulated some 350 mt of tailings with 1-3 g/t PGE (which is about 700 t PGE with Pd/Pt = 0.5-4.5)

Smelter slags: The more than 2,000 years old slag at Lavrion, Greece, stored a share of the estimated originally present 3 mt Zn content in the ore field. A portion of the slag has been reprocessed after 1875, the remainder is still there. The Kirovgrad, Krasnouralsk and Sredneuralsk smelters in the Urals had, in 1998, a cumulative reserve of 54 mt of slag that stored ~1.944 mt Zn, 308 kt Cu, 378 t Ag and 32 t Au. The Nkana slag dump in the Zambian Copperbelt has a high Co grade (~0.75%) and 1.2% Cu, containing 103 kt Cu and 64.5 kt Co. The slag is transported to Kabwe and processed in facilities remaining on site of the mined-out Broken Hill Pb-Zn deposit (Colossal Resources Corporation, Fact Sheet, 1996).

14 Higher-Grade Metamorphic Associations

14.1. Introduction

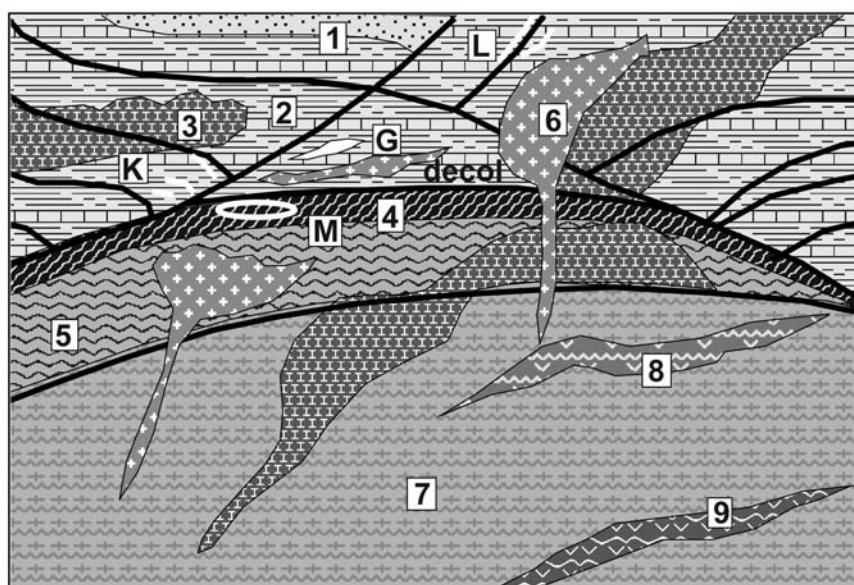
Metamorphic rocks evolve gradually from precursors exposed to increasing metamorphism, so there is no sharp boundary between metamorphosed and unmetamorphosed rocks in the field. Most of the earlier chapters, identified by names of pre-metamorphic associations, included some metamorphic equivalents as well, through the greenschist facies at least. This is a general practice of geological organization and description that puts emphasis on the initial composition and origin of rocks and related ores. In higher grade metamorphic associations, however, the metamorphic effects overwhelm the original rock characteristics and result in metamorphic homogenization: amphibolite facies metamorphosed granite, arkose, conglomerate and shale become all mineralogically uniform schist or gneiss. The progenitor has to be interpreted and the literature resorts to two sets of rock names: descriptive-metamorphic (e.g. biotite gneiss) and interpretational (e.g. meta-graywacke). Not only an interpretation might be subjective or wrong (compare the many conflicting interpretations of the Broken Hill, NSW, host assemblage; read below), but the latter is sometimes shortened to e.g. "graywacke", to save the prefix meta-: an aberration! and a source of an (often costly) confusion. In mineral exploration the emphasis is on reality, hence the metamorphic reality should take a preference in a name. This provides justification for the present chapter that cuts across boundaries previously established among the various lithologic associations, and environments in which the original rocks formed.

Metamorphism has two end-members: 1) Isochemical metamorphism, the ideal form that operates in a closed system where, theoretically, nothing is added or removed. The earlier rocks recrystallize and the constituent minerals either remain the same species (e.g. quartz, calcite, sphalerite), or change into metamorphic minerals with the same chemical composition (minus H₂O) as their progenitors (e.g. micas or sillimanite after original clay minerals); 2) Metasomatism, where substances introduced from outside replace, partially or completely, the pre-existing minerals (e.g. silicification of calcite). Even during the most isochemical load metamorphism, however, water

and some other volatiles (CO₂) leave the system and migrate out (during retrograde metamorphism they migrate back in); Walther and Wood (1986). Such fluids always carry some selectively dissolved rock-forming compounds like alkalis, silica, Ca, and trace metals but their loss in depth and gain at the higher levels is almost imperceptible and difficult to demonstrate analytically.

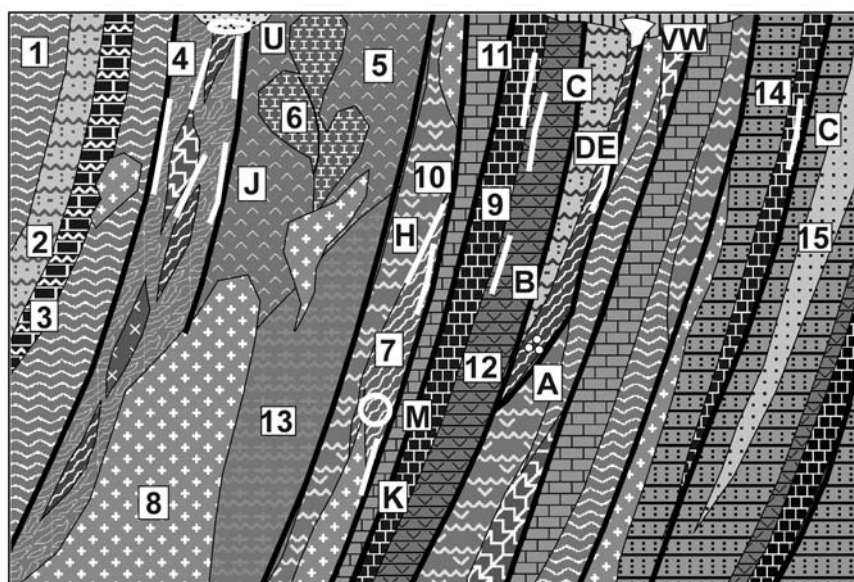
The outmigration of selected elements accelerates greatly during intracrustal melting that generates magmas (e.g. anatectic granite), and during metasomatic exchanges between the wallrocks and magmas introduced from outside. Channeling of the expelled fluids through faults and fractures greatly increases the possibility of selective accumulation of some substances to form mineral deposits. Structures: deformation, shear and high-strain zones are thus important and are the preferential sites of syn-metamorphic and later ore occurrence. The same structures, on the other hand, are also migration avenues by which substances from depth escaped into higher crustal levels causing selective impoverishment in depth, enrichment on top; Au and Cu provide the most striking examples. Some other metals, on the other hand (e.g. REE, Zr, Th, Nb) remained in depth as a residual trace elements enrichment, to reach the near-surface area by alternative routes: as a component of alkaline and carbonatitic magmas (melted in, or passing through, the enriched metamorphics), or as heavy mineral concentrates released and accumulated by supergene processes.

Varieties of metamorphic associations: Higher-grade metamorphics have formed in greater depth so they are exposed in deeply eroded crustal sections. Some occur in complexes as young as Tertiary (e.g. cores of collisional orogens, Cordilleran metamorphic core complexes, Crittenden et al (1980), Fig. 14.1; deeply eroded collisional sutures in accretionary margins and orogenic belts; Fig. 14.2), they are in minority in Paleozoic orogenic belts, abundant in Proterozoic terrains, and dominant in Archean cratons. There, the less metamorphosed supracrustals (greenstone belts) are minority erosional relics. Most high-grade metamorphics, other than the high pressure-low temperature ones (blueschist-eclogite), are Precambrian.



1. Post-tectonic clastics;
2. Pre-tectonic unmetamorphosed to slightly metamorphosed folded sediments and volcanics;
3. Pre-tectonic granitoids;
4. Mylonite band under décollement plane;
5. Mantling complex, moderately metamorphosed supracrustals;
6. Post-tectonic granites and syenites;
7. Core complex: granite gneiss, migmatite;
8. Amphibolite relics;
9. Granulite, eclogite relics; décol=décollement; G. Pb-Zn stratabound sulfides in mantling complex;

Figure 14.1. Cordilleran metamorphic core complex, rocks and ores inventory cross-section from Laznicka (2004), Total Metallogeny Site G230. Explanations (continued): K. Mn, Pb-Zn, Ag, barite, high-level veins in the upper plate; L. Pb,Zn,Ag veins in faults near granitoids; M. "Detachment-type" hydrothermal Au disseminations in breccia and phyllonite under décollement; fracture stockworks. Ore type G has the potential to contain "giant" members



1. Schist;
 2. Metaquartzite;
 3. Marble and Ca-Mg silicate gneiss;
 4. Melange-filled suture;
 5. Arc metavolcanics;
 6. Arc plutonic rocks;
 7. Alpine serpentinite;
 8. Syn- to post-collisional granites;
 9. Chert and black schist;
 10. Amphibolite;
 11. Limestone marble;
 12. Metabasalt;
 13. Migmatite to granite gneiss;
 14. Flysch turbidites;
 15. Shallow marine clastics.
- Relics of syndepositional ores: A. Podiform chromite; B. Cyprus- and Besshi-type VMS; C. Bedded Mn; D. Ni sulfides; E. PGE in ultramafics;

Figure 14.2. Deeply eroded collisional sutures, inventory of rocks and ores. From Laznicka (2004), Total Metallogeny Site G212. Explanations (continued): Syn- to Post-orogenic hydrothermal deposits. H. Cinnabar dissemination in faults; J. Mother Lode-type Au-quartz veins; K. Ni sulfide and arsenide veins in/near ultramafics; M. Chrysotile asbestos stockworks in alpine serpentinite. Mineralized regoliths (not shown): Au, alluvial placers; Ni (Fe,Mn,Co) laterite and saprolite on ultramafics; residual PGE in regolith. Ore types H, J, M, U have known "giant" members

This is even when the metamorphics are exposed in Phanerozoic orogens. There, many rocks are the product of young synorogenic metamorphism of much older rocks. The bulk of the higher-grade metamorphics are thus Precambrian (Goodwin, 1991) and this is an important consideration in metallogenesis.

Metamorphic petrogenesis and associations are extensively covered in the literature (Miyashiro, 1973; Turner, 1980; Suk, 1983; Bucher and Frey, 1994 and references therein). Laznicka (1985, Chapter 29 and 1993, Chapter 8) provided detailed inventory of metallic deposits hosted by the various metamorphic associations, but only 14 or 15 of the deposits listed there were of the "giant" magnitude. This comes as a surprise: high-grade metamorphics and associated deeply eroded granitoids, that represent some 40 to 60% of orogens and shields, contain only as many "giants" as alkaline complexes and carbonatites that make up less than 1% of terrestrial outcrop! The reasons are discussed below, but the practical consequence is that many metamorphic associations, dear to petrologists, are not even mentioned in the brief review below. A notable casualty is the blueschist-eclogite suite.

14.2. Metallogeny

One of the striking features of high-grade metamorphic metallogeny is the virtual absence of demonstrable or at least probable metamorphosed equivalents of the many common "giant"-making ore types like epithermal deposits; porphyry Cu, Au and Mo; disseminated, vein and replacement Sn; and other types. There are three possible reasons: 1) since most high-grade metamorphics are Precambrian, the "modern" ore types like epithermals and porphyries did not often form then; 2) the metamorphism destroyed and dissipated deposits formed at high crustal levels; and 3) the high level ores did form in the distant past, but were eroded away. Number 3 is the most convincing explanation as the ore type examples listed above all formed in erosion-prone settings that underwent uplift, and this follows quite convincingly from frequency of preserved ore types in geologic time. Most of the ore types that have survived high-grade metamorphism are those formed in subsiding basins such as banded iron formations, VMS's and sedex deposits (Spry et al, eds, 2000). Burial under a thick pile of younger sediments or volcanics facilitated their preservation. Not all orebodies in high-grade metamorphics, however, are metamorphosed earlier deposits. Belevtsev (1979) and Belevtsev et al (1985) distinguished three fundamental categories

of ores based on timing and origin: a) metamorphosed pre-existing deposits; b) metamorphogenic deposits formed during metamorphism; and c) ultrametamorphic deposits related to granitization.

Premetamorphic and predeformational ores: The ideal examples of metamorphosed ore deposits are banded stratiform bodies of relatively immobile metals like Fe, isochemically metamorphosed and little penetratively deformed and sheared. Banded iron formations form long, sheet-like or lens-like bodies where the original bedding is parallel with metamorphic foliation and the ore is in its original position in respect to the wallrocks. Economic orebodies often formed when the BIF thickness was doubled or tripled by folding or faulting. The ore has granoblastic texture and comprise both the original recrystallized minerals (quartz, hematite, magnetite), or minerals stable under the high-grade metamorphic conditions (e.g. Fe amphibole, Fe pyroxene), in place of Fe silicates (greenalite, chamosite). A special case of premetamorphic ores are the almost pristine layered magmatic ores (e.g. chromite, Ti-magnetite, platinoids with Fe-Ni-Cu sulfides) preserved in little internally deformed and metamorphosed rigid rock masses enveloped by high-grade metamorphics. The Stillwater complex is an outstanding example, described in Chapter 12. Other similar complexes have been, however, substantially deformed and metamorphosed to become an orthogneiss or orthogranulite merging with adjacent metamorphosed supracrustals (e.g. Fiskenaeset, Greenland).

On the other end of the spectrum of metamorphosed orebodies are those that suffered penetrative deformation and shearing, often during several phases. Banded iron formations can usually be recognized as such but sulfide deposits pose problems. The originally massive to semi-massive ores like VMS or sedex tend to be easier to interpret than vein or disseminated ores. Because of the much greater ductility of sulfides relative to their host rocks, massive sulphide lenses "invite" deformation and become the "dough" in shear- and high-strain zones. They are stretched, mylonitized, and develop the *Durchbewegung* ("kneading") textures like "ball ores" and "ductile breccias". The latter comprise variously attrition-rounded fragments of brittle wallrocks (typically siliceous gangue or pegmatite), stretched or disaggregated slivers of schist, rotated porphyroblasts like garnet, and metacrysts like pyrite and magnetite, in "paste" of the more ductile sulfides pyrrhotite, sphalerite and galena. When the physical deformation predates

metamorphic peak, the sulfides recrystallize and anneal, producing a fresh-looking mosaic of coarse crystalline sphalerite or galena with distinct tripple junction grain boundaries (e.g. at Broken Hill, NSW), sometimes with scattered porphyroblasts of garnet, biotite, staurolite or gahnite. Frequent metamorphic banding mimics syndepositional layering.

The shapes of orebodies are substantially modified and originally thick ore lenses or masses can be stretched into thin sheets conformable with schistosity, or dismembered. Features in the original footwall or hangingwall (e.g. stockworks under VMS) are transposed or lost altogether (compare Sundblad, 1980, on the Ankarvattnet Zn-Cu-Pb deposit in Sweden). Originally disseminated or stringer sulfide orebodies, still remaining so after deformation and metamorphism, are often bordered or intersected by sheets of (semi)massive "ball ore" or banded massive sulfide probably produced by syntectonic concentration of the dispersed sulfides into the most mobile structures in the system, and/or concentrated by removal of gangue minerals that increased the proportion of the sulfide residue (examples: Caraíba, Brazil and Thierry, Ontario, Cu deposits described in Laznicka, 1993).

Deposits like these are notoriously difficult to interpret. At the peak of the "stratiformity" models in the 1970s, all schistosity-conformable orebodies were automatically considered stratiform by most, although the deformational history of multiphase orebodies was often impossible to trace as far back as the F_0 (original bedding); e.g. Van der Heyden and Edgecombe (1990) for Broken Hill, NSW.

Syntectonic and synmetamorphic orebodies: Ores in this category formed by precipitation of ore minerals in a structure (typically a shear zone) shortly before, during or shortly after the metamorphic peak (synorogenic or orogenic deposits; e.g. Groves, 1993). Orebodies precipitated from newly introduced metals often overlap with remobilized earlier orebodies (pre-metamorphic ores) and this is most common in the Fe, Zn, Cu or Pb massive sulfide deposits. Deformed and metamorphosed VMS and sedex are virtually unrecognizable from mineralogically and texturally equivalent synorogenic replacements, the proportion of which has greatly increased in geologists' minds since the "age of stratiformity". The presence of unreplaced marble relics in the ore zone, Ca-Mg silicate host rocks, marble or Ca-Mg silicate horizons on strike with and in continuation of orebodies, Mn-rich haloes or gangues in Pb-Zn bodies, overlap of ore with syntectonic pegmatites

(that partly intersect the orebodies, partly form fragments in ore-cemented breccias, partly host ore stringers near sulfide masses), are some of the features suggestive of synorogenic replacement. Thompson-Ni, Vihanti Zn-Pb, Broken Hill NSW Pb-Zn-Ag, many deposits in the Bergslagen Province of Sweden, are likely candidates.

The (syn)orogenic formation of the shear-related (mostly mesothermal) gold deposits, as in greenstone belts (e.g. Groves et al., 1997) is at present the preferred model, with the formerly widespread pre-orogenic ore interpretations (like Au-exhalites) now in minority (e.g. Penczak and Mason, 1999, for the Campbell Red Lake ore zone, Ontario; Chapter 9). There are, however, only few small to medium-size gold deposits in the high-grade metamorphic assemblages.

The idea of metallic ore formation in direct response to granitization (migmatitization), as discussed by Belevtsev (1979), was locally popular in the 1960s and earlier (e.g. in Sweden, USSR), but almost forgotten since. This model has been resurrected at Challenger, a "near-large" gold deposit in the Gawler Craton of South Australia, by Tomkins and Mavrogenes (2002). There, invisible gold is dispersed in sparse sulfides (pyrrhotite, löllingite) and in bluish quartz, interpreted as a product of supply of a gold-rich quartz melt into migmatite leucosome, simultaneously with the barren silicate melt resulting from partial melting. The orebody comprises sixteen cigar-shaped flattened ore shoots in a 2.44 Ga synorogenic migmatite and the blue ore quartz overlaps with pegmatoidal mobilizate. The ore is extremely inconspicuous in the leached and oxidized shallow subcrop and was discovered by drilling a geochemical anomaly in calcrete.

Post-orogenic and post-peak metamorphic orebodies: These orebodies were emplaced at higher crustal levels following uplift and erosional unroofing of the high-grade metamorphic suites, to which they are no longer directly genetically related. The principal relationship is one of metal sources, and also structural control by old zones of weakness in the metamorphic basement. The old structures are often rejuvenated and some propagate into the youngest cover rocks. The metal source correlation between the younger, high-level and usually smaller orebodies and the larger high-grade metamorphic ore deposits is well developed in the Broken Hill, NSW, Pb-Zn-Ag ore field (Van der Heyden and Edgecombe, 1990). There, the principal orebodies had been prograde metamorphosed to granulite facies around 1.66 Ga, retrograde

metamorphosed under amphibolite facies conditions around 1.605 Ga, then again retrograded around 520 Ma at the greenschist facies level. Between 520 and 280 Ma were emplaced the postorogenic and postmetamorphic low-temperature quartz-siderite fissure veins of the Thackaringa-type.

The well-known calcite, native silver veins in **Kongsberg**, Norway (a "large" deposit of 1,400 t Ag produced; Ihlen and Vokes, 1978) formed by selective low-temperature hydrothermal silver extraction from Proterozoic Cu, Zn, Pb synorogenic sulfides in mineralized schist in shears and high-strain zones, and subsequent reprecipitation of native silver in calcite gangue as low-temperature veins in brittle faults and fissures. The process was driven by heat from intrusions (mostly diabase dikes) controlled by Permian rifting.

14.3. High-grade associations and ores

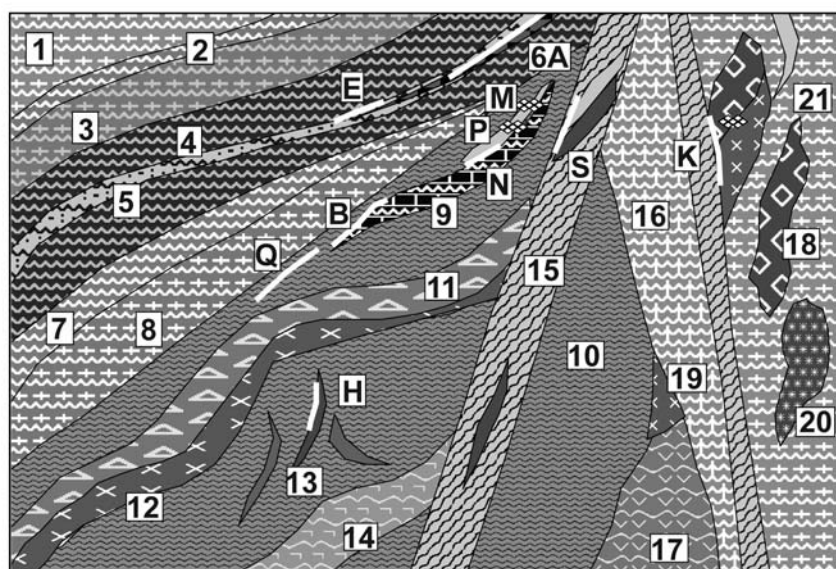
In this section are reviewed four "key" lithologic associations with the range of metamorphic grades between about upper-middle amphibolite and granulite. High pressure metamorphics (blueschist and eclogite) are not considered at all as they do not contain major metallic deposits. Although petrographic literature puts a great emphasis on metamorphic intensity and treats separately the granulite-grade rocks, this is considered impractical here as major orebodies, when they occur in granulitic rocks at all, are transitional into the amphibolite facies hosts; sometimes the host gneisses are retrograded granulites (e.g. in the Thompson Nickel belt). Because of the metamorphic homogenization that makes it often difficult to distinguish plutonic, volcanic and sedimentary rocks of similar bulk composition, terrain organization based strictly on the pre-metamorphic rock origin would be impractical for the initial field research (it comes later, through interpretation). Instead, four broad and overlapping groups, based on rock composition and style, are used here to provide framework for description of the "giant" deposits. They are: 1) Early Precambrian granite-gneiss and monotonous granulite terrains; 2) predominantly meta-sedimentary gneiss and schist terrains; 3) diverse (variegated) gneiss, Ca-Mg silicate, marble and quartzite terrains; 4) amphibolite (mafic-ultramafic) terrains; and 5) structures subjected to retrograde metamorphism and metasomatism.

1. Early Precambrian granite-gneiss and monotonous granulite terrains: Archean and many Paleoproterozoic terrains (Condie, 1981; Goodwin,

1991) are dominated by a "sea" (usually shown in pink on geologic maps) of quartzofeldspathic migmatite gradational to predominantly sodic granitoids on one side, and (hornblende) biotite gneiss on the other. These granite-gneiss terrains, considered as base of the upper continental crust (Fountain and Christensen, 1989), contain erosional relics of less intensely metamorphosed meta-volcanics (greenstones; Chapter 9) and meta-sedimentary schists. They incorporate (or rest on in terms of the original stratigraphy) old sialic nuclei and "basement complexes" (Kröner, 1984) dominated by "gray gneiss" (meta-tonalite) and sodic granitoids of an earlier generation, and relics of the more refractory rocks like metabasites and rare carbonates. Granulites, considered samples of the lower continental crust, occur in blocks believed tectonically transported from great depth (e.g. the Kapuskasing terrane, Ontario), or members of the "super-metamorphosed", Grenville-type collisional belts (Goodwin, 1991); Fig. 14.3.

These terrains as a whole are about the least mineralized settings imaginable, avoided by explorationists. Ore occurrences and several "giant" deposits occur in relics of supracrustals (e.g. greenstones) that are sometimes too small to show on a large-scale map and/or are masked by a thick tropical regolith (e.g. the Saddleback greenstone belt in Western Australia that hosts the "giant" Boddington gold deposit; Chapter 9). Orebodies also occur in mafic-ultramafic intrusions, also often too small to show or indistinct. Finally, ores may be controlled by a variety of superimposed faults, grabens, anorogenic intrusions, diatremes and platformic covers. Tropical regoliths on gneiss or granulite sometimes support lateritic bauxite deposits (e.g. Eastern Ghats, India).

2. Predominantly meta-sedimentary monotonous gneiss-schist terrains: These are more evolved components of the upper continental crust, dominated by biotite schist to gneiss to migmatite. The metamorphics grade into synorogenic peraluminous (anatectic) granites that are more potassic than their older end deeper counterparts. The old monotonous gneiss-schist outcrops are equivalent to greenstone belts and occur as supracrustal relics in the early Precambrian granite-gneiss terrains. They are also widespread in younger Proterozoic and Phanerozoic orogenic belts, especially in the higher-grade Precambrian metamorphic core massifs and belts.



1. Granite gneiss, migmatite; 2. Graphitic gneiss; 3. Garnet orthogneiss; 4. Garnet-sillimanite gneiss; 5. Metaquartzite; 6. Metamorphosed BIF; 7. Cordierite, sillimanite, garnet gneiss; 8. Augen orthogneiss; 9. Ca-Mg silicate gneiss; 10. Leptynitic granulite; 11. Gneissic anorthosite; 12. Gneissic norite; 13. Synorogenic anorthosite, hypersthene; 15. Mylonite-filled shear; 16. Retrograded granulite; 18. Relics of hypersthene; 19. Relics of gabbroids; 20. Relics of ultramafics; 21. Pegmatites of "great depths";

Figure 14.3. High-grade granulite-migmatite metamorphic complex, with relics of the more refractory rocks and with tectonites. Rocks and ores inventory cross-section from Laznicka (2004), Total Metallogeny Site G55. Explanations (continued): A. Hypersthene, magnetite, quartz BIF; B. Stratabound Mn "kodurite"; E. Broken Hill-type Pb,Zn,Ag; H. Cu in deep syntectonic gabbro, hypersthene (Okiep); K. Cu in hypersthene relics in migmatite and shears (Carafba); M. Monazite in deep level pegmatite; N. Disseminated Th minerals; P. Chrysoberyl pegmatite; Q. REE in allanite bands in pegmatite; S. Au-sulfide ores in retrograde shears. Residual deposits are not shown. Ore types E, H and K have "giant" and "near-giant" members

In the Czech Massif, one of the old blocks in the Variscan orogen of Europe, the Moldanubian metamorphics are informally divided into the "monotonous" and "diverse" (Bunte) associations (Suk, 1983). Monotonous gneiss-schist belts are usually interpreted as predominantly meta-turbidites, with which they share the paucity of mineralization. About the most interesting ore occurrences are related to pegmatites produced by intracrustal melting in the katazone, but crystallized from a melt that rose into the mesozone. Important Sn, Ta, Be, Li, Cs deposits are associated with the "rare metals" pegmatites (Chapter 10). Major deposits of Pb-Zn, Cu, U and other metals "in gneiss" are more likely related to the petrographically identical gneiss that is a member of the "diverse" suite, described below.

3. Diverse (variegated) gneiss, Ca-Mg silicate, marble, quartzite terrains: Rare Ca-Mg silicate, marble and quartzite suites appear already in Archean terrains, where they are associated with amphibolite (meta-basalt). There, they are usually interpreted as "exhalites" or metamorphosed hydrothermally altered rocks. Some are probably members of the late Archean pre-greenstone,

ripping-related suites, the equivalents of which dominate the Proterozoic intracratonic terrains (Chapter 11); the latter appear even in the granulite-metamorphosed settings (e.g. in the Highland Series of Sri Lanka; Katz, 1971). The diverse suite is most common in the old blocks and metamorphic cores of Phanerozoic orogens (e.g. the "Bunte" suite in the Czech Massif Moldanubicum; Suk, 1983); Fig. 14.4.

In all the above settings usually thin units of the diverse lithologies alternate with biotite-sillimanite paragneiss. In steeply dipping rock packages the diverse rocks have a form of ribbons, often boudinaged or dismembered. Paraamphibolite is here considered a variant of the Ca-Mg silicate rocks, whereas orthoamphibolite (metabasalt, metadiabase, metagabbro) can also occur, although the orthoamphibolite-dominated sequences are treated separately below. The rapidly alternating lithologies are usually interpreted as intracratonic graben and rift sequences. The more persistent and thick successions are considered "miogeoclinal" to platformic, although much of their counterparts remain unmetamorphosed or slightly metamorphosed (Chapter 11).

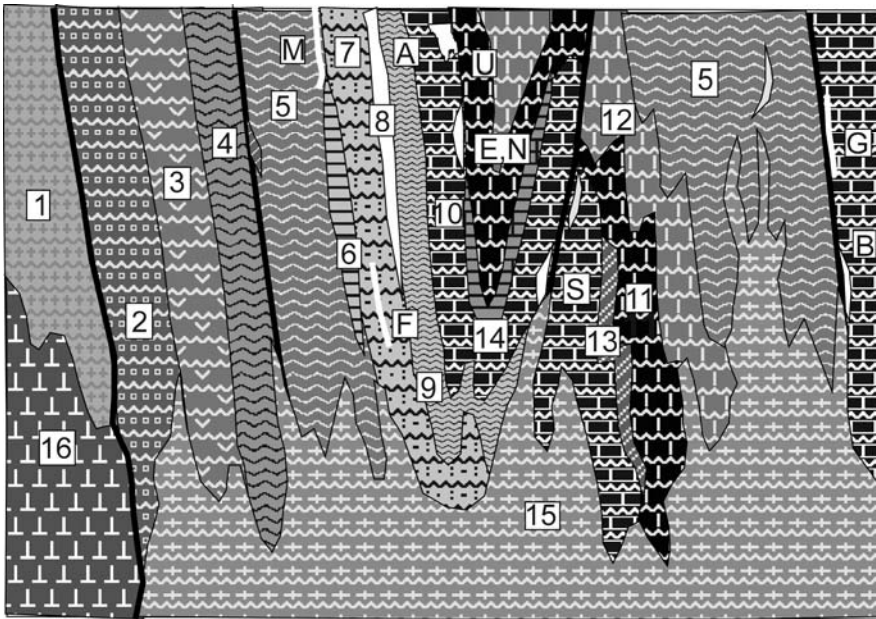


Figure 14.4. High-grade variegated metasedimentary association, rocks and ores inventory cross-section from Laznicka (2004), Total Metallogeny Site G164. Explanations (continued): ORES: A. BIF-Fe; B. Magnetite skarn; E. Mn-Zn oxides and silicates in marble; F. REE, Zr, Y, Th, Ta, Nb metasomatites in sheared gneiss (Katugin); G. Crystalline magnesite; M. Broken Hill-type Pb,Zn,Ag sulfides in aluminous gneiss and metaquartzite; N Ditto, in marble (Balmat); S. Scheelite in deep-seated skarn; U. Uraniferous phosphates in regolithic marble (Itaia). Ore types E, F, M, N and U have known "giant" and "near-giant" members

They are intruded by a variety of granitoids and gabbroids of which the early (pre- and syn-orogenic) varieties are also metamorphosed. Particularly interesting are metamorphosed alkaline magmatites and carbonatites.

Diverse sequences are the most prospective and most consistently mineralized settings among the high-grade metamorphics and they host Pb-Zn-Ag, U, some Cu, some Fe "giants" and "large" deposits.

14.4. High-grade metamorphosed banded iron formations (BIF)

Less metamorphosed BIF are usually subdivided into those in sedimentary (Superior-type) and volcanic-sedimentary (Algoma-type) host associations (Chapters 9 and 11). As there are few high-grade metamorphosed Fe "world class deposits" and as the pre-metamorphic affiliation is sometimes unclear, both varieties are considered jointly here.

In the **Labrador Iron Province** of eastern Canada (Gross and Zajac, 1983) the Paleoproterozoic (~2.15-1.85 Ga) Sokoman Iron Formation is exposed in a 950 km long, 100 km wide NNW-trending belt. Although the entire belt is

estimated to store some 10^{13} t Fe, only a fraction of this is economic to mine mainly from zones of paleo-enrichment, attributed to heated groundwaters, that survived Quaternary glacier erosion. There are presently five economically viable ore fields notable for the gradual increase of metamorphic grade from virtually zero in the north (Klein and Fink, 1976) to granulite facies in the extreme south. The southern portion of the iron province, mined in the **Wabush Lake** (Newfoundland; 4.14 bt Fe @ 30+ % Fe) and **Mount Wright** (Québec; 320 mt Fe @ 32%) iron fields, was overprinted by the 1.2 to 0.8 Ga Grenville collisional orogeny. This changed the structural grain from NNW to NE and deformed, recrystallized and metamorphosed the ores. The little metamorphosed BIF in the north comprise a spectrum of facies from oxide (hematite, magnetite) through silicate (stilpnomelane, minnesotaite) to carbonate (ankerite, siderite, dolomite), all of which show supergene enrichment in the Knob Lake district (Gross, 1968). The metamorphosed equivalents in the Grenville Province have quartz-hematite (specularite) and quartz, grünerite, actinolite, dolomite, magnetite members intercalated with marble and amphibolite (meta-

diabase), floored by garnet-kyanite schist (metamorphic equivalent of the ferruginous black shale in the north) and meta-quartzite. The principal ore mined at Wabush is a soft, friable, coarse specularite (or hematite microplate) schist, corresponding to the oxide BIF softened by supergenesis. Farther south-west, into the centre of the Grenville orogen, metamorphic intensity reaches the granulite grade. Granular quartz and hematite remain but the Fe silicates are represented by grünerite, cummingtonite, hypersthene and fayalite. The BIF is dismembered into relics that gradually lose identity and disappear.

"World class" ("large") amphibolite to granulite-metamorphosed BIF with cummingtonite and hypersthene, in the Aldan Shield of Siberia, lack supergene enrichment so they are uneconomic at present (this is in addition to the remote location). The Anshan BIF in Liaoning, NE China, is partially enriched. The 3.4-2.7 Ga BIF in the Imataca Complex near Ciudad Bolívar, in tropical SE Venezuela (Putzer, 1976; ~2.2 bt Fe @ ~55+ %), forms discontinuous relics in granite gneiss, converted into a direct shipping enriched hematite.

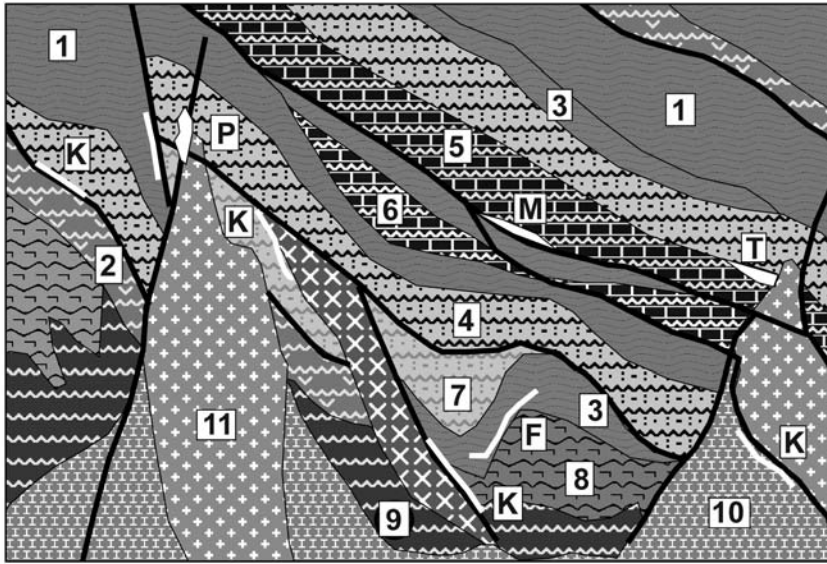
Additional "world class" high-grade metamorphosed BIF (a selection):

- Anshan, Liaoning, NE China * 3 bt Fe @ 32% * amphibolite-grade Qtz, mag, hem, amf BIF intruded by granitoids * Zitzmann, ed. (1977).
- Ciudad Bolívar, SE Venezuela * Imataca Complex * 3 bt Fe @ 55% * enriched BIF in 3.2 Ga "itabirite" * Putzer (1976), Channer et al (2005).
- Chara-Tokkin zone, central Siberia * western Aldan Shield * 3.5 Bt Fe @ 30% * non-enriched Qtz, mag, amf, opx BIF * 3.1 Ga gneiss, amphibolite, granulite, charnockite * Zitzmann, ed. (1977).
- Subgan Fe complex, central Siberia * western Aldan Shield * 1.8 bt Fe @ 35% * non-enriched Qtz, mag, amf, thin 40 km long BIF band * interbedded with Ar amphibolite * Zitzmann, ed. (1977).
- Okolovo Graben Fe zone near Minsk, Byelorussia * 1.23 bt Fe @ 30.7% * BIF buried under PZ platformic sedimentary cover * interbedded with Pp amphibolite * Zitzmann, ed. (1977).
- Simandou Fe belt, Guinea * 2.8 bt Fe @ 40% * enriched Qtz, mag, hem BIF bands and lenses * 2.95-2.75 Ga amphibolite, metaquartzite, gneiss * Wright et al. (1985).
- Nimba Fe area, NE Liberia & S Guinea * 1.2 bt @ 60% Fe * enriched 250-400 m thick Qtz, hem, (mag) BIF * Ar gneiss, amphibolite intruded by granitoids * Wright et al. (1985).

14.5. Pb-Zn-Ag sulfide orebodies in gneiss >>marble, Ca-Mg-Mn silicates: (Broken Hill-type)

Broken Hill, NSW, is so far the richest continuous Pb-Zn-Ag ore zone discovered and the type locality of the economically important Broken Hill-ore type. There are five or six "giants" of this type, some of which are multiple: that is, contain more than one metal accumulation of the "giant" magnitude (Broken Hill is a Pb "super-giant" and Zn,Ag,As,Sb and Cd "giant"; Aggeneys and Cannington are Pb & Ag "giants"). The exceptional deposits of this type, as well as several hundred of much smaller occurrences, share the principal characteristics of this type: 1) hosting by a range of high-grade metamorphics ranging from biotite or sillimanite paragneiss (rarely granulite) to schist, meta-quartzite, Ca-Mg or Mn silicate and marble; 2) conformity with the structural grain and in most cases lithology as well; 3) pre- to synmetamorphic origin; and 4) simple mineralogy dominated by galena and sphalerite with lesser pyrrhotite and pyrite. Cu sulfides and magnetite, when present in an ore field, usually form separate orebodies. The ores range from rich, coarse crystalline massive sulfides (Broken Hill, NSW) to disseminated ores in meta-quartzite (Aggeneys), and from those in entirely silicate rocks to those completely in marble (Balmat). Most ores are in meta-clastics with minor Ca-Mg-(Mn) silicates (Fig. 14.5). The Broken Hill ore, for example, has rhodonite and bustamite gangue. More complete list of characteristics has been assembled by Parr and Plimer (1993).

The "typical" Broken Hill-type representatives, mentally stripped of the metamorphic and deformational overprint, come closest to the "sedex" type (Chapters 11, 13), with pre-metamorphic lithologies corresponding to those seen at Red Dog, Rammelsberg or Howard's Pass. This assumes pre-metamorphic, synsedimentary (exhalitic) or hydrothermal-diagenetic origin, followed by high-grade metamorphism responsible for recrystallization of the common sulfides and variable remobilization. Metamorphic silicates (e.g. Ba-feldspars) and oxides (gahnite) also formed. Structural analyses of orebodies are often inconclusive and leave open the possibility that some Broken Hill-type deposits are syn- or early post-metamorphic replacements of carbonates, along shears. An important controversy results from the presence of meta-volcanics.



- 1. Schist, paragneiss;
- 2. Amphibolite; 3. Graphitic schist; 4. Metaquartzite; 5. Ca-Mg silicate gneiss; 6. Marble; 7. Arkosic gneiss; 8. Meta-rhyolite; 9. Migmatite; 10. Syn- to post-orogenic granodiorite, monzonite; 11. Ditto, granite;
- F. Stratabound Pb,Zn,Ag sulfide lenses in schist, gneiss; K. Syntectonic Cu (Co,Au) lodes in faults and shears; M. Stratabound Zn,Pb replacements in marble and Ca-Mg silicates; P. Fe oxides, Cu,U,Au; T. U,REE in allanite exoskarn

Figure 14.5. High-grade metamorphic equivalent of complex intracratonic orogenic sequences as in the Mount Isa Inlier, Eastern Succession (Queensland). Rocks and ores inventory diagram from Laznicka (2004), Total Metallogeny Site G227. Ore types F, K, M and P have known "giant" members

They are variably attributed to either the intracontinental rift or intra-arc (back-arc) setting. All the Pb-Zn-Ag "giants" are Proterozoic and two (Broken Hill and Cannington) are in the central Australian orogenic system that also includes the greenschist metamorphosed Mount Isa and almost unmetamorphosed McArthur River Pb-Zn-Ag and Century deposits (Chapter 11). The latter are often considered in the same league with Broken Hill (compare Solomon and Groves, 1994). Broken Hill, the outstanding example deposit, is described in some detail below.

Broken Hill, NSW, Pb-Zn-Ag (Johnson and Klingner, 1976; Parr and Plimer, 1997; reviews in Laznicka, 1993 and Solomon & Groves, 1994, and references therein; Cartwright, 1999). The Broken Hill gossan was discovered in 1883, in the arid lands near the western border of New South Wales, 930 km WNW of Sydney. Mining started shortly afterwards and continued ever since. Since 1889 the ore or concentrate have been smelted in, and the products shipped from, Port Pirie in South Australia, in what is the world's largest lead smelter. The published production and reserve figures vary widely but some 180 mt of high-grade ore has been produced (average grades ~11.3% Pb, 9.3% Zn, 175 g/t Ag). Haydon & McConachy (1987) mentioned an additional resource of at least 150 mt of "lower grade ore", above a cutoff of 10% Pb+Zn! There is a number of associated metals in the ore, some of

which were recovered in the smelter, others lost (Table 14.1).

Table 14.1. Summary of ore metals contents in the Broken Hill deposit

metal	minim. P+Rv x 1,000 tons	maximum P+Rv+Rc (calcul.)	range of grades
Pb	20,340	28,000	2-25% (aver. 11.3%)
Zn	24,000	31,000	2-25% (av. 9.8%)
Cu	300	450	0.1-0.2%
Ag	24	43	50-600 ppm
As	60	120	210-4000 ppm
Sb	25	57	67-420 ppm
Cd	80	120	500-800 ppm
Bi	2.2	3.5	2-48 ppm
Hg	1.02	1.6	2-5 ppm
Mn	6,000	8,000	~2.7%

Broken Hill is situated in the Curnamona Province, in the Willyama Inlier and Supergroup (Stevens, ed., 1980; Stevens et al., 1990). This is a Paleo- and Mesoproterozoic assemblage of supracrustals dated at about 1.69 Ga, mobilizates and intrusions. These have been deformed and metamorphosed under

peak granulite ("two-pyroxene") conditions around 1.6 and 1.59 Ga, followed shortly by regional retrogradation attributed to residual melts, then by several phases of shearing terminating around 460 Ma. The Willyama Supergroup is subdivided into the lower Thackaringa Group, middle Broken Hill Group and upper Sundown and Paragon Groups. Metapelitic biotite-sillimanite gneiss is the most consistent lithology throughout, the rest being various quartzofeldspathic gneisses, minor amphibolite, Ca-Mg silicate rocks, metaquartzite and magnetite quartzite. The genetic and paleoenvironmental interpretations of the quartz-feldspar lithologies are in flux (read the brief review in Cartwright, 1999). There is a general consensus that the rock progenitors include a significant proportion of volcanics, volcanoclastics and subvolcanics of bimodal and rhyodacitic composition, as well as deformed intrusions interspersed with anatectic leucogranite, affected by extensive metasomatism (e.g. albitization).

Broken Hill Complex, an informal suite of rocks that contains the main orebody and more than 60 small Pb-Zn-Ag and Cu, W, Au, U-Th, Ni-Co occurrences, crops out in a NE-trending arcuate structure about 24 km long and 3-4 km wide. This encloses package of rocks designated in traditional literature as the "Mine Sequence" (Johnson and Klingner, 1976). The latter is 2 km wide and explored to a depth of 2,000 m. Within it is the Lode Horizon ranging in width from 1 to 200 m and traceable for at least 18 km. This is a discontinuously mineralized zone of quartz-rich sillimanite gneiss, Mn-garnet quartzite with locally developed "blue quartz" lode with scattered gahnite, and irregular patches of pegmatite or pegmatitized supracrustals. Locally associated Potosi Gneiss is a porphyroblastic, low-Al, high Ca, Fe quartz, feldspar, garnet, biotite gneiss locally accompanied by a BIF. The BIF ranges from a few centimeters to 2 m in thickness, is often delicately laminated, and composed of quartz with garnet, magnetite, apatite, accessory rutile, gahnite and traces of Pb-Zn sulfides. The BIF is known from up to eight horizons, two of which are considered stratigraphic equivalents of the Pb-Zn orebodies (Johnson and Klingner, 1976).

Broken Hill Lode (Fig. 14.6) is the main massive Pb-Zn-Ag sulfide deposit. It is a continuous, NE-trending, 7,300 m long, up to 250 m wide and 850 m deep, vertical to steeply NW dipping arcuate zone of seven vertically stacked orebodies. In the central and NE portions only the No.2 and No.3 lenses are developed. The Lode plunges 15° to 60° at both ends and in a typical

cross-section it is a large drag fold. The Lode is believed to be in the overturned limb of a regional D₁ nappe fold, refolded by D₂ into tight folds with steep axial planes (Marjoribanks et al., 1980). The Lode is enclosed in the Hores Gneiss, a controversial quartz and spessartine-rich unit, considered by some as a felsic meta-volcanic, by others as a nonvolcanic arkose (Cartwright, 1999).

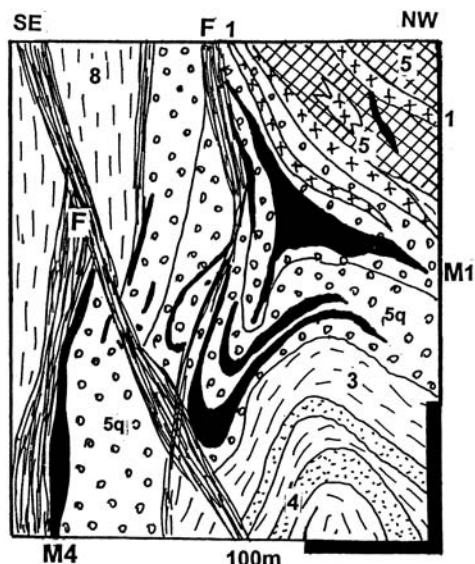


Fig. 14. 6. Broken Hill, NSW, Southern A Lode and Southern #1 Lens. Cross-section from LITHOTHEQUE No. 2854 modified after Mackenzie and Davies (1990). 1. Pp-Mp pegmatite. Pp Broken Hill Group: 3. Biotite-sillimanite gneiss; 4. Potosi Gneiss and garnet gneiss with the Broken Hill Lode; 5. Broken Hill Lode: 5b, "Banded iron formation", 5q, Garnet quartzite; 5c, Ca,Mg,Mn,Fe silicate lenses; 8. Thackaringa Group gneiss; F. Ductile shears; M1. Main Orebody of coarsely crystalline, annealed galena, sphalerite, pyrrhotite in quartz, calcite, rhodonite, bustamite, garnet gangue; M4. Sheared and retrogradely remobilized ore

The typical Lode material is a medium- to coarse-crystalline granoblastic aggregate of galena and dark brown to black sphalerite (10% Fe plus), pyrrhotite, lesser and local chalcocopyrite, arsenopyrite, tetrahedrite, löllingite and rare minerals like dyscrasite. The principal gangue minerals are quartz, calcite, Ca-Mn-Fe silicates (rhodonite, bustamite, Mn-hedenbergite, Mn or Fe garnets) with local fluorite, apatite, wollastonite, gahnite and roepperite. The grade, metals ratios and mineralogy vary slightly among the orebodies. The "classical" high-grade ore, as in the 1987 reserve of 53.8 mt in the Zinc Corporation mines, ran 8% Pb,

13% Zn and 70 g/t Ag @ 10% Zn+Pb cutoff (Mackenzie and Davies, 1990).

After the metamorphic peak the ores and their host rocks were remobilized along retrograde shears. The NE-trending Globe-Vauxhall Shear is oblique to the Broken Hill Lode and it contains several discontinuous, low-grade Pb-Zn sulfide bodies with gahnite. The north-trending De Bavay and British, and the NE-trending Main, Thompson and other shears, intersect the Lode. They are usually filled by mylonite or by sericite-chlorite phyllonite that enclose pods of unsheared ore and the host rocks, and by a variety of deformed (Durchbewegung) and subsequently recrystallized ore varieties like inclusion ore, steely galena, and remobilized veins (Lawrence, 1973). Pegmatitic patches with a light-green (Pb-rich) microcline, minor gahnite, and Pb-Zn sulfide stringers are also present.

The Broken Hill Lode has had an up to 200 m deep oxidation zone (Andrew et al., 1922; Van der Heyden and Edgcombe, 1990). At the surface, the Lode has been converted into a massive to cellular quartz with relics of garnet and some gahnite. There are abundant void fillings and coatings of goethite, Mn-oxides, coronadite, plumbojarosite and pyromorphite. Silver is enriched near the base of the oxidation zone, in the depth of 50 to 150 m, where the main Ag carrier is Br-chlorargyrite associated with coronadite, kaolinite and goethite. An irregular zone of cerussite mineralization with some malachite, azurite, smithsonite, anglesite and other minerals is between the silver zone and the hypogene sulfides. Secondary sulfides are not well developed.

The Broken Hill orebodies are interpreted by the majority of researchers as pre-metamorphic but locally remobilized after the metamorphic peak. Almost all genetic models available have been utilized by various workers, in the past 50 years, to explain the original ore formation (read the brief review in Cartwright, 1999). A minority opinion favors late syn-metamorphic origin of the Lode; the abundant carbonate gangue, some textures, skarn-like host assemblage, make selective hydrothermal replacement a tempting alternative.

The Pb-Zn-Ag deposits in the Bushmanland region of South Africa (Aggeneys; Fig. 14.7; and Gamsberg; Fig. 14.8) are the closest match of Broken Hill in terms of lithology, but the grade is lower; often much lower than what was the cutoff grade at Broken Hill!. These, and additional Pb-Zn-Ag deposits of the Broken Hill-type are briefly

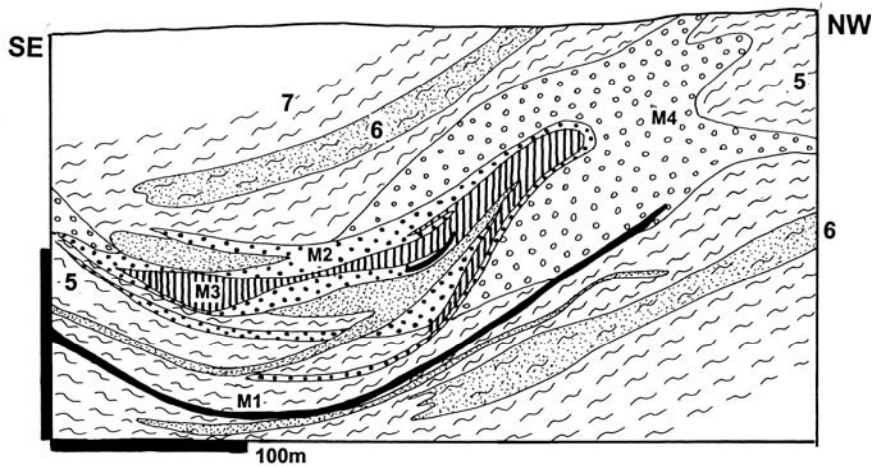
characterized below (read also a more detailed summary in Laznicka, 1993).

14.6. Zn,Pb sulfide bodies in marble and Ca-Mg silicates, and Zn-Mn oxide orebodies in marble

Balmat-Edwards district, NW New York: Zn-Pb sulfides in marble. This district, that contains the "large" Balmat deposit (deLorraine and Dill, 1982; 41 mt @ 9.4% Zn for 3.9 mt Zn, ~250 kt Pb; Fig. 14.9), is the principal representative of the "Broken Hill-type" in carbonates. It is located in the Adirondacks of NW New York State, in the polygenetic and high-grade metamorphosed Grenville province of the Canadian Shield. The NE-trending Mesoproterozoic host assemblage contains a 600 m thick band of interbedded dolomitic and lesser calcitic marble, various Ca-Mg silicate assemblages, lavender-colored crystalline meta-anhydrite and biotite-sillimanite gneiss to schist. Long and thin, intricately folded, tabular to lenticular or pod-like orebodies are generally conformable with lithology, but in detail they are controlled by structures that result from intersections of two generations of folds. The ore consists of massive to disseminated, medium to coarse-crystalline brown sphalerite, pyrite, lesser galena, pyrrhotite and minor chalcocopyrite in gangue of quartz, carbonate, diopside, tremolite, talc and locally anhydrite. Breccias of wallrock fragments embedded in ductile "paste" of sulfides are common. The same ore minerals also fill fractures in brittle rocks like clinopyroxenite.

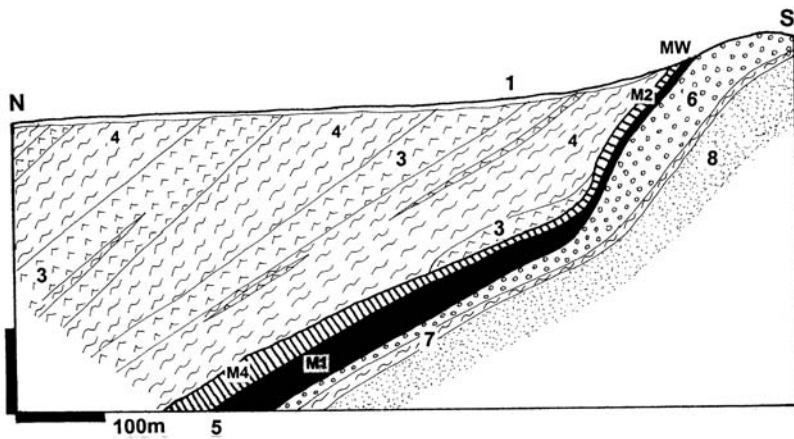
Balmat, and the smaller Edwards deposit, are interpreted as pre-metamorphic ("Irish-type"), but the primary sedimentary structures have been completely obliterated by at least four phases of ductile deformation and metamorphism. The ore has also suffered from plastic flowage, so the present position of the orebodies, dated between 1,115 and 1,005 Ma, need not correspond to their original position. There is some 100 kt of oxidized material (hemimorphite, smithsonite, cerussite) in relics left behind after Quaternary glacial erosion.

Åmmeberg (Zinkgruvan; Hedström et al., 1989; P+Rv ~40 mt containing ~1.8 mt Zn and 450 kt Pb; Fig. 14.10) is in the southernmost part of Bergslagen, 50 km south of Örebro, Sweden. It is an old mine intermittently exploited since the Middle Ages, still surviving. Åmmeberg is enclosed in rocks of the "gray leptite group" interpreted as a K-rich meta-tuffite.



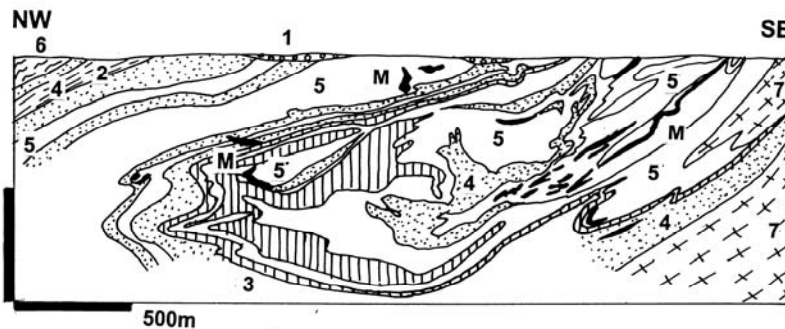
Stratabound Pb,Zn ore-bodies in Pp "Ore Schist" (Unit 5), Aggeney's Sub-group: M1. Disseminated to banded, massive sulfides in quartzite of "BIF"; M2. Ditto, sulfides in Ca-Mg silicate band; M3. Quartz-magnetite quartzite, low sulfides; M4. Garnet quartzite, sparsely scattered sulfides. 6. Metaquartzite; 7. Aluminous schist; 8. Pink quartz-feldspar gneiss

Figure 14.7. Aggeney's ore field, Black Mountain Pb-Zn deposit, Bushmanland, South Africa. Cross-section from LITHOTHEQUE No. 1933, modified from Ryan (1986)



1. Q desert cover sediments; 2.0-1.8 Ga Bushmanland Group; 3. Amphibolite; 4. Quartz-muscovite schist; 5. Gams Member sillimanite-quartz schist with three cyclic members of chemical metasediment hosting ore-bodies: MW. Gossan; M1. Main Zn layer; M4. Mn-Fe silicates-rich hangingwall; 6. "Dark Quartzite"; 7. Sillimanite schist; 8. "White Quartzite".

Fig. 14. 8. Gamsberg Zn and barite deposit, Bushmanland, South Africa. Cross-section from LITHOTHEQUE No. 1934.1. modified after Rozendaal (1986)



1. Remnants of Cm1 Potsdam Sandstone; 2-7. Mp Gouverneur Marble Fm. M. Tabular, lenticular, deformed and high-grade metamorphosed Zn,Pb sulfide replacements in marble and Ca-Mg silicates; 2. Pyritic schist; 3. Anhydrite units; 4. Dolomitic marble; 5. Ca-Mg silicate gneiss;

Figure 14.9. Balmat Zn-Pb ore field, New York, cross-section from LITHOTHEQUE No. 1841 modified after St. Joe Zinc Ltd. Staff, deLorraine and Dill (1982). Explanations (continued): 6. Mp Piseco Group biotite, sillimanite, garnet gneiss; 7. Ditto, granitic gneiss

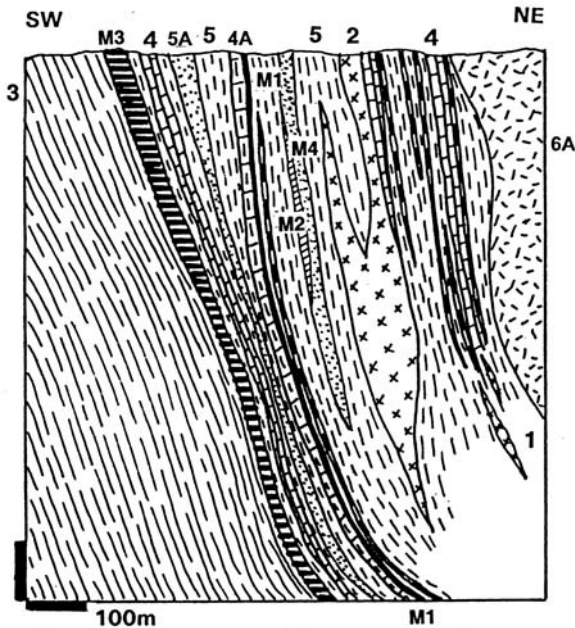


Fig. 14. 10. Åmmeberg ore field, Bergslagen, southern Sweden, Nygruvan Mine cross-section from LITHOTHEQUE No.586, modified after Hedström et al. (1989)

This is intermixed with chemical sediments, a portion of which are hydrothermally altered lithologies. The schistosity and bedding-conformable, up to 5 km long but thin (5-25 m) mineralized horizon is in a S-shaped, E-W trending and steeply north-dipping fold. It has a pink high-K orthogneiss at base, interpreted as a syndepositional hydrothermal quartz-microcline alterite. Above is the "gray leptite", interpreted as a sea-floor volcanoclastic, now garnet-biotite schist to gneiss interlayered with marble, Ca-Mg silicate rock and meta-quartzite, veined by pegmatite. At the top is the "gray gneiss group" of biotite to sillimanite gneiss, migmatite.

The ore comprises coarse crystalline massive sphalerite, galena and pyrrhotite sheets and lenses that follow the Ca-Mg silicate horizon which, in turn, has some disseminated sulfides in the footwall and relics of marble in the hangingwall. A horizon of disseminated pyrrhotite occurs above the Zn-Pb zone and, in one place, the main Zn-Pb orebody is underlaid by disseminated and stockwork chalcocopyrite in silicate marble. This is interpreted as the footwall stockwork and feeder zone of the mineralizing fluid (Hedström et al., 1989). The massive ore is texturally interchangeable with marble and replacement fabrics are widespread. Disseminated ore is locally in the hangingwall. Gahnite is quite common and there are frequent

Pp Svecofennian rocks:

1. Granite, pegmatite, aplite
2. Metadiabase (amphibolite)
3. Biotite paragneiss to migmatite
4. Calcitic and dolomitic marble
- 4A. Ca-Mg silicate gneiss to "skarn"
5. "Gray Leptite", quartzofeldspathic gneiss, ore host
- 5A. Silicified metavolcanics
- 6A. "Red Leptite"

ORES:

- M1. Stratabound band of Zn, Pb, Fe sulfides
- M2. disseminated and stringer sulfides
- M3. Stratabound zone of stringer chalcocopyrite and pyrrhotite in metaquartzite
- M4. Magnetite in silicate marble

lenses of pegmatite which, when it intersect the orebody, turns into the green Pb-rich microcline (amazonite) with stringers of galena and sphalerite. Ammeberg is close to the Broken Hill-type (Parr and Plimer, 1993).

Additional "giant" and "near-giant" Broken Hill-type Pb-Zn deposits:

- **Aggeneys ore field**, Bushmanland, South Africa * 3 major deposits, cumulative 267 mt containing 5.8 mt Pb, 3.8 mt Zn, 835 kt Cu, 7,254 t Ag. Richest Broken Hill orebody Rv 85 mt @ 3.57% Pb, 1.77% Zn, 0.34% Cu, 48.1 g/t Ag * Broken Hill style, stratabound lenses, sheets of disseminated to massive gal, sfa, pht > cpy in metaquartzite and BIF hosts * 2.07-1.8 Ga gneiss with remnants of aluminous gneiss, metaquartzite, BIF, amphibolite * Ryan et al. (1986), Fig. 14.7.
- **Gamsberg deposit**, Bushmanland, South Africa * Rc 150 mt @ 7.1% Zn, 0.55% Pb, 0.15% Cu, 5 g/t Ag for 10.65 mt Zn, 825 kt Pb * stratiform layer up to 50 m thick of disseminated to massive sfa > pyr, gal, cpy in qtz, slm, grn, gru in "BIF" band grading to qtz-hem and bar; HW enriched in Fe and Mn (some Mn-silicates); gossanous outcrop * Pp amphibolite to granulite metamorphosed banded chemical sedimentary unit enclosed in bio, slm, grn gneiss * Rozendaal (1986); Figure 14.8.
- **Rampura-Agucha deposit**, Bhilwara dist., Rajasthan, W India * Rv 61.1 mt @ 13.48% Zn,

1.57% Pb, 45 g/t Ag for 8.25 mt Zn, 960 kt Pb, 2,750 t Ag * scattered to massive, Durchbewegte sfa > gal, pyr, pht in mylonitic and phyllonitic gneiss along a steeply dipping NE shear; gossanous outcrop * 1.8 Ga graphitic bio-slm-grn gneiss to migmatite with amphibolite and Ca-Mg silicate patches * Gandhi et al. (1984).

- **Kholodnina ore zone**, central Siberia, Russia * Baiklides * 11 mt Zn + Pb, Ag * string of lenticular massive to disseminated pyr, sfa > gal, cpy, pht bodies in 30-80m thick horizon of graphitic schist (phyllonite?) and marble * Np bio, mus, grn schist to gneiss, interbeds of metaquartzite and marble * Konkin et al. (1993).
- **Cannington**, NW Queensland, Australia * Mount Isa Inlier East * Rv 44 Mt @ 11.6% Pb, 4.4% Zn, 538 g/t Ag for 5.081 mt Pb, 1.927 mt Zn, 23,564 t Ag * coarse massive stratabound lenses to bands of gal, sfa > pht, ars, cpy, tet in gangue of qzt, Kfl, cbt, hdb, fayalite, pyroxmangite in gneiss * 1.677 Ga grn-bio gneiss intruded by ~1.5 Ga granitoids * Bailey (1998).

Zn-Mn oxide and silicate deposits in marble

Franklin-Sterling, New Jersey. These unique twin deposits, about 80 km NW of New York City, are famous mineralogical localities (Palache, 1935). They are situated in the same Grenville high-grade metamorphic sequence as in Balmat, but incorporated into the Appalachian orogen (Fronde and Baum, 1974). The two former mines: **Franklin** (~22 mt @ 19.6% Zn, 8.7% Mn for 4.32 mt Zn) and the smaller **Sterling** in Ogdensburg (Johnson et al., 1990; 11 mt @ ~20% Zn, 8% Mn for 2.2 mt Zn) are now mineral collectors reserves and guest mines. The orebodies are hosted by the ~1.3 Ga old Franklin Marble, a NNE-trending, 8 km long and 330m to 500m thick, marble band interfolded with quartz-feldspar gneiss, hornblende-garnet gneiss, Ca-Mg silicate gneiss and amphibolite. Both are erosional remnants of a formerly more extensive mineralized zone, recently exhumed from beneath the unconformable Cambrian and Ordovician sedimentary cover.

The **Franklin orebody** (Fronde and Baum, 1974; Fig. 14.11) has the shape of a 25° NE-plunging synclinal trough. The marble has a disconformable contact with hornblende gneiss to amphibolite, suggestive of disharmonic fold in the more ductile marble. The polyphase deformed and metamorphosed ore lens varied in thickness between 3 and 33 m, and it consisted of thin, ore-grade layers interfolded with the sub-grade material. The footwall contact of the ore against the marble is sharp, but several meters into the footwall is a 1 to

2.7m thick layer of magnetite in matrix of graphitic calcite.

The Zn-Mn ore was composed of a medium to coarse granoblastic aggregate of black franklinite, orange-brown zincite, and willemite in coarse calcite matrix. The largest individual orebody was 600 m long, but other orebodies were much shorter and 0.3 to 10 m thick. Interbedded with the ore were marble and Ca-Mg silicate intervals composed of Mn-andradite, rhodonite, bustamite, Mn-pyroxenes and amphiboles, Ba-feldspars, magnetite and other minerals. The peak metamorphism of the ore, dated at 1.05 to 0.95 Ga, reached the upper amphibolite to granulite facies, after which a retrograde phase accompanied by mylonitization, pegmatite emplacement and partial remobilization took place mostly along the NE-trending shears and graben faults. With this was associated formation of numerous hydrothermal fracture and replacement veins and veinlets of calcite, rhodochrosite, friedelite, bementite, pyrochroite, and many rare minerals. Even greater number of rare mineral species came from remnants of regolith under unconformity.

The smaller **Sterling Zn-Mn deposit** (Johnson et al., 1990) is comparable with Franklin and about half its size. Both deposits are metamorphosed and polygenetic, but interpretation of the protolith is a major enigma tackled, as expected, by many investigators who proposed many different interpretations as follows: a) a completely in-situ oxidized Zn deposit comparable with Broken Hill; b) redeposited oxidation zone in karsted carbonate ("exotic" deposit); c) low-temperature hydrothermal replacement comparable with Vazante (Chapter 11), and others. Most recently, Johnson et al. (1990) determined the sea water-resembling ore fluid paleo-temperature as 150°C and compared the Sterling protolith with a sulfide-poor analogue of the Red Sea brine pool sediments.

14.7. Zn, Cu, Pb sulfide deposits in gneiss, schist, marble (meta-VMS?)

VMS and Besshi-type deposits in rifted island arc and backarc settings (Chapters 5, 8, 9) evolve, with increasing metamorphism, into schist and gneiss-hosted orebodies that differ from the Broken Hill-type by having Cu as a major component, and by the presence of distinct Mg (in felsics) or K, Si (in mafics) mineral assemblages, superimposed on the "regular" lithologies. These are interpreted as metamorphosed footwall alteration zones.

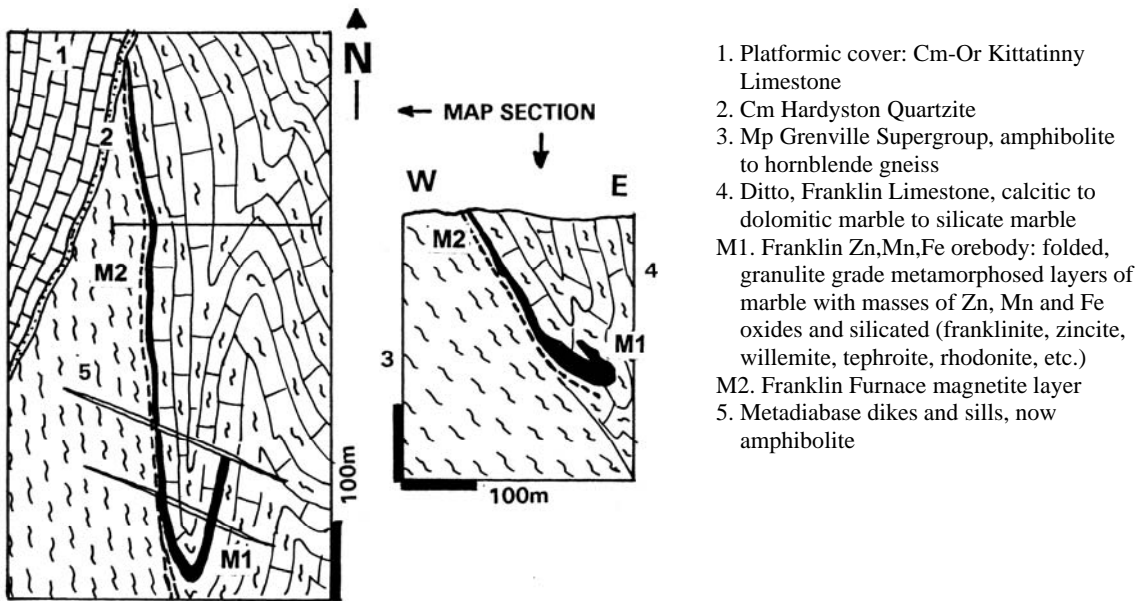


Figure 14.11. Franklin Zn, Mn deposit, New Jersey, map (left) and cross-section (right); from LITHOTHEQUE No. 1835, modified after Frondel and Baum (1974)

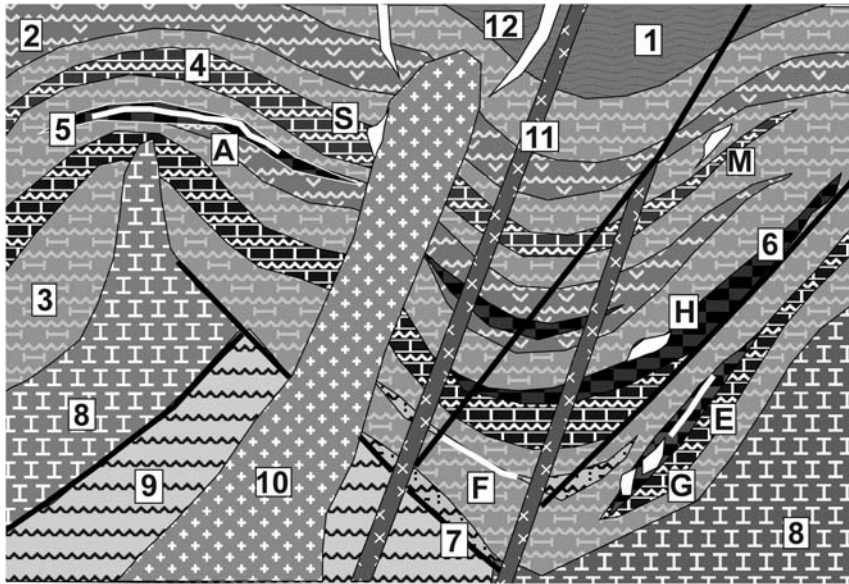
In amphibolite-grade metamorphics these include garnet, biotite, muscovite, cordierite, anthophyllite. Meta-carbonates (marble) and Ca-Mg silicate rocks are also commonly present (Fig. 14.12). Most such deposits are of small to medium size and there are no known "giants".

The Paleoproterozoic **Bergslagen Zn, Cu, Pb and Fe, Mn ore region** in central Sweden (Allen et al., 1996; also review in Laznicka, 1993, p.197-213) has a number of deposits of this type (only two "large": Falun and Garpenberg; the third, Åmmeberg, is more of the Zn-Pb Broken Hill-type; read above). Its main interpretational value is the great range of metamorphic grades, from subgreenschist (in the NW; e.g. Grythyttan; Oen et al., 1986) to upper amphibolite. This makes empirical comparison of pre- and post-metamorphic ore types possible.

Bergslagen is about 150-180 km west of Stockholm and it is a collection of numerous ~1.9 Ga felsic volcanic centers, interpreted as calderas in a back-arc setting (Allen et al., 1996), formed on the Baltic Shield basement. The dominant lithology there is "leptite", a felsic (rhyolite to rhyodacite) pyroclastic to volcanoclasti rocks with subordinate Na-basalt (spilite), metapelites, marble, Ca-Mg silicate rocks and banded iron formations. These are intruded by granitoids ranging from synvolcanic through 1.87 to 1.77 synorogenic "I-type" then "S-

type", to 1.73 post-orogenic varieties. The silicate rocks are pervasively Na-, K- and Mg-altered (sodic and potassic "leptites", skarn) and contain a myriad of small deposits of overlapping types: siliceous BIF, skarn Fe-(Mn), Fe in meta-volcanics, and massive to disseminated Fe-Zn-Cu-Pb (Magnusson, 1970). Allen et al. (1996) distinguished two types of sulfide deposits, exemplified by the two "large" deposits Falun (more widespread type) and Åmmeberg (rare).

Falun Zn, Pb, Cu, Ag, Au deposit (Geijer, 1964; Grip, 1978; 1.75 mt Zn, 595 kt Pb, 450 kt Cu, 1155 t Ag, 21 t Au) is the "flagship" of Bergslagen deposits; Fig. 14.13. It is situated in an E-W trending felsic volcanic-sedimentary belt surrounded by foliated granitoids. A portion of this belt encloses the 15 km long "Falun sulfide zone", a high-strain zone to ductile shear. The actual Falun orebody, an inactive historical mine now a mining museum, has an outcrop area of 220x370 m and 320 m deep workings. It is a 70°S plunging mass of pyrite with dispersed grains, schlieren, stringers and small monomineralic masses of sphalerite, galena and chalcopyrite. This mass of some 30 mt of ore contains relics of marble and Ca-Mg silicate rocks (skarn). The pyrite mass is enveloped by a 1-2 m thick "sköl" ("gouge"; a phyllonite) composed of biotite, chlorite, talc, amphibole, garnet, cordierite and andalusite.



- 1. Metaturbiditic biotite schist, gneiss; 2. Amphibolite; 3. Quartz-feldspar orthogneiss (leptite); 4. Marble, Ca-Mg silicate gneiss; 5. Quartz-banded BIF; 6. Skarn and skarnoid; 7. Metaquartzite, meta-arkose; 8. Synvolcanic and synorogenic granitoids; 9. Basement gneiss complex; 10. Late orogenic to post-orogenic granite; 11. Gabbro, diabase dikes; 12. Pegmatite. A. Quartz-banded BIF; E. Fe, Mn "skarn", magnetite & Mn oxide masses in Ca-Mg silicates; F. Massive stratabound Zn, Pb sulfides in gneiss;

Figure 14.12. Orthogneiss, amphibolite, marble association as in the Bergslagen, Sweden, interpreted as a "rift" or metamorphosed back-arc system. Inventory diagram from Laznicka (2004), Total Metallogeny Site G221. Explanations (continued): G. Pyritic Cu,Zn,Pb,Ag sulfidic lenses and pods in "leptite", marble or "skarn", associated with garnet-anthophyllite and cordierite alteration envelopes; H. Ditto, chalcopyrite-rich; M. Magnetite-apatite ores in dacitic orthogneiss (Grängesberg); S. Scheelite skarn, pegmatite. Ore types F and G have known "giant" or "near-giant" members

This is interpreted as the VMS footwall alteration zone (Allen et al., 1996). Outside, corresponding to the "silicified cap" of Allen et al. (1996), is an envelope of partial to complete silicification ("secondary quartzite"). Several irregular, schlieren-like bodies of disseminated and fracture-filling auriferous chalcopyrite are in the quartzite, mostly east from the pyrite mass. Allen et al. (1996) placed Falun into their "SVALS" ("stratabound volcanic-associated limestone-skarn") category. The mass of pyrite is reminiscent of the Cerro de Pasco meso-epithermal pyrite replacement (Chapter 6).

14.8. Disseminated Cu sulfide deposits in gneiss, schist and marble

Given the abundance and variety of disseminated copper deposits in both magmatic and sedimentary settings, it is logical to expect that some have been buried enough to undergo high-grade metamorphism. This is indeed the case, but metamorphic homogenization has obliterated most textural differences so that it is difficult to tell a metamorphosed porphyry-Cu from Cu-sandstone. This is further complicated by remobilization and synorogenic mineralization.

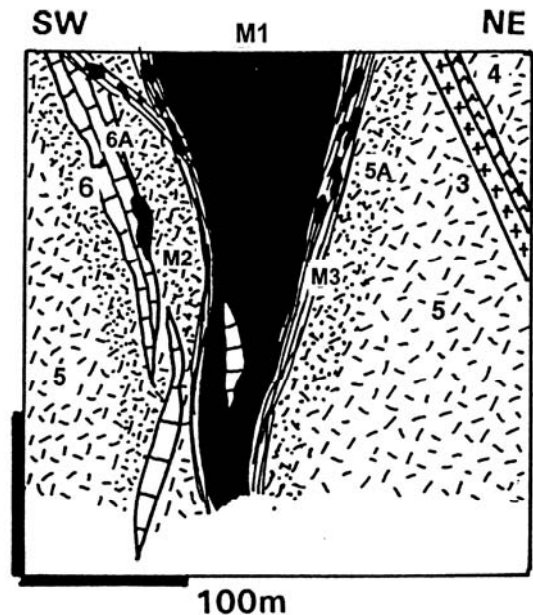


Figure 14.13. Falun orebody, Bergslagen, Sweden, cross-section from LITHOTHEQUE No. 600, based on data in Magnusson (1970). 3. Pp quartz-porphry dikes; 4. Amphibolite dikes; Pp Leptite Series: 5. Felsic metavolcanic gneiss; 5A. Ditto, Fe-Mg altered; 6. Dolomitic marble; 6A. "Skarn"; M1. Massive sulfide orebody; M2. Disseminated, stringer ore; M3. "Sköl"

The literature is ambiguous and in flux so it is best to resort to empirical characteristics. This paragraph focuses on Cu deposits in predominantly quartzofeldspathic gneiss where mafics are not directly associated.

Aitik Cu, Ag, Au deposit, Norrbotten, N. Sweden (Zweifel, 1972; Wanhainen et al., 2003; P+Rc 1.45 bt @ 0.38% Cu, 3.5 g/t Ag, 0.2 g/t Au for 5.51 mt Cu, 5,075 t Ag, 290 t Au); Fig. 14.14. Aitik is, first of all, an example of industry determination to go ahead and profitably mine an extremely low-grade deposit lacking supergene enrichment, behind Arctic Circle, in a high-wages country. Since the start of mining in 1968 the resources increased several times making Aitik the second largest Cu deposit in Europe.

The deposit is located 15 km east of the Gällivare Fe ore field, in amphibolite facies metamorphosed Paleoproterozoic intermediate volcanics and sediments, deformed by the 1.85 Ga Svecofennian orogeny. The supracrustals, dominated by hornblende gneiss to amphibolite and interpreted as meta-andesite, are interlayered with biotite schist grading to gneiss and migmatite, marble and Ca-Mg silicate rocks. They occur in the roof of, and have been intruded and locally granitized by, several generations of granitoids.

The N30°W-trending, 3 km long and 400 m wide ore zone consists of garnet-biotite schist, with K-feldspar, biotite, hornblende gneiss and porphyritic quartz monzonite in the footwall. Quartz-muscovite schist in the hangingwall is probably phyllonite, a site of ductile shear. The ore zone and its vicinity are veined and permeated by K-feldspar pegmatite. The multistage mineralization consists of disseminated, blebby and stringer chalcopyrite with some pyrite, pyrrhotite, bornite, magnetite and molybdenite. These minerals predate the peak of metamorphism and are followed by post-peak quartz-sulfide veinlets, stockworks and small massive nests, and also by mineralized pegmatites and pegmatoidal hybrids. The pre-metamorphic origin of the ore is inconclusive, although Wanhainen et al. (2003) identified high-salinity fluid inclusions suggestive, at least, of a hydrothermal origin.

Somewhat similar mineralization style is present in the **Lumwana Cu-Ag-Au district** of NW Zambia, situated 250 km west of the Copperbelt (Equinox Ltd. Annual Report, 1999; 7.42 mt Cu in three deposits). There, Neoproterozoic schist sequence, considered a high-grade metamorphic equivalent of the Lower Roan (Chapter 11), envelopes granite gneiss core of the Mombezhi

Dome (Freeman, 1991). The largest **Chimwungo** deposit has a geological resource of 892 mt @ 0.7% Cu.

In the **Ainak-Cu deposit near Kabul, Afghanistan** (Akhmadi, 1992; Rc 11.2 mt Cu) the principal host is a marble horizon, interfolded with Neoproterozoic Loikhvar Suite metamorphics. The metamorphics also include gneiss, Ca-Mg silicate rocks and amphibolite, and are exposed in an anticline cored by Neoproterozoic amphibolite, hornblende schist and gneiss. The western orebody is 1400 m long, 1100 m wide and up to 300 m thick and has zonally arranged bornite and chalcopyrite in a pegmatoid-permeated deformation zone in marble. The footwall rocks contain disseminated pyrite and pyrrhotite with some chalcopyrite and cobaltite.

In the **Singhbhum Cu belt**, Bihar, India, Cu sulfides form stringers in albitized tectonic zone superimposed on greenstone (Chapter 9).

14.9. Scheelite, uraniferous phosphates, magnesite, borates in marble and Ca-Mg silicate gneiss

Scheelite skarn

Scheelite skarns are an important source of tungsten in the non-metamorphic setting (Chapters 7 and 10), but so far no "giant" equivalent has been found in high grade metamorphic equivalents.

Seridó (Borborema) scheelite province in NE Brazil comes closest (Maranhão et al., 1986). It covers 20,000 km² in the Rio Grande do Norte and Paraíba States and it contains 677 scheelite occurrences, of which the bulk is in stratabound replacement bodies in "tactite" (skarn and Ca-Mg silicates). The host Neoproterozoic Quixaba Formation comprises discontinuous marble lenses with amphibolite, gneiss and migmatite, interfolded with rocks of the Paleoproterozoic basement complex. The largest scheelite zone is in the municipality Currais Novos (Maranhão et al., 1986; 44 kt W @ 0.4%). There, an arcuate, N-S trending, 6 km long band of two marble units is in migmatitic gneiss. The marble encloses discontinuous patches of diopside, plagioclase, vesuvianite, grossularite, epidote, tremolite, chlorite and quartz assemblage with two generations of disseminated scheelite: 1) pre- or early metamorphic fine-grained scheelite controlled by S₁ schistosity, and 2) coarse recrystallized scheelite along S₂ surfaces.

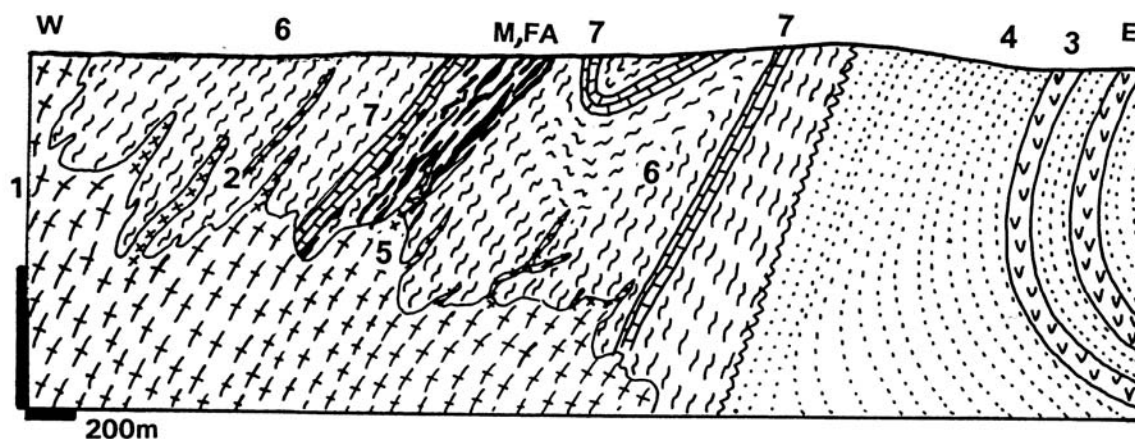


Figure 14.14. Aitik Cu, Ag, Au deposit, Norrbotten, Sweden; cross-section from LITHOTHEQUE No. 611, modified after Zweifel (1972), Boliden AB Aitik Staff materials, 1975 visit. 1. Mp postorogenic anatectic granite; 2. Pegmatite dikes and pegmatitized metamorphics; 3. Pp amphibolite; 4. Pp metaquartzite; 5. 1.89-1.85 Ga massive to foliated quartz monzonite; M in FA. Pre-orogenic or synorogenic, metamorphosed disseminated and stringer Cu,Fe sulfides in gneiss and pegmatite; FA. Ductile shear altered to garnet-biotite schist; 6. ~1.9 Ga amphibolite, hornblende gneiss, biotite schist; 7. Marble, Ca-Mg silicate gneiss

U phosphates in marble

Itataia, 170 km SW of Fortaleza in Ceará, is the largest Brazilian U deposit and also a significant phosphate mine (Mendonça et al., 1985; Angeiras, 1988; 121 kt U @ 0.16%, 18 mt P₂O₅ @ 26.35%). The host, Paleoproterozoic Itataia Group, is a shallow marine cover unit unconformably deposited over Archean basement and later incorporated into the Neoproterozoic Borborema orogen. There, it suffered high-grade metamorphism and granitic intrusion. A thick east-trending marble unit interfolded with gneiss and migmatite near a basement dome is considered site of a buried, late orogenic granite intrusion. The marble is intersected by several tongues of "episyenite" (albitized and carbonatized silicate rocks).

The phosphate and U orebodies consist of a mass of an almost monomineralic aphanitic to botryoidal, marron to yellow uraniferous collophanite, replacing karsted marble near the surface. In depth the collophanite body is underlaid by a stockwork of collophanite in marble, and by a breccia of feldspathized rock fragments in collophanite, apatite, calcite, clay minerals and zircon matrix. The U is bound in the collophanite and there are no visible U minerals. The origin of Itataia is enigmatic. Angeiras (1988) argued for hydrothermal sodic metasomatism at temperatures of 350° to 200° that formed the "episyenite", followed by formation of the uraniferous

collophanite at between 130° and 50°C. The age of mineralization is quoted as 450 Ma.

Magnesite and boron in marble

Liaodong Peninsula, NE China. ENE trending belt of Paleoproterozoic meta-carbonates (Liaohé group, especially the Dashiqiao Formation) in southern Liaoning host important deposits of crystalline magnesite (~25-30 bt @ 47% MgO in 17 major deposits) and some 77 deposits of Mg and Fe borates (~25 mt of B₂O₃); Yang Zhensheng et al. (1988); Zhang Qiusheng (1988); Peng and Palmer (2002). The 1.6 km thick magnesite-bearing sequence intruded by granitoids is a part of a 2.0 to 1.9 Ga orogen that incorporates Archean basement. It consists of dolomitic marble interlayered with tremolite, forsterite (serpentinite) or scapolite marble, amphibolite, garnet-sillimanite gneiss, and retrograde units of talc, chlorite and biotite schist. A very coarse crystalline magnesite forms up to 300m thick and 6 km long lenses in dolomite, with which they have a gradational or sharp but interfingering contact.

The borate deposits can be divided into the Mg-(suanite and szaibelyite) and Mg-Fe- (ludwigite) groups. They form lenses within the magnesian (dolomite or magnesite) marbles described above, intercalated with "leptite" and "leptynite" (orthogneiss, presumably after felsic volcanics and volcanoclastics), some of which are tourmalinized. Genetic interpretations of both the Mg and B ores

vary between the sedimentogenic models (playa lake precipitates, B derived from hot springs; Peng and Palmer, 2002) and syn- to post-orogenic carbonate replacements related to granites.

14.10. High-grade metamorphic mafic-(ultramafic)- associations

Cu sulfide deposits

In the previous group, amphibolites were present as members of an ore-bearing rock package, but not as direct ore hosts. Chalcopyrite, however, is ubiquitous in mineralogical quantities in amphibolite and there are scores of small deposits around the world, but no "giants". In two ore regions: Okiep and Caraiba, Cu sulfides are in or near small bodies of granulite facies metapyroxenite and noritoid surrounded by gneiss, migmatite and granitoids. In Okiep the mafics appear to be synorogenic intrusions shortly postdating the metamorphic peak. In Caraiba similar rocks are dismembered pre-metamorphic intrusions, later retrograded. The copper origin is controversial but now mostly considered magmatic, partly remobilized by hydrothermal processes.

Okiep (O'okiep) Cu region, Namaqualand, NW South Africa. This region, situated in the NW Cape Province around Springbok, covers about 3,000 km². It represents ~2.113 mt Cu @ 1.75% in a cumulative copper resource, intermittently mined since 1685, from 27 individual scattered deposits (Lombaard et al., 1986). The Mesoproterozoic Namaqualand metamorphic complex comprises upper amphibolite to granulite-metamorphosed supracrustal rocks intruded by several phases of synorogenic granitoids and gabbroids. Of particular interest is the 1,042 Ma mafic Koppaerberg Suite. This consists of several hundred small bodies (less than 1 km along the long axis), rather haphazardly distributed throughout the region, of which some 20% are copper-mineralized. Most are controlled by "steep structures", some by "megabreccia".

A typical "steep structure" is a "sharp antiformal structure in which the dip of the rock in the core of the structure is near vertical" (Lombaard et al., 1986). A large number of them is interpreted as piercement folds by Hälbig (1978). The "megabreccias" are pipe-like bodies with oval cross-sections, few metres to 1,000 m in diameter, and some have the form of steep dikes (Fig. 14.15). Most postdate the "steep structures".

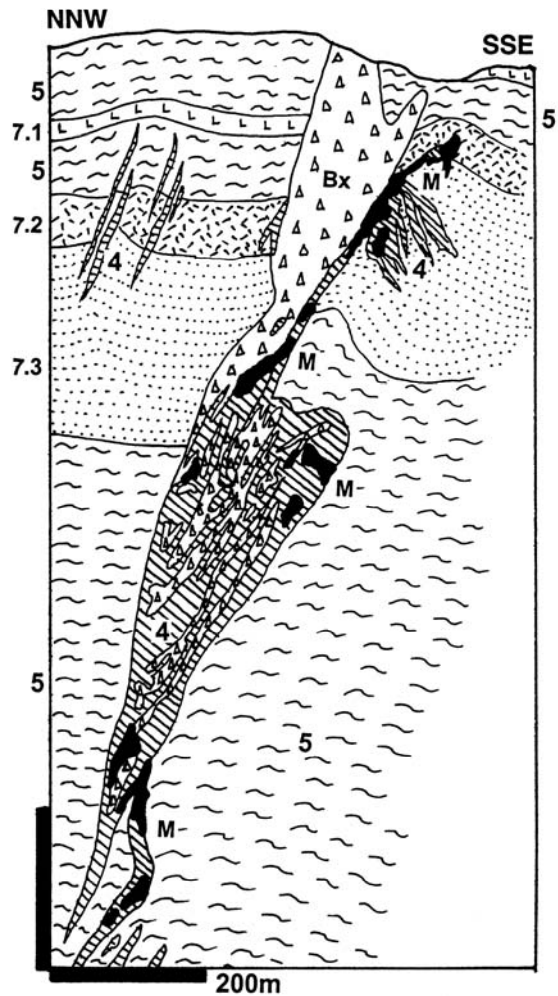


Figure 14.15. Okiep East Mine cross-section from LITHOTHEQUE No. 287, modified after Lombaard et al. (1986). 4. 1.072-1.042 Koppaerberg Suite, swarm of synorogenic anorthosite, diorite, norite > hypersthenite, leucodiorite controlled by breccia and "steep structures". M. Disseminations and stringers of Cu,Fe sulfides in and near the more mafic intrusions; Bx. Megabreccia, agmatitic steep bodies of leucogranite crowded by wallrock fragments; 5. 1.21 Ga granite gneiss; 6. 1.1 Ga S-type granite; 7. 1.8 Ga? Okiep Group: 7.1 hornblende gneiss, 7.2 "leptite", 7.3 meta-quartzite and schist

The breccia blocks have a high proportion of exotic fragments derived from above and they rest in matrix of a fine grained to pegmatitic granite, with retrograde chlorite-albite patches. The Koppaerberg Suite consists of orthopyroxene-bearing rocks that often display reverse sequence of crystallization, from oldest to youngest: diorite, anorthosite, norite, hypersthenite. The rocks are massive, resistant to deformation, fine to coarse grained and they have

sharp contacts with the steep structures. Locally they are crowded with wallrock and exotic inclusions, grading into a magmatic breccia.

The early generation of Cu deposits was exposed at the surface, then followed to depth. Such orebodies had up to 40m thick oxidation zone dominated by chrysocolla and almost no secondary sulfides. The principal hypogene ore minerals are bornite and chalcopyrite with minor and local pyrrhotite, pyrite and pentlandite. The sulfides are disseminated, in blebs, as small fracture and breccia fillings. The single largest deposit **Koparberg-Carolusberg** (Lombaard et al., 1986; Chris Beukes, oral communication, 1990; 632 kt Cu @ 1.68%) is an irregular ENE-trending subvertical segmented dike-like structure that intersects granite gneiss with units of two pyroxene granulite. The main orebody is in depth that exceeds 1,000 m and it is in brecciated anorthosite, veined by chalcopyrite and bornite mineralized hypersthene stringers.

Caraíba Cu deposit, Bahía, Brazil (Townend et al., 1980; De Lima e Silva, 1988; 1.3 mt Cu @ 1.0%, 12 kt Ni); Fig. 14.16. Caraíba open pit near Jaguarari is the largest Cu deposit in the Vale do Curaça district, in a N-S trending belt of Archean metamorphics along the eastern margin of the São Francisco Craton. In the mine are exposed unreplaced relics of ~2.9 Ga granulite facies-metamorphosed metabasites (stripes and lenses of hypersthene enveloped by "norite" and "gabbro"). The "norite" is an inhomogeneous, gneissic, hypersthene-andesine-diopside augite granoblastite gradational into clinopyroxene-plagioclase-biotite-hornblende granoblastite ("gabbro"). This is transitional into Ca-Mg silicate rocks interpreted as meta-sediments. These refractory resistors form a hybrid megabreccia that was partially retrograded into amphibole, biotite, phlogopite assemblage and veined/replaced by pink pegmatite. This all is enclosed in a regional 2.05 Ga granite gneiss complex.

Chalcopyrite > bornite, magnetite >> pentlandite and cubanite are sparsely disseminated in hypersthene and partly in the "norite" and Ca-Mg silicate envelope. The richer ores: stringers, patches and small masses of intergrown bornite and chalcopyrite are controlled by shears. The actual slip surfaces are coated or filled by a Durchbewegte "ore mylonite" gradational into a "ball ore": a breccia of attrition-rounded brittle wallrock fragments embedded in ductile sulfide matrix. The adjacent tectonized wallrocks are filled and veined by stringers of hydrothermally remobilized sulfides. The shallow oxidation zone in Caraíba yielded 5 mt

of ore @ 0.6% Cu, of mostly chrysocolla coatings and infiltrations in decomposed hypersthene.

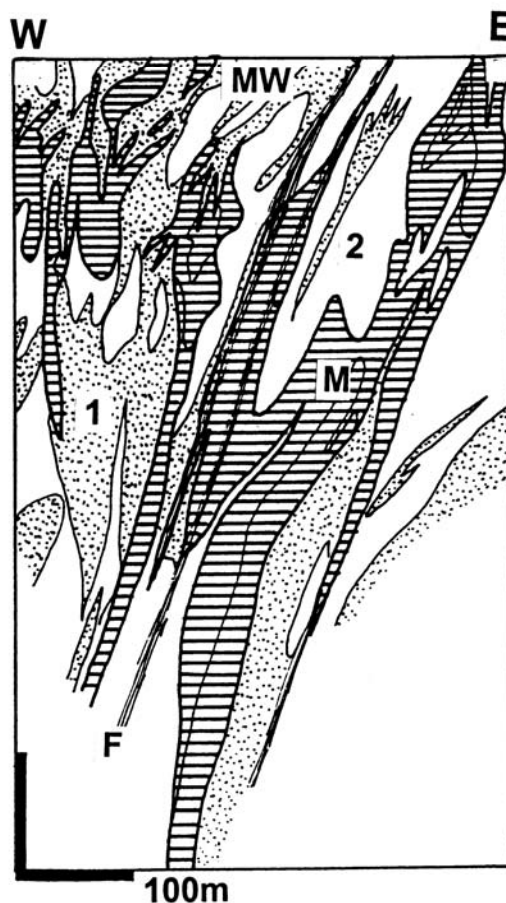


Figure 14.16. Caraíba Cu deposit, Vale do Curaça, Bahía, Brazil; cross-section from LITHOTHEQUE No. 1981 modified after Townend et al. (1980). MW. Oxidation zone, chrysocolla and malachite infiltrations and coatings; M. Scattered and stringer chalcopyrite and bornite in hypersthene and norite; massive, Durchbewegte sulfide band in shear; 1. Ar pyroxene-rich resistors enveloped and permeated by migmatite; 2. Ar granite gneiss, migmatite

Ni-Cu sulfide deposits

Synvolcanic Ni sulfide deposits in komatiitic flows and dikes (Chapter 9), Ni sulfides in gabbroids associated with plateau basalt (Noril'sk), Bushveld-type intrusions (Chapter 12), and possibly Ni in ophiolites, undergo deformation and high-grade metamorphism. In addition to this, synorogenic ores can form by hydrothermal (or "bimetasomatic"; Korzhinsky, 1974) sulfidation of the trace Ni in ultramafics, for example by sulfur displaced from

pyritic or pyrrhotitic supracrustals. As with other ore types, metamorphic homogenization weakens or obliterates the pre-metamorphic characteristics of rock suites and renders paleoenvironmental interpretations uncertain. Interestingly, there is virtually no change to the sulfide mineralogy due to metamorphism and pyrrhotite, pentlandite and chalcopyrite persist as ore minerals. The ultramafic and mafic hosts also retain their magmatic mineralogy and this contrasts with the profound change in the associated quartzo-feldspathic supracrustals.

There are several tens of Ni-(Cu) sulfide deposits in high-grade metamorphics but most are small to medium-size. Unless Jinchuan is included in this category (Chapter 12), only the Thompson Ni Belt barely clears the "giant" threshold when considered as a whole, some of its constituent deposits being of the "large" magnitude only. Selebi-Phikwe is another "large" Ni-Cu ore field.

Thompson Nickel Belt (TNB), Manitoba, Canada (Peredery et al., 1982; Bleeker, 1990; total ~5.9 mt Ni, ~200 kt Cu, ~60 kt Co). TNB is a 250 km long Ni-mineralized segment of the NE-trending contact zone between the Proterozoic Churchill Province in the NW and the Archean Superior Province in the SE, in the Canadian Shield. A component of the Trans-Hudson orogen (Hoffman, 1989), TNB is interpreted as a remobilized and retrograded granulitic Archean basement, with narrow remnants of Paleoproterozoic supracrustals. It was thrust SE onto the Superior Province, then sinistrally transpressed, sheared and cut by steep mylonite zones, and finally cut by transcurrent faults (Bleeker, 1990). The almost regularly spaced Ni deposits occur in a 2 to 10 km wide internal zone of the TNB, exposed in glacier-scoured outcrop, except for several prospects (e.g. Minago) in the SW that are concealed under Paleozoic platformic cover. Of the nine deposits/ore fields only two are "large" (Thompson and Mystery Lake). Thompson has been mined, since 1965, from an open pit and from underground mines. Mystery Lake is a low-grade resource.

Thompson (town) ore field (Peredery et al., 1982; Bleeker, 1990; P+Rv ~2.5 mt Ni @ 2.61%, 160 kt Cu @ 0.17%, 36 kt Co, 358 t Ag, 7.17 t Au plus 469 kt Ni in the Birchtree Mine). In Thompson (town) area the tectonized Archean basement is overlain by a narrow remnant of 2.1 to 1.88 Ga autochthonous "rift association" (Ospwagan Group) of amphibolite-grade metamorphics, unconformably resting on Archean meta-regolith. The rocks include equivalents of conglomerate, mature

quartzite, calcareous sediments, pelites with a minor BIF, and minor mafic-ultramafic volcanics. The latter are probably comagmatic with dismembered ultramafic sills and dikes emplaced into the supracrustals and into the reactivated basement, that are the source of the ore Ni.

The majority of Ni-(Cu,Co) deposits in the TNB are disseminations and stringers of pyrrhotite, pentlandite and lesser chalcopyrite in tectonized serpentinized peridotite or close to its contact. The ores grade into ductile to semi-brittle breccias in which sulfide stringers or masses are interstitial to attrition-rounded or angular ultramafic or sialic wallrock fragments. Many such zones are permeated by pegmatite.

The **Thompson ore field** is a 6 km long and 1,500 m deep, repeatedly deformed zone of tabular to lenticular sulfide orebodies along a schistosity-parallel horizon in biotite-sillimanite-garnet gneiss (Fig. 14.17). The gneiss is mylonitic, rich in graphite, and it encloses scattered ultramafic blocks. Bleeker (1990) differentiated among the "sedimentary" and "magmatic" sulfides, the latter further subdivided into the "intraparental" and "extraparental" varieties. The "sedimentary" sulfides, believed formed diagenetically in the pelitic gneiss progenitor, consist of pyrrhotite, minor chalcopyrite and late pyrite densely disseminated, in two horizons, in graphitic gneiss, "chert", "silicate facies BIF" or amphibolite. Most are low in Ni, but in places they constitute a "mineralized schist" with up to 10% Ni. The "intraparental" sulfides are disseminated in, or along the contact of, the ultramafic pods. These are rare in the Thompson field, but dominant in other deposits in the TNB (e.g. Pipe, Manibridge). The "extraparental magmatic sulfides" constitute the main orebodies. They are masses of pyrrhotite > pentlandite > chalcopyrite, locally gersdorffite, grading to "ore mylonite" and ductile breccias. In the ore breccia rotated and variously disaggregated wallrock fragments (pegmatite, serpentinite, biotite gneiss), with garnet, biotite, magnetite, pyrite porphyroblasts, are embedded in the ductile "paste" of sulfides. The syntectonic *Durchbewegung* fabrics are recrystallized and portion of the ore was remobilized into pegmatite (Figs. 14.18, 14.19). The "extraparental" orebodies follow, for a considerable distances, the graphitic gneiss horizon (a shear phyllonite?) between and away from the peridotite blocks. It is not clear what proportion of the Fe-Ni-Cu sulfides in the TNB are mainly physically remobilized synmagmatic ores from the ultramafics, and how many orebodies are synorogenic.

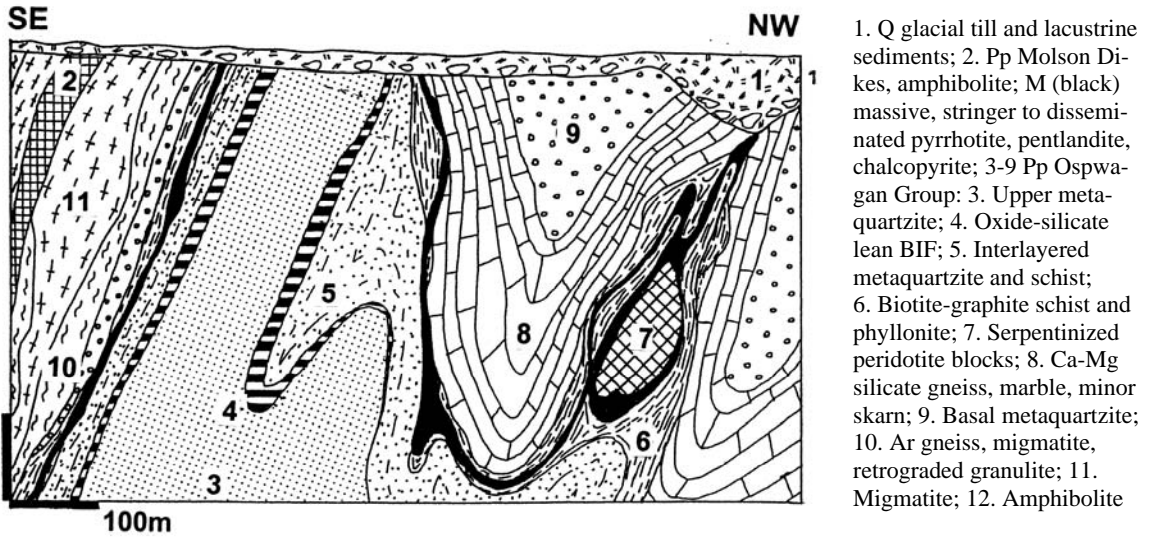


Figure 14.17. Thompson Ni mine, Manitoba, cross-section from LITHOTHEQUE No. 1553, modified after Zurbrig (1963) and INCO Ltd materials and tours

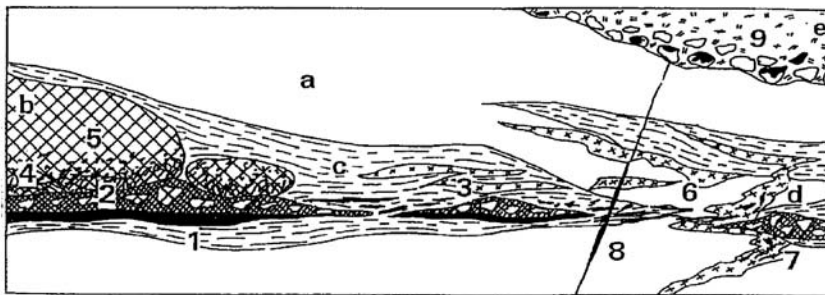
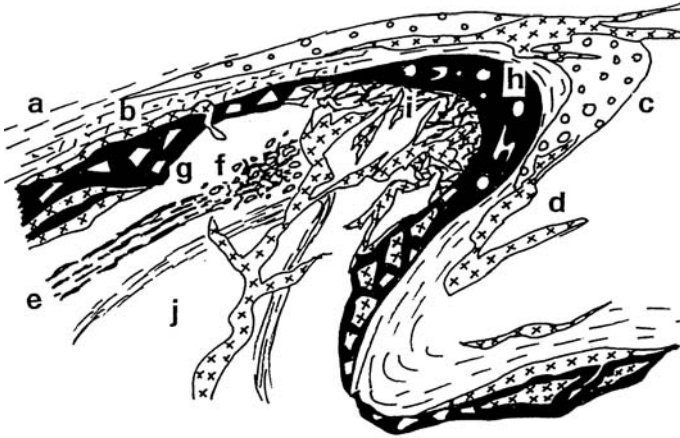


Fig. 14. 18. Thompson Mine, varieties of Fe-Ni-Cu sulfide ores from LITHOTHEQUE No. 2217 (Laznicka, 1987). a: Pp paragneiss; b: Blocks of dismembered peridotite in shear; c: Graphitic phyllonitic gneiss; d: Syntectonic pegmatite and pegmatized schist. ORES: 1. Massive to tectonically banded pyrrhotite > pentlandite > chalcopyrite; 2. Ductile ore breccia (Durchbewegung); 3. Ditto, with abundant schist and pegmatite fragments, biotite and garnet porphyroblasts; 4. sulfide fracture network in peridotite; 5. Sparsely disseminated sulfides in peridotite; 6. Sulfide stringers and bands in gneiss peneconcordant with schistosity; 7. Sulfides scattered in hybrid pegmatite; 8. Rare remobilized millerite fissure veins; e: Q glacial sediments; 9. Oxidized ore boulders at base of till

If synorogenic, the ore is most likely a product of reaction of the sedimentary sulfur in pelites with the ultramafic trace nickel.

Selebi-Phikwe Ni-Cu ore field, Botswana (Gallon, 1986; 557 kt Cu @ 0.97-1.56%, 531 kt Ni @ 0.7-1.45%, 31 kt Co) is another "large" ore field in high-grade metamorphics. Here, the host progenitor is considered a tholeiitic gabbro sill. The pre-2.66 Ga upper amphibolite to granulite facies metamorphics are members of the Limpopo orogen. Three groups of orebodies are hosted by a 14 km long, folded interval of "ore amphibolite", enveloped by biotite-hornblende gneiss. The Ni-Cu

orebodies are structurally controlled folded sheets or lenses along amphibolite contacts. The principal ore type is a ductile breccia of wallrock fragments in a mass of recrystallized pyrrhotite, with interstitial and exsolved pentlandite and chalcopyrite. The sulfides-dominated breccia with small-size rounded and rotated fragments locally changes into a megabreccia of metres-size amphibolite blocks injected by sulfides, and eventually into a disaggregated breccia in amphibolite with disseminated sulfides. As in Thompson, synorogenic pegmatite in places permeates the ore.



a. Paragneiss; b. Graphitic phyllonite rich in mostly Ni-free pyrrhotite; c. Basal metaquartzite; d. Syntectonic pegmatite; e. Ca-Mg-Fe silicate bands; f. Ditto, Fe-Ni-Cu sulfide stringers; g. Massive Durchbewegte Fe-Ni-Cu sulfide ore grading to breccia, garnet & biotite porphyroblasts in ore, angular pegmatite inclusions; h. Ditto, rotated and attrition rounded wallrock fragments in sulfide matrix; i. Hybrid pegmatite-metamorphics with sulfide stringers; j. Metaquartzite and schist.

Fig. 14. 19. Thompson Mine, varieties of the Fe-Ni-Cu sulfide ores in tectonized Pp Oswagan metamorphics and Ar gneiss. From LITHOTHEQUE No. 2218 (Laznicka, 1987)

The ore is recrystallized, annealed, and in places crowded with rotated garnet, biotite, K-feldspar and pyrite porphyroblasts. The orebodies are in places abruptly interrupted or terminated by hornblende-phlogopite schist and interspersed with biotite schist bands.

Scheelite in/near amphibolite

Showings of scheelite are frequently reported from greenstone belts and "eugeoclinal" orogens, particularly those that are higher-grade metamorphosed, interbedded with Ca-Mg silicate rocks or marble, and intruded by granite or pegmatite. The first (and so far only proven) "giant" scheelite ore field in metabasites, without conspicuously associated high-level granite, has been Felbertal in the Austrian Alps. Felbertal, found in the 1960s, is one of the few truly "greenfield" discoveries made from scrap by university geologists (Rudolf Höll from the Munich University, traversing the Alps to prove a new genetic model of "exhalative", synvolcanic scheelite; Höll and Maucher, 1976).

Felbertal-W, Austria (Höll, 1977; Thälhammer et al., 1989; Rv ~10 mt @ 0.44% W; geological Rc ~200 kt W content) is 10 km south of Mittersill, on western and eastern slopes of a glacial valley (Fig. 14.20). The scheelite ore is in Neoproterozoic to Ordovician Habachseries, a mantling complex in the Tauern Window crystalline core of the Eastern Alps. This is a polyphase metamorphosed volcano-plutonic and sedimentary succession of schist, meta-quartzite, metabasites (amphibolite,

"prasinite", hornblendite, metagabbro), albite-quartz gneiss and paragneiss. This was intruded by a Variscan Sierra Nevada-style batholith in the Carboniferous (~320 Ma), and subsequently deformed and retrograded during the Alpine orogeny (Zentralgneiss and Altkristallin) (Holzer and Stumpf, 1980).

Scheelite is broadly stratabound and distributed over a stratigraphic thickness of 200 m or more. In the Ostfeld, scheelite is very fine-grained and inconspicuous, lacking sulfides, and confined to laminated, foliation-conformable meta-quartzite bands enclosed in or alternating with hornblendite, as well as in the hornblendite. In Westfeld, Mo (powellite)-rich scheelite forms coarser porphyroblasts accompanied by pyrrhotite, chalcopyrite, molybdenite, galenobismuthite and other minerals in quartz stockworks, in several hybrid "lodes" in sheared metabasites. There appears to be a range of scheelite varieties from recrystallized synvolcanic, through remobilized, to synorogenic-vein.

This must be the world's best camouflaged underground mine quietly operating, un-noticed, under the floor of a picturesque, tourists-frequented Alpine valley.

Nuuk (Godthåb) area-W, SW Greenland. Appel and Garde (1987) described an areally extensive, but undeveloped, scheelite province in the 3.0 Ga Malene Supracrustals. These are dominated by amphibolite, surrounded by granite gneiss and intruded by 2.66 to 2.55 Ga pegmatite. Hundreds of scattered scheelite occurrences have been recorded within an area that measures 150 x 20 km.

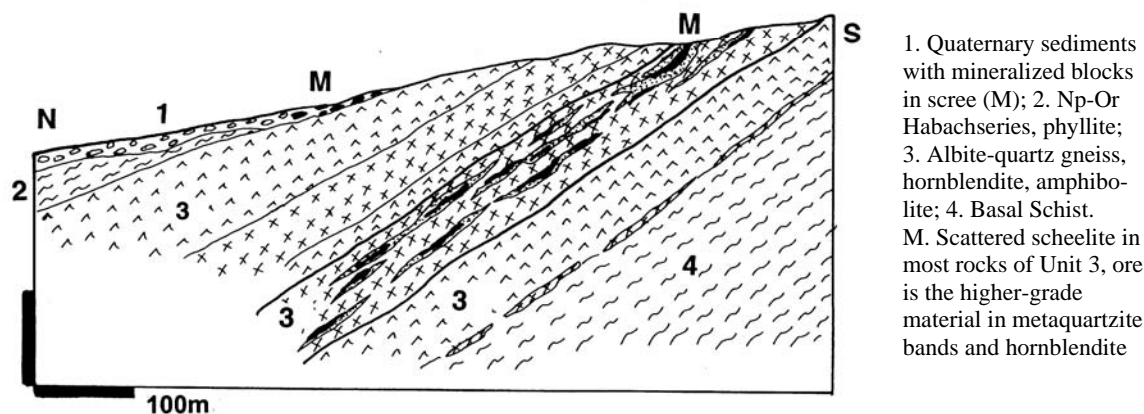


Figure 14.20. Felbertal scheelite ore field, Mittersil, Austria, Ostfeld diagrammatic cross-section. From LITHOTHEQUE No. 3089, modified after Höll (1977) and Thälhammer et al. (1989)

The most promising occurrence is only 5 km from Nuuk. Scheelite occurs as disseminated grains, strings, and laminae in zones of finely crystalline tourmaline, in up to 4 m wide zones in banded amphibolite, traceable for more than 1 km along strike. Small amounts of sulfides are associated.

Deformed and metamorphosed Bushveld-style layered intrusions

Stillwater Complex in Montana is an Archean Bushveld-style intrusion and although enclosed in granulite-facies supracrustals it remains internally virtually undeformed and unmetamorphosed, hence described in Chapter 12. Elsewhere, however, similar complexes as well as lesser differentiated mafic sills were penetratively deformed and metamorphosed so that they have the appearance of gneiss, granulite, meta-ultramafics or amphibolite that merge with the surrounding metamorphics. Recognition thus becomes difficult.

Fiskenaasset Complex 130 km SSE of Nuuk (Godthåb), Greenland, is an outstanding example which also contains a major (but not yet delineated) resource of Cr, Ti and V (Ghisler and Windley, 1967; Bridgwater et al., 1976; Myers, 1985). The Complex is a sheet-like tholeiitic layered intrusion, emplaced into mafic metavolcanics (amphibolites) in at least three phases, around 3.08 Ga. It was deformed, granulite-metamorphosed and intruded by granites at about 2.9-2.8. The intrusion is some 550 m thick in the best preserved section and it includes seven mafic-ultramafic magmatic layers. The best ore-bearing layer is the 250 m thick Anorthosite unit near the stratigraphic top of the Complex, that contains predominantly low-grade

discontinuous chromitite horizons 0.5 to 7 m thick. The disseminated Cr-spinel is scattered either in planar, equigranular bands in anorthosite, or it forms an "augen ore", where chromitite bands are interrupted by aggregates of porphyroblastic plagioclase.

14.11. Structures subjected to retrograde metamorphism and metasomatism

It has been stated above that increasing metamorphic intensity tends to obliterate many (especially textural and genetic) differences of the original rocks, resulting in metamorphic homogenization. The opposite is true when rocks, after achieving the peak metamorphic grade, undergo retrogression under lower pressure-temperature conditions, at higher crustal levels. This can be accomplished in broad high-strain zones without disruption of rock continuity (e.g. granulite converts to gneiss), or in more focused fault zones that have a much greater degree of complexity and heterogeneity, that include ore formation. The Russian literature (Kazanskii, 1972; Sviridenko, 1975; Sidorenko, ed., 1982) uses the all-embracing term "tectonomagmatic activation" for the set of tectonism-driven processes superimposed on high-grade metamorphic and magmatic complexes after their thermodynamic peak. This includes faulting, renewed (higher-level) magmatism, and hydrothermal activity. Although "activation" is useful in metallogeny as a first or second order classifier of territories, it is too broad and most ore deposits resulting from it can be treated from a different premise as well or better:

the case here. The, also Russian, class of "ore-bearing alkaline metasomatites in zones of large regional faults on crystalline basement", AMF (e.g. Kazanskii 1982), is a useful member of the "activation" category as it accommodates deposits difficult to list under a different heading. AMF comprises mostly non-sulfide, disseminated deposits of U, REE, Zr, Nb, Ta, Th, Be, Hf, sometimes Au and base metals that may mimic, or overlap with, deposits of similar metals in some granitic pegmatites (Chapter 10), alkaline magmatic complexes, and carbonatites (Chapter 12). Popular "giant" and "large" members of this class, described here under a different heading, include Salobo and Ernest Henry Cu-Ag-Au (Chapter 11) and there is a close affinity with the "iron oxide-Cu-Au-U family" (Hitzman et al., 1992).

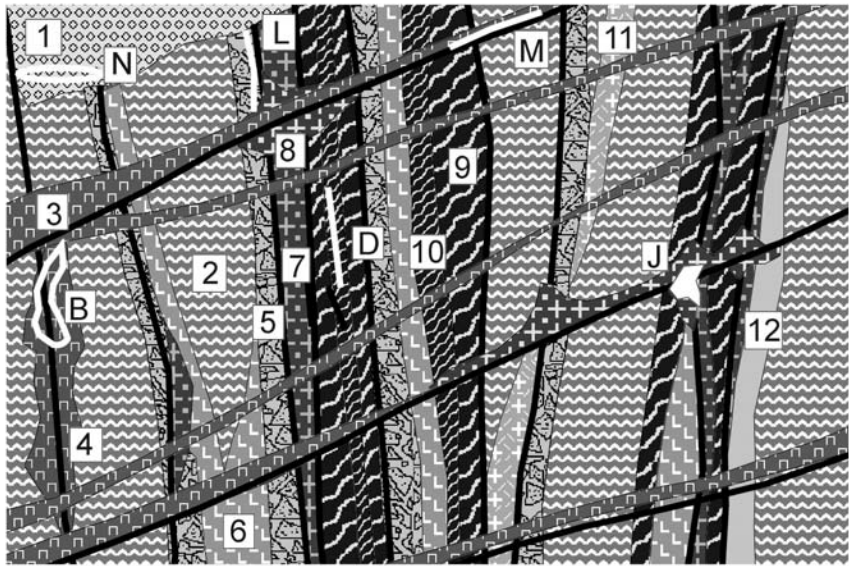
The tectonic zones emphasized here are filled by "fault rocks" (Higgins, 1971; Sibson, 1977; Wise et al., 1984) that include a variety of coarse fragmentites-breccias (reviewed in Laznicka, 1988, p. 626-690). The "typical" processes of deformation and lithogenesis took place under the brittle-ductile transition (Sibson, 1977), although the late (terminal) phases or rejuvenation events continued under the brittle conditions. The fault rocks (mylonite group, phyllonite, breccias, gouge) either remained "dry", or were replaced or infilled by various metasomatites. The metasomatism could have been "independent" (no directly apparent magmatic source) or magmatism-related; in reality potential parent magmas in depth are hard to prove. The "dry" fault rocks rarely host important metallic deposits other than superimposed veins and stockworks, for example high-level infiltrations of U oxides (Dahlkamp, 1993) but the known deposits are small. The metasomatites are more important.

The metasomatites replace/fill dilations in fault (shear) zones, partially or fully, to produce tabular (dike or sill-like) bodies gradational to stockworks and/or diffuse replacements. The continuity varies and usually a continuous fault zone controls discontinuous occurrences of metasomatites. At fault intersections, zones of intense brittle fracturing (for example, earlier ductile rocks made more brittle by an early stage metasomatism, e.g. silicification) and brecciation, the metasomatism produced subvertical columns, tongues propagating into adjacent rocks, or irregular masses reminiscent of magmatic plutons or stocks. The metasomatizing fluids attributed to metamorphic hydrotherms (produced by rock dehydration), magmatic fluids, or volatiles streaming from the mantle, had compositions comparable with fluids causing hydrothermal alteration at higher crustal levels in

granite-magmatic (e.g. porphyry Cu; Chapter 7), alkalic-magmatic (Chapter 12) or seawater-convective (e.g. VMS and spilite-keratophyre; Chapter 8) systems. The fluids reacted with the wallrocks and this (together with fluid composition and temperature) determined the metasomatite mineralogy and may have influenced the selection of ore minerals. Metasomatites in quartz-feldspathic wallrocks are dominated by microcline, albite, quartz; those in intermediate and mafic rocks have biotite, amphiboles and pyroxenes (especially the Na- equivalents). Both also include carbonatization. Metasomatites in carbonates and ultramafics are treated above. Most metasomatites resulted from multistage events and are mineralogically zoned, although zoning is often modified by overprinting (Figs. 14.21, 14.22).

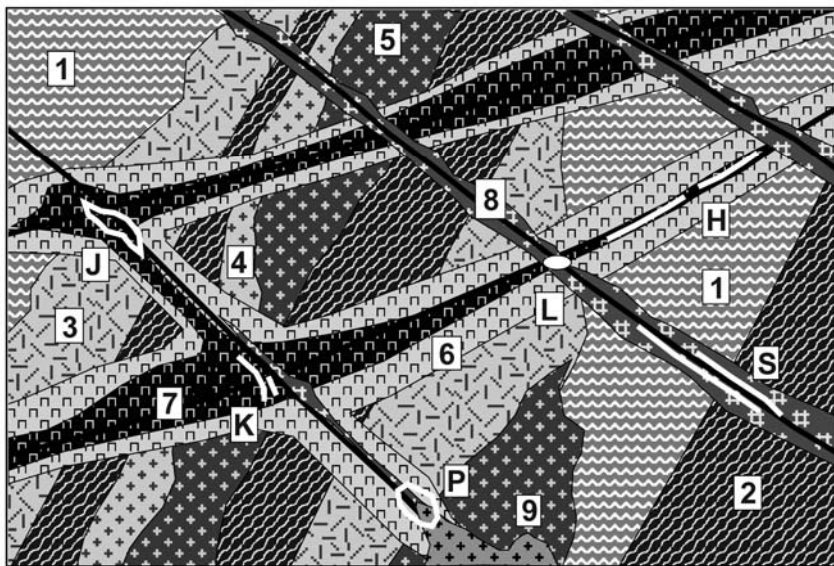
Belevtsev, ed. (1974) distinguished four typical stages of metasomatites formed in the predominantly quartz-feldspathic wallrocks in the Ukrainian Shield: 1) Early alkali metasomatism at ~600° to ~420°C dominated by microcline (K-pseudosyenite); 2) Main alkali metasomatism at ~360-250°C dominated by albitites, and early U (uraninite), Ti, Zr ores; 3) Na-ores-carbonates at ~300-150°C, of low-temperature albite, Ca-Mg carbonates, main stage pitchblende, hematite; 4) Quartz metasomatism (silicification), around 140°C, with minor associated Pb, Zn, Cu sulfides in veins. In the Fe-Mg silicates-rich wallrocks the stage 1) assemblage has also biotite, the stage 2) has amphiboles especially riebeckite, and pyroxenes aegirine, arfvedsonite. The "giant"/"large" deposits described below exemplify the Zr-Nb-Ta association in amphibole & pyroxene-rich Na metasomatites (Katugin), and the U association in albitites (Beaverlodge, Lagõa Real).

Katugin Zr, Nb, Ta deposit, Siberia (Arkhangel'skaya et al., 1993; minimum 100 mt of ore @ 2.39% Zr, 0.41% Nb, 435 ppm Ta, 167 ppm Hf). Katugin is an approximately 2.5 x 2 km large, heart-shaped complex of mineralized 1.8 Ga alkaline metasomatites, located 80 km SSE of Chara in eastern Siberia. It is situated in basement of the Paleoproterozoic Kodar-Udokan Basin, host of the "giant" Udokan Cu deposit in meta-arenites (Chapter 11). The Katugin metasomatites are located at the southern margin of the Basin, north of the Stanovoi Range Foldbelt. The immediate country rock is biotite-sillimanite gneiss to migmatite of the Archean basement, intruded by several pulses of about 2.0-1.9 Ga rapakivi granite sheets.



1. Conglomerate fill of young fault grabens; 2. Mylonitic granite gneiss; 3. Syenite and lamprophyre dikes; 4. "Episyenite"; 5. Cataclasite, breccia; 6. Metadolerite dikes; 7. Oldest feldspathic metasomatites (e.g. microcline); 8. Youngest feldspathic metasomatites (e.g. albite); 9. Mylonite; 10. Ultramylonite, blastomylonite; 11. Meta-quartz porphyry dike; 12. Meta-pegmatite. ORES: B. Disseminated uraninite in "episyenite"; D. Gold in quartz-K-feldspar metasomatite;

Fig. 14.21. Ductile faults in high-grade metamorphic or granitoid basement reactivated at shallow levels in tensional regimes; rock and ore types inventory cross-section from Laznicka (2004), Total Metallogeny Site G218. Explanations (continued): J. Disseminated uraninite in albitite; L. Carbonate-uraninite veins; M. Shandong-type gold-quartz fracture and fault veins; N. Stratabound low-temperature Au in porous conglomerate or sandstone (Balei-type). Ore types D, M and N have known "giant" members



1. Mylonitic gneiss and granitoids; 2. Mylonite, ultramylonite; 3. K-feldspar, biotite metasomatite; 4. K-feldspar altered tectonite; 5. K-feldspar solid metasomatite (feldspathite, microcline); 6. Albite-altered tectonite; 7. Albite solid metasomatite (albitite); 8. Fenite (Na-pyroxene and amphibole, nepheline); 9. Post-orogenic (anorogenic) granite; H. Cu(U) in shear albitites over mafics; J. U in albitite over feldspathic rocks; K. U, V, Sc, Zr, REE, Y, Th in albitite, carbonate, aegirine metasomatites near BIF;

Figure 14.22. Alkaline metasomatites formed in and near ductile to brittle faults and in tectono-magmatically activated regions. Materials inventory cross-section from Laznicka (2004), Total Metallogeny Site G217. Explanations (continued): L. Be in phenakite, beryl in feldspathic metasomatites; P. Fe oxides (magnetite or hematite) replacements and breccia fill, some with Cu, Au, U, REE (Olympic Dam-type); S. Nb, Ta, REE, Zr, Y, Sc, U, Th in quartz, feldspar, biotite, aegirine, arfvedsonite metasomatites in ductile shears. Ore types H, P, S have known "giant" members

These, initially possibly anorogenic granites, have been shortly afterwards "activated", that is tectonized in a Grenville-style collision front, resembling the anorthosite-rapakivi province of eastern Quebec. The Katugin deposit is in a complex of blastomylonites, blastocataclasites and augen gneiss, mainly overprinting the rapakivi and partly the basement gneiss. The fault rocks are recrystallized into amphibolite facies blastites (oligoclase, microcline, quartz, biotite, hornblende), associated with pegmatite. Alkaline metasomatites follow after another episode of mainly ductile shearing.

The alkaline ore metasomatites evolve gradually from the enclosing rocks and have an inconspicuous appearance of medium-grained gneissic granite. The central zones correspond to alkaline granosyenite with aegirine and Fe-arfvedsonite; the intermediate zones are equivalent to peralkaline granite with riebeckite and Fe-arfvedsonite; the outer zones are marked by Fe-biotite (annite). Albite is present throughout, increasing toward the center. The central zones are also richest in the ore minerals and they appear as two irregular folded "lodes" 300-400m and 100-150 m thick, respectively, traced to 1,000 m depths. Of some 40 species of disseminated ore minerals cryolite, zircon, pyrochlore, gagarinite and REE-fluorite are most widespread, and pyrochlore (0.69% in the inner zone) is the main carrier of Nb and Ta. The crystallization temperatures decreased from 650-500°C for zircon to 456-410° for gagarinite and fluorite, and 180-160°C for cryolite. The metasomatites are localized in a zone of deep regional faults and postdate intrusive activity in the area. Archangel'skaya et al. (1993) consider mantle-derived fluid as responsible for the metasomatism and mineralization.

Hydrothermal U in albitized retrograde structures in high-grade metamorphics and granitoids

There is a considerable variety of U deposits that qualify for membership in this category, although the literature groups them in many alternative ways. Dahlkamp (1993) placed the three "large" example localities into his Type 2 (Subunconformity-epimetamorphic; Beaverlodge Lake), Type 12 (Metasomatite; Zheltye Vody), and Type 12.1 (Metasomatized granite; Lagõa Real). Given a different emphasis here the "typical" unconformity-U deposits do not fit as they are not always albitized, are not always in high-grade metamorphics, are shallow, and U is believed to

have been sourced from above so they appear in Chapter 11. The Ace-Verna U zone (read below), in contrast, has been mined to a depth of 1,600 m and it is a steeply dipping linear tectonic zone that could be characterized as a "shear-U". Other deposits form irregular masses in albitized, retrograded, ductile to brittle fault rocks and they have a much lesser vertical extent.

Beaverlodge Lake (Uranium City) U district, NW Saskatchewan (Beck, 1969; Tremblay, 1978; Ward, 1984; P+Rv 34 kt U @ 0.17%). Discovered in late 1940s, this was one of the early generation of Canadian U deposits in operation before the much more productive Athabasca unconformity-U province has been discovered. The district measures 40 x 25 km along the NE axis, marked by several deep faults. The amphibolite-grade gneiss, migmatite, minor metaquartzite and marble of the Archean to Paleoproterozoic Tazin Group have been extensively reactivated during the 1.7 Ga orogeny, so they form a mosaic of blocks separated by a great variety of ductile fault rocks (mylonite, ultramylonite, blastocataclasite, kakirite, phyllonite). Many of these rocks mimic non-tectonite lithologies (e.g. "shale") and this influences reliability of especially the early geologic maps from the region. There was a truly regional-scale development of metasomatites of several generations, overprinting the tectonites and faults. Early pegmatites, K-feldspar metasomatites, biotite-altered rocks and silicified zones give way to extensive albitization followed by chlorite, hematite and carbonates. Complete albitization produced pink pseudosyenite ("aceite", after Ace mine; this term is widely used in the Russian literature, spelled "eisite"). The Tazin Group is unconformably overlaid by Mesoproterozoic Martin Formation, a "volcanic redbeds" association, preserved as erosional remnant; this provides justification for the sub-unconformity classification of the Beaverlodge deposits, although the main stage of U mineralization predate the unconformity (~1.8-1.7 Ga).

The earliest radioactive occurrences are in the early pegmatites and although uneconomic, they are considered the source of U for the later generation of ores. Of the latter, there are some 20 mostly small U deposits; the **Fay-Ace-Verna** zone was the most productive (Smith, 1986; 23.6 kt U). This is an about 5 km long zone of metasomatized mylonite and local breccias along the San Louis Fault. Silicification, chloritization and red hematitization generally predated the U mineralization, which followed, overlapping with albitization and

carbonatization. Uraninite is the main mineral at the upper levels and it forms euhedral grains, botryoidal veinlets or fragments in breccia or calcitic gangue, with brannerite present at the deep levels.

Lagoa Real-U zone, Bahía, S-C Brazil (De Oliveira et al., 1985; 80 kt U @ 0.13%). This is a retrograde metamorphosed, heavily albitized N-S trending tectonic zone in Archean gneiss with local intercalations of amphibolite, Ca-Mg silicates and intrusions of charnockite and granite, believed thrust westward over the Paleoproterozoic Eşphinhaco sequence (Lobato et al, 1983). The tectonized Archean metamorphics are overprinted

by extensive regional Na > Ca metasomatites, attributed to metamorphic fluids displaced from the sub-thrust region and reacting with the granite-gneiss at temperatures around 500°C, in a depth of about 15 km under the paleosurface. The actual host to ore at Lagoa Real, according to De Oliveira et al. (1985), is an early microcline-plagioclase metasomatite (rather than granite as stated in the review literature), overprinted by albitite. U occurs in several subparallel, SW-dipping sheets of albitite and aegirine-augite metasomatite with disseminated grains of uraninite. The multiphase mineralization culminated around 850 Ma.

15 Giant Deposits in Geological Context

15.1. Origin of the giant deposits

Concentration and accumulation of metals that successfully terminates with formation of an economic mineral deposit ranges from an instantaneous, single-stage process to a prolonged, multistage history of gradual metal addition, reconstitution and modification. The opposite, metal dispersion (Holland and Petersen, 1981), is also at work and this can take place anywhere during the ore formation history and disperse (dissipate) a promising metal enrichment or an orebody already made. The most obvious and destructive case of ore dispersal is erosion of earlier deposits. Mining, equivalent to anthropogenic erosion and denudation, is a particularly rapid and efficient process of orebody removal and dispersion, although much lower quality "remnant deposits" like dumps of low grade material, tailings or slag heaps are sometimes generated by this process, and are left for future generations (Chapter 13).

The traditional simplified classifications of ores found in textbooks and especially the forced, abbreviated groupings of ore deposits in databases do not serve the reality well. They are responsible for numerous false starts in the early stages of mineral prospectivity assessments. The problem with conventional ore classifications is that they tend to focus on a single aspect or a stage only of a more complex genetic history, leaving other equally important aspects out. Lateritic nickel deposits are usually described in chapters on weathering and placed among residual deposits. Such deposits can, however, only form when the parent rock is highly geochemically enriched in Ni as in ultramafics. The Ni/clarke of concentration (CC) relative to continental crust is substantially greater for the trace Ni enrichment in peridotite (CC=about 36) than what is the added CC of the weathering process (CC=4 to 7). The necessity of ultramafic presence in search for Ni laterites is universally known, but there are less well understood situations where ore prediction and discovery depend on a logically organized, sensitive approach that reconstructs the entire (postulated) ore history and creates a model. Woodall (1994) provided several examples, both successful and unsuccessful, of concept generation to guide mineral exploration in Australia by Western Mining Corporation. Not all metallic

deposits, "giant" as well as those of lesser magnitudes, fit well into the conventional classification groups. Of these, some established ore types based on repetitive and little varied genetic components fare better than the rest and they hold a large number of "giants" (Table 15.1). Even these reliable stalwarts are often modified by superimposed processes such as supergenesis. This sometimes determines the existence of a giant (e.g. in the form of enriched porphyry coppers; Chapter 7) where there was none before.

It is thus advisable to include and subject to scrutiny all the decisive genetic and metallogenetic (=related to setting) parameters responsible for ore formation in mineral prospectivity exercises. This can be done mentally or, increasingly, with the help of the various techniques of spatial analysis like the geographic information systems (GIS; Bonham-Carter, 1995; Burrough and McDonnell, 1998; more about it in Chapter 17). Genetic coding of the formational history of an ore deposit, where every component can be accommodated in a separate GIS layer or a mental compartment, can help. A fairly rational classification (or more correctly organization) of ore deposit types can be accomplished by quantifying, weighting and ranking these genetic components. This is applicable to all ore magnitudes, but a set of prospectivity indicators particularly favorable for the presence of "giants" can be "distilled out".

Table 15.1. Number of known "giant" and "super-giant" deposits and districts of conventional ore types (updated from Laznicka, 1999)

Epithermal Ag	3
Epithermal Au-Ag	13
Epithermal Au	7
Epithermal Pb-Zn-Ag	4
Scheelite skarn	4
Porphyry Cu-Au	6
Porphyry Cu-Mo	90
Porphyry (stockwork) Mo	17
Sedex Zn-Pb-Ag	23
VMS (volcanics-hosted massive sulfides)	22
Broken Hill (high-grade metamorphic) Pb-Zn-Ag	12
Placer Au	7

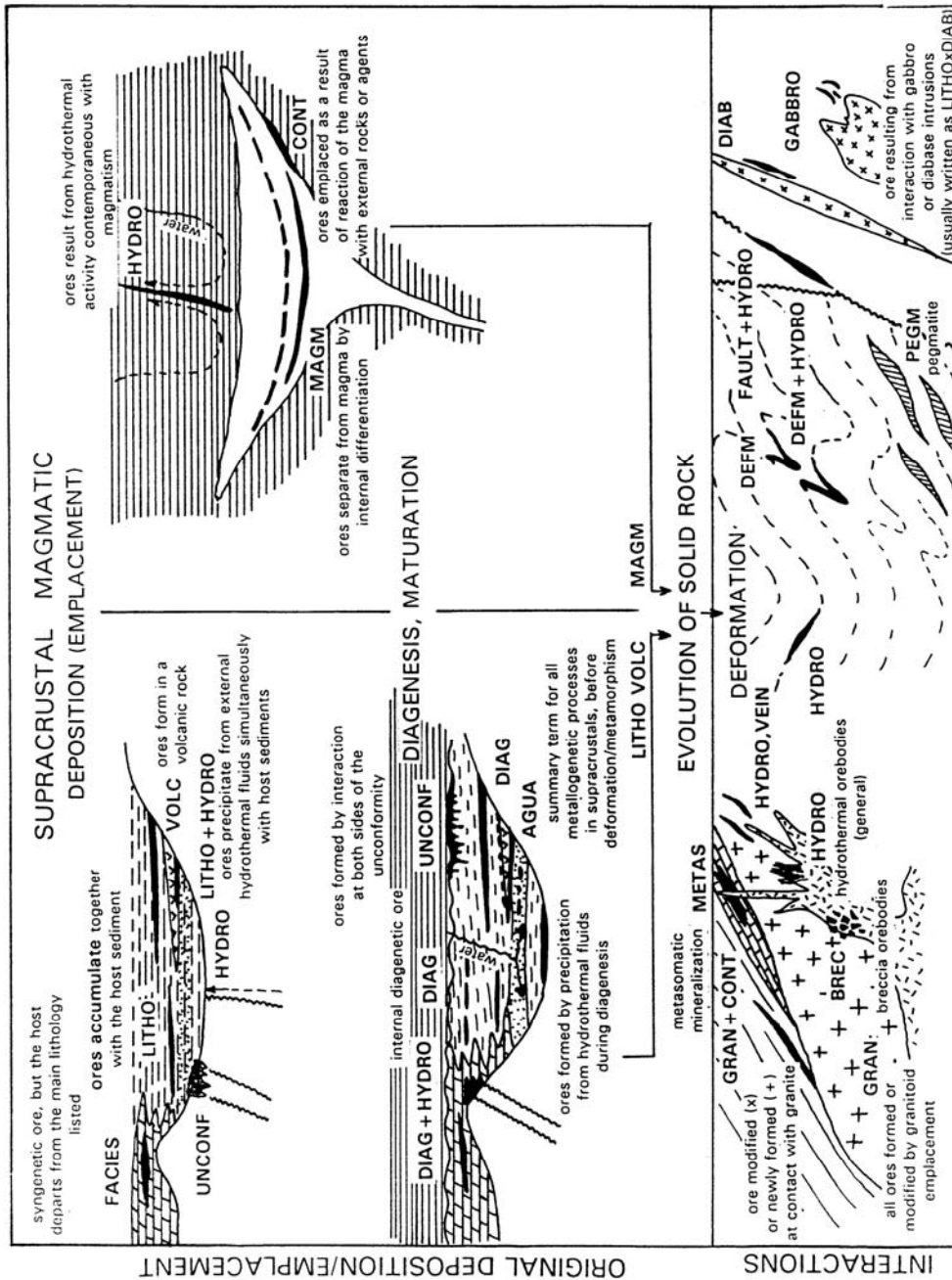
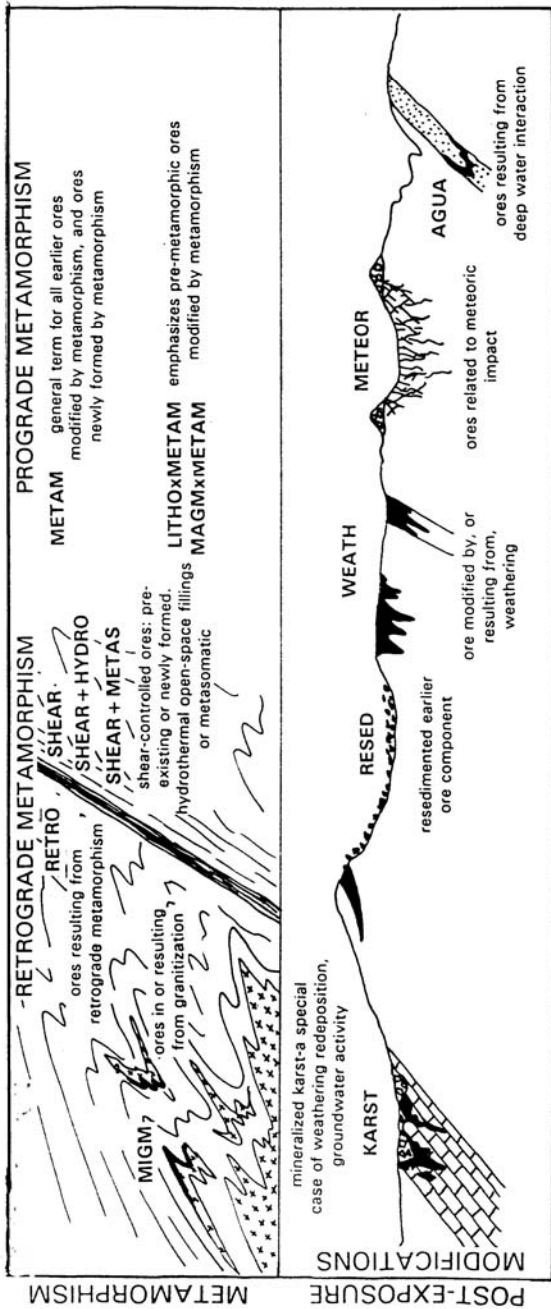


Figure 15.1. Common genetic types of metallic deposits and proposed mnemonic codes from Laznicka (1991, 1993)

15.1.1. Genetic coding and ore varieties

To provide more reality, better organization and reduce lengthy, repetitive descriptions of ore formation in databases, and to facilitate electronic retrieval and comparisons, a mnemonic code has been developed that record postulated ore history in one line (Laznicka, 1993; Fig. 15.1). An updated

version is used here for quantitative evaluation of giant deposits. Several examples: MAGM indicate a magmatic (magmatogene) deposit like the Bushveld chromitite; MAGM-HYDRO is magmatic-hydrothermal. SED indicates a sedimentary deposit (this implies syngenic and/or diagenetic metals introduction); VOLC-SED is volcanic-sedimentary, VOLC volcanogenic,



List of genetic codes in Figure 15.1.

- AQUA, ores precipitated from deeply circulating low-temperature (~50-150°C) basinal brines in aquifers
- BREC, ore in or related to breccias
- CONT, ore formed at intrusive contacts by thermal metamorphism and/or hydrothermal metasomatism (also SKARN)
- DEFM, ores controlled by deformation
- DIAB, GABBRO, ores in exocontact of diabase & gabbro intrusions, genetically related
- FACIES, ores controlled by changes in lithology and sedimentary facies
- FAULT, fault control of ore
- GRAN, granitoids related ores
- HYDRO, hydrothermal ores; EPIHYDRO, epithermal; MESOHYDRO, mesothermal
- KARST, ores in and related to karst
- LITHO, general term indicating ore (or trace metal enrichment) broadly contemporaneous with and related to the host rock
- MAGM, ores of magmatic crystallization
- MAGM-HYDRO, magmatic-hydrothermal
- METAM, ores in (higher-grade) metamorphics or generated by metamorphism
- METAM-HYDRO, metamorphic-hydrothermal ores
- METAS, metasomatic ores
- METEOR, ores produced or assisted by meteoritic impact
- MIGM, ores related to granitization
- PEGM, pegmatitic ores
- RESED, REPRECIP, resedimented and reprecipitated earlier ores
- SEDIM, sedimentary ores (also CLAST and CHEMSD)
- SHEAR, ores controlled by shear zones
- UNCONF, unconformity control
- VOLC, volcanogenic ores
- VOLC-HYDRO, volcanic-hydrothermal or EXHAL

Figure 15.1. (continued)

HYDRO hydrothermal, METAM metamorphic, WEATH weathering-generated. AQUA (equivalent to SUB-HYDRO) stands for deposits precipitated from heated basinal fluids as in the Mississippi Valley Zn-Pb type that are considered "not enough hydrothermal" but still "hotter than groundwater". LITHO is used as a general code for an unspecified, usually supracrustal barren or ore-bearing rock at

the start of ore-forming process (such a rock can be geochemically enriched in one or several metals up to the point of becoming an ore in its own way). LITHO x METAM x WEATH stands for a unspecified orebody and its host rock, later metamorphosed and modified by weathering. The fundamental categories can be further subdivided, e.g. MAGM can split into sub-categories UMAF

(ultramafic), MAFIC, GRAN (granitoid) and ALKAL (alkaline).

These are the principal genetic codes. A "simple" deposit, or one the information on which is sketchy or uncertain, can be characterized by a single mnemonic code only. METAM, used alone, stands for metamorphic ore in metamorphic rocks, which is an objectively demonstrated reality. A synmetamorphic-hydrothermal deposit would be written as METAM+HYDRO where + indicates contemporaneity of processes or conditions. If this is a post-metamorphic hydrothermal ore hosted by metamorphics, it is spelled METAM x HYDRO, where x means interaction that postdates the principal code. WEATH indicates a deposit formed or modified by weathering of an unknown or unspecified precursor. HYDRO x WEATH indicates a weathering modified hydrothermal deposit.

The basic genetic codes can easily be customized by the user, and the volume of detail increased, although this could overwhelm the relatively uncomplicated basic formula. A geological age of a process could be added (e.g. Np MAGM = Neoproterozoic magmatic) as well as a rock association, sub-category, and similar (e.g. $MAGM_{gabbro}$; = magmatic ore in/associated with gabbroids; $HYDRO_{meso}$ = mesothermal hydrothermal).

Two actual examples of "giants": Simple, usually single-stage deposits are a pleasure to interpret and organize. The **Mountain Pass** (Sulfide Queen) rare earths deposit in California is a single, thick, sharply outlined sheet of Mesoproterozoic carbonatite with densely scattered bastnäsite (Chapter 12). Its simple code would be MAGM, a more detailed code Mp MAGM_{carb}. The giant **Tomtor** rare metals field in Siberia (Epstein et al., 1994; Chapter 12; Fig. 15.2) also started as a Neoproterozoic silicate carbonatite with disseminated REE-rich apatite, monazite, pyrochlore, xenotime, florencite, bastnäsite and other minerals (Phase 1, MAGM). In Devonian the carbonatite, exposed at paleosurface, was karsted and Nb, REE, Y, Sc as well as apatite got enriched in a francolite and goethite-rich residue (Phase 2, WEATH). In Late Carboniferous the residue was mechanically reworked to form extremely rich lacustrine resistate heavy mineral beach placer (mainly monazite, xenotime, pyrochlore; Phase 3, RESED), and authigenic minerals associated with Al-phosphates have precipitated from lacustrine brines (REPRECIP). The simple genetic formula of Tomtor is thus MAGM x WEATH (or KARST) x

RESED + REPRECIP. The "involved" formula is $^{Np}MAGM_{carb} \times ^DWEATH_{karst} \times ^{Cb2}RESED_{placer} + REPRECIP_{playa\ brine}$. Perhaps this knit-picking seems overdone but it does nothing more than to substitute for genetic discussions that are a part of every paper on metallic deposits, where they take more space.

Orthogenetic (monogenetic), polygenetic, interactive and modified ores (Table 15.2)

Orthogenetic deposits result from a linear, incremental (cumulative) increase of metal(s) concentration and accumulation within a major rock-forming system. The orebodies are an integral part of such a system, and external influences on the ore formation are absent or slight. An orthomagmatic deposit, such as the layered chromitite in the Bushveld Complex or the Great Dyke (Chapter 12), results from settling of cumulate phase minerals in a preferential location within the magmatic chamber. Existence of a suitable magmatic complex is thus paramount for the occurrence of this type of deposits. Orthosedimentary ore deposits, such as the bedded Fe or Mn ores, accumulate simultaneously with the enclosing non-ore sediments, to which they are related by means of facies transitions.

Early interactive and polygenetic ore deposits form as a result of simultaneous evolution or mutual interaction of two or more rock forming systems, processes or agents. As a rule, ore deposits so created correlate with the time of interaction and they can be contemporaneous with, or younger than, their host rocks. Typical examples include the submarine-hydrothermal deposits (e.g. VMS, sedex) that are hosted by, and broadly contemporaneous with, the local sediments or volcanics but resulted from an external supply of a metal-bearing fluid.

Late modified ore deposits are the result of modification of an earlier deposit by a subsequent, superimposed enrichment process. The copper industry of the western United States owes its early 1900s origin to the existence of rich supergene chalcocite (and in places Cu silicate & carbonates) enrichment zones superimposed on the lower-grade primary ores or protores. Additional examples can be found among the weathering-reconstituted, resedimented and metamorphosed deposits, particularly the dynamically metamorphosed ones. Although interpretations of progenitors of several categories of metamorphosed deposits, like banded iron formations, are relatively error-free, they are difficult and controversial for the "Broken Hill-type" Pb-Zn-Ag deposits as the voluminous literature indicates (compare Laznicka 1993, p.1413).

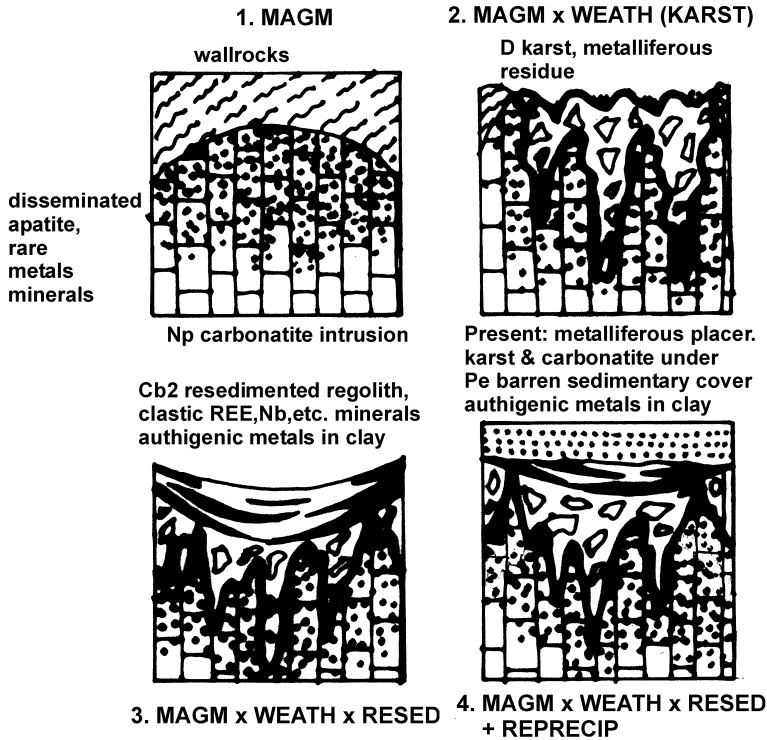


Figure 15.2. Evolution of the multiphase Nb, REE, Y, Ta, Sc mineralized, supergene-modified carbonatite Tomtor complex in the Siberian Platform. Based on data in Epstein et al. (1994)

In the latter case, it is difficult to establish as to whether the ore had been there before, or whether it was introduced, or substantially upgraded, during metamorphism. High-grade metamorphic deposits are thus treated here in their own "primary" category, even if they are the product of modification of pre-metamorphic deposits.

The style and history of metal accumulation in an ore deposit or an ore-bearing complex influence the internal uniformity and homogeneity that range from simple to highly complex (Figs. 15. 3. and 15.4). Creative interpretation of complex systems in the field, and during mining exploration, is of great importance as an initial finding of one style (e.g. a redeposited clastic ore) may result in discovery of a related style (e.g. the primary deposit). The history of "giant's" discoveries (Chapter 17) include many examples and case histories of this.

Forms of accommodation and distribution of ore metals in giant deposits (Table 15.3)

Metals in industrial ores have many forms in which they are held and distributed throughout. Apart from the styles of ore minerals' distribution, usually well

reviewed in textbooks (e.g. dispersed, disseminated, scattered, semi-massive, massive ores), it is important to consider the form in which the metals are held, as this influence the processing technology required and costs of metals recovery. The following categories can be distinguished and Table 15.3. lists examples of the corresponding "giant" deposits.

1. Native metals (Au, Cu, Ag, platinoids) are present as the principal ore mineral in the majority of Au deposits, in native copper deposits of Michigan, most PGE deposits (Merensky Reef), native Ag deposits Cobalt, Imiter and Batopilas.
2. High-metal content ore minerals other than the native metals like Au-Ag tellurides, argentite and Ag-sulfosalts, chalcocite. These minerals sometimes accumulate to form low volume, but extremely high-grade "bonanza" orebodies, some of which are of the "giant" magnitude (e.g. the Mexican silver "giants" Pachuca, Guanajuato, Zacatecas as well as the Bolivian Potosí; Comstock Lode, Hishikari gold; some chalcocite blankets over porphyry Cu; almost solid uraninite deposits like Cigar Lake and McArthur River-U; and others).
3. Average metal content ore minerals like hematite, magnetite, chalcopyrite, galena, sphalerite and others. They form the bulk of the "classical" metallic deposits of vein, replacement, exhalative and other types.

Table 15.2. Environment, process, configuration of mineral deposits showing the presence of the "giant" equivalents, orthogenetic and combined interactive deposits and sites

No	Divisions	Examples a	Examples b	Examples c
1	Atmosphere & gases; ATMOS, GAS	Industrial gases recovered from ordinary atmosphere: N ₂ , O ₂ , He, Ne, Ar, CO ₂	Synthetic products from atmosphere: nitrates, ammonia	Extracts from volcanic gases: SO ₂ , CO ₂ , H ₂ S, Cl, HCl, F, HF
2	Hydrosphere & liquids: WATER	Extracts from seawater: NaCl, Mg, Br	Extracts from some lake waters: NaCl, Na ₂ CO ₃ , Na ₂ SO ₄	Extracts from non-heated underground brines: NaCl, KCl, Na ₂ CO ₃ , Br, Li, B, H ₃ BO ₃ , W
3	Biosphere & anthroposphere BIOS, ANTHRO	Compounds and metals extracted from peat: Cu, Mn	Compounds extracted from plant ashes: I, K ₂ O	Extracts from mine tailings, slags: Au, Co, Cu, Ge, Ga, Ag
4	Weathering & pedogenesis WEATH	Metalliferous tropical regoliths (laterite & saprolite): Fe, Al, Ni, Co; kaolin & clays	Metalliferous arid regoliths (duricrusts): U, Cu, Mn; nitrates	Temperate regoliths: brick clay (nonmetallics)
5	Sedimentogenesis SEDIM or LITHO, AQUA	Metalliferous clastics: alluvial & beach placers Au, PGE, Sn, W, Fe; diamond; Ti, Zr, REE	Fine clastic to chemical sediments: bedded Fe, Mn, Al, Cu, Pb, Zn, U, V, Mo ; barite, phosphorite, pyrite	Evaporites (marine & lake): NaCl, KCl, Na ₂ CO ₃ Na, Mg sulfates, B, Li
5-6	Hydrothermal-sedimentary HYDRO+SEDIM	Zn, Pb, Ag, barite sedex		
6	Hydrothermal: general and convective; HYDRO	Hot springs to epithermal sinters, breccias, stockworks, veins, replacements Au, Ag, Pb, Zn, Cu, Sb, Hg .	Mesothermal veins, stockworks, replacements Au, Ag, Pb, Zn, Cu, Sb W, U, Fe	
6-7	Magmatic-hydrothermal MAGM+HYDRO	"Porphyry" deposits of Cu, Mo, Au, Ag, Sn, W in diorite to granite	Ore-bearing apogranites: Sn, W, Ta, Li, Cs, Rb, U. Veins, replacements in granite roof: Sn, W, Mo, Bi, U	Alkaline veins, metasomatites: Nb, REE, Be, Y, Th, U, Zr, Hf, Sc
7	Magmatic MAGM, VOLC	Mafic-ultramafic intrusions: Cr, PGE, Ni, Cu, Co, Au, Ti, Fe, V; ultramafic lavas: Ni	Rare metal granitic pegmatites: Li, Rb, Cs, Sn, Ta, Be, U	Ores in (per)alkaline systems & carbonatites: Nb, Y, Zr, REE, Th
6-8	Metamorphic-hydrothermal METAM+HYDRO	Veins, shear zones, metasomatites Mg, Fe, REE; chrysotile asbestos; Sri Lanka graphite ?	Orogenic deposits of Au, Ag, Cu, As, Sb, Hg, U	Michigan native Cu unconformity U, Au, Cu
8	Metamorphogenic METAM	Isochemical: kyanite, sillimanite, andalusite, corundum; graphite; garnets; rutile, monazite		Metasomatites: crocydolite; jadeite
9	Extra-lithospheric MANTLE METEOR	From the mantle: diamond in kimberlite & lamproite	From outer space: meteoritic Fe, Ni, Cu, PGE	

Giant metallic deposit types are shown in bold

Table 15.2. (continued from facing page on left)

No	Ortho/interactive examples	Modified deposits 1	Modified deposits 2	Bulk materials
1	Extracts from hydrocarbon ground gas: S, H ₂ S, N ₂ , He, Rn, CH ₄ , NH ₄ , Hg			atmospheric air natural (ground) gas
2	Extracts from some hydrothermal fluids: H ₃ BO ₃ , Hg, As, Au, Ag, Cu, Pb, Zn			Active hydrotherms, brines, springs
3	Extracts from general waste: Au			Waste repositories
4	Karst: bauxite, Fe oxides, Ni silicates	x METAM: emery, corundum, diaspore	x RESED: Fe oxide, bauxite gravels to clays	laterite for construction
5	Infiltrations: Cu, V, Mn, Fe late diagenetic in carbonates: Zn, Pb, Cu, U, ba, F	x WEATH: residual barite, phosphorite, Fe, Mn, Al, U x RESED: Fe, P, U, ba	x METAM: Fe(bif), Mn, Cu schists, Au-U Rand conglomerates x CONT: Mn silicates; Fe magnetite-olivine	stones & clays aggregates (sand, gravel); limestone, dolomite, gypsum
5-6		x WEATH: oxidic Pb, Zn ; Ag haloids	x METAM: Pb, Zn, Ag Broken Hill type	
6	VMS submarine massive sulfides: Fe, Cu, Zn, Pb, Au, Ag, ba	x WEATH: oxidic ores (gossans, etc.) Fe, Mn, Cu, Pb, Zn, Sb, Ag, Au, U x KARST: ditto, Fe Mn, Pb, Zn, Hg, Sb	x METAM	
6-7		x WEATH: enriched porphyries (Cu, Au), Sn-granite regoliths	x RESED: diamond, Sn, Ta placers x METAM: meta-porphry Cu	
7		x WEATH: residual Cr, PGE, Ti, Sn, Ta, Fe, Ni, Co, Mn, Mg x KARST: Nb, REE apatite on carbonatite	x RESED: Cr, PGE Ti, Sn, Ta placers x METAM: Cr, Ni, Cu, Fe, Ti, V in meta-mafics; Nb in meta-carbonatite	stones: serpentinite, gabbros, anorthosite, diorite, granitoids carbonatite, like limestone
6-8		x WEATH: residual Au (e.g. Au laterites) x RESED: Au placers		
8		x WEATH: residual corundum, andalusite x RESED: rutile, monazite placers		marbles other stones roofing slate
9		x WEATH: residual diamond x RESED: diamond placers		

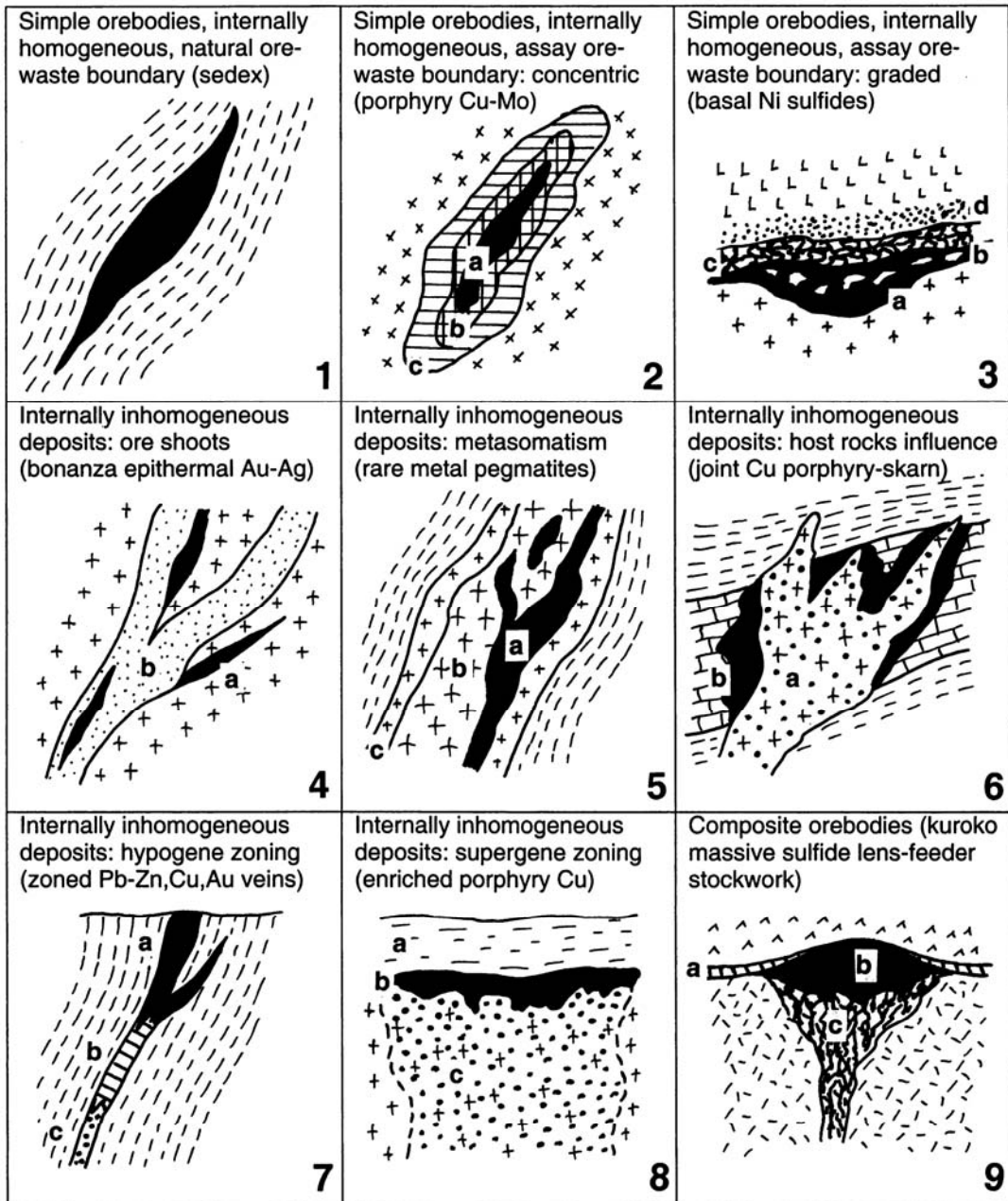


Figure 15.3. Internal uniformity (homogeneity) and complexity of the "classical" metallic deposits that include many "giants". Explanations: (2) a, average 1% Cu; b, 0.75% Cu; c, 0.5% Cu, the cutoff is 0.3% Cu; (3) a, massive basal Ni-Cu sulfides grade 7% Ni; b, breccia sulfides of 3% Ni; c, network sulfides with 1.5% Ni; d, disseminated sulfides, 0.7% Ni; (4) a, bonanza ore shoot with 500+ ppm Ag; b, mother lode quartz, ~20 ppm Ag; (5) albite metasomatic rare metals ore pegmatite; b, coarse K-feldspar pegmatite; c, wall pegmatite; (6) a, disseminated Cu sulfides in altered granodiorite; b, massive replacement Cu sulfides in exoskarn; (7) vertically zoned vein; a, Pb-Zn dominant; b, Cu dominant; c, Au dominant; (8) a, leached capping; b, chalcocite blanket, 1.5% Cu; c, porphyry Cu protore, 0.2% Cu; (9) exhalite (hydrothermal sediment marker); b, massive sulfides lens, high Zn, Pb grades; c, feeder stockwork, mainly Cu

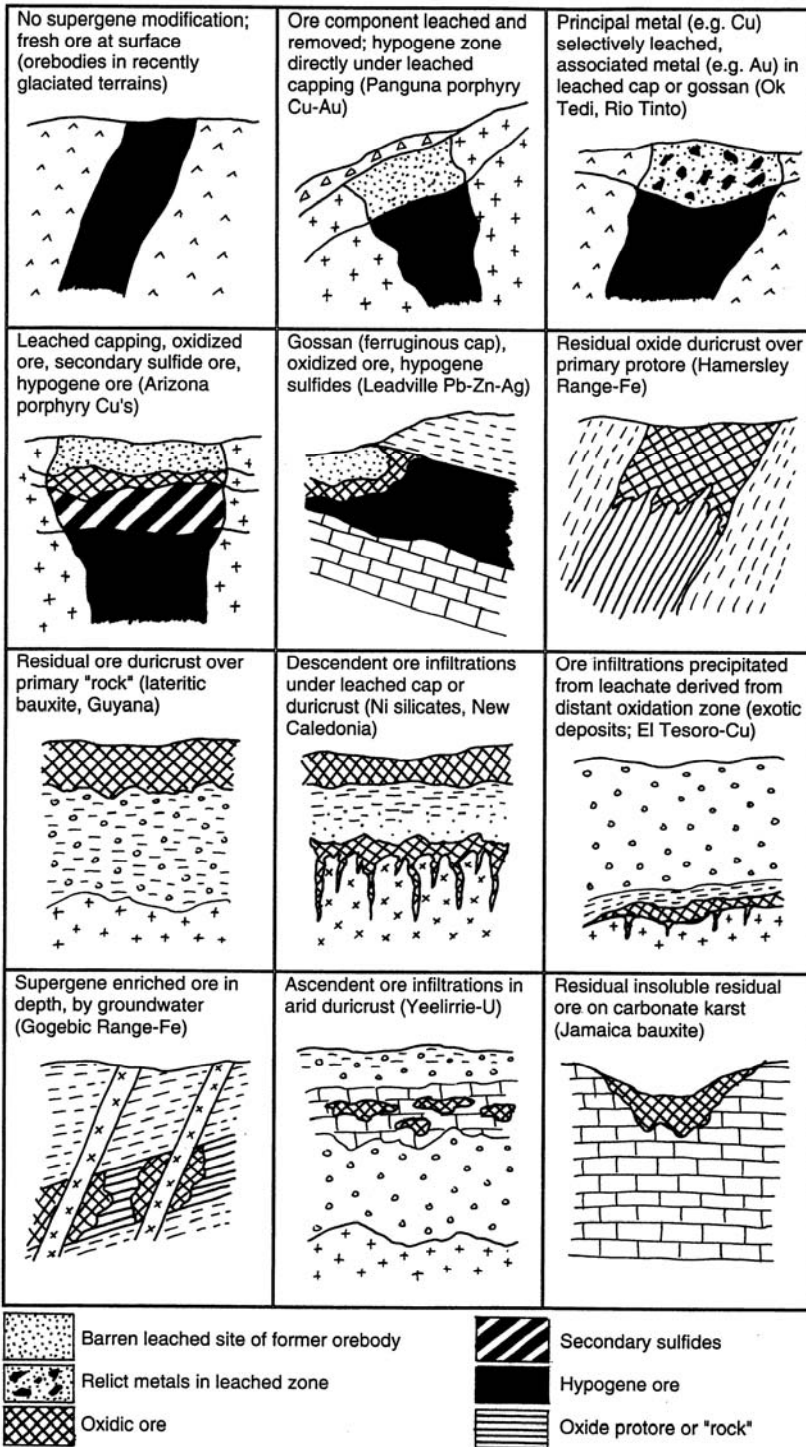


Figure 15.4. Supergene (weathering) modified primary orebodies or metalliferous rocks. Many "giants" have been substantially upgraded, or created, by this mechanism

Table 15.3. Examples of "giant" metal accumulation arranged by the categories of accommodation and distribution of the ore metals, described in text

CAT	METAL & LOCALITY	ENTITY	METAL CONTENT	TONNAGE ACC. INDEX	ORE GRADE	CLARKE OF CONC
1	Ag: Batopilas, Mexico	ore field	9,360 t	1.34x10 ¹⁰	600 ppm	8,570
	Ag: Cobalt, Ontario	ore district	14,545 t	2.08x10 ¹¹	900 ppm	12,940
	Au: Hishikari, Kyushu	ore deposit	260 t	1.04x10 ¹¹	80 ppm	32,000
	U: not available					
	Cu: Calumet-Hecla, Michigan	ore deposit	2.736 Mt	1.09x10 ¹¹	2.40 %	960
	Mn: not available					
	Fe: Disko Island, Greenland (small)					
2	Ag: Guanajuato, Mexico	ore field	31,042 t	4.43x10 ¹¹	374 ppm	5,340
	Au: Cripple Creek, Colorado	ore field	755 t	3.02x10 ¹¹	60 ppm	24,000
	U: Cigar Lake, Saskatchewan	ore deposit	137 Tt	1.01x10 ¹¹	12.2 %	71,800
	Cu: Butte Cu-Ag veins, Montana	ore field	6.80 Mt	2.72x10 ¹¹	4.00 %	1,600
	Mn: Groote Eylandt, Australia	ore deposit	222 Mt	3.08x10 ¹¹	43.0 %	597
	Fe: Kiruna, Sweden	ore deposit	2.0 Bt	4.65x10 ¹⁰	67.0 %	15.6
3	Ag: Brunswick #6 & #12, Canada	ore deposits	14,100 t	2.01x10 ¹¹	94 ppm	1,340
	Au: Central Rand Goldfield, S.A.	ore district	8,962 t	3.58x10 ¹²	8.33 ppm	3,330
	U: Grants district, New Mexico	ore district	382 Tt	2.25x10 ¹¹	0.19 %	1,120
	Cu: Bingham porphyry Cu-Mo, Utah	ore deposit	18.9 Mt	7.56x10 ¹¹	0.7 %	280
	Mn: Molango enriched ore, Mexico	ore deposit	465 Mt	6.46x10 ¹¹	27.2 %	385
	Fe: Mesabi Range enriched ore, MN	ore district	1.62 Bt	3.77x10 ¹⁰	54.0 %	12.6
4	Ag: Aggeney's, South Africa	ore field	7,823 t	1.12x10 ¹¹	39 ppm	557
	Au: Grasberg & Dalam, Indonesia	ore deposit	2,100	8.4x10 ¹¹	1.2 ppm	480
	U: Rossing, Namibia	ore field	138 Tt	8.12x10 ¹⁰	350 ppm	206
	Cu: Haib, Namibia	ore field	3.10 Mt	1.24x10 ¹¹	0.24 %	96
	Mn: Molango Mn horizon (raw), MX	ore zone	1.5 Bt	2.08x10 ¹²	10 %	138
	Fe: Mesabi Range taconite, MN	ore district	11.25 Bt	2.62x10 ¹¹	25 %	5.81
5	Ag: Bingham porphyry Cu-Mo, Utah	ore deposit	14,000 t	2.00x10 ¹¹	2.63 ppm	38
	Au: Bingham porphyry Cu-Mo, Utah	ore deposit	937 t	3.75x10 ¹¹	0.31 ppm	124
	U: Billingen-Falbygden Kolm Shale, S	metallif. horiz.	1.7 Mt	1.00x10 ¹²	213 ppm	125
	Cu: Rio Tinto pyrrhite, Spain	ore fields	400 Tt	1.00x10 ¹⁰	0.2 ppm	50
	Mn: Chamberlain nodules, S.Dakota	metallif. horiz.	5.0 Mt	6.94x10 ⁵	1.0 %	13.9
	Fe: Mesabi R., hemat. taconite/shale	metallif. horiz.	15.0 Bt	3.49x10 ¹¹	25 %	5.81

Units: t=tons, Tt=thousand tons, Mt=million tons, Bt=billion tons

- Low metal content, usually complex ore minerals and mineraloids like ilmenite for Ti, "garnierite" for Ni, pyrochlore for Nb, monazite for REE and Th, chamosite or greenalite for Fe.
- Accessory metalliferous minerals or substances in rocks that are normally sparsely distributed and uneconomic to mine, but that can be enriched by a natural process like weathering (lateritic ores) or sedimentary reworking (placers). Other forms of metals' accommodation are major or accessory nonmetallic minerals or substances (like apatite, carbon) with high trace contents of some metals (U in Florida phosphates; REE in Khibiny apatite) recoverable as a by-product.
- Major rock-forming minerals and whole rocks with exceptionally high contents of some trace metals (e.g. olivine and peridotite with 0.2-0.3% of Ni and Cr). These are the potential ores of the future.
- Waters (mainly salt, some fresh) with sub-clarke contents of metals (dissolved, sometimes in suspension), from which some metals (presently Mg) can be economically recovered under certain conditions. "High grade" metalliferous brines in the subsurface (Salton Sea) or discharging on the sea floor (e.g. some of the Red Sea "Depths").

15.1.2. Giant deposits and their genetic and host rock associations

Statistics require precise and unequivocal input, a rare commodity for ore deposits for reasons discussed above. So to provide a simplified statistical answer as to which are the most favorable "giant" ore forming processes and rock associations,

shown in Table 15.4. and in related graphs (Fig. 15.5), it has been necessary to put aside the consideration of complex genesis and concentrate on the single most important aspect only. The discussion that follows has been updated from Laznicka (1999).

About the most striking finding regarding the origin of metalliferous "giants" is the predominance of deposits, of all sizes, that precipitated from hydrous fluids (Fyfe et al., 1978). The fluid-based ore-forming regimes have been subdivided into two families:

(1) cool to low-temperature surface waters (1a), and subsurface aqueous fluids (1b). 1a-type waters are implied as an agent of sedimentogenesis and of chemical weathering in the sedimentary (SEDIM) and weathering (WEATH) categories. 1b-type fluids are responsible for the low-temperature rock diagenesis and variously heated ground water (brine) circulation credited with accumulating metals in the AQUA category.

(2) hydrothermal fluids exsolved from magmas and/or heated by magmatic and metamorphic (geothermal) systems. Hydrothermal (HYDRO) deposits make up the largest genetic family of "giant" deposits, subdivided into several lesser categories by increasing temperature (hot spring, epithermal, mesothermal, hypothermal), special magmatic association (e.g. a hydrothermal phase of alkalic intrusions), and transitionality (e.g. hydrothermal-sedimentary, i.e. ores precipitated from in-depth generated hydrothermal fluids discharged on the sea floor as in the sedimentary-exhalative [sedex] type; hydrothermal volcanic-sedimentary as in the VMS deposits).

The less controversial genetic categories embrace metalizations affiliated to magmatism in restricted sense ("MAGM"; this excludes the magmatic hydrotherms), volcanism ("VOLC"), and high-grade metamorphism ("HIMETAM", e.g. deposits of the Broken Hill-type Pb-Zn-Ag; Parr and Plimer, 1993). The metamorphic-hydrothermal vein deposits, where the agents of deposition have been hydrous fluids derived by metamorphic dehydration in depth (Goldfarb et al., 1992, 1993; Groves et al., 1982), have not been separated from the "ordinary" hydrothermal deposits ("HYDRO"; e.g. the Kalgoorlie, Timmins, Mother Lode Au deposits are entered as "HYDRO-MESO-Au"). The native copper and/or chalcocite-mineralized metabasalt flowtops as in the Keweenaw Supergroup in Michigan, interpreted as a product of precipitation of copper leached from the volcanic pile in depth by fluids released during metamorphic

dehydration and deposited at the greenschist/prehnite-pumpellyite metamorphic interface (Bornhorst et al., 1988), have been placed into the category "METAM-HYDRO-Cu".

The still enigmatic, low-temperature cinnabar deposits in sedimentary rocks, melanges and ophiolites associated with faults and folds which, because of the extremely low Hg crustal clark, have a strong presence among the giant deposits (e.g. Almadén, Spain; Idrija, Slovenia; New Almaden, California) have hitherto been treated as "hot spring", telethermal, epithermal, or exhalative metalizations. This is probably true for the deposits situated in terrains with synchronous volcanism or magma-driven geothermal circulation as in the Clear Lake region of California (the Sulfur Bank Hg deposit; Rytuba, ed., 1993), in the McDermitt Caldera, Nevada and Oregon, and partly in the Monte Amiata district of Tuscany, but it does not apply to the three Hg-giants and supergiants mentioned above.

Syn-diagenetic introduction of Hg in an externally derived fluid (related to spilitic breccias? Hernández et al., 1999) or low-temperature remobilization of cinnabar or native mercury into dilations controlled by tight folds at Almadén (Saupé, 1990) or major fault zones (Idrija, Khaidarkan; Bercé, 1958) would place these deposits into the "AQUA-Hg" category. The New Almaden Hg deposit in the Franciscan terrane of California has been interpreted by Rytuba (1996) as a product of near-surface precipitation from low-temperature, high-CO₂ fluids derived from connate waters above a thermal anomaly related to a slab window.

Hydrothermal ores and magmatic families

Hydrothermal metalizations are often spatially associated with coeval magmatic systems, but many appear independent. The last fifteen years have marked the return to the predominance of concepts linking the late magmatic and hydrothermal processes, concepts established in the pre-World War II period (Lindgren, 1933) and temporarily de-emphasized in the Age of Stratiformity in the 1970s (Burnham, 1979; Brimhall and Crerar, 1989; Candela, 1989; Hedenquist and Lowenstern, 1994).

Table 15.4. Genetic categories of the "giant" and "super-giant" metallic deposits. From Laznicka (1999), reprinted with permission from Economic Geology v. 94:4, Table 7, p. 465

Genetic category	Metal	Number of "giants" and "super-giants"	Cumulative metal tonnage
Hydrothermal-sedimentary	Au	1	3.11x10 ²
Hydrothermal volcanic/sedimentary	Ag	3	4.57x10 ⁴
Hydrothermal volcanic/sedimentary	As	1	4.50x10 ⁶
Hydrothermal volcanic/sedimentary	Au	3	1.95x10 ³
Hydrothermal volcanic/sedimentary	Cu	5	1.56x10 ⁷
Hydrothermal volcanic/sedimentary	Fe	1	1.20x10 ¹⁰
Hydrothermal volcanic/sedimentary	Pb	7	3.90x10 ⁷
Hydrothermal volcanic/sedimentary	Zn	3	5.63x10 ⁷
Hydrothermal volcanic/sedimentary	Sb	1	2.18x10 ⁵
Magmatic-alkaline	Nb	2	1.50x10 ⁷
Magmatic-alkaline	REE	2	7.50x10 ⁶
Magmatic-alkaline	Zr	2	2.60x10 ⁸
Magmatic-carbonatite	Cu	1	1.10x10 ⁷
Magmatic-carbonatite	Nb	3	8.67x10 ⁷
Magmatic-carbonatite	REE	2	5.45x10 ⁷
Magmatic-carbonatite	Th	1	1.16x10 ⁶
Magmatic-carbonatite	Y	1	3.00x10 ⁶
Magmatic-mafic	Cu	3	7.31x10 ⁷
Magmatic-mafic	Fe	1	6.60x10 ¹⁰
Magmatic-mafic	Ni	4	5.17x10 ⁷
Magmatic-mafic	PGE	6	8.91x10 ⁶
Magmatic-mafic	Ti	1	2.88x10 ⁹
Magmatic-mafic	V	1	3.71x10 ⁸
Magmatic-pegmatitic	Sn	1	5.00x10 ⁵
Magmatic-umafic	Cr	3	4.18x10 ⁹
Magmatic-umafic	Cu	1	3.42x10 ⁶
Magmatic-umafic	Ni	1	5.60x10 ⁶
Magmatic-umafic	PGE	1	1.68x10 ³
Metamorphic-hydrothermal	Cu	3	1.67x10 ⁷
Sedimentary-authigenic	Mo	1	3.20x10 ⁵
Sedimentary-authigenic	U	1	3.00x10 ⁵
Sedimentary-chemical	Fe	7	1.09x10 ¹¹
Sedimentary-chemical	Mn	8	7.16x10 ⁹
Sedimentary-chemical-(metam)	Fe	2	6.41x10 ¹⁰
Sedimentary-clastic	Au	17	5.23x10 ⁴
Sedimentary-clastic	U	1	4.84x10 ⁴
Sedimentary-evaporitic	Li	2	9.10x10 ⁶
Volcanic-diagenetic	Cu	1	4.50x10 ⁶
Volcanic-diagenetic	Li	1	2.25x10 ⁶
Weathering-residual/reworked	Sn	8	1.24x10 ⁸
Weathering-residual	Co	1	2.50x10 ⁶
Weathering-residual	Mn	1	2.75x10 ⁸
Weathering-residual	Ni	3	6.33x10 ⁷
Weathering-sulfide	Au	1	3.25x10 ²
Aqua (sub-hydrothermal)	Hg	12	7.92x10 ⁵
Aqua (sub-hydrothermal)	Pb	1	3.20x10 ⁶
Aqua (sub-hydrothermal)	Sb	1	1.75x10 ⁵
Aqua ? (sub-hydrothermal)	Cu	1	2.64x10 ⁶
Aqua-carbonate (sub-hydrothermal)	Hg	4	1.06x10 ⁵
Aqua-carbonate (sub-hydrothermal)	Pb	9	8.18x10 ⁷
Aqua-carbonate (sub-hydrothermal)	Zn	4	6.27x10 ⁷
Aqua-redox (sub-hydrothermal)	Ag	2	1.82x10 ⁵
Aqua-redox (sub-hydrothermal)	Co	2	9.51x10 ⁶

Table 15.4 (continued)

Genetic category	Metal	Number of "giants" & "super-giants"	Cumulative metal tonnage
Aqua-redox (sub-hydrothermal)	Cu	19	3.56x10 ⁸
Aqua-redox (sub-hydrothermal)	Pb	1	2.60x10 ⁶
Aqua-redox (sub-hydrothermal)	U	2	6.29x10 ⁵
Aqua-redox ? (sub-hydrothermal)	Cu	1	3.05x10 ⁶
Aqua-unconformity	U	3	5.35x10 ⁵
High-grade metamorphic	Ag	3	7.42x10 ⁴
High-grade metamorphic	Cu	1	2.50x10 ⁶
High-grade metamorphic	Pb	5	4.12x10 ⁷
High-grade metamorphic	Zn	4	5.88x10 ⁷
High-grade metamorphic	Zr	1	2.50x10 ⁷
Hydrothermal-alkaline	Nb	1	2.00x10 ⁶
Hydrothermal-alkaline	REE	1	3.60x10 ⁷
Hydrothermal-brine	Ag	1	1.09x10 ⁴
Hydro-epithermal	Ag	12	2.99x10 ⁵
Hydro-epithermal	As	1	5.44x10 ⁵
Hydro-epithermal	Au	16	7.14x10 ³
Hydro-epithermal	Pb	3	1.23x10 ⁷
Hydrothermal-hot spring	Hg	2	2.08x10 ⁴
Hydro-mesothermal	Ag	16	1.90x10 ⁵
Hydro-mesothermal	As	7	3.61x10 ⁶
Hydro-mesothermal	Au	61	3.52x10 ⁴
Hydro-mesothermal	Bi	5	5.20x10 ⁵
Hydro-mesothermal	Cd	1	1.08x10 ⁴
Hydro-mesothermal	Cu	67	7.34x10 ⁸
Hydro-mesothermal	Hg	1	3.15x10 ⁴
Hydro-mesothermal	Mo	39	2.69x10 ⁷
Hydro-mesothermal	Pb	19	5.94x10 ⁷
Hydro-mesothermal	Sb	22	6.58x10 ⁶
Hydro-mesothermal	Sn	13	1.09x10 ⁷
Hydro-mesothermal	Te	3	3.39x10 ³
Hydro-mesothermal	U	2	1.50x10 ⁶
Hydro-mesothermal	W	12	3.63x10 ⁶
Hydro-mesothermal	Zn	3	3.00x10 ⁷
Hydrothermal-sedimentary	Ag	6	5.71x10 ⁴
Hydrothermal-sedimentary	Pb	10	6.23x10 ⁷
Hydrothermal-sedimentary	Zn	7	1.07x10 ⁸

The material association between several contrasting magmatic families such as mafic-ultramafic or carbonatites on one side, and intramagmatic ore metal associations such as Cr, PGE, Ni, Fe-Ti-V or Nb-REE on the other, known for a long time, has been extended. It includes the various petrochemical families of intrusive rocks on one side, and repetitively occurring post-magmatic hydrothermal ore metal associations on the other (Abdullaev, 1964; Sattran et al., 1970; Urabe, 1985; Keith, 1986; Shaw and Guilbert, 1990; Keith and others, 1991; Blevin and Chappell, 1992). The plate tectonic model, especially its latest version that recognizes the role of displaced terranes, provides framework and a major control to magmatism and

metallogeny (Sawkins, 1990). Barton (1996) has recognized three, presumably transitional, categories of ore-depositing hydrothermal fluids in respect to magmatic systems: 1) those where magmatic fluids and heat are essential; 2) those where magmatic heat is essential and magmatic fluids problematic; 3) those where the magmatic link is problematic. The category 1) shows the best correlation between magmatic families and distinct ore metals sets. Such a correlation is useful in metallogenic predictions, and it is also extremely well pronounced among the giant and supergiant metal deposits; 182 entries in the GIANTFILE database responded positively (Table 15.5., Fig. 15.6).

Table 15.5. Giant deposits genetically related to magmatic families. From Laznicka (1999), reprinted with permission from *Economic Geology*, v. 94:4, Table 8, p. 466

Number	Magmatic family, metal	Metal content, tons	Number of deposits
1	agpaite, Nb	15×10^7	2
2	agpaite, REE	7.5×10^6	2
3	agpaite, Zr	2.6×10^8	2
4	alkaline-ultramafic, Cu	11.05×10^7	1
5	carbonatite, Nb	8.76×10^7	3
6	carbonatite, REE	5.446×10^7	2
7	carbonatite, Th	1.16×10^6	1
8	carbonatite, Y	3.0×10^6	1
9	diorite-monzonite, Ag	1.4×10^4	1
10	diorite-monzonite, Au	2.1×10^3	2
11	diorite-monzonite, Cu	3.72×10^7	4
12	Fe-tholeiite, Cr	3.47×10^9	1
13	Fe-tholeiite, Cu	7.313×10^7	3
14	Fe-tholeiite, Fe	6.6×10^{10}	1
15	Fe-tholeiite, Ni	5.172×10^7	4
16	Fe-tholeiite, PGE	8.9125×10^4	6
17	Fe-tholeiite, Ti	2.88×10^9	1
18	Fe-tholeiite, V	3.71×10^8	1
19	K-granite, Ag	2.0×10^4	1
20	K-granite, Bi	3.0×10^4	1
21	K-granite, Sn	2.23×10^7	19
22	K-granite, W	2.715×10^5	2
23	metalum granod-qz monz, Ag	31.23×10^4	3
24	metalum granod-qz monz, Au	3.343×10^3	6
25	metalum granod-qz monz, Cu	6.13×10^8	58
26	metalum granod-qz monz, Mo	2.083×10^7	30
27	metalum granod-qz monz, W	2.7×10^5	1
28	metalum granite, Bi	4.68×10^5	3
29	metalum granite, Mo	6.065×10^6	7
30	metalum granite, Sn	4.2×10^5	1
31	metalum granite, Te	8.8×10^2	1
32	metalum granite, W	1.48×10^6	2
33	MORB (mid-ocean r. basalt), Cr	3.5×10^7	1
34	peralkal granite, Li	2.25×10^6	1
35	peralkal granite, Sn	5.5×10^5	1
36	peraluminous pegmatite, Sn	5.0×10^5	1
37	peridotite, Cr	6.82×10^8	1
38	peridotite, Cu	3.417×10^6	1
39	peridotite, Ni	5.6×10^6	1
40	peridotite, PGE	1.68×10^3	1
41	syenite-trachyte, Au	7.55×10^2	1

Among the total of database entries, the most prolific host to giant and supergiant accumulations is the calc-alkaline metaluminous granodiorite-quartz monzonite association at subductive continental margins, the almost exclusive parent to the porphyry Cu-Mo deposits. Keith and Swan (1996) reviewed in detail the "Great Porphyry Copper Cluster" in Arizona, Sonora and adjacent parts of New Mexico that contains 187 known porphyry Cu-Mo districts of Mesozoic to mid-

Cainozoic age, twelve of which are of giant magnitude. They characterized the Cu-Mo orebodies as being in and marginal to biotite granodiorite stocks. The stocks are associated with hornblende-bearing precursor plutons, members of the metaluminous, calc-alkaline, Fe-Ti poor, normal Cl-F-Rb-Zr oxidized (magnetite-titanite) magma series extracted from a high-alumina quartz-kyanite eclogite in the asthenospheric wedge above the subduction (Benioff-Wadati) zone.

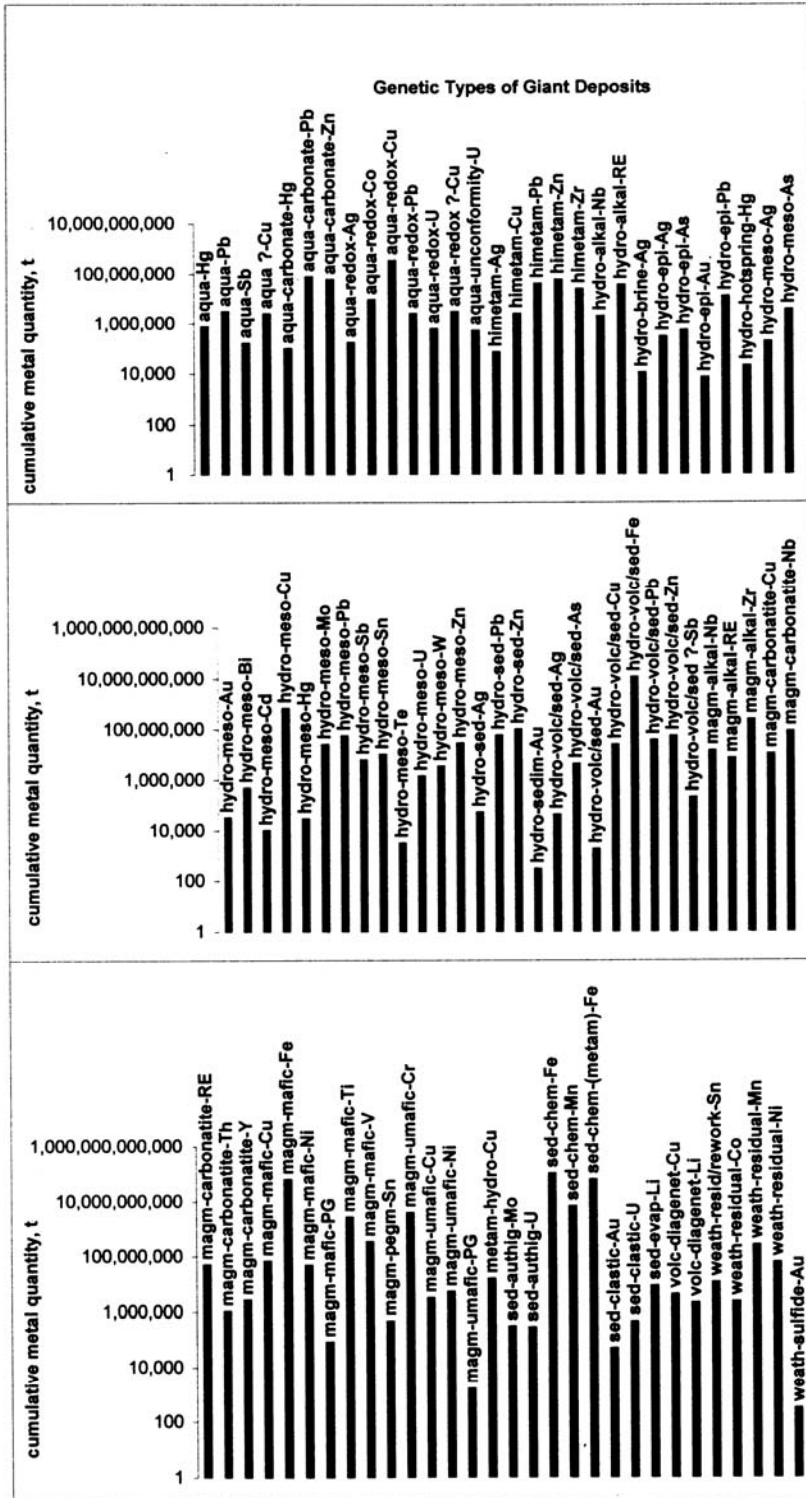


Figure 15.5. Cumulative quantities of ore metals in "giant" and "super-giant" ore deposits in the genetic classes listed in Table 15.4. Laznicka (1999), reprinted with permission from *Economic Geology* v. 94:4, Fig. 4, p.466

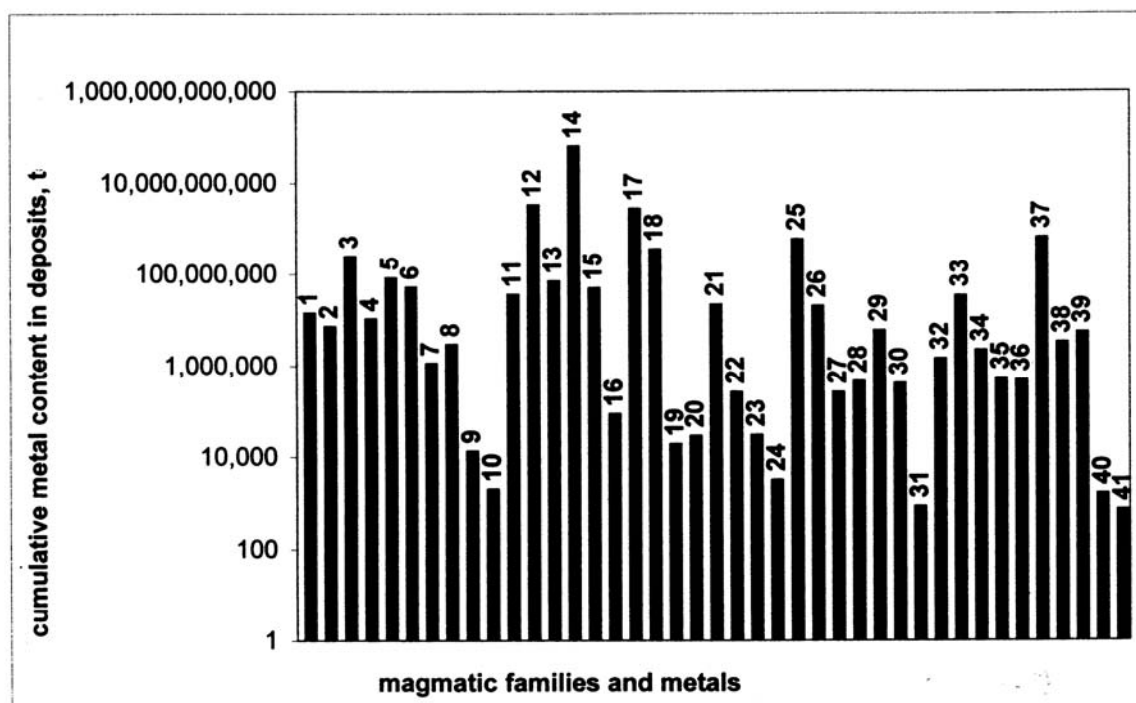


Figure 15.6. Histogram of the "giant" deposits genetically associated with the various magmatic families. The numbered columns correspond to entries in Table 15.5. Laznicka (1999), reprinted from *Economic Geology*, v. 94:4, Fig. 5, p. 467

Titley (1993), in contrast, assumed lower crustal derivation of the same magmas.

When the frequency of occurrence of giant metal accumulations is contrasted with the abundance of parent intrusions of distinct petrochemistry and origin, the most prolific single magmatic family is carbonatite. Carbonatite forms rare isolated occurrences but most frequently it participates in a joint nephelinite-carbonatite association (especially at high crustal levels; Le Bas, 1987). It also appears as a frequent extreme fractionate in agpaite suites dominated by nepheline syenitic rocks, as well as in alkaline-ultramafic suites in association with pyroxenite. Presently there are about 330 carbonatite occurrences recognized and recorded worldwide (Wooley, 1989), or perhaps 350 when the additional occurrences in the former U.S.S.R., Mongolia and China are included. Five of the carbonatites host giant or supergiant Nb, REE, Th and Cu deposits and additional eleven carbonatites host large deposits of these metals. This corresponds to 1.4% and 3.1% of the entire global inventory of carbonatites, respectively. As several carbonatites are "multiple giants" (they accommodate more than one ore metal in exceptional quantities; for example Araxá, Brazil and Tomtor, Siberia, host joint Nb, REE and Th

"giants"), the "giant" and "large" ore carbonatites account for 21 entries (records) in the GIANTDEP database. These impressive statistics suggest that any discovery of a new carbonatite has an about 4.5% chance that a "giant" or a "large" metal deposit will follow. No other class of rocks comes closer!

Alkaline rocks are substantially more abundant in the lithosphere than carbonatites, yet they are still rare rocks that are credited with occupying no more than 0.2-0.3% of the continents by area (Sørensen, ed., 1974). Nine alkaline complexes without carbonatites and twenty five complexes with carbonatites are associated with six "giant" and twelve "large" entries in the GIANTDEP database as some localities are multi-metal accumulations. This represents about 2.5% (without carbonatites) and 7% (with carbonatites) of the entire "giant/supergiant" population of metallic deposits. Alkaline and carbonatite-hosted "giants" store about 103 million tons of Nb, 72 million tons of REE, 260 million tons of Zr, 1.16 million tons of Th, 3.2 million tons of Y in potentially mineable orebodies. 11 million tons of Cu is accumulated in a single lonely "giant" carbonatite-hosted deposit Palabora, South Africa.

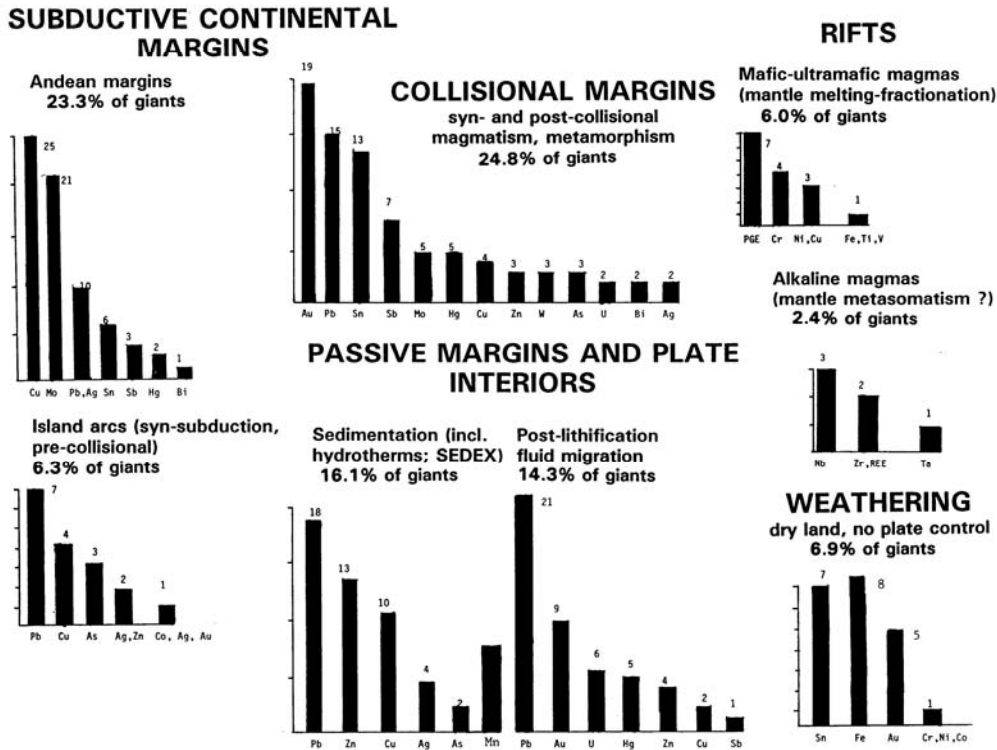


Figure 15.7. Share of the plate tectonic divisions on formation of the "giant" metallic deposits of selected metals. From Laznicka (1998), reprinted courtesy of E. Schweizerbart'sche Verlagsbuchhandlung, Stuttgart

There, the copper origin is attributed by Eriksson (1989) "to the abundance of Cu in the local crust".

15.2. Giant metallic deposits: geotectonic setting

Plate tectonics, born in 1968 (Morgan, Le Pichon) replaced the geosynclinal theory and is now the principal framework of organization of global geoscientific knowledge also applied to the ore-forming processes and ore distribution. Text- and reference books on ore deposits have been written within the plate tectonic context (Routhier, 1980; Mitchell and Garson, 1981; Hutchison, 1983; Sawkins, 1990). In this book the practically relevant version of geotectonics is the first order classifier, but the emphasis is on the rock associations that host the ores. Such rocks can be directly observed and mapped in the field and in geologically young settings. There, the cause and effect, that is the process & environment, and the type of rocks and ores that result, overlap. In geologically older, deformed and metamorphosed associations the

original setting and processes have to be interpreted and a perusal of almost every recent paper that discusses ore formation demonstrates the disunity and a short term validity of many interpretations. This is hardly of help to the practitioners in the bush so the chapters dealing with ancient rocks and ores here at times revert to the classical geotectonic divisions like eugeoclinal and miogeoclinal (referring to rock mega-associations rather than model structures, a practice retained by the U.S. Geological Survey as well). These divisions, before the appearance of plate tectonics, served the ore finder well (Bilibin, 1951). Figure 15.7. shows the preference of the "giant" and "super-giant" deposits for one of the six highly generalized plate settings, briefly summarized in Laznicka (1998).

In contrast to the early (1970s) version of "ores and plate tectonics", when the bulk of magmatism and hydrothermal activity were automatically considered coeval with subduction or rifting, a greater variety of ore formation stages is now recognized. For example, Dawson et al. (1992) distinguished the following stages of hypogene mineralization in the Meso-Cenozoic convergent

margin and orogen of the Canadian Cordillera (compare Fig. 8.2. above):

1. Pre-subduction metallogenesis, related to accretion at oceanic ridges and ocean floor sedimentation;
2. Subduction-related ores in island arc complexes (including back-arcs) and andean-type margins;
3. Collision-related ores;
4. Metallogenesis during the final, post-collision adjustments or renewed intracrustal extension.

To this should be added supergene ore formation (enriched zones, placers) that postdated each of the four stages, although largely obliterated by Quaternary glaciation (except in the ice-free region in NW Yukon where the "giant" Klondike placers survived).

15.3. Giant metal accumulations in geological time

The subject of ore formation in geological time, and the influence of evolution, has an extensive literature (e.g. Laznicka, 1973; Hutchinson, 1981; Meyer, 1981, 1988; Holland, 1984). It is also a subject widely covered in textbooks and reference books so there is no need for thorough introduction. The uneven distribution of the times of ore formation, and local clustering of deposits formed in approximately the same time, gave rise to the durable concept of metallogenic epoch. These are periods of widespread formation of ore deposits of one or more commodities and genetic types, considered within a structural or facies belt, large area or globally. The most striking periodicity of ore formation is apparent in the young orogenic belts where most of the hydrothermal deposits (e.g. porphyry Cu-Mo, hydrothermal veins and replacements with Pb-Zn-Ag, Au, W, etc.) overlap with, or shortly postdate, emplacement of granitic rocks. As most granites result from melting during subduction and from "orogenies" (=timed collisional events), named orogenies have also been used to identify metallogenic epochs. The Laramide epoch, widely developed in the American Cordillera, includes ore deposits emplaced during the late Cretaceous and early Tertiary; the Variscan Epoch in Europe comprises late Paleozoic (predominantly upper Carboniferous) deposits. The global extent of deposits formed in some metallogenic epochs is striking; for example the Laramide ores are distributed from Alaska through the Cordillera into the Andes. Laramide contemporaries form clusters within the Tethyan (Alps-Himalayas) orogen between Serbia and Iran, then through China, Japan into the

Russian Pacific Maritimes to connect with Alaska. The Oligocene-Pliocene epoch has the greatest continuity and is developed, with interruptions, throughout the Circum-Pacific and Alps-Himalayas orogenic systems.

Most metallogenic belts and provinces are dominated by deposits formed in one or more favored epochs and this experience has been utilised in exploration. Exceptions, however, are widespread. "Giant" deposits are scattered among the lesser scale deposits of corresponding types, but because of their visibility many serve as a sort of landmarks and sometimes milestones of presumed evolutionary changes

Histograms of ore formation in time, plotted for several popular ore types, often show a series of highs and lows. Two outstanding and often discussed examples are the "Superior-type" banded iron formations (80% plus formed during the interval of 2.3 to 2.8 Ga) and "U-conglomerates", the majority of which were produced in approximately the same time. The often repeated genetic rationale stresses the transition from reducing to oxidizing global atmosphere and hydrosphere in about that time (Paleoproterozoic; Holland, 1984).

As already mentioned several times before, newly formed orebodies are subject to erosion and removal and only a small percentage survive. The greatest chance to survive have orebodies emplaced in the deep subsurface, and the near-surface ores buried shortly after formation. The average global rates of erosion (higher in the rising terrains such as mountains, lower in the platform interiors) combine with the average depth of ore emplacement to determine the statistically highest incidence of exposure of orebodies found at the present erosional surface (hence a capability to be discovered by surface prospecting), called "prime times" (Laznicka, 2001). So the prime time of formation of hot spring-precipitated Au, Ag, Hg deposits (depth of emplacement between about 50 and 300 m) is Pliocene-Pleistocene (e.g. McLaughlin, California); the prime time of epithermal vein deposits (emplaced in a depth between about 300 and 1500 m) is Oligocene-Miocene (e.g. Mexican "bonanza-Ag" deposits like Guanajuato, Pachuca, Zacatecas); the majority of high-level porphyry Cu deposits formed between the end of Cretaceous and Oligocene, for example Bingham-Utah and the many deposits in Arizona and in the Cordillera Domeyko in Chile (Chuquicamata, La Escondida). The very young Cu porphyries in the High Andes (El Teniente, Rio Blanco) and Western New Guinea (Ertsberg-Grasberg, Ok Tedi) are exposed because of the higher than average rate of uplift and erosion.

Of course there are numerous exceptions of orebodies younger or older than the “prime”, but the very much older or younger examples are exceptional and usually of complex origin, or just mimicking certain features of a popular class of orebodies that makes them prone to misinterpretation. Examples of the odd deposits in terms of timing include the Archean “porphyry Cu-Mo” Coppin Gap in NW Australia and the “porphyry Cu-Au” orebodies near Timmins, Ontario; the Archean Campbell Au mine in the Red Lake district in Ontario interpreted by Penczak and Mason (1999) as metamorphosed epithermal; and others. The “prime times” of the “giant” deposits of various types, considered alone, are difficult to establish because of the limited population of examples, but in general they correlate well with timing of their lesser counterparts. Table 15.6. shows timing of the cumulative tonnages of the various metals stored in “giant” deposits. Table 15.7. gives numbers of such deposits in geological time intervals. Fig. 15.8 is a histogram based on Table 15.7. There, the “giants” are treated as a block and the peak of their formation falls into the interval of 60 to 25 Ma, an early-middle Tertiary which reflects the dominance of the “giants” by high level hydrothermal deposits. More about this below.

Is present the key to the past, or do the past deposit alert us about the ore formation possibly under way now? Hutton reversed

Do “giants” form now or, to phrase this question differently, have any giant deposits formed during the Quaternary? The answer is yes and the pre-1999 version of GIANTDEP included 7 gold placers, 2 lithium giants in playa lakes, 18 weathering-residual deposits of Fe, Sn, Co, Ni, Mn, Au (lateritic bauxites have not made it into the “giant” category because of the high crustal abundance of aluminum; the largest examples are “large”), one Quaternary hot-spring type Hg deposit (Sulfur Bank, California; Chapter 6) and one “hydro-brine”, which means a hydrothermal fluid with extremely high content of dissolved metals in the Salton Sea subsurface, California, where the silver content of 10,885 tons exceeds the “giant” threshold (Chapters 6 and 12).

Popular examples of the presently forming or recently formed hydrothermal sulfide and oxide accumulations on the sea floor in the Red Sea axial deeps, on oceanic spreading ridges (Duckworth et al., 1998); and in the back arc/interarc settings (Chapter 5) have not yet exceeded the “giant” threshold; the tonnage data released are very preliminary and based on rapid estimates. There are

more active metal-accumulating processes presently “at work” and there are “unfinalized” young metal accumulations that could reach the giant magnitude. Two examples of young metalizations are here briefly reviewed, mainly for comparative purposes.

1) The Rotokawa hot spring-epithermal gold depositing system, Taupo Zone, New Zealand. This is an active geothermal system 20 km NE of Taupo in a large hydrothermal explosion crater that itself is a lesser-order feature in a large rhyolitic caldera. There, thermal springs discharge into a shallow acid lake. It is also a site of a small bedded native sulfur deposit in lacustrine muds intermittently mined in the past (Krupp and Seward, 1987; Sinclair, 1989). Finely divided gold associated with high concentrations of As and Au sulfides and native sulfur precipitates from present springs and accumulates in bright yellow, green and orange muds that are interstratified with the monotonous gray lacustrine mud. The total demonstrable gold resource in the muds is about 250 kg at an average grade of 1 ppm Au, but Krupp and Seward (1987) have calculated that up to 370 t Au could have been transported into the region beneath the crater in the past 6,060 years by a fluid saturated with gold at 7.2 milligrams per kilogram, given the present flow rate of 5.5 kg/sec.

2) The “Intermontane Gold Anomaly” in Wyoming, Utah and Idaho. If the “Modified Placer Theory” for the origin of the Witwatersrand gold and uranium-bearing “reefs” in a braided fluvial and fan-delta system is accepted (Pretorius, 1982; Hallbauer, 1986; Minter, 1988), the next step is interpretation of the depositional basin in the time of deposition of the Central Rand Group and its structural setting. This is thought to have been a “foreland basin on the cratonward side of a collision zone” filled with molasse-like terrigenous sediments (Robb and Meyer, 1990). The first-order basin comprised at least 18 separate lesser basins resting on a block-faulted basement (Myers et al., 1990), influenced by syndepositional major thrusts verging towards the retroarc basin (Burke et al., 1986; Winter, 1994). Comparisons have been made with the more recent regions, the closest match believed to have been found in the Laramide (i.e. late Cretaceous to Eocene) Wyoming Foreland in the U.S. West, especially in the Eocene Wind River Basin (Matthews, ed., 1978; Miller et al., 1992). The Wyoming Foreland is comparable in size with the Witwatersrand. No presently economic gold accumulations hosted by the Mesozoic and Cenozoic basinal sediments have so far been developed in Wyoming Foreland.

GIANT METAL DEPOSITS IN GEOLOGICAL TIME: CUMMULATIVE TONNAGE

	Ag	As	Au	Bi	Cd	Co	Cr	Cu	Fe	Hg	Mn	Mo
Q: 0-2 Ma	20000								2100000000			1207300
T ² : 2-25 Ma	10885		8141			2500000		3300000		7000		
T ¹ : 25-60 Ma	55000		12080					180464000		242862		4068000
Cr ² : 60-100 Ma	339336	1900000	2630					382248000		20237	2210000000	19466280
Cr ¹ : 100-150Ma	20263		646					41831000		31500		1350000
J: 150-210 Ma			4255					27610000	14000000000		465000000	150000
Tr: 210-245 Ma	20000	200000	2589	260000				25932000				531000
Pe: 245-280 Ma	182000							135250000		550000		
Cb: 280-354 Ma	7000			211200						33698		162000
S-D: 354-440 Ma	17000	5500000	5558	26800				61948000		65000		
Or: 440-500 Ma	290000	2343					35000000					
Cm: 500-550 Ma	21600											320000
Np: 550-1000 Ma	8133		220000	2300	10800	9510000		227670000	31619899744		121000000	
Mp ² : 1.0-1.6 Ga	32947		1570					76081000				
Pp ² : 1.6-2.0 Ga	97307	544000	2650					52817000	62000001024		275000000	
Pp ¹ : 2.0-2.45 Ga	12900		600	22240				14098000	14166899816		4367989836	
Ar ² : 2.45-3.0 Ga	14640		51884					35000000				107000

	Nb	Ni	Pb	PG	RE	Sb	Sn	Te	Th	Ti	U	V	W	Y	Zn	Zr
		63300000					10330000									
			13830000				278000								7000000	
			19556000				398000	2398000	1000				1107240			
							158000		1160000				261310			
7875000			10725000	14460000							247000		871500	3000000		25000000
30000000			6300000	40000000	4820000						682000					
	15000000		12800000	6105												
48860000			1700000										1280000		40000000	
			24616000				565000	250000	880							
65000000			44052000		7500000		200000	2500000	1509						44570000	
			8800000		36000000		202200	457000					106000		33702000	210000000
20000000			64960000				218000								41678000	
			14400000												8000000	
85000000	7920000		21000000				2050000				300000				11000000	
	25600000		59482300	1470			500000				1735000				32275000	50000000
	88000000			76730											76684000	
				6500			446000			2880000000	484000				8088000	
												371000000			11770000	

Table 15.6. Cumulative tonnages of metals contained in "giant" and "super-giant" deposits, in geological time.

Table 15.7. Ore "giants" and "super-giants" in geological time: numbers of deposits listed in GIANTDEP 1999 version, modified from Laznicka (1999)

	Total	Ag	As	Au	Bi	Co	Cr	Cu	Fe	Hg	Li	Mn	Mo	Nb	Ni	Pb	PG	RE	Sb	Sn	U	W	Zn	Zr
No date	5	1						1					3											
Q: 0-2 Ma	23	1		8		1		1	1		2				3								6	
T ₂ : 2-25 Ma	59	2		21				14	10		1		5			4						1	1	
T ₁ : 25-60 Ma	103	19	2	5				30	3			4	26			5						4	3	1
Cr ₂ : 60-100 Ma	21	2		2				9	1				1									2		4
Cr ₁ : 100-150 Ma	26			8				5	1			1	1	1	4		1					1		2
J: 150-210 Ma	39	1	1	7	2			3					2	1	3		1		5	6	2	3		1
Tr: 210-245 Ma	14	2						5	2						1	2	1							1
Pe: 245-290 Ma	13	1			1				1				1	1	1							3	1	2
Cb: 290-354 Ma	37	1	3	9	1			7	1						7							3	1	3
S-D: 354-440 Ma	28		1	5			1							1	9		2	4	1	1	1			2
Or: 440-500 Ma	8	2														2		1		1				2
Cm: 500-550 Ma	9	1											1	1	4							1		1
Np: 550-1000 Ma	31		1	4		1		14	2		1					3						2		1
Mp: 1.0-1.6 Ga	25	3		2				6						1	1	3						1	4	3
Pp ₂ : 1.6-2.0 Ga	33	5	1	3				6	1			1			2	8	1							5
Pp ₁ : 2.0-2.45 Ga	23	1		1	1	2	2	6			2				1		4					1		1
Ar: 2.45-3.0 Ga	31	1		24				1					1				1		1			1		1

Abbreviations: PG=PGE; RE=REE;

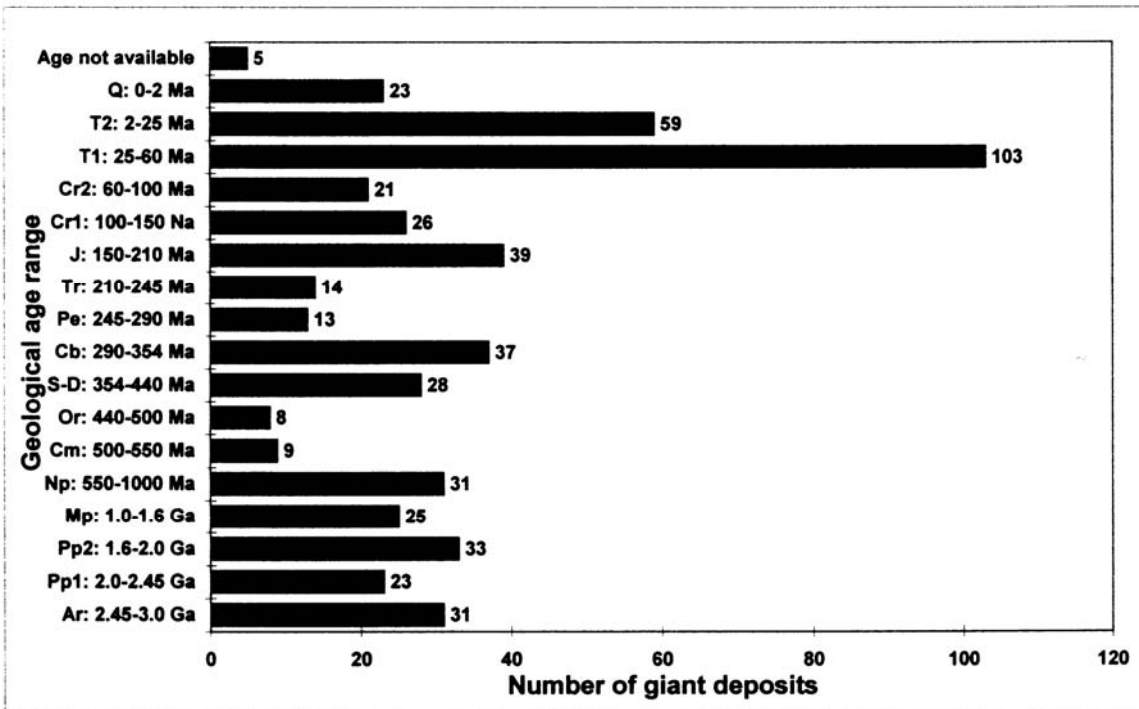


Figure 15.8. "Giant" deposits (all metals) organized by their intervals of formation, based on data in Tables 15.6. and 15.7. Laznicka (1999), reprinted with permission from Economic Geology, v. 94:4, Fig. 6, p. 470

There is, however, an extensive sub-grade, yet geochemically significant regional enrichment of gold at average concentrations between 35 and 222 ppb in several stratigraphic horizons. The Wind River Formation alone is estimated to contain 48,329 t Au at an average concentration of 0.22 g/t Au (maximum 2 g/t); the units in the Jackson Hole area of NW Wyoming probably contain 110,000 t Au at a concentration of 94 ppb Au (Antweiler and Love, 1967; Love et al., 1975) and the entire Intermontane Anomaly may store a total of 242,580 t Au (C.H. Phillips, 1985). A portion of this gold has been reworked into Quaternary alluvial sediments and the process slowly continues but it is a fine gold, largely unsuitable for recovery by traditional technology. The gold and uranium provenance appears unspectacular: just a steady but large volume erosion and reworking of the Archaean granite-greenstone basement and younger units, with portion of the U probably leached from ash that may have blanketed the area, supplied by the Laramide shoshonitic and mildly alkaline volcanoes.

“Giant” placers (Henley and Adams, 1979) have been actively forming in the Quaternary assisted by active tectonism (e.g. a steady uplift along the transpressional Alpine Fault of New Zealand that maintains steady erosion of discontinuously hydrothermally mineralized strata, possibly augmented by continuing gold precipitation at the deep levels of faults; formation of structural basins in regions undergoing block faulting or rifting) and perhaps some hitherto under-appreciated agents such as glaciation. Glaciation is about the most effective mechanism to sweep a weakly mineralized broad area and dump the material far away from the source to undergo stream reworking and gold enrichment as along the Alpine Fault in New Zealand, in Yakutia (Sacha) or in the Lena (Bodaibo) goldfields of Siberia (Bilibin, 1955).

The main problem of placers, and in fact most of the recent surficial or near-surface metal accumulations regardless of size, is the precarious preservation. Alluvial placers in particular are eroded almost as fast as they form and so are the metalized weathering crusts like laterites. The pre-Quaternary supergene ore survivors have almost always escaped dispersal thanks to a “special event” like deep downfaulting as in rifts and grabens and/or burial under lava flows or pyroclastics. Examples: The “deep leads” of the Victoria goldfields, especially Ballarat, buried under basalt; some of the Ni-saprolites in western Oregon preserved under Columbia River basalt; the fossil

enriched zones over the western United States porphyry coppers preserved under young volcanics.

A portion of the Witwatersrand “reefs” that has survived erosional removal shortly after deposition was preserved by downfaulting and under the Klipriviersberg Group basalt, almost simultaneously as it was undergoing dissection, removal and reworking (Myers et al., 1990). The Ventersdorp Contact Reef is the preserved secondary placer at the Central Rand-Klipriviersberg unconformity (McCarthy, 1994). More preservation acts followed later so that the present Rand is, in fact, a metal accumulation “that has been left behind” rather than “that was there originally”. Yet it is a substantial remnant; most other ancient deposits probably did not make it at all!

The preservation factor strongly influences the distribution of “giants” in geological time and the selection of metals and ore types as shown in Tables 15.4, 15.5. and in Figure 15.5. Apparently the “prime time” of formation of the presently exposed “giants” had been between the mid-Tertiary and late Mesozoic during which most of the high-level epithermal and “porphyry” deposits formed. A good correlation exists between the T1 ore-forming peak on Figure 15.8. and the “hydro-meso-Cu” and Mo categories on Fig. 15.5., that include the porphyry Cu-Mo or Mo. There is no substantial difference between the distribution of “giant”, and lesser size ore deposits of the same metals and types as determined by earlier studies (Meyer, 1981; Laznicka, 1993).

The preliminary results obtained by research in progress indicate that if the pattern of ore distribution in time as shown in Figure 15.8. were normalized by the usual depth of ore emplacement, combined with calculated rates of the post-emplacement tectonic and epeirogenic regimes, the statistical maxima and minima in the ore distribution would lose much of the contrast, at least through the Paleozoic. This indicates that preservation is the substantially stronger control than evolution (with the exception of some undisputable cases like the post-Silurian only occurrence of humic coals), that influences the distribution pattern of the ancient metalizations.

15.4. Why are "giants" so big and are where they are?

This section should start with the point already made before (Laznicka, 1989; Sillitoe, 1993; Phillips et al., 1996): most, if not all, metal accumulations of exceptional size, are “the end of

the spectrum" of decreasing size deposits of the same or similar types. One can hardly think about a deposit that would be qualitatively unique except perhaps Sudbury (Chapter 12.) if it is proven beyond doubt as indeed of extraterrestrial origin. Even there, however, the more than 30 Ni-Cu orebodies can also be arranged by increasing size, and the ore type is not significantly different from the magmatic deposits separated from "normal" magmas.

The "giant" ore types in general, however, range from the rare to the fairly common ones, although I doubt that there is a "one of a kind" ore type represented by a "giant" that lacks the lesser entourage. There could, however, be a gap between a "giant" and lesser deposits of a given type (e.g. among the Witwatersrand-type Au-U paleoplacers; between Palabora and lesser Cu-bearing carbonatites) although such a gap can be reduced by intense exploration. Olympic Dam, in the time of discovery in 1975, had been considered as unique. At present it is a member of the "Fe-oxides, Cu, Au, U family" (Hitzman et al., 1992) and has one or two (Prominent Hill and Carrapateena in South Australia) "large" and more than ten minor or unexplored followers in the Gawler Craton.

The reasons for "giants" formation can be treated in terms of four transitional sets of explanations that can combine in a variety of ways: 1) intensity of the process, that is genetic factors (longer, stronger) 2) metallogenetic favorability of the setting; 3) coincidence of several processes working together; 4) interaction (alias boy meets girl). Clark (1993) differentiated between genetic (i.e. related to process) and metallogenetic (i.e. related to setting) causes of ore gigantism.

Even if the most perfect condition for the formation of a "giant" had been in place and significant deposits did form, only a fraction has actually been preserved. Any regional prospectivity analysis with the purpose of predicting the possible sites of "giants" has first to review the preservation conditions. This leads to a paradox: regions with extensive and thick platformic cover sediments or basalts are mostly devoid of metals, but they preserve the potentially mineralized paleosurface beneath, undepleted by the recent erosion (and mining activity as well). Olympic Dam is one such discovery and more buried but preserved deposits are to follow.

1) Intensity of the ore accumulation process: This is comparable with optimization of a technologic process. It includes duration (length of time) of ore formation (e.g. several million years at

Chuquicamata); large volumes of magma to collect and expel trace metals combined with longevity and multiple emplacement (e.g. Ni-Cu-PGE under Noril'sk, Naldrett, 1999; Cu-Mo under Rio Blanco, Skewes and Stern, 1995); large volumes of fluid passing through the ore sites (Fyfe et al., 1978); initial trace metals enriched magma, or super-efficient fractionation (e.g. Nb, REE in carbonatites); large volumes of metalliferous rock to extract or residually enrich metals (e.g. peridotite to Ni laterite). In some presently active systems the intensity factors can be directly observed, measured and analysed, then used for ore prediction that might reveal or confirm a potentially "giant" deposit elsewhere (e.g. the active geothermal system depositing mercury at Sulfur Bank, Rytuba, ed., 1993; Ag at Salton Sea, Skinner et al., 1967; Au in Rotokawa, Krupp and Seward, 1987). In ancient ore associations the process intensity is mostly a matter of speculation, although it is sometimes believed proportional to the intensity of regional hydrothermal alteration. The latter can be determined visually and by petrographic studies, or by oxygen isotope work.

2. Favorable setting: Most ore deposits of any size are constrained by a restricted range of permissible settings in which they could have formed and where they are found, but the presence of "giants" is statistical. At even the most favorable site an orebody could only have formed if the site were "visited" by an ore forming process bringing metals from outside. An intense process and a most favorable site have a better chance to accumulate a "giant". Example of the most favorable settings include the large, permeable fracture systems as in Chuquicamata, or breccias at Rio Blanco and El Teniente; prominent deformation zones that channeled fluids (the Domeyko Fault system in the porphyry province of northern Chile; orogenic Au deposits related to the "breaks" in the Abitibi subprovince in Canada); porous or replaceable rocks under impervious screens that precipitated metals from ascending fluids; local (e.g. third order) structural basins on a generally monotonous sea floor that accumulated sedex-forming brines; aquifers; stream channels. Linear arrays of ore deposits and various features commonly associated with ore formation are often attributed to lineaments or "deep faults" (popular especially with the Russian school) that imply tapping and conducting mantle and deep crust-derived fluids to the near-surface area.

3 & 4) Coincidence and interactions: Numerous geochemical provinces with rocks systematically enriched in trace metals also carry a variety of economic deposits of the same metal, thus turning into polygenetic metallogenic provinces (metallogenesis). Several anomalously W and Sb-enriched provinces in east-central and south-east China contain a major population of "large" and "giant" deposits of the same metals (Xie and Yin, 1993). Elsewhere, as in the Carlin Trend, in Kalgoorlie (Phillips et al., 1996) and in the "Climax Mo-line" in Colorado (Wallace, 1995) the Au and Mo "giants", respectively, are attributed to multiple coincidences of various factors, some unspecified. These agents scavenged and collected metals in depth, then stripped them from the passing fluids at higher crustal levels, forcing ore deposition. Coincidence of the relatively young hydrothermal ores and old, buried deformation zones often

facilitated metal super-accumulation in the younger deposits (e.g. in the Colorado Mineral Belt). Special catastrophic events like sector collapse of volcanic edifices, as the 0.35 Ma event at Lihir Island, are credited with juxtaposition of the "porphyry" and epithermal ore depositing levels favorable for gold super-accumulation (Sillitoe, 1994).

Anomalous developments and special events in the subduction regimes are also favorites, used to justify a local super-metallogenesis. The cluster of Miocene "super-giant" Cu-Mo porphyries in Central Chile (El Teniente, Rio Blanco, Los Pelambres) is attributed to shallowing of the subduction zone and crust thickening resulting from subduction of the Juan Fernandez oceanic ridge (Skewes and Stern, 1995). Subduction of a spreading ridge in the Mesozoic is linked to the "giant" gold accumulation in SE Alaska (Juneau Au belt); Haeussler et al. (1995).

16 Giant Deposits: Industry, Economics, Politics

16.1. Historical background

Copper and gold have been known and produced since at least the 8th millennium B.C. (in the Copper, then Bronze Ages) from surface outcrops and shallow "diggings". The earliest Cu mining areas were in Cyprus, Gulf of Aqaba (Timna), Turkey and NW Iran. The principal gold diggings were in the pre-dynastic Egypt and in Sudan (Aitchinson, 1960). The source of tin, required to manufacture bronze, remains puzzling and is usually sought in Cornwall, England. The Sumerians (~3500-2000 B.C.) in Iran and the Egyptian kings (~3100-1085 B.C.) increased the Cu and Au supply from about the same areas. Boyle (1987) traced the earliest written record about gold mining in Egypt back to 3100 B.C., and this region also produced the first geological map of unknown gold workings there, dated from 1320 B.C., now in a museum in Turin. The Phoenicians (around 1000 B.C.) were Mediterranean merchants and navigators who also dealt in metals that included silver and perhaps lead. The port cities of Cádiz (southern Spain) and Cagliari (Sardinia), they established, probably shipped gold from gossans in the Rio Tinto belt (Tharsis is the oldest deposit mentioned) and silver (lead) from the Iberian Meseta, Cartagena, Iglesias and Attica workings. In the classical period after about 600 B.C. the ancient Greece was a major silver producer coming from the Lavrion mines near Athens (Chapter 7). Lavrion mining culminated during the rule of Pericles (461-429 B.C.) and it contributed to prosperity of the Athenian state that included construction of the Parthenon (Konofagou, 1980). The silver also financed the wooden Athenian navy that defeated the invading Persian fleet in the battle at Salamis.

The Romans, in the first five centuries A.D., were the first global miners (within the confines of the western Old World) producing gold in Dacia (present-day Romania; in the Apuseni Mountains of Transylvania extensive underground galleries are still preserved at Roşia Montană; read Chapter 6), tin and copper in Cornwall, gold, copper, silver and lead in southern Spain (Aitchinson, 1960). Parallel ancient mining developments had probably been taking place in China and India but there is a lack of published information. The gold mining in Hutti

and Kolar in India had been going on at least since the start of the first millennium (Boyle, 1987).

The Middle Ages, between the 5th and 16th centuries, were times of near-stagnation of the Old World mining, with few local exceptions. Although the "six metals of antiquity" (Au, Ag, Cu, Sn, Pb, Fe) were joined by several additional metals (As, Sb, Hg, Bi, Co) or their compounds utilized for a variety of purposes like pigments, poisons or alchemist's ingredients, metals were in short supply and very expensive. The scarcity of gold in Medieval Europe led to substitution of gold used for monetary purposes by silver, pioneered by the Saxon kings between A.D. 911 and 1024 (Boyle, 1987). The Erzgebirge region in Saxony (e.g. Freiberg), the adjacent Bohemia (e.g. Jáchymov, Kutná Hora), Slovakia (Banská Štiavnica) and Transylvania then in Hungary, were leaders in the medieval mining technology and proto-geological exploration recorded in the books of Agricola (1556), Lazarus Ercker (1574) and Ch. T. Delius (1773). This leadership in mining technology and related arts like mineral exploration persisted in central Europe until the mid-1800s when it moved first to Cornwall and then to North America.

The re-discovery of the Americas in 1492 was followed, shortly afterwards, by a great influx of silver and gold from the Spanish colonies (gold primarily from Chocó, Colombia and El Oro, Mexico; silver from Potosí, Bolivia and from Mexico). This became a great source of wealth to the Spanish Crown but triggered a monetary crisis in the rest of Europe and a slump in silver production. The production of iron, however, kept increasing (most of which was used for weapons manufacturing) and this culminated with the beginning of Industrial Revolution in England around 1770.

Industrial Revolution, driven by the dynamic capitalism increasingly free from feudal restrictions of the past, new technology and science, education, transportation and factory mass production of goods, greatly accelerated the rate of mineral discovery and mine development. Parallel with this was the chain of 18th and 19th century discoveries of new elements (many of which were metals) followed by industrial applications for many of them afterwards. This multiplied the variety and number of new ore deposits found and brought into

production. The exponential increase of metals supplies through the ages can be briefly demonstrated by the example quoted by Boyle (1987): of the 120,000 tons of gold produced until the end of 1985, 2% were added prior to 1492; 8% between 1492 and 1800; 20% between 1801 and 1900; 70% between 1900 and 1985. The cumulative supply growth curve is even much steeper for the newcomer metals such as Al, Ni, Mn, Mo, W, Cr and others, in wide use for a mere 100 years or so (compare also Table 1.1. and Figs. 1.1. and 1.3).

The place of giant deposits in history: The quantitative concept of giant deposits is dependent on the existence of tonnage and grade information, virtually non-existent before about the year 1900, and slowly improving to become a commonplace only after 1950. In the past reserves were not calculated for new deposits entering production and the only tonnage information available for some deposits was the cumulative metal production. Much of such information was in monetary form and to decipher it the metal values in the period and place had to be known. For this reason the reconstructed production figures quoted in the literature are incomplete, subjective and inaccurate, but at least indicative of the order of magnitude. The dominant producers of metals in the past could have rightly been considered of "world class" and they included the pre-Columbian silver producers of central Europe, gold mines of Transylvania and tin districts of Cornwall. They were joined by the Mexican and Bolivian bonanza silver deposits later.

The mines exploited early in the history were a mixture of small, medium and large deposits with few "giants", based on our present knowledge. Probably the first "giant" mined was the Sar Chesmeh porphyry Cu in Iran, the oxidation zone of which was one of the Sumerian diggings in the 3rd millenium B.C. (Aitchinson, 1960). In that time this was probably one of the many comparable diggings in the region the rest of which is now recognized as minor deposits. There was no indication then that Sar Chesmeh was of exceptional magnitude, which came only after its re-discovery in the 19th century and a modern bulk-mining development in the second half of the 20th century. We now, in retrospect, recognize the following deposits/districts mined in antiquity as of the "giant" magnitude (Fig. 16.1): Sar Chesmeh, Iran-Cu; Lavrion-Ag, Pb and possibly the Kassandra district, Greece; Rio Tinto ore field and Tharsis, Spain-Cu, Au; Cornwall, England-Sn (mainly placers) and Cu (lodes); Roşia Montană and Brad, Romania-Au; Cartagena, Linares-Ag, Pb; Almadén-Hg, all in Spain;

Rammelsberg and Freiberg, Germany-Ag, Pb; Kolar-Au in India. To this should be added the presently recognized "giants" mined early by indigenous populations and later re-discovered by European colonizers for which no written record is preserved. Remnants of old working have been mostly removed in the early stages of modern mining. The early recognized and exploited "giants" include the Mexican silver deposits (Pachuca, Guanajuato, Zacatecas), Potosí (Cerro Rico) in Bolivia and Cerro de Pasco in Perú, several sites in the African Copperbelt, and Ghana goldfields. The rapid increase of "giants" discoveries came after the year 1900, with over 40 industrial metals in existence, many exploited from multiple "giant" and some "supergiant" deposits.

"Giant" deposits in geopolitics: Compared with petroleum, metallic deposits played, in recent history, less often such a crucial role as alone triggering major wars and territory acquisition campaigns, although their deposits were certainly a welcome prize of any conquest. Before petroleum, however, minerals had been a great incentive for territorial acquisitions. In this game the size mattered, hence the "giants" of today and "world class" resources of all times played a major geopolitical role. The resource rivalry among the great powers of the day intensified during colonialism with new mineral discoveries made, although most major "giants" in colonies were discovered (or rediscovered, as many deposits had been the subject of a small scale mining by the locals, or at least the outcrops had been known to them) after colonization. Gold Coast (present Ghana), known for its gold and Malaya known for tin, both former British colonies, were known and active in the pre-colonial times. So were the great silver deposits of Mexico, Peru and Bolivia and the Colombian gold.

Most wars and military campaigns that involved "giant" metallic deposits have been fought during and after the Industrial Revolution, in times of colonization, then among the former colonies themselves. Examples include the repeated wars between Germany and France over the iron-rich Lorraine (the world-class "Minette basin") in the 2nd half of the 19th and first half of the 20th century; the 1879 Guerra del Pacífico between Chile, Perú and Bolivia over the Chilean nitrates; the annexation of the Petsamo (now Pechenga) Ni district after the 1940 U.S.S.R.-Finland war; the Hitler's campaigns in the World War 2 for possession of the Kivoi Rog and Kursk iron ore basins, and the Nikopol-Mn; the skirmishes over the Katanga Copperbelt in

the 1960s and 1970s, and the 1986 Bougainville insurgency that managed to shut down the Panguna porphyry Cu-Au "giant".

Wars are, however, only the most spectacular and bloody aspect of geopolitics and to paraphrase Clausewitz geopolitics is a war by another means. Metal "giants"-influenced restrictive geopolitics have had their expression in embargoes, blockades, nationalization of assets, politically motivated supply restrictions and price manipulation. These have been countered by a variety of measures by the adversaries. The politico-economic measures have been exercised either directly by state means, or by commandeering and subsidizing the private industry. On the positive side is the fact that some wartime needs encouraged search for substitutes for certain raw materials, or production from alternative sources.

During World War 1 Germany, denied supply of the Chilean nitrate to manufacture explosives, developed technology to synthesize nitrates from the air. During World War 2 Germany developed the technology and succeeded in large scale production of synthetic gasoline from coal, and the Allies perfected magnesium recovery from sea water. The 1940s-1950s nuclear arms race saw government agencies driving the uranium search, mining and processing; this resulted discoveries of several "giant" U deposits (e.g. Grants, Elliot Lake). Occasional political acts of kindness and cooperation to affect development of "giants" also took place, as the 1990s agreement for joint exploitation of ore fields that straddle the Chile-Argentina border (the "giants" Los Pelambres-El Pachón and Pascua-Lama).

"Giants" in political economy: Throughout the ages "world class" deposits of the day have had a great influence on the state economy and on creation of wealth (not necessarily on leaving a portion of the wealth in the mining region itself!). Throughout much of the history the mines ownership was vested with the rulers (emperors, kings, dukes, etc.) who promulgated mining laws and staffed the management and supervisory personnel. During renaissance (15th-16th centuries) and afterwards mines were sometimes franchised to local feudal enterprises or syndicates who paid royalty to the landlord, or were let to tributers. The early version of finance houses who invested in mine development and operation and marketed the products, were the "merchant princes" Fuggers of Augsburg, Germany (Ehrenberg, 1866). They, in the 15th and 16th centuries dominated the European copper, silver lead and mercury supplies through

control of the mines in Schwaz (Austria), Špania Dolina (then Hungary) and Almadén (Spain). The private capital entered the mining scene *en masse* during the Industrial Revolution and competed since with the government enterprises to achieve a near complete domination in the present age of globalization. The last pillars of total to widespread state control of mining went in the 1990s following the political changes and privatizations in the former U.S.S.R., and gradual privatization in China. Governments, however, still regulate exploration and mining, and collect taxes and royalties.

Metal mining, based on the "giant" deposits, is an important revenue earner for many national governments, as well as states, provinces and regions in larger political groupings. The revenue impact is largest in undeveloped countries where one or more "giant" mines, established and operated by foreign corporations, contribute a large share of the country GNP and export earnings. In New Guinea three presently mined "giant" Cu and Au deposits (Ok Tedi, Porgera, Lihir) contribute the bulk of the state revenues. The earlier PNG "cash cow", the Panguna porphyry Cu-Au on the island of Bougainville, has been lost to local insurgency in the 1980s. In Indonesia, the "giant" Ertsberg-Grasberg and Batu Hijau porphyry Cu-Au complexes are among the largest industrial enterprises in the country with population of 230 million. In Ghana, the five "Au giants" generate more than 80% of that country export earnings. In Zambia and DRC Congo the health of the copper and cobalt industries in the Copperbelt determines the economic health of their respective countries. The Pacific island of New Caledonia, an overseas Département of France, stores the bulk of the world's nickel. On the other hand, in the rich, industrialized countries like the United States, metal mining that used to be the initial and principal regional creator of wealth in the past (e.g. Arizona, Colorado) is on the defensive, in places on the way out, greatly overshadowed by the recreational industry. It is said that a single Colorado ski slope is worth more than a "Mo giant" like Climax or Henderson. In the "Old Europe", with its metal mining tradition, mining is virtually dead, the formerly famous "giant" mines (Rammelsberg, Freiberg, Mansfeld, Mechernich, Erzberg, Banská Štiavnica-Hodruša, Reocin, the Cornish mines, Linares, Lavrion) exhausted and reclaimed (sometimes so thoroughly that no traces of past mining are left), or converted to museums or housing developments. Some mines are still struggling, awaiting decisions (Almadén-Hg; the Iberian Pyrite Belt). There have been (or are

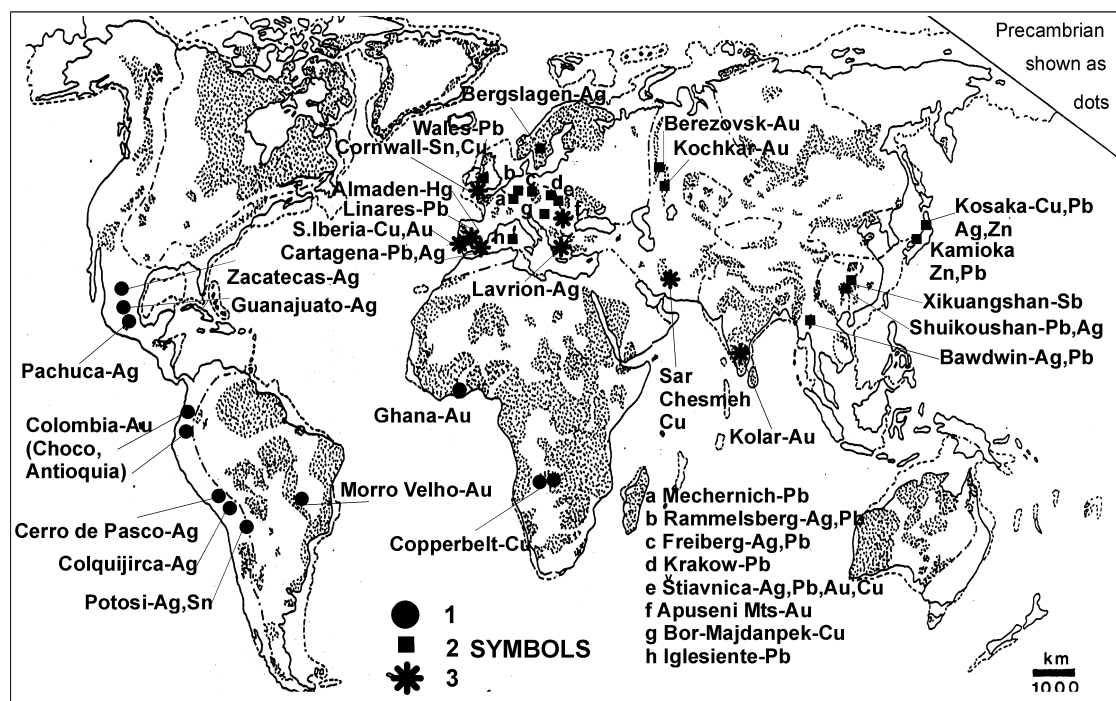


Figure 16.1. Map of deposits or districts presently recognized as of "giant" and "super-giant" magnitudes, discovered and mined before the year 1800. Symbols: 1. Deposits in former colonies, producing before 1800; 2. Pre-1800, post 1 A.D. deposits; 3. Pre-1.A.D. deposits of antiquity

planned) several recent instances of mining resurrection in the historical mining areas in Europe (e.g. Sotiel, Aljustrel in the Iberian Pyrite Belt, Roşia Montană). Some terminated in an environmental disaster (Aznalcóllar). A handful of brand new buried "giant" or "near-giant" deposits have been found in the historical districts and developed into successful mines (Corvo-Neves), or awaiting development (Las Cruces; Roşia Poieni).

16.2. Giant deposits and corporations

Automobile manufacturing and mining are both components of the same megatrend that shapes the industrialized world, so a comparison can be made. In the 1910s, when automobiles were made in small series in converted horse carriage factories or by local locksmiths, and even in the 1920s-1930s, there were close to hundred car marques in existence. New metal supplies, in the same time, were coming from hundreds of small mines, each of which held a tiny slice of the total production. In the past few decades the car manufacturers have consolidated their production facilities and 10 biggest

automakers now supply more than 80% of the global production from few large, highly efficient and automated plants. Similar trend applies to metal mining and recovery. The small number of large corporations that dominate the metal supplies prefer to have a limited number of large, high-tech, highly profitable mines than tens of small wet holes scattered around the world. Uren (2001) claims that 66% of the resource industry's wealth comes from 10% of the economic deposits. The industry objective is thus to acquire (or hold partial equity in) "world class" deposits that would maintain sustained production for a long time, as well as to dominate supply of selected commodities in order to influence the metal prices and (as they say) contribute to market stability and corporate survival. Globalization makes it possible to realize this objective almost anywhere in the world, geology permitting. Table 16-1 shows recent share of the global supply of non-fuel minerals (mostly metals) by the largest corporations. Mergers and takeovers taking place almost on a monthly basis now guarantee a rapid change of the information shown below, especially as the big players are becoming bigger and the medium-size corporations

die out. The small operators, of no interest to the "goliaths", still survive and even multiply in times of price increase.

Table 16.1. Fifteen largest corporations that controlled 37% of the Western World's non-fuel minerals mining in 1997, based on Raw Materials Data, Stockholm, 1999

Rank	Company	% of total value	main products
1	Anglo-American (incl. AngloGold, Angloplats)	8.03	Au, PGE,U
2	Rio Tinto (London)	5.53	Fe,Cu,Au
3	BHP (Broken Hill), Melbourne	4.27	Cu,Zn,Pb, Au,Ag
4	Vale do Rio Doce, Brazil	3.27	Fe>Cu,Au, Mn
5	Codelco & Enami, Chile	2.50	Cu>Mo,Ag, Au
6	Phelps Dodge, USA	1.59	Cu,Mo,Ag, Au
7	Noranda, Canada	1.57	Cu,Au,Zn
8	Freeport McMoRan	1.54	Cu,Au,Ag
9	Asarco Inc., USA	1.4%	Cu,Mo,Ag, Au,Pb,Zn
10	Cyprus Amax, USA	1.31	Cu,Mo,Ag, Au
11	Western Mining -WMC	1.21	Ni,Cu,Au, Ag,U,P,Al
12	Newmont Inc., USA	1.23	Au>Cu,Ag
13	Gencor, South Africa	1.22	Au,U
14	INCO Ltd, Canada	1.20	Ni,Cu,PGE
15	Teck Corporation, Can.	1.10	Au,Cu,Mo

Notes: The situation has changed substantially by 2005 due to mergers and takeovers. BHP+Billiton+WMC now has at least a 6.5% minerals share, becoming the world's #1 miner; Asarco is now Grupo Mexico; Newmont acquired Normandy, becoming the #1 gold producer; Teck merged with Cominco to become a major Zn,Pb,Ag producer; newcomer X-Strata took over MIM to become major Cu,Zn,Pb,Ag producer; the Zn,Pb,Ag miner Pasminco (Australia) is now Zinifex; acquisition of Placer-Dome in 2006 would make Barrick the world's largest gold miner

The market share of corporations in terms of individual commodities (metals) fluctuates, but CVRD (30%), Rio Tinto (21.4%) and BHP Billiton (14.2%) hold together 65% of the iron ore market, supplied from three "giant" Fe provinces: Carajás and Quadrilátero Ferrífero in Brazil and Hamersley Range in Australia. Four corporations (Codelco, Phelps Dodge, BHP Billiton and Rio Tinto) control about 33% of "new" copper supplies. Four corporations (Noril'sk, INCO, BHP Billiton and Falconbridge) produce 65% of world's nickel. The

market share of single corporations is still greater for producers of specialty metals of limited application that would not support a greater number of producers even when undeveloped deposits are known to exist. Examples: Brush Wellman Inc. in Delta, Utah produces ~75% of the world's beryllium; China State corporations supply ~64% of rare earths, ~80% of antimony, ~75% of tungsten; Cameco Corporation, Canada, is the major uranium player; Cyprus Amax Inc. supplies some 38% of molybdenum; Araxá, Brazil, supplies ~85% of niobium. It should be noted that contemporaneous production figures are not related to reserves and resources, although in most cases the dominant producers also own the largest metal resources. Below is a list (Table 16.2) of selected corporations and their present inventory of "giants": wholly owned or with a significant equity (33% plus; because of this, several deposits may appear more than once; China and Russia State properties are not included):

Table 16.2. Sampling of the major mining corporations and the "giant" deposits they fully own or in which they have a partial equity (early 2000s)

Corporation	Giant and world class deposits
BHP Billiton (including former WMC)	Mt. Newman (Hamersley Range)-Fe; Cannington-Zn,Pb,Ag; Escondida-Cu; Olympic Dam-Cu,U,Au;
Rio Tinto	Bingham-Cu,Mo,Au; Neves Corvo-Cu,Zn,Sn; Palabora-Cu; Escondida-Cu; Morro do Ouro-Au; Lihir-Au; Pipeline-Au; Hamersley (west)-Fe; Boron-borax; Rössing-U; Richards Bay-Ti,Zr
Anglo-American & AngloGold, Angloplats	Witwatersrand (parts)-Au,U; Tsumeb (mined out)-Cu,Pb,Zn; Aggeneys-Pb,Zn; Gamsberg-Zn,Pb;
Codelco, Chile	Potgietersrust-PGE El Teniente-Cu,Mo; Rio Blanco-Cu,Mo; El Salvador-Cu,Mo;
Placer Dome	Chuquicamata-Cu,Mo Campbell Red Lake-Au; Dome-Au; Sigma-Au; Porgera-Au; Endako-Mo; Las Cristinas-Au; La Coipa-Ag,Au; Marcopper-Cu; Zaldivar-Cu; Gibraltar-Cu
Teck Cominco	Sullivan-Pb,Zn,Ag (exhausted); Red Dog-Zn,Pb,Ag; Highland Valley-Cu; Hemlo (part)-Au
Cameco	Cigar Lake-U; McArthur River (Sask)-U; Kumtor-Au
CVRD (Rio Doce)	Quadrilátero Ferrífero (part)-Fe; Carajás-Fe; Salobo-Cu

Table 16.2. (continued)

Corporation	"Giant" and "world class" deposits
Cyprus-Amox	Sierrita-Twin Buttes-Cu,Mo; Bagdad-Cu,Mo; Globe-Miami-Cu,Mo; El Abra-Cu; Cerro Verde-Cu; Henderson-Mo; Climax-Mo; Salar de Atacama-Li
INCO	Sudbury (part)-Ni,Cu; Voisey's Bay-Ni; Thompson-Ni; Soroako-Ni; Goro-Ni
Noranda-Falconbridge	Noranda-Au,Cu (exhausted); Kidd Creek-Cu,Zn,Ag,Au; Sudbury (part)-Ni,Cu; Collahuasi-Cu
Barrick-Homestake	Homestake-Au (exhausted); Goldstrike-Au; Hemlo-Au (part); Kalgoorlie-Au (part); Round Mountain-Au; Pierina-Au; Pascua-Lama Au; El Indio-Tambo-Au,Cu; Bousquet-Au
Newmont	Carlin-Au (part); Gold Quarry-Au; Twin Creeks-Au; Yanacocha-Au; Batu Hijau-Cu,Au; Muruntau-low grade stockpile-Au
Phelps Dodge	Morenci-Cu; Santa Rita-Cu; Tyrone-Cu; Dos Pobres-Cu; Candelaria-Cu,Au; Aggeney's-Zn,Pb; El Abra-Cu
X-Strata (incl. MIM)	Mount Isa, Hilton, Ernest Fisher-Cu+Pb,Zn,Ag; McArthur River-Pb,Zn,Ag; Alumbrera-Cu,Au
Grupo Mexico	Cananea-Cu,Au,Mo; Caridad-Cu; Toquepala-Cu,Mo; El Arco-Cu
Gencor & Harmony	Witwatersrand-Au (parts); Evander-Au; Merensky Reef, 3 mines-PGE
Freeport-McMoRan	Ertzberg-Grasberg-Cu,Au; Central Florida phosphate+U

Each of the 25 or so biggest resource companies have one or more "giants" in their portfolio and in most cases it was the "giant" that made the company big and long-lasting and sustained it through the years. Some big companies are the "children" of big ore discoveries, others have become big gradually by lucky "giant" discoveries during their lifetime, or by mergers and acquisitions. The history of the presently largest resource corporation BHP-Billiton (London and Melbourne) is instructive and summarized below from Kearns (1982) plus company materials. BHP stands for Broken Hill Proprietary, named after the Australian deposit where the company had been born in 1885, but which it left in 1939. Briefly:

- 1883. Carl Rasp, a farm hand, discovered Broken Hill Pb-Zn-Ag outcrop
- 1885. Broken Hill proprietary Company was floated with initial capital of £18,000
- 1886. Two 30 t/day smelters were erected, mine market value was Au\$ 3.04 million

- 1889. Refinery, later smelter, were established at Port Pirie in South Australia; Fe ore started to be mined at Iron Knob in the Middleback Ranges initially as Pb-Zn-Ag smelter flux, later to supply Newcastle and Whyalla iron works
- 1939. Ore at the original Broken Hill lease was depleted (Au\$ 108 million extracted) and it was impossible to extend operation in the tightly held ore zone. BHP leaved Broken Hill, diversified to iron mining and smelting, eventually to become the #1 iron producer in Australia
- 1960. Australian Government lifted embargo on export of Fe ores, BHP acquired share of the Hamersley Fe Province that holds 95% of the Australian high-grade Fe reserves. The "world class" Mount Whaleback deposit there had a resource of 1.445 Bt of 65% Fe ore. Railway and port were constructed and by the year 2000 BHP shipped almost 15% of the world's Fe ore supply
- 1970s; BHP acquired Ok Tedi porphyry/skarn Cu-Au in remote Papua New Guinea, to develop later into a major environmental problem (pollution of the Fly River by tailings and heavy metals)
- 1980s; BHP acquired the "giant" Pb-Zn-Ag deposit Cannington in Queensland
- 1980s; BHP "farmed into" the newly discovered Escondida Cu "super-giant" in Chile
- 1990s; BHP acquired Magma Inc. in United States and with it the San Manuel porphyry Cu-Mo in Arizona; a wrong move, relinquished later at a loss
- 2000s; BHP merged with Billiton, originally a tin-mining company incorporated in 1860 in The Hague, but more recently a major resource corporation headquartered in London. BHP-Billiton has become the world's largest mineral resource company.

A similar history can be written about most other resource corporations, like the world's second largest Rio Tinto Ltd., originally a minor British pyrite miner in Spain. The corporation has experienced a phenomenal growth since about 1962 when it merged with the Consolidated Zinc of Australia (CRA) to acquire a portion of Broken Hill, later a portion of the Hamersley iron province (Mount Tom Price). Elliot Lake-U, Palabora-Cu, Panguna Cu-Au, Rössing-U, Escondida-Cu, Lihir-Au, Bingham-Cu,Au,Mo and a share in Olympic Dam, followed. Below is a sampling of major resource corporations born from initial or early "giant" discoveries and/or consolidation of smaller local properties:

- Anglo-American: Witwatersrand (parts)-Au, later U
- De Beers: Kimberley, diamonds
- INCO (International Nickel): Sudbury (a portion of)
- Noranda-Falconbridge: Sudbury-Ni,Cu (portion); Noranda-Cu,Au

- Teck-Cominco: Kirkland Lake-Au (portion); Sullivan Pb-Zn-Ag
- Cyprus-Amax: Climax-Mo
- Homestake (now Barrick): Homestake (Lead)-Au
- Mt. Isa Mines (now Xstrata) Mount Isa-Pb,Zn,Ag,Cu
- Newcrest: Telfer-Au; Cadia-Au,Cu
- Ivanhoe: Monywa-Cu,Au; Oyu Tolgoi-Cu,Au

The following corporations have discovered or acquired a "giant" deposit during their midlife and it contributed to a rapid growth and sustainability:

- Western Mining (now BHP): Olympic Dam-Cu, Au, U (1975)
- Kennecott (now Rio Tinto): Bingham and El Teniente-Cu, Mo, Au (pre-1970)
- Newmont: Carlin (1961), other deposits in Carlin Trend
- CVRD (Rio Doce): Serra dos Carajás-Fe
- Codelco Chile: El Teniente, Chuquicamata, El Salvador-all Cu,Mo
- Freeport McMoRan: Ertsberg, Grasberg-Cu, Au
- Xstrata: Mount Isa-Cu, Pb, Zn; McArthur River-Pb, Zn
- Navoi (Uzbekistan State): Muruntau-Au
- Noril'sk Nickel (Russia): Noril'sk-Talnakh Ni, Cu, PGE
- Cameco: Cigar Lake-U, McArthur River-U, Kumtor-Au
- Teck-Cominco: Red Dog-Zn, Pb, Ag

Loss of a life-sustaining "giant", on the other hand, can greatly reduce the worth and vitality of a corporation from which many have not recovered and either went out of business, restructured, suffered a takeover, or changed the nature of business. As in the automobile world, the "brand name" (e.g. Kennecott, Anaconda, Falconbridge) sometimes survived, but often became a different entity. The loss of a "giant" to gradual reserves depletion is a predictable matter for which a corporation can plan in good time and try to find a substitute. The Cominco's Sullivan Mine in British Columbia was in operation for 100 years, after which Red Dog has provided a long-term replacement, although the cost of transporting the concentrate from Arctic Alaska to the Trail smelter in central British Columbia has increased exponentially. The Homestake gold mine, Bingham, Sudbury, Rammelsberg, Iberian Pyrite Belt, the Mexican silver giants, Potosí and other deposits started up already in the 19th century or earlier and they enjoyed similar longevity.

The sudden, unplanned loss of a "giant" due to government/regime change, war or de-colonization,

and followed by confiscation or nationalization, beset the owners of the Zn-Pb "giants" in the Polish Silesia (e.g. Bytom), Transylvanian gold mines, much of African and South American mining corporations between 1945 and about 1980. In the 1990s and 2000 the pendulum has changed direction and a wave of privatizations crippled or eliminated some formerly powerful state mining organizations although others (Codelco Chile, Navoi Uzbekistan) have survived and prosper. Selected examples of corporation reduction or demise due to a "giant" loss follow:

- Union Minière, Katanga Copperbelt: Cu-Co properties nationalized in the 1960s-1970s
- Selection Trust, Zambian Copperbelt: properties nationalized in the 1960s-1970s
- Kennecott Chile, El Teniente-Cu, nationalized in the 1970s
- Anaconda Chile, Chuquicamata: nationalized in the 1970s
- Cerro Corporation, Cerro de Pasco and Antamina, Peru: nationalized in the 1970s
- Freeport Sulfur, Moa Bay, Cuba-Ni, nationalized in the 1960s
- Centromin Peru: Antamina, Colquijirca, etc., privatized in the 1990s
- Romanian State: Roşia Montană, privatized in the 2000s
- VEB Wismut, East Germany: Schlema, Ronneburg-U closed down after German unification in the 1990s, mutated into an environmental agency responsible for reclamation of uranium mines

There has been a gradual change of attitude of the big corporations towards the means of acquisition of exceptional metallic deposits. Until about the 1970s-1980s corporations maintained strong exploration departments staffed by top experienced geologists (the who-is-who in economic geology is rich in the names of company geologists, although some later joined the government or academia, and vice-versa). In the "golden period" of exploration the discoveries were made with the help of the hunter's instinct by enthusiastic individuals and small teams. Very senior executives did not hesitate to spend time in the bush (and, occasionally, a freezing night on an Yukon glacier when sudden fog prevented helicopter departure), or an arduous traverse through jungle to visit a discovery site. This was taking place regardless of the political system. Most "giants" found then were "in-house", joint venture, geological survey, or consultant-assisted discoveries. The boards of directors had at least one respected geologist and a large proportion of engineers, and there was a

recognition that steady exploration was a lifeblood of the corporation. This philosophy was supported by loyal shareholders. The exploration attitude of the Western Mining Corporation in Australia in the 1960s-1970s, publicized by Woodall (1983), was exemplary and they were rewarded by a series of "greenfield" discoveries like Kambalda-Ni, Yeelirrie-U and Olympic Dam-Cu, U, Au. This explorer's spirit combined with willingness to take risks and overcome formidable natural and political obstacles also follow from the story of discovery and development of Ertsberg-Grasberg in New Guinea, by Maley (1996).

The corporate attitude towards mineral exploration has changed in the "greedy 1990s" with boards of directors of many large corporations dominated by lawyers and financial experts concerned primarily with share prices and executive self-preservation. Exploration departments have been downsized or eliminated altogether, and increasingly staffed by 9 to 5 geotechnocrats. Douglas Haynes (quoted by Uren, 2001) pointed out that no giant deposit had been found worldwide between 1996 and 2001, and only four between 1992 and 1996 (an understatement; my remark). This contrasts with the regular discoveries of two or three "giants"/year until the early 1990s. Uren considered this lack of exploration success as due to exhaustion of natural targets and sharply increasing costs; corporations now counter this trend by restructuring, mergers, and acquisitions of properties found by others. The sudden availability of explored properties that included "giants", in the wake of the political changes in the communist block in the 1990s, generated a short term euphoria among the western corporations, with a vision of cornucopia and easy windfall profits based on quality deposits acquired without the risk and financial outlay of in-house exploration. This expectation has not, unfortunately, materialized.

Many large corporations these days rely on mineral discoveries being made by junior and mid-size companies whose Directors are overwhelmingly geologists (many dumped earlier by the Goliaths). Schodde (2004) argued that, between 1985 and 2003, junior companies in Australia found 36 to 44% of "major" (1 million oz Au plus) gold discoveries but only 27% of the gold amount, which seems to indicate that the Majors are (or were) better at finding the more valuable targets. The Goliaths increasingly resort to equity stakes in the junior companies or rely on "farm-in" arrangements, of which BHP-Billiton alone had 56, in 2001 (Uren, 2001). It is doubtful that the

excessive discovery expectations of the megacorporations will ever be met in the near future; BHP withdrew from joint venture with Minotaur Resources as the 1.5 mt Cu and 81 t Au Prominent Hill deposit in South Australia, still open in depth and laterally, had not been "big enough" for them.

16.3. "Giants" and economics

An exceptional metal accumulation, no matter how geochemically significant, becomes a "giant" metallic deposits only if it is suitable for, and capable of, producing commodities (metals) under given politico-economic conditions prevalent in a given territory. With the exception of the various "command economies" prevalent mainly in the near past and special temporary situations like wars, embargoes and similar, mining is an industry expected to be profitable. Economics and politics are thus the two paramount non-geological factors that can "make" any orebody into a mine, not only "giant", out of a rock or a "dirt". Mineral economics and politics is an extensive field of learning with a growing literature: try Rittenhouse (1979), Barney et al. (1980), Pye (1981), Mackenzie and Bilodeau (1984), Rudawsky (1986), McLaren and Skinner, eds. (1987), Peters (1987), Wellmer (1989), Annels (1991), White (1997), Crowson (1998 and other yearly editions). With emphasis on the geological and geochemical premises of treatment of metallic accumulations in this book, economics has been in some cases an impediment of treatment of metalliferous sites that have not (yet) made it into the industrial resources inventory.

"Geologist's values": To give a monetary meaning (a "price sticker") to the class of exceptional (and ordinary as well) metallic deposits, two sets of financial considerations are briefly described below. The first one, the "geologist's values", is artificial and it is really a simplistic approach of a geoscientist to the highly complicated problem of mine valuation. The values are derived by multiplying the ore metal quantities in a deposit by the metal price (Figures 16.3. and 16.4). Obviously this is not an exact technique as a) the metal prices fluctuate on a daily basis; b) most quoted prices apply to pure, finished metals and as the cost of metal recovery from ores varies enormously, the figures do not indicate the actual profitability. This problem can be reduced by using the prices of commodities that are not the pure metals, for which the prices have been published like Fe ore, TiO₂, chromite, alumina.

Table 16.3. Calculated "geologist's values" of metals contained in single largest deposits/districts/areas

Commodity	Largest deposit/district/area	Object	Metal content, t	Price per 1 ton, US\$	Deposit Value, US\$
Al ₂ O ₃	Boké-Gaoual, Guinea	area	7.33 bt	600	4398 b
Fe ore	Hamersley Range, rich 60% plus ore	range	39 bt	27	1053 b
TiO ₂	Bushveld Main Magnetite Seam, S. Africa	unit	668 mt	2800	1870 b
Mn	Kalahari Basin, South Africa	deposit	4.2 bt	900	3780 b
Zr conc.	Lovozero eudialyte lujavrite unit, Russia	unit	420 mt	148	62.16 b
REE	Bayan Obo, Nei Mongol, China	deposit	45 mt	4500	202 b
Chromite	Bushveld chromitite seams, South Africa	unit	11.8 bt	50	590 b
V	Bushveld Magnetite Seam, South Africa	unit	71 mt	14 k	994 b
Zn-1	Kraków-Silesia Basin, Poland	basin	40 mt	880	35.2 b
Zn-2	Broken Hill, N.S.W., Australia	ore zone	31 mt	880	27.3 b
Ni-1	New Caledonia laterite-saprolite blanket	area	50 mt	7800	390 b
Ni-2	Noril'sk-Talnakh, Russia	district	24.3 mt	7800	189 b
Cu-1	Copperbelt, DRC Congo & Zambia	ore belt	219 mt	2400	526 b
Cu-2	El Teniente, Chile	deposit	94.4 mt	2400	226 b
Co	Copperbelt, DRC Congo & Zambia	belt	11 mt	61 k	671 m
Y	Tomtor, Anabar Shield, Russia	deposit	3 mt	90 k	270 m
Nb	Seis Lagos, Brazil	deposit	48.9 mt	15 k	733 m
Ga	Brockman, Western Australia	deposit	640 t	520 k	333 m
Pb-1	Viburnum Trend, S.E. Missouri, U.S.A.	ore zone	48 mt	800	38.4 b
Pb-2	Broken Hill, N.S.W., Australia	ore zone	28 mt	800	22.4 b
Th	Araxá, Brazil	deposit	1.16 mt	70 k	81 b
Be	Spor Mountain, Utah, U.S.A	deposit	24 kt	340 k	8.16 b
Sn-1	Kinta Valley placers, Ipoh, Malaysia	area	3.10 mt	6400	19.84 b
Sn-2	Dachang, Jiangxi, China	ore field	1.65 mt	6400	10.56 b
As	Río Tinto, Spain	ore field	4.50 mt	4500	20.25 b
U	Olympic Dam, South Australia	deposit	1.40 mt	33 k	46.2 b
Ge	Tsumeb, Namibia	deposit	2,160 t	900 k	1.94 b
Ta	Ghurayyah, Saudi Arabia	deposit	93.3 kt	60 k	5.6 b
Mo	Climax, Colorado, U.S.A.	deposit	2.18 mt	0.24 %	7.68
W	Verkhnye Qairakty, Kazakhstan	deposit	880 kt	14 k	12.32 b
Tl	Meggen, Germany	deposit	960 t	90 k	86.4 m
Sb	Xikuangshan, Hunan, China	ore field	2.11 mt	3240	6.84 b
Se	Río Tinto, Spain	ore field	225 kt	7530	1.694 b
Cd	Tsumeb, Namibia	deposit	10.8 kt	2800	31 m
Bi	Shizhouyuan, Hunan, China	deposit	230 kt	7800	1.794 b
Ag-1	Lubin Kupferschiefer district, Poland	district	170 kt	170 k	28.9 b
Ag-2	Potosí (Cerro Rico), Bolivia	deposit	84 kt	170 k	14.28 b
In	Mount Pleasant, New Brunswick, Canada	ore field	100 t	112 k	11.2 m
Hg	Almadén, Spain	deposit	276 kt	9320	2.572 b
PGE	Merensky Reef, Bushveld, South Africa	unit	42 kt	15 m	630 b
Te	Cripple Creek, Colorado, U.S.A.	ore field	1000 t	10 k	10 m
Au-1	Muruntau, Uzbekistan	deposit	4300 t	12 m	51.6 b
Au-2	Central Rand Group, Witwatersrand, S. Afr.	basin	76.4 kt	12 m	917 b
Au-3	Welkom Goldfield, Witwatersrand, S. Africa	ore field	15.3 kt	12 m	183.6 b

Value of metals in deposits/districts have been calculated using commodity prices listed in Table 1.1., that in turn correspond to the approximate values in the 1980s-1990s as listed in the U.S. Geological Survey publications. The metal tonnages used are scattered in the text and tables in this book. Abbreviations: t=tons, kt=thousand tons, mt=million tons, bt=billion tons. In price columns, quoted in US \$, k=thousand, m=million, b=billion. Al, Fe, Cr, Zr prices are based on prices of commodities other than pure metals. The values apply to the pre-mining resources and some deposits listed have been mined out by now

Table 16.4. Selection of "giant" and "super-giant" deposits/districts/areas and their "geologist's values"

Deposit/area	Values of constituent ore metals, US\$	Total value
Large areas (belts) that comprise several "giant" and/or lesser size deposits		
Bushveld Complex, South Africa	Chromite, 590b; V, 994b; TiO ₂ , 1870b; PGE, 750b; Fe ore, 162b; Ni, 94b; Cu, 14.4b; Au, 10.2b	4484b
Kalahari Mn Basin, South Africa	Mn metal @ \$900/t: 3780b or Mn ore @ \$150/t	3780b 1800b
African Copperbelt	Cu, 526b; Co, 671b	1197b
Hamersley Range, W. Australia	Fe ore, 1072b	1072b
Witwatersrand Basin, S. Africa	Au (@76.4 kt), 917b; U, 19.6b	937b
Carajás Fe Plateaux, Brazil	Fe ore, 560b	650b
Noril'sk-Talnakh, Russia	Ni, 189.5b; Cu, 72b; Co, 14.6b; PGE, 42.5b	319b
Sudbury Complex, Ontario	Ni, 147b; Cu, 41b; Co, 40b; PGE, 17b; Ag, 986m; Au, 2.8b	249b
Lubin (Polish Kupferschiefer)	Cu, 163b; Ag, 29b; Zn, 44.6b; Pb, 4.2b	240b
Iberian Pyrite Belt, Spain & Portugal	Cu, 35b; Zn, 31b; Pb, 10.8b, Ag, 7.84b, Au, 11.04b, Sn, 2.24b --ditto, + As @ \$ 4500/t, 30.6b; no pyrite value included	97.7b 128.3b
Carlin Trend, Nevada	Au, 40b	40b
Timmins-Porcupine, Ontario	Au, 25.2b	25.2b
Cornwall & Devon, U.K.	Sn, 16b; Cu, 4.8b	20.8b
Hokuroku VMS dist., Japan	Zn, 4.5b; Cu, 4.9b; Pb, 1.22b; Ag, 1.65b; Au, 1.82b	14.9b
Mother Lode, California	Au, 9.64b	9.64b
Deposits, ore fields		
Araxá (Barreiro), Brazil	Nb, 300b; REE, 78.7b --ditto, plus Th, 117b; U, 4.45b	379b 500b
El Teniente, Chile	Cu, 226.6; Mo, 24.8b	251.4b
Chuquicamata, Chile	Cu, 209b; Mo, 9.97b; Ag, 6.63b	225.6b
Olympic Dam, South Australia	Cu, 110b; U, 46.2b; Au, 22.8b; Ag, 1.68b; Fe not included --ditto, plus REE content, 45b	181b 226b
La Escondida, Chile	Cu, 168b; Mo, 5b	173b
Rio Blanco-Los Bronces, Chile	Cu, 142.3b; Mo, 13.8b	156b
Kiirunavaara deposit, Sweden	Fe ore, 143b	143b
Bingham Canyon, Utah	Cu, 51.05b; Mo, 15.6b; Au, 11.5b; Ag, 6.63b	84.8b
Ertsberg-Grasberg, Indonesia	Cu, 57.12b; Au, 24b; Ag, 802m	82b
Broken Hill, NSW, Australia	Pb, 22.4b; Zn, 27.3b; Ag, 7.3b; Cu, 1.1b	58b
Muruntau, Uzbekistan	Au (4300t), 51.6b	51.6b
Antamina, Peru	Cu, 23.8b; Zn, 6.7b; Ag, 1.8b; Mo, 2.28b	34.6b
Mount Isa-Cu, Queensland	Cu, 24b; Co, 7.32b	31.32b
Climax, Colorado	Mo, 27b; W, 3.93b	31b
Red Dog, Alaska	Zn, 21.65b; Pb, 5.45b; Ag, 2.1b	29.2b
Rio Tinto ore field, Spain	Cu, 10.8b; Zn, 9.28b; Pb, 3.2b; Au, 3.0b; Ag, 2.21b	28.55b
Mountain Pass, California	REE, 28.04b	28.04b
Kalgoorlie, Golden Mile, W.A.	Au, 26.8b	26.8b
Batu Hijau, Indonesia	Cu, 18.65b; Au, 7.18b	25.8b
Butte, Montana	Cu, 17.8b; Ag, 3.42b; Au, 1.07b	22.2b
Yanacocha, Peru	Au, 21.65b; Ag not included	21.65b
Panguna, Bougainville, PNG	Cu, 14.02b; Au, 7.58b	21.6b
Kidd Creek, Ontario	Zn, 9.24b; Cu, 8.64b; Ag, 2.1b; Sn, 909m; Pb, 296m	21.2b
Potosí, Cerro Rico, Bolivia	Ag, 14.3b; Sn, 6.4b	20.7b
Obuasi, Ghana	Au, 19.8b --plus As, 5.4b	19.8b 25.2b
Goldstrike deposit, Carlin Trend	Au, 19.4b	19.4b
Cadia, NSW, Australia	Cu, 10.56b; Au, 6.9m	17.45b
Ladolam, Lihir Island, PNG	Au, 16.7b	16.7b
Cerro de Pasco, Peru	Zn, 7.56b; Pb, 2.38b; Ag, 3.44b; Cu, 2.64b	16.02b

Table 16.4. (continued)

Deposit/area	Value of constituent metals, US\$	Total value
Homestake, South Dakota	Au, 15.83b --ditto, plus As, 4.5b	15.83b 20.33b
Mount Isa Pb-Zn-Ag, Queensland	Pb, 5.92b; Zn, 5.98b; Ag, 3.04b	15.0b
Pachuca, Mexico	Ag, 7.22b; Au, 2.58b	9.8b
Navan, Ireland	Zn, 6.7b; Pb, 1.5b	8.2b
Xikuangshan, Hunan, China	Sb, 6.48b	6.48b
McArthur River, Saskatchewan	U, 6.24b	6.24b
Comstock Lode, Nevada	Au, 3.75b; Ag, 1.23b	4.98b
Almadén, Spain	Hg (276 kt), 2.57b	2.57b
Renison Bell, Tasmania	Sn, 1.84b	1.84b

Based on metal prices listed in Figure 1.1. and tonnage figures scattered in text. b=\$ billions, m=\$ millions

Despite limitations, this approach yields monetary values of ore deposits that can be ranked to answer the question of which "giant" is, or was, more valuable.

Investment (development) costs of ore deposits:

The second monetary consideration applied to orebodies is very real, and it is based on investments (mostly capital costs) required to bring a "giant" into production. As can be seen, the costs are staggering yet largely invisible to the general public, although they greatly overshadow the costs of various government programs.

The value of "giants"

This is very difficult to objectively establish in terms of mutually comparable units. Cumulative gross revenue figures of production over the life of a mine are sometimes available and so are total dividends paid and sometimes profits. Such figures are of interest for the study of economic and financial history, but are difficult to convert into metal tonnages because of fluctuating metal prices and inflation. Cumulative value of metals in ground before mining, in a deposit (the "geologist's values" introduced above) is quantitative and can be calculated for many deposits to answer the question of "which one is the dearest of them all", and what commodity to explore for. The "footprint" of the mineralized object interferes, as usually, with the credibility of conclusions as the Witwatersrand (a "basin" mineralized over some 40,000 km²) is not comparable with the 5 km² Olympic Dam, a single deposit. Needless to say the fluctuating metal prices complicate the result as does the selection of metals included in calculations. In an enargite deposit, or at many gold mines, should the value of arsenic be

included? As is usually an unrecovered penalty element the value of which to the producer is usually negative as it costs money to dispose of arsenic properly. There is, however, a limited market for arsenic and the quoted price is around \$ 4,500/t. This adds billions of dollars to the "geologist's values" of several deposits. In Table 16.4. this problem has been solved by quoting values without As as well as with As.

The "geologist's values" of selected examples of "giant" and "super-giant" deposits in Table 16.4. are based on the average commodity prices as they were in the 1980s-1990s (listed in Table 1-1), and on production/resource figures quoted throughout this book. The results are interesting, in places startling and they dispel the preconceived opinion about the relative value of ores of the various metals. The Bushveld Complex comes clearly as the most valuable repository of industrial metals. The figure in Table 16.4. exceeds \$ 4 trillion, yet this is considered conservative as it is based on the presently mineable ores rather than on the total estimated resource that includes the deep-seated ores. The trillion-plus value of the Kalahari Mn Basin comes as a surprise, as it exceeds the value of the Witwatersrand. Mn is not known for generating exploration excitement and its uses and markets are limited. The value of iron ore regions, taken for granted by most geologists except for periods of heightened demand (one is presently under way, driven by the increasing Fe ore consumption of China, Japan and Korea), greatly overshadows the more glamorous commodities like gold and silver. Copper (and molybdenum) contribute to the high values of porphyry coppers, whereas the geochemically more concentrated Pb and Zn deposits are worth much less. The Sb and Hg "super-giants" Xikuangshan and Almadén, despite

their status as the greatest local geochemical accumulations, pale into insignificance. Olympic Dam has now become the most valuable nonferrous metals deposit in Australia (\$ 181 or 226 billion), overtaking Mount Isa, Broken Hill and Kalgoorlie by a wide margin.

The 1.4 mt U stored in Olympic Dam, the world's largest uranium resource (some 35% of the world's U in past production and presently economic reserves), is worth some \$ 46 billion and increasing with the present U price recovery. Equivalent U worth in the Canadian deposits, the second most important U source, is about 40% as much. The cumulative 1945-1993 uranium production from more than 50 mined vein U deposits in the Erzgebirge and adjacent regions of Germany and the Czech Republic, some 150,000 t U (the Ronneburg deposit is not included), has a cumulative value of about \$ 3.9 billion. Almost the entire production, resulting from reckless mining, was exported to the former Soviet Union. The total cost of reclamation now borne by the German Government is in the region of \$ 12 billion (perhaps half of this is to be spent on the "black shale" and "sandstone" deposits, but additional funds are to be spent on the Czech side). The net gain over the period of almost 50 years of uranium mining in the Erzgebirge has thus been some minus 6 to 8 billion dollars.

The costs of finding and developing "giants"

Discovery costs of major metallic deposits have increased exponentially. Schodde (2004) calculated that 190 gold deposits larger than 1 million oz Au have been found in the Western World between 1985 and 2003. They contained 3,505 t Au and averaged \$150 million per discovery. Base metals cost more to find, and Uren (2001) quoted \$800 million plus as the average cost of finding a deposit with more than \$1 billion in reserve (this corresponds to about 500 kt Cu or 77 t Au). The discovery costs have about quadrupled in the past 20 years. These, of course, are the averages and some companies (or individuals) did much better, others much worse; over 95% of listed companies found nothing.

The legendary discoveries made in the past, by oldtimers traversing the bush on foot, with donkey or in canoes, generated fabulous values for negligible outlays. So Patrick Hannan's party who discovered the Kalgoorlie Golden Mile, worth some \$ 28 billion (metals in ground), probably spent about \$50k at present prices. That was in 1893. Since that time the number of deposits remaining to

be discovered at surface has been reduced to a trickle, but skill, dedication and sometimes just a good luck resulted in few spectacular recent surface finds. The skill/dedication case is exemplified by discovery of the first viable Canadian diamond field at Lac de Gras (presently Ekati Mine) by Charles Fipke's group (a multibillion value for a total outlay of less than \$ 1 million). The "luck" case goes to Al Chislett and Chris Verbiski who landed their helicopter on a rusty Labrador outcrop and discovered the Voisey's Bay Ni-Cu deposit (value around \$ 26 billion for some \$ X00,000 cost of an unrelated project). I believe there is a potential for some 5 to 10 comparable jackpot discoveries in the next 50 years made by dedicated lucky finders. More about this in the next chapter.

As it is argued below, discovery of a "giant" is a matter of statistics except for the restriction of targets to those with proven or anticipated "giants"-bearing potential. One just does not go after the "giants" only, but selects the "best" out of a population of lesser deposits (prospects) discovered. So anyone can discover a "giant" at/near the surface regardless of the size and a budget of his/her organization, although the increasing trend towards finding concealed deposits does require deeper pockets to pay for deep-reach geophysics and drilling (much of these have been done by governments and are available for free or for next to nothing). The financial outlays, however, greatly increase after feasibility, with bringing the deposit into production. The past ways where a mid-size ore field was slowly mined, with interruptions, for hundreds to thousand of years (Freiberg, Příbram) do not apply in the present "blitzkrieg"-type mining style enforced by market economics of the globalized world and the cut-throat competition (some mines of the old-fashioned type managed to survive in sheltered economies) and mega-mines are required to rapidly translate a "giant" deposit into cash. The capital costs alone are staggering and have rapidly increased from tens and hundreds of million dollars in the 1960s to 1980s (e.g. Endako-Mo, 1964, Can\$ 22m; Valley Copper-Cu, Can\$ 300m; Taylor, 1995) to billions of dollars in the past ten years. Examples follow (Table 16.5; approximate figures that include funds actually spent as well as planned).

The table does not include the "(super)-giants" where capital costs have been extended gradually, over longer period of time, or where they are dispersed among various cost items. Given the billion dollar outlays it is obvious that only the mega-corporations can sustain the truly large and

valuable properties and even there by forming consortia to share the costs and equity.

Table 16.5. Capital costs of selected projects to bring already discovered "giant" deposits into production (or to increase production)

Period	Deposit	Cost, US\$
1960	Toquepala-Cu,Mo; Perú	\$ 240m
1964	Endako-Mo, British Columbia	C\$ 22m
1970	Valley Copper-Cu, BC, Canada	C\$ 300m
1971	Gibraltar-Cu, British Columbia	C\$ 65m
1977	Cuajone-Cu,Mo; Perú	\$ 730m
1978	Bagdad-Cu,Mo; Arizona	\$ 240m
1978	Lakeshore-Cu; Arizona	\$ 200m
1979	La Caridad-Cu,Mo; Mexico	\$ 600m
1990	Windy Craggy-Cu,Co; B.C.	C\$ 400m
1990	La Escondida-Cu; Chile	\$ 2.3b
1994	Fish Lake-Cu,Au; B.C.	C\$ 460m
1994	Candelaria-Cu,Au; Chile	\$ 870m
1995	Kumtor-Au, Kyrgyzstan	\$ 452m
1995	Quebrada Blanca-Cu; Chile	\$ 360m
1995	Zaldivar-Cu; Chile	\$ 600m
1998	Collahuasi-Cu,Mo; Chile	\$ 1.8b
1999	Batu Hijau-Cu,Au; Indonesia	\$ 1.9b
1999	Century, Queensland	A\$ 850m
1999	Cerro Casale-Au,Cu; Chile	\$ 1.4b
1999	La Escondida Phase 4, Chile	\$ 1.36b
1999	Los Pelambres-Cu,Mo; Chile	\$ 1.36b
1999	El Pachón-Cu,Mo; Argentina	\$ 900m
2000	Antamina-Cu,Zn; Perú	\$ 2.3b
2001	Cerro Colorado-Cu, Chile	\$ 331m
2001	Spence-Cu; Chile	\$ 1.0b
2001	Mansa Mina (Chuquicamata)	\$ 295m
2003	La Escondida, total to date	\$ 3.7b
2004	Pascua-Lama, Au; Chile & Arg.	\$ 1.5b
2004	Ravensthorpe-Ni; W. Australia	\$ 1.05b
2004	Goro-Ni; New Caledonia	\$ 1.4b
2005	Olympic Dam, expansion	A\$ 5.0b

Several medium- to medium-large companies (capitalization \$ 200-500 million plus), however, still maintain equity in "giant" deposits they discovered or initially developed, although they tend to become targets of takeovers. In 2005, BHP-Billiton paid \$ 6.75 billion (Aus\$ 9 billion) to take over the WMC Corporation, the discoverer and operator of Olympic Dam. BHP has thus gained control of some 30% of the world's uranium resources, in times of renewed interest in nuclear energy generation.

17 Finding or Acquiring Giant Deposits

17.1. Introduction

An earlier quote stated that no "world class" deposit has been discovered in the past five years. This, of course, depends on the magnitude threshold for such deposits, and the term "discovery" is also not appropriate: it should read "announcement", as "giant" deposits enter the database only once their tonnage and grade is announced and this takes place some time after discovery. This is the cause of frequent discrepancies in recording the date of ore discovery. The "giant" Oyu Tolgoi porphyry Cu-Mo in Mongolia; new high sulfidation Au-Cu orebodies in Monywa, Burma; the Superior-deep Cu-Mo in Arizona; new "giant"-size resources at Telfer and Boddington, Western Australia; and several other deposits have been reported as discovered in this period (Table 17.1). There are thousands of new prospects in the process of exploration and resource proving, and some of them will likely turn out to be "giant". In addition to this, some existing "large" deposits or districts will achieve the "giant" rank as a result of ongoing exploration.

The reality, however, is that very recently the high rate of discovery of major ore deposits, as it had been in the 1960s through 1980s, has dropped dramatically, while the exploration expenditure increased: in case of gold from \$ 90 million per deposit with an in-situ value of \$ 1 billion plus in the 1950s and 1960s, to \$ 290 million in the 1980s and 1990s (WMC Corporation data). This, of course, reduced the return on investment so the large corporations responded by closing exploration offices (or replacing them with acquisition departments), firing the experienced staff, restructuring, takeovers and mergers. Some corporations virtually outsourced the mine finding to the junior companies (augmented by, or only made possible, by the hefty taxpayers-funded "free" assistance received from some western state geological surveys) with whom they enter into joint ventures, "farm-in" deals or straight property purchases. The underlying reasons for this are the substantial depletion of the easy-to-find deposits, the vagaries of fluctuating commodity prices, and the crippling costs of having to accommodate the ever increasing burdens of bureaucracy, environmental preservation, media-fuelled negative public perception, political correctness and a

growing list of investment risks (e.g. MacGregor, 1978; Barton, 1980; Skinner, 1993; Lonergan, 1997; Uren, 2001).

Between 1997 and 2003 the resources industry was devastated by a period of one of the historically lowest metal prices and unfriendly regulatory climates. 2004 and 2005, in turn, have seen the metal prices rebound to reach, in some cases, all time highs, which is attributed to the greatly increased demand from rapidly industrializing China and India. It remains to be seen whether this is another short-term cycle or a beginning of the impeding mineral resources crisis, predicted in the textbook of Kesler (1994) and other writers.

Except for the chance or unplanned major mineral discoveries that are extremely rare but occasionally do happen (e.g. Voisey's Bay-Ni,Cu), ore finding is the result of an increasingly more complex, costly and lengthy multidisciplinary process where the chance of success is extremely slim. This leads to a paradox: as the exploration success diminishes, corporations cut exploration expenditures that guarantees no discovery at all!

It is expected that future metal prices are going to rise sharply in line with developing shortages and this might compensate for diminishing profits. The alternative is stagnation of new metals supply leading to cannibalization of existing metals inventories (e.g. premature recycling) and a great reduction of the quality of life (especially slowing down or reversal of poverty eradication). This may lead to times reminiscent of the A.D. 700 to 1500 period, when virtually no new gold was being produced (Mullen and Parish, 1998). Skinner (1993) projected the staggering amounts of commodities required to be found, developed and supplied to keep pace with the population explosion. Diamond (2005) demonstrated by several case histories what happens when the life supports of civilizations are diminished, or entirely withdrawn.

The theater of mineral exploration is now truly global, although the regional accessibility changes rapidly with changing politics: who would have thought, in 1988, of establishing a capitalist venture and explore in countries like the former U.S.S.R, China, Mongolia or Vietnam?

Table 17.1. List of selected "giant", "super-giant", and "large" deposits/districts arranged by the year of discovery

Year	Deposit/district	Metal(s)	Disc. meth.	Notes
3000BC	Sar Chesmeh, Iran	Cu,Mo	accidental?	Visual find?, oxidic Cu gossan over porphyry Cu
2500BC	Lavrion, Greece	Ag,Pb,Zn	accidental?	Visual find of silver-rich gossan?
1100BC	Spanish Meseta (Linares)	Ag,Pb,Zn	accidental?	Ditto
? 1 AD	Kolar, Karnataka, India	Au	ditto?	Probably visual find of gold in quartz in outcrop
pre100	Rosia Montana, Romania	Au	accidental?	
~100?	Cornwall, England	Sn,Cu	ditto?	
907	Shandong goldf., China	Au	accidental?	
968AD	Rammelsberg, Germany	Ag,Pb,Zn	ditto?	Ditto ("horse hoof hit a big chunk of silver...")
1150	Mansfeld, Germany	Cu,Ag	ditto?	Visual?, oxidic Cu stained outcrops
1548	Guanajuato, Mexico	Ag,Au	local miners	Native silver diggings, mining by colonial Spain
1500s	Zacatecas, Mexico	Ag,Pb,Zn	ditto	Ditto
1522	Pachuca, Mexico	Ag,Au	ditto	Ditto
1546	Fresnillo, Mexico	Ag,Pb,Zn	ditto	Ditto
1555	San Martín, Mexico	Ag,Zn,Pb	ditto	Ditto
1500s	Cerro de Pasco, Peru	Ag,Pb,Zn	ditto	Ditto
1545	Potosí, Bolivia	Ag,Sn	ditto	Ditto
1500s	Mankayan, Lepanto	Cu,Ag	accidental?	Gossanous outcrops
1636	Michigan native Cu distr.	Cu,Ag	natives	Reported by traveller based on info from natives
1720	Mine LaMotte, Missouri	Pb,Co	government	Government expedition looking for Pb deposits
1725	Morro Velho, Brazil	Au	accidental?	Portuguese mining started on native showings
1734	Morro do Ouro, Brazil	Au	accidental?	Au in placers, ore outcrop
1784	Ridder (Leninogor), Kaz.	Pb,Zn,Ag	prospecting	Party financed by industrialist F. Ridder
1800	Central district (Santa Rita) NM	Cu,Ag,Zn, Pb	local miners	Oxidic Cu, Ag native digging, taken over by colonial Spain
1830	Itabira, MG, Brazil	Fe,Au	accidental?	Old workings in the area
1838	Balmat, New York	Pb,Zn,Ag	government	New York State geologist's report
1840	Sierra Nevada placers, California	Au	accidental, prospecting	Early nuggets found, followed by prospecting rush
1844	Lake Superior Fe, USA	Fe	accidental	Reported by W.A.Burt, US Government surveyor
1848	Joplin, Tri State, MO	Pb,Zn	accidental	Mining started on discovery outcrop
1851	Victoria goldfields, Aus.	Au	accid, prosp	Accidental nugget finds followed by prospecting
1852	Meggen, Germany	Zn,Pb,ba	ditto	Gossan recognized, relics of sulfides
1853	New Idria, California	Hg	prospecting	Oxidized ore outcrops
1856	Sudbury, Ontario	Ni,Cu	accid, govt	Reported by surveyor A.P. Salter
1860	Antamina, Peru	Cu,Zn	locals, indus	Native Cu diggings, then corporate holdings.
1863	Bingham, Utah	Au,Pb,Cu	accid,prosp	Au panned first, Pb-Zn, then Cu outcrops found
1864	Los Bronces, Chile	Cu,Mo	prospect?	
1865	White Pine, Michigan	Cu,Ag	ditto	Cu-stained ore outcrop, visual
1868	Palabora, Cu	Cu,Fe	accid, prosp	Cu-stained native diggings, recorded
1869	Murchison Range, S.Afr.	Au,Sb	prospecting	Alluv. gold panned, then Au reefs, stibnite
1869	Tintic, Utah	Ag,Cu,Pb	ditto	Visual outcrop discovery
1870	Carlin Trend, Nevada	Au,Pb	ditto	Small diggings: turquoise, traces Au; forgotten
1874	Leadville, Colorado	Ag,Pb,Zn	ditto	Au panned first, then cerussite & Ag in gossans
1874	Butte, Montana	Ag,Cu,Pc	ditto	Ag in gossan, then Cu-Ag veins found
1876	Homestake, South Dakota	Au	ditto	Gold panning near Deadwood led to ore outcrops
1877	Bisbee, Arizona	Cu,Ag	army, prosp	Army expedition, followed by prospectors; outcrop
1879	Climax, Colorado	Mo	ditto	Moly in outcrop staked as graphite prospect
1880	Tarkwa, Ghana	Au	locals, prosp	Natives diggings, gold panning
1880	Collahuasi veins, Chile	Ag,Cu,Pb	prospecting	Visual find, minor veins in later giant field
1882	Central Rand, S. Africa	Au	ditto	First traces of gold panned in the area
1882	Mount Morgan, Queensl.	Au,Cu	prospecting	Auriferous gossan found
1883	Broken Hill, NSW	Pb,Ag,Zn	accidental	Gossan found by farm hand
1883	Getchell, Nevada	Au	prospecting	Gossan found
1884	Sudbury, Ontario	Ni,Cu	accidental	Sulfides exposed in railway cut
1884	Frood Mine, Sudbury, ON	Ni,Cu	industry	Brownfield discovery in discovered ore district
1884	Coeur d'Alene, Idaho	Ag,Pb,Zn	prospecting	Visual outcrop discovery by placer miners

Table 17.1. (continued)

Year	Deposit/district	Metal(s)	Disc.meth.	Notes
1885	Ashanti gold belt, Ghana	Au	local miners	Consolidation & development of native diggings
1886	Klerksdorp, Rand, S.Afr.	Au	prospecting	Small diggings
1886	Central Rand, S. Africa	Au,U	ditto	Outcrop discovery by G. Harrison, Langlaagte farm
1888	East Rand, S. Africa	Au,U	ditto	Follow up prospecting, outcrop discovery
1888	Greenbushes, W. Austral.	Sn,Li,Ta	ditto	Placer cassiterite followed to regolithic ore outcrops
1890	Renison Bell, Tasmania	Sn	ditto	Placer cassiterite led to ore gossan
1890	Mesabi Range, Minnesota	Fe	ditto	
1892	Tsumeb, Namibia	Pb,Cu,Zn	locals,indus	Native diggings examined by corporation
1892	Sullivan, Brit. Columbia	Pb,Zn,Ag	prospecting	Gossan found
1893	Rosebery, Tasmania	Pb,Zn,Ag	prospecting	Gossan found
1893	West Rand, S. Africa	Au,U	ditto	Follow up prospecting from Central Rand, outcrop
1893	Kalgoorlie, W. Australia	Au	prospecting	Pat Hannan's party found ore outcrop
1895	Moanda, Gabon	Mn	government	First reported by government geologist
1896	Klondike, Yukon, Canada	Au	prospecting	Creek panning
1897	Dal'negorsk, Russia	Pb,Zn,Ag	government	Found by Russian government expedition
1897	Red Lake, Ontario	Au	prospecting	First gold panned, mine in 1930
1896	Pine Point, NWT, Canada	Pb,Zn	ditto	Ore boulders in drift found by gold miners
1900	Bushveld chromites, S.Af.	Cr	ditto	Chromite recognized, small diggings
1901	Bushveld magnetite	Fe	ditto	Magnetite recognized, early smelting tried
1901	Sudbury-Falconbridge	Ni,Cu	geophysics	Buried orebody indicated by dip needle (Edison)
1902	Roan Antelope, Zambia	Cu	native, pros	Prospectors led to Cu diggings by natives
1903	Ruwe mine, Katanga	Cu	ditto	Ditto, first significant mine in Katanga
1903	Chambishi, Zambia	Cu	ditto	Prospectors led to Cu diggings by natives
1903	Cobalt camp, Ontario	Ag	accidental	Silver veins intersected in railroad cuts
1904	Bingham porphyry Cu	Cu,Mo,Au	industry	Bulk mining started of porphyry Cu-Mo
1905	Santa Rita (Chino), NM	Cu,Mo	ditto	Ditto
1906	Touissit-Bou Beker, MR	Pb,Zn	accid, prosp	
1907	Zhezkazgan, Kazakhstan	Cu,Ag,Pb	industry	Old diggings developed
1909	Dome Mine, Timmins	Au	prospecting	Discovery outcrop, gold-studded quartz hummock
1910	Outokumpu, Finland	Cu,Co,Zn	prospecting	Located by tracing ore boulders in drift
1911	Kirkland Lake, Ontario	Au	ditto	Ore outcrops located
1913	San Rafael, Peru	Sn,Cu	prospecting	
1915	Flin Flon, Manitoba	Cu,Zn,Au	ditto	Gossanous outcrop of small Mandy mine found
1917	Gibralter, B.C., Canada	Cu	ditto	Orebody outcrop sighted
1820	Noril'sk I, Russia	Ni,Cu	govt, prosp	Found by Soviet Govt. prospecting expedition
1920	Panguna, Bougainville	Cu,Au	govt, prosp	
1923	Malartic-Cadillac, Quebec	Au	prospecting	Ore outcrops found
1923	Mount Isa, Queensland	Pb,Zn,Ag	ditto	Gossanous outcrop located
1923	Noranda, Quebec	Cu,Au	ditto	Outcrop discovery by Ed Horne
1925	Kal'makyr, Uzbekistan	Cu,Au	govt, prosp	Found by Soviet Govt. prospecting expedition
1925	Merensky Reef, S. Afr.	PGE	geology	Recognized as PGE ore by Hans Merensky
1925	Red Lake, Ontario	Au	prospecting	First R.L. deposit found by visual prospecting
1926	Nchanga, Zambia	Cu	locals,indus	Staked site of old native workings
1927	Balei, Russia	Au	govt, prosp	Found by Soviet Govt prospecting expedition
1934	West Wits goldfield, S.A.	Au,U	industry	Deep drill intersection based on u-g magnetics
1934	Tyrnyauz, Russia	W,Mo	govt, prosp	Found by Soviet Govt. prospecting expedition
1927-34	Bayan Obo, China	Fe,RE,Nb	prospecting	Fe ore found, later identified REE, Nb content
1935	Yellowknife, Canada	Au	ditto	Au quartz outcrops found
1936	Kempirsai, Kazakhstan	Cr	geology	Soviet state mapping and prospecting
1936	Porgera, PNG	Au	accidental	Noted by colonial government surveyor
1936	Ertzberg, Indonesia	Cu,Fe	accid, geol	Outcrop sighted by mountaneering geologist (Dozy)
1936	Akchatau, Kazakhstan	W,Mo	govt, geol	Soviet government geological expedition
1937	Cuajone, Peru	Cu,Mo	prospecting	Visual outcrop discovery
1941	Kalahari-Mn basin, S.Afr.	Mn	govt, geol	Black Rock outcrop found by geological survey
1942	Laisvall, Sweden	Pb	geol, prosp	Outcrop found by boulder tracing
1942	Jamaica bauxites	Al	government	Soil survey indicated anomalous Al
1942	Klerksdorp, Vaal Reef	Au	industry	Vaal Reef intersected by drilling

Figure 17.1. (continued)

Year	Deposit/district	Metal(s)	Disc.meth.	Notes
1943	Natal'ka, Russia	Au	govt. geol	Found by Soviet govt. geologists, Gulag connection
1944	Bakyrchik, Kazakhstan	Au	ditto	Found by Soviet govt. geologists
1945	Verkhnye Qairaqty, Kaz.	W,Mo,Bi	govt. geol	Soviet government mapping & complex exploration
1946	Welkom Goldfield, S.Afr.	Au,U	industry	Au conglomerate reefs drill intersected in depth
1947	Hilton, Queensland	Pb,Zn,Ag	industry	Drill intersection, strike extension of Mount Isa
1949	Blind River, Ontario	U	prospecting	U conglomerate discovered in outcrop
1949	Udokan, Russia	Cu	govt. geol	Visual find by Soviet government geologists
1950	Grants district, NM	U	ditto	First mineralized outcrop in Todilto Limestone
1950	Mountain Pass, California	REE	industry	Drilling found bastnäsite in area of Pb showings
1950	Evander goldfield, S.Afr.	Au	industry	Drilling intersected Au reef in depth
1951	Pima, Arizona	Cu,Mo	industry	Complex exploration
1952,3	Brunswick #6, 12, Canada	Pb,Zn,Cu	industry	EM anomaly near small Fe deposit drilled
1952-61	Hamersley Range, W.A.	Fe	prospecting	Several orebodies recorded before termination of Australian Government embargo of Fe ore export
1954	Gamsberg, S.Africa	Zn,Pb,ba	prospecting	Gossanous outcrop discovery
1954	Malmbjerg, Greenland	Mo	govt. geol.	Found by Danish government geologists
1955	Thompson Mine, Canada	Ni	industry	Drilling airborne EM anomaly
1955	Rössing, Namibia	U	industry	Proving in area with recorded U occurrences
1955	Araxa, Brazil	Nb,REE	government	Viable Nb resource identified by govt. research
1955	HYC., MacArthur R., AU	Pb,Zn	industry	Outcrop find & drilling in area of showings
1955	Weipa, bauxite, Queensl.	Al	government	Visual recognition of bauxite cliff by H. Evans
1955,68	Red Dog, Alaska	Pb,Zn,Ag	prosp, govt	Gossan first sighted from the air by bush pilot
1956	Koktenkol', Kazakhstan	W,Mo	govt, geol	Found by Soviet government geological expedition
1958	Windy Craggy, B.C., Can.	Cu,Co,Au	prospecting	Orebody outcrop visual discovery
1958	Cantung, NWT, Canada	W	prospecting	Ore outcrop found, scheelite UV identified
1959	Michiquillay, Peru	Cu,Mo	prospecting	Visual outcrop find
1959	Spor Mountain, Utah	Be,F	govt, geol	Invisible bertrandite identified in govt surveys
1960	Jinding, Yunnan, China	Pb,Zn	ditto	Found by Chinese government geologists
1960	Molango, Mexico	Mn	prospecting	Mn presence recognized in oxidized outcrop
1960	Safford, Arizona	Cu	indus, prosp	Complex industry prospecting
1960s	Aitik, Sweden	Cu,Au	ditto	Complex industry prospecting, boulder tracing
1960s	Lumwana, Zambia	Cu	prospecting	Cu stained gossans identified
1960s	Felbertal, Austria	W	university	Scheelite identified by UV on traverse by the Munich Uni school (Maucher, Höll) testing model
1961	Talnakh, Russia	Ni,Cu,PG	state indust.	Drilling intersection of anomaly, Noril'sk industry
1962	Kidd Creek, Ontario	Cu,Zn,Ag	industry	Trenching EM and geochem. anomaly in drift
1962	Carlin (Old), Nevada	Au	indust.prosp	Newmont geoch. sampling to test predictive model
1962	Thompson Creek, Idaho	Mo	ditto	Complex industry prospecting
1965	Kambalda, W. Australia	Ni	industry	WMS proved Ni sulfides under gossan found before
1965	Muruntau, Uzbekistan	Au	govt. geol	Found by Soviet govt. expedition searching for U
1965	Panguna, Bougainville	Cu,Au	indus. prosp	Gossan found visually after geochemistry
1965	Vasil'kovskoye, Kazakh.	As,Au	gov. indust	Found by Soviet govt organization searching for U
1967	Serra dos Carajas, Brazil	Fe	geol, prosp	Sighted from air during Mn search, jungle clearing
1967	J-M Reef, Stillwater, MT	PGE	indus.prosp	PGE horizon identified, geological model followed
1967	Elmwood, Tennessee	Zn,Pb	industry	Regional drilling on grid
1967	El Indio, Chile	Au,Cu	industry	Testing small local diggings
1968	Ok Tedi, PNG	Cu,Au	ditto	Cu bearing creek float traced to source
1968	Kholodnina, Russia	Pb,Zn	govt geol	Discovered during complex survey by Soviet geol.
1968	Cerro Petaquilla, Panama	Cu	UN prosp.	United Nations geoexploration, on-foot traverse
1968	Rabbit Lake, Saskatch.	U	indus.prosp	Ground check of airborne radiometric anomaly
1969	Ranger, NT, Australia	U	ditto	Drilled airborne radiometric anomaly
1970	Navan, Ireland	Zn,Pb	indus.prosp	Complex exploration based on model
1970	Mt. Emmons, Colorado	Mo	ditto	Drilling near small Pb-Zn vein deposit
1971	Jabiluka, NT, Australia	U,Au	ditto	Trenching, drilling weak radiometric anomaly
1971	Aggeneys, S. Africa	Pb,Zn,Cu	ditto	Testing Cu ox. stained outcrop known since 1920
1972	Telfer, WA, Australia	Au	ditto	Gossanous outcrops noted during regional explor.
1972	Howard's Pass, Canada	Pb,Zn	ditto	Regional reconnaissance, Zn anomalous sample

Table 17.1. (continued)

Year	Deposit/district	Metal(s)	Disc.meth.	Notes
1974	Elura, NSW, Australia	Zn,Pb,Ag	ditto	Complex exploration, drilling EM anomaly
1975	Olympic Dam, S. Austral.	Cu,U,Au	industry	Model-based complex project, drill intersected joint magnetic and gravity anomaly
1976	Itataia, Brazil	U	govt. indust	Complex exploration by Nuclebras
1977	Neves-Corvo, Portugal	Cu,Zn,Sn	industry	Complex model based exploration, drilled geophys.
1977	La Escondida, Chile	Cu	industry	Model-based, consultant guided complex search
1977	Rampura-Agucha, India	Zn,Pb	indus.prosp	Complex exploration
1977	Salobo, Carajas, Brazil	Cu,Au	govt.indust	Complex search by Docegeo
1978	Kumtor, Kyrgyzstan	Au	govt. geol	Au in drift debris traced to source by Soviet geol.
1980	Hishikari, Kyushu, Japan	Au	industry	Complex Au search, geochem., drilling
1981	Cigar Lake, Saskatch.	U	ditto	Drilling geophysical anomaly
1981	Boddington, W.Australia	Au,Al	industry	Analytical detection of gold in bauxite
1982	Gold Quarry, Carlin, NV	Au	industry	Complex testing of old showings
1982	Ladolam, Lihir Isl. PNG	Au	indus.prosp	Testing visual gossanous shore outcrops
1982	Abra, W. Australia	Pb	industry	Drilling geophysical anomaly
1982	Admiral Bay, W. Austral.	Zn,Pb	ditto	Pb,Zn found in stratigraphic and oil drill holes
1983	Yanacocha, Peru	Au,Ag	indus.prosp	Complex prospecting, model driven
1983	Hellyer, Tasmania	Pb,Zn,Ag	industry	Drill intersection of geophys. anomaly in ore field
1985	Cannington, Queensland	Pb,Zn,Ag	ditto	Complex exploration
1986	Tomtor, Russia	Nb,RE,Sc	georesearch	Testing field material by Soviet Acad. of Science
1986	Goldstrike, Carlin, NV	Au	industry	Major drillhole intersections testing shallow ore
1988	Grasberg, Indonesia	Cu,Au	industry	Drill testing outcrop in active ore field
1988	Plutonic, W. Australia	Au	indus.prosp	Complex regional exploration
1988	McArthur R., Saskatch.	U	industry	Drill testing deep anomaly
1990	Century, Queensland	Zn,Pb,Ag	indus.prosp	Complex prospecting, geoch. over ore outcrop
1991	Ujina, Collahuasi, Chile	Cu	industry	Complex exploration in ore field
1990s	Alemão, Para, Brazil	Cu,Au	ditto	Complex exploration in ore field
1990s	Pierina, Peru	Au	indus.prosp	Complex prospecting based on model
1992	Tampakan, Philippines	Cu,Au	ditto	Drilling geochemical anomaly
1997	Sadiola, Mali	Au	industry	Testing small native diggings
1998	Wabu Ridge, Indonesia	Au	ditto	Complex field exploration
2001	Oyu Tolgoi, Mongolia	Cu,Au	ditto	Complex prospecting, drilling small Cu showing
2001	Minas Conga, Peru	Au,Cu	industry	Complex prospecting
2001	Antapaccay, Peru	Cu,Au	industry	Ditto
2000s	Pebble, Alaska	Cu,Au	industry	Complex exploration, drill intersections
2000s	Roşia Poieni, Romania	Cu,Au	industry	Ditto
2000s	Monywa, Burma	Cu,Au	industry	Complex brownfields exploration in ore field
2000s	Cadia, NSW, Australia	Cu,Au	industry	New orebodies found by Newcrest in ore field
2003	Regalito, Chile	Cu	industry	Complex exploration
2004	Reko Diq, Pakistan	Cu,Au	industry	Complex exploration, drilling old showings
2005	Spinifex Ridge, W. Aus.	Mo	industry	Complex exploration follow-up, drill intersections

As at present the global mineral exploration is done predominantly by local or international corporations using the philosophy and techniques of market economy (the remaining rare exceptions include exploration by government agencies, e.g. by the Geological Survey of China), expectation of profit is the driving force although the managements and shareholders do recognize the risks involved. The area selection for exploration thus strives to assure minimum risk, although progressively higher risk has to be accepted because of the limited supply of targets. The risks are both geological and non-geological (politico-economic and environmental).

Before we put our sights on finding the future "giants", a bit of a historical Rückblick is needed.

17.2. History of discovery of giant ore deposits/districts

As already mentioned, the absolute size (tonnage) of an ore deposit was of limited relevance in the distant past when the production was very small, and reserve calculations did not exist. What mattered then was the richness of the ore, suitability for selective, labor intensive and technically

primitive mining, and ease/effectiveness of processing. Other than rich oxidation zones at surface of any derivation, hydrothermal vein and some replacement deposits supplied the bulk of the non-ferrous "classical" metals until the mid-1880s and they influenced the teaching of economic geology. Porphyry coppers mattered little unless they had a rich oxidation zone (Sar Chesmeh), and stockwork-Mo, scheelite skarns, sandstone-U were irrelevant as there was no market for elements not yet discovered.

It is a common belief that the "giant" ore deposits had been discovered early, and were the first found locally, because of their magnitude considered proportional to their striking appearance. Usually this was not the case. As for the history, only thirteen localities we now know are of the "giant" size, had been known and exploited before the rediscovery of the Americas in 1492 (Laznicka, 1997; Fig. 17.1). This number would have increased slightly if several deposits in countries and ancient civilizations that are poorly covered in the Eurocentrist literature were included (e.g. China, pre-Columbian civilizations of the Americas). After 1492, most giant discoveries (or reported rediscoveries) came from the Spanish and partly Portuguese colonies in the Americas. The rate of discovery sharply accelerated during and after the Industrial Revolution, especially between 1965 and 1990, but the number of giants' added to the global inventory has slowed down since. Has the process of giants' discovery peaked in the 1980s and are we now on the downgoing slope of a bell-shaped curve? Possibly.

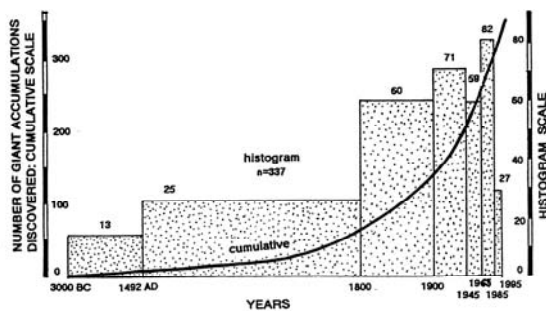


Figure 17.1. History and cumulative curve showing the timing of discovery of giant and super-giant deposits since the earliest record. N=337 entries. From Laznicka (1996, 1997), courtesy of Brill Academic Publishers

The rapid increase in the rate of discovery of giant deposits after 1800 is due to several factors, three of which have been of paramount importance. They

are: 1) increase in the number of newly discovered chemical elements; 2) industrial applications for the "new" metals and expanded applications for the "historical" metals like Au, Ag, Cu, Sn, Fe, Hg; and 3) rapidly increasing industrial production that created demand. Fig. 17.2. shows graphically that discovery peaks of deposits of the various metals coincided with surges in demand which, in turn, reflected new industrial applications.

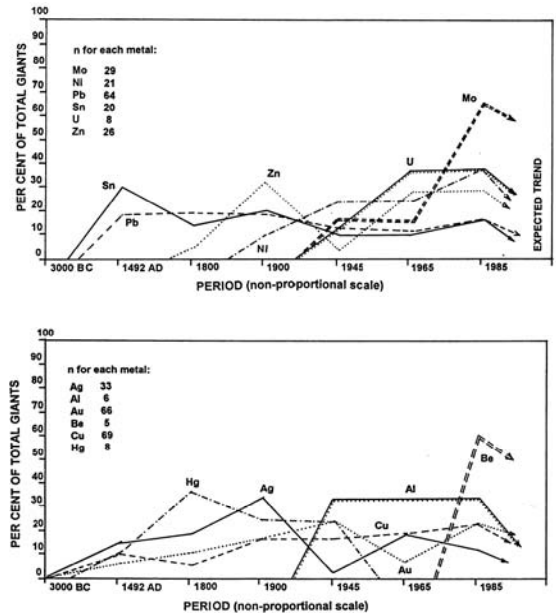


Figure 17.2. Graphs showing discovery periods of giant and super-giant deposits of twelve selected metals. From Laznicka (1996, 1997), courtesy of Brill Academic Publishers

The early discovery peak of tin correlates with the extensive use of tin utensils and containers as well as of bronze; the Hg demand in the 1800s and earlier reflects its use in gold extraction. The 1900 silver peak, coincident with Zn and Pb peaks, reflects the silver application in photography and coinage, but also increased supply of Ag as a by-product of mining the complex Zn-Pb-Ag ores (e.g. sedex, replacement) that suddenly became economic with development of new processing methods, especially flotation. Uranium discoveries peaked in the 1950s-1960s with the sudden demand for weapons and later energy applications, whereas the 1965 Mo peak coincides with the accelerated development of specialty steels. The decrease in the rate of giant Au discoveries between 1945 and 1965 is due to the economic disincentive caused by the artificially low official gold price of \$ 33/oz. Freed from this price constraint, a rush of major gold

discoveries followed in the 1970s and 1980s. This history demonstrates clearly that when demand for a metal had been created, exploration delivered. Metal shortages developed periodically (e.g. during world wars) but the world has never faced complete unavailability of a metal, so far. Although this situation will likely continue, the cornucopia of easy to find, easy to mine and easy to process metal sources seems to be coming to an end.

Ore discovery mechanisms and techniques

The mechanisms of giants' discovery have been briefly reviewed in Laznicka (1997) and there are several volumes devoted to case histories of ore finding, where many example deposits are of the "giant" magnitude (Hollister, ed., 1990, volumes 1-3; Glasson and Rattigan, eds., 1990; Hutchinson and Grauch, eds., 1991). As expected the discovery difficulty, complexity and cost kept increasing and there is a clear trend from accidental (unplanned) to simple premeditated (prospecting) to complex instrumental discoveries (Figs. 17.3, 17.4), initially at the exposed surface only, then increasingly under cover (Fig. 17.5). This progression is not linear and mutually exclusive and it is still possible to "stumble upon" a major orebody or to make discovery by simple prospecting, but the probability of success is now very low. Complex exploration programs conducted by corporations and/or governments, supported by rapidly accumulating knowledge in the public domain (literature, drill core libraries, government technical information) are now the industry standard. It is customary to distinguish between "greenfield" and "brownfield" discoveries. The former are made in areas or settings without mining history or without known deposits of the type sought (between 5 and 40 km from mine sites, in Western Australia; Flint and Rogerson, 2002), the latter are made in established mining areas: in the extension or in proximity of the known orebodies, or outside. Deposits of other than the known ore types found in the brownfield areas mark the transition to the greenfield discoveries.

Accidental discoveries: These include unintentional, unplanned finds made by lay persons who lacked advanced education or experience in geosciences or mining. It is assumed that all pre-medieval discoveries started as accidental, although once a local presence of metals had been established additional orebodies may have been found by experienced miners. Several important "discoveries" reported by European travellers, government officials or the military during the

colonial period had already been known, and sometimes mined, by indigenous populations. Examples include the major silver deposits of Mexico, Peru and Bolivia; the Chocó gold placers in Colombia, many deposits in the African Copperbelt; the El Teniente Cu "super-giant" in Chile found by a Spanish army lieutenant.

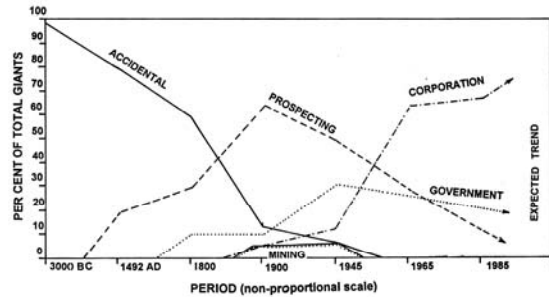


Figure 17.3. Graph showing the changing means and agent of discovery of major metallic deposits. Based on a sample of 140 "giant", "super-giant" and several "large" deposits. From Laznicka (1996, 1997), courtesy of Brill Academic Publishers

The recent and well documented accidental discoveries include Sudbury and Cobalt in Ontario; Ertsberg in Papua (Irian Jaya); and others. Sudbury and Cobalt were both discovered during excavation for railway construction in 1883 and 1903, respectively, although Ni-Cu ore samples from Sudbury area had already been collected in 1856 by a government surveyor but not followed up. Ertsberg, a Cu-oxides stained magnetite hill in what was later to become a "super-giant" Cu and Au ore field, had been first reported by a party of Dutch mountain climbers (J. Dozy) in 1936, who walked right over it (Maley, 1996). About the most recent re-discovery of an emerging gold province marked by old Roman workings is in the Rio Narcea basin in Asturias, northern Spain, now actively mined (not yet "giant"). Accidental discoveries by laypeople in outcrop have almost terminated after 1965, when the last "blank spot" on the geological map of the world has been filled. Several discoveries (not of "giant" deposits) have since been made by citizens in local excavations (e.g. wells, tunnels) and reported to the government. In Finland such reporting is actively encouraged by the government.

Discovery by prospecting: Prospecting is usually defined as an essentially non-instrumental exploration by people who lack formal specialized education and training.

Technique	prehis- tory	old ages	middle ages	Industr. Revolut.	to WW2	to 2000	future
1. Gathering at surface							
2. Visual outcrop, simple ores							
3. Ditto, complex ores, gravity							
4. Ditto, flotation							
5. Invisible ores, leaching							
6. Ores uner shallow cover							
7. Ores deep in rocks							
8. Deep seafloor ores							
9. Metals from seawater							
10. Metals from air, gases							
11. Metals bioharvesting							
12. Space mining							

Figure 17.4. Increasingly complex techniques of ore finding, mining, processing and changing industrial metal sources through history. Giant and super-giant deposits are a part of this trend

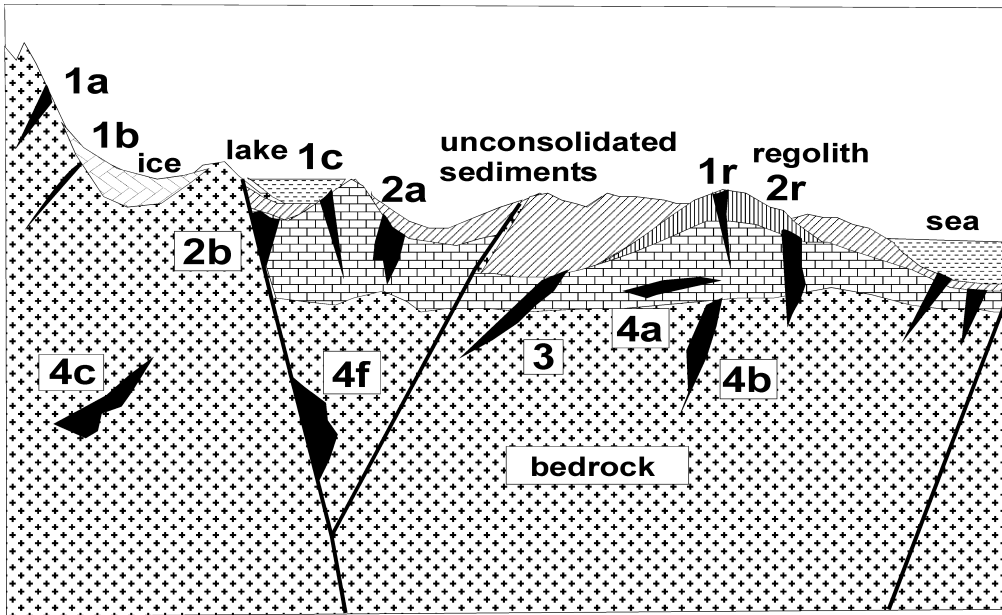
They, however, compensate by superior motivation, visual experience, and a willingness to work hard under primitive conditions. This has been the dominant means of ore discovery during several decades before and after 1900. Significant finds by the Western prospectors include the Central Rand goldfield found by George Harrison in 1882; Kalgoorlie goldfield found by Patrick Hannan's party in 1893; the Noranda camp found by Ed Horne in 1923; Hemlo goldfield proven (rather than newly discovered) by developers Don McKinnon and John Larche in 1979.

In the same category are discoveries made by government geologists traversing land on foot, in canoe, on horseback or on burros, during reconnaissance and geological mapping missions in the past 150 years. The ore occurrences they noticed have been subsequently developed by private interests. Burt first reported on the Lake Superior iron Province in 1844. The traverses of George Dawson across north-western Canada in the 1880s, that led to the discovery of the Klondike gold placers, are legendary. In the former USSR and later in China trained geologists working on foot in fairly primitive conditions made much of the post-1918 discoveries (Noril'sk in 1920, Almalyk in 1925, Tyrnyauz in 1934, Balkhash porphyry Cu province in 1936, Udokan, Kolyma goldfields, and others). Some ore discoverers, as in the Kolyma country, were made by Gulag inmates. United Nations missions found Petaquilla in Panama and

Los Pelambres in Chile. Classical individual prospecting has been much diminished by the exhaustion of visible showings at surface or under shallow cover, although geological field work continues undiminished as a part of complex, data and technology assisted projects.

Discovery during mining: This belongs to the realm of brownfield discoveries and had been, at least initially, unintentional. In addition to continuous enlargement of the original deposit as mining progressed, which often moved a lesser resource over the "giant" threshold, some of the following were often found: 1) orebodies of the same metal (e.g. Cu, Au) of different types; 2) presence of different, previously unrecognized recoverable metal(s) in the original orebodies; and 3) orebodies of different metals.

Case 1) is exemplified by the Butte ore field in Montana, established on rich chalcocite-enargite lodes the cumulative Cu content of which has eventually been exceeded by the lower-grade but greater tonnage porphyry Cu-Mo underneath. Case 2) has representation in the Bayan Obo ore field in Nei Mongol, China, discovered in 1935 and developed into an iron ore mine to feed the Baotou works. Only subsequently, by mineralogical and laboratory research, has the presence of REE and Nb been recognized, turning this deposit into the world's largest repository and producer of rare earths.



OREBODIES

1. EXPOSED AT SURFACE

- 1a In fresh rocks (e.g. recently glaciated mountains)
- 1b Ditto, under glacier ice
- 1c Under lake or sea water
- 1r In deeply weathered regolith

2. COVERED BY THIN UNCONSOLIDATED OVERBURDEN

- 2a Fresh, subaerially exposed overburden
- 2b Ditto under stream, lake, sea
- 2r Under weathered overburden

3. COVERED BY THICK UNCONSOLIDATED OVERBURDEN

4. COVERED BY (ENCLOSED IN) BEDROCK

- 4a In rocks of flat-lying platformic cover
- 4b At unconformity (nonconformity)
- 4c In basement rocks
- 4f In basement along fault that has surface exposure

Figure 17.5. The numerous sites of occurrence of metallic deposits (that include "giants" and "super-giants") exploited in the past, present and future at and under the surface. From Laznicka (2001)

Case 3) is exemplified by the metal-zoned porphyry Cu-Mo districts (e.g. Bingham), where the central Cu zone is surrounded by Pb-Zn veins or replacements; those in Bingham are cumulatively of "giant" magnitude.

Complex exploration by corporations or governments: On foot prospecting reached its limits with the gradual exhaustion of visible targets at the surface, around the mid-1990s, and has been supplemented, then almost substituted, by a complex ore search based on accumulated knowledge, application of available new technologies, and structured approach (Reedman, 1979; Peters, 1987; Chapel, 1992). This was beyond

the means of an individual prospector and has become the prevalent approach of corporations or governments. The principal exploration techniques comprise some with a long history, yet perfected in the last century. This includes drilling, documented in its primitive form from ancient Egypt (Mullen and Parrish, 1998); underground mining; heavy mineral concentrate tracing. Early geophysics (geomagnetics) was probably instrumental in recognition and utilization of the Kursk Magnetic Anomaly iron ores in Russia, later (early 1890s) in search for magnetite deposits in northern Sweden. In 1934 geophysics indicated the westerly continuation of the Central Rand gold deposits in depth. The early geoelectric experiments by T.A.

Edison contributed to discovery of the concealed Falconbridge deposit in the Sudbury district. Radiometry came late, but contributed to discovery of the first generation of post-World War 2 uranium deposits like Grants and Elliot Lake. Geochemistry, established in the 1930s by W.M. Goldschmidt, V.I. Vernadsky, and A.E. Fersman, became the state sanctioned exploration tool in the 1930s in the U.S.S.R.. With few exceptions the entire crop of the post-1950 "giants" discoveries is the result of complex, structured instrumental exploration in which, sometimes, certain components played the more important role than the others (Figure 17.6). The WMC Corporation exploration program, that culminated in discovery of the Olympic Dam five metals "(super)-giant" in 1975, provides an exemplary history. It is a pity that WMC is no longer here: it has been swallowed by a bigger fish, BHP Billiton, in 2005.

Case history of discovery and development of a "giant" deposit by a corporation, using a complex of modern techniques: Olympic Dam, South Australia.

Olympic Dam near Roxby Downs, 520 km NNW of Adelaide in South Australia (Chapter 11) is located in the sparsely inhabited arid landscape of the Precambrian Gawler Craton. It is probably the most valuable single mineral deposit discovered in the last 50 years. The deposit has a 2005 resource of 3.95 billion tons of ore and stores about 45.5 mt Cu, 1.39 mt U, 2,025 t Au, 11,700 t Ag, 20 mt of rare earths and 1.1 bt Fe (Reynolds, 2000 & WMC press release, 2005). The value of the metals in ground, at average recent prices, exceeds US\$ 181 or 226 (if REE are included) billion. This is the world's single largest deposit of uranium credited with 38% of global resources, one of ten largest copper, gold and rare earths deposits, and a significant silver and iron accumulation although not all these metals are currently recovered.

Olympic Dam is an entirely blind body of disseminated ore minerals in intensely altered breccia complex, concealed under at least 300 m thick cover of Neoproterozoic to Cambrian platformic sedimentary rocks. There are no observable or measurable indications of the ore presence at the surface and the nearest exposures of the Mesoproterozoic host sequence are more than 100 km away. This prevents direct mapping of the ore-bearing suite at surface. Olympic Dam is a greenfield discovery and an outstanding example of exploration success resulting from efforts of an enthusiastic, integrated, multi-disciplinary team of specialists and forward-looking management, blessed with a large dose of good luck.

The story of Olympic Dam discovery has been told several times by Woodall (1984, 1993), Lalor (1991), and others; the geological understanding evolves as the underground mining and exploration advance. The brief chronological review that follows is intended as a practical demonstration of a sequence of steps which,

cleverly designed and executed, may result in a major ore discovery, luck permitting.

Pre-exploration stage: Between late 1960s and mid 1980s WMC had been an innovative mining company with sustained exploration success (they discovered new Au orebodies in Norseman, Ni in Kambalda, U in Yeelirrie), and willingness to try new ideas (ore models). One such conceptual model developed by Douglas Haynes in 1972 focused on the release of trace Cu from basalts during oxidation of magnetite to hematite, followed by copper migration and local accumulation in suitable traps. The model was put to test and a search started for an Australian "basin" best responding to this model. The best match was found among the Proterozoic sequences of South Australia, some of which had supported copper mining in the past (Walleroo-Moonta, Mount Gunson).

Area selection for regional exploration: In 1973 the WMC management approved a plan to establish office in Adelaide to systematically evaluate mineral potential of four prioritized environments in the state. Materials available in the public domain were selected and studied. This included literature, archival reports and maps, geophysical/geochemical data, as well as drill core stored in the excellent South Australian government core library. Reconnaissance field visits followed, although it was soon realized that much of the area of interest had a thick younger sedimentary cover. Specialist meetings were held at frequent intervals, as well as discussions with the local government geological staff. New lines of conceptual thinking entered the project: overlapping magnetic and gravity anomalies as a means to indicate mafics concealed under young sediments (H. Rutter); lineaments, their intersections and intervening tectonic corridors as possible structural controls to ore (E.S.T. O'Driscoll). Stuart Shelf, the sediments-covered portion of the Precambrian Gawler Craton west of the Adelaide Foldbelt, has emerged as the area of priority interest in 1974 and it was selected for further exploration. A copper deposit in Mesoproterozoic basal clastics resting on oxidized mafics, similar to the existing Mount Gunson, was the anticipated target.

Regional exploration, Stuart Shelf: Photomosaics of geophysical anomalies, lineaments, known geology and existing ore occurrences were assembled and critical areas examined in the field. Unfortunately there was little to learn from outcrop because of the abundant sand dunes and cover sediments in the critical areas. Emphasis shifted to geophysics as the principal (and only) means of determining targets for stratigraphic drilling. Two targets of coinciding magnetic and gravity anomalies on the Roxby Downs pastoral station, also favorably situated in respect to the tectonic corridors, were selected and application for exploration license was made. The final well locations were refined after a seismic refraction survey (this was inconclusive, yet it correctly determined the depth to basement), and ground magnetic survey, had been completed in 1975. Drilling started shortly afterwards.

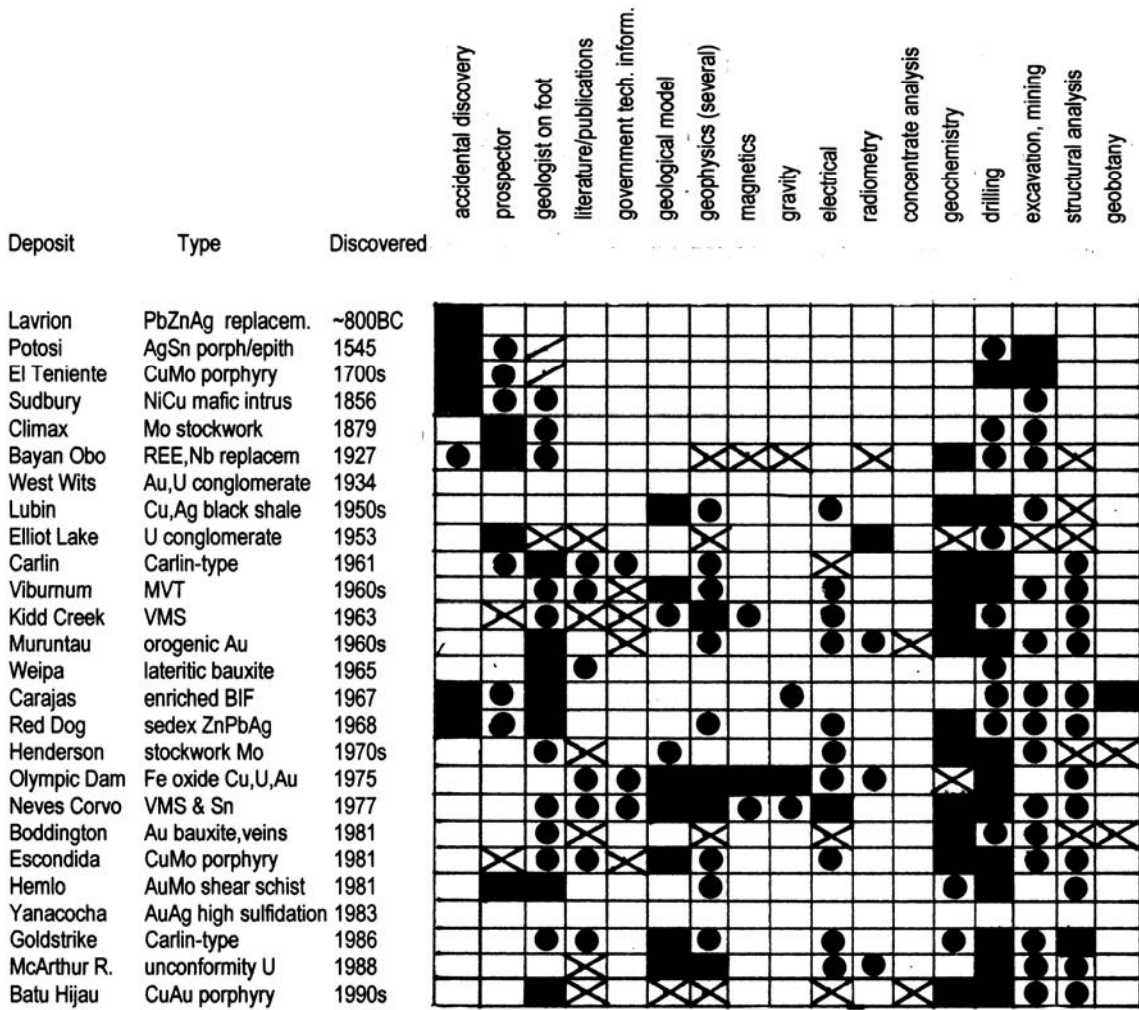


Figure 17.6. The role of the various exploration methods in discovery of selected "giant" and "super-giant" deposits. From Laznicka (2001)

Discovery: The first drill hole at Olympic Dam, RD 1, intersected 38 m of 1.05% Cu in hematitic breccias. The following eight holes were marginal, until well RD 10, drilled in November 1976, intersected 170 m of 2.12% Cu. The finely dispersed chalcocite in the drill core was not visually recognized at first, but the presence of copper was indicated by analytical results. By the end of 1976 it became obvious that a large deposit of copper, and also of gold and uranium, was discovered but more drilling was needed to outline the orebody and determine the reserves. By 1982 drilling on a 200 m grid confirmed resource of 2 billion tons of complex ore. There the Olympic Dam exploration campaign ended and the exploration team moved to the next virgin ground. Several concealed prospects of similar style (Acropolis, Wirrda Well, Oak Dam) turned out to be uneconomic. Olympic Dam then entered the next stage of the mining cycle.

Pre-production stage: The period between the late 1970s and the start of production in 1988 was occupied

by planning, financing arrangements, environmental compliance studies, reaching accommodation with the local landholders and with the Aboriginal community, feasibility studies, orebody opening and experimental mining, marketing and many other activities. The South Australian government provided valuable assistance, although numerous bureaucratic hurdles (like the Australian federal "three uranium mines" policy) required much creativity to overcome. Important dates from this period include:

- 1979: Joint venture of WMC with British Petroleum (BP) was formed (BP later merged with Rio Tinto, the present partner)
- 1982: Exploration shaft completed
- 1983: Environmental impact statement approved
- 1984: Processing pilot plant entered operation
- 1985: Feasibility study was completed

- 1986: Mine, mill, access road, aqueduct construction commenced
- 1987: Roxby Downs township and metallurgical plant construction commenced; water pipeline and service decline (ramp) were completed, and long term sales contracts signed.

Production stage: Olympic Dam has been in operation since mid-1988, producing initially 1.5 mt of ore annually, later increased to 9 mt ore/year that translates into 200 kt of refined copper, 4300 t of U_3O_8 in yellowcake, 2.4 t Au, and 14 t Ag in 1999. The hot smelter technology that produces blister copper from flotation concentrate overlaps with hydrometallurgical recovery of uranium and gold, and is followed by electrolytic refining of the raw copper. Acid plant on site produces sulfuric acid used in the leaching process and helps to keep the air clean. The cost, to 1988, to discover the orebody and to bring it into production, came to about US\$ 600 million. The workforce lives in a modern "instant town" of Roxby Downs (population about 5000), 13 km from the industrial complex. Since inception the rate of production has been several times increased and the resources doubled to the present 3.95 bt. A major production increase estimated to cost Aus\$ 5 billion is planned, following the BHP Billiton 2005 takeover.

Olympic Dam geological model: Olympic Dam is one of the few ore discoveries actually initiated by academic research; in most cases such research comes well after the ore finding. Even though the actual discovery did not exactly correspond to the original vision, it came close and it created a new exploration model that stressed the interplay of brittle breccias, extensive K-feldspathization, introduction of Fe oxides (initially magnetite, later oxidized to hematite) with the presence of disseminated Cu sulfides and U, Au, Ag and REE. Olympic Dam became a flagship of the subsequently created Fe oxides-Cu-U-Au "family" (Hitzman et al., 1992) and a target for global ore search. So far this model has proved elusive and no closely related significant orebody was discovered until 2002, when the Prominent Hill deposit, so far of the "large" magnitude only, has been discovered some 200 km NW of Olympic Dam. Several promising prospects are presently under exploration, at least one with significant early drill intersections.

Which techniques found the "giants"?

Fig. 17.4. above shows evolution of the various exploration disciplines, programs and techniques that contributed to discovery and proving of "giant" deposits in the past and (projected) likely in the future. Fig. 17.6. shows the relative importance of the exploration techniques in discovery of selected "giant" deposits. With exception of the early visual discoveries, no single technique alone has been sufficient to deliver a "giant", although one or more methods working in concert with the remainder could have been pre-eminent (e.g. the coincident gravity and magnetic anomaly that indicated

Olympic Dam). This depends on the ore type and setting and is best illustrated by case histories of successful ore discoveries described in the literature (e.g. Hollister, ed., 1990; Glasson and Rattigan, eds., 1990; Hutchinson and Grauch, eds., 1991) and frequently narrated in the mining journals.

What is the place of the "giants" in space?

The direct ore discoveries at exposed surface (Fig. 17.5) account for the majority of "giants" found so far, but by now this source has been severely depleted, especially for the ores with conspicuous appearance (e.g. green stained outcrops by oxidic Cu minerals, strong gossans). In the past a promising discovery progressed directly into the mining stage, with little long term planning. Drilling for orebody delineation and reserve calculation started only in the 20th century and became a commonplace only after 1950.

Orebody buried under shallow unconsolidated overburden like gravel, sand, glacial drift and in-situ tropical regolith have, in the past, been discovered in accidental excavations (e.g. in water well sinking, foundation excavation, railway construction; e.g. Sudbury and Cobalt) and only in the last century as a result of systematic exploration. The non-instrumental prospecting techniques (e.g. ore boulder tracing in drift, panning for heavy minerals) have been joined by exploration geochemistry (pioneered by the Soviets in the 1930s; e.g. Fersman and Vernadsky) and geophysics. The targets were excavated or drilled. Since about the 1980s the various reverse circulation, air blast and similar rapid techniques of soft overburden drilling greatly accelerated discoveries under shallow cover. The first major orebodies concealed in solid rocks were found by mining or drilling geophysical anomalies (late 1800s, Falconbridge Ni deposit near Sudbury; 1920s-1930s West Wits and Welkom goldfields in the Witwatersrand, magnetic iron in Sweden and Russia; in 1975 Olympic Dam). Exploration for ores on the sea floor started in the 1960s.

From ore finding to mining: Large number of deposits we now recognize as "giants" have had a protracted industrial history. Their outcrop could have been discovered early but no substantial work was done since, until a relatively recent period when the reserves (resources) have been determined and mining has started. Alternatively, unmined resources have been left in ground waiting for possible development later (Table 17.2).

Table 17.2. Selected "giant" and "large" deposits of metals not mined for twenty or more years after discovery.

Metal	Deposit	Tonnage	Discovered	Mined	Comments: reasons for time gap
Au	Bulyanhulu, Tanzania	420 t Au	1976	1999	Unfavourable politics (socialism) before 1985 reform
Au	Gold Quarry, Nevada	933 or 613 t Au	1935	1980	Small deposits intermittently mined; "giant" Main Zone discovered in 1979 under basin fill
Au	Kumtor, Kyrgyzstan	715 (or 450) t Au	1972	1996	Soviet planned economy until 1991, foreign investment afterwards
Au	Mokrsko, Czech Republic	100 t Au	1970s	not	Socialist planned economy until 1989, environmental objections afterwards
Au	Sukhoi Log, Russia	1200 t Au	1960s	not	Socialist planned economy until 1991, bureaucratic problems afterwards
AuAs	Vasil'kovskoye, Kazakhstan	296 (370) t Au	1970s	not	Soviet planned economy until 1991, insufficient funds; later bureaucracy prevented foreign investment; environmental problems with As
CuAu	Ertsberg, Indonesia	750 kt Cu	1936	1973	Accidental discovery poorly publicized; inaccessibility, political problems, WW II
CuAu	Monywa, Burma	~4 mt Cu	1700s	1995	Intermittent ancient workings, modern exploration only in 1980s-90s
CuNi	NW Duluth Complex, MN	26.4 mt Cu, 8 mt Ni	1960s	not	Belt of orebodies, some marginal, in environmentally sensitive area
CuAg	Udokan, Russia	20 mt Cu	1949	not	Soviet planned economy until 1991, inaccessibility before BAM railway; bureaucracy
CuAu Co	Windy Craggy, Canada	3.36 mt Cu	1958	not	Early inaccessibility & lack of funds; in 1987 development started but no mining as site placed into newly created provincial park by British Columbia government
Mo	Mount Emmons, Colorado	370 kt Mo	1970s	not	Community environmental protest, Mo oversupply
Mo	Smithers, Canada	225 kt Mo (minimum)	1956	not	Landmark site, environmental objections; Mo oversupply
PbZn	Jinding, China	10 mt Pb+Zn	1965	~2000	Planned economy, foreign investment welcome only in the 1990s
PbZn	Kholodnina, Russia	estimated 5 mt Pb+Zn	1968	not	Planned economy, remote area, limited attractiveness to investors
PGE	Hartley, Zimbabwe (Great Dyke)	4320 t PGE	1914	1997	Low grade, limited technology, low demand, political problems
PGE	Platreef, South Africa	~12 kt PGE+Au	1923	1990s	Small early mining (highgrading), then low demand; poor recoveries
REE, etc.	Katugin, Russia	10 mt+ Nb,REE, Ta	1960s	not	Planned economy, remote; now limited markets, bureaucracy
REE, etc.	Tomtor, Russia	30 mt+ REE,Nb, Sc,Y	1964	not	Planned economy, remote; now limited markets, bureaucracy
U	Jabiluka, Australia	176 kt U	1970s	not	Government "3 uranium mines" policy; environmental problems, land claims
ZnCu etc	Atlantis II Deep, Red Sea	~9.6 mt Zn	1966	not	Depth 2200 m, difficult and costly technology, presently marginal, risky; jurisdiction problems
Zn,Pb	Howard's Pass, Canada	27.5 mt Zn 11 mt Pb	1972	not	Remote (no road access), environmental problems, land claims
Zr	Ilímaussaq, Greenland	~50 mt Zr	1960s	not	Remote, environmental problems, low grade, limited markets

Abbreviations: mt=million tons of contained metal; kt=thousand tons

In the period between the initial discovery and large scale mining the ownership may have repeatedly changed as did the planned method of exploitation

and processing. Mining usually started when the time was "right", risk minimal, and reasonable return on investment expected. Examples:

Antamina-Cu, Zn in Peru had been discovered in 1860, but seriously developed only in 2001; Platereef-PGE near Potgietersrust in South Africa was recognized in 1924, but large scale mining has started only in the 1990s; San Cristobal-Pb,Ag in Bolivia had been found in 1630, and open pit mined only since the 1990s. Malmbjerg-Mo in Greenland, discovered in 1954; Mount Emmons-Mo in Colorado, discovered in 1970; Udokan-Cu in Siberia, discovered in 1949; Petaquilla-Cu in Panama, discovered in 1968; Abra-Pb in Western Australia, discovered in 1981; and several other "giants", are still waiting to become a major mine, if at all.

17.3. Acquiring giant deposits for tomorrow

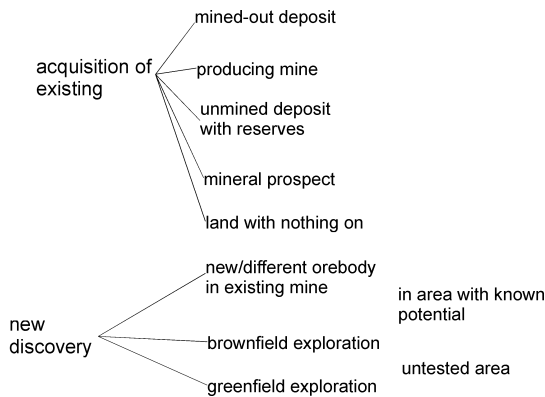
Mineral resource evaluation that terminates with a producing mine (Peters, 1987; Annels, 1991) has several successive stages. Vallée (1992) contributed the following process model targeted to greenfield gold discoveries but applicable to other metals as well, and also to deposits acquired before completed feasibility study. The stages are: 1) mineral resource assessment; 2) mineral exploration, sometimes resulting in discovery, delimitation of mineral deposit and resource estimation, but most often in failure; 3) mineral deposit appraisal: reserve calculation, mining and processing technology, feasibility study; and 4) development of mine complex and mining. Existence of "giant" deposits can be revealed in stages 2 and 3, or gradually "made" as mining progresses and extensions of the original orebodies (or new orebodies) are found in its course. This book relates mostly to Stages 1 and 2 when exploration ideas are formulated, for which it contributes the "food for thought".

Resource assessment is speculative and expected to suggest what (which commodity) to look for and acquire, where and how within the means and mission of the organization. A global, unrestricted assessment (any metal, anywhere) would likely start with an analysis of future commodity demand, price and supply trends. If, say, copper is selected, the next step would be identification of the most prolific "giants"-producing ore types assembled from the literature (e.g. following this book, the answer would be porphyry Cu, Cu-Mo or Cu-Au). A consideration should then be given to the rate of depletion of the existing "giants", rate of past discovery, discovery trends. The next step would be compilation of the existing global porphyry-Cu

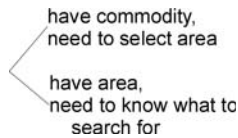
provinces and belts with consideration given to the likely degree of past exploration intensity (the least intensely explored areas are preferable) and speculation about new terrains so far without discovered deposits. The short list of selected priority areas would have to be evaluated in terms of the investment risk factors (read below), and the most favorable locations selected. In the real life there would be a parallelity of interest (many organizations thinking along similar lines), hence a strong competition, so many desired outcomes will not be available and one would have to settle for the second, third, or n-th best alternative. Evolving opportunities will have to be monitored and embraced (e.g. emergence of an organization seeking joint venture partner; expiration of mineral lease; property offered for sale; auction of properties by foreign government; sudden or gradual political change somewhere in the world), original ad-hoc ideas encouraged and evaluated. Investment in a quality consultant or experienced staff will usually pay for itself, as well as utilization of information resources outside the mainstream with which the competition is familiar; here the foreign experience or at least capability to read foreign language reports, help. An example of an "undiscovered" information bonanza eminently suitable for territory-wide (in this case the former U.S.S.R of 21 million km²) selection of areas with mineral potential, is the old Soviet Map of Magmatic Formations (Kharkevich, ed., 1968) in which the "granite-graodiorite formation" beautifully outlines areas that permit porphyry Cu-Mo presence.

"Giant" acquisition is a complex undertaking for which the large international corporations maintain departments staffed by specialists who probably do not need my advice. But many junior resource companies, even enterprising individuals and investors, can move a long distance towards this objective for a limited financial outlay, then enter into a joint venture with the "majors" once the stage that requires deep pockets has been reached (usually to start drilling, airborne geophysics, purchase properties). They might find some helpful hints here. Although crucial, favorable geology is not the only prerequisite of successful acquisition and commercialization of a major metallic deposit, it is a start. The politico-economic factors are next in importance, fully capable of derailing any masterpiece of metallogenic prediction. Case histories would fill a small library. There are three varieties of decisions to be made at the onset of a project:

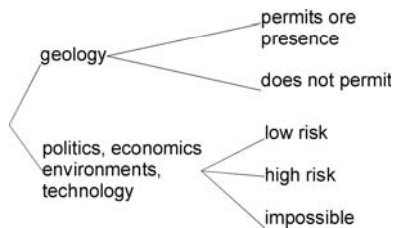
Decision 1: Acquire an existing (often "used" property) or a newly discovered one?



Decision 2: Which end to start from?



Decision 3: Risk assessment



17.3.1. Acquisition of an existing deposit

Looking for a ready-made deposit to acquire resembles shopping for a used car. "Used deposits" are not always bad and several seemingly depleted, "mined out", or "insignificant" deposits have got a new lease on life with the change of management, or mining/processing technology designed to recover metals from a different type of ore considered unprofitable during the earlier period of mining (or discovered after mine closure). "Giant" examples include the Golden Mile ore zone in Kalgoorlie, originally selectively mined from a myriad of narrow orebodies, by many operators. After depletion, the properties have been consolidated and bulk mining of the old pillars and low-grade haloes started from the Superpit, for many recent years the #1 Australian gold producer. Comparable "consolidating pits" have been established at other deposits consisting of numerous depleted small high-grade bodies enveloped by low-

grade haloes like Homestake (South Dakota), Waihi (Martha Mine), New Zealand; Dome, Ontario; Antamok, Philippines. At Muruntau, a superpit technology has been applied since the start of operations.

"Giant" producing deposits acquired in their mid-life are usually the result of politics (e.g. nationalization) or corporate manipulation. The success with the new operator varies, for better or for worse. CODELCO, the Chilean state enterprise that operates the "giant" deposits formerly owned by Kennecott and Anaconda, is considered a success story. Much of the rest in Africa and South America is not, and re-privatization has been under way for some time now.

A major unmined deposit of a desirable commodity, delineated and with reserves calculated, is considered the best candidate for acquisition. This is usually accomplished by takeover of the owner company, by a joint venture or purchase, and it is an ongoing business reported on by the mining journals. In the 1990s there appeared to have been a "once in a lifetime" opportunity to acquire a pristine major ore deposit in ground, following the political changes in the former U.S.S.R. and its satellites. There have been few success stories so far, however, and they include development and production startup in the "Au-giant" Kumtor in Kyrgyzstan by Cameco; Newmont's concession to process low-grade stockpile at Muruntau; Ivanhoe's development of the "giant" Oyu Tolgoi porphyry Cu-Au in Mongolia. Some of the coveted "giant" metal properties in Russia (Sukhoi Log-Au, Udokan-Cu), Kazakhstan (Vasil'kovskoye-Au); Uzbekistan (Dougyztau and Amantautau-Au) are still in the process of negotiation or false starts. A parallel development has been taken place in some of the left-leaning Third World countries, like Myanmar (bringing into production the "Cu-Au giant" at Monywa by Ivanhoe Mines) and Africa.

It is a common knowledge that mining and investment into mineral resources (especially metals) is a risky business, but with globalization and the advancing "New World Order" the variety of risks has multiplied. The world is heterogeneous and a large portion of it is no longer directly dominated and influenced by the few Western powers as in the times of colonialism. So the managements of the large international corporations, and the small junior companies and consultants acquiring properties abroad and overseas, are still learning. "Riskology" is now a growing business and an emerging science, and it has to be considered jointly with geology in the

international selection of mineral properties or areas to explore, and ventures to invest in.

17.3.2. International risk assessment

Given favorable geology permissive for finding certain types of metallic deposits, the potential target countries (regions) are now critically evaluated by investors or mining companies using several variables, and ranked by their investment risk factor. In 2001, the Fraser Institute in Vancouver ranked 44 countries and territories popular with explorers and investors, from the Canadian perspective, by their Investment Attractiveness Index. Ontario, Québec, Australia, Brazil and Chile occupied the first five places. In a comparable 1998 Australian ranking (Treadgold, 1998) USA, Canada and Chile won the top places whereas Papua New Guinea, India and Russia competed for the title of the most risky country to stay away from. The "risk chart" changes on the daily basis

The Australian Mining Monthly is one of the handful of media that publish regularly a world risk survey, targeted at the Australian investor (Treadgold, 1998; Table 17.3). The journal evaluates ten risk categories, each of which is given an importance weighting factor used to calculate totals for risk ranking. The weighting totals range from zero to 30: an absolutely risk-free country would earn a total of zero, the 100% risky country would be worth 30 points. Of the 20 countries considered in the 1998 Australia's Mining Monthly survey the lowest risk country, the United States, placed at the top of the middle third with 10.5 points, whereas the highest risk country, Papua New Guinea, occupied the bottom of the middle third with 19 points. Nevada (a state, not a country), the absolutely lowest risk territory in 1998 selected by other media, would be worth about 8 points, and Afghanistan, the highest risk country of the period (now superseded by Iraq), would be about 22.8 points. No part of the world is thus absolutely risky or absolutely safe and even countries that are safe heavens for tourists like Canada or Australia (compare the "map of expatriates' security", Fig. 17.7) are unsafe in some aspects of capital investment such as "green tape" (excessive environmentalism) and native land claims. The weighted risk totals, even if favorable, are of little value when a single risk category is so strong that it alone can prevent, or make extremely difficult, exploration or mining in a country. In the present day Germany, with a rather favorable weighted risk total of 11.1, the environmental factor is extremely

strong (4.5 points) so it is virtually impossible to clear the hurdle and establish a mine there.

Investment risk changes rapidly and is one of the reasons for capital volatility and profit "highgrading". Deposits that could be rapidly developed, mined out and abandoned, of commodities like gold that could be easily processed, marketed and repatriated, attract most of investment during the frequently short "windows of opportunity" when the risk decreases. More substantial long-term investments, as into integrated complexes producing base metals, require assurance of low risk, continuing risk reduction, and lasting stability of a country. There are numerous examples of events that have, suddenly or gradually, increased or reduced the exploration investment risk. The risk factors are briefly reviewed below.

Sovereign (or political) risk is exemplified by the recent events of first magnitude such as the unification of Germany in 1989 that greatly modified investment conditions in the former East Germany but changed little in the West, and the disintegration of the Soviet Union in 1991. Uncertainty in the sovereign risk sphere persists, after 14 years since independence, in Russia and even more in the former Soviet republics of Central Asia and Caucasus, but investment conditions have substantially improved in China, Vietnam, Mongolia and Laos. There are some exceptions, though, where the western companies made successful inroads even in the high investment risk countries already mentioned. A substantial sovereign risk exists even in otherwise politically stable countries like Canada and Australia, where mineral resources are the provincial or state jurisdiction. In Canada, the political orientation of provincial governments has been the main reason for the wide variation of the perceived overall risk among ten provinces and two territories, with the highest risk associated with the "socialist" provincial governments as in British Columbia of the 1980s, lowest risk with the conservative and liberal governments as in Ontario in the 1990s. Risk associated with the newly created ethnic territories such as Nunavut is difficult to assess.

Some government decisions are made to appease the various special interest groups, even if they make not much sense, and this results in refusal to permit mining or exploration. Since the 1970s the Australian government has maintained the "three mines policy" in respect to uranium, where only three mines were permitted to operate at a time, as a concession to the electorate; the 2nd largest U deposit in the country, the "giant" Jabiluka, has been idle for more than 20 years. The logic ("to stop nuclear proliferation") is hard to see served, as the demand for uranium has been fulfilled by other producers. Sweden, an environmentally enlightened country, has banned entirely uranium mining and utilization, the only major energy resource in which the country is self-sufficient. The "giant" Ranstad-U deposit has been closed.

Table 17.3. Exploration and mining risk in 25 countries for the year 1998, from the perspective of an Australian investor. Modified after Treadgold (1998); Nevada, Japan, Germany, Greenland and Afghanistan have been added

Risk weighting	4	4	3	3	3	3	2	3	2	2.5	
Category	POL	LAN	GRN	CLM	RED	SOC	INF	CIV	DIS	LAB	WT
Nevada, USA	1	1	2	2	2	1	1	1	1	1.5	8.0
USA	1	2	3	2	3	1.5	1	1	1	2	10.5
Canada	1	2	3	3	2	2	1	1	1	2	10.8
Germany	1	1	4.5	2	3	2	1	1	1	2	11.1
Japan	1	1	3	2	4	2	2	1	3	1	11.3
Chile	2	2	1.5	2	2	2	2	2	2	2	11.5
Australia	1	3	3	4	2	2	1	1	1	3	12.7
Argentina	3	2	2	2	3	2	3	2	1	2	13.2
Malaysia	3	3	2	2	3	2	2	2	2	2	14.0
Brazil	3	2	2	2	3	3	3	2	2	2	14.2
Indonesia	3	2	2	2	3	2	3	3	2	2	14.2
Mexico	3	2	2	2	2.5	2.5	3	3	2	2	14.2
Zimbabwe	3	2	2	2	3	3	3	2	2	2	14.2
Peru	3	2	2	2	2	3	3	3	3	2	14.6
Ghana	3	2	2	2	3	3	3	3	2	2	14.8
Greenland	2	4	3	3	2	2	4	1	2	2	14.8
South Africa	3	3	2	2	3	3	2	3	1	3	15.3
Tanzania	3	3	2	3	3	3	3	3	2	2	16.2
China	4	3	2	2	4	3	3	2	2	2	16.4
Philippines	3	3	2	3	3	3	3	3	3	2	16.6
Vietnam	4	3	2	2	4	3	4	2	2	3	17.3
Russia	4	3	2	2	4	3	4	3	2	3	17.9
India	4	4	3	2.5	4	3	3	3	2	3	18.4
Papua N.G.	4	3	2	4	3	3	4	4	3	2	19.0
Afghanistan	5	3	2	4	5	5	4	5	3	2	22.8

Risk weighting is from 0 (insignificant) to 5 (substantial). Abbreviations of risk categories: POL=political (sovereign) risk; LAN=land access; GRN=green tape (environmental risk); CLM=land claims; RED=red tape (bureaucracy); SOC=social risk; INF=infrastructure; CIV=civil unrest; DIS=natural disasters; LAB=labour relations. WT= weighted risk totals: 0=no risk; 30=maximum total risk

Land access, that is the permission to conduct mineral exploration and resources exploitation in a territory, is a corollary of the political risk and it depends on legislation that may rapidly change. In countries where most of the land is privately owned, the exploration access requires an agreement between the landowner and the mining company which is relatively straightforward. In countries with large tracts of public (government-owned) land such as the United States, Canada and Australia, much of the land (e.g. crown land) used to be available for exploration. This has changed in the past three decades by government land withdrawals to establish parks and natural reserves, or for transfer into ownership of the indigenous populations. Some two thirds of the state of Alaska, mostly uninhabited wilderness, have been withdrawn and mineral exploration or exploitation is completely banned in Antarctica, by international agreement.

Green tape alias environmental bureaucracy is another common cause of land withdrawal; it also fuels a rapidly growing set of rules and restrictions that require compliance at every stage of the mining cycle. Although

the western resources industry has come a long way from the often reckless ways of mining as they existed before the 1960s and has cleaned up its act as much as possible, mining still results in land modification and is resented by the public and vilified by the media. The most frustrating for the industry to deal with is the unpredictability of the withdrawal process (many land withdrawals were made after exploration money had been invested and mineral discoveries made; the Windy Craggy Cu-Co-Au "giant" in British Columbia is an often quoted example (Chapter 8).

Land claims. Human history is an endless saga of conquests in which the more aggressive, politically and technologically advanced, or expanding groups or nations invaded and incorporated territories inhabited (often sparsely) by the weaker groups. The European colonialism of the past centuries serves as the stereotype, but some non-Europeans colonized as well. In the period of de-colonization the former colonies with non-European majorities achieved independence, statehood and sovereignty over their state territories.

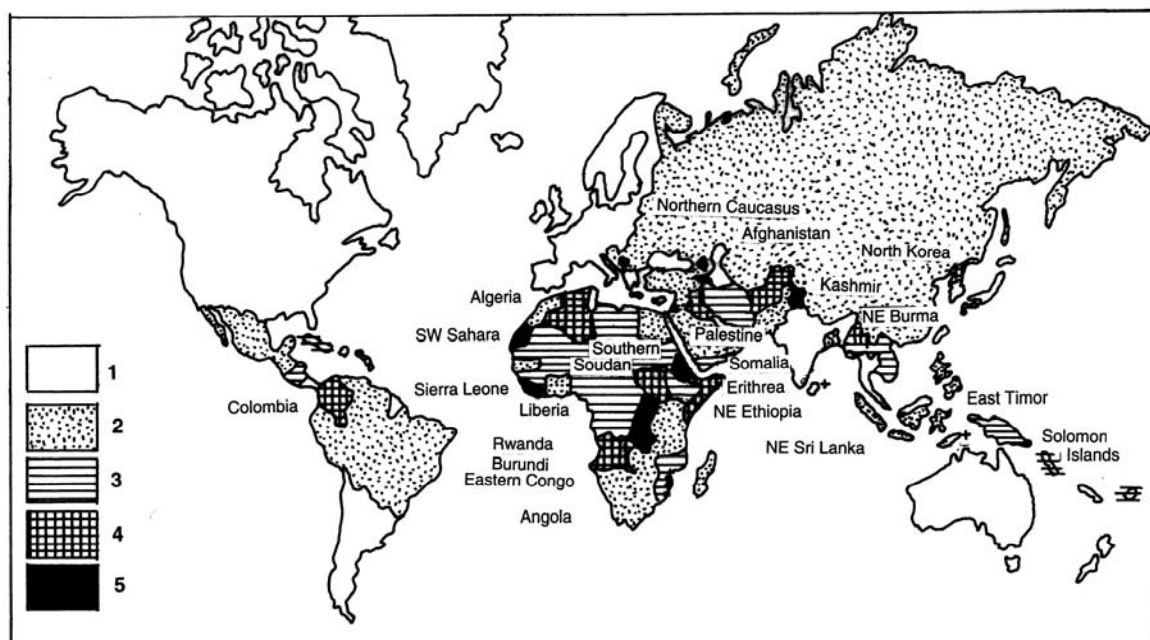


Figure 17.7. Map of the world showing distribution of lands ranked by the increasing degree of physical risk to expatriate workers and visitors resulting from political, cultural and economic factors, and to industry ability to carry on business, as they were in 2000. In 2005 Iraq and western Sudan (Dharrfur) have joined the category 5, Zimbabwe has been promoted to category 4, parts of Indonesia to category 3. It is assumed that the visitor comes from, and is accustomed to, the prevalent living and working conditions in the developed western democracies Germany, the United States, Australia, and others (Group 1). The higher risk in Group 2 is due to a degree of unpredictability resulting from the less helpful and sometimes outright corrupt officialdom; there could be entry and exit hassles, dishonest police, problems with importing and exporting objects (e.g. samples from mines), some discrimination based on race or religion, some areas out of bound, mistrust of the population. In Group 3 the above problems are multiplied as most of the member countries are or were recently ruled by non-democratic regimes, experience conflict among traditional and “western” ways or values, or suffer from regional disharmony. Group 4, in addition to problems listed under 2 and 3, suffers from severe internal repression, civil war or an armed conflict. This could be countrywide as in Afghanistan, or limited to some regions outside which the rest of country is generally safe (as in Colombia, Sri Lanka). Group 5 territories suffer, or recently suffered, or have a potential to suffer from cross-border armed conflict (war)

Native minorities, however, remained as an ethnic component in countries dominated by the former conquerors or the more recent immigrants. In most cases there had been a substantial difference in the levels of technical and political development between the settlers and the indigenous populations that has not yet disappeared after more than a century of coexistence. Indigenous societies colonized while at stone or early metal age stages of development, without written language and documents, in a sparsely populated, non-cultivated land and without permanent settlements and strong state structure, lost their unlimited ownership of land except for the delineated treaty lands and reserves. A century or more later, when the social philosophy of the western society changed profoundly, the non-assimilated remnants of the indigenous people have been encouraged to make land claims. At the present level of society development the land claims being made by native groups in Canada, Australia and the United States are processed by governments and sometimes granted when the land is

uncontested, i.e. not developed and settled by the later arrivals. Land claims are a mixed blessing to either side, but the resource industry ever in need to explore new ground is trapped in the middle. The greatest problems with land claims are overlapping applications, sluggish process extended by government timidity, “political correctness”, biased media reporting, and dubious evidence for entitlement as it is routinely based on imperfect and controversial oral history that goes back more than a century. Land claims are at present the greatest single resource investment risk in Australia (4 points out of five) and, along with “green tape”, in Canada (3 points). Chile, Indonesia, even China, do better.

Red tape, or excessive bureaucracy combined with official corruption and nepotism, has traditionally been associated with authoritative systems based on political or religious ideology (China), with successors of such systems (Russia, Mongolia), and with societies where

excessive bureaucracy is a way of life and a means of creating employment (India). All these countries have earned four demerit points out of five in the ranking. In the past decades the "bastion of free enterprise", the United States and also Canada and partly Australia, have substantially increased their red tape levels as a response to "political correctness", human rights and environmentalism. Some ministers and officials have been appointed from "disadvantaged groups" whose "progressive" ideology and good will is often counterbalanced by naivety and ignorance as to how the resource industry and national economy works. The United States have increased their red tape risk category to 3 (at par with pre-2000 Zimbabwe and Tanzania) and Canada and Australia are not far behind.

Social risk is not clearly defined and it overlaps with other categories, especially civil unrest and labor relations. Most countries are in the middle range (2 and 3 points) with the United States assessed, rather mistakenly, at 1.5.

Infrastructure includes not only transportation, the post, banks, and telephones, but also the fundamental life supports such as consumer goods distribution and medical care. It is worst in the third world and some former communist countries and best in U.S.A., Australia and Canada, clearly demonstrating that large distances are not the cause of problems. The language ability of foreign populations and institutions is an important component of infrastructure, omitted in most risk surveys, but painfully appreciated especially by the anglophone expatriate employees habitually unwilling to learn foreign languages. This severely slows down business in countries like Russia or China and an army of intermediaries is required.

Civil unrest ranges from mass demonstrations to terrorism and civil war. In many countries this is regionalized (parts of the country are quiet, parts are simmering or in the midst of a shooting war as in Iraq, Afghanistan, Colombia or parts of Sri Lanka). The risk survey is vague on this subject, singling Papua New Guinea as the only magnitude 4 recipient and awarding two points to Zimbabwe, Brazil and China. Zimbabwe has since "improved" its ranking to 4.

Natural disaster assessment appears flat, with no four points country in the list. The United States are in the low risk (#1) category which is surprising, as although disasters are not frequent (the most common ones: California earthquakes, Mississippi Basin floods, Gulf Coast hurricanes), they are the world's costliest.

Labor relations assessment shows little variation (2 or 3 points for all countries). The popularity of strikes has decreased worldwide and globalisation together with the people's capitalism and scarcity of jobs have reduced trade unions membership and union militancy.

The published risk assessments, the most recent version of which gives greater weight to terrorism and the potential for disease pandemics, provide the first, easy to get information. They scare away most potential investors who then crowd into the best rated jurisdictions producing a shortage of properties to acquire and driving prices up. Few of the intrepid companies focus on the low-ranked (or non-ranked, the majority) countries and engage in a quiet diplomacy that sometimes bear fruits. The successful Muruntau and Kumtor gold operations in otherwise inhospitable Central Asia are one "giant" exception, others are the "giants" Monywa-Au,Cu in Burma, Oyu Tolgai Cu-Au in Mongolia, Reko Diq in Pakistan, Roşia Montană-Au in Romania, Sepon Au-Cu in Laos (only "large" so far), apparently on their way to success. Several known "giants" in various parts of the world are in limbo, waiting for improvement of their investment risk count, change of politics, better solution to environmental protection, improvement of the local attitude towards mining and, of course, willingness of the owner (usually a government) to make a deal on mutually favorable terms or to permit mining. A sampling of the present "limbo giants": Waisoi-Cu,Au, Fiji; Vasil'kovskoye-Au, Kazakhstan; Sukhoi Log-Au, Russia; Ainak-Cu, Afghanistan; Panguna-Cu,Au, Bougainville; Windy Craggy-Cu,Au, Canada; Jabiluka-U, Australia; Ranstad-U, Sweden; and few others.

The above risks, substantial in their own way, do not include risks that arise from sheer dishonesty and activities devised to mislead the unsuspecting investors. The scams range greatly in magnitude, having reached a peak in the "Scam of the Century" perpetrated by the Canadian Bre-X corporation in the 1990s. A short account follows.

The Bre-X scam

The mid-1990s experienced closing years of the "longest bull market" in North American memory and between 1994 and 1997 it was extremely easy to raise funds, especially on the Toronto and Vancouver stock exchanges, and list mining exploration companies. Thousands of junior companies came to life but to qualify, they needed a mineral property. With globalization in full swing, a crop of properties was generated in exotic lands for Canadians as in the former Soviet Central Asia, Mongolia, South America and the Pacific. Indonesia, a mining investment land then rising in popularity, became of prime interest. This followed the huge Grasberg porphyry Cu-Au discovery in Papua (Irian Jaya) and there was a clear potential for epithermal deposits in the vast interiors of Kalimantan, Sumatra, Sulawesi and even in the densely populated Java. Bre-X Minerals Ltd., one of the newly bred Canadian junior

mining companies from Calgary, acquired a jungle gold property in the Mahakan River Basin in Kalimantan. The Sungai (River) Busang was the site of small scale native alluvial gold mining and its geological setting was believed similar to the Kelian deposit of the Rio Tinto corporation, a medium-size property 120 km away. Exploration at Busang, mostly reverse circulation and later diamond drilling, started in 1993, directed by the Chief Geologist John Felderhof and the Project Geologist Michael de Guzman.

A find of a "large gold deposit in Indonesia" was announced in March, 1994; by March 1996 the deposit was said to "possibly yield 30 million ounces"; the July 1996 resource estimate came to 47 million ounces, increased to 70 million ounces in February 1997, with rumors circulating about a 200 million ounce potential (=6,220 t Au). Bre-X stock followed this phenomenal rise, starting with few cents a share to reach the equivalent of \$200 at its height in May 1996. The company was then worth some \$ 6 billion and Mr. Felderhof, who gave a presentation at the 1997 Annual Prospectors and Developers Convention in Toronto, was named "exploratorist of the year".

While exploration at Busang progressed and share values kept increasing, business and political deals were being made first behind closed doors, later in full media spotlight. Several large corporations tried to buy in; Placer Dome Inc. offered \$ 4 billion. Development of a mine in Indonesia, however, required compliance with the local regulations and when these proved inflexible, members of President Soeharto's family and friends rushed to the rescue. The media accounts, especially articles in Maclean (the Canadian newsmagazine) as well as the story in TIME (April 7, 1997) reported on the greed and intrigues on both sides of the negotiating table.

The façade of the Busang riches started to crack in March 1997 when Freeport-McMoRan, the successful operator of the Ertsberg-Grasberg complex, announced that their tests showed only "insignificant amounts of gold" at the site. On March 27, 1997, Bre-X lost \$ 3 billion of market value in less than 30 minutes and the share price dived from \$ 22.44 to \$ 1.83, later to evaporate entirely. Mr. De Guzman disappeared, allegedly committing suicide by jumping from a helicopter, and Mr. Felderhof relocated to the tax haven of Grand Cayman island. The investors paid dearly for this lesson in frenzy investing.

Unfortunately, little of substance has been published about the exploration morals of the story to educate geologists; the essay by Lawrence (1997) is about the most thorough and analytical one. Apparently, De Guzman with the help of several of his Philippino fellow countrymen systematically falsified the assays by "salting" the samples going to the lab with detrital gold, purchased from native placer miners in the area. This had been done very cleverly and the results were quite consistent with geological expectations. A geological picture of Busang had been gradually created, apparently modeled on the Kelian deposit in the same mineral belt. It is uncertain as to whether Messrs. Walsh (the BreX Chairman) and Felderhof knew or suspected of what was

going on. The most worrisome thing, however, is the fact that the property was visited by teams of experts from several large mining corporations and they noticed nothing wrong! The labs reported presence of "rounded, pitted gold grains" in the samples they assayed, without anyone paying attention. Apparently De Guzman was adept on manipulation of the visiting geologists even though they had never actually seen any convincing gold mineralization either on site or in the core shed; the core itself was rarely put on display as everything was pulverized and one half of the split core was not kept as is the general practice. Yet the visiting corporate teams reported favorably!

The morning after brought a tremendous disgrace to Canadian stock exchanges for the lack of checks of companies they listed; to the international corporation that did the feasibility study based entirely on fictitious input; to the investment brokers who recommended "buy" until the very last moment. After Busang raising venture capital has become extremely difficult to impossible and scores of junior companies, many promising, have disappeared. The reporting and trading regulations are being tightened and there is a resolve of "never again". The bankrupted investors still sue for compensation and the "greatest mining scam in history" is ready to enter textbooks in mineral economics.

17.3.3. Acquiring "giants": geology perspective

Geological expertise is essential for finding new orebodies, and highly desirable in evaluation of those already found, or "used" deposits. In this paragraph the emphasis is on the new (geological) discoveries, but let us again emphasize that:

- 1) Most if not all "giant" deposits are the top of the line of lesser deposit populations.
- 2) There is no program designed, from the onset, to find "giants" only and avoid the lesser deposits, as the "giants" presence is statistical (although often a "giant" was the first deposit discovered in an area). A selection of geological targets (that is ore types, settings and rock associations) known to contain "giants", or visualized as potentially hosting exceptional deposits, should however be made at the onset of the program. In the present jargon this usually goes under the name "modelling", a "concretization" of the ore hunter's wish.
- 3) At the time of initial discovery (e.g. of a gossan, malachite stained outcrop) there is rarely an indication that the prospect represents a "giant" deposit; this tends to be revealed only gradually as the, usually drilling then mining, exploration progresses. To paraphrase Don

Mustard and others, "giants" are not found, they are made.

Mineral exploration takes place in and about the area (or property) selected and, gradually, secured (that is, having an exploration permit, contract of work, lease). As already mentioned, there is no special approach available designed to find "giants" and by-pass the lesser deposits, except for restricting the ore types sought to those with a proven "giant" record.

Where are the remaining undiscovered "giant" deposits?

For the sake of speculation, let's assume that "giant's" discovery has peaked in the late 1980s-1990s, and if this peak is a statistical mean then an equal number of "giants" (say, 600) still remains to be found. Not considering the unconventional (but very real) metal resources in and under the oceans and the low-grade materials on land (or including the latter when it is feasible to mine them), here is my educated guess about the whereabouts of the future "giants:"

Land surface: 10%-15% of the next "giants" (that is ~60-90 occurrences) will still be discovered (or "made" by augmenting resources at existing lesser deposits) at the land surface, or under shallow cover (regolith). They will include few overlooked visually conspicuous expressions of classical orebodies like gossans (as at Voisey's Bay-Ni,Cu), some probably newly exposed under receding glaciers and in erosion scars, especially in the underexplored territories. The majority of discoveries will likely be visually unobscure ore types like the Carlin-Au, metalliferous "black shales", disseminated scheelite deposits and others, including newly defined ore types. There are some emerging types of mineralization to watch, although some of them should be critically scrutinized as there is a potential for fraud. One is the "Prairie-type Au" of Feng and Abercombie (1994; read Section 13.5) of very low-temperature invisible dispersed gold replacing platformic carbonates at several places in western Canada and attributed to discharge of saline brines. Another is the hard to believe "500 mt of metallic tungsten" at ~0.01% W, presumably contained in the Ashuga regional anomaly in northern Timan, NE Russian Platform (Lisitsina and Kolokoltsev, 1996). Tungsten in the form of dispersed tungstite and scheelite there has a regional distribution in Devonian clastics resting on Mesoproterozoic carbonates and is attributed to

low-temperature fluids presumably driven by late Devonian basic magmatism, controlled by extension. Similar tungsten enrichment in sedimentary rocks is widespread in SE China, where it is overshadowed by the rich granite-related mineralized centers. It is reasonable to expect that metals other than Au and W could also occur in finely disseminated form in unexpected settings like stable platforms. With steadily decreasing average ore grades, materials with 0.1% Cu and comparably low-grades of other metals may well become acceptable ores during this century. This would extend the life of several presently mined porphyry-Cu "giants" (Titley stated that there was an enormous quantity of 0.1% Cu material under many existing porphyry coppers in the American West, like Morenci), and generate few new "giants".

Under unconsolidated cover and regolith: Between 20-30% of undiscovered "giants" will likely be found concealed under young unconsolidated covers that include Quaternary glacial sediments, especially till, in Canada, Alaska, Scandinavia and northern Russia; humid (lateritic) regolith in the tropics; arid regolith (duricrusts like calcrete); lake- and shallow sea water and bottom sediments; glacier ice. Few "giants" in this group have already been discovered in the past fifty years (e.g. Kidd Creek VMS in Ontario; Boddington-Au, Cu in Western Australia), but many more probably remain to be found. Exploration in glaciated and tropically weathered terrains is the subject of extensive research in Canada, Australia, Russia, Scandinavia and other countries. The exploration techniques already applied or proposed range from visual (e.g. tracing of trains of mineralized boulders in glaciated terrains; interpretation of relic ore textures and structures in regolith) through geochemistry to geophysical methods and geographic information systems (GIS) driven compilations.

Under solid rock cover: 19th century miners in the "giant" Ballarat placer (but not yet lode) goldfield searched for continuation of exposed lodes and for deep-lead placers, under thin cover of Cenozoic basalt flows, with variable success. There was nothing at the surface to indicate buried orebodies under the unconformity. Young volcanic flows, or ash falls or flows (including ignimbrites), cover large areas of valuable potentially mineralized ground in Tasmania, central British Columbia, western United States and Mexico, the Andes, Africa (e.g. Ethiopia), Arabia and elsewhere. Older (hydrated) flows and diabase sills obscure much of the basement in Siberia (Tunguzka Platform), India

(Deccan Trap), Brazil (Paraná Basin) and elsewhere. It is believed that the ore potential (including "giants") under the volcanics is equivalent, to only slightly inferior, to ores found at the presently exposed "bedrock" surface. Some 10-15% of future "giants" could be there.

Potentially mineralized "basement" is covered by consolidated, predominantly sedimentary platformic rocks that are several times as extensive as the volcanic cover. They are also much thicker, especially near the centers of basins where several km thick rock sequences are common. The cover sedimentary rocks contain both intraformational mineralization within (e.g. the MVT type as in the "giant" Viburnum Trend, Missouri), and also hide deposits in the basement under unconformity. Perhaps 20-30% of undiscovered "giants" could reside there, down to the depth of some 1000 m. The orebodies in the "basement" occur along sedimentary basin margins and over basement highs like domes, anticlines, ridges, horsts and similar. Olympic Dam has been discovered under 300 m plus of platformic sedimentary rocks that cover the Stuart Shelf basement high. Several "giants" have been discovered under thick platformic covers in the past by tracing folded mineralized sequences downward by drilling or geophysically. The West Wits and Welkom goldfields were intersected by drilling already in the 1930s to 1950s, where the mineralized Central Rand Group conglomerates are concealed under up to three generations of cover sequences: the Paleoproterozoic Ventersdorp basalts, Transvaal carbonates, and Mesozoic Karoo clastics. Present exploration in the Witwatersrand "gaps" has to penetrate covers exceeding 1000 m in thickness. Other than blind drilling on grid (e.g. the "random walk" that discovered the Elmwood MVT ore field in Tennessee; Callahan, 1977) or drilling based on structural interpretation, most future discoveries will result from drilling geophysical targets of ore types that provide physical response (e.g. magnetic and gravity highs that indicated Olympic Dam).

The remainder of concealed "giants" (20-30%?) will likely be discovered within the folded strata, intrusions and metamorphics in orogenic belts and

cratons. These will be most difficult to find. Contrary to the frequent opinion that, say 500m or 1000m depth levels, would contain the same frequency of mineralization as experienced in the present outcrop (e.g. Neil Williams, 1990), I believe that there is a gradual overall impoverishment in the productive ore type variety with depth and that certain highly profitable ore types like weathering-enriched ores, placers, epithermals and some porphyry deposits, rapidly disappear with increasing depth. This can be convincingly demonstrated on the example of the barren Precambrian granite-gneiss terrains and even the less eroded greenstone belts which, although locally densely mineralized, are virtually restricted to hosting BIF, VMS, "shear-Au" and rare metals pegmatite deposits only. "Under the greenstone, there is nothing", whereas under the young Andean or island arc volcanics and shallow granitoids, platformic sediments, and others, could be preserved remnants of the former basement with its own complement of mineralization. These could be fragments of Phanerozoic orogenic belts themselves resting on, or intermingled with, Precambrian greenstones or the various "rift sequences". It could be many kilometers of thickness before the unproductive granite gneiss is finally reached.

Modern exploration technology and accumulated information make it increasingly possible to detect, then intersect, many orebodies that are outside the reach of the traditional prospector, but quality people have to provide ideas and manage the process. Here is what White (1997) says: *"Exploration is about discovery of something that hitherto has been overlooked or concealed from the eyes of prospector. It requires a high degree of creativity to conceptualize, visualize, observe or find something that has escaped attention of all the skilled prospectors who went before. Exploration management is thus management of human creativity, rather than human productivity"*. This book has been written to provide the essential, yet comprehensive, factual basis for such prospectors, geologists and managers.

References

- Abbott JE, Van Vuuren CJJ, Viljoen MJ (1986) The Alpha-Gravelotte antimony ore body, Murchison greenstone belt, *in*: CR Anhaeusser, S Maske, eds, pp 321-332
- Abdulin AA, Kayopov AK, eds. (1978) Metallogeniya Kazakhstana. Rudnye Formatsii, Mestorozhdeniya Rud Medi. Nauka KazSSR, Alma Ata, 192 p.
- Abdullayev KhM (1957) Daiki i Orudneniye. Gosgeoltekhizdat, Moscow, 232 p.
- Abdullayev KhM (1964) Rudnost-Petrograficheskie Provintsii. Nedra, Moscow, 135 p.
- Abishev VM and others (1972), Geologiya, veshchestvennyi sostav rud i geokhimicheskie osobennosti Vasil'kovskovo zolotorudnovo mestorozhdeniya, *in*: N Vedernikov, ed, Geologiya, Geokhimiya i Mineralogiya Zolotorudnykh Raionov i Mestorozhdenii Kazakhstana. Kazakh Nauch-Issled Inst Miner Syr'ya, Alma-Ata, pp 107-162
- Abzalov MZ (1999) Gold deposits of the Russian North East: Metallogenic overview, *in*: PACRIM '99 Proceedings, Bali. AusIMM, pp 701-714
- Abzalov MZ, Both RA (1997) The Pechenga Ni-Cu deposits, Russia: data on PGE and Au distribution and sulfur isotope compositions. Mineralogy and Petrology, v 61, pp 119-143
- Acacia Resources (2000) Geology of the Cleo Deposit, Sunrise Dam gold mine, Laverton, Western Australia Unpublished, 7 p
- Agricola G (1556) De Re Metallica Libri XII, English translation by HC and LH Hoover (1950). Dover, New York, 638 p
- Ahlfeld FE and Schneider-Scherbina A (1964) Los Yacimientos Minerales y de Hidrocarburos de Bolivia. Bolivia Dept Nac Geol Bol 5
- Aitchinson L (1960) A History of Metals. Macdonald & Evans, London, 747 p
- Aitken JD, McMechan ME (1991) Middle Proterozoic assemblages, *in*: H Gabrielse and CJ Yorath, eds, Geology of the Cordilleran Orogen in Canada, Geology of Canada No. 4. Geol Surv of Canada, Ottawa, pp 97-124
- Akhmadi AK (1992) Gradiento-vektornye kharakteristiki zonal'nosti osnovnoi rudnoi zalezhi zapadnovo uchastka mestorozhdeniya Ainak v Afganistane. Sovetskaya Geologiya v 8
- Alderton DHM and Fallick AE (2000) The nature and genesis of gold-silver-tellurium mineralization in the Metaliferi Mountains of Western Romania. Econ Geol, v 95, pp 495-516
- Aleshin AP, Uspenskii YeN (1991) Zakonomernosti razvitiya poligennoi scheelitovoi mineralizatsii na zolotorudnom mestorozhdenii Muruntau. Geol Rud Mestor v 2
- Alexander RJ, Harper GD (1992) The Josephine ophiolite: An ancient analogue for slow- to intermediate- spreading ocean ridges. Geol Soc Spec Publ 60, London, pp 3-38
- Allcock JB (1982) Skarn and porphyry copper mineralization at Mines Gaspé, Murdochville, Quebec. Econ Geol, v 77, pp 971-999
- Allègre CJ, Poirier J-P, Humler E, Hofmann AW (1995) The chemical composition of the Earth. Earth Planet Sci Letters v 134, pp 515-526
- Allen PA, Allen JR (1990) Basin Analysis-Principles and Application. Blackwell, Oxford, 451 p
- Allen RL, Lundström I, Ripa M, Simeonov A, Christofferson H (1996) Facies analysis of a 1.9 Ga continental margin, back-arc, felsic caldera province with diverse Zn-Pb-Ag-(Cu-Au) sulfide and Fe oxide deposits, Bergslagen region, Sweden. Econ Geol v 91, pp 979-1008
- Allibone AH, Windh J, Etheridge MA, et al (1998) Timing relationships and structural controls on the location of Au-Cu mineralization at the Boddington gold mine, Western Australia. Econ Geol, v 93, pp 245-270
- Alonso RN (1988) Los boratos de salares en la Argentina. Revista de la Assoc Argentina de Geólogos Economistas, v 6, pp 11-23
- Alpers CN, Brimhall GH (1988) Middle Miocene climatic change in the Atacama desert, northern Chile: Evidence from supergene mineralizations at La Escondida. Geol Soc Amer Bull v 100, pp 1640-1656
- Altschuler ZS, Clarke RS Jr, Young EJ (1958) Geochemistry of uranium in apatite and phosphorite. US Geol Surv Profess Paper no 314-D, pp 45-90
- Alvarez AA (1999) Yacimiento Toromocho, *in*: Primer Volumen de Monografias de Yacimientos Minerales Peruanos. IIMP, Lima, pp 205-225
- Alvarez LW, Alvarez W, Asaro F, Michel HV (1980) Extraterrestrial cause for the Cretaceous-Tertiary extinction. Science v 208, pp 1095-1108
- Ambrus J (1977) Geology of the El Abra porphyry copper deposit, Chile. Econ Geol, v 72, pp 1062-1085
- Amstutz GC, Bernard AJ, eds. (1973) Ores in Sediments. Springer-Verlag, 350 p
- Anders E, Grevesse N (1989) Abundance of the elements: meteoritic and solar. Geoch Cosmoch Acta, v 52, pp 197-214
- Andersen JCO, Rasmussen H, Nielsen TFD, Ronsbo JG (1998) The Tripple Group and the Platinova gold and palladium reefs in the Skaergaard intrusion: Stratigraphic and petrographic relations. Econ Geol, v 93, pp 488-509
- Anderson C, Brooks R, Stewart R, Simcock R, Robinson B (1999) The phytoremediation and phytomining of heavy metals. PACRIM '99, Bali, AusIMM pp 127-132

- Anderson CA, Scholz EA, Strobell JD (1955) Geology and ore deposits of the Bagdad area, Yavapai County, Arizona. U.S. Geol Surv Profess Paper 278, 103 p
- Anderson IK, Ashton JH, Boyce AJ and others (1998) Ore depositional processes in the Navan Zn-Pb deposit, Ireland. *Econ Geol*, v 93, pp 535-563
- Anderson JA (1982) Characteristics of leached capping and techniques of appraisal, *in*: SR Titley, ed, *Advances in Geology of the Porphyry Copper Deposits, Southwestern North America*. Univ of Arizona Press, pp 275-295
- Andersson A, Dahlman B, Gee DG, Snäll S (1985) The Scandinavian alum shales. *Sveriges Geol Unders*, Ca 56, pp 1-50
- Andreeva OV, Golovin VA (1999) Uranium deposits and alteration processes at the late Mesozoic Tulukuev Caldera, Transbaikal region, Russia, *in*: CJ Stanley et al, eds, *Mineral Deposits: Processes to Processing*. Balkema, Rotterdam, pp 467-469
- Andrew EC, et al (1922) The geology of the Broken Hill district. *Mem Geol Surv New South Wales*, No 8, 432 p
- Andrews AJ, Owsiacki L, Kerrich R, Strong DF (1986) The silver deposits of Cobalt and Gowganda, Ontario: I Geology, petrography, and whole rock geochemistry. *Canad Journ Earth Sc*, v 23, pp 1480-1506
- Angeiras AG (1988) Geology and metallogeny of the north-eastern Brazil uranium-phosphorus province emphasizing the Itataia deposit. *Ore Geol Revs*, v 3, pp 211-225
- Anhaeusser CR (1986) Archean gold mineralization in the Barberton Mountain Land, *in*: Anhaeusser CR, Maske S, eds, pp 113-154
- Anhaeusser CR, Maske S, eds (1986) *Mineral Deposits of Southern Africa*, volumes 1 & 2. Geol Soc South Africa, Johannesburg, 2335 p
- Anhaeusser CR, Viljoen MJ (1986) Archean metallogeny in southern Africa, *in*: CR Anhaeusser, S Maske, eds, pp 33-42
- Annels AE (1984) The geotectonic environment of Zambian copper-cobalt mineralization. *Journ Geol Soc London*, v 141, pp 279-289
- Annels AE (1991) *Mineral Deposit Evaluation-a Practical Approach*. Chapman and Hall, London, 436 p
- Antrobus ESA, Brink WCJ, Brink MC, et al (1986) The Klerksdorp Goldfield, *in*: CR Anhaeusser, S Maske, eds, pp 549-598
- Antrobus ESA, Whiteside HCM (1964) The geology of certain mines in the East Rand, *in*: SH Haughton, ed, pp 125-160
- Antweiler JC, Love JD (1967) Gold-bearing sedimentary rocks in Northwest Wyoming-a preliminary report. U.S. Geol Surv Circular 541, 12 p
- Appel PWU, Garde AA (1987) Stratabound scheelite and stratiform tourmalinites in the Archean Malene supracrustal rocks, southern West Greenland. *Gronl Geol Unders, Bull* 156, 26 p
- Appold MS, Garven G (1999) The hydrology of ore formation in the Southeast Missouri District: numerical models of topography-driven fluid flow during the Ouachita orogeny. *Econ Geol*, v 94, pp 913-936
- Arambourg C, et al (1952) Les vertébrés fossiles des gisements de phosphate. *Serv Geol Maroc, Notes et Mémoires*, no 92, 396 p
- Arehart GB (1996) Characteristics and origin of sediment-hosted disseminated gold deposits: A review. *Ore Geology Revs*, v 11, pp 383-403
- Arkhangel'skaya VV, Kazanskii VI, Prokhorov KV, et al (1993) Geological structure, zonality, and formation conditions of the Katugin Ta-Nb-Zr deposit (Chara-Udokan region), Eastern Siberia. *Geol Ore Dep*, v 35, pp 100-116
- Arndt NT, Nisbet EG, eds (1982) *Komatiites*. Allen and Unwin, London, 526 p
- Arnold BW, Bahr JM, Fantucci R (1996) Paleohydrology of the Upper Mississippi Valley zinc-lead district, *in*: DF Sangster, ed, *Carbonate-Hosted Lead Zinc Deposits*, Soc Econ Geol Spec Publ 4, pp 378-389
- Arnold GO, Sillitoe RH (1989) Mount Morgan gold-copper deposit, Queensland, Australia: Evidence for an intrusion-related replacement origin. *Econ Geol* v 84, pp 1805-1816
- Arribas A Jr (1995) Characteristics of high sulfidation epithermal deposits, and their relation to magmatic fluid, *in*: JFH Thompson, ed, *Magma, Fluids and Ore Deposits*. Miner Assoc of Canada Short Course Volume 23, pp 418-454
- Arribas A Jr, Tosdal RM (1994) Isotopic composition of Pb in ore deposits of the Betic Cordillera, Spain; origin and relationship to other European deposits. *Econ Geol*, v 89, pp 1074-1093
- Ashleman JC, Taylor CD, Smith PR (1997) Porphyry molybdenum deposits of Alaska, with emphasis on the geology of the Quartz Hill deposit, Southeastern Alaska. *Econ Geol Monogr* 9, pp 334-354
- Ashley RP (1990) The Tonopah precious-metals district, Esmeralda and Nye Counties, Nevada. U.S. Geol Surv Bull 1857-H, pp H8-H13
- Ashley PM, Craw D (2004) Structural controls on hydrothermal alteration and gold-antimony mineralization in the Hillgrove area, NSW, Australia. *Mineralium Deposita*, v 39, pp 223-239
- Ashley RP, Keith WJ (1976) Distribution of gold and other metals in silicified rocks of the Goldfield mining district, Nevada, U.S. Geol Surv Profess Paper 843-B, 17 p
- Atkinson D (1995) The Glacier Gulch (Hudson Bay Mountain or Yorke-Hardy) porphyry molybdenum-tungsten deposit, west-central British Columbia. *CIM Spec Vol no* 46, pp 704-707
- Atkinson D, Baker DJ (1986) Recent developments in the geological understanding of Mactung, *in*: JA Morin, ed, *Mineral Deposits of Northern Cordillera*. CIM Spec Vol 37, pp 234-244
- Atkinson WW Jr, Einaudi MT (1978) Skarn formation and mineralization in the contact aureole at Carr Fork, Bingham, Utah. *Econ Geol*, v 73, pp 1326-1365
- Atkinson WW et al (1996) Geology and mineral zoning of the Los Pelambres porphyry copper deposit, Chile. *Soc Econ Geol Spec Publ no* 5, pp 131-156

- Auboin J (1965) Geosynclines. Elsevier, Amsterdam, 335 p
- Aubrey KV (1955) Germanium in some of the waste products from coal. *Nature*, v 176, pp 128-129
- Avila-Salinas W (1991) Petrologic and tectonic evolution of the Cenozoic volcanism in the Bolivian Western Andes. *Geol Soc Amer Spec Paper* no 265, pp 245-258
- Ayres LD, Černý P (1982) Metallogeny of granitoid rocks in the Canadian Shield. *Canad Mineralogist*, v 29, pp 439-536
- Ayres LD, Averill SA, Wolfe WJ (1982) An Archean molybdenite occurrence of possible porphyry type at Setting Net Lake, Northwestern Ontario, Canada. *Econ Geol*, v 77, pp 1105-1119
- Ayres LD, Thurston PC, Card KD, Weber W, eds (1985) Evolution of Archean Supracrustal Sequences. *Geol Assoc Canada Spec Paper* 28
- Babcock RC Jr, Ballantyne GH, Phillips H (1995) Summary of the geology of the Bingham District, Utah. *Arizona Geol Soc Digest* 20, pp 316-325
- Baccaluva L, ed (1994) Albanian ophiolites: State of the art and perspectives. *Ophioliti*, v 19, pp 1-176
- Bailes RJ, Smee BW, Blackadar DW, Gardner WD (1986) Geology of the Jason lead-zinc-silver deposit, Macmillan Pass, eastern Yukon, *in*: JA Morin, ed, *Mineral Deposits of Northern Cordillera*. *CIM Spec Vol* no 37, pp 87-99
- Bailey A (1998) Cannington silver-lead-zinc deposit, *in*: DA Berkman, DH Mackenzie, eds, pp 783-792
- Bailey EH, Everhart DL (1964) Geology and quicksilver deposits of New Almaden district, Santa Clara County, California. *U.S. Geol Surv Profess Paper* 360, 206 p
- Bailey JC, Larsen LM, Sørensen H, eds (1981) The Ilímaussaq intrusion, South Greenland. A progress report on geology, mineralogy, geochemistry and economic geology. *Rapp Grønlands Geol Unders*, no 103
- Baker EM, Kirwin DJ, Taylor RG (1986) Hydrothermal breccia pipes. *Contrib of the Econ Geol Res Unit, James Cook Univ, Townsville*, No 12, 45 p
- Bakke AA (1995) The Fort Knox "porphyry" gold deposit-structurally controlled stockwork and shear quartz vein, sulfide poor mineralization hosted by a late Cretaceous pluton, east-central Alaska. *CIM Spec Vol* 46, pp 795-802
- Baklaev YaP (1973) *Kontaktovo-Metasomaticeskije Mestorozhdeniya Zheleza i Medi na Urale*. Nauka, Moscow, 310 p
- Baksa C, Cseh-Neméth J, Csillag J, Földessy J, Zelenka T (1980) The Récsk porphyry and skarn copper deposit, Hungary, *in*: S. Janković, RH Sillitoe, eds, *European Copper Deposits*. *SGA Spec Publ* 1, Belgrade, pp 73-76
- Bakshiev IA, Savina DN, Kudryavtseva OE (1999) Alteration carbonates as zonation indicators, the Berezovsk gold deposit, Russia, *in*: CJ Stanley et al, eds, *Mineral Deposits, Processes to Processing*. Balkema, Rotterdam, pp 1379-1382
- Bally AW, Oldow JS, eds (1986) Plate tectonics, structural styles and evolution of sedimentary basins. *Geol Assoc Canada Short Course* 7, Cordillera Section, 238 p.
- Bamford RW (1972) The Mount Fubilan (Ok Tedi) porphyry copper deposit, Territory of Papua New Guinea. *Econ Geol*, v 67, pp 1019-1033
- Bankwitz E, Bankwitz P (1994) Crustal structure of the Erzgebirge, *in*: R Seltmann et al, eds, *Metallogeny of Collisional Orogens*. *Czech Geol Survey, Prague*, pp 20-34
- Banno S, Takeda H, Sato H (1970) Geology and ore deposits in the Besshi district. *IAGOD Tokyo-Kyoto meeting, Guidebook* 9, Excursion B5, 29 p
- Baragwanath W (1923) The Ballarat Goldfield. *Geol Survey of Victoria, Memoir* 14
- Barcellos da Silva (1986) Jazida de nióbio de Araxá, Minas Gerais, *in*: Schobbenhaus C, Coelho CES, eds, v 2, pp 435-453
- Bárdossy G (1982) *Karst Bauxites*. Elsevier, Amsterdam, 441 p
- Bárdossy G, Aleva GJJ (1990) *Lateritic Bauxites*. Elsevier, Amsterdam, 624 p
- Barley ME (1982) Porphyry-style mineralization associated with early Archean calc-alkaline igneous activity, Eastern Pilbara, Western Australia. *Econ Geol*, v 77, pp 1230-1235
- Barnard RM, Kistler RB (1956) Stratigraphic and structural evolution of the Kramer sodium borate body, Boron, California, *in*: JL Rau, ed, 2nd *Symposium on Salt*. *N Ohio Geol Soc*, pp 133-150
- Barnes SJ, Brand NW (1999) The distribution of Cr, Ni and chromite in komatiites, and application to exploration for komatiite-hosted nickel sulfide deposits. *Econ Geol*, v 94, pp 129-132
- Barney GO, et al (1980) *The Global 2000 Report to the President*. U.S. Government Printing Office, Washington D.C., 755 p
- Barr DA (1980) Gold in the Canadian Cordillera. *CIM Bull*, v 73, pp 59-76
- Barr DA, Fox PE, Northcote KE, Preto VA (1976) The alkaline suite porphyry deposits-a summary. *CIM Spec Volume* 15, pp 359-367
- Barra F, Ruiz J, Mathur R, Titley S (2003) A Re-Os study of sulfide minerals from the Bagdad porphyry Cu-Mo deposit, northwestern Arizona, USA. *Mineralium Deposita*, v 38, pp 585-596
- Barrett J, Hughes MN, Karavaiko GI, Spencer PA (1993) *Metal Extraction by Bacterial Oxidation of Minerals*. Ellis Horwood, New York, 191 p
- Barrie CT, Corfu F, Davis P, et al (1999) Geochemistry of the Dundonald komatiite-basalt suite and genesis of Dundead Ni deposit, Abitibi Subprovince, Canada. *Econ Geol*, v 94, pp 845-866
- Barrie CT, Hannington MD, Bleeker W (1999) The giant Kidd Creek volcanic-associated massive sulfide deposit, Abitibi Subprovince, Canada. *Reviews in Econ Geol*, v 8, pp 247-259
- Barrie CT, Hannington MD, eds (1999) *Volcanic-associated massive sulfide deposits: Processes and examples in modern and ancient settings*. *Reviews in Econ Geol*, v 8, Soc Econ Geol, Littleton CO

- Barrie CT, Hannington MD (1999) Classification of volcanic-associated massive sulfide deposits based on host-rock composition. *Reviews in Econ Geol*, v 8, pp 1-14
- Barriga FJAS, de Carvalho D, eds (1997) *Geology and VMS deposits of the Iberian Pyrite Belt*. Soc Econ Geol Guidebook Series v 27, 192p
- Bartholomé P, ed (1973) *Gisement Stratiformes et Provinces Cuprifères*. Geol Soc Belg, Liège
- Bartlett PM (1987) Republic of South Africa coastal and marine mineral potential. *Marine Mining*, v 6, pp 359-383
- Barton MD (1990) Cretaceous magmatism, metamorphism and metallogeny in the east-central Great Basin. *Geol Soc America Memoir* 174, pp 283-302
- Barton MD (1996) Granitic magmatism and metallogeny of southwestern North America. *Trans Royal Soc Edinburgh, Earth Sciences*, v 87, pp 261-280
- Barton MD, Staude J-M, Snow EA, et al (1991) Aureole Systematics, *in: Revs in Mineralogy*, v 26, Miner Soc Amer, pp 723-847
- Barton PB Jr (1980) Presidential Address: Public perspective of resources. *Econ Geol*, v 75, pp 801-905
- Barton PB Jr, Bethke PM, Roedder E (1977) Environment of ore deposition in the Creede mining district, San Juan Mountains, Colorado, Part III. Progress toward interpretation of the chemistry of the ore forming fluid for the OH vein. *Econ Geol*, v.72, pp 1-24
- Bartos PJ (2000) The pallacas of Cerro Rico de Potosi, Bolivia: A new deposit type. *Econ Geol*, v 95, pp 645-654
- Bartra R (1999) *Geologia del distrito minero Yanacocha*, *in: Primer Volumen de Monografias de Yacimientos Minerales Peruanos*. IIMP, Lima, pp 13-22
- Bass YuB, and others (1964) *Nikopol'skii Margantsevyi Rudnyi Bassein*. Nedra, Moscow, 535 p
- Bassot J-P, Morio M (1989) Morphologie et mise en place de la pegmatite kibarienne à Sn,Nb,Ta,Li de Manono (Zaire) *Chron Rech Min*, No 496, pp 41-56
- Basu PH (1982) Zawar lead-zinc deposit, India: A prototype syn-sedimentary Precambrian sulphide deposit. *Quart J Geol, Min, Metall Soc of India*, v 54, pp 78-89
- Batchelor BC (1979) Geological characteristics of certain coastal and offshore placers as essential guides for tin exploration in Sundaland, Southeast Asia. *Geol Soc Malaysia Bull*, v 11, pp 283-313
- Bateman AM (1950) *Economic Mineral Deposits*, 2nd ed. Wiley, New York, 916 p
- Bateman AM, McLaughlin DH (1920) *Geology of the ore deposits of Kennecott, Alaska*. *Econ Geol*, v 15, pp 1-80
- Bateman PC, Clark LD, Huber NK, Moore JG, Rinehart CD (1963) The Sierra Nevada Batholith—a synthesis of recent work across the central part. *U.S. Geol Surv Profess Paper* 414-D, 46 p
- Bathurst RGC (1975) *Carbonate Sediments and Their Diagenesis*, 2nd ed. Elsevier, Amsterdam, 658 p
- Batley GC, Mieziitis Y, McKay AD (1987) Australian uranium resources. *BMR Res Report* no 1, Canberra, 69 p
- Baturin GN (1982) *Phosphorites on the Sea Floor*. Elsevier, Amsterdam, 343 p
- Baturin GN (1988) *The Geochemistry of Manganese Nodules in the Oceans*. Reidel, Dordrecht, 342 p
- Baudemont D, Fedorowich J (1996) Structural control of uranium mineralization at the Dominique-Peter deposit, Saskatchewan, Canada. *Econ Geol*, v 91, pp 855-874
- Baumann L (1976) *Introduction to Ore Deposits*. Scottish Acad Press, Edinburgh, 131 p
- Beck LS (1969) Uranium deposits of the Athabasca region, Saskatchewan. *Sask Dept Miner Res, Rept* 126, 139 p
- Beck RD (1991) The image of the minerals industry. *CIM Bulletin*, v 84, pp 86-88
- Behr SH (1965) Heavy-mineral beach deposits in the Karoo System. *S Afr Geol Surv Mem* 56, 116 p
- Beisiegel V de R (1982) Carajás iron ore district. Intern Sympos on Archean and early Proter Geol Evol and Metallogeny, Salvador, pp 47-59
- Belevtsev YaN, ed (1962) *Geologia Krivoirozhskikh Zhelezorudnykh Mestorozhdenii*, 2 vols. Akad Nauk Ukr SSR, Kiev, 500 & 566 p
- Belevtsev YaN (1968) *Metamorfogennyye mestorozhdeniya*, *in: VI Smirnov, ed, Genezis Endogennykh Rudnykh Mestorozhdenii*. Nedra, Moscow, pp 648-712
- Belevtsev YaN, ed (1974) *Metallogeniya Ukrainy i Moldavii*. Nauk Dumka, Kiev, 510 p
- Belevtsev YaN, ed (1985) *Geologicheskije Osnovy Metamorfogennovo Rudoobrazovaniya*. Nauk Dumka, Kiev, 190 p
- Belevtsev YaN, Belevtsev RYA, Siroshstan RI, et al (1983) The Krivoi Rog Basin, *in: AF Trendall, RC Morris, eds, Iron Formation*. Elsevier, Amsterdam, pp 211-251
- Bell K, ed (1989) *Carbonatites-Genesis and Evolution*, Unwin Hyman, London
- Belperio A, Freeman H (2004) Common geological characteristics of Prominent Hill and Olympic Dam—implications for iron oxide copper-gold exploration model. *PACRIM Proceedings, Adelaide*, pp 115-125
- Bender F (1977) An Earth Scientist's view of metallic resources, *in: F Bender, ed, Mineral Raw Materials*. Schweizerbart, Stuttgart, pp 117-136
- Bender F (1982) Significant energy raw materials for everyone? *in: Resources for the Twenty-First Century*. U.S. Geol Surv Prof Paper 1193, pp 104-155
- Bendezú R, Fontboté L, Cosca M (2003) Relative age of Cordilleran base metal lode and replacement deposits, and high sulfidation Au-(Ag) epithermal mineralization in the Colquijirca mining district, central Peru. *Mineralium Deposita*, v 38, pp 683-694
- Benguet Corporation (1994) *Antamok mine geology (unpublished)*, 10 p
- Bennett G, Dressler BO, Robertson JA (1991) The Huronian Supergroup and associated intrusive rocks. *Ontario Geol Surv Spec Vol* 4, pt 1, pp 549-592

- Bennett VC (2004) Compositional evolution of the mantle, *in*: RW Carlson, ed, pp 493-519
- Bentor YK, ed (1980) Marine phosphorites-geochemistry, occurrence, genesis. Soc Econ Paleont Miner, Spec Publ 29, 249 p
- Bentor YK, Mart J (1984) The metallogenic map of Israel, *in*: Mém Explic de la carte Metall de l'Europe et des pays limitrophes. UNESCO, Paris, pp 537-541
- Berbeleac I, David M (1982) Native tellurium from Musariu, Brad region, Metaliferi (Metalici) Mountains, Romania, *in*: GC Amstutz, ed, Ore Genesis, the State of the Art. Springer-Verlag, Berlin, pp 283-295
- Bercé B (1958) Geologija ležišta žive Idria. Geologija, Ljubljana, v 4, pp 5-62
- Berg HC, Cobb EH (1967) Metalliferous lode deposits of Alaska. U.S. Geol Surv Bull 1246, 254 p
- Berger BR, Tingley JW, Drew LJ (2003) Structural localization and origin of compartmentalized fluid flow, Comstock Lode, Virginia City, Nevada. Econ Geol, v 98, pp 387-408
- Bergeron M (1972) Quebec iron and titanium corporation ore deposit at Lac Tio, Quebec. 24th Intern Geol Congr, Montreal, Excursion Guidebook B-09, 8 p
- Berkman DA, Mackenzie DH, eds (1998) Geology of Australian and Papua New Guinean Mineral Deposits. Austral Inst Mining Metallurgy, Monogr 22, 886 p
- Berning J (1986) The Rössing uranium deposit, South West Africa/Namibia, *in*: Anhaeuser CR, Maske S, eds, pp 1819-1832
- Berry LG, ed (1971) The silver-arsenide deposits of the Cobalt-Gowganda region, Ontario. Canad Mineralog, v 11, 429 p
- Beskin SM, Larin VN, Marin YuB (1996) The greisen Mo-W deposit of Aqshatau, Central Kazakhstan, *in*: V Shatov et al, eds, Granite-Related Ore Deposits of Central Kazakhstan and Adjacent Areas. Glagol, St. Petersburg, pp 145-154
- Bethke CM, Marshak S (1990) Brine migration across North America-plate tectonics of groundwater. Annual Reviews in Earth Planet Science, v 18, pp 287-319
- Bettles K (2002) Exploration and geology, 1962-2002 at the Goldstrike property, Carlin Trend, Nevada. Soc Econ Geol Spec Publ 9, pp 275-298
- Beukes NJ (1983) Paleoenvironmental setting of iron formations in the depositional basin of the Transvaal Supergroup, South Africa, *in*: AF Trendall, RC Morris, eds, Iron Formation: Facts and Problems. Elsevier, Amsterdam, pp 131-209
- Beukes NJ (1986) The Transvaal Sequence in Griqualand West, *in*: CR Anhaeuser, S Maske, eds, pp 819-828
- Beus AA (1968) Albitovye mestorozhdeniya, *in*: VI Smirnov, ed, Genezis Endogennykh Rudnykh Mestorozhdenii. Nedra, Moscow, pp 303-378
- Bezrukov PL, Petelin VP, Skornjakova NS (1970) Mineral'nye resursy okeana, *in*: VG Kort, ed, Tikhii Okean, v 2. Nauka, Moscow, 419 p
- Bilibin YuA (1951) Metallogenic provinces and Metallogenic Epochs, English Translation. Geol Bull, Dept Geology, Queens College, NY, 35 p
- Bilibin YuA (1955) Osnovy Geologii Rosypei. Akad Nauk SSSR, Moscow, 471 p
- Bilibina TV, Afanas'eva MA, Barkanov IV (1976) Geologiya i Metallogeniya Shchitov Drevnikh Platform SSSR. Nedra, Leningrad, 339 p
- Billington LG (1984) Geological review of the Agnew nickel deposit, Western Australia, *in*: DL Buchanan, MJ Jones, eds, Sulphide Deposits in Mafic and Ultramafic Rocks. IMM London, pp 43-54
- Binns, RA, Scott, SD (1993) Actively forming polymetallic sulfide deposits associated with felsic volcanic rocks in the eastern Manus back-arc basin, Papua New Guinea. Econ Geol, v 88, pp 2226-2236
- Bischoff JL, Piper DZ, eds (1979) Marine Geology and Oceanography of the Pacific Manganese Nodule Province. Plenum Press, NJ, 842 p
- Bissig T, Clark AH, Lee JKW, Hodgson CJ (2002) Miocene landscape evolution and geomorphologic controls on epithermal processes in the El Indio-Pascua Au-Ag-Cu belt, Chile and Argentina. Econ Geol, v 97, pp 971-996
- Bisso CB, et al (1998) Geology of the Ujina and Rosario copper porphyry deposits, Collahuasi District, Chile, *in*: TM Porter, ed, Porphyry and Hydrothermal Copper and Gold Deposits: A Global perspective. Conference Proceedings, AMF Adelaide, late addendum
- Bjørlykke A, Sangster DF (1981) An overview of sandstone-lead deposits and their relation to red-bed copper and carbonate-hosted lead-zinc deposits. Econ Geol 75th Anniv Vol, pp 179-213
- Black LP, Williams IS, Compston W (1986) Four zircon ages from one rock: the history of a 3930 Ma old granulite from Mt. Sones, Enderby Land, Antarctica. Contrib to Miner Petrol, v 94, 427-437
- Blake DH (1987) Geology of the Mount Isa Inlier and environs, Queensland and Northern Territory. Austral Bur Miner Res Geol Geophys Bulletin, no 225
- Blake DH, Etheridge MA, Page RW, Wyborn LA (1990) Mount Isa Inlier-regional geology and mineralization, *in*: FE Hughes, ed, pp 915-925
- Blake MC Jr, Morgan BA (1976) Rutile and sphene in blueschist and related high-pressure facies rocks. U.S. Geol Surv Profess Paper 959-C, pp C1-C6
- Blanchard R (1968) Interpretation of Leached Outcrops. Nevada Bureau of Mines Bull 66, 196 p
- Bleeker W (1990) Thompson area-general geology and ore deposits. 8th IAGOD Sympos, Field Trip 10 Guidebook. Geol Surv Canada Open File 2165, pp 93-125
- Blevin PL, Chappell BV (1992) The role of magma series, oxidation states and fractionation in determining the granite metallogeny of eastern Australia. Trans Royal Soc Edinburgh, Earth Sci, v 83, pp 305-317
- Blissenbach E, Nawab Z (1982) Metalliferous sediments of the seabed: The Atlantis II Deep deposits of the Red Sea, *in*: EM Borgese and N Ginsburg, eds, Ocean Yearbook. Univ of Chicago Press, v 3, pp 77-104
- Bloch S (1980) Some factors controlling the concentration of uranium in the world ocean. Geoch Cosmoch Acta, v 44, pp 373-377

- Boddington TDM (1990) Abra lead-silver-copper-gold deposit, *in*: FE Hughes, ed, pp 659-664
- Boerner DE, Milkereit B (1999) Structural evolution of the Sudbury impact structure in the light of seismic reflection data. *Geol Soc Amer Spec Paper* 339, pp 419-432
- Bogdanov BD (1983) Porphyry copper deposits of Bulgaria. *Intern Geol Review*, v 25, pp 178-188
- Bogdanov YuV, et al (1973) Stratifitsirovannye Mestorozhdeniya Medi SSSR. Nedra, Leningrad, 312 p
- Bogdanov YuV, Golubchina MN (1971) Isotopic composition of sulfur in stratified deposits of copper ores in Olekma-Vitim Mountains area. *Intern Geol Revs*, v 13, pp 1405-1417
- Bohse H, Brooks CK, Kunzendorf H (1971) Field observations on the kakortokites of the Ilímaussaq intrusion, South Greenland. *Grøn Geol Unders, Rapp No* 38, 43 p
- Bonev IK, Kerestedjian T, Atanassova R, Andrew C (2002) Morphogenesis and composition of native gold in the Chelopech volcanic-hosted Au-Cu epithermal deposit, Srednogie Zone, Bulgaria. *Mineralium Deposita*, v 37, pp 614-629
- Bonham-Carter GF (1995) Geographic Information Systems for Geoscientists: Modelling with GIS, *in*: Computer Methods in the Geosciences, v 13. Pergamon Press, New York
- Bonhomme MG, Gauthier-Lafaye F, Weber F (1982) An example of lower Proterozoic sediments: The Francevillien in Gabon. *Precamb Res*, v 18, pp 87-102
- Boni M (1985) Les gisements de type Mississippi Valley du Sud-Ouest de la Sardaigne (Italie): Une synthèse. *Chron de la rech min*, no 479, pp 7-34
- Boni M, Balassone G, Iannace A (1996) Base metal ores in the Lower Paleozoic of southwestern Sardinia, *in*: DF Sangster, ed, Carbonate-Hosted Lead-Zinc Deposits. *Soc Econ Geol Spec Publ* 4, pp 18-28
- Bonnemaison M, et al (1986) Controls on exhalative gold deposits hosted by volcanoclastic sediments in the "Schistes X", Salsigne gold district, Montagne Noire, Southern France. *Proc Gold '86, Toronto*, pp 457-469
- Bonnichsen W (1972) Southern part of Duluth Complex, *in*: PK Sims, GB Morey, eds, The Geology of Minnesota, pp 361-387
- Bonnichsen W (1975) Geology of the Biwabik Iron Formation, Dunka River area, Minnesota. *Econ Geol*, v 70, pp 319-340
- Bookstrom AA (1981) Tectonic setting and generation of Rocky Mountain porphyry molybdenum deposits. *Arizona Geol Soc Digest*, v 14, Tucson, pp 215-226
- Borg G, Kärner H, Buxton M, Armstrong R, Merwe SW (2003) Geology of the Skorpion supergene Zn deposit, southern Namibia. *Econ Geol*, v 98, pp 749-771
- Boric R, Holmgren C, Wilson NSF, Zentilli M (2002) The geology of the El Soldado manto-type Cu (Ag) deposit, central Chile, *in*: TM Porter, ed, Hydrothermal Iron Oxide Copper-gold and Related Deposits: A Global Perspective, v 2. PGC Publ, Adelaide, pp 163-184
- Bornhorst TJ, Paces JB, Grant NK, Obradovich JD, Huber NK (1988) Age of native copper mineralization, Keweenaw Peninsula, Michigan. *Econ Geol*, v 83, pp 619-625
- Borodaevskaya MB, Rozhkov IS (1974) Deposits of gold, *in*: VI Smirnov, ed, Ore Deposits of the USSR, v 3, Engl Transl, Pitman, London, pp 3-81
- Borovikov PP, L'vova IA (1962) Tipy mestorozhdenii vermikulita, ikh promyshlennoe znachenie i napravleniya dalneishikh geologorazvedochnykh rabot. *Zakon Razm Poles Iskop*, v VI, pp 470-488
- Borrok DM, Kesler SE, Boer RH, et al (1998) The Vergenoeg magnetite-fluorite deposit, South Africa, support for a hydrothermal model for massive iron oxide deposits. *Econ Geol*, v 93, pp 564-586
- Bortnikov NS, Gamyaniin GN, Alpatov VV, et al (1998) Mineralogical and geochemical features and origin of the Nezhdaninsk deposit, Sakha-Yakutia, Russia. *Geol of Ore Dep*, v 39, pp 137-156
- Both RA, Arribas A, deSaint-André B (1994) The origin of breccia-hosted uranium deposits in carbonaceous metasediments of the Iberian Peninsula: U-Pb geochronology and stable isotope studies of the Fé deposit, Salamanca Province, Spain. *Econ Geol*, v 89, pp 584-601
- Bouabdellah M, Brown AC, Sangster DF (1996) Mechanisms of formation of internal sediments at the Beddiane lead-zinc deposit, Touissit mining district, northeastern Morocco, *in*: DF Sangster, ed, Carbonate-hosted lead-zinc deposits. *Soc Econ Geol Spec Publ* 4, pp 356-363
- Boudreau AE, McCallum IS (1986) Investigations of the Stillwater Complex, III. The Picket Pin Pt/Pd deposit. *Econ Geol*, v 81, pp 1953-1975
- Bouška V (1981) Geochemistry of Coal. Academia, Prague, 284 p
- Bowden P, Black R, Martin RF, et al (1987) Nigerian alkaline ring complexes: A classic example of African Phanerozoic anorogenic mid-plate magmatism. *Geol Soc London, Spec Publ No* 30, pp 357-379
- Bower B, Payne J, DeLong W, Rebagliati CM (1995) The oxide-gold, supergene and hypogene zones at the Casino gold-copper-molybdenum deposit, west-central Yukon. *CIM Spec Vol* 46, pp 352-360
- Bownan JR, Covert JJ, Clark AH, Matheson GA (1985) The Cantung E zone scheelite skarn orebody, Tungsten, Northwest Territories: oxygen, hydrogen, and carbon isotope studies. *Econ Geol*, v 80, pp 1872-1895
- Bowring SA, Housh T (1995) The Earth's early evolution. *Science*, v 269, pp 1535-1540
- Boyle, RW (1965) Geology, geochemistry and origin of the lead-zinc-silver deposits of the Keno Hill-Galena Hill area, Yukon Territory. *Geol Survey of Canada Bull* 111, 302 p
- Boyle RW (1976) Mineralization processes in Archean greenstone and sedimentary belts. *Geol Surv Canada, Paper* 75-15
- Boyle RW (1979) The Geochemistry of Gold Deposits., *Geol Surv of Canada, Bull* 280, 584 p

- Boyle RW (1987) Gold: History and Genesis of Deposits. Van Nostrand Reinhold, New York, 676 p
- Boyle RW et al, eds (1989) Sediment-Hosted Stratiform Copper Deposits. Geol Assoc Canada, Spec Paper 36, 710 p
- Bradley WH, Eugster HP (1969) Geochemistry and paleolimnology of the trona deposits and associated authigenic minerals of the Green River Formation of Wyoming. U.S. Geol Surv Profess Paper 496-B, 71 p
- Brathwaite RL, Christie AB, Skinner DNB (1989) The Hauraki Goldfield-regional setting, mineralization and recent exploration. AusIMM Monogr 13, pp 45-56
- Braunstein J, O'Brien GD, eds (1968) Diapirism and Diapirs. AAPG Memoir 8, Tulsa, 430 p
- Breaks FW (1982) Uraniferous granitoid rocks from the Superior Province of Northern Ontario. Geol Surv Canada Paper 81-23, pp 61-69
- Breiter K (1994) Variscan rare metal-bearing granitoids of the Bohemian Massif, *in*: R Seltmann, ed, Metallogeny of Collisional Orogens. Czech Geol Survey, Prague, pp 91-95
- Bridgewater D, Keto L, McGregor VR, Myers JS (1976) Archean gneiss complex of Greenland, *in*: A Escher, WS Watt, eds, Geology of Greenland. Grøn Geol Unders, pp 19-25
- Brimhall GH Jr (1979) Lithologic determination of mass transfer mechanisms of multiple-stage porphyry copper mineralization at Butte, Montana: Vein formation by hypogene leaching and enrichment of potassium-silicate protore. Econ Geol, v 74, pp 556-589
- Brimhall GH, Crerar DA (1989) Ore fluids, magmatic to supergene. Miner Soc Amer, Revs in Mineralogy, v 17, pp 235-282
- Briskey, JA, Dingess PR, Smith F, Gilbert RC, Armstrong AK, Cole GP (1986) Localization and source of Mississippi Valley-type zinc deposits in Tennessee, USA, and comparisons with Lower Carboniferous rocks of Ireland, *in*: CJ Andrew et al, eds, Geology and Genesis of Mineral Deposits in Ireland. Irish Assoc Econ Geol, Dublin, pp 635-662
- Broadbent GC, Waltho AE (1998) Century zinc-lead-silver deposit, *in*: DA Berkman, DH Mackenzie, eds, pp 729-736
- Brobst DA, Pratt WP, eds (1973) United States Mineral Resources. U.S. Geol Surv Prof Paper 820, 722 p
- Bromfield CS (1989) Gold deposits in the Park City mining district, Utah. U.S. Geol Surv Bull 1857-C, pp C14-C26
- Brooks CK, Keays RR, Lambert DD, et al (1999) Re-Os isotope geochemistry of Tertiary picritic and basaltic magmatism of East Greenland: Constraints on plume-lithosphere interactions and the genesis of the Platinova Reef, Skaergaard Intrusion. Lithos, v 47, pp 89-108
- Brooks CK, Tegner C, Stein H, Thomassen B (2004) Re-Os and $^{40}\text{Ar}/^{39}\text{Ar}$ ages of porphyry molybdenum deposits in the East Greenland volcanic-rifted margin. Econ Geol, v 99, pp 1215-1222
- Brooks JW, Meinert LD, Kuyper BA, Lane ML (1991) Petrology and geochemistry of the McCoy gold skarn, Lander County, Nevada, *in*: GL Raines et al, eds, Geology and Ore Deposits of the Great Basin. Geol Soc Nevada, Reno, pp 419-442
- Brown AC (1971) Zoning in the White Pine copper deposits, Ontonagon County, Michigan. Econ Geol, v 66, pp 543-573
- Brown, JS, ed (1967) Genesis of Stratiform Lead-zinc-barite-fluorite Deposits in Carbonate Rocks. Econ Geol Monogr 3, 443 p
- Brown M, Díaz F, Grocott J (1993) Displacement history of the Atacama fault system 25°00'S-27°00'S, northern Chile. Geol Soc Amer Bull, v 105, pp 1165-1174
- Brown P, Kahlert B (1995) Geology and mineralization of the Red Mountain porphyry molybdenum deposit, south-central Yukon. CIM Spec Volume 46, pp 747-756
- Brummer JJ (1955) The geology of the Roan Antelope orebody. Trans Inst Min Metall, London, v 64, pp 257-318
- Bruneton P (1987) Geology of the Cigar Lake uranium deposit (Saskatchewan, Canada) Saskatchewan Geol Soc Spec Publ 8, pp 99-112
- Brunn JH (1959) Le dorsale medio-atlantique et les épanchements ophiolitiques. Comte Rendu du Soc Géol France, v 8, pp 234-236
- Bryant DG (1968) Intrusive breccias associated with ore, Warren (Bisbee) mining district, Arizona. Econ Geol, v 63, pp 1-12
- Bryant DG, Metz HE (1966) Geology and ore deposits of the Warren mining district, *in*: SR Titley and CL Hicks, eds, Geology of the Porphyry Copper Deposits, Southwestern North America. Univ of Arizona Press, Tucson, pp 189-203
- Bryner L (1969) Ore deposits of the Philippines-an introduction to their geology. Econ Geol, v 64, pp 644-666
- Bublichenko, NL, et al (1972) Printsipy i Metody Prognozirovaniya Mednokolchedannovo i Polymetalicheskovo Orudneniya. Nedra, Moscow, 256 p
- Bucher K, Frey M (1994) Petrogenesis of Metamorphic Rocks. Springer-Verlag, 318 p
- Buchwald VF (1975) Handbook of Iron Materials, 3 volumes. Univ of California Press, v 2, pp 381-398
- Buddington AF (1959) Granite emplacement with special reference to North America. Geol Soc Amer Bull, v 70, pp 671-747
- Burchfiel, BC, Cowan DS, Davis GA (1992) Tectonic overview of the Cordilleran orogen in the western United States. The Geology of North America, v G-3, Geol Soc Amer, Boulder, pp 407-479
- Burchfiel BC, Lipman PW, Zoback ML, eds (1992) The Cordilleran Orogen: Counterminous U.S. The Geology of North America, v G-3, Geol Soc Amer, Boulder, 724 p
- Burk R, Hodgson CJ, Quartermain RA (1986) The geological setting of the Teck-Corona Au-Mo-Ba deposit, Hemlo, Canada, *in*: AJ Macdonald, ed, Gold '86, pp 311-326
- Burke, K (1996) The African Plate. South African Journ of Geol, v 99, pp 339-409

- Burnham CW (1979) Magmas and hydrothermal fluids, *in*: HL Barnes, ed, *Geochemistry of Hydrothermal Ore Deposits*. Holt, Rinehart, Winston, New York, pp 71-136
- Burnol L, ed (1980) Gisements de type porphyrique et de cupoles granitiques en France. *Chron de la rech minière*, 48, 116 p
- Burnotte E, Pirard E, Michel G (1989) Genesis of gray monazites: evidence from the Paleozoic of Belgium. *Econ Geol*, v 84, pp 1417-1429
- Burns TN (1993) A new mine project-the 3000 and 3500 copper orebodies at Mount Isa. *Intern Mining Geol Conf*, Kalgoorlie, July 1993, pp 5-8
- Burrough, PA, McDonnell, RA (1998) *Spatial Information Systems and Geostatistics*. Clarendon Press, Oxford
- Burrows DR, Spooner ETC (1986) The McIntyre Cu-Au deposit, Timmins, Ontario, Canada, *in*: AJ MacDonald, ed, *Gold '86*, pp 23-39
- Burt DRL, Sheppy NR (1975) Mount Keith nickel sulfide deposits, *in*: CL Knight, ed, pp 159-168
- Bur'yak VA (1975) *Metamorfogenno-gidrotermal'nyi tip promyshlennovo zolotovo orudneniya*. Nauka, Novosibirsk, 144 p
- Bur'yak VA (1983) Features of endogenic ore deposits in carbonaceous rocks. *Proc of the 8th Quadren IAGOD Sympos*, Schweitzerbart, Stuttgart, pp 803-811
- Bur'yak VA (1987) *Formirovaniye orudneniya v uglerodsoderzhazhchich tol'shchakh*. *Izvestiya AN SSSR, Ser Geol*, No 12, pp 94-105
- Buschendorf F, Dennert H, Hannak W, et al (1971) *Geologie des Erzgang-Reviers, Mineralogie des Ganginhalts und Geschichte des Bergbaus im Oberharz*. *Geol Jahrb, BeiH No 118*, 212 p
- Bushnell SE (1988) Mineralization at Cananea, Sonora, Mexico, and the paragenesis and zoning of breccia pipes in quartzofeldspathic rock. *Econ Geol*, v 83, pp 1760-1781
- Butler BS, Burbank WS (1929) The copper deposits of Michigan. *U.S. Geol Surv Prof Paper 144*, 238 p
- Butt CRM (1988) Major uranium provinces: Yilgarn Block and Gascoyne Province, Western Australia, *in*: *Recognition of Uranium Provinces*. IAEA, Vienna, pp 273-304
- Butt CRM (1989) Genesis of supergene gold deposits in the lateritic regolith of the Yilgarn Block, Western Australia. *Econ Geol Monogr 6*, pp 460-470
- Button A (1979) Early Proterozoic weathering profile on the 2200 m.y. old Hekpoort Basalt, Pretoria Group, South Africa: Preliminary results. *Inform Circ Econ Geol Res Unit, Uni Witwatersrand*, No 133, 20 p
- Button A, Tyler N (1981) The character and economic significance of Precambrian paleoweathering and erosion surfaces in southern Africa. *Econ Geol 75th Anniv Vol*, pp 686-709
- BVSP (Basaltic Volcanism Study Project) (1981) *Basaltic Volcanism on the Terrestrial Planets*. Pergamon Press, 1286 p
- Byelous YaT, Selin, YuI (1975) The genesis of ores in the manganese basin of southern Ukraine. *Doklady AN Ukrainian SSR, Ser B*, no 8, pp 6-8
- Bykhovskii LZ, Gurvich SI, Patyk-Kara NG, Flerov IB (1981) *Geologicheskie Kriterii Poiskov Rossypei*. Nedra, Moscow, 253 p
- Bysouth GD, Wong GY (1995) The Endako molybdenum mine, central British Columbia: An update. *CIM Spec Volume 46*, pp 697-703
- Cailteux J (1974) Les sulfures du gisement cuprifère stratiforme de Musoshi, Shaba, Zaïre, *in*: P Bartholomé, ed, pp 267-276
- Caira NM, Findlay A, DeLong C, Rebagliati CM (1995) Fish Lake porphyry copper-gold deposit, central British Columbia. *CIM Spec Volume 46*, pp 327-342
- Calkins JA, Kays O, Keefer EK (1973) CRIB-the Mineral Resources Data Bank of the U.S. *Geological Survey. U.S. Geol Surv Circular 681*, 39 p
- Callahan WH (1977) The history of the discovery of the zinc deposit of Elmwood, Tennessee: Concept and consequences. *Econ Geol*, v 72, pp 1382-1392
- Cameron E (1990) Yeelirie uranium deposit, *in*: FE Hughes, ed, pp 1625-1629
- Cameron EM, ed (1983) *Uranium exploration in Athabasca Basin, Saskatchewan, Canada*. *Canad Govt Publ Centre, Ottawa*, 310 p
- Cameron EN, Jahns RH, McNair AH, Page LR (1949) Internal structure of granitic pegmatites. *Econ Geol Monogr 2*, 115 p
- Campbell IH (1998) The mantle chemical structure: Insights from the melting products of mantle plumes, *in*: I Jackson, ed, *The Earth's Mantle*. Cambridge Univ Press, pp 259-310
- Camus F (1975) Geology of the El Teniente orebody with emphasis on wall-rock alteration. *Econ Geol*, v 70, pp 1341-1372
- Camus F (1985) Los yacimientos estratoligados de Cu, Pb-Zn y Ag de Chile, *in*: J Frutos et al, eds, *Geología y Recursos Minerales de Chile*. Univ de Concepción, pp 547-635
- Canavan F (1988) Deep lead gold deposits of Victoria. *Geol Surv of Victoria Bull 62*, 101 p
- Candela PA (1989) Magmatic ore-forming fluids: Thermodynamic and mass transfer calculations of metal concentrations. *Reviews in Econ Geol*, v 4, pp 203-221
- Candela PA (1991) Physics of aqueous phase evolution in plutonic environments. *Amer Mineralogist*, v 76, pp 1081-1091
- Card KD, Poulsen KH, Robert F (1989) The Archean Superior Province of the Canadian Shield and its lode gold deposits. *Econ Geol Monogr 6*, pp 19-36
- Carlile JC, Mitchell AHG (1994) Magmatic arcs and associated gold and copper mineralization in Indonesia. *Journal of Geoch Explor*, v 50, pp 91-142
- Carlson RW, ed (2004) *Treatise on Geochemistry*, v 2 *The Mantle and Core*. Elsevier-Pergamon, 586 p
- Carmichael ISE, Turner FJ, Verhoogen J (1974) *Igneous Petrology*. McGraw-Hill, New York, 739 p
- Carpenter LG, Garrett DE (1959) Tungsten in Searles Lake. *Mining Engineering*, v 11, pp 301-303
- Carr JM (1966) Geology of the Bethlehem and Craigmont copper deposits. *CIM Special Volume 8*, pp 321-328

- Carten RB, Tayeb JM (1990) Formation of volcanic exhalative nickel sulfide deposits at a late Proterozoic spreading ridge in the proto-Arabian Shield. *Canad Journ Earth Science*, v 27, pp 742-757
- Carten RB, White WH, Stein HJ (1993) High-grade granite-related molybdenum systems: Classification and origin. *Geol Assoc Canada Spec Paper* 40, pp 521-554
- Cartwright I (1999) Regional oxygen isotope zonation at Broken Hill, New South Wales, Australia; large-scale fluid flow and implications for Pb-Zn-Ag mineralization. *Econ Geol*, v 94, pp 357-373
- Cas RAF, Wright JV (1987) *Volcanic Successions, Modern and Ancient*. Allen and Unwin, London, 528 p
- Casselman MJ, McMillan WJ, Newman KM (1995) Highland Valley porphyry copper deposits near Kamloops, British Columbia: A review and update with emphasis on the Valley deposit. *CIM Spec Volume* 46, pp 161-191
- Cathcart JB (1963) Economic geology of the Keysville Quadrangle, Florida. *U.S. Geol Surv Bull* 1128, 82 p
- Cawthorn RG, Molyneux TG (1986) Vanadiferous magnetite deposits of the Bushveld Complex, in: CR Anhaeusser, S Maske, eds, pp 1251-1266
- Cawthorn RG, Walraven F (1998) Emplacement and crystallization time for the Bushveld Complex. *Journ of Petrol*, v 39, pp 1669-1687
- CENTROMIN Ltd, Lima (1977) Property descriptions (unpublished)
- Černý P (1991) Rare element granitic pegmatites. Part I: Anatomy and internal evolution of pegmatite deposits. *Geoscience Canada*, v 18, pp 49-67
- Černý P, ed (1982) *Granitic Pegmatites in Science and Industry*. Miner Assoc Canada Short Course Handbook 8, 555 p
- Chabiron A, Cuney M, Poty B (2003) Possible uranium sources for the largest uranium district associated with volcanism: The Streltsovka Caldera (Transbaikalia, Russia). *Mineralium Deposita*, v 38, pp 127-140
- Chace FM (1948) Tin-silver veins of Oruro, Bolivia. *Econ Geol*, v 43, pp 333-382, 435-470
- Chadwick B, Crewe MA (1986) Chromite in the early Archean Akilia Association (ca 3800 m.y.), Ivisartoq region, near Godthåbsfjord, southern West Greenland. *Econ Geol*, v 81, pp 184-191
- Chaffee MA (1982) A geochemical study of the Kalamazoo porphyry copper deposit, Pinal County, Arizona, in: SR Titley, ed, *Advances in Geology of Porphyry Copper Deposits, Southwestern North America*. Univ of Arizona Press, Tucson, pp 211-226
- Chai G, Naldrett AJ (1992) Characteristics on Ni-Cu-PGE mineralization and genesis of the Jinchuan deposit, Northwest China. *Econ Geol*, v 87, pp 1475-1495
- Chalmers DI (1990) Brockman multi-metal and rare earth deposit, in: FE Hughes, ed, pp 707-710
- Chandler FW, Christie RL (1996) Stratiform phosphate, in: *Geology of Canada No 8*, *Geol Surv Canada*, pp 33-40
- Chan Quang, Clark AH, Lee JKW, Guillén JB (2003) ^{40}Ar - ^{39}Ar ages of hypogene and supergene mineralization in the Cerro Verde-Santa Rosa porphyry Cu-Mo cluster, Arequipa, Peru. *Econ Geol*, v 98, pp 1683-1696
- Channer D, Graffe E, Vielma P (2005) Geology, mining and mineral potential of southern Venezuela. *Soc Econ Geol, Newsletter No* 62, pp 14-21
- Chao ECT, Tatsumoto M, Minkin JA, Back JM, McKee EH, Ren Yingchen (1989) Multiple lines of evidence for establishing the mineral paragenetic sequence of the Bayan Obo rare earth ore deposit of Inner Mongolia, China. *Proc of the 8th Quadren IAGOD Sympos*, pp 55-73
- Chao ECT et al (1997) The sedimentary carbonate-hosted giant Bayan Obo REE-Fe-Nb ore deposit of Inner Mongolia, China. *U.S. Geol Surv Bull* 2143, 65 p
- Chapel PA (1992) *Handbook of Exploration Geophysics*. Balkema, Rotterdam, 411 p
- Chapman LH (2004) Geology and mineralization styles of the George Fisher Zn-Pb-Ag deposit, Mount Isa, Australia. *Econ Geol*, v 99, pp 233-256
- Chaykin SI (1985) Tectonic character and structural features of the KMA ferruginous siliceous formation. *Geotectonics*, v 19, pp 16-30
- Cheilletz A (2002) The giant Imiter silver deposit: Neoproterozoic epithermal mineralization in the Anti-Atlas, Morocco. *Mineralium Deposita*, v 37, pp 772-781
- Chen Guoda (1982) Polygenetic compound ore deposits and their origin in the context of regularities in crustal evolution. *Geotectonica et Metallogenia*, v 1, 27 p
- Chen Yaoqin, Zeng Bofu (1984) Geological characteristics and genesis of huge strata-bound lead-zinc ore deposit of Fankou, Guangdong. *Acta Sedimentologica Sinica*, v 2, pp 33-47
- Cheney ES (1991) Structure and age of the Cerro de Pasco Cu-Zn-Pb-Ag deposit, Peru. *Mineralium Deposita*, v 26, pp 2-10
- China Geological Survey (2004) A brief introduction to the results of the survey and assessment of mineral resources of China (1999-2003), Beijing, 10 p
- Chovan M, Hurai V, Sachan HK, Kantor J (1995) Origin of the fluids associated with granodiorite-hosted Sb-As-W mineralization at Dúbrava (Nízke Tatry Mts., western Carpathians). *Mineralium Deposita*, v 30, pp 48-54
- Christensen OD (1993) Carlin Trend geologic overview. *Soc Econ Geol Guidebook Ser*, v 18, pp 3-26
- Christiansen EH, Sheridan MF, Burt DM (1986) The geology and geochemistry of Cenozoic topaz rhyolites from the western United States. *Geol Soc Amer Spec Paper* 205, pp 189-200
- Christiansen RL, Yeats RS, et al (1992) Post-Laramide geology of the U.S. Cordilleran region. *The Geology of North America*, v G-3, *Geol Soc Amer*, Boulder, pp 261-310
- Chrt J, Bolduan H (1966) Die postmagmatische Mineralisation des Westteils der Böhmisches Masse. *Sbor Geol Věd*, LG, Prague, v 8, pp 113-192
- Clark AH (1990) The slump breccias of the Toquepala porphyry Cu (-Mo) deposit, Peru: Implications for

- fragment rounding in hydrothermal breccias. *Econ Geol*, v 85, pp 1677-1685
- Clark AH (1993) Are outsize porphyry copper deposits either anatomically or environmentally distinctive? *Soc Econ Geol Spec Publ* 2, pp 213-183
- Clark AH, ed (1995) *Giant Ore Deposits-II*. Queens Univ, Kingston, Ontario, 753 p
- Clark AH, Archibald DA, Lee AW, Farrar E, Hodgson CJ (1998) Laser probe $^{40}\text{Ar}/^{39}\text{Ar}$ ages of early- and late stage alteration assemblages, Rosario porphyry copper molybdenum deposit, Collahuasi district, I Region, Chile. *Econ Geol*, v 93, pp 326-337
- Clark GH (1990) Panguna copper-gold deposit, *in*: FE Hughes, ed, pp 1807-1816
- Clark KF, Dow RR, Knowling RD (1979) Fissure-vein deposits related to continental volcanic and subvolcanic terranes in Sierra Madre Occidental province, Mexico. *Nevada Bureau of Mines and Geol, Rept* 33, pp 189-210
- Clarke DB (1977) The Tertiary volcanic province of Baffin Bay. *Geol Assoc Canada, Spec Paper* 16, pp 445-460
- Clarke FW (1924) *The Data on Geochemistry*. U.S. Geol Survey Bull 770, 5th ed, 841 p
- Clarke M, Tittley SR (1988) Hydrothermal evolution of silver-gold veins in the Tayoltita mine, San Dumas district, Mexico. *Econ Geol*, v 83, pp 1830-1840
- Claveria RJR, Cuisson AG, Andam BV (1999) The Victoria gold deposit in the Mankayan mineral district, Luzon, Philippines. *PACRIM '99 Proceedings*, Bali, AusIMM, pp 73-80
- Cliff RA, Rickard D, Blake K (1990) Isotope systematics of the Kiruna magnetite ores, Sweden, Part 1, Age of the ore. *Econ Geol*, v 85, pp 1770-1776
- Cline JS (2001) Timing of gold and arsenic sulfide mineral deposition at the Getchell Carlin-type gold deposit, North-Central Nevada. *Econ Geol*, v 96, pp 75-90
- Cline JS (2004) Introduction to Carlin-type deposits. *Soc Econ Geol Newsletter*, Oct 2004, pp 1, 11
- Clode C, Proffett J, Mitchell P, Munajat I (1999) Relationships of intrusion, wall-rock alteration and mineralisation in the Batu Hijau copper-gold porphyry deposit. *PACRIM '99 Proceedings*, Bali, AusIMM, pp 485-498
- Clout JMF, Cleghorn JH, Eaton PC (1990) Geology of the Kalgoorlie gold field, *in*: FE Hughes, ed, pp 411-431
- Coats CJA, Snajdr P (1984) Ore deposits of the North Range, Onaping-Levack area, Sudbury, *in*: EG Pye et al, eds, *Ontario Geol Surv Spec Vol* 1, pp 327-346
- Cobbing EJ (1990) A comparison of granites and their tectonic settings from the South American Andes and the Southeast Asian tin belt. *Geol Soc Amer Spec Paper* 241, pp 193-204
- CODELCO Ltd, Rancagua (1977) *Mina El Teniente, deescription* (unpublished)
- Coleman RG (1977) *Ophiolites: Ancient Oceanic Lithosphere?* Springer-Verlag, New York, 229 p
- Coleman RG (1993) *Geologic Evolution of the Red Sea*. Oxford Univ Press, New York, 186 p
- Coleman RG (2000) Prospecting for ophiolites along the California continental margin. *Geol Soc Amer Spec Paper* 349, pp 351-364
- Coleman RG, Peterman ZE (1975) Oceanic plagiogranite. *Journ Geophys Res*, v 80, pp 1099-1108
- Collinson JD (1978) *Deserts*, *in*: HG Reading, ed, *Sedimentary Environments and Facies*. Elsevier, New York, pp 80-96
- Collenette P, Grainger D, eds (1994) *Mineral Resources of Saudi Arabia*. DMMR, Jeddah
- Colley H, Flint DJ (1995) *Metallic Mineral Deposits of Fiji*. Fiji Miner Res Dept Mem 4, Suva, 195 p
- Colvine AC, Fyon JA, Heather KB, Marmont S, Smith PM, Troop DG (1988) *Archean Lode Gold Deposits in Ontario*. Ontario Geol Surv Miscell Paper 139, 210 p
- Comer JB (1974) Genesis of Jamaican bauxite. *Econ Geol*, v 69, pp 1251-1264
- COMIBOL, Empresa Catavi (1977) *Llallagua description* (unpublished)
- COMRATE (Committee on Mineral Resources and the Environment) (1975) *Mineral Resources and the Environment*. National Acad of Sciences, Washington, DC, 348 p
- Conant LC, Swanson VE (1961) Chattanooga Shale and related rocks of central Tennessee and nearby areas. *U.S. Geol Surv Prof Paper* 357, 91 p
- Concepción RA, Cinco JC Jr (1989) Geology of the Lepanto Far Southeast gold-rich porphyry copper deposit. *Intern Geol Congr*, 28th, Washington DC, *Proceedings* v 1, pp 319-320
- Concha O, Valle J (1999) *Prospección, exploración y desarrollo del yacimiento de Cuajone*. Primer Volumen de Monografías de Yacimientos Minerales Peruanos. IIMP, Lima, pp 117-143
- Condie KC (1981) *Archean Greenstone Belts*. Elsevier, Amsterdam, 434 p
- Condie KC (1982) *Plate Tectonics and Crustal Evolution*, 2nd ed. Pergamon Press, New York
- Coney PJ (1989) Structural aspects of suspect terranes and accretionary tectonics in western North America. *Journ Struct Geol*, v 11, pp 117-125
- Conly AG, Scott SD (1998) Field evidence for synsedimentary-early diagenetic versus epigenetic origins of the Boleo Cu-Co-Zn deposit, Baja California Sur, Mexico. *Geol Assoc Canada, Miner Assoc Canada, Annual Meeting, Proceedings*, Québec '98
- Consultants Group (1986) *Correlation of uranium geology between South America and Africa*. IAEA Techn Rept Series, No 270, Vienna, 475 p
- Cook PJ (1972) Petrology and geochemistry of the phosphate deposits of Northwest Queensland, Australia. *Econ Geol*, v 67, pp 1193-1213
- Cook SS (1988) Supergene copper mineralization at the Lakeshore Mine, Pinal County, Arizona. *Econ Geol*, v 83, pp 297-309
- Cooke DL, Moorhouse WW (1968) Timiskaming volcanism in the Kirkland Lake area, Ontario, Canada. *Canad Journ Earth Sci*, v 6, pp 117-132
- Cooke DR, Cannell J, Frikken PH, Hollings P, Walshe JL (2004) *El Teniente and Rio Blanco porphyry Cu-Mo*

- deposits, Chile-giant ore formation in an active continental margin (lecture and abstract). PACRIM Congress, Adelaide, Proceedings, AusIMM, p 13
- Cooke DR, McPhail DC, Bloom MS (1996) Epithermal gold mineralization, Acupan, Baguio District, Philippines: Geology, mineralization, alteration, and the thermochemical environment of ore deposition. *Econ Geol*, v 91, pp 243-272
- Cooke DR, Simmons SF (2000) Characteristics and genesis of epithermal gold deposits. *Soc Econ Geol, Reviews in Econ Geol*, v 13, pp 163-220
- Coolbaugh DF, et al (1995) El Arco porphyry copper deposit, Baja California, Mexico. *Arizona Geol Soc Digest*, v 20, pp 525-534
- Cooper DG (1961) The geology of the Bikita pegmatite, *in*: Houghton SH, ed, *The Geology of Some Ore Deposits in Southern Africa*, 2 vols. Geol Soc S Africa, Johannesburg
- Cooper JR (1951) Geology of the tungsten, antimony and gold deposits near Stibnite, Idaho. *U.S. Geol Surv Bull* 969-F, pp 151-197
- Corbett KD (1992) Stratigraphic-volcanic setting of massive sulfide deposits in the Cambrian Mount Read Volcanics, Tasmania. *Econ Geol*, v 87, pp 564-586
- Corbett KD, Solomon M (1989) Cambrian volcanism and mineral deposits. *Geol Soc Australia, Spec Publ* 15, pp 84-153
- Corbett GJ, Leach TM (1994) SW Pacific Rim Au/Cu systems: Structure, alteration and mineralisation. Workshop notes, Townsville, 140 p
- Corbett GJ, Leach TM (1998) Southwest Pacific rim gold-copper systems: Structure, alteration and mineralization. *Soc Econ Geol, Spec Publ* 6, 234 p
- Corfu F, Andrews AJ (1987) Geochronological constraints and the timing of magmatism, deformation, and gold mineralization in the Red Lake greenstone belt, northwestern Ontario. *Canad Journ Earth Sci*, v 24, pp 1302-1320
- Corvalán J (1989) Geologic-tectonic framework of the Andean region, *in*: GE Ericksen et al, eds, pp 1-37
- Coulon C, Thorpe RS (1981) Role of continental crust in petrogenesis of orogenic volcanic associations. *Tectonophysics*, v 77, pp 79-93
- Cousins CA (1964) Additional notes on the chromite deposits of the eastern part of the Bushveld Complex, *in*: SH Houghton, ed, pp 169-182
- Cousins CA, Feringa C (1964) The chromite deposits of the western belt of the Bushveld complex, *in*: SH Houghton, ed, pp 183-201
- Coutts BP, Susanto H, Belluz N, Flint D, Edwards A (1999) Geology of the Deep Ore Zone, Ertsberg East skarn system, Irian Jaya. PACRIM '99 Proceedings, Bali, AusIMM, pp 539-547
- Coveney RM, Grauch RI, Murowchick JB (1994) The geologic setting of precious metal-bearing Ni-Mo ore beds. *Soc Econ Geol, Newsletter* No 18, pp 1-11
- Coveney RM, Murowchick JB, Grauch RI, Chen N, Glascock MD (1992) Field relations, origins and resource implications for platinumiferous molybdenum-nickel ores in black shales of South China. *Explor Min Geol*, v 1, pp 21-28
- Cowan DS, Bruhn RL (1992) Late Jurassic to early Late Cretaceous geology of the U.S. Cordillera. *The Geology of North America*, v G-3, Geol Soc of Amer, Boulder, pp 169-203
- Cowan EJ, Riller U, Schwerdtner WM (1999) Emplacement geometry of the Sudbury Igneous Complex. *Geol Soc Amer, Spec Paper* 339, pp 300-418
- Cowan JC (1968) Geology of the Strathcona ore deposit. *CIM Bulletin*, v 61, no 699, pp 38-54
- Coward MP, Ries AC, eds (1986) *Collision tectonics*. Geol Soc Spec Publ, no 19, London, pp 67-81
- Cox DP, Singer DA, eds (1986) *Mineral Deposit Models*. U.S. Geol Surv Bull 1693, 291 p
- Craig JR, Vaughan DJ, Skinner BJ (1988) *Resources of the Earth*. Prentice Hall, Englewood Cliffs, NJ, 395 p
- Craw D, Windle SJ, Angus PV (1999) Gold mineralization without quartz veins in a brittle-ductile shear zone, Macraes Mine, Otago Schist, New Zealand. *Mineralium Deposita*, v 34, pp 382-394
- Craw D, Youngson JH, Koons PO (1999) Gold dispersal and placer formation in an active oblique collisional mountain belt, Southern Alps, New Zealand. *Econ Geol*, v 94, pp 605-614
- Crawford AJ, ed (1989) *Boninites*. Unwin Hyman, London, 465 p
- Creasey SC (1980) Chronology of intrusion and deposition of porphyry copper ores, Globe-Miami district, Arizona. *Econ Geol*, v 75, pp 830-844
- Creasey SC, Quick GL (1955) Copper deposits of part of the Helvetia mining district, Pima County, Arizona. *U.S. Geol Surv Bull* 1027F, pp 301-321
- Cressman ER, Swanson RW (1964) Stratigraphy and petrology of the Permian rocks of southwestern Montana. *U.S. Geol Surv Prof Paper* 313-C, pp 275-569
- Crittenden MD Jr, Coney PJ, Davis GH, eds (1980) *Cordilleran Metamorphic Core Complexes*. Geol Soc Amer Memoir 153, 496 p
- Crocker IT (1985) Volcanogenic fluorite-hematite deposits and associated pyroclastic rock suite at Vergenoeg, Bushveld Complex. *Econ Geol*, v 80, pp 1181-1200
- Crocker IT, Martini JE, Söhnge APG (1988) The fluorspar deposits of the Republic of South Africa and Bophuthatswana. *South Afr Geol Surv Handb*, v 11, 172 p
- Cronan DS (1980) *Underwater Minerals*. Academic Press, London, 350 p
- Cronan DS, ed (2000) *Handbook of Marine Mineral Deposits*. CRC Press, Boca Raton, Florida
- Crouse RA, Černý P, Trueman DL, Burt OR (1979) The TANCO pegmatite, south-eastern Manitoba. *CIM Bulletin*, v 72, pp 142-151
- Crouzet J, et al (1979) Les gisements aurifères du Massif Central Français. *Chron de la rech minière*, no 452, pp 5-38
- Crowson P (1998) *Minerals Handbook, 1998-99*. Mining Journal Books, London
- Cruise MD (1996) Replacement origin of Crinkill Ironstone: Implications for genetic models of base

- metal mineralization, Central Ireland. *Explor and Mining Geol*, v 5, pp 241-249
- Cuadra PC (1986) Geocronologia K-Ar del yacimiento El Teniente y areas adyacentes. *Revista Geol de Chile*, No 27, pp 3-26
- Cuadra PC, Rojas GS (2001) Oxide mineralization at the Radomiro Tomic porphyry copper deposit, northern Chile. *Econ Geol*, v 96, pp 387-400
- Cuney M, Marignac C, Weisbrod A (1992) The Beauvoir topaz, lepidolite, albite granite (Massif Central, France): The disseminated magmatic Sn-Li-Ta-Nb-Be mineralization. *Econ Geol*, v 87, pp 1766-1794
- Cuney M, Raimbault L (1991) Variscan granites and associated uranium mineralizations from the North-West French Massif Central. SGA 25th Anniv Meeting, Nancy, Field Guidebook, 79 p
- Cunningham CG, et al (1982) Geochronology of hydrothermal uranium deposits and associated igneous rocks in the eastern source area of Mount Belknap volcanics, Marysvale, Utah. *Econ Geol*, v 77, pp 453-463
- Cunningham CG, Ashley RP, Chou I-M, Huang Z, Wan C, Li W (1988) Newly discovered sedimentary rock-hosted disseminated gold deposits in the People's Republic of China. *Econ Geol*, v 83, pp 1462-1467
- Cunningham CG, Austin GW, Naeser CW, Rye RO, Ballantyne GH, Stamm RG, Barker CE (2004) Formation of paleothermal anomaly and disseminated gold deposits associated with the Bingham Canyon porphyry Cu-Au-Mo system, Utah. *Econ Geol*, v 99, pp 789-806
- Cunningham CG, Zartman RE, McKee EH, Rye RO, Naeser CW, Sanjines OV, Erickson GE, Tavera FV (1996) The age and thermal history of Cerro Rico de Potosí, Bolivia. *Mineralium Deposita*, v 31, pp 374-385
- Currie KL (1974) The alkaline rocks of Canada. *Geol Surv Canada, Bull* 239
- Czamanske GK, Zientek ML, eds (1985) The Stillwater Complex, Montana: Geology and Guide. *Montana Bur Min Geol, Spec Publ* 92
- Dagger GW (1972) Genesis of the Mount Pleasant tungsten-molybdenum-bismuth deposit, New Brunswick, Canada. *Trans Inst Min Metall*, ser B, London, pp 73-102
- Dahl AR, Hagmaier JL (1974) Genesis and characteristics of the southern Powder River Basin uranium deposits, Wyoming, USA, *in: Formation of Uranium Ore Deposits*, IAEA-SM-183/5, Vienna, pp 201-218
- Dahlkamp, FJ (1993) *Uranium Ore Deposits*. Springer-Verlag, Berlin & Heidelberg, 460 p
- Daliran F, Walther J, Stuben D (1999) Sediment-hosted disseminated gold mineralization in the North Takob geothermal field, NW Iran, *in: CJ Stanley et al, eds, Mineral Deposits: Processes to Processing. Proceedings of the 5th Biennial SGA Meeting*, Balkema, Rotterdam, pp 837-840
- Dalstra H, Guedes S (2004) Giant hydrothermal hematite deposits with Mg-Fe metasomatism: A comparison of the Carajás, Hamersley, and other iron ores. *Econ Geol*, v 99, pp 1793-1800
- Dammer D, Chivas AR, McDougall I (1996) Isotopic dating of supergene manganese oxides from the Groote Eylandt deposit, Northern Territory, Australia. *Econ Geol*, v 91, pp 386-401
- Danni JCM (1976) Magmatic differentiation of the alkaline-ultrabasic intrusions in the Iporá region, South-West Goiás, Brazil, *in: Proc of the 1st Intern Symp on Carbonatites*, Poços de Caldas, pp 149-167
- Davidson A (1982) Petrochemistry of the Blatchford Lake Complex near Yellowknife, Northwest Territories. *Geol Surv Canada, Paper* 81-23, pp 71-79
- Davies GF (1998) Plates, plumes, mantle convection, and mantle evolution, *in: I Jackson, ed, The Earth's Mantle*. Cambridge Univ Press, pp 228-258
- Davies JF, Luhta LE (1978) An Archean "porphyry-type" disseminated copper deposit, Timmins, Ontario. *Econ Geol*, v 73, pp 383-396
- Davis LJ (1991) Spor Mountain beryllium deposits, Juab County, Utah, *in: VF Hollister, ed, v 3*, pp 325-332
- Dawson GL, Caessa P (2003) Geology of the Aljustrel mine area, southern Portugal, *in: GEODE, Field Workshop, The Geology of the volcanic-hosted massive sulfides in the Iberian Pyrite Belt*, Aljustrel Field Trip Guide, pp 1-23
- Dawson JB (1966) Oldoinyo Lengai-an active volcano with sodium carbonatite lava flows, *in: OF Tuttle, J Gittins, eds, Carbonatites*. Interscience, New York, pp 155-168
- Dawson JB, Garson MS, Roberts B (1987) Altered former alkalic carbonatite lava from Oldoinyo Lengai, Tanzania: Inferences for calcite carbonatite lavas. *Geology*, v 15, pp 765-768
- Dawson KM, Panteleyev A, Woodsworth GJ, Sutherland Brown A (1992) Regional metallogeny of the Canadian Cordillera, *in: H Gabrielse, CJ Yorath, eds, The Cordilleran Orogen*. *Geol of Canada*, v 4, *Geol Survey of Canada*, pp 707-768
- Dean WE (1983) Geochemistry of deep-sea manganese nodules-organic involvement, *in: WC Shanks III, ed, Cameron Volume on Unconventional Mineral Deposits*. AIME, New York, pp 123-132
- Deans T (1966) Economic mineralogy of African carbonatites; same public, *in: OF Tuttle, J Gittins, eds, Carbonatites*. Interscience, New York, pp 385-413
- deCarvalho D (1991) A case history of the Neves-Corvo massive sulfide deposit, Portugal, and implications for future discoveries. *Econ Geol Monogr* 8, pp 314-334
- Degens ET, Ross DA, eds (1969) *Hot Brines and Recent Heavy Metal Deposits in the Red Sea*. A Geochemical and Geophysical Account. Springer-Verlag, 600 p
- Degens ET, Ross DA, eds (1974) *The Black Sea-Geology, Chemistry and Biology*. Amer Assoc Petrol Geol Memoir 20, 640 p
- deHoyos MF (1988) Exploitation and concentration in the Naica mine of Compañía Fresnillo, S.A. de C.V. Cía Fresnillo, Unidad Naica, unpublished text, 8 p
- De Lima e Silva FJ, Cavalcante PRB, De Sá EP, et al (1988) Depósito de cobre do Caraíba e o distrito cuprífero do Vale do Rio Curaça, Bahía, *in: C Schobbenhaus, CES Coelho, eds, v 3*, pp 11-31
- Delius ChT (1773) *Anleitung zu der Bergbaukunst*. Wien

- Delmelle P, Bernard A (1994) Geochemistry, mineralogy, and chemical modelling of the acid crater lake of Kawah Ijen Volcano, Indonesia. *Geoch Cosmoch Acta*, v 58, pp 2445-2460
- De Lorraine WF, Dill DB (1982) Structure, stratigraphic controls, and genesis of the Balmat zinc deposits, northwest Adirondack, New York. *Geol Assoc Canada Spec Paper 25*, pp 571-596
- De Magnée I, François A (1988) The origin of the Kipushi (Cu,Zn,Pb) deposit in direct relation with a Proterozoic salt diapir. Copperbelt of Central Africa, Shaba, Republic of Zaire, *in*: GH Friedrich, PM Herzig, eds, *Base Metal Sulfide Deposits*. Springer-Verlag, pp 74-93
- Demesmaeker G (1962) La tectonique des gisements stratiformes du Roan Katangais, *in*: J Lombard, P Nicolini, eds, *Gisements Stratiformes de Cuivre en Afrique*. Symposium, 2 vols, Paris, pp 77-104
- Denson NM, Gill JR (1965) Uranium-bearing lignite and carbonaceous shale in the southwestern part of the Williston Basin—a regional study. *U.S. Geol Surv Prof Paper 463*, 75 p
- De Oliveira AG, Fuzikawa K, Moura LAM, Raposo C (1985) Provincia uranífera de Lagoa Real-Bahía, *in*: C Schobbenhaus, CES Coelho, eds, v 1, pp 105-120
- De Ronde CEJ, De Wit MJ (1994) Tectonic history of the Barberton greenstone belt, South Africa: 490 million years of Archaean crustal history. *Tectonics*, v 13, pp 938-1005
- deRoo JA (1989) The Elura Ag-Pb-Zn mine in Australia—ore genesis in a slate belt by syndeformational metasomatism along hydrothermal fluid conduits. *Econ Geol*, v 84, pp 256-278
- deSouza MM (1996) The great niobium deposit in Morro do Seis Lagos, North Brazil. 30th Intern Geol Congr Beijing, Abstract
- De Voto RH (1983) Central Colorado karst-controlled lead-zinc-silver deposits (Leadville, Gilman, Aspen, and others), a late Paleozoic Mississippi Valley-type district, *in*: The genesis of Rocky Mountain ore deposits, changes with time and tectonics. *Denver Region Explor Geol Soc*, pp 51-70
- de Vries PR (2001) Geology at Tau Lekoa Mine. Unpublished, 10 p
- Dewey JF (1980) Episodicity, sequence and style at convergent plate boundaries, *in*: DW Strangway, ed, *The Continental Crust and its Mineral Deposits*. *Geol Assoc Canada, Spec Paper 20*, pp 553-573
- Dewey JF, Bird JM (1971) Origin and emplacement of the ophiolite suite: Appalachian ophiolites in Newfoundland. *Journ Geophys Res*, v 76, pp 3179-3206
- de Wit MJ, Ashwal LD (1995) Greenstone belts: what are they? *South African Journ of Geol*, v 98, pp 505-520
- de Wit MJ, Ashwal LD, eds (1997) *Greenstone Belts*. Oxford Monogr on Geol and Geophys, v 35
- Diamond J (2005) *Collapse. How Societies Choose to Fail or Survive*. Penguin Books, London, 575 p
- Dick LA, Hodgson CJ (1982) The Mactung W-Cu(Zn) contact metasomatic and related deposits of the Northeastern Canadian Cordillera. *Econ Geol*, v 77, pp 845-867
- Diederix D (1977) The geology of the Nchanga mining licence area. NCCM Ltd, Chingola Division, unpubl, 59 p
- Dietz RS (1964) Sudbury structure as an astrobleme. *Journ Geol*, v 72, pp 412-434
- Dietz RS (1972) Sudbury astrobleme, splash-emplaced sublayer and possible cosmogenic ores. *Geol Assoc Canada, Spec Paper 10*, pp 29-40
- Dilek Y, Moores EM, Elthon D, Nicolas A, eds (2000) *Ophiolites and oceanic crust: New insights from field studies and the ocean drilling program*. *Geol Soc Amer, Spec Paper 349*, 552 p
- Dill HG, Weiser T, Bernhardt IR, Riera CR (1995) The composite gold-antimony vein deposit at Kharna (Bolivia). *Econ Geol*, v 90, pp 51-66
- Dilles JH (1987) Petrology of the Yerington Batholith, Nevada: Evidence for evolution of porphyry copper ore fluids. *Econ Geol*, v 82, pp 1750-1789
- Dilles JH, Farmer GL, Field CW (1995) Sodium-calcium alteration by non-magmatic saline fluids in porphyry copper deposits: Results from Yerington, Nevada, *in*: JFH Thompson, ed, *Magmas, Fluids and Ore Deposits*. *Miner Assoc Canada, Short Course Volume 23*, pp 309-338
- Dines HG, ed (1956) *The metalliferous mining region of South-West England*. *Mem Geol Soc, London*, 2 vols, 792 p
- Divis AF (1983) The geology and geochemistry of Philippine porphyry copper deposits, *in*: DE Hayes, ed, *AGU Geophys Monogr No 27*, pp 173-195
- Dixon JR (1998) Presidential address: Witwatersrand gold—quo vadis? *Journ South African Inst Miner Metall*, pp 213-219
- Dobrovol'skaya MG, Balashova SP, Zaozerina ON, Golovanova TI (1993) Mineral'nye paragenezisy i stadii rudoobrazovaniya v svintsovo-tsinkovykh mestorozhdeniyakh Dal'negorskovo rudnovo raiona (Yuzhnoe Primor'ye). *Geol Rud Mestorozhd*, v 35, pp 493-515
- Donaldson MJ, Leshner CM, Groves DI, Gresham JJ (1986) Comparison of Archean dunites and komatiites associated with nickel mineralization in Western Australia: Implications for dunite genesis. *Mineralium Deposita*, v 21, pp 296-305
- Donnell JR (1961) Tertiary geology and oil-shale resources of the Piceance Creek Basin between Colorado and White Rivers, Northwestern Colorado. *U.S. Geol Surv Bull 1082-L*
- Donnelly TW, Rodgers JJW (1980) Igneous series in island arcs: The northeastern Caribbean compared with worldwide arc assemblages. *Bull Volcanol*, v 3, pp 347-382
- Dorr JvN 2nd (1969) Physiographic, stratigraphic and structural development of the Quadrilátero Ferrífero, Minas Gerais, Brazil. *U.S. Geol Surv Profess Paper 641-A*, 110 p
- Dorr JvN III, Barbosa ALM (1963) Geology and ore deposits of the Itabira district, Minas Gerais, Brazil. *U.S. Geol Surv Profess Paper 341-C*, 110 p

- Doyle M (2003) Cobre Las Cruces SA, Las Cruces mineral deposit website & oral communication, 2003
- Dressler BO, Gupta VK, Muir TL (1991) The Sudbury structure, *in*: Ontario Geol Surv Spec Vol 4, Part 1, pp 593-625
- Drew LJ, Berger BR (1996) Geology and structural evolution of the Muruntau gold deposit, Kyzylkum desert, Uzbekistan. *Ore Geol Reviews*, v 11, pp 175-196
- Drew LJ, Meng Qingrun, Sun Weijun (1989) Geologic setting of iron-niobium-rare earth orebodies at Bayan Obo, Inner Mongolia, China, and a proposed regional model. *U.S. Geol Surv Circular* 1035, pp 14-15
- Drexel JF, Preiss WW, Parker AJ, eds (1993) *The Geology of South Australia*, v 1, The Precambrian. South Austr Mines and Energy, Bulletin 54, pp 51-105
- Drummond AD, Sutherland-Brown A, Young RJ, Tennant SJ (1976) Gibraltar-regional metamorphism, mineralization, hydrothermal alteration and structural development. *CIM Spec Volume* 15, pp 195-205
- Druzhinin IP (1973) *Litologiya karbonovykh otlozhenii Dzezkazganskoi vpadiny i genezis plastovykh sulfidnykh rud*. Trudy AN SSSR, Vyp 222, Nauka, Moscow, 187 p
- Drysdall AR, Jackson NJ, Ramsay CR, Douch CJ, Hackett D (1984) Rare element mineralization related to Precambrian alkali granites in the Arabian Shield. *Econ Geol*, v 79, pp 1366-1377
- du Bray EA, ed (1995) *Preliminary Compilation of Descriptive Geoenvironmental Mineral Deposit Models*. U.S. Geol Surv Open File Rept 95-831, 272 p
- Duchesne JC (1999) Fe-Ti deposits in Rogaland anorthosites (South Norway): Geochemical characteristics and problems of interpretation. *Mineralium Deposita*, v 34, pp 182-198
- Duckworth RC, Shanks WC III, Teagle DAH, Zierenberg RA (1998) High grade sediment-hosted sulfide deposits on the seafloor. *Soc Econ Geol Newsletter*, No 32, pp 20-21
- Dudkin OB (1993) Gigantskie konsentratsii fosfora v Khibinakh. *Geol Rud Mestorozhd*, v 35, pp 195-204
- Duffield WA, Sharp RW (1975) *Geology of the Sierra Foothills melange and adjacent areas, Amador County, California*. U.S. Geol Surv Prof Paper 827, pp 1-30
- Duncan RK, Willett GC (1990) Mount Weld carbonatite, *in*: FE Hughes, ed, pp 591-597
- Dunham K, Beer KE, Ellis RA, et al (1978) United Kingdom, *in*: *Mineral Deposits of Europe*, v 1. IMM/Miner Soc, London, pp 263-317
- Dymond J, et al (1973) Origin of metalliferous sediments from the Pacific Ocean. *Geol Soc Amer Bulletin*, v 84, pp 3355-3372
- Eales HV, Cawthorn RG (1996) The Bushveld Complex, *in*: RG Cawthorn, ed, *Layered Intrusions*. Elsevier, Amsterdam, pp 181-229
- Eaton GP (1982) The Basin and Range Province; origin and tectonic significance. *Annual Revs of Earth and Planet Sci*, v 8, pp 409-440
- Eaton PC, Setterfield TN (1993) The relationship between epithermal and porphyry hydrothermal systems within the Tavua caldera, Fiji. *Econ Geol*, v 88, pp 1053-1083
- Eckstrand OR (1996) Magmatic nickel-copper-platinum group elements, *in*: *Geology of Canada*, No 8. Geol Surv Canada, pp 584-605
- Eckstrand OR, Sinclair WD, Thorpe RI, eds (1996) *Geology of Canadian Mineral Deposit Types*. Geology of Canada no 8, Geol Surv Canada, 640 p
- ECMDC (The Editorial Committee of the Mineral Deposits of China) (1992) *Mineral Deposits of China*, v 2. Geol Publ House, Beijing
- Economic Geology* (1977) Special Issue 3, v 72, on Viburnum Trend
- Economic Geology* (1978) An issue devoted to the Bingham mining district, v 73, No 7
- Edwards MJ (1986) *Minera Aguilar*. *Mining Magazine*, 1986, pp 476-479
- Edwards SJ, Pearce JA, Freeman J (2000) New insights concerning the influence of water during the formation of podiform chromitite. *Geol Soc Am, Spec Pap* 349, pp 139-147
- Eganov EA, Sovetov YuK, Yanshin AL (1986) Proterozoic and Cambrian phosphorites-deposits Karatau, Southern Kazakhstan, USSR, *in*: PJ Cook and JH Shergold, eds, *Phosphate Deposits of the World*, v 1. Cambridge Univ Press, pp 175-189
- Ehrenberg R (1866) *Das Zeitalter der Fugger*. Jena
- Ehrenberg H, et al (1954) *Das Schwefelkies-Zinkblende-Schwerspatlager von Meggen (Westfalen)*. *Beih Geol Jahrb*, v 12, 352 p
- Einaudi MT (1977) Environment of ore deposition at Cerro de Pasco, Peru. *Econ Geol*, v 72, pp 893-924
- Einaudi MT (1982) Description of skarns associated with porphyry copper plutons, *in*: SR Titley, ed, *Advances in Geology of the Porphyry Copper Deposits*. Univ of Arizona Press, Tucson, pp 139-183
- Einaudi MT (1992) Ore deposits in the Oquirrh and Wasatch Mountains, Utah: Examples of large-scale water-rock interaction, *in*: Kharaka and Maest, eds, *Water-Rock Interaction*. Balkema, Rotterdam, pp 879-883
- Einaudi MT, Meinert LD, Newberry RJ (1981) Skarn deposits. *Econ Geol* 75th Anniv Vol, pp 317-391
- Einsele G (1992) *Sedimentary Basins*. Springer-Verlag, 628 p
- Elevatorski EA (1996) *Gold Resources of Asia*. Minobras, Fallbrook, California, 178 p
- El Koury W, Júnior AA (1988) Mina de estanho de Pitinga, Amazonas, *in*: C Schobbenhaus and CES Coelho, eds, v III, pp 201-211
- Elliott JE (1992) Tungsten-geology and resources of deposits in Southeastern China. *U.S. Geol Surv Bull* 1877, pp 11-20
- Emery KD (1965) Some potential mineral resources of the Atlantic continental margin. *U.S. Geol Surv Prof Paper* 525-C, pp 157-160
- Emery KD, Uchupi E (1984) *The Geology of the Atlantic Ocean*. Springer-Verlag, New York, 1050 p
- Emmons SF, Irving JD, Laughlin GF (1927) *Geology and ore deposits of the Leadville mining district, Colorado*. U.S. Geol Surv Prof Paper 148, 368 p

- Emmons WH (1913) The Enrichment of Sulphide Ores. U.S. Geol Surv Bull 529, 260 p
- Emsbo P, Hofstra AH, Lauha EA, Griffin GL, Hutchinson RW (2003) Origin of high-grade gold ore, source of ore fluid compounds and genesis of the Meikle and neighbouring Carlin-type deposits, Northern Carlin Trend, Nevada. *Econ Geol*, v 98, pp 1009-1105
- Engelbrecht CJ, Baumbach GWS, Matthyssen JL, Fletcher P (1986) The West Wits Line, *in*: CR Anhaeusser and S Maske, eds, pp 599-648
- Engell J, Hansen J, Jensen M, Kunzendorf H, Lovborg L (1971) Beryllium mineralization in the Ilímaussaq intrusion, South Greenland, with description of a field beryllometer and chemical methods. *Grønland Geol Unders*, Rapport Nr 33, 40 p
- Enns S, Thompson FHT, Stanley CR, Yarrow E (1995) The Galore Creek porphyry Cu-Au deposits, northwestern British Columbia. *CIM Spec Vol 46*
- Epstein EM, Danil'chenko NA, Postnikov SA (1994) Geology of the unique Tomtor deposit of rare metals (north of the Siberian Platform). *Geol of Ore Deposits*, v 36, pp 75-100
- Ercker L (1574) Beschreibung aller gurnemisten mineralischen Erz- und Bergwerksarten. Prague
- Eremin RA, Voroshin SV, Sidorov VA, Shaktyrov VG, Pristavko VA, Gashtold VV (1994) Geology and genesis of the Natal'ka gold deposit, Northeast Russia. *Intern Geol Rev*, v 36, pp 1113-1138
- Ericksen GE (1993) Upper Tertiary and Quaternary continental saline deposits in the central Andean region. *Geol Assoc Canada, Spec Paper 40*, pp 89-102
- Ericksen GE, Eyzaguirre VR, Urquidi FB, Salas RO (1987) Neogene-Quaternary volcanism and mineralization in central Andes. *Transact of the 4th Circum-Pacific Energy and Miner Res Conf*, Singapore, pp 537-549
- Ericksen GE, Pinochet MTC, Reinemund JA, eds (1989) Geology of the Andes and its relation to hydrocarbon and mineral resources. *Circum-Pacific Council for Energy and Mineral Resources*, Houston, 452 p
- Ericksen GE, Salas RO (1989) Geology and resources of salars in the central Andes, *in*: GE Ericksen et al, eds, 1989, pp 151-164
- Erickson RL (1973) Crustal abundance of elements and mineral reserves and resources. *U.S. Geol Surv Prof Paper 820*, pp 21-25
- Eriksson SC (1989) Phalaborwa: a saga of magmatism and miscibility, *in*: K Bell, ed, *Carbonatites, Genesis and Evolution*. Unwin Hyman, London, pp 221-254
- Ernst RE, Bell K, Ranalli G, Halls HC (1987) The Great Abitibi Dyke, southeastern Superior Province, Canada. *Geol Assoc Canada, Spec Paper 34*, pp 123-135
- Estrada CF (1975) Geología de Quellaveco. *Bol de la Soc Geol del Perú*, v 46, pp 65-86
- Ettlinger AD, Meinert LD, Ray GE (1992) Gold skarn mineralization and fluid evolution in the Nickel Plate deposit, British Columbia. *Econ Geol*, v 87, pp 1541-1565
- Eugster HP (1985) Oil shales, evaporites and ore deposits. *Geoch Cosmoch Acta*, v 49, pp 619-635
- Eugster HP, Hardie LA (1975) Sedimentation in an ancient playa-lake complex: The Wilkins Peak Member of the Green River Formation of Wyoming. *Geol Soc Amer Bull*, v 86, pp 319-334
- Eupene GS, Gee PH, Colville RG (1975) Ranger One uranium deposit, *in*: CL Knight, ed, pp 307-317
- Evans HJ (1975) Weipa bauxite deposits, Q, *in*: CL Knight, ed, pp 959-964
- Exon NF, Stewart WD, Sandy MJ, et al (1986) Geology and offshore petroleum prospects of the eastern New Ireland Basin, northeastern Papua New Guinea. *BMR Journ of Austral Geol and Geophys*, v 10, pp 39-51
- Eyles N, Miall AD (1984) Glacial facies, *in*: RG Walker, ed, *Facies Models*, 2nd ed. *Geoscience Canada Reprint Ser 1*, pp 15-38
- Fan Delian (1988) Ore deposits associated with black shale series in the central region of Hunan Province. *IAS Intern Sympos on Sedimentology Related to Miner Dep*, Beijing, *Guidebook Excursion B5*, 15 p
- Fan Delian, Ye Jie, Lui Tiebing (1992) Black shale series-hosted silver vanadium deposits of the Upper Sinian Doushantuo Formation, western Hubei Province, China. *Explor Mining Geol*, v 1, pp 29-38
- Farias NF, Saueressig R (1982) Salobo 3A copper deposit. *Sympos on Archean and Early Proterozoic Geol Evol and Metallogeny*, Salvador, pp 67-71
- Faure G (2001) *Origin of Igneous Rocks. The Isotopic Evidence*. Springer-Verlag, 496 p
- Favorskaya MA, Tomson IN, Baskina VA, Volchanskaya IK, Polyakova OP (1974) Globalnye Zakonomernosti v Razmeshchenii Krupnykh Rudnykh Mestorozhdenii. Nedra, Moscow, 192 p
- Fazakerley VW, Monti R (1998) Murrin Murrin nickel-cobalt deposits, *in*: DA Berkman, DH Mackenzie, eds, pp 329-334
- Fedikow MAF, Bezys RK, Bamburak JD, Abercombie HJ (1996) Prairie-type micro-disseminated Au mineralization-a new deposit type in Manitoba's Phanerozoic rocks (NTS 63C/14). *Manitoba Energy and Mines, Minerals Division, Report of Activities 1996*, pp 108-121
- Fedorovskii VS (1972) Stratigrafiya Nizhnego Proterozoya Khrebtov Kodar i Udokan. *Nauka, Moscow*, 130 p
- Feebrey CA, Hayashi T, Taguchi S, eds (2001) Epithermal gold mineralization and modern analogues, Kyushu, Japan. *Econ Geol Guidebook Series GB 34*, 188 p
- Feng R, Abercombie HJ (1994) Disseminated Au-Ag-Cu mineralization in the Western Canada sedimentary basin, Fort MacKay, northeastern Alberta: A new gold deposit type. *Geol Surv Canada, Current Research 1994-E*, pp 121-132
- Ferguson J (1964) Geology of the Ilímaussaq alkaline intrusion, South Greenland. *Bull Grønland Geol Unders*, v 39, 82 p
- Ferguson J, Goleby AB, eds (1980) Uranium in the Pine Creek Geosyncline. *IAEA, Vienna*, 760 p
- Ferguson KM (1999) Lead, zinc and silver deposits of Western Australia. *Geol Surv W Australia Miner Res Bull 15*, 314 p

- Ferguson SA, et al (1968) Geology and ore deposits of Tisdale Township, District of Cochrane. Ontario Dept of Mines, Geol Rept 58, 177 p
- Fernandez HE, Damasco FW, Sangalang LA (1979) Gold ore shoot development in the Antamok Mines, Philippines. *Econ Geol*, v 74, pp 606-627
- Ferrell JE (1985) Lithium, *in*: Mineral Facts and Problems, 1985 edition, U.S. Bur Mines Bull 675, pp 461-470
- Ferris GM, Schwarz MP, Heithersay P (2002) The geological framework, distribution and controls of Fe-oxide Cu-Au mineralization in the Gawler Craton, South Australia. Part 1 geological and tectonic framework, *in*: TM Porter, ed, Hydrothermal Iron Oxide Copper-gold and Related Deposits: A Global Perspective, v 2. PGC Publ, Adelaide, pp 9-31
- Fersman AYe (1933) *Geokhimiya*. 1955 reprint, Akad Nauk SSSR, Moscow, 798 p
- Field CW, Rye RO, Dymond JR, et al (1983) Metalliferous sediments of the East Pacific, *in*: WC Shanks III, ed, Cameron Volume on Nonconventional Mineral Deposits. AIME, New York, pp 133-156
- Finch WI (1967) Geology of epigenetic uranium deposits in sandstone in the United States. U.S. Geol Surv Profess Paper 538, 121 p
- Fisher DM (1996) Fabrics and veins in the forearc: a record of cyclic fluid flow at depth of < 15 km. *Geophys Monogr* 96, Amer Geophys Union, pp 75-89
- Flawn PT (1970) *Environmental Geology: Conservation, Land Use Planning, and Resource Management*. Harper and Row, New York
- Fleischer VD, Garlick WG, Haldane R (1976) Geology of the Zambian Copperbelt, *in*: KH Wolf, ed, *Geology of Stratiform and Stratabound Ore Deposits*. Elsevier, Amsterdam, v 6, pp 113-352
- Fletcher CJN (1984) Strata-bound, vein and breccia-pipe tungsten deposits of South Korea. *Trans Inst Min Metall*, Sect B, v 93, London, pp B176-B187
- Flint DJ, Rogerson R (2002) Declining greenfields exploration in Western Australia, 1996-2002, *in*: J Bowler, Ministerial inquiry into greenfields exploration in Western Australia. WA Dept of Mines and Petrol Res, pp 27-39
- Flint RF, Sanders JE, Rodgers J (1960) Diamictite, a substitute term for symmictite. *Bull Geol Soc Amer*, v 71, p 1809
- Flint S, Turner P, Jolley EJ, Hartley AJ (1993) Extensional tectonics in convergent margin basins: An example from the Salar de Atacama, Chilean Andes. *Geol Soc Amer Bull*, v 105, pp 603-617
- Floyd PA (1989) Geochemical features of intraplate oceanic plateau basalts. *Geol Soc London, Spec Publ* No 42, pp 215-230
- Floyd PA, ed (1991) *Oceanic Basalts*. Blackie and Van Nostrand Reinhold, 456 p
- Flügel E (1982) *Microfacies Analysis of Limestones*. Springer-Verlag, 633 p
- Fogwill WD (1985) Canadian and Saskatchewan uranium deposits: Compilation, metallogeny, models, exploration. *CIM Spec Vol* 32, pp 3-19
- Foley JY, Light TD, Nelson SW, Harris RA (1997) Mineral occurrences associated with mafic-ultramafic and related alkaline complexes in Alaska. *Econ Geol Monogr* 9, pp 396-449
- Fontboté L, Bendežú R (1999) The carbonate-hosted Zn-Pb San Gregorio deposit, Colquijirca district, central Peru, as part of a high sulfidation epithermal system, *in*: CJ Stanley et al, eds, *Mineral Deposits: Processes to Processing*. Balkema, Rotterdam, pp 495-498
- Foo ST, Hays RC Jr, McCormack JK (1996) Geology and mineralization in the Pipeline gold deposit, Lander County, Nevada, *in*: AR Coyner, PL Fahey, eds, *Geology and Ore Deposits of the American Cordillera*. Geol Soc Nevada, Sympos Proc, Reno, pp 95-109
- Foose MP, Bryant K (1993) *Annotated Bibliography of Metallogenic Maps*. U.S. Geol Surv Open File Rept QF 93-0208A,B
- Force ER, Cannon WF (1988) Depositional model for shallow marine manganese deposits around black shale basins. *Econ Geol*, v 83, pp 93-117
- Force ER, Eidel JJ, Maynard JB, eds (1991) *Sedimentary and Diagenetic Mineral Deposits: a Basin Analysis Approach to Exploration*. *Reviews in Econ Geol*, v 5, 216 p
- Force ER, Maynard JB (1991) Manganese: syngenetic deposits on the margins of anoxic basins, *in*: ER Force et al, eds, pp 147-157
- Ford TD (1976) The ores of the South Pennines and Mendip Hills, England—a comparative study, *in*: KH Wolf, ed, *Handbook of Stratiform and Strata-Bound Ore Deposits*, v 2. Elsevier, Amsterdam, pp 161-195
- Forrestal PJ (1900) Mount Isa and Hilton silver-lead-zinc deposits, *in*: FE Hughes, ed, pp 927-934
- Forsell P, Godin L (1980) Geology of the Kiruna area. 26th Intern Geol Congr, Guidebook, pp 143-150
- Forster DB, Seccombe PK, Phillips D (2004) Controls on skarn mineralization and alteration at the Cadia deposits, New South Wales, Australia. *Econ Geol*, v 99, pp 761-788
- Foster RP, ed (1991) *Gold Metallogeny and Exploration*. Blackie, London
- Fountain DM, Christensen NI (1989) Composition of the continental crust and upper mantle, a review. *Geol Soc Amer Memoir* 172, pp 711-742
- Fountain RC, Hayes AW (1979) Uraniferous phosphate resources of the southeastern United States. U.S. Dept of Energy Publ GJBX-110, pp 65-122
- Fouquet Y, et al (1993) Metallogenesis in back-arc environments: The Lau Basin example. *Econ Geol*, v 88, pp 2154-2181
- Fouquet Y, Herzig PM (1991) Metallogenesis and associated gold mineralization in the Lau back-arc basin, *in*: M Pagel, JL Leroy, eds, *Source, Transport and Deposition of Metals*. Balkema, Rotterdam, pp 615-618
- Fouquet Y, Wafik A, Cambor P, Mevel C, Meyer G, Gente P (1993) Tectonic setting and mineralogical and geochemical zonation in the Snake Pit sulfide deposit (Mid-Atlantic Ridge at 23°N) *Econ Geol*, v 88, pp 2018-2036

- Fourie PJ (2000) The Vergenoeg fayalite iron oxide fluorite deposit, South Africa: Some new aspects, *in*: TM Porter, ed, Hydrothermal Iron Oxide Copper-gold and Related Deposits: A Global Perspective. AMF, Adelaide, pp 309-320
- Fourie PJ, De Jager (1986) Phosphate in the Phalaborwa Complex, *in*: CR Anhaeusser, S Maske, eds, pp 2239-2253
- Forster DB, Secombe PK, Phillips D (2004) Controls on skarn mineralization and alteration at the Cadia deposits, New South Wales, Australia. *Econ Geol*, v 99, pp 761-788
- Fortuna J, Kesler SE, Stenger DP (2003) Source of iron for sulfidation and gold deposition, Twin Creeks Carlin-type deposit, Nevada. *Econ Geol*, v 98, pp 1213-1224
- Frakes L, Bolton B (1992) Effects of ocean chemistry, sea level and climate on the formation of primary sedimentary manganese ore deposits. *Econ Geol*, v 87, pp 1207-1217
- Frakes LA, Francis JE, Sykes JJ (1992) Climate models of the Phanerozoic. Cambridge Univ Press, 271 p
- Francheteau J, et al (1979) Massive deep-sea sulfide ore deposits discovered on the East Pacific Rise. *Nature*, v 277, pp 523-528
- François A (1962) Cadre tectonique général, *in*: J Lombard, P Nicolini, eds, pp 52-76
- François A (1974) Stratigraphie, tectonique et minéralisations dans l'arc cuprifère du Shaba (République de Zaïre), *in*: P Bartholomé, ed, pp 79-101
- Franklin JM (1993) Volcanic-associated massive sulfide deposits. *Geol Assoc Canada, Spec Paper 40*, pp 315-334
- Franklin JM, Lydon JW, Sangster DF (1981) Volcanic-associated massive sulfide deposits. *Econ Geol 75th Anniv Vol*, pp 485-627
- Fraser DC (1961) Cupriferous peat: Embryonic copper ore? *CIM Transact*, v LXIV, pp 301-304
- Fraser RJ (1993) The Lac Troilus gold-copper deposit, northwestern Quebec: A possible Archean porphyry copper. *Econ Geol*, v 88, pp 1685-1699
- Freeman P (1991) The Lumwana copper deposit. ZCCM Rept, unpublished, 6 p
- Freitas-Silva FH, Dardenne MA, Jost H (1991) Lithostructural control of the Morro do Ouro, Paracatú, Minas Gerais, gold deposit, *in*: EA Ladeira, ed, *Gold '91*. Balkema, Rotterdam, pp 681-683
- Fries C (1991) Pachuca-Real del Monte mining district, Hidalgo. *The Geology of North America*, v P-3, *Geol Soc Amer, Boulder*, pp 323-326
- Frimmel HE, Deane JG, Chadwick PJ (1996) Pan-African tectonism and the genesis of base metal sulfide deposits in the northern foreland of the Damara orogen, Namibia. *Soc Econ Geol, Spec Publ No 4*, pp 204-217
- Fritz WH, Cecile MP, Norford BS, Morrow D, Geldsetzer HHJ (1991) Cambrian to Middle Devonian assemblages, *in*: H Gabrielse, CJ Yorath, eds, *Geology of the Cordilleran Orogen in Canada. Geology of Canada No 4*, pp 151-218
- Frondel C, Baum JL (1974) Structure and mineralogy of the Franklin zinc-iron-manganese deposit, New Jersey. *Econ Geol*, v 69, pp 157-180
- Frutos JJ, Oyarzún MJ (1975) Tectonic and geochemical evidence concerning the genesis of El Laco magnetite lava flow deposits, Chile. *Econ Geol*, v 70, pp 988-990
- Fryer P (1996) Evolution of the Mariana convergent plate margin system. *Reviews in Geophys*, v 34, pp 89-125
- Fryer P, Hussong DM (1981) Seafloor spreading in the Mariana Trough: Results of Leg 60 drill site selection surveys. *Initial Reports Deep Sea Drilling Project*, v 60, pp 45-55
- Fryer P, Lockwood JP, Becker W, Phipps S, Todd CS (2000) Significance of serpentinite and volcanism in convergent margins. *Geol Soc Amer Spec Paper 349*, pp 35-51
- Fryklund VC, Jr (1964) Ore deposits of the Coeur d'Alene district, Shoshone County, Idaho. *U.S. Geol Surv Profess Paper 445*, 103 p
- Fu M, Changkakoti A, Krouse HR, et al (1991) An oxygen, hydrogen, sulfur and carbon isotope study of carbonate-replacement (skarn) tin deposits of the Dachang tin field, China. *Econ Geol*, v 86, pp 1683-1703
- Fyfe WS, Price NJ, Thompson AB (1978) *Fluids in the Crust*. Elsevier, Amsterdam, 383 p
- Fyon JA, Bennett G, Jackson SL, Garland MI, Easton RM (1992) Metallogeny of the Proterozoic Eon, northern Great Lakes region, Ontario, *in*: LC Thurston, ed, *Geology of Ontario. Ontario Geol Surv Spec Vol 4*, Pt 2, pp 1177-1216
- Fyon JA, Breaks FW, Heather KB, Jackson SL, Muir TL, Stott GM, Thurston PC (1991) Metallogeny of metallic mineral deposits in the Superior Province of Ontario, *in*: *Geology of Ontario, Ontario Geol Surv Spec Vol 4*, pp 1091-1174
- Gablin IF (1981) New data on formation conditions of the Dzhezkazgan copper deposit. *Intern Geol Rev*, v 23, pp 1303-1311
- Gabrielse H, Campbell RB (1992) Upper Proterozoic assemblages, *in*: H Gabrielse, CJ Yorath, eds, pp 125-150
- Gabrielse H, Yorath CJ, eds (1992) *Geology of the Cordilleran Orogen in Canada, in: Geology of Canada, No 4. Geol Surv of Canada*, 844 p
- Galley AG, Koski RA (1999) Setting and characteristics of ophiolite-hosted volcanogenic massive sulfide deposits. *Reviews in Econ Geol No 8*, pp 221-246
- Galley AG, Bailes AH, Syme EC, Bleeker W, Macek JJ, Gordon TM (1990) Geology and mineral deposits of the Flin Flon and Thompson belts, Manitoba. 8th IAGOD Sympos, Ottawa, *Field Trip 10 Guidebook, Geol Surv Canada Open File 2165*, 136 p
- Gallon ML (1986) Structural re-interpretation of the Selebi-Phikwe nickel-copper sulfide deposits, eastern Botswana, *in*: CR Anhaeusser, S Maske, eds, pp 1663-1669
- Galloway WE, Hobday DK (1983) *Terrigenous Clastics Depositional Systems-Applications to Petroleum, Coal and Uranium Exploration*. Springer-Verlag, New York, 423 p

- Galloway WE, Kreitler CW, McGowen JH (1979) Depositional and ground-water flow systems in the exploration for uranium. *Texas Bur Econ Geol*, Austin, 228 p
- Gandhi SM, Paliwal HV, Bhatnagar SN (1984) Geology and ore reserve estimates of Rampura-Agucha zinc-lead deposit, Bhilwara district, Rajasthan. *Journ Geol Soc India*, v 25, pp 689-705
- Gans PB, Mahood GA, Schermer E (1989) Synextensional magmatism in the Basin and Range Province; A case study from the eastern Great Basin. *Geol Soc Amer, Spec Paper* 233, 53 p
- Garcia JS Jr (1991) Geology and mineralization characteristics of the Mankayan mineral district, Benguet, Philippines. *Geol Surv Japan Rept* 277, pp 21-30
- Garcia Palomero F (1979) Geology of the Rio Tinto mines. *Minera Rio Tinto*, unpublished, 19 p
- Garkovets VG, Mushkin IV, Titova AP, et al (1979) Osnovnye Cherty Metallogenii Uzbekistana. *AN Uzbek SSR, Tashkent*, 272 p
- Garlick WG (1973) The Nchanga Granite. *Spec Publ Geol Soc South Africa*, pp 455-476
- Garlick WG (1967) Special features and sedimentary facies of stratiform sulfide deposits in arenites, *in: Proc 15th Inter-Univ Geol Conf*, Leicester, pp 107-169
- Garrels RM, Mackenzie FT, Hunt C (1975) *Chemical Cycles and the Global Environment*. Kaufmann, Los Angeles
- Gartz VH, Frimmel HE (1999) Complex metamorphism of an Archean placer in the Witwatersrand Basin, South Africa: The Ventersdorp Contact Reef-a hydrothermal aquifer? *Econ Geol*, v 94, pp 689-706
- Garven G, Appold MS, Toptygina VI, Hazlett TJ (1998) Hydrologic modelling of the genesis of carbonate-hosted lead-zinc ores. *Hydrogeology Journal*, v 7, pp 108-126
- Gass IG (1968) Is the Troodos massif of Cyprus a fragment of Mesozoic ocean floor? *Nature* v 220, London, pp 39-42
- Gatter I, Molnár F, Földessy J, Zelenka T, Kiss J, Szebényi G (1999) High and low-sulfidation epithermal mineralization of the Mátra Mountains, Northeast Hungary. *Econ Geol Guidebook Ser*, v 31, pp 155-170
- Gavshin VM, Zakharov VA (1996) Geochemistry of the Upper Jurassic-Lower Cretaceous Bazhenov Formation, West Siberia. *Econ Geol*, v 91, pp 122-133
- Geijer P (1964) On the origin of the Falun type of sulfide mineralization. *Geol Foren Förh*, v 86, pp 2-27
- Genkin AD, Lapatin BA, Savelyev RA, et al (1994) Gold ore in the Olympiad deposit, Yenisei Ridge, Siberia. *Geol of Ore Deposits*, v 36, pp 111-137
- Gente P, Auzende JM, Renard V, Fouquet Y, Bideau D (1986) Detailed geological mapping by submersible of the East Pacific Rise axial graben near 13°N. *Earth and Planet Sci Letters*, v 78, pp 224-236
- Geological Survey of Western Australia (1990) *Geology and Mineral Resources of Western Australia*. *WA Geol Surv Mem* 3, 827 p
- Gerasimovsky VI, Volkov VOP, Kogarko LN, Polyakov AI, Saprykina TV, Balashov YA (1966) *The Geochemistry of the Lovozero Alkaline Massif, Part 1+2*. Engl Transl, Austral Nat Univ, Canberra
- German CR, Higgs NC, Thomson J, et al (1993) A geochemical study of metalliferous sediment from the TAG hydrothermal mound, 26°08' N, Mid-Atlantic Ridge. *Journ Geophys Res*, v 98, pp 9683-9692
- Ghisler M, Windley BF (1967) The chromite deposits of the Fiskenaesset region, West Greenland. *Gronl Geol Unders*, Rept 12, 39 p
- Gibson HL, Watkinson DH, Comba CDA (1989) Subaqueous phreatomagmatic explosion breccias at Buttercup Hill, Noranda, Quebec. *Canad Journ Earth Sci*, v 26, pp 1428-1439
- Gilg HA, Frei R (1994) Chronology of magmatism and mineralization in the Kassandra mining area, Greece: The potentials and limitations of dating hydrothermal illites. *Geoch Cosmoch Acta*, v 58, pp 2107-2122
- Gill JB (1981) *Orogenic Andesites and Plate Tectonics*. Springer-Verlag, 390 p
- Gilluly J (1946) The Ajo mining district. *U.S. Geol Surv Prof Paper* 209, 112 p
- Giuliani G (1985) Le gisement de tungstène de Xihuashan (Sud-Jiangxi, Chine): Relations granites, alterations deutériques-hydrothermales, minéralisations. *Mineralium Deposita*, v 20, pp 107-115
- Giuliani G, Li YD, Sheng TF (1988) Fluid inclusion study of Xihuashan tungsten deposit in the southern Jiangxi Province, China. *Mineralium Deposita*, v 23, pp 24-33
- Glasby GP, Read AJ (1976) Deep-sea manganese nodules, *in: KH Wolf, ed, Handbook of Stratiform and Strata-Bound Ore Deposits*, v 7, Elsevier, Amsterdam, pp 295-340
- Glasson KR, Rattigan JH, eds (1990) *Geological Aspects of the Discovery of Some Important Mineral Deposits in Australia*. AusIMM, Parkville, 503 p
- Gleadow AJW, Brooks CK (1979) Fission track dating, thermal histories and tectonics of igneous intrusions in East Greenland. *Contrib Miner Petrol*, v 71, pp 45-60
- Goad RE, Mumin AH, Duke NA, Neale KL, Mulligan DL (2000) Geology of the Proterozoic iron oxide-hosted NICO cobalt-gold-bismuth, and Sue-Dianne copper-silver deposits, southern Great Bear magmatic zone, Northwest Territories, Canada, *in: TM Porter, ed, Hydrothermal Iron Oxide Copper-gold and Related Deposits: A Global Perspective*. AMF, Adelaide, pp 249-267
- Goff F, et al (1994) Gold degassing and deposition at Galeras Volcano, Colombia. *GSA Today*, v 4, No 10, pp 243-247
- Gokçe A, Spiro B (1991) Sulfur isotope study of source and deposits of stibnite in the Turhal area, Turkey. *Mineralium Deposita*, v 26, pp 30-33
- Goldfarb RJ, et al (2004) The late Cretaceous Donlin Creek gold deposit, Southwestern Alaska: Controls on epizonal ore formation. *Econ Geol*, v 99, 643-671
- Goldfarb RJ, Groves DI, Gardoll S (2001) Orogenic gold and geologic time: A global synthesis. *Ore Geol Rev*, v 13, pp 185-217

- Goldfarb RJ, Miller LD, eds (1997) Mineral Deposits of Alaska. *Econ Geol Monogr* 9, 483 p
- Goldfarb RJ, Miller LD, Leach DL, Snee LW (1997) Gold deposits in metamorphic rocks of Alaska. *Econ Geol Monogr* 9, pp 151-190
- Goldfarb RJ, Snee LW, Pickthorn WJ (1993) Orogenesis, high-T thermal events, and gold vein formation within metamorphic rocks of the Alaskan Cordillera. *Min Mag*, v 57, pp 375-394
- Goldthwait RP, Matsch CL, eds (1989) Genetic Classification of Glaciogenic Deposits. Balkema, Rotterdam, 294 p
- Gonevchuk VG, Gonevchuk GA (1995) Granitoid magmatism and related mineralization in Sikhote Alin. *Resource Geology Spec Issue* 18, Tokyo, pp 134-141
- Goodfellow WD, Franklin JM (1993) Geology, mineralogy and chemistry of sediment-hosted clastic massive sulfides in shallow cores, Middle Valley, northern Juan de Fuca Ridge. *Econ Geol*, v 88, pp 2037-2068
- Goodfellow WD, Lydon JW, Turner RJW (1993) Geology and genesis of stratiform sediment-hosted (SEDEX) zinc-lead-silver sulfide deposits. *Geol Assoc Canada, Spec Paper* 40, pp 201-251
- Goodfellow WD, McCutcheon SR, Peter JM, eds (2003) Massive sulfide deposits of the Bathurst mining camp, New Brunswick, and northern Maine. *Econ Geol Monogr* 11, 930 p
- Goodfellow WD, Zierenberg RA (1997) Genesis of massive sulfide deposits at sediment-covered spreading centres. *Geol Assoc Canada, Short Course Notes* v 13, pp 331-366
- Goodwin AM (1991) Precambrian Geology. The Dynamic Evolution of the Continental Crust. Academic Press, London, 666 p
- Goodwin AM, Monster J, Thade HG (1976) Carbon and sulfur isotope abundances in Archean iron-formations and early Precambrian life. *Econ Geol*, v 71, pp 870-891
- Goodwin AM, Thode HG, Chou CL, Karkhansis SN (1985) Chemostratigraphy and origin of the late Archean siderite-pyrite rich Helen Iron Formation, Michipicoten Belt, Canada. *Canad Journ Earth Sci*, v 22, pp 72-84
- Goossens P, Hollister VF (1973) Structural control and hydrothermal alteration pattern of Chaucha porphyry copper, Ecuador. *Mineralium Deposita*, v 8, pp 321-331
- Gorbunov GI, Yakovlev YuN, Goncharov YuV, Gorelov VA, Tel'nov VA (1985) The nickel areas of the Kola Peninsula. *Geol Surv Finland Bull* 333, pp 41-210
- Gorbunov GI, Zagorodny VG, Robonen WI (1985) Main features of the geological history of the Baltic Shield and the epochs of ore formation. *Geol Surv Finland Bull* 333, pp 17-41
- Gordey SP (1991) Devonian-Mississippian clastics of the Foreland and Omineca Belts, *in*: H Gabrielse, CJ Yorath, eds, pp 230-242
- Gordiyenko VV (1970) Mineralogiya, Geokhimiya i Genezis Spodumenovykh Pegmatitov. Nedra, Leningrad
- Gorelov VA, Turchenko SI (1997) Kola Terrain, *in*: DV Rundkvist and C Gillen, eds, Precambrian Ore Deposits of the East European and Siberian Cratons. Elsevier, Amsterdam, pp 15-50
- Gott GB, Cathrall JB (1980) Geochemical-exploration studies in the Coeur d'Alene district, Idaho and Montana. *U.S. Geol Surv Profess Paper* 1116, 63 p
- Grancea L, et al (2002) Fluid evolution in the Baia Mare epithermal gold/polymetallic district, Inner Carpathians, Romania. *Mineralium Deposita*, v 37, pp 630-647
- Grandia F, Cardellach E, Canals A (1999) Fluid mixing evidence in MVT Zn-Pb deposits related to rift stage carbonates of the Maestrat Basin, Eastern Spain, *in*: CJ Stanley et al, *Mineral Deposits: Processes to Processing*. Balkema, Rotterdam, pp 861-864
- Granger HC, Finch WI (1988) The Colorado Plateau uranium province, *in*: Recognition of Uranium Provinces. IAEA Vienna, pp 157-193
- Grant JN, Halls C, Sheppard SMF, Avila W (1980) Evolution of the porphyry tin deposits of Bolivia. *Mining Geology Spec Issue* No 8, Tokyo, pp 151-173
- Grant RW, Bite A (1984) Sudbury quartz diorite offset dikes, *in*: EG Pye et al, eds, pp 275-300
- Gray MD, Hutchinson RW (2001) New evidence for multiple periods of gold emplacement in the Porcupine mining district, Timmins area, Ontario, Canada. *Econ Geol*, v 96, pp 453-475
- Green GR, Solomon M, Walshe JL (1981) The formation of the volcanic-hosted massive sulfide ore deposits at Rosebery, Tasmania. *Econ Geol*, v 76, pp 304-338
- Green JC (1982) Geology of Keweenawan extrusive rocks. *Geol Soc Amer Mem* 156, pp 47-55
- Greene HG, Wong FL (1989) Ridge collisions along the plate margins of South America compared with those in the Southwest Pacific, *in*: GE Ericksen et al, eds, pp 39-57
- Gregor CB, Garrels RM, Mackenzie FT, Maynard JB, eds (1988) *Chemical Cycles in the Evolution of the Earth*. Wiley, New York
- Grenne T, Ihlen PM, Vokes FM (1999) Scandinavian Caledonide Metallogeny in a plate tectonic perspective. *Mineralium Deposita*, v 34, pp 422-471
- Gresham JJ, Loftus-Hills GD (1981) The geology of the Kambalda nickel field, Western Australia. *Econ Geol*, v 76, pp 1373-1416
- Grieve RAF, Masaitis VL (1994) The economic potential of terrestrial impact craters. *Intern Geol Revs*, v 36, pp 105-151
- Grieve RAF, Therriault A (2000) Vredefort, Sudbury, Chicxulub: three of a kind? *Ann Rev Earth Planet Sci* 2000, v 28, pp 305-338
- Grip E (1978) Sweden, *in*: Bowie SHU et al, eds, *Mineral Deposits of Europe*, v 1. IMM/Miner Soc, London, pp 96-198
- Groff JA, Heizler MT, McIntosh WC, Norman D (1997) $^{40}\text{Ar}/^{39}\text{Ar}$ dating and mineral paragenesis for Carlin-type gold deposits along the Getchell Trend, Nevada: Evidence for Cretaceous and Tertiary gold mineralization. *Econ Geol*, v 92, pp 601-622

- Grogan RM, Bradbury JC (1968) Fluorite zinc-lead deposits of the Illinois-Kentucky mining district, *in*: JD Ridge, ed, Ore Deposits of the United States, 1933-1967. AIME, New York, pp 370-399
- Gross GA (1968) Geology of iron deposits in Canada, v3, Iron ranges of the Labrador Geosyncline. Geol Surv Canada, Econ geol Rept 22, 179 p
- Gross GA (1980) A classification of iron formations based on depositional environments. Canad Mineralog, v 18, pp 215-222
- Gross GA (1996) Stratiform Iron, *in*: Geology of Canada No 8, Geol Surv Canada, pp 41-54
- Gross GA, Zajac IS (1983) Iron-formation in fold belts marginal to the Ungava Craton, *in*: AF Trendal, RC Morris, eds, pp 253-294
- Gross WH (1975) New ore discovery and source of silver-gold veins, Guanajuato, Mexico. Econ Geol, v 70, pp 1175-1189
- Grossi Sad JH, Torres N (1978) Geology and mineral resources of the Barreiro Complex, Araxá, Minas Gerais. Proc First Intern Sympos on Carbonatites, DNPB Brazil, pp 307-312
- Grove TL, Kinzler RJ (1986) Petrogenesis of Andesites. Ann Revs of Earth and Planet Sci, v 145, pp 417-454
- Groves DI (1972) Geology, *in*: A Century of Tin Mining at Mout Bischoff 1871-1971. Tasmania Geol Surv Bull 54, pp 165-258
- Groves DI (1993) The crustal continuum model for late-Archean lode gold deposits of the Yilgarn Block, Western Australia. Mineralium Deposita, v 28, pp 366-374
- Groves DI, Barley ME, Ho SE (1989) Nature, genesis and tectonic setting of mesothermal gold mineralization in the Yilgarn Block, Western Australia. Econ Geol Monogr 6, pp 71-85
- Groves DI, Batt WD (1984) Spatial and temporal variations of Archean metallogenic associations in terms of evolution of granitoid-greenstone terrains with particular emphasis on the Western Australian Shield, *in*: A Kröner, Greiling R, eds, Precambrian Tectonics Illustrated, pp 73-98
- Groves DI, Bettenay LF, Partington GA (1986) The giant Greenbusches pegmatite: An anomalous rare-metal pegmatite in Western Australia. Terra Cognita, v 6, p 529 (abs)
- Groves DI, Foster RP (1991) Archean lode gold deposits, *in*: RP Foster, ed, Gold Metallogeny and Exploration. Blackie, London, pp 63-103
- Groves DI, Goldfarb RJ, Gebre-Mariam M, et al (1997) Orogenic gold deposits: A proposed classification in the context of their crustal distribution and relationship to other gold deposit types. Ore Geol Revs, v 13, pp 7-28
- Groves DI, Goldfarb RJ, Robert F, Hart CJR (2003) Gold deposits in metamorphic belts: Overview of current understanding, outstanding problems, future research, and exploration significance. Econ Geol, v 98, pp 1-29
- Groves DI, Phillips GN, Ho SE, et al (1982) Controls on distribution of Archean hydrothermal deposits in Western Australia, *in*: RP Foster, ed, Gold '82. Balkema, Rotterdam, pp 689-712
- Grushevoi VG et al, eds (1971) Metallogenicheskaya Karta SSSR Mashtaba 1: 2,500,000. 16 sheets, VSEGEI Leningrad
- Gudmundsson A (2000) Dynamics of volcanic systems in Iceland: Example of tectonism and volcanism at juxtaposed hot spot and mid-ocean ridge systems. Ann Revs Earth Planet Sci 2000, v 28, pp 107-140
- Guennoc P, Pouit G, Nawab Z (1988) The Red Sea: History and associated mineralization, *in*: W Manspeizer, ed, Triassic-Jurassic rifting. Elsevier, Amsterdam, pp 957-981
- Guilbert JM, Park CF Jr (1985) The Geology of Ore Deposits. Freeman, New York, 985 p
- Guild PA, et al (1981) Preliminary Metallogenic Map of North America, 1: 5 million. U.S. Geol Survey
- Guiza R Jr (1956) El distrito minero de Guanajuato. 20th Intern Geol Congr, Mexico, Excursion A-2 and A-5, pp 141-152
- Gulbrandsen RA, Krier DJ (1980) Large and rich phosphorus resources in the Phosphoria Formation in the Soda Springs area, Southeastern Idaho. U.S. Geol Surv Bull 1494, 25 p
- Guney M, Al-Marhoun A, Nawab ZA (1988) Metalliferous sub-marine sediments of the Atlantis II-Deep, Red Sea. CIM Bulletin, Febr 1988, pp 33-39
- Gupta AK, Yagi K (1980) Petrology and Genesis of Leucite-Bearing Rocks. Springer-Verlag, 252 p
- Gustafson LB, Hunt JP (1975) The porphyry copper deposit at El Salvador, Chile. Econ Geol, v 70, pp 857-912
- Gutzmer J, Beukes NJ (1995) Fault-controlled metasomatic alteration of early Proterozoic sedimentary manganese ores in the Kalahari manganese field, South Africa. Econ Geol, v 90, pp 823-844
- Gyapong WA, Amanor J (2000) Geology/structural controls of mineralization and exploration potential of the Ashanti-Obuasi mine. Ashanti Obuasi Staff, unpublished, 8 p
- Haapala PS (1968) Fennoscandian nickel deposits, *in*: HDB Wilson, ed, Magmatic Ore Deposits. Econ Geol Monogr 4, pp 262-275
- Haeussler PJ, Bradley D, Goldfarb RJ, Snee LW, Taylor CD (1995) Link between ridge subduction and gold mineralization in southern Alaska. Geology, v 23, pp 995-998
- Hafer MR (1991) Origin and controls of deposition of the Wheal Hughes and Poona copper deposits, Moonta, S. Australia. B.Sc. Hons Thesis, Univ of Adelaide
- Hagni RD (1976) Tri-State ore deposits: the character of their host rocks and their genesis, *in*: KH Wolf, ed, Handbook of Stratiform and Strata-Bound Ore Deposits, v 6, Elsevier, Amsterdam, pp 457-494
- Hagni RD (1989) The Southeast Missouri lead district: A review. Soc Econ Geol Guidebook Ser, v 5, pp 12-57
- Hakim HD, El-Mahdy OR (1992) Sulfide assemblages and metamorphic episodes at Mahd Adh Dhahab gold mine, Kingdom of Saudi Arabia. Journ of the King Abdul-Azis Univ, Jeddah, Earth Sci, v 5, pp 153-175
- Halbach P, Blum N, Münch U, Plüger W, Garbe-Schönberg D, Zimmer M (1998) Formation and decay

- of a modern massive sulfide deposit in the Indian Ocean. *Mineralium Deposita*, v 33, pp 302-309
- Halbach P, Manheim F, Ottan P (1982) Co-rich ferromanganese deposits in the marginal seamount regions of the Central Pacific Basin. *Erzmetall*, v 35, pp 447-453
- Halbach P, Pracejus B, Märten A (1993) Geology and Mineralogy of massive sulfide ores from the Central Okinawa trough, Japan. *Econ Geol*, v 88, pp 2210-2225
- Hälbich IW (1978) Minor structures in gneisses and the origin of steep structures in the O'okiep copper district, *in*: WJ Verwoerd, ed, *Mineralization in Metamorphic Terranes*. *Spec Publ Geol Soc S Africa*, No 4, pp 297-323
- Hall CM, Kesler SE, Simon G, Fortuna J (2000) Overlapping Cretaceous and Eocene alteration, Twin Creeks Carlin-type deposit, Nevada. *Econ Geol*, v 95, pp 1739-1752
- Hall GC, Kneeshaw M (1990) Yandicoogina-Marillana pisolitic iron deposits, *in*: FE Hughes, ed, pp 1581-1586
- Hall WE, Friedman I (1963) Composition of fluid inclusions, Cave-in-Rock fluorite district, Illinois and Upper Mississippi Valley lead-zinc district. *Econ Geol*, v 58, pp 886-911
- Halliday AW (1980) The timing of early and main stage ore mineralization in southeast Cornwall. *Econ Geol*, v 75, pp 752-759
- Halls C (1994) Energy and mechanism in the magmato-hydrothermal evolution of the Cornubian batholith: A review, *in*: R. Seltmann, ed, pp 274-294
- Halls HC, Fahrig WF (1987) Mafic Dyke Swarms. *Geol Assoc Canada, Spec Paper 34*, 503 p
- Hambleton-Jones BB (1982) Uranium occurrences in the surficial deposits of southern Africa, *in*: HW Glen, ed, *Proc of the 12th CMMI Congress*, Johannesburg. *South African Inst Min Metall*, pp 123-136
- Hamilton JM (1982) Geology of the Sullivan orebody, Kimberley, B.C., Canada. *Geol Assoc Canada Spec Paper 25*, pp 597-665
- Hamilton JV, Hodgson CJ (1986) Mineralization and structure in Kolar Gold Field, India, *in*: AJ MacDonald, ed, *Gold '86*, pp 270-283
- Hamilton WB (1979) Tectonics of the Indonesian region. *U.S. Geol Surv Prof Paper 1078*, 345 p
- Hamilton WB (1995) Subduction systems and magmatism. *Geol Soc London, Spec Publ 81*, pp 3-28
- Hamilton WB, Myers WB (1967) The nature of batholiths. *U.S. Geol Survey Prof Paper 554-C*, pp 1-30
- Hancock MC, Maas R, Wilde AR (1990) Jabiluka uranium-gold deposits, *in*: FE Hughes, ed, pp 785-793
- Handley GA, Cary R (1980) Big Bell gold deposit, *in*: FE Hughes, ed, pp 211-216
- Handley GA, Henry DD (1990) Porgera gold deposit, *in*: FE Hughes, ed, pp 1717-1724
- Hanekom HJ, Van Staden CMvH, Smit PJ, Pike DR (1965) Geology of the Palabora igneous complex. *South Afr Dept of Mines, Geol Surv Mem 54*, 185 p
- Hannan KW, Golding SD, Herbert HK, Krouse HR (1993) Contrasting alteration assemblages in metabasites from Mount Isa, Queensland: Implications for copper ore genesis. *Econ Geol*, v 88, pp 1135-1175
- Hannington MD, Barrie TC, eds (1999) The giant Kidd Creek volcanogenic massive sulfide deposit, western Abitibi Subprovince, Canada. *Econ Geol Monogr 10*, 675 p
- Hannington MD, Herzig PM, Scott SD (1991) Auriferous hydrothermal precipitates on the modern seafloor, *in*: RP Foster, ed, *Gold Metallogeny and Exploration*. Blackie, London, pp 249-281
- Hannington MD, Poulsen KH, Thompson JFH, Sillitoe RH (1999) Volcanogenic gold in the massive sulfide environment. *Reviews in Econ Geol 8*, pp 325-352
- Hansen J (1968) Niobium mineralization in the Ilímaussaq alkaline complex, South-West Greenland. *23 Intern Geol Congr, Prague*, v 7, pp 263-273
- Haralyi NLE, Walde DHG (1986) Os minérios de ferro e manganês da região de Urucum, Corumbá, Mato Grosso do Sul, *in*: C Schobbenhaus, CES Coelho, eds, v 2, pp 127-144
- Harmon RS, Rapela CW, eds (1991) Andean Magmatism and its Tectonic Setting. *Geol Soc Amer Spec Paper 265*, 309 p
- Harmsworth RA, Kneeshaw M, Morris RC, Robinson CJ, Shrivastava PK (1990) BIF-derived iron ores of the Hamersley Province, *in*: FE Hughes, ed, pp 617-642
- Harper GD (1984) The Josephine ophiolite, northwestern California. *Geol Soc Amer Bull*, v 95, pp 1009-1026
- Harris DC (1986) Mineralogy and geochemistry of the Main Hemlo gold deposit, Hemlo, Ontario, Canada, *in*: AJ MacDonald, ed, *Gold '86*, pp 297-310
- Harris JF (1961) Summary of the geology of Tanganyika, part IV, Economic Geology. *Geol Surv of Tanganyika, Mem 1*, 143 p
- Harris RH, Lange IM, Krouse HR (1981) Major element and sulfur isotopic variations in the Lower Chester Vein, Sunshine Mine, Idaho. *Econ Geol*, v 76, pp 706-715
- Harris NBW, Pearce JA, Tindle AG (1986) Geochemical characteristics of collision-zone granites. *Geol Soc London, Spec Publ 19*, pp 67-81
- Harshman EN (1972) Geology and uranium deposits, Shirley Basin area, Wyoming. *U.S. Geol Surv Prof Paper 745*, 82 p
- Hart TR, Gibson HL, Leshner CM (2004) Trace element geochemistry and petrogenesis of felsic volcanic rocks associated with volcanogenic massive Cu-Zn-Pb sulfide deposits. *Econ Geol*, v 99, pp 1003-1013
- Harvey BA, Myers SA, Klein T (1999) Yanacocha gold district, northern Peru. *PACRIM '99 Proceedings*, Bali, AusIMM, pp 445-459
- Hatcher MI, Clynick G (1990) Greenbusches tantalum-lithium deposit, *in*: FE Hughes, ed, pp 599-603
- Hattori KH, Cameron EM (2004) Using the high mobility of palladium in surface media in exploration for platinum group element deposits: Evidence from the Lac des Iles region, Northwestern Ontario. *Econ Geol*, v 99, pp 157-171

- Haughton SH, ed (1964) *The Geology of Some Ore Deposits in Southern Africa*, 2 volumes. Geol Soc of S Africa, Johannesburg, 625 p
- Hawkins JW, Evans CA (1983) Geology of the Zambales Range, Luzon, Philippine Islands; ophiolite derived from an island arc-backarc basin pair. *Amer Geophys Union, Monogr* 27, pp 95-123
- Haydon RC, McConachy GW (1987) The stratigraphic setting of Pb-Zn-Ag mineralization in Broken Hill. *Econ Geol*, v 82, pp 826-856
- Haymon RM (1989) Hydrothermal processes and products on the Galapagos Rift and East Pacific Rise, *in: The Geology of North America*, v N. Geol Soc Amer, Boulder, pp 125-144
- Haynes BW, Law SL, Barton DC (1986) An elemental description of Pacific manganese nodules. *Marine Mining*, v 5, pp 239-277
- Haynes DW (2000) Iron oxide copper (-gold) deposits: Their position in the ore deposit spectrum and modes of origin, *in: TM Porter, ed, Hydrothermal Iron Oxide Copper-gold and Related Deposits: A Global Perspective*. AMF, Adelaide, pp 71-90
- Haynes DW, Cross KC, Bills RT, Reed MH (1995) Olympic Dam ore genesis-a fluid mixing model. *Econ Geol*, v 90, pp 281-307
- Heald P, Foley NK, Hayba DO (1987) Comparative anatomy of volcanic-hosted epithermal deposits: Acid-sulfate and adularia-sericite types. *Econ Geol*, v 82, pp 1-26
- Heberlein DR (1995) Geology and supergene processes: Berg copper-molybdenum porphyry, West-Central British Columbia. *CIM Spec Volume* 46, pp 304-312
- Hedström P, Simeonov A, Malmström L (1989) The Zinkgruvan ore deposit, south-central Sweden: A Proterozoic proximal Zn-Pb-Ag deposit in distal volcanic facies. *Econ Geol*, v 84, pp 1235-1261
- Heezen BC (1974) Atlantic-type continental margins, *in: CF Burk, CL Drake, eds, Geology of Continental Margins*. Springer-Verlag, pp 13-24
- Heezen BC, Hollister CD (1971) *The Face of the Deep*. Oxford Univ Press, New York, 658 p
- Hedenquist JW (1995) The ascent of magmatic fluid: Discharge versus mineralization, *in: JFH Thompson, ed, Magmas, Fluids and Ore Deposits*. Miner Assoc of Canada, Short Course v 23, pp 263-289
- Hedenquist JW, Arribas A Jr, Reynolds TJ (1998) Evolution of an intrusion-centered hydrothermal system: Far Southeast-Lepanto porphyry and epithermal Cu-Au deposits, Philippines. *Econ Geol*, v 93, pp 373-404
- Hedenquist JW, Henley RW (1985) Hydrothermal eruptions in the Waiotapu geothermal system, New Zealand: Their origin, associated breccias, and relation to precious metal mineralization. *Econ Geol*, v 80, pp 1640-1668
- Hedenquist JW, Lowenstern JB (1994) The role of magmas in the formation of hydrothermal ore deposits. *Nature*, v 370, pp 519-527
- Heijlen W, et al (2003) Carbonate-hosted Zn-Pb deposits in Upper Silesia, Poland: Origin and evolution of mineralizing fluids and constraints of genetic models. *Econ Geol*, v 98, pp 911-932
- Hein JR, et al (1985) Geological and geochemical data for seamounts and associated ferromanganese crusts in and near the Hawaiian, Johnston Island and Palmyra Island economic zones. U.S. Geol Surv Open File Report 85-292, pp 1-129
- Hein JR, Koschinsky A, Bau M, Manheim FT, Kang J-K, Roberts L (2000) Cobalt-rich ferromanganese crusts in the Pacific, *in: DS Cronan, ed, Handbook of Marine Mineral Deposits*. CRC Press, Boca Raton, pp 239-279
- Heinhorst J, Lehmann B, Seltmann R (1996) New geochemical data on granitic rocks of Central Kazakhstan, *in: V Shatov et al, eds, Granite-related deposits of Central Kazakhstan and adjacent areas*. Glagol, St. Petersburg, pp 55-65
- Heinrich CA, Neubauer F (2002) Cu-Au-Pb-Zn-Ag metallogeny of the Alpine-Balkan-Carpathian-Dinaride geodynamic province. *Mineralium Deposita*, v 37, pp 533-540
- Heinrich EW (1966) *The Geology of Carbonatites*. Rand McNally, Chicago, 555 p
- Heithersay PS, Walshe JL (1995) Endeavour 26 North, a porphyry copper-gold deposit in the Late Ordovician shoshonitic Goonumbra Volcanic Complex, New South Wales, Australia. *Econ Geol*, v 90, pp 1506-1532
- Hékinian R (1982) *Petrology of the Ocean Floor*. Elsevier, Amsterdam, 393 p
- He Lixian, Zeng Ruolan (1992) Mercury deposits of China, *in: ECMDC, eds*, pp 100-149
- Henderson FB, III (1969) Hydrothermal alteration and ore deposition in serpentinite-type mercury deposits. *Econ Geol*, v 64, pp 489-499
- Henderson JB (1970) Stratigraphy of the Archean Yellowknife Supergroup, Yellowknife Bay-Prosperous lake area, District of Mackenzie. *Geol Surv Canada Paper* 70-26, 12 p
- Henley RW, Adams J (1979) On the evolution of giant gold placers. *Trans Inst Min Metall*, London, v B89, pp 41-49
- Henneke J (1977) Die Bergwirtschaftliche Bedeutung der Blei-Zink-Erzlagerstätte Mechernich. *Glückauf*, Essen, v 38, pp 9-18
- Henry CD, Elson HB, McIntosh WC, Heitzler MT, Castor SB (1997) Brief duration of hydrothermal activity at Round Mountain, Nevada, determined from ⁴⁰Ar/³⁹Ar geochronology. *Econ Geol*, v 92, pp 807-826
- Henstock ME (1996) *The Recycling of Nonferrous Metals*. Intern Council on Metals and the Environment, Ottawa, 342 p
- Hepworth JV, Yu Hong Zhang, eds (1982) *Tungsten Geology*, Jiangxi, China. Geol Publ House, Beijing, 583 p
- Hernández A, Jébrak M, Higuera P, Oyarzún R, Morata D, Munhá J (1999) The Almadén mercury mining district, Spain. *Mineralium Deposita*, v 34, pp 539-548
- Herrington RJ, Janković S, Kozelj D (1998) The Bor and Majdanpek copper-gold deposits in the context of the Bor Metallogenic zone (Serbia, Yugoslavia), *in: TM*

- Porter, ed, Porphyry and Hydrothermal Copper and Gold Deposits, a Global Perspective. AMF, Adelaide, pp 169-178
- Herz N (1976) Titanium deposits in alkalic igneous rocks. U.S. Geol Surv Profess Paper 959-E, pp E1-E6
- Herzig PM, Hannington MD (1995) Polymetallic massive sulfides at the modern seafloor: A review. *Ore Geol Revs*, v 10, pp 95-115
- Herzig PM, Petersen S, Hannington MD (1999) Epithermal-type gold mineralization in Conical Seamount: A shallow submarine volcano south of Lihir Island, Papua New Guinea, *in*: CJ Stanley et al, *Mineral Deposits: Processes to Processing*. Balkema, Rotterdam, pp 527-530
- Hess PC (1989) *Origins of Igneous Rocks*. Harward Univ Press, Cambridge MA, 336 p
- Hester BW (1988) Silver mining in the Gowganda field, northeastern Ontario-a case history, *in*: MJ Jones, ed, *Silver; exploration, mining and treatment*. Inst Min Metall, London, Conf Proc, pp 131-146
- Heyl AV, Agnew AF, Lyons EJ, Behre CH Jr (1959) Geology of the Upper Mississippi Valley zinc-lead district. U.S. Geol Surv Prof Paper 309, 310 p
- Hezarkhani A, Williams-Jones AE, Gammons CH (1999) Factors controlling copper solubility and chalcopyrite deposition in the Sungun porphyry copper deposit, Iran. *Mineralium Deposita*, v 34, pp 770-783
- Hiemstra SA (1985) The distribution of some platinum-group elements in the UG2 chromitite layer of the Bushveld Complex. *Econ Geol*, v 80, pp 944-957
- Higgins MW (1971) *Cataclastic Rocks*. U.S. Geol Surv Profess Paper 687, 97 p
- Hills PB (1990) The Mount Lyell copper-gold-silver deposits, *in*: FE Hughes, ed, *AusIMM, Monograph 14*, pp 1257-1266
- Hilpert LS (1969) Uranium resources of northwestern New Mexico. U.S. Geol Surv Profess Paper 603, 166 p
- Hitzman MW, Beaty DW (1996) The Irish Zn-Pb-(Ba) orefield. *Soc Econ Geol, Spec Vol 4*, pp 112-143
- Hitzman MW, Oreskes N, Einaudi MT (1992) Geological characteristics and tectonic setting of Proterozoic iron oxide (Cu-U-Au-REE) deposits. *Precambrian Research*, v 58, pp 241-287
- Hitzman MW, Reynolds NA, Sangster DF, Allen CR, Carman CE (2003) Classification, genesis and exploration guides for nonsulfide zinc deposits. *Econ Geol*, v 98, pp 685-714
- Hoagland AD (1976) Appalachian zinc-lead deposits, *in*: KH Wolf, ed, *Handbook of Stratiform and Strata-bound Ore Deposits*, v 6, Elsevier, Amsterdam, pp 495-534
- Hobson GD, Tiratsoo EN (1981) *Introduction to Petroleum Geology*. Gulf Publ, Houston, 252 p
- Hodgson CJ (1989) The structure of shear-related, vein-type deposits: A review. *Ore Geol Revs*, v 4, pp 231-273
- Hodgson CJ (1989) The structure of shear-related vein-type gold deposits: A review. *Ore Geol Revs*, v 4, pp 231-273
- Hodgson CJ (1990) Uses (and abuses) of ore deposit models in mineral exploration. *Geosc Canada*, v 17, pp 79-99
- Hodgson CJ (1993) Mesothermal lode-gold deposits. *Geol Assoc Canada, Spec Paper 40*, pp 635-678
- Hodgson CJ (1995) Kitsault (Lime Creek) molybdenum mine, northwestern British Columbia. *CIM Spec Volume 46*, pp 708-711
- Hoffman PF (1989) Precambrian geology and tectonic history of North America, *in*: AW Bally, AR Palmer, eds, *The Geology of North America-An Overview*. Geol Soc Amer, Boulder, pp 447-512
- Hofmann AW (1988) Chemical differentiation of the Earth: The relationship between mantle, continental crust, and oceanic crust. *Earth Planet Sci Letters*, v 90, pp 297-314
- Hofmann AW (1997) Mantle geochemistry: The message from oceanic volcanism. *Nature*, v 385, pp 219-229
- Hofmann AW (2004) Sampling mantle heterogeneity through oceanic basalts: Isotopes and trace elements, *in*: RW Carlson, ed, *Treatise on Geochemistry*, v 2, *The Mantle and Core*. Elsevier-Pergamon, pp 61-101
- Hofstra AH and Cline JS (2000) Characteristics and models for Carlin-type gold deposits. *Reviews in Econ Geol*, v 13, pp 163-220
- Hofstra AH, Snee LW, Rye RO, et al (1999) Age constraints on Jerritt Canyon and other Carlin-type gold deposits in the western United States-relationship to mid-Tertiary extension and magmatism. *Econ Geol*, v 94, pp 769-810
- Höll R (1977) Early Paleozoic ore deposits of the Sb-W-Hg Formation in the Eastern Alps and their genetic interpretation, *in*: DD Klemm, J-H Schneider, eds, *Time and Strata-Bound Ore Deposits*. Springer-Verlag, pp 170-198
- Höll R, Maucher A (1976) The strata-bound ore deposits in the Eastern Alps, *in*: KH Wolf, ed, *Handbook of Stratiform and Strata-Bound Ore Deposits*, v 2. Elsevier, Amsterdam, pp 1-36
- Holland HD (1984) *The Chemical Evolution of the Atmosphere and Ocean*. Princeton Univ Press, 582 p
- Holland HD, Petersen U (1981) Element dispersion, element concentration, and ore deposits. *Mineral Resources Development Series*, Nat Acad Press, Washington DC, pp 39-46
- Holland HD, Petersen U (1995) *Living Dangerously: The Earth, its Resources, and the Environment*. Princeton Univ Press, 490 p
- Höllner H (1953) Der Blei- Zinkerzbergbau Bleiberg, seine Entwicklung, Geologie und Tektonik. *Carinthia*, v 11, Klagenfurt, 143 p
- Holliday JR, Wilson AJ, Blevin PL, Tedder II, Dunham PD, Pfitzner M (2002) Porphyry gold-copper mineralization in the Cadia district, eastern Lachlan gold belt, and its relationship to shoshonitic magmatism. *Mineralium Deposita*, v 37, pp 100-116
- Hollister VF (1978) *Geology of the Porphyry Copper Deposits of the Western Hemisphere*. AIME, New York, 219 p
- Hollister VF, ed (1990) *Case Histories of Mineral Discoveries*, v 2. AIME, Littleton, Colorado

- Hollister VF, Sirvas B (1974) El pórfido de cobre Michiquillay. *Bol de la Soc Geol del Perú*, v 44, pp 11-27
- Holzer HH, Stumpf EF (1980) Mineral deposits of the Eastern Alps. *Abhandl Geol Bundesanst, Wien*, v 34, pp 171-196
- Homeniuk L (2000) Kumtor gold project, Kyrgyz Republic. *CIM Bulletin*, March 2000, pp 67-72
- Honnorez J, von Herzen RP, et al (1981) Hydrothermal mounds and young ocean crust of the Galapagos: Preliminary Deep Sea Drilling results, Leg 70. *Geol Soc Amer Bull, Part I*, v 92, pp 457-472
- Hopkins H (1949) Structure at Kirkland Lake, Ontario, Canada. *Bull Geol Soc Amer*, v 60, pp 902-922
- Hosking KFG (1969) Aspect of the geology of the tin fields of Southeast Asia, *in: 2nd Techn Conf on Tin, Bangkok*, pp 39-80
- Hosking KFG (1979) Tin distribution patterns. *Geol Soc Malaysia Bull*, v 11, pp 1-70
- Hou Zengqian et al (2003) The Himalayan Yulong porphyry copper belt: Product of large-scale strike-slip faulting in Eastern Tibet. *Econ Geol*, v 98, pp 125-145
- Howell FH, Molloy JS (1960) Geology of the Braden orebody, Chile, South America. *Econ Geol*, v 55, pp 863-906
- Howland AL, Garrels EM, Jones WR (1949) Chromite deposits of Boulder River area, Sweetgrass County, Montana. *U.S. Geol Surv Bull* 948-C, pp 63-82
- Høy T (1993) Geology of the Purcell Supergroup in the Fernie west-half map area, Southeastern British Columbia. B.C. Ministry of Energy, Mines, Petrol Resources, *Bull* 84, 157 p
- Hu Shouxi, Sun Mingzhi, Yan Zhengfu, Xu Jinfang, Cao Xiaoyun, Ye Ying (1984) An important metallogenic model for W, Sn and rare granitophile element ore deposits related to metasomatically altered granites, *in: Xu Keqin, Tu Guangxi, eds, Geology of Granites and their Metallogenetic Relations*. Science Press, Beijing, pp 519-537
- Hubert C, Marquis P (1989) Structural framework of the Abitibi greenstone belt of Quebec and its implications for mineral exploration. *Geol Assoc Canada Short Course Notes*, v 6, pp 219-238
- Hubred G (1975) Deep-sea manganese nodules: A review of the literature. *Minerals Sci Engng*, v 7, pp 71-85
- Hudson, DM (2003) Epithermal alteration and mineralization in the Comstock District, Nevada. *Econ Geol*, v 98, pp 367-385
- Hughes FE, ed (1990) *Geology of the Mineral Deposits of Australia and Papua New Guinea*, 2 volumes, AusIMM, Parksville, 1828 p
- Hugon H (1986) The Hemlo gold deposits, Ontario, Canada: a central portion of a large-scale, wide zone of heterogeneous ductile shear, *in: AJ MacDonald, ed, Gold '86*, pp 379-387
- Hulbert LJ, Grégoire DC, Paktunc D, Carne RC (1992) Sedimentary nickel, zinc and platinum-group elements mineralization in Devonian black shales at the Nick property, Yukon, Canada: A new deposit type. *Explor Mining Geol*, v 1, pp 39-62
- Hulbert LJ, von Gruenewaldt G (1986) The structure and petrology of the upper and lower chromitite layers on the farm Grasvally and Zoetveld, south of Potgietersrus, *in: CR Anhaeusser, S Maske, eds*, pp 1237-1249
- Hutchinson RW (1981) Metallogenic evolution and Precambrian tectonics, *in: A Kröner, ed, Precambrian Plate Tectonics*. Elsevier, Amsterdam, pp 733-760
- Hutchinson RW (1984) Archean metallogeny: Synthesis and review. *Journ of Geodynamics*, v 1, pp 339-358
- Hutchinson RW, Grauch RI, eds (1991) *Historical Perspectives of Genetic Concepts and Case Histories of Famous Discoveries*. *Econ Geol Monogr* 8, 359 p
- Hutchinson RW, Spence CD, Franklin JM, eds (1982) *Precambrian Sulfide Deposits*. *Geol Assoc Canada Spec Paper* 25, 791 p
- Hutchison CS (1983) *Economic Deposits and their Tectonic Setting*. Macmillan, London, 365 p
- Hutchison CS (1989) *Geological Evolution of South-East Asia*. Clarendon Press, Oxford
- Hutchison CS (1996) *South-East Asian Oil, Gas, Coal and Mineral Deposits*. Clarendon Press, Oxford
- Huyck HLO (1990) The Lakeshore porphyry copper deposit, Pinal County, Arizona: Geologic setting and physical controls of mineralization. *CIM Bulletin*, May 1990, pp 77-88
- Ianovici V, Borcoş M (1982) Romania, *in: FW Dunning et al, eds, Mineral Deposits of Europe*, v 2, Southeast Europe. IMM/Miner Soc London, pp 55-142
- Ianovici V, Borcoş M, Bleahu M, et al (1976) *Geologia Munților Apuseni*. Edit Academiei, Bucharest, 580 p
- Ide FY, Kunasz IA (1990) Origin of lithium in Salar de Atacama, northern Chile, *in: GE Erickson et al, eds*, pp 165-175
- Ihlen PM, Vokes FM (1978) Metallogeny, *in: ER Neumann, ed, The Oslo Paleorift*. *Norges Geol Unders*, No 337, pp 75-90
- Ilyin AV (1989) Apatite deposits in the Khibiny and Kovdor alkaline igneous complexes, Kola Peninsula, northwestern USSR, *in: AJG Notholt, RP Sheldon, DF Davidson, Intern Geol Correl Program, Project 156-Phosphorites*, pp 485-493
- Inan EE, Einaudi MT (2002) Nukundamite (Cu_{3.38} Fe_{0.62} S₄)-bearing copper ore in the Bingham porphyry deposit, Utah: Result of upflow through quartzite. *Econ Geol*, v 97, pp 499-515
- Ineson PR (1976) Ores of the Northern Pennines, the Lake District and North Wales, *in: KH Wolf, ed, Handbook of Stratiform and Strata-Bound Ore Deposits*, v 5. Elsevier, Amsterdam, p 197-230
- Irvine WT (1972) Geological setting and mineralisation of the Pine Point lead-zinc deposit, *in: 24th Intern Geol Congr, Montreal, Excursion A24-C24 Guidebook*, pp 3-18
- Ishihara S, ed (1974) *Geology of Kuroko Deposits*. *Mining Geol Spec Issue* 6, Tokyo, 435 p
- Isozaki Y, Maruyama S, Furuoka F (1990) Accreted oceanic materials in Japan. *Tectonophysics*, v 181, pp 179-205

- Issler RS (1978) The Seis Lagos carbonatite complex. Proc of the 1st Internat Sympos on Carbonatites, Poços de Caldas, DNPB, Brasilia, pp 233-240
- Ivanova AM, Ushakov VI (1998) The resources potential of Russia's shelf zones. Minerals. Mineral'nye Resursy Rossii, 1998, pp 6-12
- Ivanova TN (1963) Mestorozhdeniya Apatita Khibinskoi Tundry. Gosgeol'tekhnizdat', Moscow, 288 p
- Izawa E, Aoki M (1992) Geothermal activity and epithermal gold mineralization in Japan. Episodes, v 14, pp 269-273
- Izawa E, Urashima Y, Ibaraki K, Suzuki R, Yokoyama T, Kawasaki K, Koga A, Taguchi S (1990) The Hishikari gold deposit: High-grade epithermal veins in Quaternary volcanics of southern Kyushu, Japan. Journ Geoch Explor, v 36, pp 1-56
- Jackson ED (1961) Primary textures and mineral associations in the ultramafic zone of the Stillwater Complex, Montana. U.S. Geol Surv Prof Paper 358, 106 p
- Jackson I, ed (1998) The Earth's Mantle. Cambridge Univ Press
- Jacob RE, Corner B, Brynard JH (1986) The regional geological and structural setting of the uraniumiferous granitic provinces of southern Africa, *in*: CR Anhaeusser, S Maske, eds, pp 1807-1818
- Jahn Bor-ming, Wu Fuyuan, Chen Bin (2000) Granitoids of the Central Asian orogenic belt and continental growth in the Phanerozoic. Trans Royal Soc Edinburgh. Earth Sci, v 91, pp 181-193
- James HL (1954) Sedimentary facies of iron formation. Econ Geol, v 49, pp 235-293
- James LP (1976) Zoned alteration in limestone at porphyry copper deposits, Ely, Nevada. Econ Geol, v 71, pp 488-512
- James LP (1978) The Bingham copper deposits, Utah, as an exploration target: History and pre-excavation geology. Econ Geol, v 73, pp 1218-1227
- James NP, Choquette PW, eds (1987) Paleokarst. Springer-Verlag, 416 p
- Janković S (1980) Porphyry copper and massive sulfide deposits in the northeastern Mediterranean. Proc 5th Quadrennial IAGOD Sympos, Schweizerbart, Stuttgart, pp 431-444
- Janković S (1982) Yugoslavia, *in*: FW Dunning et al, eds, Mineral Deposits of Europe, v 2, Southeast Europe. IMM/Miner Soc, London, pp 143-202
- Janković S, Terzić M, Aleksić D, Karamata S, Spasov T, Jovanović M, Miličić M, Mišković V, Grubić A, Antonijević I (1980) Metallogenic features of copper deposits in the volcano-intrusive complexes of the Bor district, Yugoslavia. SGA Spec Publ No 1, pp 42-49
- Jannas R, Bowers TS, Petersen U, Beane RE (1999) High-sulfidation deposit types in the El Indio district, Chile. Soc Econ Geol Spec Publ 7, pp 219-266
- Jansen LJ (1982) Stratigraphy and structure of the Mission copper deposit, Pima mining district, Pima County, Arizona, *in*: SR Titley, ed, pp 467-474
- Jarchovský T (1994) Inner structure of tin-tungsten bearing cupolas near Krásno (Slavkovský Les Mts), *in*: R Seltmann et al, eds, pp 137-141
- Jarrell OW (1944) Oxidation at Chuquicamata, Chile. Econ Geol, v 39, pp 251-286
- Jébrak M, Hernández A (1995) Tectonic deposition of mercury in the Almadén district, Las Cuevas deposit, Spain. Mineralium Deposita, v 30, pp 413-423
- Jennings DS, Jilson GA (1986) Geology and sulfide deposits of Anvil Range, Yukon. CIM Spec Vol 37, pp 319-361
- Jensen LS (1985) Stratigraphy and petrogenesis of Archean metavolcanic sequences, southwestern Ontario. Geol Assoc Canada Spec Paper 28, pp 65-87
- Jewett GA (1986) The imperatives and demands of the materials marketplace today. CIM Bulletin, Aug 1986, pp 46-50
- Jockel F (2001) Mt Weld geology and mineralization summary. Anaconda report, unpubl, 18 p
- Johansen GF (1998) The New Bendigo Goldfield. Austral Inst Geoscientists Bull 24, pp 47-51
- John DA, Ballantyne GH, eds (1997) Geology and ore deposits of the Oquirrh and Wasatch Mountains, Utah. Soc Econ Geol Guidebook 29, 256 p
- John EC (1978) Mineral zones in the Utah Copper orebody. Econ Geol, v 73, pp 1250-1259
- Johnson CA, Rye DM, Skinner BJ (1990) Petrology and stable isotope geochemistry of the metamorphosed zinc-iron-manganese deposit at Sterling Hill, New Jersey. Econ Geol, v 85, pp 1133-1161
- Johnson CM, Lipman PW, Czamanske GK (1990) H, O, Sr, Nb and Pb isotope geochemistry of the Latir volcanic field and cogenetic intrusions, New Mexico. Contrib Miner Petrol, v 104, pp 99-124
- Johnson IR, Klingner CD (1976) The Broken Hill ore deposit and its environment, *in*: CL Knight, ed, pp 476-491
- Johnson RD, McMillan NJ (1993) Petroleum. Decade of North American Geology, v D-1, Geol Soc Amer, Boulder, pp 551-554
- Johnston WD, Jr (1940) The gold quartz veins of Grass Valley, California. U.S. Geol Surv Profess Paper 194, 101 p
- Jolly WT (1974) Behavior of Cu, Zn and Ni during prehnite-pumpellyite rock metamorphism of the Keweenaw basalts, northern Michigan. Econ Geol, v 69, pp 1118-1125
- Jones CB (1990) Coppin Gap copper-molybdenum deposit, *in*: FE Hughes, ed, pp 141-144
- Jones WR, Hernon RM, Moore SL (1967) General geology of Santa Rita quadrangle, Grant County, New Mexico. U.S. Geol Surv Prof Paper 555, 144 p
- Jordan TE, Allmendinger RW (1986) The Sierras Pampeanas of Argentina; A modern analogue of Laramide deformation. Amer Journ of Science, v 286, pp 737-764
- Jovett EC (1986) Genesis of Kupferschiefer Cu-Ag deposits by convective flow of Rotliegende brines during Triassic rifting. Econ Geol, v 81, pp 1823-1837
- Jung W, Knitzschke G (1976) Kupferschiefer in the German Democratic Republic (GDR) with special reference to the Kupferschiefer deposit in the southeastern Harz Foreland, *in*: KH Wolf, ed,

- Handbook of Stratiform and Strata-Bound Ore Deposits, v 6, Elsevier, Amsterdam, pp 353-406
- Kamenov G, Macfarlane AW, Riciputi L (2002) Sources of lead in the San Cristobal, Pulacayo and Potosi mining districts, Bolivia, and a reevaluation of regional ore lead isotope provinces. *Econ Geol*, v 97, pp 573-592
- Kamona AF, Leveque J, Friedrich G, et al (1999) Lead isotopes of the carbonate-hosted Kabwe, Tsumeb, and Kipushi Pb-Zn-Cu sulfide deposits in relation to Pan African orogenesis in the Damara-Lufilian fold belt of Central Africa. *Mineralium Deposita*, v 34, pp 273-283
- Kampunzu AB, Lubola RT, eds (1991) *Magmatism in Extensional Structural Settings*. Springer-Verlag
- Kang Yougfu, Miao Shuping, Li Chongyou, Gu Juyun, Li Yidou, Wu Yongle (1992) Tungsten deposits of China, in: *ECMDC, Mineral Deposits of China*, v 2. Geol Publ House, Beijing, pp 223-293
- Kappel ES, Franklin JM (1989) Relationships between geologic development of ridge crests and sulfide deposits in the Northeast Pacific Ocean. *Econ Geol*, v 84, pp 485-521
- Karig DE (1974) Evolution of arc systems in the western Pacific. *Annual Rev in Earth and Planet Sci*, v 2, pp 51-75
- Kats AYa, Kremenetsky AA, Podkopaev OI (1998) The germanium mineral resource base of the Russian Federation. *Mineral'nye Resursy Rossii*, 1998, pp 5-9
- Katz MB (1971) The Precambrian metamorphic rocks of Ceylon. *Geol Rundschau*, v 60, pp 1523-1549
- Kay M (1951) North American Geosynclines. *Geol Soc Amer Mem* 48, 140 p
- Kay RW (1980) Volcanic arc magmas: Implications for melting, mixing model for element recycling in the crust-upper mantle system. *Journal of Geology*, v 88, pp 497-522
- Kazanskii VI (1972) Rudonosnye Tektonicheskie Struktury Aktivizirovannykh Oblastei. Nedra, Moscow, 240 p
- Kazanskii VI (1982) Evolutsiya rudonosnykh struktur dokembriya: Arkheiskye kratony i oblasti protoaktivizatsii, in: AV Sidorenko, ed, *Rudonosnye Struktury Dokembriya*. Nauka, Moscow, 766 p
- Kazanskii VI (1996) The El'kon uranium ore district in the Aldan Shield. 30th Intern Geol Congr, Beijing, Abstract volume, Paper 9-5-5
- Kazanskii VI, Omel'yanenko BI, Prokhorov KV (1978) Rudonosnye shchelochnye metasomatity v krupnykh razlomakh kristallicheskovo fundamenta, in: *Endogennoe Orudneniye Drevnikh Shchitov*. Nauka, Moscow, pp 102-144
- Kearns RHB (1982) Broken Hill, a pictorial history. Investigator Press, Adelaide, 248 p
- Keating BH, Fryer P, Batiza R, Boehlert GW, eds (1987) *Seamounts, Islands and Atolls*. Amer Geophys Union, Geophys Monogr 43, 405 p
- Ke-Chin Hsu (1943) Tungsten deposits of southern Kiangsi, China. *Econ Geol*, v 38, pp 431-474
- Keith JD, Shanks WC III, Archibald DA, Farrar E (1986) Volcanic and intrusive history of the Pine Grove porphyry molybdenum system, Southwestern Utah. *Econ Geol*, v 81, pp 553-577
- Keith, SB (1986) Petrochemical variations in Laramide magmatism and their relationships to Laramide tectonic and metallogenic evolution in Arizona and adjacent regions. *Arizona Geol Soc Digest*, v 16, pp 89-101
- Keith SB, et al (1991) Magma series and metallogeny, a case study from Nevada and environs. *Nevada Geol Soc Guidebook for Field Trips*, v 1, pp 404-493
- Keith SB, Swan MM (1996) The great Laramide porphyry copper cluster of Arizona, Sonora and New Mexico: The tectonic setting, petrology, and genesis of a world class porphyry metal cluster, in: AR Coyner, PL Fahey, eds, *Geology and Ore Deposits of the American Cordillera*, Proceedings v. III. Geol Soc of Nevada, Reno, pp 1667-1747
- Kelley KD, Jennings S (2004) A special issue devoted to barite and Zn-Pb-Ag deposits in the Red Dog District, western Brooks Range, northern Alaska. *Econ Geol*, v 99, pp 1267-1280
- Kelley KD, Romberger SB, Beaty DW, Pontius JA, Snee LW, Stein HJ, Thompson TB (1998) Geochemical and geochronological constraints on ore genesis of Au-Te deposits at Cripple Creek, Colorado. *Econ Geol*, v 93, pp 981-1012
- Kelly WC, Rye RO (1979) Geologic, fluid inclusion and stable isotope studies of the tin-tungsten deposits of Panasqueira, Portugal. *Econ Geol*, v 74, pp 1721-1822
- Kelly WC, Turneure FS (1970) Mineralogy, paragenesis and geothermometry of the tin and tungsten deposits of the eastern Andes. *Econ Geol*, v 65, pp 609-680
- Kendall CJ (1990) Ranger uranium deposits, in: FE Hughes, ed, pp 799-805
- Kennedy AK, Hart SR, Frey FA (1990) Composition and isotopic constraints on the petrogenesis of alkaline arc lavas: Lihir Island, Papua New Guinea. *Journ Geophys Res*, Ser B, v 95, pp 6929-6942
- Kent PE et al, eds (1969) *Time and Place in Orogeny*. Geol Soc London Spec Publ 3, pp 197-214
- Kenyon M (1998) Review of the Bulyanhulu gold deposit, Tanzania. *Pathways '98*, pp 41-43
- Kerr Addison Staff (1967) Kerr Addison mine, in: Pye et al, eds, 28th Intern Geol Congr, Montreal, Guidebook A39-C39, pp 34-40
- Kerr DJ, Gibson HL (1993) A comparison of the Horne volcanogenic massive sulfide deposit and intracauldron deposits of the Mine Sequence, Noranda, Quebec. *Econ Geol*, v 88, pp 1419-1442
- Kerrick R, Cassidy KF (1994) Temporal relationships of lode gold mineralization to accretion, magmatism, metamorphism and deformation-Archean to present: A review. *Ore Geol Revs*, v 9, pp 263-310
- Kerrick R, Watson GP (1984) The Macasa Mine, Archean lode gold deposit, Kirkland Lake, Ontario: Geology, patterns of alteration and hydrothermal regimes. *Econ Geol*, v 79, pp 1104-1130
- Kerswill JA (1996) Iron-formation hosted stratabound gold, in: OR Eckstrand et al, eds, *Geology of Canadian Mineral Deposits Types*. Geology of Canada no 8, pp 367-382

- Kesler SE (1994) Mineral Resources, Economics and the Environment. Macmillan, New York, 391 p
- Kesler SE (1996) Appalachian Mississippi Valley-type deposits: Paleoaquifers and brine provinces. *Soc Econ Geol Spec Publ* 4, pp 29-57
- Kesler SE, Campbell IH, Smith CN, Hall CM, Allen CM (2005) Age of the Pueblo Viejo gold-silver deposit and its significance to models for high sulfidation epithermal mineralization. *Econ Geol*, v 100, pp 253-272
- Kesler SE, Russel N, McCurdy K (2003) Trace metal content of the Pueblo Viejo precious metal deposits and their relation to other high-sulfidation epithermal systems. *Mineralium Deposita*, v 38, pp 668-682
- Kesler SE, Sutter JF, Issigonis MJ, Jones LM, Walker RL (1977) Evolution of porphyry copper mineralization in an oceanic island arc: Panama. *Econ Geol*, v 72, pp 1142-1153
- Kharkevich DC, ed (1968) *Karta Magmatischeskikh Formatsii SSSR*, 1:2,500,000. VSEGEI, Moscow, 16 sheets
- Khiltova VYa, Pleskach GP (1997) Yenisei fold belt, *in*: DV Rundkvist, C Gillen, eds, Precambrian ore deposits of the East European and Siberian Cratons. Elsevier, Amsterdam, pp 289-316
- Kidd RP, Robinson JR (2004) A review of the Kapit orebody, Lihir Island group, Papua New Guinea. PACRIM 2004 Proceedings, Adelaide, AusIMM, pp 323-331
- Kienle J, Nye CJ (1990) Volcano tectonics of Alaska, *in*: CA Wood, J Kienle, eds, Volcanoes of North America. Cambridge Univ Press, pp 8-110
- Kimberley MM (1978) Paleoenvironmental classification of iron formations. *Econ Geol*, v 73, pp 215-229
- Kimberley MM (1979) Origin of oolitic iron formations. *Journ Sedim Petrol*, v 49, pp 111-132
- Kimura ET, Bysouth GD, Drummond AD (1976) Endako. *CIM Spec Vol* 15, pp 444-454
- Kinnison JE (1966) The Mission copper deposit, Arizona, *in*: SR Titley, CL Hicks, eds, pp 281-287
- Kitrkham RV (1989) The distribution, settings and genesis of sediment-hosted, stratiform copper deposits. *Geol Assoc Canada Spec Paper* 36, pp 3-38
- Kirkham RV (1996a) Sediment-hosted stratiform copper, *in*: OR Eckstrand et al, eds, *Geology of Canada* no 8, pp 223-240
- Kirkham RV (1996b) Volcanic redbed copper, *in*: OR Eckstrand et al, eds, *Geology of Canada* no 8, pp 241-252
- Kirkham RV, Sinclair WD, Thorpe RI, Duke JM, eds (1993) Mineral Deposit Modelling. *Geol Assoc Canada Paper* 40, 770 p
- Kirwin DJ, Forster CN, Garamjov D (2003) The discovery history of the Oyu Tolgoi porphyry copper-gold deposits, South Gobi, Mongolia. *Proceedings New Generation Gold Symposium*, Perth
- Kisters AFM, Meyer FM, Znamensky SE, et al (2000) Structural controls of lode-gold mineralization by mafic dykes in late-Paleozoic granitoids of the Kochkar district, southern Urals, Russia. *Mineralium Deposita*, v 35, pp 157-168
- Klein C, Beukes NJ (1993) Sedimentology and geochemistry of the glaciogenic late Proterozoic Rapitan Iron Formation in Canada. *Econ Geol*, v 88, pp 542-565
- Klein C, Fink RP (1976) Petrology of the Sokoman Iron Formation in the Howell's River area, at the western edge of the Labrador Trough. *Econ Geol*, v 71, pp 453-487
- Klein C, Ladeira EA (2000) Geochemistry and petrology of some Proterozoic banded iron formations of the Quadrilátero Ferrífero, Minas Gerais, Brazil. *Econ Geol*, v 95, pp 405-428
- Klemme HD, Meyerhof AA, Shabab T (1970) Giant Oil and Gas Fields and Geologic Factors Affecting their Formation. AAPG Memoir 14
- Klitgord KD, Hutchinson DR, Schouten H (1988) U.S. Atlantic continental margin; structural and tectonic framework, *in*: The Geology of North America, v I-2. *Geol Soc Amer*, Boulder
- Knight FC, Videira JC (1999) The Las Cruces Project. Joint SGA-IAGOD field trip B4, London, 41 p
- Knopf A (1929) The Mother Lode system of California. *U.S. Geol Surv Profess Paper* 157, 88 p
- Knuckey MJ, Comba CDA, Riverin G (1982) Structure, metal zoning and alteration in the Millenbach deposit, Noranda, Quebec. *Geol Assoc Canada Spec Paper* 25, pp 255-296
- Kogarko IN (1987) Alkaline rocks of the eastern part of the Baltic Shield (Kola Peninsula), *in*: JG Fitton, BG Upton, eds, *Alkaline Igneous Rocks*. *Geol Soc London Spec Publ* 30, pp 531-544
- Koide M, Hodge V, Goldberg ED, Bertihe K (1988) Gold in seawater, a conservative view. *Applied Geochem*, v 3, pp 237-242
- Koistinen TJ (1981) Structural evolution of an early Proterozoic strata-bound Cu-Co-Zn deposit, Outokumpu, Finland. *Trans Roy Soc Edinburgh, Earth Sci*, v 72, pp 115-158
- Kolektiv, ČUP (1984) *Československá Ložiska Uranu*. Prague, 365 p
- Konkin VD, Ruchkin GV, Kuznetsova TP (1993) Kholodninskoe svintsovo-tsinkovo-kolchedannoe mestorozhdeniye v severnom Pribaikal'ye (Vostochnaya Sibir). *Geol Rud Mestor*, v 35, pp 3-17
- Konofagou K (1980) To Archaio Laurio kai i elliniki tekhniki paragogis tou argourou. Ekdotiki/Elladoz Publishers, Athens
- Konstantinov MM, Rosenblum IS, Strujkov SF (1993) Types of epithermal silver deposits, Northeastern Russia. *Econ Geol*, v 88, pp 1797-1809
- Kontinen A (1987) An Early Proterozoic ophiolite-the Jormua mafic-ultramafic complex, northern Finland. *Precambri Research*, v 35, pp 313-341
- Koo J, Mossman DJ (1975) Origin and metamorphism of the Flin Flon stratabound Cu-Zn sulfide deposit, Saskatchewan and Manitoba. *Econ Geol*, v 70, pp 48-62
- Koorman GJA, McLeod MJ, Sinclair WD (1986) Porphyry tungsten molybdenum orebodies, polymetallic veins and replacement bodies, and tin-bearing greisen zones in the Fire Tower zone, Mount

- Pleasant, New Brunswick. *Econ Geol*, v 81, pp 1356-1373
- Korneliusson A, Geiss H-P, Gierth E, et al (1985) Titanium ores: An introduction to a review of titaniferous magnetite, ilmenite and rutile deposits in Norway. *Norges Geol Unders Bull* 402, pp 7-23
- Kornze LD (1987) Geology of the Mercur gold mine, *in*: JL Johnson, ed, Bulk mineable precious metal deposits of the western United States, Guidebook for field trips. Geol Soc Nevada, Reno, pp 381-389
- Korzhinskii DS (1970) Theory of Metasomatic Zoning. Clarendon Press, New York Oxford, 162 p
- Korzhinskii DS, ed (1974) *Metasomatizm i Rudoobrazovaniye*. Nauka, Moscow, 363 p
- Koski RA, Clague DA, Oudin E (1984) Mineralogy and chemistry of massive sulfide deposits from the Juan de Fuca Ridge. *Geol Soc Amer Bull*, v 95, pp 930-945
- Koski RA, Lonsdale PF, Shanks WC, et al (1985) Mineralogy and geochemistry of a sediment-hosted hydrothermal sulfide deposits from the Southern Trough of Guyama Basin, Gulf of California. *Journ Geophys Res*, v 90, pp 6695-6707
- Kramers DA (1985) Magnesium, *in*: Mineral Facts and Problems, U.S. Bur of Mines, Bull 675, pp 471-482
- Kramm U, Kogarko IN (1994) Nd and Sr isotope signatures of the Khibina and Lovozero apatitic centres, Kola alkaline province, Russia. *Lithos*, v 32, pp 225-242
- Kraume E (1955) Die Erzlager des Rammelsberges bei Goslar. *Geol Jahrb Beihefte* 18, 394 p
- Krause H, Gierth E, Schott W (1985) Ti-Fe deposits in the South Rogaland Igneous Complex, with special reference to the Åna-Sira anorthosite massif. *Norges Geol Unders, Bull* 402, pp 25-37
- Kräutner HG (1977) Hydrothermal-sedimentary iron ores related to submarine volcanic rises: the Teliuc-Ghelar Type as a carbonatic equivalent of the Lahn-Dill Type, *in*: DD Klemm, H-J Schneider, eds, Time and Strata-Bound Ore Deposits. Springer-Verlag, pp 232-253
- Kravchenko SM, Laputina IP, Kataeva ZT, Krasil'nikova IG (1996) Geochemistry and genesis of rich Sc-REE-Y-Nb ores at the Tomtor deposit, northern Siberian Platform. *Geochem Internat*, v 34, pp 847-863
- Kravchenko SM, Pokrovsky BG (1995) The Tomtor alkaline ultrabasic massif and related REE-Nb deposits, northern Siberia. *Econ Geol*, v 90, pp 676-689
- Krebs W (1972) Facies and development of the Meggen Reef (Devonian, West Germany). *Geol Rundschau*, v 61, pp 647-671
- Krebs W (1981) Geology of the Meggen ore deposit, *in*: KH Wolf, ed, Handbook of Stratiform and Stratabound Ore Deposits, v 9. Elsevier, Amsterdam, pp 509-549
- Kremenetsky AA, Burenkov EK, Usova TYu, Osokin YeD (1996) Unique mineral deposits of rare elements in Russia. 30th Intern Geol Congress, Beijing, Abstracts 9-9-22
- Krendel'ev FP, Bakun NN, Volodin RN (1983) *Medistye Peshchaniki Udokana*. Nauka, Moscow, 247 p
- Křibek B (1989) The role of organic matter in the metallogeny of the Bohemian Massif. *Econ Geol*, v 84, pp 1525-1540
- Krivtsov AI, Migachev IF (1998) The placer gold initial potential and prospects of the Russian Federation. *Mineral'nye Resursy Rossii*, 1998, pp 11-15
- Kröner A (1984) Evolution, growth and stabilization of the Precambrian lithosphere. *Phys and Chem of the Earth*, v 16, pp 69-106
- Kruger FJ, Marsh JS (1982) The mineralogy, petrology and origin of the Merensky Reef cyclic unit in the western Bushveld Complex. *Econ Geol*, v 80, pp 958-974
- Krupp RE, Seward TM (1987) The Rotokawa geothermal system, New Zealand: An active epithermal gold-depositing environment. *Econ Geol*, v 82, pp 1109-1130
- Kucha H (1982) Platinum-group metals in the Zechstein copper deposits, Poland. *Econ Geol*, v 77, pp 1578-1591
- Kucha H, Przybyłowicz W (1999) Noble metals in organic matter and clay-organic matrices, Kupferschiefer, Poland. *Econ Geol*, v 94, pp 1137-1162
- Kuck PH (1985) Vanadium, *in*: Mineral Facts and Problems, U.S. Bur of Mines, Bull 675, pp 895-915
- Kudryavtsev, YuK (1996) The Cu-Mo deposits of Central Kazakhstan, *in*: V Shatov et al, eds, Granite-related Ore Deposits of Central Kazakhstan and Adjacent Areas. St. Petersburg, Glagol, pp 119-144
- Kuehn S, Ogola J, Sango P (1990) Regional setting and nature of gold mineralization in Tanzania and Southwest Kenya. *Precambrian Research*, v 46, pp 71-82
- Kuehn CA, Rose AW (1995) Carlin gold deposits, Nevada: Origin in a deep zone of mixing between normally pressured and overpressured fluids. *Econ Geol*, v 90, pp 17-36
- Kuhns RJ, Kennedy P, Cooper P, et al (1986) Geology and mineralization associated with the Golden Giant deposit, Hemlo, Ontario, *in*: AJ MacDonald, ed, Gold '86, pp 327-354
- Kurdyukov AA (1980) Lithologic control on mineralization in the Tyrnyauz deposit (Northern Caucasus). *Intern Geol Revs*, v 22, pp 318-328
- Kuyper BA (1988) Geology of the McCoy gold deposit, Lander County, Nevada, *in*: RW Schafer, JJ Cooper, PG Vikre, eds, Bulk Mineable Precious Metal Deposits of the Western United States. Geol Soc of Nevada, Reno, pp 173-186
- Kuz'menko MV, ed (1976) *Polya Redkometal'nykh Granitnykh Pegmatitov*. Nauka, Moscow, 332 p
- Kuznetsov VA, ed (1983) *Geneticheskie Modeli Endogennykh Rudnykh Formatsii*, v 1, 2. Nauka, Novosibirsk, 184 & 176 p
- Kužvart M (1990) *Kámen ve Službách Civilizace*. Academia, Prague, 293 p
- Kwak TAP (1987) *W-Sn Skarn Deposits and Related Metamorphic Skarns and Granitoids*. Elsevier, Amsterdam, 445 p

- Kwak TAP, Tan TH (1981) The geochemistry of zoning in skarn minerals at the King Island (Dolphin) mine. *Econ Geol*, v 76, pp 439-467
- Kyle JR (1981) Geology of the Pine Point lead-zinc district, *in*: KH Wolf, ed, *Handbook of Stratiform and Strata-bound Ore Deposits*, v 9. Elsevier, Amsterdam, pp 643-741
- Kyle JR, Saunders JA (1996) Metallic deposits of the Gulf Coast Basin: Diverse mineralization styles in a young sedimentary basin, *in*: DF Sangster, ed, *Soc Econ Geol Spec Publ 4*, pp 218-229
- Ladeira EA (1988) Metalogenia dos depósitos de ouro do Quadrilátero Ferrífero, Minas Gerais, *in*: C Schobbenhaus, CES Coelho, eds, v 3, pp 301-375
- Laffitte P, Rouveyrol P (1964, 1965) Carte Minière du Globe sur fond tectonique au 20,000,000^e. Notice explicative. *Annales des Mines*, Dec 1963 & Oct 1965, Paris, 27 & 33 p
- Laffitte P, et al (1970) Carte Métallogénique de l'Europe 1: 2,500,000. BRGM Orléans, UNESCO
- Lalor JH (1991) Discovery of the Olympic Dam copper-uranium-gold-silver deposit, *in*: VF Hollister, ed, *Case Histories of Mineral Discoveries*, v 3. AIME, Littleton CO, pp 219-221
- Lamb MA, Cox D (1998) New ⁴⁰Ar/³⁹Ar age data and implications for porphyry copper deposits of Mongolia. *Econ Geol*, v 93, pp 524-529
- Lamb S, Hoke L, Kennan L, Dewey J (1997) Cenozoic evolution of the Central Andes in Bolivia and northern Chile. *Geol Soc Spec Publ 121*, pp 237-264
- Landefeld LA (1988) The geology of the Mother Lode gold belt, Sierra Nevada Foothills metamorphic belt, California, *in*: G Kisvarsanyi, SK Grant, eds, *North American Conf on Tect Control of Ore Dep*, Proc, Univ of Missouri, Rolla, pp 47-56
- Landefeld LA, Silberman ML (1987) Geology and geochemistry of the Mother Lode belt, California, compared with Archean lode gold deposits, *in*: JL Johnson, ed, *Bulk Mineable Precious Metal Deposits of the Western United States*, Guidebook for field trips. Geol Soc Nevada, Reno, pp 213-222
- Landon SM (1994) Interior Rift Basins. AAPG Memoir 59, Tulsa, 276 p
- Landtwing MR, Dillenbeck ED, Leake MH, Heinrich CA (2002) Evolution of the breccia-hosted porphyry Cu-Mo-Au deposit at Agua Rica, Argentina: Progressive unroofing of magmatic-hydrothermal system. *Econ Geol*, v 97, pp 1273-1292
- Lang B (1979) The base metals-gold hydrothermal ore deposits of Baia Mare, Romania. *Econ Geol*, v 74, pp 1336-1351
- Lang JR, Stanley CR, Thompson JFH, Dunne KPE (1995) Na-K-Ca magmatic hydrothermal alteration in alkalic porphyry Cu-Au deposits, British Columbia, *in*: JFH Thompson, ed, *Magma, Fluids and Ore Deposits*. Miner Assoc Canada Short Course Notes, v 23, pp 339-366
- Langen RE, Kidwell AL (1974) Geology and geochemistry of the Highland uranium deposit, Converse County, Wyoming. *The Mountain Geologist*, v 11, pp 85-93
- Langton JM, Williams SA (1982) Structural, petrological and mineralogical controls on the Dos Pobres orebody, *in*: SR Titley, ed, pp 335-352
- Large D (2001) The geology of non-sulfide zinc deposits-an overview. *Erzmetall*, v 54, pp 264-274
- Large D, Walcher E (1999) The Rammelsberg massive sulfide Cu-Zn-Pb-Ba deposit, Germany: an example of sediment-hosted, massive sulfide mineralisation. *Mineralium Deposita*, v 34, pp 522-538
- Large RR (1992) Australian volcanic-hosted massive sulfide deposits: features, styles and genetic models. *Econ Geol*, v 87, pp 471-510
- Larin AM (1997) Batomga terrain, *in*: DV Rundkvist, C Gillen, eds, *Precambrian Ore Deposits of the East European and Siberian Craton*. Elsevier, Amsterdam, pp 227-230
- Larin AM, Ryt'sk Ye Yu, Sokolov YuM (1997) Baikal-Patom fold belt. As above, pp 317-362
- Larsen F, Chillingar GV (1979) Diagenesis in Sediments and Sedimentary Rocks. Elsevier, Amsterdam, 519 p
- Larsen LM, Sørensen H (1987) The Ilímaussaq intrusion-progressive crystallization and formation of layering in an apatitic magma, *in*: JG Fitton, BGJ Upton, eds, *Alkaline Igneous Rocks*. Geol Soc Spec Publ 30, pp 473-488
- Lasmanis R (1995) Regional geological and tectonic setting of porphyry deposits in Washington State. *CIM Spec Vol 46*, pp 77-102
- Launay de L (1913) *Traité de Métallogénie*. Gîtes Minéraux et Metalifères. Béranger, Paris, 3 volumes
- Laverov NP, Distler VV, Mitrofanov GL, Nemerov VK, Yudovskaya MA (1998) PGE mineralization at the Sukhoi Log gold deposit, eastern Siberia, Russia. 8th Intern Platinum Sympos, Series S18, Geol Soc South Africa, pp 189-195
- Lavreau J (1984) Vein and stratabound gold deposits of northern Zaïre. *Mineralium Deposita*, v 19, 158-165
- Lavric JV, Spengenberg JE (2003) Stable isotope (C,O,S) systematics of the mercury mineralization at Idrija, Slovenia: Constraints on fluid source and alteration processes. *Mineralium Deposita*, v 38, pp 886-899
- Lawrence LJ (1973) Polymetamorphism of the sulfide ores of Broken Hill, NSW, Australia. *Mineralium Deposita*, v 8, pp 211-236
- Lawrence MJ (1997) Behind Busang. The Bre-X scandal. Could it happen in Australia? *Austral Journ of Mining*, Dec 1997, pp 33-50
- Laznicka P (1973a) MANIFILE, the University of Manitoba file of nonferrous metal deposits of the world. Centre of Precambrian Studies, Univ of Manitoba, Winnipeg, 533 & 767 p
- Laznicka P (1973b) Development of non-ferrous metal deposits in geologic time. *Canad Journ Earth Sci*, v 19, pp 18-25
- Laznicka P (1983a) The search for a more realistic metallogenic map format, with reference to the Pine Creek Geosyncline. *BMR Journ of Australian Geol, Geophys*, v 8, pp 293-305
- Laznicka P (1983b) Giant ore deposits: A quantitative approach. *Global Tect and Metallogeny*, v 2, pp 41-63

- Laznicka P (1985a) *Empirical Metallogeny*. Elsevier, Amsterdam, 1794 p
- Laznicka P (1985b) Data on ore deposits: A critical review of their sources, acquisition, organization and presentation, *in*: KH Wolf, ed, *Handbook of Stratiform and Stratabound Ore Deposits*, v 11, pp 1-118
- Laznicka P (1985c) Unconformities and ores, *in*: same publication, v 12, pp 219-360
- Laznicka P (1985d) The geological association of coal and metallic ores, a review, *in*: same publication, v 13, pp 1-71
- Laznicka P (1987, 1991) *Introduction to Metallogeny and Mineral Deposits*. Course notes, Univ Heidelberg & Univ of Manitoba, 190 & 520 p
- Laznicka P (1988) *Breccias and Coarse Fragmentites*. Elsevier, Amsterdam, 840 p
- Laznicka P (1989) *Breccias and ores, part 1: History, organization and petrography of breccias*. *Ore Geol Revs*, v 4, pp 315-344
- Laznicka, P (1991, 1996) *The World of Giant Metallic Deposits, short course*. Univ of Manitoba, 280 p
- Laznicka P (1992a) Manganese deposits in the global lithogenetic system: Quantitative approach. *Ore Geol Revs*, v 7, pp 279-356
- Laznicka P (1992b) Ore deposit models, regional assessment and computerized inventory/feature retrieval system of visual images of geological materials based on Lithothèque, *in*: SC Sarkar, ed, *Metallogeny related to tectonics of the Proterozoic mobile belts*. Oxford & IBH Publ, New Delhi, pp 323-338
- Laznicka P (1993) *Precambrian Empirical Metallogeny*. Elsevier, Amsterdam, 1622 p
- Laznicka P (1996) Discovery of giant metallic deposits. 30th Intern Geol Congr Beijing, lecture
- Laznicka P (1997) Discovery of giant metal deposits and districts. *Proc of the 30th Intern Geol Congr, Beijing*, v 9, VSP Publ, pp 355-366
- Laznicka P (1998) The setting and affiliation of giant ore deposits. *Proc of the 9th Quadren IAGOD Sympos, Schweizerbart, Stuttgart*, pp 1-14
- Laznicka P (1999) Quantitative relationships among giant deposits of metals. *Econ Geol*, v 94, pp 455-472
- Laznicka, P (2001) *Metallogenic Concepts in Exploration and the Discovery of Giant Deposits*. Short course notes, Univ of Zimbabwe, 160 p
- Laznicka P (2004) *Total Metallogeny-Geosites*. AMF, Adelaide, 740 p and poster
- Laznicka P, Wilson HDB (1972) The significance of a copper-lead line in metallogeny. 24th Intern Geol Congr, Montreal, Section 4, pp 25-36
- Leach DL, Hofstra AH, Church SE, et al (1998) Evidence for Proterozoic and late Cretaceous-early Tertiary ore-forming event in the Coeur d'Alene district, Idaho and Montana. *Econ Geol*, v 93, pp 347-359
- Leach DL, Sangster DF (1993) Mississippi Valley-type lead zinc deposits. *Geol Assoc Canada Spec Paper* 40, pp 289-314
- Leach DL, Viets JG, Kozlowski A, Kibitlewski S (1996) Geology, geochemistry, and genesis of the Silesia-Cracow zinc-lead district, southern Poland, *in*: DF Sangster, ed, *Carbonate-Hosted Lead-Zinc Deposits*. *Soc Econ Geol Spec Publ* 4, pp 144-170
- Le Bas MJ (1987) Nephelinites and carbonatites, *in*: JG Fitton, BGJ Upton, eds, *Alkaline Igneous Rocks*. *Geol Soc London Spec Publ* 30, pp 53-83
- Lebedev LM (1973) Minerals of contemporary hydrotherms of Cheleken. *Geochem Internat*, v 9, pp 485-504
- Leblanc M, Petit D, Deram A, et al (1999) The phytomining and environmental significance of hyperaccumulation of thallium by *Iberis Intermedia* from southern France. *Econ Geol*, v 94, pp 109-114
- Lefebvre J-J (1989) Depositional environment of copper-cobalt mineralization in the Katangan sediments of southeast Shaba, Zaïre. *Geol Assoc Canada, Spec Paper* 36, pp 401-426
- Lefond SJ, ed (1975) *Industrial Minerals and Rocks*. AIME, New York, 5th ed, 1360 p
- Leggett JK, eds (1982) *Trench-Forearc Geology*. *Spec Publ Geol Soc London*, v 10, 576 p
- Lehmann B (1990) *Metallogeny of Tin*. Springer-Verlag, 211 p
- Lehrman NJ (1987) The McLaughlin Mine, Napa and Yolo Counties, California, *in*: JL Johnson, ed, *Bulk Mineable Precious Metal Deposits of the Western United States, Guidebook for field trips*. *Geol Soc Nevada, Reno*, pp 197-201
- Leinen M (1989) The pelagic clay province of the North Pacific Ocean. *The Geology of North America*, v N, *Geol Soc Amer, Boulder*, pp 323-335
- Leistel JM, Marcoux E, Thiéblemont D, Quesada C, Sánchez A, Almodóvar GR, Pascual E, Sáez R (1989) The volcanic-hosted massive sulfide deposits of the Iberian Pyrite Belt. *Mineralium Deposita*, v 33, pp 2-30
- Leleu M, Morikis A, Picot P (1873) Sur des minéralisations de type skarn au Laurium (Greece). *Mineralium Deposita*, v 8, pp 259-263
- Lelong F, Tardy Y, Grandin G, Trescases JJ, Boulange B (1976) Pedogenesis, chemical weathering and processes of formation of some supergene ore deposits, *in*: KH Wolf, ed, *Handbook of Stratiform and Strata-Bound Ore Deposits*, v 3. Elsevier, Amsterdam, pp 93-174
- Lentz DR (1999) Petrology, geochemistry and oxygen isotope interpretation of felsic volcanic and related rocks hosting the Brunswick 6 and 12 massive sulfide deposits (Brunswick belt), Bathurst mining camp, New Brunswick, Canada. *Econ Geol*, v 94, pp 57-86
- Leonardson RW, Rahn JE (1996) Geology of the Betze-Post gold deposits, Eureka County, Nevada, *in*: AR Coyner, PL Fahey, eds, *Geology and Ore Deposits of the American Cordillera*. *Geol Soc Nevada, Reno, Sympos Proceedings*, pp 61-94
- Leroy J (1978) The Margnac and Fanay uranium deposits of the La Crouzille district (western Massif Central, France). *Geologic and fluid inclusion studies*. *Econ Geol*, v 73, pp 1611-1634
- Leshchikov VI, Rapoport MS, Aleshin BM (1998) The mineral resource base of the Sverdlovsk Oblast. *Mineral'nye Resursy Rossii*, 1998, pp 15-25

- Leshner CM (1989) Komatiite-associated nickel sulfide deposits, *in*: JA Whitney, AJ Naldrett, eds, Ore Deposition Associated with Magmas. *Revs in Econ Geol*, v 4, pp 45-101
- Leube A, Hirdes W, Mauer R, Kesse GO (1990) The early Proterozoic Birrimian Supergroup of Ghana and some aspects of its associated gold mineralization. *Precambr Res*, v 46, pp 139-165
- Leveille R, Marshik R (1999) Candelaria and the Punta del Cobre District, Chile: VMS or epigenetic hydrothermal deposits?, *in*: Primer Volumen de Monografias de Yacimientos Minerales Peruanos, IIMP, Lima, pp 301-304
- Leventhal JS (1998) Metal-rich black shales: Formation, economic geology and environmental considerations, *in*: J Schieber et al, eds, Shales and Mudstones II. Schweizerbart, Stuttgart, pp 255-282
- Levin LE (1995) Tectonic setting of stratiform ore deposits buried in sedimentary cover of the Pacific Ocean. PACRIM '95 Proceedings, AusIMM, pp 339-355
- Levin LE, Gramberg IS, Isaev EN, eds (1993) Geology of hydrocarbon and mineral resources associated with post-Middle Jurassic sequences in the oceans and on the continents. VNII Zarubezhgeologia report, Moscow, 704 p
- Levingston KR (1972) Ore deposits and mines of the Charters Towers 1:250,000 sheet area, Queensland. *Geol Surv Queensland*, Rept 57
- Lexa J, Štohl J, Konečný V (1999) The Banská Štiavnica ore district: Relationship between metallogenetic processes and the geological evolution of a stratovolcano. *Mineralium Deposita*, v 34, pp 639-654
- Lightfoot PC (1997) Geologic and geochemical relationships between the Contact Sublayer, inclusions, and the Main Mass of the Sudbury Igneous Complex: A case study of the Whistle Mine embayment. *Econ Geol*, v 92, pp 647-673
- Lightfoot PC, Keays RR, Morrison GG, et al (1997) Geochemical relationships in the Sudbury Igneous Complex: Origin of the Main Mass and offset dikes. *Econ Geol*, v 92, pp 289-307
- Li N, Kyle JR (1997) Geologic controls of sandstone-hosted Zn-Pb (Sr) mineralization, Jinding deposit, Yunnan Province, China: A new environment for sediment-hosted Zn-Pb deposits, *in*: Pei Rongfu, ed, 30th Intern Geol Congr Beijing, Proceedings v 9, pp 67-82
- Li Yidou (1993) Poly-type model for tungsten deposits and vertical structural zoning for vein-type tungsten deposits in South China. *Geol Assoc Canada Spec Paper* 40, pp 555-568
- Liao Shifan, et al (1992) Bauxite deposits of China, *in*: ECMDC, Mineral Deposits of China, v 2. Geol Publ House, Beijing, pp 1-51
- Lightfoot PC, Keays RR, Morrison GG, et al (1997) Geologic and geochemical relationships between the contact sublayer, inclusions, and the Main Mass of the Sudbury Igneous Complex: A case study of the Whistle Mine embayment. *Econ Geol*, v 92, pp 647-673
- Lightfoot PC, Naldrett AJ, eds (1994) Proceedings of the Sudbury-Noril'sk Symposium. *Ontario Geol Surv Spec Vol* 5, 423 p
- Lightfoot PC, Naldrett AJ (1996) Petrology and geochemistry of the Nipissing gabbro: Exploration strategies for nickel, copper, and platinum group elements in a large igneous province. *Ontario Geol Surv, Study* 58, 81 p
- Lillehagen NB (1979) The estimation and mining of Gove bauxite reserves, *in*: Estimation and Statement of Mineral Reserves. AusIMM, pp 19-32
- Lilljequist R (1973) Caledonian geology of the Laisvall area, southern Norrbotten, Swedish Lapland. *Sverige Geol Unders, Ser C*, no 691, 44 p
- Lindgren W (1911) The Tertiary gravels of the Sierra Nevada of California. *U.S. Geol Surv Profess Paper* 73, 226 p
- Lindgren W (1933) *Mineral Deposits*, 4th edition. McGraw Hill, New York, 930 p
- Lindgren W, Laughlin GF (1919) Geology and ore deposits of the Tintic district, Utah. *U.S. Geol Surv Profess Paper* 107, 282 p
- Lindgren W, Ransome FL (1906) Geology and gold deposits of the Cripple Creek district, Colorado. *U.S. Geol Surv Prof Paper* 54, 516 p
- Lindsey DA (1977) Epithermal beryllium deposits in water-laid tuff, western Utah. *Econ Geol*, v 72, pp 219-232
- Lindsay DD, Zentilli M, Rojas de la Rivera J (1995) Evolution of an active ductile to brittle shear system controlling the mineralization at the Chuquicamata porphyry copper deposit, northern Chile. *Intern Geol Rev*, v 37, pp 945-958
- Lipman PW (1984) The roots of ash-flow calderas: Windows into granitic batholiths. *Journ Geophys Res*, v 89, pp 8801-8841
- Lipman PW (1992a) Ash-flow calderas as structural controls of ore deposits-recent work and future problems. *U.S. Geol Surv Bull* 2021, pp L1-L12
- Lipman PW (1992b) Magmatism in the Cordilleran United States; progress and problems, *in*: The Geology of North America, v G-3, *Geol Soc Amer, Boulder*, pp 481-514
- Lisitzin AP (1971) Sedimentation in the World Ocean. *Soc Econ Paleont and Miner, Spec Publ* 17, Tulsa, 218 p
- Lisitsina MA, Kolokoltsev VG (1996) Tungsten mineralization in sedimentary formations. 30th Intern Geol Congr, Beijing, Abstract Volume 3
- Lister GS, Davis GA (1989) The origin of metamorphic core complexes and detachment faults formed during Tertiary continental extension in the northern Colorado River region, USA. *Journ Struct Geol*, v 11, pp 65-94
- Listerud WH, Meineke DG (1977) Mineral resources of a portion of the Duluth Complex and adjacent rocks in St Louis and Lake Counties, Northeastern Minnesota. *Minnes Dept Nat Res, Div of Minerals, Rept* 93
- Litvinenko VS, Smyslov AA, Sokolovskii AK, eds (1996) *Unikal'nye Mestorozhdeniya Rossii*:

- Zakonomernosti Formirovaniya i Razmeshcheniya. Gornyi Institut, St. Petersburg, 158 p
- Liu Chang-Shi, et al (1999) An F-rich, Sn-bearing volcanic-intrusive complex in Yanbei, South China. *Econ Geol*, v 94, pp 325-342
- Livingston DL, Mauger RL, Damon PE (1968) Geochronology of the emplacement, enrichment and preservation of Arizona porphyry copper deposits. *Econ Geol*, v 63, pp 30-36
- Li Xiji, Yang Zhuang, Shi Lin, Shi Jiabin (1992) Tin deposits of China, *in*: ECMDC, Beijing, pp 150-222
- Ljunggren P, Meyer HC (1964) The copper mineralization in the Corocoro basin, Bolivia. *Econ Geol*, v 59, pp 110-125
- Llewelyn GIW (1976) Recovery of uranium from seawater, *in*: Uranium Ore Processing. IAEA, Vienna, pp 205-231
- Lloa FT, Georgel JMP, Veliz JM (1999) Los porfidos Au-Cu de Minas Conga, *in*: Primer Volumen de Monografias de Yacimientos Minerales Peruanos. IIMP, Lima, pp 177-195
- Locke A (1926) Leached Outcrops as Guides to Copper Ores. Williams and Wilkins, Baltimore, 166 p
- Logan JM, Koyanagi VM (1994) Geology and mineral deposits of the Galore Creek area (104G). B.C. ministry of Engy, Mining, Petrol Res, Victoria, Bulletin, 96 p
- Logan RG, Murray WJ, Williams N (1990) Hyc silver-lead-zinc deposit, McArthur River, *in*: FE Hughes, ed, pp 907-911
- Lombaard AF, Explor Staff O'okiep Copper Company (1986) The copper deposits of the O'okiep district, Namaqualand, *in*: CR Anhaeusser, S Maske, eds, pp 1421-1445
- Lombaard AF, Günzel A, Innes J, Krüger TL (1986) The Tsumeb lead-copper-zinc-silver deposit, South-West Africa/Namibia; same public, pp 1761-1788
- Lombard T, Niccolini P, eds (1982) Gisements Stratiformes de Cuivre en Afrique. Symposium, Paris, 2 vols, 212 & 265 p
- Lonergan W (1997) Native title, the financial time bomb. *Austral Journ of Mining*, July 1997, pp 35-42
- López VM (1939) The primary mineralization at Chuquicamata, Chile, S.A. *Econ Geol*, v 34, pp 674-711
- Loudon AG (1976) Marcopper porphyry copper deposit, Philippines. *Econ Geol*, v 71, pp 721-732
- Loukola-Ruskeeniemi K (1991) Mercury concentrations in Proterozoic black schists in Finland: Environmental and Exploration aspects, *in*: M Pagel et al, eds. Source, Transport and Deposition of Metals. Balkema, Rotterdam, pp 557-560
- Lowell JD (1968) Geology of the Kalamazoo orebody, San Manuel district, Arizona. *Econ Geol*, v 63, pp 645-654
- Lowell JD, Guilbert JM (1970) Lateral and vertical alteration-mineralization zoning in porphyry copper ore deposits. *Econ Geol*, v 65, pp 373-408
- Lozovskii VN, Cheglakov SV, Sidorenko AV (1960) Osnovnye cherty struktury Baleiskovo zolotorudnovo polya, *in*: YeT Shatalov, ed, Osnovnye Voprosy i Metody Izucheniya Struktur Rudnykh Polei i Mestorozhdenii. Gosgeoltekhizdat, Moscow, pp 608-621
- Lucas JM (1985) Gold, *in*: Mineral Facts and Problems, U.S. Bureau of Mines Bull 675, pp 323-338
- Ludden J, Hubert C, Garipey C (1986) The tectonic evolution of the Abitibi greenstone belt of Canada. *Geol Mag*, v 123, pp 153-166
- Luff WM (1977) Geology of the Brunswick #12 mine. *CIM Bulletin*, no 782, v 70, pp 109-119
- Lu Huan-Zhang, et al (2003) Mineralization and fluid inclusion study of the Shizhouyuan W-Sn-Bi-Mo-F skarn deposit, Hunan Province, China. *Econ Geol*, v 98, pp 955-974
- Lukin LI, et al (1968) Osobennosti Struktur Hidrotermal'nykh Rudnykh Mestorozhdenii v Rozlichnykh Strukturnykh Etazhakh i Yarusakh. Nauka, Moscow, 295 p
- Lydon JW (1996) Sedimentary exhalative sulfides (sedex), *in*: Geology of Canada No 8, *Geol Surv Canada*, pp 130-152
- Lydon JW, et al, eds (2000) The geological environment of the Sullivan deposit. *Geol Assoc Canada, Miner Deposits Division, Spec Volume 1*
- Lyons JJ (1988) Volcanogenic iron oxide deposits, Cerro de Mercado and vicinity, Durango, Mexico. *Econ Geol*, v 83, pp 1886-1906
- Maaløe S (1985) Principles of Igneous Petrology. Springer-Verlag
- Maaløe S, Petersen TS (1981) Petrogenesis of oceanic andesites. *Journ Geophys Res*, v 86, pp 10273-10286
- Maas R (1989) Nd-Sr isotope constraints on the age and origin of unconformity-type uranium deposits in the Alligator Rivers uranium field, Northern Territory, Australia. *Econ Geol*, v 84, pp 64-90
- Mabbutt JA (1980) Weathering history and landform development. *Journ Geoch Explor*, v 12, pp 96-107
- Macauley TN (1973) Geology of the Ingerbelle and Copper Mt deposits at Princeton, B.C. *CIM Bull for April 1973*, pp 105-112
- Macdonald C (1985) Mineralogy and geochemistry of the Sub-Athabasca regolith near Wollaston Lake. *CIM Spec Vol 32*, pp 155-158
- Macdonald GA (1968) Composition and origin of Hawaiian lavas. *Geol Soc Amer Mem 116*, pp 477-522
- Mac Donald GD, Arnold LC (1994) Geological and geochemical zoning of the Grasberg igneous complex, Irian Jaya, Indonesia. *Journ Geoch Explor*, v 50, pp 143-178
- MacGeehan PJ (1978) The geochemistry of altered volcanic rocks at Matagami, Quebec: a geothermal model for massive sulfide genesis. *Canad Journ Earth Sci*, v 15, pp 551-570
- Mac Gregor I (1978) Metals and minerals-a look at the future. *Proc 11th Commonw Min Metall Congr, Hong Kong*, pp 3-7
- MacIntyre DG (1991) SEDEX-sedimentary exhalative deposits: Ore deposits, tectonics and metallogeny of the Canadian Cordillera. *Brit Columbia Ministry of Engy, Min & Petrol Res, Paper 1991-4*, pp 25-70

- Mackenzie BW, Bilodeau ML (1984) Economics and Mineral Exploration in Australia: Guidelines for Corporate Planning and Government Policy. Austral Miner Foundation, Adelaide, 171 p
- Mackenzie DH, Davies RH (1990) Broken Hill lead-silver-zinc deposit at Z.C. mines, *in*: FE Hughes, ed, pp 1079-1084
- MacKevett EM Jr, Cox DP, Potter RW II, Silberman ML (1977) Kennecott-type deposits in the Wrangell Mountains, Alaska: High-grade copper ores near a basalt-limestone contact. *Econ Geol Monogr* 9, pp 66-89
- MacLean WH, Hoy LD (1991) Geochemistry of hydrothermally altered rocks at the Horne Mine, Noranda, Quebec. *Econ Geol*, v 86, pp 506-528
- MacLeod WN, Turner DC, Wright EP (1971) The geology of the Jos Plateau. *Geol Surv Nigeria, Bull* 32, 269 p
- Maekawa H, Shozui M, Ishii T, Fryer P, Pearce AJ (1993) Blueschist metamorphism in an active subduction zone. *Nature*, v 364, pp 520-523
- Magak'yan IG (1968) Ore Deposits. *Intern Geol Revs*, v 10, 202 p
- Magnusson NH (1970) The origin of the iron ores in Central Sweden and the history of their alterations. *Sveriges Geol Unders, Ser C, No 643*, 364 p
- Mainwaring PR, Naldrett AJ (1977) Country rock assimilation and the genesis of Cu-Ni sulfides in the Western Intrusion, Duluth Complex, Minnesota. *Econ Geol*, v 72, pp 1269-1284
- Mann AW, Horwitz RC (1979) Groundwater calcrete deposits in Australia: Some observations from Western Australia. *Journ Geol Soc Australia*, v 26, pp 293-303
- Mann AW, Webster JG (1990) Gold in the exogenic environment, *in*: FE Hughes, ed, pp 119-126
- Mao Jingwen, Goldfarb RJ, Wang Yitian, Hart CJ, Wang Zhiliang, Yang Jianmin (2004) Late Paleozoic base and precious metal deposits, East Tianshan, Xinjiang, China: Characteristics and geodynamic setting. *Episodes*, v 28, pp 23-36
- Mao Jingwen, Zhang Zuoheng, Yang Jianwin, Wang Zhiliang, Zhang Zhaochong (1999) The Ta'ergou skarn-quartz vein type tungsten deposit in the North Qilian Caledonian Orogen, NW China, *in*: CJ Stanley et al, ed, *Mineral Deposits: Processes to Processing*. Balkema, Rotterdam, pp 381-384
- Marakushev AA, Khokhlov VA (1992) A petrological model for the genesis of the Muruntau gold deposit. *Intern Geol Rev*, v 34, pp 59-76
- Maranhão R, Barreiro DS, Da Silva AP, Lima F, Pires PRR (1986) A jazida de scheelita de Brejui/Barra Verde/Boca de Lage/Zangarellhas, Rio Grande do Norte, *in*: C Schobbenhaus, CES Coelho, eds, v 2, pp 393-407
- Marcoux E, Moëlo Y, Leistel JM (1996) Bismuth and cobalt minerals as indicators of stringer zones to massive sulfide deposits, Iberian Pyrite Belt. *Mineralium Deposita*, v 31, pp 1-26
- Marcus JJ (2000) Butte, "Richest Hill on Earth" and costliest mine Superfund site. *Engin and Mining Journ*, Febr 2000, pp 31-44
- Marguis P, et al (1990) Overprinting of early, redistributed Fe and Pb-Zn mineralization by late-stage Au-Ag-Cu deposition at the Dumagami mine, Bousquet district, Abitibi, Quebec. *Canad Journ Earth Sci*, v 27, pp 1651-1670
- Marinou GP, Petrascheck WE (1956) Laurion. *Institute for Geol and Subsurf Research, Athens*, v 4, 247 p
- Marjoribanks RW, Rutland RWR, Glen RA, Laing WP (1980) The structure and tectonic evolution of the Broken Hill region, Australia. *Precambr Res*, v 13, pp 209-240
- Mark G, Oliver NHS, Williams PJ, Valenta RK, Crookes RA (2000) The evolution of the Ernest Henry Fe-oxide (Cu-Au) hydrothermal system, *in*: TM Porter, ed, *Hydrothermal Iron Oxide Copper-gold and Related Deposits: a Global Perspective*. AMF, Adelaide, pp 123-136
- Marquis P, Brown AC, Hulbert C, Rigg DM (1990) Progressive alteration associated with auriferous massive sulfide bodies at the Dumagami Mine, Abitibi greenstone belt, Quebec. *Econ Geol*, v 85, pp 746-764
- Marsaglia KM (1995) Interarc and backarc basins, *in*: CJ Busby Spera, RV Ingersoll, eds, *Tectonics of Sedimentary Basins*. Blackwell, pp 299-329
- Marsden RW, et al (1968) The Mesabi Iron Range, Minnesota, *in*: JD Ridge, ed, *Ore Deposits in the United States 1933-1967*, AIME, pp 518-537
- Marsh TM, Einaudi MT, McWilliams M (1997) $^{40}\text{Ar}/^{39}\text{Ar}$ geochronology of Cu-Au and Au-Ag mineralization in the Potrerillos district, Chile. *Econ Geol*, v 92, pp 784-806
- Marston RJ (1984) Nickel mineralization in W.A. Western Australia *Geol Surv Miner Resources Bull* 14
- Martin HJ (1964) The Bikita Tinfield. *South Rhodesia Geol Surv Bull No 58*, pp 114-132
- Martini JEJ (1986) Stratiform gold mineralization in paleosol and ironstone of early Proterozoic age, Transvaal Sequence, South Africa. *Mineralium Deposita*, v 21, pp 306-312
- Marvin RF, Witkind IJ, Keefer WM, Mehnert HH (1973) Radiometric ages of intrusive rocks in the Little Belt Mountains, Montana. *Geol Soc Amer Bull*, v 84, pp 1977-1986
- Masaitis VL (1994) Impactites from Popigay Crater. *Geol Soc Amer Spec Paper* 293, pp 153-165
- Mason B (1979) *Data of Geochemistry*, 6th edition, Chapter B, Cosmochemistry, Pt 1, Meteorites. U.S. Geol Surv Prof Paper 440-B-1, 132 p
- Masterman GJ, Cooke DR, Berry RF, Clark AH, Archibald DA, Mathur R, Walshe JL, Durán M (2004) $^{40}\text{Ar}/^{39}\text{Ar}$ and Re-Os geochronology of porphyry copper-molybdenum deposits and related copper-silver veins in the Collahuasi district, northern Chile. *Econ Geol*, v 99, pp 673-690
- Mathias BV, Clark GJ (1975) Mount Isa copper and silver-lead-zinc orebodies, Isa and Hilton Mines, *in*: CL Knight, ed, pp 351-372

- Matthews SJ, Marquillas RA, Kemp AJ, Grange FK, Gardeweg MC (1996) Active skarn formation beneath Lascar Volcano, northern Chile: A petrographic and geochemical study of xenoliths in eruption products. *Journ Metam Geol*, v 14, pp 509-530
- Mattos R, Valle J (1999) Exploración, geología y desarrollo del yacimiento Toquepala, *in*: Primer Volumen de Monografías de Yacimientos Peruanos. IIMP Lima, pp 101-116
- Maynard JB (1983) Geochemistry of Sedimentary Ore Deposits. Springer-Verlag, 305 p
- Maynard JB (1991a) Copper: product of diagenesis in rifted basins. *Reviews in Econ Geol*, v 5, pp 199-207
- Maynard JB (1991b) Uranium: syngenetic to diagenetic deposits in foreland basins. Same publication, pp 187-197
- Mazurov AK (1996) The Koktenkol' stockwork W-Mo deposit, Central Kazakhstan, *in*: V Shatov et al, eds, Granite-Related Ore Deposits of Central Kazakhstan and Adjacent Areas. Glagol, St. Petersburg, pp 155-165
- McArthur GJ, Dronseika EV (1990) Que River and Hellyer zinc-lead-silver deposits. *in*: FE Hughes, ed, Austral Inst Min Metallurgy Monogr 14, pp 1229-1230
- McBirney AR (1996) The Skaergaard Intrusion, *in*: RG Cawthorn, ed, Layered Intrusions. Elsevier, Amsterdam, pp 147-180
- McCarthy TS (1994) A review of the regional structural controls on the occurrence and character of the Ventersdorp Contact Reef. *Econ Geol Res Unit, Witwatersrand Uni, Info circular 276*, 21 p
- McCarthy TS, Stanistreet IG, Robb LJ (1990) Geological studies related to the origin of the Witwatersrand Basin and its mineralization-an introduction and a strategy for research and exploration. *South African Journ Geol*, v 93, pp 1-4
- McClay KR (1983) Structural evolution of the Sullivan Fe-Pb-Zn-Ag orebody, Kimberley, British Columbia, Canada. *Econ Geol*, v 78, pp 1398-1424
- McClay KR, Bidwell GE (1986) Geology of the Tom deposit, Macmillan Pass, Yukon. *CIM Spec Vol 37*, pp 100-114
- McConnell RB (1972) Geological development of the rift system of eastern Africa. *Geol Soc Amer Bull*, v 83, pp 2549-2522
- McCoy D, Newberry RJ, Layer P, DiMarchi JJ, Bakke A, Masterman JS, Minehane DL (1997) Plutonic-related gold deposits of interior Alaska. *Econ Geol Monogr* 9, pp 191-241
- McCracken SR, Etminan H, Connor AG, et al (1996) Geology of the Admiral Bay carbonate-hosted zinc-lead deposit, Canning Basin, Western Australia, *in*: DF Sangster, ed, Carbonate-hosted lead-zinc deposits. *Soc Econ Geol Special Publ* 4, pp 330-349
- McCready AJ, Annesley IR, Parnell J, Richardson L (1999) The uranium-carbonaceous matter association, McArthur River, Canada, *in*: Stanley et al, eds, Mineral Deposits: Processes to Processing. Balkema, Rotterdam, pp 251-254
- McCready AJ, Stumpfl EF, Lally JH, Ahmad M, Gee RD (2004) Polymetallic mineralization at the Brown's deposit, Rum Jungle mineral field, Northern Territory, Australia. *Econ Geol*, v 99, pp 257-277
- McCutcheon SR (1992) Base metal deposits of the Bathurst-Newcastle district: Characteristics and depositional models. *Explor Mining Geol*, v 1, pp 105-119
- McDonald DA, Surdam RC, eds (1984) Clastic Diagenesis. *AAPG Memoir* 37, 434 p
- McDonald EH (1985) Alluvial Mining. Chapman and Hall, London, 508 p
- McDougall JJ (1991) History of the Windy Craggy massive sulfide, B.C., Canada, *in*: VF Hollister, ed, Case Histories of Mineral Discoveries, v 3. AIME, Littleton, CO, pp 135-137
- McFarlane MJ (1976) Laterite and Landscape. *Acad Press, London*, 151 p
- McInnes M (1995) Boleo, Mexico's new copper cobalt mine. *Randol at Vancouver '95*, pp 159-168
- McInnes BIA, Cameron EM (1994) Carbonated, alkaline metasomatic melts from a sub-arc environment: Mantle wedge sample from the Tabar-Lihir-Tangafeni arc, Papua New Guinea. *Earth Planet Sci Letters*, v 122, pp 125-141
- McKee EH, Dreier JE, Noble DC (1992) Early Miocene hydrothermal activity at Pachuca-Real del Monte, Mexico: An example of space-time association of volcanism and epithermal Ag-Au vein mineralization. *Econ Geol*, v 87, pp 1635-1637
- McKee EH, Rytuba JJ, Xu Keqin (1987) Geochronology of the Xihuashan composite granitic body and tungsten mineralization, Jiangxi Province, South China. *Econ Geol*, v 82, pp 218-223
- McKelvey VE (1960) Relation of reserves of the elements to their crustal abundance. *Amer Journ Sci*, v 258-A, pp 234-241
- McKelvey VE (1986) Subsea Mineral Resources. *U.S. Geol Surv Bull* 1689-A, 106 p
- McKelvey VE, Strobell JD Jr, Slaughter AL (1986) The vanadiferous zone of the Phosphoria Formation in western Wyoming and southeastern Idaho. *U.S. Geol Surv Prof Paper* 1465, 27 p
- McKelvey VE, Williams JS, Sheldon RP, et al (1959) The Phosphoria, Park City and Shedhorn Formations in the Western Phosphate Field. *U.S. Geol Surv Profess Paper* 313-A, 47 p
- McKibben MA, Andes JP Jr, Williams AE (1988a) Active ore formation at a brine interface in metamorphosed deltaic lacustrine sediments: The Salton Sea geothermal system, California. *Econ Geol*, v 83, pp 511-523
- McKibben MA, Williams AE, Okubo S (1988b) Metamorphosed Plio-Pleistocene evaporites and the origins of hypersaline brines in the Salton Sea geothermal system, California: Fluid inclusion evidence. *Geoch et Cosmoch Acta*, v 52, pp 1047-1056
- Mc Kibben MA, Elders WA (1985) Fe-Zn-Cu-Pb mineralization in the Salton Sea geothermal system,

- Imperial Valley, California. *Econ Geol*, v 80, pp 539-559
- McKibben MA, Hardie LA (1997) Ore-forming brines in active continental rifts, *in*: HL Barnes, ed, *Geochemistry of Hydrothermal Ore Deposits*. Wiley, New York, pp 877-935
- McKinney JS, et al (1964) Geology of the Anglo-American group of mines in the Welkom area, Orange Free State Goldfield, *in*: SH Haughton, ed, pp 451-506
- McKnight ET, Fischer RP (1970) Geology and ore deposits of the Picher Field, Oklahoma and Kansas. U.S. Geol Surv Prof Paper 588, 165 p
- McLaren DI, Skinner BJ, eds (1987) *Resources and World Development*. Wiley, Chichester
- McMillan WJ (1991) Overview of the tectonic evolution and setting of mineral deposits in the Canadian Cordillera. Brit Columbia Ministry of Energy, Mines, Petrol Res, Paper 1991-4, pp 5-24
- McPhie J, Allen RL (1992) Facies architecture of mineralized submarine volcanic sequences: Cambrian Mount Read Volcanics, Western Tasmania. *Econ Geol*, v 87, pp 587-596
- Mealey GA (1996) Grasberg. Mining the Richest and Most Remote Deposit of Copper and Gold in the World, in the Mountains of Irian Jaya, Indonesia. Freeport McMoRan Inc, New Orleans, 384 p
- Megaw PKM, Ruiz J, Titley SR (1988) High-temperature, carbonate-hosted Ag-Pb-Zn(Cu) deposits of northern Mexico. *Econ Geol*, v 83, pp 1856-1885
- Meinert LD (1987) Skarn zonation and fluid evolution in the Groundhog mine, Central mining district, New Mexico. *Econ Geol*, v 82, pp 523-545
- Meinert LD (1993) Igneous petrogenesis and skarn deposits. *Geol Assoc Canada, Spec Paper* 40, pp 569-584
- Meinert LD (1995) Compositional variation of igneous rocks associated with skarn deposits-chemical evidence for a genetic conversion between petrogenesis and mineralization, *in*: JFH Thompson, ed, *Magma, Fluids and Ore Deposits*. Miner Assoc Canada, Short Course Vol 23, pp 401-418
- Meinert LD, Hedenquist JW, Satoh H, Matsuhisa Y (2003) Formation of anhydrous and hydrous skarn in Cu-Au ore deposits by magmatic fluids. *Econ Geol*, v 98, pp 147-156
- Meinert LD, Hefton KK, Mayes D, Tasiran I (1997) Geology, zonation, and fluid evolution of the Big Gossan Cu-Au skarn deposit, Ertsberg district, Irian Jaya. *Econ Geol*, v 92, pp 509-533
- Melack JM, ed (1985) *Saline lakes; Proceedings of the Third Internat Sympos on inland saline lakes*, Nairobi, Aug 1985. W Junk, Dordrecht-Boston, 316 p
- Melcher G, Grum W, Thalhammer TV, et al (1999) The giant chromite deposits at Kempirsai, Urals: Constraints from trace element (PGE, REE) and isotope data. *Mineralium Deposita*, v 34, pp 250-272
- Melchiorre EB, Enders MS (2003) Stable isotope geochemistry of copper carbonates in the NW Extension deposit, Morenci District, Arizona: Implications for conditions of supergene oxidation and related mineralization. *Econ Geol*, v 98, pp 607-621
- Mendelsohn F, ed (1961) *The Geology of the Northern Rhodesian Copperbelt*. Macdonald, London, 523 p
- Mendonça JCGS, et al (1985) Jazida de urânio de Itataia-Ceará, *in*: C Schobbenhaus, CES Coelho, eds, pp 121-131
- Meng HM, Chern K, Ho T (1937) Geology of the Kochiu tin field, Yunnan, a preliminary sketch. *Bull Geol Soc China*, v 16, pp 421-437
- Mero JL (1965) *The Mineral Resources of the Sea*. Elsevier, Amsterdam, 312 p
- MERQ-OGS (Minist de l'Energie et des Res, Québec-Ontario Geol Surv) (1983) *Lithostratigraphic Map of the Abitibi Subprovince*, 1:500,000
- Messenger PR, Taube A, Golding SD, Hartley JS (1998) Mount Morgan gold-copper deposits, *in*: DA Berkman, DH Mackenzie, eds, pp 712-722
- Metz RA, Rose AW (1966) Geology of the Ray copper deposit, Ray, Arizona, *in*: SR Titley, CL Hicks, eds, pp 177-188
- Meyer C, Shea EP, Goddard CC Jr, Staff (1968) Ore deposits at Butte, Montana, *in*: JD Ridge, ed, *Ore Deposits of the United States 1933-1967*, AIME, New York, pp 1373-1416
- Meyer C (1981) Ore-forming processes in geologic history. *Econ Geol* 75th Anniv Vol, pp 6-41
- Meyer C (1988) Ore deposits as guides to geologic history of the Earth. *Ann Revs Earth Planet Sci*, v 16, pp 147-171
- Meyer FM, Tainton S, Saager R (1990) The mineralogy and geochemistry of small-pebble conglomerate from the Promise Formation in the West Rand and Klerksdorp areas. *S Afr Journ Geol*, v 93, pp 118-134
- Meylan MA, Glasby GP, Knedler KE, Johnston JH (1981) Metalliferous deep-sea sediments, *in*: KH Wolf, *Handbook of Stratiform and Stratabound Ore Deposits*, v 9, Elsevier, Amsterdam, pp 77-178
- Miall AD (1978) Fluvial Sedimentology. *Canad Soc Petrol Geol Mem* 5, 859 p
- Middleton C, Buenavista A, Rohrlach B, Gonzales J, Subang L, Moreno G (2004) A geological review of the Tampakan copper-gold deposit, southern Mindanao, Philippines. *PACRIM 2004 Proceedings*, Adelaide, AusIMM, pp 173-187
- Mikulski SZ, Olszynski W, Speczik S, et al (1999) Primary gold deposits and occurrences in the Sudety Mts, SW Poland, *in*: CJ Stanley et al, eds, *Mineral Deposits: Processes to Processing*. Balkema, Rotterdam, pp 1419-1422
- Milburn I, Wilcock S (1998) Kunwarara magnesite deposit, *in*: DA Berkman, DH Mackenzie, eds, pp 815-818
- Milési J-P, Ledru P, Feybesse J-L, et al (1992) Early Proterozoic ore deposits and tectonics of the Birrimian orogenic belt, West Africa. *Precamb Res*, v 58, pp 305-344
- Miller RR (1988) Yttrium (Y) and other rare metals (Be, Nb, REE, Ta, Zr) in Labrador. *Newfoundland Dept Min Rept* 88-1, pp 229-245
- Miller DM, Nilsen TH, Bilodeau WL (1992) Late Cretaceous to early Eocene geologic evolution of the

- US Cordillera. The Geology of North America, v G-3, Geol Soc Amer, Boulder, pp 205-260
- Minard JP (1971) Gold occurrences near Jefferson, South Carolina. U.S. Geol Surv Bull 1334, 20 p
- Minnitt RCA (1986) Porphyry copper-molybdenum mineralization at Haib River, South West Africa/Namibia, *in*: CR Anhaeusser, S Maske, eds, pp 1567-1585
- Minter WEL (1999) Irrefutable detrital origin of Witwatersrand gold and evidence of eolian signatures. *Econ Geol*, v 94, pp 665-670
- Minter WEL, Hill WCN, Kidger RJ, Kingsley CS, Snowden PA (1986) The Welkom Goldfield, *in*: CR Anhaeusser, S Maske, eds, pp 497-539
- Minter WEL, Feather CE, Glatthaar CW (1988) Sedimentological and mineralogical aspects of the newly discovered Witwatersrand placer deposit that reflect Proterozoic weathering, Welkom Gold Field, South Africa. *Econ Geol*, v 83, pp 481-491
- Misra KC, Gratz JF, Lu C (1996) Carbonate-hosted Mississippi Valley-type mineralization in the Elmwood-Gordonsville deposits, Central Tennessee zinc district: A synthesis, *in*: DF Sangster, ed, Carbonate-Hosted Lead-Zinc Deposits. Soc Econ Geol Spec Public 4, pp 58-73
- Mitcham TW (1952) Indicator minerals, Coeur d'Alene silver belt. *Econ Geol*, v 47, pp 414-450
- Mitchell AHG (1996) Distribution and genesis of some epizonal Zn-Pb and Au provinces in the Carpathian-Balkan region. *Transact Inst Min Metall*, London, v 105, pp B 127-B 135
- Mitchell AHG, Bell JD (1973) Island arc evolution and related mineral deposits. *Journ Geology*, v 81, pp 381-405
- Mitchell AHG, Garson MS (1981) Mineral Deposits and Global Tectonic Setting. Academic Press, London, 405 p
- Mitchell AHG, Leach TM (1991) Epithermal Gold in the Philippines: Island Arc Metallogenesis, Geothermal Systems, and Geology. Academic Press, San Diego, 457 p
- Mitchell AHG, Reading HG (1986) Sedimentation and tectonics, *in*: HG Reading, ed, Sedimentary Environments and Facies, 2nd ed. Blackwell, Oxford, pp 471-519
- Mitchell RH (1986) Kimberlites. Plenum, New York
- Miyashiro A (1973) Metamorphism and Metamorphic Belts. Allen and Unwin, London, 492 p
- Mlakar I, Drovenik M (1971) Strukturne in genetske posebnosti idrijskega rudišča. *Geologija*, Ljubljana, v 14, pp 67-126
- Mlynarczyk MSJ, Sherlock RL, Williams-Jones AE (2003) San Rafael, Peru: Geology and structure of the world's richest tin lode. *Mineralium Deposita*, v 38, pp 555-567
- Moench RH, Schlee JS (1967) Geology and uranium deposits of the Laguna district, New Mexico. U.S. Geol Surv Profess Paper 519, 117 p
- Moiseyev AN (1968) The Wilbur Springs Quicksilver district (California). Example of a study of hydrothermal processes by combining field geology and theoretical geochemistry. *Econ Geol*, v 63, pp 169-181
- Molyneux TG (1970) The geology of the area in the vicinity of Magnet Heights, Eastern Transvaal, with special reference to the magnetic iron ore. *Geol Soc S Africa, Spec Publ 1*, pp 228-241
- Monger JWH, Wheeler JO, Tipper HW, Gabrielse H, Harms T, Struik LC, Campbell RB, Dodds CJ, Gehrels GE, O'Brien J (1992). Cordilleran Terranes, *in*: H Gabrielse, CJ Yorath, eds, pp 281-327
- Monteiro LVS, Bettencourt JS, Spiro B, Graça R, de Oliveira F (1999) The Vazante zinc mine, Minas Gerais, Brazil: Constraints on willemite mineralization and fluid evolution. *Explor Mining Geol*, v 8, pp 21-42
- Moolick RT, Durek JJ (1966) The Morenci district, *in*: SR Titley, CL Hicks, eds, pp 221-231
- Moon KJ (1989) Discovery of source rock of Sangdong tungsten mineralization. 28th Intern Geol Congress, Washington DC, Abstracts, v 2, p 454
- Moore CH (1989) Carbonate Diagenesis and Porosity. Elsevier, Amsterdam, 338 p
- Moore DW, Young LE, Modene JS, Plahuta JT (1986) Geologic setting and genesis of the Red Dog zinc-lead-silver deposit, western Brooks Range, Alaska. *Econ Geol*, v 81, pp 1696-1727
- Morávek P, Janatka J, Pertoldová J, Straka E, Ďurišová J, Pudilová M (1989) The Mokrsko gold deposit-the largest gold accumulation in the Bohemian Massif, Czechoslovakia. *Econ Geol Monogr 6*, pp 252-259
- Morgan GB, London D, Luedke RG (1998) Petrochemistry of late Miocene peraluminous silicic volcanic rocks from the Morococala Field, Bolivia. *Journ Petrol*, v 39, pp 601-632
- Morgan JD Jr (1976) World nonfuel mineral supply: The outlook as we approach the Twenty-first century. U.S. Geol Surv Prof Paper 1193, pp 203-215
- Morgan P, Baker BH, eds (1983) Processes of Continental Rifting. Elsevier, Amsterdam, 680 p
- Morris EM, Pasteris JD (1987) Prologue, *in*: Mantle Metasomatism and Alkaline Magmatism. Geol Soc Amer Spec Paper 215, pp 1-4
- Morris HT (1987) Tintic mining district, Utah, *in*: JL Johnson, ed, Bulk Mineable Precious Metal Deposits of the Western United States, Guidebook for Field Trips. Geol Soc Nevada, Reno, pp 390-393
- Morris HT, Lovering TS (1979) General geology and mines of the East Tintic mining district, Utah and Juab Counties, Utah. U.S. Geol Surv Profess Paper 1024, 203 p
- Morris JD, Ryan JG (2004) Subduction zone processes and implications for changing composition of the upper and lower mantle, *in*: RW Carlson, ed, pp 451-470
- Morris RC (1987) Iron ores derived by the enrichment of banded iron formation, *in*: JR Hein, ed, The Genesis of Ores and Petroleum Associated with Siliceous Deposits. Van Nostrand Reinhold, New York, pp 231-267
- Morrison G, Kary G, Handfield R, et al (1999) Intrusion-alteration-mineralization relationships in the Frieda

- River igneous complex, PNG. PACRIM '99, Bali, Proceedings. AusIMM, pp 527-533
- Morrison GG (1984) Morphological features of the Sudbury Structure in relation to an impact origin, *in*: EG Pye et al, eds, The Geology and Ore Deposits of the Sudbury Structure. Ontario Geol Surv Spec Vol 1, 603 p
- Mortensen JK (1990) Geology and U-Pb chronology of the Klondike district, West-Central Yukon Territory. *Canad Journ Earth Sci*, v 27, pp 903-914
- Mortimer C, Münchmeyer CF, Urqueta ID (1977) Emplacement of the Exotica orebody, Chile. *Inst Min Metall*, London, Transact, v 8, pp B121-B127
- Morton AC, Parson LM, eds (1988) Early Tertiary volcanism and the opening of the NE Atlantic. *Geol Soc London, Spec Publ* 39, pp 407-420
- Morton RL, Frasnklin JM (1987) Two-fold classification of Archean volcanic-associated massive sulfide deposits. *Econ Geol*, v 82, pp 1057-1063
- Morton RL, Nebel ML (1984) Hydrothermal alteration of felsic volcanic rocks at the Helen siderite deposit, Wawa, Ontario. *Econ Geol*, v 79, pp 1319-1333
- Morvai G (1982) Hungary, *in*: FW Dunning, W Mykura, D Slater, eds, Mineral Deposits of Europe, v 2. IMM/Miner Soc, London, pp 13-53
- Mossom RJ (1986) The Atok platinum mine, *in*: CR Anhaeusser, S Maske, eds, pp 1143-1153
- Motica JE (1968) Geology and uranium-vanadium deposits in the Uravan mineral belt, southwestern Colorado, *in*: JD Ridge, ed, Ore Deposits of the United States 1933-1967. AIME, New York, pp 805-813
- Mott LV, Drever JI (1983) Origin of uraniferous phosphatic beds in Wilkins Peak Member of Green River Formation, Wyoming. *AAPG Bull*, v 67, pp 70-82
- Mottl MJ (1983) Metabasalts, axial hot springs, and the structure of hydrothermal systems at mid-ocean ridges. *Geol Soc Amer Bull*, v 94, pp 161-180
- Moyle AJ, Doyle BJ, Hoogvliet H, et al (1990) Ladolam gold deposit, Lihir Island, *in*: FE Hughes, ed, pp 1793-1805
- Mpodozis C, Allmendinger RW (1993) Extensional tectonics, Cretaceous Andes, northern Chile (27°S). *Geol Soc Amer Bull*, v 105, pp 1462-1477
- Mpodozis C, Ramos V (1989) The Andes of Chile and Argentina, *in*: Ericksen et al, eds, pp 59-90
- Muir TL, Schnieders BR, Smyk MC, eds (1995) Geology and gold deposits of the Hemlo area, revised edition, *in*: Hemlo field trip guidebook, Geol Assoc/Miner Assoc Canada, Toronto '91
- Mullen TV Jr, Parrish IS (1998) Short history of man and gold. *Mining Engin*, January 1998, pp 50-56
- Müller D, Groves DI (2000) Potassic Igneous Rocks and Associated Gold-Copper Mineralization, 3rd ed. Springer-Verlag, 252 p
- Mumpton FA, ed (1986) Studies in Diagenesis. *U.S. Geol Surv Bull* 1578, 368 p
- Münchmeyer C (1996) Exotic deposits-products of lateral migration of supergene solutions from porphyry copper deposits, *in*: F Camus, RM Sillitoe, R Petersen, eds, Andean Copper Deposits: New Discoveries, Mineralization, Styles and Metallogeny. *Soc Econ Geol, Spec Publ* 5, pp 43-58
- Murillo J, Cordero G, Bustos A (1968) Geología y yacimientos minerales de la region de Potosí, v 2. *Serv Geol Bolivia, Bol* 11, 188 p
- Murphy GC (1990) Lennard Shelf lead-zinc deposits, *in*: FE Hughes, ed, pp 1103-1109
- Mustard H (1997) The Bau gold district, East Malaysia, *in*: World Gold '97. AusIMM, pp 67-77
- Mutschler FE, Mooney TC (1993) Precious metal deposits related to alkalic igneous rocks: Provisional classification, grade-tonnage data and exploration frontiers. *Geol Assoc Canada, Spec Paper* 40, pp 479-520
- Mutschler FE, Wright EG, Ludington S, Abbott JT (1981) Granite molybdenite systems. *Econ Geol*, v 76, pp 874-897
- Myers JS (1985) Archean tectonics in the Fiskenaasset region of Southwest Greenland, *in*: A Kröner et al, eds, Precambrian Tectonics Illustrated. Schweizerbart, Stuttgart, pp 95-112
- Myers JS (1988) Early Archean Narryer Gneiss Complex, Yilgar Craton, Western Australia. *Precamb Res*, v 38, pp 297-307
- Myers RE, McCarthy TS, Stanistreet IG (1990) A tectono-sedimentary reconstruction of the development and evolution of the Witwatersrand Basin, with particular emphasis on the Central Rand Group. *South Afr Journ Geol*, v 93, pp 180-201
- Naeser CW, Cunningham CG, Marvin RF, Obradovich JD (1980) Pliocene intrusive rocks and mineralization near Rico, Colorado. *Econ Geol*, v 75, pp 122-127
- Nakovnik KI (1968) Vtorichnye Kvartsity SSSR. Nedra, Moscow
- Naldrett AJ (1989a) Contamination and the origin of the Sudbury structure and its ores. *Reviews in Econ Geol*, v 4, pp 119-134
- Naldrett AJ (1989b) Magmatic Sulphide Deposits. Clarendon-Oxford Univ Press, 186 p
- Naldrett AJ (1993) Models for the formation of strata-bound concentrations of platinum-group elements in layered intrusions, *in*: RV Kirkham et al, eds, *Geol Assoc Canada Spec Paper* 40, pp 373-388
- Naldrett AJ (1997) Key factors in the genesis of Noril'sk, Sudbury, Jinchuan, Voisey's Bay and other world class Ni-Cu-PGE deposits-implications for exploration. *Austral Journ Earth Sci*, v 44, pp 283-315
- Naldrett AJ (1998) Ni-Cu-PGE ores of the Noril'sk region, Siberia: Lessons for exploration elsewhere. *Pathways '98*, pp 68-73
- Naldrett AJ (1999a) World-class Ni-Cu-PGE deposits: Key factors in their genesis. *Mineralium Deposita*, v 34, pp 227-240
- Naldrett AJ (1999b) Sudbury: Development of ideas on Sudbury geology, 1992-1998. *Geol Soc Amer, Spec Paper* 339, pp 431-442
- Naldrett AJ (2004) Magmatic Sulfide Deposits: Geology, Geochemistry, and Exploration. Springer-Verlag, 727 p
- Naldrett AJ, Asif M, Schandl E, Searcy T, Morrison GG, Binney WP, Moore C (1999) Platinum-group elements

- in the Sudbury ores: Significance with respect to the origin of different ore zones and to the exploration for footwall orebodies. *Econ Geol*, v 94, pp 185-210
- Naldrett AJ, Cameron G, von Gruenewaldt G, Sharpe MR (1987) The formation of stratiform PGE deposits in layered intrusions, *in*: I Parsons, ed, *Origin of Igneous Layering*. Reidel, Dordrecht, pp 313-397
- Naldrett AJ, Fedorenko VA, Asif M, et al (1996) Controls on the composition of Ni-Cu sulfide deposits as illustrated by those at Noril'sk, Siberia. *Econ Geol*, v 91, pp 751-773
- Naldrett AJ, Keats H, Sparkes K, Moore R (1996) Geology of the Voisey's Bay Ni-Cu-Co deposit, Labrador, Canada. *Explor Mining Geol*, v 5, pp 169-179
- Naldrett AJ, Kullerud G (1967) A study of the Strathcona Mine and its bearing on the origin of the nickel-copper ores of the Sudbury district, Ontario. *Journ Petrol*, v 8, pp 453-531
- Naldrett AJ, Rao BV, Evensen NM, Dressler BO (1985) Major and trace element and isotopic studies at Sudbury-a model for the structure and its ores. *Ontario Geol Surv Misc Paper 127*, pp 30-44
- Nanna D, Baumann M, Berentsen E, et al (1987) Getchell deposit, *in*: JL Johnson, ed, *Bulk Mineable Precious Metal Deposits of the Western United States*, Guidebook for field trips. *Geol Soc Nevada, Reno*, pp 353-356
- Naqvi SM, ed (1990) *Precambrian Continental Crust and its Economic Resources*. Elsevier, Amsterdam, 690 p
- Narkelyun LF, et al (1977) *Medistye Peschaniki i Slantsy Yuzhnoi Chasti Sibirskoi Platformy*. Nedra, Moscow, 223 p
- Nason PW, Shaw AV, Aveson KD (1982) Geology of the Poston Butte porphyry copper deposit, Pinal County, Arizona, *in*: SR Titley, ed, pp 375-386
- Nataf H-C (2000) Seismic imaging of mantle plumes. *Ann Revs Earth Planet Sci*, v 28, pp 391-417
- Needham RS (1985) A review of the distribution and controls of uranium mineralization in the Alligator Rivers uranium field, Northern Territory, Australia. *CIM Spec Vol 32*, pp 216-230
- Needham RS, Crick IH, Stuart-Smith PG (1980) Regional geology of the Pine Creek Geosyncline, *in*: J Ferguson, AB Goleby, eds, *Uranium in the Pine Creek Geosyncline*. IAEA Vienna, pp 1-22
- Nel CJ, Beukes NJ, De Villiers JPR (1986) The Mamatwan manganese mine of the Kalahari manganese field, *in*: CR Anhaeusser, S Maske, eds, pp 963-978
- Nelson CE (1988) Gold deposits in the hot spring environment, *in*: RW Schafer et al, eds, *Bulk Mineable Precious Metal Deposits of the Western United States*. *Geol Soc of Nevada, Reno*, pp 417-431
- Nelson CE (2000) Volcanic domes and gold mineralization in the Pueblo Viejo district, Dominican Republic. *Mineralium Deposita*, v 35, pp 511-525
- Nelson CH, Hopkins DM (1972) Sedimentary processes and distribution of particulate gold in the northern Bering Sea. *U.S. Geol Surv Profess Paper 689*, 27 p
- Newbery RJ, McCoy DT, Brew DA (1995) Plutonic-hosted gold ores in Alaska: Igneous vs. metamorphic origins. *Resource Geol Spec Issue 18*, Tokyo, pp 57-100
- Newberry RJ, Swanson SE (1986) Scheelite skarn granitoids: An evaluation of the roles of magmatic source and processes. *Ore Geol Revs*, v 1, pp 57-81
- Newcrest Mining Staff (1998) Cadia gold-copper deposit, *in*: DA Berkman, DH Mackenzie, eds, pp 641-646
- Newson HE (1990) Accretion and core formation in the Earth: Evidence from siderophile elements, *in*: HE Newson, JH Jones, eds, *Origin of the Earth*. Oxford Univ Press, pp 273-288
- Nicholson SW, Cannon WF, Schylz KJ (1992) Metallogeny of the Midcontinent rift system of North America. *Precamb Res*, v 58, pp 355-386
- Nie FJ (1994) Rare earth element geochemistry of the molybdenum-bearing granitoids in the Jinduicheng-Huanglongpu district, Shaanxi Province, Northwest China. *Mineralium Deposita*, v 29, pp 488-489
- Nie FJ, Bjørlykke A (1994) Lead and sulfur isotope studies of the Wulashan quartz-K feldspar and quartz vein gold deposit, southwestern Inner Mongolia, People's Republic of China. *Econ Geol*, v 89, pp 1289-1305
- Nielsen BL (1973) A survey of the economic geology of Greenland (exclusive fossil fuels). *Grøn Geol Unders, Rapp Nr 56*, 45 p
- Nielsen RL (1976) Recent developments in the study of porphyry copper geology-a review. *CIM Spec Vol 15*, pp 487-500
- Nikiforov NA (1970) Osobennosti geologicheskovo stroyeniya i razmeshcheniya orudneniya rtutno-sur'myannykh mestorozhdenii Yuzhno-Ferganskovo Poyasa, *in*: Ocherki po Geologii i Geokhemii Rudnykh Mestorozhdenii. Nauka, Moscow, pp 191-214
- Nikiforov NA, Pavlyukovich YeA, Ponomarev FI (1962) Zakonomernosti razmeshchaniya bogatyykh rtutnykh i surmyannykh rud na mestorozhdeniyakh yuznoi Fergany. *Zakon Razmesh Polez Iskop*, v 5, pp 207-228
- Nikitin VD (1968) Pegmatitovye mestorozhdeniya, *in*: VI Smirnov, Genezis Endogennykh Rudnykh Mestorozhdenii. Nedra, Moscow, pp 84-151
- Nikol'skiy AP, Naumov VP, Korobko NI (1983) Pervomaysk iron-ore deposit in the Krivoi Rog and its transformation by impact metamorphism. *Intern Geol Revs*, v 25, pp 1304-1315
- Nilsson CA (1986) Wall rock alteration at the Boliden deposit, Sweden. *Econ Geol*, v 63, pp 472-494
- Nisbet EG (1987) *The Young Earth. An Introduction to Archean Geology*. Allen and Unwin, Boston, 402 p
- Nishiwaki C, Iwafune T, Shiobara K, Sakuma T, Tono A (1970) Geology and ore deposits of the Kamioka and Hamayokokawa Mines. *IMA-IAGOD Meeting, Guidebook 7*, 40 p
- Nixon PH, ed (1987) *Mantle Xenoliths*. Wiley, New York
- Noble DC, McCormack JK, McKee EH, et al (1988) Time of mineralization in the evolution of the McDermitt Caldera complex, Nevada-Oregon, and the relation of Middle Miocene mineralization in the

- northern Great Basin to coeval regional basaltic magmatic activity. *Econ Geol*, v 83, pp 859-863
- Noble DC, Vidal CE (1990) Association of silver with mercury, arsenic, antimony and carbonaceous material at the Huancavelica district, Peru. *Econ Geol*, v 85, pp 1645-1650
- Noble JA (1950) Ore mineralization in the Homestake gold mine, Lead, South Dakota. *Geol Soc Amer Bull*, v 61, pp 221-252
- Noble SR, Spooner ETC, Harris FR (1995) Logtung: A porphyry W-Mo deposit in the southern Yukon. *CIM Spec Vol 46*, pp 732-748
- Nokleberg WJ, Bundtzen TH, Brew DA, Plafker G (1995) Metallogenesis and tectonics of porphyry copper and molybdenum (gold, silver) and granitoid-hosted gold deposits of Alaska. *CIM Spec Vol 46*, pp 103-141
- Norford BS, Orchard MJ (1985) Early Silurian age of rocks hosting lead-zinc mineralization at Howard's Pass, Yukon Territory and District of Mackenzie; local biostratigraphy of Road River Formation and Earn Group. *Geol Surv Canada Paper 83-18*
- Norman DI, Sawkins FJ (1985) The Tribag breccia pipes: Precambrian Cu-Mo deposits, Batchawana Bay, Ontario. *Econ Geol*, v 80, pp 1593-1621
- Norton JJ (1975) Pegmatite Minerals. *S Dakota Geol Surv Bull 16*, pp 132-149
- Norton JJ (1989) Gold-bearing polymetallic veins and replacement deposits-Part I: Bald Mountain gold mining region, northern Black Hills, South Dakota. *U.S. Geol Surv Bull 1857-C*, 37 p
- Oberthür T, Mumm AS, Vetter U, et al (1996) Gold mineralization in the Ashanti belt of Ghana: Genetic constraints of the stable isotope geochemistry. *Econ Geol*, v 91, pp 289-301
- O'Connor K (1999) Yacimiento polimetálico de Antamina: Historia, exploración y geología, *in: Primer Volumen de Monografías de Yacimientos Minerales Peruanos*, IIMP, Lima, pp 231-243
- O'Connor GV, Marsland LD, Barnes JFH, Cunnold GR (2001) The discovery and development of the Roşia Montană gold deposit, Transylvania, Romania. *Sympos New Generation Gold*, AMF, Adelaide, pp 33-42
- O'Connor GV, Sunyoto W, Soebari L (1999) The discovery of the Wabu Ridge gold skarn, Irian Jaya, Indonesia. *Proceedings, PACRIM '99 Congress*, Bali. AusIMM, pp 549-557
- Oen IS, Fernandez JS, Manteca JI (1975) The lead-zinc and associated ores of La Unión, Sierra de Cartagena, Spain. *Econ Geol*, v 70, pp 1259-1279
- Oen IS, de Maesschalck AA, Lustenhouwer WJ (1986) Mid-Proterozoic exhalative-sedimentary Mn skarns containing possible microbial fossils, Grythyttan, Bergslagen, Sweden. *Econ Geol*, v 81, pp 1533-1543
- Ohle EL (1996) Significant events in the geological understanding of the Southeast Missouri Lead District, *in: DF Sangster*, ed, *Soc Econ Geol Spec Publ 4*, pp 1-7
- Ohmoto H, Skinner BJ, eds (1983) *The Kuroko and Related Volcanic Massive Sulfide Deposits*. *Econ Geol Monogr 5*, 604 p
- Okita PM (1992) Manganese carbonate mineralization in the Molango district, Mexico. *Econ Geol*, v 87, pp 1345-1366
- Ollier C, Pain C (1996) *Regolith, Soil and Landforms*. Wiley, Chichester, 316 p
- Olson JC, Shawe DR, Pray LC, Sharp WN (1954) Rare-earth mineral deposits of the Mountain Pass district, San Bernardino County, California. *U.S. Geol Surv Profess Paper 261*, 75 p
- O'Neill GK (1981) 2081. A Hopeful View of the Human Future. Simon and Schuster, New York, 284 p
- O'Neill HSC, Palme H (1998) Composition of the silicate Earth: Implications for accretion and core formation, *in: I Jackson*, ed, *The Earth's Mantle*. Cambridge Univ Press, pp 3-126
- Ophuls W (1977) *Ecology and the Politics of Scarcity*. Freeman, San Francisco, 303 p
- Oreskes N, Einaudi MT (1990) Origin of rare earth element-enriched hematite breccias at the Olympic Dam Cu-U-Au-Ag deposit, Roxby Downs, South Australia. *Econ Geol*, v 85, pp 1-28
- Oreskes N, Hitzman MW (1993) A model for the origin of Olympic Dam-type deposits, *in: RV Kirkham et al*, eds, *Geol Assoc Canada Spec Paper 40*, pp 615-634
- Oreskes N, Le Grande H, eds (2001) *Plate Tectonics: An Insider's History of the Modern Theory of the Earth*. Westview Press, Boulder CO, 424 p
- Orgeval JJ, Giot D, Karoui J, Monthel J, Sahli R (1989) The discovery and investigation of the Bou Grine Pb-Zn deposit (Tunisian Atlas). *Chron rech min, spec issue 1989*, pp 53-68
- Orr TH (1995) The Mt Leyshon gold mine: geology and mineralisation. 17th IGES, May 1995, Townsville, pp 117-136
- Ossandón GC, Fréaut RC, Gustafson LB, Lindsay DD, Zentilli M (2001) Geology of the Chuquicamata Mine: A progress report. *Econ Geol*, v 96, pp 249-270
- Ossenkopf P, Helbig C (1965) Zur geologischen Aufbau der Zinnerzlagertstätte Altenberg und speziell zum Pyknitgestein. *Zeitschr f Angewandte Geol*, v 21, pp 57-67
- Ostwald J (1981) Evidence for a biogeochemical origin of the Groote Eylandt manganese ores. *Econ Geol*, v 76, pp 556-567
- O'Sullivan KN, Goode ADT (2004) Data Metallogenica-around the Pacific Rim and across the world. *PACRIM 2004 Proceedings*, Adelaide, Aus IMM, pp 199-203
- Oszczepalski S (1999) Origin of the Kupferschiefer polymetallic mineralization in Poland. *Mineralium Deposita*, v 34, pp 599-613
- Overstreet WC, White AM, Whitlow JW, Theobald PK Jr, Caldwell DW, Cuppels NP (1968) Fluvial monazite deposits in the southeastern United States. *U.S. Geol Surv Prof Paper 568*, 85 p
- Oviedo L, Fuster N, Tschischow N, Ribba L, Zuccone A, Grez E, Aguilar A (1991) General geology of La

- Coipa precious metal deposit, Atacama, Chile. *Econ Geol*, v 86, pp 1287-1300
- Owen DL, Coats CJA (1984) Falconbridge and East Mines, *in*: EG Pye et al, eds, pp 371-378
- Owen M, Tipman R (1999) Co-production of heavy minerals from oil sand tailings. *CIM Bulletin*, v 92, pp 65-73
- Ozerova NA (1981) New mercury ore belt in Western Europe. *Geol Rud Mestor*, 1981, pp 49-56
- Paarberg NL, Evans LL (1977) Geology of the Fletcher mine, Viburnum Trend, Southeast Missouri. *Econ Geol*, v 72, pp 391-397
- Padilla RAG, Tittley SR, Pimentel FB (2001) Geology of the Escondida porphyry copper deposit, Antofagasta region, Chile. *Econ Geol*, v 96, pp 307-324
- Page NJ (1977) Stillwater Complex, Montana: rock succession, metamorphism and structure of the Complex and adjacent rocks. *U.S. Geol Surv Profess Paper* 999, 79 p
- Painter MGM, Golding SD, Hannan KW, Neudert MK (1999) Sedimentologic, petrographic, and sulfur isotope constraints on fine-grained pyrite formation at Mount Isa mine and environs, Northwest Queensland, Australia. *Econ Geol*, v 94, pp 883-912
- Palache C (1935) The minerals of Franklin and Sterling Hill, NJ. *U.S. Geol Surv Profess Paper* 180, 135 p
- Pallister JS (1987) Magmatic history of Red Sea rifting: Perspective from the central Saudi Arabian coastal plain. *Geol Soc Am Bull*, v 98, pp 400-417
- Palme H, O'Neill H StC (2004) Cosmochemical estimates of mantle composition, *in*: RW Carlson, ed, pp 1-38
- Palmer AR, Wheeler JO, eds (1980s-1990s) *The Geology of North America*. *Geol Soc Amer*, Boulder; many volumes
- Panigrahi MK, Mookherjee A (1997) The Malanjhand copper (+ molybdenum) deposit, India: Mineralization from a low-temperature ore fluid of granitoid affiliation. *Mineralium Deposita*, v 32, pp 133-148
- Panteleyev A (1981) Berg porphyry copper-molybdenum deposit, British Columbia. *Ministry of Energy, Mines, Petrol Res, Bulletin* 66, 158 p
- Paone J (1970) Germanium, *in*: *Mineral Facts and Problems*. *U.S. Bur Mines Bull* 650, pp 563-571
- Papunen H, Vormaa A (1985) Nickel deposits in Finland, a review. *Geol Surv Finland Bull* 333, pp 123-143
- Parák T (1973) Rare earths in apatite iron ores of Lappland together with some data about the Sr, Th and U content of these ores. *Econ Geol*, v 68, pp 210-221
- Parák T (1975) The origin of the Kiruna iron ores. *Sveriges Geol Unders*, C 709, 209 p
- Paris J-P (1981) *Géologie de la Nouvelle Calédonie*. *Mém du BRGM*, No 113, 278 p
- Parnell J (1988) Metal enrichments in solid bitumens: A review. *Mineralium Deposita*, v 23, pp 191-199
- Parr JM, Plimer IR (1993) Models for Broken Hill-type lead-zinc-silver deposits, *in*: RV Kirkham, WD Sinclair, RI Thorpe, eds, *Mineral Deposits Modelling*. *Geol Assoc Canada, Spec Paper* 40, pp 253-288
- Paterson IA (1977) The geology and evolution of the Pinchi fault zone at Pinchi Lake, central British Columbia. *Canad Journ Earth Sci*, v 14, pp 1324-1342
- Patterson DJ, Ohmoto H, Solomon M (1981) Geologic setting and genesis of cassiterite-sulfide mineralization at Renison Bell, western Tasmania. *Econ Geol*, v 76, pp 393-438
- Patyk-Kara NG (1999) Cenozoic placer deposits and fluvial channel systems on the Arctic shelf of Siberia. *Econ Geol*, v 94, pp 707-720
- Pavillon MJ (1969) Les minéralisations plombo-zincifères de Cartagène (Cordillères bétiques, Espagne). *Mineralium Deposita*, v 4, pp 368-385
- Pearce WM, Wallace MW (2000) Timing of mineralization at the Navan Zn-Pb deposit: A post-Arundian age for Irish mineralization. *Geology*, v 28, pp 711-714
- Peacock SM (1990) Fluid processes in subduction zones. *Science*, v 248, pp 329-336
- Pearton TN (1986) The Monarch cinnabar mine: Murchison greenstone belt, *in*: CR Anhaeusser, S Maske, eds, pp 339-348
- Pearton TN, Viljoen MJ (1986) Antimony mineralization in the Murchison greenstone belt-an overview, *in*: CR Anhaeusser, S Maske, eds, pp 293-320
- Pedersen FD (1986) An outline of the geology of the Hurdal area and Nørdli granite-molybdenite deposit. *Geol Surv Sweden, Serial Ca* 59, pp 18-23
- Pei Rongfu, ed (1997) 30th Intern Geol Congress, Beijing, *Proceedings*, v 9, VSP Publ
- Penczak RS, Mason R (1999) Characteristics and origin of Archean premetamorphic hydrothermal alteration at the Campbell Gold Mine, northwestern Ontario, Canada. *Econ Geol*, v 94, pp 507-528
- Peng Qiming, Palmer MR (2002) The Paleoproterozoic Mg and Mg-Fe borate deposits of Liaoning and Jilin Provinces, Northeast China. *Econ Geol*, v 97, pp 93-108
- Percerillo A (1985) Roman comagmatic province (central Italy): Evidence for subduction-related magma genesis. *Geology*, v 13, pp 103-106
- Percival TJ, Radtke AS (1994) Sedimentary rock-hosted disseminated gold in the Alšar district, Macedonia. *Canad Mineralogist*, v 32, Pt 3, pp 649-665
- Peredery WV, Geol Staff (1982) Geology and nickel sulfide deposits of the Thompson Belt, Manitoba. *Geol Assoc Canada Spec Paper* 25, pp 165-209
- Perelló J (2003) Porphyry-style alteration and mineralization of the Middle Eocene to Early Oligocene Andahuaylas-Yauri belt, Cuzco region, Peru. *Econ Geol*, v 98, pp 1575-1605
- Perelló J, Cox D, Garamjav D, Sanjdorj S, Diakov S, Schissel D, Munkhbat TO, Oyun G (2001) Oyu Tolgoi, Mongolia: Siluro-Devonian porphyry Cu, Au-(Mo) and high-sulfidation Cu mineralization with a Cretaceous chalcocite blanket. *Econ Geol*, v 96, pp 1407-1428
- Perfit MR, Gust DA, Bence AE, Arculus RJ, Taylor SR (1980) Chemical characteristics of island-arc basalts: Implications for mantle sources. *Chem Geol*, v 30, pp 227-256
- Perichaud JJ (1980) L'antimoine, ses minerais et ses gisements. *Synthèse géologique sur les gisements du*

- Massif Central français. Chron de la réch minière, no 456
- Perkins WG (1990) Mount Isa copper orebodies, *in*: FE Hughes, ed, pp 935-941
- Pesonen PE, et al (1949) Missouri Valley manganese deposits, South Dakota. U.S. Bur Mines Rept Inv 4375, 90 p
- Peter JM, Scott SD (1988) Mineralogy, composition and fluid-inclusion microthermometry of seafloor hydrothermal deposits in the southern trough of Guaymas Basin, Gulf of California. *Canad Mineralog*, v 26, pp 567-587
- Peter JM, Scott SD (1999) Windy Craggy, Northwestern British Columbia: the world's largest Besshi-type deposit. *Reviews in Econ Geol*, v 8, pp 261-295
- Peters WC (1987) *Exploration and Mining Geology*, 2nd ed. Wiley, New York, 685 p
- Petersen CR, Rivera SL, Peri MA (1996) Chimborazo copper deposit, Region II, Chile; exploration and geology. *Soc Econ Geol, Spec Publ* 5, pp 71-80
- Petersen S, Herzig PM, Hannington MD, Jonasson IR, Arribas A Jr (2002) Submarine gold mineralization near Lihir Island, New Ireland fore-arc, Papua New Guinea. *Econ Geol*, v 97, pp 1795-1813
- Petersen U (1999) Magmatic and metallogenic evolution of the Central Andes. *Soc Econ Geol, Spec Publ* 7, pp 109-159
- Peterson NP (1962) Geology and ore deposits of the Globe-Miami district, Arizona. U.S. Geol Surv Profes Pap 342, 151 p
- Petkof B (1985) Gallium, *in*: *Mineral Facts and Problems*. U.S. Bur Mines Bull 675, pp 291-296
- Petrachenko ED (1995) Mineralization of the Kuril Island arc. *Resource Geology Spec Issue*, no 18, Tokyo, pp 271-276
- Petruk W, Moore HA, Atchison DW (1972) The Cobalt area. 24th Intern Geol Congr, Field Exc A39-C39, Guidebook, pp 11-26
- Philex Mine Staff (1994) Notes for visitors, 8 p
- Phillips CH, Gambell NA, Fountain DS (1974) Hydrothermal alteration, mineralization, and zoning in the Ray deposit. *Econ Geol*, v 69, pp 1237-1250
- Phillips GN (1986) Geology and alteration in the Golden Mile, Kalgoorlie. *Econ Geol*, v 81, pp 779-808
- Phillips GN (1987) Metamorphism of the Witwatersrand gold fields: Conditions during peak metamorphism. *Journ Metam Geology*, v 5, pp 307-322
- Phillips GN, Groves DI, Kerrich R (1996) Factors in the formation of the giant Kalgoorlie gold deposit. *Ore Geol Revs*, v 10, pp 295-317
- Phillips GN, Hughes MJ (1996) The geology and gold deposits of the Victorian gold province. *Ore Geol Revs*, v 11, pp 255-302
- Phillips GN, Hughes MJ (1998) Victorian Gold Province, *in*: DA Berkman, DH Mackenzie, eds, pp 495-506
- Phillips GN, Myers RE (1989) The Witwatersrand Gold Fields, Part II. An origin for Witwatersrand gold during metamorphism and associated alteration. *Econ Geol Monogr* 6, pp 598-608
- Pichavant M, et al (1988) The Miocene-Pliocene Macusani Volcanics, SE Peru, I & II. *Contrib to Miner Petrol*, v 100, pp 300-338
- Pichler H (1970) Italianische Vulkan-Gebiete I (Somma-Vesuv, Latium, Toscana). *Borntraeger*, 258 p
- Pichler H (1981) Italienische Vulkan-Gebiete III. *Borntraeger*, 270 p
- Picklyk DD, Rose DG, Laramie RM (1978) Canadian Mineral Occurrence Index (CANMINDEX) of the Geological Survey of Canada. *Geol Surv Canada, Paper* 78-8, 27 p
- Piestrzyński A, Vodzicki A (2000) Origin of the gold deposit in the Połkowice-West Mine, Lubin-Sierszowice mining district, Poland. *Mineralium Deposita*, v 35, pp 37-47
- Pidzhyan, GO (1975) *Medno-molibdenovaya Formatsiya Rud Armyanskoi SSR*. Akad Nauk Arm SSR, Yerevan, 312 p
- Pilote P, Joannis A, Daigneault R, Magnan M, Kirkham RV, Robert F (1998) Les gisements de type Cu-Au porphyrique Archéens du camp minier du Lac Doré, Chibougamau: Reconstruction géométrique et temporelle-potentiel du Nord Québécois. *Geol Assoc/Miner Assoc Canada, Ann Meet Québec '98, Abstracts*, A-147
- Pinsent RH, Christopher PA (1995) Adanac (Ruby Creek) molybdenum deposit, northwestern British Columbia. *CIM Spec Vol* 46, pp 712-717
- Piper DZ, Hatch GR (1989) Hydrogenous sediment, *in*: *The Geology of North America*, vol N. Geol Soc Amer, Boulder, pp 337-345
- Pirajno F (2001) *Ore Deposits and Mantle Plumes*. Kluwer Acad Publ, Dordrecht, 576 p
- Pirajno F, Preston WA (1998) Mineral deposits of the Padbury, Bryah and Yerrida Basins, *in*: DA Berkman, DH Mackenzie, eds, pp 63-70
- Pitcher WS (1978) The anatomy of a batholith. *Journ Geol Soc London*, v 135, pp 157-182
- Pitcher WS (1982) Granite type and tectonic environment, *in*: K Hsü, ed, *Mountain Building Processes*. Academic Press, London, pp 19-40
- Plafker G, Berg HC, eds (1994) *The Geology of Alaska*, *in*: *The Geology of North America*, v G1, Geol Soc Amer, Boulder
- Pohl J, Stöffler D, Gall H, Ernston K (1977) The Ries impact crater, *in*: DJ Roddy et al, eds, *Impact and Explosion Cratering*. Pergamon Press, New York, pp 343-404
- Pokalov VT (1974) Deposits of molybdenum, *in*: VI Smirnov, ed, *Ore Deposits of the USSR*, v 3, Engl Transl. Pitman, London, pp 125-179
- Pokalov VT, Semenova NV (1993) Lobash-pervoye krupnoe molibdenovoe mestorozhdeniye dokembriiskovo vozrasta (Karelia). *Geol Rud Mestorozhd*, v 35, pp 262-270
- Pokrovskaya IV, Kovrigo OA (1983) Model' formirovaniya mnogoetazhnovo vulkanogennovo polimetallicheskovo mestorozhdenia Rudnovo Altaia, *in*: VA Kuznetsov, ed, *Geneticheskie Modelli Rudnykh Mestorozhdenii*. Nedra, Moscow, pp 112-125

- Polishchuk VD, et al (1970) *Geologiya i Zheleznye Rudy KMA*. Nedra, Moscow, 438 p
- Ponce BFS, Clark KF (1988) The Zacatecas mining district: A Tertiary caldera complex associated with precious and base metal mineralization. *Econ Geol*, v 83, pp 1668-1682
- Popov PN, Vladimirov VD, Bakyrzhiev SD (1983) Strukturnaya model' poliformatsionnovo Chelopezskovo mednorudnovo polya (NRB). *Geol Rud Mestor*, No 5, pp 3-12
- Porter TM, ed (2000) Hydrothermal Iron Oxide Copper-Gold and Related Deposits, a Global Perspective. Austral Miner Found, Adelaide, 349 p
- Porter TM, ed (2002) Hydrothermal Iron Oxide Copper-Gold and Related Deposits, a Global Perspective, vol 2. PGC Publ, Adelaide, 377 p
- Pracejus B, Bolton BR (1992) Geochemistry of supergene manganese oxide deposits, Groote Eylandt, Australia. *Econ Geol*, v 87, pp 1310-1335
- Pracejus B, Bolton BR, Frakes LA (1988) Nature and development of supergene manganese deposits, Groote Eylandt, Northern Territory, Australia. *Ore Geol Revs*, v 4, pp 71-98
- Preece RK (1989) Geology and mineralization of the Northwest Extension-Summary of Activities during 1988. Phelps Dodge, Morenci, unpublished, 36 p
- Prendergast MD (1987) The chromite ore field of the Great Dyke, Zimbabwe, *in*: CW Stone, ed, pp 89-108
- Prendergast MD (1988) The geology and economic potential of the PGE-rich Main Sulfide Zone of the Great Dyke, Zimbabwe. *Geo-Platinum '87*, pp 281-291
- Prendergast MD, Jones MJ, eds (1989) Magmatic Sulfides-the Zimbabwe Volume. Inst Min Metall, London, 220 p
- Presnell RD, Parry WT (1996) Geology and geochemistry of the Barney's Canyon gold deposit, Utah. *Econ Geol*, v 91, pp 273-288
- Pretorius DA (1991) The sources of Witwatersrand gold and uranium; A continued difference of opinion. *Econ Geol, Monogr* 8, pp 139-163
- Price JG (2004) I never met a rhyolite I didn't like-some of the geology in economic geology. *Soc Econ Geol Newsletter*, April 2004, no 57, pp 1+10-13
- Price JG, Rubin JN, Henry CD, Pinkston TL, Tweedy SW, Koppelaar DW (1990) Rare-metal enriched peraluminous rhyolites in a continental arc, Sierra Blanca area, Trans-Pecos Texas; chemical modification by vapor-phase crystallization. *Geol Soc Amer, Spec Paper* 246, pp 103-120
- Proenza J, Gervilla F, Melgarejo JC, et al (1999) Al- and Cr-rich chromitites from the Mayari-Baracoa ophiolitic belt (Eastern Cuba): Consequence of interaction between volatile-rich melts and peridotites in suprasubduction mantle. *Econ Geol*, v 94, pp 547-566
- Proffett JM (2003) Geology of the Bajo de la Alumbrera porphyry copper-gold deposit, Argentina. *Econ Geol*, v 98, pp 1535-1574
- Prokin VA, Buslaev FP, Nasedkin AP (1998) Types of massive sulphide deposits in the Urals. *Mineralium Deposita*, v 34, pp 121-126
- Purdie JJ (1967) Lake Dufault Mines Ltd. CIM Centennial Field Excursion, 1967, pp 52-57
- Putzer H (1976) Metallogenetic Provinces in Südamerika. Schweizerbart, Stuttgart, 299 p
- Pye CH (1981) Profitability in the Canadian Mineral Industry. Centre for Resource Studies, Queen's Univ, 178 p
- Pye EG, Naldrett AJ, Giblin PE, eds (1984) The Geology and Ore Deposits of the Sudbury Structure. Ontario Geol Surv Spec Vol 1, 603 p
- Pyke DR (1982) Geology of the Timmins area, District of Cochrane. Ontario Geol Surv Rept 219, 141 p
- Querol FS, Lowther GK, Navarro E (1991) Mineral deposits of the Guanajuato mining district, Guanajuato, *in*: The Geology on North America, v P-3. Geol Soc Amer, Boulder, pp 403-414
- Rackley RI (1976) Origin of Western-States type uranium mineralization, *in*: KH Wolf, ed, Handbook of Stratiform and Strata-Bound Ore Deposits, v 7. Elsevier, Amsterdam, pp 89-156
- Radtke AS, Foo ST, Percival TJ (1987) Geologic and chemical features of the Cortez gold deposit, Lander County, Nevada, *in*: LJ Johnson, ed, Bulk Mineable Precious Metal Deposits of the Western United States, Guidebook for field trips. Geol Soc Nevada, Reno, pp 319-325
- Radwanek-Bak B (1985) Charakterystyka petrograficzna utlenionych rud cynku ze złóż obszaru Bolesławia i Olkusza. *Rocz Polsk Towar Geol*, v 53, pp 235-254
- Raedeke LD, Vian RW (1986) A three-dimensional view of mineralization in the Stillwater J-M Reef. *Econ Geol*, v 81, pp 1187-1195
- Ragan VM, Coveney RM Jr, Brannon JC (1996) Migration paths for fluids and northern limits of the Tri-State District from fluid inclusions and radiogenic isotopes, *in*: DF Sangster, ed, Soc Econ Geol Spec Publ 4, pp 419-431
- Rajah SS (1979) The Kinta Tinfield, Malaysia. *Geol Soc Malaysia, Bull* 11, pp 111-136
- Rajlich P (1983) Geology of Oued Mekta, a Mississippi Valley-type deposit, Touissit-Bou Bekker region, eastern Morocco. *Econ Geol*, v 78, pp 1239-1254
- Rambaud F (1969) El sinclinal carbonífero de Riotinto (Huelva) y sus mineralizaciones asociadas. *Memorias IGME*, v 71, 229 p
- Rao SR et al, eds (1995) Waste Processing and Recycling in Mineral and Metallurgical Industries. CIM, Montreal, 571 p
- Ratkin V (1995) Pre- and post-accretionary metallogeny of the southern Russian Far East. *Resource Geol, Spec Issue* No 18, Tokyo, pp 127-133
- Rautman CA (1983) Uranium deposits: A half century of exploration, *in*: SJ Boardman, ed, Revolution in the Earth Sciences. Kendall-Hunt, Dubuque, pp 344-355
- Rawlings DE, ed (1997) Biomining: Theory, Microbes and Industrial Processes. Springer-Verlag
- Ray GE, Webster ICL (1991) An overview of skarn deposits. Brit Columbia Minister of Engy, Mines, Petrol Res, Paper 1991-4, pp 213-252

- Raymond LA, ed (1984) *Melanges: Their Nature, Origin and Significance*. Geol Soc Amer Spec Paper 198, 170 p
- Reading HG, ed (1986) *Sedimentary Environments and Facies*. Blackwell, Oxford, 615 p
- Rebagliati CM, Bowen BK, Copeland DJ, Niosi DWA (1995) Keness South and Keness North porphyry gold-copper deposits, northern British Columbia. *CIM Spec Vol 46*, pp 377-396
- Redden JA, French GMcN (1989) Geologic setting and potential exploration guides for gold deposits, Black Hills, South Dakota. *U.S. Geol Surv Bull 1857-B*, pp 45-74
- Redden JA, Norton JJ, McLaughlin RJ (1982) *Geology of the Harney Peak Granite, Black Hills, South Dakota*. U.S. Geol Surv Open File Rept 82-481
- Reeve JS, Cross KC, Smith RN, Oreskes N (1990) Olympic Dam copper-uranium-gold-silver deposit, *in*: FE Hughes, ed, pp 1009-1035
- Reid DL (1979) Petrogenesis of calc-alkaline metalavas in the mid-Proterozoic Haib volcanic Subgroup, lower Orange River region. *Geol Soc S Africa, Trans*, v 82, pp 109-131
- Reid DL, Welke HJ, Erlank AJ, Moyes A (1987) The Orange River Group: A major Proterozoic calcalkaline volcanic belt in the western Namaqua Province, southern Africa. *Geol Soc London, Spec Publ No 33*, pp 327-346
- Reinhardt J, Sigleo WR, et al, eds (1988) *Paleosols and Weathering Through Geologic Time: Principles and Applications*. Geol Soc Amer Spec Paper 216, 181 p
- Retallack GJ (1986) The fossil record of soils, *in*: VP Wright, ed, *Paleosols, Their Recognition and Interpretation*. Princeton Univ Press, pp 1-57
- Reynolds LJ (2000) Geology of the Olympic Dam Cu-U-Au-Ag-REE deposit, *in*: TM Porter, ed, *Hydrothermal Iron Oxide Copper-Gold and Related Deposits: A Global Perspective*. AMF, Adelaide, pp 93-104
- Redmond PB, Einaudi MT, Inan EE, Landtwing MR, Heinrich GA (2004) Copper deposition by fluid cooling in intrusion-centered systems: New insights from the Bingham porphyry ore deposit, Utah. *Geology*, March 2004, pp 217-220
- Reedman JH (1979) *Techniques in Mineral Exploration*. Applied Science Publ, Ripple Road, 526 p
- Reeve JS, Cross RC, Smith RN, Oreskes N (1990) Olympic Dam copper-uranium-gold-silver deposit, *in*: FE Hughes, ed, pp 1009-1035
- Reimold WU, Viljoen MJ, eds (1994) Special issue on the Ventersdorp Contact Reef. *South African Journ Geol*, v 97, No 3, pp 233-386
- Reineck H-E, Singh IB (1980) *Depositional Sedimentary Environments*, 2nd ed. Springer-Verlag, 549 p
- Ren Q, Xu Z, Yang R, Qiu J (1995) The ore-forming processes of super-large molybdenum-tungsten deposits at Nannihu-Sandaozhuang in eastern Qinling Mountains, central China. *Resource Geology, Spec Issue No 18*, Tokyo, pp 179-186
- Rentsch J (1974) The Kupferschiefer in comparison with the deposits of the Zambian Copperbelt, *in*: *Gisements Stratiformes et Provinces, a Symposium*. Liège, pp 395-418
- Reshit'ko WA (1967) Platinovoe orudneniye v brachyantiklinalakh Kachanarskovo gabbro-peridotovovo massiva na Urale. *Geologiya Geofizika*, No 5, pp 33-42
- Reyes M (1991) The Andacollo strata-bound gold deposit, Chile, and its position in a porphyry copper-gold system. *Econ Geol*, v 86, pp 1301-1316
- Reynolds DG (1965) Geology and mineralization of the Salsigne gold mine, France. *Econ Geol*, v 60, pp 772-791
- Reynolds IM (1986) The mineralogy and ore petrography of the Bushveld titaniferous magnetite-rich layers, *in*: CR Anhaeusser, S Maske, eds, pp 1267-1286
- Reynolds TJ, Beane RE (1985) Evolution of hydrothermal fluid characteristics at the Santa Rita, New Mexico, porphyry copper deposit. *Econ Geol*, v 80, pp 1328-1347
- Reynolds NA, et al (2003) The Padaeng supergene nonsulfide zinc deposit, Mae Sod, Thailand. *Econ Geol*, v 98, pp 773-785
- Richards JP (1995) Alkalic-type epithermal gold deposits-a review, *in*: JFH Thompson, ed, *Magmatic Fluids and Ore Deposits*. Miner Assoc Canada, Short Course v 23, pp 367-400
- Richards JP (2003) Tectono-magmatic precursors for porphyry Cu-(Mo-Au) deposit formation. *Econ Geol*, v 98, pp 1515-1533
- Richards JP, Kerrich R (1993) The Porgera gold mine, Papua New Guinea: Magmatic hydrothermal to epithermal evolution of an alkalic-type precious metal deposit. *Econ Geol*, v 88, pp 1017-1052
- Richards TE (1986) Geological characteristics of rare-metal pegmatites of the Uis type in the Damara Orogen, South-West Africa/Namibia, *in*: CR Anhaeusser, S Maske, eds, pp 1845-1862
- Richardson DG, Birkett TC (1996a) Residual carbonatite-associated deposits, *in*: *Geology of Canada No 8*, Geol Surv Canada, pp 108-119
- (1996b) Carbonatite-associated deposits. Same public, pp 541-558
- (1996c) Peralkaline rock-associated rare metals. Same public, pp 523-540
- Rickard D (1983) Precipitation and mixing mechanisms in Laisvall-type sandstone lead-zinc deposits, *in*: G Kisvarsanyi et al, eds, *Internat Conf on Mississippi Valley-type Lead-Zinc Deposits, Proceedings Volume*, Univ of Missouri, Rolla, pp 449-458
- Rickard DT, Willden M, Marinder N-E, Donnelly TH (1979) Studies on the genesis of the Laisvall deposit. *Econ Geol*, v 74, pp 1255-1285
- Riggs SR (1991) Phosphate, *in*: *The Geology of North America*, v J, The Gulf of Mexico Basin. Geol Soc Amer, Boulder, pp 495-501
- Riggs SR, Snyder SWP, Hine AC, et al (1985) Geologic framework of phosphate resources in Onslow Bay, North Carolina continental shelf. *Econ Geol*, v 80, pp 716-738
- Ringwood AE (1975) *Composition and Petrology of the Earth's Mantle*. McGraw Hill, New York

- Ripley EM (1981) Sulfur isotopic studies of the Dunka Road Cu-Ni deposit, Duluth Complex, Minnesota. *Econ Geol*, v 76, pp 610-620
- Ripley EM, Chusi Li, Dongbok Shin (2002) Paragneiss assimilation in the genesis of magmatic Ni-Cu-Co sulfide mineralization at Voisey's Bay, Labrador; $\delta^{34}\text{S}$, $\delta^{13}\text{C}$, and Se/S evidence. *Econ Geol*, v 97, pp 1307-1318
- Ritchey JL (1987) Assessment of cobalt-rich manganese crust resources on Horizon and S.P. Lee Guyots, US Exclusive Economic Zone. *Marine Mining*, v 6, pp 231-243
- Rittenhouse PA (1979) Potash and politics. *Econ Geol*, v 74, pp 353-357
- Rivera NG (1997) The Pasco mineral belt and the metallogensis of the Cerro de Pasco mineral district. IX Congreso Peruano de Geologia, Resum Extend, v 1, Lima, pp 167-173
- Robb LJ, Charlesworth EG, Drennan GR, Gibson RL, Tongu EI (1997) Tectono-magmatic setting and paragenetic sequence of Au-U mineralization in the Archean Witwatersrand Basin, South Africa. *Austral Journ Earth Sci*, v 44, pp 353-371
- Robert F, Brown AC (1986) Archean gold-bearing quartz veins at the Sigma Mine, Abitibi greenstone belt, Quebec. Part 1. Geologic relations and formation of the vein system. *Econ Geol*, v 81, pp 578-592
- Roberts RG, Sheahan PA, eds (1988) Ore Deposit Models. *Geoscience Canada Reprint Ser*, v 3, 194 pp
- Robertson JA (1981) The Blind River uranium deposits: The ores and their setting. U.S. Geol Surv Profess Paper 1161, pp 1-23
- Robertson JA (1986) Huronian geology and the Blind River (Elliot Lake) uranium deposits. *CIM Spec Volume 33*, pp 7-43
- Robertson JA, Gould KL (1983) Uranium and thorium deposits of northern Ontario. *Ontario Geol Surv Miner Dep Circular 25*
- Robinson RF, Cook A (1966) The Safford copper district, Lone Star mining district, Graham County, Arizona, *in*: SR Titley, CL Hicks, eds, pp 251-266
- Rock NMS, ed (1991) Lamprophyres. Blackie, Glasgow
- Roden MF, Murthy VR (1985) Mantle Metasomatism. *Ann Revs Earth Planet Sci*, v 13, pp 269-296
- Rodriguez RDR (1996) Geology of Mantos Blancos mine, *in*: SM Green, E Struhsacker, eds, *Geology and Ore Deposits of the American Cordillera, Field Trip Guidebook*. Geol Soc of Nevada, Reno, pp 466-481
- Rogers DS (1982) The geology and ore deposits of the No 8 Shaft area, Dome Mine. *CIM Spec Vol 24*
- Rojas N, Perelló J, Harman P, Cabello J, Devaux C, Fava L, Etchart E (1998) Discovery of the Agua Rica porphyry Cu-Mo-Au deposit, Catamarca Province, northwestern Argentina, *in*: TM Porter, ed, *Porphyry and Hydrothermal Copper and Gold Deposits: A Global Perspective*. Confer Proceedings, AMF, Adelaide, pp 11-132
- Rollinson HR (1993) Using Geochemical Data: Evaluation, Presentation, Interpretation. Longman, London, 352 p
- Rona PA (1984) Hydrothermal mineralization at seafloor spreading centers. *Earth Sci Revs*, v 20, Elsevier, pp 1-104
- Rona PA (1988) Hydrothermal mineralization at oceanic ridges. *Canad Mineralog*, v 26, pp 431-465
- Rona PA, Scott SD, eds (1993) A special issue on seafloor hydrothermal mineralization: New perspectives. *Econ Geol*, v 88, pp 1933-2249
- Ronacher E, Richards JP, Johnston MD (1999) New mineralisation and alteration styles at the Porgera gold deposit, Papua New Guinea. PACRIM '99 Proceedings, Bali, AusIMM, pp 91-94
- Roscoe SM (1996) Paleoplacer uranium, gold, *in*: OR Eckstrand et al, eds, *Geology of Canada No 8*. Geol Surv Canada, pp 10-23
- Rösler HJ, Baumann L, Jung W (1968) Postmagmatic mineral deposits of the northern edge of the Bohemian Massif (Erzgebirge-Harz) 23th Intern Geol Congr, Prague, Guide to Excursion 22 AC, 57 p
- Rösler HJ, Lange H (1972) *Geochemical Tables*. Elsevier, Amsterdam, 468 p
- Ross JR, Travis GA (1981) The nickel sulfide deposits of Western Australia in global perspective. *Econ Geol*, v 76, pp 1291-1329
- Rostad OH (1991) Discovery of the Mount Emmons molybdenite deposit, Gunnison County, Colorado, *in*: VF Hollister, ed, *Case Histories of Mineral Discoveries*, v 3. AIME, Littleton, CO, pp 165-168
- Rota JC (1996) Gold Quarry: A geological update, *in*: SM Green, E Struhsacker, eds, *Geology and Ore Deposits of the American Cordillera, Field Trip Guidebook*. Geol Soc Nevada, Reno, pp 157-166
- Roth T, Thompson JFH, Barrett TJ (1999) The precious metal-rich Eskay Creek deposit, northwestern British Columbia. *Reviews in Econ Geol*, v 8, Soc Econ Geol, pp 357-373
- Routhier P (1963) *Les Gisements Métallifères et Principes de Recherche*. Masson, Paris, 1282 p
- Routhier P (1980) Où Sont les Métaux Pour L'avenir? *Mém du BRGM, No 105*, 410 p
- Rowan LC, Kingston MJ, Crowley JK (1986) Spectral reflectance of carbonatites and related alkalic igneous rocks: Selected samples from four North American localities. *Econ Geol*, v 81, pp 857-871
- Rowins SM, Groves DI, McNaughton NJ, Palmer MR, Eldridge CS (1997) A reinterpretation of the role of granitoids in the genesis of Neoproterozoic gold mineralization in the Telfer Dome, Western Australia. *Econ Geol*, v 92, pp 133-160
- Roy PS (1999) Heavy mineral beach placers in Southeastern Australia: Their nature and genesis. *Econ Geol*, v 94, pp 567-588
- Roy PS, Whitehouse J, Cowell PJ, Oakes G (2000) Mineral sands occurrences in the Murray Basin, southeastern Australia. *Econ Geol*, v 95, pp 1107-1128
- Rozendaal A (1986) The Gamsberg zinc deposit, Namaqualand district, *in*: CR Anhaeusser, S Maske, eds, pp 1477-1488
- Rozendaal A, Gresse PG, Scheepers R, et al (1994) Structural setting of the Riviera W-Mo deposit,

- western Cape, South Africa. *S Afr Journ of Geol*, v 97, pp 184-195
- Rubin JN, Kyle JR (1997) Precious metal mineralogy in porphyry-, skarn-, and replacement-type ore deposits of the Ertzberg (Gunung Bijih) district, Irian Jaya, Indonesia. *Econ Geol*, v 92, pp 535-550
- Rubright RD, Hart OJ (1968) Non-porphyry ores of the Bingham district, Utah, *in*: JD Ridge, ed, *Ore Deposits of the United States 1933-1967*. AIME, New York, pp 886-907
- Rudawsky O (1986) *Mineral Economics. Development and Management of Natural Resources*. Elsevier, Amsterdam, 192 p
- Rudnick RL, Fountain DM (1995) Nature and composition of the continental crust: A lower crustal perspective. *Revs of Geophys*, v 33, pp 267-309
- Rudnick RL, Gao S (2004) Composition of the continental crust, *in*: Rudnick RL, ed, pp 1-64
- Rudnick RL, ed (2004) *Treatise on Geochemistry*, v 3- The Crust. Elsevier-Pergamon, 683 p
- Rundkvist DV, ed (1978) *Kriterii Prognoznoi Otsenki Territorii na Tverdye Poleznye Iskopaemye*. Nedra, St. Petersburg, 607 p
- Rundkvist DV, ed (1981) *Rudonosnost' i Geologicheskie Formatsii Struktur Zemnoi Kory*. Nedra, St. Petersburg, 413 p
- Rundkvist IK, Bobrov VA, Smirnova TN, Smirnov MYu, Donilova MYu, Ashcheulov AA (1992) Etapy formirovaniya Bodaibinskovo zolotorudnovo raiona. *Geol Rud Mestor*, No 6, pp 3-16
- Russkikh SS, Shatov VV (1996) The Verkhnee Qairaqty scheelite stockwork deposit in Central Kazakhstan, *in*: VV Shatov et al, eds, *Granite-related ore deposits of Central Kazakhstan and adjacent areas*. Glagol, St. Petersburg, pp 167-180
- Ruvalcaba-Ruiz DC, Thompson TB (1988) Ore deposits at the Fresnillo Mine, Zacatecas, Mexico. *Econ Geol*, v 83, pp 1583-1596
- Ryan AJ (1998) Ernest Henry copper-gold deposit, *in*: DA Berkman, DH Mackenzie, eds, pp 759-768
- Ryan PJ, et al (1995) The Candelaria copper-gold deposit, Chile, *in*: Pierce FW, Bolm JG, eds, *Porphyry Copper Deposits of the American Cordillera*. Arizona Geol Soc Digest, v 20, pp 625-645
- Ryan B, Wardle R, Gower C, Nunn G (1995) Nickel-copper sulfide mineralization in Labrador: The Voisey's Bay discovery and its exploration implications. *Current Research, Newfoundland Dept Nat Res, Geol Surv Rept 95-1*, pp 177-204
- Rytuba JJ (1994) Evolution of volcanic and tectonic features in caldera settings and their importance in the localization of ore deposits. *Econ Geol*, v 89, pp 1687-1696
- Rytuba JJ (1996) Cenozoic metallogeny of California, *in*: AR Coyner, PL Fahey, eds, *Geology and Ore Deposits of the American Cordillera*. Geol Soc Nevada, Sympos Proc, Reno, pp 803-822
- Rytuba JJ, Glanzman RK (1985) Relation of mercury, uranium and lithium deposits to the McDermitt caldera complex, Nevada-Oregon, *in*: VF Hollister, ed, *Discovery of Epithermal Precious Metal Deposits*. AIME, pp 128-135
- Rytuba JJ, ed (1993) Active geothermal systems and gold-mercury deposits in the Sonoma-Clear Lake volcanic field. *Soc Econ Geol Guidebook Ser*, v 16
- Saager R, Köppel V (1976) Lead isotopes and trace elements from sulfides of Archean greenstone belts in South Africa-a contribution to the knowledge of the oldest known mineralizations. *Econ Geol*, v 71, pp 44-57
- Saegart WE, Sell JD, Kilpatrick BE (1974) Geology and mineralization of La Caridad porphyry copper deposit, Sonora, Mexico. *Econ Geol*, v 69, pp 1060-1077
- Sáez R, Almodóvar GR, Pascual E (1996) Geological constraints on massive sulfide genesis in the Iberian Pyrite Belt. *Ore Geol Revs*, v 11, pp 429-451
- Saleeby JB (1983) Accretionary tectonics of the North American Cordillera. *Annual Revs Earth Planet Sci*, v 11, pp 45-73
- Saleeby JB, Busby-Spera C, et al (1992) Early Mesozoic tectonic evolution of the western U.S. Cordillera, *in*: *The Geology of North America*, v G-3, Geol Soc Amer, Boulder, pp 107-168
- Samama JC (1968) Contrôle et modèle génétique de minéralisation en galène de type "Red-Beds". *Mineralium Deposita*, v 3, pp 261-271
- Samonov IZ, Pozharisky IF (1974) Deposits of copper, *in*: VI Smirnov, ed, *Ore Deposits of the USSR*, v 2. Engl Transl, Pitman, London, pp 106-181
- Samson SD, Patchett PJ (1991) The Canadian Cordillera as a modern analogue of Proterozoic crustal growth. *Austral Journ of Earth Sci*, v 38, pp 595-611
- Sander MV, Einaudi MT (1990) Epithermal deposition of gold during transition from propylitic to potassic alteration at Round Mountain, Nevada. *Econ Geol*, v 85, pp 285-311
- Sangster DF (1972) Precambrian volcanogenic massive sulfide deposits in Canada: A review. *Geol Surv Canada Paper 77-22*, 44 p
- Sangster DF (1996) Sandstone lead, *in*: OR Eckstrand et al, eds, *Geology of Canada No 8*, pp 220-223
- Sangster DF, Scott SD (1976) Precambrian stratabound massive Cu-Zn-Pb sulfide ores of North America, *in*: KH Wolf, ed, *Handbook of Stratiform and Stratabound Ore Deposits*, v 6, Elsevier, Amsterdam, pp 129-222
- Sangster DF, Vaillancourt PD (1980) Geology of the Yava sandstone-lead deposit, Cape Breton Island, Nova Scotia, Canada. *Geol Soc Canada, Paper 90-8*, pp 203-244
- Santana FC, Polonia JC (1982) Excursion to CVRD mines Caãe, Conceição and Picarrao. *Intern Sympos on Arch and Proter Geol Evol and Metallogeny, Salvador, Excursions Annex* pp 26-40
- Sansfaçon R (1986) The Malartic District, *in*: *Gold '86 Excursion Guidebook*, pp 100-107
- Santana FC, Polónia JC (1982) Excursion to CVRD mines: Cauê, Conceição and Piçarrão, *in*: HD Schorscher et al, eds, *ISP Symposium Excursions Annex*, pp 26-35

- Santos JOS, Groves DI, Hartmann LA, Moura MA, McNaughton NJ (2001) Gold deposits of the Tapajós and Alta Floresta Domains, Tapajós-Parima orogenic belt, Amazon Craton, Brazil. *Mineralium Deposita*, v 36, pp 278-299
- Sarkar SC (1984) Geology and ore mineralization of the Singhbhum copper-uranium belt, Eastern India. Jadavpur Univ Press, Calcutta, 263 p
- Sarkar SC, Kabiraj S, Bhattacharya S, et al (1996) Nature, origin and evolution of the granitoid-hosted early Proterozoic copper-molybdenum mineralization at Malanjkhand, central India. *Mineralium Deposita*, v 31, pp 419-431
- Sass-Gustkiewicz M, Dzułyński S, Ridge JD (1982) The emplacement of zinc-lead sulfide ores in the Upper Silesian ore district: A contribution to understanding Mississippi Valley-type deposits. *Econ Geol*, v 63, pp 1057-1068
- Satran V, et al (1966) Problémy metalogeneze Českého Masívu. *Sbor Geol Věd, LG, Prague*, v 8, pp 7-12
- Satran V, Klomínský J, Vejnar Z, Fišera M (1970) Petrometallogenic series as a source of metals of endogene ore deposits, *in: Z Poubá, M Štemprok, eds, Problems of Hydrothermal Ore Deposition. Schweizerbart, Stuttgart*, pp 78-81
- Saunders A, Tarney J (1991) Back-arc basins, *in: PA Floyd, ed, Oceanic Basalts. Blackie & Van Nostrand Reinhold*, pp 219-263
- Saunders AD, Tarney J, Stern CR, Dalziel IWD (1979) Geochemistry of Mesozoic marginal basin floor igneous rocks from southern Chile. *Geol Soc Amer Bull, Part I*, v 90, pp 237-258
- Saunders JA, Rowan EL (1990) Mineralogy and geochemistry of metallic well scale, Raleigh and Boykin Church oilfields, Mississippi, USA. *Inst Min Metall Trans*, v 99, B54-B58
- Saupé F (1990) Geology of the Almadén mercury deposit, Province of Ciudad Real, Spain. *Econ Geol*, v 85, pp 482-510
- Savard MM, Chi G, Sami T, Williams-Jones AE, Leigh K (2000) Fluid inclusion and carbon, oxygen, and strontium isotope study of the Polaris Mississippi Valley-type Zn-Pb deposit, Canadian Arctic Archipelago: Implications for ore genesis. *Mineralium Deposita*, v 35, pp 495-510
- Savory PJ (1994) Geology and grade control at ERA-Ranger Mine, Northern Territory, Australia. *AusIMM Annual Conf, Darwin*, pp 97-101
- Sawkins FJ (1990) *Metal Deposits in Relation to Plate Tectonics*, 2nd edition. Springer-Verlag, 461 p
- Schaap AD (1990) Weipa kaolin and bauxite deposits, *in: FE Hughes, ed*, pp 1669-1673
- Schaubs PM, Wilson CJL (2002) The relative roles of folding and faulting in controlling gold mineralization along the Deborah Anticline, Bendigo, Victoria, Australia. *Econ Geol*, v 97, pp 351-370
- Scheibner E, Basden H (1998) *Geology of New South Wales-Synthesis*, vol 2: Geological Evolution. *Geol Surv New South Wales, Memoir Geology 13*, 666 p
- Schlee JS (1980) A comparison of two Atlantic-type continental margins. *U.S. Geol Surv Profess Paper 1167*, 21 p
- Schmidt EA, Broch MJ, Fenne FK (1991) Geology of the Thompson Creek molybdenum deposit, Custer County, Idaho, *in: VF Hollister, ed, Case Histories of Mineral Discoveries*, v 3, AIME, Littleton, CO, pp 175-182
- Schmidt JM (1997a) Shale-hosted Zn-Pb-Ag and Cu deposits of Alaska. *Econ Geol Monogr 9*, pp 90-119
- Schmidt JM (1997b) Strata-bound carbonate-hosted Zn-Pb and Cu deposits of Alaska. *Econ Geol Monogr 9*, pp 90-119
- Schneider J, Haack U, Hein UF, et al (1999) Direct Rb-Sr dating of sandstone-hosted sphalerites from stratabound Pb-Zn deposits in the northern Eifel, NW Rhenish Massif, Germany, *in: Stanley et al, eds, Mineral Deposits: Processes to Processing. Balkema, Rotterdam*, pp 1287-1290
- Schneiderhöhn H (1941) *Lehrbuch der Erzlagerstättenkunde. Fischer-Verlag, Jena*, 858 p
- Schneiderhöhn H (1961) *Die Erzlagerstätten der Erde*, v II, Die Pegmatite. Fischer-Verlag, Stuttgart, 720 p
- Schobbenhaus C, Coelho CES, eds (1985-1988) *Principais Depósitos Minerais do Brasil*, vol 1-3. *Dep Nac Prod Miner, Comp Vale do Rio Doce, Brasilia*, 187, 501, 570 p
- Schodde RC (2004) Discovery performance of the Western World gold industry over the period 1985-2003. *PACRIM 2004 Proceedings, Adelaide. AusIMM*, pp 367-380
- Scholle PA (1978) *Carbonate Rock Constituents, Textures, Cements and Porosities. AAPG Mem 27*, 241 p
- Scholle PA, Bebout DG, Moore CH, eds (1983) *Carbonate Depositional Environments. AAPG Memoir no 33*, Tulsa
- Scholle PA, Spearing DR, eds (1982) *Sandstone Depositional Environments. AAPG Memoir 31*, Tulsa, 410 p
- Schröder E (1954) Zur Paleogeographie des Mittleren Bundsandstein bei Mechernich, Eifel. *Geol Jahrb*, v 69, pp 417-428
- Schroeter TG, ed (1995) *Porphyry Deposits of the Northwestern Cordillera of North America. CIM Spec Vol 46*, 888 p
- Schulz O (1966) Die diskordanten Erzgänge vom "Typus Bleiberg" syngenetische Bildungen, *in: Sympos Internat Giamenti Minerari delle Alpi. Petr Mitt*, v 12, pp 230-289
- Schultz RB (1991) Metalliferous black shales: accumulation of carbon and metals in cratonic basins. *Reviews in Econ Geol*, v 5, *Soc Econ Geol*, pp 171-176
- Schwartz MO (1982) The porphyry copper deposit at La Granja, Peru. *Econ Geol*, v 77, pp 482-488
- Schwartz MO, Rajah SS, Askury AK, Puthapiban P, Djaswadi S (1995) The Southeast Asia tin belt. *Earth Sci Revs*, v 38, pp 95-293

- Scott AK, Phillips KG (1990) C.S.A. copper-lead-zinc deposit, Cobar, *in*: FE Hughes, ed, AusIMM Monogr 14, pp 1337-1343
- Scott DJ, St-Onge MR, Lucas SB, Helmstaedt H (1989) The 2.0 Ga Purtuniqu ophiolite: Imbricated and metamorphosed oceanic crust in the Cape Smith Thrust Belt, northern Quebec. *Geoscience Canada*, v 16, pp 144-147
- Scott J, Collins GA, Hodgson GW (1954) Trace metals in the McMurray Oil Sands and other Cretaceous reservoirs of Alberta. *CIM Bull*, Jan 1954, pp 36-41
- Scott SD, Binns RA (1992) An actively forming volcanic-hosted polymetallic sulfide deposit in the Southeast Manus back-arc basin of Papua New Guinea (abs). *Trans Amer Geophys Union*, v 73, p 626
- Scott TM (1986) The Central Florida Phosphate District, *in*: *Geol Soc Amer, Centennial Field Guide-Southern Section*, pp 339-342
- Seedorf E, Einaudi MT (2004) Henderson porphyry-molybdenum system, Colorado: I Sequence and abundance of hydrothermal mineral assemblages, flow paths of evolving fluids, and evolutionary style. *Econ Geol*, v 99, pp 3-37
- Seedorff E (1991) Magmatism, extension, and ore deposits of Eocene to Holocene age in the Great Basin-mutual effects and preliminary proposed genetic relationships, *in*: GL Raines et al, eds, *Geology and Ore Deposits of the Great Basin*. *Geol Soc Nevada, Reno*, pp 133-178
- Segev A, Sass E (1989) Copper-enriched syngenetic dolostones as a source for epigenetic copper mineralization in sandstones and shales (Timna, Israel). *Geol Assoc Canada Spec Paper* 36, pp 647-658
- Selby D, Nesbitt BE, Muehlenbachs K, Prochaska W (2000) Hydrothermal alteration and fluid chemistry of the Endako porphyry molybdenum deposit, British Columbia. *Econ Geol*, v 95, pp 183-202
- Seltmann R (1994) Sub-volcanic minor intrusions in the Altenberg Caldera and their metallogeny, *in*: R Seltmann et al, eds, pp 198-206
- Seltmann R, Faragher AE (1994) Collisional orogens and their related metallogeny-a preface, *in*: R Seltmann et al, eds, pp 7-19
- Seltmann R, Kämpf H, Möller P, eds (1994) *Metallogeny of Collisional Orogens*. *Czech Geol Surv, Prague*, 448 p
- Seltmann R, Schilka W (1995) Late Variscan crustal evolution in the Altenberg-Teplice caldera; evidence from new geochemical and geochronological data. *Terra Nostra*, v 7-95, pp 120-124
- Semenov EI (1974) Economic mineralogy of alkaline rocks, *in*: H Sørensen, ed, *Alkaline Rocks*, pp 543-553
- Şengör AMC (1987) Tectonics of the Tethysides: Orogenic collage development in a collisional setting. *Annual Revs of Earth Planet Sci*, v 15, pp 213-244
- Şengör AMC (1992) The Palaeo-Tethyan suture: A line of demarcation between two fundamentally different architectural styles in the structure of Asia. *The Island Arc*, v 1, pp 78-91
- Şengör AMC, Natal'in BA (1996) Turcic-type orogeny and its role in the making of the continental crust. *Ann Revs of Earth and Planet Sci*, v 24, pp 263-337
- Şengör AMC, Natal'in BA, Burtman VS (1993) Evolution of the Altaid tectonic collage and Paleozoic crustal growth in Eurasia. *Nature*, v 364, pp 299-307
- Serrano L, Vargas R, Stambuk V, Aguilar C, Galeb M, Holmgren C, Contreras A, Godoy S, Vela I, Skewes MA, Stern CR (1996) The late Miocene to early Pliocene Rio Blanco-Los Bronces copper deposit, central Chilean Andes. *Soc Econ Geol Spec Publ* 5, pp 119-130
- Serykh VI (1996) Granitic rocks of Central Kazakhstan, *in*: V Shatov et al, eds, *Granite-Related Ore Deposits of Central Kazakhstan and Adjacent Areas*. *Glagol, St. Petersburg*, pp 55-65
- Sestini G (1973) Sedimentology of a paleoplacer: The gold-bearing Tarkwaian of Ghana, *in*: GC Amstutz, AJ Bernard, eds, *Ores in Sediments*. *Springer-Verlag*, pp 275-305
- Shanks WC III, Woodruff LG, Jilson GA, Jennings DS, Modene JS, Ryan MD (1987) Sulfur and lead isotope studies of stratiform Zn-Pb-Ag deposits, Anvil Range, Yukon: Basinal brine exhalation and anoxic bottom-water mixing. *Econ Geol*, v 82, pp 600-634
- Shatalov YeT, et al (1966) Printsipy i Metodika Sostavleniya Metallogenicheskikh i Prognoznykh Kart. *Nedra, Moscow*
- Shaver SA (1986) Elemental dispersion associated with alteration and mineralization at the Hall (Nevada Moly) quartz-monzonite type porphyry molybdenum deposit, with a section on comparison of dispersion patterns with those from Climax-type deposits. *Journ Geochem Explor*, v 25, pp 81-98
- Shaw HR, Jackson ED, Baragar KE (1980) Volcanic periodicity along the Hawaiian-Emperor chain. *Amer Journ Sci*, v 280A, pp 667-708
- Shcheglov AD (1967) Osnovnye cherty metallogenii zon avtonomnoi aktivizatsii. *Zakon Razmezch Polez Iskop*, v 8, pp 98-138
- Shcherba GN, et al (1972) *Geotektonogeny Kazakhstana i Redkometal'nye Orudneniye*. *Nauka Kazakh SSR, Alma Ata*, 218 p
- Shen-su Sun (1982) Chemical composition and origin of the Earth's primitive mantle. *Geoch Cosmoch Acta*, v 46, pp 179-192
- Shepherd MS (1990) Eneabba heavy mineral sand placers, *in*: EF Hughes, ed, pp 1591-1594
- Sheppard SMF (1994) Stable isotope and fluid inclusions evidence for the origin and evolution of Hercynian mineralizing fluids, *in*: R Seltmann et al, eds, *Metallogeny of Collisional Orogens*. *Czech Geol Surv, Prague*, pp 49-60
- Sheridan DM, Maxwell CH, Collier JT (1961) Geology of the Lost Creek schroëckingerite deposit, Sweetwater County, Wyoming. *U.S. Geol Surv Bull* 1087-J, pp 391-478
- Sherlock RL, Jowett EC (1992) The McLaughlin hot-spring gold-mercury deposit and its relationship to hydrothermal systems in the Coast Ranges of northern

- California, USA, *in*: Kharaka and Maest, eds, Water-Rock Interaction. Balkema, Rotterdam, pp 979-981
- Shi Mingkui, Hu Xiongwei (1988) The geological characteristics and genesis of the granite-hosted tungsten deposits at Dajishan mine, Jiangxi province, China. Proc of the 7th Quadren IAGOD Sympos, Schweizerbart, Stuttgart, pp 613-618
- Shoemaker EM (1963) Impact mechanics at Meteor Crater, Arizona, *in*: BM Middlehurst, GP Kuiper, eds, The Moon, Meteorites and Comets. Univ of Chicago Press, pp 301-336
- Shoemaker EM (1987) Meteor Crater, Arizona, *in*: Centennial Field Guide, Rocky Mountain Section. Geol Soc Amer, Boulder, pp 399-404
- Shumlyanskiy VO, Ivantyshyna OM (1998) Geological features, zonality and ore-forming solutions of the Nikitovka mercury ore field, Ukraine. Poster, Geol Assoc/Miner Assoc Canada Ann Conf, Québec '98
- Sharpe EN, MacGeehan PJ (1990) Bendigo Golodfield, *in*: FE Hughes, ed, pp 1287-1296
- Sharpe MR (1982) Noble metals in the marginal rocks of the Bushveld Complex. Econ Geol, v 77, pp 1286-1295
- Shaver SA (1986) Elemental dispersion associated with alteration and mineralization at the Hall (Nevada Moly) quartz monzonite type porphyry molybdenum deposit. Journ Geoch Explor, v 25, pp 81-98
- Shaw AL, Guilbert JM (1990) Geochemistry and metallogeny of Arizona peraluminous granitoids with reference to Appalachian and European occurrences. Geol Soc Amer Spec Paper 246, pp 317-356
- Sibbals TII (1987) Overview of the Precambrian geology and aspects of the metallogenesis of northern Saskatchewan. Sask Geol Soc Spec Publ 8, pp 1-32
- Sibson RH (1977) Fault rocks and fault mechanisms. Journ Geol Soc London, v 133, pp 191-213
- Siddeley G, Araneda R (1986) The El Indio-Tambo gold deposits, Chile. Proc of the Gold '86 Symposium, Toronto, pp 445-456
- Sidorenko AV, ed (1982) Rudonosnye Struktury Dokembriya. Nauka, Moscow, 203 p
- Sikka DB, Petruk W, Cherukupalli EN, Zheru Zhang (1991) Geochemistry of secondary copper minerals from Proterozoic porphyry copper deposit, Malanjkhanda, India. Ore Geol Revs, v 6, pp 257-290
- Sillitoe RH (1975) Lead-silver, manganese, and native sulfur mineralization within a stratovolcano, El Queva, Northwest Argentina. Econ Geol, v 70, pp 1190-1201
- Sillitoe RH (1976) Andean mineralization: A model for the metallogeny of convergent plate margins. Geol Assoc Canada, Spec Paper 14, pp 59-100
- Sillitoe RH (1977) Metallic mineralization affiliated to subaerial volcanism: A review, *in*: Volcanic Processes in Ore Genesis. Inst Min Metall/Geol Society, London, pp 99-116
- Sillitoe RH (1985) Ore-related breccias in volcanoplutonic arcs. Econ Geol, v 80, pp 1467-1514
- Sillitoe RH (1993) Giant and bonanza gold deposits in the epithermal environment: Assessment of potential genetic factors. Soc Econ Geol, Spec Publ 2, pp 125-156
- Sillitoe RH (1994) Erosion and collapse of volcanoes: Causes of telescoping in intrusion-centered ore deposits. Geology, v 22, pp 945-948
- Sillitoe RH (1995) Exploration of porphyry copper lithocaps. PACRIM '95 Proceedings, AusIMM, pp 527-532
- Sillitoe RH (2003) Iron oxide-copper-gold deposits: An Andean view. Mineralium Deposita, v 38, pp 787-812
- Sillitoe RH, Bonham HF Jr (1984) Volcanic landforms and ore deposits. Econ Geol, v 79, pp 1286-1298
- Sillitoe RH, Gappe IM Jr (1984) Philippine porphyry copper deposits: Geologic setting and characteristics. Comm for Coord of Joint Prosp for Miner Res in Asian Offshore Areas (CCOP), Nov 1984, 89 p
- Sillitoe RH, Halls C, Grant JN (1975) Porphyry tin deposits in Bolivia. Econ Geol, v 70, pp 913-927
- Sillitoe RH, Jaramillo L, Castro H (1984) Geologic exploration of a molybdenum-rich porphyry copper deposit at Mocoa, Colombia. Econ Geol, v 79, pp 106-123
- Sillitoe RH, Jaramillo L, Damon PE, Shafiqullah M, Escovar R (1982) Setting, characteristics and age of the Andean porphyry copper belt in Colombia. Econ Geol, v 77, pp 1837-1850
- Sillitoe RH, Steele GB, Thompson JFH, et al (1998) Advanced argillic lithocaps in the Bolivian tin-silver belt. Mineralium Deposita, v 33, pp 539-546
- Silva JB, Oliveira V, Matos J, Leitão JC (1997) Aljustrel and the Central Iberian Pyrite Belt. Soc Econ Geol Guidebook Series, v 27, pp 73-97
- Simmons SF, Browne PRL (2000) Hydrothermal minerals and precious metals in the Broadlands-Ohaaki geothermal system: Implications for understanding low-sulfidation epithermal environments. Econ Geol, v 95, pp 971-999
- Simon G, Kesler SE, Chryssoulis S (1999) Geochemistry and textures of gold-bearing arsenian pyrite, Twin Creeks, Nevada: Implications for deposition of gold in Carlin-type deposits. Econ Geol, v 94, pp 405-422
- Simpson TA, Gray TR (1968) The Birmingham red-ore district, Alabama, *in*: JD Ridge, ed, Ore Deposits of the United States 1933-1967. AIME New York, pp 187-206
- Sinclair B (1989) Lake Rotokaua sulphur deposit. Australas Inst Min Metall Monogr 13, pp 89-91
- Sinclair WD (1994) Tungsten-molybdenum and tin deposit at Mount Pleasant, New Brunswick, Canada: Products of ore-fluid evolution in highly fractionated granitic systems, *in*: R Seltman et al, eds, pp 410-417
- Sinclair WD, Chorlton LB, Laramée RM, Eckstrand OR, Kirkham RV, Dunne KPE, Good DJ (1999) World Minerals Geoscience Database Project: Digital databases of generalized world geology and mineral deposits for mineral exploration and research, *in*: Stanley, et al, eds, Mineral Deposits: Processes to Processing. Balkema, Rotterdam, pp 1435-1437
- Singer DA (1995) World class base and precious metal deposits: A quantitative analysis. Econ Geol, v 90, pp 88-104
- Sisson VB, Roeske SM, Pavlis TL, eds (2003) Geology of a transpressional orogen developed during ridge-

- trench interaction along the North Pacific margin. *Geol Soc Amer, Spec Paper 371*, 375 p
- Skarpelis N, Mantzos L (1990) Lead and sulfur isotope ratios from metamorphosed massive sulfide mineralization in the blueschists of Peloponnese (Greece). *Proceedings, Intern Earth Sci Congr on Aegean regions, Izmir*, pp 74-87
- Skewes MA, Holmgren C, Stern CR (2003) The Donoso copper-rich, tourmaline-bearing breccia pipe in central Chile: Petrographic, fluid inclusion and stable isotope evidence for an origin from magmatic fluids. *Mineralium Deposita*, v 38, pp 2-21
- Skewes MA, Stern CR (1996) Late Miocene mineralized breccias in the Andes of Central Chile: Sr- and Nb-isotopic evidence for multiple magmatic sources. *Soc Econ Geol, Spec Publ 5*, pp 33-42
- Skinner BJ (1993) Finding mineral resources and the consequences of mining them: Major challenges in the 21st Century. *Austral Inst Min Metall Centenary Conf, Proceedings, Adelaide*, pp 1-8
- Skinner BJ, White DE, Rose HJ Jr, Mays RE (1967) Sulfides associated with the Salton Sea geothermal brine. *Econ Geol*, v 62, pp 316-330
- Skirrow RG, Bastrakov E, Davidson G, Raymond OL, Heithersay P (2002) The geological framework, distribution and controls of Fe-oxide Cu-Au mineralisation in the Gawler Craton, South Australia. Part II-Alteration and Mineralization, *in: TM Porter, ed, Hydrothermal Iron Oxide Copper-gold and Related Deposits: a Global Perspective*, v 2. PGC Publ, Adelaide, pp 33-47
- Slack JF (1993) Descriptive and grade-tonnage models for Besshi-type massive sulfide deposits. *Geol Assoc Canada, Spec Paper 40*, pp 343-371
- Smirnov VI (1976) *Geology of Mineral Deposits*. Mir, Moscow, 520 p
- Smirnov VI, Gorzhevsky DI (1974) Deposits of lead and zinc, *in: VI Smirnov, ed, Ore Deposits of the USSR*, v 2. Engl Transl, Pitman, London, pp 182-256
- Smith DM Jr (1996) Sedimentary basins and the origin of intrusion-related carbonate-hosted Zn-Pb-Ag deposits. *Soc Econ Geol Spec Publ 4*, pp 255-263
- Smith EEN (1986) *Geology of the Beaverlodge operations of Eldorado Nuclear*. CIM Spec Vol 33, pp 95-109
- Smith GI (1979) Subsurface stratigraphy and geochemistry of late Quaternary evaporites, Searles Lake, California. *U.S. Geol Surv Prof Paper 1043*, 130 p
- Smith GA, Landis CA (1995) Intra-arc basins, *in: CJ Busby-Spera, RV Ingersoll, eds, Tectonics of Sedimentary Basins*. Blackwell, pp 263-298
- Smith JW, Milton C (1966) Dawsonite in the Green River Formation of Colorado. *Econ Geol*, v 61, pp 1029-1042
- Snyder FC, Gerdemann PE (1968) *Geology of the Southeast Missouri Lead district*, *in: JD Ridge, ed, Ore Deposits of the United States 1933-1967*. AIME, New York, pp 326-359
- Sobol F, Toscano M, Castro JA, Sáez R (1997) A field guide to the Riotinto mines. *Soc Econ Geol Fieldbook Ser, No 27*, pp 158-164
- Sobolev VS, et al (1978) Poiskovye kriterii sul'fidnykh rud Noril'skovo tipa. *AN SSSR, Sibir Otdel, Trudy 418*, 320 p
- Socolescu M (1972) Phénomènes métallogéniques dans la province de Baia Mare. *Geologija, Ljubljana*, v 15, pp 287-297
- Sokolov AL (1998) The regional and local controls on gold and copper mineralization, Central Asia and Kazakhstan, *in: TM Porter, ed, Porphyry and Hydrothermal Copper and Gold Deposits, a Global Perspective*. Austr Miner Found, Adelaide, pp 181-190
- Sokolov GA, Grigor'ev VM (1974) Deposits of iron, *in: VI Smirnov, ed, Ore Deposits of the USSR*, v1. Engl transl, Pitman, London, pp 7-113
- Sokolov YuM (1984) *Osnovy Metallogeni i Metamorficheskikh Poyasov*. Nauka, Leningrad
- Solomon M, Groves DI, Jaques AL (1994) *The Geology and Origin of Australia's Mineral Deposits*. Clarendon Press, Oxford, 951 p
- Solomon M, Heinrich CA (1992) Are high-heat producing granites essential to the origin of giant lead-zinc deposits at Mount Isa and MacArthur, Australia? *Explor Mining Geol*, v 1, pp 85-91
- Somm AF (1975) Gove bauxite deposits, *in: CL Knight, ed, Economic Geology of Australia and Papua New Guinea*, v 1. AusIMM, Monogr 5, pp 964-967
- Song Shuhe, ed (1990) *Mineral Deposits of China*, vol 1. Geol Publ House, Beijing, 355 p
- Sørensen H, ed (1974) *The Alkaline Rocks*. Wiley, New York
- Soriano C, Marti J (1999) Facies analysis of volcano-sedimentary successions hosting massive sulfide deposits in the Iberian Pyrite Belt, Spain. *Econ Geol*, v 94, pp 867-882
- Sotnikov VI, Berzina AP (1968) Nekotorye geneticheskie osobennosti medno-molibdenovoi formatsii v Altae-Sayanskoi geosinklinal'noi oblasti, *in: Rudnye Formatsii i Genezis Endogennykh Mestorozhdenii Altai-Sayanskoi Oblasti*. Nauka, Moscow, pp 40-47
- Sotnikov VI, Berzina AP, Nikitina YeI, Proskur'yakov AA, Skuridin VA (1977) *Medno-molibdenovaya Rudnaya Formatsiya*. Nauka, Novosibirsk, 424 p
- Souch BE, Podolsky T, INCO Geol Staff (1969) The sulfide ores of Sudbury: Their particular relation to a distinctive intrusion-bearing facies of the Nickel Irruptive. *Econ Geol Monogr 4*, pp 252-261
- Souther JC (1992) Volcanic regimes, *in: H Gabrielse, CJ Yorath, eds, Geology of the Cordilleran Orogen in Canada*. Geology of Canada No 4, pp 457-490
- Spencer AC (1906) The Juneau gold belt, Alaska. *U.S. Geol Surv Bull 287*, 161 p
- Sperling H (1973) *Monographien der deutschen Blei-Zink-Erzlagerstätten*, 3. Die Blei-Zink Erzganges des Oberharzes, Lieferung 2: Die Erzgänge der Erzbergwerks Grund. *Geol Jahrb, Reihe D*, 205 p
- Sperling H, Walcher E (1990) Die Blei-Zink-Erzlagerstätte Rammelsberg (ausgenommen Neues Lager). *Geol Jahrb*, v D91, pp 3-153

- Spilsbury TW (1995) The Schaft Creek copper-molybdenum-gold-silver porphyry deposit, north-western British Columbia. *CIM Spec Vol 46*, pp 239-246
- Spooner ETC (1993) Magmatic sulfide/volatile interaction as a mechanism for producing chalcophile element enriched, Archean Au-quartz, epithermal Au-Ag and Au skarn hydrothermal fluids. *Ore Geol Revs*, v 7, pp 359-379
- Spry PG, Marshall B, Vokes FM, eds (2000) *Metamorphosed and Metamorphogenic Ore Deposits. Reviews in Econ Geol*, v 11, 310 p
- Staatz MH (1979) *Geology and mineral resources of the Lemhi Pass thorium district, Idaho and Montana. U.S. Geol Surv Profess Paper 1049-A*
- Stanton RL (1972) *Ore Petrology*. McGraw Hill, New York, 713 p
- Stanton RL (1994) *Ore Elements in Arc Lavas*. Oxford Univ Press, New York, 391 p
- Štemprok M, Pivec E, Lang M, Novák JK (1995) Phosphorus in the younger granites of the Krušné Hory (Erzgebirge) Batholith, *in: J Pašava et al, eds, Mineral Deposits, from their Origin to their Environmental Impacts*. Balkema, Rotterdam, pp 535-537
- Štemprok M, Seltmann R (1994) The metallogeny of the Erzgebirge (Krušné Hory), *in: R Seltmann et al, eds, pp 61-69*
- Štemprok M, Šulcek Z (1969) Geochemical profile through ore-bearing lithium granite. *Econ Geol*, v 64, pp 392-404
- Stenger DP, Kesler SE, Peltonen DR, Tapper CJ (1998) Deposition of gold in Carlin-type deposits: The role of sulfidation and decarbonation at Twin Creeks, Nevada. *Econ Geol*, v 93, pp 201-215
- Stevens BJP (1996) Regional geology of the Broken Hill and Eurowie Blocks, *in: J Pongratz, GJ Davidson, eds, New Developments in Broken Hill-type deposits*. Univ of Tasmania, Hobart, CODES Spec Publ 1, pp 11-15
- Stevens, BPJ, ed (1980) A guide to the stratigraphy and mineralisation of the Broken Hill Block. *Rec Geol Surv NSW*, 20, 153 p
- Stevens BPJ, Barnes RG, Forbes BG (1990) Willyama Block-regional geology and minor mineralisation, *in: FE Hughes, ed, pp 1065-1072*
- Stevenson DB, Broughton DW, Cruji DR, Masson MW, Parry DE (1995) Geology and exploration history of the Amalgamated Kirkland deposit, Kirkland Lake, Ontario. *Explor and Mining Geol*, v 4, pp 187-196
- Stöffler D, Deutsch A, Avermann M, et al (1994) The formation of the Sudbury structure, Canada: Toward a unified impact model. *Geol Soc Amer, Spec Paper 293*, pp 303-318
- Stone JG (1959) Ore genesis in the Naica district, Chihuahua, Mexico. *Econ Geol*, v 54, pp 1002-1034
- Stone M, Exley CS (1985) High heat producing granites of Southwest England and their associated mineralization: A review, *in: C Halls, ed, High Heat Production (HHP) Granites, Hydrothermal Circulation, and Ore Genesis*. Inst Min Metall, London, pp 571-593
- Stone WE, Masterman EE (1998) Kambalda nickel deposits, *in: DA Berkman, DH Mackenzie, eds, pp 347-356*
- Strakhov NM (1962) *Principles of Lithogenesis*, v 2. Engl Transl, Oliver & Boyd, Edinburgh, 609 p
- Strakhov NM, Shterenberg LYe, Kalinenko VV, Tikhomirova YeS (1968) *Geokhimiya Osadochnovo Margantsevorudnovo Protsessa*. AN SSSR, Trudy, v 185, 493 p
- Strauss GK, Beck JS (1990) Gold mineralisations in the SW Iberian Pyrite Belt. *Mineralium Deposita*, v 25, pp 237-245
- Strauss GK, Gray KG (1986) Base metal deposits in the Iberian pyrite belt, *in: GH Friedrich et al, eds, Geology and Metallogeny of Copper Deposits*. Soc Geol Applied to Min Dep, Spec Publ 4, pp 304-324
- Strauss GK, Madel J, Alonso FF (1977) Exploration practice for strata-bound volcanogenic sulfide deposits in the Spanish-Portuguese pyrite belt: Geology, geophysics and geochemistry, *in: DD Klemm, H-J Schneider, eds, Time and Strata-Bound Ore Deposits*. Springer-Verlag, pp 55-93
- Stribny B, Wellmer F-W, Burgath K-P, et al (2000) Unconventional PGE occurrences and PGE mineralization in the Great Dyke: Metallogenic and Economic Aspects. *Mineralium Deposita*, v 35, pp 260-281
- Suarez M, Naranjo JA, Puig A (1990) Mesozoic "S-like" granites of the central and southern Andes: A review. *Geol Soc Amer, Spec Paper 241*, pp 27-32
- Suk M (1983) *Petrology of Metamorphic Rocks*. Elsevier, Amsterdam, 322 p
- Sullivan R (1985) Origin of lacustrine rocks of Wilkins Peak Member, Wyoming. *AAPG Bull*, v 69, pp 913-1022
- Sun SS, McDonough (1989) Magmatism in the Ocean Basins. *Geol Soc Amer Spec Publ 42*, pp 313-345
- Sundblad K (1980) A tentative "volcanogenic" formation model for the sediment-hosted Ankarvattnet Zn-Pb-Cu massive sulfide deposit, Central Swedish Caledonides. *Norges Geol Unders*, No 360, pp 211-227
- Sutherland Brown A (1976) Morphology and classification, *in: Porphyry Deposits of the Canadian Cordillera*. *CIM Spec Vol 15*, pp 44-51
- Sverjensky DA (1981) The origin of a Mississippi Valley-type deposit in the Viburnum Trend, Southeast Missouri. *Econ Geol*, v 76, pp 1848-1872
- Sverjensky D (1984) Oil field brines as ore-forming solutions. *Econ Geol*, v 79, pp 1848-1872
- Sviridenko VT (1975) *Magmaticheskie formatsii i metallogeniya stadii tektonomagmaticheskoi aktivizatsii drevnykh platform*, *in: Zakonomernosti Razmeshchaniya Poleznykh Iskopaemykh*, v XI, Nauka, Moscow, pp 122-133
- Swanson EA, Strong DF, Thurlow JG, eds (1981) *The Buchans orebodies. Fifty years of geology and mining*. Geol Assoc Canada, Spec Paper 22, pp 113-142
- Swanson RW (1973) *Geology and phosphate deposits of the Permian rocks in central western Montana*. U.S. Geol Surv Profess Paper 331-F, pp 779-785

- Sýka J, Čadek J, Blažek J, Herčík F, Chabr P, Studničná B, Veselý T (1978) Charakteristické rysy uranových a zirkonium-uranových akumulací ve svrchní křídě severních Čech. Sbor Geol Věd, LG, Prague, v 19, pp 7-33
- Symons DTA, Sangster DF (1992) Late Devonian paleomagnetic age for the Polaris Mississippi Valley-type deposit, Canadian Arctic Archipelago. *Canad Journ Earth Sci*, v 29, pp 15-25
- Symons PM, et al (1990) Boddington gold deposit, *in*: FE Hughes, ed, pp 165-170
- Tabor RW, Cady WM (1978) The structure of the Olympic Mountains, Washington-analysis of a subduction zone. U.S. Geol Surv Profess Paper 1033, 75 p
- Taira A, Katto J, Tashiro M, Okamura M, Kodama K (1988) The Shimanto belt in Shikoku, Japan-evolution of Cretaceous to Miocene accretionary prism. *Modern Geology*, v 12, pp 1-42
- Tanelli G, Lattanzi P (1985) The cassiterite-polymetallic sulfide deposits of Dachang (Guangxi, People's Republic of China). *Mineralium Deposita*, v 20, pp 102-106
- Tankard AJ, Jackson MPA, Erikson KA, et al (1982) Crustal Evolution of Southern Africa-3.8 billion years of Earth History. Springer-Verlag, New York, 523 p
- Tarkhanov AV, et al (1991) Zheltorechenskoe vanadii-skandievoye mestorozhdeniye. *Geol Rud Mestor*, v 6, pp 50-56
- Taylor CD, Premo WR, Leventhal JS, et al (1999) Greens Creek deposit, southeastern Alaska: A VMS-SEDEX hybrid, *in*: CJ Stanley et al, eds, *Mineral Deposits: Processes to Processing*. Balkema, Rotterdam, pp 597-600
- Taylor D, Dalstra HJ, Harding AE, Broadbent GC, Barley ME (2001) Genesis of high-grade hematite orebodies of the Hamersley Province, Western Australia. *Econ Geol*, v 96, pp 837-873
- Taylor G, Hughes GW (1975) Biogenesis of the Rennell bauxite. *Econ Geol*, v 70, pp 542-546
- Taylor HK (1995) Western Canadian deposits-economic perspectives, performances and prospects. *CIM Spec Vol 46*, pp 20-39
- Taylor SR (1964) Abundance of chemical elements in the continental crust. *Geoch Cosmoch Acta*, v 28, pp 1280-1281
- Taylor SR, McLennan SM (1985) *The Continental Crust: Its Composition and Evolution*. Blackwell
- Taylor SR, McLennan SM (1995) The geological evolution of the continental crust. *Revs of Geophys*, v 33, pp 241-265
- Teagle DAH, Alt JC (2004) Hydrothermal alteration of basalts beneath the Bent Hill massive sulfide deposit, Middle Valley, Juan de Fuca Ridge. *Econ Geol*, v 99, pp 561-584
- Teal L, Jackson M (1997) Geological overview of the Carlin Trend gold deposits and descriptions of recent deep discoveries, *in*: TB Thompson, ed, *Carlin-type gold deposits field conference*. *Econ Geol Guidebook Ser*, v 28, pp 3-37
- Teale GS, Lynch JE (2004) The discovery and early history of the Mt Leyshon gold deposit, North Queensland. PACRIM 2004 Congress, Adelaide, Proceedings, AusIMM, pp 385-389
- Tegart P, Allen G, Carstensen A (2000) Regional setting, stratigraphy, alteration and mineralization of the Tambo Grande VMS district, Piura Department, northern Peru. *Geol Assoc Canada, Miner Division Spec Publ No 2*, pp 375-405
- Tegengren FR (1921) The Hsi-K'uang-Shan antimony mining fields, Hsin-Hua district, Hunan. *Geol Surv China Bull 3*, pp 1-26
- Temple AK, Grogan RM (1965) Carbonatite and related alkaline rocks at Powderhorn, Colorado. *Econ Geol*, v 60, pp 672-692
- Thälhammer OAR, Stumpf EF, Jahoda R (1989) The Mittersill scheelite deposit, Austria. *Econ Geol*, v 84, pp 1153-1171
- Theodore TG, Blake DW, Loucks TA, Johnson CA (1992) Geology of the Buckingham stockwork molybdenum deposit and surrounding area, Lander County, Nevada. U.S. Geol Surv Profes Paper 798-D, D36-D40
- Theodore TG, Howe SS, Blake DW (1990) The Tomboy-Minnie gold deposits at Copper Canyon, Lander County, Nevada. U.S. Geol Surv Bull 1857-E, pp E43-E56
- Theodore TG, Orris GJ, Hammarstrom JM, Bliss JD (1991) Gold-bearing skarns. U.S. Geol Surv Bulletin 1930
- Thiry HB, Lenoble J-P, Rogel P (1977) French exploration seeks to define mineable nodule tonnages on Pacific floor. *Eng Min Journ*, July 1977, pp 86-87
- Thomas JA, Galey JT Jr (1982) Exploration and geology of the Mt Emmons molybdenite deposits, Gunnison County, Colorado. *Econ Geol*, v 77, pp 1085-1104
- Thompson JFH, Sillitoe RH, Baker T, Lang JR, Mortensen JK (1999) Intrusion-related gold deposits associated with tungsten-tin provinces. *Mineralium Deposita*, v 34, pp 323-334
- Thompson RN (1982) Magmatism of the British Tertiary Province. *Scott Journ Geol*, v 18, pp 49-107
- Thompson TB (1990) Precious metals in the Leadville mining district, Colorado. U.S. Geol Surv Bull 1857-F, pp F32-F49
- Thompson TB, Trippel AD, Dwelley PC (1985) Mineralized veins and breccias of the Cripple Creek district, Colorado. *Econ Geol*, v 80, pp 1669-1688
- Thompson TB, Teal L, Meeuwig RO (2002) Gold deposits of the Carlin Trend. Nevada Bur of Mines and Geol, Bull 111, 204 p
- Thouvenin J-M (1984) Le gisement polymétallique à Zn,Pb,Cu,Ag de Huaron (Pérou). *Chron rech min*, No 477, pp 35-54
- Thurston PC, Chivers KM (1990) Secular variation in greenstone sequence development emphasizing Superior Province, Canada. *Precamb Res*, v 46, pp 21-58
- Thurston PC, Williams HR, Sutcliffe RH, Stott GM, eds (1991, 1992) *Geology of Ontario*. Ontario Geol Surv Spec Vol 4, Pt1, Pt2, 1525 p

- Tipper GH (1914) The monazite sands of Travancore. Geol Surv India, vol 35
- Tischendorf G (1989) Silicic magmatism and metallogenesis of the Erzgebirge. Inter-Union Commission on the Lithosphere, ICL Publ No 0171. Zentralinst f Physik der Erde, Potsdam, 316 p
- Tischendorf G, Förster H-J (1990) Acid magmatism and related metallogenesis in the Erzgebirge. Geol Journ, v 25, pp 443-454
- Titly SR (1993a) Characteristics of porphyry copper occurrences in the American Southwest, *in*: RV Kirkham et al, eds, Geol Assoc Canada Spec Paper 40, pp 433-464
- Titly SR (1993b) Characteristics of high-temperature carbonate-hosted massive sulfide ores in the United States, Mexico and Peru. Geol Assoc Canada, Spec Paper 40, pp 585-614
- Titly SR, ed (1982) Advances in Geology of the Porphyry Copper Deposits, Southwestern North America. Univ of Arizona Press, Tucson, 560 p
- Titly SR, Beane RE (1981) Porphyry copper deposits, Part 1. Geologic setting, petrology, and tectogenesis. Econ Geol 75th Anniv Vol, pp 214-235
- Titly SR, Hicks CL, eds (1966) Geology of the Porphyry Copper Deposits, Southwestern North America. Univ of Arizona Press, Tucson, 287 p
- Tobey E, Schneider A, Alegria A, et al (1998) Skouries porphyry copper-gold deposit, Chalkidiki, Greece: Setting, mineralization and resources, *in*: TM Porter, ed, Porphyry and Hydrothermal Copper and Gold Deposits, a Global Perspective. Confer Proc, Perth. Austr Miner Found, Adelaide, pp 159-167
- Todd SG, et al (1982) The J-M platinum-palladium Reef of the Stillwater Complex, Montana: I Stratigraphy and petrology. Econ Geol, v 77, pp 1454-1480
- Tomkins AG, Mavrogenes JA (2002) Mobilization of gold as a polymetallic melt during pelite anatexis at the Challenger deposit, South Australia: A metamorphosed Archean gold deposit. Econ Geol, v 97, pp 1249-1271
- Tooker EW (1990) Gold in porphyry copper systems. Gold in the Bingham district, Utah. U.S. Geol Surv Bull 1857-E, pp E1-E12
- Tornos F (2003) The Tharsis mine. GEODE-GCMS, Iberian Pyrite Belt Field Trip guidebook, Apr 2003, 8 p
- Toth JR (1980) Deposition of submarine crusts rich in manganese and iron. Geol Soc Amer Bull, v 91, pp 44-54
- Tourigny G, Hubert C, Brown AC, Crepeau R (1989) Structural control of gold mineralization at the Bousquet Mine, Abitibi, Quebec. Canad Journ Earth Sci, v 26, pp 157-175
- Townend R, Ferreira PM, Franke ND (1980) Caraba, a new copper deposit in Brazil. Trans Inst Min Metall, London, v 89, pp B159-B165
- Treadgold T (1998) Playing it safe. Australia's Mining Monthly, Febr 1998, pp 27-34
- Travis GA, Woodall R, Bartram GD (1971) The geology of the Kalgoorlie Goldfield. Geol Soc Austral Spec Publ 3, pp 175-190
- Tremblay LP (1978) Uranium subprovinces and types of uranium deposits in the Precambrian rocks of Saskatchewan. Geol Surv Canada Paper 78-1A, pp 427-435
- Trendall AF (1983) The Hamersley Basin, *in*: AF Trendall, RC Morris, eds, pp 69-129
- Trendall AF, Morris RC, eds (1983) Iron Formation: Facts and Problems. Elsevier, Amsterdam, 558 p
- Trueman D (1983) Geology of the Thor Lake area. Northern Miner, Jan 19, pp B29-B30
- Trueman DL, Turnock AC (1982) Bird River greenstone belt, Southeast Manitoba: Geology and Mineral Deposits. Geol Assoc/Miner Assoc Canada, Joint Ann Meet Winnipeg, Field Trip Guidebook, 33 p
- Trumbull RB, Morteani G, Li ZL, Bai HS (1992) Gold Metallogeny in the Sino-Korean Platform. Springer-Verlag, 202 p
- Tsikos H, Beukes NJ, Moore JM, Harris C (2003) Deposition, diagenesis and secondary enrichment of metals in the Paleoproterozoic Hotazel Iron Formation, Kalahari manganese field, South Africa. Econ Geol, v 98, pp 1449-1462
- Tsikos H, Moore JM (1997) Petrography and geochemistry of the Paleoproterozoic Hotazel Iron-Formation, Kalahari manganese field, South Africa: Implications for Precambrian manganese metallogenesis. Econ Geol, v 92, pp 87-97
- Tu Guangzhi (1984) A complete but reworked Proterozoic salt formation-host rock of the Bayan Obo REE-Fe deposit, *in*: Academia Sinica, Developments in Geosciences. Science Press, Beijing, pp 255-261
- Tufar W (1992) Paragenesis of complex massive sulfide ores from the Tyrrhenian Sea. Mitteil Österreich Geol Gesselsch, v 84, pp 265-300
- Tukiainen T (1988) Niobium-tantalum mineralization in the Motzfeldt Centre of the Igaliko nepheline syenite complex, South Greenland, *in*: J Boissonvas, P Omenetto, eds, Mineral Deposits Within the European Community. Springer-Verlag, pp 230-246
- Turneure FS (1935) The tin deposits of Llallagua, Bolivia. Econ Geol, v 30, pp 14-60 & 170-190
- Turneure FS (1960) A comparative study of the major ore deposits of Central Bolivia. Econ Geol, v 55, pp 217-254, 574-606
- Turneure FS (1971) The Bolivian tin-silver province. Econ Geol, v 66, pp 215-225
- Turner FJ (1980) Metamorphic Petrology, 2nd ed. Hemisphere Publ, Washington DC, 524 p
- Turner P (1980) Continental Red Beds. Elsevier, New York, 562 p
- Turner SJ (1999) Settings and styles of high-sulfidation gold deposits in the Cajamarca region, northern Peru. PACRIM '99, Bali, Proceedings, AusIMM, pp 461-468
- Tuttle OF, Gittins J, eds (1966) Carbonatites. Interscience, New York, 591 p
- Tyson RM, Chang LLY (1984) The petrology and sulfide mineralization of the Partridge River troctolite, Duluth Complex, Minnesota. Canad Mineralogist, v 22, pp 23-38

- United Nations Development Programme (UNDP) (1987) Technical Rept No 5: Geology and Mineralization in the Baguio area, Northern Luzon. Manila, 82 p
- Unrug R (1988) Mineralization controls and source of metals in the Lufulian fold belt, Shaba (Zaire), Zambia and Angola. *Econ Geol*, v 83, pp 1247-1258
- Upton BGJ (1988) History of Tertiary igneous activity in the North Atlantic borderlands. *Geol Soc London, Spec Publ* 39, pp 429-453
- Upton BGJ, Emeleus CH (1987) Mid-Proterozoic alkaline magmatism in southern Greenland: The Gardar Province, *in*: JG Fitton, BGJ Upton, eds, *Alkaline Igneous Rocks*. *Geol Soc London, Spec Publ* 30, pp 449-471
- Ural'skaya Planovaya Komissia (1934) Mineral'nye Resursy Urala. Sverdlovsk (Yekateringurg)
- Uren D (2001) Discovery no longer the name of digging game. *The Weekend Australian*, Nov 17-18, 2001
- U.S. Geological Survey (1988) Mineral Resource Data System (MRDS), Reston, VA
- Valkovic V (1978) Trace Elements in Petroleum. PPC Books, Tulsa, OK, 269 p
- Vallée M (1992) Guide to the evaluation of gold deposits. *CIM Spec Vol* 45
- Vallée M, Raby R (1971) The Magpie titaniferous magnetite deposit. *CIM Transact*, v 74, pp 264-271
- Van Bemmelen, RW (1949) The Geology of Indonesia. 2 vols, Dutch Govt Printing Office, the Hague
- Van der Heyden A, Edgecombe DR (1990) Silver-lead-zinc deposits at South Mine, Broken Hill, *in*: FE Hughes, ed, pp 1073-1077
- Van Hise CR, Leith CK (1911) The geology of the Lake Superior region. *U.S. Geol Surv Monogr* 52, 641 p
- Van Leeuwen, TM (1994) 25 years of mineral exploration and discovery in Indonesia. *Journ Geoch Explor*, v 50, pp 13-90
- Van Staal CR, Williams PF (1984) Structure, origin and concentration of the Brunswick 12 and 6 orebodies. *Econ Geol*, v 79, pp 1669-1692
- Varentsov IM, Rakhmanov VP (1974) Deposits of manganese, *in*: VI Smirnov, ed, *Ore Deposits of the USSR*, v 1. Engl Transl, Pitman, London, pp 114-178
- Vargas CE (1970) Estudio geologico del area Llallagua. *Serv Geol Bolivia*, Bol 12
- Vázquez Guzmán F (1989) Spain, *in*: FW Dunning et al, eds, *Mineral Deposits of Europe*, vol 4/5. *Inst Min Metall London/Mineralog Soc*, pp 105-195
- Vearncombe JR, Hill AP (1993) Strain and displacement in the Middle Vale Reef at Telfer, Western Australia. *Ore Geol Revs*, v 8, pp 189-202
- Veiga MM, Schorscher HD, Fyfe WS (1991) Relationship of copper with hydrous ferric oxides: Salobo, Carajás, PA, Brazil. *Ore Geol Revs*, v 6, pp 245-255
- Velasco F, Herrero JM, Gil PP, Alvarez L, Yusta I (1994) Mississippi Valley-type, sedex, and iron deposits in Lower Cretaceous rocks of the Basque-Cantabrian basin, northern Spain, *in*: L Fontboté, M Boni, eds, *Sediment-Hosted Zn-Pb ores*. Springer-Verlag, pp 246-270
- Velasco JR (1966) Geology of the Cananea district, *in*: SR Tittley, CL Hicks, eds, pp 245-249
- Velichkin VI, Malyshev BI (1993) Olovonosnye skarny Bogemskovo massiva. *Geol Rud Mestor*, v 35, pp 16-31
- Vermaak CF (1976) The Merensky Reef-thoughts on its environment and genesis. *Econ Geol*, v 71, pp 1270-1298
- Vermaak CF (1986) Summary aspect of the economics of chromium with special reference to southern Africa, *in*: CR Anhaeusser, S Maske, eds, pp 1155-1181
- Vermaak CF, von Gruenewaldt G (1986) Introduction to the Bushveld Complex, *in*: CR Anhaeusser, S Maske, eds, pp 1021-1029
- Vessell RK, Davies DK (1981) Non-marine sedimentation in an active forearc basin. *Spec Publ Soc Econ Paleont Mineral*, Tulsa, No 31, pp 31-45
- Vial DS (1988) Mina de ouro da Passagem, Mariana, Minas Gerais, *in*: C Schobbenhaus and CES Coelho, eds, v III, pp 421-430
- Vickery NM, Buckley PM, Kellett RJ (1998) Plutonic gold deposit, *in*: DA Berkman, DH Mackenzie, eds, pp 71-80
- Vidal C, Injoque J, Sidder G, Mukasa S (1990) Amphibolitic Cu-Fe skarn deposits in the central coast of Peru. *Econ Geol*, v 85, pp 1447-1461
- Vieira EA, et al (1988) Caracterização geológico da jazida polimetálica do Salobo 3A. XXXV Cong Brasil de Geol, Belém, pp 97-111
- Vieira FWR, de Oliveira GAI (1988) Geologia do distrito aurifero de Nova Lima, Minas Gerais, *in*: C Schobbenhaus, CES Coelho, eds, v III, pp 378-391
- Vikre PG (1989) Fluid-mineral relations in the Comstock Lode. *Econ Geol*, v 84, pp 1574-1613
- Vila T, Lindsay N, Zamora R (1996) Geology of the Manto Verde copper deposit, northern Chile: A specularite-rich, hydrothermal tectonic breccia related to the Atacama Fault zone, *in*: F Camus et al, eds, *Andean Copper Deposits: New Discoveries, Mineralization, Styles and Metallogeny*. *Soc Econ Geol Spec Publ* 5, pp 157-170
- Vila T, Sillitoe RH (1991) Gold-rich porphyry systems in the Maricunga belt, northern Chile. *Econ Geol*, v 86, pp 1238-1260
- Viljoen MJ (1994) A review of regional variations in facies and grade distribution of the Merensky Reef, western Bushveld Complex, with some mining implications. XVth CMMI Congress, Johannesburg, S Afr Inst Min Metall, v 3, pp 183-194
- Viljoen MJ, Hieber R (1986) The Rustenburg section of Rustenburg Platinum Mines Limited, with reference to the Merensky Reef, *in*: CR Anhaeusser, S Maske, eds, pp 1107-1134
- Villas RN, Santos MD (2001) Gold deposits of the Carajás mineral province: Deposit types and metallogenesis. *Mineralium Deposita*, v 36, pp 300-331
- Vinokurov SF, Rybalov BL (1992) Polikronnaya rudoobrazuyushchaya sistema v uranonosnykh uglerodistykh slantsakh tsentral'noi Evropi. *Geol Rud Mestor*, 1992, pp 23-35

- Vityk MO, Krouse HR, Skakun LZ (1994) Fluid evolution and mineral formation in the Beregovo gold-base metal deposit, Transcarpathia, Ukraine. *Econ Geol*, v 89, pp 547-565
- Vlasov BP, Matyushin LV, Naumov GB (1993) Zhilnoe uranovoe mestorozhdenie Schlema-Alberoda (Rudnye Gory). *Geol Rud Mestor*, v 35, pp 205-221
- Vlasov KA, ed (1968) Geochemistry and Mineralogy of Rare Elements and Genetic Types of their Deposits, v III, Genetic Types of Rare Element Deposits. *Transl Israel Progr for Scient Transl*, Jerusalem, 915 p
- Vlasov KA, Kuzmenko MZ, Yeskova YeM (1959) the Lovozero Alkalic Massif. Engl transl, Oliver & Boyd, Edinburgh, 627 p
- Volk JA, Lauha E, Leonardson RW, et al (1996) Structural geology of the Betze-Post and Meikle deposits, Elko and Eureka Counties, Nevada, *in*: SM Green, E Struhsacker, eds, *Geology and Ore Deposits of the American Cordillera*, Field Trip Guidebook. *Geol Soc Nevada*, Reno, pp 180-202
- Volkert DF, McEwan CJA, Garay EM (1999) Pierina Au-Ag deposit, Cordillera Negra, North-Central Peru, *in*: Primer Volumen de Monografias de Yacimientos Minerales Peruanos, IIMP Lima, pp 23-25
- von Behrend (1950) Die Blei- und Zinkerz führende Imprägnations Lagerstätten im Bundsandstein am Nordrand der Eifel und ihre Entstehung. 18th Intern Geol Congr, London, Pt 7, pp 325-341
- Von Gruenewaldt G (1977) The mineral resources of the Bushveld Complex. *Minerals Sci Engn*, v 9, pp 83-118
- Von Gruenewaldt G, Hatton CJ, Merkle RKW (1986) Platinum-group element-chromitite association in the Bushveld Complex. *Econ Geol*, v 81, pp 1067-1079
- Von Gruenewaldt G, Worst BG (1986) Chromite deposits at Zwartkop chrome mine, western Bushveld Complex, *in* CR Anhaeusser and S Maske, eds, pp 1217-1227
- von Huene R, Scholl DW (1991) Observations at convergent margins concerning sediment subduction, subduction erosion, and the growth of continental crust. *Revs in Geophys*, v 29, pp 279-316
- von Stackelberg U, Marchik V, Müller P, et al (1990) Hydrothermal mineralization in the Lau and North Fiji Basins. *Geol Jahrb*, D92, pp 547-613
- Wadsworth WB (1968) The Cornelia Pluton, Ajo, Arizona. *Econ Geol*, v 63, pp 101-115
- Wagner JHF, Wiegand J (1986) The Sheba gold mine, Barberton Greenstone belt, *in*: CR Anhaeusser, S Maske, eds, pp 155-161
- Wagh AS, Pinnock WR (1987) Occurrence of scandium and rare earth elements in Jamaican bauxite waste. *Econ Geol*, v 82, pp 757-761
- Wagner PA (1929) The platinum deposits and mines of South Africa. Edinburgh, 326 p
- Wakefield J (1978) Samba: A deformed porphyry-type copper deposit in the basement of the Zambian Copperbelt. *Trans Inst Min Metall*, London, v 87, pp B43-B52
- Walker RG, ed (1984) *Facies Models*, 2nd ed. Geoscience Canada Reprint Ser 1, 317 p
- Wallace H (1981) Keweenaw geology of the Lake Superior Basin. *Geol Surv Canada*, Paper 81-10, pp 399-417
- Wallace SR (1995) Presidential address: The Climax-type molybdenite deposits: What they are, where they are, and why they are. *Econ Geol*, v 90, pp 1359-1380
- Wallace SR, Muncaster NK, Jonson DC, et al (1968) Multiple intrusion and mineralization at Climax, Colorado, *in*: JD Ridge, ed, *Ore Deposits of the United States 1933-1967*. AIME, New York, pp 605-640
- Wallis DS, Oakes GM (1990) Heavy mineral sands in eastern Australia, *in*: FE Hughes, ed, pp 1599-1608
- Walsh S (1998) Trace elements in sedimentary phosphorites. *Geol Soc Australia*, Abstracts No 49, p 454
- Walther HW (1984) Criteria on syngeneses and epigeneses of lead-zinc ores in Triassic sandstones in Germany, *in*: A Wauschkuhn et al, eds, *Syngeneses and Epigeneses in the Formation of Mineral Deposits*. Springer-Verlag, pp 212-220
- Walther JV, Wood BJ (1986) *Fluid-Rock Interaction During Metamorphism*. Springer-Verlag, 218 p
- Wanhainen C, Martinsson O (1999) Geochemical characteristics of host rocks to the Aitik Cu-Au deposit, Gällivare area, northern Sweden, *in*: CJ Stanley et al, eds, *Mineral Deposits: Processes to Processing*, Balkema, Rotterdam, pp 1443-1446
- Wänke H, Dreibus G, Jagoutz E (1984) Mantle chemistry and accretion history of the Earth, *in*: A Kröner et al, eds, *Archean Geochemistry*. Springer-Verlag
- Ward DM (1984) Uranium geology, Beaverlodge area, *in*: J Ferguson, ed, *Proterozoic Unconformity and Stratabound Uranium Deposits*. IAEA-Tecdoc 315, pp 269-284
- Ward DM (1989) Rabbit Lake project-history of exploration and general geology. *CIM Bull*, v 82, Dec 1989, pp 40-48
- Ward W, Perry OS, Griffin K, Charlewood GH, Hopkins H, MacIntosh G, Ogryzlo SP (1948) The gold mines of Kirkland Lake. *Structural geology of Canadian Ore Deposits*, pp 644-657
- Warden AJ (1970) Genesis of the Forari manganese deposit, New Hebrides. *Trans Inst Min Metall*, London, v 79, pp B30-B41
- Warnaars FW, Holmgren CD, Barassi SF (1985) Porphyry copper and tourmaline breccias at Los Bronces-Rio Blanco, Chile. *Econ Geol*, v 80, pp 1544-1565
- Warren J (1999). *Evaporites. Their Evolution and Economics*. Blackwell Science, Oxford, 438 p
- Watchorn RB (1998) Kambalda-St Ives gold deposits, *in*: DA Berkman, DH Mackenzie, eds, pp 243-254
- Waterman GC, Hamilton RL (1975) The Sar Cheshmeh porphyry copper deposit. *Econ Geol*, v 70, pp 568-576
- Watkins JS (1989) The Middle America Trench off southern Mexico. *The Geology of North America*, vol N, *Geol Soc Amer*, Boulder, pp 523-533
- Wawra CS, Bond WD, Reid RR (1994) Evidence from the Sunshine Mine for dip-slip movement during Coeur d'Alene district mineralization. *Econ Geol*, v 89, pp 515-527

- Weber F (1969) Una Série précambrienne du Gabon: le Francevillien. *Mém Serv Carte Geol Alsace-Lorraine*, v 28, 328 p
- Weber F (1973) Genesis and supergene evolution of the Precambrian sedimentary manganese deposit at Moanda (Gabon), *in*: UNESCO, Symposium Genesis of Precambrian Iron and Manganese Deposits, Kiev, pp 307-320
- Webster AE, Lutherborrow C (1998) Elura zinc-lead-silver deposit, Cobar, *in*: DA Berkman, DH Mackenzie, eds, pp 587-592
- Wedepohl KH (1971) "Kupferschiefer" as a prototype of syngenetic sedimentary ore deposits. IAGOD, Tokyo-Kyoto Conf, 1970, *Proc Spec Iss* 3, pp 268-273
- Wedepohl KH (1995) The composition of the continental crust. *Geoch Cosmoch Acta*, v 59, pp 1217-1232
- Weihed P, Bergman J, Bergstrom U (1992) Metallogeny and tectonic evolution of the Early Proterozoic Skellefte district, northern Sweden. *Precambr Research*, v 58, pp 143-167
- Weihed JB, Bergstrom U, Billstrom K, et al (1996) Geology, tectonic setting, and origin of the Paleoproterozoic Boliden Au-Cu-As deposit, Skellefte district, northern Sweden. *Econ Geol*, v 91, pp 1073-1097
- Weissberg BG (1969) Gold-silver ore grade precipitates from New Zealand thermal waters. *Econ Geol*, v 64, pp 95-108
- Weisser JD (1972) Zur Methodik der Exploration Meggen. *Schr Ges Metallhütten u Bergleute*, v 24, pp 167-186
- Welch BK, et al (1975) Mineral sand deposits of the Capel area, W.A., *in*: CL Knight, ed, *Economic Geology of Australia and Papua New Guinea*, AusIMM, pp 1070-1088
- Wellmer F-W (1989) *Economic Evaluations in Exploration*. Springer-Verlag, 163 p
- Werle JL, Ikramuddin M, Mutschler FE (1984) Allard stock, La Plata Mountains, Colorado-an alkaline rock-hosted porphyry copper-precious metal deposit. *Canad Journ Earth Sci*, v 21, pp 630-641
- Wernicke B (1992) Cenozoic extensional tectonics of the U.S. Cordillera. *The Geology of North America*, v G-3, *Geol Soc Amer, Boulder*, pp 553-582
- West RJ, Aiken DM (1982) Geology of the Sierrita-Esperanza deposit, Pima mining district, Pima County, Arizona, *in*: SR Titley, ed, pp 433-465
- Westra G, Keith SB (1981) Classification and genesis of stockwork molybdenum deposits. *Econ Geol*, v 76, pp 844-873
- Westra G, Riedell KB (1996) Geology of the Mount Hope stockwork molybdenum deposit, Eureka County, Nevada, *in*: AR Coyner, PL Fahey, eds, *Geology of Ore Deposits of the American Cordillera*. *Geol Soc Nevada Sympos Proc*, Reno, Apr 1995, pp 1639-1666
- White AH (1997) *Management of Mineral Exploration*. Austral Miner Found, Adelaide
- White DE (1981) Active geothermal systems and hydrothermal ore deposits. *Econ Geol 75th Anniv Vol*, pp 392-423
- White DE, Gonzáles JR (1946) San José antimony mines near Wadley, State of San Luis Potosí, Mexico. *U.S. Geol Surv Bull* 946-E, pp 131-153
- White DE, Roberson CE (1962) Sulfur Bank, California, a major hot spring quicksilver deposit. *Petrologic Studies (Buddington Volume)*, *Geol Soc Amer*, pp 397-428
- White JA (1994) The Potgietersrus prospect-geology and exploration history. XVth CMMI Congress, Johannesburg, v 3, *S Afr Inst Min Metall*, pp 173-181
- White RS, McKenzie D (1995) Mantle plumes and flood basalts. *Journ Geophys Res*, v 100, pp 17543-17585
- White WH, Bookstrom AA, Kamilli RJ, et al (1981) Character and origin of Climax-type molybdenum deposits. *Econ Geol 75th Anniv Vol*, pp 270-316
- White WS (1968) The native copper deposits of northern Michigan, *in*: JD Ridge, ed, *Ore Deposits of the United States 1933-1967*, AIME, New York, pp 303-325
- Whiting BH, Hodgson CJ, Mason R, eds (1993) *Giant Ore Deposits*. *Soc Econ Geol Spec Publ* 2, 404 p
- Widodo S, Manning P, Wiwoho N, Johnson L, Belluz N, Kusnanto B, Macdonald G, Edwards A (1999) Progress in understanding and developing the Kucing Liar orebody, Irian Jaya, Indonesia. *PACRIM '99 Congress, Bali, Proceedings*, Aus IMM, pp 499-507
- Wilde AR, Mernagh TP, Bloom MS, Hoffman CF (1989) Fluid inclusion evidence on the origin of some Australian unconformity-related uranium deposits. *Econ Geol*, v 84, pp 1627-1642
- Wilkerson G, Deng Q, Llavona R, Goodell P (1988) Batopilas mining district, Chihuahua, Mexico. *Econ Geol*, v 83, pp 1721-1736
- Wilkinson JFG (1982) The genesis of mid-ocean ridge basalt. *Earth Sci Revs*, v 18, pp 1-57
- Willemse J (1964) A brief outline of the geology of the Bushveld Igneous Complex, *in*: SH Haughton, ed, pp 91-128
- Willemse J (1969) The geology of the Bushveld Igneous Complex, the largest repository of magmatic ore deposits in the world. *Econ Geol Monogr* 4, pp 1-22
- Williams GJ (1965) *Economic Geology of New Zealand*. 8th Commonw Min and Metall Congr, v 4, 384 p
- Williams GE, Tonkin DG (1985) Periglacial structures and paleoclimatic significance of a late Precambrian block field in the Cattle Grid copper mine, Mount Gunson, South Australia. *Austral Journ Earth Sci*, v 32, pp 287-300
- Williams N (1990) Future direction in metallogenic research. *PACRIM '90 Congress, Proceedings*, AusIMM, p 571
- Williams VA (1990) WIM 150 detrital heavy mineral deposit, *in*: FE Hughes, ed, *AusIMM Monogr* 14, pp 1609-1614
- Williams VA (1999) Admiral Bay lead-zinc-silver deposit, *in*: KM Ferguson, ed, *Lead, zinc and silver deposits of Western Australia*. *Geol Surv W Austral Min Res Bull* 15, pp 214-220
- Willman CE, Wilkinson HE (1992) Bendigo Goldfield-Spring Gully, Golden Square, Eaglehawk. *Geol Surv Victoria Rept* 94

- Wilson AH (1982) The geology of the Great Dyke, Zimbabwe: The ultramafic rocks. *Journ Petrology*, v 23, pp 240-292
- Wilson IF (1955) Geology and mineral deposits of the Boleo copper district, Baja California, Mexico. U.S. Geol Surv Prof Paper 273, 134 p
- Wilson JL (1975) Carbonate Facies in Geologic History. Springer-Verlag, 471 p
- Wilson M, Davidson JP (1984) The relative rates of crust and upper mantle in the generation of oceanic island arc magmas. *Phil Trans Roy Soc London*, v A 310, pp 661-674
- Wilson MGC (1998) Copper, *in: Mineral Resources of South Africa*, 6th ed, Pretoria, pp 209-227
- Wilton DHC, Sinclair AJ (1988) Ore petrology and genesis of a strata-bound disseminated copper deposit at Sustut, British Columbia. *Econ Geol*, v 83, pp 30-45
- Wimmenauer W (1974) The alkaline province of central Europe and France, *in: H Sørensen*, ed, *The Alkaline Rocks*. Springer-Verlag, pp 238-271
- Win UK, Kirwin DJ (1998) Exploration, geology and mineralization of the Monywa copper deposits, central Myanmar, *in: TM Porter*, ed, *Porphyry and Hydrothermal Copper and Gold Deposits: A Global Perspective*. Confer Proc, AMF Adelaide, pp 61-74
- Windley BF, ed (1976) *The Early History of the Earth*. Wiley, London
- Wise DU et al (1984) Fault-related rocks: suggestions for terminology. *Geology*, v 12, pp 391-394
- Wodzicki A, Piestrzyński A (1994) An ore genetic model for the Lubin-Sierosowice mining district, Poland. *Mineralium Deposita*, v 29, pp 30-40
- Wolf KH (1976) Conceptual models in geology, *in: KH Wolf*, ed, v 1, pp 11-78
- Wolf, KH (1981) Terminologies, structuring and classifications in ore and host-rock petrology, *in: KH Wolf*, ed, v 8, pp 1-338
- Wolf, KH, ed (1976-1985) *Handbook of Stratiform and Strata-bound Ore Deposits*, volumes 1-14. Elsevier, Amsterdam
- Wolff F (1978) Philippinen. Rohstoffwirtschaftliche Länderberichte, v XV. Bundesanst f Geowiss, Hannover, 190 p
- Wood PC, Burrows DR, Thomas AV, Spooner ETC (1986) The Hollinger-McIntyre Au-quartz vein system, Timmins, Ontario, Canada; geological characteristics, fluid properties and light stable isotope geochemistry, *in: AJ MacDonald*, ed, pp 56-80
- Woodall R (1983) Success in Mineral Exploration: A matter of confidence. *Geoscience Canada*, v 11, pp 41-46
- Woodall R (1984) Success in Mineral Exploration: Confidence in science and ore deposit models. *Geoscience Canada*, v 11, no 3, pp 127-132
- Woodall R (1994) Empiricism and concept in successful mineral exploration. *Austral Journ Earth Sci*, v 41, pp 1-20
- Woodcock JR, Carter NC (1976) Geology and geochemistry of the Alice Arm molybdenum deposits. *CIM Spec Vol 15*, pp 462-475
- Woodsworth GJ, Anderson RG, Armstrong RL, et al (1991) Plutonic regimes, *in: H Gabrielse, CJ Yorath*, eds, *Geology of the Cordilleran Orogen in Canada*. *Geology of Canada no 4*, pp 491-531
- Woolley AR (1989) The spatial and temporal distribution of carbonatites, *in: K Bell*, ed, *Carbonatites-Genesis and Evolution*. Unwin Hyman, London, pp 149-176
- Worst BG (1960) The Great Dyke of Southern Rhodesia. *S Rhodesia Geol Surv Bull 47*, 234 p
- Wright JB, et al (1985) *Geology and Mineral Resources of West Africa*. Allen and Unwin, 187 p
- Wright VP, ed (1986) *Paleosols. Their Recognition and Interpretation*. Princeton Univ Press, 315 p
- Wright WB, et al (1968) *Iron and Steel*. U.S. Geol Surv Profess Paper 580, pp 396-416
- Wu Jiada (1993) Antimony vein deposits of China. *Ore Geol Revs*, v 8, pp 213-232
- Wu Jiada, Xiao Qiming, Zhao Shougeng (1990) Antimony deposits of China, *in: Mineral Deposits of China*, v1, Geol Publ House, Beijing, pp 209-287
- Xie Xuejing (1995) The surficial geochemical expression of giant ore deposits, *in: AH Clark*, ed, *Giant Ore Deposits II*, Queens Univ, Kingston, pp 476-485
- Xie Xuejing, Yin Binchuan (1993) Geochemical patterns from local to global. *Journ Geoch Explor*, v 47, pp 109-129
- Xu G (1996) Structural geology of the Dugald River Zn-Pb-Ag deposit, Mount Isa Inlier, Australia. *Ore Geol Revs*, v 11, pp 339-361
- Yan MZ, Hu K (1980) Geological characteristics of the Dexing porphyry copper deposits, Jiangxi, China, *in: S Ishihara, S Takenouchi*, eds, *Granitic Magmatism and Related Mineralization*. Soc Min Geol Japan, Spec Issue 8
- Yan Mei-Zhong, Wu Yong-Le, Li Chong-You (1980) Metallogenetic systems of tungsten in Southeast China and their mineralization characteristics. *Mining Geol Spec Issue 8*, Tokyo, pp 215-221
- Yang K, Mo X (1993) Characteristics of the Laochang volcanogenic massive sulfide deposit, Southwestern Yunnan, China. *Explor Mining Geol*, v 2, pp 31-40
- Yang Zhensheng, et al (1988) Structural deformation and mineralization in the early Proterozoic Liaojitite Suite, eastern Liaoning Province, China. *Precamb Res*, v 39, pp 31-38
- Yao Y, Trumbull RB, Gilg HA, Morteani G (1991) Ore genesis of the Mesozoic Niuxinshan gold deposit, eastern Hebei Province, Northeast China. *Univ Witwatersrand, Econ Geol Research Unit Inform Circul No 331*, 41 p
- Yaringaño M, Yacila C, Panéz M (1999) Historia de los exploraciones en el distrito de Colquijirca-San Gregorio, *in: Primer Volumen de Monografias de Yacimientos Peruanos*. IIMP, Lima, pp 251-273
- Yates RG, Thompson GA (1959) Geology and quicksilver deposits of the Terlingua district, Texas. *U.S. Geol Surv Prof Pap 312*
- Yeend WE (1974) Gold-bearing gravel of the ancestral Yuba River, Sierra Nevada, California. *U.S. Geol Surv Profess Paper 772*, 44 p

- Yeo GM (1981) The late Proterozoic Rapitan glaciation in the northern Cordillera. *Geol Surv Canada Paper* 81-10, pp 25-46
- Yesenov ShE, ed (1972) *Geologiya i Metallogeniya Severnovo Pribalkhas'ya*. Nauka KazSSR, Alma Ata, 267 p
- Yi Jianbin, Shan Yehua (1995) Role of post-orogenic extensional tectonics in the supergiant antimony mineralization in central Hunan Province, South China. *Geotectonica et Metallogenia*, Changsha, v 19, pp 62-70
- Young LE, St George P, Bouley BA (1997) Porphyry copper deposits in relation to the magmatic history and palimpsestic restoration of Alaska. *Econ Geol Monogr* 9, pp 306-333
- Young TP, Taylor WEG, eds (1989) *Phanerozoic Ironstones*. Geol Soc London, Spec Publ 46, 251 p
- Zarate-Del Valle PF (1996) Carbonate-hosted Sb stratiform deposits of the Sierra de Catorce, San Luis Potosi, Mexico. *Soc Econ Geol. Spec Publ No 4*, pp 298-306
- Zeegers H, Goni J, Wilhelm E (1981) Geochemistry of lateritic profiles over a disseminated Cu-Mo mineralization in Upper Volta (West Africa)-preliminary results, *in: Lateritization Processes*, Balkema, Rotterdam, pp 359-368
- Zevallos PL (1999) Yacimiento Cerro Lindo, *in: Primer Volumen de Monografias de Yacimientos Minerales Peruanos*, IIMP, Lima, pp 349-358
- Zhai Yusheng, Deng Jun, Peng Runmin (1997) Some major mineral deposits in China: their tectonic setting and deposit model characteristics. *Proc 30th Intern Geol Congr*, Beijing, v 9, pp 367-379
- Zhang Qisheng (1988) Early Proterozoic tectonic styles and associated mineral deposits of the North China Platform. *Precambr Res*, v 39, pp 1-29
- Zhang Xiao'ou, Cawood PA, Wilde SA, Liu Ruqi, Song Hailin, Li Wen, Snee LW (2003) Geology and timing of mineralization at the Cangshang gold deposit, north-western Jiaodong Peninsula, China. *Mineralium Deposita*, v 38, pp 141-153
- Zheng Mianping, Liu WWengao, Zhang Zhaoxin, Xiang Jun (1981) On the progress of the study of saline lakes in Xizang (Tibet), *in: Ann Rept Chinese Acad of Geol Sci*, 1981, Beijing, pp 84-86
- Zientek ML, Czamanske GK, Irvine TN (1985) Stratigraphy and nomenclature of the Stillwater Complex, Montana, *in: GK Czamanske, ML Zientek, eds*, pp 21-32
- Zierenberg RA, Koski RA, Morton JL, et al (1993) Genesis of massive sulfide deposits on a sediment-covered spreading center, Escanaba Trough, southern Gorda Ridge. *Econ Geol*, v 88, pp 2065-2094
- Zini A, Forlim R, Andreazza P, et al (1988) Depósito do ouro do Morro do Ouro, Paracatú, Minas Gerais, *in: C Schobbenhaus, CES Coelho, eds*, v III, pp 479-489
- Zitzmann A, ed (1977) *Iron Ore Deposits of Europe*. Bundesanst f Geowiss u Rohstoffe, Hannover
- Zolotukhin VV (1964) Osnovnye Zakonomernosti Prototektoniki i Voprosy Formirovaniya Rudonosnykh Trappovykh Intrusii. Nauka, Moscow, 176 p
- Zurbrigg HF (1963) Thompson Mine geology. *CIM Transact*, v 66, pp 227-236
- Zvezdov VS, Migachev IF, Girfanov MM (1993) Porphyry copper deposits of the CIS and the models of their formation. *Ore Geol Revs*, v 7, pp 511-549
- Zweifel H (1972) Geology of the Aitik copper deposit. *24th Intern Geol Congr*, Montreal, Sect 4, pp 463-473
- Zweng PL, Clark AH (1995) Hypogene evolution of the Toquepala porphyry copper-molybdenum deposit, Moquegua, southeastern Peru. *Arizona Geol Soc Digest*, v 20, pp 566-612

Locality Index

NOTE: Giant deposits, districts, and areas that contain "giants" are printed in bold. F (e.g. 527F) indicates page number with a figure. Please find explanation of the country codes at the end of this index

- Abbadia San Salvatore**, IT
Abitibi region, CN 45, 253-256, 254F, 255F
Abbott Springs, US 84
Abra, AU 411, 508
Abu Dhabbab, EG 312
Acupan, PH 91, 113
Adamaoua plateau, CM 440, 531
Adams Mine (Kirkland Lake), CN 262
Adanac, CN 105, 205
Adelaide, Au 3, 4, 38
Admiral Bay, AU 515
Afrikanda, RS 470
Agacapay, PE 192
Agades, NR 552
Aganozero, RS 455
Aggeneys, SA 572F, 573, 598
Agnew, Au 257
Agua Rica, AR 129, 130, 163, 183, 193, 197
Aguilar, AR 364
Aiderly-Aktogai, KZ 184, 195
Ainak, AF 577
Aitik, SW 577, 578F
Ajo, US 105, 182, 190
Akchatau (Aqshatau), KZ 208
Alaska Juneau, US 345
Alberode-Niederschlema, GE 329, 330F
Aldan (Central) Goldfield, RS 353
Aldebaran (Cerro Casale), CL 193
Alegria, BR 54, 404
Alemão, BR 292
Algarrobo, CL 117
Alice Arm, CN 105, 205
Aljustrel, PT 237, 238F
Allard stock, US 167
Allegheny, US 350
Alligator Rivers, AU 68, 414
Allouez Mine, US 438F
Almaden, SP 38, 41, 51, 54, 355, 356, 357F, 359, 615
Almadenejos, SP 357
Almalyk (Olmalyk), UZ 158, 184, 195, 197F
Alpha-Gravelotte Mine, SA 290
Alšar, MD 152
Altenberg, GE 301, 316, 317F, 324
Alto Chicama, PE 134
Altyn Topkan, TA 220
Alumbrera (Bajo de la), AR 164
Amalat Plateau, RS 552
Ambrosia Lake, US 109
Amity Point, AU 485
Åmmeberg, SW 571, 573F
Amur (Heilongjiang) placers, RS+CH 353, 543
Anarraaq deposit, US 506, 508
Andacollo, CL 183, 193
Angouran, IN 364
Anshan, CH 568
Antamok, PH 67, 91, 94, 95F, 131
Antamina, PE 168, 169, 183, 192, 214, 364
Antapacay, PE 170, **183**
Antimony Line, SA 59, 289, 290F
Apusen Mts, RO 113
Aqshatau (Akchatau), KZ 208
Arabian Shield, SB 311
Araxá, BR 37, 49, 54, 68, 474, 475F, 533, 536
Argun River (Nerchinsk), RS 365
Arizona Crater, US 57, 58
Ashanti Mine, Obuasi, GH 275, 288F
Assarel, BL 194
Athabasca Basin, CN 68, 413
Athabasca oil sands (Fort McMurray), CN 24, 26
Atlantis II Deep, Red Sea 27, 429
Atlas (Toledo), PH 195, 198F
Aurora, Utah-US 120
Aurora Mine, MN-US 400F
Ayat, KZ 489
Aznalcollar, SP 237
Baffin Island, CN 434
Bagdad, US 105, 178, 182, 190
Baguio district, PH 67, 91, 195, Baia Borša, RO 235
Baia Mare district, RO 139, 140, 364
Baigan Lake, PK 315
Bailadila, IA 404
Bailashui, CH 325
Bajo de la Alumbrera, AR 193, 197F, 183
Bakchar, RS 37, 489
Bakyrchik, KZ 350
Balei, RS 131, 134, 351
Balkhash Basin (U), KZ 552
Ballarat, AU 348, 353
Balmat-Edwards, US 571, 572F
Balmertown, CN 260, 275, 279
Balmoral-Douglas, AU 486F
Baltic Mine, US 438
Baluba, ZA 384
Banat, RO 133
Bangka Island, ID 325, 532
Bangkok, TH 22
Banpo, CH 355
Banska Štiavnica-Hodruša, SK 111, 140, 143, 364
Barberton Mountain Land, SA 256, 276
Barnes Canyon, US 148
Barit, PK 183, 194
Barza (Brad), RO 111
Basal Reef, SA 388
Batchawana (Tribag), CN 439
Bathurst-Newcastle district, CN 241
Batopilas, MX 138, 598
Battle Mountain district, US 220
Batu Hijau, ID 93, 94F, 172, 174, 184, 194
Bau, ML 141, 355
Bauchi & Jos Plateaux, NG 68
Bawdwin, BM 37, 220, 355, 365

- Bayan Obo**, CH 37, 473, 475F
 Bazhenov Formation, RS 495
Beatrix Mine, SA 388
 Beaver Brook, CN 354
 Beaverlodge (U), CN 587
Bendigo, AU 342, 343F, 349F, 351
 Belgorod, RS 404
Belitung (Billiton) Island, ID 325, 352
 Ben Lomond, AU 141
 Bent Hill, Middle Valley, Pacific Ocean 77
Beregovo, UK 37, 139
Berezovsk, RS 332, 336, 350
 Berg, CN 172, 182, **190**
Bergslagen region, SW 575
 Bernic Lake, CN 307, 309
 Besshi, JP 67, 242
 Biankouma-Touba, IV 532
Big Ben, US 205
 Bikita, ZB 307F, 310
Billingen, SW 37, 598
Bingham ore field, US 39, 67, 106, 157, 158, 160F, 164, 169, 170, 182, 187, 190, 221, 364
Bingham Canyon, US 37, 148, 598, 178, 187
Bingham Pb-Zn, US 220
 Bird Reef group, SA 389
 Birmingham (AB), US 68, 489
Bisbee, US 105, 159, 161, 163F, 169, 172, 182, 191
Black Hills region, US 308
 Black Lake, CN 67
 Blake Plateau, Atlantic Ocean 494
 Blanchford Lake Complex, CN 311
Bleiberg-Kreuth, AS 515, 516F
Blyava, RS 157, 235
Bodaibo, RS 353
Boddington, AU 272, 276, 282, 284F, 533, 537
Bogosu, GH 275
 Boke-Gaoual, GN 42, 54, 531
Boleo (Santa Rosalia), MX, 115, 116F
Boliden, SW, 120, 144, 147, 271F
Bolivian Sb belt, BO, 141
Bol'shoi Tokmak, UK, 491, 492
Bor, SER 130, 183, 194
 Borborema district, BR 310, 577
 Boron (Kramer), US 109
 Boss Mountain, CN 67
 Bou Azzer-Graara belt, MR 67
 Bou Azzer, MR 363
 Bou Grine (Jebel), TU 526
 Boulder Batholith, US 67
Bousquet, CN 147, 243, 253, 265, 269, 270F, 275
 Bozchakol', KZ 172, 174, 184, 196
Brad, RO 111, 133
 Brady Glacier, US 155
Brioude-Massiac, FR 354
Brisas, Kilometro 88, VE 275
 Brockman (REE), AU 54, 463
 Brockman IF (Fe), AU 398
Broken Hill, AU 45, 44, 54, 297, 307, 374, 532, 568-571, 570F, 618
Brown's deposit (Batchelor) AU, 411
Brunswick #6, 12, CN 37, 241, 242F, 598
 Buchans, CN 67, 247
 Buçium Tarnița, RO 183, 193
Buckingham, US 105, 206
 Buena Esperanza, CL 115
 Bulolo (Morobe Goldfield), PNG 134
 Bulong, AU 260
Bulyanhulu, TZ 276
Bunker Hill, Kellogg, US 219F
 Buribay, RS 235
 Busang, ID 645, 646
Bushveld Complex, SA 37, 49, 54, 68, 370, 444, 623
 Butte, US 37, 105, 122, 129, 130F, 157, 164, 182, 190, 220, 598
 Bwana Mkubwa, ZA 383
Bytom, PL 375

Cadia, AU 27, 167F, 169, 170, 184, 196
Cajamarca district, PE 192
 California Gulch, Leadville, US 218
Calumet-Hecla (MI), US 437, 598
Camborne-Redruth, GB 324
Campbell Red Lake Mine, Balmertown, CA 120, 147
Cananea, MX 67, 105, 163, 164F, 169, 174, 178, 182, 191
Candelaria, CL 116, 117F, 165, 193
 Cangshang, CH 335
Cannington, AU 371, 574
Cannivan (Gulch), US 205
Cantung, CA 67, 106, 157, 210, 211F
 Capel, Au 486F, 487
 Caraiba, BR 580F
Carajas (Fe), BR 263F, 531
Caridad, MX 178
 Carlin ("Old", deposit) US 150, 151F
Carlin Trend, US 106, 157, 533
 Carswell Structure, CN 57
Cartagena, SP 9, 364
Casa Grande, US 176, 182, 190
Casino, CN 105, 174, 178, 182, 189
 Catalão, BR 469, 531
Catavi (Llallagua), BO 146F
 Caê Mine, BR 401F
 Cave Hills, US 68
 Cawse, AU 260
 Central City (CO), US 67
 Central Highlands, Vietnam 440
Central Kyzyl-Kum area, UZ 552
Central Rand, SA 391, 392F, 598
 Central Tennessee, US 515
Century, AU 37, 68, 375, 376F, 508
Cerro Casale, CL 111, 166, 183, 193
Cerro Colorado, PA 105, 182, 191
 Cerro Colorado (Rio Tinto), SP 157, 176, 237, 239F, 240, 537
Cerro Colorado, CL 174, 178, 183, 192
Cerro de Pasco, PE 37, 38, 113, 122, 127, 128F, 140, 141, 142, 157, 364
 Cerro Lindo, PE 116, 247
 Cerro Negro-Diablo, CL 115
Cerro Petaquilla, PA 182
Cerro Rico (Potosi) BO 54, 68, 107, 113, 131, 144, 145F
Cerro Yanacocha, PE 124
Cerro Verde-Santa Rosa, PE 178, 183, 192
 Chador Malu, IA 423
 Chamberlain, US 25, 598
Chambishi, ZA 379, 384

- Chañarcillo, CL 363
Changpo, CH 325
 Chara-Tokkin, RS 568
 Charters Towers, AU 332, 333, 339, 351
 Chatham Rise, Pacific Ocean 494
Chatkal Range, UZ 354
Chattanooga Shale, US 30, 32, 33, 51
 Chaucha, EC 183, 191
 Chaun Bay, RS 353
 Cheleken Peninsula, TR 527
Chelopech, BL 130, 194
Chiatura, GA 491, 492
 Chibougamau, CN 262, 272, 378
 Chihuahua State, MX 119
Chilcobija Mine, BO 354
 Chililabombwe, ZA 379, 383
 Chimborazo, CL 192
Chingola, ZA 380, 383
 Chinkuashih, TW 122
Chino (Santa Rita), US 191
 Chitose, JP 67
Chulboi, TA 354
 Chukotka Peninsula placers, RS 324, 353
Chuquicamata, CL 37, 40, 108, 157, 170, 173, 174, 175, 177, 178, 183, 185, 186F, 192
Chu-Sarysu Basin, KZ 552
Choco placers, CO 353, 613
 Chorolque, BO 144
Chrzanow, PL 515
Cigar Lake, CN 414, 598
Cinovec, CZ 38, 299, 301, 310, 316, 324
 Čistá, CZ 317
Ciudad Bolívar, VE 568
 Clarion Fracture Zone, Pacific Ocean 27, 79
 Clausthal-Zellerfeld, GE 361
 Clayton Valley, US 24, 109
 Clear Hills, Swift Creek, CN 489
 Cleo-Sunrise Mine, AU 282
 Cliff Mine (MI), US 438F
Climax, US 54, 68, 106, 157, 202F, 203, 206
 Clipperton Fracture Zone, Pacific Ocean 27, 79
Cobalt, CN 363, 441, 442F, 598
 Coed-y-Brenin, GB 25, 26
Coeur d'Alene district, US 105, 218, 349, 354, 364
Collahuasi, CL 41, 44, 175, 178, 183, 192
Colombia placers, CO 353
Colorado Plateau, US 68, 552, 553
Colquijirca, PE 113, 122, 123, 126, 127, 128F, 364
 Colquiri, BO 144
Comstock Lode, US 105, 131, 136
 Concepcion del Oro, MX 67
 Condestable Mine, PE 116
Conical Seamount, PNG 97
 Cooljarloo, AU 487
Copperbelt (African), 54
 Copper Mountain-Ingerbelle, CN 158, 166
Coppin Gap, AU 204, 207, 273
 Coquimbo (Province) Mn Belt, CL 117
 Cordillera Real, BO 324
Cornwall, GB 22, 38, 68, 297, 299, 317, 321, 614
 Corocoro, BO 118
 Corriente, EC 183, 191
Cortez-Pipeline, US 196, 152
Corumba-Mutun, BR+BO, 409, 531
Corvo Neves, PT 239F
 Costerfield, AU 355
 Cove, US 148, 220
 Creede, US 139
 Creighton Mine, Sudbury, CN 458F
Crest deposit, CN 404, 406F
Cripple Creek, US 37, 54, 67, 106, 113, 131, 135, 140, 142, 167, 598
Cresson Mine (Cripple Creek), US 113
Cristalino, BR 292
Cuajone, PE 178, 183, 192
 Cuiaba, BR 277
CUMO, US 105, 206
 Currais Novos Mine, BR 577
 Cuyuna Range, US 404
 Cyprus, 9
Dachang, CH 54, 327, 355
 Dadongla, CH 359
Dajishan, CH 314
Dal'negorsk (Tetyukhe), RS 217, 362, 365
 Damiana, CL 175, 176
 Darasun, RS 332
Darling Range, AU 541
Dawson City (Klondike), CN 353, 348
 Dayong, CH 495
Dayu, CH 314
 Dead Sea, IS 25, 544
Deelkraal Mine, SA 388
 Degtyarka, RS 235
 Deputat, RS 316
 Deva, RO 133
Dexing, CH 184, 195
 Dikuluwe-Mashambo, CG 382
 Dizon, PH 67
 Draževici, BN 359
 Drummond Basin, AU 148F
Dolphin Mine, AU 212F
Dome & Preston Mines, CN 255, 275, 282
 Dominion Reef, SA 385, 386
Dongchuan, CH 384
Donlin Creek, US 84, 105, 134
 Dorotea, SW 558
Dos Pobres, US 191
 Ducktown, US 230
 Dudelange-Tetange, LX 488F
 Dugald River, AU 371, 375, 508
Dukat, RS 138
 Dulong, CH 325
Duluth Complex, US 452
 Dumagami, CN 270
 Dumont Sill, CN 256, 259
 Durango State, MX 67, 119
 Duobaoshan, CH 184, 196
Dzhezkazgan, KZ 118, 556
 Dzhugdzhur Range, RS 30
 East Hebei Fe province, CH 404
East Rand, SA 388
 Echassières, FR 318, 319F
 Eddie Creek, PNG 114, 134
Eilandsrand Mine, SA 388
El Abra Mine, CL 173, 174, 175, 177F, 182, 183, 192, 538, 539
El Arco, MX 191
 El Callao, VE 275
El Creston (Opodepe), MX 207
El Indio-Tambo, CL 67, 123, 125, 126, 157
 El Laco, CL 67, 423
 El Oro, MX 613
El Pachon, AR 163, 183, 193
El Rodeo, BO 529

- El Romeral, CL 111
El Soldado, CL 116
El Salvador, CL 164, 175, 179F, 183, 193
 El Telegrafo, CL 175
El Teniente, CL 35, 40, 54, 67, 113, 161, 162F, 162, 183, 184, 193
 El Tesoro, CL 173, 175F
 El Tofo, CL 117
 El Valle-Boinas, SP 142F
 Elatsite, BL 194
Elliot Lake, CN 49, 256, 385, 392, 394F, 541
 Elmwood, US 515
 Elsa-Keno Hill, CN 220, 364
Elura, AU 362, 363F, 365
Ely (NV), US 45, 106, 157, 169, 178, 182, 190
Emperor Mine, FJ 89, 95, 96F, 111, 131, 142, 157
Endako, CN 67, 105, 201, 202F, 205
 Eneabba, AU 487
Erdenet, MO 184, 195
 Erdenet dumps, MO 560
 Ergani Maden, TK 83
 Ernest Henry, AU 371, 419
Ertsberg-Grasberg, ID 41, 169, 188, 194, 633
 Erzberg, AS 249
 Erzgebirge, GE+CZ 22, 68, 133, 299, 300F, 321
 Escanaba Ridge, Eastern Pacific 27
Escondida (La), CL 41, 157, 172, 173, 177, 178, 540
Escondida Norte, CL 192
 Eskay Creek, CN 246
 Esperanza (Pima), US 178
 Eucla Basin, AU 487
Evander Goldfield, SA 388
Exotica (Mina Sur), CL 173, 175, 186

Fairbanks district, US 105, 108, 353
 Falconbridge Mine, CN 459
 Falcondo Mine, DR 532
 Falun, SW 575, 576F
Fankou, CH 515
Far South East deposit, PH 93, 92, 194
Faro-Anvil, CN 44, 45, 507, 508

 Fay-Ace-Verna Mines, CN 587
Feitais deposit, PT 238
Felbertal, AS 30, 107, 583, 584F
 Fenghuang-Xinhuang Anticline, CH 523
Ferghana (South) Hg-Sb belt, KS 355, 359
Fish Lake, CN 190
 Fiskenaasset, GL 584
 Fitula Mine, ZA 384
Flin Flon-Snow Lake district, CN 265
 Flin Flon ore field, CN 269
 Florida (State), US 68
Florida Land Pebble districts, US 24, 494, 512
 Forari, VT 86
 Forrestania, AU 256
 Fort Knox, US 332, 350
 Fort McMurray, CN 527, 560
 Fort Meade, US 512F
 Fortitude, US 170
Fortuna del Cobre, CL 174
 Foxtrap, CN 123
 Franklin, US 307, 574, 575F
Fredericktown, US 518
Free State (Welkom) goldfield, SA 388
Freiberg, GE 38, 361, 364
Fresnillo, MX 106, 220, 222F, 301, 302, 364
Frieda River, PNG 131, 184, 194
 Frood Mine (Sudbury), CN 459F
 Frood-Stobie ore zone, CN 459
 Furong, CH 325

 Gag Island, PNG 532
 Gai, RS 235
Galena, PE 183, 192
Galore Creek, CN 105, 158, 165, 182, 189
Gamsberg, 572F, 573
 Gaoguashan, CH 355
 Gara Djebilet, AG 489
 Gas Hills, US 554
Gaspe Copper, CN 169, 184, 196, 198F
 Gataga ore field, CN 500
Geita, TZ 276, 277
Gejiu, CH 37, 321, 323, 325, 327

George Fisher Mine, AU 371, 373, 508
 Georgina Basin, AU 494
 Geraldton, CN 277
Getchell Mine, US 105, 148, 149, 152, 156
Getchell Trend, US 67
Ghurayyah, SB 54, 68, 311F, 313
Gibraltar, CN 105, 170, 171F, 182, 190
 Gifhorn Basin, GE 489
 Gilgit, PK 194
Glacier Gulch (Smithers), CN 202F, 205
Glacier Peak, US 182, 190
 Glen Eva, AU 120, 147, 148F
Globe-Miami, US 105, 174, 182, 190
 Gogebic Iron Range, US 404
 Golconda, US 140
 Gold Acres, US 156
 Goldfield (NV), US 122
 Gold Hill (UT), US 119
Gold Quarry Mine, US 67, 150, 151
Golden Mile (Kalgoorlie), AU 281F
Goldstrike Mine, US 150, 151, 152F, 156
 Gongguan, CH 359
 Goonumbla, AU 166
 Goro, NC 232, 531, 536
Goslar (Rammelsberg), GE 505
 Gove, AU 535F
 Gowganda, CN 442F
Grants district, US 106, 551, 552F, 554, 598
Granny Smith-Sunrise, AU 276
Grasberg, ID 37, 41, 169, 170, 184, 188, 189, 194, 598
Grass Valley-Nevada City, US 106, 332, 339, 350, 447F
Grassy (King Island), AU 211, 212F
Gravelotte, SA 290
 Great Britain-coals, 550
Great Dyke, ZB 37, 68, 451, 452F
 Great Fortune (Bothaville), SA 486F
 Great Sandy Desert, AU 342
 Greenbushes, AU 308F, 310

- Greens Creek**, US 85, 105, 242
Griffith Mine (Ear Falls), CN 262
 Groningen gas field, NH 24, 25, 526
Groote Eylandt, AU 491, 492, 493F, 531, 533, 598
 Grund, GE 361, 362F
Guanajuato, MX 38, 67, 105, 131, 137, 138F, 598
 Guangdong Province, CH 152
 Gueimeishan, CH 315
 Guinaoang, PH 194
 Guinea bauxites, 11, 443
 Guizhou Province, CH 152, 358
 Guleman, TK 67
 Gulf of Persia, 22
 Gulf of California, 27
Gunung Bijih see Ertsberg
- Haib**, NM 181, 196, 273, 598
Hall (NV), US 206
 Halls Creek, AU 463
Hammersley Iron Province, AU 397, 404, 531
Hämmerlein, GE 321F
 Hanaoka, JP 45, 99
Hartley Platinum, ZB 451
Hauraki Goldfield, NZ
 Hawaii, US 79, 80
Hedley, CN 170F, 170, 334, 350
Heilongjiang (Amur) placers, CH, 353
 Hekpoort Basalt, SA 542
 Helen Fe Range, CN 264F
Hellyer, AU 348
Helvetia, US 182, 191
Hemlo, CN 45, 275, 288F
Henderson, US 68, 106, 156, 157, 203, 206
 Hiendelaencina, SP 363
Highland Valley, CN 50, 105, 182, 190, 196
 Highland U deposit (WY), US 553F, 554
 Hijaz Province, SB 9
Hillgrove, AU 67, 354, 355
Hilton Mine, AU 371, 373, 508
Hinoban, PH 91, 184, 195
Hishikari, JP 95, 132, 134, 598
 Hoboken smelter, BG 11
 Hockley Dome, US 526
 Hodruša, SK 111, 143
Hokuroku district, JP 67, 99
- Hollinger Mine** (Timmins), CN 255, 275, 281F
Homestake Mine, US 3, 275, 285, 287F
 Horizon Guyot, Pacific Ocean 80
Horne Mine, Noranda, CN 255, 265, 267, 269
 Hosokura Mine, JP 67
 Hotazel, SA 408F
Howard Pass, CN 507, 508
Hsi-Kuang-Shan (Xikuangshan), CH 352
Huancavelica, PE 142, 355, 359
 Huanuni, BO 144
Huaron Mine, PE 139, 364
Hudson Bay Mt (Smithers), CN 105, 202F, 205
H.Y.C. deposit (Mc Arthur R.), AU 374, 508
- Iberian Pyrite Belt**, SP+PT 67, 237, 238F
 Ichuno deposit, CL 175
Idrija, SV 51, 355, 358, 359F, 359
Igarape Salobo, BR 291F
 Iglesias, IT 515
 Ikuno, JP 90
Ilimaussaq, GL 37, 68, 462, 465
 Illinois-Ketucky F district, US 522
Imataca Complex, VE 568
Imiter, MR 147, 443
 Ingerbelle Mine, CN 166F
 Inspiration Mine, US 173, 174
 Intermontane Gold Anomaly (WY), US 607
Ipoh (Kinta Valley), ML 54
Irish Midlands, 530, 521F
 Island Mountain, US 83
 Itabira, BR 404
 Itataia, BR 533, 578
 Ivigut, GL 21
- J-M Reef** (Stillwater), US 454
Jabiluka, AU 415
 Jáchymov, CZ 22, 38, 68, 299, 301, 302, 613
 Jacobina, BR 385
 Jamaica bauxites, 11, 24, 86, 525F
 Jamaica red mud, 560
 Jebel Sayid, SB 68
- Jerritt Canyon, US 106, 152, 157
Jiangxi Province, CH 54, 195
Jiaodong, CH 332, 335, 351
 Jicarilla, US 108
Jinchuan, CH 37, 72, 454
Jinding, CH 558
Jinduicheng, CH 207
 Joel Mine (Free State), SA 388
 Johanngeorgenstadt, GE 22
 Johnson Island, US 27, 80
Jos & Bauchi Plateau, NG 68, 324
 Jos-Bukuru Complex, NG 312
 Juan de Fuca Ridge, Pacific Ocean 27
 Julia Creek, AU 494
Juneau Au belt, US 67, 84, 106, 350, 345
- Kabwe, ZA 378
Kachkanar Complex, RS 244
Kadamzhay, KS 353, 354F
Kadzharan, AM 183, 194
Kalahari Mn Basin, SA 41, 48, 54, 68, 407, 408F, 623
Kalamazoo-San Manuel, US 174
 Kaleçik, TK 359
Kalgoorlie, AU 47, 273, 276, 280, 624
 Kalulushi, ZA 378
 Kambalda, AU 256, 257, 258F, 276
Kambowe, CG 382, 383
 Kambowe-Kakanda tailings, 560
 Kamioka, JP 215, 362, 363F, 365
Kamoto, CG 382, 383
Kanimansoor, TA 220
Kansai, TA 220
Karamazar, TA 220, 365
 Karareis, TK 359
 Karatau, NW, KZ 494
Kassandra ore field, GR 214, 220, 364
Katugin, RS 585, 587
 Kavalerovo, RS 68, 316
 Kawai Island, US 77
Kemess, CN 182, 189
 Kemi, FN 455
Kempirsai, KZ 67, 236
 Kemuk Mountain, US 154
 Kennecott, US 85, 107, 233, 529
 Keno Hill-Elsa, CN 220, 363
 Keonjhar District, IA 45

- Kerch**, UK 37, 488, 489
 Kachkanar tailings, RS 560
 Keretti Mine (Outokumpu), FN 261
Kerr Addison Mine, CN 255, 260, 261F, 275
Keweenaw Peninsula, US 437
 Key Lake, CN 107
Khaidarkan, KS 356F, 359
 Khapcheranga, RS 316
Khibiny, RS 467F
Kholodnina, RS 574
Kidd Creek, CN 37, 44, 255, 265, 268F
 Kidston, AU 332, 333
 Kiirunavaara, SW 422, 423F
Kilo-Moto region, CG 260, 353
 King Solomon Mines, Timna, IS 38
King Island, AU 211, 212F
Kinta Valley, Ipoh, ML 54, 322F, 325, 532
Kipushi, CG 378, 410
Kirkland Lake, CN 36, 253, 275, 285, 287F
 Kiruna, SW 422F, 598
Kitwe, ZA 384
Kivu-Maniema Province, CG 324
Klerksdorp, SA 388, 390F
Klondike, CN 106, 108, 346, 348, 353, 543
 Klukwan Complex, US 244
Km 88 (Kilometro 88), VE 275
Kochbulak, UZ 134, 142
Kochiu, now Gejiu, CH 323
Kochkar, RS 332, 336, 350
Kolar, IA 260, 276, 282, 613
 Kolkhida, Caucasus 38
Kolwezi, CG 40, 382, 383
Kolya placers, RS 108, 324, 353, 543
Kokpataz, UZ 338, 350
 Koktenkol, KZ 208
 Komati River, SA 256
 Komsomolsk na Amure, RS 316, 325
 Kongsberg, NW 565
Konkola, ZA 379, 383
 Koparberg, SA 580
 Kori Kollo, BO 333
 Kosaka, JP 45, 99
 Kovdor, RS 469
Kounrad, KZ 114, 158, 163, 165, 195
Krakow-Silesia, PL 48, 54, 518, 519F
 Kramer (Boron), US 106
 Krásná Hora-Milešov, CZ 354
 Krasnoye, RS 383
Krasno, CZ 317, 324
 Krasnouralsk smelter, RS 560
Krivoi Rog, UK 57, 402, 404
Krupanj-Zajača, SER 354
 Krušné Hory (Erzgebirge), CZ+GE 299, 300F
 Kuala Langat, ML 483
Kucing Liar deposit, ID 194, 333, 351
Kumtor, KS 350
 Kununurra, AU 67
 Kunwarara, AU 233, 234F, 531, 535
Kupferschiefer (Poland), 37, 54, 68
 – (Germany) 500, 502F
 Kurgashinkan, KZ 158
Kuroko (Hokuroku) district, JP 99
Kursk Magnetic Anomaly (KMA), RS 402, 404, 531
 Kurusai, KZ 220
Katanga (Copperbelt), CG 37
 Kutná Hora, CZ 38, 363
Kyushu Island, JP 88
Kyzyl-Kum desert, UZ 338

La Caridad, MX 182, 191
La Candelaria, CL 116, 117F
 La Coipa, CL 123, 126, 166
 La Copa diatrema, CL 161
 La Crouzille, FR 329
La Escondida, CL 172, 174, 179F, 183, 192
La Fortuna, CL 183, 193
La Granja, PE 183, 191
La Lucette, FR 354
La Quinoa, PE 107, 124
La Union, SP 139, 140F, 364
La Zarza, SP 237
 Labrador Fe province, CN 404, 567
 Lac Allard, CN 304
 Lac de Gras, CN 624
 Lac Doré, CN 262
 Lac Dufault, CN 265, 266
 Lac Troilus, CN 273
Ladolam, PNG 89, 95, 96F, 111, 131
 Lady Loretta, AU 508
 Lagõa Real, BR 588
 Laguna deposit, US 108
 Lahanos, TK 116
 Lahocza deposit, HU 122, 193
Laisvall, SW 557, 558F
 Lake Cowal, AU 147
Lake George (NB), CN 354
Lake Superior Fe province, US 404
Lakeshore deposit, US 169, 182, 190
 Lamaque Mine, CN 275, 284
 Larderello, IT 24, 25
 Las Cuevas, SP, 359
Las Cristinas, VE 275
 Las Cruces, SP 237, 240, 539
 Latir, US 111
 Lau Basin, Western Pacific 27
 Laurium (Lavrion), GR 38, 217
Lavrion, GR 9, 217, 364, 559, 560, 614
Lead (Homestake Mine), US 285, 287F
Leadville, US 67, 106, 217, 218F, 364
 Lebowa territory, SA 450F
 Lee Guyots, Pacific Ocean 80
Lena Goldfield, RS 350, 353, 543
Leninogor, KZ 248, 560
 Lepanto, PH 67, 90, 91, 93, 122, 194
Letpadaung deposit, BM 194
Liaodong Peninsula, CH 578
 Liganga, TZ 305
Lihir Island, PNG 27, 81F, 82, 89, 95, 97, 110, 157
 Limousin U district, FR 329
Linares-La Carolina, SP 361, 364
 Lincoln (MT), US 350
 Linden, GT 535F
Linglong, CH 335
 Lisakovsk, RS 549
 Lisbon Valley, US 555
Llallagua, BO 47, 68, 106, 113, 144, 146F, 157, 324
 Lo Aguirre, CL 115
Lobash, RS 204, 207, 273
 Lobo, CL 166
Logtung, CN 105, 158, 205
Loolekop (Palabora), SA 468
 Lorraine Minette Basin, FR 489
Los Bronces, CL 113, 159, 162F, 193

- Los Pelambres**, CL 162F, 163, 178, 183, 193
 Los Pijiguaos, VE 531
 Lost River, US 324
 Lousal, PT 237
Lovozero Complex, RS 37, 54, 68, 462, 466
 Luanchuan County, CH 207
Luanshya, ZA 379, 384
Lubin district, PL 37, , 54, 501, 502F
Lubumbashi, CG 383
Lumwana, ZA 577
 Luzon Island, PH 88, 91
- Mačkatica**, SER 207
 Macraes, NZ 332, 340, 341F, 351
Mactung, CN 67, 106, 157, 211
Magadan region, RS 351
Magellan deposit, AU 412, 532
 Maggie Creek (Carlin Trend), US 150, 151
 Magnitogorsk, RS 220, 250
 Magpie Mountain, CN 304
 Mahd-adh-Dhahab, SB 120, 147
 Mahoning Mine (Hibbing), US 400F
Maiskoye, RS 357
Majdanpek, SER 183, 193
 Makola area, CB 24
Malanjhand, IA 159, 184, 196
Malartic, CN 255, 260, 275
Malaya tin placers, 68, 532
Malmbjerg, GL 157, 204, 207
Mamatwan Mine, SA 54
 Mangyschlag Peninsula, KZ 492
 Manhattan Hg Mine (now McLaughlin), US 141
Maniema Province, CG 532
 Manitoba, SW, CN 526
Mankayan ore field, PH 67, 88, 91, 129, 130, 184, 194
Manono-Kitotolo, CG 310, 324
Mansa Mina (MM), CL 192
Mansfeld-Sangerhausen, GE 68, 500, 502F
Mantos Blancos, CL 174, 116, 117, 193F
Manto Verde, CL 117, 118F, 174, 193
 Marcapunta deposit, PE 127
 Marcona, PE 116, 220, 423
Marcopper, PH 91
Maricunga belt, CL 166
- Marillana, AU 399
Marinduque Island, PH 91, 184, 195
 Marlborough, AU 532
 Marquette Range, US 404
 Marra Mamba IF, AU 397, 404
 Marte, CL 166
Martha Mine , Waihi, NZ 95
 Mary Kathleen, AU 328
 Marysvale (UT), US 141
Masa Valverde, SP 231
Mascot-Jefferson City, US 515
 Masugnsbyn, SW 26
 Matsumine orebody, JP 99F
 Maubach, GE 557
 Maureen, AU 141
 Mavrovouni, CY 67
Mayacmas, US 67, 105, 232, 359
Maykayan ore field, PH 161
McArthur River (Pb-Zn), AU 374, 508
McArthur River (U), CN 414
McCoy-Cove, US 148, 169F, 170
McDermitt Caldera, US 24, 111, 106, 120, 157, 359
McDonald deposit (MT), 134
McIntyre Mine, Timmins, CN 272, 275, 282
 McLaughlin Mine, US 68, 122, 141, 354
Macmillan Pass, CN 507, 508
Meade Peak, US 498
Mechernich, GE 557F
 Medet, BL 194
Meggen, GE 54, 504F, 505, 508
Mehdiabad, IN 365, 532, 540
 Meikle Mine, Carlin Trend, US 151
 Melco (UT), US 148
 Menominee, US 404
Merensky Reef, SA 37, 54, 68, 449, 450F
 Mercur, US 149
Mesabi Iron Range, US 395, 399, 404, 531, 598
 Mesel, ID 152
 Metates, MX 138
Mi Vida (Agua Rica), AR 193
Miami-Inspiration Mine, US 174F, 178
Michigan Cu district, US 68, 437
Michiquillay, PE 183
- Michipicoten Iron Range, CN 264
 Middle Valley, NE Pacific 75
 Mikhailovka, RS 403, 404
 Mina Fé, SP 328
Mina Sur (Exotica), CL 108, 173, 175F, 186, 192, 547
Minas Conga, PE 192
Mina La Motte, US 515
Minette Basin, FR+LX 68
 Mining Area C (Hamersleys), AU 404
Minnamax Mine, US 454
 Mimbula II deposit, ZA 380, 383
Mission, Pima US 168, 169F
Moa Bay, CU 232, 531
Moanda, GO 407, 533, 531
Mocoa, CO 183, 191
Moinho Mine, PT 238
 Mokrsko, CZ 332, 333
Molango, MX 491, 513, 598
Monte Amiata, IT 141, 359
Monywa, BM 113, 122, 130, 184, 194
 Moonlight (UT), US 120
 Moonta, AU 418F
Morenci-Metcalf, US 39, 106, 174, 176, 178F, 182, 191, 538, 539
Morobe Goldfield, PNG 95, 134
 Morocco, 68
Morocco, phosphates 494
Morocochoa, PE 158, 161F, 169, 217
Morro do Ouro, BR 332, 340, 341F, 350
Morro do Seis Lagos, BR 476
Morro Velho, BR 38, 260, 275, 282, 283F
 Mosaboni Mine, 291, 292F
Mother Lode, US 67, 85, 106, 332, 344, 350
Moto, CG 276
 Motzfeldt, GL 312, 465
 Mount Bischoff, AU 320
Mount Fubilan (Ok Tedi), PNG 194
Mount Emmons, US 68, 106, 204, 206
Mount Hope, US 105, 206
Mount Isa, UU 68, 371, 373F, 372F, 508

- Mount Jefferson Caldera (NV),
 US 111
 Mount Keith, AU 256, 257,
 259F
 Mount Leyshon, AU 35, 332-
 334F
 Mount Lyell, AU 249
 Mount Margaret, AU 260
 Mount Magnet, AU 277
 Mount Milligan, CN 166
Mount Morgan, AU 157, 249,
 250F
Mount Pleasant (NB), CN 54,
 209, 210F
 Mount Read Volcanics, AU 248
 Mount Skukum, CN 131
Mount Tolman, US 105, 205
 Mount Tom Price, AU 398F
 Mount Weld, AU 77, 478F
 Mount Whaleback (Newman),
 AU 404
 Mount Wright, CN 567
Mountain Pass, US 30, 44, 46,
 68, 473F, 592
Mufulira, ZA 381, 383
 Munro Township, CN 256, 262
Murchison Range, SA 260,
 289, 290F
Murdochville (Gaspé-Cu), CN
 184, 198F
 Murgul, TK 116
 Murray Basin, AU 458, 487
 Murrin Murrin, AU 260, 261F,
 532
Muruntau, UZ 48, 157, 273,
 332, 336, 337F, 350
 Musariu Nou Mine, RO 133,
 143
 Muskox Complex, CN 68
Musoshi, CG 383
Musonoi, CG 383
Muyouchang, CH 358, 359,
 523
Myutenbai, UZ 350

 Nacimiento, US 555
 Naica, MX 215F
 Nairn Anorthosite, CN 68
Nanling Range, CH 313
Nannihu-Sandaozhuang, CH
 207, 208
Natal'ka, RS 332, 338, 351
Närke, SW 496
Navan, IR 515, 520
Nchanga, ZA 380F, 383

 Ndola, ZA 383
 Nederland (CO), US 140
Nena-Frieda River, PNG 130,
 194
Nerchinsk, RS 365
New Almaden, US 67, 105,
 231F, 232, 359
New Caledonia laterites, 37,
 54, 67, 72, 531, 536
New Idria, US 105, 232, 359
Neves-Corvo, PT 237, 241, 324
Nezhdaninskoye, RS 338, 351
 Ngaoundere, CM 440
 Nicaro, CU 532
Nichkesu, KS 354
NICO, CN 420
 Niğde, TK 140
 Nigel Reef, SA 388
Niquelândia, BR 531
Nikitovka, UK 359
Nikopol, UK 68, 490, 491F, 531
 Nile Delta, EG 487
 Nimba, LI 568
 Ningshiang Fe ore type, CH 489
 Nipissing Gabbro, CN 441
 Niuxinshan, CH 335, 351
Nizhnyi Tagil, RS 155, 244
Nkana, ZA 379, 384, 560
 Nome, US 353
Noranda, CN 255, 263, 267
 Norbec deposit, CN 267F
Nördli, NW 204, 207
Noril'sk-Talnakh, RS 59, 68,
 435, 370, 560
 Northampton Sand Formation,
 GB 489
 North Dakota U coals, US 26
 North Lily Mine, Tintic, US
 216F
 Northparkes (Goonumbla), AU
 166
 North Qilian orogen, CH 315
 Novikovskoye, RS 24
 Novaya Zemlya, RS 491
 Nuuk (Godthåb), GL 583
 Nuweibi, EG 312

Oberharz district, GE 364
Obuasi, GH 275, 288F
Ok Tedi, PNG 169, 172, 176,
 177F, 184, 194, 533
 Okiep, SA 579F
 Okolovo Graben, BS 568
 Old Cadia, AU 170
Old Lead Belt, US 515, 518

 Oldoinyo Lengai, TZ 471
 Old Carlin, US 149, 150, 151F
Olimpiada, RS 332, 338, 349,
 350, 354
Olkusz, PL 515
Olmalyk (Almalyk), KZ 195,
 198F
Olympic Dam, AU 37, 40, 41,
 51, 54, 68, 298, 416F, 418,
 624, 636-638
 Olympic Peninsula, US 67
 Opalite, US 120
 Opodepe, MX 207
 Ophthalmia Range, AU 404
 Ora Banda, AU 260
 Orange Hill, US 182, 189
 Oroya smelter, PE 11
Oruro, BO 68, 113, 144, 146,
 324
 Osarizawa, JP 67, 99
Otago placers, NZ, 353
 Oued Zem, MR 513F
 Outokumpu, FN 108, 261
Oyu Tolgoi, MO 184, 196, 199F

Pachuca, MX 37, 38, 47, 67,
 105, 137
 Padaeng, TH 540, 541F
 Pajingo, AU 147, 148F
 Pakaraima Mts, GY 531
Palabora, SA 158, 468
 Palawan Island, PH 232, 531
 Palmyra Island, US 80
Panagurishte district, BL 183,
 194
 Panasqueira, PT 315, 315F
Panguna, PNG 82, 94, 184, 195
Pangushan, CH 315
Pantanos-Pedagorcito, CO
 183, 191
Park City, US 106, 220, 364
 Parral, MX 67
Pascua-Lama, CL-AR, 126
Pebble, US 105, 182, 189
 Pechenga, RS 436
 Pedernales, CL 67
 Pennines, GB 522
 Perol, PE 183, 192
 Perseverance, AU 257, 259F
 Pervomayskoye Mine, Krivoi
 Rog, UK 57
Peschanka, RS 184, 195
Petaquilla, PA 37, 105, 191
 Petsamo see Pechenga
 Pevek, RS 324

- Philex II (Santo Tomas), PH**
92F
- Phosphoria Formation**, US 68,
494
- Piaotang, CH 315
- Piceance Basin, US 24, 26, 106,
107, 545, 546F
- Picher**, US 519, 521F
- Pierina**, PE 123, 124, 125F
- Pillara Mine, AU 522, 523F
- Pilgrim's Rest, SA 152
- Pima-Mission district**, US 105,
111, 157, 169, 182, 191
- Pinares de Mayari, CU 532
- Pinchi Lake**, CN 106, 222, 359
- Pine Creek (NV)** US, 212
- Pine Grove (UT)**, US 206
- Pine Point**, CN 515, 517F
- Pipe Mine, CN 3
- Pitinga**, BR 68, 310, 318, 319,
324, 532
- Plat6 N4E Mine, Carajas, BR
263F
- Platreef**, SA 445, 448F
- Plutonic**, AU 276
- Pöhla-Hämmerlein**, GE 301,
320, 324, 328
- Pointe Noire area, CB 509
- Polaris deposit, CN 515
- Polaris Mine (ID), US 219F
- Polkowice**, PL 502
- Pongola, SA 385
- Porgera**, PNG 131, 136, 137F
- Port Dauphin, MA 487
- Port Pirie smelter, AU 11
- Post-Betze deposits**
(Goldstrike), US 151
- Poston Butte**, US 182, 190
- Potosi**, BO 37, 38, 54, 106, 157,
324, 354, 529, 613
- Potrerrillos**, CL 152, 183, 193
- Potter Mine, Munro Twp, CN
262
- Powderhorn Complex, US 469
- Prestea**, GH 275
- Preston Mine, CN 275
- Pretoria Ironstone, SA 489
- Příbram, CZ 68, 329, 330F
- Prognoz, RS 139
- Prominent Hill, AU 419
- Pueblo Viejo**, DR 122, 123,
141, 243, 244F, 533
- Pujada, Davao, PH 532
- Pulmoddai, SR 487
- Punta del Cobre, CL 116
- Que River, AU 248
- Quemont Mine, Noranda, CN
269
- Quesnellia Terrane, CN 245
- Qinglong, CH 355
- Qinling (East) belt, CH 315
- Qonyrat** see also Kounrad, KZ
163, 195
- Quadrilatero Ferrifero**, BR
401, 404, 531
- Quartz Hill**, US 12, 105, 201,
205
- Quebrada Blanca**, CL 192
- Quellaveco**, PE 178, 183, 192
- Questa**, US 106, 111, 207
- Quilon, IA 487
- Quinua**, PE 529
- Qulong (Yulong)**, CH 194
- Rabbit Lake, CN 412, 413
- Radomiro Tomic**, CL 173, 174,
175, 178, 186, 192, 539
- Radvaňovice, CZ 26
- Rajpura-Dariba, IA 37
- Rakha Mine, IA 291
- Rakkejaur**, SW 270F
- Raleigh Oilfield, US 528
- Rammelsberg**, GE 503F, 505,
508
- Rampura-Agucha**, IA 573
- Ramu River, PNG 532
- Ranger**, AU 415, 416F
- Ranong-Phuket**, TH 532
- Ranstad** deposit, SW 497F
- Rapid Creek, CN 494
- Raposos, BR 277
- Raul (Mala), PE 116
- Round Mountain**, US 131
- Ravensthorpe, AU 260
- Ray**, US 105, 178, 182, 190,
197F
- Reocin Mine**, SP 515
- Recsk**, HU 111, 122, 129, 169,
183, 193
- Red Dog**, US 68, 505, 506F,
508
- Red Lake goldfield**, CN 147,
247
- Red Mountain**, Yukon, CN
105, 205
- Red Mountain**, Rossland, CN
205
- Red Sea Graben, IS 27
- Redruth-Camborne**, GB 316,
318, 319F
- Redwell Basin, US 206
- Regalito**, CL 174, 183, 193
- Refugio**, CL 158, 166, 183, 193
- Reko Diq**, PK 194, 183
- Renison Bell**, AU 321, 325
- Rennell Island, SM 86
- Rhodes Ridge, AU 404
- Richards Bay, SA 481, 487
- Ries Crater, GE 57, 58F
- Rico, US 106, 157, 206
- Ridgeway orebody, Cadia, AU
167
- Rio Blanco-Los Bronces**, CL
40, 67, 113, 162, 183, 186,
193
- Rio Tapajos Basin**, BR 353
- Rio Tinto**, SP 37, 54, 67, 237,
240F, 533, 598
- Riviera, SA 209
- Robe River, AU 400F, 404
- Robinson district see Ely (NV),
45
- Rochester, US 157
- Rodeo**, BO 107
- Rogaland, NW 305
- Rokana**, ZA 384
- Rondônia placers**, BR 324, 532
- Ronneburg-Kauern**, GE 496,
497F
- Rosario deposit**, CL 192
- Rosebery**, AU 248, 249F
- Rosemont**, US 191
- Roşia Montană**, RO 38, 111,
131, 113, 134, 135F, 613
- Roşia Poieni**, RO 111, 133, 183,
193
- Rössing**, NM 68, 312, 598
- Rossland**, CN 205
- Rotokawa, NZ 607
- Round Mountain (NV)**, US 67,
106, 111, 122, 132
- Round Top Laccolith, US 106,
114, 118
- Rudnyi Altai**, KZ+RS 247, 248
- Rudňany**, SK 355, 359
- Ruwe**, CG 382, 383
- Săcăramb, RO 134, 142
- Sadiola Hill**, MI 275
- Sado Island, JP 67
- Safford**, US 105, 158, 182, 191
- Sagasca, CL 108, 173, 175
- Salar de Atacama**, CL 24, 25,
109

- Salar de Hombre Muerto, AR 24
 Salmon (ID), US 249
Salmon River (NS), CN 558
Salobo, BR 291F
Salsigne, FR 338, 339F, 350
Salton Sea, US 24, 106, 122, 607
 Salzgitter, GE 489
 San Antonio de Poto, PE 108
San Cristobal, BO 111, 139, 144, 364
 San Felipe, BR 532
 San Francisco del Oro, MX 106
San Gregorio orebody, PE 126, 127, 140
San Juan Basin, US 68, 552
San Manuel-Kalamazoo, US 105, 164, 171F, 174, 182, 191
San Martin, MX 106, 219, 364
 San Nicolas, MX 236
San Rafael, PE 106, 144, 146, 324
Sandaozhuan, CH 315, 207, 208
Sangdong, KO 211
 Santa Barbara Mine,
 Huancavelica, PE 142
Santa Eulalia, MX 37, 67, 106, 220, 221F, 364
Santa Rita (NM), US 106, 158, 168, 169, 178, 182, 191
Santa Rosa-Cerro Verde, PE 192
Santa Rosalia (Boleo), MX 306
 Santander, PE 515
Santo Tomas II, PH 67, 91, 92F, 184, 195
 Sam Goosly (Equity), CN 116, 147
Samarka, KZ 184, 195
 Samba, ZA 379
 São Bento, BR 277
 São Domingos, PT 237
 São João del Rei, BR 310
Sar Chesmeh, IN 9, 38, 173, 178, 183, 194, 614
 Savoyardy, KS+CH 354
 Sazare, JP 67
Schaft Creek, CN 105, 182, 189
 (Nieder)Schlema-Alberode, GE 329, 330F
 Schwaz, AS 615
 Searles Lake, US 24, 25, 109, 140, 548
Seis Lagos, BR 54, 533, 536
 Selebi-Phikwe, BW 582
Selwyn Basin, CN 495, 507
 Semail Nappe, OM 67, 75
 Sentachan, RS 354
 Serido W province, BR 577
Serra dos Carajas, BR 48, 262, 263
Serra do Urucum, BR, 404
 Serra São Felix, BR 263
 Setting Net Lake, CN 204, 273
Shaba Copperbelt, CG 382
 Shaitan-Simess, KZ 140
 Shakanai deposit, JP 99F
 Sheba-Fairview Mines, SA 276
 Sherbro placers, SL 487
 Sherman Mine, CN 262
 Shinkolobwe, CG 378
 Shirley Basin, US 554
Shizhouyuan, CH 32, 54, 147, 325, 326F, 323
 Shuikoushan, CH 365
 Shuiyinchang, CH 359
 Sibay, RS 235
 Siberian placers, RS 353
 Sierra de Gatorce, MX 141, 354
Sierra Corda, CL 192
 Sierra Madre, CU 117
 Sierra Nevada, US 106
Sierra Nevada Foothills placers, US 347, 353
 Sierra Peña Blanca, MX 141
 Sierrita, US 111
Sigma-Lamaque, CN 275, 284
Sikhote Alin, RS 57, 325
Silesia-Krakow, PL 515, 518, 519F, 532
 Silver Bell, US 111
 Silver Peak (NV), US 106
 Simandou, GN 568
 Singhbhum Copper Belt, IA 48, 290
Sipalay, PH 91, 184, 195
 Sishen, SA 404, 541
 Skellefte district, SW 265
Skorpion, NM 411, 532, 540
Skouries, GR 183, 194
 Smelter orebody, PE 127
Snake River (Yukon), CN 42, 406F
 Soda Springs, US 494
 Sokoje, KY 487
 Sora (Sorskoye), RS 207
 Soroako, ID 531
Sotiel Migollas, SP 237
 South Dakota U coals, US 26
 South Wales coalfield, GB 549
 Southern Rhodopen, GR+BL 364
 Špania Dolina, SK 615
Spence, CL 178, 183, 192
 Spor Mountain, US 106, 119, 120F, 157
Stadt Schlaining, AS 354
 Sterling Mine, US 574
Stillwater Complex, US 68, 453, 454F
 Stradbroke Island, AU 24, 28, 487
 Strange Lake, CN 54, 312, 470
 Stráž Block, CZ 552, 553F
Streltsovka, RS 111, 120, 141, 327
 Subgan, RS 568
 Sue-Dianne, CN 420
Sudbury, CN 37, 48, 57, 68, 370, 455, 456F
Sukhoi Log, RS 350
Sulfide Queen, Mountain Pass US 473
Sulfur Bank, US 68, 122F, 359
Sullivan Mine, CN 24, 37, 68, 375, 376F, 508
Sulmenev, RS 491
 Summit Lake see Howard Pass
Sungun, IN 169, 183, 194
Sunrise-Cleo deposit, AU 276, 282, 283F
Sur Sur orebody, Rio Blanco, CL 159
 Surdulica, SERB 207
 Surigao Norte, PH 531
 Sustut, CN 115
Susuman placers, RS 353
 Syrymbet, KZ 324
 Taergou, KS 315
Tahishan see Dajishan, CH 314
 Tallberg, SW 272
Talnakh, RS 54, 68
 Talvivaara, FN 261
 Tambo, CL 126
Tambo Grande, PE 247
Tampakan, PH 90, 91, 92, 111, 129, 130, 184, 195
 Tanco, Bernic Lake CN 309
 Tantramar Swamp, CN 26
 Tapira, BR 469, 470F, 531, 534
 Taranaki beaches, NZ 100
Tarkwa, GH 276, 292, 293F, 385

- Taseevka, Balei goldfield, RS**
 134
Tasna (Cerro), BO 140, 147
Tau Lekoa (Vaal Reefs), 390F
 Taupo zone, NZ 81, 121
Taurus, US 105, 182, 189
Tavua Caldera, FJ 95, 111
 Taylor Creek (NM), US 119
Tayoltita, MX 105, 138
 Taysan orebody, PH 91
Telfer, AU 152, 351, 533
 Tellnes, NW 68, 305, 306F
Tenke-Fungurume, CG 41, 383
 Terlingua, US 142
 Tesoro, CL 108
Tetyukhe (now Dal'negorsk) RS
 365
 Texas Coastal Plain U, US 552
Tharsis, SP 237, 239
 Thetford Mines, CN 28, 67
 Thierry Mine, CN 290
Thompson Creek (ID), US 105,
 206
Thompson, CN 307, 581, 582F,
 583F
 Thor Lake, CN 312
 Timagami, CN 262
Timmins-Porcupine, CN 255,
 275, 280
 Timna, IS 556
 Tincalayu, AR 109
 Tintaya, PE 169, 192
Tintic, US 106, 157, 216F, 364
Tipuani placers, BO 353
 Tiris, MU 404
 Toano Range, US 119
Toledo, PH 90, 184, 195, 198F
Tom & Jason, CN 507
 Tom Price (Mount), AU 398F,
 404
Tomtor, RS 37, 54, 476, 533,
 536, 592, 593F
 Toongi, AU 463
 Topaz Mountain (UT), US 119
Toquepala, PE 159, 163, 173,
 183, 192
Toromocho, PE 163, 192, 183
Touissit-Bou Bekker, MR+AG,
 515
 Touque, GN 531
 Toyoha, JP 99
 Trail Ridge, US 487
Trepca, Kosovo 113, 139, 141,
 364
 Tribag Mine, CN 157, 439
Tri-State district, US 68, 315,
 519
Tsumeb, NM 37, 54, 409F
Tupiza area, BO 354
 Turf Mine, Wales, GB 26
Turgai district, KZ 220, 250
Turhal, TK 353, 354
 Turquoise Ridge (NV), US 152
 Tur'ya, RS 250
Tuwu-Yandong area, CH 195
Twin Buttes, US 168, 169
Twin Creeks, US 105, 152
Tyrnyauz, KS 209
Tyrone, US 178, 182, 191
UG2 Reef, SA 68, 448F
 Uchaly, RS 235
Udokan, RS 41, 382,
 Uis tinfield, NM 308, 309F, 324
Ujina deposit, Collahuasi, CL
 175, 179F, 192
 Upper Mississippi Valley
 district, US 522
 Urad deposit, US 156, 157, 203,
 206
 Urals placers, RS 353
 Urals (North) Basin, 491
 Uravan, US 550, 551, 554
 Urna Unit, Peloponessos, GR 83
Urucum, BR 37
 Vagheena Island, SM 86
Val d'Or, CN 255, 275
 Valdez Creek, US 346
 Valkumei, RS 324
Valley Copper, CN 50
Vasil'kovskoye, KZ 37, 332,
 333F, 350
 Vazante, BR 411, 412F
Verkhnye Qairakty, KZ 37, 54,
 208
Veladero, AR 126
Veliki Krivelj, SER 169, 194,
 183
 Vergenoeg, SA 420, 421F
Veta Madre (Guanajuato),
 MX 131, 138
Viburnum Trend, US 54, 515,
 518, 519F
Victoria Goldfields, AU 156,
 348, 543, 553
 Vietnam Central Highlands, 531
Virginia City (Comstock), US
 136
 Voisey's Bay, CN 68, 303, 305,
 624
 Volkovskoye, RS 154, 254
 Vuonos deposit, FN 262
 Wabana (Bell Island), CN 489
Wabu Ridge, ID 170, 334, 351
 Wabush Lake, CN 404, 567
 Wadi Shati, LB 489
Wadley, MX 106, 353
Waihi, NZ 95, 131, 138
 Waiotapu, NZ 121
Waisoi, FJ 88, 94, 184, 195
Wales (NE) district, GB, 364
Wanshan, CH 359, 523
Wau, PNG 95, 134
 Wawa, CN 264F
 Weda Bay, ID 532
 Weipa, AU 534, 531
Welkom, SA 54, 388, 391, 393F
West Wits Line, SA 388, 390F,
 391, 393F
Western Deep Levels Mine,
 SA 393F
Westland placers, NZ 353
White Pine Mine, US 384,
 439F
 Wiluna, AU 256, 260
 WIM 150 near Horsham, AU
 485, 487
Windy Craggy, CN 67, 85, 105,
 242
 Wingellina, AU 532
 Wirralie, AU 120, 147, 148F
Witwatersrand, SA 37, 44, 49,
 57, 385, 386F, 388, 560
 Wodgina, AU 310
 Wujiaao, Hunan, CH 26, 495F
 Wulashan, CH 335
Wyoming Foreland, US 106,
 552, 554, 549
 Xiaoliugou, CH 315
 Xiaoqinling, CH 351
Xikuangshan, CH 47, 51, 54,
 351, 355
Xihuashan, CH 47, 314
 Xinglokang, CH 209
Yachishan, CH 315
Yagadnoye placer, RS 353
 Yakabindie, AU 258
Yakovlevo, RS 403, 531, 541
 Yakutia (Sacha) Republic, 324
Yanacocha, PE 107, 113, 123,
 125F, 136

Yanbei, CH 320, 325
 Yandicoogina (Yandi), AU 549
Yandong-Tuwu belt, CH 195
Yangchuling, CH 209
 Yangshikeng, CH 359
 Yawan, CH 354
 Yeelirrie, AU 547F
Yenisei Range, RS 353
 Yellow Chief deposit (UT), US 119
Yellow Pine (ID), US 105, 222, 223F, 354
Yellowknife, CN 275, 310

Yerington, US 105, 156, 169, 170, 182, 190
Yongwol, KO 207
 Youbi area, CB 24
 Yuba River, US 347
Yulong, CH 183, 194
 Yuwa-Yandong, CH 184
Zacatecas, MX 38, 67, 105, 138
 Zaglik, Caucasus, 123
Zaldivar, CL 173, 174, 178, 192
 Zarmitan, UZ 332, 350

Zarshuran, IN 152
 Zavar, IA 410
Zhezkazgan see Dzhezkazgan, KZ 68
 Zhireken, RS 207
 Zijinshan, CH 184, 195
Zinnwald, GE+CZ 299, 301, 310, 316, 324
Zloty Stok, PL 334, 350
 Zunyi, CH 495
 Zwartkop, SA 447F
Zyr'yanovsk, KZ 248

Explanations of country codes

AF	Afghanistan	GN	Guinea	NZ	New Zealand
AG	Algeria	GO	Gabon	OM	Oman
AM	Armenia	GR	Greece	PA	Panama
AR	Argentina	GY	Guyana	PE	Peru
AS	Austria	HU	Hungary	PH	Philippines
AU	Australia	IA	India	PK	Pakistan
BG	Belgium	ID	Indonesia	PL	Poland
BL	Bulgaria	IN	Iran	PT	Portugal
BM	Burma	IR	Ireland	RO	Romania
BN	Bosnia	IS	Israel	RS	Russia
BO	Bolivia	IT	Italy	SA	South Africa
BR	Brazil	IV	Ivory Coast	SB	Saudi Arabia
BS	Byelorussia	JA	Jamaica	SER	Serbia
BW	Botswana	JP	Japan	SK	Slovakia
CB	Congo-Brazzaville	KO	The Koreaes	SL	Sierra Leone
CG	Congo (DRC)	KS	Kyrgyzstan	SM	Solomon Islands
CH	China	KZ	Kazakhstan	SP	Spain
CL	Chile	LE	Libya	SR	Sri Lanka
CM	Cameroon	LI	Liberia	SV	Slovenia
CN	Canada	LX	Luxembourg	SW	Sweden
CO	Colombia	MA	Madagascar	TA	Tajikistan
CY	Cyprus	MD	Macedonia	TH	Thailand
CZ	Czech Republic	MI	Mali	TK	Turkey
DR	Dominican Republic	ML	Malaysia	TR	Turkmenistan
EC	Ecuador	MO	Mongolia	TU	Tunisia
EG	Egypt	MR	Morocco	TW	China-Taiwan
FJ	Fiji	MU	Mauritania	TZ	Tanzania
FN	Finland	MX	Mexico	UK	Ukraine
FR	France	NC	New Caledonia	US	United States
GA	Georgia	NH	Netherlands	UZ	Uzbekistan
GB	Great Britain	NG	Nigeria	VE	Venezuela
GE	Germany	NR	Niger	VI	Vietnam
GH	Ghana	NM	Namibia	VT	Vanuatu
GL	Greenland	NW	Norway	ZA	Zambia
		PNG	Papua New Guinea	ZB	Zimbabwe

Subject Index

Explanations: F (e.g. 253F) indicates Figure; T indicates Table; + indicates the subject continues beyond the page shown

- A-type granite 296
- Abitibi Subprovince 253+,
254F, 255F
- Abyssal red clay 78
- Acanthite 137
- Accidental discovery 633
- Accommodation of metals in
ores 598T
- Accreted terranes 84, 85, 225,
227
- ores 105
- Accretion 59
- metallogenesis 85
- Accretionary complex, ores 105
- Accretionary forearc 102
- margins 83
- wedge 84
- Aceite 587
- Acid sulfate alteration 122, 123
- Acquisition of existing deposit
641
- Activation 335, 584
- Active volcano, gold 110
- Adequacy of metal supplies 18
- Adularia 132, 133, 136, 137
- Advanced argillic alteration 91,
92, 123
- Aegirine 465, 467
- Ag-As-Ni-Co-Bi association
302, 329, 441, 442F
- Ag giants 131
- halides 126, 145, 214, 571
- low temperature veins 363
- native 441-443, 442F
- residual 533
- sulfosalts 138, 143, 329, 443
- Agricola 299, 613
- Agpaitic family 463, 464F, 466
- Aguilarite 138
- Airbus Industries 21
- Al from dawsonite 545
- from nepheline syenite 467
- from oil shale 26, 107
- from paleosol 542
- from phonolite 463
- Al phosphates 513
- Al, Ti from coal clays 463
- Alaska-Urals complexes 88,
154, 243-245, 244F
- Alaskite Mo-W-Bi 207
- Alaskite U 212-213
- Albite-chlorite alteration (sedex)
375, 376F
- Albite 423
- metasomatic 567, 586F, 588
- Albitized granitic cupolas 318,
319F, 320
- Algoma-type Fe 262, 263F
- Alkali basalt 77
- Alkali carbonatite 471
- Alkaline association 459+
- epithermal Au,Te 135
- forearc volcanics 84
- granitoids 461
- magmas 72
- metallogenesis 461+
- metasomatites 585, 586F
- pegmatites 466
- porphyry Cu 158, 165+, 167F
- sodic Au 136, 137F
- ultrabasic 460, 467-469
- volcanics 462, 462
- Allanite skarn 328
- Alluvial placers Au 108, 346+,
349F
- Allochthon screen (Carlin) 150
- Alpine-type orogens 295
- serpentinite 229
- Zn-Pb type 514
- Alteration zoning, porphyry Cu
164
- Alum shale 28, 493F, 496, 497F
- Aluminum see Al, and 11
- hot electrolysis 21
- wiring 21
- Alunite 122, 123
- veins 145
- Alluvial fan 108
- infiltrated Cu 176
- Alluvial mining 485
- placers 542-544F
- Alluvium 542
- Amalgam 443
- Amalgamation of terranes 154
- Americas, rediscovery 613
- Amorphous magnesite 233,
234F, 534
- Amphibolitic Cu-Fe skarn 116
- Amygdaloids-Cu 437, 438F
- Anatase 469, 470F
- Anatectic granite 154
- Ancient epithermal 147
- Ancient giants 38
- hot springs 148F
- Andalusite (alteration) 147, 165
- Andean granitoids 102
- stratovolcanoes 103
- type margins 101-103F
- Andesite hosted Cu 115
- Andesitic arc magmas 82
- Andinotype granite 153
- Anhydrite 501
- chimneys 77
- Annealed ores 570
- Anorogenic granite 297
- Anorthosite 303, 304, 253
- layered 449, 452, 454F
- Anoxic basins 490,
- Anthophyllite alteration 576F
- Anthropogenic metal sources
559, 560
- Antimony, see Sb & 21
- Antlerite 186
- Apatite, magmatic 467F
- Apogranite 310
- Appalachian Zn-Pb type 514
- Arc-trench gap 83, 84
- Archean porphyry-style
Cu,Au,Mo 2782, 273
- shoshonites 285, 286F
- VMS 264, 266F, 267F, 270F
- deformation, metamorphism
267, 269F
- Arfvedsonite 465, 466
- metasomatic 587
- Argentite 137
- Argillic lithocap 145, 147, 166
- Arid regolith 545, 546F
- Arsenian pyrite, Au 151
- Arsenic see As
- Arsenides Ni, Co 442

- Arsenopyrite veins 333F
 As-Au skarn 170F, 334
 --veins 333F, 338, 339F
 As in ironstone 488
 Asbestos 18, 230
 Ash-flow calderas 111, 113F
 Astrobleme 57
 -- paleo 456F, 457
 Asthenosphere 71, 77
 Atacamite 175
 Athabasca Basin 413, 414
 Athenian silver 613
 Athenian state 9
 Atlantic continental margin
 successions 480F
 Atlantic-type margins 430, 431F
 Au, Ag in sediments 97
 Au, anticlinal lines 342, 343F
 -- deep leads 610
 -- fine, in floodplains 347
 -- heap leach 337
 -- in black schist 338, 341, 342
 -- fault lodes 344
 -- in gossan 176, 177F, 238,
 239F, 243, 537
 -- in accretionary terranes 343-
 345
 -- in ancient Egypt 613
 -- in bauxite on greenstone 283,
 284F
 -- in conglomerates 549
 -- in glacial sediments 529
 -- in quartz conglomerate 385+
 -- in Kupferschiefer 501
 -- in melange 344
 -- in sericitic envelope 336
 -- in shears 338
 -- in silicified collapse breccia
 151
 -- in synorogenic conglomerate
 292, 293F
 -- in tailings 559, 560
 -- in thrusts 340, 341F
 -- in turbidites 340, 341F
 -- largest vein deposit 336, 337F
 -- laterites 537
 -- low grade 337, 340, 341F
 -- near dikes 338
 -- no quartz in shear 340, 341F
 -- mesothermal, global
 distribution 350, 351T, 352F
 -- paleoplaces 385+, 391
 -- placers 341, 346, 543
 -- placers, global distribution
 352F, 353T
 -- reefs in gabbro 433
 -- regoliths 537, 538
 -- residual 533, 536, 537
 -- saprolite 537, 538
 -- skarn 148, 169F, 170, 333,
 334
 -- stockwork 334F, 336
 -- submarine-hydrothermal 84
 -- veins in black clastics 339+
 -- veins in dikes 335, 336
 -- veins in turbidites 338, 339,
 342+
 Au Witwatersrand-type 385+,
 387F, 388T, 390F, 393F
 Aulacogene 430
 Aureoles 155
 Authigenesis 483
 Authigenic minerals 492
 Automobile culture 30
 Axinite 334

 Ba feldspars 574
 Back-arc 86, 87F
 Baddeleyite 468, 469
 Ball ore 377, 563, 580
 Barite giant 506
 -- sedex 503, 505
 Barrel 39
 Basal conglomerate ores 541,
 542
 Basal paleoplacer 392, 393
 Basal sequences 541
 Basalt lava fields 428
 -- in rifts 434, 432, 433F
 Basaltophile metals 82
 Basin-and-range extensions 103
 -- ores 106
 Basinal fluids 506
 -- lithofacies 507
 -- shale 504F
 -- successions 480F
 Basins and ores 49F
 Bastnasite 473-476
 Bauxite 11, 51, 439, 443
 -- in Jamaica 525F
 -- in lagoons 86
 -- residua 24
 Be hydrothermal veins 465
 -- in Andean rhyolite 119
 -- super-giant 323, 326F
 Beach placers 485F
 -- Au 346
 -- fossil 485, 486F
 Beach sands-Fe 100
 Bedded ironstone, world review
 487+T
 Bedded Mn 490+, 491TF, 493F
 -- Proterozoic 407-408F
 Bench gravels-Au 347
 Benioff zone 82, 102
 Bergakademie Freiberg 361
 Bertrandite 119, 120F
 Beryllium tuff 119, 130F
 Besshi-type 74, 75, 230, 241,
 242F, 243
 Bi super-giant 323, 326F
 BIF-aegirine 402
 BIF at gabbro contact 401
 -- high grade metamorphosed
 567, 568
 -- Na metasomatite 402
 -- riebeckite 402
 -- Superior type 394-403
 -- Superior-type, global review
 404T, 405F
 -- talc schist 402
 Bilibin's model 39, 65, 104
 Bimodal greenstones 263F,
 266F
 -- successions 235
 -- volcanism 88
 Biomining 26
 Biotechnology 26
 Bituminous shale 501
 Black clastics 339+
 -- schist in ophiolite, Ni,Zn,Cu
 261
 -- Sea 493
 -- shale 32, 28, 492, 493F
 -- shale, Cu 439F
 -- shale, trace metals 494+,T
 -- slate, Mn 408
 -- smokers 75, 77
 Blastomylonite 587
 Blueschist 83
 Bog ores 545
 Bolivia-type Sn-Ag 143+
 Bonanza Ag 214, 361, 363, 441-
 443
 -- Ag>>Au 136+
 -- Au 95
 -- Au,Ag 246
 -- shoots 132
 -- Sn>Cu vein 146
 Boninite 84
 Borates 109
 -- high-grade metamorphosed
 578
 -- in skarn 362

- Borax 109
 Boron in geothermal fluid 24
 -- in playas 109
 -- in playa brine 548
 -- skarn 221
 Boulangerite 327, 360
 Boulder tracing 108
 Boudins 340
 Br from seawater 78
 Braggite 449
 Brannerite 394, 415
 Braunite 407, 408F
 Breccia, epithermal Au-Te 135
 Breccia, impact 57
 -- pipe 163, 439
 -- pipe Fe, fluorite 420, 421F
 Bre-X scam 645, 646
 Brine pools 429
 Brochantite 186
 Brockam IF 397, 398F
 Broken Hill-type 568+, 570F,
 572F, 573F
 Bronze Age 7
 Bronzitic pegmatoid PGE 449
 Bronzite 453
 Brush Wellman 30
 Brownfield discoveries 633
 Bulk low sulfide Au-Ag 123
 -- mined Au 336
 -- mining 28, 39
 Buried Au placers 347+
 Bushveld-type intrusions 443+,
 444F
 Bustamite 568

 Ca-Mg silicates 571
 Caesium pegmatite 309
 Cahill Formation 414
 Calamine 517
 Calc-alkaline magmas 102
 -- arc magmas 88
 -- eugeoclinal orogens 245,
 246F
 -- porphyry systems 164
 -- systems 158
 Calcrete 546F, 547F
 Caldera Au-Te 95
 -- ,U 120, 327
 Calderas and ores 111T, 113F
 Caledonian-type granites 297
 California-type Hg 231F, 232
 Canadian Cordilleran orogen
 227+, 228F
 Canga 401-402
 CANMINDEX 39

 Caprocks 526
 Carbon + Au,U (Rand) 385-392
 -- vein alteration 340
 Carbonaceous hosts to Au 339+
 -- pelites 492+
 Carbonate Basinal facies 509,
 510F, 511
 Carbonate diagenesis 511
 -- facies 509, 510F
 -- platform 507, 509, 510F
 Carbonatite 469, 470+
 -- lava 471
 --, plutonic 472F
 -- regolith 472
 Carlin Trend zone 150
 Carlin-type Au 147+, 148+,
 151F
 Carnotite 551
 Carrolite 382
 Cd, Tsumeb 409F
 Central Rand Group 385+. 387F
 Central volcanic complexes 267
 Cerussite 412
 Chalcocite 176
 -- blanket 129, 176+. 178FT,
 179F, 186
 Challenger Expedition 26, 73
 Chamosite 488, 489
 Channel gravels, Au 347
 Channels, Cu infiltrations 175,
 176
 Chattanooga Shale 28, 495
 Cheap metals 49
 Chemical breccia 161
 Chemical weathering 530
 Chert 498
 Chilean nitrates 21, 107
 Chimneys Pb-Zn-Ag 212+
 Chimneys (on sea floor) 77
 China market 18
 Chkalovite 465
 Chloritic dolomite 381, 382
 Chondrite 57, 59
 --, trace metals 60T
 Chromite, metallurgical 451
 Chromitite layers 446, 447F,
 451, 453
 --, metamorphosed 584
 Cinnabar 355, 356
 --, in carbonates 522
 Civil unrest 645
 Clarke 41
 -- of concentration 41, 42, 44T
 -- values 42
 Clarkes 43T

 Clastic ores 483+
 Cleavage ore control 362, 363F
 Climax-type Mo 119, 201-204,
 202F
 Clinton-type Fe 489, 490
 Club of Rome 19
 Co in oceanic nodules, crusts 79,
 80
 -- in oceanic nodules 27
 -- in slag 560
 -- in tailings 560
 -- residual 531, 536
 Coal, metals in 26, 549
 Cobalt, see Co
 Cobar-type Zn,Pb 362, 363F
 Coffinite 412-415
 Colemanite 109
 Collisional metallogene 296
 -- orogens 295+
 -- sutures 103, 562F
 Collisions 84
 Colorado Plateau, U province
 553, 554
 Colluvium-Au 346
 Commodities 18
 Commodity prices 12, 14T
 Complex exploration 635, 636
 -- orebodies 47F
 -- Zn-Pb-Cu in carbonates 409-
 411
 Complexity of deposits 44, 49F
 Composite ore deposits 44, 46F
 Concentration factors 42
 Configuration of orebodies 46F,
 47F, 48F, 49F
 Conglomerate-Au 292, 293F,
 549
 -- Cu impregnations in 437,
 438F
 Connate waters 482
 Consumption per capita 17+
 Continental back-arc 103
 -- clastics 549
 -- crust 62+
 -- crust, clarkes 42
 -- trace metals 60T
 -- glaciation 107
 Convective systems 156
 Convergent continental margins
 82, 83, 101+
 -- basins
 Conversion, compounds to
 metals 5
 Cooperite 449
 Copper, see also Cu

- electrowinning 14
- in peat 25, 26
- shale 500-503
- Copperbelt-type Cu,Co 377+, 378F, 380F, 381F, 383F
- Co in 377+
- Cordierite (alteration) 573F
- Cordilleran Foreland 551
- granites emplaced to eugeoclinal orogens 213F
- granites in miogeoclinal setting 213F
- granitoids 153+
- metamorphic core complexes 562F
- orogens 153+, 155F
- Pb-Zn-Ag deposits 212+
- Core libraries 38
- Cornwall Cu-Sn mining 613
- type Sn 317-319F
- Corporations 616-620, 617T
- Corundum alteration 147
- Cosmic dust 57
- metals 58
- Costs of finding/developing giants 624, 625T
- Covellite 176, 186
- Cr residual 531
- resources in Bushveld 444
- Crandallite 513
- Crater lakes, Au 110
- CRIB 39
- CRIB/MRDS 36
- Critical Zone 445+, 450F
- Crocydolite 397
- Cryolite 21, 587
- Cryptomelane 490
- Cu and metabasalt 370, 371
- disseminated in carbonatite 468, 469
- in dolomite 381+
- in metaquartzite 381, 382
- in silica-dolomite 373F
- in synorogenic gabbroids 579
- in tailings 560
- in the Middle East 613
- mantos in andesite 115
- native, in basalt 473
- residual, oxidic 532, 538
- sandstone 555, 556
- skarn & porphyry Cu 169T,F
- stockwork in andesite 116
- stratabound in schist, quartzite 377+
- sulfides in marble 577
- supergene sulfides 539, 540
- cumingtonite 394, 568
- Cumulus gabbro 73
- Cupola leucogranite 208
- Curie, Pierre & Marie 22
- Cyprus-type 74, 75, 230
- Danburite 362
- Data 36
- sources 35, 36+
- Databases 35
- Data Metallogenica 37, 38
- Datolite 362
- Dawsonite 26
- Decalcification 149
- Decapitation of stratovolcano 96
- Decollement (sedex) 377
- Deep lead-Au 347
- Deep water evaporite 509
- Deformed porphyry-Cu 170, 171F
- De Launay 65
- Delineation 36
- Delius 613
- Demand reduction 19
- Deposit, ore 45
- Desalination plants 23
- Deserts 545
- Detrital ores 484+
- Devitrification of volcanic glass 108
- Diabase 440+, 441F
- Diagenesis 482
- late 511
- Diamictite Fe,Mn 403+, 405F, 409
- Diamond 462
- Diapirs 526, 527F
- in the Copperbelt 381
- Diaspore alteration 147, 165
- Diaspore bauxite 549
- Diatreme breccia 131
- and dome, Au 134, 135F
- Zn-Pb-Ag 126-128
- Diatremes and ores 113T
- Differentiated mafic-ultramafic intrusions 243, 244F
- monzogranite-Mo 200
- Dikes, granitoid 335
- Dimension of deposits 44, 50, 51
- Diorite model porphyry Cu 90, 91, 158, 165+, 166F, 167F
- Discovery during mining 634, 635
- to mining time gap 639T
- of Ertsberg 633
- Disseminated Au (Carlin) 147+
- Cu in carbonatite 158
- Cu in gneiss 577, 578F
- Cu mantos 115
- Cu in porphyries 157
- epithermal Ag-Pb 139
- Distal scheelite skarn 211
- District (ore) 45
- Diverse metamorphic association 566, 567F
- Dolerite, see diabase
- Dollar values 40
- Dollar-Thaller-Joachimsthaler 299
- Dolomite, with BIF 401
- Dolomitization 517
- Dome, rhyodacite Sn-Ag 144, 145F
- Domes (volcanic) & ores 113T, 114
- Dominion Group 386
- Dredging Au 348
- Drilling 635
- Dry plutons 168
- Ductile breccia 580
- faults 586F
- Dumortierite alteration 165
- Dune placers 485, 486F
- Dunite 469
- cumulate 256
- Duplex fault Au 340, 341F
- Durchbewegung 362, 419, 563, 580, 581-583F
- Duricrusts 546F
- Earth evolution 59
- Early finance houses 615
- Eastern Creek Volcanics 371, 373
- Eclogite 83
- Economics (giants) 620
- Edison TA 636
- Egypt, ancient-Au 613
- Egyptian kings 613
- Elements, discovery 11
- Eluvial placers 321
- Empirical Metallogeny 1
- Enargite 91-93, 122-130
- Endogreisen Be,Sn,W,Mo,Bi 323, 326F
- Endowments (metals) 48
- Enriched Algoma-type Fe 263F
- Ensialic orogens 225

- Ensimatic orogens 225
 Episyenite 578
 Epithermal As 141
 -- Au-Ag 94, 95F
 -- Bi 140, 147
 -- deposits, Andean margins 120
 -- Hg,As,Sb 142
 -- leaching 127
 -- Mo 140
 -- Pb,Zn,Ag 139+, 140F
 -- Sb 141
 -- Te 142
 -- U 141
 -- W veins 140
 Ercker, Lazarus 613
 Erzgebirge, medieval mining 613
 -- mining history 300F, 301F
 -- ores 299-302, 300F
 Eudialyte 462, 464, 456, 467
 Eugeocline 104
 Eugeoclinal 86
 -- domain 225-229, 234F
 -- orogens 82, 225+, 226F
 Euxinic basins 483, 492, 493
 Evaporite solution fronts 526
 Evaporites 509+, 510F
 -- in playas 548
 Exclusive economic zones 80
 Exhalative deposits 78
 Exhalites 82
 Exoskarn 164
 -- at pyroxenite contact 446, 448F
 Exotic Cu 539, 547
 -- deposits 108, 173, 174, 175FT, 177F
 Expanded shale 32, 33
 Exploration, changing attitudes 620
 Expressions of ore magnitude 47
 Exploration geochemistry 636
 Extinctions 57
 Extraterrestrial metals 56

 Fallback breccia 57, 455
 Fault lodes Au 335
 Fault rocks 585
 Faults, Hg minerals 358, 359F
 Favorable setting 611
 Fe-bedded deposits 483
 -- blue dust hematite 401
 -- channel gravels 399, 549
 -- enriched BIF, Superior-type 395, 396F, 398F
 -- enriched ores 530, 531
 -- in diamictites 403-406F, 405F
 -- Kiruna-type 421-423F, 422F
 -- Minette-type 488F
 -- oxides-Cu-Au 116, 117F, 292F, 292, 415+, 416F
 -- pisolith 399, 400F
 -- Rapitan-type 403-406F
 -- redeposited soft ore 549
 -- skarn 220
 -- Superior-type BIF 394-403
 -- taconite 395
 -- thermally upgraded BIF 400F
 Feldspathite-Au 335
 Fenite 460, 469
 Ferrogabbro 450, 452
 Ferromanganese crusts 27, 80
 Ferromanganese nodules 26, 27, 79
 Fissure paleokarst 409F
 Five elements association 302
 Flat subduction 102, 104
 Flood basalt 434
 Floodplain Au 347
 Florida-type phosphates 512F
 Fluctuating water tables 172
 Fluidized breccia 161, 163F
 Fluorapatite 498
 Fluorine in phosphorite 500
 Fluorite in breccia pipe 420, 421F
 Forearc 83, 84, 86
 -- deposits 105
 -- seamount, Au-Ag 97
 Footprint of orebodies 47F, 48F
 Footwall alteration (sedex) 375, 376F
 Foreland basins 103, 549
 Forelands, ores 106
 Formational fluids 482
 Foscorite 468, 469
 Fossil fuels 26
 Forsterite (Mg skarn) 168
 Fracture Au stockwork in ignimbrite 131
 Frailesca 357F
 Francolite 498
 Francevillian 408
 Franciscan Complex 83
 Franckeite 145, 146, 327
 Franklinite 574
 Freiberg Mining Academy 299, 361
 Fuggers, The 615
 Fumaroles 110, 111
 -- with Au 110
 Future metal demand 19
 -- metal sources 23F
 -- metal supply 22, 29F
 Futurists 18, 19

 Gabbro, layered 449
 -- sill 440, 441F
 -- -syenite association 460
 Gabbrodiabase sill-Ni 435, 436F
 Gagarinite 587
 Gahnite 568-571, 573
 Gallium 51, 463
 -- in bauxite residue 24
 Gardar Rift 312, 461F
 Garnet (alteration) 575
 -- quartzite 570
 Garnierite 232
 Gas as metal source 25
 Gawler Craton 417
 Ge in coal 550
 -- in Tsumeb 409
 Genetic coding 590, 591F
 -- coincidence 612
 -- types of giant deposits 593-595, 594T
 Geochemical background to ores 62
 Geochemical giants 5
 -- premise 41
 Geological ages abbreviations 4
 Geology and ore discovery 646
 Geologists' values 620, 621-623T
 Geophysics, early 635, 636
 Geopolitics, influencing giants 614, 615
 Geosynclinal model 65, 104, 225
 Geothermal systems, in rifts 122
 -- field 121, 122
 -- springs 25
 -- systems 428
 Germanium in coal 24
 -- rush 26
 Germanite 410
 Gersdorfite 442
 "Giant" deposit 5
 GIANTDEP database 36, 37, 44, 46, 47, 51
 Giant Au placers 610
 -- conventional ore types 589T
 -- deposits, definition 38-42
 -- deposits, discovery in history 631, 632F, 633

- deposits, genetic groups 598, 600T, 601T, 603F
- deposits in geological time 606, 607, 608T, 609F
- deposits in history 614
- deposits, magmatic families 599, 602T, 604F
- deposits, origin 589
- on land surface 647
- deposits in plate tectonic setting 605F, 606
- oilfields 39
- Giants discovery 628-631
- discovery techniques 633F-636
- and GNP 615
- history 613, 614, 616F
- presently forming 607-610
- magnitudes spectrum 611
- ownership 617, 616T
- thresholds 45F
- under unconsolidated cover 647
- under solid cover 647
- why so big? 610-612
- with 2 or more metals 37T
- Gibbsite 537
- GIS 39
- Glaciation and ores 529
- Glacier ore 107, 529
- Glaciogenic deposits 107
- Glaucinite 489
- Glaucinitic clay 492
- Glimmerite 468, 474
- Global metals endowments 51, 52T, 53F
- metal supplies 47
- resources 31T
- Globalization 616
- Goethite 488
- Goldfield (term) 45
- Gold-also see Au
- future demand 19F
- in seawater 23
- in a seamount 27
- rich VMS 269, 270F
- skarn 333, 334
- Gossan-Au 176
- on sea floor 74
- Grabens 426
- Grade-tonnage graphs 40
- Granoblastic texture 563
- Granophyre 433, 449
- Granite cupola 313-315
- with Sn 315-318, 317F
- Granite-greenstone terrains 251+, 251F
- Granite-related Au 331
- Sn 315+
- gneiss terrains 565
- Granitization and ores 564
- Granitoid-related ores 295+
- Granophyre 457
- Granules 483
- Granulite-migmatite complex 566F
- Graphitic gneiss-Ni 581
- Graywacke-slate, host to sedex 375, 376F
- Greece, classical 613
- Green basalts 434
- Green River Formation 545
- Green tape 643
- Green Tuff region 98F, 99F
- Greenfield discoveries 620, 633
- Greenstone basalt 262
- belt 251-253, 252F
- cycles 253
- geotectonics
- high-sulfidation As,Au,Se 271F
- Greisen 208, 314, 316, 317F
- Sn,W,Mo,Bi,Be 323, 326F, 327
- veins in skarn 323, 326F
- veins W,Mo,Be 208, 315
- Groundwater calcrete 547F
- Growth fault 374, 507, 516F, 520-522, 558
- Grunerite 394
- Gulag Archipelago 338
- Gulch placers 108, 346
- Habachseries 583, 584F
- Hafnium 463
- Halite 501
- Halmyrolysis 78
- Hausmannite 407
- Hawaiian-type islands 77
- Hawaiite 77
- Hawthorn succession 512
- Heavy heavy minerals 483
- mineral placers 484
- mineral sands 484-487, 486F, 487T
- minerals, very fine grain 485
- Hematite 488
- alteration 415-418, 587
- microplate 398
- Hemimorphite 412, 540, 541F
- Hemipelagic sediments 78, 85
- Hercynotype granites 297
- Heterolithologic breccia 162
- Hg fault lodes 355, 356F
- from natural gas 526
- global distribution 359T
- in karst 355
- in peralkaline caldera 120
- mantos 355
- replacements 355-358, 356F
- stratabound in carbonates 522, 523
- stratabound in clastics 357F
- supergiant 356, 357F
- Hierarchy of ore deposits 44, 45, 50F,T
- High-demand metals 49
- High grade metamorphic magnesite 578
- borates 578
- intracratonic orogens 569F
- rift association 576F
- VMS 574-576F
- High pressure metamorphic belts 83
- High silica rhyolite, Mo 201+, 202F
- High sulfidation Au,Ag,Zn 243, 244F
- Ag>Au 126
- Au-Ag 123-125F
- Au, Cu 125
- deposits 120-122+
- mantos Pb,Zn,Ag 128F
- and porphyry Cu-Au 91-93F, 122, 129, 130F
- pyritic Cu replacements 130
- High-temperature replacement Pb,Zn,Ag 212-221F, 215F, 216F
- Hiltaba suite 417
- Himalayan-type orogens 295
- History of metals 10F
- Hornblende, scheelite host 583
- Hornfelsed clastics 338
- Horsetail CuAu veins 129
- Hot spots 77, 430
- Hot springs 25, 120, 121+, 122F
- Hg 122F, 141
- giants 607
- Humid alluvium 542+
- regolith 534F
- tropical regolith 529+
- Hutton's law reversed 607
- Hybrid contacts, Bushveld 446

- Hydraulic fracturing 161
 Hydrocarbons 26, 511, 526
 Hydrogenous phosphorite 85
 -- sediments 78
 Hydrolytic alteration 165
 Hydrothermal breccia 161
 -- breccia pipe, Au-Ag 126
 -- eruption breccia 121
 -- karst 214, 517, 518
 -- metamorphic fluids 370
 -- U veins 302
 Hydrous skarn 210
 -- As,Au 334
 Hypersthene in BIF 569
 Hypersthenite, Cu 579F, 580F
- I-type granite 102, 296
 Ignimbrite field 114
 Ijolite 467F
 Illinois-Kentucky vein type 514
 Ilmenite, in beach sands 484, 485
 Immature ores 88
 Impact sites 57, 58F
 -- presumed 457
 -- Vredefort 385
 In situ leaching Cu 173
 Incompatible elements 71
 Indium 209
 Industrial history, Broken Hill 618T
 Industrial Revolution 9, 11, 15, 613
 Industrialization 613
 Influvium 409
 Infrastructure 645
 Instant orebodies 55
 Intensity of metal accumulation 611
 Inter-arcs 86
 Interactive ore genesis 592, 612
 Interflow conglomerate 437, 438F
 Intermontane Gold Anomaly 607, 610
 Internal homogeneity of ores 596F
 -- uniformity of ores 596F
 International Tin Council 12, 13
 Intra-arc rifting 88, 102
 Intraclasts 483
 Intracontinental rift, Mo 199, 204
 Intracratonic orogens 295+, 367+
- Intraformational paleoplacer 388-391
 Intraplate islands 77
 Intrusion-related Au 331
 Intrusive breccia 161, 163
 Investment risk 642, 643F, 644F
 Invisible gold 149, 340, 341F
 IOGC family in andesites 117
 Iridium 57
 Irish-type 503+, 516F, 521F
 Iron oxide-Cu-Au family 117, 165
 Ironstone 487, 488F
 Island arcs 81F+
 -- maturity 88
 -- metallogeny 82+
 -- terranes 227
 -- volcanic centers 88, 89F
 Isochemical metamorphism 561
 Itabirite 401, 402
- Jáchymov history 22
 Jacupirangite 469
 Jamaica bauxite 86, 525F
 Jamesonite 327
 Jasperoid 151
 -- Pb,Ba,Ag 411
 Jaspillite 394, 397
 Jiangxi-type W 313-315
 Junior companies 30
- Kakortokite 464, 465
 Kalahari Formation 407, 408F
 Karst bauxite 86, 524, 525F, 541
 Karst ores 523, 524F
 -- residual Sn 323
 Karsted carbonatite 472, 477, 478F
 Katangan Supergroup 377-382, 378F
 Kazakov theory 498
 Kennecott-type Cu 233
 Keratophyre 88
 -- tuffite 505
 Kimberlite 460
 K-Mg salts 501
 Kniest 504
 Knotten 556
 Kolm Shale 493F, 496, 497
 Komatiite association 356, 257F
 -- flows 256
 Komatiitic dunite, Ni 256, 257, 259F
 -- Ni sulfides 256, 258F
 -- peridotite 256, 257, 258F
- ultramafics 256
 Kundelungu Group 378+
 Kupferschiefer-type Cu 439F, 500-503
 Kuroko-type 90, 97, 98F, 99F
 Kutnahorite 407, 490
- Labor relations 645
 Lacustrine apatite sand 472
 -- sediments-Cu 439F
 -- sequences 544+
 -- shale 545, 546F
 Lagoons 86
 Lake beds 109
 -- Hg,U,Li,Cs 120
 Lakes 544
 Lamprophyre-Au 335
 Land access 643
 -- claims 643
 Land-Pebble phosphates 512F
 Laramide magmatic province 103
 "Large" deposits 42
 Laterite 534F
 Lateritic bauxite 439, 443, 531, 533, 535F
 -- Ni on komatiites 259-261F
 Law of the Sea 79
 Layered "dike" 451
 -- intrusions 443+, 444F, 453, 454F
 -- intrusions, alkaline 462-468
 -- mafic intrusions 433F
 Leached capping 172
 Leaching in-situ, Cu 173
 Lebowa Granite Suite 445
 Leptite 571, 576
 Leucogranite Mo,W,Bi 207
 Leucoxene 484, 485
 Li in playas 109
 -- pegmatites 308-310
 Light heavies 483
 LIL elements 72
 Listvenite 336
 Lithocap 92, 147, 165
 -- Ag-rich 144, 145F
 Lithosphere, evolution 59+, 62
 Lithospheric mantle 71
 Lithothèque 1, 3FF, 4
 Littoral 485F
 LODÉ database 36
 Lollingite 442
 London Metals Exchange 12
 Loparite 466
 Low grade ores 27, 28

- Low sulfidation 121, 131+
 -- Au 132+
 -- Au,Ag 94, 95F
 -- Au & porphyry Cu 133, 134
 -- Au-Te 134
 -- rocks associations 131
 -- and skarn Au,Cu 142F
 -- veins 131
 Lower Crustal clarkes 42
 Lower Continental Crust, trace metals 61T
 Ludwigite 578
 Lufilian Arc 377-382, 379F
 Lujavrite 462, 465
 Luzonite 91-93, 122, 128
- Maar 114
 Mafic differentiated intrusions 433F
 -- intrusions Ni,Cu 435, 436T
 -- sills 440+, 441F
 -- successions 235
 -- & ultramafic intrusions 443+, 444F
 Magma plumes 62
 -- series and ores 156, 157T
 Magmas & ores affiliation 156, 157T
 -- maturation 88
 Magmatic arc 87, 88
 -- ores 105
 -- complexes and ores, 49F
 -- families 599, 602T, 604F
 -- hydrothermal deposits 155
 -- Mo 199
 -- polarity 104
 Magnesium from sea water 21, 23
 Magnetic anomaly 402, 403
 Magnetite beach sands 100
 Magnetite in Kiruna 421+, 423F
 Magnetite layers 449
 MANIFILE 39
 Mantle 59, 71
 -- contamination 72
 -- convection 73
 -- metallogeny 72
 -- metasomatism 72
 -- plumes 59, 62, 71, 430
 -- primitive, trace metals 60T
 -- wedge 101
 Manto Pb-Zn-Ag 212+
 -- in shear Cu,Au 117, 118F
 Mantos Pb-Zn-Ag 139, 140F
 -- under ignimbrite, Au 131
- Mariana-type island arc 83
 Marine carbonates 509+
 -- clastics 481+
 -- evaporites 509+, 510F, 525+
 -- phosphorite 498
 -- placers 484, 485F
 Marra Mamba IF 397+
 Miaskitic association 463, 464F
 Massif anorthosite 303+, 304F
 -- Ni sulfides 305
 Matinenda Formation 394F
 Mature island arcs 88, 89, 90
 McKelvey formula 41
 Mediterranean bauxites 524, 525
 Megabreccia (Okiep) 579
 -- tectonic 382
 Melange 83, 229
 -- and Au 85
 Melilite 469
 Mercury from natural gas 24, 25
 Mesothermal Ag 363
 -- Ag-Sb veins 219
 -- Au 331+, 332F
 -- in greenstones 273+
 -- Pb-Zn-Ag 358+
 -- Pb-Zn veins 218-220, 219F, 222F
 -- U 328-331, 330F
 Meta-anhydrite 571
 -- anorthosite, Cr 584
 Metal belts 44
 -- endowments 35
 -- dispersion 589
 -- harvesting 25
 -- heritage 612
 -- prices 12+, 14T, 16F
 -- toxicity 22
 -- zoning around intrusions 158
 Metalliferous black shale 495F
 -- brine 122
 -- mud 27, 429
 -- sediment 77
 -- shale 28
 -- oceanic sediments 74, 79+
 Metallogene 5
 Metallogenic maps 39
 -- provinces 45
 Metallotect 45
 Metals consumption 18
 -- from rocks 28
 -- lacking giants 51
 -- of antiquity 9, 15
 -- production 35
 -- production history 17F
 -- relative values 49
- resources 35
 -- supplies 11
 -- toxicity 18
 Metaluminous granite Mo 199, 200F
 -- magmas 157
 -- plutons 104
 Metamorphic core complexes 103
 -- deposits 563
 -- metallogeny 563+
 Metamorphogenic deposits 563
 Metamorphosed Bushveld-style intrusions 584
 -- porphyry Cu 170, 171F
 Metasomatic carbonatite 470
 Metasomatism 561
 Meteor craters 58F
 Meteorite impact 56-58F
 Meteorites 57+
 Meteoritic iron 57
 Methane reductant 555
 Methods of giant's discovery 637F
 Mexico-type Ag 137+, 138F
 Mg exoskarn 168
 -- from asbestos tailings 28
 -- from sea water 615
 Microcline (metasomatic) 586F
 Micron-size Au 147+
 Microcontinent 88
 Mid-Continent Rift 438F
 Middle Ages 9
 -- metals 613
 Mine (term) 45
 -- waste 559
 Mineral Commodity Summaries 15
 Minerals Yearbook 12, 13, 15, 36
 Mining demise 615
 Minnesotaite 394
 Miogeoclinal successions 480F
 -- ores in the Cordillera 106
 Mississippi Valley-type 511, 513+, 516F, 519F, 521F
 Mn bedded carbonate 407
 -- carbonates 490
 -- grade/tonnage 56F
 -- in basinal carbonates 513
 -- in oceanic nodules, crusts 79, 80
 -- in regolith 531, 533
 -- nodules 27
 -- oxide particles 490

- oxides 490
- regolith 491, 492
- residual on plateaux 407
- Mo aplites 201
- in black shale 495
- -W skarn 205
- Modified ores 592
- MOHO 71, 72
- Molybdenum 11
- Molycorp Inc 30
- Monazite 394, 473-474
- authigenic 495
- in beach sands 484, 485
- Monolithologic breccia 187
- Monotonous schist association 565
- Monzogranite Mo 200+, 202F
- Monzodiorite porphyry-Au 96F
- Moraine Sn 107
- MORB basalts 62, 71, 72, 74, 78, 83, 88
- trace metals 60T
- Mount Isa Inlier evolution 371, 373F
- MRDS database 30
- Mudbank facies 520
- Mud volcanoes, submarine 84
- Multiple vein field 361
- Multistage ore evolution 593F
- Municipal waste 20
- Museums 38
- MVT affiliated veins 522, 523F
- global review 515T
- in reef 517
- Zn-Pb type 511, 513+, 516F, 517F, 519F
- Mylonite 585
- zones 581

- Na-alkaline Au 131
- carbonates in playa brine 548
- Native Cu 437, 438F
- Natrocarbonatite 471
- Natural disasters 645
- Nb in carbonatite 472
- residual 533, 536
- super-giants 474-477
- Nepheline 467
- syenite 11, 462-464F
- Nephelinite volcanoes 471
- "New" metals 11, 18, 19
- Ni in black shale 496
- in oceanic nodules 79, 80
- laterite 232+
- residual ores 531, 535, 536

- sulfides in basal contacts 452, 455+, 458F
- sulfides in shear 436
- sulfides in troctolite 305
- sulfides in ultramafic intrusions 454, 455
- in high-grade metamorphics 580-583, 582F
- in amphibolite 582
- in gneiss 581-583
- Ni, Cu sulfides in mafic exoskarn 435, 436F
- in plateau basalt association 434-436F
- in troctolite 452
- Ni in oceanic nodules 27
- Niobium see Nb
- Nitrates 107
- Nonconventional resources 30
- Noranda-type VMS 265-267F
- Norite 445, 449, 452, 457
- and Cu in high-grade metamorphics 579F, 580F
- Nordstrandite 26
- Noritoid 435
- No-skarn Pb-Zn replacements 216F
- No-waste mining 30
- Nuclear fission 22
- Nuggets Au 348, 349
- Numbers of giants 51
- Nyerereite 471

- Ocean floor sediments 78
- Oceanic association 227
- crust 73+, 428
- plateaux 77
- sediments 78
- spreading ridges 73-75+
- successions in orogens 233, 234F
- Offset dikes 458, 459F
- Oil shale 26, 107, 545, 546F
- Oilfield brines 522, 526, 527
- giants 39
- Old scrap 20T
- Oldest dated rocks 59
- Olympic Dam discovery 636-638
- Onaping Formation 455, 456F
- Ongeluk basalt 407
- Ooliths 483
- Oolithic ironstone 487+, 488F
- Ophiolite 74, 83
- allochthon 229, 231F

- mid-ocean 229
- suprasubduction 229
- Ore boulders in drift 107
- classifications 65, 589
- deposit (definition) 50
- district (definition) 50
- Dolomite 518
- field (definition) 50
- finding techniques 634F
- knot 45
- mylonite 580
- pegmatite 581
- shoot 50
- tonnage quotes 5
- values 40
- Orebody (definition) 50
- Organic matter 492
- Organisms 25
- Orogen 153
- Orogenic Au 331+, 332F, 339+
- in BIF 285
- global distribution 274F, 275, 276T
- in greenstones 273+, 278F, 281F, 283F
- in komatiite 260, 261F
- in metasediments 285-288F
- in syenite 285, 287F
- Orogenic belts 225
- deposits 273+
- granitoids 296+
- Sb>Au 289, 290F
- Pb-Zn 362
- Sb 349
- Orogens 295+
- Orogeny 153
- Orthogenetic ores 592
- Outokumpu Assemblage 261, 262F
- Oxidation zone 1.6 km deep 410
- Oxidic Cu 538, 539
- Oxidized skarn 210
- Sn,W,Mo,Bi,Be 323, 326F
- Ozark Uplift 517, 518

- Pallacas 107, 144, 145, 529
- Palladium 544
- Paleo-astrobleme 57, 456F, 457
- Paleo-glacials 529
- Paleokarst 523, 524F
- Paleoproterozoic ophiolite 260, 262F
- terrains 251+
- Paleoregolith 541, 542
- Paleorift 425+

- association 461F
- Paleosol 394, 541, 542
- Paleovolcanic terrains 115
- Parthenon 613
- Particulate ironstone 487+, 488F
- Paystreak, Au 347
- Pb sandstone 556, 557F, 558F
- Pb,Cu,Co in black phyllite 411
- Pb-Zn high-grade metamorphosed 568+
- hydrothermal, global distribution 364T, 365F
- mesothermal veins 358+
- in Proterozoic sedex 371-374F
- oxidation zones 214
- PGE in Alaska-Ural complexes 244
- in bronzitite pegmatoid 449, 450F
- in Kupferschiefer 501
- in layered gabbro 433
- in layered intrusions 454F
- in mafic intrusions 435, 436F
- in olivine anorthosite 454
- in pyroxenite contacts 446, 448F
- in pyroxenite layers 451, 452F
- in tailings 560
- placer 244
- Reefs (Bushveld) 448F, 450F
- resources in Bushveld 444
- Pebble dikes 216
- Pedogenic calcrete 547
- Pegmatite regolith 310
- synorogenic Cu 580
- zoning 309
- Pegmatites 305+, 306F
- synorogenic 570
- Pegmatoidal Cu ore 577, 578F
- Pelagic red clay 78
- Penetratively deformed ores 563
- Peridotite, layered 453, 454F
- Pentlandite 457, 458, 580-583
- Peralkaline rhuolite, Hg-Li-Cs-U 119
- granite 310, 311F, 312
- magmas 157
- Peraluminous leucogranite Mo 201
- rhyolite, Sn-Li-Be 118, 119
- collisional granite 300F
- granite 102, 104, 157, 323, 326F, 327
- volcanics 144, 145F
- Pericles 9, 613
- Peridotite Fe,Ni,Co in regolith 230, 232
- blocks in skarn 581-583
- Periglacial breccia 529
- Permafrost placer 348
- Perowskite 469
- Phallic porphyry Cu 158
- Philippine porphyry Cu-Au 90, 91
- Phlogopite 468
- carbonatite 474, 475F
- Phoenicians 9, 613
- Phonolite 463
- Phosphates, magmatic 468
- Phosphoria Formation 497-500, 499F
- Phosphorite 28, 32
- black shale 497, 498
- trace metals 498
- Phreatic eruptions 114
- Phreatomagmatic explosions 114
- Phyllic alteration 165
- Phyllonite 585
- Phytomining 25
- Picrite 433
- Piedmont gravels 108
- Pisolithic Mn 492, 493F
- Pitchblende 328-331
- Pitinga-type Sn 318-320, 319F
- Placer, 542
- Au 108, 346+
- types 346
- Placers, buried 543
- Plant debris 555
- Plants 26
- Plate tectonic environments 66T, 67, 69F
- and granites 67, 68T, 69F
- model 65
- Plateau basalt 434
- Platformic sequences 481F
- Platiniferous chromitite 448F
- Platinum see PGE
- Playa lakes 109
- Playas 110F, 547, 548
- Li 109
- Plumes 62
- Plutonic porphyry Cu 159
- Podiform chromite 230
- Point bar 347
- Political economy of giants 615
- risk 642
- economic factors 641
- Pollucite 309
- Polygenetic ores 592
- Polymetallic veins 358+ 362F
- Population growth 30
- Porphyry Au 96F, 136, 166, 332, 333, 334F
- Porphyry Cu 157
- architecture 158
- breccias 159+, 161, 162F, 184, 186, 187
- global distribution 182-196 181F, 196T, F, 197F
- in diatreme 188, 189F
- in geological time 180F,T
- in island arcs 90-92
- in rift setting 439
- outcrops 172
- oxidation zone 173-174F, T
- oxidic minerals 185, 186F
- Pb-Zn at fringe 129
- setting 159F
- << skarn Cu, Zn 168F
- supergene ores 173, 174F
- systems, origin 164+
- zoning 171F
- Porphyry Cu-Au, in island arcs 90-94, 92F, 93F
- and skarn 167
- Porphyry Cu-Mo and skarn 187, 188
- Porphyry deposits 157+
- Porphyry/epithermal juxtaposed 96
- Porphyry Mo 199+
- Porphyry No>Cu 200
- Porphyry Sn 143, 145, 146F
- Porphyry W-Mo 209, 210F
- Porphyry/high sulfidation overlap 91-93F, 165
- Post-industrial society 18
- Postmagmatic vein systems 302
- Post-orogenic ores 564
- Potash 25
- Potassic arc magmas 90
- alteration 164, 187, 337
- Powellite 210
- Prairie-type Au 526
- Precambrian Au,Cu,U conglomerates 386F
- granitoids 272+
- porphyry Cu-Mo 171
- stockwork Mo 204
- Pre-greenstone association 252
- Prehnite-pumpellyite alteration 434, 437, 438F

- Premetamorphic ores 563
 Preservation of ores 610
 Price of metals 12
 Product downsizing 21
 Progenitors 592
 Prograde Cu skarn 187
 -- Zn-Pb skarn 214
 Propylitic assemblage 132, 187
 Prospecting discovery 633, 634
 Proterozoic disseminated
 Cu,Au,Mo 273
 -- lithofacies 368F
 -- intracratonic basin lithofacies
 395F
 -- orogens 367+
 -- stockwork Mo 273
 -- varicolored association 378F
 Protores 27
 Province (metallogenic) 45
 Pseudoleucite 165
 Pseudosyenite (metasomatic)
 585, 586F
 Pull-apart structure 428
 Pyrite Belt 236-241
 Pyrite-enargite veins 129
 Pyrochlore 474-477, 587
 Pyrolusite 490
 Pyrophyllite 123-125
 Pyroxenite 468
 -- contact PGE deposit 446,
 448F
 -- layered 451, 452F, 453, 454F
- Quantitative maps 39
 Quartz monzonite Mo 201
 Quaternary giants 607-610
- Radioactivity, discovery 299
 Radiolarian ooze 80
 Radium 7, 18, 22
 Rank (of orebodies) 46, 50F,T
 Rapakivi 587
 Rare Earths see REE
 Rare metals pegmatite 305-309,
 306F, 307F, 308F, 309F
 Rauhaugite 471
 Reactivated Au lodes 335
 -- shears, Au 335
 Reallocated metals 12
 Reclamation costs 624
 Recycled metals 12, 19, 20, 30
 Red beds, 516F, 550F, 553
 -- Andean 118
 -- Cu 555, 556
 Redeposited bauxite 549
- Redox boundary 500-503
 -- fronts 551-555, 553F
 Red Sea Deeps 429
 Red tape 643
 Reduced skarn 210
 Reductants 551-555
 REE, Fe oxides association 474-
 475F
 -- in alkaline syenite 465-467
 -- in andean rhyolite 119
 -- in apatite 467F
 -- in carbonatite 472, 473F
 -- in Olympic Dam 418
 -- replacements 473
 -- residual 533, 536
 -- skarn 328
 -- super-giant 473-475F
 REE, Nb, Sc, Y residual on
 carbonatite 475-477
 Reef (coral) 86
 Reef package (Rand) 389, 390F
 Refabrication 20
 Refractory peridotite 74
 Regolith 528+
 -- giants in, summary 531-533T
 -- on unconformities 414
 Remobilization 571
 Replacement Pb-Zn-Ag 127,
 128F, 212+, 216F, 360+
 -- disseminated Au 147+
 -- mantos, Hg 141, 142
 -- pipes 163, 164F
 Resedimented clastics 482
 -- Mg,Fe,Ni,Co regolith 233
 -- REE,Nb,Sc regolith 476
 Reserve figures 39
 Residual disseminated Au in
 volcanics 124
 -- Mo in clay 208
 -- ores in karst 523+
 -- phosphorite 512, 513
 -- processing muds 560
 -- Sn in karst 323
 Resistate minerals 484
 Resource assessment 640
 Retrograde shears 571
 Retrograde skarn 334
 Rhodochrosite 131, 407, 490
 Rhodonite 570
 Rhyolite, andean 118
 -- U 327
 Ridge subduction 612
 Riebeckite (metasomatic) 587
 Rift basalts 428
 Rift-drift transition 428, 429F
- Rift evaporites 482
 -- lakes 544
 -- magmatism 432
 -- phase 369
 -- sequences, buried 481F, 482
 Rifted carbonate platforms 509,
 510F
 -- continental margins 430, 431F
 Rifting-initiated cycle 369, 370
 Riftogenesis, stages 426
 Rifts 425+, 427F
 -- granites 439
 -- porphyry Cu 439
 -- slightly extended 427F
 Roan Group 378-382
 Roll-type U 551-555, 553F
 Roman mining 613
 Roscoelite (alteration) 132, 136
 Rote Fäule 501
 Rotliegendes 500
 Rustenburg Layered Suite 445+
 Rutile in beach sands 484, 485
- S-type granite 102, 296
 Saddle reefs 342
 Safflorite 442
 Sag phase 369
 Saksagan Suite 402
 Salars 107, 109, 547
 Saline brines 25
 -- lakes 25, 544
 Salt diapirs 432
 -- domes 526, 527F
 Sandstone deposits 548+, 550
 -- impregnations 484
 -- Pb 556, 557F, 558F
 -- U 550-553F
 Sapolite 534F
 Sb, As, Au fault lodes 338
 Sb-Au veins 349
 Sb giants, global distribution
 354T
 Sb mantos 141, 351-354F
 Sb replacements 351-354F
 Sb super-giant 551-553
 Sc in carbonatite 476
 -- in Na-metasomatite 402
 Scandium 51
 Scapolite marble 578
 Schellenblende 517
 Scheelite, in amphibolite 583,
 584F
 -- in high-grade metamorphics
 577
 -- in metaquartzite 583

- skarn 209-212F
- skarn & Mo stockwork 209, 209
- stockwork 208
- Schistosity-conformable ores 564
- Scrap 20
- SE Asian Tin Belt 321-323
- Sea floor sulfides 27, 74, 75
 - hydrotherms 77
- Seamounts 27, 77
 - hydrotherms 84
- Sea water 22, 23, 77, 78
- Secondary metals 11, 20
 - quartzite 147, 165, 576
 - sulfides 176-179F, 185, 186F
- Sector collapse (volcano) 96
- Sedex 503F, 504F, 506F
 - barite 503-506F
 - debris flows 507
 - distal 507
 - global distribution 508T,F
 - Pb-Zn-Ag, Proterozoic 371-377, 376F
 - proximal 505
 - thrusts 506F
- Sediment-hosted Au (Carlin) 147+
- Sedimentary-exhalational 503
- Sedimentogenic literature 479
- Selenides Au,Ag 138
- Semi-mature island arcs 88
- Sericitic alteration 165
- Share of global endowment 41
- Shear-Au 338
 - Hg 222
 - Sb,Au,W 222, 223F
 - metasomatites Fe,Cu,Au 419, 585
 - zones, Au 277
- Sheeted diabase dikes 73
 - veins As,Au 333F
- Shelf 85, 481, 482
- Shoshonites in eugeoclinal orogens 245, 245F
- Shoshonitic Au-Ag setting 94-98F
 - Au-Te 131
 - porphyry Cu,Au 165
 - volcanics 89
- Siegenite 518
- Siderite 488
 - gangue 360
 - in coal 549
 - pyrite iron formation 264F
- replacements 249
- -tetrahedrite veins 219
- Silica sinter 121, 123
- Silicification (epithermal) 124, 125F, 126
- Sillimanite gneiss 568
- Simple giant 44
 - Sb-type veins 349
- Singer's terms 40
- Sinter deposits, Au 120
 - , ancient 148F
- Sites of ore occurrences 635F, 638
- Skarn, Au 333, 334
 - boron 362
 - Cu,Au,Ag 188
 - Cu-Zn 168, 214
 - REE, U 328
 - Sn,Mo,W,Bi,Be 323, 326F, 327
 - Zn-Pb 362, 363F
 - around granite cupola, Mo-W 208
 - high-grade metamorphis 577
 - complex Sn,W,Mo,Bi,Be 210
 - magnetite, Cu 188
- Slab window 102, 156
- Slope (continental) 85, 481, 482
- Smelter slag 560
- Sn-Pb-Ag sulfides 145, 146
- Sn placers 321, 322F
 - in VMS 241
 - pegmatite 308-310
 - regolith 321, 322
 - replacement in carbonate 320, 321
 - in moraine 529
 - in sedex 375-377
 - residual 532, 536
 - skarn 320, 321F
 - zoned skarn, replacement 323, 327
 - world distribution 324T, 325T, 326F
- Social risk 645
- Soda lakes 471
- Solution collapse breccia 412, 517, 518, 520
- Sooty chalcocite 176
- Sour gas 25
- Sovereign risk 642
- Sövite 471
- Spanish gold, silver mining 613
- Sperrylite 449
- Spessartite 570
- Spinifex 256
- Spodumene pegmatite 308F, 309, 310
- Spreading ridge VMS 27, 73-78, 76F
- Steenstrupine 466
- Steep structures (Okiep) 579F
- Steinmann Trinity 73
- Stibnite veins 349
- Stillwellite 328
- Stockwork Mo 199+, 208
 - global distribution 205-207 206F
 - leached cap 203
 - Mo,W,Bi 207
 - porphyry Cu 158
- Stockscheider 316
- Stone coal 26, 492
- Stratabound Au 242, 243
 - Au-As in greenstone 285-287F
 - carbonatization 282, 283F
 - silicification 152
- Strategic metals 18
- Stratovolcanoes 110
 - & ores 111T, 112F
 - porphyry Cu-Au 92
- Strike-slip displacements 84
- Strontianite 473
- Strontium 471
- Subaerial volcanism, ores 110
- Subduction 71, 72, 81F, 83, 228
 - complex 83
 - in andean margins 101, 103F, 104
 - melange 83
 - melting 153, 154
- Sublayer 57, 458F
- Submarine-exhalative 97
- Substitution 21
- Subvolcanic tonalite sill 266
- Sudbury Intrusive Complex 455, 456F
- Sulfide breccia Ni,Cu 582, 583F
 - mounds 76
- Sulfidic schist Au,Mo,Ba 288F, 289
- Sulfur 25, 511
 - from natural gas 526
 - in volcanoes 110
- Sumerians 9, 613, 614
- Super-giants 42, 51
- Supergiant oilfield 39
- Supergene enrichment 172, 185, 186

- minerals, porphyry Cu 173
- modification, porphyry Cu 171+
- modification of ores 597F
- processes 528
- sulfides 176+
- Superior-type BIF 394-403
- Suprasubduction ophiolite 86
- Sutures 106, 562F
- Suspect terranes 84
- Syenite 433
 - alkaline 462
- Syndiagenetic particles 483
- Synmetamorphic ores 564
- Synorogenic Au 339+
 - Cu 290, 291F, 292F
 - Pb-Zn 362, 363F
- Synsedimentary exhalite 484
- Syntectonic ores 564
- Synthetic gasoline 21, 615
 - nitrates 21, 615
- Synvolcanic Cu-Au 272
 - plutons 267
- Szaibelyite 578

- Ta in carbonatite 477, 478F
 - in peralkaline granite 312, 466
 - in pegmatite 308-310
- Taconite 395, 399-401, 400F
- tai index 41
- Tailings 559, 560
- Talus ores 107
- Tar sands 24, 26, 527
- Taxite 435
- Teallite 145, 146
- Technological change 21
 - ores 550
- Tectonic banding 377
- Terrace gravels 347
- Terranes, accreted 84, 85
- Terrigenous oceanic sediments 78
- Tetrahedrite-Ag 219
- Thallium 149
- Tholeiitic basalt 433, 434
- Threshold of giants 45F
- Thrust-related Hg 358, 359F
 - control (Carlin) 149+
 - and Fold belt 103
 - sheets and ores 382
 - sole breccia 382
 - parallel Au,As 338, 339F
- Thuringite 488
- Ti beach sands 484-487, 486F
 - in anorthosite 304-306F
- in perowskite 470F
- paleoplacer 485, 486F
- residual 469, 470F, 531, 534
- Tin 21
 - agreement 13
 - council 12, 13
- Titania 13, 22
- Titanite 467
- Tl enrichment 506
- Tonnage accumulation index 41, 42T
- Tonnage/grade data 36
 - units 5+
- Topaz in greisen 317
 - rhyolite 119
- Total Metallogeny 1, 2F
- Tourmaline 24, 375, 376F
 - breccia Cu 187
- Trace metals 55, 60T
- Trachyte, disseminated
 - Zr,Nb,Ta 463
- Trachytic tuff Ta,Hf,Ga 463
- Transcurrent faulting 102, 227
- Transitional crust 82
- Transported Cu oxides 173
- Transvaal Supergroup 406, 407F
- Trap (basalt) 434
- Trench 82, 102
- Troctolite 303, 304F, 452
 - PGE in 454F
- Trog und Schwelle 505
- Trona 471
- Turbidites 85
- Turbidite apron 88
 - fans 86
 - phase 369
- Turkic-type orogens 295
- Typography 21
- Tyuyamunite 551

- U collophanite 578
 - fault lodes 328-331, 330F
 - from black shale 32, 428, 495, 496, 497F
 - humate 554
 - hydrothermal remobilization from black schist 496, 497F
 - in albitite 587, 588
 - in coal 549
 - in phosphorite, 24
 - infiltrations in volcanics 108
 - in quartz conglomerate 385-394F
 - in rhyolite 120
- in rhyolite, granite cauldron 327
- leucogranite 312, 313
- metasomatites 587
- pegmatite 312, 313
- phosphates in marble 578
- residual 533
- in sea water 23
- U sandstone, global review 552T
 - infiltrations 550-555
- U skarn 328
 - sooty pitchblende in faults 414
 - in Witwatersrand conglomerate 385-391
 - in Na-metasomatites 402
- Ultramafics, trace metals 28
- Ultrametamorphic deposits 563
- Ultramylonite 587
- Unconformity 482, 541, 587
- Unconformity Uranium, 412-416F
 - and Au 415
 - As,Bi,Co,Au 420
- Unconventional metal sources 22, 24, 25T
- Undiscovered giant deposits 647
- Undepleted mantle 72
- Undervalued metals 49
- Upper continental crust trace metals 61T
- Upwelling 498, 499F
- Uraniferous lignite 108
- Uraninite 328-331, 393, 394, 412-415, 419, 585
- Uranium discovery 22
- Uranium in coal 26
- Urquhart Shale 371-374F
- Urtite 466, 457F
- U.S. Geological Survey 15

- V in black shale 495
 - in ironstone 488
 - in magnetite layers 450
 - in petroleum 24
 - in phosphorite 499
 - in tar sands 26, 527
 - in warm water phosphorite 512, 513
- Value of giant deposits 623, 624
- Vanadiferous Ti-magnetite 449
- Vanadium see V
- Variocolored sediments 550F
- Veins Pb-Zn-Ag 361, 362F

- Vein-type U 328-331, 330F
 Ventersdorp Contact Reef 389, 390F
 Ventersdorp Supergroup 388
 Vermiculite 468
 VMS deposits 230
 -- footwall stockwork 99
 -- in accretionary terranes 85
 -- in andean margins 247
 -- in back-arcs 86, 87F, 97, 98F
 -- in greenstones 264-268F
 -- in island arcs 82
 -- in orogens 235, 236F
 -- interpretation 74
 -- kuroko-type 97, 98F, 99F
 -- metamorphism 654
 -- model 74
 -- oceanic 74
 -- on seafloor 27
 -- rich in Au-Ag 243
 -- in sequentially differentiated calc-alkaline orogens 247-249F
 -- stockwork Fe,Cu,Au transition 249, 250F
 -- supergene zones 240F
 Volcanics-hosted ores 114, 115
 Volcanic landforms 110
 -- porphyry Cu 116, 158
 -- redbeds 117, 118
 Volcano sector collapse, Au 612
 Vuggy silica, Au 123-125F
- W in garnet skarn, greisen 323, 326F
 -- in playa brine 548
 Wallrock porphyry Cu 158
 Warm current phosphorite 512F, 513F
 Wars over giant deposits 614, 615
 Waste 20, 559
 Waulsortian facies 520
 Weathering-enriched carbonatite 474, 475F, 476
 Wehrlite 436
 Wessels-type Mn 407
 West Rand Group 386
 Willemite 411, 574
 Window (erosional) 150
 Witwatersrand-origin 389, 391, 607, 610
 -- Supergroup 385+, 387F
 Wolframite veins 313-315F
 World class deposits 38-40, 62
 -- thresholds 40, 41
 -- population 17
 World War I 11, 21
 -- II 18, 20, 21
 World's largest giants 51, 53F, 54F
- Young rifts 428
 Yttrium 463, 470
- Zechstein 25, 500-503
 Zincite 574
 Zinnwaldite granite 316
 Zircon beach sands 484, 485
 Zn, Mn oxides, silicates in marble 574, 575F
 -- Pb, oxidic ores 540, 541F
 -- Pb,Ag in black schist 375
 -- Pb low temperature in carbonates 513+
 -- Pb, oxidic, Proterozoic 411-412F
 -- Pb residual 532, 540
 -- Pb sulfides in marble 571, 572F, 573
 -- Pb synorogenic 375
 Zoning around porphyry Cu intrusions 158, 160F, 161Fm 164F, 168
 Zoned porphyry Cu alteration 129, 165, 187
 -- Bi,Be,Pb,Zn centers 323, 326F, 327
 Zoning, district scale 158
 Zr in alkaline intrusions 453-467
 Zr,Nb,REE,Y etc in peralkaline granite 310, 311F
 Zr,Nb,Y,Ta disseminated in trachyte 463
 Zr,REE,Nb disseminated in alkaline intrusions 462